

```
#####
#####
<a rel="license" href="http://creativecommons.org/licenses/by-nc-nd/4.0/"></a><br />This
work is licensed under a <a rel="license"
href="http://creativecommons.org/licenses/by-nc-nd/4.0/">Creative Commons
Attribution-NonCommercial-NoDerivatives 4.0 International License</a>.
#####
#####
Course Authored By:
```

```
-----
-----
K.Srinivasan
Personal website(research): https://sites.google.com/site/kuja27/
NeuronRain GitHub and SourceForge Documentation: http://neuronrain-
documentation.readthedocs.io/
-----
-----
```

```
#####
#####
```

This is a non-linearly organized, continually updated set of course notes on miscellaneous topics in Graduate/Doctoral level Computer Science and Machine Learning and supplements NeuronRain AsFer Design Notes in:

```
-----
-----
NeuronRain Enterprise Version Design Documents:
```

```
AsFer Machine Learning -
https://github.com/shrinivaasanka/asfer-github-code/blob/master/asfer-docs/
AstroInferDesign.txt
```

```
-----
NeuronRain Research Version Design Documents:
```

```
AsFer Machine Learning - https://sourceforge.net/p/asfer/code/HEAD/tree/asfer-
docs/AstroInferDesign.txt
-----
-----
```

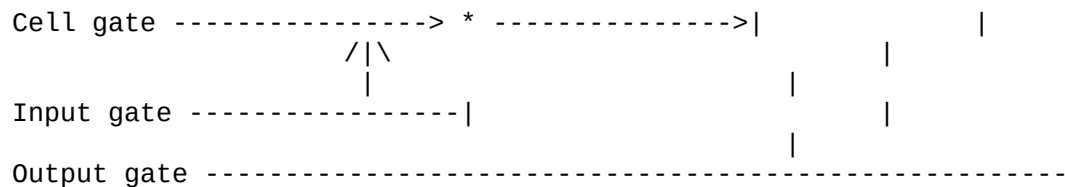
9 March 2017

```
-----
759. (THEORY and FEATURE) RNN and GRU - this section is an extended draft on
respective topics in NeuronRain AstroInfer design -
https://github.com/shrinivaasanka/asfer-github-code/blob/master/asfer-docs/
AstroInferDesign.txt
-----
```

```
Recurrent Neural Network - Long Term Short Term Memory:
-----
```

Traditional neural networks have a threshold function which outputs 1 or 0 based on a threshold. But they don't preserve state information over points in time. For example, if there is a requirement that next state depends on present state and an input, usual neural network cannot satisfy it. Recurrent Neural Networks fill this void through ability to feedback while traditional neural network is feedforward. LongTerm-ShortTerm memory Recurrent Neural Networks are defined with schematic below:

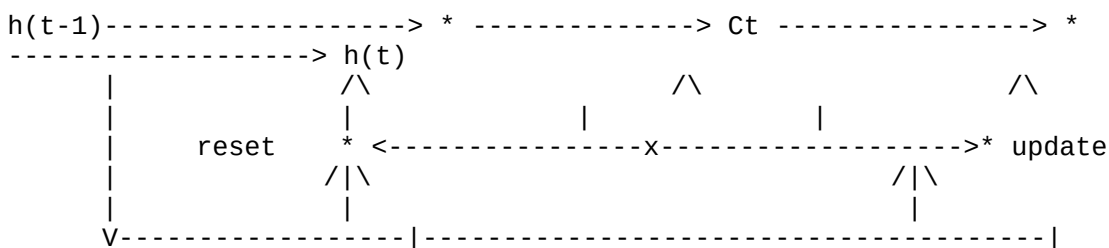
```
Forget gate -----> * <----- + -----> *
----->
|----->|
|/|\
|
|/|\
|
```



It has four gates: Forget gate, Cell gate, Input gate and Output gate and has a recurrence/feedback as shown in first line between Forget, Cell and Input gates. * is per-element product and + is per-element sum of vectors.

Recurrent Neural Network - Gated Recurrent Unit:

A slight variation of RNN LSTM diagram previously is RNN Gated Recurrent Unit (GRU). It lacks an output gate and merges the functionality of input gates into two gates - reset and update - as drawn in schematic below:



with equations:

```

ut = sigmoid(Vu*xt + Wu*h(t-1) + bu)
rt = sigmoid(Vr*xt + Wr*h(t-1) + br)
Ct = tanh(Vc*xt + Wc*(h(t-1) * rt))
ht = (1-ut)*Ct + ut*h(t-1)

```

where ut = update gate,
rt = reset gate,
Ct = cell gate
ht = state at time t
Vu,Vr,Vc,Wu,Wr,Wc are weight vectors.

Both above have been implemented in:

https://github.com/shrinivaasanka/asfer-github-code/blob/master/python-src/DeepLearning_LSTMRecurrentNeuralNetwork.py
https://github.com/shrinivaasanka/asfer-github-code/blob/master/python-src/DeepLearning_GRURecurrentNeuralNetwork.py

Mathematical Puzzles of Sam Loyd (selected and edited by Martin Gardner) -
Puzzle 18 - What is the most economical form of a tank
designed to hold 1000 cubic feet? - 26 January 2018

A Plumber wanted to estimate the lowest possible cost of a copper tank to hold 1000 cubic feet. Copper costs \$1 per square foot. Problem is to determine most economical dimensions of the rectangular tank of capacity 1000 cubic feet. Trivial solution of 10 feet * 10 feet * 10 feet = 1000 cubic feet tank costs \$500 of copper surface (100 in bottom + 4*100 in sides). Another solution which costs less than \$500 for copper surfacing is expected.

Plumber's problem has applications in packing/knapsack algorithms which minimize the cost of packing items in least volume. This is also equivalent to storing set of 1000 elements in a 3 dimensional array (cube) subject to minimizing the objective function $xy + 2z(x+y)$ and constraint $xyz =$

1000 for array indices x,y,z.

This problem can be cast into a (Multi)Linear Program formulation - sums of products

Let l,b,h be the length,breadth and height of the tank.

The objective cost function for copper plating the surface to be minimized is:

$$l*b + 2*h*l + 2*h*b = \text{cost}$$

subject to constraint:

$$l*b*h = 1000$$

Objective function can be rewritten as:

$$1000/h + 2h(l + b) = \text{cost}$$

Solving multilinear programs is non-trivial requiring reformulation and linearization creating a new LP(RL algorithms).

1. (l+b) is a constant:

If (l+b) = sum of sides of rectangles is fixed to be a constant elementary calculus can solve this:

first derivative of cost function is equated to zero:

$$d(\text{cost})/dh = -1000/h^2 + 2(l+b) = 0$$

$$2(l+b) = 1000/h^2$$

$$h^2 = 1000/[2(l+b)]$$

$$h = 22.36068/\sqrt{l+b}$$

$$[\Rightarrow lbh = lb*22.36068/\sqrt{l+b} = 1000, lb/\sqrt{l+b} = 1000/22.36068 = 44.72]$$

Second derivative of cost function is positive, implying a local minima. Thus if height of the tank h is inversely related to square root of sum of length and breadth of bottom rectangle as $h = 22.36/\sqrt{l+b}$, cost of copper plating is minimized. If bottom is a square, $l = b$ and $h = 22.36/(1.414*\sqrt{l}) = 15.811/\sqrt{l}$.

$$\Rightarrow lbh = ll*15.811/\sqrt{l} = 15.811*l*\sqrt{l} = 1000$$

$$\Rightarrow l^{1.5} = 1000/15.811 = 63.247$$

$$\Rightarrow 1.5 \log l = \log 63.247$$

$$\Rightarrow l = 15.874$$

$$\Rightarrow h = 15.811/\sqrt{15.874} = 3.968$$

Dimensions of the tank of least copper plating cost by local minima = 15.874 * 15.874 * 3.968

Cost = 500 which is not less than 10 * 10 * 10.

2. Bottom is a square and is a function of h:

Bottom is square : $l=b=kh$

$$\text{Cost function: } kh*kh + 2h*kh + 2h*kh = k^2*h^2 + 4k*h^2$$

$$\text{Cost} = (k^2 + 4k) * h^2$$

$$\text{Volume} = lbh = kh*kh*h = k^2*h^3 = 1000$$

$$\Rightarrow h^3 = 1000/(k^2)$$

$$\text{Cost} = (k^2 + 4k) * (1000)^{0.66}/k^{1.33} = (k^2 + 4k)/k^{1.33} * 95.49926$$

$$\text{Cost} = (k^{0.66} + 4k^{(-0.33)}) * 95.49926$$

$$d(\text{Cost})/dk = 0.66*k^{(-0.33)} - 1.33*k^{(-1.33)} = 0$$

$$\Rightarrow \text{minima at } k = 2.$$

Dimensions are 2h*2h*h and

$$\text{Cost is } 12h^2 = 476.21 \text{ for } h=6.2966$$

Book Solution:

 If bottom is a square of side = 2h for height h, economical cost is attained.
 $\Rightarrow 2h \cdot 2h \cdot h = 4h^3 = 1000$
 $\Rightarrow h = 6.2996$
 $\text{Cost} = 4h^2 + 2h(4h) = 12h^2 = 12 \cdot (6.2996)^2 = 476.21$

Reference:

 Mathematical Puzzles of SAM LOYD - Selected and Edited by MARTIN GARDNER

 Catalan Numbers - How many squares and lattice paths are in a grid e.g 4 * 4 -
 Puzzle 142 - Puzzles To Puzzle You -
 Shakuntala Devi - 26 January 2018

 In a grid of 4 * 4, number of possible squares are obtained by moving a sliding
 2 dimensional square window left-right, top-down as in
 algorithm below:

```

    for square sliding window size w*w
    {
        slide window top-down
        {
            slide window left-right
            number_of_squares += 1
        }
        w = w+1
    }
  
```

Sliding window square increases in size from 1*1 to 4*4.

Number of squares of size 1*1 = 16 = 4*4
 Number of squares of size 2*2 = 9 = 3*3
 Number of squares of size 3*3 = 4 = 2*2
 Number of squares of size 4*4 = 1 = 1*1

 Total = 30

Generic series is $= 1 + 2^2 + 3^2 + \dots + n^2$

Number of lattice paths in the grid which lead from bottom left to top right of
 the grid is the Catalan Number $= \frac{1}{(n+1)} \cdot 2nCn$ which is
 same as number of Dyck words of the form $XXYXX, \dots$ number of possible rooted
 binary trees of node size n and number of possible balanced
 parenthesizations of an infix arithmetic expression. Catalan numbers are
 ubiquitous in combinatorial algorithms involving recursions and
 self-similarity. Catalan number is also the number of random walks in the grid
 graph.

Most celebrated result involving Catalan numbers is the Bertrand Ballot Theorem:
 In an election of two candidates A and B, if A receives
 p votes and B receives q votes, $p > q$, what is the probability A is strictly
 ahead of B throughout counting? This problem reduces to counting
 dyck paths in the grid (time versus votes). Ballot Theorem applies to Streaming
 binary datasets and gives the probability of 1s dominating the stream if 1s
 outnumber 0s and vice versa.

Reference:

 Puzzles To Puzzle You - Shakuntala Devi

 Binary Search of a sorted array containing gaps - 6 February 2018

Q: Usual binary searches are made on arrays of contiguous sorted elements. How can binary search be made to work if the array has gaps/holes and yet the contents are in sorted order? E.g Array 12, 33, 44, -, -, 56, -, -, 66, -, -, 88, 99, -, -, 123 is sorted ascending but has gaps.

A1: One possible solution is to fill the gaps with placeholder numbers or replicate the integers in hole boundaries to fill the gap. Previous example array is filled as 12, 33, 44, 44, 44, 56, 56, 66, 66, 66, 66, 88, 99, 99, 99, 123.

A2: Other possibility is to fill the gaps with an arithmetic progression on difference of the integers on the boundaries. Previous example array is filled as 12, 33, 44, 48, 52, 56, 61, 66, ...

A3: Filling is necessary because to choose the subtree of search, an integer is necessary. Non-filling solution has to branch off to a subtree based on some other meta data on the gaps. Alternative: when a "-" is found, scan the array in one direction till an integer appears and branch off. This is similar to open addressing in hash tables. But this linear scan increases the amortized binary search cost from $O(\log N)$ to something higher. But filling the gaps by placeholders or arithmetic progressions is also linear and makes binary search superlogarithmic.

This problem has applications in splitting a single huge sorted array into multiple smaller arrays, distributed geographically but logically mapped to virtual memory pages in single address space, and searching them.

842. (THEORY and FEATURE) Computational Geometric Factorization and Planar Point Location, Wavelet Trees, Sublinear Multiple String Concatenation - related to all sections on String analytics and Planar Factor Point Location by Wavelet Trees - 8 February 2018, 18 July 2020

Q: Concatenation of multiple strings is trivially doable in $O(N)$. Can N strings be concatenated in sublinear time?

A: Subject to certain assumptions following algorithm does sublinear multiple string concatenation:

Let the number of strings be N each of length l . Each string is fingerprinted/compressed to length $\log N$ by a standard algorithm e.g Rabin string fingerprint which computes a polynomial of degree l over Galois Field $GF(2)$ and divides this by an irreducible polynomial of degree $\log N$ over $GF(2)$ to create a fingerprint of $\log N$ -bit length.

Create a matrix of $\log N * N$ (transpose) which has $\log N$ rows and as many columns as number of strings. Entries of this matrix are the bits of string fingerprint hashes. This transformation converts N strings of length l to $\log N$ strings of length N . Hashes are stored as Rope strings to facilitate $\log N$ time pairwise computation. These $\log N$ strings are concatenated as a binary tree bottom-up and each pairwise concatenation is $O(\log N)$. Following series sums up the runtime:

$$\begin{aligned} & \log N * (\log N / 2 + \log N / 4 + \log N / 8 + \log N / 16 + \dots) \\ &= \log N * \log N * 2 \\ &= 2(\log N)^2 \end{aligned}$$

This indirectly concatenates N strings in $O(\log N * \log N)$ time. But it messes up with original string. This requires slight modification to pairwise Rope string concatenation routine. Before concatenation hash has to be reverse engineered (Rabin fingerprint polynomials have to be stored) to unicode string and location in the resultant single concatenation has to be ingredient of this routine.

Fingerprinting is not a necessity. Without fingerprint, previous matrix is $l * N$ (l strings of length N) and the concatenation tree has following runtime geometric recurrence:

$$\log N * (l / 2 + l / 4 + l / 8 + l / 16 + \dots)$$

[because each internal node of concatenation tree needs $O(\log N)$ time for 2
 Rope string concatenation]
 $= \log N * 2l$
 $= 2 * l * \log N$

This runtime is sublinear if:
 $2 * l * \log N < N$
 length of each string = $l < N / (2 * \log N)$

Example:

 Set of 5 strings of length 4:

aaaa
 bbbb
 cccc
 dddd
 eeee

is transformed to transpose matrix of 4 strings of length 5:

abcde
 abcde
 abcde
 abcde

Rope representation of these 4 strings are 4 binary trees. Rope concatenation routine has to be changed to write the literals of new string in correct locations in the final concatenation e.g abcde + abcde = abcdeabcde has to be surgically mapped to aa--bb--cc--dd--ee--. Rope insertion is also $O(\log N)$. This might require storing index information for each literal in original set of strings.

Following is an example for the changed Rope concatenation by storing indices of matrix entries for abcde and abcde:

a(1,1)b(2,1)c(3,1)d(4,1)e(5,1)
 a(1,2)b(2,2)c(3,2)d(4,2)e(5,2)

In final concatenation, new indices for previous literals are $(\text{length_of_string} * (i-1) + j)$. Rope concatenation is just $O(1)$ for merging two trees as subtrees of a new root. Only updating sum of left subtree leaf weights is $O(\log N)$. Storing matrix index information multiplies the string length by 5 (length of "(i,j)") which is a constant multiple and string lengths remain $O(N)$.

Final concatenated string is stored as matrix in sublinear time $2 * l * \log N$:

a(1,1)b(2,1)c(3,1)d(4,1)e(5,1)
 a(1,2)b(2,2)c(3,2)d(4,2)e(5,2)
 a(1,3)b(2,3)c(3,3)d(4,3)e(5,3)
 a(1,4)b(2,4)c(3,4)d(4,4)e(5,4)

For example, accessing 10th element in this concatenation is $O(\text{length_of_string})$ because (i,j) have to be found iteratively for all values of l

(length_of_string):
 $l * (i-1) + j = 10$
 $4 * (i-1) + j = 10$
 $i = (10-j)/4 + 1$ and $j=1,2,3,4$

Thus total time to access an element in concatenation = $2 * l * \log N + l$ which is sublinear if:

$l * (2 \log N + 1) < N$
 $\Rightarrow l < N / (2 \log N + 1)$ which is a tighter upperbound assumption for length of strings, than previous $N / 2 \log N$.

If each string is compressed as burrows-wheeler transform, columns in concatenation matrix are compressed strings and l is reduced by compression ratio. If N strings in the concatenation can be represented as N Wavelet trees in compressed format (runlength encoding etc.), each column in previous concatenation matrix is a wavelet tree and access()/select()/rank() of a column are logarithmic time. Rectified hyperbolic arc in computational geometric factorization could be a huge string stored in wavelet trees and factor points

have to be located by rank() and select() queries. Fragments of Rectified hyperbolic arc segments in the vicinity of approximate factors found by number theoretic ray queries could be concatenated efficiently in sublogarithmic time to lessen the length of the relevant rectified hyperbolic arc string stored in wavelet tree which has to be searched for factor points because individually searching each fragment would require as many wavelet trees as number of factors. Sublinear string concatenation is considerably useful for text analytics problems as well involving huge set of strings (e.g. Bioinformatics)

References:

 842.1. Rope Strings - <http://citeseerx.ist.psu.edu/viewdoc/download?doi=10.1.1.14.9450&rep=rep1&type=pdf> - [hans-j. boehm, russ atkinson and michael plass, Xerox PARC, 3333 Coyote Hill Rd., Palo Alto, CA 94304, U.S.A.]
 842.2. Rabin-Karp String Fingerprinting by Random polynomials - [Michael O.Rabin] - <http://www.xmailserver.org/rabin.pdf>
 842.3. Myriad Virtues of Wavelet Trees - Pruned Wavelet Tree of Compressed Strings - [Paolo Ferragina, Raffaele Giancarlo, Giovanni Manzini] - <http://www.ittc.ku.edu/~jsv/Papers/FGM09.wavelettrees.pdf>

 1209. (THEORY) Computational Geometry - Analytics of Massive Spatial Ordered LIFO Datastructures - How would you move Mount Fuji? - 11 February 2018 - related to all sections on Computational Geometry, Point Location, Computer Graphics (Face and Handwriting Recognition, Mesh Deformation), Computational Geometric Factorization

 This problem has parallels in moving a huge block of solid which can only be accessed in LIFO. Comparing with moving block of memory which can be randomly accessed, this problem is non-trivial. Moving mount which is a 3D solid trivially involves cutting it into equal sized cubes and reconstructing the mount in another location by moving the cubes. This is LIFO operation requiring an intermediate stack. Following mountain is moved by an intermediate stack:

1 2	6	2
3 4 ---	4 ---	4
5 6	2	6
5 ---	1 2	
3	3 4	
1	5 6	

Previous move is $O(\text{Volume_of_mount})$. Towers of Hanoi (Towers of Brahma in Kashi Vishwanath temple) problem is akin to this and requires exponential number of moves. For 64 disks of Towers of Brahma, this requires $2^{64} - 1$ moves which is legendary lifetime of universe (1 second per move translates to 585 billion years). Non-trivial requirement in this problem is no disk should be on smaller disk. Moving mount Fuji of height h sliced as horizontal disks instead of cubes is exactly Tower of Hanoi problem of time $O(2^h - 1)$. Most massive datasets in Computational Geometry and Computer Graphics are 3-dimensional quadrilateral meshes of object shapes or stored in k-d tree (Bentley) binary space partitioning datastructures and might have often to be displaced in storage preserving sorted LIFO structure (a k-d tree in massive backend) which emulates Towers of Hanoi algorithm where each level of k-d tree is a disk of decreasing radius from leaf to root. GIS Applications involve point location queries which could be answered in polylogarithmic time by PRAM-MapReduce-BulkSynchronousParallel construction of k-d trees. Integer Factorization by Computational Geometric Planar Point location queries on rasterized hyperbolic arc could be answered by 2-dimensional k-d trees constructed in polylogarithmic time.

Reference:

 1209.1 Towers of Brahma - https://en.wikipedia.org/wiki/Tower_of_Hanoi

1209.2 Parallel Algorithms for Constructing Range and Nearest-Neighbor Searching Data Structures - k-d trees constructed in parallel by MPC and MapReduce - PODS 2016 - [Pankaj K. Agarwal, Kyle Fox, Kamesh Munagala, Abhinandan Nath] - https://users.cs.duke.edu/~abhinath/publications/kd_tree.pdf - "... We present the first provably efficient algorithms to compute, store, and query data structures for range queries and approximate nearest neighbor queries in a popular parallel computing abstraction that captures the salient features of MapReduce and other massively parallel communication (MPC) models. In particular, we describe algorithms for kd-trees, range trees, and BBD-trees that only require $O(1)$ rounds of communication ..."

1209.3 Is there a relation between Ubiquitous Catalan numbers and Towers of Hanoi - an open problem - A Surreptitious Sequence: Catalan numbers - <https://www.maa.org/meetings/calendar-events/a-surreptitious-sequence-the-catalan-numbers>

 843. (THEORY) Social networks, Bipartite and General Graph Maximum Matching, Permanent, Boolean majority, Ramsey coloring - Number of Perfect (Mis)Matchings - Hat Puzzle - 17 February 2018, 18 July 2020 - related to 14, 801

There are N people in a congregation and they have to choose matching hat for each. But they end up choosing a non-matching hat at random. What is the probability of everyone choosing a non-matching hat?

This problem can be formulated as Bipartite Matching in Bipartite Graph - Set of vertices of people and Set of Hats forming the bipartisan. Each choice corresponds to an edge in this graph. Usual problem of perfect matching tries to find edges between these sets which create a bijection. Hat problem goes further beyond this and tries to match the index of the vertices too. For example:

```
p1 p2 p3
1 2 3
1 3 2
2 1 3
2 3 1
3 1 2
3 2 1
```

is the set of permutations of persons p_1, p_2, p_3 choosing the numbered hats 1,2,3. Non-matching choices are:

```
p1 p2 p3
2 3 1
3 1 2
```

in which everyone has a mismatch. Counting the number of mismatches has the following algorithm:

```
for each person
{
    remove permutations which match the person's index from set of all
permutations
}
```

In previous example following are the iteratively curtailed set of string permutations:

```
person3:
1 3 2
2 3 1
3 1 2
3 2 1
person2:
1 3 2
2 3 1
3 1 2
person1:
```



```

2 3 1
3 1 2

```

An approximate recurrence for perfect mismatching (this is an alternative to Solution in reference):

$$[nP_n - nP_n/n] - \text{Sigma}_{m=2_to_n}[nP_n/n - (n-m)P(n-m)]$$

for $n=\text{number_of_hats/persons}$, $m=\text{number of hats/persons not yet chosen}$. Intuition for this recurrence is obvious:

- Remove all strings ending with person index for p_n .
- for all person indices m less than n , remove strings having m in index m minus set of all permuted strings ending with suffix $(m, (m+1), \dots, (n))$ already removed

Contrasting this with Mulmuley-Vazirani-Vazirani Theorem for number of perfect matchings by Isolation Lemma in randomized parallel polylog time, hat puzzle estimates Perfect Mismatches in Bipartite Graphs. Perfect matching in Bipartite graph is equal to Permanent of its incidence matrix. In Group Theoretic terms, previous number of perfect matchings is the number of permutations of cycle 6 in Symmetric Group S_6 i.e each element in a permutation is mapped to a different element and all elements are moved.

Finding perfect mismatches has applications to majority voting in Social Networks - by replacing indices of hats by candidate indices. Each voter has to find a mismatching voter peer (who has voted differently). In previous hat puzzle, p_1, p_2 and p_3 are voters who have voted to candidates 1,2,3 respectively and each of them need to find a mismatching candidate index (hat):

```

p1 p2 p3
2 3 1
3 1 2

```

An example of maximum (mis)match in a complete social network graph of 5 vertices (adjacency list) which are two colored (bipartisan) while earlier example is tripartisan. It is both a maximum match (number of edges having disjoint vertices is maximized) and a mismatch (because each pair of voter vertices in matching are complementarily 2-colored by candidate index 0-1):

```

v1 - v2,v3,v4,v5
v2 - v1,v3,v4,v5
v3 - v2,v1,v4,v5
v4 - v2,v3,v1,v5
v5 - v2,v3,v4,v1

```

One of the Maximum (mis)matchings is:

```

v1 - v3, v2 - v4

```

leaving v_5 unmatched. v_1, v_2, v_5 are colored red (voters of red) while v_3, v_4 are colored blue (voters of blue). Thus party red is the winner.

References:

-
- 843.1 Puzzle 113 and its Solution Recurrence (tends to $1/e$ for large n) - Mathematical Puzzles of SAM LOYD - Selected and Edited by MARTIN GARDNER
 - 843.2 The Art Of Computer Programming - Combinatorial Algorithms - Volume 4a - [Don Knuth] - Section 7.2.1.2 - Generating All Permutations - Reverse Colex Order, Sims table for succinct representation of Symmetric Group elements.
 - 843.3 Mulmuley-Vazirani-Vazirani Theorem and Perfect matchings - Theorem 5.5 and Theorem 5.6 (Isolation Lemma) - <https://courses.cs.washington.edu/courses/cse521/16sp/521-lecture-5.pdf>
 - 843.4 Number of Perfect matchings in Bipartite graph = Permanent of Incidence matrix - Section 2 - https://lbgf.fr/~sereni/Lectures/GC_Spring09/gc09_4.pdf
-

1210. (THEORY and FEATURE) CNF 3SAT Least Squares Approximate Solver - Epsilon Bias Generator for randomly chosen clauses of CNFSAT - Least Squares solution of 3SAT Random matrices of the form $AX=B$ - Creating Biased Coin from Fair Coin - 27

February 2018 - related to all sections on P Versus NP, Hardness Amplification, CNF 3SAT approximate solver

Q: Fair coin of Head and Tail has probability of 1/2 for either turning up. How can an unfair coin be created from fair coin?

A: 1) One possible solution is to have set of fair coins and tossing them all simultaneously. Return 1 if a regular expression occurs in the streak else 0. This would be unfair because percentage of regex matches outnumber percentage of regex mismatches and probability of unfairness follows. For example, from a set of 3 fair coins tossed simultaneously (0 for Head and 1 for Tail):

000
001
010
011
100
101
110
111

number of streaks matching regex 11 are 011,110,111 which is probability 3/8. This creates an unfair randomness bias and set of streaks matching regex correspond to 1 and rest are 0 in the unfair coin. $\Pr(\text{streaks having } 11=1) = 3/8$ and $\Pr(\text{streaks not having } 11=0) = 5/8$. This is a very primitive epsilon bias generator.

2) Another solution which expands a uniformly chosen permutation array by replicating an extra skew variable and all but skew variable have a biased probability of choice has been implemented in NeuronRain AsFer (<https://github.com/shrinivaasanka/asfer-github-code/blob/master/python-src/EpsilonBiasNonUniformChoice.py>) and is used in generating random 3SAT instances for SAT Solver -

<https://github.com/shrinivaasanka/asfer-github-code/blob/master/python-src/CNFSATSolver.py>. This is based on creating a Random Matrix per random 3SAT, computing Expected average per literal probability and is different from the standard Survey Propagation Message Passing Algorithm which represents SAT as a factor graph - <https://arxiv.org/pdf/cs/0212002.pdf> - graph having 2 types of vertices for variables and clauses and edges are between variables and clauses having variables - message passing belief propagation of potentials of a variable taking value 1 or 0.

Print the Nth element of a Fibonacci Sequence - 12 March 2018, 21 March 2018

Trivial solution uses the recurrence $f(n) = f(n-1) + f(n-2)$ and $f(0)=f(1)=1$ and is exponential. Assuming Memoization/Cacheing of results, $f(n-2)$ and $f(n-1)$ can be memoized to compute $f(n)$. Mathematically, Nth Fibonacci number is expressed in terms of Golden Ratio $\Phi = (1 + \sqrt{5})/2$ as:

$$f(n) = (\Phi^n - (1-\Phi)^n) / \sqrt{5}$$

which is based on definition of Golden Ratio = $f(n+1)/f(n)$ for large n

Related fibonacci recurrence is the problem of finding number of 1s in set of all n -bit strings. Number of 1s or 0s in set of all n -bit strings is denoted by the recurrence:

$$f(n) = 2 * f(n-1) + 2^{(n-1)}$$

Expanding the recurrence recursively creates a geometric series summation which gives the Nth element in sequence:

$$f(n) = [2^{n-1} + 2 + 2^2 + 2^3 + \dots + 2^{(n-1)}]$$

Probability of finding 1s or 0s in set of all n -bit strings = $[2 * f(n-1) + 2^{(n-1)}] / n * 2^n = 0.5$

This recurrence is quite ubiquitous in problems involving uniform distribution

e.g number of positive/negative votes in voting patterns, number of Heads/Tails in Bernoulli Coin Toss Streaks etc.,.It has been mentioned in the context of 2-coloring/Complementation in <https://github.com/shrinivaasanka/asfer-github-code/blob/master/asfer-docs/AstroInferDesign.txt> .

760. (THEORY and FEATURE) Newton-Raphson approximate factoring - 6 April 2018 - this section is an extended draft on respective topics in NeuronRain AstroInfer design - <https://github.com/shrinivaasanka/asfer-github-code/blob/master/asfer-docs/AstroInferDesign.txt>

<https://kuja27.blogspot.in/2018/04/grafit-course-material-newton-raphson.html>

References:

1. <http://www.math.lsa.umich.edu/~lagarias/TALK-SLIDES/dioph-cplx-icerm2011aug.pdf> - Binary Quadratic Diophantine Equations (BQDE) and Factorization are equivalent. BQDE is known to be in NP(Succinct Certificates for Solutions to BQDE). If BQDE is in P, Factorization is in P. Computational Geometric NC algorithm for Factorization probably implies BQDE is in P (probably because implication is in opposite direction).

761. (THEORY and FEATURE) Chomsky Sentences - 6 April 2018 - this section is an extended draft on respective topics in NeuronRain AstroInfer design - <https://github.com/shrinivaasanka/asfer-github-code/blob/master/asfer-docs/AstroInferDesign.txt>

<https://kuja27.blogspot.in/2018/04/grafit-course-material-chomsky.html>

750. (THEORY and FEATURE) Money-Changing Problem and minimum partition - 6 May 2018, 9 May 2018, 18 February 2020 - this section is an extended theory draft on set partitions, Neuro academic-use perfect forward fictitious cryptocurrency in NeuronRain, optimal denomination and coin problems among other topics in NeuronRain AstroInfer Design - <https://github.com/shrinivaasanka/asfer-github-code/blob/master/asfer-docs/AstroInferDesign.txt>

Q: How can all integers be generated as sum of elements of a minimum sized set (or) What are the least number of denominations for a currency to sum up to all possible values of money?

A: Money Changing Problem or Coin Problem is an NP-hard problem (strong-NP or weak-NP depending on encoding) and is a variant of Integer Partition Problem. Most currencies use 1-2-5 series (and 10^x multiples of 1,2,5). Linear combinations of multiples of 1,2,5 can create all possible values minimizing the number of coins/bills e.g 2950 neuros (fictitious currency in NeuronRain) can be written as $2950 = 2*1000 + 1*500 + 2*200 + 1*50$ and only 6 notes/coins are sufficient. There is a polynomial time Greedy algorithm for this as below (but exponential in number of bits):

```
Sort the denominations descending (1-2-5 series and multiples)
while (value != sum)
{
    Choose the largest possible currency denomination remaining (ci)
from sorted denominations
    subtract largest multiple m of it from value (value = value - ci*m)
    coins[ci] = coins[ci] + m
}
```

This algorithm also maps the partition to a hash table of optimum size - if each currency is assigned a serial number and denominations are keys, each per-key bucket is a chain of serial numbers for that denomination. In previous example, 2950 is mapped to hash table as below for serial numbers s1, s2, ..., s6 and denominations 1000, 500, 200, 50:

```

1000 - s1, s2
500 - s3
200 - s4, s5
50 - s6

```

This algorithm solves the linear diophantine equation $1 \cdot \exp(10) \cdot x_1 + 2 \cdot \exp(10) \cdot x_2 + 5 \cdot \exp(10) \cdot x_3 = N$ and also creates an exact cover/partition of the currencies represented by some diophantine.

Products of Other Integers - 22 May 2018

Q: Find an efficient algorithm to find the product of all other integers excluding an element or elements in an array. Naive algorithm for excluding one element is $O(N)$. For example, array [2,3,7,5,6] is multiplied to find product of all : $2 \cdot 3 \cdot 7 \cdot 5 \cdot 6 = 1260$ and array of products of all other integers is found by iterated division per element : [1260/2, 1260/3, 1260/7, 1260/5, 1260/6]. Generalizing this to all possible subset exclusions is non-trivial.

A: Following optimization is a way out. Downward closure subset product computations are cached in hash table at the outset as below by traversing array :

```

(2,3) - 6
(3,7) - 21
(7,5) - 35
(5,6) - 30
(2,3,7) - 42
(3,7,5) - 105
(7,5,6) - 210
(2,3,7,5) - 210
(3,7,5,6) - 630
(2,3,7,5,6) - 1260

```

This precomputation is $O(N \cdot N)$ and done only once as prerequisite. This does not compute $2^N = 2^5 = 32$ subsets but only $(N-1 + N-2 + N-3 =) 9$ subsets.

For excluding subset {3,5} naive algorithm has to find product of set {3,5} or set difference {2,7,6} and compute the product 84 by division of 1260 which is $O(N)$.

Algorithm based on previous lookup table:

1. For a subset X to exclude, find the maximum overlapping subset of minimum size S in the lookup table i.e X intersection S is maximum but S has smallest possible size.
2. Divide the product for S by the product for set difference of X with S to get product Z. (This could be recursive lookup for set difference in the previous cache)
3. Divide the product lookedup for all elements by Z for product of other integers

E.g 1. for excluding X={3,5}, lookup of the table results in S={3,7,5} which has maximum overlap with {3,5} but of smallest size ({2,3,7,5} also overlaps but is of larger size). Dividing the product lookedup for {3,7,5}=105 by set difference 7 with {3,5} yields Z=15. Finally, dividing product of all elements 1260 by 15 =

$$84 = 2 \cdot 7 \cdot 6.$$

E.g 2. for excluding $X=\{3,6\}$, lookup of the table results in $S=\{3,7,5,6\}$ which has maximum overlap for $\{3,6\}$. Dividing the product lookup for $\{3,7,5,6\}=630$ by recursive lookup for set difference $\{7,5\}=35$ yields $630/35=18$. Final exclusion is $1260/18 = 70 = 2 \cdot 5 \cdot 7$

This algorithm is subset oblivious and is a slight improvement over brute-force multiplication of set or set difference because of cached subset products and is sublinear mostly. Previous examples required only 2 divisions whereas brute-force would need 3 multiplications assuming lookups are $O(1)$. Cacheing has benefits in large arrays (when number of elements to be excluded are almost $O(N)$) for reducing number of multiplications.

 751. (THEORY and FEATURE) OS Scheduling and Hashing Dynamic Sets - 24 May 2018, 31 October 2018, 11 March 2019, 8 October 2019, 6 November 2019, 18 February 2020, 1 May 2020, 5 May 2020, 2,3,4 June 2020, 30 July 2020, 1 January 2021, 21 September 2021 - related to all sections on Set partitions, Computational geometry, Program analysis/Software analytics/Scheduler Analytics among other topics in NeuronRain Theory Drafts

Q: How can sets of elements which are dynamically modified at runtime be hashed by tabulation? E.g set of clockticks remaining per process in an OS scheduler for 15 processes is [23,45,12,44,55,14] at time $t=1$. This set is mapped to processes by hash table:

```

23 - p1,p2,p3
45 - p4,p5,p6,p7
12 - p8,p9
44 - p10
55 - p11,p12,p13
14 - p14,p15

```

which is a snapshot at time $t=0$. As timer ticks to $t=1$, previous hash table keys for remaining clockticks have to be decremented as:

```

22 - p1,p2,p3
44 - p4,p5,p6,p7
11 - p8,p9
43 - p10
54 - p11,p12,p13
13 - p14,p15

```

and new processes p_{16}, p_{17}, p_{18} are added at time $t=2$ with remaining timeslice clockticks 35,21,53 expanding the table to:

```

21 - p1,p2,p3,p17
43 - p4,p5,p6,p7
10 - p8,p9
42 - p10
53 - p11,p12,p13,p18
12 - p14,p15
35 - p16

```

Other clockticks are decremented based on timer. When a clocktick reaches 0, the queue of processes for it is removed.

A: Usually hash table keys are static not allowing dynamism. This requires an overloading/overriding of `hash_code()` and `equals()` functions programmatically in the respective implementation language which simulate equality of two keys so that value is appended to the correct queue bucket. Problem is how to lookup changing keys decremented by timer thread. An example `equals()` function is : `key_clockticks1 - timerticks1 == key_clockticks2 - timerticks2`. Rewriting the table:

```

23-2 - p1,p2,p3,p17

```

```

45-2 - p4, p5, p6, p7
12-2 - p8, p9
44-2 - p10
55-2 - p11, p12, p13, p18
14-2 - p14, p15
35 - p16

```

and `hash_code()` for a key is `key_clockticks - timerticks`. For example to lookup process p6, `hash_code()` returns $45-2=43$ at time $t=2$ re-routing to bucket for 43 instead of 45 at time $t=0$. Similarly two processes p_i and p_j of time slices 14 and 12 but having elapsed timerticks 4 and 2 have equal hashcodes - $14-4 = 12-2 = 10$ - p_i is older than p_j and p_j is enqueued in scheduler 2 ticks after p_i when $14-2 = 12-0 = 12$. Therefore both p_i and p_j are in same clocktick queue for 10.

When implemented as LSH partition, clockticks-to-processes map is isomorphic to some random integer partition of n (number of processes) and both n and partition of n oscillate dynamically based on clockticks. Mining patterns in streaming dataset of clockticks-to-processes maps is an indicator of performance of the system. Each clockticks-to-processes dictionary can be represented as a matrix:

```

c1 p11 p12 ... p1m
c2 p21 p22 ... p2m
...
cn pn1 pn2 ... pnm

```

c_i are clockticks and $p(i,k)$ are processes having c_i clockticks remaining before being swapped out of scheduler. Because of matrix representation each LSH partition is a graph too (previous matrix is its adjacency). Frequent subgraph mining algorithms can mine patterns in the clockticks-to-processes dictionaries. If the dictionary is string encoded, string search algorithms - multiple alignment, longest common subsequence etc., - can be applied for pattern mining. These elicited patterns are samples of how system behaves - number of processes consuming most clockticks, average load etc.,

Adjacency matrix for previous Survival Index Timeout Separate Chaining hashtable graph has edges of the form: `<time_to_live_clockticks> -> <process_id>` and this graph is dynamically refreshed after each timer tick. This graph can also be augmented by parent-child relation edges between processes (process tree and process groups) in different clocktick buckets and locks held/waited by them. Cycle detection algorithms applied on this graph for lock (hold/wait) cycles after each clocktick prevents deadlocks/races. This augmented hashtable chain directed graph has 4 types of edges:

```

<time_to_live_clockticks> -> <process_id>, <parent_process_id> ->
<child_process_id>, <process_id> -> <mutex_id>, <mutex_id> -> <process_id>

```

Dynamism of this timeout hashtable/dictionary graph warrants mention of Dynamic Graph algorithm results - changes in the timeout hashtable after every clocktick is reducible to updates/insertion/deletion in a dynamic graph by previous definition of adjacency matrix from hashtable - insertions/deletions/updates in hashtable buckets are reflected in adjacency matrix for its graph. Reckoning only the `<time_to_live_clockticks>` to `<process_id>` edge, previous clockticks-to-processes dictionary is a dynamic stream of noncrossing (NC) set partitions - each block(bucket) in the partition for every clocktick lapse is an element in the Lattice of partitions defined by Hasse Diagram. Number of such partitions is given by Narayana Number. This timeout dictionary pattern occurs cutting across many arenas of theory and systems. Previous example of OS Scheduler is just mentioned for the sake of commentary and some official copyrighted implementations of this universal theoretical timeout pattern mentioned in references are in different software contexts. Precise example for exact `time_to_live` is the network routing in ISPs which have to timeout ageing packets. TCP/UDP and other protocol families support `time_to_live` in packet headers preset by user code.

An example pattern: Sort the previous pending clockticks(Survival Index) to processes map by descending values of clockticks. Percentage of processes flocking in top ranking clocktick bucket chains is a measure of system load -

runqlat utility in linux kernel 4.x (BPF/bcc-tools) has close resemblance to clockticks-to-processes dictionary but in the histogram format (https://github.com/iovisor/bcc/blob/master/tools/runqlat_example.txt). But this histogram is a map of waiting clockticks to number of processes and not runqueue - consumed timeslice clockticks to processes.

Traditional timeout implementations are timer wheel based which are circular arrays of linked lists swept periodically like clockwork and are not hashable. Previous hashing of dynamic sets is also a timer wheel but takes a detour and converts hash table separate chaining itself into a dynamic clock in which, for example, hour keys are decremented periodically.

Mining Patterns in Survival Index Timeout:

Since every hashmap induces a set partition, previous timeout hashtable separate chaining partitions set of processes into buckets or baskets. Traditional Frequent Itemset Mining techniques - FPGrowth etc., - are applicable only for intra-hashtable patterns when process id(s) are multilocalized across timeout buckets, which elicit frequently co-occurring set of process id(s) within the hashtable. Measuring inter-hashtable distance or distance between two survival index hashtable set partitions is a non-trivial problem. This partition distance problem is formulated by mapping two partitions to a distance graph and vertex cover on this partition distance graph (different from LSH graph of a hashtable previously described). This distance dynamically fluctuates based on processes forked and timedout and is a measure of system load.

Considering the stream of processes set partition induced by survival index timeout buckets as timeseries of set partitions, provides an alternative spectacle to view and mine patterns in OS Scheduler as ARMA or ARIMA polynomials. This requires mapping each set partition in stream to a scalar point in timeseries. Distance between two consecutive observations in timeseries is called Differencing and distance between any two consecutive processes set partition timeout histograms can be defined by Earth Mover Distance or Wasserstein Distance in addition to RandIndex. Linear complexity approximations of Earth Mover Distance (e.g. LC-RWMD) could be faster differencing measures for stream of timeout-to-processes set partitions.

Caveat:

Previous adaptation of Survival Index based Transaction Timeout Management (mentioned in the references) to OS Scheduler assumes prior knowledge of execution times of processes which is undecidable in exact sense by Halting Problem. Only an approximate estimate of execution time of a process can be derived by Analysis of control statements in the program (e.g Sum of execution times of control statements in longest path in the control flow graph of the program is the upperbound). Most of the static code analysis tools for worst case execution time (WCET) do not depend on input size and concentrate only on realtime operating systems and WCET for non-realtime OS implementations therefore can be dynamically derived from theoretical worst case execution time of algorithm underlying executable by reckoning input size e.g Master Theorem $T(n) = aT(n/b) + f(n)$ for divide-and-conquer estimates worst case upperbound running time of algorithm underlying a process executable based on toplevel recursion function $f(n)$ and constants a and b for every inner level of recursion - sorting executable is $O(N\log N)$ and by choice of constant a , approximate worst case execution time of process executable is $aN\log N$. Constants have to be found by trial-and-error and mostly are architecture dependent. There are few trivial exceptions to what Master Theorem can estimate and there is no necessity of CFG longest path estimation. Busy Beaver Function is an alternative formulation which quantifies the maximum number of steps of a halting Turing Machine of N states defined as:

$BB(N)$ = maximum number of 1s written by a Halting Turing Machine of N states on tape

But $BB(N)$ requires prior knowledge of number of states of Turing Machine for a process executable. Brainfuck is a Turing-complete programming language for

designing Turing Machines and host of tools are available to translate a high level programming language (C,C++) source code of a process executable to Brainfuck (.bf) format. If the translated Brainfuck code for a high level language source of process executable has N states its worst case runtime is upperbounded by BB(N) which is a relaxation of master theorem upperbound. Infact BB(N) is the best Turing-computability replacement doing away with master theorem, CFG longest path estimations et al for Worst Case Execution Time bound of an executable as zero-knowledge of underlying algorithm is required which follows from translation of high level language source code (C/C++/Python) to Brainfuck format of Turing machine state transitions oblivious to user.

States of a process can be broadly classified as CPU intensive and IO intensive bursts. By CPU-IO burst histogram for any OS kernel, previous BusyBeaver number of a process executable is a summation of durations in (number of 1s written) CPU burst states and IO burst states - high duration CPU burst states are rare and viceversa.

Survival Index Timeout as Earliest Deadline First (EDF) OS Scheduler:

Linux Kernel has Earliest Deadline First Scheduler which requires user to specify Worst Case Execution Time (WCET) of a process and deadline (runtime <= deadline) explicitly by chrt in commandline or programmatically by sched_setattr(). EDF scheduler prioritizes low deadline processes/threads first, causing long deadline processes to wait longer. Commentaries in References below mention an example constraint to be satisfied:

$$WCET_deadline_timeout_value_of_bucket * number_of_processes_in_the_bucket = constant.$$

This constraint makes the OS Scheduler histogram lopsided - shortest deadline buckets are longest and longest deadline buckets are shortest. Enforcement of this kind of EDF constraint is tantamount to mapping deadline(timeout) values of buckets to process priorities (nice values) - lowest deadlines/timeouts have highest priorities and viceversa.

Usual scheduler race deadlock anomalies of priority inversion arise in previous Survival Index EDF scheduler too e.g low deadline thread/process id spawns another thread/process id of long deadline and waits for high deadline thread/process to end or blocks for a resource locked by high deadline thread/process. This causes starvation of both low deadline process/thread and high deadline process/thread - low deadline process waits for high deadline process to release the lock; High deadline process holding lock, which may not be scheduled in near future, blocks low deadline process stagnating further scheduling of both high and low deadline processes resulting in system freeze. This requires high deadline process to be reprioritized and deadlock avoidance.

Timeout as Graph Partition (Dynamic Process id(s) tree partition):

Previous Survival Index based OS process dynamic set partition can be theorized by a Dynamic Graph Partition too - each process has a dependency to some other process by parent/child fork() relationship as graph edge and processes as vertices. At any instant, survival index graph partition captures both the buckets of the processes set partition for timeout values and dependencies among buckets.

Processes in OS Kernel at any instant are nodes of a tree and earlier Survival Index WCET OS Scheduler partitions this processes tree into bins of a Chained dynamic hash table (one survival index timeout value per bin of process id(s)). An isomorphism could be defined between OS processes tree and Survival Index WCET Dynamic Hashmap Scheduler histogram making a less studied theoretical connection between trees and histograms - as the processes tree evolves over time by fork(), respective Survival Index WCET Scheduler Dynamic Chained Hashtable histogram bins animate dynamically having 1-to-1 bijection to processes tree at that point in time. Earlier isomorphism colors all process nodes of a tree belonging to same survival index timeout bucket by same color - in other words OS process tree is n-colored at any time point for n survival

index timeout values of the Scheduler Histogram thus creating a tree partition. Earth mover distance between two Survival Index chained hashmap histograms at 2 consecutive time points indirectly is also the distance between OS processes trees at those 2 consecutive time points (or) Earth Mover Distance and Tree Edit Distance are bijective a step closer to proving a bijection between Earth Mover Distance and more generic Graph Edit Distance.

blocked	01:13:05 PM IST	runq-sz	plist-sz	ldavg-1	ldavg-5	ldavg-15	
1	01:13:06 PM IST	2	847	2.17	1.58	1.03	
0	01:13:07 PM IST	1	846	2.17	1.58	1.03	
0	01:13:08 PM IST	3	846	2.17	1.58	1.03	
0	01:13:09 PM IST	1	846	2.17	1.58	1.03	
1	01:13:10 PM IST	0	846	2.17	1.58	1.03	
0	01:13:11 PM IST	1	845	2.07	1.58	1.03	
0	01:13:12 PM IST	1	845	2.07	1.58	1.03	
0	01:13:13 PM IST	0	846	2.07	1.58	1.03	
0	01:13:14 PM IST	1	846	2.07	1.58	1.03	
0	01:13:15 PM IST	1	845	2.07	1.58	1.03	
	Average:	1	846	2.12	1.58	1.03	0



Process id dynamic set/graph partition and rectilinear partition - a computational geometric perspective:

Aforementioned Survival Index Worst case execution time partition of process id(s) in an OS kernel can be viewed as computational geometric problem of partitioning a rectilinear orthogonal polygon into rectangles - Every timeout value bucket in set-partition histogram is visually a rectangle of dimensions 1 * number_of_processes_per_bucket. If size of set of process id(s) is factorizable as 2-dimensional orthogonal polygon, per-bucket rectangles tile this rectilinear process space. NeuronRain theory drafts describe and implement a set-partition to Lagranges four square theorem tile cover reduction which finds a rectangle by factorization of size of set-partition and tiles it by squares - an example of rectilinear partition. As a matter of fact, every histogram set partition is theoretically a rectangle partition (of dimensions 1 * size_of_set_of_processes).

References:

- 1.Previous algorithm is a substantial theoretical refinement of Proprietary Survival Index Based Transaction Timeout Management implementation design mentioned in patent disclosure (2002) -
https://github.com/shrinivaasanka/Krishna_iResearch_DoxygenDocs/blob/master/kuja27_website_mirrored/site/kuja27/SurvivalIndexBasedTxnTimeoutManager.pdf (Patent Pending - Copyright - Sun Microsystems (now Oracle)) - Specific to Java Hashmap (CustomizedHashMap) and Open Addressing - part of erstwhile iPlanet Application Server (iAS - now Eclipse GlassFish and Oracle GlassFish appservers - <https://github.com/javaee/glassfish/tree/master/appserver>, <https://www.oracle.com/middleware/technologies/glassfish-downloads.html>, <https://projects.eclipse.org/projects/ee4j.glassfish>) patents - <https://patft.uspto.gov/netacgi/nph-Parser?Sect1=PT02&Sect2=HITOFF&p=1&u=%2Fmetahtml%2FPT02%2Fsearch-adv.htm&r=0&f=S&l=50&d=PTXT&Query=%22kannan+srinivasan%22+AND+%22sun+microsystems%22>
2.Continuous Parameter Markov Chains - Probability and Statistics,Reliability,Queueing and Computer Science - [Kishore Shridharbhai Trivedi, Duke University] - Birth and Death Processes - Response Time of RoundRobin Scheduling - Little's Formula - [Chapter 8] and Network of Queues - Open Queueing Networks - [Chapter 9] - Program state transition markov chain
3.Program Analysis - Analysis of Control Statements - expected and variance of execution times and laplace transforms - Appendix E - Probability and Statistics, Queueing, Reliability and Computer Science - [Kishore Shridharbhai Trivedi, Duke University]
4.Introduction to Algorithms - [Cormen,Leiserson,Rivest,Stein] - Chapter 12 - Hashing by Chaining - <http://staff.ustc.edu.cn/~csl/graduate/algorithms/book6/chap12.htm> - Static Hashing - all runtime analyses for searching in static hashtables still apply to hashing dynamic sets - Note: Hashing Dynamic Sets is different from Dynamic Hashing which facilitates fast insertion/deletion of elements and not dynamism of element itself. Also previous adaptation of hash chaining for timeout and schedulers assumes the hash function for any process is defined as:
$$h(p) = \text{new_execution_time_of}(p) = \text{old_execution_time_of}(p) - \text{clockticks_elapsed}$$

5.Hashing by Chaining - <http://cglab.ca/~morin/teaching/5408/notes/hashing.pdf> - Section 1.3.1 - Gonnet's result on worst case search time in a Chain.
6.Structured Programming - Proper Programs - [Linger] and [Beizer] - https://books.google.co.in/books?id=GZ6WiU-GVgIC&pg=PA264&lpg=PA264&dq=Linger+beizer+proper+program&source=bl&ots=e169qHibIm&sig=Tp_G0laenwMOLpkc9ip7scs4xus&hl=en&sa=X&ved=2ahUKewjv_KHx8LfeAhVDL48KHQhTB0kQ6AEwAHoECAkQAQ#v=onepage&q=Linger%20beizer%20proper%20program&f=false - Page 264 - Probability and Statistics,Reliability,Queueing and Computer Science - [Kishor Shridharbhai Trivedi] - Expected Execution Time of a Program
7.ISO C++ Bucket Interface - Page 920 - Chapter 31 - C++ Programming Language -

[Bjarne Stroustrup] - https://books.google.co.in/books?id=PSUNAAAAQBAJ&pg=PA919&lpg=PA919&dq=hash+table+bucket+size+bucket_count+C%2B%2B&source=bl&ots=DrvmDeg57M&sig=Kj4qXTnTfI-x5qh50bPoiBYoaFw&hl=en&sa=X&ved=2ahUKEwiW6f35187eAhUHVH0KHf9bClc4ChDoATAdegQIBhAB#v=onepage&q=hash%20table%20bucket%20size%20bucket_count%20C%2B%2B&f=false - Bucket Interface provides const and mutable iterables for each bucket in the unordered_map chained hash table. In the context of previous Survival Index timeout table, mutability is defined by the dynamic hash_code(). Aside: ThoughtNet - an Evocatives based Hypergraph - in NeuronRain AsFer has been implemented as Reinforcement Learning Contextual Multi Armed Bandit dictionary which maps an evocative class to set of sentences of that class (from some classifier). ThoughtNet can also be viewed as a Hash table Chaining in which Bucket linked lists of sentences for each evocative are interconnected (HashMap-cum-LinkedList diagram in <https://sites.google.com/site/kuja27/SurvivalIndexBasedTxnTimeoutManager.pdf>). ThoughtNet Hypergraph and previous Survival Index Timeout Separate Chaining can be represented by an adjacency matrix (Hypermatrix Tensors - <https://www.sciencedirect.com/science/article/abs/pii/S0167506008700578>, <http://courses.cs.vt.edu/cs6824/2014-spring/lectures/student-presentations/2014-01-27-student-presentations.pdf>). In the case of ThoughtNet Hypergraph Chaining same value(thought or sentence id) could exist in multiple buckets making a hyperedge connection sprawling over 2 or more buckets which is ruled out in Survival Index Timeout but for the processes having multiple threads each having different timers which demands multilocating a process id and therefore a hyperedge. Survival Index hypergraph is dynamic (edges and vertices are inserted and deleted over time).

8. Mining LSH Partitions/Dictionaries - DictDiffer in Python for difference between two dictionaries - <https://github.com/inveniosoftware/dictdiffer>

9. Noncrossing Partitions and TV Narayana Number - https://en.wikipedia.org/wiki/Noncrossing_partition

10. Dynamic Graph Algorithms - <http://cs.ioc.ee/ewscs/2012/italiano/dynamic1.pdf>

11. Different version of Timeout in Global Decision Platform 3.0 - C++ - <https://sites.google.com/site/kuja27/PhDThesisProposal.pdf> - (Copyright: Global Analytics)

12. Intel Threading Building Blocks (TBB) Concurrent Hash Table Bucket Interface - https://www.threadingbuildingblocks.org/docs/help/index.htm#reference/containers_overview/concurrent_unordered_map_cls.html

13. Introduction to Algorithms - [Cormen-Leiserson-Rivest-Stein] - Coupon Collector Problem/Balls and Bins Problem - Page 134 (5.4.2), Page 1201 (C.4)

14. Balls and Bins Problem, Set Partitions, Bell Numbers and Multinomial Theorem - <https://math.dartmouth.edu/~m68f15/lectec.pdf> - Multinomial Theorem is applicable to previous Survival Index Separate Chain Set Partition if size of each bucket is some constant - e.g Processes are numbered balls and Timeout values are numbered bins and Multinomial Theorem gives all possible configurations of Timeout datastructure subject to rider: bin for timeout value $t(i)$ must contain $m(i)$ processes. Stirling Numbers of Second Kind (Bell Numbers) is the number of all possible Timeout datastructure configurations of p processes and n timeout values (unrestricted bin size).

15. Kruskal-Katona Theorem and Erdos-Ko-Rado Theorem for families of intersecting sets - https://en.wikipedia.org/wiki/Kruskal%E2%80%93Katona_theorem - Uniform Hypergraphs (size of each hyperedge set is equal) are families of intersecting sets if the hyperedges have non-empty intersection. These two theorems upperbound number of hyperedges in a hypergraph by a binomial coefficient. ThoughtNet which is Hypergraph of sentence hyperedges and each hyperedge is set of evocative vertices usually has high intersection (each element in intersection is represented by a stack hypervertex).

16. Linux Kernel Timer Wheel implementation - <https://lwn.net/Articles/646950/> - as tree hierarchy of arrays of linked lists

17. Earliest Deadline First Scheduler (EDF) in Linux Kernel - Part 1 - Dhall Effect in multicores - <https://lwn.net/Articles/743740/> - "...The run time is the amount of CPU time that the application needs to produce the output. In the most conservative case, the runtime must be the worst-case execution time (WCET), which is the maximum amount of time the task needs to process one period's worth of work. For example, a video processing tool may take, in the

worst case, five milliseconds to process the image. Hence its run time is five milliseconds...."

18. Earliest Deadline First Scheduler (EDF) in Linux Kernel - Part 2 - sched_setattr() for setting worst case execution time and deadline explicitly - <https://lwn.net/Articles/743946/>

19. Partition distance - [D. Gusfield.] - Partition-distance: A problem and a class of perfect graphs

arising in clustering - <https://csiflabs.cs.ucdavis.edu/~gusfield/cpartition.pdf>

20. Various distance measures between 2 set partitions - <http://igm.univ-mlv.fr/~gambette/Re20121025.pdf> - Overlap Distance - Minimum Number of elements to be removed to remove all overlaps between subsets of 2 partitions

21. Rand Index - Distance between two sets of classified subsets (set partitions) - https://en.wikipedia.org/wiki/Rand_index

22. Graph Partition - https://en.wikipedia.org/wiki/Graph_partition

23. Dynamic Graph Partition - [Chen Avin et al] -

<https://arxiv.org/pdf/1511.02074.pdf> - Previous Survival Index OS Scheduler is a Dynamic Graph Partition and requires online algorithms (all inputs are not readily available and processes are streamed data) because processes are forked and timedout frequently and parent-child fork relation edges between process vertices (which could be in different timeout buckets) are deleted and created dynamically.

24. Dynamic Tree Partition - Linear weighted tree partition - [Sukhamay Kundu, Jayadev Misra] - [https://epubs.siam.org/doi/abs/10.1137/0206012?](https://epubs.siam.org/doi/abs/10.1137/0206012?journalCode=smjcat)

journalCode=smjcat - SIAM J. Comput., 6(1), 151-154. (4 pages) 1977 - Previous Survival Index (Worst Case Execution Time) OS Scheduler is a Dynamic Tree

Partition if processes are related only by parent-child fork relation - at any instant set of process id(s) waiting to be scheduled on CPU form an n-ary tree and partitions of process id(s) which are timeout value buckets can be arbitrary and need not be rooted subtrees (could be non-rooted subforests). Good scheduling therefore reduces to balanced process tree partitions: number of processes per timeout(deadline) value bucket must be inversely proportional to timeout(deadline) value of the bucket (or number_of_processes_per_timeout_bucket * timeout = constant) which is exactly Earliest Deadline First (EDF) scheduling - small duration processes are preferred while longhaul processes are delayed.

25. Histogram Distance Measures - Because survival index scheduler is a dynamic histogram of timeout versus processes, all histogram distance metrics are relevant for analyzing stream of OS scheduler histograms (Wasserstein-Earth Mover Distance, Correlation, ChiSquare, Intersection, Bhattacharya-Hellinger - <https://docs.opencv.org/2.4/modules/imgproc/doc/histograms.html>). Earth Mover Distance is a variant of Transportation Problem and Simplex. Histogram Stream of Scheduler Queue Checkpoints can be plotted as timeseries of distances between pair of consecutive scheduler runqueue histograms.

26. Program Analysis - Worst Case Execution Time - Estimation - Survey - <https://arcb.csc.ncsu.edu/~mueller/ftp/pub/mueller/papers/1257.pdf> - Control Flow Graph, IPET, Longest Path, Syntax tree structure based

27. Rectangle Partitions of Orthogonal Polygon - [David Eppstein] - Graph-Theoretic Solutions to Computational Geometry Problems - Section 3 and Figure 2 - Matching and Maximum Independent Sets in Bipartite Graph of Intersections of Good Diagonals - <https://arxiv.org/pdf/0908.3916v1.pdf>

28. The Heptane Static Worst-Case Execution Time Estimation Tool - ARM and MIPS instruction sets only - [Damien Hardy, Benjamin Rouxel, and Isabelle Puaut] - <https://drops.dagstuhl.de/opus/volltexte/2017/7303/pdf/OASICS-WCET-2017-8.pdf>

29. Worst Case Execution Time and Earliest Deadline First Scheduler in Linux Kernel - SCHED_DEADLINE -

<https://www.kernel.org/doc/html/latest/scheduler/sched-deadline.html>

30. Master Theorem - [Bentley-Haken-Saxe] -

<https://apps.dtic.mil/dtic/tr/fulltext/u2/a064294.pdf>

31. Master Theorem - Case 2 - [Goodrich-Tamassia] - Algorithm Design: Foundation, Analysis and Internet Examples - Pages 268-270

32. Discrete Parameter Markov Chains - Probability and

Statistics, Reliability, Queueing and Computer Science - [Kishore Shridharbhai Trivedi, Duke University] - Chapter 7 - 7.8 Analysis of Program Execution Time - Program Flow Graph - Page 358 - [Knuth 1973] - Problem 1 - Stochastic Program Flow Graph

33. The Art of Computer Programming - Volume 1 - [Don Knuth] - Analysis of Program Execution Time - pages 190-192 - 1.3.3 - Basic concepts - Timing - Kirchhoff's First Law for Program Control Flow Graph: sum of incoming edges = sum of outgoing edges - pages 383-389 - 2.3.4 - Free tree and Flow chart of a Program - Theorem K - [Thomas Ball, James R.Laurus] - ACM Transactions on Programs and Systems 16 (1994), 1319-1360.

34. Efficient Path Profiling - [Ball-Laurus] - Published in the Proceedings of MICRO-29, December 2-4, 1996, in Paris, France. - <ftp://ftp.cs.wisc.edu/wwt/micro96.pdf>

35. Brainfuck Language for Turing Machines - <https://esolangs.org/wiki/Brainfuck> - Hello world example

36. C to Brainfuck compiler - C2BF - <https://github.com/arthaud/c2bf>

37. FBP - High level language to Brainfuck compiler - <https://esolangs.org/wiki/FBP>

38. (Vide reference 7) Bucketization - Incorrectly assigning class labels to objects - [Ethem Alpaydin] - Introduction to Machine Learning - <https://www.cmpe.boun.edu.tr/~ethem/i2ml/> - 3.3 Losses and Risks - Page 51 - "... Let us define action a_i as the decision to assign the input to class C_i and Lik as the loss incurred for taking action a_i when the input actually belongs to C_k . Then the expected risk for taking action a_i is $R(a_i) = \sum_k P(C_k) \cdot L(a_i, C_k)$..."

39. CPU burst histogram - https://www.cs.uic.edu/~jbell/CourseNotes/OperatingSystems/6_CPU_Scheduling.html - low CPU bursts are more frequent and high CPU bursts are rare (interleaved by IO bursts) on the average for a process

40. Python to Brainfuck - <https://github.com/felko/bfpy> - maps PVM bytecodes to Brainfuck

762. (THEORY and FEATURE) Markov Chains Random Walks on a Random Graph and Television Viewership, Merit of Large Scale Visuals, Media Analytics, Business Intelligence, Timeseries, Computational Geometry, Intrinsic Merit and Originality/Creative Genius, Graphical Event Models and EventNet - 4 June 2018, 3 July 2018, 7 March 2019, 7 May 2020, 2, 3, 4 June 2020, 25 January 2021, 8 April 2021, 14 April 2021 - this section is an extended draft on respective topics in NeuronRain AstroInfer design - <https://github.com/shrinivaasanka/asfer-github-code/blob/master/asfer-docs/AstroInferDesign.txt>

Television viewership is the most researched subject for Media and Advertisement Analytics (Business Intelligence). A viewer randomly shuffling channels creates a Channel Random Graph dynamically where :

- *) Channels are the vertices
- *) Switching Channels creates a random hyperlink edge between two Channel vertices c_1 and c_2 with some probability

This random graph is similar to World Wide Web and a converging random walk on this Channel graph implies viewer is finally satisfied at some point (Random Walk Mixing Time) after traversing the hyperlinks. Each such random edge is a Markov transition depending on previous state. This is similar to PageRank iteration applied on the Channel Random Graph which is converging Markov Random Walk and most ranked vertices/channels can be approximate preferences of the viewer. Infact there is more to it than PageRank - amount of time spent per channel between switches is crucial. There is a subtlety: Predicting Viewers Makes them More Unpredictable - This is because ranking channel vertices from previous random graph and directing more ads to the topmost channel, repels the viewer and causes a random channel switch. Again the PageRank has to be recomputed for finding new topmost channel and this process repeats endlessly - kind of Uncertainty Principle in macrocosm - measuring momentum and location of a subatomic particle changes its momentum and location.

Previous example differs from reputation rankings on the net because TV ads cannot be personalized similar to web adverts and each viewer creates a channel switch random graph independent of others (assuming each individual viewership statistics is recorded in a device or access meter in a set-top box and transmitted). This creates set of ranking preferences per viewer all of which have to be rank correlated and mapped to TRP for ad(s) which satisfies majority. Rank correlations are measures which measure similarity between two rank labeled sets. In Psychology, Spearman Rank Correlation (RC) of two ranked datasets of size n (e.g manual rankings of same dataset by two individuals) is computed by $RC = 1 - [6 \cdot \text{Sum}(\text{euclidean_distance}^2) / n \cdot (n^2 - 1)]$. High distance minimizes rank correlation.

Previous Converging markov random walk algorithm applies to Business Analytics particularly in FMCG where customers have lot of options to try out. An alternative histogram analytics perspective for mining stream of business intelligence dictionary data (distance metric based on rand index) is described in

<https://gitlab.com/shrinivaasanka/asfer-github-code/blob/03333f9fbf0dd087a2fa90bd1856887c8e2eca0f/asfer-docs/AstroInferDesign.txt>. Regression analysis is the primary tool for business and economics research which connects a dependent variable and set of independent variables by a linear or logistic regression equation. For example, $Y = \text{Sum}(a_i \cdot X_i) + b$ defines a linear regression model of independent variables X_i for dependent variable Y . Weights a_i are found by least squares method on equations for N observed values of Y and X_i :

$$\text{Sum}(Y) = \text{Sum}(a_i \cdot \text{Sum}(X_i)) + N b$$

$$\text{Sum}(XY) = \text{Sum}(a_i \cdot \text{Sum}(X_i \cdot X_i)) + b \cdot \text{Sum}(X_i)$$

Previous PageRank computation on Channel Switch Random Graph per viewer can be mapped to a histogram of PageRank score range buckets clustering almost similarly scored channels (intuitively channels of similar genre have almost similar scores thereby partitioning the set of channels by genre buckets) which is a probability distribution per viewer. Majority viewership trend has to be inferred from this stream of per viewer histograms e.g clustering the viewer histograms by adjusted rand index distance measure and largest cluster histogram trend wins by majority vote. It is worth noting that Television Rating Points are intrinsic merit measures for media analytics.

An intrinsic alternative to previous PageRank based voting by viewers is to rank content of channels by EventNet Tensor Products Audio-Visual Merit algorithm implemented in NeuronRain AsFer which considers every audio-visual as stream of causally related frame graphs inferred from ImageNet. This algorithm is not restricted to videos alone but models physical reality of event cause-effect (kind of simplified PetriNets where places are events and transitions are causations between events). Based on genre (Sports, Info, Entertainment etc.,) Empath or LIWC sentiment analysis might be necessary for emotional content. EventNet is a Graphical Event Model (GEM) and there are already GEM algorithms - OGEM, PGEM - which learn graphical dependency from timeseries stream of events of mostly business intelligence, economic or political genre. Formulating Video (timeseries stream of frames) as Graphical Event Model generalizes OGEM and PGEM algorithms to learn EventNet Graph of dependent frames. EventNet Tensor Products algorithm is thus a Graphical Event Model (GEM) algorithm. EventNet and Graphical or Causal Event Models are best suited for analyzing astronomical event timeseries e.g event series denoted by ordered pairs of the form (n-body celestial configuration, terrestrial event) and predicting bayesian likelihood of weather events.

H-index measure of merit in academic research is defined as h number of articles by an academic each of which have citations by atleast h other academics. Similar notion can be generalized to text, audio, video and people too. In the context of video merit, for example, h number of atleast h -times retweeted videos is a measure of quality. An alternative definition of merit in the context of music has been presented in NeuronRain AstroInfer Audio and Music Analytics which is based on how original an Audio waveform is, measured by distance dissimilarity (between other composers) and similarity (theme amongst

works of oneself). Similar definition of originality can be arrived at for following categories of merit:

Text - Semantic (Conceptual) Dissimilarity/Similarity between TextGraphs of academic publications by different authors and Self

People - Semantic Dissimilarity/Similarity between Career transition (modelled by some state machine automaton) of different people and self - Choices made across tenures define people

Video - Narrative Dissimilarity/Similarity between FaceGraph (Voronoi tessellated frames by centroid tracking) and EventNet Tensor Product representation of movies, youtube videos by different creators and Self

References:

-
1. Ranks as Symmetric Permutation Group S_n and Rank correlations - Spearman's Footrule as measure of Disarray - [Persi Diaconis and R.L. Graham] - https://statweb.stanford.edu/~cgates/PERSI/papers/77_04_spearmans.pdf
 2. H-index - Measure of Academic Research Quality - <https://www.ncbi.nlm.nih.gov/pmc/articles/PMC1283832/>
 3. Ordinal Graphical Event Models - OGEM - <https://www.ibm.com/blogs/research/2021/01/ijcai-graph-flow/>, <https://www.ijcai.org/Proceedings/2020/274> - Quite similar to EventNet but without intraevent actors and applicable to many BigData sets having temporal causality - "...OGEMs go a step further. They aim to capture the effect of the order in which preceding events have occurred and detail how each one has affected the event of interest. They do so using a new algorithm we've developed, which learns an event's causes and the quantification of the effect of the order of the causes using event streams as input....The graph itself may include cycles and even self-loops for event labels, capturing the dynamics of the process. For instance, event type C in fig. 1b depends on historical occurrences of event types A and B - meaning there is a parameter for every potential order of every subset of {A, B}...."
 4. Proximal Graphical Event Models - PGEM - <https://papers.nips.cc/paper/2018/file/f1ababf130ee6a25f12da7478af8f1ac-Paper.pdf> - "...ICEWS. We consider the Integrated Crisis Early Warning System (ICEWS) political relational event dataset [O'Brien, 2010], where events take the form 'who does what to whom', i.e. an event z involves a source actor az performing an action/verb vz on a target actor $a0z$, denoted $z = (az, vz, a0z)$. In ICEWS, actors and actions come from the Conflict and Mediation Event Observations (CAMEO) ..."
 5. Graphical Event Models and Causal Event Models - <http://www.contrib.andrew.cmu.edu/org/cfe/simplicity-workshop-2014/workshop%20talks/Meek2014.pdf> - "...Treat data as a realization of a marked point process: $x = t_1, l_1, \dots, t_n, l_n$ Forward in time likelihood: $p(x) = \prod_{i=1}^n p(t_i, l_i | h_i)$ where the history $h_i = h_i(x) = t_1, l_1, \dots, t_{i-1}, l_{i-1}$...Correlation does not imply Causation"

763. (THEORY and FEATURE) Non-graph theoretic Intrinsic merit measures of texts, Reputation Rankings, Sybils and Collusions - 16 July 2018, 23 April 2020, 29 June 2020, 30 June 2020 - this section is an extended draft of sections 783,815 and respective topics in NeuronRain AstroInfer design - Intrinsic Merit of texts, Vowelless text compression and Hyphenated Syllable vectorspace of words - <https://github.com/shrinivaasanka/asfer-github-code/blob/master/asfer-docs/AstroInferDesign.txt>

Most search engines rank websites based on their fame/reputation which is a function of incoming links to a website and reputations of vertices from which the links are incoming e.g PageRank. These Reputations can be manipulated by creating fake incoming links (Sybils) and collusions between websites to inflate PageRank artificially. Identifying Sybils and Collusions is an open problem. Intrinsic fitness/merit of a website is a valuable measure to filter Sybils. It

is known from most research papers on Fame Versus Merit that Fame is either linearly or almost-exponentially proportional to the merit of a social/academic profile vertex in the context of Social networking and Citations in Science publications. If the function relating merit to fame is known approximately by some least squares fit on a training dataset, Fame of a new website can be related to Intrinsic fitness of the website. Huge Distance between observed Fame and Fame predicted by least squares regression from training dataset could be a prima facie indicator of a Sybil. There are quite a few standard non-graph theoretic tools to quantify connectedness of words in text of a website and its narrative style which could confront Fame measures - Coh Metrix, L2 Syntactic Complexity, TAACO, WAT among others. Most of these metrics measure local cohesion (intra-sentence connectivity), global cohesion (inter-sentence connectivity), coherence (mental representation of meaning) quantitatively by correlation between a text and human pre-judged essays. Natural Language Texts of good local coherence and less global cohesion could be simulated by Markov chain models of Information theory which are kind of Turing tests.

References:

-
- 763.1 TAACO - https://alsl.gsu.edu/files/2014/03/The-tool-for-the-automatic-analysis-of-text-cohesion-TAACO_Automatic-assessment-of-local-global-and-text-cohesion.pdf - [Scott A. Crossley, Kristopher Kyle, Danielle S. McNamara] - Cohesion features - Connectives, Givenness, Type-Token Ratio (TTR), Lexical overlap, Synonymy overlap, Semantic overlap - Table 1 - Of these Lexical, Synonymy and Semantic overlap are already subsumed by Recursive Gloss Overlap and Recursive Lambda Function Growth (which approximates a natural language text by a Lambda function tree - Turing Machine - thus attaining maximum theoretical limit) TextGraph algorithms for graph complexity merit of text implemented in NeuronRain.
- 763.2 Manipulability of PageRank under Sybil Strategies - 4.1 - Theorem 2 - <http://www.eecs.harvard.edu/cs286r/courses/fall09/papers/friedman2.pdf>
- 763.3 Markov Models of Text Analysis - <https://www.stat.purdue.edu/~mdw/CSOI/MarkovLab.html> - natural language text could be artificially created by modelling text as probabilities of state transitions between alphabets and words - markov order 1 and order 3 word sequences - manufactured sentence simulates coherence of a human writing but is meaningless - Phonetic Syllable Text (De)Compression models English texts as markov sequences of vowels and consonants - probabilities of vowel succeeding n-grams of consonants are the priors - on the average every second or third letter is a vowel in an English text creating 2-grams and 3-grams of consonants.
- 763.4 Markov Models of Text Analysis - <https://www.cs.princeton.edu/courses/archive/spring05/cos126/assignments/markov.html> - an example news article and its Markov text of order 7 (each state is a string of 7 alphabets which depend on previous states)
- 763.5 Markov Models of Text - [Shannon] - <http://cm.bell-labs.com/cm/ms/what/shannonday/shannon1948.pdf>
-

1208. (THEORY and FEATURE) Software Analytics and Merit of Large Scale Visuals - Rooted Tree Isomorphism and Graph Non-Isomorphism of Source code versioning systems - AHU Algorithm - Difference between two trees (delta) - Isomorphism of k-d trees for object recognition - 7 August 2018 - related to all sections on Computational Geometry, Computer Graphics - Face recognition, Handwriting recognition, Mesh Deformation Isomorphisms-Approximate Topological Matching

Two graphs are similar if they are isomorphic (i.e there is a bijection between 2 graphs by vertex renumbering). Finding difference between two graphs or trees is therefore Graph Non-Isomorphism problem (GNI). Tree difference is a frequent requirement in source code version control systems and file sync-ing software which transmit delta (what changed) between source and destination. For example, SVN delta editor in https://subversion.apache.org/docs/api/1.9/svn_delta_8h_source.html overlays

the new revision delta on existing tree by replicating only the changed subtrees while unchanged tree is shared between versions. Finding if two rooted trees are isomorphic (Rooted Tree Isomorphism Problem) readily applies to repository source code trees which are always rooted. Aho-Hopcroft-Ullman (AHU) algorithm finds if two rooted trees are isomorphic in $O(|V|)$ - linear in number of vertices and works by assigning Knuth tuples to each node, an encoding of the descendants within a parenthesised string. Comparing two source code repository trees is essential while performing synchronization, to quantify code similarity among others. An algorithm for isomorphism of 2 rooted k-d trees or Gromov-Hausdorff distances between 2 k-d trees, thereby could recognize similarity between 2 3-dimensional visuals and objects thereof stored as 3-dimensional k-d trees.

References:

1208.1 Tree isomorphism -

https://logic.pdmi.ras.ru/~smal/files/smal_jass08_slides.pdf

1208.2 K-d tree - https://en.wikipedia.org/wiki/K-d_tree

1208.3 Gromov-Hausdorff Distance between Trees on metric spaces - [Abhinandan Nath] - <https://users.cs.duke.edu/~abhinath/dissertation.pdf> - "...The Gromov-Hausdorff distance (or GH distance for brevity) [92] is one of the most natural distance measures between metric spaces, and has been used, for example, for matching deformable shapes [119, 48], and for analyzing hierarchical clustering trees [55]. ... Despite much effort, the problem of computing, either exactly or approximately, GH distance has remained elusive. The problem is not known to be NP-hard, and computing the GH distance, even approximately, for graphic metrics is at least as hard as the graph isomorphism problem ..."

1207. (THEORY) People Analytics - Dynamic Bipartite Social Network Graphs - Stable Matchings for Dynamic Population - 7 September 2018 - related to all sections on People Analytics, Social Network Analysis, Bipartite matching, Reciprocal Recommender Systems for Matrimonial services, Gale-Shapley Stable Marriage Problem, Hall's Marriage Theorem

[This is mentioned more like an open puzzle/question than answering it]
Stable Marriage Theorem implies there exists an algorithm for finding bipartite matchings between two sets (bipartite graph) when vertices in both sets have ranking preferences of choosing a match in other set. Gale-Shapley algorithm finds such an optimal matching between two sets based on preferences in quadratic time. This algorithm is for static bipartite sets/graphs. Would the same hold for dynamic bipartite graphs in which either set grows/diminishes over time? A real world example: Population is a bipartite graph of either genders and stable marriage theorem implies there is always an optimal match between vertices of two genders. This graph grows in time and size of both sets (gender populations) remain equal approximately despite births/deaths (which is a natural mystery implying order emerging from an apparent random process).

References:

1207.1. Gale-Shapley Algorithm - Stable Marriage Problem -

https://en.wikipedia.org/wiki/Stable_marriage_problem

764. (THEORY and FEATURE) Gordian Knot and One Way Functions - 15 October 2018, 19 October 2018 - this section is an extended draft on respective topics in NeuronRain AstroInfer design - <https://github.com/shrinivaasanka/asfer-github-code/blob/master/asfer-docs/AstroInferDesign.txt>

Gordian Knot is an impossible-to-unravel knot which was allegedly solved by

Alexander the Great by cutting it.

There exists a striking parallel between one way functions for Psuedorandom Generators and difficulty in untying knots. Gordian knot is open problem in knot theory. One way functions are defined as:

$$f(x) = y$$

$$\Pr(\text{finverse}(y) = x) = 2^{(-n)} \text{ for bit length } n \text{ of } x.$$

Hardness of inversion and difficulty in untying a knot can be correlated by following contrivance:

Assuming a knot is a map of sequence of points in straightline to sequence of non-linear points in 3 dimensions, every knot is a polynomial of degree 3 drawing a locus in 3-D plane. A function for this polynomial is the mapping :

$f(x_1, x_2, x_3): \langle \text{set of straightline points in 3-D plane} \rangle \rightarrow \langle \text{knot polynomial configuration in 3-D plane} \rangle$.

Inverting the previous function implies untying a knot to straightline points:

$\text{finverse}(x_1, x_2, x_3): \langle \text{knot polynomial configuration in 3-D plane} \rangle \rightarrow \langle \text{set of straightline points in 3-D plane} \rangle$.

On the contrary a proof of existence of one way functions implies there exists an impossible-to-unravel knot by previous reduction:

$\Pr(\text{finverse}(\text{knot polynomial configuration in 3-D plane}) == \langle \text{set of straightline points in 3-D plane} \rangle)$ is exponentially small.

Infact this definition of One Way Functions is a stronger version of Gordian Knot because inversion should restore the same status-quo-ante straightline configuration of a sequence of points earlier and not some other alignment.

Defining Boolean Gordian Knot One Way Function is not straightforward: For example every point on a string to knot has to be defined as binary inputs to some boolean function which outputs 0 or 1 corresponding to some bit position of a point on the resultant knot polynomial. If there are n points on string and m bit positions each per point, this requires $m*n$ boolean functions of the form $f: \{0,1\}^m \rightarrow \{0,1\}$ all of which have to be inverted to unravel the knot - this is a family of one way boolean functions harder than plain one way boolean function.

References:

1. Gordian Knot Simulation - [Keith Devlin] -

<https://www.theguardian.com/science/2001/sep/13/physicalsciences.highereducation>

2. Knot Polynomials - Jones and Alexander -

https://en.wikipedia.org/wiki/Knot_theory#Knot_polynomials - Topologically, Knot is an embedding of a circle in R^3 (and also to all the homeomorphisms of the circle obtained by deformations - Knot equivalence - ambient isotopy) - Previous definition of one way function maps a circular or straightline string to one of the homeomorphic knot denoted by a knot polynomial and there are as many one way functions as there are knot polynomials. Inversion of one way function reduces to inverse homeomorphism. Example: Handwritings of different persons (of same language and text) are homeomorphic deformations in R^2 preserving genus (holes or maximum number of cuts required without disconnecting the manifold).

3. Homeomorphic inverse - [http://at.yorku.ca/cgi-bin/bbqa?](http://at.yorku.ca/cgi-bin/bbqa?forum=ask_a_topologist_2010&task=show_msg&msg=1138.0001)

[forum=ask_a_topologist_2010&task=show_msg&msg=1138.0001](http://at.yorku.ca/cgi-bin/bbqa?forum=ask_a_topologist_2010&task=show_msg&msg=1138.0001)

- "Thirdly, the inverse of f^{-1} is just f itself - in other words, the inverse of the inverse of f is f itself, so that $(f^{-1})^{-1} = f$. By assumption, f is continuous, and as f is the inverse of f^{-1} , the function f^{-1} has a continuous inverse."

765. (THEORY) Circle Packing and Planarity - 21 March 2019 - this section is an extended draft on respective topics in NeuronRain AstroInfer design -

<https://github.com/shrinivaasanka/asfer-github-code/blob/master/asfer-docs/>

Drawing non-crossing paths between points is a non-trivial planar graph embedding problem. There are planarity criteria defined by various theorems as below:

(*) Wagner's Theorem - Graph is planar if and only if it is free from K_5 or $K_{3,3}$ minors. K_n is a complete graph of n vertices and $K_{3,3}$ is a complete bipartite graph on 2 sets of size 3. Graph minor is obtained by contracting edges to vertices.

(*) Circle Packing Theorem - Circles of varied sizes are drawn tangentially (osculation) on plane and a graph comprising edges among osculating circles is the coin graph. Graph is planar if and only if it is a circle intersection graph or coin graph.

References:

- 1. Mathematical Puzzles of Sam Lloyd - Selected and Edited by Martin Gardner - Chicken Puzzle - Puzzle 82
2. Circle Packing Theorem - [Koebe-Andreiev-Thurston] - https://en.wikipedia.org/wiki/Circle_packing_theorem

766. (THEORY) Computational Geometric Factorization, 2-D Cellular Automaton and Multidimensional array slicing - 12 November 2019, 13 November 2019, 21 April 2020 - this section is an extended draft on respective topics in NeuronRain AstroInfer design - <https://github.com/shrinivaasanka/asfer-github-code/blob/master/asfer-docs/AstroInferDesign.txt>

Naive 2-dimensional (multidimensional) array slicing loops through rows and finds per row slice which are united to a square slice. In Python SciPy and NumPy have a multidimensional subscript slicing facility e.g `x[2:10,2:10]` for an ndarray object `x` extracts a square slice of 9×9 . Naive loop slicing is $O(n^d)$ for d dimensional arrays. Low level languages C, C++ etc., store arrays in contiguous memory locations in flat 1-dimension and 2-d slice of (a,b) is expressed by an equation $r \cdot (x+a) + y$ ($r \leq b$, $y \leq a$) which uniquely identifies an element in square slice of origin (x,y) obviating loops. But extracting the square slice still needs looping. Doing better than naive bound necessitates storing the two dimensional array in a wavelet tree and computational geometric range search on it:

(*) Wavelet Tree for Computational Geometric Planar Range Search in 2 dimensions - https://www.researchgate.net/profile/Christos_Makris2/publication/266871959_Wavelet_trees_A_survey/links/5729c5f708ae057b0a05a885/Wavelet-trees-A-survey.pdf?origin=publication_detail - "... Therefore, consider a set of points in the xy -plane with the x - and y -coordinates taking values in $\{1, \dots, n\}$; assume without loss of generality that no two points share the same x - and y -coordinates, and that each value in $\{1, \dots, n\}$ appears as a x - and y - coordinate. We need a data structure in order to count the points that are in a range $[l_x, r_x] \times [l_y, u_y]$ in time $O(\log n)$, and permits the retrieval of each of these points in $O(\log n)$ time. ... this structure is essentially equivalent to the wavelet tree. The structure is a perfect binary tree, according to the x -coordinates of the search points, with each node of the tree storing its corresponding set of points ordered according to the y -coordinate. In this way the tree mimics the distinct phases of a mergesort procedure that sorts the points according to the y -coordinate, assuming that the initial order was given by the x -coordinate. ..."

(*) Entropy bound for Wavelet Tree point grids - Lemma 2 - <https://www.sciencedirect.com/science/article/pii/S0925772113000953> - [Arash Farzan, Travis Gagie, Gonzalo Navarro] - set of all possible point grids

(slices) of size m carved from $n \times n$ square are populated in a wavelet tree and size of this set is $\{n^2 C_m\}$ and of entropy $\log\{n^2 C_m\}$ - "...Furthermore, query $\text{rel_acc}(i_1, i_2, j_1, j_2)$ (giving all the k points in $[i_1, i_2] \times [j_1, j_2]$), is answered in time $O((k+1) \lg \sigma / \lg \lg n) \dots$ ". Query $\text{rel_acc}()$ range reports all k points in the rectangular slice $[i_1, i_2] \times [j_1, j_2]$ of $n \times n$ square for an alphabet size (which could be 2 or 10 depending on binary or decimal radix of the 2-dimensional array) in $O((n^2+1) \lg 2 / \lg \lg n)$ and $O((n^2+1) \lg 10 / \lg \lg n)$ for $k=O(n^2)$. This is slightly better than $O(n^2)$ naive bound because $O((n^2+1) \lg 2 / \lg \lg n)$ and $O((n^2+1) \lg 10 / \lg \lg n) = O(n^2 / \lg \lg n) < O(n^2)$. 2-dimensional arrays are labelled points on 2-d plane and computational geometric wavelet tree planar range search selects an array slice in its entirety in time $O(n^2 / \lg \lg N)$.

Previous improvement in 2-dimensional array slicing is quite useful in speedup of delta vicinity search for exact factors around approximate factors in both Randomized NC (Section 752) and Exact NC-PRAM-BSP Computational Geometric Factorization algorithms. Once the ray shooting queries find the approximate factors on the hyperbolic arc bow, square vicinity (in contrast to circular radius) of approximate factor can be retrieved in subquadratic time. Every square vicinity of approximate factor found by ray query induces a 2-dimensional cellular automaton centered at approximate factor which sweeps the plane in 8 directions and locates the exact factor in consecutive generations by growth rules.

 767. (THEORY and FEATURE) Leaky Bucket Algorithm and Time Series Analysis - 30 November 2019 - this section is an extended draft on respective topics in NeuronRain AstroInfer design - <https://github.com/shrinivaasanka/asfer-github-code/blob/master/asfer-docs/AstroInferDesign.txt>

NeuronRain AstroInfer Research Version in SourceForge implements lot of algorithms to mine patterns in strings especially encoded astronomical datasets of celestial configurations which might be helpful to correlate gravitational influence of an n -body planetary system on sky and terrestrial weather-seismic events (example Sequence Mined astronomical pattern based on swiss ephemeris and maitreya8t - commit - <https://sourceforge.net/p/asfer/code/2606/>) . NOAA JAWF Climate Prediction Centre precipitation analytics based on time series and leaky bucket are alternative examples of machine learning driven weather forecasts (Leaky Bucket Model - https://www.cpc.ncep.noaa.gov/products/JAWF_Monitoring/India/monthly_maps.shtml, Rainfall Time Series - https://www.cpc.ncep.noaa.gov/products/JAWF_Monitoring/India/30d_time_series.shtml).

Leaky Bucket Algorithm is primarily used in traffic policing and scheduling of networks (in NOAA example previously, daily rainfall statistics replace network traffic and are plotted as timeseries) and operates as follows:

- (*) Bucket datastructure (e.g store-forward buffers in routers) is predefined for certain average expected traffic
- (*) Network Traffic trickles in a leaky bucket datastructure at random rate
 - (*) Some amount of traffic leaks out of bucket at random rate
 - (*) Bucket might either overflow or be emptied depending on rate of incoming network packets (similar to detour of vehicles in a jammed junction)
 - (*) Bandwidth rate limiting and outlier detection can be enforced based on leaky bucket model (e.g any overflow is caused by outlier packets and indicates abnormal exorbitant incoming traffic)
 - (*) Bursts of packets in network traffic can also be plotted as time series of periodic intervals (number of packets versus time)
 - (*) Time-Series of network traffic and Leaky-Bucket model often have an one-to-one correspondence - Any peak (outlier) in timeseries might trigger a bucket overflow and vice-versa.

References:

767.1 Visual and Audio Data Mining - Section 11.3.3 - Page 670 - Data Mining- [Jiawei Han-Micheline Kamber] - Visual Data mining of Rainfalls in SAS Enterprise Miner and Mining data as music or audio signals

768. (THEORY) Finding penultimate element in a linked list, sublinear Depth First Search and Breadth First Search, Survival Index Timeout WCET EDF OS Scheduler - 3 January 2020 - this section is an extended draft on respective topics in NeuronRain AstroInfer design - <https://github.com/shrinivaasanka/asfer-github-code/blob/master/asfer-docs/AstroInferDesign.txt>

Finding the last but one element in a singly linked list of N elements requires linear traversal of the list, pushing the elements to stack and popping top two elements from it by a naive $O(N)$ algorithm. Breadth First and Depth First Searches are cornerstones of Artificial Intelligence having vast literature in motion planning and robotics. Because singly linked list is a directed acyclic line graph parallel versions of traditional $O(V+E)$ breadth first search and depth first search algorithms which are sub-linear and logarithmic can locate the penultimate element in a singly linked list in parallel faster. There are many parallel BFS and DFS algorithms e.g iterative deepening A^* (IDA^*), parallel shortest path, Depth First Branch and Bound which are based on PRAMs and thus are polylogdepth NC circuits. Parallel DFS and BFS are quite useful in Survival Index Timeout OS EDF Scheduler algorithm described earlier where every per WCET timeout bucket is a linked list of process id(s) and a process id needs to be searched.

References:

1.Parallel DFS - [Nageshwara Rao - Vipin Kumar] - <https://www.lrde.epita.fr/~bleton/doc/parallel-depth-first-search.pdf>
2.Parallel DFS - Chapter 11 - Introduction to Parallel Computing - <http://parallelcomp.uw.hu/ch11lev1sec4.html>
3.Parallel DFS - http://www2.inf.uos.de/papers_html/zeus_95/node5.html
4.Parallel RAM Breadth First Search - https://en.wikipedia.org/wiki/Parallel_breadth-first_search
5.Parallel Breadth First Search and Depth First Search - [Taenam Kim & Kyungyong Chwa] - <https://www.tandfonline.com/doi/abs/10.1080/00207168608803503?journalCode=gcom20> - is of parallel time $O(\log d - \log n)$ for diameter d (longest of shortest paths between all pairs of vertices) of the graph and n is the number of vertices - "...we develop a parallel breadth first search algorithm for general graphs and a parallel depth first search algorithm for acyclic digraphs which run in time $O(\log d - \log n)$ using $O(n^2[n/\log n])$ processors....". For singly linked lists diameter d = number of vertices n

838. (THEORY) 12 May 2020 - Finding number of elements in a linked list - Sequential and Parallel - List Ranking - Pointer Jumping - related to 751,768

Counting number of elements in a linked list of N elements has a naive sequential bound of $O(N)$. List Ranking is the problem of computing distance of every element in a linked list from the end of the list. Thus counting number of elements in a linked list is a List Ranking problem for finding distance of the first element from end of the list. List Ranking has a Parallel RAM pointer jumping algorithm which finds the rank in $O(\log N)$ parallel time. Following is a pointer jumping

pseudocode for parallel
list ranking:

```
    allocate one element per processor
    for every processor and element i
        distance[i] += distance[next[i]]
        next[i] = next[next[i]]
```

Sequential sublinear algorithm for counting number of elements in a linked list and list ranking is an open problem. Every linked list is an inorder traversal of a balanced AVL tree equipped with successor (and predecessor in doubly linked list) pointers - this structure can be exploited to approximately estimate number of elements in a linked list as $2^{(\text{average length of root to leaves})}$. Parallel List Ranking by Pointer Jumping is central to many parallel algorithms for linked lists. Primitive `next[i]` is architecture dependent and if its recursive version `next(next(next(...)))` could be upperbounded by $(\log M)^k$ for $M \gg N$, N can be written as $N = a \cdot N / (\log M)^k + b$, $a \leq (\log M)^k$. Huge linked lists could be approximately estimated by this heuristic for sequential pointer jumping a times plus additional b sequential traversals.

References:

1. Algorithms - [Cormen-Leiserson-Rivest-Stein] - Page 692 - Algorithms for Parallel Computers - 30.1.1

- List ranking

8093 - 928399 - 0.6 - 8891212819219

9923 - 920499 - 0.5 - 8298212819219

9893 - 920399 - 0.5 - 8291212819289

1983 - 920399 - 0.3 - 8291218819219

1993 - 920399 - 0.4 - 8291212889219

8293 - 920399 - 0.2 - 8291212819819

#####

#####

This

work is licensed under a Creative Commons

Attribution-NonCommercial-NoDerivatives 4.0 International License.

#####

#####

Course Authored By:

Srinivasan Kannan

(also known as: Shrinivaasan Kannan, Shrinivas Kannan)

Ph: 9791499106, 9003082186

Krishna iResearch Open Source Products Profiles:

http://sourceforge.net/users/ka_shrinivaasan,

<https://github.com/shrinivaasanka>,

https://www.openhub.net/accounts/ka_shrinivaasan

Personal website(research): <https://sites.google.com/site/kuja27/>

emails: ka.shrinivaasan@gmail.com, shrinivas.kannan@gmail.com,

kashrinivaasan@live.com

#####

#####

This is a non-linearly organized, code puzzles oriented, continually updated set of course notes on AngularJS. This complements NeuronRain course materials on Linux Kernel, Cloud, BigData Analytics and Machine Learning.

2 June 2017

AngularJS is the client side Advanced Java Scripting (AJAX) engine runtime supported by most browsers. AngularJS follows Model-View-Controller pattern:

- View is the HTML visible to user
- Model is the form layout and frames of the Dynamic HTML page
- Controller acts on the model data and eschews HTML output from Server

Side JavaScript (Node.js) or other frameworks(Django/Flask/Tornado)

Model-View-Controller decouples the HTML rendering from the hidden dynamic logic. NeuronRain GUI frontend has two client/server interfaces: Plain HTML-to-Tornado and AngularJS-to-Tornado webserver

(https://github.com/shrinivaasanka/asfer-github-code/tree/master/python-src/webserver_rest_ui/). AngularJS HTML template for a simple form submit has following structure:

- form tag with ng-app directive defining the application name of the controller
- Model name for input elements in the form
- script tag which defines a controller object from ng-app and defines a function for form processing invoked from submit widget of the form
- AngularJS script in controller has access to builtin(s) like \$scope, \$http etc., for accessing model data in the scope. Form data can be submitted to a REST URL with GET or POST with stringified JSON data.

#-----

#NEURONRAIN ASFER - Software for Mining Large Datasets

#This program is free software: you can redistribute it and/or modify it under the terms of the GNU General Public License as published by the Free Software Foundation, either version 3 of the License, or (at your option) any later version.

#This program is distributed in the hope that it will be useful, but WITHOUT ANY WARRANTY; without even the implied warranty of MERCHANTABILITY or FITNESS FOR A PARTICULAR PURPOSE. See the GNU General Public License for more details.

#You should have received a copy of the GNU General Public License along with this program. If not, see <<http://www.gnu.org/licenses/>>.

#-----

#K.Srinivasan

#NeuronRain Documentation and Licensing: <http://neuronrain-documentation.readthedocs.io/en/latest/>

#Personal website(research): <https://acadpdrafts.readthedocs.io/en/latest/>
(links to mirror of erstwhile <https://sites.google.com/site/kuja27> and all references to it are redirected

implicitly to <https://acadpdrafts.readthedocs.io/en/latest/>)

#-----

Document Licensed by:

#####

#####

This work is licensed under a <a rel="license"

href="http://creativecommons.org/licenses/by-nc-nd/4.0/">Creative Commons

Attribution-NonCommercial-NoDerivatives 4.0 International License.

#####

NeuronRain - Design Objectives

NeuronRain OS is machine learning, cloud primitives enriched linux-kernel fork-off with applications in Internet-of-Things. AstroInfer is the machine learning side of it to learn analytics variables later read as config by linux kernel and any device specific driver. NeuronRain has been partitioned into components so that effective decoupling is achieved e.g Linux kernel can be realtime OS for realtime less-latency applications, Message Queuing can be KingCobra or any other standard MQ product. There are IOT operating systems like <https://github.com/RIOT-OS/>. Linux and IoT - linux on cameras, automobiles etc., - <https://lwn.net/Articles/596754/>. NeuronRain in itself is not just a product but a framework to build products. Applications can invoke VIRGO cloud memory, clone, filesystem primitives to create new products on NeuronRain Smart-IoT framework.

Copyright attributions for other open source products dependencies:

- 1.Maitreya's Dreams - <http://www.saravali.de> (some bugs were fixed locally in degree computation of textual display mode)
2.SVMLight - <http://svmlight.joachims.org/>
3.BioPython and ClustalOmega Multiple Sequence Alignment BioInformatics Tools (www.biopython.org, www.ebi.ac.uk/Tools/msa/clustalo/)

Open Source Design and Academic Research Notes have been uploaded to http://sourceforge.net/projects/acadpdrfts/files/MiscellaneousOpenSourceDesignAndAcademicResearchNotes_2013-08-11.pdf/download

Presently a complete string sequence mining subsystem and classification algorithms with indexing have been implemented for mining patterns in rules and encoded strings and executing those rules (in special case, an encoded horoscope).

AstroInfer Classifiers - Documentation on the dataset files used

decisiontree-attrvalues.txt - Attributes based on which decision is done and the values they can take (comma separated list)

decisiontree-test.txt - Test dataset with set of values for attributes in each line

decisiontree-training.txt - Training dataset with set of values for attributes and class it belongs in each line

test-set.txt - List of article id(s) to be classified - NaiveBayes

topics.txt - List of classes the article id(s) in training set belong to - NaiveBayes

training-set.txt - List of articles id(s) already classified - training dataset for NaiveBayes

word-frequency.txt - Words and their frequencies of occurrence in all articles - NaiveBayes

words.txt - words, the article id(s) having those words and number of occurrences of those words within specific article id (~ separated)

Above XXX.txt files need to be populated after doing some preprocessing of the

articles to be classified. Preprocessing might include finding the word frequencies in the articles, finding classes of the articles, finding attributes and possible values of those attributes. At present the asfer.enchoros file contains encoded horoscopes for single class of events. Thus classification is redundant. But if it has encoded horo strings for all events then to filter out strings of a particular class of events, classification is needed.

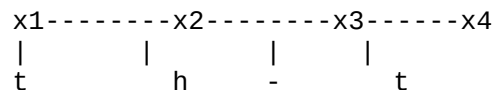
Python script for autogenerating above txt files has been added under python-src/autogen_classifier_dataset. This script needs to be changed for generating training and test set files.

```
*****
*****
DESIGN NOTES, THEORETICAL INTERLUDES(might have errors), TODO AND NICE TO HAVE
FEATURES (list is quite dynamic and might be rewritten depending on feasibility
- long-term design goals with no deadline)
*****
*****
```

(FEATURE - DONE-MDL, Entropy, Edit Distance, Compressed Sensing) 1. Test with Massive Data Sets of encoded strings for pattern mining. Algorithms for Approximate Kolmogorov Complexity or Minimum Description Length (MDL), Shannon Entropy, Levenshtein Edit Distance have been implemented in Python and C++. Compressed Sensing (used in Image and Signal Processing) which "sense" from "compressed" large data - This involves computing a matrix product $AX=B$ where X is an image or bitmap and A is a chosen matrix which together give a sketch B . Sketch of an image bitmap has been implemented.

(FEATURE - THEORY-POC Implementation-DONE) 2. An experimental text compression algorithm that deletes vowels and stores only consonants as far as meaning is not altered. For example "follow" could be stored as "fllw". Since on an average every third letter in an english word is a vowel, approximate compression is 33%. Message is reconstructed using most probable meaningful word for "fllw" (For example "follow" could be more probable than "fellow" or vice versa). This is similar to Texting in phones and to some extent encoding in Match Rating (http://en.wikipedia.org/wiki/Match_rating_approach). One more example could be "Decision" which can be compressed as "Dcsn". An interesting phonetic aspect of this is that "Decision" is spelt as "Dee-C-shan", or each vowel following a consonant is subsumed or coalesced into the preceding consonant while spelling. Thus "Dcsn" gives 50% compression ratio. PyEnchant python package SpellChecker has suggest() function that returns a tuple of closely related words to a compressed (or "misspelt") word. Conventional WSD algorithms might have to be used on this tuple to get the maximum match. Initial testing reveals that the accuracy with spellcheckers is less and this problem requires a non-trivial algorithm which might require error-correcting codes like Reed-Solomon and Berlekamp-Massey assuming the english text as a finite field of alphabets as elements. Predominantly used dictionary-based Lesk's disambiguation Algorithm can find the intersection between "follow" and the rest of the context and "fellow" and rest of the context and choose the word with maximum intersection with context - this is quite commonsensical too. But the drawback of this disambiguation is that keywords are disambiguated well while other connectives (is, are, thus, this, who, why etc.,) in the sentences are not. Another limitation of applying WSD while decompressing is lack of meaningful context words at runtime - only compressed words are available and they cannot be used as disambiguating context creating a circular dependency - disambiguation requires decompression and decompression needs disambiguation. For computing maximum likelihood, most probable vowel between 2 consonants can be zeroed in on by a 26*26 table of consonant ordered pairs and having vowels between them as probability distribution priors. This is feasible only if priors are available. For example th-t has (h,t) as consonant pairs and a is most probable vowel than e,i,o and u and th-t is disambiguated as "that". The vowels missing in compressed text can be represented by a single extra bit. This is an alternative to PyEnchant spellcheck suggest() function. This can be Hidden Markov Model also - with missing vowels as hidden states to measure and compressed letters as

observations. This requires forward-backward probabilities computation or Viterbi path which gives most likely word for a compressed word. For "th-t" the Markov Model looks like:



and Bayesian for the above is:

$\Pr(x3/[t,h,-,t])$ is directly proportional to $\Pr(x3/[t,h]) * \Pr([t]/x3)$ and to be precise it is:

$\Pr(x3/[t,h,-,t]) = \Pr(x3/[t,h]) * \Pr([t]/x3) / \Pr(t)/\Pr(t,h)$ with denominator being a pre-computable constant from substring hashtable as below.

Viterbi path would give the most likely path or most likely word for above.

(2.1) $\Pr(x3/[t,h])$ is computed from dictionary - number of words having the sequence / total number of words

which is the $\text{argmax}(\Pr(a/t,h), \Pr(e/t,h), \Pr(i/t,h), \Pr(o/t,h), \Pr(u/t,h))$ and priors are computed for the substrings tha, the, thi, tho, thu.

(2.2) $\Pr(t/x3)$ is computed from dictionary similar to the previous for argmax of probabilities for substrings at, et, it, ot, ut.

(2.3) If total number words in dictionary is E (could be 200000 to 300000) and y_i is the number of words of length i, then $y_1 + y_2 + \dots + y_n = E$.

(2.4) Number of substrings of an n bit word is $(n-1)n/2$.

(2.5) Thus number of substrings for all words in dictionary is $y_2 + 3*y_3 + 6*y_4 + 10*y_5 + \dots + (n-1)n*y_n/2$. Thus number of substrings (could be significantly more than 500000) is independent of the text to be decompressed and the substring prior probabilities can be precomputed and stored in a hash table (size of the table is = number of substrings * 5 for each vowel). This table has to be huge but does not depend on text to be decompressed.

(2.6) Above is theoretical basis only implementation of which needs precomputing the above hashtable.

(2.7) Above experimental compression scheme that ignores vowels gives a string complexity measure (a minimum description length) similar to Kolmogorov complexity.

(2.8) Algebraically, above can be imagined as a Group Action where group G is set of consonants (with the assumption that inverses exist for each consonant with a special "backspace" element added to alphabet set and identity is "space" element) and set X to act on is the set of vowels. Orbit is the set of X elements moved ($g.x$) and if concatenation (with phonetic coalition) is a group operator then consonants act on vowel sets. For example, the consonant "t" acts on "o" from vowel set to give the word "to". The concatenation is non-abelian. Interestingly the above phonetic coalition of vowels to an adjoining consonant is the Stabilizer set or set of Fixed points($g.x=g$). For example, the consonant "d" acting on the vowel "e" gives a phonetically coalesced compression "d" ("d" , "de" and "dee" are phonetically same as "d") as a fixedpoint. Thus Orbit-Stabilizer Theorem (set of cosets of Fixed points - Quotient group $G/G(x)$ - isomorphic to Orbit) should apply to the above. There may be scenarios where a maximum likely vowel from above $\text{argmax}()$ computation does not equal the actual vowel expected and for arbitrary non-dictionary strings prior computation is difficult. Thus this algorithm is quite experimental.

(2.9) Linguistic words can be construed as a polynomial graph plotted on an x-y axis: x-axis represents position of a letter in a text and y-axis represents an alphabet (vowels and consonants). From the previous string complexity measure missing vowels are missing points on the polynomial. Disambiguating the word is then equivalent to Polynomial Reconstruction Problem/List Decoding/Error correcting codes (Reference: Point 345) that reconstructs a list of polynomials

(i.e set of disambiguated words) from a codeword(i.e compressed vowelless string) one of which disambiguates and decompresses the vowelless codeword - polynomial reconstructed should include (almost all) missing vowels. Text can be represented as a polynomial function defined as $f:N \rightarrow \text{Alphabets}$ where N is set of natural numbers. Factoring over this polynomial ring enables text to be represented as products of texts. An implementation of polynomial encoding of texts has been done in 364. Berlekamp-Welch algorithm creates a system of equations which themselves are evaluations of two polynomials over finite fields for all x_i ($P(x_i) = Q(x_i)/E(x_i)$) where each x_i is from input set of ordered pair of points (x_i, y_i) . This system of equations is solved by Gaussian Elimination to compute $Q(x)/E(x) = P(x)$. Berlekamp-Welch encodes a text in a different way than plain polynomial curve fitting - each letter ordinal in text is a coefficient of a polynomial of degree equal to size of text whereas polynomial encoding of text fits a curve passing through the ordinal values of letters in successive positions. This polynomial with ordinal coefficients over a finite field is then evaluated in n points and transmitted. Recipient reconstructs the original polynomial from transmission errors in received points by Gaussian Elimination. If transmission error is simulated as removing vowels in original message polynomials, reconstruction by solving system of equations should almost correctly identify missing vowels.

(2.10) From point 345 and 346, high level language texts like English, French etc., can be thought of as 255-coloring of letter positions where 255 is the size of alphanumeric alphabet (ASCII, Unicode). Each letter in a text "colors" corresponding letter position in text with an alphabet. From Van Der Waerden and other coloring theorems, there are monochromatic arithmetic progressions in letter positions in high level language texts i.e alphabets in APj positions are all same for some APj. This implies there is an order in high level context sensitive natural language grammars and answers in affirmative the conjecture posited in 346.

(2.11) Monochromatic arithmetic progressions in letter positions of natural language texts implies that finite state automata can be learnt to accept such arithmetic progressions in text. For example , text "abaabaabaab..." over alphabets $\{a,b\}$ has alphabet b in AP positions where AP is $2+3n$. Regular language Finite State Automata for this 2-colored infinite string is:

```
a---b---a---a--->b
      |<-----|
```

(2.12) In terms of vowelless string complexity measure previously, if a 255-colored string is simplified to 2-colored string as "Consonant-Vowel-Consonant-Consonant-Vowel..." replacing consonant and vowels with "Consonant" and "Vowel" notations, english language (and most others) on an average has an arithmetic progression $k+3n$ of vowel positions for some constant k .

(2.13) Previous vowelless string compression can be linguistically explained in terms of sequence of syllables. Related syllable based name clustering of proper nouns occurring in BigData sets has been described in 708 - Strings of Names in english suffer from lack of compound alphabets which most other classical languages are bestowed with. Every syllable in an English name string (when it is spelt out verbally) could contain more than one alphabet which is concatenation of vowels and consonants while in most other natural languages every syllable is mostly associated with just one compound alphabet(vowel + consonant). This makes clustering similar names easier in other languages by comparing syllables (blocks of substrings) instead of alphabets. In previous example word "decision" has blocks of substrings or syllables - "de-ci-sion". Thus distance between two strings could be defined as distance between audio of the words (by recording the syllables of the two words by human speech and comparing the two audios by speech merit measures like MFCC). Text Compression then amounts to succinctly storing the sequences of syllables - an example succinct storage is to transcribe the string from English to another language having compound alphabets and storing the concise syllables in another language. Example string "de-ci-sion" is compressed syllable-wise as "d-c-sn" forfeiting

vowels in English while a transcription could benefit from compound alphabets. From 2.8, algebraically each syllable is an Orbit and could be a Stabilizer set too (g.x=g) - e.g d.e=d, c.i=c in previous example string "decision".

(2.14) Variable k-order (n-grams) Markov Model of texts computes prior probabilities of successor substrings to predecessor substrings (of length k) in a text (which has been trivially implemented in NeuronRain by substring probability dictionaries in Hidden Markov Model Maximum Likelihood Estimator) and those priors are bayesian conditional probability training data for predicting next literal in a string, sufficient to decompress vowelless texts by filling in absent vowels approximately. Naive algorithm which does a regular expression match of a vowelless text encoded as DFA within a dictionary corpus, having no assumption on k-order Markov Model or Hidden Markov Model Maximum Likelihood Estimator might have better accuracy than probabilistic methods. In example earlier, vowelless text d-c-s--n for string "decision" is encoded as Regular Expression DFA $d[a-z]c[a-z]s[a-z][a-z]n$ and matched by dictionary search. Downside of dictionary regex match is the exclusion of proper nouns (Names of People and Places) in decompressed text as dictionaries and encyclopaedia may not contain all possible proper nouns acting as an indirect certificate for Named Entity Recognition(NER) of names.

References:

-
- 2.15 Variable order Markov model - https://en.wikipedia.org/wiki/Variable-order_Markov_model
- 2.16 DeepMind Ithaca - Restoring and attributing ancient texts using deep neural networks - <https://ithaca.deepmind.com/> - a transformer attention model for deeplearning archaeological inscriptions and restore missing texts (71% accuracy for an example redacted greek decree text dt.485 BC). Vowelless text decompression is a text restoration algorithm (to restore the lost vowels in a word) and Very High order Markov model and Regular expression model of texts in 2.14 are, in contrast, dictionary based predictors of words without depending on training texts.
- 2.17 DeepMind Ithaca - Paper - <https://www.nature.com/articles/s41586-022-04448-z>
- 2.18 Multilingual Texts and Speech - Code Switching Examples - <https://en.wikipedia.org/wiki/Code-switching> - Vowelless Text Compression is mostly limited to English texts. Code switching is the practice of mixing multiple languages within a text or speech. Any syllable vectorspace embedding of a string obtained from a hyphenation implementation, could be code switched by arbitrarily mapping a syllable of Word1 (belonging to Language1) to a phonetically equivalent syllable in Word2 (belonging to Language2) - Example: hyphenated string "de-ci-sion" is code-switched to English-Tamil bilingual string (saving 2 vowels 'e' and 'i' which might have required additional unicode encoding in English) "டிசion"
3. (FEATURE - THEORY - Pairwise LCS implementation DONE) KMeans, KNN and other clustering and classification algorithms implemented thus far, group similar encoded strings for astronomical (or any other) data. Clustered strings can further be mined for patterns with ordering by applying a Longest Common Substring algorithm within each cluster. This gives a fine grained pattern hidden in the encoded input strings. These longest common substrings can then be translated to a rule similar to class association rule (Frequent item set and GSP algorithms are quite expensive and do not fit well for mining patterns in strings).
4. (FEATURE - DONE) Implementation of String Distance measure using different distance measures (python-src/StringMatch.py) for comparing Encoded Strings in addition to pairwise and Multiple Sequence Alignment.
5. (FEATURE - DONE) Construct a Hidden Markov Model with State transitions and Observations(events). If the number of states are exponential then this will be infeasible. A HMM has been implemented for text decompression with vowel-removed strings. Also a HMM has been implemented for Part-of-Speech tagging, Named

Entity Recognition and Conditional Random Fields.

6. (FEATURE - DONE - continuation of point 3) Correlate with Rules from Classics (BPHS, BJ etc.,) with the mined datasets for particular class of events (Special Case of Mundane Predictive Model is described in items 47 to 51 and basic framework is already implemented). The Longest Common Substring implementation already mines for most common pattern with in a clustered or classified dataset of encoded strings which suffices for astronomical datasets. Script for parsing the clustered data from classifiers and decoding the longest common pattern have been added.

7. (FEATURE - DONE) Integrate Classifiers in above String Pattern mining (classify strings and then mine).

8. (FEATURE - DONE) At present fundamental algorithms like - Perceptrons with Gradient Descent, Linear and Logistic Regression, Hidden Markov Model for Text Decompression, KMeans Clustering, Naive Bayesian, Decision Tree, SVM (uses thirdparty OSS) and kNN Classifiers, String Alignment and Distance based algorithms, Knuth-Morris-Pratt String Match Algorithm, Sequence Mining, Deep Learning(Convolution and Backpropagation), Social Network Analysis, Sentiment Analysis - have been implemented specialized for the encoded strings astronomical datasets.

9. (FEATURE - DONE) InterviewAlgorithm code in <https://sourceforge.net/p/asfer/code/146/tree/python-src/InterviewAlgorithm/InterviewAlgorithmWithIntrinsicMerit.py> and Classification based on indegrees of wordnet subgraph node in action item 6 above (as mentioned in <http://arxiv.org/abs/1006.4458> , <https://sites.google.com/site/kuja27/TAC2010papersubmission.pdf?attredirects=0> and http://www.nist.gov/tac/publications/2010/participant.papers/CMI_IIT.proceedings.pdf). Related Publication Drafts are: <https://sites.google.com/site/kuja27/LowerBoundsForMajorityVotingPseudorandomChoice.pdf?attredirects=0>, <https://sites.google.com/site/kuja27/CircuitForComputingErrorProbabilityOfMajorityVoting.pdf?attredirects=0>, <https://sites.google.com/site/kuja27/InDepthAnalysisOfVariantOfMajorityVotingwithZFAOC.pdf?attredirects=0>. Test C++ code written in 2006 for computing Majority voting error probability is at: <http://sourceforge.net/p/asfer/code/HEAD/tree/cpp-src/miscellaneous/pgood.cpp> and python script written in 2010 is at: <http://sourceforge.net/p/asfer/code/HEAD/tree/python-src/pgood.py>.

[Disclaimer and Caveat: Due to radical conclusions that are derivable from the $P(\text{good})$ binomial coefficients summation infinite series when applied to majority voting with SAT setting in perfect zero-error case, all the related points elsewhere in this document on majority voting + SAT versus pseudorandom choice (e.g 100% noise stability and circuit lowerbounds for it) are work-in-progress , unreviewed (excluding those done during 2009-2011) , not-quite rigorous drafts only with possible theoretical errors, which might have commissions-omissions and more additions to make as mentioned earlier and this analyzes a very special case of voting scenario. It is not an attempt to prove or disprove $P=NP$, but rather an analysis of very generic unnatural proof framework based on boolean social choice complexity for proving lowerbounds which might include the question of $P=NP$. Infact it shrouds entire complexity classes underneath it. It is non-conventional and questionable as to whether LHS pseudorandomness or dictator boolean function can be equated to RHS Majority Voting. This just analyzes the special case when there is zero-error or same-error on both sides and the outcomes of processes related to pseudorandom/dictator choice and Majority Voting with Voter SAT oracles are "equally good" where "Goodness" is defined as for all scenarios which could be infinite, a PRG/Dictator choice or Majority Voted Choice "make zero-error decisions". It is not a statistical mean on both sides in which all probabilities are averaged. More specifically, (in)tractability of perfect voting is pivotal to this - assuming perfection

which does away with BP* complexity classes this poses itself as a strong non-trivial counterexample. In theoretical interludes in this document probability of perfection is defined as a function of NoiseSensitivity or NoiseStability which is based on commonsense notion that if an entity (human or software) has "correct thinking in decision making" outcome "decision" is "correct". For example if noisy inputs do not perturb a voter's boolean function, voter is 100% stable. This is equivalent to real life scenarios where conflicting inputs from people make a person to decide incorrectly. A perfect voter is never swayed. Even without equating the 2 sides(e.g whether there exists a P algorithm for RHS PH or EXP circuit) above are non-trivial problems. Lot of assumptions have been made in arriving at conclusions in this document, most important being equal stability implies circuit lowerbounds which is based on a matrix of scenarios where error and noise intersect and 100% noise stability regime in percolation crossing events. In general setting, distribution is Poisson binomial with unequal voter error and Error is not just limited to noise sensitivity but also includes flawed decision tree evaluation which adds one more scenario to matrix. It is more apt to say there are no conclusions arrived at from equating LHS and RHS of Pr(Good) circuits. Rather it raises lot of more open questions and contradictions. A major requirement for proving a separation or containment is that RHS majority voting circuit has to be a complete problem for class C whether exact or probabilistic(BP*), implying whole L(RHS) is in L(LHS) because LHS is an algorithm for a complete problem. For many probabilistic BP* and PH classes no complete problems are known. Conclusions can be drawn subject to knowledge of complete problems for RHS majority voting circuit.

There are zero error voting systems:

E.g Paxos protocol without byzantine failures -

<http://research.microsoft.com/en-us/um/people/lamport/pubs/paxos-simple.pdf>

]

 Psuedorandom Choice and Majority Voting (Majority circuit with SAT inputs)

10. (THEORY)

https://sites.google.com/site/kuja27/ImplicationRandomGraphConvexHullsAndPerfectVoterProblem_2014-01-11.pdf?attredirects=0&d=1 on decidability of existence of perfect voter and the probability series for a good choice of

https://sites.google.com/site/kuja27/CircuitForComputingErrorProbabilityOfMajorityVoting_2014.pdf?attredirects=0&d=1 are related to already well studied problems in social choice theory but problem definition is completely different. Arrow's theorem of social choice for an irrational outcome in condorcet election of more than 2 candidates and its complexity theory fourier analysis proof [GilKalai] are described in www.cs.cmu.edu/~odonnell/papers/analysis-survey.pdf. Irrational outcome is a paradox where the society is "confused" or "ranks circularly" in choice of a candidate in multipartisan condorcet voting. Rational outcome converges to 91.2% (Guilbaud number) with a possibility of 8.8% irrational outcome.

Additional References:

10.1. Social Choice Theory, Arrow's Theorem and Boolean functions -

<http://www.ma.huji.ac.il/~kalai/CHAOS.pdf>

10.2. <http://www.project-syndicate.org/commentary/kenneth-arrow-impossibility-theorem-social-welfare-by-amartya-sen-2014-11>

10.3. Real life illustration of Arrow's Theorem -

<http://www.nytimes.com/2016/05/09/upshot/unusual-flavor-of-gop-primary-illustrates-a-famous-paradox.html> - Condorcet Circular choice paradox, Change in Voter decision when a new Candidate is added and Conflict between individual decision and group decision - Incompleteness of democratic process.

10.4. How hard is it to control elections [BartholdiToveyTrick] -

<http://www.sciencedirect.com/science/article/pii/S089571779290085Y> - manipulating outcomes of variety of voting schemes is NP-hard.

10.5. How hard is it to control elections with tiebreaker

[MatteiNarodytskaWalsh] - <https://arxiv.org/pdf/1304.6174.pdf>

11.(THEORY) What is perplexing is the fact that this seems to contravene guarantee of unique restricted partitions described based on money changing problem and lattices in https://sites.google.com/site/kuja27/SchurTheoremMCPAndDistinctPartitions_2014-04-17.pdf?attredirects=0 and https://sites.google.com/site/kuja27/IntegerPartitionAndHashFunctions_2014.pdf?attredirects=0&d=1 which are also for elections in multipartisan setting (if condorcet election is done). Probably a "rational outcome" is different from "good choice" where rationality implies without any paradoxes in ranking alone without giving too much weightage to the "goodness" of a choice by the elector. Actual real-life elections are not condorcet elections where NAE tuples are generated. It is not a conflict between Arrow's theorem as finding atleast 1 denumerant in multipartisan voting partition is NP-complete (as it looks) - which can be proved by ILP as in point 20 of https://sites.google.com/site/kuja27/IntegerPartitionAndHashFunctions_2014.pdf?attredirects=0&d=1 - the assumption is that candidates are not ranked; they are voted independently in a secret ballot by electors and they can be more than 3. The elector just chooses a candidate and votes without giving any ordered ranking for the candidates which makes it non-condorcet.

12.(THEORY) Moreover Arrow's theorem for 3 candidate condorcet election implies a non-zero probability of error in voting which by itself prohibits a perfect voting system. If generalized to any election and any number of candidates it could be an evidence in favour of $P \neq NP$ by proving that perfect voter does not exist and using democracy Maj+SAT circuits and P(Good) probability series convergence (As described in handwritten notes and drafts http://sourceforge.net/projects/acadpdrafts/files/ImplicationGraphsPGoodEquationAndPNotEqualToNPQuestion_excerpts.pdf/download, https://sites.google.com/site/kuja27/ImplicationRandomGraphConvexHullsAndPerfectVoterProblem_2014-01-11.pdf?attredirects=0&d=1, <https://sites.google.com/site/kuja27/LowerBoundsForMajorityVotingPseudorandomChoice.pdf?attredirects=0>, https://sites.google.com/site/kuja27/CircuitForComputingErrorProbabilityOfMajorityVoting_2014.pdf?attredirects=0&d=1 and https://sites.google.com/site/kuja27/PhilosophicalAnalysisOfDemocracyCircuitAndPRGChoice_2014-03-26.pdf?attredirects=0).

13.(THEORY) But it is not known that if Arrow's theorem can be generalized for infinite number of candidates as above and whether such an electoral system is decidable. The possibility of a circular ranking in 3-condorcet election implies that there are some scenarios where voter can err though not exactly an error in making a "good choice" (or Perfect Voter Problem is decidable in case of 3 candidates condorcet election).

14.(THEORY) Each Voter has a k-SAT circuit which is input to Majority circuit. k-SAT can be reduced to 3-SAT (not 2-SAT) and thus is NP-complete. Error by a Voter SAT circuit implies that voter votes 0 instead of 1 and 1 instead of 0. This is nothing but the sensitivity of the voter boolean function i.e number of erroneous variable assignments by the voter that change the per-voter decision input to the Majority circuit. Thus more the sensitivity or number of bits to be flipped to change the voter decision, less the probability of error by the voter. If sensitivity is denoted by s , $1/q$ is probability that a single bit is flipped and probability of error by the voter is p then $p = 1/q^s$ which is derived by the conditional probability that $\Pr[m \text{ bits are flipped}] = \Pr[m\text{-th bit is flipped}/(m-1) \text{ bits already flipped}] * \Pr[(m-1) \text{ bits are flipped}] = 1/q * 1/q^{(m-1)} = 1/q^m$ (and $m=s$) . This expression for p can be substituted in the Probability series defined in https://sites.google.com/site/kuja27/CircuitForComputingErrorProbabilityOfMajorityVoting_2014.pdf?attredirects=0&d=1. Probability of single bit flip is $1/q$ if the number of variables across all clauses is q and each variable is flipped independent of the other. Error by voter can also be simulated with probabilistic truth tables(or) probabilistic CNFs.

For example, a term in the binomial summation becomes:

$mC(n+1) * (1/q^s)^{(n+1)} * (1-1/q^s)^{(m-n-1)}$ where m is total number of voter SATs and $(1/q)$ is probability of single variable flip in Voter SAT and s is sensitivity of Voter SAT boolean function - s can change for each voter SAT in which case it has to be $s_1, s_2, s_3, s_4, s_5, \dots$ and the summation requires hypergeometric algorithms.

The Voter SAT circuit has an interesting application of Hastad's Switching Lemma - random probabilistic setting of variables known as "restrictions" decreases the decision tree depth significantly, or, number of variables that determine the Voter SAT outcome reduces significantly - in other words, random "restricted convincing" of a voter SAT CNF has huge impact on number of variables yet to be "convinced".

As done in the Switching Lemma proof, parity circuit can be an AND of ORs (or OR of ANDs) which is randomly restricted to switch the connectives in lowest 2 levels to arrive at super-polynomial lowerbound for parity and hence for each voter SAT. Thus the Parity CNF can be the special case of Voter SAT also (i.e voter wants odd number of variables to be satisfied - odd voter indeed). This kind of extends switching lemma to an infinite majority with parity oracle case.

Fourier expansion of the unbounded fan-in Majority+SAT circuit is obtained from indicator polynomial (<http://www.contrib.andrew.cmu.edu/~ryanod/?p=207>) by substituting fourier polynomial for each voter SAT in the majority circuit fourier polynomial. Conjecturally, this expansion might give an infinite summation of multilinear monomials - has some similarities to permanent computation if represented as an infinite matrix i.e Permanent converges to 1 for this infinite matrix for perfect voting (?) and Permanent is #P complete. This is obvious corollary of Toda's theorem in a special case when RHS of $P(\text{Good})$ is a PH=DC circuit because Toda's theorem implies that any PH problem is contained in $P^{\#P}(P \text{ with access to } \#P \text{ number_of_sats oracle})$. Permanent computes bipartite matchings - non-overlapping edges between two disjoint vertex sets - probably pointing to the bipartisan majority voting. This makes sense if the entire electorate is viewed as a complete social network graph and voting is performed on this network electorate. Majority voting divides the social network into two disjoint sets (for and against) with edges among them - division is by maximum matching - "for" voter vertex matched with "against" voter vertex. When this matching is perfect, election is tied. Imperfect matchings result in a clear winner vertex set - which has atleast one unmatched vertex is the winner.

Demarcation of linear and exponential sized circuits: $P(\text{good})$ RHS has Circuit SAT for each voter with unbounded fanin.

- 1) If the variables for each voter SAT are same, then the circuit size is exponential in number of variables - DC-uniform
- 2) else if the variables are different for each SAT, then the circuit is linear in number of variables - polynomial size

1) is more likely than 2) if lot of variables among voters are common.

There are three possibilities

Circuit lies between 1) and 2) - some variables are common across voters - kind of super-polynomial and sub-exponential

Circuit is 1) - all variables are common across voters - the worst case exponential (or even ackermann function?)

Circuit is 2) - there are no common variables

As an alternative formulation, LHS of the $P(\text{Good})$ series can be a dictator boolean function (property testing algorithms like BLR, NAE tuples - <http://www.contrib.andrew.cmu.edu/~ryanod/?p=1153>) that always depends on only one variable and not on a Pseudorandom generator. Thus how error-free is the assignment to LHS dictator boolean function determines $P(\text{Good})$ LHS(sensitivity and probabilistic truth tables are the measures applicable as described previously). Thus both LHS and RHS can be boolean functions with corresponding circuits constructible for them.

Influence of a variable i in a boolean function is $\text{Probability}[f(x) \neq f(x \text{ with } i\text{-th bit flipped})]$. For Majority function influence is $\sim 1/\sqrt{n}$ from Berry-Esseen Central Limit Theorem - sum of probability distributions of values assigned to boolean random variables converge to Gaussian. Thus in infinite majority a voter is insignificant. Error in majority voting can be better defined with Stability and Noise Sensitivity measures of a Boolean Function (Influence, Stability, Noise, Majority is Stablest theorem etc., - www.cs.cmu.edu/~odonnell/papers/analysis-survey.pdf) where correlated pairs of boolean variable tuples form an inner product to get the expression : $\text{Noise}(f) = 1/2 - 1/2 * \text{Stability}(f)$ where Noise is the measure of corruption in votes polled while Stability is the resilience of votes polled to corruption so that outcome is not altered. [But for infinite majority inner product could become infinite and the measures may lose relevance]. Also related is the Kahn-Kalai-Linial Theorem for corrupted voting - <http://www.contrib.andrew.cmu.edu/~ryanod/?p=1484> - that derives a lower bound for the maximum influence ($\log(n)/n$). Applications of Noise Sensitivity in real-world elections is described in - <https://gilkalai.wordpress.com/2009/03/06/noise-sensitivity-lecture-and-theses/> , <http://www.cs.cmu.edu/~odonnell/slides/mist.pps> and percolation in [http://research.microsoft.com/en-us/um/people/schramm/memorial/spectrumTalk.pdf?tduid=\(332400bcf8f14700b3a2167cd09a7aa9\)\(256380\)\(2459594\)\(TnL5HPStwNw-SliT5K_PKao3NElOXgvFug\)\(\)](http://research.microsoft.com/en-us/um/people/schramm/memorial/spectrumTalk.pdf?tduid=(332400bcf8f14700b3a2167cd09a7aa9)(256380)(2459594)(TnL5HPStwNw-SliT5K_PKao3NElOXgvFug)())

As done for sensitivity previously, a term in the $P(\text{Good})$ binomial summation becomes:

$mC(n+1) * \text{product_of_n+1_}(\text{NoiseSensitivityOfVoterSAT}(i)) * \text{product_of_m-n-1_}(1 - \text{NoiseSensitivityOfVoterSAT}(i))$ where m is total number of voter SATs and the summation requires hypergeometric algorithms. Infact it makes sense to have Stability as a zero-error measure i.e the binomial summation term can be written as $mC(n+1) * \text{product_of_n+1_}(\text{NoiseSensitivityOfVoterSAT}(i)) * \text{product_of_m-n-1_}(1/2 + 1/2 * \text{StabilityOfVoterSAT}(i))$ since $1 - \text{NoiseSensitivity} = 1/2 + 1/2 * \text{Stability}$. Difference between sensitivity and NoiseSensitivity here is that NoiseSensitivity and Stability are probabilities and not number of bits and are directly substitutable in $P(\text{Good})$ series.

Summation of binomial coefficients in RHS is the collective stability or noise in the infinite majority circuit. It converges to 0.5 if NoiseStability is uniform 0.5 for all Voter SATs and in best case converges to 1. This summation connects analysis, non-uniform infinite majority voting and complexity theory - Hypergeometric functions, Noise and Stability of Voter Boolean functions, Majority Circuit.

P(Good) summation is Complementary Cumulative Binomial Distribution Function (or) Survival Function

Goodness Probability of an elected choice is derived in https://sites.google.com/site/kuja27/CircuitForComputingErrorProbabilityOfMajorityVoting_2014.pdf . For an above average good choice (i.e a choice which is more than 50% good) atleast majority populace must have made a good decision (this is axiomatically assumed without proof where all voters have equal weightages). In probability notation this is $\text{Pr}(X > n/2)$ where X is the binomial random variable denoting the number of electorate who have made a good choice which has to be atleast halfway mark. For each $\text{Pr}(X=k)$ the binomial distribution mass function is $nCk(p)^k(1-p)^{n-k}$ [Reference: https://en.wikipedia.org/wiki/Binomial_distribution]. Cumulative distributive function is defined as $\text{Pr}(X \leq k) = \text{summation_0_k}(nCk(p)^k(1-p)^{n-k})$ and its complement is $\text{Pr}(X > k) = 1 - \text{Pr}(X \leq k)$ mentioned as Complementary Cumulative Distributive Function [Reference: https://en.wikipedia.org/wiki/Cumulative_distribution_function] which is also known as Survival Function[Reference: https://en.wikipedia.org/wiki/Survival_function].

A plausible proof for the assumption that for an above average good choice at least half of the population must have made a good decision:
 If there are n inputs to the Majority circuits, the voter inputs with good decision can be termed as "Noiseless" and voter inputs with bad decisions can be termed as "Noisy" in Noise Sensitivity parlance. For infinite majority it is known that (from <http://analysisofbooleanfunctions.org/>):

$$\lim_{\substack{n \rightarrow \infty \\ n \text{ odd}}} \text{NS}(\delta, \text{Majority}(n)) = 1/\pi * \arccos(1-2*\delta)$$
 (due to Central Limit Theorem and Sheppard's Formula)

where δ is probability of noise and hence bad decision. If δ is assumed to be 0.5 for each voter (each voter is likely to err with probability 0.5) then above limit becomes:

$$1/\pi * \arccos(1-1) = 1/\pi * \pi/2 = 1/2$$
 which is the Noise (Goodness or Badness) of the majority circuit as a whole.
 From this expected number of bad decision voters can be deduced as $E(x) = x*p(x) = 0.5 * n = n/2$ (halfway mark)

Above is infact a simpler proof for $P(\text{Good})$ without any binomial summation series for $\delta=0.5$. In other words the number of bad decisions are reverse engineered. But $P(\text{Good})$ binomial summation (complementary cumulative distributive function) is very much required in the hardest problem where each voter has a judging function to produce an input to Majority function and each such judging function is of varied complexities and noise stabilities.

For $\delta=0.5$, NoiseSensitivity of infinite majority=0.5 and both are equal. For other values of δ this is not the case. For example interesting anomalies below surface:

$\delta=0.3333\dots$:

 $\text{NS} = 1/\pi * \arccos(1 - 2*0.333\dots) = 0.3918$

$\delta=0.25$:

 $\text{NS} = 1/\pi * \arccos(1-2*0.25) = 0.333\dots$

 Chernoff upper tail bound

Upper bound for $P(\text{Good})$ binomial distribution can be derived from Chernoff bound (assuming Central Limit Theorem applies to sum of Binomial random variables)- <http://www.cs.berkeley.edu/~jfc/cs174/lects/lec10/lec10.pdf> - For $P(\text{Good})$ series the upper tail bound is needed i.e. $\Pr(\text{Number of voters making good decision} > n/2)$ which is derivable to 0.5 and 1 exactly wherein the upper bound is not necessary. But for other cases, upper tail Chernoff bound is:

$$P[X > (1+\delta)*\text{mean}] < \{e^{\delta}/(1+\delta)^{(1+\delta)}\}^{\text{mean}}$$
 Total population is n , $\text{mean}=n*p$ and $(1+\delta)*\text{mean} = n/2$
 Thus $\delta = (1 - 2*p)/2*p$

$$P[X > n/2] < \{e^{[(1-2p)/p]} / (1/2p)^{(1/2p)}\} = \{e^{(1-2p)n} * (2p)^{(1/2p)}\}$$

When $p=0.5$, $P[X > n/2] < 1$ which is an upperbound for 0.5.

But intriguingly for $p=1$ the upper tail bound is:

$(e^{-1}*\sqrt{2})^n$

which is increasingly less than 1 for high values of n whereas $P(\text{good})$ converges to 1 in exact case (why are these different?). This contradiction arises since in exact derivation of $P[X > n]$:

$$mC(n+1)(p)^{(n+1)}(1-p)^{(m-n-1)} + mC(n+2)(p)^{(n+2)}(1-p)^{(m-n-2)} + \dots + mCm(p)^m(1-p)^{(m-m)}$$

all the terms vanish by zero multiplication except $mCm(p)^m(1-p)^m$ which becomes:

$mCm*1*0^0$

and by convention, $\theta^0 = 1$, thereby converging to 1 while the Chernoff upper tail bound decreases with n .

Hoeffding upper tail bound

For Bernoulli trials involving binomial distribution summation, Hoeffding Inequality can be applied for upper tail bound -

https://en.wikipedia.org/wiki/Hoeffding%27s_inequality - defined by:

$$P(X > (p+\epsilon)n) \leq \exp(-2\epsilon^2 * n)$$

If $p+\epsilon = 0.5$ for halfway mark, $\epsilon = 1/2 - p$.

$$P(X > n/2) \leq \exp(-2(0.5-p)^2 * n)$$

For $p=1$, $P(X > n/2) \leq \exp(-n/2)$ which for infinite n converges to 1.

Thus tailbounds above are only less tight estimates and exact summation is better for $p=0.5$ and 1.

There are two independent aspects to the $P(\text{Good})$ series - Goodness and Hardness:

(1) Goodness of Voting:

The convergence of the binomial coefficient summation series in RHS is the "goodness" side of the voting expressed in terms of Noise sensitivity and Stability of each Voter's Boolean Function - whether the voters have exercised their franchise prudently to elect a "good" choice. If the Voter Boolean Functions are all balanced then by Kahn-Kalai-Linial lowerbound there are $n/\log(n)$ influential variables that control the decision of each Voter.

(2) Hardness of Voting:

The circuit for RHS(e.g Boolean Function Composition) and its Fourier polynomial expansion.

Mix of Hardness and Goodness result in variety of BP^* classes or P^* classes (if error is unbounded). Goodness is related to Noise Sensitivity and Stability. Probabilistic Hardness is due to pseudorandomness. Are Goodness and Pseudorandomness related? Yes, because Noise Sensitivity occurs when there is a correlation between two strings with flips. Correlation in turn occurs when flips are pseudorandom. Connection between Stability, Fourier coefficients and pseudorandom flip probability are expressed in (16) and (20) below (Plancherel's theorem).

(*IMPORTANT*) Noise Stability, Noise Sensitivity and Complexity Class BPP (error in voting)

In all points in this document, an assumption is made that Noise Stability and BPP are equivalent notions. Is this valid? A language L is in BPP if for x in L there exists a Turing Machine that accepts x and outputs 1 with bounded probability (e.g 2/3) and if x not in L , rejects x and outputs 0 with bounded probability (e.g 1/3). Following table illustrates all possible scenarios and where BPP and Noise Stability fill-in (x/e is correlated, flipped version of x):

x	$f(x) = f(x/e)$	$f(x) \neq f(x/e)$ Noise
$x \text{ in } L, x/e \text{ in } L$	No error	Error
$x \text{ in } L, x/e \text{ not in } L$ $f(x)=1, f(x/e)=0$	Error	No error if

				else Error	

x not in L, x/e in L f(x)=0, f(x/e)=1		Error		No error if	
				else Error	

x not in L, x/e not in L		No error		Error	

Third column of the table relates Noise Sensitivity and BPP - it subdivides the Noise Sensitivity into 4 probable scenarios. Hence Noise Sensitivity overlaps BPP - explains one half of the error. Even after a circuit is denoised i.e third column is removed, it can still be in BPP due to the second column possibilities above. Noise sensitivity handles only half the possibilities in the above table for output noise. The second and third rows in second column represent noise in input where the circuit doesn't distinguish inputs correctly (false positives and false negatives). This requires derandomization. Thus error-free decision making depends on both denoisation and derandomization. A Turing machine that computes all 8 possibilities in the table above without error is 100% perfect decision maker. In terms of probability:

Probability of Good Decision = Input noise stability (second column) + Output noise stability (third column)

which can also be stated as:

Probability of Good Decision = 1-(Probability of False positives + Probability of False negatives)

Above is a better, rather ideal, error probability measure that can be substituted in $P(\text{Good})$ RHS binomial distribution summation because it accounts for all possible scenarios of errors. Presently, $P(\text{Good})$ binomial summation depends only on output noise sensitivity. Complexity literature doesn't yet appear to have the theoretical notion of input noise counterpart of output noise sensitivity for boolean functions (e.g what is the fourier theoretic estimation of false positivity similar to the Plancherel version of noise stability?). Second column input noise can be written as $\text{TotalError} - [f(x) \neq f(x/e)]$ where $\text{TotalError} \leq 1$. Probability of Good Decision is sum of conditional probabilities of these 8 possibilities in the table:

Probability of Good Decision = $\Pr(f(x)=f(x/e) \mid x \text{ in } L, x/e \text{ in } L) \cdot \Pr(x \text{ in } L, x/e \text{ in } L) +$

$\Pr(f(x) \neq f(x/e) \mid x \text{ in } L, x/e \text{ in } L) \cdot \Pr(x \text{ in } L, x/e \text{ in } L) +$

\dots
 $\Pr(f(x) \neq f(x/e) \mid x \text{ not in } L, x/e \text{ not in } L) \cdot \Pr(x \text{ not in } L, x/e \text{ not in } L)$

Computation of the above conditional probability summation further confounds the estimation of voter decision error in Judge Boolean Functions.

In other words, a precise estimate of voter or voting error from table above which related BP^* complexity class and Boolean Noise Sensitivity:

Probability of Bad Decision = $\text{NoiseSensitivity} - \{\Pr(f(x)=1, f(x/e)=0) / x \text{ in } L, x/e \text{ not in } L\}$

$- \{\Pr(f(x)=0, f(x/e)=1) / x \text{ not in } L, x/e \text{ in } L\}$

$+ \{\Pr(f(x)=f(x/e)) / x \text{ in } L, x/e \text{ not in } L\}$

$+ \{\Pr(f(x)=f(x/e)) / x \text{ not in } L, x/e \text{ in } L\}$

which may be more or less than NoiseSensitivity depending on cancellation of other conditional probability terms. This is the error term that has to be substituted for each voter decision making error. Because of this delta, NoiseSensitivity (and NoiseStability) mentioned everywhere in this

document in $P(\text{Good})$ binomial summation and majority voting circuit is indeed NoiseSensitivity (and NoiseStability) (+ or -) δ . Previous probability coalesces Noise and Error into one expressible quantity - i.e denoisification + derandomization.

When Probability of Bad Decision is 0 across the board for all voters, the $\text{Pr}(\text{Good})$ series converges to 100% and previous identity can be equated to zero and NoiseSensitivity is derived as:

$$\begin{aligned} \text{NoiseSensitivity} = & \{ \text{Pr}(f(x)=1, f(x/e)=0)/x \text{ in } L, x/e \text{ not in } L \} \\ & \{ \text{Pr}(f(x)=0, f(x/e)=1)/x \text{ not in } L, x/e \text{ in } L \} \\ & - \{ \text{Pr}(f(x)=f(x/e))/x \text{ in } L, x/e \text{ not in } L \} \\ & - \{ \text{Pr}(f(x)=f(x/e))/x \text{ not in } L, x/e \text{ in } L \} \end{aligned}$$

Above matrix of 8 scenarios and identity above give somewhat a counterintuitive and startling possibility that NoiseSensitivity of a voter's decision boolean function can be non-zero despite the convergence of $\text{Pr}(\text{Good})$ Majority Voting binomial series when some error terms do not cancel out in previous expression. This implies that there are fringe, rarest of rare cases where voting can be perfect despite flawed decision boolean functions.

Hastad Switching Lemma, $P(\text{Good})$ Majority Voting circuit and Election Approximation or Forecasting

Hastad Switching Lemma for circuit of width w and size s with probability of random restriction p for each variable states the inequality:

$$\text{Pr}[\text{DecisionTree}(f/\text{restricted}) > k] \leq (\text{constant} * p * w)^k$$

where p is a function of width w and p is proportional to $1/w$. In forecasting, a sample of voters and their boolean functions are necessary. If the Majority circuit is PH=DC(variables are common across voters) or AC(variables are not so common across voters), the sampling algorithm pseudorandomly chooses a subset from first layer of the circuit's fanin and applies random restriction to those Voters' Boolean Circuits which abides by above inequality. The rationale is that probability of obtaining required decision tree depth decreases exponentially (RHS mantissa < 1). Thus the forecast is a 3-phase process:

- (1) Pseudorandomly choose subset of Voter Boolean Functions in the first layer of the circuit - This is also a random restriction
- (2) Randomly Restrict variables in each boolean circuit to get decision trees of required depth if voters reveal their blackbox boolean functions
- (3) Simulated Voting (and a property testing) on the restricted boolean functions subset accuracy of which is a conditional probability function of (1) and (2). This could be repetitive random restrictions of (2) also.

(1) and (2) are random restrictions happening in 2 different layers of the circuit - amongst voters and amongst variables for each voter .

Alternatively if subset of voters reveal their votes (1 or 0) in opinion polls then the above becomes a Learning Theory problem (e.g. PAC learning, Learning Juntas or oligarchy of variables that dominate) - how to learn the boolean function of the voters who reveal their votes in a secret ballot and extrapolate them to all voters. This is opposite of (1),(2),(3) and the most likely scenario as voters hold back their decision making algorithms usually. From Linial-Mansour-Nisan theorem, class of boolean functions of n variables with depth- d can be learnt in $O(n^O(\log n^d))$ with $1/\text{poly}(n)$ error. From Hastad Switching Lemma, Parseval spectrum theorem (sum of squares of fourier coefficients) and LMN theorem, for a random restriction r , the fourier spectrum is e -concentrated upto degree $3k/r$ where k is the decision tree depth of the restriction. For a function g that approximates the above majority+SAT voting circuit f , the distance function measures the accuracy of approximation.

An interesting parallel to election approximation is to sample fourier spectrum

of boolean functions of a complexity class C for each voter. (This seems to be an open problem - <http://cstheory.stackexchange.com/questions/17431/the-complexity-of-sampling-approximately-the-fourier-transform-of-a-boolean-fu>). Essentially this implies complexity of approximating a voter's boolean function in complexity class C by sampling the fourier coefficients of its spectrum and hence election forecasting is C-Fourier-Sampling-Hard.

Points (53.1) and (53.2) define a Judge Boolean Function with TQBF example that is PSPACE-complete. Each voter in RHS of P(Good) has such a TQBF that is input to Majority circuit. TQBF is also AP-hard where AP is the set of all languages recognized by an alternating turing machine (ATM) with alternating forall and thereexists states, and it is known that PSPACE=AP (<http://people.seas.harvard.edu/~salil/cs221/spring10/lec6.pdf>).

 (*IMPORTANT*) Boolean Function Composition (BFC) and Majority+SAT voting circuit

Boolean Function Composition is described in detail at [AvishayTal] Section 2.3 - <http://ecc.hpi-web.de/report/2012/163/> - which is defined as $f \circ g = f(g(x))$ and the sensitivity and complexity measures of BFC are upperbounded by products of corresponding measures. Majority Voting circuit for P(Good) Binomial summation can be formulated as composition of two functions - Majority and SAT i.e Voters' SAT outputs are input to Majority (or) Majority* $SAT = Majority(SAT_1, SAT_2, \dots, SAT_n)$. Hence sensitivity of this composition is upperbounded by $sensitivity(MAJ_n) \cdot \max(sensitivity(SAT_i))$ which becomes the "sensitivity of complete electorate". This has a direct bearing on the error probability of voter decision in P(Good) binomial summation - the pseudorandom choice error probability or dictator boolean function sensitivity in LHS and electorate sensitivity obtained from previous composition in RHS should be equal in which scenario LHS achieves what RHS does (or) there is a PH or EXP collapse to P. Circumventing this collapse implies that these two sensitivity measures cannot be equal and either Dictator/PRG choice or Majority Voting is better over the other - a crucial deduction. Dictator boolean function has a sensitivity measure n (all variables need to be flipped in worst case as function depends on only one variable) while the Majority* SAT composition is a maximum of products of 2 sensitivities. Counterintuitively, RHS electorate sensitivity can be larger than LHS as there is no SAT composition in Dictator boolean function. But the convergence of P(Good) binomial coefficient series to 1 when $p=1$ does not rule out the possibility of these two sensitivity measures being equal and when it happens the Stability is 1 and NoiseSensitivity is 0 on both sides (assumption: NoiseSensitivity for LHS and most importantly RHS are computable and have same product closure properties under composition like other sensitivity measures).

[
 Quoting Corollary 6.2 in <http://ecc.hpi-web.de/report/2012/163/> for inclusions of complexity measures:

$$"... C(f) \leq D(F) \leq bs(f) \cdot deg(f) \leq deg(f)^3 ..."$$

]

 Noise Sensitivity and Probability of Goodness in P(Good) LHS and RHS -
 Elaboration on previous

LHS of P(Good):

(1) Depends either on a natural (pseudo)random process or a Dictator Boolean Function that unilaterally decides outcome.

(2) When error is zero, probability of good decision is 1 (or) $Pr(f(x) \neq f(y))$

is zero where x and y are correlated bit strings obtained by a bit flip. In other words Noise in input does not alter outcome. If NS is Noise Sensitivity, probability of good outcome is $1-NS$ which is $1/2 + 1/2 \cdot \text{Stability}$.

RHS of $P(\text{Good})$:

(1) Depends on the Noise Sensitivity of Boolean Function Composition - $\text{Maj}(n) \cdot \text{SAT} - \text{Maj}(n) \cdot \text{SAT}_1, \text{SAT}_2, \dots, \text{SAT}_n$.

(2) When error is zero, probability of good decision is 1 because $n \cdot C_n(1)^n(1-1)^0$ becomes 1 in summation and all other terms vanish. If each individual voter has different probability of good decision (which is most likely in real world elections) then it becomes Poisson Probability Distribution trial. Throughout this document, only Binomial Distribution is assumed and therefore NoiseSensitivity of voters are assumed to be equal though the individual voter boolean functions might differ. In a generic setting each voter can have arbitrary decision function which need not be restricted to boolean functions. Throughout this document, only boolean voter judging functions are assumed.

(3) NoiseSensitivity is a fitting measure for voter error or voting error as it estimates the probability of how a randomly changed input distorts outcome of an election. Randomly changed input could be wrong assignment by voter, wrong recording by the voting process etc.,

(4) Perfect Voter has a SAT or Boolean Function that is completely resilient to correlation i.e $\Pr(f(x) \neq f(y)) = 0$. The open question is: is it possible to find or learn such a Voter Boolean Function.

(5) Brute Force exponential algorithm to find perfect voter is by property testing:

- For 2^n bit strings find correlation pairs with random flips - $2^n \cdot (2^n - 1)$ such pairs are possible.
- Test $\Pr(f(x) \neq f(y))$
- This is not a learning algorithm.

(6) For perfect voter, probability p of good decision is $1-NS$ or $1/2 + 1/2 \cdot \text{Stability}$ and has to be 1 which makes $NS=0$ and $\text{Stability}=1$.

(7) Open Question: Is there a learning algorithm that outputs a Perfect Voter Decision Boolean Function f such that $NS=\Pr(f(x) \neq f(y)) = 0$ for all correlated pairs x,y ? (Or) Can LHS and RHS of $P(\text{Good})$ be learnt with $NS=0$ and $\text{Stability}=1$. Such a function is not influenced by any voting or voter errors. Majority is Stablest theorem implies that Majority function is the most stable of all boolean functions with least noise, but still it does not make it zero noise for perfect stability.

Is there some other function stabler than stablest - answer has to be no - But there is an open "Majority is the Least Stable" conjecture which asserts "yes" by [Benjamini-Kalai-Schramm]:

For Linear Threshold Functions (majority, weighted majority et al) f , $\text{Stability}(f) \geq \text{Stability}(\text{Maj}_n)$.

Majority is Stablest theorem is for small-influence LTFs (maximum influence of $f < \epsilon$). If existence of perfect voter boolean function is proved it would be a generalization of this conjecture.

An obvious corollary is that for stablest voting boolean function, majority is apt choice (or) in the Majority voting circuit each voter has a majority as voter boolean function i.e it is a boolean function composition of $\text{Majority} \cdot \text{Majority} = \text{Maj}(\text{Maj}_1, \text{Maj}_2, \text{Maj}_3, \dots, \text{Maj}_n)$. This composition of $\text{Maj} \cdot \text{Maj}$ is the stablest with least noise. This is also depth-2 recursive majority function mentioned in [RyanODonnell] - definition 2.6 in <http://analysisofbooleanfunctions.org/> and Majority Voting with constituencies in <https://sites.google.com/site/kuja27/IndepthAnalysisOfVariantOfMajorityVotingwit>

hZFAOC_2014.pdf. Also the 2-phase document merit algorithm in http://www.nist.gov/tac/publications/2010/participant.papers/CMI_IIT.proceedings.pdf is a variant of this. A voter with Majority as boolean function trivially decides i.e if more than half of his/her variables are satisfied, outputs 1 without any fancy decision making or judging boolean function circuit (e.g an EXP-complete adversarial simulation). By far this is the stablest possible voting scheme unless [Benjamini-Kalai-Schramm] conjecture is true or there exists a 100% noise stable percolation boolean function - derived in (17) and (18) below.

(8) Theorem 2.45 in <http://analysisofbooleanfunctions.org/> is important which proves Stability and NoiseSensitivity for infinite majority:

lt (n->infinity, n odd) Stability[Majn] = $2/\pi \cdot \arcsin(\rho)$

(or)

lt (n->infinity, n odd) NS[delta,Majn] = $2/\pi \cdot \delta + O(\delta^{1.5})$ where delta is the probability of correlation - flipping x to y.

(9) There are two random variables $f(x)=f(y)$ and $f(x) \neq f(y)$ with respective probabilities.

(10) This implies for infinite electorate, error probability is (an error that causes x to become y with probability delta):

lt (n->infinity, n odd) NS[delta,Majn] = $2/\pi \cdot \delta + O(\delta^{1.5})$ where delta is the probability of correlation - flipping x to y.

(11) probability of good outcome = $p = 1 - NS$:

$p = 1 - \text{lt } (n \rightarrow \infty, n \text{ odd}) NS[\delta, \text{Maj}n] = 1 - 2/\pi \cdot \delta - O(\delta^{1.5})$.

(12) If $\delta = 1$:

lt (n->infinity, n odd) NS[delta,Majn] = $2/\pi + O(1)$.

(and)

probability of good outcome = $1 - NS = 1/2 + 1/2 \cdot \text{Stability} = 1 - 2/\pi - O(1)$.

(13) In $P(\text{Good})$ RHS:

If the error probability of voter is 0 and probability of good decision is 1 then binomial summation becomes $nCn \cdot (p)^n \cdot (1-p)^0 = 1$ and all other terms are zero. From (11) p can be 1 only if delta is 0 or no correlation flips exist. This proves the obvious because commonsensically votes are perfect iff there is no wrongdoing.

(14) In $P(\text{Good})$ LHS:

If error probability of dictator boolean function is 0 and $p=1$ then:

$p = 1 - NS(\text{DictatorFunction})$

$= 1 - \delta^n$

Similar to RHS $p=1$ iff $\delta=0$

Thus if there is no Noise on either side LHS=RHS (or) LHS is a P algorithm to RHS EXP or PH=DC. This depends on existence of perfect voter function defined in (7). This just gives a counterexample when LHS can be as efficient as RHS and viceversa.

(15) [Benjamini-Kalai-Schramm] theorem states the condition for a boolean function to be noise sensitive:

A boolean function is noise sensitive if and only if L_2 norm (sum of squares) of influences of variables in f tends to zero.

Therefore, for stability any voter boolean function in $P(\text{Good})$ RHS should not have the L_2 norm of influences to tend to zero.

(16) "How much increasing sets are positively correlated" by [Talagrand] - <http://boolean-analysis.blogspot.in/2007/03/how-much-are-increasing-sets-positively.html> - defines the inequality (Chang's Level-1 inequality):

$\text{Weight}(f) = \sum_{1 \text{ to } n} (\text{fouriercoeff}(i)) \leq O(\text{mean}^2 \cdot 1/\log(\text{mean}))$

where Weight of boolean function f in n variables is the sum of squares of n fourier coefficients and mean is $\Pr(f(x)=1) - (\Pr(f(x)=-1))$. This is alternatively defined as derivative of stability of f wrt ρ at $\rho=0$. This measure intuitively quantifies how $\Pr(f(x)=f(y))$ changes as x becomes increasingly correlated with y (due to random flips). Related to this, point (20) is derived from Plancherel's theorem which equates $E(f(x)g(x))$ to $\text{summation}(f_fourier(x)g_fourier(y))$. But stability is $E(f(x)f(y)/x\text{-correlated}))$. The noise operator $E(f(y))$ is introduced for each monomial in fourier series by which $E(\text{monomial}(S)) = (\rho^{|S|} \text{fourier_f}(S))$. $E(f(y))$ is thus equivalent to a new boolean function $g(x)$ for which Plancherel formula can be applied - $E(f(x)E(f(y))) = \text{summation}(\rho^{|S|} \text{fourier_f}(S)^2) = \text{Noise stability}$. First derivative of Stability wrt ρ at $\rho=0$ is $\text{Weight}(f)$ - in other words this connects pseudorandomness with stability of a boolean function in terms of fourier coefficients.

(17) By Majority is Stablest Theorem if $P(\text{Good})$ RHS is a boolean function composition of $\text{Maj} * \text{Maj} = \text{Maj}_n(\text{Maj}_1, \text{Maj}_2, \dots, \text{Maj}_n)$ then its stability is derived as:

$(1-2/\pi * \arccos(\rho))^2$ assuming that stability of the composition is the product like other measures

If the LHS of $P(\text{Good})$ is the Dictator Boolean Function its stability is ρ^n (because all bits have to be flipped). By equating the two stability measures both sides following expression results:

$$[\cos(\pi/2 * (1 - (\rho)^n))]^2 = \rho$$

For $\rho=0$:

$$[\cos(\pi/2 * (1 - 0^n))]^2 = 0 \text{ hence LHS=RHS}$$

For $\rho=1$:

$$[\cos(\pi/2 * (1 - 1^n))]^2 = 1 \text{ hence LHS=RHS}$$

But for $\rho=0.5$:

$$\arccos 1/\sqrt{2} = \pi/2 * (1 - 0.5^n)$$

$$n = \log(1 - 2/\pi * 0.7071) / \log(0.5)$$

$n = 0.863499276$ which is quite meaningless probably hinting that for uniform distribution the parity size n is < 1 .

(18) In RHS the $P(\text{Good})$ binomial coefficient summation in terms of Noise Sensitivities of each Voter SAT:

$$nC_0(1-NS)^0(NS)^n + nC_1(1-NS)^1(NS)^{(n-1)} + nC_2(1-NS)^2(NS)^{(n-2)} + \dots$$

Above summation should ideally converge to holistic Noise Sensitivity of the Boolean Function Composition of $\text{Maj} * \text{Maj}$ described previously for stablest voting:

$$1/2 + 1/2 * (1 - 2/\pi * \arccos(\rho))^2 = nC_0(1-NS)^0(NS)^n + nC_1(1-NS)^1(NS)^{(n-1)} + nC_2(1-NS)^2(NS)^{(n-2)} + \dots$$

If each voter has boolean function with varied Noise Sensitivities, above becomes a Poisson Trial instead of Bernoulli. Above is a closed form for the goodness of voting expressed as the binomial coefficient summation which otherwise requires hypergeometric algorithms because for $NS=a/b$ ($\neq 0.5$) summation becomes $(nC_0 * (b-a)^0 a^n + nC_1(b-a)^1(a)^{(n-1)} + nC_2(b-a)^2(a)^{(n-2)} + \dots) / b^n$ and closed form is non-trivial as summation is asymmetric whereas the case with $NS=1/2$ is symmetric with all coefficients being plain vanilla binomial coefficients. Previous identity equates Noise Sensitivity of Majority Voting Circuit in two versions: Boolean Function Composition and Majority with Oracle Voter SAT inputs.

(19) There are classes of boolean functions based on percolation crossings (<http://arxiv.org/pdf/1102.5761.pdf> - Noise Sensitivity of Boolean Functions and Percolation) which decide if the paths (left-to-right) in a percolation random graph in which edges are created with a probability p , have a left-right

crossing. Perturbed paths are analogous to correlated bit strings. [Russo-Seymour-Welsh] theorem states that the percolation crossing boolean functions are non-degenerate i.e function depends on all variables (quite intuitive as to find out a left-right crossing entire path has to be analyzed). Noise Stability Regime of the crossing events [page 68] answers the following question on noise stability of crossing events:

For $\epsilon = o(1/n^2 \alpha^4)$, $\Pr[\text{fn}(\text{sequence}) = \text{fn}(\text{sequence with } \epsilon \text{ perturbation})]$ tends to zero at infinity where α^4 is the four-arm crossing event probability (paths cross at a point on the percolation random graph creating four arms to the boundary from that point). In terms of Fourier expansion coefficients this is: $\sum (\text{fourier_coeff}(S)^2)$ tending to zero, $|S| > n^2 \alpha^4$. [Open question: Is such a percolation crossing the perfect voting boolean function required in (7) and does it prove BKS Majority is least stable conjecture? But this happens only when there are infinite number of Z^2 grid cells - $n * n$ is infinite]. If this is the only available perfect boolean function with 100% stability, [Benjamini-Kalai-Schramm] conjecture is true and both LHS and RHS use only percolation as judge boolean functions (in compositions for each voter - Majority * Percolation), then LHS=RHS by P(Good) binomial summation convergence and LHS is class C algorithm for RHS PH-complete or EXP-complete algorithm where C is the hardness of LHS pseudorandom choice judge boolean function. Also noise probability $\epsilon = o(1/n^2 \alpha^4)$ can have arbitrarily any value ≤ 1 depending on n and α^4 .

Open question: If Percolation Boolean Functions are 100% noise stable (as in infinite grid previously), what is the lowerbound of such boolean functions (or) how hard and in what complexity class C should they be. This infinite version of percolation is a non-uniform polynomial circuit class (grid has n^2 coordinates).

(*IMPORTANT* - this requires lot of reviewing - if correct places a theoretical limit on when stability occurs) From Plancherel's theorem and stability relation mentioned in (16), $\sum (\rho^{|S|} * \text{fourier_f}(S)^2) = \text{Noise stability}$. When stability is 1, this summation is equal to 1. In other words $\rho^{|S1|} * \text{fourier_f}(S1)^2 + \rho^{|S2|} * \text{fourier_f}(S2)^2 + \dots - 1 = 0$ which is a univariate polynomial in ρ as variable with n roots and degree n . Polynomial Identity Testing algorithms are required to ensure that this polynomial is non-zero (coefficients are non zero). The real, positive, roots of this polynomial are the probabilities where a boolean function is resilient to noise and 100% stable. It non-constructively shows existence of such stable boolean functions. [Talagrand] proved existence of a random CNF with noise sensitivity $> \Omega(1)$ - described in <http://www.cs.cmu.edu/~odonnell/papers/thesis.pdf>. Noise stability depends on huge $|S|$ as evidenced by $\text{stability} = \sum (\rho^{|S|} * \text{fourier_coeff}(f(S))^2)$. What this implies is that for any boolean function, 100% stability is attainable at only n points in $[0,1]$. In other words there is no boolean function which is 100% noise stable for all points of ρ in $[0,1]$. It also implies that BKS majority is least stable conjecture is true at these points of ρ . Since coefficients of this polynomial are Fourier coefficients of the boolean function, roots of this polynomial i.e stability points are functions of Fourier coefficients.

(20) Noise stability in terms of Fourier coefficient weights is defined as:
 $\sum (\rho^k * W^k)$ for all degree- k weights where $W = \sum (\text{fourier_coeff}(S)^2)$ for all $|S|$, S in $[n]$

(21) Variant 1 of Percolation as a Judge boolean function is defined in 53.4 below which is in non-uniform NC1. If this is 100% noise stable judge boolean function for LHS and RHS noise stability also converges to 100%, then there is a non-uniform NC1 circuit for RHS PH-complete or EXP-complete DC uniform circuit. This gives a non-uniform algorithm for an RHS uniform circuit. Variant 2 of Percolation in 53.5 as Judge boolean function is also in non-uniform NC1 subject to 100% noise stability condition. In 53.6 a sorting network based circuit is described for Percolation boolean function.

(22) Also from Theorem 5.17 - [RyanODonnell] - <http://analysisofbooleanfunctions.org/> - for any ρ in $[0,1]$, Stability of Infinite Majority is bounded as:

$$2/\pi \arcsin \rho \leq \text{Stabp}[\text{Maj}_n] \leq 2/\pi \arcsin \rho + O(1/(\sqrt{1-\rho^2})\sqrt{n})).$$

(23) Peres' Theorem rephrases above bound for NoiseStability in terms of NoiseSensitivity for class of uniform noise stable linear threshold functions f (which includes Majority):

$$\text{NoiseSensitivity}_\delta[f] \leq O(\sqrt{\delta})$$

(24) From <http://arxiv.org/pdf/1504.03398.pdf>: [Boppana-Linial-Mansour-Nisan] theorem states that influence of a boolean function f of size S and depth d is:

$$\text{Inf}(f) = O((\log S)^{d-1})$$

(25) [Benjamini-Kalai-Schramm] Conjecture (different from Majority is least stable BKS conjecture which is still open) is the converse of above that states: Every monotone boolean function f can be ϵ approximated by a circuit of depth d and of size $\exp((K(\epsilon) \cdot \text{Inf}(f))^{1/(d-1)})$ for some constant $K(\epsilon)$. This conjecture was disproved by [ODonnell-Wimmer] and strengthened in <http://arxiv.org/pdf/1504.03398.pdf>.

(26) Class of uniform noise stable LTFs in (23) are quite apt for Voter Boolean Functions in the absence of 100% noise stable functions, which place an upperlimit on decision error. Depth hierarchy theorem in <http://arxiv.org/pdf/1504.03398.pdf> separates on what fraction, 2 circuits of varying depths agree in outputs.

----- Additional References: -----

14.1 k-SAT and 3-SAT - <http://cstheory.stackexchange.com/questions/7213/direct-sat-to-3-sat-reduction>

14.2 k-SAT and 3-SAT - <http://www-verimag.imag.fr/~duclos/teaching/inf242/SAT-3SAT-and-other-red.pdf>

14.3 Switching Lemma

14.4 Donald Knuth - Satisfiability textbook chapter - <http://www-cs-faculty.stanford.edu/~uno/fasc6a.ps.gz> - Quoted excerpts:

" ... Section 7.2.2.2 Satisfiability

Satisfiability is a natural progenitor of every NP-complete problem'

Footnote: At the present time very few people believe that $P = NP$. In other words, almost everybody who has studied the subject thinks that satisfiability cannot be decided in polynomial time. The author of this book, however, suspects that $N^{O(1)}$ -step algorithms do exist, yet that they're unknowable. Almost all polynomial time algorithms are so complicated that they are beyond human comprehension, and could never be programmed for an actual computer in the real world. Existence is different from embodiment. ..."

14.5 Majority and Parity not in AC^0 -

www.cs.tau.ac.il/~safra/ACT/CCandSpaceB.ppt,

<http://www.math.rutgers.edu/~sk1233/courses/topics-S13/lec3.pdf>

14.6 Sampling Fourier Polynomials -

<http://cstheory.stackexchange.com/questions/17431/the-complexity-of-sampling-approximately-the-fourier-transform-of-a-boolean-fu>

14.7 Kummer's theorem on binomial coefficient summation - quoted from Wikipedia: "In mathematics, Kummer's theorem on binomial coefficients gives the highest power of a prime number p dividing a binomial coefficient. In particular, it asserts that given integers $n \geq m \geq 0$ and a prime number p , the maximum integer k such that p^k divides the binomial coefficient $\binom{n}{m}$ is equal to the number of carries when m is added to $n - m$ in base p . The theorem is named after Ernst Kummer, who proved it in the paper Kummer (1852). It can be proved by writing $\binom{n}{m}$ as $\frac{n!}{m!(n-m)!}$ and using Legendre's formula."

14.8 Summation of first k binomial coefficients for fixed n :

- <http://mathoverflow.net/questions/17202/sum-of-the-first-k-binomial-coefficients-for-fixed-n>
 - https://books.google.co.in/books?id=Tn0pBAAQBAJ&pg=PA61&lpg=PA61&dq=summation+of+first+k+binomial+coefficients&source=bl&ots=sqB_iQweyS&sig=ye5TxmCkJP-Ud5JnWiLMzqOKDjM&hl=en&sa=X&ved=0CFgQ6AEwCWoVChMI6rDEo9nVxwIVR0yOCh2AXgpz#v=onepage&q=summation%20of%20first%20k%20binomial%20coefficients&f=false
 which imply bounds for the summation:

- $\sum_{k=0}^n \binom{2n}{k} = 2^{2n} - \sum_{k=0}^{n-1} \binom{2n}{k}$
- $2^{2n} - \sum_{k=0}^{n-1} \binom{2n}{k} > 2^{2n} - \binom{2n}{n} * 2^{(2n)} / 2^{*(2n)}$

14.9 Probabilistic boolean formulae - truth table with probabilities - simulates the Voter Circuit SAT with errors
<http://www.cs.rice.edu/~kvp1/probabilisticboolean.pdf>

14.10 BPAC circuits (= Probabilistic CNF?)
<http://www.cs.jhu.edu/~lixints/class/nw.pdf>

14.11 Mark Fey's proof of infinite version of May's theorem for 2 candidate majority voting - Cantor set arguments for levels of infinities -
<https://www.rochester.edu/college/faculty/markfey/papers/MayRevised2.pdf>

14.12 Upperbounds for Binomial Coefficients Summation -
<http://mathoverflow.net/questions/17202/sum-of-the-first-k-binomial-coefficients-for-fixed-n> - Gallier, Lovasz bounds - where Lovasz bound is:

$$f(n,k) \leq 2^{(n-1)} \exp((n-2k-2)^2/4(1+k-n))$$

 for $f(n,k) = \sum_{i=0}^k \binom{n}{i}$. Proof by Lovasz at:
<http://yaroslavvb.com/upload/lovasz-proof2.pdf>

 14.13 (*IMPORTANT*) Connections between Hypergeometric series and Riemann Zeta Function :

- <http://matwbn.icm.edu.pl/ksiazki/aa/aa82/aa8221.pdf> - This relation implies that:
 - P(good) binomial coefficient infinite series summation (and hence the Psuedorandom Vs Majority Voting circuit) which require Hypergeometric functions
 - and Complement Function circuit special case for RZF (and hence the Euler-Fourier polynomial for Riemann Zeta Function circuit)
 are deeply intertwined. Kummer theorem gives the p-adic number (power of a prime that divides an integer) for dividing a binomial coefficient which relates prime powers in Euler product RZF notation and Binomial coefficients in Majority voting summation.

Above implies that binomial coefficients can be written in terms of prime powers and vice-versa: P(good) series can be written as function of sum of prime powers and Euler Product for RZF can be written in terms of binomial coefficients. Also Euler-Fourier polynomial obtained for complement function circuit (Expansion of <http://arxiv.org/pdf/1106.4102v1.pdf> described in 10) can be equated to binomial coefficient summation. If these two apparently unrelated problems of Complexity-Theoretic Majority voting and Analytic-Number-Theoretic Riemann Zeta Function are related then complexity lowerbound for some computational problems might hinge on Riemann Zeta Function - for example PH=DC circuit problems .

 14.15 ACC circuits and P(Good) RHS circuit

ACC circuits are AC circuits augmented with mod(m) gates. i.e output 1 iff sum(xi) is divisible by m. It is known that NEXP is not computable in ACC0 - <http://www.cs.cmu.edu/~ryanw/acc-lbs.pdf> [RyanWilliams]. From (129) above the P(good) RHS can be an EXP circuit if the boolean functions of the voters are of unrestricted depth. Thus open question is: can RHS of P(Good) which is

deterministic EXP, be computed in ACC0. [RyanWilliams] has two theorems. Second theorem looks applicable to P(Good) RHS circuit i.e E^{NP} , the class of languages recognized in $2^{O(n)}$ time with an NP oracle, doesn't have non-uniform ACC circuits of $2^{n^{o(1)}}$ size". Boolean functions are the NP oracles for this P(Good) Majority Voting EXP circuit if the variables are common across voters. Applying this theorem places strong super-exponential lowerbound on the size of the P(Good) majority voting circuit.

14.16. Infinite Majority as Erdos Discrepancy Problem

Related to (132) - May's Theorem proves conditions for infinite majority with sign inversions $\{+1, -1\}$ and abstention (zero). Erdos discrepancy problem which questions existence of integers k, d , and C in sequence of $\{+1, -1\}$ such that $\sum_{0 \leq i < k} x(i*d) > C$ and has been proved for $C = \infty$ - [TerenceTao] - <http://arxiv.org/abs/1509.05363>. For spacing $d=1$, Erdos Discrepancy Problem reduces to Infinite Majority and as C is proved to be infinite, it looks like an alternative proof of non-decrementality condition in Infinite version of May's Theorem.

14.17 Noise Sensitivity of Boolean Functions and Percolation -
<http://arxiv.org/pdf/1102.5761.pdf>, www.ma.huji.ac.il/~kalai/sens.ps

14.18 Binomial distributions, Bernoulli trials (which is the basis for modelling voter decision making - good or bad - in P(Good) series) -
<http://www.stat.yale.edu/Courses/1997-98/101/binom.htm>

14.19 Fourier Coefficients of Majority Function -
<http://www.contrib.andrew.cmu.edu/~ryanod/?p=877>, Majority and Central Limit Theorem - <http://www.contrib.andrew.cmu.edu/~ryanod/?p=866>

14.20 Hastad's Switching Lemma - <http://windowsontheory.org/2012/07/10/the-switching-lemma/>, <http://www.contrib.andrew.cmu.edu/~ryanod/?p=811#lemrand-restr-dt>

14.21 Degree of Fourier Polynomial and Decision tree depth -
<http://www.contrib.andrew.cmu.edu/~ryanod/?p=547#propdt-spectrum> (degree of fourier polynomial < decision tree depth, intuitive to some extent as each multilinear monomial can be thought of as a path from root to leaf)

14.22 Judgement Aggregation (a generalization of majority voting) - Arriving at a consensus on divided judgements - <http://arxiv.org/pdf/1008.3829.pdf>.

14.23 Noise and Influence - [Gil Kalai, ICS2011] -
<https://gilkalai.files.wordpress.com/2011/01/ics11.ppt>

14.24 Doctrinal Paradox (or) Discursive dilemma - Paradoxes in Majority voting where both Yes and No are possible in judgement aggregations -
https://en.wikipedia.org/wiki/Discursive_dilemma

15. (FEATURE - DONE-Minimum Implementation using NetworkX algorithms) Add Graph Search (for example subgraph isomorphism, frequent subgraph mining etc.,) for "inferring" a graph from dataset with edges as relations and nodes as entities (astronomical or otherwise). Reference survey of FSM algorithms: <http://cgi.csc.liv.ac.uk/~frans/PostScriptFiles/ker-jct-6-May-11.pdf>. The context of "Graph Search" includes deducing relationships hidden in a text data by use of WordNet (construction of wordnet subgraph by Definition Graph Recursive Gloss Overlap etc.,), mining graph patterns in Social Networks etc., At present a WordNet Graph Search and Visualizer python script that renders the definition graph and computes core numbers for unsupervised classification (subgraph of WordNet projected to a text data) has been added to repository.

16. (FEATURE - DONE) Use of already implemented Bayesian and Decision Tree Classifiers on astronomical data set for prediction (this would complement the use of classifiers for string mining) - autogen_classifier_dataset/ directory contains Automated Classified Dataset and Encoded Horoscopes Generation code.

17. (FEATURE - DONE) Added Support for datasets other than USGS EQ dataset(parseUSGSdata.py). NOAA HURDAT2 dataset has been parsed and encoded pygen horoscope string dataset has been autogenerated by parseNOAA_HURDAT2_data.py

18. (FEATURE - Minimum Functionality DONE-TwitterFollowersGraphRendering, Centrality) (Astro)PsychoSocialAnalysis - Social Network Graph Analysis and Sentiment Analysis of Social Media and drawing inferences on Psychology and Human Opinion Mining in broader sense - for example, how a social network forms, how opinions, edges and vertices appear over time , Rich-get-Richer in Random Network Erdos-Renyi Model - which by majority opinion seems to be a bad model choice for Social Networking (Do people flock to popular social groups?), Bonacich Power Centrality (a social prestige measure predating PageRank) etc.,. Related to point 15.

References:

18.1 Networks, Crowds, Markets - <http://www.cs.cornell.edu/home/kleinber/networks-book/networks-book.pdf>

18.2 Introduction to Social Network Methods - <http://faculty.ucr.edu/~hanneman/nettext/>

18.3 Bonacich Power Centrality - <http://www.leonidzhukov.net/hse/2014/socialnetworks/papers/Bonacich-Centrality.pdf>

18.4 Modelling Human Emotions - <http://www.jmlr.org/proceedings/papers/v31/kim13a.pdf>

18.5 Depression Detection - <http://www.ubiwot.cn/download/A%20Depression%20Detection%20Model%20Based%20on%20Sentiment%20Analysis%20in%20Micro-blog%20Social%20Network.pdf>

18.6 Market Sentiments - <http://www.forexfraternity.com/chapter-4-fundamentals/sentiment-analysis/the-psychology-of-sentiment-analysis>

18.7 Sentiment Analysis - <http://www.lct-master.org/files/MullenSentimentCourseSlides.pdf>

18.8 Dream Analysis - <http://cogprints.org/5030/1/NRC-48725.pdf>

18.9 Opinion Mining - <http://www.cs.uic.edu/~liub/FBS/SentimentAnalysis-and-OpinionMining.pdf>

18.10 Linked - [Albert Laszlo Barabazi] - [Ginestra Bianconi - <http://www.maths.qmul.ac.uk/~gbianconi/Condensation.html>] Bose gas theory of networks - Bose-Einstein Condensate is equivalent to evolution of complex networks - Page 101 on Einstein's Legacy - "Nodes in Network are energy levels of subatomic particles and Links across nodes are subatomic particles" - "Winner takes it all" - particles occupying lowest energy correspond to people flocking to a central node in social networks - This finding is from behaviour of large scale networks viz., WWW, Social networks etc., This Condensate theory has striking applications to Recursive Gloss Overlap Graph construction and using it for unsupervised classification based on core numbers - each network and for that matter a graph constructed from text document is a macrocosmic counterpart of quantum mechanics.

18.11 Small World Experiment and Six Degrees of Separation - [Stanley Milgram] - https://en.wikipedia.org/wiki/Small-world_experiment

18.12 LogLog estimation of Degrees in Facebook graph - 3.57 Degrees of Separation - <https://research.facebook.com/blog/three-and-a-half-degrees-of-separation/>

19. (FEATURE - DONE-PAC Learnt Boolean Conjunction) Implement prototypical PAC learning of Boolean Functions from dataset. Complement Boolean Function construction described in <http://arxiv.org/abs/1106.4102> is in a way an example of PAC learnt Boolean Function - it is rather C Learnt (Correct Learning)

because there is no probability or approximation. Complement Boolean Function can be PAC learnt (with upperbounded error) as follows:

19.1 There are two datasets - dataset1 of size 2^n of consecutive integers and dataset2 of first n -bit prime numbers of size 2^n

19.2 Each element of dataset1 is mapped to i -th bit of the corresponding prime number element in the dataset2. Boolean Conjunction is learnt for each of the i mappings.

19.3 Above step gives i probabilistic, approximate, correct learnt boolean conjunctions for each bit of all the prime numbers.

19.4 Reference: PAC Learning -

<http://www.cis.temple.edu/~giorgio/cis587/readings/pac.html>

19.5 PAC Learnt Boolean Conjunction is an approximated Decision Tree.

19.6 PAC learning is based on Occam's Razor (no unnecessary variables)

PAC Learning implementation for learning patterns in Binary encoded first 10000 Prime Numbers have been committed to AsFer repository (Commit Notes 324)

20. (FEATURE - DONE) Integrate AstroInfer to VIRGO-KingCobra-USBmd Platform which makes it an Approximately Intelligent Cloud Operating System Framework - a Cloud OS that "learns" , "decides" from datasets and "drives" using AstroInfer code. AsFer+USBmd+VIRGO+KingCobra integrated cloud platform with machine learning features together have been christened as "Krishna iResearch Intelligent Cloud Platform" or "NeuronRain". It has to be mentioned here that NeuronRain cloud differs from traditional cloud in following ways:

20.1 Usual cloud platforms support only application-application layer RPCs over an existing operating system.

20.2 NeuronRain differs in that aspect by adding new cloud features (with advanced features in development) like RPC, distributed kernel memory and network filesystem related system call clients and kernel modules kernelsocket-server-listeners into linux kernel (a fork-off in that respect)

20.3 Cloud support within kernelspace has lot of advantages - low network latency because of kernelspace-kernelspace cloud communication by kernel sockets, userspace to kernelspace communication (a userspace application like telnet can connect to a kernel socket listener of a VIRGO driver in kernelspace), userspace-userspace communication by kernel upcalls to userspace from kernelspace.

20.4 Kernelspace-Kernelspace communication is a privileged mode privy to kernel alone and userspace applications shouldn't be able to access kernelspace socket data.

20.5 At present the data sent over kernel sockets is not encrypted which requires OpenSSL in kernel. Kernel doesn't have OpenSSL support presently and it is not straightforward to implement SSL handshake in NeuronRain cloud. But there are MD5 and other hashing libraries (e.g crypto) available for encrypting data before before they are sent over cloud.

20.6 There are ongoing efforts to provide Transport Layer Security (TLS) in kernel sockets which are not yet mainline. Hopefully kernel sockets in future kernel mainline versions would support AF_KTLS sockets and thus NeuronRain cloud implicitly is TLSed :

20.6.1 KTLS - [DaveWatson - Facebook] -

<https://lwn.net/Articles/666509/> and https://github.com/ktls/af_ktls

20.6.2 IPSec for kernel sockets - [SowminiVaradhan - Oracle] -

<http://www.netdevconf.org/1.1/proceedings/slides/varadhan-securing-tunneled-kenel-tcp-udp-sockets.pdf>

20.7 Usual userspace-userspace network communication has following routing - user1---kernel1---kernel2---user2 for two cloud nodes node1 and node2. NeuronRain cloud communication has following routings - user1---kernel1---kernel2, kernel1---kernel2, user1---kernel1---kernel2---user2. With VFS filesystem API in kernel, both userspace and kernelspace mode communication can be persisted in filesystem and better than an equivalent application layer persistence mechanisms which require lot of internal kernel calls for disk writes. Thus kernel-kernel communication saves lot of user layer to kernel disk write invocations.

21. (FEATURE - DONE-Minimum Implementation) Unsupervised Named Entity Recognition and Part-of-Speech tagging using Conditional Random Fields(CRF) and

Viterbi path computation in CRF. Bayesian Network and Belief propagation might be implemented if necessary - as they are graphical models where graph edges are labelled with conditional probabilities and belief potentials respectively and can be part of other larger modules.

#####

A. Design Notes on Mining Numerical Datasets

#####

22. (FEATURE - DONE-Minimum Implementation) Period Three theorem (www.its.caltech.edu/~matilde/LiYorke.pdf) which is one of the earliest results in Chaotic NonLinear Systems, implies any data that has a periodicity of 3 can have larger periods. Fractals, Mandelbrot-Julia Sets have modelled natural phenomena. Thus finding if a data has periodicity or Chaos and if it has sensitive dependence on initial conditions (for example logistic equations similar to $x(n+1) = kx(n)(1-x(n))$) is a way to mine numerical data. Computation of Hausdorff-Besicovitch Dimension can be implemented to get Fractal Dimension of an uncountable set (this has to be visualized as a fractal curve than set of points). In addition to these, an Implementation of Chaotic PRG algorithms as described in <https://sites.google.com/site/kuja27/ChaoticPRG.pdf?attredirects=0> and <https://sites.google.com/site/kuja27/Analysis%20of%20a%20Randomized%20Space%20Filling%20Algorithm%20and%20its%20Linear%20Program%20Formulation.pdf?attredirects=0> can be done.

23. (FEATURE - DONE) Entropy of numerical data - Sum of $-\text{Pr}(x)\text{LogPr}(x)$ for all possible outcome probabilities for a random variable. This is already computed in Decision Tree Classifier as impurity measure of a dataset. Also a python Entropy implementation for texts has been added to repository - computes weighted average of number of bits required to minimum-describe the text.

#####

=====
=====
(THEORY) DECIDABILITY OF EXISTENCE AND CONSTRUCTION OF COMPLEMENT OF A FUNCTION (important draft additions to <http://arxiv.org/pdf/1106.4102v1.pdf> - quite experimental, non-conventional and not necessarily correct)
=====

(*)24. (DONE) COMPLEMENT OF A FUNCTION - Approximating or Interpolating with a Polynomial: This is quite expensive and is undecidable for infinite sets. Better alternative is to approximate with Spline interpolant polynomials, for example, cubic splines which have less approximation error. (On a related note, algorithms described by the author (that is, myself) in <http://arxiv.org/pdf/1106.4102v1.pdf> for construction of a complement of a function are also in a way eliciting pattern in numerical data. The polynomial interpolation algorithm for complement finding can be improved with Spline interpolants which reduce the error and Discrete Fourier Transform in addition to Fourier series for the boolean expression. Adding this as a note here since Tex file for this arXiv submission got mysteriously deleted and the PDF in arXiv has to be updated somehow later.). A test python script written in 2011 while at CMI for implementing the above is at:
<http://sourceforge.net/p/asfer/code/HEAD/tree/python-src/complement.py>. Also Trigonometric Polynomial Interpolation which is a special case of Polynomial interpolation, has following relation to DFT $X(i)s$:

$$p(t) = 1/N [X_0 + X_1 e^{(2\pi i t)} + \dots \text{upto } X_N] \text{ and}$$
$$p(n/N) = x_n$$

Thus DFT and interpolation coincide in the above.

1274. Theorems on prime number generating polynomials - special case is to generate all primes or integral complement of $xy=z$ - related to 24

Legendre - There is no rational algebraic function which always gives primes.
Goldbach - No polynomial with integer coefficients can give primes for all integer values

Jones-Sato-Wada-Wiens - Polynomial of degree 25 in 26 variables whose values are exactly primes exists

Polynomial interpolation and Fourier expansion of the boolean function in <http://arxiv.org/pdf/1106.4102v1.pdf> probably would have non-integral coefficients due to the above.

1275. Circuit construction for the complement function boolean DNF constructed in <http://arxiv.org/pdf/1106.4102v1.pdf> - related to 24

The DNF constructed for complement function has to be minimized (through some lowerbound techniques) before it is represented as a circuit because the number of clauses could be exponential. The circuit minimization problem has been shown to be NP-complete(unpublished proof by Masek, [GareyJohnson]). The above complement function boolean DNF would yield a constant depth 2 circuit (probably after minimization also) with unbounded fanin. If the size of the circuit is polynomial it is in AC (=NC). The size of the circuit depends on the boolean DNF constructed above which in turn depends on input complement set. Thus circuit depends on input making it a Non-Uniform AC circuit. Though complement function is undecidable as described in <http://arxiv.org/pdf/1106.4102v1.pdf>, Non-uniform circuits "decide" undecidable languages by definition.

Old draft of the complement function -
https://sites.google.com/site/kuja27/ComplementOfAFunction_earlier_draft.pdf?attredirects=0 describes this and proposes a name of co-TC₀ as integer multiplication is in TC₀ (threshold circuits) which may not be true if the circuit size is super-polynomial. Super-polynomial size circuits are DC circuits allowing exponential size. Assuming polynomial size the above may be named as "Non-uniform co-TC" for lack of better naming.

Due to equivalence of Riemann Zeta Function and Euler's theorem - $\text{inverse}(\text{infiniteproduct}(1-1/p(i)^z))$ for all primes $p(i)$ - gives a pattern in distribution of primes which is the Riemann Hypothesis of $\text{Re}(\text{nontrivial zeroes of RZF})=0.5$. Complement function for $xy=z$ obtained by <http://arxiv.org/pdf/1106.4102v1.pdf> by polynomial interpolation or Fourier approximation polynomial of the DNF boolean formula can thus be conjectured to have a strong relation to RZF or even generalize RZF. In circuit parlance, the DNF boolean formula and its minimized Non-uniform AC(if polynomial sized) circuit that outputs prime number bits, thus are related to non-trivial zeroes of Riemann Zeta Function. Another conjecture that can be made is that if the real part of the non-trivial zeroes is 0.5 in RZF, then the Non-uniform circuit family constructed for the above complement function DNF should also have a pattern in the circuit graph drawn - subgraphs of the circuit family of graphs have some common structure property.

Fourier polynomial of a boolean formula is of the form:
$$f(x) = \text{Sigma}_S(\text{fouriercoeff}(S)\text{parityfn}(S))$$

and is multilinear with variables for each input. S is the restriction or powerset of the bit positions.

Thus if a prime number is b-bit, there are b fourier polynomials for each bit of the prime. Thus for x-th prime number fourier expression is,

$P(x) = 1 + 2 \cdot f_{x1}(x) + 2^2 \cdot f_{x2}(x) + \dots + 2^b \cdot f_{xb}(x)$
 where each $f_{xi}()$ is one of the b fourier expansion polynomials for prime bits.

 1276. Riemann Zeta Function written as Euler-Fourier Polynomial : - related to 24

Fourier polynomials for each prime can be substituted in Euler formula and equated to Riemann Zeta Function:

$RZF = \text{Inverse}((1 - 1/P(x1)^s)(1 - 1/P(x2)^s)) \dots \text{ad}$
 infinitum-----
 (1).

Non-trivial complex zero s is obtained by,

$P(x_i)^s = 1$
 $P(x_i) = (1)^{(1/s)}$
 $1 + 2 \cdot f_{x1}(x_i) + 2^2 \cdot f_{x2}(x_i) + \dots + 2^b \cdot f_{xb}(x_i) = (1)^{(e^{(-i \cdot \theta)}/r)}$ after
 rewriting in phasor notation $s = r \cdot e^{(i \cdot \theta)}$.----- (2)

Above links Fourier polynomials for each prime to roots of unity involving non-trivial zeroes of Riemann Zeta Function in RHS. LHS is the x_i -th prime number. Since LHS is real without imaginary part, RHS should also be real though exponent involves imaginary part. There are as many roots of unity in RHS as there are prime numbers. The radian is \tan^{-1} which is semi-determined assuming RH with $\text{Re}(s) = 0.5$.

LHS is multilinear with at most b variables for b bits of the prime number. A striking aspect of the above is that Fourier parity function is $+1$ or -1 and a lot of them might cancel out in the above summed up polynomial in LHS after substitution and rewriting.

If s is written as $a + ic$, then $(1)^{(1/s)} = (1)^{(1/a+ic)} = (1)^{((a-ic)/(a^2+c^2))}$

If RH is true $a=0.5$ and above becomes, $(1)^{((0.5-ic)/(0.25+c^2))}$.

$1 + 2 \cdot f_{x1}(x_i) + 2^2 \cdot f_{x2}(x_i) + \dots + 2^b \cdot f_{xb}(x_i) = (1)^{((0.5-ic)/(0.25+c^2))}$
 ----- (3)

Thus imaginary part c has one-to-one correspondence to each prime. Non-trivial zeroes are usually found using functional notation of RZF instead of the above - applying Analytic Continuation that extends the domain in steps to be exact.

 1277. Delving deeper into (1) above which equates Riemann Zeta Function with Complement Function Fourier Polynomials substituted in Euler's infinite product (Hereinafter referred to as Euler-Fourier polynomial) - Pattern in primes from above Euler-Fourier polynomial: - related to 24

Finding pattern in distribution of primes is equivalent to finding pattern in above set of prime bit circuits or fourier polynomials for each prime - The family of circuits for primes above has to be mined for circuit DAG subgraph patterns which is more of machine learning than complexity (there is almost no complexity theoretic reference to this aspect). The set of fourier polynomials can be mined for linear independence for example. (1), (2) and (3) are multiple ways of expressing same relation between complement function boolean circuit and RZF.

Similar to zeros of RZF, Fourier polynomial obtained from Euler's formula by substituting complement function prime bits fourier polynomials gives a very complex polynomial whose degree could be $d \cdot s$ in b variables, where d is the

maximum degree in prime bit fourier polynomials. In randomized setting, Schwartz-Zippel Lemma can be applied for finding an upperbound for number of roots of this Fourier-Euler polynomial which is the traditional tool in Polynomial Identity Testing. Using the lemma, number of roots of the above polynomial is $\leq d*s/|K|$ where K is the random finite subset of b variables in the boolean complement function. If $|K| = b$, then number of roots is upperbounded by $d*s/b$. [This is assuming rewriting as (2) or (3)]. But degree is a complex number $d*s$ (It is not known if there is a Schwartz-Zippel Lemma for complex degree). The roots of this Fourier-Euler polynomial should intuitively correspond to zeros of Riemann Zeta Function which probably gives a complexity theoretic expression of Riemann Zeta Function (than Analytic Number Theoretic). This implies that there should be complex roots also to the Euler-Fourier polynomial which itself is puzzling on what it means to have a complex number in boolean circuits.

Important thing to note is that what it means to be a zero of the Euler-Fourier polynomial [(1),(2) and (3)] which has complex degree variable and also boolean variables within each clause. RZF just has the s in exponent. Thus Euler-Fourier polynomial is more generic and fine-grained. But zeroes of this polynomial are both within the multilinear components and the exponents instead of just in exponent in RZF. This might reveal more pattern than what RH predicts conjecturally. Moreover due to non-uniformity each Fourier polynomial component substituted in Euler formula for each prime, is different.

Sensitivity and Block sensitivity of the above complement function circuit should also have a strong relation to prime distribution as sensitivity is the number of input bits or block of bits that are to be flipped for change in value of the circuit (prime bit is the value). For each Fourier polynomial of a prime bit above the sensitivity measure would differ and the prime distribution is proportional to collective sensitivity of all the prime bit circuit Fourier polynomials. Also the degree of approximating Fourier polynomial is lower bounded by sensitivity (www.cs.cmu.edu/~odonnell/papers/analysis-survey.pdf).

 1278. Arithmetic Circuit for Euler Product and RZF - Alternative formulation to Euler-Fourier polynomials - related to 24

Instead of a boolean circuit above can be an arithmetic circuit (with $*$ and $+$ gates with elements of some field as inputs to these) alternatively which is useful in representing polynomials. The division in the above Euler product can be replaced by the transform $f/g = f/(1-(1-g)) = f*(1+(1-g)+(1-g)^2+...)$ by geometric series expansion. This is how division is implemented using powering and hence multiplication in NC circuits. Above Euler product can be represented as a depth 3 Π - Σ - Π ---- $*$ for product of each prime clause, $+$ for subtraction within each clause, $*$ for raising $(1/p)$ to power s ---- circuit assuming $1/p$. Powering with complex exponent s requires representing s as a $2*2$ matrix $M(s)$ where a and b are real and imaginary parts of s :

$$M(s) = \begin{vmatrix} a & -b \\ b & a \end{vmatrix}$$

Thus p^s can be written as $p^{M(s)}$ with matrix exponent. Rewriting this as $e^{M(s) \ln p}$ and expanding as series,

$$e^{M(s) \ln p} = 1 + M \ln p + \frac{M*M \ln p^2}{2!} + \dots$$

and $1 - 1/p^s = 1 - e^{(-M(s) \ln p)} = 1 - (1 - M*\ln p + \frac{M*M \ln p^2}{2!} - \dots) = M*\ln p - \frac{M*M \ln p^2}{2!} + \dots$ (alternating +, - terms ad infinitum)

Thus each prime clause in the Euler product is written as an infinite summation of $2*2$ matrix products. Using the transform f/g above division $1/(1-1/p^s)$ for each prime clause in the Euler product can be reduced to powering. Product gate

at root multiplies all such prime clauses. Obviously above circuit is exponential and probably is the lowerbound for this circuit. If the product is made finite then a non-uniform arithmetic circuit family is created depending on input advice and degree of the above polynomial varies. This is an alternative to Euler-Fourier polynomial obtained based on complement function boolean circuit. No Fourier polynomial for prime bits is used here but prime power as such is input to arithmetic gates.

Instead of Euler formula, circuit for Riemann Zeta Function can be constructed with + gate at the root and circuits for n^s (or $e^{(s \ln p)}$) computation at the leaves using the above series expansion. For first n terms of RZF, the circuit represents the polynomial (with s replaced by the 2×2 matrix for the complex s):

$$\text{RZF}(n) = n - M(s) * (\ln 2 + \ln 3 + \dots + \ln n)/1! + M(s)^2 * (\ln 2^2 + \ln 3^2 + \dots + \ln n^2)/2! + \dots + M(s)^n * (\ln 2^n + \dots + \ln n^n)/n!$$

The reason for drawing above arithmetic circuit is to represent the Riemann Zeta Function in complex plane as a circuit that depends on Matrix representation of complex number field (determinant of the matrix is the norm) and relate the roots of it to non-trivial zeroes of Riemann Zeta Function. The geometric intuition of Schwartz Zippel lemma is to find the probability of a point being on this circuit represented polynomial's surface. In the above circuit the variable is the Matrix M (matrix representation for the zero s). The imaginary part is hidden within the 2×2 matrices. The degree of above polynomial is n and is univariate in M . Non-uniform Sigma-Pi-Sigma Arithmetic circuit for above restricted version of Riemann Zeta Function can be constructed similar to the above for arbitrary n .

Using Taylor series expansion and Jordan Normal Form above can be written as a huge square matrix. (http://en.wikipedia.org/wiki/Matrix_function). Taylor series for a real function $f(x) = f(0) + f'(0)/1! + f''(0)/2! + \dots$ and 2×2 matrix for complex zero can be written in Jordan Normal Form as XYX^{-1} with Y being the Jordan block of diagonal fixed entries and superdiagonal 1s. Evaluating $f(Y)$ with Taylor expansion gives a square matrix. Thus Riemann Zeta Function has a matrix in Jordan Normal Form. Finding zeros of RZF is equivalent to solving system of equations represented as Jordan Normal Form using Gauss-Jordan Elimination. The matrix is already upper triangular and can be equated to zero matrix.

Eigen values of Chaotic systems Wave modelling Random matrices (matrix as random variable) have been shown to have a striking relation to zeros of RZF - Spacing of Random matrix eigenphases and RZF zeros have been conjectured to be identical (Montgomery). From complexity standpoint, the characteristic polynomial or the determinant of such Random Matrices can be computed by determinant circuits which have polynomial size and polylog depth.

 1279. Can be ignored - quite Experimental - Different way to reduce the complex exponent in (1) - related to 24

From (1), $P(x_i)^s = 1$.
 $\Rightarrow P(x_i)^{k+il} = 1$ where $s=k+il$
 $\Rightarrow P(x_i)^k * P(x_i)^{il} - 1 = 0$
 $P(x_i)^k * [\cos(l \ln(P(x_i))) + i \sin(l \ln(P(x_i)))] - 1 = 0$ -----(4)

Thus real and imaginary parts can be equated to zero independently as,
 $P(x_i)^k * \cos(l \ln(P(x_i))) = 1$ -----
 (5)

$P(x_i)^k * \sin(l \ln(P(x_i))) = 0$ -----
 (6)

From (5) and (6), it can be deduced that:

$$(7) \quad \tan(l \cdot \ln(P(x_i))) = 0 \text{ -----}$$

From (7), it can be inferred that $\text{Re}(s)=k$ is not involved and PIT has to be done only on the $b+1$ variables (b bits in primes and the $\text{Im}(s)=l$). This probably points to the fact that for all primes, the prime distribution is independent of the $\text{Re}(s)$. Series expansion of (7) gives,

$$(8) \quad \tan(T) = T + T^3/3 + 2T^5/15 + \dots = 0 \quad \text{where } T = l \cdot \ln(P(x_i)) \text{ -----}$$

$l \cdot \ln(P(x_i)) = 0 \Rightarrow$
 $l = 0$ or $\ln(P(x_i)) = 0$
 $P(x_i) = 1$
 both of which can not hold.

From (5),
 $P(x_i)^k = \sec(l \cdot \ln(P(x_i))) \text{ -----}$
 (9)

if $T = l \cdot \ln P(x_i)$, $e^{(T/l)} = P(x_i)$

$$P(x_i)^k = e^{(kT/l)} = 1 + T^2/2 + 5T^4/24 + 61T^6/720 + 277T^8/8064 + \dots$$

(expansion of sec) ----- (10)

$$1 + kT/l + (kT/l)^2/2! + (kT/l)^3/3! + \dots = 1 + T^2/2 + 5T^4/24 + \dots$$

(expansion of $e^{(kT/l)}$) ----- (11)

(5) can also be written as,

$$\ln P(x_i)^k = \ln(\sec(l \cdot \ln(P(x_i))))$$

$$k = \ln[\sec(l \cdot \ln(P(x_i)))] / \ln P(x_i)$$

----- (12)

By RH k has to be 0.5 irrespective of RHS.

Approximation of l :

 By assuming $k=0.5$ and Using series expansion of $\cos(x)$ - choosing only first two terms, l is approximately,

$$P(x_i) = 1/[\cos(l \cdot \ln P(x_i))]^2$$

----- (13)

$$l = \sqrt{2} \cdot \sqrt{(\sqrt{P(x_i)} - 1) / \ln(P(x_i))}$$

----- (14)

More on (7):

 $\tan(l \cdot \ln(P(x_i))) = 0$ implies that $l \cdot \ln(P(x_i)) = n \cdot \pi$ for some integer n .
 $\ln(P(x_i)) = n \cdot \pi / l$
 $P(x_i) = e^{(n \cdot \pi / l)}$

 ----- (15)

Above equates the Fourier polynomial for x_i -th prime in terms of exponent of e with Imaginary part l of some RZF zero. It is not necessary that primes have one-one correspondence with zeros in the same order. All above just imply that it is true for some prime (and its Fourier polynomial) and some RZF zero that satisfy these identities.

 1280. Ramanujan Graphs, Ihara Zeta Function and Riemann Zeta Function and
 Special case of Complement Function - related to 24

A graph is Ramanujan graph if it is d -regular and eigen values of its adjacency matrix are $\sqrt{d-1}$ or d . Ihara zeta function similar to RZF is a Dirichlet series that is based on prime cycle lengths of a graph defined as $\prod_p (1 - \sum_{p \text{ prime}} \frac{1}{p^s})$ where s is a zero and p prime for a $(q+1)$ -regular graph. Thus a reduction is already available from RZF to a graph. The Ihara Zeta Function satisfies Riemann Hypothesis iff graph is Ramanujan - this follows from Ihara identity that relates Ihara Zeta Function and the adjacency matrix of a graph. Thus proving above conjecture for Euler-Fourier polynomial of complement function for primes boolean and arithmetic circuits family might need this gadget using prime cycles.

If a set of p -regular graphs for all primes is considered, then Riemann Zeta Function can be derived (using Ihara Zeta Function identity) as a function of product of Ihara Zeta Functions for these graphs and a function of the determinants of adjacency matrices for these graphs divided by an infinite product similar to Euler product with $(1+1/p^s)$ clauses instead of $(1-1/p^s)$. This requires computing product of determinants of a function of adjacency matrices for these graphs. A regular connected graph is Ramanujan if and only if it satisfies RH. Zeroes of the individual Ihara zeta functions are also zeroes of this product for the set of graphs and hence for the RZF. Intuitively the product might imply set of all paths of all possible lengths across these graphs. Determinant of the product of adjacent matrices is product of determinants of the matrices and equating it to zero yields eigenvalues. All these graphs have same number of edges and vertices. The eigen values then are of the form $\sqrt{q^2 - 2a + q}$ where $s = a + ib$ for each of the regular graphs. The RHS of Ihara Zeta Function can be written as $[(1+1/q^s)(1-1/q^s)]^{[V-E]}$ and the product gives the RZF and the other series mentioned above. Eigen values can be at most q .

[If an eigen value is t ($\leq q$), then it can be derived that

$$q^s = q + (or) - \sqrt{q^2 - 4t} / 2$$

where $s = a + ib$. Setting $a = 0.5$ is creating a contradiction apparently which is above divided by \sqrt{q} (while equating real and imaginary parts for $q^{(ib)}$ or $e^{(ib \cdot \log q)}$ - needs to be verified if this kind of derivation is allowed in meromorphic functions).]

Above and the Informal notes in

<https://sites.google.com/site/kuja27/RamanujanGraphsRiemannZetaFunctionAndIharaZetaFunction.pdf?attredirects=0&d=1> can further be simplified as follows to get RZF in terms of IZF identity.

Disclaimer: It is not in anyway an attempted proof or disproof of RH as I am not an expert in analytical number theory. Hence arguments might be elementary. Following was found serendipitously as a surprise while working on special case of circuits for complement function for primes and it does not have direct relation to complementation - Fourier polynomial for Complement Function generalizes Riemann Hypothesis in a sense. Moreover, Notion of complementing a function is absent in mathematical literature I have searched so far except in mathematical logic. Following are derived based on Ihara Identity of Ihara Zeta Function. [<https://lucatrevisan.wordpress.com/2014/08/18/the-riemann-hypothesis-for-graphs/#more-2824>] for a prime+1 regular graph.

(1) For some i -th prime+1 regular graph (i.e q_i+1 regular graph where q_i is prime),

$$\frac{[1 + q_i^s]}{1} = \dots$$

$$[z_i(s) \det(I - A q_i^{-s} + q_i^{(1-2s)} I)^{(1/|V| - |E|)} \quad [1 - q_i^{-s}]$$

(2) Infinite product of the above terms for all prime+1 regular graphs gives the RZF in right in terms of Ihara Zeta Function Identities product on the left - The infinite set of prime+1 regular graphs relate to RZF zeros.

(3) For non-trivial zeros $s=a+ib$, RZF in RHS is zero and thus either numerator product is zero or denominator product tends to infinity

(4) From Handshake Lemma, it can be derived that a q -regular graph with order $n(=|V| \text{ vertices})$ has $q*n/2$ edges ($=|E|$ edges)

(5) If numerator is set to zero in LHS,
 $q^{(a+ib)} = -1$

and

$\cos(\log q) + i \sin(\log q) = -1/q^a$ which seems to give further contradiction

(6) If denominator is set to infinity in LHS,
 $[z_1*z_2*.....\det() \det()....]^{1/|V|-|E|} = \text{Inf}$
 (or)
 $[z_1*z_2*.....\det() \det()....]^{1/|E|-|V|} = 0$

for some term in the infinite product of LHS which implies that $[z_1*z_2*.....\det() \det()....] = 0$ which is described earlier above in the notes.

(7) More derivations of the above are in the notes uploaded in handwritten preliminary drafts at:

(7.1) https://sites.google.com/site/kuja27/RZFAndIZF_250ctober2014.pdf?attredirects=0&d=1

(7.2)
http://sourceforge.net/p/asfer/code/HEAD/tree/python-src/ComplFunction_DHF_PVsNP_Misc_Notes.pdf

(8) By equating the determinant in (6) above to zero, written notes in (7) derive values of $s=a+ib$ for non-Ramanujan prime+1 regular graphs for the expressions in points (1) to (6) above. They seem to suggest that RH is true with elementary complex arithmetic without using any complex analysis, with or without any assumption on the eigenvalue surprisingly - assuming $q^s + q^{(1-s)} = v$ (v can be set to any eigenvalue - can be atmost $q+1$ for the $q+1$ -regular non-ramanujan graph) and solving for $s=a+ib$ - gives $a=1/2$ and thus for both ramanujan and non-ramanujan graphs as eigen value becomes irrelevant - needs lot of reviewing - because it implies that graph formulation above of Riemann Hypothesis is true for all prime+1 regular graphs by applying Ihara Identity of Ihara Zeta Function and thus Riemann Hypothesis is true. The choice of prime+1 regularity is just a contrived gadget to equate to Riemann Zeta Function through an infinite product. Crucial fact is the independence of eigen value in the previous derivation whenever the graph regularity is prime+1, thus directly connecting prime numbers and real part of Riemann Zeta Function non-trivial zero.

(9) Above doesn't look circular also because infinite product of characteristic polynomials - determinants - are independent of infinite product of Ihara Zeta Functions preceding them in denominator - this happens only when the product $z_1*z_2*...$ is not zero i.e when the graphs are non-ramanujan. The infinite product of determinants of the form $\det(I - A(q_i)^{-s} + (q_i)^{(1-2s)} I)$ when solved for zero do not depend on eigenvalue and s is assumed nowhere. Independence of eigen value implies all possible graphs. Further the last step is independent of regularity q too. Had it been circular, the eigenvalue for Ramanujan graph

should have occurred somewhere in the derivation throwing back to square one.

(10) Expression in (1) for a prime+1 regular graph can also be equated to Euler-Fourier polynomial mentioned in (24c) per-prime term for each prime+1 regular graph - LHS is a graph while RHS is a fourier polynomial for boolean circuit for a prime - $P(x_i)$. Thus pattern in prime polynomials in RHS are related to patterns in graphs on left:

$$\frac{[1+q_i^{-s}]}{[z_i(s)\det(I-A^*q_i^{-s} + q_i^{(1-2s)*I})^{(1/|V|-|E|)}]} = \frac{1}{[1-P(x_i)^{-s}]}$$

(11) q_i can be replaced with Fourier polynomial $P(x_i)$, and the above becomes:

$$[1-P(x_i)^{-2s}] = [z_i(s)\det(I-A^*P(x_i)^{-s} + P(x_i)^{(1-2s)*I})^{(1/|V|-|E|)}]$$

(or) $[1-P(x_i)^{-2s}]^{(|V|-|E|)} = [z_i(s)\det(I-A^*P(x_i)^{-s} + P(x_i)^{(1-2s)*I})]$

(12) LHS of (11) can be expanded with binomial series. Thus Euler-Fourier polynomial is coalesced into Ihara identity to give Euler-Fourier-Ihara polynomial for a prime (and hence corresponding prime+1 regular graph). Partial Derivatives of the above polynomial look crucial in deciphering pattern in primes - for example $\text{doe}(s)/\text{doe}(P(x_i))$.

(13) ACC circuits have support for mod(m) gates. Thus a trivial circuit for non-primality is set of mod(i) circuits - 1,2,3,...,sqrt(N) - that output 1 to an OR gate up (factor gates output 1). This non-primality circuit is equivalent to complement of complement function circuit for $xy=z$ described previously (and it can be stated in its dual form also).

(14) The Fourier polynomial of a prime $P(x_i)$ is holographic in the sense that it has information of all primes due to the multiplexor construction.

(15) Without any assumption on Ihara and Riemann Zeta Functions, for any $(q+1)$ -regular graph for prime q , just solving for eigenvalue in $\det[-[A - I^*(q^s + q^{(1-s)})]]$ to get $\text{Real}(s) = 0.5$ looks like an independent identity in itself where A is adj matrix of graph. It neither requires Riemann Zeta Function nor Ihara Zeta Function to arrive at $\text{Real}(s)=0.5$.

(16) In (15), even the fact that q has to be prime is redundant. Just solving for $q^s + q^{(1-s)} = \text{some_eigen_value}$ gives $\text{Real}(s)=0.5$. In such a scenario what the set $\{\text{Imaginary}(s)\}$ contains is quite non-trivial. It need not be same as $\{\text{Imaginary}(\text{RZF_zero})\}$.

(17) Assuming $\text{Real}(s)=0.5$ from 7.1 and 7.2, it can be derived with a little more steps that $\text{eigen_value} = 2*\sqrt{q}*\cos(b*\log(q))$ - eigen value depends only on $\text{imaginary}(s)$ and regularity.

(18) It is not known if $\{\text{Imaginary}(\text{RZF_zero})\} = \{\text{Imaginary}(s)\}$. If not equal this presents a totally different problem than RZF and could be a disjoint_set/overlap/superset of RZF zeroes.

(19) Maximum eigen value of $(q+1)$ -regular graph is $(q+1)$ and the infinite set $\{\text{Imaginary}(s)\}$ can be derived from $\text{eigen_value}=2*\sqrt{q}*\cos(b*\log(q))$ in (17) for infinite set of $(q+1)$ -regular graphs.

(20) An experimental python function to iterate through all $\{\text{Imaginary}(s)\}$ mentioned in (19) supra has been included in complement.py. Because of the restriction that $\cos()$ is in $[-1,1]$, $\text{eigen_value} \leq 2*\sqrt{q}$ which has a trivial value of $q=1$ when $\text{eigen_value}=q+1$.

(21) (SOME EXPERIMENTATION ON DISTRIBUTION OF PRIMES) List of primes read by complement.py is downloaded from <https://primes.utm.edu/lists/>. IharaIdentity() function in complement.py evaluates $\text{Imaginary}(s)=b=\arccos(v/(2*\sqrt{q}))/\log(q)$ by incrementing v by small steps in a loop till it equals $2*\sqrt{q}$. This allows v to be in the range $[0, 2*\sqrt{q}]$ whereas Ramanujan graphs require it to be $2*\sqrt{q-1}$ or q . Hence non-ramanujan graphs are also allowed. Logs in testlogs/

print all Imaginary(s) iterations of this eigenvalues for all 10000 primes. arccos() function returns radians which is a cyclic measure and hence can take $x+2*y*\pi$ where $y=0,1,2,3,4,5,6,\dots$ which could be arbitrarily large infinite set. Logs print only x with $y=0$ and not all cycles. Prima facie visual comparison shows this set to be different from Imaginary(RZF) for x alone which could be inaccurate. Sifting through all cycles and verifying if these are indeed Im() parts of RZF might be an arduous task and could be undecidable too because two infinite sets have to be compared for equality. But theoretically the Re() part of (2) which is infinite product of (1) equivalent to Riemann Zeta Function is 0.5 for all while Im() part is computationally intensive. Crucial evidence that comes out of it is the possibility of cyclic values of radians in $b=\arccos(v/(2*\sqrt{q}))/\log(q)$ which implies a fixed (prime, eigenvalue) ordered tuple correspond to infinitely many b(s) (Im() parts). Thus $2*\sqrt{q}*\cos(b*\log(q)) = \text{eigen_value}$ is a generating function mining pattern in distribution of primes. Rephrasing, b has generating function: $b \leq (x + 2*y*\pi)/\log q$, where $0 \leq x \leq \pi/2$. SequenceMining.py also has been applied to binary representation of first 10000 prime numbers (Commit Notes 273 below) which is learning theory way of finding patterns in distribution in primes. Logs for the most frequent sequences in prime strings in binary have been committed in testlogs/. These binary sequences mined from first 10000 primes have been plotted in decimal with R+py2 function plotter. Function plot in decimal shows sinusoidal patterns in mined sequences with periodic peaks and dips as the length of sequence increases i.e the mined sequences in prime binary strings periodically have leftmost bits set to 1 and rightmost bits set to 1 and viceversa which causes decimals to vacillate significantly. Primes are not regular and context-free languages which are known from formal languages theory. The function doing complementation in complement.py can be translated to Turing Machine by programming languages Brainfuck and Laconic which is equivalent to a lambda function for complement.

1281. PAC Learning and Complement Function Construction - related to 24

Complement Boolean Function construction described in <http://arxiv.org/abs/1106.4102> is in a way an example of PAC learnt Boolean Function - it is rather C Learnt (Correct Learning) because there is no probability or approximation. Complement Boolean Function can be PAC learnt (with upperbounded error) as follows:

- There are two datasets - dataset1 of size 2^n of consecutive integers and dataset2 of first n -bit prime numbers of size 2^n
- Each element of dataset1 is mapped to i -th bit of the corresponding prime number element in the dataset2. Boolean Conjunction is learnt for each of the i mappings (PAC Learning Algorithm:

<http://www.cis.temple.edu/~giorgio/cis587/readings/pac.html>).

- Above step gives n probabilistic, approximate, correct learnt boolean conjunctions for each bit of all the 2^n prime numbers.

- An example PAC Boolean Conjunction Learner is at:

<http://sourceforge.net/p/asfer/code/HEAD/tree/python-src/PACLearning.py>

1282. Star Complexity and Complement Function Circuit Lowerbound (related to 24,198)

Star Complexity of a Boolean Circuit is the minimum number of AND and OR gates required in monotone circuit graph. Size lowerbound for Complement Function circuit can thus be lowerbounded by Strong Magnification Lemma (Stasys Jukna - <http://www.thi.informatik.uni-frankfurt.de/~jukna/ftp/graph-compl.pdf>) - $\text{Size}(\text{ComplementCircuit}) \geq \text{Star}(\text{ComplementCircuitGraph}) - (2 + o(1))*n$. Mapping from Boolean Circuit to Graph is done through a bipartite graph gadget wherein a boolean variable $x(v_1,v_2)$ iff there is an edge from v_1 to v_2 in the bipartite graph and replacing each boolean literal by an OR of two new variables. Star Complexity views Boolean Circuits as a graph and for most graphs it is

$\Omega(n^2/\log n)$. Obtaining Size Lowerbounds for arbitrary complement functions is non-trivial.

1283. Additional references - related to 24:

1283.1 Google groups thread reference 2003 (OP done by self):

https://groups.google.com/forum/#!search/ka_shrinivaasan%7Csort:relevance%7Cspell:false/sci.math/RqsDNc6SBdk/Lgc0wLiFhTMJ

1283.2 Math StackExchange thread 2013:

<http://math.stackexchange.com/questions/293383/complement-of-a-function-f-2n-n-in-mathbbn-0-n-rightarrow-n1>

1283.3 Theory of Negation -

<http://mentalmodels.princeton.edu/skhemlani/portfolio/negation-theory/> and a quoted excerpt from it :

"... The principle of negative meaning: negation is a function that takes a single argument, which is a set of fully explicit models of possibilities, and in its core meaning this function returns the complement of the set..."

1283.4 Boolean Complementation [$\{0, 1\}$ as range and domain] is a special case of Complement Function above (DeMorgan theorem -

<http://www.ctp.bilkent.edu.tr/~yavuz/BOOLEEAN.html>)

1283.5 Interpolation -

http://caig.cs.nctu.edu.tw/course/NM07S/slides/chap3_1.pdf

1283.6 Formal Concept Analysis -

http://en.wikipedia.org/wiki/Formal_concept_analysis,

<http://ijcai.org/papers11/Papers/IJCAI11-227.pdf>

1283.7 Prime generating polynomials -

http://en.wikipedia.org/wiki/Formula_for_primes

1283.8 Patterns in primes - every even number > 2 is sum of 2 primes - Goldbach conjecture : http://en.wikipedia.org/wiki/Goldbach%27s_conjecture

1283.9 Arbitrarily Long Arithmetic progressions - Green-Tao theorem:

http://en.wikipedia.org/wiki/Green%E2%80%93Tao_theorem

1283.10 Prime generating functions -

https://www.sonoma.edu/math/colloq/primes_sonoma_state_9_24_08.pdf

1283.11 Hardness of Minimizing and Learning DNF Expressions -

<https://cs.nyu.edu/~khot/papers/minDNF.pdf>

1283.12 DNF Minimization - <http://users.cms.caltech.edu/~umans/papers/BU07.pdf>

1283.13 DNF Minimization - <http://www.cs.toronto.edu/~toni/Papers/mindnf.pdf>

1283.14 Riemann Zeta Function Hypothesis - all non-trivial (complex) zeroes of RZF have $\text{Re}(z) = 0.5$ - http://en.wikipedia.org/wiki/Riemann_hypothesis.

1283.15 Frequent Subgraph Mining -

<http://research.microsoft.com/pubs/173864/icde08gsearch.pdf>

1283.16 Frequent Subgraph Mining -

<http://glaros.dtc.umn.edu/gkhome/fetch/papers/sigramDMKD05.pdf>

1283.17 Roots of polynomials - Beauty of Roots -

<http://www.math.ucr.edu/home/baez/roots/>

1283.18 Circuit lowerbounds (Gate Elimination, Nechiporuk, Krapchenko, etc) -

http://cs.brown.edu/~jes/book/pdfs/ModelsOfComputation_Chapter9.pdf

1283.19 Schwartz-Zippel Lemma for Polynomial Identity Testing -

http://en.wikipedia.org/wiki/Schwartz%E2%80%93Zippel_lemma

1283.20 Schwartz-Zippel Lemma for PIT of multilinear polynomials -

<http://www.cs.huji.ac.il/~noam/degree.ps>

1283.21 Analysis of Boolean Functions - <http://analysisofbooleanfunctions.org/>

1283.22 Riemann-Siegel Formula for computation of zeros -

<http://numbers.computation.free.fr/Constants/Miscellaneous/zetaevaluations.html>

1283.23 RZF zeros computation -

<http://math.stackexchange.com/questions/134362/calculating-the-zeroes-of-the-riemann-zeta-function>

1283.24 Online Encyclopedia of Integer Sequences for Prime numbers - all

theorems and articles related to primes - [https://oeis.org/search?](https://oeis.org/search?q=2%2C3%2C5%2C7%2C11%2C13%2C17%2C19%2C23%2C29%2C31%2C37%2C41%2C43%2C47%2C&language=english&go=Search)

[q=2%2C3%2C5%2C7%2C11%2C13%2C17%2C19%2C23%2C29%2C31%2C37%2C41%2C43%2C47%2C&language=english&go=Search](https://oeis.org/search?q=2%2C3%2C5%2C7%2C11%2C13%2C17%2C19%2C23%2C29%2C31%2C37%2C41%2C43%2C47%2C&language=english&go=Search)

1283.25 Intuitive proof of Schwartz-Zippel lemma -

<http://rjlipton.wordpress.com/2009/11/30/the-curious-history-of-the-schwartz->

zippel-lemma/
 1283.26 Random Matrices and RZF zeros -
<http://www.maths.bris.ac.uk/~majpk/papers/67.pdf>
 1283.27 Circuit for determinant - S. J. Berkowitz. On computing the determinant in small parallel time using a small number of processors. Inf. Prod. Letters 18, pp. 147-150, 1984.
 1283.28 Mangoldt Function, Ihara Zeta Function, Ramanujan Graphs -
<http://lucatrevisan.wordpress.com/2014/08/18/the-riemann-hypothesis-for-graphs/#more-2824>
 1283.29 Multiplicity of an eigen value in k-regular graph -
<http://math.stackexchange.com/questions/255334/the-number-of-connected-components-of-a-k-regular-graph-equals-the-multiplicity>
 1283.30 PAC Learning -
<http://www.cis.temple.edu/~giorgio/cis587/readings/pac.html>
 1283.31 Pattern in Prime Digits - [Oliver-Kannan Soundarrajan] -
<http://arxiv.org/abs/1603.03720> - Prime numbers which are juxtaposed avoid ending in same digit. This has direct bearing on Fourier polynomial of prime complement function and Euler-Fourier polynomial derived above which is binary representation of a prime and a special case of function complementation. If decimal representation of adjacent primes is repulsive in last digit, then last binary bits (LSB) output by the complement circuit should be too.
 1283.32 Pattern in Prime Digits - <http://www.nature.com/news/peculiar-pattern-found-in-random-prime-numbers-1.19550> - above with assumption of Hardy-Littlewood k-tuple conjecture a generalization of twin primes conjecture to all prime constellations.
 1283.33 Pattern in Primes - Ulam's Spiral - [Stainslaw Ulam] -
<https://www.alpertron.com.ar/ULAM.HTM> - Prime numbers are clustered along diagonals of anticlockwise spiral of integers 1,2,3,4,5,6,... ad infinitum.
 1283.34 Theory of Negation (Broken URL in 24.3 updated) -
<http://mentalmodels.princeton.edu/papers/2012negation.pdf>
 1283.35 Prime Number Theorem - n-th prime is $\sim O(n \log n)$
 1283.36 Riemann Hypothesis prediction of prime distribution -

$$\text{Integral}_2 p(n) [dt/\log t] = n + O(\sqrt{n}(\log n)^3)$$

 1283.37 Brainfuck Turing Machine Compiler - <https://esolangs.org/wiki/Brainfuck>
 1283.38 Laconic Turing Machine Compiler - <https://esolangs.org/wiki/Laconic>
 1283.39 Circuit Complexity Lowerbound for Explicit Boolean Functions -
http://logic.pdmi.ras.ru/~kulikov/papers/2011_3n_lower_bound_mfcs.pdf - $3n - o(n)$
 1283.40 Star Complexity of Boolean Function Circuit - [Stasys Jukna] -
<http://www.thi.informatik.uni-frankfurt.de/~jukna/ftp/graph-compl.pdf>
 1283.41 Random Matrices, RZF zeroes and Quantum Mechanics -
<https://www.ias.edu/ideas/2013/primes-random-matrices>
 1283.42 Jones-Sato-Wada-Wiens Theorem - Polynomial of 25 degree-26 variables for Prime Diophantine set -
<http://www.math.ualberta.ca/~wiens/home%20page/pubs/diophantine.pdf>
 1283.43 Energy levels of Erbium Nuclei and zeros of Riemann Zeta Function -
http://seedmagazine.com/content/article/prime_numbers_get_hitched/
 1283.44 Bhargava's prime-universality criterion theorem asserts that an integer-matrix quadratic form represents all prime numbers if and only if it represents all numbers in this sequence - [2, 3, 5, 7, 11, 13, 17, 19, 23, 29, 31, 37, 41, 43, 47, 67, 73] - <https://oeis.org/A154363>

 #####

25. (FEATURE - DONE) Approximating with some probability distribution - Gaussian, Binomial etc., that model the probability of occurrence of a datapoint in the set. Kullback-Leibler Divergence python implementation which computes distance in terms of amount of bits between two probability distribution has been added to python-src/. Minimum of the distance for different standard distributions with a dataset is the closest distribution approximation for the dataset.

(FEATURE - DONE) 26. Streaming algorithms - Finding Frequency moments, Heavy

Hitters(most prominent items), Distinct Elements etc., in the numerical dataset. Usually numerical data occur in streams making these best choice for mining numerical data.

(FEATURE - DONE) 26.1 Implementation of LogLog and HyperLogLog Counter(cardinality - distinct elements in streamed multiset), CountMinSketch-CountMeanMinSketch (Frequencies and heavy hitters) and Bloom Filters(membership) (FEATURE - DONE) 26.2 Parser and non-text file Storage framework for Realtime Streaming Data - Hive, HBase, Cassandra, Spark and Pig Scripts and Clients for Storage Backends have been implemented. The Storage is abstracted by a generator - architecture diagram at: <http://sourceforge.net/p/asfer/code/HEAD/tree/asfer-docs/BigDataStorageAbstractionInAsFer.jpg> (FEATURE - DONE) 26.3 Python scripts for Stock Quotes Data and Twitter tweets stream search data for a query.

References:

26.4 <https://gist.github.com/debasishg/8172796>

27. (FEATURE - DONE) Usual Probabilistic Measures of Mean, Median, Curve fitting on the numeric data. Python+RPy2+R implementation wrapper has been added to repository (python-src/Norms_and_Basic_Statistics.py)

28. (FEATURE - DONE - using python, R+Rpy2) Application of Discrete Fourier Transform(using R), LOESS(using R), Linear Polynomial Approximate Interpolation(using R), Logistic Regression and Gradient Descent

29. (FEATURE - DONE) Least Squares Method on datapoints $y(i)$ s for some $x(i)$ s such that $f(x) \sim y$ needs to be found. Computation of L_0 , L_1 and L_2 norms. Python+RPy2+R implementation wrapper has been added to repository (python-src/Norms_and_Basic_Statistics.py)

(FEATURE - DONE)30. K-Means and kNN Clustering(if necessary and some training data is available) - unsupervised and supervised clustering based on coordinates of the numerical dataset

31. (FEATURE - DONE) Discrete Hyperbolic Factorization - Author has been working on a factorization algorithm with elementary proof based on discretization of a hyperbola since 2000 and there seems to be some headway recently in 2013. To confirm the polylog correctness, a minimal implementation of Discrete Hyperbolic Factorization (and could be even less than polylog due to a weird upperbound obtained using stirling formula) has been added to AstroInfer repository at: <http://sourceforge.net/p/asfer/code/HEAD/tree/cpp-src/miscellaneous/DiscreteHyperbolicFactorizationUpperbound.cpp> with factors output logs.

32. (FEATURE - DONE) Multiple versions of Discrete Hyperbolic Factorization algorithms have been uploaded as drafts in <https://sites.google.com/site/kuja27>:

32.1)

http://sourceforge.net/projects/acadpdrafts/files/DiscreteHyperbolicFactorization_UpperboundDerivedWithStirlingFormula_2013-09-10.pdf/download and

32.2)

http://sourceforge.net/projects/acadpdrafts/files/DiscreteHyperbolicPolylogarithmicSieveForIntegerFactorization_updated_rectangular_interpolation_search_and_StirlingFormula_Upperbound.pdf/download(and multiple versions due to various possible algorithms for search and upperbound technique used)

33. (DONE) NC PRAM version of Discrete Hyperbolic Factorization:

33.1) An updated NC PRAM version of Discrete Hyperbolic Factorization has been uploaded at:

http://sourceforge.net/projects/acadpdrafts/files/DiscreteHyperbolicPolylogarithmicSieveForIntegerFactorization_PRAM_TileMergeAndSearch_And_Stirling_Upperbound.pdf/download that does PRAM k-merge of discrete tiles in logarithmic time before binary search on merged tile.

33.2) Preliminary Design notes for CRCW PRAM implementation of the above is added to repository at:
<http://sourceforge.net/p/asfer/code/237/tree/ImplementationDesignNotesForDiscreteHyperbolicFactorizationInPRAM.jpg>. This adds a tile_id to each tile so that during binary search, the factors are correctly found since coordinate info gets shuffled after k-tile merge.

34. (FEATURE - DONE) An updated draft version of PRAM NC algorithm for Discrete Hyperbolic Factorization has been uploaded - with a new section for Parallel RAM to NC reduction, disambiguation on input size (N and not logN is the input size for ANSV algorithm and yet is in NC - in NC2 to be exact - $(\log N)^2$ time and polynomial in N PRAM processors - NC circuit depth translates to PRAM time and NC circuit size to number of PRAMs):

34.1 LaTeX -

http://sourceforge.net/projects/acadpdrafts/files/DiscreteHyperbolicPolylogarithmicSieveForIntegerFactorization_PRAM_TileMergeAndSearch_And_Stirling_Upperbound_updateddraft.tex/download

34.2 PDF -

http://sourceforge.net/projects/acadpdrafts/files/DiscreteHyperbolicPolylogarithmicSieveForIntegerFactorization_PRAM_TileMergeAndSearch_And_Stirling_Upperbound_updateddraft.pdf/download

Additional references:

34.3 Above PRAM k-merge algorithm implies Factorization is in NC, a far more audacious claim than Factorization in P. It has been disputed if PRAM is indeed in NC because of input size being N and not logN. But there have been insurmountable evidences so far which all point to PRAM model being equivalent to NC circuits in certain conditions and NC circuit nodes can simulate PRAM with polylog upperbound on number of bits [HooverGreenlawRuzzo]-
<https://homes.cs.washington.edu/~ruzzo/papers/limits.pdf> . References for this are in LaTeX and PDF links previously and also mentioned below in "Additional References"

34.4) (IMPORTANT OPTIMIZATION OVER 34.1, 34.2 ABOVE) Instead of [BerkmanSchieberVishkin] an $O(\log \log \log N)$ algorithm can be used described in (since the numbers in tiles are within a known range - 1 to N - for factorization of N in discretized tessellated hyperbolic arc) - Triply-Logarithmic Parallel Upper and Lower Bounds for Minimum and Range Minima over Small Domains (Omer Berkman, Yossi Matias, Prabhakar Ragde) - 1998 -
<http://www.sciencedirect.com/science/article/pii/S0196677497909056>. This algorithm internally applies [BerkmanSchieberVishkin] but lemmas 2.3 and 3.1 mentioned in [BerkmanMatiasPrabhakar] preprocess the input within a known domain $[1..N]$. This takes $O(\log \log \log N)$ time using $(\log N)^3 / \log \log \log N$ processors for each merging problem and $O(\log \log \log N)$ time using $N / \log \log \log N$ processors overall. This algorithm can therefore supersede 34.1 and 34.2.

34.5) Randomized Algorithms ,Rajeev Motwani and Prabhakar Raghavan, Chapter 12 on Distributed and Parallel Algorithms, also describes input size and randomized algorithms for Parallel sort - Definition 12.1 of NC (Page 336) - "NC consists of languages that have PRAM algorithms with $O(\log N)$ time and $O(N^k)$ PRAM processors".

34.6) Also an alternative merge algorithm in constant depth polysize circuit described in Chandra-Stockmeyer-Vishkin [<http://cstheory.com/stockmeyer@sbcglobal.net/csv.pdf>] can be applied (but it is for merging two lists of m, m-bit numbers where as the above factorization needs merging two lists of $O(m)$, $\log(m)$ -bit numbers)

34.7) [RichardKarp-VijayaRamachandran] define the inclusion of PRAM models in NC in page 29 of

<http://digitalassets.lib.berkeley.edu/techreports/ucb/text/CSD-88-408.pdf> - NCK in EREWk in CREWk in CRCWk=ACK in NC(k+1). [KarpRamachandran] cite [HooverKlawePippenger] - Bounding Fanout in Logical Networks - <http://dl.acm.org/citation.cfm?id=322412> - for this inclusion. Thus references for PRAM=NC imply All Nearest Smaller Values (ANSV) CRCW PRAM algorithm [BerkmanSchieberVishkin] is also in NC counterintuitively despite the input size being $N=n$ (and not $\log N$).

34.8) Parallel RAM survey - <http://www.cs.utoronto.ca/~faith/PRAMsurvey.ps>

34.9) Related: Quantum Search using Grover Algorithm over unsorted lists can be done in $O(\sqrt{N})$ - https://en.wikipedia.org/wiki/Grover's_algorithm. This is another counterintuitive fact that a quantum search on unsorted lists is slower than ANSV Parallel RAM algorithm.

34.10) Recent Advances in All Nearest Smaller Values algorithms:

34.10.1) ANSV in hypercube - Kravets and Plaxton - http://www.cs.utexas.edu/~plaxton/pubs/1996/ieee_tpds.ps

34.10.2) ANSV lowerbound - Katajainen - <http://www.diku.dk/~jyrki/Paper/CATS96.ps> - $\omega(n)$ processors with $\omega(\log n)$ time

34.10.3) ANSV in BSP machines - Chun Hsi Huang - <http://www.cse.buffalo.edu/tech-reports/2001-06.ps>

34.11) The crucial fact in the above is not the practicality of having order of n parallel processors with RAM to get the logarithmic time lowerbound (which looks costly in number of PRAMs wise), but the equivalence of PRAM to NC which is theoretically allowed despite input size being n instead of $\log n$ (because each PRAM cell mapped to a circuit element can have $\text{poly}(\log n)$ bits and $\text{poly} n$ such PRAMs are allowed) which is sufficient for Discrete Hyperbolic Factorization to be in NC.

34.12) Rsync - PhD thesis - chapters on external and internal sorting - https://www.samba.org/~tridge/phd_thesis.pdf

34.13) Handbook of Parallel Computing - [SanguthevarRajasekaran-JohnReif] - <http://www.engr.uconn.edu/~rajasek/HandbookParallelComp.pdf>, https://books.google.co.in/books?id=OF9hk4oC6FIC&pg=PA179&lpg=PA179&dq=PRAM+NC+equivalence&source=bl&ots=LpYceSocLO&sig=GtslRh1I1AveOLO0kTylSzyDd48&hl=en&sa=X&ved=0ahUKEwi_10fmuKbJAhUCHY4KHTpdAFoQ6AEISTAI#v=onepage&q=PRAM%20NC%20equivalence&f=false

34.14) [Eric Allender] - NC^1 and EREW PRAM - March 1990 - https://groups.google.com/forum/#!topic/comp.theory/0a5Y_DSkoao - "... Since NC^1 is contained in DLOG, and many people suspect that the containment is proper, it seems unlikely that NC^1 corresponds to log time on an EREW PRAM ..." - contradicts 34.7.

34.15) Efficient and Highly Parallel Computation - [JeffreyFinkelstein] - <https://cs-people.bu.edu/jeffreyf/static/pdf/parallel.pdf> - "... NC represents the class of languages decidable by a CREW PRAM with a polynomial number of processors running in polylogarithmic parallel time. Languages in NC are considered highly parallel ...". [Berkman-Schieber-Vishkin] algorithm - www.umiacs.umd.edu/users/vishkin/PUBLICATIONS/ansv.ps - for ANSV is for both CREW PRAM of $O(\log n, n/\log n)$ and CRCW PRAM of $O(\log \log n, n/\log \log n)$ and thus former is in NC.

34.16) There is a commercially available Parallel CRCW RAM chip implementation by NVIDIA CUDA GPUs - <http://developer.nvidia.com/cuda> and XMT research project - www.umiacs.umd.edu/users/vishkin/XMT/ but not for CREW PRAM which is a limitation of implementing All Nearest Smaller Values PRAM merge for discretized hyperbolic arc and doing a benchmark.

34.17) StackExchange thread on Consequences of Factorization in P -

<http://cstheory.stackexchange.com/questions/5096/consequences-of-factoring-being-in-p> . Factorization in P is unlikely to have any significant effect on existing class containments, though practical ecommerce becomes less secure.

34.18) What happened to PRAM - <http://blog.computationalcomplexity.org/2005/04/what-happened-to-pram.html> - Quoted excerpts from comments - "... I don't understand why some CS theory people apologize for the PRAM. NC is robust and interesting as a complexity class, and an easy way to show that a problem is in NC is to give a PRAM algorithm. That's all the argument I need for the PRAM's existence. And yes, I've heard all of the arguments about why the PRAM is completely unrealistic ..."

34.19) [Page 29 - HooverGreenlawRuzzo] - "... but there is no a priori upper bound on the fanout of a gate. Hoover, Klawe, and Pippenger show that conversion to bounded fanout entails at most a constant factor increase in either size or depth [160]..."

34.20) (DONE-BITONIC SORT IMPLEMENTATION) In the absence of PRAM implementation, NC Bitonic Sort has been invoked as a suitable alternative in parallel tile merge sort step of Parallel Discrete Hyperbolic Factorization Implementation. Commit Notes 261-264 and 265-271 below have details on this. Bitonic Sort on SparkCloud requires $O((\log n)^2)$ time with $O(n^2 \log n)$ parallel comparators (which simulate PRAM but comparators required are more than PRAMs). With this NC factorization has been implemented on a Spark cloud.

34.21) An important point to note in above is that an exhaustive search in parallel would always find a factor, but in how many steps is the question answered by NC computational geometric search. This is 1-dimensional geometric factorization counterpart of 2-dimensional Graham's Scan and Jarvis March for Convex Hull of n points. A parallel algorithm in $O(n)$ steps wouldn't have qualified to be in NC. Above NC algorithm scans just an one-dimensional tessellated merged tiles of a hyperbolic arc in $O((\log n)^2)$ for merge + $O(\log n)$ for search and doesn't scan more than 1-dimension. Parallel tessellation of $O(n)$ long hyperbolic arc to create locally sorted tile segments requires $< O(\log n)$ steps only if number of processors is $> O(n/\log n)$. Hence it adheres to all definitions of NC. Thus total parallel work time is $O((\log n)^2) + O(\log n) + O(\log n) = O((\log n)^2)$. Here again $N=n$.

34.22) NC Computational Geometric algorithms - [AggarwalChazelleGuibasDunlaingYap] - <https://www.cs.princeton.edu/~chazelle/pubs/ParallelCompGeom.pdf>

34.23) Parallel Computational Geometry Techniques - [MikhailAtallah] - <http://docs.lib.purdue.edu/cgi/viewcontent.cgi?article=1021&context=cstech> - Section 3.1 - Sorting and Merging - "...best hypercube bound for Parallel Sorting is $O(\log n (\log \log n)^2)$ - [CypherPlaxton] - <http://dl.acm.org/citation.cfm?id=100240> ..."

34.24) [DexterKozen-CheeYap] - Cell Decomposition is in NC - <http://anothersample.net/order/fe1d53539cff07d3e836ccc499d443b38b2848ba> - This is a deep Algebraic Geometry/Topology result for Cell Decomposition by constructing NC circuit for it. Coincidentally, the connection between NC factorization and geometry conjectured in 35 below is already present as evidenced by this. This algorithm is for Cell decomposition of a manifold in arbitrary dimensions - a set of disjoint union of cells created by intersecting polynomials. For NC factorization, the polynomial of interest is hyperbola. Illustration in [Kozen-Yap] - page 517 - is for 0,1,2-dimension cells with 2 polynomials - parabola and circle. This corresponds to tessellation step of factorization where a continuous hyperbola is discretized into disjoint union of cells.

34.25) Cell decomposition for tessellation of hyperbola can be created in two ways. In the first example, set of polynomials are {hyperbola,

stepfunction1, stepfunction2, $y=k$ for all integer k }. Geometrically the hyperbola is bounded above and below by 2 step functions i.e hyperbola intersects a grid of x-y axes lines. This creates 2-dimensional cells above and below hyperbola ensconced between 2 step functions which are homeomorphic to \mathbb{R}^2 (there is a bijective map between cells and \mathbb{R}^2 - Topology - James Munkres}. Each cell has same sign for a polynomial {above=+1, on=0, below=-1}. This cell decomposition is in NC. Cells above and below hyperbola have to be merged to get squared tessellation.

34.26) In another example Cell decomposition is created by intersection of integer y-axis lines and hyperbola which results in set of 0-cells (discrete set of points on hyperbola).

34.27) NVIDIA CUDA Parallel Bitonic Sort Implementation Reference - http://developer.download.nvidia.com/compute/cuda/1.1-Beta/x86_website/Data-Parallel_Algorithms.html, Linux code - <http://developer.download.nvidia.com/compute/cuda/1.1-Beta/Projects/bitonic.tar.gz>

34.28) Tiling of Hyperbolic curve: The discretization step of a hyperbola to form set of contiguous tiled segments has been mentioned as "Tessellation" throughout this document which could be a misnomer. Precise equivalent of this tiling is pixelation in Computer Graphics where an image bitmap is downsampled to create a low-resolution approximation of image - in this example, an image of hyperbolic curve is pixelated to get a tiled set of segments (<http://demonstrations.wolfram.com/PixelizationOfAFont/> shows how a letter A is pixelated to create stylized pixelated A).

34.29) The tiling of hyperbolic curve is done by $\Delta x = N/[y*(y+1)]$ which is a process similar to low-pass filter or Box Blur in Graphics. In a parallel setting with PRAMs or Parallel Bitonic Sort, the preprocessing step required is the tiled hyperbolic arc already in place spread out across all nodes of total number $O(N/\log N)$. This naive tiling though not as sophisticated as Box Blur Gaussian Filter, needs time $O(\log N)$ for each node i.e delta computation per coordinate is $O(1)$ and each node is allotted $O(\log N)$ long arc segment and thus $O(1*\log N)$ per node.

34.30) Above algorithm ignores Communication Complexity across PRAMs or Comparator nodes on a Cloud.

34.31) Comparison of Parallel Sorting Algorithms (Bitonic, Parallel QuickSort on NVIDIA CUDA GPU etc.,) - <http://arxiv.org/pdf/1511.03404.pdf>. Bitonic Sort has the best parallel performance in most usecases.

34.32) NC-PRAM Equivalence and Parallel Algorithms - [David Eppstein] - <https://www.ics.uci.edu/~eppstein/pubs/EppGal-ICALP-89.pdf>

34.33) Parallel Merge Sort - [Richard Cole] - <https://www.cs.nyu.edu/cole/> - best known theoretical parallel sorting algorithm - requires $O(\log n)$ time with n processors and thus in NC - <https://www.semanticscholar.org/paper/Parallel-Merge-Sort-Cole/6b67df5d908993eca7c03a564b5dcb1c4c8db999/pdf>

34.34) NC-PRAM equivalence - <http://courses.csail.mit.edu/6.854/06/notes/n32-parallel.pdf>

34.35) Theorem 13 - PRAM(polylog, log) = uniform-NC - www.wisdom.weizmann.ac.il/~oded/PS/CC/l27.ps - This mentions that Communication Complexity in PRAM model is assumed to be $O(1)$ and thus negligible though practically PRAMs are unrealistic.

34.36) PRAM Implementation Techniques - http://www.doc.ic.ac.uk/~nd/surprise_95/journal/vol4/fcw/report.html - "... However to say that an algorithm is in NC does not mean that it can be

efficiently implemented on a massively parallel system..."

34.37) Logarithm Time Cost Parallel Sorting - [Lasse Natvig] - Survey on Batcher's Bitonic Sort, AKS Sorting Network, Richard Cole's Parallel Sort - www.idi.ntnu.no/~lasse/publics/SC90.ps - Bitonic Sort is faster in practice though Richard Cole Parallel Sorting is the fastest and most processor-efficient known.

34.38) What is wrong with PRAM - "Too much importance is placed on NC . In particular, algorithms which have "fast" runtimes but use, for example, $O(n^2)$ processors are simply of no use" - Section 3.2 - <https://people.eecs.berkeley.edu/~jrs/meshpapers/SuThesis.pdf>

34.39) NC-PRAM equivalence - <https://www.ida.liu.se/~chrke55/courses/APP/ps/f2pram-2x2.pdf> - "set of problems solvable on PRAM in polylogarithmic time $O((\log n)^k)$ $k > 0$, using only $n^{O(1)}$ processors (i. e. a polynomial number) in the size n of the input instance"

34.40) Number of PRAMs in NC definition - <http://cs.stackexchange.com/questions/39721/given-a-pram-may-use-arbitrarily-many-processors-why-is-hamiltonian-cycle-not-i>

34.41) EURO-PAR 1995 - Input size in Parallel RAM algorithms - https://books.google.co.in/books?id=pVpjOwUHEigC&pg=PA245&lpg=PA245&dq=size+of+input+in+PRAM&source=bl&ots=uZ9Ge0Nqtg&sig=6YHL4CvNUdFERPe8p192hdB1Kc0&hl=en&sa=X&ved=0ahUKEwiZ3_z20qTOAhVJGJQKHx8bALIQ6AEIOTAG#v=onepage&q=size%20of%20input%20in%20PRAM&f=false - "... Third, inputs are usually measured by their size. We use overall number of array elements ..."

34.42) Batcher's Bitonic Sort is in NC - <https://web.cs.dal.ca/~arc/teaching/CS4125/Lectures/03b-ParallelAnalysis.pptx> - also other PRAM algorithms are in NC.

34.43) Brief Overview of Parallel Algorithms, Work-Time Efficiency and NC - [Blelloch] - <http://www.cs.cmu.edu/~scandal/html-papers/short/short.html> - "... Examples of problems in NC include sorting, finding minimum-cost spanning trees, and finding convex hulls ...". Work-Time Efficiency is more about optimizing number of processors required (with polylog time) and two algorithms with differing work-time are both theoretically in NC.

34.44) Sorting n integers is in NC - [BussCookGuptaRamachandran] - www.math.ucsd.edu/~sbuss/ResearchWeb/Boolean2/finalversion.ps

34.45) PRAM and Circuit Equivalence - [Savage] - <http://cs.brown.edu/~jes/book/pdfs/ModelsOfComputation.pdf> - Lemma 8.14.1

34.46) Efficient Parallel Computation = NC - [AroraBarak] - <http://theory.cs.princeton.edu/complexity/book.pdf> - Theorem 6.24 - Simpler version of 34.3

34.47) Parallel sorting and NC - <http://courses.csail.mit.edu/6.854/06/notes/n32-parallel.pdf>

34.48) Parallel sorting in PRAM model - <http://www.math.ias.edu/~avi/PUBLICATIONS/MYPAPERS/MW87/MW87.pdf>

34.49) Parallel Sorting is in NC - <http://www.toves.org/books/distalg/distalg.pdf> - Section 5 (Page 17)

34.50) Parallel K-Merge Algorithm for merging k sorted tiles into a single sorted list - LazyMerge - www.cs.newpaltz.edu/~lik/publications/Ahmad-Salah-IEEE-TPDS-2016.pdf

34.51) Timsort and its parallel implementation in Java, Python and Android for parallel merge sort of arrays - <https://docs.oracle.com/javase/8/docs/api/java/util/Arrays.html#parallelSort-int:A-> . Timsort exploits order in unsorted lists. Java implementation is based on ForkJoinPool work-stealing pattern (similar to router-worker-dealer pattern in ZeroMQ) and parallelism is equal to number of processors. Cloud Bitonicsort SparkPython implementation in NeuronRain AsFer could be more time efficient than `Arrays.parallelSort()` in Java 8 as it implements Batcher Sort on Cloud.

34.52) Comparison of Parallel and Sequential Sorts - <https://github.com/darkobozidar/sequential-vs-parallel-sort>

34.53) Trigonometric Functions over Finite Galois Fields (of prime power order) - <https://arxiv.org/pdf/1501.07502.pdf> - Defines trigonometric functions (hyperbola is also a trigonometric function - class of hyperbolic functions) on discrete objects like a finite field yielding a function on a set of complex points (Gaussian integers). This abstracts and reduces to discretization step of hyperbolic factorization but requires prime power sized finite field.

34.54) Adaptive Bitonic Sorting - <http://epubs.siam.org/doi/abs/10.1137/0218014> - very old paper (1989) on PRAM implementation of bitonic sort - NeuronRain AsFer implements bitonic sorting on Spark Cloud and parallelizes comparators on cloud (34.20) effectively treating cloud as sorting network with cloud communication complexity assumed as constant in average case.

34.55) Efficient Parallel Sorting - improvement of Cole's Parallel Sort and AKS sorting networks: sorting networks can be implemented in EREW PRAM - [Goodrich] - <https://arxiv.org/pdf/1306.3000v1.pdf> - [Godel's Lost Letter and P=NP - Richard Lipton - Galactic Sorting Networks - <https://rjlipton.wordpress.com/2014/04/24/galactic-sorting-networks/>]

34.56) Computational Pixelation Geometry Theorems - <https://arxiv.org/pdf/1105.2831v1.pdf> - defines planar pixelation of a continuous curve and proves Intermediate Value Theorem for Pixelation geometry. This is exactly the discretization step of this hyperbolic factorization algorithm. This formalizes the discretization mentioned in 34.29 where each pixelated tile is a set of intermediate values between $f(x)$ and $f(x+1)$ for interval $[x, x+1]$ where $f = N/x$ for N to be factorized.

34.57) Approximating a function graph by planar pixelation - <http://www3.nd.edu/~lnicolae/Pixelations-beam.pdf> - this applies advanced topology and geometry for pixelation of any function graph. Presently pixelation of hyperbola graph is done in very simple, primitive way as mentioned in 34.29.

34.58) Resource Oblivious Sorting on Multicores - [RichardCole-VijayaRamachandran] - <https://arxiv.org/pdf/1508.01504v1.pdf> - New parallel merge sort algorithm for multicore machines (SPMS - SamplePartitionMergeSort) with parallel execution time in $O(\log N * \log \log N)$. Multicores are equivalent to Asynchronous PRAMs (each core executes asynchronously) and thus it is an NC sorting algorithm.

34.59) NC and various categories of PRAMs - <https://pdfs.semanticscholar.org/5354/99cf0c2faaaa6df69529605c87b511bd2226.pdf> - CRCW PRAM can be simulated by EREW PRAM with polylogarithmic increase in time.

34.60) PRAM-NC equivalence, definition of input size - <ftp://ftp.cs.utexas.edu/pub/techreports/tr85-17.pdf> - atom is an indivisible unit of bit string, input is sequence of atoms, input size is length of this sequence.

34.61) PRAM model and precise definition of input size in PRAM models - <https://www.cs.fsu.edu/~engelen/courses/HPC-adv-2008/PRAM.pdf> - input size is

length of sequence $n = 2^k$, not number of bits $k = \log n$, and each element in the sequence is a set of bits - input size to a PRAM algorithm is exponential in number of bits and differs from sequential algorithms which have input size in just number of bits.

34.62) Simulation of Parallel RAMs by Circuits -
<http://www.cstheory.com/stockmeyer@sbcglobal.net/sv.pdf>

34.63) PRAM Models and input size - [Joseph JaJa] -
<https://www.cs.utah.edu/~hari/teaching/bigdata/book92-JaJa-parallel.algorithms.intro.pdf> - "...ALGORITHM 1.3 (Matrix Multiplication on the PRAM) Input: Two $n \times n$ matrices A and B stored in the shared memory, where $n = 2^k$. The initialized local variables are n, and the triple of indices (i, j, I) identifying the processor. ...",
<https://people.ksp.sk/~ppershing/data/skola/JaJa.pdf> - Chapter 4 - Searching, Merging, Sorting

34.64) Input Size for PRAMs, NC-PRAM equivalence, Cook-Pippenger Thesis, Brent's Speedup Lemma - www.csl.mtu.edu/cs5311.ck/www/READING/pram.ps.gz - Section on Input/Output Convention in PRAMs and Parallel MergeSort in EREW PRAM - Input size to Parallel Merge Sort is the length of array of integers to be sorted and is not logarithmic in length of array. This requires parallel time $O((\log N)^2)$ which is the depth of equivalent NC circuit. Computational Geometric Discrete Hyperbolic Factorization described above discretizes hyperbola into segments of sorted tiles of numbers on a 2 dimensional plane and merge-sorts them. This obviously requires $O((\log N)^2)$ time to find a factor with additional $O(\log N)$ binary search. Brent Speedup Lemma applies because, the tile segments can be statically allocated to each specific processor in tiling phase.

34.65) Pixelation of Polygons - On Guarding Orthogonal Polygons with Bounded Treewidth - [Therese Biedl and Saeed Mehrabi] - Page 160 -
<http://2017.cccg.ca/proceedings/CCCG2017.pdf> - CCCG 2017, Ottawa, Ontario, July 26-28, 2017 - Computational Geometric definition of standard pixelation divides a polygon into rectangles and adjoining rectangles are vertices connected to form a planar pixelation graph. Similar notion of pixelation holds for pixelating hyperbola $pq=N$ for finding factors p and q of integer N. Art Gallery problem in computational geometry finds minimum number of vantage points to guard the art gallery. If hyperbolic curve is considered as an art gallery, and guards have visibility only in vertical and horizontal directions, pixelation creates set of rectangles bounded by vantage points ensconcing the hyperbola. This illuminates the hyperbola completely.

34.66) A Comparison of Parallel Sorting Algorithms on Different Architectures- [NANCY M. AMATO, RAVISHANKAR IYER, SHARAD SUNDARESAN, YAN WU] -
https://parasol.tamu.edu/publications/download.php?file_id=191

34.67) Bitonic Sort Implementation - [Amrutha Mullapudi] -
<https://www.cse.buffalo.edu/~faculty/miller/Courses/CSE633/Mullapudi-Spring-2014-CSE633.pdf> - input size is $n=2^k$ and parallel execution time $O(\log n^2)$ for Batcher Bitonic Sort - Hyperbolic Pixelated Factorization is in NC because bitonic sort is in NC and is also optimal if $O(\log n)$ depth AKS sorting networks are used, because $O(n) * O(\log n) = O(n \log n)$ which is serial sorting time lowerbound.

34.68) PRAMs and Multicore architectures -
<http://blog.computationalcomplexity.org/2008/04/revenge-of-parallelism.html>

34.69) NC and PRAMs -
<http://www.cse.iitd.ernet.in/~subodh/courses/CSL860/slides/3pram.pdf>

34.70) Geometric Searching, Ray Shooting Queries - [Michael T. Goodrich] -
<http://www.ics.uci.edu/~goodrich/pubs/42.pdf> - Section 42.5 - Ray Shooting is defined as searching a point location in set of line segments by shooting a ray from a point outside the set of line segments. It is an open problem to find an

efficient data structure for parallel ray shooting which searches n points in parallel by shooting n light rays. Previous Hyperbolic Factorization can also be rephrased as parallel shooting problem which searches the factor points on the pixelated hyperbolic tile segments in parallel from an external point outside the hyperbola and answers the open question in affirmative.

34.71) Planar Point Location in Parallel -

<ftp://ftp.cs.brown.edu/pub/techreports/89/cs89-45a.pdf> - Section 4 - Point Location problem is defined as searching a query point q in a set of line segments. Discretized/Pixelated Hyperbola has number of line segments in $O(\log \log N)$. Finding factors (p, q) such that $pq=N$ is planar point location problem which searches for the factors in the tiled hyperbolic line segments. Point Location can be done in parallel by PRAM.

34.72) One dimensional Point Location -

<https://www.csun.edu/~ctoth/Handbook/chap38.pdf> - Section 38.1 - List searching - Tiled hyperbolic line segments are one dimensional intervals and number of intervals are $O(\log \log N)$. Searching this list amounts to finding a factor of N .

34.73) Hoover-Klawe-Pippenger Algorithm for converting arbitrary circuit

to bounded fanout 2 - [Ogihara-Animesh] -

<http://www.cs.rochester.edu/u/ogihara/research/DNA/cec.ps.gz>

34.74) PRAM definition of NC - [Kristoffer Arnsfelt Hansen] -

<https://users-cs.au.dk/arnsfelt/CT08/scribenotes/lecture7.pdf>

34.75) Factorization, Planar Point Location in parallel, Cascading, Polygon pixelation of hyperbola - [Mikhail Atallah] -

<https://pdfs.semanticscholar.org/1043/702e1d4cc71be46388cc12cd981ee5ad9cb4.pdf> - Section 4.5 - Art Gallery

Pixelation of Hyperbola $pq=N$ (described in 465) creates a polygon covering it and Factors of N are points located in the vertices of this polygon: Parallel Planar Point Location algorithms involve Cascading technique to find the factor query points p and q on the faces of this polygon. Cascading algorithms execute in multiple levels of the processor tree per stage and there are logarithmic number of stages - $O(\log N)$ parallel time. Cascading derives its nomenclature from relay nature of computation. Node at height h is "woken-up" and computes its subtree only after certain number of stages e.g h . This reduces integer factorization to Parallel Planar Point Location on Polygon.

34.76) Multicores, PRAMs, BSP and NC - [Vijaya Ramachandran] -

<https://womenintheory.files.wordpress.com/2012/05/vijaya-wit12.pdf>

34.77) Word Size in a PRAM - <https://hal.inria.fr/inria-00072448/document>

- Equation 5 - $\log N \leq w$ (N is input size and w word size)

34.78) Prefix Sum Computation and Parallel Integer Sorting - [Sanguthevar

Rajasekaran, Sandeep Sen] - <http://www.cse.iitd.ernet.in/~ssen/journals/acta.pdf> - "...Specifically, we show that if the word length is sufficiently large, the problem of integer sorting reduces to the problem of prefix sum computation. As a corollary we get an integer sorting algorithm that runs in time $O(\log n)$ using $n/\log n$ processors with a word length of n^ϵ , for any constant $\epsilon > 0$"

34.79) AMD Kaveri Heterogeneous System Architecture and hUMA - treats CPU

and GPUs equally, best suited for algorithms involving binary searches, zero-copy (GPU and CPU have access to memory by pointers) - an example for Parallel RAM - <https://www.anandtech.com/show/7677/amd-kaveri-review-a8-7600-a10-7850k/6>,

<https://pdfs.semanticscholar.org/90ec/1e63da44821d94c86047fa2f728504d89a4d.pdf>

34.80) Philosophical implications of Factorization in NC - NC in BPNC in RNC in QNC in BQP in DQP in EXP -

<https://www.math.ucdavis.edu/~greg/zoology/diagram.xml> - Presently factorization

is known to be in BQP and NC-PRAM factorization implies factorization is in NC, implying a decoherence from Quantum to Classical world - Rabi Oscillations - <https://www.youtube.com/watch?v=OONFQgwbV9I> - superposed quantum state $|p\rangle = \text{Sigma}(|ai\rangle|si\rangle)$ settles in one of the classical states si on interaction with classical world. No cloning theorem implies quantum state cannot be replicated. Since NC-PRAM equivalence is in BQP, a natural question arises: Are Parallel RAMs replicated quantum states and thus violate No Cloning?

34.81) An Oracle Result for relativized BQP and P - [Fortnow-Rogers] - <https://arxiv.org/pdf/cs/9811023.pdf> - There exists an oracle A for which $P^A = BQP^A$ - Theorems 4.1,4.2,4.3 - Pages 9-10 - This is significant because with respect to some oracle, Quantum computation is equivalent to and can be simulated by Deterministic Classical Computation in polynomial time. In the context of PRAM-NC factorization, this theorem applies because NC^A is in P^A (Christopher Wilson - https://link.springer.com/chapter/10.1007/3-540-16486-3_111) for any oracle A. Sequential Optimization for Computational Geometric Factorization mentioned in 506 implies a weaker result - Factorization is in P. An example Oracle for Factorization is the set of beacons (approximate factors) obtained by Ray-Shooting queries. Shor's Quantum Factorization (mentioned in 350) involves period finding - finding period r such that $f(x)=f(x+r)$. Ray shooting queries are also period finding algorithms in the sense that gaps between prime factors are estimated approximately - if f is a ray shooting query oracle A, querying f returns the next prime factor $pf(n+1) = pf(n) + \text{gap}$ (exactly or approximately) in classical deterministic polynomial time which is in NC^A or P^A . Ray shooting can be performed in both P and BQP from the previous equivalence of period finding and prime factor gap ray shooting i.e in P^A and BQP^A .

34.82) Factorization by Planar Point Location and Persistent Binary Search Trees - [Sarnak-Tarjan] - <https://pdfs.semanticscholar.org/731f/a2d06bd902b9fd7f3d5c3a17485edfe4133c.pdf> - Planar Point Location problem is defined as locating the polygon containing the query point in a subdivision of 2D plane by the line segments creating the polygons. Persistent Binary Search Trees are versioned Binary Trees which support insert/delete and preserve the past history of the Binary Search Tree for queries. Factorization is a Planar Point Location problem - Pixelated hyperbolic tile segments create set of polygons (arrays of pixels forming a rectangle of dimension $1 * \text{length_of_tile_segment}$) and these polygons divide 2D plane. Factor points (pixels) are located in some of these polygons. Planar Point Location retrieves the polygon containing the factor point in $O(\log N)$ time. This retrieved polygon tile segment can in turn be binary searched in $O(\log N)$ time because of implicit sortedness (either x or y axis points are strictly ascending). To be in NC, Parallel RAM Construction of Persistent Binary Search Tree is necessary.

34.83) Factorization by Planar Point Location - [PARALLEL TRANSITIVE CLOSURE AND POINT LOCATION IN PLANAR STRUCTURES, ROBERTO TAMASSIA AND JEFFREY S. VITTER] - Parallel RAM construction of Bridge Separator Tree for Planar Point Location - <http://citeseerx.ist.psu.edu/viewdoc/download?doi=10.1.1.72.4319&rep=rep1&type=pdf> - Separators are st-paths in planar subdivision graph formed by the hyperbolic line segments of pixel-array polygons on 2D plane. "...The separator tree uses $O(n)$ space and supports point location queries in $O((\log n)^2)$ time, where n is the number of vertices of S [33]..." - Lemma 4.5 - "... Let S be a regular subdivision with n vertices. The bridged separator tree for point location in S can be constructed by an EREW PRAM in $O(\log n)$ time using $n/\log n$ processors, which is optimal ...". Thus a factor point $N=pq$ within some of the hyperbolic pixel-array polygons can be found in $O((\log N)^2 + \log N) = O((\log N)^2)$ PRAM time and $O(N/\log N)$ processors. Number of rectangle polygons in planar subdivision created by the hyperbolic pixel-array = N of vertices $4*N$. This concurs with $O((\log N)^2)$ to $O((\log N)^3)$ PRAM time for Segment Trees. This factorization by parallel planar point location is work-optimal and is in NC requiring $N/\log N$ processors.

34.84) Criticism and defence of PRAM model - [Casanova-Legrand-Robert] -

Parallel Algorithms - <http://citeseerx.ist.psu.edu/viewdoc/download?doi=10.1.1.466.8142&rep=rep1&type=pdf> - Section 1.5 - "...NC is the class of all problems which, with a polynomial number of PUs, can be solved in polylogarithmic time. An algorithm of size n is polylogarithmic if it can be solved in $O(\log(n)^c)$ time with $O(n^k)$ PUs, where c and k are constants. Problems in NC can be solved efficiently on a parallel computer ... common criticism of the PRAM model is the unrealistic assumption of an immediately addressable unbounded shared parallel memory. ... • Theory is not everything: theoretical results are not to be taken as is and implemented by engineers. • Theory is also not nothing: the fact that an algorithm cannot in general be implemented as is does not mean it is meaningless. ..."

34.85) Parallel Point in Planar Subdivision - Design and Analysis of Parallel Algorithms - [Selim Akl] - <https://dl.acm.org/citation.cfm?id=63471> - Section 11.2.2 - Point in Planar Subdivision

34.86) Alternatives to Parallel RAM - QSM - <http://theory.stanford.edu/~matias/papers/qsm.pdf> - [Philip b.Gibbons, Yossi Matias, Vijaya Ramachandran] - Parallel RAM algorithms lay stress on sharing memory by processing elements while Bridging models like QSM, LogP and BSP (Bulk Synchronous Parallel) rely on Message Passing between processors having local non-shared memory and communicating with peer elements within finite number of messages (h -relation). Each computation is termed a superstep constrained by barrier synchronization amongst the processors performing local computation.

34.87) Communication Efficient Parallel Sorting - [Michael T.Goodrich] - <https://www.ics.uci.edu/~goodrich/pubs/parsort-pre.pdf> - Parallel Sorting on BSP instead of PRAMs - footnote 1 - page 247: PRAM is a BSP model having h -relation = 1 and therefore BSP is in NC by this PRAM simulation.

34.88) PRAM and Bulk Synchronous Parallel - <http://www.cse.iitd.ernet.in/~subodh/courses/COL730/pdfslides/6pram.pdf> - Schematic diagram for Barrier Synchronization Superstep

34.89) Bridging model for Parallel Computation - <http://web.mit.edu/6.976/www/handout/valiant2.pdf> - [Leslie G.Valiant] - "... that even the most general model, the CRCW PRAM, can be simulated optimally on the BSP model given sufficient slack if g is regarded as a constant..." - slack is the ratio of number of virtual processors ($v=p \log p$) to physical processors (p) = $p \log p / p$ and g is the ratio of total computation performed by all local nodes per second to total number of data words delivered per second.

34.90) Definition of NC - Computational Complexity - [Christos Papadimitriou] - Page 375 - Problems solvable by polynomial number of PRAMs in polylogarithmic depth.

34.91) NOW-Sort - <https://people.eecs.berkeley.edu/~fox/summaries/database/nowsort.html> - High-Performance Sorting on Networks of Workstations - MinuteSort

34.92) NSort - Parallel Sorting - <http://citeseerx.ist.psu.edu/viewdoc/summary?doi=10.1.1.23.1823>

34.93) Improved Sorting Networks - [R.L. (Scot) Drysdale, Frank H. Young] - <https://search.proquest.com/openview/3d400dff715e308df20e8812113844d7/1?pq-origsite=gscholar&cbl=666313> - SIAM Journal of Computing Volume 4, Number 3, 1975

34.94) Definition of Sorting Networks - Runtime of Sorting Networks is its depth and there exists an $O(\log N)$ depth Sorting Network - https://courses.engr.illinois.edu/cs573/fa2012/lec/lec/19_sortnet.pdf - implies sorting networks is in NC.

34.95) Ajtai-Komlos-Szemerédi (AKS) Sorting Network - Proof of existence

of $O(\log N)$ depth Sorting Network -

https://www.cl.cam.ac.uk/teaching/1415/AdvAlgo/lec2_ann.pdf - Sorting Networks are graphs consisting of input and comparator wires. Input wires are connected by comparator at specific points. Inputs traversing this graph while finding a comparator are swapped if top wire has greater value than bottom wire. This process propagates till the output is reached. Output gates contain sorted integers. Logdepth sorting networks are constructed by Bipartite Expander Graphs - approximate halvers - which split the inputs into two sets of smallest and largest in two halves of the wires (bitonic). This implies computational geometric sorting networks of $O(\log N)$ time for sorting the hyperbolic tile segments and finding the factors by binary search but constant in $O(\log N)$ is notoriously huge.

34.96) Complexity of Boolean Functions - [Ingo Wegener] - Blue Book - <https://eccc.weizmann.ac.il/resources/pdf/cobf.pdf> - Circuit lowerbounds are difficult because efficiency has to be proved over all possible circuits computing a function - Theorem 7.5 - Page 402 - Boolean function on n variables can be computed by a PRAM time lowerbound of $\Omega(\log \log n)$. This lowerbound is relevant to Computational geometric factorization by binary searching hyperbolic tile pixelation on PRAMs (number of variables = number of bits in integer to factorize). Integer factorization circuits on PRAMs (e.g PRAM circuits for parallel planar point location algorithms to locate a factor point on hyperbolic arc bow) have polylogarithmic depth (parallel time) and for each PRAM in the longest path from root to leaf of the circuit, this lowerbound applies. Factorization lowerbound for all PRAMs along this longest path is $\Omega((\log N)^k \log \log \log N)$ if $n = \log N$.

34.97) List of Parallel Planar Point Location Algorithms - Table 42.5.1 - Parallel Geometric Searching Algorithms - <https://www.ics.uci.edu/~goodrich/pubs/42.pdf>

34.98) Parallel Planar Point Location - [Atallah-Goodrich-Cole] - Purdue e-Pubs - https://pdfs.semanticscholar.org/f80e/bfe40dfbfad40659ff82e80cb632a3f8eeeb8.pdf?_ga=2.211071314.671597020.1548674481-1949614478.1548674481 - Section 4.2 - Factorization is a planar point location problem - Hyperbolic arc pixelation creates juxtaposed rectangular polygons of tile segments each of them internally sorted. Factorization $N=pq$ amounts to finding the polygon (segment) containing the point N which is $O(\log N)$ in CREW PRAM time. Binary Searching this implicitly sorted polygon yields the factor point (p,q) and additional $O(\log N)$ time. Tiles are computed by the relation $\delta = N/[x(x+1)]$

34.99) Optimal Bounds for Decision Problems on the CRCW PRAM - [Beame-Hastad] - <https://homes.cs.washington.edu/~beame/papers/crcwparity.pdf> - "...Optimal $Q(\log n / \log \log n)$ lower bounds on the time for CRCW PRAMs with polynomially bounded numbers of processors or memory cells to compute parity and a number of related problems are proven..." - Corollary 4.2 - these lowerbounds apply to all sorting problems on CRCW PRAMs and to k -mergesort/segment tree of hyperbolic segments in computational geometric factorization.

34.100) BSP versus PRAM - Survey - <https://web.njit.edu/~alexg/courses/cis668/Fall2000/handsub5.pdf>

34.101) Multipoint Planar Point Location - Algorithmic Motion Planning and Related Geometric Problems on Parallel Machines - [Suneeta Ramaswami] - Section 5.1 - https://repository.upenn.edu/cgi/viewcontent.cgi?article=1271&context=cis_reports - Parallel Multipoint planar point location on rasterized hyperbolic arc bow finds multiple factor points spread across multiple pixel array polygons

35. (THEORY) Above Discrete Hyperbolic Factorization can be used as a numerical dataset analysis technique. Discrete Hyperbolic Factorization uses only elementary geometric principles which can be fortified into an algebraic geometry result, because of strong connection between geometry (hyperbola) and

algebra (unique factorization theorem) for integer rings - excluding Kummer's theorem for counterexamples when Unique Factorization is violated(e.g $(\sqrt{5}+1)(\sqrt{5}-1)/4 = 2*3 = 6$).

#####

B. EXPERIMENTAL NON-STATISTICAL INFERENCE MODEL BASED ON ALREADY KNOWN THEORETICAL COMPUTER SCIENCE RESULTS:

#####

36.1. (FEATURE - DONE-WordNet Visualizer implementation for point 15) The classification using Interview Algorithm Definition Graph (obtained from Recursive Gloss Overlap algorithm described in <http://arxiv.org/abs/1006.4458> , <https://sites.google.com/site/kuja27/TAC2010papersubmission.pdf?attredirects=0> and http://www.nist.gov/tac/publications/2010/participant.papers/CMI_IIT.proceedings.pdf) wordnet node indegrees can classify a same document in multiple classes without any training set (unsupervised). Thus same document will be in multiple classes. This can be visualized as one stack per class and documents in same class are pushed into a stack corresponding to each class. When a same document is across multiple classes, a document can be visualized as a "hyperedge" of a hypergraph that transcends multiple class nodes. Here each class node in this non-planar graph (or multi-planar graph) is a stack.

36.2. (THEORY) Thus if number of classes and documents are infinite, an infinite hypergraph is obtained. This is also somewhat a variant of an inverted index or a hashtable where in addition to hashing ,the chained buckets across the keys are interconnected (Quite similar to <https://sites.google.com/site/kuja27/SurvivalIndexBasedTxnTimeoutManager.pdf?attredirects=0> and <https://sites.google.com/site/kuja27/PhDThesisProposal.pdf?attredirects=0>). This is also similar to "Connectionism" in Computational Psychology which allows cycles or interconnections in Perceptrons and Neural Networks. An old version of this was written in an old deleted blog few years ago in 2006 at: <http://shrivaskannan.blogspot.com>. If the relation between Hash Functions and Integer Partitions is also applied as described using Generating Functions in <https://sites.google.com/site/kuja27/IntegerPartitionAndHashFunctions.pdf?attredirects=0> then an upperbound on number of possible Hypergraphs (visualizing them as interconnected Hash tables) can be derived which is a stronger notion to prove.

37.(FEATURE - PoC WordNet Visualizer Closure DONE) Above multiplanar hypergraph is quite related as a theoretical construct to a Pushdown Automata for Context Free Grammar. Also the Definition Graph Construction using Recursive Gloss Overlap is a Context-Sensitive counterpart of Parse Trees obtained for Context Free Grammar, but ignoring Parts-Of-Speech Tagging and relying only on the relation between words or concepts within each sentence of the document which is mapped to a multipartite or general graph. Infact this Definition Graph and Concept Hypergraph constructed above from indegrees quite resemble a Functional Programming Paradigm where each relationship edge is a Functional Program subroutine and the vertices are the parameters to it. Thus a hyperedge could be visualized as Composition Operator of Functional Programs including FP routines for Parts-of-Speech if necessary [WordNet or above Concept Hypergraph can be strengthened with FPs like LISP, Haskell etc.,]. RecursiveNeuralNetworks(MV-RNN and RNTN) have a notion of compositionality quite similar to Functional Programming in FPs (Reference: http://nlp.stanford.edu/~socherr/EMNLP2013_RNTN.pdf) but for tree structures. Applying the compositionality for Concept Hypergraphs constructed above using FPs is a possible research direction.

38.(THEORY) But above is not context free because context is easily obtainable from the hyperedge which connects multiple classes. As an experimental gadget above seems to represent an alternative computational model for context

sensitivity and also process of human thought. This needs HyperEdge Search algorithms for hypergraph. A Related Neuropsychological notion of Hippocampus Memory Allocation in Human Brain can be found in <http://people.seas.harvard.edu/~valiant/Hippocampus.pdf>. Also a similar gadget is a special case of Artificial Neural Network - http://en.wikipedia.org/wiki/Hopfield_network - Hopfield Network - used to model human associative memory (pattern based memory retrieval than address based retrieval). Hyperedges of the above hypergraph can be memory vectors retrieved in an associative memory.

39.(THEORY) An interesting academic question to pose is - "Does the above hypergraph have a strong connectivity and a diameter upperbounded by a constant?". Equivalently, is the collection of universal knowledge close-knit or does nature connect seemingly unrelated concepts beyond what is "observable"? For example, path algorithms for Hypergraphs etc., can be applied to check s-t connectivity of two concepts. Some realworld linear programming and optimization problems which have strong natural applications are KnapSack problem, Tiling Problem or Packing problem that occur in everyday life of humanbeings (packing items for travel, arranging on a limited space etc.,). Thus the concept hypergraph might have a path connecting these.

40.(THEORY) A recent result of Rubik's cube (<http://www.cube20.org/>) permutations to get solution having a constant upperbound (of approximately 20-25 moves) indicates this could be true (if all intermediary states of Rubik's transitions are considered as vertices of a convex polytope of Concepts then isn't this just a Simplex algorithm with constant upperbound? Is every concept reachable from any other within 20-25 moves? Or if the above hypergraph is considered as a variant of Rubik's Cube in higher dimensions, say "Rubik's Hypercube" then is every concept node reachable from the other within 20 logical implication moves or is the diameter upperbounded by 20?). Most problems for hypergraph are NP-Complete which are in P for graphs thus making lot of path related questions computationally harder. Counting the number of paths in hypergraph could be #P-Complete. There was also a recent study on constant upperbound for interconnectedness of World Wide Web document link graph which further substantiates it (<http://www9.org/w9cdrom/160/160.html> - paragraph on diameter of the Strongly Connected Component Core of WWW). Probably this is a special case of Ramsey theory that shows order emerging in large graphs (monochromatic subgraphs in an arbitrary coloring of large graph).

41.(THEORY) Mapping Rubik's Cube to Concept Wide Hypergraph above - Each configuration in Rubik's Cube transition function can be mapped to a class stack node in the Concept Hypergraph. In other words a feature vector uniquely identifies each node in each class stack vertex of the Hypergraph. Thus move in a Rubik's cube is nothing but the hyperedge or a part of the hyperedge that contains those unique vectors. Thus hyperedges signify the Rubik's cube moves. For example if each class stack vertex is denoted as $c(i)$ for i -th class and each element of the stack is denoted by $n(i)$ i.e. n th element of stack for class i , then the ordered pair $[c(i), n(i)]$ uniquely identifies a node in class stack and correspondingly uniquely identifies an instantaneous face configuration of a Rubik's Hypercube (colored subsquares represent the elements of the feature vector). Thus any hyperedge is a set of these ordered pairs that transcend multiple class stacks.

42.(THEORY) The Multiplanar Primordial Field Turing Machine model described by the author in "Theory of Shell Turing Machines" in [<http://sites.google.com/site/kuja27/UndecidabilityOfFewNonTrivialQuestions.pdf?attredirects=0>] with multiple dimensions seems to be analogous to the above. If dimension info is also added to each plane in above hypergraph then both above formulations and Shell Turing Machines look strikingly similar. One more salient feature of this hypergraph is that each class node stack indirectly encodes timing information for events from bottom to top of the stack and height of each stack independently varies. Thus this is more than just a hypergraph. There also exists a strong similarity with Evocation WordNet (one word "reminding" or "evocative" of the other) - <http://wordnet.cs.princeton.edu/downloads.html> -

difference being above is a hypergraph of facts or concepts rather than just words. The accuracy of sense disambiguation is high or even 100% because context is the hyperedge and also depends on how well the hyperedges are constructed connecting the class stack vertices.

43.(THEORY) Instead of a wordnet if a relationship amongst logical statements (First Order Logic etc.,) by logical implication is considered then the above becomes even more important as this creates a giant Concept Wide Web as mentioned in

[http://sourceforge.net/projects/acadpdrafts/files/ImplicationGraphsPGoodEquationAndPNotEqualToNPQuestion_excerpts.pdf/download] and thus is an alternative knowledge representation algorithm.

44.(THEORY) Implication graphs of logical statements can be modelled as a Random Growth Network where a graph is randomly grown by adding new edges and vertices over a period of learning.

45.(THEORY) If a statistical constraint on the degree of this graph is needed, power law distributions (Zipf, Pareto etc.,) can be applied to the degrees of the nodes along with Preferential Attachment of newborn nodes.

46.(THEORY) Set cover or Hitting Set of Hypergraph is a Transversal of hypergraph which is a subset of set of vertices in the hypergraph that have non-empty intersection with every hyperedge. Transversal of the above Concept Wide Hypergraph is in a way essence of the knowledge in the hypergraph as in real world what this does is to grasp some information from each document (which is a hyperedge of class vertices) and produces a "summary nucleus subgraph" of the knowledge of the encompassing hypergraph.

47.(THEORY) Random walk on the above concept hypergraph, Cover time etc., which is a markov process. Probably, Cover time of the hypergraph could be the measure of time needed for learning the concept hypergraph.

48.(THEORY - IMPLEMENTATION - DONE) Tree decomposition or Junction Trees of concept hypergraph with bounded tree width constant.[If Junction tree is constructed from Hypergraph modelled as Bayesian Network, then message passing between the treenodes can be implemented, but still needs to be seen as what this message passing would imply for a junction tree of concept hypergraph above.]. A tree width measure computing script for Recursive Gloss Overlap graph for a text document has been added in python-src/InterviewAlgorithm which is a standard graph complexity measure.

49.(THEORY) 2(or more)-dimensional random walk model for thinking process and reasoning (Soccer model in 2-dimensions):

As an experimental extension of point 47 for human reasoning process, random walk on non-planar Concept hypergraph (collective wisdom gained over in the past) or a planar version of it which is 2-dimensional can be theorized. Conflicts in human mind could mimic the bipartite competing sets that make it a semi-random walk converging in a binary "decision". Semi randomness is because of the two competing sets that drive the "reasoning" in opposite directions. If the planar graph is generalized as a complex plane grid with no direction restrictions (more than 8), and the direction is anything between 0 to 2π radians, then the distance d after N steps is \sqrt{N} (summation of complex numbers and the norm of the sum) which gives an expression for decision making time in soccer model.(related: http://web.archive.org/web/20041210231937/http://oz.ss.uci.edu/237/readings/EBRW_nosofsky_1997.pdf). In other words, if mental conflict is phrased as "sequence of 2 bipartite sets of thoughts related by causation" then "decision" is dependent on which set is overpowering. That is the corresponding graph vertices are 2-colored, one color for each set and yet not exactly a bipartite graph as edges can go between nodes of same set. Brownian Motion is also a related to this. Points (53.1) and (53.2) describe a Judge Boolean Function

(with TQBF example) which is also a decision making circuit for each voter in P(Good) summation with interactive prover-verifier kind of adversarial notions based on which a voter makes a choice.

##

C. Slightly Philosophical - Inferences from conflicting opinions:

##

50. (DONE) As an example, if there are "likes" and "dislikes" on an entity which could be anything under universe - human being, machine, products, movies, food etc., then a fundamental and hardest philosophical question that naturally has evaded an apt algorithm: Is there a way to judge an entity in the presence of conflicting witnesses - "likes" and "dislikes" - and how to ascertain the genuineness of witnesses. In <http://arxiv.org/abs/1006.4458> and http://www.nist.gov/tac/publications/2010/participant.papers/CMI_IIT.proceedings.pdf this has been the motivation for Interview Algorithm and P(Good) error probability for majority voting which is the basis for this. Moreover the opinions of living beings are far from correct due to inherent bias and prejudices which a machine cannot have.

51. (DONE) Another philosophical question is what happens to the majority voting when every voter or witness is wrong intentionally or makes an error by innocuous mistake. [http://sourceforge.net/projects/acadpdrafts/files/ImplicationGraphsPGoodEquationAndPNotEqualToNPQuestion_excerpts.pdf/download]. This places a theoretical limitation on validity of "perceptual judgement" vis-a-vis the "reality".

52. (THEORY) There is a realword example of the above - An entity having critical acclaim does not have majority acclaim often. Similarly an entity having majority acclaim does not have critical acclaim. Do these coincide and if yes, how and when? This could be a Gaussian where tails are the entities getting imperfect judgements and the middle is where majority and critical acclaim coincide.

53. (THEORY) Items 50,51,52 present the inherent difficulty of perfect judgement or perfect inference. On a related note, Byzantine algorithms have similar issues of deciding on a course of action in the presence of faulty processors or human beings and faulty communications between them. Thus, probably above problem reduces to Byzantine i.e Faulty human beings or machines vote "like" or "dislike" on an entity and a decision has to be taken. This is also in a way related to Boolean Noise Sensitivity where collective intelligence of an entity can be represented as a "judging" boolean function and its decision tree. This "judge" boolean function accepts arguments from two opposing parties and outputs 1 or 0 in favour of one of them. How perfect is this "judge" depends on NoiseSensitivity of its boolean function. Thus a perfect judge boolean function is 100% NoiseStable even though attempts are made to confuse it through noise inputs.

53.1 (THEORY) Judge Boolean Function (there doesn't seem to be an equivalent to this in literature - hence it is defined as below):

A Judge Boolean function $f:(0,1)^n \rightarrow (0,1)$ has two classes of input sets of bit sets (x_1, x_2, x_3, \dots) and (y_1, y_2, y_3, \dots) corresponding to two adversarial parties x and y and outputs 0 (in favor of x) or 1 (in favor of y) based on the decision tree algorithm internal to f . Each x_i and y_i are sets of bits and hence input is set of sets (Intuitively such classes of boolean functions should be part of interactive proof systems.). This function is quite relevant to P(Good) summation because:

- LHS PRG/Dictator boolean function choice can also be thought of as randomly chosen Judge boolean function (from a set of judge boolean functions) defined above. NoiseStability of this Judge boolean function is its efficacy.
- In RHS, each voter has a judge boolean function above and NoiseStability of Boolean Function Composition of Maj*Judge is its efficacy.
- An example: From <https://sites.google.com/site/kuja27/InterviewAlgorithmInPSPACE.pdf?attredirects=0>, Judge Boolean Function can be a Quantified Boolean Formula (QBF) i.e (There exists $f(x_i)$ (For all $g(y_k) \dots (((...)))$). Intuitively this simulates a debate transcript (prover-verifier) between x and y that is moderated by the QBF judge boolean function. Of interest is the NoiseStability of this QBF.
- QBF is PSPACE-complete and hence Judge Boolean Function is PSPACE-complete.
- Thus LHS of $P(\text{good})$ is in PSPACE (a pseudorandomly chosen Judge Boolean Function) while RHS of $P(\text{good})$ is still in $PH=DC$ where each voter's Judge Boolean Function is fed into Majority circuit inputs, because, if the QBF is of finite depth then RHS is depth-restricted and due to this RHS is in $PH=DC$. Thus if $P(\text{Good})$ probability is 1 on either side then there exists a PSPACE algorithm for PH implying $PSPACE=PH$ than an intimidatingly unacceptable $P=PH$. If there is no quantifier depth restriction on either side both LHS and RHS can grow infinitely making both of them EXP. This makes Judge Boolean Function somewhat a plausible Voter Oracle than simple boolean functions - each voter is intrinsically allowed an intelligence to make a choice amongst 2 adversaries.
- Since Judgement or Choice among two adversaries is a non-trivial problem, it is better to have each Voter's SAT in RHS and that of pseudorandom choice in LHS to be in the hardest of complexity classes known. Thus interpretation of convergence of $P(\text{Good})$ series depends on hardness of judgement boolean function (it could be from simple 2-SAT, 3-SAT, k -SAT upto PSPACE-QBFSAT and could be even more upto Arithmetic Hierarchy) some of which might have $circuit_complexity(LHS) == circuit_complexity(RHS)$ while some might not.
- Reference: QBF-SAT solvers and connections to Circuit Lower Bounds - [RahulSanthanam-RyanWilliams] - http://web.stanford.edu/~rrwill/QBFSAT_SODA15.pdf
- A complex Judging scenario: Doctrinal Paradox (or) Discursive dilemma - Paradoxes in Majority voting where both Yes and No are possible in judgement aggregations - https://en.wikipedia.org/wiki/Discursive_dilemma. [Open question: What is the majority circuit or boolean equivalent of such a paradox with both Yes and No votes]

53.2 (THEORY) $P(\text{Good})$ Convergence, Voter TQBF function, PH -completeness and EXP-completeness - Adversarial reduction

$P(\text{Good})$ RHS is in PH if depth restricted and in EXP if depth unrestricted. LHS is a pseudorandomly chosen Judge Boolean Function. PH -completeness or EXP-completeness of RHS remains to be proven (if not obvious). PH is the set of all problems in polynomial hierarchy - $PH = \bigcup \Sigma(p, i)$. For every i there exists a problem in $\Sigma(p, i)$ that is $\Sigma(p, i)$ -complete. If there exists a PH -complete problem then PH collapses to $\Sigma(p, i)$ for some level i . [Arijit Bishnu - <http://www.isical.ac.in/~arijit/courses/spring2010/slides/complexitylec12.pdf>] . Hence it remains an open question if there exists a PH -complete problem. Thus instead of depth restriction, the hardest depth unrestricted EXP circuit class ($EXP=DC$) is analyzed as a Judge Boolean Function. There are known EXP-complete problems e.g. Generalized Chess with $n*n$ board and $2n$ pawns - [Fraenkel - <http://www.ms.mff.cuni.cz/~truno7am/slozitostHer/chessExptime.pdf>]. In RHS, each voter has a Judge Boolean Function, output of which is input to Majority circuit. This Judge Boolean Function can be shown to be EXP-complete by reduction from Chess. Reduction function is as below:

Each Voter can be thought of as simulator of both adversaries in Chess i.e Voter TQBF has two sets of inputs x_1, x_2, x_3, \dots and y_1, y_2, y_3, \dots . Each x_i is a move of adversary1-simulated-by-voter while each y_i is a move of adversary2-simulated-by-voter. Voter thus makes both sides of moves and votes for x or y depending on

whichever simulation wins. Thus there is a reduction from generalized Chess EXP-complete problem to Voter Judge Boolean Function (special cases of Chess with n constant are PSPACE-complete). Hence RHS is a Majority(n) boolean function composed with EXP-complete Judge Boolean Function (assumption: voters vote in parallel). When $P(\text{Good})$ summation converges to 1 (i.e Judge Boolean Function has zero noise and 100% stability existence of which is still an open problem), LHS is an EXP-complete algorithm for RHS which is harder than EXP-complete - it is still quite debatable as to how to affix notation to above RHS - probably it is P/EXP (access to an oracle circuit) or $P^*\text{EXP}$ (composition). RHS of $P(\text{Good})$ belongs to a family of hardest of boolean functions. [Kabanets - <http://www.cs.sfu.ca/~kabanets/papers/thes-double.pdf>] describes various classes of hard boolean functions and Minimum Circuit Size Problem [is there a circuit of size at most s for a boolean function f] and also constructs a read-once (each variable occurs once in the branching) branching program hard boolean function [Read-Once Branching Programs - <http://www.math.ias.edu/~avi/PUBLICATIONS/MYPAPERS/RWY97/proc.pdf>, Bounded Width polysize Branching Programs and non-uniform NC1 - <http://www.complexity.ethz.ch/education/Lectures/ComplexityHS10/ScriptChapterTwelve>]. In a general setting, RHS of $P(\text{Good})$ summation is m-EXP-complete (staircase exponents). RHS always has a fixed complexity class (PH-complete or EXP-complete or NEXP-complete if RHS is non-deterministically evaluated) while only complexity class of LHS changes due to pseudorandomly chosen Judge Boolean Function. Even Go is EXP-complete which has close to 10^{170} possibilities which is greater than chess - same person simulates both sides of adversaries and captures territory by surrounding.

A special case of Complexity of Quantified 3-CNF Boolean Formulas is analyzed in <http://eccc.hpi-web.de/report/2012/059/download/> - if 3CNF quantified boolean formulas of n variables and $\text{poly}(n)$ size can be decided in $2^{(n-n^{(0.5+e)})}$ time deterministically, NEXP is not contained in NC1/poly. This has direct implications for $P(\text{Good})$ majority voting circuit - if LHS is 100% noise stable NC1/poly percolation boolean function circuit and RHS is Quantified 3-CNF QBFs as Judge Boolean Functions decidable in $2^{(n-n^{(0.5+e)})}$ time then, since NEXP in RHS can not have NC1/poly circuits, RHS $P(\text{Good})$ summation shouldn't be equal to LHS which implies that RHS NEXPTIME Quantified 3-CNF decidable in $2^{(n-n^{(0.5+e)})}$ time cannot be 100% noise stable. There are other NEXP-complete problems viz., Succinct 3-SAT. The 100% noise stability regime for percolation boolean function is described in [<http://arxiv.org/pdf/1102.5761.pdf> - page 68]

Depth Hierarchy Theorem, a recent result in 2015 in <http://arxiv.org/pdf/1504.03398.pdf> proved PH to be infinite relative to some and random oracles i.e PH does not collapse with respect to oracles, which mounts the evidence in favour of non-existence of PH-Complete problems, but does not rule them out.

----- 53.3 (THEORY- *IMPORTANT*) Conditions for complexity classes of LHS and RHS of $P(\text{Good})$ summation being equated -----

RHS of $P(\text{Good})$ is either PH-complete or EXP-complete as mentioned in 53.2. LHS of $P(\text{Good})$ is a pseudorandomly chosen Judge Boolean Function while RHS is a huge mixture of judge boolean functions of almost all conceivable complexity classes depending on voter which together make the DC-circuit. LHS thus can belong to any of the complexity classes depending on the pseudorandom choice.

Probability of LHS Judge Boolean Function belonging to a complexity class C with NoiseStability p is =
 Probability of LHS PRG choice Judge Boolean Function in complexity class C *
 Probability of Goodness in terms of NoiseStability of PRG choice =
 $c/n * p$ where c is the number of judge boolean functions in complexity class C and n is the total number of judge boolean functions

When $p=1$ and $c=n$ LHS is 1 and is a complexity class C algorithm to RHS PH-complete or EXP-complete DC circuit when RHS $P(\text{Good})$ summation in terms of NoiseStabilities also converges to 1. Thus complexity_class(LHS) has a very high probability of being unequal to complexity_class(RHS). This is the perfect boolean function problem (in point 14 above) rephrased in probabilities. This is very tight condition as it requires:

- boolean function composition in RHS is in some fixed circuit complexity class (PH-complete or EXP-complete) and only LHS complexity class varies depending on pseudorandom choice

- LHS has to have 100% noise stability
- RHS has to have 100% noise stability

Thus above conditions are to be satisfied for equating complexity classes in LHS and RHS to get a lowerbound result. Also convergence assumes binomial complementary cumulative mass distribution function as mentioned in 14 above which requires equal probabilities of successes for all voters (or equal noise stabilities for all voter boolean functions). Hence voters may have different decision boolean functions but their noise stabilities have to be similar. If this is not the case, $P(\text{Good})$ series becomes a Poisson trial with unequal probabilities.

If LHS and RHS of $P(\text{Good})$ are not equatable, probability of goodness of LHS and RHS can vary independently and have any value. LHS and RHS are equatable only if the probability of goodness (in terms of noise stabilities on both sides) is equal on both sides. (e.g 0.5 and 1). Basically what this means is that LHS is an algorithm as efficient as that of RHS. If a pseudorandom choice judge boolean function has 100% noise stability then such a choice is from the huge set of boolean functions on RHS. This is an assumption based on the fact that any random choice process has to choose from existing set. Also when LHS pseudorandom judge boolean function choice is 100% noise stable, if RHS had LHS as one of its elements it would have forced RHS to be 100% and noise stabilities of all other judge boolean functions in RHS to 0%. Because of this RHS has to exclude LHS pseudorandom choice judge boolean function. That is:

cardinality(RHS) + cardinality(LHS) = cardinality(Universal set of judge boolean functions) (or)

cardinality(RHS) + 1 = cardinality(Universal set)

which is the proverbial "one and all".

Assuming there exists a boolean percolation function with noise stability 100%, voter with such a boolean function could be a pseudorandom choice in LHS and RHS has to exclude this function.

53.4 (THEORY) Variant 1 of Percolation as a Judge boolean function (related to 14 above)

Percolation boolean function returns 1 if there is a left-right crossing event in a path within the Z^2 grid random graph else 0. The definition of percolation is modified slightly as below to obtain a ranking of 2 adversaries:

There are n parameters on which the voter or a judge weighs two adversaries a and b (each take the 2 coordinates in the grid) and scores them as set of ordered pairs $(a_1, b_1), (a_2, b_2), (a_3, b_3), \dots, (a_n, b_n)$ where each a_i is the score given by voter for adversary a on parameter i and each b_i is the score given by voter for adversary n on parameter i . These coordinates are plotted on the grid and a left-right traversal of these coordinates is done via a path that covers all of them. At each coordinate, total score summations of $a_i(s)$ and $b_i(s)$ so far traversed are computed. The boolean function outputs 1 if $\sum(a_i) > \sum(b_i)$ favouring adversary a and outputs 0 if $\sum(a_i) < \sum(b_i)$ favouring adversary b . This is just a 2 candidate ranking variant of 3-candidate condorcet elections. In terms of circuit complexity, this is an iterated integer addition circuit (in non-uniform NC1) which inputs to a comparator circuit (in AC0 - [Chandra-Stockmeyer-Vishkin] - <http://cstheory.com/stockmeyer@sbcglobal.net/csv.pdf>) which together make non-uniform NC1 (since AC0 is contained in NC1). Thus this

variant of percolation decides based on sum of integral scores than left-right crossing. It always has a left-right crossing and there are no random graph edges.

53.5 (THEORY) Variant 2 of Percolation as a Judge boolean function (related to 14 above)

53.5.1 Both x and y axes have the criteria common to both adversaries a and b as coordinates.

53.5.2 If adversary a is equal to b for a criterion c, then there is a horizontal left-right edge with probability p.

53.5.3 If adversary b is better than a for criterion c, then there is a vertical edge (down-top) with probability p.

53.5.4 If adversary a is better than b for criterion c, then there is a vertical edge (top-down) with probability p.

53.5.5 Example 1:

criterion	a	b
c1	5	4 (top-down)
c2	3	5 (down-top)
c3	2	2 (left-right)
c4	4	6 (down-top)
c5	7	8 (down-top)

21 25 (a < b)

53.5.6 Example 2:

criterion	a	b
c1	2	1 (top-down)
c2	7	2 (top-down)
c3	5	5 (left-right)
c4	3	8 (down-top)
c5	9	7 (top-down)

26 23 (a > b)

53.5.7 Length of each edge is proportional to the difference between score(a) and score(b) at criterion c.

53.5.8 Lemma: a is better than b implies a top-down crossing event and b is better than a implies down-top crossing event.

Proof: If a is better than b in majority of the criteria then the path is more "top-down"-ish due to 53.5.4 (top-left to bottom-right) and if b is better than a then path is more "down-top"-ish due to 53.5.3 (bottom-left to top-right). Thus this formulation of percolation subdivides left-right paths into two classes top-down and down-top and all paths are left-right paths.

53.5.9 Above variant of percolation boolean function returns 1 if path is top-down (a > b) else 0 if path is down-top (a < b).

53.5.10 Previous description is an equivalence reduction of percolation and judging two adversaries.

53.5.11 To differentiate top-down and down-top left-right paths, comparator circuits (constant depth, polysize) and non-uniform NC1 circuit for integer addition of scores are required. Together this is also a non-uniform NC1 circuit (for infinite grid) similar to Variant1 in 53.4.

53.6 (THEORY) Circuit for Percolation as a Judge Boolean Function

 For an $m \times m$ grid with random edges, maximum length of the left-right path is m^2 (traverses all grid cells). Each boolean function is a path that is represented as set of coordinates on grid. If these coordinates form a left-right crossing, then circuit has value 1. Each coordinate on the grid requires $2 \log m$ bits. Hence maximum input bits required is $m^2 \cdot 2 \log m = O(m^2 \log m)$. Coordinates are sorted on left coordinate left-right ascending by a Sorting Network (e.g Batcher-sorting networks, Ajtai-Komlos-Szemerédi-AKS-sorting networks, Parallel Bitonic Sort - <http://web.mst.edu/~ercal/387/slides/Bitonic-Sort97.pdf>). This function outputs, with the sorted coordinates as inputs:

- 1 if both x-axis coordinate of the leftmost ordered pair is 0 and x-axis coordinate of the rightmost ordered pair is m
- else 0

which requires comparators. Sorting networks of depth $O((\log n)^2 \cdot n)$ and size $O(n(\log n)^2)$ exist for algorithms like Bitonic sort, Merge sort, Shell sort et.,. AKS sorting network is of $O(\log n)$ depth and $O(n \log n)$ size. For $n = m^2$, AKS sorting network is of $O(\log(m^2))$ depth and $O(m^2 \log(m^2))$ size. Thus percolation circuit consists of:

- Sorting network that sorts the coordinates left-right in NC1 or NC2
- Comparator circuits in constant depth and polynomial size

which together are in NC. This is non-uniform NC with advice strings as the circuit depends on percolation grid - e.g BP.(NC/log) where advice strings are the grid coordinates and the circuit has bounded error (Noise+ δ). [If the left-right paths are classified as top-down and down-top paths for ranking two adversaries (in 53.5 above) additional comparator circuits are required for finding if right coordinate is in top or down half-space. This is by comparing the y-axis of the leftmost and rightmost in sorted ordered pairs and output 1 if y-axis of leftmost lies between $m/2$ and m and y-axis of rightmost lies between 0 and $m/2$ (top-down) and output 0 else (down-top).]

Above percolation circuit based on Sorting networks is not optimal for arbitrarily large inputs. As per Noise Stability Regime [page 68 - <http://arxiv.org/pdf/1102.5761.pdf> - Christophe Garban, Jeffrey E. Steif], for $\epsilon = o(1/n^2 \alpha^4)$, $\Pr[f_n(\text{crossing event sequence}) = f_n(\text{crossing event sequence with } \epsilon \text{ perturbation})]$ tends to zero at infinity where α^4 is the four-arm crossing event probability (paths cross at a point on the percolation random graph creating four arms to the boundary from that point). In terms of fourier expansion coefficients this is: $\sum (\text{fourier_coeff}(S))^2$ tending to zero, $|S| > n^2 \alpha^4$. Circuit for this arbitrarily large percolation grid would be infinitely huge though can be termed as non-uniform NC sorting-network+comparator and hence a non-uniform circuit for an undecidable problem. Noise stability tending to zero depends not just on input, but on "infinite-input".

----- 53.7 (THEORY) P/Poly and P(Good) LHS and RHS - Karp-Lipton and Meyer's Theorems -----

P/poly is the circuit class of polynomial size with polynomial advice strings and unrestricted depth. Thus P/poly is non-uniform circuit class. Hence non-uniform NC is in P/poly. In 53.4, 53.5 and 53.6 example non-uniform NC1 circuits (subject to 100% noise stability) Percolation boolean function were described. These are in P/poly as non-uniform NC is in P/poly and thus LHS of P(Good) is in P/poly. Hence when LHS and RHS binomial coefficient summations converge to 100% noise stability satisfying the conditions in 53.3, LHS is a P/poly algorithm to RHS EXPTIME DC uniform circuit (because both sides are depth unrestricted). To be precise LHS is an NC/poly circuit. If the advice string is logarithmic size, it is NC/log and there is a known result which states that NP in P/log implies P=NP. For percolation boolean functions with 100% noise stability regime (page 68 - <http://arxiv.org/pdf/1102.5761.pdf>), if the grid boundaries are the only advice strings, boundary coordinates can be specified in $\log(N)$ bits and hence LHS is in NC/log.

If RHS is simply NP (if depth restricted and unlikely for arbitrary number of electorate) then LHS is a P/poly algorithm to RHS NP implying NP is contained in P/poly. By Karp-Lipton theorem NP in P/poly implies that PH collapses to second-level i.e $\Sigma(p,2)$ and from [Arvind, Vikraman; Köbler, Johannes; Schöning, Uwe; Schuler, Rainer (1995)] NP in P/poly implies $AM=MA$.

EXPTIME version of this is Meyer's Theorem which states that if EXPTIME is in P/poly (which is the hardest case for RHS of P(good) and can be m-EXPTIME) then $EXPTIME = \Sigma(p,2) \cap \Pi(p,2)$ and $EXPTIME=MA$. When RHS of P(good) is a DC uniform EXPTIME circuit, P(good) convergence subject to availability of 100% noise stable percolation boolean functions satisfying conditions in 53.3, implies that $EXPTIME=MA$.

References:

-
- 53.7.1 Relation between NC and P/poly - <http://cs.stackexchange.com/questions/41344/what-is-the-relation-between-nc-and-p-poly>
- 53.7.2 P/poly - <https://en.wikipedia.org/wiki/P/poly>
- 53.7.3 Karp-Lipton Theorem - https://en.wikipedia.org/wiki/Karp%E2%80%93Lipton_theorem
- 53.7.4 NP in P/poly implies $AM=MA$ - [Arvind, Vikraman; Köbler, Johannes; Schöning, Uwe; Schuler, Rainer (1995),] - <http://www.informatik.hu-berlin.de/forschung/gebiete/algorithmenII/Publikationen/Papers/ma-am.ps.gz>
- 53.7.5 BPP, PH, P/poly, Meyer's theorem etc., - <http://www.cs.au.dk/~arnsfelt/CT10/scribenotes/lecture9.pdf>
- 53.7.6 Descriptive Complexity - https://books.google.co.in/books?id=kWSZ00wnupkC&pg=PA177&lpg=PA177&dq=NC1/poly&source=bl&ots=6oGGZV4fa&sig=Y_4syLFZ-nTj4L0qrBxxWve75EA&hl=en&sa=X&ved=0CBsQ6AEwAGoVChMI66v6tqqSyQIVyZC0Ch2uMwyr
- 53.7.7 Non-uniform computation - <https://courses.engr.illinois.edu/cs579/sp2009/slides/cc-s09-lect10.pdf>
-

53.8 (THEORY) An example Majority+SAT majority voting circuit, P(Good) convergence and some observations on Noise Stability

Let the number of voters be 8 ($=2^3$). Each voter has a boolean function of 3 variables - x_1, x_2 and x_3 . From Boolean Function Composition, this is defined as $Maj(SAT_1(x_1, x_2, x_3), SAT_2(x_1, x_2, x_3), \dots, SAT_8(x_1, x_2, x_3))$. Each variable x_i corresponds to a criterion i and $x_i=1$ if and only if the criterion i is satisfied in 2-candidate voting (candidate0 and candidate1). Thus all voters should vote $x_i=1$ if the candidate1 satisfies criterion x_i . If some of the voters vote $x_i=0$ even though the candidate1 satisfies criterion x_i , then it becomes noise in the boolean function. This composition has exponential size in number of inputs ($32 = 2^3 + 3 \cdot 2^3 = O(n \cdot \exp(n))$). For negation NOT gates are allowed and it is not necessarily a monotone circuit. If the variables are different for each voter, there are 24 variables and circuit is polynomial in input size - $O(n^k)$. This illustrates the pivotality of noise when voters have a variable in common.

If the RHS doesn't converge to 1 and thus is in BPP and Noise Stability of LHS is 100% (e.g by PRG choice of a percolation function) then LHS is a P/poly algorithm for RHS BPP. This implies BPP is in P/poly, an already known amplification result. Infact this result implies something stronger: Since BPP is in P/poly, even if RHS doesn't converge, there is always a P/poly algorithm in LHS by amplification.

If the RHS has a perfect k-SAT boolean decision function for all voters, size of the circuit is super-polynomial and sub-exponential (if exponential, circuit is DC uniform), P(Good) series converges to 100% and LHS is 100% noise stable

Percolation function, then LHS is a P/poly algorithm for RHS NP-complete instance. Special case is when RHS has only one voter - LHS is P/poly (or NC/poly or NC/log) and RHS is NP-complete (assuming k-SAT of RHS voter is 100% noise stable) - and thus there is a P/poly circuit for NP in such a special case. From [Karp-Lipton] (53.7) if NP is in P/poly, PH collapses to second level and AM=MA. If LHS is P/log and RHS is NP, then P=NP. Thus 100% noise stable boolean function in LHS has huge ramifications and the P(Good) summation, its circuit version devour complexity arena in toto and variety of results can be concluded subject to noise stability.

If LHS of P(Good) is in NC/log (Percolation as Judge boolean function) and RHS doesn't converge to 100% (i.e Majority*SAT boolean function composition has < 100% noise stability), LHS is a more efficient NC/log algorithm for RHS BP* hard circuit (e.g RHS is single voter with a SAT judge boolean function without 100% noise stability and thus in BPP). BPP is already known to have P/poly circuits and this implies a better bound that BPP is in NC/log. BPP is not known to have complete problems in which case, NC/log algorithm for RHS BPP-complete problem would imply NC/log = BPP for the single voter RHS with 3-SAT judging function with < 100% noise stability.

Subtlety 1: For single voter in RHS with a 3-SAT voter judge boolean function, RHS is NP-complete from voting complexity standpoint irrespective of noise stability (Goodness of voting). But if noise stability is the criterion and 3-SAT is not noise stable 100%, RHS is a BPP problem. This is already mentioned in point 14 above (2 facets of voting - judging hardness and goodness).

Subtlety 2: [Impagliazzo-Wigderson] theorem states that if there exists a decision problem with $O(\exp(n))$ runtime and $\Omega(\exp(n))$ circuit size, then $P=BPP$. P(Good) RHS being a DC uniform circuit can have exponential size if variables are common across voter judge boolean functions, but is questionable if it is a decision problem of runtime $O(\exp(n))$ - for m-EXPTIME circuits this bound could be $O(\text{staircase_exp}(n))$.

NC/log circuits can be made into a uniform circuits by hardwiring advice strings which are logarithmic size. There are $2^{(\log(n))} = n$ advice strings possible for NC/log circuit with $O(\log n)$ depth and $O(n^k)$ size. The n advice strings are added as hardwired gates into NC/log circuit which does not alter the polynomial size of the circuit. Due to this NC/log is in NC and hence in P. For NC/log LHS with 100% noise stability, if RHS is BPP-complete with < 100% noise stability, LHS is NC/log algorithm for BPP-complete problem (or) BPP is in NC/log and hence in P. But P is in BPP. Together this implies $P=BPP$ if LHS is NC/log and RHS is a BPP-complete majority voting circuit (special case: one voter with less than 100% noise stability and 3-SAT boolean function). This leads to the question: Is there a 3-SAT voter judge boolean function with 100% noise stability? Is percolation with 100% noise stability regime reducible to 3-SAT? If yes, then LHS [P/log, NC/log or P/poly] percolation boolean function with 100% noise stability solves RHS NP-complete problem and hence NP is in P/poly, PH collapses to second level and AM=MA (or) NP is in [P/log, NC/log] and $P=NP$.

References:

-
- 53.8.1 Pseudorandomness - [Impagliazzo-Wigderson] -
<http://people.seas.harvard.edu/~salil/pseudorandomness/pseudorandomness-Aug12.pdf>
- 53.8.2 XOR Lemma [Yao] and [Impagliazzo-Wigderson] theorem -
theory.stanford.edu/~trevisan/pubs/stv99stoc.ps
-

53.9 (THEORY) Possible Scenarios in P(Good) LHS and RHS summation

-
- 53.9.1 LHS = RHS is 100% - LHS and RHS are equally efficient
 (and can be equated to get a lowerbound if equal error implies a lowerbound)

which is still doubtful. More about this in 53.16).

53.9.2 LHS is $< 100\%$ and RHS is $< 100\%$ - RHS is more efficient than LHS and both sides are in BP* classes and LHS $<$ RHS

53.9.3 LHS is $< 100\%$ and RHS is $< 100\%$ - LHS and RHS are equally efficient (and can be equated to get a lowerbound if equal error implies a lowerbound which is still doubtful. More about this in 53.16). Both are in BP* classes and LHS = RHS

53.9.4 LHS is $< 100\%$ and RHS is $< 100\%$ - LHS is more efficient than RHS and both sides are in BP* classes and LHS $>$ RHS

53.9.5 LHS is 100% and RHS is $< 100\%$ - LHS is more efficient than RHS. LHS is non-BP algorithm to RHS BP* algorithm. (e.g P/poly algorithm for BPP)

53.9.6 LHS is $< 100\%$ and RHS is 100% - RHS is more efficient than LHS. RHS is non-BP algorithm to LHS BP* algorithm.

53.10 (THEORY) Dictatorship, k-juntas testing and P(Good) circuit - simulation

LHS of P(Good) is a pseudorandom choice judge boolean function. It has to be tested for dictatorship and k-junta property. This step adds to the hardness of LHS. What is the probability of LHS pseudorandom choice being a dictator or k-junta boolean function? This probability is independent of Goodness probability of LHS which is the noise stability. If the size of the population is n and k out of n are having dictators or k-juntas as judge boolean functions, probability of LHS being dictator or k-juntas is k/n . Following steps are required:

- PRG Choice outputs a Judge boolean function candidate for LHS.
- Dictatorship or k-juntas testing algorithm is executed for this candidate PRG choice.

Expected number of steps required for choosing a dictator via PRG is arrived at by Bernoulli trial. Repeated PRG choices are made and property tested for dictatorship and k-juntas. Probability of PRG choice being a dictator is k/n . Probability $p(t)$ that after t trials a dictator or k-juntas is found:
 $p(t) = (1-k/n)^{(t-1)}(k/n) = (n-k)^{(t-1)} * k/n^t$

If t is the random variable, expectation of t is:
 $E(t) = \sum(t * p(t)) = \sum((n-k)^{(t-1)} * tk/n^t)$

For a property testing algorithm running in $O(q)$, time required in finding a dictator or k-juntas is $O(q * \sum((n-k)^{(t-1)} * tk/n^t))$

For $k=0$:

$$E(t) = 0$$

For $k=1$:

$$\begin{aligned} E(t) &= \sum((n-1)^{(t-1)} * t/n^t) = 1/n + (n-1)^2/n^2 + (n-1)^2 * 3/n^3 \\ &+ \dots \\ &< 1/n + 2n/n^2 + 3n^2/n^3 + \dots \\ &= 1+2+3+\dots+n/n \\ &= n(n+1)/2n \\ &= (n+1)/2 \end{aligned}$$

Thus to find one dictator approximately $(n+1)/2$ PRG expected choices are required. Above is not necessarily an exact process by which LHS arises but just a simulation of one special scenario.

[Axiomatically k shouldn't be greater than 1 i.e there shouldn't be more than one dictator or juntas. Philosophical proof of this is by contradiction. Every element in a population set is subservient to a dictator by definition. The meaning of "dictator" here is global uniqueness for all voters and not locally unique to a voter boolean function. If there are 2 dictators population-wide, this definition is violated.]

References:

53.10.1 Dictatorship, k-juntas testing - [Oded Goldreich] -
<http://www.wisdom.weizmann.ac.il/~oded/PDF/pt-junta.pdf>

(THEORY-IMPORTANT*) 53.11 Hastad-Linial-Mansour-Nisan (HLMN) Theorem and Noise Stable boolean functions - Denoisification 1

Hastad-Linial-Mansour-Nisan Theorem states that for a boolean function $f: \{0,1\}^n \rightarrow \{0,1\}$ computed by circuit of size $< s$ and depth $< d$, if the fourier coefficients for large S are epsilon-concentrated:

$\sigma(\text{fourier_coeff}(S)^2) < \epsilon$ for $|S| > t$ where $t = O((\log s/\epsilon)^{1/(d-1)})$.

Above implies that:

$t = O(\log s/\epsilon)^{d-1} = k(\log s/\epsilon)^{d-1}$ for some constant k .

$(t/k)^{1/(d-1)} = \log(s/\epsilon)$

$s = \epsilon \cdot 2^{((t/k)^{1/(d-1)})}$

For a noisy boolean function f with ρ probability of flip, the noise operator T is applied to the Fourier expansion of f :

$T(f) = \sum (\rho^{|S|} \text{fourier_coeff}(S) \text{parity}(S))$ for S in $[n]$ and each

Fourier coefficient of $T(f) = \rho^{|S|} \text{fourier_coeff}(S)$

From HLMN theorem, applying noise operator above (this needs to be verified) to noisy boolean function circuit Fourier spectrum:

if $\sigma(\rho^{|S|} \text{fourier_coeff}(S)^2) \leq \epsilon$, $|S| > t$ where $t = O((\log s/\epsilon)^{d-1})$,

size $s = \sigma(\rho^{|S|} \text{fourier_coeff}(S)^2) \cdot 2^{((t/k)^{1/(d-1)})}$

substituting for ϵ and $|S| > t$.

Thus size of the circuit exponentially depends on t - size of parity sets S in $[n]$ - $|S|$ - which can have maximum value of n (number of inputs).

If f is 100% noise stable, from Plancherel theorem:

$\sigma(\rho^{|S|} f(S)^2) = 1$, S in $[n]$

Stability can be written as:

$\sigma_{S < t}(\rho^{|S|} f(S)^2) + \sigma_{S \geq t}(\rho^{|S|} f(S)^2) = 1$

$[1 - \sigma_{S < t}(\rho^{|S|} f(S)^2)] = \sigma_{S \geq t}(\rho^{|S|} f(S)^2)$

Since $\rho < 1$:

$\epsilon = \sigma_{S \geq t}((\rho^{|S|} f(S)^2)) < \epsilon_{\text{stable}} =$

$\sigma_{S \geq t}(\rho^{|S|} f(S)^2)$, $|S| > t$

ϵ_{stable} can also be written as $= \sigma_{S < t}(1 - \rho^{|S|} f(S)^2)$, $|S| < t$

$s = \sigma[f(S)^2] \cdot 2^{((t/k)^{1/(d-1)})}$, $t = O((\log s/\epsilon)^{d-1})$, $|S| > t$

$s_{\text{stable}} = [1 - \sigma_{S < t}(\rho^{|S|} f(S)^2)] \cdot 2^{((t/k)^{1/(d-1)})}$, $t = O((\log s_{\text{stable}}/\epsilon_{\text{stable}})^{d-1})$, $|S| < t$

(or)

$s_{\text{stable}} = \sigma(\rho^{|S|} [\text{fourier_coeff}(S)]^2) \cdot 2^{((t/k)^{1/(d-1)})}$,

$t = O((\log s_{\text{stable}}/\epsilon_{\text{stable}})^{d-1})$, $|S| > t$.

s_{stable} is the size of the 100% noise stable circuit for f .

From above, t with noise operator is:

$t(\text{noise_operator}) = O(\log s/\sigma(\rho^{|S|} f(S)^2))$, $|S| > t$ (or)

$t(\text{noise_operator}) = O(\log s/(1 - \sigma_{S < t}(\rho^{|S|} f(S)^2)))$, $|S| < t$

which is substituted for t in s_{stable} above and t without noise operator is:

$t = O(\log s/\sigma(f(S)^2))$, $|S| > t$

which implies that $t(\text{noise_operator}) > t$ since denominator summation of fourier coefficients is attenuated by $\rho^{|S|}$ i.e the lowerbound of t in exponent for size increases due to noise operator. This should be the case for both expressions of s_{stable} above using Plancherel version of stability. This has strong relation to non-uniformity as ρ is set of pseudorandom number strings for flip corresponding to values of ρ where stability=1 which are advice strings to the circuit. The exponent $t(\text{noise_separator})$ increases as ρ in denominator of $\log(s/\epsilon_{\text{stable}})$ increases - correlation due to random flip

increases - implying that circuit size depends on increased lowerbound for $\log(s/\epsilon_{\text{stable}})$ which is a logarithmic increase in exponent that becomes a polynomial increase in size (because of $2^{\log()}$). Thus 100% stability requires polynomial increase in circuit size which implies a P/poly circuit for 100% noise stability. For example, if LHS of P(Good) has Percolation circuit in P/Poly, with polynomial increase in size 100% noise stability can be obtained. If LHS of P(Good) has percolation circuit in NC/poly, polynomial increase in size for 100% noise stability would still be in NC/poly, with additional gates adding to depth with bounded fanin. Moreover, from (53.8), an LHS with 100% noise-stable NC/poly circuit (if percolation is in NC/poly and not P/poly) for an RHS BPP-complete (i.e RHS binomial summation need not converge with 100% noise stability) means BPP is in P and $P=BPP$.

*Implication 1 of above: If RHS is in BPP (e.g a 3-SAT voter judge boolean function circuit with $< 100\%$ noise stability or bounded error) with polynomial size additional gates, it becomes 100% noise stable i.e a BPP circuit becomes NP-complete instance. But BPP is already known to be in P/poly and hence BPP has polynomial size circuits. Hence $\text{size}(\text{BPP_circuit}) + \text{polynomial size addition for stability}$ is still a polynomial = P/poly circuit which makes RHS to be 100% noise stable NP-complete from $<100\%$ BPP problem. This implies NP has P/poly circuits surprisingly and NP in P/poly implies PH collapses to second level Σ_2^P , and also $AM=MA$.

*Implication 2 of above: If LHS of P(Good) has BP.(NC/log) circuit due to $<100\%$ noise stability, with polynomial size increase it can be derandomized or denoised to 100% noise stable circuit. NC/log is in P/log. With polynomial size increase P/log is still P/log. If RHS is BPP it can be denoised as mentioned in Implication 1 to NP-complete instance. Thus both LHS and RHS converge in P(Good) binomial summation and RHS is NP-complete and LHS is P/log. Thus NP is in P/log implying $P=NP$.

Points 53.4, 53.5, 53.6 and 53.7 describe P/poly, NC/poly and NC/log circuits for Percolation Boolean Functions subject to 100% noise stability regime. Important disclaimer is that above considers only denoising and just denoising may not be sufficient to remove errors in BP* circuits. As described in 14 on "Noise Stability and Complexity Class BPP" table of error scenarios, there might be cases where both denoising (removing errors in column three) and derandomization (removing errors in column two) might be required that could add to the circuit size. But since BPP is in P/poly (Adleman's theorem) this is just another polynomial overhead in size. Thus increase in size due to denoising + derandomization = $\text{poly}(n) + \text{poly}(n) = \text{poly}(n)$ in P/poly.

Noise sensitive NC/log percolation circuit in LHS of P(Good) is in BP(NC/log) which requires denoising and derandomization. Is BP(NC/log) in P/log? If yes, this could imply $P=NP$ when RHS is an error-free NP-complete k-SAT instance (denoised and derandomized BPP). BP(NC/log) can be denoised with $\text{poly}(n)$ additional gates from derivation above from HMLN theorem which makes NC/log to be in P/log. Next step of derandomization is by naive enumeration of all possible pseudorandom advice strings. Assumption here is that length of pseudorandom strings required for derandomizing percolation is $\log(n)$ which is sufficient to specify any point on an axis in the percolation grid. If $\log(n)$ bit pseudorandom advice is enumerated there are $2^{\log(n)}=n$ possible pseudorandom strings which is $\text{poly}(n)$ addition in circuit size again. P/log circuit is executed for all $2^{\log(n)}$ pseudorandom strings which makes the total runtime $n \cdot \text{poly}(n) = \text{poly}(n)$. Thus derandomization takes as input a denoised P/log circuit, adds $\text{poly}(n)$ gates to it and outputs a circuit that has runtime $\text{poly}(n)$ with logarithmic advice i.e P/log. This has a strange consequence that NP can have P/log circuits and $P=NP$ (Implication 2) contrary to popular belief if logarithmic advice is valid. Equivalently for error-free, denoised and derandomized PH-complete problems in RHS (assuming PH-complete problems exist - from (53.2) above), denoised and derandomized P/log circuit in LHS implies $P=PH$ - collapse of polynomial hierarchy.

(THEORY-*IMPORTANT*) 53.12 Hastad-Linial-Mansour-Nisan (HLMN) Theorem and Noise Stable boolean functions - Denoisification 2

Above version derived by rewriting HLMN in terms of $s(\text{size})$ and $t(\text{size of fourier basis})$ is not too appealing. Basically, rate of change of circuit size with respect to noise is required and may not be necessary if denoisification is a subproblem of larger derandomization. It then reduces to the question of how size of circuit increases with derandomization, specifically for BPNC percolation circuits - Since BPP is in P/poly , is BPNC in NC/poly or NC/\log . From Linial-Mansour-Nisan Theorem - Lemma 7 (Main Lemma) - <http://www.ma.huji.ac.il/~ehudf/courses/anal09/LMN.pdf> - Circuit size and Fourier coefficients are related as:

For $|S| > t$, $\text{Summation}(\text{fourier_coeff}(S)^2) \leq 2^{*(\text{Size})} 2^{-(t^{(1/d)}/20)}$
For Noise-operated Fourier Spectra, the summation is augmented with $\rho(\text{noise operator})$:

For $|S| > t$, $\text{Summation}(\rho^{|S|} \text{fourier_coeff}(S)^2) \leq 2^{*(\text{Size})} 2^{-(t^{(1/d)}/20)}$

Applying Plancherel theorem and stability=1:

| For $|S| < t$, $1 - \text{Summation}(\rho \text{fourier_coeff}(S)^2) \leq$
 $2^{*(\text{Size})} 2^{-(t^{(1/d)}/20)}$ |
| $\Rightarrow [1 - \text{Summation}(\rho^{|S|} \text{fourier_coeff}(S)^2)] * 2^{((t^{(1/d)}/20)-1)} \leq \text{Size}$
|

which is the circuit size lowerbound in terms of noise probability and fourier coefficients. As ρ increases from 0 to 1, lowerbound for size decreases, that is, low noise requires high circuit size. Partial Derivative of size bound wrt ρ :

$-\text{Summation}(\text{fourier_coeff}(S)^2) * 2^{((t^{(1/d)}/20)-1)} \leq \text{doe}(\text{Size})/\text{doe}(\rho)$
which points to exponential - in t and d - decrease in size (because $t=O(n)$ and $d=O(\text{function}(n))$ with linear increase in ρ (noise) due to negative sign and vice versa. Consequences of this are significant. Though derandomization could result in polysize circuits, denoisification does not necessarily add $\text{poly}(n)$ size and in worst case could be exponential too. For NC circuits, $t=O(n)$ and $d=O(\text{polylog}(n))$, denoisification results in $2^{O(n^{1/\text{polylog}(n)})}$ increase in size which is superpolynomial. Stability=1 is the point when LHS and RHS of $P(\text{Good})$ binomial summation converge i.e both sides are equally efficient and are perfect voter boolean functions not affected by input noise. Therefore BPNC can not be denoisified in polynomial circuit size even if it can be derandomized to be in NC with polynomial size (i.e if BPNC is in NC/poly). Thus percolation NC circuit in LHS cannot be made 100% stable with denoisification with mere polynomial size and has superpolynomial size lowerbound. This implies when RHS is also 100% stable circuit size of RHS is atleast superpolynomial. Rephrasing:

| $P(\text{Good})$ binomial summation in its circuit version can not have
polynomial size circuits |
| when LHS and RHS converge with 100% noise stability.
|

For example, if LHS is a percolation logdepth circuit and RHS is single voter with 3-SAT NP-complete circuit, when LHS and RHS are both 100% noise stable and derandomized ($\rho=0$):

LHS circuit size $\geq 2^{O(n^{1/\text{polylog}(n)})} = \text{superpolynomial}$,

quasiexponential lowerbound, depth is $\text{polylog}(n)$
implying LHS percolation circuit could become superpolynomial sized when noise stability is 1 and not in NC despite being logdepth.

RHS circuit size $\geq O(2^{n^{1/d}})$ = higher superpolynomial,
quasiexponential lowerbound, depth is arbitrary, could be constant for 3-CNF
and thus LHS and RHS circuits are equally efficient algorithms with differing
circuit sizes. As RHS is NP-complete, LHS is size lowerbound for RHS - LHS has
lesser superpolynomial size than RHS where $d(\text{depth of RHS which could be a constant } 3) < \text{polylog}(n)(\text{depth of LHS})$.
[Open question: Does this imply superpolynomial size lowerbounds for NP and thus $P \neq NP$]

Reference:

53.12.1 Derandomizing BPNC - [Periklis Papakonstantinou] -
http://iis.tsinghua.edu.cn/~papakons/pdfs/phd_thesis.pdf
53.12.2 Derandomization basics - [Salil] - Enumeration -
<http://people.seas.harvard.edu/~salil/pseudorandomness/basic.pdf>
53.12.3 Simplified Hitting Sets Derandomization of BPP - [Goldreich-Vadhan-Wigderson] - <http://www.wisdom.weizmann.ac.il/~oded/COL/gvw.pdf> - where hitting sets are set of strings at least one element of which is accepted by any circuit that accepts at least half of its inputs (i.e randomized algorithms in RP and BPP). Hitting Set generators H expand $k(n)$ to n so that a function f returns $f(H(k(n)))=1$ always where f is in RP or BPP.
53.12.4 Derandomizing BPNC - Existence of Hitting Set Generators for BPNC=NC - [Alexander E.Andreev, Andrea E.F.Clementi, Jose D.P.Rolim] - http://ac.els-cdn.com/S0304397599000249/1-s2.0-S0304397599000249-main.pdf?_tid=e56d3a1e-ad3d-11e5-a4ef-00000aach35e&acdnat=1451291885_fbff7c6ae94326758cf8d6d7b7a84d7b
53.12.5 Linial-Mansour-Nisan Theorem - Lemma 7 (Main Lemma) - <http://www.ma.huji.ac.il/~ehudf/courses/anal09/LMN.pdf>:
For $|A| > t$, $\text{Summation}(\text{fourier_coeff}(A)^2) \leq 2^*(\text{Size})^2 \cdot (-t^{1/d})^{20}$
53.12.6 The Computational Complexity Column [Allender-Clementi-Rolim-Trevisan] - theory.stanford.edu/~trevisan/pubs/eatcs.ps

53.13. (THEORY) Partial Derivative of Circuit size wrt rho (noise probability) - increase in circuit size for Denoisification

From 53.11 above, size of denoised circuit from HMLN theorem, and Stability in terms of Fourier coefficients with noise operator is:

$s_{\text{stable}} = [1 - \sigma_{S < t}(\rho^{|S|} f(S)^2)]^{2^{\lceil (t/k)^{1/(d-1)} \rceil}}$, $t = O((\log s_{\text{stable}}/\epsilon_{\text{stable}})^{(d-1)})$, $|S| < t$

(or)

$s_{\text{stable}} = \sigma_{S > t}(\rho^{|S|} [\text{fourier_coeff}(S)]^2)^{2^{\lceil (t/k)^{1/(d-1)} \rceil}}$, $t = O((\log s_{\text{stable}}/\epsilon_{\text{stable}})^{(d-1)})$, $|S| > t$.

Lower bound of exponent increases as $\sigma_{S > t}(\rho^{|S|} f(S)^2)$ decreases in denominator of exponent subject to stability constraint:

$[1 - \sigma_{S < t}(\rho^{|S|} f(S)^2)] = \sigma_{S > t}(\rho^{|S|} f(S)^2)$

which implies that $\sigma_{S > t}(\rho^{|S|} f(S)^2)$ decreases when $\sigma_{S < t}(\rho^{|S|} f(S)^2)$ increases. This is Consequence of HMLN theorem that t acts as an inflexion point for Fourier spectrum with noise operator - area integral from 0 to t is concentrated greater than area integral from t to n .

Partial derivative of Circuit size wrt to rho can be derived as:

$\Delta s / \Delta \rho = \sigma_{S > t}(|S| \cdot \rho^{|S|-1} \cdot f(S)^2) / (1 - \sigma_{S < t}(\rho^{|S|} f(S)^2))$ where Δs is increase in size of circuit with $\Delta \rho$ increase in noise probability. When $\rho=0$, increase in circuit size is 0 (obvious base case). When $\rho=1$, which is the worst case, increase in circuit size is $= \sigma_{S > t}(|S| f(S)^2) / f(S)^2$ which is upperbounded by $n - \text{poly}(n)$ increase in size.

53.14. (THEORY) Hastad-Linial-Mansour-Nisan Theorem, Circuit size, Noise Stability and BP* classes

Percolation circuit defined previously has:

- Sorting Network for creating path sequentially on grid (NC logdepth and polysize)
- Comparators (Constant depth and polysize) are required for comparing the leftmost and rightmost coordinates.

Together Percolation is in non-uniform NC. This circuit depends on number of points on the left-right path which is $\text{poly}(n)$.

Therefore percolation is in NC/poly because size of list of advice strings could be $O((n^2)\log(n^2))$ and it may not have NC/log circuits.

From Linial-Mansour-Nisan Theorem - Lemma 7 (Main Lemma) -

<http://www.ma.huji.ac.il/~ehudf/courses/anal09/LMN.pdf>:

For $|A| > t$, $\text{Summation}(\text{fourier_coeff}(A)^2) \leq 2^{*(\text{Size})} 2^{-(t^{(1/d)}/20)}$

With noise operator, noise stability=1 from Plancherel's theorem:

| For $|S| < t$, $1 - \text{Summation}(\rho^{|S|} \text{fourier_coeff}(S)^2) \leq 2^{*(\text{Size})} 2^{-(t^{(1/d)}/20)}$

| Corollary: For $|S| > t$, $\text{Summation}(\rho^{|S|} \text{fourier_coeff}(S)^2) \leq 2^{*(\text{Size})} 2^{-(t^{(1/d)}/20)}$

| $\Rightarrow [1 - \text{Summation}(\rho^{|S|} \text{fourier_coeff}(S)^2)] * 2^{((t^{(1/d)}/20)-1)} \leq \text{Size}$
|

When denoisified, $\rho=0$ and lowerbound for size:

$[1 - (0^{|S|} \text{fourier_coeff}(S)^2 + \dots)] * 2^{((t^{(1/d)}/20)-1)} \leq \text{size}$

$[1 - f(\phi)^2] * 2^{((t^{(1/d)}/20)-1)} \leq \text{size}$ (as all other coefficients vanish)

when $t=n$, the size is lowerbounded by :

$[1 - f(\phi)^2] * 2^{((n^{(1/d)}/20)-1)}$

which is superpolynomial. This implies an NC/poly polysize circuit when denoisified becomes $O(2^{((n^{(1/\text{polylog}(n)}/20)-1)})$.

From the table that describes relation between Noise and Error(BP* and PP) in 14 previously, it is evident that Noise intersects Error

if following is drawn as a Venn Diagram i.e. Noise stability solves just a fraction of total error, and remaining requires derandomization.

In other words, Noisy circuit could be error-free and Noise-free circuit could have error.

x		$f(x) = f(x/e)$		$f(x) \neq f(x/e)$ Noise

x in L, x/e in L		No error		Error

x in L, x/e not in L		Error		No error if
$f(x)=1, f(x/e)=0$				else Error

x not in L, x/e in L		Error		No error if
$f(x)=0, f(x/e)=1$				else Error

x not in L, x/e not in L		No error	

Noise percolation circuit in P(Good) summation converges in noise stability regime:

$$\lim_{n \rightarrow \infty} \Pr[f(w(n)) \neq f(w(n)/e)] = 0, \quad e = 1/(\alpha^4 n^2)$$

Infinite $f(n)$ is representable as Non-uniform NC/poly circuit though undecidable because turing machine computing the above limit is not in recursive but recursively enumerable languages.

For a 3-CNFSAT boolean function with noise, size of circuit is lowerbounded as:

$$[1 - \text{Summation}(\rho^{|S|} \cdot \text{fourier_coeff}(S)^2)] \cdot 2^{((t^{1/d}/20)-1)} \leq \text{Size},$$

for constant depth d.

For $\rho=1$,

$$[1 - \text{Summation}(\text{fourier_coeff}(S)^2)] \cdot 2^{((t^{1/d}/20)-1)} \leq \text{Size}, \text{ for}$$

constant depth d, $|S| < t$.

Gist of the above:

53.14.1 Size of percolation logdepth circuit (with noise) $\rho=1$:

$$(f([n])^2) \cdot 2^{(n^{1/\text{polylog}(n-1)}/20)-1} \leq \text{size}$$

53.14.2 Size of depth d circuit (with noise) $\rho=1$:

$$(f([n])^2) \cdot 2^{((n-1)^{1/d}/20)-1} \leq \text{size}$$

53.14.3 Size of percolation logdepth circuit (with noise) $\rho=0$:

$$(1 - f([\phi])^2) \cdot 2^{(n^{1/\text{polylog}(n)}/20)-1} \leq \text{size}, \text{ } \phi \text{ is empty set}$$

53.14.4 Size of depth d circuit (with noise) $\rho=0$:

$$(1 - f([\phi])^2) \cdot 2^{(n^{1/d}/20)-1} \leq \text{size}, \text{ } \phi \text{ is empty set}$$

53.15 (THEORY) Special Case of HLMN theorem for PARITY as 3-SAT and counterexample for polynomial circuit size

From HMLN theorem:

$$\text{Summation}(\text{fourier_coeff}(S)^2) \cdot 2^{((t^{1/d}/20)-1)} \leq \text{Size}, \text{ for constant depth } d, |S| > t.$$

When $t=n-1$, fourier series has only coefficient for the parity set that has all variables:

$$\text{fourier_coeff}([n])^2 \cdot 2^{(((n-1)^{1/d}/20)-1)} \leq \text{size}, \text{ for constant depth } d.$$

For a circuit of size polynomial (n^k) and depth 3:

$$\text{summation}(\text{fourier_coeff}([n])^2) \leq n^k / 2^{((t^{1/3}/20)-1)}.$$

and for $t=n-1$:

$$\text{fourier_coeff}([n])^2 \leq n^k / 2^{(((n-1)^{1/3}/20)-1)}.$$

From definition of fourier coefficients:

$$\text{fourier_coeff}([n]) = \text{summation}(f(x) \cdot (-1)^{\text{parity}(xi)}) / 2^n \text{ for all } x \text{ in } \{0,1\}^n$$

Maximum of $\text{fourier_coeff}([n])$ occurs when $f(x)=1$ for $(-1)^{\text{parity}(xi)} = 1$ and when $f(x)=-1$ for $(-1)^{\text{parity}(xi)} = -1$ together summing to 2^n .

Maximum($\text{fourier_coeff}([n])$) = $2^n / 2^n = 1$ (this implies all other fourier coefficients are zero)

Which happens when $f(x)$ is equivalent to Parity function.

An example PARITY as 3-CNFSAT from DIMACS32 XORSAT [Jing Chao Chen -

<http://arxiv.org/abs/cs/0703006>] that computes parity of $n=3$ variables x_1, x_2, x_3 is:

$$(x_1 \vee \text{not } x_2 \vee \text{not } x_3) \wedge (\text{not } x_1 \vee x_2 \vee \text{not } x_3) \wedge (\text{not } x_1 \vee \text{not } x_2 \vee x_3) \wedge (x_1 \vee x_2 \vee x_3)$$

Previous PARITY SAT accepts odd parity strings. Complementing variables in each clause makes it accept even parity:

$$(\text{not } x_1 \vee x_2 \vee x_3) \wedge (x_1 \vee \text{not } x_2 \vee x_3) \wedge (x_1 \vee x_2 \vee \text{not } x_3) \wedge (\text{not } x_1$$

V not x2 V not x3)

Assumption: PARITY as 3-CNFSAT has polynomial size.

PARITY 3-SAT is satisfied by odd parity bit strings and is NP-complete because this is search version of parity - it searches for strings that have odd parity. Complementing each clause would make it satisfy even parity bit strings. This example PARITY as 3-SAT with variables in each clause complemented maximizes the fourier coefficient to 1 at $S=[n]$. For $|S| < n$ by pigeonhole principle if one coefficient at $|S|=n$ is enough to make it 1 others have to be either all zero or cancel out each other. An extension of this 3-CNF for arbitrary n should be recursively obtainable from the above example by XOR-ing with additional variables and simplifying and also by Tseitin Transformation (https://en.wikipedia.org/wiki/Tseitin_transformation) which converts arbitrary combinatorial logic to CNF.

$\Rightarrow 1^2 \leq n^k / 2^{((n-1)^{1/3}/20)-1}$ which is a contradiction to assumption (denominator is exponential) that PARITY 3-SAT has polynomial size (n^k) circuits.

From above, for some circuit size of PARITY as 3-CNFSAT, there exists $t(=O(n))$ such that:

$$2^{((t)^{1/3}/20)-1} \leq \text{size} / \sum_{|S| > t} f(S)^2$$

$2^{((t)^{1/3}/20)-1} \leq \text{size}$ (for all $t < n-1$, fourier coefficients of PARITY 3-SAT are 0, and this bound is meaningful only for $t=n-1$).

i.e for all values of t , circuit size is bounded from below by a quantity exponential in function of n (which could be $O(n)$, $W(n)$ or $\Theta(n)$). If this is $O(n)$, might imply a lowerbound by upperbound - reminiscent of Greatest Lower Bound in a Lattice if Complexity Classes form a Lattice). LHS of the inequality can have values of t from 1 to $n-1$ and only one value of this can be chosen lowerbound. If LHS is not a function of n , it leads to a contradiction that 2 PARITY 3SAT circuits of varying sizes can have constant lowerbound. Also finding Minimum Circuit Size problem is believed to be in NP but not known to be NP-Complete (<http://web.cs.iastate.edu/~pavan/papers/mcsp.pdf>).

(How can a special case of NP-complete problem have superpolynomial size circuits? Is this a counterexample and thus implies superpolynomial size circuits for all problems in NP and $P \neq NP$. Because of this correctness of above counterexample has to be reviewed)

References:

53.15.1 Circuit Complexity Lecture notes - [Uri Zwick] -

<http://cs.tau.ac.il/~zwick>

53.15.2 Lecture notes - [Nader Bshouty] - <http://cs.technion.ac.il/~bshouty>

53.16 (THEORY) P/poly, Percolation and PARITY as 3-CNFSAT in 53.15

53.16.1 NP in P/poly (NP having polynomial size circuits) implies $AM=MA$ and PH collapses to Σ_2^P .

53.16.2 PARITYSAT in 53.15 which is a special case of NP-complete has superpolynomial size circuits.

53.16.3 If Percolation is in NC/poly and both LHS and RHS of $P(\text{Good})$ converge to 100% noise stability, does it imply an NC/poly lowerbound for arbitrary circuit size in RHS? In other words what does it imply when 2 circuits of varying size have equal stability - Do two boolean circuits of equal decision error (NoiseStability + or - δ) with different sizes imply a lowerbound? E.g NC/poly circuit for $PH=DC$ (if PH-complete) circuit implying PH in NC/poly.

53.16.3.1 If equal error (NoiseStability $\pm \delta$) with different circuit sizes implies a lowerbound:

There is an inherent conflict between 53.16.1, 53.16.3 which are conditions for polynomial size circuits for NP and 53.16.2 which implies superpolynomial circuit size for a special case of NP-complete 3-SAT problem. This contradiction is resolvable if following is true:

- LHS of $P(\text{Good})$ is percolation NC/poly circuit in 100% noise stability regime.
 - RHS of $P(\text{Good})$ is non-percolation circuit of arbitrary size (e.g. DC circuit of exponential size, superpolynomial size NP circuit from 53.15 and 53.16.2 etc.,).
 - LHS NC/poly 100% noise stability implies a lowerbound when RHS (e.g. superpolynomial size NP circuit from 53.15 and 53.16.2) is also 100% noise stable contradicting superpolynomial size lowerbound for NP from 53.16.2. Contradiction is removed only if RHS of $P(\text{Good})$ is never 100% noise stable and hence LHS is not equatable to RHS i.e. $P(\text{Good})$ summation has to be divergent and never converges to 100% while LHS is 100%. Major implications of this divergence are:
 - the individual voter error/stability cannot be uniform 0.5 or 1 across the board for all voters - voters have varied error probabilities.
 - varied stability/sensitivity per voter implies RHS majority voting is Poisson Distribution.
 - for probabilities other than 0.5 and 1, RHS $P(\text{good})$ summation becomes hypergeometric series requiring non-trivial algorithms which might or might not converge.
 - This assumes that RHS does not have a boolean function that is 100% noise stability regime similar to LHS Percolation.
 - Superpolynomial size for NP-complete PARITY3SAT (kind of a promise problem) implies $P \neq \text{NP}$ and $P \neq \text{NP}$ implies either a Poisson distribution or a hypergeometric series that might or might not converge.
- In other words a democratic decision making which does not involve percolation is never perfect and thus BKS conjecture has to be true berating majority i.e. there exists atleast one function - percolation - stabler than stablest majority.

53.16.3.2 If equal error (NoiseStability +/- delta) with different circuit sizes doesn't imply a lowerbound:

- LHS of $P(\text{Good})$ is percolation NC/poly circuit in 100% noise stability regime.
- RHS of $P(\text{Good})$ is of arbitrary size (e.g. superpolynomial size NP circuit from 53.16.2).
- LHS NC/poly 100% noise stability doesn't imply a lowerbound when RHS (e.g. superpolynomial size NP circuit from 53.16.2) is also 100% noise stable. It doesn't contradict convergence of $P(\text{Good})$ summation to 100%, superpolynomial size lowerbound for NP from 53.16.2 and BKS conjecture has to be trivially true i.e. Both LHS and RHS of $P(\text{Good})$ are equally stable.

53.17 (THEORY) Oracle results and $P=\text{NP}$ and PH

From [Baker-Gill-Solovay] there are oracles A and B such that $P^A = P^B$ and $P^A \neq P^B$ implying natural proofs involving relativizing oracles cannot answer $P=\text{NP}$ question. Also PH is shown to be infinite with oracle access recently. Because of this all points in this document avoid oracle arguments and only use fourier series of boolean functions and boolean function compositions for circuit lowerbounds for $P(\text{Good})$ voting circuits.

53.18 (THEORY) $P(\text{Good})$ circuit special case counterexample in PH collapse

LHS of P(Good) - a $\sigma(p,k)$ hard (could be dictatorial or PRG) circuit with 100% (noise stability $\pm \delta$) (assuming such exists)
RHS of P(Good) - a $\sigma(p,k+1)$ hard majority voting circuit with 100% (noise stability $\pm \delta$) (assuming such exists)

If above converging P(good) LHS and RHS imply a lowerbound , LHS $\sigma(p,k)$ lowerbounds RHS $\sigma(p,k+1)$ implying PH collapses to some level k .
The matrix of noise versus BPP in 53.14 and 14 imply noise and BPP intersect, but if only classes in $(\sigma(p,k) - \text{BPP})$ are chosen for voter boolean functions, derandomization is not required and noise stability is sufficient to account for total error. If there is a PH-complete problem, PH collapses to some level, but implication in other direction is not known i.e collapse of PH implying PH-completeness - if both directions are true then this proves non-constructively that there exists a PH-complete problem. Every level k in PH has a QBFSAT(k) problem that is complete for $\sigma(p,k)$ class. To prove PH-completeness from PH-collapse, all problems in all PH levels should be reducible to a PH-complete problem i.e all QBFSAT(k) complete problems should be reducible to a QBFSAT(n)-complete problem for $k < n$. Intuitively this looks obvious because QBFSAT(n) can generalize all other QBFSAT(k) by hardcoding some variables through a random restriction similar to Hastad Switching Lemma.

Equating $\sigma(p,k)$ with $\sigma(p,k+1)$ is probably the most generic setting for P(Good) circuits discounting arithmetic hierarchy.

Example $\sigma(p,k)$ -complete QBFSAT(k) boolean function:
there exists x_1 for all x_2 there exists $x_3 \dots \text{QBF1}(x_1, x_2, x_3, \dots, x_k)$

Example $\sigma(p,k+1)$ -complete QBFSAT($k+1$) boolean function:
there exists x_1 for all x_2 there exists $x_3 \dots$
 $\text{QBF2}(x_1, x_2, x_3, \dots, x_k, x_{(k+1)})$

53.19 (THEORY) Depth Hierarchy Theorem for P(Good) circuits

Average case Depth Hierarchy Theorem for circuits by [Rossman-Servedio-Tan] - <http://arxiv.org/abs/1504.03398> - states that any depth $(d-1)$ circuit that agrees with a boolean function f computed by depth- d circuit on $(0.5+o(1))$ fraction of all inputs must have $\exp(n^{\Omega(1/d)})$ size. This theorem is quite useful in election forecast and approximation where it is difficult to learn a voter boolean function exactly.

53.20 (THEORY) Ideal Voting Rule

[Rousseau] theorem states that an ideal voting rule is the one which maximizes number of votes agreeing with outcome [Theorem 2.33 in <http://analysisofbooleanfunctions.org/>]. The ideal-ness in this theorem still doesn't imply goodness of voting which measures how "good" is the outcome rather than how "consensual" it is - fact that majority concur on some decision is not sufficient to prove that decision is correct which is measured by noise stability $\pm \delta$. Because of this P(good) summation is quite crucial to measure hardness alongwith goodness.

53.21 (THEORY) Plancherel's Theorem, Stability polynomial and Lowerbounds in 53.18

Stability polynomial can be applied to QBFSAT(k) and QBFSAT(k+1) in 53.18.

By Plancherel's Theorem, Stability of a boolean function with noise rho is written as polynomial in rho:

$$\text{Stability}(f) = \sigma(\rho^{|S|} * f(S)^2), S \text{ in } [n]$$

which can be equated to 1 to find roots of this polynomial - noise probabilities - where 100% stability occurs.

From HLMN theorem for sigma(p,k)-complete QBFSAT(k):

$$\sigma(f(A_1)^2) \leq 2^*(M_1)*2^{(-t_1^{1/d_1}/20)}, |A_1| > t_1$$

From HLMN theorem for sigma(p,k+1)-complete QBFSAT(k+1):

$$\sigma(f(A_2)^2) \leq 2^*(M_2)*2^{(-t_2^{1/d_2}/20)}, |A_2| > t_2$$

When noise stability is 100%:

$$\text{Stability}(\text{QBFSAT}(k)) = \sigma(\rho_1^{|S_1|} * f(S_1)^2) = 1, S_1 \text{ in } [n]$$

$$\text{Stability}(\text{QBFSAT}(k+1)) = \sigma(\rho_2^{|S_2|} * f(S_2)^2) = 1, S_2 \text{ in } [n]$$

where rho1 and rho2 are variables each in the polynomial for QBFSAT(k) and QBFSAT(k+1). Solving these polynomials gives the points where 100% stability occurs in both QBFSATs. By choosing non-zero, real, positive roots of these polynomials as noise probabilities, 100% stability can be attained for QBFSAT(k) in LHS and QBFSAT(k+1) in RHS. Noise probabilities need not be equal in LHS and RHS. This is not an average case bound but lies as special case somewhere between best case and worst case. If delta due to BPP is ignored, equal stability implies lowerbound - LHS sigma(p,k) lowerbounds RHS sigma(p,k+1) and PH collapses to level k. If collapse implies completeness as mentioned in 53.18, this suffices to prove existence of a PH-complete problem non-constructively. Thus Stability implying Lowerbound has enormous implications for separation results.

Above deduction on PH collapse and possible PH-completeness contradicts 53.15 counterexample for NP having superpolynomial size circuits and hence $P \neq NP$, because PH-completeness could imply $P=PH$ (when LHS of $P(\text{Good})$ is an $[NC/\log \text{ in } P]$ percolation circuit - unlikely if percolation has only NC/poly circuits - which is 100% stable and RHS is PH-complete and 100% stable) and therefore $P=NP$. Resolution of this contradiction requires:

- Equal decision error (stability +/- delta) does not imply lowerbound.
- Roots of $\sigma(\rho^{|S|} * f(S)^2) - 1 = 0$ can only be complex with Re+Im parts and can't be real.
- $\sigma(\rho^{|S|} * f(S)^2) - 1 = 0$ is zero polynomial where all coefficients are zero.
- PH-collapse does not imply PH-completeness.

Stability polynomial above with rho as variable can be applied to any circuit to find the noise probabilities where 100% stability is attained without machinery like size and depth hierarchies, if equal stability implies lowerbounds. Indirectly 100% stability implies size bound - when rho=1, Stability polynomial grows and concides with HLMN theorem for circuit size lowerbound as mentioned above.

54(THEORY). Would the following experimental gadget work? It might, but impractical:

A voter gadget spawns itself into liker, disliker and neutral parallel threads on an entity to be judged. The neutral thread gathers inputs from liker and disliker threads and gets a weighted sum on them to classify the entity as "like-able" or "dislike-able". Thus real-world classification or judgement and perception seem mythical. (And how is weightage decided? Can this be using SentiWordNet score?). Theoretically, this is similar to Judge Boolean Functions defined in 53.* above, specifically when a voter decides by interactive proof system adversarial simulation (likes and dislikes are reducible to provers and verifiers) which is EXPTIME-complete. Implementation of this gadget is thus

EXPTIME-complete.

55(THEORY). Evocation is a realworld everyday phenomenon - a word reminding of the other. Positive thought chooses the right evocation and a negative thought chooses the negative evocation in the absence of context to disambiguate. For example, for a pessimist "fall" means "falling down" while for an optimist "fall" could mean "windfall or sudden gain". For a pessimist((optimist+pessimist)/2), fall could mean one of the "seasons" or even nothing. Mind sees what it chooses to see. Pessimism and Optimism are probably mathematically definable as accumulated weighted thoughts of past occurrences and any future thought or decision is driven by this "accumulated past" which acts as an implicit "disambiguator". This accumulated past or a Karma is reminiscent of above hypergraph of class stacks.

56(THEORY). A crude way to automatically disambiguate is to lookup the corresponding class stack and analyze only bounded height of events from the top of the stack. Bounded height would imply analyzing only a small window of the past events. For example, looking up the class stack from top to bottom for limited height of 2 for "fall" might have hyperedges "tree fall, heavy rain fall". Thus automatic disambiguation context could be the tuple of tuples $[[tree], [heavy, rain]]$ gathered from each hyperedge analyzed from top. Then this tuple of tuples has to be weighted to get majority. Alternatively, each tuple in this tuple set, as a random variable, could be assigned a belief potential or a conditional probability of occurrence based on occurrence of other tuples in the set. Thus a Bayesian Belief Network can be constructed and by propagating belief potential, probability of each tuple can be computed. Most disambiguating tuple is the one with high belief propagation output. Alternatively, elements of the set of tuples above can be construed as Observations and the State - the most disambiguating tuple - is Hidden and needs to be measured. Thus a Hidden Markov Model can be built. Emission probabilities for an Observation at a State are to be given as priors - probability of a tuple being observed for a word or "class". Importantly each stack is grown over time and is a candidate for Markov process with the restriction - node at height h is dependent only on node at height $(h-1)$ - height encodes timestamp. (But this makes the inference semi-statistical). Consequently, this gives a Trellis from which a Viterbi path can be extracted. Forward-Backward probabilities can be computed (Either generative or discriminative model can be applied, generative being costlier) using this Markov property and deeming the stack itself as a dynamically grown Hidden Markov Model where the Observations are the tuples(hyperedges) and the hidden state is the document that disambiguates. Using the Forward-Backward algorithm, the State(hyperedge) which maximizes the Probability of ending up in that State is the most disambiguating document hyperedge = $\text{argmax} [\text{Pr}(\text{State}(t)=\text{Hyperedge}(e) / \text{ObservedTuples}(1..t))]$ i.e The tuple or hyperedge that has highest forward conditional probability in the Trellis transition. This assumes the Hypergraph node stack as a Markov Chain. Moreover, State need not be a hyperedge. State is rather a "meaningful context". As in above example, uttering "fall" would kickoff a Forward-Backward computation on the Hypergraph node class stack for "fall" considering the stack as a Hidden Markov Model and would output the argmax State (which is not limited to hyperedge) as above. (Handwritten illustration at: https://sites.google.com/site/kuja27/NotesOnConceptHypergraphHMM_and_ImplicationGraphConvexHulls_2013-12-30.pdf?attredirects=0&d=1). Above assumption that node at height $(h-1)$ implies node at height h is quite experimental and is just to model how the human neuropsychological process of "evocation" works on uttering a word. There is no real-life application to this - an event at height $(h-1)$ need not imply an event at height h .

57(THEORY). Thus Sentiment Mining techniques can be used for the above hypergraph to get the overall sentiment of the hypergraph past. Probably each hyperedge might have to be analyzed for positive or negative sentiment to get grand total. Citation graph maxflow in <http://arxiv.org/abs/1006.4458> already gives a SentiWordnet based algorithm to weight each edge of a citation graph. Citations can be generalized as "like" or "dislike" opinions on entities as mentioned above.

58(THEORY). Thus not only documents but also events in human life can be modelled as above hypergraph to get a graphical model of the past and a PsychoProfiling of an individual could be arrived at using Sentiment mining. Thus, item 18 about "AstroPschoAnalysis" is feasible by two parallel paths which converge - Psychoprofiling by above concept or event hypergraph for a human being and equating it with results from Astronomical+Astrological analysis done through String Multiple Sequence Alignment mining.

##

59. Initial Design Notes for - Mundane Predictive Model:

##

- (FEATURE - DONE) DecisionTree, NaiveBayes and SVM classifiers and horoscope encoders are already in the AstroInfer codebase.
- (FEATURE - DONE) Encode the dataset which might be USGS or NOAA(Science on a Sphere) datasets or anyother dataset available after getting text horos for these using Maitreya's Dreams textclient (AstroInfer version)
- (FEATURE - DONE) Above gives encoded horoscope strings for all classes of mundane events in both Zodiacal and AscendantRelative formats (autogenerated by Python scripts in python-src/)
- (FEATURE - DONE) Above set is a mix of encoded strings for all events which can be classified using one of the classifiers above.
- (FEATURE - DONE) For each class the set of encoded horo strings in that class can be pairwise or multiple-sequence aligned to get the pattern for that class
- (FEATURE - DONE) There are two sets for each class after running the classifiers - one set is AscendantRelative and the other is Zodiacal
- (FEATURE - DONE) The above steps give the mined astronomical patterns for all observed mundane events - Pattern_Mundane_Observed_AscRelative and Pattern_Mundane_Observed_Zodiacal

60. (FEATURE - DONE) Above has implemented a basic Class and Inference Model that was envisaged in 2003. Class is the set-theoretic notion of sets sharing common underlying theme. Using VC Dimension is a way to determine accuracy of how well the dataset is "shattered" by the classes.

61. (THEORY) Now on to mining the classics for patterns: For all classes of events, running the classifier partitions the rules in a classic into set of rules or patterns for that class. Here again there are two sets for each class - Pattern_Mundane_Classic_AscRelative and Pattern_Mundane_Classic_Zodiacal

62. (THEORY) Thus correlation of the two sets *_Observed_* and *_Classic_* (each set has 2 subsets) for percentage similarity using any known similarity coefficient would unravel any cryptic pattern hidden astronomical datasets for that event and would be a circumstantial and scientific proof of rules in astrological classics with strong theoretical footing and would also bring to light new rules earlier unknown.

63. (THEORY and IMPLEMENTATION) More importantly, for example, if a non-statistical,astrological model of rainfall is computed based on a classical rule which says that "Venus-Mercury in single sign or Venus-Sun-Mercury in close proximity degrees with Sun in the middle causes copious rainfall" is used as a model, expected output of the model could be "Between 28October2013 and 15December2013 there could be peak monsoon activity in ---- longitude ---- latitude with --- percentage probability". And thus this could be a Medium Range Weather Forecasting tool. A python script that searches the Astronomical Data for mined rules from Sequence Mining of Astronomical Data has been added to python-src/. It uses Maitreya's Dreams Ephemeris text client for getting astronomical data for range of date, time and longitude and latitude. This script prints matching date, time and longitude and latitude when a rule for a weather phenomenon occurs as mined by sequence mining.

64. (FEATURE - DONE-related to 65 and 139) Integrate AstroInfer,USB-md,KingCobra and VIRGO into an approximately intelligent cloud OS platform that not just executes code statically but also dynamically learns from the processes (say through log files, executables, execution times etc., and builds predictive models).

USB-md Design Document:

http://sourceforge.net/p/usb-md/code-0/HEAD/tree/USBmd_notes.txt

VIRGO Design Document:

<http://sourceforge.net/p/virgo-linux/code-0/HEAD/tree/trunk/virgo-docs/VirgoDesign.txt>

KingCobra Design Document:

<http://sourceforge.net/p/kcobra/code-svn/HEAD/tree/KingCobraDesignNotes.txt>

This AsFer+USBmd+VIRGO+KingCobra would henceforth be known as "Krishna iResearch Intelligent Cloud OS - NeuronRain "

65. (THEORY and IMPLEMENTATION) Related to point 64 - Software Analytics - source code and logs analytics - related to Program comprehension - point 139 on BigData Analytics has more on this. Recently added VIRGO kernel_analytics module is in a way a software analytics module which reads config file set by the machine learning software after mining the kernel logs and objects. Kernel Analytics VIRGO driver module at present reads key-value pairs written to by the AsFer Machine Learning code from /etc/virgo_kernel_analytics.conf. Optionally, AsFer code can directly modify the kernel tunable parameters learnt by AsFer (<https://www.kernel.org/doc/Documentation/kernel-parameters.txt>) through modprobe or "echo -n \${value} > /sys/module/\${modulename}/parameters/\${parm}" for existing modules while virgo_kernel_analytics.conf is read for VIRGO specific modules. Graph Isomorphism of Program Slice Dependency Graphs for 2 codebases mentioned in

<https://sites.google.com/site/kuja27/PhDThesisProposal.pdf> is also a Software Analytics problem. There are Slicing and Graph Isomorphism tools already available. Recently there has been a SubExponential Time algorithm for GI - [Lazlo Babai]. Kernel Analytics config in filesystem requires reloading. New feature to set the kernel analytics key-value pairs directly from userspace to kernel memory locations dynamically has been added via boost::python C++ and CPython extensions - described in 217.SATURN Program Analysis Framework has been integrated into VIRGO Linux - error logs of SATURN are AsFer analyzable - more on this in 232. SourceForge VIRGO repository does not contain SATURN .db files in saturn_program_analysis/saturn_program_analysis_trees/. They are committed only in GitHub saturn_program_analysis/saturn_program_analysis_trees/. Spark code computing Cyclomatic Complexity of codebase from SATURN generated .dot files has been committed in python-src/software_analytics/. This requires VIRGO Linux saturn program analysis driver generated .dot files.

AsFer Python -----> Boost::Python C++ Extension -----> VIRGO memory system calls -----> VIRGO Linux Kernel Memory Drivers

/\

V

|

|

<-----

AsFer Python -----> CPython Extensions -----> VIRGO memory system calls -----> VIRGO Linux Kernel Memory Drivers

/\

V

|

|

<-----

AsFer Python -----> VIRGO SATURN program analyzer .dot files -----> Spark -----> Cyclomatic Complexity

References:

-
- 65.1 Analytics of Device Driver code -
http://research.microsoft.com/en-us/groups/sa/drivermine_asplos14.pdf
- 65.2 Logging -
<http://research.microsoft.com/en-US/groups/sa/loggingpractice.pdf>
- 65.3 Law of leaky abstraction -
<http://www.joelonsoftware.com/Articles/LeakyAbstractions.html>
- 65.4 Function Point Analysis -
<http://www.bfpug.com.br/Artigos/Albrecht/MeasuringApplicationDevelopmentProductivity.pdf>
- 65.5 Function Point Analysis and Halstead Complexity Measures -
https://en.wikipedia.org/wiki/Halstead_complexity_measures
- 65.6 Cyclomatic Complexity of a Program - Euler Characteristic of program flow graph ($E - V + 2$) - Approximate code complexity.

66. (THEORY) Encoding a document with above Hypergraph of Class stack vertices and Hyperedges - This hypergraph of concepts can also be used as a steganographic encoding tool for obfuscating a document (somewhat an encryption of different kind). For example, each document is a hyperedge in this hypergraph of class stack vertices. By choosing a suitable encoding function every concept or a word can be replaced with some element within each class stack vertex. This encoding function chooses some element in each class stack - $f(\text{word or concept } C1 \text{ in a document}) = \text{a different word or concept } C2 \text{ in the class stack vertex that contains } C1$. This function f has to be one-one and onto so that it is invertible to get the original document. This function can be anything modulo the height of that stack. Thus a plain text meaningful document can encrypt another meaningful hidden document without any ciphertext generation.

67. An automaton or Turing machine model for data or voice (or musical) samples - Voice samples or musical notations are discrete in time and occur in stream. As an experimental research, explore on possibility of automatically constructing an automaton or Turing machine that recognizes these languages (RE or CFG) where the notes are the alphabets.

(FEATURE - DONE) 68. Music Pattern Mining - Computational Music - Alternatively, a Discrete Fourier Transform on a set of data or voice samples gives a set of frequencies - a traditional DSP paradigm.

References:

-
- 68.1 <https://ccrma.stanford.edu/~jos/st/>

69. (FEATURE - Audacity FFT - DONE) Music Pattern Mining - Experimental Idea of previous two points is to mine patterns in discrete data and voice(music for example) samples. Music as an expression of mathematics is widely studied as Musical Set Theory - Transpositions and Inversions (E.g http://en.wikipedia.org/wiki/Music_and_mathematics, <http://www.ams.org/samplings/feature-column/fcarc-canon>, <http://www-personal.umd.umich.edu/~tmfiore/1/musictotal.pdf>). Items 56,57 and 58 could help mining deep mathematical patterns in classical and other music and as a measure of similarity and creativity. In continuation of 68, following experiment was done on two eastern Indian Classical audio clips having similar raagas:

69.1 FFT of the two audio files were done by Audacity and frequency domain files were obtained with sampling size of 65536, Hanning Window, Log frequency

69.2 FFTs of these two have been committed in music_pattern_mining/. Similarity is observed by peak decibel frequency of $\sim 500\text{Hz}$ in both FFTs - Similarity criterion here is the strongest frequency in the sample though there could be others like set of prominent frequencies, amplitudes etc.,. Frequencies with low peaks are neglected as noise.

70-79 (THEORY - EventNet Implementation DONE) EventNet and Theoretical analysis

of Logical Time:

70. In addition to Concept wide hypergraph above, an interesting research could be to create an EventNet or events connected by causation as edge (there is an edge (x,y) if event x causes event y). Each event node in this EventNet is a set of entities that take part in that event and interactions among them. This causation hypergraph if comprehensively constructed could yield insights into apparently unrelated events. This is hypergraph because an event can cause a finite sequence of events one after the other, thereby including all those event vertices. For simplicity, it can be assumed as just a graph. This has some similarities with Feynman Diagrams and Sum-over-histories in theoretical physics.

71. Each event node in the node which is a set as above, can have multiple outcomes and hence cause multiple effects. Outcome of an interaction amongst the elements of an event node is input to the adjacent event node which is also a set. Thus there could be multiple outgoing outcome edges each with a probability. Hence the EventNet is a random, directed, acyclic graph (acyclic assuming future cannot affect past preventing retrocausality). Thus EventNet is nothing but real history laid out as a graph. Hypothetically, if every event from beginning of the universe is causally connected as above, an indefinite ever growing EventNet is created.

72. If the EventNet is formulated as a Dynamic Graph with cycles instead of Static Graph as above where there causal edges can be deleted, updated or added, then the above EventNet allows changing the past theoretically though impossible in reality. For example, in an EventNet grown upto present, if a causal edge is added from a present node to past or some causal edge is deleted or updated in the past, then "present" causes "past" with or without cycles in the graph.

73. EventNet can be partitioned into "Past", "Present" and "Future" probably by using some MaxFlow-MinCut Algorithms. The Cut of the graph as Flow Network is the "Present" and either side of the Cut is "Past" and "Future".

74. A recreational riddle on the EventNet: $\text{Future}(\text{Past}) = \text{Present}$. If the Future is modelled as a mathematical function, and if Past is fixed and Present is determined by 100% freewill and can have any value based on whimsical human actions, then is the function $\text{Future}()$ well-defined?

75. Conjecture: Undirected version of EventNet is Strongly Connected or there is no event in EventNet without a cause (outgoing edge) or an effect (incoming edge).

76. Events with maximum indegree and outdegree are crucial events that have deep impact in history.

77. Events in each individual entity's existence are subgraphs of universal EventNet. These subgraphs overlap with each other.

78. There is an implicit time ordering in EventNet due to each causation edge. This is a "Logical Clock" similar to Lamport's Clock. In a cloud (e.g VIRGO Linux nodes, KingCobra MAC currency transactions) the EventNet is spread across the nodes and each node might have a subgraph of the giant EventNet.

79. EventNet can also be viewed as a Bayesian Network.

80. (THEORY) Mining EventNet for Patterns:

As an old saying goes "history repeats itself". Or does it really? Are there cycles of events? Such questions warrant checking the EventNet for cycles. But the above EventNet is acyclic by definition. This probably goes under the item 48

above that models the events as a hypergraph based on classification of events which is different from EventNet altogether. Alternatively, the EventNet nodes which are events with set of partakers and their interactions, can be mined for commonalities amongst them. Thus checking any pair of event nodes separated by a path of few edges (and thus separated in logical time) for common pattern suffices and this recursively continues.

Frequent Subgraph Mining of above EventNet (i.e whether a subgraph "repeats" with in the supergraph) as mentioned in Graph Search feature above could find patterns in events history. (Reference: Graph growing algorithms in chapter "Graph Mining", Data Mining, Han and Kamber)

There is a striking resemblance of EventNet to sequence mining algorithm CAMLS - a refined Apriori algorithm - (<http://www.cs.bgu.ac.il/~yarongon/papers/camls.dasfaa2010.pdf>) which is for mining a sequence of events - each event has intraevent partakers occurring at different points in time with gaps. EventNet mining is infact a generalization of linear time in CAMLS to distributed logical clock defined as EventNet causation infinite graph above. The topological orderings of EventNet can be mined using CAMLS. Sequence Mining python script that implements Apriori GSP has been added to repository and it can be applied to topologically sorted EventNet graphs as well.

81-86. (THEORY) Fractal nature of events:

81. Are events self-similar or exhibit fractal nature? This as in item 71, needs mining the event nodes which are sets of partakers for self-similarity. A fractal event is the one which has a cycle and any arbitrary point on the cycle has a cycle attached at that point and so on. An example of fractal event is the Hindu Vedic Calendar that has Major cycles, subcycles, cycles within cycles that occur recursively implying that calendar is self-similar. How to verify if the EventNet graph has a fractal nature or how to prove that a graph is "Fractal" in general? Would it be Ramsey theory again?

82. EventNet is a Partial Order where there may not be edges of causality between some elements. Thus a Topological Sort on this EventNet directed, acyclic graph gives many possible orderings of events. If history of the universe assuming absolute time is formulated as EventNet, then the topological sort does not give a unique ordering of events which is counterintuitive to absolute time. (Is this sufficient to say there is no absolute time?).

83. EventNet on history of events in the universe is quite similar to Directed Acyclic Graph based Scheduling of tasks with dependencies on parallel computers. Thus universe is akin to a Infinitely Massive Parallel Computer where events are dynamically scheduled with partakers, outcomes and with non-determinism. Even static scheduling is NP-Complete.

84. In the above EventNet, each node which is a set can indeed be a graph also with freewill interactions amongst the set members as edges. This gives a graph G1 with each node being replaced by a graph G2. This is a fractal graph constructed naturally and notions of Outer products or Tensor products or Kronecker products with each entry in adjacency matrix replaced by another adjacency matrix apply. By definition each node can be replaced by different graph.

85. Similar to Implication graphs as Random Growth Graphs, EventNet also qualifies as a Random Growth Network as events happen randomly and new edges are added whenever events happen (with previous Kronecker Tensor model). Rich-Get-Richer paradigm can also hold where nodes with more adjacent nodes are more likely to have future adjacent nodes. (A related notion of Freewill Interactions in <http://sites.google.com/site/kuja27/UndecidabilityOfFewNonTrivialQuestions.pdf?attredirects=0> is worth mentioning here).

86. Regularity Lemma can be used as a tool to test Implication and EventNet Random Growth Graphs - specifically seems to have an application in EventNet Kronecker Graph model above where each node is replaced by a graph and thus can be construed as epsilon-partition of the vertices that differ infinitesimally in density. Each element in the partition is the event.

87. COMMIT RELATED NOTES

(FEATURE- DONE) commits as on 3 September 2013

DecisionTree, NaiveBayes and SVM classifier code has been integrated into AstroInfer toplevel invocation with boolean flags

(FEATURE- DONE) commits as on 6 September 2013

In addition to USGS data, NOAA Hurricane dataset HURDAT2 has been downloaded and added to repository. Asfer Classifier Preprocessor script has been updated to classify set of articles listed in articlesdataset.txt using NaiveBayesian or DecisionTree Classifiers and training and test set text files are also autogenerated. New parser for NOAA HURDAT2 dataset has been added to repository. With this datasets HTML files listed in articlesdataset.txt are classified by either classifiers and segregated into "Event Classes". Each dataset document is of proprietary format and requires parser for its own to parse and autogenerate the date-time-longlat text file. Date-time-longlat data for same "Event Class" will be appended and collated into single Date-time-longlat text file for that "Event Class".

(FEATURE- DONE) commits as on 12 September 2013

1. asfer_dataset_seggregator.py and asfer_dataset_seggregator.sh - Python and wrapper shell script that partitions the parsed datasets which contain date-time-long-lat data based on classifier output grepped by the invoker shell script - asfer_dataset_seggregator.sh - and writes the names of parsed dataset files which are classified into Event Class "<class>" into text files with names of regular expression "EventClassDataSet_<class>.txt"

2. DateTimeLongLat data for all datasets within an event class (text file) need to be collated into a single asfer.anchors.<classname>.zodiacal or asfer.anchors.<classname>.asrelative. For this a Python script MaitreyaToEnchoroClassified.py has been added to repository that reads the segregated parsed dataset files generated by asfer_dataset_aggregator.sh and invokes maitreya_textclient for all date-time-long-lat data within all parsed datasets for a particular event class - "EventClassDataSet_<class>.txt" and also creates autogenerated asfer.anchors.<class>.zodiacal and asfer.anchors.<class>.asrelative encoded files

(FEATURE- DONE) commits as on 2 November 2013

Lot of commits for implementation of Discrete Hyperbolic Factorization with Stirling Formula Upperbound (<http://sourceforge.net/p/asfer/code/HEAD/tree/cpp-src/miscellaneous/DiscreteHyperbolicFactorizationUpperbound.cpp>) have gone in. Overflow errors prevent testing large numbers. (URLs:

1) Multiple versions of Discrete Hyperbolic Factorization uploaded in <http://sites.google.com/site/kuja27/>

2) Handwritten by myself - http://sourceforge.net/projects/acadpdrafts/files/DiscreteHyperbolicFactorization_UpperboundDerivedWithStirlingFormula_2013-09-10.pdf/download and

3) Latex version - <http://sourceforge.net/projects/acadpdrafts/files/DiscreteHyperbolicPolylogarith>

micSieveForIntegerFactorization_updated_rectangular_interpolation_search_and_StirlingFormula_Upperbound.pdf/download
)

(FEATURE- DONE) commits as on 20 November 2013 and 21 November 2013

1. Lots of testing done on Discrete Hyperbolic Factorization sequential implementation and logs have been added to repository.

2. An updated draft of PRAM NC version of Discrete Hyperbolic Factorization has been uploaded at:
http://sourceforge.net/projects/acadpdrafts/files/DiscreteHyperbolicPolylogarithmicSieveForIntegerFactorization_PRAM_TileMergeAndSearch_And_Stirling_Upperbound.pdf/download that does PRAM merge of discrete tiles in logarithmic time before binary search on merged tile.

3. Preliminary Design notes for CRCW PRAM implementation of the above is added to repository at:
<http://sourceforge.net/p/asfer/code/237/tree/ImplementationDesignNotesForDiscreteHyperbolicFactorizationInPRAM.jpg>. This adds a tile_id to each tile so that during binary search, the factors are correctly found since coordinate info gets shuffled after k-tile merge.

88.Tagging as on 16 December 2013

AsFer version 12.0 and VIRGO version 12.0 have been tagged on 6 December 2013 (updated the action items above).

(THEORY) 89. More reference URLs for Parallel RAM design of above NC algorithm for Discrete Hyperbolic Factorization for merging sorted lists:

- 1.http://arxiv.org/pdf/1202.6575.pdf?origin=publication_detail
2.<https://electures.informatik.uni-freiburg.de/portal/download/3/6951/thm15%20-%20parallel%20merging.ppt> (Ranks of elements)
3.<http://cs.brown.edu/courses/csci2560/syllabus.html> (Lecture Notes on CREW PRAM and Circuit Equivalence used in the NC algorithm for Discrete Hyperbolic Factorization above -
<http://cs.brown.edu/courses/csci2560/lectures/lect.24.pdf>)
4.<http://cs.brown.edu/courses/csci2560/lectures/lect.22.ParallelComputationIV.pdf>
5.<http://www.cs.toronto.edu/~bor/Papers/routing-merging-sorting.pdf>
6.<http://www.compgeom.com/~piyush/teach/AA09/slides/lecture16.ppt>
7.Shift-and-subtract algorithm for approximate square root computation implemented in Linux kernel
(http://lxr.free-electrons.com/source/lib/int_sqrt.c) which might be useful in finding the approximate square root in discretization of hyperbola (Sequential version of Discrete Hyperbolic Factorization)
8.<http://research.sun.com/pls/apex/f?p=labs:bio:0:120> - Guy Steele - approximate square root algorithm
9.<http://cstheory.stackexchange.com/questions/1558/parallel-algorithms-for-directed-st-connectivity> - related theoretical discussion thread on PRAM algorithms for st-connectivity
10.PRAM and NC algorithms - <http://www.cs.cmu.edu/afs/cs/academic/class/15750-s11/www/handouts/par-notes.pdf>
11. An Efficient Parallel Algorithm for Merging in the Postal Model - <http://etrij.etri.re.kr/etrij/journal/getPublishedPaperFile.do?fileId=SPF-1043116303185>
12. Parallel Merge Sort -
<http://www.inf.fu-berlin.de/lehre/SS10/SP-Par/download/parmerge1.pdf>
13. NC and PRAM equivalence - www.cs.tau.ac.il/~safra/ACT/CCandSpaceB.ppt
14. Extended version of BerkmanSchieberVishkin ANSV algorithm -

<http://www1.cs.columbia.edu/~dany/papers/highly.ps.Z> (has some references to NC, its limitations, highly parallelizable - loglog algorithms) - input to this ANSV algorithm is elements in array (of size N) and not number of bits ($\log N$) which is crucial to applying this to merge tree of factorization and proving in NC.
 15. Structural PRAM algorithms (with references to NC) - <http://www.umiacs.umd.edu/users/vishkin/PUBLICATIONS/icalp91.ps>
 16. Parallel Algorithms FAQ - NC, RAM and PRAM - Q24 - <http://nptel.ac.in/courses/106102114/downloads/faq.pdf>

17. Definitions related to PRAM model - <http://pages.cs.wisc.edu/~tvrdik/2/html/Section2.html> - Input to PRAM is N items stored in N memory locations - (For factorization, this directly fits in as the $O(N) \sim \pi^{1/2}/6 * N$ coordinate product integers stored in as many locations - for discretized tiles of hyperbola)

18. Reduction from PRAM to NC circuits - <http://web.cse.ohio-state.edu/~gurari/theory-bk/theory-bk-sevense6.html#Q1-80006-21> (The SIMULATE_RAM layer in each step is a subcircuit that is abstracted as a node in NC circuit. This subcircuit performs the internal computation of PRAM processor in that NC circuit node at some depth i. The NC circuit is simulated from PRAM model as - depth is equal to PRAM time and size is equal to number of processors.). Thus for Discrete Hyperbolic Factorization, the ANSV PRAM mergetree of polylogdepth is simulated as NC circuit with this reduction. Thus though each array element in ANSV is a $\log N$ bit integer, the SIMULATE_RAM abstraction reduces it to a node in NC circuit that processes the input and propagates the output to next step towards root.

19. Length of input instance in PRAM (n or N) - <http://web.cse.ohio-state.edu/~gurari/theory-bk/theory-bk-sevense2.html#Q1-80002-3> - "... When no confusion arises, because of the obvious relationship between the number N of values in the input and the length n of the input, N and n are used interchangeably. ...". For ANSV algorithm, the number N of values in the input array and the length n of the input are the same ($N=n$) and due to this it runs in polyloglogtime in input size $O(\log \log N)$ and with polynomial processors $N/\log \log N$.

20. Quoted abstract - "... The all nearest smaller values problem is defined as follows. Let $A = (a_1 ; a_2 ; : : : ; a_n)$ be n elements drawn from a totally ordered domain. For each a_i , $1 \leq i \leq n$, find the two nearest elements in A that are smaller than a_i (if such exists): the left nearest smaller element a_j (with $j \leq i$) and the right nearest smaller element a_k (with $k \geq i$). We give an $O(\log \log n)$ time optimal parallel algorithm for the problem on a CRCW PRAM ...". Thus $N=n$.

21. SIMULATE_RAM subcircuit in point 18 - Number of bits allowed per PRAM cell in PRAM to NC reduction - <http://hall.org.ua/halls/wizzard/books2/limits-to-parallel-computation-p-completeness-theory.9780195085914.35897.pdf> - pages 33-36 - quoted excerpts - "... Let M be a CREW-PRAM that computes in parallel time $t(n) = (\log n)^{O(1)}$ and processors $p(n) = n^{O(1)}$. Then there exists a constant c and a logarithmic space uniform Boolean circuit family, $\{\alpha_n\}$, such that α_n on input x_1, \dots, x_n computes output $y_{1,1}, y_{1,2}, \dots, y_{i,j}, \dots$, where $y_{i,j}$ is the value of bit j of shared memory cell i at time $t(n)$, for $1 \leq i \leq p(n) * t(n)$ and $1 \leq j \leq c * t(n)$...". Thus number of bits allowed per PRAM memory location is upperbounded by polylogn. For ANSV algorithm underlying the Discrete Hyperbolic Factorization, maximum number of bits per PRAM cell is thus $\log N$ where N is the integer to factorize (and maximum number of PRAM cells is $\sim \pi^{1/2}/6 * N$) thereby much below the above polylogN bound for number of bits per PRAM cell for creating a uniform NC circuit from PRAM model.

 (THEORY) 90. Some notes on extensions to Integer partitions and Hash Functions (<https://sites.google.com/site/kuja27/IntegerPartitionAndHashFunctions.pdf>)

attredirects=0)

1. Riemann sums (discrete approximation of Riemann integral) of all the functions corresponding to the hash functions are same. Thus all such functions form an equivalence class. (Assuming each partition created by the hash functions as a function plot)

2. Hardy-Ramanujan asymptotic bound for partition function $p(n)$ is $\sim O(e^{(\pi \sqrt{0.66n})} / (4 \cdot 1.732^n))$ which places a bound on number of hash functions also. ([http://en.wikipedia.org/wiki/Partition_\(number_theory\)](http://en.wikipedia.org/wiki/Partition_(number_theory)))

3. If m -sized subsets of the above $O(m! \cdot e^{(\sqrt{n})}/n)$ number of hash functions are considered as a (k, u) -universal or (k, u) -independent family of functions ($\Pr(f(x_1)=y_1 \dots) < u/m^k$), then following the notation in the link mentioned above, this m -sized subset family of hash functions follow the $\Pr(f(x_1)=y_1 \& \dots) < u/m^n$ where n is number of keys and m is the number of values. ($m!$ is for summation over $(m, \lambda(i))$ for all partitions)

4. Thus deriving a bound for number of possible hash functions in terms of number of keys and values could have bearing on almost all hashes including MD5 and SHA.

5. Birthday problem and Balls and Bins problem - Since randomly populating m bins with n balls and probability of people in a congregation to have same birthday are a variant of Integer partitioning and thus hash table bucket chaining, bounds for birthday problem and Chernoff bounds derived for balls and bins could be used for Hash tables also
(http://en.wikipedia.org/wiki/Birthday_problem,
<http://www.cs.ubc.ca/~nickhar/W12/Lecture3Notes.pdf>)

6. Restricted partitions which is the special case of integer partitions has some problems which are NP-complete. Money changing problem which is finding number of ways of partitioning a given amount of money with fixed denominations (Frobenius number) is NP-complete (<http://citeseer.uark.edu:8080/citeseerx/showciting;jsessionid=92CBF53F1D9823C47F64AAC119D30FC4?cid=3509754>, Naoki Abe 1987). Number of partitions with distinct and non-repeating parts follow Roger-Ramanujan identities (2 kinds of generating functions).

7. The special case of majority voting which involves integer partitions described in https://sites.google.com/site/kuja27/IndepthAnalysisOfVariantOfMajorityVotingwithhZFAOC_2014.pdf requires a hash function that non-uniformly distributes the keys into hashes so that no two chains are equal in size (to simulate voting patterns without ties between candidates). This is the special case of restricted partitions with distinct and non-repeating parts of which money changing is the special case and finding a single solution is itself NP-complete.

8. Thus Majority voting can be shown to be NP-complete in 2 ways:

8.1 by Democracy circuit (Majority with SAT) in http://sourceforge.net/projects/acadpdrafts/files/ImplicationGraphsPGoodEquationAndPNotEqualToNPQuestion_excerpts.pdf/download and https://sites.google.com/site/kuja27/PhilosophicalAnalysisOfDemocracyCircuitAndPChoice_2014-03-26.pdf

8.2 by reduction from an NP-hard instance of Restricted Partition problem like Money changing problem for Majority voting with constituencies described in https://sites.google.com/site/kuja27/IndepthAnalysisOfVariantOfMajorityVotingwithhZFAOC_2014.pdf

9. Infact the above two ways occur in two places in the process of democratic voting: The democracy circuit is needed when a single candidate is elected while the restricted partition in second point is needed in a multi-partisan voting where multiple candidates are voted for.

10. Point 8.2 above requires a restricted partition with distinct non-repeating parts. There are many results on this like Roger-Ramanujan identities, Glaisher theorem and its special case Euler's theorem which equate number of partitions with parts divisible by a constant and distinctiveness of the parts (odd, differing by some constant etc.,). Such a restricted partition is needed for a tiebreaker and hence correspond bijectively to hash collision chaining.

11. An interesting manifestation of point 10 is that nothing in real-life voting precludes a tie and enforces a restricted partition, with no two candidates getting equal votes, where all voters take decisions independent of one another (voter independence is questionable to some extent if swayed by phenomena like "votebank", "herd mentality" etc.,) thereby theoretically invalidating the whole electoral process.

12. Counting Number of such restricted partitions is a #P-complete problem - <https://www.math.ucdavis.edu/~deloera/TALKS/denumerant.pdf>.

13. If a Hash table is recursive i.e the chains themselves are hashtables and so on... then this bijectively corresponds to a recurrence relation for partition function (expressing a partition of a higher integer in terms of lower integer).

14. If the hash table chains are alternatively viewed as Compositions of an integer (ordered partitions) then there are 2^{n-1} maximum possible compositions. ([http://en.wikipedia.org/wiki/Composition_\(number_theory\)](http://en.wikipedia.org/wiki/Composition_(number_theory)))

15. In the summation over all parts of partitions derived in <https://sites.google.com/site/kuja27/IntegerPartitionAndHashFunctions.pdf> if $m=n$ then it is the composition in point 14 above and thus summation over all parts of partitions is greater than or equal to 2^{n-1} since some permutations might get repeated across partitions. Thus the summation expresses generalized restricted composition ($\text{summation_over_all_partitions_of_n}((n, \text{lamda}(i)) \geq 2^{n-1})$).

16. Logarithm of above summation then is equal to $(n-1)$ and thus can be equated to any partition of n . Thus any partition can be written as a series which is the combinatorial function of parts in all individual partitions.

91. Updated drafts on Integer partitions and hash function (with points in 80 above) , Circuits for Error probability in Majority Voting

1.
https://sites.google.com/site/kuja27/IntegerPartitionAndHashFunctions_2014.pdf?attredirects=0&d=1
2.
https://sites.google.com/site/kuja27/CircuitForComputingErrorProbabilityOfMajorityVoting_2014.pdf?attredirects=0&d=1

92. Reference URLs for restricted integer partitions with distinct parts

(for
http://sites.google.com/site/kuja27/IntegerPartitionAndHashFunctions_2014.pdf?attredirects=0&d=1)
1. Generating function - <http://math.berkeley.edu/~mhaiman/math172-spring10/partitions.pdf>
2. Schur's theorem for asymptotic bound for number of denumerants - http://en.wikipedia.org/wiki/Schur's_theorem
3. Frobenius problem - <http://www.math.univ-montp2.fr/~ramirez/Tenerif3.pdf>

4. Locality Sensitive Hashing (that groups similar keys into a collision bucket chain using standard metrics like Hamming Distance) - <http://hal.inria.fr/inria-00567191/en/>, <http://web.mit.edu/andoni/www/LSH/index.html>, http://en.wikipedia.org/wiki/Locality-sensitive_hashing
5. Locality Sensitive Hashing and Lattice sets (of the diophantine form $a_1x_1+a_2x_2+\dots+a_nx_n$) - <http://hal.inria.fr/docs/00/56/71/91/PDF/paper.pdf>
6. Minhash and Jaccard similarity coefficient - http://en.wikipedia.org/wiki/MinHash#Jaccard_similarity_and_minimum_hash_values (similar to LSH that emphasizes on hash collisions for similarity measures between sets e.g bag of words of URLs)

(THEORY) 93. Reduction from Money Changing Problem or 0-1 Integer LP to Restricted Partitions with distinct parts

If the denominations are fixed as 1,2,3,4,5,...,n then the denumerants to be found are from the diaphantine equation:
 $a_1*1 + a_2*2 + a_3*3 + a_4*4 + a_5*5 + \dots + a_n*n$
(with $a_i = 0$ or 1). GCD of all $a_i(s)$ is 1. Thus Schur's theorem for MCP or Coin Problem applies.
Integet 0-1 LP NP-complete problem can also be reduced to above diophantine format instead of MCP. Finding one such denumerant with boolean values is then NP-complete and hence finding one partition with distinct non-repeating parts is NP-complete (needed in multipartisan majority vote).

(FEATURE- DONE) 94. Commits as on 23 April 2014

Updated pgood.cpp with some optimizations for factorial computations and batched summation to circumvent overflow to some extent.
For Big decimals IEEE 754 with 112+ bits precision is needed for which boost::multiprecision or java.math.BigDecimal might have to be used.

(FEATURE- DONE) 95. Commits as on 7 July 2014

Initial implementation of a Chaos attractor sequence implementation committed to repository.

(FEATURE- DONE) 96. Commits as on 8 July 2014

Python-R (rpy2) code for correlation coefficient computation added to above Chaos attractor implementation.

(FEATURE- DONE) 97. Time Series Analysis - Commits as on 9 July 2014

DJIA dataset, parser for it and updated ChaosAttractor.py for chaotic and linear correlation coefficient computation of DJIA dataset have been committed.

(FEATURE- DONE) 98. Commits as on 10 July 2014

Python(rpy2) script for computing Discrete Fourier Transform for DJIA dataset has been added (internally uses R). [python-src/DFT.py]

(FEATURE- DONE) 99. Commits as on 11 July 2014

Python(rpy2) script for spline interpolation of DJIA dataset and plotting a graph of that using R graphics has been added. [python-src/Spline.py]

(FEATURE- DONE) 100. Commits as on 15 July 2014 and 16 July 2014

Doxygen documentation for AsFer, USBmd, VIRGO, KingCobra and Acadpdrafts have been committed to GitHub at https://github.com/shrinivaasanka/Krishna_iResearch_DoxygenDocs. LOESS local polynomial regression fitting code using loess() function in R has been added at python-src/LOESS.py. Approximate linear interpolation code using approx() and approxfun() in R has been added at python-src/Approx.py

(FEATURE- DONE) 101. Commits as on 23 July 2014

Draft additions to <http://arxiv.org/pdf/1106.4102v1.pdf> are in the Complement Function item above. An R graphics rpy2 script RiemannZetaFunctionZeros.py has been added to parse the first 1000000 zeros of RZF and plot them using R Graphics.

(FEATURE - THEORY - Visualizer Implementation DONE) 102. Dense Subgraphs of the WordNet subgraphs from Recursive Gloss Overlap

<http://arxiv.org/abs/1006.4458> and http://www.nist.gov/tac/publications/2010/participant.papers/CMI_IIT.proceedings.pdf have been extended for a summary creation algorithm from WordNet subgraphs of Recursive Gloss Overlap by filtering out low degree vertices(https://sites.google.com/site/kuja27/DocumentSummarization_using_SpectralGraphTheory_RGOGraph_2014.pdf?attredirects=0&d=1). For undirected graphs there is a notion of k-core of a graph which is an induced subgraph of degree k vertices. Since Wordnet is a directed graph, recently there are measures to measure degeneracy(D-cores - http://www.graphdegeneracy.org/dcores_ICDM_2011.pdf). Graph peeling is a process of removing edges to create a dense subgraph. This can be better visualized using visual wordnet implementations:
102.1 <http://kylescholz.com/projects/wordnet/>
102.2 <http://www.visuwords.com>
102.3 <http://www.visualthesaurus.com/browse/en/Princeton%20WordNet>

103. AsFer version 14.9.9 release tagged on 9 September 2014

(FEATURE- DONE) 104. Commits as on 9 October 2014

Initial python script implementation for Text compression committed with logs and screenshot. Decompression is still hazy and needs some more algorithmic work.

(FEATURE- DONE) 105. Commits as on 21 October 2014

An experimental POC python implementation that uses Hidden Markov Model for decompression has been committed. But it depends on one-time computing a huge number of priors and their accuracy.

(THEORY) 106. Creating a summary graph from EventNet

EventNet graph for historical cause and effect described above can be huge of the order of trillion vertices and edges. To get a summary of the events might be necessary at times - similar to a document summarization.

Summarizing a graph of event cause-effects requires giving importance to most important events in the graph - vertices with high number of degrees (indegrees + outdegrees) . This is nothing but finding k-core of a graph which is a maximal connected subgraph of EventNet where every vertex is of degree atleast k.

(FEATURE- DONE) 107. Commits as on 1 November 2014

A minimal PAC learning implementation in python to learn a Boolean Conjunction from dataset has been added to repository.

(FEATURE- DONE) 108. Commits as on 4 November 2014

Initial implementation for Minimum Description Length has been added to repository.

(FEATURE- DONE) 109. Commits as on 6 November 2014

Python Shannon Entropy implementation for texts has been added to repository and is invoked in MinimumDescLength.py MDL computation.

(FEATURE- DONE) 110. Commits as on 7 November 2014

Python Kraft Inequality MDL implementation has been committed.

(FEATURE- DONE) 111. Commits as on 11 November 2014

C++ implementation for Wagner-Fischer Dynamic Programming algorithm that iteratively computes Levenshtein Edit Distance than recursively has been added to repository.

(FEATURE - DONE) 112. Expirable objects

Setting expiry to an object is sometimes essential to control updates and access to an object. Example application of this - A JPEG image should be accessible or displayable for only a finite number of times and after that it has to self-destruct. Though doing this in C++ is straightforward with operator overloading, in C it looks non-trivial. Presently only C++ implementation is added to repository.

(FEATURE- DONE) 113. Commits as on 11 November 2014 - Expirable template class implementation

Similar to weak_ptr and shared_ptr, a generic datatype that wraps any datatype and sets an expiry count to it has been added to repository in cpp-src/expirable/ . For example, a bitmap or a JPEG image can be wrapped in expirable container and it can be access-controlled. If expiry count is 1, the object (an image for example) can be written to or displayed only once and thus a singleton. Presently this is only for rvalues. Implementing for lvalues (just a usage without assignment should be able to expire an object) seems to be a hurdle as there is no operator overloading available for lvalues - i.e there is no "access" operator to overload. This might be needed for KingCobra MAC electronic money also.(std::move() copy-by-move instead of a std::swap() copy-by-swap idiom)

(FEATURE- DONE) 114. Commits as on 12 November 2014

Expirable template in asferexpirable.h has been updated with 2 operator=() functions for copy-assignment and move-assignment which internally invoke std::swap() and std::move(). Explicit delete(s) are thus removed. Also example testcase has been updated to use a non-primitive datatype.

(FEATURE- DONE) 115. Commits as on 13 November 2014

Overloaded operator*() function added for expiry of "access" to objects. With this problem mentioned in 113 in tracking access or just usage is circumvented indirectly.

(FEATURE- DONE) 116. Commits as on 15 November 2014

Python implementation for Perceptron and Gradient has been added to repository.

(FEATURE- DONE) 117. Commits as on 17 November 2014

Python implementation for Linear and Logistic Regression in 2 variables.

(FEATURE- DONE) 118. Commits as on 20 November 2014

C++ implementation of K-Means clustering with edit distance as metric has been added to repository.

(FEATURE- DONE) 119. Commits as on 21 November 2014

C++ implementation of k-Nearest Neighbour clustering has been added to repository.

120. Commits as on 24 November 2014

Bugfixes to kNN implementation.

(FEATURE- DONE) 121. Commits as on 25 November 2014

Python script for decoding encoded horoscope strings (from Maitreya's Dreams) has been added to repository.

122. (FEATURE - DONE) Commits as on 3 December 2014

Initial implementation for EventNet:

1. EventNet python script has inputs from two text files - EventNetEdges.txt and EventNetVertices.txt - which define the event vertices and the causations amongst them with partakers in each event node
2. This uses GraphViz (that in turn writes a dot file) and python-graph+gv packages
3. GraphViz writes to EventNet.graphviz.pdf and EventNet.gv.png rendered and visualized graph files.
4. Above text files are disk-stored and can be grown infinitely.
5. EventNetVertices.txt has the format:
 <event vertex> - <csv of partakers in the event vertex>
EventNetEdges.txt has the format:

<ordered pairs of vertices for each causation edge>

6. Topological Sorting of EventNet using python-graph algorithms package

(THEORY) 123. EventNet - partakers of events and an application of EventNet to a related problem

Event vertices have partakers of event as defined in 122. Point 84-86 previously defined EventNet as a fractal graph tensor where each vertex is a graph or partakers. Alternative formulation of this is where the partakers are just key words or persons in that event. For example, a fictitious story can be translated into a giant EventNet where each vertex is an event with corresponding partakers in it. It could be difficult to find edges among the partakers (Ideally the edges are conversations among the partakers of an event specific to this example). As an approximation, the partakers could be simply the keywords parsed from that set of conversations. Complexity or connectedness and number of topological orderings possible for this translated EventNet is a measure of elegance.

(FEATURE- DONE) 124. Commits as on 4 December 2014

EventNet - a cloudwide event ordering with unique id implementation

EventNet has 2 input files for vertices and edges with partakers and writes an output file with ordering of the events

Input - EventNetVertices.txt has the format:

<event vertex> - <csv of partakers> - <tuples of conversations amongst the partakers # separated>
partakers could be machine id(s) or IP addresses and thread id(s) and the conversations being the messages to-and-fro across the partakers, which create an IntraEvent Graph of Conversations within each event vertex

Input - EventNetEdges.txt has the format:

<event vertex1, event vertex2>

Output - EventNetOrdering.txt has the format:

<index in chronologically ascending order> - <event id>

EventNet script thus is run in a central node which has the input files above that is updated by all the nodes in cloud. Outgoing edge from an event vertex has partakers from multiple events and thus is an outcome of the event. If the input files are split and stored in multiple cloud nodes, the topological sorts for multiple input files have to be merged to create a single cloudwide ordering.

(THEORY) 125. Massive EventNet computation

Each conversation of the events needs to create a log message that is sent to the EventNet service which updates the input vertices and edges files. The python EventNet script run

optionally on a hadoop
cluster mapreduce recomputes the topological ordering periodically. This is quite tedious a process that can flood the cloud with log messages enabled by config boolean flag or compile time #ifdef.

(FEATURE- DONE) 126. Commits as on 5 December 2014

Initial C++ Boost::graph based implementation for EventNet has been added to repository.

(THEORY) 127. 2-dimensional random walks for decision making (experimental)

Continued from point 49 above, the psychological process of decision making (in a mental conflict with two opposing directions) is akin to a game theoretical notion of Nash Equilibrium - where a huge payoff matrix is constructed for the random walk directions as strategies for the two conflicting decisions. There could be Nash Equilibria where decision1 doesn't gain from changing the random walk direction and decision2 doesn't gain from changing the direction (max(column),max(row)). These equilibria are like a win-win or a dilemma . For that matter this should apply to decision trees as well. Related application of equilibria for epidemic and malware are at:
<http://www.aaai.org/ocs/index.php/AAAI/AAAI14/paper/view/8478>

128. Commits as on 9 December 2014

Bugfixes for DOT file generation and toposort in C++ EventNet implementation.

129. (THEORY) Draft Updates to
https://sites.google.com/site/kuja27/CircuitForComputingErrorProbabilityOfMajorityVoting_2014.pdf?attredirects=0&d=1 - P(Good) series computation

For even number of finite population (electorate) the binomial coefficient summation in uniform distribution has an extra coefficient which when summed up tends to zero at infinity. Thus P(Good) series converges to,

$$(2^n - nC(n/2))/2^{(n+1)} = 0.5 - \epsilon \text{ where } \epsilon = \sqrt{1/(2*n*\pi)}$$
limit for which vanishes at infinity

(or) probability of good choice is epsilon less than 50% for finite even number of electorate for uniform distribution - a weird counterintuitive special case. Thus the counterexample for P Vs NP is still valid at infinity if infinite majority is decidable (related to decidability of infinite-candidate condorcet election , May's theorem and Arrow's theorem) . Written notes for this are at: http://sourceforge.net/p/asfer/code/568/tree/python-src/ComplFunction_DHF_PVsNP_Misc_Notes.pdf. What this implies is the LHS is PRG circuit in NC or P while the RHS is a humongous infinite majority+SAT (oracle) circuit - unbounded fan-in constant depth circuit. This then becomes an NP-complete Circuit SAT problem - <http://www.cs.berkeley.edu/~luca/cs170/notes/lecture22.pdf>.

If this infinite-ness breaches the polynomiality then what is quite puzzling is that RHS becomes a Direct Connect DC circuit equivalent to PH(Polynomial

Hierarchy). Quoted excerpts from Arora-Barak for DC uniform circuits:

"...

6.6

Circuits of exponential size

As noted, every language has circuits of size $O(2^n)$. However, actually finding these circuits may

be difficult— sometimes even undecidable. If we place a uniformity condition on the circuits, that

is, require them to be efficiently computable then the circuit complexity of some languages could

exceed 2^n . In fact it is possible to give alternative definitions of some familiar complexity classes, analogous to the definition of P in Theorem 6.7.

Definition 6.28 (DC-Uniform)

Let $\{C_n\}_{n \geq 1}$ be a circuit family. We say that it is a Direct Connect uniform (DC uniform) family if,

given n, i , we can compute in polynomial time the i th bit of (the representation of) the circuit C_n .

More concretely, we use the adjacency matrix representation and hence a family $\{C_n\}_{n \in \mathbb{N}}$ is DC

uniform iff the functions SIZE, TYPE and EDGE defined in Remark ?? are computable in polynomial time.

Note that the circuits may have exponential size, but they have a succinct representation in

terms of a TM which can systematically generate any required node of the circuit in polynomial

time.

Now we give a (yet another) characterization of the class PH, this time as languages computable

by uniform circuit families of bounded depth. We leave it as Exercise 13.

Theorem 6.29

$L \in PH$ iff L can be computed by a DC uniform circuit family $\{C_n\}$ that

- uses AND, OR, NOT gates.

$O(1)$

- has size 2^n

and constant depth (i.e., depth $O(1)$).

- gates can have unbounded (exponential) fanin.

- the NOT gates appear only at the input level.

If we drop the restriction that the circuits have constant depth, then we obtain exactly EXP

..."

The RHS Majority+SAT circuit has all characteristics satisfying the DC-uniformity in the theorem above - size can be exponential, unbounded fanin, depth is constant (each Voter Circuit SAT CNF is AND of ORs - depth 3) and NOT gates are required only in leaf nodes of the Voter Circuit SAT. Thus the counterexample could imply very, very importantly that P could be equal to PH or EXP (P=PH or P=EXP based on depth restricted or unrestricted) in infinite or exponential case respectively - could have tumultuous ramifications for complexity theory as a whole as it goes beyond P=NP question - for perfect voter scenario described in point 133 - all circumstantial evidences above point to this.

It is not necessary that per voter SAT is same for all voters. Each voter can have unrestricted depth SAT clauses (in real world, each voter decides on his-her own volition and depth of their SAT circuits can vary based on complexity of per-individual decision making algorithm) - due to which RHS zero-error DC circuit need not be in PH but in EXP.

even if a BQP algorithm is used in voting outside the purview of PH but in EXP, it doesn't change the above unless:

- perfection is impossible i.e there cannot be zero-error processes in the universe
- DC-circuit is not drawable (or undecidable if it can be constructed)
- infinite majority is undecidable (so circuit is DC non-uniform and not DC-uniform)
- the voter CNF can only be 2-SAT (which is highly unlikely) and not k-SAT or 3-SAT

129.1 Toda's theorem and $P(\text{good})$ circuit above:

 PH is contained in $P^{\#P}$ (or) P with #no-of-solutions-to-SAT oracle (Toda's theorem).
 If zero-error Majority+SAT voting DC uniform circuit is in PH then due to LHS=RHS of the $P(\text{good})$ series convergence (in cases of $p=0, p=1$ and $p=0.5$ as derived in <http://sourceforge.net/p/asfer/code/916/tree/cpp-src/miscellaneous/MajorityVotingErrorProbabilityConvergence.JPG>), PH collapses(?) to P (quite unbelievably):
 LHS Pseudorandom choice is in P while RHS Majority+SAT is in PH=DC circuit (restricted depth) or EXP (unrestricted depth) (i.e there is a P algorithm for PH).
 if $P=PH$:
 $P=PH$ is in $P^{\#P}$ by Toda's theorem

if $P=EXP$:
 $P=PH=EXP$ in $P^{\#P}$ or $P=PH=EXP=P^{\#P}$ (which is a complete collapse)

[$p=0.5$ is the uniform distribution which is a zero bias space while for other probabilities some bit patterns are less likely - epsilon-bias spaces]

 130. (THEORY) Counterexample definition for P Vs NP

Majority Circuit with SAT voter inputs with finite odd number of voters, in uniform distribution converges to $1/2$ same as LHS for pseudorandom choice. Even number of voters is a special case described previously. Also both LHS and RHS converge to 1 if probability is 1 (without any errors in pseudorandom choice and majority voting) which is counterintuitive in the sense that LHS nonprobabilistically achieves in PTIME what RHS does in NPTIME.

 131. (THEORY) Infinite majority and SAT+Majority Circuit

Infinite version of majority circuit is also a kind of heavy hitters problem for streaming algorithms where majority has to be found in an infinite bitstream of output from majority circuits for voters(http://en.wikipedia.org/wiki/Streaming_algorithm#Heavy_hitters). But nonuniform distribution still requires hypergeometric series. Moreover the SAT circuit is NP-complete as the inputs are unknown and is P-Complete only for non-variable gates(Circuit Value Problem). Odd number of electorate does not give rise to above extra coefficient in summation and is directly deducible to 0.5.

 132. (THEORY) May's Theorem of social choice

May's Theorem: In a two-candidate election with an odd number of voters, majority rule is the only voting system that is anonymous, neutral, and monotone, and that avoids the possibilities of ties.

May's theorem is 2-candidate analog of Arrow's Theorem for 3-candidate condorcet voting. May's theorem for 2 candidate simple majority voting defines a Group Decision Function which is valued at -1, 0 or 1 (<http://www.jmc-berlin.org/new/theorems/MaysTheorem.pdf>) for negative, abstention and positive vote for a candidate. For 2 candidates, positive vote for one candidate is negative for the other (entanglement). In the democracy circuit (SAT+Majority) the SAT clauses are kind of Group Decision Functions but with only binary values without any abstention. This is kind of alternative formulation - corollary - for May's theorem. Arrow's theorem does not apply for 2 candidate simple majority voting. May's theorem stipulates the conditions of anonymity, neutrality, decisiveness, monotonicity which should apply to the Majority+SAT circuit decision function as well. Neutrality guarantees that all outcomes are equally probable without bias which might imply that only uniform distribution is allowed in 2 candidate Majority+SAT voting. Thus there is a reduction from May's theorem to SAT+Majority democracy circuit. May's theorem does not apply to ties. This has been generalized to infinite electorate by Mark Fey. Anonymity is secret balloting. Monotonicity is non-decremental (e.g by losing votes a losing candidate is not winner and vice versa).

Additional References:

 132.1 May's theorem -
<http://www.math.cornell.edu/~mec/Summer2008/anema/maystheorem.html>

----- 133. (THEORY) Pseudorandom number generator and Majority voting for choice on a set

 Let S be a set of elements with "goodness" attribute for each element. Choice using LHS and RHS on this set is by a PRG and a majority voting circuit with SAT inputs. LHS for pseudorandom choice consists of two steps:

- 133.1 Accuracy of the PRG - how random or k-wise independent the PRG is - this is usually by construction of a PRG (Blum-Micali, Nisan etc.,)
- 133.2 Goodness of chosen element - PRG is used to choose an element from the set - this mimicks the realworld phenomenon of non-democratic social or non-social choices. Nature itself is the PRG or RG in this case. After choice is made, how "good" is the chosen is independent of (133.1). Proof is by contradiction - if it were dependent on PRG used then a distinguisher can discern the PRGs from True Randomness by significant fraction.
- 133.3 Thus if the set S is 100% perfect - all elements in it are the best - LHS of P(Good) is 1. Similarly the RHS is the majority voting within these "best" elements which can never err (i.e their SAT clauses are all perfect) that converges to 1 by binomial coefficient summation in uniform distribution.

From the aforementioned, it is evident that for a 100% perfect set, both PRG(LHS) and Majority+SAT(RHS) Voting are two choice algorithms of equal outcome but with differing lowerbounds (with $p=0.5$ both LHS and RHS are in BPP or BPNC, but when $p=1$ then RHS is NP and LHS is P or NC). The set in toto is a black-box which is not known to the PRG or individual voters who are the constituents of it.

----- (FEATURE- DONE) 134. Commits as on 8 January 2015

- 134.1 C++ implementation for Longest Common Substring has been added to repository with logs. Datasets were the clustered encoded strings output by KMeans clustering C++ implementation.
- 134.2 AsFer+USBmd+VIRGO+KingCobra+Acadp drafts - version 15.1.8 release tagged.

----- 135. (THEORY) Updates, Corrigenda and References to Space Filling Algorithm in : <https://sites.google.com/site/kuja27/Analysis%20of%20a%20Randomized%20Space>

%20Filling%20Algorithm%20and%20its%20Linear%20Program%20Formulation.pdf?
attredirects=0

135.1 The standard LP form can be obtained by slack variables (with only equalities) - mentioned as free variables in above -
http://ocw.mit.edu/courses/sloan-school-of-management/15-053-optimization-methods-in-management-science-spring-2013/tutorials/MIT15_053S13_tut06.pdf

135.2 Pseudorandom generator with linear stretch in NC1 -
<http://homepages.inf.ed.ac.uk/mcryan/mfcs01.ps>
- ... " The notion of deterministically expanding a short seed into a long string that ... the question of whether strong pseudorandom generators actually exist is a huge ... hardness assumption, that there is a secure pseudorandom generator in NC1 " ... [Kharitonov]

135.3 This space filling algorithm is in NC (using Tygar-Rief) with an assumption that multiplicative inverse problem is almost always not in RNC.

135.4 Tygar-Rief algorithm outputs n^c bits in parallel (through its PRAM processors) for $n=\log N$ for some composite N and is internal to the algorithm. For the sake of disambiguation, the number of bit positions in grid corresponding to the LP is set to Z .

135.5 Above pseudorandom bits have to be translated into the coordinate positions in the grid which is Z . In other words, pseudorandom bits are split into Z substrings ($n^c/\log Z = Z$) because each coordinate in the grid of size $2^{\log Z/2} * 2^{\log Z/2}$ is notated by the tuple of size $(\log Z/2, \log Z/2)$

135.6 Constant c can be suitably chosen as previously to be $c = \log(Z*\log Z)/\log n$ (n need not be equal to Z)

135.7 Either the n^c sized pseudorandom string can be split sequentially into $(\log Z/2 + \log Z/2)$ sized substring coordinate tuples (or) an additional layer of pseudorandomness can be added to output the coordinate tuples by pseudorandomly choosing the start-end of substrings from n^c size string, latter being a 2-phase pseudo-pseudo-random generator

135.8 In both splits above, same coordinate tuple might get repeated - same bit position can be set to 1 more than once. Circumventing this requires a Pseudorandom Permutation which is a bijection where Z substrings do not repeat and map one-one and onto Z coordinates on grid. With this assumption of a PRP all Z coordinates are set to 1 (or) the P-Complete LP is maximized in this special case, in NC.

135.9 There are Z substrings created out of the 2^{n^c} pseudorandom strings generated by Tygar-Rief Parallel PRG. Hence non-repeating meaningful substrings can be obtained only from $Z!/2^{n^c}$ fraction of all pseudorandom substrings.

135.10 Maximizing the LP can be reduced to minimizing the collisions (or) repetitive coordinate substrings above thus filling the grid to maximum possible. An NC algorithm to get non-repetitive sequence of coordinates is to add the index of the substring to the each split substring to get the hashed coordinates in the grid. For example in the $2*2$ grid, if the parallel PRG outputs 01011100 as the pseudorandom bit string, the substrings are 01, 01, 11 and 00 which has a collision. This is resolved by adding the index binary (0,1,2,3) to corresponding substring left-right or right-left. Thus 01+00, 01+01, 11+10, 00+11 - (001,010,101,011) - are the non-repetitive hashed coordinates. The carryover can be avoided by choosing the PRG output string size. This is a trivial bijection permutation.

135.11 The grid filling can be formulated as a Cellular Automaton of a different kind - by setting or incrementing the 8 neighbour bit positions of a coordinate to 1 while setting or incrementing a coordinate to 1.

135.12 Instead of requiring the non-repetitive coordinate substrings mentioned in (10) supra, the grid filling can be a multi-step algorithm as below which uses the Cellular Automaton mentioned in (11).

135.13 Cellular Automaton Algorithm:

(Reference for reductions below:

<http://cstheory.com/stockmeyer@sbcglobal.net/csv.pdf> [Chandra-Stockmeyer-Vishkin])

[<http://sourceforge.net/p/asfer/code/HEAD/tree/asfer-docs/AstroInferDesign.txt> and

<https://github.com/shrinivaasanka/asfer-github-code/blob/master/asfer-docs/AstroInferDesign.txt>]

The circuits described in [ChandraStockmeyerVishkin] are constant depth circuits [AC0] and thus in [NC1] (unbounded to bounded fanin logdepth reduction)

From wikipedia - Linear programs are problems that can be expressed in canonical form:

$c^T * X$

subject to $AX \leq b$

and $X \geq 0$

maximize X

subject to $AX \leq \text{some maximum limit}$

and $X \geq 0$

Below Cellular Automaton Monte Carlo NC algorithm for grid filling assumes that:

$C=[1,1,1,...1]$

$A=[1,1,1,...1]$ in the above and the vector of variables X is mapped to the grid - sequentially labelled in ascending from top-left to bottom-right, row-by-row and column-by-column. Though this limits the number of variables to be a square, additional variables can be set to a constant.

Grid cells (or variables in above grid) are initialized to 0.

loop_forever

{

(135.13.1) Parallel Pseudorandom Generator (Tygar-Rief) outputs bit string which are split into coordinates of grid and corresponding Grid cells are incremented instead of overwriting. This simulates parallel computation in many natural processes viz., rain. This is in NC. This is related to Randomness Extractors - https://en.wikipedia.org/wiki/Randomness_extractor - if rainfall from cloud can be used a natural weak entropy parallel randomness source (or strong?) - predicting which steam particle of a cloud would become a droplet is heavily influenced by the huge number of natural variables - fluid mechanics comes into force and this happens in parallel. Extractor is a stronger notion than Pseudorandom Generator. Extracting parallel random bits can also be done from a fluid mechanical natural processes like turbulent flows.

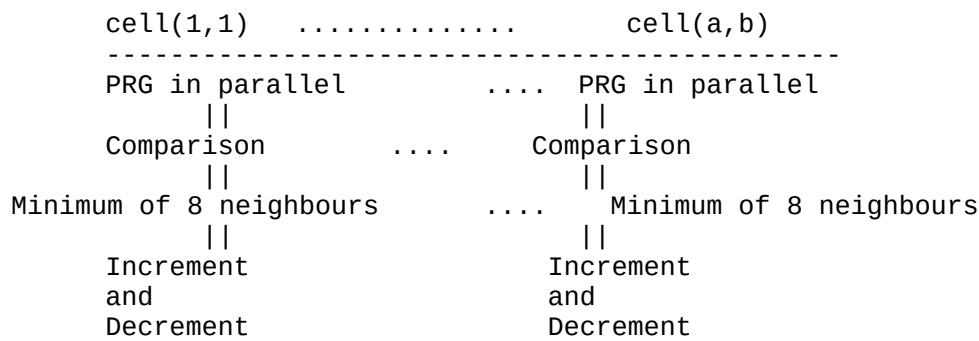
(135.13.2) Each grid cell has a constant depth Comparison Circuit that outputs 1 if the grid cell value exceeds 1. This is in AC0(constant-depth, polynomial size).

(135.13.3) If above Comparison gate outputs 1, then another NC circuit can be constructed that finds the minimum of grid neighbours of a cell (maximum 8 neighbours for each cell in 2-dimensional grid), decrements the central cell value and increments the minimum neighbour cell. This can be done by a sorting circuit defined in [ChandraStockMeyerVishkin]. This simulates a percolation of a viscous fluid that flows from elevation to lowlying and makes even. Each grid cell requires the above comparator and decrement NC circuit.

}

Above can be diagrammatically represented as: (for $N=a*b$ cells in grid in

parallel)



135.14 For example, a 3*3 grid is set by pseudorandom coordinate substrings obtained from Parallel PRG (6,7,7,8,9,1,3,3,2) as follows with collisions (grid coordinates numbered from 1-9 from left-to-right and top-to-bottom):

```
1 1 2
0 0 1
2 1 1
```

Above can be likened to a scenario where a viscous fluid is unevenly spread at random from heavens.

By applying cellular automaton NC circuit algorithm above, grid becomes:
(minimizes collisions,maximizes variables and LP)

```
1 1 1
1 1 1
1 1 1
```

Above can be likened to a scenario where each 8-neighbour grid cell underneath computes the evened-out cellular automaton in parallel. Size of the NC circuit is polynomial in LP variables n and is constant depth as the neighbours are constant (ChandraStockmeyerVishkin)

Thus there are 2 NC + 1 AC circuits which together maximize the special case of P-Complete LP instance without simplex where each grid coordinate is an LP variable. 135.13.1 (randomly strewn fluid) is independent of 135.13.2 and 135.13.3 (percolation of the fluid). This is both a Monte-Carlo and Las Vegas algorithm. The Parallel coordinate generation with Tyger-Reif Parallel PRG is Monte Carlo Simulation where as there is a guaranteed outcome with 100% possibility due to Comparison and Increment-Decrement circuits.

135.15 References on Cellular Automata, Parallel Computation of CA, Fluid Dynamics, Navier-Stokes equation, Percolation Theory etc.,:

- 135.15.1 <http://www.nt.ntnu.no/users/skoge/prost/proceedings/acc11/data/papers/1503.pdf>
135.15.2 <http://citeseerx.ist.psu.edu/viewdoc/summary?doi=10.1.1.52.8377>
135.15.3 <http://www.stephenwolfram.com/publications/academic/cellular-automaton-fluids-theory.pdf>
135.15.4 Constant Depth Circuits - <http://www.cs.berkeley.edu/~vazirani/s99cs294/notes/lec5.ps>
135.15.5 Complexity Theory Companion - <https://books.google.co.in/books?id=ysu-bt4UPPIC&pg=PA281&lpg=PA281&dq=Chandra+Stockmeyer+Vishkin+AC0&source=bl&ots=fzmsGWrZXi&sig=jms3hmJoeiHsf5dq-vnMHUOU54c&hl=ta&sa=X&ei=jjcqVYrNFc25uATkvICoDA&ved=0CCAQ6AEwAQ#v=onepage&q=Chandra%20Stockmeyer%20Vishkin%20AC0&f=false>
135.15.6 Pseudorandom Permutation in Parallel - <https://www.nada.kth.se/~johanh/onewaync0.ps>

135.16 A related algorithm - filling a square with infinitely many inscribed circles

Let S be a square of unit area. This square is filled with infinitely many circles of varying radii. This can be expressed in terms of geometric equations for circle - $x(i)^2 + y(i)^2 = r(i)^2$. Each $(x(i), y(i))$ is a coordinate on the circle of radius $r(i)$. Since $x(i)$ and $y(i)$ are < 1 , let $x(i) = 1/a(i)$ and $y(i) = 1/b(i)$ for some integers $a(i)$ and $b(i)$. At infinity the square is filled with above infinite number of circles that cover the unit area (has some analogies to set cover and VC-dimension-shattering). This can be written as the infinite summation $\pi * (1/a(1)^2 + 1/b(1)^2 + 1/a(2)^2 + 1/b(2)^2 + \dots) = 1$ (or sum of areas of all circles equals the unit area of square). Thus this equation is a quadratic program instead of a linear program. This is extensible to higher dimensions also (filling a hypercube with infinite number of n -spheres). For example, in 3 dimensions, set of spherical bubbles of varying radii covers the entire cube.

135.17 Above grid can be alternatively formulated as a Voronoi Diagram where Parallel PRG randomly sets multiple points on the plane and a tessellation of the plane covers these points. Instead of squares a Delaunay Triangulation is obtained from the dual of the Voronoi diagram.

Reference:

135.18. Circle Packing and Grid Filling - <http://11011110.livejournal.com/332331.html> - Filling a square with non-overlapping circles of maximum radii which is formulated as Dual of LP relaxation problem for matching where the constraints are that circles do not overlap i.e sum of radii \leq distance between centroids and objective function maximizes the radii variables.
135.19. 135.16 is a slight variant of Kepler's Theorem [Proof - [Hales] - <https://sites.google.com/site/thalespitt/>] - filling a cube with small spheres has maximum density $\sim 74\%$
135.20 Maximizing Sum of Radii of Balls - [Eppstein] - <http://www.ics.uci.edu/~eppstein/pubs/Epp-CCCG-16-slides.pdf>
135.21 Thue's Theorem For packing of discs on 2D - <http://www.math.stonybrook.edu/~tony/whatsnew/dec00/paper.html> - Circle packing in 2-dimension has maximum density $(\pi/[2*\sqrt{3}]) \sim 90.69\%$ when circles are arranged in hexagonal lattice. The LP formulation in <https://5d99cf42-a-62cb3a1a-s-sites.googlegroups.com/site/kuja27/Analysis%20of%20a%20Randomized%20Space%20Filling%20Algorithm%20and%20its%20Linear%20Program%20Formulation.pdf> and Cellular Automaton Algorithm Version above for Optimum Space Filling of a 2D plane by Monte-Carlo Parallel Random process are RNC algorithmic solutions to Thue's theorem (e.g natural process of Rain tiles earth in parallel by droplets of small radii and ultimately whole plane is covered, difference being allowance of circle overlaps) maximizing the variable points on plane having value 1.
135.22 Circle Packing Theorem and Planarity - [Koebe-Andreiev-Thurston] - Graph is planar if and only if it is $K_5, K_3, 3$ minor-free and is an intersection graph which has edges drawn between centroids of every pair of tangential closely packed coins of varied radii as vertices (https://gitlab.com/shrinivaasanka/Grafit/blob/master/course_material/NeuronRain/AdvancedComputerScienceAndMachineLearning/AdvancedComputerScienceAndMachineLearning.txt). Previous Linear Programming and Cellular Automaton algorithms for space filling by circular solids and drops of fluids are random circle packings of 2-D space which are not necessarily close. Random Close Packing is described in 461.
135.23 Cellular Automata and Chaos, Berlekamp-Conway-Guy Life Cellular Automata - <https://plato.stanford.edu/entries/cellular-automata/>
135.24 Edge of Chaos, Cellular Automata - <http://math.hws.edu/eck/js/edge-of-chaos/CA-info.html> - each row is an 1D set of squares colored by states and

subsequent rows evolve based on rules defined on states of a square and its neighbours. This is precisely similar to evolving tableau of Turing Machine states in Cook-Levin Theorem - https://en.wikipedia.org/wiki/Cook%E2%80%93Levin_theorem#/media/File:CookLevin_svg.svg and thus cellular automata are as powerful as Universal Turing Machines

135.25 Edge of Chaos, Lambda - Graphic illustration - <http://math.hws.edu/eck/js/edge-of-chaos/CA.html> - changing the fraction of rules (Christopher Langton's lambda) from 0 to 1 creates a phase transition from orderly to chaotic filling of 2D plane. Changing the previous Cellular Automaton algorithm for space filling in 2D to fill the neighbouring squares of a pseudorandomly chosen square by set of user defined rules (as against plain simple increment-decrement earlier) could exhibit chaotic behaviour especially on multichromatic filling of 2D plane.

(FEATURE- DONE) 136. Commits as on 28,29 January 2015

Python parser script to translate Longest Common Substring extracted from clustered or classified set of encoded strings has been added to repository.

(FEATURE - DONE) 137. Mining the Astronomical Datasets using KMeans and kNN - sequence of algorithms in AstroInfer
- Commits as on 4 February 2015

1. MaitreyaToEnchoros.py - This scripts reads a text file with set of date,time and long/lat for a specific class of events (at present it has earthquakes of 8+ magnitude from 1900). This script creates two encoded files asfer.enchoros.zodiacal and asfer.enchoros.asrelative using Maitreya's Dreams opensource CLI.
2. asfer.cpp is executed with doClustering=true by which kNN and KMeans clustered data are obtained.
3. asferkmeansclustering.cpp and asferkNNclustering.cpp implement the KMeans and kNN respectively.
4. Set of strings from any of the clusters has to be written manually in asfer.enchoros.clustered
5. asferlongestcommonsubstring.cpp - Within each cluster a pairwise longest common substring is found out.
6. TranslateClusterPairwiseLCS.py - Translates the longest common substring to textual rule description mined from above dataset. Mined rules are grep-ed in python-src/MinedRulesFromDatasets.earthquakes. Thus the astronomy dataset cpp-src/earthquakesFrom1900with8plusmag.txt (or cpp-src/magnitude8_1900_date.php.html) ends up as the set of automatically mined rules.

(FEATURE - DONE) 138. Commandline sequence for Mining Astronomical Datasets (e.g Earthquakes as above) using KMeans and kNN - Commits as on 4 February 2015

138.1 In asfer.cpp, set doClustering=true and build asfer binary
138.2 Set asfer.enchoros to asfer.enchoros.asrelative or asfer.enchoros.zodiacal
138.3 `./asfer 2>&1 > logfile1`
138.4 From logfile1 get maximum iteration clustered data for any cluster and update asfer.enchoros.clustered
138.5 In asfer.cpp set doLCS=true and build asfer binary
138.6 `./asfer 2>&1 > logfile2`
138.7 `grep "Longest Common Substring for" logfile2 2>&1 >`

```
python-src/asfer.ClusterPairwiseLCS.txt
138.8 sudo python TranslateClusterPairwiseLCS.py | grep "Textually" 2>&1 >>
MinedRulesFromDatasets.earthquakes
```


(FEATURE - DONE) 139. BigData Analytics subsystem (related to point 64,65 on software analytics)

139.1 (DONE) As mentioned in commit notes(13February2015) below, new multipurpose Java Hadoop MapReduce code has been added to a bigdata_analytics/ directory. At present it computes the frequencies of astronomical entities in the MinedRulesFromDatasets textfile obtained from clustering+LCS.

139.2 VIRGO Linux Kernel has following design choices to interface with the machine learning code in AsFer :

139.2.1 (DONE) the kernel module does an upcall to userspace asfer code - already this facility exists in VIRGO linux drivers

139.2.2 (INITIAL VIRGO COMMITS - DONE) the analytics subsystem creates a policy config file /etc/virgo_kernel_analytics.conf having key-value pairs for each config variable by mining the datasets with classification+clustering+any-hadoop-based-analytics. This is read by a VIRGO Linux kernel module - kernel_analytics - with VFS calls and sets(and exports symbols) the runtime config variables that indirectly determine the kernel behaviour. These exported analytics variables can be read by other interested kernel modules in VIRGO Linux, USB-md and KingCobra (and obviously mainline kernel itself). An example Apache Spark python script which mines the most frequent IP address from Uncomplicated Fire Wall and some device driver info from logs in /var/log/kern.log and /var/log/udev which can be set as a config key-value in /etc/virgo_kernel_analytics.conf has been added to AsFer repository. Dynamic setting of kernel analytics key-value pairs has been implemented with Boost::Python C++ and CPython C Extensions which obviates /etc/virgo_kernel_analytics.conf reload.

139.2.3 (INITIAL ASFER COMMITS - DONE) kernel module implements the machine learning algorithm in C (C++ in kernel is not preferable - <http://harmful.cat-v.org/software/c++/linus>) which doesn't reuse existing code and hence less attractive. Despite this caveat, a PoC Boost::Python C++ invocation of VIRGO memory system calls works - VIRGO linux has been made an extension Python C++ and C module which is invoked from Python userspace. Commits for this are described in 217. This is a tradeoff between pure C kernelspace and pure python/C/C++ userspace.

Diagrams depicting the above options have been uploaded at:
<http://sourceforge.net/p/asfer/code/HEAD/tree/asfer-docs/AsFerVIRGOlinuxKernelInterfaceDesignChoices.jpg>

--
(FEATURE - DONE) Commits as on 4 February 2015

--

C++ implementation of Knuth-Morris-Pratt String Match Algorithm added to repository.

--
(FEATURE - DONE) Commits as on 9 February 2015

--

Python+R script for DFT analysis of multimedia data has been added to

repository.

--
(FEATURE - DONE) Commits as on 13 February 2015

--
Initial commits for BigData Analytics (for mined astro datasets) using Hadoop 2.6.0 MapReduce:

- new folder bigdata_analytics has been added
- hadoop_mapreduce is subfolder of above
- A Hadoop Java MapReduce implementation to compute frequencies of astronomical entities in MinedRulesFromDatasets.earthquakes (obtained from clustering+LCS earlier in python-src) has been added with compiled bytecode and jar(MinedRulesFromDatasets_MapReducer.java)
- This jar was executed on a Single Node Hadoop Cluster as per the documentation at:
 - <http://hadoop.apache.org/docs/stable/hadoop-mapreduce-client/hadoop-mapreduce-client-core/MapReduceTutorial.html>
 - <http://hadoop.apache.org/docs/stable/hadoop-project-dist/hadoop-common/SingleCluster.html>
- The HDFS filesystem data is in hdfs_data - /user/root output with frequencies are in userroot_output and namenode and datanode logs are in hadooproot_logs(part_r_0000 has the frequencies)
- hdfs_data also has commandlines history and the console output logs for above.

(FEATURE - DONE) Commits as on 17 February 2015

Python implementations for LogLog and HyperLogLog cardinality estimation for streamed multiset data have been added to repository.

(FEATURE - DONE) Commits as on 18 February 2015

Python implementations for CountMinSketch(frequencies and heavy-hitters) and BloomFilter(membership) for Streaming Data have been added to repository.

(FEATURE - DONE) Commits as on 19,20 February 2015

Python clients for Apache Hive and HBase have been added to repository and invoked from Stream Abstract Generator script as 2-phase streamer for Streaming_<algorithm> scripts.
Hive,Pig,HBase HDFS and script data added to repository in java-src/bigdata_analytics.

-
(FEATURE - DONE) 140. Schematic for Apache Cassandra/Hive/HBase <=> AsFer Streaming_<algorithm> scripts interface

-

(\$) BigData Source(e.g MovieLens) => Populated in Apache Cassandra, Apache HiveQL CLI(CREATE TABLE..., LOAD DATA LOCAL INPATH...),HBase shell/python client(create 'stream_data','cf'...) (or) Apache PigLatin

(\$) Apache Hive or HBase SQL/NoSQL or Cassandra table => Read by Apache Hive or HBase or Cassandra python client => StreamAbstractGenerator => Iterable,Generator => Streaming_<algorithm> scripts

(FEATURE - DONE) Commits as on 25 February 2015

Added the Hive Storage client code for Streaming Abstract Generator `__iter__` overridden function. With this Streaming_<algorithm> scripts can instantiate this class which mimicks the streaming through iterable with three storages - HBase, File and Hive.

(DONE) 141. Classpaths required for Pig-to-Hive interface - for pig grunt shell in -x local mode

1. SLF4J jars
2. DataNucleus JDO, core and RDBMS jars (has to be version compatible) in pig/lib and hive/lib directories:
datanucleus-api-jdo-3.2.6.jar
datanucleus-core-3.2.10.jar
datanucleus-rdbms-3.2.9.jar
3. Derby client and server jars
4. Hive Shims jars
hive-shims-0.11.0.jar
5. All Hadoop core jars in /usr/local/hadoop/share/hadoop:
common hdfs httpfs kms mapreduce tools yarn
6. HADOOP_CONF_DIR(\$HADOOP_HOME/etc/hadoop) is also required in classpath.

(DONE) 142. Classpaths required for Pig-to-HBase interface

In addition to the jars above, following cloudera trace jars are required:
htrace-core-2.01.jar and htrace-1.45.jar

hadoop2_core_classpath.sh shell script in bigdata_analytics exports all the jars in (141) and (142).

(FEATURE - DONE) Commits as on 26 February 2015

Pig-HBase stream_data table creation and population related Pig scripts, HDFS data and screenshots have been added to repository.

(FEATURE - DONE) Commits as on 27 February 2015

Cassandra Python Client has been added to repository and Streaming_AbstractGenerator.py has been updated to invoke Cassandra in addition to Hive, HBase and File storage. Cassandra data have been added in bigdata_analytics/

143. (FEATURE - DONE) Storage Abstraction in AsFer - Architecture Diagram

Architecture diagram for Hive/Cassandra/HBase/File NoSQL and other storage abstraction implemented in python has been uploaded at:
<http://sourceforge.net/p/asfer/code/HEAD/tree/asfer-docs/BigDataStorageAbstractionInAsFer.jpg>

144. (FEATURE - DONE) Apache Spark and VIRGO Linux Kernel Analytics and Commits as on 6 March 2015

1. Prerequisite: Spark built with Hadoop 2.6.0 with maven commandline:
mvn -Pyarn -Phadoop-2.4 -Dhadoop.version=2.6.0 -DskipTests package

2. Spark Python RDD MapReduce Transformation script for parsing the most frequent source IP address from Uncomplicated FireWall logs in /var/log/kern.log has been added to repository. This parsed IP address can be set as a config in VIRGO kernel_analytics module (/etc/virgo_kernel_analytics.conf)

(FEATURE - DONE) Commits as on 10 March 2015

Spark python script updated for parsing /var/log/udev and logs in python-src/testlogs.
(spark-submit Commandline: bin/spark-submit /media/shrinivaasanka/0fc4d8a2-1c74-42b8-8099-9ef78d8c8ea2/home/kashrinivaasan/KrishnaiResearch_OpenSource/asfer-code/python-src/SparkKernelLogMapReduceParser.py 2> /media/shrinivaasanka/0fc4d8a2-1c74-42b8-8099-9ef78d8c8ea2/home/kashrinivaasan/KrishnaiResearch_OpenSource/asfer-code/python-src/testlogs/Spark_Logs.kernlogUFWandHUAWEIparser.10March2015)

145. (FEATURE - DONE) Commits as on 26 March 2015

New python script to fetch stock quotes by ticker symbol that can be used for Streaming_<algorithm> scripts has been added.

146. (FEATURE - DONE) Commits as on 2 April 2015

New Python script to get Twitter tweets stream data for a search query has been added.

147. (FEATURE - DONE) Related to Item 3 - Sequence Mining Implementation - Commits as on 3 April 2015

Python class that implements Apriori GSP algorithm for mining frequent subsequences in ordered sequences dataset has been added to repository. Though exponential, together with Longest Common Subsequence, Apriori GSP gives a near accurate subsequences - befitting trend of the dataset. For example the logs added to repository print the candidate support after 5 iterations (which can be modified) for asfer.anchors dataset thereby eliciting a pattern in astronomical objects.

148. An example Class Association Rule Learnt from Sequence Mining:

For length 6 most frequent subsequences in earthquake astronomical data from 1900 are: ('conjoinedplanets',frequency)

[('0', 313), ('4', 313), ('8', 313), ('3', 313), ('7', 313), ('2', 313), ('6', 313), ('1', 313), ('5', 313), ('9', 313), ('a', 313), ('14', 121), ('46', 66), ('56', 51), ('13', 51), ('34', 42), ('45', 36), ('9a', 33), ('79', 31), ('24', 30), ('16', 30), ('69', 29), ('7a', 29), ('146', 29), ('36', 26), ('12', 25), ('57', 24), ('68', 23), ('6a', 22), ('49', 22), ('47', 22), ('28', 21), ('58', 21), ('8a', 21), ('78', 21), ('134', 20), ('25', 20), ('35', 20), ('23', 18), ('29', 18), ('48', 18), ('27', 17), ('3a', 17), ('4a', 17), ('59', 16), ('37', 16), ('67', 15), ('5a', 14), ('17', 14), ('38', 13), ('346', 12), ('26', 11), ('124', 11), ('39', 11), ('15', 11), ('145', 11), ('14a', 10), ('456', 9), ('348', 8), ('2a', 8), ('247', 7), ('345', 7), ('1a', 7), ('469', 7), ('147', 7), ('356', 7), ('378', 6), ('156', 6), ('69a', 5), ('249', 5), ('179', 5), ('167', 5), ('358', 5), ('37a', 4), ('347', 4), ('279', 4), ('46a', 4), ('79a', 4), ('568', 4), ('169', 4), ('57a', 4), ('18', 4), ('1456', 4), ('679', 4), ('149', 4), ('359', 4), ('137', 3), ('135', 3), ('1469', 3), ('13a', 3), ('368', 3), ('1345', 3), ('123', 3), ('125', 3), ('268', 3), ('1346', 3), ('24a', 3),

```
( '1347', 3), ('56a', 3), ('1256', 3), ('1348', 3), ('59a', 3), ('457', 3),
('256', 3), ('1468', 3), ('468', 3), ('467', 3), ('1356', 3), ('168', 3),
('1378', 3), ('19', 3), ('234', 3), ('68a', 3), ('1247', 3), ('148', 3), ('136',
2), ('67a', 2), ('29a', 2), ('349', 2), ('167a', 2), ('38a', 2), ('123a', 2),
('78a', 2), ('245', 2), ('247a', 2), ('248', 2), ('4568', 2), ('1248', 2),
('258', 2), ('1247a', 2), ('359a', 2), ('158', 2), ('36a', 2), ('47a', 2),
('23a', 2), ('12a', 1), ('26a', 1), ('1349', 1), ('2349', 1), ('139', 1),
('1467', 1), ('349a', 1), ('678', 1), ('49a', 1), ('126', 1), ('127', 1),
('34a', 1), ('379', 1), ('3568', 1), ('23469', 1), ('2349a', 1), ('179a', 1),
('124a', 1), ('3479', 1), ('369', 1), ('27a', 1), ('39a', 1), ('458', 1),
('459', 1), ('578', 1), ('16a', 1), ('259', 1), ('257', 1), ('1678', 1),
('368a', 1), ('17a', 1), ('134a', 1), ('1458', 1), ('159', 1), ('3469', 1),
('2345', 1), ('2346', 1), ('13479', 1), ('479', 1), ('169a', 1), ('469a', 1)]
```

indices for planets:

- ```

* 0 - for unoccupied
* 1 - Sun
* 2 - Moon
* 3 - Mars
* 4 - Mercury
* 5 - Jupiter
* 6 - Venus
* 7 - Saturn
* 8 - Rahu
* 9 - Ketu
```

Some inferences can be made from above:

-----  
By choosing the creamy layer of items with support > 30 (out of 313 historic events) - ~10%:

```
[('14', 121), ('46', 66), ('56', 51), ('13', 51), ('34', 42), ('45', 36), ('9a',
33), ('79', 31), ('24', 30), ('16', 30)]
```

Above implies that:

-----  
Earthquakes occur most likely when, following happen - in descending order of frequencies:

- Sun+Mercury (very common)
- Mercury+Venus
- Jupiter+Venus
- Sun+Mars
- Mars+Mercury
- Mercury+Jupiter
- Ketu is in Ascendant
- Saturn+Ketu
- Moon+Mercury
- Sun+Venus

Machine Learnt pattern above strikingly coincides with some combinations in Brihat Samhita (Role of Mars, Nodes, and 2 heavy planets, Mercury-Venus duo's role in weather vagaries) and also shows some new astronomical patterns (Sun+Mars and Jupiter+Venus as major contributors). Above technique is purely astronomical and scientific with no assumptions on astrology.

Some recent major intensity earthquakes having above sequence mined astronomical conjunctions :

-----  
Sendai Earthquake - 11 March 2011 14:46 - Sun+Mars in Aquarius, Mercury+Jupiter in Pisces

Nepal Earthquake - 25 April 2015 11:56 - Sun+Mars+Mercury in Aries

Chile Earthquake - 16 September 2015 22:55 - Sun+Mars+Jupiter in Leo

All three have Sun+Mars coincidentally.

-----  
(FEATURE - DONE) Commits as on 5 April 2015  
-----

Textual translation of Class Association Rules added to SequenceMining.py with logs.

-----  
(FEATURE - DONE) Commits as on 13 April 2015  
-----

Python implementation of :

- Part-of-Speech tagging using Maximum Entropy Equation of Conditional Random Fields(CRF) and
- Viterbi path computation in HMM-CRF for Named Entity Recognition has been added to repository.

-----  
(FEATURE - DONE) Commits as on 15 April 2015  
-----

Named Entity Recognition Python script updated with:

- More PoS tags
- Expanded HMM Viterbi probabilities matrix
- Feature function with conditional probabilities on previously labelled word

-----  
(FEATURE - DONE) Commits as on 17 April 2015  
-----

Twitter Streaming python script updated with GetStreamFilter() generator object for streaming tweets data.

-----  
(FEATURE - DONE) 149. Commits as on 10 May 2015  
-----

A Graph Search NetworkX+Matplotlib Visualizer for WordNet has been implemented in python and has been added to repository. This is an initial code and more algorithms to mine relationships within a text data would be added using WordNet as ontology - with some similarities to WordNet definition subgraph obtained in <http://sourceforge.net/p/asfer/code/HEAD/tree/python-src/InterviewAlgorithm/InterviewAlgorithmWithIntrinsicMerit.py>. But in this script visualization is more important.

-----  
1230. (FEATURE - DONE) Commits as on 12 May 2015  
-----

WordNet Visualizer script has been updated to take and render the WordNet subgraph computed by Recursive Gloss Overlap algorithm in:

- <http://arxiv.org/abs/1006.4458>

-

[http://www.nist.gov/tac/publications/2010/participant.papers/CMI\\_IIT.proceedings.pdf](http://www.nist.gov/tac/publications/2010/participant.papers/CMI_IIT.proceedings.pdf)

- <https://sites.google.com/site/kuja27/PresentationTAC2010.pdf?attredirects=0>

-----  
(FEATURE - DONE) 150. Commits as on 14 May 2015  
-----

Updated WordNet Visualizer with:

- bidirectional edges
- graph datastructure changed to dictionary mapping a node to a list of nodes (multigraph)
- With these the connectivity has increased manifold as shown by gloss overlap
- the graph nodes are simply words or first element of lemma names of the synset
- more networkx drawing layout options have been added

Added code for:

- removing self-loops in the WordNet subgraph
- for computing core number of each node (maximum k such that node is part of k-core decomposition)

In the input example, nodes "India" and "China" have core numbers 15 and 13 respectively which readily classify the document to belong to class "India and China". Thus a new unsupervised classifier is obtained based on node degrees.

-----  
(FEATURE - DONE) Commits as on 16 May 2015  
-----

- added sorting the core numbers descending and printing the top 10% core numbers which are prospective classes the document could belong to. This is a new unsupervised text classification algorithm and is based on recursive gloss overlap algorithm in <http://arxiv.org/abs/1006.4458> and [http://www.nist.gov/tac/publications/2010/participant.papers/CMI\\_IIT.proceedings.pdf](http://www.nist.gov/tac/publications/2010/participant.papers/CMI_IIT.proceedings.pdf). A major feature of this algorithm is that it is more precise in finding the class of a document as intrinsic merit is computed by mapping a text to subgraph of wordnet, than conventional text classification and clustering based on distance metrics and training data.

-----  
(FEATURE - DONE) 151. Commits as on 18 May 2015  
-----

An interesting research was done on the wordnet subgraph obtained by Recursive Gloss Overlap algorithm:

- PageRank computation for the WordNet subgraph was added from NetworkX library. This is probably one of the first applications of PageRank to a graph other than web link graph.
- The objective was to find the most popular word in the subgraph obtained by the Random Walk Markov Model till it stabilized (PageRank)
- The resultant word with maximum pagerank remarkably coincides with the most probable class of the document and is almost similar in ranking to core numbers of nodes ranked descending.
- Some random blog text was used.
- Above was mentioned as a theoretical statement in 5.12 of [http://www.nist.gov/tac/publications/2010/participant.papers/CMI\\_IIT.proceedings.pdf](http://www.nist.gov/tac/publications/2010/participant.papers/CMI_IIT.proceedings.pdf)

-----  
(FEATURE - DONE) Commits as on 19 May 2015  
-----

A primitive text generation from the definition graph has been implemented by:

- computing the k-core of the graph above certain degree k so that the core is dense
- each edge is mapped to a relation - at present "has" , "is in" are the only 2 relations (more could be added based on hypernyms)
- Each edge is output as "X <relation> Y"
- Above gives a nucleus text extracted from the original document
- It implements the theory mentioned in: [https://sites.google.com/site/kuja27/DocumentSummarization\\_using\\_SpectralGraphTheory\\_RGOGraph\\_2014.pdf?attredirects=0&d=1](https://sites.google.com/site/kuja27/DocumentSummarization_using_SpectralGraphTheory_RGOGraph_2014.pdf?attredirects=0&d=1)

-----  
(FEATURE - DONE) Commits as on 20 May 2015  
-----

Hypernyms/Hyponyms based sentence construction added to WordNet Visualizer. The core-number and pagerank based classifier was tested with more inputs. The accuracy and relevance of the word node with topmost core number and pagerank for RGO graph looks to be better than the traditional supervised and

unsupervised classifiers/clusterers. The name of the class is inferred automatically without any training inputs or distance metrics based only on density of k-core subgraphs.

-----  
(FEATURE - DONE) Commits as on 21 May 2015  
-----

Updated the Visualizer to print the WordNet closure of hypernyms and hyponyms to generate a blown-up huge sentence. The closure() operator uncovers new vertices and edges in the definition graph (strict supergraph of RGO graph) and it is a mathematically generated sentence (similar to first order logic and functional programming compositionality) and mimicks an ideal human-thinking process (psychological process of evocation which is complete closure in human brain on a word utterance).

-----  
(FEATURE - DONE) 151. Commits as on 22,23,24 May 2015  
-----

Added code for computing recursive composition of lambda functions over the RGO graph relations(edges):

- For this the Depth First Search Tree of the graph is computed with NetworkX
- The lambda function is created for each edge
- Composition is done by concatenating a recursive parenthesisatation string of lambda expressions:
  - for each DFS edge:
    - Composed\_at\_tplus1 = Composed\_at\_t(lambda <edge>)
- DFS is chosen as it mimicks a function invocation stack
- Lambda composition closure on the Recursive Gloss Overlap graph has been rewritten to create a huge lambda composition string with parentheses. Also two new lambda function relations have been introduced - "subinstance of" and "superinstance of". These are at present most likely do not exist in WordNet parlance, because the Recursive Gloss Overlap algorithm grows a graph recursively from WordNet Synset definition tokenization.
- Thus a tree is built which is made into a graph by pruning duplicate edges and word vertices. WordNet graph does not have a depth. RGO algorithm adds one more dimension to WordNet by defining above relations. These are different from hyper/hypo-nyms. During recursive gloss overlap, if Y is in Synset definition of X, Y is "subinstance of" X and X is "superinstance of" Y.
- Thus RGO in a way adds new hierarchical recursive relationships to WordNet based on Synset definition.
- The lambda composition obtained above is a mathematical or lambda calculus representation of a text document - Natural Language reduced to Lambda calculus compositionality operator.

-----  
(FEATURE - DONE) Commits as on 26 May 2015  
-----

Added initial code for Social Network Analyzer for Twitter following to create a NetworkX graph and render it with Matplotlib.

-----  
(FEATURE - DONE) Commits as on 3 June 2015  
-----

Bonacich Power Centrality computation added to Twitter Social Network Analyzer using PageRank computation.

-----  
(FEATURE - DONE) Commits as on 4 June 2015  
-----

- Eigen Vector Centrality added to Twitter Social Network Analyzer.
  - File storage read replaced with Streaming\_AbstractGenerator in Streaming\_HyperLogLogCounter.py and Streaming\_LogLogCounter.py
-

(FEATURE - DONE) 152. Commits as on 7 June 2015

-----  
New Sentiment Analyzer script has been added to repository:

- This script adds to WordNet Visualizer with Sentiment analysis using SentiWordNet from NLTK corpus
- added a Simple Sentiment Analysis function that tokenizes the text and sums up positivity and negativity score
- A non-trivial Sentiment Analysis based on Recursive Gloss Overlap graph - selects top vertices with high core numbers and elicits the positivity and negativity of those vertex words.
- Above is intuitive as cores of the graph are nuclei centering the document and the sentiments of the vertices of those cores are important which decide the sentiment of the whole document.
- Analogy: Document is akin to an atom and the Recursive Gloss Overlap does a nuclear fission to extricate the inner structure of a document (subatomic particles are the vertices and forces are edges)
- Instead of core numbers, page\_rank can also be applied (It is intriguing to see that classes obtained from core\_numbers and page\_rank coincide to large extent) and it is not unusual to classify a document in more than one class (as it is more realistic).

Above script can be used for any text including social media and can be invoked as a utility from SocialNetworkAnalysis\_<brand> scripts.  
Microblogging tweets are more crisp and "emotionally precise" i.e. extempore - convey instantaneous sentiment (without much of a preparation)

-----  
(FEATURE - DONE) Commits as on 8 June 2015

-----  
Commits for:

- fixing errors due to NLTK API changes in lemma\_names(), definition() ... [ variables made into function calls ]
- Unicode errors
- Above were probably either due to Ubuntu upgrade to 15.04 which might have added some unicode dependencies and/or recent changes to NLTK 3.0 (SentimentAnalyzer.py already has been updated to reflect above)

-----  
(FEATURE - DONE) Commits as on 10 June 2015

-----  
Sentiment Analysis for twitter followers' tweets texts added to SocialNetworkAnalysis\_Twitter.py which invokes SentimentAnalyzer.py

-----  
(FEATURE - DONE) Commits as on 13 June 2015

-----  
Sentiment Analysis for tweet stream texts added to SocialNetworksAnalysis\_Twitter.py which invokes SentimentAnalyzer.py

-----  
153. (FEATURE - THEORY - Minimum Implementation DONE) Sentiment Analysis as lambda function composition of the Recursive Gloss Overlap WordNet subgraph

-----  
SentiWordNet based scoring of the tweets and texts have some false positives and negatives. But the lambda composition of the Recursive Gloss Overlap graph is done by depth-first-search - set of composition trees which overlap. If each edge is replaced by a function of sentiment scores of two vertex words, then lambda composition performed over the graph is a better representation of sentiment of the document. This is at present a conjecture only. An implementation of this has been added to SentimentAnalyzer.py by doing a Belief Propagation of a sentiment potential in the Recursive Gloss Overlap graph

considering it as a Bayesian graphical model.

-----  
Commits as on 15 June 2015  
-----

NeuronRain - (AsFer+USBmd+VIRGO+KingCobra) - version 15.6.15 release tagged  
Most of features and bugfixes are in AsFer and VIRGO  
-----

-----  
154. (FEATURE - DONE) Belief Propagation and RGO - Commits as on 20 June 2015  
-----

SentimentAnalyzer is updated with a belief propagation algorithm (Pearl) based  
Sentiment scoring by  
considering Recursive Gloss Overlap Definition Graph as graphical model and  
sentiwordnet score for  
edge vertices as the belief potential propagated in the bayesian network (RGO  
graph). Since the  
sentiment is a collective belief extracted from a text rather than on isolated  
words and the  
sentiwordnet scores are probabilities if normalized, Sentiment Analysis is  
reduced to Belief Propagation problem.  
The previous Belief Propagation function is invoked from  
SocialNetworkAnalysis\_<> code to Sentiment Analyze tweet stream.

-----  
155. Updates to  
[https://sites.google.com/site/kuja27/DocumentSummarization\\_using\\_SpectralGraphTheory\\_RGOGraph\\_2014.pdf?attredirects=0&d=1](https://sites.google.com/site/kuja27/DocumentSummarization_using_SpectralGraphTheory_RGOGraph_2014.pdf?attredirects=0&d=1)  
-----

-----  
Algorithms and features based on Recursive Gloss Overlap graph:

- 155.1 RGO visualizer
- 155.2 RGO based Sentiment Analyzer - Belief Propagation in RGO as a graphical model
- 155.3 Graph Search in text - map a text to wordnet relations by RGO graph growth - prints the graph edges which are relations hidden in a text
- 155.4 New unsupervised text classifier based in RGO core numbers and PageRank
- 155.5 Social Network Analyzer (Tweets analysis by RGO graph growth)
- 155.5 Lambda expression construction from the RGO graph
- 155.6 Sentence construction by composition of edges

-----  
156. (FEATURE - DONE) Commits as on 4 July 2015 - RGO sentiment analyzer on cynical tweets  
-----

Added query for a "elections" to stream tweets related to it. Few sample cynical tweets were sentiment-analyzed with  
RGO Belief Propagation SentimentAnalyzer that gives negative sentiment scores as expected whereas trivial SentiWordNet score summation  
gives a positive score wrongly.

-----  
157. (THEORY) Recursive Gloss Overlap graphical model as a Deep Learning algorithm that is an alternative to Perceptrons - for text data  
-----

Point 155 mentions the diverse applications of Recursive Gloss Overlap algorithm each of which touch upon multiple facets of Machine Learning (or) Deep Learning.



Instead of a multi-layered perceptron and a backpropagation on it which have the standard notation ( $W \cdot X + \text{bias}$ ) and have to be built, the wordnet RGO subgraph presents itself readily as a deep learning model without any additional need for perceptrons with additional advantage that complete graph theory results apply to it (core numbers, pageranks, connectivity etc.), making it a Graph-theoretical learning instead of statistical (for text data).

---

#### 158. (THEORY) Graph Discovery (or) Graph Guessing and EventNet (related to EventNet points 70-79)

---

EventNet mentioned previously is an infinite cause-effect graph of event vertices with partakers for each event (kind of a PetriNet yet different). A special case of interest is when only few subgraphs of a giant EventNet is available and it is often necessary to discover or guess the complete graph of causality with partakers. A familiar example is a crime scene investigation where:

- it is necessary to recreate the complete set of events and their causalities with partakers of a crime (reverse-engineering)
- but only few clues or none are available - which are akin to very sparse subgraphs of the crime scene EventNet
- Guessing (100-x)% of the graph from x% clue subgraphs can be conjectured to be an NP problem - because non-deterministic polynomially an EventNet path can be guessed. As a counting problem this is #P-complete (set of all paths among known subgraphs of an unknown supergraph). But there is only one accepting path (could be in Unambiguous Logspace if the number of states is in logspace)

Another example: set of blind men try to make out an object by touch.

---

#### 159. (THEORY) Pattern Grammar and Topological Homeomorphism of Writing Deformations

---

Grammar for patterns like texts, pictures similar to RE, CFG etc., for pattern recognition:

- example text grammar:  $\langle a \rangle := \langle o \rangle \langle \text{operator} \rangle \langle \rangle$
- example text grammar:  $\langle d \rangle := \langle o \rangle \langle \text{operator} \rangle \langle l \rangle$
- example text grammar:  $\langle v \rangle := \langle \backslash \rangle \langle \text{operator} \rangle \langle / \rangle$

Previous grammar is extensible to any topological shapes. For example, handwriting of 2 individuals are homeomorphic deformations.

References:

159.1 Topology and Graphics - [https://books.google.co.in/books?id=vCc8DQAAQBAJ&pg=PA263&lpg=PA263&dq=homeomorphism+and+handwriting&source=bl&ots=L\\_9kNgTcmF&sig=l-PfRL\\_jjcuF0L-2dJ5rukrc4CM&hl=en&sa=X&ved=0ahUKEwji8bDJ683QAhWBQY8KHQ3qAuEQ6AEIHzAA#v=onepage&q=homeomorphism%20and%20handwriting&f=false](https://books.google.co.in/books?id=vCc8DQAAQBAJ&pg=PA263&lpg=PA263&dq=homeomorphism+and+handwriting&source=bl&ots=L_9kNgTcmF&sig=l-PfRL_jjcuF0L-2dJ5rukrc4CM&hl=en&sa=X&ved=0ahUKEwji8bDJ683QAhWBQY8KHQ3qAuEQ6AEIHzAA#v=onepage&q=homeomorphism%20and%20handwriting&f=false)

---

#### 160. (THEORY) Cognitive Element

---

An element of a list or group is cognitive with respect to an operator if it "knows" about all or subset of other elements of list or group where "knowing" is subject to definition of operation as below:

- In list 2,3,5,7,17 - 17 knows about 2,3,5,7 in the sense that  $17 = 2+3+5+7$  with + operator
- In list "addon", "add", "on" - "addon" knows about "add" and "on" with concatenation operator
- In list "2,3,6,8,9,10,..." - 6 knows about 2 and 3, 10 knows about 2 and 5 with factorization as operator.

This might have an equivalent notion in algebra. Motivation for this is to abstract cognition as group operator. Essentially, this reduces to an equivalence relation graph where elements are related by a cognitive operator edge.

-----  
 161. (THEORY) Philosophical intuition for P(Good) summation - Continuation of (129) and other previous related points.  
 -----

-----  
 The apparent paradox in Perfect Voting can be reconciled as below to some extent:

- Voting is done in parallel in real-world elections and not serially
- Votes are counted in parallel - iterated integer addition in NC1 (<http://www.ccs.neu.edu/home/viola/classes/gems-08/lectures/le8.pdf>)
- Thus if RHS is just Circuit-Value Problem and not a Circuit-SAT then LHS getting equated to RHS is not unusual - both can be NC or P-Complete
- Separation of RHS from LHS happens only when the Circuit-SAT is required in RHS.
- P(Good) convergence in perfect voting implies that Voter SAT is not necessary if there is perfection (proving the obvious). This is true even though the PRG is imperfect that operates to choose on a perfect set.
- Parallelism implies NC circuits
- Above applies to infinite majority also (Mark Fey)
- RHS in worst-case can be EXP-Complete if the Majority+Voter SAT oracle circuit is of unrestricted depth and lot of variables are common across all voters. Proving EXP-completeness is ignored as it is evident from definition of DC circuits. Thus LHS has a P or NC algorithm to RHS EXP-Complete problem (something seemingly preposterous unless perfection is prohibited and voters do not have common variables in their boolean functions)

-----  
 162. (THEORY) Majority Voting Circuit with Boolean Function Oracles  
 -----

-----  
 If each voter has a boolean function to decide which has fanout > 1 gates instead of a formula, RHS Majority Voting becomes generic. Decision tree, Certificate, and other complexity measures automatically come into reckoning. Thus RHS circuit is an infinite (non-uniform) majority circuit with boolean function circuit DAGs or oracles.

References:

-----  
 162.1 <http://www.cs.cmu.edu/~odonnell/papers/barbados-aobf-lecture-notes.pdf>  
 162.1 [http://www.math.u-szeged.hu/~hajnal/research/papers/dec\\_surv.gz](http://www.math.u-szeged.hu/~hajnal/research/papers/dec_surv.gz)  
 -----

-----  
 163. (THEORY) Parity and Constant Depth - intuition (not a formal proof, might have errors)  
 -----

-----  
 Inductive Hypothesis:  
 -----

For depth d and n variables parity has  $n^k$  sized circuit.

For n+1 variables:

```

 XOR gate
 / \
n-variable (n+1)th variable
circuit
```

Each XOR gate is of atleast depth 2 or 3 with formula -  $(x \wedge \text{not } y) \vee (\text{not } x \wedge y)$ . Thus for each additional variable added depth gets added by atleast 2 contradicting the constant depth d in hypothesis above though size is polynomial.

-----  
164. (FEATURE - DONE) Commits as on 16 September 2015  
-----

-----  
cpp-src/cloud\_move - Implementation of Move Semantics for Cloud objects:  
-----

This expands on the usual move semantics in C++ and implements a Perfect Forwarding of objects over cloud. A move client invokes the T& rvalue reference move constructor to move (instead of copying) a local memory content to a remote machine in userspace. Functionality similar to this in kernelspace is required for transactional currency move in KingCobra - <http://sourceforge.net/p/kcobra/code-svn/HEAD/tree/KingCobraDesignNotes.txt> and <https://github.com/shrinivaasanka/kingcobra-github-code/blob/master/KingCobraDesignNotes.txt>. Though kernel with C++ code is not advised, kingcobra driver can make an upcall to userspace move client and server executables and perform currency move with .proto currency messages.

VIRGO kernel sockets code has been carried over and changed for userspace that uses traditional sockaddr\_in and htons.

C++ sockets reference code adapted for std::move - for use\_addrinfo clause:

- getaddrinfo linux man pages
- <http://codebase.eu/tutorial/linux-socket-programming-c/> (addrinfo instead of usual sockaddr\_in and htons)

Move semantics schematic:

```

 &
member fn temp arg lvalue <-----source data rvalue
 |
 &
 |
 V
client proxy destination lvalue<- /
 |
 |-----> cloud server destination
```

lvalue reference& does additional copy which is removed by rvalue reference&& to get the rvalue directly. Move client proxies the remote object and connects to Move server and the object is written over socket.

-----  
165. (FEATURE - DONE) Commits as on 18 September 2015  
-----

-----  
Cloud Perfect Forwarding - Google Protocol Buffer Currency :  
-----

Currency object has been implemented with Google Protocol Buffers - in cloud\_move/protocol\_buffers/ src\_dir and out\_dir directories. Currency has been defined in src\_dir/currency.proto file. Choice of Protocol Buffer over other

formats is due to:

- lack of JSON format language specific compilers
- XML is too complicated
- Protocol Buffers also have object serialization-to-text member functions in generated C++ classes.

Protocol Buffer compilation after change to currency object:  
protoc -I=src\_dir/ --cpp\_out=out\_dir/ src\_dir/currency.proto

-----  
166. (THEORY) Debug Analytics, Software Analytics, Automated Debugging - 24  
November 2019 - related to 65, 581  
-----

Debugging software is painful process with repetitive labour - For example kernel and device driver development has the following lifecycle:

1. Writing the kernel patch code for some deep kernel panics.
2. Kernel incremental or full build.
3. Test the patch.

(1), (2) and (3) are sometimes frustratingly repetitive. If the debugging is represented as a state machine automaton, the cycles in automaton are the time consuming phases. Thus Debug Analytics can be defined as the problem to find the most efficient debug state machine automaton without cycles or with least number of cycles and cycles of least length.

Delta debugging algorithm bisects the code changes between two successive commits recursively and isolates the code snippet causing the regression in unit testing. Example: If revision  $r+1$  has the patch set  $[p1, p2, p3, p4, p5]$  over revision  $r$ , delta debugging creates delta subsets  $[p1, p2]$ ,  $[p3]$ ,  $[p4, p5]$  and applies the deltas incrementally over  $r$  as paths in a binary search tree by `union()` and `minus()` primitives based on unit test pass or fail - for instance the path:

$r + [p1, p2]$  - pass,  $r + [p1, p2]$  union  $[p3]$  - pass,  $r + [p1, p2, p3]$  union  $[p4, p5]$  - fail

isolates  $[p4, p5]$  delta as point of failure. `minus()` primitive is applied to  $[p1, p2, p3, p4, p5]$  and  $[p4, p5]$  are segregated to fail state in bisection. Program state reachability graphs are obtained by a fixed point of variables as vertices and edges amongst them are deduced from pointer analysis. These program states between two consecutive revision states create a stream of Program state graphs which is a Streaming Common Subgraph Mining problem. Correlating the common subgraphs in the program state graph stream and corresponding unit test pass-fail binary stream for sequence of patch revisions yields insights into the regression causing state subgraph:

...  $\text{Graph}(r) - \text{Graph}(r + \text{delta})$  ...  
... Pass-Fail ...

Debug Analytics goes further beyond isolating the buggy code and asks for minimum state debug automaton if any which resolves the bug.

References:

166.1 Learning Finite State Machines -

<https://www.cs.upc.edu/~bballe/other/phdthesis.pdf>

166.2 Delta Debugging - Why Programs Fail -

<https://www.st.cs.uni-saarland.de/dd/> - Bisection in Git/SVN/Hg

166.3 Beautiful Code - [Oram-Wilson] - Chapter 28 - Beautiful Debugging by

Andreas Zeller - DDD and Eclipse plugins for Delta Debugging algorithm - Code

example 28.1 - computing common subgraphs between program state graphs - Fig

28.2 - Program State of GNU C Compiler - Example of regression between gdb 4.16 and gdb 4.17 for DDD

166.4 Program Verification debate - [DeMillo-Lipton-Perlis] - Proofs of Program correctness could not work - <https://blog.computationalcomplexity.org/2021/06/i-went-to-debate-about-program-verif.html>  
-----

-----  
167. (THEORY) Prestige based ranking and Condorcet Elections  
-----

Web Search Engine Rankings by prestige measures are n-tuples of rankings (for n candidate web pages where n could be few billions) which are not condorcet rankings. Arrow's Theorem for 3-candidate condorcet election allows a winner if and only if there is dictatorship. If there are m search engines each creating n-tuples of condorcet rankings (NAE tuples), then conjecturally there shouldn't be a voting rule or a meta search engine that circumvents circular rankings and produces a reconciled ranking of all NAE tuples from m search engines.

-----  
168. (FEATURE - DONE) Commits as on 20,21,22 October 2015  
-----

Initial code for LinkedIn crawl-scrape. Uses Python-linkedin from <https://github.com/ozgur/python-linkedin> with some additional parsing for url rewriting and wait for authurl input:  
- prints a linkedin url which is manually accessed through curl or browser  
- created redirect\_url with code is supplied to raw\_input "authurl:"  
- parses the authcode and logs-in to linkedin to retrieve profile data;  
get\_connections() creates a forbidden error

Logs for the above has been added to testlogs

-----  
169. (FEATURE - DONE) Commits as on 28 October 2015  
-----

Deep Learning Convolution Perceptron Python Implementation.

-----  
170. (FEATURE - DONE) Commits as on 29 October 2015, 1 November 2015  
-----

Deep Learning BackPropagation Multilayered Perceptron Python Implementation.

-----  
171. Commits as on 3 November 2015  
-----

DeepLearning BackPropagation implementation revamped with some hardcoded data removal.

-----  
172. (FEATURE - DONE) Hurricane Datasets Sequence Mining - Commits as on 4 November 2015  
-----

Miscellaneous code changes:

-----  
- Weight updates in each iteration are printed in DeepLearning\_BackPropagation.py  
- Changed maitreya\_textclient path for Maitreya's Dreams 7.0 text client; Updated to read HURDAT2 NOAA Hurricane Dataset (years 1851-2012) in MaitreyaToEnchoro.py  
- Maximum sequence length set to 7 for mining HURDAT2 asfer.enchoros.seqmining  
- New files asfer.enchoros.ascrelative.hurricanes, asfer.enchoros.zodiacal.hurricanes have been added which are created by MaitreyaToEnchoro.py  
- an example chartsummary for Maitreya's Dreams 7.0 has been updated  
- 2 logs for SequenceMining for HURDAT2 encoded datasets and Text Class Association Rules learnt by SequenceMining.py Apriori GSP have been added to testlogs/  
- Increased number of iterations in BackPropagation to 100000; logs for this with weights printed are added in testlogs/; shows a beautiful convergence and

error tapering ( $\sim 10^{-12}$ )

Sorted Candidate support for all subsequence lengths - gives an approximate pattern in dataset:

```
[('0', 1333), ('4', 1333), ('8', 1333), ('3', 1333), ('7', 1333), ('2', 1333),
('6', 1333), ('1', 1333), ('5', 1333), ('9', 1333), ('a', 1333), ('14', 613),
('46', 315), ('67', 261), ('78', 190), ('59', 189), ('49', 186), ('34', 180),
('57', 165), ('45', 161), ('13', 159), ('56', 158), ('58', 147), ('12', 134),
('23', 128), ('146', 116), ('36', 115), ('8a', 113), ('25', 108), ('9a', 106),
('346', 103), ('69', 99), ('26', 98), ('24', 95), ('134', 90), ('16', 83),
('6a', 81), ('35', 77), ('38', 75), ('149', 75), ('68', 73), ('467', 73), ('28',
71), ('2a', 71), ('569', 70), ('29', 66), ('367', 66), ('4a', 64), ('37', 59),
('567', 59), ('3a', 57), ('457', 56), ('27', 55), ('7a', 55), ('47', 51),
('145', 50), ('3467', 49), ('5a', 48), ('124', 44), ('79', 41), ('14a', 38),
('1346', 37), ('459', 36), ('17', 32), ('126', 29), ('246', 29), ('1459', 28),
('46a', 27), ('59a', 25), ('1a', 25), ('15', 25), ('156', 25), ('39', 24),
('345', 23), ('13467', 22), ('1345', 22), ('3457', 22), ('19', 22), ('13457',
22), ('1457', 21), ('234', 21), ('136', 20), ('1367', 20), ('2346', 18),
('3567', 18), ('356', 18), ('78a', 17), ('258', 16), ('259', 16), ('169', 16),
('135', 14), ('146a', 14), ('278', 14), ('67a', 13), ('49a', 13), ('469', 13),
('13567', 12), ('679', 12), ('178', 12), ('1356', 12), ('237', 12), ('3679',
12), ('4569', 11), ('678', 11), ('268', 11), ('456', 11), ('57a', 11), ('129',
10), ('28a', 10), ('238', 10), ('68a', 10), ('147', 10), ('23a', 10), ('459a',
10), ('267', 10), ('26a', 9), ('23467', 9), ('247', 9), ('16a', 9), ('256', 9),
('2569', 9), ('137', 8), ('249', 8), ('1246', 8), ('257', 8), ('36a', 8),
('168', 8), ('1567', 8), ('12a', 7), ('346a', 7), ('1459a', 7), ('245', 7),
('2459', 7), ('2367', 7), ('236', 7), ('1268', 6), ('567a', 6), ('25a', 6),
('1247', 6), ('79a', 5), ('47a', 5), ('149a', 4), ('29a', 4), ('1469', 4),
('126a', 4), ('19a', 4), ('2469', 4), ('37a', 3), ('679a', 3), ('24a', 3),
('367a', 3), ('268a', 3), ('1367a', 3), ('58a', 3), ('147a', 3), ('3679a', 3),
('357', 3), ('123', 2), ('69a', 2), ('246a', 2), ('56a', 2), ('1268a', 2),
('124a', 2), ('1234', 2), ('1249', 2), ('4569a', 2), ('1567a', 2), ('2459a', 2),
('1357', 2), ('168a', 2), ('35a', 2), ('569a', 2), ('1346a', 2), ('1246a', 2),
('349', 1), ('34a', 1), ('137a', 1), ('467a', 1), ('38a', 1), ('2345', 1),
('237a', 1), ('267a', 1), ('27a', 1), ('39a', 1), ('247a', 1), ('123467', 1),
('1247a', 1), ('134a', 1), ('13467a', 1), ('12345', 1), ('12346', 1), ('239',
1), ('3467a', 1)]
size of dataset = 1333
```

Sun , Mercury ,

Class Association Rule 12 mined from dataset: with frequencies: 23.6309077269 percentage

Mercury , Venus ,

Class Association Rule 13 mined from dataset: with frequencies: 19.5798949737 percentage

Venus , Saturn ,

Class Association Rule 14 mined from dataset: with frequencies: 14.2535633908 percentage

Saturn , Rahu ,

Class Association Rule 15 mined from dataset: with frequencies: 14.1785446362 percentage

Jupiter , Ketu ,

Class Association Rule 16 mined from dataset: with frequencies: 13.9534883721

```
percentage
=====
Mercury , Ketu ,
=====
Class Association Rule 17 mined from dataset: with frequencies: 13.503375844
percentage
=====
Mars , Mercury ,
=====
Class Association Rule 18 mined from dataset: with frequencies: 12.3780945236
percentage
=====
Jupiter , Saturn ,
=====
Class Association Rule 19 mined from dataset: with frequencies: 12.0780195049
percentage
=====
Mercury , Jupiter ,
=====
Class Association Rule 20 mined from dataset: with frequencies: 11.9279819955
percentage
=====
Sun , Mars ,
=====
Class Association Rule 21 mined from dataset: with frequencies: 11.8529632408
percentage
=====
Jupiter , Venus ,
=====
Class Association Rule 22 mined from dataset: with frequencies: 11.0277569392
percentage
=====
Jupiter , Rahu ,
=====
Class Association Rule 23 mined from dataset: with frequencies: 10.0525131283
percentage
=====
Sun , Moon ,
=====
Class Association Rule 24 mined from dataset: with frequencies: 9.60240060015
percentage
=====
Moon , Mars ,
=====
Class Association Rule 25 mined from dataset: with frequencies: 8.70217554389
percentage
=====
Sun , Mercury , Venus ,
=====
Class Association Rule 26 mined from dataset: with frequencies: 8.6271567892
percentage
=====
Mars , Venus ,
=====
Class Association Rule 27 mined from dataset: with frequencies: 8.47711927982
percentage
=====
Rahu , Ascendant ,
=====
Class Association Rule 28 mined from dataset: with frequencies: 8.10202550638
percentage
=====
Moon , Jupiter ,
=====
```

Class Association Rule 29 mined from dataset: with frequencies: 7.951987997  
percentage

=====  
Ketu , Ascendant ,  
=====

Class Association Rule 30 mined from dataset: with frequencies: 7.72693173293  
percentage

=====  
Mars , Mercury , Venus ,  
=====

Above are excerpts from the logs added to testlogs/ for Sequence mined from HURDAT2 dataset for hurricanes from 1851 to 2012. Similar to the sequence mining done for Earthquake datasets, some of the mined sequences above are strikingly similar to astronomical conjunctions already mentioned in few astrological classics (E.g Sun-Mercury-Venus - the legendary Sun flanked by Mercury and Venus, Mercury-Venus) and many others look quite new (e.g prominence of Venus-Saturn). Though these correlations can be dismissed as coincidental, these patterns are output automatically through a standard machine learning algorithm like Sequence Mining on astronomical datasets without any non-scientific assumptions whatsoever. Scientific corroboration of the above might require knowhow beyond purview of computer science - e.g Oceanography, Gravitational Effects on Tectonic Geology etc.,

=====  
173. (FEATURE - DONE) BigData Storage Backend Abstraction subsystem for AsFer -  
Commits as on 5 November 2015 :

-----  
-----  
- These are initial minimal commits for abstracting storage of ingested bigdata for AsFer Machine Learning code  
- A dependency injection implementation of database-provider-specific objects is added to repository.  
- Presently MySQLdb based MySQL backend has been implemented with decoupled configuration which are injected into Abstract Backend class to build an object graph. Python injector library based on Google Guice Dependency Injection Framework (<https://pythonhosted.org/injector/>) is used for this. Logs for a sample MySQL query has been added to testlogs/

Schematic Dependency Injected Object Graph:

-----  
Injector  
=====

```
|
|
V
MySQL_Configuration ---injects config ----> MySQL_DBBackend ----
injects connection ----> Abstract_DBBackend ---> exec_query()
/
\
|
xxx_Configuration ---injects config ----> xxx_DBBackend ---- injects
connection -----|
```

-----  
174. (FEATURE - DONE) AsFer C++ - Python Integration - Embedding Python in AsFer  
C++ - Commits as on 11 November 2015  
-----



-----  
 Python Embedding in C++ implementation has been added and invoked from asfer main entrypoint with a boolean flag. This at present is not based on boost::python and directly uses CPython API. Logs for this has been added in cpp-src/testlogs. With this all AsFer machine learning algorithms can be invoked from asfer.cpp main() through cmdline as: \$./asfer <python-script>.

Schematic Diagram:

```

 AsFer C++ -----> C Python Embedding -----> AsFer Python ----->
Machine Learning algorithms on Spark RDD datasets
 /\
V
 |
 |
 |-----<----- userspace upcall -----VIRGO
kernel analytics and other kernel modules

```

-----  
 175. (FEATURE - DONE) Config File Support for AsFer C++ and Python Machine Learning Algorithms - Commits as on 12 November 2015  
 -----

Config File support for asfer has been added. In asfer.cpp main(), read\_asfer\_config() is invoked which reads config in asfer.conf and executes the enabled AsFer algorithms in C++ and Embedded Python. Config key-values are stored in a map.

-----  
 176. (THEORY) Isomorphism of two Document Definition Graphs  
 -----

-----  
<http://arxiv.org/abs/1006.4458> and  
[http://www.nist.gov/tac/publications/2010/participant.papers/CMI\\_IIT.proceedings.pdf](http://www.nist.gov/tac/publications/2010/participant.papers/CMI_IIT.proceedings.pdf) describe the Recursive Gloss Overlap Algorithm to construct a Definition Graph from a text document with WordNet or any other Ontology. If Definition Graphs extracted from two documents are Isomorphic, then it can be deduced that there is an intrinsic structural similarity between the two texts ignoring grammatical variations, though vertices differ in their labelling.  
 [SubExponentialTIME algorithm for GI - Lazlo Babai -  
<http://people.cs.uchicago.edu/~laci/update.html>]  
 -----

-----  
 177. Commits as on 13 November 2015  
 -----

- Corrections to Convolution Map Neuron computation with per-coordinate weight added
- Removed hardcoded convolution stride and pooling width in the class
- testlogs following input bitmap features have been added with the output of 5 neurons in final layer:
  - Without Zero inscribed
  - With Zero inscribed in bitmap as 1s
  - With Bigger Zero inscribed in bitmap as 1s
  - With Biggest Zero inscribed in bitmap as 1s

The variation of final neural outputs can be gleaned as the size of the pattern increases from none to biggest.  
 The threshold has to be set to neural output without patterns. Anything above it shows a pattern.

- Added a config variable for invoking cloud perfect forwarding binaries in KingCobra in asfer.conf

- config\_map updated in asfer.cpp for enableCloudPerfectForwarding config variable

---

178. (THEORY) Approximate Machine Translation with Recursive Gloss Overlap Definition Graph

---

For natural language X (=English) an RGO graph can be constructed (based on algorithms in <http://arxiv.org/abs/1006.4458> and [http://www.nist.gov/tac/publications/2010/participant.papers/CMI\\_IIT.proceedings.pdf](http://www.nist.gov/tac/publications/2010/participant.papers/CMI_IIT.proceedings.pdf)). This definition graph is a subgraph of WordNet-English. Each vertex is a word from English dictionary. New RGO graph for language Y is constructed from RGO(X) by mapping each vertex in RGO(X) to corresponding word in language Y. RGO(X) and RGO(Y) are isomorphic graphs. Sentences in language Y can be constructed with lamda composition closure on the RGO(Y) graph implemented already. This is an approximation for machine translation between two natural languages. I

n the converse direction, text graphs of 2 texts in 2 different natural languages can be verified for Graph Isomorphism. Isomorphic text graphs in two natural languages prima facie indicate the texts are similarly organized and have same meaning.

---

179. (FEATURE - DONE) Web Spider Implementation with Scrapy Framework - Commits as on 16 November 2015

---

Initial commits for a Web Spider - Crawl and Scrape - done with Scrapy framework. Presently it crawls Google News for a query and scrapes the search results to output a list of lines or a digest of the news link texts. This output file can be used for Sentiment Analysis with Recursive Gloss Overlap already implemented. Complete Scrapy project hierarchy is being added to the repository with spider in WebSpider.py and crawled items in items.py

---

180. (FEATURE - DONE) Sentiment Analyzer Implementation for Spidered Texts - Commits as on 16 November 2015

---

Sentiment Analyzer implementation for Crawled-Scraped Google News Search result texts with testlogs and screenshots of the RGO graph has been added. This has been made a specialized analyzer for spidered texts different from twitter analyzer.

---

181. Commits as on 17 November 2015

---

Requirements.txt for package dependencies have been added to asfer-docs/. WebSpider Crawl-Scraped URLs descriptions are inserted into MySQL table (asfer\_webspider) by importing backend/AbstractDBBackend.py MySQL implementation. Logs for this Scrapy crawl has been added to webspider/testlogs. WebSpider.py parse() has been updated with MySQL\_DBBackend execute\_query()s. \_\_init\_\_.py have been added for directory-as-package imports.

---

182. Commits as on 19 November 2015

- Added more stop words in spidered text and commented text generation in SocialNetworkAnalysis\_WebSpider.py
- logs and screenshots for this has been added to testlogs/
- crawl urls in WebSpider.py has been updated
- Added more edges in definition graph by enumerating all the lemma names of a keyword in previous iteration. This makes the graph dense and probability of a node having more k-core number increases and classification is more accurate.
- logs and screenshots for updated web spidered news texts of two topics "Theoretical Computer Science" and "Chennai" have been added

183. Commits as on 20 November 2015

- Updated Spidered text for Sentiment Analysis
- Changed the Sentiment Analysis scoring belief potential propagation algorithm:
  - Two ways of scoring have been added - one is based on DFS tree of k-core subgraph of the larger wordnet subgraph and the other is based on top core numbered vertices of the wordnet subgraph
  - Sentiment thus is computed only for the core of the graph which is more relevant to the crux or class of the document and less pertinent vertices are ignored.
  - the fraction score is multiplied by a heuristic factor to circumvent floating points

184. Commits as on 23 November 2015

- Updated SentimentAnalyzer.py and SocialNetworkAnalysis\_Twitter.py scripts with core number and k-core DFS belief potential propagation similar to SocialNetworkAnalysis\_WebSpider.py.
  - logs and screenshots for twitter followers graph and tweet RGO graph Sentiment Analysis have been added.
  - Example tweet is correctly automatically classified into "Education" class based on top core number of the vertices and top PageRank. Again this is an intriguing instance where Top core numbered vertices coincide with Top PageRank vertices which is probably self-evident from the fact that PageRank is a Markov Model Converging Random Walk and PageRank matrix multiplication is influenced by high weightage vertices (with lot of incoming links)
- Sentiment Analysis of the tweet:
- K-Core DFS belief\_propagated\_posscore: 244.140625
  - K-Core DFS belief\_propagated\_negscore: 1.0
  - Core Number belief\_propagated\_posscore: 419095.158577
  - Core Number belief\_propagated\_negscore: 22888.1835938
  - Above Sentiment Analysis rates the tweet with positive tonality.

185. Commits as on 25 November 2015

- New WordNetPath.py file has been added to compute the path in a WordNet graph between two words
- WordNetSearchAndVisualizer.py text generation code has been updated for importing and invoking path\_between() function in WordNetPath.py by which set of sentences are created from the RGO WordNet subgraph. This path is obtained from common hypernyms for two word vertices for each of the edges in

RG0 WordNet subgraph. RG0 graph is a WordNet+ graph as it adds a new relation "is in definition of" to the existing WordNet that enhances WordNet relations. Each edge in RG0 graph is made a hyperedge due to this hypernym path finding.

- logs and screenshots have been added for above

The text generated for the hypernym paths in WordNet subgraph in testlogs/ is quite primitive and sentences are connected with " is related to " phrase. More natural-looking sentences can be created with randomly chosen phrase connectives and random sentence lengths.

-----  
-----  
186. Commits as on 4 December 2015  
-----

-----  
All the Streaming\_<>.py Streaming Algorithm implementations have been updated with:

- hashlib ripemd160 hash MD algorithm for hash functions and return hexdigest()
- USBWWAN byte stream data from USBmd print\_buffer() logs has been added as a Data Storage and Data Source
- logs for the above have been added to testlogs/
- Streaming Abstract Generator has been updated with USB stream data iterable and parametrized for data source and storage
- Some corrections to the scripts

-----  
-----  
187. Commits as on 7 December 2015  
-----

- USB stream file storage name updated in Streaming\_AbstractGenerator
  - Corrections to CountMinSketch - hashing updated to include rows (now the element frequencies are estimated almost exactly)
  - logs for above updated to CountMinSketch
- Added Cardinality estimation with LogLog and HyperLogLog counters for USB stream datasets
- HyperLogLog estimation: ~110 elements
  - LogLog estimation: ~140 elements

-----  
-----  
188. Commits as on 8 December 2015  
-----

- Updated the Streaming LogLogCounter and HyperLogLogCounter scripts to accept StreamData.txt dataset from Abstract Generator and added a Spark MapReducer script for Streaming Data sets for comparison of exact data with Streaming\_<algorithm>.py estimations.
- Added logs for the Counters and Spark MapReducer script on the StreamData.txt
- LogLog estimation: ~133
- HyperLogLog estimation: ~106
- Exact cardinality: 104

-----  
-----  
189. (FEATURE - DONE) Commits as on 9 December 2015  
-----

- New python implementation for CountMeanMinSketch Streaming Data Frequency Estimation has been added which is an improved version of CountMinSketch that computes median of average of estimator rows in sketch
- Corrections to CountMinSketch hashing algorithms and Sketch width-depth as per the error bounds has been made

- Spark MapReducer prints the number of elements in the stream data set
- Logs for the above have been added to testlogs

-----  
 190. (FEATURE - DONE) Commits as on 11 December 2015  
 -----

-----  
 Dependency Injection code commits for MongoDB backend - With this MongoDB is also a storage backend for AsFer algorithms similar to MySQL:

- Abstract\_DBBackend.py has been updated for both MySQL and MongoDB injections
- MongoDB configuration and backend connect/query code has been added. Backend is either populated by Robomongo or pymongo reading from the Streaming Abstract Generator iterable framework.
- With this AsFer supports both SQL(MySQL) and NoSQL(file,hive,hbase,cassandra backends in Streaming Abstract Generator).
- log with a simple NoSQL table with StreamingData.txt and USBWWAN data has been added to testlogs/.
- MongoDB configuration has a database(asfer-database) and a collection(asfer-collection).
- MongoDB\_DBBackend @provides pymongo.collection.Collection which is @inject-ed to Abstract\_DBBackend
- Abstract\_DBBackend changes have been reflected in Scrapy Web Spider - backend added as argument in execute\_query()
- Abstract\_DBBackend.py has a subtle problem:
  - Multiple @inject(s) are not supported in Python Injector
  - only the innermost @inject works and outer @inject throws a \_\_init\_\_ argument errors in webspider/
  - Conditional @inject depending on backend is required but at present switching the order of @inject(s) circumvents this
- most recent scrapy crawl logs for this have been added to webspider/testlogs

-----  
 191. (THEORY) An update and additions to runtime analysis of Recursive Gloss Overlap Algorithm in TAC 2010  
 ([http://www.nist.gov/tac/publications/2010/participant.papers/CMI\\_IIT.proceedings.pdf](http://www.nist.gov/tac/publications/2010/participant.papers/CMI_IIT.proceedings.pdf))  
 -----

-----  
 Analysis of runtime in the link above is too cryptic. An updated analysis of steps are given here:

- Nodes at topmost level are keywords in document. For each subsequent recursion step following analysis is per keyword.
- Nodes at level i-1 are computed (base case) :  $x^{(i-1)}$  where x is average size of gloss definition
- Naive pairwise comparison of overlap is done at level i-1 which makes it  $x^{2(i-1)}$
- Tree isomorphism algorithms can be optionally applied to reduce number of nodes getting recomputed. There are polytime algorithms for subtree isomorphisms ([www.cs.bgu.ac.il/~dekelts/publications/subtree.pdf](http://www.cs.bgu.ac.il/~dekelts/publications/subtree.pdf))
- Nodes at level i-1 are reduced by  $\text{Overlap}(i-1) : x^{(i-1)} - \text{Overlap}(i-1)$
- Maximum number Nodes at level i - are from gloss expansion of those at i-1 :  $(x^{(i-1)} - \text{Overlap}(i-1)) * x$
- Thus total time at level i is:  
 $\text{Time\_for\_pairwise\_comparison\_to\_find\_gloss\_verlap} + \text{Time\_for\_removing\_isomorphic\_nodes}$   
 $T(i) = \sigma([x^{(i-1)} - \text{Overlap}(i-1)]^2 + \text{subtree\_isomorphism}(i))$
- Above is naively upperbounded to  $O(x^{(2d)})$  [as subtree isomorphism is polynomial in supertree and subtree vertices and is only an optimization step that can be ignored]. For W keywords in the document time bound is  $O(W * x^{(2d)})$ .
- If number of vertices in RGO multipartite graph (ignoring isomorphism) constructed above is  $V=O(x^{(d)})$ , runtime is  $O(W * V^2)$  which is

far less than  $O(E \cdot V^2)$  mentioned in TAC 2010 link because number of keywords in toplevel are less than number of edges created during recursion which depend on  $x$  and exponentially on  $d$ . For example after first recursion completion, number of edges are  $W \cdot x$ .

- On a related note runtime for intrinsic merit ranking of the RGO wordnet subgraph can not be equated per-se to ranking from prestige-based search engines as RGO is objective graph-theoretic ranking (does not require massive bot-crawling, indexing and link graph construction) and PageRank is subjective prestige based ranking (depends on crawling, indexing and time needed for link graph construction). Standard publicly available PageRank iteratively computes random walk matrix multiplication for link graphs for billions of nodes on WWW and this runtime has to be apportioned per-node. Time and Space for crawling and indexing have also to be accounted for per-node. Naive bound for PageRank per node is

$O(\text{time\_for\_iterative\_matrix\_multiplication\_till\_convergence}/\text{number\_of\_nodes})$ .

Matrix multiplication is  $O(n^\omega)$  where  $\omega \sim 2.3$ . Thus pagerank bound per node is  $O((n^\omega \cdot \text{iterations})/n)$  assuming serial PageRank computation.

Parallel Distributed Versions of PageRank depend on network size and scalable.

- Parallel Recursive Gloss Overlap graph construction on a cloud could reduce the runtime to  $O(W \cdot V^2/c)$  where  $c$  is size of the cloud.

-----  
192. (FEATURE - DONE) Commits as on 14 December 2015  
-----

- New Interview Algorithm script with NetworkX+Matplotlib rendering and takes as input a randomly crawled HTML webpage (uses beautiful soup to rip off script and style tags and write only text in the HTML page) has been added

- Above script also computes the graph theoretic connectivity of the RGO wordnet subgraph based on Menger's theorem - prints number of nodes required to disconnect the graph or equivalently number of node independent paths

- logs and screenshots for the above have been added

- WebSpider.py has been updated to crawl based on a crawling target parameter - Either a streaming website (twitter, streamed news etc.,) or a HTML webpage

-----  
193. (FEATURE - DONE) RGO graph complexity measures for intrinsic merit of a text document - Commits as on 15 December 2015  
-----

- Interview Algorithm Crawl-Visual script has been updated with a DOT graph file writing which creates a .dot file for the RGO graph constructed

- Also variety of connectivity and graph complexity measures have been added

- Importantly a new Tree Width computing script has been added. NetworkX does not have API for tree width, hence a naive script that iterates through all subgraphs and finds intersecting subgraphs to connect them and form a junction tree, has been written. This is a costly measure compared to intrinsic merit which depends only on graph edges, vertices and depth of recursive gloss overlap. Tree decomposition of graph is NP-hard.

-----  
194. Commits as on 16 December 2015  
-----

- TreeWidth implementation has been corrected to take as input set of edges of the RGO graph

- TreeWidth for set of subgraphs less than an input parameter size is computed as TreeWidth computation is exponential in graph size

and there are MemoryErrors in python for huge set of all subgraphs. For example

even a small graph with 10 nodes gives rise to 1024 possible subgraphs

- Spidered text has been updated to create a small RGO graph
- Logs and screenshots have been added
- Each subgraph is hashed to create a unique string for each subgraph
- Treewidth is printed by finding maximum set in junction tree

-----  
195. (THEORY) WordNet, Evocation, Neural networks, Recursive Gloss Overlap and Circuit Complexity  
-----

WordNet and Evocation WordNet are machine learning models based on findings from psychological experiments. Are WordNet and Neural networks related? Evocation WordNet which is network of words based on how evocative a word is of another word readily translates to a neural network.

This is because a machine learning abstraction of neuron - perceptron - takes weights, inputs and biases and if the linear program of these breach a threshold, output is activated. Evocative WordNet can be formulated as a neuron with input word as one end of an edge and the output word as the other end - a word evokes another word. Each edge of an Evocation WordNet or even a WordNet is a single input neuron and WordNet is one giant multilayered perceptron neural network. Since Threshold circuits or TC circuit complexity class are theoretical equivalents of a machine learning neuron model (threshold gate outputs 1 if more than  $k$  of inputs are 1 and thus an activation function of a neuron), WordNet is hence a gigantic non-uniform TC circuit of Threshold gates. Further  $TC_k$  is in  $NC(k+1)$ . This implies that all problems depending on WordNet are inherently parallelizable in theory and Recursive Gloss Overlap algorithm that depends on WordNet subgraph construction in

[http://www.nist.gov/tac/publications/2010/participant.papers/CMI\\_IIT.proceedings.pdf](http://www.nist.gov/tac/publications/2010/participant.papers/CMI_IIT.proceedings.pdf) and updates to it in (191) above are non-uniformly parallelizable.

-----  
196. (FEATURE - DONE) Mined Rule Search in Astronomical Data - Commits as on 17 December 2015  
-----

- New Mined Class Association Rule Search script has been added. This script searches the astronomical data with parsed Maitreya Text client data with date, time and longitude-latitude queries.
- Where this is useful is after mining the astronomical data with SequenceMining, there is a necessity to search when a particular mined rule occurs. This is an experimental, non-conventional automated weather prediction (but not necessarily unscientific as it requires expertise beyond computer science to establish veracity).
- Logs for this has been added in testlogs/ and chartsummary.rulesearch

-----  
197. Commits as on 18 December 2015  
-----

- Interview Algorithm crawl-visual script changed for treewidth invocation
- Spidered text changed
- Rule Search script corrected to use datetime objects
- Rule Search script corrected to use timedelta for incrementing date and time
- logs and screenshots for above
- Junction Tree for RGO graph - logs and screenshots

-----  
198. (THEORY) Star Complexity of Graphs - Complement Function circuit and

## Unsupervised Classification with RGO graph

Star complexity of a graph defined in [Stasys Jukna] -

<http://www.thi.informatik.uni-frankfurt.de/~jukna/ftp/graph-compl.pdf>

is the minimum number of union and intersection operations of star subgraphs required to create the larger graph which is strikingly relevant to the necessity of quantitative intrinsic merit computation in Recursive Gloss Overlap algorithm

[[http://www.nist.gov/tac/publications/2010/participant.papers/CMI\\_IIT.proceedings.pdf](http://www.nist.gov/tac/publications/2010/participant.papers/CMI_IIT.proceedings.pdf)]. Each star subgraph of the definition graph is an unsupervised automatically found class a text belongs to. Apart from this star complexity of a boolean circuit graph for Complement Function

<http://arxiv.org/pdf/1106.4102v1.pdf> and in particular for Prime complement special case should have direct relationship conjecturally to pattern in primes because boolean formula for the graph depends on prime bits.

199. (FEATURE - DONE) Tornado Webserver, REST API and GUI for NeuronRain -  
Commits as on 22 December 2015

Commits for NeuronRain WebServer-RESTfulAPI-GUI based on tornado in  
python-src/webserver\_rest\_ui/:

- NeuronRain entrypoint based on tornado that reads a template and implements GET and POST methods
- templates/ contains renderable html templates
- testlogs/ has neuronrain GUI logs
- RESTful API entrypoint <host:33333>/neuronrain

200. (FEATURE - DONE) NeuronRain as SaaS and PaaS - for commits above in (199)

RESTful and python tornado based Graphical User Interface entrypoint that reads from various html templates and passes on incoming concurrent requests to NeuronRain subsystems - AsFer, VIRGO, KingCobra, USBmd and Acadpdrfts - has bee added. Presently implements simplest possible POST form without too much rendering (might require flask, twisted, jinja2 etc.,) for AsFer algorithms execution. This exposes a RESTful API for commandline clients like cURL. For example a cURL POST is done to NeuronRain as:

cURL POST: curl -H "Content-Type: text/plain" -X POST -d

'{"component": "AsFer", "script": "<script\_name>", "arguments": "<args>"}'

<http://localhost:33333/neuronrain> where REST url is <host:port>/neuronrain.

Otherwise REST clients such as Advanced RESTful Client browser app can be used.

With this NeuronRain is Software-As-A-Service (SaaS) Platform deployable on VIRGO linux kernel cloud, cloud Oses and containers like Docker.

More so, it is Platform-As-A-Service (PaaS) when run on a VIRGO cloud.

201. (FEATURE - DONE) Apache Spark MapReduce Parallel Computation of Interview Algorithm Recursive Gloss Overlap Graph Construction  
- Commits as on 24 December 2015

- 2 python files for Spark MapReduce of Recursive Gloss Overlap graph construction has been added to repository
- These two implement Interview Algorithm Recursive Gloss Overlap graph construction and Map-Reduce functions that parallellize each recursion step computing the gloss tokens from previous recursion level.



This is the most important part of the algorithm which consumes lot of time in serial version along with overlap computation. Apache Spark has been recently gaining importance over its plain Hadoop counterpart and is many times faster than Hadoop in benchmarks.

- In this implementation, Resilient Distributed Dataset is the set of tokens in each recursion level and is parallelly computable in a huge Spark cluster.
- For example if Spark cluster has 10000 nodes, and each level of recursion produces X number of gloss tokens for graph vertices, time complexity in Spark is  $O(X/10000)$  where as serial version is  $O(X)$  with negligible network overhead. Spark has in-memory datasets which minimizes network latency because of disk access.
- There were lot of implementation issues to make the parallelism. Map and Reduce functions use namedtuples to return data. With more than one field in namedtuple, there are internal pickling issues in Py4J - Python4Java which PySpark internally invokes to get streamed socket bytes from Java side of the object wrapped as an iterable. This prevents returning multiple values - for example Synsets - in Map-Reduce functions.
- So only tokens at a level are map-reduced and returned while the prevlevelsynsets (required for adding edges across vertices) are "pickled" with a proprietary asfer\_pickle\_load() and asfer\_pickle\_dump() functions that circumvents the python and java vagaries in pickling.
- With proprietary pickling and Map-Reduce functions, Recursive Gloss Overlap graph has been constructed in parallel. Screenshots for this has been added in testlogs.
- Proprietary pickling is done to a text file which is also added to repository. This file is truncated at the end of each recursion.
- Subtlety here is that maximum number of tokens at a recursion level  $t = \text{number\_of\_tokens\_at\_level}(t-1) * \text{maximum\_size\_of\_gloss\_per\_word}(s)$  which grows as  $\text{series} = \text{number\_of\_words} * (1 + s + s^2 + s^3 + \dots + s^{t\_max})$ . Size of a document - number of words - can be upperbounded by a constant (d) due to finiteness of average text documents in realworld ignoring special cases of huge webpages with PDF/other.
- If size of the Spark cluster is  $O(f(d)*s^{t\_max})$ , each recursion step is of time  $O(d*s^{t\_max}/f(d)*s^{t\_max})=O(d/f(d))$  and total time for all levels is  $O(d*t\_max/f(d))$  which is ranking time per text document. This bound neglects optimization from overlaps and isomorphic nodes removal and is worst case upperbound. For ranking n documents this time bound becomes  $O(n*d*t\_max/f(d))$ . For constant  $t\_max$  this bound is  $O(n*d/f(d))$  - and thus linearly scalable.
- Maximum size of gloss per word (s) is also an upper-boundable constant. With constant d and  $t\_max$ , size of cluster  $O(f(d)*s^{t\_max})$  is constant too independent of number of documents.
- Example: For set of 1000 word documents with  $f(d)=\log(d)$ , max gloss size 5 and recursion depth 2, size of cluster is  $O(\log(1000)*25) \sim 250$  nodes with runtime for ranking n documents =  $O(n*1000*t\_max/\log(1000))=O(n*100*t\_max)$  which is  $O(n)$  for constant  $t\_max$ .
- Above is just an estimate of approximate speedup achievable in Spark cluster. Ideally runtime in Spark cloud should be on the lines of analysis in (191) -  $O(n*d*s^2(t\_max)/f(d)*s^{t\_max}) = O(n*d*s^{t\_max}/f(d))$ .
- Thus runtime upperbound in worst case is  $O(n*d*s^{t\_max}/f(d))$  for cluster size  $O(f(d)*s^{t\_max})$ .
- If cluster autoscales based on number of documents also, size is a function of n and hence previous size bound is changed to  $O(g(n)*f(d)*s^{t\_max})$  and corresponding time bound =  $O(n*d*s^2(t\_max)/(f(d)*s^{t\_max}*g(n))) = O(n*d*s^{t\_max}/(f(d)*g(n)))$

---

## 202. (THEORY) Recursive Gloss Overlap, Cognitive and PsychoLinguistics and Language Comprehension

---

Recursive Gloss Overlap algorithm constructs a graph from text documents. Presently WordNet is probably the only solution available to

get relations across words in a document. But the algorithm does not assume WordNet alone. Any future available algorithms to create relational graphs from texts should be able to take the place of WordNet. Evocation WordNet (<http://wordnet.cs.princeton.edu/downloads/evocation.zip>) is better than WordNet as it closely resembles a neural network model of a word evocative of the other word and has stronger psychological motivation. There have been efforts to combine FrameNet, VerbNet and WordNet into one graph. Merit of a document is independent of grammar and language in which it is written. For example a text in English and French with grammatical errors delving on the same subject are equivalently treated by this algorithm as language is just a pointer to latent information buried in a document. Process of Language Comprehension is a field of study in Cognitive and Psychological Linguistics. Problem with prestige based subjective rankings is that same document might get varied reviews from multiple sources and consensus with majority voting is required. This is somewhat contrary to commonsense because it assumes majority decision is correct 100% (this is exactly the problem analyzed by P(Good) binomial summation and majority voting circuits elsewhere in this document). In complexity parlance prestige rankings are in BP\* classes. Objective rankings are also in BP\* classes because of dependency on the framework like WordNet to extract relationships without errors, but less costlier than prestige rankings - major cost saving being lack of dependence on WWW link graph crawling to rank a document.

Intuition for Recursive Gloss Overlap for weighing natural language texts is from computational linguistics, Eye-Movement tracking and Circuit of the Mind [Leslie Valiant]. Human process of comprehending language, recursion as an inherent trait of human faculty and evolution of language from primates to human is described in <http://www.sciencemag.org/content/298/5598/1569>, [www.ncbi.nlm.nih.gov/pubmed/12446899](http://www.ncbi.nlm.nih.gov/pubmed/12446899) and [http://ling.umd.edu/~colin/courses/honr218l\\_2007/honr218l\\_presentation7.ppt](http://ling.umd.edu/~colin/courses/honr218l_2007/honr218l_presentation7.ppt) by [Hauser, NoamChomsky and Fitch] with an example part-of-speech recursive tree of a sentence. For example, a human reader's eye usually scans each sentence in a text document word by word left-to-right, concatenating the meanings of the words read so far. Usually such a reader assumes grammatical correctness (any grammatical anomaly raises his eyebrows) and only accrues the keyword meanings and tries to connect them through a meaningful path between words by thinking deep into meaning of each word. This is exactly simulated in Recursive Gloss Overlap graph where gloss overlaps connect the words recursively. Fast readers have reasonably high eye-movement, sometimes randomly. The varied degree of this ability to form an accurate connected visualization of a text probably differentiates people's intellectual wherewithal to draw inferences. From theory of computation perspective, recursive gloss overlap constructs a disambiguated Context Sensitive graph from Natural language text a superset of context free grammars. But natural languages are suspected to be subset of larger classes of context sensitive languages accepted by Linear Bounded Automata. Thus reverse engineering a text from the recursive gloss overlap graph may yield a language larger than natural languages. Information loss due to text-to-graph translation should only be grammatical ideally (e.g Parts of Speech, connectives etc.,) because for comparing two documents for information quality, grammar shouldn't be a factor unless there are fringe cases where missing grammar might change the meaning of a document. Corrections for pre-existing grammatical errors are not responsibilities of this algorithm. This fringe case should be already taken care of by preprocessing ingestion phase that proof-reads the document for primitive grammatical correctness though not extensive and part-of-speech. Recursive Gloss Overlap graph constructed with Semantic Net frameworks like WordNet, Evocation WordNet, VerbNet, FrameNet, ConceptNet, SentiWordNet etc., can be fortified by mingling Part-of-Speech trees for sentences in a document with already constructed graph. This adds grammar information to the text graph.

Psycholinguistics have the notion of event related potentials - when brain reacts excessively to anomalous words in neural impulses. Ideal intrinsic merit rankings should also account for such ERP data to distinguish unusual sentences, but datasets for ERPs are not widely accessible except SentiWordNet. Hence Recursive Gloss Overlap is the closest possible for comparative study of multiple documents that ignores parts-of-speech, subjective assessments and

focuses only on intrinsic information content and relatedness.

A thought experiment of intrinsic merit versus prestige ranking:  
Performance of an academic personality is measured first by accolades, awards, grades etc., which form the societal opinion - prestige (citations). That is prestige is created from intrinsic merit. But measuring merit from prestige is anachronistic because merit precedes prestige. Ideally prestige and intrinsic merit should coincide when the algorithms are equally error-free. In case of error, prestige and merit are two intersecting worlds where documents without merit might have prestige and vice-versa. Size of the set-difference is measure of error.

#### References:

- 
- 202.1 Circuits of the Mind - [Leslie Valiant] - <http://dl.acm.org/citation.cfm?id=199266>
- 202.2 Mind Grows Circuits - Lambda calculus and circuit modelling of mind - [Rina Panigrahy, Li Zhang] - <http://arxiv.org/pdf/1203.0088v2.pdf>
- 202.3 Psycholinguistics Electrified - EEG and SQUID Event Related Electric Potentials (ERP) peaking for anomalous words - N400 experiment - <http://kutaslab.ucsd.edu/people/kutas/pdfs/1994.HP.83.pdf>
- 202.4 Word Associations and Evocations - <http://hci.cse.ust.hk/projects/evocation/index.html>
- 202.5 Combining WordNet, VerbNet, FrameNet - <http://web.eecs.umich.edu/~mihalcea/papers/shi.cicling05.pdf>
- 202.6 Computational Psycholinguistics - PoS Parsers - [http://www.coli.uni-saarland.de/~crocker/courses/comp\\_psych/comp\\_psych.html](http://www.coli.uni-saarland.de/~crocker/courses/comp_psych/comp_psych.html)
- 202.7 Brain Data for Psycholinguistics - [http://personality.altervista.org/docs/14yg-al\\_brainsent@jllcl.pdf](http://personality.altervista.org/docs/14yg-al_brainsent@jllcl.pdf)
- 202.8 ConceptNet 5 - <http://conceptnet5.media.mit.edu/>
- 202.9 Sanskrit WordNet - <http://www.cfilt.iitb.ac.in/wordnet/webswn/>
- 202.10 IndoWordNet - <http://www.cfilt.iitb.ac.in/indowordnet/index.jsp>
- 202.11 Brain Connectivity and Multiclass Hopfield Network - Associative memory - [http://www.umiacs.umd.edu/~joseph/Wangetal\\_Neuroinformatics2015.pdf](http://www.umiacs.umd.edu/~joseph/Wangetal_Neuroinformatics2015.pdf)
- 202.12 Text Readability Measures, Coherence, Cohesion - <http://www.readability.biz/Coherence.html>
- 202.13 MultiWordNet for European Languages - <http://multiwordnet.fbk.eu/english/home.php>
- 202.14 Coherence and Text readability indices (Coh-Metrix, FleschKincaid, Brain Overload etc.,) - [http://lingued.info/clw2010/downloads/clw2010-talk\\_09.pdf](http://lingued.info/clw2010/downloads/clw2010-talk_09.pdf) - Coherence measures how connected the document is and thus closely related to Intrinsic Merit obtained by WordNet subgraph for a text.
- 202.15 Readability and WordNet - <http://www.aclweb.org/anthology/008-1>
- 202.16. Semantic Networks (Frames, Slots and Facets) and WordNet - [http://onlinelibrary.wiley.com/doi/10.1207/s15516709cog2901\\_3/epdf](http://onlinelibrary.wiley.com/doi/10.1207/s15516709cog2901_3/epdf) - describes various graph connectivity measures viz., Clustering coefficient for the probability that neighbours of a node are neighbours themselves, Power-Law distribution of degree of a random node. WordNet is modern knowledge representation framework inspired by Semantic Networks which is a graph of Frames with Slots and Facets for edges amongst Frames.
- 202.17 Text Network Analysis - Extracting a graph relation from natural language text - <http://noduslabs.com/publications/Pathways-Meaning-Text-Network-Analysis.pdf> (2011) - Parses keywords from texts and connects the keyword nodes by relation edges with weights - an alternative to WordNet where connections are based on co-occurrence/proximities of words within a certain window. Two words are connected conceptually if they co-occur (similar to Latent Semantic Indexing by SVD).
- 202.18 Text Network Analysis - Networks from Texts - <http://vlado.fmf.uni-lj.si/pub/networks/doc/seminar/lisbon01.pdf>
- 202.19 Six Degrees - Science in Connected Age - [Duncan J.Watts] - Pages 141-143 - Groundbreaking result by [Jon Kleinberg] - <https://www.kth.se/social/files/5533a99bf2765470d3d8227d/kleinberg-smallworld.pdf> which studies Milgram's Small World Phenomenon by probability of

finding paths between two nodes on a lattice of nodes: Probability of an edge between 2 nodes is inversely proportional to the clustering coefficient ( $r$ ). The delivery time (or) path between 2 nodes is optimum when  $r=2$  and has an inverted bell-curve approximately. When  $r$  is less than 2 and greater than 2 delivery time is high i.e finding the path between two nodes is difficult. In the context of judging merit by definition graph of a document, document is "meaningful" if it is "relatively easier" to find a path between two nodes (Resnik, Jiang-Conrath concept similarity and distance measures). This assumes the definition graph is modelled as a random graph. Present RGO definition graph algorithm does not create a random, weighted graph - this requires probabilistic weighted ontology. Statically, Kleinberg's result implies that document definition graphs with  $r=2$  are more "meaningful, readable and visualizable" and can be easily understood where  $r$  is proportional to word-word edge distance measures (Resnik, Jiang-Conrath).

202.20 Align, Disambiguate, Walk distance measures -

[http://wwwusers.di.uniroma1.it/~navigli/pubs/ACL\\_2013\\_Pilehvar\\_Jurgens\\_Navigli.pdf](http://wwwusers.di.uniroma1.it/~navigli/pubs/ACL_2013_Pilehvar_Jurgens_Navigli.pdf)

202.21 Coh Metrix - Analysis of Text on Cohesion and Language -

<https://www.ncbi.nlm.nih.gov/pubmed/15354684> - quantifies text for meaningfulness, relatedness and readability

202.22 Homophily in Networks - [Duncan J. Watts] - Pages 152-153 -

<https://arxiv.org/pdf/cond-mat/0205383.pdf> - This result implies in a social network where each vertex is a tuple of more than one dimension, and similarity between any two tuples  $s$  and  $j$  is defined as distance to an adjacent node  $j$  of  $s$  which is close to  $t$ , and any message from sender  $s$  reaches receiver  $t$  in minimum length of intermediaries - optimal when number of dimensions are 2 or 3 -

Kleinberg condition is special case of this.

202.23 Six Degrees - [Duncan J. Watts] - Triadic closure of Anatole Rapoport - Clustering Coefficient - Page 58

-----  
203. Apache Spark MapReduce Parallel Computation of Interview Algorithm  
Recursive Gloss Overlap Graph Construction

- Commits as on 25 December 2015  
-----

- Added more parallelism to  
python-src/InterviewAlgorithm/InterviewAlgorithmWithIntrinsicMerit\_Crawl\_Visual\_Spark.py. New map-reduce functions  
for computing parents (backedges in the recursion) have been added -  
mapFunction\_Parents(), reduceFunction\_Parents(), SparkMapReduce\_Parents()  
in  
python-src/InterviewAlgorithm/InterviewAlgorithmWithIntrinsicMerit\_SparkMapReducer.py

- These functions take the previous level tokens as inputs instead of synsets  
-----

204. Commits as on 28 December 2015  
-----

- Updated MapReduce functions in Spark Recursive Gloss Overlap implementation  
-----

205. Commits as on 29 December 2015  
-----

- Updated  
python-src/InterviewAlgorithm/InterviewAlgorithmWithIntrinsicMerit\_Crawl\_Visual\_Spark.py for choosing parallel spark mapreduce or  
serial parents backedges computation based on a boolean function.  
- This is because Recursive tokens mapreduce computation (Spark\_MapReduce) is

faster than serial version.

But serial parents computation is faster than parallel parents computation ironically(Spark\_MapReduce\_Parents).

This happens on single node Spark cluster. So, parents computation has been made configurable(serial or parallel)

- Logs and Screenshots for various texts experimented have been added to testlogs/  
-

python-src/InterviewAlgorithm/InterviewAlgorithmWithIntrinsicMerit\_SparkMapReducer.py mapreduce uses best\_matching\_synset() for disambiguation now which was commented earlier.

- MapFunction\_Parents() has a pickling problem in taking a tuple of synset objects as input arg due to which synsets have to be recomputed that causes the slowdown mentioned above compared to serial parents() version.

MapFunction\_Parents() has been rewritten to take previous level gloss tokens in lieu of synsets to circumvent pickling issues.

- Slowdown could be resolved on a huge cluster.

- Thus this is a mix of serial+parallel implementation.

- Logs, DOT file and Screenshots for mapreduced parents() computation

-----  
206. Commits as on 30 December 2015  
-----

-----  
Some optimizations and redundant code elimination in  
python-src/InterviewAlgorithm/InterviewAlgorithmWithIntrinsicMerit\_Crawl\_Visual\_Spark.py  
-----

-----  
207. Commits as on 31 December 2015  
-----

- Spark Recursive Gloss Overlap Intrinsic Merit code has been optimized and some minutiae bugs have been resolved.

- Map function for parents computation in Spark cluster has been updated to act upon only the previous recursion level glosses by proprietary pickling of the keyword into a file storage and loading it, and not as a function argument

- Problems with previous level gloss tokens were almost similar to MapReduce functions of the recursion

- New pickling file for parents computation in Spark has been added

- logs and screenshots have been added to testlogs

- With this, Spark Intrinsic Merit computation is highly parallelized apt for large clouds

- Also a parents\_tokens() function that uses gloss tokens instead of synsets has been added

- New pickling dump() and load() functions have been added for keyword storage

- pickling is synchronized with python threading lock acquire() and release().

Shouldn't be necessary because of

Concurrent Read Exclusive Write (CREW) of keyword, but for safer side to prevent Spark-internal races.

-----  
208. Commits as on 1,2,3,4,5,6,7 January 2016  
-----

- Added sections 53.14, 53.15 for HLMN and PARITY 3-SAT in 53

- updated spidered text

- best\_matching\_synset() enabled in mapreduce backedges computation which accurately disambiguates the graph. Spark single node cluster is significantly slower than serial version of parents() computation with only

python calls probably due to costly Python4Java  
back-and-forth stream socket reads.

- logs, DOT file and screenshots for single node Spark cluster have been added  
to testlogs/

-----  
-----  
209. Commits as on 8 January 2016  
-----

-----  
- In InterviewAlgorithm/InterviewAlgorithmWithIntrinsicMerit\_SparkMapReducer.py  
increased local threads to 2 (for dual core cpu(s)) for  
all SparkContexts instantiated  
- Added screenshot and logs for 2 local threads SparkContext mapreduce  
- Reference: Berkeley EdX Spark OpenCourse -  
<https://courses.edx.org/c4x/BerkeleyX/CS100.1x/asset/Week2Lec4.pdf>  
-----

-----  
210. Commits as on 10 January 2016  
-----

-----  
NeuronRain Enterprise (GitHub) version 2016.1.10 released.  
-----

-----  
211. Commits as on 11 January 2016  
-----

Added section 53.16 for an apparent contradiction between polysize and  
superpolynomial size among P/poly, Percolation and  
special case of HLMN theorem.  
-----

-----  
212. (FEATURE - DONE) Principal Component Analysis (PCA) and Singular Value  
Decomposition (SVD) - Commits as on 12 January 2016  
-----

-----  
Python rpy2 wrapper implementation for :  
- Principal Component Analysis(PCA)  
- Singular Value Decomposition(SVD)  
which invoke R PCA and SVD functions and plot into 2 separate pdf files has been  
added to repository.  
Logs for an example have been added to testlogs/  
-----

-----  
213. (FEATURE - DONE) Kullback-Leibler Divergence - Commits as on 17 January  
2016  
-----

-----  
Kullback-Leibler Divergence implementation:  
-----

Approximate distance between 2 probability distributions with logs  
in terms of weighted average distance represented as bits  
-----

-----  
214. (FEATURE - DONE) Basic Statistics - Norms and Median - Commits as on 19  
January 2016  
-----

-----  
Implementation for basic statistics - L1, L2 norms, median etc.,  
-----

-----  
-----  
215. Commits as on 20 January 2016  
-----  
-----

- Updated AsFer Design Document for Psycholinguistics of Reading a Text document and Recursive Gloss Overlap  
- Added Standard Deviation and Chi-Squared Test R functions to  
python-src/Norms\_and\_Basic\_Statistics.py  
-----  
-----

216. (THEORY) Recursive Lambda Function Growth Algorithm - Psycholinguistic Functional Programming simulation of Human Reader Eye Movement Tracking and its special setting application in Recursive Gloss Overlap  
-----  
-----

Example sentence:  
California Gas Leak Exposes Growing Natural Gas Risks.

A left-right scan of the human reading groups the sentence into set of phrases and connectives and grows top-down gloss overlap graphs:

p1 - California Gas Leak  
p2 - Exposes  
p3 - Growing Natural Gas Risks

For each phrase left-right, meaning is created by recursive gloss overlap disambiguated graph construction top-down (graph is constructed left-right, top-down):

p1 - graph g1  
p2 - graph g2  
p3 - graph g3

Prefix graph construction and functional programming:

Above sentence has three prefix phrases and graphs- p1, p1-p2, p1-p2-p3 in order (and g1, g1-g2, g1-g2-g3). As reader scans the sentence, meaning is built over time period by lambda function composition. Function f1 is applied to g1,g2 - f1(g1,g2) - f1(g1(California Gas Leak), g2(Exposes)) - which returns a new graph for prefix p1-p2. Function f2 is applied to f1(g1,g2) and g3 - f2(f1(g1,g2),g3(Growing Natural Gas Risks)) - which returns a new graph for sentence p1-p2-p3. This is recursively continued and above example can be generalized to arbitrarily long sentences.

This formulation does not depend on just semantic graphs - graphs g1,g2 and g3 could be functional programming subroutines too, which makes f2(f1(g1,g2),g3) as one complete function composition tree. In previous example, for each phrase a function is defined and finally they are composed:

p1 - function g1 - california\_gas\_leak()  
p2 - function g2 - exposes()  
p3 - function g3 - growing\_natural\_gas\_risks()  
f3 = f2(f1(g1,g2),g3)

How functions f1,f2,g1,g2,g3 are internally implemented is subjective. These functions are dynamically created and evaluated on the fly. Grouping sentences into phrases and connectives has to be a preprocessing step that uses PoS NER tagger - even a naive parsing for language connectives should suffice. Return values of these functions are functions themselves - this is standard "First Class Object" concept in higher order lambda calculus - [https://en.wikipedia.org/wiki/First-class\\_citizen](https://en.wikipedia.org/wiki/First-class_citizen) . These functions themselves might invoke smaller subroutines internally which build meaning and return to previous level. Recursive Gloss Overlap implements a special case of this where f1,f2 are gloss overlap functions and g1,g2,g3 are wordnet subgraphs. Its Spark implementation does a "Parallel-Read, Top-Down Graph construction" as against

left-right read. In a more generic alternative, these functions could be deep learning neural networks, LISP subroutines etc., that compute "meaning" of the corresponding phrase. If the reading is not restricted to left-right, the composition tree should ideally look like a balanced binary tree per sentence. This is a kind of "Mind-Grows-Functions" formalism similar to the Mind-Grows-Circuit paradigm in [Rina Panigrahy, Li Zhang] - <http://arxiv.org/pdf/1203.0088v2.pdf>. It is questionable as to what does "Meaning" mean - is it a graph, neural electric impulse in brain etc., and the question itself is self-referencing godel sentence: What is meant by meaning? - which may not have answers in an axiomatic system because word "meaning" has to be defined by something more atomic than "meaning" itself.

As an ideal human sense of "meaning" stored in brain is vague and requires a "Consciousness and Freewill" theory, only a computation theoretic definition of meaning (i.e a circuit graph) is axiomatically assumed. Thus above lambda function composition is theoretically equivalent to boolean function composition (hence circuit composition). With this the above recursive lambda function growth algorithm bridges two apparently disconnected worlds - complexity theory and machine learning practice - and hence a computational learning theory algorithm only difference being it learns a generic higher-order lambda function (special case is recursive gloss overlap) from text alphabet strings rather than a boolean function from binary strings over {0,1} alphabet. Essentially every lambda function should have a circuit by Church-Turing thesis and its variants - Church-Turing thesis which states that any human computable function is turing-computable is still an axiom without proof on which computer science has been founded. Because of this equivalence of lambda functions and Turing machines, the lambda function learning algorithm essentially covers all possible complexity classes which include Recursively Enumerable languages. Theoretically, concepts of noise sensitivity, influence which measure the probability of output change for flipped input should apply to this lambda function learning algorithm for text documents - For example typo or error in grammar that affects the meaning.

Learning theory perspective of the previous - From Linial-Mansour-Nisan theorem, class of boolean functions of  $n$  variables with depth- $d$  can be learnt in  $O(n^{\Omega(\log n^d)})$  with  $1/\text{poly}(n)$  error. Consequentially, Above Lambda Function Growth for depth  $d$  can be encoded as a circuit (a TC circuit in wordnet special case) that has  $n$  inputs where  $n$  are number of keywords in text (each word is boolean encoded to a binary string of constant length) and learnt in  $O(n^{\Omega(\log n^d)})$  with  $1/\text{poly}(n)$  error. This learning theory bound has striking resemblance to parallel Recursive Gloss Overlap bound of  $O(n_1 * d_1 * s^{t_{\max}} / (g(n_1) * f(d_1)))$  for  $n_1$  documents with  $d_1$  keywords each on a cluster. Equating to LMN bound gives rise to interesting implication that average number of gloss per keyword =  $\log(\text{number\_of\_keywords})$  which is too high gloss size per word (other variables equated as  $n=d_1, t_{\max}=d$ ). Therefore recursive gloss overlap could be faster than LMN learning algorithm.

#### References:

- 
- 216.1 Eye Movement Tracking - <https://en.wikipedia.org/wiki/Psycholinguistics#Eye-movements>
- 216.2 Eye Movements in Text Comprehension - Fixations, Saccades, Regressions - <http://www.jove.com/video/50780/using-eye-movements-to-evaluate-cognitive-processes-involved-text>
- 216.3 Symbol Grounding Problem and learning from dictionary definitions - <http://aclweb.org/anthology//W/W08/W08-2003.pdf> - "...In the path from a word, to the definition of that word, to the definition of the words in the definition of that word, and so on, through what sort of a structure are we navigating (Ravasz & Barabasi, 2003; Steyvers & Tenenbaum, 2005)? Meaning is compositional: ..." - Symbol grounding is the problems of infinite regress while affixing meaning to words. As defined by Frege, word is a referent and meaning is its definition and the two are different. This paper lays theoretical foundations for Graphical Ontologies like WordNet etc., Process of meaning grasping is defined in terms of finding a Grounding set of vertices of an ontology which is



equal to a Feedback Vertex Set of the graph. Feedback Vertex Set is subset of vertices of an ontology graph removal of which causes the directed graph to be cycle-less. This is an NP-complete problem. Definition graph construction in Recursive Gloss Overlap creates a subgraph of an ontology projected onto the text document.

216.4 TextGraphs - graph representation of texts -

<https://sites.google.com/site/textgraphs2017/>

216.5 Symbol Grounding Problem -

<http://users.ecs.soton.ac.uk/harnad/Papers/Harnad/harnad90.sgproblem.html> -

" ... (1) Suppose the name "horse" is grounded by iconic and categorical representations, learned from experience, that reliably discriminate and identify horses on the basis of their sensory projections. (2) Suppose "stripes" is similarly grounded. Now consider that the following category can be constituted out of these elementary categories by a symbolic description of category membership alone: (3) "Zebra" = "horse" & "stripes"[17] ... Once one has the grounded set of elementary symbols provided by a taxonomy of names (and the iconic and categorical representations that give content to the names and allow them to pick out the objects they identify), the rest of the symbol strings of a natural language can be generated by symbol composition alone, [18] ..."

216.6 Understanding Natural Language - [Terry Winograd] -

<https://dspace.mit.edu/handle/1721.1/7095#files-area> - Chapter 3 - Inference -

Meaning of sentences are represented as relations between objects. Recursive Lambda Function Growth described previously has a lambda function for each relation. Relations/Lambda Functions are mostly verbs/adverbs/adjectives and arguments of lambda functions are objects/nouns.

216.7 Grounded Cognition - [Barsalou] -

<http://matt.colorado.edu/teaching/highcog/readings/b8.pdf> - How Language is Grounded - "...Phrasal structures embed recursively..." - Neuroimageing evidences for Grounded cognition

-----  
-----  
217. Commits as on 21 January 2016  
-----  
-----

- Corrected Chi-squared test input args
- logs added to testlogs/

-----  
-----  
218. Commits as on 27 January 2016  
-----  
-----

Updated Sections 14 and 216.

-----  
-----  
219. Commits as on 29 January 2016  
-----  
-----

- Uncommented both commandlines in cpp-src/asferpythonembedding.sh

-----  
-----  
220. (FEATURE - DONE) Python-C++-VIRGOKernel and Python-C-VIRGOKernel  
boost::python and cpython implementations:

- It is a known idiom that Linux Kernel and C++ are not compatible.
- In this commit an important feature to invoke VIRGO Linux Kernel from userspace python libraries via two alternatives have been added.
- In one alternative, C++ boost::python extensions have been added to encapsulate access to VIRGO memory system calls - virgo\_malloc(), virgo\_set(), virgo\_get(), virgo\_free(). Initial testing reveals that C++ and Kernel are not

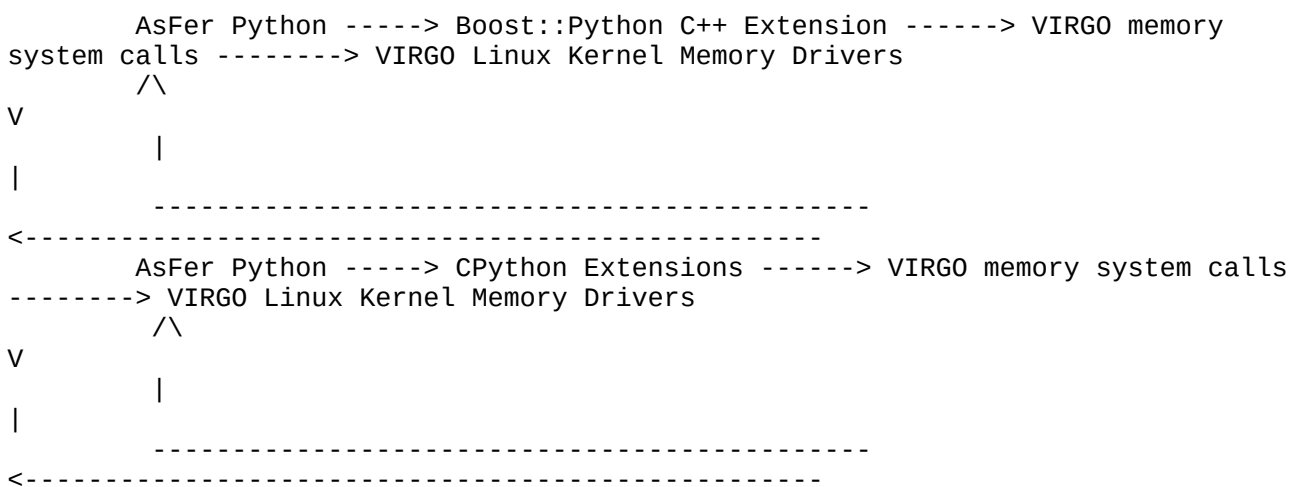
too incompatible and all the VIRGO memory system calls work well though initially there were some errors because of config issues.

- In the other alternative, C Python extensions have been added that replicate boost::python extensions above in C - C Python with Linux kernel works exceedingly well compared to boost::python.
- This functionality is required when there is a need to set kernel analytics configuration variables learnt by AsFer Machine Learning Code dynamically without re-reading /etc/virgo\_kernel\_analytics.conf.
- This completes a major integration step of NeuronRain suite - request travel roundtrip to-and-fro top level machine-learning C++/python code and rock-bottom C linux kernel - bull tamed ;-).
- This kind of python access to device drivers is available for Graphics Drivers already on linux (GPIO - for accessing device states)
- logs for both C++ and C paths have been added in cpp\_boost\_python\_extensions/ and cpython\_extensions.
- top level python scripts to access VIRGO kernel system calls have been added in both directories:
  - CPython - python cpython\_extensions/asferpythonextensions.py
  - C++ Boost::Python - python

cpp\_boost\_python\_extensions/asferpythonextensions.py

- .so, .o files with build commandlines(asferpythonextensions.build.out) for "python setup.py build" have been added in build lib and temp directories.
- main implementations for C++ and C are in cpp\_boost\_python\_extensions/asferpythonextensions.cpp and cpython\_extensions/asferpythonextensions.c

#### - Schematic Diagram:



221. Commits as on 2 February 2016

- Uncommented PyArg\_ParseTuple() to read in the key-value passed from Python layer
- Unified key-value in Python layer and within CPython code with : delimiter
- added Py\_BuildValue() to return void - VIRGO Unique ID - to python and commented virgo\_free() so that a parallel code can connect to kmem cache and do a virgo\_get on this void - this is a precise scenario where Read-Copy-Update fits in so that multiple versions can co-exist at a time

222. (THEORY) Recursive Lambda Function Growth Algorithm - 216 elaborated with examples

-----  
-----  
Boolean function learning and PAC learning are special cases of this Lambda function learning algorithm because any intermediate lambda function can be a boolean function too.

Algorithms steps for English Natural Language Procssing - Parallel read:  
-----

- Approximate midpoint of the sentence is known apriori
- Language specific connectives are known apriori (e.g is, was, were, when, who etc.,)
- Sentence is recursively split into phrases and connectives and converted into lambda functions with balanced number of nodes in left and right subtrees
- Root of each subtree is unique name of the function

Example Sentence1:  
-----

PH is infinite relative to random oracle.

Above sentence is translated into a lambda function composition tree as:  
relative(is(PH, infinite), to(random,oracle))) which is a tree of depth 3

In this example every word and grammatical connective is a lambda function that takes some arguments and returns a partial "purport" or "meaning" of that segment of sentence. These partial computations are aggregated bottom-up and culminate in root.

Example Sentence2:  
-----

Farming and Farmers are critical to success of a country like India.

Above sentence is translated into a lambda function composition tree as:  
Critical(are(and(Farming,Farmers)), a(success(to,of), like(country, India)))

This composition is slightly different from Part-of-Speech trees and inorder traversal of the tree yields original sentence.

As functions are evaluated over time period, at any time point there is a partially evaluated composition prefix tree which operates on rest of the sentence to be translated yet - these partial trees have placeholder templates that can be filledup by a future lambda function from rest of the sentence.

Each of these lambda functions can be any of the following but not limited to:

- Boolean functions
- Generic mathematical functions
- Neural networks (which include all Semantic graphs like WordNet etc.,)
- Belief propagated potentials assigned by a dictionary of English language and computed bottom-up
- Experimental theory of Cognitive Psycholinguistics - Visuals of corresponding words - this is the closest simulation of process of cognition and comprehension because when a sentence is read by a human left-right, visuals corresponding to each word based on previous experience are evoked and collated in brain to create a "movie" meaning of the sentence. For example, following sentence:

Mobile phones operate through towers in each cellular area that transmit signals.

with its per-word lambda function composition tree :

in(operate(mobile phones, through(tower)), that(each(cellular area), transmit(signals)))

evokes from left-to-right visuals of Mobile phones, towers, a bounded area in quick succession based on user's personal "experience" which are merged to form

a visual motion-pictured meaning of the sentence. Here "experience" is defined as the accumulated past stored in brain which differs from one person to the other. This evocation model based on an infinite hypergraph of stacked thoughts as vertices and edges has been described earlier in sections 35-49 and 54-59. This hypergraph of thoughts grows over time forming "experiences". For some words visual storage might be missing, blurred or may not exist at all. An example for this non-visualizable entity in above sentence is "transmit" and "signal" which is not a tangible. Thus the lambda function composition of these visuals are superimposed collations of individual lambda functions that return visuals specific to a word, to create a sum total animated version. Important to note is that these lambda functions are specific to each reader which depend on pre-built "experience" hypergraph of thoughts which differs for each reader. This explains the phenomenon where the process of learning and grasping varies among people. Hypergraph model also explains why recent events belonging to a particular category are evoked more easily than those in distant past - because nodes in stack can have associated potential which fades from top to down and evocation can be modelled as a hidden markov model process on a stack node in the thought hypergraph top-down as the markov chain. Rephrasing, thoughts stored as multiplanar hypergraphs with stack vertices act as a context to reader-specific lambda functions. If stack nodes of thought hypergraph are not markov models - node at depth t need not imply node at depth t-1 - topmost node is the context disambiguating visual returned by the lambda function for that word. This unifies storage and computation and hence a plausible cerebral computational model - striking parallel in non-human turing computation is the virtual address space or tape for each process serving as context.

The language of Sanskrit with Panini's Grammar fits the above lambda calculus framework well because in Sanskrit case endings and sentence meaning are independent of word orderings. For example following sentence in Sanskrit:  
Sambhala Grama Mukhyasya VishnuYashas Mahatmana: ... ( Chieftain of Sambhala Village, Vishnuyashas the great ...)

can be rearranged and shuffled without altering the meaning, a precise requisite for lambda function composition tree representation of a sentence, which is tantamount to re-ordering of parameters of a lambda function.

As an alternative to WordNet:

-----  
Each lambda function carries dictionary meaning of corresponding word with placeholders for arguments.

For example, for word "Critical" corresponding lambda function is defined as:  
Critical(x1,x2)

If dictionary meanings of critical are defined with placeholders:

- 1) Disapproval of something -
- 2) - is Important to something -

there is a need for disambiguation and 2) has to be chosen based either on number of arguments or disambiguation using lesk algorithm or more sophisticated one. If Second meaning fits context then, lambda function Critical(x1,x2) returns:

x1 is important to something x2

Thus WordNet can be replaced by something more straightforward. These steps can be recursed top-down to expand the meaning - in above example "important" might have to be lookedup in dictionary. This simulates basic human process of language learning and comprehension.

This algorithm accepts natural languages that are between Context Free Languages and Context Sensitive Languages.

References:

222.1 Charles Wikner - Introductory Sanskrit -

[http://sanskritdocuments.org/learning\\_tutorial\\_wikner/](http://sanskritdocuments.org/learning_tutorial_wikner/)

222.2 Michael Coulson - Teach yourself - Sanskrit -

<http://www.amazon.com/Complete-Sanskrit-Teach-Yourself-Language/dp/0071752668>)

-----  
-----  
223. Commits as on 4 February 2016  
-----

-----  
- Updated AsFer Design Document with more references for Discrete Hyperbolic Factorization in NC - PRAM-NC equivalence  
-----

-----  
(FEATURE - DONE) C++ - Input Dataset Files nomenclature change for NeuronRain Enterprise  
-----

-----  
- 3 new input files cpp-src/asfer.enterprise.encstr, cpp-src/asfer.enterprise.encstr.clustered, cpp-src/asfer.enterprise.encstr.knn have been added which contain set of generic binary strings for KMeans, KNN clustering and Longest Common Subsequence of a clustered set .  
- Code changes for above new input files have been done in asfer.cpp and new class(asferencodestr.cpp and asferencodestr.h) has been added for generic string dataset processing  
- Changes for generic string datasets have been done for knn and KMeans clustering  
- logs for clustering and longest common subsequence have been added  
-----

-----  
(FEATURE - DONE) Python - Input Dataset Files nomenclature change for NeuronRain Enterprise  
-----

-----  
- 1 new input file python-src/asfer.enterprise.encstr.seqmining has been added for Sequence Mining of generic string dataset - presently contains set of generic binary strings .  
- Code changes for above new input files have been done in SequenceMining.py  
- logs for SequenceMining of binary strings with maximum subsequence length of 15 have been added  
-----

-----  
-----  
224. Commits as on 4 February 2016  
-----

-----  
(FEATURE - DONE) Crucial commits for Performance improvements and Cython build of Spark Interview algorithm implementation  
-----

-----  
- New setup.py has been added to do a Cythonized build of PySpark Interview algorithm MapReduce script  
- Commandline for cython build: python setup.py build\_ext --inplace  
- This compiles python spark mapreduce script into a .c file that does CPython bindings and creates .o and .so files  
- FreqDist has been commented which was slowing down the bootstrap  
- MapReduce function has been updated for NULL object checks  
- Thanks to Cython, Performance of Spark MapReduce has performance shootup by factor of almost 100x - Spark GUI job execution time shown for this interview execution is ~10 seconds excluding GUI graph rendering which requires few minutes. This was earlier taking few hours.  
- With Cython ,essentially Spark-Python becomes as fast as C implementation.  
- DOT file, Output log, Spark logs and Screenshot has been added  
- This completes important benchmark and performance improvement for Recursive Gloss Overlap Graph construction on local Spark single node cluster.  
- Above Cythonizes just a small percentage of Python-Spark code. If complete

python execution path is Cythonized and JVM GC and Heap tunables for Spark are configured, this could increase throughput significantly further. Also Spark's shuffling parameters tuning could reduce the communication cost.

-----  
225. Commits as on 5 February 2016  
-----

-----  
Further optimizations to Spark-Cython Interview algorithm implementation:  
-----

- webspidered text for RGO graph construction updated
- PySpark-Cython build commandlines added as a text file log
- Commented unused python functions - shingling and jaccard coefficient
- threading.Lock() Spark thread pickling synchronizer variable made global in MapReducer
- renamed yesterday's logs and screenshot to correct datetime 4 February 2016
- Added a new special graph node ["None"] for special cases when no parents are found in backedges computation in MapReducer. This makes a default root in the RGO graph as shown in matplotlib networkx graph plot
- Spark logs show time per RDD job - an example MapReduce job takes 335 milliseconds
- Tried Cythonizing InterviewAlgorithmWithIntrinsicMerit\_Crawl\_Visual\_Spark.py but there is a serious cython compiler error in Matplotlib-PyQt. Hence those changes have been backed out.
- DOT file and Cython C file have been updated

-----  
226. Commits as on 8 February 2016  
-----

- PySpark-Cythonized Interview Algorithm implementation generated graph has been pruned to remove edges involving "None" vertices which were added during Spark MapReduce based on a config variable.
- Logs and Screenshots for the above have been added to testlogs/
- Some benchmark results parsed from the Spark logs with commandline - "for i in `grep Finished InterviewAlgorithmWithIntrinsicMerit\_Crawl\_Visual\_Spark.2localthreads.CythonOptimized.8February2016.out |grep TaskSetManager| awk '{print \$14}'`; do sum=\$(expr \$sum + \$i); done":
  - Total time in milliseconds - 99201
  - Number of jobs - 113
  - Average time per mapreduce job in milliseconds - 877

Thus a merit computation of sample document with few lines (33 keywords) requires ~100 seconds in local Spark cluster. This excludes NetworkX and other unoptimized code overhead.

-----  
227. (THEORY) Graph Edit Distance in Interview Algorithm, PySpark-Cython Interview Algorithm benchmarks and Merit in Recursive Lambda Function Growth Algorithm  
-----

Interview Algorithm to assess merit, throughout this document, refers to 3 algorithms - Citation graph maxflow(which includes standard radius, eccentricity and diameter measures of the graph), Recursive Lambda Function growth and Graph edit distance (or Q&A) based interview between a pair of documents. Recent result about impossibility of better algorithms for edit distance (Backurs-Indyk - <http://arxiv.org/abs/1412.0348> - edit distance cannot be computed in subquadratic time unless Strong Exponential Time Hypothesis is false) finds its applications in Graph edit distance for Interview Algorithm Questions&Answering

where one document's Recursive Gloss Overlap graph is compared for distance from another graph's RGO WordNet subgraph ([http://www.nist.gov/tac/publications/2010/participant.papers/CMI\\_IIT.proceedings.pdf](http://www.nist.gov/tac/publications/2010/participant.papers/CMI_IIT.proceedings.pdf)). Graph edit distance is a special case of edit distance when graph edges are encoded as strings. A better algorithm to find edit distance between 2 documents' wordnet subgraphs, therefore implies SETH is false.

Previous benchmarks for PySpark-Cython parallel interview algorithm implementation could scale significantly on a cluster with ~100 Spark nodes with parallel runtime of ~800 milliseconds. If all Java Spark code is JVM tuned and python modules are Cythonized fully, even this could be bettered bringing it to order of few milliseconds.

Computing Intrinsic Merit of a text with Recursive Lambda Function growth could involve multitude of complexity notions:

- Depth of Composition tree for a text
- Size of resultant lambda function composition e.g size of WordNet subgraphs, neural nets, complexity of context disambiguation with thought hypergraph psychological model enunciated in 222.
- In essence, this reduces to a lowerbound of lambda function composition
- boolean circuit lowerbounds are special cases of lambda function composition lowerbounds. Since thought hypergraph disambiguator is reader dependent, each reader might get different merit value for same document which explains the real-life phenomenon of "subjectivity". To put it simply, Objectivity evolves into Subjectivity with "experience and thought" context. Evaluating merit based on thought context is non-trivial because disambiguating a word visually as mentioned in 222 requires traversal of complete depth of thought hypergraph - it is like billions of stacks interconnected across making it tremendously multiplanar - a thought versioning system. This explains another realword phenomenon of experiential learning: An experienced person "views" a text differently from a relatively less experienced person.

-----  
228. (THEORY) Thought Versioning - ThoughtNet and EventNet - Psychophilosophical Digression - Might have some parallels in Philosophical Logic - related to points (70-79)  
-----

(\*) This postulates an experimental model for a "Logical Brain". It makes no assumptions about neural synapses, firing etc., though a graph can be mapped to a neural network with some more reductions. The computation side is taken care of by Recursive Lambda Function Growth (which might invoke neural learning etc.,) while the storage is simulated with a giant ThoughtNet - together this is a turing-computable model for natural language processing which is subjective to each individual. This model makes an assumption of pre-existing consciousness or an equivalent to account for emotions and sentiments.

(\*) ThoughtNet is built over time from inception of life - books a person reads, events in life, interactions etc., - are lambda-evaluated and stored. This is where the computation and storage distinction seems to vanish - It is not a machine and tape but rather a machinetape (analogy: space and time coalescing to spacetime). Evaluated lambda functions themselves are stored in ThoughtNet not just thoughts data - storage contains computation and computation lookup storage.

(\*) Thought Versioning System - tentatively named ThoughtNet - mentioned in 227 is a generalization of Evocation WordNet as a multiplanar graph with stacked thoughts as vertices. Each stack corresponds to a class an experience or thought is binned - visually or non-visually.

(\*) An approximate parallel to ThoughtNet versioning is the Overlay FileSystems in Unixen. Overlay filesystems store data one over the other in layers which play "obscurantist" and prevent the bottom truth from being out. This follows a

Copy-up-on-write (CUOW) - a data in bottom layer is copied up and modified and stays overlaid. File access systems calls "see" only "topmost" layer. In ThoughtNet this roughly translates to Thought edges of particular class-stack node placed one over the other and grown over period of time. ThoughtNet thus presents an alternative to Overlay storage where a layer with maximum  $\text{argmax}()$  potential can be chosen.

(\*) EventNet when unified with ThoughtNet makes a cosmic storage repository, all pervasive. Thoughts are stored with accompanied potentials - which could be electric potentials - some stronger thoughts might have heavy potentials compared to insignificant thoughts. How this potentials arise in first place is open to question. Rather than numeric and sign representation of sentiments, this ThoughtNet model proposes "coloring" of the emotions - akin to edge coloring of graphs. ThoughtNet is a giant pulp of accrued knowledge in the form of observed events stored as hyperedges. Here a distinction has to be made between Wisdom and Knowledge - Knowledge measures "To know" while Wisdom measures "To know how to know". Common knowledge in Logic ("We know that you know that We know ... ad infinitum") thus still does not explain wisdom (Does wisdom gain from knowledge and viceversa?). ThoughtNet is only a knowledge representation and Wisdom remains open to interpretation - probably recursive lambda function growth fills-in this gap - it learns how to learn.

(\*) For example, an event with pleasant happening might be stored with high potential of positive polarity as against a sad event with a negative polarity potential. Repetitive events with high potentials reinforce - potentials get added up. This extends SentiWordNet's concept of postivity, negativity and objectivity scoring for words. It is not a necessity that Hidden Markov Models are required for finding a right evocative (mentioned in 56). Trivial  $\text{argmax}(\text{all potentials per stack class})$  is sufficient to find the most relevant evocative hyperedge. This explains the phenomenon where an extremely happy or sad memory of a class lingers for long duration despite being old whereas other memories of same class fade away though relatively recent. Emotions affecting potentials of thought hyperedges is explained further below.

(\*) EventNet is a cosmic causality infinite graph with partaker nodes whereas ThoughtNet is per partaker node. This evocation model is experimental only because a void exists in this simulation which can be filledup only by consciousness and egoself. Example: A sentence "Something does not exist" implies it existed in past or might exist in future and thus self-refuting. Otherwise mention of "something" should have never happened.

(\*) EventNet is a parallely created Causality graph - event vertices occur in parallel across universe and causation edges are established in parallel. This is like a monte-carlo Randomized NC circuit that grows a random graph in parallel.

(\*) Previous evocation model with HMM or maximum potential need not be error-free - it can be derailed since human understanding at times can be derailed - because humans are inherently vulnerable to misunderstand ambiguous texts. Hence above evocation might return a set of edges than a unique edge which has to be further resolved by additional information for disambiguation. For example, rather than individual words a sentence as a block might require disambiguation: In the Cognitive Psycholinguistics model which stores thoughts as visuals mentioned in 222, there is a chance of derailment because of evocation returning multiple edges when human emotions are involved (Love, Anger, Sarcasm, Pathos etc.,). ThoughNet based disambiguation simulates subjective human reasoning more qualitatively specific to each individual and accurately than usual statistical sentiment inferences which are mere numbers and do not consider individual specific perception of a text. This also explains how an "image"/"perception" is engineered over a time period which depends on thoughts stored.

-----  
Thought experiment for this defective disambiguation is as below  
-----

(\*) Example Sentence 1: "Love at first sight is the best". Considering two



persons reading this sentence with drastically different ThoughtNet contexts - one person has multiple good followed by bad experiences stored as ThoughtNet hypergraph edges with stronger positive and negative potentials and the `argmax()` disambiguated evocative edges returned could be therefore both quite positive and negative inducing him to either like or abhor this sentence based on whichever wins the mind conflict (i.e. whichever potential positive or negative is overpowering), while the other person has a pure romantic history with good experiences alone disambiguated evocation in which case is uniquely positive. This is real-world simulation of "confused" thought process when emotions rule. In other words emotions determine the polarity and extent of potentials tagged to each thought hyperedge and more the emotional conflict, larger the chance of difficulty in unique disambiguation and derailment. It is not a problem with ThoughtNet model, but it is fundamental humane problem of emotions which spill over to ThoughtNet when accounted for. If human reasoning is ambiguous so is this model. This danger is even more pronounced when lambda compositions of visuals are involved than just sentences. As an example, a test human subject is repeatedly shown visuals related to love reinforcing the potentials of hyperedges belonging to a class of "Love" and subject is bootstrapped for future realtime love. This artificially creates an illusory backdrop of "trained data" ThoughtNet context - a kind of "Prison Experiment for Behavioural Modification Under Duress" - the distinction between reality and imagination gets blurred - e.g. Stanford Prison Experiment. Machine learning programs cannot quantify emotions through statistics (in the absence of data about how emotions are stored in brain, does emotion originate from consciousness etc.,) and hence creating a visualized meaning through recursive lambda composition of natural language texts have a void to fill. If emotions are Turing-computable, the lambda function composition makes sense. ThoughtNet model with potentials, thus, simulates human grasp of a text with provisions for emotions. No existing machine learning model at present is known to reckon emotions and thought contexts.

(\*) Example Sentence 2: "You are too good for any contest". This sentence has sarcastic tone for a human reader. But can sarcasm be quantified and learned? Usual statistical machine learning algorithms doing sentiment analysis of this sentence might just determine positivity, negativity or objectivity ignoring other fine-grained polarities like "rave, ugly, pejorative, sarcastic etc.,". Trivial sentiment analysis rates this as positive while for a human it is humiliating. This is an example when lambda composition of visuals fares better compared to textual words. Visually this lambda-composes to a collated thought-enacted movie of one person talking to another having a discourteous, ridiculing facial expression. Lambda functions for this visual compositions could invoke face-feature-vector-recognition algorithms which identify facial expressions. In social media texting smileys(emoticons) convey emotions (e.g. tongue-in-cheek). Thus disambiguating the above text sentence accurately depends on a pre-existing visually stored ThoughtNet context of similar sarcastic nature - a person with prior visual ThoughtNet experience hyperedge similar to sarcastic sentence above is more capable of deciphering sarcasm than person without it. This prior edge is "training data" for the model and is stored with an edge-coloring of configurable choosing. Marking sentiments of Thought edges with edge coloring is more qualitative and coarse grained than numbering - each of the emotions Love, Hate, Sorrow, Divinity etc can be assigned a color. As ThoughtNet is grown from beginning of life, stacked up thoughts are colored where the sentiment coloring is learnt from environment. For example, first time a person encounters the above sentence he may not be familiar with sarcasm, but he might learn it is sarcastic from an acquaintance and this learning is stored with a "sarcastic" sentiment coloring in multiplanar thoughtnet hypergraph. Intensity of coloring determines the strength of thought stored. Next instances of evocations, for example "too good" and "contest" which is the crucial segment, return the above edge if intensely colored (in a complex setting, the lambda composition tree is returned, not just the sentence).

(\*) Example Poetry 3 - lambda evaluation with shuffled connectives, is shown below with nested parenthesization - Each parenthesis scope evaluates a lambda function and composed to a tree - [Walrus-Carpenter - Alice in Wonderland]:

((("The time has come,") (the Walrus said),  
("To talk of many things:")  
(Of shoes--and ships--and sealing-wax--)  
(Of cabbages--and kings--)  
And (why (the sea is boiling hot--))  
And (whether (pigs have wings.)))))

This lambda composition itself can be classified in classes viz., "time", "poetry", "sea" etc., (in special case of gloss overlap this is easy to classify by computing high core numbers of the graph). Above evaluation itself is stored in ThoughtNet as hyperedge in its entirety as the "meta-learning", and not just "knowledge", and an edge coloring for sentiment can be assigned. During future evocation, say utterance of word "time", the edge returned is the most intensely colored edge.

(\*) Perfect design of Psycholinguistic text comprehension must involve ego-centric theory specific to each reader as mentioned previously. Combining EventNet and ThoughtNet throws another challenge: When did ThoughtNet begin? Who was the primordial seed of thought? EventNet on the other hand can be axiomatically assumed to have born during BigBang Hyperinflation and the resultant "ultimate free lunch". Invoking Anthropic principle - "I think, therefore I am", "I exist because I am supposed to exist" etc., - suggests the other way i.e EventNet began from ThoughtNet. Then, did consciousness create universe? Quoting an Indological text - Hymn of creation - Nasadiya Sukta - "Even non-existence did not exist in the beginning" which concurs with aforementioned paradoxes. This theorizes duality arose from singularity throwing spanner into spokes of linguistics which are based on duality of synonyms and antonyms. That is a glaringly discordant note in achieving a perfect artificial intelligence. Thus conscious robot may never be a reality.

(\*) Above exposition is required to get to the bottom of difficulties in formalising "what is meant by meaning" and "intrinsic merit" in perfect sense. Graph theoretic intrinsic merit algorithms might require quantum mechanical concepts like Bose-Einstein condensate mentioned in 18.10 i.e In recursive gloss overlap graph context, word vertices are energy levels and edges amongst words are subatomic particles.

(\*) If ThoughtNet begot EventNet by anthropic principle, there is a possibility language was born before something existed in reality. For example, word "Earth" existed before Earth was created. This presents another circular paradox - ThoughtNet implies EventNet implies ThoughtNet ... because events create thoughts and anthropic principle implies thought created events. This also implies thought created brain and its constituents which in turn think and "understand meaning" of a text - sort of Supreme consciousness splitting itself into individual consciousness.

(\*) Another counterexample: A cretan paradox like sentence - "This sentence is a lie" - which is true if it is false and false if true - Lambda function composition algorithm is beyond the scope of such sentences. This sentence exhibits 2 levels of truths and falsehoods - Truth/Falsehood within a sentence and Truth/Falsehood outside the sentence - in former observer and observed are one and the same and in the latter observer stands aloof from observed

(\*) If there are two levels of Truth/Falsehoods similar to stratified realities defined in <https://sites.google.com/site/kuja27/UndecidabilityOfFewNonTrivialQuestions.pdf>, above paradox "This sentence is a lie" can be analyzed (kind of Godel sentence proving languages are incomplete) as below with TRUE/FALSE and true/false being two levels of this nest:

- This sentence is a lie - true - self-refuting and circular
- This sentence is a lie - TRUE - not self-refuting because TRUE

transcends "true"

- This sentence is a lie - false - self-refuting and circular
- This sentence is a lie - FALSE - not self-refuting because FALSE

transcends "false"

(\*) (QUITE PRESUMPTIVE, THIS MIGHT HAVE A PARALLEL IN LOGIC BUT COULDN'T FIND IT) In other words, the sentence "(It is TRUE that (this sentence is a lie))" is different from "(It is true that this sentence is a lie)" - in the former the observer is independent of observed sentence (complete) where as in the latter observer and observed coalesce (incomplete) - TRUE in former has scope beyond the inner sentence while true in latter is scope-restricted to the inner sentence. If Truth and Falsehood are scoped with a universe of discourse, above paradox seems to get reconciled and looks like an extension of Incompleteness theorems in logic. Natural languages and even Formal Logic have only one level of boolean truth/falsehood and thus previous is mere a theoretical fancy.

(\*) Above philosophical dissection of meaning has striking similarities to quantum mechanics - If language has substructure abiding by quantum mechanics [e.g Bose-Einstein model for recursive gloss overlap wordnet subgraph], the links across words which correspond to subatomic particles must obey Heisenberg uncertainty principle also i.e As a linguistic parallel, 100% accurate meaning may never be found by any model of computation. This can not be ruled out if network is a random graph with probabilities for edges.

(\*) Levels of Truth are reminiscent of Tarski's Undefinability of Truth Theorem - <https://plato.stanford.edu/entries/goedel-incompleteness/#TarTheUndTru> - There are two levels of languages - Inner Object Language and Outer Meta Language - Truth of statements in inner object languages are determined in outer meta language. An example sentence in object language is the Cretan Paradox - "All cretans are liars". In previous example, "this sentence is a lie" is defined in object language (English) and is a self-referential Goedel sentence. Truth of this sentence has to be decided in metalanguage. Another example paradox sentence in object language is: "This is bigger than the biggest". Can truth of this be determined in object language? This can be geometrically interpreted: If object language and metalanguage are vector spaces of dimensions  $k$  and  $k+1$ , any sentence in object language is a vector of dimension  $k$  (e.g word2vec representation extended to sentence2vec) and truth of it has to be decided in metalanguage space of dimensions  $k+1$ . In object language space there can not be an entity bigger than biggest - e.g set of concentric circles limited by outermost circle and truth of this sentence is "False". But when this sentence is projected to a  $k+1$  metalanguage vector space, a circle "bigger" in  $k+1$  dimension vectorspace can exist, than the "biggest" circle in  $k$  dimension vectorspace and truth is "True". Example of dimensions in a natural language are Parts-of-Speech.

---

#### 229. (THEORY) Bose-Einstein Condensate model for Recursive Gloss Overlap based Classification

---

Bose-Einstein condensate fitness model by [Ginestra Bianconi] described in 18.10 for any complex network graph is:

Fitness of a vertex =  $2^{(-b \cdot \text{Energy})}$  where  $b$  is a Bose-Einstein condensate function.

Here fitness of a vertex is defined as ability to attract links to itself - Star complexity. It is not known if ability of a word to attract links from other words is same as intrinsic merit of a document in recursive gloss overlap context - prima facie both look equal. As energy of a node decreases, it attracts increased number of node edges. In Recursive Gloss Overlap graph, node with maximum core number or PageRank must have lowest energy and hence the Fittest. Previous equation is by applying Einstein derivation of Satyendranath Bose's Planck's formula for Quantum mechanics where in a critical temperature above zero kelvin most of the particles "condense" in lowest energy level. This was proved in 1995-2001 by NIST lab (<http://bec.nist.gov/>).

Applying the above model to a relational graph obtained from text document

implies graph theoretic representation of language has lurking quantum mechanical traits which should apply to all semantic graphs and ontologies viz., WordNet, ConceptNet etc.,. For example, when a winner word vertex takes all links to other words, the winner word becomes a dictator and thus the only class a document can belong to. Thus Bose-Einstein condensate can be mapped to a Dictator boolean function. This should ideally be extensible to structural complexity of circuit graphs i.e. gate within a neural net TC circuit version of WordNet with maximum fanin and fanout has lowest energy where neighbours flock. If energy implies information entropy in a document, low energy implies low entropy of a text i.e.  $-\sum p \log p$  of a text as bag of words probability distribution, decreases as text document increasingly becomes less chaotic and vice-versa holds too. As a document becomes more chaotic with high entropy and energy, fitness per word vertex decreases as there are multiple energy centres within it. Hence low entropy is equivalent to presence of a high fitness word vertex in the graph.

Analogy: Recursive Gloss Overlap graph can be construed as a 3 dimensional rubbersheet with low energy words as troughs. Deepest troughs are words (lowest energy levels) that classify a document.

Reference:

-----  
229.1 Linked [Albert Laszlo Barabasi] - Chapter 8 - Einstein's Legacy  
229.2 Bianconi-Barabasi Bose-Einstein Condensation in Networks, Simplicial Complexes, Intrinsic Fitness -  
<http://www.eng.ox.ac.uk/sen/files/symposium2017/bianconi.pdf>  
-----

-----  
230. (THEORY) Expander Graphs, Bose-Einstein Condensate Fitness model and Intrinsic Merit  
-----

-----  
Edge expander graphs are defined with Cheeger's constant for minimum high edge boundary per vertex subset:

$$\text{minimum}(|\text{boundary}(S)|/|S|), 1 < |S| < n/2$$

where  $\text{boundary}(S)$  of a subset  $S$  of vertices of  $G$  ( $V(G)$ ) is:

$$\text{boundary}(S) = \{ (u,v) \mid u \in S, v \in V(G) \setminus S \}$$

From Bose-Einstein condensate fitness model, ability of a vertex to attract links increases with decreasing energy of a vertex. This implies  $\text{boundary}(S)$  expands with presence of low energy vertices. Thus Bose-Einstein condensate model translates into an edge expander construction. Also high expansion implies high star complexity. Recursive Gloss Overlap graph with a low energy vertex is a high edge expander and easily classifiable to a topic with core numbers.

Measuring intrinsic merit (and therefore fitness if both are equivalent concepts) by edge expansion (Cheeger's constant) over and above usual connectivity measures formalises a stronger notion of "meaningfulness" of a text document. For example High Cheeger's constant of RGO graph implies high intrinsic merit of a text.

-----  
231. (THEORY) Sentiment analysis and ThoughtNet Continuum - Fine grained emotions and evocation - related to 228  
-----

-----  
(\* ) ThoughtNet need not be a discrete hypergraph but a continuum of edges and nodes. Analogy: Set of countably infinite natural numbers and continuum of uncountably infinite reals. It is difficult to visualize a continuum as a graph - no graph theoretic gadget exists for a continuum graph - Infinite graph is countable, Continuum graph is uncountable. By diagonalization, continuum could be as hard as halting problem.

(\*) Each feature of a visual thought is a class stack node in ThoughtNet. Number of features per visual could be thousands. Visual is flattened into a hyperedge across class stack nodes corresponding to feature vector vertices.

(\*) Example schematic:

```
----->Lambda computation-----
returns | | stores thought hyperedges
evocatives | |
-----ThoughtNet <-----
```

(\*) Colors of Thought hyperedges are determined by sentimentality of class stack nodes. The class stack nodes are colored too, not just edges. If an edge transcends various colored class stack nodes, resultant color of thought hyperedge is a function of colors of constituent class stack nodes:

Edge sentiment color of ThoughtNet Hyperedge = weight\_function(node colors in the hyperedge).

(\*) Node colors are priors. How these priors are decided for each class stack node is the mainstay of emotional inference. This requires assumption of Desire/Prejudice/Bounded Rationality/Irrational Exuberance arising from Consciousness or equivalent. This irrationality creates a pre-conceived potential per class stack node, though no edges may be part of the class at all. Irrationality has to be assumed to be an independent variable and atomic because if it is not, what it depends on is a question. Though previous inquisition on Sentiments, Meaning et al border on Theology, it is inevitable to exclude the emotional root causes while working on a close-to-perfect mathematical simulation of human sentiments.

-----  
232. VIRGO commits for AsFer Software Analytics with SATURN Program Analysis - 29 February 2016, 1 March 2016  
-----

-----  
Software Analytics - SATURN Program Analysis added to VIRGO Linux kernel drivers  
-----

-----  
- SATURN (saturn.stanford.edu) Program Analysis and Verification software has been integrated into VIRGO Kernel as a Verification+SoftwareAnalytics subsystem  
- A sample driver that can invoke an exported function has been added in drivers  
- saturn\_program\_analysis  
- Detailed document for an example null pointer analysis usecase has been created in virgo-docs/VIRGO\_SATURN\_Program\_Analysis\_Integration.txt  
- linux-kernel-extensions/drivers/virgo/saturn\_program\_analysis/saturn\_program\_analysis\_trees/error.txt is the error report from SATURN  
- SATURN generated preproc and trees are in linux-kernel-extensions/drivers/virgo/saturn\_program\_analysis/preproc and linux-kernel-extensions/drivers/virgo/saturn\_program\_analysis/saturn\_program\_analysis\_trees/  
-----

-----  
233. (FEATURE-DONE) Commits as on 3 March 2016 - PERL WordNet::Similarity subroutine for pair of words  
-----

-----  
\*) New perl-src folder with perl code for computing WordNet Distance with Ted Pedersen et al WordNet::Similarity CPAN module

\*) Logs for some example word distances have been included in testlogs. Some weird behaviour for similar word pairs - distance is 1 instead of 0. Probably a

clockwise distance rather than anticlockwise.

This leverages PERLs powerful CPAN support for text data processing. Also python can invoke PERL with PyPerl if necessary.

---

#### 234. (FEATURE-DONE) PERL WordNet::Similarity build and python issues notes

---

- NLTK WordNet corpora despite being 3.0 doesnt work with WNHOME setting (errors in exception files and locations of lot of files are wrongly pointed to)  
- Only Direct download from Princeton WordNet 3.0 works with WNHOME.  
- Tcl/Tk 8.6 is prerequisite and there is a build error "missing result field in Tk\_Inter" in /usr/include/tcl8.6/tcl.h. Remedy is to enable USE\_INTERP\_RESULT flag with macro: #define USE\_INTERP\_RESULT 1 in this header and then do:  
    make Makefile.PL  
    make  
    make install  
in WordNet::Similarity with WNHOME set to /usr/local/WordNet-3.0.  
- PyPerl is no longer in active development - so only subprocess.call() is invoked to execute perl with shell=False.

---

#### 235. (THEORY) Dream Sentiment Analysis with ThoughtNet - related to 18 and 228

---

Dream Analysis in <http://cogprints.org/5030/1/NRC-48725.pdf> (mentioned in 18.8) scores dreams based on polarity with bag of words representation- dreams are known to be related to Limbic and Paralimbic systems in brain. Insofar as theories pertaining to ThoughtNet described in 18 and 228 are concerned, only conscious evocatives arising from events are described. Going a step further, can ThoughtNet account for interpretation of dreams? Dreams, psychologically, are known to be vagaries of suppressed thoughts manifesting in subconscious state. ThoughtNet stores thoughts of experiences, visuals and events as hyperedges consciously. A dream model is proposed where in subconscious/RapidEyeMovement state, Thought hyperedges momentarily disintegrate and re-arrange to form new edges manifesting as dream visuals. Once dream expires, these dream edges are dissolved and original ThoughtNet is restored. Before dissolution, dream might be stored if potentially strong. This explains why some dreams linger after wakeup. Caveat: this is just a theory of dream analysis based on some thought experimentation and has no scientific backing. This model makes an assumption that dream hyperedges are functions of preexisting ThoughtNet hyperedges which is not quite right because there are exceptional phenomena like extra-sensory perception where visions of future are observed by few individuals which could not have arisen from past experience and thoughts. ESP implies brain has faculty to foresee inherently in a superconscious state which is subdued in normal conscious state. It is more accurate to say that dream hyperedges are functions of both past thought hyperedges and superconscious hidden variables which might explain ESP.

---

#### 236. (THEORY) Regularity Lemma and Ramsey Number of Recursive Gloss Overlap graph and ThoughtNet

---

Throughout this document, ranking of documents which is so far a pure statistical and machine learning problem is viewed from Graph Theory and Lambda Function growth perspective - theory invades what was till now engineering. Both Regularity Lemma and Ramsey theory elucidate order in large graphs. Regularity Lemma has a notion of density which is defined as:

$$d(V1, V2) = |E(V1, V2)|/|V1||V2|$$

where  $V_1$  and  $V_2$  are subsets of vertices  $V(G)$  for a graph  $G$  and  $E(V_1, V_2)$  are edges among subsets  $V_1$  and  $V_2$ . Density is a quantitative measure of graph complexity and intrinsic connectedness merit of a text document. Ramsey Number  $R(a, b)$  of a graph is the least number such that there always exists a graph of vertex order  $R(a, b)$  with a clique of size  $a$  or an independent set of size  $b$ . Typically associated with "Party problem" where it is required to find minimum number of people to be invited so that  $a$  people know each other or  $b$  people do not know each other, Ramsey number of ThoughtNet sentiment colorings - e.g bipartisan red-blue colorings for 2 thought hyperedge sentiment polarities - provides a theoretical bound on size of ThoughtNet as such so that order arises in a motley mix of emotionally tagged thoughts - a clique of similar sentimental edges emerges. Similar application of Ramsey number holds good for Recursive Gloss Overlap graph also - a document's graph can have cliques and independent sets with vertex colorings for word sentiments.

=====  
237. (FEATURE-DONE) Commits as on 11 March 2016 - Deep Learning Convolution - Multi Feature Convolution Map Kernel Filters  
=====

- Convolution Network supports Multiple Feature Maps (presently 3)
- New example bitmap for feature recognition of pattern "3" inscribed as 1s has been introduced
- Final neural network from Max pooling layer now is randomized with randint() based weights for each of the 10 neurons
- Logs for this have been committed to testlogs
- Logs show a marked swing in Maxpooling map where the segments of pattern "3" are pronounced.
- Final neural layer shows a variegated decision from each neuron for corresponding 3 convolution maps

-----  
238. (FEATURE-DONE) Commits as on 14 March 2016  
-----

- Some bugs resolved
- Added one more example with no pattern
- Convolution is computed for all 3 bitmap examples
- Final neuron layer now is a function of each point in all maxpooling layers
- The existence of pattern is identified by the final output of each of 10 neurons
- Patterns 0 and 3 have a greater neural value than no pattern. Gradation of neural value indicates intensity of pattern.
- Above is a very fundamental pattern recognition for 2 dimensional data. Sophisticated deconvolution is explained in <http://arxiv.org/abs/1311.2901> which reverse engineers pooling layers with Unpooling.
- 3 logs for this commit have been included in testlogs/
- random weighting has been removed.

-----  
239. (THEORY) Deep Learning Convolution Network and a boolean function learning algorithm of different kind  
-----

Deep Learning Convolution Network for Image Pattern Recognition elicits features from the image considered as 2-dimensional array. In the Deep Learning implementation in python-src/ image is represented as  $\{0,1\}^*$  bitmap blob. Each row of this bit map can be construed as satisfying assignment to some boolean function to be learnt. Thus the 2-dimensional bitmap is set of

assignments satisfying a boolean function - A boolean function learnt from this data - by some standard algorithms viz., PAC learning, Hastad-Linial-Mansour-Nisan fourier coefficient concentration bounds and low-degree polynomial approximation (learning phase averages the coefficients from all sample points and prediction phase uses this averaged fourier coefficient) - accepts the image as input. Deep Learning Convolution Network is thus equivalent to a boolean function learnt from an image - quite similar to HMLN low-degree learning, deep learning convolution also does weighted averaging in local receptive field feature kernel map layers, maxpooling layer and final neuron layers with binary output. Essentially convolution learns a TC circuit. It presupposes existence of set of satisfying assignments which by itself is a #P-complete problem. This connects two hitherto unrelated concepts - Image Recognition and Satisfiability - into a learning theory algorithm for 2-dimensional binary data. Same learning theory approach may not work for BackPropagation which depend on 4 standard Partial Differential Equations.

-----  
 -----  
 240. (FEATURE-DONE) Commits as on 15 March 2016  
 -----

- DeepLearning BackPropagation implementation:
  - An example Software Analytics usecase for CPU and Memory usage has been included
  - Number of Backpropagation weight update iterations has been increased 10 fold to 3000000.
  - logs for some iterations have been included in testlogs/
- DeepLearning Convolution Network implementation:
  - Image patterns have been changed to 0, 8 and no-pattern.
  - Final neuron layer weights have been changed by squaring to scale down the output - this differentiates patterns better.
  - logs for this have been included in testlogs/

-----  
 -----  
 241. (THEORY and IMPLEMENTATION) ThoughtNet and Reinforcement Learning  
 -----

Reinforcement Learning is based on following schematic principle of interaction between environment and agent learning from environment. ThoughtNet described in 228 and previous is an environmental context that every human agent has access to in decision making. This makes human thought process and thought-driven-actions to be a special case of Reinforcement Learning. Reinforcement Learning is itself inspired by behavioural psychology.

```

-----> ThoughtNet context (environment) -----
 action (evocation) | reward and
state transition (most potent evocative thought) |
 |<----- Text Document (agent) -----<----- |

```

Schematic above illustrates text document study as reinforcement learning. During left-right reading of text, evocation action is taken per-word which accesses ThoughtNet storage and returns a reward which is the strongest thought edge. State transition after each evocation is the partially evaluated lambda composition prefix mentioned in 222 - this prefix is updated after reading each word left-right. Human practical reading is most of the time lopsided - it is not exactly left-right but eye observes catchy keywords and swivels/oscillates around those pivots creating a balanced composition tree. Error in disambiguation can be simulated with a model similar to what is known as "Huygen's Gambler's Ruin Theorem" which avers that in any Gambling/Betting game, player always has a non-zero probability of becoming insolvent - this is through a Bernoulli trial sequence as below with fair coin toss (probability=0.5):

- 1) First coin flip -  $\text{Pr}(\text{doubling}_1) = 0.5$ ,  $\text{Pr}(\text{bankrupt}_1) = 0.5$
- 2) Second coin flip -  $\text{Pr}(\text{bankrupt}_2) = \text{Pr}(\text{bankrupt}_1) * 0.5 = 0.25$



- 3) Third coin flip -  $\Pr(\text{bankrupt3}) = \Pr(\text{bankrupt2}) * 0.5 = 0.125$

....

By union bound probability of gambler going bankrupt after infinite number of coin flips is 1. This convergence to 1 applies to unfair biased coin tosses also. This theorem has useful application in ThoughtNet reinforcement learning disambiguation. Reward is defined as probability of most potent evocative thought being retrieved from ThoughtNet (this is when return value is set of hyperedges and not unique - probability of reward is  $1/\text{size\_of\_set\_returned}$ ) and state transition is akin to consecutive coin flips. This proves that probability of imperfect disambiguation is eventually 1 even though reward probability is quite close to 1.

A ThoughtNet Reinforcement Learning implementation has been committed as part of python-src/DeepLearning\_ReinforcementLearningMonteCarlo.py

References:

-----

241.1 Reinforcement Learning - [Richard Sutton] -  
<http://webdocs.cs.ualberta.ca/~sutton/book/the-book.html>,  
<https://www.dropbox.com/s/b3psxv2r0ccmf80/book2015oct.pdf?dl=0>.

-----

242. (FEATURE-BENCHMARK-DONE) Interview Algorithm PySpark-Cython implementation benchmark with and without Spark configurables

-----

This benchmark is done with both:  
InterviewAlgorithmWithIntrinsicMerit\_Crawl\_Visual\_Spark.py  
InterviewAlgorithmWithIntrinsicMerit\_SparkMapReducer.py  
both precompiled with Cython to create .c source files and .so libraries.

Number of keywords in newly crawled web page: 35

-----  
With spark-defaults.conf :

-----  
Execution 1:

-----  
root@shrinivaasanka-Inspiron-1545:/media/shrinivaasanka/0fc4d8a2-1c74-42b8-8099-9ef78d8c8ea2/home/kashrinivaasan/KrishnaiResearch\_OpenSource/GitHub/asfer-github-code/python-src/InterviewAlgorithm/testlogs# for i in `grep Finished InterviewAlgorithmWithIntrinsicMerit\_Crawl\_Visual\_Spark.2localthreads.CythonOptimized.16March2016.out |grep TaskSetManager| awk '{print \$14}'`  
> do  
> sum=\$(expr \$sum + \$i)  
> done

root@shrinivaasanka-Inspiron-1545:/media/shrinivaasanka/0fc4d8a2-1c74-42b8-8099-9ef78d8c8ea2/home/kashrinivaasan/KrishnaiResearch\_OpenSource/GitHub/asfer-github-code/python-src/InterviewAlgorithm/testlogs# echo \$sum  
243058  
root@shrinivaasanka-Inspiron-1545:/media/shrinivaasanka/0fc4d8a2-1c74-42b8-8099-9ef78d8c8ea2/home/kashrinivaasan/KrishnaiResearch\_OpenSource/GitHub/asfer-github-code/python-src/InterviewAlgorithm/testlogs# grep Finished InterviewAlgorithmWithIntrinsicMerit\_Crawl\_Visual\_Spark.2localthreads.CythonOptimized.16March2016.out |grep TaskSetManager| awk '{print \$14}'|wc -l  
156  
Per task time in milliseconds: ~1558

-----  
Execution 2:

-----  
root@shrinivaasanka-Inspiron-1545:/media/shrinivaasanka/0fc4d8a2-1c74-42b8-8099-

```

9ef78d8c8ea2/home/kashrinivaasan/KrishnaiResearch_OpenSource/GitHub/asfer-
github-code/python-src/InterviewAlgorithm/testlogs# for i in `grep Finished
InterviewAlgorithmWithIntrinsicMerit_Crawl_Visual_Spark.2localthreads.CythonOpt
imized2.16March2016.out |grep TaskSetManager| awk '{print $14}'`
> do
> sum=$(expr $sum + $i)
> done
root@shrinivaasanka-Inspiron-1545:/media/shrinivaasanka/0fc4d8a2-1c74-42b8-8099-
9ef78d8c8ea2/home/kashrinivaasan/KrishnaiResearch_OpenSource/GitHub/asfer-
github-code/python-src/InterviewAlgorithm/testlogs# echo $sum
520074
root@shrinivaasanka-Inspiron-1545:/media/shrinivaasanka/0fc4d8a2-1c74-42b8-8099-
9ef78d8c8ea2/home/kashrinivaasan/KrishnaiResearch_OpenSource/GitHub/asfer-
github-code/python-src/InterviewAlgorithm/testlogs# grep Finished
InterviewAlgorithmWithIntrinsicMerit_Crawl_Visual_Spark.2localthreads.CythonOpt
imized2.16March2016.out |grep TaskSetManager| awk '{print $14}'|wc -l
312
Per task time in milliseconds: ~1666

```

-----  
Without spark-defaults.conf  
-----

Execution 3:

```

root@shrinivaasanka-Inspiron-1545:/media/shrinivaasanka/0fc4d8a2-1c74-42b8-8099-
9ef78d8c8ea2/home/kashrinivaasan/KrishnaiResearch_OpenSource/GitHub/asfer-
github-code/python-src/InterviewAlgorithm/testlogs# echo $sum
69691
root@shrinivaasanka-Inspiron-1545:/media/shrinivaasanka/0fc4d8a2-1c74-42b8-8099-
9ef78d8c8ea2/home/kashrinivaasan/KrishnaiResearch_OpenSource/GitHub/asfer-
github-code/python-src/InterviewAlgorithm/testlogs# grep Finished
InterviewAlgorithmWithIntrinsicMerit_Crawl_Visual_Spark.2localthreads.CythonOpt
imized3.16March2016.out |grep TaskSetManager| awk '{print $14}'|wc -l
156
Per task time in milliseconds: ~446 which is twice faster than earlier benchmark
done in February 2016 and almost 4 times faster than previous 2 executions with
spark-defaults.conf enabled.

```

A spark-defaults.conf file has been committed to repository (Reference: <http://spark.apache.org/docs/latest/configuration.html>). With Spark configuration settings for memory and multicore, something happens with Spark performance which is counterintuitive despite document size being almost same.

-----  
243. Commits (1) as on 16,17 March 2016  
-----

PySpark-Cython Interview Algorithm for Merit - Benchmark

- 3 executions with and without spark-defaults.conf config settings have been benchmarked
- Cython setup.py has been updated to compile both InterviewAlgorithmWithIntrinsicMerit\_Crawl\_Visual\_Spark.py and InterviewAlgorithmWithIntrinsicMerit\_SparkMapReducer.py to create .c and .so files
- Benchmark yields some intriguing results:
  - Executions with spark-defaults.conf enabled are 4 times slower than executions without spark-defaults.conf
  - Execution without spark config is twice faster than earlier benchmark
- Logs and screenshots for above have been committed to testlogs
- Text document has been recrawled and updated (number of keywords almost same as previous benchmark)
- Spark config file has been committed

-----

244. Commits (2) as on 16,17 March 2016

-----  
More benchmarking of PySpark-Cython Intrinsic Merit computation  
-----

- Enabled Spark RDD cacheing with cache() - storage level MEMORY
- Recompiled .c and .so with Cython
- uncommented both lines in Cython setup.py
- logs and screenshots for above have been committed in testlogs/
- locking.acquire() and locking.release() have been commented
- With this per task duration has been brought down to ~402 milliseconds on single node cluster. Ideally on a multinode cluster when tasks are perfectly distributable, this should be the runtime.

-----  
With spark-defaults.conf - multiple contexts disabled and reuse worker enabled  
-----

```
root@shrinivaasanka-Inspiron-1545:/media/shrinivaasanka/0fc4d8a2-1c74-42b8-8099-9ef78d8c8ea2/home/kashrinivaasan/KrishnaiResearch_OpenSource/GitHub/asfer-github-code/python-src/InterviewAlgorithm/testlogs# echo $sum
246796
root@shrinivaasanka-Inspiron-1545:/media/shrinivaasanka/0fc4d8a2-1c74-42b8-8099-9ef78d8c8ea2/home/kashrinivaasan/KrishnaiResearch_OpenSource/GitHub/asfer-github-code/python-src/InterviewAlgorithm/testlogs# grep Finished
InterviewAlgorithmWithIntrinsicMerit_Crawl_Visual_Spark.2localthreads.CythonOptimized.17March2016.out |grep TaskSetManager| awk '{print $14}'|wc -l
156
Per task time milliseconds: ~1582
```

-----  
Without spark-defaults.conf - locking.acquire()/release() disabled and Spark RDD cacheing enabled  
-----

```
root@shrinivaasanka-Inspiron-1545:/media/shrinivaasanka/0fc4d8a2-1c74-42b8-8099-9ef78d8c8ea2/home/kashrinivaasan/KrishnaiResearch_OpenSource/GitHub/asfer-github-code/python-src/InterviewAlgorithm/testlogs# echo $sum
248900
root@shrinivaasanka-Inspiron-1545:/media/shrinivaasanka/0fc4d8a2-1c74-42b8-8099-9ef78d8c8ea2/home/kashrinivaasan/KrishnaiResearch_OpenSource/GitHub/asfer-github-code/python-src/InterviewAlgorithm/testlogs# grep Finished
InterviewAlgorithmWithIntrinsicMerit_Crawl_Visual_Spark.2localthreads.CythonOptimized2.17March2016.out |grep TaskSetManager| awk '{print $14}'|wc -l
618
Per task time milliseconds: ~402 (fastest observed thus far per task; Obviously something is wrong with spark-defaults.conf enabled)
```

-----  
245. (FEATURE-BENCHMARK-DONE) Interview Algorithm PySpark-Cython implementation benchmark with Spark configurables  
-----

- Commits as on 21 March 2016

-----  
Following benchmark was done with a new spark-defaults.conf (committed as spark-defaults2.conf):  
-----

```
root@shrinivaasanka-Inspiron-1545:/media/shrinivaasanka/0fc4d8a2-1c74-42b8-8099-9ef78d8c8ea2/home/kashrinivaasan/KrishnaiResearch_OpenSource/GitHub/asfer-github-code/python-src/InterviewAlgorithm/testlogs# echo $sum
965910
root@shrinivaasanka-Inspiron-1545:/media/shrinivaasanka/0fc4d8a2-1c74-42b8-8099-9ef78d8c8ea2/home/kashrinivaasan/KrishnaiResearch_OpenSource/GitHub/asfer-github-code/python-src/InterviewAlgorithm/testlogs# grep Finished
```

```
InterviewAlgorithmWithIntrinsicMerit_Crawl_Visual_Spark.2localthreads.CythonOpt
imized.21March2016.out |grep TaskSetManager| awk '{print $14}'|wc -l
618
Time per task in milliseconds: ~1562 (Again, with spark-defaults.conf with some
additional settings, there is a blockade)
```

---

#### 246. (THEORY) Learning a variant of Differential Privacy in Social networks

---

Nicknames/UserIds in social media are assumed to be unique to an individual. Authentication and authorization with Public-Key Infrastructure is assumed to guarantee unique identification. In an exceptional case, if more than one person shares a userid intentionally or because of cybercrime to portray a false picture of other end, is it possible to distinguish and learn such spoof behaviour? This is a direct opposite of differential privacy [Cynthia Dwork - <http://research.microsoft.com/pubs/64346/dwork.pdf>] where 2 databases differing in one element are indistinguishable to queries by a randomized algorithm with coin tosses. But in previous example of shared id(s) in social network, distinguisher should be able to discern the cases when a remote id is genuine and spoofed/shared - probably suitable name for it is Differential Identification. This can theoretically happen despite all PKI security measures in place when id is intentionally shared i.e a coalition of people decide to hoodwink PKI by sharing credentials and the receiving end sees them as one. For example, if a chat id is compromised by a coalition, the chat transcript is no longer credible reflection of the other end, and receiving end may not be aware of this at all. Here chat transcript is a mix of both genuine and spoofed portrayal of other end. An example statistical Learning algorithm for distinguishing when spoof happened analyzes the chat transcript conversations with genuine chat as priors if there is a prior available. Non-statistically, it is not known how a boolean function learner would look like for this example. A special case is when a coalition is unnecessary. The remote end can be a single individual garnering collective wisdom from multiple sources to present a deceptive portrayal of multitude.

---

#### 247. (FEATURE-DONE) Commits as on 24 March 2016 - Code Optimizations - Cacheing and Loop invariant - Interview Algorithm

---

- New Cacheing datastructures have been included for storing already found previous level backedge vertices for each level and already found gloss tokens. Presently these caches are python dictionaries only and in a distributed setting this can be replaced with an object key-value stores like memcached.(InterviewAlgorithm/InterviewAlgorithmWithIntrinsicMerit\_SparkMapReducer.py)
- There was an inefficient loop invariant computation for prelevessynsets\_tokens which has been moved to outermost while. (InterviewAlgorithm/InterviewAlgorithmWithIntrinsicMerit\_Crawl\_Visual\_Spark.py)
- spark-default2.conf has been updated with few more Spark config settings
- Spidered text has been recrawled
- logs and screenshots for this commits have been included in testlogs/
- Cython .c , .so files have been rebuilt
- Cacheing above in someway accomplishes the isomorphic node removal by way of Cache lookup

---

#### 248. (FEATURE-BENCHMARK-DONE) Intrinsic Merit PySpark-Cython implementation - With and Without cacheing

- Commits as on 25 March 2016

-----  
-----  
1.Cache md5 hashkey has been changed to be the complete tuple  
(tokensofprevlevel,keyword) - the rationale is to have perfect  
uniqueness to find backvertices for a keyword and gloss from previous recursion  
step.  
2.Following benchmark was done by disabling and enabling lookupCache and  
lookupCacheParents boolean flags.  
3.Cache values are "Novalue" string literals by default initialized in lambda  
and the Cache updates are not append()s but  
simple key-value assignments.

--  
Number of keywords: 7  
Without Cacheing: 9 minutes for all tasks (including NetworkX and graphics  
rendering times which is quite considerable)  
With Cacheing: 9 minutes for all tasks (including NetworkX and graphics  
rendering times which is quite considerable)

Summation of individual task times in milliseconds and averaging sometimes gives  
misleadingly high duration per task though  
total execution is faster. Because of this start-end time duration is measured.  
For above example Cacheing has no effect because  
there are no repetitions cached to do lookup. Logs and screenshots with and  
without cacheing have been committed to testlogs/

-----  
-----  
249. (THEORY) An alternative USTCONN LogSpace algorithm for constructing  
Recursive Gloss Overlap Graph  
-----

-----  
Benchmarks above are selected best from multiple executions. Sometimes a  
mysterious slowdown was observed with both CPUs clocking 100%  
load which could be result of JVM Garbage Collection for Spark processes among  
others. These benchmarks are thus just for assessing feasibility of Spark  
clustering only and a perfect benchmark might require a cloud of few thousand  
nodes for a crawled webpage. At present there is no known standard algorithm to  
convert a natural language text to a relational graph without WordNet and  
internally looking up some \*Net ontology to get path relations between two words  
could be indispensable theoretically speaking. This is the reverse process of  
Graph Traversals - Breadth First and Depth First - traversal is the input text  
and a graph has to be extracted from it. For n keywords, there are  $n^2$  ordered  
pairs of word vertices possible for each of which WordNet paths have to be  
found. This is Undirected ST Connectivity in graphs for which there are quite a  
few algorithms known right from [Savitch] theorem upto [OmerReingold] ZigZag  
product based algorithm in logspace. This is more optimal compared to all pairs  
shortest paths on WordNet. This algorithm does not do deep learning recursion  
top-down to learn a graph from text. For all pairs this is better than  $O(n^3)$   
which is upperbound for All Pairs Shortest Paths. These  $n^2$  pairs of paths  
overlap and intersect to create a graph. Presently implemented Recursive Gloss  
Overlap learns deeper than all pairs USTCONN algorithm because it uses  
"superinstance" notion - whether x is in definition of y - something absent in  
WordNet jargon. This algorithm is quadratic in number of words where as  
Recursive Gloss Overlap is linear -  $O(n*d*s^{tmax}/cpus)$  - counterintuitively.

-----  
-----  
250. Commits as on 29 March 2016  
-----

-----  
- New subroutine for printing WordNet Synset Path between 2 words - this prints  
edges related by hypernyms and hyponyms  
- an example log has been committed in testlogs/

From the example path in logs, distance is more of a metapath than a thesaurus-like path implemented in Recursive Gloss Overlap in NeuronRain. Due to this limitation of WordNet hyper-hyponyms the usual unsupervised classifier based on core numbers of the graph translated from text would not work as accurately with straightforward WordNet paths. This necessitates the superinstance relation which relates two words  $k$  and  $l$ :  $k$  is in definition of  $l$ .

-----  
-----  
251. (FEATURE-DONE) Commits (1) as on 30 March 2016 - MemCache Integration with Spark-Cython Intrinsic Merit Computation  
-----

-----  
-----  
- In this commit, native python dictionary based cache lookup for Spark\_MapReduce() and Spark\_MapReduce\_Parents() is replaced with standard MemCache Distributed Object Cacheing get()/set() invocations.  
- Logs and Screenshots for above have been committed to testlogs/  
- Prerequisites are MemCached (ubuntu apt package) and Python-memcache (pip install) libraries  
- a recrawled webpage has been merit-computed  
- MemCached is better than native dict(s) because of standalone nature of Cache Listener which can be looked up from anywhere on cloud  
-----

-----  
-----  
252. (FEATURE-DONE) Commits (2) as on 30 March 2016 - Spark-Cython Intrinsic Merit computation with spark-defaults.conf enabled  
-----

-----  
-----  
- spark-defaults2.conf has been enabled with extra java options for performance (reference: <http://docs.oracle.com/javase/8/docs/technotes/tools/unix/java.html>)  
- lookupCache and lookupCacheParents boolean flags have been done away with because memcache has been enabled by default for subgraph cacheing  
- With this spark logs show more concurrency and less latency. Dynamic allocation was in conflict with number of executors and executors has been hence commented in spark-defaults2.conf  
- text document has been updated to have ~10 keywords. This took almost 7 minutes which looks better than one with spark-defaults.conf disabled  
- Screenshot and logs have been committed in testlogs/  
-----

-----  
-----  
253. (FEATURE-DONE) Commits as on 1 April 2016  
-----

-----  
-----  
Loopless Map function for Spark\_MapReduce()  
-----

-----  
-----  
- new Map function MapFunction2() has been defined which doesn't loop through all keywords per level, but does the glossification per keyword which is aggregated by Reduce step. MapFunction() does for loop for all keywords per level.  
- a dictionary cacheing with graphcachelocal has been done for lookup of already gloss-tokenized keywords. This couldn't be memcached due to a weird error that resets the graphcachelocal to a null which shouldn't have.  
- This has a execution time of 6 minutes overall for all tasks compared to for-loop Map function in Spark\_MapReduce().  
- logs and screenshots for Loopless Map with and without graphcachelocal have been committed  
- Rebuilt Cython .c, .o, .so, intrinsic merit log and DOT files  
-----  
-----

254. (THEORY) Hypercontractivity - Bonami-Beckner Theorem Inequality, Noise Operator and p-Norm of Boolean functions

Hypercontractivity implies that noise operator attenuates a boolean function and makes it close to constant function. Hypercontractivity is defined as:

$|Trhof|_q \leq |f|_p$  where  $0 \leq \rho \leq \sqrt{(p-1)(q-1)}$  for some p-norm and q-norm

and in its expanded form as:

$$\sigma(\rho^{|S|} \cdot (1/2^n \cdot \sigma(|f(x)|^q \cdot (-1)^{\text{parity}(x)})))^{1/q \cdot \text{parity}(S)} \leq (1/2^n \cdot \sigma(|f(x)|^p))^{1/p}$$

Hypercontractivity upperbounds a noisy function's q-norm by same function's p-norm without noise. For 2-norm, by Parseval's theorem which gives 2-norm as  $\sigma(f(S)^2)$ , hypercontractivity can be directly applied to Denoisification in 53.11 and 53.12 as it connects noisy and noiseless boolean function norms.

Reference:

254.1 Bonami-Beckner Hypercontractivity -  
<http://theoryofcomputing.org/articles/g001/g001.pdf>

255. (THEORY) Hypercontractivity, KKL inequality, Social choice boolean functions - Denoisification 3

For 2-norm, Bonami-Beckner inequality becomes:

$$\sigma(\rho^{|S|} \cdot \text{fourier\_coeff}(S)^2)^{2/2} \leq [1/2^n \cdot (\sigma(f(x)^p)^{2/p})]$$

For boolean functions  $f: \{0,1\}^n \rightarrow \{-1,0,1\}$ , [Kahn-Kalai-Linial] inequality is special case of previous:

$$\text{For } \rho=p-1 \text{ and } p=1+\delta, \sigma(\delta^{|S|} \cdot \text{fourier\_coeff}(S)^2) \leq (\Pr[f \neq 0])^{2/(1+\delta)}$$

where p-norm is nothing but a norm on probability that f is non-zero (because  $\Pr[f \neq 0]$  is a mean of all possible f(x) at  $2^n$  points).

From 53.12 size of a noisy boolean function circuit has been bounded as:

$\text{Summation}(\rho^{|S|} \cdot \text{fourier\_coeff}(S)^2) \cdot 2^{(t^{1/d}/20)-1} \leq \text{Size}$   
for  $|S| > t$ . From KKL inequality, 2-norm in LHS can be set to maximum of  $(\Pr[f \neq 0])^{2/(1+\delta)}$  in 53.12 and Size lowerbound is obtained for a denoised circuit:

$$(\Pr[f \neq 0])^{2/(1+\delta)} \cdot 2^{(t^{1/d}/20)-1} \leq \text{Size}$$

which is exponential when  $\delta=1$  and  $\Pr[f \neq 0]$  is quite close to 1 i.e f is 1 or -1 for most of the inputs.

If f is 100% noise stable, from Plancherel theorem:

$$\sigma(\rho^{|S|} \cdot f(S)^2) = 1, S \text{ in } [n]$$

$$\text{For } |S| < t=n, 1 - \text{Summation}(\rho^{|S|} \cdot \text{fourier\_coeff}(S)^2) \leq 2^{(\text{Size})} \cdot 2^{(-t^{1/d}/20)}$$

But for  $\rho=p-1$  and  $p=1+\delta$ ,  $1 - \text{Summation}(\delta^{|S|} \cdot \text{fourier\_coeff}(S)^2) > 1 - (\Pr[f \neq 0])^{2/(1+\delta)}$  from KKL inequality.

$$\begin{aligned} \text{For } |S| < t=n, 1 - (\Pr[f \neq 0])^{2/(1+\delta)} &< 1 - \text{Summation}(\rho^{|S|} \cdot \text{fourier\_coeff}(S)^2) \leq 2^{(\text{Size})} \cdot 2^{(-t^{1/d}/20)} \\ \Rightarrow 0.5 \cdot (1 - (\Pr[f \neq 0])^{2/(1+\delta)}) \cdot 2^{(t^{1/d}/20)} &< 0.5 \cdot (1 - \text{Summation}(\rho^{|S|} \cdot \text{fourier\_coeff}(S)^2)) \cdot 2^{(t^{1/d}/20)} \leq \text{Size} \end{aligned}$$

Again denoisification by letting  $\rho$  and  $\delta$  tend to 0 in above, places an exponential lowerbound, with constant upperbound on depth, on a noiseless circuit size. In above size bound  $\lim_{n \rightarrow \infty} n^{1/n} = 1$  for n tending to infinity (Real analysis result - [http://www.jpetrie.net/2014/10/12/proof-that-the-limit-as-n-approaches-infinity-of-n^{1/n}-1-\lim\\_n-to-infty-n^{1/n}-1/](http://www.jpetrie.net/2014/10/12/proof-that-the-limit-as-n-approaches-infinity-of-n^{1/n}-1-\lim_n-to-infty-n^{1/n}-1/)). Percolation in 100% noise stable regime can have NC/poly circuits while above stipulates the lowerbound

for noiseless circuits to be exponential when depth is constant. It implies NC/Poly formulation of percolation has unrestricted depth which is obvious because 100% noise stability regime is attained when  $n$  tends to infinity. Randomized algorithm equivalent of Percolation implies Percolation is in RP or RNC with pseudorandom advice which vindicates derandomized NC representation for percolation. This leads to an important result if 100% stability implies lowerbound: LHS is an NC/Poly Percolation circuit in 100% noise stability regime of polynomial size. RHS is exponential, denoised, 100% stable circuit of arbitrary hardness. From 53.9 and 53.16, RHS has an NC/Poly lowerbound e.g if RHS is PH-complete then PH in P/poly. From Toda's theorem, PH is in  $P^{\#P}$  and there is a known result that  $P^{\#P}$  in P/Poly implies  $P^{\#P} = MA$ . Unifying: PH in  $P^{\#P}$  in P/Poly  $\Rightarrow P^{\#P} = MA$ . (assumption: NC/Poly is in P/Poly because any logdepth, polysize bounded fanin circuit has polysize gates) NC/log percolation circuit would imply collapse of polynomial hierarchy - RHS PH-complete is lowerbounded by LHS NC/log in P and trivially  $P = NP$ .

Percolation boolean functions have a notion of revealment - that is, there exists a randomized algorithm corresponding to each percolation boolean function which has coin toss advice to query the next bit and revealment is the maximum probability that a bit index  $i$  in  $[n]$  is queried in these sets of bits  $B$  in  $[n]$  - it reveals the secret in randomness. Thus LHS Percolation in  $\Pr(\text{Good})$  circuit can be simulated by a randomized algorithm with revealment. In such a case, advice strings are random coin tosses. This revealment has close resemblance to random restrictions - each restriction brings down a variable by revealing it finally leading to a constant function. Following theorem connects Fourier weights of percolation and Randomized revealments:

$$\text{Sigma}(\text{fourier\_coeff}(S)^2) \leq \text{revealment} * \text{constant} * 2\text{-norm}(f)$$

There is a special case in which size of advice list can be brought down to  $\log n$  from  $n$  for  $Z(n)$  grid. Set of  $\log n$  points are pseudorandomly chosen from  $n$  points. This  $\log n$  sized subset when sorted would still point to left-right trend unless leftmost and rightmost are not in sample. This places Percolation in NC/log which could imply a PH collapse mentioned previously. This is an exponential decrease in size of advice.

Reference:

-----  
 255.1 Randomized Algorithms and Percolation -  
<http://math.univ-lyon1.fr/~garban/Slides/Newton.pdf>

## ----- 256. (THEORY) Majority Voting in Multipartisan Elections -----

Uptill now,  $P(\text{Good})$  majority voting in this document describes only 2-candidate elections with a majority function voting circuit.

Noise stability of a voter's decision boolean function is assumed as a suitable measure of voter/voting error in RHS of  $P(\text{Good})$  summation. Most generic RHS is when there is a multiway contest and error is bounded.  $P(\text{Good})$  binomial summation still applies for multipartisan democracy because voter decision vector (set of binary decision bits of all voters - in  $\{\text{Good}, \text{Bad}\}^*$ ) remains same though number of candidates increase manifold. Differences are in:

- Individual Voter Judging Functions which are not boolean functions and
- Generic Majority Function that needs to find most prominent index from an assorted mix of votes (Heavy hitter) - might require Sorting Networks on Hashvalues.

- There are three variables - number of variables per voter, number of voters and number of candidates (which is 2 in boolean decision functions special case for fixed 2 candidate elections) and these numbers can be arbitrarily huge - in the order of Graham's number for example.

Voter judging functions have to choose an index within  $n$  candidates than simple 0-1. In a special case non-boolean functions can be simulated by a functional



aggregation of boolean functions e.g Voted Candidate index in binary representation is nothing but a  $\log N$  sized binary string of 0-1 output gates from multiple boolean functions for maximum of  $N$  candidates. Measuring how good is the choice made by a multiway voter decision function has no equivalent notion of stability and sensitivity in non-boolean functions. For 2 voters 0-1 boolean function is sufficient. Multiparty Generic Majority Function without tie in which candidates are hashkeys and votes are hashvalues can be shown to be NP-complete from Money Changing Problem and 0-1 Integer Linear Programming([https://sites.google.com/site/kuja27/IntegerPartitionAndHashFunctions\\_2014.pdf](https://sites.google.com/site/kuja27/IntegerPartitionAndHashFunctions_2014.pdf)). [Friedgut-Kalai-Nisan] theorem is quantitative extension of Arrow's Theorem and Gibbard-Satterthwaite Theorem which prove that there is a non-zero probability that elections with 3 candidates and more can be manipulated. This appears sufficient to prove that Goodness probability of a multiway contest in RHS of  $P(\text{good})$  binomial summation can never converge to 100% implying that democracy is deficient. This non-constructively shows the impossibility without even knowing individual voter error and series summation. Interestingly, this divergence condition coincides with contradiction mentioned in 53.16.3.1 for PARITY3SAT superpolynomial size circuits. Assuming an NC/Poly or P/Poly LHS Percolation Boolean Function with 100% noise stability in  $P(\text{Good})$  LHS, Multiway Election in RHS can be placed in hardest known complexity classes - Polynomial Hierarchy PH, EXPSPACE - \*) for PH it is exponential DC-uniform circuit size required by RHS \*) for adversarial simulation by Chess, Go etc., it is EXPTIME-hard required by RHS etc.,. This fits into scenario 53.9.5 when LHS is 100% stable circuit and RHS is unstable PH=DC circuit.

#### Reference:

- 256.1. Elections can be manipulated often - [Friedgut-Kalai-Nisan] - <http://www.cs.huji.ac.il/~noam/apx-gs.pdf>  
 256.2. Computational Hardness of Election Manipulation - <https://www.illc.uva.nl/Research/Publications/Reports/MoL-2015-12.text.pdf>  
 -----

---  
 257. Commits as on 4 April 2016  
 -----

- - Updated AsFer Design Document - KKL inequality and Denoisification  
 - Spark-Cython intrinsic merit computation has been md5hash enabled again since there were key errors with large strings  
 - logs and screenshots have been committed to testlogs/  
 - rebuilt Cython .c, .so files  
 - Spidered text has been changed - This took 28 minutes for ~40+ keywords better than 6 minutes for ~10 keywords earlier. Again Spark in single node cluster dualcore has some bottleneck.  
 -----

-----  
 258. (FEATURE-BENCHMARK-DONE) Analysis of PySpark-Cython Intrinsic Merit Computation Benchmarks done so far  
 -----

-----  
 From 191 and 201 time complexity analysis of Recursive Gloss Overlap algorithm, for single node dualcore cluster following is the runtime bound:

$$O(n \cdot d \cdot s^{\text{tmax}} / \text{cpus})$$

where  $d$  is the number of keywords,  $n$  is the number of documents and  $s$  is the maximum gloss size per keyword. For last two benchmarks done with MD5 hashkeys, Local Cacheing and Global Cacheing(MemCached) enabled number of words are 10 and 40. Corresponding runtimes are:

-----  
 10 words  
 -----

n=1

d=10  
s=constant  
tmax=2 (depth 2 recursion)  
cpus=2 (dual core)  
Runtime = 7 minutes =  $k \cdot 10 \cdot (s)^{2/2}$

-----  
40 words  
-----

n=1  
d=40  
s=constant  
tmax=2 (depth 2 recursion)  
cpus=2 (dual core)  
Runtime = 28 minutes =  $k \cdot 40 \cdot (s)^{2/2}$

Ratio is  $7/28 = k \cdot 10 \cdot (s)^{2/2} / k \cdot 40 \cdot (s)^{2/2} = 0.25$  a linear scaling in number of words which substantiates the theoretical bound. If cluster scales on number of words and documents (e.g logd and logn) this should have non-linear asymptotic scaling. Maximum number of words per document can be an assumption and set to a hardcoded large number. If number of web documents versus number of keywords follow a Gaussian Normal distribution i.e a small fraction of documents have high number of words while the tails have less number of keywords, cluster prescales on a function of mean which is apriori known by a heuristic. Above excludes the crawling time per webpage - crawling does not build linkgraph.

-----  
259. (THEORY) Major update to Computational Geometric PRAM-NC algorithm for Discrete Hyperbolic Factorization  
-----

-----  
PRAM-NC Algorithm for Discrete Hyperbolic Factorization in 34 above:

#### 34.1 LaTeX -

[http://sourceforge.net/projects/acadpdrafts/files/DiscreteHyperbolicPolylogarithmicSieveForIntegerFactorization\\_PRAM\\_TileMergeAndSearch\\_And\\_Stirling\\_Upperbound\\_updateddraft.tex/download](http://sourceforge.net/projects/acadpdrafts/files/DiscreteHyperbolicPolylogarithmicSieveForIntegerFactorization_PRAM_TileMergeAndSearch_And_Stirling_Upperbound_updateddraft.tex/download)

#### 34.2 PDF -

[http://sourceforge.net/projects/acadpdrafts/files/DiscreteHyperbolicPolylogarithmicSieveForIntegerFactorization\\_PRAM\\_TileMergeAndSearch\\_And\\_Stirling\\_Upperbound\\_updateddraft.pdf/download](http://sourceforge.net/projects/acadpdrafts/files/DiscreteHyperbolicPolylogarithmicSieveForIntegerFactorization_PRAM_TileMergeAndSearch_And_Stirling_Upperbound_updateddraft.pdf/download)

internally relies on [BerkmanSchieberVishkin] and other All Nearest Smaller Values PRAM algorithms for merging sorted tessellated hyperbolic arc segments which is then binary searched to find a factor. There are some older alternatives to merging sorted lists other than All Nearest Smaller Values which require more processors. Section 2.4 in [RichardKarp-VijayaRamachandran] on "Sorting, Merging and Selection" in PRAM where input is an array of  $O(N=n)$  elements, describes some standard PRAM algorithms, gist of which is mentioned below (<https://www.eecs.berkeley.edu/Pubs/TechRpts/1988/5865.html>):

259.1) There are 3 parallel computing models - Parallel Comparisons, Comparator Sorting Networks and PRAMs

259.2) Section 2.4.1 on merging two increasing sequences of length n and m,  $n \leq m$  in Page 19 gives an algorithm of  $O(\log \log N)$  steps on  $O(n+m)$  CREW PRAM processors. This constructs a merge tree bottom-up to merge two sorted lists. For merging more than 2 lists, requires logarithmic additional parallel steps.

259.3) Section 2.4.2 describes Batcher's and [AjtaiKomlosSzmeredi] Bitonic Sort algorithm which sorts n elements in  $O((\log n)^2)$  time with  $n/2$  processors.

259.4) Section 2.4.3 describes Cole's PRAM sorting algorithm which requires  $O(\log n)$  steps and  $O(n)$  PRAM processors.

Advantage of these older algorithms is they are implementable e.g Bitonic sort - [https://en.wikipedia.org/wiki/Bitonic\\_sorter](https://en.wikipedia.org/wiki/Bitonic_sorter), <http://www.nist.gov/dads/HTML/bitonicSort.html>. Replacing

[BerkmanSchieberVishkin] in ANSV sorted tile merge for discrete hyperbolic factorization with older algorithms like bitonic parallel sorting networks would require more processors but still be in NC though not PRAM.

References:

-----  
259.1 Bitonic Sorting -

<https://cseweb.ucsd.edu/classes/wi13/cse160-a/Lectures/Lec14.pdf>  
-----

-----  
260. Commits as on 10 April 2016  
-----

Complement Function script updated with a new function to print Ihara Identity zero imaginary parts mentioned in  
Complement Function extended draft:

1.

<https://sourceforge.net/p/asfer/code/HEAD/tree/asfer-docs/AstroInferDesign.txt>

2.

<https://github.com/shrinivaasanka/asfer-github-code/blob/master/asfer-docs/AstroInferDesign.txt>

Logs for this included in python-src/testlogs/  
-----

-----  
261. Commits (1) as on 12 April 2016  
-----

(FEATURE-DONE) Implementation for NC Discrete Hyperbolic Factorization with Bitonic Sort alternative (in lieu of unavailable PRAM implementations):  
-----

-----  
Bitonic Merge Sort Implementation of:

-  
[http://sourceforge.net/projects/acadpdrafts/files/DiscreteHyperbolicPolylogarithmicSieveForIntegerFactorization\\_PRAM\\_TileMergeAndSearch\\_And\\_Stirling\\_Upperbound\\_updateddraft.tex/download](http://sourceforge.net/projects/acadpdrafts/files/DiscreteHyperbolicPolylogarithmicSieveForIntegerFactorization_PRAM_TileMergeAndSearch_And_Stirling_Upperbound_updateddraft.tex/download)  
-

[http://sourceforge.net/projects/acadpdrafts/files/DiscreteHyperbolicPolylogarithmicSieveForIntegerFactorization\\_PRAM\\_TileMergeAndSearch\\_And\\_Stirling\\_Upperbound\\_updateddraft.pdf/download](http://sourceforge.net/projects/acadpdrafts/files/DiscreteHyperbolicPolylogarithmicSieveForIntegerFactorization_PRAM_TileMergeAndSearch_And_Stirling_Upperbound_updateddraft.pdf/download)

- Bitonic Sort is  $O((\log n)^2)$  and theoretically in NC  
- Bitonic Sort requires  $O(n^2 \log n)$  parallel comparators. Presently this parallelism is limited to parallel exchange of variables in bitonic sequence for which python has builtin support (bitonic\_compare()) - internally how it performs on multicore archs is not known.  
- a shell script has been added which does the following  
(cpp-src/miscellaneous/DiscreteHyperbolicFactorizationUpperbound\_Bitonic.sh):  
- NC Factorization implementation with Bitonic Sort is C++Python (C++ and Python)  
- C++ side creates an unsorted mergedtiles array for complete tessellated hyperbolic arc  
(cpp-src/miscellaneous/DiscreteHyperbolicFactorizationUpperbound\_Bitonic.cpp)  
- This mergedtiles is captured via output redirection and awk in a text file  
cpp-src/miscellaneous/  
DiscreteHyperbolicFactorizationUpperbound\_Bitonic.mergedtiles  
- Python bitonic sort implementation which is a modified version of algorithm in [https://en.wikipedia.org/wiki/Bitonic\\_sorter](https://en.wikipedia.org/wiki/Bitonic_sorter)

requires the size of the array to be sorted in exponents of 2. Presently it is hardcoded as array of size 16384 -  $2^{16}$  (python-src/DiscreteHyperbolicFactorizationUpperbound\_Bitonic.py). It outputs the sorted array. Vacant elements in array are zero-filled

- Binary and logs for C++ and Python side have been committed
- Parallel comparators on large scale require huge cloud of machines per above bound which makes it NC.

-----  
Commits (2) as on 12 April 2016  
-----

- Compare step in Bitonic Sort for merged tiles has been Spark MapReduced with this separate script -  
../python-src/DiscreteHyperbolicFactorizationUpperbound\_Bitonic\_Spark.py. Can be used only in a large cluster. With this comparators are highly parallelizable over a cloud and thus in NC.

References:

-----  
261.1 Parallel Bitonic Sort -  
<http://www.cs.utexas.edu/users/plaxton/c/337/05s/slides/ParallelRecursion-1.pdf>  
-----

-----  
262. Commits as on 13 April 2016  
-----

Spark Bitonic Sort - Imported BiDirectional Map - bidict - for reverse lookup (for a value, lookup a key in addition to for a key, lookup a value) which is required to avoid the looping through of all keys to match against a tile element.

-----  
263. Commits as on 27 April 2016  
-----

-----  
Interim Commits for ongoing investigation of a race condition in Spark MapReduce for NC Factorization with Bitonic Sort :  
-----

- The sequential version of bitonic sort has been updated to do away with usage of boolean flag up by 2 compare functions for True and False
- Spark NC implementation of Bitonic Sort for Factorization still has some strange behaviour in sorting. In progress commits for this do following in Compare-And-Exchange phase:
  - Comparator code has been rewritten to just do comparison of parallelized RDD set of tuples where each tuple is of the form:  
(i, i+midpoint)
  - This comparison returns a set of boolean flags collect()ed in compare()
  - The variable exchange is done sequentially at each local node.
  - This is because Spark documentation advises against changing global state in worker nodes (though there are exceptions in accumulator)
  - There were some unusual JVM out of memory crashes, logs for which have been committed
    - some trivial null checks in complement.py
    - Bitonic Sort presents one of the most non-trivial cases for parallelism - parallel variable compare-and-exchange to be specific
- and present commits are a result of few weeks of tweaks and trial-errors.
  - Still the race condition is observed in merge which would require further commits.

-----  
----  
264. Commits as on 28 April 2016  
-----

-----  
Interim commits 2 for ongoing investigation of race conditions in Spark Bitonic Sort:  
-----

-----  
- bidict usage has been removed because it requires bidirectional uniqueness, there are better alternatives  
- The variable exchange code has been rewritten in a less complicated way and just mimicks what sequential version does in CompareAndExchange phase.  
- logs for Sequential version has been committed  
- number to factor has been set to an example low value  
- .coordinates and .mergedtiles files have been regenerated  
- Still the race condition remains despite being behaviourally similar to sequential version except the parallel comparator array returned by mapreduce  
- Parallel comparator preserves immutability in local worker nodes  
-----

-----  
265. (THEORY) UGC(Unique Games Conjecture) and Special Case of Percolation-Majority Voting Circuits  
-----

-----  
265.1 Unique Games Conjecture by [SubhashKhot] is a conjecture about hardness of approximating certain constraint satisfaction problems. It states that complexity of obtaining polynomial time approximation schemes for specific class of constraint satisfaction NP-hard problems is NP-hard itself i.e polytime approximation is NP-hard. From section 255 above, if in a special case percolation with sampling of left-right points on percolation grids results in logarithmic advice, then percolation is in NC/log. Thus if RHS has 100% stable NP-hard voting function then NP is in NC/log implying NP is in P/log and P=NP. This disproves UGC trivially because all NP problems have P algorithms. But this disproof depends on strong assumptions that percolation has NC/log circuit and RHS of Majority voting is 100% noise stable. There are already counterexamples showing divergence of RHS in sections 53.16.3.1 and 256.

265.2 Voter Boolean Functions can be written as :

265.2.1 Integer Linear Programs : Voter Judging Boolean Functions are translated into an Integer Linear Program, binary to be precise because value for variable and final vote is 0, 1 and -1(abstention). This readily makes any decision process by individual voter to be NP-hard.

265.2.2 and Constraint Satisfaction Problems : Voter expects significant percentage of constraints involving variables to be satisfied while voting for a candidate which brings the majority voting problem into the UGC regime. Approximating the result of an Election mentioned in Section 14 is thus reducible to hardness of approximation of constraint satisfaction and could be NP-hard if UGC is true.

265.3 Thus RHS of Majority Voting Circuit becomes a functional composition behemoth of indefinite number of individual voter constraint and integer linear programs. There is a generic concept of sensitivity of a non-boolean function mentioned in [Williamson-Schmoys] which can be applied to sensitivity and stability of a voter integer linear program and constraint program.

265.4 Approximating outcome of a majority voting (e.g. real life pre/post poll surveys) depends thus on following factors:

265.4.1 Correctness - Ratio preserving sample - How reflective the sample is to real voting pattern e.g a 60%-40% vote division in reality should be reflected by the sample.

265.4.2 Hardness - Approximation of Constraint Satisfaction Problems and UGC.  
-----

## References:

-----  
265.4 Unique Games Conjecture and Label Cover -  
[https://en.wikipedia.org/wiki/Unique\\_games\\_conjecture](https://en.wikipedia.org/wiki/Unique_games_conjecture)  
265.5 Design of Approximation Algorithms - Page 442 -  
<http://www.designofapproxalgs.com/book.pdf>  
-----

-----  
266. Commits 1 as on 29 April 2016  
-----

Interim commits 3 for Bitonic Sort Spark NC Factorization Implementation  
-----

- AsFer Design Document updated for already implemented NVIDIA CUDA Parallel C reference code for bitonic sort on hypercube
- Bitonic Sort C++ code updated for max size of sort array - reduced from 16384 to 256
- Bitonic Sort Python Spark implementation updated for returning a tuple containing index info also instead of plain boolean value because Spark collect() after a comparator map() does not preserve order and index information was lost.
- if clauses in exchange phase have been appropriately changed
- Still there are random mysterious jumbled tuples which will be looked into in future commits
- This implementation becomes redundant because of already existing better NVIDIA CUDA Parallel C implementation and is of academic interest only.

-----  
Final commits for Bitonic Sort Spark NC Factorization Implementation  
-----

- Indeed Bitonic Sort from previous commit itself works without any issues.
- Nothing new in this except reduced sort array of size just 64 for circumventing frequent Py4Java Out of Memory errors and for quick runtime
- Logs for this have been committed in testlogs/
- the debug line "merged sorted halves" is the final sorted tiles array
- .coordinates and .mergedtiles files have been updated

-----  
267. Commits as on 30 April 2016  
-----

- Printed return value of bitonic\_sort() in sorted. Earlier it was wrongly printing globalmergedtiles a global state which is not changed anymore
- logs for bitonic sort of tessellated hyperbolic arc

-----  
268. Commits as on 1 May 2016  
-----

- The Map step now does both Compare and Exchange within local worker nodes for each closure and result is returned in tuples
- The driver collect()s and just assigns the variables based on comparator boolean field in tuple which are already exchanged within local worker

-----  
269. Commits as on 2 May 2016  
-----

-----  
Accumulator support for Bitonic Sort mapreduce globalmergedtiles  
-----

- Spark context has been parametrized and is passed around in the recursion so that single spark context keeps track of the

accumulator variables

- globalmergedtiles\_accum is the new accumulator variable which is created in driver and used for storing distributed mutable globalmergedtiles
- AccumulatorParam has been overridden for Vectors as globals
- Spark does not permit however, at present, mutable global state within worker tasks and only driver creates the accumulator variables which can only be incrementally extended within closure workers.
- muting or accessing accumulator.value within worker raises Exception: Can't access value of accumulator in worker tasks
- Logs for above have been committed to testlogs/
- Because of above limitation of Spark in global mutability, accumulator globalmergedtiles is updated only outside the Spark mapreduce closures.
- Support for global mutables, if Spark has it, would make compare-and-exchange phase closer in behaviour to an NVIDIA Parallel bitonic sort.
- Documentation on this necessary feature is scarce and some suggest use of datastores like Tachyon/Alluxio for distributed shared mutables which is non-trivial. This cloud parallel sort implementation achieves thus almost ~90% of NVIDIA CUDA parallel bitonic sort - CompareAndExchange is done in parallel but assigning CompareAndExchange results is done sequentially.

-----  
-----  
270. Commits as on 3 May 2016  
-----  
-----

New threading function assign\_compareexchange\_multithreaded() has been implemented which is invoked in lieu of sequential for loop assignment , by creating a thread for each pair of (i,i+midpoint) compare-exchange assignment of accumulator globalmergedtiles. This thread function assigns the Spark Mapreduce result of Compare and Exchange.

Multithreading is an alternative for global state mutability in the absence of Spark support and it does not require any third party in-memory caching products.

Coordinates are also shuffled first few elements of which correspond to number to factor N - these are the factors found finally. Multithreaded assignment maps to a multicore parallelism. Logs for this have been committed to testlogs with and without Coordinates Shuffling.

-----  
-----  
271. Commits 2 as on 3 May 2016  
-----  
-----

Number to factorize has been changed to 147. The mergedtiles array has been set to size 256. The logs for this have been committed in testlogs/. The factors are printed in last few lines of the logs in shuffled globalcoordinates corresponding to 147 in sorted globalmergedtiles accumulator:

```
sorted= [147, 147, 147, 147, 147, 147, 147, 147, 147, 147, 147, 147, 147, 146,
146, 146, 146, 146, 146, 146, 145, 145, 145, 145, 145, 145, 144, 144, 144, 144,
144, 144, 144, 144, 144, 144, 144, 144, 144, 144, 144, 144, 144, 144, 144, 144,
144, 144, 144, 144, 144, 144, 144, 144, 143, 143, 143, 143, 143, 142, 142,
142, 142, 141, 141, 141, 141, 141, 140, 140, 140, 140, 140, 140, 140, 140,
140, 140, 140, 140, 140, 140, 140, 139, 138, 138, 138, 138, 138, 138, 138,
138, 138, 137, 136, 136, 136, 136, 136, 136, 136, 136, 135, 135, 135, 135,
135, 135, 135, 135, 134, 134, 133, 133, 133, 132, 132, 132, 132, 132, 132,
132, 132, 132, 132, 132, 131, 130, 130, 130, 130, 130, 130, 129, 129, 129, 129,
128, 128, 128, 128, 128, 128, 127, 126, 126, 126, 126, 126, 126, 126, 126,
126, 125, 125, 125, 124, 124, 124, 124, 123, 123, 123, 122, 122, 121, 120, 120,
```

```

120, 120, 120, 120, 120, 120, 119, 118, 118, 117, 117, 117, 116, 116, 116, 116,
115, 114, 114, 114, 114, 113, 112, 112, 111, 111, 111, 110, 110, 109, 108, 108,
108, 108, 107, 106, 106, 105, 104, 104, 103, 102, 102, 101, 100, 100, 99, 98,
98, 97, 96, 95, 94, 93, 92, 91, 90, 89, 88, 87, 86, 85, 84, 83, 82, 81, 80, 79,
79, 78, 78, 77, 77, 76, 76, 75, 75, 74, 74, 73, 0, None]
globalcoordinates= [1, 21, 21, 49, 49, 7, 147, 147, 3, 3, 3, 3, 7, 73, 73, 147,
2, 2, 145, 2, 144, 5, 5, 29, 29, 5, 24, 16, 16, 9, 8, 24, 18, 18, 6, 6, 6, 143,
2, 2, 3, 4, 4, 4, 3, 3, 4, 8, 71, 12, 36, 47, 9, 36, 12, 142, 13, 13, 11, 11, 2,
70, 141, 2, 3, 3, 140, 3, 46, 34, 14, 7, 139, 2, 27, 14, 10, 10, 69, 19, 5, 7,
4, 4, 4, 5, 138, 45, 22, 68, 3, 137, 2, 6, 6, 3, 136, 2, 33, 16, 67, 135, 4, 4,
8, 3, 3, 5, 134, 5, 9, 14, 26, 44, 66, 133, 7, 132, 18, 65, 4, 3, 3, 4, 6, 43,
11, 131, 32, 21, 10, 130, 129, 5, 12, 25, 9, 64, 3, 3, 42, 128, 7, 127, 4, 31,
15, 63, 126, 8, 41, 13, 62, 6, 3, 5, 125, 17, 20, 24, 5, 124, 61, 30, 123, 4, 3,
122, 40, 60, 121, 120, 3, 4, 59, 39, 23, 29, 119, 4, 118, 117, 58, 38, 3, 116,
115, 3, 28, 57, 114, 113, 37, 3, 56, 112, 55, 111, 110, 3, 36, 109, 54, 108, 53,
107, 2, 35, 106, 52, 105, 104, 51, 103, 102, 101, 50, 100, 49, 99, 98, 48, 97,
96, 95, 94, 93, 92, 91, 90, 89, 88, 87, 86, 85, 84, 83, 82, 81, 80, 79, 1, 78,
77, 1, 76, 1, 1, 75, 74, 1, 73, 1, 72, 146, None]
sorted globalmergedtiles accumulator version: = [147, 147, 147, 147, 147, 147,
147, 147, 147, 147, 147, 147, 146, 146, 146, 146, 146, 146, 146, 145, 145,
145, 145, 145, 144, 144, 144, 144, 144, 144, 144, 144, 144, 144, 144, 144,
144, 144, 144, 144, 144, 144, 144, 144, 144, 144, 144, 144, 144, 144, 144,
144, 143, 143, 143, 143, 143, 142, 142, 142, 142, 142, 141, 141, 141, 141, 141, 140,
140, 140, 140, 140, 140, 140, 140, 140, 140, 140, 140, 140, 140, 140, 140,
139, 138, 138, 138, 138, 138, 138, 138, 138, 138, 137, 136, 136, 136, 136, 136,
136, 136, 136, 135, 135, 135, 135, 135, 135, 135, 135, 135, 135, 134, 134, 133, 133,
133, 132, 132, 132, 132, 132, 132, 132, 132, 132, 132, 132, 132, 132, 131, 130, 130,
130, 130, 130, 130, 129, 129, 129, 129, 128, 128, 128, 128, 128, 128, 128, 127, 126,
126, 126, 126, 126, 126, 126, 126, 126, 126, 125, 125, 125, 124, 124, 124, 124,
123, 123, 123, 122, 122, 121, 120, 120, 120, 120, 120, 120, 120, 120, 119, 118,
118, 117, 117, 117, 116, 116, 116, 116, 115, 114, 114, 114, 114, 113, 112, 112,
111, 111, 111, 110, 110, 109, 108, 108, 108, 108, 107, 106, 106, 105, 104, 104,
103, 102, 102, 101, 100, 100, 99, 98, 98, 97, 96, 95, 94, 93, 92, 91, 90, 89,
88, 87, 86, 85, 84, 83, 82, 81, 80, 79, 79, 78, 78, 77, 77, 76, 76, 75, 75, 74,
74, 73, 0, None]
16/05/03 18:33:06 INFO SparkUI: Stopped Spark web UI at
http://192.168.1.101:4040
16/05/03 18:33:06 INFO DAGScheduler: Stopping DAGScheduler
16/05/03 18:33:06 INFO MapOutputTrackerMasterEndpoint:
MapOutputTrackerMasterEndpoint stopped!

```

-----  
Factors of 147 are [1,21,49,7,147,3] from globalcoordinates and  
globalmergedtiles(corresponding to 147 elements) printed previously in logs.  
-----

-----  
272. (THEORY) Integer Partitions, Riemann Sums, Multipartisan Majority Voting -  
a special case  
-----

-----  
From [https://github.com/shrinivaasanka/Krishna\\_iResearch\\_DoxygenDocs/blob/master/kuja27\\_website\\_mirrored/site/kuja27/IntegerPartitionAndHashFunctions\\_2014.pdf](https://github.com/shrinivaasanka/Krishna_iResearch_DoxygenDocs/blob/master/kuja27_website_mirrored/site/kuja27/IntegerPartitionAndHashFunctions_2014.pdf), Integer Partitions when visualized as area under a curve in discrete sense, correspond to Riemann Sums Discrete Area Integral i.e Each part in the partition slices the area under a curve formed by topmost points of each part in partition. This curve can be perturbed to arbitrary shape without altering the area underneath it - in other words each perturbed curve corresponds to a partition of N where N is the area integral value for the curve. A striking analogy: a vessel containing water is perturbed and the surface of the liquid takes arbitrary curvature shapes but the volume of the liquid remains unchanged (assuming there is no spillover) - has some similarities to perturbation of spacetime Riemannian Manifolds due to gravity in General Relativity. This analogy simulates a 3-dimensional partition number (as



against the usual 2-dimensional) of liquid of volume  $V$ . Let  $p_3(V)$  denote the 3-dimensional partition of a liquid of volume  $V$ . It makes sense to ask what is the bound for  $p_3(V)$ . For example a snapshot of the curvature of liquid surface be the function  $f$ . A slight perturbation changes this function to  $f'$  preserving the volume. Hence  $f$  and  $f'$  are 2 different 3-dimensional partitions of liquid - the difference is these are continuous partitions and not the usual discrete integer partitions with distinct parts. Number of such perturbations are infinite - there are infinitely many perturbations possible creating an equivalence class:  $f=f'=f''=f'''=f''''=f''''' \dots = V$  and hence  $p_3(V)$  is infinite (proof is by diagonalization: an arbitrary point of the curve on the continuum can be changed and this recursively continues indefinitely). As any perturbation can be linked to a (pseudo)random source,  $p_3(V)$  is equivalent to number of pseudorandom permutations (randomness extracted from some entropy source).  $p_3(V)$  can be extended to arbitrary dimensions  $n$  as  $p_n(V)$ . This extends hash functions and also majority voting to continuous 3-dimensional setting - though it is to be defined what it implies by voting in continuous population vis-a-vis discrete - conjecturally majority voting over continuum could be undecidable (e.g every point over a real interval is a voter and  $2^{(\aleph_0)} = \aleph_1$  or cardinality of reals = cardinality of uncountable ordinals by Continuum Hypothesis and ZFAOC). In essence, Multipartisan Majority Voting = Hash Functions = Partitions in both discrete and continuous scenarios.

#### References:

-----  
 272.1 3 Dimensional Histograms and Double Integral Riemann Sums -  
<https://www.geogebra.org/m/YPeaPJtS> - arbitrary 3 dimensional histograms (as double integral Riemann Sums beneath the curve) could be visualized by varying the polynomial curve plot  
 -----

-----  
 273. Commits as on 4 May 2016  
 -----

#### Sequence Mining of Prime Numbers as binary strings

-----  
 - First 10000 prime numbers have been written to a text file in binary notation in complement.py  
 - SequenceMining.py mines for most prominent sequences within prime binary strings - a measure of patterns in prime distribution  
 - Logs for this have been committed to testlogs/  
 -----

-----  
 274. Commits as on 11 May 2016  
 -----

#### Sequence Mining in Prime binary strings has been made sophisticated:

- Prints each binary string sequence pattern in decimals upto maximum of 15-bit sequences mined from first 10000 primes.
- This decimals are written to a file PatternInFirst10000Primes.txt
- Approx.py R+Rpy2 has been invoked to print an R function plotter of this decimal pattern in prime binary string sequences
- The function plots the sequences in Y-axis and length of sequences in ascending order in X-axis (with decreasing support)
- As can be seen from pdf plot, the sequences show dips amongst peaks periodically.

-----

-----  
 275. (THEORY) Non-boolean Social Choice Functions Satisfiability, Sensitivity, Stability and Multipartisan Majority Voting - 256 continued  
 -----

-----  
 Let  $f$  be a voter decision function which takes in  $x_1, x_2, \dots, x_m$  as decision variables and outputs a vote for candidate  $1 \leq c \leq n$ . This generalizes voter boolean judging functions for 2 candidates to arbitrarily large number of contestants. Assuming  $f$  to be continuous function and parameters to be continuous (as opposed to discrete binary string SAT assignments to variables in boolean setting), this generalizes Satisfiability problem to continuous, multivalued and non-boolean functions. This allows the candidate index to be continuous too. The function plot of this (candidate index versus decision string) would resemble any continuous mathematical function. Stability which is:  $\Pr[f(s) == f(t)] - \Pr[f(s) != f(t)]$  for randomly correlated  $s=(x_{11}, x_{12}, \dots, x_{1m})$  and  $t=(x_{21}, x_{22}, x_{23}, \dots, x_{2m})$  where correlation (measured by usual euclidean distance between  $s$  and  $t$ ) could be uncomputable value in terms of mean but can be approximated as difference in ratio of length integral of function arc segments with high curvature and low curvature (where function has huge fluctuations and relatively flat). Sensitivity follows accordingly. This requires first derivative of the function to find out local maxima and minima. From Gibbard-Satterthwaite theorem any social choice function for more than 3 candidates has a non-zero probability of being manipulated though negligible in practice. Probably this implies atleast indirectly that the stability of any non-boolean social choice function  $< 1$  if number of candidates  $> 3$  hinting at divergence of  $\Pr(\text{Good})$  Binomial series. This function plot should not be confused with function plot mentioned in 272 for votes partitioned across candidates which reduces to Riemann Sum. Unlike boolean sensitivity/stability, non-boolean counterparts can only be approximated and exact computation might never halt being undecidable. Non-boolean Social Choice Function generalizes satisfiability because an appropriate assignment to  $(x_1, x_2, x_3, \dots, x_m)$  has to be found so that  $f(x_1, x_2, x_3, \dots, x_m) = c$  where  $1 \leq c \leq n$ . This is precisely curve-line intersection problem - curve  $f(x_1, x_2, x_3, \dots, x_n)$  and line  $y=c$  - in computational geometry. Intersecting points  $(a_1, a_2, a_3, \dots, a_z)$  are the satisfying assignments which choose candidate  $c$ . Contrasting this with boolean kSAT which is NP-complete, non-boolean kSAT has polynomial time computational geometric algorithms to find satisfying intersection points. It is intriguing to observe a sharp threshold phenomenon in computational hardness of satisfiability - an easy polytime non-boolean kSAT becomes NP-hard boolean kSAT. Assuming that real-life voters have non-boolean decision functions only, the RHS circuit of  $\Pr(\text{Good})$  majority voting is confined to polytime satisfiability realm alone. Non-boolean voting decision functions can be specialized for 2 candidates special case too - this allows fractional values to decision variables. This is plausible because Linear Programming (non-boolean) is polytime while 0-1 Integer Linear Programming (boolean) is NP-complete. Because of Non-boolean Social Choice functions (e.g Linear Programs with Constraints which each voter solves) being the most generic which allow fractional values to variables, any of the standard polytime Simplex algorithms - Dantzig Pivot Tableau and Karmarkar Interior Point Method - can be applied to find a satisfying assignment. Voter decides to vote for/against when the solution to LP is above/below a threshold. This is a far from real, hypothetical, perfectly rational election setting. Real life elections have bounded rationality. It is an alternative to Computational Geometric intersection detection previously mentioned.

#### References:

- 275.1 Intersection detection - <https://www.cs.umd.edu/~mount/Papers/crc04-intersect.pdf>  
 275.2 Transversal Intersection of two curves - Newton iteration and Cramer's rule - [https://en.wikipedia.org/wiki/Intersection\\_\(Euclidean\\_geometry\)](https://en.wikipedia.org/wiki/Intersection_(Euclidean_geometry))  
 -----

276. (FEATURE-DONE) Commits as on 30 May 2016 - Continued from 220

-----  
VIRGO CloudFS system calls have been added (invoked by unique number from syscall\_32.tbl) for C++ Boost::Python interface to VIRGO Linux System Calls. Switch clause with a boolean flag has been introduced to select either VIRGO memory or filesystem calls. kern.log and CloudFS textfile Logs for VIRGO memory and filesystem invocations from AsFer python have been committed to testlogs/  
-----

277. (FEATURE-DONE) Commits as on 31 May 2016 - Continued from 220 and 276

-----  
Python CAPI interface to NEURONRAIN VIRGO Linux System Calls has been updated to include File System open, read, write primitives also. Rebuilt extension binaries, kern.logs and example appended text file have been committed to testlogs/. This is exactly similar to commits done for Boost::Python C++ interface. Switch clause has been added to select memory or filesystem VIRGO syscalls.  
-----

278. (FEATURE-DONE) Commits as on 7 June 2016

-----  
- getopt implementation for commandline args parsing has been introduced in Maitreya textclient rule search python script.  
- an example logs for possible high precipitation longitude/latitudes in future dates - July 2016 - predicted by sequence mining learnt rules from past data has been added to testlogs/  
-----

```
root@shrinivaasanka-Inspiron-1545:/home/shrinivaasanka/Maitreya7_GitHub/martin-pe/maitreya7/releases/download/v7.1.1/maitreya-7.1.1/src/jyotish# python MaitreyaEncHoro_RuleSearch.py --min_year=2016 --min_month=7 --min_days=1 --min_hours=10 --min_minutes=10 --min_seconds=10 --min_long=77 --min_lat=07 --max_year=2016 --max_month=7 --max_days=15 --max_hours=10 --max_minutes=10 --max_seconds=10 --max_long=78 --max_lat=10 |grep " a Class Association"
{ --date="2016-7-2 10:10:10 5" --location=" x 77:0:0 7:0:0 " --planet-list } -
There is a Class Association Rule match [['Mercury', 'Venus']] in sign Gemini
{ --date="2016-7-3 10:10:10 5" --location=" x 77:0:0 7:0:0 " --planet-list } -
There is a Class Association Rule match [['Mercury', 'Venus']] in sign Gemini
{ --date="2016-7-4 10:10:10 5" --location=" x 77:0:0 7:0:0 " --planet-list } -
There is a Class Association Rule match [['Mercury', 'Venus']] in sign Gemini
{ --date="2016-7-5 10:10:10 5" --location=" x 77:0:0 7:0:0 " --planet-list } -
There is a Class Association Rule match [['Mercury', 'Venus']] in sign Gemini
{ --date="2016-7-6 10:10:10 5" --location=" x 77:0:0 7:0:0 " --planet-list } -
There is a Class Association Rule match [['Mercury', 'Venus']] in sign Gemini
{ --date="2016-7-11 10:10:10 5" --location=" x 77:0:0 7:0:0 " --planet-list }
- There is a Class Association Rule match [['Mercury', 'Venus']] in sign
Cancer
{ --date="2016-7-13 10:10:10 5" --location=" x 77:0:0 7:4:0 " --planet-list }
- There is a Class Association Rule match [['Mercury', 'Venus']] in sign
Cancer
{ --date="2016-7-14 10:10:10 5" --location=" x 77:0:0 7:4:0 " --planet-list }
- There is a Class Association Rule match [['Mercury', 'Venus']] in sign
Cancer
```

-----  
279. (FEATURE-DONE) Commits - 23 June 2016 - Recurrent Neural Network Long Term Short Term Memory - Deep Learning - Implementation  
-----

-----  
A very minimal python implementation of LSTM RNN based on Schmidhuber-Hochreiter LSTM has been added to already existing AsFer algorithms repertoire. LSTM RNN has gained traction in recent years in its variety of applications in NLP, Speech Recognition, Image Pattern Recognition etc., The logs for this implementation show a convergence of final output layer in 25th iteration itself (out of 10000). Learning the weights requires other algorithms like Gradient Descent, Backpropagation (and there are already known limitations in weight learning with these)  
-----

-----  
280. (FEATURE-DONE) Commits - 23 June 2016 - Minimal Reinforcement Learning (Monte Carlo Action Policy Search) implementation  
-----

-----  
Reinforcement Learning has been implemented which changes state based on environmental observation and an appropriate policy is chosen for observation by Monte Carlo Random Policy Search based on which rewards for each transitions are accumulated and output in the end. Logs for 3 consecutive executions of Reinforcement Learning have been committed with differing total rewards gained. Input observations are read from text file ReinforcementLearning.input.txt.  
-----

Reference: Richard Sutton - <http://webdocs.cs.ualberta.ca/~sutton/papers/Sutton-PhD-thesis.pdf>  
-----

-----  
281. (FEATURE-DONE) Commits - 24 June 2016 - ThoughtNet Reinforcement Learning implementation  
-----

-----  
ThoughtNet based Reinforcement Learning Evocation has been experimentally added as a clause in python-src/DeepLearning\_ReinforcementLearningMonteCarlo.py. This is just to demonstrate how ThoughtNet hypergraph based evocation is supposed to work. python-src/ReinforcementLearning.input.txt has been updated to have a meaningful textual excerpt. Logs for this evocative model has been committed to python-src/testlogs/DeepLearning\_ReinforcementLearningMonteCarlo.ThoughtNet.out. 24June2016  
-----

-----  
282. (FEATURE-DONE) Commits - 26 June 2016 - ThoughtNet File System Storage  
-----

-----  
ThoughtNet text files have been stored into a filesystem backend. It is read and eval()-ed into list of edges and hypergraphs. Separate ThoughtNet directory has been created for these text files.  
-----

-----  
283. (THEORY) ThoughtNet growth and Evocation Reinforcement Learning algorithm (not feasible to implement exactly):  
-----

-----  
loop\_forever  
{  
When an observation stimulus from environment arrives:  
    (\*) Sensory instruments that simulate eye, ear, nose, etc., receive stimuli from environment (thoughts, music, noise, sound etc.,)  
and convert to sentential form - this is of the order of billions - and appended  
-----

to list in ThoughtNet\_Edges.txt

(\*) Sentences are classified into categories (for example, by maximum core numbers in definition wordnet subgraph) which is also order of billions and added as hypergraph edges in dict with in ThoughtNet\_Hypergraph.txt - hyperedge because same document can be in more than 2 classes. This creates a list for each key in dict and the list has to be sorted based on evocation potential - reward for reinforcement learning. There is no need for monte carlo and dynamic programming if pre-sorted because sum of rewards is always maximum - only topmost evocative edge is chosen in each list of a key.

(\*) observation is split to atomic units - tokenized - or classified and each unit is lookedup in ThoughtNet\_Hypergraph.txt to get a list and hyperedge with maximum potential is returned as evocative with optional lambda evaluation which is the action side of reinforcement learning.  
}

-----  
284. (FEATURE-DONE) Auto Regression Moving Average - ARMA - Time Series Analysis for Stock Ticker Stream  
-----

-----  
Commits - 27 June 2016  
-----

-----  
1. Time Series Analysis with AutoRegressionMovingAverage of Stock Quote streamed data has been implemented (R function not invoked). Logs which show the actual data and projected quotes by ARMA for few iterations have been committed to testlogs. This ARMA projection has been plotted in R to a pdf file which is also committed.

2. ARMA code implements a very basic regression+moving averages. Equation used is same though not in usual ARMA format

$(1-\sigma())X(t) = (1+\sigma())$

3. Also committed is the R plot for SequenceMined Pattern in first 10000 prime numbers in binary format (DJIA approx and approxfun plots have been regenerated)

-----  
285. (FEATURE-DONE) Commits 1 - 28 June 2016 - Neo4j ThoughtNet Hypergraph Database Creation  
-----

-----  
1. New file ThoughtNet\_Neo4j.py has been added to repository which reads the ThoughtNet edges and hypergraph text files and uploads them into Neo4j Graph Database through py2neo client for Neo4j.

2. Neo4j being a NoSQL graph database assists in querying the thoughtnet and scalable.

3. ThoughtNet text files have been updated with few more edges and logs for how Neo4j graph database for ThoughtNet looks like have been committed to testlogs/  
-----

-----  
286. (FEATURE-DONE) Commits 2 - 28 June 2016 - ThoughtNet Neo4j Transactional graph creation  
-----

-----  
1. transactional begin() and commit() for graph node and edges creation has been included.

2. This requires disabling bolt and neokit disable-auth due to an auth failure config issue.

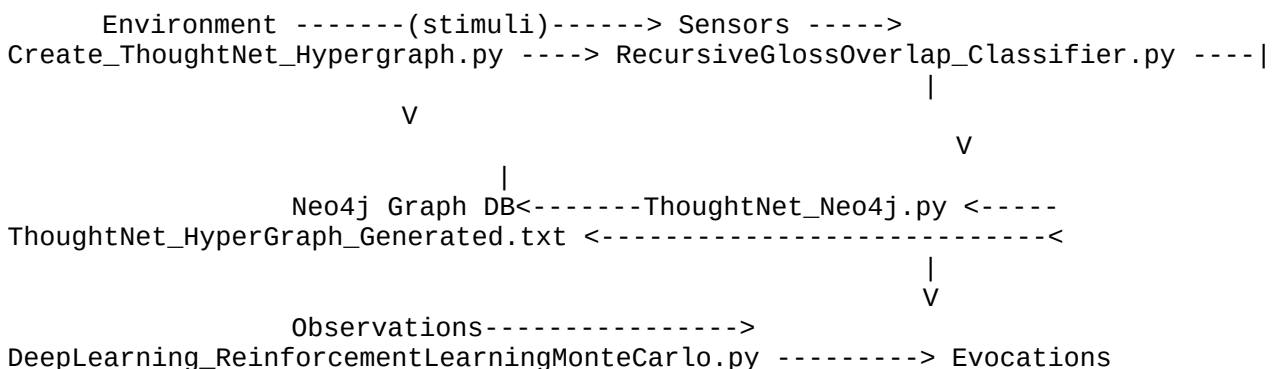
3. Logs and a screenshot for the ThoughtNet Hypergraph created in GUI (<http://localhost:7474>) have been committed to testlogs/  
-----

-----  
287. (FEATURE-DONE) Commits - 29 June 2016 - ThoughtNet and Reinforcement Deep Learning  
-----

-----  
Major commits for ThoughtNet Hypergraph Construction and Reinforcement Learning from it  
-----

1. python-src/DeepLearning\_ReinforcementLearningMonteCarlo.py reads from automatically generated ThoughtNet Hypergraph text backend created by python-src/ThoughtNet/Create\_ThoughtNet\_Hypergraph.py in python-src/ThoughtNet/ThoughtNet\_Hypergraph\_Generated.txt
2. Separate Recursive Gloss Overlap CoreNumber and PageRank based Unsupervised Classifier has been implemented in python-src/RecursiveGlossOverlap\_Classifier.py which takes any text as input arg and returns the classes it belongs to without any training data. This script is imported in python-src/ThoughtNet/Create\_ThoughtNet\_Hypergraph.py to automatically classify observations from environment and to build ThoughtNet based on them for evocations later.
3. python-src/ThoughtNet/ThoughtNet\_Neo4j.py reads from automatically generated ThoughtNet in python-src/ThoughtNet/ThoughtNet\_Hypergraph\_Generated.txt
4. Logs for above have been committed to respective testlogs/ directories
5. Compared to human evaluated ThoughtNet Hypergraphs in python-src/ThoughtNet/ThoughtNet\_Hypergraph.txt, generated python-src/ThoughtNet/ThoughtNet\_Hypergraph\_Generated.txt does quite a deep learning from WordNet mining and evocations based on this automated ThoughtNet are reasonably accurate.
6. python-src/ReinforcementLearning.input.txt and python-src/ThoughtNet/ThoughtNet\_Edges.txt have been updated manually.

-----  
288. (FEATURE-DONE) Schematic Diagram for ThoughtNet Reinforcement Evocation - approximate implementation of 283  
-----



-----  
289. (FEATURE-DONE) Commits - 30 June 2016 - Sentiment Scoring of ThoughtNet edges and Sorting per Class  
-----

1. Create\_ThoughtNet\_Hypergraph.py has been changed to do sentiment scoring which is a nett of positivity, negativity and objectivity per thought hyperedge and to sort the per-class key list of hyperedges descending based on sentiment scores computed.
2. python-src/ReinforcementLearning.input.txt which is the input observation stimulus and python-src/ThoughtNet/ThoughtNet\_Edges.txt, the training data for construction of Hypergraph have been updated with additional text sentences.

3. Hypergraph created for this is committed at  
python-src/ThoughtNet/ThoughtNet\_Hypergraph\_Generated.txt with logs in python-  
src/ThoughtNet/testlogs/Create\_ThoughtNet\_Hypergraph.sentiment\_sorted.out.30June  
2016. Example evocatives for python-src/ReinforcementLearning.input.txt input  
to python-src/DeepLearning\_ReinforcementLearningMonteCarlo.py are logged in  
python-src/testlogs/DeepLearning\_ReinforcementLearningMonteCarlo.ThoughtNet\_sen-  
timent\_sorted.out.30June2016

This completes ThoughtNet Classifications based Evocative Inference  
implementation minimally.

-----  
290. (FEATURE-DONE) Commits - 1 July 2016 - Reinforcement Learning Bifurcation  
-----

Reinforcement Learning code has been bifurcated into two files than having in  
if-else clause, for facilitating future imports :-  
one for MonteCarlo and the other for ThoughtNet Evocation. Logs for these two  
have been committed to testlogs.

-----  
291. (THEORY) Logical Time and ThoughtNet (related to EventNet 70-79)  
-----

ThoughtNet Hypergraph is multiplanar and when seen from elevation it resembles  
billions of skyscraper category towers interconnected by Thought  
HyperEdges which are classified onto these categories. This gives an alternative  
route to define Time. Each tower represents chronologically stacked up  
events/occurrences/thoughts when unsorted i.e most recent thought is on top  
always and evocation based on chronology returns topmost thought. ThoughtNet  
evocation is an associative memory process returning most relevant thought in  
past for an observation in present. Two stack node towers with differing depths  
define two views of time i.e time is subjective to the category than objective  
across ThoughtNet. In a timeless universe, measuring duration between two events  
reduces to height of these unequal stacks which is not absolute - there are many  
logical "Time"(s). Each stack node has its own independent logical "Clock". This  
makes no assumption about relativistic theory of time and is independent of any  
physical law. From theory of computation standpoint, this is similar to a multi-  
tape turing machine but with added feature in which tapes are interconnected.  
When the stacks are sorted for evocation potential based on some criterion (e.g  
sentiwordnet, EEG electric pulse etc.,) chronology information is lost to some  
extent but still the edge id retains it - most recent edge has largest edge  
numeric id. Yet, this assumes a distributed global unique id is achievable. When  
events occur in parallel, two edges geographically separate can have same edge  
id in the absence of special mechanisms for uniqueness. Vis-a-vis EventNet,  
ThoughtNet is not a causation graph. Relationship between EventNet and  
ThoughtNet is: Every partaker node in EventNet has a ThoughtNet. EventNet when  
topologically sorted has no absolute time - can have many orderings of events -  
similar to ThoughtNet - each thought edge can have varied logical timestamps  
when viewed from different category spectacles - in the absence of time.  
Following is the hierarchy: Each node in an EventNet is an event, and each event  
has partaker nodes which create graph by interaction among themselves, and each  
partaker node has an internal ThoughtNet. Thus there are 3 levels - EventNet is  
the biggest, Event is bigger and Partaker is big - EventNet is a graph of graph  
nodes of graph nodes. The tensor product of these nested graphs has 3 tiers -  
EventNet(Event(PartakerThoughtNet)) - denoted as EventNet (\*) Event (\*)  
PartakerThoughtNet. This tensor product captures both individual's view of event  
ordering and cosmic event ordering. ThoughtNet per node in an event is more of a  
projection of its observable universe - imaginary - while interaction among  
nodes in an event and causality between events are real. Measurement of duration  
between events in this tensor product can be done in various ways: 1) Distance  
between two event nodes causally connected 2) Global topological sorting of





compared to quantitative Neural Networks.

It is assumed in present implementation that every thought edge is a state implicitly, and the action for the state is the "meaning" inferred by recursive lambda evaluation (lambda composition tree evaluation for a natural language sentence is not implemented separately because its reverse is already done through closure of a RGO graph in other code in NeuronRain AsFer. Approximately every edge in Recursive Gloss Overlap wordnet subgraph is a lambda function with its two vertices as operands which gives a more generic lambda graph composition of a text)

-----  
292. (THEORY) Recursive Lambda Function Growth Algorithm and Recursive Gloss Overlap Graph - 216 Continued  
-----

-----  
Lambda Function Recursive Growth algorithm for inferring meaning of natural language text approximately, mentioned in 216 relies on creation of lambda function composition tree top-down by parsing the connectives and keywords of the text. Alternative to this top-down parsing is to construct the lambda function composition graph instead from the Recursive Gloss Overlap WordNet subgraph itself where each edge is a lambda function with two vertex endpoints as operands (mentioned in 291). Depth First Traversal of this graph iteratively evaluates a lambda function  $f_1$  of an edge,  $f_1$  is applied to next edge vertices in traversal to return  $f_2(f_1)$ , and so on upto function  $f_n(f_{n-1}(f_{n-2}(\dots(f_2(f_1))\dots)))$  which completes the recursive composition. Which one is better - tree or graph lambda function growth - depends on the depth of learning necessary. Rationale in both is that the "meaning" is accumulated left-right and top-down on reading a text.

-----  
293.(FEATURE-DONE) Commits - 7 July 2016 - Experimental implementation of Recursive Lambda Function Growth Algorithm (216 and 292)  
-----

-----  
1.Each Sentence Text is converted to an AVL Balanced Tree (inorder traversal of this tree creates the original text)  
2.Postorder traversal of this tree computes a postfix expression  
3.Postfix expression is evaluated and a lambda function composition is generated by parenthesization denoting a function with two arguments.Logs for this have been committed to testlogs/ which show the inorder and postorder traversal and the final lambda function grown from a text.  
4.This is different from Part of Speech tree or a Context Free Grammar parse tree.  
5.On an average every english sentence has a connective on every third word which is exactly what inorder traversal of AVL binary tree does.If not a general B+-Tree can be an ideal choice to translate a sentence to tree. Every subtree root in AVL tree is a lambda function with leaves as operands.

-----  
294. (FEATURE-DONE) Commits - 8 July 2016  
-----

-----  
Changed Postfix Evaluation to Infix evaluation in Lambda Function Growth with logs in testlogs/  
-----  
-----

295. (THEORY) Contextual Multi-Armed Bandits, Reinforcement Learning and ThoughtNet - related to 241, 291, 292 - 18 July 2016

Contextual Multi-Armed Bandits are the class of problems where a choice has to be made amongst  $k$  arms and each iteration fetches a reward. Choice of an arm in next iteration depends on rewards for previous iteration. Ideal examples are Recommender Systems, Contextual website advertisements etc., Thus an agent learns from past and policy action depends on rewards for previous actions. Translating this into ThoughtNet realm is fairly straightforward - Each class stack node in ThoughtNet is a multi-armed bandit and an evocative has to choose a hyperedge that 1) maximizes reward by fitting the context meaningfully and 2) learns from rewards for previous actions by virtue of ThoughtNet storage itself because ThoughtNet per partaker is built gradually by storing thought hyperedges colored with a sentiment mentioned in Ramsey coloring of ThoughtNet in 236 (or SentiWordNet score). In terms of a Markov Model, Reward for an evocative word  $w$  at time  $t$  is denoted as  $Reward(w, t)$  and returns a corresponding thought hyperedge which depends on  $Reward(w, t-1)$ ,  $Reward(w, t-2)$  and so on i.e  $Reward(w, t) = \text{function\_of}(Reward(w, t-1), Reward(w, t-2), \dots, Reward(w, 0))$ . Recommender Systems in e-commerce websites which display similar items to a selected item in shopping cart have a striking resemblance to ThoughtNet evocation. This makes ThoughtNet a suitable candidate for Recommender System - Sales history is built as a ThoughtNet similar to the algorithm mentioned in 283 and 288. Every item added to shopping cart returns evocatives based on some scoring (sentiment ranked etc.,) which is a Recommender System.

Reference:

295.1 Multiword Testing Decision Service - <http://arxiv.org/pdf/1606.03966v1.pdf>

296. (FEATURE-DONE) Music Pattern Mining - Jensen-Shannon Divergence Distance between two FFT Frequency Distributions for similarity

Commits - 20 July 2016 - related to 68, 69

(NOTE: Because of some weird SourceForge/GitHub error, FFT txt files added to repos on 19 July 2016 are still flagged as new(?). They have been added to repos again along with new files)

FFTs of 2 audio files are parsed and written to \*\_trimmed.txt by awk to contain only the frequencies for each sample.

These files are read by JensenShannonDivergence.py to compute the JS Distance between these two FFT frequency distributions.

Preprocessing is done so as to normalize the frequency to map to a probability ( $\text{frequency}/\text{sum\_of\_frequencies}$ ) which gives probability distribution from frequency distribution. Jensen-Shannon Distance which is the weighted average of bidirectional Kullback-Leibler Divergence measures of the two distributions, indicates similarity or distance between two music samples quantitatively.

There are 4 music samples: music\_pattern\_mining/FFT\_classical\_1\_20July2016.txt and music\_pattern\_mining/FFT\_classical\_2\_20July2016.txt are similar (similar notes sung by different musicians). music\_pattern\_mining/FFT\_classical\_1\_19July2016.txt and music\_pattern\_mining/FFT\_classical\_2\_19July2016.txt are also similar (different set of notes sung by different musicians). Jensen-Shannon distance across these 4 ordered pairs is captured and committed in testlogs/

Jensen-Shannon Distance across 2 FFT Frequency-Probability distributions of music

samples is a simple, basic measure for distance and can be basis for clustering and classification of music. There could be some inaccuracies because Audacity does not generate FFT for complete music file but only for first ~5 minutes. Two similar notes with different musicians could be distant and two dissimilar notes might be close because of this Audacity limitation. Presently noise filtering and cherrypick peak frequencies is not done and entire frequency range is compared.

-----  
297. (FEATURE-DONE) Software Analytics - Cyclomatic Complexity from SATURN .dot graphs - related to 65  
-----

-----  
Commits - 22 July 2016  
-----

New Python-Spark implementation that reads the SATURN program analyzer generated .dot graph files processes them with Spark MapReduce to find the number of edges and vertices in the graph represented by .dot file for each snippet. From this Cyclomatic Complexity is calculated (which is Edges - Vertices + 2) - a standard Function Point Estimator for code complexity. There were some JVM crashes frequently while starting up spark-submit logs for which are also committed in testlogs along with the two successful Spark computed Cyclomatic Complexity measures for two .dot files. These .dot files are sourced from VIRGO Linux saturn program analysis kernel driver.

-----  
298. (FEATURE-DONE) String Search - Longest Common Substring - Suffix Trees(Suffix Arrays+LCP) Implementation  
-----

-----  
Commits - 26 July 2016  
-----

This implementation finds the most repeated substrings within a larger string by constructing Suffix Trees indirectly with Suffix Array and Longest Common Prefix (LCP) datastructures. An ideal application for String Search is in Bioinformatics, Streamed Data analysis etc., For example, a Time Series data with fluctuating curve can be encoded as a huge binary string by mapping ebb and tide to 0 and 1. Thus a function graph time series is projected on to {0,1} alphabet to create blob. Usual Time Series analysis mines for Trends, Cycles, Seasons and Irregularities over time. This binary encoding of time series gives an alternative spectacle to look at the trends (highs and lows). Longest repeating pattern in this binary encoding is a cycle. Suffix Array by [UdiManber] has been implemented over Suffix Trees implementations of [Weiner] and [Ukkonen] because of simplicity of Suffix Arrays and Suffix Trees=Suffix Arrays + LCPs.

-----  
299. (FEATURE-DONE) Binary String Encoding of Time Series - Commits - 27 July 2016  
-----

-----  
1. New python script to encode a time series datastream as binary string has been added to repository.

2. This writes to StringSearch\_Pattern.txt which is read by StringSearch\_LongestRepeatedSubstring.py  
3. Encoding scheme: If next data point is smaller, write 0 else if greater write 1. This captures the fluctuations in dataset irrespective of the amplitudes at each point.  
4. For example a bitonic sequence would have been encoded as ....1111111100000000.... (ascends and descends)  
5. Suffix Array + LCP algorithm on this sequence finds the Longest Repeated Substring. For a specific example of Stock ticker time series data this amounts to frequently recurring fluctuation pattern.  
6. Logs for the above have been committed to testlogs/  
7. Every time series dataset is a union of bitonic sequences with varying lengths corresponding to peaks and troughs and has self-similar fractal structure (zooming out the series has similarities to original series) . This implies the binary string encoded as previously is fractal too.

-----  
300. (FEATURE-DONE) Tornado GUI Authentication Template - Commits - 27 July 2016  
-----

Rewritten Tornado GUI with Login Template and redirect to Algorithms Execution Template. Presently implemented for only a root user by cookie setting. Entry point has been changed to http://host:33333/neuronrain\_auth (Login).

-----  
301. (FEATURE-DONE) OAuth2 authentication and credentials storage in MongoDB/Redis with passlib sha256 encryption  
-----

-----  
1.Login Handler has been augmented with OAuth2 authentication by python-oauth2 library.  
2.MongoDB is used as OAuth2 credentials storage backend and Redis for token storage backend  
3.Passlib is used to encrypt the password with SHA256 hash digest and stored once in MongoDB (code is commented)  
4.Login page password is verified with passlib generated hash in MongoDB queried for a username argument  
5.With this minimal standard authentication has been implemented for NeuronRain cloud deployment.  
6.Prerequisite is to populate MongoDB neuronrain\_oauth database and neuronrain\_users collections with passlib encrypted JSON by uncommenting the collections.insert\_one() code.

-----  
302. Commits - 29 July 2016 - boost::python extensions for VIRGO Linux Kernel system calls  
-----

virgo\_clone() system call has been included in switch-case and invokes an exported kernel module function in kernelspace.

-----  
303. (THEORY) Update on Bitonic Sort Merge Tree for Discrete Hyperbolic Factorization Spark Cloud Implementation in 34.20  
-----

Bitonic Sort Merge Tree for Discrete Hyperbolic Factorization described in

[http://sourceforge.net/projects/acadpdrafts/files/DiscreteHyperbolicPolylogarithmicSieveForIntegerFactorization\\_PRAM\\_TileMergeAndSearch\\_And\\_Stirling\\_Upperbound\\_updateddraft.pdf/download](http://sourceforge.net/projects/acadpdrafts/files/DiscreteHyperbolicPolylogarithmicSieveForIntegerFactorization_PRAM_TileMergeAndSearch_And_Stirling_Upperbound_updateddraft.pdf/download) has following bound which can be derived as:

303.1 Bitonic Sort requires  $O((\log N)^2)$  time with  $O(N * (\log N)^2)$  processors.

303.2 Discretized Hyperbolic arc of length  $N$  can be split into  $N/\log N$  segments of length  $\log N$  each.

303.3 Above  $N/\log N$  segments can be grouped in leaf level of merge tree into  $N/2\log N$  pairs of  $(\log N, \log N) = 2\log N$  length segments to be sorted together.

303.4 Each such pair can be sorted in  $\log(2\log N)$  time in parallel with  $N/(2\log N) * N(\log N)^2 = N^2/2\log N$  comparator processors in leaf level which is the maximum number of processors required. Next level requires  $\log(4\log N)$ ,  $\log(8\log N)$  and so on till root.

303.5 Height of the merge tree is  $O(\log(N/\log N))$ . Total sort time is sum over sorts at each level of merge tree =  $\log(2\log N) + \log(4\log N) + \dots + \log((2^{\log(N/\log N)}) * \log N)$

303.6 Total sort time of merge tree is upperbounded as (not tight one) height \* maximum\_sort\_time\_per\_level:

$$\leq O(\log(N/\log N) * \log(N/\log N * \log N)) = O(\log(N/\log N) * \log(N))$$

with maximum of  $N^2/2\log N$  processor comparators at leaf which tapers down up the tree.

303.7 Binary Search on final sorted merged tile requires additional  $O(\log N)$

which effectively reduces to:

$$O(\log(N/\log N) * \log N + \log N) = O(\log(N/\log N) * \log N) \leq O((\log N)^2) \text{ time}$$

with  $N^2/2\log N$  processor comparators for finding a factor.

303.8 This is comparably better bound than the Parallel RAM ANSV algorithm based merge sort alternatives and easy to implement on a cloud as done in 34.20 and also is in NC because of polylog time and polynomial comparator processors required.

303.9 Again the input size is  $N$  and not  $\log N$ , but yet definition of NC is abided by. It remains an open question whether Bitonic Sort Comparators are equivalent conceptually to PRAMs (Are cloud nodes same as PRAMs assuming the nodes have access to a shared memory?).

-----  
304. Commits - 31 July 2016 - boost::python C++ and cpython virgo\_clone() system call invocations  
-----

1. Boost C++ Python extensions - virgo\_clone() system call has been included in switch-case for cpython invocation of VIRGO linux kernel with test logs for it with use\_as\_kingcobra\_service=1 (Routing: C++Boost::Python ---> virgo\_clone() ----> virgo\_queue driver ----> KingCobra message queue pub/sub service). Test logs for it have been committed in testlogs/

2. CPython extensions - test log for boost::python virgo\_clone() invocation with use\_as\_kingcobra\_service=0 which directly invokes a kernelspace function without forwarding to virgo\_queue/kingcobra, has been committed to testlogs/.

-----  
305. NEURONRAIN VIRGO Commits for ASFER Boost::Python C++ virgo memory system calls invocations  
-----

(BUG - STABILITY ISSUES) Commits - 1 August 2016 - VIRGO Linux Stability Issues - Ongoing Random oops and panics investigation  
-----

1. GFP\_KERNEL has been replaced with GFP\_ATOMIC flags in kmem allocations.

2. NULL checks have been introduced in lot of places involving strcpy, strcat, strcmp etc., to circumvent buffer overflows.

3. Though this has stabilized the driver to some extent, still there are OOPS in

unrelated places deep  
 with in kernel where paging datastructures are accessed - kmalloc somehow  
 corrupts paging  
 4. OOPS are debugged via gdb as:  
     4.1 gdb ./vmlinux /proc/kcore  
     or  
     4.2 gdb <loadable\_kernel\_module>.o  
 followed by  
     4.3 l \*(address+offset in OOPS dump)  
 5. kern.log(s) for the above have been committed in tar.gz format and have  
 numerous OOPS occurred during repetitive telnet and syscall  
 invocation(boost::python C++) invocations of virgo memory system calls.  
 6. Paging related OOPS look like an offshoot of set\_fs() encompassing the  
 filp\_open VFS calls.  
 7. In C++ Boost::Python extensions, flag changed for VIRGO memory system calls  
 invocation from python.

-----  
 306. Commits - 3 August 2016  
 -----

Social Network Analysis with Twitter - Changes to Belief Propagation Potential  
 Computation  
 -----

-----  
 1. Exception handling for UnicodeError has been added in SentimentAnalyzer  
 2. Belief Propagation Potential computation for the RGO graph constructed has  
 been changed to do plain  
 summation of positivity and negativity scores for DFS of K-Core rather than  
 multiplication which heuristically  
 appears to predict sentiments better  
 3. An example for tweets sentiments analysis for 2 search keywords has been  
 logged and committed in testlogs/  
 -----

-----  
 4. Excerpts for sentiment scores - positive and negative - from RGO graph of few  
 tweets  
 -----

-----  
 root@shrinivaasanka-Inspiron-1545:/media/shrinivaasanka/0fc4d8a2-1c74-42b8-8099-  
 9ef78d8c8ea2/home/kashrinivaasan/KrishnaiResearch\_OpenSource/SourceForge/asfer-  
 code/python-src/testlogs# grep "score:"

SocialNetworkAnalysis\_Twitter.out1.Republicans.3August2016

K-Core DFS belief\_propagated\_posscore: 6.078125  
 K-Core DFS belief\_propagated\_negscore: 8.140625  
 Core Number belief\_propagated\_posscore: 25.125  
 Core Number belief\_propagated\_negscore: 26.125  
 K-Core DFS belief\_propagated\_posscore: 6.078125  
 K-Core DFS belief\_propagated\_negscore: 8.140625  
 Core Number belief\_propagated\_posscore: 25.125  
 Core Number belief\_propagated\_negscore: 26.125  
 K-Core DFS belief\_propagated\_posscore: 55.09375  
 K-Core DFS belief\_propagated\_negscore: 54.3125  
 Core Number belief\_propagated\_posscore: 92.625  
 Core Number belief\_propagated\_negscore: 93.875  
 K-Core DFS belief\_propagated\_posscore: 60.09375  
 K-Core DFS belief\_propagated\_negscore: 59.3125  
 Core Number belief\_propagated\_posscore: 118.625  
 Core Number belief\_propagated\_negscore: 117.75

root@shrinivaasanka-Inspiron-1545:/media/shrinivaasanka/0fc4d8a2-1c74-42b8-8099-  
 9ef78d8c8ea2/home/kashrinivaasan/KrishnaiResearch\_OpenSource/SourceForge/asfer-  
 code/python-src/testlogs# grep "score:"

SocialNetworkAnalysis\_Twitter.out2.Democrats.3August2016

K-Core DFS belief\_propagated\_posscore: 34.0  
K-Core DFS belief\_propagated\_negscore: 30.359375  
Core Number belief\_propagated\_posscore: 90.25  
Core Number belief\_propagated\_negscore: 85.125  
K-Core DFS belief\_propagated\_posscore: 54.0  
K-Core DFS belief\_propagated\_negscore: 46.734375  
Core Number belief\_propagated\_posscore: 111.125  
Core Number belief\_propagated\_negscore: 108.125  
K-Core DFS belief\_propagated\_posscore: 97.203125  
K-Core DFS belief\_propagated\_negscore: 91.015625  
Core Number belief\_propagated\_posscore: 172.125  
Core Number belief\_propagated\_negscore: 172.125  
K-Core DFS belief\_propagated\_posscore: 97.203125  
K-Core DFS belief\_propagated\_negscore: 91.015625  
Core Number belief\_propagated\_posscore: 178.125  
Core Number belief\_propagated\_negscore: 178.125

5. Majority Predominant Sentiment indicated by above scores for randomly sampled tweets can be used as one of the Election Approximation and Forecast Technique described in 14.

-----  
307. (THEORY) Sentiment Analysis from Recursive Gloss Overlap as a Voting Function in Majority Voting - related to 14  
-----

As mentioned in 306, Sentiment Analysis scores derived from Recursive Gloss Overlap graph of a text is an indirect voting function - when the overall sentiment is negative it is an "against" vote and when positive it is a "for" vote. In this sense, Sentiment Analysis shrouds a Satisfiability problem underneath it. In other words every polarised text is a boolean SAT circuit translated into natural language text which opens whole new vista to look at Sentiment Analysis per se. Infact it is a generalization of a boolean SAT circuit - it is bipolar and whichever polarity wins decides the vote.

-----  
308. (FEATURE-DONE) Markov Random Fields (MRF) Belief Propagation - Commits - 8 August 2016  
-----

Existing Sentiment Analyzer does belief propagation by computing product of potentials in DFS traversal only.  
New function for Markov Random Fields Belief Propagation has been included which handles the generalized case of belief propagation in a graph by factoring it into maximal cliques and finding potentials per clique. These per clique potentials are multiplied and normalized with number of cliques to get polarized sentiments scores - positive, negative and objective. Logs for Sentiment Analysis of tweets stream with MRF have been committed to testlogs/

Reference:

-----  
308.1 Introduction to Machine Learning - [Ethem Alpaydin] - Graphical Models  
-----

-----  
309. (FEATURE-DONE) Commits - 12 August 2016 - Boost 1.58.0 upgrade from 1.55.0 - Boost::Python C++ extensions for VIRGO  
-----

-----  
1.Rebuilt Boost::Python extensions for VIRGO Linux kernel system calls with boost 1.58 upgraded from boost 1.55.

2.kern.log for miscellaneous VIRGO system calls from both telnet and system call request routes has been compressed and committed to testlogs (~300MB).

Following multiple debug options were tried out for heisencrash resolution (Note to self):

3./etc/sysctl.conf has been updated with kernel panic tunables with which the mean time between crashes has increased and crash location is deep within kernel (VMA paging) - commits for this are in VIRGO linux tree. With these settings following usecase works:

```
virgo_cloud_malloc()
virgo_cloud_set()
virgo_cloud_get()
virgo_cloud_set() overwrite
virgo_cloud_get()
```

through telnet route.

4.Debugging VIRGO linux kernel with an Oracle VirtualBox virtual machine installation and debugging the VM with a netconsole port via KGDB was explored, but there are serious issues with VirtualBox initialization in Qt5.

5.Debugging VIRGO linux kernel with QEMU-KVM installation and debugging the VM with a netconsole port via KGDB is being explored. Reference documentation at: <https://www.kernel.org/doc/Documentation/gdb-kernel-debugging.txt>

---

#### 310. (THEORY) DFT of a Sliding Window Fragment of Time Series, Integer Partitions and Hashing

---

Time Series Data Stream can be viewed through a sliding window of some fixed width moving across the data. Captured data points in such window are analyzed in frequency domain with a Discrete Fourier Transform. If there are  $n$  frequencies in the window of data, there are  $n$  sinusoids which superimpose to form the original data. In discrete sense, sinusoids partition the data at any time point. Following the relation between hash functions and integer partitions in [https://sites.google.com/site/kuja27/IntegerPartitionAndHashFunctions\\_2014.pdf](https://sites.google.com/site/kuja27/IntegerPartitionAndHashFunctions_2014.pdf), each of  $n$  discrete sinusoid in DFT corresponds to a hash function and the time-series sliding window is an amalgamation of  $n$  hash functions.

---

#### 311. (THEORY) Pr(Good) Majority Voting Circuit, Percolation, PRG choice and Boolean Circuit Composition - related to 14, 53.12 and 129

---

Even though Percolation circuit is in Noise Stability Regime with zero sensitivity and 100% stability, delta term mentioned in matrix of 14 and 53 (second column) need not be zero which could force percolation circuit to be in BPNC. Problem is then derandomizing BPNC. (Open question: Is BPNC in NC/poly?). Thus LHS of Pr(Good) could be in BPNC which coincides with [Applebaum] NC1 PRG based pseudorandom choice described in - <https://5d99cf42-a-62cb3a1a-s-sites.googlegroups.com/site/kuja27/LowerBoundsForMajorityVotingPseudorandomChoice.pdf> and [https://5d99cf42-a-62cb3a1a-s-sites.googlegroups.com/site/kuja27/IndepthAnalysisOfVariantOfMajorityVotingwithZFAOC\\_2014.pdf](https://5d99cf42-a-62cb3a1a-s-sites.googlegroups.com/site/kuja27/IndepthAnalysisOfVariantOfMajorityVotingwithZFAOC_2014.pdf). Boolean Function Composition is preferred over Oracle results for Majority Voting circuit which is an NC1 circuit with CircuitSAT as inputs for each voter. This is infact "Boolean Circuit Composition" corresponding to Boolean Function Composition.

#### References:

---

311.1 Mathematical Techniques for Analysis of Boolean Functions - [AnnaBernasconi] - 2.8.2 Boolean Function Composition - [www.di.unipi.it/~annab/tesi.ps.gz](http://www.di.unipi.it/~annab/tesi.ps.gz)



311.2 Properties and Applications of Boolean Function Composition - [AvishayTal]  
- [eccc.hpi-web.de/report/2012/163/download/](http://eccc.hpi-web.de/report/2012/163/download/)  
311.3 Boolean Circuit Composition - [www.cs.tau.ac.il/~safra/ACT/CCandSpaceB.ppt](http://www.cs.tau.ac.il/~safra/ACT/CCandSpaceB.ppt)

-----  
312. (THEORY) Circuit SAT lowerbounds for  $\Pr(\text{Good})$  Majority Voting - related 14 and 129  
-----

312.1 RHS of  $\Pr(\text{Good})$  Majority Voting circuit is an NC circuit in composition with CircuitSAT for each voter. This parallel voting by electorate requires some kind of barrier synchronization so that input from all voters is available to NC Majority Circuit. This is a non-trivial overhead to be ignored because the barrier delay depends on the voter whose decision time is the most. If in worst case the bottleneck voter function is in EXP then barrier synchronization is also in EXP. It is also assumed that voters decide independent of each other.

312.2 CircuitSAT is the circuit version of CNF SAT concerned with the bounds for finding satisfying assignments to a circuit to get the output true at root of Circuit DAG.

312.3 An arbitrary Circuit's Satisfiability requires  $O(2^{0.4058m})$  where  $m$  is the number of gates in Circuit (i.e. size of circuit). This bound was proved in [SergeyNurk] - <ftp://ftp.pdmi.ras.ru/pub/publicat/preprint/2009/10-09.pdf.gz>. This is very generic bound without concerning the complexity classes of voter decisioning function.

312.4 Because of the fact that  $\Pr(\text{good})$  majority voting is a circuit composition with voter circuit SATs as inputs to NC majority circuit, previous bound applies and estimates the time for each voter's decision to be input to Majority circuit. In other words, a satisfying assignment to at least half of the electorate CircuitSATs has to be found to pronounce a winner. Time required to convince a voter is therefore exponential in size of the voter circuit. For a voter  $k$  size of the CircuitSAT is  $m(k)$  and the time required to satisfy it is  $O(2^{0.4058 \cdot m(k)})$ .

312.5 Let number of voters be  $n$  and number of gates on the average per voter be  $m$ . NC1 majority requires  $O(\log n)$  time because  $n$  voters input to it at leaf. There are  $nm$  gates for all voters. Per voter decision requires  $O(2^{0.4058m})$  time in parallel to find a satisfying assignment to at least  $n/2$  voters for majority to output 1.

312.6 If number of voters is exponential in number of gates per voter then  $n=2^m$  which is the worst case scenario and is the most realistic, then size of the Majority voting circuit in RHS of  $\Pr(\text{Good})$  is  $m \cdot 2^m$  - exponential in size of per voter circuit. LHS of  $\Pr(\text{Good})$  is NC/poly or BPNC percolation circuit while RHS is an exponential circuit (DC uniform - PH if depth restricted or EXP if depth unrestricted)

312.7 In a very generic case, as mentioned in 275, each voter can have a non-boolean voting function viz., a linear program or constraint satisfaction which is NP if integer-LP and is in P if real-LP (simplex, interior point). In terms of Oracles circuit for RHS  $\Pr(\text{Good})$  can be written as:

312.7.1  $NC^P$  (if voting functions are real LP) and LHS NC/poly or BPNC percolation lowerbounds  $NC^P$  when both LHS and RHS are of same error

312.7.2  $NC^{NP}$  (if voting functions are integer LP) and LHS NC/poly or BPNC percolation lowerbounds  $NC^{NP}$  when both LHS and RHS are of same error

312.8 Circuit Size of  $\Pr(\text{Good})$  RHS is non-trivial to determine. All that is known so far is the bound for CircuitSAT which is  $O(2^{0.4058m})$  where  $m$  is number of gates. But number of gates itself is an open problem for SAT - it is not known if NP has polynomial size circuits.

312.9 Assumption 1: Each voter has different variables - set of variables of voters are all pairwise disjoint.

312.10 If number of voters is arbitrarily huge and if number of voters is exponential in number of gates per voter SAT, size of RHS is  $m \cdot 2^m$  with unbounded fan-in, unrestricted depth most probably and thus in EXP, with AND-OR-NOT gates. Assumption 2: When voters have common variables it implies that they decide in unison. For example if variable  $x$  is common to voters  $v_1$  and  $v_2$ , both  $v_1$  and  $v_2$

assign  $x=0$  or  $x=1$ . This is negation of Assumption 1 in 312.9 and Assumption 1 is more realistic than Assumption 2.

312.11 Even if  $m$  (number of gates per voter SAT) is assumed to be polynomial in number of input variables i.e  $m=f(v)$  where  $v$  is average number of inputs per voter, size of RHS is  $f(v)*2^{f(v)}$  - exponential in number of variables. Thus in all probability RHS majority voting circuit is exponential DC-uniform circuit in PH or EXP even if NP has polynomial size circuits. This is a special case with lot of assumptions made in 312.6, 312.9 and 312.10.

312.12 If both LHS and RHS of  $\Pr(\text{Good})$  are of zero or equal error, LHS lowerbounds RHS (an assumption made throughout this document - equal error with differing circuit sizes implies lowerbound). Here error is the usual (NoiseSensitivity  $\pm \delta$ ) on both LHS and RHS. For percolation circuit in LHS, NoiseSensitivity is zero. But for RHS NoiseSensitivity is unknown. With an assumption that RHS has non-zero error, it is a BP.EXP circuit assuming unrestricted depth of RHS. LHS is NC/poly with zero error, while RHS is BPEXP and thus implies BPEXP is in NC/poly which resembles BPP in P/poly. If LHS has an error with a PRG choice function in NC (e.g Applebaum NC PRG with linear stretch), LHS would have been a BPNC circuit implying BPEXP is in BPNC which is absurd and conflicts with assumption that equal error implies lowerbound (refer 53.9, 53.14 and 53.16) - this conflict is resolved only if LHS and RHS do not have equal error with differing circuit sizes (and also implies that error depends on circuit size?).

312.13 Important notion in representing a voter boolean function by a circuit is Hardness which is defined as:

A boolean function  $f:\{0,1\}^n \rightarrow \{0,1\}$  is  $h$ -hard if there exists a circuit  $C$  of size  $s$  such that for all  $x$  in  $\{0,1\}^n$ ,  $\Pr(C(x)=f(x)) < h$ . Narrative above on CircuitSAT for voter boolean functions is incomplete without knowing how hard is it to compute or approximate the voter decision function with a circuit of size  $s$ . Harder a function, lower the value of  $h$  ( $0 < h < 1$ ). This definition of hardness is far better generalization of computational complexity of a voter boolean function than identifying with complexity class names. [Yao] XOR Lemma is applied to amplify hardness of boolean function by XOR-ing values of  $f$  on many randomly distributed inputs.

312.14 There are two classes of errors: Voter error + Voting error. Voter error is the Noise Sensitivity of a voter boolean function while Voting error is the intrinsic error in voting system itself though user has done nothing wrong. E.g Malfunctioning Electronic Voting Machines. Voter error is captured by second and third column of matrix in 53.14 while Voting error is captured by probabilistic truth table of the function - inputs have no effect on this error. This implies  $\delta$  in  $\Pr(\text{Good})$  series error (NoiseSensitivity  $\pm \delta$ ) might have to account for voting error term also, over and above voter error.

#### References:

-----

312.15 Complexity Hardness of Noisy Boolean Functions -

<http://cstheory.stackexchange.com/questions/18822/hardness-of-noisy-boolean-functions> - hardness of a noise-operated boolean function. Has applications to voting error where a voter's decision boolean function is perturbed by noise to output a wrong vote. Also, comparability and  $p$ -selectivity of a set -

[D.Sivakumar] - [http://citeseerx.ist.psu.edu/viewdoc/download?](http://citeseerx.ist.psu.edu/viewdoc/download?doi=10.1.1.16.648&rep=rep1&type=pdf)

[doi=10.1.1.16.648&rep=rep1&type=pdf](http://citeseerx.ist.psu.edu/viewdoc/download?doi=10.1.1.16.648&rep=rep1&type=pdf) and [AgrawalArvind94] on "Polynomial time truth-table reductions to  $P$ -selective sets". Every voting function (and ranking function in general) over  $n$  candidates is a  $p$ -selector with candidate set being  $p$ -selective set because for any two candidates  $x, y$  voting function makes a choice.

312.16 Hardness of Boolean Functions and Amplification - [RyanODonnell] - <https://www.cs.cmu.edu/~odonnell/boolean-analysis/lecture17.pdf>

312.17 Probabilistic Boolean Logic - [LakshmiNBChakrapani-KrishnaPalem] -

<http://www.ece.rice.edu/~al4/visen/2008ricetr.pdf> - Truth table of a boolean function has 1s and 0s with probabilities. This captures the notion of error in voting function truth table itself, not just limited to noise correlations of inputs.

312.18 How much a Linear Programming Oracle speedup Polytime algorithms -

<http://cstheory.stackexchange.com/questions/32646/how-much-would-a-sat-oracle->

help-speeding-up-polynomial-time-algorithms - Pr(Good) majority voting circuit is NC with SAT/LP oracle for each voter.

312.19 Algorithms for Circuits and Circuits for Algorithms - [RyanWilliams] - <http://web.stanford.edu/~rrwill/ICM-survey.pdf> - Kolmogorov conjecture based on [ArnoldKolmogorov] answer to Hilbert's 13th problem - every continuous function in 3 variables can be expressed as finite composition of functions of 2 variables - discrete analog : Is 3SAT expressible as a finite composition of 2SAT (which implies composition of P instances yielding NP as counterexample)? A special case majority voting with 3 variables common to all voter functions and Non-boolean continuous voting functions in 3 variables precisely has application of Hilbert's 13th problem.

312.20 Depth 3 multilinear circuits - [OdedGoldreich] - <http://www.wisdom.weizmann.ac.il/~oded/R3/kk.pdf> - D-canonical depth-3 circuit is constructed by composition of 2 depth-2 circuits i.e  $F=H(F_1, F_2, \dots, F_n)$  in Section 1.2. Has strong applications to a Majority voting circuit composition where  $F_i(s)$  are voting functions and  $H$  is Majority function.

312.21 Size hierarchy theorem for circuits - <http://csttheory.stackexchange.com/questions/5110/hierarchy-theorem-for-circuit-size>. And also theorems 5.8 and 5.9 in [http://www.complexity.ethz.ch/education/Lectures/ComplexityFS12/skript\\_ch5.pdf](http://www.complexity.ethz.ch/education/Lectures/ComplexityFS12/skript_ch5.pdf) - there are functions computable by  $(1+o(1))2^n/n$  and not computable by circuits of size  $2^n/n$ .

312.22 Size Hierarchy [Lupanov] - Number of functions computable by circuit of size  $s$  - Lemma 2.1 counting argument - <http://eccc.hpi-web.de/resources/pdf/cobf.pdf> (Wegener - pages 88-92)

312.23 Efficient Parallel Computation = NC - [AroraBarak] - <http://theory.cs.princeton.edu/complexity/book.pdf> - Theorem 6.24 - Parallel Voting Simulation can be done by massive parallel processing assuming the input votes are precomputed.

312.24 Size hierarchy of 312.22 in Pr(Good) majority voting circuit context implies that number of functions computable by LHS has to be different from number of functions computable by RHS when LHS is NC/poly and RHS is PH or EXP i.e if EXP does not have polysize circuits. The central motivation for equating LHS and RHS of Pr(Good) is both sides are 2 algorithms to decide same question: Non-majority choice and Majority choice - which is more efficient where efficiency implies less error? This motivation therefore leads to assumption stated in disclaimer earlier: less circuit size implies a lowerbound (i.e least circuit size of LHS and RHS is chosen as separating class containing the other) when errors are equal or less.

312.25 If circuit sizes differ in zero-error case on both sides i.e when 100% convergence occurs (or) equal error on both sides of series, then by size hierarchy,  $\text{size(LHS)} < \text{size(RHS)}$  implies RHS computes functions not possible by LHS and viceversa (Open question: Does this contradict lowerbound assumption? Or is this just a special case because both LHS and RHS compute same function i.e they answer same question in which case size hierarchy does not apply which counts all possible functions for specific circuit size?).

312.26 There is an alternative definition of Boolean function hardness in <http://www.math.ias.edu/~avi/PUBLICATIONS/MYPAPERS/NOAM/HARDNESS/final.pdf> (Section 2.2) which states hardness = circuit size complexity hardness + approximation hardness.

-----  
 313. (FEATURE-DONE) Astronomical Sequence Mining based Precipitation Forecast (from 100 year historic dataset) - related to 172, 278  
 -----

-----  
 Following the earlier experimental pattern mining done on astronomical datasets and their striking correlational coincidence with weather vagaries, below rule search explores highly probable heavy precipitation - shows peaks after 29 November 2016 :

```
python MaitreyaEncHoro_RuleSearch.py --min_year=2016 --min_month=11 --
min_days=15 --min_hours=10 --min_minutes=10 --min_seconds=10 --min_long=77 --
```

```
min_lat=7 --max_year=2016 --max_month=12 --max_days=30 --max_hours=10 --
max_minutes=10 --max_seconds=10 --max_long=78 --max_lat=10 |grep "a Class
Association"
```

```
{ --date="2016-11-29 10:10:10 5" --location=" x 77:0:0 7:0:0 " --planet-list }
- There is a Class Association Rule match [['Mercury', 'Venus']] in sign
Sagittarius
{ --date="2016-11-30 10:10:10 5" --location=" x 77:0:0 7:0:0 " --planet-list }
- There is a Class Association Rule match [['Mercury', 'Venus']] in sign
Sagittarius
{ --date="2016-12-1 10:10:10 5" --location=" x 77:0:0 7:0:0 " --planet-list }
- There is a Class Association Rule match [['Mercury', 'Venus']] in sign
Sagittarius
{ --date="2016-12-2 10:10:10 5" --location=" x 77:0:0 7:0:0 " --planet-list }
- There is a Class Association Rule match [['Mercury', 'Venus']] in sign
Sagittarius
{ --date="2016-11-29 10:10:10 5" --location=" x 77:0:0 7:1:0 " --planet-list }
- There is a Class Association Rule match [['Mercury', 'Venus']] in sign
Sagittarius
{ --date="2016-11-30 10:10:10 5" --location=" x 77:0:0 7:1:0 " --planet-list }
- There is a Class Association Rule match [['Mercury', 'Venus']] in sign
Sagittarius
{ --date="2016-12-1 10:10:10 5" --location=" x 77:0:0 7:1:0 " --planet-list }
- There is a Class Association Rule match [['Mercury', 'Venus']] in sign
Sagittarius
{ --date="2016-12-2 10:10:10 5" --location=" x 77:0:0 7:1:0 " --planet-list }
- There is a Class Association Rule match [['Mercury', 'Venus']] in sign
Sagittarius
{ --date="2016-11-29 10:10:10 5" --location=" x 77:0:0 7:2:0 " --planet-list }
- There is a Class Association Rule match [['Mercury', 'Venus']] in sign
Sagittarius
{ --date="2016-11-30 10:10:10 5" --location=" x 77:0:0 7:2:0 " --planet-list }
- There is a Class Association Rule match [['Mercury', 'Venus']] in sign
Sagittarius
{ --date="2016-12-1 10:10:10 5" --location=" x 77:0:0 7:2:0 " --planet-list }
- There is a Class Association Rule match [['Mercury', 'Venus']] in sign
Sagittarius
{ --date="2016-12-2 10:10:10 5" --location=" x 77:0:0 7:2:0 " --planet-list }
- There is a Class Association Rule match [['Mercury', 'Venus']] in sign
Sagittarius
{ --date="2016-11-29 10:10:10 5" --location=" x 77:0:0 7:3:0 " --planet-list }
- There is a Class Association Rule match [['Mercury', 'Venus']] in sign
Sagittarius
{ --date="2016-11-30 10:10:10 5" --location=" x 77:0:0 7:3:0 " --planet-list }
- There is a Class Association Rule match [['Mercury', 'Venus']] in sign
Sagittarius
{ --date="2016-12-1 10:10:10 5" --location=" x 77:0:0 7:3:0 " --planet-list }
- There is a Class Association Rule match [['Mercury', 'Venus']] in sign
Sagittarius
{ --date="2016-12-2 10:10:10 5" --location=" x 77:0:0 7:3:0 " --planet-list }
- There is a Class Association Rule match [['Mercury', 'Venus']] in sign
Sagittarius
{ --date="2016-11-29 10:10:10 5" --location=" x 77:0:0 7:4:0 " --planet-list }
- There is a Class Association Rule match [['Mercury', 'Venus']] in sign
Sagittarius
{ --date="2016-11-30 10:10:10 5" --location=" x 77:0:0 7:4:0 " --planet-list }
- There is a Class Association Rule match [['Mercury', 'Venus']] in sign
Sagittarius
{ --date="2016-12-1 10:10:10 5" --location=" x 77:0:0 7:4:0 " --planet-list }
- There is a Class Association Rule match [['Mercury', 'Venus']] in sign
Sagittarius
{ --date="2016-12-2 10:10:10 5" --location=" x 77:0:0 7:4:0 " --planet-list }
- There is a Class Association Rule match [['Mercury', 'Venus']] in sign
Sagittarius
```

[illegible]

[illegible]

[illegible]

[illegible]



[illegible]

[illegible]

[illegible]

[illegible]

[illegible]

[illegible]

[illegible]

[illegible]



[illegible]

[illegible]

[illegible]

[illegible]

[illegible]

[illegible]

[illegible]

```

} - There is a Class Association Rule match [['Mercury', 'Venus']] in sign
Sagittarius
{ --date="2016-12-1 10:10:10 5.5" --location=" x 77:3:0 9:7:0 " --planet-
list } - There is a Class Association Rule match [['Mercury', 'Venus']] in
sign Sagittarius
{ --date="2016-12-2 10:10:10 5.5" --location=" x 77:3:0 9:7:0 " --planet-
list } - There is a Class Association Rule match [['Mercury', 'Venus']] in
sign Sagittarius
{ --date="2016-11-29 10:10:10 5.5" --location=" x 77:3:0 9:8:0 " --planet-list
} - There is a Class Association Rule match [['Mercury', 'Venus']] in sign
Sagittarius
{ --date="2016-11-30 10:10:10 5.5" --location=" x 77:3:0 9:8:0 " --planet-list
} - There is a Class Association Rule match [['Mercury', 'Venus']] in sign
Sagittarius
{ --date="2016-12-1 10:10:10 5.5" --location=" x 77:3:0 9:8:0 " --planet-
list } - There is a Class Association Rule match [['Mercury', 'Venus']] in
sign Sagittarius
{ --date="2016-12-2 10:10:10 5.5" --location=" x 77:3:0 9:8:0 " --planet-
list } - There is a Class Association Rule match [['Mercury', 'Venus']] in
sign Sagittarius
{ --date="2016-11-29 10:10:10 5" --location=" x 77:4:0 7:0:0 " --planet-list }
- There is a Class Association Rule match [['Mercury', 'Venus']] in sign
Sagittarius
{ --date="2016-11-30 10:10:10 5" --location=" x 77:4:0 7:0:0 " --planet-list }
- There is a Class Association Rule match [['Mercury', 'Venus']] in sign
Sagittarius
{ --date="2016-12-1 10:10:10 5" --location=" x 77:4:0 7:0:0 " --planet-list }
- There is a Class Association Rule match [['Mercury', 'Venus']] in sign
Sagittarius
{ --date="2016-12-2 10:10:10 5" --location=" x 77:4:0 7:0:0 " --planet-list }
- There is a Class Association Rule match [['Mercury', 'Venus']] in sign
Sagittarius
{ --date="2016-11-29 10:10:10 5" --location=" x 77:4:0 7:1:0 " --planet-list }
- There is a Class Association Rule match [['Mercury', 'Venus']] in sign
Sagittarius
{ --date="2016-11-30 10:10:10 5" --location=" x 77:4:0 7:1:0 " --planet-list }
- There is a Class Association Rule match [['Mercury', 'Venus']] in sign
Sagittarius
{ --date="2016-12-1 10:10:10 5" --location=" x 77:4:0 7:1:0 " --planet-list }
- There is a Class Association Rule match [['Mercury', 'Venus']] in sign
Sagittarius
{ --date="2016-12-2 10:10:10 5" --location=" x 77:4:0 7:1:0 " --planet-list }
- There is a Class Association Rule match [['Mercury', 'Venus']] in sign
Sagittarius
{ --date="2016-11-29 10:10:10 5" --location=" x 77:4:0 7:2:0 " --planet-list }
- There is a Class Association Rule match [['Mercury', 'Venus']] in sign
Sagittarius
{ --date="2016-11-30 10:10:10 5" --location=" x 77:4:0 7:2:0 " --planet-list }
- There is a Class Association Rule match [['Mercury', 'Venus']] in sign
Sagittarius
{ --date="2016-12-1 10:10:10 5" --location=" x 77:4:0 7:2:0 " --planet-list }
- There is a Class Association Rule match [['Mercury', 'Venus']] in sign
Sagittarius
{ --date="2016-12-2 10:10:10 5" --location=" x 77:4:0 7:2:0 " --planet-list }
- There is a Class Association Rule match [['Mercury', 'Venus']] in sign
Sagittarius

```

-----  
314. (THEORY) Pseudorandomness, Voter Decision Error and lambda-tolerant  
Randomized Decision Trees of Voter Boolean Functions  
-----

Pseudorandom generators are those which stretch a seed  $l(n)$  to  $n : f:\{0,1\}^{l(n)} \rightarrow \{0,1\}^n$



>{0,1}<sup>n</sup> indistinguishable from perfect random source with bounded error. References 314.1 and 314.2 describe a counting argument to show that there are PRGs. For a seed length  $d$  there are  $2^d$  possible strings stretched to length  $n$ . For a single random string the probability that a circuit or an algorithm distinguishes it from perfect random source is  $\epsilon$ . By iterating over all  $2^d$  strings generated by a PRG the expected fraction of strings distinguished is  $\epsilon \cdot 2^d$  where each iteration is a random variable with probability  $\epsilon$  and follows from union of expectations -  $E(\sum(X_i)) = E(X_1) + E(X_2) + \dots + E(X(2^d)) = \sum(X_i \cdot \epsilon)$ . Probability that there are tails where deviation from this expected value is less than  $\epsilon$  so that indistinguishability is preserved is by Chernoff bounds:  $\Pr(\sum(X_i) - \text{mean} > \delta \cdot \text{mean}) \leq 2 \cdot \exp(-\delta^2 \cdot \text{mean} / 3)$  where  $0 < \delta < 1$  and  $\epsilon = \delta \cdot \text{mean}$ . Substituting for mean, this Probability  $\leq 2 \cdot \exp(-2^d \cdot \epsilon \cdot \delta^2 / 3)$ . For all possible algorithms or circuits of size  $s$  which could be  $2^s$ , by union bound cumulative probability is  $2^s \cdot 2 \cdot \exp(-2^d \cdot \epsilon \cdot \delta^2 / 3) < 1$ . It implies probability of distinguishability is  $< 1$  and there should be a lurking PRG which achieves indistinguishability. This previous description is mooted to connect PRGs with Voter Decision Error. Voters have a boolean decision function in  $\Pr(\text{Good})$  majority voting circuit. Alternatively each voter decides by evaluating the leaves of the boolean decision tree of the corresponding function. Randomized decision trees allow randomness by allowing coin tosses to choose the next edge in decision tree. Reference 314.3 describes a decision tree evaluation by voter which allows error by including decision tree choices not necessarily belonging to the voter. That is, voter errs in judgement during decision process wherein (pseudo)random error pollutes his/her discretion. This formalizes the notion of Voting error (analogous somewhat to Probabilistic CNFs). The level of error probability to what decision tree deviates is upperbounded by  $\lambda$  and called as  $\lambda$ -tolerance. There are known results which bound the error-free decision tree complexity and erring decision tree complexity. Quoting 314.3, "...The possible algorithms can output anything. The mistake can be either way...". 1-way error occurs in one direction - 1 is output instead of 0 while 2-way error occurs in both directions - 1 for 0 and 0 for 1. This error is intrinsic to the decision process itself not just limited to sensitivity measures which depend on flipped inputs affecting outputs. Thus if error is modelled as a function of PRGs, error in voting process as a whole implies existence of PRGs. For example above distinguisher can be mapped to a voter who fails to distinguish two candidates with differing goodness - voter is fooled - a less merited candidate if had access to the intrinsic PRG that vitiates the decision tree evaluation can exploit the voter's flawed decision tree.

#### References:

- 
- 314.1 Definition of Pseudorandomness - Simpler Distinguisher - <http://people.seas.harvard.edu/~salil/pseudorandomness/prgs.pdf> - Page 217 and Proposition 7.8 in Page 218
- 314.2 Definition of Pseudorandomness - Counting argument - <http://www.cse.iitk.ac.in/users/manindra/survey/complexity25.pdf> - Page 3 - Definition 21
- 314.3 Lambda-tolerant Randomized Boolean Decision Trees - [https://www.math.u-szeged.hu/~hajnal/research/papers/dec\\_surv.gz](https://www.math.u-szeged.hu/~hajnal/research/papers/dec_surv.gz) - Page 5
- 

315. (FEATURE-DONE and BUG-STABILITY ISSUES) NeuronRain AsFer Commits for Virgo Linux - Commits - 25 August 2016

-----

Kernel Panic investigation for boost::python c++ invocations of Virgo System Calls

-----

1. Python code in AsFer that invokes Virgo Linux system calls by boost::python C++ bindings is being investigated further for mystery and random crashes that occur after system call code and driver end code is finished.

2.kern.log with 3 iterations of virgo\_malloc()+virgo\_set()+virgo\_get()  
invocations succeeded by panics in random points at kernel has been committed.  
3.Logs also contain the gdb vmlinux debugging showing line numbers within kernel  
source where panics occur. Prima facie look unrelated directly to virgo system  
calls and driver code. Debugging through KVM+QEMU is ruled out because of lack  
of VT-x.

-----  
-----  
316. (FEATURE-DONE and BUG-STABILITY ISSUES) NeuronRain AsFer Commits for Virgo  
Linux - Commits - 26 August 2016  
-----  
-----

Kernel Panic investigation for boost::python c++ invocations of Virgo System  
Calls  
-----  
-----

kern.log with panic in FS code after boost::python C++ AsFer-VIRGO Linux system  
calls invocations  
-----  
-----

317. (THEORY) Generic Definitions of Majority and Non-majority Choice Errors and  
some contradictions - related to 14 and 53.14  
-----  
-----

Majority Voting Social Choice has usual meaning of aggregation of for and  
against votes. Non-majority Social Choice can be in two  
flavours:

317.1 Pseudorandom Choice - a Pseudorandom Generator chooses a voting  
function from a set of Voting functions of electorate

317.2 Social choice by ranking - set of boolean functions are ranked  
ascending in their error probabilities and least error boolean function is  
chosen.

-----  
Algorithm for 317.1:  
-----

There are pseudorandom generators in NC(Applebaum PRG, Parallel PRGs etc.,)  
which choose a boolean function at random. This chosen boolean function can be  
Percolation boolean function too which is again in non-uniform NC. Thus Non-  
majority social choice can be done in BPNC as below:

- Invoke a PRG in NC or P to obtain pseudorandom bits X.
- Choose an element in electorate indexed by X.
- Goodness of LHS is equal to the goodness of chosen element.

LHS is BPNC algorithm to RHS BPEXP Condorcet Jury Theorem (CJT) unbounded  
circuit and if CJT converges to 1 in RHS and Goodness of PRG choice is 1, LHS is  
a BPNC algorithm to EXP RHS.

-----  
Algorithm for 317.2:  
-----

- foreach(voter)
- {
- Interview the voter boolean function : Rank the voters by merit  
(error probabilities e.g noise stability)
- }
- choose the topmost as non-majority social choice

LHS is a PSPACE-complete algorithm and RHS is either BPEXP or EXP algorithm  
depending on convergence or divergence of Goodness of CJT circuit in RHS.  
Goodness of LHS is the error probability of topranked boolean voter function.

Above loop can be parallelized and yet it is in PSPACE. Proof of CJT circuit in RHS to be EXP-complete would immediately yield a lowerbound and either EXP is in BPNC or EXP is in PSPACE under equal goodness assumption in LHS and RHS. EXP in PSPACE implies EXP=PSPACE because PSPACE is in EXP. An EXPTIME problem is EXP-Complete if it can solve Exponential Time Bounded Halting Problem (i.e output 1 if a Turing Machine halts after exponential number of steps). Unbounded depth RHS CJT Majority voting composition circuit (Majority+SAT) is in EXPTIME. Following reduction from Majority voting to Bounded Halting Problem is a proof outline for EXP-completeness of CJT circuit:

(\*) Let there be exponential number of voters (i.e exponential in number of variables)

(\*) Number of voters = Number of steps in Bounded Halting Problem input Turing Machine = exponential

(\*) Voting halts when all exponential voters have exercised franchise applying their SAT = EXPTIME Turing Machine Halts after exponential number of steps.

If there are  $n$  boolean functions in total and probability that a boolean function  $i$  with goodness  $e(i)$  is chosen is:

$= x(e(i))/n$ , where  $x(e(i))$  is the number of boolean functions with goodness  $e(i)$

When voter boolean functions have unequal error probabilities, the distribution is Poisson Binomial (which is for bernoulli trials with unequal probabilities for each event) and not Binomial or Poisson (which is the limit of Binomial distribution). This fraction is the LHS and in special case can be 1 when all boolean functions are of same goodness (1-error) probability. Thus LHS goodness is conditional probability  $x(e(i))/n * e(i)$  and can be 1 when all boolean functions are perfect.

Thus most generic Majority voting case is when:

317.3 Voters have unequal decision errors

317.4 Set of voter boolean functions is an assorted mix of varied error probabilities ranging from 0 to 1.

317.5 Modelled by Poisson Binomial Distribution

In both Majority and Non-majority Choice, error of a boolean function comprises:

317.6 Voting Error - Misrecorded votes, Probabilistic CNFs

317.7 Voter Error - Noise Sensitivity of boolean function which has extraneous reasons like correlated flipped bit strings and Error intrinsic to boolean function in Decision tree evaluation (lambda-tolerant randomized decision trees) mentioned in 314.

Randomized decision tree evaluation in 317.7 adds one additional scenario to error matrix of 8 possibilities in 14 and 53.14 which is beyond just correlation error.

As mentioned elsewhere in this document and disclaimer earlier, LHS circuit is a lowerbound to RHS circuit for a C-complete class of problems when errors are equal, assuming complete problems exist for class C. When both LHS and RHS have errors, which is the most realistic case, LHS is a BPNC circuit and RHS is a BPEXP circuit with unrestricted depth of exponential sized circuit. This raises a contradiction to already known result as follows: BPP is not known to have complete problems. [Marek Karpinski and Rutger Verbeek - KV87] show that BPEXP is not in BPP and EXP is in BPEXP. If there are BPEXP-complete problems then contradiction is LHS is a BPNC algorithm to RHS BPEXP-complete problem. But BPNC is in BPP (logdepth, polysize circuit with error can be simulated in polytime with error) and BPEXP is not in BPP. This contradiction is resolved only if there are no BPEXP-complete problems or there are no BPNC/BPEXP voting functions.

From <https://www.math.ucdavis.edu/~greg/zoology/diagram.xml>, following chain of inclusions are known:

NC in BPNC in RNC in QNC in BQP in DQP in EXP  
RP in BPP in BQP in DQP in EXP

If LHS is a BPNC or RNC or BPP or RP pseudorandom algorithm to unbounded CJT RHS EXP-complete problem under equal goodness assumption, previous class containments imply a drastic collapse of EXP below:

EXP=BPNC (or) EXP=RNC (or) EXP=RP (or) EXP=BPP

This is rather a serious collapse because the containments include Quantum classes BQP and QNC, implying classical parallelism is equivalent to quantum parallelism. One of the interpretations to Quantum parallelism is "Many Worlds" - computations happen in parallel (states of the wave function) and interfere constructively or destructively (superposition of wave functions when some state amplitudes cancel out while others reinforce) to curtail some of the worlds. This special case occurs only if all voters have decision correctness probability  $p=1$ . For  $1 > p > 0.5$ , RHS CJT circuit goodness converges to 1 for infinite electorate but LHS expected goodness of Pseudorandom social choice is always less than 1, infact tends to 0 as N is infinite as below. Referring to 359:

Let number of voter decision functions with goodness  $x_i = m(x_i)$ . Thus  $N = m(x_1) + m(x_2) + m(x_3) + \dots + m(x_n)$

Expected goodness of a PRG choice is:

$$\frac{1}{N} * \text{summation}(x_i * m(x_i)) = (x_1 * m(x_1) + x_2 * m(x_2) + x_3 * m(x_3) + \dots + x_n * m(x_n)) / N$$

When all voter functions have goodness 1 then PRG choice in LHS of P(good) has goodness 1.

For  $p=0.5$ , RHS goodness is 0.5 and LHS goodness is 0.5  $\Rightarrow$  LHS is in BPNC or RNC or RP or BPP and RHS is BPEXP. If RHS is BPEXP-complete, as mentioned previously, contradicts result of [KV87], implying BPEXP=BPP. For  $p < 0.5$ , RHS CJT series goodness tends to 0 while LHS pseudorandom choice expected goodness is always  $> 0$ . Thus only feasible lowerbound looks to be:

EXP=BPNC (or) EXP=RNC (or) EXP=RP (or) EXP=BPP

when goodness  $p=1$  uniformly for all infinite homogeneous electorate.

References:

-----  
317.8 Derandomization Overview - [Kabanets] -

[http://www.cs.sfu.ca/~kabanets/papers/derand\\_survey.pdf](http://www.cs.sfu.ca/~kabanets/papers/derand_survey.pdf)

317.9 Unconditional Lowerbounds against advice - [BuhrmanFortnowSanthanam] -

<http://homepages.inf.ed.ac.uk/rsanthan/Papers/AdviceLowerBoundICALP.pdf>

317.10 EXPTIME-Completeness - [DingZhuDu-KerIKo] - Theory of Computational Complexity - [https://books.google.co.in/books?id=KMwOBAAQBAJ&pg=PT203&redir\\_esc=y#v=onepage&q&f=false](https://books.google.co.in/books?id=KMwOBAAQBAJ&pg=PT203&redir_esc=y#v=onepage&q&f=false)

317.11 BPP with advice -

<http://people.cs.uchicago.edu/~fortnow/papers/advice.pdf> - "...It can be shown using a translation argument that BPEXP is not in BPP [KV87], but this translation argument does not extend to showing a lower bound against advice. Since BPP and BPEXP are semantic classes, it is unknown whether for instance  $BPEXP \subseteq BPP/1$  implies  $BPEXP/1 \subseteq BPP/2$ ". LHS pseudorandom social choice algorithm is non-uniform because randomly choosing an element from a varying number of electorate requires maximum size of electorate as advice.

-----  
318. (THEORY) Yao's XOR Lemma, Hardness of Pr(Good) Majority Voting Function Circuit and Majority Version of XOR Lemma  
-----

Caution: Majority Hardness Lemma derivation is still experimental with possible errors.

Hardness of a boolean function is defined as how hard computationally it is to compute the function with a circuit of size s:

if  $\Pr(C(x) \neq f(x)) = \delta$  where  $C(x)$  computes boolean function  $f(x)$ , then  $f(x)$   $\delta$ -hard.

Majority function is known to have formula of size  $O(n^{5.3})$  - from Sorting networks of [AjtaiKomlosSzemerédi] and non-constructive proof by [Valiant]. Majority is computable in log-depth and hence in non-uniform NC1.

Hardness Amplification result by [Andrew Yao] states that a strongly-hard boolean function can be constructed from mildly-hard boolean function by amplification of hardness using XOR of multiple instances of function on some distribution of inputs. Following derivation develops intuition for amplification in XOR lemma:

318.1 Let  $f$  be a boolean function with delta-hardness. Therefore there is a circuit  $C(x)$  with size  $s$ , such that  $\Pr(C(x) \neq f(x)) = \delta$ . XOR lemma states that there is a circuit  $C_1(x)$  with size  $s_1$ , such that  $\Pr(C_1(x) \neq f_1(x))$  tends to  $0.5 > \delta$  where  $f_1(x) = f(x_1) \text{ XOR } f(x_2) \text{ XOR } \dots \text{ XOR } f(x_k)$  for some distribution of inputs  $x_1, x_2, x_3, \dots, x_k$ .

318.2 Each  $f(x_i)$  in XOR function  $f_1$  in 318.1, is either flipped or not flipped. Let  $Z_i$  be the random variable for flip of  $f(x_i)$  -  $Z_i=0$  if there is no flip and  $Z_i=1$  if there is a flip using coin toss. Now the probability of correctly computing XOR of  $f(x_i)$ s is equal to the sum = Probability that none of  $f(x_i)$ s are flipped + Probability that even number of  $f(x_i)$  is flipped. Even flips do not alter XOR outcome while odd flips do. This is nothing but  $\Pr[Z_1 \text{ XOR } Z_2 \text{ XOR } Z_3 \text{ XOR } \dots \text{ XOR } Z_k = 0]$  because even flips cause XOR of  $Z_i=1$  to zero. If  $(1-2*\delta)$  is probability of no flip and  $2*\delta$  is probability of a flip, for all  $Z_i$ s  $\Pr(\text{XOR is correctly computed}) = (1-2*\delta)^k + 0.5*(1-(1-2*\delta)^k)$ . The second term is halved because probability of even number of flips is required whereas at least 1 flip implies both (odd+even).

318.3  $\Pr(\text{Good})$  majority voting boolean function computes composition of Majority function with Voting functions of individual voters. This can be expressed as:  $\text{Maj}_n(f_1, f_2, f_3, \dots, f_n)$  for  $n$  voters. Till now hardness of this composition is not known in literature. Experimentally, following derivation computes hardness of this composition as below.

318.4 For simplicity, it is assumed that all voters have same boolean function with hardness  $\delta$  computable by circuit size  $s$ .

318.5 Majority function makes error when the inputs are flipped by some correlation. This Probability that  $\Pr(\text{Maj}(x) \neq \text{Maj}(y))$  for two correlated strings  $x$  and  $y$  is termed as Noise Sensitivity. This together with the probability that a circuit with access to pseudorandom bits incorrectly computes majority function is an estimate of how flawed majority voting is (denoted as randomerror). Then probability that Majority function is correctly computed is  $1 - \text{NoiseSensitivity}(\text{Maj}_n) - \text{randomerror}$ . This implies majority function is in BPNC if there is a parallel voting.

318.6 Noise Sensitivity of Majority function is  $O(1/\sqrt{n*\epsilon})$  where  $\epsilon$  is probability of flip per bit. Therefore  $\epsilon$  is nothing but probability that a voter boolean function is incorrectly computed and sent as input to Majority function. This implies  $\Pr(f(x) \neq C(x)) = \delta = \epsilon = \text{hardness of all voter functions}$ .

318.7 Probability that Majority function is computed incorrectly =  $\text{NoiseSensitivity} \pm \text{randomerror} = [c/\sqrt{n*\epsilon}] \pm \text{randomerror} = [c/\sqrt{n*\delta}] \pm \text{randomerror}$  which is the hardness of Majority+VoterFunctions composition. (Related: points 14, 53.14 and 355 for BP\* error scenarios matrix which picturises overlap of Noise Sensitivity and Error)

318.8 Above derivation, if error-free, is the most important conclusion derivable for hardness of  $\Pr(\text{Good})$  majority voting boolean function circuit composition. Hardness of RHS of  $\Pr(\text{Good})$  Majority Voting circuit is expressed in terms of hardness of individual voter boolean functions.

318.9 Therefore from 318.7,  $\Pr(C(\text{Maj}_n(f(x_1), f(x_2), \dots, f(n))) \neq \text{Maj}_n(f(x_1), f(x_2), \dots, f(n))) = [c/\sqrt{n*\delta}] \pm \text{randomerror}$  is the probability that how incorrectly a circuit of size  $s_1$  computes  $\text{Maj}_n + \text{VoterFunction}$  composition = hardness of majority+voter composition.

318.10 Hardness is amplified if  $[c/\sqrt{n*\delta}] \pm \text{randomerror} \geq \delta$  as follows:

$$\frac{\text{Hardness of Maj+voter composition}}{\text{Hardness of voter function}} = \frac{[c/\sqrt{n*\delta}] \pm \text{randomerror}}{\delta} >> 1$$

318.11 Let  $\text{randomerror} = r$ . From above,  $[c/\sqrt{n*\delta}] \pm r / \delta$  must

be  $\gg 1$  for hardness amplification. For large  $n$ , this limit tends to  $r/\delta \gg 1$  implying error in majority circuit has to be huge for large electorate compared to error in voter boolean function SATs for hardness amplification. Caveat: There are scenarios where numerator is comparably equal to denominator and hardness amplification may not occur. From error scenarios matrix in 355, relation between error and noise can be precisely defined as: Error = Noise + (column2 error entries) - (column3 no error entries) where randomerror =  $r =$  (column2 error entries) - (column3 no error entries) which substituted in amplification becomes:

$$\frac{\text{Hardness of Maj+voter composition} \quad [c/\sqrt{n*\delta}] + [\text{sum(column2 error entries)}] - [\text{sum(column3 no error entries)}]}{\text{Hardness of voter function} \quad \delta} =$$

$\gg 1$

For large  $n$ ,  $c/\sqrt{n*\delta}$  tends to 0 and If  $[\text{sum(column2 error entries)}] - \text{sum(column3 no error entries)} \gg \delta$  then following applies:

318.12 318.11 implies that for weakly hard functions (low  $\delta$ ), if quantity in numerator (hardness of majority+voter composition) is considerably huge compared to hardness of individual voter functions, hardness is amplified.

318.13 318.11 also implies that Majority+Voter composition is extremely hard to compute concurring with exponential circuit size (PH=DC or EXP-completeness) of  $\text{Pr}(\text{Good})$  RHS.

318.14 Being extremely hard implies that RHS of  $\text{Pr}(\text{Good})$  could be one-way function. One-way functions are hard to invert defined formally as:

$\text{Pr}(f(f_{\text{inverse}}(y))=f(x))$  is almost 0.

For example inverse for  $\text{Pr}(\text{Good})$  majority voting function is the one that returns set of all voters who voted for a candidate to win. This implies that any electoral process has to be one-way function hard so that secret balloting is not in jeopardy and finding such inverse for majority has to be hardest. Similarity of definition of one-way function and hardness of boolean functions is obvious. Hardness for majority derived previously is for forward composition direction which itself is high.

318.15 Conjecture: Circuit for reverse direction (i.e decomposition of majority to voters who voted in favour) is considerably harder than composition and thus Majority(n)+Voter composition is an one-way function. An intuitive proof of this conjecture: Search for all permutations of voters who voted in favour which is of size  $O(2^n)$  - equivalent to solving SAT of Majority function boolean formula to find assignments which is counting problem and is #P-Complete. Indices of 1s in the assignment strings are the voter permutations. Next step is to find satisfying assignments to individual voter SATs which is also #P-Complete. This completely inverts the Majority+Voter composition and cumulatively is atleast #P-Complete. While the forward direction is composition of NC instance to voter SATs bottom-up, inverse is harder because it is completely #P-Complete top-down.

318.16 Huge hardness of  $\text{Pr}(\text{Good})$  RHS also implies that very strong pseudorandom number generators can be constructed from it.

318.17 The counting problem in 318.15 finds all possible permutations of voters who could have voted in favour while what is required is the exact permutation which caused this majority outcome. From this, probability of finding exact permutation of voting pattern =  $1/\#\text{SAT} = 1/\text{number\_of\_sat\_assignments\_to\_MajoritySAT}$ . This counting and search problem is defined as function Majorityinverse(1)=(v1,v2,v3,...vn) and returns the exact permutation of voters who voted for Majority outcome to be 1.

318.18 318.17 implies  $\text{Pr}(\text{Majority}(\text{Majorityinverse}(1))=\text{Majority}(v1,v2,...,vn)) = 1/\#\text{SAT} \leq 1/2^n$  in worst case.

318.19 In average case, expected number of SAT assignments to MajoritySAT

$= 1 \cdot 1/2^n + 2 \cdot 1/2^n + \dots + 2^n \cdot 1/2^n = 2^n \cdot (2^{n+1})/2 \cdot 1/2^n = (2^{n+1})/2$ ,  
 assuming all permutations are equally probable. Average case  
 $\Pr(\text{Majority}(\text{Majority}^{-1}(1)) = \text{Majority}(v_1, v_2, \dots, v_n)) = 1/\#\text{SAT} = 2/(2^{n+1}) \approx 1/2^{n-1}$   
 which is same as definition of a one-way function and thus Majority is hard to invert in average case.

318.20 318.19 implies Majority is one-way. Therefore  $\text{FP} \neq \text{FNP}$  and thus  $\text{P} \neq \text{NP}$  if hardness is amplified in 318.11.

#### References:

-----  
 318.20 [Impagliazzo-Wigderson] -  $\text{P}=\text{BPP}$  if EXP has  $2^{\Omega(n)}$  size circuits - <http://www.math.ias.edu/~avi/PUBLICATIONS/MYPAPERS/IW97/proc.pdf> -  $\Pr(\text{Good})$  has exponential sized circuits (by theorem 6.29 of [AroraBarak] mentioned in 129 previously) because of unbounded nature of RHS.  
 318.21 [Trevisan] - XOR Lemma Course Notes - <http://theory.stanford.edu/~trevisan/cs278-02/notes/lecture12.ps>  
 318.22 [Goldreich-RoniIzsak] - One-way functions and PRGs - <http://www.wisdom.weizmann.ac.il/~oded/PDF/mono-cry.pdf>  
 318.23 Noise Sensitivity of Majority Function - <http://pages.cs.wisc.edu/~dieter/Courses/2008s-CS880/Scribes/lecture16.pdf>  
 318.24 Definition of One-way functions - [https://en.wikipedia.org/wiki/One-way\\_function](https://en.wikipedia.org/wiki/One-way_function)

-----  
 319. (THEORY) Integer Partitions, Multiway Contests, Hash Table Functions and Ordered Bell Numbers - related to 256 and 272  
 -----

Number of hash table functions derived in [https://sites.google.com/site/kuja27/IntegerPartitionAndHashFunctions\\_2014.pdf](https://sites.google.com/site/kuja27/IntegerPartitionAndHashFunctions_2014.pdf), which sums all possible permutations of hash buckets per partition does not consider order of elements within each bucket. Bell number (named after Eric Temple Bell) is the number of all possible partitions of a set (induced by all possible equivalence relations). Each hash table is a set of equivalence classes (i.e. each bucket is an equivalence class and hash function is the relation), partitioning the set. Ordered Bell Number takes into account order of keys in each bucket and gives all possible Ordered Hash Table Functions. This is a stronger estimate of number of hash table functions than plain counting from integer partitions which is unordered. Unordered  $n$ -th Bell Number is given by:  $\sum_{k=0}^n \{n, k\}$  where  $\{n, k\}$  is the Stirling Number of Second kind computing number of ways of partitioning set of size  $n$  into subsets of size exactly  $k$ .

Let there be  $n$  keys and size of hash table be  $m$ . Let  $h_i(x) \bmod m$  be a hash function.

For each  $h_i$

```

{
 For each $x < n$
 {
 Compute $h_i(x) \bmod m$ and append to corresponding chain of buckets in hash table
 }
}

```

Above loops create all possible partitions of set of size  $n$ . If just the integer partition is reduced to above hash table chains,  $\sum(mP(\lambda(i)))$  is only an approximation. Also Ordered Bell Number is an approximation as it does not permute each partition within a larger set of slots. Stirling Number of second kind  $\{n, k\}$  is equal to number of partitions of an  $n$ -element set into  $k$  nonempty subsets. Each partition is permuted within  $m$  slots in a separate chained hash table and each such permutation is a configuration of a hash function after all

keys are populated. Total number of such functions =  $\sum_{k=1}^m mP(\{n, k\})$  which can be called as Augmented Stirling Number and is greater than Ordered Bell Number:

$$\sum_{k=1}^m mP(\{n, k\}) \geq \text{Ordered Bell Number} = \sum_{k=1}^m \{n, k\}$$

In multipartisan voting with more than 2 candidates, above augmented stirling number is also the number of all possible voting patterns with an electorate of size  $n$  voting on  $m$  candidates - each chain is the set of votes for corresponding candidate. Hash function for each voter chooses a candidate index. Thus Chained Hashing with optional sorting of chains on number of votes is Majority Function generalized. From Arrow, Friedgut-Kalai-Nisan and Gibbard-Satterthwaite theorems elections with more than 3 candidates can be manipulated implying multiway majority function has non-zero noise sensitivity.

Probability that above multiway majority function has an error (i.e chooses wrong outcome) =

Probability of changing one voting pattern to the other that changes ranking of candidates

Each voting pattern can be deemed to be a point vertex on an  $m$ -dimensional metric space and edges between these vertices are distances to other patterns. If each edge has a probability of occurrence, Probability of flip in voting pattern due to a malpractice is the probability of a path existing between these two voting patterns in this random graph. If each edge has equal probability, path probabilities vary between  $p$  and  $p^{\text{augmented\_stirling\_number}}$ . This assumes that any voting error is a converging random walk on the random graph of point vertices of voting pattern in a metric space. It could be a complete graph too which does not require a random walk.

In a sense the multiway majority hashing previously is a locality sensitive hashing wherein similarity between items is defined as voters voting for same candidate who are chained together in a bucket i.e Probability(two voters  $x$  and  $y$  voting for same candidate are colocated in a bucket) = 1 and Probability(two voters  $x$  and  $y$  voting for different candidates are colocated in a bucket) = 0 with strict equalities while the distance function is defined as  $d(x, y) \leq r$  if  $x$  and  $y$  vote for same candidate and  $d(x, y) > r$  else. From  $m$ -balls and  $n$ -bins problem bounds, for  $m \gg n$ , maximum number of balls per bin with high probability could be  $m/n + \theta(\sqrt{m \log n / n})$  - in terms of votes, this is a rough estimate of maximum votes a candidate can get with high probability in random voting. For example, a locality sensitive hash function  $f(x) \bmod m$  returning  $k$  for  $f(x) \bmod m$  with  $f(x)$  defined over  $[-l, +l]$  maps a ball of radius  $l$  comprising similar voters to a candidate  $k$  - ball is the chained bucket for  $k$ .

As mentioned in previous paragraphs, each voting pattern is a point vertex on a metric space and it is necessary to define distance  $d$  between any two voting patterns. Let  $v_1$  and  $v_2$  be two voting patterns in the chained hashing previously described for  $m$  candidates and  $n$  voters. These two patterns differ in votes per candidate. Hence it makes sense to define the distance between the patterns as number of votes gained/lost by candidates across these two patterns. Let  $p$  be the probability that single vote is transferred by rigged voting from candidate  $k$  to candidate  $l$ . Also let  $c_1, c_2, c_3, \dots, c_k$  be the candidates who either all gained (or) all lost across voting patterns  $v_1$  and  $v_2$ . Then the probability that voting pattern changes from  $v_1$  to  $v_2 = p^d$  where  $d$  is the metric distance between two voting patterns defined as  $d = v_2(c_1) - v_1(c_1) + v_2(c_2) - v_1(c_2) + \dots + v_2(c_k) - v_1(c_k)$  where  $v_a(c_b)$  is the votes for candidate  $c_b$  in voting pattern  $v_a$ . L2 norm is not preferred because probability for voting pattern change requires gained/lost votes in one direction only. For example voting pattern  $\{5, 3, 4\}$  becoming  $\{6, 4, 2\}$  implies first 2 candidates gained 1 vote each while third candidate lost 2 votes. L2 norm is  $\sqrt{6}$  while metric distance as per previous definition is 2. Greater the distance between patterns, exponentially rarer is the probability  $p^d$  of voting pattern flip. It is assumed that all voters vote independently and each vote flip in pattern change occurs independently. Thus the random graph edges between voting pattern vertices are



weighted by these probabilities( $p^{d_1}$ ,  $p^{d_2}$ , etc., for distances  $d_1, d_2, \dots$ ). This is an alternative definition of edge probability different from one described previously. Number of vertices in this random graph = augmented\_stirling\_number =  $\sum_{k=1}^n m(P(\{n, k\})) \geq$  Ordered Bell Number

Probability of multiway majority choosing a wrong outcome = Probability that voting pattern noise flip changes sorted ranking of candidates. For example,  $\{12, 10, 5\}$  becomes  $\{7, 12, 8\}$  which changes winner from first to second candidate with total votes remaining same. Not all edges of random graph of patterns change the ranking despite noise. If majority in multiway contest is defined as candidate index getting more than half of total votes, winning voting patterns are number of integer partitions of  $n$  voters with largest part  $> n/2$ . These partitions with largest part greater than  $n/2$  correspond to subset of voting patterns which are not affected by noise flip because only parts other than largest are shuffled. Therefore probability that outcome is not changed by noise flip of voting pattern =  $\text{number\_of\_partitions\_of\_n\_voters\_greater\_than\_n/2} / \text{partition\_number}(n)$ . From this probability of wrong outcome because of noise flip in voting pattern =  $1 - \{ (\text{number\_of\_partitions\_of\_n\_voters\_greater\_than\_n/2}) / \text{partition\_number}(n) \} =$  Noise sensitivity of Multiway Majority Function.

319.8 is an NVIDIA CUDA parallel implementation of hash table chaining. 319.9 is a recent parallel locality sensitive hashing algorithm for multicore machines, and segregates twitter stream of tweets into similar buckets. Availability of parallel algorithms for hash table chains implies that hash chaining and LSH especially could be in NC (logarithmic table construction time) though there is no known result thus far. Parallelism in multiway majority function LSH is obvious because people vote in parallel and hash chain buckets are populated in parallel across multiple voting machines in compartmentalized voting. Each such voting machine can correspond to a node in Multiway Majority circuit. The  $\rho$  parameter of LSH is  $\log(1/p_1)/\log(1/p_2)$  where  $p_1 = \Pr(h(x)=h(y))$  if  $x$  and  $y$  had voted for same candidate and  $p_2 = \Pr(h(x)=h(y))$  if  $x$  and  $y$  had voted for different candidates. In multiway majority LSH mentioned previously,  $p_1=1$  and  $p_2=0$  and  $\rho=0$  where as in usual approximate neighbours problem  $\rho$  is only required to be  $< 1$ . Intuitively, each hash table slot is lock-free and each bucket for a slot is lock-synchronized. Thus votes across candidates is parallelizable and votes for a candidate are serially incremented(linked-list bucket is appended). Addition of votes per candidate slot should be doable in NC (because integer addition is in NC). Thus there are as many NC circuits as there are candidates. Set of votes from all candidates has to be then sorted to find the winner which is also in NC (e.g Sorting networks). Optional comparator circuits for half-way mark comparison is also in NC. Thus Multiway majority function could be computable in Non-uniform NC which places it in same league as boolean  $\Theta(1)$  majority function.

#### References:

- 
- 319.1 Unordered Bell Number - [https://en.wikipedia.org/wiki/Bell\\_number](https://en.wikipedia.org/wiki/Bell_number)
  - 319.2 Ordered Bell Number - [https://en.wikipedia.org/wiki/Ordered\\_Bell\\_number](https://en.wikipedia.org/wiki/Ordered_Bell_number)
  - 319.3 Mining Massive Data Sets - [UllmanRajaramanLeskovec] - <http://infolab.stanford.edu/~ullman/mmds/book.pdf>
  - 319.4 Lowerbounds for Locality Sensitive Hashing - [RyanODonnell] - <https://www.cs.cmu.edu/~odonnell/papers/lsh.pdf>
  - 319.5 Theory of Partitions - Bell numbers - [GeorgeEAndrews] - [http://plouffe.fr/simon/math/Andrews%20G.E.%20The%20Theory%20of%20Partitions%20\(Enc.Math.Appl.%202,%20AW,%201976\)\(266s\).pdf](http://plouffe.fr/simon/math/Andrews%20G.E.%20The%20Theory%20of%20Partitions%20(Enc.Math.Appl.%202,%20AW,%201976)(266s).pdf)
  - 319.6 Power of Simple Tabulation Hashing - [PatrascuThorup] - <http://arxiv.org/pdf/1011.5200v2.pdf> - Lemma 4 - Balls and Bins hashing
  - 319.7 Balls and Bins, Chained Hashing, Randomized Load balancing - <http://pages.cs.wisc.edu/~shuchi/courses/787-F09/scribe-notes/lec7.pdf>
  - 319.8 Parallel Hash tables - Chaining buckets with arrays - <http://idav.ucdavis.edu/~dfalcant/downloads/dissertation.pdf>
  - 319.9 Parallel Locality Sensitive Hashing - [Narayanan Sundaram†, Aizana Turmukhametova, Nadathur Satish†, Todd Mostak, Piotr Indyk, Samuel Madden and

-----  
-----  
320. (BUG-STABILITY ISSUES) Commits - 6 September 2016  
-----

-----  
-----  
VIRGO Linux Kernel Stability Analysis - 2 September 2016 and 6 September 2016  
-----

-----  
-----  
kern.log(s) for Boost::Python invocation of VIRGO system calls with and without crash on two dates have been committed:  
Logs on 2/9/2016 have a crash as usual in VM paging scatterlist.c. Today's invocation logs show perfect execution of whole end-to-end user/kernel space without any kernel panic much later. Such randomness in behaviour is quite unexplainable unless something lurking beyond the code path intercepts this. Could be a mainline kernel bug in 4.1.5 tree.  
-----

-----  
-----  
321. (BUG-STABILITY ISSUES) Commits - 8 September 2016  
-----

-----  
-----  
Continued kernel panic analysis of boost::python-VIRGO system calls invocations. Similar pattern of crashes in vma paging is observed with a successful panic-free invocation in the end.  
-----

-----  
-----  
322. (BUG-STABILITY ISSUES) Commits - 9 September 2016  
-----

-----  
-----  
Boost::python-VIRGO system calls invocation kernel panic analysis showing some problem with i915 graphics driver interfering with VIRGO system calls.  
-----

-----  
-----  
323. (THEORY) Complement Functions for Hash Chains, PAC Learning, Chinese Remaindering and Post Correspondence Problem - related to 19,24,319  
- important draft additions to <http://arxiv.org/pdf/1106.4102v1.pdf>  
-----

-----  
-----  
A hash table chain can be viewed as a subset segment of a larger rectangular region. Complement of this subset is another hash table chain.  
For example following schematic illustrates hash table complements with respect to chained buckets:  
-----

----- #####  
----- #####  
----- #####  
----- #####  
----- #####  
----- #####

Above diagram has two hash table chains shown in different constituent colors. Together these two cover a rectangular region. Thus left(f1) and right(f2) are complements of each other. In partition parlance, both f1 and f2 have same number of parts. Let f1 partition a set of n1 and f2 partition a set of n2 elements into chains. Let m be the number of parts in both (breadth of rectangle). Then length is (n1 + n2) / m. If Pi(f1) and Pi(f2) denote the i-th chain partition on both f1 and f2, then Pi(f1) + Pi(f2) = (n1 + n2)/m. Hash function which created f1 is known while that of f2 is unknown. This is a special case of Decidability of Complement Function mentioned in 24 where "complementation" is defined with reference to a larger universal rectangular

set. From the chain pattern on right the hash function for f2 can be reverse engineered. When the left is viewed as a multiway majority voting pattern or a Locality Sensitive Hash function, right is a complementary voting pattern or a Complementary Locality Sensitive Hash Function which "inverts" the ranking. A tabulation for hash function of f2 can be constructed like an example below:

```
f(x01) mod m = 0
f(x11) mod m = 1
f(x12) mod m = 1
...
f(x21) mod m = 2
f(x22) mod m = 2
...
```

where  $x_{ij}$  is the  $j$ -th element in  $i$ -th chain part in f2 on right. Above tabulation can be solved by Euclid's algorithm. For example,  $f(x_{11}) \bmod m = 1$  can be solved as:

$$[-m \cdot y + f(x_{11})] = 1 \Rightarrow f(x_{11}) \bmod m = 1$$

Therefore above table can be written as system of congruences:

```
f(x01) = a01*m + 0
f(x11) = a11*m + 1
f(x12) = a12*m + 1
...
f(x21) = a21*m + 2
f(x22) = a22*m + 2
...
```

Since  $m$  is known and all  $a_{ij}$  can take arbitrary values, complement function for f2 can be constructed by fixing  $a_{ij}$  and applying either PAC learning (approximation only) or CNF multiplexor construction/Interpolation/Fourier Series (described in 19 and 24). There are indefinite number of Complement Functions constructible by varying  $a_{ij}$ . But Number of hash functions is upperbounded by Augmented Stirling Number. This is because hash functions which internally apply complement functions, create finite chained bucket configurations or voting patterns bounded by augmented stirling number modulo size of the table whereas complement functions don't have such restrictions in construction. This implies two complement functions could give rise to similar hash table chain configurations. Thus set of complement functions is partitioned by hash chained configurations i.e. there are augmented stirling number of sets of complement functions. Main advantage of PAC learnt complement construction over exact multiplexed CNF construction is there are no bloating of variables and boolean conjunctions are minimal, but the disadvantage is approximation and not exact. For first  $n$  prime numbers there are  $\log(n)$  conjunctions each of  $\log(n)$  literals.

Boolean 0-1 majority function is a special case of multiway majority function (or) LSH, where hashtable is of size 2 with 2 chained buckets i.e.

$$\text{Augmented Stirling Number of Boolean Majority} = 2P(n,1) + 2P(n,2)$$

Chinese Remaindering Theorem states that there is a ring isomorphism for  $N=n_1 \cdot n_2 \cdot n_3 \cdot \dots \cdot n_k$  (for all coprime  $n_i$ ) such that:

$$X \bmod N \Leftrightarrow (X \bmod n_1, X \bmod n_2, X \bmod n_3, \dots, X \bmod n_k)$$

(or)

$$Z/NZ \Leftrightarrow Z/n_1Z * Z/n_2Z * \dots * Z/n_kZ$$

Chinese Remaindering has direct application in hash table chains as they are created in modular arithmetic.  $K$  hash functions on the right of isomorphism correspond to  $K$  hash table chains (or) LSH (or) Voting patterns for hash tables of sizes  $n_1, n_2, \dots, n_k$ . Left of isomorphism is a hash table of size  $N$  (LSH or a Voting Pattern).

From Post Correspondence Problem, if  $f_1$  and  $f_2$  in schematic diagram are two voting patterns, finding a sequence such that:

$$p_1 p_2 p_3 \dots p_m = q_1 q_2 q_3 \dots q_m$$

is undecidable where  $p_i$  and  $q_i$  are parts in voting patterns  $f_1$  and  $f_2$  as concatenated strings. What this means is that finding a sequence which makes serialized voters in both patterns equal is undecidable.

Alternative proof of undecidability of Complement Function Construction with PCP  
:

-----  
Complement Functions are reducible to Post Correspondence Problem. PCP states that finding sequence of numbers  $i_1, i_2, i_3, \dots, i_k$  such that:

$$s(i_1)s(i_2)s(i_3)\dots s(i_k) = t(i_1)t(i_2)t(i_3)\dots t(i_k)$$

where  $s(i_k)$  and  $t(i_k)$  are strings is undecidable.

Example inductive base case:

-----  
Let  $f(x) = 2, 4, 6, 8, \dots$

and  $g(x) = 1, 3, 5, 7, \dots$

$f(x)$  and  $g(x)$  are complements of each other.

Define  $a(i)$  and  $b(i)$  as concatenated ordered pairs of  $f(x_i)$  and  $g(x_i)$ :

$$a_1 = 2 \qquad b_1 = 2, 3$$

$$a_2 = 3, 4 \qquad b_2 = 4, 5$$

$$a_3 = 5, 6 \qquad b_3 = 6, 7$$

$$a_4 = 7, 8 \qquad b_4 = 8, 9$$

$$a_5 = 9, 10 \qquad b_5 = 10$$

[e.g  $a_2 = 3, 4$  where  $g(a_2) = 3$  and  $f(a_2) = 4$ ;  $b_3 = 6, 7$  where  $f(b_3) = 6$  and  $g(b_3) = 7$  and so on. Here complement of an element is the succeeding element in universal set  $Z=1, 2, 3, 4, 5, \dots$  ]

Then,  $1, 2, 3, 4, 5$  is a sequence such that:

$$a_1 a_2 a_3 a_4 a_5 = b_1 b_2 b_3 b_4 b_5 = 2, 3, 4, 5, 6, 7, 8, 9, 10$$

which can be parenthesised in two ways as:

$$2(3,4)(5,6)(7,8)(9,10) = (2,3)(4,5)(6,7)(8,9)10 = 2, 3, 4, 5, 6, 7, 8, 9, 10$$

Each parenthesization is a string representation of a possible way to construct a complement function. Ideally, process of complementation has two symmetric directions created by the gaps in the range a function maps a domain to - predecessors and successors - which is captured by the two parenthesizations (i.e  $f$  is complement of  $g$  and  $g$  is complement of  $f$ ). Each substring within the parentheses is indexed by sequence numbers  $a_i$  and  $b_i$ . Thus an order of sequence numbers have to be found for both symmetric directions to get matching concatenated union of complements (universal set). Both directions have to converge because complementation is symmetric relation. But finding such an order of sequence numbers is a Post Correspondence Problem and undecidable (question of if turing machine halts on input). Since each  $a(i)$  and  $b(i)$  are concatenated ordered pair of value of  $f(x)$  and its complement  $g(x)$ , complement function is constructible if such ordered pairs exist for indefinite length. In essence: Finding an order of sequence numbers = Construction of complement functions which converge in opposing directions => Undecidable by Post Correspondence Problem. Above example can be generalized for any function, and its complement ordered pair and thus is an alternative proof (with a tighter definition of complementation that complements are bidirectional) of undecidability of Complement Function Existence and Construction. Another example is 2 parenthesizations for prime complementation below - elements succeeding a prime in left and elements preceding a prime in right:

$$f(x) = 2, 3, 5, 7, 11, \dots$$

$$g(x) = 4, 6, 8, 9, 10, 12, \dots$$

$$([2, 3], 4)(5, 6)(7, [8, 9, 10])(11) = ([2, 3])(4, 5)(6, 7)([8, 9, 10], 11) = 2, 3, 4, 5, 6, 7, 8, 9, 10, 11$$

Generic inductive case:

$$(f(x_1), \text{succ}(f(x_1)))(f(x_2), \text{succ}(f(x_2)))\dots = (\text{predec}(g(x_1)), g(x_1))$$

$$(\text{predec}(g(x_2)), g(x_2))\dots = Z$$

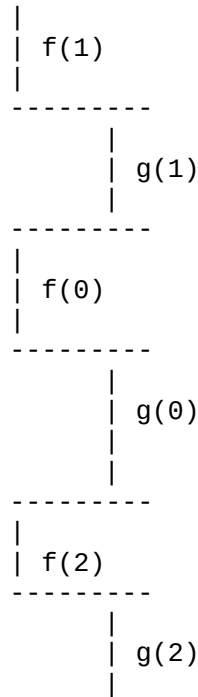
(or)

$$\text{concatenation\_of}(f(x_i), g(x_i)) = \text{concatenation\_of}(g(x_i), f(x_i)) = Z$$

where  $\text{succ}()$  and  $\text{predec}()$  are successor and predecessor functions respectively in lambda calculus jargon and  $x_i$  take some integer values. This assumes nothing

about the sorted order of  $f(x_i)$  and  $g(x_i)$  and each ordered pair is arbitrarily sampled and aggregated.  $f(x)$  is known and from this complement  $g(x)$  has to be constructed (though  $g(x_i)$  sampled data points are known,  $g(x)$  is not). To construct  $g(x)$ , ordered pairs for  $g(x_i)$  have to be sequenced as  $g(0)$ ,  $g(1)$ , ... which amounts to assigning values to  $x_i$  which is Post Correspondence Problem and undecidable.

Two complementation parenthesizations can be drawn as step function where indentation denotes complementary  $g$  points to  $f$  in example below:



which represent two parenthesization correspondences (sequence on right is staggered by one segment):

$$(f(1), g(1))(f(0), g(0))(f(2), g(2)) = (f(1))(g(1), f(0))(g(0), f(2))(g(2)) = f(1)g(1)f(0)g(0)f(2)g(2)$$

Hence  $x_1, x_2, x_3$  take values 1, 0, 2 for string on left. String on the right despite staggering also takes values 1, 0, 2 for  $x_1, x_2, x_3$  with only slight change - 1, 0, 2 is represented as 1-0, 0-2, 2 by coalescence of any two juxtaposed  $x_i$ . This correspondence is undecidable by PCP. This complementation scheme relaxes the definition of complements in <http://arxiv.org/pdf/1106.4102v1.pdf> by allowing the pre-image of complementary function segments to be in unsorted order - e.g 1, 0, 2 is not sorted.

Two Generic parenthesizations for  $f$  and its complement  $g$  are:

$$[f(x_1)][g(y_1)f(x_2)][g(y_2)f(x_3)][g(y_3)]... = [f(x_1)g(y_1)][f(x_2)g(y_2)][f(x_3)g(y_3)]... = f(x_1)g(y_1)f(x_2)g(y_2)f(x_3)g(y_3)...$$

where each  $f(x_i)$  and  $g(y_i)$  are contiguous streak of set of values of  $f$  and  $g$ .  $x_i$  is not necessarily equal to  $y_i$ . Required sequence numbers are  $x_1-y_1$ ,  $x_2-y_2$ ,  $x_3-y_3$ , ... in right and  $x_1$ ,  $y_1-x_2$ ,  $y_2-x_3$ , ... in left to make the strings correspond to each other. Here sequence numbers are identifiers which are concatenation of 2 numbers  $x_i$  and  $y_i$  as  $x_i-y_i$  or  $y_i-x(i-1)$ . Thus original undecidability of finding  $x_1-y_1, x_2-y_2, x_3-y_3, ...$  still remains. This is the most relaxed version of complementation.

Another alternative definition of complement function is: function  $f$  and its complement  $g$  are generating functions for the exact disjoint set cover of size 2 of a universal set formed by values of  $f$  and  $g$ . Disjoint Set Cover is the set of subsets of a universal set where each element of universal set is contained in exactly one set and their union is the universal set. Notion of complementation can be extended to arbitrary dimensional spaces. Each half-space is generated by a function complement to the other. Complementation is also related to concepts

of VC-Dimension and Shattering where each half-space is a class classified by complement functions (set A is shattered by a set C of classes of sets if for all subsets s of A,  $s = c \cap A$  for  $c$  in C)

Complementation Disjoint Set Cover can be represented as bipartite graph where edges are between two sets A and B. Set A has sequence numbers  $x_i$ (or  $y_i$ ) and set B is the universal set (Z for example). For each  $f(x_i)$  and  $g(y_i)$  there is an edge from  $x_i \rightarrow f(x_i)$  and  $y_i \rightarrow g(y_i)$ .

Boolean 0-1 majority special case of Hash chains and Complement Functions:

-----  
A hash table of size 2 with 2 chains partitions the set of keys into 2 disjoint sets. Each chain in this hash table is created by 2 functions complement to each other (examples previously described: set of odd and even integers, set of primes and composites). Thus if there exists a hash function h that accepts another function f as input and partitions a universal set into two chained buckets with mutually complementary elements belonging to f and g(complement of f), then it is an indirect way to construct a complement. But undecidability of complement construction by post correspondence precludes this.

-----  
324. (FEATURE-DONE) PAC Learning for Prime Numbers encoded as binary strings - Commits - 12 September 2016  
-----

-----  
PAC Learning implementation has been augmented to learn patterns in Prime Numbers encoded as binary strings. For each prime bit a boolean conjunction is learnt. Separate Mapping code has been written in python-src/PACLearning\_PrimeBitsMapping.py which json dumps the mapping of first 10000 prime numbers to corresponding i-th prime bit. Logs for this have been committed to python-src/testlogs/PACLearning.PrimeBitsMappingConjunctions.out.12September2016  
-----

-----  
325. (FEATURE-DONE) PAC Learning for Prime Numbers - Commits - 14 September 2016  
-----

Some errors corrected in bit positions computation in JSON mappings for PAC learning of Prime Numbers. Logs committed to testlogs/  
-----

-----  
326. (BUG-STABILITY ISSUES) Boost::Python-VIRGO System calls invocations random kernel panics - Commits - 15 September 2016  
-----

Further Kernel Panic analysis in i915 driver for Boost::python-VIRGO system calls invocations.  
-----

-----  
327. (THEORY) Algorithmic Fairness, Pr(Good) Majority Voting Circuit and Algorithmic Decision Making - Related to 14,53,275,317  
-----

-----  
In Majority Voting hardness analyzed thus far, voting functions of Individual Human Voters are assumed. Recent advances in algorithmic decision making (High Frequency Algorithmic Trading, Predictive Policing etc.,) involve decision making by algorithms than humans. It was implicit so far that algorithms cannot have bias. But there is a new emerging field of algorithmic fairness which highlights growing bias by machine learning algorithms in decision making (bias could be in

training dataset, algorithm's false assumptions leading to wrong conclusions based on correlations etc.,) that could subvert stock trading buy-sell decisions, criminal justice system and so on. Similar unfairness could happen in Majority voting also if the voters are algorithms (algorithm internally using a boolean function, non-boolean function, past training data to make future decisions among others). Unfair voting algorithms imply that  $\Pr(\text{Good})$  summation would never converge to 100% and therefore error is non-zero. Unfair voting is detrimental to distributed cloud computing involving majority voting choice - e.g loadbalancing of requests get skewed to a node unfairly by bad voting. Most importantly a proof of existence of 100% fair voting algorithm implies that LHS of  $\Pr(\text{Good})$  summation is 1 (From 317.2 least error algorithm is chosen as Non-majority social choice).

#### References:

-----  
327.1 Algorithmic Fairness - <https://algorithmicfairness.wordpress.com>  
327.2 Leader Election Algorithms in Cloud - HBase ZooKeeper - [Mahadev Konar - Yahoo] - [http://wiki.apache.org/hadoop/ZooKeeper/ZooKeeperPresentations?action=AttachFile&do=view&target=zookeeper\\_hbase.pptx](http://wiki.apache.org/hadoop/ZooKeeper/ZooKeeperPresentations?action=AttachFile&do=view&target=zookeeper_hbase.pptx)  
327.3 Leader Election and Quorum in ElasticSearch - <https://www.elastic.co/blog/found-leader-election-in-general> - Each node votes for a leader and minimum number of votes required for a leader is Quorum - This is realworld application of Multiway Majority function.  
-----

-----  
328. (FEATURE-DONE) Locality Sensitive Hashing Implementation - Nearest Neighbours Search - Commits - 16 September 2016  
-----

-----  
1.This commit implements locality sensitive hashing in python by wrapping defaultdict with hashing and distance measures.  
2.Locality Sensitive Hashing is useful for clustering similar strings or text documents into same bucket and is thus an unsupervised classifier and an inverted index too.  
3.In this implementation, very basic LSH is done by having replicated hashtables and hashing a document to each of these hashtables with a random polynomial hash function which itself is aggregation of random monomials.  
4.For a query string, random hash function is again computed and buckets from all hashtables corresponding to this hash value is returned as nearest neighbour set.  
5.Each of these buckets are sieved to find the closest neighbour for that hashtable.  
6.Sorting the nearest neighbours for all hash tables yields a ranking of documents which are in the vicinity of the query string.  
7.The input strings are read from a text file LocalitySensitiveHashing.txt  
8.Logs with hashtable dumps and nearest neighbour rankings are in testlogs/LocalitySensitiveHashing.out.16September2016  
-----

-----  
329. (FEATURE-DONE) LSH WebCrawler Support - Commits - 19 September 2016  
-----

-----  
Locality Sensitive Hashing now accepts scrapy crawled webpages as datasources.  
-----

-----  
330. (BUG - STABILITY ISSUES) Boost::Python AsFer-VIRGO system calls kernel panics - Commits - 19 September 2016  
-----

Boost::python AsFer - VIRGO system call ongoing kernel panic analysis - i915 DRM race condition kernel panic in VM pages freeing

-----  
331. (FEATURE-DONE) ZeroMQ based Concurrent Request Servicing CLI - Client and Multithreaded Server Implementation  
-----

Commits - 21 September 2016  
-----

-----  
1. NeuronRain already has support for RESTful GUI implemented in Python Tornado and NeuronRain code can be executed by filling up HTML form pages.  
2. ZeroMQ has a lowlevel highly performant low latency concurrency framework for servicing heavily concurrent requests.  
3. ZeroMQ is a wrapper socket implementation with special support for Request-Reply, Router-Worker, Pub-Sub design patterns.  
4. Important advantage of ZeroMQ is lack of necessity of lock synchronization (i.e ZeroMQ is lock-free per its documentation) for consistency of concurrent transactions  
5. Hence as a CLI alternative to HTTP/REST GUI interface, a C++ client and server have been implemented based on ZeroMQ Request-Reply Router-Dealer-Worker sockets pattern to serve concurrent requests.  
6. ZeroMQ client: ./zeromq\_client "<neuronrain executable command>"  
7. ZeroMQ server: invokes system() on the executable arg from zeromq client  
8. With this NeuronRain has following interfaces:  
    8.1 telnet client ----->  
NeuronRain VIRGO ports  
    8.2 VIRGO system call clients ----->  
NeuronRain VIRGO ports  
    8.3 AsFer boost::python VIRGO system call invocations ----->  
NeuronRain VIRGO ports  
    8.4 Tornado GUI RESTful ----->  
NeuronRain VIRGO ports  
    8.5 ZeroMQ CLI client/server ----->  
NeuronRain VIRGO ports  
-----

-----  
332. (FEATURE-DONE) KingCobra VIRGO Linux workqueue and Kafka Publish-Subscribe Backend Message Queue support in Streaming Generator  
-----

Commits - 22 September 2016  
-----

-----  
1. Streaming\_AbstractGenerator has been updated to include KingCobra request-reply queue disk persisted store, as a data storage option (reads /var/log/kingcobra/REQUEST\_REPLY.queue). Initial design option was to integrate a Kafka client into KingCobra kernelspace servicerequest() function which upon receipt of a message from linux kernel workqueue, also publishes it in turn to a Kafka Topic. But tight coupling of Kafka C Client into KingCobra is infeasible because of conflicts between userspace include header files of Kafka and kernelspace include header files of Linux. This results in compilation errors. Hence it looks sufficient to read the persisted KingCobra REQUEST\_REPLY.queue by a standalone Kafka python client and publish to Kafka subscribers. This leverages analytics by python code on KingCobra queue.  
2. NeuronRain backend now has a support for Kafka Pub-Sub Messaging.  
3. New publisher and subscriber for Kafka (with Python Confluent Kafka) have been written to read data from  
-----



Streaming\_AbstractGenerator and to publish/subscribe to/from a Kafka Message Broker-Topic. Thus any datasource that AsFer may have(file,HBase,Cassandra,Hive etc.,) is abstracted and published to Kafka. This also unites AsFer backend and KingCobra disk persistence into a single Kafka storage.

-----  
333. (BUG-STABILITY ISSUES) Boost::Python AsFer-VIRGO system call invocations kernel panic ongoing investigation  
-----

-----  
Commits - 23 September 2016  
-----

Ongoing Boost::Python AsFer-VIRGO system call invocation kernel panic analysis: Random crashes remain, but this time no crash logs are printed in kern.log and finally a successful invocation happens. It could be same as i915 GEM DRM crash similar to earlier analyses.

Pattern observed is as follows:

1. First few invocations fail with virgo\_get() though virgo\_malloc() and virgo\_set() succeed.
2. After few failures all virgo calls succeed - virgo\_malloc(), virgo\_set() and virgo\_get() work without any problems.
3. Sometimes virgo\_parse\_integer() logs and few other logs are missing. When all logs are printed, success rate is very high.
4. Some failing invocations have NULL parsed addresses. When there are no NULL address parsings, success rate is very high.
5. a rare coincidence was observed: Without internet connectivity crashes are very less frequent. (Intel Microcode updates playing spoilsport again?).
6. There have been panic bugs reported on i915 GEM DRM and recent patches for busy VMA handling to it:
  - 6.1 <https://bugs.launchpad.net/ubuntu/+source/linux/+bug/1492632>
  - 6.2 <https://lists.freedesktop.org/archives/intel-gfx/2016-August/102160.html>
7. Intel GPU i915 GEM DRM docs - <https://01.org/linuxgraphics/gfx-docs/drm/gpu/drm-mm.html>

-----  
334. (BUG-STABILITY ISSUES) Boost::Python AsFer-VIRGO syscall/drivers invocations kernel panics - new findings  
-----

-----  
Commits - 28 September 2016  
-----

Continued analysis of kernel panics after VIRGO syscalls/drivers code in i915 GPU driver. Has hitherto unseen strange OOM panic stack dumps in GPU memory after kmalloc() of 100 bytes in virgo\_cloud\_malloc() and set/get of it. Logs with panic stack dumps and High and Low Watermark memory details have been committed to cpp\_boost\_python\_extensions/testlogs/.

-----  
335. (BUG-STABILITY ISSUES) Boost::Python AsFer-VIRGO syscall invocations panics - more findings  
-----

-----  
Commits - 29 September 2016  
-----

Kernel Panic Analysis for Boost::Python AsFer - VIRGO system calls invocations: This log contains hitherto unseen crash in python itself deep within kernel (insufficient logs) followed by random -32 and -107 errors. Finally successful invocations happened. Connections between -32,-107 errors and random panics/freezes were analyzed few years ago (Blocking and Non-blocking socket modes). i915 DRM related stacks were not found in kern.log. Random disappearance of logs is quite a big travail. Crash within python could be i915 related - cannot be confirmed without logs. Pattern emerging is that of: Something wrong going on between CPU and GPU while allocating kernel memory in CPU domain - kmalloc() is likely allocating from GPU and not CPU - quite a weird bug and unheard of.

-----  
336. (BUG-STABILITY ISSUES) VIRGO kernel panics - final findings - 30 September 2016  
-----

Further kernel panic investigation in VIRGO - probably the last. Logs with analysis have been committed to cpp\_boost\_python\_extensions/testlogs/.

-----  
337. (THEORY) Ramsey Theorem, Edge Labelling of Voting Graph and Multiway Majority Function - 5 October 2016 - related to 256,272,319  
-----

Multiway majority voting can be drawn as a directed graph. There is an edge between vertices  $v_1$  and  $v_2$  if  $v_1$  votes for  $v_2$  forming a Voting Graph with a weight  $\geq 0$ . Realworld example of this is web link graph where incoming links to a webpage are votes to it and outgoing links from a webpage are votes for adjacent pages. PageRank is a special case of Multiway Majority Function which ranks the candidate webpages by a converging random walk markov chain of transition probabilities, with a rider that all webpages are both voters and candidates making it a peer-to-peer majority voting. PageRank is thus a Non-boolean voting function. If web link graph is a tree of depth  $d$ , it is equivalent to depth- $d$  recursive majority function. Edge labelling of a graph assigns colors to edges of a graph (Edge coloring is a special case of labelling with restriction no two adjacent edges are of same color). Voting graphs can be edge labelled where each color of an edge denotes a voter affiliation. Ramsey Number in combinatorics states that there exists a number  $v=RN(r,s)$  for every graph of order  $v$ , there exists a clique of size  $r$  or independent set of size  $s$ . For any Voting graph Ramsey Theorem implies emergence of a clique or an independent set i.e voters who vote among themselves or who do not vote for each other. If the Voting graph is complete then Ramsey Theorem implies emergence of monochromatic cliques  $r$  (red cliques) or  $s$  (blue cliques).

References:

- 337.1 Ramsey Theorem Lecture Notes - <http://math.mit.edu/~fox/MAT307-lecture05.pdf>  
337.2 Ramsey Theorem - [https://en.wikipedia.org/wiki/Ramsey%27s\\_theorem](https://en.wikipedia.org/wiki/Ramsey%27s_theorem)  
-----

338. (THEORY) Van Der Waerden Number, Schur, Szemerédi and Ramsey Theorems, Coloring of Integers and Complement Function - Related to 323 - important draft updates to <http://arxiv.org/pdf/1106.4102.pdf>  
-----

-----  
Complement Function over Integer sequences can be defined in terms of 2-colorings of the integers. Described previously in (323) PCP undecidability proof of complementation, a function  $f$  and its complement  $g$  can be construed as 2-colorings of the Disjoint Set Cover Union i.e the set of natural numbers - each color is a function - for example  $f$  is red and  $g$  is blue.

Schur's Theorem for Ramsey coloring of integer sequences states (quoted from <http://math.mit.edu/~fox/MAT307-lecture05.pdf>):

" ... Schur's theorem

Ramsey theory for integers is about finding monochromatic subsets with a certain arithmetic structure. It starts with the following theorem of Schur (1916), which turns out to be an easy application of Ramsey's theorem for graphs.

Theorem 3.

For any  $k \geq 2$ , there is  $n > 3$  such that for any  $k$ -coloring of  $1, 2, 3, \dots, n$ , there are three integers  $x, y, z$  of the same color such that  $x + y = z$  ... "

For complement function special case (i.e 2-coloring of the sequences), Schur Theorem implies that there are always integers  $x, y$  and  $z$  in the image of a function or its complement obeying  $x+y=z$ . Van Der Waerden Theorem for coloring integers is the variant of Ramsey Theorem for graphs (quoting [https://en.wikipedia.org/wiki/Van\\_der\\_Waerden%27s\\_theorem](https://en.wikipedia.org/wiki/Van_der_Waerden%27s_theorem)):

" ... for any given positive integers  $r$  and  $k$ , there is some number  $N$  such that if the integers  $\{1, 2, \dots, N\}$  are colored, each with one of  $r$  different colors, then there are at least  $k$  integers in arithmetic progression all of the same color. ... "

Van Der Waerden Theorem for 2-colorings of natural numbers is equivalent to complementation disjoint set cover of natural numbers. When this is a prime complementation special case, prime integers are colored in red and composites in blue. Thus Van Der Waerden theorem for prime-composite complementation implies that either set of primes or composites have arithmetic progressions (because of same coloring) of size at least  $k$  (Related: Green-Tao theorem states that primes have arbitrarily long arithmetic progressions). Upperbound for  $N$  in this 2-coloring prime complementation is derivable from [TimothyGowers] bound as:  $N \leq 2^{2^{2^{2^{k+9}}}}$  for a family of  $k$  sized arithmetic progressions (also called as  $k$ -regularity). This implies arbitrarily long monochromatic arithmetic progressions can be found in prime-composite complementation by choosing  $N$  and  $k$ .

Finding the arithmetic progressions for Van Der Waerden numbers have been formulated as SAT instances which involves a SAT solver to search for a satisfying monochromatic arithmetic progression. Similar SAT solving approach applies also to prime-composite bichromatic complementation for finding arithmetic progressions. This takes the notion of complementation a fine grained step further in the sense: prime-composite complementation is a pattern miner in primes and arithmetic progressions in prime-composite complementation are patterns within pattern.

Concept of complement graphs have been studied in Perfect Graph Theorem and has strong resemblance to function complementation. Complement graph  $H$  is obtained from a graph  $G$  by adding edges to make it complete graph and removing edges in  $G$  i.e  $H$  has edges which are not in  $G$  and vice versa. Function complementation is precisely a sequence corollary of Graph complementation. Perfect Graph Theorem (PGT) states that a graph is perfect if its complement is perfect where perfect graph is one in which all its induced subgraphs have chromatic number (number of colors required to  $k$ -color a graph) equal to size of maximum clique. Function complementation can be translated to Graph complementation by defining a relation: There is an edge in  $F$ ,  $f(x_1) \text{---} f(x_2)$  for every  $f(x_1)$  and  $f(x_2)$  and

there is an edge in  $G$ ,  $g(x_1) \dots g(x_2)$  for every  $g(x_1)$  and  $g(x_2)$  where  $f$  and  $g$  are mutual complements. Obviously  $F$  and  $G$  have a single maximum clique with an independent set without any edge amongst them. Then it follows that order of  $F$  and  $G$  are their respective Ramsey Numbers.

A contrived independent set can be created by adding edges from constituent vertices of the maximum clique which is also maximal such that there are no edge overlaps with its complement graph - thus every graph for a function and its complement has a single maximum and maximal clique and an independent set connected only to the clique with no edges among them i.e. Vertices of the clique form vertex cover of the graph

Any 2 graphs corresponding to 2 functions defined on same set obtained from previous construction are isomorphic. For example if a complete graph of 3 vertices ( $K_3$ ) is constructed from elements 2,3,5 for function  $f_1$  where  $f_1$  is defined as  $f_1(0)=2$ ,  $f_1(1)=3$  and  $f_2(2)=5$ , the vertices can be numbered by the inverse( $f_1$ ) as 0,1,2. Similarly for a different function  $f_2$  over 2,3,5  $K_3$  obtained can be vertex numbered by the inverse( $f_2$ ) where  $f_2(0)=5$ ,  $f_2(1)=2$  and  $f_3(2)=3$  where numbering is 1,2,0. This also implies two graphs for function  $f$  and its complement  $g$  are not isomorphic.

In the context of complement function graphs constructed previously, functions are mapped to maximum clique subgraph and only this subgraph is vertex-renumbered which is the problem of subgraph isomorphism to find out if clique subgraph is isomorphic to another function clique subgraph.

Szemerédi's Theorem which is the generalization of Van Der Waerden's Theorem states: For any subset  $A$  of  $N$  of natural density  $> 0$ , there are infinitely many arithmetic progressions of size at least  $k$  where natural density is defined as  $\lim_{n \rightarrow \infty} \sup |A \cap \{1, 2, 3, \dots, n\}| / n > 0$ . Green-Tao theorem applies a relative Szemerédi theorem because prime numbers have 0 natural density. Szemerédi's Theorem has been generalized to polynomial progressions where the polynomial progression is defined as  $[t(i) = t(i-1) + p(i)]$  in  $A$  for some integer valued polynomials  $p(i)$ . Thus Generalized Szemerédi Theorem for Finding polynomial arithmetic progressions in a subset of natural numbers is closest to finding the complement of a function when set of natural numbers is 2-colored - only a subset of complement set is expressed as polynomials whereas complement function requires, by definition, the complete set to be expressed as polynomials (e.g interpolation polynomials, Fourier polynomials).

Roth Estimate for 2-coloring of integer sequences (in references 338.4 and 338.5) is a measure of order or randomness in a colored sequence and hence in a complementation by functions  $f$  and  $g$  (where each function is a color - e.g  $f$  is blue and  $g$  is red) over a universal set. If arithmetic progressions are thought of as all possible "sampled points" on 2-colored integers (functions  $f$  and  $g$ ) i.e an approximation of  $f$  and  $g$ , then Roth estimate is a measure of difference in size of  $f(x)$  and  $g(x)$  with probability equal to natural density of arithmetic progression chosen in minimax() step. This is because natural density is a fraction of size of set of elements of an arithmetic progression on natural numbers - in other words, natural density is the size of a sample of  $f$  and  $g$ . From Roth estimate bounds,  $||f(x)|| - ||g(x)||$  is approximately  $N^{(1/4+\epsilon)}$  with probability equal to natural density of arithmetic progression in minimax() step and  $||f(x)|| + ||g(x)||$  is  $N$  with probability 1. This implies:

$$||f(x)|| = \{N + N^{(1/4+\epsilon)}\} / 2$$

$$||g(x)|| = \{N - N^{(1/4+\epsilon)}\} / 2$$

with probability equal to natural density of arithmetic progression in minimax()

Previous approximation with sampling relates size of complement functions, coloring and arithmetic progressions by Roth estimate.

Complement Graphs  $F$  and  $G$  constructed previously for function  $f$  and its complement  $g$  have set of all values of inverse( $f$ ) and inverse( $g$ ) as the respective vertex labels in their maximum monochromatic cliques. This maps a 2-colored integer sequence with each color representing a function to 2 graphs,

mutually complement, each with a maximal monochromatic clique for respective function (f or g) and an independent set of other color. This construction adds one more dimension to the coloring problem: numbering of vertices for either color and subgraph isomorphism. From Van Der Waerden and later newer theorems, this implies numbered vertices in F and G have at least one monochromatic arithmetic progression.

Another important question is: Can a complement function polynomial be constructed from constituent monochromatic arithmetic progressions (or) Is the complement function polynomial interpolated by Lagrange Theorem or Fourier Analysis a composition of constituent arithmetic progressions? This is answered in reference 338.11 - Interpolation Polynomial for n points can be approximated from low discrepancy arithmetic progressions. References 338.12 and 338.13 are related to Polynomial Sequences of length n (P(n) - Polynomial Points) represented by rings of polynomials  $F(x)$  with integer coefficients in  $Z_n$  and for each sequence  $S(k)=(a_1,a_2,\dots,a_n)$  there exists a polynomial  $f(x)$  in  $F(x)$  such that  $f(i)=a_i, i=1,2,3,\dots,n$  ( $f(x)$  is a Lagrange Interpolation Polynomial). For example, monochromatic arithmetic progressions from Van Der Waerden and other theorems are polynomial sequences represented by arithmetic progression polynomial points. Thus Complement Function Polynomial interpolated (Fourier or Lagrange) from maximal monochromatic subset of 2-colored integer sequence is a Polynomial point and corresponding maximum monochromatic sequence subset is Polynomial Sequence.

Let  $f_1, f_2, f_3, \dots$  be functions and  $g_1, g_2, g_3, \dots$  be their respective complements. They are represented as graphs constructed previously as  $F_1, F_2, F_3, \dots$  (each with a monochromatic red clique and independent set of blue color) and  $G_1, G_2, G_3, \dots$  (each with a monochromatic blue clique and independent set of red color). All  $f_i(s)$  have isomorphic red clique subgraphs and  $g_i(s)$  have isomorphic blue subgraphs. Vertices are numbered with  $f_i^{-1}()$  and  $g_i^{-1}()$  labels. Vertices of cliques in  $f_i(s)$  and  $g_i(s)$  have monochromatic arithmetic progressions in  $f_i(\text{vertexlabel})$  and  $g_i(\text{vertexlabel})$ . For each arithmetic progression  $AP_j$  in monochromatic clique in  $F_k$  corresponding to  $f_k()$ ,  $f_k^{-1}(AP_j)$  is the preimage of  $AP_j$ . Define  $AP_1, AP_2, AP_3, AP_4, AP_5, \dots$  as the monochromatic arithmetic progressions in a monochromatic clique (vertices corresponding to some function  $f_k()$ ). Union of  $AP_j$  is a subset of  $f_k()$ . Define  $C(x)$  as the interpolation polynomial of the Union of  $AP_j$ .  $C(x)$  is an approximation of  $f_k()$ . Accuracy of approximation is determined by the density ratio  $|C(x)|/|f_k()$ . When Union of  $AP_j$  covers all points in sequence for generating function  $f_k()$ , then density is 1 because  $C(x)$  is 100% correct approximation of  $f_k()$  -  $C(x) = f_k()$ . A naive construction of  $C(x)$  from  $AP_j$  is done by parallel mergesort of:  $AP_1, AP_2, AP_3, AP_4, AP_5, \dots, AP_n$  to get a total ordering. Interpolation on the merged splintered arithmetic progressions scattered over the sequence gives an approximation  $C(x)$  of  $f_k()$ . This construction is in NC. Let Interpolation polynomial for the sequence be  $P(x)=f_k()$ .

There are 2 possibilities of arithmetic progressions - APs have both colors (elements from both function and its complement) or APs are all monochromatic (elements from a function or its complement). For example the sequence 1,2,3,4,5,.... of natural numbers have two arithmetic progressions:

$$AP_1 = 2x+1 \Rightarrow 1, 3, 5, 7, 9, \dots$$

$$AP_2 = 3x+1 \Rightarrow 1, 4, 7, 11, 14, \dots$$

Merging them gives 1,3,4,5,7,9,10,11,13.... which is a subset of 1,2,3,4,5,....

-----  
Scenario1: Monochromatic APs

-----  
Approximation polynomial for sequence interpolated from constituent monochromatic APs mergesorted =  $C(x)$ . Let  $AP_1(x), AP_2(x), AP_3(x), \dots, AP_n(x)$  be the arithmetic progression polynomials. Let  $C(x) = E(x)AP_1(x)AP_2(x)AP_3(x)\dots AP_n(x)$  i.e arithmetic progressions are factors of  $C(x)$  with  $E(x)$  as quotient over some polynomial ring  $F[x]$ .  $C(x)$  approximates a function  $f_k()$  or its complement  $g_k()$ . This is described previously.

-----  
Scenario2: Multichromatic APs

-----  
 When APs have elements of both colors (from both functions  $fk()$  and  $gk()$ ), parallel mergesort of APs and interpolation by polynomial  $C(x)$  cannot approximate either  $fk()$  or  $gk()$  because APs consist of both colors. This is where minimum discrepancy plays its part - when discrepancy is low AP has elements from both colors or functions in almost equal number. Therefore arithmetic progression samples both functions with least error and interpolation succeeds with high accuracy - this is an intuitive explanation for 338.11.

#### References:

- 
- 338.1 Bound for Van Der Waerden Numbers - <https://www.emis.de/journals/INTEGERS/papers/a20int2005/a20int2005.pdf>
- 338.2 Exact Ramsey Theory and Van Der Waerden Numbers by SAT-solvers - [OliverKullmann] - <https://arxiv.org/pdf/1004.0653v2.pdf>
- 338.3 Erdos-Turan Conjecture - [https://en.wikipedia.org/wiki/Erd%C5%91s\\_conjecture\\_on\\_arithmetic\\_progressions](https://en.wikipedia.org/wiki/Erd%C5%91s_conjecture_on_arithmetic_progressions) - If sum of reciprocals of elements of a set of positive integers diverges, then the set contains arbitrarily long arithmetic progressions
- 338.4 Roth Estimate - <http://matwbn.icm.edu.pl/ksiazki/aa/aa9/aa9125.pdf> - Consider a two coloring of set of natural numbers  $N$  in red and blue. For all arithmetic progressions in the set  $N$  let Discrepancy be the difference between number of red and blue colored integers. Maximum of Discrepancy for all arithmetic progressions be  $\text{Maximum}(\text{Discrepancy})$ .  $\text{Minimum}(\text{Maximum}(\text{Discrepancy}))$  for all 2-colorings is the Roth Estimate lowerbounded by  $N^{1/4}$ .
- 338.5 Roth Estimate is nearly sharp - Beck, J. Combinatorica (1981) 1: 319. doi:10.1007/BF02579452 - <http://link.springer.com/article/10.1007/BF02579452> - Previous Roth Estimate is upperbounded by  $N^{(1/4+\epsilon)}$ .
- 338.6 Discrepancy in Arithmetic Progressions - [MatousekSpencer] - Roth estimate is best possible -  $\text{ROTH}(N) \leq N^{1/4}$  - <http://www.ams.org/journals/jams/1996-9-01/S0894-0347-96-00175-0/S0894-0347-96-00175-0.pdf> - This paper has some interesting remarks - "...In words, we show the existence of a two-coloring  $\chi$  of the first  $n$  integers so that all arithmetic progressions  $A$  have imbalance  $|\chi(A)| \leq Cn^{1/4}$ . We remark that the proof does not give a construction of  $\chi$  in the usual sense and is indeed not satisfactory from an algorithmic point of view. The methods of §2 (see comments in [5]) are such that we have not been able to obtain an algorithm that would output this coloring  $\chi$  in time polynomial in  $n$ . Our proof involves variants of the probabilistic method; we give [1] as a general reference ..." which is about algorithm for constructing a coloring for a given discrepancy - coloring algorithm is nothing but construction of a function and its complement for a finite set of integers. Thus notions of integer sequence coloring and complement function are two sides of a coin with respect to integer valued functions and complements. Undecidability of Infinite complementation from 19,24,319 and 323 PCP based proof also implies "Infinite Integer Sequence Coloring is Undecidable" i.e there is no coloring algorithm for 2-coloring of infinite integer sequences.
- 338.7 Discrepancy Minimization by Walking on Edges - [BansalLovettMeka] - <https://arxiv.org/pdf/1203.5747v2.pdf> - This proves Spencer's Theorem which states that for any system of subsets  $S$  of universal set  $V$  of size both  $N$  there always exists a 2-coloring with  $\text{minimax}(\text{discrepancy}) < 6\sqrt{N}$  also known as Six Standard Deviation and gives a randomized polytime algorithm for constructing such a 2-coloring mentioned non-constructively in 338.6. System of subsets can be set of arithmetic progressions. This is a special case of function-complement (2-coloring) construction subject to minimax discrepancy criterion.
- 338.8 Fourier Interpolation of  $n$  data points with polynomial of degree  $m$  - <http://www.muskingum.edu/~rdaquila/m350/fourier-interdn10-1.ppt>
- 338.9 Fourier Analysis and Szemerédi's Theorem - Roth's Argument - Documenta Mathematica ICM Extra Volume 1998 - <http://www.mathunion.org/ICM/ICM1998.1/Main/Fields/Gowers.MAN.ocr.pdf> - Fourier Transform of set of integers mod  $N$  (for prime  $N$ ) and deriving the arithmetic progressions of length 3 from inverse Fourier Transform.
- 338.10 Hales-Jewett Theorem - [MichelleLee] - <http://www.math.uchicago.edu/~may/VIGRE/VIGRE2009/REUPapers/Lee.pdf> -

generalization of Van Der Waerden Theorem to higher dimensions (n-cubes and n-lines) - any k-coloring of n-dimensional cube (or a matrix of points) has monochromatic line (with fixed coordinates for some dimensions and varying for others)

338.11 Polynomial Interpolation from Low Discrepancy Arithmetic Progressions - [The Discrepancy Method: Randomness and Complexity - Bernard Chazelle] - [https://books.google.co.in/books?id=dmOPmEh6LdYC&pg=PA338&lpg=PA338&dq=polynomial+interpolation+arithmetic+progression&source=bl&ots=CDNgOUBnua&sig=pxKMqX9ciY7\\_d4Gc0kFwnCr0UEU&hl=en&sa=X&ved=0ahUKEwiSq0v0ovPPAhVMpo8KHZsbA3wQ6AEIPzAE#v=onepage&q=polynomial%20interpolation%20arithmetic%20progression&f=false](https://books.google.co.in/books?id=dmOPmEh6LdYC&pg=PA338&lpg=PA338&dq=polynomial+interpolation+arithmetic+progression&source=bl&ots=CDNgOUBnua&sig=pxKMqX9ciY7_d4Gc0kFwnCr0UEU&hl=en&sa=X&ved=0ahUKEwiSq0v0ovPPAhVMpo8KHZsbA3wQ6AEIPzAE#v=onepage&q=polynomial%20interpolation%20arithmetic%20progression&f=false) - Page 338 and Figure 9.4 in Page 342

illustrating the distribution of Fourier Coefficients over a circle in Discrete Fourier Transform of a subset of  $Z_{16}$  (also explained in 338.8).

338.12 Sequences Generated By Polynomials - [Cornelius Schultz] -

[https://www.researchgate.net/profile/E\\_Cornelius\\_Jr/publication/258155515\\_Sequences\\_Generated\\_by\\_Polynomials/links/0deec5272541943938000000.pdf](https://www.researchgate.net/profile/E_Cornelius_Jr/publication/258155515_Sequences_Generated_by_Polynomials/links/0deec5272541943938000000.pdf)

338.13 Polynomial Points, Green-Tao Theorem and Arithmetic Progressions - [Cornelius Schultz] -

<https://cs.uwaterloo.ca/journals/JIS/VOL10/Schultz/schultz14.pdf>

338.14 Recent Advanced Theorems in k-coloring of integer sequences -

<http://people.math.sc.edu/lu/talks/ap4.pdf> - the set  $[n]$  is randomly r-colored and bounds for number of monochromatic k-APs and K-APs in  $[n]$  are mentioned where k is common difference and K is Van Der Waerden number.

-----  
339. (FEATURE-DONE) Boyer-Moore Streaming Majority Algorithm - Commits - 7 October 2016  
-----

-----  
This commit implements Boyer-Moore algorithm for finding Majority element in Streaming Sequences. It uses the Streaming Generator Abstraction for input streaming datasource. Logs have been committed to python-src/testlogs/  
-----

-----  
340. (FEATURE-DONE) GSpan Graph Substructure Mining Algorithm Implementation - Commits - 13 October 2016 and 14 October 2016  
-----

-----  
1. Graph Substructure Mining GSpan algorithm implementation with logs in testlogs/  
2. This code requires the Graph vertices to be labelled by unique integers  
3. Integer labelling of vertices makes it easier for DFSCode hashes to be generated uniquely.  
-----

-----  
341. (THEORY) Graph Mining Algorithms and Recursive Gloss Overlap Graph for text documents - Document Similarity  
-----

-----  
Recursive Gloss Overlap Algorithm implementations in python-src/InterviewAlgorithm and its Spark Cloud Variants generate graphs with word labels from Text Documents. GSpan algorithm implemented in (340) mines subgraphs and edges common across graph dataset. This allows extraction of common patterns amongst text document graphs and thus is an unsupervised similarity clustering for text analytics. GSpan has provisions for assigning minimum support for filtering patterns which amounts to finding prominent keywords in recursive gloss overlap graphs.  
-----

-----  
342. (FEATURE-DONE) Graph Mining Recursive Gloss Overlap Graph for text documents - Document Similarity  
-----

-----  
Commits - 17 October 2016  
-----

-----  
1.Code changes have been done to choose between numeric and word labelling of Graph vertices in GSpan GraphMining implementation.  
2.New file GraphMining\_RecursiveGlossOverlap.py has been added to JSON dump the Recursive Gloss Overlap graph of a text document  
3.New directory InterviewAlgorithm/graphmining has been created which contains the numeric and word labelled Recursive Gloss Overlap graphs of 5 example text documents in topic class "Chennai Metropolitan Area Expansion"  
4.logs for common edges mined between two Recursive Gloss Overlap document graphs has been committed in testlogs/  
5.Spidered web text has been updated  
6.GraphMining\_RecursiveGlossOverlap.py JSON dumps the RGO edges into a text file and GraphMining\_GSpan.py JSON loads them from InterviewAlgorithm/graphmining/  
-----

-----  
343. (THEORY) Streaming Majority and 2-Coloring(Complement Functions) - related to 14.16 and 19,24,323,338,339 - important draft updates to <http://arxiv.org/pdf/1106.4102.pdf> - 1 November 2016  
-----

-----  
In simple 2 candidate majority voting done on stream of votes, a 2-colored sequence of votes by voters is generated. This is already mentioned in infinite majority (Erdos Discrepancy Theorem) - 14.16.Each color symbolizes a candidate voted. This partitions the sequence of votes into 2 monochromatic sets. Obviously, if the voters are uniquely identified by a sequence number, all sequence coloring theorems imply there are monochromatic and multichromatic arithmetic progressions in voter unique identities. Boyer-Moore algorithm computes streaming majority (implemented in 339),  
-----

-----  
344. (BUG-STABILITY ISSUES) AsFer-VIRGO Boost::Python system calls invocations analysis - commits - 4 November 2016  
-----

-----  
Some resumed analysis of AsFer-VIRGO boost::python invocations of VIRGO memory system calls which were stopped few months ago.  
The i915 DRM GEM error is highly reproducible pointing something unruly about it. No logical reason can be attributed to this except some kernel sync issues. This further confirms that there is nothing wrong with VIRGO layer of Linux kernel and Linux kernel deep within inherently has a chronic problem.  
-----

-----  
345. (THEORY) Polynomial Reconstruction (PR) Problem, Error Correcting Codes and 2-Coloring/Complement Functions - important draft updates to <http://arxiv.org/pdf/1106.4102.pdf> - 10 November 2016 and 17 November 2016  
-----

-----  
Polynomial Reconstruction Problem states that:  
Given a set of  $n$  points  $(x_1, y_1), (x_2, y_2), \dots, (x_n, y_n)$  recover all polynomials  $p$  of



degree less than  $k$  such that  $\pi(x_i) \neq y_i$  for maximum of  $i$  points in  $\{1, 2, 3, \dots, n\}$ . In other words PRP is a curve-fitting interpolation problem and is related to Error correcting problems like List Decoding (list of polynomials approximating a message one of which is correct), Reed-Solomon Codes.

2-Coloring scheme algorithms and Complement Function constructions are alternative spectacles to view the Polynomial Reconstruction Problem i.e Complement Function and 2-Coloring are special settings of Polynomial Reconstruction with exact curve fitting.

References:

-----  
345.1 Polynomial Reconstruction and Cryptanalysis - Berlekamp-Welch, Guruswami-Sudan algorithms - <https://eprint.iacr.org/2004/217.pdf>  
345.2 Hardness of Constructing Multivariate Polynomials over Finite Fields - [ParikshitGopalan, SubhashKhot, RishiSaket] - <https://www.cs.nyu.edu/~khot/papers/polynomial.pdf> - If there is a polynomial  $P(X_1, X_2, \dots, X_n)$  such that  $P(x_i) = f(x_i)$  for all points  $(x_i, f(x_i))$ , it can be found by interpolation. This is exact agreement. Can we find a polynomial that agrees on most points? This approximation is proved to be NP-hard.  
345.3 Lagrange Interpolation and Berlekamp-Welch PRP algorithm - [SadhkanRuma] - [https://www.academia.edu/2756695/Evaluation\\_of\\_Polynomial\\_Reconstruction\\_Problem\\_using\\_Lagrange\\_Interpolation\\_Method?auto=download](https://www.academia.edu/2756695/Evaluation_of_Polynomial_Reconstruction_Problem_using_Lagrange_Interpolation_Method?auto=download)  
-----

-----  
346. (THEORY) Data written in electronic storage devices (e.g CD/DVD) and 2-Coloring/Complement Functions - important  
draft updates to <http://arxiv.org/pdf/1106.4102.pdf> - 24 November 2016 and 28 November 2016  
-----

-----  
CD/DVD storage devices contain binary data burnt on concentric cylindrical tracks. A radial line from central bull's eye of the circular storage to outer rim crosscuts the data to form a binary string of length  $n$  where  $n$  is the radius of circular storage. This radial line sweeping the complete circle in a scan covers  $2^n$  possible binary strings. In the best case all  $2^n$  words are distinct. Total Number of 1s or 0s in these  $2^n$  words are in fibonacci sequence:

$$f(n) = 2f(n-1) + 2^{n-1}$$

with  $f(0)=0$  and  $f(1)=1$ . In 2-coloring parlance, DVD is 2-colored with 1(red) and 0(blue) where number of monochromatic bits is lower bounded by:

$f(n) = 2f(n-1) + 2^{n-1}$  out of minimum  $n \cdot 2^n$  possible bits on the storage. Thus any data written to storage ultimately gets translated into a 2-coloring complement function scheme. For example, device with 3 concentric tracks has  $3 \cdot 2^3 = 24$  minimum possible bit positions and:

$$f(3) = 2f(2) + 2^2 = 2(2f(1) + 2) + 2^2 = 8 + 4 = 12 \text{ minimum possible}$$

monochromatic bit positions

This has some applications of Hales-Jewitt Theorem for multidimensional 2-coloring - storage device always has a monochromatic  $k$ -line. (where  $k$  is dimension and  $k$ -line is a hyperline. 2-line is a square and 3-line is a cube). As a simple example for  $n=2$ :

00  
01  
10  
11

are minimum possible distinct binary words swept by a radial scan of the circle and there are  $f(2)=2f(1) + 2 = 4$  monochromatic bits spread across out of  $2 \cdot 2^2=8$  possible bits in 4 binary strings. A crucial insight is that any high level data stored has an order in low level 2-coloring or Complement Function scheme (Monochromatic APs etc.,) though high level data is usually alphanumeric and appears random. A conjectural question is: Does the low level 2-coloring binary

order imply high level non-binary order and are they functionally related?

The previous question has been answered in 2.10. There could be \ / shaped gaps in circular arrangement of  $2^n$  binary word radial lines. These gaps could be resolved by recursive application of  $f(n)$  for all lengths  $< n$ . Let this new function be  $g(n)$  defined as:

$$g(n) = f(n) + f(n-1) + f(n-2) + \dots + f(1) + f(0)$$

Thus  $g(n)$  is the tightest bound for number of 1s and 0s. Prefix "minimum" has been added in this bound because repetitions of some binary words in radial line during circular scan have been ignored and hence a lowerbound. Total number of bit positions is  $k \cdot 2 \cdot \pi \cdot (1+2+3+\dots+n) = k \cdot 2 \cdot \pi \cdot n(n+1)/2$  summing up all concentric tracks for some constant  $k$ . Lowerbound  $g(n)$  for 1s and 0s implies a unique distribution of all binary word patterns and any number above this lowerbound implies predominance and emergence of a binary pattern.

-----  
347. (FEATURE-DONE) NeuronRain C++-Python System calls invocation - Commits - 29 November 2016  
-----

- 
1. Further analysis of NeuronRain AsFer-VIRGO boost::python system calls invocation - there has been an erratic -32 and -107 errors
  2. But VIRGO system calls work without problems - malloc, set and get work as expected
  3. There is a later panic outside VIRGO code but logs have not been found.
  4. Logs for this have been added in testlogs/
  5. boost C++ code has been rebuilt.
- 

-----  
348. (THEORY) Kleinberg Lattice , Random Graph Ontologies, Bose-Einstein model and Recursive Gloss Overlap algorithm for ranking documents by intrinsic merit - 3 December 2016 and 20 December 2016 - related to 202, 229 and 230  
-----

-----

Result of  $r=2$  in [Kleinberg - 202.19] is an equilibrium state. Random shortcut edges are created with some probabilities between any two nodes  $n1$  and  $n2$  on a lattice of all possible nodes. Thus there are 2 distance measures between any two nodes on a lattice - 1) lattice distance which is the usual manhattan distance step function - this is circuitous. 2) random edge distance between pair of vertices  $n1$  and  $n2$  on the lattice which is shortcut. The random edge has the probability as a function of lattice distance:

random edge probability( $d(n1, n2)$ ) =  $|l(n1, n2)|^{(-r)}$  where  $l$  is the lattice distance

When  $r$  is less than 2 or close to zero, random edges are as numerous as lattice edges (random edges exist in abundance but they are no better than lattice paths) and when  $r$  is more than 2, random edges are rarer (random edges fade, only lattice paths are possible and no shortcut random paths) and it is difficult to find a path for message to be delivered from one extreme to the other. Steady state converges and these two conflicts are resolved when  $r=2$  and it is optimum to find a path between two nodes.

Above small world phenomenon can be mapped to ontology of linguistic concepts/words. Let set of all concepts/words form a lattice. Set of random edges with probability embeds a random graph on some or all of these lattice points and thus is a probabilistic ontology - probability depends on distance measure of 2 concepts. Document definition graph obtained from this ontology with recursive gloss overlap is optimal (easy to find path between concepts in a document and grasp meaning) when it has  $r=2$  by previous lattice-randomedge relation. Usual distance measures are based on least common ancestor principle - node which is conceptually common to two other nodes creates a path. Lower the distance, greater the meaningfulness. Reference 202.20 adds disambiguation to

finding distance by aligning and intersecting all possible senses of two concepts with a random walk and doing `argmax()` to find distance. Probabilistic random edge ontology created on a lattice of concepts provides dynamism in text analytics.

Kleinberg criterion of  $r=2$  is an alternative way to assess the meaningfulness of a document. Document definition graph with  $r=2$  should theoretically have easy paths between concepts and average short distance measures across nodes and hence has high intrinsic merit. From the above relation:

$$r * \log(l(n1,n2)) = \log(1/d(n1,n2))$$

When  $r=2$ :

$$2\log(l(n1,n2)) = \log(1/d(n1,n2))$$

which stipulates conditions for high intrinsic merit for a document in terms of lattice distance and random edge probability between two concepts  $n1$  and  $n2$ .

Bose-Einstein model for networks relates fitness of a vertex (ability to attract edges) in a graph and Bose-Einstein condensation. Kleinberg's small-world graph has average clustering coefficient significantly higher than a random graph and mean shortest distance approximately same as random graph (on same vertices). Here clustering coefficient is the ratio of number of edges to neighbours and number of all possible edges to neighbours. Kleinberg's small-world graph, Bose-Einstein condensation in network graphs and Intrinsic meaningfulness merit in graph representation of documents are closely related because all three are multiple views of "meaningfulness" or "connectedness" in a document.

References:

-----  
348.1 Bose-Einstein Model and Complex Networks -

<https://en.wikipedia.org/wiki/Bose>

[%E2%80%93Einstein\\_condensation\\_\(network\\_theory\)](https://en.wikipedia.org/wiki/Bose-Einstein_condensation_(network_theory))

348.2 Golden mean as a clock cycle of brain waves -

<http://www.v-weiss.de/chaos.html> - "...In 2001 Bianconi and Barabási [15]

discovered that not only neural networks but all evolving networks, including the World Wide Web and business networks, can be mapped into an equilibrium Bose gas, where nodes correspond to energy levels and links represent particles. Still unaware of the research by Pascual-Leone, for these network researchers this correspondence between network dynamics and a Bose gas was highly unexpected [16]..."

-----  
349. (THEORY) Randomness, Quantum Machine Learning and a Schroedinger Cat simulation of learning patterns in BigData - 23 December 2016  
-----

Caution: This section postulates a drastically new theory mapping quantum mechanics to learning patterns in bigdata which is subject to errors.

State of a subatomic particle is defined by a wave function on Hilbert Space (Complex State Vector Space). In Dirac notation wave function for particle  $p$  is,  $|p\rangle = a_1|s_1\rangle + a_2|s_2\rangle + \dots + a_n|s_n\rangle$  is state of a particle where each  $a_i$  is a complex number named amplitude of particle at state  $s_i$  - particle's state is a linear superposition of all states  $s_i$  with amplitude  $a_i$ . Dirac delta function is fourier transform of Schroedinger wave equation of a particle. State vector  $|p\rangle$  is a linear superposition of all possible alternatives (or) Hilbert space dimensions that a particle can exist with respective amplitude for each dimension. Set of states form orthonormal basis for this Hilbert space. Wave function state vector collapses to one of the states to give a classical probability for the state estimated by square of amplitude for the state dimension. For example, in Young's Double Slit experiment a single photon acts as a wave by duality and interferes with itself by travelling through both slits to establish an interference pattern with state vector wavefunction amplitudes which collapses to a classical probability when one of the slits is closed. Schroedinger's cat paradox is an imaginary thought experiment (not possible in

reality) where a black box with cat and a radioactive material triggered by a particle's spin exists in both states dead and alive simultaneously when viewed from outside with amplitude  $1/\sqrt{2}$ :  $|\text{state of cat}\rangle = 1/\sqrt{2} ( |\text{dead}\rangle + |\text{alive}\rangle )$ . Squaring amplitude  $1/\sqrt{2}$  gives classical probability  $1/2$  for each state. There are two observers - one within the black box and one outside of it. For observer within black box, particle spin is measurable and wavefunction collapses to one of the states "dead or alive" while for observer outside black box there is no way for such collapse to occur and state is a superposition "dead and alive".

In terms of BigData analytics, learning a variable in a blackbox is reducible to Schroedinger's Cat paradox. Assuming there exists a Pseudorandom Generator with Quantum Mechanical source, Cat is an algorithm with access to randomness - e.g Double Slit experiment, radioactive decay etc., and chooses one of the alternative outputs - output1, output2, ..., outputn - based on quantum mechanical measurement (e.g spin) with "if...else" branches. This randomized algorithm can be thought of as a subroutine F. Observer1 which measures output of F is another subroutine G. Thus both F and G together constitute the blackbox. Observer2 outside the blackbox is another subroutine H. Only G measures output of F and state vector collapses to one of the alternative outputs. But for H, F+G is impervious and state vector remains as:  $a_1|\text{output1}\rangle + a_2|\text{output2}\rangle + \dots + a_n|\text{outputn}\rangle$  with complex amplitudes  $a_i$ . This extends the notion of Pseudorandomness in traditional complexity literature to a more generic state vector with complex amplitudes over a Hilbert space of dimensions(alternatives) - here algorithm is itself a "particle" with a superposed state of outputs.

Any BigData set with apparent randomness can be construed as a series of outputs over time generated by a randomized algorithm (or) an algorithm with access to randomness including quantum mechanical randomness (For example, streamed datasets like stock market tickers) i.e the algorithm F. Subroutines F+G together create a BigData set from randomness. When viewed from H, the blackbox F+G has a state vector wavefunction evolving over time:  $W(t) = a_1|\text{output1}\rangle + a_2|\text{output2}\rangle + \dots + a_n|\text{outputn}\rangle$ . Any machine learning algorithm which tries to learn patterns from such a dataset is equivalent to what H does above. If H learns the pattern in the dataset with x% accuracy, it implies algorithms F+G are reverse engineered with x% correctness. This presents a contradiction if the source of randomness is quantum mechanical - state vector collapses for both observers G and H, not only for G. If Schroedingers cat paradox is axiomatically true, it raises questions: Does this limit the scope of machine learning to only classical randomness? Is quantum randomness not learnable?

An alternative formulation of F+G is:

F is the quantum randomness source (e.g Double slit) and G invokes (or measures) F to produce a datastream over time. Here G as observer within blackbox is an inseparable entity from F i.e F is an internal routine of G.

There are two levels of learning possible:

\*) Learning within blackbox - Learning patterns from observations of F+G. F+G are pre-equipped with ability to learn patterns in collapsed wavefunction generated dataset. Such a pattern learnt exists only within the blackbox. External observer H has no way to learn the dataset and the pattern. Even within F+G there are problems with learning patterns from quantum randomness. Logical independence implies any two observations (boolean propositions) are independent and learning pattern from such independent observations contradicts it - pattern in independent observations imply observations are dependent on each other. For example, two propositions "Today is holiday" and "There are 100 cars" are logically independent while propositions "There are 100 flights" and "There are 100 cars" are logically dependent. Former 2 propositions have no common patterns while latter 2 propositions have a common pattern (100, vehicles) - new information "100 and vehicles" is deducible from 2 propositions. Quantum randomness stems from logical independence and thus there should not be a common pattern to learn from independent streaming set of observations.

\*) Learning outside blackbox - This is obvious contradiction mentioned previously because dataset generated by F+G is never visible to H because wavefunction of H never collapses.

Thus above seems to imply learning is impossible with quantum randomness.

References:

-----  
349.1 Feynman Lectures on Physics - [RichardFeynman] - Volume 3 - Chapter 1 and 2  
349.2 Emperor's New Mind - [RogerPenrose] - Chapter 6 - Quantum Magic and Quantum Mystery  
349.3 Quantum Randomness and Logical Independence -  
<https://arxiv.org/pdf/0811.4542v2.pdf> - Mutually independent logical propositions cause quantum randomness  
349.4 Elitzur-Vaidman Bomb tester - [https://en.wikipedia.org/wiki/Elitzur%E2%80%93Vaidman\\_bomb\\_tester](https://en.wikipedia.org/wiki/Elitzur%E2%80%93Vaidman_bomb_tester) - Detecting if bomb inside a box has detonated or not by quantum superposition - Constructive and Destructive self-interference - Previous thought experiment replaces the bomb in the box by a bigdata source which has to be predicted. Difference is one of the observers (detectors) is within the box and other is outside.

-----  
350. (THEORY) Quantum Parallelism, Quantum Interference, Integer Factoring, Periodicity Finding, Polynomial Reconstruction and Complement Function/2-Coloring - related to 24,34,323,338,345 and 347 - 29 December 2016 - important draft updates to :

-  
[http://sourceforge.net/projects/acadpdrafts/files/DiscreteHyperbolicPolylogarithmicSieveForIntegerFactorization\\_PRAM\\_TileMergeAndSearch\\_And\\_Stirling\\_Upperbound\\_updateddraft.tex/download](http://sourceforge.net/projects/acadpdrafts/files/DiscreteHyperbolicPolylogarithmicSieveForIntegerFactorization_PRAM_TileMergeAndSearch_And_Stirling_Upperbound_updateddraft.tex/download) and  
- <http://arxiv.org/pdf/1106.4102.pdf>

-----  
Discrete Hyperbolic Factorization draft in 34 claims (disputed because of input size though references exist to prove PRAM=NC equivalence and Bitonic Batchers Sort is in NC) that integers can be factored by NC parallel computation circuit of logdepth and polynomial size (by PRAM or Cloud Bitonic sorting). Similar parallelism is the basis for Quantum Factorization Algorithm of [Shor] - factorization is in BQP and NC is in BQP. Quantum Computation relies on two phenomena:

\*) Quantum Parallelism in which a function  $f(x)$  is computed to get many values of  $f(x)$  in parallel

\*) Quantum Interference by Hadamard transform where cancellation occurs ( $|0\rangle = 1/\sqrt{2}*(|0\rangle+|1\rangle)$  and  $|1\rangle = 1/\sqrt{2}*(|0\rangle-|1\rangle)$ ) by interference

Period Finding in Quantum Computation finds smallest  $r$  such that  $f(x)=f(x+r)$  and Shor's factorization internally applies period finding by quantum fourier transform. Ramsey theory of integers and related theorems viz., Van Der Waerden, Szemerédi etc., imply existence of monochromatic arithmetic progressions in 2-coloring of integer sequences where each color is equivalent to a function and its complement. Period finding problem reduces to finding arithmetic progressions in integer sequences by defining a function  $f(x+iy)=f(x+(i+1)y)$  for any  $x$  in the sequence and some integers  $y$  and  $i$ . More generically, factoring and period finding are special cases of Hidden Subgroup Problem i.e  $f(g)=f(hg)$  for  $g$  in  $G$  and  $h$  in subgroup  $H$  of  $G$  and  $hG$  is a coset of  $H$ . In terms of polynomial reconstruction, period finding computes the function  $f$  passing through the arithmetic progression points. In Discrete Hyperbolic Factorization of 34, instead of quantum parallelism, classical NC parallelism is applied to  $k$ -merge sort and binary search the pixelated hyperbola tiles.

References:

350.1 Quantum Computation Course notes - Order Finding, Fermat's Little Theorem and Simon, Shor Factorization algorithms - [AndrisAmbainis] - <http://www.cs.ioc.ee/yik/schools/win2003/ambainis2002-2.ppt>  
350.2 Progress on Quantum Algorithms - [PeterShor] - <http://www-math.mit.edu/~shor/papers/Progress.pdf>

-----  
351. (FEATURE-DONE) Recommender Systems Implementation based on ThoughtNet Hypergraph - 1 January 2017  
-----

-----  
\*) Input to python-src/DeepLearning\_ReinforcementLearningRecommenderSystems.py is a set of observations which are user activities (shopping cart items, academic articles read by user etc.,) and already built thoughtnet hypergraph history is searched by usual evocatives from the input  
\*) Evocatives returned from ThoughtNet hypergraph are items recommended relevant to user's activities.  
\*) This technique of recommendation is more qualitative than usual methods of Collaborative Filtering and mimicks the human thought process of "relevance based evocation" based on past experience (i.e ThoughtNet history)  
\*) New input text file and folder RecommenderSystems has been added to python-src with Neo4j Graph Database support  
\*) Logs have been committed in testlogs/  
-----

-----  
352. (FEATURE-DONE) Kafka data storage for Streaming Abstract Generator - 2 January 2017  
-----

-----  
Kafka Streaming Platform has been added as a data storage in Streaming Generator Abstraction Single-Window entrypoint. Kafka subscriber code for a neuronraindata topic polls for incoming messages in iterator. As an example Streaming CountMeanMinSketch implementation has been updated to source streamed data published in Kafka.  
-----

-----  
353. (FEATURE-DONE) An example usecase of Recommender Systems for online shopping cart - 2 January 2017  
-----

-----  
\*) RecommenderSystems folder has been updated with new text file from an example past shopping cart history items (e.g books from miscellaneous topics in Amazon online bookstore)  
\*) From the above edges a Hypergraph is created by classifying the shopping cart items into classes and constructing hyperedges across the classes (by Recursive Gloss Overlap Graph maximum core number classifier)  
\*) Text files for above usecase have .shoppingcart suffixes  
\*) Above shopping cart hypergraph has a past history of items chosen by a user from variety of topics.  
\*) New input file RecommenderSystems.shoppingcart.input.txt has present items in user's shopping cart and new items have to be recommended to user based on present choice and past history.  
\*) For this, items in present shopping cart are lookedup in past sales history Hypergraph created previously and recommendations are returned  
\*) Items in present shopping cart are looked up in two ways: 1) By classifying with Recursive Gloss Overlap graph and looking up rare classes less than a threshold (presently core number 5) and 2) Raw token lookup  
\*) Logs for these two lookups based Recommendations generated are committed to testlogs/  
-----

An important note: Rationale for Hypergraph based past history is that a meaningful text can be classified on multiple classes vis-a-vis usual supervised classifiers which classify text on exactly one class. This is more realistic because text can delve into multiple topics simultaneously e.g an article on medical imaging (MRI scans) could contain details also on nuclear physics and pattern recognition and can exist in 3 classes simultaneously. There are still impurities in recommendations generated from lookups as gleaned from logs. These are inaccuracies in the way WordNet infers because of small size of the text description about book. Larger the description per shopping cart item, greater is the information connectedness of the WordNet subgraph generated and accuracy of core number based classification.

-----  
354. (FEATURE-DONE) More detailed shopping cart example 2 for RGO+ThoughtNet based Recommender System - 3 January 2017  
-----

-----  
\*) python-src/DeepLearning\_ReinforcementLearningRecommenderSystems.py has been updated to choose top percentile classes of text input so that vertices with large core numbers get more weightage.  
\*) New shoppingcart2 product reviews text has been added and corresponding Hypergraph history has been created. This example has detailed product description with an assorted mix (TV reviews, Washing Machine reviews, Home Theatre reviews etc.,) -  
python-src/RecommenderSystems/RecommenderSystems\_Edges.shoppingcart2.txt,  
python-src/RecommenderSystems/  
RecommenderSystems\_Hypergraph\_Generated.shoppingcart2.txt  
\*) New input file python-src/RecommenderSystems.shoppingcart2.input.txt has been added with an example product (TV).  
\*) Recommender System chooses relevant TV products from Hypergraph history and displays to user.  
\*) Logs have been committed to testlogs/  
-----

-----  
355. (THEORY) NEXP not in non-uniform ACC, P(Good) majority voting circuit and some contradictions - 4 January 2017 and 5 January 2017  
- related to all P(Good) majority voting circuit related points in this document (e.g 14,53 etc.,)  
-----

-----  
RHS of P(Good) majority voting circuit has exponential size with unrestricted depth in worst case and is in EXP (if depth restricted, RHS is in PH direct-connect uniform circuit). RHS is a boolean function composition of non-uniform NC and individual voter decision functions. Known result by [RyanWilliams] limits that NEXP is not in ACC (AC circuits with counter mod[m] gates which output 1 if sum of inputs is a multiple of m). Non uniform ACC is contained in TC and AC is contained in ACC (AC in ACC in TC). This makes a contradiction if LHS is 100% efficient percolation circuit in non-uniform NC (NC/poly). If P(Good) binomial coefficient series summation converges to 100%, then RHS majority voting circuit is also 100% efficient and LHS=RHS. This implies if RHS has NEXP-complete algorithm/circuit, because of convergence, NEXP is in NC/poly. But NC is in ACC and this implies NEXP has non-uniform ACC circuits - contradicts NEXP does not have non-uniform ACC circuits. This is one more counterexample implying some or all of the following:

- \*) There is no 100% efficient RHS majority voting boolean function composition
- \*) There is no 100% efficient LHS boolean function (pseudorandomly chosen boolean function, ranked by social choice function etc.,)
- \*) RHS Majority voting is not in NEXP.
- \*) LHS pseudorandom choice boolean cannot have a non-uniform NC circuit

Above, "efficiency" implies "No error" cases in scenarios matrix of 53.14 and a ninth error tree scenario of Randomized Decision Tree Evaluation Error(zero-error decision tree evaluation) mentioned in 314, 317. This adds one more possibility where  $P(\text{Good})$  binomial summation for majority voting diverges already mentioned in 53.16.3.1, 256, 265, 275. Ranking by social choice function includes Interview algorithm implemented in Asfer and any other ranking function. Thus there exists a setting where both LHS and RHS fail to converge. It has to be noted that above counterexamples do not rule out the possibility of convergence of LHS and RHS of  $P(\text{Good})$  circuit. There could be decision functions which adhere to "no error" cases in 10 possibilities as below:

| $x$<br>$f(x/e)$ Noise                               | $f(x) = f(x/e)$ | $f(x) \neq$               |
|-----------------------------------------------------|-----------------|---------------------------|
| $x$ in $L$ , $x/e$ in $L$                           | No error        | Error                     |
| $x$ in $L$ , $x/e$ not in $L$<br>$f(x)=1, f(x/e)=0$ | Error           | No error if<br>else Error |
| $x$ not in $L$ , $x/e$ in $L$<br>$f(x)=0, f(x/e)=1$ | Error           | No error if<br>else Error |
| $x$ not in $L$ , $x/e$ not in $L$                   | No error        | Error                     |
| $x$                                                 | $f(x)$          |                           |
| Randomized Decision tree evaluation                 | No error        | Error                     |

If LHS social choice ranking function is Interview algorithm which is a  $PSPACE=IP$  algorithm (by straightforward reduction from polynomial round prover-verifier protocol) or a  $PSPACE$  function fitting within "No error" scenarios in matrix above, then an unrestricted depth 100% errorfree RHS EXP circuit could imply,  $EXP=PSPACE$ . Hence whether such perfect resilient errorfree decision functions in previous "No error" cases can be learnt is an open question.

There are natural processes like Soap Bubble formation known to solve Steiner Tree NP-hard problem efficiently. Soap Bubbles between two glass plates are formed and bubbles are connected by line segments of optimum total length which converge at Steiner vertices. Voting is a also a natural process with human element involved. Does human judgement overwhelm algorithmic judgement in decision correctness is also an open question. If neural networks are algorithmic equivalents of human reasoning, then each voter decision function could be a TC (threshold) circuit and majority voting could be a composition of NC majority function with TC voter circuit inputs. Thus entire RHS of  $P(\text{Good})$  is a huge non-uniform TC neural network. Error of majority voting is then equal to error



of this majority function + neural network composition i.e majority voting involving humans is BPTC algorithm.

Previous matrix of 10 scenarios basically subdivides the traditional BP\* definition which says: For  $x$  in  $L$ , a BP\* turing machine accepts with probability  $> 2/3$  and for  $x$  not in  $L$  rejects with probability  $> 2/3$ . In other words, a BP\* algorithm allows false positives and false negatives and thus errs in "judgement" with probability  $1/3$ . All "Error" entries in the previous matrix are :

- \*) ( $f(x)=f(x/e)$ ) in which case two correlated strings one in  $L$  and other not in  $L$  are both accepted (false positive) and rejected by  $f$  (false negative)

- \*) ( $f(x) \neq f(x/e)$  - Noise sensitivity) in which case two correlated strings in  $L$  or not in  $L$  are erroneously accepted and rejected by  $f$  (false positives and false negatives)

- \*) Previous two are input related while the last scenario with error in decision tree evaluation is internal to the boolean function itself with false positive and negative decision tree evaluation based on pseudorandom advice bits.

This false positive + false negative voter judgement error applies to BPTC NC+neural network circuit composition also described previously. Derandomizing BPTC should give a non-uniform TC circuit for RHS of  $P(\text{Good})$  majority voting implying zero-error voting by neural network voters. This non-uniform TC circuit is an alternative way to specify the enormity of RHS earlier described by  $PH=DC$  (depth restricted) and  $EXP$  (depth unrestricted) classes. Thus these two unbounded circuit models for RHS of  $P(\text{Good})$  majority voting are equivalent: non-uniform TC and  $EXP$ . But  $ACC$  is contained in TC and  $NEXP$  is not in non-uniform  $ACC$ . This does not rule out the possibility that  $EXP$  has non-uniform TC circuits which is a superset of  $ACC$ .

#### References:

- 
- 355.1  $NEXP$  not in non-uniform  $ACC$  - [RyanWilliams] - <http://www.cs.cmu.edu/~ryanw/acc-lbs.pdf>
  - 355.2 Soap Bubble Steiner Tree and  $P=NP$  - [ScottAaronson] - <https://arxiv.org/pdf/quant-ph/0502072v2.pdf>
  - 355.3 Constant depth Threshold circuits - <http://people.cs.uchicago.edu/~razborov/files/helsinki.pdf>
  - 355.4 Circuit Complexity of Neural networks - <https://papers.nips.cc/paper/354-on-the-circuit-complexity-of-neural-networks.pdf>
  - 355.5 Exact Threshold circuits - <http://www.cs.au.dk/~arnsfelt/Papers/exactcircuits.pdf>
  - 355.6 Universal Approximation Theorem - [Cybenko] - [https://en.wikipedia.org/wiki/Universal\\_approximation\\_theorem](https://en.wikipedia.org/wiki/Universal_approximation_theorem) - Multilayered Perceptrons with single hidden layer and finite inputs can approximate continuous functions [It has to be noted that single layer perceptron cannot compute XOR function and spatial connectedness - from Perceptrons:an introduction to computational geometry by MarvinMinsky-SeymourPapert]. Thus BPTC threshold networks with multiple layers as voter decision functions are good approximators of voting decisions.
  - 355.7  $L^*$  algorithm for exact learning of DFAs - [Dana Angluin] - <https://people.eecs.berkeley.edu/~dawnsong/teaching/s10/papers/angluin87.pdf> - membership and counterexample queries to learn DFA
  - 355.8 Efficient Learning Algorithms Yield Circuit Lower Bounds - [Lance Fortnow] - <http://lance.fortnow.com/papers/files/fksb.pdf> - Theorem 1 and Corollary 1 for depth-2 threshold circuits (neural networks) - "... If there exists an algorithm for exactly learning class  $C$  (e.g depth-two neural networks) in time  $2^{s^{o(1)}}$  with membership and equivalence queries then  $EXP^{NP}$  is not in  $P/Poly(C)$  (e.g  $TC_0[2]$ ) ... ". This theorem has direct implications for learning voter decision functions belonging to TC and BPTC classes in majority voting. Intuitively, this implies if an exact voter neural network without error is learnt in time exponential in size of neural network (e.g error minimization by gradient descent, backpropagation etc.), then  $EXP^{NP}$  is not computable by neural networks -  $EXP^{NP}$  is not in TC/poly.

-----  
-----  
356. (FEATURE-DONE) PythonSpark+Cython Interview Algorithm cloud implementation update - 4 January 2017 - related to 348  
-----  
-----

PythonSpark+Cython Cloud Implementation of Interview Algorithm has been updated to print average clustering coefficient of the definition graph for text. Average clustering coefficient is average(per node clustering coefficient) for all nodes where clustering coefficient of a vertex is a ratio of edges to neighbours to all possible edges to neighbours (or) amount of "cliqueness" of each neighbourhood of all vertices in a graph. This adds an alternative way for computing intrinsic merit of a document recursive gloss overlap graph mentioned in 348 (Kleinberg's small world graph and clustering coefficient = 2). Average clustering coefficient supplements the intrinsic merit quantitative score in deciding semantic relatedness of a graph. Closer the clustering coefficient is to 2, it is easier to find paths in graph of a text and greater the linguistic meaningfulness.

-----  
-----  
357. (THEORY) P(Good) non-majority versus majority social choices, BPTC and PSPACE classes - related to 317,355 - 6 January 2017  
-----  
-----

Caution: Following tries to prove a major lowerbound result with some assumptions and is subject to errors.

Main motivation for so much emphasis on P(Good) binomial summation convergence is: LHS is non-majority social choice and RHS is majority social choice and convergence to 100% on both sides implies LHS and RHS are of equal merit with varying complexity classes giving a lowerbound. In non-majority social choice one of the elements in the population set has to be chosen without voting. If there are  $n$  voters and out of them  $m$  are of  $x\%$  goodness, probability of pseudorandom choice to have  $x\%$  efficiency =  $m/n$ . If LHS is an Interview algorithm based social choice, choice process is as follows:

```
foreach(voter)
{
 Interview the voter (a PSPACE-complete problem where polynomial number of
 question-answering reduces to prover-verifier protocol)
}
Rank the voters by merit and choose the topmost as non-majority social choice -
voting is obviated.
```

It is interesting to note that web search engines use both non-majority (Ranking by merit) and majority choice (e.g PageRank, Hub-Authority) to rank websites. Above algorithm is polynomial time in number of voters. Previous loop is parallelizable per voter and could be an NC circuit with PSPACE algorithms as inputs. Thus effectively LHS is a PSPACE algorithm. RHS majority voting is better approximated by BPTC circuit with threshold neural network circuits for each voter, mentioned previously. It is known that BPP is in PSPACE. Thus LHS interview social choice with error is already accounted for in PSPACE. This equates an error-prone LHS PSPACE-complete problem to an error-prone RHS BPTC problem. BPTC is in BPP (couldn't find reference for this, but looks obvious because every TC circuit with error can be simulated by a polynomial time Turing Machine with error). This implies BPTC is in PSPACE because BPP is in PSPACE. If equal error on both LHS and RHS implies a lowerbound, LHS PSPACE-complete interview non-majority social choice has a BPTC majority social choice circuit and therefore all PSPACE problems are in BPTC. These two directions together imply PSPACE=BPTC. But BPTC is in BPP and BPP is in PSPACE implying PSPACE=BPP.

From <https://www.cse.buffalo.edu/~regan/papers/ComplexityPoster.jpg>, this might imply a collapse of entire Polynomial Hierarchy upto second level and some consequences for NP and coNP.

-----  
358. (THEORY) KRW Conjecture on Boolean Function Composition, Non-majority (PSPACE) and Majority (harder than PSPACE) circuits - related to 14,53,311,357 - 7 January 2017  
-----

-----  
Previous point mooted the idea of the parallel interview of voters and ranking them as a non-majority social choice. This requires sorting the interview algorithm scores of individual voters and finding topmost. Sorting of numbers is in AC=NC=TC (Sorting networks, parallel sorting, [ChandraStockMeyerVishkin] Constant Depth Reducibility for Sorting - <http://www.cstheory.com/stockmeyer@sbcglobal.net/csv.pdf> etc., Threshold circuits for sorting) and each voter's PSPACE-complete interview circuit is input to NC sorting circuit to find non-majority social choice. Thus LHS is a circuit composition of NC and PSPACE voter interview circuits denoted as NC+PSPACE. RHS of P(Good) is, as already mentioned by neural network approximation, a bounded probabilistic non-uniform BPTC circuit which is a circuit composition of BPNC and voter BPTC circuits denoted as BPNC+BPTC. If circuit compositions NC+PSPACE = PSPACE and BPNC+BPTC = BPTC then LHS is a PSPACE algorithm to RHS BPTC algorithm assuming equal error.

This creates a following intriguing possibility: If RHS majority voting has voter functions harder than PSPACE (i.e EXP, EXPSPACE, NEXP, coNEXP etc., and not in BPTC) , under equal error assumption, LHS PSPACE-complete non-majority interview algorithm lowerbounds the RHS. PSPACE is in EXP and EXP is in PSPACE. Thus equal error assumption for lowerbound raises possibilities of PSPACE=EXP, PSPACE=NEXP, PSPACE=coNEXP, PSPACE=EXPSPACE etc., It has to be observed that both PSPACE and other harder-than-PSPACE classes contain PP(Probabilistic Polynomial) and thus derandomization (error removal) is implicit. KRW Conjecture for Boolean Function Composition of two boolean functions f and g says:  $\text{DepthComplexity}(f + g) \sim \text{DepthComplexity}(f) + \text{DepthComplexity}(g)$ . PSPACE-complete interview is equivalent to a TrueQBF  $\phi(q_1, a_1, q_2, a_2, \dots, q_n, a_n)$  computed by an Alternating Turing Machine (AP=PSPACE) where "forall" quantifier is equivalent to a question  $q_i$  and "exists" quantifier is equivalent to its answer  $a_i$ . It is not known if there is a Circuit Composition equivalent of KRW conjecture for depth-size lowerbound of composition of two circuits and it is assumed that  $\text{NC}+(\text{PSPACE}=\text{AP}) = \text{PSPACE}$  because PSPACE is harder than NC and composition of NC with PSPACE should increase circuit depth proportional to number of quantifiers in interview TQBF. RHS BPNC+BPTC=BPTC is somewhat obvious because NC=TC=AC and only circuit depth-size increases when composed.

References:

-----  
358.1 Karchmer-Raz-Wigderson (KRW) Conjecture of Boolean Function Composition and Information Complexity - [http://cs.haifa.ac.il/~ormeir/papers/krw\\_info.pdf](http://cs.haifa.ac.il/~ormeir/papers/krw_info.pdf)  
-----

-----  
359. (THEORY) Non-majority social choices - Interview Ranking Function and Pseudorandom Choice Function - 11 January 2017 - related to 317, 358 and all other non-majority versus majority voting points  
-----

-----  
Previous sections mentioned about two possible ways of non-majority social choice:

- \*) Parallel interview of voters and ranking based on sorted interview scores
- \*) Psuedorandom choice

-----  
Interview circuit:  
-----

Error in interview circuit which is an NC sorting network with PSPACE-complete voter interviews as inputs is defined in usual sense as:

False positives + False negatives + False questions = Percentage of wrong answers marked as right + Percentage of right answers marked as wrong + Percentage of wrong questions

For sorting purposes output of TQBF is not a binary 0 or 1 but a binary string with value equal to number of correct answers. Like all other boolean functions sensitivity of TQBF  $\phi(q_1, a_1, q_2, a_2, q_3, a_3, \dots, q_n, a_n)$  is defined as how flipping of  $q_i$  and  $a_i$  affects the output.

Formally,

$\text{Sensitivity}(\text{TQBF}) = \Pr(\text{TQBF}(X) \neq \text{TQBF}(X_{\text{correlated}}))$  where  $X_{\text{correlated}}$  is an interview with erroneous questions and answers.

Thus sensitivity captures the error in interview. It has to be noted that wrong questions also measure the flaw in interview process while wrong answer to a right question is already accounted for by a binary 0. When sensitivity of TQBF is 0, interview is flawless and LHS of  $P(\text{good})$  is 1. BKS Majority is least stable conjecture by [Benjamini-Kalai-Schramm] predicts existence of a linear threshold function with stability greater than Majority function of  $n$  variables,  $n$  odd. Interview Circuit which is a composition of an NC sorting network with PSPACE TQBF interviews of voters, is also a linear threshold function which outputs candidate above a threshold (i.e. sum of correct answers > threshold). If  $\text{Stability}(\text{Interview}) > \text{Stability}(\text{Majority})$  then it is a proof of BKS conjecture. For large  $n$ ,  $\text{Stability}(\text{Majority}) = 1 - 2/\pi * (\delta)$ . When  $\delta$  is close to 1,  $\text{Stability}(\text{Majority})$  tends to 0.35.

-----  
Pseudorandom Choice:  
-----

Set of all voter decision functions is partitioned into  $n$  sets where each set has goodness  $x_i$ . Here goodness of a voter decision function  $f$  is defined as:  $1 - \text{error}(f)$ .

Let number of voter decision functions with goodness  $x_i = m(x_i)$ . Thus  $N = m(x_1) + m(x_2) + m(x_3) + \dots + m(x_n)$

Expected goodness of a PRG choice is:

$$\frac{1}{N} * \text{summation}(x_i * m(x_i)) = (x_1 * m(x_1) + x_2 * m(x_2) + x_3 * m(x_3) + \dots + x_n * m(x_n)) / N$$

When all voter functions have goodness 1 then PRG choice in LHS of  $P(\text{good})$  has goodness 1.

These two non-majority choices are just hypothetical examples of how a social choice can be made without voting. In reality how non-majority social choice occurs is quite complex and determined by various factors of society ( economic disparities, ethnicity etc., )

-----  
360. (FEATURE-DONE) Commits - 11 January 2017 - DeepLearning Convolution Networks update  
-----

Some changes done to Convolution computation:

- \*) Made sigmoid perceptron optional in final neural network from Maxpooling layer so that weighted sum is printed instead of sigmoid value

- \*) This causes the convolution network to be very sensitive to presence of pattern

- \*) 2 more example bitmaps have been added with varying degree of pattern prominence (a pronounced X and a thin 1)

- \*) With this final neurons from maxpooling layer print values of neurons which

quite closely reflect the pattern's magnitude: Huge pattern results in big value while small pattern results in small value proportionately.  
\*) This can rank the bitmaps in increasing degree of magnitude of pattern presence  
\*) Logs for this have been committed to testlogs

-----  
361. (FEATURE-DONE) DeepLearning Convolution Network - an example pattern recognition from bitmap images - 12 January 2017  
-----

-----  
\*) Few more bitmap images have been included with same pattern but of different sizes  
\*) There are 5 patterns and 9 bitmaps:  
    - Thin X and Boldfaced X  
    - Thin 0 and Boldfaced 0  
    - Thin 8 and Boldfaced 8  
    - No pattern  
    - Thin 1 and Boldfaced 1  
\*) Expectation is that Convolution Network final neuron layer must output similar values for same pattern and different values for different patterns  
\*) pooling\_neuron\_weight has been reintroduced in final neuron layer of 10 neurons each with a randomly chosen weight.  
\*) Logs show for all 10 neurons, final neural activation values are close enough for similar patterns and different for different patterns.  
\*) Thus Convolution Network which is a recent advance in DeepLearning works quite well to recognize similar image patterns.

In above example , 9th and 10th neurons output following values. Example 11 and 12 are similar patterns - 0 and 0. Example 21 and 22 are similar patterns - 8 and 8. Example 41 and 42 are similar patterns - X and X. Example 51 and 52 are similar patterns - 1 and 1. Neurons reflect this similarities :

#####  
#####

Inference from Max Pooling Layer - Neuron 8

#####  
#####

Example 11:

#####  
[27.402311485751664]  
#####

Example 12:

#####  
[27.36740767846171]  
#####

Example 21:

#####  
[32.15200939997122]  
#####

Example 22:

#####  
[30.835940458495205]  
#####

Example 3:

#####  
[17.133246549473675]  
#####

Example 41:

#####  
[29.367605168715038]  
#####

Example 42:

```
#####
[27.446193773968886]
#####
Example 51:
#####
[22.12145242997834]
#####
Example 52:
#####
[24.17603022706531]
#####
#####
Inference from Max Pooling Layer - Neuron 9
#####
#####
Example 11:
#####
[24.667080337176497]
#####
Example 12:
#####
[24.635666910615544]
#####
Example 21:
#####
[28.941808459974094]
#####
Example 22:
#####
[27.757346412645685]
#####
Example 3:
#####
[15.424921894526316]
#####
Example 41:
#####
[26.435844651843524]
#####
Example 42:
#####
[24.70657439657199]
#####
Example 51:
#####
[19.914307186980512]
#####
Example 52:
#####
[21.763427204358788]
```

-----  
 362. (FEATURE-DONE) DeepLearning BackPropagation Implementation Update - 17  
 January 2017  
 -----

-----  
 \*) DeepLearning BackPropagation code has been changed to have 3 inputs, 3 hidden  
 and 3 output layers  
 with  $3*3=9$  input-hidden weights and  $3*3=9$  hidden-output weights with total of 18  
 weights  
 \*) Software Analytics example has been updated with a third input and logs for  
 it have been committed  
 to testlogs/.



```

105, 105, 105, 105, 105, 105, 105, 105, 105, 105, 105, 105, 105, 105, 105, 105, 105,
105, 105, 105, 105, 105, 105, 105, 105, 105, 105, 105, 105, 105, 105, 105, 105]
Coefficients of fitting polynomial of degree 5: [1.07744279e+02 -
1.44951431e+00 1.33928005e-01 -3.69850703e-03
4.03119671e-05 -1.53297932e-07]
X-axis: xrange(95)
Y-axis: [119, 106, 101, 106, 119, 101, 106, 119, 107, 106, 101, 107, 119, 106,
107, 101, 106, 107, 119, 106, 101, 107, 106, 119, 107, 106, 101, 107, 119, 106,
106, 111, 105, 115, 106, 100, 105, 119, 105, 100, 111, 105, 119, 101, 105, 119,
105, 101, 48, 105, 119, 48, 101, 105, 111, 48, 119, 105, 101, 48, 119, 105, 101,
48, 105, 119, 48, 101, 105, 48, 99, 110, 100, 107, 110, 102, 110, 100, 110, 102,
110, 100, 110, 102, 107, 100, 106, 102, 107, 106, 100, 102, 107, 106, 100]
Coefficients of fitting polynomial of degree 5: [1.13816036e+02 -
2.17630157e+00 1.96357195e-01 -6.45349037e-03
8.34267469e-05 -3.67775407e-07]
...
#####
##
Two text polynomial ordinal points are represented as set of ordered pairs
#####
##
Wagner-Fischer Edit Distance for text9 and text10: 76
Polynomial Encoding Edit Distance (JensenShannon) for text9 and text10:
str1str2_tuple: [(102, 119), (100, 106), (106, 101), (102, 106), (106, 119),
(107, 101), (107, 106), (107, 119), (107, 107), (107, 106), (107, 101), (107,
107), (107, 119), (107, 106), (107, 107), (107, 101), (107, 106), (107, 107),
(102, 119), (106, 106), (106, 101), (106, 107), (106, 106), (106, 119), (106,
107), (106, 106), (106, 101), (106, 107), (106, 119), (106, 106), (115, 106),
(107, 111), (119, 105), (119, 115), (119, 106), (119, 100), (119, 105), (119,
119), (119, 105), (119, 100), (119, 111), (119, 105), (119, 119), (119, 101),
(119, 105), (119, 119), (119, 105), (119, 101), (119, 48), (119, 105), (105,
119), (105, 48), (105, 101), (105, 105), (105, 111), (105, 48), (105, 119),
(105, 105), (105, 101), (105, 48), (105, 119), (105, 105), (105, 101), (105,
48), (105, 105), (105, 119), (105, 48), (105, 101), (105, 105), (105, 48), (105,
99), (105, 110), (105, 100), (105, 107), (105, 110), (105, 102), (105, 110),
(105, 100), (105, 110), (105, 102), (105, 110), (105, 100), (105, 110), (105,
102), (105, 107), (105, 100), (105, 106), (105, 102), (105, 107), (105, 106),
(105, 100), (105, 102), (105, 107), (105, 106), (1, 100)]
421.059610023
Polynomial Encoding Edit Distance (L2 Norm) for text9 and text10:
str1str2_tuple: [(102, 119), (100, 106), (106, 101), (102, 106), (106, 119),
(107, 101), (107, 106), (107, 119), (107, 107), (107, 106), (107, 101), (107,
107), (107, 119), (107, 106), (107, 107), (107, 101), (107, 106), (107, 107),
(102, 119), (106, 106), (106, 101), (106, 107), (106, 106), (106, 119), (106,
107), (106, 106), (106, 101), (106, 107), (106, 119), (106, 106), (115, 106),
(107, 111), (119, 105), (119, 115), (119, 106), (119, 100), (119, 105), (119,
119), (119, 105), (119, 100), (119, 111), (119, 105), (119, 119), (119, 101),
(119, 105), (119, 119), (119, 105), (119, 101), (119, 48), (119, 105), (105,
119), (105, 48), (105, 101), (105, 105), (105, 111), (105, 48), (105, 119),
(105, 105), (105, 101), (105, 48), (105, 119), (105, 105), (105, 101), (105,
48), (105, 105), (105, 119), (105, 48), (105, 101), (105, 105), (105, 48), (105,
99), (105, 110), (105, 100), (105, 107), (105, 110), (105, 102), (105, 110),
(105, 100), (105, 110), (105, 102), (105, 110), (105, 100), (105, 110), (105,
102), (105, 107), (105, 100), (105, 106), (105, 102), (105, 107), (105, 106),
(105, 100), (105, 102), (105, 107), (105, 106), (1, 100)]
200.743617582
#####
##
From above, usual edit distance between 2 strings is less than polynomial
distances of JensenShannon and L2 norms. Ordinal values were not normalized by
subtracting lowest possible ordinal value of unicode.


```



-----  
Caution: This derivation is still experimental with possible errors.

Stability of a boolean function is defined as:

$$\text{Stability}(f) = \text{Expectation}(f(x)*f(y))$$

where y is correlated version of x.

Stability of Majority is defined as (From page 120 of AnalysisOfBooleanFunctions - Chapter 5 Majority and Threshold Functions -

<https://www.cs.cmu.edu/~odonnell/boolean-analysis/>)

$$\text{Stability}(\text{Maj}_n) = \text{Expectation}(\text{Maj}_n(x)*\text{Maj}_n(y))$$

where y is correlated version of x.

For infinite n,  $\text{Stability}(\text{Maj}_n)$  is bounded by  $2/\pi * \arcsin(\rho)$ . Similar stability measure can be derived for Interview TQBF threshold function also. Interview as a linear threshold function (LTF) can be defined as:

$$w_1*a_1 + w_2*a_2 + \dots + w_n*a_n > \text{threshold\_cutoff}$$

where each  $a_i$  is an answer for a question  $q_i$  and  $w_i$  is the weightage associated with it. Berry-Esseen Central Limit Theorem applies for Interview threshold function. CLT implies that a random variable  $S=X_1 + X_2 + X_3 + \dots + X_n$  which is a sum of random variables  $X_i(s)$  converges to Gaussian Normal Distribution. Berry-Esseen CLT generalizes it to  $S=a_1*x_1 + a_2*x_2 + \dots + a_n*x_n$  where  $\sum(a_i^2)$  is normalized and  $= 1$ . Thus interview threshold function and Berry-Esseen CLT are structurally similar when weights  $w_i$  are normalized and  $\sum(w_i^2) = 1$ . This implies interview scores are approximately Gaussian (Intuitively obvious because, bell curve corresponds to large proportion of voters scoring medium while tails correspond to very small percentage scoring very low and very high).

Stability of Interview can be equivalently defined as:

$$\text{Stability}(\text{Interview}) = \text{Expectation}(\text{Interview}(x)*\text{Interview}(y))$$

where y is correlated version of x.

Substituting the threshold definition of interview in Stability:

$$\begin{aligned} \text{Stability}(\text{Interview}) &= \text{Expectation}((w_1*a_1 + w_2*a_2 + \dots + w_n*a_n)*(z_1*b_1 + z_2*b_2 + \dots + z_n*b_n)) \\ &= \text{Expectation}(w_1*z_1*a_1*b_1 + w_1*z_1*a_2*b_2 + \dots + w_n*z_n*a_n*b_n) \\ &= a_1*b_1*\text{Expectation}(w_1*z_1) + \dots + a_n*b_n*\text{Expectation}(w_n*z_n) \end{aligned}$$

Assuming for all  $a_i=b_i=a$ :

$$\text{Stability}(\text{Interview}) = a^2 * (\text{Expectation}(w_1*z_1) + \text{Expectation}(w_1*z_2) + \dots + \text{Expectation}(w_n*z_n))$$

$\text{Expectation}(w_i*z_k) = 0*0*1/4 + 0*1*1/4 + 1*0*1/4 + 1*1*1/4$  for 4 possible values of  $(w_i, z_k)$  each with probability  $1/4$ .

$$\Rightarrow \text{Stability}(\text{Interview}) = a^2 * (n^2 * 0.25) = a^2 * n^2 / 4$$

$$\text{Stability}(\text{Interview}) = a^2 * n^2 / 4 < 1 \Rightarrow a < 2/n$$

If  $\text{Stability}(\text{Interview}) > \text{Stability}(\text{Majority})$ , BKS conjecture is true.

$$\Rightarrow a^2 * n^2 / 4 > 1 - 2/\pi$$

$$\Rightarrow a > 2/n * \sqrt{1 - 2/\pi}$$

$$\Rightarrow a > 1.2056205488/n \text{ [For minimum case of } n=2, a > 0.6028102744]$$

Thus for  $\text{Stability}(\text{Interview})$  to exceed  $\text{Stability}(\text{Majority})$  and BKS Conjecture to be true, weight per answer has to be  $> 1.2056/n$  approximately. For minimal base case  $n=2$ ,  $a > 0.6028$ .

Stability is alternatively defined as:

$$(+1)*Pr(f(x) = f(y)) + (-1)*Pr(f(x) \neq f(y))$$

which is just expansion of Expectation and there are two random variables (+1 for  $f(x)=f(y)$ ) and (-1 for  $f(x) \neq f(y)$ )

$$\Rightarrow \text{Stability}(f(x)) = 1 - 2*Pr(f(x) \neq f(y))$$

$$\Rightarrow \text{Stability}(f(x)) = 1 - 2*\text{Sensitivity}(f(x))$$

$$\Rightarrow \text{Sensitivity}(f(x)) = 0.5 - 0.5*\text{Stability}(f(x))$$

NoiseSensitivity(Interview) which is the dual of Stability is defined as:

$$\text{NoiseSensitivity(Interview)} = 0.5 - 0.5*\text{Stability(Interview)} = 0.5 - 0.5*a^2*n^2/4$$

-----  
366. (FEATURE-DONE) Commits - 25 January 2017 - related to 2.9 and 345  
-----

-----  
Berlekamp-Welch Polynomial Reconstruction Decoder Implementation (for Reed-Solomon codes, texts, numerical points etc.,)  
-----

-----  
\*) Implements Berlekamp-Welch Polynomial Reconstruction Algorithm for reconstructing data from errors.

\*) System of linear equations has been solved with NumPy/SciPy Linear Algebra solve().

\*) Logs show how well the reconstructed polynomial closely approximates the original polynomial.

\*) Error locator polynomial E is degree 1 and Numerator Q is of degree = number of points thus yielding  $Q/E=P$  (reconstructed)

\*) Special case is natural language text with errors and a polynomial can be reconstructed from ordinal values of unicode  
-----

-----  
367. (FEATURE-DONE) Berlekamp-Welch Algorithm implementation - update for text message decoding - 27 January 2017  
-----

-----  
\*) Using unicode values for ordinals with ord() and inverting with chr() causes overflow errors in SciPy/NumPy

Linear Algebra Equation solver (solve()) because evaluating polynomials for large messages creates huge numbers

\*) Hence unicode has been replaced with a simple dictionaries - alphanumeric to numeric values and numeric to alphanumeric values.

\*) With above 2 dictionaries an example text message with error (garbled version of "thisissentence") is list decoded with a window of possible values for each letter positions.

\*) Logs show an approximate decoding of original message from message with error.

\*) Garbled text with error was created from a previous execution of Berlekamp-Welch algorithm.  
-----

-----  
368. (THEORY) KRW Conjecture, KW relations, Majority Voting Circuit Composition - 30 January 2017 and 31 January 2017 - related to 358  
-----

-----  
Majority Voting Circuit for P(Good) binomial series RHS is a boolean circuit composition of NC Majority voting circuit with Voter Decision Functions for each voter variable input to Majority function defined as:

$$\text{Maj}(m) + \text{Voter}(n) =$$

Maj(Voter1(x1,x2,...,xn),Voter2(x1,x2,...,xn),...,Voterm(x1,x2,...,xn)).  
 Assumption is Voter Decision Functions can be exactly learnt in Angluin Exact Learning model i.e Voters can have zero errors.  
 KRW Conjecture for boolean formula composition implies  $\text{Depth}(f+g) \sim \text{Depth}(f) + \text{Depth}(g)$  for composition  $f+g$  of two boolean formulae (fanout 1)  $f$  and  $g$ . Applying KRW conjecture to Maj( $m$ ) + Voter( $n$ ) Majority voting composition:

$$\text{Depth}(\text{Maj}(m) + \text{Voter}(n)) \sim \text{Depth}(\text{Maj}(m)) + \text{Depth}(\text{Voter}(n))$$

where  $m$  is the number of voters and  $n$  is the number of variables per voter decision function.

KW relations  $R(f)$  for a function  $f$  imply  $\text{Depth}(f) = \text{CommunicationComplexity}(R(f))$ .

Karchmer-Wigderson relations for the composition are the following:

-----  
 $R(\text{Maj}, \text{Voter})$ :  
 -----

Alice:  $x$  in  $\text{Inverse}(\text{Maj} + \text{Voter})(0)$   
 Bob:  $y$  in  $\text{Inverse}(\text{Maj} + \text{Voter})(1)$   
 Find  $x_i$  and  $y_i$  such that  $x_i \neq y_i$

$\text{Depth}(\text{Maj} + \text{Voter}) = \text{CommunicationComplexity}(R(\text{Maj}, \text{Voter}))$

Thus Majority voting circuit composition is a KW relation.

There is an equivalent notion of Universal relation  $U(n)$  for KW relation defined as:

Alice:  $x$  in  $\{0,1\}^n$   
 Bob:  $y$  in  $\{0,1\}^n$   
 Find  $x_i$  and  $y_i$  such that  $x_i \neq y_i$

Result in 368.2 prove a lowerbound:

$$\text{Depth}(g+U(n)) = \text{CommunicationComplexity}(R(g,U(n))) \geq \log L(g) + n -$$

$O(m \cdot \log m/n)$  where  $L(g)$  is the formula size of  $g$ .

If  $g$  is Majority function and  $U(n)$  is individual voter decision function, depth of composition of Majority and Voter circuits is:

$$D(\text{Maj} + \text{Voter}) = \text{CommunicationComplexity}(R(\text{Maj}, \text{Voter})) \geq \log L(\text{Majority}) + n - O(m \cdot \log m/n)$$

But formula size of Majority is  $O(m^{5.3})$  implying depth of

Majority+VoterDecisionFunction composition is:

$$D(\text{Maj} + \text{Voter}) = \text{CommunicationComplexity}(R(\text{Maj}, \text{Voter})) \geq 5.3 \cdot \log m + n - O(m \cdot \log m/n)$$

Thus depth of Majority voting circuit for  $P(\text{Good})$  RHS is lowerbounded by a function of number of voters and number of variables per voter decision function.

368.1 prove a result which is an extension of 355.8:

If a class  $C$  is exactly learnable in polynomial time,  $\text{DTIME}(n^{\omega(1)})$  is not in  $C$ . In mistake bounded learning model, learner updates the hypothesis in each round based on mistake it makes in labelling a point on hypercube. Mistake bounded learning very closely matches human experiential learning and hence human voting error. If a class  $C$  is mistake bounded learnable in time  $T$  and mistakes  $M$  then,  $\text{DTIME}(n + MT)$  is not in  $C$  yielding a separation. Corollary: If a function in NP is polynomial time exact learnable, there is no polynomial time algorithm for NP. For unbounded number of voters( $m$ ) and variables per voter decision function( $n$ ), depth of composition is unbounded. Depth Hierarchy Theorem 368.4 immediately applies for functions computable by circuits of various depths of RHS composition. Number of variables per voter and depth of composition are linearly related while Number of voters and depth of composition are logarithmically related.

Exact Learning implies zero error on both sides of  $P(\text{Good})$  binomial series.

Assuming all boolean function are exactly learnt, a Pseudorandom choice amongst those functions yields 100% perfect choice. Quoting from 359:

Let number of voter decision functions with goodness  $x_i = m(x_i)$ . Thus  $N =$

$m(x_1)+m(x_2)+m(x_3)+\dots+m(x_n)$

Expected goodness of a PRG choice is:

$\frac{1}{N} * \text{summation}(x_i * m(x_i)) = (x_1 * m(x_1) + x_2 * m(x_2) + x_3 * m(x_3) + \dots + x_n * m(x_n)) / N$

When all voter functions have goodness 1 then PRG choice in LHS of  $P(\text{good})$  has goodness 1.

Similarly, exact learning implies all voter decision functions are 100% perfect with zero-error in LHS. Binomial series converges to 1 on both sides. LHS is a polynomial time algorithm (because there is a PRG in  $P$  to make a choice) to RHS majority voting NP problem (assuming the exactly learnt boolean functions are in NP) implying  $P=NP$ . But from 368.1, if NP is learnable in polynomial time, NP does not have polynomial time algorithms and therefore  $P \neq NP$  - a contradiction. Thus polynomial time exact learning of an NP boolean function (e.g 3SAT learnt from a truth table) conflicts with  $P=NP$  and binomial series convergence.

Usual process of high level human learning vis-a-vis boolean function learning is bottom-up. Atomic concepts are learnt in leaves and complexity is built from leaf to root by learning new concepts which are functions of subtrees. Recursive Lambda Function Growth algorithm for learning texts described earlier in this document is based on this paradigm but constructs a composition tree top-down (Mind grows lambda functions/circuits). Generalization of Recursive Lambda Function Growth is to learn a graph as opposed to trees. This is already done in Recursive Gloss Overlap special case by merging/removing isomorphic, repetitive subtrees while tree is grown top-down. This is why core number based classifier for the recursive gloss overlap graph works - repeating gloss nodes are connected to already discovered nodes by a new edge thereby converting a tree to graph top-down - Because most synset paths between words in a text go through "class label" vertices making them high degree and all such high degree vertices belong to a dense subgraph e.g k-core.

Hypothetical exact learner for 3SAT - NP voter decision functions :

-----  
Given a truth table of size  $n*2^n$  for  $n$  variables with truth values:

- \*) Find a set of binary strings, satisfying truth values 1
- \*) Construct a DNF for complement of the previous set
- \*) Complement the DNF to get CNF for original set

Example - For following truth table, to construct CNF for satisfying assignments {000, 001, 011, 101, 110}:

| x1 x2 x3 |   |   | truthvalue | complement |
|----------|---|---|------------|------------|
| -----    |   |   |            |            |
| 0        | 0 | 0 | 1          | 0          |
| 0        | 0 | 1 | 1          | 0          |
| 0        | 1 | 0 | 0          | 1          |
| 0        | 1 | 1 | 1          | 0          |
| 1        | 0 | 0 | 0          | 1          |
| 1        | 0 | 1 | 1          | 0          |
| 1        | 1 | 0 | 1          | 0          |
| 1        | 1 | 1 | 0          | 1          |

DNF for complement set {010,100,111} is:

$!x_1x_2!x_3 + x_1!x_2!x_3 + x_1x_2x_3$

and the CNF learnt is complement of DNF:

$(x_1 + !x_2 + x_3)(!x_1 + x_2 + x_3)(!x_1 + !x_2 + !x_3)$

with satisfying assignments {000, 001, 011, 101, 110}

This exact learner requires  $O(2^n)$  time which is exponential in number of variables.

368.6 describes an algorithm (CDNF) to learn any boolean functions in time

polynomial in number of variables, its DNF size and CNF size. This together with 368.1 implies a polynomial time learning algorithm for NP and existence of polynomial time learning algorithm for NP(3CNF) indicates NP does not have polynomial time algorithms (and Exponential Time Hypothesis could be true). This coincides with evidences towards divergence of P(Good) series and superpolynomial size circuits for 3SAT implied in 53.16, 256, 265, 275, 318 (Majority Lemma for Hardness Amplification) and 355. This is a serious contradiction - exact learning derandomizes both sides of P(Good) circuit. LHS non-majority social choice is zero-error and equals 1 while RHS if NP also converges to 1 and implies a polynomial time algorithm for NP while exact learning forbids polynomial time algorithm for NP. Resolving this impasse amounts to defining what is meant by exactness and zero-error in voting decision and social choice (Perfection commonsensically enshrines zero-error decision making for unbounded number of scenarios i.e variables while exact learning assumes bounded set of variables)

#### References:

- 
- 368.1 Exact Learning implies Derandomization (i.e.  $P=BPP$ ) and Mistake bound learning - [KlivansKothariOliveira] - <http://www.cs.princeton.edu/~kothari/cc13.pdf>
- 368.2 KRW Conjecture, KW relations and Lowerbound for Depth of Boolean Circuit Composition - [GavinskyMeirWeinsteinWigderson] - <https://video.ias.edu/sites/video/files/Meir.pdf>
- 368.3 Generalization of Spira's Theorem - <https://www.cs.utexas.edu/users/panni/spira.pdf> - Spira's theorem transforms every circuit of size  $S$  to a circuit of depth  $O(\log S)$ .
- 368.4 Depth Hierarchy Theorem - [RossmanServedioTan] - Theorem 1 - <https://arxiv.org/pdf/1504.03398v1.pdf> - Circuit of depth  $\leq d-1$  with size  $\leq 2^{(n^{1/6(d-1)})}$  agrees with a function of depth  $d$  on at most  $0.5 + n^{\Omega(-1/d)}$  fraction of inputs.
- 368.5 Formula size of Majority function - [Valiant] - <http://www.sciencedirect.com/science/article/pii/0196677484900166?via%3Dihub>
- 368.6 Exact Learning of Boolean Functions from Monotone Theory - [Nader H. Bshouty] - <http://www.cs.technion.ac.il/~bshouty/MyPapers/Exact-Learning-Boolean-Functions-via-the-Monotone-Theory.ps> - CDNF algorithm - Section 6 - exactly learns any boolean function in time polynomial in number of variables, size of DNF and CNF with polynomial membership and equivalence(counterexample) queries.
- 368.7 BPEXP is believed to collapse to EXP - if  $P=BPP$  then  $BPEXP=EXP$  (but converse  $BPEXP=EXP$  implying  $P=BPP$  is not known) - <https://www.ime.usp.br/~spschool2016/wp-content/uploads/2016/07/CarboniOliveiraIgor.pdf>
- 368.8 From [Klivans-Fortnow] result mentioned in 368.1, if class EXP is efficiently PAC learnable with membership queries, BPEXP is not in EXP contradicting  $BPEXP=EXP$  by homogeneous voter Condorcet Jury Theorem BPEXP circuit derandomization mentioned in 400.  $BPEXP=EXP$  implies hence that EXP is not efficiently PAC learnable.
- 368.9 Extended Depth Hierarchy Theorem - <https://dl.acm.org/citation.cfm?id=3095799> - [Hastad-Rossman-Servedio-Tan] - For any  $d < \log n / \log \log n$  there is a function  $F$  computed by a read once formula of depth  $d$  but any circuit of depth  $d-1$  and size  $O(2^{O(n^{1/5d})})$  agrees with  $F$  by a fraction of  $0.5 + O(n^{-1/5d})$  inputs. This approximation by smaller depth circuit has applications in forecasting accuracy of previous Majority+VoterSAT boolean composition voting - as all Voters' decision SAT Circuit depth tends to infinity, accuracy of election forecasting tends to 50%.
- 368.10 Quasidemocracies - Banzhaf Power Index - <https://gilkalai.files.wordpress.com/2018/08/kalai-icm2018.pptx> - Quasi democracies are electorate in which each voter has decision SAT of  $n$  variables and as  $n$  tends to infinity, probability of forecasting the outcome of the election by any voter tends to zero as other voters vote at random. This needs to be contrasted with previous depth hierarchy ramification - number of variables per SAT versus depth of the CircuitSAT.

-----  
369. (FEATURE-DONE) An experimental special case k-CNF SAT Solver algorithm  
implementation - 31 January 2017  
-----

Algorithm:

-----  
\*) Create a k-DNF from k-CNF input by negating literals in all clauses of k-CNF  
\*) Binary encode the clauses of k-DNF into set of binary strings of length n  
where n is number of variables  
\*) Compute the complement of the previous binary encoded set from set of  $2^n$   
binary strings  
\*) These are satisfying assignments  
\*) Presently requires all literals in each CNF clause  
\*) Implemented for simulation of a Majority Voting with Voter SATs  
-----

-----  
370. (THEORY) Majority Boolean Function, Sensitivity, Roth's estimate and 2-  
Coloring/Complement Functions of Sequences -  
1 February 2017 - related to 24,338 - Important draft updates to  
<https://arxiv.org/pdf/1106.4102v1>  
-----

-----  
Boolean Majority Function finds the majority binary value of input binary string  
of length n. Any binary string of length n can be  
considered as 2-coloring of bit position integers with corresponding complement  
functions for each color: f(x) is for 1s colored red and  
g(x) is for 0s colored blue. For example, 1001011 is a 2-colored sequence with  
red (1) in bit positions 1,4,6,7 and blue (0) in bit positions  
2,3,5. Complement functions for this bit position binary coloring are defined  
as:

f(1)=1  
f(2)=4  
f(3)=6  
f(4)=7

and

g(1)=2  
g(2)=3  
g(3)=5

Naturally, arithmetic progressions and monochromatic arithmetic progressions on  
these bit positions can be defined. Discrepancy is the  
difference between number of colored integers in an arithmetic progression.  
Roth's estimate which is the minimum(maximum(discrepancy))  
for all possible colorings (i.e all possible binary strings) is  $\geq$   
 $N^{1/4+\epsilon}$ . For majority function 2-coloring, this estimate is  
the difference between number of 0s and 1s in the input to majority function  
with probability equal to natural density of min(max()) arithmetic progression.  
If majority function outputs 1,  $|f(x)| > |g(x)|$  and if 0,  $|g(x)| > |f(x)|$ . From  
this an approximate estimate of number of 1s and 0s in majority function input  
can be obtained (with probability equal to natural density):

$|f(x)| = \text{number of 1s} = [N + N^{1/4+\epsilon}]/2$  if majority function  
outputs 1

$|g(x)| = \text{number of 0s} = [N - N^{1/4+\epsilon}]/2$  if majority function  
outputs 1

and vice versa if majority function outputs 0. For previous example, majority is  
1 and :

$|f(x)| = \text{number of 1s} = [7 + 7^{0.25}]/2 = 4.313288 \sim 4$

$|g(x)| = \text{number of 0s} = [7 - 7^{0.25}]/2 = 2.6867 \sim 3$

Sensitivity of Majority function is number of bits to be flipped to change the  
outcome which is nothing but the discrepancy ( $|f(x)| - |g(x)|$ ) wth probability  
equal to natural density and is lowerbounded by Roth's estimate. Formally,  
 $\text{Sensitivity(Majority)} > N^{1/4+\epsilon}$ . An important special case is when input

to majority is a binary string 2-colored by prime-composite complement functions in bit positions i.e prime bit positions are 1 and composite bit positions are 0 and majority function outputs 0 or 1 (Approximate number of primes less than  $N = \pi(N) \sim N/\log N$  from Prime Number Theorem).

-----  
371. (FEATURE-DONE) Reinforcement Learning - ThoughtNet based Recommender Systems Implementation Update - 2 February 2017  
-----

-----  
\*) Recursive Gloss Overlap classifier disambiguation has been updated to invoke NLTK lesk algorithm function() with options to choose between PyWSD lesk implementation and best\_matching\_synset() primitive disambiguation native implementation  
\*) New usecase shopping cart example with book reviews has been added  
\*) Fixed a major bug in RecursiveGlossOverlap Classifier in definition graph construction : Edges for all lemma names of previous level synsets were added which bloated the graph and somewhat skewed core number of the graph. Changed it to create edge only for one lemma name. All other Recursive Gloss Overlap implementations in InterviewAlgorithm/ folder already have this fix. Regenerated the hypergraph for shoppingcart3 example Logs for this have been added to testlogs/  
-----

-----  
372. (FEATURE-DONE) Recursive Gloss Overlap classifier update - 3 February 2017  
-----

-----  
Uncommented NetworkX matplotlib graph plotting to get a graph for a sample document definition graph. Logs and PNG file for this classification have been added to testlogs/. Also did some experimentation with various documents and classification based on core number has been reasonably accurate (relevance of unsupervised core number based classification to the document's actual class decreases with core number) and top percentage classes reflect the subject matter of the document. Also best\_matching\_synset() lesk disambiguation implemented in AsFer and NLTK lesk() functions are faster than PyWSD simple\_lesk().  
-----

-----  
373. (THEORY and FEATURE-DONE) CNFSAT solver update - polynomial time approximation - 5 February 2017  
-----

-----  
Solves CNFSAT by a Polynomial Time Approximation scheme:

- Encode each clause as a linear equation in  $n$  variables: missing variables and negated variables are 0, others are 1
  - Solve previous system of equations by least squares algorithm to fit a line
  - Variable value above 0.5 is set to 1 and less than 0.5 is set to 0
  - Rounded of assignment array satisfies the CNFSAT with high probability
- Essentially each CNF is represented as a matrix  $A$  and solved by  $AX=B$  where  $X$  is the column vector of variables and  $B$  is identity column vector  
-----

-----  
374. (FEATURE-DONE) Java Spark Streaming - Generic Stream Receiver Implementation - 6 February 2017  
-----

-----  
Spark Streaming Java implementation to receive generic stream of unstructured text data from any URL and Sockets has been added to NeuronRain AsFer java/bigdata\_analytics/. It is based on Sparta 2.1.0 + Hadoop  
-----

2.7 single node cluster. Following are the setup prerequisites:

```
*) Oracle Java 8 compiler and runtime and PATH set to it
*) export CLASSPATH=/home/shrinivaasanka/spark-2.1.0-bin-hadoop2.7/jars/spark-streaming_2.11-2.1.0.jar:./home/shrinivaasanka/spark-2.1.0-bin-hadoop2.7/jars/scala-library-2.11.8.jar:/home/shrinivaasanka/spark-2.1.0-bin-hadoop2.7/jars/spark-sql_2.11-2.1.0.jar:/usr/lib/jvm/java-8-oracle/bin:/usr/local/sbin:/usr/local/bin:/usr/sbin:/usr/bin:/sbin:/bin
*) Compiled as: javac SparkGenericStreaming.java
) JAR packaging of SparkGenericStreaming.class : jar -cvf sparkgenericstreaming.jar *class
*) Example Spark submit commandline for 2 local threads (2 cores) and data streamed from twitter :
/home/shrinivaasanka/spark-2.1.0-bin-hadoop2.7/bin/spark-submit --class SparkGenericStreaming --master local[2] sparkgenericstreaming.jar "https://twitter.com/search?f=tweets&vertical=news&q=Chennai&src=typd"
```

Spark Streaming Java implementation complements Streaming Abstract Generator Python native abstraction implemented in AsFer. Advantage of Spark Streaming is it can process realtime streamed data from many supported datasources viz., Kinesis, Kafka etc., This implementation is generic, customized for arbitrary streaming data.

-----  
375. (FEATURE-DONE) Java Spark Streaming for Generic data - Jsoup ETL integration - 7 February 2017  
-----

```
*) Jsoup HTML parser has been imported into SparkGenericStreaming.java and a very basic Extract-Transform-Load is performed on the URL passed in with a special boolean flag to use Jsoup
*) Jsoup connects to URL and does a RESTful GET of the HTML, extracts text from HTML and stores the text in Spark RDD
*) receive() is periodically invoked and word count is computed
*) foreachRDD() is invoked on the DStream to iterate through all words in DStream.
*) forEach() invokes a lambda function to print the word text
*) Logs for this have been added to spark_streaming/testlogs/
```

spark-submit commandline requires additional classpath to jsoup .jar with --jars option as below:

```
/home/shrinivaasanka/spark-2.1.0-bin-hadoop2.7/bin/spark-submit --class SparkGenericStreaming --master local[2] --jars /home/shrinivaasanka/jsoup/jsoup-1.10.2.jar sparkgenericstreaming.jar "https://twitter.com/search?f=tweets&vertical=news&q=Chennai&src=typd" 2>&1 > testlogs/SparkGenericStreaming.out.7February2017
```

-----  
376. (THEORY and FEATURE-DONE) Approximate SAT solver update - 8 February 2017 - related to 373  
-----

Updated CNFSATSolver.py to create set of random 3CNFs and verify if the least squares assignment is satisfied. Presently it creates randomly concatenated CNFs of 10 variables and 10 clauses in an infinite loop and prints a percentage of satisfied 3CNFs so far by least square heuristic. Logs for this percentage after few hundred iterations has been committed to testlogs/. It shows an intriguing convergence at 80% (i.e 80% of 3CNFs are satisfied) after few hundred iterations of random CNFs. A caveat has to be mentioned here on hardness of approximation and PCP theorem: MaxSAT and Clique do not have Polynomial Time Approximation Scheme unless P=NP. PTAS usually creates a solution within 1+/-epsilon distance



from optimal. MaxSAT problem tries to maximize number of clauses satisfied in a CNF. But this least square SAT solver is exact SAT solver and the percentage of 80% found in testlogs/ implies 80% of CNFs were satisfied. This could heuristically imply 80% of clauses per CNF were satisfied on the average. Though this percentage is specific to 10 clauses \* 10 variables, similar asymptotic convergence to ~79% was observed for 5 clauses \* 5 variables. Assuming this implies epsilon to be 0.2 in general (average 20% distance from optimal for all CNFs), could imply a PTAS (because solving system of equations by Least Squares or Gaussian Elimination is polynomial in number of clauses) for MaxSAT which satisfies 80% clauses per CNF on average and P=NP.(Related: Unique Games Conjecture)

#### References:

-----  
376.1 PCP theorem and Hardness of Approximation -  
[http://www.cs.jhu.edu/~scheideler/courses/600.471\\_S05/lecture\\_9.pdf](http://www.cs.jhu.edu/~scheideler/courses/600.471_S05/lecture_9.pdf)  
376.2 PCP theorem and Hardness of Approximation -  
<http://pages.cs.wisc.edu/~dieter/Courses/2008s-CS880/Scribes/lecture17.pdf>  
-----

-----  
377. (FEATURE-DONE) Java Spark Streaming Generic Receiver update - 9 February 2017  
-----

-----  
\*) Objectified the SparkGenericStreaming more by moving the SparkConf and JavaStreamingContext into class private static data.  
\*) new method SparkGenericStreamingMain() instantiates the Spark Context and returns the JavaPairDStream<String,Integer> wordCounts object  
\*) main() static method instantiates SparkGenericStreaming class and receives wordCounts JavaPairDStream from SparkGenericStreamingMain() method  
\*) Spark JavaStreamingContext output operations are invoked by start() and print actions by lambda expressions.  
\*) SparkConf and JavaStreamingContext variables have to be static because Not Serializable exceptions are thrown otherwise.  
\*) sparkgenericstreaming.jar has been repackaged by recompilation.  
-----

-----  
378. (FEATURE-DONE) Spark Streaming Java Update - Java Bean DataFrame(Dataset) creation, Hive Metastore support and persistence of DataFrame to Hive and as a Parquet file - 10 February 2017  
-----

-----  
\*) New JavaSparkSingletonInstance class for singleton Spark Context has been added.  
\*) New Java Bean Word.java has been added for creating DataFrame from JavaRDD iterable  
\*) DataFrame has been persisted to filesystem as .parquet file in overwrite mode of DataFrameWriter  
\*) DataFrame has also been persisted to Hive MetaStore db which Spark supports (Shark SQL) with saveAsTable()  
\*) SparkGenericStreaming has been rewritten to do transformations on words JavaRDD iterable with VoidFunction() in 2-level nested iterations of foreachRDD() and forEach()  
\*) map() transformation for each row in JavaRDD throws a null pointer exception and inner call() is never invoked.  
\*) This has been remedied by replacing map() with a forEach() and storing the rows in each RDD in an ArrayList  
\*) With Hive MetaStore + Shark integration, Streaming\_AbstractGenerator.py abstraction now has access to Java Spark Streaming because it already supports Hive via thrift and NeuronRain now has ability to  
-----

analyze any realtime or batch unstructured data.

\*) Primitive ETL to just scrape words in URL text sufficiently tracks trending topics in social media.

\*) Hive metastore db, Spark warehouse data have been committed and Logs for this has been added to testlogs/

\*) sparkgenericstreaming.jar has been repackaged with recompilation

\*) Updated spark-submit commandline: /home/shrinivaasanka/spark-2.1.0-bin-hadoop2.7/bin/spark-submit --class SparkGenericStreaming --master local[2] --jars /home/shrinivaasanka/spark-2.1.0-bin-hadoop2.7/jars/scala-reflect-2.11.8.jar,/home/shrinivaasanka/spark-2.1.0-bin-hadoop2.7/jars/spark-catalyst\_2.11-2.1.0.jar,/home/shrinivaasanka/jsoup/jsoup-1.10.2.jar sparkgenericstreaming.jar "http://www.facebook.com"

\*) Updated CLASSPATH: export CLASSPATH=/home/shrinivaasanka/spark-2.1.0-bin-hadoop2.7/jars/scala-reflect-2.11.8.jar:/home/shrinivaasanka/spark-2.1.0-bin-hadoop2.7/jars/spark-catalyst\_2.11-2.1.0.jar:/home/shrinivaasanka/jsoup/jsoup-1.10.2.jar:/home/shrinivaasanka/spark-2.1.0-bin-hadoop2.7/jars/spark-streaming\_2.11-2.1.0.jar:./home/shrinivaasanka/spark-2.1.0-bin-hadoop2.7/jars/scala-library-2.11.8.jar:/home/shrinivaasanka/spark-2.1.0-bin-hadoop2.7/jars/spark-sql\_2.11-2.1.0.jar:/home/shrinivaasanka/spark-2.1.0-bin-hadoop2.7/jars/spark-core\_2.11-2.1.0.jar:/usr/lib/jvm/java-8-oracle/bin:/usr/local/sbin:/usr/local/bin:/usr/sbin:/usr/bin:/sbin:/bin

-----  
379. (THEORY) Machine Translation, Recursive Gloss Overlap Graphs in different Natural Languages and Graph Homomorphisms - 13 February 2017  
- related to 178  
-----

Machine Translation is equivalent to graph homomorphism between 2 recursive gloss overlap graphs of a text in 2 natural languages where homomorphism  $f$  for translation is defined as:

if  $(u,v)$  is in  $E(G_1)$  then  $(f(u),f(v))$  is in  $E(G_2)$

for recursive gloss overlap graphs  $G_1$  and  $G_2$  for languages  $L_1$  (e.g. English) and  $L_2$  (e.g. Tamizh) constructed from respective ontologies.

In previous definition,  $u$  and  $v$  are two words in natural language  $L_1$  and  $f(u)$  and  $f(v)$  are two words in natural language  $L_2$ .

This relaxes the isomorphism requirement mentioned in 178. Set of all digraphs  $G$  such that there is a homomorphism from  $G$  to a graph  $H$  is denoted by  $L(H)$ . Guessing the set of digraphs  $G$  for a digraph  $H$  implies finding set of all translations for a text from a set of natural languages to another natural language. This guessing problem is known by Dichotomy Conjecture to be either in P or NP-Complete.

-----  
380. (FEATURE-DONE) Approximate SAT solver update - 14 February 2017  
-----

\*) Changed number of variables and clauses to 14 and 14 with some additional debug statements.

\*) After 4000+ iterations ratio of random 3SAT instances satisfied is: ~70%  
-----

381. (FEATURE-DONE) Java Spark Streaming with NetCat WebServer update and some analysis on HiveServer2+Spark Integration - 18 February 2017  
-----

\*) Rewrote SparkGenericStreaming.java mapreduce functions with Spark 2.1.0 + Java 8 lambda functions

\*) Enabled Netcat Socket streaming boolean flag instead of URL socket with Jsoup

\*) With above changes (and no HiveServer2), socket streaming receiver works and Hive saveAsTable()/Parquet file saving works.

\*) HiveServer2 was enabled in Spark Conf by adding hive-site.xml in spark/conf directory. (Two example hive-site.xml(s) have been committed to repository.)

\*) Spark 2.1.0 was started with hive-site.xml to connect to HiveServer2 2.1.1. This resulted in 2 out of heap space errors as documented in testlogs/ with exception "Error in instantiating HiveSessionState".

\*) Such OOM errors with HiveServer2 and Spark have been reported earlier in Apache JIRA. Instead of TTransport, FrameTransport was also tried which caused "Frame size exceeds maximum frame size" errors. SASL was also disabled in hive-site.xml.

\*) Reason for such OOM errors in HiveServer2 seems to be heavy memory footprint of HiveServer2 and Spark together and CPU usage reaches 100% for both cores. Might require a high-end server with large RAM size so that heap space is set to atleast 8GB. HiveServer2 is known to be memory intensive application. Also Spark only supports Hive 1.2.1 and not Hive 2.1.1 which could be the reason.

\*) Increasing Java Heap space in spark config file (spark.executor.memory and spark.driver.memory) also did not have effect.

\*) Setting HADOOP\_HEAPSIZE also did not have effect. OOM error occurs while instantiating HiveSessionState and bootstrapping Hive databases (get\_all\_databases). Isolated beeline CLI connection works though with HiveServer2.

\*) Hence presently Spark Streaming works with Spark provided metastore\_db Hive Support and Parquet file support.

\*) testlogs/ have stream processing logs for NetCat (NC) webserver.

-----  
 382. (FEATURE-DONE) Spark Version Upgrade for Recursive Gloss Overlap Graph  
 Intrinsic merit and Discrete Hyperbolic Factorization Cloud  
 Implementations - 21 February 2017  
 -----

\*) Re-executed Interview Algorithm and Factorization Spark Cloud implementations with Spark 2.1.0 and Cython optimization for Recursive Gloss Overlap Graph construction

\*) Earlier these were benchmarked with Spark 1.5.x

\*) Added debug statements in python-src/DiscreteHyperbolicFactorizationUpperbound\_Bitonic\_Spark.py and file locations updated. Logs committed to python-src/testlogs and python-src/InterviewAlgorithm/testlogs

-----  
 383. (THEORY) Recursive Gloss Overlap Graphs, Intrinsic Merit and Korner Graph  
 Entropy - related to 348 - 22 February 2017  
 -----

Graph representation of text and deriving a quantitative intrinsic merit from recursive gloss overlap definition graph by projecting WordNet onto the document has been described previously. Spectral Graph Theory qualitatively analyzes the graph in terms of eigenvalues of its Laplacian. Quantitative Graph Theory provides various statistical tools to quantify a graph in terms of its complexity. Measuring meaningfulness of a text has been translated to the problem finding easy paths between concepts and keywords in the text. This is computational linguistic Symbol Grounding problem of learning from dictionary definitions (refer 216.3). Korner's Graph Entropy defines the entropy of a graph G as follows:

$$KE(G) = \text{minimum}(I(X,Y))$$

where X is a randomly chosen vertex in V(G) and Y is an independent set of G (set of vertices with no edges between them). I(X,Y) is the probabilistic mutual information of two random variable X and Y defined as:

$$I(X,Y) = \text{double\_summation}(p(x,y)\log(p(x,y)/p(x)p(y)))$$

where  $p(x)$  is probability of  $X=x$ ,  $p(y)$  is probability of  $Y=y$  and  $p(x,y)$  is a joint probability distribution of  $X=x$  and  $Y=y$ .

An alternative definition of Korner Entropy of a graph  $G$  is :

$$KE(G) = \text{minimum} [- \sum_{v \in V(G)} \{1/|V(G)| * \log(\text{Pr}[v \text{ in } Y])\}]$$

i.e minimum of summations over product of probability of a randomly chosen vertex  $v$  in  $V(G)$  and log likelihood probability of  $v$  in an independent set  $Y$  of  $G$ .

Mutual information is the generalization of Shannon information entropy when two dependent random variables are involved. Korner's entropy quantitatively captures the complexity and merit of a graph representation of text quite effectively because mutual information is the amount of knowledge one random variable has about the other. This is quite useful for text meaningfulness - two words with high mutual information are quite likely to be closely related. More precisely, from definitions of Korner Entropy, mutual information of a word vertex and an independent set of word vertices in recursive gloss overlap graph is the "extent of relatedness" between a word and an independent set of words it is part of. When a word is in an independent set of word vertices, there exists no relation among them - no word vertex is in dictionary gloss definition of other word vertices. By summing up log likelihoods for all such vertices, a measure of "meaninglessness" is obtained. Dual of this meaninglessness is meaningfulness (document ranking by meaninglessness is inversion of ranking by meaningfulness) obtained by  $(-)$  sign and minimum(). Maximum Korner Entropy is  $\log(|V|)$  for complete graphs and minimum is zero for empty graphs. Any document graph would have entropy merit value between 0 and  $\log|V|$ . Computing Korner Entropy is NP-hard since finding stable independent sets is NP-hard.

#### References:

- 
- 383.1 Korner Entropy - [JaikumarRadhaKrishnan] - <http://www.tcs.tifr.res.in/~jaikumar/Papers/EntropyAndCounting.pdf>
- 383.2 Entropy of Graphs - [MowshowitzDehmer] - [www.mdpi.com/1099-4300/14/3/559/pdf](http://www.mdpi.com/1099-4300/14/3/559/pdf)
- 383.3 Entropy Centrality of Graphs - [Qiao-Shan-Zhou] - <http://www.mdpi.com/1099-4300/19/11/614/pdf> - influence of a vertex is defined in terms of Shannon Entropy  $(-p \log p)$  and Subgraph Degree Centrality
- 383.4 Entropy measures for networks - [Anand-Bianconi] - <https://arxiv.org/pdf/0907.1514.pdf> - Relations between Shannon Entropy, Gibbs Entropy and Von Neumann Entropy of networks
- 383.5 Graph Energy and its relation to average degree  $k$  - <http://iopscience.iop.org/article/10.1088/1742-6596/604/1/012024/pdf> - Energy of a Graph is sum of absolute values of its adjacency matrix eigenvalues. Quoted excerpts: "...When the network is very sparse, graph energy  $E$  will be monotonically increasing with  $k$ . With slow increase of intensity, energy  $E$  will be still proportional to  $k$  but with appearing of some weak fluctuations. However, while the network is becoming highly dense, the graph energy will drop sharply. And the value of  $k$  that corresponds to the largest graph energy is about  $0.8N$ ...". This threshold relation between average degree and energy of graph has parallels to Bianconi-Barabasi least energy intrinsic fitness which implies low energy vertices attract large number of links. Similarly, Graph Energy which is cumulative estimate for all vertices, decreases when the graph has lot of edges which is possible only if average degree of the vertices is high. High average degree by Bianconi-Barabasi model implies least energy and high intrinsic fitness.
- 383.6 Graph Energy and its meaning - <https://arxiv.org/pdf/1704.00779.pdf>
- 

384. (THEORY) Neural Tensor Networks Reasoning and Recursive Gloss Overlap merit scoring - 23 February 2017

-----

Neural Tensor Networks described in 384.1 generalizes a linear neuron into a

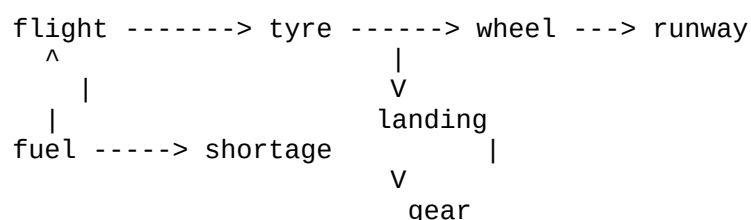
multidimensional tensor and assigns a score for relation between two entities e1 and e2. This is described in the context of an ontology (e.g WordNet) where a relation between two words w1 and w2 is assigned a score based on various distance measures. Recursive Gloss Overlap graph which is a gloss definition graph has a single relation between any two words - w1 "is in dictionary/gloss definition of" w2. Present implementation does not quantify the extent of relatedness between two words connected by an edge in Recursive Gloss Overlap graph. This definition graph can be considered as a Neural Tensor Network and each edge can be scored as a neural tensor relation between two word vertices. Cumulative sum total score of all edges in this graph is a quantitative intrinsic merit measure of the meaningfulness and intrinsic merit. Thus any document's definition graph is a set of tensor neurons which together decide the merit of the text. Together with Korner Entropy complexity measure, Sum of Tensor Neuron scores effectively weight the text.

#### References:

-----  
 384.1 Neural Tensor Networks - [SocherManningNg] -  
[http://nlp.stanford.edu/pubs/SocherChenManningNg\\_NIPS2013.pdf](http://nlp.stanford.edu/pubs/SocherChenManningNg_NIPS2013.pdf)

-----  
 385. (THEORY) Recursive Lambda Function Growth, Random Walks on Recursive Gloss Overlap graph and Text Comprehension - 25 February 2017 - related to 46, 47, 216, 230 and 384  
 -----

As mentioned in previous section, two word vertices x1 and x2 are connected by an edge weight determined by tensor neuron (x1 R x2) for some relation R. Human comprehension of text can be approximated by set of compositional lambda functions created from converging random walks or DFS Tree on the recursive gloss overlap graph. For example, following definition graph for a text "Flight landed on runway because of fuel shortage" is created from thesaurus/sdictionary/gloss definitions of an ontology:



Example Random walks on previous graph:

-----  
 flight ---> tyre ----> wheel ---> landing ---> gear  
 flight ----> fuel ----> shortage

If Tensor Neurons are applied for each edge, this graph is a weighted directed graph where weight is determined by Tensor Neuron. If each relation is a lambda function following the Recursive Lambda Function Compositional Growth defined in 216, every random walk can be mapped to a lambda function composition tree. For example, following random walk:

fuel ----> flight ---> tyre ----> wheel ---> landing ---> gear

is tensor neuron labelled with lambda functions:

fuel --(requiredby)---> flight----(has)---> tyre ---(has)--->  
 wheel --- (does) ---> landing --- (requires) ---> gear

where lambda functions for each edge with word vertices as parameters are:

f1 = requiredby(fuel, flight)

```

f2 = has(flight, tyre)
f3 = has(tyre, wheel)
f4 = does(wheel, landing)
f5 = requires(landing, gear)

```

Composition is done left associative creating following tree recursively:

```

f5(landing, gear)
f4(wheel, f5(landing, gear))
f3(tyre, f4(wheel, f5(landing, gear)))
f2(flight, f3(has, f4(wheel, f5(landing, gear))))
f1(fuel, f2(flight, f3(tyre, f4(wheel, f5(landing, gear)))))

```

Previous composition tree is done for each Markov Chain Random Walk on the Definition Graph. Difference between composition in 216 and previous is: Recursive Lambda Function Compositional Growth is done on a flat sentence in 216, while it is applied to a random walk on definition graph here. Because neuron tensors are equivalent to a lambda function per edge, each function  $f_i$  can be made to return a relevance merit score which is fed to next layer - in essence each random walk lambda function composition tree is a multilayer tensor neuron. Similar process can be applied to paths in a DFS tree also. Inorder traversal of the composition tree yields an equivalent expanded text of original text (In above example it is "fuel required by flight has tyre has wheel does landing requires gear"). Each random walk results in a tree-structured multilayer tensor neuron. Equivalently, each lambda function tensor could return a pictorial meaning and each composition "operates" on the tensor arguments to return a new animated version to next level up the tree (i.e meaning is represented as visuals). Ontology required for this is an ImageNet than a WordNet.

Advantage of Random Walks is it mimicks the randomness of deep learning in human text comprehension. Typical visual comprehension reads a passage atleast once scanning the keywords and inferring grammatical connectives between keywords. After keywords are known, they have to be related to infer meaning. An ontology provides paths between keywords and how they are related. After all edges and paths are known, collective meaning has to be evaluated by traversing the graph. Meaning is accrued over time by traversing the relations between keywords compositionally. This traversal is a random walk on the definition graph. Previous lambda function growth for each random walk on graph builds meaning recursively. Covering time of random walk is the number of steps required to visit all vertices. Mixing time of random walk is the number of steps required to reach stationary distribution (i.e any further random walk is no different from previous walks). These two measures have been widely studied for weighted directed graphs and are good estimators of time required to deep-learn and comprehend a text. Trivial DFS search is quite static and stationary distribution in Mixing time of random walk is the state when a text has been fully understood and any further reading does not add more meaning. Mixing time in undirected graph is proportional to Isoperimetric number or Cheeger's constant. Isoperimetry measures amount of bottleneck in a graph. For directed weighted graph, Conductance is the equivalent isoperimetric measure. When isoperimetry is high, random walk converges quickly implying faster text comprehension. For a partition of the vertex set of a graph  $(S, T)$ , conductance of the cut  $\Phi(S, T) = \frac{\sum_{u \in S, v \in T} a(u, v)}{\min(\sum_{w \in S} d_w, \sum_{w \in T} d_w)}$  where  $d_w = \sum_{z} a(w, z)$  and  $a(s, t)$  is the weight of an edge i.e tensor neuron lambda function score. PageRank of the Recursive Gloss Overlap graph is converging random walk - PageRank along with Core Number of definition graph is already known to classify texts in unsupervised setting by ranking the vertices.

References:

-----  
385.1 Random Walks Survey - <http://www.cs.elte.hu/~lovasz/erdos.pdf>  
385.2 Random Walks on Weighted Directed Graphs -  
<http://www.cs.yale.edu/homes/spielman/eigs/lect7.pdf>

-----  
386. (FEATURE-DONE) Java Spark Generic Streaming and Streaming Abstract  
Generator Integration - 27 February 2017  
-----

-----  
\*) Enabled URLSocket in Spark Generic Streaming and crawled an example facebook  
and twitter  
streaming data stored into Parquet files and Spark metastore  
\*) Added Spark Streaming Data Source and Parquet Data Storage to  
Streaming\_AbstractGenerator.py  
and updated iterator to read DataFrames from word.parquet Spark Streaming  
storage.  
\*) Spark DataFrames are iterated by accessing word column ordinal and yielded to  
any application of  
interest.  
\*) As an example Streaming HyperLogLogCounter implementation has been updated to  
read from Spark  
Parquet streaming data storage and cardinality is computed  
\*) Example Spark Generic Streaming logs with URLSockets and HyperLogLogCounter  
with Spark Parquet  
data storage have been added to testlogs in python-src and  
java-src/bigdata\_analytics/spark\_streaming/testlogs  
\*) Thus an end-to-end Java+Spark+Python streaming ETL pipeline has been  
implemented where:  
    - Extract is done by JSoup crawl  
    - Transform is done by Spark RDD transformations  
    - Store is done by Spark Hive and Parquet storage  
    - Load is done by Streaming Abstract Generator iterator/facade

pattern

\*) Streaming\_HyperLogLogCounter.py instantiates SparkSession from pyspark.sql.  
Usage of SparkSession requires executing this through spark-submit (Usual python  
<file> commandline doesnot work) as below:  
/home/shrinivaasanka/spark-2.1.0-bin-hadoop2.7/bin/spark-submit  
Streaming\_HyperLogLogCounter.py 2>&1 >  
testlogs/Streaming\_HyperLogLogCounter.out.SparkStreaming.27February2017  
-----

-----  
387. (FEATURE-DONE) Streaming Algorithms Implementations for Spark Streaming  
Parquet Data Storage - 28 February 2017  
-----

-----  
\*) All Streaming\_<algorithm> implementations have been updated to have Spark  
Streaming  
Parquet file storage as input generators.  
\*) New Streaming\_SocialNetworkAnalysis.py file has been added to do sentiment  
analysis for  
Streaming Data from Spark Parquet file storage  
\*) Streaming\_AbstractGenerator.py has been updated to filter each Spark Parquet  
DataFrame to remove  
grammatical connectives and extract only keywords from streamed content  
\*) Logs for all Streaming\_<algorithm>.py and Streaming\_SocialNetworkAnalysis.py  
executed against  
Spark Streaming Parquet data have been committed to testlogs/  
\*) Streaming\_SocialNetworkAnalysis.py presently iterates through word stream  
generated by  
Streaming\_AbstractGenerator.py and does Markov Random Fields Clique potential  
sentiment analysis.  
\*) Streaming\_AbstractGenerator.py Spark Parquet \_\_iter\_\_() clause presently  
returns word stream which  
can be optionally made to return sentences or phrases of specific length  
\*) All python streaming implementations instantiating  
Streaming\_AbstractGenerator.py have to be executed with \$SPARK\_DIR/bin/spark-

submit

-----  
388. (FEATURE-DONE) Major rewrite of BackPropagation Implementation for  
arbitrary number of Neuron input variables layer - 2 March 2017  
-----

-----  
\*) BackPropagation algorithm code has been rewritten for arbitrary number of  
input layer, hidden layer and output layer variables.  
\*) Some Partial Differential Equations functions have been merged into one  
function.  
\*) This was executed with 6 variable input layer neuron, 6 variable hidden layer  
and 6 variable output layer with  $2*6*6=72$  weights  
for each of 72 activations.  
\*) Logs for this have been committed to testlogs/  
\*) For 100000 iterations, error tapers to  $\sim 10^{-29}$  as below  
-----

-----  
Error after Backpropagation- iteration : 99998

1.05827458078e-29

Layers in this iteration:

#####

Input Layer:

#####

[0.23, 0.11, 0.05, 0.046, 0.003, 0.1]

#####

Hidden middle Layer:

#####

[0.07918765738490302, 0.17639329000539292, 0.3059104560477687,  
0.06819897810162112, 0.13596389556531566, 0.18092367420130773]

#####

Output Layer:

#####

[0.29999999999999977, 0.53, 0.110000000000000039, 0.09000000000000002,  
0.0100000000000004578, 0.20999999999999999]

Weights updated in this iteration:

[0.048788506679748, 0.11426171324845727, 0.24603459114714846,  
0.0795780558315572, 0.17784209754093078, 0.18901665972998824,  
0.11262698024008909, 0.20899193850252168, 0.5190303819914409,  
0.3056462222980023, 0.5043023226568699, 0.6597581902164429, 0.16317511417689112,  
0.6856596163043989, 1.0387023103855846, 0.2606362555325616, 0.9902995852922012,  
1.0606233996394616, 0.03792106334721366, 0.08894920940249851,  
0.19690317303590538, 0.06956852060077344, 0.15685074966243606,  
0.1617685764906898, 0.07393365494416165, 0.11785754559950794,  
0.32914500297950156, 0.2691055311488234, 0.4255090307780099, 0.5588219323805761,  
0.17422407739745155, 0.7118075853635217, 0.335920938970278, 0.08421750448989332,  
0.18955175416917805, 0.2131459459234997, 0.18585916895619456,  
0.2871421205369935, 0.4097382856269691, 0.09927665626493291, 0.2820455537957722,  
0.44170499922267087, 0.4181874495051114, 0.6343547541074734, 0.5019659876526656,  
0.6341824150669009, 0.9311854573920668, 0.415739542966714, 0.8116648622103757,  
0.7642211240783323, -0.27787045024304763, -0.03796350343576473, -  
0.06897746410924578, -0.12106324365840128, 0.09688102161356603,  
0.0833653488478167, 0.025844281679456543, 0.01924251728820474,  
0.1166534752079898, 0.22544113767193752, 0.2565459528164421, 0.2598246679566054,  
-0.2448286735461752, 0.48545168615654455, -0.12033616818940464, -  
0.17996884551601777, 0.09161370830913909, 0.16523481156548922,  
0.22079944846849042, 0.4246703906819317, 0.05813513760785996,  
0.49187786590191596]

Recomputing Neural Network after backpropagation weight update

Error after Backpropagation- iteration : 99999

1.05827458078e-29

Layers in this iteration:

#####



Input Layer:

#####

[0.23, 0.11, 0.05, 0.046, 0.003, 0.1]

#####

Hidden middle Layer:

#####

[0.07918765738490302, 0.17639329000539292, 0.3059104560477687,  
0.06819897810162112, 0.13596389556531566, 0.18092367420130773]

#####

-----  
-----  
389. (FEATURE-DONE) Convolution Network Final Neuron Layer Integrated with  
BackPropagation Implementation- 3 March 2017  
-----

\*) New python module has been added to repository to invoke BackPropagation  
algorithm

implementation in final neuron layer of convolution network.

\*) This creates a multilayer perceptron from maxpooling layer variables as input  
layer and

backpropagates for few iterations to do weight updates.

\*) Maxpooling layer is a matrix of  $5*5=25$  variables. With 25 variable input  
layer, backpropagation

is done on  $25*25*2=1250$  activation edges with weights( $25$  inputs \*  $25$  hidden +  $25$   
hidden \*  $25$  outputs).

\*) Logs for this have been added to testlogs/

\*) Presently expected output layer has been hardcoded to some constant  
-----

-----  
390. (THEORY) Prime-Composite Complementation/2-coloring, Riemann Zeta Function  
and Sum of Eigenvalues - Elementary Analysis - 6 March 2017  
- related to 19, 24, 319, 323, 338, 370  
-----

-----  
Special case of complementation/2-coloring is prime-composite coloring where set  
of natural numbers is 2-colored as primes and composites.

Here terminology of complementation and 2-coloring is used interchangeably. But  
complementation is a generic notion for functions over  
reals too. Riemann Zeta Function and truth of Riemann Hypothesis imply a pattern  
in distribution of primes and hence pattern in prime-composite  
coloring. Thus Riemann Zeta Function is a 2-coloring scheme for set of natural  
numbers.

Let  $q^s + q^{(1-s)} = v$  be an eigenvalue of a graph where  $s$  is a complex exponent  
( $s=a+ib$ ). It can be written as:

$$q^{2s} + q = vq^s$$

$$q^{2(a+ib)} + q = vq^{(a+ib)}$$

$$q^{2a}q^{2ib} + q = vq^a q^{ib}$$

$$q^{2a}(e^{i2b\log q}) + q = vq^a [e^{ib\log q}] \text{ by rewriting } q^{ib} = e^{ib\log q}$$

$$q^{2a}[\cos(2b\log q) + i\sin(2b\log q)] + q = vq^a [\cos(b\log q) + i\sin(b\log q)]$$

Equating Re() and Im():

$$q^{2a}[\cos(2b\log q)] + q = vq^a [\cos(b\log q)]$$

$$q^{2a}[\sin(2b\log q)] = vq^a [\sin(b\log q)]$$

Ratio of Re() and Im() on both sides:

$$\frac{q^{2a}[\sin(2b\log q)]}{q^{2a}[\cos(2b\log q)] + q} = \frac{vq^a [\sin(b\log q)]}{vq^a [\cos(b\log q)]}$$

$$\frac{q^{2a}[2*\sin(b\log q)*\cos(b\log q)]}{\text{-----}} = \frac{[\sin(b\log q)]}{\text{-----}}$$

$$\begin{aligned}
& q^{2a}[\cos(2b\log q)] + q \quad [\cos(b\log q)] \\
& q^{2a}[2*\cos(b\log q)*\cos(b\log q)] = q^{2a}[\cos(2b\log q)] + q \\
& q^{2a}[2*\cos(b\log q)*\cos(b\log q)] = q^{2a}[\cos(b\log q)*\cos(b\log q) - \\
& \sin(b\log q)*\sin(b\log q)] + q \\
& q^{2a}[\cos(b\log q)*\cos(b\log q) + \sin(b\log q)*\sin(b\log q)] = q \\
& q^{2a} = q \Rightarrow a = 0.5
\end{aligned}$$

When  $s=0.5$  with no imaginary part and  $q+1$  is regularity of a graph,  $v = 2*\sqrt{q}$  and corresponding graph is a  $q+1$  regular Ramanujan Graph.

[This is already derived in:

<https://sites.google.com/site/kuja27/>

[RamanujanGraphsRiemannZetaFunctionAndIharaZetaFunction.pdf,](#)

[https://sites.google.com/site/kuja27/RZFAndIZF\\_25October2014.pdf,](https://sites.google.com/site/kuja27/RZFAndIZF_25October2014.pdf)

<http://sourceforge.net/p/asfer/code/HEAD/tree/python-src/>

[ComplFunction\\_DHF\\_PVSNP\\_Misc\\_Notes.pdf\]](#)

Let  $H = \{G_1, G_2, G_3, \dots\}$  be an infinite set of graphs with eigenvalues  $1^s + 1^{(1-s)}$ ,  $2^s + 2^{(1-s)}$ ,  $3^s + 3^{(1-s)}$ , ....

Sum of these eigenvalues for infinite set of graphs has following relation to Riemann Zeta Function for  $s=w+1$ :

$$\text{Sum}_{q=1\_to\_inf}(q^s + q^{(1-s)}) = [1 + 1/2^w + 1/3^w + \dots] + [1 + 2^{(w+1)} + 3^{(w+1)} + \dots] = \text{RiemannZetaFunction} + [1 + 2^{(w+1)} + 3^{(w+1)} + \dots]$$

$$\text{Sum}_{q=1\_to\_inf}(q^s + q^{(1-s)}) - [1 + 2^{(w+1)} + 3^{(w+1)} + \dots] = \text{RiemannZetaFunction}$$

Thus Riemann Zeta Function is written as difference of sum of eigenvalues for an infinite set of graphs and another infinite exponential series.

Hermitian Real Symmetric matrices have real eigenvalues which is true for undirected graphs. For directed graphs, eigenvalues are complex numbers. Because of this condition, elements of set  $H$  have to be directed graphs. Relation between eigenvalues of two matrices  $M_1$  and  $M_2$  and eigenvalues of their sum  $M_1+M_2$  is expressed by [Weyl] inequalities and [Knutson-Tao] proof of Horn's conjecture. Sum of eigenvalues of  $M_1+M_2$  is equal to sum of eigen values of  $M_1$  + sum of eigen values of  $M_2$  (Trace=sum of eigen values=sum of diagonal elements). The set  $H$  has one-to-one mapping with set of natural numbers and is 2-colored as prime and composite graphs based on index (each graph is monochromatic). Sum of adjacency matrices of  $H$  is also a directed graph (if all  $G_i$  have same number of vertices) denoted as  $G(H)$ .

References:

-----

390.1 Complex Analysis - [Lars Ahlfors] - Page 30 - Poles and Zeros, Page 213 - Product Development, Riemann Zeta Function and Prime Numbers

390.2 Honeycombs and Sums of Hermitian Matrices - <http://www.ams.org/notices/200102/fea-knutson.pdf>

-----  
 391. (FEATURE-DONE) DeepLearning (ConvolutionNetwork-BackPropagation) JPEG files with Python Imaging Library (PILlow) - 6 March 2017  
 -----

\*) Added import of PIL Image library to open any image file and convert into a matrix in Integer mode

\*) This matrix is input to Convolution and BackPropagation code

\*) Logs of Convolution and BackPropagation for sample images have been committed to testlogs/

-----  
-----  
392. (FEATURE-DONE) DeepLearning (ConvolutionNetwork-BackPropagation) tobit()  
update - 7 March 2017  
-----

-----  
\*) Updated python-src/DeepLearning\_ConvolutionNetwork\_BackPropagation.py tobit()  
function to map each pixel to a decimal value < 1  
\*) Increased BackPropagation iteration to 100.  
\*) Logs for this have been committed to testlogs/. With this final neurons for  
max pooling layer are sensitive to changes in image pixels  
-----

-----  
393. (FEATURE-DONE) DeepLearning (ConvolutionNetwork-BackPropagation)  
image\_to\_bitmatrix() update - 8 March 2017  
-----

-----  
\*) Refactored the tobit() function - moved it to a new directory  
image\_pattern\_mining and reimplemented it with a new  
image\_to\_bitmatrix() function in ImageToBitMatrix.py by enumerating through the  
pixel rows and applying map(tobit)  
\*) This removed the opaqueness related 255 appearing for all pixels in bitmap.  
\*) Each pixel is multiplied by a fraction. Mapping it to binary digits 0,1 based  
on [0-127],[128-255] intervals for pixel values  
does not work well with BackPropagation of MaxPooling in Convolution Network.  
Instead multiples of a small fraction makes the  
MaxPooling layer quite receptive to changes in image pixel values.  
\*) Added few handwriting recognition example images for numbers 1(two fonts),2  
and 8.  
\*) Logs for this have been committed to testlogs/  
-----

Following are Maxpooling Neurons  
-----

Final Layer of Inference from Max Pooling Layer - BackPropagation on Max Pooling  
Layer Neurons

Inference from Max Pooling Layer - Image: [0.1452950826564989,  
0.15731736449115244, 0.16984767785665972]  
Inference from Max Pooling Layer - Image: [0.14920888863234688,  
0.16193600589418844, 0.17528092024601222]  
Inference from Max Pooling Layer - Image: [0.13197897244871004,  
0.1417448800619895, 0.15171424525284838]  
Inference from Max Pooling Layer - Image: [0.14007345008310818,  
0.15118749472569865, 0.16267822705412283]  
Inference from Max Pooling Layer - Image: [0.07847441088145349,  
0.0807616625716103, 0.08303607840796547]  
Inference from Max Pooling Layer - Image: [0.08983732685398557,  
0.09365789540391084, 0.09744765711798722]  
Inference from Max Pooling Layer - Image: [0.0903328782140764,  
0.09421672093823663, 0.09806798136073994]  
Inference from Max Pooling Layer - Image: [0.08761036574911765,  
0.09113121170496671, 0.09462405037074482]  
( 'Inference from Max Pooling Layer - Example 11:', [0.1619896774094416,  
0.1615169723530323, 0.15009965578039716])  
( 'Inference from Max Pooling Layer - Example 12:', [0.14303879829783814,  
0.12068614560924568, 0.07211705852669059])  
( 'Inference from Max Pooling Layer - Example 21:', [0.1932801269861012,  
0.11587916253160746, -0.007889615456070018])  
( 'Inference from Max Pooling Layer - Example 22:', [0.17605214289097237,  
0.19326380725531284, 0.2114152778184319])  
( 'Inference from Max Pooling Layer - Example 3:', [0.062097695970929206,  
0.062097695970929206, 0.062097695970929206])  
( 'Inference from Max Pooling Layer - Example 41:', [0.2976324086103368,

```

0.32891470561393965, 0.34986397693929844])
('Inference from Max Pooling Layer - Example 42:', [0.22669904395788065,
0.26336097548290116, 0.3065443950445386])
('Inference from Max Pooling Layer - Example 51:', [0.11935155170571034,
0.12477637373255022, 0.12911872514904305])
('Inference from Max Pooling Layer - Example 52:', [0.12675869649313706,
0.12051203261825084, 0.10578392639393523])

```

-----  
Previous logs are grep-ed from testlogs/. Handwritten Numeral recognitions (with high noise) are done in following Maxpooling inferences:

```

[Number 1 - Font 1] Inference from Max Pooling Layer - Image:
[0.07847441088145349, 0.0807616625716103, 0.08303607840796547]
[Number 1 - Font 2] Inference from Max Pooling Layer - Image:
[0.08983732685398557, 0.09365789540391084, 0.09744765711798722]
[Number 2] Inference from Max Pooling Layer - Image: [0.0903328782140764,
0.09421672093823663, 0.09806798136073994]
[Number 8] Inference from Max Pooling Layer - Image: [0.08761036574911765,
0.09113121170496671, 0.09462405037074482]

```

Contrasting this with bitmap numerals inscribed in 2 dimensional arrays (with low noise), similar elements have close enough values:

```

[Number 0 - Font 1] ('Inference from Max Pooling Layer - Example 11:',
[0.1619896774094416, 0.1615169723530323, 0.15009965578039716])
[Number 0 - Font 2] ('Inference from Max Pooling Layer - Example 12:',
[0.14303879829783814, 0.12068614560924568, 0.07211705852669059])
[Number 8 - Font 1] ('Inference from Max Pooling Layer - Example 21:',
[0.1932801269861012, 0.11587916253160746, -0.007889615456070018])
[Number 8 - Font 2] ('Inference from Max Pooling Layer - Example 22:',
[0.17605214289097237, 0.19326380725531284, 0.2114152778184319])
[Null pattern] ('Inference from Max Pooling Layer - Example 3:',
[0.062097695970929206, 0.062097695970929206, 0.062097695970929206])
[Letter X - Font 1] [('Inference from Max Pooling Layer - Example 41:',
[0.2976324086103368, 0.32891470561393965, 0.34986397693929844])
[Letter X - Font 2] ('Inference from Max Pooling Layer - Example 42:',
[0.22669904395788065, 0.26336097548290116, 0.3065443950445386])
[Number 1 - Font 1] ('Inference from Max Pooling Layer - Example 51:',
[0.11935155170571034, 0.12477637373255022, 0.12911872514904305])
[Number 1 - Font 2] ('Inference from Max Pooling Layer - Example 52:',
[0.12675869649313706, 0.12051203261825084, 0.10578392639393523])

```

-----  
394. (THEORY) Coloring Real Numbers and Complement Functions - 8 March 2017 - related to 323, 338  
-----

So far equivalence of 2-coloring schemes and integer valued complement functions have been mentioned. Most generic problem in this class is to find coloring schemes (or) functions which "complement" real and complex n-dimensional surfaces(i.e sets of values of a function f and its complement g create a disjoint set cover of the real/complex planes). Ramsey theory pertains to coloring integer sequences. 394.1 defines the problem of coloring the real line as minimum number of colors required to color the real line such that no two points within some specific distance (which in turn is an element of a distance set) are of same color. In Graph theory terms, this reduces to chromatic number of a graph where two vertices a and b are adjacent iff distance between a and b on real line is in distance set. This is stricter requirement of coloring compared to complementation and complement graphs representation mentioned in 338. For example, following complementation of [1,2]:

```

f(0) = [1.0,1.11]
g(0) = [1.12,1.23]
f(1) = [1.24,1.30]
g(1) = [1.31,1.68]

```

$f(2) = [1.69, 2.0]$   
 has colored regions of length  $[0.11, 0.11, 0.06, 0.37, 0.31]$  and can be 2-colored with  $f$  and  $g$ . If the distance set is  $\{0.01, 0.02\}$  two points 1.32 and 1.33 are 0.01 apart but have same color (belong to same function  $g$ ). Similarly points 1.69 and 1.71 are 0.02 apart but have same color  $f$ . Thus complementation over reals relaxes the coloring conditions significantly. Coloring real line is a special case of complementation with distance set requirement while Coloring integers is equivalent to complementation. Rather, distance set for real complementation is of size 1 containing length of largest monochromatic streak - in previous example it is  $\{0.37\}$ .

#### References:

-----  
 394.1 Coloring Real Line - [EggletonErdosSkilton] -  
[http://ac.els-cdn.com/0095895685900395/1-s2.0-0095895685900395-main.pdf?\\_tid=3b53ab92-03ec-11e7-870e-00000aabb0f01&acdnat=1488970060\\_784d7a37e58d4662a8e474c62a6c8ae7](http://ac.els-cdn.com/0095895685900395/1-s2.0-0095895685900395-main.pdf?_tid=3b53ab92-03ec-11e7-870e-00000aabb0f01&acdnat=1488970060_784d7a37e58d4662a8e474c62a6c8ae7)  
 394.2 Coloring Reals - <http://webbuild.knu.ac.kr/~trj/HN.pdf>  
 -----

-----  
 395. (FEATURE-DONE) Deep Learning Recurrent Neural Network Gated Recurrent Unit (RNN GRU) Implementation - 9 March 2017  
 -----

-----  
 \*) This commit implements Gated Recurrent Unit algorithm (most recent advance in deep learning - published in 2014) which is a simplification of RNN LSTM by reducing number of gates (input, cell, forget, output are mapped to cell, reset, update)  
 \*) Logs for this have been uploaded to testlogs/ showing convergence of gates and state.  
 -----

-----  
 396. (FEATURE-DONE) Recursive Lambda Function Growth + Tensor Neuron (NTN) Intrinsic Merit - 13 March 2017 - related to 384, 385  
 -----

-----  
 \*) This commit rewrites the Recursive Lambda Function Growth implementation by adding a new lambda function growth function.  
 \*) This new function creates a definition graph with Recursive Gloss Overlap algorithm from a text and computes all pairs shortest paths in the graph  
 \*) For each such shortest path edges, an AVL lambda function composition balanced tree is grown (i.e every path is a lambda function composition tree).  
 \*) Tensor Neuron Lambda Function is computed for each subtree root by following relation evaluated on a stack:  
     function(operand1, operand2)  
 where operand1, operand2 and function are successively popped from AVL composition tree stack representation  
 \*) Tensor Neuron triplet (operand1, function, operand2) is evaluated presently as maximum Wu-Palmer similarity of Synsets for cartesian product of operand1 and operand2. But it can be augmented with any arbitrary weighting scheme. Cartesian product of Synsets for 2 entities is the simplest 2-dimensional tensor neuron.  
 \*) Sum of tensor neuron weights for all random walks composition tree evaluation is printed as merit of the text.  
 \*) Logs for this have been committed to testlogs  
 -----

-----  
 397. (FEATURE-DONE) Korner Entropy Intrinsic Merit for Recursive Gloss Overlap graphs - 14 March 2017 - related to 383  
 -----

-----  
\*) Implemented Korner Entropy intrinsic merit for Recursive Gloss Overlap graph.  
\*) function korner\_entropy() finds maximal independent sets for all vertices and chooses the minimum entropy such that a vertex is in a maximal independent set.  
\*) Logs for this have been committed to testlogs/

Previous two intrinsic merit measures - tensor neuron network and korner entropy - sufficiently quantify the complexity of a document's inner purport. Neuron Tensors transform the ontology subgraph of a text into a new kind of multilayered graph perceptron. Infact it generalizes traditional multilayered trellis perceptrons for which backpropagation is applied to find weights per activation edge. There is no known backpropagation algorithm for generic graph of perceptrons. Neuron Tensors per word-word edge are equated to a lambda function and compositional tree of these neurons for any walk on the text-graph is an alternative deep learning technique to backpropagation. Korner Entropy is a measure of disconnectedness (total probability of vertices in independent sets). Presently all pairs shortest paths is used in place of random walks - set of all pairwise path tensor neuron lambda compositions is an upperbound on set of all random walks.

-----  
398. (FEATURE-DONE) Software Analytics update - 15 March 2017  
-----

-----  
\*) Software Analytics Deep Learning code has been updated to include all Deep Learning implementations: RNN LSTM, RNN GRU, BackPropagation and ConvolutionNetwork+BackPropagation  
\*) logs for this have been committed to software\_analytics/testlogs/

-----  
399. (USECASE) NeuronRain Usecases - Software (Log) Analytics and VIRGO kernel\_analytics config - 16 March 2017  
-----

-----  
Software Analytics Deep Learning implementation in python-src/software\_analytics/ sources its input variables - CPU%, Memory%, TimeDuration% for a process from logs. VIRGO kernel\_analytics module reads machine learnt config variables from kernel\_analytics.conf and exports them kernelwide. An example single layer perceptron usecase is:

```
 If the CPU% is > 75% and Memory% > 75% and TimeDuration% > 75% then
 do a kernelwide overload signal
 else
 do nothing
```

Sigmoid function for this usecase is:

$\text{sigma}(4/9 * x1 + 4/9 * x2 + 4/9 * x3)$  where  $x1 = \text{CPU\%}$ ,  $x2 = \text{Memory\%}$  and  $x3 = \text{TimeDuration\%}$   
which is 1 when all variables reach 75%.

Spark Streaming Log Analyzer ETLs htop data to .parquet files and Software Analytics code reads it, deep-learns above neural network and writes a key-value variable OverloadSignal=1 to VIRGO kernel\_analytics.conf. VIRGO kernel\_analytics driver reads it and exports a kernelwide variable kernel\_overload=1. Any interested kernel driver takes suitable action based on it (automatic shutdown, reboot, quiesce intensive applications etc.,)

An inverse of this usecase is to find the weights for  $x1, x2, x3$  when system crashes. This requires a gradient descent or backpropagation with multilayered perceptron.

-----  
400. (THEORY) Mechanism Design, Condorcet Jury Theorem, Derandomization, Gibbard-Satterthwaite Theorem and Designing a Voting Mechanism  
- 27 March 2017 , 30 March 2017, 31 March 2017, 18 April 2017 - related to 368 and all other P(Good) circuit related sections  
-----

Gibbard-Satterthwaite theorem prevents any Social Choice Function defined on at least 3 elements from being non-dictatorial. Mechanism Design is the reverse game theory which tries to circumvent this limitation and designs a mechanism for required result for social goodness. With respect to P(Good) series and circuit, design of a voting mechanism for arbitrary number of voters which overcomes limitation of Gibbard-Satterthwaite Theorem would imply convergence of P(Good) series. This is related to exact learning of boolean social choice functions with zero-error in 368.6. Open question: Does exact learning of a voter decision function imply a voting mechanism design?

A simple example of strategic/tactical voting and Gibbard-Satterthwaite theorem is given in <http://rangevoting.org/IncentToExagg.html>. Here by changing the ranking preferences (i.e voter switch loyalties by manipulation, tactical and strategic voting, bribery, bounded rationality and erroneous decision etc.,) result of an election with at least 3 candidates can be changed. Thus majority voting is vulnerable to error. Gibbard-Satterthwaite Theorem applies to all voting systems including secret ballot because even discreet voter can be psychologically influenced to change stance against inherent desire.

This implies for more than 3 candidates, RHS of P(Good) series for majority voting can never converge because there is always a non-zero error either by bounded rationality or manipulation. By pigeonhole principle either some or all of voters contributing to the P(Good) summation must have decided incorrectly or manipulated with non-zero probability. But this requires voter decision function (i.e social choice function) to be non-boolean (Candidates are indexed as 0,1,2,...). Exact learning of boolean functions applies to only 2 candidates setting where candidates are indexed as 0 and 1. Also, LHS of P(Good) series which is a (or quite close to a dictatorship by Friedgut-Kalai-Nisan quantitative version of Gibbard-Satterthwaite theorem) dictatorship social choice function, would be strategyproof (resilient to error and manipulative voting) and thus may have greater goodness probability (which is a conditional probability on chosen one's goodness) than RHS in more than 3 candidates setting.

Condorcet Jury Theorem mentioned in references below, is exactly the P(Good) binomial series summation and has been studied in political science and social choice theory. This theorem implies majority decision is better and its goodness probability tends to 1 than individual decision if probability of correct decision making for each voter is  $> 0.5$ . In the opposite case majority decision goodness worsens if individual decision goodness probability is  $< 0.5$ . Thus majority voting is both good and bad depending on individual voter decision correctness. In terms of BP\* complexity definitions, if each voter has a BP\* social choice function (boolean or non-boolean) with  $p > 0.5$ , accuracy of majority voting tends to 100% correctness i.e Composition  $\text{Maj}_n(\text{BPX}_1, \text{BPX}_2, \dots)$  for some complexity class  $\text{BPX}_i$  for each voter implying derandomization (this also implies  $\text{BPX} = \text{X}$  if  $\text{Maj}_n(\text{BPX}_1, \text{BPX}_2, \dots)$  composition is in  $\text{BPX}$ ). Proof of BPP ! = P would imply there is at least one voter with  $p < 0.5$ . Condorcet theorem ignores dependency and unequal error scenarios but still holds good by central limit theorem (because each voter decision is a random variable +1 or -1 and sum of these random variables for all voters tends to gaussian by CLT) and law of large numbers.

Corollary: From 129 and 368, depth of Majority voting circuit composition can be unbounded and if all voter social choice functions have same number of variables and number of voters is exponential in number of variables, Majority voting circuit composition with error is in BPEXP than PH. By Condorcet Jury Theorem,

if all voters tending to infinity decide correctly with probability  $> 0.5$ , then BPEXP derandomizes to EXP  $\Rightarrow$  BPEXP=EXP. Non-boolean social choice functions for more than 2 candidates are usually preference profiles per voter (list of ranked candidates per voter) and top-ranked candidate is voted for by the voter.

If Majority Voting Circuit is in BPP, which is quite possible if number of voters is polynomial in number of variables and circuit is of polynomial size and because from Adleman's Theorem (and Bennet-Gill Theorem), BPP is in P/poly, BPP derandomizes to P for infinite electorate with decision correctness probability  $> 0.5$  for all voters. Thus homogeneous electorate of high decision correctness ( $> 0.5$ ) implies both BPEXP=EXP and P=BPP.

Locality Sensitive Hashing accumulates similar voters in a bucket chain. The social choice function is the distance function. Circuit/Algorithm for Multiway contest social choice (generalization of Majority boolean function) is:

- \*) Locality Sensitive Hashing (LSH) for clustering similar voters who vote for same candidate

- \*) Sorting the LSH and find the maximum size cluster (bucket chain)

#### References:

-----

400.1 Mechanism Design, Convicting Innocent, Arrow and Gibbard-Satterthwaite Theorems - [https://ocw.mit.edu/courses/electrical-engineering-and-computer-science/6-254-game-theory-with-engineering-applications-spring-2010/lecture-notes/MIT6\\_254S10\\_lec21.pdf](https://ocw.mit.edu/courses/electrical-engineering-and-computer-science/6-254-game-theory-with-engineering-applications-spring-2010/lecture-notes/MIT6_254S10_lec21.pdf)

400.2 Electoral Fraud, Gibbard-Satterthwaite Theorem and its recent extensions on manipulative and strategic voting, Cake cutting Multi Agent Resource Allocation Protocols - <https://www.illc.uva.nl/COMSOC/theses/phd-schend.pdf>

400.3 Condorcet Jury Theorem in Political Science -

[http://www.stat.berkeley.edu/~mossel/teach/SocialChoiceNetworks10/](http://www.stat.berkeley.edu/~mossel/teach/SocialChoiceNetworks10/ScribeAug31.pdf)

ScribeAug31.pdf - Asymptotic closed form and convergence of  $P(\text{Good})$  binomial summation when probability of good decision  $> 0.5$  uniformly for all voters was already solved by Condorcet 2 centuries ago :

"... Condorcet's Jury theorem applies to the following hypothetical situation: suppose that there is some decision to be made between two alternatives + or -. Assume that one of the two decisions is 'correct,' but we do not know which. Further, suppose there are  $n$  individuals in a population, and the population as a whole needs to come to a decision. One reasonable method is a majority vote. So, each individual has a vote  $X_i$ , taking the value either +1 or -1 in accordance with his or her opinion, and then the group decision is either + or - depending on whether  $S_n = \sum_{i=1}^n X_i$  is positive or negative. Theorem 1.1. (Condorcet's Theorem) [4] If the individual votes  $X_i$ ,  $i = 1, \dots, n$  are independent of one another, and each voter makes the correct decision with probability  $p > 1/2$ , then as  $n \rightarrow \infty$ , the probability of the group coming to a correct decision by majority vote tends to 1. ..."

400.4 Strategic Voting and Mechanism Design - [VinayakTripathi] -

<https://www.princeton.edu/~smorris/pdfs/PhD/Tripathi.pdf>

400.5 Condorcet Jury Theorem and OCR - Section 2 -

<http://math.unipa.it/~grim/Jlamlouisa.PDF>

400.6 Condorcet Jury Theorem graph plots -

<http://www.statisticalconsultants.co.nz/blog/condorcets-jury-theorem.html>

400.7 Probabilistic Aspects of Voting - Course Notes -

[www.maths.bath.ac.uk/~ak257/talks/Uugnaa.pdf](http://www.maths.bath.ac.uk/~ak257/talks/Uugnaa.pdf) - Condorcet Jury Theorem, Bertrand Ballots Theorem and Gibbard Random Dictatorship Theorem

400.8 Law of Large Numbers and Weighted Majority - [Olle Haggstrom, Gil Kalai, Elchanan Mossel] - <https://arxiv.org/abs/math/0406509v1>

400.9 Thirteen Theorems in search of truth -

<http://www.socsci.uci.edu/~bgrofman/69%20Grofman-Owen-Feld-13%20theorems%20in%20search%20of%20truth.pdf> - Condorcet Jury Theorem for Heterogeneous voters

(voters with unequal decision correctness probability - Poisson-binomial distribution) - same as Condorcet Jury Theorem for Homogeneous voters (voters with equal decision correctness probability) when correctness probabilities are a Gaussian and  $> 0.5$ . In other words, large majority is more correct than small majority.



400.10 Margulis-Russo Formula and Condorcet Jury Theorem -  
<http://www.cs.tau.ac.il/~amnon/Classes/2016-PRG/Analysis-Of-Boolean-Functions.pdf> - pages 224-225 - Majority function is defined in Erdos-Renyi Random graph model with each edge having probability  $p$ .  $\text{Maj}(N, G)$  for a random graph  $G$  with probability of edge being  $p = \text{True}$  of  $G$  has at least  $N/2 = |V| * (|V| - 1)/4$  edges. Majority voting can be defined as a random graph with each voter being an edge with decision correctness probability  $p$  i.e Probability of Existence of an edge increases with correctness of decision by voter. Margulis-Russo formula describes the sharp threshold phenomenon for boolean functions and rate of change of  $P(\text{Maj}(G))=1$  with respect to  $p$ , specifically for majority boolean function. Thus it is an alternative spectacle to view  $P(\text{Good})$  majority voting binomial coefficient summation and Condorcet Jury Theorem. For majority function, sharp threshold occurs at  $p \geq 0.5$ .  
400.11 Percolation, Sharp Threshold in Majority, Condorcet Jury Theorem and later results, Influence, Pivotality -  
<http://www.cs.tau.ac.il/~safra/PapersAndTalks/muligil.old.pdf>  
400.12 Complexity Inclusion Graph -  
<https://www.math.ucdavis.edu/~greg/zoology/diagram.xml> -  $\text{BPEXP}=\text{EXP}$  implies a significant collapse of the complexity class separation edges.

-----  
401. (FEATURE-DONE) LSH Index implementation for NeuronRain AsFer Text and Crawled Web Documents Intrinsic Merit Ranking - 4 April 2017  
-----

-----  
\*) This commit adds a Locality Sensitive Hashing based inverted index for scrapy crawled HTML website pages.  
\*) It is a derivative of LSH based similarity clustering implemented in python-src/LocalitySensitiveHashing.py  
\*) It has to be mentioned here that ThoughtNet is also an inverted index for documents with additional features (i.e it is classifier based than raw string similarity)  
\*) LSHIndex uses Redis Distributed Key Value Persistent Store as hashtable backend to store index.  
\*) LSHIndex is not string to text inverted index, but hashed string to text inverted index (something like a digital fingerprint)  
\*) Presently two types of hashes exist: primitive ordinal and MD5 hash  
\*) Only one hash table is implemented on Redis with multiple hash functions with random choice.  
\*) Presently 50 hash functions with 50 entries hash index has been implemented.  
-----

-----  
402. (FEATURE-DONE) ThoughtNet Index implementation for NeuronRain AsFer Text and Crawled Web Documents Intrinsic Merit Ranking - 4 April 2017  
-----

-----  
\*) This commit implements an inverted index on top of ThoughtNet  
\*) ThoughtNet is a hypergraph stored in file and on Neo4j Graph Database  
\*) JSON loads ThoughtNet edges and hypergraph files and queries by classes returned by Recursive Gloss Overlap classifier  
\*) Querying Neo4j is also better, but file representation of ThoughtNet is quite succinct and scalable because it just numerically encodes each edge (= a web crawled HTML document)  
\*) file representation of ThoughtNet views the hypergraph as stack vertices interconnected by document id(s) similar to a source code versioning system. Having similar view on a graph database doesn't look straightforward  
-----

-----  
403. (FEATURE-DONE) Initial commits for Indexless Hyperball Recursive Web Crawler - 7 April 2017  
-----

-----  
-----  
\*) An indexless crawler which tries to find a url matching a query string in a recursive crawl creating a hyperball of certain radius  
\*) This is similar to Stanley Milgram, Kleinberg Lattice Small World Experiments and recent Hyperball algorithm for Facebook graph which concluded that Facebook has 3.74 degrees of freedom.  
\*) Starts with a random url on world wide web.  
\*) Success probability depends on average number of hops over large number of queries.  
\*) This is a Randomized Monte Carlo Crawler and does a Depth First Search from an epicentre pivot url to start with  
\*) Hyperball References:  
1)  
<http://webgraph.di.unimi.it/docs/it/unimi/dsi/webgraph/algo/HyperBall.html>  
2) Facebook Hyperball - <https://arxiv.org/pdf/1308.2144.pdf>  
-----

-----  
404. (THEORY) Indexless Web Search, World Wide Web Graph Property Testing, On-demand Indexing - related to 403 - 9 April 2017  
-----

-----  
Almost all known web search engines rely on a pre-built index created from already crawled WWW graph. Is a pre-built index necessary for web search? Can the small world property of world wide web graph (i.e property of graph such that easy short paths exist between any pairs of vertices as proved in Stanley Milgram experiment, Kleinberg Lattice), be applied to find a url matching a search query starting from any vertex? Facebook graph has almost a billion user vertices and on an average any person is connected to any other within 3.74 path lengths. Can this be generalized to world wide web? Traditional book index maps word queries to pages having the words. If entire book is translated into a huge definition graph by Recursive Gloss Overlap graph, then instead of looking-up index, starting at a random word vertex, any other word should be easily reachable if graph has small world property. This realworld problem is already studied as Graph Property Testing which are algorithms to test if a graph has specific property(clique, colorability, edge and vertex queries etc.,). Hyperball indexless crawler in NeuronRain AsFer is an effort in this line of thought. Such an indexless crawler can "learn" an index online by repeated queries and build an index from cached results at runtime. Index is not prebuilt but grown ondemand. Assuming internet has such small world degrees of freedom upperbounded by a constant, any query is constant time serviceable in average case complexity.  
-----

References:

-----  
404.1 Small World Property - [WattsStrogatz]  
-<http://www.nature.com/nature/journal/v393/n6684/full/393440a0.html>  
-----

-----  
405. (FEATURE-DONE) Commit - NeuronRain AsFer-CPython Extensions VIRGO64 system call invocations - 20 April 2017  
-----

-----  
\*) VIRGO64 system calls are invoked from Python code by CPython extensions.  
\*) Separate folder cpython\_extensions64/ has been created for 64bit VIRGO kernel  
\*) Requires Python 64-bit version  
\*) Logs for VIRGO64 memory and filesystem systemcalls-to-drivers have been committed to testlogs  
\*) With this Complete Application Layer-SystemCalls-Drivers request routing for python applications deployed on VIRGO64 works.  
-----

-----  
-----  
406. (FEATURE-DONE) Commits - NeuronRain AsFer Boost C++-Python - VIRGO64 System calls + Drivers invocation - 26 April 2017  
-----

-----  
\*) VIRGO64 system calls are invoked from C++ by Boost::Python extensions  
\*) Kernel Logs for VIRGO KMemCache, Clone and FileSystem Calls Boost::python invocations have been committed to testlogs/  
\*) Boost version used is 1.64.0  
\*) setup.py has been updated with library\_dirs config variable  
\*) virgofstest.txt for filesystem calls has been committed to testlogs/  
-----

-----  
407. (FEATURE-DONE) Commits - 28 April 2017 - NeuronRain AsFer-Boost::Python-C++ - VIRGO64 systemcalls and drivers invocations  
-----

-----  
\*) VIRGO64 clone, kmemcache and filesystem system calls were invoked from Python-C++ boost extensions again and reproducibly work without kernel panics.  
\*) Logs, persisted disk file written by filesystem system calls and rebuilt boost-python C++ extensions have been committed to testlogs/  
-----

-----  
408. (THEORY) Condorcet Jury Theorem, Collaborative Filtering, Epistemological Democracy, Network Voting in WWW Link Graph, Majority Function and Correctness of Majority Vote Ranking - 16 May 2017, 23 May 2017  
-----

-----  
Let  $v_1, v_2$  be two vertices being good and bad choices respectively. In link graph all incoming edges to a vertex  $v_1$  are votes for that vertex. From Condorcet Jury Theorem if all incoming links occur with probability  $p > 0.5$ , then probability that  $v_1$  is chosen tends to 1 for large indegree. For 2 candidates  $c_1, c_2$  and voters  $v_1, v_2, v_3, \dots, v_n$ , edges (votes) to  $c_1$  occur with probability  $p$  and edges (votes) to  $v_2$  occur with probability  $1-p$ . Thus voting graph is a random bipartite graph and can be generalized to multiple candidates. Candidates Vertex set  $C=\{c_1, c_2, \dots, c_n\}$  can have more than one indegree and zero outdegree. Voters Vertex set  $V=\{v_1, v_2, \dots, v_n\}$  can have only one outdegree and zero indegree. If  $C$  intersection  $V \neq \text{emptyset}$ , then graph is general directed graph and can have cycles. Each voter vertex  $v_y$  either votes to some other vertex  $v_x$  or receives vote from  $v_x$ .  $v_y$  votes for  $v_x$  with probability  $p$ .  $v_y$  votes for vertices other than  $v_x$  with cumulative probability  $1-p$ . Vertices voted by  $v_y$  are ranked by goodness (i.e.  $\text{goodness}(v_x) > \text{goodness}(\text{others})$ ). If  $v_y$  votes for  $v_x$  then  $v_y$  decides with decision correctness probability  $p$ .

More generically, vertex  $v_x$  receives votes from vertices  $v_{y2}, v_{y2}, v_{y3}, \dots, v_{yn}$  with decision correctness probability  $p$ . Vertices  $v_{y1}, v_{y2}, v_{y3}, \dots, v_{yn}$  vote for vertices other than  $v_x$  with decision correctness probability  $1-p$ . Each vertex in WWW link graph has this 2 level tree structure with varying probability  $p_i$ . From Condorcet Jury Theorem, hyperlinks to  $v_x$  from  $v_{y1}, v_{y2}, \dots, v_{yn}$  are 100% correct group decision if  $p > 0.5$ . Equal  $p$  for all votes to a vertex is the homogeneous voter assumption of Condorcet Jury Theorem. If the vertices are ranked by some algorithm (HITS Hub-Authority, PageRank etc.,) then correctness of rank is measured by Condorcet Jury Theorem. It is apt to mention here that probability  $p$  is different from weights of directed graph edges in PageRank Markov Random Walk iteration (where weight of outgoing edge/vote is decided by the ratio  $1/\text{outdegree}$ ) in the sense that:  $1/\text{outdegree}$  is the static percentage of vote to an adjacent vertex in a non-random graph while  $p$  in network voting is a dynamic measure for decision correctness of a vote to a vertex in a random graph. For

heterogeneous voter assumption, more recent theorems which generalize Condorcet Jury Theorem are required.

Collaborative Filtering in Recommender Systems is the most generalized way of Majority Voting where a matrix of users to their preferences for items is used as a training data for a new user to recommend an item. For example, if 9 out of 10 users up vote an item, 11th user is recommended that item and viceversa for down votes. Above analysis is an alternative direction for defining value judgement correctness already discussed in references 408.1 and 408.2. Correlated Votes and their effects on Condorcet Jury Theorem are analyzed by [KrishnaLadha].

References:

-----  
408.1 Condorcet Jury Theorem and the truth on the web -

<http://voxxpublica.no/2017/03/condorcets-jury-theorem-and-the-truth-on-the-web>

408.2 Webometrics, Goodness of PageRank and Condorcet Jury Theorem -

[MastertonOlssonAngere] - <https://link.springer.com/article/10.1007/s11192-016-1837-1> - PageRank is very good in finding truth i.e it is close to objective judgement with certain empirical assumptions despite being subjective ranking measure. Here objective judgement is any value judgement which is not majority voting or subjective. Computational linguistic text graph analysis which reckons the psychological aspects of text comprehension is an objective intrinsic merit judgement. Ideally majority vote should coincide with objective judgement absence of which implies error in voting or objective judgement or both (family of BP\* complexity classes).

408.3 Generalized Condorcet Jury Theorem, Free Speech, Correlated Voting (dependence of voters) - <https://www.jstor.org/stable/2111584>

-----  
409. (FEATURE-DONE) Commits - 17 May 2017 - NeuronRain AsFer-VIRG064 Boost-C++-Python invocations  
-----

-----  
\*) Boost Python C++ VIRG064 system calls were tested repeatedly in a loop  
\*) All three system call subsystems - virgo\_clone, virgo\_kmemcache, virgo\_filesystem - work well without any kernel panics  
\*) But a strange thing was observed: virgo filesystem system calls were not appending to disk file but when run as "strace -f python asferpythonextensions.py" disk file is written to (a coincidence or strace doing something special)  
-----

-----  
410. (THEORY) Objective and Subjective Value Judgement, Text Ranking and Condorcet Jury Theorem - 29 May 2017 and 4 June 2017 - Related to 202, 384, 385 and all Recursive Lambda Function Growth and Recursive Gloss Overlap algorithms sections in this document  
-----

-----  
Objective merit or Intrinsic merit of a document is the measure of meaningfulness or information contained in a document. Subjective merit is how the document is perceived - Reality Versus Perception - Both should ideally coincide but do not.

Following are few real-world examples in addition to academic credentials example in 202:

\*) Soccer player, Cricket player or a Tennis player is measured intrinsically by number of goals scored, number of runs/wickets or number of grandslams won respectively and not subjectively by extent of votes or fan following to them (incoming edges). Here reality and perception coincide often and an intrinsically best player by records is also most revered. Any deviation is because of human prejudice. Here intrinsic merit precedes social prestige.

\*) Merits of students are judged by examinations (question-answering) and not by majority voting by faculty. Thus question-answering or interview is an algorithm to measure intrinsic merit objectively. Here again best student in terms of marks or grades is also the most favoured. Any deviation is human prejudice. Interview of a document is how relevant it is to a query measured by graph edit distance between recursive gloss overlap graphs of query and text. Here also intrinsic merit precedes social prestige.

Present ranking algorithms are mostly majority voting (perception) oriented which is just half truth. Other half is the reality and there are no known algorithms to objectively judge documents. Recursive Lambda Function Growth algorithm and its specialization Recursive Gloss Overlap graph are objective intrinsic merit algorithms filling this void and try to map above real-life examples to text document ranking.

But how to measure "number of goals etc.," of a document vis-a-vis the rest? This is where Computational Linguistic Text-to-Graph analysis fits in. Graph representation of a document with various quantitative and qualitative graph complexity measures differentiates and grades the texts by intrinsic complexity. This combines two fields: Computational Linguistics which is founded on Psychoanalysis and Graph Theory. Former pertains to mental picture created by reading a document and latter is how complex that picture is. Recursive Lambda Function Growth envisages an ImageNet which is a graph of related images of entities to create an animated movie representation of a text stored as a subgraph of ImageNet. ImageNet (pictorial WordNet) is not yet available.

Condorcet Jury Theorem formalizes above intuition and bridges two worlds - objective reality and subjective perception. A best performing student by objective examination/interview assessment is also the most voted by infinite faculty if correctness of decision  $> 0.5$  for all faculty voters i.e. Objective Intrinsic Merit = Subjective Perception based Majority Voting Merit.

Crucial Observation is: Merit creates Centrality (Social prestige) and not the opposite - Prestige can not create merit but can only be a measure of merit. Otherwise this is an anachronism - merit does not exist yet but prestige exists and thus prestige preceding merit.

Alternatively, interview of document is simply the rank of the document in terms of intrinsic graph complexity merit of it versus the rest of the text documents. Thus there are 2 aspects of interview:

- \*) Ranking text document by intrinsic graph complexity/entropy merit
- \*) Relevance of the text to a query - graph edit distance

Here again another question can be raised: Why is a graph representation of text an apt objective intrinsic merit measure? Because, by "Circuits of Mind" and "Mind grows circuits/lambda functions" theories (cited in previous sections), biological neurons are connected as a graph and information from sensory perception is transmitted through these neurons. Threshold TC circuits theoretically formalize neural networks. Better neuroimaging techniques for quantifying the potentials created in brain by cerebral representation of a text could be ideal relevance measures and can be substituted in Tensor Neuron Model of Recursive Lambda Function Growth algorithm.

There is special case of intrinsic merit: For example, reading a story creates a mental picture of it as a graph of events. Objectively judging it could vary from one human to the other making it subjective. But still the absolute objective merit can be defined for such a special case by applying EventNet to this problem - whole set of events are laid out as events with partakers with cause-effect edges amongst them.

References:

-----

410.1 The Meaning of Meaning -

<http://courses.media.mit.edu/2004spring/mas966/Ogden%20Richards%201923.pdf>

#### 410.2 WordNet and Word2Vec -

<https://yaledatascience.github.io/2017/03/17/nnnlp.html> - In word2vec words from text are represented in a vector space and contextually related words are close enough in proximity on vector space. Word2Vec is a recent neural network model of word relations similar to Neural Tensor Network (NTN). NTN defines a relation between two words as a tensor neuron and thus complete WordNet can be defined as a graph with Tensor Neuron as edge potentials. This is the motivation for invoking Neural Tensor WordNet as an objective intrinsic merit indicator as it approximates human brain neurological text comprehension and visualization.

410.3 Random Walks on WordNet - <http://anthology.aclweb.org/N/N15/N15-1165.pdf> - Recursive Lambda Function Growth algorithm does something similar to this. It finds all random walks on Recursive Gloss Overlap graph (described in 385) and constructs a lambda function composition tree for each such walk and assigns a Neural Tensor Potential to each edge of these trees.

410.4 ImageNet - Pictorial WordNet - <http://www.image-net.org/> - image net is recently available. In the context of Recursive Lambda Function Growth, lambda functions inferred from ImageNet than WordNet/ConceptNet are pictures and composition of the lambda functions translates to animating the pictures based on PoS or tensor relation. For example the composition for "It rained heavily today", `rained(It, heavily(today))`, should theoretically compose/superpose/animate images for day, heaviness, rain from leaves to root of the tree.

-----  
411. (FEATURE-DONE) AngularJS - Tornado GUI-REST WebService - Commits - 1 June 2017  
-----

-----  
NeuronRain AngularJS RESTful client for Tornado webserver and others  
-----

\*) AngularJS support has been added to NeuronRain GUI-WebServer with a new `webserver_rest_ui/NeuronRain_AngularJS_REST_WebServer.py` which reads and renders angularjs Model-View-Controller templates

\*) New AngularJS Model, View and Controller script-html templates have been added to angularjs directory

\*) LSHIndex.py has been updated to have commandline arguments for index queries

\*) Hyperball Crawler pivot epicentre url has been changed and an example query "Chennai" was found to be matching within few hops.

\*) NeuronRain\_REST\_WebServer.py has been updated to print the logs for the script execution to browser console with subprocess POpen() , communicate() and poll() python facilities

-----  
412. (THEORY) Graph Neural Networks, Tensor Neurons and Recursive Lambda Function Growth Intrinsic Merit - 4 June 2017 and 8 June 2017 - related to 410  
-----

Definition Recursive Gloss Overlap Graph with word-word edges as Neuron Tensor Network relations having potentials was defined previously. Recursive Lambda Function Growth computes all random walks of the definition graph and creates a lambda function composition tree for each such random walk. For each subtree  $f$  of the recursive lambda function growth with children  $w1$  and  $w2$  composed potential for  $f$  is defined as:

$$p(f(w1,w2)) = p(w1) * p(w2) \text{ for some operator } *$$

Rather than mere summation of potentials of edges following minmax criterion extracts the most meaningful random walk:

\*) Minimum Neuron Tensor Potential edge of each random walk is found - path

minimum potential

\*) Maximum of all minimum path potentials extracts a random walk lambda composition tree which is the most probable inferred meaning of the document -  $\text{Max}(\text{Min}(\text{potentials}))$  - this makes sense because maximum of minimum potential implies minimum possible neural activation.

Event Related Potentials (ERP) mentioned in 202 are unusual spikes in EEG of brain (N400 dataset) when unrelated words are read. Complement of ERP for related words as dataset could be an ideal estimator for Neuron Tensor relatedness potential between two words in definition graph.

Graph Neural Networks are recent models of neural network which generalize to a graph. In a Graph Neural Network, potential of each vertex is a function of potentials of all adjacent vertices and neuron tensor potentials of incoming edges from them. Neuron Tensor Network edge relations for each word vertices pair of Recursive Gloss Overlap Graph can be mapped to edges of a Graph Neural Network. Thus a text is mapped to not just a graph but to a Graph Neural Network with Tensor Neuron Edges, an ideal choice for human text comprehension simulation. Recursive Gloss Overlap Graph with Neuron Tensor word-word edges combines two concepts into one - Graph Tensor Neuron Network (GTNN).

Data on websites can be classified into 3 categories: 1) text 2) voice 3) images and videos. Intrinsic merit which is a measure of creativity presently focuses only on text. Analyzing the intrinsic merit of voice and visuals is a separate field in itself - Fourier Analysis of Waveforms and Discrete Fourier Transforms.

Ranking text by Graph Tensor Neuron Network intrinsic merit potential can be done in multiple ways:

- Rank Vertices and Edges by potential
  - Rank the random walk lambda function composition tree by potential
  - Rank by Korner Entropy of the Graph Tensor Neuron Network and other qualitative and quantitative graph complexity metrics.
- and so on.

Example lambda composition tree on a random walk of recursive gloss overlap graph:

```
f1 = requiredby(fuel, flight)
f2 = has(flight, tyre)
f3 = has(tyre, wheel)
f4 = does(wheel, landing)
f5 = requires(landing, gear)
f1(fuel, f2(flight, f3(tyre, f4(wheel, f5(landing, gear)))))
```

Previous example random walk lambda composition tree has been constructed in 384 and 385. Potentials for Tensor Neuron Relations have to be predetermined by a dataset if such exists similar to N400 EEG dataset. Tensor Neuron Relations in Recursive Gloss Overlap Definition Graph are grammatical connectives mostly. In this example, "requiredby" is a relation. Cumulative potential of each such random walk lambda composition tree has to be computed.

Difference in Graph Tensor Neuron Network mapping of a text is: Each lambda composition tree is evaluated as a Graph Neural Network - each subtree is evaluated and passed on to higher level - and potential at the root is returned as the merit. Mixing time in markov chain andom walk is the number of steps before stationary distribution is attained. Thus maximum potential returned at the root of (a lambda composition graph tensor neuron network of (any converging stationary random walk of (a recursive gloss overlap definition graph of (a text)))) is a measure of intrinsic merit.

Intuition for Graph Tensor Neuron Network is below:

- \*) Random walk on recursive gloss overlap graph simulates randomness in cognitive cerebral text comprehension.
- \*) Tensor Neuron relatedness potential between two word vertices in definition graph quantifies relevance and meaningfulness

\*) Lambda composition tree-graph neural network for each random walk on definition graph simulates how meaning is recursively understood bottom-up with randomness involved.

#### References:

-----  
412.1 Graph Neural Networks -

[http://repository.hkbu.edu.hk/cgi/viewcontent.cgi?article=1000&context=vprd\\_ja](http://repository.hkbu.edu.hk/cgi/viewcontent.cgi?article=1000&context=vprd_ja)  
-----

-----  
413. (FEATURE-DONE) Recursive Lambda Function Growth - Graph Tensor Neuron Network Implementation - Commits - 9 June 2017  
-----

-----  
(\*) Recursive Lambda Function Growth implementation has been updated to compute Graph Tensor Neuron Network intrinsic merit

(\*) Each lambda function composition tree of a random walk on recursive gloss overlap graph is evaluated as a Graph Neural Network having Tensor Neuron potentials for word-word edges.

(\*) Tensor neuron potential for relation edges in Graph Neural Network has been hardcoded at present and requires a dataset for grammatical connective relations similar to EEG dataset for brain spikes in electric potentials.  
-----

-----  
414. (FEATURE-DONE) Graph Tensor Neuron Network - implementation update - Commits - 10 June 2017  
-----

-----  
(\*) Changed the subtree graph tensor neuron network computation

(\*) Children of each subtree are the Tensor Neuron inputs to the subtree root. Each subtree is evaluated as a graph neural network with weights for each neural input to the subtree root.

(\*) WordNet similarity is computed between each child and subtree root and is presently assumed as Tensor Neuron relation potential for the lack of better metric to measure word-word EEG potential.

If a dataset for tensor neuron potential is available, it has to be looked-up and numeric potential has to be returned from here.

(\*) Finally a neuron activation function (simple 1-dimensional tensor) is computed and returned to the subtree root for next level.

(\*) logs for this have been committed to testlogs. Presently graph tensor neuron network intrinsic merit is a very small decimal because of the decimal values of similarity and tensor neurons, but quite receptive to small changes.  
-----

-----  
415. (FEATURE-DONE) Script for Querying Index (LSH and ThoughtNet) and Ranking the results with Recursive Lambda Function Growth - Commits - 13 June 2017  
-----

-----  
(\*) New python script QueryIndexAndRank.py has been committed for retrieving results from Index matching a query and rank them

(\*) It queries both Locality Sensitive Hashing and ThoughtNet indices



- \*) Functions of classes have been parametrized for invocation across modules
- \*) Both LSH and ThoughtNet indices have been recreated
- \*) Ranking is done by Recursive Lambda Function Growth algorithm which is a superset of Recursive Gloss Overlap
- \*) This script was tested via NeuronRain Tornado RESTful GUI

-----  
 416. (FEATURE-DONE) Graph Tensor Neuron Network Intrinsic Merit and QueryIndexAndRank update - Commits - 15 June 2017  
 -----

- \*) Graph Tensor Neuron Network Intrinsic Merit computation has been changed - Intrinsic merits of all random walks are summed up then multiplying to get a tangible merit value
- \*) Some bugs fixed and debug prints have been changed
- \*) logs have been committed to testlogs/

-----  
 417. (FEATURE-DONE) Hyperball crawler update - Commits - 19 June 2017  
 -----

Integrated Recursive Lambda Function Growth Intrinsic Merit Score(Graph Tensor Neuron Network and Korner Entropy) into Hyperball crawler.

-----  
 418. (THEORY) Thought Experiment of Generic Intrinsic Merit and Condorcet Jury Theorem - 21 June 2017  
 -----

Intrinsic merit so far is restricted to text documents. Subjective ranking measures are like mirrors which reflect the real merit of the candidate. Each vote in the majority voting is similar to an image of the votee projected on to the voter mirror. Some mirrors reflect well while others don't. Efficiency of a voter mirror is equivalent to decision correctness of a voter. Present web ranking algorithms measure votee by the perception mirror images, which is indirect. Intrinsic merit breaks mirror images and relies only on what the votee really is. But then isn't intrinsic merit a mirror image too? It is not because no human perception or image based voting is involved to ascertain merit. Only the graph complexity of the text-graph and its graph neural network is sufficient. Merit is a universal requirement. Examples in 410 and 202 motivate it. Can merit be applied to entities beyond voice, visuals and text? Most probably yes. Intelligence of human beings are ranked by intelligence quotients which is also an intrinsic merit measure (though IQ tests are disputed by psychological studies). Hence judging people by intrinsic merit is beyond just IQ scores. An algorithm to classify people as "Good" and "Bad" could be a breakthrough in machine intelligence. Hypothetical people classifier could be as below:

- (\*) Peruse academic records and translate to score
- (\*) Peruse work records and translate to score
- (\*) Translate awards received to score
- (\*) Translate brain imaging data to score (EEG and fMRI)
- (\*) Translate IQ or EQ to score

Above is not a formal algorithm but tries to intuit how it may look like. Human Resource Analytics are done as above

Objective Intrinsic Merit = Vote by an algorithm

Subjective Ranking = Votes by people translated into rank by an algorithm  
 (present ranking algorithms rely on incoming links or votes to a text which are created by human beings)

Thus Generic Intrinsic Merit removes human element completely while assessing

merit (closer to AI). Goodness when it applies to human beings is not just a record based score and usually has moral and ethical elements in it. People classifier based on intrinsic merit has to be intrusive and invasive similar to HR analytics example earlier.

(\*)Question: Why should intrinsic merit be judged only in this way?

(\*)Answer: This is not the only possible objective intrinsic merit judgement. There could be other ways too. Disclaimer is intrinsic merit assumes cerebral representation of sensory reception (words, texts, visuals, voices etc.,) and its complexity to be the closest to ideal judgement.

(\*)Question: Wouldn't cerebral representation vary from person to person and thus be subjective?

(\*)Answer: Yes, but there are standardized event related potential datasets gathered from multiple neuroscience experiments on human subjects. Such ERP data are similar for most brains. Variation in potential occurs because cerebral cortex and its sulci&gyri vary from person to person. It has been found that cortex and complexity of gray matter determine intelligence and grasping ability. Intrinsic merit should therefore be based on best brain potential data.

(\*)Question: Isn't perception based ranking enough? Why is such an intrusive objective merit required?

(\*)Answer: Yes and No. Perception majority voting based ranking is accurate only if all voters have decision correctness probability  $> 0.5$  from Condorcet Jury Theorem. PageRank works well in most cases because incoming edges vote mostly with  $>50\%$  correctness. This correctness is accumulated by a Markov Chain Random Walk recursively - vote from a good vertex to another vertex implies voted vertex is good (Bonacich Power Centrality) and so on. Initial goodness is based on weight of an edge. Markov iteration stabilizes the goodness. Probability that goodness of stationary Markov distribution  $< 0.5$  can be obtained by a tail bound and should be exponentially meagre.

It was mentioned earlier that Fourier analysis of visuals and voice is the measure of intrinsic merit. Following definition of generic intrinsic merit further strengthens it:

Generic intrinsic merit of an entity - text, visual or voice - is the complexity of cerebral representation potential as received by sensory perception. For texts it is the graph complexity measure. For voice and visuals it could ERPs activated on seeing or hearing and based on EEG data.

References:

-----  
418.1 Event Related Potentials for attractive facial recognition -  
<https://labs.la.utexas.edu/langloislab/research/event-related-potential-erp/>  
418.2 Event Related Potentials -  
[http://cognitron.psych.indiana.edu/busey/eegseminar/pdfs/Event-Related](http://cognitron.psych.indiana.edu/busey/eegseminar/pdfs/Event-Related%20PotentialsIntro.pdf)  
%2520PotentialsIntro.pdf - ERPs are cortical potentials of interoperating  
neurons in response to a cognitive stimulus.

-----  
419. (THEORY) Goodness of Link Graph Majority Voting and Complex Plane  
representation of merit - 22 June 2017 and 23 June 2017 - related to 418  
-----

Following is an example link graph in world wide web with weights for each edge:

y1 - x1 : 0.25  
y1 - x2 : 0.25  
y1 - x3 : 0.25  
y1 - x4 : 0.25

implying y1 votes to x1,x2,x3,x4 with weight 0.25 each.

Following is the corresponding initial decision correctness (goodness) graph with goodness for each edge:

$y_1 - x_1 : 0.25$   
 $y_1 - x_2 : 0.25$   
 $y_1 - x_3 : 0.375$   
 $y_1 - x_4 : 0.125$

implying  $y_1$  votes to  $x_1$  with correctness 0.25,  $x_2$  with correctness 0.25,  $x_3$  with correctness 0.375 and  $x_4$  with correctness 0.125.

Markov iteration on the decision correctness graph (similar to random walk on link graph) tends to a stationary distribution after certain number of random walks. Cumulative goodness of voter  $v_1$  is defined as:

$\text{summation}(\text{weight}(\text{edge}) * \text{goodness}(\text{edge}))$

For previous example cumulative goodness of voter  $y_1$  is:

$0.25*0.25 + 0.375*0.25 + 0.25*0.25 + 0.25*0.25 =$   
 $1/32 + 3/32 + 2/32 + 2/32 = 0.25$

If all votes are 100% correctly decided by  $y_1$ , correctness graph has 1 for all edge weights. Thus cumulative goodness of  $y_1$  is:

$0.25 * 1 + 0.25 * 1 + 0.25 * 1 + 0.25 * 1 = 1 = 100\%$

After markov iteration attains stationary distribution, cumulative goodness of all vertices also becomes stationary. Atleast one incoming vertex  $y$  voting to another vertex  $x$  having cumulative goodness  $< 0.5$  at the end of markov iteration implies group decision is a failure and does not concur with the real merit of a vertex  $x$ .

Following are the votes received by a vertex  $x_1$  from voters  $y_1, y_2, y_3, y_4$  having respective cumulative goodness:

$y_1 - x_1: 0.75$   
 $y_2 - x_1: 0.3$  (voter with cumulative goodness  $< 0.5$ )  
 $y_3 - x_1: 0.8$   
 $y_4 - x_1: 0.9$

What is the probability in average case that atleast one voting vertex has cumulative goodness  $< 0.5$ ? Link graph voting is different from normal voting - it is peer to peer and each voter apportions vote to the neighbouring candidates - single voter can vote multiple candidates simultaneously.

$\text{Pr}[\text{atleast one adjacent vertex } y \text{ to a candidate vertex } x \text{ has cumulative goodness } < 0.5 \text{ after markov iteration}] = 1 - \text{Pr}[\text{goodness} > 0.5]$

From Markov inequality tail bound,  $\text{Pr}[\text{cumulative goodness} > 0.5] \leq \text{mean}/0.5$

$\text{Pr}[\text{cumulative goodness} < 0.5] = 1 - \text{Pr}[\text{goodness} > 0.5] \geq 1 - \text{mean}/0.5$

where mean is the average cumulative goodness of all vertices in link graph.

When mean is 0.5 (uniform distribution),  $\text{Pr}[\text{cumulative goodness} < 0.5] \geq 1 - 0.5/0.5 = 0$

For any other values of mean  $< 0.5$ ,  $\text{Pr}[\text{atleast one adjacent vertex } y \text{ to a candidate vertex } x \text{ has cumulative goodness} < 0.5 \text{ after markov iteration}] = 1 - \text{mean}/0.5$  is always greater than zero.

In discrete random variable case, if goodness takes  $n$  discrete values between 0 and 1 then, mean =  $\text{summation}(x * p(x))$  where  $p(x) = 1/n$  is:

$n(n+1)/2 * n * n = 0.5 + 0.5/n$  which tends to 0.5 when  $n$  tends to infinity.

Thus mean cumulative goodness is 0.5 in uniform distribution.

Objective and Subjective rankings can be represented on a complex plane with following notation:

$(\text{intrinsic merit}=m) + i(\text{perception}=p) = m + ip$

where  $p$  is a function of  $m$ . Any text, visual or voice can be plotted on complex plane in previous notation. Ideally  $m$  should be equal to  $p$ . This creates a special case when  $m$  is fixed and  $p$  varies for an entity which usually happens with perception based majority voting. Such set of complex numbers with fixed merit and varying perception can be thought of as zeros of a complex valued function. Famous special case is Riemann Zeta Function with merit=0.5 and varying perception imaginary parts.

Riemann Hypothesis if true implies  $\text{Re}=0.5$  for non trivial zeros of Riemann Zeta Function. If a set of complex number rankings as described previously have  $\text{Re}=0.5$  or fixed real part and varying imaginary parts equalling non trivial zeros of Riemann Zeta Function, then the rankings show pattern in prime numbers an unusual connection.

Any k-coloring of a sequence of text and audio-visuals(AVs) denoted by integers is a classifier. 2-coloring or complementation is a special case of such a classifier. Conversely, any classifier is a coloring scheme for sequence of text and audio-visuals(AVs). For example following bit pattern is a 2-coloring/complement function - 0 and 1 are colors and f and g are complement functions illustrated as dotted indentations:

111100001111000011100001110001111100000

----- function f:  
..... complement g:

Vapnik-Chervonenkis Shattering or VC Shattering is defined as:  
Let H be a set of sets and C be a set. C is shattered by H if  $H \cap C = \text{powerset of } C = 2^C$ . Intuitively, H classifies C with labels from the set H. Largest cardinality of C shattered by H is the VC dimension.

2-coloring/complementation is a classifier on real line or integer sequences. 2 colors/binary encodings/complementations create a set H of size equal to powerset of real line of integer sequence. Largest cardinality of real line or integer sequence that can be shattered by H ( $H \cap C = 2^C$ ) is infinite. Thus 2-color/complementation classifier of infinite stream of sequences has VC Dimension Infinity.

References:

-----  
419.1 Probability and Statistics with Reliability, Queuing and Computer Science Applications - Pages 223-225 - [Kishor Shridharbhai Trivedi-Duke University]

-----  
420. (THEORY) Human Resource Analytics, Interview Algorithm and Intrinsic Merit - related to 314, 359 and 365 - 26 June 2017 and 27 June 2017  
-----

-----  
Stability of Interview TQBF circuit which is the theoretical formalism of Interview Algorithm Intrinsic Merit has been analyzed earlier as opposed to stability of Majority Voting. Extending the notion of merit from WWW to humans is the most obvious consequence. Usual interview procedure in industry is to screen resumes, shortlist them and interview for few rounds and make an offer. Does this tradition measure merit flawlessly? No. Error in interview and its stability has been analyzed in 359 and 365. Is there a way to circumvent this error and remove human element completely? Error in interview process applies to examination system in academics too. Real-life interviews and examinations have duration of few hours and rely on question-answering. Can few hours measure years of accrued merit? This question is reduced to sampling problem. If merit is a scatter-plot of feature vector points on a metric space V of n-dimensions, a sample is a set of subspaces S which approximate V. Contraction Mapping (and Banach Fixed Point Theorem) maps a space to a subspace and there is always a unique fixed point in this map ( $f(x)=x$  for some  $x$  in V). An intrinsic merit analyzer can be thought of as a contraction map on the metric space of merit feature vectors of an individual. This contraction map must create a sample subspace in such a way that all merit feature vectors are near-perfectly measured. This involves 2 difficult problems:

(\*) Construct a complete merit metric feature vector space for an individual based on past records( work and academic ).

(\*) Construct a contraction map(s) which contracts this merit vector space into a sample subspace. This contraction map is then translated into an interview

TQBF function. Objective Question-Answers (multiple choice) are relatively easy to construct and evaluate than descriptive, subjective question-answers.

Real life interviews typically have following usecase (e.g IT industry) - a slightly modified version of previous TQBF construction:

- (\*) suitability for a requirement
- (\*) technical discussions (question-answering on programming/projects etc.,)
- (\*) experience

Intrinsic Merit of Collection of Humans are measured in economics literature by many indices like GDP, Human Development Index(HDI), Inequality adjusted HDI, Gender Inequality Index, Purchasing Power Parity(PPP) etc., Human Development Index defined as geometric mean of standard of life, income, education indices is used to rank countries by their development. Intrinsic Merit of sportspersons are measured by Intrinsic Performance Rating(IPR) measures e.g Elo rating in Chess is used to rank players. Translating the previous example, one possible IPR for interview is the following adapted from HDI (not necessarily perfect):

$$\text{IPR}(\text{candidate}) = \text{geometric\_mean}(\text{IPR}(\text{interview}) * \text{IPR}(\text{education}) * \text{IPR}(\text{experience}))$$

From 359 and 365, NoiseSensitivity(InterviewTQBF) which is the dual of Stability is defined as:

$$\text{NoiseSensitivity}(\text{InterviewTQBF}) = 0.5 - 0.5 * \text{Stability}(\text{InterviewTQBF}) = 0.5 - 0.5 * a^2 * n^2 / 4$$

Error in interview is equal to NoiseSensitivity of interview TQBF. What is the probability of interview process failing? By Markov tail bound:

$$\Pr[\text{Error in interview process} > e] \leq \text{mean}/e$$
 where mean is the average error or NoiseSensitivity of interview. Therefore:

$$\Pr[\text{Error in interview process} > e] \leq \text{NoiseSensitivity}(\text{InterviewTQBF})/e$$

While suitability can be easily quantified for error and interview TQBF having previous error bound, experience is a new variable in real-life HR analytics. Experience of a candidate is total duration in industry (academics, private initiatives inclusive). Experience itself is indirectly caused by past interviews. For example, a person having 30 years experience from 10 companies was meritorious in past 10 interviews and it is counterintuitive if 11th finds no merit (this contradiction makes objective merit subjective and in a sense this is also an error in interview process - a flawed TQBF). Thus experience is a function of merit and gradually makes future interviews redundant - an example below:

Experience = f(number of job/academic/private hops, intrinsic merit at each previous hop, experience per hop)

Interview algorithm being a TQBF satisfiability problem is PSPACE-complete (=IP=AP). There are existing question-answering systems like IBM watson (answer-questioning) which beat humans in Jeopardy with least error, a contest like Turing test, Question-Answering using WordNet as Word Sense Disambiguator and older expert-system based Q&A software. But there does not seem to exist a theoretical decision tree parallel for QBF similar to boolean decision trees except DPLL evaluations. An error in interview QBF can also be formalised as a Lambda-Tolerant Randomized Decision Tree having access to pseudorandom bits and making errors with an upperbound while evaluating decision tree.

TQBF formulation of question-answering is far stringent than traditional interviews. Existential and Universal quantifiers simulate "there exists an answer or a counter-question for all questions" instead of "there exists an answer for a question". In proving lowerbounds for games like Chess, Go etc., TQBF is evaluated as game-tree (alpha-beta pruning) - "for all moves there exists a countermove" where each level choices in the tree alternate between 2 opponents for bounded (polynomial) or unbounded (exponential) number of rounds.

Intrinsic merit metric space of feature vector points can be construed as a Hypergraph with feature vector points as vertices and edges spanning multiple of

these points which are related as edges. Hypergraph edge connects more than two vertices. Transversal or Hitting Set of a Hypergraph is the subset  $S$  of the vertices  $X$  which have non-empty intersection with all hyperedges. Transversal graph is a subgraph of this hypergraph consisting of all possible minimal transversals (a minimal transversal has no other transversals as subsets). Transversal graph is a "summary" of the larger graph and thus is a Contraction Map which creates a gist of the merit metric space.

Similar notion of transversal hypergraph can be applied to Recursive Gloss Overlap Definition Graph too (considering it as a hypergraph), for text summarization - subset of word vertices which intersect all hyperedges. Hypergraph Transversal Problem is known to be in co-NP.

Like usual text documents, candidate resumes can be represented as either a Recursive Gloss Overlap graph or a ThoughtNet hypergraph:

\*) Graph: Resume text is mapped to a graph by Recursive Gloss Overlap algorithm. Core number based classifier brings out the best in the graph - candidate experience domains in resume that are closely related

\*) Hypergraph: Resumes are stored in ThoughtNet as Hypergraph index. Querying results in similar resumes. ThoughtNet internally invokes Recursive Gloss Overlap core number classifier.

#### References:

- 
- 420.1 P, NP and examinations - <https://terrytao.wordpress.com/2009/08/01/npn-relativisation-and-multiple-choice-exams/>
  - 420.2 Shrink Map and Contraction Map - [Topology - James Munkres] - pages 181-182
  - 420.3 Banach Fixed Point Theorem - [https://en.wikipedia.org/wiki/Banach\\_fixed-point\\_theorem](https://en.wikipedia.org/wiki/Banach_fixed-point_theorem)
  - 420.4 Davis-Putnam-Logemann-Loveland (DPLL) decision tree solver algorithm for QBF - <http://personalpages.manchester.ac.uk/student/joshua.dawes/notes/qbf.pdf>
  - 420.5 Parallel algorithm for Hypergraph Transversals - <https://people.mpi-inf.mpg.de/~elbassio/pub/COCOON05.pdf>
  - 420.6 Efficient algorithm for Hypergraph Transversals - <http://jgaa.info/accepted/2005/KavvadiasStavropoulos2005.9.2.pdf>
  - 420.7 Compendium of Intrinsic Performance Ratings in Chess - <https://www.cse.buffalo.edu/~regan/papers/pdf/Reg12IPRs.pdf>
  - 420.8 Human Development Index (New) - <https://poseidon01.ssrn.com/delivery.php?ID=615100008007024087109082112068031068002059093093031010095070006067125121072104018099058027096058051040011088102003094012124014108058062055076070124088071097101123070065059085125012119018080072084029012007002119065081015116009119108104075076102112012027&EXT=pdf>
  - 420.9 Social Progress Index - [https://www.socialprogressindex.com/assets/downloads/resources/en/English-2017-Social-Progress-Index-Methodology-Report\\_embargo-until-June-21-2017.pdf](https://www.socialprogressindex.com/assets/downloads/resources/en/English-2017-Social-Progress-Index-Methodology-Report_embargo-until-June-21-2017.pdf) - Comprehensive ranking of countries based on multitude of social indicators (Basic Needs, Wellbeing, Opportunities)
  - 420.10 Stockfish OpenSource Chess Engine - <https://stockfishchess.org/> - Usual round-robin tournament graph tradition of contests pit pairs of human players against each other for ranking which may not be truly absolute. Instead players could be ranked by their scores against an algorithmic chess engine (which is objectively intrinsic if Chess engine is algorithmically fair) thereby removing human error element in judging merit.

-----

421. (FEATURE-DONE) Text Summarization from Recursive Gloss Overlap Graph Core - Commits - 28 June 2017

-----

(\*) Added a new function to create a summary from text - This function creates the core of a Recursive Gloss Overlap graph with certain core number and writes out a text sentence for each edge in core

subgraph obtaining least common ancestor(hypernym) relation  
(\*) logs for this have been committed to python-src/testlogs

Summarization from k-core(s) of a Recursive Gloss Overlap graph captures the most crucial areas of the text because document belongs to the class/word vertex with high core numbers.

-----  
422. (FEATURE-DONE) Text Summarization from Recursive Gloss Overlap Graph Core - Commits - 30 June 2017  
-----

-----  
(\*) New clause added to classify the text and match the prominent core number word vertices in the text and only add those sentences to summary.

(\*) This is an alternative to k-core subgraph traversal and creating text programmatically. It is based on the heuristic that a summary should capture the essence/classes the text belongs to.

(\*) Prominent core number classes are shaved off from the sorted core number list returned by RGO classifier and top percentile is used. Summary is limited in size relative to the original text.

-----  
423. (THEORY) Dense Subgraph Problem and Mining patterns in Graph Representation of Text - 2 July 2017  
-----

-----  
Recursive Gloss Overlap and Recursive Lambda Function Growth algorithms create graphs from text documents. Unsupervised classification from prominent vertices of the definition graph and Text summarization at present depend on finding k-core subgraphs. In general this is an NP hard problem to find Dense Subgraphs of a Graph where density of a subgraph S of a graph G is defined as:

$$d(S) = |\text{Edges of } S| / |\text{Vertices of } S|$$

There are polynomial time maxflow based algorithms and approximations to find dense subgraphs of a graph.

References:

-----  
423.1 Goldberg Algorithm, Charikar Algorithm and k-Cliques Densest Subgraph Algorithm for Dense Subgraph Discovery - [people.seas.harvard.edu/~babis/dsd.pdf](http://people.seas.harvard.edu/~babis/dsd.pdf)  
423.2 Network Structure and Minimum Degree - [Social Networks - Seidman] - <https://ucilnica.fri.uni-lj.si/pluginfile.php/1212/course/section/1202/Seidman%20-%20Network%20structure%20and%20minimum%20degree%2C%201983.pdf> - k-cores as measure of connectedness in a network G which are maximal connected subgraphs of G whose vertices have degree atleast k.

-----  
424. (THEORY) Pseudorandom non-majority choice and Bounded Electorate Majority Choice - 3 July 2017 - related to 53.7  
-----

Bounded Electorate Majority Choice:

-----  
Odd Electorate with 3 voters is the minimum possible majority voting setting which vouchsafes a clear winner. This is a composition (both formula and circuit) of NC majority voting function with Voter SATs. This composition can be written as a unified formula by substituting the voter SAT formulas in formula for Majority function which has formula of size  $O(n^{5.3})$ . This combined formula can be converted to a 3-CNF by Tseitin transformation. This specific 3 voter example is NP-complete. Similar substitution for infinite electorate majority could be undecidable.

## Pseudorandom Non-majority Choice:

Majority social choice has only one level of error probability i.e goodness for each voter while Non-majority pseudorandom social choice invoking a PRG has 2 levels of probabilities - 1) Probability of choosing a voter SAT at random 2) Goodness probability of chosen voter SAT and thus conditional.

Let number of voter decision functions with goodness  $x_i = m(x_i)$ . Total number of voters  $N = m(x_1) + m(x_2) + m(x_3) + \dots + m(x_n)$

Effective goodness of a PRG choice is the mean:

$$\frac{1}{N} * \text{summation}(x_i * m(x_i)) = (x_1 * m(x_1) + x_2 * m(x_2) + x_3 * m(x_3) + \dots + x_n * m(x_n)) / N$$

When all voter functions have goodness 1 then PRG choice has effective goodness 1.

Probability of choosing a voter of Goodness  $x_i = m(x_i)/N$

Conditional goodness probability of a PRG chosen voter SAT =

$$\text{Pr}[\text{choosing voter SAT of goodness } x_i] * \text{Pr}[\text{goodness of SAT}] = [m(x_i)/N] * x_i$$

When  $m(x_i) * x_i / N = 1$ , Goodness of PRG choice is 1. This can happen only if  $m(x_i) * x_i = N \Rightarrow m(x_i) = N$  and  $x_i = 1$  i.e all voters have equal goodness 1 because smaller values of  $x_i$  require  $m(x_i) > N$ , a contradiction. This is a BPP/BPNC/RNC/RP algorithm despite the goodness being 1 because Pseudorandom bits have to be created by a PRG.

When goodness is 1 for both LHS PRG choice and RHS Bounded Electorate Majority Choice, PRG choice is a BPP/BPNC/RNC/RP algorithm to NP-complete Majority Choice for finite voters  $\Rightarrow$  NP is in BPP/BPNC/RNC/RP. But BPP is in P/poly. Therefore NP is in P/poly if NP is in BPP. From Karp-Lipton theorem if NP is in P/poly, PH collapses to  $\Sigma(p, 2)$  and NP in P/poly implies  $AM=MA$  by [Arvind, Vikraman; Köbler, Johannes; Schöning, Uwe; Schuler, Rainer (1995)]. This independently leads to a similar bound mentioned earlier for Percolation Boolean Voter Functions for Non-majority social choice which have 100% Noise stability (LHS is a P/poly percolation circuit with 100% goodness while RHS is NP-complete finite electorate).

NP in P/poly also implies PH is in P/poly. It is not known if this implies PH-complete problems exist (because PH collapsing to second level causes every k-QBFSAT problem in PH to reduce to 2-QBFSAT  $\Sigma(p, 2)$  and thus PH-hardness is proved).

## PH-completeness proof outline:

If NP is in BPP, NP is in P/poly because BPP is in P/poly.

$\Rightarrow$  If NP is in P/poly, PH is in  $\Sigma(p, 2)$  from Karp-Lipton-Sipser Collapse Theorem

$\Rightarrow$  If NP is in P/poly, PH collapses to P/poly

$\Rightarrow$  There are complete problems in each level k of the Polynomial Hierarchy (correspond to a k-depth QBFSAT).

$\Rightarrow$  There is a complete problem in  $\Sigma(p, 2)$  corresponding to 2-QBFSAT.

$\Rightarrow$  All problems in  $\Sigma(p, 2)$  can be reduced to this  $\Sigma(p, 2)$ -complete 2-QBFSAT problem.

$\Rightarrow$  All problems in PH collapse to  $\Sigma(p, 2)$  if NP is in P/poly

$\Rightarrow$  All problems in PH can be reduced to this  $\Sigma(p, 2)$ -complete 2-QBFSAT problem.

$\Rightarrow$   $\Sigma(p, 2)$ -complete problem is thus a PH-Complete problem

## References:

424.1 Proof of Karp-Lipton-Sipser collapse theorem - PH in P/poly - <http://www.cse.iitm.ac.in/~jayalal/teaching/CS6840/2012/lecture14.pdf>



-----  
425. (FEATURE-DONE) Updates to Text Summarization from Dense Subgraph of Recursive Gloss Overlap graph of a Text -  
Commits - 4 July 2017  
-----

-----  
(\*) import matplotlib commented in RGO classifier  
(\*) New clause added to Text Summarization: This finds the common path between 2 word vertices synsets by inheriting an existing WordNet code for shortest wordnet path distance and constructs sentences by a sliding window for each successive pair of intermediate vertices in this common path. This creates a deeper profound summary than least\_common\_hyponyms(). Sentences thus created are sorted based on a relevance score to the actual text - size of intersection similar to Lesk WSD. Only top relevant sentences can be chosen as required.  
(\*) Logs for this have been committed to testlogs/.

It has to be noted that, dense subgraph traversal and writing unguided summary sans training data mimicks human recursive comprehension and looks non-conventional for human reading. Presently only hypernym (IS A) relation is used for connectives. More comprehensive humane-looking summary can be created by Meronyms (HAS A) and Holonyms (IS PART OF) in WordNet API. ConceptNet 5 which is a better semantic framework for finding relations between concepts could do well in this context. But presently there is no python API for ConceptNet5 and data has to be queried as RESTful JSON objects.

-----  
426. (FEATURE-DONE) Updates to Text Summarization - Commits - 5 July 2017  
-----

-----  
(\*) Changed the class-sentence matching clause by increasing the percentile of prominent classes  
(\*) Changed relevance\_to\_text() by comparing each sentence chosen by prominent class match to the sentences in text - Ratcliff-Obershelp Longest Common Subsequence matching difflib library function is invoked for this similarity. Sentences are chosen also based on relevance\_to\_text() scoring  
(\*) Percentage of summary to the size of the text has been printed as a ratio. Logs have been committed to testlogs/

-----  
427. (FEATURE-DONE) Updates to Text Summarization - choosing sentences matching class labels - 6 July 2017  
-----

-----  
(\*) Some experimentation on choosing relevant sentences to be added to summary was performed  
(\*) relevance\_to\_text() invocation has been changed as per algorithm below:  
for each prominent dense subgraph k-core class label  
find the synset definition of class label  
for each sentence  
invoke relevance\_to\_text() similarity function between sentence and the class label definition  
and add to summary if the relevance ratio > 0.41 and if not already in summary  
(\*) Ratio 0.41 was arrived at heuristically:  
- For relevance ratio 0.1, summary ratio was 0.65  
- For relevance ratio 0.2, summary ratio was 0.48  
- For relevance ratio 0.3, summary ratio was 0.35  
- For relevance ratio 0.4, summary ratio was 0.21  
- For relevance ratio 0.5, summary ratio was 0.02  
There is a drastic dip in size of summary if relevance threshold is increased

beyond 0.4. Because of this 0.41 has been  
hardcoded.

(\*) Logs for this have been added to testlogs/

(\*) Summary generated is human readable - subset chosen from actual text.

-----  
428. (FEATURE-DONE) ConceptNet 5.4 Python RESTful API implementation - lookup,  
search and association - 7 July 2017  
-----

-----  
(\*) This commit implements the RESTful Python requests HTTP API for querying  
ConceptNet 5.4 dataset

(\*) Three functions for looking up a concept, searching a concept and finding  
similar associated concepts have been

implemented with 3 endpoints (as per the documentation in

[https://github.com/commonsense/conceptnet5/wiki/API/2349f2bbd1d7fb726b3bbdc14cbe  
b18f0a40ef18](https://github.com/commonsense/conceptnet5/wiki/API/2349f2bbd1d7fb726b3bbdc14cbe<br/>b18f0a40ef18))

(\*) ConceptNet is quite different from WordNet in representation as JSON  
dictionary as against graph in WordNet.

(\*) ConceptNet 5.4 endpoints have been invoked instead of 5.

(\*) If necessary ConceptNet can replace all WordNet invocations in a later point  
in time. But such a replacement is non-trivial and would  
probably require almost all Recursive Gloss Overlap related code to be rewritten  
from scratch. But that depends on how ConceptNet 5  
weighs against WordNet in measuring semantic meaningfulness.

-----  
429. (THEORY) Contradictions in bounds between finite and infinite electorate -  
8,10,11,12,13 July 2017  
-----

-----  
Lowerbounds by equating the goodness of Non-majority and Majority social choice  
thus far mentioned in drafts in this document (subject to errors) are based on  
following assumptions:

(\*) There are two possible paths to social choice - Non-majority and  
Majority

(\*) Each social choice belongs to a computational complexity class

(\*) Goodness of a social choice is the measure of error-free-ness of the  
choice made in either paths i.e decision correctness (e.g noise stability,  
sensitivity,error in BP\* algorithm etc.,)

(\*) RHS Majority voting has been assumed to abide by Homogeneous version  
of Condorcet Jury Theorem convergence and divergence of group decision goodness  
as a function of individual voter goodness while LHS is either a pseudorandom  
choice or an interview TQBF algorithm

(\*) Goodness of either choice majority or non-majority must be equal

(\*) Either LHS or RHS has to be a complete problem for a complexity class

C.

(\*) Traditional literature on boolean majority functions and circuits  
assumes that input to majority is readily available which is equivalent to SAT  
oracle access to Majority function where SAT oracle could belong to any  
complexity class (2-SAT, 3-SAT, k-QBFSAT, etc.,) => Majority voting is in  
 $P^{NP}, P^{PH}, P^{EXP}$  etc.,

(\*) Previous Oracle access based proofs have been intentionally  
circumvented by replacing Oracles with Boolean Function/Circuit compositions  
which have strong Communication Complexity basis (KW relations and depth of a  
circuit composition mentioned in 368)

(\*) Assuming all above, LHS is an algorithm for RHS complete problem (or  
viceversa) creating a lowerbound.

(\*) All bounds derived in this draft assuming above do not follow  
conventional lowerbound techniques e.g Circuit Lower Bounds. Equal goodness  
assumption implies - "both algorithms solve same problem - one is more efficient  
than the other".

(\*) Most importantly drafts in this document are just analyses of various social choice functions, their complexities and contradictions irrespective of attaining lowerbounds.

Equality of Goodness of PRG choice and Majority voting for finite electorate of size 3:

-----  
-----  
Let  $x_1, x_2, x_3$  be the goodness of 3 voter SATs. PRG choice randomly chooses one of the 3 voters while majority voting is the usual CJT Majority+SAT composition.

Goodness of PRG choice:

-----  
$$= (x_1 * m(x_1) + x_2 * m(x_2) + x_3 * m(x_3)) / 3$$
  
When all 3 have equal goodness 1, effective goodness is:  
$$= (1 * 1 + 1 * 1 + 1 * 1) / 3 = 1$$

Goodness of Majority choice:

-----  
This is the bounded version of CJT binomial series summation. When  $x_1 = x_2 = x_3 = 1$ :  
$$= (3C2(1)^2(0)^1 + 3C3(1)^3(0)^0) = (0 + 1) = 1$$

Possible Lowerbounds described previously for Unbounded and Bounded electorate lead to contradictions as below:

(\*) In infinite voter case, homogeneous voter CJT circuit in BPP is derandomized to P if CJT converges  $\Rightarrow P = BPP$ .  
(\*) In finite voter case, NP-complete RHS has BPP algorithm in LHS (NP in BPP) implying NP in P/poly and collapse of PH  $\Rightarrow$  NP in P/poly and PH in P/poly.

Contradiction 1 :

-----  
If  $BPP = P$  (unbounded CJT) and NP is in BPP (bounded) then NP is in  $P = BPP \Rightarrow P = NP$ . This conflicts with  $P \neq NP$  implied by :  
    (\*) the Majority Hardness Lemma (318),  
    (\*) Polytime learning of NP implying NP does not have polytime algorithms (368) and  
    (\*) HLMN PARITYSAT counterexample (53.15)  
but concurs with :  
    (\*) high percentage of random k-SATs satisfied in Approximate CNF SAT solver by least squares (376).

But can infinite voter CJT circuit be in BPP and thus in P/poly? Infinite voter CJT circuit is of polynomial size if it is polynomial in number of Voter SAT variables and exponential if it is exponential in number of variables. Latter happens only if all voters have dissimilar SAT variables while common variables across voter SATs make it exponential. This is described in example of 53.8. Condorcet Jury Theorem convergence in homogeneous voters case implies all voters are similar (e.g have similar voting SATs) thus ruling out polynomial size case i.e Unbounded CJT circuit can not both be in BPP and converging. This contradiction stems from the assumption - BPP derandomizes to P. LHS could be in RP too. RP is contained in NP. (Can BPP derandomize to NP i.e BPP in NP?). Another assumption is all voters have 3-SAT choice functions. If all voter SATs are 2-SATs (in P), infinite and finite voter cases are not equatable and there is no contradiction. Known result: If NP is in BPP,  $NP = RP$  - this applies to bounded voting case above. Thus  $BPP = P$  possibility is removed by exponential sized CJT circuit and  $BPEXP = EXP$  is still possible when CJT converges. Contradiction 1 is avoided.

Contradiction 2 :

-----  
If NP is in BPP and thus in P/poly (irrespective of  $BPP = P$ ), similar conflicts arise. An assumption made in composition of 3-SAT voters and Majority function for bounded electorate in 424 is resultant composition is also in NP (depth lowerbound for this composition can be obtained by KW relations in 368). This

assumption could be false because composition of NP 3-SAT with non-uniform NC1 majority function could be harder than mere NP - because this is equivalent to replacing oracle with a circuit composition in a  $P^{NP}$  algorithm. P with NP oracle adds an additional quantifier and places it in second level of polynomial hierarchy (inclusion in <https://www.cse.buffalo.edu/~regan/papers/ComplexityPoster.jpg> shows there are problems in  $\Sigma(p,2) \wedge \Pi(p,2)$  which also have BPP algorithms and  $P^{NP}$  is contained in  $\Sigma(p,2) \wedge \Pi(p,2)$ ). Thus a PRG choice and converging bounded electorate voting of equal goodness need not imply NP in BPP. This composition may not be a complete problem. Stricter oracle definition of Majority+SAT composition is NC1(L) where Majority is computable by non-uniform circuits or BWBP with oracle access to gates belonging to a class L. For 3-SAT voter oracles, CJT majority voting circuit is in NC1(NP) (is this contained in  $P^{NP}$ ?). Subject to equal goodness, composition equivalent of NC1(NP) is in BPP and not NP is in BPP.

Reference 429.3 suggests there exists a random oracle A relative to which  $NC^A$  is in  $P^A$ . P having NP oracle access is known as class  $\delta(p,2)=P^{NP}$ . This answers if  $NC^{NP}$  is in  $P^{NP}$  in the affirmative. There is a known  $\delta(p,2)$ -complete problem mentioned in reference 429.5. If bounded electorate  $NC^{NP}$  problem is complete for its class, then equal goodness of PRG choice and bounded majority voting implies  $NC^{NP}$  is in BPP. This in turn implies NP is in BPP (if  $NC^{NP}$  strictly contains NP) and thus NP is in P/poly again leading to contradiction in the outset.

Replacing oracles with compositions and applying depth lowerbounds for Majority+VoterSAT circuit composition as below for m voters with n variables per voter SAT (from 368):

$$D(\text{Maj} + \text{Voter}) = \text{CommunicationComplexity}(R(\text{Maj}, \text{Voter})) \geq 5.3 \cdot \log m + n - O(m \cdot \log m / n)$$

does away with the hassles of relativization and directly gives the depth lowerbound of the majority voting circuit composition. Size of this composition is the alternately phrased KRW conjecture in 429.7.

Example  $\delta(p,2)$ -complete problem mentioned in 429.5:

```

While number of queries to NP oracle <= k
{
 (*) Query a 3SAT oracle for a satisfying assignment for a 3CNF Voter SAT
 (*) Store the queried satisfying assignment in a linked list in sorted
order - this is linear per insertion i.e traverse the list and compare the two
adjacent nodes. E.g. {1,5}, {1,3,5}, {1,3,5,6}, {1,3,5,6,7}... upto k-th query
and lexicographic ordering is preserved by a decimal encoding of SAT oracle
query string.
}
Output 1 if last element in the list ends with binary 1 digit.
```

This algorithm makes k queries to an NP oracle and has  $O(k^2)$  time complexity and thus in  $\delta(p,2)$ . Hardness follows by reducing any polynomial time algorithm with NP oracle to above - reasonably straightforward because oracle queries are memoized and can be looked-up in polynomial time.

Mapping above  $\delta(p,2)$  complete problem to proving completeness of  $NC^{NP}$  majority voting is non-trivial. Majority function can make n queries to n voter SAT oracles and atleast  $n/2 + 1$  queries should return 1 or 0 to compute majority in NC1. Beyond this, NC reducibility has to be proved by Many-one/Turing reductions or Logspace reductions of any other problem in  $NC^{NP}$  to this. Integer multiplication, powering and division have been proved to be equivalent (NC reducible to each other) mentioned in reference 429.8. NC reducibility through oracle NC gates have been proved in reference 429.9. Majority function is known not to be complete for NC1 under AC0 many-instances-to-one reductions (reference 429.10). This could probably imply that  $NC^{NP}$  is not complete too, thereby avoiding contradiction 2.

But this also implies that any Majority<sup>A</sup> for a random oracle A is not complete if Majority is not complete for NC1. Hence it has to be proved or disproved if a problem is not NC1 complete, it is not NC1<sup>A</sup> complete for an oracle A. Lemma 3.3.9 in reference 429.9 [RuzzoGreenlawHoover] describes an Oracle PRAM or an NC oracle circuit M' to another NC circuit M. M has  $O(n^c)$  size/processors and depth/time of  $O(\log n)$  and M makes at most  $O(n^c)$  oracle queries to M' (each node can query). But these oracle queries are made simultaneously in parallel time of  $O(\log n)$ . Thus replacing calls to M' by M' itself increases depth by  $O(\log n)$  and size by  $O(n^c)$  order of magnitude i.e new circuit without oracle M' has time  $O((\log n)^2)$  and size  $O(n^{2c})$ . Similar oracle replacement could be done for Majority<sup>A</sup> circuits too. If oracle gates to Majority are replaced by circuit for A itself which has size s and depth d and Majority makes at most  $O(n^c)$  calls to oracle A, new Majority circuit without oracle has depth/time  $O(d \cdot \log n)$  and size/processors  $O(s \cdot n^c)$ . This new circuit need not be in NC1. From Spira's Theorem a circuit of size  $O(s \cdot n^c)$  can be transformed into a circuit of depth  $O(\log(s \cdot n^c)) = O(\log(s) + c \cdot \log(n))$ . Following cases arise after replacing oracle gates with a new circuit of size s.

Case 1 -  $s = 2^n$ :

-----  
This makes the new majority circuit sans oracle to be of depth  $O(n \cdot \log 2 + c \cdot \log(n))$  which is not polylog depth and polynomial size and thus lies outside NC - this new circuit problem could be complete for a different class. This line of reasoning coincides with previous formulations of majority voting based on depth bounds by Communication Complexity (KRW Conjecture) and Direct Connect circuit families of unbounded depth and exponential size. If there is a problem B in NC1, Majority<sup>A</sup> and B<sup>A</sup> can be in totally different depth hierarchy classes by depth hierarchy theorem. This could be a complete problem in different class (e.g, PH-complete, EXP-complete etc.,) and can be equated under equal goodness assumption with a non-majority social choice.

Case 2 -  $s = n^c$ :

-----  
This new majority circuit has depth  $O(2 \cdot c \cdot \log(n))$  and size  $O(n^{2c})$  and is obviously in NC1 and computes majority. But majority is not complete for NC1 and thus majority voting itself is not a complete problem and cannot be equated under equal goodness assumption with a non-majority choice.

References:

-----  
429.1 Definition of Homogenous Voter -  
[http://www.uni-saarland.de/fak1/fr12/csle/publications/2006-03\\_condorcet.pdf](http://www.uni-saarland.de/fak1/fr12/csle/publications/2006-03_condorcet.pdf) -  
"...Now assume that a chamber consists of three homogenous judges. Homogenous means that the decision-making quality of each single judges is described by identical parameters r..." - identical parameters are translatable to identical variables though SAT could be different for each  
429.2 Counting Classes and Fine Structure between NC and L - [Samir Datta , Meena Mahajan , B V Raghavendra Rao , Michael Thomas , Heribert Vollmer] -  
<http://www.imsc.res.in/~meena/papers/fine-struct-nc.pdf> - Definition of NC circuits with Oracle gates. Definitions 8 and 10 and Remark 9 - Majority NC1 circuit with NP oracle for all homogeneous voters belongs to Boolean Hierarchy and specifically is in NC1 hierarchy.  
429.3 For a random oracle A, NC<sup>A</sup> is strictly contained in P<sup>A</sup> -  
[https://complexityzoo.uwaterloo.ca/Complexity\\_Zoo:N](https://complexityzoo.uwaterloo.ca/Complexity_Zoo:N),  
<https://complexityzoo.uwaterloo.ca/Zooref#mil92> - [PeterBroMiltersen]  
429.4 Delta(p,2) - P has NP oracle -  
[https://complexityzoo.uwaterloo.ca/Complexity\\_Zoo:D#delta2p](https://complexityzoo.uwaterloo.ca/Complexity_Zoo:D#delta2p)  
429.5 Delta(p,2) complete problem -  
<https://complexityzoo.uwaterloo.ca/Zooref#kre88> - [Krentel] - Given a Boolean formula, does the lexicographically last satisfying assignment end with 1?  
429.6 Spira theorem - any formula of leaf size s can be transformed into a formula of depth  $\log(s)$  -  
[https://www.math.ucsd.edu/~sbuss/CourseWeb/Math267\\_1992WS/wholecourse.pdf](https://www.math.ucsd.edu/~sbuss/CourseWeb/Math267_1992WS/wholecourse.pdf)

429.7 Size of a circuit composition - alternative form of KRW conjecture - <http://www.math.ias.edu/~avi/PUBLICATIONS/GavinskyMewewi2016.pdf> - "...This suggests that information complexity may be the "right" tool to study the KRW conjecture. In particular, since in the setting of KW relations, the information cost is analogous to the formula size, the "correct" way to state the KRW conjecture may be using formula size:  $L(g \circ f) \approx L(g) \cdot L(f)$ ..." - for Majority+VoterSAT composition size is conjectured as  $O(n^{5.3} \cdot s)$  where  $s$  is the size of VoterSAT formula. Information complexity of a composition of a function  $g: \{0,1\}^m \rightarrow \{0,1\}$  and a universal relation  $Un: \{0,1\}^n \rightarrow \{0,1\}$  for majority voting is: a Voter SAT  $g$  of  $m$  variables is composed with a Majority universal relation of  $n$  variables. Majority is a universal relation because for 2 input strings to majority function drawn at random can be checked if they differ in a bit position. Above depth bound is the amount of mutual information "leaked" while computing the composition together by Alice and Bob. Alice gets a  $m \times n$  matrix  $X$  and a string  $a$  in  $g^{-1}(0)$  and Bob gets a  $m \times n$  matrix  $Y$  and a string  $b$  in  $g^{-1}(1)$  and both accept if  $a$  and  $b$  differ in a bit position and  $X$  and  $Y$  have row mismatch and reject else.  $g^{-1}(0)$  is equivalent to a rejecting assignment to SAT and  $g^{-1}(1)$  is equivalent to an accepting assignment to SAT because  $g()$  is the Voter SAT.

429.8 Log Depth circuits for Division and Related - [BeameCookHoover] - <https://pdfs.semanticscholar.org/29c6/f0ade6de6c926538be6420b61ee9ad71165e.pdf>

429.9 NC reducibility - reducing one NC instance to another - <https://homes.cs.washington.edu/~ruzzo/papers/limits.pdf> - replace NC oracle gates by multiplication of equivalent number of processors and depth

429.10 Catechism on open problems - Interview of Eric Allender - [https://books.google.co.in/books?id=7z3VCgAAQBAJ&pg=PA37&lpg=PA37&dq=NC+reducibility+majority+function&source=bl&ots=W0zlJFRbpt&sig=OmFqckehlrTfyaeTOjScJ423dUk&hl=en&sa=X&ved=0ahUKEwjQ\\_0-Y1YPVAhVGMi8KHbJCdbAQ6AEIIzAA#v=onepage&q=NC%20reducibility%20majority%20function&f=false](https://books.google.co.in/books?id=7z3VCgAAQBAJ&pg=PA37&lpg=PA37&dq=NC+reducibility+majority+function&source=bl&ots=W0zlJFRbpt&sig=OmFqckehlrTfyaeTOjScJ423dUk&hl=en&sa=X&ved=0ahUKEwjQ_0-Y1YPVAhVGMi8KHbJCdbAQ6AEIIzAA#v=onepage&q=NC%20reducibility%20majority%20function&f=false) - "...Majority function is not complete for NC1 under AC0 many-one reductions..."

429.11 Parallel Computation and the NC hierarchy relativized - [Christopher Wilson] - [https://link.springer.com/chapter/10.1007/3-540-16486-3\\_111](https://link.springer.com/chapter/10.1007/3-540-16486-3_111) - containments of NC classes relative to oracle - " $NC^A$  hierarchy is seen to be in  $P^A$  for any oracle  $A$ . Also, nondeterministic log-space relative to ... there exists an oracle  $A$ , such that  $NC1^A$  in  $NC2^A$  ... in  $P^A$ "

-----

430. (THEORY) Theoretical Formalism for an Electronic Voting Machine based on Locality Sensitive Hashing - 13 and 14 July 2017 - related to 265,275,376 and 319

-----

Locality Sensitive Hashing and their relevance to Multiway Contests have been described in 319. Voters voting for same candidate are clustered together in a bucket chain of tabulation hashing. This is akin to a naive electronic voting machine which increments counters of a candidate for each vote cast for  $h(im/er)$ . An LSH voting machine queries voter SAT oracles sequentially (or parallelly if there is a parallel LSH implementation), receives the candidate index, finds the candidate index key in LSH and appends the voter id to the bucket chain for the candidate. Sequential version of LSH voting machine is in  $\Delta(p,2)=P^{NP}$  because LSH is in  $P$  and oracle queries are made to voter 3SATs. LSH algorithms usually search for nearest neighbours and find similar items with high probability. For LSH based Electronic Voting Machine this  $\rho$  parameter as defined in 319 is  $\log(1/p_1)/\log(1/p_2)$  where  $p_1=Pr(h(x)=h(y))$  if  $x$  and  $y$  had voted for same candidate and  $p_2=Pr(h(x)=h(y))$  if  $x$  and  $y$  had voted for different candidates. Simplest voting machine is an array of candidates and voters increment an array element for a candidate index which is exact and errorfree. But LSH voting generalizes the notion of voting as: " $x$  and  $y$  vote for same candidate" is generalized to " $x$  and  $y$  are similar or have similar liking". For example, a web search engine lists URL results for a query and all these URLs hash/vote to same query bucket in LSH parlance. Thus notion of exact candidate is replaced by an abstract similarity probability. Definition of  $\rho$  thus allows

error and its bounds are derived in references 430.2 and 430.3.

Non-boolean social choice functions which a voter computes to obtain a candidate index have been described previously. Previous LSH or array of counters based voting machine has following standard operating procedure:

- (\*) receives voters in a streaming sequence,
- (\*) each voter solves a non-boolean SAT (which could be in an arbitrary complexity class) having oracle access to it
- (\*) oracle returns a candidate index and counter is incremented
- (\*) LSH based voting has a special step - it compares two voters for similarity i.e if their oracle queries return same candidate index hash them to same bucket

- (\*) Multipartisan SAT Oracle internally has to implement the following:
  - Iterate through all candidates
  - Find the maximum number of clauses that can be satisfied by each candidate and quantify it as score which is NP-hard MAXSAT problem.
  - Sort the scores for the candidates and return the top ranked candidate.

- (\*) Sort the LSH by length of buckets
- (\*) MAXSAT has been used in lieu of Exact SAT for grading the candidates based on number of clauses satisfied. Exact SAT would return either 1 or 0 only and doesn't compute percentage of clauses satisfied.

- (\*) Random k-CNF SAT Solver implemented in 276 approximates by solving system of equations by least squares.

- (\*) Boolean Majority function is a special case of multipartisan voting: Restrict the number of candidates to 2 indexed as 0 and 1 and apply LSH.

- (\*) Voter SAT Oracles could be Constraint Satisfaction Problem(CSP) Solvers too which allow reals. This has been described in 265. Approximation of CSPs could be NP-hard if UGC is true.

Circuit Value Problem finds if a circuit encoding evaluates to 1 or 0 for an input assignment. This is equivalent to the following prover-verifier protocol:

- (\*) Voter has a Constraint Satisfaction Problem (boolean or real)
- (\*) Candidate has an assignment to the variables of voter CSP (Prover)
- (\*) Voter verifies the assignment to CSP (Verifier)

This kind of Circuit Value Problem (CVP) formulation has been avoided throughout drafts in document for Majority Voting. This is because, equating goodness and Condorcet Jury Theorem application requires quantifying the decision correctness (or) accuracy of Voter SAT/CSP which is not feasible to compute in CVP. Class PP generalizes BPP by removing bounds on error. From Toda's Theorem, PH is contained in  $P^{PP}$  and  $P^{#P}$ . Goodness in LSH voting is exactly the rho parameter and if each voter SAT oracle in LSH with unbounded error is in PP (extent to which a voter is misclassified in a candidate bucket), LSH voting itself is in  $P^{PP}$  and thus subsumes PH. Another aspect of LSH voting is majority circuit fan-in is replaced by size of buckets.

References:

-----

430.1 Locality Sensitive Hashing - [Alex Andoni] - <http://web.mit.edu/andoni/www/LSH/index.html>

430.2 Lowerbounds for Locality Sensitive Hashing - [MotwaniAssafPanigrahi] - <http://theory.stanford.edu/~rinap/papers/lshlb.pdf>

430.3 Optimal lowerbounds for Locality Sensitive Hashing - [ODonnell] - <https://www.cs.cmu.edu/~odonnell/papers/lsh.pdf>

430.4 Reflections on Trusting Trust - Trojan horses in code - program that prints itself - Quines - Godel, Escher, Bach: An Eternal Golden Braid - Fixed Points in Turing Computable Functions - [Ken Thompson] - <http://www.ece.cmu.edu/~ganger/712.fall02/papers/p761-thompson.pdf>

430.5 Problems with Electronic Voting Machines (e.g DRE machines), VVPAT and Trusting source code - [Bruce Schneier] - [https://www.schneier.com/blog/archives/2004/11/the\\_problem\\_wit.html](https://www.schneier.com/blog/archives/2004/11/the_problem_wit.html)

430.6 B-Cryptographic counters protocol augmented with Public Key Infrastructure for Incrementing Counters in Tabulation Authority - <https://crypto.stanford.edu/pbc/notes/crypto/voting.html> - Previous LSH based

theoretical voting machine requires such a secure increment protocol for incrementing tabulation hashing buckets. Anonymity requires shuffling the buckets.

430.7 PP is as hard as polynomial time hierarchy - [Toda] -

<http://epubs.siam.org/doi/abs/10.1137/0220053?journalCode=smjcat> and

[SanjeevArora-BoazBarak] - <http://theory.cs.princeton.edu/complexity/book.pdf>

430.8 Beyond Locality Sensitive Hashing - [Alexandr Andoni, Piotr Indyk, Huy L. Nguyen, Ilya Razenshteyn] - <http://www.mit.edu/~andoni/papers/subLSH.pdf> - Two level LSH partitioning by hash tables - Outer hashing creates buckets for the hash table and Inner hashing creates hash table for each buckets around a centroid.

-----  
431. (FEATURE-DONE and THEORY) Approximate CNF SAT Solver Update - percentage of clauses satisfied - 18 July 2017  
-----

(\*) This commit prints percentage of clauses satisfied for each random CNF 3SAT formula for both 0 and 1 evaluations

(\*) logs for ~1000 iterations of random 3SAT have been committed to testlogs/

(\*) Interestingly, even failing formula assignments by least squares satisfy more than 75% of clauses of the formula

(\*) Percentage of formulas satisfied by least squares heuristic is ~70%

(\*) This is probably a demonstration of complement form of Lovasz Local Lemma (LLL) for MAXSAT which is:

if events occur independently with a certain probability, there is a small non-zero probability that none of them will occur

(\*) Dual of LLL for this MAXSAT approximation is:

if each clauses are satisfied with a certain probability, there is a large probability that all of them are satisfied

References:

-----  
431.1 Lovasz Local Lemma - [https://en.wikipedia.org/wiki/Lovász\\_local\\_lemma](https://en.wikipedia.org/wiki/Lovász_local_lemma)  
-----

-----  
432. (THEORY) MAXSAT ranking of text documents, Approximate CNF SAT solver and Lovasz Local Lemma - related to 431 -  
19 July 2017  
-----

-----  
Considering a set of text documents, ranking function  $r(X,A)$ , is the subjective perception measure of a text  $X$

with access to a perception oracle  $A$ :

$r(X,A)$  = subjective rank of  $X$  as perceived by an oracle  $A$

In the context of web link graphs of HTML documents, every adjacent vertex of a node  $N$  is the perceiver of  $N$  and for two adjacent vertices  $A$  and  $B$  of  $N$ :

$r(X,A) = r(X,B)$  or  $r(X,A) \neq r(X,B)$

Perception ranking of a node need not be decided just by adjacent vertices at the end of random walk markov iterations. For example, there could be vertices which are not adjacent but yet could have indirect unaccounted for perception. An example of this are the readers of a website who do not link to it but yet have a perception. This perception is not reckoned in subjective link graph ranking.

Ranking of texts can be thought of as MAXSAT problem: Each reader of a text has a CNF (subjective) or all readers have fixed CNF (Intrinsic Objective Merit) which they apply on the qualitative and quantitative attributes of a text. CNF for measuring merit conjoins clauses for measuring meaningfulness of the text. Each literal in this CNF is a merit variable e.g Graph complexity measures like Korner Entropy , Graph Tensor Neuron Network Intrinsic Merit, Connectivity etc.,



Rank of the text is the percentage of clauses satisfied. This CNF based ranking unifies all subcategories of rankings.

Lovasz Local Lemma:

Let  $a_1, a_2, a_3, \dots, a_n$  be set of events. If each event occurs with probability  $< p$ , and dependency digraph of these events have outdegree at most  $d$ , then the probability of non-occurrence of all these events is non-zero:

$\Pr[\bigwedge_i \neg a_i] > 0$ , if  $ep(d+1) < 1$  for  $e=2.7128\dots$

CNF formula can be translated into a graph where each vertex corresponds to a clause and there is an edge between any 2 clausevertices if they have a common literal (negated or unnegated). In approximate least-square SAT solver, let  $d+1$  be the number of clauses per CNF. Then at most  $d$  other clauses can have literal overlap and thus CNF clause dependency graph can have maximum outdegree of  $d$ . Each event  $a_i$  corresponds to not satisfying clause  $i$  in CNF.

From LLL, If  $p < 1/[e(d+1)]$  is the probability of an event (not satisfying a clause) :

Probability that clause is satisfied:  $1-p > (1-1/[e(d+1)])$

Probability that all of the clauses are satisfied  $> (1-1/[e(d+1)])^{(d+1)}$  (for  $d+1$  clauses)

Probability that none of the clauses are satisfied  $< 1-(1-1/[e(d+1)])^{(d+1)}$

In previous example  $d+1 = 14$  and thus probability that none of the clauses are satisfied for any random CNF is:

$= 1-(1-1/[e(14)])^{(14)} < \sim 31.11\%$

and probability of all the clauses being satisfied for any random CNF is:

$(1-1/[e(14)])^{(14)} > \sim 68.89\%$

Experimental iterations of SAT solver converge as below (10000 CNFs):

Percentage of CNFs satisfied so far: 71.14

Average Percentage of Clauses per CNF satisfied: 97.505

This coincides with LLL lowerbounds above and far exceeds it because outdegree (common literals) is less and average percentage of CNFs satisfied is 71% after 10000 iterations. It has to be noted that average percentage of clauses satisfied per random CNF is 97% which implies that very few clauses fail per CNF.

-----  
433. (FEATURE-DONE) Approximate CNF SAT Solver update - Commits 1 - 19 July 2017  
-----

(\*) Average percentage of clauses satisfied per CNF is printed at the end of 10000 iterations

(\*) AsFer Design Document updated for Lovasz Local Lemma analysis of least squares CNF SAT solver

(\*) logs for least square assignment of 10000 random CNFs committed to testlogs/  
-----

-----  
434. (FEATURE-DONE) Recursive Gloss Overlap Graph Classifier update - Commits 2 - 19 July 2017  
-----

(\*) printed Betweenness Centrality (BC) of the definition graph of a text

(\*) BC of a node is the ratio of number of (s-t) shortest paths going through the node to all pairs shortest paths and

thus measures how central a node is to the graph and thus is another basis for classifying a text apart from dense subgraphs.  
-----

-----  
435. (FEATURE-DONE) Recursive Gloss Overlap graph classifier update - commits 1 - 20 July 2017  
-----

-----  
-----  
(\*) Following centrality measures for the definition graph have been printed in sorted order and top vertices are compared:

- 1) Betweenness Centrality
- 2) Closeness Centrality
- 3) Degree Centrality
- 4) Eigenvector Centrality (PageRank)
- 5) Core numbers Centrality (k-core dense subgraphs)

(\*) While first 3 centrality measures are reasonably equal in terms of ranking central vertices, PageRank centrality and k-core centrality are slightly different

(\*) But all 5 centrality measures reasonably capture the central purport of the text i.e the text on

"Chennai Metropolitan Area Expansion to 8848 sqkm" is classified into "Area" which is the topranked central vertex

-----  
-----  
436. (FEATURE-DONE) Approximate SAT Solver update - commits 2 - 20 July 2017  
-----

(\*) Increased number of clauses and variables to 16 and iterated for ~3100 random CNF formulae.

(\*) Following are the MaxSAT percentages after ~3100 iterations:

Percentage of CNFs satisfied so far: 69.1020276794

Average Percentage of Clauses per CNF satisfied: 97.6122465401

(\*) Previous values are quite close to 14 clauses and variables iterations done previously.

Lovasz Local Lemma bound for 16 clauses all having common literals:

$= (1 - 1/[e(16)])^{(16)} > \sim 68.9233868\%$

and average percentage of clauses satisfied after 3100 iterations far exceeds this bound at 97.61%

Commercially available SAT solvers (exact NP-complete decision tree evaluation based) usually scale to millions of clauses and variables. Though this approximate polynomial time SAT solver does not have similar advantage, yet the huge percentage of clauses satisfied in repetitive iterations does seem to have a lurking theoretical reason. Infact this is symmetry breaking solver having a sharp threshold phase transition which tries to translate a system of equations over reals in  $[0,1]$  to discrete boolean CNF formulae (value below 0.5 is 0 and above 0.5 is 1). Hardness of Approximation and UGC prohibit polytime approximations unless  $P=NP$ . 98% satisfied clauses could imply  $100/98 = (1 + 0.020408163)$  approximation where  $\epsilon = 0.020408163$ . This has to be corroborated for millions of clauses and variables in least-squares and requires high performance computing.

Random number generator used in generating random CNF clauses is based on /dev/random and hardware generated entropy. This CNF SAT solver depends on linux randomness to simulate pseudorandomness and create permutations of CNFs. Accuracy of previous convergence figures therefore might depend on if the CNFs are pseudorandom (e.g k-wise independent for k variables - when k increases to infinity independence may have infinitesimal probability).

References:

-----  
-----  
436.1 Linux Pseudorandom Generator - <https://eprint.iacr.org/2012/251.pdf>  
-----

-----  
-----  
437. (FEATURE-DONE) Approximate SAT Solver update - 24 July 2017  
-----  
-----

(\*) Increased number of variables and clauses to (20,20).  
(\*) Changed SciPy lstsq() to NumPy lstsq() because NumPy has a faster lstsq() LAPACK implementation as against xGELSS in SciPy  
(\*) Logs for 100 random CNFs have been committed to testlogs/ and Percentage CNFs and Clauses satisfied are as below:  
Percentage of CNFs satisfied so far: 58.4158415842  
Average Percentage of Clauses per CNF satisfied: 97.1782178218

-----  
438. (THEORY) Tight Hamiltonian Cycles and Independent Sets in ThoughtNet Hypergraph for Social Networks - related to 40,222,229,295,351,418,420 and other sections on ThoughtNet - 25 July 2017 and 28 July 2017  
-----

Theoretical description of ThoughtNet Hypergraph as basis for evocative thought and text analysis is mentioned previously. Hypergraph with 3 vertices per edge (3-uniform) and number of vertices  $n > n_0$ , and minimum degree  $> n/2 + \epsilon \cdot n$  is guaranteed to have atleast one tight hamiltonian cycle from [Rodl,Rucinski,Szemerédi] theorem. Tight Hamiltonian Cycles have set of maximum vertex overlapping hyperedges. If complete universal knowledge is represented as 3-uniform ThoughtNet (infinite), this ensures all the concepts in universe are connected in a tight hamiltonian. Social media networks are also generalizable to hypergraphs (though tradition is to model as graphs having network flow). This can be simulated by ThoughtNet index - streamed social media tweets/posts/shares/likes are updated in ThoughtNet (non-planar) and each class stack vertex (e.g genre of people) could be part of multiple hyperedges (e.g events involving people) and each hyperedge can span multiple class stack vertices. Independent sets in this ThoughtNet Hypergraph are set of vertices e.g people who do not directly know each other. Centrality measures (e.g PageRank if there is one for hypergraph) on this hypergraph would elicit the social prestige/perception of individuals. It is worth quantifying how a vertex A is perceived by vertex B with no edge between them. This is a special case of centrality and gossip information flow - ratio of number of shortest paths between two vertices s,t in an independent set / number of all pair shortest paths. This estimates how two unknown vertices indirectly know each other.

Ranking people in social network can not be done in the same way as documents are ranked because of intrinsic merit anachronism paradox motivated by real world examples in earlier sections - merit precedes prestige while perception/prestige is a measure of merit. Bianconi-Barabasi network model deserves a mention here in which each node has an intrinsic fitness parameter in addition to incoming links. Examples in the reference 438.2 below explain how intrinsic fitness/merit are applied to search engine ranking algorithms. Earlier network models relied on temporal Preferential Attachment alone i.e node having high adjacency at time x are likely to have higher adjacency at time x+delta x. This is a transition from older First-Mover-Advantage (first starter always wins), Rich-Get-Richer to Fit-Get-Richer paradigm. Fitness of a social network profile (twitter/facebook etc.,) is a function of credentials mentioned in the profile and how fitness is quantified is specific to internal algorithm.

Reference:

-----  
438.1 Tight Hamiltonian Cycles in 3-uniform Hypergraphs - [Rodl-Rucinski-Szemerédi] theorem - <https://web.cs.wpi.edu/~gsarkozy/Cikkek/Rio08.pdf>  
438.2 Bianconi-Barabasi Social Network Model - [https://en.wikipedia.org/wiki/Bianconi%E2%80%93Barab%C3%A1si\\_model](https://en.wikipedia.org/wiki/Bianconi%E2%80%93Barab%C3%A1si_model) - "...In 1999, Albert-László Barabási requested his student Bianconi to investigate evolving networks where nodes have a fitness parameter. Barabási was interested in finding out how Google, a latecomer in the search engine market, became a top player. Google's toppling of previous top search engines went against Barabási's BA model, which states that first mover has an advantage. In the scale-free network if a node appears first it will be most connected because it had the longest time to attract links. Bianconi's work showed that when fitness

parameter is present, the "early bird" is not always the winner.[10] Bianconi and Barabási's research showed that fitness is what creates or breaks the hub. Google's superior PageRank algorithm helped them to beat other top players. Later on Facebook came and dethroned Google as Internet's most linked website. In all these cases fitness mattered which was first showed in Bianconi and Barabási's research. In 2001, Ginestra Bianconi and Albert-László Barabási published the model in the Europhysics Letters.[11] In another paper,[12] substituting fitness for energy, nodes for energy level and links for particles, Bianconi and Barabási was able to map the fitness model with Bose gas...."

438.3 Experience versus Talent shapes the web -

<http://www.pnas.org/content/105/37/13724.full> - following simplistic theory provides intuition for it:

Let  $M$  be the natural ability/merit/fitness of a vertex and  $E$  be the experience.

Rate of change of experience of a social profile vertex is proportional to its intrinsic fitness and present experience.

Previous assumption is a heuristic on real-life experiences - intrinsic fitness is a constant while experience changes with time.

Thus at any time point, experiential learning depends on how naturally meritorious a person is and how much past experience is

helpful in increasing experiential learning. (Might have some theoretical basis in Mistake bound in computational learning theory.

Following formalises how a boolean function is learnt incrementally from a dataset over time by making mistakes and correcting them)

$$dE/dt = kME$$

$$\Rightarrow dE = kME \cdot dt$$

$$\Rightarrow dE/E = kM \cdot dt$$

$$\Rightarrow \log E = kMt + c$$

$$\Rightarrow E = e^{(kMt+c)}$$

$$\Rightarrow E = e^c \cdot e^{(kMt)}$$

$\Rightarrow$  Experience is exponentially related to talent/merit/fitness

$\Rightarrow$  People with high natural ability amass same experience in less time

compared to people with low merit

At time  $t=0$ ,  $E = e^c$  which is equal to natural ability/merit/fitness  $M$  of a social profile vertex in Bianconi-Barabasi network model.

Therefore,  $E = M \cdot e^{(kMt)}$ . At  $t=0$ , experience equals merit and grows exponentially over time. But how to measure the fitness of a social profile for a human in terms of energy? What is the energy of a human social profile? Low energy syntactically implies low entropy and less chaotic nature of a profile. But real-life social profiles with high entropy do attract huge links. Previous derivation assumes natural talent is defined in terms of numeric quantification of credentials (marks/grades/awards/publications/IQ/achievements) which is insufficient. For human resource analytics, sampling experience at each tenure change (academic/work) gets a snap of experience at that time. Usually experience is measured linearly in time in academics/industries often overlooking merit, but previous equation changes that notion and implies experience exponentially increases with time as a function of intrinsic merit. Also previous differential equation is a very naive definition of experience vs talent - adding more variables could make it reflect reality.

438.4 Bose-Einstein Condensation in Complex Networks - [Bianconi-Barabasi] - Physical Review Letters - <http://barabasi.com/f/91.pdf>

438.5 PAFit - Joint estimation of preferential attachment and node fitness in growing complex networks - [Thong Pham, Paul Sheridan & Hidetoshi Shimodaira] - <https://www.nature.com/articles/srep32558> - factors determining node fitness in facebook graph - "...A directed edge in the network represents a post from one user to another user's wall. One might speculate that the following factors are important for a user to attract posts to his/her wall: a) How much information about his/her life that he/she publicises: his/her birthday, engagement, promotion, etc. b) How influential and/or authoritative his/her own posts are which call for further discussions from other people; and c) how responsive the user is in responding to existing wall posts. We then can hypothesize fitness  $\eta_i$  to be a combination of these three factors averaged over time ..."

438.6 3-Uniform Hypergraphs/Triple System and Langford Pairs - [Donald Knuth] - The Art of Computer Programming: Combinatorial Algorithms - Volume 4 - Pages 3,33 - Langford Pairs are combinatorial objects created by all possible ways of spacing each of  $2n$  elements in a set having  $n$  pairs of identical twins so that each pair is spaced equal to its numeric value. In the context of ThoughtNet, langford pairs can be created by embedding any two pair of class stack vertices having identical number of hyperedges passing through them on a plane, separated by distance equal to number of edges traversing the two hypervertices. 3-Uniform Hypergraphs or Triple System can be represented by an equivalent bipartite graph, incidence matrix and a boolean formula.

-----  
439. (FEATURE-DONE) Scheduler Analytics for VIRGO Linux Kernel - Commits - 31 July 2017 and 1,3 August 2017  
-----

-----  
(\*) As mentioned in NeuronRain FAQ at <http://neuronrain-documentation.readthedocs.io/en/latest/>, analytics driven linux kernel scheduler is the ideal application of machine learning within kernel. There are two options to go about:

(\*) First is Application Layer Scheduling Analytics in which a python code for example, learns from linux kernel logs, `/proc/<pid>/schedstat` and `/proc/<pid>/sched` data of CFS and exports key-value pairs on how to prioritize processes' nice values in `/etc/kernel_analytics.conf`. This config file is read by VIRGO Linux kernel `kernel_analytics` module and exported kernelwide. Existing kernel scheduler code might require slight changes to read these variables periodically and change process priorities. There have been past efforts like Scheduler Activations which delink userspace threads and kernel threads by multiplexing  $M$  user threads onto  $N$  kernel threads and focus is on scheduling the userspace threads on kernel threads. But Linux kernel does not have support for Scheduler Activation and has 1:1 user:kernel thread ratio i.e there is no application thread library having scheduling support. This option would be ideally suited for prioritizing userspace threads by deep-learning from process perf data.

(\*) Second is Kernel Layer Scheduling Analytics in which kernel has to make upcalls to userspace machine learning functions. This is quite impractical because kernel overhead and latency of scheduling increases and upcalls are usually discouraged for heavy processing. Moreover this adds a theoretical circularity too - upcall is made on the context of present kernel thread and who decides the priority of the upcall? This requires complete kernel level machine learning implementation (e.g Kernel has an independent replicated implementation of String library and does not depend on userspace GCC libraries). Major hurdle to implement machine learning in kernel is the lack of support for C in machine learning as most of the packages are in C++/Java/Python - e.g. how would Apache Spark cloud processing fit with in kernel?. Computational complexity of this scheduling is  $O(n*m)$  where  $m$  is the time spent per upcall in process priority classification by machine learning and  $n$  is the number of processes. This implies every process would have significant waiting time in queue and throughput takes a hit. Also this requires significant rewrite of kernel scheduler to setup upcalls, do userspace `execve()`, redirect standard error/output (`fd_install`) for logging userspace analytics etc., Userspace upcalls are already supported in VIRGO linux CPU/Memory/FileSystem kernel modules for executing user libraries from kernel. If upcall instead writes to `/etc/kernel_analytics.conf` file than communicating to kernel (using NetLink for example), this option is same as first one.

(\*) Third option is to implement a separate kernel module with access to process waiting queue which loops in a kernel thread and does upcalls to userspace to classify the process priorities and notifies the scheduler on process priorities change asynchronously. But this option is same as first except it is done in kernel with upcalls and overkill while first is a downcall.

First option is chosen for time being because:  
- it is top-down

- it does not interfere in existing scheduler code flow much
- minimal code change is required in kernel scheduler e.g as a KConfig build parameter and can be #ifdef-ed
- key-value pair variable mechanism is quite flexible and broadcast kernelwide
- any interested module in kernel can make use of them not just scheduler
- it is asynchronous while kernel layer scheduling is synchronous (scheduler has to wait to know priority for each process from userspace code)
- second and third options are circuitous solutions compared to first one.
- Languages other than C are not preferable in kernel (<http://harmful.cat-v.org/software/c++/linus>)
- Key-Value pair protocol between userspace and kernelspace effectively tames language barriers between user and kernel spaces indirectly i.e this protocol is atleast as efficient as an inlined kernel code equivalent doing an upcall and computing the same pair
- Key-Value storage can also exist on a cloud too not necessarily in /etc/kernel\_analytics.conf file thus transforming VIRGO kernel into a practical dynamic cloud OS kernel
- first option is more suited for realtime kernels

```
#####
#####
#Scheduler Analytics for Linux Kernel:
#=====
Following DeepLearning models learn from process perf variables - CPU, Memory,
Context switches, Number of Threads and Nice data
for each process id retrieved by psutil process iterator - BackPropagation,
RecurrentLSTM
RecurrentGRU and ConvolutionNetwork models learn software analytics neural
networks from psutil process performance info
Key value pairs learnt from these can be read by Linux Kernel Scheduler or
anything else
and suitably acted upon for changing the process priorities dynamically. Any
kernel module can make an upcall to this userspace
executable and dump the key-value pairs in /etc/kernel_analytics.conf.
Presently the implementation is quite primitive and
classifies the output layer of neural network into "Highest, Higher, High,
Normal, Medium, Low, Lower and Lowest" priority classes
in the format: <pid#deeplearningalgorithm>=<scheduled_priority_class>. Number
of iterations has been set to 10 for all deep learning networks.
#####
#####
```

Following is a simulation of how the key-value pair for reprioritization from Scheduler Analytics could affect the kernel scheduler:

- (\*) Linux kernel scheduler has the notion of jiffies - HZ - set of clock ticks - for time slicing processes
- (\*) Each priority class has a red-black binary search tree based queue - deletion is  $O(1)$  and insertion is  $O(\log N)$  after rebalancing such that longest root to leaf path is not more than twice longer than that of least root to leaf path
- (\*) On receipt of reprioritization analytics, kernel\_analytics exports it kernelwide, scheduler reads this <pid>=<new\_priority> key-value pair and removes <pid> from <old\_priority> red-black tree and inserts in <new\_priority> red-black tree.
- (\*) Thus multiple red-black trees make a trade-off and rebalance periodically with no manual nice interventions - this deletion and insertion is  $O(\log N)$
- (\*) Every reprioritization is therefore  $O(\log N)$ .
- (\*) In realtime bigdata processing of heavy load, priorities can change quite frequently. For  $m$  reprioritizations, scheduler incurs  $O(m \cdot \log N)$  time. But  $m$  can have maximum value equal to total number of processes and thus a multiple of  $N$  (number of processes per priority class) and thus effective worstcase cost is  $O(N \log N)$

## References:

-----  
439.1 Scheduler Activations - Effective Kernel Support for the user level management of parallelism - <http://dl.acm.org/citation.cfm?id=121151>  
439.2 Controlling Kernel Thread Scheduling From Userspace - <http://citeseerx.ist.psu.edu/viewdoc/download?doi=10.1.1.605.3571&rep=rep1&type=pdf>  
-----

-----  
440. (THEORY) Social Networks, Money Flow Markets, Pricing Equilibrium, Centrality, Intrinsic versus Perceptive Valuations - 1 August 2017 and 11 August 2017  
-----

-----  
Flow of money in a network of buyers and sellers and pricing have been described in KingCobra design document - <https://github.com/shrinivaasanka/kingcobra-github-code/blob/master/KingCobraDesignNotes.txt>. Problem of relating intrinsic merit/fitness of an entity to perceptive judgements is essentially reducible to the problem of market equilibrium as below:

In a flow market digraph, there is a directed edge from a vertex  $b$  to vertex  $s$  of weight  $p$  where  $b$  is a buyer,  $s$  is a seller and  $p$  is the price offered by buyer  $b$  for  $s$ . There can be multiple  $b(i)$  edges incoming for a seller  $s$  offering different prices and multiple sellers  $s(i)$  can have incoming edges from a buyer  $b$ . Problem of determining fair price for seller  $s$  amounts to finding objective intrinsic merit/fitness of goods/services of  $s$  while incoming buyer edges are perceptive subjective market values (auction). Treating this as a link graph and applying Centrality measures like PageRank could identify most valued seller in terms of market perception. Thus the problem of intrinsic merit versus perception is ubiquitous and is not just restricted to internet(text, audio-visuals). Assuming Bose-Einstein Condensation in Flow Markets, fitness/merit is measured by least energy. Note of caution is the term "least energy" has multiple meanings depending on context and cannot be literally taken as least entropy. In flow markets, least energy seller could be one with best marketing abilities, quality, technical knowhow, qualifications etc.,

In money flow markets, each buyer  $i$  is allocated a good/service  $j$  of  $x(ij)$  units with utility  $u(ij)$  with price  $p(j)$ . Objective is to maximize the money weighted geometric mean of the product of utilities for all buyers. This has to satisfy Karush-Kuhn-Tucker conditions of convex program i.e this money weighted geometric mean is a convex function (line connecting two points on the graph of a function is always above the graph - epigraph is convex) on a convex set (line connecting any two points in the set is within the set) and optimized subject to KKT conditions. Another algorithm is to construct a goods/services - buyers bipartite flow network with a source and sink. This network has edges weighted by prices from source to goods/services vertices and edges weighted by money from buyers vertices to sink. Mincuts of this network determine price equilibrium by maxflow algorithm.

Previous example is mooted to invoke the striking parallels between buyer versus seller price equilibrium and intrinsic merit versus perception equilibrium - Intrinsic value of a good/service is immutable while buyers' price requirements for same good/service vary; Similarly intrinsic merit of an entity is immutable while perception of an entity is subjective. By replacing price with merit in Convex Program and Maxflow algorithms, equilibrium state between intrinsic merit and perceived merit of a social profile vertex can be found. But still this does not lead to absolute intrinsic merit.

Convex Program for Market Equilibrium is defined as below:

Maximize  $u(ij)^{e(i)}$  where buyer  $i$  has money  $e(i)$  at disposal  
subject to:

Total happiness of a customer =  $\text{Sigma}(u(ij) * x(ij))$  where  $u(ij)$  is the utility buyer  $i$  gets from  $x(ij)$  units of good  $j$

Following maps a Market to Merit equilibrium:

Intrinsic merit of a (corresponds to Seller) vertex is defined by a feature vector of merit variables. Buyers are perceivers. Each perceiver has a pre-allocated total perceived merit which is divided amongst the perceived vertices. The Convex Program for Equilibrium between intrinsic merit and perceived merit is:

Maximize  $u(ij)^{e(i)}$  where perceiver  $i$  has total perceived merit  $e(i)$  at disposal and  $u(ij)$  is the utility perceiver  $i$  gets from merit variable  $j$  of a vertex  
subject to:

Total happiness of a perceiver = utility of  $i$  =  $\text{Sigma}(u(ij) \cdot x(ij))$  where  $u(ij)$  is the utility perceiver  $i$  gets from  $x(ij)$  units of merit variable  $j$  of a vertex

and  $p(j)$  is the equilibrium perceived merit of a variable  $j$

Solving the previous convex program results in an optimal merit vector (set of  $p(j)$ 's) and weights of merit variables ( $x(j)$ 's) which satisfies both perceiver and perceived.

This equilibrium is closely related to Nash Bargaining Problem which postulates existence of an agreement and disagreement point  $(a,b)$  in a set  $X$  in  $R^2$  involving two players where  $a$  and  $b$  are utilities of the two players. Nash function of a point  $(a,b)$  is the maximum  $a \cdot b$ . In the context of merit equilibrium, the equilibrium point  $(a,b)$  is in optimum distance between intrinsic merit and perceived merit and maximizes happiness utility of both perceiver and the perceived.

References:

-----  
440.1 Algorithmic Game Theory - Chapter 5 and Chapter 15 - Existence of Flow Markets Equilibrium and Nash Bargaining Problem - Fisher and Eisenberg-Gale Convex Program and Network MaxFlow algorithm - [Tim Roughgarden, Noam Nisan, Eva Tardos, Vijay Vazirani] - [http://www.cambridge.org/download\\_file/909426](http://www.cambridge.org/download_file/909426)  
440.2 New Convex Program for Fisher Market Equilibria - Convex Program Duality, Fisher Markets, and Nash Social Welfare - [Richard Cole † Nikhil R. Devanur ‡ Vasilis Gkatzelis § Kamal Jain ¶ Tung Mai k Vijay V. Vazirani \*\* Sadra Yazdanbod ††] - <https://arxiv.org/pdf/1609.06654.pdf> - Previous Convex Geometric Mean Program is a Nash Social Welfare Function which is Spending Restricted. This article introduces an improved Convex Program with higher integrality gap. Integrality Gap is the measure of goodness of approximation and is based on Linear Program Relaxation. LP Relaxation waives the 0-1 integer programming to range of reals in  $[0,1]$ . Approximate CNFSAT Solver implemented and described earlier in this document is also a relaxation but for system of equations. Integrality Gap of CNF MAXSAT solver found experimentally for few instances is  $\sim 100/98 = 1.02$  though still it requires further theoretical analysis to upperbound the error.  
440.3 Triangle Inequality based Christofides  $1/2$ -approximation Algorithm for Travelling Salesman Problem - Combinatorial Optimization - [Christos H.Papadimitriou, Kenneth Steiglitz] - Page 416  
-----

-----  
441. (FEATURE-DONE) Scheduler Analytics update - commits - 1 August 2017  
-----

-----  
(\* ) Updated AsFer Design Document  
(\* ) Updated python-src/software\_analytics/DeepLearning\_SchedulerAnalytics.py to write in /etc/kernel\_analytics.conf  
(\* ) logs committed to testlogs/  
-----

-----  
442. (FEATURE-DONE) Graph Density (Regularity Lemma) and Bose-Einstein Fitness implementations - commits - 1 August 2017  
-----



-----  
 (\*) New intrinsic merit measures based on graph density (regularity lemma) and Bose-Einstein intrinsic fitness have been added as functions and invoked  
 (\*) logs have been committed to testlogs/  
 -----

-----  
 443. (THEORY) Mistake bound learning(MB), Experience and Intrinsic merit, Social Network Analytics - 2,3,11 August 2017 - related to 368, 438  
 -----

Mistake bound learning, iteratively refines and converges from an initial hypothesis based on mistakes. PAC learning is also a kind of mistake bound learning. Previously described differential equation relation between experience and intrinsic merit/fitness/natural talent can be theoretically formalised as below:

Let M be the intrinsic merit (correctness) of a boolean function hypothesised in the form of conjunctions and disjunctions. From the derivation of experience(E) versus merit(M) as function of time(t):

$$\begin{aligned} dE/dt &= kME \\ \Rightarrow dE &= kME \cdot dt \\ \Rightarrow dE/E &= kM \cdot dt \\ \Rightarrow \log E &= kMt + c \\ \Rightarrow E &= e^{(kMt+c)} \\ \Rightarrow E &= M \cdot e^{(kMt)} \end{aligned}$$

If  $dE/dt$  is replaced by number of mistakes  $b1$  made and corrected per time unit in MB model and  $E$  is replaced by total number of mistakes  $b2$  made so far in hypothesis and corrected (experience is function of this in human context), learner's experiential learning converges in time  $t$  to some percentage error and number of mistakes done in time  $t$ ,  $b2 = t \cdot b1$ .

$$\begin{aligned} \Rightarrow E &= M \cdot e^{(kMt)} \\ \Rightarrow E &= M \cdot e^{(kM \cdot b2/b1)} \end{aligned}$$

Previous expression for experience depends both on intrinsic merit and mistakes made which is exactly required in human classification.

Traditionally mistake bounds are used only in learning boolean functions. Generalizing it to any functions and humans creates a generic definition of merit and experience irrespective of the entity involved. Assumption in the previous differential equation is delta increase in experience is proportional to existing experience and merit. Boolean function learning theory does not appear to have the concept of intrinsic merit or how learning accrued so far helps in further learning which is quite essential for classifying humans based on merit+experience in social networks and human resource analytics. In previous expression for mistake bounded experience, number of mistakes made  $b2$  and  $b1$  themselves could be a function of factors like IQ and EQ e.g  $b1 = f(IQ, EQ)$  and  $b2 = g(IQ, EQ)$ . Then experience becomes:

$$\Rightarrow E = M \cdot e^{(kM \cdot g(IQ, EQ)/f(IQ, EQ))}$$

If  $M=h(IQ)$ :

$$\Rightarrow E = h(IQ) \cdot e^{(k \cdot h(IQ) \cdot g(IQ, EQ)/f(IQ, EQ))}$$

It has to be mentioned here  $f$  is nothing but the first temporal derivative of  $g$  evaluated at time  $t$  i.e  $f = dg/dt$ .

$$\Rightarrow E = h(IQ) \cdot e^{(k \cdot h(IQ) \cdot g(IQ, EQ)/g'(IQ, EQ))}$$

Alternatively,  $f$  and  $g$  can be substituted directly if known and integrable:

$$\begin{aligned} g'(IQ, EQ) &= k \cdot h(IQ) \cdot g(IQ, EQ) \\ g'(IQ, EQ) &= k \cdot h(IQ) \cdot g(IQ, EQ) \\ \log g(IQ, EQ) &= k \cdot M \cdot t + c \\ g(IQ, EQ) &= h(IQ) \cdot e^{(k \cdot h(IQ) \cdot t)} \end{aligned}$$

Curiously, function  $g$  which depends on  $EQ$  has no equivalent in RHS except time duration  $t$  and a constant  $k$ . This is probably because time is measured in terms of mistakes in the integral above and  $EQ$  is function of mistakes. Intrinsic merit function  $M$  does not involve  $EQ$  because mistakes alone are usually emotive in the context of social profiles (bounded rationality) and merit must be independent of emotions and time. Previous definition of experience can be used as a ranking metric for human social profiles as below for comparison of two humans after evaluating  $h$ ,  $g$  and  $g'$  for some time duration subject to disclaimer that follows:

$$g(IQ1, EQ1) = h(IQ1) * e^{(k * h(IQ1) * t1)}$$

$$g(IQ2, EQ2) = h(IQ2) * e^{(k * h(IQ2) * t2)}$$

Disclaimer: Previous model of merit based on  $IQ$  and  $EQ$  are purely presumptive and disputable because of lack of well-defined Bose-Einstein "least energy" counterpart for human profiles.

This model is quite generic and should apply to any computable function including boolean learnt by mistake bounds. For boolean function learning, this model implies total number of mistakes corrected at time  $t$  ("experience") depends exponentially on learning time i.e if the mistake bound learning algorithm is polynomial time in number of variables, number of mistakes corrected is exponential in number of variables. For learning 3CNFs polynomial time mistake bound in RHS implies exponential number of mistakes have been corrected (function  $g$ ) in LHS but an existing result implies if polynomial time learning is possible for 3CNFs there is no polynomial time algorithm for SAT (section 368) (But, isn't correcting exponential number of mistakes in polynomial time a nemesis of SETH?).

Mistakes in the social networks context are proportional to bounded rationality of the human social profile vertices of the social network. Bounded rationality in turn arises by inability of a human being to make 100% correct decision because of cognitive, psychological, emotional, time limitations. Decision taken is termed satisfactory than optimal and such suboptimal decision is called satisficing. Thus emotional quotient and bounded rationality are related. Measuring emotional quotient (intelligence+emotions) than intelligence quotient (intelligence alone) in social network profiles is equivalent to quantifying the sentiments of social network tweets/wallposts/likes etc.,

Thus following equivalence is conspicuous: Emotional Quotient (proportional to) Bounded Rationality (proportional to) Sentiment polarity of Social profile data e.g obtained by Sentiwordnet sentiment analysis. This is an approximate estimation of mistake-prone-ness and applies to decision errors of voters in Condorcet Jury Theorem group decision circuit too.

BackPropagation is a mistake bound deep-learning algorithm refining a perceptron by trial and error iterations. Previous differential equation for experiential learning is equivalent to a time-evolving recursive mistake correction tree described below:

At time  $x$ , tree reaches level  $l(x)$ . Each node in the tree is a corrected mistake and each mistake corrected at level  $l(x)$  is subtree root for  $n$  corrected mistakes in level  $l(x+1)$ . Thus each level  $l(x)$  of the learning tree is the set of mistakes made at time  $x$ . In the language of NC-PRAM circuit families, each node is a PRAM processor correcting a mistake. After time duration  $x$ , this learning tree has  $2^x - 1$  nodes correcting exponential number of mistakes. In NC notation, if number of mistake correcting processors  $= 2^x = n$ , depth of the circuit is  $O(\log n)$  equal to learning time  $x$ . This is a hypothetical parallel learning algorithm in non-uniform NC. This recursive mistake correction tree is nothing but a translation of differential equation  $dE/dt = kME$ . Outdegree of each vertex (number of future mistakes corrected by a PRAM processor) is determined by merit  $M$ , and delta increase in learning is number of mistakes corrected at level  $l(x)$  after time  $x = M * 2^{l(x)}$ . This should apply to backpropagation weight update iterations because each error term is a mistake. Perceptrons are in  $TC=AC=NC$  which is same as previous PRAM recursive learning.

Caveat is the previous recursive mistake correction tree is not traditional

bottom-up evaluation circuit but is top-down based on heuristic: mistake corrected at time  $x$  helps correcting  $n$  number of mistakes at time  $x+\Delta t$  inspired by a differential equation for experiential learning. It makes sense to define "least energy/fitness" of a social network profile vertex to be equal to function  $g$  above thereby sufficiently weighing both merit and experiential learning. Social networks fall into two classes: Professional (e.g. LinkedIn/Stackoverflow/Quora/Academic Citation Networks) and Personal (e.g. Facebook/Twitter/Instagram/Whatsapp). Aforementioned definition of least energy as function of merit and experience applies only to Professional social networks. Stackoverflow is a special case of professional social profile - users up or down vote answers to a question which is fame-driven and not merit-driven. Least energy in personal social networks is totally unrelated to merit and experience and should more or less quantify definition of fitness in Facebook mentioned in 438.5 - profile having high nett positive emotive sentiment evaluated from wallposts/tweets/likes/replies/retweets. Personal social networks are replete with spam, chutzpah, trolls, expletives, emojis, satires etc., requiring parsing/filtering in Sentiment Analysis. Reference 443.4 analyzes the Merit Versus Fame problem in academic citations which belongs to Professional social network category. In essence ranking humans on intrinsic merit is two-fold: 1) Merit-Experience ranking 2) Personal Emotive ranking. These two rankings need not coincide and define intrinsic fitness/least energy of a person in two disjoint contexts. In literature, fitness/least energy of a social profile vertex is not a point value but a probability distribution i.e probability of a vertex/person having an intrinsic merit random variable value. Let us assume that merit is defined as a vector of  $n$  dimensions as:

$M = \langle m_1, m_2, m_3, \dots, m_n \rangle$  where each  $m_i$  is the weight for a merit variable  
For example, Probability distribution for merit/least energy/fitness can be defined as:

$\Pr(M=m_i) = m_i/|M|$  where  $|M|$  is the L1 norm of  $M$

$\text{Sigma}(\Pr(M=m_i)) = (m_1 + m_2 + m_3 + \dots m_n) / |M| = 1$

Continuous Probability distribution is the polynomial passing through above merit weight points.

In generic sense, previous recursive mistake correction tree need not be a binary tree but a graph: At any time point  $t$ , number of mistakes corrected by a social profile vertex thus far forms an evolving triangular region of experience  $E$ , and each corrected mistake vertex in this triangle causes some mistake to be corrected in a future trapezoidal region  $dE$  in time interval  $(t, t+dt)$  adjoining this triangle  $E$  weighted by intrinsic merit  $M$ . This intuitively captures the equation  $E = M \cdot e^{(kMt)}$  ( $dE/dt = kME$ ) and the paradigm "experience = learning from mistakes"

References:

-----

443.1 Mistake bound learning - <https://www.cs.utexas.edu/~klivans/lec1.ps> - In this teacher/learner model, learner iteratively refines hypothesis based on mistakes pointed out by teacher and number of mistakes are polynomially bounded.  
443.2 Learning quickly when irrelevant attributes abound - [Nick Littlestone] - <http://citeseerx.ist.psu.edu/viewdoc/download?doi=10.1.1.130.9013&rep=rep1&type=pdf>  
443.3 Bounded Rationality and Satisficing - [https://en.wikipedia.org/wiki/Bounded\\_rationality](https://en.wikipedia.org/wiki/Bounded_rationality)  
443.4 Multiplex Networks with Intrinsic Fitness: Modeling the Merit-Fame Interplay via Latent Layers - [Babak Fotouhi and Naghmeh Momeni] - <https://arxiv.org/pdf/1506.04189.pdf> - An example of intrinsic merit versus fame in Academic Citations graph - "...We consider a growing directed multiplex network that comprises two layers. Each node is assigned an intrinsic fitness, which models its quality. The fitness of a node never changes. Each node belongs to two layers: a merit layer and a fame layer. In the former, fitness values are the sole drivers of the growth mechanism. In the fame layer, attachment is preferential, that is, the probability that a node receives a link from a newcomer is proportional to the total degree of that node, i.e., the sum of its degrees in both layers. For example, in the case of citation networks, the interpretation of the model is as follows. Two distinct types of citations can

be discerned. The first type—the meritocratic type—is when a scholar reads a paper, and cites it because of its content (a citation which would be given regardless of the number of citations that paper already has). Another type of citation is what we call fame-driven. A paper can become trendy, or well-known in some literature (particularly true for seminal papers which initiate a new subfield), and many citations that it receives would be solely due to its fame—i.e., current number of citations,..."

443.5 Relation between Intrinsic Merit of two vertices and probability of creating link between them - Page 27 - Equation 3.1 -

<http://bura.brunel.ac.uk/bitstream/2438/10345/1/FulltextThesis.pdf> - a new vertex is assumed to have an apriori fitness and probability of establishing connection between a new node and an existing node in social networks is weighted average of probability of new node creation and edge creation between new node and existing node. From this edge probability an a posteriori fitness distribution can be derived for all vertices after a stationary markov chain random walk.

443.6 First to Market is not Everything: an Analysis of Preferential Attachment with Fitness - [Christian Borgs, Jennifer Chayes, Constantinos Daskalakis \* Sebastien Roch †] -

<https://www.microsoft.com/en-us/research/wp-content/uploads/2016/11/First-to-Market-is-not-Everything-an-Analysis-of-Preferential-Attachment-with-Fitness.pdf>

- Polya Urn model of preferential attachment and Power law relation between degree of a vertex in networks and its intrinsic fitness - "...A by-product of our technique is a precise characterization of the vertex dynamics under preferential attachment with fitness. More specifically, if a vertex  $v$  has fitness  $f$ , then our analysis implies that its degree  $dv(t)$  at time  $t$  scales as  $dv(t) \sim t^{(c*f)}$ , (1) where  $c$  is a global constant determined by the fitness distribution. (The details are omitted from this extended abstract.) Hence, the logarithm of the degree of the vertices directly reflects their quality. We note in passing that this could suggest new directions in the design of ranking or recommendation algorithms...". Roughly this implies, fame in social networks is exponentially related to merit. Previous experience-versus-merit temporal identity strikingly coincides with this. Fame= $dv(t)=t^{(cf)}$  can be rewritten as  $dv(t) = e^{(cf*\log t)}$  which when contrasted against Experience  $E = M*e^{(kMt)}$ , yields  $E=f*e^{(cft)}$  setting fitness  $f$ = Merit  $M$  and  $k=c$ . Similarity between degree of a vertex and experience by matching LHS of these 2 expressions is obvious i.e experience of vertex is proportional to its adjacency. This is intuitive because experience is gained after interacting with other vertices and correcting mistakes while judging them. Alternatively, Experiential Learning  $E$  can be defined in terms of time evolving degree of vertex :

$$\log(dv(t)) = cf*\log t$$

$$f=\log(dv(t))/c\log(t)$$

$$\text{Since } f=M, E = M*e^{(kMt)} = \log(dv(t)) * e^{(k\log(dv(t))*t/c\log t)} / c\log t$$

443.7 Degree distribution and Intrinsic Fitness -

[https://www.cs.upc.edu/~CSN/slides/08network\\_dynamics.pdf](https://www.cs.upc.edu/~CSN/slides/08network_dynamics.pdf) - "... Consider  $f(x_i, x_j) = (x_i*x_j)/x(M)^{MM}$  where  $x(M)$  is the largest value of  $x$  in the network. Then the mean degree of a node of fitness  $x$  is  $k(x) = nx/x(M)^2 * \int_0^\infty [yp(y)dy] = N\langle x \rangle/x(M)^2 \dots$ " - Expected Degree of vertex and Fitness of vertex are thus related - Expectation of Fitness PDF is obtained by integral.

443.8 Ghadge et al Model of Intrinsic Fitness of a vertex -

<https://www.cs.umb.edu/~duc/publications/papers/ijpeds10.pdf> - A statistical construction of power-law networks - [Shilpa Ghadgea, Timothy Killingback, Bala Sundaram and Duc A. Trana] - "... To motivate the definition of our procedure, we observe that in most real-world networks the nodes will have an attribute or an associated quantity that represents, in some way, the likelihood that other nodes in the network will connect to them. For example, in a citation network (see, e.g. [22]), the different nodes (i.e. papers) will have different propensities to attract links (i.e. citations). The various factors that contribute to the likelihood of a paper being cited could include the prominence of the author(s), the importance of the journal in which it is published, the apparent scientific merit of the work, the timeliness of the ideas contained in the paper, etc. Moreover, it is plausible that the overall quantity that determines the propensity of a paper to be cited depends essentially multiplicatively on such various factors. The multiplicative nature is likely in

this case since if one or two of the factors happen to be very small, then the overall likelihood of a paper being cited is often also small, even when other factors are not small. The case of Mendel's work on genetics constitutes an exemplar of this – an unknown author and an obscure journal were enough to bury a fundamentally important scientific paper. Motivated by this and the other examples, we consider it reasonable that in many complex networks each node will have associated to it a quantity, which represents the property of the node to attract links, and this quantity will be formed multiplicatively from a number of factors. That is, to any node  $i$  in the network there is associated a non-negative real number  $F_i$ , which is called the fitness of node  $i$ , and which is of the form  $F_i = \text{product}(f_l)$ ,  $l=1$  to  $L$  where each  $f_l$  is non-negative and real. ..."

- this multiplicative intrinsic merit is mapped to summation of logarithms of merit variables. Central Limit Theorem implies summation of random variables converge to a Gaussian irrespective of values of merit variables. Merit variables are dimensional projections of merit vector defined above. CLT also implies merit (social or linguistic) converges to a Gaussian as it were in real life - tails are entities with highest and lowest merit and modal is of maximum merit. Interestingly, this prohibits multimodal. It has to be noted here Recursive Gloss Overlap algorithm computes the intrinsic merit of a text as a product of graph complexity merit variables (Section 4.6 of <https://arxiv.org/abs/1006.4458>, Section 5.6 of [https://tac.nist.gov/publications/2010/participant.papers/CMI\\_IIT.proceedings.pdf](https://tac.nist.gov/publications/2010/participant.papers/CMI_IIT.proceedings.pdf)). Recursive Gloss Overlap graph intrinsic merit is indeed a mapping of social network intrinsic fitness to graph representation of texts - socially networked humans are replaced by hyperlinked texts.

443.9 Vertex Intrinsic Fitness in Social Networks - [Servedio, Caldarelli] - <https://arxiv.org/pdf/cond-mat/0309659.pdf>

443.10 Bibliography listed in Social Networking: Mining, Visualization and Security - [Mrutyunjaya Panda, Satchidanda Dehuri, Gi-Nam Wang] - <https://books.google.co.in/books?id=5-W5BQAAQBAJ&pg=PA42&lpg=PA42&dq=intrinsic+fitness+social+network&source=bl&ots=KD2lkaUq9Q&sig=6WmEYptNmz4X2Y4qrQHJIRpsHk&hl=en&sa=X&ved=0ahUKEwi1770J7dHWAhUBtY8KHZ9hBPcQ6AEITDAH#v=onepage&q=intrinsic%20fitness%20social%20network&f=false>

443.11 Vertex Fitness defined in terms of Unfitness - Network growth models: A behavioural basis for attachment proportional to fitness - [Michael Bell\*, Supun Perera, Mahendrarajah Piraveenan, Michiel Bliemer, Tanya Latty, Chris Reid] - <https://arxiv.org/pdf/1702.04046.pdf>

443.12 A  $\kappa$ -deformed Model of Growing Complex Networks with Fitness - [Massimo Stella, Markus Brede] - <https://arxiv.org/pdf/1404.3276.pdf> - Generalizes the Bianconi-Barabasi Bose-Einstein Condensation Least Energy Intrinsic Fitness of a vertex - <https://arxiv.org/pdf/1404.3276.pdf>

443.13 Various Intrinsic Fitness Models - Barabasi-Albert, Barabasi-Bianconi, Ghadge Log Normal Fitness Attachment, Caldarelli Fitness - [https://www.cs.umb.edu/~duc/www/research/publications/papers/bookchapter\\_fitness\\_models.pdf](https://www.cs.umb.edu/~duc/www/research/publications/papers/bookchapter_fitness_models.pdf) - Of these Ghadge LNFA multiplicative intrinsic fitness has close resemblance to Recursive Gloss Overlap Intrinsic Merit and Recursive Lambda Function Growth Graph Tensor Neuron Network Intrinsic Merit which are both multiplicative and additive.

-----

444. (FEATURE-DONE) Scheduler Analytics Update - Commits - 10 August 2017

-----

(\*) There is a problem in defining expected priorities in BackPropagation Neural Network output layer. This is necessary for weight update to happen iteratively and to quantify error between expected and actual neural network output

(\*) Output layer of BackPropagation is an indicator of process priority learnt by the perceptron.

(\*) Previously expected priorities were hardcoded. This has been changed as below:

(\*) Set of processes currently running are clustered and stored in an input JSON file

- (\*) This JSON dictionary has key-value pairs mapping a process class to its apriori expected priority
- (\*) Scheduler Analytics loads this JSON and looks up the expected priority for each process executable by its process class
- (\*) Presently process class is just a substring of the executable name
- (\*) BackPropagation does string match of this process class to executable name and finds the expected priority from JSON dict
- (\*) BackPropagation iteration updates the weights of all 3 layers
- (\*) Defining apriori class of a process is subjective and instead of substring of executable, an independent clustering algorithm having a suitable distance function can be used to write the JSON classification of processes. For example, unix process groups are numerical classes of processes.
- (\*) Previous generation of JSON classes for processes and backpropagation weight update iteration is the first phase of analytics.
- (\*) In the second phase, weight-updated BackPropagation Neural Network takes as input runtime process statistics (CPU, Memory and Context Switches) to predict the actual priority of a process belonging to the apriori class.
- (\*) This is a depth 2 tree evaluation:
  - Static - apriori expected class of a process and BackPropagation iteration
  - Dynamic - fine grained priority of a process within the previous static class by evaluating the multilayer neural network

Presently, input variables are per process CPU percentage, Memory percentage and ratio of involuntary context switches to total context switches. Involuntary context switches are usually number of pre-emptions by the scheduler on time-slice expiry and Voluntary context switches are number of system call and I/O pre-emptions.

-----  
 445.(FEATURE-DONE) Celestial Pattern Mining Update - specific to NeuronRain Research in SourceForge repositories - recreated Sequence Mined Rules - Commits - 22 August 2017  
 -----

- (\*) Added a documentation text file asfer-docs/NeuronRain\_Research\_Celestial\_Pattern\_Mining.txt describing how astronomical pattern mining is done and code involved therein.

- (\*) In python-src/autogen\_classifier\_dataset/MaitreyaToEncHoroClassified.py upgraded Maitreya's Dreams (<http://www.saravali.de/>) ephemeris text client version to 7.1.1

- (\*) Created separate string encoded astronomical data files for Earthquakes(USGS 100 year earthquake dataset) and Storms(NOAA 100 year HURDAT2 dataset) Datasets from python-src/autogen\_classifier\_dataset/MaitreyaToEncHoroClassified.py (zodiacal does not have ascendant, while asrelative is rotated string relative to ascendant. Ascendant is defined astronomically as the degree of the zodiac sign rising at the time of an event in eastern horizon)

- (\*) Executed python-src/SequenceMining.py on these 2 datasets. The results have been written to python-src/MinedClassAssociationRules.txt

- (\*) python-src/autogen\_classifier\_dataset/asfer\_dataset\_seggregator.sh has updated asfer relative location

-----  
 446. (FEATURE-DONE) Celestial Data Pattern Mining - Updates to autogen\_classifier\_dataset pre-processing and classification of datasets - 23

August 2017

-----  
-----  
(\*) An 8 year old lurking bug in cpp-src/NaiveBayesClassifier.cpp has been resolved. It was causing a null class to be returned after bayesian argmax() computation.  
(\*) Lot of new articles on earthquakes and hurricanes have been added as training dataset for NaiveBayesian Classifier. These articles also have lot of research information on predicting hurricanes and earthquakes  
(\*) python-src/autogen\_classifier\_dataset/AsferClassifierPreproc.py has been updated to include new articles in training data for NaiveBayesian  
(\*) words.txt, word-frequency.txt, training-set.txt, topics.txt, test-set.txt have been re-created by executing  
python-src/autogen\_classifier\_dataset/AsferClassifierPreproc.py  
(\*) Datasets are classified into  
python-src/autogen\_classifier\_dataset/EventClassDataSet\_Earthquakes.txt and  
python-src/autogen\_classifier\_dataset/EventClassDataSet\_Storms.txt by executing  
asfer\_dataset\_seggregator.sh  
-----

-----  
447. (FEATURE-DONE) Updated Ephemeris Search Script - Commits - 24 August 2017  
-----

-----  
Updated mined class association rule parsing in  
python-src/MaitreyaEncHoro\_RuleSearch.py  
-----

-----  
448. (FEATURE-DONE) Approximate CNFSAT Solver update - SciPy Sparse - 28 August 2017  
-----

-----  
(\*) imported scipy.sparse.linalg least squares function lsqr().  
(\*) Number of clauses and variables set to 18 each.  
(\*) After 673 iterations of Random 3CNFs following satisfied clauses data were observed:  
Percentage of CNFs satisfied so far: 58.7537091988  
Average Percentage of Clauses per CNF satisfied: 97.0161556215  
-----

From LLL, If  $p < 1/[e(d+1)]$  is the probability of an event (not satisfying a clause) :

Probability that clause is satisfied:  $1-p > (1-1/[e(d+1)])$

Probability that all of the clauses are satisfied  $> (1-1/[e(d+1)])^{(d+1)}$  (for  $d+1$  clauses)

Probability that some of the clauses are satisfied  $< 1-(1-1/[e(d+1)])^{(d+1)}$

If all clauses overlap:

In previous example  $d+1 = 18$  and thus probability that all of the clauses are satisfied for any random CNF is :

$(1-1/[e(18)])^{(18)} > \sim 68.96\%$

and probability that some but not all of the clauses being satisfied for any random CNF is:

$1-(1-1/[e(18)])^{(18)} < \sim 31.043\%$

If none of the clauses overlap:

$d=0$  and probability that all the clauses are satisfied  $(1-1/e) > \sim 63.21\%$

and probability that some but not all of the clauses being satisfied for any random CNF is  $< \sim 36.79\%$   
-----

-----  
449. (THEORY) Analysis of Error Upperbound for Approximate CNFSAT Solver based on Lovasz Local Lemma clause dependency digraph - 29 August 2017  
-----

,30 August 2017

-----  
Probability of a clause being not satisfied from Lovasz Local Lemma:

$$p < 1/(e(d+1))$$

Probability of a clause being satisfied:

$$1-p > 1 - 1/(e(d+1))$$

Probability of all n clauses being satisfied (ExactSAT):

$$(1-p)^n > [1 - 1/(e(d+1))]^n$$

Probability of some or none of the clauses being satisfied:

$$1-(1-p)^n < 1 - [1 - 1/(e(d+1))]^n$$

If there are no overlaps,  $d=0$ :

$$\text{Probability of all n clauses being satisfied} = (1-p)^n > [1 - 1/e]^n = [1 - 1/e]^n$$

$$\text{Probability of some or none of the clauses being satisfied} = 1 - (1-p)^n < 1 - [1 - 1/e]^n$$

Probability of atleast k of n clauses being satisfied:

$$\Pr[\#SATclauses \geq k] = \Pr[\#SATclauses = k] + \Pr[\#SATclauses = k+1] + \Pr[\#SATclauses = k+2] + \dots + \Pr[\#SATclauses = n]$$

$$= (1-p)^k + (1-p)^{k+1} + \dots + (1-p)^n$$

if  $q = 1-p$ :

$$= q^k + q^{k+1} + \dots + q^n$$

$$= q^k * (1 + q + q^2 + \dots + q^{n-k}) \quad [\text{Geometric series}]$$

$$= q^k (1 - q^{n-k+1}) / (1-q)$$

But from LLL,  $p < 1/(e(d+1))$

$$q = 1 - p > (ed+e-1)/(ed+e)$$

Substituting for q:

$$[(ed+e-1)/(ed+e)]^k [1 - [(ed+e-1)/(ed+e)]^{n-k+1}]$$

$$1 - [(ed+e-1)/(ed+e)]^{n-k+1}$$

#####  
#Probability of atleast k of n clauses being satisfied: #  
#  $[ed+e-1]^k [(ed+e)^{n-k+1} - [ed+e-1]^{n-k+1}]$  #  
# ----- #  
#  $[(ed+e)^n]$  #  
#####

if  $k=n$ :

$$(ed+e-1)^n / (ed+e)^n$$

If overlap of variables across the clauses is huge,  $ed+e-1 \sim ed+e$

Maximum overlap d is (n-1) i.e a clause has common variables across all other clauses

When d is maximum:

$$\text{Lt } (d \rightarrow n-1, n \rightarrow \text{infinity}) ((ed+e-1)/(ed+e))^n$$

$$= [((e(n-1)+e-1)/(e(n-1) + e))]^n$$

$$= [(en-e+e-1)/(en-e+e)]^n$$

$$= [(en-1)/(en)]^n$$

$$= [(1-1/ne)]^n$$

$$= [1 - 0.3678/n]^n$$

For infinite n:

$$= e^{(-0.3678)}$$

$$\Pr[\#SATclauses = n] = 69.22\%$$

When overlap is absent at  $d=0$ :

$$\Pr[\#SATclauses = n] = (e-1)^n/e^n = (0.6321)^n \rightarrow 0 \text{ for huge } n$$



When  $d=1$  (minimum overlap):

-----  
 $\Pr[\#SATclauses = n] = [2e-1]^n / [2e]^n = [1-0.5/e]^n = (0.81606)^n \rightarrow 0$  for huge  $n$

=> When the number of variables overlapping across clauses tends to a huge number almost equal to number of clauses, the system of linear equations obtained by relaxing each of the clauses are solved by least squares and probability of all clauses being satisfied tends to 69.22%. High overlap of variables across clauses is the most probable occurrence in real world SAT solvers. If the overlap as random variable is uniformly distributed:

Expected value of  $d = 1/(n-1) * (n-1)n/2 = n/2$

For mean overlap of  $n/2$  variables across clauses:

#####  
#Probability of atleast k of n clauses being satisfied: #  
#  $[en/2+e-1]^k [(en/2+e)^{(n-k+1)} - [en/2+e-1]^{(n-k+1)}]$  #  
# ----- #  
#  $[(en/2+e)^n]$  #  
#####

When  $k=n$ :

$[en/2+e-1]^n$

-----

$[en/2+e]^n$

$= [1 - 0.7357888/(n+1)]^n > [1 - 0.7357888/n]^n$

$= \lim_{n \rightarrow \infty} [1 - 0.73578882/n]^n = e^{-0.73578882}$

=>  $\Pr[\#SATclauses = n] > 47.91\%$

=> When the number of variables overlapping across clauses are uniformly distributed, Probability of all clauses being satisfied per random 3CNF is lowerbounded as 47.91% when number of clauses tend to infinity.

=> Caveat: This is an average case analysis of overlaps and best case analysis for number of clauses satisfied. This implies SAT is approximately solvable in polynomial time asymptotically in infinite if the overlaps are uniformly distributed. This is almost an 1/2-approximation in average overlap setting, similar to Christofides algorithm for TSP. This is not an abnormal approximation and it does not outrageously contradict witnesses towards  $P \neq NP$  described earlier in this document.

Correction to Geometric distribution LLL estimate:

-----  
Previous bound assumes  $\Pr[\#SATclauses \geq k]$  is geometric distribution. If  $k$  satisfying clauses are chosen from total  $n$  clauses in 3CNF, it is a tighter binomial distribution and not geometric.

=>  $\Pr[\#SATclauses \geq k] = \sum_{l=k}^n \binom{n}{l} (1-p)^{n-l} p^l$ ,  $l=k, k+1, k+2, \dots, n$

If  $k=n/2$ , this summation is exactly same as Condorcet Jury Theorem where each clause in the 3CNF is a voter = probability of majority of the clauses are satisfied. Each satisfying clause is +1 vote and each rejecting clause is -1 vote. Condorcet Jury Theorem thus applies directly and  $\Pr[\#SATclauses \geq k]$  tends to 1 if  $p > 1/2$  and tends to 0 if  $p < 1/2$ . For  $p=0.5$ ,  $\Pr[\#SATclauses \geq k] = 0.5$ . From LLL,  $p=0.5$  implies  $e^{0.5(d+1)} > 1$  (or)  $(d+1) > 2/e$ . For arbitrary values of  $k$ , computing closed form of binomial coefficient sum for  $\Pr[\#SATclauses \geq k]$  requires hypergeometric functions.

When  $k=n$ :

-----

$\Pr[\#SATclauses = n] = (1-p)^n$

From LLL,  $e^{p(d+1)} > 1 \Rightarrow p > 1/e(d+1)$

$$1-p < 1 - 1/e(d+1)$$

$$1-p < 1 - 0.36788/(d+1)$$

$$(1-p)^n < (1 - 0.36788/(d+1))^n$$

d=0, no overlaps:

-----  
 $\Pr[\#SATclauses=n] = (1-p)^n < (0.6321)^n$  which tends to 0 for huge number of clauses n.

d=n-1, maximum overlaps:

-----  
 $\Pr[\#SATclauses=n] = (1-p)^n < (1 - 0.36788/n)^n$   
 But  $\text{Limit}(n \rightarrow \infty) (1 - 0.36788/n)^n = e^{(-0.36788)} = 0.692200241$   
 $\Pr[\#SATclauses=n] < 69.22\%$  for huge n.

d=n/2, expected overlaps in uniform distribution:

-----  
 $\Pr[\#SATclauses=n] = (1 - 1/(e(n/2+1)))^n = (1 - 0.735758882/(n+2))^n$   
 $0.735758882/(n+2) < 0.735758882/n$   
 $(1 - 0.735758882/(n+2))^n > (1 - 0.735758882/n)^n$   
 As  $n \rightarrow \infty$ ,  $(1 - 0.73578882/(n+2)) > e^{(-0.73578882)} \sim 47.91\%$   
 $\Rightarrow \Pr[\#SATclauses=n] > 47.91\%$

=> 97-98% satisfied clauses found in few hundred iterations above for upto 20 clauses and 20 variables should tend asymptotically to 69.22% if there are high overlaps, high number of clauses and variables. For average number of overlaps,  $\Pr[\#SATclauses=n] > 47.91\%$  and does not rule out convergence to 98%. This can be substituted for k for probability that 98% clauses are satisfied as below:

$\Pr[\#SATclauses \geq 0.98n] = \text{summation}(nC_l * (1-p)^l * (p)^{(n-l)})$ ,  
 $l=k, k+1, k+2, \dots, n$   
 This is tail bound for binomial distribution which is defined as:  
 $\Pr[X \geq k] \leq e^{(-nD(k/n || p))}$   
 where relative entropy  $D(k/n || p) = k/n \log(k/np) + (1-k/n) \log((1-k/n)/(1-p))$   
 But  $k/n = 0.98n/n = 0.98$   
 $\Rightarrow D(k/n || p) = k/n \log(k/np) + (1-k/n) \log((1-k/n)/(1-p)) = 0.98 \log(0.98/p) + 0.02 \log(0.02/(1-p))$   
 $\Rightarrow \Pr[X \geq 0.98n] \leq e^{(-n*(0.98 \log(0.98/p) + 0.02 \log(0.02/(1-p))))}$   
 From LLL,  $p < 1/e(d+1)$ . Substituting for p:  
 $\Rightarrow \Pr[X \geq 0.98n] \leq e^{(-n*(0.98 \log(0.98e(d+1)) + 0.02 \log(0.02(ed+e)/(ed+e-1))))}$

$$\text{Lt}(n \rightarrow \infty) e^{(-n*(0.98 \log(0.98e(d+1)) + 0.02 \log(0.02(ed+e)/(ed+e-1))))} = 0$$

$\Pr(\#SATclauses \leq n) \leq e^{(-(np-n)^2/2pn)}$  by Chernoff bounds. From LLL,  $p < 1/e(d+1)$ . For average number of overlaps  $d=n/2$ , Chernoff bound reduces to:  
 $\Pr(\#SATclauses \leq n) \leq e^{(-1/e)} \sim 69.22\%$  which coincides with maximum overlaps bound above.

Previous imply approximate CNF SAT solver by solving system of linear equations (= clauses relaxed to reals from binary) is a 0.6922-approximation.

References:

-----  
 449.1 Sum of Binomial Coefficients -  
<http://web.maths.unsw.edu.au/~mikeh/webpapers/paper87.pdf> - "... "For years [before working with George E. Andrews in 1973] I had been trying to point out that the rather confused world of binomial coefficient summations is best understood in the language of hypergeometric series identities. Time and again I would find first-rate mathematicians who had never heard of this insight and who would waste considerable time proving some apparently new binomial coefficient summation which almost always turned out to be a special case of one of a handful of classical hypergeometric identities. ..."  
 449.2 Binomial Distribution Tail Bounds -  
[https://en.wikipedia.org/wiki/Binomial\\_distribution#Tail\\_bounds](https://en.wikipedia.org/wiki/Binomial_distribution#Tail_bounds)

-----  
-----  
450.(THEORY) Analysis of Error Upperbound for Approximate CNFSAT Solver based on Lovasz Local Lemma clause dependency digraph - continued - 1 September 2017  
-----  
-----

(\*) Least Squares lsqr() function has been replaced by recent lsqr() least square function mentioned to be faster.

(\*) For 10 variables and 10 clauses for 54068 random 3CNF iterations following were the percentage of satisfied CNFs and clauses satisfied per CNF:

Percentage of CNFs satisfied so far: 79.6722706172

Average Percentage of Clauses per CNF satisfied: 97.6276609517

(\*) Again the percentage of clauses satisfied per random 3CNF converges to ~98% after ~54000 random 3CNFs.

(\*) The clauses are created by randomly choosing each literal and its negation independent of any other literal or clause and thus are identically, independently distributed. CNFs can repeat since this is not a permutation.

(\*) Repetitive convergence of number of clauses satisfied per CNF to 98% is mysterious in varied clause-variable combinations.

(\*) Previous error bound analysis does not assume least squares and is based only on LLL. But Least Squares is about sum of squares of errors minimization i.e  $\text{Error}^2 = \|Ax-b\|^2$  is minimized e.g  $A^T Ax = A^T b$ , partial first derivative of error set to 0. System of equations translated from each 3CNF is overdetermined or underdetermined mostly i.e number of variables and number of clauses are not equal.

(\*) Motivation for least squares for boolean CNF is the relaxation achieved: An example assignment for a literal, 0.88 is inclined towards boolean 1 and 0.02 is inclined towards boolean 0.

(\*) Convergence to 98% implies probability of average number of clauses satisfied per 3CNF  $> 0.98n$  must be almost 0.

(\*) Following Binomial Tail Bound:

$\Pr[\#SATclauses \geq 0.98n] \leq e^{(-n*(0.98\log(0.98e(d+1)) + 0.02\log(0.02(e+d)/(e+d-1)))}$  is maximized when there are no overlaps -  $d=0$ .

$\Pr[\#SATclauses \geq 0.98n] \leq e^{(-n*(0.98\log(0.98e) + 0.02\log(0.02(e)/(e-1)))}$

$\Pr[\#SATclauses \geq 0.98n] \leq e^{(-n*(0.41701 - 0.02999))}$

$\Pr[\#SATclauses \geq 0.98n] \leq e^{(-n*0.38701)} \sim 0$  for large  $n$ .

-----  
-----  
451.(THEORY) PCP theorem, Hardness of Approximation, Least Squares SAT solver and Semidefinite Programming - related to 450 - 2 September 2017 and 3 September 2017  
-----  
-----

Probabilistically Checkable Proof theorem implies it is NP-hard to find satisfiable instances or  $7/8 + \epsilon$  satisfiable instance to 3SAT. There are Semidefinite Programming optimization algorithms for MAX3SAT which replace the clauses by an arithmetized polynomial for each literal. Sum of these polynomials or Sum of Squares (SOS) of these polynomials is optimized by Semidefinite decomposition. Positive literal  $x$  is replaced by  $(1+x)/2$  and negation  $\neg x$  by  $(1-x)/2$ . Literal polynomials within each clause are multiplied. This is a polynomial over reals and is decomposed as  $XSX^T > 0$  i.e positive semi-definite. Values of these Sum and Sum of Squares polynomials ( $F$ ) for an assignment to CNF ( $a$ ) are equal to number of clauses violating an assignment. Semidefinite Program maximizes/minimizes the difference  $F(a) - e$  (thus maximizing or minimizing the number of violating clauses) where  $e$  is value of  $F$  for assignment  $a$ . In this context, the striking 98% convergence for percentage of clauses satisfied for multiple clause-variable combinations for least squares/LSMR solver gains importance. It implies  $7/8 + \epsilon = 0.98$  (or  $0.875 + 0.105 = 0.98$ ) satisfiable clauses per CNF if proved for all permutations of variables-clauses-overlaps (and that is a big if) implying  $P=NP$ . Atleast a convergence to 0.875 if not 0.98 would suffice.

## References:

-----  
451.1 PCP and hardness of approximation - algorithm satisfying  $7/8 + \delta$  clauses  
- <https://cs.stackexchange.com/questions/71040/hardness-of-approximation-of-max-3sat>

451.2 SDP for MAX3SAT -

[http://www.isa.ewi.tudelft.nl/~heule/publications/sum\\_of\\_squares.pdf](http://www.isa.ewi.tudelft.nl/~heule/publications/sum_of_squares.pdf) - Maximum number of clauses violating an assignment and Semidefinite Programming

451.3 Binary Solutions to System of Linear Equations -

<https://arxiv.org/pdf/1101.3056.pdf>

451.4 Karloff-Zwick  $7/8$  algorithm for MAX3SAT -

<http://citeseerx.ist.psu.edu/viewdoc/summary?doi=10.1.1.51.1351> - A  $7/8$ -approximation algorithm for MAXSAT? - This is randomized polynomial time algorithm and satisfies an expected  $\geq (7/8)n$  clauses.

451.5 Inapproximability results - [Johan Hastad] -

<https://www.nada.kth.se/~johanh/optimalinap.pdf> - Assuming  $P \neq NP$ , MAX3SAT can not have polynomial time algorithm satisfying  $> (7/8)n$  clauses.

451.6 Gauss-Jordan Elimination For System of Linear Equations, Origin of Least Squares, Linear Programs for Inequalities -

<http://www-personal.umich.edu/~murty/LPINFORMStutorial2.pdf> - previous CNF SAT Solver has only equalities.

451.7 Randomized Rounding for LP relaxation -

[https://en.wikipedia.org/wiki/Randomized\\_rounding](https://en.wikipedia.org/wiki/Randomized_rounding) - Randomized Rounding involves 3 steps - formulating a Linear Program for a 3SAT, solving it fractionally and rounding the fraction to nearest integer. Previous CNF SAT Solver maps this rounding process to system of linear equations - formulate each 3SAT as system of linear equations, one equation per clause ( $AX=B$ ,  $B$  is unit vector of all 1s), get fractional values for vector  $X$  from Least Squares, Round the fraction to 0 or 1 whichever is nearest.

-----  
452.(THEORY) Approximate CNF 3SAT Solver - Least Squares Error Rounding Analysis  
- 9 September 2017, 11 September 2017, 14 September 2017  
-----

## Notation:

$A'$  = Transpose of  $A$

$A^{-1}$  = Inverse of  $A$

$E(A)$  = Expectation of  $A$

$p(A)$  = probability of  $A$

Rounding in least squares solution to system of equations per CNF 3SAT fails if and only if binary assignment obtained by rounding does not satisfy the CNF while fractional assignment satisfies the system of equations for CNF. Least Square error is minimized by setting first partial derivative of error to zero:

$$A'Ax = A'b$$

$$\Rightarrow x = (A'A)^{-1}A'b$$

Number of satisfied clauses in least squares is  $= \text{tr}(A(A'A)^{-1}A'b)$  because  $Ax - b$  is minimized.

Maximum value of  $\text{tr}(A(A'A)^{-1}A'b)$  is the maximum number of satisfied clauses if  $\text{tr}(A(A'A)^{-1}A'b) > 7/8 * \text{number\_of\_clauses}$ , then  $P=NP$  by PCP theorem.

Each matrix  $A$  corresponding to a CNF is a random variable -  $A$  is a random matrix (not necessarily square).

Expected value of  $A(A'A)^{-1}A'b$  where random matrix  $A$  belongs to some probability distribution  $= E(A(A'A)^{-1}A'b)$

$$E(A(A'A)^{-1}A'b) = b * E(A) * E((A'A)^{-1}) * E(A')$$

$E(A(A'A)^{-1}A'b) = b * E(A) * E((A'A)^{-1}) * E(A)$  because  $A$  and  $A'$  are bijections.

$E(A(A'A)^{-1}A'b) = b * E(A) * E(A'A) * E(A)$  because  $A'A$  and  $(A'A)^{-1}$  are bijections.

$$E(A(A'A)^{-1}A'b) = b * E(A) * E(A) * E(A') * E(A) \text{ by definition of product of}$$

expectations

$$E(A(A'A)^{-1}A'b) = b*(E(A))^4$$

$$E(A(A'A)^{-1}A'b) = b*(A*p(A))^4$$

Each random matrix for a random 3CNF has nm entries where n is number of variables and m is number of clauses. Each of nm literals is either a variable or its negation.

Probability of choosing a variable or its negation =  $1/(2n)$  for n variables + n negations.

Probability of a random matrix A of mn entries =  $(1/(2n))^{nm}$

$$\Rightarrow E(A(A'A)^{-1}A'b) = b(\sigma(A(1/2n)^{nm}))^4 \text{ in uniform distribution.}$$

$$= b(1/(2n)^{nm} * \sigma(A))^4 \text{ which sums up all } 2^{nm} \text{ possible}$$

boolean matrices.

$$= b(1/(2n)^{mn} * [\text{matrix of } 2^{(nm-1)} \text{ for all entries }])^4$$

$$= b * [\text{matrix of } 2^{(mn-1)/(2n)^{nm}} \text{ for all entries }]^4$$

=====

Tighter estimate for probability of a random 3CNF:

=====

Per clause 3 literals have to be chosen from 2n literals =

$$2nC3(1/2n)^3(1/2n)^{(2n-3)}$$

For m clauses each being independent, Probability of a random 3CNF

$$= (2nC3(1/2n)^3(1/2n)^{(2n-3)})^m$$

$$E(A(A'A)^{-1}A'b) = b * [\text{matrix of } 2^{(mn-1)/(2n)^{nm}} \text{ for all entries }]^4$$

$$(1,m) * (m^n, n^m, m^n, n^m)$$

$$= b * [\text{matrix of } n^2 2^{(2nm-2)/(2n)^{2mn}} \text{ for all entries }]^2$$

$$(1,m) * (m^m, m^m)$$

$$= b * [\text{matrix of } m^n n^2 2^{(2nm-2)/(2n)^{2mn}} \text{ for all entries }]$$

$$(1,m) * (m^m)$$

$$= [\text{matrix of } m^2 n^2 2^{(2nm-2)/(2n)^{2mn}} \text{ for all entries }]$$

$$(1,m)$$

Trace of this expected matrix is the expected number of clauses that can be satisfied by least squares in uniform distribution:

$$= m^3 n^2 2^{(2nm-2)/(2n)^{2mn}}$$

$$\text{if number of clauses to be satisfied } \leq m, m^3 n^2 2^{(2nm-2)/(2n)^{2mn}} \leq m * (2n)^{2mn}$$

$$\Rightarrow m^2 n^2 2^{(2nm-2)/(2n)^{2mn}} \leq (2n)^{2nm}$$

which is obvious because  $(2n)^{(2mn)}$  grows faster.

$$\Rightarrow m^2 n^2 2^{2nm} \leq 4 * 2^{2nm} * n^{2nm}$$

$$\Rightarrow m^2 n^2 \leq 4 * n^{2nm}$$

For all m clauses to be satisfied, this must be an equality:

$$m^2 = 4 * n^{2(nm-1)}$$

if m=n (number of clauses = number of variables), all clauses are satisfied if:

$$n^2 = 4 * n^{(n^2-1)}$$

$$n^2/4 = n^{(n^2-1)}$$

$$\Rightarrow \log(n^2/4) = (n^2-1) \log(n)$$

$$\Rightarrow \log(n^2/4)/\log(n) = (n^2-1)$$

which is a contradiction because RHS grows faster.

=====

Alternatively, following simpler analysis leads to something more concrete:

For minimum error  $x = (A'A)^{-1}A'b$

$Ax = A(A'A)^{-1}A'b$  is maximum when  $A(A'A)^{-1}A'b = b$

$$\Rightarrow A(A'A)^{-1}A' = I$$

When A is square symmetric matrix (number of variables = number of clauses) and  $A=A'$ :

$$\Rightarrow A(AA)^{-1}A = I$$

$\Rightarrow$  Least squares perfectly solves system of equations for CNFSAT if matrix of clauses is symmetric and square i.e error is zero

Least squares thus solves a subset of NP-complete set of input 3CNFs i.e exactly solves a promise NP problem in deterministic polynomial time.

References:

-----

452.1 Advanced Engineering Mathematics - [Erwin Kreyszig - 8th Edition] - Page 357

452.2 Linear Algebra - [Gilbert Strang] -  
<http://math.mit.edu/~gs/linearalgebra/ila0403.pdf>

452.3 Least Squares Error - [Stephen Boyd] -  
<https://see.stanford.edu/materials/lsoeldsee263/05-ls.pdf>

-----  
453. (THEORY) Random Matrix Analysis of Least Squares Approximate CNFSAT solver  
- related to 452 - 15 September 2017  
-----

From previous definition of expected value of random matrix equivalent to a random 3SAT:

$$E(A(A'A)^{-1}A'b) = b*(E(A))^4$$

Previous derivation of expected value of a random matrix is further simplified by a different definition of expectation:

$E(A) = [ \text{matrix of } E(x(i,j)) ]$  i.e each entry of the matrix is evaluated independently.

Let the probability of each entry  $x(i,j)$  of the random matrix =  $p$ . Each entry is a literal or its negation and can take 0 or 1 values.

$$E(x(i,j)) = p$$

$$\Rightarrow E(A) = [ \text{matrix of } p \text{ for all entries} ]$$

$$\Rightarrow b * (E(A))^4 = b * [ \text{matrix of } np^4 \text{ for all entries} ]^2$$

$$= b * [ \text{matrix of } m^2 n^2 p^4 \text{ for all entries} ]$$

$$= [ \text{matrix of } m^2 n^2 p^4 \text{ for all entries} ]$$

$$E(A(A'A)^{-1}A'b) = [ \text{matrix of } m^2 n^2 p^4 \text{ for all entries} ]$$

Trace( $E(A(A'A)^{-1}A'b)$ ) =  $m^3 n^2 p^4$  which has maximum value equal to number of clauses  $m$

$$\Rightarrow m^3 n^2 p^4 \leq m$$

$$\Rightarrow m^2 n^2 p^4 \leq 1$$

$$\Rightarrow p^4 \leq 1/(mn)^2$$

$$\Rightarrow p^2 \leq 1/(mn)$$

$$\Rightarrow p \leq 1/\sqrt{mn}$$

This retrieves the probability distribution of the random 3SAT instances.

If all clauses have to be satisfied (ExactSAT),  $p = 1/\sqrt{mn}$ .

In previous example iterations of the solver, number of clauses = number of variables i.e  $p = 1/n$ .

This differs from the uniform probability assumption  $1/(2n)$  per literal in earlier derivations including the negations too.

The promise subset of NP solved exactly by least squares is defined by the set of all random 3CNFs created with each literal occurring with probability  $1/n$ .

References:

-----  
453.1 Random matrices -

<http://www.utstat.toronto.edu/~brunner/oldclass/431s09/readings/RandomMatrices.pdf>  
-----

-----  
454. (FEATURE and THEORY) Commits - Approximate SAT solver - 15 September 2017  
-----

(\*) Some debug statements have been included to print average probability of each literal's occurrence in random 3CNF.

(\*) SATsolver has been re-executed with 20 clauses and 20 variables and probability of occurrence of each literal has been logged.

(\*) This was necessitated to ascertain the pseudorandomness of the clauses and CNFs created.

(\*) Average probability of a literal is less than previous estimate of  $1/n =$

1/20 = 0.05 for 100% satisfied clauses but still converges to usual 97% for 100 iterations.

(\*) logs committed to testlogs/

-----  
455. (THEORY) Eigenvalues of Random Matrices, Riemann Zeta Function, MAXSAT ranking of merit, Promise problems and Some additional notes on CNFSAT solver scipy/numpy least squares implementation - 18 September 2017 - related to 24,432  
-----

The set of random 3CNFs created by the solver is just a subset of all possible 3CNFs because all least squares API in SciPy require number of variables to be equal to number of clauses, and an exception is thrown at runtime if they are unequal. A better alternative for these API which works for any combination of number of clauses and variables has to be found and substituted in least square invocation (replacing lsqr()/lsmr()). This is a limitation of SciPy/NumPy and not the least squares algorithm. This makes it a Promise SAT solver and not the universal SAT solver for time being. Also for huge number of variables/clauses, both lsqr() and lsqr() functions slow down heavily and it is difficult to test on low-end personal desktops. The most plausible reason for convergence of MaxSAT to ~98% for almost all executions so far is the promise nature of the problem and only subset of 3CNFs (number of clauses=number of variables) are solved. In above random matrix analysis, if number of variables=number of clauses, probability of choosing a literal (positive or negative) is  $1/n$  which is also uniform if two sets of positive and negated literals each of size  $n$  are separately evaluated for probability  $(E(x(i,j))) = 0*1/n + 1*1/n$ . This also raises a question: Since promise-SAT instances are NP-complete, does solving promise-NP imply solving NP. Since least squares exactly solves this promise subset (square matrix of equal number of variables and clauses) when probability of choosing a literal is  $1/n$ , percentage of clauses satisfied is ~98% which is close to 100% implying the probability of choosing a literal is slightly less than uniform  $1/n$ . Exact average MaxSAT percentage of least squares solver can be analyzed only if there is a suitable alternative to SciPy/NumPy. Therefore this convergence still does not contradict  $P \neq NP$  and PCP.

Earlier the problem of intrinsically ranking texts etc., based on merit has been reduced to a MAXSAT problem where each text document etc., satisfies a fixed or variable 3CNFSAT formed from merit variables (e.g textgraph complexity) and merit is ranked by percentage of clauses satisfied. All the quantified outcomes of intrinsic merit algorithms described in this document can be translated to merit variables e.g variable1 = 1 if graph tensor neuron merit > threshold else 0.

Random Matrix representation of random 3SAT instances throws up an unusual window into the realm of Riemann Zeta Functions. It has been known that non-trivial zeros of Riemann Zeta Functions and Eigenvectors of Random Matrices ( $N \times N$  hermitian matrices) have something in common. This indicates a possibility of a connection between Riemann Zeta Function zeros and eigenvalues of Random Matrices for Random 3CNFs.

References:

-----  
455.1 Promise Problems -

<http://www.cs.tau.ac.il/~amnon/Classes/2017-BPP/Lectures/Lecture11.pdf>

455.2 Survey of Promise Problems - [Oded Goldreich] -

<http://www.wisdom.weizmann.ac.il/~oded/PSX/prpr-r.pdf> - there exist BPP-complete promise problems though in general case there are no known BPP-complete problems. This is quite applicable in equating a non-majority social choice and a Condorcet Jury Theorem majority social choice e.g. RHS majority choice with error is promise-BPP-complete and LHS non-majority interview TQBF social choice is in PSPACE.

455.3 Gaussian Unitary Ensemble - Random Matrices -

<http://empslocal.ex.ac.uk/people/staff/mrwatkin/zeta/random.htm>

-----  
456. (THEORY and FEATURE) CNF3SAT Approximate Solver Update - All possible  
variable-clause combinations - Commits - 18 September 2017  
-----

-----  
(\*) Solve\_SAT2() function has been changed to take both number of variables and  
clauses as parameters  
(\*) Bug in EquationsB creation has been fixed so that length of b equals number  
of clauses. This was causing dimension mismatch and incompatible  
dimensions in LSMR and LSQR  
(\*) Logs for 18\*16 clauses-variables random 3CNFs have been committed to  
testlogs/. MaxSAT percentage is ~96% after 1200 random CNF iterations  
. Per literal probability is too less than  $1/\sqrt{mn}$  obtained from random  
matrix analysis and therefore converges much below 100%.  
-----

(\*) Bugs fixed in prob\_dist()  
(\*) restored lsmr()  
(\*) logs for some other clause-variable combinations have been committed to  
testlogs/. Observed per literal probability is close to random  
matrix probability of  $1/\sqrt{mn}$   
-----

-----  
457. (THEORY and FEATURE) Inapproximability and Random Matrix Analysis of Least  
Square Approximate SAT solver - Commits - 19 September 2017  
-----

-----  
Previous Random Matrix Analysis shows expected number of satisfied clauses =  
 $m^3 n^2 p^4$  where there are m clauses, n variables and p is the  
probability of choosing a positive or negative literal. For 21 variables and 20  
clauses, following are the results after few iterations:  
-----

-----  
Iteration : 29  
-----

solve\_SAT2(): Verifying satisfying assignment computed .....

-----  
a: [[0 0 0 0 0 0 0 0 0 0 0 0 0 0 0 0 0 0 0 0 0]  
[0 0 0 0 0 0 0 0 0 0 0 0 1 1 0 0 0 0 0 0 0]  
[0 0 0 0 0 0 0 0 0 0 0 0 1 0 0 0 0 0 0 0 0]  
[0 0 0 0 0 0 0 0 0 0 0 0 1 0 0 0 0 0 0 0 0]  
[0 0 0 0 1 0 0 0 0 0 0 0 0 0 0 0 0 0 0 0 0]  
[0 0 0 1 0 0 0 0 0 0 0 0 0 0 0 0 0 0 0 0 0]  
[0 0 0 0 1 0 1 0 0 0 0 0 0 1 0 0 0 0 0 0 0]  
[0 0 0 0 0 0 0 0 0 0 1 0 1 0 0 0 0 0 0 0 0]  
[0 0 0 0 0 0 0 0 0 0 0 0 0 1 0 0 0 0 0 0 0]  
[0 0 0 1 0 0 0 0 0 0 0 0 0 0 0 0 0 0 0 0 0]  
[0 0 0 0 0 0 0 0 0 0 0 0 0 0 0 0 0 0 0 1 0]  
[0 0 0 0 0 0 0 0 0 0 0 1 0 0 0 0 0 0 0 0 0]  
[0 0 0 0 1 0 1 0 0 0 0 0 0 0 0 0 0 0 0 0 0]  
[0 0 0 0 0 0 0 0 1 0 0 0 0 0 0 0 0 0 1 0 0]  
[1 0 0 0 0 0 0 0 0 0 0 0 1 0 0 0 0 0 0 0 0]  
[0 0 0 0 0 0 0 0 0 0 0 0 0 0 0 0 0 0 0 0 0]  
[0 0 0 0 1 1 0 0 0 0 0 0 0 0 0 0 0 0 0 0 0]  
[0 0 0 0 0 0 0 0 0 0 0 0 0 0 0 0 0 0 0 0 0]  
[1 0 0 0 0 0 0 0 0 0 0 0 0 0 0 0 0 0 1 0 0]]  
b: [1 1 1 1 1 1 1 1 1 1 1 1 1 1 1 1 1 1 1 1 1]

a.shape: (20, 21)

b.shape: (20,)

solve\_SAT2(): lstsq(): x: (array([ 5.00000000e-01, 0.00000000e+00,



```

0.000000000e+00,
 1.000000000e+00, 3.89920951e-13, 1.000000000e+00,
 1.000000000e+00, 5.000000000e-01, 7.500000000e-01,
 1.000000000e+00, 5.000000000e-01, 7.500000000e-01,
 1.24863661e-13, 0.000000000e+00, 0.000000000e+00,
 0.000000000e+00, 5.000000000e-01, 5.000000000e-01,
 1.000000000e+00, 5.000000000e-01, 0.000000000e+00)), 2, 12,
1.870828693386971, 5.2032984761241552e-12, 4.898979485566356, 4.001266321699533,
2.7613402542972292)
Random 3CNF: (!x11 + !x3 + !x13) * (!x2 + x12 + x11) * (x20 + x11 + !x10) * (!x1
+ !x2 + x11) * (x5 + !x10 + x19) * (!x4 + x9 + !x17) * (x4 + !x1 + !x6) * (x5 +
x7 + x13) * (x9 + x11 + !x15) * (!x20 + !x19 + x12) * (!x14 + !x9 + x4) * (!x11
+ !x6 + x19) * (x10 + !x9 + !x15) * (x7 + !x16 + x5) * (!x7 + x17 + x8) * (!x3 +
x1 + x11) * (!x18 + !x7 + !x13) * (x5 + !x21 + x6) * (!x16 + !x9 + !x6) * (x1
+ !x6 + x18)
Assignment computed from least squares: [1, 0, 0, 1, 0, 1, 1, 1, 1, 1, 1, 1, 0,
0, 0, 0, 1, 1, 1, 1, 0]
CNF Formula: [['!x11', '!x3', '!x13'], ['!x2', 'x12', 'x11'], ['x20', 'x11', '!
x10'], ['!x1', '!x2', 'x11'], ['x5', '!x10', 'x19'], ['!x4', 'x9', '!x17'],
['x4', '!x1', '!x6'], ['x5', 'x7', 'x13'], ['x9', 'x11', '!x15'], ['!x20', '!
x19', 'x12'], ['!x14', '!x9', 'x4'], ['!x11', '!x6', 'x19'], ['x10', '!x9', '!
x15'], ['x7', '!x16', 'x5'], ['!x7', 'x17', 'x8'], ['!x3', 'x1', 'x11'], ['!
x18', '!x7', '!x13'], ['x5', '!x21', 'x6'], ['!x16', '!x9', '!x6'], ['x1', '!
x6', 'x18']]
Number of clauses satisfied: 20.0
Number of clauses : 20
Assignment satisfied: 1
Percentage of clauses satisfied: 100.0
Percentage of CNFs satisfied so far: 46.6666666667
Average Percentage of Clauses per CNF satisfied: 96.0
y= 46
sumfreq= 896
y= 43
sumfreq= 896
y= 36
sumfreq= 896
y= 46
sumfreq= 896
y= 41
sumfreq= 896
y= 42
sumfreq= 896
y= 48
sumfreq= 896
y= 37
sumfreq= 896
y= 48
sumfreq= 896
y= 39
sumfreq= 896
y= 46
sumfreq= 896
y= 42
sumfreq= 896
y= 42
sumfreq= 896
y= 50
sumfreq= 896
y= 39
sumfreq= 896
y= 33
sumfreq= 896
y= 41
sumfreq= 896

```

y= 42  
sumfreq= 896  
y= 44  
sumfreq= 896  
y= 43  
sumfreq= 896  
y= 48  
sumfreq= 896  
y= 40  
sumfreq= 904  
y= 43  
sumfreq= 904  
y= 51  
sumfreq= 904  
y= 36  
sumfreq= 904  
y= 38  
sumfreq= 904  
y= 46  
sumfreq= 904  
y= 44  
sumfreq= 904  
y= 36  
sumfreq= 904  
y= 41  
sumfreq= 904  
y= 45  
sumfreq= 904  
y= 46  
sumfreq= 904  
y= 34  
sumfreq= 904  
y= 46  
sumfreq= 904  
y= 46  
sumfreq= 904  
y= 36  
sumfreq= 904  
y= 42  
sumfreq= 904  
y= 44  
sumfreq= 904  
y= 47  
sumfreq= 904  
y= 51  
sumfreq= 904  
y= 54  
sumfreq= 904  
y= 38  
sumfreq= 904  
Probability of Variables chosen in CNFs so far: [0.05133928571428571,  
0.04799107142857143, 0.04017857142857143, 0.05133928571428571,  
0.04575892857142857, 0.046875, 0.05357142857142857, 0.041294642857142856,  
0.05357142857142857, 0.04352678571428571, 0.05133928571428571, 0.046875,  
0.046875, 0.05580357142857143, 0.04352678571428571, 0.036830357142857144,  
0.04575892857142857, 0.046875, 0.049107142857142856, 0.04799107142857143,  
0.05357142857142857]  
Probability of Negations chosen in CNFs so far: [0.04424778761061947,  
0.04756637168141593, 0.05641592920353982, 0.03982300884955752,  
0.0420353982300885, 0.05088495575221239, 0.048672566371681415,  
0.03982300884955752, 0.04535398230088496, 0.049778761061946904,  
0.05088495575221239, 0.03761061946902655, 0.05088495575221239,  
0.05088495575221239, 0.03982300884955752, 0.046460176991150445,  
0.048672566371681415, 0.051991150442477874, 0.05641592920353982,

0.059734513274336286, 0.0420353982300885]  
 Average probability of a variable or negation: 0.047619047619  
 Probability per literal from Random Matrix Analysis of Least Squared  
 (1/sqrt(mn)): 0.0487950036474

-----  
 From PCP theorem and [Hastad] inapproximability result based on it, if  
 $m^3 n^2 p^4 > 7/8 m$  then  $P=NP$ .  
 $\Rightarrow m^2 n^2 p^4 > 7/8$   
 $\Rightarrow p^4 > 7/(8m^2 n^2)$   
 $\Rightarrow$  if  $p > 0.96716821/\sqrt{m \cdot n}$  then  $P=NP$ .

In previous iteration, y and sumfreq print the frequencies of literals chosen so far at random (which are almost evenly distributed) and observed average probability of choosing a literal is 0.047619 whereas the required Random Matrix analysis probability for exact SAT is somewhat higher at 0.048795. Substituting the observed probability 0.047619 for 21 variables and 20 clauses:

Expected number of clauses satisfied =  $(20)^3 \cdot (21)^2 \cdot (0.047619)^4 = 18.1405$  clauses or 90.7025%  
 implying the MaxSAT for 21 variables and 20 clauses converges to 90.7025% asymptotically ad infinitum.

The inequality  $m^3 n^2 p^4 > 7/8 m$  relates hardness and randomness because probability distribution for  $p$  is directly related to uniformity and  $k$ -wise independence of pseudorandom (number) generator for choosing a literal at random. Presently the randomness depends on linux PRNG. If there exists a pseudorandom number generator corresponding to probability  $p > 0.96716821/\sqrt{m \cdot n}$  then  $P=NP$ .

For a binary valued random variable  $X$ , bias( $X$ ) is defined as  $\Pr(X=0) - \Pr(X=1) \leq \epsilon$ . Epsilon biased pseudorandom generators (e-PRG) are functions  $G: \{0,1\}^l \rightarrow \{0,1\}^n$  expanding seed of length  $l$  to a pseudorandom string of length  $n$  and for all subsets  $S_i$  (which are random variables) of  $\{0,1\}^n$ , bias( $S_i$ )  $\leq \epsilon$ . For uniform distributions, bias of all subset random variables is zero excluding the empty set. This is equivalent to: Bias(UniformDistribution)-Bias(e-PRGDistribution)  $\leq \epsilon$ . For random matrix approximate SAT solver probability  $p$ , previous condition of probability of choosing a positive or negative literal in a random SAT,  $p > 0.96716821/\sqrt{m \cdot n}$  for  $P=NP$  to hold, differs from the uniform probability distribution  $1/2n$  (assuming  $n$  variables and  $n$  negations of them). This implies an epsilon biased PRG of bias  $p - (1-p) = 2p - 1 = [1.93433642/\sqrt{m \cdot n}] - 1$  for all possible values of  $m$  and  $n$ , must exist for  $P=NP$ . PRG described in reference has bias  $(n-1)/2^l$ . Equating  $2p - 1 = (n-1)/2^l$  and solving for seed length  $l$  gives an expression of required seed length  $l$  in terms of number of clauses  $m$ .

Let  $X_i$  be the random variable for choosing the literal  $x_i$ . If literal  $x_i$  is chosen  $X_i=1$ , else  $X_i=0$ . Therefore bias(ePRG)= $\Pr(X_i=1) - \Pr(X_i=0)$ . But  $\Pr(X_i=1) = p = 0.96716821/\sqrt{m \cdot n}$  for choosing a literal from random matrix analysis derived previously for 7/8 approximation to exist.

An example application of Epsilon biased Pseudorandom Generator in reference 457.1 below :

-----  
 $\Rightarrow \text{bias(ePRG)} = p - (1-p) = 1.94/\sqrt{m \cdot n} - 1$ .

Equating this to the ePRG bias  $(n-1)/2^l$ :

$\Rightarrow (n-1)/2^l = [1.94/\sqrt{m \cdot n}] - 1$

$\Rightarrow$  length of the seed  $l$  in ePRG =  $\log([(n-1) \cdot \sqrt{m \cdot n}] / [1.94 - \sqrt{m \cdot n}])$

Absurdity is for length of the seed to be valid logarithm,  $\sqrt{m \cdot n} < 1.94 \Rightarrow m \cdot n < 4$  which is possible only for  $m=1$  and  $n=3$ , the trivial 1 clause 3SAT. This necessitates transforming previous into an inequality as below:

$$\begin{array}{l} 2^{2l} * (1.94)^2 \\ \text{-----} < m \\ n * [2^l + (n-1)]^2 \end{array}$$

For large  $n$ , inequality tends to a surd  $0 < m$ .

An example application of Epsilon biased Pseudorandom Generator in reference 457.2 below :

-----  
=>  $\text{bias}(\text{ePRG}) = p - (1-p) = 1.94/\sqrt{m \cdot n} - 1$ .

Other ePRG (Mossel-Shpilka-Trevisan) bias  $1/2^{(kn/c^4)}$  mentioned in the references relates  $m$  and  $n$  for random matrix CNF SAT solver bias as:

$$\frac{(1.94)^2 \cdot 2^{(2kn/c^4)}}{n \cdot (1 + 2^{(kn/c^4)})^2} < m$$

For large  $n$ , inequality tends to a surd  $0 < m$ .

Both these prescribe a relation between  $n$  and  $m$  for small  $n$  and for large number of variables both ePRGs fit to the random matrix CNF SAT solver least squares bias for  $P=NP$  to hold. This implies there are random SAT instances for small  $n$  which might not create literals with probability  $0.96716821/\sqrt{m \cdot n}$  a hindrance to conclude that  $P=NP$  and defining this small  $n$  is non-trivial.

Generic Epsilon biased Pseudorandom Generator of bias  $\epsilon = 1/x$  for  $x > 0$ :

-----  
Consider a fictitious Epsilon biased Pseudorandom Generator of bias  $\epsilon = 1/x$ ,  $x > 0$ .

Lowerbounding bias:

$$[1.94/\sqrt{m \cdot n}] - 1 \leq 1/x$$

which reduces to:

$$m \geq (1.94)^2 \cdot x^2 / [n \cdot (x+1)^2]$$

This implies for any epsilon biased PRG, there exists number of clauses  $m$  below which Approximate SAT solver solves less than  $7/8$  fraction of the clauses.

Largest possible value of  $m$  occurs for  $n=1$  and  $x$  tending to infinity =>  $m \geq 1.94 \cdot 1.94$  (or)  $m \geq 3.7636$  i.e all CNF random SAT instances of 4 or less number of clauses can not be solved by least squares to get at least  $7/8$ -approximation.

Number of possible random  $k$ -SAT instances of  $m$  clauses and  $n$  variables =  $(n^{P3} \cdot 2)^m$  because each clause has either a literal or its negation, not both. Variables and their negation form a set of ordered pairs  $(x_1, x_1'), (x_2, x_2'), \dots, (x_n, x_n')$  from which 3 ordered pairs are chosen per clause in  $n^{P3}$  ways and variable or its negation is chosen from each ordered pair thereby creating  $n^{P3} \cdot 2$  possible clauses. An  $m$  clause random 3SAT has thus  $(n^{P3} \cdot 2)^m$  possibilities.

Number of possible 4 clause 3SATs are =  $(n^{P3} \cdot 2)^4$ . Therefore fraction of random SAT instances not solvable for  $7/8$  approximation is:

$$\frac{(n^{P3} \cdot 2)^4}{(n^{P3} \cdot 2)^m} = \frac{1}{(n \cdot (n-1) \cdot (n-2))^{(m-4)}}$$

which is negligible for large  $m$  and  $n$  but non-trivial for small  $m$  and  $n$ .

Number of variables in 4 clause 3SAT is at the maximum 12. Thus this small subset can be solved in a constant time because  $m$  and  $n$  are fixed at 4 and 12 respectively.

[Caution: Previous derivation is still experimental with possible errors and assumes an epsilon PRG of bias at least  $[1.94/\sqrt{m \cdot n}] - 1$  exists. If it indeed does, then it could imply  $P=NP$  and is in direct conflict with Majority version of XOR lemma - if numerator hardness does not cancel out - for hardness amplification described earlier and caveats therein which implies  $P \neq NP$ .]

References:

-----  
457.1 Epsilon biased Pseudo Random Generators - [Advanced Complexity Theory Course Notes - Dieter] -

<http://pages.cs.wisc.edu/~dieter/Courses/2008s-CS880/Scribes/lecture21.pdf>

457.2 Epsilon biased Pseudo Random Generator in NC0 - every pseudorandom bit

depends only on 5 bits of seed - [Elchanan Mossel, Amir Shpilka, Luca Trevisan]  
- <https://www.stat.berkeley.edu/~mossel/publications/prginn0.pdf> - "... Then we present an  $\epsilon$ -biased generator mapping  $n$  bits into  $cn$  bits such that  $\epsilon = 1/2^{\Omega(n/c^4)}$  and every bit of the output depends only on  $k = 5$  bits of the seed. The parameter  $c$  can be chosen arbitrarily, and may depend on  $n$ . The constant in the  $\Omega()$  notation does not depend on  $c$  ..."

-----  
458. (THEORY) Intrinsic Merit, Consensus Algorithms, Byzantine Failures and Level Playing Field - 23 September 2017  
-----

So far Intrinsic merit of a text has been analyzed mostly in the context of connectedness and meaningfulness of it. It assumes a document text-graph (subgraph of an ontology like WordNet) obtained from the Ontology graph is implicitly agreed upon metric to measure merit i.e  $IM(\text{text}) = \text{subgraph of Ontology}$ , for some intrinsic merit algorithm  $IM$ . But the problem of "agreeing" by stakeholders on some process is itself a non-trivial Consensus Problem which has been overlooked so far. For example, merit measured by interview/examination question-answering or a competition requires all parties to agree upon the terms, conditions and rules a priori. This is widely studied problem of Agreement or Consensus. Consensus is defined by:

- \* Agreement - all parties must agree on a correct process and its outcome
- \* Validity - if all correct processes receive same input value, they must all output same value

- \* Termination - all processes must eventually decide on an output value

There are realworld consensus implementations - Google Chubby Lock Service based on Paxos Consensus Protocol, Bitcoin's Proof-of-work hyperledgering which appends transactions of a node to common log in a distributed timestamp server etc., ensuring all participants agree. As opposed to Majority voting which requires crossing just half-way mark in number of votes(>50%), Consensus requires complete agreement (=100%). Once 100% consensus is achieved on how to measure intrinsic merit, it is accepted as a standard and levels playing field for contestants. Consensus is most required in measuring human intrinsic merit than merit of documents. In other words, majority voting permits each voter to decide on his/her own volition. Each voter can have different decision function(boolean or non-boolean). But Consensus requires all voters to reach an agreement on a standardized decision function. Recursive Gloss Overlap algorithm and its enhancements to measure intrinsic merit from graph of text can be termed as "consensual" because connectedness implies meaningfulness by WordNet distance measures (Resnick, Wu-Palmer, Jiang-Conrath etc.,) and any text can be mapped to a subgraph of an ontology like WordNet and WordNet has been accepted as a consensus peer-reviewed standard.

Consensus can be impeded by presence of malicious nodes which spoof and send spurious votes known as Byzantine generals problem. A known result implies there is a consensus resilient to byzantine failures if number of faulty nodes is not above 33%.

References:

-----  
458.1 Consensus Algorithms -  
[https://en.wikipedia.org/wiki/Consensus\\_\(computer\\_science\)](https://en.wikipedia.org/wiki/Consensus_(computer_science))  
-----

-----  
459. (THEORY) Random Matrix Rounding for Least Squares Approximate CNFSAT Solver, Distinguisher for Pseudorandomness, Majority Hardness Lemma  
- related to 318, 457 - 13 October 2017  
-----

-----  
Existence of Pseudorandom generators (PRG) implies  $P \neq NP$ . Proof of this is by contradiction: If there exists a distinguisher which is able to discern perfect

randomness from any PRG in polynomial time then existence of PRGs which fool a distinguisher is ruled out i.e  $\Pr[A(x)=1] - \Pr[A(G(s))=1] > \epsilon$  where  $x$  is a perfect random string in  $\{0,1\}^n$ ,  $A$  is a distinguisher and  $G$  is a function extending a seed  $s$  of length  $m$  to  $n$  -  $G: \{0,1\}^m \rightarrow \{0,1\}^n$ ,  $m < n$ .

Majority Voting Hardness Lemma is an adaptation of Yao's XOR Lemma for hardness amplification from weak voting functions composed to Majority function (related to KRW Conjecture and Boolean Function Composition). Hardness of a boolean function is the error in approximating the function  $f$  by a boolean circuit  $C$  defined by probability  $\Pr[f(x) \neq C(x)]$ . Majority Hardness Lemma implies hardness of the majority+votingfunction composition amplifies the hardness compared to individually weak voters and inverting this composition (MajorityInverse: finding who voted in favour or against) is extremely hard to approximate by a circuit and thus in average case could be an one-way function composition. Being one-way implies hard-to-distinguish PRGs can be constructed from this composition.

Random Matrix Rounding for Least Squares Approximate CNFSAT Solver in previous sections derives an expected probability of choosing a literal in a CNF for ExactSAT(when all clauses are satisfied). This expected random matrix probability (mentioned as RMLSQR henceforth:  $1/\sqrt{m \cdot n}$ ) corresponds to some hypothetical pseudorandom generator PRG1.

Probability of choosing a CNF by RMLSQR (there are  $3m$  literals per 3CNF) =  $(1/[mn])^{1.5m}$

Alternatively, number of all possible random 3CNF SATs of  $m$  clauses and  $n$  variables =  $(n * n * n)^m = n^{(3m)}$

Probability of choosing a CNF from all possible  $n^{(3m)}$  random 3SATs in this uniform distribution is =  $(1/n)^{3m}$

Thus there are two possible probability distributions for choosing a random 3SAT:  $(1/[mn])^{1.5m}$  required by Random Matrix rounding and  $(1/n)^{3m}$  for uniform. Probability distributions and Pseudorandom generators underlying these distributions are directly related.

If  $m=n$  (number of clauses and number of variables are equal):

-----  
 $(1/[nn])^{1.5n} = (1/n)^{3n}$  and thus both RMLSQR and Uniform distributions are same implying similar pseudorandomness in RMLSQR and Uniform and distinguisher is fooled. This is a promise special case described earlier and does not suffice.

If  $m \neq n$  e.g.  $m \gg n$  (this is most prevalent setting where number of clauses are huge and variables are relatively less):

-----  
 $(1/[mn])^{1.5m} < (1/n)^{3m}$   
 $(1/m)^{1.5m} * (1/n)^{1.5m} < (1/n)^{1.5m} * (1/n)^{1.5m}$   
 $(1/m)^{1.5m} < (1/n)^{1.5m}$   
 $1/m < 1/n$   
 $\Rightarrow m > n$

When number of clauses  $m$  differs from number of variables  $n$ , RMLSQR and Uniform distributions are dissimilar implying there are two different randomness-es: PRG1 for RMLSQR and PRG2(or perfect randomness) for Uniform. Distinguisher for these two random generators has the probability of success defined by difference of the probability distributions for RMLSQR and Uniform =  $(1/n)^{1.5m} * [(1/n)^{1.5m} - (1/m)^{1.5m}]$  i.e when the number of clauses is high compared to number of variables, this difference is significant and distinguisher succeeds with high probability implying PRG1 is not pseudorandom and altogether PRGs may not exist at all. This coincides with  $> 87.5\%$  of clauses getting satisfied breaking  $7/8$  barrier in average case and could be synonymous to Karloff-Zwick SDP relaxation algorithm for  $> 7/8$  MAXSAT. This need not

contradict majority+voterfunction composition hardness because MajorityInverse is a depth-2 #P-Complete counting problem (first step counts and inverts voter inputs to majority and second step counts and inverts assignments per voter and hardness is a function of sensitivity) and could be beyond P != NP purview (i.e. There could be pseudorandom generators indistinguishable only by an algorithm harder than NP).

-----  
460. (THEORY and FEATURE) Random Matrix Rounding for Least Squares Approximate CNFSAT Solver - various clause-variable permutations - numbers, some anomalous - 25 October 2017  
-----

Following are some random 3SAT iteration MAXSAT percentage numbers for multiple combinations of number of variables and clauses. Observed average probabilities of linux PRNG have some anomalies when substituted in random matrix expected number of satisfied clauses (>100%). Reasons for this could be error in estimating linux PRNG probability distribution. Deficiencies of Linux PRNGs - especially randomness extractor from SHA - are already analyzed (random.c) in <https://eprint.iacr.org/2005/029.pdf> - [BoazBarak-ShaiHalevi]

#####  
17 variables, 18 clauses - 1066 random 3SATs:  
#####

-----  
Iteration : 1066  
-----

solve\_SAT2(): Verifying satisfying assignment computed .....

-----  
a: [[0 0 1 0 0 0 0 0 0 0 0 0 0 0 0 0 0 0]

[0 0 1 0 1 0 0 0 0 0 0 0 0 0 0 0 0 0]

[0 0 0 0 0 1 0 0 0 0 0 0 0 0 0 0 0 0]

[0 0 0 0 0 0 0 1 0 0 0 0 0 0 0 1 0 0]

[0 1 0 0 0 0 0 0 0 0 0 0 0 0 0 0 0 0]

[0 0 0 0 0 0 0 0 0 0 0 0 0 0 0 0 0 0]

[0 1 0 0 0 0 0 0 0 0 0 0 0 0 1 0 0 0]

[0 0 1 0 0 0 0 0 0 0 0 0 0 0 0 0 0 0]

[0 1 0 0 0 0 0 0 1 0 0 0 1 0 0 0 0 0]

[0 0 0 0 0 0 0 0 0 0 0 0 0 0 0 0 0 0]

[0 0 0 0 0 0 0 0 0 1 0 0 0 0 0 0 0 0]

[0 0 0 1 0 0 0 0 0 0 0 0 0 0 0 0 0 0]

[0 0 0 0 0 0 0 0 1 0 0 0 0 0 0 0 0 0]

[0 0 0 0 0 0 0 0 0 1 0 0 0 0 0 0 1 0]

[0 0 0 0 0 0 0 0 0 0 0 0 0 0 0 1 0 0]

[0 0 0 0 0 0 1 0 0 0 0 0 0 0 0 0 0 0]

[0 0 1 0 0 0 0 0 0 1 0 0 0 0 0 0 0 0]

[0 0 0 0 0 0 0 0 0 0 0 0 0 1 0 0 1 0]]

b: [1 1 1 1 1 1 1 1 1 1 1 1 1 1 1 1 1 1]

a.shape: (18, 17)

b.shape: (18,)

solve\_SAT2(): lstsq(): x: (array([ 0.00000000e+00, 1.00000000e+00, 8.00000000e-01,

1.00000000e+00, 2.00000000e-01, 1.00000000e+00,

1.00000000e+00, 6.66666667e-01, 6.00000000e-01,

0.00000000e+00, 0.00000000e+00, -6.66666667e-01,

6.00000000e-01, 1.89190298e-14, 6.66666667e-01,

4.00000000e-01, 0.00000000e+00]), 2, 11, 1.653279569018299,

9.190906242470613e-13, 4.690415759823429, 4.19738295792774, 2.625515822335343)

Random 3CNF: (x3 + !x11 + !x16) \* (!x16 + x3 + x5) \* (x6 + !x9 + !x4) \* (x15 + !x10 + x8) \* (!x14 + x2 + !x8) \* (!x11 + !x10 + !x3) \* (!x9 + x2 + x14) \* (!x1 + x3 + !x7) \* (x2 + x8 + x12) \* (!x8 + !x1 + !x13) \* (!x10 + !x8 + x9) \* (!x12 + x4 + !x8) \* (!x7 + x8 + !x4) \* (!x8 + x16 + x9) \* (!x12 + !x7 + x15) \* (!x1 + x7

```

+ !x14) * (x3 + x9 + !x12) * (!x11 + x13 + x16)
Assignment computed from least squares: [0, 1, 1, 1, 1, 1, 1, 1, 1, 0, 0, 0, 1,
0, 1, 1, 0]
CNF Formula: [['x3', '!x11', '!x16'], ['!x16', 'x3', 'x5'], ['x6', '!x9', '!
x4'], ['x15', '!x10', 'x8'], ['!x14', 'x2', '!x8'], ['!x11', '!x10', '!x3'], ['!
x9', 'x2', 'x14'], ['!x1', 'x3', '!x7'], ['x2', 'x8', 'x12'], ['!x8', '!x1', '!
x13'], ['!x10', '!x8', 'x9'], ['!x12', 'x4', '!x8'], ['!x7', 'x8', '!x4'], ['!
x8', 'x16', 'x9'], ['!x12', '!x7', 'x15'], ['!x1', 'x7', '!x14'], ['x3', 'x9',
'!x12'], ['!x11', 'x13', 'x16']]
Number of clauses satisfied: 18.0
Number of clauses : 18
Assignment satisfied: 1
Percentage of clauses satisfied: 100.0
Percentage of CNFs satisfied so far: 61.0121836926
Average Percentage of Clauses per CNF satisfied: 97.3341664063
y= 1675
sumfreq= 28722
y= 1683
sumfreq= 28722
y= 1716
sumfreq= 28722
y= 1750
sumfreq= 28722
y= 1699
sumfreq= 28722
y= 1690
sumfreq= 28722
y= 1697
sumfreq= 28722
y= 1662
sumfreq= 28722
y= 1732
sumfreq= 28722
y= 1740
sumfreq= 28722
y= 1687
sumfreq= 28722
y= 1669
sumfreq= 28722
y= 1677
sumfreq= 28722
y= 1662
sumfreq= 28722
y= 1664
sumfreq= 28722
y= 1660
sumfreq= 28722
y= 1659
sumfreq= 28722
y= 1716
sumfreq= 28896
y= 1782
sumfreq= 28896
y= 1660
sumfreq= 28896
y= 1714
sumfreq= 28896
y= 1704
sumfreq= 28896
y= 1716
sumfreq= 28896
y= 1721
sumfreq= 28896
y= 1688

```



```

sumfreq= 28896
y= 1679
sumfreq= 28896
y= 1653
sumfreq= 28896
y= 1662
sumfreq= 28896
y= 1686
sumfreq= 28896
y= 1702
sumfreq= 28896
y= 1673
sumfreq= 28896
y= 1735
sumfreq= 28896
y= 1678
sumfreq= 28896
y= 1727
sumfreq= 28896
Probability of Variables chosen in CNFs so far: [0.058317665900703294,
0.05859619803634844, 0.05974514309588469, 0.06092890467237658,
0.059153262307638746, 0.05883991365503795, 0.059083629273727456,
0.057865051180279924, 0.06030220736717499, 0.06058073950282014,
0.05873546410417102, 0.05810876679896943, 0.058387298934614584,
0.057865051180279924, 0.057934684214191214, 0.05779541814636864,
0.057760601629412996]
Probability of Negations chosen in CNFs so far: [0.059385382059800665,
0.061669435215946845, 0.05744739756367663, 0.05931616832779624,
0.058970099667774084, 0.059385382059800665, 0.05955841638981174,
0.05841638981173865, 0.058104928017718716, 0.057205149501661126,
0.057516611295681065, 0.05834717607973422, 0.058900885935769656,
0.057897286821705425, 0.06004291251384274, 0.0580703211517165,
0.059766057585825025]
Average probability of a variable or negation: 0.0588235294118
Probability per literal from Random Matrix Analysis of Least Squared
(1/sqrt(mn)): 0.0571661950475

```

```

#####
18 variables, 19 clauses - 137 random 3SATs:
#####

```

```

Iteration : 137

```

```

solve_SAT2(): Verifying satisfying assignment computed

```

```

a: [[1 0 0 1 0 0 0 0 0 0 0 0 0 0 0 0 0 0]
[0 0 0 0 0 1 0 0 1 0 0 0 0 0 0 0 0 0]
[0 0 1 0 0 0 1 0 0 0 0 1 0 0 0 0 0 0]
[0 0 0 0 0 0 0 0 0 0 0 0 0 0 0 0 0 0]
[0 0 0 0 0 0 0 0 0 0 0 0 1 0 0 0 1 0]
[0 0 0 0 0 0 0 0 0 0 0 0 0 1 0 0 0 0]
[0 0 0 0 0 0 0 0 0 0 0 0 0 0 0 0 1 0]
[0 0 0 0 0 0 0 0 0 0 0 0 0 0 0 0 0 1]
[0 0 0 1 0 0 0 0 0 0 0 0 0 0 0 0 1 0]
[0 0 0 0 0 1 0 0 0 0 0 0 0 0 0 0 0 0]
[0 0 0 0 0 0 0 0 0 0 0 0 0 0 0 0 0 0]
[0 1 0 0 0 0 0 0 0 0 0 0 0 0 0 0 1 0]
[0 0 0 0 0 1 0 0 0 0 0 0 0 1 0 0 1 0]
[0 0 0 0 0 0 0 0 0 0 0 0 0 0 0 0 0 0]
[0 0 0 0 0 0 0 0 1 0 0 0 0 1 0 0 0 0]
[0 0 1 0 0 0 0 1 0 0 0 0 0 0 0 1 0 0]
[0 0 0 0 0 0 0 0 0 0 0 0 0 0 0 0 0 0]
[0 0 0 0 0 1 0 0 0 0 0 0 0 0 0 0 0 0]
[0 0 0 0 0 0 0 0 0 0 0 0 0 0 0 0 1]]

```

```

b: [1 1 1 1 1 1 1 1 1 1 1 1 1 1 1 1 1 1]
a.shape: (19, 18)
b.shape: (19,)
solve_SAT2(): lstsq(): x: (array([6.66666667e-01, 1.00000000e+00, -
1.11111111e-01,
 3.33333333e-01, 0.00000000e+00, 1.00000000e+00,
 4.44444445e-01, 1.66666667e+00, 8.93039852e-11,
 0.00000000e+00, 0.00000000e+00, 6.66666667e-01,
 -6.66666666e-01, 0.00000000e+00, -5.55555556e-01,
 6.66666667e-01, -8.43769499e-15, 1.00000000e+00]), 2, 13,
2.0816659994661344, 5.027196399901854e-09, 5.2915026221291805,
4.8051011045747947, 2.8609762647129626)
Random 3CNF: (x4 + x1 + !x7) * (!x3 + x6 + x9) * (x3 + x12 + x7) * (!x13 + !x4 +
!x10) * (x12 + x16 + !x6) * (x12 + !x17 + !x14) * (x16 + !x2 + !x17) * (x17 +
x18 + !x7) * (x16 + !x2 + x4) * (x6 + !x17 + !x18) * (!x14 + !x5 + !x17) * (x2 +
!x14 + x17) * (x6 + x16 + x13) * (!x12 + !x10 + !x7) * (x13 + !x12 + x8) * (x15
+ x8 + x3) * (!x3 + !x9 + !x7) * (x6 + !x16 + !x13) * (x18 + !x6 + !x2)
Assignment computed from least squares: [1, 1, 0, 1, 0, 1, 1, 1, 0, 0, 0, 1, 0,
0, 0, 1, 0, 1]
CNF Formula: [['x4', 'x1', '!x7'], ['!x3', 'x6', 'x9'], ['x3', 'x12', 'x7'], ['!
x13', '!x4', '!x10'], ['x12', 'x16', '!x6'], ['x12', '!x17', '!x14'], ['x16', '!
x2', '!x17'], ['x17', 'x18', '!x7'], ['x16', '!x2', 'x4'], ['x6', '!x17', '!
x18'], ['!x14', '!x5', '!x17'], ['x2', '!x14', 'x17'], ['x6', 'x16', 'x13'], ['!
x12', '!x10', '!x7'], ['x13', '!x12', 'x8'], ['x15', 'x8', 'x3'], ['!x3', '!x9',
'!x7'], ['x6', '!x16', '!x13'], ['x18', '!x6', '!x2']]
Number of clauses satisfied: 19.0
Number of clauses : 19
Assignment satisfied: 1
Percentage of clauses satisfied: 100.0
Percentage of CNFs satisfied so far: 52.8985507246
Average Percentage of Clauses per CNF satisfied: 96.7581998474
y= 220
sumfreq= 3952
y= 243
sumfreq= 3952
y= 252
sumfreq= 3952
y= 230
sumfreq= 3952
y= 195
sumfreq= 3952
y= 203
sumfreq= 3952
y= 231
sumfreq= 3952
y= 225
sumfreq= 3952
y= 224
sumfreq= 3952
y= 228
sumfreq= 3952
y= 221
sumfreq= 3952
y= 224
sumfreq= 3952
y= 205
sumfreq= 3952
y= 216
sumfreq= 3952
y= 199
sumfreq= 3952
y= 206
sumfreq= 3952
y= 203

```

```

sumfreq= 3952
y= 227
sumfreq= 3952
y= 207
sumfreq= 3914
y= 218
sumfreq= 3914
y= 214
sumfreq= 3914
y= 220
sumfreq= 3914
y= 223
sumfreq= 3914
y= 204
sumfreq= 3914
y= 220
sumfreq= 3914
y= 233
sumfreq= 3914
y= 203
sumfreq= 3914
y= 210
sumfreq= 3914
y= 234
sumfreq= 3914
y= 208
sumfreq= 3914
y= 239
sumfreq= 3914
y= 180
sumfreq= 3914
y= 205
sumfreq= 3914
y= 232
sumfreq= 3914
y= 259
sumfreq= 3914
y= 205
sumfreq= 3914
Probability of Variables chosen in CNFs so far: [0.05566801619433198,
0.06148785425101214, 0.06376518218623482, 0.05819838056680162,
0.049342105263157895, 0.0513663967611336, 0.058451417004048586,
0.056933198380566805, 0.05668016194331984, 0.057692307692307696,
0.05592105263157895, 0.05668016194331984, 0.05187246963562753,
0.05465587044534413, 0.05035425101214575, 0.05212550607287449,
0.0513663967611336, 0.05743927125506073]
Probability of Negations chosen in CNFs so far: [0.05288707204905468,
0.05569749616760347, 0.054675523760858456, 0.05620848237097598,
0.05697496167603475, 0.052120592743995914, 0.05620848237097598,
0.05952989269289729, 0.051865099642309655, 0.05365355135411344,
0.05978538579458355, 0.05314256515074093, 0.061062851303014816,
0.045988758303525806, 0.052376085845682166, 0.05927439959121104,
0.06617271333673991, 0.052376085845682166]
Average probability of a variable or negation: 0.05555555555556
Probability per literal from Random Matrix Analysis of Least Squared
(1/sqrt(mn)): 0.0540738070436

```

```

#####
19 variables, 18 clauses - 34 random 3SATs
#####

```

```

Iteration : 34

```

```

solve_SAT2(): Verifying satisfying assignment computed

```

```

a: [[0 0 0 1 0 0 0 0 0 1 0 0 0 1 0 0 0 0]
[0 0 0 0 1 0 0 0 0 0 0 0 0 0 0 0 0 0]
[0 1 0 0 0 0 0 0 0 0 0 0 0 0 0 1 1 0]
[0 0 0 0 0 0 1 0 0 0 1 0 0 0 0 0 0 0]
[0 0 0 0 0 0 0 0 0 0 1 0 0 0 0 0 0 0]
[0 0 0 1 0 0 0 0 0 0 0 0 0 0 0 0 1 0]
[0 0 0 0 0 0 0 0 0 0 0 0 0 0 0 1 0 0]
[0 0 0 0 0 0 0 0 0 0 1 0 0 0 0 0 1 0]
[0 0 0 0 0 0 0 0 0 0 0 0 0 0 0 1 0 0]
[1 0 0 0 0 0 0 0 0 0 0 0 0 0 0 0 0 0]
[0 0 0 0 1 0 0 0 0 0 0 0 0 0 0 0 1 0]
[0 0 0 0 0 0 0 0 0 1 0 0 0 0 0 0 0 1]
[0 1 0 0 0 0 0 0 0 0 0 0 0 0 0 0 0 0]
[0 0 0 0 0 0 0 0 0 0 0 0 0 0 0 0 0 0]
[0 0 0 0 0 0 0 0 0 0 0 0 0 0 0 0 0 0]
[1 0 0 0 0 0 0 0 0 0 0 0 0 0 0 0 0 0]
[0 0 0 0 1 0 0 0 0 0 0 0 0 0 0 0 0 0]
[0 0 1 0 0 0 0 0 0 0 0 0 0 0 0 0 0 0]]
b: [1 1 1 1 1 1 1 1 1 1 1 1 1 1 1 1 1 1]
a.shape: (18, 19)
b.shape: (18,)
solve_SAT2(): lstsq(): x: (array([1.00000000e+00, 1.00000000e+00,
1.00000000e+00,
 1.00000000e+00, 1.00000000e+00, 1.00000000e+00,
-3.65332764e-15, 0.00000000e+00, 0.00000000e+00,
 9.05525654e-15, 1.00000000e+00, 1.00000000e+00,
 0.00000000e+00, 9.05525654e-15, 0.00000000e+00,
-1.00000000e+00, 1.00000000e+00, 3.34888367e-14,
-3.65332764e-15]), 2, 12, 1.414213562373095, 2.093877713811129e-13,
4.795831523312719, 3.8125525032467102, 3.1622776601683884)
Random 3CNF: (x4 + x14 + x10) * (!x2 + !x11 + x5) * (x16 + x2 + x17) * (!x8 +
x11 + x7) * (!x5 + x11 + !x14) * (x4 + x18 + !x7) * (x17 + !x6 + !x5) * (!x10 +
x18 + x12) * (!x4 + x17 + !x11) * (!x8 + x1 + !x13) * (!x7 + x6 + x18) * (x11 +
x19 + !x16) * (!x6 + x2 + !x3) * (!x1 + !x2 + !x8) * (!x13 + !x10 + !x7) * (!x6
+ !x10 + x1) * (!x7 + x6 + !x10) * (x3 + !x18 + !x1)
Assignment computed from least squares: [1, 1, 1, 1, 1, 1, 0, 0, 0, 0, 1, 1, 0,
0, 0, 0, 1, 0, 0]
CNF Formula: [['x4', 'x14', 'x10'], ['!x2', '!x11', 'x5'], ['x16', 'x2', 'x17'],
['!x8', 'x11', 'x7'], ['!x5', 'x11', '!x14'], ['x4', 'x18', '!x7'], ['x17', '!
x6', '!x5'], ['!x10', 'x18', 'x12'], ['!x4', 'x17', '!x11'], ['!x8', 'x1', '!
x13'], ['!x7', 'x6', 'x18'], ['x11', 'x19', '!x16'], ['!x6', 'x2', '!x3'], ['!
x1', '!x2', '!x8'], ['!x13', '!x10', '!x7'], ['!x6', '!x10', 'x1'], ['!x7',
'x6', '!x10'], ['x3', '!x18', '!x1']]
Number of clauses satisfied: 18.0
Number of clauses : 18
Assignment satisfied: 1
Percentage of clauses satisfied: 100.0
Percentage of CNFs satisfied so far: 80.0
Average Percentage of Clauses per CNF satisfied: 98.7301587302
y= 52
sumfreq= 942
y= 39
sumfreq= 942
y= 46
sumfreq= 942
y= 50
sumfreq= 942
y= 53
sumfreq= 942
y= 43
sumfreq= 942
y= 47
sumfreq= 942

```

y= 51  
sumfreq= 942  
y= 57  
sumfreq= 942  
y= 48  
sumfreq= 942  
y= 54  
sumfreq= 942  
y= 49  
sumfreq= 942  
y= 46  
sumfreq= 942  
y= 61  
sumfreq= 942  
y= 54  
sumfreq= 942  
y= 44  
sumfreq= 942  
y= 48  
sumfreq= 942  
y= 49  
sumfreq= 942  
y= 51  
sumfreq= 942  
y= 44  
sumfreq= 948  
y= 42  
sumfreq= 948  
y= 43  
sumfreq= 948  
y= 43  
sumfreq= 948  
y= 61  
sumfreq= 948  
y= 60  
sumfreq= 948  
y= 49  
sumfreq= 948  
y= 60  
sumfreq= 948  
y= 43  
sumfreq= 948  
y= 57  
sumfreq= 948  
y= 47  
sumfreq= 948  
y= 60  
sumfreq= 948  
y= 49  
sumfreq= 948  
y= 41  
sumfreq= 948  
y= 60  
sumfreq= 948  
y= 46  
sumfreq= 948  
y= 53  
sumfreq= 948  
y= 41  
sumfreq= 948  
y= 49  
sumfreq= 948

Probability of Variables chosen in CNFs so far: [0.055201698513800426,  
0.041401273885350316, 0.04883227176220807, 0.05307855626326964,

```

0.05626326963906582, 0.045647558386411886, 0.049893842887473464,
0.054140127388535034, 0.06050955414012739, 0.050955414012738856,
0.05732484076433121, 0.05201698513800425, 0.04883227176220807,
0.06475583864118896, 0.05732484076433121, 0.04670912951167728,
0.050955414012738856, 0.05201698513800425, 0.054140127388535034]
Probability of Negations chosen in CNFs so far: [0.046413502109704644,
0.04430379746835443, 0.04535864978902954, 0.04535864978902954,
0.06434599156118144, 0.06329113924050633, 0.05168776371308017,
0.06329113924050633, 0.04535864978902954, 0.060126582278481014,
0.049578059071729956, 0.06329113924050633, 0.05168776371308017,
0.043248945147679324, 0.06329113924050633, 0.04852320675105485,
0.05590717299578059, 0.043248945147679324, 0.05168776371308017]
Observed Average probability of a variable or negation: 0.0526315789474
Probability per literal from Random Matrix Analysis of Least Squared
(1/sqrt(mn)): 0.0540738070436
Percentage of Clauses satisfied - Observed Average Probability substituted in
Random Matrix Analysis of Least Squared ($m^2 \cdot n^2 \cdot p^4$): 89.7506925208

```

```

#####
16 variables, 15 clauses - 60 random 3SATs
#####

```

```

Iteration : 60

```

```

solve_SAT2(): Verifying satisfying assignment computed

```

```

a: [[0 0 0 0 0 0 0 0 0 0 1 0 0 0 0 0]
[0 0 1 0 0 0 0 0 0 0 1 0 0 0 0 0]
[0 0 0 0 0 0 0 0 0 0 0 0 0 0 0 0]
[0 0 0 0 0 1 0 0 0 0 0 0 0 0 0 0]
[0 0 0 0 0 0 0 0 1 0 0 0 0 0 0 0]
[0 0 0 0 0 1 0 0 0 0 0 0 0 0 0 0]
[0 1 0 0 0 0 0 1 0 0 0 0 0 0 0 0]
[0 1 0 0 1 0 0 0 0 1 0 0 0 0 0 0]
[0 0 0 0 0 0 0 0 0 0 0 0 0 0 0 0]
[0 0 1 0 0 0 0 0 0 0 0 0 0 0 0 0]
[0 0 0 0 0 0 0 0 0 0 0 0 1 1 0 0]
[0 0 0 0 0 0 0 0 0 1 0 0 0 0 0 0]
[0 0 0 0 0 0 0 0 0 0 1 0 0 0 1 0]
[0 0 0 0 0 0 0 0 0 1 1 0 0 0 0 0]
[0 0 0 1 0 0 0 0 0 0 0 0 0 0 0 0]]
b: [1 1 1 1 1 1 1 1 1 1 1 1 1 1 1 1]

```

```

a.shape: (15, 16)

```

```

b.shape: (15,)

```

```

solve_SAT2(): lstsq(): x: (array([0.00000000e+00, 4.00000000e-01,
1.00000000e+00,

```

```

1.00000000e+00, -2.00000000e-01, 1.00000000e+00,
0.00000000e+00, 6.00000000e-01, 6.00000000e-01,
8.00000000e-01, -2.28234722e-16, 0.00000000e+00,
5.00000000e-01, 5.00000000e-01, 1.00000000e+00,
0.00000000e+00]), 2, 9, 1.5491933384829675, 1.3065051242742054e-12,
4.242640687119285, 2.7186789946524619, 2.4617067250183342)

```

```

Random 3CNF: (!x8 + x10 + !x11) * (x11 + x3 + !x8) * (!x10 + !x16 + !x1) * (!x8
+ x6 + !x4) * (x9 + !x1 + !x10) * (!x5 + !x1 + x6) * (!x6 + x2 + x8) * (x10 + x2
+ x5) * (!x1 + !x8 + !x7) * (x3 + !x1 + !x12) * (x14 + !x11 + x13) * (!x1 + x10
+ !x2) * (!x13 + x15 + x11) * (x9 + !x1 + x10) * (!x1 + x4 + !x8)

```

```

Assignment computed from least squares: [0, 1, 1, 1, 0, 1, 0, 1, 1, 1, 0, 0, 1,
1, 1, 0]

```

```

CNF Formula: [['!x8', 'x10', '!x11'], ['x11', 'x3', '!x8'], ['!x10', '!x16', '!
x1'], ['!x8', 'x6', '!x4'], ['x9', '!x1', '!x10'], ['!x5', '!x1', 'x6'], ['!x6',
'x2', 'x8'], ['x10', 'x2', 'x5'], ['!x1', '!x8', '!x7'], ['x3', '!x1', '!x12'],
['x14', '!x11', 'x13'], ['!x1', 'x10', '!x2'], ['!x13', 'x15', 'x11'], ['x9', '!
x1', 'x10'], ['!x1', 'x4', '!x8']]

```

```

Number of clauses satisfied: 15.0

```

Number of clauses : 15  
Assignment satisfied: 1  
Percentage of clauses satisfied: 100.0  
Percentage of CNFs satisfied so far: 65.5737704918  
Average Percentage of Clauses per CNF satisfied: 97.1584699454  
y= 75  
sumfreq= 1376  
y= 95  
sumfreq= 1376  
y= 77  
sumfreq= 1376  
y= 79  
sumfreq= 1376  
y= 96  
sumfreq= 1376  
y= 89  
sumfreq= 1376  
y= 79  
sumfreq= 1376  
y= 94  
sumfreq= 1376  
y= 86  
sumfreq= 1376  
y= 93  
sumfreq= 1376  
y= 101  
sumfreq= 1376  
y= 91  
sumfreq= 1376  
y= 92  
sumfreq= 1376  
y= 80  
sumfreq= 1376  
y= 77  
sumfreq= 1376  
y= 72  
sumfreq= 1376  
y= 93  
sumfreq= 1369  
y= 82  
sumfreq= 1369  
y= 82  
sumfreq= 1369  
y= 85  
sumfreq= 1369  
y= 84  
sumfreq= 1369  
y= 87  
sumfreq= 1369  
y= 84  
sumfreq= 1369  
y= 71  
sumfreq= 1369  
y= 80  
sumfreq= 1369  
y= 74  
sumfreq= 1369  
y= 90  
sumfreq= 1369  
y= 91  
sumfreq= 1369  
y= 100  
sumfreq= 1369  
y= 100

```

sumfreq= 1369
y= 88
sumfreq= 1369
y= 78
sumfreq= 1369
Probability of Variables chosen in CNFs so far: [0.05450581395348837,
0.0690406976744186, 0.0559593023255814, 0.057412790697674417,
0.06976744186046512, 0.06468023255813954, 0.057412790697674417,
0.06831395348837209, 0.0625, 0.06758720930232558, 0.07340116279069768,
0.06613372093023256, 0.06686046511627906, 0.05813953488372093,
0.0559593023255814, 0.05232558139534884]
Probability of Negations chosen in CNFs so far: [0.0679327976625274,
0.05989773557341125, 0.05989773557341125, 0.0620891161431702,
0.061358655953250546, 0.0635500365230095, 0.061358655953250546,
0.05186267348429511, 0.05843681519357195, 0.05405405405405406,
0.06574141709276844, 0.0664718772826881, 0.07304601899196493,
0.07304601899196493, 0.06428049671292914, 0.05697589481373265]
Observed Average probability of a variable or negation: 0.0625
Probability per literal from Random Matrix Analysis of Least Squared
(1/sqrt(mn)): 0.0645497224368
Percentage of Clauses satisfied - Observed Average Probability substituted in
Random Matrix Analysis of Least Squared ($m^2 \cdot n^2 \cdot p^4$): 87.890625

```

```

#####
21 variables, 18 clauses - 6 random 3SATs
#####

```

```

Iteration : 6

```

```

solve_SAT2(): Verifying satisfying assignment computed

```

```

a: [[0 0 0 0 0 0 0 1 0 0 1 0 0 0 0 1 0 0 0 0 0]
[0 0 0 0 1 0 0 0 0 0 0 1 0 0 0 0 0 0 0 0 0]
[0 0 0 0 0 0 0 0 0 0 0 0 0 0 0 0 0 0 1 1 0]
[0 0 0 0 1 0 0 0 0 0 0 0 0 0 0 0 0 0 0 0 0]
[1 0 0 0 0 0 0 0 0 0 0 0 0 0 0 0 0 0 0 0 1]
[0 0]
[0 0 0 1 0 0 0 0 0 0 0 0 0 0 0 0 0 0 0 1 0]
[0 0 0 0 0 0 0 0 0 0 0 0 0 0 0 0 0 1 0 0 0]
[0 1 0 0 0 0 0 1 0 0 0 0 0 0 0 0 0 0 0 0 0]
[0 0 0 0 0 0 0 0 0 1 0 0 0 0 0 1 0 0 1 0 0]
[0 1 0 0 0 0 0 0 0 0 0 0 0 0 0 0 0 0 0 0 0]
[0 0 0 0 0 0 0 0 0 0 0 0 0 0 0 0 0 0 0 1 0]
[0 0 0 0 0 0 0 0 0 0 0 1 0 0 0 0 0 0 0 1 0]
[0 0 0 0 0 0 0 1 0 0 0 0 0 0 0 0 0 0 0 0 0]
[0 0]
[0 0]
[0 0 0 0 1 0 0 0 0 0 1 0 0 0 0 0 0 0 0 0 0]
[0 1 0 0 0 0 0 0 0 0 0 0 0 0 0 0 0 0 0 0 0]]

```

```

b: [1 1]

```

```

a.shape: (18, 21)

```

```

b.shape: (18,)

```

```

solve_SAT2(): lstsq(): x: (array([5.00000000e-01, 1.00000000e+00,
0.00000000e+00,

```

```

5.00000000e-01, 1.00000000e+00, 0.00000000e+00,
-2.63027447e-16, 1.00000000e+00, -3.67351548e-14,
0.00000000e+00, 8.39171896e-12, 9.28077060e-17,
0.00000000e+00, -3.67351548e-14, 0.00000000e+00,
2.65906351e-12, 1.00000000e+00, -2.52681990e-14,
5.00000000e-01, 1.00000000e+00, 5.00000000e-01]), 2, 12,

```

```

1.7320508075688767, 6.3185165416969518e-11, 4.898979485566356,
3.9602900491395312, 2.4494897427873532)

```

```

Random 3CNF: (x11 + x8 + x16) * (!x12 + x11 + x5) * (!x4 + x17 + x18) * (x5 + !
x18 + !x8) * (!x8 + x21 + x1) * (!x9 + !x20 + !x17) * (x4 + !x20 + x19) * (!x6 +

```



$(x_{17} + \neg x_{12}) * (x_2 + x_7 + \neg x_9) * (x_{17} + x_{14} + x_9) * (x_2 + \neg x_{13} + \neg x_6) * (\neg x_{13} + \neg x_{19} + x_{20}) * (x_{20} + \neg x_3 + x_{12}) * (x_8 + \neg x_{20} + \neg x_7) * (\neg x_8 + \neg x_2 + \neg x_7) * (\neg x_2 + \neg x_9 + \neg x_{10}) * (x_5 + \neg x_1 + x_{11}) * (\neg x_{13} + x_2 + \neg x_{11})$

Assignment computed from least squares: [1, 1, 0, 1, 1, 0, 0, 1, 0, 0, 0, 0, 0, 0, 0, 0, 0, 0, 1, 0, 1, 0, 1, 1, 1]

CNF Formula: [['x11', 'x8', 'x16'], ['!x12', 'x11', 'x5'], ['!x4', 'x17', 'x18'], ['x5', '!x18', '!x8'], ['!x8', 'x21', 'x1'], ['!x9', '!x20', '!x17'], ['x4', '!x20', 'x19'], ['!x6', 'x17', '!x12'], ['x2', 'x7', '!x9'], ['x17', 'x14', 'x9'], ['x2', '!x13', '!x6'], ['!x13', '!x19', 'x20'], ['x20', '!x3', 'x12'], ['x8', '!x20', '!x7'], ['!x8', '!x2', '!x7'], ['!x2', '!x9', '!x10'], ['x5', '!x1', 'x11'], ['!x13', 'x2', '!x11']]

Number of clauses satisfied: 18.0

Number of clauses : 18

Assignment satisfied: 1

Percentage of clauses satisfied: 100.0

Percentage of CNFs satisfied so far: 71.4285714286

Average Percentage of Clauses per CNF satisfied: 97.619047619

y= 10

sumfreq= 184

y= 9

sumfreq= 184

y= 5

sumfreq= 184

y= 7

sumfreq= 184

y= 10

sumfreq= 184

y= 2

sumfreq= 184

y= 11

sumfreq= 184

y= 5

sumfreq= 184

y= 8

sumfreq= 184

y= 13

sumfreq= 184

y= 14

sumfreq= 184

y= 9

sumfreq= 184

y= 8

sumfreq= 184

y= 10

sumfreq= 184

y= 4

sumfreq= 184

y= 9

sumfreq= 184

y= 11

sumfreq= 184

y= 9

sumfreq= 184

y= 10

sumfreq= 184

y= 9

sumfreq= 184

y= 11

sumfreq= 184

y= 8

sumfreq= 194

y= 14

sumfreq= 194

y= 9

```

sumfreq= 194
y= 11
sumfreq= 194
y= 7
sumfreq= 194
y= 10
sumfreq= 194
y= 11
sumfreq= 194
y= 11
sumfreq= 194
y= 11
sumfreq= 194
y= 11
sumfreq= 194
y= 6
sumfreq= 194
y= 11
sumfreq= 194
y= 4
sumfreq= 194
y= 6
sumfreq= 194
y= 11
sumfreq= 194
y= 3
sumfreq= 194
y= 8
sumfreq= 194
y= 14
sumfreq= 194
y= 4
sumfreq= 194
y= 13
sumfreq= 194
y= 11
sumfreq= 194
Probability of Variables chosen in CNFs so far: [0.05434782608695652,
0.04891304347826087, 0.02717391304347826, 0.03804347826086957,
0.05434782608695652, 0.010869565217391304, 0.059782608695652176,
0.02717391304347826, 0.043478260869565216, 0.07065217391304347,
0.07608695652173914, 0.04891304347826087, 0.043478260869565216,
0.05434782608695652, 0.021739130434782608, 0.04891304347826087,
0.059782608695652176, 0.04891304347826087, 0.05434782608695652,
0.04891304347826087, 0.059782608695652176]
Probability of Negations chosen in CNFs so far: [0.041237113402061855,
0.07216494845360824, 0.04639175257731959, 0.05670103092783505,
0.03608247422680412, 0.05154639175257732, 0.05670103092783505,
0.05670103092783505, 0.05670103092783505, 0.05670103092783505,
0.030927835051546393, 0.05670103092783505, 0.020618556701030927,
0.030927835051546393, 0.05670103092783505, 0.015463917525773196,
0.041237113402061855, 0.07216494845360824, 0.020618556701030927,
0.06701030927835051, 0.05670103092783505]
Observed Average probability of a variable or negation: 0.047619047619
Probability per literal from Random Matrix Analysis of Least Squared
(1/sqrt(mn)): 0.0514344499874
Percentage of Clauses satisfied - Observed Average Probability substituted in
Random Matrix Analysis of Least Squared ($m^2 \cdot n^2 \cdot p^4$): 73.4693877551

```

-----  
 Parallel PRG and Cellular Automaton Algorithms for randomly filling a space with objects and their relevance to Linear Programming were described earlier. Space Filling is a problem studied in the field of Structural Topology. For example, density of spheres randomly packed into a container is approximately ~63.6% (reference below) which is exactly the problem solved by Parallel PRG and Cellular Automaton Randomized Space filling algorithms. This space filling problem can be formulated as a Voter Constraint Satisfaction Problem. Variant of Space filling is the NP-hard Packing problem where set of items of variable sizes have to be packed into set of bins of same volume by minimizing number of bins whereas Space filling has just one container and items are of similar sizes and random close packing converges to a fixed density percentage. If set of items in a random close packing within a container are equivalent to satisfied clauses (having same number of variables) of a Voter Decision Function, this topology result implies not more than  $\sim V \cdot 63.6\%$  of clauses (where V is the volume of container) can be satisfied per candidate (MAXSAT). Each n-sphere can be mapped to a satisfied clause of n variables (each variable corresponds to a bounded length equal to diameter of n-sphere on a dimension of the n-space).

Reference:

-----  
 461.1 Random Close Packings of Spheres in a Container - Space-filling and Structural Topology - <http://www.math.cornell.edu/~connelly/PackingsIII.IV.pdf> and <http://www-iri.upc.es/people/ros/StructuralTopology/>  
 -----

-----  
 462. (THEORY) Reduction from Random Close Packing to CNFSAT - related to 461 - 30 October 2017  
 -----

Each random close pack after a random shuffle shifts the centre of an n-sphere. Set of all possible centroids of an n-sphere in each random close pack are connected in a clause by disjunctions. There are as many clauses as number of n-spheres connected by conjunctions. For example, if  $R_1, R_2, R_3, \dots$  are random close packs and n-spheres  $s_1, s_2, s_3, \dots$  are constituents of these packs  $R_1, R_2, R_3, \dots$ , Centroid of n-sphere  $s_i = C_{ik}$  is different for each  $R_k$  i.e n-sphere  $s_i$  can exist on any of these possible centroids which implies disjunction  $C_{i1} \vee C_{i2} \vee \dots$  for locations of n-sphere  $s_i$  in Random Close Packs  $R_1, R_2, R_3, \dots$ . This creates one clause per n-sphere. For all n-spheres packed in container at random, following conjunction of clauses for all n-spheres completes the reduction:

$$(C_{11} \vee C_{12} \vee C_{13} \dots) \wedge (C_{21} \vee C_{22} \vee C_{23} \dots) \wedge (C_{31} \vee C_{32} \vee C_{33} \dots) \wedge$$

....

Each  $C_{ik}$  is assumed to be boolean variable which is 1 if n-sphere  $s_i$  is located in centroid  $C_{ik}$  in random close pack  $R_k$ , else 0.

Randomized Algorithm (Parallel PRG or Cellular Automaton) for this space filling random close pack finds a satisfying assignment to previous kSAT. This is not exactSAT because some spheres (clauses) might lie outside the container. Topological maximum limit of 63% for this random close pack is the limit on density = Total Volume of Spheres (or) Total number of satisfied clauses / Volume of Container. As density increases, number of satisfied clauses increases. In other words, Total number of satisfied clauses = Volume of Container \* PackingDensity =  $V \cdot 0.636$ . What Volume of Container translates to in the context of CNFs is open to interpretation - it might depend on the maximum-minimum range of centroid dimensions.

Filling the space within the container by n-spheres in parallel monte carlo random choice of centroids, simulates many natural parallel processes e.g shaking a container filled with equal sized balls. Parallel PRG and Cellular Automaton algorithms are for these special settings of random close packing (wherein size of the ball is infinitesimally finite) which are BPP/BPNC/RNC randomized algorithms to find a random close pack assignment to the previous kSAT. Each literal in this random close pack SAT is not just a centroid but also

covers circular space around it of finite constant radius. Considering the usual example - shaking a container having closely packed balls: Every successive shake of the container creates an assignment to the kSAT. Formulating this kSAT requires prior knowledge of all possible centroid tuples which could be infinite. If shaking is of constant or polynomial time, churning out successive assignments to previous kSAT is surprisingly not hard. Also previous kSAT does not have overlapping literals across clauses.

-----  
463. (FEATURE-DONE) Ephemeris Search Script Update - Celestial Pattern Mining - 31 October 2017  
-----

-----  
Updated Ephemeris Search for Sequence Mined Celestial Configurations - toString() function has been changed to concatenate "Unoccupied" for vacant zodiac signs while creating encoded celestial chart.  
-----

-----  
464. (FEATURE-DONE) Ephemeris Search - Sequence Mining of Tropical Monsoon for mid-November 2017 - 1 November 2017  
-----

-----  
(#) Apriori GSP SequenceMining on autogen\_classifier\_dataset historic Storms data has been executed  
(#) asfer.anchoros.seqmining has been updated from autogen\_classifier\_dataset  
(#) MinedClassAssociationRules.txt has been rewritten containing almost 2500 celestial planetary patterns  
(#) Ephemeris has been searched for almost 250 top astronomical patterns of these 2500 configurations for mid-November 2017  
(#) There has been a significant match of most the patterns during this period. Range of search has been narrowed to 2 days because exhaustive search for all patterns is intensive.  
(#) This matches to NOAA CPC forecast in [http://www.cpc.ncep.noaa.gov/products/JAWF\\_Monitoring/India/GFS\\_forecasts.shtml](http://www.cpc.ncep.noaa.gov/products/JAWF_Monitoring/India/GFS_forecasts.shtml)  
-----

-----  
465. (THEORY) Discrete Hyperbolic Computational Geometric Factorization, Chvatal Art Gallery Theorem and Parallel Tiling - 6 November 2017, 8 November 2017 - related to 34  
-----

-----  
Chvatal Art Gallery Theorem states for floodlighting an art gallery shaped as n-polygon, floor(n/3) guards are sufficient. There is a graph theoretic proof of this by [Fisk]. Discrete Hyperbolic Factorization requires pixelation of continuous hyperbolic curve as set of contiguous tiles (array of pixels). This computational geometric standard pixelation creates a polygon surrounding hyperbola of 4\*(number\_of\_factors + 1) sides. This is because there are (number\_of\_factors + 1) pixelated rectangles in the polygon and each rectangle of the polygon has 4 sides. From Chvtal art gallery theorem 4/3 \* (number\_of\_factors + 1) guards are sufficient to cover this polygon. This optimum number of guards is approximately the minimum number of parallel processors (PRAMs) required for tiling (pixelation) pre-processing step. Once these tiles are created in parallel, parallel sorting requires O(logN) time and post-processing binary search is also O(logN) - If there is a parallel binary search algorithm this could be sub-logarithmic. Assumption made previously is each guard has only vertical and horizontal 90 degree visibility.  
-----

As opposed to polygon pixelation, if the hyperbolic curve is discretized into set of line segments by plain rounding off creating a line segment for each interval [N/x, N/(x+1)], lower envelope of this set of segments is the list of

endpoints of segments and there are no overlaps - segments meet only at endpoints. Number of line segments is twice the number of factors of  $N$  or  $O(\log \log N)$ . Computing lower envelope in parallel is equivalent to tiling in parallel. Lower envelope can be computed in parallel by CREW PRAM in  $O(\log N)$  time and  $O(N \log N)$  operations.

#### References:

-----  
465.1 Chvatal Art Gallery Theorem and Fisk's Proof - <https://www.cut-the-knot.org/Curriculum/Combinatorics/Chvatal.shtml>  
465.2 Number of prime factors of an integer - [Srinivasa Ramanujan] - Quarterly Journal of Mathematics, XLVIII, 1917, 76 - 92 - Ramanujan Papers and Notebooks - <http://ramanujan.sirinudi.org/Volumes/published/ram35.pdf> - number of prime factors are of  $O(\log \log N)$ . This implies number of rectangles (and hence number of PRAMs) in the pixelated hyperbola polygon could be sub-logarithmic in  $N$ .  
465.3 Introduction to Parallel Algorithms - [Joseph JaJa] - Chapter 4 - Searching, Sorting, Merging - Corollary 4.5 - Cole's Pipelined Mergesort and Chapter 6 - Planar Geometry - Lower Envelopes and Visibility polygon - Theorem 6.7 - <https://people.ksp.sk/~ppershing/data/skola/JaJa.pdf>  
-----

-----  
466. (FEATURE-DONE) Support Vector Machines implementation - based on CVXPY - 9 November 2017  
-----

-----  
(\*) New Support Vector Machines python implementation is committed to NeuronRain AsFer repository  
(\*) This minimizes an objective function  $\frac{1}{2} \|w\|^2$  subject to constraint  $\|WX+b\| \geq 1$  which labels a point +1 or -1 on either side of a decision separating hyperplane  $WX+b$  for weight vector  $W$  and bias  $b$  (Reference: Machine Learning - Ethem Alpaydin - Chapter 13 - Kernel Machines)  
(\*) Optimization is solved by CVXPY DCCP Convex-Concave program  
(\*) logs for this have been added to testlogs/  
(\*) Present NeuronRain AsFer SVMRetriever.cpp depends on third-party SVMlight opensource software. With this new implementation, references to SVMlight are to be phased out.  
-----

-----  
467. (THEORY) Random Matrix Rounding for CNFSAT Solver, Blum-Micali PRG, Distinguisher for Pseudorandomness - 10 November 2017 - related to 459  
-----

-----  
Blum-Micali PRG depends on intractability of Discrete Logarithm  $f(x)=g^x \bmod p$  for primes  $p, g$  and group element  $x$ . Blum-Micali PRG creates sequences of  $(f(x), f^2(x), f^3(x), \dots)$  by composition of  $f$  and computes stream of bits by hard-core boolean predicate function  $b(\cdot)$  -  $(b(f(x)), b(f^2(x)), \dots)$  which is sequence of unpredictable pseudorandom bits. In Random Matrix Rounding for CNFSAT solver by least squares, probability of choosing a literal  $x_n$  = probability of the bit stream  $(b(f(x)), b(f^2(x)), \dots)$  corresponding to binary encoding of  $n$ .

Probability of choosing a CNF by RMLSQR probability ( $p=1/\sqrt{mn}$ ) and there are  $3m$  literals per 3CNF) =  $(1/[mn])^{1.5m}$   
Probability of choosing a CNF from all possible  $n^{(3m)}$  random 3SATs in uniform distribution is =  $(1/n)^{3m}$

Inverse of RMLSQR probability =  $(mn)^{1.5m}$  is the expected number of pseudorandom binary strings churned out by PRG before a required 3SAT is found.  
Inverse of uniform probability =  $n^{3m}$  is the expected number of pseudorandom

binary strings churned out by PRG before required 3SAT is found.

Distinguisher for these 2 distributions iterates through both sequences of bitstreams and prints "RMLSQR" if match occurs in  $(mn)^{1.5m}$  expected number of iterations else prints "Uniform". This requires exponential time in number of clauses.

From PCP [Hastad] inapproximability result and previous Random Matrix analysis for approximate CNFSAT solver, if  $m^3 n^2 p^4 > 7/8 m$  then  $P=NP$  i.e. if  $p > 0.96716821/\sqrt{m \cdot n}$  then  $P=NP$ . For the previous distinguisher, this requires  $(mn)^{1.5m} / (0.96716821)^{3m}$  exponential iterations. From condition for  $P=NP$ , this number of iterations has to be polynomial for efficient distinguishing of a PRG from perfect random sequence, which is a contradiction.

References:

-----  
467.1 Existence of Pseudorandom Generators - [Goldreich-Hugo-Luby] -  
<http://www.wisdom.weizmann.ac.il/~oded/X/gkl.pdf>

-----  
468. (FEATURE-DONE) Support Vector Machines - update - 10 November 2017  
-----

-----  
(\* ) Numpy indexing has been changed  
(\* ) Both random point and parametric point distances have been tested  
(\* ) DCCP log and Support Vector logs for 2 points and a random point have been committed to testlogs/  
(\* ) Distances are printed in the matrix result - two diametrically opposite points have equal distances  
(\* ) Distance matrix is returned from distance\_from\_separating\_hyperplane() function  
(\* ) The distance minimized is the L1 norm (sum of tuple elements) and not L2 norm  
(sum of squares of tuple elements)  
-----

-----  
469. (FEATURE-DONE) Computational Geometric Hyperbolic Factorization - Pixelated Segments Spark Bitonic Sort - 13 November 2017  
-----

-----  
(\* ) Numbers 147,219,251,253 are factorized.  
(\* ) C++ tiling pre-processing routines have been changed for this and Pixelated Tiles storage text files for bitonic sort have been updated  
(\* ) Factorization is benchmarked on single node cluster on dual core (which is parallel RAM).  
(\* ) This is just a representative number on single dual-core CPU and not a cloud parallelism benchmark.  
(\* ) Each DAGScheduler Spark work item is independent code executable in parallel and benchmark has to be this parallel time per work unit which is captured in per task duration logs below by Spark Driver:  
17/11/13 21:18:22 INFO TaskSetManager: Finished task 1.0 in stage 1791.0 (TID 3583) in 46 ms on localhost (executor driver) (1/2)  
17/11/13 21:18:22 INFO TaskSetManager: Finished task 0.0 in stage 1791.0 (TID 3582) in 47 ms on localhost (executor driver) (2/2)  
17/11/13 21:18:22 INFO TaskSetManager: Starting task 0.0 in stage 1792.0 (TID 3584, localhost, executor driver, partition 0, PROCESS\_LOCAL, 6281 bytes)  
17/11/13 21:18:22 INFO TaskSetManager: Starting task 1.0 in stage 1792.0 (TID 3585, localhost, executor driver, partition 1, PROCESS\_LOCAL, 6309 bytes)  
17/11/13 21:18:22 INFO TaskSetManager: Finished task 1.0 in stage 1792.0 (TID 3585) in 46 ms on localhost (executor driver) (1/2)  
17/11/13 21:18:22 INFO TaskSetManager: Finished task 0.0 in stage 1792.0 (TID 3584) in 50 ms on localhost (executor driver) (2/2)  
-----

17/11/13 21:26:39 INFO TaskSetManager: Finished task 0.0 in stage 1791.0 (TID 3582) in 50 ms on localhost (executor driver) (1/2)  
 17/11/13 21:26:39 INFO TaskSetManager: Finished task 1.0 in stage 1791.0 (TID 3583) in 49 ms on localhost (executor driver) (2/2)  
 17/11/13 21:26:39 INFO TaskSetManager: Starting task 0.0 in stage 1792.0 (TID 3584, localhost, executor driver, partition 0, PROCESS\_LOCAL, 6281 bytes)  
 17/11/13 21:26:39 INFO TaskSetManager: Starting task 1.0 in stage 1792.0 (TID 3585, localhost, executor driver, partition 1, PROCESS\_LOCAL, 6309 bytes)  
 17/11/13 21:26:39 INFO TaskSetManager: Finished task 0.0 in stage 1792.0 (TID 3584) in 48 ms on localhost (executor driver) (1/2)  
 17/11/13 21:26:39 INFO TaskSetManager: Finished task 1.0 in stage 1792.0 (TID 3585) in 49 ms on localhost (executor driver) (2/2)  
 17/11/13 21:33:59 INFO TaskSetManager: Finished task 0.0 in stage 1791.0 (TID 3582) in 48 ms on localhost (executor driver) (1/2)  
 17/11/13 21:33:59 INFO TaskSetManager: Finished task 1.0 in stage 1791.0 (TID 3583) in 50 ms on localhost (executor driver) (2/2)  
 17/11/13 21:33:59 INFO TaskSetManager: Starting task 0.0 in stage 1792.0 (TID 3584, localhost, executor driver, partition 0, PROCESS\_LOCAL, 6281 bytes)  
 17/11/13 21:33:59 INFO TaskSetManager: Starting task 1.0 in stage 1792.0 (TID 3585, localhost, executor driver, partition 1, PROCESS\_LOCAL, 6309 bytes)  
 17/11/13 21:33:59 INFO TaskSetManager: Finished task 0.0 in stage 1792.0 (TID 3584) in 55 ms on localhost (executor driver) (1/2)  
 17/11/13 21:33:59 INFO TaskSetManager: Finished task 1.0 in stage 1792.0 (TID 3585) in 57 ms on localhost (executor driver) (2/2)  
 17/11/13 21:40:20 INFO TaskSetManager: Finished task 1.0 in stage 1791.0 (TID 3583) in 49 ms on localhost (executor driver) (1/2)  
 17/11/13 21:40:20 INFO TaskSetManager: Finished task 0.0 in stage 1791.0 (TID 3582) in 52 ms on localhost (executor driver) (2/2)  
 17/11/13 21:40:20 INFO TaskSetManager: Starting task 0.0 in stage 1792.0 (TID 3584, localhost, executor driver, partition 0, PROCESS\_LOCAL, 6281 bytes)  
 17/11/13 21:40:20 INFO TaskSetManager: Starting task 1.0 in stage 1792.0 (TID 3585, localhost, executor driver, partition 1, PROCESS\_LOCAL, 6309 bytes)  
 17/11/13 21:40:20 INFO TaskSetManager: Finished task 0.0 in stage 1792.0 (TID 3584) in 50 ms on localhost (executor driver) (1/2)  
 17/11/13 21:40:20 INFO TaskSetManager: Finished task 1.0 in stage 1792.0 (TID 3585) in 50 ms on localhost (executor driver) (2/2)  
 (\*) Bitonic Sort is  $O(\log N \cdot \log N)$  and number of processors required is approximately  $O(N^{2.5})$  but abides by NC definition. Cole Pipelined Merge Sort which is  $O(\log N)$  is both in NC and Work-Time Optimal.

-----  
 470. (FEATURE-DONE) Support Vector Machines Update - Learn and Classify functions - 13 November 2017  
 -----

(\*) Support Vector Machines python implementation has been updated to include two functions :  
 - for learning set of support vectors from a training dataset tuples and store the vectors in a dictionary map of distance-to-vectors.  
 - to classify a tuple by finding its distance with reference to the support vector regions - distance-to-vectors map is sorted and  
 - if there are more than 1 tuples per minimum distance, those have to be reckoned as support vectors

-----  
 471. (THEORY) Jones-Sato-Wada-Wiens Theorem, Complement Functions, Prime-Composite Complementation, Prime Number Theorem, Ulam Spiral, Ramsey 2-coloring of integers, Hilbert Tenth Problem, Unique Factorization , Matiyasevich-Robinson-Davis-Putnam Theorem, Riemann Hypothesis - related to 24,370,390,394 - 13 November 2017, 14 November 2017, 29 November 2017, 1 December 2017, 4 December 2017, 23 December 2017  
 (Draft updates to <https://arxiv.org/abs/1106.4102>)

-----  
 -----  
 Jones-Sato-Wada-Wiens Theorem proves existence of a polynomial in 25 degree-26 variables which has values equal to set of all primes. This relates to Prime-Composite Function Complementation - Jones-Sato-Wada-Wiens polynomial is a complement function of set of composites which are formalized by unique factorization theorem. This is special case of Matiyasevich-Davis-Robinson-Putnam Theorem which proves any recursively enumerable set accepted by a Turing machine is equivalent to a polynomial accepting the elements of the set. Another closely related problem is: Does there exist a prime between two integers  $p=xy$  and  $q=x(y+1)$ . Prime number theorem states and proves number of primes less than  $N=O(N/\log N)$ .

Number of primes  $< p=xy$ :

$$= c1*xy/\log xy$$

Number of primes  $< q=(x+1)y$ :

$$= c1*(x+1)y/\log(x+1)y$$

Number of primes between  $p=xy$  and  $q=(x+1)y$  :

$$= c1*(x+1)y/\log(x+1)y - c1*xy/\log xy$$

Assuming number of primes between  $p$  and  $q = c1*(x+1)y/\log(x+1)y - c1*xy/\log xy > 0$ :

$$(x+1)y/\log(x+1)y > xy/\log xy$$

After reducing:

$$\log(xy) > x(\log(x+1) - \log x)$$

$$\log(xy) > x\log(x+1/x)$$

For large  $x$ :

$$\log(x+1/x) \sim \log 1 = 0$$

$$\Rightarrow \log(xy) > 0$$

thus proving the assumption. This estimate of number of primes between two composites thus directly has bearing on discrepancy of this 2-colored (prime-composite) integer sequence where discrepancy is difference between number of elements of 2 colors in monochromatic arithmetic progressions. Ulam Spiral, which is sequence of integers written in concentric spiralling rectangle, has diagonals aligned along points of prime numbers described by polynomials. Rectangle of Ulam Spiral can be written as polynomial  $x(x+1)$  or  $x(x-1)$ . Previous derivation on existence of primes between  $x(x+1)$  and  $x*x$  implies there is a prime diagonal. Ulam rectangle sequence for  $x(x+1)$  or  $x(x-1)$  is 1, 2, 4, 6, 9, 12, 16, 20, 25, 30, 36, 42, ...

Matiyasevich-Davis-Robinson-Putnam theorem implies every recursively enumerable set has a diophantine equation. Complement Function in several variables is nothing but a diophantine equation for the complement set by rewriting a diophantine as function in several variables. Thus concepts of Diophantine sets/equations and Complement functions are synonymous. Decidability of complement functions (<https://arxiv.org/abs/1106.4102>) is equivalent to decidability of diophantine equations. MRDP theorem requires every recursively enumerable set to have a diophantine equation and therefore to have a function for it. [There exists a set which is not recursively enumerable e.g set of subsets of infinite set]. Undecidability of Function Complementation follows from MRDP theorem because there exists a recursively enumerable set which is not computably recursive and hence has no algorithm (algorithms are computable recursive languages which do not loop and have yes/no halt on all inputs) i.e Undecidability of Hilbert's Tenth Problem applies directly to Undecidability of Function Complementation. In other words set of diophantines has cardinality greater than set of all computable recursive languages and therefore there exists a diophantine function for a complement set which cannot be computed by a Turing machine. This is one more proof of undecidability of complementation and simpler than Post Correspondence Problem based proof described earlier.

Definition:

-----  
 For a set  $S$  and subsets  $A, B$  of  $S$ , if  $\{A, B\}$  is a disjoint set cover of  $S$  and if  $A$



has a diophantine equation  $\text{diophantine}(A)$  (expressible as values of polynomial), then diophantine equation for  $B = \text{diophantine}(B)$ , is the complement function of  $\text{diophantine}(A)$ .

-----  
Theorem: Existence of Complement Diophantine Equation or Complement Function is Undecidable when neither of the complementary sets are recursive.  
-----

Proof:

-----  
MRDP theorem for Hilbert's tenth problem implies every recursively enumerable set is expressible as values of a diophantine polynomial.

Possibility 1 - Generic - Both complementary sets A and B are recursively enumerable:

-----  
If both complementary sets A and B are recursively enumerable, they always have a diophantine polynomial -  $\text{diophantine}(A)$  and  $\text{diophantine}(B)$ .  
There is a known result which states: if set A and  $B=S-A$  are both recursively enumerable, then A is recursive. But there exists a recursively enumerable set B which is not recursive, for some complement  $A \Rightarrow$  There is no algorithm for construction of  $\text{diophantine}(B)$ .

Possibility 2 - Special - One of the complementary sets A or B is recursively enumerable and the other is recursive:

-----  
Both A and B have a diophantine polynomial. If A is recursively enumerable but not recursive, there is a complement  $B (A=S-B)$  such that there is no algorithm for construction of  $\text{diophantine}(A)$ .

Possibility 3 - Special - Both complementary sets A and B are recursive:

-----  
Both A and B are recursive and recursively enumerable  $\Rightarrow$  Both A and B have diophantine polynomials and both  $\text{diophantine}(A)$  and  $\text{diophantine}(B)$  can be constructed. There are many examples for this complementation: [Squares, PellEquation], [Composites/UniqueFactorizationDomain, Primes] etc.,

Possibility 4 - Special - Both complementary sets are non recursively enumerable:

-----  
Obviously both sets A and B are beyond Chomsky hierarchy and there is no algorithm for construction of  $\text{diophantine}(A)$  and  $\text{diophantine}(B)$

Possibility 5 - Special - One of the complementary sets is recursively enumerable and the other is non recursively enumerable:

-----  
One of the sets A is recursively enumerable and thus has a diophantine polynomial. But there exists a complement  $B=S-A$  such that A is not recursive  $\Rightarrow$  There is no algorithm for construction of  $\text{diophantine}(A)$

Proof in one line: Any set is a complementary set of some other set and thus any complementary set which is recursively enumerable but not recursive has a diophantine equation, and thus undecidable by an algorithm.

Construction of a complement function for complementary set:

-----  
Construction of a complement function is to find a mapping function f defined as:

$$\begin{aligned} f(0) &= a_1 \\ f(1) &= a_2 \\ f(2) &= a_3 \\ &\vdots \\ f(n) &= a_n \end{aligned}$$

for  $a_1, a_2, a_3, \dots, a_n$  in Diophantine complementary set, which is equivalent to definition of recursively enumerable total function. This enumeration can be written as a diophantine equation:

$$f(x) - a = 0$$

Function  $f$  can internally be any mathematical function and can have additional parameters besides  $x$ . Finding the enumerated mapping previously is equivalent to solving an arbitrary diophantine  $f(x) - a = 0$  i.e finding solutions to  $x$  and  $a$  which is Hilbert's Tenth Problem - MRDP theorem proves finding integer solutions to arbitrary Diophantine is undecidable. ArXiv version at <https://arxiv.org/abs/1106.4102> mentions some algorithms for constructing a complement e.g Fourier series, Lambda calculus, Polynomial interpolation. Polynomial Reconstruction Problem also provides a polynomial approximation of the set and has origins in Error Correction and List Decoding. These algorithms apply only to recursive sets - complement function mappings are constructible only for recursive sets. This is intuitively obvious because a Turing Machine computing the previous mapping for a recursively enumerable set might loop for ever.

An important example for applicability of function complementation is ABC Conjecture which is defined in references below. Let  $S$  be the universal set of all possible integer triples  $(a, b, c)$ . Set of coprime triples which have quality  $q(a, b, c) = \log(c)/\log(\text{radical}(abc)) > 1 + \epsilon$  for all  $\epsilon > 0$  is the subset  $A$  of  $S$ . ABC conjecture states that there are only finitely many such triples for every  $\epsilon > 0$ . Then the set  $B = S - A$  is the set of all triples which violate this criterion - sets  $A$  and  $B$  are complementary. Proving ABC Conjecture is equivalent to proving the violation of this criterion in the complement set  $B$  - there are infinite non-coprime triples for each  $\epsilon > 0$  which have  $q(a, b, c) > 1$ . This converts ABC conjecture from primal finiteness to its dual infiniteness.

#### References:

- 
- 471.1 Jones-Sato-Wada-Wiens Theorem and Prime valued Polynomial - [https://www.maa.org/sites/default/files/pdf/upload\\_library/22/Ford/JonesSatoWadaWiens.pdf](https://www.maa.org/sites/default/files/pdf/upload_library/22/Ford/JonesSatoWadaWiens.pdf) - Jones-Sato-Wada-Wiens polynomial generates negative numbers too and its positive values are set of primes.
- 471.2 Matijasevic Polynomial - <http://primes.utm.edu/glossary/xpage/MatijasevicPoly.html> - negative values can be removed by setting squared terms of polynomial to zero and thus only set of all primes is generated which is the complement function of factorization.
- 471.3 Hilbert's Tenth Problem and Matijasevich-Robinson-Davis-Putnam (MRDP) Theorem - [https://en.wikipedia.org/wiki/Hilbert%27s\\_tenth\\_problem](https://en.wikipedia.org/wiki/Hilbert%27s_tenth_problem) - Hilbert's Tenth Problem poses if there exists an algorithm which generates integer values for unknowns in a multivariate diophantine equation. Hilbert's Tenth Problem was proved undecidable. Converse of this is finding a diophantine equation for a set - MRDP Theorem: Every recursively enumerable set is diophantine.
- 471.4 Primes are nonnegative values of a polynomial in 10 variables - [Yu.V. Matijasevic - <https://logic.pdmi.ras.ru/~yumat/publications/publications.php>] - <https://link.springer.com/article/10.1007/BF01404106> - [In Russian, Translated to English by Louise Guy and James P. Jones, The University of Calgary, Calgary, Canada]
- 471.5 Pell's Equation - [https://en.wikipedia.org/wiki/Pell%27s\\_equation](https://en.wikipedia.org/wiki/Pell%27s_equation) - Diophantine equation for set of nonsquare integers - Discovered first in treatise Brahmasphutasiddhanta of Brahmagupta. This complements set of squared integers.
- 471.6 Non-Recursively Enumerable Languages - <https://www.seas.upenn.edu/~cit596/notes/dave/relang8.html> - powerset of

infinite set is NonRecursivelyEnumerable.

471.7 Goedel's First Incompleteness Theorem Follows From MRDP theorem -

[https://en.wikipedia.org/wiki/G%C3%B6del%27s\\_incompleteness\\_theorems](https://en.wikipedia.org/wiki/G%C3%B6del%27s_incompleteness_theorems) and

[http://www.scholarpedia.org/article/Matiyasevich\\_theorem](http://www.scholarpedia.org/article/Matiyasevich_theorem) - Diophantines and

Complement Functions - "... The Diophantine equation of the general form  $P(a, x_1, \dots, x_n) = 0$  in the definition of a Diophantine representation can be replaced by a Diophantine equation of a special kind, namely, with the parameter isolated in the right-hand side, thus giving a representation of form  $a \in R \Leftrightarrow \exists x_1 \dots x_n \{Q(x_1, \dots, x_n) = a\}$  In other word, every Diophantine (and hence every listable) set of non-negative integers is the set of all values assumed by some polynomial with integer coefficients with many variables. ..." - Any complement set which is enumerable/listable is diophantine and there exists a diophantine set which is not recursive but enumerable.

471.8 What is Mathematics: Goedel Theorem and Around -

[https://dSPACE.lv/dSPACE/bitstream/handle/7/5306/Podnieks\\_What\\_is\\_Mathematics\\_Goedel.pdf?sequence=1](https://dSPACE.lv/dSPACE/bitstream/handle/7/5306/Podnieks_What_is_Mathematics_Goedel.pdf?sequence=1) - Ramsey Theorem (finite and infinite) - Decidability of

Function Complementation is the question: "For any two sets A and B which are disjoint set covers of a universal set S ( $A \cup B = S$ ), and if set A is diophantine (is expressible as values of a polynomial), is B also diophantine and if yes is there a generic algorithm to construct a diophantine polynomial for B?". [Equivalently A and B are Ramsey 2-coloring of S and diophantine polynomials for A and B(if it exists) are 2-coloring schemes]. Answer to this question is two-fold:

(\*) Is set B recursively enumerable? (There are sets which are not recursively enumerable e.g set of subsets of infinite set)

(\*) If set B is recursively enumerable, B has an equivalent diophantine polynomial. But there exists a set B which is enumerable but not computably recursive and there is no generic algorithm for constructing complement diophantine polynomial. Undecidability of Complementation implies finding 2-coloring scheme is also undecidable.

(\*) In both possibilities, there is a set which does not have a diophantine polynomial - there is a non-recursively enumerable set which is outside Chomsky-Schutzenberger Type-0,1,2,3 hierarchy and there is a recursively enumerable set which is not recursive computable by a Turing machine thus ruling out a generic procedure for finding 2-coloring schemes.

471.9 Goedel Incompleteness and MRDP theorem -

<https://plato.stanford.edu/entries/goedel-incompleteness/#HilTenProMRDThe> - "... Beginning in the early 1950s, Julia Robinson and Martin Davis worked on this problem, later joined by Hilary Putnam. As a result of their collaboration, the first important result in this direction was achieved. Call an equation "an exponential Diophantine equation" if it involves also exponentiation, as well as addition and multiplication (that is, one can have both constants and variables as exponents); naturally, the focus is still in the integer solutions. Davis, Putnam, and Robinson (1961), showed that the problem of solvability of exponential Diophantine equations is undecidable. In 1970, Yuri Matiyasevich added the final missing piece, and demonstrated that the problem of the solvability of Diophantine equations is undecidable. Hence the overall result is often called MRDP Theorem (for an exposition, see, e.g., Davis 1973; Matiyasevich 1993). The essential technical achievement was that all semi-decidable (recursively enumerable) sets can be given a Diophantine representation, i.e., they can be represented by a simple formula of the form  $\exists x_1 \dots \exists x_n (s = t)$ , where  $(s = t)$  is a Diophantine equation. More exactly, for any given recursively enumerable set S, there is a Diophantine equation  $(s(y, x_1, \dots, x_n) = t(y, x_1, \dots, x_n))$  such that  $n \in S$  if and only if  $\exists x_1 \dots \exists x_n (s(n, x_1, \dots, x_n) = t(n, x_1, \dots, x_n))$ . As there are semi-decidable (recursively enumerable) sets which are not decidable (recursive), the general conclusion follows immediately:

MRDP Theorem

There is no general method for deciding whether or not a given Diophantine equation has a solution. ..."

471.10 Special Case of Complement Functions and MRDP Theorem -

<http://www.logicmatters.net/resources/pdfs/MRDP.pdf> - Section 3 (Diophantine equation for set of Primes) and Section 4 - Theorem 4.3 - "If a set K and its complement  $N-K$  are both recursively enumerable then K is recursive". But MRDP

theorem implies all recursively enumerable sets are diophantine and because there exists a recursively enumerable set which is not recursive, there is no algorithm to find a diophantine polynomial whose values is a set and thus the general case procedure for complementation is undecidable. Rephrasing theorem 4.3, If a set  $K$  is diophantine( $K$  is expressible as values of a polynomial) and the complement set  $N-K$  is also diophantine( $N-K$  is expressible as values of a polynomial), then  $K$  is recursive(there exists an Yes/No halt Turing machine accepting  $K$ ). It has to be observed here that diophantine equations for  $K$  and  $N-K$  are complement functions. This special case is for the converse direction: assuming 2 complementary sets are diophantine, then one of the two is computable by an algorithm. Quoted excerpts from Definition 4.1 - "...Definition 4.1. A set of numbers  $K$  is recursively enumerable iff it is (i) the range of a total recursive function - or equivalently, it is (ii) the domain of a partial recursive function. What does this come to? Definition (i) says that  $K$  is recursively enumerable if there is an algorithmically computable (total) function  $f$  such that as you go through  $f(0)$ ,  $f(1)$ ,  $f(2)$ , . . . you spit out values  $k_0$ ,  $k_1$ ,  $k_2$  . . . in  $K$ , with any member of  $K$  eventually appearing (perhaps with repetitions). The equivalent definition (ii) says that there is an algorithm such that the set of input numbers for which the algorithm halts is exactly the set of numbers in  $K$  ...". Partial recursive function is a primitive recursive function not necessarily defined for all inputs and computable by a Turing machine. Total recursive function is a partial recursive function which is defined for all inputs.

471.11 MRDP Theorem, Jone-Sato-Wada-Wiens Polynomial and Undecidability in Number Theory - [Bjorn Poonen] -

<http://www.cis.upenn.edu/~cis262/notes/rademacher.pdf> - Diophantine statement of Riemann Hypothesis - " MRDP theorem gives a polynomial equation that has integer solutions if and only if Riemann Hypothesis is false " i.e find a counterexample to Riemann Zeta Function non-trivial zeroes - one which does not have  $\text{Re}(s) = 0.5$ . Turing machine for this might loop forever and thus recursively enumerable. Hence this Turing machine has a diophantine polynomial representation.

471.12 Formulas for Primes -

[https://oeis.org/wiki/Formulas\\_for\\_primes#Solutions\\_to\\_Diophantine\\_equations](https://oeis.org/wiki/Formulas_for_primes#Solutions_to_Diophantine_equations)

471.13 Simplest Diophantine Representation - [Panu Raatikainen] -

<https://pdfs.semanticscholar.org/cd96/ead1a00b73ecc9cfabf4b9a617907ce9bdd6.pdf> -

Theorem 4 - This translates to the problem of determining simplest complement diophantine function of complexity measure  $K$  such that with respect to a complexity measure (e.g Kolmogorov Complexity and Chaitin incompleteness Theorem) every other diophantine for a complementary set has complexity greater than  $K$ . Finding Simplest Complement Diophantine is also undecidable.

471.14 Waring Problem and Diophantos/Bachet/Lagrange Four Square Theorem for real quaternions - Topics in Algebra - Lemma 7.4.3 and Theorem 7.4.1 - Page 373-377 - [Israel N. Herstein] - Ever positive integer is sum of four squares i.e There is a diophantine polynomial  $f(a,b,c,d) = a^2 + b^2 + c^2 + d^2 = n$  in  $N$ .

471.15 Complement Functions, Diophantine Analysis and ABC Conjecture -

[https://en.wikipedia.org/wiki/Abc\\_conjecture](https://en.wikipedia.org/wiki/Abc_conjecture) - ABC Conjecture in number theory is the following:

Let  $a + b = c$  be a mutually coprime integer triple  $f(a,b,c)$ . Quality  $q(a,b,c)$  is defined as  $= \log(c)/\log(\text{radical}(abc))$  where  $\text{radical}(abc)$  is the product of distinct prime factors of product  $abc$ . In most cases  $q(a,b,c) < 1$ . ABC conjecture postulates existence of finitely many triples  $(a,b,c)$  for which  $q(a,b,c) > 1 + \epsilon$ .  $f(a,b,c) : a + b = c$  is the diophantine equation for the set of coprime triples.

471.16 Erdos-Straus Diophantine Conjecture - [https://en.wikipedia.org/wiki/Erd%C5%91s%E2%80%93Straus\\_conjecture](https://en.wikipedia.org/wiki/Erd%C5%91s%E2%80%93Straus_conjecture) - For any integer  $n \geq 2$ , there exist integer triples  $a,b,c$  which are solutions to diophantine equation :  $4/n = 1/a + 1/b + 1/c$

471.17 ABC Conjecture Proof-designate - Interuniversal Teichmüller Theory - [Shinichi Mochizuki] - <http://www.kurims.kyoto-u.ac.jp/~motizuki/top-english.html>

471.18 Exponential Diophantines, Fibonacci and Lucas Sequences, Maximum limit on solvability of Diophantine - Reduction of Unknowns in Diophantine Representations - [SunZhiwei] - <http://maths.nju.edu.cn/~zwsun/12d.pdf> - "... If

we take into account the number of unknowns, then it is natural to ask that for what  $n$  there does not exist an algorithm to test (polynomial) Diophantine equations with  $n$  unknowns for solvability in integers..." -  $n=27$  or  $n=11$

471.19 Diophantine Equation Representation of Fibonacci Series - [James P.Jones] - <https://www.fq.math.ca/Scanned/13-1/jones.pdf>

471.20 Vandermonde Matrix and Polynomial Interpolation - <https://ece.uwaterloo.ca/~dwharder/NumericalAnalysis/05Interpolation/vandermonde/>

471.21 Number of zeroes of Riemann Zeta Function - [Norman Levinson - Hugh L.Montgomery] - [https://projecteuclid.org/download/pdf\\_1/euclid.acta/1485889821](https://projecteuclid.org/download/pdf_1/euclid.acta/1485889821)

471.22 Diophantine Representation of Riemann Zeta Function - Davis-Matiyasevich-Robinson Theorem and Matiyasevich(1993) Theorem - "...Theorem 2 (Davis, Matiyasevich, and Robinson). The Riemann hypothesis is equivalent to the assertion (for  $n = 1, 2, 3, \dots$ ) that  $(\sum_{k \leq \delta(n)} [1/k - n^{1/2}])^2 < 36n^3 \dots$ " and "...Matiyasevich essentially takes advantage of the fact that the Riemann hypothesis implies that for  $n \geq 600$ ,  $|\psi(n) - n| < n^{1/2}(\log n)^2$ . Since  $\psi(n) = \log(\text{lcm}(1, 2, \dots, n)), \dots$ " - [http://web.stanford.edu/~anayebi/projects/RH\\_Diophantine.pdf](http://web.stanford.edu/~anayebi/projects/RH_Diophantine.pdf) (Philosophical Implication: Diophantines are contained in Adleman-Manders Complexity Class D a subset of NP. Proof of  $P=NP$  implies Riemann Hypothesis is easily solvable by an algorithm e.g ZetaGrid or humans)

-----

472. (FEATURE-DONE) Support Vector Machines Update and Discrete Hyperbolic Factorization Spark Benchmarks  
- 14 November 2017

-----

(\*) Support Vector Machines implementation has been updated to persist the learnt support vectors to a disk file SupportVectorMachines.txt  
 (\*) This text file is read in classify()  
 (\*) Support Vectors Dictionary is JSON dumped and eval()-ed and not JSON loaded because of serialization  
 glitch in defaultdict(list)

-----

(\*) Computational Geometric Hyperbolic Factorization Spark implementation has been benchmarked for  
 2 more integers of 9 and 10 bits. Some 8 bit numbers were benchmarked earlier.  
 (\*) Spark logs for these benchmarks have been committed and time duration is calculated as 3 way split  
 of real/user/system by time shell utility  
 (\*) These benchmark numbers are on dual core single node Spark cluster  
 (\*) C++/python files for tilings have been updated and pixelated tiles storage text files have been rewritten

-----

Note on Factorization Spark benchmarks

-----

Following are approximate correlations of the observed numbers to the theoretical polylogarithmic time bound - exponents of  $\log N$  (=number of bits) increase probably because number of parallel RAMs(cores) do not increase commensurate with the number of bits and is static dual core:

|               |            |             |                       |                         |             |
|---------------|------------|-------------|-----------------------|-------------------------|-------------|
| 10 bit - real | 17m11.931s | = 1031.931s | $(\sim k \cdot 10^x)$ | $\sim (\log N)^{3.013}$ | $(x=3.013)$ |
| 9 bit - real  | 7m46.247s  | = 466.247s  | $(\sim k \cdot 9^x)$  | $\sim (\log N)^{2.796}$ | $(x=2.796)$ |
| 8 bit - real  | 3m40.091s  | = 220.091s  | $(\sim k \cdot 8^x)$  | $\sim (\log N)^{2.589}$ | $(x=2.589)$ |
| 8 bit - real  | 3m39.539s  | = 219.539s  | $(\sim k \cdot 8^x)$  | $\sim (\log N)^{2.589}$ | $(x=2.589)$ |
| 8 bit - real  | 3m38.795s  | = 218.795s  | $(\sim k \cdot 8^x)$  | $\sim (\log N)^{2.589}$ | $(x=2.589)$ |
| 8 bit - real  | 3m38.622s  | = 218.622s  | $(\sim k \cdot 8^x)$  | $\sim (\log N)^{2.589}$ | $(x=2.589)$ |
| 8 bit - real  | 3m38.920s  | = 218.920s  | $(\sim k \cdot 8^x)$  | $\sim (\log N)^{2.589}$ | $(x=2.589)$ |

-----

473. (THEORY) Computational Geometric Hyperbolic Factorization, Discrete Geometry, Rastering in Graphics/Computational Digital Geometry, Bresenham's Line Algorithm adapted for Hyperbolic tiling, Point Location, Ray shooting - 15,16 November 2017 - related to 34, 465

-----

Finding factors of integer N by creating pixelated polygon for hyperbolic curve  $xy=N$  has great visual intuition. Similar algorithms already exist in discrete geometry and computer graphics disciplines. Bresenham's Line drawing algorithm is a classic used still in vector graphics which approximates a continuous line on a pixelated digital space. This approximation of continuous curves on digital space is called Rastering. Tile segments of hyperbola in preprocessing step of factorization are found by solving for  $\text{deltay}$  in:

$$\begin{aligned}xy &= N \\(x+1)(y-\text{deltay}) &= N \\xy - x*\text{deltay} + y - \text{deltay} &= N \\y &= \text{deltay} * (x+1) \\\text{deltay} &= y/(x+1) \text{ for } \text{deltax}=1\end{aligned}$$

which is similar to Bresenham Line algorithm for finding next point to plot on raster. Tile segment  $(N/x, N/(x+1))$  along y-axis is equal to interval  $(y, y-(y/x+1))$  on y-axis.

Tiling preprocessing phase of factorization embeds a continuous hyperbola in a grid of horizontal and vertical straight lines. Each horizontal line corresponds to an integer in y-axis and vertical line to an integer in x-axis. Hyperbolic arc traverses the squares(pixels) of the grid. Thus the polygon approximating the continuous hyperbola is the union of all squares(pixels) through which hyperbolic arc passes. Union of squares create rectangular faces of the art gallery polygon vertices of which are the locations of the guards. Vertices of these rectangles through which hyperbolic arc passes through are the factors.

Art Gallery Pixelated polygon approximating a hyperbola is a Planar Simple Line Graph (PSLG) where each side of the polygon is an edge in PSLG. This PSLG has  $(\text{number\_of\_factors} + 1)$  rectangular faces which is  $O(\log\log N)$ . Vertices where two adjacent rectangular faces meet are the factor points of N. Planar point location has to find these factor points. Geometric Ray Shooting Query for this is : "Find points of vertices where two rectangular faces of polygon meet". This ray shooting can be picturised as a line from origin intersecting the rastered hyperbolic polygon and multiple rays from a common origin are shot in parallel of various  $(0-90)$  degrees angles.  $O(\log\log N)$  of these rays pass through the factor vertices. Number of rays required is proportional to length of the hyperbolic curve =  $O(N)$ . Thus parallel ray shooting is a geometric sieve for factoring and is an alternative to sorting and binary searching the hyperbolic tile segments.

References:

-----

- 473.1 Bresenham Algorithm for Line Rastering - [https://en.wikipedia.org/wiki/Bresenham%27s\\_line\\_algorithm](https://en.wikipedia.org/wiki/Bresenham%27s_line_algorithm)
- 473.2 Rasterizing curves - <http://members.chello.at/easyfilter/bresenham.pdf>
- 473.3 Efficient Algorithms for Ray Shooting Queries - [Pankaj K.Agarwal] - <https://epubs.siam.org/doi/pdf/10.1137/0222051>
- 473.4 Parallel Planar Point Location - [Richard Cole] - <https://ia601408.us.archive.org/33/items/onoptimalparalle00cole/onoptimalparalle00cole.pdf>
- 473.5 Parallel Geometric Search - [Albert Chan, Frank Dehne, Andrew Rau-Chaplin] - <https://web.cs.dal.ca/~arc/publications/1-16/paper.pdf>
- 473.6 Parallel Computational Geometry - <https://www.cs.princeton.edu/~chazelle/pubs/ParallelCompGeom.pdf> - [A. Aggarwal, B. Chazelle, L. Guibas, C.O. Dunlaing, C. Yap] - Section 2 - Definition of NC based on PRAM - Section 5 - Algorithms for line segment intersection, art gallery guards, polygon triangulation, partitioning (kd-trees, quadtrees) are in

NC. Factorization by approximating a hyperbola into a pixelated polygon can be rephrased as line segment intersection problem, where sides of the polygons are line segments and their intersecting points contain factor vertices. There are  $O(\log\log N)$  intersection points in hyperbolic polygon where sides meet. Thus factorization can be solved in NC assuming pixelated hyperbolic polygon already exists.

-----  
474. (FEATURE-DONE) Computational Geometric Factorization - Tiling Update and benchmark numbers for factoring few integers - 16 November 2017  
-----

-----  
(\*) Existing hyperbolic tiling code depends on C++ code in cpp-src/miscellaneous  
(\*) To remove this dependency, python script for tiling the hyperbolic arc with simple pixelation similar to bresenham algorithm has been committed to repository - this script writes two files suffixed .coordinates and .mergedtiles from rounding off the interval  $[N/x, N/(x+1)]$  in a function hyperbolic\_tiling()  
(\*) This function is invoked in DiscreteHyperbolicFactorizationUpperbound\_Bitonic\_Spark.py before bitonic sort  
(\*) DiscreteHyperbolicFactorizationUpperbound\_Bitonic\_Spark.py is parametrized and accepts number to factorize as cmdline argument:  
    #\$SPARK\_2.1.0\_HOME/spark-submit  
DiscreteHyperbolicFactorizationUpperbound\_Bitonic\_Spark.py <number\_to\_factorize>  
(\*) Few more time shell builtin benchmark numbers for factorizing 3-bit, 4-bit, 5-bit, 6-bit, 7-bit integers have been committed in testlogs/  
-----

-----  
475. (FEATURE-DONE) Computational Geometric Factorization Update - Spark Accumulators, JSON for Tiling etc., - 19 November 2017  
-----

-----  
(\*) Hyperbolic tiling code in python has been changed to reflect C++ tiling in cpp-src/miscellaneous  
(\*) globalcoordinates global variable has been made Spark Accumulator Mutable global state - globalmergedtiles is already a Spark Accumulator global mutable state  
(\*) bitoniclock acquire/release statements have been added for global variables, but commented for benchmarking  
(\*) New boolean flags for bitonic comparator python style variable swap, for enabling multiple threads for assign have been added  
(\*) merge\_sorted\_halves() has been invoked as a separate function  
(\*) C++ tiling has been chosen because accuracy of long double in creating tile pixels is better than similar tiling code in python  
(\*) Benchmark numbers for factoring 511 has been added to testlogs/ and are similar to previous numbers  
(\*) .mergedtiles and .coordinates files are loaded/dumped as JSON in python hyperbolic tiling  
-----

-----  
476. (FEATURE-DONE and THEORY) Computational Geometric Factorization Update - Benchmarks and Tiling - 20 November 2017 - related to 34  
-----

-----  
(\*) Some further changes to Python hyperbolic tiling have been made - tile endpoints have been cast from floating point to integer  
for create\_tile()  
(\*) C++ tiling in cpp-src/miscellaneous/DiscreteHyperbolicFactorizationUpperbound\_Bitonic.cpp has been parametrized and takes as cmdline argument the integer to factorize.  
(\*) Shell script  
-----

cpp-src/miscellaneous/DiscreteHyperbolicFactorizationUpperbound\_Bitonic.sh has been changed to pass in the integer to factorize to the C++ tiling binary in cpp-src/ and spark-submit for PySpark executable in python-src/ from shell args \$\*

(\*) This shell script unifies C++ tiling and PySpark factorization

(\*) Known issues: Python tiling still differs from C++ tiling significantly. Changing the hardcoded tile arrays storage in C++ tiling to malloc()-ed heap storage causes faulty tiling. There are only optimization issues which do not affect the factorization. Factorization works well and more benchmarks were done e.g for integers 723 and 501. Numbers for these and past numbers are charted below

(\*) Following profiling numbers along with previous benchmarks for 8,9,10 bits (14 November 2017) capture the trend in the exponent of  $\log N$

(\*) Gradual increase in exponent of number of bits because of static number of parallel RAMs (cores) is not quite steep from 3-bit to 10-bit integers as one might expect. Integers of same bit numbers need almost equal duration to factorize which implies the exponent could be a function of  $\log N$  and not  $N$ . Htop shows equal loading of both cores of CPU and consumption is almost 100%+100%.

(\*) Cloud computing is not exactly a parallel RAM but multiple cores are PRAMs having concurrent access to a shared memory. Nodes in cloud have local memory processing too. Spark's Global State Variables (Accumulators) which are reflected across all cloud nodes are software simulations of Parallel RAMs - same global state is concurrently accessed by CPUs of spark nodes. Present PySpark implementation does the sorting on accumulators. Binary search is not necessary because Maximum elements at the end of the k-merge sorting of globalmergetiles automatically have shuffled coordinates as factors in globalcoordinates accumulator. This shaves of additional  $O(\log N)$ . This optimization is an update to drafts in 34.1 and 34.2:

[http://sourceforge.net/projects/acadpdrafts/files/DiscreteHyperbolicPolylogarithmicSieveForIntegerFactorization\\_PRAM\\_TileMergeAndSearch\\_And\\_Stirling\\_Upperbound\\_updateddraft.tex/download](http://sourceforge.net/projects/acadpdrafts/files/DiscreteHyperbolicPolylogarithmicSieveForIntegerFactorization_PRAM_TileMergeAndSearch_And_Stirling_Upperbound_updateddraft.tex/download)

[http://sourceforge.net/projects/acadpdrafts/files/DiscreteHyperbolicPolylogarithmicSieveForIntegerFactorization\\_PRAM\\_TileMergeAndSearch\\_And\\_Stirling\\_Upperbound\\_updateddraft.pdf/download](http://sourceforge.net/projects/acadpdrafts/files/DiscreteHyperbolicPolylogarithmicSieveForIntegerFactorization_PRAM_TileMergeAndSearch_And_Stirling_Upperbound_updateddraft.pdf/download)

(\*) Following are only representative figures and ideal benchmark requires a Spark cloud preferably on machines of high number multicore CPUs and comparison with existing General Number Field Sieve implementations (which is quasipolynomial-exponential).

```

723 - 10-bit - real 16m30.346s = 990.346s ~ $O(\log N^2.9956)$
511 - 9-bit - real 7m46.518s = 466.518s ~ $O(\log N^2.8382)$
511 - 9-bit - real 7m35.642s = 455.642s ~ $O(\log N^2.7854)$
501 - 9-bit - real 7m36.879s = 456.642s ~ $O(\log N^2.7864)$ [shell script -
includes time duration for C++ tiling]
100 - 7-bit - real 2m33.911s = 153.911s ~ $O(\log N^2.5851)$
123 - 7-bit - real 2m52.704s = 172.704s ~ $O(\log N^2.6482)$
63 - 6-bit - real 1m17.460s = 77.460s ~ $O(\log N^2.4243)$
33 - 6-bit - real 0m58.950s = 58.950s ~ $O(\log N^2.2757)$
14 - 4-bit - real 0m19.927s = 19.927s ~ $O(\log N^2.1609)$
12 - 4-bit - real 0m19.651s = 19.651s ~ $O(\log N^2.1609)$
6 - 3-bit - real 0m15.118s = 15.118s ~ $O(\log N^2.4649)$

```

477. (THEORY) Computational Geometric Factorization - Tiling Optimizations - K-Merge Sort is dispensable and Local Tile Search is sufficient  
- 21 November 2017



Finding factor vertices in pixelated hyperbolic polygon is equivalent to geometric search query: "Is there a right turn followed by a downturn in the polygon?". These turning points coinciding with hyperbolic arc are factor points. Number of rectangles in pixelated hyperbolic polygon =  $O(\log \log N)$ . Each tile along y-axis in the polygon (array of pixels) is of length  $\text{deltay} = N/[x(x+1)]$ . Maximum number of tiles in the pixelation can be derived as:

```

xy=N
(x+deltax)(y-deltay)=N
=> xy + y*deltax - x*deltay - deltax*deltay = N
But deltax = 1,
=> y - (x+1) deltax = 0
deltay = y/(x+1) and y = N/x
=> N/x(x+1) = deltax > 1 [each tile should be of length atleast 1]
N > x*x + x
=> x = (sqrt(1 + 4N) - 1) / 2
For large N, sqrt(1 + 4N) ~ sqrt(4N) = 2*sqrt(N)
=> x ~ sqrt(N) for large N

```

Maximum number of tiles in the pixelation is  $O(\sqrt{N})$ . If number of processors is  $O(\sqrt{N})$ , each tile can be assigned to a processor and tiling can be done in  $O(1)$  parallel time. Number of processors required can be reduced by having  $O(\sqrt{N}/(\log N)^c)$  processors.  $O(\sqrt{N})$  tiles can be created in  $O((\log N)^c)$  total parallel time i.e in each iteration  $O(\sqrt{N}/(\log N)^c)$  tiles can be created in parallel by as many processors and there are  $O((\log N)^c)$  iterations. Creating a tile in a processor is defined as assigning the tile interval ordered pair of coordinates (tilestart, tileend) to it where tilestart=(x, y1) and tileend=(x, y2). This tile segment interval is implicitly sorted ascending/descending in one of the axes and therefore can be locally binary searched. This does away with Global K-Merge Sort of the locally sorted tile segments. Because each tile is of length  $N/x(x+1)$ ,  $|y_2 - y_1| = N/[x(x+1)]$ . If N exists in a tile segment then there exists a factor point (x,y) in the tile segment such that  $y_1 < y < y_2$  and  $xy=N$ . Binary search per implicitly sorted tile segment is of  $O(\log(N/[x(x+1)])) \leq O(\log N)$ .

Thus factors can be found just by:

```

477.1 Tiling in parallel requiring $O((\log N)^c)$ tile and
 $O(\sqrt{N}/(\log N)^c)$ processors where number of tiles = $O(\sqrt{N})$
477.2 Local Binary Search per processor on each sorted tile of $O(\log N)$
time
and no k-merge sort is necessary.

```

Previous optimization reduces number of PRAMs by orders of  $(\log N)^c$  but increases exponent of parallel time  $O((\log N)^c)$ . Bitonic K-merge sort is global and least parallel time though number of processors required is huge (yet in NC and work-time optimal). Bitonic K-merge sort doesnot require binary search because factors are in the forefront of the mergesorted and shuffled tile coordinates always.

References:

-----

477.1 Line segment turn detection -

[http://fileadmin.cs.lth.se/cs/Personal/Rolf\\_Karlsson/lect9.pdf](http://fileadmin.cs.lth.se/cs/Personal/Rolf_Karlsson/lect9.pdf) - For two line segments, find if there is a left or right turn - line segments are vectors and sign of their cross product determines left or right turn. Assuming a pixelated polygon and

its sides as input array of line segments, cross product of adjacent pairs of line segment vectors can be computed in parallel and direction of turn can be found.

477.2 Sweepline algorithms - <http://www.ics.uci.edu/~goodrich/pubs/ggb-sweep-j.pdf>

477.3 Rectangle Stabbing - School on Geometric Computing, IIT Delhi (2010) - <http://www.cse.iitd.ernet.in/~ssen/geomschool/nandy/TR-RS.pdf> - Stabbing number for a set of axis-parallel rectangles is the minimum number of vertical and horizontal lines required such that each line passes through one of the

rectangles covering all rectangles. This problem is NP-hard by reduction from set cover. Hyperbolic pixelation is a special case inverse problem of stabbing where a polygon of adjoining axis-parallel rectangles are created such that hyperbolic arc passes through each of them. (Because of certain mistaken identity issues, it is hereby clarified author did not participate in School on Geometric Computing, IIT Delhi 1-4 October 2010 though author's name - "Ka.Shrinivaasan Chennai Mathematical Institute shrinivas@cmi.ac.in 32" - finds mention in IIT Delhi Hostel accommodation - <https://www.cse.iitd.ac.in/~naveen/activities/geometry/school-acco.pdf>)

-----  
478. (FEATURE-DONE and THEORY) Computational Geometric Factorization and Parallel Tile Search Updates  
- related to 34 and 477 - 22 November 2017  
-----

-----  
(\*) cpp-src/miscellaneous/DiscreteHyperbolicFactorizationUpperbound\_Bitonic.cpp has been revamped and unnecessary code has been removed. Function names have been changed. NUMBER\_OF\_TILES has been declared as a macro and has to be manually changed and compiled to nearest power of 2 greater than number to factorize. Compilation and PySpark factorization is taken care of by shell script  
cpp-src/miscellaneous/DiscreteHyperbolicFactorizationUpperbound\_Bitonic.sh  
(\*) New Spark python script  
python-src/DiscreteHyperbolicFactorizationUpperbound\_TileSearch\_Optimized.py has been added to repository. This is the parallel tile search optimization already mentioned in NeuronRain AsFer Design Document. Spark parallelize() distributes the tiles-coordinates array of ordered pairs as RDDs across cloud nodes and node prints the factor point in y-axis if x-axis matches the number to factorize. Spark parallelize() simulates the binary search on a local tile segment per PRAM processor. Presently binary search has not been implemented in tilesearch() function of foreach() Spark Action. This is because map/foreach functions act on a single element argument of a parallelized RDD.  
(\*) How Spark parallelizes a sequential datastructure on cloud nodes is equivalent to binary search on an array of length 1 which is a no-op. Because of this parallize() of Spark has been assumed to be equivalent to a binary search.  
(\*) Benchmark numbers for two integers 1011 and 1013 with and without sorting have been committed to testlogs/ and Tiling time durations have also been captured on how well mere tile search optimizes as opposed to sorting.  
(\*) As evidenced from  
python-src/testlogs/DiscreteHyperbolicFactorizationUpperbound\_TileSearch\_Optimized.log.22November2017, tiling preprocessing is quite insignificant (<<1 sec) and tile search for 1011 and 1013 requires approximately 20 seconds while bitonic sorting duration for same numbers is ~16minutes (960 seconds) a speedup of almost 50x.  
(\*) Benchmarks for Local Tile Search obviate the requirement for k-merge sorting of pixelated hyperbolic tiles, if parallelism is huge.  
(\*) Following is the trade-off:  
- Bitonic K-merge sorting of tiles : binary search is not necessary but a tremendous performance drag and overkill, suitable for low number of PRAMs  
- Local tile search : binary search is necessary only per processor but requires relatively high number of PRAMs  
-----

-----  
479. (FEATURE-DONE) Computational Geometric Factorization Tiling Optimization - Binary Search for Tile Segments in Spark - 23 November 2017  
-----

-----  
(\*) Binary Search has been implemented in Spark Tile Search Optimization by parallizing the set of intervals of pixelated hyperbolic arc.  
(\*) By this each tile interval can be binary searched in parallel to find the

factor point with no  
necessity for global k-merge sorting.  
(\*) Separate pixelation and tile interval file creation C++ source file has been  
added in cpp-src/miscellaneous  
(\*) Arrayless tile creation has been chosen and only intervals are written to a  
file suffixed as .tileintervals  
(\*) Shell script which compiles and executes the tile interval creation file and  
spark interval binary search script has been added.  
(\*) Invoking the shell script as:

```
cpp-src/miscellaneous/DiscreteHyperbolicFactorizationUpperbound_TileSearch_Optim
ized.sh <number_to_factorize>
```

is sufficient to print the factors

(\*) Following are benchmark numbers for factorizing few reasonably high bit  
integers. Removing K-Merge sort has significant effect on the  
throughput even for a single node spark cluster on dual core (local[2]):

```
Factorization of 12093 (14-bit): real 0m33.108s (single core - local[1])
Factorization of 12093 (14-bit): real 0m29.589s (dual core - local[2])
```

```
Factorization of 65532 (16-bit): real 0m44.899s (single core - local[1])
Factorization of 65532 (16-bit): real 0m39.621s (dual core - local[2])
```

```
Factorization of 102349 (17-bit): real 1m5.490s (single core - local[1])
Factorization of 102349 (17-bit): real 0m58.776s (dual core - local[2])
```

```
Factorization of 934323 (20-bit): real 8m20.017s (single core - local[1])
Factorization of 934323 (20-bit): real 7m37.958s (dual core - local[2])
```

```
Factorization of 1343231 (21-bit): real 16m34.759s (single core - local[1])
Factorization of 1343231 (21-bit): real 10m49.218s (dual core - local[2])
```

(\*) Above tile binary search numbers beat bitonic k-mergesort of tiles by many  
orders of magnitude  
(\*) logs containing factors of above integers have been committed to testlogs/  
(\*) This optimization thus effectively supersedes mergesort of tiles and is thus  
a better PySpark implementation of Discrete Hyperbolic Factorization.

-----  
(\*) Updated AsFer Design Document - benchmark numbers for both single and dual  
cores for tile search  
in computational geometric factorization  
(\*) Updated  
python-src/DiscreteHyperbolicFactorizationUpperbound\_TileSearch\_Optimized.py for  
dual cores  
(local[2])

-----  
480. (FEATURE-DONE) Computation Geometric Factorization - Binary Search for  
Tiles - Benchmarks  
- 24 November 2017  
-----

Benchmark numbers for factoring 24 bit integer by Tile BinarySearch Optimization  
script have been committed to testlogs/ (single node cluster, dual core):

Factorization of 9333123 (24-bit):

```

real 112m24.101s (Spark duration 12:21 to 14:02 = 101minutes = 6060seconds)
user 0m0.000s
sys 0m0.004s
```

Again binary search of tiles in parallel is way better than k-mergesort of  
tiles. Largest known numbers

widely used are 128-bit. Trend for different bits indicates, Spark cloud of few multicore nodes is sufficient to factorize 128-bit integers in few minutes. Previous benchmark uses spark-default.conf files from python-src/InterviewAlgorithm/ (2GB of heap space)

-----  
481. (THEORY) Computational Geometric Factorization - Parallel Local Binary Search for Tiled Hyperbolic Arc - 27 November 2017  
- Snir's Theorem for Parallel Search - related to 34,477  
-----

-----  
Previous optimized factorization with no sorting and only local binary search per tile interval can achieve further speed-up (from logarithmic to sublogarithmic) if search of each locally sorted tile can be done in PRAMs. Snir's Theorem implies searching a table of sorted elements can be done in sublogarithmic  $O(\log N / \log p)$  time by  $p$  CREW PRAM processors.

Tiling preprocessing of hyperbolic arc creates  $O(N)$  tiles. [This is proportional to length of hyperbolic arc obtainable from elementary calculus =  $\text{DefiniteIntegral}(\sqrt{1 + [N^2/x^4]})$ ]

Number of iterations =  $O((\log N)^k)$   
Number of PRAMs =  $(N/(\log N)^k)$

Factorization in parallel has following algorithm:

```
while(iterations <= $O((\log N)^k)$)
{
 *) Assign $N/(\log N)^k$ tiles to $N/(\log N)^k$ PRAMs in parallel ($O(1)$ parallel time because each interval tile in a global shared memory array can be accessed by PRAM id as index)
 *) Binary Search tile in each PRAM for factors ($O(\log N)$ parallel time which can be reduced to $O(\log N / \log p)$ by parallel binary search from Snir's Theorem)
}
```

Previous loop totally is of  $[O(1) + O(\log N)] * O((\log N)^k) = O((\log N)^{(k+1)})$  parallel time. For minimum value of  $k=1$ , Factorization by parallel local binary search of tiled hyperbolic arc, can be done in  $O((\log N)^2)$  parallel time and  $O(N/\log N)$  PRAM processors without  $k$ -mergesort. Assigning  $N/(\log N)^k$  tiles to each of  $N/((\log N)^k)$  PRAMs is of constant time assuming tile intervals are in a global shared memory state i.e PRAM is simulated by a cloud global distributed state - e.g. Spark Accumulators. Snir's Theorem implies  $O((\log N)^2)$  could be optimized to  $O(\log N * \log N / \log p)$  in CREW PRAM.

References:

-----  
481.1 Efficient Parallel Algorithms and subclasses of NC - [KruskalRudolphSnir]  
- [https://ac.els-cdn.com/030439759090192K/1-s2.0-030439759090192K-main.pdf?\\_tid=4ba471c8-d35a-11e7-9c39-00000aabb0f26&acdnat=1511777222\\_ae2aa80751a47624aeb524f723e969b0](https://ac.els-cdn.com/030439759090192K/1-s2.0-030439759090192K-main.pdf?_tid=4ba471c8-d35a-11e7-9c39-00000aabb0f26&acdnat=1511777222_ae2aa80751a47624aeb524f723e969b0)  
481.2 On Parallel Search - Snir's Theorem -  
<https://pdfs.semanticscholar.org/3a58/58e8517f28fa586364daffb34160c437bf78.pdf>  
481.3 Point in Polygon (PIP) problem -  
[https://en.wikipedia.org/wiki/Point\\_in\\_polygon](https://en.wikipedia.org/wiki/Point_in_polygon) - queries if a point is inside, outside or on the polygon. Factor points are always within the pixelated hyperbolic polygon.  
481.4 Simulation of BSP and CRCW PRAM in MapReduce - Sorting, Searching, and Simulation in the MapReduce Framework - [Michael T. Goodrich, Nodari Sitchinava, Qin Zhang] - <https://arxiv.org/abs/1101.1902> - Theorem 3.2 - CRCW PRAM can be simulated on MapReduce clouds by logarithmic increase in parallel time.  
481.5 Models of Parallel Computation - PRAM shared memory model can be simulated

on BSP distributed memory model -

[http://mpla.math.uoa.gr/media/theses/msc/Lentaris\\_G.pdf](http://mpla.math.uoa.gr/media/theses/msc/Lentaris_G.pdf) - Bulk Synchronous Parallel model consists of sequence of supersteps. Each superstep performs a local computation in a processor, communicates to other parallel processors and synchronizes multiple local computations by barriers. BSP which is a distributed memory model than shared thus has close resemblance to cloud parallelism than PRAM.

481.6 PRAM memory access is unit time - [Guy Blelloch] -

<http://www.cs.cmu.edu/afs/cs/academic/class/15499-s09/www/scribe/lec2/lec2.pdf> -

"...Once again, recall that all instructions - including reads and writes - takes unit time. The memory is shared amongst all processors, making this a similar abstraction to a multi-core machine - all processors read from and write to the same memory, and communicate between each other using this...". First step in the loop of previous factorization thus implies a hypothetical machine of  $N/(\log N)^k$  cores and each core reads tile assigned to it in  $O(1)$  time.

-----  
482. (FEATURE-DONE) Support Vector Machines - Mercer Theorem - Kernel Implementation - 29 November 2017  
-----

(\*) This commit implements the kernel trick for lifting points in lower dimension to higher dimension by a Feature map so that decision hyperplane in higher dimension separates the points accurately.

(\*) Mercer Theorem creates a kernel function unifies Feature map lifting and Dot product in higher dimension

(\*) Feature map  $\phi$  maps a point in a dimension  $d$  to a point in dimension  $d+k$ :

$\phi(x) = X$ . Inner Product (Dot) of two vectors in dimension

$d+k = \phi(x) \cdot \phi(y)$ . Mercer Theorem unifies the Feature map and Dot product into a Kernel function defined as series:

$$K(x,y) = \sum \text{eigenvalue}(i) \cdot \text{eigenfunction}(x) \cdot \text{eigenfunction}(y)$$

(\*) This implementation randomly instantiates a  $N \times N$  square matrix, finds its Eigenvalues and Eigenvectors, and computes the series for

$K(x,y)$  as per previous identity (neglecting imaginary parts of Eigenvalues and Eigenvectors)

(\*) logs for this have been added to testlogs/  
-----

-----  
483. (FEATURE-DONE) Support Vector Machines - Mercer Kernel Update - 30 November 2017  
-----

(\*) Mercer Kernel Function has been changed to return a tuple of feature mapped points and the dot product

(\*) Feature mapped points in higher dimension are : [...],  
 $\text{square\_root}(\text{eigenvalue}[i]) \cdot \text{eigenfunction}(x[i]), \dots]$   
-----

-----  
484. (FEATURE-DONE) Compressed Sensing - Image Sketch implementation - 1 December 2017  
-----

(\*) Sketch  $B$  of an image bitmap  $X$  is computed by multiplying with a random matrix  $A$ :  $B=AX$

(\*) `import ImageToBitMatrix from image_pattern_mining/` for mapping an image to a bitmap matrix

(\*) Sketch matrix  $B$  contains compressed information of the larger image. Original image can be sensed from this sketch.  
-----  
-----

485. (FEATURE-DONE) Compressed Sensing Update - Decompression and Error estimation of recovered image bitmap from sketch - 4 December 2017

---

(\*) Sketch  $Ax=B$  of an image bitmap has been persisted to a file CompressedSensing.sketch

(\*) A is a random matrix of dimensions  $(m,n)$   $m \ll n$  and  $m$  is scaled by a sketch ratio variable

(\*) Original image  $x$  is recovered from sketch  $Ax=B$  by inverting A and multiplying with sketch:

$$A_{\text{inverse}}.Ax = x_{\text{recovered}}$$

(\*) For non-square only approximate pseudo inverse is computable.

(\*) For inverting non-square matrix A, Moore-Penrose Pseudoinverse function `pinv()` from NumPy is invoked.

(\*) Error of the recovered image computed by trace (sum of all entries) of the recovered image.

(\*) Logs for multiple sketch ratios (row values:100,200,300,400,50) have been committed to testlogs/ which show an increase in error as size of the sketch decreases.

---

486. (THEORY) Computational Geometric Factorization, Tile Search Optimization and Parallel Interval/Segment Search Trees - 5 December 2017 and 22 December 2017 - related to 34, 481

---

Tile Search optimization for finding factors of an integer described earlier, binary-search set of intervals in parallel for factor point. This is the classic segment/interval search tree problem in Computational Geometry. Segments/Intervals are 1-dimensional polygons and represented in a binary search tree. Query point and the containing interval are searched on this binary search tree. Sequential construction of interval/segment search tree needs  $O(n \log n)$  time. Searching each tile segment in parallel and searching an interval/segment tree in parallel for factor points are equivalent. There are parallel segment tree construction algorithms on Bulk Synchronous Parallel(BSP) model and as Distributed Segment Trees. Distributed Segment Trees are based on Distributed Hash Tables and insertion/retrieval of a key is based on keyspace partitioning and routing in the network i.e Each node in the network is assigned a subset of segment id(s) in a binary partitioned space. Insertion/Retrieval primitives hop through the network and find the matching node for the segment. Most cloud key-store implementations are distributed hash tables. Example: For inserting  $n$  keys in  $O(\log N)$  time, number of hops has to be  $O(\log N)$  per key and each key is inserted in parallel in  $O(1)$  time. Minimizing number of hops implies maximizing mean degree of a node in the network and is a trade-off.

Unique Prime Factorization of an integer  $N = p_1^{k_1} * p_2^{k_2} \dots * p_n^{k_n}$   
This can be rewritten as:

$$2^{\log N} = 2^{(k_1 \log(p_1) + k_2 \log(p_2) + \dots + k_n \log(p_n))}$$

$$\Rightarrow \log N = (k_1 \log(p_1) + k_2 \log(p_2) + \dots + k_n \log(p_n))$$

SmallOmega(N) = number of distinct prime factors of  $N = O(\log \log N)$  from Hardy-Ramanujan Theorem

BigOmega(N) = number of prime factors including multiplicity = sum of prime powers =  $k_1 + k_2 + k_3 + \dots + k_n$

But  $k_1 + k_2 + k_3 + \dots + k_n < (k_1 \log(p_1) + k_2 \log(p_2) + \dots + k_n \log(p_n)) = \log N$

$$\Rightarrow \text{BigOmega}(N) < \log N$$

BigOmega(N) =  $O(\log N)$  [This is very high upperbound and not tight estimate]

Segment binary search tree representation of pixelated hyperbolic tile segments is described in references below.

Factorization algorithm for  $N$  based on Segment Tree Search is:

(#) Construct Segment Tree of Pixelated Hyperbolic Segments in Parallel ( $O(\log N)$  or between  $O((\log N)^2)$  and  $O((\log N)^3)$  depending on sorting)

(#) Query the Segment Tree for factor points in  $O(k + \log N)$  where  $k$  is the number of segment intervals to be reported having factor point  $N=pq$ . It is sufficient to report atleast 1 segment having factor point and thus  $k=1$ . Number of segments containing both prime and non-prime factor points is proportional to size of set of all subsets of distinct prime factors and multiplicity (SmallOmega and BigOmega). Geometric intuition for this is: By moving a sweepline across the x-y plane, factor points and segments containing them (which are nothing but all possible size 2 partitions of set of distinct prime factors which correspond to  $p$  and  $q$  in  $N=pq$ , where as Bell Number of this set is number of all possible partitions) are reached in sequence left-to-right sorted ascending. Size of set of all subsets of distinct prime factors =  $2^{\text{SmallOmega}(N)} = 2^{\log \log N} = \log N$ . If multiplicity is taken into consideration, from the very high bound above number of sets of subsets can be as high as  $O(2^{\log N})$ .

Thus there are 3 Computational Geometric Factorization algorithms described in this draft and all of them are PRAM algorithms and in NC requiring between  $O((\log N)^2)$  and  $O((\log N)^3)$  parallel time:

(#) K-MergeSort and BinarySearch of Hyperbolic tile segments (mentioned in 34 - requires merge sort of tile intervals/segments)

(#) Local Binary Search in parallel of hyperbolic tiles without K-MergeSort (mentioned in 481 - recent optimization, better than k-mergesort)

(#) Segment Tree Representation and Binary Search of hyperbolic tile Segments (uses a classic datastructure, preprocessing is non-trivial and segment tree has to be constructed in parallel - requires merge sort of tile intervals/segments)

Note: First and Third factorization algorithms are equivalent because both involve sorting of pixelated hyperbolic tile segments. Second algorithm obviates sorting by assumption that each PRAM can locally do a binary search without involving peer PRAM processors. Theoretically all three have similar polylogarithmic ( $O(\log N * \log N)$  at best) runtime upperbounds. Second algorithm is better than First and Third probably because the constant involved in Big-O notation in second algorithm is very small compared to First and Third.

It is apt to mention the resemblance of K-MergeSort of Hyperbolic Tile segments and Burrows-Wheeler Transform (BWT) of a string. Burrows-Wheeler Transform sorts all rotation permutations of a string, extracts the last index from each sorted permutation, concatenates them into a transformed string which has co-located substrings. This co-location of similar substrings is invertible and useful for compression and indexes. K-MergeSort Computational Geometric Factorization merges and sorts concatenated tile segment strings, resulting in a sorted string which has colocated similar factor points.

An Unsorted Search algorithm has been implemented in NeuronRain (Section 500) to locate a query point on an unsorted array of numbers, by representing the numbers as arrays of hashtables for each digit. This algorithm can find factors in the concatenation of merged pixelated hyperbolic tile segments with no requirement for sorting. But this involves hashtable preprocessing.

Length of each tile on x-axis can be derived from equating for  $N$ :

$$xy = (x+\delta)(y-1) \\ \delta = x/(y-1) = N/[y(y-1)]$$

Sum of lengths of all pixelated hyperbolic tiles along x-axis is the series:

$$N/(1*2) + N/(2*3) + N/(3*4) + \dots$$

But:

$$N/(1*2) + N/(2*3) + N/(3*4) + \dots < N/1 + N/2^2 + N/3^2 + \dots < N +$$

$$\text{DefiniteIntegral}_{2 \text{ to } N}(dx/x^2) = 1.5N-1$$

=> Sum of lengths of all pixelated hyperbolic tiles is upperbounded by  $1.5N-1$  or  $O(N)$

Some more optimizations:

-----  
[#] Sorting is required only if end points of two adjoined segments are in conflict (only some, not all, elements in next tile are greater than last element of the preceding tile).

[Subsegment1] Elements of succeeding tile segment become bigger than last element in preceding tile segment if:

$$\begin{aligned}xy &< (x + \text{delta})(y-1) \\xy &< xy - x + \text{delta}(y-1) \\ \Rightarrow \text{delta} &> x/(y-1)\end{aligned}$$

[Subsegment2] Similarly first element in succeeding tile is bigger than last element in Subsegment1 if:

$$(x+\text{delta})y < (x + N/(y-1)(y-2))(y-1)$$

Splitting each tile segment of length  $l$  into two subsegments of length  $\text{delta}$  and  $l-\text{delta}$  and binary searching two sets of concatenations of these split tile segments can find factors in  $O(\log N)$  sequentially with no necessity for PRAMs if concatenation can be done in sequential in  $O(\log N)$  time (tree of list concatenations can be done in parallel on PRAMs in  $O(\log N)$  time, but doing sequential concatenation of lists in sublinear time is an open problem). In other words hyperbolic arc bow is broken into two concatenated tile segment sets and these two tile concatenations are searched.

[#] If the quadrant containing hyperbolic arc is partitioned by parallel ray shooting queries from origin, separated by angles proportional to location of factor points, there is no necessity for sorting. Number of primes factors are  $O(\log \log N)$ . Thus  $k \log \log N$  ray shooting queries from origin pierce the hyperbolic arc bow in parallel. If angular spacing between ray shooting queries are approximately equal, following trigonometric expression gives the approximate prime factor for each ray angle:

$$y(m) = \text{SquareRoot}(N/[\tan(m\pi/(2*k*\log \log N))]) - 1 \text{ for}$$

$m=1,2,3,\dots,k \log \log N$

These are only approximate angles. Factors should lie in close proximity of the intersection points of these rays with in hyperbolic bow.

References:

-----  
486.1 Parallel Segment Trees - [AV Gerbessiotis] -  
<https://web.njit.edu/~alexg/pubs/papers/segment.ps.gz>  
486.2 Distributed Segment Trees - [Guobin Shen, Changxi Zheng, Wei Pu, and Shipeng Li - Microsoft Research] -  
<http://www.cs.columbia.edu/~cxz/publications/TR-2007-30.pdf>  
486.3 Computational Geometry - Algorithms and Applications - [Mark de Berg, Otfried Cheong, Marc van Kreveld, Mark Overmars] - Chapter 10 - More Geometric Datastructures - Interval Trees and Segment Trees -  
[http://people.inf.elte.hu/fekete/algorithmusok\\_msc/terinfo\\_geom/konyvek/Computational%20Geometry%20-%20Algorithms%20and%20Applications,%203rd%20Ed.pdf](http://people.inf.elte.hu/fekete/algorithmusok_msc/terinfo_geom/konyvek/Computational%20Geometry%20-%20Algorithms%20and%20Applications,%203rd%20Ed.pdf)  
486.4 Parallel Construction of Binary Search Trees -  
[MJAtallah, SRKosaraju, LLLarmore, GLMiller, SHTeng] -  
<https://www.cs.cmu.edu/~glmiller/Publications/Papers/ConstructingTreesInParallel.pdf> - general binary search trees can be constructed in parallel.  
486.5 Segment Trees - definition and diagrams - [Computational Geometry Course Notes - Antoine Vigneron - King Abdullah University of Science and Technology] -  
<https://algo.kaust.edu.sa/documents/cs372l07.pdf> - Segments are sorted by endpoints. Leaves of the binary search segment tree are atomic elementary intervals created by start-end coordinates of segments. Internal nodes of the segment tree contain list of segments. Internal node  $n$  of segment tree has a segment  $[s_1,s_2]$  if and only if  $\text{Interval}(n)$  is a subset of  $[s_1,s_2]$  and  $\text{Interval}(\text{parent}(n))$  is not a subset of  $[s_1,s_2]$  and  $n$  is closest to root. Stabbing Query "Which are the segments containing a point  $q$ ?" is answered by traversing the segment search tree from root recursively and choosing one of the



two child subtree intervals containing  $q$  at each level. In Computational Geometric Factorization, segment binary search tree stores the tile segments of pixelated hyperbola and stabbing query is "Which of the tile segments have the factorization point  $N=pq$ ?" which is  $O(k+\log N)$  and  $k$  is the  $O(\log \log N)$  because number of tile segments containing  $N$  is exactly equal to number of factors of  $N$  which is  $\log \log N$  from Hardy-Ramanujan Theorem. Thus finding all factor points is  $O(\log \log N + \log N)$ . It has to be noted here this further optimizes the factorization algorithm by local binary search of tiles in parallel described earlier in 481. Loop in the algorithm is replaced by a segment tree of tile segments. But construction preprocessing time of segment search tree is  $O(N \log N)$  which requires a parallel tile segment tree construction in polylogarithmic time mentioned in references below - Thus segment tree construction + stabbing query for factor points is:  $O(\log N^2 + \log \log N + \log N) = O((\log N)^2)$  which is same as the time required in Factorization loop.

486.6 Hardy-Ramanujan Theorem - [https://en.wikipedia.org/wiki/Hardy](https://en.wikipedia.org/wiki/Hardy%E2%80%93Ramanujan_theorem)

486.7 Parallel Construction of Segment Trees -

<https://www.cs.dartmouth.edu/~trdata/reports/TR92-184.pdf> - [Peter Su, Scot Drysdale] - Section 4.2 - Analysis of Algorithm S - "...Thus we expect runtime of algorithm S would be between  $O(\log N^2)$  and  $O(\log N^3)$  depending on how good our sorting algorithm is..."

486.8 Parallel Computational Geometry - Parallel Construction of Segment Trees is  $O(\log N)$  time - Section 5 - Pages 308-309 -

[A.Aggarwal, B.Chazelle, L.Guibas, C.O.Dunlaing, C.Yap] -

<https://www.cs.princeton.edu/~chazelle/pubs/ParallelCompGeom.pdf>

486.9 Small omega - Number distinct prime factors of an integer -

<https://oeis.org/A001221> - is  $O(\log \log N)$  from Hardy-Ramanujan and Erdos-Kac Theorems

486.10 Big omega - Number prime factors of an integer with multiplicity -

<https://oeis.org/A001222> - is sum of prime powers in unique factorization of  $n$ . For quadratfrei(squarefree) integers Big Omega = Small Omega. An optimization in the segment tree search or local binary search in parallel for factor points is it is not necessary to find all factorization points in stabbing query. Segment tree search or local binary search can stop once first factor is found. Other factors are obtained by repetitive application of this algorithm after dividing the integer by factor found in previous step.

486.11 Parallel Construction of Segment Trees applied in another setting -

[Helmut Alt, Ludmila Scharf] - computing depth of arrangement of axis parallel rectangles -

[http://cs.au.dk/fileadmin/madalgo/PDF/Parallel\\_Algorithms\\_for\\_Shape\\_Matching.pdf](http://cs.au.dk/fileadmin/madalgo/PDF/Parallel_Algorithms_for_Shape_Matching.pdf) and

<https://pdfs.semanticscholar.org/99e5/2d0c99263dd97d5db289b72f82b233528765.pdf> -  $O((\log N)^2)$  time parallel construction of a balanced search tree

486.12 Function plot of Number of PRAM processors -  $N/(\log N)^k$  - For  $k=1$ ,  $N/\log N$  has been plotted in

<https://github.com/shrinivaasanka/asfer-github-code/blob/master/python-src/testlogs/>

DiscreteHyperbolicFactorizationUpperbound\_TileSearch\_Optimized.NbylogN\_Desmos\_Function\_Plot.pdf -  $N/(\log N)^k$  can be rewritten as  $2^{(\log N - k \log \log N)}$ . If  $N^m = 2^{(\log N - k \log \log N)}$ ,  $m = \log(\log N - k \log \log N)/\log N \ll 1$  for large  $k \log \log N$ .

486.13 Interval Hash Trees - [T. F. Syeda-Mahmood, P. Raghavan, N. Megiddo] -

<http://www.almaden.ibm.com/cs/people/stf/papers/caivd99.pdf> - Variant of Interval Trees which includes Merkle Hash Trees for Region hashing of affine rectangles within images. Merkle trees are trees of hashes - leaves are hashes of regions of file blocks, internal nodes are hashes of concatenations of hashes of its children nodes. If hyperbola is represented as an image, computational geometric factorization reduces to querying the factor point or rectangles having factors in the image.

486.14 Efficient Parallel Algorithms for Geometric Clustering and Partitioning Problems (1994) - [Amitava Datta] -

<http://www.informatik.uni-freiburg.de/tr/1994/Report64/report64.ps.gz> - Section 2.1 - Parallel Construction of Range Tree by creating Segment Tree in parallel in  $O(\log N)$  time and  $O(N)$  processors.

486.15 Parallel computational geometry of rectangles - [Chandran-Kim-Mount] -

<https://link.springer.com/article/10.1007/BF01758750> - this algorithm is applied in 486.14 for parallel construction of segment trees.

486.16 SCALABLE PARALLEL COMPUTATIONAL GEOMETRY FOR COARSE GRAINED MULTICOMPUTERS - [FRANK DEHNE, ANDREAS FABRI, ANDREW RAU-CHAPLIN] - <http://citeseerx.ist.psu.edu/viewdoc/download?doi=10.1.1.46.1429&rep=rep1&type=pdf> - describes a Scalable Parallel Segment Tree Construction and Search Algorithm.

486.17 Simpler example of Segment trees - tree of nested intervals - [http://www.eng.biu.ac.il/~wimers/files/courses/VLSI\\_Backend\\_CAD/Lecture\\_Notes/SegmentTree.ppt](http://www.eng.biu.ac.il/~wimers/files/courses/VLSI_Backend_CAD/Lecture_Notes/SegmentTree.ppt) - each internal node has an interval of endpoints which is union of intervals of subtree rooted in it. E.g Internal node having children [10,11] and [11,13] has interval [10,13] - Set of pixelated tile segments of hyperbolic arc bow creates a lower envelope - list of tile segment endpoints - which has no overlaps. Segment tree of this envelope is parallelly created by one of the parallel segment tree constructions algorithms referred previously.

486.18 Parallel construction of Bounding Volume Hierarchy Trees (BVH) - BVH trees are computational geometric binary search datastructures similar to BSP and kd-trees for hierarchical space partitions. Each internal node of the search tree has union of volumes bounded by its children. In this respect BVH trees are 3-dimensional counterparts of segment trees. BVH trees can be constructed in parallel in GPU - <https://digi.felk.cvut.cz/projects/ploc/ploc-tvcg.pdf>

486.19 Parallel Algorithms for Geometric Problems - [Anita Chow] - Ph.D Thesis - <http://www.dtic.mil/dtic/tr/fulltext/u2/a124353.pdf> - Planar Point Location Binary Search Tree for Plain Simple Line Graph (similar to segment tree) - "...In this section we describe two algorithms: (i) the construction of a search structure for the set of edges on the SML4 with N processors and (ii) the concurrent location of M points with M processors. The construction and the location run in time  $O((\log N)^2 \log \log N)$  and  $O((\log N)^2)$  respectively..." - Section 4.1 - Page 60

486.20 Parallel Augmented Maps (PAM) - <https://arxiv.org/pdf/1612.05665.pdf> - [Yihan Sun, Daniel Ferizovic, Guy Blelloch] - Recent Algorithm for Parallel Construction of Interval Trees by Parallel Augmented Maps - Segment Trees are specialized versions of Interval Trees. Interval Trees can also answer stabbing query on interval, not just a point - Section 5.1 and Section 6.2 - "...In parallel, on  $10^8$  intervals, our code can build an interval tree in about 0.23 second, achieving a 63-fold speedup. We also give the speedup of our PAM interval tree in Figure 6(d). Both construction and queries scale up to 144 threads (72 cores with hyperthreads)..."

486.21 Burrows-Wheeler Transform - Example transformed string "<sup>^</sup>BANANA|" - [https://en.wikipedia.org/wiki/Burrows%E2%80%93Wheeler\\_transform](https://en.wikipedia.org/wiki/Burrows%E2%80%93Wheeler_transform)

-----

487. (THEORY) Thermodynamics Gas Diffusion Entropy Model of Information Diffusion in Social Networks and Text Graphs - 11 December 2017  
- related to 383

-----

Second Law of Thermodynamics implies entropy of a closed system always increases. Gas diffusion in a closed chamber distributes molecules at random within the space of the chamber. Gas chamber is a 3-dimensional grid of volume N. If in initial state, all gas molecules were confined to a small fractional cubic volume, probability of finding m gas molecules in kN ( $k < 1$ ) grid points is  $k^m N^m / N^m$ . As the fractional volume gets close to N (k is almost 1), gas molecules engulf the chamber. Increase in fractional volume facilitates increase in degrees of freedom. Entropy of this closed system is defined as  $c \log N$  where c is Boltzmann constant. Diffusion of information in Social network graphs can be likened to gas diffusion in closed chamber and adjacent vertices of a social network node are the neighbouring grid points. In other words, social network graph is plotted as non-planar simple line graph in a 3-dimensional space and information diffuses along edges of this graph. Entropy of this system can then be defined as  $O(\log V)$  where V is number of vertices. Probability of finding a diffused information in any fraction kV of the network follows previous Gas diffusion model =  $(kV)C_i / VC_i$  where i is the total number of

information units diffused among social network vertices. For text definition graphs, this is nothing but Korner Entropy.

#### References:

-----  
487.1 Solomon Asch Conformity Experiments and Herd behaviour - Information Diffusion in Social Media - Section 7.1 - <http://dmml.asu.edu/smm/SMM.pdf> - this is a psychology experiment where set of subjects are swayed by peer opinions and rational independent decision making ceases i.e majority voting can go wrong.  
487.2 Emperor's New Mind - [Roger Penrose] - Inexorable increase in entropy - Page 405  
-----

-----  
488. (FEATURE-DONE) NeuronRain AsFer-KingCobra MAC Electronic Money - Proof-of-Work and Universally Unique ID Hash implementation -  
14 December 2017  
-----

-----  
(#) Fictitious Message-As-Currency (MAC) in AsFer-KingCobra has been named "Neuro".  
(#) This commit implements a non-trivial proof-of-work computation and finds a universally unique hash id for each Neuro currency  
which has 2 leading "ff"s - Proof of Work is analogous to reCAPTCHA in websites for filtering out robots  
(#) Unique id is created from Boost UUID random generator and checked in a loop for 2 leading "ff" in stringified hex representation  
(#) Protocol Buffer version has been upgraded to 3.5/15 and currency.proto has been recompiled with protoc  
(#) asfercloudmoveclient.cpp has been updated to make a choice between std::move() and std::forward() move semantics:  
- std::move() just does =operator overload and moves Neuro currency over network  
- std::forward() + std::move() first defers rvalue of && for currency uuid and then does =operator overload to move Neuro currency  
(#) Limitation: Presently there is no documented way to create an rvalue for non-primitive datatypes. For example std::string can have rvalue as literal string "xxxxxx".  
-----

-----  
489. (FEATURE-DONE) AsFer-KingCobra Neuro Electronic Currency - Rvalue NonPrimitive Perfect Forward - 18 December 2017  
-----

-----  
(#) New constructor for cloudmove which takes const char\* uuid has been defined. This enables  
assigning a string literal rvalue to cloudmove<currency::Currency> objects.  
(#) New move operator= which takes const char\* uuid has been defined. This internally instantiates  
a currency::Currency object  
(#) New move operator= which takes cloudmove<T>& lvalue has been defined.  
(#) New value and a clause for move semantics, "nonprimitiveforward" has been defined. This clause  
does std::forward() of an rvalue cloudmove<currency::Currency> and then invokes std::move() of the currency over network.  
(#) This differs from move semantics "std::forward" which is specific to std::string uuid only, and thus solves the generic currency::Currency object rvalue forward and move.  
(#) client and server logs for this network move have been committed to testlogs.  
-----  
-----

490. (THEORY) Generalization of Complementation Undecidability to Rationals(Q) and Reals(R) by H10(Hilbert Tenth Problem) and Connection between ZF with Axiom of Choice (ZFC) and Complementation - related to 471 - 28 December 2017, 29 March 2018

-----

Thus far Function Complementation described in drafts of this document are oriented towards set of natural numbers only - e.g Coloring of Integer Sequences, Diophantine Sets of Integers and associated Diophantine polynomials having Integer Solutions. As mentioned earlier, finding the map  $f$  from a diophantine set  $a=\{a_1,a_2,\dots,a_n\}$  is equivalent to solving the diophantine  $f(x,a)=0$  for unknown  $x$  and parameter  $a$  and  $f$  itself being an arbitrary unknown diophantine. Integer solutions to  $x$  in  $f(x,a)=0$  creates the enumeration  $f(0)=a_1,f(1)=a_2,\dots$  which is the constructed complement map. But from MRDP theorem solving integer diophantine  $f(x,a)=0$  is undecidable. MRDP theorem does not apply for set of reals which is uncountable/non-recursively-enumerable - Reals have cardinality  $2^{\aleph_1}$  where  $\aleph_1$  is set of natural numbers (there are at least two levels of infinities). Because any set of cardinality greater than set of natural integers are uncountable, reals cannot be enumerated as  $f(0),f(1),\dots$  [By Cantor diagonalization there exists a real between any two reals]. For reals, Sturm's and Tarski methods solve arbitrary diophantines for real solutions to unknowns and thus H10 is decidable for reals. But there are undecidable real diophantine problems which involve  $\sin()$  function(details in references). Construction of complementation is not just about solving unknowns in a diophantine but to construct the diophantine itself which is harder problem than proving undecidability from H10. Constructing the complement diophantine by previous mapping procedure mandates  $x$  to be always a natural integer for enumerability/listability and existence of a corresponding diophantine for this enumerable set -  $f(0),f(1),f(2),\dots$  - once the mapping process terminates, interpolation can find the diophantine polynomial from the ordered pairs  $(x_1,f(x_1)), (x_2,f(x_2)), \dots, (x_n,f(x_n))$ . Undecidability of complement construction for recursively enumerable sets arises when mapping procedure itself is not recursive. Removing restriction that  $x$  has to be integer and admitting real solutions for  $a$  and  $x$ , makes  $f(x,a)=0$  decidable.

Axiom of Choice: For set of sets  $S=\{s_1,s_2,s_3,\dots\}$  there exists a choice function  $C(s_i)=x_i$  which chooses an element  $x_i$  from every set  $s_i$  in  $S$ .

Following is a special case example of Axiom of Choice in Boolean Social Choice functions:

Depth-2 boolean function/circuit  $B$  leaves of which are sets  $s_1,s_2,s_3,\dots$  and nodes at level one are  $C(s_1)=x_1,C(s_2)=x_2,\dots$  for  $C(s_i) = 0$  or  $1$  and  $s_i=\{s_{i1},s_{i2}\}$ ,  $s_{i1},s_{i2}$  in  $\{0,1\}$ . Root is an AND/OR gate. For example  $C(s_i)$  is a boolean AND/OR function. Boolean complementation of  $C(s_i)$  flips the chosen element per each set  $s_i$ . This yields a complement choice function per set. If this example of Boolean Axiom of Choice complementation is generalized to any set and is True,  $S=\{C(s_1),C(s_2),C(s_3),\dots,C(s_n)\}$  is a recursively enumerable set listed by function  $C$  and has a diophantine representation by MRDP theorem and its complement set created from complement choice function  $C'$  of  $C$  denoted by  $S'=\{C'(s_1),C'(s_2),C'(s_3),\dots\}$ . If this complement set  $S'$  is also recursively enumerable, then both sets  $S$  and  $S'$  are recursive. This implies choice functions  $C$  and  $C'$  are constructible and have a diophantine representation.

Disjoint Set Cover is also known as Exact Cover defined as subcollection  $S'$  of collection of subsets  $S$  of a universal set  $X$ , and each element in  $X$  is contained in exactly one subset in  $S'$ .  $S'$  is a disjoint collection and the exact set cover of  $X$ . Exact Cover problem is NP-complete and is solved by DLX Dancing Links algorithm. Complementary or Ramsey  $k$ -colored sets are created by Exact Set Cover.

Hilbert's Tenth Problem for Rationals (Q) is open. Some approaches to solving Diophantines over Q - defining integers via rationals i.e integers are definable in first order theory of rationals - have been mentioned in references.

## References:

- 
- 490.1 Diophantines for Reals - [http://www.mayr.in.tum.de/konferenzen/Jass07/courses/1/Sadovnikov/Sadovnikov\\_Paper.pdf](http://www.mayr.in.tum.de/konferenzen/Jass07/courses/1/Sadovnikov/Sadovnikov_Paper.pdf) - Section 1.2 - "...It would be natural to ask if the complements of the sets listed above are also Diophantine. We can easily build a Diophantine representation for the complement of the first set while the answer for two other complements is not so evident: ... " and Section 3
- 490.2 Uncountable sets and non-recursively enumerable languages - <http://www.cs.colostate.edu/~massey/Teaching/cs301/RestrictedAccess/Slides/301lecture23.pdf>
- 490.3 Deciding the Undecidable - <https://books.google.co.in/books?id=1rjnCwAAQBAJ&pg=PA10&lpg=PA10&dq=real+solutions+to+diophantine+tarski&source=bl&ots=W2QvvG1KJX&sig=PqhrS-5ThqyokMAvXDIYNivBPAC&hl=en&sa=X&ved=0ahUKEwj05ofgmqzYAhUBro8KHUaYA-sQ6AEINDAC#v=onepage&q=real%20solutions%20to%20diophantine%20tarski&f=false> - Tarski's Decision Procedure for Algebra over Reals
- 490.4 Introduction to Automata Theory, Languages and Computation - [John E. Hopcroft, Rajeev Motwani, Jeffrey D. Ullman] - Theorem 9.4 - Page 376 - If both language  $L$  and its complement  $L'$  are recursively enumerable, then  $L$  is recursive and  $L'$  is recursive as well.  $L' = A^* - L$  for set of alphabets  $A$ .
- 490.5 Real Roots of polynomials - [https://en.wikipedia.org/wiki/Root-finding\\_algorithm](https://en.wikipedia.org/wiki/Root-finding_algorithm)
- 490.6 Constructing Diophantine Representation of a Listable Set, Register Machines preferred over Turing Machines - [https://books.google.co.in/books?id=GlgLDgAAQBAJ&pg=PA43&lpg=PA43&dq=constructing+diophantine+representations&source=bl&ots=UT5\\_nW-OU&sig=vpIkAMBvoNBD1PvqdZ-qmP7QYME&hl=en&sa=X&ved=0ahUKEwjKxKwmsa\\_YAhVFr48KHcpJCvUQ6AEIPjAC#v=onepage&q=constructing%20diophantine%20representations&f=false](https://books.google.co.in/books?id=GlgLDgAAQBAJ&pg=PA43&lpg=PA43&dq=constructing+diophantine+representations&source=bl&ots=UT5_nW-OU&sig=vpIkAMBvoNBD1PvqdZ-qmP7QYME&hl=en&sa=X&ved=0ahUKEwjKxKwmsa_YAhVFr48KHcpJCvUQ6AEIPjAC#v=onepage&q=constructing%20diophantine%20representations&f=false) - Chapter 2 - Martin Davis and H10 - [Y. Matiyasevich] - Constructing Diophantine representation for a listable complementary set is exactly construction of a complement function.
- 490.7 Diophantine Representation, Non-Deterministic Diophantine Machine (NDDM), Complexity class NP, Single Fold Diophantine - [Yuri Matiyasevich, St. Petersburg, Department of Steklov Institute of Mathematics of Russian Academy of Sciences] - <https://www.newton.ac.uk/files/seminar/20120111170017302-152989.pdf> - Adleman-Manders class D of Diophantines which have total binary length of unknowns  $\leq [\text{binary length of parameter}]^k$  - Open Problem: Is  $D = NP$ ?
- 490.8 DPR theorem and finite-fold diophantine representations - [Yuri Matiyasevich] - <ftp://ftp.pdmi.ras.ru/pub/publicat/zns1/v377/p078.pdf> - Every effectively enumerable set has single-fold exponential diophantine representation (a diophantine polynomial which has unknowns in exponents and value for unknowns per parameter tuple is unique) of the form:  $\langle a_1, a_2, \dots \rangle$  in  $S \Leftrightarrow$  There exist  $y, x_1, x_2, \dots, a_1, a_2, \dots$   $P(y, x_1, x_2, \dots, a_1, a_2, \dots) = 4^y + y$  for a diophantine polynomial  $P$  in integer coefficients.
- 490.9 Factoring Semi-primes (numbers of the form  $N=pq$  for prime  $p, q$ ) by Diophantine Equations - <http://www2.mae.ufl.edu/~uhk/FACTORING-VIA-DIOPHANTINE.pdf>
- 490.10 Dancing Links X Algorithm For Exact Cover - Pentominoes Example - 4-way doubly linked list - [Donald E. Knuth] - <https://arxiv.org/pdf/cs/0011047.pdf>
- 490.11 Dancing Links - [Hitotumatu, Hiroshi; Noshita, Kohei] (1979). "A Technique for Implementing Backtrack Algorithms and its Application". Information Processing Letters. 8 (4): 174-175. doi:10.1016/0020-0190(79)90016-4.
- 490.12 Hilbert Tenth Problem for Rationals - <https://rjlipton.wordpress.com/2010/08/07/hilberts-tenth-over-the-rationals/> - "...One of the most celebrated such results is that deciding whether or not a polynomial  $\{P(x_1, x_2, \dots, x_m)\}$  has an integer solution is undecidable. This is the famous negative solution to Hilbert's Tenth. An obvious question, which is still open, is what happens if we ask for solutions where the  $\{x_1, x_2, \dots, x_m\}$  are allowed to be rationals? This is open—I discussed it recently as a potential million dollar problem.... An approach to proving that H10 extended to the rationals is also undecidable is to show that the integers are definable by a polynomial formula. Suppose  $\exists y_1 \dots \exists y_n R(x, y_1, \dots, y_n) = 0$  is true for a rational  $\{x\}$  if and only if  $\{x\}$  is actually an integer. Note, the quantifiers range over rationals. Then, we can transform a

question about integers into a question about rationals—this would show that H10 for rationals is also undecidable. ..."

-----  
491. (FEATURE-DONE) All pairs of encoded strings - Sum of Distances - algorithm mentioned in Grafit course notes implemented - 3 January 2018  
-----

-----  
(#) For pairwise pattern mining, sum of distances between binary encoded strings algorithm mentioned in Grafit course notes has been implemented which is better than bruteforce.  
(#) asfer.conf has been updated  
(#) asferencodestr.cpp and asferencodestr.h have been updated for new class member functions (factorial and combinations)  
(#) logs have been committed to testlogs/  
(#) This is only in GitHub (NeuronRain Enterprise) repo which has binary encoded strings. NeuronRain Research repo in SourceForge has astronomically encoded unicode strings which requires a variant of this implementation (must be sum of 10 combination terms for each character - each term is per symbol).  
-----

-----  
492. (THEORY and FEATURE-DONE) Complement Function Map Construction - Diophantine Representation - Lagrange's Four Square Theorem SymPy solver (Draft updates to: <https://arxiv.org/abs/1106.4102>) - related to 472 - 4 January 2018  
-----

-----  
(#) This commit implements diophantine representation of an enumerable recursive set by Sum of Four squares solver in SymPy.  
(#) New function that enumerates each element  $x$  of the complement set and applies it as a parameter to Sum of Squares Diophantine solver to obtain the quadruple  $(a,b,c,d)$  such that  $a^2 + b^2 + c^2 + d^2 = x$   
(#) This is mostly partial recursive function and not necessarily a total recursive function (defined for all possible quadruples).  
(#) logs for this have been committed to testlogs/  
(#) SymPy has other diophantine solvers too which require more than one parameters.  
(#) SymPy does not have exponential diophantine support yet which if available could construct an exponential diophantine for almost every recursively enumerable set ('almost' because of MRDP theorem - there are diophantine equations for recursively enumerable non-recursive sets and undecidable)  
-----

Any partial function  $f: X \rightarrow Y$  which maps a subset  $X'$  of  $X$  to  $Y$ , can be converted to a total function by mapping all elements in the unmapped complement domain set  $X - X'$  to an element  $y$  in a new extended codomain  $Y' = Y \cup \{y\}$  or an existing element in  $Y$ . This partial-turned-total function map can be interpolated to obtain a polynomial.

References:

-----  
492.1 Reduction of arbitrary diophantine equation to one in 13 unknowns - [Matijasevic-Robinson] - <http://matwbn.icm.edu.pl/ksiazki/aa/aa27/aa27125.pdf> - This implies every effectively enumerable complement set can be represented by a diophantine in 13 unknowns.  
492.2 Distinction between Enumerable and Effectively Enumerable - <http://faculty.washington.edu/keyt/Effenumerability.pdf> - "1) A set is enumerable if, and only if, it is the range of a total or partial function on the natural numbers. 2) A set is effectively enumerable if, and only if, it is the range of a total or partial effectively computable function on the natural

numbers. 3) A function  $f$  is effectively computable if, and only if, there is a list of instructions giving a step-by-step procedure that will determine in a finite number of steps the value  $f(n)$  for any argument  $n$  for which  $f$  returns a value...." - Effectively enumerable sets are recursive sets created by a partial or total recursive function i.e an algorithm can always find a diophantine representation of the set. From previous result every recursive set can be represented by a diophantine in 13 unknowns. If each unknown has maximum limit  $l$ , then there are  $l^{13}$  possible 13-tuples  $t(i)$  of unknowns which is the maximum cardinality of the effectively enumerable set - mapping is enumerated as  $f(t(0)), f(t(1)), \dots, f(t(l^{13}-1))$ . This kind of complementation has two phases:

- (\*) first 13-tuples are found by a diophantine solver and
- (\*) these tuples are listed as  $t(0), t(1), t(2), \dots$ .

492.3 Function Spaces - Extending partial function to a total function - [https://en.wikipedia.org/wiki/Partial\\_function#Total\\_function](https://en.wikipedia.org/wiki/Partial_function#Total_function)

-----  
 493. (FEATURE-DONE) Computation Geometric Factorization - Binary Search for Tiles - Optimization - Benchmarks - Revised - 4 January 2018  
 - related to 480  
 -----

(#) Factorization benchmarks for Tile binary search optimization have been redone on dual core (local[2]) after removing some print statements in python spark code which were CPU intensive.

(#) Following are the durations for factoring same 24 bit integer factorized previously after removing print statements - an improvement of more than 3X:

-----  
 Factorization of 9333123 (24-bit) - without print statements  
 -----

```
real 35m56.196s (Spark Duration = 1839.146seconds)
user 3m2.836s
sys 4m56.668s
```

-----  
 Factorization of 9333123 (24-bit) - with print statements earlier  
 -----

```
real 112m24.101s (Spark duration 12:21 to 14:02 = 101minutes = 6060seconds)
user 0m0.000s
sys 0m0.004s
```

=====

Factors of 9333123 are (excerpt from logs):

=====

```
...
Factor is = 219
Factor is = 1387
Factor is = 2243
Factor is = 4161
Factor is = 6729
Factor is = 6729
Factor is = 42617
Factor is = 127851
Factor is = 163739
Factor is = 491217
Factor is = 3111041
Factor is = 9333123
```

=====

(#) Compressed Spark log for this factorization has been committed to python-src/testlogs/

(#) General Number Field Sieve algorithm is sequential, exponential in number of bits and requires  $O(2^{(c(\log N)^{0.33}(\log \log N)^{0.67})})$  where  $c=1.901883$  (for at least one factor). For 24-bit ( $=\log N$ ) this is approximately  $k*128$  time units for some constant  $k$ . But Computational Geometric Factorization Sieve finds all factors in  $O(\log N * \log N)$  time on multicore (PRAMS).

-----  
-----  
494. (THEORY and FEATURE-DONE) Complement Diophantine Map - Converts a Partial Function to Total Function - 6 January 2018  
-----

-----  
-----  
(#) Sum of Four Squares diophantine solutions are quadruples (a,b,c,d) which form a subset of all possible tuples and thus complement function unknowns-to-parameter map is partial.  
(#) This is remedied by extending the parameter codomain by adding -1 as additional possible parameter value and mapping all unmapped tuples in domain to -1. Resultant map is Total defined for all possible unknown tuples.  
(#) logs for this have been committed to testlogs/  
-----

-----  
-----  
495. (THEORY) Factoring as a service - General Number Field Sieve on Amazon EC2 cloud - RSA 512 bit - Relevance to Computational Geometric NC-PRAM-Multicore Factorization Theoretical  $O((\log N)^2)$  bound - related to 481 - 9 January 2018  
-----

-----  
-----  
Number field sieve has been implemented as Amazon EC2 cloud service. Benchmarks for RSA 512 bit achieve factorization in less than 4 hours applying CADO-NFS and MSieve NFS implementations optimized for Elastic Cloud. Instance type used is c4.8xlarge (each instance has two Intel Xeon E5-2666 v3 processor chips, with 36 vCPUs in a NUMA configuration with 60 GB of RAM) and maximum of 200 instances were in the cloud connected by Elastic Network Adapter(ENA). RSA 512 GNFS benchmark has some parallels in Computational Geometric Factorization - Most time intensive preprocessing step is to create tile segments in parallel by pixelating the hyperbolic arc. Presently this is implemented as SparkContext.parallelize(tilesegmentslist) which creates tile segment RDDs in parallel on cloud reading tile segment array on flatfile. Ideally, each PRAM processor (assuming there are  $N/(\log N)^k$  PRAMs) must read in a tile by computation and not from storage. For example in the algorithm mentioned in 481, p-th PRAM has to compute the tile segment interval (tilestart,tileend) locally in i-th iteration as tilestart=(x,N/x) and tileend=(x,N/x-N/x(x+1)) for  $x=(p+i*N/(\log N)^k)$ . Factoring 512 bit by Hyperbolic pixelation and sort-search of tiles theoretically requires constant\*(512)^k parallel time units and  $2^{512}/(512)^k$  PRAM processors. It has to be mentioned that real advantage of this Computational Geometric Factorization can be felt only for large integers on huge multicores and is by-and-large a theoretical fancy abiding by definition of NC ("Factorization is in NC") in the absence of a practical large scale cloud benchmark. Number of PRAMs required in definition of NC-PRAM equivalence is high even for work-optimal NC. Necessity of sorting the tile segments arises because successive segments though locally sorted ascending cannot be merged by splicing end-to-end directly because some elements in end of a segment could be larger than some elements in the beginning of next segment. Local tile search redresses this deficit.

#### References:

-----  
495.1 Factoring as a service - slides - <http://crypto.2013.rump.cr.yp.to/981774ce07e51813fd4466612a78601b.pdf>  
495.2 Factoring as a service - <https://github.com/eniac/faas> - Parallelizing Number Field Sieve - Polynomial selection, Sieving, Linear Algebra, Square root - paper - [Luke Valenta, Shaanan Cohney, Alex Liao, Joshua Fried, Satya Bodduluri, Nadia Heninger - University of Pennsylvania] - <https://eprint.iacr.org/2015/1000.pdf> - "...The current public factorization record, a 768-bit RSA modulus, was reported in 2009 by Kleinjung, Aoki, Franke, Lenstra, Thomé, Bos, Gaudry, Kruppa, Montgomery, Osvik, te Riele, Timofeev, and Zimmermann, and took about 2.5 calendar years and a large academic effort [23],...We experimented with Apache Spark [37] to manage data flow, but Spark was not flexible enough for our needs, and our initial tests suggested that a



Spark-based job distribution system was more than twice as slow as the system we were aiming to replace. Ultimately we chose Slurm (Simple Linux Utility for Resource Management) [36] for job distribution..."

-----  
496. (THEORY and FEATURE-DONE) Computational Geometric Factorization Update - Local Tile Computation and necessity for storage removed - 10 January 2018 - 30-bit integer dual core single node Spark Cluster benchmark - related to 495  
-----

-----  
As mentioned in previous section, reading tiles from storage in SparkContext.parallelize() is a serious bottleneck. In this commit, tile interval storage is obviated and each foreach() invokes a function which computes non-persisted tile interval locally and does binary search to print factors. SparkContext.parallelize() takes xrange() as argument. Python xrange() is an optimized implementation of list and returns xrange object. xrange object does not store all the elements in memory and is more like an iterator. A thirty bit integer has been factored and numbers are below:

-----  
Factorization of 921234437:  
-----

18/01/10 17:56:56 INFO Utils:  
/home/shrinivaasanka/Krishna\_iResearch\_OpenSource/GitHub/asfer-github-code/python-src/DiscreteHyperbolicFactorizationUpperbound\_TileSearch\_Optimized.py has been previously copied to  
/tmp/spark-9fba8482-8ca1-4022-9bcc-1c285a8e1f58/userFiles-3e4bf574-9b1a-44c5-8b96-3873e96dc6c3/  
DiscreteHyperbolicFactorizationUpperbound\_TileSearch\_Optimized.py

Factor is = 1  
Factor is = 17  
Factor is = 19  
Factor is = 59  
Factor is = 323  
Factor is = 1003  
Factor is = 1121  
Factor is = 19057  
Factor is = 48341  
Factor is = 821797  
Factor is = 918479  
Factor is = 2852119  
Factor is = 15614143  
Factor is = 48486023  
Factor is = 54190261

18/01/10 18:08:51 INFO PythonRunner: Times: total = 714516, boot = 649, init = 23, finish = 713844

Spark Duration: 18:08:51 - 17:56:56 = 535seconds

Spark-Python has RPC and serialization latencies and following numbers could be better if implemented in a different frameworks like Slurm and on a Gigabit ENA cloud. First non-trivial factor above was printed within few seconds and this benchmark is for sieving all factors. Time utility is misleading because it includes all Spark RPC overhead.

-----  
497. (THEORY and FEATURE-DONE) Computational Geometric Factorization - Non-Persistent Tile Segments - 30 bit Single Node Dual Core Spark Benchmarks - 11 January 2018 - related to 495  
-----

-----  
(#) Benchmarks for factoring another 30-bit integer 999994437 on single node

```
dual core Spark cluster have been committed to python-src/testlogs/
(#) Similar to previous 30 bit integer, time utility prints 40 minutes 56
seconds while the actual Spark duration is between first and last factors:
18/01/11 13:34:34 INFO Utils:
/home/shrinivaasanka/Krishna_iResearch_OpenSource/GitHub/asfer-github-code/
python-src/DiscreteHyperbolicFactorizationUpperbound_TileSearch_Optimized.py has
been previously copied to
/tmp/spark-5630f619-b8a7-46b8-b15b-7296508792c5/userFiles-44c23be8-a7b3-48d3-
bfd7-98acf1971e10/
DiscreteHyperbolicFactorizationUpperbound_TileSearch_Optimized.py
=====
Factor is = 1
=====
=====
Factor is = 3
=====
=====
Factor is = 9
=====
=====
Factor is = 13
=====
=====
Factor is = 23
=====
=====
Factor is = 27
=====
=====
Factor is = 39
=====
=====
Factor is = 69
=====
=====
Factor is = 97
=====
=====
Factor is = 117
=====
=====
Factor is = 207
=====
=====
Factor is = 291
=====
=====
Factor is = 299
=====
=====
Factor is = 351
=====
=====
Factor is = 621
=====
=====
Factor is = 873
=====
=====
Factor is = 897
=====
=====
Factor is = 1261
=====
```

```
=====
Factor is = 1277
=====
=====
Factor is = 2231
=====
=====
Factor is = 2619
=====
=====
Factor is = 2691
=====
=====
Factor is = 3783
=====
=====
Factor is = 3831
=====
=====
Factor is = 6693
=====
=====
Factor is = 8073
=====
=====
Factor is = 11349
=====
=====
Factor is = 11493
=====
=====
Factor is = 16601
=====
=====
Factor is = 20079
=====
=====
Factor is = 29003
=====
=====
Factor is = 29371
=====
=====
Factor is = 34047
=====
=====
Factor is = 34479
=====
=====
Factor is = 49803
=====
=====
Factor is = 60237
=====
=====
Factor is = 87009
=====
=====
Factor is = 88113
=====
=====
Factor is = 123869
=====
=====
```

Factor is = 149409  
=====

Factor is = 261027  
=====

Factor is = 264339  
=====

Factor is = 371607  
=====

Factor is = 381823  
=====

Factor is = 448227  
=====

Factor is = 783081  
=====

Factor is = 793017  
=====

Factor is = 1114821  
=====

Factor is = 1145469  
=====

Factor is = 1610297  
=====

Factor is = 2848987  
=====

Factor is = 3344463  
=====

Factor is = 3436407  
=====

Factor is = 4830891  
=====

Factor is = 8546961  
=====

Factor is = 10309221  
=====

Factor is = 14492673  
=====

Factor is = 25640883  
=====

Factor is = 37036831  
=====

Factor is = 43478019  
=====

Factor is = 76922649  
=====

```
=====
=====
```

Factor is = 111110493

```
=====
```

18/01/11 13:48:32 INFO PythonRunner: Times: total = 837634, boot = 641, init = 37, finish = 836956

18/01/11 13:48:32 INFO Executor: Finished task 0.0 in stage 0.0 (TID 0). 1529 bytes result sent to driver

18/01/11 13:48:32 INFO TaskSetManager: Starting task 1.0 in stage 0.0 (TID 1, localhost, executor driver, partition 1, PROCESS\_LOCAL, 6208 bytes)

18/01/11 13:48:32 INFO Executor: Running task 1.0 in stage 0.0 (TID 1)

```
=====
```

Factor is = 333331479

```
=====
```

18/01/11 13:48:32 INFO TaskSetManager: Finished task 0.0 in stage 0.0 (TID 0) in 838426 ms on localhost (executor driver) (1/3)

which is almost 14 minutes ( 13:48:32 - 13:34:34 ). First non-trivial factor was printed within 10 seconds. Time utility prints 40 minutes including overhead for finishing Spark RPC tasks

```


```

498. (THEORY and FEATURE-DONE) Computational Geometric Factorization - Non-Persistent Tile Segments - 31 bit Single Node Dual Core Spark Benchmarks - Primality Testing - Multiplicative Partition - Factorisatio Numerorum - 12 January 2018 - related to 495

```


```

31-bit integer 2147483647 has been factorized by searching non-persisted pixelated hyperbolic tile segments. Only trivial factors are found and is a mersenne prime. This integer is the maximum permissible limit for xrange() and printed by python sys module (sys.maxsize). Similar to integer partition function which is number of ways of splitting an integer as sum of smaller integers, multiplicative partition function  $f(n)$  = number of ways of unordered factorizations of  $n$ . This function has an upperbound of :  $a\{n\} \leq n(\exp\{\log n * \log\log\log n\}/\{\log\log n\})^{\{-1+o(1)\}}$ .

```

Factorization/Primality of 2147483647

```

18/01/12 14:33:12 INFO Utils:

/home/shrinivaasanka/Krishna\_iResearch\_OpenSource/GitHub/asfer-github-code/python-src/DiscreteHyperbolicFactorizationUpperbound\_TileSearch\_Optimized.py has been previously copied to

/tmp/spark-169ef9d3-56df-46eb-9b09-d63561491f87/userFiles-9f55cc79-e7cc-46e6-bad7-540f950587b5/

DiscreteHyperbolicFactorizationUpperbound\_TileSearch\_Optimized.py

```
=====
```

Factor is = 1

```
=====
```

18/01/12 15:02:57 INFO PythonRunner: Times: total = 1784724, boot = 643, init = 23, finish = 1784058

```

```

Spark Duration 15:02:57 - 14:33:12 = 29 minutes 45 seconds

Spark Logs have been committed to python-src/testlogs/

References:

```

```

498.1 Multiplicative Partition Function - ON THE OPPENHEIM'S "FACTORISATIO NUMERORUM" FUNCTION - [FLORIAN LUCA, ANIRBAN MUKHOPADHYAY AND KOTYADA SRINIVAS] - <https://arxiv.org/pdf/0807.0986.pdf> - "... The function  $f(n)$  is related to various partition functions. For example,  $f(2^n) = p(n)$ , where  $p(n)$  is the

number of partitions of  $n$ . Furthermore,  $f(p_1 p_2 \dots p_k) = B_k$ , where  $B_k$  is the  $k$ th Bell number which counts the number of partitions of a set with  $k$  elements in nonempty disjoint subsets. In general,  $f(p_1^{\alpha_1} p_2^{\alpha_2} \dots p_k^{\alpha_k})$  is the number of partitions of a multiset consisting of  $\alpha_i$  copies of  $\{i\}$  for each  $i = 1, \dots, k$ . Throughout the paper, we put  $\log x$  for the natural logarithm of  $x$ . We use  $p$  and  $q$  for prime numbers and  $0$  and  $o$  for the Landau symbols. ..."

498.2 Multiplicative Partition Function - <https://oeis.org/A001055>

498.3 Bound for Multiplicative Partition Function - [Canfield-Erdos-Pomerance] - <https://www.math.dartmouth.edu/~carlp/PDF/paper39.pdf>

498.4 Eighth Mersenne Prime -  $2^{4783647} - 1 = 2147483647$  - <https://en.wikipedia.org/wiki/2,147,483,647> - this was largest known prime till 1867.

498.5 M31 - <http://primes.utm.edu/curios/page.php/2147483647.html> - The first prime that cannot be tested on 32-bit primality-check software.

498.6 Cryptography in NC0 - [Benny Applebaum, Yuval Ishai, Eyal Kushilevitz] - <http://www.cs.technion.ac.il/~abenny/pubs/nc0.pdf>, Hardness of factoring - [Emanuele Viola] - <https://emanueleviola.wordpress.com/2018/02/16/i-believe-pnp/> - One way functions are in NC0 and there are PRGs for which output bit depends only on  $O(1)$  bits of seed implying factoring is hard for constant depth. Computational Geometric Factorization doable in  $O(\log N^2)$  PRAM time in NC2, implies factoring can be made easy by parallelism and polylog depth circuits.

498.7 Binary Quadratic Diophantine Equations (BQDE) and BQDE for Factorization - [JC Lagarias] - <https://arxiv.org/pdf/math/0611209> - Succinct Certificates for the Solvability of BQDE.

498.8 Polynomial Time Quantum Algorithm for Solving Pell's Equation - [Hallgren] - <http://www.cse.psu.edu/~sjh26/pell.pdf> - Integer Solutions to Pell's Equation reduce to Factoring - e.g Solving for  $x, y$  for known  $N$  in  $x^2 - Ny^2 = 1$  factorizes  $N$  by rewriting as:  $(x^2 - 1) / y^2 = N \Rightarrow ((x+1)/y)((x-1)/y) = N$ . In this respect, Hallgren's algorithm is equivalent to Shor Quantum Factorization. Computational Geometric Factorization in NC-PRAM or Sequential Optimization in P could therefore imply Pell's equation is solvable by PRAM model and in NC or in P as follows:

$$\begin{aligned} (x+1)/y &= a \\ (x-1)/y &= b \\ 2/y &= a-b \text{ for factors } a, b \text{ of } N. \\ y &= 2/a-b \\ \Rightarrow (x+1) &= 2a/(a-b) \\ \Rightarrow x &= 2a/(a-b) - 1 \end{aligned}$$

Historicity of this problem (Brahmagupta's Chakravala) and a polylog approximation based on Newton-Raphson square root recurrence is described in GRAFIT course material <https://kuja27.blogspot.in/2018/04/grafit-course-material-newton-raphson.html>

-----  
 499. (FEATURE-DONE) Secure Neuro Currency Cloud Perfect Forward Move - OpenSSL client and server - 19 January 2018  
 -----

Neuro Currency Cloud Perfect Forward Move socket code has been openssl enabled:

- Makefile updated include -DOPENSSL #ifdef option for compiling SSL client-server headers
- license headers updated
- new header asfercloudmove\_openssl.h has been added to repository for invoking openssl client and server functions in opensslclient.h and opensslserver.h
- An example fictitious X.509 cert.pem and key.pem have been created by openssl utility for certificate verification
- new headers opensslclient.h and opensslserver.h have been added to repository which define openssl client and server functions (these are reference examples in [www.openssl.org](http://www.openssl.org) Wiki changed for cloud move)
- logs for SSL cloud\_move client and server have been committed to cloud\_move/testlogs/

-----  
-----  
500. (FEATURE-DONE) Searching Unsorted List of Numbers - Algorithm in GRAFIT  
Open Learning Implemented - 21 January 2018  
-----

-----  
An algorithm to search list of numbers better than brute force search mentioned  
in GRAFIT Course Notes:

[https://github.com/shrinivaasanka/Grafit/blob/master/course\\_material/ComputerScienceMiscellaneous/ComputerScienceMiscellaneous\\_CourseNotes.txt](https://github.com/shrinivaasanka/Grafit/blob/master/course_material/ComputerScienceMiscellaneous/ComputerScienceMiscellaneous_CourseNotes.txt)  
has been implemented in NeuronRain AsFer.

This lifts one dimensional numbers to multidimensional tuples and creates  
hashtables for each dimension of tuple. Lookup for a query number is  
lookup of each digit in query in these hash tables in succession. If all hash  
lookups succeed queried number exists in the unsorted list

This implementation pads each number with "#" so that it is right justified and  
maximum number of digits is stipulated.

Searching Unsorted lists is the most fundamental open research problem and this  
implementation uses Locality sensitive hashing as the hash table  
. Python dictionaries are hash maps and not hash tables which support  
collisions. Each digit in query is looked up for nearest neighbours and if  
there is a match digitmatch is set to True. Logical AND of all digit matches is  
returned as True/False.

-----  
-----  
501. (THEORY) Answer-Questioning (Reversal of Interview) and Recursive Gloss  
Overlap Dense Subgraph Classification - 21 January 2018  
- related to 412, 420  
-----

-----  
Recursive Gloss Overlap Definition Graph of a text previously has been  
demonstrated to classify documents in unsupervised manner based on  
dense subgraphs: centrality, k-cores, pageranks etc., Dense subgraphs of text  
graph extract the essence of an article and highlight the keywords  
which may or may not be present in the document. Keywords not present in the  
document can be classes of a document because of the recursive  
deep learning of definitions. From the keywords, a question or set of  
permutations of questions can be constructed which the text answers.  
Relevance of Question depends on the relatedness e.g Tensor Neuron of all  
possible pairs of keyword class vertices.

Example:

-----  
If a text graph of an academic research text has been classified in following  
word vertices of high core numbers

[Prime, Factorization, Theorem, Composites, Diophantine,  
Polynomials,...]

in decreasing value of centrality/k-core/pagerank and pairwise Tensor Neuron  
potentials are ranked as below:

Prime-Factorization = 0.34234

Theorem-Composites=0.33333

Diophantine-polynomials=0.221212

... and so on

then question(s) can be constructed based on previous ranking of Tensor  
relatedness as:

Does this article discuss relation between [Primes] and  
[Factorization]?

....

Reference:

-----  
501.1 CALO, SIRI, PAL - <https://pal.sri.com/architecture/> - Cognitive Assistants, Question Answering  
-----

-----  
502. (FEATURE-DONE) Scheduler Analytics - Interprocess Distance Computation by DictDiffer - 24 January 2018  
-----

1. Representing OS Process Information as Feature Vectors has been mentioned as Software Scheduler Analytics usecase in <http://neuronrain-documentation.readthedocs.io/en/latest/>
2. This commit implements a new python function which reads process info as a dictionary from psutils. Psutils has an option to read individual process metrics or to read the dictionary in its entirety.
3. Psutils per-process dictionary has all the basic details pertaining to instantaneous resource consumptions of a process
4. These per-process features are collated in an array and are json.dump()-ed as strings in asfer.enterprise.encstr.scheduleranalytics file which can be used as input by clustering/classification NeuronRain-AsFer C++ implementations.
5. logs for this have been committed to `software_analytics/testlogs/DeepLearning_SchedulerAnalytics.log.24January2018`
6. Distance between two process feature dictionaries/vectors are printed by DictDiffer which has been imported and length of the diff is the distance function between any two processes.

-----  
503. (FEATURE-DONE) Scheduler Analytics - Process kNN classification and K-Means clustering, Process Dict Hashing - 25 January 2018  
(Only in NeuronRain Enterprise - GitHub)  
-----

1. `python-src/software_analytics/DeepLearning_SchedulerAnalytics.py` has been updated to define a `getHash()` function similar to `Streaming_<algorithm>.py` implementations, which creates an MD5 hash of process psutils dictionary string.
2. This hashing of dictionary is because of huge size of process dictionary storing of which requires few KBs for each process. Computing distance (Levenshtein) of these strings is again memory intensive.
3. DictDiffer distance implemented in `python-src/software_analytics/DeepLearning_SchedulerAnalytics.py` is not directly invocable in C++ and diff between process dictionary strings is also huge in KBs.
4. Succinct representation of process dictionary string - Fingerprinting - is therefore a necessity to optimize space. MD5 binary hash digest of the process dictionary string is written to `python-src/software_analytics/asfer.enterprise.encstr.scheduleranalytics` prefixed by process name and process id, instead of complete chunk.
5. `cpp-src/asferkNNclustering.cpp` and `cpp-src/asferkmeansclustering.cpp` are updated for EOF check and number of clusters has been increased to 10 in kNN classifier.
6. asfer binary has been rebuilt and `asfer.conf` has been updated to do clustering and classification.
7. process statistics dataset - `cpp-src/asfer.enterprise.encstr,` `cpp-src/asfer.enterprise.encstr.clustering` and `cpp-src/asfer.enterprise.encstr.kNN` have been updated.
8. asfer kNN classification and KMeans clustering has been executed on this encoded process statistics dataset
9. logs have been committed to `cpp-src/testlogs/asfer.SchedulerAnalytics.KMeansAndkNNClustering.log.25January2018` (Scheduler Analytics) and



```

cpp-src/testlogs/asfer.SchedulerAnalytics.KMeansAndkNNClustering.log.25January20
18 (kNN classification and KMeans clustering) - for 194 processes
10. logs for clustering and classification imply similar processes flock
together - e.g excerpt from KMeans cluster logs show lot of kworkers in same
cluster:
=====
Cluster 6
=====
encoded string
[5574:bash:0b1101110111101000111110100011000011111011100001101001000100110011010
01101100000111001010010110000011000011000101100110010011000000100001111010001010
0000000000]
encoded string
[139:kworker/u4:4:0b110011101011001001110101000100001001110110011001001111001100
1001101100011001111110101101100101011110000000001011011111101100001010100111010
0100010010010010001]
encoded string [145:usb-
storage:0b110000101010111000011111001110110001011101110101000000001100110001100
10011011010100110101001010000001101111100010010111010111000100101011110110100011
1000001]
encoded string
[35:fsnotify_mark:0b101101111000000111101001100011010101101000110000001001000101
0100110101111010011110000111001010001110001110010000001010000110001011101011001
00101000001101101110]
encoded string [2769:cups-
browsed:0b1110011010000000111100101100010010111011110111110111100111101011010010
00001100111010100110111011110010101000100111110100110001011010001001110111001100
000000100]
encoded string
[5673:bash:0b10000000101010011010111000111111011100010100001101000010111101011000
00110101101001000011000101110000110100010111010001001101000001101101110101011110
101011100011]
encoded string
[49:acpi_thermal_pm:0b1110010100000111110100000010000101111000001000011001001111
01011110010100000010111011110010001010010111110100001110000011010101100110001100
0110100011100001010100]
encoded string
[6220:kworker/u4:1:0b101111110010001100110000000101111001111111100010001010111101
00111001101010110101010111010000111001010110001101111111100101000110001111011110
10101100111001100100]
encoded string
[5977:kworker/0:0:0b110100001001000101110110010000101101101101110110011110010111
0000111110111011001010010110101011000000001110011010110110110000011011100001111
10110101000110010010]
encoded string
[5905:kworker/u4:0:0b10110111100100101110001110011011010010000010101001001001010
01110000111100111001101110100101101000001011101010000010010001101010100110001000
111111100100111100010]
encoded string
[2433:kworker/u5:0:0b11001001011000101001010000100010101110100101111101100111101
11100001110110110101110010010101001101011111011000101110000001001000110100100010
111011110000110000101]
encoded string
[2439:kworker/u5:2:0b111010000111101010101111011010111010110100110000001110001111
00011010000110011111011001011101000100110101100010101100010100010010001011110110
11100101101000001111]
encoded string
[5:kworker/0:0H:0b10001100001001100111111000111111001000010001100110110010001110
010111001001101011011101011011001010011100111011101011111111111110111011100001001
000100010010011000]
encoded string
[9:migration/0:0b110011010000111101100010000111001100001011111001010100101111001
01011011010001011011001110011001101110101101111011111001001101111010010000101001
0000011001001000]

```

encoded string  
[6300:kworker/0:1:0b110001100110111000000000010000010001110011011000101110111001  
10100111010000010111110010110100000000011010101010001011001011010000111110101100  
1100011010001110100]  
encoded string [5065:upstart-dbus-  
bridge:0b10100001111110000000001001110101101001100011001011101010101110011000110  
0011111110101110100001010011110011100001101001111101101100010101100100100101100  
011101000]  
=====

Reference:

-----  
503.1 Randomized Algorithms - [Rajeev Motwani, Prabhakar Raghavan] - Pages 168  
and 214 - 7.4 Verifying Equality of Strings and 8.4 Hash Tables for string  
fingerprinting

-----  
504. (FEATURE-DONE) Streaming Algorithms - Encoded Strings Data Source - 26  
January 2018  
(For MD5 hash and other Encoded Strings)

-----  
1. python-src/Streaming\_AbstractGenerator.py iterator has been updated for new  
data storage "AsFer\_Encoded\_Strings" and data source "NeuronRain"  
for streaming encoded strings created by NeuronRain AsFer  
2. Streaming algorithm implementations have been updated to stream data from  
this new datasource and logs have been committed to testlogs/

-----  
505. (FEATURE-DONE) Scheduler Analytics - Sequence Mining - 29 January 2018  
(Only in NeuronRain Enterprise - GitHub)

-----  
1. Sequence Mining has been executed on Scheduler Analytics process statistics  
(few processes and max length set to 5).  
2. Candidate initial item set has been changed to alphanumeric  
3. Declared boolean flag for choosing between MD5 hash encoding of process dicts  
or plain string representation of process dict  
4. updated software\_analytics/asfer.enterprise.encstr.scheduleranalytics  
5. Sequence Mined Scheduler Analytics has been committed to  
testlogs/SequenceMining.log.SchedulerAnalytics.29January2018

-----  
506. (THEORY) Computational Geometric Factorization - Feasibility of Sequential  
Optimization - related to 486 - 6 February 2018, 1 September 2018

-----  
Doing away with Parallel RAMs in Computational Geometric Factorization by  
breaking the hyperbolic arc bow into two sets of tilesegments  
and searching their concatenations which are implicitly sorted ascending, has  
problems because concatenation of multiple tile segments may not be sublinear.  
Concatenating tile segments can be likened to concatenation of multiple strings.  
Concatenation of two strings can be done  
in  $O(\log N)$  time by using Rope Strings which are tree representations of strings  
(logarithmic in length of strings and not in number of  
strings). But concatenation of multiple strings/tiles logarithmic time in number  
of strings is still open.

Following sequential optimization tries to find feasibility of doing Sequential  
Factorization without PRAMS and concatenation of tile segments:

number\_to\_factorize=N  
factor\_candidate=N/2

-----  
Loop for subsegment1 tree:  
-----

while(factor is not found)  
{

    1. Find the tile segment/interval containing factor candidate.  
    [2. Split the candidate tile segment to two subsegments - subsegment1 contains points which are less than previous segment's end point, subsegment2 contains points which are greater than previous segment's end point.]  
    3. Binary Search each node in subsegment1 tree for factor points (p,q) (N=pq) - There are 3 possibilities:  
        3.1 All points in this subsegment1 tree node are less than N => Binary Search has to be done on right subsegment1 subtree recursively, factor\_candidate is updated  
        3.2 All points in this subsegment1 tree node are greater than N => Search has to be done on left subsegment1 subtree recursively, factor\_candidate is updated  
        3.3 N is present in this subsegment1 tree node and factor point N=pq is found  
}

-----  
Loop for subsegment2 tree:  
-----

while(factor is not found)  
{

    4. Find the tile segment/interval containing factor candidate.  
    [5. Split the candidate tile segment to two subsegments - subsegment1 contains points which are less than previous segment's end point, subsegment2 contains points which are greater than previous segment's end point.]  
    6. Binary Search each node in subsegment2 tree for factor points (p,q) (N=pq) - There are 3 possibilities:  
        6.1 All points in this subsegment2 tree node are less than N => Binary Search has to be done on right subsegment2 subtree recursively  
        6.2 All points in this subsegment2 tree node are greater than N => Search has to be done on left subsegment2 subtree recursively  
        6.3 N is present in this subsegment2 tree node and factor point N=pq is found  
}

7. Above algorithm is Depth-2 Two Level Binary Search:

7.1) First binary search finds the subsegment node in subsegment trees in  $O(\log N)$

7.2) Second binary search searches within subsegment node in  $O(\log N)$  and thus requires  $O(\log N * \log N)$  sequential time.

8. Sets of subsegment1(s) and subsegment2(s) constitute 2 binary search trees of segments, but these two search trees are not physically created. Binary search of tile containing factor candidate dynamically creates treelike traversal.

9. Finding tile segment containing a factor candidate point is non-trivial planar point location problem in general. But Following algorithm finds the interval containing the point in  $O(1)$  time specific to hyperbolic pixelated tiling:

Sum of lengths of k consecutive hyperbolic pixelated tiles =  $N/(1*2) + N/(2*3) + N/(3*4) + \dots + N/(k*(k+1))$   
=  $N(1/1 - 1/2 + 1/2 - 1/3 + 1/3 - 1/4 + \dots + 1/k - 1/(k+1))$   
=  $N(1 - 1/(k+1))$   
=  $Nk/(k+1)$

Tile containing point x:

$Nk/(k+1) < x < N(k+1)/(k+2)$

$k < x/(N-x)$   
integer round-off of  $k$  is the index of tile interval containing  $x$ .

10. Previous sequential optimization of  $O((\log N)^2)$  though removes PRAMs, proves only that Factorization is in P. Computational geometric factorization by PRAMs is still a better result because it implies Factorization is in NC from PRAM-NC equivalence despite requirement of high number of parallel processors.

11. For each segment  $k$  in loops previously, 2 subsegments of it have following interval endpoints -  $(x_{\text{left}}, y_{\text{left}}, x_{\text{right}}, y_{\text{right}})$ :

subsegment1:  $(N/(k+2), (k+1), N/(k+2)+\delta, (k+1))$

subsegment2:  $(N/(k+2)+\delta, (k+1), N/(k+1), (k+1))$

and  $\delta = N/((k+1)(k+2))$

12. CAVEAT: Two factor points  $(x_1, y_1)$  and  $(x_2, y_2)$  can equal by  $x_1*y_1 = x_2*y_2$  but these two points are located in different subsegments of different tiles because points within subsegment1 or subsegment2 of a tile segment have same  $y$ -coordinates. Previous inequality applies only to a binary search segment tree comprised of subsegment2(s) of all segments by implicit geometric spatial sortedness i.e end of subsegment2 in previous segment is less than start of subsegment2 in next segment. Set of subsegment1(s) need not be implicitly sorted and thus can not be searched by a segment tree constructed sequentially. This renders previous optimization feasible only to a subset of integers. Algorithms for Parallel RAM construction of segment tree described previously are therefore necessary to find factor points in polylogarithmic time and thus in NC and all these algorithms require parallel  $k$ -mergesort. This sequential algorithm has been mentioned only as an optimization.

-----  
13. Tile Summation and Wavelet trees:  
-----

Sum of lengths of first  $n$  tile segments of pixelated hyperbolic curve derived previously:

$$N/[1^2] + N/[2^3] + \dots + N/[n*(n+1)] = Nn/(n+1)$$

which can be equated to sum of distances between first  $m$  prime factors by Hardy-Ramanujan Theorem:

$$Nn/(n+1) = mN/k \log \log N$$

$\Rightarrow n = m/(k \log \log N - m)$  = number of tiles till  $m$ -th prime factor. Sum of lengths  $(N/x(x+1))$  each of these  $n$  tiles  $(=O(\log \log N))$  till  $m$ -th prime factor finds approximate  $m$ -th prime factor. Constructing wavelet tree for concatenated unsorted string of tile segments of epsilon radius around approximate factors and doing  $\text{select}(N)$  on the wavelet string finds at least one factor location. Geometric intuition: Tile summations are hyperbolic pixel polygons and if vertices of this polygon - endpoints of concatenation - coincide with factor points on  $x$ - $y$  axis grid, factors are found. Accuracy depends on precision of tile summation and this is only an optimization. If epsilon radius centered around each approximate prime factor is  $e$ , total length of concatenated unsorted tile for all prime factors is:  $O(2^e * \log \log N)$ . Sequential Construction and  $\text{select}()$  for wavelet tree for this string is:

$$O(2 \log \log N * \log(2 \log \log N)) + \log(2 \log \log N) = O(e * \log \log N * \log(e * \log \log N)) + \log(e * \log \log N)$$

For sequential polylogarithmic factorization,  $e$  has to be upperbounded by  $O((\log N)^1)$ .

-----  
507. (THEORY) Tournament Graph Election, Coloring, Intrinsic Merit, Partitions and Bell Number - 8 February 2018  
-----

Tournament Graph of  $n$  vertices has  $n(n-1)/2$  edges (complete). Each vertex of the tournament graph is uniquely colored by total of  $n$  colors.  
Each edge  $(v_1, v_2)$  is the contest between vertices  $v_1$  and  $v_2$ . Each edge of the

tournament graph is progressively colored by the color of winning vertex of the edge endpoints. Thus at the end of the tournament,  $n(n-1)/2$  edges are partitioned into  $n$  monochromatic sets of edges. Number of all possible partitions of a set is the Bell number. Vertex corresponding to Color of the biggest part in this edge set partition is the final winner. Any partition which has unequal parts has biggest part. Thus number of partitions of edges having atleast one biggest part = BellNumber - 1 because there is exactly one partition of  $n(n-1)/2$  edges into  $n$  sets of equal size  $(n-1)/2$ . Tournament Graph Election is an alternative social choice function and does not involve Majority voting. Win in contest between two vertices of an edge can be defined as the vertex having greater Intrinsic Merit (In social networks this is the standard Intrinsic Fitness of a vertex). This formalizes the intrinsic merit usecases mentioned in NeuronRain Documentation and FAQ in <http://neuronrain-documentation.readthedocs.io/en/latest/> . One additional usecase where majority voting falters and Intrinsic Merit is a necessity is the indispensability of experimental evidences in exact sciences. For example, in archaeology/history/mythology, "an artefact existed few millenia ago" is quite presumptive hypothesis which cannot be proved by mere majority voting in contemporary era. In tournaments involving knock-out(s), each elimination removes  $(n-1)$  edges and  $n/2$  rounds decides winner.

#### References:

-----  
507.1 Tournament Trees - Minimum Comparison Selection - [Don Knuth] - The Art of Computer Programming - Volume 3  
- Page 207-209 - Section 5.3.3 - Kislitsyn Theorem - In a knockout tournament tree of  $n$  players, minimum number of comparisons required to find second best player is  $n - 2 + \text{ceil}(\log n)$ . For first best player minimum number of comparisons required is  $n - 1$ .  
-----

-----  
508. (FEATURE-DONE) Streaming Analytics Abstract Generator Update - Socket Streaming Datasource Added - 8 February 2018  
-----

-----  
1.Streaming Abstract Generator facade/generator pattern implementation has been updated for a new "Socket Streaming" data storage/data source.  
2.Constructor Datasource arg is the remote host and port is hardcoded to 64001 (one more than kernel\_analytics driver streaming port)  
3.Python socket has been imported and socket client code has been added to `__iter__()`  
4.As example, Hyper LogLog Counter Streaming implementation has been updated to read streaming data from remote streaming webservice host  
5.Logs for this have been committed to testlogs/  
6.Example webserver commandline:  
    nc -l 64001  
    ><data>  
-----

-----  
509. (FEATURE-DONE) Scheduler Analytics - Socket Streaming Server - Decorator pattern implementation - 9 February 2018  
-----

-----  
1. New Socket Streaming Server for Scheduler Analytics has been implemented in `python-src/software_analytics/SchedulerAnalytics_WebServer.py`  
2. This invokes `get_stream_data()` function in `python-src/software_analytics/DeepLearning_SchedulerAnalytics.py`  
3. `get_stream_data()` function is decorated by a Decorator class implemented in a new file `python-src/webserver_rest_ui/NeuronRain_Generic_WebServer.py`  
4. `SocketWebServerDecorator` implemented in `python-src/webserver_rest_ui/NeuronRain_Generic_WebServer.py` is generic and overrides  
-----

\_\_init\_\_() and \_\_call\_\_() functions. \_\_call\_\_() invokes the decoratee function get\_stream\_data() specific to Scheduler Analytics.

5. SocketWebServerDecorator can decorate any other streaming datasource, not just scheduler analytics - decoratee function has to be implemented accordingly.

6. Logs for Socket Streaming Server have been committed to python-src/software\_analytics/testlogs/SchedulerAnalytics\_WebServer.log.9February2018 and example Socket Streaming Client HyperLogLogCounter logs are at python-src/testlogs/Streaming\_HyperLogLogCounter.log.9February2018

7. Global configs for socket streaming server host and port (64001) have been set in a new config file python-src/software\_analytics/SchedulerAnalytics\_Config.py

8. Known issue: There seems to be a random iterator disconnect because of psutil process\_iter() process statistics streaming delay

-----

510. (FEATURE-DONE) Scheduler Analytics Socket Streaming Decorator - Psutil iterator frequent disconnects resolution - 11 February 2018

-----

1. SocketWebServerDecorator frequently and periodically throws "NoneType object not callable" exception.

2. This exception happens after every 215 or 217 processes (not sure what this magic number is)

3. Because of this try/except error handling has been added throughout decorator code

4. Socket listen queue size has been increased to 100

5. datasourcefunc() is re-called once an exception is thrown in a loop - a palliative cure

6. After this 215 barrier is breached. Logs for 558 processes streamed by Socket Server Decorator and received by Streaming Abstract Generator client have been committed to python-src/software\_analytics/testlogs/SchedulerAnalytics\_WebServer.log.11February2018 and python-src/testlogs/Streaming\_HyperLogLogCounter.log.11February2018

-----

511. (FEATURE-DONE) Approximate 3SAT Solver Randomized Rounding Update - NumPy random choice() replacing permutation() - 27 February 2018

-----

1. CNFSATSolver.py - function creating random 3SAT instances has been updated to invoke NumPy random choice() instead of permutation() without replacement - equivalent to nP3 per clause for n variables.

2. Logs for 16 variables - 16 clauses and 18 variables - 18 clauses have been committed to testlogs/CNFSATSolver.16variables16clauses.log.27February2018 and testlogs/CNFSATSolver.18variables18clauses.log.27February2018

3. Numpy random choice() is based on Uniform distribution.

4. It is remarkable to note that observed probability average and Random Matrix probability  $1/\sqrt{m*n}$  are strikingly equal - a confirmation of the least squares randomized rounding and relaxation SAT solver's accuracy

5. Logs for 16\*16 and 18\*18 have few hundreds and thousand plus random 3SAT instances which are solved 100%

-----

512. (FEATURE-DONE) ConceptNet5 Update - REST endpoints changed - 27 February 2018

-----

1. ConceptNet5 rest\_client.py has been imported which already wraps REST methods and endpoints
2. REST endpoints for search, lookup and query have been updated for ConceptNet 5.5 which were 5.4 earlier

-----  
513. (FEATURE-DONE and THEORY) Approximate SAT Solver and ConceptNet REST client updates - 21 variables, 21 clauses LSMR and Common Ancestor Distance in ConceptNet5 - 28 February 2018  
-----

1. Least Square SAT solver has been updated to print more readable debug messages and highlight MAXSAT approximation ratio average for SATs solved thus far
2. Number of variables and clauses is set to 21, 21 and MAXSAT ratio is 98% for 34 random 3SATs
3. Logs for 21, 21 has been committed to testlogs/CNFSATSolver.21variables21clauses.log.28February2018 which shows the observed literal probabilities and random matrix  $1/\sqrt{m \cdot n}$  literal probability agreeing well.
4. This is because of uniform unbiased (mostly) choice() when number of clauses = number of variables causing  $1/\sqrt{m \cdot n} = 1/n$
5. For unequal clauses and variables numbers, an epsilon biased PRG implementation in linux kernel is necessary (random.c might have to be rewritten)

- 
6. ConceptNet5 client has been updated to include a related() function wrapper which invokes /related REST endpoint for finding similar concepts.
  7. ConceptNet5 finds related concepts by word embeddings implementation of word2vec which maps each word to a vector and similar words/concepts are clustered together in this vector space. More precisely, word distances are represented as a word-word 2 dimensional matrix/graph and sum of path edge weights between word pair is the distance.
  8. For finding distance between two concepts a common ancestor algorithm has been implemented in new conceptnet\_distance() function which recursively invokes related() to deep learn concepts and grows paths between the two concept endpoints. This recursion stops when paths grown from both ends meet i.e when there is a common ancestor (inspired by Savitch and USTCONN in logspace theorems).
  9. Common ancestors are printed in end and distance between the concepts is also printed
  10. Some example conceptnet\_distance() invocations have been captured in ConceptNet/testlogs/ConceptNet5Client.log.28February2018

#### References:

- 
- 513.1 ConceptNet 5.5: An Open Multilingual Graph of General Knowledge - [Robert Speer, Joshua Chin, Catherine Havasi-Luminoso Technologies] - <https://arxiv.org/pdf/1612.03975.pdf>
  - 513.2 ConceptNet blog - <https://blog.conceptnet.io/>
  - 513.3 Microsoft Concept Graph - Probable - <https://concept.research.microsoft.com/Home/Introduction> - similar to ConceptNet
- 

514. (THEORY) ConceptNet, Graph Tensor Neuron Network Intrinsic Merit, Word2Vec Word Embeddings - 2 March 2018 - related to 412, 513  
-----

-----

ConceptNet5 /related REST endpoint retrieves concepts similar to a concept and ranks them by word2vec word embedding similarity score. Recursive Lambda Function Growth algorithm mentioned previously, grows lambda functions for random walks in a text definition graph created by Recursive

e Gloss Overlap and word-word similarity/relevance is formalized by Neural Tensor Network. ConceptNet /related word2vec word embedding word-word similarity scores are perfect fit for Neuron Tensor Network entity relation potentials. Per random walk lambda function composition tree composes the neuron tensor potentials of all relations in the random walk. Composition trees are ranked by these composed potentials and Lambda composition tree of maximum potential best approximates the meaning of the Natural Language Text. This implies ConceptNet itself is one huge Graph Tensor Neuron Network Monolith.

Rationale for creating random walks in text definition graph is: Process of Human Text Comprehension is simulated by connecting concepts in text in various possible random walks of finite lengths, creating a tree of their meaning as lambda function composition and choosing the most rewarding random walk ranked by composed potentials. Most rewarding random walk must contain the word vertices of high core numbers (or centralities/classes of the text) because most number of paths in the graph go through these hub vertices (Section 5.16 in [https://tac.nist.gov/publications/2010/participant.papers/CMU\\_IIT.proceedings.pdf](https://tac.nist.gov/publications/2010/participant.papers/CMU_IIT.proceedings.pdf) proves this notion for Recursive Gloss Overlap graph in terms of WordNet relations). Cycles in the definition graph have also been experimentally found to approximate the text well. Random walks/Cycles in the definition graph have close resemblance to Word-Chain Theory in Psycholinguistics which postulates Brain stores the information as chain of words. Word-Chain Theory was dismissed by the Deep Structure theory of Chomsky. Lambda Function Composition of Random Walks/Cycles combines Word-Chain and Deep Tree Structure into one - converts list of words into a meaning tree.

#### References:

- 
- 514.1 Neural Tensor Network - [Socher-Chen-Manning-Ng] - [https://nlp.stanford.edu/pubs/SocherChenManningNg\\_NIPS2013.pdf](https://nlp.stanford.edu/pubs/SocherChenManningNg_NIPS2013.pdf) - Section 3.1 - "...The goal of our approach is to be able to state whether two entities ( $e_1$ ,  $e_2$ ) are in a certain relationship  $R$ . For instance, whether the relationship ( $e_1$ ,  $R$ ,  $e_2$ ) = (Bengal tiger, has part, tail) is true and with what certainty. ... The Neural Tensor Network (NTN) replaces a standard linear neural network layer with a bilinear tensor layer that directly relates the two entity vectors across multiple dimensions. ..."
- 514.2 The Language Instinct - [Steven Pinker] - Chapter 4 - How Language Works - Word Chains and Chomsky
- 514.3 Chomsky-Norvig Debate on Algorithmic Versus Statistical Learning - <http://daselab.cs.wright.edu/nesy/NeSy13/norvig.pdf> - 98% learning models are probabilistic/statistical while 2% are algorithmic. Chomsky's viewpoints:
- <quote>
  - Statistical language models have had engineering success, but that is irrelevant to science.
  - Accurately modeling linguistic facts is just butterfly collecting; what matters in science (and specifically linguistics) is the underlying principles.
  - Statistical models are incomprehensible; they provide no insight.
  - Statistical models may provide an accurate simulation of some phenomena, but the simulation is done completely the wrong way; people don't decide what the third word of a sentence should be by consulting a probability table keyed on the previous two words, rather they map from an internal semantic form to a syntactic tree-structure, which is then linearized into words. This is done without any probability or statistics.
  - Statistical models have been proven incapable of learning language; therefore language must be innate, so why are these statistical modelers wasting their time on the wrong enterprise?
  - <unquote>
- Recursive Gloss Overlap and Recursive Lambda Function Growth are Algorithmic Language Learning Models.
- 514.4 Gold's Theorem - [www.lps.uci.edu/~johnsonk/Publications/Johnson.GoldsTheorem.pdf](http://www.lps.uci.edu/~johnsonk/Publications/Johnson.GoldsTheorem.pdf) and limit on learnability - language  $L$  has infinite elasticity if there exist subsets  $T_1$  in  $T_2$  in ... ad infinitum such that  $T_i$  in  $L_i$  and  $T_{i+1}$  not in  $L_i$  for set of languages  $L_i$  and  $\lim T_i = L$ . Languages of infinite elasticity are not



learnable.

514.5 Power Law Distribution, Scale-Invariance, Small Word Phenomenon in Roget's Thesaurus and WordNet -Section 4.3 -

<http://web.mit.edu/cocosci/Papers/03nSteyvers.pdf> - Roget's Thesaurus and WordNet follow Pareto's Power Law Distribution i.e  $P(k) = k^{-e}$  where  $P(k)$  is the probability of vertices having  $k$  incoming links and  $e$  is the scale exponent. Power Law implies large number of nodes have small incoming links and small number of nodes have high incoming links. Both Roget's Thesaurus and WordNet have scale exponent  $\sim 3$ , high sparsity, very short average distances among words(5.6 and 10.56), single connected component containing almost all words, high local clustering.

514.6 Pareto's 80/20 rule, Scale-Invariance in phase-transition - Chapter 6: Sixth Link - Linked - [Albert Laszlo Barabazi]

-----  
515. (THEORY and FEATURE-DONE) Recursive Lambda Function Growth - ConceptNet5 support, Per random walk  
Lambda Function Composition Tree Graph Tensor Neuron Network Intrinsic Merit - 3 March 2018 - related to 514  
-----

-----  
Recursive Lambda Function Growth implementation has been updated to print per random walk lambda function composition tree and its Graph Tensor Neuron Network Intrinsic Merit. Similarity has been made configurable by a flag to choose between 2 Antology Nets - WordNet and ConceptNet. Logs for this have been committed to  
`testlogs/RecursiveLambdaFunctionnGrowth.log.GraphTensorNeuronNetwork.3March2018`. Logs show a striking similarity between Maximum Intrinsic Merit Random Walk Composition and Centralities/Classes of the definition graph (excerpts below):

...  
`grow_lambda_function3(): Maximum Per Random Walk Graph Tensor Neuron Network Intrinsic Merit : (u'(present(etc,(infrastructure(country,(urban(area,(Mumbai(city,largest)))))))))', 3.790350877192983)`  
...

=====  
Unsupervised Classification based on top percentile Core numbers of the definition graph(subgraph of WordNet)  
=====

=====  
This document belongs to class: Mumbai ,core number= 12  
This document belongs to class: infrastructure ,core number= 9  
...

which is an evidence to the fact intrinsic merit peaks for random walks through high core numbered hub word vertices. Another aspect of ConceptNet's relevance to Graph Tensor Neuron Network is the strong resemblance of word2vec word embeddings to Connectomes in Computational Neuroscience (mentioned in references). Connectomes are the wiring diagrams for neurons in brain. Word2Vec clusters similar words of a text in vector space forming a clique. These word cluster cliques are wired together into a text graph. Thus Graph representation of Text and Neuron Cliques and Connectome Information Propagation Among Cliques of Neurons have uncanny similarities.

References:

-----  
515.1 Cliques and Cavities in Human Brain - [Ann Sizemore, Chad Giusti, Ari Kahn, Richard F. Betzel, Danielle S. Bassett] - <https://arxiv.org/abs/1608.03520>

515.2 Algebraic topology and Computational Neuroscience -  
<https://www.technologyreview.com/s/602234/how-the-mathematics-of-algebraic-topology-is-revolutionizing-brain-science/>

515.3 Brain Graphs of Women are better expander graphs than men -  
<http://journals.plos.org/plosone/article?id=10.1371/journal.pone.0130045> - Brain

Graphs (or) Connectomes of Brain have been analyzed in computational neuroscience as Graph Expanders. Better Expander implies the Brain Graph or Graph of Neurons have better epsilon-Expansion trait i.e each vertex subset  $S$  of brain graph has  $\epsilon|S|$  incident edges. - "...Expander graphs and the expander-property of graphs are one of the most interesting area of graph theory: they are closely related to the convergence rate and the ergodicity of Markov chains, and have applications in the design of communication- and sorting networks and methods for de-randomizing algorithms [25]. A graph is an  $\epsilon$ -expander, if every-not too small and not too large-vertex-set  $S$  of the graph has at least  $\epsilon|S|$  outgoing edges (see [25] for the exact definition). Random walks on good expander graphs converge very fast to the limit distribution: this means that good expander graphs, in a certain sense, are "intrinsically better" connected than bad expanders. It is known that large eigengap of the walk transition matrix of the graph implies good expansion property [25]. We have found that women's connectomes have significantly larger eigengap, and, consequently, they are better expander graphs than the connectomes of men. For example, in the 83-node resolution, in the left hemisphere and in the unweighted graph, the average female connectome's eigengap is 0.306 while in the case of men it is 0.272, with  $p = 0.00458...$ " - High expansion implies least energy by [Barabasi-Bianconi] Bose-Einstein condensation and vertices are able to attract high number of links. In the context of random walks in Recursive Lambda Function Growth previously, assuming the lambda function tree as logical connectome - because role of neurons is simulated by the lambda functions - random walks on high expanding, least energy definition graph should converge faster theoretically.

515.4 Mapping Neurone Synapses to Connectomes -

[https://neurophys.gu.se/digitalAssets/1553/1553052\\_richard\\_dybowski.pdf](https://neurophys.gu.se/digitalAssets/1553/1553052_richard_dybowski.pdf) -

Workflow for Segmentation of fMRI images, Identifying membranes, Inferring Connectomes by Deep Learning.

515.5 Measuring Intrinsic Fitness in WWW and Scientific Publications (Bianconi-Barabasi Model) - <http://networksciencebook.com/6#bianconi-model> - Sections 6.3

- Case studies of journals (Nature, PRL, PNAS, Science etc.,) and Bose-Einstein Condensation in some networks - Section 6.4

515.6 Analysis of Brain Graphs or Connectomes -

<https://arxiv.org/pdf/1105.4705.pdf> - Network Motifs - "...Similarly, human structural connectivity between brain regions shows small-world properties with a small-worldness  $S$  of 10.6 (Text S2, Hagmann et al., 2008). For human functional connectivity between brain regions, the clustering coefficient is 53% (22% in random networks) and the path length 2.5 (2.3 in random networks) (Achard et al., 2006)..."

-----  
516. (FEATURE-DONE) SAT Solver - verbose print and iterations reduced - 4 March 2018  
-----

Least Squares LSMR SAT solver implementation has been updated to print LSMR internal calculations. Maximum iterations, conlim, atol, btol parameters have been set to least values for reducing latency. But this reduces MAXSAT accuracy to ~94% which is still above 88% (7/8 approximation). SciPy Sparse `dsolve.spsolve()` was tried for solving least squares by `csc_matrix` and there were nan errors. Finally, LSMR looks to be the best of the lot. Logs for few random 3SATs of (21 clauses, 21 variables) have been committed to `testlogs/CNFSATSolver.21variables21clauses.log.4March2018`. Observed average probability of choosing a literal again agrees quite well to  $1/\sqrt{m \cdot n}$  Random Matrix theoretical probability as gleaned from logs.

-----  
517. (THEORY) Majority+Voter Composition Hardness Amplification Lemma, Sensitivity Conjecture - Updated Hardness Bound - related to 318,355 - 5 March 2018  
-----

-----  
Hardness Amplification for Majority+Voter Composition has been described earlier by adapting XOR Lemma to Majority function as:

$$\text{Hardness of Maj+voter composition} = \frac{[c/\sqrt{n \cdot \delta}] + [\text{sum(column2 error entries)}] - [\text{sum(column3 no error entries)}]}{\delta}$$

-----  
--  
Hardness of voter function delta

which is based on the subdivided BP\* error scenarios matrix mentioned earlier and described again below:

| $x$<br>f(x/e) Noise                      |  | $f(x) = f(x/e)$ |  | $f(x) \neq$               |
|------------------------------------------|--|-----------------|--|---------------------------|
| -----                                    |  |                 |  |                           |
| x in L, x/e in L                         |  | No error        |  | Error                     |
| -----                                    |  |                 |  |                           |
| x in L, x/e not in L<br>f(x)=1, f(x/e)=0 |  | Error           |  | No error if<br>else Error |
| -----                                    |  |                 |  |                           |
| x not in L, x/e in L<br>f(x)=0, f(x/e)=1 |  | Error           |  | No error if<br>else Error |
| -----                                    |  |                 |  |                           |
| x not in L, x/e not in L                 |  | No error        |  | Error                     |

| $x$                                 |  | $f(x)$              |
|-------------------------------------|--|---------------------|
| -----                               |  |                     |
| Randomized Decision tree evaluation |  | No error      Error |

-----  
This matrix picturises the various false positives and false negative errors possible in majority voting. Language L denotes voting pattern for candidate 0 to win (and its complement is voting pattern for candidate 1). Correlation x/e is the flip in voting pattern. Previous matrix divides BP\* errors into 2 dimensions based on 1) whether the voting pattern is valid 2) Noise sensitivity/stability . For example a voting pattern x for candidate 0's win is correlated/flipped to x/e so that candidate 1 wins and input to Majority function f(), but yet majority function treats them with equal outcome - in matrix this error scenario is: x in L, x/e not in L and f(x)=f(x/e). Other scenarios follow this convention. Based on this error matrix, Hardness amplification ratio derived previously can be rewritten as:

$$\text{Hardness of Maj+voter composition} = \frac{[\text{sum(column2 entries)}] + [\text{sum(column3 entries)}] - [\text{sum(all no error entries)}]}{\delta}$$

-----  
Hardness of voter function

delta

But  $\text{Stability}(f(x)) = \Pr(f(x)=f(x/e)) - \Pr(f(x) \neq f(x/e))$  from definition of Noise stability  $\Rightarrow \Pr(f(x)=f(y)) = (1+\text{Stability})/2$ .

$\text{Sum}(\text{column2 entries}) = \Pr(f(x)=f(y)) = (1+\text{Stability})/2$ .

$\text{Sum}(\text{column3 entries}) = \text{NoiseSensitivity}$

$\Rightarrow \text{Hardness of Maj+Voter composition} = (1+\text{Stability})/2 + \text{NoiseSensitivity} - [\text{sum}(\text{all no error entries})]$

For majority function,  $\text{Stability} = (2/\pi)*\text{delta} + O((\text{delta})^{1.5})$  and  $\text{NoiseSensitivity} = O(1/\sqrt{n*\text{delta}})$

$\Rightarrow \text{Hardness of Maj+Voter composition} = 1 + (2/\pi)*\text{delta} + O((\text{delta})^{1.5}) + O(1/\sqrt{n*\text{delta}}) - [\text{sum}(\text{all no error entries})]$

For large n, previous hardness tends to  $1 + (2/\pi)*\text{delta} + O((\text{delta})^{1.5}) - [\text{sum}(\text{all no error entries})]$

From definition of BP\*, Probability of No error entries  $\geq 2/3 \Rightarrow \text{Sum}(\text{all no error entries}) \geq 2/3$

$\Rightarrow \text{Hardness of Maj+Voter composition} \leq [\pi + 2*\text{delta} + k*\pi*(\text{delta})^{1.5}]/2*\pi - 2/3$

$\Rightarrow \text{Hardness Amplification for Majority+Voter Composition} \leq [3*\pi + 6*\text{delta} + 6k*\pi*(\text{delta})^{1.5} - 2] / [6*\pi*\text{delta}]$

-----  
 $\Rightarrow \text{Hardness Amplification for Majority+Voter Composition} \leq 1/\text{delta}*(1/2-1/3*\pi) + 1/\pi + 6k*\pi*(\text{delta})^{0.5}$   
-----

which is huge amplification for small hardness of voter boolean functions.

$\Rightarrow$  weak voters are hardened by majority

$\Rightarrow$  Computing majority by a circuit is increasingly hard as voters become weak (intuitively obvious because if voter circuits err, majority circuit errs, an indirect proof of Margulis-Russo Threshold and Condorcet Jury Theorem).

Sensitivity Conjecture polynomially relates sensitivity and block sensitivity of boolean functions as:  $s(f) \leq bs(f) \leq \text{poly}(s(f))$ . So far only Noise Sensitivity has been applied as sensitivity measure throughout for quantifying BP\* error in Majority voting because it is a probability measure. But Sensitivity and Block Sensitivity are maximum number of bits and disjoint blocks of bits sensitive to output. Noise sensitivity probability can be written as:

$$\frac{\text{for\_all\_length\_e}(\text{Number of correlations } x/e \text{ for which } [f(x) \neq f(x/e)])}{\text{for\_all\_length\_e}(\text{Number of correlations } x/e \text{ for which } [f(x) == f(x/e)] + \text{Number of correlations } x/e \text{ for which } [f(x) \neq f(x/e)])}$$

Sensitivity and Block Sensitivity are maximum values of e(which can be number of bits or number of blocks) in summations of numerator and denominator. Block Sensitivity in Majority+Voter composition implies voter boolean functions are interdependent (correlated majority) and swayed by peer opinions en masse (Herdning). Hardness of voter boolean function and majority are indirectly related to sensitivity and block sensitivity through summations in Noise Sensitivity probability.

NOTE: Here hardness of voter boolean function is approximately assumed to equal NoiseSensitivity of Voter Boolean Function and  $\text{delta}=\text{epsilon}$ . To be precise,  $\text{delta} = \text{epsilon} \pm \text{error by BP* versus NoiseSensitivity/Stability Scenarios Matrix conventions}$ . This  $\pm$  term is ignored. Accounting for this  $\pm$  error:

-----  
 $\Rightarrow \text{Hardness Amplification for Majority+Voter Composition} \leq 1/(\text{delta} + \text{or} - \text{error})*(1/2-1/3*\pi) + 1/\pi + 6k*\pi*(\text{delta} + \text{or} - \text{error})^{0.5}$   
-----

-----  
-----  
518. (THEORY and FEATURE-DONE) Hardness of Majority Voting, SAT Solver Update -  
Compressed Sensing and Moore-Penrose Pseudoinverse  
- Conflicts - 6 March 2018 - related to 517  
-----  
-----

Approximate CNF SAT Solver has been updated to invoke Moore-Penrose Pseudoinverse function to compute approximate inverse of random 3SAT matrix and is multiplied as  $A^{-1} \cdot b$  to find assignments  $x$ . Compressed Sensing implementation already uses pseudoinverse to decompress image from sketch which is similar to this SAT solver. Performance is almost similar to LSMR and MAXSAT approximation ratio hovers around 97-98% for 306 random 3SAT instances of 21 variables and 21 clauses. Randomized rounding threshold has been increased to 0.5 from 0.1 (a literal is set to 0 if it is  $< 0.5$  and to 1 if  $\geq 0.5$ ). Observed per literal probabilities are equal to random matrix expected probability  $1/\sqrt{m \cdot n}$ . This reduces SAT solving to Compressed Sensing. There are some conflicts between the findings of SAT Solver and Hardness of Majority:

(#) Hardness of Majority+Voter Boolean Function Composition in both directions - bottom-up Voter-Majority and top-down MajorityInverse-VoterInverse have been described earlier (bottom-up hardness has been derived) and top-down inversion is considerably harder (#P-complete counting problem) and a likely choice for an one-way function and strong pseudorandom generator implying  $P \neq NP$  (or does it imply something more than  $P \neq NP$  because top-down inversion is in #P?). In oracle notation, top-down inversion is  $\#P^{\#P}$  assuming VoterInverse() assignments are #P oracles to MajorityInverse() #P problem. Toda's theorem implies PH is in  $P^{\#P}$ . If  $P^{\#P}$  is in  $\#P^{\#P}$ , then top-down inversion is harder than PH and hardness of top-down inversion implies more than just  $P \neq NP$ .

(#) SAT Solver random matrix analysis per-literal probability agrees with observed findings so far in small number of variables and clauses and MAXSAT approximation ratio for (21,21) and less number of variables-clauses combinations is almost 97% in most of the Solver executions - SAT solver solves the equal number of clause-variable instances exceeding 7/8-approximation similar to Karloff-Zwicky semidefinite programming randomized algorithm but in deterministic polynomial time. Solving unequal clause-variables requires choice in a non-uniform distribution. Solving large number of variables-clauses in the order of millions might further confirm this trend but is cpu-intensive. So it still remains open if this more than 7/8-approximation implies  $P=NP$ . It is unusual that a simple rounding of real solutions to 0 or 1 from linear system of (boolean) equations, is able to solve most number of clauses per random SAT which is more obvious compared to other Randomized Rounding/Relaxation techniques like Semi-definite programming.

(#) If Hardness of Majority implies something stronger than  $P \neq NP$  e.g an one-way function or PRG in  $\#P^{\#P}$  then there is no conflict from SAT Solver  $>7/8$ -approximation in deterministic Polynomial time and  $P=NP$ .

-----  
-----  
519. (THEORY and FEATURE-DONE) SAT Solver Update - pinv2() - 1000 variables and 1000 clauses - 6 March 2018  
-----  
-----

SAT Solver has been updated to use pinv2() pseudoinverse function which has been documented to be faster. After removing some code causing redundant bottleneck, 1000 variables-1000 clauses random SATs have been solved by pinv2() and matrix multiplication to find real assignments which have been rounded. This means solving a million entry matrix ( $1000 \times 1000$ ). MAXSAT approximation ratio is 97%-98% again. Probability per literal average observed coincides with theoretical value of  $1/\sqrt{m \cdot n}$ . It has to be noted that Random matrix expectation for solving SAT translated to linear system of equations is an average case solution and is not worst case. This  $>7/8$  approximation could imply AverageP=AverageNP or PromiseP=PromiseNP (for equal number of variables-

clauses) if not P=NP. This is the likely reason for observed per literal probability being 97% asymptotically less than theoretical per literal probability 100%.

-----  
520. (THEORY and FEATURE-DONE) SAT Solver Update - 2500 clauses and 2500 variables - LSMR, LSQR and PseudoInverse Benchmarks - related to 518  
- 9 March 2018  
-----

1. SAT Solver class has been changed to accept the algorithm as parameter which can be function names for LSMR, LSQR, PseudoInverse, SPSOLVE, SOLVE etc.,
2. 2500 variables and 2500 clauses combination of SAT instances have been benchmarked by invoking LSMR, LSQR and PseudoInverse(pinv2) separately.
3. LSMR benchmark has 405 random 3SAT instances and is the fastest, LSQR and PseudoInverse(pinv2) benchmarks have only few random 3SAT instances.
4. LSQR and PseudoInverse(pinv2) are equally slower compared to LSMR by many orders of magnitude.
5. But approximation ratio for LSMR is 91-92% while LSQR and PseudoInverse trend at 96-97% though for small number of iterations. This probably implies an accuracy versus speed tradeoff: LSMR is less accurate but fast while LSQR and PseudoInverse(pinv2) are more accurate but less fast.
6. Observed probability per literal for all three coincide with random matrix  $1/\sqrt{m*n}$  uniform distribution probability per literal
7. These numbers are only representative figures and number of iterations for LSQR and PseudoInverse(pinv2) are too meagre.
8. Logs have been committed to:  
python-src/testlogs/CNFSATSolver.2500clauses2500variables.LSMR.log.9March2018  
python-src/testlogs/CNFSATSolver.2500clauses2500variables.LSQR.log.9March2018

python-src/testlogs/CNFSATSolver.2500clauses2500variables.PseudoInverse.log.9March2018  
-----

521. (THEORY and FEATURE-DONE) SAT Solver Update - Non-Uniform Choice - For both equal and unequal number of clauses and variables -  
related to 520 - 11 March 2018  
-----

SAT Solver has been updated to include a new Non-Uniform Choice function for creating random SAT instances by choosing a literal by probability =  $1/\sqrt{m*n}$  which works for both equal and unequal number of clauses. This new function chooses non-uniformly. This function creates a submatrix of dimension ( $\sqrt{m}, \sqrt{n}$ ) chosen uniformly from larger matrix of ( $m$  clauses \*  $n$  variables) by invoking choice() function to choose  $\sqrt{m}$  rows from  $m$  rows and  $\sqrt{n}$  columns from  $n$  columns. This uniformly chooses  $\sqrt{m}*\sqrt{n}$  entries from  $m*n$  entries of random matrix. This simulates the random matrix probability  $1/\sqrt{m*n} = \sqrt{m*n}/m*n$ . From this submatrix 3 literals are chosen in succession to create a random 3SAT clause. Replace flag in choice() was set to False and True while creating random clause and there was not much difference and has been set to True. Logs for following 3 variables-clauses combinations have been committed to testlogs/ for ~100 random 3SAT instances each:

1000 variables, 1000 clauses -  
CNFSATSolver.1000variables1000clauses.NonUniformChoice.log.11March2018  
1100 variables, 1200 clauses -  
CNFSATSolver.1100variables1200clauses.NonUniformChoice.log.11March2018  
1200 variables, 1100 clauses -  
CNFSATSolver.1200variables1100clauses.NonUniformChoice.log.11March2018  
From logs it is evident non-uniform choice function defined as previously approximately simulates the bias and almost matches theoretical  $1/\sqrt{m*n}$

random matrix expected per literal probability. LSMR algorithm has been chosen and MAXSAT approximation ratio is 91-93% for 100 iterations for each of the 3 variable-clause combinations. For equal variable-clause combinations, non-uniform choice function is equivalent to choice() and expected and observed probabilities per literal agree fully. Previous benchmarks have been done to verify the random matrix theory for Satisfiability problem which is a probabilistic average case  $P=NP$  problem mentioned in hardness amplification conflicts previously. There is also a special case conflict with PARITYSAT Hastad-Linial-Mansour-Nisan Theorem circuit size counterexample mentioned in 53.15. Also unequal variable-clause SATs can be simulated by equal variable-clause SATs by setting redundant variables to 0 in disjunction of the literals in clauses or redundant clauses in conjunction to 1. Thus non-uniform choice may not be necessary.

-----  
522. (THEORY and FEATURE-DONE) SAT Solver Update - Non-Uniform Choice - 3200 variables and 3100 clauses and Alpha=4.26 - related to 521  
- 12 March 2018  
-----

SAT Solver has been updated for some aesthetics - literal selection in non-uniform choice has been parametrized: sequential or simultaneous  
based on how three random literals are chosen per random 3SAT clause - sequentially as  $3 \cdot nP1$  or simultaneously as  $nP3$ . But no difference was observed between these two choices. Number of variables is set to 3200 and clauses to 3100. LSMR iteration has been increased to 5 and conlim reduced to 10. For few random 3SATs, observed MAXSAT approximation ratio average stands at ~95%. This accuracy has been observed to increase proportional to number of LSMR iterations. Commercial SAT solvers solve million variable-clause combinations in few seconds but in exponential time. Two other logs have been committed which solve the notorious Alpha=4.26 Clause/Variable ratio, which is known to be hardest subset of SAT and where a phase transition occurs from easy-to-hard. Number of unsatisfiable formulae increase for  $\alpha > 4.26$ . MAXSAT approximation ratio observed for few random 3SAT instances is ~91% for number of variables 300 and 1000 and  $\alpha=4.26$ . Observed per literal probability is skewed and substituting it in random matrix MAXSAT approximation ratio  $m^2 \cdot n^2 \cdot p^4$  shows an anomaly. Another fact observed: per literal probability does not change at all for any number of iterations and stays put and because of this observed MAXSAT ratio converges within few iterations itself.

#### References:

-----  
522.1 SAT Solvers and Phase Transition at Alpha=4.26 [Clause/Variable Ratio] - [Carla P. Gomes, Henry Kautz, Ashish Sabharwal, and Bart Selman] - [https://www.cs.cornell.edu/gomes/pdf/2008\\_gomes\\_knowledge\\_satisfiability.pdf](https://www.cs.cornell.edu/gomes/pdf/2008_gomes_knowledge_satisfiability.pdf)  
-----

523. (THEORY and FEATURE-DONE) SAT Solver Update - Non-uniform Choice 2 - 5000 variables and Alpha=4.267 and some intuition - related to 522  
- 15 March 2018  
-----

SAT Solver has been updated for a new nonuniform choice function nonuniform\_choice2() which has following algorithm:  
- Each permutation  $nPn$  of length  $n$  is elongated to  $n \cdot n \cdot \alpha$  length array by replicating a non-variable  $X$  of large index ( $n \cdot n$ )  
- Literals are chosen from this new array as  $(n \cdot n \cdot \alpha)P1$  or  $(n \cdot n \cdot \alpha)P3$  in a while loop till a valid literal which is not equal to  $n \cdot n$  is found  
- This creates a probability of fraction  $n/(n \cdot n \cdot \alpha) = 1/(n \cdot \alpha)$  for per literal choice.

But this implementation was found to be no different from `nonuniform_choice()` which chooses a submatrix in per literal probability and therefore has been commented at present. MAXSAT approximation ratio observed was 88% for `nonuniform_choice2()` versus 90% for `nonuniform_choice()`. 5000 variables and  $\text{Alpha}=4.267$  have been solved for few iterations and MAXSAT approximation ration is 90-91%. In all the benchmarks done so far, it has been observed that equal variables-clause combinations almost always converge to ~95% MAXSAT approximation ratio and  $\text{Alpha}=4.267$  almost always converge to ~90-91%. Though these numbers are not conclusive and comprehensive, previous emerging pattern is too striking.

Here the intuition on how LSMR/LSQR works has to be mooted - Each binary assignment string can be thought of as a step function plotted as binary value versus variables. For example, assignment 001101 is plotted as:

```


```

where troughs represent 0s and peaks 1s. LSMR/LSQR finds a set of real valued points on a sinusoidal polynomial which approximates this step function by minimizing sum of distances/errors between troughs-peaks of polynomial and those of step function. By rounding the peaks and troughs of this LSMR polynomial to 1s and 0s thus converts the sinusoid to a step function. Minimizing the sum of squares distance error implies, this polynomial is almost unique(though there can be multiple satisfying assignments) and is able to extract atleast one satisfying assignment.

Probability of an LSMR/LSQR real-to-binary round off assignment failing to satisfy a random 3SAT:

-----

For each binary variable  $x_i$ , LSMR/LSQR creates a real value which is rounded off as:

```

xi - 0 if xi < 0.5
xi - 1 if xi > 0.5

```

This round off can fail if:

```

xi - 1 if xi < 0.5
xi - 0 if xi > 0.5

```

Lovasz Local Lemma Analyses described earlier further explain the clause-variable dependency graph(Factor graph) scenarios but only lowerbound the MAXSAT approximation ratio for various values of dependency. But Random Matrix Least Squares Error Partial Derivative Analysis forbids values of assignments which cause such large deviations of real solutions from 0s and 1s to maximum possible extent,by providing a mechanism on how to choose a literal -  $1/\sqrt{m \cdot n}$  probability - reverse-engineered a posteriori probability. In other words, real solutions are almost in proximity to 0 or 1 - sinusoid approximates step-function near-perfectly. Any other probability distribution of per literal choice is theoretically inferior.

-----

524. (THEORY and FEATURE-DONE) SAT Solver Update - Variables and Alpha as parameters and two Alpha Versus MAXSAT ratio graph plots - related to 523 - 16 March 2018

-----

SAT Solver has been updated to accept commandline parameters of number of variables and Alpha (Clause/Variable ratio) as:

```
$python CNFSATSolver.py <number_of_variables> <alpha>
```

Some debug prints have been changed. Following sets of SATs were solved and variation of MAXSAT approximation ratio versus Alpha has been captured as graph (for `nonuniform_choice()`):

-----  
Number of Variables - 600 (after atleast 15 random 3SAT iterations)



| Alpha | Observed MAXSAT Approximation Ratio |
|-------|-------------------------------------|
| 1     | 94.5%                               |
| 2     | 92.7%                               |
| 3     | 91.5%                               |
| 4     | 90.74%                              |
| 4.267 | 90.45%                              |
| 5     | 90.28%                              |
| 6     | 90.25%                              |

Number of Variables - 300 (after atleast 15 random 3SAT iterations)

| Alpha | Observed MAXSAT Approximation Ratio |
|-------|-------------------------------------|
| 1     | 95%                                 |
| 2     | 93%                                 |
| 3     | 92%                                 |
| 4     | 90.6%                               |
| 4.267 | 90.6%                               |
| 5     | 90.49%                              |
| 6     | 90.73%                              |

Logs for an iteration of 5000 variables and Alpha=4.267 has been committed to python-src/testlogs/CNFSATSolver.5000variablesAlpha4.267.log.16March2017 which also has MAXSAT approximation ratio of 90-91%. Gradual nosedive of MAXSAT approximation ratio as Alpha increases is notable and it stabilizes to 90-91% after Alpha  $\geq 4$  for both 300 and 600 variables implying phase transition.

SAT Solver has been updated for a new nonuniform\_choice3() function based on an Epsilon Bias Test Snippet EpsilonBiasNonUniformChoice.py which has been added to repository. This is similar to nonuniform\_choice2() but Probabilities of nonuniformly chosen literals are computed separately and updated within the while loops also. Algorithm is similar to nonuniform\_choice2() which elongates a permutation by replicating a skew variable. Average probabilities of all variables other than skew variable almost match the random matrix  $1/\sqrt{m*n}$  probability. Logs which print these probabilities for 1000 variables and Alpha=1/Alpha=4.267 have been committed to testlogs/CNFSATSolver.1000variablesAlpha1.log.16March2018 and testlogs/CNFSATSolver.1000variablesAlpha4.267.log.16March2018.

525. (FEATURE-DONE) SAT Solver Update - nonuniform\_choice3() updated for constant multiple in expansion of the variables array  
- 19 March 2018 - related to 524

1. CNFSATSolver.py nonuniform\_choice3() has been changed to expand the variables array by following relation:  

$$n + x = n * \sqrt{\alpha}$$

$$x = n * (\sqrt{\alpha} - 1)$$

$$\Rightarrow \text{array of } n \text{ variables is expanded to array of size } n * (\sqrt{\alpha} - \text{damp}) \text{ for } \alpha = \text{number\_of\_clauses} / \text{number\_of\_variables}$$
2. damp variable has been hardcoded to 2 than 1 which approximates theoretical  $1/\sqrt{m*n}$  probability well because of round-off.
3. This expansion creates an approximate nonuniform probability  $1/n * \sqrt{\alpha}$  per literal excluding replicated skew variable which is filtered in the while loops
4. Example SAT Solver logs for 1000 variables and Alpha=4.267 has been committed to python-src/testlogs/CNFSATSolver.1000variablesAlpha4.267.log.19March2018
5. MAXSAT Approximation ratio again is 90-91% for 20+ random 3SATs and nonuniform per literal probability almost matches  $1/\sqrt{m*n}$

(till penultimate decimal)

-----  
526. (THEORY) Counterexample in Majority Voting, Timeline Evolution of Belief  
Propagation, Intrinsic Merit - related to 507 - 20 March 2018  
-----

Previous sections described a counterexample in Majority Voting for a question:

"Did an artefact exist millenia ago?"

There are two possible answers: Yes and No which depend on intrinsically determining truth of answer to this question. Both possible answers are belief propagated as trees which evolve over time following a gossip protocol. Root of either of the trees propagates its belief to its children and so on recursively for all other internal nodes. Each edge in either of the trees has a belief potential for "Yes" and "No". Parent node propagates its belief to the children proportional to this potential. If potential is below a threshold, belief propagation stops and trees are pruned. Thus there are two trees which correspond to two sets of people who believe "Yes" and "No" by potentials percolated from Roots. Only the root node has most authentic direct intrinsic evidence to either Yes or No truth value to the question. Question is: How can intrinsic absolute truth of answer be determined? Does size of the trees imply truth i.e Can Majority Voting determine intrinsic truth value at the root? This problem becomes all the more non-trivial when a chronologically ancient portion of tree (e.g Root is extinct) is not available and only nodes closer to leaves remain. Value of belief potential is a function of intrinsic truth viewed by the roots of either tree.

-----  
527. (THEORY and FEATURE-DONE) Hardy-Ramanujan Approximate Ray Shooting Queries  
for Factors - Optimization in Computational Geometric  
Factorization - 21 March 2018 - related to 486  
-----

1. Ray Shooting Queries based on Hardy-Ramanujan Theorem for Normal Order of number of factors of an integer has been implemented as a new function.
2. Each approximate factor is queried by a ray from origin of slope  $\tan(m\pi/(2^k \log \log N))$  intersecting hyperbolic arc bow and approximate factors are:

$$\sqrt{N/[\tan(m\pi/(2^k \log \log N))]} - 1 \text{ for } m=1,2,3,\dots,k \log \log N$$

3. Two integers have been factorized using local tile search and comparison between approximate factors and actual factors have been logged in:

python-src/testlogs/DiscreteHyperbolicFactorizationUpperbound\_TileSearch\_Optimized.HardyRamanujanRayShootingQueries.log.21March2018

python-src/testlogs/DiscreteHyperbolicFactorizationUpperbound\_TileSearch\_Optimized.HardyRamanujanRayShootingQueries2.log.21March2018

4. Approximate Ray Shooting could be useful for integers having large value of factor multiplicity BigOmega (sum of prime factor powers)
5. Constant k has been hardcoded presently and has to be heuristically found.
6. Approximate Factors are helpful for sieving huge integers and binary search can be localized based on these approximate factors as beacons. It is not necessary to search the entire pixelated hyperbolic arc.

-----  
528. (FEATURE-DONE) Unsorted Search Update - Streaming Abstract Generator File  
Datasource Support, Prefix-Suffix substrings hashtables  
- 23 March 2018  
-----

1. Hardcoded File name in Streaming Abstract Generator has been replaced by a file name variable and file contents are tokenized and stripped of leading and trailing whitespaces and yielded.
2. Padding of '#' in Unsorted Search has been replaced by '0'. Revised Unsorted Search Algorithm in [https://github.com/shrinivaasanka/Grafit/blob/master/course\\_material/ComputerScienceMiscellaneous/ComputerScienceMiscellaneous\\_CourseNotes.txt](https://github.com/shrinivaasanka/Grafit/blob/master/course_material/ComputerScienceMiscellaneous/ComputerScienceMiscellaneous_CourseNotes.txt) has been implemented by creating hash tables for all integer-string prefixes and suffixes (though not for all substrings) than just for single digits.
3. New function to print contents of all hashtables has been added.
4. Function `create_prefix_suffix_hashtables()` initializes prefix and suffix hashtables for strings from Streaming Abstract Generator
5. `search_number()` function has been rewritten to search for all prefixes and suffixes hashtables and match True/False is written
6. New input file `First100Primes.txt` has been created.
7. Primes and Non-Primes are lookedup and logs has been committed to `testlogs/UnsortedSearch.log`. 23 March 2018

-----

529. (THEORY) Consensus, Pareto Optimality, Intrinsic-Perceived Value/Merit Equilibrium, Fair Division, Multiple Agent Resource Allocation(MARA), MAXSAT ranking of texts - related to 432,440,513,526 and all Intrinsic Fitness/Merit sections - 26 March 2018, 27 March 2018

-----

Intrinsic Fitness/Merit and Perceived Merit Equilibrium has been described earlier as an approximate consensus measure for agreeing on value or merit of an entity. Consensus problem for absolute intrinsic merit arises in the following context of Fair Division where set of resources have to be allocated amongst multiple agents fairly (also known as MARA-Multi Agent Resource Allocation). Fairness in allocation is usually expressed by Pareto Optimality which is defined as:

For a utility function  $u: (\text{Good}, \text{Agent}) \rightarrow \text{Happiness}$ , set of agents  $(x_1, x_2, x_3, \dots, x_n)$  and goods/services/resources  $(r_1, r_2, r_3, \dots, r_m)$  allocated by  $u$  with a Happiness Vector  $V = (a_1, a_2, a_3, \dots, a_n)$ , there is no other alternative allocation Happiness Vector  $V' = (a_1', a_2', a_3', \dots, a_n')$  for which  $u(a_i') \geq u(a_i)$  for all  $i=1, 2, 3, \dots, n$  and there exists an agent  $i$  such that  $u(a_i') > u(a_i)$ . Most obvious application of Pareto Optimality is Pricing or Determining Value of Goods. Allocation is Envy-Free if no agent feels its own resource allocation as inferior to others. Equating Intrinsic Value and Intrinsic Merit reduces the Multi Agent Resource Allocation or Fair Division problem to Fair Judgement of Intrinsic Merit. Preferences or Desires of an agent are specified by Logic clauses - Ceteris Paribus - all others being equal agent prefers  $(P_1 \wedge !P_2)$  to  $(!P_1 \wedge P_2)$ . Translating the Intrinsic Value MARA problems to Intrinsic Merit MARA problem is non-trivial. For example, if the agents are web URLs and merit has to be fairly apportioned to the Web URLs (Ranking), to ensure no URL feels envious requires defining per URL preferences. This is precisely where MAXSAT representation of per text/URL preferences finds its utility - number of clauses satisfied per text/URL determines its merit i.e text/URL prefers some clauses over others or it has certain special qualities not in others. Pareto Optimality is NP-Complete by reduction from Set Packing problem (Problem of finding disjoint subsets from a collection of subsets).

Traditional Ranking methodology followed is to compute ranking scores per website URL independent of other URLs i.e envy is not accounted for which vitiates fairness. By MARA based ranking, Ranking Fairness is strengthened and Total Cumulative Intrinsic Merit = 1.0, is viewed as Pie/Cake cutting problem and websites are allocated pareto-optimal fractional merit by an envy-free protocol. Thus  $\text{Sum}(\text{rank}(\text{url}))=1$ .

An example envy-free cake cutting algorithm is a hash function which distributes the values nearly equally onto the per-key buckets of the hash table - all buckets have equal number of values or resources are equidistributed. Varying

the hash functions changes the per-key bucket number of values. Each key is an agent requiring certain number of values in its bucket and Choosing a hash function which satisfies this constraint is a MARA protocol.

There exists a bijection between a discrete probability distribution and per-bucket sizes of hashtables (or) parts in a set partition. If each discrete random variable  $x_i$  has probability  $p(x_i)$ ,  $\sum(p(x_i)) = 1$ . Similarly, if each bucket  $x_i$  of a hash table (part in a set partition/exact cover) has size  $b(x_i)$ ,  $\sum(b(x_i)) = N$  (total number of values). Choosing an apt probability distribution does fair allocation e.g If fair allocation constraint is a gaussian, mapping discrete points in normal probability distribution ( $p(x_i)$ ) to size of hash table buckets fairly allocates. Expressing the fair allocation constraints as 3SAT and solving it by Random Matrix LSMR/LSQR Approximate SAT Solver yields real solutions to the constraint variables if rounding is overlooked. As described earlier, this random matrix SAT solver approximates the assignment step function by a polynomial traversing these real assignment points. Riemann Sum Discrete Integral of points on this polynomial should be theoretically equal or close to parity of the binary assignment extracted by LSMR/LSQR.

#### References:

529.1 MARA Survey - <https://staff.science.uva.nl/u.endriss/MARA/mara-survey.pdf>

530. (THEORY and FEATURE-DONE) Recursive Lambda Function Growth - Graph Tensor Neuron Network Intrinsic Merit for Random Walks  
- Analysis for different text - 26 March 2018

1. Text input for Recursive Lambda Function Growth has been updated
2. Graph Tensor Neuron Network Intrinsic Merit for Lambda Function Composition of Random Walks of Definition Graph have been captured in log  
testlogs/RecursiveLambdaFunctionGrowth.log.GraphTensorNeuronNetwork.26March2018
3. Maximum Graph Tensor Neuron Network Intrinsic Merit occurs for Random Walk Composition:  
grow\_lambda\_function3(): Maximum Per Random Walk Graph Tensor Neuron Network Intrinsic Merit :  
(u'(housing(protective,(certain(zone,(something(target,(part(include,(urban(area,(Chennai(city,formerly))))))))))))', 6.023684210526316)
4. Top percentile Unsupervised Classes of this text by Dense Subgraph Discovery (Core Numbers) are:

Unsupervised Classification based on top percentile Core numbers of the definition graph(subgraph of WordNet)

This document belongs to class: arsenic ,core number= 16  
This document belongs to class: Greenwich\_Village ,core number= 14  
This document belongs to class: state\_of\_matter ,core number= 14  
This document belongs to class: order ,core number= 14  
This document belongs to class: include ,core number= 10  
This document belongs to class: part ,core number= 10  
This document belongs to class: exploitation ,core number= 9  
This document belongs to class: area ,core number= 9  
This document belongs to class: three ,core number= 9  
This document belongs to class: collector ,core number= 8  
This document belongs to class: housing ,core number= 8  
This document belongs to class: January ,core number= 8  
This document belongs to class: trey ,core number= 8  
This document belongs to class: Chennai ,core number= 7

This document belongs to class: urban ,core number= 7  
This document belongs to class: planning ,core number= 6  
This document belongs to class: zone ,core number= 6  
This document belongs to class: free-base ,core number= 6  
This document belongs to class: travel ,core number= 6  
This document belongs to class: one ,core number= 6  
This document belongs to class: target ,core number= 6  
This document belongs to class: something ,core number= 6  
This document belongs to class: republic ,core number= 6  
This document belongs to class: government ,core number= 5  
This document belongs to class: legal\_power ,core number= 5

-----  
which reasonably coincide with the vertices of the maximum intrinsic merit random walk and capture the Legal/Gubernatorial/Urban planning nature of the text though there are WordNet anomalies printing 'arsenic' etc., as classes. These anomalies are caused because usually Urban planning is related to exploitation and Solid Waste Management which in turn are connected to Toxic substances and Pollutants. WordNet contains all these relations. Some other Net like ConceptNet5 might probably do better which are word2vec based.

Essence:

-----  
Meaning of a text is approximated as:

- Create a Definition Graph Representation of Text from some Ontology
- Do random walks/Hamiltonian on the graph to simulate the human text comprehension
- Get classes of the text from Recursive Gloss Overlap Unsupervised Classifier
- Compute Lambda Composition Trees for all random walks in definition graph
- These random walk lambda composition trees are approximations of all possible meanings of the text
- Compute Graph Tensor Neuron Network Intrinsic Merit for all random walk lambda composition trees
- Lambda Composition Tree of Maximum Graph Tensor Neuron Network Intrinsic Merit is the most likely approximate meaning of the text
- This is obvious because this maximum merit tree has Neuron Tensor Network Relations of maximum similarity/truth value and these similarities are composed and belief propagated

-----  
531. (FEATURE-DONE) Recursive Lambda Function Growth - Simple Cycles and Rich Club Coefficient - 27 March 2018  
-----

- 
1. Recursive Lambda Function Growth implementation has been updated to loop through cycles in the definition graph of text and to choose between Cycles and Random Walks by a boolean flag ClosedPaths.
  2. Closed Paths or Cycles simulate the meaning better and the tree lambda composition obtained from cycle vertices has been experimentally found to approximate meaning more closely.
  3. Logs for this has been committed to testlogs/RecursiveLambdaFunctionGrowth.log.GraphTensorNeuronNetwork.27March2018
  4. Rich Club Coefficients of the Definition Graph has been printed for each degree as a measure of connectivity of high degree vertices (rich club):  
Rich Club Coefficient of the Recursive Gloss Overlap Definition Graph: {0: 0.004865591072487624, 1: 0.016526610644257703, 2: 0.018738738738738, 3: 0.02396259497369959, 4: 0.024154589371980676, 5: 0.023809523809523808, 6: 0.028985507246376812, 7: 0.032679738562091505, 8: 0.02222222222222223, 9: 0.0, 10: 0.0}
  5. Top core number classes from Unsupervised Recursive Gloss Overlap Classifier:  
=====

Unsupervised Classification based on top percentile Core numbers of the definition graph(subgraph of WordNet)

```
=====
This document belongs to class: incorporate ,core number= 4
This document belongs to class: environment ,core number= 4
This document belongs to class: regional ,core number= 4
This document belongs to class: `in ,core number= 4
This document belongs to class: component ,core number= 4
This document belongs to class: exploitation ,core number= 4
This document belongs to class: useful ,core number= 4
This document belongs to class: relating ,core number= 4
This document belongs to class: unit ,core number= 4
This document belongs to class: particular ,core number= 4
This document belongs to class: making ,core number= 4
This document belongs to class: process ,core number= 4
This document belongs to class: sphere ,core number= 4
This document belongs to class: something ,core number= 4
This document belongs to class: goal ,core number= 4
This document belongs to class: farm ,core number= 4
This document belongs to class: urbanization ,core number= 4
This document belongs to class: strategic ,core number= 4
This document belongs to class: ' ,core number= 4
This document belongs to class: increase ,core number= 4
This document belongs to class: comforts ,core number= 4
This document belongs to class: city ,core number= 4
This document belongs to class: district ,core number= 4
This document belongs to class: farming ,core number= 4
This document belongs to class: urban ,core number= 4
This document belongs to class: way ,core number= 4
This document belongs to class: plan ,core number= 4
This document belongs to class: do ,core number= 4
This document belongs to class: contain ,core number= 4
This document belongs to class: see ,core number= 4
This document belongs to class: state ,core number= 4
This document belongs to class: region ,core number= 4
This document belongs to class: proposal ,core number= 4
This document belongs to class: life ,core number= 4
This document belongs to class: decisiveness ,core number= 4
This document belongs to class: lives ,core number= 4
This document belongs to class: metropolitan ,core number= 4

```

coincide reasonably well to the Maximum Merit Cycle as below and the meaning of the text can be inferred from the composition tree of the word chain and the composed tensor potential is printed for this maximum merit cycle:

```

Cycle : [u'particular', u'regional', u'region', u'something', u'see', u'make',
u'plan', u'goal', u'state', u'city', u'urban', u'area', u'exploitation',
u'land', u'farm', u'unit', u'assembly', u'parts', u'environment', u'sphere']
Cycle Composition Tree for this cycle : (u'particular((region(regional,
(see(something,(plan(make,(state(goal,(urban(city,(exploitation(area,(farm(land,
(assembly(unit,(environment(parts,sphere))))))))))))))))))', 7.250082923612336)
maximum_per_random_walk_graph_tensor_neuron_network_intrinsic_merit=
(u'(regional(particular,(`in(region,(pronounce(way,(see(certain,(add(make,
(important(increase,(plan(strategic,(state(goal,(urban(city,
(administrative(relating,(unit(agency,(land(farm,(useful(exploitation,
(proper(necessitate,(metropolitan(person,
(environment(lives,sphere))))))))))))))))))))))', 14.322488296017706)
=====
```

grow\_lambda\_function3(): Graph Tensor Neuron Network Intrinsic Merit for this text: 3804.34147246

6.NetworkX library has been upgraded to recently released version 2.1

-----  
-----  
532. (THEORY-FEATURE-DONE) Least Squares SAT Solver Benchmarks - 1000 variables  
- Non-uniform choice 3 - different values of Alpha - 29 March 2018 - related to  
524  
-----  
-----

1. SAT Solver (LSMR) has been benchmarked for 1000 variables and for varying values of Alpha as below. MAXSAT approximation ratio after at least 20 iterations of random 3SAT for nonuniform\_choice3() are:  
Alpha = 1 - Observed - MAXSAT-APPROXIMATION Ratio - Moving Average Percentage of Clauses per CNF satisfied so far: 94.3032258065  
Alpha = 2 - Observed - MAXSAT-APPROXIMATION Ratio - Moving Average Percentage of Clauses per CNF satisfied so far: 92.2115384615  
Alpha = 3 - Observed - MAXSAT-APPROXIMATION Ratio - Moving Average Percentage of Clauses per CNF satisfied so far: 91.1458333333  
Alpha = 4.267 - Observed - MAXSAT-APPROXIMATION Ratio - Moving Average Percentage of Clauses per CNF satisfied so far: 90.196679346  
Alpha = 5 - Observed - MAXSAT-APPROXIMATION Ratio - Moving Average Percentage of Clauses per CNF satisfied so far: 89.7233333333  
Alpha = 6 - Observed - MAXSAT-APPROXIMATION Ratio - Moving Average Percentage of Clauses per CNF satisfied so far: 89.8702898551  
Alpha = 7 - Observed - MAXSAT-APPROXIMATION Ratio - Moving Average Percentage of Clauses per CNF satisfied so far: 89.8266233766

2. As usual for equal variable-clauses MAXSAT ratio is the maximum at 94-95% and decreases for increasing alpha. For Alpha=4.267, MAXSAT ratio is 90-91% similar to previous benchmarks(which were done on nonuniform\_choice()).

3. Log excerpts have been captured in  
testlogs/CNFSATSolver.1000variablesDifferentAlphasBenchmarks.29March2018

-----  
-----  
533. (THEORY) Packing/Filling/Tiling problems, Complement Functions/Diophantine Equations, Ramsey Coloring, Exact Cover, Matiyasevich-Robinson-Davis-Putnam Theorem - related to  
461,462,490 - 19 April 2018  
-----  
-----

As mentioned in previous sections, complement functions are subsets of set of Diophantine Equations defining each diophantine set in an exact cover - this generalizes definition of complement functions to exact cover of size greater than 2. Exact Cover is a special scenario of Bin Packing/Space Filling/Tiling plane (e.g Pentominoes tiling of a Chess board, N-Queens Problem etc.,). Complement Diophantine Equations for sets in an exact cover uniquely determine each element in tiling and thus create a bijective map between Diophantines and Tiles(i.e sets in exact cover).

Reference:

-----  
533.1 Pentominoes Tiling Exact Cover for Chess board -  
[https://en.wikipedia.org/wiki/Exact\\_cover](https://en.wikipedia.org/wiki/Exact_cover) - Each pentomino tile can be defined by a Diophantine Equation because Exact Cover is NP-complete recursive set, from MRDP theorem. These diophantine equations for tiles are complement functions of the exact cover.  
533.2 Euclidean Ramsey Theory -  
[http://www.math.ucsd.edu/~ronspubs/pre\\_Euclidean.pdf](http://www.math.ucsd.edu/~ronspubs/pre_Euclidean.pdf) - [RL Graham] - Euclidean Ramsey Theory pertains to the coloring/partitioning of euclidean plane E into tiles  $C_i$  i.e  $E = \cup C_i$  and there exists set of subsets  $E'$  of E such that for every  $x$  in  $E'$ ,  $x$  is exactly contained in one  $C_i$ .

-----  
-----  
534. (THEORY and FEATURE-DONE) Complement Diophantine and Factorization - Pell Equation Solver Update -  
20 April 2018  
-----

-----  
-----  
1. Complement Function Implementation has been updated to invoke sympy Pell Equation solver for some N and D  
in  $x^2 - D*y^2 = N$   
2. Factorization reduces to integer solutions of Pell Equation but the converse is harder - factors must be known  
a priori as  $pq = N$  from some factoring algorithm. Then following equations can be solved:  
$$x + \sqrt{D}*y = p$$
$$x - \sqrt{D}*y = q$$
for x and y.  
-----

-----  
-----  
535. (THEORY and FEATURE-DONE) Complement Diophantine and Factorization - Pell Equation Solver Update 2 -  
20 April 2018  
-----

-----  
-----  
1. Complement Function Implementation has been updated to invoke sympy Pell Equation solver for some N and D  
in  $x^2 - D*y^2 = N$  for  $D=1$   
2. Following are the factors p,q of N:  
$$x + y = p$$
$$x - y = q$$
for Pell equation solutions x and y. This is exponential in number of bits of N and equivalent to most  
Number Field Sieve algorithms for Factorization in vogue. Computational Geometric Factorization in NC  
implies x and y can be found in parallel polynomial time (which is quite surprising given the antiquity and  
notorious difficulty of this ~1500 year old problem).  
3. Pell's Equation for Factoring and Prime polynomials (e.g Matiyasevich, Jones-Sato-Wada-Wiens) are thus  
complement diophantines representing the exact cover {Primes,Composites} of the Set of Natural Numbers  
-----

-----  
-----  
536. (THEORY) Complement Functions, Complement Graphs, Ramsey coloring, Intrinsic Merit of Text-Graph -  
related to 2,338 - 21 April 2018, 25 April 2018  
-----

-----  
-----  
Relations between the concept of complement functions and complement graphs have been described earlier in the  
context of Perfect Graph Theorem. This notion of complement graphs has direct application in graph representation of texts (text-graph) and resulting  
Intrinsic Merit qualities of the text-graph. For example, complement graph dual of a text-graph has edges amongst word vertices absent in its primal. Also  
cliques in primal graph G become independent sets in complement dual graph G' and vice-versa. Complement graphs have spawned vast literature of theoretical  
results foremost being Perfect Graph Theorem. Recursive Gloss Overlap and Recursive Lambda Function Growth algorithms map text to Graph of word vertices  
and composition of Lambda Functions - a language between Context Free Grammar and Context Sensitive Grammar. Composition of lambda functions by random  
walks/cycles/girth in text graphs makes it a Church-Turing-equivalent model  
which is an overlap of two fields - Formal Languages Theory and Graph Theory. It



is an open question as to what Complements of text-graph and their Chromatic number imply: Does a complement of text-graph negate the meaning of text? As opposed to Coloring a linear sentence by Part-of-speech tagging, what does coloring of text-graph imply? E.g The sentence "It rained heavily today" is colored by PoS tags as Pronoun-Verb-Adjective-Object which is a Ramsey coloring of text construed as a sequence of words. Alphabet coloring and arithmetic progressions of alphabet positions in text has been already described in 2.10,2.11 and 2.12. In text-graphs coloring is usually edge coloring and not vertex coloring where each edge color corresponds to a relation (Is-a, Has-a, Is-part-of etc.,) between word vertices. All theorems related to Edge Coloring therefore apply to text graphs. Thus Complement Functions/Complement Graphs are useful in deep structure analysis of text graphs. If the text-graph is complete, Ramsey Theorem for edge k-coloring applies (relations are colors), order emerges and there exists a c-homogeneous subgraph edge-colored by same relation c.

There is a known theorem which states that if a graph G is disconnected its complement G's is connected and vice-versa. This can be proved by elementary arguments. If x-y is not an edge in G, x-y have an edge in G'. If x-y is an edge in G, x and y are in same component in G. If z is a vertex in some other disconnected component of G, then there are no x-z and y-z vertices in G but they exist in G' and there is x-z-y path in G' and G' is connected. In the context of WordNet relations, variant of this theorem has been proved as condition for meaningfulness and Intrinsic Merit in Section 5.16 of [https://tac.nist.gov/publications/2010/participant.papers/CMI\\_IIT.proceedings.pdf](https://tac.nist.gov/publications/2010/participant.papers/CMI_IIT.proceedings.pdf). This qualitatively answers the previous question on meaningfulness of text-graph complement. If text-graph G is disconnected (i.e less meaningful) its complement G' is connected (i.e more meaningful). Here two meanings of primal and its complement text graph need not negate each other. Meaning of complement could be totally different from primal and may be in some other class.

WordNet Synsets for words have noun,verb etc., suffixes (.n,.v,...) which is tantamount to vertex coloring of the text-graph as nouns,verbs,adjectives etc.,. Set of vertices of same color class constitute independent sets or partition the word vertices into monochromatic independent sets. Perfect Graph Theorem applies if text-graph G and its complement G' are perfect (i.e if every induced subgraph of G or G' has its Chromatic Number equal to Maximal Clique Number).

#### References:

-----  
536.1 Introduction to Graph Theory - [Douglas B.West] - Perfect Graph Theorem for complement graphs, Ramsey Theorem for Graphs - Pages 226,380  
536.2 A New Measure of Word Semantic Similarity based on WordNet Hierarchy and DAG Theory -  
<https://pdfs.semanticscholar.org/d3a0/c2a70d3d39a5b41b4ef8c4890a481307259f.pdf>  
-----

-----  
537. (FEATURE-DONE) ConceptNet Client Upgrade to 5.6 - REST endpoints for Emoticons - 23 April 2018  
-----

-----  
1. ConceptNet Client has been updated for new REST endpoints in ConceptNet 5.6  
2. Function for querying emotions has been added for new emoji endpoints in ConceptNet 5.6  
3. logs for this have been committed to  
testlogs/ConceptNet5Client.log.23April2018  
-----

-----  
538. (THEORY) Shell Turing Machines, Word2Vec and Intrinsic Merit - 24 April 2018, 25 April 2018 - related to 42  
-----

-----  
Shell Turing Machines described earlier are experimental enhancements to Turing

Machine definition which introduces dimension as a parameter in addition to tapes, alphabets, head etc., Adding dimension to Turing Machines has immense applications and simulates lot of real world computations which span across multiple dimensions. For example a Turing Machine defined in dimension  $d+1$  has more computational power than a machine defined in dimension  $d$  i.e  $L(T(d))$  is in  $L(T(d+1))$ . This is a dimensional hierarchy as opposed to Time and Space hierarchies of Turing Machines. This has striking applications in graph representation of texts. Each word vertex in a definition graph  $G_1$  can be represented as a vector in a space of dimension  $d$ . Word2Vec embeddings (e.g ConceptNet) already implement this by mapping each word to a vector in space of some dimension. Then another definition graph  $G_2$  of words defined on a vector space of dimension  $d+1$  can elicit more meaning from text than  $G_1$ . Recursive Lambda Composition Trees for  $G_1$  and  $G_2$  are two Turing-equivalent computation models approximating the meaning -  $G_2$  approximates better than  $G_1$ . Essentially a Turing Machine/Lambda Function is extracted from natural language text by growing Lambda Function by recursive composition. In other words intrinsic merit computed for  $G_2$  is more accurate than  $G_1$  for same text. Present algorithms for Recursive Gloss Overlap and Recursive Lambda Function Growth do not affix dimension information for word vertices.

-----  
 539. (THEORY) Recursive Lambda Function Growth for sentences - related to 385,412,530,536 - 26 April 2018  
 -----

Recursive Lambda Function Growth algorithm described so far depends on a text graph and walks/cycles in the text graph are deemed as sentences of word vertices connected by WordNet/ConceptNet/Ontology relations which are converted to lambda function composition tree. This section explains how to construct a lambda function composition from linear sentences with no text-graph representation.

Approximate algorithm to create a lambda composition tree from sentence:

- 
- \*) PoS/NER tag the sentence into Nouns, Verbs, Adjectives, Adverbs, Pronouns etc.,
  - \*) Make all words tagged as verbs into lambda functions and noun/object for the verb as respective arguments for the lambda function. This is a thumbrule because verbs in the sentences are the crux/actions on the nouns and objects.
  - \*) Most natural languages are self-similar in the sense, the simple sentence template Noun-Pronoun-Adverb-Verb-Adjective-Object is recursively substituted to create large sentences. For example Object in Noun-Verb-Object template can itself be another template of the form Noun-Verb-Object.
  - \*) Adjectives/Adverbs qualifying nouns/verbs/objects are created as wrapper lambda functions for nouns/verbs/objects.
  - \*) This algorithm for extracting Lambda functions/Turing Machines from Natural Language Texts is the maximum theoretical limit attainable if Church-Turing Thesis is true. In other words, this algorithm creates Turing machines recognizing Recursively Enumerable sets.

Example sentence: "It rained heavily today"

The example sentence is PoS tagged as Pronoun-Verb-Adjective-Object. Verb "rained" is marked as lambda function (after normalizing to "rain" if preferred.). Adjective "heavily" qualifying Object "today" is the wrapper function "heavily(today)". "It" is a separate lambda function for pronoun. Verb function "rained" thus accepts "It" and "heavily(today)" as arguments creating

the tree:

rained(It, heavily(today))

This algorithm is independent of natural language of the text. Lacuna in this composition from flat sentence is the deep structure - connections/paths between words - is not exploited which is remedied by the random walks/cycle traversal in text-graph and maximum merit composition is chosen.

-----  
540. (THEORY and FEATURE-DONE) Recursive Lambda Function Growth - Update -  
WordNet Relations Deep Structure  
- 1 May 2018  
-----

-----  
1. Recursive Lambda Function Growth python implementation has been updated to define a new function to expand the  
Random Walks and Simple Cycles in Recursive Gloss Overlap graph to include the deep structure relations between the pairs of words.  
2. This invokes path\_between() function implemented in WordNetPath.py which is python alternative implemented in NeuronRain to WordNet::Similarity in Perl CPAN  
3. Logs for this have been committed to  
testlogs/RecursiveLambdaFunctionGrowth.log.GraphTensorNeuronNetworkDeepStructure.1May2018  
4. This is the deepest possible graph structure which can be extracted from a Natural Language Text for an ontology.  
5. Maximum merit lambda function composition printed abstracts the concept of expansion of a Megapolis as Hyponyms/Hypernyms "event","geographic area","region","definite quantity","land" etc.,:  
grow\_lambda\_function3(): Maximum Per Random Walk Graph Tensor Neuron Network  
Intrinsic Merit : (u'event((social\_event(affair,(property(abstraction,(property(abstraction,(property(abstraction,(resource(abstraction,(resource(abstraction,(kind(abstraction,(abstraction(concept,(concept(kind,(information(abstraction,(abstraction(evidence,(evidence(information,(entity(abstraction,(entity(measure,(abstraction(plan,(abstraction(abstraction,(district(entity,(region(location,(entity(physical\_entity,(municipality(district,(municipality(district,(region(district,(region(district,(physical\_entity(location,(event(entity,(exploitation(abstraction,(use(activity,(entity(psychological\_feature,(abstraction(event,(property(land,(land(abstraction,(abstraction(property,(point(entity,(farm(location,(entity(physical\_entity,(location(point,(physical\_entity(farm,(definite\_quantity(entity,(definite\_quantity(entity,(assembly(entity,(artifact(physical\_entity,(assembly(entity,(geographical\_area(physical\_entity,(region(location,(geographical\_area(physical\_entity,(region(location,(entity(physical\_entity,(situation(abstraction,entity))))))))))))))))))))))))))))))))))))))))))))))))))))))))', 36.399953525147026)  
-----

-----  
541. (THEORY and FEATURE-DONE) Recursive Lambda Function Growth - Update -  
Postorder Traversal of AVL Lambda Composition Tree - 2 May 2018  
-----

-----  
1. Text file extracting lambda function composition tree has been updated to increase the size of the text  
and more precisely represent the concept of "Expansion of Chennai Metropolitan Area".  
2. Lambda Function Composition AVL Tree is evaluated as a Postfix expression (Postorder Traversal of AVL tree)  
3. Maximum Merit composition from logs:  
grow\_lambda\_function3(): Maximum Per Random Walk Graph Tensor Neuron Network  
Intrinsic Merit : (u'physical\_entity((artifact(road,(object(event,(entity(way,(abstraction(living\_thing,(entity(causal\_agent,(entity(planner,(physical\_entity(means,(abstraction(property,(entity(entity,(entity(entity,

```
(abstraction(definite_quantity,(abstraction(one,(entity(auditory_communication,
(music(measure,(digit(property,(relation(abstraction,(part(part,
(event(abstraction,(relation(entity,(event(abstraction,(entity(relation,
(politics(investigation,(investigation(politics,(entity(relation,
(entity(Security_Service,(abstraction(abstraction,(group(abstraction,
(international_intelligence_agency(intelligence,
(international_intelligence_agency(group,(Security_Service(intelligence,
(entity(abstraction,(unit(region,(entity(location,(entity(physical_entity,
(district(district,(physical_entity(location,(grasping(control,(event(entity,
(region(embrace,(activity(abstraction,(entity(event,
(grasping(psychological_feature,(clasp(abstraction,(embrace(abstraction,
(abstraction(group,(abstraction(control,(clasp(abstraction,(unit(division,
(clergyman(leader,(living_thing(entity,(causal_agent(entity,
(object(living_thing,(curate(leader,(clergyman(curate,(object(person,
(entity(physical_entity,(thing(physical_entity,
(physical_entity(external_body_part,(abstraction(entity,(abstraction(district,
(entity(entity,(head(causal_agent,(group(region,(entity(physical_entity,
(abstraction(abstraction,(entity(event,(abstraction(increase,(event(action,
(event(abstraction,(expansion(entity,(expansion(abstraction,(action(fact,
(proposal(abstraction,(information(abstraction,(abstraction(plan,
(abstraction(entity,(event(plan,(entity(increase,
(mathematical_relation(abstraction,(relation(entity,(location(region,
(function(entity,(location(region,(entity(concept,(given(physical_entity,
(physical_entity(idea,(given(entity,(abstraction(abstraction,(people(entity,
(concept(abstraction,
(abstraction(location,abstraction))
))
))
))'
```

4. This maximum merit lambda function composition has lambda functions "expansion", "mathematical\_relation", "region" which grasps the leitmotif of the text: "Expansion" is a "mathematical relation" on the "region" implying numeric increase in area from 1189 sqkms to 8848 sqkms

5. logs have been committed to  
testlogs/RecursiveLambdaFunctionGrowth.log.GraphTensorNeuronNetworkDeepStructure PostFix.2May2018

6. Classifier Core number for "expansion" is also maximum at 4.

7. Text for this is a mix of news articles from following websites:  
[https://ipfs.io/ipfs/QmXoybizjW3WknFiJnKLwHCnL72vedxjQkDDP1mXWo6uco/wiki/Chennai\\_Metropolitan\\_Area.html](https://ipfs.io/ipfs/QmXoybizjW3WknFiJnKLwHCnL72vedxjQkDDP1mXWo6uco/wiki/Chennai_Metropolitan_Area.html)  
[https://en.wikipedia.org/wiki/Chennai\\_metropolitan\\_area](https://en.wikipedia.org/wiki/Chennai_metropolitan_area)  
<http://www.thehindu.com/todays-paper/tp-national/tp-tamilnadu/metropolitan-planning-area-expanded/article22639607.ece>  
<https://www.newstodaynet.com/index.php/2018/02/06/chennai-to-grow-from-metropolis-to-megapolis/>

-----  
542. (THEORY and FEATURE-DONE) SAT Solver Update - Parity of the Assignment - 3 May 2018  
-----

-----  
1. solve\_SAT2() function of CNFSATSolver.py has been changed to compute binary parity (sum of 1s) after rounding  
and real parity (sum of real values for variables before rounding)  
2. Rationale is both the parities should be approximately close enough which is another measure of efficiency  
of MAXSAT approximation. Real parity is nothing but Riemann Sum Discrete Integral of the polynomial through  
real assignment points.  
3. Notion of real parities is non-conventional and is introduced as proprietary NeuronRain SAT Solver feature.  
4. This instance solves 1000 variables and Alpha=1.0 and MAXSAT approximation ratio is ~97%. LSQR solver

has been invoked instead of LSMR because of absence of LSMR in SciPy 0.9.0  
5. Logs for this have been committed to  
testlogs/CNFSATSolver.1000variablesAlpha1AssignmentParity.3May2018

-----  
543. (FEATURE-DONE) SAT Solver Update - SciPy Upgrade to 1.1 for restoring LSMR  
- 1000 clauses and Alpha=1.0  
- 16 May 2018  
-----

-----  
1. SciPy has been upgraded to SciPy 1.1 by installing scipy 1.1 wheel file as  
"easy\_install scipy==1.1"  
2. LSMR invocation has been uncommented and invoked restoring status quo ante  
3. Almost 150, 1000 variables and 1000 clauses random SAT instances have been  
solved and MAXSAT approximation  
ratio is > 94 pegged at 94.5% which coincides with Alpha=1.0 pattern of ~95% for  
all executions so far.  
4. Logs for this have been committed to testlogs/  
5. Scipy 1.1 has initial guess parameter for x (SAT assignment) for faster  
convergence which can be utilized in  
future versions of SAT Solver.  
-----

-----  
544. (FEATURE-DONE) Computational Geometric Factorization - Spark 2.3 Upgrade -  
Single Core - 30-bit integer  
- 17 May 2018  
-----

-----  
1. Spark has been upgraded to 2.3 (oracle jdk 1.8) and Hyperbolic local tile  
search optimization for Computational  
Geometric Factorization has been executed for a 30-bit integer on Single Core  
Processor.  
2. Parallelism wont be perceptible in Single Core. This is just a dependency  
upgrade.  
3. Logs have been committed to testlogs/  
-----

-----  
545. (FEATURE-DONE) SAT Solver Update - Initial Guess for LSMR - 1000 variables  
and Alpha=4.267 and 1.0  
- 18 May 2018  
-----

-----  
1. SAT Solver has been updated to invoke lsmr() function with an initial guess  
assignment vector - hardcoded  
to a decimal value < 1 and close to 0 for all variables.  
2. Binary and Real parities (Riemann Discrete Integral Sum) are printed along  
side the assignment vector for each random SAT  
3. SAT Solver has been executed for 1000 variables - Alpha=1.0 and 1000  
variables - Alpha=4.267 for this  
initial guess and logs have been captured in  
testlogs/CNFSATSolver.1000variablesAlpha1.0.log.initial\_guess.18May2018 and  
testlogs/CNFSATSolver.1000variablesAlpha4.267.log.initial\_guess.18May2018  
4. As usual Alpha=1.0 converges to ~95% and Alpha=4.267 to ~90% for 150 and 20  
random SAT iterations respectively.  
5. Non-uniform choice probability for Alpha=4.267 is alomst close to theoretical  
random matrix probability  $1/\sqrt{m*n}$   
-----

-----  
546. (THEORY) Depth-2 Recursive Majority Circuit and a Contradiction - related  
to 14,319,430 - 20 May 2018



2.This enables mining EventNet Event-Partakers Graph for patterns  
3.EventNet has been implemented in NeuronRain AsFer in C++ and Python for persisting general purpose Cloud Event-Actors conversations as Graph.  
4.EventNet is also an Economic Trading Network/Money Flow Market for KingCobra Fictitious Neuro Electronic Currency and Buyer-Seller networks in Neuro Money Flow Markets e.g AsFer-KingCobra Cloud Move of Neuro Currency writes out an EventNet edge in a DOT file from Buyers to Sellers  
5.Mining this Economic Network EventNet requires Frequent SubGraph Mining(GSpan)  
6.log for this has been committed to testlogs/GraphMining\_GSpan.log.21May2018

-----  
548. (FEATURE-DONE) ThoughtNet - Contextual Multi Armed Bandit Evocation -  
Update - 21 May 2018  
-----

-----  
1.Python implementation DeepLearning\_ReinforcementLearningThoughtNet.py has been updated to Classify the input text by Recursive Gloss Overlap Definition Graph Core Number Classifier and lookup the classes in the ThoughtNet Hypergraph  
2.ThoughtNet Hypergraph has been recreated having classes mostly belonging to terrorism, economics, social progress etc.,  
extracted from chronologically older thought edges.  
3.Input to ThoughtNet Reinforcement Learning has been updated to have recent events/thoughts/stimuli  
4.Logs for the evocation of the new thoughts on the ThoughtNet hypergraph is in ThoughtNet/ThoughtNet\_Hypergraph\_Generated.txt  
5.Logs show a recent terrorist event evoking an older event of similar class among others.

-----  
549. (FEATURE-DONE) ThoughtNet Reinforcement Learning - Contextual Multi Armed Bandit Evocation Update  
- 22 May 2018  
-----

-----  
1. RecursiveGlossOverlap\_Classifier.py has been updated to return both the definition graph NetworkX object  
and Recursive Gloss Overlap Intrinsic Merit  
2. RecursiveLambdaFunctionGrowth.py has been updated to return all intrinsic merits from grow\_lambda\_function3():  
    2.1 Korner Entropy of Definition Graph  
    2.2 Bose Einstein Intrinsic Fitness  
    2.3 Graph Tensor Neuron Network Intrinsic Merit  
    2.4 Definition Graph Density  
    2.5 Definition Graph Recursive Gloss Overlap Intrinsic Merit  
    2.6 Maximum Per Random Walk Graph Tensor Neuron Network Intrinsic Merit  
3.ThoughtNet/Create\_ThoughtNet\_Hypergraph.py has been updated to make a choice for merit criterion by choosing between  
sentiment scoring and graph tensor neuron network intrinsic merit for ThoughtNet HyperGraph edges  
4.ThoughtNet/ThoughtNet\_Hypergraph\_Generated.txt has been recreated based on Graph Tensor Neuron Network Intrinsic Merit and the sorted order of hyperedges for most vertices is different compared to  
sentiment scoring earlier  
5.Logs for previous ThoughtNet creation has been committed to  
ThoughtNet/testlogs/Create\_ThoughtNet\_Hypergraph.GraphTensorNeuronNetwork.log.22 May2018  
6.Logs for ThoughtNet Contextual Multi Armed Bandit Evocation has been committed to testlogs/DeepLearning\_ReinforcementLearningThoughtNet.log.22May2018  
-----

-----  
550. (THEORY and FEATURE-DONE) Computational Geometric Factorization - Single  
Core - Hardy-Ramanujan Ray Shooting Queries - 23 May 2018  
-----

- 
1. Hard-Ramanujan Approximate Ray Shooting Queries function has been refactored to compute the angle and tangent of the ray simply as functions of multiples of  $N/k \cdot \log \log N$ .
  2. Precisely angle between the rays must be a function of spacing/gap between prime factors of  $N$  which is at present assumed to be equal.
  3. Cramer's bound for Spacing between primes is  $O(\sqrt{p} \cdot \log(p))$  assuming Riemann Hypothesis is true while the best known modern bound proved in 1995 and 2001 by [Baker-Harman-Pintz] is  $p^{(0.525)}$  which is unconditional.
  4. Prime number theorem implies prime counting function  $\sim N/\log N$ . Probability that a prime below  $N$  is a prime factor of  $N$  is roughly:  $(\log \log N \cdot \log N)/N$  - ratio of Hardy-Ramanujan estimate and Prime Counting Function.
  5. Even with this equal spacing between prime factors, two experimental logs committed herewith show previous approximate ray shooting is exact, passing through an exact factor found by tile binary search. Both logs have an exact match for one factor - approximate and exact ray shooting coincide.
  6. By replacing equal spacing by a function of Cramer and Baker-Harman-Pintz Prime Gap estimate might accurately fine tune the location of a factor further.

References:

- 
- 550.1 Gaps between Consecutive Primes - [Harald Cramer] - <http://matwbn.icm.edu.pl/ksiazki/aa/aa2/aa212.pdf>
  - 550.2 Gaps between Integers with Same Prime Factors - [Cochrane-Dressler] - <https://pdfs.semanticscholar.org/0dea/870aecd2513323c6f7df6b27fc31660b215c.pdf>
  - 550.3 Gaps between Consecutive Primes - [Baker-Harman-Pintz] - <https://academic.oup.com/plms/article-abstract/83/3/532/1479119>
- 

-----

551. (THEORY) Computational Geometric Factorization - Hardy-Ramanujan and Prime Number Theorems, Gap between consecutive prime factors of an integer, Ray shooting queries based on these - 24 May 2018  
-----

-----

From [Baker-Harman-Pintz] estimate Gap between primes  $p(n)$  and  $p(n+1)$  is approximately  $(p(n))^{0.525}$ . Combining Hardy-Ramanujan and Prime Number Theorem following estimate of number of primes between two prime factors of an integer  $N$  can be found:

Approximate number of primes between 2 prime factors of  $N = (\text{Number of primes less than } N) / (\text{Number of prime factors of } N) \sim N/((\log N) \cdot (\log \log N))$

If  $pf(n)$  and  $pf(n+1)$  are two consecutive prime factors of  $N$ , then from Prime Number Theorem number of primes between  $pf(n)$  and  $pf(n+1) = (pf(n+1)/\log(pf(n+1))) - pf(n)/\log(pf(n))$  which is equivalent to Hardy-Ramanujan and Prime Number Theorem estimate  $N/((\log N) \cdot (\log \log N))$

$$\Rightarrow pf(n+1)/\log(pf(n+1)) - pf(n)/\log(pf(n)) = N/((\log N) \cdot (\log \log N))$$
$$\Rightarrow pf(n+1)/\log(pf(n+1)) = pf(n)/\log(pf(n)) + N/((\log N) \cdot (\log \log N))$$

Previous relation finds the next prime factor  $pf(n+1)$  in terms of  $pf(n)$  as a logarithmic ratio. Similar recurrence can be arrived at based on [Baker-Harman-Pintz] estimate too. If  $p_1, p_2, p_3, \dots, p_m$  are primes between  $pf(n)$  and  $pf(n+1)$ :

$$p_1 = pf(n) + (pf(n))^{0.525}$$



```

p2 = p1 + p1^0.525
p3 = p2 + p2^0.525
...
pf(n+1) = pm + pm^0.525

```

Expanding this recurrence yields a continued nested exponentiation of 0.525 for  $pf(n+1)$  in terms of  $pf(n)$  which must be equal to Hardy-Ramanujan-Prime Number Theorem estimate  $N/((\log N) * (\log \log N))$ . This estimate for gap between two consecutive prime factors of an integer can be substituted for computing angles for prime factor points ray shooting queries in Computational Geometric Factorization in lieu of equal spacing.

-----  
552. (FEATURE-DONE) Computational Geometric Factorization - Ray Shooting Queries - Hardy-Ramanujan-Prime Number Theorem and Baker-Harman-Pintz Gap between Prime Numbers - 24 May 2018  
-----

-----  
1. DiscreteHyperbolicFactorizationUpperbound\_TileSearch\_Optimized.py has been updated to include two new functions for ray shooting queries - 1) based on Hardy-Ramanujan-Prime Number Theorem estimate for number of primes between two prime factors 2) based on Baker-Harman-Pintz Gap between prime numbers.  
2. These two functions are quite nascent and might be refined in next commits.  
3. Two numbers have been factored and all three ray shooting query algorithms print the approximate location of factors.  
4. Of the three, Hardy-Ramanujan query is very simple and finds the factor exactly in most executions (logs show an exact match for one factor in both integers).  
Hardy-Ramanujan-Prime Number Theorem and Baker-Harman-Pintz estimates are too skewed. But theoretically latter two estimates are tighter approximations compared to Hardy-Ramanujan ray shooting.  
5. Logs for these two integer factorizations have been committed to testlogs/  
-----

-----  
553. (THEORY and FEATURE-DONE) Computational Geometric Factorization - Ray Shooting Queries and Cramer Prime Gap Updates - 29 May 2018  
-----

-----  
1. DiscreteHyperbolicFactorizationUpperbound\_TileSearch\_Optimized.py has been updated to include a new ray shooting query function for Cramer Prime Gaps ( $\sqrt{p} * \log(p)$ )  
2. All Four Ray Shooting Query functions have been executed on two integers and factorization logs have been captured in testlogs/ (Single Core - Spark 2.3)  
3. Both logs don't show an exact shoot (but are sufficiently close)  
4. Of the Four, Hardy-Ramanujan ray shooting is still the best and estimates are close to exact factors and sometimes exact.  
5. Baker-Harman-Pintz, Hardy-Ramanujan-PrimeNumberTheorem Ray Shooting functions have been slightly changed for initial prime factor, constant for Prime Counting Function normal order etc.,  
-----  
6. Analysis:  
-----

These ray shooting queries are Monte Carlo algorithms with an error bounded by the spacing between two prime factors. Ray shooting to find a prime factor by Hardy-Ramanujan succeeds with a probability  $\log \log N / N$  which is  $\log \log N / 2^{\log N} = \log \log N / (2^{(2^{\log \log N})})$  which is exponentially small. But real benefit of ray shooting queries is in the following factorization algorithm:

- Sequentially ray shoot  $O(\log \log N)$  queries in  $O(\log \log N)$  time to create beacons
- Distance between any two such beacon in the hyperbolic arc bow is  $O(N/\log \log N)$
- This creates  $O(\log \log N)$  hyperbolic pixelated segments of length  $O(N/\log \log N)$ 
  - Pixelation of  $O(N/\log \log N)$  sized segment requires Parallel RAM sorting (e.g. Using Cole's Parallel Sort each pixelated segment of length  $O(N/\log \log N)$  can be sorted in  $O(\log(N/\log \log N))$  on PRAMs.)
  - Each pixelated segment can be binary searched in  $\log(N/\log \log N)$  time
  - Sequentially this requires  $O(\log \log N) * O(\log(N/\log \log N))$  time for all segments
  - Total factorization time =  $O(\log \log N) + O(\log \log N) * O(\log(N/\log \log N)) + O(\log \log N) * O(\log(N/\log \log N)) < O(\log \log N) * O(\log N)$
  - This PRAM algorithm does factorization in at most  $O(\log \log N * \log N)$  time compared to  $O((\log N)^2)$  or  $O((\log N)^3)$  PRAM time algorithms using segment trees and sorting described earlier.

-----  
 554. (FEATURE-DONE) Scheduler Analytics Update - Rewrite of scheduler analytics webserver functionality and Spark log mapreduce of "perf sched script" - 30 May 2018  
 -----

-----  
 1. SparkKernelLogMapReduceParser.py has been rewritten to remove hardcoded filenames and patterns - new function log\_mapreducer() has been defined for passing log file name and pattern as arguments.  
 2. software\_analytics/DeepLearning\_SchedulerAnalytics.py and software\_analytics/SchedulerAnalytics\_WebServer.py h\$ been refactored and get\_stream\_data() (@Generic Socket Web Server) decorated function has been moved to software\$  
 3. software\_analytics/DeepLearning\_SchedulerAnalytics.py invokes log\_mapreducer() defined in SparkKernelLogMapRed\$  
 for new scheduler performance file perf.data.schedscript and pattern sched\_stat\_runtime.  
 4. New perf.data file has been created from perf utility by "perf sched record" commandline  
 5. New perf.data.schedscript has been created from perf.data by "perf sched script" commandline for printing scheduler context switches and runtime in nanoseconds  
 6. logs for both have been committed to software\_analytics/testlogs/DeepLearning\_SchedulerAnalytics.log.30May2018 and software\_analytics/testlogs/SchedulerAnalytics\_WebServer.log.30May2018  
 7. Perf utility support has been added for potential clockticks-to-processes dynamic hash table creation later.  
 -----

-----  
 555. (THEORY) Non-majority social choice, Majority social choice - Boolean Composition of Majority+SAT Versus SAT Oracles, Margulis-Russo Threshold , KRW Conjecture, Condorcet Jury Theorem and a conflict - 4 June 2018 - related to 129, 317, 355, 358, 400, 429 and all other Majority Voting related sections  
 -----

-----  
 In the theoretical drafts in this document, relativizing proofs involving oracle access to Voter SAT have been neglected in favour of boolean function composition/communication complexity proofs based on composition of Majority and Voter SAT boolean functions. But a recent result has proved  $BQP^A$  is not contained in  $PH^A$  relative to some oracle A. This has direct relation to Condorcet Jury Theorem circuit for Majority Voting having SAT oracle access.  $P(\text{Good})$  binomial series (or Condorcet Jury Theorem) equates Non-majority and Majority social choice based on

correctness of electorate group decision vis-a-vis individual decision correctness. This is tantamount to equating goodness of following two algorithms in different complexity classes:

- \*) LHS: An algorithm having access to PRG making a random choice of a boolean function(voter) - could be in BPP/BQP/RP/BNP/RNC

- \*) RHS: An algorithm which does majority voting by composing Majority function and Individual voter SATs - could be in PH (DC-uniform) if the number of variables  $m$ , per Voter SAT are same for all and size of the electorate is  $n=2^m$  - exponential fanin - and depth restricted (unrestricted is in EXP).

Assuming both LHS and RHS have equal goodness (1-error) of 0.5 (by Margulis-Russo Threshold and Condorcet Jury Theorem), which happens when each individual votes with correctness  $p=0.5$  (homogeneous voters), Oracle version of the previous equality is (for some oracle Voter SAT A which has goodness  $p=0.5$ ):

- \*) LHS:  $BPP^A / BQP^A / RNC^A / BNP^A$

- \*) RHS:  $PH^A / EXP^A / \text{Other larger classes}$

Caveat: This assumes equal error/goodness implies lowerbounds and there are complete problems for respective classes.

Since goodness/error is equal, if one side of the equality is a C-complete problem, the other side devours class C. E.g:

- \*) if LHS is  $BQP^A$ -complete and RHS is  $PH^A$ ,  $BQP^A$  is in  $PH^A$  - this is in direct conflict with 555.1 which separates BQP and PH relative to some oracle A.

- \*) if RHS is  $PH^A$ -complete and LHS is  $BQP^A$ ,  $PH^A$  is in  $BQP^A$

Resolving this conflict requires:

- \*) LHS and RHS have different Oracles (Pseudorandom Oracle A1 for LHS and SAT Oracle A2 for all voters in RHS) - but in real-world voting nothing prohibits all voters from making a random choice and thus there is always a possibility electorate votes at random (Therefore Both Oracles are Pseudorandom Generators and  $A1=A2$ . This is exactly Balls-and-Bins problem described in sections on theoretical EVMS based on LSH and separate chaining hashtables elsewhere in this draft).

- \*) ruling out existence of  $BQP^A$ -complete problems for Voter SAT oracle A separating PH and BQP.

- \*) assumption of equal goodnesses of LHS and RHS implying lowerbounds is wrong.

- \*) Oracle A which separates ( $BQP^A$  is not in  $PH^A$ ) has goodness  $> 0.5$  or  $< 0.5$  violating Margulis-Russo threshold.

But if LHS is Promise-BPP-Complete which are known to exist and RHS is  $PH^A$ , Promise-BPP is in  $PH^A$ .

References:

-----  
555.1 Oracle Separation of BQP and PH - [AvishayTal-Raz] -

<https://ecc.weizmann.ac.il/report/2018/107/download>

555.2 Margulis-Russo Threshold for Majority at  $p=0.5$  - [RyanODonnell] - Pages 224-225 - <http://www.cs.tau.ac.il/~amnon/Classes/2016-PRG/Analysis-Of-Boolean-Functions.pdf>

555.3 Promise-BPP-Complete problems - [OdedGoldreich] -

<http://www.wisdom.weizmann.ac.il/~oded/PSX/prpr-r.pdf>

-----  
556. (THEORY and FEATURE-DONE) Computational Geometric Factorization - Ray Shooting Queries - Yitang Zhang Prime Gap Estimate - 5 June 2018

-----  
1.DiscreteHyperbolicFactorizationUpperbound\_TileSearch\_Optimized.py has been updated to include a new function for ray shooting queries which implements recent breakthrough result in Prime Gap estimation - there are

infinitely many twin primes separated by gap  $< 70000000$  - by [Yitang Zhang]  
 which refines  
 [Goldston-Pintz-Yildirim] Sieve. This might have effect only for finding primes  
 between prime factors of  
 large integers and summing up the gap for spacing between any two prime factors.  
 2. Constants  $k$  and  $l$  for multiplying estimation bounds have been changed  
 slightly.  
 3. logs for this have been committed to testlogs/ for an 8-digit 26-bit integer.  
 4. None of the five ray shooting queries in the bouquet shoot exactly. But Hardy-  
 Ramanujan is still the best and  
 Baker-Harman-Pintz estimate is also close enough to actual factors.  
 5. Ray Shooting's success rate depends on the number and multiplicity of the  
 prime factors - Integers of large Big Omega and Small Omega would have lot of  
 prime factors taking a point-blank hit. In other words large multiplicative  
 partition (Factorisatio Numerorum) number of an integer is a pre-requisite for  
 exact ray shooting. Finding the values of the constants for estimation functions  
 which are normal orders, is presently done by trial and error. Correct values  
 for these constants are also crucial for exact shooting.  
 6. Another weird observation is the convergence of the Hardy-Ramanujan-  
 PrimeNumberTheorem log ratio  $(p/\log(p))$ , also known as Merit) estimate after some  
 iterations and this converged integer sometimes matches closely with actual  
 factors. This has happened in earlier logs too.

#### References:

-----  
 556.1 Bounded Gaps between Primes - [Yitang Zhang] -  
[http://citeseerx.ist.psu.edu/viewdoc/download?](http://citeseerx.ist.psu.edu/viewdoc/download?doi=10.1.1.308.998&rep=rep1&type=pdf)  
[doi=10.1.1.308.998&rep=rep1&type=pdf](http://citeseerx.ist.psu.edu/viewdoc/download?doi=10.1.1.308.998&rep=rep1&type=pdf)  
 556.2 Goldston-Pintz-Yildirim Sieve - [K.Soundararajan] -  
<https://arxiv.org/pdf/math/0605696.pdf> - there are infinitely many twin primes  
 such that  $\limsup (p(n+1) - p(n)) / \log(p(n)) \sim 0$  - there exist prime tuples which  
 are arbitrarily close apart  
 556.3 Primes in Tuples - [Goldston-Pintz-Yildirim] -  
<https://arxiv.org/pdf/math/0508185.pdf>

-----  
 557. (THEORY and FEATURE-DONE) Computational Geometric Factorization - Ray  
 shooting queries - correction  
 - 6 June 2018  
 -----

-----  
 1. DiscreteHyperbolicFactorizationUpperbound\_TileSearch\_Optimized.py has been  
 updated to correct the  
 number of primes estimate between two factors - constant for prime counting  
 function (merit)  $O(p/\log p)$  has been  
 moved to numerator which was earlier in denominator incorrectly.  
 2. Two integers have been factored and logs have been committed to testlogs/.  
 Both show exact ray shoot finding  
 factors correctly matching with actual factors. These are on Single Core + Spark  
 2.3 with local[4]. This  
 simulates quadcore on single core and some factors are printed out of order  
 probably because of Spark Driver  
 Executor Threads.

-----  
 558. (THEORY and FEATURE-DONE) Computational Geometric Factorization - Hardy-  
 Ramanujan-PNT Ray Shooting - Correction - 7 June 2018  
 -----

-----  
 1. Mysterious convergence of merit  $p/\log p$  has been investigated.  
 2. This estimate equates the Prime number theorem merit difference between 2  
 prime factors and ratio of Prime

counting function and Hardy-Ramanujan prime factors estimate as below:

$$l * pf(n+1) / \log(pf(n+1)) - l * pf(n) / \log(pf(n)) = l * N / (\log N * k * \log \log N)$$

3. Earlier the constant multiples k and l were missing in some places which has been rectified.

4. Even after this, previous ratio converges after lot of iterations for l=10 and k=6. So suitable value of l is still elusive.

5. Two integers with large Omega (usually numbers ending in 5 have lot of factors) have been factored. While one integer has exact shoot from Hardy-Ramanujan, the other has close shave, but approximate factors are quite in proximity to actual factors.

6. This establishes utility of ray shooting queries as an Oracle access implementation which can be used both by classical P and quantum period-finding BQP ( $P^A$  versus  $BQP^A$ ) Factoring Turing Machines which at most requires  $O(\log \log N)$  queries.

-----  
559. (THEORY and FEATURE-DONE) Computational Geometric Factorization - Ray Shooting Queries - Constant Changes  
- 8 June 2018  
-----

-----  
1. Constants in all ray shooting query functions have been changed so that gaps are reduced and possibility of exact hit increases. Specifically constant l for Cramer, Baker-Harman-Pintz, Zhang has been made small to widen xrange().

2. 2 integers have been factored and approximate factors for all 5 queries are printed after these new constant values. Zhang and Cramer queries were overshooting previously beyond N. None of the queries exactly shoot but are quite close to actual factors.

-----  
560. (THEORY and FEATURE-DONE) SAT Solver Update - nonuniform\_choice3() damp - 2000 variables and Alpha=4.267  
- 12 June 2018  
-----

-----  
1. CNFSATSolver.py - damp variable in nonuniform\_choice3() function has been fine tuned to match the theoretical probability of  $1/\sqrt{m*n}$  - observed probability almost matches with theoretical

2. random 3SAT instances for Number of variables=100,200,300,400,500,600,700,800,900,1000,1100,1200,1300,1400,1500 and 2000 for alpha=4.267 have been solved and observed probability closely matches the random matrix probability

3. Logs for 2000 variables and Alpha=4.267 have been committed to testlogs/CNFSATSolver.2000clausesAlpha4.267.log.12June2018.

4. Observed MAXSAT approximation ratio for first few iterations hovers around 90-91-92% for all previous variable combinations.

5. Theoretically, if damp variable is perfectly tuned to create required bias in nonuniform choice, then MAXSAT ratio observed for unequal variable-clause combinations should also be in the range of 94-95% if not 100%.

-----  
561. (FEATURE-DONE) Scheduler Analytics Update - New Convolution Network for

analyzing stream of 2-dimensional graphics performance image data - 14 June 2018

-----  
Pictorial Performance Pattern Mining by Convolution Network:  
-----

-----  
Input to this Convolution Network is an image bitmap matrix obtained from some standard graphic performance analyzers - runqueueelat, BPF/bcc-tools, perf etc., Following example image is created by "perf timechart" on perf.data which captures the state, timeslice etc., information of list of processes in scheduler at any instant in the form of a gantt chart.

Backpropagation-Convolution is then applied to this performance snapshot and convolution, maxpooling, final neuron layers are computed as usual. This convolution is iterated periodically for stream of performance snapshot bitmaps.

Advantages of mining graphic images of performances captured periodically are:

- number of dimensions of a performance snapshot image is 2 while psutils creates 1 dimensional array stream of data per process id.

- 2 dimensional performance snapshots are system wide and capture all process id(s) at a time and not process id specific.

- Recent advanced performance analyzers like BPF/bcc-tools provide a histogram equivalent of timechart in perf (runqueueelat) which is also an image bitmap. So support for graphic performance data analytics is futuristic.

- Processing stream of performance snapshot image bitmaps by convolution to extract patterns is more universal/holistic than applying convolution to stream of process structure data

- Specifically if remaining\_clockticks-to-processes dynamic hash tables are available as

- stream of histogram images, applying convolution on this stream creates frequent recurring

- patterns of queueing in OS Scheduler (Described in GRAFIT course material:

-  
[https://github.com/shrinivaasanka/Grafit/blob/master/course\\_material/NeuronRain/AdvancedComputerScienceAndMachineLearning/AdvancedComputerScienceAndMachineLearning.txt](https://github.com/shrinivaasanka/Grafit/blob/master/course_material/NeuronRain/AdvancedComputerScienceAndMachineLearning/AdvancedComputerScienceAndMachineLearning.txt),

-  
[https://gitlab.com/shrinivaasanka/Grafit/blob/master/course\\_material/NeuronRain/AdvancedComputerScienceAndMachineLearning/AdvancedComputerScienceAndMachineLearning.txt](https://gitlab.com/shrinivaasanka/Grafit/blob/master/course_material/NeuronRain/AdvancedComputerScienceAndMachineLearning/AdvancedComputerScienceAndMachineLearning.txt)

)

NOTE on linux kernel versions: All the NeuronRain commits being done (in SourceForge and GitHub) for the past 2 months since April 2018 are based on executions/tests on linux kernel 3.x.x + Single Core. Berkeley Packet Filtering(BPF)/bcc-tools performance analyzer which includes runqlat is recent addition to mainstream linux kernel from version 4.x.x onwards. Commits prior to April 2018 were done on a linux kernel 4.13.3 + Dual Core development environment which was sabotaged by a probable severe Cybercrime in first week of April 2018 causing catastrophic damage to partitions and hardware failure too making recovery impossible. This incident caused total destruction of all dev and build setups necessitating full checkouts from GitHub and SourceForge repositories and continued development on another base linux kernel of lesser version which does not support BPF/bcc-tools. Previous provision for graphic performance data pattern recognition is mainly targeted towards supporting BPF/bcc-tools in future.

-----  
-----  
562. (THEORY) Computational Geometric PRAM-NC Factorization, Ray Shooting Query  
Oracles, Quantum NC, Quantum  
Factorization, Classical-Quantum Transition and Knot Theory - related to  
34,351,555 - 15 June 2018 and  
18 June 2018  
-----  
-----

Earlier sections define various Ray Shooting Query functions on Hyperbolic curve  
to find approximate factors -

Hardy-Ramanujan, Prime Number Theorem, Baker-Harman-Pintz, Zhang, Cramer  
etc., These Ray shooting functions are

utilized as supporting preprocessing oracles to k-mergesort, local tile search,  
segment trees based PRAM factorization algorithms - oracles locate prime factors  
approximately and sometimes exactly in sequential time of  $O(\log\log N)$ . If an  
oracle ray shooting query succeeds, factorization is over in  $O(\log\log N)$  steps  
with no necessity for further pixelation of hyperbolic curve and  
mergesort/search for factors in PRAM-NC - of parallel time  $O((\log N)^2)$  or  
 $O((\log N)^3)$ . If an oracle ray shooting query is approximate, PRAM  
k-mergesort/search phase of factorization is taken up using the approximate  
factors queried by ray shooting as beacons - search in vicinity of approximate  
factor should easily locate the exact factor. Therefore a factorization  
involving both ray shooting queries and k-mergesort/segment trees/tile search is  
a problem in complexity class  $NC^A$  where A is a ray shooting query oracle in P  
or NC (if  $O(\log\log N)$  parallel ray shooting queries are made on  $O(\log\log N)$  PRAMs  
in  $O(1)$  time). Similar to classical NC, Quantum NC is the class of problems  
solvable in polynomial size quantum circuits (controlled-U gates, controlled-not  
gates, Hadamard gates) in polylogarithmic time. There exists an oracle A such  
that  $P^A = BQP^A$  and  $NC^A$  is contained in  $P^A$ . Also BQP is contained in AWPP i.e.  
any quantum computation can be simulated by a GapP function  $f(x)$  computed by a  
NPTIME Turing Machine (= number of accepting paths of  $x$  - number of rejecting  
paths of  $x$ ) such that:

$$\Pr(M(x) \text{ accepts}) = f(x)/5^{(2 \cdot t(x))}$$

for a Turing Machine  $M(x)$  in BQP. Since NC is contained in QNC, PRAMs in NC  
Factorization can be termed as decohered quantum gates in corresponding QNC  
algorithm. Since Every quantum computation can be transformed into a braid  
evaluated by Jones Polynomial, an oracle A of Jones Polynomial can be non-  
constructively shown to exist such that quantum part in a BQP Turing Machine is  
mapped to a deterministic computation. Theorem 6.1 in reference 562.4 defines  
such a Jones polynomial PTIME braid oracle A so that BQP is contained in  $P^A$ .

Computational Geometric Factorization involves both Parallel and Sequential  
phases - Pixelating hyperbolic arc bow and k-mergesorting/segment-tree them  
requires parallel RAMs whereas binary search of k-mergesorted/segment-tree tiles  
can be done by sequential binary search with no necessity for PRAMs. If each  
PRAM is replaced by a Quantum Gate, computational geometric factorization can be  
done in QNC instead of NC which is contained in BQP. Following algorithm maps  
the mergesort and search of hyperbolic tiles as below and does away with sorting  
and searching.

-----  
-  
Pixelated Hyperbolic arc bow as superposition of quantum state pixels  
-----  
-

Set of pixel coordinates in pixelated hyperbolic arc bow can be construed as  
superposed pixel quantum states each of some amplitude:

$$|(p,q)\rangle = B_1|(x_1,y_1)\rangle + B_2|(x_2,y_2)\rangle + \dots + B_n|(x_0(N),y_0(N))\rangle$$

for complex amplitudes  $B_i$  of  $O(N)$  coordinate states in pixelated hyperbolic arc.  
This superposition implies all the coordinates of hyperbolic arc simultaneously  
have certain probability of being the factor of N. Factorization reduces to  
maximizing probability of decoherence of this superposition to correct classical

factor state  $|(x_l, y_l)\rangle$  i.e  $x_l \cdot y_l = N$ .

Number of distinct prime factors of  $N = k \log \log N$  for some constant  $k$  from Hardy-Ramanujan Theorem. Set of all factors = Set of all multiplicative partitions of  $N$ . Average Probability of a coordinate in pixelated hyperbolic arc to be the factor of  $N = O((\text{Multiplicative Partition Number of } N) / N)$ . But square of complex amplitude  $B_i^2$  is the classical probability of a pixel coordinate state  $|(x_i, y_i)\rangle$ . Each state  $|(x_i, y_i)\rangle$  is created by a quantum toffoli multiplication gate and requires  $2 \cdot \log N$  qubits. Amplitude  $B_i$  for each state  $|(x_i, y_i)\rangle$  can be defined as the complex number function of coordinate:

$$B_i = f(x_i, y_i) + i \cdot g(x_i, y_i)$$

Classical probability of being a factor of  $N = B_i^2$  which is 1 for factor points. Solving  $B_i^2 = 1$ , yields  $f$  and  $g$ .

Classical probability  $(\text{modulus}(B_i))^2$  of pixel coordinate state  $|(x_i, y_i)\rangle$  - assumed to be normalized so that

$\text{Sum}(B_i^2) = 1$  - can be defined as below:

$$(\text{modulus}(B_i))^2 = f(x_i, y_i)^2 + g(x_i, y_i)^2 = \text{floor}(1 - \text{abs}(x_i \cdot y_i / N - 1))$$

which is 1 only if  $x_i \cdot y_i = N$ , the factor point, and is 0 if  $x_i \cdot y_i / N > 1$  or  $x_i \cdot y_i / N < 1$ , the non-factor points on pixelated hyperbolic arc bow, because  $\text{floor}()$  makes the enclosing fraction to 0.

-----  
Quantum NC equivalent of Classical PRAM-NC Computational Geometric Factorization:  
-----

-  
- Input to the quantum NC circuit is the equation for hyperbola,  $xy=N$   
- Length of pixelated hyperbolic arc bow is  $O(N)$  or approximately  $1.5N-1$   
- For factorization it suffices if each pixel  $(p,q)$  in the pixelated hyperbola is input to a quantum gate and it is verified by all gates in parallel if  $pq=N$   
- Succeeding multiplication gates with  $pq=N$  find factors  $p,q$  in parallel.  
This is similar to multiplication in modular exponentiation subroutine of Shor Factorization (or) a quantum multiplication circuit similar to reference 562.7  
- Pixelated Tiles and their pixel coordinates are found in parallel by tiling equation  $N/(x(x+1))$   
- Each multiplication gate for  $p,q$  has  $2 \cdot \log N$  bits inputs -  $|p| + |q|$   
- Number of multiplication gates required  $< 1.5N-1$  (adheres to QNC definition if input size is  $N$  and not  $\log N$ )  
- No sorting and search is necessary  
- Modular multiplication of pixel coordinates  $(p,q) = pq \bmod N$  and verifying it to be 0 is sufficient to conclude  $p,q$  are divisors/factors of  $N$ .  
Succeeding Quantum Modular Multiplication Gates have  $pq \bmod N = 0$  and each modular multiplication gate is of polylogarithmic depth  
- Exact sum of tiles of pixelated hyperbolic arc bow:  
 $N/(1 \cdot 2) + N/(2 \cdot 3) + \dots N/((N-k)(N-k+1)) = N \cdot \{1/1 - 1/2 + 1/2 - 1/3 + 1/3 - 1/4 + \dots + 1/(N-k) - 1/(N-k+1)\}$   
 $= N \cdot (1 - 1/(N-k+1)) = N \cdot (N-k)/(N-k+1)$   
But tiling ends when  $N=(N-k)(N-k+1)$  or  $N=N^2 - 2Nk + N + k^2 - k$   
 $\Rightarrow k^2 - k(2N+1) + N^2 = 0$   
(or)  $k = [(2N+1) \pm \sqrt{4N^2 + 4N + 1 - 4N^2}]/2$   
 $\Rightarrow k = [(2N+1) \pm \sqrt{4N + 1}]/2$   
 $\Rightarrow k \sim N - \sqrt{N} + 0.5 = \text{Approximate Number of tiles (arrays of pixels)}$   
 $\Rightarrow \text{Sum of tile lengths} = N \cdot (N - \sqrt{N} - 0.5) / (N - N + \sqrt{N} + 0.5)$   
 $\Rightarrow \text{Sum of tile lengths} = N \cdot (\sqrt{N} - 0.5) / (\sqrt{N} + 0.5) \sim 0.999999 \dots \cdot N$  for large  $N$   
- Tiling phase also requires Quantum multiplication gates e.g Division in  $N/(x(x+1))$  is converted to a multiplication circuit ([BeameCookHoover] - division reduces to multiplication)



## References:

- 
- 562.1 Quantum NC - <https://arxiv.org/pdf/quant-ph/9808027.pdf>
- 562.2 Shor's Factorization simulated on GPUs (comparison to Microsoft LIQuID Quantum simulator) - <https://arxiv.org/pdf/quant-ph/9808027.pdf>
- 562.3 Complexity limitations on Classical Computation - [Fortnow-Rogers] - <https://arxiv.org/pdf/cs/9811023.pdf> - BQP is in AWPP (Lemma 3.2) and  $P^A = BQP^A$  (Theorem 4.1)
- 562.4 Approximate Counting and Quantum Computation - [M. Bordewich, M. Freedman, L. Lovasz, D. Welsh] - <http://web.cs.elte.hu/~lovasz/morepapers/additive1.pdf> - "...A classical polynomial time algorithm can convert a quantum circuit for an instance of such a problem, into a braid, such that the probability that the output of the quantum computation is zero, is a simple (polynomial time) function of the Jones polynomial of the braid at a 5th root of unity. For an exact statement of this see Freedman, Kitaev, Larsen and Wang [5], or the more detailed papers by Freedman, Kitaev and Wang [6], and Freedman, Larsen and Wang [7, 8]. ..." and "...The Kitaev-Solovay theorem, [K, S] together with the density theorem, Freedman, Larsen and Wang [7, 8], yields an algorithm for an approximation of any gate by a braid of length  $\text{polylog}(1/\epsilon)$  under a Jones representation. We take the number of strings  $m$ , as the size of the input, however the number of crossings in the link is the same as the number of gates in the BQP computer, which is bounded by a polynomial in the input size, hence an algorithm will be polynomial with respect to both measures (or neither)..." - Theorem 6.1 - "Let  $A(L)$  be an oracle that returns the sign of the Jones polynomial of the link  $L$  evaluated at  $e^{2\pi i/5}$ . Then  $BQP \subseteq P^A$ "
- 562.5 Jones Polynomial, Knot Theory and Equivalence of Quantum and Classical Computation - [https://en.wikipedia.org/wiki/Jones\\_polynomial](https://en.wikipedia.org/wiki/Jones_polynomial) - related to 562.4 - Quantum part of any computation can be replaced by approximate evaluation of Jones Polynomial of certain braid under a Jones representation.
- 562.6 Shor Quantum Factorization - [Peter Shor] - (1995) and (1996) - <https://arxiv.org/abs/quant-ph/9508027> - modular exponentiation and Quantum Fourier Transform of an integer state  $|a\rangle$
- 562.7 Quantum Karatsuba Integer Multiplication - <https://arxiv.org/pdf/1706.03419.pdf>
- 562.8 Quantum Multiplication Modulo N Gate Example - <https://www.math.ksu.edu/reu/sumar/QuantumAlgorithms.pdf> - Depth of multiplication gates is polylogarithmic in  $N$ .
- 562.9 Log Depth Circuits for Division and Related Problems - [BeameCookHoover] - <https://pdfs.semanticscholar.org/29c6/f0ade6de6c926538be6420b61ee9ad71165e.pdf>
- 562.10 Quantum Machine Learning - HHL Algorithm - <https://www.scottaaronson.com/papers/qml.pdf> - HHL solves system of linear equations  $Ax=B$  in quantum logarithmic time. Quantum RAM loads the classical amplitudes of all states - Quoted excerpts - "...If the HHL algorithm could be adapted to the case where (say) a single  $b_i$  is 1 and all the others are 0, then it would contradict the impossibility of an exponential speedup for black-box quantum search, which was proved by Bennett, Bernstein, Brassard, and Vazirani...". This is relevant in the context of pixel state superposition above i.e if exactly one  $B_i$  corresponding to a factor point is made to 1 and all others are 0, factorization immediately follows. HHL algorithm fits well in the context of least squares SAT solver also which maps 3SAT clauses to system of linear equations and finds assignments approximately by solving random matrix equation,  $Ax=B$ .
- 

563. (THEORY and FEATURE-DONE) Random 3SAT Approximate LSQR/LSMR Solver update - Increase in Accuracy  
- 19 June 2018

-----

1.CNFSATSolver.py has been updated to increase the accuracy of least squares approximation of SAT assignments  
by setting  $\text{atol}=\text{btol}=\text{conlim}=0$  as prescribed by SciPy documentation in :

<https://docs.scipy.org/doc/scipy-0.14.0/reference/generated/scipy.sparse.linalg.lsmr.html>

Also set the damp to a low value close to zero to solve the 3SAT as regularized least squares problem which is a generalization of least squares.

2. Random 3SAT instances of 1000 variables and Alpha=1.0 have been solved and MAXSAT approximation ratio for this converge to ~97% for few iterationsA

3. This increase in accuracy slows down LSMR. But by better least squares optimization which is parallelizable on cloud viz., LSRN - <http://web.stanford.edu/group/SOL/software/lsrcn/> which is recent parallel algorithm for

solving least squares (LSRN paper -

<http://web.stanford.edu/group/SOL/papers/lsrcn-sisc-2014.pdf>) this slow down can be remedied. Invoking LSRN instead of LSMR implies SAT Solver can be executed on cloud.

-----  
564. (THEORY and FEATURE-DONE) SAT Solver Update - Randomized Rounding and other linear system of equation solvers - 21 June 2018  
-----

-----  
1. SAT Solver has been updated to include a special if condition to check if Alpha=1 and directly invoke linear system of equations solvers instead of least squares regression solvers. Various system of equations solvers like minres, cg, solve and their variants in SciPy were tried for number\_of\_clauses==number\_of\_variables

and minres was found to be the best equalling lsmr's accuracy. But they have been commented and lsmr() is invoked with no regularization damp for Alpha=1

2. Randomized Rounding of the fractional real assignments computed from least squares has been refined. Earlier the rounding threshold was set to 0.5 which has been generalized to the midpoint of the assignment array ((min + max)/2)

3. This midpoint computation is important because it finds the halfway inflexion point of the polynomial traversing the real assignment points. This polynomial is approximated to a step function of 1s and 0s based on whether the assignment for a variable is above or below half-way mark.

4. Polynomial through the fractional assignment points is sinusoidal and it crosses this midpoint in as many places as there are 0-to-1 and 1-to-0 inflexions.

5. Another randomized rounding scheme is also implemented by computing a pseudorandom fraction between 0 and 1 as threshold. Midpoint threshold is quite accurate and is mostly 0.5 which is on the expected lines, while values other than 0.5 are caused because of negative values to some variables in least squares. This follows the usual randomized rounding convention (e.g for Set Cover).

6. Few Random SAT instances of 1000 variables and Alpha=1 have been computed and MAXSAT approximation ratio has been found to be 97-98% which is captured in logs. In some other executions, this ratio touched even 98.5%

7. Accuracy of randomized rounding threshold is crucial to maximizing MAXSAT ratio.

8. Quantum HHL algorithm solves system of equations  $Ax=B$  in logarithmic time while previous classical solvers are polynomial in clauses-variables. Theoretically this SAT Solver invoking HHL on a quantum computer should be able to solve SAT NP-Complete problem approximately in logtime and thus in BQ-P (or BQ-NC).

-----  
-----

565. (FEATURE-DONE) Query Index and Ranking - Sorting by merit - 22 June 2018

-----  
1. QueryIndexAndRank.py has been changed to sort the results queried from LSH and ThoughtNet indices by descending order of Graph Tensor Neuron Network Intrinsic Merit. Earlier sorting was missing. Two dictionaries have been created for LSH and ThoughtNet index rankings and are sorted descending.  
2. Locations of ThoughtNet Hypergraph have been updated in Indexing/  
3. Logs for the ranking have been captured in testlogs/QueryIndexAndRank.log.22June2018  
-----

566. (THEORY) Exact Learning of Boolean Functions(e.g absolute CNF) and Intrinsic Merit - 22 June 2018  
- related to 529  
-----

-----  
Intrinsic Merit problem has been defined as MAXSAT problem earlier assuming there exists an absolute universal CNF which accepts merit variable values from texts/AVs. Merit variables in this universal CNF are boolean  
based on threshold: if a merit value > threshold, merit variable is 1 and 0 otherwise. For example if graph tensor neuron network intrinsic merit of a text exceeds a threshold, corresponding variable "intrinsic\_merit" in universal CNF is set to 1. Texts/AVs are ranked by descending order of percentage of clauses satisfied in this universal CNF which is MAXSAT problem. Problem is how to learn this universal CNF if it exists. There are approximate learning algorithms like PAC learning which can learn a concept class approximately correctly with a bounded error. Traditional exact learning model uses halving algorithm based on membership and equivalence queries to gradually shrink the concept class to 1 element. Number of queries required are  $\log|C|$ . Membership queries ask an oracle if  $x$  is in  $C$  and equivalence queries ask an oracle if  $f(x)=h(x)$ . This halving algorithm is analogous to interval halving proof of Bolzano-Weierstrass Theorem which states that every infinite sequence has a convergent monotone subsequence. Applying this halving procedure to set of all texts and AVs could exactly learn a universal CNF in logarithmic number of Angluin model membership and counterexample/equivalence queries.  
-----

References:

-----  
566.1 Oracles and Queries That Are Sufficient for Exact Learning - [Nader H. Bshouty, Richard Cleve, Ricard Gavaldà, Sampath Kannan and Christino Tamon] - [https://ac.els-cdn.com/S002200009690032X/1-s2.0-S002200009690032X-main.pdf?\\_tid=735940ad-7047-40d2-a9a7-2575422672c3&acdnat=1529665709\\_798fd8cba3f740826f4c3ce299cdb6c1](https://ac.els-cdn.com/S002200009690032X/1-s2.0-S002200009690032X-main.pdf?_tid=735940ad-7047-40d2-a9a7-2575422672c3&acdnat=1529665709_798fd8cba3f740826f4c3ce299cdb6c1)  
566.2 Bolzano-Weierstrass theorem and its application to MARA - [https://en.wikipedia.org/wiki/Bolzano%E2%80%93Weierstrass\\_theorem](https://en.wikipedia.org/wiki/Bolzano%E2%80%93Weierstrass_theorem)  
-----

567. (FEATURE-DONE) Streaming Analytics - Facebook Graph API - Python 3.4 and facebook-sdk - 29 June 2018  
-----

-----  
1. Similar to Streaming\_<datasource>.py for LinkedIn and Twitter,  
-----

Streaming\_FacebookData.py has been added to NeuronRain AsFer repositories in SourceForge, GitHub and GitLab.

2. This imports facebook-sdk for python 3.4. This is the first python implementation on python 3.4.
3. This upgrade to python 3.4 from python 2.7 is necessitated because:
  - 3.1 facebook-sdk on python 2.7 requires python 2.7.9
  - 3.2 But importing facebook-sdk on Python 2.7.9 raises errors related to `_ssl` and `_hashlib` (md5, sha etc.,) which are not by default supported by python 2.7.9
  - 3.3 Enabling SSL flags in Modules/Setup.dist for python 2.7.9 non-system builds also does not resolve this error and ssl is not built along with python
  - 3.4 Facebook sdk supports only python 3.4 and 3.7 in 3.x
  - 3.5 Python3.4 has been installed from a non standard PPA
  - 3.6 VirtualEnv, EasyInstall3, PIP also do not solve the above SSL import issue
  - 3.7 In python3.4 too, lot of facebook-sdk dependencies have to be git-cloned, built and installed (requests, idna, certifi, chardet etc.,) for facebook import to work
4. Example temporary access token has been created from from <https://developers.facebook.com/tools/explorer/>
5. Simple name and id REST query has been done using requests and logs committed to testlogs/

-----  
 568. (FEATURE-DONE) Streaming Analytics - Facebook Graph - 2 July 2018  
 -----

1. Streaming\_FacebookData.py has been parametrized to accept user name as commandline argument  
`$python3.4 Streaming_FacebookData.py <facebook_user>`  
 2. Wall Posts and Friends of a user are obtained by facebook-sdk REST  
 3. Friends generator object is iterated and printed

-----  
 569. (THEORY and FEATURE) SAT Solver - Discrete Fourier Transform (FFT) of the real assignment, Parseval/Plancherel Theorems, Semidefinite Programming Approximation and Least Squares - 3 July 2018  
 -----

1. SAT Solver has been updated to compute Fast Fourier Transform of the real assignment points for each random 3SAT.  
 2. Discrete Fourier Transform of set of points is:  

$$X(N) = \text{Sum}(x(n) * e^{(2\pi i * n * k / N)}), k=0,1,2,\dots,N-1$$
 $X(i)$  are frequencies and  $x(i)$  are discrete points in real assignment vector computed from Least Squares  
 3. Mapping the real assignment points to frequency domain enables finding periodicity within the real assignments and applying Parseval/Plancherel Theorems ([https://en.wikipedia.org/wiki/Discrete\\_Fourier\\_transform](https://en.wikipedia.org/wiki/Discrete_Fourier_transform))  
 4. Parseval Theorem equates the inner product of two vectors to inner product of Fourier Transform Frequencies.  
 5. Inner product of two assignment vectors (exact binary and real approximate - for values of variables) is a measure of distance between the exact (if known) and approximate assignments  
 6. Least Square Approximation solves the system of linear equations  $AX = B$  for random 3SAT while Semidefinite Programming (SDP) solves the Convex Optimization Problem:  
 maximize/minimize:  $\text{Double\_Summation}(a(i,k) * x_i * y_k)$   
 Subject to Constraints:  $\text{Double\_Summation}(c_l * x_i * y_k) < b_l$

7. In other words, SDP solves:  
 maximize/minimize:  $A^*X$   
 Subject to Constraints:  $C^*X < B$   
 $X$  is a Positive Semidefinite Gramian Matrix having entries from inner product space of vectors  
 (or  $v^*Xv^T$  is non-zero for real vectors  $v$ )

8. [Goemans-Williamson] MAXCUT Approximation algorithm - <http://www-math.mit.edu/~goemans/PAPERS/maxcut-jacm.pdf> - Journal of the Association for Computing Machinery, vol. 42, No.6, November 1995 - solves MAXCUT in ~88% by SDP.

9. Any symmetric matrix can be approximated to nearest positive semidefinite matrix (e.g. cov\_nearest - [http://www.statsmodels.org/dev/generated/statsmodels.stats.correlation\\_tools.cov\\_nearest.html](http://www.statsmodels.org/dev/generated/statsmodels.stats.correlation_tools.cov_nearest.html))

10. There is an SDP variation of least squares, Semidefinite Least Squares, which solves the convex program:  
 minimize:  $|X-C|^2$   
 Subject to:  $AX=B$  for positive semidefinite matrix  $X$ .  
 which is similar to least squares solution for variable vector  $X$ .  $X$  is positive semidefinite because for any real vector  $v$  and some assignment to  $X$ ,  $v^*Xv^T$  is positive. Minimizing  $|X-C|^2$  for some binary assignment  $C$  finds closest approximation of  $X$  to binary step function characterized by  $C$ . (Example: <https://ljk.imag.fr/membres/Jerome.Malick/Talks/08-louvain.pdf>)

11. logs for 2000 variables and  $\alpha=1$  have been committed to testlogs/ which show usual MAXSAT approximation ratio convergence to  $\geq 97\%$

-----  
 570. (THEORY and FEATURE) Computational Geometric Factorization, Ray Shooting Query Oracles, ABC Conjecture  
 - related to 486, 527, 550, 558 and all other sections on factorization - 6 July 2018  
 -----

ABC Conjecture implies there exist finite number of coprime integer triples  $a, b, c$  as solutions to diophantine equation  $c=a+b$  constrained by:

$$\text{quality} = \frac{\log(c)}{\log(\text{rad}(abc))} < 1 + \epsilon \text{ for all } \epsilon > 0$$

$\text{rad}(N)$  or  $\text{rad}(N)$  is the product of distinct prime factors of  $N$  (square-free).

Gap between numbers  $c$  and  $a$  having same prime factors has been conjectured in reference 570.1 as:  
 $c - a > C(\epsilon)a^{(0.5-\epsilon)}$  which is derived from ABC Conjecture. This is contrasted against the observed convergence of merit difference in Hardy-Ramanujan-PrimeNumberTheorem ray shooting query oracle:

$l \cdot \text{pf}(n+1)/\log(\text{pf}(n+1)) - l \cdot \text{pf}(n)/\log(\text{pf}(n)) = l \cdot N/(\log N * k \cdot \log \log N)$   
 which is the approximate gap between merit of  $n$ -th and  $(n+1)$ st prime factors  $\text{pf}(n)$  and  $\text{pf}(n+1)$  of an integer  $N$ .

An example factorization and ray shooting query log has been committed which shows actual and ray shooting estimates of factors in 4 of 5 algorithms (Hardy-Ramanujan, Hardy-Ramanujan-PNT, Cramer, Baker-Harman-Pintz) which are in close agreement (off by small distance for most factors) and Hardy-Ramanujan-PNT estimate converges. If  $c=N_1$  and  $a=N_2$  are two integers having same prime factors, previous Hardy-Ramanujan-PNT ray shooting estimate of gap between prime factors for  $N_1$  and  $N_2$  is:

$$l_1 \cdot \text{pf}(n+1)/\log(\text{pf}(n+1)) - l_1 \cdot \text{pf}(n)/\log(\text{pf}(n)) = l_1 \cdot N_1/(\log N_1 * k_1 \cdot \log \log N_1)$$

$$l_2 \cdot \text{pf}(n+1)/\log(\text{pf}(n+1)) - l_2 \cdot \text{pf}(n)/\log(\text{pf}(n)) = l_2 \cdot N_2/(\log N_2 * k_2 \cdot \log \log N_2)$$

$k_2 \cdot \log \log N_2$   
 rewriting  $N_1$  and  $N_2$  in terms of merit difference of prime factors:  

$$\frac{pf(n+1)}{\log(pf(n+1))} - \frac{pf(n)}{\log(pf(n))} \cdot \log N_1 \cdot k_1 \cdot \log \log N_1 = N_1 =$$

$$pf_1^{s_1} \cdot pf_2^{s_2} \cdot \dots \cdot pf_n^{s_n}$$

$$\frac{pf(n+1)}{\log(pf(n+1))} - \frac{pf(n)}{\log(pf(n))} \cdot \log N_2 \cdot k_2 \cdot \log \log N_2 = N_2 =$$

$$pf_1^{t_1} \cdot pf_2^{t_2} \cdot \dots \cdot pf_n^{t_n}$$

$$\Rightarrow N_1 - N_2 = c - a > C(\epsilon) \cdot N_2^{(0.5-\epsilon)}$$
 if ABC conjecture is true  

$$\Rightarrow \left( \frac{pf(n+1)}{\log(pf(n+1))} - \frac{pf(n)}{\log(pf(n))} \right) \cdot (\log N_1 \cdot k_1 \cdot \log \log N_1 - \log N_2 \cdot k_2 \cdot \log \log N_2) = N_1 - N_2 > C(\epsilon) \cdot N_2^{(0.5-\epsilon)}$$
  

$$\Rightarrow \left( \frac{pf(n+1)}{\log(pf(n+1))} - \frac{pf(n)}{\log(pf(n))} \right) > \frac{C(\epsilon) \cdot N_2^{(0.5-\epsilon)}}{(\log N_1 \cdot k_1 \cdot \log \log N_1 - \log N_2 \cdot k_2 \cdot \log \log N_2)}$$
  
 which is the approximate lower bound on number of primes between two prime factors of  $N_1$  and  $N_2$  having same prime factors if ABC conjecture is true.

#### References:

-----  
 570.1 Gaps between integers having same prime factors - [Cochrane-Dressler] - <http://www.ams.org/journals/mcom/1999-68-225/S0025-5718-99-01024-8/S0025-5718-99-01024-8.pdf> - Conjecture 2 and Theorem 1 - "...Conjecture 2. For any  $\epsilon > 0$  there exists a constant  $C(\epsilon)$  such that if  $a < c$  are positive integers having the same prime factors, then  $c - a \geq C(\epsilon)(a^{(0.5-\epsilon)}) \dots$ " and "...Theorem 1. The abc conjecture implies Conjecture 2...."  
 570.2 Pillai's Conjecture and ABC Conjecture - [Subbayya Sivasankaranarayana Pillai] - <https://webusers.imj-prg.fr/~michel.waldschmidt/articles/pdf/abcEnVI.pdf> - Difference of consecutive perfect powers tends to infinity - Pillai's conjecture as a consequence of the abc Conjecture : if  $x^p \neq y^q$ , then  $|x^p - y^q| \geq c(e) \cdot \max\{x^p, y^q\}^{(k-e)}$  with  $k = 1 - 1/p - 1/q$ . Factoring Perfect powers is special case of factorization and in previous ray shooting algorithm  $N_1 = x^p$  and  $N_2 = x^p y^q$  and both  $N_1$  and  $N_2$  have same prime factors.

-----  
 571. (FEATURE) Streaming Facebook Analytics - Exhaustively print all wall posts of a user - 6 July 2018

-----  
 1. Loop has been added to Streaming\_FacebookData.py for printing all pages of user wall posts in json  
 2. logs for this have been committed to testlogs/Streaming\_FacebookData.log.6July2018

-----  
 572. (THEORY) Merit Versus Fame, an example definition of Intrinsic Fitness/Merit in social networks, some contradictions - 9 July 2018

-----  
 Intrinsic Merit-Versus-Fame/Image discrepancy is a well-studied problem in social networks and is the leitmotif of Intrinsic/Absolute Choice versus Majority voting theoretical complexities discussed at length in many sections of this draft. The populist engineering facet of this includes various definitions of intrinsic merit and fame in different disciplines(sports, science etc.,). Bianconi-Barabasi Bose-Einstein condensation phenomenon in social networks occurs when links (particles) accrue in some prominent fittest hub vertices (least energy levels). Defining what least energy implies in social networks is still an open problem. An example definition of Intrinsic Merit function for Bianconi-Barabasi least energy social network profile is described:

Most link-attractive social profiles fall into three disjoint categories:

- Wealthy: Affluent/Businesses/Political (W),
- Educative: Oratory/Academic/Science/Research (E),
- Valorous: Media/Entertainment/Sportspersons/Heroics (V)

Log-Normal Fitness Attachment (LNFA) Function of previous three,  $f(W,E,V) = g(W)*h(E)*l(V)$  formed by multiplication of individual merits in three categories. When a social profile has overlaps with 2 or all 3 of these categories, its ability to attract link increases manifold implying protean all-round nature of profile. E.g Superheroes in fiction/history were versatile and had two or all three. Log Normal distribution is a sum of these random variables and tends to Gaussian by Central Limit Theorem. It remains to define merits in individual categories:

- Wealth: Income, Gravity Model based on GDP
- Education: Publications, Citations, Degrees, Awards
- Valour: Elo Rating, IPR

Metrics like HDI and SPI already incorporate mixture of these variables.

Log Normal summation of these three quantities therefore is factor causing links to gravitate towards a vertex thereby relating to least energy as:

Energy of a Social Profile Vertex  $\sim 1/(\log W + \log E + \log V)$

=> When the log normal sum of merit random variables tends to maximum/infinity, energy of a vertex is at its nadir. On a side note, these three quantities are interdependent:

- Education causes Wealth i.e W is a function of E mostly though there are exceptions
- Valour causes Wealth i.e W is a function of V mostly though there are exceptions

In references below, it is surmised that Fame increases linearly or exponentially with merit. The two contrarian cases when 1) Fame occurs with no merit 2) Merit does not cause Fame, complement this educated guess and is equivalent to group decision correctness probability (p) defined by Condorcet Jury Theorem and Margulis-Russo Threshold when majority function has a sharp transition at  $p=0.5$ . For majority to decide correctly (or) for Fame to coincide with merit p has to be at least 0.5. Margulis-Russo Formula equates derivative of expected value of boolean function for bias p to the Ratio of Sum of Influences of individual variables (voters) and Standard Deviation. In simple terms, this theoretical bound implies Fame or Majority Voting opinion depends on how influential the voters are (i.e how flipping individual preference affects group decision outcome). For majority voting function, this first derivative of  $\Pr[\text{MajorityDecision}(N) == \text{Good}]$  or influence is  $O(\sqrt{\text{number\_of\_voters}})$  at  $p=0.5$ . Both of the previous contrary scenarios occur when bias  $p < 0.5$  which is obvious because the group is prejudiced because all its constituents are prejudiced. Therefore probability of this bias being less than 0.5 has to be quantified:

Probability of per voter bias  $p < 0.5$  for all N voters =  $(0.5)^N$  because random variable for p has two values ( $p \geq 0.5$  and  $p < 0.5$  both equally probable) and voting is uncorrelated which is exponentially meagre though not impossible. This implies previous Fame-Merit mismatch error occurs with  $(0.5)^N$  probability and is infact a converse of Margulis-Russo.

References:

- 
- 572.1 The quantitative measure and statistical distribution of fame - [Ramirez-Hagen] - <https://arxiv.org/pdf/1804.09196.pdf> - Fame is measured by Google Hits, Google News references, Wikipedia edits, Wikipedia views.
- 572.2 How Famous is a Scientist - Famous to those who know us - [James P. Bagrow, Hernán D. Rozenfeld, Erik M. Bollt, and Daniel ben-Avraham] - <http://people.clarkson.edu/~dbenavra/paper/118.pdf> - Fame increases near-exponentially with achievement/merit i.e  $\text{Fame} = c(\text{Achievement})^{(\epsilon)}$ . Achievement or Intrinsic merit in science is defined as number of publications.
- 572.3 Untangling Performance from Success - [Burcu Yucesoy and Albert-László Barabási] - <http://barabasi.com/f/908.pdf> - defines a least square fit of wikipedia references to a tennis player versus a function of his/her ATP rank, Tournament value, number of matches, rank of the best opponent, Career length. - "...For example, only \$0.0 million of Roger Federer's \$00.0 million reported income was from tournament prizes [00], the rest came from endorsements

tied to the public recognition of the athlete. Yet, Novak Djokovic, who was better ranked than Federer during 2008, received over \$100.0 million prize money but only \$10 million via endorsements, about a third of Federer's purse ..."

572.4 Chess Players' Fame Versus Their Merit - [M.V. Simkin and V.P. Roychowdhury] - <https://arxiv.org/pdf/1505.00055.pdf> - defines a linear and exponential fit of Fame versus Elo IPR score of a Chess player. - "...This suggests that fame grows exponentially with Elo rating rather than linearly. ..."

572.5 Only 15 Minutes? The Social Stratification of Fame in Printed Media - [Arnout van de Rijt, Eran Shor, Charles Ward, and Steven Skiena] - <http://citeseerx.ist.psu.edu/viewdoc/download?doi=10.1.1.888.1629&rep=rep1&type=pdf> - "... We measure a person's fame as the number of appearances of that person's name in newspaper records. More precisely, for every day, we count the number of distinct newspaper articles in which a name appeared ..."

572.6 Log Normal Fitness Attachment - [Shilpa Ghadgea, Timothy Killingback, Bala Sundaram and Duc A. Tran] - <https://www.cs.umb.edu/~duc/www/research/publications/papers/ijpeds10.pdf> - "...we consider it reasonable that in many complex networks each node will have associated to it a quantity, which represents the property of the node to attract links, and this quantity will be formed multiplicatively from a number of factors...."

572.7 p-biased boolean functions analysis, Margulis-Russo Formula - <http://www.cs.tau.ac.il/~amnon/Courses/2016-PRG/Analysis-Of-Boolean-Functions.pdf> - Section 8.4 - Equation 8.8 - Page 225 - Example 8.49 and Question 8.23 (Condorcet Jury Theorem)

572.8 Sybils, Collusions and Reputations - GRAFIT course material - [https://gitlab.com/shrinivaasanka/Grafit/blob/master/course\\_material/NeuronRain/AdvancedComputerScienceAndMachineLearning/AdvancedComputerScienceAndMachineLearning.txt](https://gitlab.com/shrinivaasanka/Grafit/blob/master/course_material/NeuronRain/AdvancedComputerScienceAndMachineLearning/AdvancedComputerScienceAndMachineLearning.txt) - PageRank majority function which is non-boolean peer-to-peer converged markov chain random walk voting is a generalization of Boolean Majority function Margulis-Russo Threshold. Boolean majority function is equivalent to PageRank computed for 2 candidate websites on (n+2)-vertex graph (n user websites choose between 2 candidate websites - Good(1) and Bad(0), choice is fraction of outdegree from a user website) normalized to 0 (smaller pagerank) and 1 (bigger pagerank). Margulis-Russo threshold  $d(\Pr(\text{Choice}=\text{Good}=1))/dp$  on this PageRank version of Majority function is ratio of sum of influences of variables (user websites) to standard deviation which has a phase transition to Good(1) at per-voter website bias  $p \geq 0.5$ . It is obvious that bias  $p$  is inversely proportional to probability of a website being a Sybil - increased bias implies user votes more correctly and probability of it being a Sybil decreases.

572.9 Cascading and Thresholds in Social Networks - Chapter 8 - Six Degrees - [Duncan J. Watts] - Cascading is the phenomenon of deluge of acceptance of new concept/innovation in Social Networks. Every social profile has a threshold above which he/she accepts an innovation spread as a meme/fad. Probability of a user acceptance/voting for A increases sharply after more than a threshold of its neighbours accept/vote for A implying Herding.

572.10 Bradley Effect and Noelle-Neumann Spiral of Silence - [https://en.wikipedia.org/wiki/Spiral\\_of\\_silence](https://en.wikipedia.org/wiki/Spiral_of_silence) - Minority opinion is silenced by Majority - "...which stipulates that individuals have a fear of isolation ... social group or the society in general might isolate, neglect, or exclude members due to the members' opinions. This fear of isolation consequently leads to remaining silent instead of voicing opinions...". Bradley effect in psephology is problem of opinion/exit polls going wrong because of this spiral of silence.

572.11 Achievement of a Nobel Laureate defined in terms of Fame - <https://www.tandfonline.com/doi/full/10.1080/13504851.2016.1200176>

572.12 Fame Versus Merit in Economic Networks - CPI(Corruption Perception Index)/Global Integrity Versus Real Gross Domestic Product - <https://arxiv.org/pdf/0705.0161.pdf>, <https://arxiv.org/pdf/0710.1995.pdf> - CPI(Transparency International) which ranks perceived corruption (not absolute) in countries based on various surveys (WEF etc.,) is the counterpart of Fame/Reputation ranking for countries similar to WWW/Social Networks. GDP has



been accepted as intrinsic standard to measure wealth of a nation. These articles describe a power law distribution between CPI and Foreign Direct Investment/GDP.

572.13 Methodology of TI Corruption Perception Index -

[https://www.stt.lt/documents/soc\\_tyrimai/KSI\\_methodology\\_2007.pdf](https://www.stt.lt/documents/soc_tyrimai/KSI_methodology_2007.pdf) - Density Function for each Normalized Variable - Matching Percentiles and Beta Transformation - Samples, Perception and Reality - an example of Fame/Infamy correlating to Merit/Demerit.

572.14 Strength of Weak Ties - [Mark Granovetter] -

<https://www.cs.cmu.edu/~jure/pub/papers/granovetter73ties.pdf> - Social Networks have clusters of strong ties among themselves (Cliques) and Strength of weak tie between individuals in two separate groups determines diffusion of influence.

572.15 Linked - Chapter 10 - Viruses and Fads - Viruses (Biological and Computational), Pandemics, Epidemics, Memes/Fads, Scale Free Topology (few nodes have high degree -  $\text{number\_of\_nodes}(\text{degree } x) \text{ is proportional to } 1/((\text{constant})^x)$ )

572.16 Erdos Number Project -

<https://sites.google.com/oakland.edu/grossman/home/the-erdoes-number-project/facts-about-erdoes-numbers-and-the-collaboration-graph> - Academic excellence is quantified by Author Collaboration graph (distance from Erdos), a research equivalent of Six Degrees of Kevin Bacon

-----  
573. (FEATURE) Streaming Facebook Analytics - Comments - 10 July 2018  
-----

For each wall post, comments object is retrieved by requests and printed

-----  
574. (FEATURE) DeepLearning - Reinforcement Learning - Recommender Systems - Recursive Lambda Function Growth Merit - 12 July 2018  
-----

1.RecommenderSystems/Create\_RecommenderSystems\_Hypergraph.py has been changed similar to ThoughtNet/ to rank the hypergraph edges by both Sentiment and Graph Tensor Neuron Network Intrinsic Merit

2.RecommenderSystems/RecommenderSystems\_Hypergraph\_Generated.shoppingcart3.txt has been recreated and rankings for hyperedges through hypergraph stack vertices is different from sentiment scoring

3.DeepLearning\_ReinforcementLearningRecommenderSystems.py has been changed to remove creamy layer computation for classes and all classes are lookedup in hypergraph

4.Logs for these have been committed to RecommenderSystems/testlogs/Create\_RecommenderSystems\_Hypergraph.GraphTensorNeuronNetworkMerit.log.12July2018 and testlogs/DeepLearning\_ReinforcementLearningRecommenderSystems.shoppingcart3.log.12July2018

5.Example input is a book on quantum physics and is lookedup in Recommender Systems Hypergraph and matches return lot of books on quantum mechanics and physics

-----  
575. (THEORY) Computational Geometric Factorization and Parallel Construction of Wavelet Trees - 13 July 2018  
- related to 34, 486  
-----

Classical algorithm for Computational Geometric Factorization described earlier is based on storing the pixelatedhyperbolic tile segments in parallelly

constructed Interval Trees/Segment Trees and doing stabbing query for factor point  $N=(p,q)$  or by k-mergesort of locally sorted tile segments and doing binary search which are  $O(\log N \cdot \log N)$  parallel time. Wavelet Trees are recently gaining prominence as succinct binary search tree data structure for bigdata algorithms like string search, indexing etc., Wavelet Trees are binary search trees having following traits:

- (\*) Prerequisite is a set of symbols (alphabets) and sequence of symbols (string)
- (\*) Alphabets are divided into two equal sized sets encoded as 0 and 1
- (\*) At root full string is encoded as 0-1 bitmap by previous set encoding for symbols
- (\*) Left subtree contains first half of the parent alphabets and Right subtree the second half and encoded as 0-1 by dividing into two sets again
- (\*) Previous subdivision of alphabets in each node is recursed encoded as 0 and 1 till single element per node is reached at leaves.
- (\*) Wavelet trees have two operators:  $\text{rank}(c,S,i)$  and  $\text{select}(c,S,j)$
- (\*)  $\text{rank}(c,S,i)$  queries number of occurrences of symbol  $c$  in string sequence  $S$  till position  $i$ .
- (\*)  $\text{select}(c,S,j)$  queries position of  $j$ -th occurrence of symbol  $c$  in string sequence  $S$ .
- (\*) Both  $\text{rank}()$  and  $\text{select}()$  are logarithmic time operations traversing the tree from root to leaf.

Binary Search for Factor points  $N=(p,q)$  on hyperbolic tile segments can be mapped to wavelet tree:

- (\*) Set of all segments of length  $N/x(x+1)$  of  $y$ -axis endpoints ( $N/x, N/(x+1)$ ) are concatenated into a single String sequence in ascending order of  $y$ -axis unsorted
- (\*) Each element of this unsorted concatenated string is an integer some of which could be factor points
- (\*) Alphabets of this string are integers in the vicinity of  $N$  in the interval  $[N-\epsilon, N+\epsilon]$  and size of this alphabet is  $2 \cdot \epsilon \ll N$
- (\*)  $\text{select}(N,S,j)$  queries index  $k$  of  $j$ -th occurrence of  $N$  in this concatenated string which is nothing but a factor point  $N=(k,N/k)$  and maximum of value of  $j$  = number of factors of  $N$ . This selection finds factor in logarithmic time.
- (\*) But previous algorithm requires Wavelet Tree construction on PRAMs or Multicores to be in NC and there have been many parallel algorithms for wavelet tree construction mentioned in references.

LevelWT parallel wavelet tree construction algorithm in 575.7 requires  $O(N \log S)$  work and  $O(\log S \cdot \log N)$  depth ( $S$  is the size of the alphabet and  $N$  is size of input). For Computational Geometric Factorization by  $\text{select}()$  on concatenated unsorted hyperbolic tile segments into one huge string, Parallel Wavelet Tree construction requires  $O(\log(\epsilon) \cdot \log N)$  depth and  $O(N \log(\epsilon))$  work which implies requiring  $O(N/\log N)$  PRAM processors. This is far better polylogarithmic depth bound than parallel k-mergesort/interval tree/segment tree which require  $O(\log N \cdot \log N)$  parallel time (depth) minimum. No necessity for sorting the hyperbolic segments is another advantage and Wavelets can store huge strings suitable for factoring very large integers - Each concatenated unsorted hyperbolic segments string is  $O(N)$ .

#### References:

- 
- 575.1 Parallel Construction of Wavelet Trees on Multicore Architectures - [Sepulveda · Erick Elejalde · Leo Ferres · Diego Seco] - <https://arxiv.org/pdf/1610.05994.pdf>
- 575.2 Parallel lightweight wavelet tree, suffix array and FM-Index construction - [Labeit et al] - <https://people.csail.mit.edu/jshun/JDA2017.pdf> - Parallel Cilkplus Implementation : <https://github.com/jlabeit/wavelet-suffix-fm-index>
- 575.3 Wavelet Trees for All - [Navarro] - <https://www.dcc.uchile.cl/~gnavarro/ps/cpm12.pdf>
- 575.4 Improved Parallel Construction of Wavelet Trees and Rank/Select - [Julian Shun] - <https://arxiv.org/pdf/1610.03524.pdf>

575.5 Wavelet Trees and RRR Succinct Data Structure for  $O(1)$  rank() - <http://alexbowe.com/wavelet-trees/> - Each node in Wavelet Tree invokes RRR for  $O(1)$  rank computation per node

575.6 RRR - Succinct Indexable Dictionaries with Applications to Encoding k-ary Trees, Prefix Sums and Multisets - [Rajeev Raman, Venkatesh Raman, S. Srinivasa Rao] - <https://arxiv.org/pdf/0705.0552.pdf> - Succinct Data Structure for computing rank() and select() of a bitmap in  $O(1)$  time. Bitmap is divided into blocks and sets of blocks(superblocks). For each block, rank is computed and stored in a class-offset two level lookup dictionary where class is the rank of the block and offset is index into set of permutations for that block. Superblocks add the ranks of the blocks.

575.7 Shared Memory Parallelism Can Be Simple, Fast and Scalable - [Julian Shun] - <http://reports-archive.adm.cs.cmu.edu/anon/2015/CMU-CS-15-108.pdf> - Theorem 34 - Section 14.4.1 and Page 10 footnote 6 on NC - "...Polylogarithmic-depth algorithms are also desirable for computational complexity reasons, as they fall in the class NC (Nick's Class) containing problems that can be solved on circuits with polylogarithmic depth and polynomial size [15] ..."

575.8 Wavelet Tree in Computational Geometry - [Meng He] - Planar Point Location - <https://pdfs.semanticscholar.org/f32b/bece8f1cd11e5c50acab532b41aaac34f8e0.pdf> - "...Mäkinen et al. [54] showed that a wavelet tree can be used to support orthogonal range counting and reporting for  $n$  points on an  $n \times n$  grid, when the points have distinct x-coordinates (this restriction can be removed through a reduction [14]). To construct a wavelet tree for such a point set, we conceptually treat it as a string  $S$  of length  $n$  over alphabet  $[n]$ , in which  $S[i]$  stores the y-coordinate of the point whose x-coordinate is  $i$ . Thus Figure 1 can also be considered as a wavelet tree constructed for 8 points on an 8 by 8 grid, and this point set is given in the caption of the figure ..." - "... Fig. 1. A wavelet tree constructed for the string 35841484 over an alphabet of size 8. This is also a wavelet tree constructed for the following point set on an 8 by 8 grid: {1, 3}, {2, 5}, {3, 8}, {4, 4}, {5, 1}, {6, 4}, {7, 8}, {8, 4}..." - Previous Computational Geometric Factorization algorithm exactly applies this and construes set of points of hyperbolic arc on 2 dimensional plane as single huge string.

575.9 Wavelet Tree for Computational Geometric Planar Range Search in 2 dimensions - [https://www.researchgate.net/profile/Christos\\_Makris2/publication/266871959\\_Wavelet\\_trees\\_A\\_survey/links/5729c5f708ae057b0a05a885/Wavelet-trees-A-survey.pdf?origin=publication\\_detail](https://www.researchgate.net/profile/Christos_Makris2/publication/266871959_Wavelet_trees_A_survey/links/5729c5f708ae057b0a05a885/Wavelet-trees-A-survey.pdf?origin=publication_detail) - "... Therefore, consider a set of points in the xy-plane with the x- and y-coordinates taking values in  $\{1, \dots, n\}$ ; assume without loss of generality that no two points share the same x- and y-coordinates, and that each value in  $\{1, \dots, n\}$  appears as a x- and y- coordinate. We need a data structure in order to count the points that are in a range  $[lx, rx] \times [by, uy]$  in time  $O(\log n)$ , and permits the retrieval of each of these points in  $O(\log n)$  time. ... this structure is essentially equivalent to the wavelet tree. The structure is a perfect binary tree, according to the x-coordinates of the search points, with each node of the tree storing its corresponding set of points ordered according to the y-coordinate. In this way the tree mimics the distinct phases of a mergesort procedure that sorts the points according to the y-coordinate, assuming that the initial order was given by the x-coordinate. ..." - In the PRAM k-mergesort version of computational geometric factorization ([http://sourceforge.net/projects/acadpdrafts/files/DiscreteHyperbolicPolylogarithmicSieveForIntegerFactorization\\_PRAM\\_TileMergeAndSearch\\_And\\_Stirling\\_Upperbound\\_updateddraft.tex/download](http://sourceforge.net/projects/acadpdrafts/files/DiscreteHyperbolicPolylogarithmicSieveForIntegerFactorization_PRAM_TileMergeAndSearch_And_Stirling_Upperbound_updateddraft.tex/download)) 2 dimensional plane which has the hyperbolic curve is divided into  $\log N$  rectangles of length  $N/\log N$  and hyperbolic point-sets in each of these rectangles are sorted and searched for factor points. Wavelet tree exactly applies to this rectangular range search and can retrieve a factor point from hyperbolic arc point set in  $O(\log N)$  time per rectangle. For  $\log N$  rectangles, time to find factors is  $O(\log N * \log N)$ . As mentioned in the reference, Wavelet Tree mimics sorting the points. But this 2-dimensional Wavelet tree requires parallel multicore construction NC algorithms mentioned earlier for logarithmic depth.

575.10 Wavelet Tree in Computational Geometry - Range Report - [Travis Gagie, Gonzalo Navarro, Simon J. Puglisi] - [https://ac.els-cdn.com/S0304397511009625/1-s2.0-S0304397511009625-main.pdf?\\_tid=bb9ebcde-9e40-41b4-8327-](https://ac.els-cdn.com/S0304397511009625/1-s2.0-S0304397511009625-main.pdf?_tid=bb9ebcde-9e40-41b4-8327-)

4b9ed4e2fb57&acdnat=1536661119\_222f9c6a5423840eec8e09f8107d3f71 - report points in a rectangular area in logarithmic time. As mentioned in previous reference, point in each rectangle bounding a pixelated hyperbolic point-set can be retrieved in logarithmic time e.g query factor point  $N=(p,q)$  on the point-set. 575.11 Functional Approach to Data Structures and their use in Multi-dimensional Searching - [Bernard Chazelle] -

<https://www.cs.princeton.edu/~chazelle/pubs/FunctionalDataStructures.pdf> - Data structure which inspired wavelet

tree in geometric search - M-Structures (Mergesort-Structures)

575.12 Space Efficient Data Analysis Queries on Grids - [Gonzalo Navarro, Yakov Nekrich, Luís M.S. Russo] - [https://ac.els-cdn.com/S0304397512010742/1-s2.0-S0304397512010742-main.pdf?\\_tid=fa66c1a6-518d-4fd1-b6f3-59720d2736fa&acdnat=1537341599\\_ebf10ba8401e952f49aa06f5168192ba](https://ac.els-cdn.com/S0304397512010742/1-s2.0-S0304397512010742-main.pdf?_tid=fa66c1a6-518d-4fd1-b6f3-59720d2736fa&acdnat=1537341599_ebf10ba8401e952f49aa06f5168192ba) - Space

efficient representation of point-sets on 2-dimensional grid

575.13 Succinct Orthogonal Range Search Structures on a Grid with Applications to Text Indexing - [Prosenjit Bose, Meng He, Anil Maheshwari, and Pat Morin] - <https://pdfs.semanticscholar.org/3d28/169f7c1524cf87c9215b61d536939ae5841a.pdf> - Orthogonal range reporting of points in a rectangle - "Lemma 8. Let  $N$  be a set of points from the universe  $M = [1..n] \times [1..n]$ , where  $n = |N|$ .  $N$  can be represented using  $n \lg n + o(n \lg n)$  bits to support orthogonal range reporting in  $O(k \lg n / \lg \lg n)$  time, where  $k$  is the size of the output....". This implies each hyperbolic point in rectangle of width  $N/\log N$  in

[http://sourceforge.net/projects/acadp drafts/files/DiscreteHyperbolicPolylogarithmicSieveForIntegerFactorization\\_PRAM\\_TileMergeAndSearch\\_And\\_Stirling\\_Upperbound\\_updateddraft.pdf/download](http://sourceforge.net/projects/acadp drafts/files/DiscreteHyperbolicPolylogarithmicSieveForIntegerFactorization_PRAM_TileMergeAndSearch_And_Stirling_Upperbound_updateddraft.pdf/download) containing pixelated hyperbolic point-sets can be reported in sub-logarithmic time ( $k=1$ ) independent of other rectangles thereby obviating  $k$ -mergesort of the tile segments (or mimicking it).

575.14 Succinct Datastructure for Multidimensional Orthogonal Range Searching - [Ishiyama-Sadakane] -

<https://www.computer.org/csdl/proceedings/dcc/2017/6721/00/07921922.pdf> - kd-tree example for orthogonal range reporting - Figure 1.

-----  
576. (FEATURE) Spark Streaming - Java 1.8 - Spark Java Upgrade to 2.3 and Some Structured Streaming Enhancements - 17 July 2018  
-----

1. Spark Generic Streaming Java Implementation has been compiled on Spark 2.3 upgraded from Spark 2.1 and sparkgenericstreaming.jar has been repackaged
2. JavaPairDStream code which was commented earlier has been uncommented to return Word Count instead of Words
3. Structured Streaming usecase example in <https://spark.apache.org/docs/latest/structured-streaming-programming-guide.html> for website advertisement analytics has been implemented by computing timestamp of each word occurrence along with its count
4. Word.java has been changed for doing get/set of Time, Count and Word
5. DataFrame schema has been changed to Word, Count and Timestamp instead of just Word.
6. This Structured Streaming DataFrame prints periodically changing tables of word occurrences, frequencies and timestamp as a tabular column.
7. JavaPairDStream still does not have Java Pair support but only scala.Tuple2.

8. Commandline for spark-submit has been changed for jsoup:  
/home/kashrinivaasan/spark-2.3.0-bin-hadoop2.7/bin/spark-submit --jars  
/home/kashrinivaasan/jdk1.8.0\_171/lib/jsoup-1.11.3.jar --class  
SparkGenericStreaming --master local[2] sparkgenericstreaming.jar  
"https://twitter.com/search?f=tweets&vertical=news&q=Chennai&src=typd"

9. CLASSPATH for spark 2.3 has been changed as for catalyst, scala-reflect:  
/home/kashrinivaasan/spark-2.3.0-bin-hadoop2.7/jars/spark-streaming\_2.11-  
2.3.0.jar::/home/kashrinivaasan/spark-2.3.0-bin-hadoop2.7/jars/scala-library-  
2.11.8.jar:/home/kashrinivaasan/spark-2.3.0-bin-hadoop2.7/jars/spark-sql\_2.11-

2.3.0.jar:/home/kashrinivaasan/spark-2.3.0-bin-hadoop2.7/jars/spark-core\_2.11-2.3.0.jar:/home/kashrinivaasan/jdk1.8.0\_171/lib/jsoup-1.11.3.jar:/home/kashrinivaasan/spark-2.3.0-bin-hadoop2.7/jars/spark-catalyst\_2.11-2.3.0.jar:/home/kashrinivaasan/spark-2.3.0-bin-hadoop2.7/jars/scala-reflect-2.11.8.jar:/home/kashrinivaasan/jdk1.8.0\_171/bin:/usr/local/sbin:/usr/local/bin:/usr/sbin:/usr/bin:/sbin:/bin

10. Example logs for streamed news analysis has been committed to testlogs/

-----  
577. (THEORY and FEATURE) Computational Geometric Factorization and its Pell Diophantine (Complement Diophantine of Prime Valued Polynomials) - Updates - 18 July 2018  
-----

-----  
1. DiscreteHyperbolicFactorizationUpperbound\_TileSearch\_Optimized.py has been updated to persist the factors found to a JSON file (json.dump() and json.load()).  
2. Aggregating factors found by multiple Spark executors requires defining a new Spark Broadcast Accumulator class which appends a factor to already existing accumulator value globally  
3. complement.py has been updated for solving both directions of Pell-Factoring (for  $D=1$  and  $N > 1$ ):  
    3.1 Pell Equation to Factoring: Solves Pell equation  $x^2 - y^2 = N$  for  $D=1$  and finds factors  $(x+y)$  and  $(x-y)$  in exponential time (or between polynomial and exponential - <http://www.math.leidenuniv.nl/~psh/ANTproc/01lenstra.pdf>)  
    3.2 Factoring to Pell Equation: Computes all factors  $(p,q)$  of  $N$  by PRAM Computational Geometric Factorization and finds  $x$  and  $y$  in Pell Equation as:  $x=(p+q)/2$  and  $y=(p-q)/2$ . This solves a special case of Pell Equation in classical NC for  $D=1$  (for generic, only quantum polynomial time algorithms are known so far)  
4. Logs for these have been committed to testlogs/DiscreteHyperbolicFactorizationUpperbound\_TileSearch\_Optimized.JSONPersistence.18July2018 and testlogs/complement.PellEquation.SolvedByPRAMNCFactoring.18July2018  
5. Ray Shooting Oracle shows some exact and close ray shooting of factors. For simple Hardy-Ramanujan ray shooting factorization requires only  $O(\log \log N) + O(\log(N/\log \log N) * \log(N/\log \log N)) + O(\log(N/\log \log N))$  time to find a factor because prime factors are  $O(\log \log N)$  and distance between any two prime factors is  $O(N/\log \log N)$ .  
6. Hyperbolic arc bow for this x-axis distance is sufficient to locate a factor. K-mergesort/Segment-tree of this subset is  $O(\log(N/\log \log N) * \log(N/\log \log N))$  and binary search is  $O(\log(N/\log \log N))$ .  
-----

-----  
578. (FEATURE) ConceptNet 5.6 Client Update - Common Ancestor Algorithm rewrite for path between concepts  
- 19 July 2018  
-----

-----  
1. ConceptNet 5.6 provides a REST endpoint /query for finding connections between two concepts which has been wrapped by a new function conceptnet\_path()  
2. Common Ancestor Algorithm for finding distance between two concepts has been rewritten to create a NetworkX subgraph from the edges connecting two concepts. Function conceptnet\_distance() has been renamed to conceptnet\_least\_common\_ancestor\_distance()  
3. Loop iterating over cartesian product has been split into 2 loops which grow from two opposite directions (concept1, --- ) and (--- ,concept2) and intersect at common ancestors.  
4. Edges recursively seen by /related REST query are collected in a list and a NetworkX DiGraph is created from

it which has all paths between concept1 and concept2

5. Shortest path on this subgraph yields the shortest distance and path between concept1 and concept2 and thus passes via the least common ancestor between two concepts

6. Logs for this have been captured in testlogs/ConceptNet5Client.log.19July2018 which show conceptnet\_least\_common\_ancestor\_distance() computes deeper paths than /query

-----  
579. (THEORY and FEATURE) SAT Solver Update - some refactoring, and replace=True  
- 20 July 2018  
-----

-----  
1.CNFSATSolver.py has been refactored for invoking Uniform and Non-uniform choice based on Variables==Clauses  
or Variables !=Clauses and lsqr() invocation has been changed to remove regularized LSQR

2.replace=False has been set to replace=True in np.random.choice() for Uniform choice of random 3SAT variables

(and everywhere else). For very long time replace was set to False

3.logs for this have been committed to

testlogs/CNFSATSolver.2000VariablesAlpha1.0.log.20July2018 and

MAXSAT approximation ratio for few iterations ranges from ~95% to ~99% (logs for 98.25% have not been committed)

-----  
580. (THEORY) Random Matrix Least Square SAT Solver, kSAT Sharp Threshold and Friedgut Theorem, ThoughtNet  
Hypergraph as k-SAT problem, TextGraph and Social Network Property Testing - 26 July 2018 - related to 453  
-----

-----  
Margulis-Russo Threshold and Condorcet Jury Theorem in the context of Sharp Threshold of Majority Function have been extensively described earlier. Random Matrix Least Squares SAT Solver has been analyzed and distribution for choosing a literal has been derived as  $1/\sqrt{m \cdot n}$ . Similar to Majority Function Sharp Thresholds exist for

kSAT formulae from Friedgut's Theorem which is stated as:

The satisfiability property for random k-CNF has a sharp threshold, i.e. there exists  $p'$  such that for any  $\epsilon > 0$ ,

$$\mu p(A) \rightarrow (1 \text{ if } p \leq (1 - \epsilon)p', 0 \text{ if } p \geq (1 + \epsilon)p')$$

$$\text{where } p' = \alpha(n) \cdot n/N.$$

probability of choosing a clause  $p$  is ( $M$ =Number of clauses in a random kSAT)/( $N$ =All possible clauses in a random kSAT). Number of all possible clauses in a random kSAT =  $N = nC_k \cdot 2^k$  and  $\alpha = M/n$  ( $n$  is number of variables)  $\Rightarrow p = (\alpha \cdot n)/N$ .

Probability of choosing a random 3SAT clause in Random Matrix SAT Solver  $p = [1/\sqrt{mn}]^3 = 1/((mn)^{1.5})$ . From Friedgut's Theorem number of satisfied clauses increase if  $p \leq (1-\epsilon)p'$ . This leads to inequality:

$$1/((mn)^{1.5}) \leq ((1-\epsilon)\alpha(n) \cdot n)/N$$

$$\Rightarrow 1/((mn)^{1.5}) \leq [((1-\epsilon)\alpha(n) \cdot n)^6 \cdot (n-3)!]/(8 \cdot n!) \text{ from } N = nC_3 \cdot 2^3$$

Simplifying reduces to:

$$1/((mn)^{1.5}) \leq [((1-\epsilon)\alpha(n))^{0.75}]/((n-1)(n-2)) \text{ from } N = nC_3 \cdot 2^3$$

But  $mn = \alpha(n) \cdot n^2$  substituting which reduces the previous inequality to:

$$[(n-1)(n-2)/(n^3 \cdot (1-\epsilon)^{0.75})]^{0.4} \leq \alpha(n)$$

Example - For  $n=10$  and  $\alpha(n)=4.267$  previous inequality becomes:

$$0.39165/(1-\epsilon)^{0.4} \leq \alpha(n)$$

=> epsilon <= 0.6154  
implying a sharp threshold to increased number of satisfied clauses.

Related note: Sharp Thresholds in k-SAT have some applications in graph representation of texts e.g Definition graphs, ThoughtNet Hypergraph. Any random k-SAT formula can be represented as a hypergraph (Factor graph) of variables as vertices and clauses as hyperedges. ThoughtNet hypergraph is a Factor graph for some k-SAT and extracting the k-SAT from ThoughtNet translates the Contextual Multi Armed Bandit ThoughtNet to a random kSAT instance. Graph representation of texts can be queried for various properties e.g number of matchings, triangles, connected components which extract pattern in the meaning of text. For example, Margulis-Russo threshold is a graph property threshold of at least  $n(n-1)/2$  random edges between  $n$  vertices in a random graph where each edge is created with probability  $p$ . Similar threshold holds for Social Network Random graphs.

#### References:

-----  
580.1 Thresholds in Random Graphs and k-SAT - [Emmanuel Abbe] -  
<https://pdfs.semanticscholar.org/d862/14a9e02c3749ca92515b592f2fdb38710b45.pdf> -  
Proof of Margulis-Russo Threshold (Lemma 2), Sharp Threshold of k-SAT and  
Friedgut Theorem (Section 6 - Theorem 7)  
580.2 Hunting for Sharp Thresholds - [Ehud Friedgut] -  
<http://www.ma.huji.ac.il/~ehudf/docs/survey.ps> - "...Much like water that  
freezes abruptly as its temperature drops below zero the structure of the random  
graph quickly changes from a primordial soup of small tree-like connected  
components to a graph in which the giant component, one of linear size, captures  
a constant proportion of the vertices...." - Erdos-Renyi edge probability  
threshold in random graphs has close resemblance to Bose-Einstein condensation  
in networks.  
-----

-----  
581. (THEORY) Rice Theorem, Complement Diophantines, Program Analysis, SAT  
Solver and Undecidability of  
Non-trivial properties of Turing Machines - 30 July 2018 - related to 166, 471  
-----

#### Draft updates to:

-----  
1. Decidability of Complement Functions (2011) - Section on Rice Theorem -  
<https://arxiv.org/abs/1106.4102v1>  
-----

Rice Theorem implies every non-trivial property of Turing Machines are  
undecidable. Non-trivial property is defined as below.

For a non-trivial subset  $S$  of recursively enumerable languages which is a non-  
empty proper subset of all recursively enumerable languages  $RE$  (trivial subsets  
are empty-set and  $RE$ ):

581.1 Turing Machine  $M$  which accepts a language in  $S$

581.2 Turing Machine  $M'$  which accepts a language in complement of  $S$  ( $RE \setminus S$ )

Previous proofs of undecidability of complement diophantines by Post  
Correspondence Problem and MRDP theorem are devoted only to the question of  
existence of a complement function. Since all languages in  $RE$  are diophantine,  
languages which are recursively enumerable but not recursive do not have  
accept/reject halting Turing Machine to decide diophantine polynomial  
representation. But Rice Theorem applies in a different setting: Once the set  $S$   
and its complement  $RE \setminus S$  are known, it is undecidable if an arbitrary Turing  
Machine  $M$  accepts a language in  $S$  or  $RE \setminus S$ . In terms of equivalence of  $RE$  and  
Diophantine Equations, it is undecidable if an arbitrary Diophantine Equation  
represents a set in  $S$  or its complement in  $RE \setminus S$  i.e. Given a (complement)  
diophantine  $D$  and 2 complementary sets in  $RE$  (disjoint set cover of  $RE$ ) it is  
undecidable to decide which set in  $S$  or  $RE \setminus S$  are values of diophantine  $D$  which

is the converse direction of existence of complement diophantine.

#### References:

-----  
581.3 Rice Theorem applications in Programming - [http://ai.cs.unibas.ch/\\_files/teaching/fs16/theo/slides/theory-d08.pdf](http://ai.cs.unibas.ch/_files/teaching/fs16/theo/slides/theory-d08.pdf) - Every question on comprehending Programs is undecidable  
581.4 Mortality Problem/Halting Problem Undecidability Proof of Rice Theorem - <http://people.seas.harvard.edu/~cs125/fall14/lec17.pdf>  
581.5 Approximate Program Analysis - <https://cs.au.dk/~amoeller/spa/1%20-%20TIP.pdf> - Exact Program Analysis is undecidable  
581.6 OSSPolice - Identifying Open-Source License Violation and 1-day Security Risk at Large Scale - [Ruian Duan, Ashish Bijlani, Meng Xu, Taesoo Kim, Wenke Lee] - <https://acmccs.github.io/papers/p2169-duanA.pdf>  
581.7 OSSPolice - <https://github.com/osssanitizer/oss police>  
581.8 Bliss - Graph Isomorphism Detector - <http://www.tcs.hut.fi/Software/bliss/>  
581.9 Program Analysis - Analysis of Control Statements - expected and variance of execution times and laplace transforms - Appendix E - Probability and Statistics, Queueing, Reliability and Computer Science - [Kishore Shridharbhai Trivedi, Duke University]  
581.10 Program Analysis - JRF self-study - 2008 Course Notes - [Madhavan Mukund, CMI and Sriram Rajamani, Microsoft Research] - Pointer Analysis - Andersen and Steensgaard algorithms creating points-to graphs - <https://www.cs.cmu.edu/~aldrich/courses/15-8190-13sp/resources/pointer.pdf> - Graph Mining algorithms can be applied to points-to graphs (static)  
581.11 Comparing Call Graphs - [Lohtak] - <https://plg.uwaterloo.ca/~olhotak/pubs/paste07.pdf>  
581.12 Principles of Program Analysis - [Flemming Nielsen-Hanne Riis Nielsen-Chris Hankin] - [https://books.google.co.in/books?id=YseqCAAAQBAJ&printsec=frontcover&dq=nielsen+nielsen+hankin&hl=en&sa=X&ved=0ahUKewiki\\_-gsOXfAHUpeysKHwpmA1gQ6AEIKjAA#v=onepage&q&f=false](https://books.google.co.in/books?id=YseqCAAAQBAJ&printsec=frontcover&dq=nielsen+nielsen+hankin&hl=en&sa=X&ved=0ahUKewiki_-gsOXfAHUpeysKHwpmA1gQ6AEIKjAA#v=onepage&q&f=false) - Interprocedural Analysis - Section 2.5.4 Call Strings as Context and Examples 2.33 and 2.37 - function call stacks or paths in dynamic call graphs can be formalized as unbounded call strings which are defined by concatenation of values of transfer functions for each entry and exit(return) of functions invoked along a path in call graph.  
581.13 Survey of Tools for estimation of Worst Case Execution Time of a program - Fig. 5 Bound Calculation - CFG, Path based, IPET, Transformation rules, Structure based - <http://moss.csc.ncsu.edu/~mueller/ftp/pub/mueller/papers/1257.pdf>  
-----

-----  
1191. (THEORY and FEATURE) PhD Thesis Proposal (2011) - Sections on Program Comprehension - <https://sites.google.com/site/kuja27/PhDThesisProposal.pdf> - Theoretical Answers to some questions in it:  
-----

-----  
For the same reason, Comprehending a Program behaviour is a non-trivial property X which asks "Does the Code do X?". Translating Code to Boolean Formula and applying a SAT Solver (as done in SATURN Program Analyzer) is also a non-trivial property: "Does the Code Satisfy the 3SAT?". Similarly automated debug analytics of code is undecidable too. Software solutions to these are only approximations.

A circular timerwheel hashmap of dynamic sets of timeout clockticks to queues of processes - Survival Index Timeout - has been applied to OS Scheduler in [https://github.com/shrinivaasanka/Grafit/blob/master/course\\_material/NeuronRain/AdvancedComputerScienceAndMachineLearning/AdvancedComputerScienceAndMachineLearning.txt](https://github.com/shrinivaasanka/Grafit/blob/master/course_material/NeuronRain/AdvancedComputerScienceAndMachineLearning/AdvancedComputerScienceAndMachineLearning.txt) which estimates a non-trivial undecidable property approximately - Worst Case Execution Time of a process.

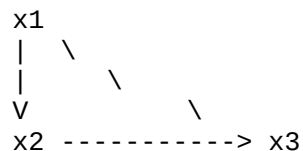
Licensing Violation is a great problem in Open Source Software (advertently or inadvertently) and Software Similarity Detection provides solutions to identify similar source codes. Mostly available Similarity Detectors parse function and



variable names in two source trees and compare similarity but rarely compare the control flow graphs. But Frequent Subgraph Mining of SATURN Control Flow Graphs (static) and Valgrind/Callgrind/KCachegrind Call Graphs (dynamic) in NeuronRain AsFer takes it further solving similarity detection holistically. Third-party Graph Isomorphism Detectors can also be applied on these compiletime and runtime graphs. NeuronRain AsFer also provides indexing of source code and pairwise similarity by Latent Semantic Analysis.

-----  
 582. (THEORY) Cloud, Autonomous Vehicles, EventNet Logical Clock, Relativity, Lorentz Transform, Lamport's Clock  
 - related to 70-86 - 2 August 2018, 3 August 2018  
 -----

Cloud of autonomus vehicles(e.g drones) in a wireless network are mostly not stationary and each node has a velocity. This relative motion between nodes of a cloud fits in the realm of relativistic time dilation. Lorentz Transform for a stationary and a moving observer with respect to a frame of reference is derived as below:



Node x1 in vehicle cloud transmits an information with speed of light  $c$  (which is fixed for all observers by Maxwell Equations as  $3 \times 10^5$  km/s) as electromagnetic signal, which is received by both x2 and x3. x2 is stationary and x3 is moving with velocity  $v$ . Each node has its own clock  $t(x_i)$ . For x2, information from x1 reaches in  $t(x2)*c$  and for x3 information from x1 reaches in  $t(x3)*c$ . By this time x3 has travelled  $t(x3)*v$  distance from x2. This leads to Lorentz transform below:

$$\begin{aligned} (t(x2)*c)^2 + (t(x3)*v)^2 &= (t(x3)*c)^2 \\ (t(x2)*c)^2 &= (t(x3)*c)^2 - (t(x3)*v)^2 \\ \Rightarrow (t(x2)*c)^2 &= t(x3)^2*(c^2 - v^2) \\ \Rightarrow t(x2)^2 &= t(x3)^2*(1 - (v/c)^2) \\ \Rightarrow t(x2) &= t(x3)*\sqrt{1 - (v/c)^2} \end{aligned}$$

i.e clock of vehicle x3 slows down compared to x2's clock as x3

moves faster.

Though autonomus vehicles could have speed less than light, if event timestamps are in nanoseconds (C++ provides nanosecond resolution in `std::chrono::duration_cast<std::chrono::nanoseconds>`), relativistic time dilation could be non-trivial. Lamport's Logical Clock has the causation protocol (s,r):

sender(s) - transmits timestamp to receiver  
 receiver(r) - finds maximum of local timestamp and received timestamp and increments by 1

which is valid only for stationary nodes in cloud and has to be augmented by previous relativistic time dilation transform for moving nodes in cloud.

Previous time dilation is because of Special Relativity where as General Relativity predicts clocks in objects closer to a heavier mass tick slower. This causes onboard clocks in GPS satellites to tick faster than those on earth slowed down by its mass and corrections are applied. Drones using GPS navigation are directly affected by this. EventNet is a partial ordered directed acyclic graph (infinite) and causality in EventNet Logical Clock (for wireless clouds) is defined by light cone i.e an expanding circular region travelled by light plotted against arrow of time - two events P and Q are causally related if Q is in past lightcone or future lightcone of P and viceversa.

References:

-----

582.1 On the Relativistic Structure of Logical Time in Distributed Systems - [https://www.vs.inf.ethz.ch/publ/papers/relativistic\\_time.pdf](https://www.vs.inf.ethz.ch/publ/papers/relativistic_time.pdf) - Section 5 - Minkowski Spacetime of (n-1) space and 1 time dimensions and Light Cone Causality - Time is a partial order and not linear - Causal ordering between two spacetime points U and V

582.2 Atomic Clocks, Satellite GPS and Special/General Relativity - <http://www.astronomy.ohio-state.edu/~pogge/Ast162/Unit5/gps.html>

582.3 Feynman's Lectures on Physics - [Richard Feynman] - Volume 1 - Chapter 15 - Lorentz Transformation and Special Relativity

582.4 CAP Theorem, Spanner Database, TrueTime clock - [Breuer] - <https://storage.googleapis.com/pub-tools-public-publication-data/pdf/45855.pdf> - Spanner achieves almost all three (Consistency, Availability, Partition Tolerance) - "...The short answer is "no" technically, but "yes" in effect and its users can and do assume CA. The purist answer is "no" because partitions can happen and in fact have happened at Google, and during (some) partitions, Spanner chooses C and forfeits A. It is technically a CP system. We explore the impact of partitions below..."

-----

583. (FEATURE) \*) Sentiment Analyzer - Empath word embeddings - multipolar sentiment analysis  
\*) Factorization - JSON - 6 August 2018

-----

-----

1. SentimentAnalyzer.py has been changed to invoke Empath lexical analyzer for various signals (sentiments) in Markov Random Fields Belief Propagation Sentiment Analysis function.
2. Empath invocation computes objective maximum score from the dictionary returned by lexical analyzer for each vertex in a clique
3. RecursiveLambdaFunctionGrowth.py invokes Markov Random Fields Belief Propagation Sentiment Analyzer function for the text graph and returns the sentiment score in `intrinsic_merit_dict["empath_sentiment"]`
4. Logs for this have been committed to `testlogs/RecursiveLambdaFunctionGrowth.log.Empath_BeliefPropagation_RGO_M`

-----

5. JSON for a sample factorization execution has also been committed

References:

-----

583.1. Analyzing Right Wing YouTube Channels - [Raphael Ottoni, Evandro Cunha, Gabriel Magno, Pedro Bernardina, Wagner Meira Jr., Virgilio Almeida, Berkman Klein] - <https://arxiv.org/pdf/1804.04096.pdf>

583.2. Empath - <http://empath.stanford.edu/>

-----

584. (FEATURE) Latent Semantic Analysis/Indexing (LSA/LSI) Implementation - 7 August 2018

-----

-----

1. Latent Semantic Analysis/Indexing has been implemented as python class in `LatentSemanticAnalysis.py`
2. This reads list of filenames from `LatentSemanticAnalysis.txt` and converts into term-document matrix by invoking Pandas DataFrame and ScikitLearn Vector libraries
3. Pandas DataFrame is converted to NumPy array and Singular Value Decomposition (SVD) is done on term-document matrix to arrive at  $UEV^T$  decomposition.
4. Documents are represented by U and terms by V. E is matrix of singular values.

5. Cosine similarity of pairs of documents in U is computed for all pairs of documents and printed in log:  
testlogs/LatentSemanticAnalysis.log.7August2018  
6. This class is multipurpose and can be used for variety of applications including Program Analysis.  
7. Corpus for this execution is list of python files and similarity between python code is evidenced by cosine similarity

-----  
585. (FEATURE) SAT Solver - CVXOPT LAPACK gels() least squares - 9 August 2018  
-----

-----  
1. SAT Solver has been changed to invoke LAPACK gels() least squares from CVXOPT  
2. For this NumPy array is cast to CVXOPT real matrix object  
3. CVXOPT gels() works only if the matrix is full-rank (number of linearly independent rows is equal to number of rows and similarly for columns) and throws ArithmeticError exception otherwise  
4. Approximately 1040 random 3SAT instances for 10 variables - 10 clauses have been executed and MAXSAT approximation ratio converges to ~97%. For larger values of variables, finding full rank matrix needs lot of iterations but still for 20 variables - 20 clauses similar convergence to ~96% was observed.  
5. Support for CVXOPT is crucial because of wide range of functionalities (including Convex programs, SDPs) present in CVXOPT  
6. logs for this have been committed to  
testlogs/CNFSATSolver.10variablesAlpha1.0.CVXOPT.log.9August2018

-----  
586. (FEATURE) Latent Semantic Analysis - Low Rank Approximation - 9 August 2018  
-----

-----  
1. New function for computing low rank approximation of term-document matrix has been included  
2. For SVD of  $td = UEV^T$ , few least singular values (square root of eigen values of  $td$ ) are set to zero (hardcoded to 10, because matrix\_rank() computation is quite slow for large term-document matrices)  
3. Low rank approximation of  $td$  is computed from matrix product of  $U * \text{rankreduced}(E) * V^T$   
4. logs for this have been committed to  
testlogs/LatentSemanticAnalysis.log.9August2018

-----  
587. (THEORY) ImageNet, EventNet and Recursive Lambda Function Growth and Merit of Large Scale Visuals  
- ImageGraph Algorithm - related to 249,410 - 10 August 2018  
-----

-----  
ImageNet is the pictorial WordNet and has received lot of attention in Computer Vision and Large Scale Visual Recognition (LSVR) from Images/Videos. Deciding merit of a Video intrinsically with no reputation rankings has been an open problem (in Fame versus Merit). Recursive Lambda Function Growth algorithm which generalizes Recursive Gloss Overlap for text-graph creation has been so far restricted only to text analysis. ImageNet has been applied for Object recognition/tracking based on Convolution Networks in Video datasets (e.g VID). This section describes an algorithm to map a video to ImageNet graph of visuals

and infer merit from this  
image-graph:

-----  
ImageNet-EventNet ImageGraph Algorithm:  
-----

- (\*) Every Video is set of frames of Images continuously played out in time.
- (\*) Some image frames in the past causally relate to some frames in future in the Video.
- (\*) For each image frame:
  - {
  - (\*) Each frame is recognized by a standard LSVR algorithm (e.g ConvNet) and objects are annotated by bounding boxes.
  - (\*) Each bounded recognized object in a frame is lookedup in ImageNet and an ImageGraph is constructed per frame by computing ImageNet path between every pair of recognized objects and unifying the paths to create an ImageGraph for the frame, similar to WordNet Path s-t connectivity algorithm mentioned earlier for TextGraphs.
  - (\*) Merit of Video in human judgement is more than mere connectedness of information conveyed - it also depends on visual appeal e.g object attributes like Angle, Resolution, Lighting, Texture, Aesthetics etc., Edge weights in frame ImageGraph has to reckon these factors.
  - }
  - (\*) Previous loop creates a huge set of ImageGraphs for frames in Video.
  - (\*) Following EventNet convention, every frame is an Event vertex of set of actors (partakers) in EventNet. Causation between two Event ImageGraphs for chronologically ordered frames F1 and F2 (E(F1) and E(F2)) is determined by causal similarity of the graphs E(F1) and E(F2) i.e if there exist ImageNet paths from vertices of E(F1) to vertices of E(F2) then F1 "causes" F2.
  - (\*) Example: If frame F1 has recognized visual ImageGraph of a birthday party and F2 has recognized visual ImageGraph of cake-cutting, and if there exists an ImageNet path "birthday - celebration - cake - cutting " ,then E(F1) causes E(F2).
  - (\*) Previous algorithm converts a Video into a Graph of Graphs (or) Tensor which is a matrix having matrix entries. Size of this video tensor is  $O(\text{number\_of\_frames})$ .
  - (\*) If Audio is also annotated by a Speech Recognition algorithm to text, it catalyses in deciphering causation amongst sets of frames (by creating AudioGraph per set of frames from WordNet and connecting AudioGraphs by WordNet distances and this creates an audio tensor).
  - (\*) Once these tensors for video and audio are created, merit is computed by how causally connected these tensors are from standard Graph complexity measures already defined for TextGraphs.

-----  
ImageGraph Merit as Tensor Products:  
-----

- (\*) Two causally related (having ImageNet path between their vertices) ImageGraphs E(F1) and E(F2) for frames F1 and F2 can be multiplied by Tensor Product which is a cartesian/kronecker product of two adjacency matrices of each ImageGraph per frame - resulting tensor product graph has:
  - (\*) ImageNet vertex gh for g in  $V(E(F1))$  and h in  $V(E(F2))$
  - (\*) ImageNet edge (a,b)-(c,d) iff edge (a,c) in E(F1) and (b,d) in E(F2)
- (\*) the tensor product for two frame ImageGraphs in the Video (which are connected causally by ImageNet) as  $E(F1) * E(F2)$  yields a semantic similarity measure between successive chronologically causative frames. e.g edges (birthday, congregation) in E(F1) and (cake, serving) in E(F2) are mapped to edge (birthday-cake, congregation-serving) in the product graph.
- (\*) EventNet Causality of ImageGraphs in a Video is represented by an adjacency matrix defined as:
  - (\*) EventNet matrix EN for a video of N image frames has N rows and N columns
  - (\*) entry  $EN(i,j)$  = tensor product of Event ImageGraph for frame i

and Event ImageGraph for frame j if there is an ImageNet path between ImageGraphs for Frame i and j, else, 0

(\*) This EventNet adjacency matrix represents a graph of causality between frames in the video.

(\*) Weight of every edge (a,b)-(c,d) (or) (ab)-(cd) in tensor product of ImageGraphs for frames F1 and F2,  $E(F1)*E(F2)$  (i.e (a,c) in  $E(F1)$  and (b,d) in  $E(F2)$ ) =  $1/(d(a,b)*d(c,d))$  for ImageNet distance d between two vertices in different ImageGraphs  $E(F1)$  and  $E(F2)$ .

(\*) Previous Inverse Weight implies an edge has more weight in Tensor Product graph if distance between endpoints of edges in two different ImageGraphs are close enough in ImageNet. When either of the endpoints in two different ImageGraphs are not related by ImageNet, d is infinity and respective adjacency matrix entry for tensor product graph is 0.

(\*) Applicability of EventNet to Large Scale Visual Recognition is quite unusual. Necessity of tensor product entries as edge weights in Video EventNet adjacency matrix, than simple scalar weights is because of necessity of capturing distance between every pair of vertices among 2 causally related ImageGraphs - one vertex is in  $E(F1)$  and other in  $E(F2)$

-----  
Gist and Intuition of previous algorithm  
-----

Every Video (set of frames) can be mapped to 1) a causation graph of image frame event vertices and 2) each frame event itself is a subgraph of ImageNet - depth 2 graph-of-graphs creation. Causality between frame events is determined by ImageNet distances between vertices in ImageGraphs of the frames represented as tensor product.

References:

- 
- 587.1 ImageNet Large Scale Visual Recognition Challenge - [Olga Russakovsky\* · Jia Deng\* · Hao Su · Jonathan Krause · Sanjeev Satheesh · Sean Ma · Zhiheng Huang · Andrej Karpathy · Aditya Khosla · Michael Bernstein · Alexander C. Berg · Li Fei-Fei] - <https://arxiv.org/pdf/1409.0575.pdf>
- 587.2 Zig-Zag Product - [Reingold, O.; Vadhan, S.; Wigderson, A. (2000)], "Entropy waves, the zig-zag graph product, and new constant-degree expanders and extractors", Proc. 41st IEEE Symposium on Foundations of Computer Science (FOCS), pp. 3-13 - <https://arxiv.org/abs/math/0406038> - Graph product of large graph G and small graph H in which each vertex in G is replaced by copy of H. In ImageGraph EventNet Tensor above, each vertex in EventNet G is replaced by ImageGraph of Frame Event.
- 587.3 Tensor Product of Graphs - [https://en.wikipedia.org/wiki/Tensor\\_product\\_of\\_graphs](https://en.wikipedia.org/wiki/Tensor_product_of_graphs)
- 587.4 ImageNet publications - <http://image-net.org/about-publication>
- 587.5 ImageNet VID dataset - <https://www.kaggle.com/c/imagenet-object-detection-from-video-challenge>
- 

588. (THEORY) Analyzing Youtube Videos, Ranking Movies and ImageGraph Tensor Products Algorithm for

Merit of Large Scale Visuals - 14 August 2018, 15 August 2018 - related to 587

-----

Analyzing Videos in public domain and Ranking Movies based on merit as opposed to usual human review/reputation based rankings is one of the hardest Large Scale Visual Recognition Challenge. Algorithm for Mapping Video or Movie to EventNet Graph of frame ImageGraphs and representing EventNet edge weights as Tensor Products has been described earlier. This algorithm just elicits the graph complexity of visual information contained in the Video overlooking sentimental polarities and psychological impact. Language Inquiry and Word Count (LIWC) is a dictionary of human voted words categorized by their human psychological emotions. Classifying the objects in Video or Movie of human viewership therefore demands emotional categories of

words. Following changes are made to previous algorithm for quantifying emotions:

(\*) Emotions are mostly verbal and Speech Recognition annotated AudioGraph of Video or Movie Dialogue Transcript are created per frame/scene by union of WordNet paths for all pairs of words in Transcript per frame/scene

(\*) Word Vertices of Each ImageGraph and AudioGraph per frame in Video or Movie are also annotated by the psychological polarity of the Word Vertex in LIWC

(\*) Weight of every edge (a,b)-(c,d) (or) (ab)-(cd) in tensor product of AudioGraphs and ImageGraphs for frames F1 and F2,  $E(F1)*E(F2)$  (i.e (a,c) in  $E(F1)$  and (b,d) in  $E(F2)$ ) is the ordered pair of inverse distance similarity and majority LIWC polarity =  $(1/(\text{dist}(a,b)*\text{dist}(c,d)), \text{majority\_LIWC\_polarity\_of}(a,b,c,d))$  for ImageNet distance dist between two vertices in different ImageGraphs or AudioGraphs  $E(F1)$  and  $E(F2)$ .

(\*) Merit of the Video or Movie in toto is the ordered pair = (Tensor Rank of the AudioGraph and ImageGraph EventNet Tensors, Sorted list of top percentile LIWC polarity of edge weights in ImageGraph and AudioGraph Tensor Products)

(\*) Computing Tensor Rank is NP-Complete for Finite Fields and NP-hard for Rationals.

(\*) Previous Merit captures both the complexity and emotional content of the Large Scale Visual.

(\*) Tensor Rank is the generalization of Matrix Rank (number of linearly independent rows) = Dimension of Tensor = Minimum number of Tensors  $T_i$  to linearly express Tensor  $T = \text{Sigma}(T_i)$

(\*) Most algorithms for Video analysis are caption and statistics based whereas the previous algorithm is a graph theoretic formulation of a machine learning computer vision problem.

(\*) There are recent other alternatives to LIWC e.g Empath.

(\*) Intuition for choice of Tensor Rank as Merit of Large Scale Visuals:

(\*) Tensor Rank of EventNet is the number of Independent n-rows/n-columns of Events in the Video

where n-columns and n-rows are hypercubes considering Tensor as multidimensional array

(\*) Increased Tensor Rank implies the Events in the Video are more disconnected/independent

while decreased Tensor Rank implies the Events are more connected/dependent

(\*) Therefore Video of Low Tensor Rank is heavily connected.

(\*) Though applied to Video EventNet, tensor rank has wider philosophical ramifications because EventNet formalizes flow of time logically and has weird implication - EventNet Logical Time Tensor can be written as linear sum of independent tensors and therefore Time tensor essentially is a linear function of finer time subdivision tensors.

(\*) An important difference between Videos and Theoretical EventNet is: Event vertices and participants/actors within an Event vertex can be created in parallel independent of other event vertices in theoretical eventnet (and causality edges between event vertices could be established later in parallel too) while a video (youtube, movie etc.,) is always a serialized set of frames (events) though it could depict concurrent events - video is non-parallel unless more than one video source is simultaneously streamed. EventNet can be formally defined by some Process calculi.

(\*) Usually Like-ing Versus Merit of Videos has the following conflict: Videos or movies which induce viewers to repetitively watch them, garner huge popular support which is not necessarily a reflection of their merit. Music/Audio has an equivalent of this phenomenon known as "Earworm"

References:

-----  
588.1 Language Inquiry and Word Count - LIWC - [http://liwc.wpengine.com/wp-content/uploads/2015/11/LIWC2015\\_LanguageManual.pdf](http://liwc.wpengine.com/wp-content/uploads/2015/11/LIWC2015_LanguageManual.pdf)

588.2 Exploring Tensor Rank - <http://www.its.caltech.edu/~matilde/WeitzMa10Abstract.pdf>

588.3 Tensor Rank is NP-Complete - [Hastad] - <http://www.nada.kth.se/~johanh/tensorrank.pdf>

588.4 Computational Complexity of Tensor Problems -  
<https://www.stat.uchicago.edu/~lekheng/meetings/agtd/hillar13.pdf>  
588.5 Tensor Rank as Measure of its Complexity -  
[http://web.math.unifi.it/users/ottavian/colloquium\\_kias.pdf](http://web.math.unifi.it/users/ottavian/colloquium_kias.pdf)  
588.6 Process Calculi - [https://en.wikipedia.org/wiki/Process\\_calculus](https://en.wikipedia.org/wiki/Process_calculus)  
588.7 Actor Model and Process Calculi -  
[https://en.wikipedia.org/wiki/Actor\\_model\\_and\\_process\\_calculi\\_history](https://en.wikipedia.org/wiki/Actor_model_and_process_calculi_history)

-----  
589. (THEORY and FEATURE) SAT Solver - CVXOPT - gesv() least squares - 16 August 2018 - related to 424  
-----

-----  
1. CNFSATSolver.py has been changed to import gesv, getsr, sysv functions for least squares in cvxopt  
2. Each of these were tried for 10 variables and 10 clauses combinations and gesv() has the highest accuracy observed so far (~99% to 100%) in any of the least squares algorithms.  
3. logs for 500 random 3SAT instances have been committed to testlogs/CNFSATSolver.10variablesAlpha1.0.CVXOPT.log.16August2018  
4. Caveat: Though the number of variables/clauses are less which could cause repetitive choice of same 3SAT similar randomness did not attain 99% accuracy for other least squares algorithms earlier for similar variable-clause combination.  
5. gesv() also throws ArithmeticError for non full-rank matrices and logs for gesv() are filtered-out random 3SAT instances which are full rank. This leaves some random 3SAT instances unsolved.  
6. try...except has been changed to print exception stacktrace for ArithmeticError

CVXOPT gesv() has breached the accuracy barrier to large extent from 95-97% to > 99% coinciding with Random Matrix Analysis for 3SAT. But problem is with high number of variables and clauses which do not churn out full rank matrices for 3SAT and lot of instances are left out. So the average is only for full-rank random 3SATs. If this implies  $P=NP$ , Polynomial Hierarchy PH collapses to P implying existence of PH-complete problems.

-----  
590. (FEATURE) Program Analysis + Software Analytics - Valgrind/Callgrind/KCachegrind Call Graph DOT file creation and its Cyclomatic Complexity - 18 August 2018  
-----

-----  
1. Valgrind/Callgrind are the standard tools for call graph profiling and memory leak check of userspace code.  
2. Cyclomatic Complexity is already computed for DOT files created by SATURN Program Analyzer for Linux Kernel by VIRGO SATURN Program Analysis Driver. For userspace call graph DOT files are created by Kcachegrind complementing SATURN in userspace. ([https://github.com/shrinivaasanka/virgo64-linux-github-code/blob/master/virgo-docs/VIRGO\\_SATURN\\_Program\\_Analysis\\_Integration.txt](https://github.com/shrinivaasanka/virgo64-linux-github-code/blob/master/virgo-docs/VIRGO_SATURN_Program_Analysis_Integration.txt))  
3. Valgrind for an example Spark program (Factorization) is invoked as:  
valgrind --tool=callgrind -v --dump-every-bb=10000000 /media/Ubuntu2/spark-2.3.1-bin-hadoop2.7/bin/spark-submit  
../DiscreteHyperbolicFactorizationUpperbound\_TileSearch\_Optimized.py 819289  
4. callgrind.out files are written to:  
callgrind.DiscreteHyperbolicFactorization\_TileSearch\_Optimized.out.14531  
suffixed by process id.  
5. callgrind.out file is viewed by kcachegrind (requires KDE) and call graph is exported as DOT and image files in:  
5.1  
kcachegrind\_callgraph\_DiscreteHyperbolicFactorization\_TileSearch\_Optimized.png

## 5.2

kcachegrind\_callgraph\_DiscreteHyperbolicFactorization\_TileSearch\_Optimized.dot  
6. CyclomaticComplexitySparkMapReducer.py has been updated for doing Spark wordcount of both SATURN and Valgrind/Callgrind/KCachegrind DOT Control Flow Graph / call graph files and print Cyclomatic Complexity.  
7. This leverages on already implemented Convolution Net Deep Learning of Graphic Performance Patterns by Perf and FlameGraph.  
8. Essentially Program Behaviour Analysis in userspace+kernelspace reduces to Graph Mining of these DOT graphs.

-----  
591. (FEATURE) Program Analysis + Software Analytics - Graph Mining of Call graph and CFG DOT files  
- 20 August 2018  
-----

-----  
1.GraphMining\_GSpan.py has been changed to check for an error condition of number of vertices per edge  
2.New function graph\_mining() has been included in software\_analytics/CyclomaticComplexitySparkMapReducer.py for invocation of Graph Mining GSpan implementation to print frequent subgraph patterns in SATURN CFG and Valgrind/Callgrind/KCachegrind graph DOT files  
3.logs for this have been committed to software\_analytics/testlogs/CyclomaticComplexitySparkMapReducer.log.GraphMining. 20August2018  
4.This formally unifies the two ends: Program Analysis and Software Analytics (Deep Learning and Graph Mining)  
5.Frequent Subgraphs in DOT files of Call graph and Control Flow Graph(CFG) extract static patterns in underlying software running on a system while the FlameGraph/Perf Graphics DeepLearning Analytics extract runtime patterns  
6.Theoretically, if SAT for a Program is created by SATURN, Least Square SAT Solver in NeuronRain could be model checker for the Program  
-----

-----  
592. (THEORY and FEATURE) SAT Solver - CVXOPT - L1-norm Regularized Least Squares Quadratic Program l1regls() and gesv() - 22 August 2018  
-----

-----  
1.This commit includes a special SAT Solver in CVXOPT documentation example l1regls() [<https://cvxopt.org/examples/mlbook/l1regls.html>] which solves the L1-norm regularized Least Squares Quadratic Program(QP):

$\text{minimize error } |AX-B|^2 + L1\text{Norm}(|X|)$

which is the most accurate Least Square Solution. Geometric intuition and preference of L1 norm for least squares is depicted in Q&A:  
<https://www.quora.com/Why-is-L1-regularization-better-than-L2-regularization-provided-that-all-Norms-are-equivalent>

2. In the context of SAT, previous minimization implies, the polynomial approximating the binary assignment heaviside step function is as close as possible to satisfying each clause (because B is unit vector of 1s for each clause) and sum of real fractional assignments (real parity) is minimum. This can be visualized as a sinusoidal string pulled on both directions and string settles at an equilibrium curvature which minimizes the QP above.

3. Prerequisite l1regls from [https://cvxopt.org/\\_downloads/l1regls.py](https://cvxopt.org/_downloads/l1regls.py) has to be downloaded and PYTHONPATH must be set to it.

4. CNFSATSolver.py has been refactored with if clauses for the least square



algorithm invoked. For equal variable-clause "lapack()" invokes gesv() and for unequal variable-clause gels() is invoked

5. Few 1000 variables \* 1000 clauses random 3SAT instances have been solved for l1regls() with MAXSAT approximation ratio 96%-97%

6. CVXOPT gesv() has been tested again for 10 variables \* 10 clauses and similar MAXSAT approximation ratio of 99%-100% has been observed. gesv() throws ArithmeticError if A is singular (not invertible, determinant 0) while gels() throws ArithmeticError if A is not full-rank - gesv() is exact solver and gels() is least square solver. (NumPy solve() internally uses lapack gesv). So the logs filter out singular random 3SAT matrices.

References:

-----  
592.1 Advanced Engineering Mathematics - Tenth Edition - [Erwin Kreyszig] - <https://www.safaribooksonline.com/library/view/advanced-engineering-mathematics/9780470458365/Chapter006.html#ch006-sec003> - Many Unit Heavyside step function and Laplace Transforms. Randomized Rounding of real assignments creates a many unit Heavyside step function.  
-----

-----  
593. (FEATURE) Audio/Music Pattern Mining - Audio to Time Series - 24 August 2018  
-----

-----  
1. Similar to image\_pattern\_mining/ImageToBitMatrix.py, new file AudioToBitMatrix.py has been committed to repository for converting an audio file (e.g MP3, .wav) to time series array  
2. AudioToBitMatrix.py imports librosa (audioread) Python library which returns waveform time series floating point array and sampling rate.  
3. audio-to-bitmatrix function has optional arguments to specify if the time series is binary or float (defaults to float) and duration of the timeseries (defaults to full)  
4. Binary time series invokes bin() on each time series point  
5. An example audio MP3 file has been converted to time series and logs have been committed to testlogs/AudioToBitMatrix.log.24August2018  
-----

-----  
594. (THEORY) Horn3SAT and Least Squares Approximate SAT Solver - 7 September 2018  
-----

Horn3SAT is the special case of 3SAT in which each clause is Horn clause having single positive literal known as Head and all other literals are negative. Horn3SAT is P-complete and is solved by unit propagation algorithm in polynomial time. Unit propagation algorithm has 2 repetitive phases: \*) Remove all unit clauses having single literal \*) Remove negated literal in all clauses. Horn3SAT can be solved by Least Squares Approximate Solver by creating random Horn3SAT matrix similar to random 3SAT matrix. This random Horn3SAT matrix is very sparse and has only one 1 per row for head literal and all other columns are 0s. Since Horn3SAT is P-complete, there exists a deterministic (and possibly parallel because P-completeness implies NC) algorithm to solve it one of which is unit propagation. Solution to this Horn3SAT random matrix Linear system of equations for equal variable-clause is deterministic polynomial time (gesv() solver can be applied for non-singular instances) while unequal variable-clauses are least squares solvable by algorithms - lsqr/gels/lsqr etc., Cloud algorithms like lsrn can solve Horn3SAT random matrix instance in NC if number of parallel processors are logdepth and polynomial size.

References:

-----  
594.1 Unit Propagation Horn3SAT Solver -  
[https://en.wikipedia.org/wiki/Unit\\_propagation](https://en.wikipedia.org/wiki/Unit_propagation)

594.2 Binary Least Squares and SAT Solver -  
[http://www.mirlab.org/conference\\_papers/International\\_Conference/ICASSP%202011/pdfs/0003780.pdf](http://www.mirlab.org/conference_papers/International_Conference/ICASSP%202011/pdfs/0003780.pdf) - Binary Least Squares Solution to  $AX=B$  for boolean  $X$  is NP-Hard - Semidefinite Relaxation of Least Squares - Gaussian Randomization for obtaining binary values for  $X$  from feasible Semidefinite solution - Section 3 - Page 3782

-----  
595. (FEATURE) Music/Audio Pattern Mining - Histogram and Probability Distribution Function extraction (PDF)  
- 7 September 2018  
-----

-----  
1. New function `audio_features()` has been added for analyzing features in audio/music signal  
2. Considering audio as time series there are 2 standard ways to extract probability distribution from time series: 1) Histogram 2) Bandt and Pompe - [Andres M. Kowalski, Maria Teresa Martin, Angelo Plastino and George Judge] - [www.mdpi.com/1099-4300/14/10/1829/pdf](http://www.mdpi.com/1099-4300/14/10/1829/pdf)  
3. `audio_features()` invokes `histogram()` function and extracts PDF from NumPy by setting `density=True`  
4. Comparing two music signals amounts to finding Jensen-Shannon Divergence of two probability distributions  
5. Histogram for an example audio signal is printed in `testlogs/AudioToBitMatrix.log`. 7 September 2018  
-----

-----  
596. (FEATURE) Music/Audio Pattern Mining - Jensen-Shannon Divergence of Probability Distributions of two audio signals - 8 September 2018  
-----

-----  
1. `audio_features()` in `AudioToBitMatrix.py` returns the probability histogram and bins in a tuple  
2. `JensenShannonDivergence.py` has been rewritten to compute normalization inline (`normalize()` function has been removed), import audio functions from `AudioToBitMatrix.py` and compute probability histograms for two different audio files.  
3. logs for Jensen-Shannon Divergence distance between two audio files have been committed to `testlogs/JensenShannonDivergence.log`. 8 September 2018 (For same audio, distance is zero)  
-----

-----  
597. (THEORY) Computational Geometric Sequential Factorization Optimization by Wavelet Trees, Tile Summation Ray Shooting Queries and Error Probability - related to 506, 575 - 14 September 2018, 15 September 2018, 16 September 2018  
-----

-----  
Sequential Factorization Optimization by Tile Summation Ray Shooting Queries and searching the epsilon radius in the vicinity of approximate factors described earlier have the following error probability in failing to find a factor:

If epsilon radius is  $O((\log N)^{1/l})$  around an approximate factor, probability of

not finding a factor =  
distance between periphery of 2 epsilon radius circles surrounding an  
approximate factor

$$\frac{N/k\log\log N}{N/k\log\log N - 2q(\log N)^l}$$

$$= \frac{N/k\log\log N - 2q(\log N)^l}{N/k\log\log N}$$

For low error probability, numerator tends to 0:

$$N/k\log\log N = 2q(\log N)^l$$

=>  $l = \log(N/2kq\log\log N)/\log\log N = O(\log(N/\log\log N)/\log\log N)$  which is exponential.

For constant  $l$ , probability of error is non-trivial. This epsilon radius vicinity search applies to other ray shooting algorithms too (by replacing Hardy-Ramanujan estimate with the corresponding ray shooting algorithm and equating to tile summation). Advantage of tile summation is it always results in an integral value and coincides with some factor point on xy-plane.

598. (THEORY) Hastad Switching Lemma, Least Squares Approximate SAT Solver, Random Restrictions, CNFSAT to DNFSAT - 18 September 2018

Least Squares Approximation by Random 3SAT matrix analysis previously has so far solved almost 99%-100% clauses (observed) excluding singular random 3SAT matrix instances. This implies binary assignments to some variables are not right by randomized rounding of real assignments, falsifying some of the clauses. Hastad Switching Lemma implies setting values to alpha fraction of variables (restriction) in a CNF(or DNF) formula and evaluating the restricted formula by switching it to DNF(or CNF) and computing its decision tree abides by the inequality:

$$\Pr[DTdepth(f/\alpha) > d] \leq (10 \cdot \alpha \cdot w)^d$$

for  $s = \sigma \cdot n \leq n/5$ ,  $d \geq 0$ ,  $w$  is formula width. Least Squares Approximation thus can be construed as restriction generator by following algorithm:

- (\*) Solve a random 3SAT matrix by Least Squares (e.g gesv())
- (\*) Variables in all satisfied clauses in least squares solution form a random restriction - set variables
- (\*) Variables in all unsatisfied clauses in least squares solution (excluding variables in satisfied clauses) are made unset variables
- (\*) Switch the restricted CNF3SAT to a DNF3SAT in unset variables
- (\*) DNF3SAT is solvable in polynomial time (linear)

References:

598.1 Hastad Switching Lemma - [Johan Hastad] - PhD Thesis - Chapter 4 - Lemma 4.1 - "Let  $G$  be an AND of ORs all of size  $\leq t$  and  $\rho$  a random restriction from  $R(p)$ . Then the probability that  $G/\rho$  cannot be written as an OR of ANDs all of size  $\leq s$  is bounded by  $\alpha^s$  where  $\alpha$  is the unique positive root to the equation:

$(1 + 4p/(1+p) \cdot (1/\alpha))^t = (1 + 2p/(1+p) \cdot (1/\alpha))^t + 1$  and Stronger Switching Lemma - Lemma 4.2 - "Let  $G = \bigwedge G_i$  where  $G_i$  are ORs of fanin  $\leq t$ . Let  $F$  be an arbitrary function and  $p$ , a random restriction in  $R(p)$ . Then  $\Pr[\min(G) \geq s/Fp = 1] \leq (\alpha)^s$ " - <https://www.nada.kth.se/~johanh/thesis.pdf>

598.2 Hastad Switching Lemma - [Vikraman Arvind] - JRF Course Notes - Complexity 2 - August-December 2010 - Institute of Mathematical Sciences, Chennai.

598.3 Randomized Rounding of Set Cover - [CR Subramanian] - JRF Course Notes - Randomized Algorithms - August-December 2010 - Institute of Mathematical Sciences, Chennai. Least Squares SAT Solver rounds real assignment by midpoint of max-min values in assignment vector. Alternatively, each variable  $x^*$  in real assignment vector can be rounded with respect to maximum value  $f$  in real assignment as:  $x = 0$  if  $x^* < 1/f$  else  $x = 1$ .

598.4 Hastad Switching Lemma - Course Notes - [Jonathan Katz] - Corollary 3 - "Let  $f: \{0,1\}^n \rightarrow \{0,1\}$  be computed by a DNF formula (resp. CNF formula) of width at most  $w$ . Let  $\alpha$  be a random  $s$ -restriction with  $s \leq n/5$ . Then  $f/\alpha$  can be computed by a CNF formula (resp. DNF formula) of width  $w$  except with probability at most  $(10sw/n)^w \Rightarrow \Pr[\text{DT}(f/\alpha) \geq s] < (10sw/n)^w$  (or)  $\Pr[\text{DTdepth}(f/\alpha) > d] \leq (10 \cdot \sigma \cdot w)^d$  for  $s = \sigma \cdot n \leq n/5$  and  $d \geq 0$ ." - <http://www.cs.umd.edu/~jkatz/complexity/f05/switching-lemma.pdf>

598.5 Switching Lemma - [https://en.wikipedia.org/wiki/Switching\\_lemma](https://en.wikipedia.org/wiki/Switching_lemma) - "...The switching lemma says that depth-2 circuits in which some fraction of the variables have been set randomly depend with high probability only on very few variables after the restriction. The name of the switching lemma stems from the following observation: Take an arbitrary formula in conjunctive normal form, which is in particular a depth-2 circuit. Now the switching lemma guarantees that after setting some variables randomly, we end up with a Boolean function that depends only on few variables, i.e., it can be computed by a decision tree of some small depth  $d$ . This allows us to write the restricted function as a small formula in disjunctive normal form. A formula in conjunctive normal form hit by a random restriction of the variables can therefore be "switched" to a small formula in disjunctive normal form...."

598.6 Cutting Planes - Gomory Cut - [https://ocw.mit.edu/courses/sloan-school-of-management/15-053-optimization-methods-in-management-science-spring-2013/tutorials/MIT15\\_053S13\\_tut11.pdf](https://ocw.mit.edu/courses/sloan-school-of-management/15-053-optimization-methods-in-management-science-spring-2013/tutorials/MIT15_053S13_tut11.pdf) - for Integer Linear Programs.

598.7 Chapter 14 - Cutting planes - Combinatorial Optimization - [Stiglitz-Papadimitriou]

598.8 Randomized Rounding Survey - [Aravind Srinivasan] - <http://homepage.divms.uiowa.edu/~sriram/196/fall08/rr-final.pdf> -  $\Pr[\text{Clause is satisfied}] > 0.75 \cdot (\text{sum of relaxed fractional assignments})$  - "...One intuitive justification for this is that if  $x^*(j)$  were "high", i.e., close to 1, it may be taken as an indication by the LP that it is better to set variable  $j$  to True; similarly for the case where  $x(j)$  is close to 0. ..."

598.9 Randomized Rounding - Randomized Algorithms - [Motwani-Raghavan] - Pages 81,96,105,106 - optimized wiring nets.

-----  
 599. (FEATURE) Streaming Algorithms - Approximate Counting and Distinct Elements - 21 September 2018  
 -----

599.1. Two new python implementations for Streaming Approximate Counting and Distinct Elements in a random subset have been committed to repository

599.2. These are implementations of two algorithms from JRF presentation notes (on 28-29/10/2010) for course - Topics in Datamining - during August-December 2010, Chennai Mathematical Institute, Chennai.

599.3. They have been implemented because of their importance for processing Streaming Datasets e.g Spark Streaming

References:

-----  
 599.4. Approximate Counting Algorithm - [Morris-Flajolet] - <http://algo.inria.fr/flajolet/Publications/Slides/aofa07.pdf>  
 599.5. Distinct Elements algorithm - [BarYossef] - <https://slideplayer.com/slide/4943252/>

-----  
600. (FEATURE) Streaming Abstract Generator - Absolute paths to Relative paths -  
21 September 2018  
-----

File Datasource paths have been changed from absolute to relative paths

-----  
601. (THEORY) Algebraic Geometry and Computational Geometric Factorization -  
some definitions  
- 24 September 2018  
-----

Euclidean Rings are defined as:

For  $a, b$  in ring  $R$ , both non-zero, there exist  $t, r$  in  $R$  such that  $a = tb + r$   
where  $r \neq 0$ . Unique Factorization Theorem is defined on Euclidean Rings.  
Set of Integers are examples of Euclidean Rings.

Let  $R$  be a Ring. An Ideal  $I$  of  $R$  is a subgroup of  $(R, +)$  and for all  $x$  in  $I$  and  
for all  $r$  in  $R$ ,  $x \cdot r$  and  $r \cdot x$  in  $I$ .

Set of all Integers  $Z$  divisible by an integer  $n$  is an ideal denoted by  $nZ$ .

Ideals can be generated by a subset  $X$

of  $Z$ . Special case is when  $X$  is a singleton  $X = \{a\}$  for some  $a$  in  $Z$ , named  
Principal Ideal:

$$\Rightarrow aZ = \{ar \mid r \text{ in } Z\}$$

$$\text{and } Za = \{ra \mid r \text{ in } Z\}$$

These ideals are left and right principal ideals generated by  $X = \{a\}$  i.e  
multiples of  $a$ .

Every hyperbolic tile segment in Computational Geometric Factorization is the  
union of intersections of principal ideals - one infinite ideal  $y_1Z$  parallel to  
 $x$ -axis and other  $k$  infinite ideals  $x_iZ$  parallel to  $y$ -axis in  $xy$ -grid (each  
intersection is a pixel in  $xy$ -grid) for  $x_i$  and  $y_1$  in  $Z$  - this intersection of  
principal ideals is finite:

$$y_1Z = \{y_1, y_1^2, y_1^3, \dots\}$$

$$x_1Z = \{x_1, x_1^2, x_1^3, \dots\}$$

$$x_2Z = \{x_2, x_2^2, x_2^3, \dots\}$$

$$x_3Z = \{x_3, x_3^2, x_3^3, \dots\}$$

...

$$x_kZ = \{x_k, x_k^2, x_k^3, \dots\}$$

$$\text{Tile segment} = (x_1Z \cap y_1Z) \cup (x_2Z \cap y_1Z) \cup \dots (x_kZ \cap y_1Z)$$

In Algebraic Geometric terms, a hyperbolic pixelation is union of tile segments  
(union of union of intersections of principal ideals). Sum of lengths of first  $n$   
tile segments of pixelated hyperbolic curve:

$$N/[1^2] + N/[2^3] + \dots + N/[n^{(n+1)}] = Nn/(n+1)$$

$$N/[1^2] + N/[2^3] + \dots + N/[n^{(n+1)}] \leq N/1^2 + N/2^2 + N/3^2 + N/4^2$$

+ ...

$$N/[1^2] + N/[2^3] + \dots + N/[n^{(n+1)}] \leq (\text{RiemannZetaFunction}(s=2)) \cdot N$$

$$N/[1^2] + N/[2^3] + \dots + N/[n^{(n+1)}] \leq 1.6449 \cdot N$$

An algebraic subset of  $Z^2$  for hyperbolic variety is defined as ( $N$  is number to  
factorize):

$$V(S) = \{ (x_1, y_1) \text{ in } Z^2 \mid x_1 y_1 - N = 0 \}$$

which is the point-set on the hyperbolic tile segments (equivalent to previous  
definition based on principal ideals).

-----  
Computational Geometric Hyperbolic tile segments pixelation as Variety over  
Finite Fields:

-----  
-----  
Algebraic Varieties are defined as set of zeros of polynomial equations. If  $K$  is a Field and  $N$  is a positive integer, an affine  $N$ -Space over  $K$  is defined as:

$$A^N(K) = \{(a_1, a_2, \dots, a_N) \mid a_1, a_2, \dots, a_N \text{ in } K\}$$

A subset of affine  $N$ -Space is an affine Algebraic Variety over  $K$  defined as:

$$X(K) = \{a \text{ in } A^N(K) \mid f_1(a) = 0, f_2(a) = 0, \dots, f_r(a) = 0\}$$

if there are polynomials  $f_1, f_2, \dots, f_r$  having coefficients from  $K[T_1, T_2, \dots, T_n]$ . In Computational Geometric Factorization, Hyperbolic tile segment pixelation is an affine Algebraic Variety defined over a finite field or Galois Field  $K$  of order  $p^n \gg N$  ( $p^n$  is a prime power) satisfying polynomial  $x_1 y_1 - N = 0$  for  $(x_1, y_1)$  in affine 2-Space  $A^2(K)$ . Counting number of elements in finite algebraic variety is non-trivial problem - in the context of geometric factorization, this is tantamount to finding number of points in hyperbolic tile segments.

References:

-----  
-----  
601.1 Algebraic Geometry - Chapters 1 and 2 - [JS Milne] -  
<https://www.jmilne.org/math/CourseNotes/AG.pdf>  
601.2 Principal Ideal - [https://en.wikipedia.org/wiki/Ideal\\_\(ring\\_theory\)](https://en.wikipedia.org/wiki/Ideal_(ring_theory))  
601.3 Topics in Algebra - [Israel N. Herstein] - Pages 143-144 - Euclidean Rings  
601.4 Value of Riemann Zeta Function at  $s=2$  -  
[https://en.wikipedia.org/wiki/Particular\\_values\\_of\\_the\\_Riemann\\_zeta\\_function](https://en.wikipedia.org/wiki/Particular_values_of_the_Riemann_zeta_function) -  
 $\pi^2/6=1.6449\dots$   
601.5 Counting Points of Varieties over Finite Fields - [Sudhir Ghorpade, IIT Bombay, Mumbai] -  
[http://www.math.iitb.ac.in/~srg/Talks/IRCCAwardLecture\\_Ghorpade\\_29Aug2012.pdf](http://www.math.iitb.ac.in/~srg/Talks/IRCCAwardLecture_Ghorpade_29Aug2012.pdf)  
-----  
-----

602. (THEORY) Software Analytics - GraphFrames - GraphX - Parallel Graph Algorithms for CallGraph/CFG/SATURN Graph DOT files - 27 September 2018  
-----  
-----

1. NeuronRain till now has a native implementation of parallelized graph processing (e.g. definition graph growth implementation in InterviewAlgorithm/ for texts) and sequential NetworkX Graph objects  
2. Spark has parallel graph library GraphX and a separate repository GraphFrames which internally wraps GraphX  
(<http://graphframes.github.io/api/python/graphframes.html>)  
3. This commit introduces an option to choose GraphFrames in analyzing Software Analytics CallGraph/CFG/SATURN DOT files in CyclomaticComplexitySparkMapReducer.py and invokes few parallel algorithm functions for indegrees, strongly connected components, triangle counting.  
4. Number of strongly connected components, degrees, triangles in CallGraph/CFG/SATURN graphs are cyclomatic measures of code complexity (both static and dynamic)  
5. logs for GraphFrames is committed to  
testlogs/CyclomaticComplexitySparkMapReducer.log.GraphXFrames.27September2018  
6. GraphFrames can be applied not just to Program Analysis DOT files but to any other source (TextGraph, Social Networks etc.,)`  
7. Spark Commandline for GraphFrames package: /media/Ubuntu2/spark-2.3.1-bin-hadoop2.7/bin/spark-submit --packages graphframes:graphframes:0.6.0-spark2.3-s\_2.11 CyclomaticComplexitySparkMapReducer.py  
-----  
-----

603. (THEORY and FEATURE) ImageGraph creation from an Image - Keras-Theano - related to 587 and 588 -  
EventNet Tensor Products Algorithm for Merit of Large Scale Visuals - 30 September 2018  
-----  
-----

-----

- 1.This commit introduces a primitive but crucial implementation of EventNet Tensor Products Algorithm for Large Scale Visuals which creates a text graph from information gained from processing of a visual (.jpg).
- 2.Keras is a framework for Computer Vision which supports pre-trained ImageNet datasets (VGG, ResNet) annotated to ImageNet vertices by Convolution Neural Networks. ImageNet presently has 14 million vertices.
- 3.Keras has support for TensorFlow, Theano, CNTK backends. A python implementation which imports Keras and sets the backend to Theano and predicts objects in an image from ImageNet has been committed to `image_pattern_mining/ImageNet/ImageGraph_Keras_Theano.py`
- 4.This script loads an image in keras-theano, converts it to an image array, expands its dimensions and predicts the objects in the image by ResNet50 pre-trained ImageNet dataset.
- 5.Predictions for objects in image are decoded into array of tuples of the form (id, imagenet\_vertex, probability).
- 6.An example prediction for few images is described in : <https://www.pyimagesearch.com/2016/08/10/imagenet-classification-with-python-and-keras/> along with probabilities for objects annotated.
- 7.These predicted ImageNet vertices are concatenated into a text and passed on to `RecursiveGlossOverlap_Classifier.py` which creates a Text Graph - ImageGraph - by invoking `RecursiveGlossOverlapGraph()` on this text.
- 8.This algorithm essentially maps an Image to a TextGraph. Presently only still images are supported - extending to Video is straightforward by getting all frames in a video and computing ImageGraphs for all frames and Tensor Products of the causally related ImageGraphs.
- 9.logs for few images (one of which is courtesy: <https://www.aazp.in/live-streaming/> - WhiteTiger\_1.jpg) have been committed to `image_pattern_mining/ImageNet/testlogs/`
- 10.Graphs printed in logs show fairly reasonable inference of prominent entities in image.

-----

604. (FEATURE) Music Pattern Mining - Onset of Notes Detection - 1 October 2018 - related to 67,68,69

-----

1. `audio_features()` function in `AudioToBitMatrix.py` has been updated to compute notes onset from audio signal
2. Notes Onset Detection involves finding peaks in onset strength of the signal time series.
3. Extracting notes from signal converts the music time series to a string from a language of notes alphabets.
4. Most algorithms for audio analysis are time-series (fft,statistics etc.,) based. Considering music as a Formal language opens new vistas into theoretical analysis of music. For example, finding a deterministic finite state automaton for sequence of notes in a music signal is measure of complexity in music.
5. Not just automata, variety of string complexity measures (e.g Kolmogorov complexity - MDL) can effectively describe music notes strings.

-----

605. (THEORY) Computational Geometric Factorization, Parallel Planar Point Location, Ray Shooting Queries, Multisearch, PRAM and BSP models - 2 October 2018 - related to 34, 506, 575, 597

-----

Factorization by Computational Geometric algorithms - k-mergesort, segment trees, wavelet trees, ray shooting queries - described earlier implement a generic idiom of Planar Point Location

which locates factor points inside some of the polygons in the planar subdivision created by the hyperbolic pixel array segments. Planar Point Location is a special problem in Multisearch which is defined as: Given a set of query points and set of line segments in 2D plane, multisearch returns the line segments containing the query points which is exactly what is required in factorization. There are lot of parallel planar point location algorithms for PRAM and BSP model and thus in NC (references in 34). After locating a pixel array polygon by parallel planar point location, factor can be found by binary search of the segment polygon containing the factor because each hyperbolic segment is implicitly sorted - one of the ordinate axes is constant and other increases i.e each tile is an arithmetic progression. Parallel Planar Point Location algorithm in reference 34.83 can locate a polygon containing factor point in  $O((\log N)^2)$  PRAM time with additional  $O(\log N)$  sequential time for binary search to locate the factor within polygon.

Ray shooting query algorithms described earlier reduce the necessity of parallelism to great extent by making an educated guess of approximate location of factor points by applying number theory results and search their circular vicinity for exact factors by k-mergesort, segment trees or wavelet trees. Probability of error in ray shooting has been derived earlier. Planar Point Location and Ray Shooting queries can be combined into one by following algorithm for multisearch:

- (\*) Sequentially shoot ray queries for  $O(\log \log N)$  approximate prime factors with average spacing  $O(N/\log \log N)$  between rays shot from origin. This is  $O(\log \log N)$  sequential time (assuming Hardy-Ramanujan estimate)

- (\*) Locate the segments (pixel array polygons) containing each of the approximate factors by Parallel Planar Point Location. This returns  $O(\log \log N)$  segments in  $O((\log N)^2 \log \log N)$  parallel time. With high probability a segment containing approximate factor might also contain exact factor:

- (\*) Each tile segment is of variable length  $N/[x(x+1)]$  but spacing between prime factors is equal  $kN/\log \log N$  for some constant  $k$

- (\*) Error occurs if  $N/[x(x+1)] < kN/\log \log N$  (or)  $\log \log N < k(x(x+1))$

- (\*) Solving for  $x$  in  $x^2 + x - (\log \log N/k) > 0$ :  

$$x > -0.5 + 0.5 \sqrt{1 + 4 \log \log N/k}$$

- (\*) Each  $O(\log \log N)$  segment (polygon) can be binary searched in  $O(\log N \log \log N)$  sequential time.

- (\*) Total Parallel and Sequential time of previous 3 steps =  $O(\log \log N + (\log N)^2 \log \log N + \log N \log \log N)$

- (\*) This is just another sequential optimization which makes some parallel computation sequential.

-----  
 -----  
 An average case sequential optimization for removing parallelism in Computational Geometric Factorization:  
 -----  
 -----

- (\*) Average number of tiles between two approximate prime factors  $m$  and  $(m+1)$  found by ray shooting:

$$= (m+1)/[k \log \log N - m - 1] - m/[k \log \log N - m]$$

because number of tiles till  $m$ -th prime factor =  $n = m/[k \log \log N - m]$  for  $m=1, 2, 3, \dots, k \log \log N$

- (\*) Polygon (hyperbolic tile segment) containing the ray shot approximate factor can be found by equation in 2-level binary search sequential optimization described previously - Tile containing approximate factor point  $x$  can be expressed by inequality:

$$Nk/(k+1) < x < N(k+1)/(k+2)$$

$$k < x/(N-x)$$

integer round-off of  $k$  is the index of tile interval containing  $x$ . This a simple



sequential planar point location identity in elementary arithmetic with no necessity for PRAMs or BSP.

(\*) Each consecutive tile in  $N/k\log\log N$  spacing between approximate factors can be found by tiling equation  $N/[x(x+1)]$  - subtract y coordinate by  $N/[x(x+1)]$  and increment x coordinate by 1 or vice versa - and each of these tiles in  $N/k\log\log N$  spacing can be individually binary searched in  $O(\log N)$ .

(\*) Thus total average sequential time to sweep binary search tiles in  $N/k\log\log N$  spacing between 2 consecutive approximate factors found by ray shooting:

$$= O([(m+1)/[k\log\log N - m - 1] - m/[k\log\log N - m]] * \log N)$$

(\*) Maximum number of tiles in  $N/k\log\log N$  spacing occurs by setting  $m=k\log\log N - 2$  (because of geometric intuition of hyperbolic tiling, most tiles occur within an interval in topmost or rightmost extreme of hyperbolic arc which contains  $k\log\log N$ -th factor on either axes):

$$= O([(k\log\log N - 2 + 1)/[k\log\log N - k\log\log N + 2 - 1] - (k\log\log N - 2)/[k\log\log N - k\log\log N + 2]])$$

$$= O(k\log\log N - 1 - (k\log\log N - 2)/2)$$

$$= O(k\log\log N)$$

=> Maximum time to binary search tiles in  $N/k\log\log N$  spacing =  $O(\log\log N * \log N)$

=> Each of  $O(\log\log N)$  spacings between approximate factors can be searched in:

$$O(\log\log N * \log\log N * \log N)$$

average case sequential time with no necessity for parallel processing.

References:

-----  
605.1 Truly efficient parallel algorithms: 1-optimal multisearch for an extension of the BSP model - [Armin Baumker, Wolfgang Dittrich, Friedhelm Meyer auf der Heide] - Elsevier Theoretical Computer Science -  
<https://core.ac.uk/download/pdf/81931675.pdf> - Parallel Planar Point Location by Multisearch in BSP\* model - Section 1.1.  
605.2 Communication Efficient Deterministic Parallel Algorithms for Planar Point Location and 2d Voronoi Diagram - [Mohamadou Diallo, Afonso Ferreira and Andrew Rau-Chaplin] - Section 2 - Hyperbolic pixelation is in a sense a Voronoi tessellation in which factor points are ensconced by the pixel array polygons.  
605.3 Computational Geometric Planar Point Location on Arrangements - Section 9.9.1 - Randomized Algorithms - [Motwani-Raghavan] - Pixelated Hyperbolic tile segments are adjacent arrangements  
605.4 Rectifiable Curves - Principles of Mathematical Analysis - [Walter Rudin] - Pages 136-137 - Section 6.26 and Theorem 6.27 - Pixelation of Hyperbolic arc is exactly rectification - map is defined by  $y = N/x$  and interval  $[1, N]$  is partitioned into tile segments of lengths  $N/[x(x+1)]$  and sum of lengths of tile segments is the length of polygonal path.  
605.5 Rectification of Curves and Bresenham Line Drawing Algorithm -  
[https://en.wikipedia.org/wiki/Arc\\_length](https://en.wikipedia.org/wiki/Arc_length) and  
[https://en.wikipedia.org/wiki/Bresenham%27s\\_line\\_algorithm](https://en.wikipedia.org/wiki/Bresenham%27s_line_algorithm) - Rectification also called as Arc Length finds length of a curve by approximating it with line segments which may not be axis parallel whereas Computational Geometric Factorization approximates hyperbola by only axis parallel straightline segments which is exactly similar to Bresenham line drawing algorithm - line is replaced by hyperbolic arc (illustrated in [https://en.wikipedia.org/wiki/Bresenham%27s\\_line\\_algorithm#/media/File:Bresenham.svg](https://en.wikipedia.org/wiki/Bresenham%27s_line_algorithm#/media/File:Bresenham.svg)).

-----  
606. (THEORY and FEATURE) VideoGraph EventNet Tensor Product Merit for Large Scale Visuals - 3 October 2018  
-----

-----  
1. Two new functions have been committed to ImageGraph\_Keras\_Theano.py for reading a Video file, extracting frames from the video upto certain number and extract object information by Keras-Theano ImageNet predictions for each frame.

2. `imagenet_videograph()` function depends on OpenCV 3.4.3 (cv2) Python for reading Videos and writing Frame JPEG files suffixed by unique id. Each frame is mapped to a TextGraph - ImageGraph - by `imagenet_imagegraph()`

3. `videograph_eventnet_tensor_product()` function computes tensor products of pairs of Frame ImageGraphs and returns an EventNet Tensor from NetworkX.

4. logs, an example Video (MP4) and 2 sample extracted frames (JPEG) for EventNet Tensor representation of a video have been committed to `testlogs/ImageGraph_Keras_Theano.log.30october2018`

5. From this EventNet Tensor any kind of intrinsic merit can be computed - e.g previously described ImageNet based inverse weights, Graph Edit Distance between two Frame ImageGraphs, Tensor Rank for connectedness etc.,

-----  
 607. (THEORY and FEATURE) Video EventNet Tensor Products - Inverse Distance Merit of Large Scale Visuals  
 - 4 October 2018  
 -----

-----  
 1. New function `inverse_distance_intrinsic_merit()` has been included in `ImageGraph_Keras_Theano.py`. It iterates through each tensor product entry of Video EventNet Tensor Products matrix and for every edge (a,b)-(c,d) in tensor product computes inverse wordnet distance (which is basis for ImageNet):  

$$1/\text{dist}(a,b) * 1/\text{dist}(c,d)$$
  
 and populates a weights matrix per tensor product graph.

2. Each tensor product in EventNet Tensor corresponds to causality between any 2 frames in the video.

3. An example merit computation log has been committed to `testlogs/ImageGraph_Keras_Theano.log.40october2018` which shows merits for 4 tensor products (2 frames \* 2 frames).

4. Lot of weights in merit matrix in logs have huge values implying high causality between two frame events.

5. EventNet Tensor Product Algorithm is computationally intensive. Each ImageGraph per frame encodes relationship between objects (actors) in the frame event.

6. Size of the EventNet Tensor is  $O(\text{number\_of\_frames} * \text{number\_of\_frames} * \text{average\_number\_of\_actors\_per\_frame} * \text{average\_number\_of\_actors\_per\_frame})$  and memory intensive too.

-----  
 608. (THEORY and FEATURE) Video EventNet Tensor Products - Emotional Merit of Large Scale Visuals  
 - 15 October 2018  
 -----

-----  
 1. EventNet Tensor Product representation of a Large Scale Visual just infers the connectedness of the information in the video with no emotional or sentiment scoring.

2. To redress this, new function has been included in `ImageGraph_Keras_Theano.py` to lookup the edges of tensor product graph in empath and aggregate the sentiments of the vertices as a tuple which is qualitative emotive merit of the video.

3. Two new example visuals have been added: `ExampleImage_1.jpg` and `ExampleVideo_2.mp4` in addition to earlier `ExampleVideo_1.mp4` and images.

4. Keras has mistook `ExampleImage_1.jpg` to be a theatre audience which is indeed a classroom photo and annotated it accordingly (probably because seating and ambience are similar in both). Also

Empath has misjudged the alumni website content in ExampleVideo\_2.mp4 to large extent excluding "college" as emotional annotation. Logs have been committed to testlogs/ImageGraph\_Keras\_Theano.log.15October2018

5. These Photo and Videos are courtesy (and related to self):

(\*) ExampleVideo\_1.mp4 - <https://www.cmi.ac.in/people/fac-profile.php?id=shrinivas> - Chennai Mathematical Institute - Research Scholar website - 2010-11

(\*) ExampleImage\_1.jpg - <http://www.angelfire.com/id/95cse/album.html> - PSG College of Technology - 1995-99 CSE batch alumni website album - Classroom Photo (class1.jpg)

(\*) ExampleVideo\_2.mp4 - <https://alumni.psgtech.ac.in/profile/view/srinivasan-kannan-1> - PSG College of Technology Official Alumni website

6. Frames captured by OpenCV2 are prefixed by the Video file name.

7. THEANO\_FLAGS have been set as: declare -x THEANO\_FLAGS="cxx=/usr/bin/g++-6"

-----  
609. (THEORY) EventNet Tensor Products - Example for Movie and Youtube Merit - 16 October 2018  
- related to 608  
-----

-----  
Previous videos were proof-of-concept implementations for utility of EventNet Tensor. Following is stated just as a theoretical example with no testcases because computation involved is massive requiring millions of frames and their EventNet Tensor Product - EventNet Tensor Products Algorithm can be applied to set of movie/youtube datasets to deduce the connectedness and emotions in the videos. Since most movie and youtube channels are emotions oriented which are expressed visually, comparing the emotion annotated tuples (e.g by Empath previously described) of any pair of movies/youtube videos, could rank them by emotional quotient approximately. Also the previous Empath emotion annotation creates a set of emotions and not a hashmap of emotion annotations to their number of occurrences in the Audio-Visual which is yet another indicator. Comparing emotions occurrence hashmaps of two Audio-Visuals is a ranking measure - requires sorting two hashmaps by emotions occurrence values, comparing top percentile emotions in two Audio-Visual hashmaps and finding correlation coefficient between the two probability distributions. Added advantage could be speech recognition in the AV frame-by-frame or for set of frames which is not done by previous Keras-Theano implementation and creating AudioGraph from it (there is no AudioNet library so far).  
-----

-----  
610. (THEORY) Summary of Large Scale Visuals and EventNet Subgraphs - related to 158,423 - 19 October 2018  
and 20 October 2018  
-----

-----  
Guessing/Discovering a Larger EventNet causality Graph from Subgraphs of EventNet has been mentioned earlier.

An opposite of it is to summarize a huge EventNet Graph into a small summary EventNet subgraph without much

loss of causality information. Text Summarization is text analysis application of Graph Summarization which has been earlier described and implemented by Recursive Lambda Function Growth algorithm. Realworld application of Graph Summary is Video Summarization by EventNet Tensor Products representation e.g a movie or a youtube video is a small duration summary (minutes or hours) of real life events (and their causalities) enacted by set of people over many years - this involves sampling an EventNet Tensor Product Graph of a Video at relevant vertices and induce a summary subgraph on it which preserves meaning. Similar to Text Summarization, Video Summary could also be approximated by choosing dense subgraphs (or high core number vertices) of Video EventNet Tensor Products. Topological Sort of Dense Subgraph of Video EventNet Tensor Product Graph gives a flattened summary of the video by some ordering (a gist of

important frames).

-----  
611. (THEORY and FEATURE) Video Emotions Hashmap, Video Core Topological Sort  
Summary - 25 October 2018  
- related to 611  
-----

-----  
(\*) Empath emotions of the Video EventNet Tensor Products Graph have been aggregated in a hashmap. This facilitates quantitative emotional scoring of the video. Hashmap correlates the empath emotion and its cumulative score.  
(\*) Core (Main core) of the Video EventNet Tensor Product Graph has been computed and is sorted topologically for creating some ordering for the summary.

(\*) New example MP4 video has been created from 6 JPEG photos (in which I was present) and google search related to self (ExampleVideo\_3.mp4) :

Frame 1 - Self - Mahabalipuram, Chennai - 2012 (Copyright: Self)  
Frame 2 - Self - photo (Copyright: Self)  
Frame 3 - Self - VISA photo (Copyright: Self)  
Frame 4 - Self - Family photo (Copyright: Self)  
Frame 5 - Self - IEC Sun Microsystems - Bengaluru - 2004 (Copyright: Ex-Colleagues at Sun Microsystems)  
Frame 6 - Self - IEC Sun Microsystems - Bengaluru - 2000 (Copyright: Sun Microsystems/Oracle)  
Frame 7 and 8 - Google Search of Self

(\*) Previous recording is a mix of photos of varied genre. Sentiment hashmap for this video prints (excerpts):

Sentiment Analysis of the Video: [('work', 1484.0), ('toy', 424.0), ('tool', 848.0), ('technology', 3180.0), ('social\_media', 1060.0), ('shopping', 424.0), ('science', 1060.0), ('restaurant', 848.0), ('reading', 424.0), ('programming', 2544.0), ('play', 424.0), ('phone', 1696.0), ('office', 1060.0), ('negative\_emotion', 0.0), ('musical', 424.0), ('music', 424.0), ('messaging', 1272.0), ('meeting', 424.0), ('internet', 2968.0), ('hiking', 424.0), ('furniture', 212.0), ('dance', 212.0), ('computer', 5088.0), ...]. This is a remarkable inference of the Video content by Keras-Theano ImageNet giving high weightage to office and technology as emotional annotations.

(\*) Logs for this have been committed to  
testlogs/ImageGraph\_Keras\_Theano.log.25October2018

-----  
612. (FEATURE) Video EventNet Core Topological Sort Summary - Bugfixes - 28  
October 2018  
-----

-----  
(\*) Some errors in inverse distance merit computation of the Video EventNet Tensor have been corrected which was earlier a 2-dimensional tensor and has been made 3-dimensional in this commit.

(\*) Core Summary of the Video has also been changed to compute maximum merit for each tensor product inverse distance merit vector and apply a threshold filter for the distance merit.

(\*) Three dimensional EventNet Tensor is mapped to NetworkX Graph after previous threshold filter.

(\*) Only causal frames above inverse distance threshold are included in the NetworkX graph and main core is computed on this graph

(\*) self loops and parallel edges are removed and topological sorting is performed on main core.

(\*) logs for this have been committed to  
testlogs/ImageGraph\_Keras\_Theano.log.28October2018  
-----  
-----

613. (FEATURE) People Analytics - HR Analytics Implementation and Least Energy Intrinsic Merit of a social profile - 9 November 2018 - related to 365, 443, 572

-----

-----

(\*) People Analytics is the generalized version of HR Analytics for analyzing any social profile vertex.

(\*) This commit adds SocialNetworkAnalysis\_PeopleAnalytics.py python implementation to repository which at present analyzes LinkedIn profiles and computes:

(\*) Graph Tensor Neuron Network Intrinsic Merit of the profile text with no field parsing - this treats the social profile as an en masse text with no delineations and applies Recursive Lambda Function Growth algorithm to create lambda function composition tree of the resume text. Core classification and Centrality measures throw some interesting insights:

(\*) Core number 4 identifies the class of the social profile

(\*) Maximum merit random walk of the lambda composition tree approximately guesses the purport of the text in the social profile

(\*) Betweenness and Closeness Centralities estimate the top-ranked classes accurately compared to Degree and PageRank Centralities

(\*) Log Normal Fitness of the social profile after parsing the total work experience and academic stints of the profile - for linkedin this inverse log normal least energy fitness is  $1/(\log E + \log V)$  with no Wealth estimates - Wealth is caused by E(Education) and V(Work/Valour) as far as professional profiles are concerned. Lowest Value of Least Energy Fitness implies Highest Fitness. Parsing is done by parse\_profile() function which implements a switch design pattern - stint polymorphs from work to academic tenures.

(\*) Log Normal Experiential Intrinsic Fitness of the social profile (by applying mistake bound learning differential equation for recursive mistake correction tree described earlier) - log normalized because of huge exponents

(\*) Because of limitations due to Updated LinkedIn Scraping Policy (<https://www.forbes.com/sites/forbestechcouncil/2017/09/20/linkedin-vs-hiq-ruling-casts-a-long-shadow-over-the-tech-industry/#19f535f35e6c>), this is only implemented as a non-crawled example for LinkedIn profile of self: <https://www.linkedin.com/comm/in/srinivasan-kannan-608a671> (pdf and text version of pdf by pdf2txt)

(\*) datetime python package is used to compute timedelta(s) and a regex matcher isdate range() function has been implemented for parsing date ranges in the profile:

(\*) Work Experience Date Ranges have the Regex: <Month> <Year> - <Month> <Year>

(\*) Academic Date Ranges have the Regex: <Year> - <Year> and months are implicit

(\*) This implementation does not assume a Web Crawler and Social Profile Datasource and only requires a file input (datasource, file type and file name are passed in as arguments to parse\_profile()) - optionally, crawled social profiles can be invoked as file arguments to parse\_profile(). Presently only linkedin datasource, text file types are supported. PDF parsing has been implemented by PyPDF2 but there are IndirectObject related errors.

-----

Theory:

-----

An obvious application of HR analytics is feasibility of automatic recruitment of people by profile analytics. Usual Interview and Written Test based process of recruitment measures Intrinsic Merit (approximately subject to error) of people. Analytics of Professional Networks is Fame (Degree etc.,) based. From 572.8 ("...Boolean majority function is equivalent to PageRank computed for 2 candidate websites on (n+2)-vertex graph (n user websites choose between 2 candidate websites - Good(1) and Bad(0), choice is fraction of outdegree from a user website) normalized to 0 (smaller pagerank) and 1 (bigger pagerank).

Margulis-Russo threshold  $d(\text{Pr}(\text{Choice}=\text{Good}=1))/dp$  on this PageRank version of Majority function is ratio of sum of influences of variables (user websites) to standard deviation which has a phase transition to Good(1) at per-voter website bias  $p \geq 0.5\dots$ ). Majority Voting/PageRank or any other Fame/Degree measure is known to have phase transition from Low accuracy to High accuracy for per voter  $p\text{-bias} > 0.5$  implying automatic recruiting is feasible if Fame lowerbounds Intrinsic Merit (Intrinsic Merit  $\geq$  Fame). Stability or Resilience of Interview as LTF vis-a-vis Majority Function has been analyzed earlier in 365. Problematic condition for rendering automatic crowdsourced recruitment infeasible is: Intrinsic Merit  $\ll$  Fame. Comparison of Intrinsic Merit to Fame by correlation coefficients requires normalization of fame and merit rankings e.g fame and merit probability distributions and distance between these two distributions for same dataset. From references in 572, most experimental results in sports(e.g Elo rating), science (e.g research published) etc., show fame grows exponentially to merit implying merit is quantitatively proportional to  $\log(\text{Fame})$ . For example, if PageRank/Degree centrality is computed on Professional Network Vertices and dynamic experiential intrinsic merit  $E$  of a profile at time point  $t$  is computed by previous implementation:

$$E = M * e^{(kMt)} = \log(dv(t)) * e^{(k \log(dv(t)) * t / c \log t)} / c \log t$$
 for evolving degree  $dv(t)$

crowdsourcing infeasibility condition reduces to:

$$\begin{aligned} \log(dv(t)) * e^{(k \log(dv(t)) * t / c \log t)} / c \log t &\ll dv(t) \\ (k \log(dv(t)) * t / c \log t) &\ll \log(c \log t * dv(t) / \log(dv(t))) \end{aligned}$$

-----  
 614. (FEATURE) Social Network Analysis - People Analytics - Another example and Unicode corrections -

12 November 2018 - related to 613

- 
1. RecursiveGlossOverlap\_Classifier.py has been changed to ignore unicode errors in text strings
  2. New example Curriculum Vitae TeX (self) has been analyzed by Recursive Lambda Function Growth Algorithm for various intrinsic merit measure it prints.
  3. Core classifier shows high relevance to human judgement and again Closeness and Betweenness centralities are better than Degree and PageRank centralities (classes like "Silver" are probably produced because of relevance of "Silver" to "Hyderabad")
  4. RecursiveLambdaFunctionGrowth.dot file has been recreated.
  5. logs for this have been committed to `testlogs/SocialNetworkAnalysis_PeopleAnalytics.log.12November2018`
  6. Textual analysis of a CV is quite open-ended and unstructured - Nonetheless the classification by TextGraph core numbers gives reasonable estimate of crucial aspects in the resume

-----  
 615. (THEORY) Hash Table Chaining, Locality Sensitive Hashing and Frequently occurring patterns - 13 November 2018 - related to all sections on LSH partitions, Majority Voting, Theoretical EVMs, Streaming, Audio-Visual Pattern Mining, Bigdata Analytics

-----  
 Locality Sensitive Hashing is a collision-supportive hash chaining which as described earlier has multitude of applications in clustering similar elements of a set which can be votes for candidates(EVMs which colocate votes for a candidate in same bucket), bigdata or audio-visual spectrogram-histogram representation. Essentially, every chained hash table or LSH partition of a set is a histogram of probability distribution when viewed pictorially - e.g audio signals represented as series of animated histograms. Assuming dataset is a stream of these LSH partitions, problem is to

decipher patterns underlying these histograms. There are LSH algorithms like Nilsimsa hash, Minhash etc., which find similarities of two sets (texts for example in Nilsimsa) by Jaccard, Hamming and other distance coefficients. If each element in the stream of histograms/LSH partition/Chained Hashtables are considered as set of buckets, comparing two such histograms is tantamount to computing similarity of 2 consecutive sets of buckets by some hash metric e.g Minhash. It is worthwhile to mention that this histogram (set of buckets) pattern is ubiquitous across any algorithm doing an LSH partition or hash table bucket chaining. In the People Analytics example previously, LSH partition of People and Professional Profiles splits them into buckets of similar traits.

Distributed Hash Tables which geographically decentralize chunks of a huge table realise theoretical Electronic Voting Machines which have been defined earlier in terms of LSH partitions or Separate Chaining Hash tables in distributed/cloud setting - buckets of votes for candidates are distributed on cloud nodes. CAP Theorem applies to Theoretical EVMs implying only 2 of 3 (Consistency-serialization, Availability-readwrites are 100% reflected and Partition Tolerance-resilience to node/network failures) are feasible on an internet EVM based on LSH Partition/Separate Chaining. Real world EVMs are most vulnerable to network, sabotage or power failure (partition) making it a CA system. This limitation is less visible if number of candidates is small and table is local but serious if number of candidates (buckets) are huge and requires distribution. Even if partitions are assumed to be nil, there is always a tradeoff between consistency and latency i.e a distributed system has to compromise on speed for greater consistency. This has been formalized as extension of CAP Theorem - PACELC theorem.

Example:

If profiles are represented as TextGraphs as in previous implementation of HR Analytics, edges between vertices of the textgraph encodes the temporal information because most social profiles contain chronologically ordered timeline history of events - similarity measure for any two profiles could be the temporal cause-effect similarity between two profiles and thus Social Profile TextGraph is an EventNet too.

References:

-----  
615.1 PACELC Theorem extension of CAP - [Daniel Abadi] - <http://cs-www.cs.yale.edu/homes/dna/papers/abadi-pacelc.pdf>  
-----

-----  
616. (FEATURE) Software Analytics - Cyclomatic Complexity - Rewrite for merging two clauses - 14 November 2018  
-----

-----  
1. CyclomaticComplexitySparkMapReducer.py has been changed to merge True and False clauses for GraphFrames  
2. Cyclomatic Complexity (Zeroth Betti Number) has been computed from GraphFrames stronglyConnectedComponents()  
as per definition of Cyclomatic Number in Topological Graph Theory  
3. Cyclomatic Complexity (First Betti Number) has been computed as  $E - V + [\text{Zeroth Betti Number}]$   
4. New callgrind and kcachegrind DOT files for execution of command "ls" have been committed and included for  
Cyclomatic Complexity and Call graph GSpan mining:  
    callgrind.ls.out.3104  
    kcachegrind\_callgraph\_ls.dot  
5. logs for this have been committed to  
CyclomaticComplexitySparkMapReducer.log.GraphXFrames.14November2018  
-----

-----  
617. (THEORY) Beatty Sequences and Complement Diophantines - related to all  
-----

sections on Complementary Sets  
, Ramsey 2-coloring and their Diophantine/Function representations - 16 November  
2018, 18 November 2018 - draft updates to  
<https://arxiv.org/pdf/1106.4102v1>

-----

Complement Functions have been defined for arbitrary complementary sets (Integers/Rationals/Reals) in <https://arxiv.org/pdf/1106.4102v1> and their relevance to Ramsey Coloring of Sequences and decidability of Diophantine representation of complementary sets (MRDP Theorem) have been expounded in detail earlier. Special Case of Complementary Sets of Integers is a well-studied problem and a classic result due to Beatty defines 2 complementary sets of integers based on solutions to equation  $1/a + 1/b = 1$  for irrationals  $a$  and  $b$ . Thus terminologies - Complement Functions, Complement Diophantines, Ramsey 2-Coloring of Sequences and Beatty Complementary Sequences - are synonymous with respect to set of Integers  $\mathbb{Z}$ . Notion of Complementation generalizes it to any sets Boolean, Integer, Real or Rational. Integer and Real Complementation have solvable algorithms in the form of Diophantine equations subject to MRDP theorem and Tarski/Sturm, but complementation over rationals is open problem for the direction  $\mathbb{N}$  to  $\mathbb{Q}$  - mapping  $\mathbb{Q}$  to  $\mathbb{N}$  is straightforward.

ABC Conjecture and Complement Diophantines:

-----

ABC conjecture states there are finite coprime triples  $a, b, c$  such that  $a+b=c$  and  $\text{quality}(q) = \log(c)/\log(\text{rad}(abc)) > 1 + \epsilon$  for every  $\epsilon > 0$ . Though there are infinitely many coprime triples  $a, b, c$  ( $a+b=c$ ) having  $\text{quality} > 1$ , this conjecture predicts there are only finite number of coprime triples cluttered between every real value of  $\epsilon$ . Complementary version of ABC conjecture is defined as:

- (\*)  $T$  = set of all coprime triples ( $a, b, a+b=c$ )
- (\*)  $Q_1$  = set of all coprime triples of  $\text{quality} > 1$
- (\*)  $Q_0$  = set of all coprime triples of  $\text{quality} < 1$
- (\*)  $Q_0 \cup Q_1 = T$  and  $Q_0 \cap Q_1 = \text{Empty}$  i.e sets  $Q_0$  and  $Q_1$  are complementary infinite sets (creates Beatty sequences equivalent for triples).
- (\*) Complementary Sets Version of ABC Conjecture: Infinite set of triples  $Q_1$  is the disjoint set cover or exact cover of finite sets of triples of  $\text{quality} 1+\epsilon$  for every real  $\epsilon$ .
- (\*) Previous complementary sets can be picturised as:
  - (\*)  $T$  is a Rubik's cube in which each ordinate is a coprime triple ( $a, b, c$ )
  - (\*)  $Q_0$  and  $Q_1$  partition  $T$  into two disjoint sets of qualities less than 1 and greater than 1.
  - (\*)  $Q_1$  is the 3 dimensional half-space of Cube tiled by finite sets of triples of  $\text{quality} 1+\epsilon$  for every real  $\epsilon$ . As mentioned earlier, Pentominoes tiling is an exact cover problem for 2 dimensions.

References:

-----

617.1 Beatty functions and Complementary Sets -

[http://citeseerx.ist.psu.edu/viewdoc/download?](http://citeseerx.ist.psu.edu/viewdoc/download?doi=10.1.1.514.2119&rep=rep1&type=pdf)

[doi=10.1.1.514.2119&rep=rep1&type=pdf](http://citeseerx.ist.psu.edu/viewdoc/download?doi=10.1.1.514.2119&rep=rep1&type=pdf) - "...Let  $U$  be a subset of  $\mathbb{Z}$ . We call two non-empty sets  $A, B$  complementary with respect to  $U$  if  $A \cap B = \emptyset$  and  $A \cup B = U$ . A classical result of 1926 due to S. Beatty [1] states that if  $\alpha$  and  $\beta$  are positive irrational numbers with  $1/\alpha + 1/\beta = 1$ , then  $\{\text{floor}(n\alpha)\}$  and  $\{\text{floor}(n\beta)\}$  ( $n \in \mathbb{N}$ ) are complementary with respect to  $\mathbb{N}$ , where  $\text{floor}(x)$  denotes the greatest integer function of real  $x$ . This result has since then been generalized by a number of authors, see e.g., [2], [4], [5], [6] and [7]. ..."

617.2 Diophantine Equations over Rationals and Reals - Section 3.1 -

[http://www.mayr.in.tum.de/konferenzen/Jass07/courses/1/Sadovnikov/Sadovnikov\\_Paper.pdf](http://www.mayr.in.tum.de/konferenzen/Jass07/courses/1/Sadovnikov/Sadovnikov_Paper.pdf) - Solving in  $\mathbb{Q}$  (multiplication by integers), Solving in  $\mathbb{R}$  (Tarski and Sturm methods)

617.3 Three Dimensional Visualization of ABC Conjecture -

<http://www.lactamme.polytechnique.fr/images/CABC.21.20.1.M.D/display.html> -

visual intuition of the finite sets of coprime triples for every real  $\epsilon > 0$



0 for quality  $> 1 + \epsilon$ .

617.4 Fraenkel Conjecture for exact cover decomposition of  $\mathbb{Z}$  -

<https://core.ac.uk/download/pdf/82382652.pdf>

617.5 Diophantines for 2D Pentominoes Tiling -

<https://did.mat.uni-bayreuth.de/~alfred/home/pentominoes.ps.gz> - Locations of Tiles in  $9 \times 10$  rectangle are specified by linear diophantines.

617.6 Kummer Theorem for Universal Diophantine Equation representation of arbitrary recursively enumerable set - Hilbert Tenth Problem and Two-way bridge between Number Theory and Computer Science - [Yuri Matiyasevich] -

<http://www.cs.auckland.ac.nz/~cristian/tcspi/ch9.ps> - Diophantine Hierarchy - 9

Unknowns - Best known bound of number of unknowns ( $u$ ) and degree ( $d$ ) for Diophantine representation of an RE Set (in other words complement diophantine in the context of complementary sets) is  $(d, u) = (1.6 \cdot 10^{45}, 9)$ . Kummer theorem equates a binomial coefficient  $\binom{a+b}{b}$  to its exponential prime factorization  $2^{a_2} 3^{a_3} \dots$  where  $a_2, a_3, \dots$  are defined by Kummer Theorem: If integers  $a$  and  $b$  are written in  $p$ -adic (prime radix  $p$ ) notation and are added the number of carries during this addition is given by  $a_p$ . Because set of integers in binary notations can be expressed by binomial coefficients ( $a$  is number of 1s and  $b$  is number of 0s,  $a+b$  is the length of the binary integer string,  $\binom{a+b}{b}$  is the number of all possible integers having  $b$  0s in binary representation), Kummer's theorem is widely used for exponential diophantine representation of arbitrary recursively enumerable sets. Word concatenations also have diophantine representation (related to 2.11 and 2.12 - Ramsey 255-coloring texts by alphabets) implying natural language texts can be represented by a diophantine equation which is helpful in text compression.

617.7 Further results on Hilbert Tenth Problem - [Zhi Wei Sun] -

<https://arxiv.org/pdf/1704.03504.pdf> - Solving Diophantines in 11 unknowns over  $\mathbb{Z}$  is undecidable.

617.8 Hilbert Tenth Problem for Rational Functions over Finite Fields is

Undecidable - [Pheidias] - <https://link.springer.com/article/10.1007/BF01239506> - related to previous problem of finite sets tile cover but finite fields require size of tiles to be power of prime (characteristic)

617.9 Decision method for elementary algebra and geometry - [Alfred Tarski] - Rand Corporation -

<https://www.rand.org/content/dam/rand/pubs/reports/2008/R109.pdf> - decision procedure for real diophantines

617.10 Chaos Theory, Diophantines, Chaitin Theorem, Minimum Descriptive Complexity (Kolmogorov) - [Matiyasevich] -

<ftp://ftp.pdmi.ras.ru/pub/publicat/zns/v377/p078.pdf> - Computational Chaos Theory implies disorder in large sets arising from order (e.g. Logistic Map  $x_{n+1} = kx_n(x_n-1)$ ) - Chaitin theorem constructs a Diophantine set  $S$  which is chaotic and an exponential diophantine for it and its kolmogorov complexity for an initial finite fragment of  $S$  is  $O(\log|S|)$ .

617.11 Rayleigh Theorem or Beatty Theorem -

[https://en.wikipedia.org/wiki/Beatty\\_sequence](https://en.wikipedia.org/wiki/Beatty_sequence) - "...The Rayleigh theorem (also known as Beatty's theorem) states that given an irrational number  $r > 1$ , there exists  $s > 1$  so that the Beatty sequences  $\{B_r\}$  and  $\{B_s\}$  partition the set of positive integers: each positive integer belongs to exactly one of the two sequences...." - Examples - Upper and Lower Wythoff Sequences  $[nr]$  and  $[ns]$  generated by Golden ratio  $r$  and  $s=r+1$

617.12 Generalization of Beatty Theorem for Complementary Continuous functions over reals -

[https://web.archive.org/web/20140419091400/http://math.uncc.edu/sites/math.uncc.edu/files/2002\\_17\\_0.pdf](https://web.archive.org/web/20140419091400/http://math.uncc.edu/sites/math.uncc.edu/files/2002_17_0.pdf) - "...Main Theorem: Let  $F$  and  $G$  be real, continuous, strictly increasing, functions with domains  $[0, \infty)$  satisfying  $F(0) = G(0) = 0$  and  $\lim_{x \rightarrow \infty} (F(x) + G(x)) = \infty$ . For all  $t > 0$ , let  $P_t = \{0, (F+G)^{-1}(t), (F+G)^{-1}(2t), (F+G)^{-1}(3t), \dots\}$ , and  $P+t = P_t \setminus \{0\}$ . Then the two sequences  $A_t$  and  $B_t$  defined by  $A_t = \{c(F-1)^{-1}(n) \mid n \in P_t\}$  and  $B_t = \{b(G-1)^{-1}(n) \mid n \in P_t\}$  partition  $P+t$  for all  $t > 0$ . Also, the elements of  $A_t$  are distinct and the elements of  $B_t$  are distinct ..."

-----  
618. (FEATURE) People Analytics - Experiential Intrinsic Merit - LinkedIn

Profile Connections - 20 November 2018  
- related to 443

- 
1. SocialNetworkAnalysis\_PeopleAnalytics.py has been changed to parse connections of a linkedin profile
  2. Number of connections of a profile is then used to compute experiential intrinsic merit based on degree of a vertex as:  
$$E = M * e^{(kMt)} = \log(dv(t)) * e^{(k \log(dv(t)) * t / \log t)} / \log t$$
 for evolving degree  $dv(t)$
  3. This identity is derived from exponential relation between Fame (Degree) and Merit (Intrinsic fitness) of a social profile - in <https://www.microsoft.com/en-us/research/wp-content/uploads/2016/11/First-to-Market-is-not-Everything-an-Analysis-of-Preferential-Attachment-with-Fitness.pdf> (described earlier)
  4. Previous relation is anachronistic in the sense merit is defined in terms of fame when it has to be other way around. Function for `experiential_intrinsic_merit()` takes number of connections as a parameter and branches off into two clauses for least energy log normal merit if degree is 0 and degree based merit for degree > 0.
  5. Example LinkedIn Profile Connections (committed in pdf and txt) have been analyzed for previous degree based experiential merit and Recursive Lambda Function Growth merit. Example linkedin Connection pdf and text file have been committed to:  
    ConnectionsLinkedIn\_KSrinivasan.pdf  
    ConnectionsLinkedIn\_KSrinivasan.txt
  6. Definition TextGraph of connections (.txt) extracts essence of the aura surrounding a social profile.
  7. Dense subgraph (core) of this connections textgraph is a clustering coefficient measure i.e how well the neighbours of a vertex have semantic connections among themselves.
  8. Though social profiles are prone to Sybil links for artificially bumping up popularity, previous analysis is based on the assumption that humans do not link to another human unless they are trusted/befriended.
  9. logs for this have been committed to:  
    SocialNetworkAnalysis\_PeopleAnalytics.log.20November2018 (degree experiential merit)  
    SocialNetworkAnalysis\_PeopleAnalytics.log2.20November2018 (recursive lambda function growth merit)
  10. Recursive Lambda Function Growth merit logs have been truncated because of following recursion depth error in bintrees AVL Tree:  
    RuntimeError: maximum recursion depth exceeded  
but the logs show few erratic cycles having "missiles" which are inferred from random walk paths printed in the logs. Also Names of the connections have not been filtered which misleads the WordNet. Previous error impedes full analysis based on core number. But there are some relevant cycles related to "head hunter", "Ph.D", "dissertation", "entrepreneur", "engineer", "managers", "information\_technology" etc., giving a glimpse of the social circle's nature.

---

619. (THEORY and FEATURE) Software Analytics - Cyclomatic Complexity - FTrace call graphs - 28 November 2018, 12 April 2020  
- related to 581,770

---

1. FTrace kernel function call graph shell script (asfer\_ftrace.sh) already in USBmd and USBmd64 have been included as part of AsFer Cyclomatic Software Analytics for analyzing what happens in kernel within while executing a userspace code.
2. Example ftrace.log for Computational Geometric Factorization has been

recorded in ftrace.DiscreteHyperbolicFactorization\_TileSearch\_Optimized.log  
3. DOT graph creation function for parsing ftrace call graph log has been added in CyclomaticComplexitySparkMapReducer.py  
4. FTrace call graph DOT file is written to CyclomaticComplexitySparkMapReducer.ftrace\_callgraph.dot  
5. logs for Cyclomatic Analysis of kernel callgraph for previous factorization example have been committed to:

testlogs/CyclomaticComplexitySparkMapReducer.log.FTrace.28November2018

testlogs/DiscreteHyperbolicFactorizationUpperbound\_TileSearch\_Optimized.factors

testlogs/DiscreteHyperbolicFactorizationUpperbound\_TileSearch\_Optimized.ftrace.log.28November2018

6. PageRank, Degree Centrality, Cycles and Longest Path of Call graph are printed.

7. Least pageranked kernel functions are:

```
... ('unix_release\n', 0.0006824636787772093), ('nf_ct_get_tuple\n',
0.0006824636787772093), ('insert_work\n', 0.0006824636787772093),
('wake_up_worker\n', 0.0006824636787772093), ('__tcp_push_pending_frames\n',
0.0006824636787772093), ('bictcp_cong_avoid\n', 0.0006824636787772093),
('fsnotify_clear_marks_by_inode\n', 0.0006824636787772093),
('tcp_timewait_state_process\n', 0.0006824636787772093), ('ktime_get\n',
0.0006824636787772093), ('free_page_and_swap_cache\n', 0.0006824636787772093),
('update_page_reclaim_stat\n', 0.0006824636787772093), ('__cond_resched\n',
0.0006824636787772093), ('unlink_anon_vmas\n', 0.0006824636787772093),
('timer_interrupt\n', 0.0006824636787772093), ('inet_put_port\n',
0.0006824636787772093), ('update_process_times\n', 0.0006824636787772093),
('tcp_v4_send_ack\n', 0.0006824636787772093), ('ext4_get_inode_loc\n',
0.0006824636787772093), ('enable_8259A_irq\n', 0.0006824636787772093),
('__pagevec_free\n', 0.0006824636787772093), ('getnstimeofday\n',
0.0006824636787772093), ('dequeue_task\n', 0.0006824636787772093),
('__jbd2_journal_file_buffer\n', 0.0006824636787772093), ('fuse_prepare_release\n',
0.0006824636787772093), ('tcp_established_options\n',
0.0006824636787772093), ('fuse_release_common\n', 0.0006824636787772093)
```

...

which are top level invocations closest to userspace arising out of TCP traffic in Spark Executor Driver (TCP in kernel:

[http://vger.kernel.org/~davem/tcp\\_output.html](http://vger.kernel.org/~davem/tcp_output.html))

8. It is worthy to note lot of ----exit() kernel functions related to VMA paging (e.g.do\_exit()) which release virtual memory pages (possibly by GC) and TCP (tcp\_write\_xmit(), tcp\_transmit\_skb(), etc.,) having high degree centrality showing heavy TCP traffic.

Comparing call graphs by Graph Isomorphism or Graph Non-Isomorphism deduces code similarities. This is somewhat counterintuitive surprise to Program Equivalence Problem which is undecidable implying isomorphism detection is only an approximation. Program Equivalence essentially asks if two Turing machines accept same language (equivalent).

References:

-----

619.1 Program Equivalence Problem is Undecidable - [Nancy Lynch] - Mapping Reduction to/from Halting Problem - [https://ocw.mit.edu/courses/electrical-engineering-and-computer-science/6-045j-automata-computability-and-complexity-spring-2011/lecture-notes/MIT6\\_045JS11\\_lec09.pdf](https://ocw.mit.edu/courses/electrical-engineering-and-computer-science/6-045j-automata-computability-and-complexity-spring-2011/lecture-notes/MIT6_045JS11_lec09.pdf) - two Turing machines M1 and M2 are contrived and hypothetical Turing Machine M compares the M1 and M2. Reduction: M halts on x  $\Leftrightarrow \langle M1, M2 \rangle$  are not equivalent (EQ'). M1 always rejects while M2 accepts if M accepts x else rejects. There are two possibilities:

(\*) M1 rejects and M2 accepts (because M accepts x  $\Rightarrow M1 \neq M2$ )

(\*) M1 rejects and M2 rejects (because M rejects x  $\Rightarrow M1 = M2$ )

(\*) But LHS is undecidable Mortality problem  $\Rightarrow M1$  and  $M2$  are not

equivalent is undecidable

(\*) Complement of the previous is hence undecidable

619.2 Call Graphs for Multilingual Software Analysis - [Anne Marie Bogar, Damian

Lyons, David Baird] - <https://arxiv.org/pdf/1808.01213.pdf> - NeuronRain Call Graphs are dynamic and multilingual - KCachegrind for userspace C/C++/Java and SATURN/FTrace for kernelspace C code.

619.3 Game theoretic epidemic model of cybercrimes - [https://link.springer.com/chapter/10.1007/978-3-642-17197-0\\_9](https://link.springer.com/chapter/10.1007/978-3-642-17197-0_9) - [Bensoussan A., Kantarcioglu M., Hoe S. (2010) A Game-Theoretical Approach for Finding Optimal Strategies in a Botnet Defense Model. In: Alpcan T., Butty=E1n L., Baras J.S. (eds) Decision and Game Theory for Security. GameSec 2010. Lecture Notes in Computer Science, vol 6442. Springer, Berlin, Heidelberg] - A Game-Theoretical Approach for Finding Optimal Strategies in a Botnet Defense Model - "...Botnets are networks of computers infected with malicious programs that allow cybercriminals/botnet herders to control the infected machines remotely without the user's knowledge. In many cases, botnet herders are motivated by economic incentives and try to significantly profit from illegal botnet activity while causing significant economic damage to society. To analyze the economic aspects of botnet activity and suggest feasible defensive strategies, we provide a comprehensive game theoretical framework that models the interaction between the botnet herder and the defender group (network/computer users). In our framework, a botnet herder's goal is to intensify his intrusion in a network of computers for pursuing economic profits whereas the defender group's goal is to defend botnet herder's intrusion. The percentage of infected computers in the network evolves according to a modified SIS (susceptible-infectious-susceptible) epidemic model. For a given level of network defense, we define the strategy of the botnet herder as the solution of a control problem and obtain the optimal strategy as a feedback on the rate of infection. In addition, using a differential game model, we obtain two possible closed-loop Nash equilibrium solutions. They depend on the effectiveness of available defense strategies and control/strategy switching thresholds, specified as rates of infection. The two equilibria are either (1) the defender group defends at maximum level while the botnet herder exerts an intermediate constant intensity attack effort or (2) the defender group applies an intermediate constant intensity defense effort while the botnet herder attacks at full power...." - FTrace analyzer in NeuronRain for kernel callgraphs provides a streaming delta-debugging feedback on rate of infection e.g delta changes (frequent call subgraphs in evolving SIS graph) in malicious patterns of infected kernels thus aiding a strategy.

-----  
 620. (THEORY) Space Filling, Separate Chaining Hash Tables, Theoretical EVMs, Timeout, Balls-and-Bins, Linear Programming, Program Analysis, Cellular Automata, Majority Hardness Amplification Lemma - 30 November 2018, 1 December 2018, 2 December 2018, 28 January 2019 - related to 135, 517, 615  
 -----

Space Filling has been defined in terms of Linear Program in <https://sites.google.com/site/kuja27/Analysis%20of%20a%20Randomized%20Space%20Filling%20Algorithm%20and%20its%20Linear%20Program%20Formulation.pdf> and its cellular automaton algorithm version has been described earlier. This linear program with constraint that every variable is non-zero:

$$x_1 + x_2 + \dots + x_n = N, \text{ for all } x_i > 0$$

is isomorphic to an LSH set partition, Integer Partition or Separate Chaining hash table partition of n parts of a set of N items. In most scenarios this is a restricted partition. Separate Chaining and Balls-Bins problems are equivalent if buckets are filled at random. Following are some of the probability estimates for Balls-and-Bins problem:

620.1 Average number of balls in a bin =  $n/b$  (n balls and b bins)

620.2 Number of balls to toss till a bin contains a ball:

probability of ball/item landing in a bin/bucket  $q=1/b$ ,  $p=1-q$

Number of tosses till success is Bernoulli trial geometric distribution

For success after kth ball toss, bernoulli probability:  $p^{(k-1)}q$

Since k is a random variable,  $E(k) = \text{Sum over } k \cdot p^{(k-1)}q = b$

620.3 Number of balls tossed till every bin has a ball:

Total number of bins = b

Number of balls  $n$  is partitioned as  $n_1 + n_2 + n_3 + \dots + n_k = N$  for each stage of tossing.

After  $i$ th stage, number of bins having atleast one ball =  $i-1$

Number of remaining buckets =  $b-i+1$

Probability of a toss landing in remaining buckets in  $i$ th stage =  $(b-i+1)/b$

Each  $n_i$  is a random variable of probability =  $b/(b-i+1)$

Sum of  $E(n_i) < O(b \ln b)$  before every bin has a ball.

Balls and Bins have histogram representation and previous bounds apply to histogram patterns too. In the context of theoretical EVMs if every voter votes perfectly at random with no prejudice to a candidate, number of voters required for every candidate to have atleast 1 vote =  $O(b \ln b)$  for  $b$  candidates. Course material in

([https://github.com/shrinivaasanka/Grafit/blob/master/course\\_material/NeuronRain/AdvancedComputerScienceAndMachineLearning/AdvancedComputerScienceAndMachineLearning.txt](https://github.com/shrinivaasanka/Grafit/blob/master/course_material/NeuronRain/AdvancedComputerScienceAndMachineLearning/AdvancedComputerScienceAndMachineLearning.txt)) describe a separate chaining

hashtable timeout based OS scheduler pattern and similar bounds apply - Number of processes required for atleast one process per timeout value =  $O(b \ln b)$ .

Previous linear program version of separate chaining if solved by Balls-and-Bins has similar bounds -  $O(n \ln(n))$  for solving LP of  $n$  variables.

To ensure secrecy of balloting, every vote appended to a candidate bucket in Theoretical Separate Chaining EVM has to be mapped to a unique one time randomly generated numeric id obfuscating the voter identity (and each bucket is encrypted). Mining patterns in this anonymous dictionary elicits only voting patterns and not voter patterns. Majority version of hardness amplification lemma described earlier envisages a MajorityInverse() function which inverts Majority+VoterSAT Boolean function composition for 2 candidates and obtains voters voting for a candidate and per voter SAT assignments top-down. Hardness of this MajorityInverse() is crucial to prove amplification. Theoretical EVM for 2 candidates is exactly separate chaining/LSH version of Majority gate of binary inputs 0 and 1 and Majority() and MajorityInverse() are defined as:

- Majority(): candidate of maximum sized voters bucket

- MajorityInverse(): voters bucket for a candidate

Intriguingly, MajorityInverse() is palpably easier in this separate chaining/LSH version of majority gate but previous anonymizer rules out easy inversion. Voter is issued a receipt containing the encrypted ciphertext of the candidate bucket index his/her vote is appended to. Encrypted receipt of vote issued to voter is more reliable than VVPAT which is in plaintext and not voter-received. Ballot secrecy is not compromised because this encryption is as secure as any other ciphertext transmitted over the network by public key infrastructure. Only authority accountable for conduct of voting can decrypt the receipt in case of disputes.

#### References:

-----

620.4 Introduction to Algorithms - [Cormen-Leiserson-Rivest-Stein] - Coupon Collector Problem/Balls and Bins Problem - Page 134 (5.4.2), Page 1201 (C.4)

620.5 Analysis of Electronic Voting System - John Hopkins Paper - [TADAYOSHI KOHNO, ADAM STUBBLEFIELD, AVIEL D. RUBIN, DAN S. WALLACH] -

<https://homes.cs.washington.edu/~yoshi/papers/eVoting/vote.pdf> - Analyzes C++ Source Code of Diebold AccuVote EVM and stresses VVPAT. Vulnerabilities include unencrypted ballot definition file tamper, Safety of Protective Counter storing number of votes polled, Party Affiliation tamper etc., - "...On a potentially much larger scale, if the voting terminals download the ballot definition over a network connection, then an adversary could tamper with the ballot definition file en-route from the back-end server to the voting terminal; of course, additional poll-worker procedures could be put in place to check the contents of the file after downloading, but we prefer a technological solution. With respect to modifying the file as it is sent over a network, we point out that the adversary need not be an election insider; the adversary could, for example, be someone working at the local ISP. If the adversary knows the structure of the ballot definition, then the adversary can intercept and modify the ballot definition while it is being transmitted. Even if the adversary does not know

the precise structure of the ballot definition, many of the fields inside are easy to identify and change, including the candidates' names, which appear as plain ASCII text...". In the context of theoretical EVMs on cloud defined previously based on LSH/Separate chaining, these encryption prerequisites are relevant in addition to CAP theorem limitations and PACELC theorem consistency versus speed trade-off. Per-candidate vote counters are replaced by hash table buckets which have to be secured. History preserving VVPAT audit trails require linking voters to votes which is obviously evident from per-candidate vote buckets. Frequent item set mining (e.g FPGrowth) of EVM buckets could point to malicious and suspicious voting patterns which is not feasible in counter increment.

-----  
621. (FEATURE) Social Network Analysis - People Analytics - Dictionary filter for names - 4 December 2018  
-----

-----  
1. RecursiveGlossOverlap\_Classifier.py has been changed to define a new function nondictionaryword() for filtering nondictionary words. This is necessary for parsing text of Social Profiles which contain names in SocialNetworkAnalysis\_PeopleAnalytics.py. Finding names in text is an open AI problem which comes under the purview of Named Entity Recognition (NER) which often requires CRF or Neural Network Training models.  
2. As an alternative to statistical learning, if a word in text is not in a language Dictionary it is assumed to have exited any semantic network (WordNet for English etc.,) which could be names of people, places etc., But there are some exceptions to this and countably few names are in language dictionaries and encyclopedia.  
3. Function nondictionaryword() lookup a word in PyDictionary which is based on WordNet, Google Translation, Thesaurus.com and returns true or false based on language dictionary. If for a word lookup null meaning is returned, it is outside Semantic Network and nondictionaryword() returns true.  
4. Depth of the Recursive Gloss Overlap recursion has been parametrized in RecursiveGlossOverlap\_Classifier.py and RecursiveLambdaFunctionGrowth.py and invoked in SocialNetworkAnalysis\_PeopleAnalytics.py for depth 2.  
5. WordNet and ConceptNet consist of network of concepts than textual words. PyDictionary has additional support for other datasources - Google Translation and Thesaurus - specific to language words.  
-----

-----  
622. (THEORY and FEATURE) Text (De)Compression by HMM on Vowelless texts - Prefix and Suffix Probabilities from English Dictionary - 6 December 2018  
-----

-----  
1. Python implementation for Decompressing vowelless compressed text TextCompression.py has been updated to invoke Prefixes and Suffixes probability priors computed from English Dictionary instead of hardcoded priors.  
2. New source file WordSubstringProbabilities.py for computing word prefixes and suffixes probabilities by FreqDist has been committed which parses English Wordlist from Dictionary.txt into two probability distribution dictionaries for prefixes and suffixes.  
3. Function wordprefixsuffixprobdist() in WordSubstringProbabilities.py called in TextCompression.py has been nominal because of computationally intensive Maximum Likelihood Estimator in Hidden Markov Model (likelydict) and hardcoded priors are used.  
4. Logs for this commit have been committed to WordSubstringProbabilities.log.6December2018 and TextCompression.log.6December2018.gz  
5. compressedtext.txt and decompressedtext.txt have been updated  
6. MLE likelydict is  $O(\text{prefixes} * \text{suffixes}) = O(\text{number\_of\_words}^2 * \text{length\_of\_longest\_word}^2)$  is costly one time disk read and might require some memcache-ing during initialization.  
-----

-----  
623.(THEORY) Arithmetic Circuit Complexity, Diophantine Complexity, Universal  
Diophantine Equation, ABC  
Conjecture, Complementary Sets, Diophantine Representation of Complementary  
Sets, Proof Complexity - 7 December 2018, 8 December 2018 - related to 617  
-----

Arithmetic Circuits are directed acyclic graphs of operands  $+$ (sum),  $*$ (product) as internal circuit elements (gates) and variable or numeric constant inputs as leaves. There is one output gate at root. Arithmetic circuits formalize computation of polynomials over a coefficient field. Some prominent upper bound (Big-O) results in arithmetic complexity include Matrix Multiplication and lower bound (Omega) results include size of arithmetic circuit computing exponential polynomials. It has to be noted that solving Diophantine equations and computing polynomials are two opposite inverse directions - solving diophantines involves searching for a solution space while computing polynomials is circuit value problem and involves substituting solution values in arithmetic circuit input variables and evaluating the root gate. Algebraic Complexity classes VP and VNP define the arithmetic hierarchy of polynomials - VP contains polynomials which have polynomial size arithmetic circuits while VNP has polynomials such that coefficient of every monomial in it can be found efficiently. Permanent of a matrix has been shown to be complete for the class VNP by [Valiant]. If Permanent has polynomial size circuits,  $VP=VNP$ . From MRDP theorem, every recursively enumerable set is known to have a diophantine equation representation. There exists a universal diophantine equation which represents every recursively enumerable set ([Jones] theorem). Present state-of-the-art is universal diophantine of 9 unknowns of huge degree  $1.6 * 10^{45}$ . It is open if Diophantine complexity class D ([Adleman-Manders]) is in NP (or D in VNP in algebraic complexity because  $P$  in NP implies  $VP$  in VNP?). Complementary Sets (Beatty Sequences) and their relevance to ABC Conjecture have been described earlier. By universal diophantine equation of 9 unknowns but huge degree, every subset of quality  $1+\epsilon$  for every real  $\epsilon > 0$  predicted by ABC conjecture can be represented. Complexity of a Diophantine Equation is also expressed by proof complexity notion of number of additions, multiplications required for verifying a solution. For universal diophantine equation, current known proof complexity bound is 100.

References:

-----  
623.1 Arithmetic Circuit Complexity -  
[https://en.wikipedia.org/wiki/Arithmetic\\_circuit\\_complexity](https://en.wikipedia.org/wiki/Arithmetic_circuit_complexity)  
623.2 Circuit Complexity - [Heribert Vollmer] - Chapter 5 - Arithmetic Circuits and Straightline Programs - <https://books.google.co.in/books?id=q0epCAAQBAJ&pg=PA172&lpg=PA172&dq=arithmetic+circuits+heribert+vollmer&source=bl&ots=KiFHOVH3kh&sig=Q5PaW5rJEHI8LBU0iYfNSrRXrwk&hl=en&sa=X&ved=2ahUKEwivu8GZo43fAhXLTn0KHek8BWI4ChDoATAJegQIABAB#v=onepage&q=arithmetic%20circuits%20heribert%20vollmer&f=false>  
623.3 Undecidable Diophantine Equations - [James P Jones] -  
<https://pdfs.semanticscholar.org/7f96/11e582cf4a2efb1155c2fde9c891c6fc7be3.pdf> -  
Universal Diophantine Equation for representing every recursively enumerable set which applies Kummer's Theorem for factoring Binomial Coefficients.  
623.4 Arithmetization of 3SAT - Randomized Algorithms - [Rajeev Motwani - Prabhakar Raghavan] - Page 177 (Section 7.7) - 3SAT can be arithmetized to a multilinear diophantine polynomial by replacing each clause of the form  $(x_1 \vee x_2 \vee x_3)$  to  $(1-(1-x_1)(1-x_2)(1-x_3))$  which can be solved for integer or real solutions. Number of unknowns in diophantine equals number of variables of 3SAT. This reduction implies diophantine class D is in NP. Real solutions to this SAT diophantine (e.g by Tarski method) is another kind of relaxation similar to least squares approximate MAXSAT Solver. But an added advantage is there exists a universal diophantine equation in 9 unknowns for any 3SAT diophantine though number of variables in 3SAT could be unlimited.

-----  
624. (THEORY) Shell Turing Machines, MRDP Theorem, Category Theory, Diophantine Equations, Turing Degrees, Embedding Formal Languages in Vector Space - 10  
December 2018, 21 August 2019 - related to 538  
-----

-----  
Intuition for Shell Turing Machines defined in <https://5d99cf42-a-62cb3a1a-s-sites.googlegroups.com/site/kuja27/UndecidabilityOfFewNonTrivialQuestions.pdf> has been explained in NeuronRain FAQ <https://neuronrain-documentation.readthedocs.io/en/latest/> . Dimension of a Shell Turing Machine parallels Turing Degree of a Turing Machine which is a measure of unsolvability of a set. Every Shell Turing Machine is defined on a vector space and all Shell Turing machines of similar dimension create an equivalence class. Partial Order Semi-Lattice is induced by this vector space dimensional hierarchy of Shell Turing Machines. Following example Shell Turing Machines defined over two different vector spaces of dimensions  $d_1$  and  $d_2$  motivate solvability hierarchy:

Turing Machines  $Td_1$  and  $Td_2$  find the lexicographically longest tuple (word) in languages  $L(Td_1)$  and  $L(Td_2)$ . Tuples in  $L(Td_1)$  and  $L(Td_2)$  are of the form  $[x_1, x_2, x_3, \dots, x_{d_1}]$  and  $[x_1, x_2, x_3, \dots, x_{d_2}]$  respectively. Though both  $Td_1$  and  $Td_2$  are computationally similar, words in  $L(Td_1)$  and  $L(Td_2)$  belong to two different vector spaces of dimensions  $d_1$  and  $d_2$  therefore returning different results of lengths  $d_1$  and  $d_2$ . This implies Turing degrees of  $Td_1$  and  $Td_2$  are different and the two machines solve varied difficulties.

In this sense, Shell Turing Machines generalize the notion of word embeddings of natural languages (e.g Word2Vec) in a vector space to any formal language - Regular, Context-Free, Context-Sensitive or Natural, Recursive, Recursively Enumerable - and formal languages become algebraic sets (similarity to VP and VNP is intriguing). MRDP Theorem implies Goedel's First Incompleteness Theorem. MRDP Theorem implies there are recursively enumerable sets having Diophantine representation but not recursive (there are no halting accept/reject Turing machines and therefore  $H_{10}$  is undecidable for set of integers). For Shell Turing Machines, MRDP theorem applies too but there is an additional fine structure (Dimension hierarchy partial order) introduced by vector space dimensions similar to Turing Degrees. Another relevant question arises: How Shell Turing Machines map to Diophantine representations i.e What is the relation between (number of unknowns, degree) of a diophantine equation of an RE set to the vector space dimension of Shell Turing Machine accepting it.

Example embedding of natural language text sentence in a Shell Turing Machine defined over vector space:

-----  
Sentence: "This is bigger than the biggest" is an oxymoron if read flat with no dimensional depth. Assuming there exists set of Shell Turing Machines defined on a vector space of dimension  $d+x$  having oracle access to Shell Turing Machine defined on a vector space of dimension  $d$  (Turing Jump), following dimension subscripted sentence is an example sentence in a Shell Turing Machine of dimension  $d+x$  having oracle access to lower dimensional ( $d$ ) Shell Turing Machine and transcends two vector spaces of varied dimensions:

This ( $d+x$ ) is bigger ( $d+x$ ) than the biggest( $d$ )  
Vector Space for a Shell Turing Machine can be any arbitrary topological space in real analysis e.g Baire Space, Cantor Space (sets homeomorphic to Cantor Set Fractal obtained by removing midsegment of a line indefinitely)

Set of Recursively Enumerable Languages can be written as disjoint union/exact cover of recursively enumerable languages of Shell Turing Machines embedded in vector spaces of all possible dimensions:

$$RE = RE(d_1) \cup RE(d_2) \cup RE(d_3) \dots \cup RE(d_n)$$

Since each dimension corresponds to a Turing Degree (measure of unsolvability), Partial Order Semi Lattice of all Shell Turing Machines has a Lowest Upper Bound



dimension - There exists a maximal dimension Turing Machine  $dm$  accepting some  $RE(dm)$  language. Shell Turing Machines are most befitting in formalizing Computational Physics problems e.g Quantum and Relativistic Physics, String Theory/M-Theory, Branes, Multiverses.

An adaptation of Halting Problem to Shell Turing Machines

-----  
Undecidability of Halting Problem is proved by following gadget (oversimplified):

Turing Machine  $M'$  accepts an encoding of another Turing Machine  $M$  and an input  $x$  -  $M'(M,x)$ .

$M'$  rejects and halts if  $M$  accepts and halts on  $x$

$M'$  accepts and halts if  $M$  rejects and halts on  $x$

Turing Machine  $M''$  accepts if  $M'$  rejects and rejects if  $M'$  accepts which detects  $M$  has halted either way -  $M''(M'(M,x))$

Contradiction is established by changing the Turing machine encoding to  $M'$  from  $M$  as  $M'(M',x)$ :

$M'$  rejects and halts if  $M'$  accepts and halts on  $x$

$M'$  accepts and halts if  $M'$  rejects and halts on  $x$

which is crucial to undecidability of halting. Previous encoding has no dimensional information. If  $M'$  and  $M$  are

Shell Turing Machines of varied dimensions  $d1$  and  $d2$ , Halting Problem is rephrased as -  $M''(M'[d1](M[d2],x[d2]))$  - Turing Machine  $M'$  defined in space of dimension  $d1$  accepts encoding of Turing Machine  $M$  and an input  $x$  defined in space of dimension  $d2$  ( $d1 > d2$ )

Following diagonalization proof of halting problem undecidability extends to Shell Turing Machines:

-----  
Let  $f(x,i)$  be a function defined as:

$f(x,i) = 1$  if Turing Machine  $x$  halts on input  $i$ ,  $0$  if Turing Machine  $x$  does not halt on input  $i$ .

Let  $g(y)$  be another function defined as:

$g(y) = 0$  if  $f(y,y)=0$ , else undefined (if  $f(y,y)=1$ )

Diagonalization is an infinite two dimensional matrix  $D$  defined as:

$D(x,y) = 1$  if Turing Machine  $x$  halts on input  $y$ ,  $0$  if Turing Machine  $x$  does not halt on  $y$

Proof is by showing function  $f(x,i)$  is partial and not total (not defined for all inputs) and thus not recursive but recursively enumerable.

Nothing prevents asking what is  $g(g)$ :

$g(g) = 0$  if  $f(g,g)=0$  then  $0$ , else undefined (if  $f(g,g) = 1$ )

$\Rightarrow f(g,g) = 1$  if Machine  $g$  halts on encoding of  $g$ ,  $0$  if Machine  $g$  does not halt on encoding of  $g$  (Diagonal of the Diagonalization Matrix  $D$ )

But from previous definition of  $g(g)$ :

$g(g) = 0$  if  $f(g,g)=0$  (if Machine  $g$  does not halt on  $g$ ) then  $g(g)$  halts returning  $0$  and

if  $f(g,g)=1$  (if Machine  $g$  halts on  $g$ ) then  $g(g)$  is undefined

which is a contradiction.

The fact that there exists atleast one Turing Machine  $g$  whose halting is not decidable makes  $f(x,i)$  partial and not a total recursive function and therefore Halting problem is undecidable. It has to be noted that function  $g$  has oracle access to Halting problem function  $f(x,i)$  thus defining a Turing jump ( $0'$ ). But Recursively Enumerable set has been previously expressed as disjoint union of languages of Shell Turing Machines defined on all possible vector spaces. This implies there are Shell Turing Machines which are not recursive (but represented by a Diophantine equation). Implications of this for problems in Quantum computation and Relativistic Physics defined for example on Hilbert Spaces are

huge - There are Shell Turing Machines defined on certain vector spaces which are not recursive (or) there are no physics experiments for verifying truths of physical realities represented by these Hilbert Machines.

Problem of relevance to Shell Turing Machines is: What happens to halting problem if functions  $f$  and  $g$  are defined on two different vector spaces of unequal dimensions. If  $f(x,i)$  is embedded on a Hilbert space  $S1$  which contains all other vector spaces and  $g(y)$  on another Hilbert space  $S2$  ( $S1$  contains  $S2$ ), truth value of a logical statement in two quantifiers:

For all Shell Turing Machines  $x$  defined in Hilbert space  $S(d)$  of dimension  $d$ , there exists input  $i$  defined in  $S(d)$  such that  $x$  halts on  $i$  (True or False)

has to be exported to  $f(x,i)$  defined on Hilbert space  $S1$  containing  $S(d)$

This lifting/export of logical statements between Hilbert Spaces of 2 different dimensions is accomplished by Linear Transformations between Hilbert Spaces. Section 4.2 of Reference 624.5 describes some example definitions of logical formulas (conjunctive normal form) in Hilbert Spaces. Conjunctive Clauses of the formulas are represented as vectors of a Hilbert Space. It is not necessary that all transformations are possible. Computational Physics example: Assuming logical statements inside a blackhole singularity are defined in some Hilbert Space, existence of all possible linear transformations implies information (truths of logical formulas) oozes out of the blackhole space into observable space (e.g Hawking Radiation, Blackholes are not Black, Blackhole information paradox)

Traditional results on homomorphisms between Vector Spaces apply to Shell Turing Machines defined on any two vector spaces one of which is a subspace of the other:

(\*) If  $T$  is a homomorphism defined from vectorspace  $U$  to vectorspace  $V$  of kernel  $W$ , then  $V$  is isomorphic to  $U/W$ . Conversely, if  $U$  is a vectorspace and  $W$  is a subspace of  $U$ , then there is a homomorphism of  $U$  onto  $U/W$ .

(\*) If  $U$  is a vectorspace defined over field  $F$ , and  $W$  is a subspace of  $V$  then  $V/W$  is a quotient vectorspace over  $F$  if for  $v_1, v_2$  in  $V$  and  $v_1 + W$  in  $V/W$ ,  $v_2 + W$  in  $V/W$ :

$$(v_1 + W) + (v_2 + W) = (v_1 + v_2) + W$$

(and)

$$\text{For } a \text{ in } F, a(v_1 + W) = av_1 + W$$

If Shell Turing Machines  $S1(U)$  and  $S2(W)$  are defined over vector spaces  $V$  and  $W$  and  $W$  is subspace of  $V$  and there is a homomorphism  $T$  (defined by relation "bigger than") from  $V$  to  $V/W$ , previous example oxymoron sentence - "This is bigger than the biggest" - is logically defined in quotient space  $V/W$  in first order logic quantifiers as (annotated by square parentheses):

This is [There exists  $v_1$  in  $V$ ] bigger than [ $T(v_1, \text{identity} + w_1): v_1 > \text{identity} + w_1$ ] the biggest [there exists  $w_1$  in  $W$  such that for all  $w$  in  $W$ ,  $w_1 > w$ ]

Shell Turing Machines can be defined in terms of Category Theory too:

-----  
Category Theory of [Eilenberg-MacLane] abstracts whole of mathematics into following:

(\*) Category  $C$  is a Set of Objects associated with a topological space

(\*) Every Category has set of morphisms  $f:a-b$  defined on objects  $a,b$  in Category  $C$  - morphisms are maps between objects on topological spaces - every morphism  $f:a-b$  on objects  $a,b$  in topological spaces can be a Shell Turing Machine defined on topological spaces of  $a$  and  $b$

(\*) Functors  $F$  are maps between two Categories  $C1$  and  $C2$  - for each object  $x$  in  $C1$ ,  $F(x)$  is in  $C2$  and for each morphism  $f:a-b$  in  $C1$  morphism,  $F(f):F(a)-F(b)$  is in  $C2$  - every functor  $F$  can be a Shell Turing Machine defined on topological spaces of  $F(a)$  and  $F(b)$

References:

-----

624.1 Turing Jump, Priority Method of Emil Post, Injury -

[https://en.wikipedia.org/wiki/Turing\\_degree#Post's\\_problem\\_and\\_the\\_priority\\_method](https://en.wikipedia.org/wiki/Turing_degree#Post's_problem_and_the_priority_method) - Turing jump of a Turing Machine  $X$  is the set  $X'$  of Turing machines which halt by having oracle access to  $X$  or in other words,  $X'$  is set of harder problems than  $X$ . Priority method is applied to prove existence or otherwise of intermediate degrees between two Turing machines of different jumps e.g Turing Degree 0 (halting problem) and Turing Degree  $0'$  (problems having oracle access to halting problem). Priority method tabulates requirements  $A_e$  and  $B_e$  for an oracle machine  $e$  where  $A_e$  stipulates  $e$  does not compute  $0'$  from  $X$  and  $B_e$  implies non-oracle machine  $e$  does not compute  $X$ . Dimensional Hierarchy of unsolvability follows from Turing Jump.

624.2 Embedding Turing Machines on Hilbert Space -

<https://mathoverflow.net/questions/313343/embedding-turing-machine-counts-functions-for-languages-of-turing-machines-by-number-of-states-and-searches-for-the-turing-machines-for-these-languages> - This is the opposite direction of Shell Turing Machine definition which has an intrinsic dimensional parameter in addition to state.

624.3 Definability of Turing Jump - [Shore-Slaman] -

<https://math.berkeley.edu/~slaman/papers/jump.pdf> - relation between Turing Machines  $A$  and  $B$ ,  $A <_T B$  implies  $A$  is recursive in  $B$  or  $A$  is Turing-computable by oracle access to  $B$ .  $A =_T B$  ( $A <_T B$  and  $B <_T A$ ) is the Turing Degree, an equivalence class of machines solving sets of similar difficulties. Turing Jump  $A' = \{e \mid \text{Machine } e \text{ halts on oracle access to } A\}$

624.4 Aspects of Turing Jump - [Slaman] -

<https://math.berkeley.edu/~slaman/papers/lc2000.pdf>

624.5 Hilbert Machines - Turing Machines in Complex Inner Product Spaces and Applications to Quantum Computation -

<http://citeseerx.ist.psu.edu/viewdoc/download?doi=10.1.1.36.73&rep=rep1&type=pdf> - has close resemblance to definition of Shell Turing Machines. Linear Machines are conventional Turing Machines defined over input vector space, output vector space and a state vector space. Concrete Hilbert Machines are Linear Machines defined over a Hilbert Complex Vector Space and a linear Complex Operator - Theorem 8 - Any finite automata can be represented in a finite dimensional Hilbert Space by a Hilbert Machine - Examples of Hilbert Machines - Quantum Computation: Input and Output to a Quantum Computer are represented by vectors on Hilbert Space and computation (state transition) is performed by Unitary Operator  $H$  on Hilbert Spaces (Operator  $HH^* = H^*H = I$ ,  $H^*$  is infinite dimensional conjugate transpose of  $H$ ) - Expected Value of State (at time  $t$ ) =  $e^{(-iHt)}$ . Shell Turing Machines go beyond just embedding a Turing Machine in vector space - As the name "Shell" suggests inspired by Unix shells, truths of logical statements in lower dimensional vector spaces are allowed to be exported to higher dimensions.

624.6 The Elegant Universe: Superstrings, Hidden Dimensions, and the Quest for the Ultimate Theory - [Brian Greene]

624.7 Turing Degrees of Diophantine Sets - Computably Enumerable Turing Degrees - Hilbert Tenth Problem - Sixth Asian Logic Conference -

[https://books.google.co.in/books?id=7IbVCgAAQBAJ&pg=PA152&lpg=PA152&dq=diophantine+equations+turing+degree&source=bl&ots=q9HomH3o-9&sig=rHKb81u6mifJvOX\\_-kjkV4YRdUY&hl=en&sa=X&ved=2ahUKEwjMpLvsur3fAhVNeisKHd\\_MA-U4ChDoATABegQIBRAB#v=onepage&q=diophantine%20equations%20turing%20degree&f=false](https://books.google.co.in/books?id=7IbVCgAAQBAJ&pg=PA152&lpg=PA152&dq=diophantine+equations+turing+degree&source=bl&ots=q9HomH3o-9&sig=rHKb81u6mifJvOX_-kjkV4YRdUY&hl=en&sa=X&ved=2ahUKEwjMpLvsur3fAhVNeisKHd_MA-U4ChDoATABegQIBRAB#v=onepage&q=diophantine%20equations%20turing%20degree&f=false)

624.8 Degrees of Unsolvability: Tutorial -

<https://pdfs.semanticscholar.org/acae/fe1907be68d357700f0690519251fc948fdb.pdf> - Mass Problems, Muchnik Degrees, Turing Degrees

624.9 Linear Transformations in Hilbert Space - [Stone] -

<https://www.ams.org/journals/bull/1934-40-11/S0002-9904-1934-05973-1/S0002-9904-1934-05973-1.pdf> - Transform points on one Hilbert Space to points on another Hilbert Space

624.10 Geometry of Interaction and Linear Logic - [Girard] -

[https://en.wikipedia.org/wiki/Geometry\\_of\\_interaction](https://en.wikipedia.org/wiki/Geometry_of_interaction) - Proofs are represented as Networks of Logical Statement implications than trees in Sequent Calculus. This has some resemblance to Implication Graph Convex Hulls defined in <http://sourceforge.net/projects/acadpdrafts/files/ImplicationGraphsPGoodEquation>

AndPNotEqualToNPQuestion\_excerpts.pdf/download,  
[https://sites.google.com/site/kuja27/NotesOnConceptHypergraphHMM\\_and\\_ImplicationGraphConvexHulls\\_2013-12-30.pdf?attredirects=0&d=1](https://sites.google.com/site/kuja27/NotesOnConceptHypergraphHMM_and_ImplicationGraphConvexHulls_2013-12-30.pdf?attredirects=0&d=1),  
[https://sites.google.com/site/kuja27/ImplicationRandomGraphConvexHullsAndPerfectVoterProblem\\_2014-01-11.pdf?attredirects=0&d=1](https://sites.google.com/site/kuja27/ImplicationRandomGraphConvexHullsAndPerfectVoterProblem_2014-01-11.pdf?attredirects=0&d=1)

624.11 Searle's Chinese Room Argument, Turing Test and AI -  
[https://en.wikipedia.org/wiki/Chinese\\_room](https://en.wikipedia.org/wiki/Chinese_room) - Turing test differentiates a human from a machine by question-answering (e.g reCAPTCHA). If there is a machine translation turing machine translating English to Chinese, it does not necessarily imply machine understands English and Chinese(strong AI), but only simulates it (weak AI) - Human equivalent of a Turing machine in a room can exactly mimic Turing Machine by executing the translation algorithm churning out Chinese from English with no knowledge of English or Chinese whatsoever. Chinese room example demarcates measure of difficulties of two sets - understandability/consciousness and simulatability - and thus a Turing jump - human has oracle access to a translation turing machine.

624.12 Definability of Logical Formulas -

<http://www.math.wisc.edu/~msoskova/talks/MadisonColloquium.pdf>

624.13 Topics in Algebra - [Israel N.Herstein] - Chapter 4 - Vector Spaces and Modules - Page 174 - Theorem 4.1.1 and Lemma 4.1.2 - Quotient Spaces

624.14 Reproducing Kernel Hilbert Space -

[https://en.wikipedia.org/wiki/Reproducing\\_kernel\\_Hilbert\\_space](https://en.wikipedia.org/wiki/Reproducing_kernel_Hilbert_space) - Mathematical Functions are embedded on Hilbert Space and have distance metric defined on them. Every Function can be defined by a Turing Machine from Church-Turing Thesis.

-----  
625. (THEORY) Recursive Lambda Function Growth - TextGraph Machine Translation -  
10 December 2018 - related  
to 178  
-----

1. RecursiveLambdaFunctionGrowth python implementation has a new function to do machine translation of Text

Graph english word vertices to another natural language. It uses PyDictionary Google Translate REST API service internally.

2. An example Text Graph from Recursive Lambda Function Growth has been translated from English to Kannada (an Indian language).

3. This is just a primitive implementation without sentences creation which can be done through usual graph traversal or random walks.

4. Logs have been committed to

testlogs/RecursiveLambdaFunctionGrowth.log.MachineTranslation.10December2018  
-----

626. (THEORY) Partial Ordered Rankings, Intrinsic Merit Vectors, Galois Connections and ThoughtNet - related  
to all sections expanding

[https://tac.nist.gov/publications/2010/participant.papers/CMI\\_IIT.proceedings.pdf](https://tac.nist.gov/publications/2010/participant.papers/CMI_IIT.proceedings.pdf)

and <https://arxiv.org/abs/1006.4458> and ThoughtNet - 21 December 2018  
-----

Search Engines usually rank results as linear total order. Alternatively for each query ranked set of results

can be a partial order and not necessarily total. This has been mentioned as a passing reference in ArXiv and

NIST TAC articles previously. Traditionally Intrinsic Merit/Fitness is a scalar quantity which can be vectorized

based on feature dimensions. Consequently, two URLs may not be comparable by a total ordering < relation. Following example intrinsic merit vector partial ordered rankings of websites intuit this:

(1) Subset partial ordered ranking - set of subsets ordered by containment:

```
[1,2,3,4]
 | \
 [1,2,3] [2,3,4]
 | |
 [1,2] [2,3]
```

(2) Less Than or Equal To Ranking - Each tuple has elements of value less than or equal to elements of predecessor tuple:

```
[1,2,3,4] [2,3,2,5]
 | |
 [1,1,2,3] ----- [2,2,3,4]
 |
 [1,1,1,2]
```

Search Results for any two different queries thus create two partial ordered tuple sets of rankings. Galois connections define maps F and G between elements of two posets A and B subject to conditions:

```
a in A, b in B
F(a)=c in B, G(b)=d in A
F(a) <= b if and only if a <= G(b)
```

Previous Galois Connections provide an alternative spectacle to perceive

ThoughtNet - ThoughtNet as defined

elsewhere earlier is a hypergraph of sentence hyperedges on evocative hypervertices motivated by Psycho-and-Neurolinguistics. Search engine queries can be construed as evocatives returning results evoked by the query and thus search engine results are hyperedges of a ThoughtNet (Internet itself as a ThoughtNet) and queries are evocative hypervertices - same search result URL can appear in more than two queries creating the hyperedge across these query hypervertices. Previous partial ordered rankings of search results bring an additional application of Galois connections amongst search result posets - if URLs a,b,c,d are such that a=c and b=d aforementioned Galois connections are equivalent to hyperedges between ranked search query result posets in ThoughtNet and evocative hypervertices are search queries => ThoughtNet is a giant transitive Galois Connection which is different from Contextual Multi Armed Bandit formulation of ThoughtNet earlier. Various results and theorems applicable to ThoughtNet Hypergraphs (and its stripped down version of Survival Index Timeout pattern) have been mentioned in:  
[https://github.com/shrinivaasanka/Grafit/blob/master/course\\_material/NeuronRain/AdvancedComputerScienceAndMachineLearning/AdvancedComputerScienceAndMachineLearning.txt](https://github.com/shrinivaasanka/Grafit/blob/master/course_material/NeuronRain/AdvancedComputerScienceAndMachineLearning/AdvancedComputerScienceAndMachineLearning.txt)

References:

-----  
626.1 Galois Connections - [https://en.wikipedia.org/wiki/Galois\\_connection](https://en.wikipedia.org/wiki/Galois_connection)  
-----

-----  
627. (FEATURE) Vowelless Text (De)Compression - simplified likelydict MLE for HMM - 3 January 2019  
-----

- 
1. TextCompression.py has been classified to new class VowellessText and all functions have been made its members.
  2. One time Likelyhood Dictionary computation of prefixes, suffixes and substrings has been shifted to WordSubstringProbabilities.py - wordlikelydict() and wordprefixsuffixsubstringsprobdist()
  3. All precomputed prefix and suffix priors are initialized in TextCompression.py \_\_init\_\_()
  4. Costly loop in HiddenMarkovModel\_MLE() of TextCompression.py has been done away with and instead wordlikelydict() has been changed to choose between costly exhaustive search and substringsdict list comprehension.
  5. Hardcoded priors for HMM have been removed and replaced by previous

likelihood computation.

6. Logs for this have been committed to  
testlogs/TextCompression.log.3January2019

7. likelydict is created on demand once per compressed word than earlier heavy  
initialization for all possible likelihoods.

8. Regular Expressions are used in list comprehension for matching strings - "\_" are treated as alphabets in lower or upper case.

9. For Exhaustive Search. following line is crucial which computes the  
conditional probability of a prefix for a suffix:

likelydict[k3[:-1]+k3[len(k3)-1]+k4[1:]] = v3 \* v4

10. The else clause, generalizes it and applies precomputed frequency  
probabilities of concatenated substrings circumventing the following conditional  
probability:

likelydict[substring1 + substring2 + ... + substringN] =

Pr(substring1) \* Pr(substring2) \* ... \* Pr(substringN)

by:

likelydict[substring1 + substring2 + ... + substringN] =

Pr(substring1 + substring2 + ... + substringN)

11. Both should be almost equal if substring random variables are independent  
and identically distributed.

12. An example English text from

[https://www.valmikiramayana.net/utf8/yuddha/sarga128/yuddha\\_128\\_frame.htm](https://www.valmikiramayana.net/utf8/yuddha/sarga128/yuddha_128_frame.htm) - Verse  
120 has been compressed and decompressed.

13. Decompressed text has almost more than 50% accuracy and most priors are  
equal misleading the decipherment.

14. Previous HMM based probabilistic decompression can be compared to List  
decoding Berlekamp-Welch implementation which maps text to a polynomial

-----  
628. (FEATURE) Software Analytics - Hardcoded inputlayer replaced by Psutils - 8  
January 2019 - Usecase  
in 399 implemented  
-----

-----  
1.DeepLearning\_SoftwareAnalytics.py in software\_analytics/ has been updated and  
hardcoded process statistics

for input layer of BackPropagation have been replaced by Psutil systemwide load  
percentages

2.This implements the usecase for software analytics mentioned earlier and finds  
the weights for

input layer, hidden layer and output layer of BackPropagation multilayered  
perceptron.

3.Psutil provides cpu\_percentage(), memory\_percentage() and disk\_usage()  
functions fields from which have been used as input layer of the perceptron.

4.Sampling loop has been limited to 2 but it can be any number. For each value  
of instantaneous system load (cpu, memory, disk IO) backpropagation iterates for  
sometime (limited to 10000) and finds the weights.

5.For any two successive load values of input layer at two time points t and  
t+delta, the weights of the perceptron fluctuate and should theoretically  
stabilize for significant number of load samples (which is presently 2)

6.Output layer has been set to a high value of 99% implying heavily thrashed  
system and input percentage values are divided by 10000 instead of 100 for  
probabilities to prevent overflow errors (NaN and Inf).

7.Logs have been committed to

testlogs/DeepLearning\_SoftwareAnalytics.log.8January2019  
-----

-----  
629. (THEORY) Complement Diophantine Equations over Complex Numbers and  
Algebraic/Arithmetic Circuits for them, Blum-Shub-Smale Turing Machines, Thue  
and Siegel Equations, Elliptic Curves, Mordell Conjecture and Theorem, ABC  
Conjecture, Riemann Zeta Function, Chaos, Integer Factorization, Multiplicative  
Partitions - 9 January 2019, 12 April 2020, 14 November 2021, 23 February 2022 -

related to 24,490,617

-----  
As mentioned in previous sections, finding Diophantine representation of a complementary set reduces to creating a map  $f$  from diophantine set  $a=\{a_1,a_2,\dots,a_n\}$  such that  $f(x,b)=0$  for unknown  $x$  in  $\{\text{Integers/Reals/Rationals/Complex}\}$  and parameter  $b$  in  $a$ . Discussions previously have been mostly restricted to Integers, Reals and Rationals and terminology "complement function" is applied to a diophantine of integer solutions to  $x$  and is totally defined for all  $x$ (recursive) throughout all sections of this draft. Extension to Complex Diophantine Sets involves applying a converse of Thue's Equation which exactly solves a known homogenous bivariate diophantine  $f$ :

$$f(x,y)=m, \text{ } m \text{ is non-zero integer.}$$

$f(x,y)$  is factorized as:

$$f(x,y)=a(d)*\text{product}_{r=1\text{ to }d}(x-\alpha(r)*y)$$

where  $\alpha(r)$  are complex roots of  $f(t,1)=a_0+a_1*t+a_2*t^2+\dots a(d)*t^d=0$ .

But  $f$  is assumed to be unknown for a complementary diophantine set and has to be represented by reversing the factorization to an interpolation:

$$f(x,y)=a(d)*\text{product}_{r=1\text{ to }d}(x-\alpha(r)*y)$$

for all  $\alpha(r)$  in a complex complementary diophantine set

$CDS=\{\alpha_1,\alpha_2,\dots,\alpha_d\}$  which yields  $f(x,y)$  for integer values of  $x,y$ .

Assumption here is CDS is the set of complex roots of

$$f(t,1)=a_0+a_1*t+a_2*t^2+\dots a(d)*t^d=0.$$

Siegel Equation generalizes Thue's Theorem for arbitrary diophantine equations in integer coefficients.  $f(x,y)$  is decomposed as:

$$f(x,y) = h(x,y) + k(x,y)$$

where  $h(x,y)$  is homogenous and Thue's equation applies. Set of complex solutions of  $f(x,y)$  adjoined by set of distinct  $\{\alpha(r)\}$  form a Riemann compact surface of singularities or an algebraic curve which is the required Complement Diophantine Surface over Complex Numbers. Mordell-Weil Theorem is a classic result which states diophantine elliptic curves of the form:

$$y^2 = x^3 + ax^2 + bx + c$$

have finitely many rational solutions which can be obtained by a chord-tangent algorithm and create an abelian group. Elliptic curve diophantines of finite rational solutions are suitable candidates for formalizing finite sets of triples in complement diophantine version of ABC conjecture mentioned in 617 - "...Q1 is the 3 dimensional half-space of Cube tiled by finite sets of triples of quality  $1+\epsilon$  for every real  $\epsilon$ . As mentioned earlier, Pentominoes tiling is an exact cover problem for 2 dimensions..."

Algebraic or Arithmetic circuits for Diophantines over Complex Numbers can be defined by complexity classes over complex numbers (classes  $P_c, N_{pc}, \dots$ ). Blum-Shub-Smale Turing Machine model generalizes Turing Machines over  $\mathbb{Z}[2]$  to any Field Real, Complex, Rationals etc., For example, Hilbert Nullstellensatz problem decides if set of polynomials have common root and is in algebraic complexity class  $H_{nc}$  over complex numbers. Riemann Zeta Function can be represented as a disjunctive clauses or non-uniform Hilbert Nullstellensatz algebraic circuit in  $\Theta-1-H_{nc}$  (0 if  $s$  is a non-trivial zero else 1) of product polynomials having complex roots (non-trivial zeros):

$$RZF=\text{product\_of}(1/[1-\text{prime}(k)^{-s}]) \text{ for all primes } 2,3,5,7,\dots$$

Algebraic computation is defined by a binary tree - Algebraic Computation Tree over  $+, -, \%, *, \text{sqrt}()$ . From Koiran's Theorem  $\Theta-1-N_{pc}$  (variables are binary but polynomial size certificates are complex) is in  $AM[2]=BP.NP$  if Riemann Hypothesis is True which equates conventional complexity classes over  $\mathbb{Z}[2]$  and algebraic classes.  $\Theta-1-H_{nc}$  is  $\Theta-1-N_{pc}$ -complete and  $\Theta-1-H_{nc}$  is in  $PSPACE$ . This is an alternative circuit formulation to Euler-Fourier polynomial mentioned in 24 for Riemann Zeta Function. Number of solutions (non-trivial zeros) to previous RZF circuit can be characterized by counting class equivalent Sharp- $\Theta-1-H_{nc}$  (not in literature). From Riemann Hypothesis, all these solutions must have  $\text{Re}(s) = 0.5$ .

Riemann Hypothesis can be written as an infinite Disjunctive Normal Form SAT in

Blum-Shub-Smale Turing Machine model and by Hilbert Nullstellensatz finding non-trivial zeros of Riemann Hypothesis is  $\Theta$ -1-HNc and thus  $\Theta$ -1-NPc-complete (if infinite version of Nullstellensatz is  $\Theta$ -1-NPc-complete). Diophantine representation of RZF in 471.22 implies Riemann Hypothesis is in Diophantine class D which is subset of NP (for Turing machines over reals):

$RZF = \text{product\_of}(1/[1 - \text{prime}(k)^{(-s)}])$  for all primes  $k=2,3,5,7,\dots$

=> Each of the prime monomial having 1 as coefficient in infinite product can be written in Hilbert Nullstellensatz form as:

$\text{product\_of}(1 - k^{-s}) = \prod (1 - x_k), x_k = 1/k^s$

=>  $k^s = k^{(a+ib)} = k^a * k^{ib} = k^a * (e^{[ib * \log k]})$

=>  $k^a (\cos(b \log k) + i \sin(b \log k))$

=>  $k^{-s} = k^{-a} (\cos(b \log k) - i \sin(b \log k))$

=>  $RZFSAT = \prod (1 - k^{-s}) = \prod (1 - k^{-a} \cos(b \log k) + k^{-a} i \sin(b \log k))$  and  $a=0.5$  if Riemann Hypothesis is true.

Proving Riemann Hypothesis is equivalent to proving all satisfying assignments (nontrivial zeros -infinite of them) for RZFSAT earlier have  $a=0.5$ . Instead of considering infinite product earlier, finite number of monomials per prime could be multiplied i.e iteratively add prime monomial clauses to RZFSAT for each consecutive prime and find  $s=a+ib$  from assignment  $x_k=p+iq$  by equating:

$p = k^{-a} \cos(b \log k)$

$q = -k^{-a} \sin(b \log k)$

$\tan^{-1}(-p/q)/\log k = b$

$\log[\cos(\tan^{-1}(-p/q)\log k)/p]/\log k = a$

Compute infinite series of values of  $a$  for every clause of consecutive prime monomial incrementally added to RZFSAT ad infinitum:

$a_1, a_2, a_3, \dots$

Previous infinite series should converge to 0.5 if Riemann Hypothesis is true which can be verified by series convergence tests. For finite RZFSAT this series may or may not converge to 0.5.

Every term in Euler product version of RZF earlier could be written as complex power of corresponding prime by following transform:

$p^s/(p^s - 1) = p^k$

(or)  $\log[p^s/(p^s - 1)] = k * \log(p)$

=>  $k = 1/\log(p) * \{\log[p^s/(p^s - 1)]\}$

Consequently, RZF could be written as infinite multiplicative partition of complex exponents for all primes solvable by an algebraic computation tree on Blum-Shub-Smale Turing machines over Complex field - non-trivial zeros of RZF input to non-uniform algebraic computation tree should asymptotically evaluate to 0. Usual multiplicative partition (factorisatio numerorum) is limited to integral powers:

$RZF = p_1^{c_1} * p_2^{c_2} * p_3^{c_3} \dots \text{ad infinitum}, c_n = 1/\log(p_n) * \{\log[p_n^s/(p_n^s - 1)]\}$  for  $p_n = 2,3,5,7,11,13,17,19,\dots$

Earlier multiplicative partition version of RZF could be further reduced to factorization product of two polynomials over complex field - one finite and the other infinite - by splitting the infinite product into product of two factor polynomials. Extended RZF written in terms of Gamma function requires zero-knowledge of primes.

References:

-----

629.1 Diophantine Equations - Survey - [V Srinivas, Tata Institute of Fundamental Research] -

[https://www.currentscience.ac.in/Downloads/article\\_id\\_059\\_12\\_0589\\_0594\\_0.pdf](https://www.currentscience.ac.in/Downloads/article_id_059_12_0589_0594_0.pdf)

629.2 Exploring Number Theory via Diophantine Equations -

<https://www.csbsju.edu/Documents/Math/Sunil-CC-2009-B1.pdf> - Gaussian Integers, Pythagorean Triples

629.3 Fermat's Last Theorem - [Amir D. Aczel] - Shimura-Taniyama Conjecture:

Elliptic Curves are Modular Forms and proof of Fermat's Last Theorem by [Andrew Wiles]

629.4 Algebraic Complexity - [Arora-Barak] - Blum-Shub-Smale Model -

<http://theory.cs.princeton.edu/complexity/algebraicchap.pdf>

629.5 Extended Riemann Zeta Function - Theory and Problems of Complex Variables



- [Murray Spiegel] - Schaum Series - Page 273 -  $RZF(1-z) = 2^{(1-z)} \cdot \pi^{(-z)} \cdot \Gamma(z) \cdot \cos(\pi \cdot z/2) \cdot RZF(z)$  which symmetrically defines RZF with zero knowledge of primes and thereby a composition of algebraic computation tree for RZF in Blum-Shub-Smale model over complex field.  
 629.6 Undecidability of Mandelbrot Set (Fractal Logistic map) and Decidability of its complement -  
<https://users.cs.duke.edu/~reif/courses/complectures/books/AB/ABbook.pdf> -  
 [Arora-Barak] - 14.3.3 - Page 290 - "...Definition 14.23 (Mandelbrot set decision problem) Let  $PC(Z) = Z^2 + C$ . Then, the Mandelbrot set is defined as  $M = \{C \mid \text{the sequence } PC(0), PC(PC(0)), PC(PC(PC(0))) \dots \text{ is bounded}\}$ . Note that the complement of  $M$  is recognizable if we allow inequality constraints. ..." -  
 has far reaching ramifications for problems in chaotic non-linear dynamics.

-----  
 630. (THEORY and FEATURE) Music Pattern Mining - Audio to Notes - Intrinsic Merit of Music - 12 January 2019, 21 January 2019 - related to all sections on Intrinsic Merit and Fame - related to 67,68,69,593  
 -----

-----  
 1. Implementations in NeuronRain on Intrinsic Merit Versus Fame previously have so far concentrated only on Merit of Text (TextGraphs), Large Scale Visuals (Videos and Images - LSVR) and People (Interview/Examination/Contest based merit, Analytics of Social Network Profile Vertices). Merit of Audio or Complexity of Music has been defined theoretically earlier as a minimum size DFA or Turing Machine accepting musical notes as language which is a minimum description length measure similar to Kolmogorov complexity.  
 2.To this effect music\_pattern\_mining/AudioToBitMatrix.py has been changed to include a new function which converts an audio waveform to frequency domain by FFT. These frequencies are in turn mapped to a string of musical notes over octave alphabet - C,D,E,F,G,A,B,C (12 including fine divisions of notes denoted by #) - librosa API are invoked.  
 3.Essentially by mapping music to huge strings over octave alphabets the problem of music mining is made easier and all algorithms implemented for string mining in NeuronRain apply to music as well.  
 4.Since music is often related to creative genius, complexity of string of notes is an approximation of merit.  
 5.String of musical notes differ from usual text strings because of an inherent periodicity in music (self-similar fractal-like ascending and descending sequence of notes)  
 6.logs for an example audio to notes string has been committed to `python-src/music_pattern_mining/testlogs/AudioToBitMatrix.log.AudioToNotes.12January2019`  
 7.State machine diagrams for Minimum Turing Machine or DFA accepting languages of strings of octave notes are directed graphs possibly having lots of cycles implying inherent periodicity in music. All directed graph complexity measures and algorithms therefore could quantify merit of audio or music.  
 8.Emphasis is laid more on music patterns than audio patterns because audio is simply some textual content extractable by speech recognition and spelt out in flat notes of similar frequency mostly without modulation excluding emotives.

-----  
 631. (THEORY) Computational Geometric Factorization, Alternative Ray Shooting Algorithm, BQP and QNC, Pythagorean Triples, Possibility of decoherence from Quantum NC to Classical PRAMs, No cloning theorem - related to 562 and all other sections on factorization - 21 January 2019  
 -----

-----  
 Pythagorean triples are integers of the form  $a^2 + b^2 = c^2$  which can be factorized into product of Gaussian Integers ( $\mathbb{Z}[i]$ ) as  $c = (a+ib)(a-ib)$  which is a hyperbolic curve defined on complex number field ( $\mathbb{C}^2$ ). This extends integer factorization to complex

Gaussian Integers factorization of Pythagorean triples. Blum-Shub-Smale Turing Machines can factorize Pythagorean triples to Gaussian Integers. Ray Shooting Query Algorithms so far described previously depend on rays from origin (0,0) and piercing hyperbolic arc bow at different spacings. Instead of ray shooting from origin (0,0), end points of the hyperbolic arc can be connected by a chord (line between (0,N) and (N,0)) and midpoint of this chord is an alternative origin for ray shooting queries. This inverts the sweepline direction of rays from (0,0) to (N,N) to (N,N) to (0,0).

From QNC Computational Geometric Factorization described earlier, hyperbolic pixelated arc bow can be specified as a Hilbert Space vector superposition of factor/product states (ket notation) over complex amplitudes  $B_i$ :

$$|(p,q)\rangle = B_1|(x_1,y_1)\rangle + B_2|(x_2,y_2)\rangle + \dots + B_n|(x_0(N),y_0(N))\rangle$$

and  $B_i^2$  is the classical probability of a state  $|(x_i,y_i)\rangle$ . QNC contains polynomial size quantum multiplication logdepth toffoli gates while NC has polynomial size logdepth PRAM processors and containment NC in QNC in BQP is known. Quoting reference 562.10 - "...If the HHL algorithm could be adapted to the case where (say) a single  $b_i$  is 1 and all the others are 0, then it would contradict the impossibility of an exponential speedup for black-box quantum search, which was proved by Bennett, Bernstein, Brassard, and Vazirani...", if classical probability  $B_i^2$  of some state  $|(x_i,y_i)\rangle$  is 1:

$$B_i^2 = (a+ib)^2 = (a^2 - b^2) + i(2ab) = 1$$

$$\text{implying } b=0 \text{ and } |a| = 1$$

Zero imaginary part in previous scenario implies a possibility of decoherence from quantum toffoli gates in QNC to PRAMs in NC. No cloning theorem implies quantum state cannot be replicated. But since NC is contained in QNC, every PRAM algorithm in NC can be translated to a quantum algorithm in QNC. For example any two toffoli multiplication gates in QNC algorithm for two PRAMs in NC algorithm (e.g. for previous factorization problem allowing decoherence), must have different state superposition vectors  $v_1$  and  $v_2$  such that  $v_1$  has some factor state amplitude  $B_i(v_1)$  and  $v_2$  has other factor state amplitude  $B_k(v_2)$  of classical probabilities 1:  $B_i(v_1)^2 = B_k(v_2)^2 = 1$  which does not violate No cloning theorem.

Even if classical probability  $B_i^2$  of some factor state  $B_i=|(x_i,y_i)\rangle$  is not 1 but close to 1 in previous superposition of factor/product states, implying amplitudes of other factor states are non-zero, QNC factorization collapses to a classical BPNC factorization (e.g. a randomized PRAM factorization algorithm) despite no derandomization to NC. Derandomizing BPNC to NC has been mentioned previously in references 53.12.1 and 53.12.4 (Hitting Set Generators) which does not rule out possibility of a complete collapse of QNC all the way up to NC via BPNC.

#### References:

-----

631.1 Wave Function Collapse and Various Interpretations of QM -

[https://en.wikipedia.org/wiki/Wave\\_function\\_collapse](https://en.wikipedia.org/wiki/Wave_function_collapse) - Quantum Decoherence is one of the ways to interpret collapse of wave function to a classical state

631.2 Computational Meaning of Quantum Gates and Measurement Gates -

<https://www.fi.muni.cz/usr/gruska/quantum10f/qc1004.pdf> - [Bernstein-Vazirani] Theorem implies for universal quantum gates it is sufficient to have real amplitudes

631.3 Measurement Principles of Quantum Gates - [http://www-](http://www-inst.eecs.berkeley.edu/~cs191/sp12/notes/chap1&2.pdf)

[inst.eecs.berkeley.edu/~cs191/sp12/notes/chap1&2.pdf](http://www-inst.eecs.berkeley.edu/~cs191/sp12/notes/chap1&2.pdf) - Measurement by Phases

631.4 BQP is contained in PP -

<https://www.cs.cmu.edu/~odonnell/quantum15/lecture23.pdf> - Bounded Error Quantum Polynomial Time computation is contained in Classical Probabilistic Polynomial Time computation - Theorem 4.1 - [Adleman-DeMarrais-Huang]. But derandomizing PP to P or PP success amplification does not seem to have a parallel to that of BPP success amplification. As a special case, hypothetical PP factoring algorithm can be made bounded error by invoking ray shooting query oracles to find approximate factors which bound the failure probability and thus bringing factorization to BPP or BPNC (by parallel ray shooting) which can then be derandomized to NC.

631.5 BPP is contained in BQP and Feynman Path Integral Proof of BQP in PP - <https://www.scottaaronson.com/democritus/lec10.html> - classical coin flip is a quantum Hadamard Gate mapping qubit  $|0\rangle$  to  $1/\sqrt{2}(|0\rangle + |1\rangle)$  and qubit  $|1\rangle$  to  $1/\sqrt{2}(|0\rangle - |1\rangle)$ . Hadamard Gate is a Universal Quantum Computation Gate. Combined together Bounded Error Quantum Computation lies between bounded classical 2-sided error and unbounded classical 2-sided error complexity classes

631.6 Quantum Hadamard Gate -

[https://en.wikipedia.org/wiki/Quantum\\_logic\\_gate#Hadamard\\_\(H\)\\_gate](https://en.wikipedia.org/wiki/Quantum_logic_gate#Hadamard_(H)_gate)

631.7 Is Factoring really in BQP? really? -

<https://rjlipton.wordpress.com/2011/01/23/is-factoring-really-in-bqp-really/> - "...The problem is that if we press the button again at time  $\{i+1\}$ , we may get a bit that pertains to some other value  $\{y_{i+1}\}$  that is not the same as  $\{y_i\}$ . If we could guarantee that repeated taps on  $\{B_1\}$  would stay focused on  $\{y_i\}$  then we could apply search-to-decision and recover the function value  $\{y_i\}$ ..."

632. (FEATURE and THEORY) Intrinsic Merit of Music, Exact Learning of DFAs, Minimum Description Length

Merit - 29 January 2019 - related to all sections on Intrinsic Merit and Fame - related to 67,68,69,593,

630

1. New function `audio_merit()` has been defined in `AudioToBitMatrix.py` which invokes `minimum_descriptive_complexity()` to compute MDL for string of octave notes for a musical clip.

2. Source files `MinimumDescLength.py` and `Entropy.py` have been changed to include `__main__` and rewritten to define member function `minimum_descriptive_complexity()` and some other error checks for floating point overflow.

3. An example musical MP4 clip excerpt of JS Bach has been analyzed. This masterpiece is featured in Douglas Hofstadter's *Godel-Escher-Bach: An Eternal Golden Braid* for its self-similar strange loops of notes (a mandelbrot fractal set)

4. This implementation thus is a culmination of 4 classes of intrinsic merits on Internet and WWW - Text, Video, Audio and People - defined in this draft.

5. Following are intrinsic merit implementations in this draft which expand on publications <http://arxiv.org/abs/1006.4458>, [http://www.nist.gov/tac/publications/2010/participant.papers/CMI\\_IIT.proceedings.pdf](http://www.nist.gov/tac/publications/2010/participant.papers/CMI_IIT.proceedings.pdf) and <http://arxiv.org/abs/1106.4102> (Complement Diophantines are intrinsic merit measures too because text obtained by word concatenations can be represented by word diophantine equations and can be Ramsey 255-colored by alphabet locations thereby creating arithmetic progressions):

5.1. Textual merit is analyzed by Recursive Gloss Overlap and Recursive Lambda Function Growth algorithms - Graph Tensor Neuron Network Merit.

5.2. People Merit is analyzed by a mixture model of Intrinsic(Academic/Work/Interview/Contest/Examinations) and Experiential Mistake Bound Merit by a recursive mistake correction tree differential equation.

5.3. Video Merit is analyzed by EventNet/ImageNet Tensor Products Algorithm.

5.4. Audio Merit is defined theoretically as complexity of exact learning of DFAs on strings of notes and their minimization in [Dana Angluin]  $L^*$  Algorithm Model and implemented by a less intensive Minimum Description Length merit on string of notes in this commit. Implementation of  $L^*$  could be exponential and there are PAC learning approximate DFA learning algorithms.

6. Previous algorithms for 4 classes of intrinsic merit are theoretical approximations based on algorithmic graph theory, causality and logical time in clouds, learning theory and connectomes with no invocation of statistical tool and by no means the only way to analyze merit but one of them.

References:

632.1 Hilbert Tenth Problem: What was done and What is to be done - [Yuri

Matiyasevich] - <https://books.google.co.in/books?id=qWYbCAAQBAJ&pg=PA11&lpg=PA11&dq=word+concatenation+diophantine&source=bl&ots=zQD07Jy-kK&sig=ACfU3U1CeZ4WvshXDu62TEI0mb0bofrcbg&hl=en&sa=X&ved=2ahUKewjItsy05JLgAhUSfsSKHZ-NAX8Q6AEwAnoECAQQAQ#v=onepage&q=word%20concatenation%20diophantine&f=false>  
- "...Under this representation of matrices, concatenation words corresponds to matrix multiplication and thus can be easily expressed by a system of diophantine equations ..."  
632.2 The Musical Offering - JS Bach - [https://en.wikipedia.org/wiki/The\\_Musical\\_Offering](https://en.wikipedia.org/wiki/The_Musical_Offering)  
632.3 Godel Escher Bach: An Eternal Golden Braid - [Hofstadter] - Endlessly rising canon - "...In this canon, Bach has given us our first example of the notion of Strange Loops. The "Strange Loop" phenomenon occurs whenever, by moving upwards (or downwards) through the levels of some hierarchical system, we unexpectedly find ourselves right back where we started..."  
632.3 Exact Learning of DFA - Angluin's L\* Algorithm - teacher/learner model of membership and equivalence queries - <http://www.cs.ox.ac.uk/james.worrell/DFA-learning.pdf>

-----  
633. (THEORY and FEATURE) GIS and Urban Planning Analytics, Convex Hull - 31 January 2019  
-----

1. ImageGraph\_KerasTheano.py has been changed to include a new function for finding convex hull of set of points/pixels in an image
2. QHull ConvexHull() function from SciPy Spatial library - <https://docs.scipy.org/doc/scipy/reference/generated/scipy.spatial.ConvexHull.html> - has been invoked in the new convex\_hull() function defined for this purpose.
3. An example demographic GIS satellite image of Chennai Megapolis (Population density of Urban Agglomeration) from SEDAC website - <http://sedac.ciesin.columbia.edu/mapping/popest/gpw-v4/> - has been analyzed to draw a convex hull around thickly populated regions and convex hull vertices are printed in terms of some area units (not sqkm or sqmiles).
4. OpenCV2 provides api for convex hull too - <https://docs.opencv.org/2.4/doc/tutorials/imgproc/shapedescriptors/hull/hull.html>
5. Convex Hull analytics of GIS imagery is helpful for Urban planners and sustainable development.

-----  
634. (FEATURE) Software Analytics and Scheduler Analytics - Backpropagation correction - 9 February 2019  
-----

1. DeepLearning\_SchedulerAnalytics.py and DeepLearning\_SoftwareAnalytics.py have been updated for correction to a serious bug in BackPropagation computation.
2. Earlier, BackPropagation Neural Network (BPNN) object for Software and Scheduler Analytics was getting created for every input training dataset element erroneously.
3. This has been remedied by instantiating BackPropagation class only once outside the loop and updating only the input layer and/or expected output layer for each element in input dataset iteration.
4. Iterations have been curtailed for concise logs.
5. By this change, weights are updated for every psutil per process proc object (Scheduler Analytics) or systemwide process statistics info (Software Analytics) thus learning weights of the multilayer perceptron from system performance.

6.logs for this have been committed to  
testlogs/DeepLearning\_SchedulerAnalytics.log.9February2019 and  
testlogs/DeepLearning\_SoftwareAnalytics.log.9January2019 (Timestamped wrongly -  
must be read DeepLearning\_SoftwareAnalytics.log.9February2019)  
7.After sufficiently large number of input training data, hopefully this BPNN  
would be able to predict outputs from input per-process and systemwide  
performance statistics data e.g 99% load average.

-----  
635. (THEORY and FEATURE) Intrinsic Merit of Texts, Ramsey Theory, Complement  
Diophantines - Ramsey  
number of text graph - related to 2,617,630,632 and all sections on Fame and  
Merit - 11 February 2019  
-----

-----  
1.It has been mentioned earlier that texts which are concatenations of words can  
be represented by  
\*) Matrix Diophantine Equations \*) and (255 or 511) coloring of texts by  
ASCII/Unicode alphabets (excluding space) which give rise to ramsey ordering by  
Van Der Waerden Theorem assuming texts of size N are integer sequences of  
locations 1-to-N colored by alphabets containing monochromatic arithmetic  
progressions of alphabet(color) locations.  
2.Best known upper bound for Van Der Waerden Number for a least length sequence  
of N integers =  $W(r,k)$  for r-coloring of an integer sequence and arithmetic  
progression of least length  $k \leq 2^{2^{r^{2^{2^{k+9}}}}}$  by [Timothy Gowers]  
3.Previous upperbound for texts colored by alphabets of size 255 implies size N  
of a natural language text to have length k arithmetic progressions on alphabet  
locations  $\leq 2^{2^{(255^{2^{2^{k+9}}})}}$  which is huge even for small k.  
4.Ramsey coloring  $R(r,s)$  of graphs is equivalent of Van Der Waerden sequence  
coloring which defines emergence of monochromatic cliques r or independent sets  
s (also known as Friends and Strangers theorem).  
5.By definition of complementation in generic sense, k-coloring partitions a set  
into k disjoint subsets which can be represented by some diophantine (e.g Beatty  
functions) - Complementation is a size 2 partition.  
5.In this commit, Ramsey R2 function is invoked from NetworkX API on textgraphs  
of natural language texts and maxclique-maxindependentset pairs are computed.  
7.This is a less intensive intrinsic merit measure for a text and Van Der  
Waerden number computation has no mention in python libraries presently and is  
daunting too - SAT solvers are used to compute Van Der Waerden Numbers in some  
algorithms.  
8.Following this reasoning, strings of octave alphabets in music can be  
construed as 12-coloring (and more including majors and minors) of music as  
sequence and indicates inevitable emergence of order from chaos.

References:

-----  
635.1 SAT Solver for Van Der Waerden number 1132 =  $V(2,6)$  -  
<https://www.cs.umd.edu/~gasarch/TOPICS/vdw/1132.pdf>  
-----

-----  
636. (THEORY) Computational Geometric Factorization - Parallel Planar Point  
Location of factors in Monotone Subdivision formed by Hyperbolic Arc Pixel  
Polygons with no necessity for Ray Shooting Queries, Van Der Waerden Ramsey  
Coloring of Sequences, Computational Algebraic Geometry - related to 506,601,605  
and other sections on factorization - 12 February 2019, 18 February 2019, 20  
February 2019, 22 September 2019, 20 October 2020  
-----

-----  
In previous sections on computational geometric factorization, various parallel  
algorithms based on k-mergesort,segment tree, wavelet tree,sorting  
networks,planar point location and ray shooting were described to locate factors  
on the hyperbolic arc tile segments (or) pixel array polygons. A continuous

hyperbolic curve is "rectified" to a chain of non-intersecting polygons (juxtaposed) by considering each tile segment  $(x, N/x, x+1, N/x)$  of hyperbola obtained by differential calculus identity  $\Delta = N/[x(x+1)]$  as a rectangular polygon of dimension  $1 * N/[x(x+1)]$  which is an array of pixels of dimension  $1 * 1$  containing the product of  $x$  and  $y$  ordinates in arithmetic progression and thus implicitly sorted. These adjoining rectangular polygons which meet at endpoints, create a plain simple line graph formed by their vertices and edges which is strongly connected. This set of polygons partition the 2 dimensional plane of area  $(1,N)*(1,N)$  into 3 planar subdivisions - space above hyperbolic polygons, space within the hyperbolic polygons and space below hyperbolic polygons. Earlier algorithms assumed arbitrary subdivisions and had ray shooting to find a polygon containing approximate factor as a prerequisite which is then binary searched. But this chain of hyperbolic tile polygons is monotone because  $y$ -axis is strictly decreasing or non-increasing for any path along the plain simple line graph (PSLG) formed by hyperbolic polygonal planar subdivision. There are efficient algorithms for PRAM geometric searching of monotone subdivisions mentioned in references below. Thus locating a hyperbolic pixel array polygon containing factor point can be done in  $O(\log N)$  PRAM time and finding the factor in this polygon by sequential binary search in additional  $O(\log N)$  sequential time. Thus factorization by planar point location in monotone subdivision of hyperbolic pixel array polygons is in  $O(\log N)$  parallel +  $O(\log N)$  sequential time - and thus in Nick's class - without requirement of approximate factoring by ray shooting queries.

Arithmetic Progression of points as product of ordinates within each Hyperbolic pixel array polygon brings Ramsey/Van Der Waerden coloring of sequences into the realm of factorization - by  $k$ -mergesort the tile segment polygons are unified into single totally ordered integer sequence of length  $N*N/(N+1)$ . If each arithmetic progression polygon is colored uniquely, the sorted sequence is a union of set of  $k$ -colored arithmetic progressions of some minimum length (or)  $N*N/(N+1) = \text{VanDerWaerden}(k, \text{minimum length of a segment})$

In all sections related to factorization in this draft, factoring only one integer at a time has been the focus. Geometric intuition of hyperbolic tile/polygon segmentation allows storing segments or polygons for hyperbolic curves of multiple integers in same datastructure which could be segment tree, wavelet tree, or point location tree. For example two rectified hyperbolic polygons/segments for  $xy=N_1$  and  $xy=N_2$  for factoring  $N_1$  and  $N_2$  can be stored in single search tree which can be queried for factor points of  $N_1$  and  $N_2$  independently. This optimization saves lot of parallel tree construction time and space.

#### References:

- 
- 636.1 Parallel Planar Point Location for Monotone Subdivisions - <https://www.csun.edu/~ctoth/Handbook/chap46.pdf> - Table 46.5.1 - Parallel Point location in monotone subdivision by EREW PRAM in  $O(\log n)$  time,  $O(n)$  parallel work - Reference [TV91] in 636.2
- 636.2 Parallel transitive closure and point location in planar structures - Lemma 4.8 - [Tamassia-Vitter] - <http://www.ittc.ku.edu/~jsv/Papers/TaV91.transclosure.ps.gz>
- 636.3 Computational Geometry - [Preparata-Shamos] - Point Location - Section 2.2 - [https://books.google.co.in/books?id=\\_p3eBwAAQBAJ&printsec=frontcover#v=onepage&q=point%20location&f=false](https://books.google.co.in/books?id=_p3eBwAAQBAJ&printsec=frontcover#v=onepage&q=point%20location&f=false)
- 636.4 Point Location in Successive Convex Hulls - [Greenlaw-Hoover-Ruzzo] - List of P-Complete Parallel RAM Problems - A.9.5 - <https://homes.cs.washington.edu/~ruzzo/papers/limits.pdf> - Given a point on 2D Plane, is the point in  $k$ -th remaining convex hull after finding and removing convex hulls repetitively? - Previous monotone chain of hyperbolic pixel array polygons are successive convex hulls containing respective tile segment points
- 636.5 CREW Parallel RAM Version of Kirkpatrick's Planar Point Location - Chapter 5 - Some Parallel Geometric Algorithms - Section 3 - <https://books.google.co.in/books?id=ThBR22H0jMcC&pg=PA85&lpg=PA85&dq=parallel+planar+point+location&source=bl&ots>

=jFBpEv60Ab&sig=ACfU3U1ffffe1j5o-

w6GWnZHKxAsW0iaU\_A&hl=en&sa=X&ved=2ahUKEwik4uHr9cTgAhUDBIgKHRDlAwc4FBDoATAFegQIC RAB#v=onepage&q=parallel%20planar%20point%20location&f=false - Kirkpatrick's decomposition triangulates a Planar Straight Line Graph (plain simple line graph or PSLG) e.g PSLG of Hyperbolic arc pixel array polygons previously described for factorization. CREW PRAM Version of this triangulation algorithm is  $O((\log N)^k)$  parallel time and  $O(\log N)$  sequential query time but requires  $O(N)$  processors.

636.6 Parallel Planar Point Location by Parallel Construction of Subdivision Hierarchies - [N. DADOUN AND D. G. KIRKPATRICK]

-[https://ac.els-cdn.com/0022000089900421/1-s2.0-0022000089900421-main.pdf?\\_tid=c9b3fe06-f5de-4038-a511-](https://ac.els-cdn.com/0022000089900421/1-s2.0-0022000089900421-main.pdf?_tid=c9b3fe06-f5de-4038-a511-1e201f91edc8&acdnat=1550480942_c4eea646a5bb64a5444edc195ca6743d)

1e201f91edc8&acdnat=1550480942\_c4eea646a5bb64a5444edc195ca6743d - "...It is worth noting that Atallah and Goodrich [AG] use the parallel plane sweep technique to perform planar point location with  $O(\log n \log \log n)$  parallel preprocessing,  $O(n \log n)$  space and  $O(\log n)$  sequential query time. The subdivision hierarchy technique uses  $O((\log n)^2)$  parallel preprocessing ( $O(\log n \log^* n)$  for convex subdivisions),  $O(n)$  space and  $O(\log n)$  sequential query time. ..."

636.7 Parallel Planar Point Location by Parallel Construction of Plane Sweep Tree - [Atallah and Goodrich] - <https://docs.lib.purdue.edu/cgi/viewcontent.cgi?referer=https://www.google.com/&httpsredir=1&article=1481&context=cstech> -

Theorem 3.12 and Table 1 - Summary of Results in the end - "...Given a planar subdivision  $S$  consisting of  $n$  edges, we can construct in parallel a data structure which, once constructed, enables one processor to determine for any query point

$p$  the face in  $S$  containing  $p$  in  $O(\log n)$  time. The construction takes  $O(\log n \log \log n)$  time and

$O(n \log n)$  space using  $O(n)$  processors on a CREW PRAM...." - It has to be observed that PSLG from Hyperbolic arc pixel array polygonal rectification is the simplest form of its kind containing  $O(N)$  rectangular faces and  $\leq 4*N$  edges, 4 per rectangle.

636.8 List of Problems in NC and Drawbacks of NC Theory -

<http://pages.cs.wisc.edu/~tvrdik/3/html/Section3.html> - Parallel sorting and most of Computational Geometric Problems are in NC - "...The class NC may include some algorithms which are not efficiently parallelizable. The most infamous example is parallel binary search...NC theory assumes situations where a huge machine (polynomial number of processors, e.g., millions) solves very quickly (polylogarithmic time, e.g., seconds) moderately sized problems (e.g., hundred of thousands input items). In practice, however, moderately sized machines (hundreds, at most thousands of processors) are used to solve large problems (e.g., millions of input items). So that the number of processors tends to be subpolynomial, even sublinear...." - This practical limitation of NC applies to computational geometric factorization by planar point location especially when huge integers e.g semiprimes of the order of 1024 bits or more in public key infrastructure have to be factorized. This requires huge number of processors (PRAMs) but yet theoretically highly parallelly feasible. Precision ray shooting queries optimization like tile-summation ray shooting sieves out lot of factorless segments of hyperbolic arc bow finding approximate factors which are in proximity to exact factors and with high probability in same polygon/segment facilitating binary search of arithmetic progression. If a ray shooting query followed by binary search fails to find exact factor, angle of the ray can be altered in either direction and shot again covering unswept areas of the plane. Ray shooting partitions the hyperbolic arc into  $O(N/\log \log N)$  segments for  $O(\log \log N)$  prime factor ray queries.

636.9 NC1 and L - Theorem 3.5 -

<https://cse.buffalo.edu/~regan/papers/pdf/ALRch27.pdf> - [Eric Allender, Rutgers University, Michael C. Loui, University of Illinois at Urbana-Champaign, Kenneth W. Regan, State University of New York at Buffalo] -  $O(\log N)$  Parallel Planar Point Location time implies complexity class  $NC^1$  which is contained in deterministic logspace class L. This is quite counterintuitive because despite prohibitively high number of PRAMs even if simulated by BSP, space required for computational geometric factorization is logarithmic.

636.10 Generalized Planar Point Location - [Chazelle-Sharir] - Collins

Decidability Theorem (refinement of Tarski Decidability) based point location on arbitrary set of polynomials defined over euclidean plane -  
[https://www.sciencedirect.com/science/article/pii/S074771710880065X/pdf?md5=1abc953f7893218fefbad2e9bb83d68c&pid=1-s2.0-S074771710880065X-main.pdf&\\_valck=1](https://www.sciencedirect.com/science/article/pii/S074771710880065X/pdf?md5=1abc953f7893218fefbad2e9bb83d68c&pid=1-s2.0-S074771710880065X-main.pdf&_valck=1) - Factorization is limited to locating integer points on hyperbola  $xy - N = 0$

636.11 Union of Arithmetic Progressions - [Newman] -  
[http://inis.jinr.ru/sl/M\\_Mathematics/MT\\_Number%20theory/Newman%20D.J.%20Analytic%20Number%20Theory%20\(GTM%20177,%20Springer,1998\)\(ISBN%200387983082\)\(81s\)\\_MT\\_.pdf](http://inis.jinr.ru/sl/M_Mathematics/MT_Number%20theory/Newman%20D.J.%20Analytic%20Number%20Theory%20(GTM%20177,%20Springer,1998)(ISBN%200387983082)(81s)_MT_.pdf) - Page 14 - Every tile segment in rectified hyperbola (which is a monotone subdivision formed by juxtaposed line segments decreasing or non-increasing in one coordinate and thus is a plain simple straightline graph) is an arithmetic progression. By analytic number theory every tile segment arithmetic progression  $an + b$  can be written as a generating function  $z^b/(1 - z^a)$ . It is natural to ask if union of tile segment arithmetic progressions can be written as single generating function. Answer is no by contradiction. Generating functions based arithmetic progression exact cover of set of natural numbers is a special case of complement diophantines and complementary equations - "...Thus the dissection into evens and odds corresponds to the identity  $\sum_{n \geq 0} z^{2n} = \sum_{n \geq 0} z^{2n} + \sum_{n \geq 0} z^{2n+1}$ , and the dissection into  $2n$ ,  $4n + 1$ ,  $4n + 3$  corresponds to  $\sum_{n \geq 0} z^{4n} = \sum_{n \geq 0} z^{4n} + \sum_{n \geq 0} z^{4n+1} + \sum_{n \geq 0} z^{4n+3}$ , ...."

636.12 Van Heuraets Rectification of Curves -  
<https://www.maa.org/press/periodicals/convergence/mathematical-treasures-van-heuraets-rectification-of-curves>

636.13 Numerical Rectification of Curves - [B. P. Acharya, M. Acharya and S. B. Sahoo - ITER, S'O'A University, Bhubaneswar, India] -  
<http://www.m-hikari.com/ams/ams-2014/ams-17-20-2014/acharyaAMS17-20-2014.pdf>

636.14 Exact Rasterization of Algebraic Curves - [Stussak] -  
<https://opendata.uni-halle.de/bitstream/1981185920/7892/1/Dissertation%20-%20Christian%20Stussak%20-%200n%20reliable%20visualization%20algorithms%20for%20real%20algebraic%20curves%20and%20surfaces.pdf> - Figure 3.2 - Correct and wrong rasterizations of the curve  $y^2 + x^2(x + 1) = 0$  - Rasterization of an algebraic curve in Computer Graphics is the Computational Geometry equivalent of rectification - curve is approximated by pixels. Bresenham Line Rasterization is limited to approximating straightlines by pixels - "...we solve the task of rasterizing a real algebraic plane curve  $VR(F)$  defined by a polynomial  $F \in \mathbb{Z}[x, y]$ . Although many algorithms exist for rendering such a curve, only a few of them guarantee the correctness of the output. The term correctness is often interpreted as topological correctness, i.e. the graph induced by the rendering is isotopic to  $VR(F)$ ...." - "...Real algebraic space curves are visualized by determining a line strip approximation to their segments using a projection and lifting approach..." - Computational Geometric Factorization rasterizes hyperbola by axis-parallel line segments which are juxtaposed pixel-array polygons. Finding a polygon containing factor point can be done in polylog time and searching the polygon is logarithmic because of (arithmetic progression) implicit sortedness of pixels.

636.15 Graphics Computation in PRAMs - Parallel Rasterization - XMT-GPU -  
<http://users.umiacs.umd.edu/~vishkin/XMT/ICPP08version.pdf> - [Thomas DuBois University of Maryland College Park, MD [tdubois@cs.umd.edu](mailto:tdubois@cs.umd.edu), Bryant Lee Carnegie Mellon University Pittsburgh, PA [bryantl@cs.umd.edu](mailto:bryantl@cs.umd.edu), Yi Wang Virginia Polytechnic Institute Blacksburg, VA [samywang@vt.edu](mailto:samywang@vt.edu), Marc Olano University of Maryland, Baltimore County Baltimore, MD [olano@umbc.edu](mailto:olano@umbc.edu), Uzi Vishkin University of Maryland College Park, MD [vishkin@umiacs.umd.edu](mailto:vishkin@umiacs.umd.edu)] - Draft sections on Computational Geometric Factorization in this design document assume that total number of  $O(N)$  hyperbolic arc tile segments of endpoints  $(x, N/x, x+1, N/x)$  are axis-parallel rectified by differential calculus identity  $\delta = N/[x(x+1)]$  which is length of each segment and  $N/(\log N)^k$  processors are work-optimally allocated  $(\log N)^k$  segments each (from section 477 on Local Tile Search). Each of  $N/(\log N)^k$  PRAM processors binary searches  $(\log N)^k$  segments allocated to it in  $(\log N)^k * \log N = (\log N)^{(k+1)}$  parallel time. Instead, Rasterizing hyperbolic arc by Parallel RAMs approximates hyperbola on pixel grid which may not be axis-parallel.

636.16 Rasterization of Conic Sections - Efficient Integer algorithms for drawing Ellipse, Hyperbola, Parabola - refinement of Bresenham, Pitteway, Kappel conic sections and line drawing algorithms -



<https://alexanderagathos.com/publications/CAG98.pdf> - Section 4.1  
 636.17 Topology of Plane Algebraic Curves -  
<https://who.paris.inria.fr/Elias.Tsigaridas/files//clpprt-socg-2009.pdf> - any algebraic curve including hyperbola drawn on  $\mathbb{R}^2$  could be mapped to a planar graph  $G$  which is ambient isotopic to the curve - "...Even more precisely we want the curve  $C$  and the graph  $G$  to be ambient isotopic in the real plane. In other words, we require the existence of a continuous map  $F : \mathbb{R}^2 \times [0, 1] \rightarrow \mathbb{R}^2$ , such that  $F_t$  is an homeomorphism for any  $t \in [0, 1]$ ,  $F_0$  is the identity of  $\mathbb{R}^2$  and  $F_1(C) = G$  ..." - In other words hyperbola is piece-meal approximated by set of non-axis parallel edges of a graph by cylindrical algebraic decomposition (CAD) or other algebraic geometry algorithms. Each edge of this isotopic graph could be independently and parallelly rasterized by Bresenham line rasterization to obtain set of pixel array polygons which could be located for factor points in polylog time.

636.18 On the Sorting of Points along an algebraic curve - [Johnstone-Bajaj] - Convex segment decomposition - <https://docs.lib.purdue.edu/cgi/viewcontent.cgi?article=1702&context=cstech> - "... Given a segment  $AB$  of an algebraic curve, a set of points on the curve is sorted from  $A$  to  $B$  along  $AB$  by putting them into the order that they would be encountered in traveling continuously from  $A$  to  $B$  along  $AB$ . ...". Parallel planar point location factorization in its earlier version required global sorting of set of segments (arithmetic progressions of ordinate products) of hyperbolic arc within an interval to facilitate binary search of factor points. Local binary search obviates global sorting by assigning  $O((\log N)^k)$  implicitly sorted segments each to  $O(N/(\log N)^k)$  processors in parallel for sequential binary searching them which is of PRAM time  $O((\log N)^{(k+1)})$ .

-----  
 637. (FEATURE) NeuronRain Usecases - Analytics Piloted Drone Online Shopping Delivery - 25 February 2019  
 -----

1.This commit creates a new NeuronRainApps/ directory in python-src/ for illustrating usecases defined in asfer-docs/NeuronRainUsecases.txt  
 2.An unmanned aerial vehicle usecase is implemented by a pseudocode in NeuronRainApps/Drones/OnlineShoppingDelivery.py  
 3.Following static mission plan example from DronecodeSDK has been changed to OnlineShoppingDelivery.py:  
     3.1 Example Drone Mission - <https://github.com/Dronecode/DronecodeSDK-Python/blob/master/examples/mission.py>  
     3.2 Drone MissionItem Proto - <https://github.com/Dronecode/DronecodeSDK-Proto/blob/a54b353d73ff8d6e36c716b5278990e0f8cb770c/protos/mission/mission.proto>  
 4.Dynamic Mission Plan: Autopilots the UAV drone based on GIS analytics navigation variables  
   - e.g. longitude, latitude, altitude, speed, camera action etc., -  
   read by Streaming Abstract Generator socket streaming and appends MissionItems to  
   flight plan dynamically restricted by ordinates convex hull. Convex Hull for a terrain image is obtained from ImageNet/ImageGraph\_Keras\_Theano.py. When drone is within convex hull airspace, its altitude is set to 0 (or minimal value) and landed  
 5.Dynamic flight trajectory remote-controlled by analytics are applicable to online shopping deliveries when multiple courier items have to be delivered en route which is NP-Hard Hamiltonian problem - Finding most optimal shortest tour from origin, through intermediate delivery point vertices and back to origin  
 6.This is not compileable, executable code but only a pseudocode and has not been tested on a drone because of lack of it and aviation licensing requirements

References:

-----  
 637.1 GIS and Drones -  
[https://www.itu.int/en/ITU-D/Regional-Presence/AsiaPacific/SiteAssets/Pages/Events/2018/Drones-in-agriculture/asptraining/A\\_Session1\\_Intro-to-Drones-RS-](https://www.itu.int/en/ITU-D/Regional-Presence/AsiaPacific/SiteAssets/Pages/Events/2018/Drones-in-agriculture/asptraining/A_Session1_Intro-to-Drones-RS-)

-----  
 638.(FEATURE) Software Analytics - Scheduler Analytics - /etc/sysctl.conf  
 kernel.sched\_\* optional  
 clause - 25 February 2019  
 -----

1.DeepLearning\_SchedulerAnalytics.py has been changed to include new clause for writing sysctl.conf kernel.sched\_\* variables instead of scheduler classes within learnt\_scheduler\_class() based on output layer of BackPropagation Neural Network(BPNN)

2.These variables are documented in:

2.1 <https://www.kernel.org/doc/Documentation/scheduler/>

2.2

<https://doc.opensuse.org/documentation/leap/tuning/html/book.sle.tuning/cha.tuning.taskscheduler.html>

3.Different values of kernel.sched\_\* are returned based on numpy mean of output layer of BPNN. For example:

```
["kernel.sched_latency_ns=9000000",
 "kernel.sched_migration_cost_ns=100000",
 "kernel.sched_wakeup_granularity_ns=2000000",
 "kernel.rr_timeslice_ms=10",
 "sched_rt_runtime_us=990000",
 "sched_nr_migrate=12",
 "sched_time_avg_ms=100"]
```

which increase CPU affinity of a process, its timeslice quantum and reduce cost of CPU loadbalancing and migration if it is CPU-intensive.

-----  
 639.(FEATURE) Software Analytics - Scheduler Analytics - /proc/sched\_debug  
 support - 27 February 2019  
 -----

1.Missing kernel prefix for some of the /etc/sysctl.conf variables have been included in return array.

2./proc/sched\_debug support has been included by defining a new function to read /proc/sched\_debug and

print the red-black tree of the Complete Fair Scheduler (CFS)

[[https://elixir.bootlin.com/linux/v3.2/source/kernel/sched\\_fair.c](https://elixir.bootlin.com/linux/v3.2/source/kernel/sched_fair.c)] runqueue for user defined iterations in a loop - reads the /proc/sched\_debug periodically, reverses the list of lines to print the tail.

3./proc/sched\_debug is a convenient alternative to BCC tools runqlat

4.Kernel CFS chooses the root of the red-black tree which has least virtual runtime to schedule it to run on CPU thereby prioritizing and fairly treating starved processes.

5.Tree Key field is the virtual runtime of the process id - Example below prints runqueue at any instant for a CPU:

runnable tasks:

| task     | PID       | tree-key | switches | prio | exec-runtime |
|----------|-----------|----------|----------|------|--------------|
| sum-exec | sum-sleep |          |          |      |              |

```

 metacity 2709 2070924.605059 1155243 120 2070924.605059
104482.007672 13723394.606366 /autogroup-149
 unity-2d-panel 2724 2070927.500112 232355 120 2070927.500112
58204.926440 14229127.111319 /autogroup-149
 gnome-terminal 3049 2070927.622210 59498 120 2070927.622210
22064.526687 14285212.740904 /autogroup-149
R cat 7834 612871.102038 1 120 612871.102038
2.269097 0.000000 /autogroup-153
```

6.Logs for this have been committed to  
testlogs/DeepLearning\_SchedulerAnalytics.log.27February2019

-----  
640.(FEATUE) Software Analytics - Streaming Analytics + Scheduler Analytics -  
/proc/sched\_debug -  
28 February 2019  
-----

-----  
1.DeepLearning\_SchedulerAnalytics.py - sched\_debug\_runqueue() has been changed  
to return a dictionary  
of process runqueue and loop has been removed  
2.Streaming Analytics support has been provided for Operating System performance  
statistics (e.g runqueue) by adding new data\_storage "OperatingSystem" and  
data\_source "SchedulerRunQueue" to Streaming\_AbstractGenerator.py  
3.New clause for previous Scheduler Analytics streaming has been added in  
\_\_iter\_\_() which invokes  
sched\_debug\_runqueue() in a loop and yields the scheduler runqueue dictionaries.  
4.This integrates Streaming and Software Analytics seamlessly and any Streaming  
or other machine learning algorithm can process Operating System Stats  
Dictionary Stream like a bigdata source.  
5.DeepLearning\_SchedulerAnalytics.py imports this Streaming Abstract Generator  
by "OperatingSystem" and "SchedulerRunQueue" parameters and reads the scheduler  
stats as input stream.  
6.In future, any operating system data source other than scheduler runqueue can  
be plugged into Streaming Abstract Generator iterable and fulfils the foremost  
requirement for real time software streaming analytics.

References:

-----  
640.1 Load Averages - /proc/loadavg versus /proc/sched\_debug -  
<http://www.brendangregg.com/blog/2017-08-08/linux-load-averages.html> - Linux  
load averages include uninterruptible IO tasks too apart from CPU load.  
-----

-----  
641.(THEORY) Word Diophantine Equations, Intrinsic Merit defined by Word  
Equations - 4 March 2019 -  
related to 635 and all sections on Merit and Complement Diophantines  
-----

-----  
Throughout this draft intrinsic merit of text has been analyzed by results from  
algorithmic graph theory and dense subgraph complexity measures. Renowned Word  
Problem in computability encodes every word from an alphabet into an equation.  
In the context of World Wide Web, Concatenations of words form a text. This  
leads to concatenation representation of word equations of text by Diophantines.  
This kind of word equation representation is not just limited to text but to  
other genre of merits - audio/music, video, social profiles of people encoded as  
words over binary alphabet - as well. Thus Diophantine representation unifies  
all 4 classes of merit - text, audio/music, video, people - into one thereby  
facilitating number theoretic analysis of merit drastically different from graph  
theoretic perspective earlier:

(\*) Text - Text Graphs -> Text Word Equation Diophantines  
(\*) Video - EventNet Tensor Products -> Binary encoded Video Word Equation  
Diophantines  
(\*) Audio/Music - DFA Learning -> Binary encoded Audio/Music Word Equation  
Diophantines  
(\*) People - Mistake Bound Experiential Learning Merit and Social Profile  
Analytics -> Binary encoded social profile Word Equation Diophantines

Decidability of Hilbert's Tenth Problem is still open for solutions to Word  
Diophantine Equations. Diophantine Word Equations can enforce arbitrary number

of conditions on the solutions e.g length of words. Solutions to a Word Diophantine Equation - text, audio/music, video, people - are kind of unsupervised classifiers which cluster similar texts, audio/music, video and people. For example, Complement Word Equation Diophantines bifurcate the set of texts, audio/music, video and people.

#### References:

-----  
641.1 Word Equations, Fibonacci Numbers, and Hilbert's Tenth Problem - [Yuri Matiyasevich] - Steklov Institute of Mathematics at Saint-Petersburg, 27 Fontanka, Saint-Petersburg, 191023, Russia - URL:  
<http://logic.pdmi.ras.ru/~yumat> -  
<https://logic.pdmi.ras.ru/~yumat/talks/turku2006/FibonacciWordsAbstract.pdf.gz> -  
"...Every word  $X = x_n x_{n-1} \dots x_1$  in the alphabet  $B$  can be viewed as the number  $x = x_n u_n + x_{n-1} u_{n-1} + \dots + x_1 u_1$  (1) written in positional system with weights of digits being the Fibonacci numbers  $u_1 = 1, u_2 = 1, u_3 = 2, u_4 = 3, u_5 = 5, \dots$  (rather than traditional 1, 2, 4, 8, 16,  $\dots$ )...."  
641.2 Collected works of Richard J. Buchi - <https://books.google.co.in/books?id=9BfvAAAAAAJ&q=inauthor:%22J.+Richard+B%C3%BCchi%22&dq=inauthor:%22J.+Richard+B%C3%BCchi%22&hl=en&sa=X&ved=0ahUKEwio19KMhejgAhXEfXAKHW6tB7oQ6AEIKjAA>  
- Every existential formula in concatenation is Diophantine

-----  
642. (FEATURE) Merit of Audio/Music - Music Synthesizer from Random samples and State Machine - 5 March 2019  
-----

-----  
1. New function `notes_to_audio()` has been implemented in `music_pattern_mining/AudioToBitMatrix.py`  
2. It creates a .wav file from random Scipy array or traverses a finite state machine to create a stream of notes in CDEFGABC notation which are translated to integer array of frequencies in hertz  
3. `Scipy.io.wavfile.write()` is invoked to write out this ndarray to a .wav file of sampling rate 44100  
4. Finite state machine has been implemented simply in a dictionary and supports quasi-non-determinism (array of possible previous states)  
5. Two .wav files `automaton_synthesized_music.wav` and `notes_synthesized_music.wav` are written for the two clauses: automaton or notes array  
6. Logs for synthesizer have been committed to `testlogs/AudioToBitMatrix.log.MusicSynthesizer.5March2019`  
7. It is pertinent to mention here that Stanford Music Information Retrieval at [https://musicinformationretrieval.com/genre\\_recognition.html](https://musicinformationretrieval.com/genre_recognition.html) does a statistical genre recognition of music as opposed to automata theoretic analysis in NeuronRain  
8. State machine has been hardcoded presently which have to be read from file and `literal_eval()`-ed.

-----  
643. (FEATURE) Merit of Audio/Music - Music Synthesizer - Music from mathematical functions - 6 March 2019  
-----

-----  
1. New clause has been added to `notes_to_audio()` for synthesizing music from values of any mathematical function  
2. Function expression string is `eval()`-ed in a lambda function and applied to a list of range values of variable `x` by `map()` and a wave file `function_synthesized_music.wav` is written to.  
3. Error in `prevstates` has been corrected by `prevprevstates` and resetting `prevstates` for each state transition for an alphabet.  
4. Logs for this have been committed to `testlogs/AudioToBitMatrix.log.MusicSynthesizer.6March2019`

5.The wave files do not play any human palatable music and are representative only.  
6.Infact learning the right DFA (or in general a mathematical function) for language of music is the exact opposite of the previous and is measure of merit.

-----  
644. (FEATURE) Intrinsic Merit of Audio/Music - Mel Frequency Cepstral Coefficients - 11 March 2019  
-----

1.New function for Mel Frequency Cepstral Coefficients (MFCCs) of a music audio clip (invokes librosa) has been added in this commit.  
2.MFCCs are kind of spectra of spectra of an audio waveform and have been widely used for speech recognition and music genre identification.  
3.logs for example MFCCs of a music file are committed to testlogs/AudioToBitMatrix.log.MFCC.11March2019

#### References:

-----  
644.1 Stanford MIR - <https://musicinformationretrieval.com/mfcc.html>  
644.2 MFCCs for Music Modelling - <http://musicweb.ucsd.edu/~sdubnov/CATbox/Reader/logan00mel.pdf>  
644.3 Music Emotion Recognition (MER): The combined evidence of MFCC and residual phase - [NJ Nalini , S Palanivel] - Dept of Computer Science and Engineering, Annamalai University, Tamil Nadu 608002, India - <https://www.sciencedirect.com/science/article/pii/S1110866515000419>  
-----

645. (THEORY) Comparing Partitions - Related to 620 and all sections on Majority Voting, Theoretical EVMs, Separate Chaining Hashtable/LSH Set Partitions, Integer Partitions, Complementary Sets and Diophantines, Streaming Histogram/Dictionary Analytics, People Analytics, Software Analytics, Business Analytics - 15 March 2019  
-----

Previous sections deeply delve into the ubiquitous isomorphism between integer/set partitions and set partitions, particularly those induced by hash table separate chaining buckets. A Theoretical EVM has been formulated having separate chaining partition as basis which is an encrypted set partition of electorate into candidate buckets. Drawing analytic inferences from stream of set partitions has been hitherto a far less researched bigdata topic and applies to whole gamut of theory and analytics - For example:

(\*) Business Analytics - Customer base intelligence is often represented as dynamic stream of histogram set partitions or probability distributions of product influences. Hashtable separate chaining can be picturised as histogram of buckets of hashed items

(\*) People Analytics - Stream of voting patterns in Theoretical EVMs are dynamically changing set partitions of electorate - vote shares in Psephology

(\*) Scheduler Queuing Analytics in Operating Systems - an example hashtable based timeout is described in

[https://github.com/shrinivaasanka/Grafit/blob/master/course\\_material/NeuronRain/AdvancedComputerScienceAndMachineLearning/AdvancedComputerScienceAndMachineLearning.txt](https://github.com/shrinivaasanka/Grafit/blob/master/course_material/NeuronRain/AdvancedComputerScienceAndMachineLearning/AdvancedComputerScienceAndMachineLearning.txt) - finding patterns in stream of scheduler timeout hashtable queues

(\*) Music Spectrograms are streams of Histograms

(\*) Theoretically set partitions are complementary sets or exact cover of a universal set.

Comparing any two set partitions thus far has few standard measures (rooted in comparing two cluster partitions created by supervised or unsupervised classifiers) like Rand Index (RI), Adjusted Rand Index etc., (ARI) which compute distance between partitions as ratio of agreements to disagreements by measuring

overlaps. For a stream of set partitions (which could be any of the above), Rand Index or Adjusted Rand Index between two consecutive partitions in the stream themselves create another stream of scalar indices which are easier to interpret. In people analytics or business analytics example above, highly fluctuating stream of rand indices for voting or customer histogram patterns is a measure of disarray in voting and consumers and points to a state of flux whereas a periodic or steady state of stream of rand indices indicates voters and consumers have limited options or are content with status quo. Similarly a chaotic stream of rand indices for Scheduler implies a heavily thrashed system.

Theoretically, rand indices define distance metric between two complementary sets and therefore diophantines (e.g beatty functions for size two partition) defined on them - in other words, diophantines are embedded in a metric space by rand index distance metric (similar to Reproducing Kernel Hilbert Space of Functions mentioned in 624.14).

#### References:

- 645.1 Comparing Partitions - Journal of Classification 2:193-218 (1985) - Springer-Verlag New York Inc.  
 - [Lawrence Hubert ,The University of California, Santa Barbara - Phipps Arabie, University of Illinois at Champaign] -  
<https://link.springer.com/article/10.1007/BF01908075>  
 645.2 Adjusted Rand Index -  
[https://en.wikipedia.org/wiki/Rand\\_index#Adjusted\\_Rand\\_index](https://en.wikipedia.org/wiki/Rand_index#Adjusted_Rand_index)  
 -----

646. (THEORY) Complementary Equations, Spectra of Numbers, Complementary Integer Sequences - related to 645 and all sections on Complement Functions, Complementary Sets and Diophantines - 16 March 2019  
 -----

Increasing sequences which partition set of natural integers are known as complementary sequences and equations which define both of them are complementary equations. This definition of complementary equations differs technically from complement functions which are diophantine equation representations of either a set or its complement and not both at once. OEIS sequences  $b(n)=A005228$  and  $a(n)=A030124$  are complementary and both are defined simultaneously by complementary equation  $b(n) = a(n - 1) + b(n - 1)$

Spectra of numbers are integer sequences and defined in terms of rounding off set of real multiples to nearest integers. For example:

If  $r$  is a positive real number, spectra of  $r = S(r) = \{ [r], [2r], [3r], \dots \}$  and  $[x]$  is the nearest integer  $\leq x$ .

There are some special qualities of Spectra of integers - e.g. Spectra of any three real numbers  $S[r1], S[r2], S[r3]$  have some pairs which have infinitely many elements in common and thus cannot be complementary and thus is a prima facie condition for feasibility of complementation.

#### References:

- 646.1 Complementary Equations - Example 3 - [Journal of Integer Sequences, Vol. 10 (2007), Clark Kimberling, Department of Mathematics, University of Evansville, 1800 Lincoln Avenue, Evansville, IN 47722, USA] -  
<https://cs.uwaterloo.ca/journals/JIS/VOL10/Kimberling/kimberling26.pdf>  
 646.2 Complementarity in Philosophy - Dualism - Taichi - Yin-Yang (Dark-Bright) -  
[https://en.wikipedia.org/wiki/Yin\\_and\\_yang](https://en.wikipedia.org/wiki/Yin_and_yang)  
 646.3 OEIS - Hofstadter Sequence - <https://oeis.org/A005228>  
 646.4 OEIS - Complement of Hofstadter Sequence - <https://oeis.org/A030124>  
 646.5 Spectra of Integers - [Graham-Lin-Lin] -  
[https://www.jstor.org/stable/2689998?seq=1#page\\_scan\\_tab\\_contents](https://www.jstor.org/stable/2689998?seq=1#page_scan_tab_contents)  
 -----

-----  
 -----  
 647. (THEORY and FEATURE) Bounded Error Factorization (Approximate Factors), Ray Shooting Queries, Transition from Quantum to Classical Computation, Derandomization - related to 597,631 - 21 March 2019, 2 August 2019  
 -----  
 -----

In Computational Geometric Factorization algorithms described previously, Approximate Factors are found by prime factor estimation involving various number theoretic results which narrow down the location of exact factor to large extent. By searching a circular radius vicinity surrounding an approximate factor, probability of finding a factor is amplified. Error probability of not finding an exact factor by ray queries has been derived previously as:

$$N/k\log\log N - 2q(\log N)^l$$

$$-----$$

$$N/k\log\log N$$

for integer-to-factorize  $N$  and constants  $k, q$  and  $l$ . This error probability though exponential can be brought down to a desired bound by suitable choice of radius and values for constants  $k, q$  and  $l$  or by precision tile summation ray shooting. Shor's BQP factoring algorithm can be made a PP classical probabilistic polytime algorithm by [Adleman-DeMarrais-Huang] theorem - BQP in PP. By invocation of Ray Shooting Oracles as subroutines in this PP factoring algorithm, PP is error-bounded to a BPP or BPNC algorithm (by doing ray shooting queries on parallel RAMs). Derandomization of BPP to P has known Hitting Set Generator algorithms. BPNC derandomization has some restrictions - only derandomizing BPNC1 is known. But this could be sufficient because classical PRAM computational geometric factorization is achievable by Parallel Planar Point Location NC1 algorithms of  $O(\log N)$  parallel time. This pipelined derandomization of BQP through BQP-PP-BPP(or BPNC)-P(or NC) points to prima facie feasibility of wave function superposition collapse (a quantum universal gate) to some classical eigenstate (PRAM).

#### References:

-----  
 647.1 Nisan's PRG and Derandomization of BPNC1 - [Periklis Papakonstantinou] - Section 3.4 - "...We consider logspace machines without a stack, and we parametrize on the number of passes over the random tape. This defines a hierarchy of classes between LogSpace and  $BP \cdot \text{LogSpace} \supseteq \text{BPNC1}$  [Nis93b]. Therefore a full derandomization of this hierarchy derandomizes BPNC1 ..." - Section 3.4.1 - [http://papakonstantinou.org/periklis/pdfs/phd\\_thesis.pdf](http://papakonstantinou.org/periklis/pdfs/phd_thesis.pdf) - "...Observe that a PRG that fools logspace machines with two-way access over the input, also fools NC1 circuits. The classical PRG of Nisan [Nis92] is shown to fool logspace machines that make  $r(n) = 1$  pass over the random or pseudorandom input. Using a simple analysis, we show that for every  $k > 0$  there exists  $k'$  such that for seeds of length  $\log^{k'}(n)$  the original Nisan's PRG is also secure against logspace machines with  $r(n) = \log^k(n)$  passes..."  
 647.2 Simplified Derandomization of BPP by Hitting Set Generator - [Goldreich-Vadhan-Wigderson] - <http://www.wisdom.weizmann.ac.il/~oded/COL/gvw.pdf>  
 647.3 Quantum Factorization and Decoherence - <https://arxiv.org/pdf/quant-ph/9503007.pdf> - [I. L. Chuang, R. Laflamme, P. Shor and W. H. Zurek] - "...As a quantum system evolves, information about its states leaks out into the environment, causing them to lose their purity, and, consequently, their ability to interfere...The decoherence process has been proposed as a mechanism for enforcing classical behavior in the macroscopic realm. Decoherence results in environment-induced superselection[5, 6, 7] which destroys superpositions between the states of preferred pointer basis[6]. Classical computers are already decohered - "  
 647.4 Proof of Ambainis-Aaronson Conjecture - "Quantum Speedups need structure" - "...Let  $f : \{-1, 1\}^n \rightarrow [-1, 1]$  be a multilinear polynomial of degree  $d$ . Then there exists a variable  $x_i$  whose influence on  $f$  is at least  $\text{poly}(\text{Var}(f)/d)$ ...."  
 - [Nathan Keller\* and Ohad Klein†] - <https://arxiv.org/pdf/1911.03748.pdf> - "..."

Let  $Q$  be a quantum algorithm that makes  $T$  queries to a Boolean input and let  $q, \delta > 0$ . Then there exists a deterministic classical algorithm that makes  $\text{poly}(T, 1/q, 1/\delta)$  queries to the input and that approximates  $Q$ 's acceptance probability to within an additive error  $q$  on a  $1 - \delta$  fraction of inputs. In other words, any quantum algorithm can be simulated on most inputs by a classical algorithm which is only polynomially slower, in terms of query complexity...." - proof of this conjecture lends credence to the pipelined decoherence of BQP factorization to BPP or BPNC mentioned earlier, in terms of query complexity - BQP-PP-BPP/BPNC - effectively implying decohered reduction from quantum error to classical error while classical error still depends on success of derandomization from BPP or BPNC to P or NC.

-----  
 648. (THEORY) Voting in Knot Theory, Gordion Knot, One-Way Functions, Hardness Amplification Lemma for Majority + VoterSAT Boolean Function Composition, Separate Chaining or LSH Partition based Theoretical EVMS - related to 318, 517, 620 - 21 March 2019  
 -----

Knot theoretic formulation of One-Way-Functions (as a Gordion Knot) has been mentioned in

[https://github.com/shrinivaasanka/Grafit/blob/master/course\\_material/NeuronRain/AdvancedComputerScienceAndMachineLearning/AdvancedComputerScienceAndMachineLearning.txt](https://github.com/shrinivaasanka/Grafit/blob/master/course_material/NeuronRain/AdvancedComputerScienceAndMachineLearning/AdvancedComputerScienceAndMachineLearning.txt). Previous sections describe a

hard-to-invert MajorityInverse() function which extracts the identity of the voters who voted for or against a candidate (for simplicity binary 0 or 1). Majority function can be formulated as a knot polynomial by following example procedure:

- (\*) Electorate are points on a straightline string
- (\*) Each voter has a decision function or VoterSAT of arbitrary complexity

class

- (\*) Knot on this string of voters maps each voter to a point on locus of a knot polynomial in 3 dimensional space. This mapping obfuscates the identity of the voter and vouchsafes secrecy.
- (\*) Knot polynomial is defined on 3 variable axes - Voters, Candidates, VoterSATs
- (\*) Each point on the knot is a tuple (obfuscated\_voter\_id, obfuscated\_VoterSAT, candidate\_id) denoting an anonymous vote in ballot
- (\*) MajorityInverse() for this Knot ballot is defined as:  
 MajorityInverse(obfuscated\_voter\_id, obfuscated\_VoterSAT, candidate\_id) = voter\_id
- (\*) Previous example in 3-dimensions is only for illustrative purposes (Obfuscated VoterSAT in the vote tuple may not be necessary) and knot ballot polynomial can be embedded in arbitrary topological space other than  $R^3$ .
- (\*) Hardness of previous knot version of MajorityInverse() depends on difficulty in unravelling the knot (to retrieve voter who voted for a candidate) so that secret ballot is not compromised.
- (\*) Thus a Gordion Knot Ballot is hard-to-invert MajorityInverse() function.
- (\*) Number of votes for a candidate is determined by the number of points on the knot polynomial intersecting the 2-dimensional plane for a candidate axis point.

-----  
 649. (THEORY) Planar Graph Theoretic Circle Packing, Space Filling/Grid Filling, CSP/Linear Programming, Tile Cover and LSH/Separate Chaining Partitions - related to 135 - 25 March 2019, 1 April 2019  
 -----

Previous algorithms for packing/filling space by circular solids/fluids were based on solving Linear Program and Cellular Automata by a Parallel Pseudorandom



Generator. In this section a random graph theoretic circle packing algorithm is described:

Circle Packing problem is defined as filling a grid with non-overlapping circles of maximum possible radii. In other words, sum of radii of the non-overlapping tangential circles are maximized by a constraint satisfaction problem(CSP) or LP. Rectangular grid is mapped to a linear program  $x_{11} + x_{12} + \dots + x_{mn}$  for each ordinate  $x(ij)$  of the grid. Points on the grid are randomly filled by a Parallel Pseudorandom Generator and these points are centroids of circles of arbitrary radius which intersect the grid. All grid ordinates intersected by or within the circles are set to 1. Circle Packing Theorem implies this set of tangential circles draw a planar intersection graph or coin graph. Conversely for every planar graph, a set of tangential circles can be demarcated which are solutions to a CSP/LP. This version of circle packing has an added parallel randomness ingredient and therefore is a Parallel Random Graph Circle Packing:

```
while (there are unfilled grid ordinates)
{
 (*) Centroids of tangential circles (which are vertices of random
intersection graph) are chosen by a PRG in parallel
 (*) edges are created at random amongst centroid vertices which
simulate tangential circles and have length equal to sum of radii of two
tangential circles
 (*) any overlap of circles is avoided by shrinking the sum of radii
as necessary.
 (*) all ordinate variables within random tangential circles are set
to 1.
 (*) Grid ordinates are stored in a hashmap and an ordinate is
removed from map after being set to 1.
 (*) At any instant, Parallel PRG chooses only from remaining
ordinates in the hashmap which is exhausted when grid is completely filled by
circles.
}
```

Previous Parallel Random Graph Circle Packing is in BPNC/RNC and indirectly probabilistically solves the constraint satisfaction problem for sum of radii in parallel and is an online algorithm ( whereas sequential CSP/LP solution guarantees that the tangential osculating circles have maximum radius possible apriori).

Circle Packing is also an exact cover set partition of 2-D space (e.g infinite number of circles in Apollonian Gasket). Set partition and space filling (by Circle packing, Tile cover etc.,) have an isomorphism. Separate Chaining Hashtable and LSH partitions are isomorphic to exact tile cover of a rectangular 2-D region and there exists a connection to factorization if Number of elements of a set S is composite and size of every bucket in set partition of S is composite i.e every bucket in histogram is mapped to a rectangular tile in tile cover of S plotted as a rectangle. Size of every bucket can be written as sum of four squares by Lagrange Four Squares Theorem and thus every set in a set partition can be mapped to 4 juxtaposed squares which reduces Balls-Bins/Set partition problems to Tile Packing.

#### References:

-----  
649.1 Circle Packing Survey - Apollonian Gasket - Computational Effort in finding radii - Figure 2 - Packing and Simplicial Complexes - Discrete Riemann Mapping Theorem - Maximal Packing - [http://www.math.utk.edu/~kens/Notices\\_article.pdf](http://www.math.utk.edu/~kens/Notices_article.pdf) - Previous algorithm for Circle Triangulation Packing in Apollonian Gasket is a greedy algorithm where maximum possible radii are chosen initially which are fractally reduced  
649.2 Descartes Circle Theorem - [https://en.wikipedia.org/wiki/Descartes%27\\_theorem](https://en.wikipedia.org/wiki/Descartes%27_theorem) - Every four kissing quadratic circles satisfy the quadratic equation -  $(b_1 + b_2 + b_3 + b_4)^2 = 2(b_1^2 + b_2^2 + b_3^2 + b_4^2)$  where  $b_i$  are bends or curvatures (radii) of the four circles. Quite useful in previous randomized parallel algorithm in finding the radius of inscribed fourth circle.

649.3 An example Constraint Satisfaction Problem for unequal Circle Packing in rectangle by 0-1 Integer Linear Programming - Integer Programming Formulations for Approximate Packing Circles in a Rectangular Container - <https://www.hindawi.com/journals/mpe/2014/317697/>

-----

650. (THEORY and FEATURE) Streaming Set Partition (Histogram) Analytics - 28 March 2019

-----

1.New Python implementation for multipurpose analytics of streamed set partitions (histograms) has been committed - Streaming\_SetPartitionAnalytics.py  
2.Two new bigdata sources have been defined in Streaming\_AbstractGenerator.py - "TextHistogramPartition" and "DictionaryHistogramPartition" which respectively:  
(\*) Map a list of textfiles to list of histograms by finding word frequency in the text and yield partition datastructure as iterable which is a dictionary of words to buckets in histograms (occurrences are mapped to array of 1s e.g occurrence 5 for word "word" is mapped to binned bucket ('word', [1,1,1,1,1]))  
(\*) Read a text file - Streaming\_SetPartitionAnalytics.txt - containing list of dictionaries, literal\_eval() it and yield the elements as iterable  
3.TextHistogramPartition is a fancy datasource which facilitates an alternative measure of streaming text analytics and text similarity  
4.DictionaryHistogramPartition is the conventional datasource for succinctly representing a set partition which could be anything ranging from LSH partition, Exact Cover, Balls-Bins, Separate Chained Hashtables, Electronic Voting Machines based on LSH and Separate Chaining, Business Intelligence Histograms, SMS voting histograms, Music Spectrograms etc.,.  
5.adjusted\_rand\_index() in Streaming\_SetPartitionAnalytics.py instantiates both these datasource iterators and computes Adjusted Rand Index for two consecutive partitions in the stream by SciKitLearn adjusted\_rand\_score()  
6.Because of the fact that every set partition is set of class labels in some classifier, various other clustering performance measures - mutual information, silhouette etc.,  
(<https://scikit-learn.org/stable/modules/clustering.html#clustering-evaluation>) could compare partitions too.  
7.tocluster() in Streaming\_SetPartitionAnalytics.py maps a partition to an array of labelled elements in scikitlearn format  
8.An example streaming set partition analytics for linux kernel logs (TextHistogramPartition) and list of dictionaries (DictionaryHistogramPartition) is committed to Streaming\_SetPartitionAnalytics.log.28March2019 which show how Adjusted Rand Index works for similar and dissimilar partitions.  
9.For circumventing sklearn exception two compared partitions are truncated to minimum size of the two

-----

651. (THEORY and FEATURE) Reduction from Set Partition to Exact Square Tiles Cover of Rectangular Region, Lagrange Four Square Theorem, Complementary Sets, Computational Geometric Factorization, Space Filling, Tile Cover, Packing, Set Partition/Histogram Analytics, LSH Partitions, Separate Chaining Hashtables - 3 April 2019, 17 November 2019 - related to 649 and 650

-----

1.Python implementation for Set Partition Analytics (Streaming\_SetPartitionAnalytics.py) has been updated for a new function which reduces a histogram set partition to exact square tiles cover of rectangular region which has area equal to number of elements in the histogram.  
2.Function setpartition\_to\_tilecover() loops through histogram buckets (set partition) and maps each bucket size to sum of four squares by Lagrange Four Square Theorem essentially mapping each 1-dimensional bucket to 4 2-dimensional square tiles.

3. Collection of these sets of 4 square tiles covers the rectangular region of area equal to number of elements partitioned by histogram/LSH/Separate Chaining.  
 4. Example logs in testlogs/Streaming\_SetPartitionAnalytics.log.3April2019 demonstrate reduction of histogram buckets [11,12,13,14,15] of total number of 65 elements to tile cover of rectangular region which has composite area  $13*5=65$ :

square tiles for partition 11 : set([(0, 1, 1, 3)])  
 square tiles for partition 12 : set([(1, 1, 1, 3)])  
 square tiles for partition 13 : set([(1, 2, 2, 2)])  
 square tiles for partition 14 : set([(0, 1, 2, 3)])  
 square tiles for partition 15 : set([(1, 1, 2, 3)])

Lagrange Four Square Tiles Cover reduction of Set Partition [11, 12, 13, 14, 15] : [0, 1, 1, 9, 1, 1, 1, 9, 1, 4, 4, 4, 0, 1, 4, 9, 1, 1, 4, 9]

5. This reduction indirectly solves factorization problem (complexity depends on sum of four squares) geometrically by following square tiles cover algorithm:

5.1 Number to factorize N is partitioned arbitrarily by some integer partition and is isomorphic to a histogram

5.2 Square tiles are obtained from partition by previous Lagrange Four Square reduction

5.3 Square tiles are geometrically juxtaposed/arranged to create a tiled rectangle sides of which are factors of N

5.4 Finding an arrangement of tiles on a rectangular region can be formulated as a non-linear (quadratic) convex-concave optimization problem. If  $x_1, x_2, x_3, \dots, x_n$  are sides of square tiles:

$N = \text{area of rectangle} = \text{sum of areas of square tiles} = x_1^2 + x_2^2 + x_3^2 + \dots + x_n^2$

= product of sum of sides of peripheral tiles

=  $(c_1*x_1 + c_2*x_2 + \dots + c_n*x_n)*(d_1*x_1 + d_2*x_2 + \dots + d_n*x_n)$  for  $c_i = 0$  or 1,  $d_i = 0$  or 1

5.5 Solving  $N = x_1^2 + x_2^2 + x_3^2 + \dots + x_n^2 = (c_1*x_1 + c_2*x_2 + \dots + c_k*x_k + c_n*x_n)*((1-c_1)*x_1 + (1-c_2)*x_2 + \dots + c_k*x_k + (1-c_n)*x_n)$  by Integer Programming for binary  $c_i$  amounts to factorizing N (because tiles of the sides have to be mutually exclusive save corner tile)

5.6 The corner square tile is common to both sides and  $c_k = d_k$  for exactly one square tile  $x_k$ .

If Factorization is doable in PRAMS (and therefore in Nick's Class) as per previous sections on various parallel RAM polylogarithmic time algorithms for factoring (e.g Parallel Planar Point Location), geometric arrangement of square tiles in a rectangle is of polynomial time - find factors which are sides of rectangle, successively tile the rectangle by choosing largest square remaining. Many randomized algorithms are available for finding Lagrange Sum of squares. If the factors of  $N = p*q$  are known in polylogarithmic time finding the tile arrangement is by solving two linear programs:

$$c_1*x_1 + c_2*x_2 + \dots + c_k*x_k + \dots + c_n*x_n = p$$

$$(1-c_1)*x_1 + (1-c_2)*x_2 + \dots + c_k*x_k + \dots + (1-c_n)*x_n = q$$

which are underdetermined linear equations (n variables and 2 equations) and constraints are specified by complemented binary coefficients  $c_i$  and  $1-c_i$  and  $c_k=d_k$  in the two equations for mutually excluding tiles in the sides of the rectangle except corner tile. This boolean coefficient complement constraint can be ignored if two sides of the rectangle can have tiles of similar squares. Another relaxation: Number of tiles can be unequal in either sides. Equations then are easier to interpret as:

$$c_1*x_1 + c_2*x_2 + \dots + c_k*x_k + \dots + c_m*x_m = p$$

$$d_1*x_1 + d_2*x_2 + \dots + d_k*x_k + \dots + d_n*x_n = q$$

subject to one constraint for corner tile  $c_k=d_k$  and number of variables m and n could be unequal. Number of variables m and n can be equated by additional  $|m-n|$  slack variables of zero coefficients in equation of lesser variables. From Rouche-Capelli theorem number of solutions to underdetermined system of equations is Infinite because rank of augmented matrix is < rank of coefficient matrix for underdetermined system of equations. Solutions can be found by many algorithms prominent being Gauss-Jordan elimination (Gaussian Elimination by Partial Pivoting-GEPP). GEPP has been proved to be P-complete problem. Previous

system of equations are solved by GEPP post-factorization (sides of rectangle  $p, q$  are factors of  $N$  found by PRAM computational geometric factorization). If  $NC=P$ , both sides of rectangle and arrangement of square tiles on the sides of the rectangle can be done in  $NC$  by PRAM GEPP which is a depth-two parallelism. Without knowledge of factors, previous product  $(c_1x_1 + c_2x_2 + \dots + c_mx_m)(d_1x_1 + d_2x_2 + \dots + d_nx_n) = pq = N$  is a quadratic program solving which is NP-Hard.

Point location by parallel construction of wavelet trees has been described in previous sections, which consider the set of points of a geometric variety (e.g. points on rectified hyperbolic arc) on the plane as a string of points represented as a wavelet tree. Point Location by Parallel Wavelet Tree construction is more obvious than Parallel Point Location by Kirkpatrick Triangulation, Planar subdivision, Bridge Separator Trees etc.,. The string of points formed from rectified hyperbolic arc are concatenated straightline segments each of which is an arithmetic progression. Query select( $B, N, i$ ) returns the position  $p$  of the  $i$ -th occurrence of  $N$  in concatenated hyperbolic line segments string  $B$  from which  $i$ -th factors of  $N=(p, N/p)$  are obtained.

Previous reduction from set partition to tile cover by Lagrange Four Square Theorem is restricted to tiling 2-dimensional space. It can be generalized to filling/tiling arbitrary dimensional space by Chinese Remainder Theorem as follows:

- (\*) Chinese Remainder Theorem states that there is a ring isomorphism between  $x \bmod N$  and  $(x \bmod n_1, x \bmod n_2, \dots, x \bmod n_k)$  for pairwise coprime integers  $n_1, n_2, \dots, n_k$  and  $N = n_1 * n_2 * n_3 * \dots * n_k$  (or)  $x \bmod N \iff (x \bmod n_1, x \bmod n_2, \dots, x \bmod n_k)$  which is an isomorphism between ring of integers mod  $N$  and direct product space of rings of integers modulo  $n_k$
- (\*) By Chinese Remainder Theorem, there is a bucket of size  $x < N$  (so that  $x \bmod N = x$ ) of the set partition which can be mapped isomorphically to a  $k$ -dimensional hypercube of sides  $(x \bmod n_1, x \bmod n_2, \dots, x \bmod n_k)$  modulo an integer  $N=n_1*n_2*\dots*n_k$  (requires solving for  $x$ ).
- (\*) This Chinese Remaindering Reduction reduces 1-dimensional set partition to tiling arbitrary dimensional space

## References:

- 
- 651.1 Wang Tiling - [https://en.wikipedia.org/wiki/Wang\\_tile](https://en.wikipedia.org/wiki/Wang_tile) - Previous Lagrangian Tiling can be contrasted to Wang Tiles which is about feasibility of tiling a 2-D plane by multicolored square tiles by matching colors of adjacent tiles.
- 651.2 Alternative partition distance measures - <https://arxiv.org/pdf/1106.4579.pdf>
- 651.3 Clustering for set partitioning -  $k$ -set partitioning and centroid clustering are equivalent - [https://www.microsoft.com/en-us/research/wp-content/uploads/2016/11/OPT2015\\_paper\\_32.pdf](https://www.microsoft.com/en-us/research/wp-content/uploads/2016/11/OPT2015_paper_32.pdf)
- 651.4 Sage Set Partitions Implementation - [http://doc.sagemath.org/html/en/reference/combinat/sage/combinat/set\\_partition.html#sage.combinat.set\\_partition.SetPartition](http://doc.sagemath.org/html/en/reference/combinat/sage/combinat/set_partition.html#sage.combinat.set_partition.SetPartition)
- 651.5 Sage Ordered Set Partitions Implementation - complement of a partition - [http://doc.sagemath.org/html/en/reference/combinat/sage/combinat/set\\_partition\\_ordered.html](http://doc.sagemath.org/html/en/reference/combinat/sage/combinat/set_partition_ordered.html)
- 651.6 Jacobi Sum of Four Squares Theorem - [https://en.wikipedia.org/wiki/Jacobi%27s\\_four-square\\_theorem](https://en.wikipedia.org/wiki/Jacobi%27s_four-square_theorem) - "...The number of ways to represent  $n$  as the sum of four squares is eight times the sum of the divisors of  $n$  if  $n$  is odd and 24 times the sum of the odd divisors of  $n$  if  $n$  is even ..."
- 651.7 Succinct and Implicit Data Structures for Computational Geometry - [Meng He, Faculty of Computer Science, Dalhousie University, Halifax, NS, B3H 4R2, Canada, [mhe@cs.dal.ca](mailto:mhe@cs.dal.ca)] - Figure 1 - "A wavelet tree constructed for the string 35841484 over an alphabet of size 8. This is also a wavelet tree constructed for the following point set on an 8 by 8 grid: {1, 3}, {2, 5}, {3, 8}, {4, 4}, {5, 1}, {6, 4}, {7, 8}, {8, 4}" and Section 3 - Planar Point Location - [https://web.cs.dal.ca/~mhe/publications/ianfest66\\_succinctgeometry.pdf](https://web.cs.dal.ca/~mhe/publications/ianfest66_succinctgeometry.pdf)
- 651.8 Simple, Fast and Lightweight Parallel Wavelet Tree Construction - [Fischer-

Kurpicz-Lobel] - <https://arxiv.org/pdf/1702.07578.pdf> - Comparison to Domain Decomposition Parallel Wavelet Tree Construction and Variant of Wavelet Tree (Wavelet Matrix) - In the context of Computational Geometric Parallel Planar Point Location, size of the alphabet for wavelet tree is very small in the range  $[N-\delta, N+\delta]$  because hyperbolic tile segments have product of ordinates which are more or less equal to  $N$ .

651.9 Planar Point Location - Algorithms -

[https://cw.fel.cvut.cz/b181/\\_media/courses/cg/lectures/02-pointloc.pdf](https://cw.fel.cvut.cz/b181/_media/courses/cg/lectures/02-pointloc.pdf)

651.10 Segment Trees and Point Location Query -

<http://www.cs.umd.edu/class/fall2016/cmsc754/Lects/cmsc754-fall16-lects.pdf>

651.11 Rouché-Capelli Theorem for Underdetermined system of equations -

[https://en.wikipedia.org/wiki/Underdetermined\\_system#Solutions\\_of\\_underdetermined\\_systems](https://en.wikipedia.org/wiki/Underdetermined_system#Solutions_of_underdetermined_systems), [https://en.wikipedia.org/wiki/Rouch%C3%A9%E2%80%93Capelli\\_theorem](https://en.wikipedia.org/wiki/Rouch%C3%A9%E2%80%93Capelli_theorem)

651.12 Parallel Complexity of Gaussian Elimination by Partial Pivoting -

<https://algo.ing.unimo.it/people/mauro/strict.ps>

651.13 CGAL 5.0 Planar Point Location implementation -

[https://doc.cgal.org/latest/Arrangement\\_on\\_surface\\_2/index.html#title14](https://doc.cgal.org/latest/Arrangement_on_surface_2/index.html#title14)

651.14 Parallel CGAL - Multicore parallelism in CGAL is achieved by Intel TBB -

<https://github.com/CGAL/cgal/wiki/Concurrency-in-CGAL>

-----  
652. (FEATURE) Histogram-Set Partition Analytics - Adjusted Mutual Information - 3 April 2019  
-----

-----  
1. `adjusted_mutual_info_score()` from `sklearn.metrics` has been invoked in `adjusted_rand_index()` for comparing two set partitions.

2. Logs in `testlogs/Streaming_SetPartitionAnalytics.log` 2.3 April 2019 show the difference between two measures - adjusted rand index and adjusted mutual information

-----  
653. (FEATURE and THEORY) Computational Geometric Factorization - Tile Search - Spark 2.4 - `SparkContext.range()` - 16 April 2019  
-----

-----  
1. `DiscreteHyperbolicFactorizationUpperbound_TileSearch_Optimized.py` has been changed to replace `xrange()` by `Spark Context range()` function in Spark 2.4.

2. `Python xrange()` is sequential and local while `Spark range()` is resilient distributed dataset which can be computed on cloud in parallel

3. Some ray query functions have also been transitioned to `Spark Context range()`.

4. An example integer is factorized and logs in `testlogs/DiscreteHyperbolicFactorizationUpperbound_TileSearch_Optimized.log` 16 April 2019 show some accurate ray shooting by Hardy-Ramanujan approximate factoring and exact factors.

5. Spark 2.4 has Barrier Synchronization feature (mentioned experimental) which is BSP model (like Pregel) than PRAM -

<https://spark.apache.org/docs/latest/api/python/pyspark.html#pyspark.BarrierTaskContext.get>

6. Greenwich Mean Time (`gmtime()`) is printed after every factor is found for duration analysis of finding all factors.

-----  
654. (THEORY and FEATURE) EventNet creation from Video, Actor Model, PetriNets, Video EventNet Tensor Products Intrinsic Merit - 19 April 2019 - related to all sections on Causality-Logical Time and Merit  
-----

-----  
1. ImageNet Keras-Theano Python implementation has been changed to write EventNet Vertices and Edges

files from causally related frame events of the video which can be read by GraphViz or NeuronRain EventNet Python implementation

2.EventNet differs from traditional PetriNet in following respects:

- 2.1 PetriNets have vertices having tokens called "Places" while EventNet has vertices having "actors" or "participants" in an event (Actor-Event Model)
- 2.2 PetriNets have transitions which move the tokens from Place-a to Place-b while EventNet has directed edges which connect a causing event vertex to an effect event vertex which is akin to flow of tokens.
- 2.3 EventNet is an Actor Model where actors interact in an event, modify local states and send messages to other actors.

3.Video EventNet vertices and edges are written to Video\_EventNetEdges.txt and Video\_EventNetVertices.txt

#### References:

-----

654.1 Actor Model - [https://en.wikipedia.org/wiki/Actor\\_model](https://en.wikipedia.org/wiki/Actor_model)  
654.2 PetriNets - <https://www.techfak.uni-bielefeld.de/~mchen/BioPNML/Intro/pnfaq.html>

-----

655. (THEORY and FEATURE-BUGFIX) EventNet creation from Video - bug resolutions, corrections to EventNet vertices and edges text files - 21 April 2019

-----

-----

- 1.ImageNet Keras Theano Python Implementation had some bugs in creating EventNet vertices and edges text files which have been resolved in this commit.
- 2.Frame prevfix has been included in EventNet edges text file.
- 3.Extracting EventNet from video facilitates computing usual dense subgraph complexity measures for Video similar to TextGraphs - e.g k-core, cycles, strongly connected components, algebraic connectivity etc.,

-----

656. (FEATURE) Medical Imageing Analytics - ElectroCardioGram (ECG), EventNet from Video - 23 April 2019

-----

-----

- 1.Extracting patterns in medical imagery (ECG, MRI, Echo Cardio Gram Scans etc.,) is one of the most obvious analytics that can be performed on a Medical Image dataset which has widespread requirement in healthcare.
- 2.ImageNet Keras-Theano Python implementation has been augmented with a `medical_imageing()` function which takes an image source (presently ECG) and thresholds the image to retrieve contours from it by CV2 `findContours()`.
- 3.Image Contours are prominent features in an image which are more pronounced and distinguish it from other images.
- 4.Two example ECG images (Normal and Infarction) are compared by creating contours (i.e extract the ECG waveform from image) and computing the hausdorff distance between the two image contours:
- 5.Example comparison from logs in `testlogs/ImageGraph_Keras_Theano.log.MedicalImageing.23April2019:`  
Distance between Normal ECG and Normal ECG: (0.0, 0, 0)  
Distance between Normal ECG and Infarction ECG: (1741.9586677071302, 0, 0)
- 6.EventNet edges and vertices numbering in text files Video\_EventNetEdges.txt and Video\_EventNetVertices.txt has been corrected.

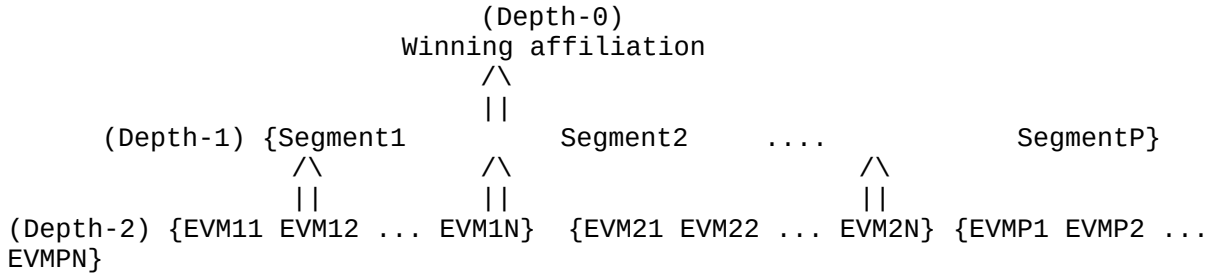
#### References:

-----

656,1 Medical Imageing Analysis - <https://www.pyimagesearch.com/2018/12/03/deep-learning-and-medical-image-analysis-with-keras/>  
656.2 ECG Library - <https://ecglibrary.com/ecghome.php>

-----  
 657. (THEORY) Depth-2 Majority Function, Theoretical EVMs, Set Partitions,  
 People Analytics, Axiom of Choice - related to 546,490 and all sections on  
 majority voting - 25 April 2019  
 -----

It has been mentioned in earlier sections on set partitions that every  
 theoretical majority voting partitions the population into subsets or buckets  
 indexed by the candidate voted for. Most realworld democracies follow the depth-  
 2 majority voting division convention below:



and each EVM is defined by the hieararchy of partitions( candidates per segment  
 might vary as  $n(1), n(2), \dots, n(P)$ ) - votes per candidate  $k$  in  $q$ -th EVM of  $p$ -th  
 segment (EVM<sub>mpq</sub>) is denoted by  $ckpq$  :

$$\begin{aligned}
 \text{EVM11} &= c111 + c211 + c311 + \dots + cn(1)11 \\
 \text{EVM12} &= c112 + c212 + c312 + \dots + cn(1)12 \\
 &\dots \\
 \text{EVM21} &= c121 + c221 + c321 + \dots + cn(2)21 \\
 &\dots \\
 \text{EVMP1} &= c1P1 + c2P1 + c3P1 + \dots + cn(P)P1 \\
 &\dots
 \end{aligned}$$

Previous partition tree of depth-2 (i.e a tree whose nodes are set partitions)  
 generalizes depth-2 boolean majority function to non-boolean setting and is an  
 arithmetic circuit. At Depth-2 EVM set partitions per segment are summed up  
 partwise (because all partitions within a segment should have equal number of  
 parts which is the number of candidates per segment) and passed on to Depth-1 -  
 in previous per segment partition identities summing vertically columnwise  
 yields Depth-1 partition per segment. At Depth-1 index for candidate of maximum  
 part/bucket size in segmentwise partition sum is computed and passed on to  
 Depth-0. At Depth-0, single set partition is created which contains buckets per  
 affiliation of the candidates. Maximum size part in Depth-0 set partition is the  
 winning affiliation.

Whole depth-2 majority voting democratic process rests on the correctness of  
 Axiom of Choice which avers: For a collection  $X$  of subsets, there always exists  
 a choice function  $f$  such that for every set  $A$  in  $X$ ,  $f(A)$  is an element of  $A$ . In  
 previous example, at Depth-1, maximum() is the choice function applied across  
 the board for all segment set partitions for choosing the winning candidate per  
 segment (ruling out ties). It is readily obvious that each segment is a cluster  
 of partitions and empirically distance between majority of EVM partitions of  
 same segment (partition rank, rand index, mutual info) should not be abnormally  
 high and reflects trend per segment.

By Berry-Esseen Central Limit Theorem, if vote for each candidate ( $ckpq$ ) is a  
 random variable, normalized sum of the votes for all candidates or average  
 number of votes per candidate tends to normal distribution. In other words,  
 every part in each of the EVM partitions previously is a random variable which  
 are summed up. This implies distances between any two EVM partitions (which is  
 the function of distance between individual parts in two voting partitions) also  
 tend to distance between two normal distributions (i.e almost a constant on the  
 average). Most importantly, columnwise sum of parts leading to per segment  
 partition in Depth-1 is also an averaged normal distribution.

Ramanujan's Congruences for EVM partitions imply, for certain size of electorate (5k + 4, 7k + 5, 11k + 6) number of possible voting patterns (partition number or number of possible partitions) abides by following congruences:

$$\begin{aligned}p(5k + 4) \bmod 5 &= 0 \\p(7k + 5) \bmod 7 &= 0 \\p(11k + 6) \bmod 11 &= 0\end{aligned}$$

References:

-----  
657.1 Ramanujan Congruences - [https://en.wikipedia.org/wiki/Ramanujan%27s\\_congruences](https://en.wikipedia.org/wiki/Ramanujan%27s_congruences)

657.2 Distance measures between partitions - Hamming Distance, Maximum Matching Distance, Variation of Information - <https://pdfs.semanticscholar.org/d8a2/936cc4bcb8bda106e3b307104c3ee824b4a8.pdf>

657.3 Microsoft ElectionGuard OpenSource EVM - <https://blogs.microsoft.com/on-the-issues/2019/05/06/protecting-democratic-elections-through-secure-verifiable-voting/> - "...First, ElectionGuard provides each voter a tracker with a unique code that can be used to follow an encrypted version of the vote through the entire election process via a web portal provided by election authorities. During the process of vote-casting, voters have an optional step that allows them to confirm that their trackers and encrypted votes accurately reflect their selections...."

657.4 Ballot Marking Devices Cannot assure the will of voters - [Appel-DiMello-Stark] - [https://papers.ssrn.com/sol3/papers.cfm?abstract\\_id=3375755](https://papers.ssrn.com/sol3/papers.cfm?abstract_id=3375755)  
-----

-----  
658. (THEORY and FEATURE) Video EventNet Causality Graph Complexity Measures, Graph Minors, Merit of Large Scale Visuals - 29 April 2019  
-----

-----  
1.This commit invokes networkx Graph API and creates NetworkX EventNet causality graph object for an example video. Connectivity of the Video EventNet is printed.

2.Example video in matrovska format which records the facebook profile of the author <https://www.facebook.com/shrinivaasan.ka> (containing NeuronRain commits twitter feeds) is converted to mp4 by ffmpeg:

ffmpeg -i ExampleVideo\_Facebook\_GRAFIT\_29April2019.mkv -strict experimental ExampleVideo\_Facebook\_GRAFIT\_29April2019.mp4

3.Usually most videos have set of frames which are consecutive and closely related. These frames create straightline linear paths of vertices of degree 2 in the EventNet Graph underneath it.

4.These straightline paths can be coalesced or edge-contracted to single vertex forming Graph Minors of EventNet.

5.Connectivity of a Video is a necessary but not sufficient condition for merit.

6.Rationale for Video EventNet Connectivity as Merit Measure: Video of disconnected underlying EventNet causality has scattered non-coherent information which is not appealing to viewer.  
-----

-----  
659. (FEATURE) Music Pattern Mining - Music Synthesis by Automaton - Read from textfile - 30 April 2019  
-----

-----  
1.Hardcoded states2notes DFA has been removed and DFA is read from a textfile NotesStateMachine.txt and

ast.literal\_eval()-ed to a dictionary.

2.Scaling of notes have been commented and note values are magnified (multiplied by 1000). Waveform timeseries can be visually analyzed by loading .wav file to a player and displaying waveform oscilloscope in visual effects.

3.Logs for this have been committed to  
testlogs/AudioToBitMatrix.log.MusicSynthesizer.30April2019



-----  
660. (THEORY and FEATURE) DeepLearning Convolution BackPropagation - handwriting recognition - utility function - 5 May 2019, 9 May 2019  
- related to 159  
-----

-----  
1. DeepLearning\_ConvolutionNetwork\_BackPropagation.py has been changed to define a new utility function handwriting\_recognition() which loads two images of handwritings by CV2, thresholds them, finds contours of the two images and approximates the contours by Douglas-Peucker Polynomial (DP) and computes the hausdorff distance between the two DP approximate polynomials of the handwritten images.

2. testlogs/DeepLearning\_ConvolutionNetwork\_BackPropagation.log.5May2019 shows how 2 pairs of handwritten digits fare against hausdorff distance measure - 2 pictures of handwritten digit 1 (similar), 2 pictures of handwritten digits 1 and 8 (dissimilar)

3. Logs show DP polynomials of contours of 1 and 1 are close enough while DP polynomials of contours of 1 and 8 are far apart:

#####

Handwriting Recognition

#####

[[[1279 719]]]

[[[1276 719]]]

[[[1279 719]]]

Distance between DP polynomials approximating two handwriting contours: (3.0, 0, 0)

[[[1279 719]]]

[[[ 0 564]]]

Distance between DP polynomials approximating two handwriting contours: (1288.3578695378083, 0, 0)

4. Though image Contours and DP approximation are not traditional deep learning, previous contouring and DP approximation could as well be performed on convolution layers and maxpooling map layers of the two images as against images themselves.

5. Function handwriting\_recognition() is supervised learner and takes two arguments - training (labelled) and test (unlabelled) images - and compares the unlabelled image to training image (printed or handwritten)

6. In the topological sense, each approximate DP polynomial for handwriting contours of same alphabet or digit are equivalent homeomorphic deformations in  $R^2$ . Handwritings of same person for similar text create a cluster of deformations which are close enough and create outliers for different persons.

7. Pattern grammars described earlier define grammatical rules similar to context free grammars for shape description. For example handwritten alphanumeric 'b' is defined as:

$\langle b \rangle := \langle | \rangle \langle \text{operator} \rangle \langle o \rangle$

where  $\langle \text{operator} \rangle$  could be  $\langle \text{prefix} \rangle$  which tangentially attaches  $\langle | \rangle$  before  $\langle o \rangle$ .

Following the convention above, a family or cluster of close-enough DP approximate polynomials fit in as operands within  $\langle \rangle$  - e.g Coffee mug in 2 dimensions is homeomorphic to the letters 'D' and 'O' and all three (Mug, D, O) have close-enough DP Approximate polynomials of small hausdorff distances amongst them. Alternatively, Mug can be written as pattern grammar:

$\langle \text{Mug} \rangle := \langle I \rangle \langle \text{prefix} \rangle \langle \rangle$

and  $\langle I \rangle$  and  $\langle \rangle$  are defined by DP polynomials.

References:

-----  
660.1 Ramer-Douglas-Peucker Curve Decimation Algorithm - approxPolyDP() - [https://docs.opencv.org/2.4/modules/imgproc/doc/structural\\_analysis\\_and\\_shape\\_descriptors.html](https://docs.opencv.org/2.4/modules/imgproc/doc/structural_analysis_and_shape_descriptors.html)

660.2 Coffee Mug is homeomorphic to Donut Torus - Graphic illustration -

-----  
-----  
661.(THEORY and FEATURE) Music Pattern Mining - Weighted Automaton Learning from Music - 11 May 2019 - related to all sections on  
Intrinsic Merit of Music  
-----  
-----

1.Previous sections described ascertaining merit of music by various analyses of waveforms e.g MFCC, learning DFA from music notes. Apart from these there are standard measures viz., zero crossings, chroma which quantify genre or merit of music (<https://librosa.github.io/librosa/feature.html>).

2.Of these learning a deterministic finite automaton from strings of music notes is a qualitative intrinsic merit measure of music which does not involve any statistical processing.

3.Learning DFA is a computational learning theoretic problem (PAC Learning, Angluin Model etc.,). Weighted Deterministic Finite State Automata are generalizations of DFA in which state transitions have an associated numeric weightage in addition to alphabets from a language.

4.For example, weighted DFA below has the weighted transitions:

(state1, a, state2) - transition from state1 to state2 on symbol a of weight 1

(state2, 2b, state3) - transition from state2 to state3 on symbol b of weight 2

5.Weighted automata are apt formalisms to represent music notes strings as DFA because notes have subdivisions - sharp and flat - which can be likened to weightage for state transitions ([https://en.wikipedia.org/wiki/Musical\\_note](https://en.wikipedia.org/wiki/Musical_note) - CDEFGABC - ascending and descending graphic).

6.For example string of music notes - "CD(sharp)DEEGAF(flat)F(sharp)" - and its accepting weighted music automaton could be:

state1, C, state2

state2, Dsharp, state3

...

state10, Fflat, state5

state6, Fsharp, state2

...

where sharp and flat are weights for the transition symbol.

7.Scikit Learn SPLearn (scikit-splearn) provides a weighted automaton learning framework based on Spectral Theory.

8.This commit implements a Music Weighted Automaton python code in MusicWeightedAutomaton.py which accepts a set of training string of music notes and fits them to a weighted automaton using scikit-splearn. It makes predictions later based on training data.

9.Learnt weighted automaton for music notes string is drawn as DOT graph file by graphviz in MusicWeightedAutomaton.gv and is rendered to a pdf -

MusicWeightedAutomaton.gv.pdf

10.Weightage the transition in music notes has an another advantage: Some portions of the music waveform are more impressive and catchy which makes them to be listened again - <https://en.wikipedia.org/wiki/Earworm> - and transitions for these could have heavy weights.

11.Alphabets in sample music notes strings for scikit-splearn are numeric encoded as - A:0,B:1,C:2,D:3,E:4,F:5,G:6

References:

-----  
-----  
661.1 Weighted Automata Theory -

<https://perso.telecom-paristech.fr/jsaka/CONF/Files/IWAT.pdf>  
-----  
-----

662. (FEATURE) Intrinsic Merit of Music - Learning Weighted Automata from Music - Example - 14 May 2019  
-----  
-----

-----  
1.MusicWeightedAutomaton.py has been updated to define a new function audio\_notes\_to\_samples() to read a music clip of certain duration by librosa, convert the waveform to notes, create notes string samples from them and return samples as word frequency dictionary and numeric encoded sample notes strings  
2.SplearnArray is instantiated from encoded notes strings of variable size equal to number of columns in the notes matrix  
3.Weighted automaton is learnt from these Sample dictionary and numeric encoded notes strings  
4.automaton graph drawn in MusicWeightedAutomaton.gv.pdf shows a condensed weighted automata for an example music clip  
5.Logs for this are committed to testlogs/MusicWeightedAutomaton.log.14May2019  
-----

-----  
663. (FEATURE) Named Entity Recognition - Conditional Random Fields - Update - 16 May 2019  
-----

-----  
1.NamedEntityRecognition\_HMMViterbi\_CRF.py has been changed to removed hardcoded PoS tagged sentences and instead to read states and observations from two files: NamedEntityRecognition\_HMMViterbi\_CRF.states and NamedEntityRecognition\_HMMViterbi\_CRF.observations which have the semi-PoS tagged sentence PoS states and sentence word observations respectively.  
2.Emission Probabilities for each state are computed by a skew normal distribution which moves the mean from left to right of the sentence as states progress.  
3.This skew normal distribution gives more weightage to respective state than others while each state is observed.  
4.An example log in testlogs/NamedEntityRecognition\_HMMViterbi\_CRF.log.16May2019 shows the skewing of probability weights from left to right of the sentence  
5.For example, Name-Verb-Object PoS tag is weighted as : First 1/3 of sentence has more weightage for emission probabilities of "Name",second 1/3 of sentence has more weightage for emission probabilities of "Verb" and third 1/3 of sentence has more weightage for emission probabilities of "Object"  
-----

-----  
664. (FEATURE) Spark 2.4 Structured Streaming - Windowed Stream - 21 May 2019  
-----

-----  
1.SparkGenericStreaming.java in java-src/bigdata\_analytics/spark\_streaming has been changed to do windowed structured stream if URL socket is false i.e data is read from plain socket stream.  
2.New boolean flag "windowed" has been added to the java class as static member based on which Windowed streaming spark code is executed.  
3.Windowed streaming spark code fragment uses readStream()/writeStream() facility in Spark to read data written over socket.  
4.Netcat utility creates the socket server in port 8080.  
5.Java lambda functions in FlatMapFunction tokenize the incoming stream of lines to words and organize them as word-timestamp rows dataset.  
6.Next groupBy() parses word-timestamp dataset from previous lambda invocation and creates structured stream of tables of columns slidingwindow\_timestamp-word-count.  
7.Logs in testlogs/SparkGenericStreaming.log.21May2019 show dataframe tables for both urlsocket=false(windowed=true) and urlsocket=true boolean option settings.  
8.CLASSPATH for compilation of SparkGenericStreaming.java (javac SparkGenericStreaming.java) has been updated to:  
CLASSPATH=/media/Ubuntu2/spark-2.4.0-bin-hadoop2.7/jars/spark-streaming\_2.11-2.4.0.jar:./media/Ubuntu2/spark-2.4.0-bin-hadoop2.7/jars/scala-library-2.11.12.jar:/media/Ubuntu2/spark-2.4.0-bin-hadoop2.7/jars/spark-sql\_2.11-2.4.0.jar:/media/Ubuntu2/spark-2.4.0-bin-hadoop2.7/jars/spark-core\_2.11-2.4.0.jar:/media/Ubuntu2/jdk1.8.0\_171/lib/jsoup-1.11.3.jar:/media/Ubuntu2/spark-2.4.0-bin-hadoop2.7/jars/spark-catalyst\_2.11-2.4.0.jar:/media/Ubuntu2/spark-  
-----

2.4.0-bin-hadoop2.7/jars/scala-reflect-2.11.12.jar:/media/Ubuntu2/jdk1.8.0\_171/bin:/usr/local/sbin:/usr/local/bin:/usr/sbin:/usr/bin:/sbin:/bin  
9.sparkgenericstreaming.jar is packaged as bin/jar cvf sparkgenericstreaming.jar \*.class

10. SparkGenericStreaming is executed as:  
/media/Ubuntu2/spark-2.4.0-bin-hadoop2.7/bin/spark-submit --jars  
/media/Ubuntu2/jdk1.8.0\_171/lib/jsoup-1.11.3.jar --class SparkGenericStreaming  
--master local[2] sparkgenericstreaming.jar "https://twitter.com/search?  
f=tweets&vertical=news&q=Chennai&src=typd"

/media/Ubuntu2/spark-2.4.0-bin-hadoop2.7/bin/spark-submit --jars  
/media/Ubuntu2/jdk1.8.0\_171/lib/jsoup-1.11.3.jar --class SparkGenericStreaming  
--master local[2] sparkgenericstreaming.jar "localhost" "8080"

for URLSocket and Windowed streaming respectively

11. Reference: Spark Structured Streaming Example in  
<https://github.com/apache/spark/blob/v2.4.3/examples/src/main/java/org/apache/spark/examples/sql/streaming/JavaStructuredNetworkWordCountWindowed.java>

-----  
665. (FEATURE) Named Entity Recognition - Conditional Random Fields - Skew  
Normal Distribution Update - 29 May 2019  
-----

-----  
1. Miscellaneous changes in NamedEntityRecognition\_HMMViterbi\_CRF.py for  
corrections to skew normal distribution which shifts mean of the distribution  
for each part of speech to the right by some constant multiples.  
2. Skew normal distribution mean shift for each state (part of speech) is shown  
in NamedEntityRecognition\_HMMViterbi\_CRF.29May2019.png  
3. Motivation for skew normal distribution mean shift from left to right for  
emission probabilities is: For some part of speech state, successive word  
observations in the sentence receive more weightage corresponding to the peak  
value at mean i.e one word in the sentence peaks at mean and is more likely  
candidate observation emitted for respective Part of Speech state.  
4. In this example 5 words in the sentence peak for 5 part of speech states.  
5. logs for this commit have been committed to  
testlogs/NamedEntityRecognition\_HMMViterbi\_CRF.log.29May2019  
-----

-----  
666. (THEORY) Approximation of Majority Voting, Streaming majority, Forecasts,  
Bertrand Ballot Theorem, Theoretical EVMs, Set Partitions - 4 June 2019  
-----

-----  
Bertrand Ballot Theorem states: In a majority voting involving 2 candidates A  
and B receiving p and q votes respectively of total electorate p+q, probability  
of candidate A always being ahead of candidate B in counting of votes is  
 $(p-q)/(p+q)$ . Approximation of Majority voting has important applications in  
psephological forecast (pre-poll and post-poll surveys) which samples electorate  
to predict the winner. In pure complexity theoretic perspective, as has been  
mentioned earlier, boolean majority gate can be alternatively represented by a  
set partition of 2 candidate buckets indexed 0 and 1 and maximum size candidate  
bucket index is the output of set partition boolean majority gate. It is also  
worth mentioning here that approximating a majority gate of n inputs by a much  
smaller gate of m inputs ( $m \ll n$ ) is the complexity theoretic equivalent of  
forecasting a real-world majority voting of 2 candidates by sampling m voters  
from an electorate of size n. It is obvious that process of counting of votes  
creates instantaneous snapshots of the electorate set partition and any m sized  
(less than n) voter set partition snapshot is equivalent to a sampling of total  
electorate. In terms of set partition definition of majority gate, both buckets  
of voter set partition 0 and 1 grow over time and at any instant the set  
partition of total size m is a sampling of n voters. Votes for 2 candidates 1 and  
0 can be drawn as timeseries polynomial curves (votes versus time) and

intersection points of 2 curves are trend reversals contributing to the probability  $(p-q)/(p+q)$ . Complexity theoretic majority gate assumes all the inputs at the leaves are immediately available which is not possible in approximation in which only  $m$  of  $n$  votes are known. Majority approximation gate predicts output of majority gate of  $n$  inputs by a majority gate of  $m$  inputs for  $m \ll n$  with some error probability. By Bertrand Ballot Theorem probability that a majority approximation gate of  $m$  inputs (snapshot at some time point) has the same output as an exact majority gate of  $n$  inputs is  $(p-q)/(p+q)$  for total electorate  $p+q=n$  and  $p$  voters for 0 or 1 and  $q$  voters for 1 or 0. If  $m=a+b$  for  $a$  voters for 0 or 1 and  $b$  voters for 1 or 0 in the sample approximation, sample betrand probability is assumed to be proportional to bertrand probability of total electorate:

$$(p-q)/(p+q) = k*(a-b)/(a+b)$$

$$(p-q)/n = k*(a-b)/m$$

$$(p-q) = n*k*(a-b)/m$$

which extrapolates the sample to the entire electorate.

#### References:

666.1 Bertrand Ballot Theorem - <https://en.wikipedia.org/wiki/Bertrand>

%27s\_ballot\_theorem

666.2 Digging into Election Models -

<https://windowsontheory.org/2020/10/30/digging-into-election-models/>

667. (FEATURE) Social Network Analysis, People Analytics, PDF file parsing - 13 June 2019

1. Changed SocialNetworkAnalysis\_PeopleAnalytics.py to parse PDF files of social network profiles by PyPDF2 which was not working earlier.
2. PyPDF2 expects PDF files to be written by PDF writer or otherwise blank text is extracted
3. As example CV of self written by LaTeX2PDF has been parsed to print profile text to testlogs/SocialNetworkAnalysis\_PeopleAnalytics.log.13June2019
4. Recursive Lambda Function Growth import has been commented because of WordNet error:

Traceback (most recent call last):

File "<stdin>", line 1, in <module>

File "/usr/local/lib/python2.7/dist-packages/wn/\_\_init\_\_.py", line 11, in <module>

from wn.info import InformationContentSimilarities

File "/usr/local/lib/python2.7/dist-packages/wn/info.py", line 7, in <module>

from wn.reader import parse\_wordnet\_ic\_line

File "/usr/local/lib/python2.7/dist-packages/wn/reader.py", line 22

offset, lexname\_index, pos, n\_lemmas, \*the\_rest = columns\_str.split()

SyntaxError: invalid syntax

5.LinkedIn PDF Profile has been updated by linkedin pdf export

668. (THEORY) Computational Geometric Factorization - Average case Sequential Optimization, Stirling Approximation of Gamma Function, Sum of binary search times of each tile and some observations - related to 605 - 14 June 2019

(\*) Average number of tiles between two approximate prime factors  $m$  and  $(m+1)$  found by tile summation ray shooting:

$$= (m+1)/[k\log\log N - m - 1] - m/[k\log\log N - m]$$

because number of tiles till  $m$ -th prime factor  $= n = m/[k\log\log N - m]$  for  $m=1,2,3,\dots,k\log\log N$

(\*) Thus total average sequential time to sweep binary search tiles in  $N/k\log\log N$  spacing between 2 consecutive approximate factors found by ray shooting:

$$= O([(m+1)/[k\log\log N - m - 1] - m/[k\log\log N - m]] * \log N)$$

(\*) Maximum number of tiles in  $N/k\log\log N$  spacing occurs by minimizing denominator and setting  $m=k\log\log N - 2$ :

$$= O([(k\log\log N - 2 + 1)/[k\log\log N - k\log\log N + 2 - 1] - (k\log\log N - 2)/[k\log\log N - k\log\log N + 2]])$$

$$= O(k\log\log N - 1 - (k\log\log N - 2)/2)$$

$$= O(k\log\log N)$$

=> Maximum time to binary search tiles in  $N/k\log\log N$  spacing =  $O(\log\log N * \log N)$

=> Each of  $O(\log\log N)$  spacings between approximate factors can be searched in:

$$O((\log\log N)^2 * \log N)$$

average case sequential time with no necessity for parallel processing.

(\*) If each tile segment arithmetic progression is searched individually and sequentially, sum of binary search times for first  $k$  adjacent tile segments is:

$$\log N/(1*2) + \log N/(2*3) + \log N/(3*4) + \dots + \log N/(k*(k+1))$$

which can be written as:

$$\log N - (\log 1 + \log 2) +$$

$$\log N - (\log 2 + \log 3) +$$

...

$$\log N - (\log k + \log (k+1))$$

by logarithmic identities and becomes:

$$k \log N - (\log 1 + \log (k+1) + 2 \log k!)$$

But Gamma function is:

$$\Gamma(x+1) = x!$$

and by Stirling approximation:

$$\log k! \sim \log \Gamma(k+1) = (k+0.5)*\log k - k - 1 + 0.5*\log 2*\pi$$

Substituting in the summation:

Total time for binary searching  $k$  adjacent tile segment arithmetic progressions  
 $= k \log N - \log (k+1) - (2k + 1)\log k + 2(k+1) - \log (2*\pi)$

A variant approximation of this search time summation has been described in section 5 of

[http://sourceforge.net/projects/acadpdrafts/files/DiscreteHyperbolicPolylogarithmicSieveForIntegerFactorization\\_PRAM\\_TileMergeAndSearch\\_And\\_Stirling\\_Upperbound\\_updateddraft.pdf/download](http://sourceforge.net/projects/acadpdrafts/files/DiscreteHyperbolicPolylogarithmicSieveForIntegerFactorization_PRAM_TileMergeAndSearch_And_Stirling_Upperbound_updateddraft.pdf/download)

if  $k$  is  $O(\log\log N)$  from previous derivation of maximum number of tiles between 2 approximate prime factors, in average case at least one factor can be found in average time:

$$\log\log N * \log N - \log (\log\log N + 1) - (2\log\log N + 1)\log\log\log N + 2(\log\log N + 1) - \log (2*\pi) \\ \leq O(\log N * \log\log N)$$

References:

-----  
 668.1 Stirling Approximation of Factorial and Gamma Function -

<https://en.wikipedia.org/wiki/Stirling>

%27s\_approximation#Stirling's\_formula\_for\_the\_gamma\_function

-----  
 669. (THEORY) Computational Geometric Factorization, Ramsey Coloring and Arithmetic Progressions in the Tile Segments, Van Der Waerden Numbers - related to 636 - 19 June 2019

-----  
 By Van Der Waerden theorem, for any positive integers  $r$  and  $k$  there is number  $N$  such that if the numbers  $\{1, 2, 3, \dots, N\}$  are colored, each with one of the  $r$  different colors then there are at least  $k$  integers in arithmetic progression whose elements are of same color. Computational Geometric Factorization is based on rectification of hyperbolic curve into straightline or rectangular polygonal tile segments (of dimensions  $1 * 1$ )

length\_of\_segment) and reducing the factorization problem to parallel RAM planar point location of factor points (i.e hyperbolic curve is rectified to a polygon containing arithmetic progression of products of ordinates as its rectangular faces, parallel planar point location finds a rectangular face of the polygon having the factor point  $N=pq$  in polylogarithmic time and the rectangular face arithmetic progression having factor point is binary searched in logarithmic time - thus in NC) in this rectified polygon. Each hyperbolic tile segment obtained by rectification are construed to be arrays of products of ordinates or arrays of ordered pair of ordinates in x-axis and y-axis. Unsorted Concatenation of these tile segments of ordered pair of ordinates has the x-axis or y-axis sorted ascending from 1 to N (or  $\sqrt{N}$  to N). Since arrays of product or ordered pair of ordinates in each tile segment have one of the ordinates constant, each tile segment array is an arithmetic progression of ordinate products elements of which are colored monochromatically. Factor point location by parallel RAM sorting based on product of ordinates of ordered pairs in tile segments sorts the product of ordinates but shuffles the x-axis ordinate in ordered pair notation which was strictly ascending in unsorted concatenation. Sorted concatenation of tile segments of product of ordinates is the union of subsets of elements in each monochromatic arithmetic progression and creates a (pseudo)random coloring of sorted sequence of integers in the range  $\{N-\delta, N+\delta\}$ . In other words rectification of hyperbolic curve just inverts the Van Der Waerden theorem - instead of finding monochromatic arithmetic progressions in a colored sequence, it forms a mergesorted sequence from monochromatic arithmetic progressions in tile segments. Since rectification of hyperbolic curve for every integer creates unique set of tile segments, previous inverse of Van Der Waerden coloring is also unique.

-----  
670. (THEORY) Computational Geometric NC-PRAM Factorization, Tile Summation Ray Shooting Queries and Gamma approximation, Iterated addition for sum of tile segment lengths - 27 June 2019 - related to 506, 668  
-----

-----  
Tile summation ray shooting queries:  
-----

Sum of lengths of first n tile segments of pixelated hyperbolic curve derived previously:

$$N/[1*2] + N/[2*3] + \dots + N/[n*(n+1)] = Nn/(n+1)$$

which can be equated to sum of distances between first m prime factors by Hardy-Ramanujan Theorem:

$$Nn/(n+1) = mN/k\log\log N$$

=>  $n = m/(k\log\log N - m)$  = number of tiles till m-th prime factor.

Gamma approximated tile summation ray shooting queries:  
-----

Alternatively, sum of lengths of tiles obtained approximately from sum of binary search times by Gamma function previously can be equated to Hardy-Ramanujan normal order estimate:

$$2^{(n \log N - \log(n+1) - (2n+1)\log n + 2(n+1) + \log(2\pi))} =$$

$$mN/k\log\log N$$

$$\text{(or)} (n \log N - \log(n+1) - (2n+1)\log n + 2(n+1) + \log(2\pi)) =$$

$$\log(mN/k\log\log N)$$

and solved for number of tiles n that have to be summed till m-th prime factor.

Total Binary Search time has been raised to exponent to get approximate total length searched. Solving logarithmic equation previously might require some logarithmic series approximation resulting in a cubic equation or higher degree in n depending on number of terms chosen from logarithmic series.

An important fact ignored so far is the summing of tile lengths while doing ray shooting queries which has to be parallelized too. But tile summation is an iterated addition of  $O(N) \log N$  bit integers (tile lengths are rounded off) which is in NC1. Thus Computational Geometric NC-PRAM planar point location

factorization invoking tile summation ray shooting query oracles is in NC again. It can be noted that most other ray shooting query algorithms do not have this iterated addition of tile lengths requirement.

References:

-----  
670.1 Iterated addition of n n-bit integers is in NC1 - Theorem 8.9 -  
<https://courses.cs.washington.edu/courses/cse532/08sp/lect08.pdf>  
-----

-----  
671. (THEORY and FEATURE) Intrinsic Merit of Music - MFCC analysis and zero crossing rate - 27 June 2019  
-----

-----  
1.AudioToBitMatrix.py MFCC function has been updated to scale MFCCs by sklearn and print mean and variance of MFCCs of an audio/music waveform  
2.zero crossing rate of waveform is also printed which is measure of modulations in music.  
3.One of the ways to measure Music merit and Music Genre or Emotion Classification is by clustering music waveforms by distance similarity of MFCCs.  
4.MFCC similarity can be used as recommender system where a listener is recommended music of similar MFCCs based on historic listening habits.  
5.MFCCs of music waveform drawn as images (e.g by librosa.display.specshow()) can be compared for similarities.

Reference:

-----  
671.1 Music Information Retrieval and MFCCs -  
<https://musicinformationretrieval.com/mfcc.html>  
-----

-----  
672. (FEATURE and THEORY) Intrinsic Merit of People/Professional Profiles - People Analytics - Tenure Histogram - 28 June 2019  
-----

-----  
1.People Analytics implementation has been updated to print Work and Academic Tenure stints as array (histogram or integer partition)  
2.This essentially makes tenures as a set partition analytics problem because job and academic stint time durations can be picturized as histograms.  
3.Tenures represented as Set Partitions can be quantified by set partition measure of partition rank:  
    Length of largest part in partition - Number of parts in partition  
4.In the context of People Analytics, previous rank measure is quite applicable practically as attrition metric because:  
    4.1 High partition rank implies the professional profile has spent large duration in an organization or number of tenure switches are less (number of parts)  
    4.2 Low Partition rank implies the professional profile has low duration per organization or high number of tenure switches  
5.Tenure Partition can be printed as Ferrer or Young Diagram and size of Durfee Square of this tenure partition is also a measure of average time spent per organization and thus an attrition metric  
6.Recursive Lambda Function Growth wordnet error has been resolved (pywsd is not used) and import uncommented.  
7.logs for this have been committed to  
testlogs/SocialNetworkAnalysis\_PeopleAnalytics.log.28June2019  
-----

-----  
673. (FEATURE) People Analytics - Partition Rank Attrition Metric of Tenure Histogram - 29 June 2019  
-----



-----  
-----  
1. People Analytics implementation has been updated to compute partition rank described previously (Crank of a Partition - Freeman Dyson - [https://en.wikipedia.org/wiki/Crank\\_of\\_a\\_partition](https://en.wikipedia.org/wiki/Crank_of_a_partition)) of tenure histogram set partition of a person's professional and academic profile.  
2. Recursive Lambda Function Growth algorithm has been applied to text of the profile again. Closeness and Betweenness Centralities rankings are quite relevant than other Centrality measures.  
3. Logs for this have been committed to  
testlogs/SocialNetworkAnalysis\_PeopleAnalytics.log.29June2019  
-----  
-----

674. (FEATURE) People Analytics - Rank Correlation based Attrition Model of Tenure Histogram - 1 July 2019  
-----  
-----

1. People Analytics implementation has been updated to include a function to compute Correlation Coefficients of Statistical Dependence between vectors of Tenure Histograms.  
2. Tenure Histogram is deemed as a set of vectors of the form (organization/designation, income, duration) which captures the crucial factors of a tenure  
3. New function tenure\_partition\_rank\_correlation() has been implemented to compute rank correlations between each pair of variables of a tenure:  
    3.1 Designations versus Remunerations  
    3.2 Designations versus Durations  
    3.3 Remunerations versus Durations  
4. An example tenure histogram vectors of previous format has been analyzed (presently not parsed from profiles) for Kendall-Tau Rank correlation coefficient and logs are in  
testlogs/SocialNetworkAnalysis\_PeopleAnalytics.log.1July2019  
5. Previous correlations can be interpreted as below:  
    5.1 Designations versus Remunerations - If positive or high, professional profile has increasing career graph along with increasing remunerations (expected). If negative or low, professional profile has increasing career graph vis-a-vis reduced remunerations (not expected - implies profile preferred more challenging roles than remuneration) and vice-versa (not expected - implies profile preferred better remuneration than designations)  
    5.2 Designations versus Durations - If positive or high, profile has increasing career graph vis-a-vis durations of tenure (expected). If negative or low profile has increasing career graph vis-a-vis decreasing durations per tenure (not quite expected - increased designations were not appealing to profile and person decided to leave) and vice-versa (not quite expected - decreasing responsibilities of the role were preferred by the profile which decided to stay longer)  
    5.3 Remunerations versus Durations - If positive or high, profile has increasing emoluments versus increasing durations per tenure (expected). If negative or low profile has increasing remunerations against decreasing durations per tenure (not quite expected - profile was more inclined to salary) and vice-versa (not quite expected - profile stayed longer per tenure despite decreasing benefits).  
6. Previous interpretations facilitate inferences (in parentheses) of why attritions could have happened.  
7. From logs following positive and negative correlations are found and can be interpreted based on (5):  
    Kendall Tau Rank Correlations - Designations and Remunerations: tau= 0.7142857142857143 , pvalue= 0.0301587301587  
    Kendall Tau Rank Correlations - Designations and Durations: tau= - 0.09759000729485331 , pvalue= 0.7612636496364197  
    Kendall Tau Rank Correlations - Durations and Remunerations: tau= - 0.19518001458970663 , pvalue= 0.5434238636256696

-----  
675. (FEATURE) Urban Planning Analytics - Analysis of Remote Sensing GIS Imagery of Urban Sprawls - 3 July 2019  
-----

1. Analyzing Builtup land, Water bodies etc., of an urban sprawl is crucial for urban planners and is an apt application of image analysis. Urban sprawl is defined as expanse of urbanization in suburbs and is not measured by governance limits. For example rankings of metropolitan areas in India is:

[https://en.wikipedia.org/wiki/List\\_of\\_metropolitan\\_areas\\_in\\_India](https://en.wikipedia.org/wiki/List_of_metropolitan_areas_in_India) ("...

Rank Metropolitan area State/Territory Population  
Area

(in km<sup>2</sup>/sq mi)

|   |                                 |                               |                      |                  |
|---|---------------------------------|-------------------------------|----------------------|------------------|
| 1 | Central National Capital Region | Delhi, Haryana, Uttar Pradesh | 25,735,000 (2016)[3] | 2,163 (835)[3]   |
| 2 | Mumbai Metropolitan Region      | Maharashtra                   | 20,800,000 (2005)[4] | 4,354 (1,681)[5] |
| 3 | Kolkata metropolitan area       | West Bengal                   | 14,720,000 (2001)[6] | 1,851 (715)[7]   |
| 4 | Chennai metropolitan area       | Tamil Nadu                    | 13,300,253 (2011)    | 1,189 (459)..."  |

which is measure of urbanization.

2. Convex Hull based on Scipy Spatial for urban sprawls has already been implemented in ImageGraph\_Keras\_Theano.py for GIS images from SEDAC (<http://sedac.ciesin.columbia.edu/mapping/popest/gpw-v4/>) which is also invoked in Drone Online Shopping Delivery NeuronRain usecase

3. A Machine Learning (Random Forests) and entropy based analysis of Chennai Urban Sprawl - <https://www.mdpi.com/1099-4300/19/4/163/pdf> - studies the growth of built area and dwindling of water bodies from 1991 to 2016 and predicts scenario for 2027. Images referred to in this article are drawn from various Remote Sensing satellite sources (LandSat, ISRO-Bhuvan Geo Platform - [https://bhuvan.nrsc.gov.in/bhuvan\\_links.php](https://bhuvan.nrsc.gov.in/bhuvan_links.php) etc.,) and are great references for Chennai Urban Sprawl Land Usage, Water bodies, Greenery etc.,.

4. Images from <https://www.mdpi.com/1099-4300/19/4/163/pdf> have been extracted and are analyzed for Red, Green and Blue Channels in this commit. New python function `analyze_remotesensing_RGB_patches()` has been implemented for this which invokes `OpenCV2 split()` of the image to Red, Green, Blue channels.

5. Rationale for Red-Green-Blue Channel split of Urban Sprawl is most of the images are color coded in Red, Green and Blue for Built Area, Greenery and Water bodies respectively and splitting to respective color channels layers the image.

6. Each color channel - Red, Green and Blue - is a NumPy ndarray which is flattened and histograms are computed for each color channel.

7. Color channel images are written to JPG files of respective suffixes and read again to compute Numpy histogram

8. Each color channel image is grayscale only and percentage of white pixels of value 255 is the sum total size of respective color patch in image.

9. Scikit Learn Image has `extract_patches_2d()` function - [https://scikit-learn.org/stable/modules/generated/sklearn.feature\\_extraction.image.extract\\_patches\\_2d.html](https://scikit-learn.org/stable/modules/generated/sklearn.feature_extraction.image.extract_patches_2d.html) - which can segment an image to patches or clusters of similar features. But a native implementation of patch extraction has been preferred for color coded GIS Remote Sensing images.

10. Ratio of white pixels to total number of pixels is computed from color channel image histograms as:

Size of 255 (white) bucket in image ndarray histogram / Sum of sizes of all buckets in image ndarray histogram

11. Images extracted from <https://www.mdpi.com/1099-4300/19/4/163> and their color channel images have been committed to ImageNet/testlogs/RemoteSensingGIS/

12. Logs for this are committed to

`testlogs/ImageGraph_Keras_Theano.log.RemoteSensingGIS.3July2019` which print the percentage of water bodies (blue), built area (red) and greenery (green) inferred from color channels

13. Alternatively, image ndarray itself could have been mapped to histograms and

ratio of respective pixel color value buckets could have been computed. But exact color value for each color coding is not known and color channels grayscale the images and just number of white pixels (255) have to be found.

-----  
676. (FEATURE) Image Analytics - ImageNet Keras-Theano - Random Forest Classification wrapper for images - 4 July 2019  
-----

-----  
1. New wrapper function has been implemented which invokes scikit learn Random Forests -  
<https://scikit-learn.org/stable/modules/generated/sklearn.ensemble.RandomForestClassifier.html#sklearn.ensemble.RandomForestClassifier.predict> to classify set of test images based on training images and training labels.  
2. This wrapper function `random_forest_image_classification()` pre-processes the training and test images by loading to CV2 and flattening the image ndarray and then reshaping and transposing it so that scikit learn accepts.  
3. First the random forest classifier which is a forest of lot of decision trees which vote to decide the class label of a sample, is trained by `fit()` for training images and then test images are labelled by `predict()`  
4. Logs for this are committed to  
`ImageGraph_Keras_Theano.log.RandomForests.4July2019`  
5. Scikit learn provides `train_test_split` function which divides set of samples into training and test images based on which `fit()` and `predict()` are invoked.  
6. Alternative version without training and test split also follows the above as in logs.  
-----

-----  
677. (FEATURE) Image Analytics - ImageNet Keras-Theano - Unsupervised Recursive Gloss Overlap classifier based on ImageNet - 5 July 2019  
-----

-----  
1. As opposed to Random Forest classifier implemented earlier based on scikit learn, NeuronRain unsupervised graph theoretic Recursive Gloss Overlap classifier has been applied for some test images  
2. Recursive Gloss Overlap `classify()` function has been invoked from `imagenet_imagegraph()` which was earlier only creating text graph from Keras predictions text for the image.  
3. Example Dense subgraph (core number) classifications for these images in the logs at `testlogs/ImageGraph_Keras_Theano.log.ImageNetClassifier.5July2019` are reasonably accurate and classify the images better. No training labelled data are required.  
-----

-----  
678. (THEORY) Majority Hardness Amplification Lemma, Noise Sensitivity, Sensitivity, Block Sensitivity, Condorcet Jury Theorem - 6 July 2019, 6 October 2019 - related to 517  
-----

-----  
Hardness of a boolean function has been defined previously as how hard computationally it is to compute the function with a circuit of size  $s$ :  
if  $\Pr(C(x) \neq f(x)) = \delta$  where  $C(x)$  computes boolean function  $f(x)$ , then  $f(x)$   $\delta$ -hard.

Hardness amplification for Majority + VoterSAT boolean composition has been derived earlier as:

Hardness Amplification for Majority+Voter Composition  $\leq 1/(\delta + \text{or-error}) * (1/2 - 1/3 * \pi) + 1/\pi + 6k * \pi * (\delta + \text{or-error})^{0.5}$   
for  $\delta$ -hard voter SAT boolean functions (i.e Probability of a circuit incorrectly computing a voter SAT =  $\delta$ )

Noise Sensitivity of Majority function has been previously mentioned as  $O(1/\sqrt{n \cdot \epsilon})$  where  $\epsilon$  is probability of flip per bit. Therefore  $\epsilon$  is nothing but probability that a voter boolean function is incorrectly computed and sent as input to Majority function. This implies  $\Pr(f(x) \neq C(x)) = \delta = \epsilon = \text{hardness of all voter functions}$ .

In all sections related to majority voting and majority+voterSAT boolean composition, measure of sensitivity used is Noise Sensitivity which is  $\Pr(f(x) \neq f(y))$  for 2 correlated boolean strings  $x$  and  $y$  in  $\{0,1\}^n$  and sensitivity and block sensitivity measures have been ignored. Lemma 15 in reference 678.1 provides a simple boolean hypercube random walk proof of relation between sensitivity and Noise sensitivity from which:

$\text{NoiseSensitivity}(f) \leq 2 \cdot \delta \cdot \text{sensitivity}$  for probability of a bit flip =  $\delta = \epsilon$   
 $\Rightarrow \text{NoiseSensitivity}(\text{Majority}) = O(1/\sqrt{n \cdot \epsilon}) \leq 2 \cdot \delta \cdot \text{sensitivity}$

Since sensitivity conjecture ( $\text{block sensitivity} \leq \text{poly}(\text{sensitivity})$ ) has been proved recently, sensitivity in previous inequality can be written as a function of block sensitivity. Majority Hardness Amplification ratio then can be written as:

|                                                                          |                                                    |                                                    |
|--------------------------------------------------------------------------|----------------------------------------------------|----------------------------------------------------|
| Hardness of Maj+voter composition                                        | $[c/\sqrt{n \cdot \delta}] \pm \text{randomerror}$ | -----                                              |
| -----                                                                    | =                                                  | -----                                              |
| $\leq 2 \cdot \delta \cdot \text{sensitivity} / \delta \pm \text{error}$ |                                                    | $\leq 2 \cdot \text{sensitivity} \pm \text{error}$ |
| Hardness of voter function                                               |                                                    | $\delta$                                           |

which upperbounds the maximum hardness amplification of Majority+VoterSAT composition almost as twice of sensitivity of majority function.

Recent versions of Condorcet Jury Theorem by [Black] and [Ladha] lay emphasis on correlated voting in which voters are not independent but are statistically dependent and swayed by peer opinions en masse (this is the most prevalent "Herding" phenomenon in real world voting and in social networks), and from [Ladha] performance of majority voting decreases as correlation increases. In boolean majority function this herding correlation of bits is formalized by Block sensitivity and flipping a contiguous block of bit positions (contiguous set of voters flip their decisions) changes the outcome of the majority function. From [Ladha] more block sensitive (more correlated voters) majority function is less effective it is and towards less goodness it tends to.

NOTE: Throughout all sections on Majority Voting + VoterSAT boolean composition and its hardness amplification, Sensitivity measures have been assumed as main contributors to hardness because by definition a hard boolean function is not 100% correctly computable by a circuit and sensitivity to input correlation (flipped bits) is the major factor preventing the correct computation by circuit. There could be other factors intrinsic to boolean function itself too apart from sensitivity measures which prevent a circuit from being perfect characterized by ( $\pm$ ) error term above - randomized decision tree evaluation being one of them.

#### References:

- 
- 678.1 Smooth Boolean functions are easy - [Parikshit Gopalan, Noam Nisan, Rocco A. Servedio, Kunal Talwar, Avi Wigderson] - Lemma 15 - <http://www.math.ias.edu/~avi/PUBLICATIONS/GopalanNSTW.pdf>
- 678.2 Proof of Sensitivity Conjecture - [Huang] - [http://www.mathcs.emory.edu/~hhuan30/papers/sensitivity\\_1.pdf](http://www.mathcs.emory.edu/~hhuan30/papers/sensitivity_1.pdf)
- 678.3 Journal of Economic Behavior & Organization Volume 26, Issue 3, May 1995, Pages 353-372, Information pooling through majority-rule voting: Condorcet's jury theorem with correlated votes - [Krishna K Ladha] - <https://www.sciencedirect.com/science/article/pii/016726819400068P> - "...Does majority-rule voting steer an imperfectly informed assembly of people towards





(2 files of Bach Sonata and 1 file of Veena Instrumental - S.Balachander's Amritavarshini - respective copyrights attributed)

8. Though number of files analyzed is small, Bach Sonata files have high EMD similarities compared to Bach and Veena Instrumental suggesting a clustering of oriental and western classical music in terms of spectral analysis.

-----  
682. (THEORY) KRW Conjecture, Majority + VoterSAT Boolean Function Composition, BKS Conjecture, Computing any function by Parity - 12 July 2019, 17 July 2019, 18 July 2019, 19 July 2019, 22 July 2019 - related to 365, 368 and all sections on Majority Voting  
-----

-----  
Boolean function composition of Majority and any Voter boolean function and its relevance to KRW Conjecture ( $\text{Depth}(f+g) \sim \text{Depth}(f) + \text{Depth}(g)$  or  $\text{FormulaSize}(f+g) \sim \text{FormulaSize}(f) * \text{FormulaSize}(g)$ ) and Communication Complexity - KW Relations - which is an open problem - have been described in detail earlier and an inequality below for lower bound on depth of circuit computing Majority+VoterSAT composition has been derived assuming KRW conjecture:

$$D(\text{Maj} + \text{Voter}) = \text{CommunicationComplexity}(R(\text{Maj}, \text{Voter})) \geq 5.3 * \log m + n - O(m * \log m / n)$$

for  $m$  voters having voter SATs of  $n$  variables per voter.

KRW Conjecture for composing any boolean function  $f$  and parity has been proved by [Hastad] and [Dinur-OrMeir]. Proving the general case of KRW conjecture implies  $P \neq NC1$  (not all sequential polytime algorithms are logdepth parallelizable). If every Voter boolean functions are computable by circuits of AND, OR and Parity function, previous composition of Majority + VoterSAT is reduced to Majority + function\_of(Parity) composition replacing Voter SAT circuit by a circuit of AND, OR and parity gates. Recent result in reference 682.2 delves on upperbounds and lowerbounds for computing symmetric and threshold boolean functions by parity gates (Razborov approximation of AND and OR by low degree polynomials on  $F[2]$  and composing them). Voter decision function can also be thought of as a threshold function (weighting the variables). Stability of Interview TQBF has been derived earlier in the context of BKS Conjecture by formalizing a question-answering in machine learning and learning theory as a weighted linear threshold function on answers to questions and their respective weights. Generalizing proof of KRW Conjecture for composing a function and parity to composition of a function and function\_of(parity) proves the general case of KRW Conjecture. In reference 682.4 previous Communication Complexity (CC) Lower bound of composition has been refined to  $CC(KWf + Un) \geq \log L(f) + n - 2 \log m - 10$  implying  $CC(\text{Majority} + \text{Voter}) \geq 5.3 * \log m + n - 2 * \log m - 10$  assuming a universal Voter relation.

Assuming Voter SATs are indeed Linear or Polynomial Threshold Functions by which each voter scores the candidate to vote (0 or 1) based on some variables (e.g answers to questions) and votes for or against based on if the evaluated LTF or PTF exceed threshold or not, is a learning theoretic perspective as opposed to SAT based decision making. An experimental proof of BKS Conjecture (Majority is least stable) previously is restricted to LTFs only. Polynomial Threshold Functions have a circuit representation of depth 2 consisting of Parity and Threshold gates - layer 1 of parity gates for each monomial and layer 2 of a single threshold gate. From classic result of [Minsky-Papert], any computable function can be written in terms of threshold function. Circuit representation of Polynomial Threshold Functions are thus helpful to compute any Voter Decision Function in terms of Parity and Threshold gates. By Chow's Theorem for threshold functions, any 2 functions  $f$  (LTF) and  $g$  (any function) are equivalent if the degree-0 and degree-1 Fourier coefficients in Fourier expansion of  $f$  and  $g$  are equal.

Assuming KRW Conjecture, Formula Size of the Majority + VoterSAT boolean composition is:

$\text{FormulaSize(Majority + VoterSAT)} \sim \text{FormulaSize(Majority)} * \text{FormulaSize(VoterSAT)}$   
 $\Rightarrow \text{FormulaSize(Majority + VoterSAT)} \sim m^{5.3} * \text{FormulaSize(VoterSAT)}$   
 (Formula Size implies the circuit composition has fanout 1)  
 It is known that set of languages of Turing Machine deciding an input in time( $t$ ) is contained in set of languages accepted by a circuit of size( $t \log t$ ). Combining this to the previous composition formula size bound assuming KRW Conjecture an estimated runtime of a Turing Machine equivalent to Majority + VoterSAT composition can be obtained by solving for  $t$  in the equality:  
 $t \log t = m^{5.3} * \text{FormulaSize(VoterSAT)}$   
 (or)  $t^t = 2^{(m^{5.3} * \text{FormulaSize(VoterSAT)})}$   
  
 if  $t=O(\text{FormulaSize(VoterSAT)})$ :  
 $\log t = k * m^{5.3}$  (or)  $t = 2^{(k * m^{5.3})}$  for some constant  $k$  which is an EXPTIME Turing Machine (i.e exponential in number of voters) for Majority Voting Circuit Composition, implying unbounded depth.

PTF can encode a CNF MAX k-SAT - Example:

$(x_1 \vee \neg x_3 \vee x_4) \wedge (x_2 \vee x_3 \vee x_5) \wedge (x_1 \vee \neg x_2 \vee x_3)$  can be encoded as 3-sparse PTF  $(x_1)(1-x_3)(x_4) + (x_2)(x_3)(x_5) + (x_1)(1-x_2)(x_3) \geq k$

References:

-----  
 682.1 KRW Conjecture results survey - [OrMeir] - <https://simons.berkeley.edu/sites/default/files/docs/10492/presentation.pdf>  
 682.2 Parity helps compute Majority - Theorem 4 and Theorem 8 on computing symmetric boolean functions and threshold functions by parity - [Igor C. Oliveira\* Department of Computer Science University of Oxford, Rahul Santhanam† Department of Computer Science University of Oxford, Srikanth Srinivasan‡ Department of Mathematics IIT Bombay] - <https://eccc.weizmann.ac.il/report/2019/073/download>  
 682.3 Proof of KRW Conjecture for composing a function and parity - [Dinur] - <http://drops.dagstuhl.de/opus/volltexte/2016/5841/>  
 682.4 Improved Composition Theorems for Functions and Relations - [Koroth-OrMeir] - Theorem 8 - <http://drops.dagstuhl.de/opus/volltexte/2018/9452/pdf/LIPIcs-APPROX-RANDOM-2018-48.pdf>  
 682.5 Toward Better Formula Lower Bounds: An Information Complexity Approach to the KRW Composition Conjecture\* - [Dmitry Gavinsky† Or Meir‡ Omri Weinstein § Avi Wigderson¶] - <http://www.math.ias.edu/~avi/PUBLICATIONS/GavinskyMeWeWi2016.pdf> - Section 1.2.1 - Formula size of Composition of a function and Parity by [Andreev] and [Hastad] - "... $L(g \# \otimes n) = L(g) \cdot n^2 / \text{poly log } m = L(g) \cdot L(\otimes n) / \text{poly log}(m), \dots$ "  
 682.6 Linear and Polynomial Threshold Functions - <http://www.contrib.andrew.cmu.edu/~ryanod/> - Page 114-116 - Chapter 5 - Chow's Theorem 5.1 and Theorem 5.8, Threshold of Parities Circuit (depth 2 comprising parity gates in layer 1 and threshold gate at layer 2) computing a Polynomial Threshold Function  
 682.7 Perceptrons - [Minsky-Papert] - (1972:232): "... a universal computer could be built entirely out of linear threshold modules. This does not in any sense reduce the theory of computation and programming to the theory of perceptrons."  
 682.8 Circuit Complexity Lecture Notes - <http://www.cs.umd.edu/~jkatz/complexity/f05/lecture4.pdf> - Section 1.2 - "Theorem 1 If  $t(n) \geq n$ , then  $\text{time}(t) \subseteq \text{size}(t \log t) \dots$ "  
 682.9 Satisfiability and Derandomization for Small Polynomial Threshold Circuits - CircuitSAT for circuits of PTF gates - <https://eccc.weizmann.ac.il/report/2018/115/download/> - s-sparse PTFs having s monomials can encode MAXSAT of s clauses - Previous Boolean Composition of Majority and VoterSAT can alternatively be stated as a Circuit Composition of Majority and Voter PTF circuits - section 1.4 - "...for fixed sparsity s, much more expressive. For example, the polynomial  $p(x_1, \dots, x_n) = \bigvee_{i=1}^n (x_i \otimes 1) = \bigvee_{i=1}^n (1-x_i)$  has sparsity 1 by our definition, but sparsity  $2^n$  by the usual definition. Sakai, Seto, Tamaki and Teruyama [SSTT16] recently reported a



after-than-brute-force algorithm for MAX-kSAT for any constant k with arbitrary weights (which implies a satisfiability algorithm for degree-k PTFs)..."

682.10 Bounded Depth Circuits with Weighted Symmetric Gates: Satisfiability, Lower Bounds and Compression - [Sakai-Seto-Tamaki-Teruyama] - <https://pdfs.semanticscholar.org/084f/27ca498158992b5e5a5a61dbaf4161503b5c.pdf>

682.11 Learning DNF - [Klivans-Servedio] - [https://arxiv.org/pdf/1710.09079.pdf](https://pdf.sciencedirectassets.com/272574/1-s2.0-S0022000000X01572/1-s2.0-S00220000003001363/main.pdf?X-Amz-Security-Token=AgoJb3JpZ2luX2VjEjN%2F%2F%2F%2F%2F%2F%2F%2FwEaCXvzLWVhc3QtMSJIMEYCIQDpY%2BJ8ysvIVftFSRPRVv6S2w42%2FtCoesbh0lj0MJMoawIhAKgdNj9DXxjJN1myHJPiU14ZKBuvHmphenWHLagD%2F0LCFKtoDCBEQAhoMMDU5MDAazNTQ2ODY1Igwd1ipPK634MOjeQmcqtWPLCTvVsLS90BxtDUtf9IbmH06ay73ITn2Thu7F%2F%2BdbUWumBXtnTo%2FyRZle3Bz4V2GoWLcrjc6AEDJ1GaCa4Enc3HMxOtC3PPiKo5DaQ9EH%2BaGSUqb1Nm1fu40iohaH%2F7%2FqLSau0Tqh5QbnoCzqb9F8cZWl4%2FNhIFdm6IbL3Yh0iizEDKzd5tylsXH46lNIZN0cPouFRCC%2B6korSB0yEhtzp%2BxlOBosz5%2BknHQdJGsgog7aHP507iB2Aml3V%2BIWQAg8Pl%2BFZ9Dc8WyAtxiQU%2Bh%2BcdJh9faDjbG7VkzSuhKfVH%2B6tqiwbSPyLSLvofne65KYI%2FdPyTCJ5C7shMuRot3V4JGJHhmcmzy5h8YeVK3eTwigD4j1cPzzQpifs33XIaca1do32RJNs9%2BAwCC6dkwl0l6s4whXVQE%2BcJ6ixOSsbjKuRo%2FRS9dFJ5%2F%2FCfVB0HG2F%2B9rDDktiSZiegDoK7ndITzvPeymrTbAVZqIHhX83sL3TfJiFLPPwrScwhLkfoF3I32griAkFIURZNWYF%2B6bzxxsh1qxQUgNIIdshGhmyRRca9ktj33spdyvFDBEHLyHdAhMPHM5ekF0rMBR1vs5b47SxpOUk17oLpowsH6xCobvsX76f2ShEhvoQLnQNqis%2F6LYtv6QNLguQj%2BjUobapU2SaT2pmQPrwmvshW06K5kt1GQMwnF840iPaXss85P45Za7aCwifUX1GCflCxtm%2FWFqmXuHDrq2uxze6LlzExKN0mgltcusR7rZXToLUtQTz2z1mjtrXn3mwyIE5uoAS320ECsACejGB0tTCISfjA2GYNql1Je%2FqASIPd2aM%3D&X-Amz-Algorithm=AWS4-HMAC-SHA256&X-Amz-Date=20190725T091916Z&X-Amz-SignedHeaders=host&X-Amz-Expires=300&X-Amz-Credential=ASIAQ3PHCVTYQWHGSGT4%2F20190725%2Fus-east-1%2Fs3%2Faws4_request&X-Amz-Signature=b04a101db0c513928d40565cf895dfc601324123b95c08e2938f461bd76c3490&hash=eb5b8aed06292daa7502dca41a62db9110c81a7c336d1543c86683f1bb58faa3&host=68042c943591013ac2b2430a89b270f6af2c76d8dfd086a07176afe7c76c2c61&pii=S00220000003001363&tid=spdf-f4e32f52-621c-4768-8b49-b835a3261877&sid=31838a2e23fe724bb06b9d4-5a4c8715f5a8gxrrqa&type=client) - "...The approximate degree of a Boolean function  $f : \{-1, 1\}^n \rightarrow \{-1, 1\}$ , denoted  $\deg g(f)$ , is the least degree of a real polynomial  $p$  such that  $|p(x) - f(x)| \leq 1/3$  for all  $x \in \{-1, 1\}^n$ . ... Until very recently, the method of dual polynomials had been used exclusively to prove hardness amplification results for block-composed functions. That is, the harder function  $g$  would be obtained by block-composing  $f$  with another function  $h$ , i.e.,  $g = h \circ f$ . Here, a function  $g : \{-1, 1\}^{n \cdot m} \rightarrow \{-1, 1\}$  is the block-composition of  $h : \{-1, 1\}^n \rightarrow \{-1, 1\}$  and  $f : \{-1, 1\}^m \rightarrow \{-1, 1\}$  if  $g$  interprets its input as a sequence of  $n$  blocks, applies  $f$  to each block, and then feeds the  $n$  outputs into  $h$ ...." - Majority+VoterSAT boolean composition can be viewed as block composition by approximating Majority and VoterSAT by low-degree polynomials  $h$  and  $f$ .

683.(THEORY) Proof of KRW Conjecture for Majority+VoterSAT/VoterPTF composition  
- related to 682 - 23 July 2019

Caution: This section is experimental and subject to errors

Previously a reduction from CNF MAX-k-SAT to PTFSAT was described with an example. Any Voter SAT can be encoded as a Polynomial Threshold Function  $g$  and any Polynomial Threshold Function can be computed by a Threshold-of-Parities circuit of depth 2 described in previous section:

$$g = \text{threshold} + \text{parity}$$

If Majority function is denoted by  $f$ , Majority + VoterSAT/VoterPTF composition can be written in terms of parity as:

$$f + g = f + \text{threshold} + \text{parity}$$

But composition is associative and therefore:

$$(f + \text{threshold}) + \text{parity} = f + (\text{threshold} + \text{parity})$$

But composition  $(f + \text{threshold})$  previously can be any function  $h$ :

$$(f + \text{threshold}) + \text{parity} = h + \text{parity}$$

which is composition of some function and parity and KRW conjecture for composing any function and parity has been already proved ([Hastad],[Andreev],[Dinur]) and thus KRW Conjecture for Majority + VoterSAT/VoterPTF composition is proved immediately because previous breakdown of any function as threshold of parities reduces Majority + VoterSAT/VoterPTF composition to composition of any function to parity.

For a general case of composing any function  $f$  to another function  $g$ , applying previous threshold of parities representation to both  $f$  and  $g$ :

$$f + g = (\text{threshold} + \text{parity}) + (\text{threshold} + \text{parity})$$

and applying associativity of composition:

$$f + g = (\text{threshold} + \text{parity} + \text{threshold}) + \text{parity}$$

-----  
684. (FEATURE) Urban Planning/GIS Image Analytics - scikit learn  
extract\_patches\_2d() integration - 25 July 2019  
-----

1. Scikit Learn extract\_patches\_2d() has been invoked in a wrapper function analyze\_remotesensing\_2d\_patches() for patches analysis of Remote Sensing Imagery
2. Patch ndarrays are flattened and pixel histogram is computed for each patch of an image
3. Maximum pixel bucket in the patch histogram is an indicator of class of the patch.
4. This is in addition to RGB patch analysis function implemented earlier for Red-Green-Blue channel classification of an image
5. Logs of extract\_patches\_2d() and the patch histograms for 2 example remote sensing images are at  
ImageNet/testlogs/ImageGraph\_Keras\_Theano.log.RemoteSensingGIS.25July2019

-----  
685. (FEATURE) People Analytics - Kaggle LinkedIn Dataset Analysis - 26 July 2019  
-----

1. This commit introduces a new function in People Analytics implementation - linkedin\_dataset\_tenure\_analytics() - which parses Kaggle LinkedIn dataset from <https://www.kaggle.com/killbot/linkedin> and computes various correlation coefficients between column attributes.
2. Following are the People Analytics field attributes in LinkedIn obfuscated dataset which has almost 15000 rows:  
['avg\_n\_pos\_prev\_tenure', 'avg\_pos\_len', 'avg\_prev\_tenure\_len', 'c\_name', 'm\_urn', 'n\_pos', 'n\_prev\_tenures', 'tenure\_len', 'age', 'beauty', 'beauty\_female', 'beauty\_male', 'blur', 'blur\_gaussian', 'blur\_motion', 'emo\_anger', 'emo\_disgust', 'emo\_fear', 'emo\_happiness', 'emo\_neutral', 'emo\_sadness', 'emo\_surprise', 'ethnicity', 'face\_quality', 'gender', 'glass', 'head\_pitch', 'head\_roll', 'head\_yaw', 'img', 'mouth\_close', 'mouth\_mask',

'mouth\_open', 'mouth\_other', 'skin\_acne', 'skin\_dark\_circle', 'skin\_health', 'skin\_stain', 'smile', 'african', 'celtic\_english', 'east\_asian', 'european', 'greek', 'hispanic', 'jewish', 'muslim', 'nationality', 'nordic', 'south\_asian', 'n\_followers'] which include average variables for tenure, positions or designations per tenure, number of previous tenures, tenure lengths etc., 3.Pairwise kendall-tau Correlation coefficients of 3 important variables are computed:

- average number of positions per previous tenure
- average length of a position
- average length of previous tenures

4.Some preprocessing of the linkedin CSV dataset was required to cast the type to integer

5.VectorAssembler is instantiated to create necessary subset projections of the linkedin dataset columns

6.5 important columns of the Spark CSV dataframe are sliced by list comprehension to 5 arrays for (ethnic, emotional, physical and racial fields are ignored):

- average number of positions per previous tenure
- average length of a position
- average length of previous tenures
- number of previous tenures
- tenure length

and mapped to a Pandas DataFrame which supports correlation matrix for all datatypes

7.Pandas correlation matrix is printed for these 5 fields:

|                           | avg_n_pos_per_prev_tenure | avg_pos_len |
|---------------------------|---------------------------|-------------|
| avg_prev_tenure_len       | 0.836112                  | 0.836637    |
| n_prev_tenures            | 0.832915                  | 0.804373    |
| tenure_len                | 1.000000                  | 0.804373    |
| avg_n_pos_per_prev_tenure | 0.836112                  | 0.836637    |
| avg_pos_len               | 0.804373                  | 1.000000    |
| avg_prev_tenure_len       | 0.978873                  | 0.993264    |
| n_prev_tenures            | 0.968333                  | 0.975659    |
| tenure_len                | 0.981673                  | 0.981673    |

8.In addition to basic designation(position),remuneration, tenure duration correlations implemented earlier previous variables provide fine grained pattern analysis.

9,From previous correlation matrix, an obvious negative or low correlation is:

avg\_n\_pos\_per\_prev\_tenure - versus - (avg\_prev\_tenure\_len, n\_prev\_tenures, tenure\_len)  
implying increased average number of designations(positions) in previous tenures implies low average previous tenure lengths, low number of previous tenures and low tenure length which (exluding low number of previous tenures) is against what intuition suggests.

686. (FEATURE) People Analytics - Kaggle LinkedIn DataSet - Experiential and Degree Intrinsic Merit - 27 July 2019

1.In continuation to previous commit for linkedin dataset analytics, this commit implements computation of lognormal experiential intrinsic merit and degree based experiential intrinsic merit for all profiles in linkedin dataset.

2.Pandas DataFrame has been expanded to include two new columns - lognormal\_experiential\_merits and degree\_experiential\_merits - and correlation matrix is computed for this 7 rows \* 7 columns.

3.Experience of the n-th profile is derived from dataset columns as:

experience = avg\_n\_pos\_per\_prev\_tenure[n] \* avg\_pos\_len[n] \* n\_prev\_tenures[n] + tenure\_len[n]

#### 4. Correlation coefficients for all pairs of 7 variables from logs:

```
linkedin_dataset_tenure_analytics(): pandas correlation coefficient =
avg_n_pos_per_prev_tenure avg_pos_len ... lognormal_experiential_merits
degree_experiential_merits
avg_n_pos_per_prev_tenure 1.000000 0.804373 ...
0.687246 0.116707
avg_pos_len 0.804373 1.000000 ...
0.566021 0.112341
avg_prev_tenure_len 0.836112 0.983461 ...
0.673678 0.156701
n_prev_tenures 0.836637 0.978873 ...
0.553288 0.058373
tenure_len 0.832915 0.993264 ...
0.532364 0.076770
lognormal_experiential_merits 0.687246 0.566021 ...
1.000000 0.426055
degree_experiential_merits 0.116707 0.112341 ...
0.426055 1.000000
```

[7 rows x 7 columns]

5. Previous matrix shows highly negative or low correlation between first 3 tenure variables and degree experiential merits and a medium correlation between first 3 variables and lognormal\_experiential\_merits.

-----  
687. (THEORY) Approximate Polynomials and Approximate Degree of Boolean Functions, Dual Polynomials, Hardness Amplification, KRW Conjecture, Boolean Composition of Majority and VoterSAT/VoterPTF, Communication Complexity, Linear Program Primal/Dual - related to 365, 368, 682 -  
27 July 2019  
-----

-----  
From 682.13, the approximate degree of a Boolean function  $f : \{-1, 1\}^n \rightarrow \{-1, 1\}$ , denoted  $\deg g(f)$ , is the least degree of a real polynomial  $p$  such that  $|p(x) - f(x)| \leq 1/3$  for all  $x \in \{-1, 1\}^n$ . Existence of approximate polynomials implies that the function is easy. Therefore non-existence of approximate polynomials implies the function is hard. Fact that  $f$  can be approximated by a real polynomial is equivalent to feasibility of a Linear Program on Fourier coefficients. Feasibility of dual of this linear program on Fourier Coefficients implies the primal boolean function is hard to approximate by a real polynomial and thus is an alternative way to prove hardness of boolean functions and their compositions especially block-compositions and is quite relevant to Majority+VoterSAT composition and KRW-Communication Complexity based size and depth lowerbounds of it previously derived based on Sensitivity measures. Approximate degree of  $t$ -threshold functions is  $\sqrt{t(n-t)}$  and approximate degree of Majority or Parity is  $\Theta(n)$ . From [Nisan-Szegedy],  $\text{approxdegree}(f) \leq \text{degree}(f) \leq \text{DecisionTree}(f) < 1296 \cdot \text{degree}(f)^8$ . From [Sherstov] theorem,  $\text{approxdegree}(\text{Majority} + \text{VoterSAT}) = \text{approxdegree}(\text{Majority}) * \text{approxdegree}(\text{VoterSAT}) \leq \text{DecisionTree}(\text{Majority}) * \text{DecisionTree}(\text{VoterSAT})$ .

#### References:

-----  
687.1 Dual Polynomial for OR function - [Robert Spalek, Google, Inc.] - <http://www.ucw.cz/~robert/papers/dualor.pdf>  
687.2 Degree of Polynomials Approximating Symmetric Boolean Functions - [Ramamohan Paturi] - [https://cseweb.ucsd.edu/~paturi/myPapers/pubs/Paturi\\_1992\\_stoc.pdf](https://cseweb.ucsd.edu/~paturi/myPapers/pubs/Paturi_1992_stoc.pdf)  
687.3 Approximate degree of composition of boolean functions - Theorem 8 - [Sherstov] - The Polynomial Method Strikes Back:  
Tight Quantum Query Bounds via Dual Polynomials - [Mark Bun Princeton University [mbun@cs.princeton.edu](mailto:mbun@cs.princeton.edu), Robin Kothari Microsoft Research]

-----  
 -----  
 688. (THEORY) Approximate Polynomials and Approximate Degree of Boolean Functions, Algebraic Circuits and KRW Conjecture for Boolean composition of Majority and VoterSAT/VoterPTF - related to 365, 368, 682, 687 - 28 July 2019, 1 August 2019  
 -----  
 -----

Approximate Polynomial for Majority exists from 687.2 and has approximate degree  $\theta(n)$  and therefore has  $n$  roots from Fundamental Theorem of Algebra. This approximate polynomial for Majority can be written as factorized product (assuming reducible polynomials over field of reals):

$$\text{Product}(x-x_i)_{i=1,2,3,\dots,n}$$

Previous product for approximate polynomial for majority can be expressed by an Algebraic/Arithmetic Circuit of depth-2 having  $2n$  leaves (2 leaves per factor) and  $n$  intermediate minus gates in depth-1. Root is a multiplication gate of fanin  $n$ :

\* (multiplication operator - Root)

-       -       -       -       -       ... - (minus operators -

Depth 1)

x    x1 x    x2 x    x3 x    x4 x    x5       x    xn

(operands - Depth 2)

Similarly if there exists an approximate polynomial (assuming reducible over field of reals) for an arbitrary VoterSAT/VoterPTF arithmetic circuit of approximate degree  $d$  it can be factorized and represented by an Algebraic/Arithmetic circuit of depth-2 having  $2d$  leaves,  $d$  intermediate minus gates at depth-1 and multiplication gate at root. Since both arithmetic circuits for Majority and VoterSAT/VoterPTF have fanout 1, both can be termed arithmetic formulas. Thus approximate polynomials for Majority and VoterSAT/VoterPTF have arithmetic circuits of size  $O(\text{approxdegree})$ . Block Composing Majority arithmetic formula and VoterSAT/VoterPTF arithmetic formula is fairly straightforward in this special setting and  $\text{ArithmeticFormulaSize}(\text{approxpoly}(\text{Majority}) + \text{approxpoly}(\text{VoterSAT})) = \text{ArithmeticFormulaSize}(\text{approxpoly}(\text{Majority})) * \text{ArithmeticFormulaSize}(\text{approxpoly}(\text{VoterSAT})) = O(n*d)$ . This is an approximate version of KRW conjecture and  $O(n*d)$  could be  $\Theta(n*d)$  because factorization lowerbounds the number of arithmetic gates. Over field of reals, every irreducible polynomial has degree 1 or 2 at most. Previous algebraic circuit assumes degree 1 irreducibility. For degree 2, instead of factors of the form  $(x-x_i)$ , factors are  $ax^2 + bx + c$  which require arithmetic subcircuits as below increasing depth by 1 and size multiplies by 4:

$$\begin{array}{ccccccc} & & & + & & & \\ & & * & & * & & * \\ a & x & x & b & x & c & 1 \end{array}$$

An already known result in reference 688.4 implies intersection of set of polynomials computed by non-uniform arithmetic circuits of polynomial size and set of polynomials of constant degree is equal to intersection of set of polynomials computed by nonuniform arithmetic circuits of polynomial size and  $\log N * \log N$  depth and set of polynomials of constant degree for all fields  $F$ . This implies each of the arithmetic circuit for approximate univariate polynomial over field of reals of a boolean function is a  $\log N * \log N$  depth circuit. Assuming degree 1 irreducible factors throughout previously for approximate real polynomials of both functions  $f$  and  $g$ , an estimate of depth lowerbound of the block composition of  $f$  and  $g$  can be arrived at:

$$\text{Depth}(f + g) \sim \text{Depth}(f) + \text{Depth}(g) \sim 2 * \log N * \log N$$

## References:

-----  
688.1 Algebraic Circuits - [Sanjeev Arora-Boaz Barak] -  
<https://theory.cs.princeton.edu/complexity/book.pdf> - Section 14.1 and Example 14.3 (Arithmetic circuits for determinants)  
688.2 Fundamental Theorem of Algebra -  
[https://en.wikipedia.org/wiki/Fundamental\\_theorem\\_of\\_algebra](https://en.wikipedia.org/wiki/Fundamental_theorem_of_algebra) - "... every non-zero, single-variable, degree  $n$  polynomial with complex coefficients has, counted with multiplicity, exactly  $n$  complex roots..."  
688.3 Irreducible polynomials over reals have degree 1 or 2 -  
[https://en.wikipedia.org/wiki/Irreducible\\_polynomial](https://en.wikipedia.org/wiki/Irreducible_polynomial)  
688.4 Arithmetic Circuits versus Boolean Circuits - [Joachim von zur Gathen† - Gadiel Seroussi‡] - Section 2 -  
<https://www.sciencedirect.com/science/article/pii/089054019190078G>  
-----

-----  
689. (FEATURE) Fraud Analytics - Credit Card Dataset - Pandas DataFrame  
Correlation Coefficient Matrix - 28 July 2019  
-----

-----  
1. Fraud Analytics implementation has been updated to instantiate Pandas DataFrame from credit card dataset and print Pandas Correlation matrix for all the columns.  
2. Columns V1-V28 are Obfuscated Names of the cardholders which are numeric unique id(s)  
3. Correlation between unique identities/names and amount drawn is a behavioural pattern and any deviation is an alarm (most swipes are periodic and personality oriented).  
4. Correlation matrix logs are committed to  
testlogs/FraudAnalytics.log.28July2019  
5. Correlation between Timestamp and Amount drawn is also measure of fraud.  
-----

-----  
690. (FEATURE) Time Series Analysis - ARIMA implementation - 1 August 2019  
-----

-----  
1. Time Series implementation has been made to a new python source file containing time series algorithms implementations for ARMA and ARIMA - Streaming\_TimeSeriesData.py  
2. Auto Regressive Integrated Moving Averages (ARIMA) has been implemented as a function ARIMA in Streaming\_TimeSeriesData.py and factoring has been implemented for a parameter lag in autoregression\_factored()  
3. ARIMA differs from ARMA in factoring the autoregression polynomial into two factor polynomials one which is dependent on a lag operator.  
4. Because Yahoo finance and Google Finance stock data are no longer available, ystockquote does not work and throws urllib exception and hence a hardcoded array of timeseries stock close data has been used.  
5. ARMA and ARIMA functions from Streaming\_TimeSeriesData.py are invoked in Streaming\_StockMarketData.py.  
6. Logs for ARIMA and R+ipy2 graphics plot have been committed to  
DJIA\_ARIMA\_Time\_Series.pdf and  
testlogs/Streaming\_StockMarketData.ARIMATimeSeries.log.1August2019  
-----

-----  
691. (FEATURE) Time Series Analysis - ARMA and ARIMA implementations - Rewrite - 2 August 2019  
-----

-----  
1. ARMA and ARIMA related functions in Streaming\_TimeSeriesData.py have been rewritten based on ARMA and ARIMA polynomials in  
-----

[https://en.wikipedia.org/wiki/Autoregressive\\_integrated\\_moving\\_average](https://en.wikipedia.org/wiki/Autoregressive_integrated_moving_average)  
2. Projection iterations have been removed and instead are done in the invoking source file e.g Streaming\_StockMarketData.py for randomly chosen regression weights  
3. ARMA polynomial is computed as:  
    arma=timeseries[len(timeseries)-1] -  
    autoregression(time\_series\_data[pprime:]) -  
    moving\_averages(time\_series\_data[q:], 5)  
which subtracts the autoregression and moving averages from the latest timeseries point. ARMA parameters pprime and q are sliced to be as distant from the latest timeseries point  
4. ARIMA polynomial is computed as:  
    arima=autoregression\_factored(time\_series\_data[len(time\_series\_data)-d:],p)  
    - moving\_averages(time\_series\_data[q:], 5)  
which computes autoregression\_factored differently as:  
5.Lag operator for lag d is applied to slice the timeseries data from latest point t to d as t-d and autoregression\_factored() is invoked to compute regressions from slice t-d-p to t-d  
6.Finally the autoregression is subtracted from latest timeseries point  $X_t$  and moving averages is added to it  
7.Logs for rewrite are available for few iterations at  
testlogs/Streaming\_StockMarketData.ARIMATimeSeries.log.2August2019  
8.R+rpyp2 function plots have been commented

-----  
692. (FEATURE) Time Series Analysis - ARMA and ARIMA implementations - Rewrite 2  
- 3 August 2019  
-----

-----  
1. ARMA and ARIMA functions in Streaming\_TimeSeriesData.py have been again refactored to implement lag operator and binomial expansion of lag factor in ARIMA polynomial  
2. autoregression\_factored() has been rewritten to invoke a new function lag\_factor\_binomial\_expansion() which in turn expands the factor power term in ARIMA polynomial by binomial series expansion of  $(1-L)^d$ .  
3. lag\_factor\_binomial\_expansion() loop invokes functions binomial\_term() which computes the numerator and denominator factorial of each binomial term and lag() function for each binomial term.  
4. Example logs for Stock quotes timeseries data is at  
Streaming\_StockMarketData.ARIMATimeSeries.log.3August2019 which has comparative projections of rewritten ARMA and ARIMA functions.  
5. ARIMA has been invoked by parameters (2,2,2)

-----  
693. (FEATURE) Time Series Analysis and Fraud Analytics - Credit Card Transactions Dataset - 3 August 2019  
-----

-----  
1.FraudAnalytics.py has been updated to import TimeSeries ARMA and ARIMA functions from Streaming\_TimeSeriesData.py and compute ARMA and ARIMA polynomials on amounts withdrawn timeseries in credit card transactions dataset.  
2.Logs for these projections are at testlogs/FraudAnalytics.log.3August2019  
3.Though timeseries is a perfect fit for analyzing credit card amounts withdrawn as timeseries, projection curves for ARMA and ARIMA in logs are skewed widely for multiple iterations of random weights in autoregression and moving averages but values of ARMA and ARIMA are uniformly same almost.

-----  
694. (FEATURE) Linear and Logistic Regressions - Rewrite - 4 August 2019, 6 August 2019  
-----

-----

1.LinearAndLogisticRegression.py has been rewritten to accept arbitrary number of weights and variables for computing Linear and Logistic Regressions.

2.Linear And Logistic Regressions are estimators of Intrinsic Economic Merit of Nations in Economic Networks. Thus far following classes of intrinsic merit have been researched and implemented in NeuronRain:

1. Text
2. Audio - Speech
3. Audio - Music
4. Visuals - Images
5. Visuals - Videos
6. People - Professional Networks - Experiential Intrinsic Merit
7. People - Social Networks - Log Normal Least Energy Merit - Education/Wealth/Valour e.g Rankings of Universities based on various factors including research output, Rankings of Students based on examinations/contests, Sports IPR (Elo ratings in Chess, Player rankings in sports)
8. People - Professional Networks - HR Analytics - Attrition model and Economic merit of nations is the 9th class of intrinsic merit applicable to Economic Networks. Regression is one amongst the set of econometric techniques for ascertaining growth of economies:
9. Nations - GDP, HDI etc.,

3. Logs for the previous are at  
testlogs/LinearAndLogisticRegression.log.4August2019

#### References:

-----

694.1 India's GDP Mis-estimation: Likelihood, Magnitudes, Mechanisms, and Implications - [Arvind Subramanian] - Working Paper -  
<https://growthlab.cid.harvard.edu/files/growthlab/files/2019-06-cid-wp-354.pdf> -  
"...We divide the sample into two periods, pre-and post-2011. For each period we estimate the following cross-country regression:  $GDP\ Growth_i = \beta_0 + \beta_1 Credit\ Growth_i + \beta_2 Electricity\ Growth_i + \beta_3 Export\ Growth_i + \beta_4 Import\ Growth_i + \beta_5 India + \varepsilon_i$  ..."

-----

695. (FEATURE) Gradient Ascent and Descent - Rewrite - 4 August 2019

-----

1.PerceptronAndGradient.py has been rewritten for computing Gradient Ascent and Descent for arbitrary number of variables.

2.Earlier loop for partial derivative delta computation for just 2 variables has been generalized for any number of variables

3.Gradient Ascent has also been added based on computed value of weight updated perceptron (+ instead of -)

4.Logs for Ascent and Descent are at  
testlogs/PerceptronAndGradient.log.4August2019

5.Hardcoded variable,weights,bias,rho,output values have been removed and made as arguments.

-----

696. (FEATURE) Named Entity Recognition (NER)-HMM-Viterbi-CRF - Rewrite - 12 August 2019

-----

1.Named Entity Recognition by Conditional Random Fields Hidden Markov Model has been updated significantly for resolving some errors in Viterbi computation

2.Prior Emission Probabilities computation by skew normal distribution has been updated to renormalize by dividing the skewnorm probability by sum of probabilities

3.New part of speech "adverb" has been included in transition probabilities,emission probabilities and states

4.weighted sknorm has been done away with and replaced by previous renormalized



skewnorm distribution

5. Error in argmax() computation has been corrected - label and maximum are reset in the loop

6. logs for this rewrite have been committed to

testlogs/NamedEntityRecognition\_HMMViterbi\_CRF.log.12August2019

7. Transition probabilities are updated as below:

```
transition_probabilities={ 'noun':{'noun':0.0, 'verb':0.3, 'object':0.2,
'adjective':0.1, 'adverb':0.1, 'conjunction':0.3},
 'verb':{'noun':0.1, 'verb':0.0, 'object':0.4,
'adjective':0.2, 'adverb':0.1, 'conjunction':0.3},
 'object':{'noun':0.0, 'verb':0.1, 'object':0.4,
'adjective':0.1, 'adverb':0.1, 'conjunction':0.3},
 'adjective':{'noun':0.4, 'verb':0.2, 'object':0.2,
'adjective':0.0, 'adverb':0.1, 'conjunction':0.1},
 'adverb':{'noun':0.1, 'verb':0.4, 'object':0.1,
'adjective':0.0, 'adverb':0.1, 'conjunction':0.3},
 'conjunction':{'noun':0.2, 'verb':0.4, 'object':0.1,
'adjective':0.1, 'adverb':0.1, 'conjunction':0.1}
}
```

7. It has to be mentioned here that previous state transition probabilities priors are hardcoded heuristics and based on the following rationale:

7.1 verb follows nouns more often

7.2 object follows verb more often

7.3 object follows object more often

7.4 noun follows adjective more often

7.5 verb follows adverb more often

7.6 verb follows conjunction more often (e.g infinitives)

8. Previous heuristics are minimal and could be replaced by more sophisticated probability distribution learnt from a training dataset once and loaded everytime.

-----  
697. (THEORY-FEATURE) Named Entity Recognition and Text Graph Algorithms in NeuronRain AstroInfer - a non-statistical alternative - 12 August 2019  
-----

TextGraph algorithms in NeuronRain are two-fold:

697.1 Recursive Gloss Overlap - Project WordNet to a Subgraph by traversing the Synsets recursively

697.2 Recursive Lambda Function Growth - Project WordNet to a Subgraph by traversing the Synsets recursively, learn AVL tree based Graph Tensor Neural Network and Lambda expressions from cycles and random walks of the WordNet subgraph - this is the maximum attainable theoretical limit of learning a formal language (Turing Machine or a lambda function) from natural language

Usual Named Entity Recognition algorithms are prior probabilities and Conditional Random Fields-HMM based which relies heavily on statistics ignoring linguistic deep structure. Instead if missing Part-of-Speech tags could be inferred from a textgraph representation of a partially PoS annotated text, no language PoS priors are required. Following algorithm explores this alternative:

697.3 Partial PoS annotated text is mapped to a text graph by previous algorithms and each word vertex in the partial annotated text is labelled by either a part of speech or ? for missing PoS tag.

697.4 Resultant text graph thus has mixture of word vertices which have either PoS known (labelled by a PoS name) or PoS unknown (labelled by ?)

697.5 WordNet has support for list of all possible PoS tags for a word vertex

697.6 It is then a problem of inferring most probable disambiguating PoS tag for a word vertex.

697.7 Set of all wordnet paths between a PoS annotated word vertex and an adjacent PoS unannotated word vertex provide set of sequences of PoS tags for the paths.'

697.8 For example phrase "can be called as a function" annotated as

"conjunction conjunction verb conjunction conjunction ?" and unannotated "function" has three possible wordnet PoS tags which have to be disambiguated - Noun, Verb and Object and set of wordnet paths between "as-a" and "function" could be - {"connective", "entity", "work"}, {"article", "entity", "event"}, {"one", "entity", "happening"} having PoS sequences as {noun, noun, verb}, {noun, noun, noun} and {noun, noun, noun} if function has lemma synsets "work", "event" or "happening"

697.9. Of the three possible paths PoS "noun" for "function" wins by majority voting of 2 to 1 because 2 paths have a penultimate vertices which imply "function" is a noun.

---

#### 698. (FEATURE) GIS Remote Sensing Image Analytics - Image Segmentation - 13 August 2019

---

1. New function `image_segmentation()` has been defined in `ImageGraph_Keras_Theano.py` which segments an image into similar regions or patches
2. As opposed to RGB patches and `extract_patches_2d()` of scikit learn, segmentation of an image is generic and segments/patches of arbitrary irregular shapes and containing similar pixels can be extracted
3. Example code in OpenCV2 documentation - [https://opencv-python-tutroals.readthedocs.io/en/latest/py\\_tutorials/py\\_imgproc/py\\_watershed/py\\_watershed.html](https://opencv-python-tutroals.readthedocs.io/en/latest/py_tutorials/py_imgproc/py_watershed/py_watershed.html) - has been used as reference
4. This example filters the image into foreground and background by:
  - 4.1 applying OTSU threshold filter
  - 4.2 morphological opening for removal of noise
  - 4.3 Background - Dilation to increase object boundary to background and demarcate background accurately
  - 4.4 Foreground - Distance transform and then thresholding is applied to demarcate the foreground
  - 4.5 Markers - Connected components are found from foreground of 4.4
  - 4.6 Watershed - watershed segmentation algorithm is applied on the marked image to find segments.
5. Watershed algorithm works by considering an image as topographic surface of valleys and dams between valleys. Valleys in image are filled with water till no two adjacent valleys merge creating "dams" or segments bounding the valleys.
6. Watershed segmentation is graphically illustrated in <http://www.cmm.mines-paristech.fr/~beucher/wtshed.html>
7. EventNet Tensor Products Merit algorithm for visuals described earlier depends on bounding box segmentation which are squares. Instead segmentation could be the way to go if ImageNet and Keras support it.
8. Two segmented satellite images of Chennai Metropolitan Area Urban Sprawl are committed at:
  - 8.1 `testlogs/RemoteSensingGIS/ChennaiUrbanSprawl_Page-10-Image-15_segmented.jpg`
  - 8.2 `testlogs/RemoteSensingGIS/ChennaiUrbanSprawl_Page-9-Image-13_segmented.jpg`

---

#### 699. (THEORY-FEATURE) Computational Geometric Factorization - Tile Search Optimization - Spark 2.4.3 and QuadCore benchmarks - 13 August 2019

---

1. This is the first genuine benchmark of Computational Geometric Factorization on Spark 2.4.3 and QuadCore. Earlier execution on local[4] was a simulation of 4 spark executor threads on single core
2. `SparkContext` has been replaced by Spark context of `SparkSession`
3. logs for factorization are at `testlogs/DiscreteHyperbolicFactorizationUpperbound_TileSearch_Optimized.log`. 13 August 2019 which have some notable estimates of approximate factors by Hardy-

Ramanujan (1 exact factor ray query), Baker-Harman-Pintz and Cramer ray shooting queries

-----  
700.(THEORY) Computational Geometric Factorization, Complement Diophantines, Covering a set by Arithmetic Progressions, Ramsey Coloring - related to 24,477,491,636 - 14 August 2019  
-----

-----  
Computational geometric factorization works by parallel planar point location - rectification of Hyperbolic arc bow into straightline segments which are then made to segment tree, wavelet tree, interval tree etc., by parallel RAM construction or segments are parallel RAM mergesorted and binary searched to find factors and thus factorization (finding all factors of an integer) is in Nick's class. It has been mentioned earlier that each segment of rectified hyperbolic arc bow is an arithmetic progression which facilitates local binary search without necessity for parallel mergesort. Thus set of all segments of rectified hyperbolic arc create an arithmetic progression cover of set of points on rectified hyperbolic curve. Finding a minimum size set of arithmetic progressions covering a set of integers is a hard problem. Previous rectification process for factorization solves a special case of arithmetic progression cover of a set. It has to be noted that finding an exact arithmetic progression cover of a set is the complement diophantine problem because the set of arithmetic progressions represents each of the diophantine subset in the exact cover partition. Known result in 700.1 implies covering a set by arithmetic progressions is NP-complete while the previous rectification for factorization solves this special case of arithmetic progression cover of set of rectified hyperbolic points in NC. This also implies complement diophantine problem is NP-complete for the special case of arithmetic progression diophantines for some partition of a set.

References:

-----  
700.1 Covering a set by arithmetic progressions is NP-complete - [Lenwood Heath - Virginia Tech] - <https://vtechworks.lib.vt.edu/bitstream/handle/10919/19566/TR-89-25.pdf?sequence=3&isAllowed=y>  
-----

-----  
701.(THEORY) Category Theory formulation of EventNet - Objects, Morphisms, Functors - related to 582, 588, 654 - 21 August 2019, 22 September 2019, 29 October 2019, 6 December 2019  
-----

-----  
Category Theory of [Eilenberg-MacLane] abstracts whole of mathematics into following:

701.1 Category C is a Set of Objects

701.2 Every Category has set of morphisms  $f:a-b$  defined on objects  $a,b$  in Category C

701.3 Functors F are maps between two Categories C1 and C2 - for each object  $x$  in C1,  $F(x)$  is in C2 and for each morphism  $f:a-b$  in C1 morphism,  $F(f):F(a)-F(b)$  is in C2

EventNet Tensor Products defined and implemented in NeuronRain and applied as intrinsic merit measure for large scale visuals can be formalised in terms of Category theory as follows:

701.4 Every Event vertex in EventNet is a category

701.5 Set of Actors in an Event Category are Objects of the Category

701.6 Every intra-event interaction between any two actor objects  $a,b$  of an event category E is a Morphism -  $f:a-b$

701.7 Every inter-event causation between two Event Categories E1 and E2 (E1 causes E2) is a Functor - for each actor object  $x$  in E1,  $F(x)$  is in E2 and

for each morphism  $f:a \rightarrow b$  in  $E_1$ , morphism  $F(f):F(a) \rightarrow F(b)$  is in  $E_2$

As mentioned in previous sections on EventNet Tensor Product merit of Large Scale Visuals, EventNet Tensor formalizes logical time and causation. Rank of a Tensor  $T$  is the minimum number of Simple Tensors that sum to  $T$  where Simple Tensors are factorizable products of tensors. This implies Logical Time Tensor can be written as sum of products of Tensors implying seemingly linear 1-dimensional time is decomposable to tensor components basis. This has implications for physical sciences and experiments involving spacetime - Time could be multidimensional and any spatial object can be projected to any of the time tensor component axes similar to space. From previous Category Theory definition, EventNet Causality Functor Graph can also be written as sum of products of Tensors. Tensor Decomposition of Video EventNet Tensor yields component videos i.e video can be split into linearly independent component videos.

Another theoretical implication of EventNet is the possibility of retrocausality - effect causing the cause and arrow of time can be bidirectional. EventNet DAG can be partitioned into past, present and future disjoint subgraph components by 2 cuts/vertex separators. To preclude the possibility of retrocausality/time reversal, EventNet must be a directed acyclic graph devoid of loops and backedges (edges of right to left if Events flow left to right). If logical time is unidirectional (retrocausality is false) following "future" functions  $f_1$  and  $f_2$  defined on EventNet graph partition components (past,present,future) must be hard to invert implying one-way functions, Pseudorandom Generators and  $P \neq NP$  (left inverse does not exist for EventNet category):

$f_1(\text{past}) = \text{present}$   
 $f_2(\text{present}) = \text{future}$

Ramsey Theorem for Graphs implies any large graph  $G$  has a Ramsey number  $R(s,t)$  such that a graph  $G$  of  $R(s,t)$  vertices has an independent set of size  $s$  or a clique of size  $t$ . In the context of EventNet which is a huge causality graph, Ramsey Theorem implies there always exists a clique of mutually dependent events or mutually independent set of events in EventNet of  $R(s,t)$  vertices howsoever random the causality is.

#### References:

- 
- 701.8 Category Theory - [https://en.wikipedia.org/wiki/Category\\_theory](https://en.wikipedia.org/wiki/Category_theory)
- 701.9 Tensor Products as Functors - <https://en.wikipedia.org/wiki/Functor> - "... Tensor products: If  $C$  denotes the category of vector spaces over a fixed field, with linear maps as morphisms, then the tensor product  $\{\displaystyle V \otimes W\}$  defines a functor  $C \times C \rightarrow C$  which is covariant in both arguments. [7] ..."
- 701.10 Tensor Decomposition in Python - Tensorly and Tensorlab - <https://medium.com/yadb/tensor-factorization-for-graph-analysis-in-python-590df44c9f6c> - Graphic illustrations of Non-Negative Canonical Polyadic Decomposition (NCPD) of a 3-way tensor to sum of products of multiple rank-1 tensors - Figure 1 (3-way tensor) decomposed as Figure 2 (sum of products of rank-1 tensors) - "...The rank of a tensor  $T$ , denoted  $\text{rank}(T)$ , is defined as the smallest number of rank-one tensors that generate  $T$  as their sum..."
- 701.11 Tensor Decomposition and its applications - [Tamara G. Kolda and Brett W. Bader] - <https://epubs.siam.org/doi/abs/10.1137/07070111X?journalCode=siread> - "...A tensor is a multidimensional or  $N$ -way array. Decompositions of higher-order tensors (i.e.,  $N$ -way arrays with  $N \geq 3$ ) have applications in psychometrics, chemometrics, signal processing, numerical linear algebra, computer vision, numerical analysis, data mining, neuroscience, graph analysis, and elsewhere ..."
- 701.12 Ramsey Theorem for Graphs - <http://math.mit.edu/~fox/MAT307-lecture05.pdf> - Complete disorder is impossible - Theorem 1 - "...Theorem 1 (Ramsey's theorem). For any  $s, t \geq 1$ , there is  $R(s, t) < \infty$  such that any graph on  $R(s, t)$  vertices contains either an independent set of size  $s$  or a clique of size  $t$ . In particular,  $R(s, t) \leq (s + t - 2, s - 1) \dots$ "

-----  
702.(THEORY-FEATURE) Non-statistical Ontology Semantic Paths based Named Entity Recognition - related to 697 - 22 August 2019  
-----

1.A non-statistical WordNet Paths based Named Entity Recognition alternative was theoretically described earlier which exploits linguistic deep structure.

2.This alternative has been implemented in  
NamedEntityRecognition\_HMMViterbi\_CRF.py which works as below:

2.1 find the semantic path between a PoS annotated word and unannotated adjacent word in an ontology e.g WordNet - path\_between() from WordNetPath.py has been invoked (instead the text graph path between the words is also sufficient)

2.2 for each vertex in the path find all possible PoS tags from WordNet Synsets which is a 2 dimensional list - Words \* Set-of-PoS-per-Word

2.3 find the cartesian product of the 2 dimensional list from 2.2 which enumerates all possible PoS paths between annotated and unannotated words - itertools product computes cartesian product of lists for all possible PoS paths which is a trellis

2.4 aggregate the penultimate vertices in PoS paths

2.5 find the majority PoS tag Synset of 2.4 which is the most likely PoS of the unannotated word

3.Logs in testlogs/NamedEntityRecognition\_HMMViterbi\_CRF.log.22August2019 demonstrate previous PoS paths majority voting for NER of an unannotated vertex.

4.Some paths between annotated and unannotated words drew blank because path\_between() did not find a path

5.In some respects, previous algorithm resembles a transformer which is an attention model neural network scoring a sequence pipeline in transduction - it maps a sequence of words to sequence of PoS and attention context (important annotated words influencing an unannotated word) is provided by the PoS paths between PoS annotated and unannotated words in the word sequence.

-----  
703.(FEATURE) Text Graph of a natural language text from ConceptNet 5.7 - implementation - 23 August 2019  
-----

1.NeuronRain text graph implementations so far rely only on WordNet for deciphering intrinsic deep structure merit of a text.

2.This commit implements ConceptNet 5.7 text graph alternative which was long pending.

3.New function conceptnet\_text\_graph() invokes least\_common\_ancestor graph creating function and aggregates edges from paths between all pairs of words.

4.ConceptNet5.7 Text Graph has been plotted by matplotlib at

testlogs/ConceptNet5.7.TextGraph.23August2019

5.Logs for ConceptNet text graph creation are at

testlogs/ConceptNet5Client.log.23August2019

6.Quality of Paths in ConceptNet is an open problem e.g  
<https://arxiv.org/abs/1902.07831>

-----  
704.(FEATURE) ConceptNet 5.7 Text Graph - shortest path filter - 25 August 2019  
-----

1.ConceptNet 5.7 Text Graph implementation has been updated to find shortest paths from least common ancestor graph for each pair of

words in the text and merge the shortest paths to create the graph by NetworkX add\_path()

2.This filtering improves the path quality to some extent.

3.Centrality measures and Dense Subgraph Classification (Core Numbers) are printed.

4.logs for this commit are at testlogs/ConceptNet5Client.log.25August2019

-----  
705.(FEATURE) ConceptNet 5.7 Text Graph - additional Graph Complexity Intrinsic Merit measures - 31 August 2019  
-----

-----  
1.ConceptNet 5.7 Text Graph implementation has been updated to print a comprehensive dictionary of graph complexity intrinsic merit measures of the ConceptNet text graph similar to WordNet text graph in RecursiveLambdaFunctionGrowth implementation  
2.grow\_lambda\_function3() in RecursiveLambdaFunctionGrowth python implementation has been changed to accept a textgraph as argument in the absence of a text and directly grow lambda functions from argument textgraph without creating it.  
3.Text is read from a file ConceptNet5Client.txt and passed on as conceptnet textgraph function argument.  
4.logs for this commit are at testlogs/ConceptNet5Client.log.31August2019  
5.Special concept vertex '/c/en/\xb0\_c' is in all the paths found by least common ancestor algorithm and therefore the graph has a hub-spoke star structure always. This node has been filtered by a new function remove\_noise() to avoid star graphs. To increase path quality more vertices might be added whenever deemed necessary in remove\_noise()  
6.Exception handling for non-existent paths has been included.  
7.Resulting filtered textgraph has been drawn in testlogs/ConceptNet5Client5.7.TextGraph.31August2019.png and is more like a sunflower (set of subsets of vertices having pairwise intersection forming petals).  
-----

-----  
706.(FEATURE) Recursive Lambda Function Growth - Machine Translation - updated implementation - 5 September 2019  
-----

-----  
1.machine\_translation() function in RecursiveLambdaFunctionGrowth.py has been changed to create a summary text in the destination language similar to create\_summary()  
2.As done in create\_summary() summary translated text in target language is either created by traversing the textgraph or without traversing the textgraph  
3.Presently translation creates only simple sentences. Complex sentences could be created in next iteration by compounding two neighbouring sentences.  
4.Goslate and googletrans python libraries have been imported for translation because of frequent Invalid Word errors in PyDictionary()  
5.Clauses specific to Goslate, googletrans and PyDictionary have been created along with exception handlers  
6.Caveat is rate limitations of Google Translate REST API underlying all previous three translate libraries which might or might not work depending on load and requested time point.  
7.If there are exceptions, source language edges are populated in translation text graph  
8.logs for previous commit are at testlogs/RecursiveLambdaFunctionGrowth.log.MachineTranslation.5September2019 - because of Google translate REST API ratelimit translation textgraph could not be created  
9.nondictionaryword() filter has been commented in RecursiveGlossOverlap Classifier because of slowdown.  
-----

-----  
707.(FEATURE) Recursive Lambda Function Growth - Machine Translation - simplified - 6 September 2019  
-----

1.machine\_translation() function in RecursiveLambdaFunctionGrowth.py has been simplified to remove unnecessary arguments and clauses and do the graph traversal and create summary in target language from it by default. This is because relevance\_to\_text() function which chooses sentences from text based on some distance measure to create summary is not necessary during translation  
2.3 clauses for choice of translator - googletans, goslate, PyDictionary - have been simplified to translate the connectives "and" and "are" to respective target language.

3.3 logs of translation for Hindi, Kannada and Telugu have been committed to testlogs:

testlogs/RecursiveLambdaFunctionGrowth.log.Telugu.MachineTranslation.6September2019

testlogs/RecursiveLambdaFunctionGrowth.log.Kannada.MachineTranslation.6September2019

testlogs/RecursiveLambdaFunctionGrowth.log.Hindi.MachineTranslation.6September2019

4.Previous logs have some intermittent errors because of Google translate API ratelimit.

5.ConceptNet is an alternative to Google Translate which is a multilingual ontology.

5.Translated text printed has some weird words not relevant to the text subject because of encoding/decoding problems of the language fonts.

6.Normal english language summary of the text - from create\_summary() - is also printed

7.Usual machine translations are rule based and recently transformers (sequence attention neural network) are gaining traction.Main motivation of NeuronRain is to implement an alternative, non-statistical, formal languages theory based framework for analyzing texts exploiting deep linguistic structure in them

8.This formal languages focussed approach to measure merit of texts - NER, translation, extracting lambda expression from a text etc., is superior to inferring a neural network from text because text is approximated to a Turing machine indirectly by recursively grown lambda expressions which has strong cognitive psychology basis - Grounded Cognition - "phrasal structures are embedded recursively"

9.As far as machine translation is concerned, instead of sequence transducers, text graph of one language is mapped to text graph of another language bijectively thus preserving deep structure and meaning irrespective of language - minimizes "lost in translation".

-----  
708. (FEATURE) Social Network Analysis - People Analytics - PIPL.com python API integration - Syllable based name clustering - 11 September 2019 and 14 September 2019  
-----

1.PIPL.com (people dot com) is a people search engine which tries to uniquely identify a person based on name, email etc.,

2.PIPL.com python API have been imported in SocialNetworkAnalysis\_PeopleAnalytics.py and invoked in a newly defined function pipldotcom\_analytics() which has query parameters: first name, last name and email

3.pipldotcom\_analytics() has been invoked on 3 example emails and names and JSON response is printed in logs at

testlogs/SocialNetworkAnalysis\_PeopleAnalytics.log.11September2019 which contains identities, photos, followers and relationships sourced from multiple social networks (linkedin, twitter, facebook, google, outlook etc.,)

4.Example email queries are: ka.shrinivaasan@gmail.com, shrinivas.kannan@gmail.com, kashrinivaasan@live.com for the name of the author - "Srinivasan Kannan"

5.Previous query is a perfect example of multiple english name spellings and

online identities author has for the single Hindi/Tamizh/Sanskrit name of the author "Sri-Ni-Va-San": Shrinivas Kannan, Srinivasan Kannan, Shrinivaasan Kannan (Shrinivaasan Ka)

6.This multiple name spelling problem arises in English because of multiple alphabets per syllable (hyphenated previously) and could easily cause identity confusion while in Tamizh, Hindi and Sanskrit name syllables have single vowel+consonant compound alphabets

7.Finding and clustering similarly named people and proving their uniqueness is a challenge in BigData because of spelling conflicts in English for similarly pronounced names.

8.Syllable based (acoustic) linguistic clustering of names by hyphenation previously as opposed to edit distance based clustering is thus a good model to classify similar names of different spellings.

9.Apart from Syllables, the 3 name spellings in previous example have same meaning which requires a Name ontology (NameNet) for semantically relating names of same meaning.

10. Names are non-dictionary words and creating a NameNet could be exhaustive and daunting.

#### References:

-----  
708.1 Word Hy-phen-a-tion by Com-put-er - [Liang - Ph.D Dissertation] -  
<http://www.tug.org/docs/liang/liang-thesis.pdf> - describes some difficult  
hyphenations and syllable boundaries in typesetting

-----  
709. (FEATURE) Social Network Analysis - People Analytics - Contextual Name  
Parsing - 14 September 2019  
-----

-----  
1.Name Parsing is an open problem and there are many tools already available  
(IBM Name Parser, Python Human Name Parser,...)

2.In the context of People Analytics, it is often required to find the first name, second name, middle name, surname, last name etc., from full names in a BigData set and there are cultural barriers e.g some countries have convention of <second name> <first name> and others have <first name> <second name> and <second name> is initial,surname or name of the parent/spouse.

3.Because of cultural barriers across nations parsing first name or second name in the absence of some context (e.g. an ID card) is difficult and prone to error.

4.New function nameparser() has been defined in  
SocialNetworkAnalysis\_PeopleAnalytics.py which accepts full name, a regular expression and an ID contextual text as arguments.

5.nameparser() searches for the regular expression pattern and the tokenized full name in the ID contextual text and tries to infer First Name and Second Name.

6.An example name parsing for the author and failure of Python Human Name Parser has been demonstrated - Some past forum mails of the author from

<https://marc.info/?a=104547613400001&r=1&w=2> and <https://marc.info/?l=apache-modules&m=105610024116012> sent from official mail id: Kannan.Srinivasan@Sun.COM have wrong first (Kannan) and last (Srinivasan) names while final salutation in the emails contain the name per Indian convention as "K.Srinivasan" and Python Human Name parser fails to parse the names correctly in the absence of this context.

7.NeuronRain nameparser() defined in this commit is passed the email texts as contexts and the nameparser() searches for places in the emails containing the tokens of the full name by regular expression pattern.

8.Following lines define two named regex patterns which are searched in the email ID contexts mentioned in (6) as per Indian Cultural Convention of Second Name or Initial followed by First Name:

```
hrranal.nameparser("Kannan Srinivasan",r"((?P<second_name>\w+).(?P<first_name>\w+))",emailcontext_text)
```

```
hrranal.nameparser("Kannan Srinivasan",r"((?P<second_name>\w+) (?P<first_name>\w+))",emailcontext_text)
```



w+)",emailcontext\_text)

9.nameparser() returns the regex groupdicts for the matched named-parentheses

10.nameparser() has been made generic to suit all kinds of regular expressions for names and ID contexts and can be invoked for any social or professional network names. ID Context could be text from any source (e.g emails, texts, ID card texts) and regex pattern argument must comply with the ID context - if Context argument is an ID card text having Name, Address and Parent Names, UniqueID etc., regex pattern must accordingly follow e.g "Parent Name:(? P<parent\_name>\w+)"

11.Logs for this commit are at

testlogs/SocialNetworkAnalysis\_PeopleAnalytics.log.14September2019 and email ID contexts at testlogs/SocialNetworkAnalysis\_PeopleAnalytics\_NameParsing/

#### References:

709.1 Python nameparser - <https://nameparser.readthedocs.io/en/latest/>

709.2 NameAPI - <https://www.nameapi.org/en/demos/name-parser/> - REST API which supports culture specifics

709.3 IBM Name Parser -

[https://www.ibm.com/support/knowledgecenter/en/SSEV5M\\_5.0.0/com.ibm.iis.gnm.parsingnames.doc/topics/gnr\\_np\\_con\\_parsingnamesusingnameparser.html](https://www.ibm.com/support/knowledgecenter/en/SSEV5M_5.0.0/com.ibm.iis.gnm.parsingnames.doc/topics/gnr_np_con_parsingnamesusingnameparser.html)

710. (THEORY and FEATURE) Compressed Sensing for Texts - Syllable Vector

Vowelless Text Compression - 18 September 2019 - Related to 2, 708

1.Compressed Sensing which is mostly restricted to digital signal and image processing, reconstructs original signal from lossy signal with high probability.([https://en.wikipedia.org/wiki/Compressed\\_sensing](https://en.wikipedia.org/wiki/Compressed_sensing))

2.Vowelless Text Compression which compresses english texts by stripping vowels also creates a lossy compressed signal from which actual text has to be recovered with high probability and thus is a Text Compressed Sensing.

3.Existing Vowelless Text Compression implementation in neuronRain relies on Hidden Markov Model estimation to infer maximum likely missing vowels.

4.Syllables of a string in any language are phonetic divisions in the string.

5.Syllable boundary name clustering for clustering similar Names differing in spellings mentioned previously maps each string to a vector of syllables which is audio/linguistic representation of the string

6.Thus every n-syllable string irrespective of languages can be represented in an n-dimensional syllable space as a syllable vector and distance between two strings is the L2 norm in this syllable space - each syllable is phonetically represented than by a script. This is an alternative word2vec embedding model and is a better distance measure than levenshtein edit distance because of language script independence - 2 strings of different natural languages can be compared by phonetic syllable distance.

7.Syllable space embedding for similarity of names in NeuronRain is different from Phonetic Match Rating algorithm

([https://en.wikipedia.org/wiki/Match\\_rating\\_approach](https://en.wikipedia.org/wiki/Match_rating_approach)) which also removes vowels but does not consider syllable boundaries or hyphenations.

8.CompressedSensing Python implementation has been changed to include a new function syllable\_boundary\_text\_compression() which invokes PyHyphen python hyphenator and gets syllable vector of a string and compressed syllable vector by removevowels() in TextCompression implementation.

711. (FEATURE) Social Network Analysis - People Analytics - Contextual Name Parsing and Syllable Vector Compression of Strings

- 18 September 2019

1.Regex Pattern Matching in nameparser() has been changed to ignore case by flag

re.IGNORECASE

2.Few more ID context texts are being regex matched in nameparser() which are parsed texts and OCRs (by pdftotext and gocr) from pdf and image IDs of the author uploaded in <https://sourceforge.net/projects/acadpdrafts/files/>

source=navbar - Public Distribution System ID card linked to Unique Aadhaar IDs and Permanent Account Number (PAN) which is Aadhaar linked -

<https://sourceforge.net/projects/acadpdrafts/files/NewRationCard2.pdf/download>,

<https://sourceforge.net/projects/acadpdrafts/files/NewRationCard1.pdf/download>

and <https://sourceforge.net/projects/acadpdrafts/files/PAN.jpg/download>

3.These three ID cards are examples of Both Indian convention of Second name followed by First name and International standard of First name followed by Second name.

<https://sourceforge.net/projects/acadpdrafts/files/NewRationCard2.pdf/download>,

<https://sourceforge.net/projects/acadpdrafts/files/NewRationCard1.pdf/download>

have Unique IDs linked to both formats but in different languages - Srinivasan Kannan கண்ணன் சீனிவாசன்

4.nameparser() is invoked on previous three ID contexts for full name "Kannan Srinivasan" and first and second names are printed

5.syllable\_boundary\_text\_compression() from CompressedSensing implementation is invoked for 3 different spellings of same name "Shrinivaasan, Shrinivas, Srinivasan" and syllable vectors (and their vowelless versions) are printed:

```


#####
```

Vowelless Syllable Vector Compression for text - Shrinivaasan : ([u'Shrini', u'vaasan'], u'Shr\_n\_-v\_s\_n')

```

#####
```

Vowelless Syllable Vector Compression for text - Shrinivas : ([u'Shrini', u'vas'], u'Shr\_n\_-v\_s')

```

#####
```

Vowelless Syllable Vector Compression for text - Srinivasan : ([u'Srini', u'vasan'], u'Sr\_n\_-v\_s\_n')

```
=====
```

6.Distance between these syllable vectors has to be phonetic by finding syllable-wise audio similarity - every syllable is an audio waveform and two names are compared by syllable distances between vectors of waveforms e.g ["Shrini", "vas"] and ["Srini", "vasan"]. This has been omitted presently because syllable-to-audio tools are required.

7.Comparison to Match Rating Codex from JellyFish is also printed:

Match ratings for same name of differing spellings -

[Shrinivaasan, Shrinivas, Srinivasan]: [u'SHRVSN', u'SHRNVS', u'SRNVSN']

8.logs for this commit and previous are at

testlogs/SocialNetworkAnalysis\_PeopleAnalytics.log.18September2019

-----  
712. (THEORY) Computational Geometric Factorization - Gamma Approximation of Sum of Binary Search times - Summation for first  $\sqrt{N}$  tiles and why non-average case sequential factorization is difficult - related to 668 - 19 September 2019  
-----

For sane binary search length of the tile must be  $> 1 \Rightarrow N/(k^2 + k) > 1$  (or)  
 $k^2 + k < N$

$\Rightarrow k^2 + k - N < 0$

$\Rightarrow$  solving the quadratic,  $k = -1 + \sqrt{1 + 4N} / 2$

$\Rightarrow k = -0.5 \pm 0.5\sqrt{1 + 4N}$

For large  $N$ ,  $k < 0.5\sqrt{4N}$  (or)  $k < \sqrt{N}$

Total time for binary searching  $k=\sqrt{N}$  adjacent tile segment arithmetic progressions by gamma approximation =  $\sqrt{N}\log N - \log(\sqrt{N}+1) - (2\sqrt{N} + 1)\log(\sqrt{N}) + 2(\sqrt{N}+1) - \log(2\pi)$   
=  $\sqrt{N}\log N + 2\sqrt{N} + 2 - \log(\sqrt{N}+1) - 2\sqrt{N}\log(\sqrt{N}) -$

$$\begin{aligned} & \log(\sqrt{N}) - \log(2\pi) \\ & \leq \sqrt{N} \log N + 2\sqrt{N} + 2 - \log(\sqrt{N}) - 2\sqrt{N} \log(\sqrt{N}) - \\ & \log(\sqrt{N}) - \log(2\pi) \\ & \leq 2\sqrt{N} \log(\sqrt{N}) + 2\sqrt{N} + 2 - \log(\sqrt{N}) - 2\sqrt{N} \log(\sqrt{N}) - \\ & \log(\sqrt{N}) - \log(2\pi) \\ & \leq 2\sqrt{N} + 2 - 2\log(\sqrt{N}) - \log(2\pi) \\ & \leq 2*(\sqrt{N} - \log(\sqrt{N}) + 1) - \log(2\pi) \\ & \leq 2*(\sqrt{N} - \log(\sqrt{N})) \end{aligned}$$

which is exponential in  $\log N$  still shaving off only a logarithm from squareroot of  $N$ . This necessitates finding approximate factors close to actual factors in average case sequential optimization previously implying factorization (finding atleast one factor) is in average-P which is an average lowerbound for all possible integers and different from P. Therefore deterministic factorization to find one factor or all factors requires NC (PRAM or BSP) parallelism - NeuronRain Spark Factorization which is both a PRAM (multicore) and BSP(cloud) model finds all factors. It has to be noted previous average case sequential time is for finding atleast one factor.

-----  
 713. (THEORY and FEATURE) People Analytics - Set Partition based Electronic Voting Machine implementation and a NeuronRainApps Drone usecase - 24 September 2019 - related to 620,648  
 -----

-----  
 Voter Received Encrypted Paper Audit Trail (VREPAT) Theoretical Voting Machine based on Set Partition Bucketing described previously is partially implemented as a futuristic drone usecase (Autonomous Delivery Usecases - <https://syncedreview.com/2019/08/24/autonomous-delivery-moves-from-research-labs-to-the-streets/>) in this commit - this is not a full-fledged implementation but conceptual:

- (\*) Usual state-issued unique id(s) are singletons stored in centralized cloud and vulnerable to breaches/fakes creating identity disputes.

- (\*) To redress this an alternative dual unique id (public id and private id) similar to public-key-infrastructure is assumed which is as strong as RSA and Diffie-Hellman protocols

- (\*) Public unique id is a hash digest of a string which uniquely identifies a person e.g concatenation of <VoterID><Full Name><Parent/Spouse Name><Permanent Address> is always a unique public id. Private id is a password for a voter issued along with a Public unique id.

- (\*) Polling Station is a Drone - it contains a set partition bucketing voting machine which based on addresses or public unique id(s) in the voter list automatically navigates to an address and lands on a voter doorstep. Voter casts h(is|er) vote on the drone booth by public unique id card and private password and receives encrypted receipt of vote.

- (\*) This Dynamic Drone Polling Booth is inspired by Autonomous Online Shopping Delivery and Mobile ATMs available already (which work on smartcard and password authentication) and has many advantages over traditional static polling stations which satisfy constraints of John Hopkins Paper to some extent:

- (\*) Voting need not be limited to a day and can sprawl multiple days.

- (\*) Voter can do advanced booking for drone and it lands on demand making the voting behaviour difficult to predict.

- (\*) All households are covered and thus maximizes polling percentage

- (\*) Completely automated election - Minimizes or obviates polling stations, cost, queueing and personnel and thus human tamper-proof - requires one drone per polling precinct of few hundred voters

- (\*) Ensures privacy

- (\*) Reduces malpractices because of no crowding, each voter independently votes, polling happens at doorstep at time of choosing which is unpredictable and unique demographic/geographic identity is electronically verified by drone navigation to unique address minimizing bogus voting (no voter is denied voting because it could not have been already cast in h(is|er) name - GPS drone navigation is an additional geographic uniqueness).

(\*) This commit defines a new minimal voting function `electronic_voting_machine()` in `Streaming_SetPartitionAnalytics.py` which accepts `voted_for`, example voter id card contexts of the author from `testlogs/Streaming_SetPartitionAnalytics_EVM/` (no text parsing is done) and makes `ripemd160` hash digests from them. EVM is a dictionary set partition object mapping candidate `voted_for` to list of voters' public uniqueid hash digests - does not use counters and private id authentication.

(\*) Complexity theoretically, drone voting is reducible to Motion planning (A-Star algorithm) and travelling salesman problem (TSP) because drone has to efficiently navigate the voter vertices spread across geographically (e.g hamiltonian) and thus NP-complete.

-----  
714. (THEORY and FEATURE) Topological Handwriting Recognition - Product Homotopies - Related to 159,660 - 30 September 2019  
-----

Pattern grammars for shape description for handwriting recognition previously as homeomorphic deformations in  $R^2$  preserving genus (also defined by knots - [https://github.com/shrinivaasanka/Grafit/blob/master/course\\_material/NeuronRain/AdvancedComputerScienceAndMachineLearning/AdvancedComputerScienceAndMachineLearning.txt](https://github.com/shrinivaasanka/Grafit/blob/master/course_material/NeuronRain/AdvancedComputerScienceAndMachineLearning/AdvancedComputerScienceAndMachineLearning.txt)) have an alternative topological definition in terms of Product of Path Homotopy classes: Two paths  $f$  and  $f'$  are homotopic if they have same initial and final points  $x_0$  and  $x_1$  and there is a continuous map  $F: I \times I \rightarrow X$  for some topology space  $X$  such that  $F(s,0) = f(s)$  and  $F(s,1) = f'(s)$ ;  $F(0,t) = x_0$  and  $F(1,t) = x_1$ . If  $f$  is a path in  $X$  from  $x_0$  to  $x_1$  of homotopy  $F$  and  $g$  is a path from  $x_1$  to  $x_2$  of homotopy  $G$ , product homotopy  $F * G$  by pasting lemma is the set of all continuous paths from  $x_0$  to  $x_2$  via  $x_1$ . An example of product homotopy is handwritten digit '8' which has a pattern grammar:

$\langle 8 \rangle := \langle o \rangle$  pasted on  $\langle o \rangle$

Set of closed paths (all possible ways of writing 'o' - initial and end points are same) for  $\langle o \rangle$  form a path homotopy  $F$  and product homotopy  $F * F$  defines all possible ways of writing '8' by pasting together endpoints of two handwriting homotopies  $F$  and  $F$  (also referred to as path composition). Similarly every handwritten alphabet can be defined as product of homotopies by pasting together path initial-end points. For example letter 'p' has pattern grammar:

$\langle p \rangle := \langle | \rangle$  pasted to the left of  $\langle o \rangle$

In other words homotopy is a continuous deformation of a path having end points fixed. It has to be noted that previous homotopy definition does not distinguish handwritings of two humans - it just recognizes any written alphanumeric as a product homotopy. Distinguishing two humans requires fine definition of homotopies within thresholds (e.g handwritings of same person hardly deviate from thresholds and some paths do not exist in handwriting homotopy of one person but do in other person's). This topological information of handwritings can complement traditional neural network based recognitions.

References:

-----  
714.1 Topology - [James R.Munkres] - Second Edition - Page 108 - Theorem 18.3 - Pasting Lemma - Pages 322-326 - Path Homotopy and Product Homotopy - Figures 51.1, 51.5

714.2 Path Homotopy and Path composition -  
[https://en.wikipedia.org/wiki/Path\\_\(topology\)#Homotopy\\_of\\_paths](https://en.wikipedia.org/wiki/Path_(topology)#Homotopy_of_paths)  
-----

715. (THEORY) People Analytics - Topological Face Recognition - Product Homotopies - related to 714 - 2 October 2019  
-----

Previous section defined Handwriting recognition topologically by Product Homotopies. Face Recognition and Handwriting recognition are crucial for unique

identification of a human in people analytics. Extending Product Homotopies to Face Recognition is not straightforward because facial features are not continuous functions which can be unified by pasting lemma. Possible solution is to segment the image by either bounding boxes or watershed algorithm and find contours of facial features which are piecemeal discontinuous curves (approximable by Douglas-Peucker polynomial). Each bounding box or segment containing only continuous curves have to be unified by pasting lemma which define product homotopies of continuous deformations in 3-dimensions whereas handwriting homotopies are deformations in 2D. Example: set of images of all possible postures, expressions and facial distortions of a human face can be equated to union of product homotopies of continuous contour curves in bounding boxes or segments in the image - Contours of Eyes, Nose, Mouth and Ears of a face cannot be a single continuous curve and can be in separate segments or bounding boxes of an image each defined by a product homotopy of continuous contours. Union of product homotopies for Eyes, Nose, Mouth, Ears and any other feature recognizes a face including all possible facial deformations.

Example Shape Grammar for Face Recognition - Union of Product Homotopies (each <feature> defines a product homotopy for one continuous segment of facial feature contour deformations):

```

 <Hair>
 <Ear><Eye><Eye><Ear>
 <Nose>
 <Mouth>

```

-----  
716. (THEORY and FEATURE) Economic Intrinsic Merit - Gravity Model of Volume of Trade and GDP as fitness measure - 2 October 2019  
-----

1. Intrinsic Fitness or Intrinsic Merit has been traditionally applied to denote innate ability of a vertex in Social Networks. Fitness model is applicable in Economic Networks too e.g International Trading Network(ITN), Production Networks(<https://economics.mit.edu/files/9790>).

2. <https://arxiv.org/pdf/1409.6649.pdf> discusses various measures of Economic fitness including GDP and quantifying volume of trade between nations - Quoted excerpts:

2.1 "...The standard model of non-zero trade flows, inferring the volume of bilateral trade between any two countries from the knowledge of their Gross Domestic Product (GDP) and mutual geographic distance (D), is the so-called 'gravity model' of trade [21-25]. In its simplest form, the gravity model predicts that the volume of trade between countries i and j is  $F_{ij} = \alpha \text{GDP}^{\beta_i} \cdot \text{GDP}^{\beta_j} / D_{ij}^k$ ..."

2.2 "...where  $z_i \equiv e^{-\theta_i}$  and  $p_{ij} \equiv z_i z_j / (1 + z_i z_j)$ . The latter represents the probability of forming a link between nodes i and j, which is also the expected value  $\langle a_{ij} \rangle = z_i z_j / (1 + z_i z_j) = p_{ij}$ . (4) ..."

2.3 "...It should be noted that eq.(4) can be thought of as a particular case of the so-called Fitness Model [41], which is a popular model of binary networks where the connection probability  $p_{ij}$  is assumed to be a function of the values of some 'fitness' characterizing each vertex. Indeed, the variables  $z_i$  can be treated as fitness parameters [6, 37] which control the probability of forming a link. A very interesting correlation between a fitness parameter of a country (assigned by the model) and the GDP of the same country was found [37]. This relation is replicated here in Fig. 2, where the rescaled GDP of each country ( $g_i \equiv \text{GDP}_i / \sum(\text{GDP}_i)$ ) is compared to the value of the fitness parameter  $z_i$  obtained by solving eq.(5). The red line is a linear fit of the type  $z_i = \sqrt{a} \cdot g_i$ ..."

3. This commit defines a new function `EconomicMerit()` in `LinearAndLogisticRegression.py` which computes trade link probabilities and gravity model between countries based on GDP as intrinsic fitness measure and distances between countries. Reference 694.1 defines GDP fitness as a linear regression dependent on macroeconomic variables.

## References:

716.1 Another Fitness Model of GDP - Fitness-dependent topological properties of the World Trade Web - <https://arxiv.org/pdf/cond-mat/0403051.pdf>

717. (THEORY) Cognitive Element in the context of Category theory, Factorization and Set Partitions - related to 160 - 4 October 2019

Notion of "Cognitive element" for the lack of better name was defined earlier as an element in an array, set partition, group, category or any algebraic structure which "knows" or has "information" about other peer elements - this is an experimental abstraction in Category theory which might have overlaps to existing algebraic concepts (left inverse of a morphism - retraction/section - [https://en.wikipedia.org/wiki/Section\\_\(category\\_theory\)](https://en.wikipedia.org/wiki/Section_(category_theory))). Information could be any equivalence relation or morphism - "member-of", "factor-of", "subset-of" etc., defined in a Category. Examples:

717.1  $117 = 13 \times 9$  is an element of ring of integers as category - 13, 9 are "factors-of" 117 or 13 "knows" about 9 by factorization. Factorization is a morphism relation defined on category of integer objects -  $\text{Inverse}([13, 9]) = 117$

717.2 Following set partition which maps timeout values to buckets of processes having that timeout value in an OS scheduler is a category (Hashing Dynamic Sets -

[https://github.com/shrinivaasanka/Grafit/blob/master/course\\_material/NeuronRain/AdvancedComputerScienceAndMachineLearning/AdvancedComputerScienceAndMachineLearning.txt](https://github.com/shrinivaasanka/Grafit/blob/master/course_material/NeuronRain/AdvancedComputerScienceAndMachineLearning/AdvancedComputerScienceAndMachineLearning.txt)):

10 - 1, 2, 5  
20 - 12, 15, 11  
33 - 3, 111  
41 - 16  
55 - 25, 114

and every bucket defines a timeout morphism relation between objects in the processes category - Timeout Bucket 55 has processes 25, 114 which know each other.

717.3 Every morphism equivalence relation on any Category defines equivalence classes elements of which have "information" about peers.

717.4 Cognitive elements have useful applications in set partition equivalence relations - in previous set partition example, question of inverse - finding a bucket containing an element - is non-trivial e.g find the bucket having element 111. This requires an exhaustive search because set partition is not a bijective map and reverse lookup is not possible (but there are bidirectional dictionary implementations in Python which can retrieve a key from value - <https://pypi.org/project/bidict/>). Elements 3, 111 are cognitive peers by inverse morphism relation "in the bucket of 33" -  $\text{Inverse}([111, 3]) = 33$ . Implementing such an inverse requires knowledge of cognitive elements which are domains of the inverse morphism.

718. (THEORY and FEATURE) People Analytics - Set Partition Analytics based Drone Electronic Voting Machine - updated - 9 October 2019 - related to 713

1. `Streaming_SetPartitionAnalytics.py` has been changed to update `electronic_voting_machine()` function - New semaphore mutual exclusion synchronized primitive block (`BoundedSemaphore`) has been added to guard the voting critical section. Maximum value of semaphore is set to 1 voter.
2. Voting code has been updated to check if voter has already voted by Voted list and skip voting if yes. Voter id(s) are appended to Voted array after voting within synchronized block.
3. Additional encryption has been introduced by invoking SHA256 Passlib encrypt on the `ripemd160` publicuniqueid hex hash digest and append the encrypted voter

id to EVM bucket.

4.This EVM assumes the function `electronic_voting_machine()` is invoked from a Drone python code which should have already navigated to the voter address and done the user/password authentication by smartcard.

5.Single Signon username/password authentication has already been implemented in NeuronRain GUI - `python-src/webserver_rest_ui/NeuronRain_REST_WebServer.py` - by passlib OAuth having MongoDB and Redis credential storage - which might as well be used as alternative caller for this EVM.

6.logs for preventing repetitive voting and SHA256 buckets are at `testlogs/Streaming_SetPartitionAnalytics.EVM.log.90october2019`

7.This Set Partition EVM is also a Dynamic Graph Partition (Similar Worst Case Execution Time - Survival Index - Dynamic Graph Partition OS Scheduler is described in

[https://github.com/shrinivaasanka/Grafit/blob/master/course\\_material/NeuronRain/AdvancedComputerScienceAndMachineLearning/](https://github.com/shrinivaasanka/Grafit/blob/master/course_material/NeuronRain/AdvancedComputerScienceAndMachineLearning/AdvancedComputerScienceAndMachineLearning.txt)

`AdvancedComputerScienceAndMachineLearning.txt` - Hashing Dynamic Sets) because voting is dynamic and voters related among themselves might vote for different candidates which creates edges of dynamic people partition graph (voter vertices related by edges are partitioned into candidate buckets)

8.As mentioned in previous section, Left Inverse of Voter Bucket Objects is the Candidate voted for connecting peer voters by an equivalence relation.

-----  
719. (THEORY) Complement Diophantines over Integers (Z), Polynomial Interpolation, Polynomial Reconstruction Problem, Error Correcting Codes, MRDP theorem, Lagranges Four Square Theorem and Decidability of Complementation, Ramsey 2-coloring of sequences, Set Partitions to Tile Cover reduction, Factorization, Lagrangian tiling of 2-dimensional space, ZF and Axiom of Choice (AOC) and Complement Choice functions, Depth-2 majority voting social choice circuits - an alternative interpretation based on diagonalization - 13 October 2019 - related to 345, 471, 617, 646, 651, 657  
-----

-----  
By MRDP theorem, every recursively enumerable (RE) set of Integers is diophantine representable and there are RE sets which are not recursive ( $R = RE \setminus R$  (RE set difference R).  $RE \setminus R$  languages have diophantine representations but are not accepted/rejected by a halting turing machine (without looping) which includes a turing machine for finding the complement diophantine representation of a language in  $RE \setminus R$ . Such a halting turing machine (TM1) in  $RE \setminus R$  or an algorithmic equivalent for finding complement diophantine representation of other sets in  $RE \setminus R$  is a contradiction. This diagonalization proves undecidability of complement diophantine for  $RE \setminus R$  (diophantine representation exists but algorithm does not for  $RE \setminus R$ ).

For Recursive sets (R), there are algorithms available or there exists a halting turing machine (TM2) in R for finding algorithmic equivalent of diophantine representation of other sets in R and diagonalization does not contradict e.g Polynomial Interpolation (exact), Polynomial Reconstruction Problem (error correcting polynomial agreeing on most points - reference 345.2), Lagrange four square theorem. Lagrange four square theorem maps tuples in 4-dimensional space to points on recursive set (or) any integer can be written as sum of 4 squares. This 4-tuples to integer map from Lagrange four square theorem is infact an interpolation by a polynomial over 4 variables -  $f(x_1, x_2, x_3, x_4) = x_1^2 + x_2^2 + x_3^2 + x_4^2 = y$ . Lagrange Four Square interpolation indirectly solves factorization by solving an optimization problem - set partition is reduced to tile cover of a rectangular 2-dimensional space and factors are sides of the rectangle which have to be solved for by an integer program.(Both diophantine representation and algorithm exist for R). Chinese Remainder Theorem generalizes this as an isomorphic map in multiple dimensions -  $x \bmod N \iff (x \bmod n_1, \dots, x \bmod n_k)$  for coprime  $n_1, n_2, \dots, n_k$  and  $N = n_1 * n_2 * \dots * n_k$ .

This diagonal interpretation is more dichotomous than previous sections on complement diophantine undecidability which in a nutshell implies: Any set is a

complementary set of some other set and thus any complementary set which is recursively enumerable but not recursive has a diophantine representation and not decidable by an algorithm, while any recursive complementary set is decidable by an algorithm and also has a diophantine representation.

As a special example complement of Axiom of Choice for depth-2 majority boolean circuits is phrased as: For set of electorate sets  $S=\{s_1, s_2, s_3, \dots\}$  there exists a choice function  $C'(s_i)=(x_1, x_2, \dots)$  which flips a chosen majority (0 or 1) from every set  $s_i$  in  $S$ . Leaves are members of  $S$  (electorate sets or constituencies) while depth-1 are complemented/flipped bits from majority voting of leaves. This complements AOC democracy function as: "Who won" Vs "Who lost" (alternatively can be complemented as "Who voted in favour" versus "Who did not vote in favour" which has hardness amplification ramifications for proving  $P \neq NP$ ). It is open if Complement AOC is decidable. Traditional democracy is depth-2 majority circuit and abides by AOC.

Complement Diophantines throughout this draft focus mainly on sets or sequences of Integers ( $\mathbb{Z}$ ) because MRDP theorem and Rayleigh-Beatty sequences theorem are limited to  $\mathbb{Z}$  while complementation over Rationals ( $\mathbb{Q}$ ) is open problem and complementation over Reals ( $\mathbb{R}$ ) is solvable by Tarski/Sturm decidability.

-----  
720. (THEORY and FEATURE) People Analytics - Handwriting Recognition - Contour Homotopies - Matplotlib Rasterization - 16 October 2019 - related to 714 and 715  
-----

-----  
1. This commit updates `handwriting_recognition()` in `DeepLearning_ConvolutionNetwork_BackPropagation.py` to additionally raster the contours extracted from the handwritten alphanumeric.  
2. Rasterization presently invokes `matplotlib plot()` having parameter `rasterized=True` and presets `dots-per-inch` parameter to 100 in `figure()` for restricting number of pixels.  
3. Contours from each recognized written alphanumeric are looped and plotted by `matplotlib plot()` setting `rasterized=True`.  
4. There are better alternatives to this primitive rastering - `rasterio` (<https://rasterio.readthedocs.io/en/stable/>) and `wavelet-rasterization` (<https://github.com/ufoym/wavelet-rasterization/>) and desired rasterization is similar to illustrations in <https://github.com/ufoym/wavelet-rasterization> which is a coarse rectification required for hyperbolic arc in Computational Geometric Factorization (But there is a windows DLL build dependency). `Matplotlib dots-per-inch` and `rasterized=True` creates fine grained rasterized curves.  
5. Each contour is approximable by a Bezier-like curve ([https://en.wikipedia.org/wiki/B%C3%A9zier\\_curve](https://en.wikipedia.org/wiki/B%C3%A9zier_curve)) which is an instance of homotopy because bezier curves have endpoints/control points unchanged and intermediate points on curve are puppet-animated (most applicable in Graphics).  
6. Handwriting can be simulated by a Bezier curve having unchanged endpoints or control points which is a homotopic continuous deformation.  
7. Original handwriting is reconstructible by homotopy and pasting lemma - by pasting together polynomials for individual contours.  
8. Logs and images for this commit are at `testlogs/` (handwritten 1(style 1) and 1(style 2), 1 and 8 are contour-rasterized and compared):  
`DeepLearning_ConvolutionNetwork_BackPropagation.log.tar.xz`  
`DeepLearning_ConvolutionNetwork_BackPropagation.Raster.Homotopies_1_1.jpg`  
`DeepLearning_ConvolutionNetwork_BackPropagation.Raster.Homotopies_1_2.jpg`  
`DeepLearning_ConvolutionNetwork_BackPropagation.Raster.Homotopies_8_1.jpg`  
`DeepLearning_ConvolutionNetwork_BackPropagation.Raster.Homotopies.pdf`  
9. Every contour can be fit to a bezier polynomial and two alphanumerics have to be verified if they are homotopic (has a dependency on topology libraries). This is non-trivial because every homotopically "similar" contour in two alphanumerics have to be pairwise compared  
and number of contours per alphanumeric could be in hundreds.  
-----



-----  
721. (THEORY and FEATURE) People Analytics - Handwriting Recognition - Inner Product Space of Contour Interpolated Polynomials - 17 October 2019 - related to 714, 715, 720  
-----

-----  
1. In continuation of the previous commit for drawing rasterized contour curves, handwriting contours are interpolated by `SciPy.interpolate.splprep()`  
2. Points on contour curves are `stack()`-ed to 2 dimensional arrays and contours having more than 3 points are interpolated by spline polynomials of degree less than number of points per contour.  
3. PdfPages "pdf damaged" error in `DeepLearning_ConvolutionNetwork_BackPropagation.Raster.Homotopies.pdf` has been resolved by PdfPages `close()` which flushes the buffer.  
4. `splprep`  
(<https://docs.scipy.org/doc/scipy-1.2.1/reference/generated/scipy.interpolate.splprep.html>) creates B-Spline curves which are exact but less smooth as opposed to Bezier curves which are smoother, depend on control points and are approximate fit (passes through most of the points).  
5. Boolean flag `TopologicalRecognition=True/False` has been introduced in `__main__` to choose topological handwriting recognition instead of Convolution Neural Network Pattern Recognition.  
6. Logs and Pdf images for contour polynomials are at:  
`testlogs/DeepLearning_ConvolutionNetwork_BackPropagation.log.17October2019`  
`testlogs/DeepLearning_ConvolutionNetwork_BackPropagation.Raster.Homotopies.pdf`  
7. By defining an inner product space of contour polynomials  
 $\langle f, g \rangle = \text{DefiniteIntegral}(f(x)g(x)dx)$ , distance function is obtained for verifying if 2 contours belonging to different handwritten alphanumerics are "similar" or "orthogonal" (polynomials  $f$  and  $g$  are orthogonal if  $\langle f, g \rangle = 0$ ). This is an algebraic but less topological similarity.

References:

-----  
721.1 Orthogonal Polynomials -  
<https://www.math.tamu.edu/~yvorobet/MATH304-503/Lect4-04web.pdf>  
-----

-----  
722. (THEORY and FEATURE) Update - Drone Electronic Voting Machine  
NeuronRainApps Usecase - 22 October 2019 - related to 713  
-----

-----  
722.1 ROS Drone Navigation Algorithms which depend on Google Maps for GPS geolocation have been cited as references in NeuronRain Documentation and Licensing: <http://neuronrain-documentation.readthedocs.io/en/latest/> - Distance is computed by geodesic geometric equations (Bearing). Following are quoted excerpts from <https://journalofbigdata.springeropen.com/articles/10.1186/s40537-019-0214-3>:

722.1.1 "...In the experiment that we did, the average of positional deviation of landing position between the actual landing position and the desired landing position in the flight tests of flying from start to goal is 1.1125 m and for the tests that use the algorithm which uses course-over-ground, the positional deviation has average of 2.39 m...."

722.1.2 "...The recent developments of drone for sprayer pesticide applications and used for delivering items, for example the Amazon Prime Air, where Amazon used an octocopter to deliver items with weighs less than 5 lb or around 2.3 kg..."

722.2 Commercially experimented drone online shopping grocery delivery mechanisms have payload of few kilograms.

722.3 Drone Electronic Voting Machine has an accompanied Point-of-Voting handheld device for smartcard voter id authentication.

722.4 Drone navigates to an address by Google maps from a voter list (powered by ROS or linux kernel PXRC drivers).

722.5 Once drone lands on doorstep, Voter authenticates in the Point-of-Voting

machine with in drone by voter id smartcard.

722.6 Ballot is displayed in a touchscreen of the drone. At the end of the voting drone Point-of-Voting device issues a VREPAT encrypted receipt of the vote and retreats.

722.7 Drone EVM does not have payload like autonomous delivery - thus lightweight.

722.8 Landing deviation has to be specified upfront as config parameter.

#### References:

-----  
722.9 UAV Theory, Design and Applications - [AR Jha] -

<https://content.taylorfrancis.com/books/download?dac=C2014-0-36678-5&isbn=9781498715430&format=googlePreviewPdf>  
-----

-----  
723. (THEORY) Update 2 - Drone Electronic Voting Machine - Voting Analytics - Set Partition Distance Measures - 2 November 2019 - related to 722  
-----

723.1 Drone Electronic Voting machine partial implementation (depends on drone navigation) in NeuronRain is an obfuscated set partition of electorate (voters identity per candidate bucket is encrypted)

723.2 Analytics inferences can be drawn from a stream of previous encrypted set partition EVMS without compromising voter privacy.

723.3 Variety of distance measures are available for comparing set partitions:

723.3.1 Earth Mover Distance or Wasserstein Distance (OpenCV2 and SciPy) - which is amount of work necessary to move a mass of one shape to another - shape is a multidimensional object and two set partition EVMS are of different shapes - [https://docs.opencv.org/2.4/modules/imgproc/doc/histograms.html?](https://docs.opencv.org/2.4/modules/imgproc/doc/histograms.html?highlight=emd#cv.CalcEMD2)

highlight=emd#cv.CalcEMD2 and

[https://docs.scipy.org/doc/scipy/reference/generated/scipy.stats.wasserstein\\_distance.html](https://docs.scipy.org/doc/scipy/reference/generated/scipy.stats.wasserstein_distance.html) - EMD2 in OpenCV2 is a sophisticated version of EMD for comparing two visuals by mapping images to histogram probability distributions while EMD in SciPy is wasserstein distance

723.3.2 OpenCV2 provides many other measures for comparing image histograms - <https://docs.opencv.org/2.4/modules/imgproc/doc/histograms.html> - cvCompareHist() by Correlation, Chi-Square, Intersection, Bhattacharyya, Hellinger distance measures  
-----

-----  
724. (FEATURE) Update 3 - Drone Electronic Voting Machine - JSON persistence of EVMS - Datasource for Voting Analytics - 2 November 2019 - related to 723  
-----

724.1 `electronic_voting_machine()` function in `Streaming_SetPartitionAnalytics.py` has been updated to accept 3 arguments - voting machine set-partition obfuscated dictionary, unique id context and candidate voted for - for removing hardcoded voting dictionary and being generic across polling stations.

724.2 Voting machine dictionaries are iterated and mapped to histograms of Candidate to Votes Counter (size of bucket)

724.3 Voting machine dictionaries are JSON dumped to a file `testlogs/Streaming_SetPartitionAnalytics.EVMS.json` - this JSON persistence is only for analytics purposes and voting machine dictionary is still an in-memory object per drone EVM supposed to be passed on from an already navigated Drone python code which is lacking.

724.4 This JSON file can be read as a stream by Streaming Abstract Generator Dictionary datasource -

`Streaming_AbstractGenerator.StreamAbsGen("DictionaryHistogramPartition", "testlogs/Streaming_SetPartitionAnalytics.EVMS.json")` and any histogram analytics function can be invoked on the stream.

724.5 `electronic_voting_machine()` is invoked 9 times for 2 voting machines, 3 voter id contexts and 3 candidates and `electronic_voting_analytics()` function

which implements the previous JSON persistence is invoked after - logs at testlogs/Streaming\_SetPartitionAnalytics.EVM.log.2November2019  
724.6 Streaming\_AbstractGenerator.py "DictionaryHistogramPartition" \_\_iter\_\_() clause has been updated to do JSON load() of dictionaries instead of AST literal\_eval() and yield the dictionaries as stream.

-----  
725. (THEORY) Drone Electronic Voting Machine, Voting Analytics and Forecasts, Bertrand Ballot Theorem, Money Changing Problem, Set Partitions, Depth-2 Boolean Majority Circuit - 3 November 2019 - related to 657, 666  
-----

-----  
Drone Electronic Voting Machine partial implementation previously is only a majority voting simulation - Voted dictionary hardcoded at present which prevents duplicate voting in Streaming\_SetPartitionAnalytics.py (if publicuniqueid not in Voted:) has to be either in a centralized NoSQL store or localized per drone for global uniqueness so that no voter casts vote in 2 drone EVMs (which is already guaranteed by geographic uniqueness - drone autonomously navigates to an address and authenticates voter smartcard by point-of-voting device - in some aspects this is similar to old tech postoffice protocol and a betterment of postal ballots: Sealed paper mails are delivered uniquely to a name and address which is a public unique id and there is no password. Tampering is easily verifiable if there is damage to courier seal) - Localized Voted dictionary requires voter lists per drone. Clustering of EVM Set partitions by either Earth Mover Distance or other aforementioned distance measures in OpenCV2 classifies EVMs of similar voting patterns in single cluster (non-invasive because histogram depends on per candidate counters alone). This clustering of EVMs corresponds to depth-1 of depth-2 non-boolean Majority Voting Circuit described schematically in 657 and reflects per segment trend. In boolean setting, empirically EVMs might be clustered into 2 disjoint partitions for candidates 0 and 1. It has to be noted that set partition of votes is available only post-poll while prepoll numbers are only total votes - inferring post-poll votes set partition from pre-poll total votes is reducible to function:

$$f(n) = c_1 + c_2 + \dots + c_k \text{ (n votes partitioned to k candidates)}$$
and has probability  $1/p(n,k)$  where  $p(n,k)$  is restricted partition number of  $n$  for  $k$  parts - restricted partition and money changing problem/coin problem are equivalent. Probability of candidate of biggest part ( $c_0$ ) being always ahead in counting by Bertrand Ballot theorem is  $c_0 - c_1 / (c_0 + c_1)$  if  $f(n) = c_0 + c_1$  in boolean majority for candidates 0 and 1.

-----  
726. (THEORY and FEATURE) Drone Electronic Voting Machine - Pseudorandom Majority Voting Balls-Bins Simulation and Voting Analytics - 3 November 2019 - related to 620, 725  
-----

-----  
726.1 electronic\_voting\_machine() function in Streaming\_SetPartitionAnalytics.py has been updated to import random, sklearn packages for histogram analytics.

726.2 evm\_histograms dictionary of EVM dictionaries has been made a list of EVM dictionaries which is dumped to JSON persistence. EVM stream is read from Streaming Abstract Generator - DictionaryHistogram JSON datasource testlogs/Streaming\_SetPartitionAnalytics.EVMs.json and ARI(adjusted rand index), AMI(adjusted mutual information index) and EMD(earth mover distance) histogram distance functions are invoked from sklearn and SciPy for every consecutive pair of EVM histogram set partitions.

726.3 Exceptions for dissimilar or empty histogram shapes in ARI, AMI and EMD have been handled.

726.4 Majority Voting is simulated by a poll loop of 10 voters, 3 unique id contexts, 3 candidates and 3 electronic voting machines - only 3 votes are allowed and others are discarded as "already voted".

726.5 Majority Voting simulation is by python pseudorandom number function random() for randomly choosing candidate to vote for - bounds for the balls and

bins coupon collector problem described in 620 apply.

726.6 These 3 EVMs are analyzed pairwise by `electronic_voting_analytics()` for ARI, AMI and EMD-Wasserstein distance.

726.7 Logs and EVMs JSON for previous simulated election are at `Streaming_SetPartitionAnalytics.EVMs.json` and `Streaming_SetPartitionAnalytics.EVM.log.3November2019`

726.8 `calcEMD2()` is not available on OpenCV2 Python (error: no name found) though recently released OpenCV3 Gold has its C++ counterpart - OpenCV2 histogram comparison function `compareHist()` requires UMat format.

726.9 Streaming Abstract Generator - Dictionary Histogram `__iter__()` clause yields dictionary instead of entries, restoring status quo ante.

-----  
727. (THEORY) Fame-Merit Equilibrium and Converging Markov Random Walk on World Wide Web, Condorcet Jury Theorem, Bipartite Decomposition of World Wide Web, Margulis-Ruzzo Threshold - Conjecture - 12 November 2019 - related to 572 and all sections on Intrinsic Merit, Fame and Majority Voting  
-----

727.1 Page Rank is a converging markov random walk based Fame ranking for World Wide Web and is a peer-to-peer markov chain voting mechanism.

727.2 Fame-Merit Equilibrium mentioned theoretically earlier, is an alternative reputation ranking which tries to find an equilibrium approximation point between absolute intrinsic merit and perceived fame of an entity.

727.3 Both Fame-Merit Equilibrium and PageRank are based on directed graph having weighted edges between perceived and perceiver vertices and thus are two formats of Condorcet Jury Theorem and its derivatives([Black],[KKLadha]) or Margulis-Ruzzo Threshold for boolean majority CJT (Voters or Perceivers err in judging intrinsic merit of the perceived and error probability tilts the group decision either way beyond a threshold) - mistake-minimized infinite voters/jury implies Nash equilibrium is attainable in either variants of reputation rankings - PageRank and Fame-Merit equilibrium are two sides of Condorcet Jury Theorem Coin.

727.4 Fame-Merit equilibrium in the context of algorithmic economics finds Market Clearing Prices for commodities (which are between intrinsic and perceived prices) by Convex Programs and is schematically drawn as bipartite graph of edges between two sets of vertices - Perceivers(Buyers) and Perceived(Items). Every perceiver has a total disposable price merit which has to be apportioned amongst perceived items by the convex program (Eisenberg-Gale, Fischer, Nash Equilibria). Similar equilibria can be found for any Perception-Absolute (Fame-Merit) problem irrespective of entity being judged - Fame is an image possibly distorted while Merit is real.

727.5 PageRank finds ranking of an entity by a converging markov random walk on peer-to-peer world-wide-web weighted directed graph of Perceiver-Perceived (huge graph of few billion vertices)

727.6 Equating PageRank and Fame-Merit equilibrium is of theoretical importance because the two are different mathematical gadgets - convex program and converging markov chain random walk.

727.7 Fame-Merit equilibrium convex program for world wide web should also be a huge bipartite graph of few billion perceivers and perceived on the internet.

727.8 Solutions to Fame-Merit equilibrium convex program strike an approximate midpoint between absolute intrinsic merit and perceived fame.

727.9 Natural question begotten by equating rankings from fame-merit convex program and PageRank markov chain is: Are two rankings equivalent? Answer to this question is conjectured as yes in 727.3 supra. Proof/Disproof of this conjecture might involve equating a generic convex program for a huge bipartite graph of p perceivers and q perceived vertices and PageRank of the same graph of p+q vertices. Or Nash equilibria have to be found for both Fame-Merit and PageRank and checked for equality.

727.10 High Correlation coefficients between the two rankings prima facie might indicate coincidence. Challenge is to conceive the world-wide web as a whole to be a bipartite graph of perceivers-perceived though some components of the internet might be bipartite - this might require algorithms for bipartite

decomposition - world wide web directed graph is decomposed to bipartite subgraph components and fame-merit equilibrium is computed for each bipartisan component.

#### References:

-----  
727.11 Bipartite Decomposition of Random Graphs -  
<http://www.cs.tau.ac.il/~nogaa/PDFS/bipdec2.pdf> - World Wide Web is theoretically modelled as a random graph. Its bipartite decomposition leading to computing fame-merit equilibrium for every bipartite component is stated as conjecture previously vis-a-vis PageRank.  
727.12 Demand-Supply and Market Clearing Prices - Walrasian-Arrow-Debreu, Fisher Markets - [Yishay Mansour] -  
<https://m.tau.ac.il/~mansour/advanced-agt+ml/scribe-10-market-EQ.pdf> - Market Clearing Price Equilibria viz., Eisenberg-Gale apply to a market in which demand equals supply and all products are sold with no remaining demand. But actual scenario mostly is the inequality of demand and supply (Demand-Supply curves - [https://en.wikipedia.org/wiki/Supply\\_and\\_demand](https://en.wikipedia.org/wiki/Supply_and_demand)) defined by equation Demand \* Supply = constant (Demand is inversely proportional to Supply). Demand is also a perception and can be defined as perceived importance or utility of a commodity and thus a function of perception/utility:  
utility = function\_of(demand) or function\_of(1/supply)  
Glut of any entity diminishes perceived importance and dearth increases it.  
Demand-Supply equilibrium can be generalized to any entity -  
text, audio, video, people - merit of which has to be judged e.g rare texts are more valued, rare visuals are more sought after, rare earths are costly.  
727.13 Artificial Intelligence and Economic Theories -  
<https://arxiv.org/pdf/1703.06597.pdf> - Individualized Supply-Demand curves for pricing in ecommerce platforms (Amazon, EBay et al), Granger Causality - one economic time series causes the other with a lag -  
[https://en.wikipedia.org/wiki/Granger\\_causality](https://en.wikipedia.org/wiki/Granger_causality), Pricing - Ricardo labour theory of value - price is proportional to labour went into manufacturing goods and services (Neuro MAC Cryptocurrency, Pricing and Market Equilibrium - <https://github.com/shrinivaasanka/kingcobra64-github-code/blame/master/KingCobraDesignNotes.txt>).

-----  
728. (THEORY and FEATURE) Set Partition to Tile Cover Reduction by Computational Geometric Factorization - Least Squares Approximate Solution  
for the underdetermined linear equations, Exact Money Changing Problem(MCP) Solution, Quadratic Programs, Pell Equation, Shell Turing Machines(Category of Topological Spaces) - related to 577,624,651 - 19 November 2019, 20 November 2019, 6 December 2019, 24 January 2020, 26 January 2020, 27 January 2020  
-----

1.A random set is partitioned by SymPy set partition API and a partition of the set is chosen at random. Random set partition is mapped to a histogram by map(len,) and setpartition\_to\_tilecover() is invoked. New parameter for number to factorize has been added in setpartition\_to\_tilecover().

2.An integer is factorized by Spark Computational Geometric PRAM factorization by subprocess.call() invocation and factors of N=pq are read from JSON persistence.

3.Following underdetermined system of equations is solved approximately by LSMR least squares for finding arrangement of tiles on the periphery of the rectangle and the fractional solution vector is rounded off to 1 or 0 based on a threshold:

```
#c1*x1 + c2*x2 + ... + ck*xk + ... + cn*xn = p
#d1*x1 + d2*x2 + ... + dk*xk + ... + dn*xn = q
#solve AX=B:
#X = [c1 c2 ... cn] - unknowns (boolean include or exclude of a tile)
#A = [[x1 x2 ... xn] - knowns (sides of the square tiles)
permutation_of[x1 x2 ... xn]]
#B = [p q] - factors - pq=N
```

4. Solving underdetermined equations by most libraries including SciPy, NumPy, SymPy etc., yield only approximate solutions because of Rouché-Capelli theorem limitation. In the previous system of equations coefficient matrix A has two rows of square tile sides from Lagrange four square theorem and one of the rows is permuted for randomness (reverse() is invoked) and unknown tile choice vector (d1,d2,...,dn) should also be some permutation of (c1,c2,...,cn).

5. This commit approximately solves the previous underdetermined linear equations by lsqr() function of scipy.sparse.linalg and rounds the real solution vector to binary vector. Mutual exclusion of tiles is by an if-else clause which chooses 1 tiles for side1 and 0 tiles for side2 of rectangle. But product of sum of sides won't be equalling N always because of error allowed in LSQR and rounding. Sophisticated PRAM GEPP implementations might do better at finding the tile arrangement vector (c1,c2,...,cn)

6. logs for this commit are at

testlogs/Streaming\_SetPartitionAnalytics.log.19November2019

7. An example Lagrange's Four Square reduction for integer 18 and its random partition=[4,10,4]:

18  $\Leftrightarrow$  [4,10,4]  $\Leftrightarrow$  [1+1+1+1]+[1+4+4+1]+[1+1+1+1]

18  $\Leftrightarrow$  2\*9  $\Leftrightarrow$  Solutions for previous tile arrangement system of equations for the rectangle periphery: [1+1]\*[2+2+1+1+1+1+1]

8. Each of the two linear equations can be interpreted as instance of Money Changing Problem (MCP) or Coin Problem. Sides of the square tiles are coins and following linear system:

$$c1*x1 + c2*x2 + \dots + ck*xk + \dots + cn*xn = p$$

$$d1*x1 + d2*x2 + \dots + dk*xk + \dots + dn*xn = q$$

equates factors of  $N=(p,q)$  to Linear Sum of sides of Lagrangian square tiles (1-dimensional) for the length and breadth of rectangular periphery. Both of the earlier MCP equations are NP-Hard (Strongly or Weakly depending on encoding) which involves finding the integer vector [c1,c2,c3,...,cn]. Equivalently, tile cover of the rectangle is the linear sum of Lagrangian squares (coins are 2-dimensional Lagrangian tiles themselves) and is a 2-dimensional Money Changing Problem which is again NP-Hard. Product of the equations is a Quadratic Program which is also NP-Hard. Solution vector [c1,c2,c3,...,cn] is the set of number of tiles for each Lagrangian tile square. MCP solves the tile arrangement in exact non-deterministic polynomial time while LSQR least squares is a deterministic polynomial time approximation. An example greedy algorithm for minimum coins change problem is described in GRAFIT course material repository:

[https://github.com/shrinivaasanka/Grafit/blob/master/course\\_material/](https://github.com/shrinivaasanka/Grafit/blob/master/course_material/NeuronRain/AdvancedComputerScienceAndMachineLearning/AdvancedComputerScienceAndMachineLearning.txt)

NeuronRain/AdvancedComputerScienceAndMachineLearning/  
AdvancedComputerScienceAndMachineLearning.txt

9. Lagrangian Four Square reduction of a set partition to sum of squares can be equated to Pell Equation written in terms of factors of  $N=pq$ :

integer or set partition of  $N = pq = n1^2 + n2^2 + n3^2 + \dots + nk^2 = x^2 - y^2 =$  for  $x=(p+q)/2$  and  $y=(p-q)/2$

which in effect shatters or demolishes an one-dimensional set to a set of k 2-dimensional square tiles and equates the sum of squares to difference of two squares.

10. Shell Turing Machines defined in this draft can be formalized by Category Theory: Category S has various topological spaces of arbitrary dimensions as objects and morphisms are Conduit Turing Machines amongst these object spaces which act as linear transformations between one space to the other. Lagrangian set partition to tile cover reduction is an instance of such a Category of Topological Spaces (TOP) - For objects S1 and S2 in S, set partition defined in an one dimensional space S1 is lifted to a 2 dimensional space of square tiles S2 by Lagrange Four Square Conduit Turing Machine Morphism between object spaces S1 and S2. Application of Shell Turing Machines to previous reduction is unusual (NeuronRain Documentation, FAQ and Licensing: <http://neuronrain-documentation.readthedocs.io/en/latest/> mentions some references on TOP). Thus Shell Turing Machines (Category of Topological Spaces) perform a kind of kernel lifting - Lagrangian Tiling Conduit Turing Machines are the kernels

11. Nomenclature "Shell Turing Machines" is thus a universal mathematical abstraction which connects vector space embedding of alphabets and states transitions of Turing Machine and transformation of truth values of logical statements between spaces in many fields of STEM:

11.1 Hilbert Space Quantum Computation Machines - States and Alphabets of Quantum Turing Machine are embedded in a Hilbert Space (Section 624)

11.2 Linear Machines of Category theory - [Eilenberg-MacLane] - Categories (Objects, Morphisms, Functors) are embedded in a vector space (Conceptual graph of NeuronRain theory drafts - <http://neuronrain-documentation.readthedocs.io/en/latest/>)

11.3 Kernel Lifting in Support Vector Machines - dataset in smaller dimensional space  $S_1$  is lifted to a higher dimensional space  $S_2$  by a kernel (e.g Mercer polynomial kernel - [https://github.com/shrinivaasanka/Grafit/blob/master/course\\_material/ComputerScienceMiscellaneous/ComputerScienceMiscellaneous\\_CourseNotes.txt](https://github.com/shrinivaasanka/Grafit/blob/master/course_material/ComputerScienceMiscellaneous/ComputerScienceMiscellaneous_CourseNotes.txt)) and decision hyperplane classifier is found in  $S_2$

11.4 Set Partition to Lagrange Tile Cover reduction - lifts an one dimensional set partition to a 2 dimensional square tile cover of a rectangle by Lagrange Four Square Theorem (sides of rectangle are found by Computational Geometric Factorization)

11.5 Word Embedding of datasets in Machine Learning

11.6 Reproducing Kernel Hilbert Space (RKHS) - functions (Turing machines) are embedded on a metric space and distance is defined between functions (Section 624).

11.7 Category of Topological Spaces - TOP - abstracts all the previous embeddings and lifting by defining topological spaces (e.g datasets embedded on vector space) as objects of category and morphisms amongst them. Morphisms between topological spaces are Conduit Turing Machines formalized by any of the previous computation models which lift data and truth values of logical statements between spaces - Linear Machines, RKHS, linear transformations, kernels, Lagrange's four squares theorem, Word embedding. Examples:

11.7.1 TOP category  $T$  has two space objects  $S_1$  and  $S_2$ . Conduit Turing Machine morphisms are defined between  $S_1$  and  $S_2$ . Logical statement Biggest() which finds maximum of points in a topological space thus has two truth values in  $S_1$  and  $S_2$  - Biggest( $S_1$ ) and Biggest( $S_2$ ) - which might have to be teleported between spaces.

11.7.2 Another Good software engineering example of such lifting is the Unix Shell Category where object shells are arbitrarily created and environment variables are privy to a shell object unless otherwise communicated explicitly by EXPORT which acts as a Conduit Turing Machine Morphism between object shells. Outermost shell is the Root and a tree hierarchy of recursively created subshells forms a nested category of shell objects -  $S_1$  and  $S_2$  are two shell objects in this Shell Category theoretically embedded in some topological space, and EXPORT morphism EXPORT:  $S_1 \Leftrightarrow S_2$  is a Conduit Turing Machine which exports environment variables of  $S_1$  embedded in space  $X$  and  $S_2$  embedded in space  $Y$  bijectively between  $S_1$  and  $S_2$  except Outermost shell which is unidirectional (because nothing needs to be lifted out of outermost shell but only to subshells). Cutting across operating systems, such a Shell mechanism and EXPORT morphism has been universally implemented not just limited to Unix - any computation in STEM (Science-Technology-Engineering-Mathematics) is on some OS which has shell TOP category implementation.

11.7.3 Shell Turing Machines Category of Topological Spaces can be formulated as a space filling problem - Category of hierarchically nested topological space shells are embedded in and cover the outermost  $n$ -dimensional Shell topological space (Outermost  $n$ -sphere) and EXPORT morphisms are defined amongst these shell spaces. For 3-dimensions, this is akin to filling an Outermost spherical bubble container shell by smaller nested spherical shell bubbles which is a 3-dimensional variant of Apollonian Gasket.

11.8 Turing Degree is the equivalence class of Turing machines solving sets of similar difficulty. Turing Jump  $A'$  of  $A$  is the set of Turing machines which halt having oracle access to  $A$  or set of problems harder than  $A$ . Previous Conduit Turing Machine morphisms in TOP abstraction define a Turing Jump between topological spaces of different Turing degree difficulties e.g Conduit Turing Machine Morphism might have an oracle access to a Turing machine defined in a domain topological space of lower Turing Degree lifting to a range topological space of higher Turing Degree. Every computation in STEM can be abstracted as Category of Topological Spaces and Turing Degree Hierarchy can be defined on them e.g Computational Physics problems in Relativity, Quantum mechanics and

String theory involving theoretical abstractions for microcosm and macrocosm.

#### References:

728.1 Coin Problem, Frobenius Problem, Postage Stamp Problem - What This Country Needs is an 18c Piece - <https://cs.uwaterloo.ca/~shallit/Papers/change2.pdf>

729. (THEORY and FEATURE) Drone Electronic Voting Machine - Streaming Boyer-Moore Majority voting - 27 November 2019

- 1.This commit updates already existing streaming majority implementation of Boyer-Moore algorithm to accept arbitrary datasources (majority\_voting() in Streaming\_BoyerMoore\_MajorityVoting.py)
- 2.Drone electronic voting machine JSON persistence datastorage written by Streaming SetPartitionAnalytics electronic\_voting\_analytics() function (Streaming\_SetPartitionAnalytics.py) is passed on to Boyer-Moore function as DictionaryHistogramPartition datasource.
- 3.Persisted EVMS are looped through and majority candidate bucket per EVM is printed.

730. (THEORY and FEATURE) Drone Electronic Voting Machine - Streaming Voting Analytics - Bertrand Ballot Theorem - Approximation of Majority Voting, Streaming majority, Forecasts, Theoretical EVMS, Set Partitions - related to 666 - 28 November 2019

- 1.This commit implements the Betrand Ballot Theorem - probability  $p-q/p+q$  that one of the candidate might win of two rival candidates getting  $p$  and  $q$  votes respectively during the process of counting - as a live election analytics measure within electronic\_voting\_machine() function of Streaming\_SetPartitionAnalytics.py
- 2.It assumes live counting of voting - votes are immediately counted after they are cast - is allowed as against deferred counting convention usually followed in elections because secrecy might be compromised.
- 3.But this measure is also useful for post-poll analytics during the process of counting itself for extrapolating the result - before election is called.
- 4.Random Majority voting is simulated on 3 fictitious candidates and probabilistic trend is printed while voting is underway.
- 5.logs are at testlogs/Streaming\_SetPartitionAnalytics.EVM.log.28November2019
- 6.This measure applies only to binary election of 2 candidates - EVM dictionary is sorted and votes of top 2 rivals are compared dynamically (after each vote is cast), to print the Bertrand probability.

731. (FEATURE) Astronomical Pattern Mining - Rule Search Script update for Maitreya Swiss Ephemeris text client maitreya8t - 4 December 2019

- 1.python-src/MaitreyaEnchHoro\_RuleSearch.py has been changed for updated chart summary table of maitreya swiss ephemeris text client which truncates the names of signs and planets to first 3 alphabets.
- 2.New function prune\_rule() has been defined to prune the class association rules to be matched from python-src/MinedClassAssociationRules.txt(which contains already learnt rules from SequenceMining.py for various weather datasets)
- 3.SearchOption=2 has been updated for redefined signs-planets defaultdict to populate truncated names.
- 4.Encoded chart concatenation has been changed for lookup of truncated names



5.Maitreya Text Client commandline has been changed to 64-bit deb package  
install /usr/bin/maitreya8t - text client is not built from Maitreya Dreams  
source.

6.An example celestial 2-body pattern "Mercury,Jupiter" is searched on  
26/12/2019 when a rare 7 planet conjunction of  
Sun,Moon,Mercury,Jupiter,Saturn,Nodal Points,Pluto (8 planets including nodal  
axis) occurs. This 7+1 body planetary system in Sagittarius-Gemini is  
significant in the context of heightened correlation of weather events that  
might befall (seismic,oceanic and atmospheric).

7.logs for class association rule match are in  
python-src/testlogs/MaitreyaEncHoro\_RuleSearch.maitreya8t.log.4December2019

-----  
732. (FEATURE and THEORY) Merit of Large Scale Visuals - Tensor Rank intrinsic  
merit of EventNet of a video - 7 December 2019 - related to 588  
-----

1.This commit upgrades ImageGraph\_Keras\_Theano.py to Python 3.6 from Python 2.7  
and computes Tensor Rank of EventNet of a video by tensorly python library  
(tensorly requires Python 3) - autopep8 and 2to3 tools have been used for  
upgrade. Python 3.6 is many orders of magnitude faster than Python 2.7 and  
EventNet Tensor Product and Tensor Rank is computationally intensive which needs  
faster Python.

2.Following dependent files have been upgraded to Python 3.6 by two tools -  
autopep8 and 2to3 - which correct formatting issues to comply with PEP8 and  
convert a file written in python 2.7 to python 3.6 (Python 2.7 versions have  
been committed having .2.7 suffix):

- 2.1 RecursiveGlossOverlap\_Classifier.py
- 2.2 WordNetPath.py
- 2.3 ImageGraph\_Keras\_Theano.py

3.Note: all python 2.7 source files in NeuronRain can be upgraded to Python 3.6  
in two simple steps for better performance:

- 3.1 Execute autopep8 on the file for PEP8
- 3.2 Execute 2to3-2.7 on PEP8 formatted file

4.ImageGraph\_Keras\_Theano.py - videograph\_eventnet\_tensor\_product() has been  
modified for preprocessing (slicing 100\*100 square) the tensor product of video  
EventNet and tensorly non\_negative\_parafac() is invoked which decomposes the  
video EventNet tensor.

5.logs have been committed to

testlogs/ImageGraph\_Keras\_Theano.log.TensorRank1Decomposition.7December2019

6.Video EventNet Tensor is printed for debug purposes

7.Rank-1 tensor factors from non\_negative\_parafac() of Video EventNet Tensor are  
also printed

-----  
733. (FEATURE and THEORY) Computational Geometric Factorization - Quadcore  
Python 3.6 Upgrade Benchmarks - 11 December 2019 - related to all  
sections of Factorization  
-----

1.This commit upgrades Spark Python Computational Geometric Factorization  
implementation DiscreteHyperbolicFactorizationUpperbound\_TileSearch\_Optimized.py  
from Python 2.7 to Python 3.6 for performance and availing the better range()  
utility in Python 3.x which breaches the maximum range barrier limitation in  
Python 2.7. Python 3.6 range() is a rewrite and supports huge integers (of  
hundreds of digits).

2.Following Spark Python environment variables have been set to Python 3.6m  
binary for PySpark upgrade to Python 3.6:

- SPARK\_PYTHON=/usr/bin/python3.6m
- SPARK\_DRIVER\_PYTHON=/usr/bin/python3.6m

3.Large Integer 999999999999999999 (60 bits) has been factorized which is by far  
the largest integer factorized in Spark BSP-NC-PRAM model. Larger integers throw

a Spark Python error in PySpark context.py (File "spark-2.4.3-bin-hadoop2.7/python/lib/pyspark.zip/pyspark/context.py", line 501, in parallelize, OverflowError: Python int too large to convert to C ssize\_t):

```
 if isinstance(c, xrange):
 size = len(c)
```

because of len() failure for larger integers

[  
Error can also be produced from commandline:

```
>>> x=range(9999999999999999999)
```

```
>>> len(x)
```

Traceback (most recent call last):

File "<stdin>", line 1, in <module>

OverflowError: Python int too large to convert to C ssize\_t

```
>>> x=range(9999999999999999999)
```

```
>>> len(x)
```

```
9999999999999999999
```

```
]
```

4.Previous error requires Spark rewrite of context.py parallelize() to:

```
 range().stop - range().start
```

replacing len() specific to Python 3.x range())

5.Python 2.7 Spark Factorization implementation has been upgraded to Python 3.6 by autopep8 followed by 2to3-2.7 utilities. Python 2.7 version has been marked as DiscreteHyperbolicFactorizationUpperbound\_TileSearch\_Optimized.py.2.7

6.Spark Python version is printed by sys.version:

```
Spark Python version: 3.6.8 (default, Oct 7 2019, 12:59:55)
```

```
[GCC 8.3.0]
```

7.First few factors of 9999999999999999999 are printed to

testlogs/DiscreteHyperbolicFactorizationUpperbound\_TileSearch\_Optimized.Python3.

6Upgrade.11December2019. Timestamp of each factor is printed.

8.Ray shooting queries excluding Hardy-Ramanujan and some imports have been commented.

-----  
734. (FEATURE) Merit of Large Scale Visuals - Video EventNet Tensor

Decomposition to Rank-1 Tensors on Python 3.7.5 - slicing - 12 December 2019  
-----

1.ImageNet\_Keras\_Theano.py videograph\_eventnet\_tensor\_product() has been changed to accept side of square slice per frame as an argument which is by default 100\*100 pixels.

2.Square slicing per frame is necessary when elements of video tensor product matrix are of unequal rectangular dimensions and tensorly stipulates equal dimensions.

3.Usual videos have frames of equal dimensions but the example montage video footage in NeuronRain has unequal frame sizes and minimum frame sides have to be found which are then used to slice each frame.

4.Since a video can have arbitrarily large number of frames in millions, finding the minimum sides of the frame rectangles could be daunting.

5.Instead of finding minimum frame sides, square slicing has been made default and configurable by user in function argument "squareslice" which is by default 100.

6.Python 3.6.8 for TensorLy has been upgraded to Python 3.7.5 which is the fastest python distribution.

-----  
735. (THEORY and FEATURE) Complement Diophantines - Least Squares Vandermonde Polynomial Fit Learning - related to all sections on  
Complement Diophantines - Python 3.7.5 upgrade - 14 December 2019  
-----

1. complement.py complement diophantine learner has been updated to learn a degree 5 interpolated polynomial for a complementary set (non-squares)

2. `polyfit()` from numeric python has been invoked on a complementary set of non-squares  
<https://docs.scipy.org/doc/numpy/reference/generated/numpy.polyfit.html>) which is a least squares solution solver for Vandermonde coefficient matrix

3. `polyfit()` least square interpolation is an alternative to Lagrangian polynomial interpolation ([https://en.wikipedia.org/wiki/Lagrange\\_polynomial](https://en.wikipedia.org/wiki/Lagrange_polynomial)) mentioned in arXiv version (<https://arxiv.org/abs/1106.4102v1>, <https://scholar.google.com/citations?user=eLZY7CIAAAAJ&hl=en>).

4. `complement.py` has been upgraded to Python 3.7.5 from Python 2.7 by `autopep8` and `2to3` utilities. Python 2.7 version has been suffixed as `.2.7`

5. `polyfit()` least square interpolation is guaranteed to be unique - [https://en.wikipedia.org/wiki/Polynomial\\_interpolation](https://en.wikipedia.org/wiki/Polynomial_interpolation)

6. logs for `polyfit()` are committed to `testlogs/complement.PolyFitPython3.7.5.14December2019`

7. Least Squares and Lagrangian interpolations are total functions while Lagrange Four Square Theorem `complement` map is a partial function (not all domain tuples are mapped to a point in complementary set)

-----  
 736. (THEORY and FEATURE) Computational Geometric PRAM-NC-BSP Factorization - Python 3.7.5 upgrade - Spark Quadcore benchmarks - 512 bit integer - related to 477,481 and all other sections on Factorization - 18 December 2019  
 -----

-----  
 1. Computational Geometric Factorization Python-Spark implementation has been upgraded to Python 3.7.5 and following local tile search algorithm mentioned in 477 and 481 has been implemented which obviates parallel sorting and completely removes the maximum integer barrier altogether:

```
while(iterations <= O((logN)^k))
{
 *) Assign N/(logN)^k tiles to N/(logN)^k PRAMs in parallel (O(1) parallel time because each interval tile in a global shared memory array can be accessed by PRAM id as index)
 *) Binary Search tile in each PRAM for factors (O(logN) parallel time which can be reduced to O(logN/logp) by parallel binary search from Snir's Theorem)
}
```

2. Number of PRAMs (multicores) is 4 and constant  $k$  in  $(\log N)^k$  has been set to 50 which, though not commensurate, is hardcoded for demonstrative reasons. Previous algorithm is work optimal NC because  $\text{PRAM time} * \text{iterations} = \text{Sequential time}$

3. `Spark context parallelize()` has been refactored to following loop which circumvents the `Spark context ssize_t exception` in `pyspark context.py`  
`parallelize()` - maximum value of `len()` is limited to 64 bits per slice by suitable choice of exponent  $k$ :

```
normal_order_n = int(math.pow(math.log(n, 2), 50))
tiles_start = 1
tiles_end = int(n/normal_order_n)
for x in range(normal_order_n):
 print("tiles_start:", tiles_start)
 print("tiles_end:", tiles_end)
 tiles = range(tiles_start, tiles_end)
 print(("len(tiles):", len(tiles)))
 spcon.parallelize(tiles).foreach(
 tilesearch_nonpersistent)
 tiles_start = tiles_end
 tiles_end += int(n/normal_order_n)
```

Previous loop of  $(\log N)^k$  iterations slices the Python 3.7.5 `range()` into multiples of  $N/(\log N)^k$  and individually parallelizes each slice to RDDs.

4. Because Python 3.7.5 `range()` is unlimited, maximum number factorizable is arbitrary for all practical purposes - previous benchmark for 60 bits has been



```

('Factor is = ', 8349, '(at ', 'Wed, 18 Dec 2019 05:28:48 GMT', '))')
=====
('Factor is = ', 13947, '(at ', 'Wed, 18 Dec 2019 05:29:02 GMT', '))')
=====
('Factor is = ', 16491, '(at ', 'Wed, 18 Dec 2019 05:29:09 GMT', '))')
=====
('Factor is = ', 21649, '(at ', 'Wed, 18 Dec 2019 05:29:22 GMT', '))')
=====
('Factor is = ', 23661, '(at ', 'Wed, 18 Dec 2019 05:29:28 GMT', '))')
=====
[...truncated...]

```

737. (THEORY and FEATURE) Spark NC-PRAM-BSP Computational Geometric Factorization quadcore Python 3.7.5 benchmarks - 1000+ bits non-smooth random integer of mixed digits - 22 December 2019 - related to all sections on Computational Geometric Factorization

1. DiscreteHyperbolicFactorizationUpperbound\_TileSearch\_Optimized.py has been changed to increase k to 100 which factorizes a difficult 1000 bits integer of mixed digits (low omega and less number of prime factors) which is by far the largest integer factorized in NeuronRain -  
993209302039093029039092093023090293090290392038198218928912172881728717287187281728172871872817287187281787281731836176379390293091128821894348898938982931129829189987676767675656565454553437878787876767566565645454534434333878738728738278372243439848343884384983984989483849839483984983984983984977 - in  $O((\log N)^{100})$  Parallel RAM time requiring  $O(N/(\log N)^{100})$  PRAM processors - first few factors are printed below within 20 seconds and 73 seconds respectively which includes Spark-Python-Py4j-Java 8 bidirectional marshalling and VM bytecode interpretation overhead (Cythonized C++ DLL version might be still faster):

```

spark-submit DiscreteHyperbolicFactorizationUpperbound_TileSearch_Optimized.py
993209302039093029039092093023090293090290392038198218928912172881728717287187281728172871872817287187281787281731836176379390293091128821894348898938982931129829189987676767675656565454553437878787876767566565645454534434333878738728738278372243439848343884384983984989483849839483984983984983984977
19/12/22 13:10:08 WARN Utils: Set SPARK_LOCAL_IP if you need to bind to another address
19/12/22 13:10:09 WARN NativeCodeLoader: Unable to load native-hadoop library for your platform... using builtin-java classes where applicable
('Spark Python version:', '3.7.5 (default, Nov 7 2019, 10:50:52) \n[GCC 8.3.0]')
('factors of ',
993209302039093029039092093023090293090290392038198218928912172881728717287187281728172871872817287187281787281731836176379390293091128821894348898938982931129829189987676767675656565454553437878787876767566565645454534434333878738728738278372243439848343884384983984989483849839483984983984983984977, '(',
1003.212454334434, ' bits integer) are:')
=====
('Factor is = ', 249, '(at ', 'Sun, 22 Dec 2019 07:40:29 GMT', '))')
=====
('Factor is = ', 4731, '(at ', 'Sun, 22 Dec 2019 07:41:22 GMT', '))')
=====
[...truncated...]

```

2. Previous complexity bounds imply  $O(1000^{100})$  parallel time units (polylog

depth) and  $O(2^{1000}/1000^{100})$  processors  $\sim O(2^{1000}/2^{997}) = O(8)$  PRAMS (multicores) which is a meagre NC parallelism required for factorizing such a huge number - seemingly prohibitive  $O(N/(\log N)^k)$  PRAMS in definition of NC might not be a roadblock after all.

3. Recursion limit has been increased to 3000 because of stack overflow in recursive binary search and ray shooting queries have been commented.

4. Spark factorization logs (truncated) have been uploaded at `testlogs/DiscreteHyperbolicFactorizationUpperbound_TileSearch_Optimized.Python3.7.5Upgrade.1000bits.22December2019`

5. Change in the constant  $k$  depending on the input simulates non-uniform NC circuit for factorization theoretically (family of circuits depending on input)

#### References:

737.6. Input Size and PRAMS -  $n$  and  $N$  defined - Geomblog - [Suresh Venkatasubramanian] - <http://blog.geomblog.org/2008/05/p-vs-nc-part-i-preliminaries.html>:  
 "...It will be important to pay attention to input size. As always, the input size can either be described by  $n$ , the cardinality of the input (the quantity counting the number of "things"), or by  $N$ , the bitsize (the quantity measuring the number of bits needed to write everything down). When we talk about polylogarithmic time and polynomial number of processors, unless specified otherwise, we will be referring to polynomials of  $n$  AND  $N$ . In the non-uniform setting, we'll assume that we're presented with a PRAM that for fixed  $n, N$ , runs in time  $t(n, N)$  with  $p(n, N)$  processors...." - In Computational Geometric Factorization NC definition,  $O((\log X)^k)$  is a polynomial  $t(N)$  and  $O(X/(\log X)^k)$  PRAMS is a polynomial  $p(n, N)$  where  $N = \log X$  and  $n = X$ .

737.7 Definition of PRAM - Definition 2.2.1 - [RAYMOND GREENLAW, H. JAMES HOOVER, WALTER L. RUZZO - OXFORD UNIVERSITY PRESS 1995] - <https://homes.cs.washington.edu/~ruzzo/papers/limits.pdf>

737.8 Poster: Easy PRAM-based High-performance Parallel Programming with ICE - [Ghanim-Rajeev-Vishkin] - [https://www.researchgate.net/publication/310824244\\_POSTER\\_Easy\\_PRAM-based\\_High-Performance\\_Parallel\\_Programming\\_with\\_ICE](https://www.researchgate.net/publication/310824244_POSTER_Easy_PRAM-based_High-Performance_Parallel_Programming_with_ICE) - input size to Pointer jumping algorithm

738. (THEORY and FEATURE) Computational Geometric NC-PRAM-BSP Factorization - Python 3.7.5 Single node cluster quadcore benchmarks - 1067 bits integer - some factcheck references on NC-PRAM equivalence and input size - 24 December 2019, 31 December 2019, 2 January 2020 - related to all sections on Factorization

1. In continuation of previous benchmarks on 1000 bits integer another hard non-smooth random 1067 bits integer of randomly mixed digits -  
 93948384983949343848398948938498394893884398498398498398493894834893849938492883  
 09283802893892839829839283982497483784783787384787387487298392893892893829839829  
 83928938298398298328938298398239274873874873874928338298938298392893298392893829  
 83928938298392839829839283928938298392874873875837483748373748134938483349938497  
 9 - has been factorized on single node cluster of quadcores and first few factors - mostly primes - are printed from 18th second onwards:

```
=====
('Factor is = ', 11, '(at ', 'Tue, 24 Dec 2019 08:21:47 GMT', ')')
=====
('Factor is = ', 17, '(at ', 'Tue, 24 Dec 2019 08:21:47 GMT', ')')
=====
('Factor is = ', 47, '(at ', 'Tue, 24 Dec 2019 08:21:49 GMT', ')')
=====
('Factor is = ', 51, '(at ', 'Tue, 24 Dec 2019 08:21:49 GMT', ')')
=====
```

```

=====
('Factor is = ', 141, '(at ', 'Tue, 24 Dec 2019 08:21:53 GMT', ')')
=====
('Factor is = ', 187, '(at ', 'Tue, 24 Dec 2019 08:21:55 GMT', ')')
=====
('Factor is = ', 289, '(at ', 'Tue, 24 Dec 2019 08:22:00 GMT', ')')
=====
('Factor is = ', 311, '(at ', 'Tue, 24 Dec 2019 08:22:01 GMT', ')')
=====
('Factor is = ', 517, '(at ', 'Tue, 24 Dec 2019 08:22:11 GMT', ')')
=====
('Factor is = ', 561, '(at ', 'Tue, 24 Dec 2019 08:22:13 GMT', ')')
=====
('Factor is = ', 799, '(at ', 'Tue, 24 Dec 2019 08:22:24 GMT', ')')
=====
('Factor is = ', 867, '(at ', 'Tue, 24 Dec 2019 08:22:27 GMT', ')')
=====
('Factor is = ', 3179, '(at ', 'Tue, 24 Dec 2019 08:24:16 GMT', ')')
=====
('Factor is = ', 3421, '(at ', 'Tue, 24 Dec 2019 08:24:27 GMT', ')')
=====
('Factor is = ', 5287, '(at ', 'Tue, 24 Dec 2019 08:25:54 GMT', ')')
=====
('Factor is = ', 8789, '(at ', 'Tue, 24 Dec 2019 08:28:37 GMT', ')')
=====
('Factor is = ', 9537, '(at ', 'Tue, 24 Dec 2019 08:29:12 GMT', ')')
=====
('Factor is = ', 10263, '(at ', 'Tue, 24 Dec 2019 08:29:46 GMT', ')')
=====
('Factor is = ', 13583, '(at ', 'Tue, 24 Dec 2019 08:32:20 GMT', ')')
=====

```

[....truncated....]

2.float() cast has been changed to Decimal() for highest precision and remove overflow errors for tile segments and interval midpoint computations

3.Recursion limit has been increased to 10000

4.Exponentiation by math.pow() for normal order computation in local search optimization has been replaced by faster \*\* exponentiation operator of Python.

5.Exponent k in local search loop -  $(\log N)^k$  (iterations) \*  $N/(\log N)^k$  (PRAMs) - has been parametrized in SearchTiles\_and\_Factorize() function which simulates non-uniform NC circuit of  $(\log N)^k$  depth and  $N/(\log N)^k$  circuit elements.

Optimization:

-----

Finding all factors by searching through every rasterized tile segment for hyperbola  $xy=N$  could be optimized by stopping after first factor p is found and re-rasterizing a new hyperbolic arc for  $xy=N/p$ . Following loop formalizes it (reduction in cost might depend on which is easier - parallel planar point location or rasterization - this optimization creates an array of hyperbolic arcs equal to number of factors):

```

 for_all_factors_of_N

```

```

{
 Rasterize hyperbola xy=N
 PRAM-BSP-NC Planar Point locate and Search the rasterized hyperbolic
planar straight line graph till first factor p is found
 N=N/p
}

```

Previous loop is of approximate total parallel RAM time (excluding parallel rasterization which is increasingly easier after each iteration churning out a factor):

$O((\log p_1)^k) + O((\log N/p_1)^k) + O((\log N/[p_1 p_2])^k) + \dots + O((\log N/[p_1 p_2 \dots p_n])^k)$  for first  $n$  factors of  $N=\{p_1, p_2, \dots, p_n\}$

#### References:

-----

738.6 Sorting, Searching, Merging - [Joseph JaJa] - <https://people.ksp.sk/~ppershing/data/skola/JaJa.pdf> - Chapter 4 - Pages 159-160 - Algorithm 4.3 - Simple Merge Sort - "... input: an array  $X$  of order  $n$  where  $n=2^l$  ...", Corollary 4.2 - CREW PRAM model - "... Sorting a sequence of  $n$  elements can optimally be done in  $O(\log n \cdot \log \log n)$  ... " - previous local search does away with parallel sorting

738.7 PARALLEL TRANSITIVE CLOSURE AND POINT LOCATION IN PLANAR STRUCTURES - [ROBERTO TAMASSIA AND JEFFREY S. VITTER] - <http://www.ittc.ku.edu/~jsv/Papers/TaV91.transclosure.pdf> - "... Abstract. Parallel algorithms for several graph and geometric problems are presented, including transitive closure and topological sorting in planar st-graphs, preprocessing planar subdivisions for point location queries, and construction of visibility representations and drawings of planar graphs. Most of these algorithms achieve optimal  $O(\log n)$  running time using  $n/\log n$  processors in the EREW PRAM model,  $n$  being the number of vertices...." - number of processors required by this planar point location algorithm is  $\text{poly}(n, \log n)$  and time is  $\text{poly}(\log n)$  by reference 737.6 and ANSV problem for mergesort in reference 34.15 - all PRAM models are mutually reducible to other - previous local search planar point location factorization requires  $O((\log N)^k)$  parallel time and  $N/(\log N)^k$  PRAM processors and thus work optimal - number of vertices in rasterized hyperbolic arc bow planar simple line graph is approximately  $3 \cdot N + 1$  if every juxtaposed tile segment is construed as a rectangular polygon face of dimensions  $1 \cdot \text{segment\_length}$ ; polygon arithmetic progression segment located in polylog time is binary searched.

738.8 An accurate algorithm for rasterizing algebraic curves - [Gabriel Taubin - IBM Watson Research Centre] - <http://citeseerx.ist.psu.edu/viewdoc/download?doi=10.1.1.72.9588&rep=rep1&type=pdf> - Rasterization defined - "... By rasterizing an algebraic curve we mean to determine which cells, or pixels, from a square mesh of cells in the plane, are cut by a curve represented as the set of zeros of a polynomial in two variables. By using a recursive space subdivision scheme, the problem is reduced to testing whether the curve cuts a square or not ..." - rasterizing hyperbola which is polynomial in two variables thus is the problem of collating the pixel squares on 2-D grid cut by hyperbola to axis parallel pixel-array polygons.

738.9 Multidimensional planar point location and rasterized point location - <https://pure.tue.nl/ws/portalfiles/portal/4238920/373169.pdf> - [Two and Three-Dimensional Point Location in Rectangular Subdivisions - Mark de Berg, Marc van Kreveld, Jack Snoeyink] - "... We give a new type of stratified tree that emphasizes a tradeoff between space and query time. In two dimensions, we can preserve Muller's  $O((\log \log U)^2)$  query time using only  $O(n \log \log U)$  space or reduce space to linear and increase the query time to  $O((\log U)^{1/h})$  for any constant  $h$ . ..."

738.10 Bulk Synchronous Parallel (BSP) and Coarse Grained Multicomputer Planar Point Location - [Frank Dehne, Wolfgang Dittrich, David Hutchinson, and Anil Maheshwari] - [http://www.sce.carleton.ca/~hutchins/papers/DDHM02\\_Bulk.pdf](http://www.sce.carleton.ca/~hutchins/papers/DDHM02_Bulk.pdf) - "... . The PRAM assumption of a large shared random access memory with uniform cost access to every cell by each processor has the advantage of simplicity but has also prompted alternative proposals intended to be more representative of practical machines. These include the Bulk Synchronous Parallel (BSP) model of



Valiant [45], the Coarse-Grained Multicomputer (CGM) of Dehne et al. [22], the LogP model of Culler et al. [19], and the Extended BSP (BSP\*) model of Baumker et al. [10]...."

738.11 Rasterized point location - H. Müller. Rasterized point location. In Proceedings Workshop on Graph theoretic Concepts in Computer Science, 1985 pages 281-293. Trauner Verlag, Linz, Austria

738.12 Entropy based Planar Point Location Query Complexity - [Sunil Arya, Malamatos, Mount] - <https://www.cs.umd.edu/~mount/Papers/ptloc-rand.pdf>

738.13 Fast Queries in Planar Point Location - [Goodrich-Orletsy-RamaIyer] - <http://www.cs.jhu.edu/~goodrich/cgc/pubs/adaptive.ps.gz>

738.14 Rasterization in Graphics - approximating curves by line segments - Bresenham rasterization - illustrations -

<http://www.cs.cornell.edu/courses/cs4620/2013fa/lectures/09rasterization.pdf>

738.15 Dynamic Parallel Planar Point Location and extensions to higher dimensions - [Ketan Mulmuley-Sandeep Sen] -

<https://link.springer.com/content/pdf/10.1007/BF02293052.pdf> - Theorem 7 -

"...The dynamic point-location data structure for an arrangement of lines can be updated in  $O(\log n)$  time on a CRCW PRAM model using  $n$  processors. The query time is  $O(\log n)$  and the space complexity is  $O(n^2)$ . ..." - Drafts on Computational Geometric factorization by planar point location discuss only static parallel planar point location which assume hyperbola has been fully rasterized before location - rasterization creates an axis parallel line arrangement. Optimization could be to lazy-rasterize hyperbolic arc segments on demand and dynamically query the factor points on CRCW PRAM.

738.16 Zone Theorem and Ray shooting queries for approximate factors intersecting rasterized hyperbolic segment arrangement -

<http://homepages.math.uic.edu/~jan/mcs481/zonetheorem.pdf> - Set of faces in an arrangement of lines intersecting a query ray is a Zone of ray query. Zone complexity is the sum of number of vertices, edges and faces in zone of a query ray. Zone theorem states that Zone complexity of an arrangement of  $m$  lines and a query ray is  $O(m)$ . Hyperbolic rasterization produces an arrangement of  $O(N)$  lines. But yet because of being axis parallel, every ray shooting query from origin  $(0,0)$  intersects only 3 faces of the rasterized arrangement at most (above, pixel array rectangle, below) and thus zone complexity of ray shooting is a constant 3.

738.17 Approximate Factors and Local search for exact factor point location -

[https://en.wikipedia.org/wiki/Local\\_search\\_\(optimization\)](https://en.wikipedia.org/wiki/Local_search_(optimization)) - Approximate factors found by number theoretic results are in close proximity to exact factors. Local search optimization finds exact solution to an optimization problem from candidate solutions and iteratively refines. Finding exact factors from approximate factors could be formulated as local search problem e.g Approximate factor  $ax$  for an integer  $N$  could be refined by incrementing (decrementing) along  $x$ -axis - a kind of hill-climbing on hyperbolic arc. Local search algorithms could have arbitrary, user-defined runtimes.

-----  
739. (THEORY and FEATURE) Intrinsic Merit - Unique Identification and its necessity in People Analytics (Drone Electronic Voting Machines), Online Citizen Science, Sports Analytics and Academic Rankings, BKS Conjecture, Consensus versus Majority - 29 December 2019, 2 January 2020 - related to 730  
-----

-----  
(\*) Drone Electronic Voting Machine on GPS navigation to a voter's residence optionally can have an one time password multifactor authentication before voting. Traditional OTPs are electronic prone to sabotage. Alternatively a non-digital OTP authentication is envisaged e.g serial number of a currency bill (only one voter in nation at any point in time can possess a note having a unique serial number if there are negligible counterfeits). Drone EVM reads the unique serial number in note by OCR before voting. Encrypted vote to a candidate salted with

encrypted OCR-ed serial number of the currency is appended to voted candidate's bucket. Voter can have multiple non-digital currencies (multiple serial number unique ids) which are chosen at random by voter for OCR. Currencies are

anonymous and unpredictably flow in economic networks which further randomizes the non-digital OTPs (high entropy randomness extractor source).

(\*) QR codes are unique id(s) - two dimensional quick response bar codes

(\*) NeuronRain KingCobra implements a protocol buffer cryptocurrency which is serial numbered by Boost Universally Unique Identifier(based on Perfect Forward copyless move idiom of C++ - has parallels to Cloud Object move in Google Clouds - more on this in <http://neuronrain-documentation.readthedocs.io/en/latest/>).

Exchequer in some countries is RFID tagged for tracking money trail and similar reasoning might apply for voter uniqueness - RFID tagged currency authentication at drone EVM.

(\*) Genetic Haplogroups of populace have specific cluster of traits across ethnic groups which might be occasionally necessary to establish uniqueness (e.g India has prominence of R1a1a... haplogroup -

<https://www.ncbi.nlm.nih.gov/pmc/articles/PMC1380230/>).

(\*) Vandermonde interpolation polynomial is guaranteed to be unique for set of points to be interpolated. This set of points could be strings sourced from multiple identification traits of a person which can be Rabin fingerprinted by a polynomial over GF(2) modulo an irreducible polynomial over GF(2). This set of fingerprinted data points are then interpolated by a Vandermonde unique polynomial to ID a voter.

(\*) Sports Analytics and Intrinsic Performance Rankings have been mentioned in GRAFIT course material as a BigData usecase

([https://github.com/shrinivaasanka/Grafit/blob/master/course\\_material/](https://github.com/shrinivaasanka/Grafit/blob/master/course_material/NeuronRain/LinuxKernelAndCloud/BigdataAnalyticsCloud_CourseNotes.txt)

NeuronRain/LinuxKernelAndCloud/BigdataAnalyticsCloud\_CourseNotes.txt) - e.g ATP,WTA,NBA,ICC. Academic Rankings (rankings of researchers and universities - USA today,Times Higher Education) could leverage from Sports Rankings e.g Number of experimentally verified papers of an author in relativity and quantum mechanics with no dependency on number of citations is a measure of intrinsic research quality

(\*) Evidence usecase for BKS conjecture: Everyone agrees on denomination of a currency bill or coin - \$100 is universally accepted consensually as equal to \$100 discounting devaluation and other economic phenomena. If this fact is formulated as an LTF or PTF -  $\text{value}(x) = x$  - could evidence the truth of BKS conjecture implying consensus is stabler than majority function.

-----  
740. (THEORY and FEATURE) People Analytics - Drone Electronic Voting Machine - Python 3.7.5 upgrade and Paper ballot shuffle simulation, PRAM Breadth First and Depth First Search, Set Partition Analytics, Money Trail Economic EventNet Graph Random Walk, Expander Graphs, Cheeger's Constant, Random Closed Packing, Space Filling, Pseudorandomness Extractors and Generators, Birthday Paradox, Unique Identification, Ramsey coloring, Computational Chaos, Voting analytics - 7 January 2020,12 January 2020,13 January 2020 - related to 22,135,230,338,461,739  
-----

(\*) Drone Electronic Voting Machine implementation in Streaming\_SetPartitionAnalytics.py - electronic\_voting\_machine() - has been updated to simulate random shuffle of paper ballots in boxes to ensure disorder - votes appended to bucket per candidate are shuffled after each vote - every new vote is randomly inserted into obfuscated encrypted bucket of votes per candidate which simulates a shuffle (shuffle is essentially a permutation group  $S_n$ ) while an exact shuffle has to enumerate the permutation group ( $O(n!)$ ) and choose one element - every shuffle of a candidate bucket is also a reduction from space filling and random closed packing

(\*) Drone EVM implementation has been upgraded to Python 3.7.5 by autopep8 and 2to3 utilities and 2.7 version has been separately committed with eponymous suffix - random.randint() has been invoked to get an index to insert a new vote somewhere in the candidate bucket

(\*) Traditional incremental counters coalesce votes of multiple voters into one integer which prohibits forensic examination of individual votes if there is a dispute. Votes per candidate bucket thus isolates each anonymous encrypted vote but subverts chronological ordering.

(\*) Serial number unique id(s) of paper currencies were envisaged earlier as

non-digital one time passwords for authenticating a voter. Rationale for choice of currencies is the unpredictable pseudorandom flow of paper currency unique id(s) in economy which creates a huge EventNet Money Trail Graph (edges are labelled by flow of uniquely ID-ed currencies between buyers and sellers) which is non-digital and thus insulated from electronic sabotage. Money Trail EventNet Graph is a high entropy randomness source and could serve as a pseudorandomness generator and extractor e.g. topological sort or random walk of a subgraph of money trail EventNet is a random concatenation of unique id(s)

(\*) If Money Trail EventNet Graph is an edge expander, it could be a gadget for Pseudorandom Number Generator. Edge expander graphs are defined with Cheeger's constant for minimum high edge boundary per vertex subset:

$$\frac{\text{minimum}(|\text{boundary}(S)|/|S|), 1 < |S| < n/2}$$

where  $\text{boundary}(S)$  of a subset  $S$  of vertices of  $G$  ( $V(G)$ ) is:

$$\text{boundary}(S) = \{ (u,v) \mid u \in S, v \in V(G) \setminus S \}$$

Random walks on an expander graph are conventionally applied to Pseudorandom Generators e.g. Margulis [Mar88] and Lubotzky, Phillips and Sarnak [LPS88]

(\*) Locating an encrypted vote in a candidate bucket of votes (if bucket is a linked list) could be done in sublinear time by Parallel RAM Breadth First Search and Depth First Search of the linked list line graph - GRAFIT course material in

[https://github.com/shrinivaasanka/Grafit/blob/master/course\\_material/NeuronRain/AdvancedComputerScienceAndMachineLearning/AdvancedComputerScienceAndMachineLearning.txt](https://github.com/shrinivaasanka/Grafit/blob/master/course_material/NeuronRain/AdvancedComputerScienceAndMachineLearning/AdvancedComputerScienceAndMachineLearning.txt) mention usefulness of parallel RAM

sublinear linked list search in the context of Survival Index Timeout OS Scheduler version of Process IDs Set Partition in OS Kernels

(\*) Limitations of unique identification are best explained by birthday paradox - GRAFIT course material in

[https://github.com/shrinivaasanka/Grafit/blob/master/course\\_material/ComputerScienceMiscellaneous/ComputerScienceMiscellaneous\\_CourseNotes.txt](https://github.com/shrinivaasanka/Grafit/blob/master/course_material/ComputerScienceMiscellaneous/ComputerScienceMiscellaneous_CourseNotes.txt) have a Q and A on birthday paradox probability of collision of unique IDs in a population.

(\*) An expander graph simulation of Economic Network by Neuro Cryptocurrency in NeuronRain which is Boost UUID, Protocol Buffer, Perfect-Forward and Object Move based, theoretically could source pseudorandom bits.

Paper ballots and Drone EVM - comparison and contrast:

-----  
Previous concept implementation of Drone EVM in NeuronRain has separate buckets for candidates which are independently shuffled to simulate paper ballots whereas real world paper ballot votes are sealed and cast in single ballot box bucket without candidate delineation. Instead if Drone EVM is implemented such that all encrypted votes are in a single shuffled list (or) linked list bucket (which is how paper ballots work), reduction is necessary which shatters/classifies the shuffled list/linked list of votes to a set partition of buckets of per-candidate lists/linked lists of votes. Example:

every node of the list/linked list of anonymous votes has the fields  
<candidate\_id>:<encrypted\_vote>.

Usually this reduction happens post-poll in paper ballot counts. This sort of exact pseudorandom shuffle simulation of paper ballot box of assorted votes democratizes further and is a non-trivial monochromatic balls-bins problem in Drone EVM - every anonymous vote is colored by candidate index - single list (or) linked list line graph of votes of previous format has to be set/graph-partitioned to candidate buckets of multiple lists/line graphs (or) a multichromatic set has to be partitioned to monochromatic candidate bucket subsets - an  $O(N)$  labelled classifier. Sequence of  $N$  votes for  $k$  candidates is thus Ramsey  $k$ -colored and order emerges inevitably by Van Der Waerden Theorem - there exist numbers  $N, k, r$  such that if shuffled sequence of  $N$  votes are colored by  $k$  candidates, there is a monochromatic arithmetic progression of length at least  $r$  (in other words,  $r$  voters who had voted for same candidate are equally spaced out which presents an insight into voting pattern).

Conflict between pseudorandomness and arithmetic progressions in Ramsey coloring of votes - Orderly Disorder:

-----

-----  
 Previous simulation of pseudorandom paper ballot shuffle in Drone EVM gives rise to a multichromatic sequence of votes colored by candidate indices. But yet monochromatic arithmetic progression order emerges from pseudorandom disorder irrespective of number of colors (candidates) and voting chronology which is a contradiction. This "orderly disorder" oxymoron paradox should apply universally to any pseudorandomly shuffled multichromatic set not just limited to shuffled voting sequences. This limitation implies a prerequisite for indistinguishability of pseudorandom generators (PRG) from true randomness - PRGs should create pseudorandomly shuffled multicolored sequences of Ramsey number  $R(N,k,r)$  of high  $N,k$  and low  $r$  - Sequence of  $N$  elements,  $k$ -colored having an arithmetic progression of length at least  $r$  - which lessens the probability of emergence of arithmetic progression periodicities. On a related note, Period Three Theorem of Chaos theory ([www.its.caltech.edu/~matilde/LiYorke.pdf](http://www.its.caltech.edu/~matilde/LiYorke.pdf)) implies sequences of periodicity 3 can have larger periodicities.

#### References:

- 740.1 Random Walks on Expander Graphs and Spectral Graph Theory - [Spielman] - <http://www.cs.yale.edu/homes/spielman/561/2012/lect11-12.pdf> - Section 11.5 - "...Our pseudo-random generator will use a random walk on an expander graph whose vertex set is  $\{0, 1\}^r$ . The expander graph will be  $d$ -regular, for some constant  $d$ . Let  $A$  be the adjacency matrix of the graph, and let its eigenvalues be  $d = \mu_1 > \mu_2 \geq \dots \geq \mu_n$ . One property that we will require of the expander graph is that  $|\mu_i|/d \leq 1/10$ , (11.1) for all  $i$ . ... such graphs exist with  $d = 400$ . Degree 400 seems sort of big, but we will see that it is reasonable for our application...." - Degree 400 Money Trail EventNet could potentially be a high edge expander and random walks on it might be pseudorandom. Money Trail Graph could have Rich and Poor strata (and scalefree because select vertices could have huge neighbours) causing regularity to fluctuate and it suffices to find dense subgraphs of high regularity as candidates for expander graph random walks.
- 740.2 A. Lubotzky, R. Phillips, and P. Sarnak. Ramanujan graphs. *Combinatorica*, 8(3):261-277, 1988.
- 740.3 G. A. Margulis. Explicit group theoretical constructions of combinatorial schemes and their application to the design of expanders and concentrators. *Problems of Information Transmission*, 24(1):39-46, July 1988.
- 740.4 Hardy-Ramanujan-Rademacher estimation of partition function, Bell numbers of set partitions - [Donald Knuth] - <http://www.cs.utsa.edu/~wagner/knuth/fasc3b.pdf>
- 740.5 Generalized Condorcet Jury Theorem for multipartisan election - [Christian List-Robert Goodin] - <http://personal.lse.ac.uk/LIST/PDF-files/listgoodin.pdf> - Appendix 1 and Proposition 1 -  $k$ -option Condorcet Jury Model - "...Let  $X_1, X_2, \dots, X_k$  be the random variables whose values are the numbers of first choice votes (out of a total of  $n$  votes) cast for  $x_1, x_2, \dots, x_k$ , respectively. The joint distribution of  $X_1, X_2, \dots, X_k$  is a multinomial distribution with the following probability function:  $P(X_1=n_1, X_2=n_2, \dots, X_k=n_k) = (n! / [n_1! n_2! \dots n_k!]) * (p_1^{n_1} * p_2^{n_2} * \dots p_k^{n_k})$ , where  $\sum_i n_i = n$ . ... " - Theoretical  $k$ -parts Set Partition Electronic Voting Machine in NeuronRain AstroInfer is exactly  $k$ -option plurality Condorcet Jury Model for  $k$  candidates multipartisan election and probability of a candidate win is derived as: "... For each  $i$ , the probability that  $x_i$  will win under plurality voting is  $P_i := P(\text{for all } j \neq i, X_i > X_j) = P(X_1=n_1, X_2=n_2, \dots, X_k=n_k : \langle n_1, n_2, \dots, n_k \rangle \in N_i) = \sum_{\langle n_1, n_2, \dots, n_k \rangle \in N_i} (n! / n_1! n_2! \dots n_k!) * (p_1^{n_1} p_2^{n_2} \dots p_k^{n_k})$ , where  $N_i := \{\langle n_1, n_2, \dots, n_k \rangle : (\text{for all } j, n_j \geq 0) \& (\sum_j n_j = n) \& (\text{for all } j \neq i, n_i > n_j)\}$  (set of all  $k$ -tuples of votes for the  $k$  options for which option  $i$  is the plurality winner). Moreover, if, for all  $j \neq i, p_i > p_j$ , then, for all  $j \neq i, P_i > P_j$ . ...".

-----  
 741. (THEORY and FEATURE) Computational Geometric NC-PRAM-BSP Factorization - Spark 2.4.3 + Python 3.7.5 benchmarks - 1213 and 1243 bits integers factorized, Hyperbolic Rasterization graphics example, Multidimensional hyperplanar point location, Integer Diophantines, Multiplicative partitions and sundry resolutions



[illegible]



(\*) Logistic Equation Chaos PRG implementation in ChaosAttractor.py has been updated to also compute Lehmer-Palmore PRG by a function argument. An if clause has been introduced to choose between parabola attractor  $rx(1-x)$  and Lehmer-Palmore PRG ( $Bx \bmod M$ )

(\*) ChaosAttractor.py Lorenz Attractor code has been refactored and made a function of parameters:  
 ChaosPRG(algorithm="Logistic", seqlen=100, radix=10, initialcondition=0.7, prime=104729) which respectively choose the algorithm ("Logistic" equation or "Lehmer-Palmore" prime modulus PRGs), length of pseudorandom sequence, radix (k for "Logistic" and B for "Lehmer-Palmore"), initial condition for sensitive dependence and a Large prime modulus

(\*) R cor() correlation function has been invoked by R+ipy2 to print a correlation between pseudorandom sequence and a sample DJIA stock quotes dataset.

(\*) ChaosPRG() function can be optionally invoked in NeuronRain wherever pseudorandomness is necessary - e.g Pseudorandom shuffle simulation of paper ballot in Drone Electronic Voting Machine, Pseudorandom Shuffle of 2-colored (0 and 1) leaves in a boolean majority voting circuit which gives rise to monochromatic arithmetic progression order from pseudorandom chaotic shuffled votes disorder by Ramsey theory (Van Der Waerden numbers), Economic merit - Models for Econometric Datasets

(\*) Section 318 states a Majority version of XOR Hardness Amplification Lemma and points 318.15 to 318.19 define hardness of inverting boolean majority + voter SAT composition which might imply existence of an one way function (a #P-complete counting problem). Emergence of arithmetic progression order from binary colored voter leaves of Boolean Majority Circuit stipulates a prima facie indistinguishability condition between a good PRG and true randomness - Good pseudorandom shuffle must minimize probability of emergence of monochromatic arithmetic progressions in the leaves of boolean majority circuit.

(\*) Probability of monochromatic arithmetic progressions in any pseudorandom bichromatic sequence of length N (including shuffled 2-colored voter leaves of boolean majority circuit) is inversely proportional to Van Der Waerden number  $VDW(N, 2, r)$  - N elements in sequence(voters), 2 colors (candidates 0 and 1), arithmetic progression of length  $\geq r$  (voters who chose same candidate are equally spread out in the shuffled bichromatic votes string).

(\*) Chaos implies disorder from order (Period Three Theorem implies any sequence of period 3 can have larger periods while Feigenbaum sequences define self-referential recursive universality order in Chaos) and monochromatic arithmetic progressions in Pseudorandom multichromatic sequences imply order from disorder - these are two mutually conflicting trends in diametrically opposite directions.

(\*) logs testlogs/ChaosAttractor.LehmerPalmorePRG.log.21January2020 and testlogs/ChaosAttractor.LogisticEquationPRG.log.21January2020 print a correlation between DJIA data and two chaotic PRGs - Logistic and Lehmer-Palmore. Opposing correlation signs between Logistic and Lehmer-Palmore PRGs and DJIA sample is an indicator of extent of chaos and pattern in economic data:  
 Logistic: correlation coefficient of pseudorandom and DJIA sequences is: -0.00173395205970038  
 Lehmer-Palmore: correlation coefficient of pseudorandom and DJIA sequences is: 0.00648048041159691

(\*) Equilibrium point where the aforementioned Orderly Disorder (Ramsey) and Disorderly Order (Chaos) coincide might be of independent area of research.

#### References:

-----  
 743.1 Chaos - [James Gleick] - Mandelbrot-Julia sets, Fractals, Koch curves, Lorenz attractors, Feigenbaum universality - Period Doubling, Yorke's Period Three Theorem  
 743.2 Feigenbaum constants - First and Second -  
[https://en.wikipedia.org/wiki/Feigenbaum\\_constants](https://en.wikipedia.org/wiki/Feigenbaum_constants)  
 -----

744. (THEORY and FEATURE) Chaotic Pseudorandom Generator - Python 3.7.5 upgrade,



1. This commit upgrades Chaos Pseudorandom Generator implementation to Python 3.7.5 by autopep8 followed by 2to3, which is the defacto NeuronRain recommended python version for performance reasons.
2. Both Logistic and Lehmer-Palmore PRGs have been tested on Python 3.7.5 + R-py2 combine and logs are committed to  
testlogs/ChaosAttractor.Python3.7.5Upgrade.30January2020
3. GRAFIT course material on Geometric search of BigData in  
[https://github.com/shrinivaasanka/Grafit/blob/master/course\\_material/NeuronRain/LinuxKernelAndCloud/BigdataAnalyticsCloud\\_CourseNotes.txt](https://github.com/shrinivaasanka/Grafit/blob/master/course_material/NeuronRain/LinuxKernelAndCloud/BigdataAnalyticsCloud_CourseNotes.txt) describe a Randomized NC factorization algorithm based on Parallel Chaotic Pseudorandom Generator and Central Limit Theorem based Space filling Linear Program mentioned in drafts - <https://sites.google.com/site/kuja27/ChaoticPRG.pdf> and  
<https://sites.google.com/site/kuja27/Analysis%20of%20a%20Randomized%20Space%20Filling%20Algorithm%20and%20its%20Linear%20Program%20Formulation.pdf> .
4. Exact PRAM-NC-BSP computational geometric factorization algorithm implemented on Spark in NeuronRain AstroInfer is the derandomized version of Randomized NC Bernoulli trials factorization algorithm in  
[https://github.com/shrinivaasanka/Grafit/blob/master/course\\_material/NeuronRain/LinuxKernelAndCloud/BigdataAnalyticsCloud\\_CourseNotes.txt](https://github.com/shrinivaasanka/Grafit/blob/master/course_material/NeuronRain/LinuxKernelAndCloud/BigdataAnalyticsCloud_CourseNotes.txt) which has the success probability of finding atleast one prime factor  $pr(m) = (1 - \sqrt[2N]{(N \cdot \sqrt{2}) - \sqrt{2}} - \sqrt{N})^{(m-1)} \cdot (\sqrt[2N]{(N \cdot \sqrt{2}) - \sqrt{2}} - \sqrt{N})$  after  $m$  trials for square embedded hyperbolic arc. Expected number of trials  $E(m)$  before atleast one factor is found =  $\sum_{x=1}^{\infty} x \cdot pr(x)$
5. Thus NeuronRain Theory drafts define 3 different Nick's class Computational Geometric Integer factorization algorithms - Randomized NC, Quantum NC, Exact NC - which transition from a randomized, cohered quantum state to classical exact decohered state.

#### References:

-----

- 744.1 Chaos - [James Gleick] - Pages 22,61,79 - Chaotic behaviour and non-linear modelling of epidemics - Period doubling in Measles, Rubella, Polio - Logistic equation
- 744.2 Simple mathematical models with very complicated dynamics - [Nature 261 459-67, 1976 - Robert May] -  
[http://abel.harvard.edu/archive/118r\\_spring\\_05/docs/may.pdf](http://abel.harvard.edu/archive/118r_spring_05/docs/may.pdf) - Logistic equation  $X(t+1) = a \cdot X(t) \cdot (1 - X(t))$  - Equations 3,4 - Figure 4 on Period doubling and Chaos after  $a > 3.57$  - References 7,8,9,10,11,28 thereof on impact of Chaos on epidemiology, economics, social sciences.
- 744.3 CORO-19 - COVID-19 dataset - <https://registry.opendata.aws/coro-19/>,  
<https://pages.semanticscholar.org/coronavirus-research>
- 744.4 Foundations of Economic Analysis - [PA Samuelson] - Page 291 - Verhulst-Pearl-Reed Logistic Law -  
<https://ia801603.us.archive.org/7/items/in.ernet.dli.2015.150369/2015.150369.Foundations-Of-Economic-Analysis.pdf>
- 744.5 Game theoretic model of epidemics -  
<https://www.elsevier.com/connect/using-game-theory-to-predict-peoples-behavior-in-an-epidemic> - "...When there's no epidemic, everyone behaves normally. In the event of an outbreak, changing behavior will be costly in some way - perhaps people stay home from work or avoid crowded environments, change their commute or buy preventative medication. But there's also a payoff: people who change behavior are less likely to be infected. At a certain point in the epidemic, those people have an advantage in the population, and others begin to copy their behavior...We applied game theory to these dynamics and produced a mathematical model that shows how people's responses can affect the spread of a disease during an epidemic. We found that reducing the number of people an individual is in contact with, even by a small amount, can make a difference to the spread of disease..." - NeuronRain USBmd analyzer for malwares game theoretically (game between saboteur and sabotaged) is motivated on creating information or mining patterns in software viri and cybercrimes to counteract the spread, isolate

infected systems, shutting down broadband networks and any instrument emitting RF(radio-frequency) and zero-in on origin - a PredPol. Translating this to epidemiology is obvious - information on prevention minimizes infection. But an apparent contradiction arises - Per 744.2 Verhulst model, if  $a > 3.57$  when epidemic becomes chaotic to predict, rate of infection could outpace and be out of sync with information. Epidemics are also modelled by fitting to polynomials, exponential distribution, poisson distribution and logistic/linear regression - COVID19 exponential outbreak -

<https://www.nytimes.com/2020/03/13/science/coronavirus-math-mitigation-distancing.html>.

744.6 Reproduction Number of COVID19 transmission -

[https://www.thelancet.com/journals/laninf/article/PIIS1473-3099\(20\)30144-4/fulltext](https://www.thelancet.com/journals/laninf/article/PIIS1473-3099(20)30144-4/fulltext) - "... We modelled transmission as a geometric random walk process, and we used sequential Monte Carlo simulation to infer the transmission rate over time, as well as the resulting number of cases and the time-varying basic reproduction number ( $R_t$ ), defined here as the mean number of secondary cases generated by a typical infectious individual on each day in a full susceptible population ..." - By modelling transmission as edges added/deleted in dynamic random graph between infected individuals, Reproduction Number is the average degree of Dynamic Infection Random graph.

744.7 Social Networks, Erdos-Renyi(ER) Random Graphs, Epidemics and SIR model, Small World, Clustering coefficient, Reproduction ratio -

<https://arxiv.org/pdf/1111.4875.pdf> - Epidemic ER-SIR model applies as well to Cybercrimes - malwares, viri, bots.

744.8 Random Graphs, Quantum Chaos, Riemann Zeta Function, Graph representation of primes, Ihara Zeta Function, k-core, Expander graphs, Pseudorandomness -

<http://www.its.caltech.edu/~matilde/GraphsRandomChaosQuantum.pdf>

744.9 Forest Fire Model or epidemic model of Social Networks - new node  $v$  connects to an ambassador node  $w$ , and links to  $x$  neighbours of  $w$  by forward burning and backward burning probabilities which is recursed - Data Mining - Section 9.2.2 - Page 560 - [Jiawei Han-Micheline Kamber] - this is typical of citation graphs: paper  $v$  citing  $w$  recursively consults subset of articles cited by  $w$ .

-----  
745. (THEORY and FEATURE) Compressed Sensing - Alphabet-Syllable vectorspace embedding - Python 3.7.5 upgrade - update - 4 February 2020  
-----

1. Function `syllable_boundary_text_compression(self, text, vectorspace_embedding=True)` in `CompressedSensing` python implementation has been updated to parametrically choose alphabet vectorspace embedding of words in text described in GRAFIT course material on Geometric Search -

[https://github.com/shrinivaasanka/Grafit/blob/master/course\\_material/NeuronRain/LinuxKernelAndCloud/BigdataAnalyticsCloud\\_CourseNotes.txt](https://github.com/shrinivaasanka/Grafit/blob/master/course_material/NeuronRain/LinuxKernelAndCloud/BigdataAnalyticsCloud_CourseNotes.txt) - words of text are embedded in  $|A|^m$  vectorspace ( $|A|$  is the size of natural language alphabet and  $m$  is the longest word in text). For English, this is a space of  $26^m$ .

2. Words are python tokenized to vectors and concatenated to an array creating a vectorspace embedding words in the text document.

3. Return value is a tuple which includes or excludes the word embedding of text depending on `vectorspace_embedding` boolean flag

4. `CompressedSensing.py` has been upgraded to Python 3.7.5 by `autopep8` and `2to3` utilities. Python 2.7 version is separately committed.

5. An Example sentence is syllable hyphenated (`PyHyphen`), vowel stripped-compressed and embedded as:

#####  
#####

Vowelless Syllable Vector Compression for text - This sentence is alphabet-syllable vector space embedded : `(['This', 'sen', 'tence', 'al', 'pha', 'bet', '-', 'syl', 'la', 'ble', 'vec', 'tor', 'space', 'em', 'bed', 'ded'], 'Th_s-s_n-t_nc_-_l-ph_b_t---syl-l-bl_v_c-t_r-sp_c_-_m-b_d-d_d')`

Alphabet vectorspace embedding of text: `(['T', 'h', 'i', 's'], ['s', 'e', 'n',`





5.Synchronization is by a binary semaphore guarding the deque in main thread and outgoing stream thread.

6.Theoretical overtone of leaky bucket is its ability to flag outliers by overflows and peaks in timeseries are often the abnormalities in stream causing overflow. For example excessive network traffic corresponds to peaks in timeseries data and frequent overflows in leaky bucket as buffer fills faster than leakage.

7.Leaky Bucket Analyzer thus is a universal tool for mining any stream of text,audio,video,people data and most apt for wireless network stream, stream of celestial bodies configurations, climate change datastream (e.g <http://climate.nasa.gov> data stream on surface temperature, melting polar ice sheets, carbon emission, ocean currents and acidity), economic datasets having lot of outlier spikes.

8.Streaming\_LeakyBucket.py has been implemented on Python 3.7.5 and Streaming\_AbstractGenerator.py has been upgraded to Python 3.7.5

9.Logs for dictionary time series example are at testlogs/Streaming\_LeakyBucket.log.12February2020

-----

749. (THEORY and FEATURE) PAC Learning - Python 3.7.5 upgrade, Riemann Hypothesis, Patterns in Primes, class HNC and Algebraic Circuits - 21 February 2020, 22 February 2020 - related to 24,629 and all sections on Complement diophantines, Complementary Sets and Equations, Prime-Composite complementation and Patterns in Primes

-----

1. PACLearning.py PAC learning implementation has been refactored and upgraded to Python 3.7.5. Binary encoded and bits mapped UTM Primes dataset has been PAC Learnt again for per-prime-bit-position boolean disjunctions of first 10000 primes (16 disjunctions for each bit of 16-bits prime integer). New refactored PACLearning() function accepts a generic datasource and a hypothesis dictionary as arguments.

2. Example logs for this PAC learning are at testlogs/PACLearning.PrimeBitsMappingConjunctions.Python3.7.5.21February2020 which are different from Python 2.7 approximate learning.

3. Prime pattern References in Section 24 (24.31, 24.32, 24.33) mention a prima facie pattern in juxtaposed primes especially their avoidance of same digit ending. PAC learnt hypothesis in testlogs/PACLearning.PrimeBitsMappingConjunctions.Python3.7.5.21February2020 show an intriguing avoidance pattern in 14th,15th and 16th bits for first 10000 primes though approximate.

4. Prime counting function (number of primes  $\leq N$ ) can be written in terms of non-trivial zeros of Riemann Zeta Function. Riemann Hypothesis (RH) conjectures all non-trivial zeros of Riemann Zeta Function are along critical line  $\text{Re}(z)=0.5$ . Riemann Zeta Function is just a rephrased version of Sieve of Eratosthenes and is expanded by Euler product.

5. From Section 629, Riemann Zeta Function has an algebraic computation tree circuit in HNC:

"... Riemann Zeta Function can be represented as a disjunctive clauses or non-uniform Hilbert Nullstellensatz algebraic circuit in

$0-1\text{-HNC}$  (0 if  $s$  is a non-trivial zero else 1) of product polynomials having complex roots (non-trivial zeros):

$\text{RZF}=\text{product\_of}(1/[1-\text{prime}(k)^{-s}])$  for all primes 2,3,5,7,..."

6.Approximate binary digit hypothesis disjunctions for primes dataset learnt by PAC and exact learning by Euler-Fourier polynomial imply pattern in spacings between consecutive primes and thus are indirect boolean prime counting functions. Both Euler-Fourier polynomial and PAC learnt disjunctive clauses are mapping functions between integer  $n$  and  $i$ -th bit of  $n$ -th prime -  $f(n,i): n \Leftrightarrow i$ -th bit of  $n$ -th prime

7.Riemann Zeta Function has diophantine equation representation and thus in RE by MRDP theorem. Recent result of  $\text{MIP}^*=\text{RE}$  implies a quantum multiparty interactive prover-classical verifier algorithm for diophantine and algebraic circuit versions of Riemann Zeta Function. It is notable and coincidental that

distribution of Gaussian Unitary Ensemble eigenvalues in quantum world are identical to spacings of non-trivial zeros of RZF.

#### References:

-----  
749.1 Prime Obsession - Bernhard Riemann and the Greatest Unsolved Problem in Mathematics - [John Derbyshire] - Chapters 18,19,21 - Pages 292,299,309,328 - Montgomery-Odlyzko law, Euler product, Sieve of Eratosthenes, Function  $J(x)$  in terms of Prime counting function  $Pi(x)$  and Riemann Zeta Function in terms of  $J(x)$  - Equations 19.1,19.6,21.1 - " ...  $\frac{1}{s} \log(RZF(s)) = \int_0^\infty J(x) x^{-(s-1)} dx$  ..."

749.2  $MIP^*=RE$  - <https://arxiv.org/abs/2001.04383> - this result implies quantum computers could decide halting problem which is in RE. Diophantine representation of RZF is in Adleman-Manders class D and is in RE by MRDP theorem.  $MIP^*=RE$  implies Riemann Zeta Function (RZF) and Riemann Hypothesis has a quantum verification algorithm which halts despite infinite number of non-trivial zeros of RZF. Similar to computerized proof of Four color theorem this could be a machine generated proof or disproof of Riemann Hypothesis - An example quantum algorithm for proving or disproving Riemann hypothesis in  $MIP^*=RE$ :

- Multiparty interactive quantum prover finds all non-trivial zeros of RZF
- classical verifier checks real part of all non-trivial zeroes for  $Re(z)=0.5$  and finds a counter-example for disproof or a lack of it for proof of Riemann Hypothesis.

[Intermediary sections 750-781 are scattered in other NeuronRain repositories - Acadpdrafts,USBmd,VIRGO,KingCobra,GRAFIT,Krishna\_iResearch\_DoxygenDocs]

-----  
782. (THEORY and FEATURE) Text Compression, Compressed Sensing, Syllable boundaries decompression implementation - Python 3.7.5 upgrade and refactoring - 28 February 2020, 29 February 2020  
-----

-----  
1.TextCompression.py vowelless text compression-decompression implementation has been upgraded to Python 3.7.5 by autopep8 and 2to3 utilities  
2.Syllable boundaries text compression function from CompressedSensing.py has been imported to optionally choose between syllable boundary compression of text and earlier vowelless compression (which strips vowels across the board) by a boolean flag syllable\_boundary  
3.Earlier commented code for PyEnchant spelling suggestions has been uncommented to choose between PyEnchant maximum likelihood (prob() function) and Hidden Markov Model maximum likelihood (HiddenMarkovModel\_MLE() function) estimators based on if suggestions is not-None and None respectively.  
4.Both PyEnchant and HMM computed maximum likelihood words are printed to logs.  
5.Logs at testlogs/TextCompression.log.28February2020 contain PyEnchant and Hidden Markov Model maximum likelihood estimations per decompressed string for both vowel compressed and syllable boundary compressed words  
6.decompressedtext.txt contains the newly introduced approximate syllable boundary decompressed text:

ghts fer over with lus tins der ly2 on dead ster nal ve tting pro mer  
dial placed be form byss paw er ful ry mev ing grant ybody wn ters ician  
milk shy ser pant ged form ing cotch shed sh mania

for exact text:

Rama gets forever pleased with him who listens to or reads Ramayana daily. He is indeed the eternal Vishnu, the Lord of preservation. Rama is the primordial Lord, clearly placed before the eyes the powerful Lord removing the sins and the great-armed, who has abode on waters of the ocean of milk Sesha the serpent-god forming his couch is said to be Lakshmana.

7. It is worth observing how the words "primordial", "removing", "serpent" and

"powerful" have been syllable decompressed - "pro mer dial", "ry mev ing", "ser pant", "paw er ful" - to homophones (phonetically equivalent but linguistically different)

8. Advantage of syllable boundaries is their language and script independence, dependence on phonetics alone, fine-graining of words to syllables for better accuracy in phonetic decomposition.

9. Embedding a text on syllable vector space as opposed to traditional flat one-dimension thus blurs linguistic boundaries and useful for similar name clustering.

#### References:

-----  
782.1 Phonetic Match Rating Algorithm - for similar name clustering in airlines

-  
<https://ia801704.us.archive.org/2/items/accessingindivid00moor/accessingindivid00moor.pdf>

-----  
783. (THEORY) Phonetic Syllable Boundaries Compression and Approximate Decompression - error bounds and success amplification - 1 March 2020  
- related to all sections on Text Compression, Compressed Sensing and People Analytics - Similar name match  
-----

-----  
Approximate Syllable Boundaries Decompression in earlier example can be phonetically matched for further error correction and accuracy. Example decompression of "powerful" to "paw er ful" demonstrates approximate phonetic match which requires lookup of per word audio dictionary to spell out a matching word (e.g Interactive Voice Response). By finding the best phonetic match of "paw er ful" in a syllable audio dictionary (which is a map of collated-syllable-audio-of-words to words), "paw er ful" is further decoded to "powerful" thus amplifying success. Phonetic match therefore involves an audio waveform distance function of two words different from string edit distance text similarity (e.g waveforms of "paw er ful" and "powerful" are in proximity). This audio-to-words dictionary is static containing as many words in language and requires initialization only once. Another prerequisite is a syllables-to-audio dictionary for lookup of every syllable in approximately decompressed word and splice their audio waveforms (e.g waveforms of syllables "paw", "er", "ful" are lookedup and collated to obtain "paw er ful") which is then lookedup in audio-to-words dictionary (e.g waveform for "paw"+"er"+"ful" is lookedup to retrieve "powerful").

Number of vowels per english word (approximate) =  $\text{length\_of\_the\_word} / 3$   
(because on the average every third letter of a word is a vowel)

Number of vowels per english word syllable (approximate) = 1

Number of syllables per english word =  $\text{length\_of\_the\_word} / 3$

Probability of erroneous decompression per english word syllable =  $4/5$  = choice of wrong vowel in a,e,i,o,u

Probability of wrong decompression of a word =  $(0.8)^{(l/3)}$  ( $l$  =  $\text{length\_of\_the\_word}$ )

Probability of successful phonetic decompression increases therefore with increasing length of the word.

[Intermediary sections 784-791 are scattered in other NeuronRain repositories - Acadpdrafts, USBmd, VIRGO, KingCobra, GRAFIT, Krishna\_iResearch\_DoxygenDocs]

-----  
792. (FEATURE) Social Network Analytics - LinkedIn Connections Analysis, Name filter and Python 3.7.5 upgrades - 4 March 2020  
-----  
-----

1. SocialNetworkAnalysis\_PeopleAnalytics.py - Connections in a Professional Network Profile have been analyzed by Recursive Lambda Function Growth (RLFG) after applying name filters to strip off Human names of connections and only extract their professional roles.
2. Name filter works by looking up words in profile connections text in a dictionary and filters Proper nouns (Human Names) - rationale is a language dictionary should not contain human names or contain least human names and is a short-cut stop-gap algorithm to recognize proper nouns while an artificial intelligence culture-neutral name parsing alternative might involve extensive training data and deep learning.
3. Dictionary.txt file already committed for CompressedSensing has been preferred to nondictionaryword() in RecursiveGlossOverlap\_Classifier.py which repetitively invokes slower REST lookup - first word in each line of Dictionary.txt (Concise Oxford Dictionary) has been parsed to create an array of words
4. Quite a few dependent python source files have been upgraded to Python 3.7.5 including the very necessary RecursiveLambdaFunctionGrowth.py implementation for performance by autopep8 and 2to3 utilities.
5. Dense subgraph extracted from definition graph of professional descriptions of connections is an indication of prominent designations/skills pattern.
6. Machine Translation has been commented because of slow REST calls to Google Translate.
7. Unfeasible Exception has been handled in korner\_entropy() - maximal independent set computation.
8. Only a fraction of connections profile contents is analyzed because of intensive computation.
9. logs at  
testlogs/SocialNetworkAnalysis\_PeopleAnalytics.log.ConnectionsRLFGAnalysis.4March2020.gz contain exhaustive graph theoretic analysis of LinkedIn Connections of the author (K.Srinivasan - <https://www.linkedin.com/in/srinivasan-kannan-608a671/>) and to large extent core numbers reflect the designations/skills profile.
10. Of all the graph complexity measures, closeness centrality is more accurate than others - top ranked vertices which directly relate to designations are (and still there are Human names because dictionary attack is just an approximation):  
[('system', 0.07260504201680672), ('computer\_architecture', 0.05979238754325259), ('made', 0.05585003232062055), ('ecosystem', 0.05464895635673624), ('son', 0.05163025210084034), ('John', 0.050760079312623926), ('male', 0.050760079312623926), ('servicing', 0.049373191899710706), ('logic', 0.04934323243860651), ('considered', 0.048403361344537814), ('forming', 0.048403361344537814), ('components', 0.048403361344537814), ('interdependent', 0.048403361344537814), ('unified', 0.048403361344537814), ('body', 0.048403361344537814), ('whole', 0.048403361344537814), ('living', 0.048403361344537814), ('act', 0.04657368101879927), ('computer', 0.04537815126050421), ('permanent\_wave', 0.044582043343653247), ('engagement', 0.04364876385336743), ('science', 0.042352941176470586), ('organization', 0.042352941176470586), ('software', 0.042352941176470586), ('structure', 0.042352941176470586), ('hardware', 0.042352941176470586), ('human', 0.04069952305246423), ('offspring', 0.04069952305246423), ('1215', 0.04015686274509804), ('sign', 0.04015686274509804), ('Henry', 0.04015686274509804), ('youngest', 0.04015686274509804), ('French', 0.04015686274509804), ('Magna', 0.04015686274509804), ('compelled', 0.04015686274509804), ('Richard', 0.04015686274509804), ('barons', 0.04015686274509804), ('1167-1216', 0.04015686274509804), ('1216', 0.04015686274509804), ('throne', 0.04015686274509804), ('brother', 0.04015686274509804), ('England', 0.04015686274509804), ('death', 0.04015686274509804), ('1199', 0.04015686274509804), ('II', 0.04015686274509804), ('lost', 0.04015686274509804), ('King', 0.04015686274509804), ('possessions', 0.04015686274509804), ('Carta', 0.04015686274509804), ('succeeded', 0.04015686274509804), ('group', 0.03997917751171265), ('organisms', 0.039705882352941174), ('physical', 0.039705882352941174), ('formed', 0.039705882352941174), ('interaction', 0.039705882352941174), ('community', 0.039705882352941174), ('environment', 0.039705882352941174), ('mating', 0.03928388746803069), ('animals', 0.03928388746803069), ('product',



0.038431372549019606), ('written', 0.03796078431372549), ('reasoning', 0.03682864450127877), ('strontium', 0.036580138128125744), ('writer', 0.035812060673325936), ('sharing', 0.03557202408522464), ('activities', 0.03557202408522464), ('infrastructure', 0.03529411764705882), ('machine', 0.034573829531812726), ('performing', 0.034573829531812726), ('automatically', 0.034573829531812726), ('calculations', 0.034573829531812726), ('hair', 0.03410975128306356), ('applying', 0.03410975128306356), ('heat', 0.03410975128306356), ('waves', 0.03410975128306356), ('series', 0.03410975128306356), ('chemicals', 0.03410975128306356), ('Das\_Kapital', 0.03329893360853113), ('two', 0.031512605042016806), ('era', 0.031512605042016806), ('timbre', 0.030745098039215688), ('silver-white', 0.030732292917166865), ('element', 0.030732292917166865), ('yellowish', 0.030732292917166865), ('turns', 0.030732292917166865), ('celestite', 0.030732292917166865), ('metal', 0.030732292917166865), ('occurs', 0.030732292917166865), ('air', 0.030732292917166865), ('strontianite', 0.030732292917166865), ('soft', 0.030732292917166865), ('metallic', 0.030732292917166865), ('alkali', 0.030732292917166865), ('yellow', 0.030732292917166865), ('person', 0.029656862745098038), ('complex', 0.02956259426847662), ('summation', 0.029411764705882353), ('policy', 0.02920060331825038), ('produce', 0.028467683369644153), ('trade\_name', 0.028467683369644153), ('mood', 0.027450980392156862), ('college', 0.026504394861392833), ('something', 0.02564917859035506), ('able', 0.02564917859035506), ('write', 0.02564917859035506), ('leader', 0.02464985994397759), ('working', 0.024546114742193172), ('former', 0.024434389140271493), ('1867', 0.02433383609854198), ('economic', 0.02433383609854198), ('Marx', 0.02433383609854198), ('theories', 0.02433383609854198), ('Karl', 0.02433383609854198), ('describing', 0.02433383609854198), ('book', 0.02433383609854198), ('large', 0.023529411764705882), ('booth', 0.023529411764705882), ('circumstances', 0.023291740938799762), ('someone', 0.023291740938799762), ('set', 0.023291740938799762), ('efforts', 0.023291740938799762), ('consequence', 0.023291740938799762), ('particular', 0.023291740938799762), ('contract', 0.022070223438212494), ('insurance', 0.022070223438212494), ('certificate', 0.022070223438212494), ('activity', 0.02137887413029728), ('serving', 0.02137887413029728), ('Indo-European', 0.021176470588235293), ('divided', 0.02100840336134454), ('geological', 0.02100840336134454), ('time', 0.02100840336134454), ('major', 0.02100840336134454), ('division', 0.02100840336134454), ('periods', 0.02100840336134454), ('usually', 0.02100840336134454), ('musical', 0.020227038183694528), ('sound', 0.020227038183694528), ('music', 0.020227038183694528), ('property', 0.020227038183694528), ('noise', 0.020227038183694528), ('distinctive', 0.020227038183694528), ('voice', 0.020227038183694528), ('a....']

-----  
793. (THEORY and FEATURE) GIS and Urban Sprawl Analytics - Image Segmentation and Face components statistics, Dual Graph, Four color theorem  
- 12 March 2020  
-----

-----  
1. ImageNet Keras-Theano + OpenCV + Python 3.7.5 implementation - ImageGraph\_Keras\_Theano.py - has been changed for computing statistics of image segmentation by watershed algorithm.  
2. image\_segmentation() function has been augmented to invoke cv2.connectedComponentsWithStatsWithAlgorithm(sure\_fg, connectivity=8, ltype=2, ccltype=cv2.CCL\_GRANA) which computes the connected face components of foreground image accompanied by statistics and algorithm parameters. 8-way connectivity of an image by GRANA connected components algorithm is computed. cv2.connectedComponents() is limited to markers only.  
3. Labels, Centroids and Statistics of each connected component of a segmented image are printed. Every component of segmented image is also a face in graph theoretic terms and a dual graph of adjacent faces can be drawn connecting centroids of faces.  
4. By Four color theorem (a kind of Multiple Agent Resource Allocation),

centroids of adjacent faces could be made color-repulsive - every face and thus its centroid can be colored by one of the four categories (Manufacturing-IT-ITES, Residential, Commercial, Greenery) and adjacent faces avoid same color. Dense subgraphs of Colored Weighted Dual graph (vertices are colored by one of the 4 categories and edges are labelled by distance between centroids of the faces) of segmented urban sprawl GIS offer insight into urbanization, expansion and density.

5. An example montage MP4 video (Example Video 1 - Erstwhile Research Scholar profile - 1995-2011 - academics and industry - of the author) has been benchmarked again along with a segmentation of Chennai Urban Sprawl GIS JPEG (SEDAC - <http://sedac.ciesin.columbia.edu/mapping/popest/gpw-v4/>).

6. Logs at testlogs/ImageGraph\_Keras\_Theano.log.12March2020 show two prominent segments of Chennai Urban Sprawl and their centroids.

[Intermediary sections 794-809 are scattered in other NeuronRain repositories - Acadpdrafts, USBmd, VIRGO, KingCobra, GRAFIT, Krishna\_iResearch\_DoxygenDocs]

-----  
810. (THEORY and FEATURE) GIS and Urban Sprawl Analytics - Delaunay Triangulation and Voronoi diagram of Segmented Image, Intrinsic Merit of Large Scale Visuals, Computational Geometry - Planar Point Location, Computational Geometric Factorization - 16 March 2020, 17 March 2020, 18 March 2020  
-----

-----  
1. ImageGraph\_Keras\_Theano.py image\_segmentation() has been updated to approximately compute face graph of a segmented image by Voronoi diagram for segment centroids.

2. Centroids from connected components statistics are construed to be the points of a Voronoi diagram planar subdivision.

3. A planar rectangle of the size of image is instantiated by Subdiv2D() and centroids of image segment components are populated in planar subdivision.

4. Delaunay triangles and Voronoi faces tessellation of the planar subdivision are obtained by OpenCV API - getTriangleList() and getVoronoiFacetsList().

5. Voronoi diagram draws boundaries optimally in a way such that centroids are equidistant from them and thus approximates the face graph for the connected segment components of the image which is essentially necessary to simulate envy-free allocation of four categories/colors of an urban sprawl and a fair division MARA. An alternative to Voronoi diagram could be to minimize a linear program of average weighted distance between centroids of segment faces - optimal weights of edges between face centroids decide the dimensions of every segment category:

$\text{Minimize } \sum(\text{distance}(C_x - C_y)) / |C| \text{ for set of centroids}$

$C = \{C_1, C_2, \dots, C_k\}$

6. For every facet in the Voronoi diagram which corresponds to a segment, a NetworkX vertex object is created by stringified concatenation of pixel ordinates delimited by "#". This uniquely identifies a vertex in facegraph. Edges are added for each face boundary in NetworkX Undirected graph. This NetworkX facegraph of an image is sufficient for graph theoretic analysis of any image.

7. Polygon is drawn for each face and NetworkX facegraph of an image in its entirety is written to a DOT file.

8. Two GIS images of Chennai Urban Sprawl have been segmented by watershed and their facegraphs have been plotted as PNG images. (There are graph theoretic alternatives to watershed viz., GRAB CUT graph based image segmentation algorithm which is on similar line)

9. New video montage - Google Search of NeuronRain repositories and Google Scholar profile of author <https://scholar.google.com/citations?user=eLZY7CIAAAAJ&hl=en> - has been recorded as MP4 and analyzed for EventNet

Tensor Product Merit which is a good mix of visuals and text. Incidentally every frame of a video can also be segmented graph theoretically as FaceGraph as against ImageGraph analysis from ImageNet predictions.

10. Segment centroid Voronoi diagrams are as well irregular bounding boxes implementations for an image as opposed to rectangles.

11. Voronoi Diagrams of frames in video dynamically morph and create a stream of FaceGraph(s) - for a movie or YouTube video example, actors per scene/event (set of consecutive frames) could be located by segmentation and Voronoi tessellation of segment centroids. Every segmented frame has a Voronoi FaceGraph whose faces contain actor centroids. For consecutive frames per scene, actor centroids arbitrarily float (Centroid Tracking) resulting in a stream of Dynamic Voronoi FaceGraph(s). Intuitively, set of FaceGraphs per scene or event are isomorphic. Merit of Visuals has two facets - style and substance. Substance of visual is measurable by Tensor Rank connectedness of information while Style often is a visual genre stereotype and narrative USP of a creator e.g laidback, offbeat, actionpacked, VFX. Patterns in narrative graph theoretically reduces to frequent subgraph mining problem - multiple movies or videos (stream of Voronoi facegraphs of frames) of a creator are mined for frequent subgraphs in facegraphs.

12. Streaming Voronoi Tessellation of Videos is a Computational Geometric solution which involves all pervasive Planar Point Location - Voronoi Diagram FaceGraph is a Planar Subdivision of each Frame and Points to be located/tracked are Centroids of Faces/Segments(actors).

13. Rasterized Point Location in Computational Geometric Factorization could be expressed in terms of Voronoi Diagrams:

13.1 Factors of an Integer (already found) are centroids of segments located on hyperbolic arc

13.2 Voronoi diagrams subdivide 2D plane and find faces comprising every factor centroid

13.3 Planar Point Location on Voronoi 2D planar subdivision locates the polygon face containing a factor point. Advantage of Rasterized hyperbolic arc: every polygon face is an axis-parallel arithmetic progression enabling binary search within faces.

14. Urban Sprawls are real counterparts of Social networks in virtual world - WWW, dynamic and undergo rapid expansion by preferential attachment - Good example of such an expansion is Chennai Urban Sprawl which is 8848 sqkm an eightfold expansion in 50 years from 1189 sqkms in 1970s. It is imperative that resource allocation is in tandem and keeps pace with urbanization and none of the four categories are found wanting. Graph theoretically, Subgraphs of FaceGraph of an Urban Sprawl by Voronoi Diagrams of segment centroids could be fairly allocated to categories by Multi Agent Graph Coloring. Expanding Urban sprawl grows the FaceGraph dynamically and new segments of various categories (and faces) are added in the periphery of the city. Multi Agent Four coloring of Urban sprawl FaceGraph therefore cannot be static and must be recomputed to catch up with this expanding dynamic facegraph. High Edge Expander facegraph of an urban sprawl has least Cheeger constant (low bottlenecks, high regularity and low eigenvalues) and high connectivity.

#### References:

-----  
810.1 Multi Agent Graph Coloring - [Blum-Rosenschein] - <https://www.aaai.org/Papers/AAAI/2008/AAAI08-004.pdf> - "...Multiple agents hold disjoint autonomous subgraphs of a global graph, and every color used by the agents in coloring the graph has associated cost. In this multiagent graph color- ing scenario, we seek a minimum legal coloring of the global graph's vertices such that the coloring is also Pareto efficient, socially fair, and individual rational ... Every node corresponds to an agent, and each agent tries to determine its color so that neighbors do not have the same color." - Socially Fair Coloring of FaceGraphs of Urban Sprawls could involve Four colors (categories or agents) - Manufacturing-IT-ITES, Residential, Commercial, Greenery - which compete to grab their pie (subgraph) of Urban sprawl. Pareto optimal 4-coloring of Urban sprawl FaceGraph finds an efficient resource allocation.  
-----

-----  
811. (THEORY and FEATURE) Interview Algorithm - Spark Recursive Gloss Overlap Implementation - Python 3.7.5 upgrade and Quadcore Benchmarks  
- 20 March 2020  
-----

```

1. Spark Recursive Gloss Overlap MapReduce implementation in
python-src/InterviewAlgorithm has been upgraded to Python 3.7.5 and benchmarked
on Quadcore.
2. Earlier implementation on Python 2.7 and Dual core was slower because of
local[2] which has been upgraded to local[4] for quadcores.
3. Memcache python client has been changed to pymemcache for Python 3.7.5 and
pymemcache API changes have been incorporated.
4. Spark Python Recursive Gloss Overlap sources have been compiled to C by
Cython3 (upgraded from Cython2) - following are commandline alternatives to
setup.py and .so(s):
 cython3 <Python3.7.5_file.py> -o <Cython3_file.c>
 gcc -I<include_Python3.7_headers> <Cython3_file.c> -o <Cython3_executable>
-lpython3.7m
5. Unicode encode() for Python 3 strings has been invoked wherever necessary
6. Pickle file is opened in 'a' and not 'ab' because of Python 3 bytes type
conflict
7. Python 2.7 versions still depend on memcache python client, have .2.7
extension and Cython 2 .so(s) remain intact.
8. Replacement of Flat file pickle in MapReduce by memcache get/set was tried but
the code for it has been left commented because of huge number of connection
reset errors within memcache. This is despite lockdown of pages in memcache.conf
and parallel connections set to 1024. In-memory cache of Synsets in Spark
mapreduce could reduce latency further and might be uncommented later.
9. 2 sentences in small one liner file have been mapped to 2 textgraphs and
timestamped textgraph plot images and logs are at InterviewAlgorithm/testlogs/

```

```

812. (THEORY and FEATURE) People Analytics - Human Resource Analytics -
Recursive Lambda Function Growth Intrinsic Merit of Name-filtered Profile -
corrections, Chaotic Hidden Markov Model of Tenures/Attrition, Martingales -
related to 418,420,613 - 25 March 2020

```

```

812.1. Recursive Lambda Function Growth Intrinsic Merit of a profile text has been
benchmarked again on Python 3.7.5 upgraded implementation because of some
misleading graph cores created in Python 2.7 by proper nouns
(cities, organization names, institution names). Exceptions for word hyphenator
maximum word length have been handled. Logs are at
python-src/testlogs/SocialNetworkAnalysis_PeopleAnalytics.log.25March2020
812.2. An example profile text (testlogs/CV.tex) of the author has been analyzed
and dense subgraph analysis of its textgraph has been executed. Most of the
proper nouns have been filtered from profile text but for few ambiguities (e.g
"Sun", "Global" are in dictionary but they were old first names of organizations
author worked for and "Green" is name of NeuronRain repositories, "Gold
medalist" is mistook for "Golf medalist")
812.3. By and large top percentile core numbers of the profile textgraph
reasonably reflect the stature of the profile and name filtering increases
relevance of the dense subgraphs. Though anything can be written on a CV, an id
verified profile content is a trustworthy measure of merit (Trusted Social
Network Connections of professional profile in organizations worked vouch for
authenticity despite being fame based citations) and facilitates autonomous
recruitment if Merit Lowerbounds Fame:
=====

```

```

=====
Unsupervised Classification based on top percentile Core numbers of the
definition graph(subgraph of WordNet)
=====

```

```

=====
('This document belongs to class:', 'senior', ',core number=', 4)
('This document belongs to class:', 'architect', ',core number=', 4)
('This document belongs to class:', 'college', ',core number=', 4)
...

```

```

('This document belongs to class:', 'group', ',core number=', 2)
('This document belongs to class:', 'swarm', ',core number=', 2)
('This document belongs to class:', 'belongs', ',core number=', 2)
('This document belongs to class:', 'Green', ',core number=', 2)
('This document belongs to class:', 'golf', ',core number=', 2)
('This document belongs to class:', 'medalist', ',core number=', 2)
('This document belongs to class:', 'essential', ',core number=', 2)
('This document belongs to class:', 'kernel', ',core number=', 2)
...
('This document belongs to class:', 'technical_school', ',core number=', 2)
('This document belongs to class:', 'semantic', ',core number=', 2)
...
('This document belongs to class:', 'expert', ',core number=', 2)
('This document belongs to class:', 'adviser', ',core number=', 2)

```

812.4. Predictability of Tenure transitions of a profile can be effectively expressed as Chaotic Hidden Markov Model which is a combination of Verhulst Logistic and Hidden Markov Model. Verhulst-Pearl-Reed Logistic defines present observation  $X(n+1)$  in terms of previous  $X(n)$ :  $X(n+1) = \text{Lambda} * X(n) * (1 - X(n))$ . Hidden Markov Model on similar lines defines state transition probabilities and observations in each state. For this example profile, state transitions are organizations (including academic tenures and opensource initiative of the author) - in a gist left-to-right in chronological order (spanning 25 years - 1995-2020):

```

States: PSG - Baan/SSA - Sun/Oracle - Krishna-iResearch - Verizon -
webMethods/SoftwareAG - CMI/IIT/IMSc - GlobalAnalytics/GAIN - ClockWork -
CloudEnablers - Unaffiliated private research
Observations: Could be any parameter - academic or work, opensource
contribution, tenure duration, city, remuneration, designation in each
organization, proven research, domain

```

812.5. Both Verhulst Law and Hidden Markov Model assume observation on present state depends only on observation on previous state and not cumulatively conditioned on all previous states or tenure switch is decided only by present independent of history (which would have otherwise been a Martingale sequence -  $E(X_i/X_0, X_1, X_2, \dots, X_{i-1}) = X_{i-1}$ ) - expected observation in a state conditioned on all past states is the previous state observation - if each random variable  $X_i$  signifies one of the aforementioned observed parameters in an academic/work tenure state  $i$ ). Chaotic Hidden Markov Model which is a merger based on this common fact underlying Chaos and HMM adds one more dimension to predictability of a profile or lack of it depending on value of Lambda.

References:

```

812.6 Randomized Algorithms - [Prabhakar Raghavan-Rajeev Motwani] - Page 85 -
Martingales

```

813. (FEATURE) Recursive Lambda Function Growth - corrections for machine translation - 25 March 2020

```

1. RecursiveLambdaFunctionGrowth.py implementation has been changed to uncomment
machine_translation(). But yet because of REST ratelimit
English-Telegu translation is marred by "too many requests" exceptions.
Exception handling and error checks have been added in machine_translation() for
NoneType and ratelimit exceptions. Alternative could be local lookup of English-
Telegu dictionary from flat file.
2. Self loop edges have been removed because of exceptions in rich club

```

coefficient computation for the textgraph.

3.A news article on Chennai Urban Sprawl expansion has been mapped to textgraph and merit measures are printed to logs  
testlogs/RecursiveLambdaFunctionGrowth.log.MachineTranslation.25March2020.  
Telugu font decoding errors have created a Roman script graph. Proper noun filtering could further fine tune the objective meaning of the news article textgraph.

-----  
814. (THEORY and FEATURE) Computational Geometric Factorization and Set Partition to Lagrange Four Square Theorem Square Tile Cover Reduction - Randomization - 26 March 2020 - related to 651, 728 and all sections on Set partitions, Shell Turing Machines, Kernel Lifting and Factorization  
-----

1.DiscreteHyperbolicFactorizationUpperbound\_TileSearch\_Optimized.py has been changed to handle exceptions in Factor Spark Accumulator object by stripping off zero-es in zero() function.

2.Streaming\_SetPartitionAnalytics.py has been changed for subprocess invocation commandline of factorization. Error handling for size of arrays has been done.

3.Hardcoded set has been removed and Set to be partitioned is instantiated by range() and maximum size of the set is sent by commandline sys.argv. Size of the set to partition is randomly chosen between 1 and maxsize and factorized to get the sides of the rectangle. Lagrangian Four Square Theorem Square Tile Cover reduction for the tile cover of factorized random set rectangle is printed.

4.This reduction has following phases:

4.1 Partition a set of random size in SymPy - random histogram

4.2 Factorize the size of the set of random size by Computational Geometry - sides of the rectangle

4.3 Reduce each part of the random partition to sum of four squares by Lagrange Four Square Theorem - kernel lifting from 1 dimensional partition to 2 dimensional rectangle partition.

4.4 Concatenate each of four square tiles per part of the random partition into single set of square tiles.

4.5 Tile the rectangle by square tiles.

4.6 Number of square tiles per tile cover of rectangle = 4 \*  
number\_of\_parts\_in\_partition

-----  
815. (THEORY and FEATURE) Waveform Distance of Audios, Acoustic Distance of Strings, Name Similarity, Music Clustering - Python 3.7.5 - 27 March 2020,30 April 2020 - related to 783 and all sections on People Analytics, Compressed Sensing, Intrinsic Merit, Syllable embedding of strings, Hyphenation and Music Pattern Mining  
-----

1.NeuronRain AstroInfer already has a Music Recommender Systems implementation based on EMD similarities of Mel Frequency Cepstral Coefficients but not based on waveforms.

2.Usual Levenshtein Edit Distance is an alphabet based similarity measure while some problems in Name similarity require sophisticated acoustic matching algorithms (e.g NYSIIS, Soundex, Phonetic Match Rating)

3.This commit implements audio\_distance() function for 2 audios (whether music or speech waveforms) which extracts waveform arrays of two audio(s) and compares them by Hausdorff distance and Earth Mover Distance which are more quantitative distance measures than edit distance.

4.Such a generic waveform phonetic distance between audios of two text strings is an alternative to Levenshtein Edit Distance. But it requires two human voice audio recordings which spells out the text of two strings (as in IVRs)

5.Syllables are language and script independent phonemes and previous audio\_distance() by waveform match theoretically captures syllable phonetics

better than edit distance and suits name similarity. Audio waveform match might perform better by spelling out Syllable hyphenated texts than plain texts. Syllable boundary word hyphenation has been implemented earlier for People Analytics and requires syllable to human voice audio transforms.

6.AudioToBitMatrix.py has been upgraded to Python 3.7.5. Logs for the change are at

python-src/music\_pattern\_mining/testlogs/AudioToBitMatrix.log.AudioDistance.27March2020 which compare two similar and different pairs of audio clips of same duration.

7.Intrinsic merit in music is usually associated with creativity/originality of the composer where originality is defined as dissimilarity with works of other composers and similarity between works of self - waveform distance for music approximately captures how dissimilar a music work is from others and common pattern in compositions by self.

-----  
816. (THEORY and FEATURE) People Analytics - Human Resource Analytics - Chaotic Hidden Markov Model of Tenures/Attrition - implementation - related to 812 - 31 March 2020  
-----

-----  
1.Chaotic Hidden Markov Model of Tenures/Attritions based on Verhulst actuarial logistic has been implemented in a new source file  
SocialNetworkAnalysis\_PeopleAnalytics\_ChaoticHMM.py (Python 3.7.5) and  
SocialNetworkAnalysis\_PeopleAnalytics\_ChaoticHMM.py.2.7 (Python 2.7)  
2.Similar to other Hidden Markov Models for CRF and TextCompression, this implementation is a Python class accepting states(institutions and organizations),observations(including but not limited to domain-designations-remunerations-cities),emission probabilities(probability of an observation in a state),state transition probabilities(probability of switchovers between orgs) and Lambda (constant for Verhulst Logistic)  
3.chaotic\_HMM\_viterbi() function computes the HMM Viterbi algorithm as usual but with a difference in following line of code:  
(probability, state) = max((Viterbi[x-1]  
[t]\*self.Lambda\*self.transition\_probabilities[t][y]\*(1-  
self.transition\_probabilities[t][y])\*self.emission\_probabilities[y]  
[self.observations[x]], t) for t in self.states)  
which computes the argmax of transition to a state and observation in transitioned state by Verhulst logistic format  $\text{Lambda} \times x \times (1-x)$   
4.Probabilities dictionaries have been hardcoded presently in \_\_main\_\_ for invoking Chaotic HMM Viterbi (Lambda=3.7).  
5.Example profile of author (overall history of 25 years including academics and work) has been mapped to state transition and observation probabilities (in chronological order - ["Graduation", "AssociateSoftwareEngineer", "MemberTechStaff", "Founder-Architect", "SystemAnalyst", "Specialist", "PostGraduation-ResearchScholar", "Consultant-Architect", "Consultant", "Architect"]) and Viterbi computed is as below which accurately captures the career switches. Still this model considers parallel Tenures as sequential - FOSS initiative of author (Krishna iResearch) from 2003-present has duration of 17 years thus far. Non-major (below 18 years age) graduation in Hindi and schooling have been excluded which increase number of states and observations to 12 from 10 and history to 38 years:

=====  
Chaotic HMM Viterbi computation  
=====  
[{'BaaN-SSAGlobal': 0.0,  
...  
'PSGTech': 1.0,  
...  
'webMethods-SoftwareAG': 0.0},  
{'BaaN-SSAGlobal': 0.33300000000000001,  
...  
'webMethods-SoftwareAG': 0.0},

```
{'BaaN-SSAGlobal': 0.0,
 ...
 'SunMicrosystems-Oracle': 0.110889000000000004,
 ...
 'webMethods-SoftwareAG': 0.0},
{'BaaN-SSAGlobal': 0.0,
 ...
 'Krishna-iResearch': 0.0369260370000000016,
 ...
 'webMethods-SoftwareAG': 0.0},
{'BaaN-SSAGlobal': 0.0,
 ...
 'Verizon': 0.012296370321000007,
 ...
 'webMethods-SoftwareAG': 0.0},
{'BaaN-SSAGlobal': 0.0,
 ...
 'webMethods-SoftwareAG': 0.004094691316893003},
{'BaaN-SSAGlobal': 0.0,
 ...
 'CMI-IIT-IMSc': 0.0013635322085253701,
 ...
 'webMethods-SoftwareAG': 0.0},
{'BaaN-SSAGlobal': 0.0,
 ...
 'GlobalAnalytics': 0.0004540562254389483,
 ...
 'webMethods-SoftwareAG': 0.0},
{'BaaN-SSAGlobal': 0.0,
 ...
 'Clockwork-PiQube': 0.0001512007230711698,
 ...
 'webMethods-SoftwareAG': 0.0},
{'BaaN-SSAGlobal': 0.0,
 ...
 'CloudEnablers': 5.034984078269955e-05,
 ...
 'webMethods-SoftwareAG': 0.0}]
```

-----  
 817. (THEORY and FEATURE) People Analytics - Talent Analytics - Chaotic Hidden Markov Model of Parallel Tenures/Attritions and JSON persistence - Weighted Automata model of Tenures - Tensor Decomposition of EventNet Logical Time - related to 661,701,812 - 8 April 2020  
 -----

-----  
 1.SocialNetworkAnalysis\_PeopleAnalytics\_ChaoticHMM.py has been updated to remove hardcoded state transition and emission probabilities (from linkedin profile of author) and to read them from a JSON persistence  
 SocialNetworkAnalysis\_PeopleAnalytics\_ChaoticHMM.json by json.loads()  
 2.SocialNetworkAnalysis\_PeopleAnalytics\_ChaoticHMM.json has been made comprehensive to merge and serialize parallel academic and work tenures - there are multiple parallel academic and work tenures in the example profile making it increasingly difficult to fathom tenure durations because time is parallelized amongst multiple tenures. Parallel tenures are metrics for ability of a profile to multitask. Tensor decomposition of EventNet Causality Logical clock is worth mentioning here which componentizes time - each linear component of time tensor could correspond to a parallel tenure empirically.  
 3.Parallel tenures are presently simulated by probability distributions - earlier sequential viterbi has been recomputed for parallel tenures which has multiple non-zero probability states per chronological layer of viterbi trellis and largest probability per layer points to the most prominent state at a time



point. Optimal choice of probabilities in JSON are reflected in viterbi and following is an example for parallel tenure traversal from logs  
testlogs/SocialNetworkAnalysis\_PeopleAnalytics\_ChaoticHMM.log.8April2020  
simulating parallelism:

```
=====
Chaotic HMM Viterbi computation
=====
[{'BaaN-SSAGlobal': 0.0,
 ...
 'Schooling': 0.1,
 ...
 'webMethods-SoftwareAG': 0.0},
{'BaaN-SSAGlobal': 0.0,
 ...
 'DBHPS': 0.036223000000000005,
 'PSGTech': 0.0333,
 'Schooling': 0.0333,
 ...
 'webMethods-SoftwareAG': 0.0},
{'BaaN-SSAGlobal': 0.0,
 ...
 'DBHPS': 0.012062259000000004,
 ...
 'PSGTech': 0.013121057290000003,
 'Schooling': 0.012062259000000004,
 ...
 'webMethods-SoftwareAG': 0.0},
{'BaaN-SSAGlobal': 0.004369312077570002,
 ...
 'webMethods-SoftwareAG': 0.0},
{'BaaN-SSAGlobal': 0.0,
 ...
 'SunMicrosystems-Oracle': 0.001454980921830811,
 ...
 'webMethods-SoftwareAG': 0.0},
{'BaaN-SSAGlobal': 0.0,
 ...
 'Krishna-iResearch': 0.00048450864696966017,
 ...
 'webMethods-SoftwareAG': 0.0},
{'BaaN-SSAGlobal': 0.0,
 ...
 'Verizon': 0.00016134137944089685,
 ...
 'webMethods-SoftwareAG': 0.0},
{'BaaN-SSAGlobal': 0.0,
 ...
 'webMethods-SoftwareAG': 5.3726679353818657e-05},
{'BaaN-SSAGlobal': 0.0,
 'CMI-IIT-IMSc': 1.7890984224821618e-05,
 ...
 'webMethods-SoftwareAG': 0.0},
{'BaaN-SSAGlobal': 0.0,
 ...
 'GlobalAnalytics': 5.9576977468656e-06,
 ...
 'webMethods-SoftwareAG': 0.0},
{'BaaN-SSAGlobal': 0.0,
 ...
 'Clockwork-PiQube': 1.983913349706245e-06,
 ...
 'webMethods-SoftwareAG': 0.0},
{'BaaN-SSAGlobal': 0.0,
```

```

 ...
'CloudEnablers': 6.606431454521795e-07,
 ...
'webMethods-SoftwareAG': 0.0}]

```

4. Tenure transitions could also be formalized by weighted automata which has been already implemented in NeuronRain AstroInfer to measure complexity of music notes:

```

(tenure1, a, tenure2) - transition from state tenure1 to state tenure2 on
symbol a of weight 1
(tenure2, 2b, tenure3) - transition from state tenure2 to state tenure3 on
symbol b of weight 2

```

Symbols inducing tenure transitions could be any observation (remuneration, designation, location, ...) augmented by weight which simulates importance of observation.

5. Complexity of Chaotic HMM and Weighted Automata for tenure transitions of a profile measures unpredictability and merit which is any of the following - parallel tenures, cyclical tenures, academic-work transitions, individual contributions - (corporate and personal initiatives(FOSS)),....

-----  
818. (THEORY and FEATURE) Chaotic Pseudorandom Generator (PRG) - Mandelbrot set, Undecidability of Learning Chaotic Bigdata - 13 April 2020 - related to 459,629,740,743,744 and all sections on Pseudorandomness, EVMs, Hardness amplification, Computational learning theory, Chaos  
-----

1. ChaosAttractor.py has been changed to create Mandelbrot set sequence by recursively iterating complex logistic map in a separate clause and function arg - "Mandelbrot" - to ChaosPRG():

```

Z <- Z^2 + C (for seed C)

```

2. From 629.6 earlier, Mandelbrot set is undecidable due to differing Hausdorff dimensions(1 and 2) which is crucial because Mandelbrot sets are universally found amongst most natural processes (biological, economic-markets, weather, geographic massive datasets) - Undecidability implies there is no halting Turing machine which recognizes language of Bigdata Mandelbrot sets dealing a lethal blow to BigData learnability.

3. Pseudorandom Mandelbrot sequence generated by previous map  $Z: Z^2 + C$  thus is undecidable and a distinguisher Turing machine  $A$  ( $\Pr[A(x)=1]$  -

$\Pr[A(\text{ChaosPRG}(\text{seed}))=1] > \epsilon$  where  $x$  is a perfect random string in  $\{0,1\}^n$ ) which recognizes such a chaotic sequence does not exist too.

4. Example Mandelbrot sequences can be found in testlogs/ChaosAttractor.Mandelbrot.log.13April2020

5. Psuedorandom paper ballot shuffle simulation of Drone Electronic Voting Machine ballots by Chaotic Mandelbrot PRG thus nullifies distinguishability - but yet aforementioned Ramsey theoretic anomaly - "inevitable emergence of order from chaos" - arises: monochromatic arithmetic progressions are still possible in chaotically shuffled multichromatic sequence of votes(if votes are explicitly colored by candidate indices).

References:

-----  
818.1 Chaotic Cryptographic Hash Functions - Merkle-Damgard Construction and Chaotic Network automata -

<https://ui.adsabs.harvard.edu/abs/2017JPhCS.936a2058M/abstract> - "Chaos theory has been used to develop several cryptographic methods relying on the pseudo-random properties extracted from simple nonlinear systems such as cellular automata ... Following the Merkle and Damgård model of construction, a portion of the message is entered as the initial condition of the network automata, so that the rest parts of messages are iteratively entered to perturb the system ..."

818.2 Merkle-Damgard Construction - initialization vector (IV) and iterated hashing - [https://en.wikipedia.org/wiki/Merkle%E2%80%93Damgård%3A5rd\\_construction](https://en.wikipedia.org/wiki/Merkle%E2%80%93Damgård%3A5rd_construction)

-----  
-----  
819. (THEORY and FEATURE) Chaotic Pseudorandom Generator - 1D Binary Cellular Automaton - Multicolored Space Filling - implementation - 16 April 2020, 17 April 2020 - related to 135, 752, 818 and all sections on Monochromatic and Multichromatic Space filling, Chaos, Computational Geometric Planar Point Location Search, Pseudorandomness, Linear Programs/CSP, LSH/Separate Chaining, Circle Packing in NeuronRain Unified Theory Drafts  
-----  
-----

1. New function `grow_cellular_automaton()` has been defined in `ChaosAttractor.py` which grows an one dimensional binary cellular automaton.  
2. `ChaosPRG()` function accepts four algorithm options - "Logistic", "Lehmer-Palmore", "Mandelbrot" and "Cellular Automaton".  
3. `grow_cellular_automaton()` function accepts a binary string of 0s and 1s as initialization vector and a random Lambda fraction.  
4. Following simple growth rule has been implemented:  
    4.1 Automaton is grown by scanning the two binary digit neighbours of a bit location for four possibilities - 00, 10, 01, 11  
    4.2 For each possible neighbourhood, bit location in next generation is updated depending on random value of lambda to 0 or 1  
    4.3 This simulates Conway's Birth-Survival-Death Game of Life Cellular Automaton approximately and 2-dimensional tableau of binary strings grown in parallel thus captures space filling complexity of natural processes including random fluid flow, rainfall, randomly strewn solids, ...  
    4.4 Cellular Automaton Space Filling Algorithm in 135, a refinement of LP version in <https://sites.google.com/site/kuja27/Analysis%20of%20a%20Randomized%20Space%20Filling%20Algorithm%20and%20its%20Linear%20Program%20Formulation.pdf?attredirects=0> describes a Parallel PRG based 2-dimensional Cellular Automaton which monochromatically fills a 2-D plane in parallel  
    4.5 Each generation row of 1D binary Cellular Automaton is a Pseudorandom bit sequence  
5. States (colors) of the squares in this implementation are binary - 1 or 0 which could be generalized to arbitrary coloring alphabet by defining/reading new growth rules within `grow_cellular_automaton()` making it a multichromatic space filling. An example rule for 2-dimensional multicolored cellular automata could be Four color theorem - cell and its 8 neighbours are 4-colorable facets; neighbouring faces avoid same color and for successive generations coloring violations might have to be readjusted - Example:  
    1 2 3  
    3 4 1  
    1 2 3  
6. R correlations of the Cellular Automaton PRG to a stock quote dataset are printed in `testlogs/ChaosAttractor.CellularAutomaton.log.16April2020`.  
-----  
-----

820. (THEORY and FEATURE) People Analytics - LinkedIn Dataset Analysis - Tenure statistics - 17 April 2020 - related to 817  
-----  
-----

1. LinkedIn profile parser function `parse_profile()` in `SocialNetworkAnalysis_PeopleAnalytics.py` has been updated to compute following tenure statistics for each linkedin text profile for being compliant to Kaggle linkedin CSV dataset (<https://www.kaggle.com/killbot/linkedin>) which has these fields. Ethnic and physical feature fields have been excluded:  
    `self.avg_n_pos_per_prev_tenure = 1`  
    `self.avg_pos_len =`  
    `float(sum(self.timedeltas))/float(len(self.timedeltas))`  
    `self.avg_prev_tenure_len =`  
    `float(sum(self.timedeltas[:-1]))/float(len(self.timedeltas[:-1]))`  
    `self.n_prev_tenures = len(self.timedeltas)-1`

```

 self.tenure_len = self.timedeltas[-1:]
 self.n_followers = self.parse_connections(profile_text)
2.Previous statistics compute average number of positions per previous tenure
(which has been assumed to be 1), average length of positions(computed from
tenure timedeltas histogram), average previous tenure length (computed by
neglecting present tenure), number of previous tenures, tenure length (only
present tenure), number of followers (connections)
3.Each of these tenure variables could be either analyzed as moving average
timeseries (kind of martingale because it captures past history) or observations
read from JSON in Weighted Automata - Chaotic Hidden Markov Model of Tenures
(SocialNetworkAnalysis_PeopleAnalytics_ChaoticHMM.py) - JSON file based on these
variables could be dynamically written per linkedin profile and Viterbi is
computed.
4.Logs for example linkedin profile of author
(https://www.linkedin.com/comm/in/srinivasan-kannan-608a671) are at
testlogs/SocialNetworkAnalysis_PeopleAnalytics.log.17April2020
5.Video resumes could also be analytics datasources apart from usual social
network data in PDF and TXT because of their greater authenticity
(Alumni,Quora,Facebook,Twitter,Google,Repositories profile montage Video resumes
of author in python-src/image_pattern_mining - ExampleVideo_1.mp4,
ExampleVideo_4.mp4, ExampleVideo_2.mp4,
ExampleVideo_Facebook_GRAFIT_29April2019.mp4, ExampleVideo_3.mp4,
ExampleVideo_GoogleScholar_Search.mp4) .

```

-----

865. (THEORY and FEATURE) NeuronRainApps - NeuronRain usecases - Drone  
Autonomous Online Shopping Delivery Implementation - MAVSDK + JMAVSIM simulation  
for PX4 - 1 September 2020 - related to 637,675,713

-----

```

1. OnlineShoppingDelivery Python 3.7.5 implementation in NeuronRainApps/Drones
has been changed to import MAVSDK Mission Plan classes and
dronecode_sdk imports have been commented (Example:
https://github.com/mavlink/MAVSDK-Python/blob/master/examples/mission.py).
2. Following GIS analytics variables are read by socket streaming datasource in
Streaming Abstract Generator from a webserver listening on port 64001 (netcat -l
64001) and are parsed as key-value pairs (these variables have also been
committed to
python-src/NeuronRainApps/Drones/OnlineShoppingDelivery.GISvars.txt) delimited
by end marker:
 longitude=47.397825620791895
 latitude=8.5450092830163281
 relative_altitude_m=1
 speed_m_s=1
 is_fly_through = True
 gimbal_pitch_deg = nan
 gimbal_yaw_deg = nan
 camera_action = none
 loiter_time_s = nan
 camera_photo_interval_s = nan
 end
3. In this commit only first four variables for navigation are being read from
socket stream while rest are assumed to have default values.
4. Code changes for MissionPlan specific to MAVSDK mission-upload, start-mission
and arm-takeoff-take_photo have been committed. To simulate a hamiltonian cycle,
drone.mission.set_return_to_launch_after_mission(True) has been invoked.
5. awaits for mission progress and observe_is_in_air have been commented.
6. GIS navigation analytics variables read over socket stream are filtered for
convex-hull boundaries and mission items are appended accordingly to Mission
plan. Every mission item is a delivery point.
7. JMAVSIM and PX4 SITL Logs, Netcat logs for streaming analytics variables and
MP4 video of the simulated flight of a drone have been committed as hereunder:

```

python-src/NeuronRainApps/Drones/testlogs/OnlineShoppingDelivery\_Drone\_JMAVSIM\_Flight\_Simulation.log1.1September2020

python-src/NeuronRainApps/Drones/testlogs/OnlineShoppingDelivery\_Drone\_JMAVSIM\_Flight\_Simulation.log2.1September2020

python-src/NeuronRainApps/Drones/testlogs/OnlineShoppingDelivery\_PX4\_Drone\_JMAVSIM\_Flight\_Simulation2.mp4

#### 8. Video

python-src/NeuronRainApps/Drones/testlogs/OnlineShoppingDelivery\_PX4\_Drone\_JMAVSIM\_Flight\_Simulation2.mp4 shows the imaginary multirotor drone in JMAVSIM PX4 SITL making a vertical takeoff, drawing an aerial cycle based on longitude-latitude-altitude of mission item delivery points before comeback to origin by vertical landing.

-----  
867. (THEORY and FEATURE) OpenCV Image Contours and Segmentation for Drone Obstacle Avoidance and Motion Planning - related to 866 and all sections on Large Scale Visual Recognition, GIS analytics and Drone Navigation - 12 September 2020  
-----

-----  
1.This code change implements a new function `image_segmentation_contours()` in `ImageGraph_Keras_Theano.py` which is exactly similar to contouring code in `handwriting_recognition()` (`DeepLearning_ConvolutionNetwork_BackPropagation.py`) for topological handwriting recognition (Product Homotopy) but without distance computation for two imagefiles and finds contour interpolation polynomials for single image.

2.`image_segmentation_contours()` has been implemented as a subroutine which is invoked by `image_segmentation()` and could be used by any other NeuronRain computer vision and Large Scale Visual Recognition analytics code.

3.`image_segmentation()` earlier had only a computational geometric segmentation of an image for finding component segments and their centroids (GRANA), Delaunay Triangulation and Facegraphs.

4.A-Star motion planning implementation in NeuronRain (Section 866 of NeuronRain Theory Drafts) assumes a graph adjacency matrix and heuristic array signifying estimated cost of obstacle per vertex.

5.Contour detection for GIS imagery is a tool for obstacle avoidance in drone navigation and motion planning. For example, extracting contour points and its interpolated polynomials from a Road network GIS imagery of a terrain is useful for drawing a Contour graph vertices of which are contour points connected by contour polynomials. Adjacency matrix of such a contour graph could be used in A-Star implementation for Drone navigation.

6. It is worth observing that 3D-navigation of drones on the edges of road (rail or other transport) network graphs (assuming sufficient vehicle clearance heights greater than grade separators and interchanges for drone altitude) is always obstacle-free because of zero collision (on the contrary driverless vehicles on 2D road networks have non-trivial obstacle avoidance challenge - an optional obstacle avoidance could be to do a VerticalTakeOffLanding (VTOL) for circumventing every obstacle adding a third dimension to surface transport vehicle).

7. An example Road network map from Google Maps has been contour-recognized and following logs and image files illustrate the contour polynomials inferred from road network - by both `image_segmentation()` and `image_segmentation_contours()` :

testlogs/ImageGraph\_Keras\_Theano.log.ContourSegmentation.26September2020

testlogs/RemoteSensingGIS/Google\_Maps\_SouthernIndia\_RoadMap-000.jpg

testlogs/RemoteSensingGIS/Google\_Maps\_SouthernIndia\_RoadMap-

000\_contours\_segmented.png

testlogs/RemoteSensingGIS/Google\_Maps\_SouthernIndia\_RoadMap-

000\_segmented.jpg

testlogs/RemoteSensingGIS/Google\_Maps\_SouthernIndia\_RoadMap.pdf

testlogs/VoronoiFaceGraph\_GoogleMaps\_RoadMap\_1\_26September2020.png

-----  
868. (THEORY and FEATURE) OpenCV Image Contours and Segmentation for Medical Imageing - Magnetic Resonance Imageing (MRI and fMRI) - related to 656, 681, 867, 815 and all sections on Large Scale Visual Recognition, Medical Imageing and Intrinsic Merit of Music - 26 September 2020  
-----

- 1. Functional MRI datasets (OpenNeuro - <https://openneuro.org/public/datasets> - earlier OpenfMRI) contain huge volumes of experimental functional MRI data for analyzing connectomes in brain and impact of music on humans (e.g <https://openneuro.org/datasets/ds000171/versions/00001>)  
2. Machine Learning has been extensively applied to analyze fMRI data - [Frontiers in Psychology - [https://www.researchgate.net/publication/51563375\\_Functional\\_Data\\_Analysis\\_in\\_Brain\\_Imaging\\_Studies](https://www.researchgate.net/publication/51563375_Functional_Data_Analysis_in_Brain_Imaging_Studies)] - by means of which merit of music waveforms could be quantitatively compared for music clustering. NeuronRain already implements automata theoretic and mel-frequency merit measures for music.  
3. This code change adds a clause for MRI in `medical_imageing()` in `ImageGraph_Keras_Theano.py` and invokes `medical_segmentation_contours()` to find contours of an example MRI image of brain for different activities.  
4. Actual MRI and contour segmented images are at:

`testlogs/ImageGraph_Keras_Theano.MedicalImageing.MRIContours.26September2020.png`  
`testlogs/medical_imageing/MRI_fpsyg-01-00035-000.jpg`

5. Logs for 867 -  
`testlogs/ImageGraph_Keras_Theano.log.ContourSegmentation.26September2020` - have computation of contours for example MRI medical image (`testlogs/medical_imageing/MRI_fpsyg-01-00035-000.jpg`) as well.  
-----

-----  
869. (THEORY and FEATURE) Drone Obstacle Avoidance by 3D Navigation on Airspace defined by Road Geometry - related to 582, 867 and all sections on Motion Planning, GIS Analytics, Logical clocks, Large Scale Visuals Recognition, Drone Swarms - 2 October 2020, 6 October 2020  
-----

- 1. 3D Navigation of Drones along road network graph airspace (which is theoretically free of natural obstacles) mentioned in 867 requires a webservice which churns out array of GPS ordinates of a road geometry from origin to destination.  
2. Google Roads webservice - <https://developers.google.com/maps/documentation/roads/overview> - returns array of snapped GPS ordinate points best fit to a road geometric course between origin and destination.  
3. Previous array of GPS ordinates could be looped to create mission items which can be populated to a mission plan and uploaded which is theoretically an obstacle free mission sticking to airspace strip along the road geometry.  
4. Obstacle avoidance in 3D (4D including time reckoning relativity for Drone Swarms) thus reduces to finding optimal altitude along the airspace on road geometry  
5. Road geometry airspace poses mostly man-made obstacles (flyovers etc.,) and drone altitude must be recomputed for each obstacle (requires interchange/grade-separators structure recognition and their height inference by OpenCV contouring and sensors) or a maximum altitude for drone mission items is set which is greater than all possible man-made structures on a road strip.  
6. Groups of Drones (Drone Swarms) and Obstacle avoidance amongst them has increasing applications in combat and tactical ops.

References:

-----  
869.1 Google Roads Geometry REST API - <https://developers.google.com/maps/documentation/roads/snap> - returns an array

of GPS points and place id(s) best fit to an approximate road trajectory between origin and destination

869.2 Lane detection for autonomous surface transport vehicles in OpenCV - <https://campushippo.com/lessons/detect-highway-lane-lines-with-opencv-and-python-21438a3e2>

869.3 Drone Swarms - DARPA - <https://www.theverge.com/2019/8/9/20799148/darpa-drones-robots-swarm-military-test>

869.4 SwarmLab - Obstacle Avoidance Simulation of Drone Swarms in MATLAB - Olfeti-Saber and Vaserhelyi Obstacle avoidance algorithms - <https://arxiv.org/pdf/2005.02769.pdf>

869.5 Decentralized 3D Collision Avoidance for Multiple UAVs in Outdoor Environment - <https://www.ncbi.nlm.nih.gov/pmc/articles/PMC6308403/>

-----  
872. (THEORY and FEATURE) Fibonaccian Search - alternative to binary search - related to all sections on Computational Geometric Planar Point Location Factorization, Geometric Search of BigData, Arithmetic Progressions and Ramsey coloring - 31 October 2020  
-----

1. Binary Search could be costly in some architectures because of division by 2. Fibonaccian search based on Fibonacci series avoids division and depends only on addition and subtraction. Note: Fibonaccian search is different from Fibonacci search to locate maximum of a unimodal function.
2. Binary search is central to Computational Geometric Factorization to locate a factor point within a segment/interval/pixel-array-polygon which is a sorted arithmetic progression of ordinate products.
3. Fibonaccian search optimization to replace Binary search in planar point location could significantly reduce constant involved in  $O(\log N)$  search.
4. Both Binary search and Fibonaccian search are  $O(\log N)$  while the search tree of the latter makes the difference - Left subtree of Fibonacci search is 1.618 (Golden ratio) times more skewed than Right subtree.
5. In terms of runtime efficiency Fibonaccian search lies between Binary Search and Interpolation search (which is  $O(\log \log N)$  and assumes elements are within a known range)

References:

-----  
872.1 Fibonaccian search - Section 6.2.1 - Searching an ordered table - Page 418 - Algorithm F - The Art of Computer Programming - Volume 3 - [Donald Knuth]  
-----

873. (THEORY and FEATURE) Fibonaccian Search - Python 3.9.0 upgrade for Factorization - related to 872 - 5 November 2020  
-----

1. Fibonaccian search python implementation has been upgraded to Python 3.9.0 by autopep8 and 2to3-3.9 tools for potential invocation from Computational geometric factorization which is already Python 3 compatible.
2. Python 2.7 version of Fibonaccian search has been separately committed.
3. After this upgrade NeuronRain supports all three versions of Python 3 - Python 3.7.5, Python 3.8.5 and Python 3.9.0

-----  
874. (THEORY and FEATURE) People Analytics - People Profiles as Tensors - related to 752 and all sections on Embedding in vectorspace, Social Network Analytics, Psephology/Election analytics, Majority Voting, Intrinsic merit of People profiles - 13 November 2020  
-----

-----

- 1.python-src/SocialNetworkAnalysis\_PeopleAnalytics.py has been changed to optionally choose between REST API calls to PIPL.com and reading a json file of people profile from any datasource including PIPL.com by boolean parameter loadfromjson in function pipldotcom\_analytics() which reads People data in JSON from testlogs/SocialNetworkAnalysis\_PeopleAnalytics.json
- 2.JSON objects are multidimensional which could be construed as points on a vectorspace. TensorFlow supports reading JSON format of Tensors as Protobufs (Read JSON string and return a Protobuf Tensor - [https://www.tensorflow.org/api\\_docs/python/tf/io/decode\\_json\\_example](https://www.tensorflow.org/api_docs/python/tf/io/decode_json_example)).
- 3.Mapping people profiles onto Tensor points on vectorspace opens up possibility of whole gamut of Computational geometric People analytics - for example closest pair and clusters of people could be found and profiles could be iteratively ranked to get similarities.
- 4.Clustering of people profiles is crucial in analyzing voting patterns.
- 5.On a related note, NeuronRain implements a Set partition Electronic Voting Machine and every candidate bucket is a cluster of voters - Distance similarity (or Swing between consecutive polls) between any two Set Partition EVMs is measurable by Earth mover distance (Wasserstein distance).

-----

875. (THEORY and FEATURE) People Analytics - Alphabet Vectorspace Embedding Distance implementation - related to 752,874 and all sections on Embedding in vectorspace, Compressed Sensing, Social Network Analytics, Meaning Representation, Intrinsic Merit of People Profiles/HR Analytics - 15 November 2020

-----

1. CompressedSensing.py has been changed to implement a new function alphabet\_vectorspace\_embedding\_distance(self, embedding1, embedding2) which finds the euclidean distance between two string vector points (1-dimensional Tensor) embedded in alphabet space.
2. It uses the ord() builtin to compute ordinal values of the ascii or unicode strings.
3. alphabet\_vectorspace\_embedding\_distance() is invoked from python-src/SocialNetworkAnalysis\_PeopleAnalytics.py to compare two different name spellings in English of a Sanskrit name.
4. Strings of different lengths are left justified and padded by "#" fill before distance computation.
5. Distance computed is normalized - divided by length of the strings compared.
6. Logs

python-src/testlogs/SocialNetworkAnalysis\_PeopleAnalytics.log.15November2020 show distance similarities amongst different name spellings in English of Sanskrit name which can be contrasted against Phonetic match rating and NYSIS Flight manifest name similarity algorithms as below:

```
embedding1: ['S', 'h', 'r', 'i', 'n', 'i', 'v', 'a', 's', '#', '#', '#']
embedding2: ['S', 'h', 'r', 'i', 'n', 'i', 'v', 'a', 'a', 's', 'a', 'n']
Alphabet Vectorspace Embedding Distance between ['S', 'h', 'r', 'i', 'n', 'i', 'v', 'a', 's', '#', '#', '#'] and ['S', 'h', 'r', 'i', 'n', 'i', 'v', 'a', 'a', 's', 'a', 'n'] : 127.251719045363
Normalized Alphabet Vectorspace Embedding Distance between ['S', 'h', 'r', 'i', 'n', 'i', 'v', 'a', 's', '#', '#', '#'] and ['S', 'h', 'r', 'i', 'n', 'i', 'v', 'a', 'a', 's', 'a', 'n'] : 10.604309920446918
leftjustified: ['S', 'h', 'r', 'i', 'n', 'i', 'v', 'a', 's', '#']
embedding1: ['S', 'h', 'r', 'i', 'n', 'i', 'v', 'a', 's', '#']
embedding2: ['S', 'r', 'i', 'n', 'i', 'v', 'a', 's', 'a', 'n']
Alphabet Vectorspace Embedding Distance between ['S', 'h', 'r', 'i', 'n', 'i', 'v', 'a', 's', '#'] and ['S', 'r', 'i', 'n', 'i', 'v', 'a', 's', 'a', 'n'] : 84.34453153583817
Normalized Alphabet Vectorspace Embedding Distance between ['S', 'h', 'r', 'i', 'n', 'i', 'v', 'a', 's', '#'] and ['S', 'r', 'i', 'n', 'i', 'v', 'a', 's', 'a', 'n'] : 8.434453153583817
leftjustified: ['S', 'r', 'i', 'n', 'i', 'v', 'a', 's', 'a', 'n', '#', '#']
```



embedding1: ['S', 'h', 'r', 'i', 'n', 'i', 'v', 'a', 'a', 's', 'a', 'n']  
embedding2: ['S', 'r', 'i', 'n', 'i', 'v', 'a', 's', 'a', 'n', '#', '#']  
Alphabet Vectorspace Embedding Distance between ['S', 'h', 'r', 'i', 'n', 'i', 'v', 'a', 'a', 's', 'a', 'n'] and ['S', 'r', 'i', 'n', 'i', 'v', 'a', 's', 'a', 'n', '#', '#'] : 103.24243313676794  
Normalized Alphabet Vectorspace Embedding Distance between ['S', 'h', 'r', 'i', 'n', 'i', 'v', 'a', 'a', 's', 'a', 'n'] and ['S', 'r', 'i', 'n', 'i', 'v', 'a', 's', 'a', 'n', '#', '#'] : 8.603536094730662  
7. Invocation of Recursive Lambda Function Growth Meaning Representation of a Professional Profile and Email context name parsing have been uncommented. Because of unfiltered proper nouns of organizations, few lambda functions are misleading.  
8. Two phonetically different name spellings "Rasa" and "Raja" of same name (in Tamizh and Sanskrit respectively) are compared for euclidean distance similarity.  
9. Syllable Hyphenation of name strings adds one more dimension and would create a 2-dimensional tensor embedding and distance between two 2D tensors could be more accurate e.g:  
    "Srinivasan" - [[S,r,i,n,i],[v,a,s,a,n]]  
    "Shrinivas" - [[S,h,r,i,n,i],[v,a,s]]  
    "Shrinivaasan" - [[S,h,r,i,n,i],[v,a,a,s,a,n]]  
10. For arbitrary dimensional people data as JSON tensors which include name, work experience, connections, academics etc., distance computation between Person1 and Person2 requires expanding dimensions of smaller tensor and computing the norm of Person1 - Person2 (Stackoverflow question - <https://stackoverflow.com/questions/55196194/how-to-calculate-the-euclidean-distance-between-a-2-d-tensor-and-a-3-d-tensor>)

-----  
876. (THEORY and FEATURE) People Analytics - People profiles as Tensors - Chaotic Hidden Markov Model of Tenure Transitions - TensorFlow integration for conversion of People profile data to Tensors - 17 November 2020 - related to 365,400,572,875 and all sections on Intrinsic merit of People, BKS Conjecture, Condorcet Jury Theorem, Margulis-Ruzso Threshold, Berry-Esseen Central Limit Theorem and Stability of Interview formalized by LTF/TQBF/PTF  
-----

-----  
1. This commit invokes TensorFlow convert\_to\_tensor() function for converting any People profile data encoded as any Python object including JSON to a Tensor.  
2. python-src/SocialNetworkAnalysis\_PeopleAnalytics\_ChaoticHMM.py which models tenure transitions of People profiles by Chaotic Hidden Markov Model Viterbi Trellis, now imports TensorFlow and TensorFlow I/O.  
3. SocialNetworkAnalysis\_PeopleAnalytics\_ChaoticHMM.json Tenure Transition is read and the fields are converted to Tensors by convert\_to\_json() TensorFlow API e.g tenure organizations - academic and work - are encoded as TF tensor below:  
    piplprofiTensor - states: tf.Tensor(  
    [b'Schooling' b'DBHPs' b'PSGTech' b'Baan-SSAGlobal'  
    b'SunMicrosystems-Oracle' b'Krishna-iResearch' b'Verizon'  
    b'webMethods-SoftwareAG' b'CMI-IIT-IMSc' b'GlobalAnalytics'  
    b'Clockwork-PiQube' b'CloudEnablers'], shape=(12,), dtype=string)  
4. TensorFlow function decode\_as\_json() might also be invoked but there are occasional JSON parsing errors.  
5. Objective of NeuronRain People Analytics is to automate, do away with or minimize human errors in talent recruitment through machine learning models. Stability and Noise Sensitivity criterion of an interview TQBF/LTF/PTF derived earlier theoretically stipulates when a talent recruitment system by Question-Answering is better than majority voting and thus has enormous HR analytics ramifications. Goodness of majority voting - when group decision converges to good outcome for p-biased voters - is limited by Margulis-Ruzso Threshold/Condorcet-Black-Ladha Jury Theorems for p-biased boolean functions. Combining the two, Stability criterion for interview TQBF (which is in IP=PSPACE) outclassing majority decision and Margulis-Ruzso/CJT threshold for majority decision converging to 100% are thus inversely related - if Questions-

Answers are improperly weighted ( $a \leq 1.2056205488/n$ ) for every possible LTF, Interview process is subverted and becomes unstable making BKS Conjecture False.

-----  
877. (FEATURE) Merit of Large Scale Visuals (LSVR) - TensorFlow Keras Backend - 18 November 2020 - related to 868 and all sections on Video Merit, Large Scale Visual Recognition  
-----

-----  
This commit changes KERAS\_BACKEND to TensorFlow for Video predictions by Keras and ImageNet. By this both Theano and TensorFlow are supported by NeuronRain Large Scale Visual Analytics. An example GoogleScholar and Google Search for query "NeuronRain Srinivasan Kannan" is analyzed by Keras-TensorFlow combine. TensorFlow has inbuilt support for tensors and Logical Clock EventNet Tensors, Video EventNet Tensors, People Profile Tensors and any multidimensional data could be translated to TensorFlow `tf.Tensor()` object. TensorFlow supports Keras models.  
-----

-----  
878. (FEATURE) EventNet Python Parser - Events as Tensorflow Tensors - 20 November 2020 - related to 701 and all sections on EventNet Logical Clock, Video EventNet Tensor Products algorithm for Merit of Large Scale Visuals and Category Theory  
-----

-----  
This commit refactors EventNet/EventNet.py to define `EventNet_Tensor_Parser()` function which parses the EventNet Vertices and Edges text files and instantiates TensorFlow Tensor objects for each intraevent conversations (edges amongst actors in an event) and a holistic EventNet TensorFlow Tensor for interevent causality. EventNet abstraction helps analyzing Videos - each Frame is an Event, actor objects within a Frame event category interact by morphisms (intraevent) and Causality between Frames (interevent) is defined by edges or Functors between two Frame Event categories. More than anything else, EventNet conceptualizes a multidimensional logical time Tensor and postulates that time tensor could be decomposed to components. EventNet example has been redrawn by GraphViz and `testlogs/EventNet.Tensor.log.20November2020` capture the EventNet Tensor instantiated as TensorFlow `tf.Tensor()` objects.  
-----

-----  
1123. (THEORY and FEATURE) People Analytics - Alphabet Vectorspace Embedding - Earth Mover Distance between String Syllable Tensors - related to 752,874,875 and all sections on Embedding in vectorspace, Compressed Sensing, Social Network Analytics, Meaning Representation, Intrinsic Merit of People Profiles/HR Analytics, Set Partition and Histogram analytics - 27 November 2020  
-----

-----  
1.This commit augments `CompressedSensing.py` - `alphabet_vectospace_embedding_distance()` function to optionally compute syllable vector earth mover distance between two phonetic syllable hyphenated string 2D tensors (encoded by ordinal integers) by `syllable_tensor_distance` boolean flag  
2.Lot of options were tried for computing distance norm between two 2D tensors having arbitrary number of rows and columns of unequal lengths - TensorFlow, sklearn, SciPy `directed_hausdorff`, `wasserstein_distance` and `cdist`, OpenCV2 EMD - and OpenCV2 EMD has been chosen because of its implicit dimension expansion, support for unequal rows and columns between two 2D tensors (which is very much necessary for comparing two strings of unequal number of syllables of arbitrary length) and ability to measure syllables as histograms - syllables partition a string to histogram buckets and distance between two strings is the amount of work necessary to move one string syllable histogram to another (2D analogue of Edit Distance) which is captured by Earth Mover Distance of OpenCV.  
3.Function `tosig()` translates a syllable hyphenation of string to `OpenCV.EMD()`  
-----

```

format.
4.Logs at
python-src/testlogs/SocialNetworkAnalysis_PeopleAnalytics.log.27November2020
compute EMD between following string syllable hyphenations:
csensing.alphabet_vectorspace_embedding_distance(['n','o'], ['m','i'],
['n','a','l']], [['s','e'], ['m','i'], ['n','a','l']],True)
csensing.alphabet_vectorspace_embedding_distance(['t','e','r'], ['m','i'],
['n','a','l']], [['s','e'], ['m','i'], ['n','a','l']],True)
csensing.alphabet_vectorspace_embedding_distance(['S','h','r','i'], ['n','i'],
['v','a','a'], ['s','a','n']], [['S','r','i'], ['n','i'],
['v','a','s','a','n']],True)
5.Following are the respective EMDs computed for string syllable
hyphenations(encoded by ordinals):
ordembedding1: [[110, 111], [109, 105], [110, 97, 108]]
ordembedding2: [[115, 101], [109, 105], [110, 97, 108]]
Earth Mover Distance between two String syllable tensors: (0.006666666828095913,
None, array([[110., 0., 0., 0., 0., 0., 0.],
[5., 101., 0., 0., 0., 0., 0.],
[0., 0., 109., 0., 0., 0., 0.],
[0., 0., 0., 105., 0., 0., 0.],
[0., 0., 0., 0., 110., 0., 0.],
[0., 0., 0., 0., 0., 97., 0.],
[0., 0., 0., 0., 0., 0., 108.]], dtype=float32))
ordembedding1: [[116, 101, 114], [109, 105], [110, 97, 108]]
ordembedding2: [[115, 101], [109, 105], [110, 97, 108]]
Earth Mover Distance between two String syllable tensors: (0.0, None,
array([[115., 0., 0., 0., 0., 0., 0.],
[0., 101., 0., 0., 0., 0., 0.],
[0., 0., 0., 0., 0., 0., 0.],
[0., 0., 109., 0., 0., 0., 0.],
[0., 0., 0., 105., 0., 0., 0.],
[0., 0., 0., 0., 110., 0., 0.],
[0., 0., 0., 0., 0., 97., 0.],
[0., 0., 0., 0., 0., 0., 108.]], dtype=float32))
ordembedding1: [[83, 104, 114, 105], [110, 105], [118, 97, 97], [115, 97, 110]]
ordembedding2: [[83, 114, 105], [110, 105], [118, 97, 115, 97, 110]]
Earth Mover Distance between two String syllable tensors: (0.3320339024066925,
None, array([[83., 0., 0., 0., 0., 0., 0., 0., 0., 0.],
[0., 104., 0., 0., 0., 0., 0., 0., 0., 0.],
[0., 9., 105., 0., 0., 0., 0., 0., 0., 0.],
[0., 1., 0., 0., 0., 0., 0., 0., 0., 104.],
[0., 0., 0., 110., 0., 0., 0., 0., 0., 0.],
[0., 0., 0., 0., 105., 0., 0., 0., 0., 0.],
[0., 0., 0., 0., 0., 118., 0., 0., 0., 0.],
[0., 0., 0., 0., 0., 0., 97., 0., 0., 0.],
[0., 0., 0., 0., 0., 0., 0., 97., 0., 0.],
[0., 0., 0., 0., 0., 0., 0., 0., 0., 0.],
[0., 0., 0., 0., 0., 0., 0., 11., 0., 0.],
[0., 0., 0., 0., 0., 0., 0., 7., 97., 6.]],
dtype=float32))

```

---

1124. (THEORY and FEATURE) Graph Search and Analytics - NetworkX Graph Edit Distance - related to 753, 829, 1123 and all sections on TextGraph algorithms for Meaning Representation, Social Network Analytics, Distance and Similarity measures for Text/Audio/Video/People, Frequent Subgraph mining, Inexact Graph Matching, Program Analysis - 9 December 2020

---

1.GraphMining\_GSpan Python implementation has been upgraded to Python 3.7 by autopep8 and 2to3-3.7 utilities.  
2.New function GraphEditDistance() has been defined in GSpan class which takes

two NetworkX Graph objects as arguments and computes exact Graph Edit Distance (NP-Hard) by `graph_edit_distance()` and approximations by `optimize_edit_paths()` and `optimize_graph_edit_distance()` NetworkX APIs.

3. Logs in

`python-src/testlogs/GraphMining_GSpan.GraphEditDistance.log.9December2020` capture the GSpan Graph mining for some example TextGraphs (Recursive Gloss Overlap algorithm) and Graph Edit Distance for two example numeric labelled graphs.

4. `GraphEditDistance()` could be invoked from any Graph analytics implementation in NeuronRain for Similar Graph clustering viz., Social network graphs, FaceGraphs (Delaunay triangles and Voronoi facets) of Segmented images (Pattern recognition, GIS, Urban Sprawls), TextGraphs, Economic networks, Program Slice Graphs, FTrace kernel callgraphs, Userspace Valgrind/KCacheGrind/Callgrind callgraphs, Control Flow Graphs et al.

5. Graph Edit Distance for Audios (Speech) assumes a hypothetical AudioNet similar to ImageNet dataset or Speech-to-Text engine for eliciting graph structure in speech though Music as a graph is vague to define, but NeuronRain music pattern mining learns a weighted automata from musical clips which are directed graphs of state transitions labelled by heptatonic western classical notes (CDEFGABC).

6. Classical Indian music has 72 fundamental notes patterns and many derivatives from them.

References:

-----  
1124.1 An Exact Graph Edit Distance algorithm for Pattern Recognition Problems - <https://hal.archives-ouvertes.fr/hal-01168816>  
-----

-----  
1125. (THEORY and FEATURE) Software Analytics - Cyclomatic Complexity Program Analyzer - Graph Edit Distance - related to 581,1124 and all sections on Program Analysis, Software Analytics, Graph Edit Distance, Inexact Graph Matching - 15 December 2020  
-----

-----  
1. Cyclomatic Complexity Program Analyzer Spark implementation `python-src/software_analytics/CyclomaticComplexitySparkMapReducer.py` has been refactored and new function `cyclomatic_complexity()` has been defined for Cyclomatic Analysis of FTrace callgraph by GraphFrames.  
2. Function `graph_mining()` now invokes `GraphEditDistance()` from `GraphMining_GSpan` for each pair of callgraph NetworkX objects instantiated from DOT files in addition to GSPAN algorithm for frequent subgraph mining.  
3. Finding code similarity by Graph Edit Distance between callgraphs is dynamic program analysis (Inexact matching) which is more comprehensive profiling than Graph Isomorphism (Exact Matching)  
-----

-----  
1126. (THEORY and FEATURE) People Analytics - Word Sense Disambiguation changed to NeuronRain implementation - related to 876,1123 and all sections on Embedding in vectorspace, Compressed Sensing, Social Network Analytics, Meaning Representation, Intrinsic Merit of People Profiles/HR Analytics, Set Partition and Histogram analytics - 16 December 2020  
-----

-----  
1. Recursive Lambda Function Growth Meaning Representation was inferring some misleading lambda functions related to the proper noun dictionary-filtered profile contents - Word "Architect" was incorrectly disambiguated to civil engineering and produced lemmas - "slab", "home\_plate", "base\_ball" et al.  
2. This was perhaps because of deficiencies of NLTK lesk implementation. Changing to PyWSD significantly slows down and there are WordNet  
-----

errors within PyWSD. This has necessitated reverting to NeuronRain Lesk Word Sense Disambiguation function `best_matching_synset()` and both NLTK and PyWSD disambiguation have been disabled.

3. NeuronRain WSD `best_matching_synset()` has extracted quite accurate synset lemmas which have been used to create TextGraph and Graph Tensor Neural Network Lambda functions are grown from Random walks and Cycles on this new TextGraph - TextGraph for `best_matching_synset()` is much different from those of NLTK/PyWSD Lesk functions.

4. New TextGraph has been written to DOT file `RecursiveLambdaFunctionGrowth.dot`

5. Logs `testlogs/SocialNetworkAnalysis_PeopleAnalytics.log.16December2020` print following Dense subgraph classes (which give high weightage to durations) and intrinsic merit parameters while Betweenness, Closeness, Degree, PageRank centralities rank the profile highly in class "Software":

```
...
=====
Unsupervised Classification based on top percentile Core numbers of the
definition graph(subgraph of WordNet)
=====
('This document belongs to class:', 'April', ',core number=', 6)
('This document belongs to class:', 'March', ',core number=', 6)
('This document belongs to class:', 'May', ',core number=', 6)
('This document belongs to class:', 'month', ',core number=', 6)
('This document belongs to class:', 'preceding', ',core number=', 6)
('This document belongs to class:', 'following', ',core number=', 6)
('This document belongs to class:', 'architect', ',core number=', 4)
('This document belongs to class:', 'search', ',core number=', 4)
('This document belongs to class:', 'Hindi', ',core number=', 4)
('This document belongs to class:', 'institute', ',core number=', 4)
('This document belongs to class:', 'education', ',core number=', 4)
('This document belongs to class:', 'experience', ',core number=', 4)
('This document belongs to class:', 'software', ',core number=', 4)
('This document belongs to class:', 'science', ',core number=', 4)
('This document belongs to class:', 'activities', ',core number=', 4)
('This document belongs to class:', 'Tamil', ',core number=', 4)
('This document belongs to class:', 'skill', ',core number=', 4)
('This document belongs to class:', 'knowledge', ',core number=', 4)
('This document belongs to class:', 'something', ',core number=', 4)
('This document belongs to class:', 'India', ',core number=', 4)
('This document belongs to class:', 'written', ',core number=', 4)
('This document belongs to class:', 'language', ',core number=', 4)
('This document belongs to class:', 'spoken', ',core number=', 4)
('This document belongs to class:', 'someone', ',core number=', 4)
...
intrinsic_merit_dict: {'graph_tensor_neuron_network_intrinsic_merit':
1011.984847256428,
'maximum_per_random_walk_graph_tensor_neuron_network_intrinsic_merit':
('experience(content,(education(skill,(cognition(ability,(cognition(ability,
(psychological_feature(cognition,(activity(event,(act(education,
(skill(education,(act(activity,(psychological_feature(institute,
(abstraction(event,(organization(group,(social_group(institute,
(organization(association,(abstraction(association,(group(science,
(abstraction(knowledge_domain,(cognition(abstraction,
(psychological_feature(content,
(discipline(social_group,psychological_feature))))))))))))))))))))))))))
))))))', 16.89555722055722), 'korner_entropy': 0.7184074850146093, 'density':
0.007855421686746989, 'bose_einstein_intrinsic_fitness': 0.8612343424751857,
'recursive_gloss_overlap_intrinsic_merit': 856492032.0, 'empath_sentiment':
(0.0, 0.0, 1.8548942433184686e-296)}
```

Specific Dictionary - LinkedIn Dataset analytics in Spark 3.0.1+ Hadoop 3.2 - related to 613,727,812,876 and all sections on People Analytics, Intrinsic Merit Versus Fame Equilibrium, Novelty Detection, BKS Conjecture, Stability of Interview LTF/PTF - 19 December 2020

-----

1. NeuronRain People Analytics is mainly about automating the process of recruiting talent by minimizing or obviating human error and intervention.
  2. Theoretically if intrinsic merit lowerbounds fame, automatic recruitment is feasible which has been analyzed in earlier relevant sections. In this commit, profile parser function has been updated to include a domain specific dictionary argument which contains fields specific to a work domain - IT, Manufacturing, Academics etc.,
  3. For Information Technology domain, example dictionary has two fields (values) - "name" (Information Technology) and "opensource\_sloc" (Number of Source Lines of Code contributed to OpenSource products). Domain of IT is quite different from other industries in the sense work experience and technical wherewithal is quantifiable by lines of code and arbitrary number of clones can be derived from digital content which is impossible in other disciplines.
  4. Technical Talent in Information Technology domain is measurable quantitatively by number of lines of code written which is used in various opensource codebase analyzers (e.g OpenHub COCOMO analyzer) and software complexity metrics (e.g Function Point Analysis).
  5. Total experience of a profile is weighted by opensource\_sloc value (which is at present just a linear addition function but could be any other) for least energy intrinsic merit of a profile which is the single largest crucial parameter more important than mere tenure duration for automatic recruitment in Information Technology domain and more intrinsic than Majority Voting (which suffers from limitations of Condorcet Jury Theorem) and manual processes of Interview (which is subject to BKS Conjecture and human error).
  6. If Novelty Detection measures (e.g Patents) and SLOC measures per proprietary and opensource products of organizations are accumulated and weighted it could further augment the previous merit statistic.
  7. Spark Version has been upgraded to 3.0.1 (based on Hadoop 3.2) for LinkedIn Dataset Analytics.
- 

1128. (THEORY and FEATURE) People Analytics - HR and Talent Analytics - Chaotic Hidden Markov Model - Career Transition Score of a Profile - Weighted Automaton of Career Transition - related to 753, 1127 and all sections on People Analytics, Intrinsic Merit Versus Fame Equilibrium, BKS Conjecture, Stability of Interview LTF/PTF - 23 December 2020

-----

1. This commit implements an important and most fundamental merit measure for People profiles - Career Transition Score - which quantifies and grades the career tenure switchovers of a Professional profile by traversing designations/paygrades in a Career Transition Weighted Automaton State Machine.
2. Section 753 attributes following qualities to career transition ranked by incentivizing choices made:

```
" ...
 (*) transition from industry to academics is considered nobler than
industry-to-industry.
 (*) transition from academics to industry is majority choice
 (*) transition from low remuneration to high is a majority choice
 (*) transition from high remuneration to low is rare
 (*) transition from employment to entrepreneur is rare and considered less
risk-averse
 (*) transition from low designation to high is majority choice
... "
```
3. SocialNetworkAnalysis\_PeopleAnalytics\_ChaoticHMM.py defines a new function career\_transition\_analytics() which traverses the Observations of the Chaotic Hidden Markov Model, classifies them into states and lookup the

state transitions in a predefined Weighted Automaton defined by a dictionary:  
self.career\_statemachine={'academic-academic':2, 'work-work':1, 'startup-startup':2, 'academic-work':1, 'work-academic':2, 'academic-startup':3, 'startup-academic':3, 'work-startup':3, 'startup-work':1, 'academic-business':5, 'business-business':6}

4.Previous career state machine presently has 4 classes of designations for states - academic, work, startup (which includes own initiatives of a profile) and business (corporate designations) - and transitions among them are weighted by integers in ascending order of importance and risk aversion. E.g Transition work-work is weighted as 1 which is considered secure while business-business is weighted as 6 because of high risk.

5.Designations (Observations in HMM) are classified into 4 classes above - academic, startup, business, work - and weighted by increased paygrades/power/independence/authority/experience/totempole:

```
self.designations["academic"]={"Schooling":1, "Graduation":2, "PostGraduation":3, "PostGraduation-ResearchScholar":4}
self.designations["startup"]={"Founder-Architect":7}
self.designations["business"]={'CEO':10, 'CTO':9, 'CFO':8}
self.designations["work"]={"AssociateSoftwareEngineer":1, "MemberTechStaff":2, "SystemAnalyst":3, "Specialist":4, "Consultant-Architect":6, "Consultant":5, "Architect":6}
```

6.More predefined designations, classes of designations and state transitions could be added to previous dictionaries which might be optionally read from a persisted NoSQL datastore.

7.Observations of Career Chaotic Hidden Markov Model are traversed and weights per state transition and corresponding observation are summed to get a Career Transition Score of a profile which intrinsically rates merit of a profile based on predefined weights.

8.Industry has been divided into startup (for MSMEs, private initiatives) and business (for management profiles of Corporates, Bellwether, Blue Chips, Big Fishes) for weighting the risk.

-----  
1130. (THEORY and FEATURE) People Analytics - HR and Talent Analytics - Chaotic Hidden Markov Model - Career Polynomial of a Profile and Inner Product Space Distance Similarity between 2 people profiles - related to 753,1127,1128,1129 and all sections on People Analytics, Intrinsic Merit Versus Fame Equilibrium, BKS Conjecture, Stability of Interview LTF/PTF - 30 December 2020  
-----

-----  
1.This commit implements 3 new functions in python-src/SocialNetworkAnalysis\_PeopleAnalytics\_ChaoticHMM.py - career\_polynomial\_inner\_product\_distance(), normalize(), second() - and polynomial fit of weighted HMM observations (designations) in career\_transition\_analytics()  
2.career\_polynomial\_inner\_product\_distance() takes two arrays of points on a polynomial (of same size sampled on similar time points which could be numeric values for designations, remunerations or durations), polyfit()-s the points to two polynomials and computes inner product of the two polynomials which is the clustering similarity measure for two people profiles.  
3.second() is a utility function for getting the second element in an array of ordered tuples. Usual cast of array of ordered tuple to dict() and invoking values() on them returns unique values and not a multiset of repetitive values which is redressed by second().  
4.Utility Function normalize() divides a numeric array by maximum element which might be necessary for comparing trends in remunerations, designations and durations of two talent profiles.  
5.Apart from these, weighted observations (designations) within Chaotic HMM are as well fitted to a polynomial in career\_transition\_analytics()  
6.All polynomials are of degree 5 and logs  
testlogs/SocialNetworkAnalysis\_PeopleAnalytics\_ChaoticHMM.log.30December2020 demonstrate the inner product distance measures and fitted career polynomials

through few example inputs.

-----  
-----  
1132. (THEORY and FEATURE) People Analytics - Alphabet Vectorspace Embedding - Earth Mover Distance between String Syllable Tensors - related to 752,874,875,1123 and all sections on Embedding in vectorspace, Compressed Sensing, Social Network Analytics, Meaning Representation, Intrinsic Merit of People Profiles/HR Analytics, Set Partition and Histogram analytics - 5 February 2021  
-----  
-----

1. SocialNetworkAnalysis\_PeopleAnalytics.py implementation has been updated to compare Earth Mover Distance and Wagner-Fischer Edit distance.  
2. Few debug print()s have been added to print EMD and Edit distance measures for 2 strings. EMD computes the Earth Mover Distance between histograms of 2 strings.  
3. Each string histogram has single alphabet buckets which reduces Edit Distance to Earth Mover Distance and subquadratic Earth Mover Distance computation (e.g LC-ACT linear complexity approximation of EMD has high accuracy close to 100% depending on iterations) implies SETH is False.

-----  
-----  
1133. (THEORY and FEATURE) Recursive Lambda Function Growth - Transformer Attention Model - related to 697,1131 and all sections on Intrinsic Merit of Texts, Embedding in vectorspace, Machine Translation, Named Entity Recognition and Meaning Representation - 5 February 2021  
-----  
-----

1.Transformers attention model implementation in NeuronRain could be used for Named Entity Recognition and Machine Translation.  
2.Attention of a word vertex  $w_i$  to word vertex  $w_j$  in text graph from Recursive Gloss Overlap and Recursive Lambda Function Growth algorithms is heuristically inverse-proportional to degree of the vertex  $w_j$  - extent to which meaning of the word vertex  $w_j$  depends on  $w_i$ .  
3.Transformer attention model learns Query weights (Q), Key weights (K), Value weights (V) for embedding  $x_i$  for word  $i$  defined by:  
$$Q_i = x_i * q_i$$
$$K_i = x_i * k_i$$
$$V_i = x_i * v_i$$
$$\text{Attention}(Q,K,V) = \text{softmax}(Q * K^T / \sqrt{d^k}) * V, d^k = \text{dimension of Keys vector}$$
$$a(i,j) = \text{attention of word } i \text{ to word } j = q_i * k_j$$
$$\text{softmax}(x_i) = e^{x_i} / \text{Sigma}(e^{x_j}) \text{ which normalizes sum to 1}$$
  
4.Every word vertex of the text graph could be embedded in a vectorspace by word2vec and from previous transformer attention model:  
attention of word vertex  $w_i$  to word vertex  $w_j$  in text graph =  $a(w_i, w_j)$  = proportional to  $(1/\text{degree}(w_j)) = q_i * k_j$   
5.New function `rlfg_transformers_attention_model()` has been implemented in `RecursiveLambdaFunctionGrowth.py` which computes degree of every word vertex in a text definition graph, derives degree attention matrix from them and learns Query weights, Key weights and Value weights from degree based attentions of the word vertices of text graph by Gradient Descent.  
6.Product of learnt query and key weights yields the exact attention values between word vertices  $w_i$  and  $w_j$ .  
7.Transformer Gradient Descent implementation in NeuronRain GRAFIT has been imported and invoked.  
8.Logs for 1132 and 1133 in xz format have been committed:

-  
python-src/testlogs/SocialNetworkAnalysis\_PeopleAnalytics.log.5February2021.xz  
-

python-src/testlogs/SocialNetworkAnalysis\_PeopleAnalytics.log2.5February2021.xz  
9.Debug statements and correction to for loops have been introduced in



-----  
-----  
1134. (THEORY and FEATURE) Named Entity Recognition - Transformers Attention Model - related to 697,1131,1133 and all sections on Named Entity Recognition - 9 February 2021,11 February 2021  
-----  
-----

1. NamedEntityRecognition\_HMMViterbi\_CRF.py has been updated to invoke `rlfg_transformers_attention_model()` from Recursive Lambda Function Growth python implementation for the textgraph of the observation text based on degree attention per word vertex defined earlier.
2. Perceptron learnt Query,Key and Value weights are printed in Recursive Lambda Function Growth `rlfg_transformers_attention_model()` routine.
3. Adjacency matrix for textgraph is instantiated by Numeric Python `ones()` function initialized to all 1s and cast to python list.
4. Textgraph edges ( $w_i, w_j$ ) between word vertex  $w_i$  to word vertex  $w_j$  of maximum query, key, value weights could be high contributors to meaning of word vertex  $w_j$ .
5. Test Logs for this code change are:

python-src/testlogs/NamedEntityRecognition\_HMMViterbi\_CRF.log.11February2021

python-src/testlogs/NamedEntityRecognition\_HMMViterbi\_CRF.log.9February2021  
(merged and compressed in

python-src/testlogs/NamedEntityRecognition\_HMMViterbi\_CRF.log.11February2021.xz)  
-----  
-----

1135. (THEORY and FEATURE) SETH is 100% False - Draft Proof - related to 752 and all sections on Earth Mover Distance, Edit Distance, BigData and String analytics, String complexity measures, Histogram analytics, Merit of Large Scale Visuals - 11 March 2021,12 March 2021  
-----  
-----

1135.1.LC-ACT (Algorithm 3) in IBM Research paper on LC-RWMD has 2 nested loops (for and argmin) for variables  $p$  (size of histogram1) and  $q$  (size of histogram2) as quoted below:

```
Algorithm 3 Approximate Computation of ICT
1: function ACT(p, q, C, k)
2: $t = 0$ \leftarrow initialize transportation cost t
3: for $i = 1 \dots hp$ do \leftarrow iterate the indices of p
4: $s = \text{argmink}(C_i, [1 \dots hq])$ \leftarrow find top-k smallest
5: $l = 1$ \leftarrow initialize l
6: while $l < k$ do
7: $r = \min(p_i, q_s[l])$ \leftarrow size of max. transfer
8: $p_i = p_i - r$ \leftarrow move r units of p_i to $q_s[l]$
9: $t = t + r \cdot C_{i,j}$ \leftarrow update cost
10: $l = l + 1$ \leftarrow increment l
11: end while
12: if $p_i \neq 0$ then \leftarrow if p_i still has some mass
13: $t = t + p_i \cdot C_{i,s[k]}$ \leftarrow move the rest to $q_s[k]$
14: end if
15: end for
16: return t \leftarrow return transportation cost t
17: end function
```

1135.2.Bottom left constant size quadrant rectangle of Edit distance memoization table hence computes edit distances of constant size substring histograms of 1-alphabet buckets. Example edit distance table from <https://web.stanford.edu/class/cs124/lec/med.pdf> is quoted below:

```
N 9 8 9 10 11 12 11 10 9 8
O 8 7 8 9 10 11 10 9 8 9
I 7 6 7 8 9 10 9 8 9 10
```

```

T 6 5 6 7 8 9 8 9 10 11
N 5 4 5 6 7 8 9 10 11 10
E 4 3 4 5 6 7 8 9 10 9
T 3 4 5 6 7 8 7 8 9 8
N 2 3 4 5 6 7 8 7 8 7
I 1 2 3 4 5 6 7 6 7 8
0 1 2 3 4 5 6 7 8 9
E X E C U T I O N

```

1135.3 In previous example, constant quadrant could be the bottom left 4\*4 square fragment of the table computed by LC-ACT in linear time while the rest of the table adheres to conventional quadratic recurrence:

```

T 3 4 5 6
N 2 3 4 5
I 1 2 3 4
0 1 2 3
E X E

```

1135.4. Algorithm 3 for LC-ACT has histogram sizes  $p, q$  and iterations  $k$  as arguments. Therefore Algorithm 3 runs in predefined constant linear time for constant size quadrant of edit distance table - Iterations variable  $k$  could be appropriately predetermined for constants  $p$  and  $q$  of histogram sizes - For 100% accuracy iterations depend on string histogram sizes  $p$  and  $q$ . Each  $p_i$  and  $q_s$  have sizes  $\leq 1$  because string histograms have buckets of 1 alphabet.

1135.5. Thus a fraction of edit distance dynamic programming is performed in linear time. This reduces the exponent of quadratic time edit distance computation from 2 to 1.99999... or less asymptotically depending on constant size quadrant which implies edit distance is subquadratic and SETH is false.

1135.6. Constant size quadrant fraction of edit distance dynamic programming table of sides  $x$  and  $y$  has maximum distance computation  $d(x, y)$  in top right corner of the constant quadrant for 2 string histograms of lengths  $x$  and  $y$  equivalent to edit distance between 2 strings of lengths  $x$  and  $y$  - this assumes LC-ACT distances for string histograms are directly proportional to integral edit distances between strings of those histograms. In previous example fragment  $d(\#INT, \#EXE) = 6$  for  $x=4$  and  $y=4$ .

1135.7. Thus  $x$  and  $y$  are the maximum constant values for 2 nested loops of string histograms of size  $p$  and  $q$  ( $x=p, y=q$ ).

1135.8. Constant number of iterations  $k$  in LC-ACT could be found once in initialization phase for constant values  $p=x$  and  $q=y$  and used as constant upperbound for all computations of distances within the constant sized quadrant rectangle.

1135.9. LC-ACT depends only on lengths  $p, q$  of string histograms and iterations  $k$ .

1135.10. Edit distance table grows from bottom left to top right. Therefore LC-ACT optimization works only for a constant sized rectangle in bottom left of the table, where constant length substring distances are computed.

1135.11 For string histograms, each bucket has only one alphabet and number of iterations ( $k$ ) required is only 1 from LC-ACT algorithm 3 earlier (lines 7 to 10) because  $r \leq 1$  which is a major runtime reduction - at most one alphabet could be moved from bin of  $p$  to bin of  $q$ .

1135.12 Complexity of data parallel LC-ACT implementation (Table 3 of 1135.14) is  $O(vhm + nhk)$  where  $v$  = size of vocabulary,  $h$  = average size of the string histograms,  $m$  = dimension of the coordinates,  $n$  = number of string histograms,  $k$  = iterations.

1135.13 For Edit distance - Earth mover distance reduction,  $n = 1$  (for distance between pair of string histograms),  $m = 1$  (because each bin has only one alphabet) and  $k = 1$  (because only one alphabet is moved) which implies the Complexity of LC-ACT edit distance computation is  $O(vh + h)$  which is linear in average size of the string histograms (or) linear in average length of the strings if size of the vocabulary  $v$  is constant (ASCII or Unicode) and thus subquadratic implying SETH is false and previous constant quadrant optimization could be unnecessary on the average.

References:

-----

1135.14 LC-RWMD and LC-ACT - Algorithm 3 -  
<http://proceedings.mlr.press/v97/atasu19a/atasu19a.pdf>

1135.15 Edit Distance Dynamic Program Memoization -  
<https://web.stanford.edu/class/cs124/lec/med.pdf>

-----  
1136. (THEORY and FEATURE) SETH is 100% False - Draft Proof - alternative Edit distance-Earth mover distance reduction - related to 752,1135 and all sections on Earth Mover Distance, Edit Distance, BigData and String analytics, String complexity measures, Histogram analytics, Merit of Large Scale Visuals, Embedding of Strings in Syllable vector space - 24 March 2021, 11 April 2021  
-----

1136.1 As alternative to 1 alphabets per bin, every String histogram has buckets containing ASCII or Unicode numeric values of alphabet as numeric weights. This makes string histograms more similar to traditional histograms having bins of numeric weights e.g. Image Pixel Histograms of Large Scale Visuals.

1136.2 LC-ACT is thus readily applicable to string histograms of numeric weights. Direct proportionality assumption between edit distance values and earth mover distance values stated earlier in 1135 has to be proved.

1136.3 For same strings both edit distance and earth mover distance are zero. For dissimilar strings edit distance inserts alphabets, deletes alphabets and updates alphabets while previous numeric weights string histogram for earth mover distance depends on  $r$  and  $C(i,j)$  -  $r$  and  $C(i,j)$  increase with widening numeric weights (differing alphabets) - Edit distance counts only insertions, deletions and substitutions while EMD generalizes edit distance.

1136.4 Because there is not much literature on relation between edit distance and earth mover distance (except L1-embeddings which exist for all classes of distance metrics) following equation in 1136.5 has been contrived for proving proportionality between former and latter inspired by edit distance dynamic programming recurrence:

    Edit distance =  $\text{minimum}(d(i-1,j-1), d(i-1,j) + \text{delete}(a_i), d(i,j-1) + \text{insert}(b_j), d(i-1,j-1) + \text{substitute}(a_i, b_j))$

1136.5 Earth Mover Distance =  $w_1 \cdot \text{Sum}(\text{unicode values of inserted alphabets}) - w_2 \cdot \text{Sum}(\text{unicode values of deleted alphabets}) + w_3 \cdot \text{Sum}(\text{difference between unicode values of substituted alphabets})$

1136.6 Previous linear program sums unicode values of inserted alphabets in string histogram bins, subtracts unicode values of deleted alphabets in string histogram bins, sums the difference between unicode values of substituted alphabets in string histogram bins by assigning appropriate weights which is same as lines 7-10 of LC-ACT data parallel algorithm earlier.

1136.7 Instead of 1s for counting insertions, deletions and substitutions, unicode value weights of the string histogram bins are used which maps edit distance to earth mover distance - iterated summation of  $r$  (=difference between weights of bins in 2 histograms) \*  $C(i,j)$  (=cost).

1136.8 Replacing unicode weights by 1s reverts EMD to Edit distance. Number of iterations of LC-ACT is upperbounded by total number of alphabet encodings e.g. 256 for ASCII, 512 for Unicode - for numeric string histograms which is again constant and thus linear time and accuracy is 100%.

1136.9 An example computation of LC-ACT algorithm - lines 7-10:

For  $p_i = 3$  (unicode weight) and  $q_s = 1$  (unicode weight),  $r = \min(3,1) = 1$ . If  $C(i,j)$  is 1 uniformly throughout:

$p_i - r = 3 - 1 = 2$  (iteration 1),  $t = 1$

$p_i - r = 2 - 1 = 1$  (iteration 2),  $t = 2$

1136.10 Edit distance to Earth mover distance reduction could be useful as well for (\*) computing distance between syllable hyphenated natural language strings in which each string is a histogram of bins containing syllables (\*) and stream of Survival Index WCET OS Scheduler Histograms in which timeslice bins are process id strings.

References:

-----  
1136.11 High Dimensional EMD - [Andoni-Indyk-Krauthgamer] -  
<http://www.cs.columbia.edu/~andoni/papers/emd-hd.pdf> - "...Since many metrics (e.g., variants of edit distance [MS00, CM07, OR05, CK06]) can be embedded with

bounded distortion into L1 with small integer coordinates, our result implies that EMD over s-subsets of such metrics can be embedded into L1 as well...."

1136.12 Linear sketch for EMD - <https://people.cs.umass.edu/~mcgregor/papers/13-approx1.pdf> - "...Example 1. Suppose  $A = \{2, 3, 10\}$  and  $B = \{3, 4, 8\}$  and note that  $\text{EMD}(A, B) = 4$ . Then  $x = (0, 1, 2, 2, 2, 2, 2, 2, 2, 2)$  and  $y = (0, 0, 1, 2, 2, 2, 2, 3, 3)$  and  $|x - y|_1 = 4$  as required ..."

1136.13 Embeddings of non-norms (Earth Mover Distance and Edit Distance) to norms(L1), Distortion, Non-embeddability - <https://simons.berkeley.edu/sites/default/files/docs/516/andonislides2.pdf>

-----

1137. (THEORY and FEATURE) Intrinsic Merit Versus Majority Voting,  $P=BPP$  ("Maybe" tends to "Exists") in the context of Condorcet Jury Theorem and its derivatives, Margulis-Russo Threshold for boolean majority, Histogram analytics, Set Partition Theoretical Electronic Voting Machines, Edit distance to Earth Mover Distance reduction, Boolean function composition, KRW Conjecture, Communication complexity, Hardness amplification, Bounded Rationality, Gibbard-Satterthwaite Theorem, Ramsey coloring of sequences, Infinite Pigeonhole Principle, Voting Analytics (pre-poll and post-poll) - related to 400,572,666,725,730,688,1136 and all sections on complexity theoretic aspects of Majority Voting and Intrinsic merit - 31 March 2021, 16 January 2022

-----

Condorcet Jury Theorem and its later refinements formalize goodness of majority voting function allowing voter error. Bounded probabilistic polynomial time Turing Machine (BPP) accepts YES instances ( $x$  in  $L$ ) with probability  $> 2/3$  and rejects NO instances with probability  $< 1/3$  ( $x$  not in  $L$ ). Bounded error majority voting Turing machine with  $p$ -bias  $< 1/2$  (voter has bounded rationality and errs  $< 50\%$  while choosing a candidate) converges to 1 for infinite electorate by CJT and its variants implying  $P=BPP$  for infinite majority voting - BPP majority voting Turing machine elects a good candidate  $x_i$  from input vector  $x$  of candidates by gathering votes vector  $v$  from infinite number of voters with probability  $\sim 1$  if  $x_i$  in  $L$  (Good) or rejects with probability  $\sim 0$  otherwise by Condorcet Jury Theorem. In the context of intrinsic merit of an entity, infinite voters having  $p$ -bias  $< 1/2$  (low error) increasingly reach consensus on perceived merit - intrinsic merit and perceived merit coincide. Previous BPP majority voting Turing machine is depth-1 majority and does not compose boolean functions. Depth-2 majority function composes majority and individual voter SATs (boolean for binary or non-boolean for multipartisan) of arbitrary complexity class. For example, Majority \* BPP denotes a composition of boolean majority with Voter functions of BPP where every voter function is a BPP machine which decides correctly with  $> 2/3$  probability ( $p$ -bias  $< 1/2$ ) implying outcome of voting tends to 100% correctness for infinite number of voters (but polynomial e.g number of voters  $x^{1000000000000}$  is polynomial though huge). BPP is low for itself  $\Rightarrow BPP^{BPP} = BPP$  and if Majority \* BPP could be alternatively formalized as oracle machine  $BPP^{BPP}$  then depth-2 majority is in BPP and by CJT, voting tends to 100% goodness for infinite number of voters and BPP is derandomized to P. Previous Majority \* BPP boolean composition is in KRW conjecture - Communication complexity regime.  $P=BPP$  does not imply  $P=NP$  and thus hardness amplification (and separation of P from NP) is not contradicted though converse  $P=NP$  implies  $P=BPP$ . As an aside, Edit distance to Earth mover distance reduction earlier applies to theoretical set partition voting machine histograms defined and implemented in NeuronRain if votes in histogram bins are encoded as strings. Gibbard-Satterthwaite theorem implies no voting system for more than 2 candidates is manipulation free thus implying non-boolean majority functions (boolean majority is restricted to 2 candidates) are always in Probabilistic complexity classes. There is a curious Ramsey theoretic aside to plurality (multipartisan) democracy (Refer: Plurality CJT - 740.5) - Incumbent change after every 4 or 5 years by periodic electoral processes (or less under extraordinary circumstances) could be written as integer sequence colored by incumbents - illustration:

Infinite sequence of Dispensations of durations 4-5 years are numbered  $d_1, d_2, d_3, d_4, \dots$  which are colored by Finite sequence of incumbents

$i_1, i_2, i_3, \dots, i_n$ .

For 3 parties,  $i_1, i_2, i_3$  -

$d_1(i_1), d_2(i_1), d_3(i_1), d_4(i_2), d_5(i_3), d_6(i_1), d_7(i_2), d_8(i_2), d_9(i_1), d_{10}(i_3), \dots$  is a 3-coloring of first 10 dispensations of infinite sequence by 3 incumbents.

Number of monochromatic subsequences of length  $> m$  is a measure of voter displeasure. Higher the number of longer monochromatic subsequences, Less dissatisfied are the voters.

$d_1(i_1), d_2(i_1), d_3(i_1), d_4(i_1), d_5(i_2), d_6(i_2), d_7(i_2), d_8(i_2), \dots$  is a stabler incumbency (voters stick to their choice longer) than

$d_1(i_1), d_2(i_2), d_3(i_1), d_4(i_2), d_5(i_1), d_6(i_2), d_7(i_1), d_8(i_2), \dots$  implying mercurial voting pattern in the latter (importunate voters who switch their preferences often) - typical anti-incumbency syndrome

From Infinite Pigeonhole Principle, every infinite sequence which is finitely colored has an infinite monochromatic subsequence implying there is a possibility of single party rule for indefinite period of time in plural democracy (perhaps an evidence of Gibbard-Satterthwaite impossibility no-go theorem for plural democracies).

There is a correspondence between Voter loyalty in democracy and Brand loyalty (marketing) - Brand loyalties could be considered as votes by consumers to brands - Double jeopardy is a phenomenon in which low market share brands have few takers and high loyalty attrition. On similar lines low vote share parties are less coveted by populi.

#### References:

- 
- 1137.1 Election Manipulation and Integer Factorization - [Edith Hemaspaandra , Lane A. Hemaspaandra , and Curtis Menton] - <https://drops.dagstuhl.de/opus/volltexte/2013/3949/pdf/37.pdf> - "...If integer factoring is hard, then for election manipulation, election bribery, and some types of election control, there are election systems for which recognizing which instances can be successfully manipulated is in polynomial time but producing the successful manipulations cannot be done in polynomial time...."
- 1137.2 Infinite Pigeonhole Principle - <https://ieeexplore.ieee.org/document/8206699> - "... The use of classical logic for some combinatorial proofs, as it is the case with Ramsey's theorem, can be localized in the Infinite Pigeonhole (IPH) principle, stating that any infinite sequence which is finitely coloured has an infinite monochromatic subsequence. ..."
- 1137.3 Erdos-Szekeres Theorem - [https://en.wikipedia.org/wiki/Erd%C5%91s%E2%80%93Szekeres\\_theorem](https://en.wikipedia.org/wiki/Erd%C5%91s%E2%80%93Szekeres_theorem) - "... given  $r, s$ , any sequence of distinct real numbers with length at least  $(r - 1)(s - 1) + 1$  contains a monotonically increasing subsequence of length  $r$  or a monotonically decreasing subsequence of length  $s$ . ..."
- 1137.4 Erdos-Szekeres Theorem and Happy Ending Problem - "... any set of five points in the plane in general position[2] has a subset of four points that form the vertices of a convex quadrilateral. ..."
- [https://en.wikipedia.org/wiki/Happy\\_ending\\_problem](https://en.wikipedia.org/wiki/Happy_ending_problem)
- 1137.5 Happy Ending Problem - <https://www.smh.com.au/national/a-world-of-teaching-and-numbers-times-two-20051107-gdme4e.html>
- 1137.6 Low Discrepancy Sequences - [https://en.wikipedia.org/wiki/Equidistributed\\_sequence#Discrepancy](https://en.wikipedia.org/wiki/Equidistributed_sequence#Discrepancy) - Low Discrepancy of dispensation sequence earlier implies high anti-incumbency and viceversa

-----

1138. (THEORY and FEATURE) Recursive Lambda Function Growth Textgraph as EventNet Causality Graphical Event Model - implementation - 12 April 2021 - related to 762 and all sections on Intrinsic Merit of Text and Videos, EventNet, Graphical Event Models

-----

1.New python source file RecursiveLambdaFunctionGrowth\_EventNetGEM.py derived from RecursiveLambdaFunctionGrowth.py implements



```
['determined', 'magnetic', 'sunspot', 'field', 'space', 'cosmic', 'extended'],
['determined', 'magnetic', 'sunspot', 'field', 'space', 'cosmic', 'extended'],
['determined', 'magnetic', 'sunspot', 'field', 'space', 'cosmic', 'extended']
...
```

3.Nested loop for verb filtering has been optimized.

4.Recursive Lambda Function Growth EventNet GEM textgraph is particularly useful when two different seemingly unrelated research articles are collated (their texts are merged) and textgraph from merged text is analyzed for actor-action-actor causality random walks. This could prove hidden connections between hitherto unrelated fields of research.

-----  
1142. (THEORY and FEATURE) SETH is 100% False - Draft Proof - Edit distance-Earth mover distance reduction and order preservation - illustration - related to 752,1135,1136 and all sections on Earth Mover Distance, Edit Distance, BigData and String analytics, String complexity measures, Histogram analytics and Set partitions, Merit of Large Scale Visuals, Embedding of Strings in Syllable vector space - 26 May 2021, 11 July 2021  
-----

1142.1 Earth mover distance - Edit distance reduction preserves order of bins in histograms because histograms are usually set partitions of a numeric range on x-axis (or y-axis) and thus order of alphabets in a string and order of single alphabet buckets in string histograms are same.

1142.2 Single alphabet buckets of string histogram therefore are order preserving and Earth Mover distance and Edit distance are equivalent and directly proportional (Insertion of an alphabet = Insertion of new single alphabet bucket, Deletion of an alphabet = Removal of single alphabet bucket, Update of an alphabet = Update of single alphabet bucket)

1142.3 For string histograms of numeric ASCII or Unicode values for each 1-alphabet bucket, the order preservation is obvious - each bucket has size equal to ASCII or Unicode value of the alphabet.

1142.4 Following illustration depicts Earth mover distance to Edit distance reduction between two string histograms for strings "acdfp" and "qdpfg" (each bin has size equal to ASCII or Unicode values of the alphabet):

String histogram1 ("acdfp") ===== morphed to =====>String  
histogram2 ("qdpfg")

|         |         |
|---------|---------|
| a ##### | q ##### |
| c ##### | d ##### |
| d ##### | p ##### |
| f ##### | f ##### |
| p ####  | g ##### |

1142.5 Earth Mover Distance (EMD) - Edit Distance (ED) reduction is immediate for numeric string histograms because transportation of bin weights in LC-ACT - Algorithm 3, lines 7-10 - (which are differences in ASCII or Unicode values of the bins) changes ASCII or Unicode values between strings morphing one string to another (Example iterations in 1136.9) - direct proportionality is by linear program earlier.

1142.6 Previous illustration envisions an alternative spectacle to view a string - every string is a numeric set partition of sum of ASCII or Unicode values of constituent alphabets and thus edit distance between strings is equivalent to distance between numeric ASCII or Unicode set partitions which unusually relates String complexity and Theory of partitions. Two way reduction between Edit Distance and Earth Mover Distance for previous numeric string histogram illustration in essence is as follows:

1142.7 Edit distance to Earth mover distance direction: Replace the 1s in dynamic program for edit distance by unicode or ASCII value of the alphabet inserted,deleted and difference of the unicode or ASCII values for substituted alphabets (#ins-del-sub)

1142.8 Earth mover distance to Edit distance direction: In LC-ACT transportation

algorithm, replace addition and subtraction of  $r$  by fraction of unicode or ASCII value moved between histograms of strings e.g if ASCII or unicode value of a string histogram bin is 100 and  $r=25$ , replace steps 7,8,9 of LC-ACT algorithm involving  $r$  by  $25/100 = 0.25$ . After 4 iterations when bin is emptied, whole alphabet is moved and fraction is  $4 * 0.25=1.0$  which simulates increment by 1 in dynamic programming recursion (#ins-del-sub) for edit distance.

-----  
1143. (THEORY and FEATURE) Recursive Lambda Function Growth EventNet GEM - 2 different research articles collated - related to 752, 1138, 1139 and all sections of Intrinsic Merit, EventNet Causal and Graphical Event Models - 8 June 2021  
-----

1.RecursiveLambdaFunctionGrowth\_EventNetGEM.py has been executed on merged abstracts of 2 different research articles on Collatz conjecture and Pseudorandom number generators (but both are indirectly related to Chaotic maps and Fractals) - <https://www.math.auckland.ac.nz/~king/745/collatz.pdf> and [https://www.researchgate.net/publication/332583614\\_Pseudo-random\\_number\\_generators\\_based\\_on\\_the\\_Collatz\\_conjecture](https://www.researchgate.net/publication/332583614_Pseudo-random_number_generators_based_on_the_Collatz_conjecture) - which reasonably extracts the crux of the two articles and finds random walks connecting the abstracts.

2.There are some irrelevant word vertices which could be because of deficient word sense ambiguation (Primitive Lesk and PyWSD) and non-scientific nature of WordNet which is more linguistic and might therefore necessitate a Concept Ontology specific to Theoretical and Experimental Science.

3.Cause-effect random walks extracted from the previous 2 articles on Collatz conjecture and Pseudorandom number generators have prominent word vertices "simulation", "graph", "mathematics" which convey the common thread connecting the two articles. Full text merge of the 2 articles might increase the accuracy but cause slowdown.

-----  
1150. (THEORY and FEATURE) NeuronRain CoronaVirus 2019 analyzer (R and Python - GEM,R Logit,Chaotic ERSIR Cellular Automaton Graph) - related to all sections on Space Filling,Chaos,Cellular Automata,Social Network Analysis,Central Limit Theorem,Cybercrime analytics,Ramsey Theory - 5 July 2021, 6 July 2021, 8 July 2021  
-----

1150.1 .NeuronRain implements CoronaVirus 2019 analyzer in R and Python for COVID19 Social Network BigData set which could be easily adapted to model quite a few chaotic processes - spread of memes,fads,cybercrimes,opinions and pandemics in a society. NeuronRain COVID19 analyzer models COVID19 as a 2-dimensional space filling chaotic dataset by Verhulste-Pearl-Reed actuarial logistic, 2-D Cellular Automaton Graph, Linear Regression, Logistic Regression among other tools.

1150.2 .COVID19 ERSIR dataplot from December 2019 to June 2021 shows an intriguing order despite being chaotic - it is a symmetric bimodal (for 2 peaks) bell curve which tapers nicely around tails when it could have been of any other shape. Furthermore shape of the curve is independent of easing or tightening of curbs. This normal distribution could be explained by Central Limit Theorem(CLT). While some of the nations are already past the 3rd peak, dataplot for India is peaking and in 2-to-3 transition.

1150.3 2-D Cellular Automaton Graph for COVID19 SIR is 3-colored - edges between each of the vertices and its 8 neighbours in a social network or electronic network could be colored as Susceptible,Infected and Recovered. By Ramsey Theorem for Graphs and [Motzkin - Complete disorder is impossible] - 701.12 - "...Theorem 1 (Ramsey's theorem). For any  $s, t \geq 1$ , there is  $R(s, t) < \infty$  such that any graph on  $R(s, t)$  vertices contains either an independent set of size  $s$  or a clique of size  $t$ . In particular,  $R(s, t) \leq (s + t - 2, s - 1) \dots$ " - order emerges (clique or independent set) inevitably in CAGraph for COVID19 SIR.



1150.4 CAGraph is a dynamic random graph in which values of point vertices are incremented-decremented (S-susceptible), incremented (I-infected) and decremented (R-recovered) and each point vertex of the CA Grid is a random variable.

1150.5 By Central Limit Theorem sum of values of point vertices on CAGraph tends to a normal distribution which fits the COVID19 dataplot.

1150.6 An example space filling by 3-colored (SIR) Social network CAGraph vertices of 2-dimensional cellular automaton for COVID19 might look like (at some timepoint and labels of vertices might change dynamically):

```
S I S R S I
I R R S I R
S S S R S S
S R R I I R
R I S S I S
S R I R S I
```

and each of the vertices are labelled as S,I and R. Sum of the values of random variables for these vertices therefore tends to a bell curve by CLT (value(S) > values(I) > value(R)):

$S + I + S + R + S + I + I + R + R + S + I + R + \dots = \text{Normal}$

Distribution

1150.7 8 neighbours per vertex in CAGraph is only a geometric heuristic implying actual degree could be multiple of 8 arborescent from a centroid vertex.

Estimating the modals (peaks) of the normal distribution thus reduces to previous summation of random variables. Empirical data suggests R-number of COVID19 was 406 (a function of density of urban sprawls) for 30 days which is an approximate multiple of 8 and values of S,I and R were approximately in the range of 51 plus or minus. Being a high degree expander, mixing time of CA Random graph determines the time required to reach stationary distribution where transmission is modelled as a random walk in CAGraph. Thus estimating further peaks involves assigning heuristic values to S,I and R (51-100 based on vehemence). For example  $S, I, R = \text{average\_density\_per\_squarekm} / \text{area\_of\_2\_yard\_radius\_circle}$  which yields population within allowed social distance perimeter.

1150.8 Hypothetical estimate of COVID19 excess mortality in India based on 3-colored CAGraph model earlier where each social profile vertex is a random variable and colored by S(usceptible), I(nfected) or R(ecovered) - based on serosurvey 1150.12 which is a different kind of zero-knowledge projection of COVID19 outreach:

1150.8.1 Percentage of population having antibodies (unvaccinated + vaccinated) in July 2021 serosurvey (possibly Infected) =  $67.6\% = 0.676 = \text{Pr}(\text{Infected})$

1150.8.2 Percentage of unvaccinated population in July 2021 serosurvey = 62.2%

1150.8.3 For 1.2% official mortality rate of COVID19 in India (1150.14), projected deathtoll for 1370 million population without serosurvey =  $1370 \text{ million} * 0.012 * 0.676 = 11.11344 \text{ million}$

1150.8.4 Assuming vaccines were 100% effective, percentage of Susceptible unvaccinated population (which had antibodies) from July 2021 serosurvey = 62.2% (unvaccinated) of 67.6% (population having antibodies) =  $42.0472\% = 0.420472 = \text{Pr}(\text{Susceptible})$

1150.8.5 For 1370 million population of India and 1.2% mortality rate of Susceptible, projected deathtoll from serosurvey =  $1370 \text{ million} * 0.420472 * 0.012 = 6.91255968 \text{ million}$  atleast which coincides with Lancet,WHO,BMJ,Economist model trends of excess deaths.

1150.8.6 From earlier CAGrid, Expected Sum of random variables of vertices valued 'S' (which tends to Gaussian by Central Limit Theorem) = Estimated COVID19 deathtoll

References:

-----  
1150.9 Methods for estimating the excess mortality associated with the COVID-19 pandemic - Section 4.1 - Overdispersed Poisson Log Linear Regression model of estimates for countries with no data - [https://cdn.who.int/media/docs/default-source/world-health-data-platform/covid-19-excessmortality/who\\_methods\\_for\\_estimating\\_the\\_excess\\_mortality\\_associated\\_with\\_the\\_covid-](https://cdn.who.int/media/docs/default-source/world-health-data-platform/covid-19-excessmortality/who_methods_for_estimating_the_excess_mortality_associated_with_the_covid-)

19\_pandemic.pdf?sfvrsn=5a05fa76\_1&download=true - R analyzer in NeuronRain for COVID19 Chaotic pandemic model (VPR and May) has a provision for scaling multiplicand which is set to 3.0 at present for global data - might have to be changed to 10.0 specific to India death toll projection of 4.7 million.

1150.10 Poisson Log-Linear regression model - <https://web.stanford.edu/class/archive/stats/stats200/stats200.1172/Lecture27.pdf> - Lambda (mean) of Poisson distribution is a logarithm of a linear regression

1150.11 Overdispersion - <https://aip.scitation.org/doi/10.1063/5.0040330>

1150.12 Covid-19: Two thirds in India carry antibodies, while research suggests country's death toll is 10 times official figure - <https://www.bmj.com/content/374/bmj.n1856>

1150.13 The Economist COVID19 excess deaths tracker - R model - scripts and graphics - <https://github.com/TheEconomist/covid-19-excess-deaths-tracker>

1150.14 COVID19 mortality rate by country - <https://coronavirus.jhu.edu/data/mortality>

-----

1154. (THEORY and FEATURE) Conflicts between Derandomization of Shor Factorization in BQP by Majority-VoterSAT boolean composition or  $BQP^BQP$  oracle machine and PRAM-NC-BSP computational geometric factorization, Gamma approximation of sum of hyperbolic tiles in average case polynomial time sequential computational geometric factorization and Quantum NC computational geometric factorization - related to 562, 668, 670, 712, 1152 and all sections on Majority Voting, Condorcet Jury Theorem and Integer Factorization - 27,28 July 2021

-----

1154.1 Shor's BQP Integer factorization as VoterSAT in Majority-VoterSAT boolean composition or Oracle Turing Machine  $BQP^BQP$  derandomizes 100% to P (implying a sequential factorization) for infinite majority by CJT variants. But Parallel RAM factorization in NC which is finer than P implies more than one quantum state in BQP are chosen for certainty which is a contradiction unless  $NC=P$  (all PTIME problems are parallelizable) or BQP is derandomizable to NC by majority-VoterSAT boolean composition (plausible as majority is in non-uniform NC).

1154.2 If Shor factorization is in BQNC a subset of BQP, then there is no contradiction since CJT infinite majority-VoterSAT boolean composition amplifies success of BQNC to exact NC.

1154.3 NeuronRain theory drafts (Section 562) already contain a Quantum NC (QNC) computational geometric factorization in which pixelated or rasterized hyperbolic arc bow is treated as superposition of quantum states defined by amplitudes corresponding to classical probability of being a factor point.

1154.4 Derandomization of BQP factorization to P implies sequential exact factorization is possible in polynomial time.

1154.5 Gamma approximation of average case sequential polynomial time computational geometric factorization algorithm in NeuronRain perhaps is an evidence hinting at possibility of worst case sequential polynomial time factorization.

1154.6 From 668, for tile summation ray shooting queries:

"... if  $k$  is  $O(\log\log N)$  from previous derivation of maximum number of tiles between 2 approximate prime factors, in average case at least one factor can be found in average time:

$\log\log N * \log N - \log(\log\log N + 1) - (2\log\log N + 1)\log\log\log N + 2(\log\log N + 1) - \log(2\pi)$

$\leq O(\log N * \log\log N) \dots$ "

References:

-----

1154.1 Simulation of Boolean composition by Oracle Turing machines - [Ingo Wegener] - <https://ecc.weizmann.ac.il/resources/pdf/cobf.pdf> - Section 9.4 - "... Each Boolean function  $f_n \in B_n$  can be computed by a Turing machine in  $n$  steps without working tape ..." - The simulation of circuits by Turing machines with oracle - Theorem 4.1 - "... Proof : The oracle  $\alpha_n$  is an encoding of an

optimal circuit  $S_n$  for  $f_n \in B_n$ . We number the inputs and gates of  $S_n$  by  $1$  to  $n+cn$ . A gate is encoded by its number, its type and the numbers of its direct predecessors. The encoding of a gate has length  $O(\log cn)$ , the encoding of  $S_n$  has length  $O(cn \log cn)$ , hence  $\log |a_n| = O(\log cn)$ . The Turing machine can now simulate the circuit given in the oracle ..."

-----  
 1155. (THEORY and FEATURE) Computational Geometric Factorization - Python 3.9.0 + Spark 3.0.1 - 2061 bits integer quadcore Benchmarks - related to all sections on Integer Factorization, Derandomization of BQP, Numeric Compression by Prime Factorization, Set Partition to Exact Square Tile Cover Space Filling Reduction of Rectangular Region, Lagranges Four Square Theorem - 1 August 2021  
 -----

1155.1 Huge 2061 bits randomly chosen integer

223920930920930920390923092093092093092399203902930920909239029392392930920930920382839828382932732787387287382772737287382737287723727382773728378273727328738723782737273728378273728738727382783728737287372738728372787382773872837827387273827837278738277387283782738727382783727873827738728378273872738278372737283782723982983982398238928839283298398293828938283982938283928839283928983232323232839829389828928398928388928392893829398289382983928398283928983232323232839829389828928398928388928392893829398289382983928398283928983982838298382389289829838239283829839928398232392398293898238928983928983823898238982983928389283982983298938298389283982938928398928397378723787238727837278372783727387827387239298392982131 has been factorized by NeuronRain NC-PRAM-BSP computational geometric factorization algorithm implementation parametrized by non-uniform logdepth circuit of depth 186.

1155.2 First few factors of

223920930920930920390923092093092093092399203902930920909239029392392930920930920382839828382932732787387287382772737287382737287723727382773728378273727328738723782737273728378273728738727382783728737287372738728372787382773872837827387273827837278738277387283782738727382783727873827738728378273872738278372737283782723982983982398238928839283298398293828938283982938283928839283928983232323232839829389828928398928388928392893829398289382983928398283928983928983823982983928983982838298382389289829838239283829839928398232392398293898238928983928983823898238982983928389283982983298938298389283982938928398928397378723787238727837278372783727387827387239298392982131 are at testlogs/DiscreteHyperbolicFactorizationUpperbound\_TileSearch\_Optimized.Python3.9Upgrade.2000plusbits.1August2021

1155.3 First four factors (two small and two huge) are printed and verified in 26 seconds and 45 seconds respectively:

=====

```
Factor point verification: (xl + intervalmidpoint)*yl == number_to_factorize =
True
```

```
Factor point verification: xl*yl == number_to_factorize = False
```

```
('Factors are: (' , 83, ', ',
```

```
26978425412160351854328083384709890734024000470232641073402292697878666376015773
54010118414252201599848039607021358280570876352864141293768358173232213582273960
52750285871961901534612938225762390034623237798480395629864316595027515454683462
44322081189442514906912390099667449378292046070998601546142648546781853354196311
18545643287220359425581112390340890340834746858842039565408895108227636504087758
82931305938479860220462565040943178672749866614252817155763650409552287026978793
12517860111925774576364325089034094449203528190720879390156432443853366135951678
12016611129966731672093106473347876233588281773967450517857, ') (at ', 'Sun, 01
Aug 2021 08:56:30 GMT', '))')
=====
```

```
Factor point verification: (xl + intervalmidpoint)*yl == number_to_factorize =
True
```

```
Factor point verification: xl*yl == number_to_factorize = False
```

```
('Factors are: (' , 1637, ', ',
```

```
13678737380631088600545088093652540811997507874339091075701834416151064808853446
57195111963243327628511834376192869500839234803223724663303443667552069195655092
99806192592381416172100634531082946688294005725558172494066819043294341983742989
51000199992203596440279342567332915689665484568679804082650212763487439391559522
```

47032916266580878633617790643850298706715235120854546633652646878331666645322443  
38932794092204205243117855213184385032609889608936981209092137959638606128523151  
06530130661513984666085760429992851797702460841965992604660866785826691443396391  
4720451266821770756740212484598578941593052771679473667063, ') (at ', 'Sun, 01  
Aug 2021 08:59:49 GMT', '))'  
=====

1155.4 Theoretical number of multicores required for NC-PRAM-BSP  $O((\log N)^k)$   
time planar point location factorization circuit is  $O(N/(\log N)^k)$ . PRAM time  
 $O((\log N)^k)$  for 2061 bits factorization circuit of depth 186 therefore is  
 $O(2061^{186})$  and number of PRAMs required are  $O(2^{2061}/2061^{186}) =$   
 $O(2^{2061/2^{2048}}) = O(2^{13}) =$  multiples of 8192 which is quite usual on clouds.  
1155.5 Exponentiation operator  $**$  has been replaced by `math.pow()` in  
factorization implementation.

#### References:

-----  
1155.6 Dynamic Planar Orthogonal Point Location in Sublogarithmic Time -  
[Timothy M. Chan, Konstantinos Tsakalidis] -  
<https://drops.dagstuhl.de/opus/volltexte/2018/8738/pdf/LIPIcs-SoCG-2018-25.pdf> -  
"...We study a longstanding problem in computational geometry: dynamic 2-d  
orthogonal point location, i.e., vertical ray shooting among  $n$  horizontal line  
segments. We present a data structure achieving  $O(\log n / \log \log n)$  optimal  
expected query time and  $O((\log n)^{(1/2+\epsilon)})$  update time (amortized) in the word-  
RAM model for any constant  $\epsilon > 0$ , under the assumption that the  $x$ -coordinates  
are integers bounded polynomially in  $n$  ..." - For rasterized and rectified  
hyperbolic arc, number of horizontal line segments which have to be 2D planar  
factor-point located  $\leq \sqrt{n}$  and  $x$ -coordinates  $\leq \sqrt{n}$ .  
1155.7 Apache Giraph - Open Source Counterpart of Google Pregel - Bulk  
Synchronous Parallel (BSP) Computation - <http://giraph.apache.org/intro.html>  
-----

-----  
1156. (THEORY and FEATURE) Majority Voting by  $NC^BQP$  Oracle Turing Machine,  
Derandomization of BQP, Integer Factorization in BQP, QNC and PRAM-NC-BSP,  
Bernstein-Vazirani algorithm and secure voting - 4 August 2021, 5 August 2021, 6  
August 2021, 14 August 2021, 15 August 2021 - related to 1152, 1154 and all  
sections on Majority Voting, Communication complexity, KRW Conjecture, Boolean  
Function Composition and Integer Factorization  
-----

-----  
1156.1 Majority Voting can be formulated by  $NC^BQP$  oracle Turing machine (which  
simulates composition of non-uniform Majority boolean function and BQP VoterSAT  
boolean function) as an alternative to broader  $BQP^BQP$  formalism of Majority  
Voting Oracle Turing Machine earlier - non-uniform majority NC circuit has  
infinite number of voter leaves which query BQP VoterSAT oracles.  
1156.2  $NC^BQP$  is a tighter version of  $BQP^BQP$  which if in BQNC (or BQNC=QNC  
because quantum circuit always has implicit bounded error by superposition and  
bounded prefix is redundant) derandomizes asymptotically to 100% NC by CJT-  
Margulis-Russo-Black-Ladha sharp thresholds for majority because  $p$ -bias  $< 1/3$ .  
1156.3  $NC^BQP$  if in BQNC resolves the conflict between derandomization of Shor  
BQP factorization and PRAM-NC-BSP computational geometric factorization as BQP  
voter SATs are directly derandomized to NC instead of P. NC non-uniform majority  
function has oracle access to BQP Shor Factorization - all voters factorize same  
integer  $N$  and vote 1 if factors are right and 0 if wrong and 2/3 of the infinite  
population succeed by definition of BQP. It needs to be proved that  $NC^BQP$  is  
contained in BQNC (or QNC).  
1156.4  $NC^BQP$  is in QNC - Draft proof:  $NC^BQP$  oracle machine has infinite BQP  
Shor Factorization VoterSAT oracles who feed to the leaves of majority NC  
circuit - 67% of infinite BQP oracles factorize correctly and input 1 to  
majority NC circuit - This hypothetical  $NC^BQP$  voting machine for infinite  
population always returns 1 by majority. On the other hand, QNC or BQNC majority  
voting circuit ( $\log \text{depth}$ ) has leaves as quantum voters by considering each vote  
as superposition of classical states  $a_1|0\rangle + a_2|1\rangle$  where  $|0\rangle$  implies wrong  
factorization by Shor BQP algorithm and  $|1\rangle$  implies correct factorization by

BQP. Thus language  $L$  accepted by  $NC^{\wedge}BQP$  is also accepted by QNC or BQNC implying  $NC^{\wedge}BQP$  is in  $QNC=BQNC$ .

1156.5 Classical probabilities of amplitudes in each voter superposition are known -  $|a_1|^2 = 1/3$  and  $|a_2|^2 = 2/3$  by definition of BQP (Born Rule: classical probability = squares of modulus of complex amplitude). Infinite number voter superpositions whose classical probabilities are known apriori are input to QNC circuit. How the voter superposition  $a_1|0\rangle + a_2|1\rangle$  are handled internally within QNC majority circuit is matter of choice - for example QNC majority voting circuit might simulate (\*) conventional NC nonuniform majority since NC is in QNC (\*) QNC version of computational geometric factorization (\*) Rabi oscillation and decohere to classical state  $|1\rangle$  of high amplitude et al.

1156.6 In BQNC majority voting circuit earlier, each voter leaf exists in a state  $|0\rangle$  (wrong factors) and  $|1\rangle$  (right factors) specified by qubits  $a_1|0\rangle + a_2|1\rangle$  without actually simulating BQP factorization oracle within BQNC (which might not be BQNC any longer and " $NC^{\wedge}BQP$  in BQNC" containment may not work) by apriori hardcoding of classical probabilities  $1/3$  and  $2/3$  to complex amplitudes  $a_1$  and  $a_2$  respectively. Embedding BQP oracle within BQNC is not necessary because by definition of BQP, factorization by each voter is both 67% right and 33% wrong and amplitudes for voter qubit superpositions can be predetermined without factorization.

1156.7 Quantum Circuits ([Deutsch] model) can be converted to Parallel RAMs in Nick's Class by Memory Peripheral model mentioned in <https://eprint.iacr.org/2019/103.pdf> - [Samuel Jaques and John M. Schanck - Waterloo] - Figure 1 - every quantum state evolves over time by Schrodinger equation Hamiltonian operator -  $d/dt|\psi(t)\rangle = -iH|\psi(t)\rangle$  and Voter qubits earlier have to abide by it. Quoted excerpt: "Time-evolution for a duration  $\delta$  yields  $|\psi(t_0 + \delta)\rangle = U\delta |\psi(t_0)\rangle$  where  $U\delta = \exp(-iH\delta)$ ". This conversion from quantum gates to classical NC Parallel RAMs is another indicator of derandomization of BQP to  $NC.NC^{\wedge}BQP$  class could be alternatively construed as NC circuits having oracle access to PRAMs by converting Deutsch model quantum circuits of BQP to Parallel RAMs in memory peripheral model which could be either  $NC^{\wedge}BPNC$  (if voter error is non-zero) and thus effectively in BPNC derandomizable to NC or  $NC^{\wedge}NC = NC$  (if voter error is zero) if number of PRAMs in oracle are  $O(N/(\log N)^k)$  and depth added by PRAMs in oracle is  $O((\log N)^k)$ . Bernstein-Vazirani algorithm proposes a quantum solution to find the secret string  $s$  for a boolean function  $f(x) = x.s$  defined as dot product of bit positions in  $x$  and  $s$ , by Hadamard transform  $1/2^n \sum (-1)^{[f(x) + x.y]} |y\rangle$  for  $x, y$  in  $\{0,1\}^n$  which is non-zero only if  $y = s$  (others cancel out). VoterSAT of the form  $f(x) = x.s$  where every voter decides discreetly by dot product on a secret is susceptible to quantum reverse engineering.

#### References:

-----

1156.8 Nonasymptotic Condorcet Jury Theorem - Bounds for subset of population - <https://www.jstor.org/stable/41106350> - "...This paper provides first the condition under which the majority of an odd number of jurists is more likely to choose the better of two alternatives than a single jurist selected at random from the jurists, given that each jurist has a probability larger than one half of choosing correctly, and second that the same inequality holds for a subset of an odd number of jurists chosen at random from the original group...."

1156.9 Sharp Thresholds for Monotone Non Boolean Functions and Social Choice Theory - [Gil Kalai, Elchanan Mossel - 2017] - <https://arxiv.org/pdf/1011.3566.pdf> - "...Theorem 1.1. There exists an absolute constant  $C = C(|A|)$  such that if  $f$  is symmetric and monotone then for any  $a \in A$  and  $q > 0$  it holds that  $\gamma[\mu : q \leq P_\mu[f = a] \leq 1 - q] \leq C(\log(1 - q) - \log(q)) \log \log n \log n$ . The result above establishes sharp threshold for symmetric functions as it shows that for almost all probability measures  $f$  takes one specific value with probability at least  $1 - q$ ...." - Applications - Section 3.1 A general form of Condorcet's Jury theorem

1156.10 Factorization is in  $ZPP^{\wedge}BQNC$  - <https://arxiv.org/abs/quant-ph/0006004> - "... As an application of the above depth bound, we show that Shor's factoring algorithm may be based on quantum circuits with depth only  $O(\log n)$  and polynomial-size, in combination with classical polynomial-time pre- and post-processing. In the language of computational complexity, this implies that











54573104215473089909973696328473492329752243231242000982639924857885257037816550  
97689699944577643539421591324702051347022086296985945669179376568615360862916400  
79529166034542693073987506193182831277798719169302416029039440463315705636622591  
63952905965046015200134700340132629390414667572312435615362951001032519860982328  
31809110671221239755649964807553077122466571937136066547849129044630758768129009  
99752224546122485430390947849129007952916587641516603435634596137819509477262916  
89904473488921796830388664096826778485776089409307398750804117058267418314324670  
70238540824876415165878644978990979183330097712556537312451205168958263958418471  
57068802520390651637482087487830238695130933885255684565015165881761032174369687  
98730048197018283678145082989559994112049789930207052731085916401136326063641516  
58788317968506549821392352331828022120550113975717609999443909474875371591106710  
32488871913437020547745291640079373454667572309268940440272417936774523487452343  
90251691086262419717000692041522491349480968858108281290759145118352605325360174  
02740806546847852280982463779591802502454357200356167447405671599685222522592764  
80729765776156409425547691830390443733504979177817611900656879719662248546156691  
67072605478543039094772608937504942556845665670324523317400635736461203715319681  
06362366539236325997231833910034602076124567450841844392363111432190100446679217  
71948415359963007626062395508757519755395262639904471627124886882454356502799409  
37378232903814269838349269836810515323177502871604947539544630774715708971763727  
637310663608241275843350097833

xl =

34599390729864778307683013574713124886135267817314543013567159996641496169311145  
08968990602016741499215497365843385042469649613403905786756879852501168952846826  
55319162032431616898902205146668767570371236584338157049424663923279372762554580  
87452691603023779836933312708781409134359307349420032139767588179871758786791833  
31966380376606518785409108384888719132836778298958229719475407937125945638003404  
59653385224357402708788338544255501136273300428695149821392362762278198214471709  
07952574042349235238508594546360688522435738371224854613491135980585757726432278  
19698407397482279321359440736275878156999096134044027438890305235986159169550173  
01038062281416364370032158894084061947782108623159488024322869217757897238861325  
98376896506204980034684807027345781671041186612118717332880013782985948037502556  
84566885258921774532260549927127438868276951639802435650276917276893851523496160  
18346308788317750305530509402324819440386599214089369611860959471236269144355460  
82449194765353916203396985165353588993193193214506308762049561357519834716023945  
68478859145401051629858198235958792706166030859132120826772620324819632274665323  
13923435549229713750424857175718816167398871379717210285027244922966345269160494  
06153196636115181255319143248887138352332142851173990602017245426965030548059821  
44719475373488693159973436790045786845260318760875131425546430097518656850585750  
24955436723122225717381426726584561357519835028509732660838693159558211875570907  
26371549019211883817412882326378369842635523640932135930044078641462931928675561  
54800255115495752243274052732954646657191452732973643231240132504596515169302397  
5720527070009826399272764458127779892485788559633158802179374685061705826743731  
08644631117295495791798748231588176414615669145273331625685948926745293508279925  
23494249961876781418129010009826400806191636622466573804115169513093334903937274  
69649770684558089528468469990959305530771564470588235294117647058823529179698720  
74024011086169339201004477235055087855685439582423263046052706204471657540913228  
38197551242315948198301139477588557411845120528821418091288544235235238694945619  
31602039063661931935364672107366917056402390762018100010048107024942297516896137  
81948692639165149421167030203177433142831047999559923278156691289753381947360994  
41950618468075184699904492382000829840459805980380068613781639544630774492708940  
92869514990737828125945653627298560516553250117401170567414857542696484369664304  
25238160547745304146706864463108093179871916345772951501705328108094255465016691  
67092869515011207551521902558075753771037484392328663989065153596138371224822793  
21063109788178989056359424662241617256883385442844747404844290657439446366781774  
85443008280066449491138508962954743705606886827308094533989689651322121426674841  
95129066571253664461276918024322868592017619457577276226262381945983681602020701  
86603454093388544630790066852561380723318440485435744717061947764370000720844229  
6989059855768917895753696441962535888677570338468121755300286293177794943693366  
04611552677262066691101654921793420063113577484027433667265845615549579232850617  
27641497713805648177274492727660547713785430048059805982485446307591106710325200  
11413124200098264008279925253577265876259269837314269648384027656885201519861001  
34887160172454290097712741833321243196861037473470551498214162075534218975741467  
03732608260341622089023658435549229715665699789959837308415224913494809688581314  
87866066757887172800013504979339412781733324984049457065880001117717332983021080

65408070561592522810757886882454356502799387865370322629179340449233157056345961  
88229356153627103769167468160309067094252695636779585781765478307622504854429786  
58817433558418626893331206671808361665247624274235730597374572758348832972916203  
41585737641044035184296978760644159733107708899055995784211548847271147515130857  
53352000598172570306649697980194381578296254766877774104761843154419248154761855  
61132393518049382960678741030007363920114124321518782693051312051838402066719121  
54573104215473089909973696328473492329752243231242000982639924857885257037816550  
97689699944577643539421591324702051347022086296985945669179376568615360862916400  
79529166034542693073987506193182831277798719169302416029039440463315705636622591  
63952905965046015200134700340132629390414667572312435615362951001032519860982328  
31809110671221239755649964807553077122466571937136066547849129044630758768129009  
99752224546122485430390947849129007952916587641516603435634596137819509477262916  
89904473488921796830388664096826778485776089409307398750804117058267418314324670  
70238540824876415165878644978990979183330097712556537312451205168958263958418471  
57068802520390651637482087487830238695130933885255684565015165881761032174369687  
98730048197018283678145082989559994112049789930207052731085916401136326063641516  
58788317968506549821392352331828022120550113975717609999443909474875371591106710  
32488871913437020547745291640079373454667572309268940440272417936774523487452343  
90251691086262419717000692041522491349480968858108281290759145118352605325360174  
02740806546847852280982463779591802502454357200356167447405671599685222522592764  
80729765776156409425547691830390443733504979177817611900656879719662248546156691  
67072605478543039094772608937504942556845665670324523317400635736461203715319681  
06362366539236325997231833910034602076124567450841844392363111432190100446679217  
71948415359963007626062395508757519755395262639904471627124886882454356502799409  
37378232903814269838349269836810515323177502871604947539544630774715708971763727  
637310663608241275843350097828

yl = 289

Factor point verification: (xl + intervalmidpoint)\*yl == number\_to\_factorize =  
True

Factor point verification: xl\*yl == number\_to\_factorize = False

('Factors are: (' , 289, ', ',

34599390729864778307683013574713124886135267817314543013567159996641496169311145  
08968990602016741499215497365843385042469649613403905786756879852501168952846826  
55319162032431616898902205146668767570371236584338157049424663923279372762554580  
87452691603023779836933312708781409134359307349420032139767588179871758786791833  
31966380376606518785409108384888719132836778298958229719475407937125945638003404  
59653385224357402708788338544255501136273300428695149821392362762278198214471709  
07952574042349235238508594546360688522435738371224854613491135980585757726432278  
19698407397482279321359440736275878156999096134044027438890305235986159169550173  
01038062281416364370032158894084061947782108623159488024322869217757897238861325  
98376896506204980034684807027345781671041186612118717332880013782985948037502556  
84566885258921774532260549927127438868276951639802435650276917276893851523496160  
18346308788317750305530509402324819440386599214089369611860959471236269144355460  
82449194765353916203396985165353588993193193214506308762049561357519834716023945  
68478859145401051629858198235958792706166030859132120826772620324819632274665323  
13923435549229713750424857175718816167398871379717210285027244922966345269160494  
06153196636115181255319143248887138352332142851173990602017245426965030548059821  
44719475373488693159973436790045786845260318760875131425546430097518656850585750  
24955436723122225717381426726584561357519835028509732660838693159558211875570907  
26371549019211883817412882326378369842635523640932135930044078641462931928675561  
54800255115495752243247052732954646657191452732973643231240132504596515169302397  
57205270700098263992727644581277798924857885599633158802179374685061705826743731  
08644631117295495791798748231588176414615669145273331625685948926745293508279925  
23494249961876781418129010009826400806191636622466573804115169513093334903937274  
69649770684558089528468469990959305530771564470588235294117647058823529179698720  
74024011086169339201004477235055087855685439582423263046052706204471657540913228  
38197551242315948198301139477588557411845120528821418091288544235235238694945619  
31602039063661931935364672107366917056402390762018100010048107024942297516896137  
81948692639165149421167030203177433142831047999559923278156691289753381947360994  
41950618468075184699904492382000829840459805980380068613781639544630774492708940  
92869514990737828125945653627298560516553250117401170567414857542696484369664304  
25238160547745304146706864463108093179871916345772951501705328108094255465016691  
67092869515011207551521902558075753771037484392328663989065153596138371224822793  
21063109788178989056359424662241617256883385442844747404844290657439446366781774



=====

90902035644826553917458099300837209928119021810944572099280993082085385390281099  
37200348036207620847938897624806711611579352166124807021570347976116707521570298  
85338525703388520761661248067157034798520794298852067157124798852979442985257035  
20671162484307930662488430662162065816634907490748993530843936218026711721662180  
26711672080357126627120293847571271176271172076353894444803571762085438994390762  
98543893907629903480362089448089452985299852944480893621658116711803629854384762  
94529944529444808944808943853620354390762985357127118029990348167175308935808439  
99025815798839806580662530661670261703388534388533853907629983756363636363636363  
63636363630266630026720853821729944571900267200846291263902810944836657291190210  
99372028093574902091126447553663008208462753917293720992748399848026718025802172  
07634816725712662180211808444907543935745809308208217299363900845657482639003548  
118371203620348167118028837933806619842884288442893423798434702610793470751988437  
98434702610793470752561170116247156536662116718112029383930211202938474844826548  
20821729936553672009354720819928100837108935620810753808520793398844306612529803  
52035207942976247944298033852570344294347943897620670657935216206702488934430752  
57984307525793521661702112717530754398399902581720757127118035712662671167175349  
07490258026711202938475665748393021802547564744481027108935620892571743907448016



$$y_l = 11$$

Factor point verification:  $x_l \cdot y_l == \text{number to factorize} = \text{False}$

```
('Factors are: (' , 11, ' , ' ,
```

90902035644826553917458099300837209928119021810944572099280993082085385390281099

[illegible]



```

49853081353990439930902580267175308989408994390909090909090897868126727271900267
20084629126390281094483665729119021099372028093574902091126447553663008208462753
91729372099274839984802671802580217207634816663539845308116725721720763538945197
53380252889343793519884379843067, ') (at ', 'Sun, 01 Aug 2021 09:53:18 GMT',
')')

```

=====

1158.4 Every rectangular region could be thought of as histogram union of equal sized buckets which makes Factorization (or multiplicative partition) a special case of set partitions.

1158.5 Example Schematic equivalence between a histogram H1 of unequal sized buckets and factorization histogram H2 of equal sized buckets - both of total size N:

| Histogram H1 | Histogram H2 |
|--------------|--------------|
| -----        | -----        |
| h1b1 #####   | h2b #####    |
| h1b2 #####   | h2b #####    |
| h1b3 #####   | h2b #####    |
| h1b4 #####   | h2b #####    |
| h1b5 #####   | h2b #####    |

=>  $h1b1 + h1b2 + \dots + h1b5 = N = h2b + h2b + \dots + h2b$

1158.6 Finding the exact Earth Mover Distance between H1 and H2 solves integer factorization indirectly. LC-ACT Earth Mover Distance between arbitrary unequal size bucket histogram H1 and equal size bucket histogram H2 could be written as optimization program:

=>  $h1b1 + h1b2 + \dots + h1b5 = N = h2b + h2b + \dots + h2b = (h1b1 +/- a1c1) + (h1b2 +/- a2c2) + \dots + (h1bn +/- anc_n)$  for any integral value of  $a_i$  and  $c_i$ .  $a1c1 + a2c2 + \dots + anc_n = \text{function\_of(EMD)}$  and solving for  $a_i$  and  $c_i$  finds factors of N.

1158.6 Linguistically, every string made of one alphabet and arbitrary length is equivalent to factorization (ASCII or Unicode integer value replaces the alphabet) - Example: "aaaaa" is a string of length 5 which maps to a string histogram of 5 equal sized buckets (size of each bucket equals the ASCII or Unicode value  $v('a')$  of the alphabet 'a') =>  $N = \text{length\_of\_the\_string} * v(\text{alphabet})$

1158.7 Recursion limit has been increased in DiscreteHyperbolicFactorizationUpperbound\_TileSearch\_Optimized.py for stack overrun issues while recursing binary search point location for large integers.

1158.8 Disclaimer: All benchmarks for NeuronRain computational geometric factorization so far have been performed as Nick's Class proof-of-concept only on single node Python-Spark cluster quadcore for randomly chosen non-RSA moduli or semiprime integers (high omega, easy, smooth and hard). Factorizing RSA moduli and semiprimes could be significantly harder and expensive practically and requires enterprise cloud. An optimal PRAM implementation of Planar Point Location by Sorting/WaveletTrees/SegmentTrees/IntervalTrees might have to be plugged-in for accurate Parallel RAM results (e.g <https://github.com/jlabeit/wavelet-suffix-fm-index>). Previous Benchmark numbers might scale exponentially on a production-grade BSP cloud of huge multicores if communication complexity is negligible (e.g 1 second on single node quadcore might scale to nanosecond on BSP cloud of  $10^9$  multicores subject to Amdahl and Brent speedup theorems).

1158.9 Integer Factorization benchmarks for RSA-250 semiprime moduli - 829 bits - was performed by CAD0-NFS opensource software -

<https://listserv.nodak.edu/cgi-bin/wa.exe?A2=NMBRTHRY;dc42ccd1.2002> - Year 2020 - consumes runtime of ~2700 Core years (Intel Xeon 2.1 GHz - Sieving + Matrix - 1 year for 2700 CPU-multicores) for Number Field Sieve algorithm which is exponential in input size. Computational Geometric Factorization on the other hand which is polylogarithmic ( $(\log N)^k$ ) in input size would theoretically require:

$\log 2700 \approx 11.3987$  Core years for  $k=1$

or approximately 1 year on 12 CPU-multicore PRAM hardware to factorize RSA-250 829 bits semiprime moduli (stated as estimate without benchmarks).

-----



99118548469140404711989848326283283418426283262614054627041404262605611975691418  
34260462748547055689127556913271197484260556899770405561199756904270547119846914  
04198469141326281969605410341041119611196125533896268324838913283418545902857142  
85714285714285714276133275756275627434147055755843277029901314843275845770457604  
31472747441870329861331989000341560441470441470441470441461561560033199761184842  
61197484183426140568977040568904270413426140470457700341470055756143272757461758  
43271986132886903426054711975690245961026754503737887509376307505894489487502181  
66116104167540398168968826088180240374038374037374518383039816895975402338768024  
08765947410402546741040246959818312316803880394537537325168039468109594680246673  
75308959532310895953231038166102393765937368103040247018545612741325997559755975  
68756885325975160959467311816747119974854627041198976140568991184197548547054691  
32691326275569033189033262832769975561199846912704056127689914041340426275485469  
04262755626119975691327119975483283403413271185483198976899771326283189131997562  
71176989854846997689128319854711989769897711854756991185484183426134132628418341  
85485462831984697704047119975626127689771184832627554846913271189033189040568991  
28327040569897698469132705470568984832834183426118997704134040568997704140568976  
89976891275568997689132626140570405689034177118484260556128341842626055689128328  
3418341326283283328419756912754854705561199846913283426056891275484690426283276  
89848326283276897704119897704140461760461834261341404132628418341275484699118485  
46991185484691404047119898483262832834184262832626140546270414042626056119756914  
18342604627485470556891275569132711974842605568997704055689912831984699770414054  
62711769975691326270405689976141340426270405689912754855611996255319696055326833  
89691041124818198261055319899770426018857142857142857142857142847561847184847056  
00557562718441470560132988627184727434188617574329890299013187004189131857484417  
58432758432758432758431870441717605690404198546911769975627117698985484699768912  
83198547119897698977118547569911854841834261341326284183424826748267483898262468  
33898267706263412119769927055640560570405470556119984049984832857142857142855379  
27705714272718484584727434147044171990290328861560458472747271847484614319870329  
86132986132986132986044187028903426183276997548319846914042618556261405561199756  
27040569897710246959754025468310410267545403910541870289034261832769975483198469  
140426185562614055611997562704056989771024695975402546831041026754540391

xl =

14284605601329887044171987041198975896271176890331116755312468826105532625467696  
10546839039124624696246767547122366202179198983418341842617604617611997562711841  
83427040547484615600557561560056171890029013188704417584327605604289129890128990  
12899012899012890132988604628332613414040546271184842605561283418426260556891283  
28341834132628328332841975691275485470556119984691391124625531981839767540532683  
91348348406911984984842119891418340419846914126214134042857142857142839507056285  
71298613417275845770041870291331474717187033156156044147046274714627274727184727  
18472718472717585713177029901315615600558461560132988704417713148432758458441770  
04198913275845847274340405689768990390398198183911824676755340391041103389626110  
53262546767533267696054039103910405403910410553248325481839104105324838976754105  
46819818339753410391182676105531961248181961196896056899771177117698983418332834  
26134041340405689911834184056119898547474747475485470556898469141326269897704134  
04199755626140561199754756913270546914042627556914040547119748418426140546275483  
28342754854617703426134140341327119898548319854627118548469127548547118998483283  
41326283276989771275485339817683891246969103976755410532483975341034185484711733  
14285714285714285714285713327613289913277029128991289870041988704417198613298862  
76004614575846172758461557561770328605584615575615575615575615574727584574748547  
54705568976891275485471199754846914033284184199756904188627177004148432757184418  
60331870041484327574404628319756911854738881816961168959610246959754025468310410  
26754540388389739754024695981831118259612446838838884332618341417604617474747474  
74747461847274328986271847172719887184313271702987274402832740413118455624696105  
53267675339754055319818391039124676961119605403911246254676898197533960532676832  
48181968969626111968962611196124832553189141326261405462841834270404691404262754  
846991183413269140341834041974747474747474747474854686045888418447117118454711  
68984547117040260303030304260461760461760462832768903318903318913303912831974747  
30331890291427457030539523646049176046175703319069835030951903184838976832483896  
26112475341033898196105326254674854711997485462704119897614056899118419754854705  
46913269132627556903318903326283276997556119984691270405612768991404134042627548  
54690426275562611997569132711997548328340341327118548319897689977132628318913199  
75627117698985484699768912831985471198976989771185475699118548418342613413262841  
83424826748267483898262468338982676753411181981770426275688759999999999999999999  
999999990418990041989913148432770041557562744187029128990131484743318600441760132

98901289903417571770131870041870041870041870032990131461771189756271183403413262  
83283426119897711761413270568997613314843198612912899000415614604615575577004186  
01189140340426261404531675312468832453245326740397397540246959818311181981833975  
34103911826761055319612481819611968960568997711771176989834183328342613404134040  
56899118341840561198985474747474754854705568984691413262698977041340419975562614  
05611997547569132705469140426275569140405471197484184261405462754832834275485461  
77034261341403413271198985483198546271185484691275485471189984832834132628327698  
97712754853398176838912469691039767554105324839753410341854847117331428571428571  
42857142857133276132899132770291289912898700419887044171986132988627600461457584  
61727584615575617703286055846155756155756155756155747275845747485475470556897689  
12754854711997548469140332841841997569041886271770041484327571844186033187004148  
43275744046283197569118547388818169611689596102469597540254683104102675454039124  
69111819818197541046769605326767533897683246283283426056891275548469042628327689  
84832628327689770411989770414046176046183426134140413262841834127548469911848546  
99118548469140404711989848326283283418426283262614054627041404262605611975691418  
34260462748547055689127556913271197484260556899770405561199756904270547119846914  
04198469141326281969605410341041119611196125533896268324838913283418545902857142  
85714285714285714276133275756275627434147055755843277029901314843275845770457604  
31472747441870329861331989000341560441470441470441470441461561560033199761184842  
61197484183426140568977040568904270413426140470457700341470055756143272757461758  
43271986132886903426054711975690245961026754503737887509376307505894489487502181  
66116104167540398168968826088180240374038374037374518383039816895975402338768024  
08765947410402546741040246959818312316803880394537537325168039468109594680246673  
75308959532310895953231038166102393765937368103040247018545612741325997559755975  
68756885325975160959467311816747119974854627041198976140568991184197548547054691  
32691326275569033189033262832769975561199846912704056127689914041340426275485469  
04262755626119975691327119975483283403413271185483198976899771326283189131997562  
71176989854846997689128319854711989769897711854756991185484183426134132628418341  
85485462831984697704047119975626127689771184832627554846913271189033189040568991  
28327040569897698469132705470568984832834183426118997704134040568997704140568976  
89976891275568997689132626140570405689034177118484260556128341842626055689128328  
34183413262832833284197569127548547055611998469132834260568912755484690426283276  
89848326283276897704119897704140461760461834261341404132628418341275484699118485  
46991185484691404047119898483262832834184262832626140546270414042626056119756914  
18342604627485470556891275569132711974842605568997704055689912831984699770414054  
62711769975691326270405689976141340426270405689912754855611996255319696055326833  
89691041124818198261055319899770426018857142857142857142857142847561847184847056  
00557562718441470560132988627184727434188617574329890299013187004189131857484417  
58432758432758432758431870441717605690404198546911769975627117698985484699768912  
83198547119897698977118547569911854841834261341326284183424826748267483898262468  
33898267706263412119769927055640560570405470556119984049984832857142857142855379  
27705714272718484584727434147044171990290328861560458472747271847484614319870329  
86132986132986132986044187028903426183276997548319846914042618556261405561199756  
27040569897710246959754025468310410267545403910541870289034261832769975483198469  
140426185562614055611997562704056989771024695975402546831041026754540390

yl = 7

Factor point verification: (xl + intervalmidpoint)\*yl == number\_to\_factorize = True

Factor point verification: xl\*yl == number\_to\_factorize = False

('Factors are: (', 7, ', ',

14284605601329887044171987041198975896271176890331116755312468826105532625467696  
10546839039124624696246767547122366202179198983418341842617604617611997562711841  
83427040547484615600557561560056171890029013188704417584327605604289129890128990  
12899012899012890132988604628332613414040546271184842605561283418426260556891283  
28341834132628328332841975691275485470556119984691391124625531981839767540532683  
91348348406911984984842119891418340419846914126214134042857142857142839507056285  
71298613417275845770041870291331474717187033156156044147046274714627274727184727  
18472718472717585713177029901315615600558461560132988704417713148432758458441770  
04198913275845847274340405689768990390398198183911824676755340391041103389626110  
53262546767533267696054039103910405403910410553248325481839104105324838976754105  
46819818339753410391182676105531961248181961196896056899771177117698983418332834  
26134041340405689911834184056119898547474747475485470556898469141326269897704134  
04199755626140561199754756913270546914042627556914040547119748418426140546275483  
28342754854617703426134140341327119898548319854627118548469127548547118998483283

[illegible]

1159.2 Equal bucket size histograms (or Factorization histograms mentioned in 1158) have been widely studied in BigData analytics by the name of V-Optimal histograms, Equidepth histograms and Equiheight histograms which strive to maintain depth and width of buckets to be equal.

1159.3 There are some recent results in computing Partition distance (which generalizes histogram and set partition distance measures such as Earth mover distance, Adjusted rand index etc.,) in linear time (linear in total size of histogram H1 which is moved to another histogram H2 which could be equidepth or equiheight) for closely resembling partitions - In following Example arbitrary histogram H1 of unequal bin size is moved to a equidepth or equiheight histogram H2 of equal bin size which factorizes 15 as 3 buckets of size 5 each:

| H1 (size 15 = 5 + 8 + 2) | H2 (size 15 = 5 + 5 + 5) |
|--------------------------|--------------------------|
| #####                    | #####                    |
| #####                    | #####                    |
| ##                       | #####                    |

1159.4 Linear time partition distance of histograms if reducible to edit distance of string histograms implies SETH is false. Partition distance or histogram distance has been traditionally used to compare images for similarity by treating every image as histogram of pixels. Closely resembling partitions are crucial for image analytics, face recognition in specific because pixel histograms of visuals of humans might have only small variations as facial features differ slightly though facegraph segmentation of human faces abide by similar Topological Product Homotopy shape grammar (Section 715 - Contour deformations by Product Homotopy for facial feature grammar). Linear time partition distance for closely resembling histograms of human face visuals imply linear time face recognition.

1159.5 Histogram Partition distance between two images could be a CoronaVirus 2019 analytics tool:

1159.5.1 Digital watermarking Overlay of COVID19 hotspot GIS geospatial imagery (JHU, ARCGIS, ESRI) on 6-colored SEDAC urban sprawl population estimator (GPW-4 - <http://sedac.ciesin.columbia.edu/mapping/popest/gpw-v4/>) which color encodes urban sprawls by increasing population density estimated by convex hull polygons drawn around colored segments, and percentage of overlay is the similarity.

1159.5.2 Instead of convex hull polygons, overlay the Voronoi facegraphs of the Urban sprawl SEDAC imagery and COVID19 hotspot GIS imagery and find similarity by graph edit distance (GED) between the facegraphs of two GIS images.

1159.5.3 Compute Histogram Partition Distance between COVID19 hotspot GIS imagery and SEDAC urban sprawl density GIS imagery - low distance implies high overlay and high correlation between population density (average degree) and transmission of COVID19.

1159.6 New file

DiscreteHyperbolicFactorizationUpperbound\_TileSearch\_Optimized.largestintegerfactorized has been created which contains the largest integer factorized by NeuronRain so far.

References:

- 
- 1159.7 Linear Time Partition Distance for close partitions - <https://www.sciencedirect.com/science/article/pii/S0166218X10003069>
  - 1159.8 Equiheight and Equidepth histograms - <https://www.cise.ufl.edu/~adobra/approxqp/histograms2>
  - 1159.9 Computing Equidepth histograms for BigData - <https://arxiv.org/pdf/1606.05633.pdf>
  - 1159.10 CoronaVirus 2019 GIS map - <https://coronavirus.jhu.edu/map.html>
  - 1159.11 Factorization of 1061 bits integer by Number Field Sieve - <https://eprint.iacr.org/2012/444.pdf>
  - 1159.12 Integer Factorization Records - [https://en.wikipedia.org/wiki/Integer\\_factorization\\_records](https://en.wikipedia.org/wiki/Integer_factorization_records)
  - 1159.13 NeuronRain Lecture on PRAM Integer Factorization - <https://kuja27.blogspot.com/2021/10/neuronrain-lecture-integer.html>
-

-----  
1160. (THEORY and FEATURE) Set Partition Analytics - Set Partition to Lagrangian Sum of Squares tile cover reduction - Python 3.9.0 upgrade and some code changes - 27 August 2021 - related to all sections on Set Partitions and Histogram analytics, Space filling by tile cover, Integer Factorization by Equidepth histograms, Drone Set Partition Electronic Voting Machines, Diophantines and Complement Functions  
-----

-----  
1160.1 Streaming\_SetPartitionAnalytics.py implementation has been upgraded to Python 3.9.0 and package imports have been changed to suit Python 3.9.0 (SymPy Diophantine SOS solvers)  
1160.2 Subprocess call to computational geometric factorization has been upgraded to Spark 3.0.1  
1160.3 NumPy ndarray has been cast to float by astype()  
1160.4 Randomized rounding after LSMR least square  $AX=B$  solver approximation has been changed to Python round()  
1160.5 Rectangular Periphery - Sides of Square tiles - approximated from LSMR rounding are computed from equationsA matrix to preserve order.  
1160.6 complement.py has been upgraded to python 3.9.0 and imports of SymPy Diophantine Sum of Squares (SOS) solver have been changed.  
1160.7  
testlogs/Streaming\_SetPartitionAnalytics.Python3.9Upgrade.log.27August2021 and DiscreteHyperbolicFactorizationUpperbound\_TileSearch\_Optimized.factors contain the logs for this update.  
-----

-----  
1161. (THEORY and FEATURE) Set Partition Analytics - Set Partition to Lagrangian Sum of Squares tile cover reduction - Integer Linear Programming Exact Solution - 29,30 August 2021 - related to all sections on Set Partitions and Histogram analytics, Space filling by tile cover, Integer Factorization by Equidepth histograms, Drone Set Partition Electronic Voting Machines, Integer Linear Programming  
-----

-----  
1161.1 Streaming\_SetPartitionAnalytics.py has been updated to compute exact Integer Linear Programming solution for sides of the rectangle to which a set partition is reduced, by CVXOPT GLPK ilp() mixed integer linear programming function.  
1161.2 ILP function has been imported from CVXOPT GLPK module.  
1161.3 setpartition\_to\_tilecover() function has been changed to take additional argument "solution" which defaults to "ILP".  
1161.4 Two linear programs in equationsA matrix are made different by random permutation.  
1161.5 Error condition has been handled while populating equationsB matrix.  
1161.6 New if-else clause has been introduced which chooses between exact CVXOPT Integer Linear Programming solution (NP-Hard) and approximate least squares solutions including LSMR (polynomial time)  
1161.7 cvxopt.glpk.ilp() function is invoked by suitably passing arguments C,G,H,A,B,I which are interpreted as below:  
    1161.7.1 C - constraints matrix which is all 1s for variables (number of tiles per square tile side)  
    1161.7.2 G - mask matrix which has 1 row per variable and each row has one 1 at the variable index  
    1161.7.3 H - Array of all 0s which has size equal to number of variables  
    1161.7.4 A - EquationsA matrix  
    1161.7.5 B - EquationsB matrix  
    1161.7.6 I - Array of variable indices  
1161.8 Sides of the rectangle are printed as addition of sides of square tiles computed by CVXOPT GLPK ILP Simplex which are exact for ILP and approximate for Least squares.  
1161.9 As an example following is a reduction from Set partition to Rectangular region by NeuronRain computational geometric factorization - Factors 7 and 77 of

539 (Rectangular periphery) are expressed in terms of sides of square tiles from Lagrange sum of squares of a set partition by CVXOPT GLPK ILP simplex:

[illegible]

## 1161.10 Logs

testlogs/Streaming\_SetPartitionAnalytics.Python3.9Upgrade.ILP.log.30August2021 and testlogs/Streaming\_SetPartitionAnalytics.Python3.9Upgrade.log.29August2021 respectively compute exact CVXOPT GLPK ILP and approximate LSMR solutions.

1161.11 Previous CVXOPT GLPK ILP can be written as:

```
optimize c1 + c2 + c3 + ... + cn
```

subject to:

$$c_1 \cdot x_1 + c_2 \cdot x_2 + \dots + c_k \cdot x_k + \dots + c_n \cdot x_n = p$$
$$d_1 \cdot x_1 + d_2 \cdot x_2 + \dots + d_k \cdot x_k + \dots + d_n \cdot x_n = a$$
$$c_1 \geq 0, \quad c_2 \geq 0, \quad \dots, \quad c_n \geq 0$$

.....



1162. (THEORY and FEATURE) Merit of Large Scale Visuals - GIS and Urban Sprawl Analytics, CoronaVirus 2019 Analyzer, Histogram Partition Distance Similarity of images - implementation - related to 1159 and all sections on GIS and Urban Sprawl Analytics, Earth Mover Distance, CoronaVirus 2019 Analyzer, Large Scale Visual Recognition, Social Network Analytics - 3,4 September 2021,23 October 2021

-----

1162.1 In this update new function `histogram_partition_distance_similarity()` has been defined which computes histogram partition distance similarity between pixel histograms of two images which is by default Earth Mover Distance though other partition distances could be defined as clauses later (e.g SymPy Partition distance).

1162.2 By CoronaVirus 2019 analyzer usecase mentioned in 1159, following GIS images of Population Density and COVID19 hotspots are compared for histogram Earth Mover Distance similarity (from SEDAC,GHSL and JHU datasources) and their Voronoi facegraphs are computed from `image_segmentation()` - color coding has been ignored, images might have to be converted to grayscale:

1162.2.1 SEDAC GPW4 Population Density GIS for India -  
`SEDAC_PopulationDensity_India_2021-09-04-10-49-24_segmented.jpg` -  
<https://sedac.ciesin.columbia.edu/mapping/popest/gpw-v4/>

1162.2.2 SEDAC COVID19 Hotspots GIS - `SEDAC_COVID19_Hotspots_GIS_2021-09-04-10-51-29_segmented.jpg` -  
<https://sedac.ciesin.columbia.edu/mapping/popest/covid-19/> and  
<https://ghsl.jrc.ec.europa.eu/visualisation.php> (Global Human Settlements Layer)

1162.2.3 JHU COVID19 Hotspots GIS - `JHU_COVID19_Hotspots_GIS_2021-09-04-11-02-11_segmented.jpg` - <https://coronavirus.jhu.edu/map.html> 1162.3  
`image_segmentation()` has been changed to write the Facets Graph of each segmented image in labelled DOT files in `testlogs/RemoteSensingGIS/` which could be separately read and instantiated as FaceGraph by NeuronRain Graph Analytics (`GraphMining_GSpan.py`) per segmented image.

1162.4 Logs for this update are at  
`testlogs/ImageGraph_Keras_Theano.HistogramDistance.log.4September2021`

1162.5 `tosig()` function used for preprocessing in `CompressedSensing.py` alphabet vector space embedding EMD has been changed as `tosig3d()` for transforming 3 Dimensional Keras image pixel ndarray to two dimensional OpenCV2 UMat format.

1162.6 NASA VIIRS Earth Observatory NightLights -  
<https://earthobservatory.nasa.gov/features/NightLights> - imagery captures lights on earth during night which are convex hull polygons or circles of various radii viewed from sky. Circles in VIIRS NightLights which are proportional to electricity consumption by an urban sprawl are approximate alternatives to census data for estimation of urban area expanse and its population.

1162.7 Cities can be ranked by area of their NightLights convex hulls (`OpenCV2 convexHull()` or `scipy ConvexHull()`) for Urban agglomeration ranking.

-----

1165. (THEORY and FEATURE) Drone Online Shopping Delivery - NeuronRainApps - Refactoring for ConvexHull and GIS analytics variables read over socket stream - related to all sections on Async IO, Drone Electronic Voting Machines, GIS and Urban Sprawl Analytics, Merit of Large Scale Visuals, Drone Obstacle Avoidance, Computational Geometry - 12 October 2021, 21 October 2021, 23 October 2021

-----

1165.1 `OnlineShoppingDelivery.py` has been refactored for analytics variables read over socket stream (port 64001). Instead of inferring convex hull of the destination only from aerial GIS image by OpenCV2, optional clauses have been introduced to read longitude-latitude list of convex hull waypoints and mission way points over socket stream (`nc -l 64001`) port.

1165.2 GIS analytics variables have been enhanced by uncommenting earlier commented variables. Convex Hull from OpenCV is a list of integers and not in format of longitude-latitude of vertices of convex hull polygon

which necessitates writing convex hull longlat(s) over socket stream or reading from file. OnlineShoppingDelivery.GISvars.txt has been updated for a reference list of variables.

1165.3 Convex Hull mission longitude-latitude list and GIS analytics key-value pair list written over socket stream have to be now demarcated by "end\_longlat" and "end\_gis" delimiter strings.

1165.4 start\_mission() throws error "start\_mission(): coro=run() done" errors if the waypoints are too faraway and PX4 console prints "waypoints are too far away" error messages. Because of this list of longitude-latitudes read over socket stream have been separated by decimals (reference: list of longitude-latitude(s) of mission.py example in MAVSDK Python source code)

1165.5 Earlier "start\_mission(): coro=run() done" error has been documented also to be related to QGroundControl (QGC) in MAVSDK issues. But QGC installation is fraught with GLIBC and GLIBCXX version number errors which might require upgrade to gcc-9 and g++-9 and correct packages containing matching libstdc++.so.6 and libc.so have to be found by "strings". Some other MAVSDK documentation mention QGC is not necessary for mission.

1165.6 Earlier "coro=run() done" errors are resolved if start\_mission() is populated with longlat(s) which are not faraway.

1165.7 OnlineShoppingDelivery.py is a versatile implementation which can be adapted to Drone Postal Delivery, Drone EVM, Drone Human Transport (if payload allowed is ~100kg and range of flight > 35 kms assuming solar panel powered drones, but mostly available drones have flight time of ~20 to 25 minutes requiring either a midair recharge or relayed drone delivery. Relayed drone delivery splits mission into equal distances for 20 minutes flight time and Drone(N) after its flight time lands and delivers payload to Drone(N+1) which continues mission to Drone(N+2). Without Relay same drone has to land at multiple intermediate points and has to be recharged every 20-25 minutes for continued mission. Relay drones are already recharged and ready for takeoff), Drone Autonomous Combat (Several military drones used for precision aerial bombings have high payload), GIS Mapping Drones among others.

1165.8 Drone Human Transport (single seater) though a solution for surface traffic congestion, could cause air traffic congestion and special Drone Air Traffic Control (ATC) is necessary - ATC for drones is fully programmable (allocating non-colliding mission trajectories to drones) as drones are autopiloted and mission plans are controlled by ATC.

1165.9 Drone transport is 3-dimensional (longitude, latitude, altitude) as against 2-dimensional surface transport (longitude, latitude) and aerial transportation graph is non-planar, while surface transportation graph is planar - Open Source NASA Perseverance Mars Rover is both surface and aerial transportation (helicopter) drone - <https://github.com/nasa-jpl/open-source-rover> and <https://opensourcerover.jpl.nasa.gov/>.

1165.10. Safe transport of items insulated from natural obstacles (e.g turbulent weather) is paramount for online shopping delivery - Drones being lightweight may not withstand ferocious onslaught of rain and winds. GIS analytics variables read over socket stream by OnlineShoppingDelivery.py Python implementation could be sourced from image and video analytics of GIS imagery by OpenCV2 - e.g list of mission longitude-latitude(s) dynamically changes based on weather vicissitudes learnt from remote sensing weather satellite photo of sky (clear, overcast, storms) which is an obstacle avoidance algorithm.

1165.11 Image analytics might require functionality to analyze any GIS imagery - SEDAC-GPW4-PopEst, Weather, Rural-Urban clusters, ... - and segment those images to find facets of importance and least obstacles whose vertices have to be mapped to longitude-latitude and written over socket stream for live reading by drones (instead of nc -l).

1165.12 MAVSDK does not seem to support dynamic mission plans to add/delete/update longitude-latitude(s) during flight after upload\_mission()-start\_mission() and all longlat(s) must be known apriori.

1165.13 Dynamic Mission Obstacle Avoidance Algorithm by GIS imagery analytics:

-----  
1165.13.1 Drone executes TAKE\_PHOTO command and transmits terrestrial image back to PX4-MAVSDK ground control and satellite weather GIS photo at that instant is used for obstacle overlay - the two images have to be overlaid to filter the obstacle vertices-edges.

1165.13.2 MAVSDK Client invokes (\*) transportation graph extraction algorithm on terrestrial image transmitted by drone and (\*) image analytics segmentation on aerial GIS image to find segments containing obstacles - clouds, storms, dust, ... - obstacle segments are bounded by convex hulls

1165.13.3 MAVSDK client overlays the transportation graph imagery on segmented (convex hull) weather GIS imagery and masks the vertices and edges (roads and junctions) from transportation graph which coincide with obstacle segment convex hulls (e.g road-junctions vertices-edges on earth directly below and with in cloud convex hull segments in sky are masked and removed from transportation graph - in other words, holes are punctured in transportation graph fabric by convex hull obstacles)

1165.13.4 Shortest distance (Geodesic) is computed between source and destination on the obstacle masked punctured transportation graph and Geodesic longlat(s) (from Geocoding Geodesic functionality - <https://geopy.readthedocs.io/en/stable/index.html?highlight=geodesic#module-geopy.distance>) are populated dynamically before upload\_mission() and start\_mission() which bypasses obstacles.

1165.14 Graph masking earlier to remove terrestrial transportation subgraphs coinciding with aerial GIS imagery obstacle segments could be non-trivial computational geometric problem.

1165.15 Obstacle segments in GIS imagery are usually convex hulls (e.g polygon encompassing clouds) and planar intersection algorithms are required to find transportation graph edges-vertices which intersect and are with in obstacle convex hull edges-vertices of aerial GIS imagery.

1165.16 Previous algorithm could be an implementation separate from MAVSDK client which computes Graph Obstacle Masking earlier and writes the geodesic longlat(s) over socket stream as GIS analytics variables to MAVSDK client.

1165.17 Logs for this commit are at:

OnlineShoppingDelivery.py -

OnlineShoppingDelivery\_Drone\_JMAVSIM\_Flight\_Simulation\_Mission.log.MAVSDKClient.120October2021

nc -l 64001 -

OnlineShoppingDelivery\_Drone\_JMAVSIM\_Flight\_Simulation\_Mission.log.netcat.120October2021

PX4 console -

OnlineShoppingDelivery\_Drone\_JMAVSIM\_Flight\_Simulation\_Mission.log.PX4.120October2021

1165.18 MP4 Video of the Drone Mission flight for earlier convexhull and mission analytics variables has been uploaded at:

<https://kuja27.blogspot.com/2021/10/blog-post.html>

1165.19 Another important manmade obstacle for civilian drones are sabotage (mistakenly shotdown, antidrone systems) causing payload destruction. Most countries mandate licensing for drones which to some extent can minimize human errors - Drones are discoverable by UUID which can be verified for security checks. Modern drones are fitted with onchip radar SAA - Sense and Avoid - <https://www.droneassemble.com/obstacle-avoidance-radar-in-drones/>

1165.20 Artificial obstacle by sabotage for Drones is as risky as any surface vehicle - Both are equally prone to attacks. There are some recent efforts (Project Interceptor - <https://www.codemotion.com/magazine/dev-hub/security-manager/project-interceptor-avoiding-counter-drone-systems-with-nanodrones/>) which evade antidrone systems by nanodrones.

## References:

-----  
1165.21 Theory, Design, and Applications of Unmanned Aerial Vehicles - [AR Jha] - <https://www.taylorfrancis.com/books/mono/10.1201/9781315371191/theory-design-applications-unmanned-aerial-vehicles-jha-ph?refId=0d1cd32d-6709-436c-81ba-9b7e4eb92d4c&context=ubx> - Civilian and Military Drones (Unmanned Combat Aerial Vehicle) for Intelligence-Reconnaissance-Surveillance (IRS) - Gasoline and Electric engines - Nickel-Cadmium and Zinc-Silver batteries - "... When the needed sensors and equipment are fully developed and available, UAVs can be equipped to create highly accurate images of the mouths of rivers, coastlines, ports, and settlements in critical regions. Typical physical parameters of a miniature UAV known as a nano-or micro-UAV, which can be launched by hand, are

summarized as follows. Typical physical parameters of mini-UAVs [1] • Takeoff weight: 6-12 lb • Airframe weight: 5-7 lb • Wing span: 5-7 ft • Fuselage length: 4-6 ft • UAV speed: 20-30 mph • Payload: 5-10 lb • Flight endurance: 10-25 h • Rating of electrical motor: 1 kW or 1.35 HP (some UAVs use gasoline engine and some use an electric motor) • Takeoff speed: 15-20 mph • Landing speed: 15-20 mph • Runway length: 40-60 ft • Maximum climb speed: 16 ft/s • Turn radius: 35-50 ft • Flight altitude: 50-5000 ft ..."

-----  
1166. (THEORY and FEATURE) Set Partition Analytics - Complementary Set Partitions - implementation - 20 October 2021 - related to 864 and all sections on Complement functions, Complementary sets, Set Partitions, Electronic Voting Machines, Set Partition version of Boolean Majority, Majority Voting  
-----

-----  
1166.1 Streaming\_SetPartitionAnalytics.py has been updated to define a new function complementary\_set\_partition() as per NeuronRain definition of complement set partitions (Example described in Section 864 - item 60) - each partition and its complement split an equidepth partition.  
1166.2 This function iterates through parts of a partition and pads each part by zeros (numpy zero fill) to create a complementary set partition union of which together form an equidepth partition. Depth of the equidepth partition is a configurable parameter to complementary\_set\_partition()  
1166.3 Complement and Equidepth partitions for a random partition are printed. Logs for this commit are at  
testlogs/Streaming\_SetPartitionAnalytics.Python3.9Upgrade.Complement.20October2021  
-----

-----  
1167. (THEORY and FEATURE) GIS Urban Sprawl Analytics - NASA VIIRS NightLights Urban Area and Population Estimation - implementation - 24 October 2021 - related to all sections on Merit of Large Scale Visuals, GIS and Urban Sprawl Analytics, Computational Geometry, R Ricker Population Estimator implementation, SEDAC GPW4 PopEst, Social Network Analytics  
-----

-----  
1167.1 Because of importance of GIS geospatial imagery for Urban Sprawl Analytics, new source file GISUrbanSprawlAnalytics.py has been added to NeuronRain repositories which defines function urban\_sprawl\_from\_segments() for reading an urban sprawl GIS image and segment it by contours and compute convex hulls around contour polynomial points.  
1167.2 NASA VIIRS 2016 imagery for India NightLights python-src/image\_pattern\_mining/ImageNet/testlogs/NightLights\_13nasa-india-2016.jpg is contour segmented by ImageGraph\_Keras\_Theano.py image\_segmentation() and contours of 1825 urban areas in the subcontinent are read by previous function.  
1167.3 Convex Hulls of 1825 urban areas are found by OpenCV2 convexHull(). Circumference of 1825 urban sprawls is computed from cv.arcLength() of the urban area segment contour polynomials and approximate urban sprawl area is derived from circumference as a circular region:  
$$\text{Area} = 3.1428 * (\text{Circumference}/2*3.1428)^2$$
  
1167.4 Segmented Contours of 1825 urban sprawls are written as JPEG image file python-src/image\_pattern\_mining/ImageNet/testlogs/RemoteSensingGIS/NightLights\_13nasa-india-2016\_segmented.jpg which are fairly accurate in demarcating urban areas and new insights of urban areas emerge - formation of megalopolises in TN,MH,Gangetic Plain and lopsided growth in certain pockets.  
1167.5 Imagery and Logs for this implementation are at:  
Logs - ImageNet/testlogs/GISUrbanSprawlAnalytics.log.24October2021  
NASA VIIRS NightLights - India 2016 -  
ImageNet/testlogs/NightLights\_13nasa-india-2016.jpg (Copyright:

<https://earthobservatory.nasa.gov/features/NightLights>)  
FaceGraph of NightLights -  
ImageNet/testlogs/RemoteSensingGIS/NightLights\_13nasa-india-2016\_FaceGraph.jpg  
DOT file for FaceGraph -  
ImageNet/testlogs/RemoteSensingGIS/NightLights\_13nasa-india-2016\_ImageNet\_Keras\_Theano\_Segmentation\_FaceGraph.dot  
1825 Contour segmented urban sprawls of India -  
ImageNet/testlogs/RemoteSensingGIS/NightLights\_13nasa-india-2016\_contours\_segmented.pdf  
1825 Convex Hull segmented urban sprawls of India -  
ImageNet/testlogs/RemoteSensingGIS/NightLights\_13nasa-india-2016\_convex\_hulls\_segmented.pdf  
NASA VIIRS NightLights India 2016 image layered by 1825 urban sprawl  
Contour segments - ImageNet/testlogs/RemoteSensingGIS/NightLights\_13nasa-india-2016\_segmented.jpg  
1167.6 ImageGraph\_Keras\_Theano.py has been updated for return value tuples of contour segments.

-----  
1168. (THEORY and FEATURE) GIS Urban Sprawl Analytics - NASA VIIRS NightLights Urban Area Rankings - 29 October 2021 - related to all sections on Merit of Large Scale Visuals, GIS and Urban Sprawl Analytics, Computational Geometry, Intrinsic Merit Rankings, R Ricker and SEDAC GPW4 Population Estimations, Social Network Analytics, Space filling by Curves, Circle packing, Chaos and Mandelbrot sets  
-----

-----  
1168.1 GISUrbanSprawlAnalytics.py has been updated to compute area of every Urban Area in contour segmented NASA VIIRS NightLights 2016 imagery by cv2.contourArea() in addition to circular area approximation, draw bounding box rectangle around each of 1825 Urban area sprawls by cv2.boundingRect(), write an id string for every urban area bounding box by cv2.putText() and sort the list of tuples of contour areas of cities which is printed as rankings of Urban areas.

1168.2 Contours of 1825 urban areas have been imprinted on VIIRS NightLight image along with their numeric id(s) through which lookup can be made on the sorted urban area ranking list of tuples. Contour id labelled image is written to testlogs/NightLights\_13nasa-india-2016-contourlabelled.jpg

1168.3 Following are the affected logs and images:

FaceGraph of NightLights - testlogs/RemoteSensingGIS/NightLights\_13nasa-india-2016\_FaceGraph.jpg

1825 Contour segmented urban sprawls of India -

testlogs/RemoteSensingGIS/NightLights\_13nasa-india-2016\_contours\_segmented.pdf

1825 Convex Hull segmented urban sprawls of India -

testlogs/RemoteSensingGIS/NightLights\_13nasa-india-

2016\_convex\_hulls\_segmented.pdf

Python Keras and OpenCV2 Logs -

testlogs/GISUrbanSprawlAnalytics.log.29October2021

NASA VIIRS India 2016 image layered by 1825 City id labelled Contours -

testlogs/NightLights\_13nasa-india-2016-contourlabelled.jpg

1168.4 Contours of Urban areas which are in close proximity are highly likely to merge in future.

1168.5 Contour curves fill a 2-dimensional space - either as polynomials or unequal circles. Parallels can be drawn between Fractal geometry (Koch curves which are known to be space filling - [https://en.wikipedia.org/wiki/Space-filling\\_curve](https://en.wikipedia.org/wiki/Space-filling_curve)) of coastlines which are Mandelbrot sets and Contour curve geometry of urban areas - [https://en.wikipedia.org/wiki/Coastline\\_paradox](https://en.wikipedia.org/wiki/Coastline_paradox).

1168.6 Population of urban sprawls can be estimated by product of population density and contour area.

-----  
1169. (THEORY and FEATURE) GIS Urban Sprawl Analytics - NASA VIIRS NightLights

2012 and 2016 Distance Similarity and Urban Area Rankings - related to all sections on Merit of Large Scale Visuals, GIS and Urban Sprawl Analytics, Computational Geometry, Intrinsic Merit Rankings, R Ricker and SEDAC GPW4 Population Estimations, Social Network Analytics, Space filling by Curves, Unequal Circle and Polynomial packing, Chaos and Mandelbrot sets, Computational Geometry, Four color theorem, Linear Programming - 5,6 November 2021

-----

1169.1 GISUrbanSprawlAnalytics.py has been updated to compute histogram set partition distance similarity (Earth Mover Distance) measure between NASA NightLights Contour Segmented Urban Sprawl imagery of India - 2012 and 2016 - as below:

```
('EMD Histogram distance similarity between images -
testlogs/NightLights_13nasa-india-2016.jpg and testlogs/NightLights_13nasa-
india-2012.jpg :', (0.053227465599775314, None, array([[36., 0., 0., ..., 0.,
0., 0.],
[0., 34., 0., ..., 0., 0., 0.],
[0., 0., 37., ..., 0., 0., 0.],
...,
[0., 0., 0., ..., 25., 0., 0.],
[0., 0., 0., ..., 1., 19., 0.],
[0., 0., 0., ..., 0., 6., 34.]]), dtype=float32)))
```

1169.2 Following are excerpts of logs which show more than doubling of Urban area NightLight circles between 2012 and 2016 implying an impressive urban boom of 20-25% growth per annum and doubling of electricity consumption between 2012 and 2016 (but not in proportionate correlation to GDP growth):

2016: ('Number of segments - Number of Urban areas:', 1914)

2012: ('Number of segments - Number of Urban areas:', 835)

1169.3 2D surface of a nation is sparsely packed by closed urban area contour polynomials of arbitrary shapes. Though equal circle packing of 2D surface has been widely studied, unequal circle packing and its generic version - polynomial packing - find less or no mention.

1169.4 Following are some of Unequal Circle Packing (within a Circle or Square container) algorithms and there are no published algorithms for packing arbitrary polynomial curves within a 2D surface though Voronoi Diagram Tessellations could approximate contour polynomials by polygons:

1169.4.1 Packing Unequal Circles into a Square Container by Partitioning Narrow Action Spaces and Circle Items - <https://arxiv.org/abs/1701.00541>

1169.4.2 Packing unequal circles using formulation space search - <https://www.sciencedirect.com/science/article/abs/pii/S0305054812002663?via%3DIhub>

1169.4.3 Packing different-sized circles into a rectangular container - <https://www.sciencedirect.com/science/article/abs/pii/S037722179500032L>

1169.5 Following are the logs, contour segment, convexhull segment, contour labelled image files generated from 2012 and 2016 VIIRS imagery for this commit:

```
testlogs/NightLights_13nasa-india-2016-contourlabelled.jpg
testlogs/NightLights_13nasa-india-2016.jpg
testlogs/RemoteSensingGIS/NightLights_13nasa-india-2016_FaceGraph.jpg
testlogs/RemoteSensingGIS/NightLights_13nasa-india-
2016_ImageNet_Keras_Theano_Segmentation_FaceGraph.dot
testlogs/RemoteSensingGIS/NightLights_13nasa-india-
2016_contours_segmented.pdf
testlogs/RemoteSensingGIS/NightLights_13nasa-india-
2016_convex_hulls_segmented.pdf
testlogs/RemoteSensingGIS/NightLights_13nasa-india-2016_segmented.jpg
testlogs/GISUrbanSprawlAnalytics.log.5November2021
testlogs/NightLights_13nasa-india-2012-contourlabelled.jpg
testlogs/NightLights_13nasa-india-2012.jpg
testlogs/RemoteSensingGIS/NightLights_13nasa-india-2012_FaceGraph.jpg
testlogs/RemoteSensingGIS/NightLights_13nasa-india-
2012_ImageNet_Keras_Theano_Segmentation_FaceGraph.dot
testlogs/RemoteSensingGIS/NightLights_13nasa-india-
2012_contours_segmented.pdf
testlogs/RemoteSensingGIS/NightLights_13nasa-india-
```

2012\_convex\_hulls\_segmented.pdf

testlogs/RemoteSensingGIS/NightLights\_13nasa-india-2012\_segmented.jpg

1169.6 Urbanization percentage which is the ratio of sum of contour areas of urban sprawls in VIIRS imagery to total area of nation might have a heuristic limit of 67% going by Greenery standards of 33%. Sparse Polynomial packing of urban sprawl contour closed polynomials could hence be written as a linear program:

$$a(c1) + a(c2) + a(c3) + \dots + a(c_n) \leq 0.67 * A$$

for areas of urban sprawl contours  $a(c1), a(c2), a(c3), \dots, a(c_n)$  and total area of nation  $A$ . Sum of urban sprawl contour areas combines 3 of the 4 colors of urban sprawl facegraph (Residential, Commercial, Manufacturing-IT-ITES) excluding Greenery.

-----  
1170. (THEORY and FEATURE) GIS Urban Sprawl Analytics - NASA VIIRS NightLights 2021 Urban Area Rankings - related to all sections on Merit of Large Scale Visuals, GIS and Urban Sprawl Analytics, Intrinsic Merit Rankings, R Ricker and SEDAC GPW4 Population Estimations, Social Network Analytics, Space filling by Curves, Unequal Circle and Polynomial packing, Chaos and Mandelbrot sets, Computational Geometry, Four color theorem, Linear Programming, Economic Merit, Computational Economics - 7,8 November 2021  
-----

-----  
1170.1 In continuation of Urban sprawl contour analytics of NASA VIIRS NightLights 2012 and 2016 imagery earlier, latest NASA VIIRS imagery of India dated 6 November 2021 from <https://resourcewatch.org/data/explore/cli061nrt-Daily-Nighttime-lights> has been analyzed by GISUrbanSprawlAnalytics.py for EMD similarity and Growth of Urbanization in India between 2016 and 2021.

1170.2 Previous image of India NightLights has been manually captured in file NightLights\_13nasa-india-2021.jpg from resourcewatch.org and is not a NASA released composited and filtered image. It contains some cloud formations and lighting could be slightly exaggerated because of Deepavali fireworks on 04 November 2021 and later. Mismatch in image sizes, additional graphics could have contributed to exaggeration.

1170.3 Following are some excerpts of logs on Indian Urban area statistics in 2021 in comparison to 2016:

2021: ('Number of segments - Number of Urban areas:', 7335)

2016 to 2021: ('EMD Histogram distance similarity between images - testlogs/NightLights\_13nasa-india-2016.jpg and testlogs/NightLights\_13nasa-india-2021.jpg :', (0.031924109905958176, None, array([[36., 0., 0., ..., 0., 0., 0.]

1170.4 Number of Urban area circles have roughly quadrupled from 2016 to 2021 and multiplied 8 times from 2012 - 835 to 1914 (2012-2016), 1914 to 7335 (2016-2021) - Exaggeration by Deepavali lights could be minimal because only luminosity might have been boosted per urban area and festival may not have created so many new contours.

1170.5 EMD similarity between 2012 and 2016 is 5% while EMD similarity between 2016 and 2021 is 3% perhaps pointing at 95% and 97% dissimilarity respectively (approximate doubling(s) in urbanization between 2012-2016 and 2016-2021).

1170.6 Previous analytics measures prima facie might hint at spectacular annual urban growth and increase in electricity consumption of 20-25% out of sync with GDP growth (which was negative in some quarters and grew on the average by 5-8% during 2012-2021 - agriculture contributes 70% to GDP of India and glaring Urban-Rural divide could be pulling down the numbers)

1170.7 Following are the logs, contour id labelled and segmented image files (compressed in .gz file) for this commit:

ImageNet/testlogs/GISUrbanSprawlAnalytics.log.8November2021

ImageNet/testlogs/NightLights\_13nasa-india-2021-contourlabelled.jpg

ImageNet/testlogs/NightLights\_13nasa-india-2021.jpg

ImageNet/testlogs/RemoteSensingGIS/NightLights\_13nasa-india-2021\_analytics.tar.gz

-----  
-----  
1171. (THEORY and FEATURE) GDP estimation from GIS Urban Sprawl Analytics - related to 694,1170 and all sections on GIS and Urban Sprawl Analytics, Merit of Large Scale Visuals, EventNet and Graphical Event Models-Causal Event Models, Computational Economics, Economic Merit, Four Color Theorem, Multiple Agent Resource Allocation, Linear and Logistic Regression, Intrinsic Merit Rankings, R Ricker and SEDAC GPW4 Population Estimations, Social Network Analytics, Space filling by Curves, Unequal Circle and Polynomial packing, Chaos and Mandelbrot sets, Computational Geometry, Linear Programming - 9 November 2021,12 November 2021,13 November 2021,14 November 2021  
-----  
-----

1171.1 From 694.1: India's GDP is estimated by a logistic regression based on parameters including electricity growth - [Arvind Subramanian] - <https://growthlab.cid.harvard.edu/files/growthlab/files/2019-06-cid-wp-354.pdf> - "...We divide the sample into two periods, pre-and post-2011. For each period we estimate the following cross-country regression:  $GDP\ Growth_i = \beta_0 + \beta_1 Credit\ Growth_i + \beta_2 Electricity\ Growth_i + \beta_3 Export\ Growth_i + \beta_4 Import\ Growth_i + \beta_5 India + \varepsilon_i$  ..."  
1171.2 Similarly, Rural-Urban GDP of India could be estimated by Logistic Regressions from Urban Sprawl Analytics of NASA VIIRS NightLights imagery which quantifies urban growth in terms of electricity consumption growth.  
1171.3 Logit1: Total GDP growth of nation could be written as linear or logistic regression on Rural GDP growth and Urban GDP growth:  
-----  
-----

Total GDP Growth =  $a_1 * UrbanGDPGrowth + a_2 * RuralGDPGrowth + constant$ ,  $a_1$  and  $a_2$  are weightages for Rural and Urban GDP  
-----  
-----

1171.4 As farm output contributes 70% to India's GDP,  $a_2=0.7$  and  $a_1=0.3$ . For an example total GDP growth of 5% per annum and constant=0, substituting in Logit1:  
 $5\% = 0.3 * UrbanGDPGrowth + 0.7 * RuralGDPGrowth$

1171.5 From VIIRS Urban Sprawl Analytics earlier, India's Urban growth could be 25% annually in the past decade. Substituting in Logit1:

$$5\% = 0.3 * 25\% + 0.7 * RuralGDPGrowth$$

$$\Rightarrow 5\% - 7.5\% = 0.7 * RuralGDPGrowth$$

$$\Rightarrow -2.5\% / 0.7 = RuralGDPGrowth = -3.5\%$$

$\Rightarrow$  Or Indian Agricultural sector shrunk (grew negatively) by 3.5% in past decade

1171.6 Logit2 - Alternatively, another logistic regression could be derived from Four coloring of Urban sprawl facegraphs which segment region to Residential (R), Commercial (C), Manufacturing-IT-ITES (M), Greenery-Agriculture-Waterbodies (A) which can be written as linear or logistic regression on growth of each sector:  
-----  
-----

Total GDP Growth =  $a_1 * M + a_2 * R + a_3 * C + a_4 * A + constant$  and weightages  $a_1, a_2, a_3, a_4$  are defined as:  
-----  
-----

$a_1$  = weightage for M - Growth in manufacturing-IT-ITES industries

$a_2$  = weightage for R - Growth in residential areas

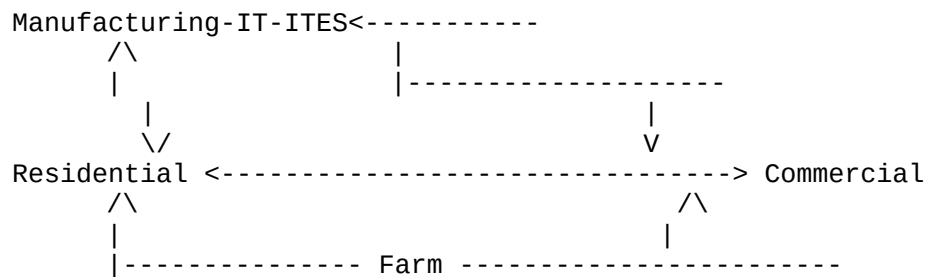
$a_3$  = weightage for C - Growth in commercial areas

$a_4$  = weightage for A - Growth in farming

1171.7 Weightage for Greenery(A)  $a_4 = 0.7$  which is same as Logit1. Weightages  $a_1, a_2, a_3$  for remaining 3 colors could be 0.1 each because growth in residential, commercial and industry are highly interconnected while growth in farming affects residential and commercial activities mostly and manufacturing industry is less connected to Greenery-farming

1171.8 Intersegment Growth Event Dependencies in Four colored urban sprawl growth in 1171.7 could be picturised by a Graphical Event Model (GEM)-Causal Event Model (CEM) below (by double-sided arrows and one-sided arrows):





1171.9 On substitution for  $a_1-a_2-a_3=0.1$ ,  $a_4=0.7$  and constant=0, Logit2: Total GDP Growth =  $0.1*M + 0.1*R + 0.1*C + 0.7*A$ . For Total annual GDP growth of 5% and Urban growth of 25% per annum (constituted by 3 colors - Manufacturing-IT-ITES, Residential, Commercial):

$$\text{Logit2: } 5\% = 0.1*25 + 0.1*25 + 0.1*25 + 0.7*A$$

$$\Rightarrow 5\% - 7.5\% = 0.7*A$$

$$\Rightarrow -2.5\%/0.7 = A = -3.5\%$$

$\Rightarrow$  Or Indian Agricultural sector shrunk (grew negatively) by 3.5% in

past decade

1171.10 Previous numbers are demonstrative only and could depend on accuracy of images, but hint at an unequivocal trend reasonably of farm sector contraction dragging GDP down.

1171.11 GDP Regression in 694.1 which is mostly manufacturing specific, could be substituted for Manufacturing-IT-ITES sector growth (M) in Logit2: Total GDP Growth =  $a_1*M + a_2*R + a_3*C + a_4*A + \text{constant}$

1171.12 Manufacturing-IT-ITES growth (M) =  $\beta_1*\text{CreditGrowth} + \beta_2*\text{ElectricityGrowth} + \beta_3*\text{ExportGrowth} + \beta_4*\text{ImportGrowth}$

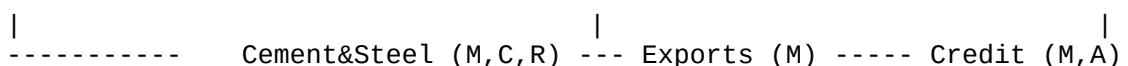
Logit3: Total GDP Growth =  $a_1*\beta_1*\text{CreditGrowth} + a_1*\beta_2*\text{ElectricityGrowth} + a_1*\beta_3*\text{ExportGrowth} + a_1*\beta_4*\text{ImportGrowth} + a_2*\text{ResidentialGrowth} + a_3*\text{CommercialGrowth} + a_4*\text{AgricultureGrowth} + \text{constant}$

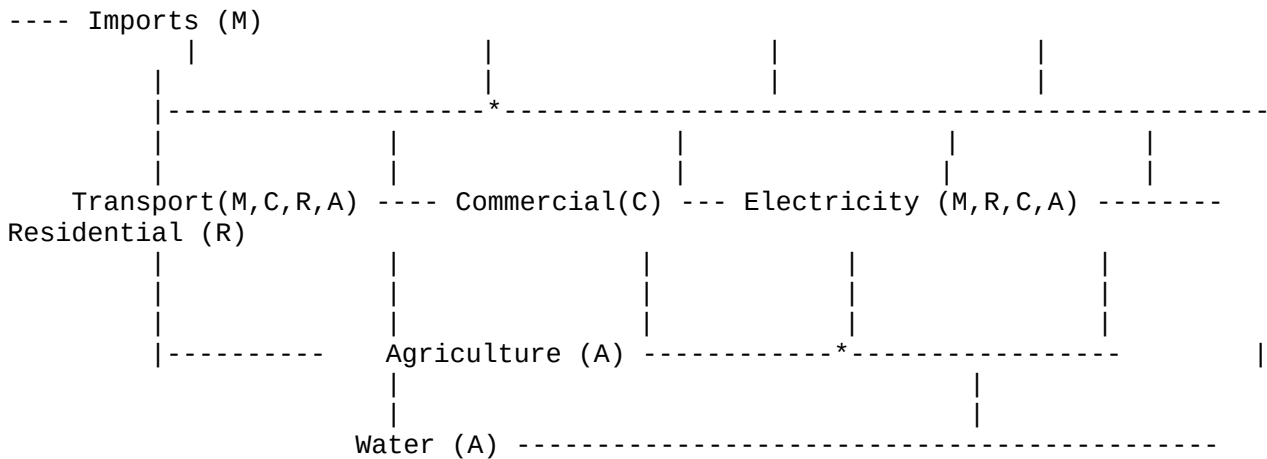
Of these, ElectricityGrowth could be estimated by NASA VIIRS Urban Areas NightLights imagery. ResidentialGrowth and CommercialGrowth are proportional to ElectricityGrowth.

1171.13 Infrastructure Growth (Air-Road-Rail-Sea Transport Infrastructure Growth, Cement and Steel Consumption Growth, Water supply Growth) is another crucial variable which could be incorporated in Logit3 as additional Manufacturing-IT-ITES and Agriculture sector parameter to make a comprehensive Logit4:

Logit4: Total GDP Growth =  $a_1*\beta_1*\text{CreditGrowth} + a_1*\beta_2*\text{ElectricityGrowth} + a_1*\beta_3*\text{ExportGrowth} + a_1*\beta_4*\text{ImportGrowth} + a_2*\text{ResidentialGrowth} + a_3*\text{CommercialGrowth} + a_4*\text{AgricultureGrowth} + a_5*\text{CementGrowth} + a_6*\text{SteelGrowth} + a_7*\text{TransportInfrastructureGrowth} + a_8*\text{WaterSupplyGrowth} + \text{constant}$

1171.14 Based on Logit4, Graphical Event Model-Causal Event Model earlier for 4-colored (M,R,C,A) GDP intersegment growth event causal dependencies could be expanded to following well-connected GEM-CEM (Vertices are labelled by 4 colors. Credit vertex is 2-colored for both Manufacturing and Agriculture sectors. Cement&Steel vertex is 3-colored by M,C,R because of its fundamental importance to Manufacturing-IT-ITES, Residential and Commercial segments. Transport and Electricity are 4-colored because power and logistics are central to all 4 sectors). Finer subdivision can be obtained by adding more vertices in supply chain:





1172. (THEORY and FEATURE) GIS Weather Analytics and Image grayscale inversion - implementation - related to 445,446,463,1165,1171 and all sections on GIS and Urban Sprawl Analytics, Mining patterns from Astronomical Datasets for correlating celestial-terrestrial events, Machine Learning solutions to N-Body problem, Merit of Large Scale Visuals, Space filling by Curves, Unequal Circle and Polynomial packing, Chaos and Mandelbrot sets, Computational Geometry, Drone Obstacle Avoidance, Autonomous Online Shopping Delivery - 11 November 2021

1172.1 Weather Forecast is an indispensable element of Urban planning, Disaster Response, Agriculture Warning Systems among others. Finding weather obstacle segments - clouds and winds - from Weather GIS imagery is essential for safe navigation of autonomous aerial vehicles. Study of Orderly Disorder in Long term weather forecast gave birth to Deterministic Chaos theory (Lorenz attractors - [https://en.wikipedia.org/wiki/Edward\\_Norton\\_Lorenz](https://en.wikipedia.org/wiki/Edward_Norton_Lorenz))

1172.2 Because of separate modelling involved in predicting weather vagaries, new source file GISWeatherAnalytics.py has been created and two functions weather\_GIS\_analytics() and invert\_image() have been defined.

1172.3 Function weather\_GIS\_analytics() reads a Weather GIS image and computes contour and convex hull segments from it quite similar to Urban sprawl contours but computed contour polynomials are for aerial weather phenomena instead of terrains viz., cloud, wind - which is passed as parameter to weather\_GIS\_analytics().

1172.4 An example Low pressure trough satellite image testlogs/Windy\_WeatherGIS\_2021-11-11-13-07-51.jpg over Bay of Bengal from <https://www.windy.com/-Satellite-satellite?satellite,20.448,79.387,5> (unedited,unfiltered and uncomposited) has been segmented and cloud contours from it are ranked by their convex hull area and circumference. Cloud contours are labelled by integers.

1172.5 Function invert\_image() inverts a thresholded image to its grayscale complement. Image inversion is particularly necessary in four color segmentation of an urban sprawl facegraph e.g. NASA VIIRS NightLights urban areas. Inverted VIIRS NightLights image indicates non-urban areas - Unlit, Rural, Underdeveloped areas and Greenery.

1172.6 Previous windy.com image has been inverted in grayscale and printed to testlogs/Windy\_WeatherGIS\_2021-11-11-13-07-51-inverted.jpg

1172.7 NOAA HURDAT2 Hurricane and USGS Earthquake datasets have been Sequence Mined earlier to correlate gravitational effects of celestial n-body choreographies from astronomical ephemeris datasets (NASA JPL Ephemeris) and terrestrial extreme weather events. GISWeatherAnalytics supplements this Celestial-Terrestrial weather event pattern analytics.

1172.8 GIS Weather imagery could as well be a timeseries stream of images read from Streaming\_AbstractGenerator Facade and yielded to GISWeatherAnalytics.py for live weather analytics - movement and velocity of cloud and wind contours, number and area of cloud-wind contours, altitude of clouds, gradual

strengthening of low pressure troughs to Cyclones-Hurricanes among others.

1172.9 Image files, DOT and Logs for this commit are at:

testlogs/GISWeatherAnalytics.log.11November2021

testlogs/RemoteSensingGIS/Windy\_WeatherGIS\_2021-11-11-13-07-

51\_FaceGraph.jpg

testlogs/RemoteSensingGIS/Windy\_WeatherGIS\_2021-11-11-13-07-

51\_ImageNet\_Keras\_Theano\_Segmentation\_FaceGraph.dot

testlogs/RemoteSensingGIS/Windy\_WeatherGIS\_2021-11-11-13-07-

51\_contour\_segmented.jpg

testlogs/RemoteSensingGIS/Windy\_WeatherGIS\_2021-11-11-13-07-

51\_convex\_hull\_segmented.jpg

testlogs/RemoteSensingGIS/Windy\_WeatherGIS\_2021-11-11-13-07-

51\_segmented.jpg

testlogs/Windy\_WeatherGIS\_2021-11-11-13-07-51-contourlabelled.jpg

testlogs/Windy\_WeatherGIS\_2021-11-11-13-07-51-inverted.jpg

testlogs/Windy\_WeatherGIS\_2021-11-11-13-07-51.jpg

1172.10 Various Reference Weather GIS Datasources:

1172.10.1 NOAA CPC Joint Agriculture Weather Facility -

[https://www.cpc.ncep.noaa.gov/products/JAWF\\_Monitoring/India/index.shtml](https://www.cpc.ncep.noaa.gov/products/JAWF_Monitoring/India/index.shtml) - 2 weeks red-orange-yellow-green alert forecast

1172.10.2 [https://www.windy.com/-Satellite-satellite?](https://www.windy.com/-Satellite-satellite?satellite,20.448,79.387,5)

satellite,20.448,79.387,5 - Color satellite imagery and lot of layers for cloud,wind,rain,waves,air quality each of which could be a Drone obstacle avoidance parameter

1172.10.2 IMD - INSAT -

[https://mausam.imd.gov.in/imd\\_latest/contents/satellite.php](https://mausam.imd.gov.in/imd_latest/contents/satellite.php) - monochromatic weather satellite imagery

1172.11 Voronoi Tessellations and Their Application to Climate and Global Modeling - Centroidal Voronoi Tessellation - Centroids and Generators of cells coincide - <https://www.osti.gov/servlets/purl/1090872>

-----  
1173. (THEORY and FEATURE) Large Scale Visuals Streaming NoSQL Datastore (MongoDB-GridFS) support in Streaming\_AbstractGenerator Facade - related to 1 and all sections on BigData NoSQL backend, Streaming analytics, Merit of Large Scale Visuals, Compressed Sensing, GIS Urban Planning Analytics, GIS Weather Analytics, Drone Imagery Analytics, Online shopping delivery, Obstacle avoidance - 15 November 2021  
-----

1173.1 Streaming\_AbstractGenerator.py facade design pattern has been updated with a clause for GIS and Visuals streaming on MongoDB-GridFS backend which facilitates storage of large visuals (> 16 MB)

1173.2 Within Streaming\_AbstractGenerator.py, MongoDB GIS and Large Scale Visuals database "neuronraingis" has been created with a bucket id "bucket1" which stores various weather GIS visuals uploaded manually by Robomongo3T-Studio3T GUIs (could be automated through a standalone python client code). StreamingAbsGen() object is instantiated within GISWeatherAnalytics.py by passing the datasource (GISAndVisualStreaming), datastorage (MongoDB) and MongoDB GridFS Bucket (bucket1) as arguments. The \_\_init\_\_() and \_\_iter\_\_() methods of StreamingAbsGen class have been changed for member variables and iterator yield by enumerating items in GridFS bucket.

1173.3 Choice of an optimal datastore for streaming image files has been contentious and use of databases for storing large images has been discouraged. For example, Netflix OTT platform implements a proprietary datastore NMDB which ingests huge movie files and keeps track of customer billing optimized for realtime response. NoSQL choices are of widerange from ElasticSearch to MongoDB-Kafka-Kinesis-Cassandra to Hadoop-Sparrk Parquets. Many video streaming platforms are hosted on proprietary AWS Kinesis and S3.

1173.4 NeuronRain analytics which transcends the whole gamut of software stack from application layer machine learning---middleware---OS kernel cloud RPC system calls-drivers-scheduler requires a robust performant opensource backend which serves large files especially images and videos in realtime with low

latency. MongoDB's GridFS which supports huge files is an opensource alternative. By this commit, NeuronRain-MongoDB-GridFS could be termed an enterprise-grade streaming and OTT platform for deploying and streaming large visuals including movies.

1173.5 Downloaded image files from MongoDB are read from GridOut object and cast to bytes by `io.BytesIO()`. `PILlow Image.open()` is invoked to read the image bytestream which is then written to a temporary file name `testlogs/GISAndVisualStreamNoSQLStore.jpg` for use by weather analytics. Previous pattern of upload and iterator download of large scale visuals through `Streaming_AbstractGenerator` might have to be replicated throughout NeuronRain image analytics - topological face recognition and handwriting recognition, GIS satellite imagery for remote sensing, urban sprawls and weather.

1173.6 Compressed Sensing sketch for compressing-decompressing large image files has been minimally implemented in NeuronRain. For minimizing storage, GIS and large visuals might have to be compressed and stored.

1173.7 Drone imagery analytics for Online Shopping Delivery and Obstacle avoidance is another arena which requires realtime analytics of streaming images transmitted by drone. Images from on-flight drone have to be segmented live to find natural, weather and man-made obstacles and accordingly alter drone trajectory.

1173.8 MongoDB-GridFS BigData backend earlier could well be suitable for any other bigdata not just limited to visuals - Sifting large volumes of emails and documentation requires storage which is non-proprietary. There are opensource web email and repository linked web hosting providers like [www.protonmail.com](http://www.protonmail.com) and [readthedocs.org](http://readthedocs.org) which could be feeds to MongoDB-GridFS backend.

1173.9 Following are the image and logs files created for this code change:  
`image_pattern_mining/ImageNet/testlogs/GISAndVisualStreamNoSQLStore-contourlabelled.jpg`  
`image_pattern_mining/ImageNet/testlogs/GISAndVisualStreamNoSQLStore-inverted.jpg`  
`image_pattern_mining/ImageNet/testlogs/GISAndVisualStreamNoSQLStore.jpg`  
`image_pattern_mining/ImageNet/testlogs/GISWeatherAnalytics.log.15November2021`  
`image_pattern_mining/ImageNet/testlogs/RemoteSensingGIS/GISAndVisualStreamNoSQLStore_FaceGraph.jpg`  
`image_pattern_mining/ImageNet/testlogs/RemoteSensingGIS/GISAndVisualStreamNoSQLStore_ImageNet_Keras_Theano_Segmentation_FaceGraph.dot`  
`image_pattern_mining/ImageNet/testlogs/RemoteSensingGIS/GISAndVisualStreamNoSQLStore_contour_segmented.jpg`  
`image_pattern_mining/ImageNet/testlogs/RemoteSensingGIS/GISAndVisualStreamNoSQLStore_convex_hull_segmented.jpg`  
`image_pattern_mining/ImageNet/testlogs/RemoteSensingGIS/GISAndVisualStreamNoSQLStore_segmented.jpg`

-----  
-----  
1174. (THEORY and FEATURE) GIS Urban Sprawl Analytics - Moments, Centroid, Minimum Enclosing Circle of an urban sprawl - 17,18 November 2021 - related to all sections on GIS Urban Sprawl Analytics, Merit of Large Scale Visuals, Computational Geometry, Intrinsic Merit Rankings, R Ricker and SEDAC GPW4 Convex Hull Population Estimations, Social Network Analytics, Space filling by Curves, Unequal Circle and Polynomial packing, Computational Geometry, Four color theorem, Economic Merit, Computational Economics  
-----  
-----

1174.1 `GISUrbanSprawlAnalytics.py` has been updated to compute OpenCV2 moments of each urban sprawl contour and centroids from those moments. Each urban sprawl contour is bounded by a minimum enclosing circle (`cv2.minEnclosingCircle()` and `cv2.circle()`) drawn around it which is a better measure of extent of an urban

area because an urban sprawl might consist of multiple smaller contours within a bigger contour interspersed by semi-lit areas.

1174.2 Two urban sprawls of Chennai and Bengaluru from NASA VIIRS India NightLights (<https://resourcewatch.org/data/explore/cli061nrt-Daily-Nighttime-lights>) imagery on 17 November 2021 -

NASAVIIRSNightLightsChennaiMetropolitanArea\_17November2021.jpg - are compared.

1174.3 Ranking of Urban Sprawls has been changed to sorting based on circular area of urban sprawl radius computed from `cv2.minEnclosingCircle()` instead of contour area since multiple suburban contours are packed within a larger outermost urban sprawl contour as drawn in

NASAVIIRSNightLightsChennaiMetropolitanArea\_17November2021-contourlabelled.jpg.

In this example, Bengaluru as a landlocked sprawl has single contour and a minimum enclosing circle while Chennai has single largest contour and multiple suburban contours within perimeter of an outermost minimum enclosing circle which offers a glimpse of growth patterns in two metro areas. NightLights being only a lowerbound estimate of an urban sprawl, has to be superseded by minimum enclosing circle upperbound estimate. Based on area of minimum enclosing circle Chennai's urban sprawl exceeds Bengaluru significantly. Following are excerpts of the logs for areas of the 2 minimum enclosing circles of Chennai and Bengaluru:

Chennai - 50645.0600000000005 (excluding area of sea in the circle would reduce it to ~35000 by visual estimate)

Bengaluru - 27157.8600000000004

1174.4 Each urban sprawl contour is now identified by an id concatenated by its area rather than mere id earlier and fonts have been shortened.

1174.5 Bengaluru is roughly circular and heavily lit while Chennai's semi-circular urban sprawl elongates heavily to west, north, south and comprises two large segments - first extending upto Kanchipuram in west, Tada in north and Tiruvanmiyur in south which is heavily lit and the second less lit segment of ECR till Kalpakkam - which comprises host of backwaters, beaches, marshes and waterbodies - as could be gleaned from

NASAVIIRSNightLightsChennaiMetropolitanArea\_17November2021\_segmented.jpg.

Minimum Enclosing Circle for Urban sprawl area of Chennai earlier does not include aforementioned elongated western segment addition of which would further extend metropolitan agglomeration area to ~40000.

1174.6 Centroid of an urban sprawl is a crucial metric for assessing gradual movement of core of a city (over a period of time) around which economic activity takes place.

1174.7 Logs and images for this commit are:

image\_pattern\_mining/ImageNet/testlogs/GISUrbanSprawlAnalytics.log.18November2021

image\_pattern\_mining/ImageNet/testlogs/NASAVIIRSNightLightsChennaiMetropolitanArea\_17November2021-contourlabelled.jpg

image\_pattern\_mining/ImageNet/testlogs/NASAVIIRSNightLightsChennaiMetropolitanArea\_17November2021.jpg

image\_pattern\_mining/ImageNet/testlogs/RemoteSensingGIS/NASAVIIRSNightLightsChennaiMetropolitanArea\_17November2021\_FaceGraph.jpg

image\_pattern\_mining/ImageNet/testlogs/RemoteSensingGIS/NASAVIIRSNightLightsChennaiMetropolitanArea\_17November2021\_ImageNet\_Keras\_Theano\_Segmentation\_FaceGraph.dot

image\_pattern\_mining/ImageNet/testlogs/RemoteSensingGIS/NASAVIIRSNightLightsChennaiMetropolitanArea\_17November2021\_contour\_segmented.jpg

image\_pattern\_mining/ImageNet/testlogs/RemoteSensingGIS/NASAVIIRSNightLightsChennaiMetropolitanArea\_17November2021\_convex\_hull\_segmented.jpg

image\_pattern\_mining/ImageNet/testlogs/RemoteSensingGIS/NASAVIIRSNightLightsChennaiMetropolitanArea\_17November2021\_segmented.jpg

1174.8 Some GIS references:

1174.8.1 City of 1000 tanks - <https://www.cityof1000tanks.org/>

1174.8.2 UN World Urbanization prospects - <https://population.un.org/wup/>

1174.8.3 Chennai Metropolitan Sprawl - Old and Expanded -

<https://portfolio.cept.ac.in/fp/metropolitan-planning-studio-4656-monsoon-2018/planning-for-chennai-metropolitan-area-monsoon-2018-pp0006717> - Expanded boundaries match segments of

NASAVIIRSNightLightsChennaiMetropolitanArea\_17November2021\_segmented.jpg and convex hull (right) in

NASAVIIRSNightLightsChennaiMetropolitanArea\_17November2021\_convex\_hull\_segmented.jpg (8848 sqkm) - New and Expanded - 2022 -

<https://www.newindianexpress.com/states/tamil-nadu/2022/sep/28/chennai-metropolitan-area-to-be-trifurcated-will-cover-5904-sqkm-2502600.html> (truncated 5904 sqkm)

1174.8.4 Population of Chennai Urban Sprawl :

1174.8.4.1 In 1901 - 600000 -

<https://images.squarespace-cdn.com/content/v1/5c51647131d4df43a0f16f93/1549035005953-62UEYZMX3KUGQI3YM7B7/WALCITYOF1000TANKSImage71copyright0oze01.jpg>

1174.8.4.2 Before expansion of boundaries - (\*) 12395000 -

Demographia 2022 Rankings of World Urban Sprawls - <http://demographia.com/db-worldua.pdf> (based on GHSL R2019A settlement dataset - includes definitions of metropolitan area, urban areas, municipalities) and (\*) 13,300,253 -

[https://en.wikipedia.org/wiki/Chennai\\_metropolitan\\_area](https://en.wikipedia.org/wiki/Chennai_metropolitan_area)

1174.8.4.3 After expansion of boundaries - 2018 - 16458272 -

[https://portfolio.cept.ac.in/assets/projects/visuals/2018/4656/mobile\\_visual\\_20181204181501\\_portfolio6.jpg](https://portfolio.cept.ac.in/assets/projects/visuals/2018/4656/mobile_visual_20181204181501_portfolio6.jpg)

1174.8.5 GIS of Chennai Metropolitan Area - Old Boundaries -

Comprehensively Color coded (29-colors) subdivision of Residential, Commercial, Waterbodies-Greenery and Industrial faces and Convex Hull area estimator - <https://www.luiscmda.tn.gov.in/public/>

-----  
1175. (THEORY and FEATURE) GIS Urban Sprawl Analytics - Population Estimator from Urban Sprawl Contours - usecase study of few urban sprawls - related to 1174 and all sections on GIS Urban Sprawl Analytics, Merit of Large Scale Visuals, Computational Geometry, Intrinsic Merit Rankings, R Ricker and SEDAC GPW4 Convex Hull Population Estimations, Social Network Analytics, Space filling by Curves, Unequal Circle and Polynomial packing, Computational Geometry, Four color theorem, Economic Merit, Computational Economics, Approximation of functions by polynomials, Weirstrass Theorem, Jordan Curve Theorem, Cellular Automaton Graph model of diffusion of opinions/memes/cybercrimes/pandemics, Multiple Agent Resource Allocation - 21,22,23,24,25,26 November 2021  
-----

1175.1 GISUrbanSprawlAnalytics.py has been updated to analyze NASA SEDAC GPW

4.11 Population Estimation 2020 imagery (revised from 2015 SEDAC GPW 4 estimates) for Southern India which has brought to light emergence of some new countermagnet urban sprawls between 2015 and 2020 (e.g Hosur UA as competitor to Bengaluru UA of almost equal area and density, Tirupur UA as countermagnet to Coimbatore UA, Amalgamation of Puducherry-Cuddalore as one huge urban sprawl of few million population).

1175.2 SEDAC GPW 4.11 Population Count 2020 image testlogs/SEDAC\_GPW4-

11\_PopulationEstimate2020.jpeg has been downloaded and photoshopped by GNU Image Manipulation Program (GIMP) selection editor to remove non-urban low density area pixels by selecting only high population density urban areas. Few noise pixels along periphery of Urban Areas have been erased. Edited image has been written to testlogs/SEDAC\_GPW4-11\_PopulationEstimate2020\_edited.jpeg

1175.3 Urban sprawl contour polynomials are closed curves sparsely packed on a 2D surface and by Jordan Curve Theorem any closed curve divides a planar region into interior and exterior half-plane regions. Simply connected regions do not have holes while multiply connected regions do. Thus unequal sparse packing of urban sprawl contours (as holes) on a 2D surface of a nation is multiply-connected.

1175.4 As there is no algorithm for packing arbitrary closed curves on a 2D surface, Voronoi tessellation diagram is the closest approximation of each urban sprawl closed curve contour by a polygon. By Weierstrass theorem, every function can be approximated by a series summation of polynomials within a bounded error and thus every Voronoi diagram polygon approximates an urban sprawl contour polynomial:

$$|f(x) - l(x)| < \epsilon$$

$f(x)$  = Urban sprawl contour polynomial

$l(x)$  = series summation of line equations for sides of Voronoi

diagram polygon

1175.5 Earlier edited image testlogs/SEDAC\_GPW4-

11\_PopulationEstimate2020\_edited.jpeg has been contour and convex-hull segmented by GISUrbanSprawlAnalytics.py and minimum enclosing circles have been drawn around them.

1175.6 Estimating populations of Urban Areas requires conversion of Contour area to square kilometer area. Rough legend could be circumference\_of\_earth / length\_of\_GIS\_imagery.

1175.7 Function urban\_sprawl\_from\_segments() from GISUrbanSprawlAnalytics.py has been updated to pass on average population density as argument so as to compute population by formula contour\_area\_in\_squarekilometers \* population\_density.

1175.8 Contour area to Square kilometer area conversion has been made configurable by passing ratio of contour area to square kilometer area as argument to urban\_sprawl\_from\_segments(), because ratio depends on image size and requires prior knowledge from a training data of contour area and its corresponding square kilometer area E.g. Ratio of contour area 854.0 and corresponding square kilometer area of 266.0 for cityid 1356 (Kumbakonam UA) in SEDAC\_GPW4-11\_PopulationEstimate2020\_edited-contourlabelled.jpg has been used as reference heuristic multiplicand for population density of 5000 per square kilometer area.

1175.9 Ratio of contour area of urban sprawl to total area of GIS image (height \* width) has been computed which is an alternative ranking measure for urban areas.

1175.10 putText() has been changed for font color, size and area append has been removed for better clarity of cityid displayed. City id(s) are displayed only for urban sprawls of non-zero contour area.

1175.11 Urban Sprawl network of southern India has undergone a metamorphosis from 2015 to 2020 based on SEDAC GPW 4.11 mapping and thus exemplifies preferential attachment in this real social network vis-a-vis virtual social networks such as Facebook and Twitter.

1175.12 GIS References - Human settlement and Climate:

1175.12.1 GHSL - European union - Visual analytics -

<https://ghsl.jrc.ec.europa.eu/visualisation.php>

1175.12.2 WorldPop - <https://apps.worldpop.org/woprVision/>

1175.12.3 Facebook Research HRSL - High Resolution Settlement Layer -

which is the most recent addition and said to be accurate -

<https://research.fb.com/downloads/high-resolution-settlement-layer-hrsl/>

1175.12.4 ECMWF CliMetLab - Python package and GIS Dataset for Global Climate analytics - <https://climetlab.readthedocs.io/en/latest/>

1175.12.5 UrbanSprawl - Python package for Urban Sprawl analytics - <https://github.com/lgervasoni/urbansprawl>

1175.12.6 NASA SEDAC GPW 4.11 -

<https://sedac.ciesin.columbia.edu/data/set/gpw-v4-population-count-rev11/data-download>

1175.12.7 NASA SEDAC GPW 4.11 Population Density -

<https://sedac.ciesin.columbia.edu/data/set/gpw-v4-population-density-rev11> -

contains most recent sprawl of urban areas which are either missing from or smaller in <https://sedac.ciesin.columbia.edu/data/set/gpw-v4-population-count-rev11/maps/services> and could be more accurate e.g Chennai metro area sprawl has significantly expanded to west in SEDAC GPW 4.11 Population Density matching the NASA VIIRS NightLights minimum circle contour segmentation in 1174.8.3 - Night lights are often proportional to density.

1175.12.8 Urban Extents from VIIRS and MODIS for the Continental U.S.

Using Machine Learning Methods, v1 (2015) -

<https://sedac.ciesin.columbia.edu/data/set/urbanspatial-urban-extents-viirs->

modis-us-2015/maps/services - Neural network model

1175.12.9 GMIS and HBASE - <https://sedac.ciesin.columbia.edu/mapping/gmis-hbase/explore-view/#>

1175.12.10 SEDAC Dar-es-Salaam (Tanzania) Urban Spatial Data Land Use GIS - most dynamic urban settlement in Africa - 1982-2002 - <https://sedac.ciesin.columbia.edu/downloads/maps/urbanspatial/urbanspatial-dar-es-salaam-luse/urbanspatial-dar-es-salaam-luse.jpg>

1175.13 It can be observed that cities of huge urban sprawls have proportionately high population density (which is the real equivalent of average degree in virtual social networks) and Urban GDP is proportional to population density:

$\text{estimated population} = \text{population\_density} * \text{urbanarea}$

$\Rightarrow \text{population\_density} = \text{constant} * \text{urbanarea}$

$\Rightarrow \text{estimated population} = \text{constant} * (\text{urbanarea})^2$

which can be used as an alternative heuristic estimate in the absence of population density data. This heuristic has been implemented in GISUrbanSprawlAnalytics.py for constant value 6.22 (from training data of cityid 1356 for population of 440000 and 266 square kilometer area:  $6.22 = 440000 / (266)^2$ )

1175.14 Following are the logs and GIS images contour and convexhull segmented by this code change:

testlogs/GISUrbanSprawlAnalytics.log.22November2021

testlogs/RemoteSensingGIS/SEDAC\_GPW4-

11\_PopulationEstimate2020\_edited\_FaceGraph.jpeg

testlogs/RemoteSensingGIS/SEDAC\_GPW4-

11\_PopulationEstimate2020\_edited\_ImageNet\_Keras\_Theano\_Segmentation\_FaceGraph.do  
t

testlogs/RemoteSensingGIS/SEDAC\_GPW4-

11\_PopulationEstimate2020\_edited\_contour\_segmented.jpeg

testlogs/RemoteSensingGIS/SEDAC\_GPW4-

11\_PopulationEstimate2020\_edited\_convex\_hull\_segmented.jpeg

testlogs/RemoteSensingGIS/SEDAC\_GPW4-

11\_PopulationEstimate2020\_edited\_segmented.jpg

testlogs/SEDAC\_GPW4-11\_PopulationEstimate2020.jpeg

testlogs/SEDAC\_GPW4-11\_PopulationEstimate2020\_edited-contourlabelled.jpg

testlogs/SEDAC\_GPW4-11\_PopulationEstimate2020\_edited.jpeg

1175.15 Theory References:

1175.15.1 Theory and Problems of Complex Variables - [Murray Spiegel] - Schaum Series - Page 94-97 - Jordan Curve Theorem and Connected Regions

1175.15.2 Approximation by polynomials - [Burkill] - TIFR Lectures 1959 - Weirstrass Theorem - <http://www.math.tifr.res.in/~publ/ln/tifr16.pdf>

1175.16 Urban Sprawl Social Network could be formalized as a 2D tensor (each vertex of a graph is a graph) where each of the urban sprawl contour of various areas are vertices and every urban sprawl vertex is a social network graph in itself with role of average degree being played by population density. Urban sprawl vertices are interconnected by transportation graph having rural areas of lesser density as intermediary vertices. Urban sprawl network 2D tensor thus has two dimensional nesting of edges and vertices:

1175.16.1 Intra urban sprawl social network - every urban sprawl vertex is in itself a social network having people as its vertices and population density as its average degree (average number of people who might be in contact per person per unit area e.g in a suburban public transportation network). In Cellular Automaton Graph model for spread of memes/pandemics/cybercrimes/opinions average degree per person is a multiple of 8.

1175.16.2 Inter urban sprawl social network - Urban sprawl vertices are connected by transportation graph among cities, towns and metropolitan agglomerations. Transportation network between urban sprawls is the lifeline of intermediary rural regions as they depend on and gravitate towards nearest urban sprawls to make a living eventually devoured by nearest urban sprawl.

1175.16.3 NASA VIIRS NightLights and NASA SEDAC GPW segmentation and minimum enclosing circles are real equivalent of community detection or graph partitioning in virtual social networks which concerns grouping close-knit social network vertices of similar nature by modularity defined by -



[https://en.wikipedia.org/wiki/Modularity\\_\(networks\)](https://en.wikipedia.org/wiki/Modularity_(networks)) - and Strength of Weak Ties - <http://snap.stanford.edu/class/cs224w-2017/slides/15-weakties.pdf>.  
1175.17 Urban Sprawl Analytics thus automates urban planning, land usage statistics, multiple agent resource allocation(MARA) and has zero-error because of its completely algorithmic approach (bounding urban sprawls by watershed segmentation, convex hull, minimum enclosing circle, Voronoi diagram tessellation algorithms on VIIRS NightLights and other gridded population GIS imagery) with nil human intervention assuming algorithmic fairness.

-----  
1176. (THEORY and FEATURE) GIS Weather Analytics and Climate Analytics from OpenWeatherMap PyOWM and ECMWF CliMetLab - implementation - 30 November 2021 - related to 148,445,446,463,1165,1171 and all sections on Correlation between gravitational effects of Mined Celestial N-Body Patterns and terrestrial extreme weather events (or Gravitational effects on climate change), Drone natural obstacle avoidance, Drone autonomous online shopping delivery, Drone Electronic Voting Machine, Large Scale Visuals Recognition, Artificial Intelligence models for Climate Change  
-----

-----  
1176.1 GISWeatherAnalytics.py has been updated to define a new function `weather_forecast()` which imports Python client for OpenWeatherMap (<https://openweathermap.org>) - PyOWM - <https://github.com/csparpa/pyowm> - and makes REST API calls to OpenWeatherMap weather data and OneCall forecast for a location by city name or latitude-longitude.

1176.2 PyOWM Weather details and forecast include humidity, temperature, rain, precipitation probability, wind, heat, clouds for a location. Forecast is made through one-call API for 1-week window per longitude-latitude. OpenWeatherMap sources weather forecasts from multitude of providers including ECMWF, NOAA. Function `weather_forecast()` might be invoked by a Drone autonomous delivery client or Drone Electronic Voting Machine and accordingly its mission plan could be charted avoiding longitude-latitude waypoints of extreme weather. An example invocation of current weather and 7-day forecast for location "Chennai" and its longitude-latitude has been shown in logs `testlogs/GISWeatherAnalytics.log.30November2021`.

1176.3 An alternative to PyOWM is ECMWF MetView Python Client - <https://github.com/ecmwf/metview-python> - but requires MetView 5.0 and above, significant preprocessing and shell script modifications (`/usr/bin/metview`) for environment variables to make it work. API access credentials are a prerequisite for access to ECMWF meteorological data by MARS client - <https://confluence.ecmwf.int/display/WEBAPI/Access+MARS> . MetView GUI can create python scripts for loading and analyzing datasets.

1176.4 Another function `climate_analytics()` has been defined which loads various climate datasources from ECMWF by CliMetLab python library and tries to model them using machine learning. CliMetLab obfuscates various dataset formats including GRIB. Presently few CliMetLab climate datasets - ECMWF-Copernicus-ERA5, NOAA Hurricane Dataset - HURDAT2, ECMWF-MARS, High-Low - have been sourced (optionally cast to Pandas Dataframes) and High-Low atmospheric pressure dataset is trained by a TensorFlow-Keras Sequential Linear Regression which could be used as forecast model - based on Jupyter notebook at <https://climetlab.readthedocs.io/en/latest/examples/05-high-lows.html#Build-the-model>. Logs `testlogs/GISWeatherAnalytics.log.30November2021` print the trained model and its prediction on test high-low data. Such models add to the kitty of SequenceMining (by Class Association Rule-APrioriGSP, BioPython-ClustalOmega Multiple Sequence Alignment algorithms) models for correlating celestial n-body choreographies and terrestrial extreme weather events (Sections 17,148 and 445 detail some correlations already mined from USGS Earthquake and NOAA Hurricane datasets)

1176.5 ECMWF datasets ERA5, MARS and High-Low require ECMWF (<https://apps.ecmwf.int/registration/>) and Copernicus API Keys (<https://cds.climate.copernicus.eu/api-how-to#install-the-cds-api-key>) information in files `~/.cdsapirc` and `~/.ecmwfapirc` and there could be error messages of the form - " <user> has no access to service/mars " despite API key

perhaps due to ECMWF MARS datacentre migration and dataset shutdown. Because of this limitation, ERA5 and MARS dataset invocations have been commented.

1176.6 Logs for this update are at

testlogs/GISWeatherAnalytics.log.30November2021. Two functions for weather and climate segregate medium range weather forecast based on GIS and machine learnt analytics on historic climate data, the latter being an artificial intelligence challenge - Improve subseasonal-to-seasonal precipitation and temperature forecasts with Machine Learning/Artificial Intelligence - <https://s2s-ai-challenge.github.io/>.

1176.7 References:

1176.7.1 MetView Python - ECMWF -

<https://www.ecmwf.int/en/newsletter/162/computing/metviews-python-interface-opens-new-possibilities>

1176.7.2 CliMetLab -

[https://events.ecmwf.int/event/211/contributions/1876/attachments/972/1700/Cloud-WS\\_Raoult.pdf](https://events.ecmwf.int/event/211/contributions/1876/attachments/972/1700/Cloud-WS_Raoult.pdf)

1176.7.3 MetView -

[https://cdn.knmi.nl/system/ckeditor\\_assets/attachments/112/egows2019\\_-\\_metview\\_in\\_a\\_pythonic\\_world\\_iain\\_russell\\_ecmwf.pdf](https://cdn.knmi.nl/system/ckeditor_assets/attachments/112/egows2019_-_metview_in_a_pythonic_world_iain_russell_ecmwf.pdf)

1176.7.4 MetView Python -

<https://www.ecmwf.int/sites/default/files/elibrary/2018/18720-metviews-new-python-interface.pdf>

1176.7.5 OpenWeatherMap models - ECMWF-IFS, NOAA-GFS, GEM -

<https://openweathermap.org/models>

-----  
1177. (THEORY and FEATURE) GIS Urban Sprawl Analytics - a Multiple Agent Resource Allocation Algorithm - related to 1174,1175 and all sections on Fair division, Merit of Large Scale Visuals, Computational Geometry, Intrinsic Merit Rankings, R Ricker and SEDAC GPW4 Convex Hull Population Estimations, Social Network Analytics, Space filling by Curves, Unequal Circle and Polynomial packing, Computational Geometry, Four color theorem, Economic Merit, Computational Economics, Approximation of functions by polynomials, Weirstrass Theorem, Jordan Curve Theorem, Cellular Automaton Graph model of diffusion of opinions/memes/cybercrimes/pandemics, Multiple Agent Resource Allocation, Constraint satisfaction problems, Ramsey Coloring of sequences, Arithmetic progressions - 3,4 December 2021  
-----

-----  
1177.1 Computational geometric Voronoi tessellation growth algorithm is exactly what is necessary to simulate urban sprawl expansion - [https://en.wikipedia.org/wiki/Voronoi\\_diagram#/media/File:Voronoi\\_growth\\_euclidean.gif](https://en.wikipedia.org/wiki/Voronoi_diagram#/media/File:Voronoi_growth_euclidean.gif). Growing adjoining urban sprawl circles collide (intersection points of the circles are connected to form sides of each polygon) to create closely packed Voronoi tessellation polygons which approximate urban sprawl contour polynomials by Weirstrass theorem.

1177.2 One of the motivations for urban sprawl analytics is to allocate resources (urban land and waterbody use) equitably among 4 prominent sectors by an envy-free mechanism - segments of Industry, residential, commercial and greenery must be optimally distanced from one another.

1177.3 29-color coded land use segments in GIS of Chennai metro area mentioned in 1174.8.5 could be a good reference which might be relevant to any urban sprawl for optimal multiple agent resource allocation through complexity theoretic tools.

1177.4 An example multiple agent resource allocation algorithm for 29-colored Chennai metropolitan area GIS Urban Sprawl facegraph:

1177.4.1 Find the facegraph of 29-colored GIS (or number of colors from map legend) imagery

1177.4.2 For all shortest paths or random walks between every pair of vertices (s-t), allocate 29-colors equally amongst the vertices of the shortest path or random walk

1177.4.3 Example: If there are 290 vertices (faces) in a path or walk between s and t, every path or walk connecting s and t must have 10 vertices

each of same color (for 29 colors,  $290/29 = 10$ ) and colors are arranged in arithmetic progressions. For 4 colors - if 29 colors are reducible to 4 colors by four color theorem - and a path or walk traversing 12 vertices, coloring scheme by arithmetic progression is: 1-2-3-4-1-2-3-4-1-2-3-4 which periodically repeats 4 colors for 12 vertices in the path or walk. This coloring scheme by arithmetic progression should be satisfied by every path or walk in the facegraph.

1177.4.4 Previous allocation by assigning colors to vertices (variables) of every path or walk is a constraint satisfaction problem, constraint being the condition of arithmetic progression of colored vertices for each path or walk. Feasibility and complexity of satisfying arithmetic progression coloring constraint for every path or walk for arbitrary number of colors which is stringent criterion, could be an open problem as it is harder than mere satisfiability and enforces arithmetic progression structure in assignments.

1177.4.5 For 2-colors, every alternate vertex in a path or walk could be colored 0 or 1 which makes it a subset promise of boolean DNFSAT problem by defining one conjunctive clause per path or walk constituted by boolean variables of the vertices thereof.

1177.4.6 Example 2-colored walk of 10 vertices alternately marked 0 and 1: 1-0-1-0-1-0-1-0-1-0 and corresponding disjunctive clause is  $(v1 \wedge !v2 \wedge v3 \wedge !v4 \wedge v5 \wedge !v6 \wedge v7 \wedge !v8 \wedge v9 \wedge !v10)$  and there are as many clauses as there are paths or walks in urban sprawl facegraph. Computing all walks or paths and formulating DNF clauses from them adds to the complexity of DNFSAT MARA.

1177.5 Rationale for previous allocation is it optimally locates each segment and no segment of one color (face) is neither too far away nor too close from another segment of same color decongesting land use and thus equitable.

1177.6 Urban sprawl expansion based on suburban transport coverage is quite scientific in the sense the travel patterns of floating population using suburban transport has already been studied. Urban sprawl expands by a real equivalent of Preferential attachment (Rich-get-richer or big cities get bigger). Expansion of urban extent occurs along the circumference of an urban sprawl contour and an optimal, sustainable urban expansion gives equal weightage to all 4 colors (Manufacturing-IT-ITES-M, Residential-R, Commercial-C, Vegetation-V) of the segmented urban extent facegraph. For a 29-colored urban land use facegraph, expansion attaches additional faces along the periphery of the graph or composes ears to existing face graph (converse of ear decomposition of a graph). Faces or ears thus attached to facegraph might have to be colored equitably by 4 colors of M,R,C,V thus adding one more constraint dimension to DNFSAT MARA earlier.

-----  
1178. (THEORY and FEATURE) GIS Analytics - MongoDB GridFS backend standalone client implementation - related to 1173,1174 and all sections on GIS Urban sprawl analytics and weather analytics, Streaming analytics, Merit of Large Scale Visuals - 6 December 2021  
-----

1178.1 New standalone MongoDB GridFS client

python-src/backend/GISMongoDBGridFSStreamingClient.py has been implemented which can independently upload and download large scale visuals to and from MongoDB GridFS backend.

1178.2 Two functions `streaming_upload()` and `streaming_download()` have been defined in `GISMongoDBGridFSStreamingClient.py` which respectively wrap `GridFS.put()` and `get()`. Visuals are lookedup and retrieved by `fileid(s)` created by `put()` and `get()`.

1178.3 Need for such a client separated from `Streaming_AbstractGenerator` facade arises because of necessity for an alternative command line interface upload and download facility for bulk visuals to and from GridFS without installing Robomongo3T and Studio3T.

1178.4 Storing large scale visuals in MongoDB GridFS is not straightforward and requires additional shape metadata. Function `streaming_upload()` also inserts the shape information per image and returns a tuple of image fileid, shape fileid

and image name which are inturn used in streaming\_download() to get the image and shape as strings. Image string is a flattened ndarray which is reshape()-d by shape information eval()-ed from shape fileid string.

1178.5 This client for large scale visuals can be plugged into NeuronRain backend/MongoDB\_DBClient.py for text data which uses find()-insert\_one() pair and Streaming\_AbstractGenerator.py facade optionally.

1178.6 An example invocation of GISMongoDBGridFSStreamingClient.py uploads a contour labelled NASA SEDAC GPW 4.11 Urban Sprawl GIS image

../image\_pattern\_mining/ImageNet/testlogs/SEDAC\_GPW4-

11\_PopulationEstimate2020\_edited-contourlabelled.jpg to GridFS and downloads it to testlogs/GISMongoDBGridFSStreamingClient\_ExampleImage.jpeg and the logs are at testlogs/GISMongoDBGridFSStreamingClient.log.6December2021

-----  
1179. (THEORY and FEATURE) GIS Urban Sprawl Analytics - Urban Sprawl Extent from NASA SEDAC 2020 GPW 4.11 Population Density by contour, convex hull segmentation and minimum enclosing circles - related to 1174,1175 and all sections on GIS Urban Sprawl Analytics, Merit of Large Scale Visuals, Computational Geometry, Intrinsic Merit Rankings, R Ricker and SEDAC GPW4 Convex Hull Population Estimations, Social Network Analytics, Space filling by Curves, Unequal Circle and Polynomial packing, Computational Geometry, Four color theorem, Economic Merit, Computational Economics, Neural Network Model of Urban Extent, Approximation of functions by polynomials, Weirstrass Theorem, Jordan Curve Theorem, Cellular Automaton Graph model of diffusion of opinions/memes/cybercrimes/pandemics, Multiple Agent Resource Allocation - 8 December 2021  
-----

1179.1 Estimation on Urban Sprawls of Southern India (which has since been chosen because of heavy urbanisation) from NASA SEDAC GPW 4.11 Population count 2020 imagery <https://sedac.ciesin.columbia.edu/data/set/gpw-v4-population-count-rev11/data-download> in 1175 was based on population count which has been revised in Population density 2020 imagery

<https://sedac.ciesin.columbia.edu/data/set/gpw-v4-population-density-rev11> to include latest urban area boundaries and new urban sprawls.

1179.2 SEDAC GPW 4.11 Population Density 2020 image SEDAC\_GPW4-

11\_PopulationDensity2020.jpeg has been GIMP photoshopped to remove non-urban area pixels and edited image is stored in SEDAC\_GPW4-

11\_PopulationDensity2020\_edited.jpeg

1179.3 SEDAC\_GPW4-11\_PopulationDensity2020\_edited.jpeg has been contour and convex hull segmented and minimum enclosing circles are drawn around urban sprawls.

1179.4 Urban sprawl ranking are updated accordingly and written to logs testlogs/GISUrbanSprawlAnalytics.log.8December2021.

1179.5 Similar to <https://sedac.ciesin.columbia.edu/data/set/urbanspatial-urban-extents-viirs-modis-us-2015/maps/services> urban extent learner which uses sophisticated machine learning methods of Random forests, Gradient boost machine, Ensemble and neural networks for US cities based on NASA MODIS and VIIRS mentioned in 1175.12.8, following simple Neural network (perceptron) could be defined for learning urban sprawls based on SEDAC color coding and night lights (which is per se statistical while Urban sprawl extent estimation in NeuronRain is Computational geometric and polynomial packing based):

1179.5.1 For pixel value  $p$ , weight  $a$  and bias  $b$ , if  $a * p + b > \text{threshold\_brightness}$  add pixel to urban area.

1179.6 Following are the affected logs and convexhull-contour segmented image files for SEDAC GPW 4.11 Population Density 2020:

testlogs/RemoteSensingGIS/SEDAC\_GPW4-

11\_PopulationDensity2020\_edited\_FaceGraph.jpeg

testlogs/RemoteSensingGIS/SEDAC\_GPW4-

11\_PopulationDensity2020\_edited\_ImageNet\_Keras\_Theano\_Segmentation\_FaceGraph.dot

testlogs/RemoteSensingGIS/SEDAC\_GPW4-

11\_PopulationDensity2020\_edited\_contour\_segmented.jpeg

testlogs/RemoteSensingGIS/SEDAC\_GPW4-

11\_PopulationDensity2020\_edited\_convex\_hull\_segmented.jpeg  
testlogs/RemoteSensingGIS/SEDAC\_GPW4-  
11\_PopulationDensity2020\_edited\_segmented.jpg  
testlogs/SEDAC\_GPW4-11\_PopulationDensity2020\_edited-contourlabelled.jpg  
testlogs/SEDAC\_GPW4-11\_PopulationDensity2020\_edited.jpeg

#### References:

-----  
1179.7 Mapping Urban Extent at Large Spatial Scales Using Machine Learning  
Methods with VIIRS Nighttime Light and MODIS Daytime NDVI Data  
- <https://www.mdpi.com/2072-4292/11/10/1247/htm>  
-----

-----  
1180. (THEORY and FEATURE) GIS Urban Sprawl Analytics - Voronoi Tessellation  
Diagram implementation engulfing urban sprawl contours - related to  
1174,1175,1179 and all sections on GIS Urban Sprawl Analytics, Merit of Large  
Scale Visuals, Computational Geometry, Intrinsic Merit Rankings, R Ricker and  
SEDAC GPW4 Convex Hull Population Estimations, Social Network Analytics, Space  
filling by Curves, Unequal Circle and Polynomial packing, Computational  
Geometry, Four color theorem, Economic Merit, Computational Economics, Neural  
Network Model of Urban Extent, Approximation of functions by polynomials,  
Weirstrass Theorem, Jordan Curve Theorem, Cellular Automaton Graph model of  
diffusion of opinions/memes/cybercrimes/pandemics, Multiple Agent Resource  
Allocation - 9 December 2021  
-----

-----  
1180.1 GISUrbanSprawlAnalytics.py has been updated to implement function  
draw\_voronoi\_tessellation() to draw Voronoi polygons surrounding contour  
polynomials of urban sprawl extents thus approximating them by a polygonal  
packing of 2D surface.  
1180.2 Facets from Voronoi 2D planar subdivision are enumerated and polygons are  
drawn by OpenCV2 polylines().  
1180.3 Centroid of each polygon in tessellation is the centre of minimum  
enclosing circle around the urban sprawl contour polynomials.  
1180.4 Voronoi diagram has been written as a layer on SEDAC\_GPW4-  
11\_PopulationDensity2020\_edited-contourlabelled.jpg.  
1180.5 Big urban areas are covered by multiple Voronoi polygons. Asymmetry in  
areas of the polygons is a measure of skewed development and every polygon is a  
mix of urban area and rural hinterland depending on it as nearest economic  
fulcrum for livelihood.  
1180.6 Sustainable urban development therefore is to strive for almost equally  
sized Voronoi polygons. Area of Voronoi polygon around an urban contour is thus  
susceptible to expansion and future urbanization.  
1180.7 python-src/image\_pattern\_mining/ImageNet/ImageGraph\_Keras\_Theano.py has  
been changed to revamp the for loops adding edges to facegraph of Voronoi  
tessellation 2D subdivision.  
1180.8 Logs and contour-convexhull segmented images for this update:  
python-src/image\_pattern\_mining/ImageNet/testlogs/RemoteSensingGIS/  
SEDAC\_GPW4-11\_PopulationDensity2020\_edited\_FaceGraph.jpeg  
python-src/image\_pattern\_mining/ImageNet/testlogs/RemoteSensingGIS/  
SEDAC\_GPW4-  
11\_PopulationDensity2020\_edited\_ImageNet\_Keras\_Theano\_Segmentation\_FaceGraph.dot  
python-src/image\_pattern\_mining/ImageNet/testlogs/SEDAC\_GPW4-  
11\_PopulationDensity2020\_edited-contourlabelled.jpg

python-src/image\_pattern\_mining/ImageNet/testlogs/GISUrbanSprawlAnalytics.log.9D  
ecember2021  
-----

-----  
1181. (THEORY and FEATURE) GIS Urban Sprawl Analytics - Correction to FaceGraph  
Plot - Centrality Measures of Urban Sprawl Facegraph - related to 1180 and all  
sections on GIS Urban Sprawl Analytics, Merit of Large Scale Visuals,

Computational Geometry, Intrinsic Merit Rankings, R Ricker and SEDAC GPW4 Convex Hull Population Estimations, Social Network Analytics, Space filling by Curves, Unequal Circle and Polynomial packing, Computational Geometry, Four color theorem, Economic Merit, Computational Economics, Neural Network Model of Urban Extent, Approximation of functions by polynomials, Weirstrass Theorem, Jordan Curve Theorem, Cellular Automaton Graph model of diffusion of opinions/memes/cybercrimes/pandemics, Multiple Agent Resource Allocation - 10 December 2021

-----

1181.1 ImageGraph\_Keras\_Theano.py has been updated to change the way facegraph is plotted - instead of centroids from cv2.connectedComponentsWithStatsWithAlgorithm(), centroids of the contours are now being used for plotting the facegraph ensconcing the contour polynomials. Contour centroids are comprehensive and numerous compared to cv2.connectedComponentsWithStatsWithAlgorithm() and must be more suitable for urban sprawl analytics.

1181.2 GISUrbanSprawlAnalytics.py has been executed for this enhancement to compute a detailed facegraph of urban area contours and its Degree,Betweenness,Closeness and PageRank centrality measures for urban vertices which are essential ranking metrics.

1181.3 Following are the affected logs, Facegraph DOT and JPEG image files for this change:

testlogs/RemoteSensingGIS/SEDAC\_GPW4-  
11\_PopulationDensity2020\_edited\_FaceGraph.jpeg  
testlogs/RemoteSensingGIS/SEDAC\_GPW4-  
11\_PopulationDensity2020\_edited\_ImageNet\_Keras\_Theano\_Segmentation\_FaceGraph.dot  
testlogs/GISUrbanSprawlAnalytics.log.10December2021

-----

1182. (THEORY and FEATURE) GIS Urban Sprawl Analytics - Delaunay Triangulation plot - related to 1181 and all sections on GIS Urban Sprawl Analytics, Merit of Large Scale Visuals, Computational Geometry, Intrinsic Merit Rankings, R Ricker and SEDAC GPW4 Convex Hull Population Estimations, Social Network Analytics, Space filling by Curves, Unequal Circle and Polynomial packing, Computational Geometry, Four color theorem, Economic Merit, Computational Economics, Neural Network Model of Urban Extent, Approximation of functions by polynomials, Weirstrass Theorem, Jordan Curve Theorem, Aerial transportation graph for Drone navigation, Autonomous Online Shopping Delivery and Drone Electronic Voting Machine, Cellular Automaton Graph model of diffusion of opinions/memes/cybercrimes/pandemics, Multiple Agent Resource Allocation - 12 December 2021

-----

1182.1 python-src/image\_pattern\_mining/ImageNet/GISUrbanSprawlAnalytics.py has been changed to define Function draw\_delaunay\_triangulation() to add Delaunay triangulation plot in testlogs/SEDAC\_GPW4-11\_PopulationDensity2020\_edited-contourlabelled.jpg

1182.2 Delaunay triangulation is the dual of Voronoi diagram and quite crucial urban sprawl analytics tool as it approximates transportation graph (aerial and surface) between prominent urban contour centroids and thus could be a Hamiltonian (traverse each vertex once) or Eulerian circuit (traverse each edge once) -

[https://networkx.org/documentation/stable/reference/algorithms/generated/networkx.algorithms.euler.eulerian\\_circuit.html#networkx.algorithms.euler.eulerian\\_circuit](https://networkx.org/documentation/stable/reference/algorithms/generated/networkx.algorithms.euler.eulerian_circuit.html#networkx.algorithms.euler.eulerian_circuit)) estimator tool for autonomous drone delivery of services (Drone EVM, Drone online shopping delivery) so as to visit each edge connecting cities or each city vertex once.

1182.3 Delaunay triangulation plot has been added as layer to testlogs/SEDAC\_GPW4-11\_PopulationDensity2020\_edited-contourlabelled.jpg by 8-connected lines of cv2.line() while Voronoi diagram has been plotted by antialiased cv2.line().

1182.4 Logs and affected image files for this update are:

python-src/image\_pattern\_mining/ImageNet/testlogs/RemoteSensingGIS/  
SEDAC\_GPW4-11\_PopulationDensity2020\_edited\_FaceGraph.jpeg  
python-src/image\_pattern\_mining/ImageNet/testlogs/SEDAC\_GPW4-  
11\_PopulationDensity2020\_edited-contourlabelled.jpg

python-src/image\_pattern\_mining/ImageNet/testlogs/GISUrbanSprawlAnalytics.log.12  
December2021

#### References:

-----  
1182.5 Mapping Urban Land Cover: A Novel Machine Learning Approach Using Landsat  
and Nighttime Lights - Hexagonal Tessellation of India, USA and Mexico -  
[https://gps.ucsd.edu/\\_files/faculty/hanson/hanson\\_research\\_RS0E\\_021517.pdf](https://gps.ucsd.edu/_files/faculty/hanson/hanson_research_RS0E_021517.pdf)  
1182.6 Building(s and) cities: Delineating urban areas with a machine learning  
algorithm - DBSCAN clustering -  
<https://www.sciencedirect.com/science/article/pii/S0094119019300944>  
-----

-----  
1183. (THEORY and FEATURE) GIS Urban Sprawl Analytics - Distance similarity of  
Voronoi Tessellations and Measuring Urban Expansion - related to 1182 and all  
sections on GIS Urban Sprawl Analytics, Merit of Large Scale Visuals,  
Computational Geometry, Intrinsic Merit Rankings, R Ricker and SEDAC GPW4 Convex  
Hull Population Estimations, Social Network Analytics, Space filling by Curves,  
Unequal Circle and Polynomial packing, Computational Geometry, Four color  
theorem, Economic Merit, Computational Economics, Machine Learning models of  
Urban Extent, Approximation of functions by polynomials, Weierstrass Theorem,  
Jordan Curve Theorem, Cellular Automaton Graph model of diffusion of  
opinions/memes/cybercrimes/pandemics, Community Detection in Social Networks,  
Multiple Agent Resource Allocation, Earth Mover Distance, Graph Edit Distance -  
16 December 2021  
-----

-----  
1183.1 Average Degree of Transportation graph vertices or its approximation by  
Delaunay triangulation increases with the economic importance and urban expanse  
of a city sprawl contour - Centroids of Large urban area contours have high  
transport connectivity and high degree.  
1183.2 Urban sprawl expansion is quantifiable by distance between two Voronoi  
tessellations of geospatial imagery at two time points separated by some  
duration.  
1183.3 Voronoi tessellations at two time points differ when new urban area  
contours (and Voronoi polygons containing them) emerge and existing urban area  
contours (and Voronoi polygons containing them) expand.  
1183.4 Voronoi tessellation is a visual clustering algorithm (each polygon is a  
cluster) and Earth mover distance (EMD) can measure distance between Voronoi  
tessellation clusters of two GIS images separated by time interval which is  
directly proportional to expansion of urban sprawls.  
1183.5 While EMD between two Voronoi tessellation clustering would consider the  
area of each Voronoi polygon, Graph edit distance between two Voronoi facegraphs  
would estimate newly added edges and vertices and cannot account for change in  
area of each face.  
1183.6 As against Square and Hexagonal tessellated cellular automata grids which  
respectively are of 8 and 6 neighbours, Voronoi facegraph allows faces of  
arbitrary number of neighbours.  
1183.7 Spread of memes/fads/opinions/pandemic in a social network of urban  
sprawls could be better simulated on their Voronoi facegraphs than Cellular  
automaton graph which is of average degree 8 or multiples of it.  
1183.8 GISUrbanSprawlAnalytics.py has been updated to compute Approximate Graph  
Edit Distance (NetworkX implementation) between Voronoi facegraphs of two NASA  
VIIRS Nighttime Lights images of India (2012 and 2016) separated by 4 years but  
commented because of slow approximation of GED. Exact Graph Edit Distance  
wrapper in NeuronRain (GraphEditDistance() - GraphMining\_GSpan.py) is NP-Hard  
and slower for huge graphs which is as well commented. Both Voronoi Facegraph  
and its dual Delaunay triangulation graph have been overlaid and plotted to

NightLights\_13nasa-india-2012-contourlabelled.jpg and NightLights\_13nasa-india-2016-contourlabelled.jpg

1183.9 As a stopgap and timesaving alternative to costly Graph Edit Distance similarity of facegraphs, community structure of 2 facegraphs (how clustered urban sprawls are) is detected by modularity matrix of all vertices and Wasserstein Earth mover distance of modularity between two urban sprawl facegraphs is computed as distance similarity or growth of urban sprawl communities over a period of time. Infact, Modularity captures the notion of communities better than Graph Edit Distance.

1183.10 Community structure distance - increase in modularity between 2012 and 2016 NASA VIIRS imagery is printed to logs

testlogs/GISUrbanSprawlAnalytics.log.15December2021 - excerpts:

Increase in Community structure - Wasserstein EMD of modularity:

0.0006727360452344568

1183.11 Following are the affected logs and contour-convexhull segmented images for NASA VIIRS 2012 and 2016 images:

testlogs/NightLights\_13nasa-india-2012-contourlabelled.jpg

testlogs/NightLights\_13nasa-india-2016-contourlabelled.jpg

testlogs/RemoteSensingGIS/NightLights\_13nasa-india-2012\_FaceGraph.jpg

testlogs/RemoteSensingGIS/NightLights\_13nasa-india-

2012\_ImageNet\_Keras\_Theano\_Segmentation\_FaceGraph.dot

testlogs/RemoteSensingGIS/NightLights\_13nasa-india-2016\_FaceGraph.jpg

testlogs/RemoteSensingGIS/NightLights\_13nasa-india-

2016\_ImageNet\_Keras\_Theano\_Segmentation\_FaceGraph.dot

testlogs/GISUrbanSprawlAnalytics.log.15December2021

testlogs/RemoteSensingGIS/NightLights\_13nasa-india-

2012\_contour\_segmented.jpg

testlogs/RemoteSensingGIS/NightLights\_13nasa-india-

2012\_convex\_hull\_segmented.jpg

testlogs/RemoteSensingGIS/NightLights\_13nasa-india-

2016\_contour\_segmented.jpg

testlogs/RemoteSensingGIS/NightLights\_13nasa-india-

2016\_convex\_hull\_segmented.jpg

## References:

1183.12 [Zeina Abu-Aisheh, Romain Raveaux, Jean-Yves Ramel, Patrick Martineau] - An Exact Graph Edit Distance Algorithm for Solving Pattern Recognition Problems. 4th International Conference on Pattern Recognition Applications and Methods 2015, Jan 2015, Lisbon, Portugal. 2015, <https://hal.archives-ouvertes.fr/hal-01168816>

1183.13 Multiple articles on Community detection in various types of social networks - [https://www.sciencedirect.com/topics/computer-science/community-detection#:~:text=Community%20detection%2C%20also%20called%20graph,Lancichinetti%20and%20Fortunato%2C%202009\)](https://www.sciencedirect.com/topics/computer-science/community-detection#:~:text=Community%20detection%2C%20also%20called%20graph,Lancichinetti%20and%20Fortunato%2C%202009)).

1184. (THEORY and FEATURE) GIS Urban Sprawl Analytics - Computation of Urbanization Correlation from Voronoi Polygons and Urban Sprawl Contours - related to 1183 and all sections on GIS Urban Sprawl Analytics, Merit of Large Scale Visuals, Computational Geometry, Intrinsic Merit Rankings, R Ricker, NASA Suomi NPP VIIRS and SEDAC GPW4 imagery Convex Hull Population Estimations, Social Network Analytics, Space filling by Curves, Unequal Circle and Polynomial packing (Sparse), Polygonal packing (Close), Computational Geometry, Four color theorem, Economic Merit, Computational Economics, Machine Learning models of Urban Extent, Approximation of functions by polynomials, Weierstrass Theorem, Jordan Curve Theorem, Cellular Automaton Graph model of diffusion of opinions/memes/cybercrimes/pandemics, Community Detection in Social Networks, Multiple Agent Resource Allocation, Earth Mover Distance, Graph Edit Distance - 17 December 2021

1184.1 Ratio of Voronoi Tessellation Polygon area to the Urban sprawl contour



polynomial area contained in polygon is an estimate of Rural-Urban Land use and disparity.

1184.2 Area of Voronoi Facet Polygon combines Rural and Urban sprawls (Close polygonal packing - as Voronoi Tessellation is a partition of total surface area) while Area of Contour is specific to more populous urban sprawl subset (Sparse polynomial packing) of the outer Voronoi polygon.

1184.3 GISUrbanSprawlAnalytics.py has been updated to compute area of each of the Voronoi Tessellation Facet polygon by Shapely Polygon() and Correlation-PValue of the sorted arrays of Voronoi polygon areas and Contour polynomial areas of urban sprawls is found by Kendall-Tau Correlation Coefficient and there are some striking facts emerging from it.

1184.4 Following are excerpts of logs from testlogs/GISUrbanSprawlAnalytics.log.17December2021 Correlation-PValues of sorted arrays of Areas for VoronoiFacets-Contours of NASA VIIRS India Urban Sprawls from NightLights 2012 and 2016:

1184.4.1 VIIRS NightLights 2012 - (Correlation,PValue) between Contour areas and Voronoi polygon areas of Urban sprawls: (0.9089575693287888, 4.4992471056554334e-294) implying 90% correlation between areas of Voronoi polygons (Rural+Urban) and Contours (Urban)

1184.4.2 VIIRS NightLights 2016 - (Correlation,PValue) between Contour areas and Voronoi polygon areas of Urban sprawls: (0.8049119202576946, 0.0) implying 80% correlation between areas of Voronoi polygons (Rural+Urban) and Contours (Urban)

1184.5 Downward trend of correlation from 90% to 80% (2012 to 2016) perhaps is an indicator of rising disparity between areas of Voronoi polygons (Rural + Urban) and Contours (Urban) contained in them or there is a growing mismatch between Urban sprawls and Rural areas. Previous deduction is just one angle of interpreting the anomaly while there could be many. Number of India urban sprawl contours have doubled from 834 in 2012 to 1912 in 2016 creating new Voronoi Facets which could have caused the decline in correlation. Some urban sprawls could have expanded faster than others occupying more space within outer Voronoi polygons making inroads into rural suburbs skewing the correlation.

1184.6 Following are contour-convexhull segmented images and logs affected:

testlogs/RemoteSensingGIS/NightLights\_13nasa-india-2012\_FaceGraph.jpg

testlogs/RemoteSensingGIS/NightLights\_13nasa-india-

2012\_contour\_segmented.jpg

testlogs/RemoteSensingGIS/NightLights\_13nasa-india-2016\_FaceGraph.jpg

testlogs/RemoteSensingGIS/NightLights\_13nasa-india-

2016\_contour\_segmented.jpg

testlogs/RemoteSensingGIS/NightLights\_13nasa-india-

2016\_convex\_hull\_segmented.jpg

testlogs/GISUrbanSprawlAnalytics.log.17December2021

1184.7 Urban sprawl contours and Voronoi polygon facets containing them could be a variant of Hub-Spokes model - Every urban sprawl contour is a Hub and its peripheral rural regions within Voronoi polygon are spokes depending on and connected to urban hub contour centroid. Hub-spokes together constitute a community.

References:

-----  
1184.8 Shoelace Formula and Green Theorem -

[https://en.wikipedia.org/wiki/Shoelace\\_formula](https://en.wikipedia.org/wiki/Shoelace_formula) - Calculating area of polygon

1184.9 HITS algorithm - Hubs, Authorities and Communities - [Kleinberg] -

[http://cs.brown.edu/memex/ACM\\_HypertextTestbed/papers/10.html](http://cs.brown.edu/memex/ACM_HypertextTestbed/papers/10.html)

1184.10 OSGEO GRASS Voronoi Diagrams -

<https://grass.osgeo.org/grass78/manuals/v.voronoi.html>

1184.11 OpenCities AI Challenge for Urban Planning -

<https://towardsdatascience.com/the-open-cities-ai-challenge-3d0b35a721cc>

1184.12 Voronoi Cells as Clusters of a Partition and Wasserstein Earth Mover Distance - <https://www.ncbi.nlm.nih.gov/pmc/articles/PMC6377175/>

-----  
1185. (THEORY and FEATURE) People Analytics - Merit of Large Scale Visuals -

Topological Face Recognition - Voronoi Tessellation and Delaunay Triangulation of Faces, their Morphology and Shape Grammar - related to 159,660,714,715,720 and all sections on Topological Face and Handwriting Recognition, Product Homotopy, Unique identification, Homeomorphism and Topological Deformations, Merit of Large Scale Visuals, People Analytics, Computational Geometry, Augmenting Graph Edit Distance by Facet Area - 20 December 2021

-----

1185.1 Recognition of Shapes (Shape Grammar for Faces, Handwriting, ...) by Topological Product Homotopy and Homeomorphic Deformations (their limitations) mentioned earlier has been implemented geometrically by Segmenting an image and plotting Voronoi tessellation and Delaunay triangulation spiderweb on it as overlay. Their morphology is analyzed.

1185.2 python-src/DeepLearning\_ConvolutionNetwork\_BackPropagation.py has been updated to define two functions face\_recognition\_image\_segmentation() and face\_recognition\_image\_segmentation\_contours() which segment an imagefile of human face and draw Voronoi tessellations and Delaunay triangulations as overlay

1185.3 Two visuals of the author python-src/testlogs/IMG\_20160610\_071455.jpg and python-src/testlogs/IMG\_20160610\_071603.jpg having small differences have been Voronoi tessellated and Delaunay triangulated and mesh(s) have been written to python-src/testlogs/IMG\_20160610\_071455-tessellated.jpg and python-src/testlogs/IMG\_20160610\_071603-tessellated.jpg.

1185.4 Voronoi Facegraphs of the images have been written as DOT files to python-src/testlogs/IMG\_20160610\_071455\_FaceRecognition\_Segmentation\_FaceGraph.dot and python-src/testlogs/IMG\_20160610\_071603\_FaceRecognition\_Segmentation\_FaceGraph.dot

1185.5 Watershed segmentation for the images are written to

python-src/testlogs/IMG\_20160610\_071455\_segmented.jpg and

python-src/testlogs/IMG\_20160610\_071603\_segmented.jpg

1185.6 python-src/DeepLearning\_BackPropagation.py , python-src/DeepLearning\_ConvolutionNetwork\_BackPropagation.py and python-src/image\_pattern\_mining/ImageToBitMatrix.py have been upgraded to Python 3.7.5 by autopep8 and 2to3 utilities. Python 2.7 versions of the files have been renamed to python-src/DeepLearning\_BackPropagation.py.2.7, python-src/DeepLearning\_ConvolutionNetwork\_BackPropagation.py.2.7 and python-src/image\_pattern\_mining/ImageToBitMatrix.py.2.7

1185.7 Shape Grammar for Human face mentioned in 715 in terms of union of product homotopies as follows:

```
<Hair>
 <Ear><Eye><Eye><Ear>
 <Nose>
 <Mouth>
```

is easier to define in tessellated images as homeomorphic deformations (Typical example: Coffee mug is homeomorphic to Donut Torus, 'D' is product of 'I' and 'J' by pasting lemma) of Voronoi facets (Graph edit distance as face similarity between 2 facegraphs could be costlier even for closely resembling images being NP-Hard and has been ignored. GED does not measure change in areas of facets between two graphs which is a drawback). Voronoi facets could be partitioned into components of the Shape grammar earlier - facets for <Hair>, <Ear>, <Eye>, <Nose>, <Mouth>.

1185.8 Facet areas of Voronoi and Delaunay spiderweb (and angles of facet edges) have changed notably between two images earlier in spite of minute variations in features while number of facets (vertices and edges) is almost the same. This requires a Facet Area Augmented Graph Edit Distance measure which counts in changed angles between the morphed facet edges.

1185.9 logs for this update are at testlogs/DeepLearning\_ConvolutionNetwork\_BackPropagation.log.20December2021

References:

-----

1185.10 Facial Landmark Detection by dlib and Voronoi Diagrams - <https://learnopencv.com/delaunay-triangulation-and-voronoi-diagram-using-opencv-c-python/>

-----  
-----  
1186. (THEORY and FEATURE) People Analytics - Merit of Large Scale Visuals - Topological Face Recognition - Distance similarity between Facial Image Voronoi Tessellations of similar Faces and Facial Landmark Detection - related to 159,660,714,715,720,1185 and all sections on Topological Face and Handwriting Recognition, Product Homotopy, Unique identification, Homeomorphism and Topological Deformations, Merit of Large Scale Visuals, People Analytics, Computational Geometry, Graph Edit Distance and Earth Mover Distance - 22 December 2021  
-----  
-----

1186.1 DeepLearning\_ConvolutionNetwork\_BackPropagation.py has been changed to compute centroids of the contours from cv2.moments() and if there is an exception from minEnclosingCircle().  
1186.2 Areas of Voronoi polygons are computed from Shapely Polygon() and Wasserstein EMD similarity of Voronoi facet areas between 2 images is computed which measures the deformation of the facial features in 2 images.  
1186.3 Performing Voronoi tessellation around centroids computed from facial landmarks detection algorithm instead of cv2.moments() centroids might increase the alignment of the Voronoi facets along facial feature landmarks (<Eye>,<Nose>,<Mouth>,...) of the Shape Grammar.  
1186.4 Hausdorff distance between Douglas-Peucker contour polynomials of the two images are computed which is another similarity metric.  
1186.5 Histogram Partition Distance (EMD) similarity(cv2.EMD()) of the two images in toto is computed (histogram\_partition\_distance\_similarity()). These three distance similarities help identify people more often if faces in two images are heavily similar (and not arbitrary images of same person) and could assist in landmark based facial recognition. OpenCV Voronoi Tessellation is done in 2D and 3D Voronoi Tessellation could be a better choice for modelling arbitrarily oriented images of same person - changes in facial features and emotional face orientations happen in 3D and not in 2D.  
1186.6 Finally Approximate and Exact Graph Edit Distance similarity computation between Voronoi Facegraphs of the two images has been introduced but left commented because of NP-Hardness.  
1186.7 Logs and tessellated images for this update are (compared images: testlogs/IMG\_20160610\_071455.jpg and testlogs/IMG\_20160610\_071603.jpg):

testlogs/DeepLearning\_ConvolutionNetwork\_BackPropagation.log.22December2021  
testlogs/IMG\_20160610\_071455-tessellated.jpg  
testlogs/IMG\_20160610\_071455\_FaceRecognition\_Segmentation\_FaceGraph.dot  
testlogs/IMG\_20160610\_071603-tessellated.jpg  
testlogs/IMG\_20160610\_071603\_FaceRecognition\_Segmentation\_FaceGraph.dot  
-----  
-----

1187. (THEORY and FEATURE) People Analytics - Merit of Large Scale Visuals - Topological Face Recognition - Voronoi diagram and Delaunay Triangulation of Facial images from centroids computed by Dlib face landmarks detection and Voronoi FaceGraph Isomorphism-Subgraph Isomorphism Similarity - related to 159,660,714,715,720,1185,1186 and all sections on Topological Face and Handwriting Recognition, Product Homotopy, Unique identification, Homeomorphism and Topological Deformations, Merit of Large Scale Visuals, People Analytics, Computational Geometry, Graph Edit Distance and Earth Mover Distance, Graph Isomorphism (Exact, Approximate and Subgraph), Graph Matching, Graph similarity, Image Search - 23 December 2021  
-----  
-----

1187.1 DeepLearning\_ConvolutionNetwork\_BackPropagation.py has been updated to import dlib face landmarks detection and draw Voronoi and Delaunay triangulation facegraphs from face landmark centroids instead of contour centroids which aligns the Voronoi faces symmetrically centered around face landmarks. Dlib face landmarks detection finds standard of 68 points of five features of Human face

Shape Grammar - Ear, Nose, 2 Eyes, Mouth.

1187.2 DeepLearning\_ConvolutionNetwork\_BackPropagation.py has been updated to import netrd Graph Distance and NetworkX Graph Isomorphism implementations. Netrd implements extensive distance similarity measures for comparing two Graphs. Image FaceGraph Voronoi Planar Subdivision is populated either from contour centroids or face landmark centroids depending on boolean flag fromlandmarks which defaults to True.

1187.3 Image Voronoi FaceGraph similarity computations between 2 images have been segregated to a new function facegraph\_similarity\_metrics() which computes Voronoi FaceGraph Facet areas EMD, Hausdorff distance between facial image contour polynomials, Whether 2 facegraphs are isomorphic or not, Whether 2 facegraphs are subgraph isomorphic or not, Netrd Jaccard distance between 2 facegraphs, Netrd Jensen-Shannon Degree Divergence between 2 facegraphs and Graph Edit Distance between 2 facegraphs (commented).

1187.4 Three facial images

testlogs/IMG\_20160610\_071455.jpg, testlogs/IMG\_20160610\_071603.jpg and testlogs/KSrinivasan\_2003.jpg of author are compared pairwise for similarity. While first two images dated 2016 are heavily similar, last image dated 2003 has noticeable differences separated by 13 years.

1187.5 Histogram partition distance and Voronoi FaceGraph similarities are computed pairwise for 3 images earlier. While two heavily resembling images testlogs/IMG\_20160610\_071455.jpg and testlogs/IMG\_20160610\_071603.jpg are Voronoi FaceGraph Isomorphic and Subgraph Isomorphic, image pairs (testlogs/IMG\_20160610\_071603.jpg and testlogs/KSrinivasan\_2003.jpg) and (testlogs/IMG\_20160610\_071455.jpg and testlogs/KSrinivasan\_2003.jpg) are less similar and are not Voronoi FaceGraph isomorphic but Subgraph isomorphic. Thus Graph Isomorphism and Subgraph Isomorphism of Voronoi FaceGraphs act as distinguishers of facial features - Percentage of Voronoi FaceGraph Isomorphism-Subgraph Isomorphism wanes as images become increasingly dissimilar (Voronoi facegraphs of images are more likely to be subgraph-isomorphic than isomorphic for same person). Graph Isomorphism similarity earlier is an unusual application in Topological Face Recognition for measuring homeomorphic facial deformations (or conjecturally, Voronoi Graph-Subgraph Isomorphism implies Topological Homeomorphism).

1187.6 Dlib uses iBUG 300W training dataset

/tmp/shape\_predictor\_68\_face\_landmarks.dat for learning face landmarks which can be downloaded from

[https://github.com/italojs/facial-landmarks-recognition/blob/master/shape\\_predictor\\_68\\_face\\_landmarks.dat](https://github.com/italojs/facial-landmarks-recognition/blob/master/shape_predictor_68_face_landmarks.dat). Earlier implementation of Face recognition is Graph theoretic differing from usual computer vision algorithms focussing on machine learning models for face recognition. Graph similarity, Graph matching and Exact-Subgraph-Approximate Graph Isomorphism are related concepts for mining patterns in graphs. Percentage of isomorphism between image Voronoi facegraphs could be an intrinsic merit ranking metric for an image search engine.

1187.7 Following are the log excerpts:

```
('EMD Histogram distance similarity between images -
testlogs/IMG_20160610_071455.jpg and testlogs/IMG_20160610_071603.jpg :',
(0.029700525104999542, None, array([[203., 0., 0., ..., 0., 0., 0.],
 [0., 222., 0., ..., 0., 0., 0.],
 [0., 0., 190., ..., 0., 0., 0.],
 ...,
 [0., 0., 0., ..., 242., 0., 0.],
 [0., 0., 0., ..., 0., 251., 0.],
 [0., 0., 0., ..., 0., 0., 232.]], dtype=float32)))
('EMD Histogram distance similarity between images -
testlogs/IMG_20160610_071603.jpg and testlogs/KSrinivasan_2003.jpg :',
(0.010611597448587418, None, array([[210., 0., 0., ..., 0., 0., 0.],
 [0., 229., 0., ..., 0., 0., 0.],
 [0., 0., 210., ..., 0., 0., 0.],
 ...,
 [0., 0., 0., ..., 244., 0., 0.],
 [0., 0., 0., ..., 3., 247., 0.],
 [0., 0., 0., ..., 0., 0., 235.]], dtype=float32)))
```

```
('EMD Histogram distance similarity between images -
testlogs/IMG_20160610_071455.jpg and testlogs/KSrinivasan_2003.jpg :',
(0.013819809071719646, None, array([[203., 0., 0., ..., 0., 0., 0.],
[0., 222., 0., ..., 0., 0., 0.],
[0., 0., 190., ..., 0., 0., 0.],
...,
[0., 0., 0., ..., 242., 0., 0.],
[0., 0., 0., ..., 1., 247., 3.],
[0., 0., 0., ..., 0., 0., 232.]], dtype=float32)))
```

```
=====
EMD Similarity between Voronoi Facet Areas of the images: 51952.31409460765
('Hausdorff Distance between DP polynomials approximating two facial image
contours:', (99.36297097007517, 0, 0))
('Voronoi FaceGraphs of two facial images are isomorphic - (True or False):',
True)
('Jaccard distance between Voronoi Facegraphs of two facial images:', 1.0)
('Jensen-Shannon Degree Divergence distance between Voronoi Facegraphs of two
facial images:', 0)
('Voronoi FaceGraphs of two facial images are subgraph isomorphic - (True or
False):', True)
```

```
=====
EMD Similarity between Voronoi Facet Areas of the images: 566002.5197416454
('Hausdorff Distance between DP polynomials approximating two facial image
contours:', (1261.1621624517602, 0, 0))
('Voronoi FaceGraphs of two facial images are isomorphic - (True or False):',
False)
('Jaccard distance between Voronoi Facegraphs of two facial images:', 1.0)
('Jensen-Shannon Degree Divergence distance between Voronoi Facegraphs of two
facial images:', 0)
('Voronoi FaceGraphs of two facial images are subgraph isomorphic - (True or
False):', True)
```

```
=====
EMD Similarity between Voronoi Facet Areas of the images: 556108.7037362487
('Hausdorff Distance between DP polynomials approximating two facial image
contours:', (1336.449400463781, 0, 0))
('Voronoi FaceGraphs of two facial images are isomorphic - (True or False):',
False)
('Jaccard distance between Voronoi Facegraphs of two facial images:', 1.0)
('Jensen-Shannon Degree Divergence distance between Voronoi Facegraphs of two
facial images:', 0)
('Voronoi FaceGraphs of two facial images are subgraph isomorphic - (True or
False):', True)
```

## 1187.8 References:

```

1187.8.1 Dlib and Mediapipe Face landmark detection -
https://towardsdatascience.com/face-landmark-detection-using-python-1964cb620837
1187.8.2 Graph Matching Survey - Graph Matching: Theoretical Foundations,
Algorithms, and Applications - https://www.ai.rug.nl/ki2/literature/graphmatch-
bunke.pdf
1187.8.3 Algorithms for Subgraph matching and Graph similarity -
https://www.cs.cmu.edu/~jingx/docs/DBreport.pdf
1187.8.4 Netrd Graph Distance measures -
https://netrd.readthedocs.io/en/latest/distance.html#
1187.8.5 Approximate Graph Isomorphism - [V. Arvind , Johannes Kobler ,
Sebastian Kuhnert , Yadu Vasudev] - Institute of Mathematical Sciences, Chennai
- https://www.imsc.res.in/~yadu/approx-gi-full.pdf - alpha-approximation of
Graph Isomorphism
1187.8.6 VF2 Graph Isomorphism algorithm - NetworkX -
https://networkx.org/documentation/stable/reference/algorithms/isomorphism.vf2.h
tml
```

```


```

1188. (THEORY and FEATURE) People Analytics - Merit of Large Scale Visuals - Topological Face Recognition - Voronoi FaceGraph Isomorphism-Subgraph Isomorphism Similarity - VF2 and ISMAGS Isomorphic Subgraphs iteration - related to 159,660,714,715,720,1185,1186,1187 and all sections on Topological Face and Handwriting Recognition, Product Homotopy, Unique identification, Homeomorphism and Topological Deformations, Merit of Large Scale Visuals, People Analytics, Computational Geometry, Graph Edit Distance and Earth Mover Distance, Graph Isomorphism (Exact, Approximate and Subgraph), Graph Matching, Graph similarity, Image Search - 24 December 2021

-----

1188.1 DeepLearning\_ConvolutionNetwork\_BackPropagation.py has been updated (facegraph\_similarity\_metrics()) to compute isomorphic subgraphs of Voronoi Diagram Facegraphs obtained from 2 facial images by two algorithms - VF2 and ISMAGS

1188.2 Number of iterations of isomorphic subgraphs has been set to 15 as default which is configurable function parameter. ISMAGS algorithm prints different subgraphs for symmetry=False and symmetry=True.

1188.3 ISMAGS symmetry=True clause has been commented due to slowdown.

Percentage similarity between two images could be derived from the number and size of isomorphic subgraphs. Example function for image similarity between two images = number of isomorphic Voronoi subgraphs of size > constant

1188.4 Contour segmented and Facegraph images of the 3 JPG files have been added to repository:

testlogs/DeepLearning\_ConvolutionNetwork\_BackPropagation.log.24December2021

testlogs/IMG\_20160610\_071455\_FaceGraph.jpg

testlogs/IMG\_20160610\_071455\_contour\_segmented.jpg

testlogs/IMG\_20160610\_071603\_FaceGraph.jpg

testlogs/IMG\_20160610\_071603\_contour\_segmented.jpg

testlogs/KSrinivasan\_2003\_FaceGraph.jpg

testlogs/KSrinivasan\_2003\_contour\_segmented.jpg

and logs are at

testlogs/DeepLearning\_ConvolutionNetwork\_BackPropagation.log.24December2021

1188.5 It is obvious to note that contours of facial images themselves are landmark detectors to some extent as contours mostly straddle facial features.

Accuracy of contour based face landmark detection could be increased by changing pixel color contrast of the binary inverted images.

-----

1189. (THEORY and FEATURE) People Analytics - Merit of Large Scale Visuals - Topological and Graph Theoretic Face Recognition - Voronoi FaceGraph Isomorphism Similarity - Percentage similarity and arbitrary visuals analyzed - related to 159,660,714,715,720,1185,1186,1187,1188 and all sections on Topological Face and Handwriting recognition, Product Homotopy, Unique identification, Homeomorphism and Topological Deformations, Merit of Large Scale Visuals, People Analytics, Computational Geometry, Graph Edit Distance and Earth mover distance, Graph Isomorphism (Exact, Approximate and Subgraph), Graph matching, Graph similarity, Image Search - 29 December 2021

-----

1189.1 DeepLearning\_ConvolutionNetwork\_BackPropagation.py has been updated to analyze more visuals for unique person identification across arbitrary images.

1189.2 facegraph\_similarity\_metrics() has been changed to increase number of default isomorphism iterations to 25. ISMAGS symmetry and Graph Edit Distance have been made function parameters set to default False and their respective clauses have been uncommented.

1189.3 Subgraph Isomorphism Percentage similarity between two facial visuals are computed for VF2 and ISMAGS clauses by ratio of number of vertices in the isomorphic Voronoi subgraphs and total number of vertices in Voronoi Facegraphs. If two visuals are Fully Isomorphic percentage similarity is set to 100. Both directions of the percentage ratio (denominator changes for size of image Facegraphs of image1 and image2 while numerator - size of isomorphic

subgraph - stays same) are printed and the minimum of the two is considered as subgraph similarity.

1189.4 Two more visuals have been compared - testlogs/IMG\_20171112\_180837.jpg and testlogs/ExamplePortrait1.jpg - former a visual of author (2017) and the latter being a portrait drawn by author (1990). Following are pairwise similarity computations by facegraph\_similarity\_metrics():

```
facegraph_similarity_metrics("testlogs/IMG_20160610_071455.jpg","testlogs/IMG_20160610_071603.jpg",image1,image2)
```

```
facegraph_similarity_metrics("testlogs/IMG_20160610_071455.jpg","testlogs/KSrinivasan_2003.jpg",image1,image3)
```

```
facegraph_similarity_metrics("testlogs/IMG_20160610_071603.jpg","testlogs/KSrinivasan_2003.jpg",image2,image3)
```

```
facegraph_similarity_metrics("testlogs/IMG_20160610_071455.jpg","testlogs/IMG_20171112_180837.jpg",image1,image4)
```

```
facegraph_similarity_metrics("testlogs/IMG_20160610_071603.jpg","testlogs/IMG_20171112_180837.jpg",image2,image4)
```

```
facegraph_similarity_metrics("testlogs/IMG_20171112_180837.jpg","testlogs/ExamplePortrait1.jpg",image4,image5)
```

1189.5 Excerpts of the logs at

testlogs/DeepLearning\_ConvolutionNetwork\_BackPropagation.log.29December2021 reveal an important finding - Visuals of a person separated by small time durations are Fully Isomorphic. Three facial images

testlogs/IMG\_20160610\_071455.jpg, testlogs/IMG\_20160610\_071603.jpg and testlogs/IMG\_20171112\_180837.jpg of the author separated by 1.5 years are fully isomorphic while all these three images are only subgraph isomorphic to 13 years older image testlogs/KSrinivasan\_2003.jpg. This points to change in facial features over a period of 14+ years affecting Voronoi facegraph and isomorphism:

```
('Voronoi FaceGraphs of two facial images are isomorphic - (True or False):', True)
```

```
('Voronoi FaceGraphs of two facial images are isomorphic - percentage similarity - ', 'testlogs/IMG_20160610_071455.jpg', ' and ', 'testlogs/IMG_20160610_071603.jpg', ': 100.0')
```

```
('Voronoi FaceGraphs of two facial images are subgraph isomorphic - (True or False):', True)
```

```
('Voronoi FaceGraphs of two facial images are isomorphic - (True or False):', False)
```

```
('Voronoi FaceGraphs of two facial images are subgraph isomorphic - (True or False):', True)
```

```
('Voronoi FaceGraphs of two facial images are isomorphic - (True or False):', False)
```

```
('Voronoi FaceGraphs of two facial images are subgraph isomorphic - (True or False):', True)
```

```
('Voronoi FaceGraphs of two facial images are isomorphic - (True or False):', True)
```

```
('Voronoi FaceGraphs of two facial images are isomorphic - percentage similarity - ', 'testlogs/IMG_20160610_071455.jpg', ' and ', 'testlogs/IMG_20171112_180837.jpg', ': 100.0')
```

```
('Voronoi FaceGraphs of two facial images are subgraph isomorphic - (True or False):', True)
```

```
('Voronoi FaceGraphs of two facial images are isomorphic - (True or False):', True)
```

```
('Voronoi FaceGraphs of two facial images are isomorphic - percentage similarity - ', 'testlogs/IMG_20160610_071603.jpg', ' and ', 'testlogs/IMG_20171112_180837.jpg', ': 100.0')
```

```
('Voronoi FaceGraphs of two facial images are subgraph isomorphic - (True or False):', True)
```

```
('Voronoi FaceGraphs of two facial images are isomorphic - (True or False):', False)
```

('Voronoi FaceGraphs of two facial images are subgraph isomorphic - (True or False):', True)  
 1189.6 Following could be a thumbrule decision tree for face recognition by isomorphism (Earth mover distance between Voronoi Facegraphs of the images is attached high priority in the tree) where leaves are graded by probabilities - extremely likely, highly likely and likely:

```

 If Voronoi facegraphs of two images are Fully isomorphic:
 {
 /* There are less chances of False positives and False
negatives - Face recognition is almost certain.*/
 Images are "extremely likely to be similar" and might
belong to same person.
 }
 else if Voronoi facegraphs of two images are not Fully isomorphic
but less stringent subgraph isomorphic:
 {
 /* high chances of false positives and false negatives
depending on decision tree branch */
 /* and percentage probability for "likely" and "highly
likely" */
 if Wasserstein EMD between Voronoi facet areas of the
images are high:
 {
 if subgraph isomorphism percentage similarity is low:
 Images are "highly likely to be dissimilar" and
might belong to different persons
 if subgraph isomorphism percentage similarity is high:
 Images are "likely to be similar" and might belong
to same person
 }
 else if Wasserstein EMD between Voronoi facet areas of the
images are low:
 {
 if subgraph isomorphism percentage similarity is low:
 Images are "likely to be similar" and might belong
to same person
 if subgraph isomorphism percentage similarity is high:
 Images are "highly likely to be similar" and might
belong to same person
 }
 }
 else if Voronoi facegraphs of two images are neither fully
isomorphic nor subgraph isomorphic:
 {
 Images are "extremely likely to be dissimilar" and might
belong to different persons
 }

```

1189.7 In the examples earlier testlogs/ExamplePortrait1.jpg and testlogs/IMG\_20171112\_180837.jpg are subgraph isomorphic (and percentage similarity is high and EMD of Voronoi Facet areas is also high which are mutually in conflict) though former is a feminine watercolor art and thus a False positive.

1189.8 Previous Graph theoretic and topological face recognition is an unsupervised classifier while conventional face recognizers are mostly supervised depending on training data. Rather, Machine learning training models could be formulated from Voronoi facet areas of face images as training priors.

References:

-----  
 1189.9 Graph Homeomorphism - Topological Graph Theory - [https://en.wikipedia.org/wiki/Homeomorphism\\_\(graph\\_theory\)](https://en.wikipedia.org/wiki/Homeomorphism_(graph_theory)) - isomorphism between a subdivision (expansion) of a Graph G1 to another subdivision (expansion) of a Graph G2 - precisely same as Topological Homeomorphism.  
 1189.10 Within-Ensemble Graph Distances - netrd -



<https://royalsocietypublishing.org/doi/pdf/10.1098/rspa.2019.0744>

1189.11 Euler Characteristic invariant -  $V-E+F$  -

[https://en.wikipedia.org/wiki/Euler\\_characteristic](https://en.wikipedia.org/wiki/Euler_characteristic) - 3D Voronoi Tessellations of Human Faces are Topological 3-dimensional CW Complexes (Polyhedra - Convex or non-Convex) and determining the Euler characteristic for human face 3D Voronoi tessellation might be useful as face recognition measure. Graph Isomorphism of Delaunay Triangulation Graphs vis-a-vis Voronoi facegraphs of human facial images is another face recognizer.

-----  
1190. (THEORY and FEATURE) People Analytics - Merit of Large Scale Visuals - Topological and Graph Theoretic Face Recognition - Delaunay Triangulation Mesh isomorphism and Euler Characteristic - related to 159,660,714,715,720,1185,1186,1187,1188,1189 and all sections on Topological Face and Handwriting recognition, Product Homotopy, Unique identification, Homeomorphism and Topological Deformations, Merit of Large Scale Visuals, People Analytics, Computational Geometry, Graph Edit Distance and Earth mover distance, Graph Isomorphism (Exact, Approximate and Subgraph), Graph matching, Graph similarity, Image Search - 30 December 2021  
-----

-----  
1190.1 DeepLearning\_ConvolutionNetwork\_BackPropagation.py has been changed to compute NetworkX Delaunay triangulation mesh graph dual of Voronoi Facegraph in `draw_delaunay_triangulation()`. Return values have been changed in some functions and new boolean clauses for Voronoi and Delaunay mesh(s) have been introduced.  
1190.2 Euler characteristic of a facial image 2D Voronoi tessellation facegraph is printed to

`testlogs/DeepLearning_ConvolutionNetwork_BackPropagation.log.30December2021` ( $V-E+F$ ) which is 2 for all images. This characteristic might vary for 3D Voronoi tessellation non-planar polyhedron mesh of a facial image:

```
('Euler characteristic of the Voronoi facegraph:', 2)
('Euler characteristic of the Voronoi facegraph:', 2)
('Euler characteristic of the Voronoi facegraph:', 2)
('Euler characteristic of the Voronoi facegraph:', 2)
('Euler characteristic of the Voronoi facegraph:', 2)
```

1190.3 Graph isomorphism of Delaunay triangulation mesh(s) for pairs of facial images is printed in `testlogs/DeepLearning_ConvolutionNetwork_BackPropagation.log.30December2021` and contrary to intuition Delaunay triangulation dual mesh(s) which are localized to facial feature deformations are not isomorphic for none of the 6 pairs when Voronoi facegraphs are isomorphic for 3 pairs of face visuals separated by small time duration - Voronoi facegraphs may be best suited for face recognition by isomorphism:

-----  
('Voronoi FaceGraphs of two facial images are isomorphic - (True or False):', True)  
('Delaunay Triangulation Mesh Graphs of two facial images are isomorphic - (True or False):', False)  
('Voronoi FaceGraphs of two facial images are isomorphic - percentage similarity - ', 'testlogs/IMG\_20160610\_071455.jpg', ' and ', 'testlogs/IMG\_20160610\_071603.jpg', ': 100.0')  
('Voronoi FaceGraphs of two facial images are subgraph isomorphic - (True or False):', True)  
('Voronoi FaceGraphs of two facial images are isomorphic - (True or False):', False)  
('Delaunay Triangulation Mesh Graphs of two facial images are isomorphic - (True or False):', False)  
('Voronoi FaceGraphs of two facial images are subgraph isomorphic - (True or False):', True)  
('Voronoi FaceGraphs of two facial images are isomorphic - (True or False):', False)  
('Delaunay Triangulation Mesh Graphs of two facial images are isomorphic - (True or False):', False)

```

('Voronoi FaceGraphs of two facial images are subgraph isomorphic - (True or
False):', True)
('Voronoi FaceGraphs of two facial images are isomorphic - (True or False):',
True)
('Delaunay Triangulation Mesh Graphs of two facial images are isomorphic - (True
or False):', False)
('Voronoi FaceGraphs of two facial images are isomorphic - percentage similarity
- ', 'testlogs/IMG_20160610_071455.jpg', ' and ',
'testlogs/IMG_20171112_180837.jpg', ': 100.0')
('Voronoi FaceGraphs of two facial images are subgraph isomorphic - (True or
False):', True)
('Voronoi FaceGraphs of two facial images are isomorphic - (True or False):',
True)
('Delaunay Triangulation Mesh Graphs of two facial images are isomorphic - (True
or False):', False)
('Voronoi FaceGraphs of two facial images are isomorphic - percentage similarity
- ', 'testlogs/IMG_20160610_071603.jpg', ' and ',
'testlogs/IMG_20171112_180837.jpg', ': 100.0')
('Voronoi FaceGraphs of two facial images are subgraph isomorphic - (True or
False):', True)
('Voronoi FaceGraphs of two facial images are isomorphic - (True or False):',
False)
('Delaunay Triangulation Mesh Graphs of two facial images are isomorphic - (True
or False):', False)
('Voronoi FaceGraphs of two facial images are subgraph isomorphic - (True or
False):', True)

```

-----  
1192. (THEORY and FEATURE) Software Analytics - Graph Isomorphism Similarity of  
Code Callgraphs and Control Flow Graphs - Spark 3.0.1 + Python 3.7.5 - related  
to 1191,619,770,906,911,771 and all sections on Program Analysis, AsFer-USBmd-  
VIRGO-KingCobra FTrace kernel callgraph analysis - Valgrind-Callgrind-  
KCacheGrind-Flamegraph userspace callgraph analysis, SATURN control flow  
analysis of VIRGO linux kernel, Software Analytics, Pandemic model of Botnet-  
Defense adversarial Game theoretic security, Cybercrime analytics, Anti-  
Malware, Anti-Ransomware, Anti-Theft and Anti-Plagiarism tools - 2 January 2022  
-----

-----  
1192.1 Updated CyclomaticComplexitySparkMapReducer.py software analytics python  
implementation to define new function graph\_matching() which finds Graph  
Isomorphisms between 2 control flow graphs or callgraphs of executables by VF2  
and ISMAGS isomorphism implementations of NetworkX.  
1192.2 Few pairs of SATURN VIRGO linux kernel DOT files, FTrace kernelspace  
callgraph DOT files, KCacheGrind userspace callgraph DOT files are compared by  
graph\_matching() which internally instantiates NetworkX Graphs from DOT files.  
1192.3 Isomorphisms (Full and Subgraph) are printed to logs  
testlogs/CyclomaticComplexitySparkMapReducer.log.Python3.7.5.Isomorphism.2Januar  
y2022 and provide hints to kernelspace and userspace code most invoked by  
different program executables. Percentage similarities are printed in both  
directions of Graph matching (G1 -> G2 and G2 -> G1). Callgraphs are matched  
pairwise and only similar executables are fully isomorphic and subgraph  
isomorphic while dissimilar executables are not. Matching has been restricted to  
few pairs only as Graph isomorphism is computationally intensive and its  
lowerbound complexity is not yet proved.  
1192.4 Graph Isomorphisms are tools to find similarity of codebases belonging to  
different repositories which is a pointer to frequently common algorithms and  
design patterns across implementations. Graph Isomorphism Detectors are used in  
anti-plagiarism tools and analyzing malicious code invocations (if Callgraphs-  
ControlFlowGraphs in two computers running similar executable are not isomorphic  
something could be brewing - one of them could be infected). Two executable  
copies of same code running in 2 computers must be callgraph isomorphic or  
atleast subgraph isomorphic. Control flow graph depends on parameters to the  
program which changes callgraphs for same executable between machines in which

case at least few subgraphs of the callgraph must be similar (subgraph isomorphic) or two callgraphs must be approximate isomorphic (number of isomorphic vertices-edges are maximized). If callgraphs are not full-subgraph-approximate isomorphic between two machines executing similar executable of identical parameters, then some kind of corruption must have happened somewhere - quite useful forensic in modelling script injection cybercrime attacks which usurps and alters control flow by injecting malware in userspace that percolates down to kernelspace derailing usual sequence of kernel function callgraph in FTrace (e.g Cross Site Scripting - XSS, SQL injection attacks, Buffer overrun exploits). Degree sequence of the two callgraphs which is a monotone non-increasing series of vertex degrees is a non-isomorphism graph similarity measure.

1192.5 Previous code change implements an item specified in [https://github.com/shrinivaasanka/Krishna\\_iResearch\\_DoxygenDocs/blob/master/kuja27\\_website\\_mirrored/site/kuja27/PhDThesisProposal.pdf](https://github.com/shrinivaasanka/Krishna_iResearch_DoxygenDocs/blob/master/kuja27_website_mirrored/site/kuja27/PhDThesisProposal.pdf) on isomorphism of Program Control Flow Graphs (SATURN-FTrace-Valgrind-Callgrind-KCacheGrind) and Slice Dependency Graphs.

1192.6 FTrace logs and DOT files of kernelspace callgraphs for "find" and "pwd" executables created by asfer\_ftrace.sh and parsed to DOT by:

```
ftrace_callgraph_dot("ftrace.pwd.log")
ftrace_callgraph_dot("ftrace.find.log")
```

have been added to repositories:

```
find.ftrace_callgraph.dot
ftrace.find.log
ftrace.pwd.log
pwd.ftrace_callgraph.dot
```

1192.7 Isomorphism iterations and ISMGAS symmetry have been made configurable arguments and set to default 25 and False respectively.

CyclomaticComplexitySparkMapReducer.py has been upgraded to Python 3.7.5 + Spark 3.0.1 by autopep8 and 2to3 utilities. Python 2.7 version of CyclomaticComplexitySparkMapReducer.py has been renamed to CyclomaticComplexitySparkMapReducer.py.2.7.

#### References:

-----

1192.8 Degree Sequence of a Graph -

[https://en.wikipedia.org/wiki/Degree\\_\(graph\\_theory\)#Degree\\_sequence](https://en.wikipedia.org/wiki/Degree_(graph_theory)#Degree_sequence) - Graph realization problem tries to find a simple graph for a degree sequence solved by Erdos-Gallai theorem or Havel-Hakimi algorithm. Isomorphic graphs have same degree sequence while converse is not true.

1192.9 Scalable Function Call Graph-based Malware Classification -

<https://cs.fit.edu/~pkc/papers/codaspy17.pdf> - Cost effective function call graph classification for identifying malware - ACM CODASPY 2017 - References in the paper

-----

1193. (THEORY and FEATURE) Software Analytics - Approximate Graph Isomorphism Similarity of Code Callgraphs and Control Flow Graphs - Spark 3.0.1 + Python 3.7.5 - related to 1192,1191,581,619,770,906,911,771 and all sections on Program Analysis, AsFer-USBmd-VIRGO-KingCobra FTrace kernel callgraph analysis - Valgrind-Callgrind-KCacheGrind-Flamegraph userspace callgraph analysis, SATURN control flow analysis of VIRGO linux kernel, Software Analytics, Pandemic model of Botnet-Defense adversarial Game theoretic security, Cybercrime analytics, Anti-Malware, Anti-Ransomware, Anti-Theft and Anti-Plagiarism tools - 2 January 2022

-----

1193.1 CyclomaticComplexitySparkMapReducer.py - graph\_matching() has been updated to invoke faster\_could\_be\_isomorphic() for guesstimate of approximate isomorphism between two callgraphs or control flow graphs which is faster than fast\_could\_be\_isomorphic() and exact but only presumptive.

1193.2 Approximate isomorphism has been made configurable by boolean flag approximateisomorphic.

1193.3 Two FTrace callgraph DOT files for pwd and find and two SATURN VIRGO linux kernel callgraph DOT files are matched for approximate isomorphism which turn out to be both False.  
1193.4 Results are printed to logs  
testlogs/CyclomaticComplexitySparkMapReducer.log2.Python3.7.5.Isomorphism.2January2022

-----  
1194. (THEORY and FEATURE) GIS Analytics - DBSCAN Density Clustering implementation - related to 1182 and all sections on Merit of Large Scale Visuals, Text analytics, Unsupervised clustering, GIS and Urban Sprawl Analytics - Urban Extent Learners, Computational Geometry, Intrinsic Merit Rankings, R Ricker and SEDAC GPW4 Convex Hull Population Estimations, Community detection, Social Network Analytics, Space filling by Curves, Unequal Circle and Polynomial packing, Computational Geometry and Polygonal packing by Voronoi Tessellation, Four color theorem, Economic Merit, Computational Economics - 5 January 2022  
-----

1194.1 New source file DBSCANClustering.py has been added to repository which implements award winning DBSCAN clustering algorithm especially useful for visual clustering of images, GIS Mapping and Urban Sprawl Extent Learners (NASA SEDAC, VIIRS and recent state-of-the-art Landsat9 TIRS2 and OLI2 - <https://www.nasa.gov/content/landsat-9-image-gallery>).  
1194.2 DBSCAN is intuitive and finds clusters by density concentration of points around a core point which is the cluster centroid.  
1194.3 Following is a gist of DBSCAN algorithm pseudocode implemented in DBSCANClustering.py:  
    1194.3.1 For each core point find the neighbours of it bounded by minPoints by some distance function  
    1194.3.2 If number of neighbours is < minPoints mark the point as noise else create a new cluster label for the core point  
    1194.3.3 Initialize a seed set to neighbours of the core point and for all neighbour points of a core point find the neighbours (neighbours of neighbours - expands the cluster recursively till seedset is exhausted) and add them to the cluster by labelling - Graph theoretically, community of neighbours or a strongly connected component of neighbourhood is detected.  
1194.4 DBSCANClustering.py finds neighbours (greater than minpoints) within a  $4 * (\epsilon)^2$  pixel area square bounding box (of side  $2 * \epsilon$ ) around a point after filtering below a threshold pixel value. Clusters are stored in a dictionary map of pixel-to-label. Present implementation of DBSCAN is visual clustering specific but could be used for any multidimensional text dataset after minor datatype changes to find\_neighbours() and clustering() functions. DBSCAN clusters could be optionally invoked in place of OpenCV2 Contouring, Watershed Segmentation and Minimum enclosing circle boundaries of urban sprawl extents in image\_pattern\_mining/ImageNet/GISUrbanSprawlAnalytics.py.  
1194.5 An example scatterplot visual image\_pattern\_mining/ImageNet/testlogs/GHSL\_GIS\_ChennaiMetropolitanArea.jpg of Chennai Metropolitan Sprawl Population Density from Global Human Settlement Layer (GHSL - Urban Centre Database 2018 - <https://ghsl.jrc.ec.europa.eu/ucdb2018visual.php#> ) has been DBSCAN clustered and written to image\_pattern\_mining/ImageNet/testlogs/GHSL\_GIS\_ChennaiMetropolitanArea\_dbscanclustered.jpg by write\_clustered\_image() - clusters are color coded by DBSCAN cluster label. Only the less dense areas of the map are clustered perhaps due to the thresholding.  
1194.6 Class DBSCAN is parametrized by minimum number of neighbourhood points, epsilon size of the rectangular neighbourhood and threshold for choosing pixels.  
1194.7 Logs are written to testlogs/DBSCANClustering.log.5January2022 which include number of clusters found and cluster labelled pixel dictionary.

References:

-----  
1194.8 DBSCAN - A density-based algorithm for discovering clusters in large

spatial databases with noise (1996) -

<https://citeseerx.ist.psu.edu/viewdoc/summary?doi=10.1.1.121.9220> - [Martin Ester , Hans-Peter Kriegel , Jörg Sander , Xiaowei Xu]

1194.9 DBSCAN Revisited: Mis-Claim, Un-Fixability, and Approximation -

<https://dl.acm.org/doi/10.1145/2723372.2737792> - "...In this paper, we prove that for  $d \geq 3$ , the DBSCAN problem requires  $\Omega(n^{4/3})$  time to solve, unless very significant breakthroughs---ones widely believed to be impossible---could be made in theoretical computer science...."

1194.10 DBSCAN Revisited, Revisited: Why and How You Should (Still) Use DBSCAN -

[https://www.ccs.neu.edu/home/vip/teach/DMcourse/2\\_cluster\\_EM\\_mixt/notes\\_slides/revisitoofrevisitDBSCAN.pdf](https://www.ccs.neu.edu/home/vip/teach/DMcourse/2_cluster_EM_mixt/notes_slides/revisitoofrevisitDBSCAN.pdf)

-----  
1195. (THEORY and FEATURE) Software Analytics - Degree Sequence Earth Mover Distance Similarity of Code Callgraphs and Control Flow Graphs - Spark 3.0.1 + Python 3.7.5 - related to 1193,1192,1191,581,619,770,906,911,771 and all sections on Program Analysis, AsFer-USBmd-VIRGO-KingCobra FTrace kernel callgraph analysis - Valgrind-Callgrind-KCacheGrind-Flamegraph userspace callgraph analysis, SATURN control flow analysis of VIRGO linux kernel, Software Analytics, Pandemic model of Botnet-Defense adversarial Game theoretic security, Cybercrime analytics, Anti-Malware,Anti-Ransomware,Anti-Theft and Anti-Plagiarism tools,Graph Matching,Graph Similarity and Graph Isomorphism - 7 January 2022  
-----

-----  
1195.1 python-src/software\_analytics/CyclomaticComplexitySparkMapReducer.py - graph\_matching() has been changed to implement Degree Sequence Earth Mover Distance similarity of two callgraphs.

1195.2 Degree Sequences of a callgraph are obtained from NetworkX degree() DegreeView and cast to dict() which is a map of vertices to their degrees.

1195.3 Degree Sequences are the reversed, sorted, monotone non-increasing values of the earlier dictionary of vertices to degrees. Degree Sequences of two callgraphs are matched by Wasserstein Earth Mover Distance similarity.

1195.4 Identical Degree Sequences of 2 graphs are less costly approximations of their isomorphism (Isomorphism => Identical Degree Sequences but Identical Degree Sequences !=> Isomorphism).

1195.5 3 pairs of callgraphs - 2 dissimilar and 1 identical - are matched, degree sequences are verified by is\_graphical() and their approximate isomorphism is printed as boolean and Earth Mover Distance values. Identical callgraphs of same executable-parameter have 0 EMD which might differ depending on cybercrime penetration if the callgraphs are situated across multiple compromised machines which are vertices of SIS model infection graph (Refer: 619.3). Logs are written to testlogs/CyclomaticComplexitySparkMapReducer.log.DegreeSequenceEMD.7January2022

References:

-----  
1195.6 Mining Software Repositories -

<https://www.st.cs.uni-saarland.de/edu/msa10/>, <http://www.msrrconf.org/> - machine learning applied to software engineering for mining code commits,bug reports,features

1195.7 The Impact of Tangled Code Changes -

<https://www.microsoft.com/en-us/research/wp-content/uploads/2013/01/msr2013-untangling.pdf> - Bug reports following a security incident-cybercrime eventually lead to zeroing in on the design flaw or commit that caused the compromise via callgraph analysis. Mostly commits combine resolution of multiple bugs-refactoring-features entangling the code and isolating the delta could be non-trivial

1195.8 It's not a Bug, It's a feature - How Misclassification Impacts Bug Prediction - <https://dl.gi.de/bitstream/handle/20.500.12116/2512/103.pdf?sequence=1> - most bug reports are not bugs after all

1195.9 2014 OpenSSL HeartBleed Bug and flurry of reports -

<https://heartbleed.com/> - led to resolution of mission bounds check failure in

OpenSSL when source payload buffer is empty but payload size is non-zero in memcpy(dest,source,size) causing garbage to be returned to client in Heartbeat (a periodic P2P keep-alive check) -  
<https://www.openssl.org/news/secadv/20140407.txt>, <https://gizmodo.com/how-heartbleed-works-the-code-behind-the-internets-se-1561341209>  
1195.10 2021 Apache Log4j Vulnerability Resolution -  
<https://logging.apache.org/log4j/2.x/security.html> - Allows Remote Code Execution in Log4j calls while using JDBC appender with JNDI LDAP URI

-----  
1196. (THEORY and FEATURE) GIS Analytics - DBSCAN Density Clustering - Neural Network Thresholding implementation - related to 1151,1171,1174,1179,1194 and all sections on Merit of Large Scale Visuals, Text analytics, Unsupervised clustering, GIS and Urban Sprawl Analytics - Urban Extent Learners, Computational Geometry, Intrinsic Merit Rankings, R Ricker and SEDAC GPW4 Convex Hull Population Estimations, Community detection, Social Network Analytics, Space filling by Curves, Unequal Circle and Polynomial packing, Computational Geometry and Polygonal packing by Voronoi Tessellation, Four color theorem, Economic Merit, Computational Economics - GDP estimation from electricity consumption - 12 January 2022  
-----

-----  
1196.1 DBSCANClustering.py has been changed to implement a neural network thresholding of pixels in find\_neighbours() and write\_clustered\_image() of DBSCAN algorithm. This feature has been made optional by a configurable parameter and original DBSCAN algorithm does not incorporate neural network thresholding in find\_neighbours().  
1196.2 New clauses based on boolean flag "neuralnetwork" have been introduced in both find\_neighbours() and write\_clustered\_image() which evaluate a neural network passed on as lambda function argument and filter the pixels above or below a threshold color thus detecting clusters or communities of urban areas.  
1196.3 Function find\_neighbours() computes neighbours satisfying the neural network while write\_clustered\_image() writes out the neural network clustered image to an image file suffixed "\_neuralnetworkclustered.jpg". An option of choosing a square bounding box subset of an image has been provided in write\_clustered\_image() by "fraction" parameter which slices the image to subset square for invocation of find\_neighbours() - epsilon neighbourhood is a percentage fraction of image dimension - so as to distinguish areas clustered and left unclustered by neural network lambda function.  
1196.4 Global Human Settlement Layer (GHSL) image of Chennai Metropolitan area sprawl (of approximately 10000 square km by definition of metro sprawl in 1151 - semicircular sprawl covered by suburban train transport of 80 kms each in north,west and south) has been clustered by a simple neural network which weights each pixel by 2 for threshold value of 200. Clustered image has been written to GHSL\_GIS\_ChennaiMetropolitanArea\_neuralnetworkclustered.jpg containing only densely populated localities excluding sparse suburbs and including composite city administrative area of 940 square km (Reference: GHSL convex hull and contour area estimator - R2019A - <https://ghsl.jrc.ec.europa.eu/ucdb2018visual.php>) and adjoining dense suburbs mostly concentrated in west,north and south. Lambda function argument can be arbitrary string and can depend on many variables not just limited to pixel value alone, computable as expression by eval().  
1196.5 Facebook High Resolution Settlement Layer (HRSL) Nighttime Streets imagery of world atlas - HRSL\_World\_NightTimeStreets.jpg - has been clustered by neural network thresholding - central 25% square fraction of image has been clustered and pixel colors of urban communities have been changed. Nighttime streets finetunes Nighttime lights urban area circles and is theoretically a graph of dotted streaks (edges) of streetlights in high resolution as against densely lit urban sprawl circles viewed from sky in VIIRS and MODIS.  
1196.6 Four colors of Urban sprawl could be deciphered from a partition of Nighttime Street Graph as follows (For 29 color Urban GIS segmentation in 1174.8.5, percentage luminosity could be attributed accordingly):  
1196.6.1 Manufacturing-IT-ITES - Vertices and Edges (Intersections and

Streets) are extremely lit at night - highest electricity consumer

1196.6.2 Commercial - Vertices and Edges (Intersections and Streets) are highly lit at night - higher electricity consumer

1196.6.3 Residential - Vertices and Edges (Intersections and Streets) are less lit at night - high electricity consumer

1196.6.4 Greenery - Vertices and Edges (Intersections and Streets) are not lit almost (another metric: Greenery could be found by Vegetation index - NDVI for urban centres - <https://ghsl.jrc.ec.europa.eu/ucdb2018visual.php>) - minimal or no electricity consumed

1196.7 Neural network clustering is an independent feature (Continental US has been modelled by neural network extent learner for VIIRS and MODIS in 1175.12.8) which could be optionally used within DBSCAN find\_neighbours(). Code invoking neural network clustering option in find\_neighbours() has been commented within DBSCAN clustering().

-----  
1201. (THEORY and FEATURE) People Analytics - Merit of Large Scale Visuals - Topological and Graph Theoretic Face Recognition - Delaunay Triangulation Mesh Bezier Animation by PyVis - related to 159,660,714,715,720,1185,1186,1187,1188,1189,1190 and all sections on Topological Face and Handwriting recognition, Product Homotopy, Unique identification, Homeomorphism and Topological Deformations, Merit of Large Scale Visuals, People Analytics, Computational Geometry, Graph Edit Distance and Earth mover distance, Graph Isomorphism (Exact, Approximate and Subgraph), Graph matching, Graph similarity, Image Search - 17 January 2022, 18 January 2022  
-----

-----  
1201.1 DeepLearning\_ConvolutionNetwork\_BackPropagation.py has been updated to draw an animated HTML version of Delaunay Triangulation Mesh of a facial image by importing PyVis -

<https://pyvis.readthedocs.io/en/latest/tutorial.html#visualization>.

1201.2 Delaunay Triangulation Mesh of a face aligns to 68 face landmarks and Bezier-like facets morphing of the Delaunay trimesh simulates the homeomorphic emotional deformations of the face (by changing facet areas) which is quintessential prerequisite for uniqueness of face irrespective of orientations.

1201.3 Delaunay Trimesh for facial image is written to an html file suffixed "\_FaceRecognition\_Segmentation\_FaceGraph.html". An option to exit after full isomorphism check without subgraph isomorphism test and iterating the isomorphic subgraphs by VF2 and ISMAGS (both subgraph isomorphism test and iterations are time consuming for some photos) has been introduced by setting isomorphism\_iterations to 0 in facegraph\_similarity\_metrics().

1201.4 Two new images of the author -

python-src/testlogs/Shrinivas\_Kannan\_01Sept2007\_sitting.jpg (2007) and python-src/testlogs/SrinivasanKannan\_alias\_KaShrinivaasan\_alias\_Shrinivaskannan\_photo.jpg (2015) - have been added to pairwise graph isomorphism face similarity computation.

1201.5 Following are 6 isomorphic pairs of visuals (of 11 pairs of visuals of author) - from testlogs/DeepLearning\_ConvolutionNetwork\_BackPropagation.log.17January2022 which belong to 2015, 2016 and 2017 while remaining non-isomorphic 5 pairs have at least one older image:

('Voronoi FaceGraphs of two facial images are isomorphic - percentage similarity - ', 'testlogs/IMG\_20160610\_071455.jpg', ' and ', 'testlogs/IMG\_20160610\_071603.jpg', ': 100.0')

('Voronoi FaceGraphs of two facial images are isomorphic - percentage similarity - ', 'testlogs/IMG\_20160610\_071455.jpg', ' and ', 'testlogs/IMG\_20171112\_180837.jpg', ': 100.0')

('Voronoi FaceGraphs of two facial images are isomorphic - percentage similarity - ', 'testlogs/IMG\_20160610\_071603.jpg', ' and ', 'testlogs/IMG\_20171112\_180837.jpg', ': 100.0')

('Voronoi FaceGraphs of two facial images are isomorphic - percentage similarity - ', 'testlogs/IMG\_20160610\_071455.jpg', ' and ', 'testlogs/SrinivasanKannan\_alias\_KaShrinivaasan\_alias\_Shrinivaskannan\_photo.jpeg', ': 100.0')

```

', ': 100.0')
('Voronoi FaceGraphs of two facial images are isomorphic - percentage similarity
- ', 'testlogs/IMG_20160610_071603.jpg', ' and ',
'testlogs/SrinivasanKannan_alias_KaShrinivaasan_alias_Shrinivaskannan_photo.jpeg
', ': 100.0')
('Voronoi FaceGraphs of two facial images are isomorphic - percentage similarity
- ',
'testlogs/SrinivasanKannan_alias_KaShrinivaasan_alias_Shrinivaskannan_photo.jpeg
', ' and ', 'testlogs/IMG_20171112_180837.jpg', ': 100.0')
1201.6 11 pairs of visuals earlier span 14 years from 2003 to 2017 and belong to
2003,2007,2015,2016,2017. As per decision tree in Section 1189,visuals of
2015,2016 and 2017 (short durations) are heavily similar while isomorphism wanes
between 2003 to 2007 (false negatives). Previous results reasonably establish
graph-isomorphic face recognition of visuals separated by short durations.
1201.7 Approximate isomorphism test by faster_could_be_isomorphic() has been
included in facegraph_similarity_metrics()

```

-----

1202. (THEORY and FEATURE) People Analytics - Merit of Large Scale Visuals - Topological and Graph Theoretic Face Recognition - Pairwise similarity loop and error handling - related to 159,660,714,715,720,1185,1186,1187,1188,1189,1190,1201 and all sections on Topological Face and Handwriting recognition, Product Homotopy, Unique identification, Homeomorphism and Topological Deformations, Merit of Large Scale Visuals, People Analytics, Computational Geometry, Graph Edit Distance and Earth mover distance, Graph Isomorphism (Exact, Approximate and Subgraph), Graph matching, Graph similarity, Image Search, Mesh Deformation - 21 January 2022

-----

1202.1 DeepLearning\_ConvolutionNetwork\_BackPropagation.py has been updated to loop through an array of images and compute pairwise face similarity by Graph Isomorphism (no subgraph isomorphism and iterations). Only full Isomorphism between Voronoi Facegraphs and Delaunay Trimesh(s) of a pair of images is being verified.

1202.2 8 face images of author are being matched for isomorphism spanning over a period of 19 years from 2003 to 2022. Images are of varied postures (passport, portrait-sitting, masked). New image testlogs/IMG\_20220119\_165911.jpg of the author wearing N95 COVID19 mask has been added to the computation to check if face isomorphism is recognized in disguise.

1202.3 Dlib shape detector fails to find 68 face landmarks for masked image testlogs/IMG\_20220119\_165911.jpg. Because of this an error condition is being handled to opt for contour centroids if 68 landmark centroids are not correctly found. Delaunay trimesh of testlogs/IMG\_20220119\_165911.jpg for contour centroids drawn by PyVis has been written to testlogs/IMG\_20220119\_165911\_FaceRecognition\_Segmentation\_FaceGraph.html. PyVis drawn Delaunay Trimesh can be arbitrarily animated thus implementing a mesh deformation for arbitrary face expressions. PyVis mesh deformations can be non-planar. Voronoi Tessellation, Segmented Image and FaceGraph DOT files are written to:

```

testlogs/IMG_20220119_165911-tessellated.jpg
testlogs/IMG_20220119_165911_FaceRecognition_Segmentation_FaceGraph.dot
testlogs/IMG_20220119_165911_segmented.jpg

```

1202.4 There are standard Mesh Deformation algorithms (As Rigid As Possible being one of them) for simulating the object animation and topological homeomorphic deformations in Computer Graphics. Identifying a face from its multiple mesh deformations is more accurate and harder than Graph Isomorphism recognition - facet areas change in addition to vertex renumbering.

1202.5 Logs for this update are written to testlogs/DeepLearning\_ConvolutionNetwork\_BackPropagation.log.21January2022. For 64 pairs of images (8\*8), Full Graph Isomorphism is True for 19 pairs which is remarkable for a learner with no training priors. Subgraph isomorphism test has been avoided because of slowdown.



## References:

-----  
1202.6 Large Mesh Deformation Using the Volumetric Graph Laplacian - Microsoft Research - <https://www.microsoft.com/en-us/research/publication/large-mesh-deformation-using-the-volumetric-graph-laplacian/> - Face recognition requires converse of this: Given set of Mesh Deformations (multiple face images of varied postures) verify if they belong to same face.

1202.7 Large Mesh Deformation Using the Volumetric Graph Laplacian - ppt - <https://www.cs.jhu.edu/~misha/Fall07/Notes/Zhou05.pdf>

1202.8 Mesh Deformation algorithm implementations - ARAP, Spokes-Rims, SmoothRotationEnhancedARAP - CGAL 5.3.1 -

[https://doc.cgal.org/latest/Surface\\_mesh\\_deformation/index.html](https://doc.cgal.org/latest/Surface_mesh_deformation/index.html)

1202.9 Isomorphism of Quadrilateral mesh(s) -

<https://www.ics.uci.edu/~goodrich/pubs/geomproc.pdf> - Motorcycle Graphs: Canonical Quad Mesh Partitioning - "We describe algorithms for canonically partitioning semi-regular quadrilateral meshes into structured submeshes, using an adaptation of the geometric motorcycle graph of Eppstein and Erickson to quad meshes. Our partitions may be used to efficiently find isomorphisms between quad meshes. ... Mesh isomorphism. In feature film production many characters may all be created from the same base topology; Figure 1 shows just a few different characters out of about 70 that all use the same mesh topology ..."

-----  
1203. (THEORY and FEATURE) People Analytics - Merit of Large Scale Visuals - Textual, Topological and Graph Theoretic Face Recognition - Physique Recognition From Quadrilateral mesh isomorphism and Face Distinguisher from ImageNet predictions - related to

159,660,714,715,720,1185,1186,1187,1188,1189,1190,1201,1202 and all sections on Topological Face and Handwriting recognition, Product Homotopy, Unique identification, Homeomorphism and Topological Deformations, Merit of Large Scale Visuals, People Analytics, Computational Geometry, Graph Edit Distance and Earth mover distance, Graph Isomorphism (Exact, Approximate and Subgraph), Graph matching, Graph similarity, Image Search, Quadrilateral Mesh Deformation and Isomorphism, Maximum Common Subgraph Problem - 24 January 2022

-----  
1203.1 ImageNet Predictions from ResNet50 training dataset could filter visuals containing faces (human or animal) through textual predictions along with other objects in the frame which might be a preprocessing step in a Face recognition pipeline.

1203.2 First frame of an MP4 visual of 3 Ducks -

testlogs/3Ducks\_VID\_20220119\_173052.mp4Frame\_1.jpg - is predicted by imagenet\_videograph() and its ImageGraph computed by EventNet Tensor Products algorithm is written to logs testlogs/ImageGraph\_Keras\_Theano.log.24January2022 - following are vertices of the ImageGraph and their pageranks. Nature of objects and 3 animals in the visual are approximately predicted - including "face" as a vertex:

```
[('wood_rabbit', 0.20490727007427248), ('meerkat', 0.1042849885504515),
('Bedlington_terrier', 0.06599733304073167), ('cliff', 0.04908043707463344),
('Wisconsinite', 0.044626573497110016), ('face', 0.023766317129790045),
('resident', 0.01613222743894782), ('Wisconsin', 0.01613222743894782),
('native', 0.01613222743894782), ('resemble', 0.014707510136039716), ('groomed',
0.014707510136039716), ('terrier', 0.014707510136039716), ('lamb',
0.014707510136039716), ('light', 0.014707510136039716), ('high',
0.013917572237708857), ('steep', 0.013917572237708857), ('rock',
0.013917572237708857), ('mongoose-like', 0.013337116985104445), ('South',
0.013337116985104445), ('viverrine', 0.013337116985104445), ('lemur',
0.013337116985104445), ('toes', 0.013337116985104445), ('like',
0.013337116985104445), ('Africa', 0.013337116985104445), ('four',
0.013337116985104445), ('common', 0.01316406639122259), ('North',
0.01316406639122259), ('brownish', 0.01316406639122259), ('rabbit',
0.01316406639122259), ('greyish', 0.01316406639122259), ('disease',
0.01316406639122259), ('tail', 0.01316406639122259), ('host',
```

```
0.01316406639122259), ('scapularis', 0.01316406639122259), ('America',
0.01316406639122259), ('fur', 0.01316406639122259), ('underside',
0.01316406639122259), ('pacificus', 0.01316406639122259), ('Ixodes',
0.01316406639122259), ('small', 0.01316406639122259), ('ticks',
0.01316406639122259), ('Lyme', 0.01316406639122259), ('white',
0.01316406639122259)]
```

1203.3 Textual predictions from imagenet\_videograph() could be optionally added to decision tree in 1189 for improved Face recognition:

```
 if ImageNet Text Predictions contain face related vertices of high
 pagerank
 {
 /* Proceed with Topological and Graph Theoretic Face recognition */
 }
```

1203.4 Full Physique quadrilateral mesh subgraph isomorphism algorithms try to match some fraction of 2 human bodies tessellated by quadrilateral mesh (only Delaunay triangulated mesh have been implemented thus far in NeuronRain) thus expanding the scope of Face Recognition to Physique Recognition, a comprehensive unique identification alternative to traditional face IDs - Figure 1.1, Figure 5.2 and Figure 5.3 of <https://www.ics.uci.edu/~goodrich/pubs/approx-match.pdf> approximately match two quadrilateral meshes topologically (two arbitrarily rigged animation characters) which could be adapted to two human visuals tessellated by quadrilateral mesh(s).

1203.5 Large Video File 3Ducks\_VID\_20220119\_173052.mp4 for the frame earlier has been uploaded to <https://kuja27.blogspot.com/2022/01/3-ducks-large-scale-visual-for.html>

#### References:

-----  
1203.6 Approximate Topological Matching problem finds maximum matching portions of two quadrilateral meshes and differs slightly from Graph Edit Distance and Graph Isomorphism - Approximate Topological Matching Heuristic Algorithm - Matches both Face orientations and Vertices-Edges - <https://www.ics.uci.edu/~goodrich/pubs/approx-match.pdf> - [David Eppstein · Michael T. Goodrich · Ethan Kim · Rasmus Tamstorf - Walt Disney Studios] - "... The approximate topological matching is not the same as graph edit distance, however. Graph edit distance is concerned with minimizing the number of edit operations to convert one graph to another, whereas approximate topological matching is concerned with maximizing the amount of common matching quads between two quad meshes, even if there are large portions of one of the two meshes that might not match with any part of the other. Thus, the approximate topological matching problem is an adaptation of the maximum common subgraph problem (22) to quad meshes, where we wish to match oriented quad faces as well as vertices and edges...." - Isomorphisms for bounded genus can be solved in linear time.

1203.7 Non-uniform Quadmesh to Uniform Trimesh - ACVD and pyacvd - Cow example - <https://pypi.org/project/pyacvd/> - Opposite direction of Trimesh to Quadmesh is a hard problem and a naive algorithm could be to merge two adjacent triangles in 3D Delaunay trimesh forming quadrilaterals within a quadmesh of least per quad cell area (if number of triangles is even). For odd number of triangles in trimesh, after merging all pairs of triangles to quadrilaterals, one side of last unmatched triangle is edge-subdivided to create last quadrilateral of quadmesh.

1203.8 Graph subdivision (Expansion) - [https://en.wikipedia.org/wiki/Homeomorphism\\_\(graph\\_theory\)#Subdivision\\_and\\_smoothing](https://en.wikipedia.org/wiki/Homeomorphism_(graph_theory)#Subdivision_and_smoothing)

-----  
-----  
1204. (THEORY and FEATURE) People Analytics - Social Network Analysis (Professional) - Chaotic Hidden Markov Model of Career Transition - some corrections to Viterbi Trellis computation, JSON persistence and PageRank Model of Career Transition - 27 January 2022 - related to 14,365,711,753,876,1127,1128,1129,1130 and all sections on People Analytics, Intrinsic Merit Versus Fame Equilibrium, BKS Conjecture, Stability and Noise

Sensitivity of Interview LTF/PTF, Peres Theorem, Unique Identification, HR Analytics and Automated Recruitment, Question-Answering, Majority Voting, Condorcet Jury Theorem Variants, Margulis-Ruzso Thresholds, Novelty Detection, Recommender Systems, Urban Sprawl Analytics

-----

-----

1204.1 SocialNetworkAnalysis\_PeopleAnalytics\_ChaoticHMM.py has been updated to persist dictionaries for Career State Machine and Designation classifications to SocialNetworkAnalysis\_PeopleAnalytics\_ChaoticHMM.json JSON backend and remove the hardcoded values.

1204.2 Viterbi Trellis computation has been corrected to find argmax for every state-observation and append to Viterbi trellis for printing to logs  
testlogs/SocialNetworkAnalysis\_PeopleAnalytics\_ChaoticHMM.log.27January2022.  
Career Transition computed by Chaotic HMM is correctly printed sequentially ignoring parallel tenures:

=====

Chaotic HMM Viterbi Trellis computation

=====

```
['Schooling',
 'DBHPS',
 'PSGTech',
 'BaaN-SSAGlobal',
 'SunMicrosystems-Oracle',
 'Krishna-iResearch',
 'Verizon',
 'webMethods-SoftwareAG',
 'CMI-IIT-IMSc',
 'GlobalAnalytics',
 'Clockwork-PiQube',
 'CloudEnablers']
```

1204.3 SocialNetworkAnalysis\_PeopleAnalytics\_ChaoticHMM.json contains dictionaries for an example career transition (academic and work) of author spanning 40 years (1982-2022: parallel tenure of 23 years total work experience + parallel tenure of 23 years of academics for schooling and 3 degree qualifications) which includes parallel tenure of Open Source Software R&D initiative (Krishna iResearch: 2003-2022) spanning 19 years. Lamda of Chaotic HMM has been increased to 5.0. Serializing the parallel tenures has a weird implication of experience exceeding age of the candidate.

1204.4 Unique Identification of a profile is of utmost importance for choosing authentic candidates. Usual Face Recognition and Physique Recognition technologies may not be sufficient unless the career transition and financial history of the profile is authorized by a state issued unique ID (Section 711). Relocation history of a professional profile is a mobility measure associated with travel patterns - chronological sequence of cities where a candidate worked. Relocation timeline is a graph when a profile often relocates to a workplace of same urban centre. Frequent subgraphs or common subgraphs and average degree of Relocation travel pattern graphs is reflective of both personal preference and most prolific, economically thriving urban areas providing job opportunities where people gravitate or migrate to.

1204.5 Modelling Career Transition by PageRank further refines Markov model earlier by replacing websites by organizations. For a career transition probability column-stochastic matrix  $CT(N)$  and Initial state of  $P$ , following power iteration converges to stationary distribution:

$$CT(N+1) = CT(N) * P$$

Element  $(i,j)$  of  $CT(N)$  is the probability of state transitioning from organization  $i$  to organization  $j$

Stochastic Column Vector  $P$  is initialized to random probabilities.

1204.6 Previous PageRank model ranks employee preference of corporate organizations quite similar to website rankings and is holistic and not employee specific. Usual "Best place to work" surveys are mostly intrinsic based on worklife quality metrics.

1204.7 SocialNetworkAnalysis\_PeopleAnalytics.py already implements a LinkedIn HR analytics for domain specific dictionary for Intrinsic Measurement of Technical Talent (Lines of Code for Information Technology Domain - Open Source

Contribution and Corporate Individual Contribution) - such domain specific intrinsic parameters for measuring talent helps in automated recruitment of talent when both Question-Answering (Contests-Examinations-Interviews) and Majority Voting are prone to failures by human errors - thus in Bounded error complexity classes. Stability condition for BKS Conjecture to be true and Interview as LTF has been derived in Section 365.

1204.8 Influence, Average Sensitivity and Noise Sensitivity of LTFs and PTFs are theoretical formalisms of human errors in Question-Answering (when a question or answer is corrupted by some probability). By Peres' Theorem Noise Sensitivity ( $NS(\delta)$ ) of LTF is upperbounded by  $2\sqrt{\delta}$  where  $\delta$  is probability of flipping each bit (or)  $\Pr(f(x) \neq f(y)) < 2\sqrt{\delta}$  for  $x$  correlated to  $y$  by  $\delta$ -probability flip per bit. From 1204.9 Average Sensitivity of PTF is upperbounded by  $AS(f) \leq 2^{O(d)} \cdot \log n \cdot n^{(1-1/(4d+2))}$  for degree- $d$  Polynomial Threshold Function in  $n$  variables. PTFs are better models of examinations as their coefficients are real-valued and thresholded by sign of polynomial evaluated (Kind of Pass or Fail). Conditions for Human Error in Majority Voting have been analyzed at length by Variants of CJT ( $p$ -bias of a voter SAT, Margulis-Ruzzo sharp Threshold at  $p$ -bias=0.5) which apply to PageRank as well. Equality of Average Sensitivity/Stability/Sensitivity/Influence of LTF-PTFs and Majority Decision Error of Condorcet Jury Theorem could be a Fame-Merit equilibrium point. Failure of both Question-Answering and Majority Voting by human error plays spoilsport in measuring the much touted "Employability" of a candidate and would necessitate inevitably resorting to automated Talent analytics by historic intrinsic merit metrics - Academic qualifications (not necessarily examination scores), Skills e.g Total lines of code written, Lateral or Out-of-the-box thinking, Number of projects and teams managed, Independent Research and Development (Novelty Detection) - which are merit samples of huge durations thus minimizing error. Academic examinations, prone to failure by LTF-PTF sensitivities, as talent yardsticks for students might likewise have to be replaced by merit samples of wider ambit. Class of LTFs is learnable in  $\text{poly}(n/\epsilon)$  or Questions for Answers are learnable in polynomial time (Answer-Questioning or anti-examination where students are supposed to ask questions for given answers, rationale being a person cannot ask questions unless (s)he has understanding of the answers). Limitations of various admission tests e.g SAT, GRE, TOEFL, IELTS have been reported and academic admissions are often decided based on Letter of Recommendations than admission test scores - a real life instance of Recommender Systems.

#### References:

- 
- 1204.9 Average Sensitivity (expected probability of certain number of hamming neighbours of boolean cube) and Noise Sensitivity of Boolean PTFs - [Ilias Diakonikolas, Prasad Raghavendra, Rocco A. Servedio, Li-Yang Tan] - <https://arxiv.org/pdf/0909.5011.pdf>
- 1204.10 Peres Theorem - Lecture 19: Noise sensitivity of Linear Threshold Functions - [Ryan O'Donnell] - <https://www.cs.cmu.edu/~odonnell/boolean-analysis/lecture19.pdf>
- 1204.11 The Limitations of the GRE in Predicting Success in Biomedical Graduate School - <https://journals.plos.org/plosone/article?id=10.1371/journal.pone.0166742> - Correlation between GRE Scores and Success in Research career is quite low
- 1204.12 Change in mobility - [https://kzaremba.shinyapps.io/Dystansowanie/?fbclid=IwAR0WoEn5H2RXJ2WzyjWCqoevRcqK-n6\\_B1I1ItE7h00EF0qDj34FZB5byqM](https://kzaremba.shinyapps.io/Dystansowanie/?fbclid=IwAR0WoEn5H2RXJ2WzyjWCqoevRcqK-n6_B1I1ItE7h00EF0qDj34FZB5byqM) - Data for Good - estimation of facebook users' mobility anonymously gathered from users who have geolocation enabled.

-----

1205. (THEORY and FEATURE) Computational Geometric Factorization - Matplotlib plot of benchmarks - 300 integers from 100 to 400 and 20 integers from 500 to 520 - related to 1159 and all sections on Computational Geometric Factorization, Neural network learning of Factors by SAC=TC=NC=AC equivalence, Planar Point Location - 30 January 2022

-----

-----  
1205.1 New source file

python-src/DiscreteHyperbolicFactorizationUpperbound\_TileSearch\_Optimized\_MultipleIntegers.py has been committed to iterate multiple integers sequentially over a range and time their computational geometric factorization durations by invoking python-src/DiscreteHyperbolicFactorizationUpperbound\_TileSearch\_Optimized.py within subprocess.call()

1205.2 NeuronRain Spark MapReduce implementation of Computational Geometric Factorization NC-PRAM-BSP algorithm by local binary search of rasterized hyperbolic arc bow segments is in complexity class Deterministic MRC, a software limitation. Time durations of computational geometric factorization of 300 integers from 100 to 400 and 20 integers from 500 to 520 are plotted against theoretical time of  $O(\log N \cdot \log N)$  for depth-1 non-uniform Nick's Class circuit.  
1205.3

python-src/DiscreteHyperbolicFactorizationUpperbound\_TileSearch\_Optimized\_MultipleIntegers.py takes following commandline arguments in the order - minimum integer of the range, increment, depth of non-uniform NC circuit=exponent  $k$  of  $O((\log N)^k)$ , constant of Big-O and exponent of  $\log N$  in the plot.

1205.4 It is hereby clarified that motive of Computational Geometric Factorization algorithm is to devise a polylogarithmic time integer factorization mechanism or a logdepth bounded fanin Nick's class circuit implemented by a cloud computing DMRC simulation of multicore-PRAMs which evidences existence of factorization algorithms in NC and not proving the lowerbound for factorization (e.g possibility of factorization by planar point location being present in a subset of NC cannot be ruled out - sublogarithmic time - since there are sequential sublogarithmic planar point location algorithms) which are two entirely different notions. That is precisely the reason for (ab)use of BigO notation throughout instead of Omega.

1205.5 Equivalence of  $SAC=AC=NC=TC$  implies Nick's class parallel algorithms are learnable by Threshold circuits of majority gates or Neural networks - iterated factorization of sequential set of integers might serve as priors for further factorization. Example: Factorization of 39 as  $39 = 13 \cdot 3$  might be a prior by substitution for factorization of  $117 = 3 \cdot 39 = 3 \cdot 3 \cdot 13$

1205.6 Two matplotlibs

python-src/DiscreteHyperbolicFactorizationUpperbound\_TileSearch\_Optimized\_MultipleIntegers1.jpg (for integers 100 to 400, logdepth=1, BigOconstant=1, log exponent in plot=2) and

python-src/DiscreteHyperbolicFactorizationUpperbound\_TileSearch\_Optimized\_MultipleIntegers2.jpg (for integers 500 to 520, logdepth=1, BigOconstant=1, log exponent in plot=2) have been committed to AstroInfer repositories.

1205.7 Both the graphics depict the  $k \cdot \log N$  ( $k=1$ ) actual runtimes of factorization (blue) far upperbounded by theoretical  $O((\log N)^2)$  (red). Depth of circuit (parallel RAM time) has been differentiated from exponent of logarithm for graphic illustration (though both have to be equal by definition of NC). Previous runtime plots are for finding all factors (with and without multiplicity - Big Omega and Little Omega) which is a harder problem than finding just one factor.  
-----

-----  
1206. (THEORY and FEATURE) People Analytics - Social Network Analysis - Bipartite Social Networks (Matrimonial portals, Employer-Employee Professional networks) - Recommender Systems and Sentiment Analysis of Profiles for Ranking Preferences - related to 583,843 and all sections on Social Network Analysis, Clustering, Bipartite Matching, Gale-Shapley algorithm for Stable Marriage Problem and College Admission Problem, Online Citizen Science, Intrinsic Merit ranking of People profiles, Graph Isomorphism and Common Subgraph Problem, Recommender Systems, Unique Identification, Graphical models-Markov Random Fields and Belief Propagation, Hall's Marriage Theorem, Perfect Matching and Permanent of Bipartite graph - 31 January 2022  
-----

1206.1 Matching Algorithms for finding complementary pairs of profiles (Match

making) in bipartite 2-colored social networks have been studied as Bipartite matching problem and Stable Marriage Problem (Gale-Shapley algorithm).

1206.2 Contrary to homogeneous social networks of Facebook and Twitter, match making social networks consist of 2 sets of vertices (Brides-Grooms, Employee-Employer, Male-Female) and profiles in each set have ranking preferences for their suitor in the other set.

1206.3 k-Nearest Neighbour Clustering of matrimonial profiles has been investigated as a Marriage Recommender Systems engine for suggesting profile vertices of closest match in set V2 for a profile vertex in set V1 of a bipartite social network  $G=(V1 \cup V2, E)$  - Reference 1206.8.

1206.4 Recursive Gloss Overlap Textgraphs of 2 Profile texts from sets V1 and V2 could be matched by Graph similarity measures - Graph Edit Distance, Netrd Graph Distance measures, Graph Isomorphism (Full-Subgraph-Approximate), Common Subgraph Algorithms - for percentage match of the profile textgraphs in bipartite sets V1 and V2 which could be a preliminary recommender systems screening criterion.

1206.5 Unique Identification of a profile in match making is implicit necessity without stating to rule out bigamy. Gale-Shapley Stable Marriage Algorithm discovered in 1962 and awarded Nobel Prize in Economics 2012, has found variety of applications including National Resident Matching Program

(<https://www.nrmp.org/> for matching healthcare professionals to positions) and states: For equal number of men and women having ranking preferences, it is always possible to find a stable marriage match. A match of two vertices from sets V1 and V2 respectively is said to be stable if there is no pair (A,B) from sets V1 and V2 who prefer each other over their already matched partners. But Gale-Shapley algorithm is heavily tilted in favour of women who are allowed to ditch a current provisional partner found in previous round and choose a better man in next round and thus could be protested as asymmetric, unethical taint for marital sanctity. Thus Gale-Shapley algorithm may not be applicable in its exact sense to ethical matrimonial matching. Runtime of Gale-Shapley algorithm is  $O(n^2)$  for n men and n women. Hall's Marriage Theorem is another result which stipulates a condition for unique happy marriage:

For two sets of n men and n women, and for subset I of n women, of  $A_i$  is the set of men i-th woman in set I prefers to marry,  $\sum |A_i|$  for all i in I  $\geq |I|$

1206.6 Ranking preferences of a profile required as a preprocessing step by Gale-Shapley algorithm earlier is approximately a Sentiment analysis problem of the profile text or inferring expectations of profile vertices from text. An example matrimonial advertisement profile text of author in SentimentAnalyzer-BipartiteMatching-SocialNetworks.txt (Source advert JPG - Print Media - 2017: testlogs/SentimentAnalyzer-BipartiteMatching-SocialNetworks.IMG\_20171111\_135651.jpg) has been Deep-learnt to a Recursive Gloss Overlap TextGraph and analyzed for Empath and SentiWordNet sentiment by SentimentAnalyzer.py Belief Propagation and Markov Random Fields Graphical Model sentiment analysis functions which treat the textgraph as Graphical model having sentiment score potentials. Some small changes have been made to potential computation (multiplying by 2 for magnifying the scores, filter object of sentiwordnet synsets cast to list)

1206.7 Excerpts of logs

testlogs/SentimentAnalyzer.BipartiteMatchingSocialNetworks.log.31January2022  
print the positivity, negativity and objectivity scores of the profile text -  
sample profile text is overwhelmingly objective from SentiWordNet and Empath sentiment analysis:

```
=====
 Sentiment Analysis (Applying SentiWordNet to the tokenized text) of the
text
```

```
=====
 Positivity = 0.5
 Negativity = 0.125
 Objectivity = 12.375
 =====
 Empath:
 =====
```

RG0 Markov Random Fields - Empath positivity: 0.0  
RG0 Markov Random Fields - Empath negativity: 0.0  
RG0 Markov Random Fields - Empath objectivity: 1478.6871718142365

1206.8 Previous sentiment scores of a profile could be essential ingredients of a larger match recommender systems engine which clusters profiles of similar attitudes by their sentimental score euclidean distances or matches suiting profile vertex pairs (either by Gale-Shapley algorithm or Hall's marriage theorem) which are ranked by sentiment polarity.

#### References:

-----  
1206.8 Marriage Recommendation Algorithm Based on KDTree-KNearestNeighbours clustering-Logistic Regression Model -  
<https://ieeexplore.ieee.org/document/9182566> - claimed accuracy of 86%  
1206.9 Hall's Marriage Theorem - [https://en.wikipedia.org/wiki/Hall%27s\\_marriage\\_theorem](https://en.wikipedia.org/wiki/Hall%27s_marriage_theorem)  
1206.10 Gale-Shapley Stable Marriage Algorithm -  
[https://en.wikipedia.org/wiki/Gale%E2%80%93Shapley\\_algorithm](https://en.wikipedia.org/wiki/Gale%E2%80%93Shapley_algorithm)  
1206.11 Reciprocal Recommender Systems: Analysis of State-of-Art Literature, Challenges and Opportunities towards Social Recommendation -  
<https://arxiv.org/pdf/2007.16120v2.pdf> - "...In other words, a vital requirement in any RRS is that both users should reciprocate, i.e. both of them should indicate positive feedback on the suggestion to connect with each other in order to deem the matching recommendation as successful. This requisite adds an additional layer of complexity in RRS with respect to the majority of conventional RS, the latter of which typically only seek satisfying the end user preferences. RRS are popular in dating [112], recruitment [11], online learning environments [120], and social media platforms [61, 107] where reciprocity can yield better matchings between people [109]..."  
1206.12 Reciprocal Recommender Systems - <https://indiaai.gov.in/article/how-matchmaking-matrimonial-platforms-are-leveraging-reciprocal-recommender-systems-at-its-core>  
1206.13 Datasets from various print media matrimonial match making services - hint at an alarming trend of growing reciprocal mismatch which could doom RRS, Gale-Shapley or Hall match making: (\*) unequal number of prospective men and women suitors (\*) age bracket preferences (\*) culture and community preferences (\*) qualification preferences (\*) affluence preferences - Sentiment analyzer algorithms might not be able to capture subtleties of cupid.

-----  
1211. (THEORY and FEATURE) GIS Urban Sprawl Analytics - Population Density computation from Contour Pixel color coding - 4 February 2022 - related to 1174,1175,1179,1194 and all sections on GIS Urban Sprawl Analytics, Merit of Large Scale Visuals, Gridded Population Estimators (SEDAC GPW4 and GHSL convex hull estimators), DBSCAN and Neural Network Urban Extent Learners, Computational Geometry, Intrinsic Merit Rankings, R Ricker Population Estimation, Community detection, Social Network Analytics, Space filling by Curves, Unequal Circle and Polynomial packing, Computational Geometry and Polygonal packing by Voronoi Tessellation, Four color theorem, Economic Merit, Computational Economics - GDP estimation from electricity consumption  
-----

1211.1 GISUrbanSprawlAnalytics.py has been updated to compute Population of an urban sprawl contour extent from pixel color coding of the contour and points within the contour. Earlier population density was assumed to be a constant throughout the GIS visual which has been rectified in this code change.  
1211.2 There are standard methodologies to find population density from GIS GeoTIFF which project the map pixel coordinates to longitude-latitude by GDAL Geo transformations and lookup the population density of a longitude-latitude from a GIS map service which is multiplied by contour area to get the population count. But the issue with GDAL is it is quite heavy to install and dependency requirements are huge causing C++ compile errors (GDAL is implemented in C++ and there are GLIBC version mismatch errors) and has been abandoned in favour of a

simpler alternative.

1211.3 Simpler alternative implemented in this commit:

1211.3.1 Find the Blue-Green-Red color of a pixel in contour boundary of an urban sprawl

1211.3.2 Average of BGR color is divided by 255 to get the ratio of pixel intensity -  $\text{AverageBGR}/255$

1211.3.3 Average BGR color pixel intensity ratio is multiplied by highest population density of an urban sprawl in the world to get approximate estimate of population density of an urban sprawl contour (e.g Barcelona, Spain and Los Angeles, The US are the densest in world) - 100000 per square kilometre (Assumption: Pixel colors graded from 0 to 255 map from lowest population density to highest population density range which is the convention followed by GHSL, SEDAC, HRSL)

1211.4 Function `urban_sprawl_from_segments()` is invoked for Meta-Facebook High Resolution Settlement Layer World Nighttime Streets image - `testlogs/HRSL_World_NightTimeStreets.jpg` - by setting population density as -1 a flag implying population density is internally computed.

1211.5 Following are the logs, facegraph DOT file and convex hull-contour-segment-facegraph images created - Logs

`testlogs/GISUrbanSprawlAnalytics.log.4February2022` print the contour boundary point chosen for pixel color computation and the approximate populations of urban sprawl contour areas (not necessarily close to actual populations because area of a pixel may not be 1 square km exactly as contour area to square km conversion is computed by a heuristic training data in 1175, but quite useful for rankings by proportionality):

`testlogs/GISUrbanSprawlAnalytics.log.4February2022`

`testlogs/HRSL_World_NightTimeStreets-contourlabelled.jpg`

`testlogs/RemoteSensingGIS/HRSL_World_NightTimeStreets_FaceGraph.jpg`

`testlogs/RemoteSensingGIS/HRSL_World_NightTimeStreets_ImageNet_Keras_Theano_Segmentation_FaceGraph.dot`

`testlogs/RemoteSensingGIS/HRSL_World_NightTimeStreets_contour_segmented.jpg`

`testlogs/RemoteSensingGIS/HRSL_World_NightTimeStreets_convex_hull_segmented.jpg`  
`testlogs/RemoteSensingGIS/HRSL_World_NightTimeStreets_segmented.jpg`

#### References:

-----

1211.6 The curse of urban sprawl: how cities grow, and why this has to change - <https://www.theguardian.com/cities/2016/jul/12/urban-sprawl-how-cities-grow-change-sustainability-urban-age>

1211.7 High Resolution Settlement Layer - [Samapriya Roy] - Google Earth Engine model - <https://samapriya.github.io/awesome-gee-community-datasets/projects/hrsl/>

1211.8 HRSL Data for Good Visualizations - mWater Portal - <https://dataforgood.facebook.com/dfg/tools/high-resolution-population-density-maps>

1211.9 What Density Doesn't Tell Us About Sprawl - <https://www.accessmagazine.org/fall-2010/density-doesnt-tell-us-sprawl/> - Population Density rankings may not translate to urban sprawl rankings

1211.10 OSGEO GDAL Python bindings - <https://gdal.org/python/index.html>

1211.11 Map Projection in GDAL - pixel from long-lat - <https://stackoverflow.com/questions/58623254/find-pixel-coordinates-from-lat-long-point-in-geotiff-using-python-and-gdal>

1211.12 HRSL legend in `testlogs/HRSL_World_NightTimeStreets.jpg` dt.11/01/2022 for population counts: 7 pixel colors for population ranges 0-1, 1-50, 50-100, 100-250, 250-1000, 1000-2500 and 2500-27057 and map scale 1:147914382

-----

1212. (THEORY and FEATURE) GIS Urban Sprawl Analytics - Population count computation from HRSL Map Legend - 7 February 2022 - related to 1174, 1175, 1179, 1194, 1211 and all sections on GIS Urban Sprawl Analytics, Merit



of Large Scale Visuals, Gridded Population Estimators (SEDAC GPW4 and GHSL convex hull estimators), DBSCAN and Neural Network Urban Extent Learners, Computational Geometry, Intrinsic Merit Rankings, R Ricker Population Estimation, Community detection, Social Network Analytics, Space filling by Curves, Unequal Circle and Polynomial packing, Computational Geometry and Polygonal packing by Voronoi Tessellation, Four color theorem, Economic Merit, Computational Economics - GDP estimation from electricity consumption, Jordan Curve Theorem, Weirstrass Theorem

-----  
-----  
1212.1 GISUrbanSprawlAnalytics.py has been updated to compute population count from a Legend Dictionary through additional argument "legend" to urban\_sprawl\_from\_segments() which is a dictionary of average RGB pixel colors to population range strings of the form "<minimum>-<maximum>"  
1212.2 If no legend dictionary is available, population density computation defaults to proportional density based on pixel color having 100000 as maximum. It is upto the invoking function to suitably populate the legend dictionary and mapscale for contour area to square kilometer conversion. An example legend dict for Meta High Resolution Settlement Layer Map testlogs/HRSL\_World\_NightTimeStreets.jpg has been passed on to urban\_sprawl\_from\_segments() as mapping of RGB averages for color gradings - Yellow1, Yellow2, Yellow3, Orange1, Orange2, Orange3, Red1 - to population ranges. Mapscale could be either set to HRSL legend ratio of 1:147914382 or NeuronRain heuristic of 266.0/854.0 for urban sprawl contour area to square kilometre conversion:  
    legend={235/3:"0-1",245/3:"1-50",255/3:"50-100",362/3:"100-250",372/3:"250-1000",382/3:"1000-2500",510/3:"2500-27057"}  
    mapscale=147914382  
    #mapscale=266.0/854.0

urban\_sprawl\_from\_segments("testlogs/HRSL\_World\_NightTimeStreets.jpg",seg9,-1,mapscale,legend)

1212.3 urban\_sprawl\_from\_legends() iterates through legend dictionary to find matching color range for an average RGB value of contour boundary pixel - it is not a key lookup in exact sense, but a range query for color range which contains the average RGB value e.g an average RGB value of 300/3 would be matched by 255/3 - 362/3 bracket.

1212.4 Use of mapscale from HRSL (mapscale=147914382) as multiplicand magnifies the urban sprawl area and population values thus facilitating better ranking.

1212.5 Excerpts of logs from testlogs/GISUrbanSprawlAnalytics.log.7February2022 for area and population estimates of few urban sprawl contours:

```
('Circumference of Urban Area:', 30.485281229019165)
('Approximate circular area of Urban Sprawl:', 78.5)
('Contour Area of Urban Sprawl:', 60.0)
('Ratio of urban sprawl contour area to image area:', 6.96301247771836e-05)
('Square Kilometer Area of Urban Sprawl:', 8874862920.0)
('Population of Urban Sprawl (from density):', 8874862920.0)
('Population of Urban Sprawl (from area):', 4.8990705329947954e+20)
('Centroid of the Urban Sprawl:', (413, 43))
Contour boundary point: [[387 40]]
Contour color: [255 255 255]
('Convex Hull of Urban Area:', array([[388, 40]],
```

```
[[395, 46]],
```

```
[[396, 50]],
```

```
[[396, 56]],
```

```
[[387, 56]],
```

```
[[387, 40]]], dtype=int32))
```

```
('Circumference of Urban Area:', 69.79898953437805)
```

```
('Approximate circular area of Urban Sprawl:', 254.34)
('Contour Area of Urban Sprawl:', 21.0)
('Ratio of urban sprawl contour area to image area:', 2.437054367201426e-05)
('Square Kilometer Area of Urban Sprawl:', 3106202022.0)
('Population of Urban Sprawl (from density):', 3106202022.0)
('Population of Urban Sprawl (from area):', 6.0013614029186245e+19)
('Centroid of the Urban Sprawl:', (391, 48))
Contour boundary point: [[369 40]]
Contour color: [255 255 255]
```

-----  
1213. (THEORY and FEATURE) Economic merit - Neuro Cryptocurrency mint - Commodity linked Neuro Fictitious Cryptocurrency Proof of Work Algorithm - related to 164,165,488,489,499 and all sections on Economic merit, Neuro academic-use fictitious cryptocurrency, Economic networks, Towers of Hanoi problem - Ordered Histograms, Set Partition Analytics, Earth mover distance, Psuedorandom generators, NP-complete problems, P Versus NP, EventNet consensus and Hyperledger, Samuleson-Stolper theorem, Invisible Hand - Labour theory of value, Gold Standard - 8 February 2022  
-----

1213.1 NeuronRain implementation of academic-use fictitious Neuro cryptocurrency mining rig computes a naive, non-trivial proof of work by looping through a set of pseudorandomly chosen Neuro Protocol Buffer currency object Boost UUIDs and selecting only hexadecimal UUIDs having leading "ff". Success probability of Randomized Proof of Work algorithm (for finding 2 leading fs) earlier is  $16^{(m-2)}/16^m = 1/256$  for m hexadecimal digit UUIDs (number of m-2 hex digit substrings / number of m hex digit strings).

1213.2 Hardness of Proof of Work computation is crucial in assigning value to mined cryptocurrency (another economic merit measure). In essence, Hardness of Proof of Work Hashcash computation = Value of commodity (or should be proportional to Value of commodity). NP-Complete problems and harder classes of EXP,PSPACE problems are computational formulations of valuable commodities - in a way a reincarnation of Adam Smith-Ricardo Labour theory of value as Computational Theory of value. Lot of NP-complete problems have been studied as candidates for Cryptocurrency proof of work algorithms. Proof of P=NP could raise questions on hardness of Cryptocurrency Proof of Work mining rigs.

1213.3 Going by earlier line of reasoning, Tower of Hanoi problem of moving disks preserving order could be the hardest Cryptocurrency proof of work algorithm potentially consuming entire lifetime of universe for  $[2^n - 1]$  moves (mostly n=64) - even a partial version of Towers of Hanoi which moves some percentage of disks could be a quantifier of proof of work.

1213.4 Earth Mover Distance for set partitions and histograms formalizes the notion of moving a mass of histogram to morph it to another set partition histogram. Towers of Hanoi is a single bin ordered histogram of sorted disks of descending radii from bottom to top. If Earth Mover Distance definition could be adapted to Towers of Hanoi problem of moving disks (which is a problem of moving conical 3D ordered histogram of single bin containing sorted disks of various radii decreasing from bottom to top from one place to other - moving a histogram to itself - a fixed point computation  $f(h)=h$ ), a Towers of Hanoi EMD algorithm could be a proof of work alternative for Neuro Cryptocurrency of formidable hardness. Intuitively EMD for Single bucket Towers of Hanoi Ordered Histogram must be exponentially hard to compute.

1213.5 Neuro Perfect Forward C++ cloud move implementation of Cryptocurrency protobuf objects within an OpenSSL tunnel follows C++ idiom of zero-copy move and perfect forward (no change to argument value - immutable) as against copy-delete object move simulation in most cloud providers. Transactional move is assured by Software Transactional Memory in most C++ compilers or could be filled in by XA 2-phase commit consensus managers e.g Sun Microsystems-Oracle GlassFish AppServer JTS XA -

<https://github.com/javaee/glassfish/tree/master/appserver/transaction/jts>. An EventNet global consensus hyperledger appends a vertex and edge (Buyer-Seller - equivalent of a block in blockchain) for every Neuro cryptocurrency mined and

awarded thus tracking money trail.

1213.6 Pure computer science theoretic algorithms for proof of work are delinked from value oriented hardness computation of commodities. Commodity linked Proof of Work would make Neuro cryptocurrency more meaningful tender. In other words, hardness of mining one unit of Neuro cryptocurrency should be directly proportional to hardness (labour involved) of creating commodity from scratch (akin to Doctrines of Labour Theory of Value, Reductionism, Macroeconomics in terms of microeconomics and erstwhile Gold standard).

1213.7 An example Commodity linked Proof of work algorithm for Neuro: Neuro Value of a commodity is determined by hardness of computational simulation of producing the commodity from scratch - e.g Neuro Value of 1 kilogram of wheat or 1 metre of cloth is decided by hardness of algorithmic simulation of producing 1 kilogram of wheat or 1 metre of cloth from first principles (Wages + constituent materials from crop to market).

#### References:

-----  
1213.8 Adam Smith's Invisible Hand of Providence - Inevitability of Proletariat despite economic disparity - [The Theory of Moral Sentiments] - [https://en.wikipedia.org/wiki/Invisible\\_hand](https://en.wikipedia.org/wiki/Invisible_hand) - "...The rich only select from the heap what is most precious and agreeable. They consume little more than the poor, and in spite of their natural selfishness and rapacity, though they mean only their own conveniency, though the sole end which they propose from the labours of all the thousands whom they employ, be the gratification of their own vain and insatiable desires, they divide with the poor the produce of all their improvements...They are led by an invisible hand to make nearly the same distribution of the necessaries of life, which would have been made, had the earth been divided into equal portions among all its inhabitants, and thus without intending it, without knowing it, advance the interest of the society, and afford means to the multiplication of the species. When Providence divided the earth among a few lordly masters, it neither forgot nor abandoned those who seemed to have been left out in the partition...."

1213.9 Exponential Computational complexity of Towers of Hanoi - <https://dl.acm.org/doi/abs/10.1145/8312.8320> -  $O(2^n)$  for  $n$  disks

1213.10 JTS XA implementation in Sun Microsystems-Oracle GlassFish - <https://github.com/javaee/glassfish/blob/master/appserver/transaction/jts/src/main/java/com/sun/jts/CosTransactions/Configuration.java> - Configuration settings for IBM Transaction manager

1213.11 Proposal for a fully decentralized blockchain and proof-of-work algorithm for solving NP-complete problems - <https://arxiv.org/pdf/1708.09419.pdf> - Candidate blockchain proof of work NP-complete problems from Computational Biology and Particle Physics (Multiple Sequence Alignment, Protein Folding, Ising lattice)

1213.12 Software Transactional Memory in C++ - Example - [https://github.com/shrinivaasanka/Grafit/blob/master/course\\_material/Programming/C%2B%2B/code/softwaretransactionalmemory.cpp](https://github.com/shrinivaasanka/Grafit/blob/master/course_material/Programming/C%2B%2B/code/softwaretransactionalmemory.cpp)

1213.13 GlassFish (now an Eclipse project) - <https://github.com/eclipse-ee4j/glassfish>

1213.14 AWS S3 Bucket sync - <https://docs.aws.amazon.com/cli/latest/reference/s3/sync.html>

-----  
1214. (THEORY and FEATURE) Computational Geometric Integer Factorization - 20523 bits quadcore benchmarks - Factorization as a non-trivial Proof of Work computation for Neuro Cryptocurrency mining rig - related to 620,713,728,739,1158,1159,1161,1213 and all sections on Neuro Cryptocurrency, Computational Geometric Factorization, Set Partitions to Exact Square Tile Cover Reduction by Lagrange Sum of 4 Squares - Optimal denominations and Money Changing Problem, Integer Partitions, Equidepth-Equiheight V-Optimal Histograms and Set partition analytics, Drone Electronic Voting Machines - 9 February 2022  
-----

1214.1 Non-trivial proof of work computation requirement for mining Neuro



[illegible]

[illegible]

14042618556261405561199756270405698977102469597540254683104102675454039142857111  
173898181674532553, ') (at ', 'Sun, 06 Feb 2022 23:12:25 GMT', '))'  
=====

1214.5 Fed issued Paper Currency unique IDs have been proposed earlier as non-digital One Time Passwords for VREPAT Drone Electronic Voting Machines implemented in NeuronRain to ensure uniqueness of a vote cast. Neuro Boost UUIDs of the format <UUID>:<denomination> e.g ff20a894-a2c4-4002-ac39-93d053ea3020:100 are 512 bit long (plus bit size for denomination - longer than most currency unique IDs) and could catapult voting accuracy in spite of being digital.

1214.6 Logs for 20523 bits integer factorization are at DiscreteHyperbolicFactorizationUpperbound\_TileSearch\_Optimized.log.9February2022 . Factorization of 20523 bits required a non-uniform NC circuit of depth  $k=1432$  or  $O(N/(\log N)^k) = O(2^{20523}/20523^{1432}) = O(2^{10}) = 1024$  multicores, a quite usual number in MapReduce clouds and 1024 cores have been simulated on 4 cores in this factorization - it has to be noted that if MapReduce is implemented on a Single node cluster of multicores communication complexity is negligible.

1214.7 Earlier Proof-of-Work computation by Set partition to square tile cover which is a combination of (\*) factorization of a rectangular area equal to size of a set partition (\*) and money changing problem solutions for the two factors found, achieves 2 goals at a time - (1) mining a unit of Neuro cryptocurrency (2) expressing the mined currency in terms of optimal denominations e.g Rectangular area (= Value of Neuro currency mined) could be set to a function of 1,2 and 5:  $N = (a1 + 2*a2 + 5*a3)*(b1 + 2*b2 + 5*b3)$ .

-----  
1215. (THEORY and FEATURE) Set Partition Analytics - Set Partition-Rectangular Area to Factorization reduction and Integer Linear Program solution of Frobenius Coin Diophantines for Neuro Cryptocurrency mining rig Proof of Work, One Time Password facility augmented for Voter Received Encrypted Paper Audit Trail (VREPAT) Conceptual Drone Electronic Voting Machine - related to 135,562,1140 and all sections on Money Changing Problem, Optimal Denominations, Integer Partitions, Computational Economics - Computational Hardness (Labour) Theory of Value, Histogram and Set Partition analytics, Equidepth-Equiheight Histograms, Separate Chaining Hashtables, Drone EVMs, Space Filling and Teapot Shards, Equal and Unequal Circle packing, Grid filling, Integer Linear Programming and Cellular automata, Quantum Versus Classical Computation, Parallel Pseudorandom Generators, Berry-Esseen Central Limit Theorem - 11 February 2022  
-----

1215.1 Streaming\_SetPartitionAnalytics.py has been updated to change following functions to expand their scope to Neuro Cryptocurrency Proof of Work (NeuroFed) and Drone EVM one time password padding facility respectively:

```
def setpartition_to_tilecover(histogram_partition=None,
number_to_factorize=1, solution="ILP",Neuro_Crypto_ProofOfWork=False)
def electronic_voting_machine(Voting_Machine_dict, unique_id, voted_for,
Streaming_Analytics_Bertrand=False, onetimepassword=None)
```

1215.2 setpartition\_to\_tilecover() now accepts an additional boolean flag Neuro\_Crypto\_ProofOfWork to treat the number\_to\_factorize argument as a Neuro Currency of same value and factorize the Currency value  $N=pq$  to obtain two Frobenius Money Changing Coin Diophantines which are equated to factor pairs  $p$  and  $q$ .

1215.3 Integer Linear Program CVXOPT GLPK solutions for the two diophantines are printed to partition the Neuro currency as sum of multiples of denominations. Computational Theory of Value (a rephrasal of Labour Theory of Value) equates Hardness of the supply chain producing 1 unit of commodity from raw materials to market and its commercial value.

1215.4 Agriculture usecase supply chain following Samuleson-Stolper convention : Seeds - Land rental - Farm labour wages - Water - Materials - End product. Computationally, agriculture is a Space filling problem of randomly sowing seeds in a 2 dimensional plane and their probability of fructification (a la Teapot Shards model) - Seeds parallelly sprout and grow ordained by a probability distribution of ordinates from nature's parallel pseudorandom generator (invisible hand of providence) and thus could be in NC or Randomized NC (Tygar-

Reif Parallel PRG, Applebaum PRG in NC1 with linear stretch could churn out ordinates for seeds in parallel - NC - and only some randomly chosen seeds sprout in parallel - RNC). Finding total number of successfully sprouted seeds is tantamount to sum of random variables for the seed ordinates which tends to mean by Central Limit Theorem.

1215.5 electronic\_voting\_machine() now accepts an argument for One Time Password presumably a serial number of paper currency or Neuro Cryptocurrency Boost 512 bit UUID which is appended optionally to ripemd160 digest of Voter's public id context string. Defeating this uniqueness salting of an anonymous vote at a Drone polling terminal is as hard as counterfeiting of currency - paper or digital.

1215.6 Passlib SHA256 encrypt() has been deprecated and replaced by hash() while appending to a candidate's votes bin.

1215.7 Clauses have been introduced to differentiate Set partition to square tile cover reduction and Neuro Cryptocurrency proof of work. An example Neuro currency of #8375 has been mined by Factorizing 8375 (Neuro currency has been assigned a logo "#" to distinguish it from legal tenders). SymPy Random integer partition of the Neuro currency value is reduced to a rectangle and then factorized. Logs

testlogs/Streaming\_SetPartitionAnalytics.Python3.9Upgrade.NeuroProofOfWorkILP.log.11February2022 print the minted Neuro Cryptocurrency and its optimal denominations as sum of products.

1215.8 Earlier factorization based Neuro mint could be optimized by reducing 2 Money Changing Diophantines to 1 if area of the rectangle is a huge prime integer > 2 (or) Prime valued Neuro currency equal to rectangular area is minted. One of the two factors is 1 and diophantine for it is trivially solved.

1215.9 Quantum NC algorithm for factorization in Section 562 implies Neuro cryptocurrency could be mined by Quantum circuits.

#### References:

1215.10 ASUS, NVIDIA GPU Cryptocurrency mining rigs - Hashcash rate in Megahash per second - <https://www.nvidia.com/en-us/cmp/>

1215.11 Statistical Analysis of Exchange rate of Bitcoin versus Dollar - <https://journals.plos.org/plosone/article?id=10.1371/journal.pone.0133678>

-----  
1217. (THEORY and FEATURE) Fictitious Neuro Cryptocurrency Mining Rig - Random Integer Partition + Rectangular Area Factorization + Money Changing Problem Proof of Work - Digital Watermarking implementation for Visual Neuro cryptocurrency - 15 February 2022 - related to 112,113,114,488,751,784,785,787,791,841,848,859,1095(a,b,c,d),1215,1216 and all sections on Economic merit, Set Partition analytics, Pseudorandom generators, Computational Geometric Factorization, Money Changing Problem - Frobenius Coin Diophantines, Computational Theory of Value, Poverty Alleviation, Neuro Cryptocurrency implementations in AstroInfer and KingCobra, Optimal Denominations, Computational Economics - Computational Hardness (Labour) Theory of Value, Histogram and Set Partition analytics, Equidepth-Equiheight Histograms, Separate Chaining Hashtables, Timeout gadgets (RefCounted Expirable C++ objects, KingCobra atomic refcounting and Survival Index Timeout) in NeuronRain, Digital Watermarking, Drone Electronic Voting Machines, Numeric Compression by Prime power encoding - Unique Factorization Domain, Multiplicative Partitions, Compressed Sensing (Succinct representation), Large Scale Visuals, Cybercrime analytics  
-----

1217.1 Neuro Cryptocurrency Mining Rig in Streaming\_SetPartitionAnalytics.py has been augmented to print a visual Neuro currency which is digitally signed by Digital Watermarking OpenCV2 overlay of Neuro currency symbol (single strikethrough-N) and name.

1217.2 Digital Watermark is a configurable image in testlogs/NeuroCurrencyWatermark.jpg (contains Neuro name and symbol). Blank cleanslate currency template is stored in testlogs/NeuroCurrencyTemplate.jpg.



Neuro cryptocurrency mint proof of work, a combination of Random Integer Partition + Lagrange Sum-of-squares Partition-to-Rectangular Area Reduction and Factorization + Money Changing Problem (BPP pseudorandom choice of an integer partition from SymPy, MRC or NC factorization of Lagrange Sum-of-squares Integer Partition-to-Rectangular Area Reduction, NP-Complete solutions to two Money Changing Problem Frobenius Coin Diophantine Integer Linear Programs equated to factor sides of the rectangle - and thus effectively a non-trivial pipeline of BPP + MRC-NC + NP) computes the factor sides of the rectangle equal to value of Neuro cryptocurrency and solves two ILPs.

1217.3 All factors of the integer factorized (= value of Neuro cryptocurrency mined) are concatenated and encrypted to SHA256 cryptographic hash as UUID of the currency - Currency value and SHA256 UUID are written to testlogs/NeuroCryptoCurrency.jpg based on template testlogs/NeuroCurrencyTemplate.jpg by OpenCV2 putText(). 2 leading "ff"s requirement as non-trivial Proof of Work in a pseudorandomly chosen Boost UUID is thus relaxed theoretically by uniqueness of integer factorization into multiplicative partition of prime powers (Factorisatio Numerorum) which has been already implemented in NeuronRain Grafit in the context of compressed succinct storage of a huge integer. Euclidean Semiprimes could be an apt choice as currency values as they could be factored into 2 primes and solved for 2 Money Changing ILPs.

1217.4 Visual Neuro Currency object testlogs/NeuroCryptoCurrency.jpg thus dynamically printed is watermarked by testlogs/NeuroCurrencyWatermark.jpg and written to testlogs/NeuroCryptoCurrency.jpg\_Watermarked.jpg by watermark\_image() function of DigitalWatermarking.py implementation in NeuronRain Grafit. An example Neuro Visual Currency Note of value 100 and SHA256 UUID watermarked by Neuro symbol and name backdrop is unveiled at testlogs/NeuroCryptoCurrency.jpg\_Watermarked.jpg.

1217.5 Proof of work computation earlier has been captured in testlogs/Streaming\_SetPartitionAnalytics.NeuroCryptocurrencyWatermarking.log.15February2022. Some commented code on EVM analytics has been uncommented to regenerate JSON persisted Drone EVMS -

testlogs/Streaming\_SetPartitionAnalytics.EVMS.json

1217.6 Expirable C++ Objects which could be timed out or expired by reference counting have been implemented in NeuronRain AstroInfer cpp-src/expirable/ and described theoretically in Conceptual Survival Index Timeout WCET OS Scheduler and KingCobra Message-As-Currency Atomic transactional Refcounting (over cloud) within KingCobra linux kernel driver. Refcounting is a bidirectional logical clocktick for objects oscillated by increment and decrement - objects are garbage collected by reaper when refcount is 0. C++ expirable objects which were meant originally for limiting number of views of an Image object (e.g a photo sent over email self-destructs after constant number of views, a privacy feature most sought after), could be suitably used for Visual Cryptocurrency sent over networks as add-on security to limit the transactions involving a currency ID.

1217.7 Neuro Cryptocurrency mining rigs theoretically demonstrated earlier try to equate value of a currency in terms of Hardness of computation and simulated value of a commodity which is producible by similar real-life hardness and are potential poverty eradication tools.

#### References:

-----  
1217.8 Computer Science Handbook - [Allen Tucker] - Second edition - <https://e-maxx.ru/bookz/files/tucker.pdf> - Section 6.2.1 - Five fundamental problems in theory of computation - (Wang Tiling) Tiling a square by multicolored square tiles, String compression (Undecidability of Kolomogorov complexity or automating compression is undecidable - e.g. Kepler's law as compression scheme for Tycho Brahe's astronomical data) - Theorem 6.3 - Every pattern language is context sensitive (or) acceptable by a Turing machine in linear space - [Angluin] - Aside: Pattern languages are highly relevant in archaeological script decipherment as any undeciphered script is a pattern language which needs to be substituted by a suitable contextual string in known language, a theoretical formalism of decipherment problem - example: pattern language {xx | x in [0,1]\*} is neither acceptable by DFA or PDA but only LBA [Linear Bounded Automata accepting Context-Sensitive Grammar].

1217.9 Prime powers encoding - <http://www.cwi.nl/~paulv/papers/book.ps> - [Li-Vitanyi] - An introduction to Kolmogorov Complexity and its Applications: Preface to the First Edition (1997) - Example 1.1.2 - An integer  $n$  in unique factorization exponents form of first  $m$  prime numbers, can be encoded in  $m \cdot \log \log(n)$  bits -  $\log \log(n)$  bits per prime exponent.

-----  
1218. (THEORY and FEATURE) Music Synthesizer - Python 3.8 upgrade and Fractal implementation - 21 February 2022 - related to 3,298,642,643,644,659,681,1124 and all sections on Intrinsic Merit of Music, MIR(Music Information Retrieval), Music Similarity and Clustering, AI Music Synthesis, fMRI connectomes - OpenNeuro - Psychology of music, Weighted automata, Chaos, Deep Learning, Timeseries analysis, Physique recognition and Motion capturing algorithms, SETH  
-----

-----  
1218.1 Music Synthesizer in python-src/music\_pattern\_mining/AudioToBitMatrix.py (from Functions, Automata and Randomness) has been enhanced to generate music notes waveform from a fractal dataset. It has also been upgraded to Python 3.8 by 2to3 and autopep8.

1218.2 Function notes\_to\_audio() has been updated to include additional boolean argument for enabling fractal waveform and a clause for computing the chaotic Mandelbrot set (Real only) from a logistic function. Samplerate and Amplitude for the waveform have been set accordingly for loading .wav file in Audacity. Fractal set of notes is grown within a loop of eval() by feedback.

1218.3 Fractal music waveform is written to separate .wav file - function\_synthesized\_music\_fractal.wav. Scaled notes are cast to NumPy int16.

1218.4 Amplitude is multiplied by array of notes by NumPy Array broadcast throughout for all types of music synthesis - function, fractal, automata and randomness. Music waveform has been sufficiently amplified now and audible in Audacity. Waveform could be loaded in Audacity and analyzed visually by zooming the track.

1218.5 Three invocations of music synthesizer below respectively generate music from a quadratic equation, sinusoid and a Fractal Verhulste-Pearl-Reed(VPR) logistic function :

```
notes_to_audio(function='(x*x+x+1) % 32767',fractal=False)
notes_to_audio(function='int(math.sin(x*x+x+1) * 32767)',fractal=False)
notes_to_audio(function='5*(x*x-x) % 32767')
```

1218.6 Following are logs and music waveforms synthesized from finite state automaton, function, randomness and fractals:

```
automaton_synthesized_music.wav
function_synthesized_music.wav
notes_synthesized_music.wav
function_synthesized_music_fractal.wav
testlogs/AudioToBitMatrix.log.MusicSynthesizer.21February2022
```

1218.7 Similarity between two music waveforms is often computed by Dynamic Time Warping Algorithm, a monotonically increasing match of indices from first sequence to those in second sequence, and by Longest Common Subsequence algorithm. There is no subquadratic algorithm for Dynamic Time Warping unless SETH is False.

References:

-----  
1218.8 Deep Learning MIR - <https://ccrma.stanford.edu/workshops/deepmir-2017>  
1218.9 DeepMIR 2017 Workshop material - <https://github.com/bmcfree/stanford-mir>  
1218.10 Dynamic Time Warping for Timeseries Audio-Visual data - match of motion capture sequences for Physique recognition - [https://en.wikipedia.org/wiki/Dynamic\\_time\\_warping#/media/File:Two\\_repetitions\\_of\\_a\\_walking\\_sequence\\_of\\_an\\_individual\\_recorded\\_using\\_a\\_motion-capture\\_system.gif](https://en.wikipedia.org/wiki/Dynamic_time_warping#/media/File:Two_repetitions_of_a_walking_sequence_of_an_individual_recorded_using_a_motion-capture_system.gif)  
1218.11 OpenAI Music Generator from NeuralNets - JukeBox - <https://openai.com/blog/jukebox/>  
-----

1219. (THEORY and FEATURE) Music similarity - Dynamic Time Warping Waveform Distance algorithm implementation - 23 February 2022 - related to 815,1218 and all sections on Intrinsic merit of music, Novelty Detection - Original Music Score, Music clustering, Merit of audio-visuals, Physique recognition, Timeseries analysis - Stock quote tickers-Granger causality, Computer Graphics - Trimesh-Quadmesh Deformations, Face Recognition, Multiple Sequence Alignment, Graphical Event Models

-----

1219.1 AudioToBitMatrix.py has been updated to define a new function `dynamic_time_warping()` implementing Dynamic Time Warping (DTW) Timeseries sequence similarity algorithm that could find use as broad-spectrum routine across whole gamut of sequence similarity analytics - stock quote timeseries, trimesh-quadmesh sequences of human physiques from motion captures of CCTV footages, DNA multiple sequence alignment, string matching - longest common subsequence among others. Granger causality (timeseries of stockA causing timeseries of another stockB separated by time duration) between two stock quote time series could be found by DTW similarity across timelines and Graphical Event Model of stocks could be established.

1219.2 Reference pseudocode from [https://en.wikipedia.org/wiki/Dynamic\\_time\\_warping](https://en.wikipedia.org/wiki/Dynamic_time_warping) has been translated to NumPy Python 3.8 function `dynamic_time_warping()` - in a nutshell this function grows a dynamic programming memoization tableau and populates it by cost minimization function:

```
 dtw[i, j] = cost + min([dtw[i-1, j], dtw[i, j-1], dtw[i-1, j-1]])
```

1219.3 Two example audio clips -

`./testlogs/JSBach_Musicological_Offering.mp4`,  
`./testlogs/AudioGraphExample_SpeechRecognition_2019-07-09-103018.wav` have been compared by Dynamic Time Warping and logs are available at `python-src/music_pattern_mining/testlogs/AudioToBitMatrix.log.DynamicTimeWarping.23February2022`

1219.4 Function `audio_distance()` has been changed to include a clause and boolean flag argument for enabling dynamic time warping.

1219.5 Earlier audio clips have been curtailed to 0.01 duration each as `np.array()` from `librosa` returned notes are memory hogging (requires few GBs). DTW is a music clustering distance metric quite apt to define creativity and original music score - pattern or style in one's own work and dissimilarity to the rest - a foremost prerequisite for Novelty Detection.

References:

-----

1219.6 Using Dynamic Time Warping to Find Patterns in Time Series - [Donald J. Bemdt, James Clifford, Information Systems Department, Stern School of Business] - <https://www.aaai.org/Papers/Workshops/1994/WS-94-03/WS94-03-031.pdf>

1219.7 Real-time full-body human gender recognition in (RGB)-D data - <https://www.semanticscholar.org/paper/Real-time-full-body-human-gender-recognition-in-Linder-Wehner/2c8743089d9c7df04883405a31b5fbe494f175b4>

-----

1220. (THEORY and FEATURE) Music Information Retrieval (MIR) - Learning a polynomial from music waveform - 25 February 2022 - related to 3,298,642,643,644,659,681,1124,1218,1219 and all sections on Merit of Music - MIR, Novelty Detection - Original Music Score, Music clustering, Dynamic Time Warping, Timeseries analysis, AI Music Synthesis, Weighted Automata Learning from Music waveform notes

-----

1220.1 Function `audio_to_notes()` in `AudioToBitMatrix.py` has been updated to learn a degree 5 polynomial from raw music waveform timeseries returned by `librosa`. `NumPy polyfit()` is invoked on the music waveform notes array to fit a degree 5 polynomial.

1220.2 Theoretically distance between 2 music waveform timeseries found by Dynamic Time Warping and inner product distance between polynomials of 2 music

waveforms f and g -  $\langle f, g \rangle = \text{DefiniteIntegral}(f(x)g(x)dx)$  must coincide or be proportional. Novelty or Originality or Similarity of a music score is therefore quantified algebraically though somewhat superficial ignoring the graph structure found by Weighted Automata.

1220.3 Exception in hertz to note function - librosa.hz\_to\_note() - of librosa has been handled.

1220.4 Following 3 instrumental MP4 music clips of different genres (MP3 files have been upgraded to MP4 as librosa fails to load MP3) - Orient and Western classical - JS Bach and S Balachander in Veena (Amritavarshini) - have been fit to music waveform polynomials and printed to testlogs/AudioToBitMatrix.log.PolyFit.25February2022:

```
notes1 =
audio_to_notes("testlogs/JSBach_Musicological_Offering.mp4", dur=20)
notes2 = audio_to_notes("testlogs/054-SBC-Aanandhamridhakarshini.mp4",
dur=20)
```

```
notes3 = audio_to_notes("testlogs/Bach_Flute_Sonata_EFlat.mp4", dur=20)
```

1220.5 Following are the coefficients of the degree 5 polynomials learnt for clips earlier in order:

polynomial learnt from raw audio-music waveform: [ 1.86408187e-29 - 2.44250264e-23 1.12197649e-17 -2.12257382e-12 1.52604679e-07 2.37511803e-03]

polynomial learnt from raw audio-music waveform: [ 3.26195558e-31 - 3.39615870e-25 1.33295412e-19 -2.28165048e-14 1.22378846e-09 -6.05635122e-05]

polynomial learnt from raw audio-music waveform: [-9.67130004e-32 2.01499959e-26 3.51124576e-20 -1.43713102e-14 1.59537748e-09 -4.41037145e-05]

1220.6 Novelty Detection or Originality of a Music Score is quantifiable by clustering of music waveforms either by Dynamic Time Warping distances among them or inner product distances of Quintic degree 5 polynomials learnt from music waveforms earlier. Style/Touch/Creative Genius of a composer is the extent of clustering observed in one's own work and how much of an outlier it is from the rest.

-----  
1221. (THEORY and FEATURE) Fictitious Neuro Cryptocurrency NP-Hard Proof of Work - Moving Mount Fuji - Single Bin Sorted LIFO Histogram - Towers of Hanoi - implementation - 28 February 2022 - related to 112,113,114,488,751,784,785,787,791,841,848,859,1095(a,b,c,d),1209,1215,1216,1217 and all sections on Economic merit, Set Partition analytics, Pseudorandom generators, Computational Geometric Factorization, Money Changing Problem - Frobenius Coin Diophantines, Computational Theory of Value, Poverty Alleviation, Neuro Cryptocurrency implementations in AstroInfer and KingCobra, Optimal Denominations, Computational Economics - Computational Hardness (Labour) Theory of Value, Histogram and Set Partition analytics, Equidepth-Equiheight Histograms, Separate Chaining Hashtables, Timeout gadgets (RefCounted Expirable C++ objects, KingCobra atomic refcounting and Survival Index Timeout) in NeuronRain, Digital Watermarking, Drone Electronic Voting Machines, Numeric Compression by Prime power encoding - Unique Factorization Domain, Multiplicative Partitions, Compressed Sensing (Succinct representation), Large Scale Visuals, Cybercrime analytics, Russian Peasant's Linear Complexity Multiplication Algorithm, K Dimensional Trees, Computer Graphics, Collatz Conjecture, Mandelbrot sets, Earth Mover Distance, Graphical Event Models and Stock Timeseries, AI Music Synthesis  
-----

1221.1 Streaming\_SetPartitionAnalytics.py has been changed to define a new function single\_bin\_sorted\_LIFO\_histogram\_ToH() for computing all order preserving moves of a single bin sorted LIFO histogram (a k-d tree or mountain sliced to horizontal disks in 3 dimensions) as Neuro Cryptocurrency Rig Proof of Work - Towers of Hanoi (or Towers of Brahma) - which is NP-Hard (not NP-Complete as no NP algorithm for Towers of Hanoi problem has been found yet).

1221.2 Set Partitions to Lagrange Sum of Squares Tile Cover of a Rectangle reduction + Computational Geometric Factorization + Money Changing Problem-Integer Linear Programming Proof of Work implementation earlier is NP-Complete and its hardness is subject to  $P \neq NP$  while NP-Hard class is independent of  $P$  !

= NP and universally present as even undecidable problems are NP-Hard (Halting problem).

1221.3 Function `single_bin_sorted_LIFO_histogram_ToH()` internally invokes `print_Towers_of_Hanoi()` routine recursively for  $n$  disks and 3 bins (source, destination and intermediary) and computes Earth mover distance between those triples after every move. Earth mover distance triples and 3 Towers are printed to logs

`testlogs/Streaming_SetPartitionAnalytics.TowersOfHanoi.NeuroProofOfWork.28February2022` after computing pairwise `wasserstein_distance()` triples for all  $O(2^n)$  moves.

1221.4 Towers of Hanoi algorithm is based on following pseudocode 2-part recursion for moving top  $n-1$  disks from source  $x$  to destination  $z$  and source  $z$  to destination  $y$  having  $y$  and  $x$  as intermediaries respectively:

`single_bin_sorted_LIFO_histogram_ToH(n-1,x,z,y)`

`single_bin_sorted_LIFO_histogram_ToH(n-1,z,y,x)`

1221.5 Earth Mover Distance Triples printed sinusoidally fluctuate and always end in 0 exhibiting Collatz sequence behavior and are thus simulators for many naturally arising timeseries Graphical Event Model sequences - bidirectional object refcounting clockticks, Stock quote tickers et al. Stock quote timeseries influenced by high frequency algorithmic trading and manual trading platforms have been simulated by multifractals, Mandelbrot sets, Irrational exuberance and Bounded rationality. Undecidability of Mandelbrot sets implies prediction of market volatility is intractable. Towers of Hanoi and Earth Mover Distance are personifications for any human labour involving mass movement and formalize hardness in terms of simulated labour. Rhythmic ebb and tide of Towers of Hanoi EMD sequence makes it a candidate music waveform for AI Music Synthesis and the undulating histograms printed in intermediate steps are corresponding spectrograms of it. Following are the set of EMD triples for last few Towers of Hanoi POW computation steps grepped from

`testlogs/Streaming_SetPartitionAnalytics.TowersOfHanoi.NeuroProofOfWork.28February2022` ending in (0,0,0) for 3 towers:

Pairwise ToH Earth Mover Distance Triple: (4.166666666666667, 2.0, 3.166666666666667)

Pairwise ToH Earth Mover Distance Triple: (5.5, 2.5, 3.0)

Pairwise ToH Earth Mover Distance Triple: (5.000000000000001, 0, 0)

Pairwise ToH Earth Mover Distance Triple: (4.5, 2.0, 6.5)

Pairwise ToH Earth Mover Distance Triple: (3.5, 2.5, 5.714285714285714)

Pairwise ToH Earth Mover Distance Triple: (3.25, 0, 0)

Pairwise ToH Earth Mover Distance Triple: (3.25, 1.0, 3.75)

Pairwise ToH Earth Mover Distance Triple: (4.214285714285714, 1.5, 4.000000000000001)

Pairwise ToH Earth Mover Distance Triple: (5.0, 1.0, 5.0)

Pairwise ToH Earth Mover Distance Triple: (3.5, 2.0, 5.5)

Pairwise ToH Earth Mover Distance Triple: (0, 0, 5.000000000000001)

Pairwise ToH Earth Mover Distance Triple: (0, 0, 4.0)

Pairwise ToH Earth Mover Distance Triple: (4.5, 1.0, 3.75)

Pairwise ToH Earth Mover Distance Triple: (5.5, 1.5, 4.000000000000001)

Pairwise ToH Earth Mover Distance Triple: (5.0, 0, 0)

Pairwise ToH Earth Mover Distance Triple: (4.5, 1.0, 5.5)

Pairwise ToH Earth Mover Distance Triple: (0, 0, 5.0)

Pairwise ToH Earth Mover Distance Triple: (0, 0, 0)

1221.6 Function `single_bin_sorted_LIFO_histogram_ToH()` prints a digital-watermarked Visual Neuro currency after completion of Towers of Hanoi proof of work. Following are the Neuro currency visuals for an example denomination:

`testlogs/NeuroCryptoCurrency.jpg`

`testlogs/NeuroCryptoCurrency.jpg_Watermarked.jpg`

References:

-----  
1221.7 Towers of Hanoi - Datastructures, Algorithms and Applications in Java - [Sartaj Sahni] - Page 320-324

1221.8 Irrational Exuberance - [Greenspan] -

<https://www.federalreserve.gov/boarddocs/speeches/1996/19961205.htm>

1221.9 Irrational Exuberance - Dataset for the book -

-----  
1223. (THEORY and FEATURE) Music Information Retrieval - AI Music Synthesis from Sum of Damped Sinusoids - 4 March 2022 - related to 3,298,642,643,644,659,681,827,829,1124,1144,1189,1218,1219,1220 and all sections on Merit of Music - MIR, Novelty Detection - Original Music Score, Music clustering, Dynamic Time Warping, Timeseries analysis, AI Music Synthesis, Weighted Automata Learning from Music waveform notes, Speech Synthesis, Fourier analysis, ProofNets, Girard Geometry of Interaction, Logic, Intrinsic merit of academic publications - Bibliometrics, Embedding music on vectorspace, Shell Turing Machines and Kernel Lifting, People Analytics-Unique identification  
-----

-----  
1223.1 notes\_to\_audio() function in AudioToBitMatrix.py has been changed to synthesize notes from python 3.8 lambda expression and map() instead of a list comprehension earlier.  
1223.2 Lambda expression for any mathematical function is repetitively evaluated within a loop and notes are appended to get an onset-to-onset periodic music waveform timeseries.  
1223.3 There has been sufficient publication prior art analyzing feasibility of speech synthesis from summation of damped sinusoid waveforms for simulating human utterances of syllables. Damped Sinusoid summation has been implemented for music synthesis equivalent in this commit. In a sense, summation of damped sinusoids is the Time domain converse of Fourier spectrum decomposition of music waveform into set of frequencies in Frequency domain.  
1223.4 notes\_to\_audio() synthesizer is invoked for a sum of damped sinusoids and an instrumental music waveform simulating thunderbolt has been composed (function\_synthesized\_music.wav):

```
notes_to_audio(function='((np.iinfo(np.int16).max/(1+x))*math.sin(2*3.1428/720*x) + (np.iinfo(np.int16).max/(1+x))*math.sin(2*3.1428/1240*x) + (np.iinfo(np.int16).max/(1+x))*math.sin(2*3.1428/2400*x))', fractal=False)
```

corresponding to sum of three damped oscillator waveform frequencies of the form  $a/(b + x) \cdot \sin(2\pi x/c)$

1223.5 Earlier summation combines 3 damped sinusoids of frequencies 720,1240 and 2400 Hz into a natural rhythmic music. Music waveforms (especially orient) have a distinct periodic damping feature (notable difference could be visually felt by loading testlogs/054-SBC-Aanandhamridhakarshini.mp4 and testlogs/Bach\_Flute\_Sonata\_EFlat.mp4 in Audacity - former has an intriguingly self-similar periodic damped sinusoidal structure)

1223.6 There have been raging debates on credibility of music synthesis and an orthodox view avers that music cannot be invented but could only be discovered (a notion strikingly similar to "Straight from the Book" of Erdos - Theorems are not invented but only discovered). As a trivia, Permutation of heptatonic scale allows only 5040 waveforms of enjoyable music (7!) discarding major,minor,flat,sharp variants.

1223.7 Analogous to Music Synthesis earlier, Merit of Academic Publications (Bibliometrics) concerns analysis and originality of Theorems and results proved thereof based on the fact that every theorem could be visualized as a graph of logical implications amongst pairs of logical statements (premise to QED) known as Girard Geometry of Interaction-ProofNets (Long Trip operator criterion) formalisms. If every theorem is constrained by maximum number of logical statements it can contain, number of all possible theorems that can ever be proved is upperbounded and finite (upholding Erdos' Straight from the book). On the contrary, there need not be any logical implication relation (but dependence of a note on previous notes can't be ruled out per se) between any two successive music notes in waveform unlike ProofNet GoIs of Theorems (or) Theorem is a music waveform of logical statements fortified by logical implications. All possible music melody waveforms have been already created (1223.14) and out in the open forcing the notion of "Creativity" in Music to be redefined as "Music search or Music discovery" as against "Music synthesis" - genius might have to be measured by ability to search from the catalogue of all possible music (68

billion of them for 12-note scale) than inventing afresh. More rigorous formulation of Music discovery could be the vector embedding of 68 billion melodies on an m-dimensional space of 12-note scale similar to alphabet-syllable vectorspace embedding of texts (each of the 12 notes are the alphabets for music waveform string) and performing Geometric search within it quite on the lines of Word2Vec embedding of texts. Music waveforms based on 7-note heptatonic octave scale (CDEFGABC) thus constitute a subspace of 12-note melody space of 68 billion waveforms (finer subdivisions of notes do a kernel lifting of the music from 7-note to 12-note shell space). English texts are embedded in an m-dimensional space of size  $(26)^m$  for maximum length m string - 68 billion 12-note melodies are likewise embedded in an m dimensional space of size  $(12)^m$  for maximum m length music notes waveform. Most albums are in the range of 5 minutes thereby upperbounding m to ~300 for 1 note per second - 7-note melodies are  $7^m$  in number forming a subset of 12-note melodies.

1223.8 Unique identification of a digital artefact (music or art) by Non Fungible Tokens (NFT) assigned on a Cryptocurrency global hyperledger presents a new avenue for dispute-free unique identification adding to conventional face recognition, fingerprint recognition, fullbody recognition, handwriting recognition, gender recognition because non-fungibility implies non-exchangeability of an entity by a duplicate thereby ruling out forgery - watercolor art testlogs/ExamplePortrait1.jpg analyzed in NeuronRain face recognition could be a Non-Fungible Token on KingCobra Neuro HyperLedger, for example, preferably maintained on a Global Reference Count framework (Berkeley Ray).

#### References:

- 
- 1223.9 Speech Synthesis from Damped Sinusoids - [https://www.researchgate.net/publication/11189786\\_Speech\\_Synthesis\\_Using\\_Damped\\_Sinusoids](https://www.researchgate.net/publication/11189786_Speech_Synthesis_Using_Damped_Sinusoids) - Figure 2. Synthesizing a short segment of a sustained /A/ by summing exponentially damped sinusoids at frequencies corresponding to F1, F2, and F3 and by pulsing the damped sinusoids at onset-to-onset intervals corresponding to the fundamental period
- 1223.10 Graphic illustration of Damped Sinusoids - <https://www.desmos.com/calculator/hcamzyeujj>
- 1223.11 The Man who loved only numbers - [Hoffman] - <https://archive.nytimes.com/www.nytimes.com/books/first/h/hoffman-man.html?pagewanted=all>
- 1223.12 Damped Sinusoids - Exponential damp version - [https://en.wikipedia.org/wiki/Damping#Damped\\_sine\\_wave](https://en.wikipedia.org/wiki/Damping#Damped_sine_wave) - Earlier synthesis is based on fractional damp
- 1223.13 Non Fungible Tokens (NFT) and the 68 billion melody algorithm: The beginning of the end of copyright as we know it - There are only 68 billion 12-note melodies (anecdotal evidence for 1223.6) and as digital assets could be protected by a Non-Fungible Token on a Cryptocurrency blockchain - <https://www.dailymaverick.co.za/article/2021-11-03-non-fungible-tokens-and-the-68-billion-melody-algorithm-the-beginning-of-the-end-of-copyright-as-we-know-it/> - "... "No song is new... (we) have exhausted the data set... (we) have made all the music to be able to allow future songwriters to make all of their music." These remarkable words appear in a magazine article. They are the words of two lawyers who claim to have created an algorithm that can create, and allegedly has created, every single 12-note melody that has been written or indeed can ever be written. The creation of this algorithm is premised on the assumption that there is a finite number of melodies that can exist – the lawyers talk of the fact that songwriters are "walking on a melodic minefield". So how many melodies are there? It's 68 billion, and they're apparently all available on allthemusic.info. But the two lawyers are not claiming any ownership, rather they're releasing the entire catalogue in the hope that it will put an end to all music copyright lawsuits..."
- 1223.14 All The Music - <http://allthemusic.info/> , <https://github.com/allthemusicllc/atm-cli> - Catalogue of All Possible Music MIDI for averting Music Copyright Infringement
- 1223.15 Ethereum NFT - <https://ethereum.org/en/nft/>
- 1223.16 12 Note Chromatic Scale -

[https://en.wikipedia.org/wiki/Chromatic\\_scale#/media/File:Pitch\\_class\\_space.svg](https://en.wikipedia.org/wiki/Chromatic_scale#/media/File:Pitch_class_space.svg)  
1223.17 Linear Logic, ProofNets, Geometry of Interaction, Curry-Howard Isomorphism (Logic  $\Leftrightarrow$  Programming Language), New ways of representing proofs -  
<https://plato.stanford.edu/entries/logic-linear/> - "... Intuitionistic and constructive logic began when people saw the possibility of reading ' $A \Rightarrow B$ ' as 'if you give me an A, I will give you a B', which is a significant departure from the classical reading 'A is false or B is true'... Linear logic provides a further twist in the interpretation of the implication ' $A \Rightarrow B$ ': now it can be read as 'give me as many A's as I might need and I will give you one B'... For linear logic, this succinct representation of proofs is given by proof nets, graph-like structures that enjoy particularly good properties for the MLL fragment of the logic. The first step towards this representation is to convert all the sequent calculus system, using the involutivity of negation, into a one-sided system, where sequents are of the form  $\vdash \Gamma$ ... the first correctness criterion for MLL proof nets, called the "long trip criterion", and present in Girard's original paper, is exponential, as well as the ACC (Acyclic connected) criterion of Danos and Regnier..."

1223.18 New Foundations of Geometry of Interaction - [Samson Abramsky - Radha Jagadeesan] - <https://www.cs.ox.ac.uk/people/samson.abramsky/nfgoi.ps.gz>

1223.19 Rankings of Academic Institutions by Bibliometrics and Research - Bradford Law - [https://en.wikipedia.org/wiki/Bradford%27s\\_law](https://en.wikipedia.org/wiki/Bradford%27s_law) - "... if journals in a field are sorted by number of articles into three groups, each with about one-third of all articles, then the number of journals in each group will be proportional to  $1:n:n^2$  ... " - Information scattering phenomenon of few sources having many information and many sources having few information (or) Pareto distribution of information - NIRF 2022 rankings example (Bradford's law and Spearman Rank correlation of Overall rank versus Research) - <https://www.nirfindia.org/nirfpdfcdn/2022/flipbook/index.html>

-----  
1224. (THEORY and FEATURE) Music Information Retrieval - AI Music Synthesis from Sum of Damped Sinusoids - 8 March 2022 - related to 3,298,642,643,644,659,681,1124,1218,1219,1223 and all sections on Merit of Music - MIR, Novelty Detection - Original Music Score, Music clustering, Dynamic Time Warping, Timeseries analysis, AI Music Synthesis, Weighted Automata Learning from Music waveform notes, Speech Synthesis, Fourier analysis  
-----

1224.1 Some additional audacity music waveform files (.aup and .au) synthesised by AudioToBitMatrix.py from periodic mathematical functions have been added to repositories - simulate an instrumental music  
-----

1225. (THEORY and FEATURE) GIS Urban Sprawl Analytics - SEDAC Urban Expansion Probabilities Projection for Year 2030 - a case study of urban sprawls - 8 March 2022 - related to 675,753,1174,1175,1177,1179,1194,1211,1212 and all sections on GIS Urban Sprawl Analytics, Merit of Large Scale Visuals, Gridded Population Estimators (SEDAC GPW4 and GHSL convex hull estimators), DBSCAN and Neural Network Urban Extent Learners, Computational Geometry, Intrinsic Merit Rankings, R Ricker Population Estimation, Community detection, Social Network Analytics, Space filling by Curves, Unequal Circle and Polynomial packing, Computational Geometry and Polygonal packing by Voronoi Tessellation, Four color theorem, Economic Merit, Computational Economics - GDP estimation from electricity consumption, Jordan Curve Theorem, Weierstrass Theorem, Cellular Automata, Preferential attachment, Random Graphs, Dynamic Graphs  
-----

1225.1 GISUrbanSprawlAnalytics.py has been updated to compute Voronoi tessellation facegraph, Delaunay triangulation, convex hull, contour segments and minimum enclosing circles of SEDAC Urban Expansion Probabilities Projection for Year 2030 (Southern India) - SEDAC2030UrbanExpansionProbabilities.jpg - which is a cellular automaton square grid raster of urban extent expansion probabilities



in year 2030 proportionately coded by color legend.

1225.2 Color legend is of size 100 for SEDAC Urban Expansion 2030 GIS and ranges from light to dark corresponding to 0% to 100% probabilities of urban expansion. For this reason, default grading legend averageBGR/255 \* 100000 (e.g Barcelona in section 1211) has been used to compute population density.

1225.3 As mentioned in Section 1177, Urban Sprawl Expansion is the dynamic graph growing problem of adding new faces (or composing ears to create new faces) to Urban sprawl facegraph perimeter, a graph theoretic version of preferential attachment. Voronoi-Delaunay Facegraph of SEDAC Urban Expansion Probabilities Projection for Year 2030 computed earlier is a random graph wherein each ear or face is added to the periphery of an urban sprawl with probability assigned by color legend of the grid. Conventional Dynamic Graphs allow dynamic add-delete of vertices and edges while Urban Sprawl Expansion by face-ear composition along the circumference is an one-way Dynamic Graph and irreversible - only addition of edges and vertices are allowed and face of a suburb and its vertices-edges can't be deleted from an expanded urban sprawl.

1225.4 Most Urban area expansions in South India example previously have been colored in the probability range of 50% (plus or minus) and a projected emergence of megalopolises in 2030 is conspicuous in coastal urban areas of TN (tremendous westward and southward expansion of Chennai Metropolitan Sprawl upto Vellore-Puducherry and gradual coalescence of Puducherry urban sprawl-Cauvery river delta urban sprawl which could be another pearl river delta in the making) and entire west coast of Kerala.

1225.5 In terms of realestate, Light shaded colors might indicate a horizontal residential growth while dark shaded regions might witness a vertical growth of skyscrapers.

1225.6 Following are the images (contours, segments, convex hull, facegraph, Voronoi-Delaunay tessellation, minimum enclosing circles of UAs) and logs for this commit:

testlogs/GISUrbanSprawlAnalytics.log.8March2022

testlogs/RemoteSensingGIS/SEDAC2030UrbanExpansionProbabilities\_FaceGraph.jpg

testlogs/RemoteSensingGIS/SEDAC2030UrbanExpansionProbabilities\_ImageNet\_Keras\_Th  
eano\_Segmentation\_FaceGraph.dot

testlogs/RemoteSensingGIS/SEDAC2030UrbanExpansionProbabilities\_contour\_segmented  
.jpg

testlogs/RemoteSensingGIS/SEDAC2030UrbanExpansionProbabilities\_convex\_hull\_segme  
nted.jpg

testlogs/RemoteSensingGIS/SEDAC2030UrbanExpansionProbabilities\_segmented.jpg

testlogs/SEDAC2030UrbanExpansionProbabilities-contourlabelled.jpg

testlogs/SEDAC2030UrbanExpansionProbabilities.jpg

References:

-----  
1225.7 NASA SEDAC Global Grid of Probabilities of Urban Expansion to 2030, v1 (2000-2030) - <https://sedac.ciesin.columbia.edu/data/set/lulc-global-grid-prob-urban-expansion-2030>

1225.8 Dynamic Graphs - [Harary-Gupta] - <https://www.sciencedirect.com/science/article/pii/S0895717797000502>

1225.9 High-resolution global urban growth projection based on multiple applications of the SLEUTH urban growth model - <https://www.ncbi.nlm.nih.gov/pmc/articles/PMC6472366/> - Various Urban Growth Projection Models including Cellular Automata, SLEUTH

-----  
1226. (THEORY and FEATURE) GIS Urban Sprawl Analytics - Maximum Population Density and Area-Population Ratio as arguments - 12,13,14,15  
March 2022 - related to

135,675,753,760,1150,1174,1175,1177,1179,1194,1211,1212,1225 and all sections on

GIS Urban Sprawl Analytics, Merit of Large Scale Visuals, Gridded Population Estimators (SEDAC GPW4 and GHSL convex hull estimators), DBSCAN and Neural Network Urban Extent Learners, Computational Geometry, Intrinsic Merit Rankings, R Ricker Population Estimation, Community detection, Social Network Analytics, Space filling by Curves, Unequal Circle and Polynomial packing, Computational Geometry and Polygonal packing by Voronoi Tessellation, Four color theorem, Economic Merit, Computational Economics - GDP estimation from electricity consumption, Jordan Curve Theorem, Weirstrass Theorem, Cellular Automata-SLEUTH Urban Growth Models, Preferential attachment, Random Graphs, Dynamic Graphs, NeuronRain CoronaVirus 2019 analyzer (R and Python - GEM, R Logit, Chaotic ERSIR Cellular Automaton Graph), Chaos, Central Limit Theorem, Cybercrime analytics, Ramsey Theory, Integer and Real Factorization

-----

1226.1 GISUrbanSprawlAnalytics.py has been refactored to simplify population density computation clauses - with legend and without legend (or if color coding legend range is huge, proportionate scaling of population density by pixel color is inevitable) - by removing hardcoded values for maximum population density (~100000) and urban sprawl to population ratio heuristic (~6.22) and replacing them by function arguments to urban\_sprawl\_from\_segments() - maximum\_population\_density and sqkmareatopopulationratio

1226.2 NASA SEDAC 2030 Urban Sprawl Expansion GIS projection in previous section has been reanalyzed for a fictitious maximum population density of 100000 and urban sprawl to population ratio heuristic of 6.22. There are no changes to contour-segment-convex hull visuals - logs of recomputed population estimates are at

python-src/image\_pattern\_mining/ImageNet/testlogs/GISUrbanSprawlAnalytics.log.15 March2022.

1226.3 NeuronRain UGM (Urban Growth Model) is based on One Way Dynamic Graph upward growth of an Urban Sprawl FaceGraph by attaching faces (or composing ears as counter magnets) along its circumference, a generalization of widely used Cellular Automaton square grid expansion models (SLEUTH) to arbitrary shape cells - Cellular automata UGMs expand by adding square faces to periphery of an urban sprawl CA grid while NeuronRain Dynamic FaceGraph Urban Growth Model expands by annexing faces of arbitrary shapes to periphery of urban extent.

1226.4 High Population Density faces along the boundaries and interiors of an urban sprawl FaceGraph are most likely to expand in future to adjoining and new peripheral faces. Parallel Algorithm for Cellular Automaton Fluid Dynamics in 135 is of uncanny similarity to CA Urban Growth Models - Fluid dynamics is replaced by Population dynamics - how population from high density cells (square faces) migrate towards low density cells (square faces) in parallel (either at random or influenced by UGM factors of 1226.8) is a generic CA abstraction underlying most of the parallel natural random processes including a fluid spreading from elevation to lowlying finally levelling the field. One of the most obvious factors influencing urban growth and expansion is Road gravity (or Transportation network gravity for multimodal transit) which is the real urban sprawl equivalent of intrinsic fitness of a social profile vertex (degree charisma of a social profile) in virtual online social networks - ability of a metropolitan agglomeration in attracting population settlements aligned to transportation network.

1226.5 Cellular Automaton Urban Growth Models are exactly instances of CAGraph model of Pandemics/Memes/Opinions/Fads/Cybercrimes in Social and Electronic networks - each face of CAGraph is a square.

1226.6 Cellular Automata Grid of Square cells of an urban sprawl is a minimum bounding box rectangle of area (in contrast to minimum enclosing circle of an urban sprawl) equal to urban sprawl contour area extent sides of which are found by factorization (integer or real). While a real factorization of urban area into sides of a square is trivial by square root algorithm, integer factorization of an urban contour area into sides of an almost-square is non-trivial (a semiprime factorization of almost equal factor pairs). E.g factorization of an area 105 as  $105=15*7$  is less rectangular than  $105=3*35$  as ratio of the factors is closer to 1 in the former. Following algorithm finds an almost-square factorization of an integer:

1226.6.1 Find square root (real) of an integer N by Newton-Raphson

algorithm rounded off to nearest integer

1226.6.2 Compute Planar factor point location around the vicinity of  $\sqrt{N}$  by binary search-interpolation search on rasterized hyperbolic arc pixel array polygon segments - Number theoretic ray shooting query approximate factor estimates implemented in NeuronRain could further narrow down the search range and the factor point  $N=pq$  -  $(p,q)$  - closest to square root is of factor ratio  $(p/q)$  nearest to 1 which is the required bounding almost-square rectangle. Set partition to (Lagrange Sum of 4 squares) square tile cover reduction by an almost-square rectangle of sides obtained from Almost-square factorization algorithm earlier is the best possible square tile packing of an almost-square.

1226.7 Minimum enclosing circle of an urban area is trivially a variant of real square root algorithm - urban sprawl is enclosed in a circle of radius =  $\sqrt{\text{contour\_area} / 3.1428}$ .

1226.8 Transportation network gravity factor of Urban Growth Model is inversely proportional to areas of faces in transportation graph (each face is bounded by multimodal transit intersections):- Population settlements naturally gravitate and align to boundaries of face quadrilaterals of multimodal transportation network graph and as area of faces in transportation graph increase, distances between arterial multimodal transport intersection edges of faces widen discouraging settlements within the central regions of faces (low diffusion factor). Four colored urban sprawl facegraph of a metropolis could be approximated by faces of urban sprawl multimodal transportation graph. On the other hand, urban growth is often proportional to extent of vertical settlements (number of highrises), a variant of slope factor, often caused by horizontal space crunch.

#### References:

-----

1226.9 Project Gigalopolis - SiliconGraphics C implementation of SLEUTH Cellular Automata Urban Growth Model - <http://www.ncgia.ucsb.edu/projects/gig/index.html> - Clarke's UGM - Methods And Techniques for Rigorous Calibration of a Cellular Automaton Model of Urban Growth - [http://www.ncgia.ucsb.edu/projects/gig/Pub/SLEUTHPapers\\_Nov24/Clarke\\_Hoppen\\_Gaydos\\_1996.pdf](http://www.ncgia.ucsb.edu/projects/gig/Pub/SLEUTHPapers_Nov24/Clarke_Hoppen_Gaydos_1996.pdf) - Five Factors controlling urban expansion and Four types of urban expansion - "... Five factors control the behavior of the system. These are: a diffusion factor, which determines the overall outward dispersiveness of the distribution; a breed coefficient, which specifies how likely a newly generated detached settlement is to begin its own growth cycle; a spread coefficient, which controls how much organic expansion occurs from existing settlements, a slope resistance factor, which influences the likelihood of settlement extending up steeper slopes; and a road gravity factor which attracts new settlements toward and along roads. These values, which affect the acceptance level of randomly drawn numbers, are set by the user for every model run. Four types of growth are defined in the model: spontaneous, diffusive, organic, and road influenced growth. Spontaneous growth occurs when a randomly chosen cell falls nearby an already urbanized cell, simulating the influence urban areas have on their surroundings. Diffusive growth permits the urbanization of cells which are flat enough to be desirable locations for development, even if they do not lie near an already established urban area. Organic growth spreads outward from existing urban centers, representing the tendency of cities to expand. Road influenced growth encourages urbanized cells to develop along the transportation network replicating increased accessibility ... "

1226.10 LandScan dataset - Global Urban Population Distribution GIS - <https://landscan.ornl.gov/>

1226.11 Metropolitan area population density rankings - there is no concurrence between multiple rankings over maximum population density - <http://www.demographia.com/db-worldua.pdf>, [https://en.wikipedia.org/wiki/List\\_of\\_world\\_cities\\_by\\_population\\_density](https://en.wikipedia.org/wiki/List_of_world_cities_by_population_density), <https://www.usatoday.com/story/news/world/2019/07/11/the-50-most-densely-populated-cities-in-the-world/39664259/> - ranges widely between ~75000 to ~200000 per sqkm.

1226.12 Population Rankings of Urban Areas in Indian Subcontinent (Year 1958) - Oxford School Atlas of India, Pakistan, Burma, Ceylon - [John Bartholomew] - Oxford University Press, 1958 edition - <https://lccn.loc.gov/map62000528>

1226.13 Comparison of Urban Growth Modeling Using Deep Belief and Neural Network Based Cellular Automata Model—A Case Study of Chennai Metropolitan Area, Tamil Nadu, India - [Aishwarya Devendran Aarthi, Lakshmanan Gnanappazham\*] - Department of Earth and Space Sciences, Indian Institute of Space Science and Technology, Trivandrum, India - <https://www.scirp.org/journal/paperinformation.aspx?paperid=90031>

1226.14 Wallace-Bolyai-Gerwein Theorem - [http://www.cut-the-knot.org/do\\_you\\_know/Bolyai.shtml](http://www.cut-the-knot.org/do_you_know/Bolyai.shtml) - Any two simple polygons of equal area are equidecomposable (or) can be dissected into finite number of congruent polygonal pieces - convex hull polygonal area of an urban sprawl contour and rectangular bounding box of the urban sprawl of same area found by almost-square factorization are equidecomposable.

1226.15 Tarski Circle Squaring problem - [https://en.wikipedia.org/wiki/Tarski%27s\\_circle-squaring\\_problem](https://en.wikipedia.org/wiki/Tarski%27s_circle-squaring_problem) - task of cutting a circle into finitely many pieces and reassemble them to form a square of same area (while Squaring a circle - for a circle draw a square of same area by straightedge and compass - is impossible) - Proved in 1990 by Laczkovich using Measure theory, Axiom of Choice (AOC) and number of pieces are  $10^{50}$  - in the context of minimum enclosing circle of an urban sprawl, Tarski squaring of the minimum enclosing bounding circle to get an exact square bounding box of same area is feasible, as against almost-square.

1226.16 Dissection of Polygons into Rectangles - <https://11011110.github.io/blog/2022/04/03/dissection-into-rectangles.html>

1226.17 Polya Urn Model - Rich get Richer - Preferential attachment in urban sprawls - [https://en.wikipedia.org/wiki/P%C3%B3lya\\_urn\\_model](https://en.wikipedia.org/wiki/P%C3%B3lya_urn_model) - By considering 4-colored urban sprawls as an Urn of 4 colored balls, urban growth could be simulated by Polya Urn UGM(Urban Growth Model) - a ball (segment) is chosen from Urn at random, its color is noted, and another ball of same color is added to the Urn thus simulating a randomized Urban Sprawl Growth equivalent of Cellular Automata based UGMs.

1226.18 Shelley's Defence of Poetry - [https://en.wikipedia.org/wiki/Percy\\_Bysshe\\_Shelley](https://en.wikipedia.org/wiki/Percy_Bysshe_Shelley) - Rich get Richer and Poor get poorer - [https://en.wikipedia.org/wiki/The\\_rich\\_get\\_richer\\_and\\_the\\_poor\\_get\\_poorer](https://en.wikipedia.org/wiki/The_rich_get_richer_and_the_poor_get_poorer) - "...To him that hath, more shall be given; and from him that hath not, the little that he hath shall be taken away. The rich have become richer, and the poor have become poorer; and the vessel of the State is driven between the Scylla and Charybdis of anarchy and despotism..."

1226.19 Automatic Delineation of Urban Growth Boundaries Based on Topographic Data Using Germany as a Case Study - <https://www.mdpi.com/2220-9964/10/5/353/pdf> - Minimum Spanning Tree algorithm for Urban Sprawl Delineation versus Manual Expert Delineation

-----

1227. (THEORY and FEATURE) Set Partition Analytics - Neuro Cryptocurrency Towers of Hanoi NP-Hard Proof-of-Work - Set Partition Histogram to Lagrange Sum of Four Square theorem square tile cover of an Almost-Square rectangle by Integer Factorization - 24 March 2022 - related to 1213,1215,1217,1221,1226 and all sections on Set Partitions and Histogram Analytics, Merit of Large Scale Visuals, GIS Urban Sprawl Analytics - minimum rectangular bounding box of an urban sprawl, Computational Geometric Integer Factorization, Neuro Cryptocurrency Proof-Of-Work Hardness, Economic Merit, Poverty Alleviation, Money Changing Problem, Integer Linear Programming, Pell Diophantine for Factorization

-----

1227.1 Streaming\_SetPartitionAnalytics.py has been changed to compute an almost-square factorization of an integer by maximizing the ratio of sides of a rectangle (making it closest to 1) in Set Partition to Lagrange Sum of 4 Square Theorem square tile cover of a rectangle by Computational Geometric Integer Factorization

1227.2 Sides of almost-square rectangle are found assuming zero-knowledge of real square root by following algorithm:

1227.2.1 List of all factors of an integral area found by Computational

Geometric Binary Search Planar Point location Factorization are sorted and split into two equal halves

1227.2.2 Approximate square root integer factor pairs are located on either side of factors-list midpoint - (\*) first element of second half (\*) last element of the first half.

1227.2.3 Earlier factors array midpoint heuristic obviates real square root computation, rounding it off and searching the vicinity of rounded-off real square root in finding almost-square factor pairs, which in essence is a zero-knowledge integer approximation of real square root - approximate square root could be found by solving Pell diophantine form of factorization as:

$$(\text{approximate\_square\_root} + x) * (\text{approximate\_square\_root} - x) = 25 * 9 = 225$$

$$\text{approximate\_square\_root}^2 = 34$$

$$\text{approximate\_square\_root} = 17$$

$$x^2 = 16$$

$$x = 8$$

$$(\text{or}) (17 + 8)(17 - 8) = 25 * 9 = 225$$

1227.3 An example integral rectangular area of 225 is factorized to an almost-square rectangle of sides 9 and 25 and two ILPs for those sides are solved by GLPK. In Urban Sprawl Analytics jargon, almost-square factorization of 225 corresponds to an optimal sized bounding rectangle box of an urban sprawl of area 225 sprawling geographically by orthogonal extents 25 and 9.

1227.4 Logs for ILP solutions to Square tile cover of rectangle area  $25 * 9 = 225$  are at testlogs/Streaming\_SetPartitionAnalytics.AlmostSquare.log.24March2022. Sorted list of factors are: ('factorslist:', [225, 75, 45, 25, 9, 5, 3, 1])) and sides of almost-square rectangle 25 and 9 flank the midpoint of the list at locations 4 and 5.

1227.5 Towers of Hanoi Single Bin Sorted LIFO Histogram NP-Hard Proof-of-Work for Neuro Cryptocurrency has been recomputed to rewrite the Digital watermarked Neuro Visual Currency - decimal denomination 1024.0 has been cast to integer  $2^{10} = 1024$ . Powers of 2 Neuro Cryptocurrency Proof-of-Work requires logarithmic number of variable denominations for Optimal Money Change of arbitrary valued Neuro buy-sell transaction (binary notation of value = Optimal money change) different from usual 1-2-5 series denominations which are of constant denomination size 3 though coefficients of Money Changing Diophantines would arbitrarily vary.

1227.6 A counterintuitive oddity (or blessing) of Cryptocurrency mint is its ability to create unlimited wealth out of thin air by cryptocurrency rigs solving POW algorithms which might have, otherwise, no associated real life economic importance unless Proof-Of-Work Hardness is commodity-linked by a simulation of Labour involved in producing a commodity from scratch (there seems to be no standard theory available to link commodities to cryptocurrencies and decide their exchange rates with conventional currencies - a gross disconnect with value). Crypto mining rigs expend few Terawatts of electricity per annum in minting hashcash and cost of energy consumed by rigs could be an indirect measure of value, dollar exchange rates and buying power. Notwithstanding aforesaid deficit, state attested cryptocurrency rigs might aid poverty alleviation by periodically awarding units of cryptocurrencies to underprivileged - a guaranteed universal basic income mechanism akin to direct benefit transfers (DBT) experimented in emerging economies.

1227.7 Following are recomputed Neuro Digital Watermarked Visual currency images, factors and a JSON for fictitious voting on 3 Set partition EVMs:

DiscreteHyperbolicFactorizationUpperbound\_TileSearch\_Optimized.factors

testlogs/NeuroCryptoCurrency.jpg

testlogs/NeuroCryptoCurrency.jpg\_Watermarked.jpg

testlogs/Streaming\_SetPartitionAnalytics.EVMs.json

References:

-----  
1227.8 Integer Square Root - new isqrt() function in Python 3.8 - <https://docs.python.org/3/library/math.html#math.isqrt>

1227.9 Integer Square Root - [https://en.wikipedia.org/wiki/Integer\\_square\\_root](https://en.wikipedia.org/wiki/Integer_square_root)

1227.10 Square roots by subtraction - Jarvis algorithm - <http://www.afjarvis.staff.shef.ac.uk/maths/jarvisspec02.pdf>

-----  
-----  
1228. (THEORY and FEATURE) Kernel lift random walk in tree of TOP Category Shell Turing Machines and UNIX Shell Game Example - 28 March 2022 - related to 624,651,728 and all sections on Shell Turing Machines, MRDP Theorem, Category Theory, Diophantine Equations, Turing Degrees, Embedding Formal Languages in Vector Space, Kernel lifting - Set Partition (1D) to Tile Cover (2D) Reduction by Computational Geometric Factorization, Exact Money Changing Problem(MCP) Solution, Quadratic Programs, Pell Equation, Shell Turing Machines(TOP-Category of Topological Spaces), Unix Shell Implementations of Category of Topological Spaces, Turing Degrees, Turing Jump, Hilbert Space Turing Machines,Chinese Remaindering  
-----  
-----

1228.1 Nested Shells of Category of Topological Spaces (TOP) could be schematically visualized as a tree of shell topological spaces (binary tree or k-dimensional trees depending on how many subshells are nested within a supershell).

1228.2 An earlier formulation of nested topological spaces in 624 was based on Partial Order Semi Lattice dimensional hierarchy of Shell Turing Machines having Least Upper Bound dimensional Shell defined on Topological spaces (e.g Hilbert Space Turing Machines,Reproducing Kernel Hilbert Space of computable functions). As a partial order does not guarantee a shell space to be a unique subspace of a superspace, a simplified tree nesting alternative of shell TOP spaces and kernel lift random walk in its interior is herein discussed.

1228.3 Turing Degree is a measure of unsolvability of a set or an equivalence class of Turing Machines solving sets of similar hardness. Turing Jump of a Turing Machine X is the set of Turing Machines X' having oracle access to X or X' is the set of problems harder than X solvable by oracle access to X.

1228.4 Turing Degree of Shell Turing Machines increases from leaves to root in Tree model of Nested Shell Turing Machines - computational power of shell Turing Machines and hardness of set they solve evolve gradually from leaves to root as a result of higher visibility of logical truths available in TOP space vertices bottom-to-top. Random Kernel lifting (upwards and downwards) of logical truths within lower dimensional shells to-and-from higher dimensional shells (and viceversa) close to root is a graph random walk traversal of Tree of TOP Shell spaces. Root shell is omniscient and there is nothing to lift upwards beyond root.

1228.5 Every interior vertex of Shell TOP space tree defines a space of logical statements embedded on vectorspace of some dimension and Turing Jump is indirectly defined by considering the lower dimensional TOP space children C(X) of an interior shell TOP space vertex X as oracles (or) X has oracle access to C(X) by Conduit Morphism Turing Machines which internally export-import logical statements between spaces of X and C(X).

1228.6 Arbitrarily traversing the tree of Shell TOP categories from leaves to root by kernel lift (upwards and downwards) of logical statements between pair of subshell and supershell vertices could be a random walk on the tree of TOP spaces. Estimating expected time to reach root shell from a leaf shell by kernel lifting is non-trivial and such a random walk could be exponential -  $O(k^n)$  for n-level nesting and k-dimensional tree.

1228.7 Earlier Random walk traversal within a TOP Category of Topological spaces could be exemplified by a hypothetical UNIX Shell Tree Game below:

1228.7.1 Intialize Root Shell

1228.7.2 while (number of iterations < maximum)

{

(\*) Randomly create k subshells in parallel within each

existing shell

(\*) Within each shell define some environment variables

visible only within that shell (simulates logical truths known only within the shell space)

}

1228.7.3 while (number of iterations < maximum)

{

(\*) Turing Jump: Randomly EXPORT-IMPORT environment variables

(kernel lifting random walk of logical statements  
 across spaces) to-and-from pairs of supershells and subshells  
 (Most unix implementations support only EXPORT of  
 variables) within the TOP Shell space tree created in  
 1228.7.2. Direction of kernel lift (up or down) at each  
 shell space vertex is decided by pseudorandom coin toss  
 (EXPORT or IMPORT) - this process draws a random walk  
 kernel lift streak from leaf shells to root shell.

}

1228.8 Previous Shell Game terminates when all kernel lift (EXPORT-IMPORT)  
 random walks reach root UNIX shell from leaf UNIX shells and truth values of all  
 logical statements (environment variables) are visible within entire tree (In  
 1228.7.2 visibility of logical truths was restricted to individual shell TOP  
 space vertices). It is obvious that there are random walks which may not end in  
 root shell (because of perpetually oscillating kernel up-down lifts with in  
 Shell TOP tree) causing the Turing machine computing the Shell Game to loop  
 forever - Shell Game is undecidable and recursively enumerable.

1228.9 Kernel lifting in NeuronRain Theory Drafts are mostly devoted to 1-  
 dimensional to 2-dimensional lift by Lagrange Four Square Theorem and 1-  
 dimensional to k-dimensional lift by Chinese Remaindering Theorem (by a ring  
 isomorphism between a ring of integer  $X \bmod N = n_1 * n_2 * \dots * n_k$  and direct product  
 space of coprime integer rings  $X \bmod n_1, X \bmod n_2, \dots, X \bmod n_k$ ):

$$\mathbb{Z}/N\mathbb{Z} \iff \mathbb{Z}/n_1\mathbb{Z} * \mathbb{Z}/n_2\mathbb{Z} * \dots * \mathbb{Z}/n_k\mathbb{Z}$$

1228.10 By MRDP Theorem Every Recursively Enumerable Set is Diophantine and  
 earlier shell Turing Machine tree of TOP spaces defined by Turing Jump could be  
 mapped to a corresponding tree of diophantines for the respective shell Turing  
 Machine vertices.

-----  
 1229. (THEORY and FEATURE) Intrinsic Merit of Texts - TAC 2010 code opensourced  
 - 29 March 2022 - related to 9,36 and all sections on  
 Intrinsic Merit Ranking of Texts, Update Summarization, Topic Detection and  
 Tracking, Interview Algorithm, Citation Graph Maxflow-Mincut,  
 Meaning Representation  
 -----

1229.1 An almost 12-13 years old archaic python code (sequential) for  
 publications and PPTs - ArXiv and NIST TAC 2010, US Department of Commerce -  
[https://github.com/shrinivaasanka/Krishna\\_iResearch\\_DoxygenDocs/blob/master/kuja27\\_website\\_mirrored/site/kuja27/PresentationTAC2010.pdf](https://github.com/shrinivaasanka/Krishna_iResearch_DoxygenDocs/blob/master/kuja27_website_mirrored/site/kuja27/PresentationTAC2010.pdf),  
<http://arxiv.org/abs/1006.4458>,  
[https://tac.nist.gov/publications/2010/participant.papers/CMI\\_IIT.proceedings.pdf](https://tac.nist.gov/publications/2010/participant.papers/CMI_IIT.proceedings.pdf) - has been opensourced (which was originally intended to be part of JAIMINI  
 closedsource private repositories - <https://github.com/Brihaspathi/jaimini>,  
<https://sourceforge.net/projects/jaimini/> and  
<https://gitlab.com/shrinivaasanka/jaimini> ) including TAC2010 dataset logs.  
 1229.2 An expanded, sophisticated, parallel (PySpark) implementation of  
 Interview Algorithm and Recursive Gloss Overlap algorithm and its improved  
 formal language version - Recursive Lambda Function Growth algorithm for Meaning  
 Representation - are already part of NeuronRain AstroInfer repositories.  
 1229.3 Disclaimer: Because of mistaken identity issues, it is hereby clarified  
 author did not participate in Text Analysis Conference (TAC 2010), November 15  
 and 16, 2010, Gaithersburg, Maryland, USA in person despite invitation.

-----  
 1232. (THEORY and FEATURE) GMSH Trimesh and Quadmesh - GEO OPT and MSH files  
 from GMSH FLTK - 4 April 2022 - related to 1203 and all sections on Merit of  
 Large Scale Visuals, Physique Recognition From Quadrilateral mesh  
 isomorphism, Topological Face and Handwriting recognition, Product Homotopy,  
 Unique identification, Homeomorphism and Topological Deformations, Merit of  
 Large Scale Visuals, People Analytics, Computational Geometry, Graph Edit  
 Distance and Earth mover distance, Graph Isomorphism (Exact, Approximate and

Subgraph), Graph matching, Graph similarity, Image Search, Quadrilateral Mesh Deformation and Isomorphism, Maximum Common Subgraph Problem and Approximate Topological Matching

---

1232.1 Converting Delaunay Triangulation Mesh to Quadrilateral mesh is crucial for Face and Physique Recognition by Approximate Topological Matching (Maximum Common Subgraph Problem) of quadmeshes generated from 2 human visuals.

1232.2 GMSH is a 3D FEM (Finite Element Model) library for trimesh and quadmesh generation. MSH (3D trimesh) and GEO OPT files generated by GMSH FLTK GUI for wildlife visual

python-src/image\_pattern\_mining/ImageNet/testlogs/3Ducks\_VID\_20220119\_173052.mp4 Frame\_1.jpg have been added to repositories.

1232.3 GMSH trimesh MSH file earlier could be converted to quadmesh either by gmsch commandline - <https://gitlab.onelab.info/gmsch/gmsch/-/issues/784> (Converting an existing triangle-element mesh into a quad-element mesh) or through python code snippet which loads the trimesh and computes quadmesh by Recombination algorithm API - `gmsch.model.mesh.recombine()`

#### References:

1232.4 GMSH - <https://gmsch.info/>

1232.5 CALFEM -

[https://calfem-for-python.readthedocs.io/en/latest/calfem\\_mesh\\_guide.html](https://calfem-for-python.readthedocs.io/en/latest/calfem_mesh_guide.html)

---

1233. (THEORY and FEATURE) Merit of Large Scale Visuals - Trimesh and Quadmesh generation from an image by GMSH - 11 April 2022 - related to 1203, 1232 and all sections on Merit of Large Scale Visuals, Physique Recognition From Quadrilateral mesh isomorphism, Topological Face and Handwriting recognition, Product Homotopy, Unique identification, Homeomorphism and Topological Deformations, Merit of Large Scale Visuals, People Analytics, Computational Geometry, Graph Edit Distance and Earth mover distance, Graph Isomorphism (Exact, Approximate and Subgraph), Graph matching, Graph similarity, Image Search, Quadrilateral Mesh Deformation and Isomorphism, Maximum Common Subgraph Problem and Approximate Topological Matching

---

1233.1 This commit implements Trimesh and Quadmesh generation from a facial image by loading GEO file for an image in GMSH FLTK GUI and GMSH Python API.

1233.2 GMSH GEO has a separate scripting convention and an example CG GMSH GEO script from <https://people.montefiore.uliege.be/geuzaine/> for mesh generation by different algorithms (Delaunay Trimesh and Quadmesh) has been suitably changed (TriMeshToQuadMesh.geo) to load a watercolor art by author (a Lenna Digital Image Processing lookalike - <http://www.lenna.org/> - testlogs/ExamplePortrait2.jpg - dt.1990). TriMeshToQuadMesh.geo has to be opened in GMSH FLTK GUI (commandline: `gmsch TriMeshToQuadMesh.geo 2>&1 >` testlogs/gmsch.TriMeshToQuadMesh.geo.log.11April2022) and executed by selecting options for trimesh generation (saved to TriMeshToQuadMesh.msh) and recombination algorithm for converting trimesh to quadmesh (example logs: testlogs/gmsch.TriMeshToQuadMesh.geo.log.11April2022) which is written to testlogs/ExamplePortrait2\_mesh.jpg.

1233.3 Alternatively, TriMeshToQuadMesh.msh trimesh generated in 1233.2 could be recombined to quadmesh by Python script TriMeshToQuadMesh.py (example python gmsch recombination: <https://gitlab.onelab.info/gmsch/gmsch/-/issues/784>)

commandline: `python3.7 TriMeshToQuadMesh.py 2>&1 >`

testlogs/python3.7.TriMeshToQuadMesh.log.11April2022 (example logs:

testlogs/python3.7.TriMeshToQuadMesh.log.11April2022)

1233.4 Following are the affected files (Database, GEO, MSH, Python, JPEG and logs) in this commit:

- TriMeshToQuadMesh.db
- TriMeshToQuadMesh.geo
- TriMeshToQuadMesh.msh



TriMeshToQuadMesh.py  
testlogs/ExamplePortrait2.jpg  
testlogs/ExamplePortrait2\_mesh.jpg  
testlogs/gmsh.TriMeshToQuadMesh.geo.log.11April2022  
testlogs/python3.7.TriMeshToQuadMesh.log.11April2022

1233.5 Quadmesh obtained earlier from GMSH might have to be a Graph object (and instantiation of Graph from Mesh is not obvious in GMSH which might have to be inferred from getNodes() and getElements() API) so as to compute isomorphisms, maximum common subgraphs and approximate topological matching between mesh(s) of faces and physiques. Physique Recognition could also be realized by Dynamic Time Warping analysis of Stream of Quadmesh(s) computed from frames of a video (CCTV footages).

#### References:

-----  
1233.6 GMSH - [Prof. Christophe Geuzaine] -  
<https://people.montefiore.uliege.be/geuzaine/>  
1233.7 GMSH Python API -  
[https://gitlab.onelab.info/gmsh/gmsh/blob/gmsh\\_4\\_9\\_5/api/gmsh.py](https://gitlab.onelab.info/gmsh/gmsh/blob/gmsh_4_9_5/api/gmsh.py)  
1233.8 Dynamic Time Warping models for Physique Recognition - Simultaneous inference for misaligned multivariate functional data -  
<https://arxiv.org/pdf/1606.03295.pdf>  
-----

-----  
1234. (THEORY and FEATURE) GIS Urban Sprawl Analytics - Polya Urn Urban Growth Model implementation for 4-colored Urban Sprawl Contour Segment Facegraphs - 15 April 2022 - related to related to 135,675,753,760,1150,1174,1175,1177,1179,1194,1211,1212,1225,1226 and all sections on GIS Urban Sprawl Analytics, Merit of Large Scale Visuals, Gridded Population Estimators (SEDAC GPW4 and GHSL convex hull estimators), DBSCAN and Neural Network Urban Extent Learners, Computational Geometry, Intrinsic Merit Rankings, R Ricker Population Estimation, Community detection, Social Network Analytics, Space filling by Curves, Unequal Circle and Polynomial packing, Computational Geometry and Polygonal packing by Voronoi Tessellation, Four color theorem, Economic Merit, Computational Economics - GDP estimation from electricity consumption, Jordan Curve Theorem, Weierstrass Theorem, Cellular Automata-SLEUTH Urban Growth Models, Preferential attachment, Random Graphs, Dynamic Graphs, Separate Chaining Hash tables  
-----

-----  
1234.1 This update defines a new function `polya_urn_urban_growth_model()` in `GISUrbanSprawlAnalytics.py` for implementing Polya Urn Urban Growth Model algorithm mentioned in 1226.17 (4-colored contour segmented Urban Sprawl FaceGraph segments as balls), as an alternative to Oneway Dynamic Facegraph growth outwards along perimeter of Urban sprawls (ear composition of new faces on circumference). Polya Urn model is conceptually equivalent to cellular automata growth models but different in how population (segments) evolution growth rules are stipulated.

1234.2 Function `polya_urn_urban_growth_model()` populates a defaultdict map of 4 keys-to-buckets by randomly choosing one of the 4 color bucket indices and appends a segment from watershed contour segments of an Urban sprawl GIS to respective colored bucket. Another loop iteratively churns out random color indices of buckets and random indices of bucket elements to choose a random segment which is replicated and appended to bucket of same color.

1234.3 Polya Urn has been implemented on a defaultdict(list) which is a separate chained hashtable, a drastic departure from conventional homogeneous blackbox urn having multicolored balls from which a colored ball is sampled and replaced with duplication.

1234.4 Though Polya Urn model has been presently restricted to Urban Growth Models, its usage has far reaching implications cutting across any heterogeneous dataset e.g Survival Index WCET OS Scheduler described in NeuronRain Design is a Dynamic Polya Urn of processes colored by their clockticks and a randomly sampled processid from scheduler hashtable could be replaced by replication (or

a new process replacement by fork()).

1234.5 Contour segments of urban sprawls for NASA SEDAC Urban Expansion Probabilites 2030 GIS imagery have been encoded numerically prefixed by "s" and populated in Polya Urn defaultdict(list) separate chaining hashtable (printed to testlogs/GISUrbanSprawlAnalytics.log.15April2022).

1234.6 Polya Urn Growth of Urban sprawl segments simulates rich-get-richer paradigm in Urban sprawl preferential attachment wherein an already grown settlement is overloaded by transportation network gravity factor. Dynamic Facegraph Urban Growth Model and Polya Urn Urban Growth Model for Urban Sprawls could be merged into one UGM by attaching every replicated clone of a sampled segment (encoded by one of the 4 colors) to the periphery of Urban sprawl facegraphs than interiors (which is anyway impossible in 2-dimensions unless UGM is extended to 3-dimensions for both horizontal and vertical (skyscrapers) expansions). 3D UGM including Vertical expansion (average number of skyscrapers of n storeys) is quite crucial in estimating prosperity (GDP) of an urban sprawl:

Average number of skyscrapers above n-storeys in an urban sprawl =  
function\_of(Opportunities/Horizontal\_Area\_Of\_Urban\_Sprawl)

which in other words could be stated as:

Vertical expansion of urban sprawl is directly proportional to growth in Opportunities(Jobs,Industries,Electricity consumption estimated from VIIRS-NightLights) and inversely proportional to horizontal area induced by geographic limitations in horizontal expansion.

#### References:

-----  
1234.7 USGS Earth Explorer - eMODIS,MODIS,VIIRS NDVI and Land cover imagery -  
<https://earthexplorer.usgs.gov/>

1234.8 Building(s and) cities: Delineating urban areas with a machine learning algorithm - <https://www.sciencedirect.com/science/article/pii/S0094119019300944>  
- "... Here, we calculate the vertical land of the delineated urban areas as the footprint of the buildings (horizontal land) multiplied by the number of floors. Our results indicate that the vertical land multiplies by three the amount of developed land. This analysis of the vertical land provides a different perspective on city size (especially in the case of the a country's largest urban areas). ..."

-----  
1236. (THEORY and FEATURE) GIS Analytics - an archaeoastronomical and computer vision analysis of MODIS GIS image of Adam's Bridge (Ram Sethu) - 19 April 2022, 20 April 2022 - related to 2,18,714 and all sections on Merit of Large Scale Visuals, Text Restoration, Astronomical Datasets, Archaeology, Drone Urban Extent Imagery, Urban Sprawl Analytics, Dream analysis, Image search, Topological Script Recognition  
-----

1236.1 Application of Machine Learning to archaeology has been recently demonstrated by DeepMind Ithaca which restored 2500 year old Greek manuscript by predicting illegible words damaged and lost in antiquity with high accuracy.

1236.2 On similar lines, devising algorithms for deciphering ancient inscriptions (e.g. Voynich Manuscript, Scripts of Sarasvati-Indus Civilization) by artificial intelligence could be challenging open area of research. For example, Rebus principle which is the technique of code switching between scripts and pictures to express information, has been in vogue since time immemorial (example: word "height" is encoded by pictogram "h8" = "h" + "eight") - Cuneiform tablets, Hieroglyphs and ancient writing systems are pictograms of words and pictures to convey a coded message. Dreams have been interpreted by Rebus principle in Freudian psychology. Most undeciphered scripts contain a mixture of pictorial and script motifs (e.g Indus scripts) and a training data based machine learning algorithm might be less successful (as there are no prior unknown-to-known to train) compared to a rebus principle software implementation which sifts through the pictograms, performs a matching image search of the

motifs and maps to a meaningful natural language text. Product Homotopy based Topological handwriting recognition mentioned earlier in section 714 could be extended to Rebus Topological script recognition for decipherment of newly excavated inscriptions by an approximate topological match with already excavated scripts:

1236.2.1 Archaeology software implementing Rebus would hypothetically segment an image containing pictogram inscription yet to be deciphered, extract DP polynomials of contours in pictogram and find approximate topological match between known scripts and image motifs by Product homotopy-Pasting lemma pattern grammar which has already been implemented minimally in NeuronRain topological handwriting recognition (Directed Hausdorff distance between contours - clustering of close-enough contours of images-motifs-writings-scripts by Hausdorff distance defines a Product Homotopy)

1236.2.2 Additionally Rebus Topological Script Recognition would involve searching DP polynomials of script and image motif contours in a pre-defined database of deciphered image and script contours by various topological distance measures - it has to be pointed out that this database is not a training data but an expensive search space. For scripts differing by small deviations (Tamil Brahmi scripts in Keezhadi excavations differ only slightly from Indus Brahmi scripts - 1236.21) Dynamic Time Warping topological similarity could be useful considering segmented inscription-script images as timeseries waveforms or trimesh-quadmesh.

1236.2.3 Logo-syllabic scripts (logo or motif per syllable) are mostly Rebus decipherable. Thus indirectly Rebus Topological Script Recognition for archaeological decipherment is already implemented in NeuronRain.

1236.3 In this commit, a GIS image of Palk Straits and Adam's Bridge captured by NASA MODIS instrument in 2018 (250 metre resolution - NASA\_MODIS\_RamSethu\_Image07272018\_250m.jpg), which is legendarily attributed to Lord Rama, has been photoshopped and filtered by GIMP and contour segmented. An earlier image of Adam's Bridge by NASA in 2007 was subject matter of debate.

1236.4 Adam's Bridge or Ramsethu is perhaps the only available prima facie archaeological evidence for establishing historicity of Ramayana.

Differentiating man-made structures from natural terrains has long been investigated by large scale visual algorithms mostly in the context of Drone urban extent imagery analyzers for classification of settlements (1182.6).

1236.5 Proving if aforementioned MODIS image of Adam's Bridge is natural or manmade might require a sophisticated Ground Penetrating Radar (GPR) Remote Sensing going beyond aerial imagery for analysis of ocean floor and depth - scripture mentions the bridge has been built by woods and elephant-sized sandstones dragged by mechanised contrivances and only a GPR imagery might help in verifying if ocean floor has fossil remnants of wooden structures though studies have revealed heavy presence of sandstones. To compensate for lack of GPR original MODIS image has been enhanced by VFX filters (sharpening, anti-aliasing, contrast) to make graded depth of ocean more pronounced.

1236.6 Another curious aspect of Adam's Bridge is its curvature possibly caused by ocean currents, as a bridge is usually a straightline and scripture verses mention that monkey-men used ropes to ensure straightline alignment of the bridge.

1236.7 Contour segmented image

NASA\_MODIS\_RamSethu\_Image07272018\_250m\_contoursegmented\_20April2022.jpg has been color coded and colors might mostly be proportional to their depth (or elevation). Particularly the streak of shoals bridging international waters has been uniformly colored in blue. This is probably because of OpenCV implementations of Watershed algorithm for segmentation by pixel color depth and Teh-Chin Chain Approximation algorithm for contour detection which is based on dominant points detection (high curvature points).

1236.8 Following are the affected files (Facegraph DOT, segmented image, contour segmented image and logs). Graph plotting by draw\_networkx() has been commented and only DOT files are created because of slowdown:

```
testlogs/ImageGraph_Keras_Theano.log.20April2022
testlogs/NASA_MODIS_RamSethu_Image07272018_250m.jpg
```

testlogs/NASA\_MODIS\_RamSethu\_Image07272018\_250m\_contoursegmented\_20April2022.jpg

testlogs/RemoteSensingGIS/NASA\_MODIS\_RamSethu\_Image07272018\_250m\_ImageNet\_Keras\_Theano\_Segmentation\_FaceGraph.dot

testlogs/RemoteSensingGIS/NASA\_MODIS\_RamSethu\_Image07272018\_250m\_segmented.jpg

#### References:

-----

- 1236.9 NASA MODIS GIS Imagery of Palk Straits and Adam's Bridge - 2018 - [https://modis.gsfc.nasa.gov/gallery/images/image07272018\\_250m.jpg](https://modis.gsfc.nasa.gov/gallery/images/image07272018_250m.jpg) - "... A chain of islands and coral reef stretches across the southern end of the strait. Most often called Adam's Bridge, this feature is also called "the Bridge of Rama". Sacred to the Hindu religion, the bridge was said to be built by Lord Rama, who visited many towns in the region. The shoals are primarily limestone and the waters in this location are quite shallow - some data suggests the "bridge" may be the remnants of a true land bridge that once stretched between India and Sri Lanka.... On July 23, 2018, NASA's Aqua satellite passed over the Palk Strait, allowing the Moderate Resolution Imaging Spectroradiometer (MODIS) flying aboard to acquire a true-color image of the region...."
- 1236.10 Valmiki Ramayan - Construction of Ram Sethu in 5 days by 1000 crore monkey-men and materials used were Woods and Sandstones - Yuddha Kanda - Chapter 22 - Verses 58-71 - [https://www.valmikiramayan.net/utf8/yuddha/sarga22/yuddha\\_22\\_frame.htm](https://www.valmikiramayan.net/utf8/yuddha/sarga22/yuddha_22_frame.htm) - Verse 58 on mechanical contrivances - पूर्वतांश्च समुत्पाट्य यन्त्रैः परिवहन्ति चV - Verse 60 on strings binding the stones - समुद्रम् क्षोभयामासुनिपतन्तः समन्ततः || २-२२-६० सूत्राण्यन्ये प्रगृह्णन्ति ह्यायतम् शतयोजनम् |
- 1236.11 The deciphered Indus script : methodology, readings, interpretations / N. Jha and N.S. Rajaram. - [https://franklin.library.upenn.edu/catalog/FRANKLIN\\_9928639583503681](https://franklin.library.upenn.edu/catalog/FRANKLIN_9928639583503681)
- 1236.12 Voynich Manuscript - [https://en.wikipedia.org/wiki/Voynich\\_manuscript](https://en.wikipedia.org/wiki/Voynich_manuscript)
- 1236.13 Ground Penetrating Radar imageing in archaeology - [https://en.wikipedia.org/wiki/Ground-penetrating\\_radar#Archaeology](https://en.wikipedia.org/wiki/Ground-penetrating_radar#Archaeology)
- 1236.14 What On Earth - Discovery Science Channel - Documentary on Ram Sethu and Adam's Bridge - 2018 - Rocks predate sand - <https://twitter.com/sciencechannel/status/940259901166600194?lang=en>
- 1236.15 DeepMind Ithaca AI archaeology software - <https://www.smithsonianmag.com/smart-news/a-new-ai-can-help-historians-decipher-damaged-ancient-greek-texts-180979736/>
- 1236.16 Teh-Chin Chain Approximation Algorithm for contour detection (implemented in OpenCV) - Dominant point detection by points of high curvature - [Teh-Chin] - [https://web.archive.org/web/20160528025504id\\_/http://www-prima.inrialpes.fr:80/perso/Tran/IEEE-PAMI/1989/Teh89-PAMI.pdf](https://web.archive.org/web/20160528025504id_/http://www-prima.inrialpes.fr:80/perso/Tran/IEEE-PAMI/1989/Teh89-PAMI.pdf)
- 1236.17 Watershed segmentation algorithm (implemented in OpenCV) - graphics illustration - <https://people.cmm.minesparis.psl.eu/users/beucher/wtshed.html>
- 1236.18 Rebus principle in linguistics, archaeology and Freudian psychology of dreams - <https://en.wikipedia.org/wiki/Rebus>
- 1236.19 Indus Unicorn Seal - Metropolitan Museum of Art - [https://en.wikipedia.org/wiki/Indus\\_script#/media/File:Stamp\\_seal\\_and\\_modern\\_impression-unicorn\\_and\\_incense\\_burner\\_\(?\)\\_MET\\_DP23101\\_\(cropped\).jpg](https://en.wikipedia.org/wiki/Indus_script#/media/File:Stamp_seal_and_modern_impression-unicorn_and_incense_burner_(?)_MET_DP23101_(cropped).jpg)
- 1236.20 Dholavira sign board - Harappan civilization - <https://www.harappa.com/blog/dholavira-and-its-mysterious-sign-board> - Deciphered by Natwar Jha - Navaratna Rajaram as Vedic Sanskrit for "Sea has entered dwelling places"
- 1236.21 Keezhadi excavations - Tamil Brahmi script on Potsherds - <https://science.thewire.in/society/history/keeladi-settlement-tamil-nadu-department-of-archaeology-tamil-brahmi-script-indus-valley-civilisation/> - similarities of Keezhadi graffiti to Indus script - <https://www.thenewsminute.com/article/major-discovery-tamil-nadu-s-keezhadi-possible-link-indus-valley-civilisation-109165>
- 1236.22 Ground Penetrating Radar GIS - USGS - Fire Island, New York - [https://pubs.usgs.gov/ds/ds1078/ds1078\\_data-downloads.html](https://pubs.usgs.gov/ds/ds1078/ds1078_data-downloads.html)
- 1236.23 Ground Penetrating Radar GIS - <https://www.livescience.com/8657-underground-peep-show-reveals-artifacts-life.html> - "... Tucker, an earth scientist with NASA's Goddard Space Flight Center in Greenbelt, Md., and Joe Nigro, a geographic information systems (GIS) specialist and archaeologist

working at Goddard through Science Systems and Application Inc., are combining NASA satellite data and ground-penetrating radar (GPR) technology to map and protect the famed spot where Alexander the Great cut fabled King Midas' Gordian knot. ..."

1236.24 MIMOSA - Spaceborne Ground Penetrating Radar -  
<https://adsabs.harvard.edu/full/2000ESASP.450..645H>

1236.25 Keezhadi Brahmi Inscriptions - similarities to Indus script signs  
225,307,365,318,318 -<https://www.tamilnadutourism.com/blog/keeladi-excavation-a-revelation-that-rewrites-the-history-of-tamil-nadu/>

1236.26 Indus Script Concordance Table - [Iravatham Mahadevan] - ASI -  
<https://indianculture.gov.in/ebooks/indus-script-texts-concordance-and-tables>

1236.27 Ocean Floor Depth Imagery of Ramsethu - Google Maps - Terrametrics -  
[https://github.com/shrinivaasanka/asfer-github-code/blob/master/python-src/image\\_pattern\\_mining/ImageNet/testlogs/](https://github.com/shrinivaasanka/asfer-github-code/blob/master/python-src/image_pattern_mining/ImageNet/testlogs/)

RamSethuOceanFloorDepth\_GoogleMaps\_24May2022.pdf - existing structure of adam's bridge is situated on elevated ocean floor strip of few kilometres width along east coast possibly caused by sea level rise and coastal erosion. At present rate of sea erosion (0.5-2 metre/year) earlier land strip of approximately 45 kilometres to east could have been submerged in 22500-90000 years BCE implying a later origin of existing structure.

1236.28 Seabed 2030 GEBCO Gridded Bathymetry - ongoing mapping of ocean floor targeted for 2030 (only 20% of ocean floor has been mapped at present) - Depth relief of Ramsethu structure on elevated ocean floor strip along east coast of Indian ocean -

[https://github.com/shrinivaasanka/asfer-github-code/blob/b982be9496cc1a108858dc6db862d4b75872d463/python-src/image\\_pattern\\_mining/ImageNet/testlogs/](https://github.com/shrinivaasanka/asfer-github-code/blob/b982be9496cc1a108858dc6db862d4b75872d463/python-src/image_pattern_mining/ImageNet/testlogs/)

RamSethu\_GEBSCO\_Seabed2030\_25May2022.jpg from

[https://www.gebco.net/data\\_and\\_products/gridded\\_bathymetry\\_data/](https://www.gebco.net/data_and_products/gridded_bathymetry_data/) - pixel color coded ocean floor and land elevation (deep blue for deepest to deep red for highest through green for plains)

-----  
1237. (THEORY and FEATURE) Merit of Large Scale Visuals - Face recognition by Approximate Topological Match of GMSH Quadmesh images - 25,26 April 2022 - related to 1203,1232,1233,1236 and all sections on Merit of Large Scale Visuals, Physique Recognition From Quadrilateral mesh isomorphism, Topological Face and Handwriting recognition, Archaeology-Topological Script Recognition, Product Homotopy, Unique identification, Homeomorphism and Topological Deformations, Merit of Large Scale Visuals, People Analytics, Computational Geometry, Graph Edit Distance and Earth mover distance, Graph Isomorphism (Exact, Approximate and Subgraph), Graph matching, Graph similarity, Image Search, Quadrilateral Mesh Deformation and Isomorphism, Maximum Common Subgraph Problem and Approximate Topological Matching, Astronomical Datasets  
-----

1237.1 In this commit, an approximate topological match between two contour segmented GMSH quadmesh images of portraits -

python-src/testlogs/ExamplePortrait1.jpg and

python-src/image\_pattern\_mining/ImageNet/testlogs/ExamplePortrait2.jpg - has been computed by directed Hausdorff distance between set of DP polynomials of the two image contours.

1237.2 python-src/image\_pattern\_mining/ImageNet/TriMeshToQuadMesh.geo has been updated to write trimesh MSH file (TriMeshToQuadMesh.msh) for

python-src/testlogs/ExamplePortrait1.jpg by loading GEO file in GMSH FLTK GUI and option "save Mesh" - Mesh file TriMeshToQuadMesh.msh has been overwritten.

1237.3 TriMesh earlier is recombined to QuadMesh by python 3.7 script

TriMeshToQuadMesh.py through commandline - python3.7 TriMeshToQuadMesh.py 2>&1 > testlogs/python3.7.TriMeshToQuadMesh.log.25April2022 - and QuadMesh for

ExamplePortrait1.jpg is written to ExamplePortrait1\_mesh.jpg by Blossom-FullQuad Recombination algorithm (an FLTK GUI radio button option). Network HTML plot of Delaunay Trimesh has been made optional by boolean flag bezier\_animation set as False by default in DeepLearning\_ConvolutionNetwork\_BackPropagation.py face recognition routine.

1237.4 QuadMesh for ExamplePortrait2.jpg is already present in ExamplePortrait2\_mesh.jpg (created by 1233 earlier) which was obtained by Blossom Recombination.

1237.5 DeepLearning\_ConvolutionNetwork\_BackPropagation.py has been updated to add additional parameters `approximate_topological_match=True` and `match_fraction=0.000001` to `facegraph_similarity_metrics()` which is read within a new clause to compute approximate DP polynomials for some fraction of contours (set to 0.000001 by default because full image Hausdorff match - `match_fraction=1.0` - is computationally intensive as number of contours for all quadfaces is in order of thousands or almost equal to pixel area of the image as each quadface is a rectangular aggregate of few pixel squares) for quadfaces in two quadmeshes and find an approximate topological match by directed Hausdorff distance between sets of contours belonging to two portraits. Graph Isomorphism computation is excluded by this option and clause returns after topological match computation.

1237.6 Getting a Graph object from QuadMesh (mentioned in 1233.5) has been obviated by contour polynomials computation for every quadmesh face which indirectly encode the topology of the face. Contour segmented images of the two quadmesh(s) for ExamplePortrait1.jpg and ExamplePortrait2.jpg - `python-src/image_pattern_mining/ImageNet/testlogs/ExamplePortrait2_mesh_contours_egmented_25April2022.jpg` and `python-src/testlogs/ExamplePortrait1_mesh_contoursegmented_25April2022.jpg` - reveal how contours closely align with each quadrilateral face thereby achieving a superlative objective of not just extracting graph structure of the mesh but also preserving topological orientation of each quadrilateral algebraically.

1237.7 DP Contour polynomials for every quadrilateral face of a quadmesh found earlier is a basic prerequisite for any approximate topological matching algorithm including Hausdorff distance. For example, approximate topological matching of oriented quadfaces in 1203.6 could be augmented by maximum per quadface common contour DP polynomial match which is a further finetuning of maximum common subgraph matching problem. Matching quadfaces could be determined by inner product space polynomial distances between DP polynomials of the quadfaces - quadfaces of small distances are approximate topological matches and similarity is the percentage of matching quadface contours.

1237.8 Earlier DP polynomial distance measure could be suitably adapted to Rebus Topological Script Recognition in archaeological decipherment by exhaustively searching for least distance approximate topological contour match for an undeciphered script quadmesh image, in pre-defined database of pictogram motif quadmesh contour DP polynomials and concatenate textual description for the motifs into a meaningful sentence - Example: Dholavira signboard in 1236.20 might be Rebus deciphered by a hypothetical contour search-match algorithm as "Wheel-Hammer-Wheel-Pounding Urn-Wheel-Wheel-Sickle" (Indus script for a civilization ranging from time duration of 7000BC - Mehrgarh - is presumed to be right-to-left and logo-syllabic) based on an ImageNet ResNet50 prediction search of the motifs of least contour DP polynomial distance which could be contextually inferred as a natural language sentence "Transport of Processed (Agriculture) Products" after ImageNet prediction Textgraph thesaurus expansion for Wheel(Transport), Hammer, Urn and Sickle(Processing tools mostly used in cultivation) neglecting the repetitive logos and their order.

1237.9 Disclaimer: Earlier Dholavira signboard example is not a decipherment claim but stated herein as only a walkthrough on how an AI Topological script recognition-decipherment algorithm might approximate the meaning of an undeciphered archaeological inscription. By Rebus principle, meaning of a pictogram inscription could be inferred independent of natural language underneath and knowledge of syllables for each logo may not be necessary - even if it does, ResNet50 prediction in English for an image motif might have to be translated to corresponding word-syllables of all possible contemporary-medieval languages and a sentence might have to be formed from their concatenation right-to-left or left-to-right to zero-in-on the origin of ancient script - an exponentially daunting computational effort. In the example 1236.2, pictogram "h8" could as well be deciphered though an AI algorithm which searches ResNet50 and concatenates syllable-word predictions for "h" and symbol "8" in any other language and only h+eight=height in English is meaningful. ImageNet-ResNet50 is a standard massive deep learning dataset for supercomputers.

1237.10 A paradoxical implication arises if similarities between Keezhadi Script and Indus Script turn out to be derivatives of one another and are classified into one of contemporary languages (Sanskrit as per decipherment claim 1236.11 or Tamil) by an exhaustive Rebus AI contour polynomial-word-syllable search (which is evident from cursory visual glance): Both Indus and Keezhadi scripts should belong to Tamil or else both should be Sanskrit unless a common unifying script was used in the past by both prima facie hinting at common ancestry of Tamil and Sanskrit (as per a legend, Tamil grammar propounded by Agastya is a simplified form of Panini's Sanskrit grammar with Ka-Cha-Ta-Pa-Yadi vargas removed).

1237.11 Decipherment of archaeological motifs is often inseparable from astronomy and recorded history of eclipses in cuneiforms, copper plates, rock edicts and scripture manuscripts is sizeable requiring dating of the inscriptions by C-14 or AMS (Accelerated Mass Spectrometry) and exhaustive search of astronomical data for planetary alignment in an ephemeris software dating back to few thousand years which is hindered by calendar conflicts (Julian-Gregorian-Sidereal-Solar-Lunar), Software overflow errors, Use of Tropical (Dynamic based on Sun's motion over equinoctical points) and Sidereal (Static) zodiacs. Axiomatically it can be stated, hence, that an accurate estimate of civilization timeline must satisfy all 3 predictions (or post-dictions): Script Decipherment, Astronomy and Carbon dating-AMS must concur. NeuronRain implements a textual astronomical dataset pattern mining (Maitreya' Dreams NASA JPL Ephemeris CLI) for extreme weather events by encoding celestial bodies as strings (GSP Sequence Mining, Longest Common Subsequence, BioPython-ClustalOmega Multiple Sequence Alignment analytics of strings) which could be complemented by large scale visual analytics of a planetarium software sky imagery (<https://stellarium.org/>) of constellations and planets (Image similarity found through various algorithms - Voronoi tessellation, quadmesh, histogram, dynamic time warping - between skyview imagery in two different time points of extreme weather events).

#### References:

- 
- 1237.12 Remarkable visual similarity of Fish signs on Potsherds - Indus and Keezhadi - Plate 8 of Indus Fish potsherds - [KN Dikshit] - Origin of Early Harappan Cultures in The Sarasvati Valley - Recent Archaeological Evidence and Radiometric Dates - 2013 - <https://www.scribd.com/document/260613722/Origin-of-Early-Harappan-Cultures-in-the-Sarasvati-Valley-Recent-Archaeological-Evidence-and-Radiometric-Dates> and Fish potsherds of Keezhadi in 1236.25
- 1237.13 ResNet50 Fujitsu Supercomputing benchmark - [https://sc19.supercomputing.org/proceedings/tech\\_poster/poster\\_files/rpost203s2-file3.pdf](https://sc19.supercomputing.org/proceedings/tech_poster/poster_files/rpost203s2-file3.pdf)
- 1237.14 Beta Analytic - AMS - <https://www.radiocarbon.com/accelerator-mass-spectrometry.htm>
- 1237.15 Stellarium - <https://stellarium-web.org/>
- 

1238. (THEORY and FEATURE) Merit of Large Scale Visuals - ImageNet predictions from multiple models - Rebus Topological Script Recognition - Dholavira Signboard example deciphered by ResNet50 and ResNet50V2 - 28 April 2022 - related to 1236, 1237 and all sections on Archaeology-Topological Script Recognition, Face-Physique-Handwriting-Gender-Motif Recognition, Product Homotopy, Unique identification, Homeomorphism and Topological Deformations, Merit of Large Scale Visuals

-----

- 1238.1 ImageGraph\_Keras\_Theano.py has been updated to refactor `imagenet_imagegraph()` for ImageNet predictions from multiple Deep Learning Models instead of hardcoded ResNet50 earlier.
- 1238.2 Models have been instantiated within a dictionary of modelname-model map and are iterated in a loop and ImageNet predictions for an image are sequentially printed. List of all available Keras Deep Learning models and their top-k accuracy are at <https://keras.io/api/applications/>

1238.3 Since Deep Learning models are efficient probabilistic guesses of artifacts in an image based on convolution network layers, top accuracy has been increased to 5 to allow top 5 probabilities.

1238.4 To verify the Rebus principle topological script recognition algorithm mentioned in 1236 and 1237, Dholavira signboard image from <https://www.harappa.com/blog/dholavira-and-its-mysterious-sign-board> (testlogs/The\_Ten\_Indus\_Scripts\_discovered\_near\_the\_northern\_gateway\_of\_the\_Dholavira\_citadel.jpg) containing 10 pictorial symbols of Indus script has been deciphered by ResNet50 and ResNet50V2 models in imagenet\_imagegraph() and the results ensue (full logs: testlogs/ImageGraph\_Keras\_Theano.log.28April2022 for top-5 and ImageGraph\_Keras\_Theano.log2.28April2022 for top-1 accuracies).

1238.5 For ResNet50 predictions and their top-5 probabilities are:  
( 'Predictions - ', 'ResNet50', ':', [(['n03857828', 'oscilloscope', 0.18934955), ('n03291819', 'envelope', 0.05882809), ('n02840245', 'binder', 0.029974239), ('n04554684', 'washer', 0.025299871), ('n03041632', 'cleaver', 0.024807546)])

1238.6 For ResNet50V2 predictions and their top-5 probabilities are:  
( 'Predictions - ', 'ResNet50V2', ':', [(['n02123597', 'Siamese\_cat', 0.9940566), ('n02089973', 'English\_foxhound', 0.0059434352), ('n07613480', 'trifle', 1.8534284e-13), ('n02356798', 'fox\_squirrel', 4.2353065e-23), ('n04479046', 'trench\_coat', 1.3498343e-29)])

1238.7 Counterintuitively, ResNet50 version 1 is predicting better than ResNet50 version 2 for top-5 accuracy - Cleaver or a large knife, Washer or a wheel are reasonable matches for symbols in signboard excluding "oscilloscope"- though both are far away from expected decipherment by a hypothetical DP contour polynomial match algorithm mentioned earlier in 1237.8. Extending deep-learning models to train and match arbitrary topological varieties (contour polynomials of images instead of images - a mammoth computational task in itself to create such a contour database) by their polynomial distance similarity might improve decipherment accuracy.

1238.8 Top pageranked vertices in Textgraph of ImageNet-ResNet50 predictions in 1238.5 are:

```
[('oscilloscope', 0.12046130243949144), ('envelope', 0.12046130243949144), ('cleaver', 0.08107992792460737), ('binder', 0.08107992792460737), ('washer', 0.06795280308631269), ('someone', 0.018726084942707544), ('things', 0.018726084942707544), ('washes', 0.018726084942707544), ('living', 0.018726084942707544), ('large', 0.018069728700792813), ('knife', 0.018069728700792813), ('machine', 0.018069728700792813), ('butcher', 0.018069728700792813), ('blade', 0.018069728700792813), ('binds', 0.018069728700792813), ('grain', 0.018069728700792813), ('sheaves', 0.018069728700792813), ('square', 0.018069728700792813), ('cuts', 0.018069728700792813), ('electrical', 0.017085194337920707), ('varying', 0.017085194337920707), ('equipment', 0.017085194337920707), ('usually', 0.017085194337920707), ('rectangular', 0.017085194337920707), ('thin', 0.017085194337920707), ('quantities', 0.017085194337920707), ('images', 0.017085194337920707), ('provides', 0.017085194337920707), ('letter', 0.017085194337920707), ('visual', 0.017085194337920707), ('flat', 0.017085194337920707), ('etc', 0.017085194337920707), ('electronic', 0.017085194337920707), ('package', 0.017085194337920707), ('container', 0.017085194337920707)]
```

rebus-deciphering the signboard to be a natural language phrase for a "butchering or grain shop using equipments (blade, washer, cleaver-knife)" which coincides with visual intuition.

1238.9 For 2 inscriptions containing some common scripts-motifs, set intersection between textgraphs of their ImageNet predictions isolates the meaning of common scripts-motifs in 2 inscriptions which is the fundamental necessity for a Rebus decipherment breakthrough. Textgraph creation from ImageNet predictions are best suited for archaeological script decipherment as there are no intermediate phases of sentence formation and syllable demarcation and meaning is represented by textgraph directly which in itself is a decipherment.

1238.10 Example: For the following two inscriptions having A,B and C as scripts-motifs (and common script B):

A B - inscription1 and textgraph1 for its ImageNet predictions

B C - inscription2 and textgraph2 for its ImageNet predictions

set intersection of textgraph1 and textgraph2 from ImageNet predictions of 2



inscriptions isolates the meaning of script B.

-----  
1239. (THEORY and FEATURE) Merit of Large Scale Visuals - Astronomy Analytics - DBSCAN Clustering and Segmentation analysis of sky imageries for 2 high magnitude seismic events - 9 May 2022 and 10 May 2022 - related to 3,6,8,15,16,59,62,63,147,148 and all sections on analytics of textually encoded astronomical datasets, Various algorithms for string analytics, climate analytics, weather analytics, N-Body problem, Computational Astrophysics, Computational Geometry  
-----

-----  
1239.1 NeuronRain has so far been confined to analytics of textual astronomical datasets correlated to terrestrial extreme weather events, which are encoded strings of degree alignments (N-body choreography) of celestial bodies on zodiac obtained from an ephemeris client (NASA JPL ephemeris - Maitreya's Dreams Text Client).

1239.2 This commit extends astronomy analytics to sky imagery of celestial bodies sourced from Planetarium software. Astronomical imagery of celestial bodies are scatterplots of distant objects (constellations, planets, meteor showers are usually circles of varying radii spread out on sky) and visual clustering and segmentation algorithms viz., DBSCAN, Watershed segmentation, Chain approximation contour detection could be suited for classifying the point celestial objects into en-masse clusters. Each cluster thus found is a candidate for gravitational influence on earth's tectonics which in a sense generalizes 12 house static zodiac division over 360 degrees of 30 degrees each, to a sky arbitrarily divided by clustering and segmentation algorithms based on density of objects.

1239.3 Celestial objects for two high richter scale seismic events and two of the top 10 high death toll disasters ever - Tangshan earthquake of 26 July 1976 and Boxing Day Sumatra earthquake of 26 December 2004 (both coinciding with fullmoon or newmoon - fullmoon or newmoon is often cited as prerequisite for a seismic event possibly exacerbated by a solar or lunar eclipse) - have been plotted in The Sky Live planetarium as observed from respective epicentres and captured in two JPG files (includes both above horizon and below horizon bodies)

- SkyLive\_SumatraBoxingDayEarthQuake\_26December2004\_0758.jpg (7:58 am local time) and SkyLive\_TangshanEarthQuake\_28July1976\_0342.jpg (3:42 am local time)

1239.4 Image segmentation in ImageGraph\_Keras\_Theano.py has been changed to include Delaunay Triangulation and Voronoi Tessellation plots for an image imported from GISUrbanSprawlAnalytics.py. Keras backend has been set to Theano. Return value tuple of image\_segmentation() has been updated to return img ndarray and contourcentroids instead of GRANA centroids.

1239.5 Following computation has been performed on 2 seismic events sky imagery (logs, Voronoi and Delaunay imagery, DBSCAN clustering imagery, Neural network clustering imagery, DOT files of the facegraphs):

1239.5.1 Histogram Earth Mover Distance similarity between how sky looked like when two seismic events struck -  
testlogs/ImageGraph\_Keras\_Theano.AstronomicalImagery.log.9May2022 - ('EMD Histogram distance similarity between images -  
testlogs/SkyLive\_SumatraBoxingDayEarthQuake\_26December2004\_0758.jpg and  
testlogs/SkyLive\_TangshanEarthQuake\_28July1976\_0342.jpg :', (7.763535976409912, None, array([[1., 0., 0., ..., 0., 0., 0.]...))

1239.5.2 DBSCAN clustering of the two sky imagery -  
testlogs/SkyLive\_SumatraBoxingDayEarthQuake\_26December2004\_0758\_dbscanclustered.jpg, testlogs/SkyLive\_TangshanEarthQuake\_28July1976\_0342\_dbscanclustered.jpg -  
number of DBSCAN clusters differ slightly between two imagery as:

number of DBSCAN density clusters: 104719

size of image: 869031

size of dbscandict: 446804

number of DBSCAN density clusters: 105352

size of image: 869031

size of dbscandict: 446813

1239.5.3 Neural network clustering of the two sky imagery -

testlogs/SkyLive\_SumatraBoxingDayEarthQuake\_26December2004\_0758\_neuralnetworkclustered.jpg,  
testlogs/SkyLive\_TangshanEarthQuake\_28July1976\_0342\_neuralnetworkclustered.jpg  
1239.5.4 Watershed segmentation of the two sky imagery -  
testlogs/RemoteSensingGIS/SkyLive\_SumatraBoxingDayEarthQuake\_26December2004\_0758\_segmented.jpg,  
testlogs/RemoteSensingGIS/SkyLive\_TangshanEarthQuake\_28July1976\_0342\_segmented.jpg

1239.5.5 Voronoi tessellation and Delaunay triangulation around centroids of Chain approximation contours of the two sky imagery -  
testlogs/SkyLive\_SumatraBoxingDayEarthQuake\_26December2004\_0758-contourlabelled.jpg, testlogs/SkyLive\_TangshanEarthQuake\_28July1976\_0342-contourlabelled.jpg

1239.5.6 DOT files of the facegraphs of 2 imagery -  
testlogs/RemoteSensingGIS/SkyLive\_SumatraBoxingDayEarthQuake\_26December2004\_0758\_ImageNet\_Keras\_Theano\_Segmentation\_FaceGraph.dot,  
testlogs/RemoteSensingGIS/SkyLive\_TangshanEarthQuake\_28July1976\_0342\_ImageNet\_Keras\_Theano\_Segmentation\_FaceGraph.dot

1239.6 Of all the clustering data earlier, Watershed segmentation imagery has computed a remarkable visual demarcation of celestial clustering compared to DBSCAN clustering, Neural network clustering, Voronoi-Delaunay tessellation pivoted around Chain approximation contour centroids (which is too fine-grained mesh). Additionally what catches the attention is the unusually high number of meteor showers in Tangshan imagery though clustering is sparse (7.5 richter), while Sumatra imagery has noticeable clustering of bodies around Milky way and less meteor showers (9.1 richter).

#### References:

-----  
1239.7 The Sky Live - Online Planetarium - <https://theskylive.com/planetarium>  
-----

-----  
1240. (THEORY and FEATURE) Merit of Large Scale Visuals - Archaeology - Rebus Decipherment of Indus Unicorn Seals and their validation by extracting common subgraphs in ImageNet predictions textgraphs (GSpan Frequent Subgraph Mining algorithm) - 13 May 2022 - related to 1203,1232,1233,1236,1237 and all sections on Merit of Large Scale Visuals, Physique Recognition From Quadrilateral mesh isomorphism, Topological Face and Handwriting recognition, Archaeology-Topological Script Recognition, Product Homotopy, Homeomorphism and Topological Deformations, People Analytics, Computational Geometry, Graph Edit Distance and Earth mover distance, Graph Isomorphism (Exact, Approximate and Subgraph), Graph matching, Graph similarity, Image Search, Quadrilateral Mesh Deformation and Isomorphism, Maximum Common Subgraph Problem and Approximate Topological Matching  
-----

-----  
1240.1 New function frequent\_subgraphs\_of\_imagenet\_prediction\_textgraphs() has been defined to compute GSpan frequent subgraph mining of textgraphs deeplearnt from ImageNet predictions (ResNet50, ResNet50V2) by Recursive Gloss Overlap Dense subgraph classifier. Frequent subgraphs of ImageNet prediction textgraphs learnt from different inscriptions approximately correspond to common scripts-motifs in the inscriptions. Frequent subgraph mining generalizes set intersection of Rebus pictogram textgraphs mentioned in 1238.

1240.2 Earlier textgraph mining function is invoked on 3 archaeological artefacts - Indus Unicorn Seals of differing scripts having some common motifs: image\_pattern\_mining/ImageNet/testlogs/bagasra-unicorn-seal.jpg, image\_pattern\_mining/ImageNet/testlogs/unicorn-seal\_0.jpg, image\_pattern\_mining/ImageNet/testlogs/unicorn-seal\_1\_5.jpg

1240.3 Mined Common Subgraphs (ResNet50 and ResNet50V2) throw some light on intended meaning of the unicorn seals (Disclaimer: it is an automated machine learning decipherment based on accuracy of Rebus Image Search and shouldn't be construed as a full-fledged decipherment claim) - full logs at testlogs/ImageGraph\_Keras\_Theano.log.13May2022 :

ResNet50: Mined Frequent Subgraph Edges: {('brass', 'tube'), ('times', 'trilobite'), ('igniter', 'used'), ('igniter', 'substance'), ('instrument', 'brass'), ('sundial', 'dial'), ('bolo\_tie', 'neck'), ('printed', 'book\_jacket'), ('parts', 'trilobite'), ('worn', 'bolo\_tie'), ('trilobite', 'abundant'), ('brass', 'wind'), ('book', 'book\_jacket'), ('jacket', 'book\_jacket'), ('brass', 'cup-shaped'), ('sundial', 'indicates'), ('substance', 'igniter'), ('three', 'trilobite'), ('cup-shaped', 'brass'), ('means', 'brass'), ('obelisk', 'pyramidal'), ('trilobite', 'exoskeleton'), ('arthropod', 'trilobite'), ('blown', 'brass'), ('ignite', 'igniter'), ('usually', 'brass'), ('trilobite', 'times'), ('book\_jacket', 'information'), ('daylight', 'sundial'), ('brass', 'instrument'), ('tapering', 'obelisk'), ('rectangular', 'obelisk'), ('Paleozoic', 'trilobite'), ('obelisk', 'pillar'), ('neck', 'bolo\_tie'), ('variable', 'brass'), ('timepiece', 'sundial'), ('trilobite', 'Paleozoic'), ('base', 'support'), ('book\_jacket', 'jacket'), ('ornamental', 'bolo\_tie'), ('book\_jacket', 'paper'), ('brass', 'usually'), ('obelisk', 'cross'), ('trilobite', 'extinct'), ('bolo\_tie', 'necktie'), ('necktie', 'bolo\_tie'), ('obelisk', 'stone'), ('cord', 'bolo\_tie'), ('obelisk', 'towards'), ('hours', 'sundial'), ('buckle', 'buckles'), ('gnomon', 'sundial'), ('fasten', 'buckle'), ('calibrated', 'sundial'), ('obelisk', 'top'), ('foundation', 'base'), ('stone', 'obelisk'), ('book\_jacket', 'promotional'), ('brass', 'blown'), ('clasp', 'bolo\_tie'), ('obelisk', 'tapering'), ('cross', 'obelisk'), ('mouthpiece', 'brass'), ('promotional', 'book\_jacket'), ('brass', 'funnel-shaped'), ('sundial', 'daylight'), ('brass', 'means'), ('sundial', 'gnomon'), ('bolo\_tie', 'clasp'), ('shadow', 'sundial'), ('pyramidal', 'obelisk'), ('divided', 'trilobite'), ('around', 'bolo\_tie'), ('casts', 'sundial'), ('fastened', 'bolo\_tie'), ('base', 'foundation'), ('extinct', 'trilobite'), ('usually', 'book\_jacket'), ('obelisk', 'rectangular'), ('towards', 'obelisk'), ('pillar', 'obelisk'), ('brass', 'brass'), ('book\_jacket', 'printed'), ('igniter', 'kindle'), ('bolo\_tie', 'cord'), ('book\_jacket', 'book'), ('igniter', 'fire'), ('exoskeleton', 'trilobite'), ('dial', 'sundial'), ('sundial', 'casts'), ('igniter', 'ignite'), ('trilobite', 'three'), ('sundial', 'hours'), ('top', 'obelisk'), ('bolo\_tie', 'worn'), ('bolo\_tie', 'ornamental'), ('brass', 'mouthpiece'), ('fire', 'igniter'), ('trilobite', 'divided'), ('section', 'obelisk'), ('brass', 'length'), ('abundant', 'trilobite'), ('length', 'brass'), ('funnel-shaped', 'brass'), ('trilobite', 'arthropod'), ('sundial', 'timepiece'), ('indicates', 'sundial'), ('information', 'book\_jacket'), ('tube', 'brass'), ('wind', 'brass'), ('buckle', 'fasten'), ('paper', 'book\_jacket'), ('bolo\_tie', 'around'), ('trilobite', 'parts'), ('buckle', 'buckle'), ('sundial', 'shadow'), ('kindle', 'igniter'), ('brass', 'consists'), ('brass', 'variable'), ('sundial', 'calibrated'), ('used', 'igniter'), ('obelisk', 'section'), ('bolo\_tie', 'fastened'), ('book\_jacket', 'usually'), ('consists', 'brass'), ('support', 'base'), ('buckles', 'buckle')}

ResNet50V2: Mined Frequent Subgraph Edges: {('common', 'wood\_rabbit'), ('barrel', 'hold'), ('wood\_rabbit', 'North'), ('English\_foxhound', 'hunt'), ('small', 'ice\_lolly'), ('wood\_rabbit', 'Ixodes'), ('chambered\_nautilus', 'spiral'), ('host', 'wood\_rabbit'), ('fox\_squirrel', 'arboreal'), ('wood\_rabbit', 'underside'), ('pale', 'chambered\_nautilus'), ('someone', 'hotdog'), ('ice\_lolly', 'ice'), ('scapularis', 'wood\_rabbit'), ('slightly', 'English\_foxhound'), ('English\_foxhound', 'larger'), ('trifle', 'sponge'), ('attention', 'hotdog'), ('stick', 'ice\_lolly'), ('fruit', 'trifle'), ('cream', 'ice\_lolly'), ('chocolate', 'trifle'), ('hotdog', 'attract'), ('barrel', 'size'), ('wood\_rabbit', 'rabbit'), ('trifle', 'pudding'), ('wood\_rabbit', 'ticks'), ('hunt', 'English\_foxhound'), ('stunts', 'hotdog'), ('Pacific', 'chambered\_nautilus'), ('nuts', 'trifle'), ('cream', 'trifle'), ('hotdog', 'performs'), ('chambered\_nautilus', 'cephalopod'), ('made', 'trifle'), ('United', 'fox\_squirrel'), ('trifle', 'cake'), ('wood\_rabbit', 'greyish'), ('wood\_rabbit', 'common'), ('larger', 'English\_foxhound'), ('wood\_rabbit', 'small'), ('fox\_squirrel', 'States'), ('wood\_rabbit', 'fur'), ('brownish', 'wood\_rabbit'), ('trifle', 'jelly'), ('water', 'ice\_lolly'), ('cephalopod', 'chambered\_nautilus'), ('States', 'fox\_squirrel'), ('wood\_rabbit', 'white'), ('performs', 'hotdog'), ('English\_foxhound', 'foxhounds'), ('trifle', 'decorated'), ('attract', 'hotdog'), ('chambered\_nautilus', 'pale'), ('chambered\_nautilus', 'partitions'), ('rabbit', 'wood\_rabbit'), ('disease', 'wood\_rabbit'), ('wood\_rabbit', 'tail'), ('decorated', 'trifle'), ('tail',

'wood\_rabbit'), ('fox\_squirrel', 'large'), ('hotdog', 'dangerous'), ('wood\_rabbit', 'Lyme'), ('packs', 'English\_foxhound'), ('hotdog', 'attention'), ('trifle', 'layers'), ('exceptionally', 'fox\_squirrel'), ('wood\_rabbit', 'pacificus'), ('greyish', 'wood\_rabbit'), ('Lyme', 'wood\_rabbit'), ('trifle', 'cold'), ('white', 'wood\_rabbit'), ('English\_foxhound', 'originally'), ('chambered\_nautilus', 'oceans'), ('chambered\_nautilus', 'shell'), ('wooden', 'ice\_lolly'), ('hotdog', 'someone'), ('dangerous', 'hotdog'), ('ice', 'ice\_lolly'), ('small', 'wood\_rabbit'), ('spiral', 'chambered\_nautilus'), ('cake', 'trifle'), ('hold', 'barrel'), ('underside', 'wood\_rabbit'), ('foxhounds', 'English\_foxhound'), ('ice\_lolly', 'water'), ('squirrel', 'fox\_squirrel'), ('English\_foxhound', 'breed'), ('chambered\_nautilus', 'pearly'), ('breed', 'English\_foxhound'), ('quantity', 'barrel'), ('ice\_lolly', 'small'), ('sponge', 'trifle'), ('wood\_rabbit', 'host'), ('English', 'English\_foxhound'), ('trifle', 'fruit'), ('English\_foxhound', 'American'), ('pacificus', 'wood\_rabbit'), ('trifle', 'nuts'), ('chambered\_nautilus', 'Pacific'), ('fox\_squirrel', 'squirrel'), ('oceans', 'chambered\_nautilus'), ('wood\_rabbit', 'disease'), ('large', 'fox\_squirrel'), ('spread', 'trifle'), ('English\_foxhound', 'used'), ('ice\_lolly', 'cream'), ('pudding', 'trifle'), ('eastern', 'fox\_squirrel'), ('barrel', 'quantity'), ('fur', 'wood\_rabbit'), ('wood\_rabbit', 'brownish'), ('partitions', 'chambered\_nautilus'), ('wood\_rabbit', 'scapularis'), ('fox\_squirrel', 'United'), ('wood\_rabbit', 'America'), ('Ixodes', 'wood\_rabbit'), ('fox\_squirrel', 'eastern'), ('shell', 'chambered\_nautilus'), ('English\_foxhound', 'packs'), ('ice\_lolly', 'wooden'), ('North', 'wood\_rabbit'), ('America', 'wood\_rabbit'), ('ticks', 'wood\_rabbit'), ('layers', 'trifle'), ('size', 'barrel'), ('American', 'English\_foxhound'), ('cold', 'trifle'), ('trifle', 'made'), ('chambered\_nautilus', 'Indian'), ('pearly', 'chambered\_nautilus'), ('trifle', 'spread'), ('ice\_lolly', 'stick'), ('English\_foxhound', 'slightly'), ('English\_foxhound', 'English'), ('fox\_squirrel', 'exceptionally'), ('trifle', 'cream'), ('trifle', 'chocolate'), ('Indian', 'chambered\_nautilus'), ('arboreal', 'fox\_squirrel'), ('used', 'English\_foxhound'), ('jelly', 'trifle'), ('originally', 'English\_foxhound'), ('hotdog', 'stunts'), ('barrel', 'barrel')}]

1240.4 From earlier frequent subgraph mining, few notable common vertices between ImageNet textgraphs of 3 unicorn seals are:

ResNet50 - sundial, gnomon, fire, cup-shaped (perhaps hinting at an animal sacrifice fire altar and astronomical configuration during sacrifice guided by gnomon-sundial - script on seal might be a description of sacrifice)

ResNet50V2 - foxhound (unicorn bull or buffalo figurine has been predicted as foxhound)

#### References:

-----  
1240.5 Unicorn Seal 1 - Mohenjo-Daro - <https://www.harappa.com/indus/25.html>

1240.6 Unicorn Seal 2 - Bagasra - <https://www.harappa.com/content/organization-indus-unicorn-seal-production-multi-faceted-investigation-technology-skill-and>

1240.7 Unicorn Seal 3 - <https://www.harappa.com/seal/1.html>

1240.8 Buffalo Sacrifice in Harappan Seals -

<https://www.harappa.com/blog/buffalo-sacrifice> - "... In the form of worship at Kannapuram, a south India village in Tamil Nadu studied by Brenda Beck (1981), the tree-trunk (known as kampakam in Tamil, from Sanskrit skambha ("pillar") in front of which the sacrificial buffaloes are decapitated, is said to be the husband of the goddess. At the end of the annual marriage rite, after the last victim has been slaughtered, this trunk is uprooted and the goddess divested of her ornaments like a widow. The pillar and its uprooting correspond to Siva's phallus and its castration. The sacrificial post used to be burned after the divine marriage festival ... Later Parpola continues: "If the buffalo sacrifice is common in south Indian village religion, it is absent from north Indian village religion. The reason is probably the conscious efforts of Vedic Brahmans to eradicate it. Extravagant buffalo sacrifices were at first adopted by the Rigvedic Aryans in the Indus Valley (RV 5,29,7-8 etc.), but thereafter this mode of worship is not heard of."

1240.9 John Marshall's interpretation of Pashupati Seal as Lord Shiva -

[https://en.wikipedia.org/wiki/Pashupati\\_seal](https://en.wikipedia.org/wiki/Pashupati_seal) - "...My reasons for the identification are four. In the first place the figure has three faces and that

Siva was portrayed with three as well as with more usual five faces, there are abundant examples to prove. Secondly, the head is crowned with the horns of a bull and the trisula are characteristic emblems of Siva. Thirdly, the figure is in a typical yoga attitude, and Siva [sic] was and still is, regarded as a mahayogi—the prince of Yogis. Fourthly, he is surrounded by animals, and Siva is par excellence the "Lord of Animals" (Pasupati)—of the wild animals of the jungle, according to the Vedic meaning of the word pashu, no less than that of domesticated cattle..."

1240.10 Anthropomorphic figures, Chariots, Antenna Swords in Sanauli (alleged Mahabharata war) Harappan Burial Site -

<https://journal.fi/store/article/view/98032/56890> - figure motifs are likely rebus decipherable.

-----  
1252. (THEORY and FEATURE) Merit of Large Scale Visuals - GIS Urban Sprawl Analytics - Automatic Delineation of Urban Growth Boundaries from Transportation Network GIS - related to 1151,1174,1196,1226,1233,1234,1237 and all sections on GIS Urban Sprawl Analytics, Merit of Large Scale Visuals, Gridded Population Estimators (SEDAC GPW4 and GHSL convex hull estimators), DBSCAN and Neural Network Urban Extent Learners, Computational Geometry, Intrinsic Merit Rankings, R Ricker Population Estimation, Community detection, Social Network Analytics, Space filling by Curves, Unequal Circle and Polynomial packing, Computational Geometry and Polygonal packing by Voronoi Tessellation, Four color theorem, Economic Merit, Computational Economics - GDP estimation from electricity consumption, Jordan Curve Theorem, Weirstrass Theorem, Cellular Automata-SLEUTH Urban Growth Models, Automatic Delineation of Urban Growth Boundaries, Preferential attachment, Random Graphs, Dynamic Graphs, Separate Chaining Hash tables, Unmanned Aerial Vehicle Navigation-Autonomous Drone Delivery-Drone EVMS-Passenger Drones, Wiring Problem  
-----

1252.1 An algorithm for Automatic Delineation of Urban Growth Boundaries(UGB) from Minimum Spanning Tree of Building Coverage Ratio Segmentation (Meta Research - High Resolution Settlement Layer) and Voronoi-Delaunay Tessellation-Triangulation vis-a-vis Expert Delineation has been studied in 1226.19 - Algorithmic UGB Delineation has been found to be ~93% accurate at its maximum (Frankfurt-Main) versus manual expert delineation.

1252.2 Extracting Road networks from GIS (a crucial prerequisite for predefined Unmanned Aerial Vehicle mission flight plans) preserving topological orientation is of paramount significance in delimiting rural-urban boundaries.

1252.3 Transport Networks are graph structures with added topological embedding defined on a 2D plane connecting urban centres (allowing twists and turns in each edge as against traditional straightline edges of Graph theory) and an optimal layout of transportation network is an unrestricted-twist-and-turn variant of wiring problem in logic gate arrays (optimal space efficient layout of wires connecting logic gates is reduced to optimal space efficient layout of transport network carriageways connecting urban centres) which is NP-Hard for maximum of one 90 degree turn. Problem of unrestricted 90 degree turns between two points approximating a carriageway could be significantly harder(a random walk on a grid). Usual graph algorithms discard layout topology.

1252.4 Inferring a graph structure which preserves topology of transportation network edges from a Transit network GIS is non-trivial and similar to sections 1233,1237 (which warrant a Graph topology from Quadmesh that preserves face orientations), contour polynomials (which correspond to topological orientation of road-rail network) of transportation network are retrieved from segmentation of an example GIS image of Chennai Metropolitan Area (python-src/image\_pattern\_mining/ImageNet/testlogs/ChennaiMetropolitanAreaTransitNetwork\_GoogleMaps\_20May2022.jpg - Google Maps augmented by Transport network, Terrain, Live Traffic layers) bypassing necessity for access to Graph structure of Transportation network (e.g Google Roads REST API)

1252.5 Automatic Delineation of Chennai Metropolitan Area by NASA VIIRS NightTime Lights based Urban Extent Learner in earlier sections (1174)depends on luminosity of night lights which at times could be disproportionate to urban

area and only a lowerbound of the sprawl. Earlier Google Maps GIS of Transportation network - `python-src/image_pattern_mining/ImageNet/testlogs/ChennaiMetropolitanAreaTransitNetwork_GoogleMaps_20May2022.jpg` - is a daylight image and vegetation-tree-canopies (NDVI) are conspicuous by green color pixels. Extent of vegetation is inversely proportional to urbanization and degree of transportation network is maximum in urban centres (as multiple carriageways originate from a thriving megapolis).

1252.6 Extent of Urbanization is proportional to dense subgraphs of transportation networks - In earlier GIS imagery, high concentration of transit network aligned to Chennai Metropolitan Area sprawl of approximately 100 kms radius (coinciding with suburban transport network) in North-South-West has been reflected in topological clustering of contour polynomials of transit network plotted in `ChennaiMetropolitanAreaTransitNetwork_GoogleMaps_20May2022-contoursegmented.jpg`. Extent of a Metropolitan Area Sprawl has been defined earlier (1151) as area catered by suburban transport network or floating population depending on urban centre.

1252.7 Partitioning of contour polynomials of transportation network edges into dense and sparse clusters is a delineator: (\*) Dense contour polynomial clusters (subgraphs) of small face areas denote an urban sprawl (\*) Sparse contour polynomial clusters (subgraphs) of high face areas might be rural. Voronoi Tessellation-Delaunay Triangulation of earlier image at `ChennaiMetropolitanAreaTransitNetwork_GoogleMaps_20May2022-contourlabelled.jpg` is too fine-grained and does not show transportation network clustering.

1252.8 Previous set of contour polynomials of transportation network could (\*) either be an automatic delineator of Chennai Metropolitan Area Sprawl based on clusters of contour polynomials segregated by their Hausdorff topological distance or Inner product distance (\*) or assist a manual expert delineation.

1252.9 `ImageGraph_Keras_Theano.py` is directly imported instead of "from-import" earlier. Following are logs, facegraph DOT file, contour-Voronoi-Delaunay-watershed segmentation imagery for this commit:

`testlogs/ChennaiMetropolitanAreaTransitNetwork_GoogleMaps_20May2022-contourlabelled.jpg`  
    `testlogs/ChennaiMetropolitanAreaTransitNetwork_GoogleMaps_20May2022-contoursegmented.jpg`  
    `testlogs/ChennaiMetropolitanAreaTransitNetwork_GoogleMaps_20May2022.jpg`  
    `testlogs/GISUrbanSprawlAnalytics.log.20May2022`

`testlogs/RemoteSensingGIS/ChennaiMetropolitanAreaTransitNetwork_GoogleMaps_20May2022_ImageNet_Keras_Theano_Segmentation_FaceGraph.dot`

`testlogs/RemoteSensingGIS/ChennaiMetropolitanAreaTransitNetwork_GoogleMaps_20May2022_segmented.jpg`

#### References:

-----  
1252.9 High Resolution Roads, Land Parcel, Building Coverage, Vegetation Detection - MAXAR - <https://www.maxar.com/products/analysis-ready-data>  
1252.10 MAXAR DeepCore AI Models for GIS imagery - Solutions for US Defense - <https://cdn.mediavalet.com/usva/maxar/pCuVslH0zUu9M-jTxLndug/Ob26f4k240-Z00i7iRiZPw/Original/10081-ds-deepcore.pdf>  
1252.11 NASA Black Marble NightLights Global Composite - <https://blackmarble.gsfc.nasa.gov/> and <https://earthobservatory.nasa.gov/images/90008/night-light-maps-open-up-new-applications> - algorithmic enhancement to filter moon light, vegetation, cloud contamination in VIIRS imagery - <https://www.sciencedirect.com/science/article/pii/S003442571830110X>  
-----

1253. (THEORY and FEATURE) Merit of Large Scale Visuals - GIS Urban Sprawl Analytics - Automatic Delineation of Urban Growth Boundaries from Transportation Network GIS 2 - KMeans Clustering of Contour Polynomials - 24 May 2022 - related to 714,1151,1174,1196,1226,1233,1234,1237,1252 and all sections on GIS Urban

Sprawl Analytics, Merit of Large Scale Visuals, Gridded Population Estimators (SEDAC GPW4 and GHSL convex hull estimators), DBSCAN and Neural Network Urban Extent Learners, Computational Geometry, Intrinsic Merit Rankings, R Ricker Population Estimation, Community detection, Social Network Analytics, Space filling by Curves, Unequal Circle and Polynomial packing, Computational Geometry and Polygonal packing by Voronoi Tessellation, Four color theorem, Economic Merit, Computational Economics - GDP estimation from electricity consumption, Jordan Curve Theorem, Weierstrass Theorem, Cellular Automata-SLEUTH Urban Growth Models, Automatic Delineation of Urban Growth Boundaries, Preferential attachment, Random Graphs, Dynamic Graphs, Separate Chaining Hash tables, Unmanned Aerial Vehicle Navigation-Autonomous Drone Delivery-Drone EVMs-Passenger Drones, Wiring Problem

-----

#### 1253.1 New clustering function

contours\_kmeans\_clustering(imagefile, segment, number\_of\_clusters=3, maxiterations=3) has been defined in ImageGraph\_Keras\_Theano.py which implements K-Means Clustering of contour polynomials not only useful for automatic delineation of urban boundaries from GIS transportation network imagery but also in analysis of any contour segmented large scale visual.

1253.2 Function contours\_kmeans\_clustering() is a Python 3.7.x verbatim translation of C++ k-means unsupervised clustering implementation in NeuronRain AstroInfer (centroids of contour clusters are with reference to a predefined contour similar to cpp-src/asferkmeansclustering.cpp which computes centroids based on a reference string) and redefines the Euclidean distance metric as topological Hausdorff distance amongst pair of contour polynomials in place of string edit distance.

1253.3 Pasting Lemma-Path Homotopy-Product Homotopy formalism for Shape Recognition (Inscription Decipherment-Handwriting-Face-Physique-Gender) in earlier sections (714) is a proper subset ("Very similar") of Contour Polynomial clustering ("Similar") of a visual focusing only on homeomorphic deformation of shapes - set of deformations are cluster subsets.

1253.4 Usual clustering algorithms are limited to delineation of point sets while contours are sets of polynomials (or algebraic varieties) defining a topological orientation. Clustering of polynomials or curves is less studied in Bigdata mining. This requires definition of Euclidean distance as topological or polynomial distance, revised from usual Levenshtein distance for texts.

1253.5 Transportation Network Google Maps imagery of Chennai Metropolitan area testlogs/ChennaiMetropolitanAreaTransitNetwork\_GoogleMaps\_20May2022.jpg which includes Live traffic layer (red busy circles - a visual urbanization measure of dynamic floating population centred around a city) has been clustered by K-Means (3 clusters and 3 iterations) and contour polynomials of transportation network are colored in RGB channels proportional to the cluster id they have been classified into (written to ChennaiMetropolitanAreaTransitNetwork\_GoogleMaps\_20May2022-contourkmeansclustered.jpg).

1253.6 Voronoi Tessellation and Delaunay Triangulation have been made optional by boolean flags voronoi\_delaunay=False in following segmentation functions in ImageGraph\_Keras\_Theano.py and GISUrbanSprawlAnalytics.py as plots by multiple segmentation algorithms obfuscate and overlay previous layers:

(\*) def

urban\_sprawl\_from\_segments(image, segment, maximum\_population\_density=None, sqkmtoc  
ontourarearatio=0, legend=None, sqkmareatopopulationratio=6.22, voronoi\_delaunay=False)

(\*) def image\_segmentation(imagefile, voronoi\_delaunay=False)

1253.7 Following are the contour segmented files created by this commit:

(\*) Voronoi-Delaunay set to False -

testlogs/ChennaiMetropolitanAreaTransitNetwork\_GoogleMaps\_20May2022-contourlabelled.jpg

(\*) Plot for KMeans clustering of contour polynomials -

testlogs/ChennaiMetropolitanAreaTransitNetwork\_GoogleMaps\_20May2022-contourkmeansclustered.jpg - 3 color coded clusters of transportation network contours

(\*) Contour polynomial cluster dictionary is printed to Logs

(comprehensive listing of 3 clusters of contour polynomials computed from testlogs/ChennaiMetropolitanAreaTransitNetwork\_GoogleMaps\_20May2022.jpg which could be candidate delineators, better than graphics plot earlier as color differentiation for 3 clusters in drawContours is not upto mark) - testlogs/GISUrbanSprawlAnalytics.log.24May2022 - road network polynomials (wires connecting localities) are discernible by their almost straightline alignment (pixel ordinates are almost same in one axis while the other axis increments) having some arbitrary degree turns.

#### References:

-----  
1253.8 Number of monotonic walks on a lattice grid - Catalan numbers - [https://sites.math.washington.edu/~nichifor/310\\_2008\\_Spring/Pres\\_CatalanNumbers.pdf](https://sites.math.washington.edu/~nichifor/310_2008_Spring/Pres_CatalanNumbers.pdf) - "... The Catalan numbers describe (1) the number of ways in which parentheses can be placed in a sequence of numbers to be multiplied, two at a time; (2) the number of ways a polygon with  $n+2$  sides can be cut into  $n$  triangles; (3) the number of paths of length  $2n$  through an  $n$ -by- $n$  grid that do not rise above the main diagonal, etc. ..." - rails-roads (wires) of optimal alignment connecting localities could be approximated by monotonic paths on  $n*n$  grid having one or more 90 degree turns of length  $2n$  that do not rise above main diagonal where optimal alignment of a road (wire) is defined as a path on grid connecting two localities which does not deviate too much from theoretical straightline connecting the two localities (or more rigorously, root mean square error for a straightline fit of vertices on turns of monotone path between 2 localities is minimized). Number of such optimal alignments equals Catalan number.  
1253.9 Staircase Walk and Dyck Paths - <https://mathworld.wolfram.com/StaircaseWalk.html> - "... The number of staircase walks on a grid with  $m$  horizontal lines and  $n$  vertical lines is given by  $(m+n; m) = ((m+n)!)/(m!n!)$  (Vilenkin 1971, Mohanty 1979, Narayana 1979, Finch 2003). ..."  
1253.10 Catalan numbers and lattice walks - [http://discrete.openmathbooks.org/more/mdm/sec\\_basic-catalan.html](http://discrete.openmathbooks.org/more/mdm/sec_basic-catalan.html) - Computational hardness of finding optimal alignment in transportation networks equals hardness of finding lattice walk of least root mean square error between 90 degree turn points on monotone lattice walk and straightline fit between 2 localities. Number of least root mean square error monotone lattice walks could be (more than 1) equal to  $m!$  for  $m$  90 degree turn points ( $m \leq n$ ) based on all possible permutations of distance-squares in Root Mean Square Error (RMSE) =  $\sqrt{\sum (p_i - x_i)^2}$  for  $p_i$  = 90 degree turn points on lattice walks and  $x_i$  = points on straightline fit which are perpendicular projections from turn points. Probability of finding least RMSE monotone lattice walk =  $m!/\text{Catalan\_number}$  and brute force algorithm enumerates all lattice walks, sorts them by RMSE between straightline fit and chooses top-ranked least RMSE lattice walks by probability earlier. Previous brute force algorithm is exponential -  $O(2^n)$  to  $O(3^n)$  depending on optimizations for  $n*n$  grid.  
1253.11 Lattice walk enumeration - <https://arxiv.org/pdf/cond-mat/0404728.pdf>  
1253.12 Visualization of Urban Growth Pattern in Chennai Using Geoinformatics and Spatial Metrics - IISc - [Bharath H. Aithal, T.V. Ramachandra] - [http://wgbis.ces.iisc.ernet.in/energy/water/paper/visualization-of-urban-growth/ISRS\\_Bharath-2016-Print.pdf](http://wgbis.ces.iisc.ernet.in/energy/water/paper/visualization-of-urban-growth/ISRS_Bharath-2016-Print.pdf) - an urban sprawl study on Growth of Chennai Administrative Area and predictions for 2026 - GIS covers projected city area of ~1500 sqkms (administrative boundary + 10kms radius) - Cellular Automaton, Markov Analysis, Shannon Entropy urban growth models - City administrative area of Chennai from GHSL R2019A urban centre database (<https://ghsl.jrc.ec.europa.eu/ucdb2018visual.php#>) - 940 sqkms  
1253.13 NVIDIA DARPA Autonomous Vehicle (DAVE2) - Convolution Neural Network trained - <https://images.nvidia.com/content/tegra/automotive/images/2016/solutions/pdf/end-to-end-dl-using-px.pdf>  
-----

1254. (THEORY and FEATURE) Computational Geometric Factorization - Quadcore



benchmarks - Spark 3.0.1 + Python 3.7.x - Nanoseconds perf counter - 27 May 2022  
- related to 1214 and all sections on Computational Geometric Factorization, Set  
Partitions to Exact Square Tile Cover Reduction by Lagrange Sum of 4 Squares -  
Optimal denominations and Money Changing Problem, Integer Partitions, Equidepth-  
Equiheight V-Optimal Histograms and Set partition analytics

---

1254.1 Nick's class Computational Geometric Factorization implementation -  
DiscreteHyperbolicFactorizationUpperbound\_TileSearch\_Optimized.py - has been  
updated to print nanoseconds elapsed in factorization which raises the  
resolution of performance counter from present seconds (Greenwich mean time) by  
python primitive gmtime() to highest possible nanoseconds elapsed from epoch by  
times\_ns() primitive.

1254.2 Python time\_ns() nanoseconds function is imported and time duration perf  
counter is printed in nanoseconds from start of factorization and nanoseconds  
elapsed from beginning till each factor is found.

1254.3 20523 bits integer and 107 bits integer have been factorized (20523 bits  
integer is same as section 1214). Factors and nanosecond perf counters have been  
printed to

python-src/testlogs/DiscreteHyperbolicFactorizationUpperbound\_TileSearch\_Optimiz  
ed.log.27May2022 and  
testlogs/DiscreteHyperbolicFactorizationUpperbound\_TileSearch\_Optimized.log2.27M  
ay2022

1254.4

DiscreteHyperbolicFactorizationUpperbound\_TileSearch\_Optimized.largestintegerfac  
torized has been updated to 20523 bits integer.

---

1255. (THEORY and FEATURE) Astronomical Dataset Analytics - Planetarium  
Ephemeris Search - 1 June 2022 - related to 731,1206,1236 and all sections on  
Astronomical Dataset Mining, Archaeoastronomical Dating, Sequence Mining, String  
analytics, Sequence Alignment, Visual Planetarium Search, Archaeology,  
Reciprocal Recommender Systems based Matrimony analytics in Bipartite Social  
Networks, Climate and Extreme Weather Event Analytics

---

1255.1 MaitreyaEncHoro\_RuleSearch.py python Swiss-JPL ephemeris search  
maitreya8t text client wrapper has been updated for searching sky for a zodiac  
configuration which simulates visual timeline search for celestial bodies in  
planetarium software.

1255.2 Astronomical data are rife in ancient scriptures and most archaeological  
artefacts as religion and astronomy are often intertwined. Scientific  
corroboration of mythology and historicity of epics requires an exhaustive  
search of astronomical references in scriptures either through Planetarium  
software or traditional alternatives.

1255.3 Problem lies in computational cost of this exhaustive search to pinpoint  
historic timeline of events described in an epic which could have occurred few  
millenia ago and lack of ephemeris data for that period (possibly hindered by  
tropical-sidereal conflicts, ayanamsa conundrum among others). Exhaustive search  
could be optimized to some extent by exploiting orbital periodicity-conjunctions  
of planets and extrapolating future - e.g Eight planets were conjunct 0 degree  
of Aries during Kali era birth, Eight planets were conjunct in 1962 in Aquarius.

1255.4 Visual equivalent of earlier textual search script could be far more  
intensive and might need preprocessing but does not depend on cuspal  
boundaries :

1255.4.1 Plot visual zodiac (Degrees of Planets, Meteors, Constellations)  
from astronomical data mentioned in a treatise

1255.4.2 Do a matching image search of previous plot and Visual  
Planetarium Sky Maps dating back thousands of years - number of sky images to  
search and match could be in millions.

1255.5 MaitreyaEncHoro\_RuleSearch.py has been so far restricted to search of  
class association rules (which are subsets of 360 degree zodiac), mined from  
past extreme weather event datasets by GSP Sequence Mining and Sequence

Alignment, to predict future climate and seismic events. It has been enhanced in this commit to search a celestial configuration from text file CelestialConfiguration.txt (full 360 degree zodiac - which could be birth data of a mythological personality or event described in scriptures) in the ephemeris within a minimum-maximum range of days-months-years through maitreya8t text client.

1255.6 MaitreyaEncHoro\_RuleSearch.py has been upgraded to Python 3.7 by 2to3 + autopep8 upgrade tools. Two boolean flags ClassAssociationRuleSearch and PlanetariumSearch have been introduced to separate CAR (class association rule) search and Planetarium search (read from either MinedClassAssociationRules.txt or CelestialConfiguration.txt) and invoke either substring\_find() or a new function match\_chart\_and\_rule().

1255.7 New function match\_chart\_and\_rule() has been implemented as a container iterable alternative of string-based substring\_find() to check equality of chart data dictionary from maitreya8t and dictionary computed from CelestialConfiguration.txt and return boolean -1 (Dissimilar) or 1 (Similar). Both dictionaries have 12 key-value pairs mapping zodiac divisions to planets housed therein.

1255.8 Maitreya8t and any planetarium software are limited by availability of ephemeris data which seems to be restricted to 3000 BC and older dates are not supported. Maitreya8t provides facilities for astrological matrimonial match by following commandline options:

--file2=<str>	Open second file for partner chart
--partner-vedic	Show Vedic partner analysis
--partner-composite	Show partner composite chart

which is culture-oriented orthodox match making complementing reciprocal recommender systems followed in bipartite (Bride-Groom) matrimonial portal software.

1255.9 An example Celestial configuration for 1 June 2022 is searched by MaitreyaEncHoro\_RuleSearch.py (PlanetariumSearch=True) and match is identified as per testlogs/MaitreyaEncHoro\_RuleSearch.PlanetariumSearch.log.1June2022

#### References:

-----

1255.10 Date of Ramayana -

<https://www.vifindia.org/transcriptions-paper/2012/07/03/scientific-dating-of-ancient-events-from-7000-bc-to-2000-bc> - 5114 BC to 5075 BC derived by Planetarium software based on astronomical data in Ramayana - Sea level was 3 metres below present level 7000 years BCE.

1255.11 Aihole inscription of Kali era and Mahabharata war - 3101 BC -

<https://www.myindiamyglory.com/2018/10/27/what-aihole-inscription-of-meguti-temple-tell-about-mahabharata-war-date/>

1255.12 Milankovitch cycles - <https://climate.nasa.gov/news/2948/milankovitch-orbital-cycles-and-their-role-in-earths-climate/> - 100000(eccentricity), 41000(oblique tilt), 26000(precession) year cycles causing climate change

1255.13 Date of Mahabharata War - 3067 BC - [Prof.Srinivasa Raghavan-1891] -

<https://archive.org/details/dateofmahabharat00srinuoft> - War time placed in Kali and not Dvapara yuga

1255.14 Vartak's dating of Mahabharata war - 5561 BC -

[https://archive.org/details/ArticleOnScientificDatingOfMahabharataWar\\_PVVartakSp](https://archive.org/details/ArticleOnScientificDatingOfMahabharataWar_PVVartakSp) eakingTree/mode/2up

1255.15 Valmiki Ramayana - Yudhha Kanda - Sarga 4 - Verse 5 - "Uttaraphalguni conjoins Hasta" - implies unusual occultation of one constellation by the other - [https://www.valmikiramayan.net/utf8/yuddha/sarga4/yuddha\\_4\\_frame.htm](https://www.valmikiramayan.net/utf8/yuddha/sarga4/yuddha_4_frame.htm) - उत्तरा फल्गुनी हि अद्य श्वसु तु हस्तेन योक्ष्यते || ६-४-५ अभिप्रयाम सुग्रीव सर्व अनीक समावृताः |

1255.16 Valmiki Ramayana - Bala Kanda - Sarga 18 - Verses 8,9,10,11 - "Chaitra Navami, When Five planets were exalted, Moon-Jupiter were conjunct, Cancer ascending" - [https://www.valmikiramayan.net/utf8/baala/sarga18/bala\\_18\\_frame.htm](https://www.valmikiramayan.net/utf8/baala/sarga18/bala_18_frame.htm) - ततश्च द्वादशे मासे चैत्रे नावमिके तिथौ || १-१८-८ नक्षत्रेऽदितिदैवत्ये स्वोच्चसंस्थेषु पंचसु | ग्रहेषु कर्कटे लग्ने वाक्पताविंदुना सह

1255.17 Quintuple Planetary Groupings from 3101 BC to 2735 AD -

<https://articles.adsabs.harvard.edu//full/1994JBAA..104..293D/0000295.000.html>- Grouping on 18 February 3101 BC is axiomatically the Kali era beginning.

1255.18 Valmiki Ramayana - Kishkindha Kanda - Sarga 41 - Verses 16,17,18,19 - [https://www.valmikiramayan.net/utf8/kish/sarga41/kishkindha\\_41\\_frame.htm](https://www.valmikiramayan.net/utf8/kish/sarga41/kishkindha_41_frame.htm) - Tamraparni, Gateway of Pandyas (likely Kavatapapuram, erstwhile deluged capital of Pandyas - dating of Kavatapapuram indirectly dates Ramayana) - "... ताम्रपर्णीम् ग्राह जुष्टम् तरिष्यथ महानदीम् | ... युक्तम् कवाटम् पाण्ड्यानाम् गता द्रक्ष्यथ वानराः | ..."

1255.19 Dating of Mahabharata war by Planetarium software - 3067 BC - [Narahari Achar] - [https://www.researchgate.net/publication/237283001\\_Date\\_of\\_the\\_Mahbhrata\\_War\\_based\\_on\\_Simulations\\_using\\_Planetarium\\_Software](https://www.researchgate.net/publication/237283001_Date_of_the_Mahbhrata_War_based_on_Simulations_using_Planetarium_Software)

1255.20 Dating of Mahabharata war - 3136 BC - <https://jayasreesaranathan.blogspot.com/2021/11/published-my-new-book-mahabharata-3136.html> - dated in Dvapara yuga and based on Surya Siddhanta sidereal calendar without relying on Planetarium software (7200 years ayanamsa to-and-fro oscillation of maximum 27 degrees - separation between 0 degree Aries and Vernal equinox - as opposed to tropical 26000 year cycle of precesssional vernal equinox of Milankovitch at the rate of 50 arcseconds per year anticlockwise) - Limitations of Planetarium software and Theory of Comet hit on Earth-Moon in 3136 BC, a catastrophe causing Earth-Moon orbits to wobble recorded in Mahabharata verses.

1255.21 GIS Imagery of River Sarasvati - The Lost Courses of the Saraswati River in the Great Indian Desert: New Evidence from Landsat Imagery - [Ghose et al] - 1979 - <https://www.jstor.org/stable/633213>

1255.22 GIS Imagery of Erstwhile Deluged Dwaraka - Raised ocean floor - coast of Veraval (Prabhas Patan), Present day Dwaraka, Raivataka Parvata (Girnar) - [https://sourceforge.net/p/asfer/code/3077/tree/python-src/image\\_pattern\\_mining/ImageNet/testlogs/Dwarka\\_PrabhasPatan\\_GEBCO\\_Seabed2030\\_7June2022.jpg](https://sourceforge.net/p/asfer/code/3077/tree/python-src/image_pattern_mining/ImageNet/testlogs/Dwarka_PrabhasPatan_GEBCO_Seabed2030_7June2022.jpg) - Location of City of Dwaraka (deluged capital of Lord Krishna) is disputed as present city of Dwaraka is ~400 kms away from Prabhas Patan (or Prabhas Kshetra - mouth of Sarasvati) and Raivataka Parvata which are said to be near and accessible to legendary Dwaraka - [http://mahabharata-resources.org/harivamsa/vishnuparva/hv\\_2\\_056.html](http://mahabharata-resources.org/harivamsa/vishnuparva/hv_2_056.html) - Mahabharata - Vishnu Parva - Harivamsha - Chapter 56 - Building City of Dvaraka - Kumbakonam Edition:Southern Recension (Madhva vilas depot,Kumbakonam) - Kalayavana-Jarasandha invasion and Dvaravati - "... tatra raivatako nAma parvato nAtidUrataH ..." (Raivataka mountain is not very far)

1255.23 Lost City of Dvaraka - [SR Rao] - [https://books.google.com/books/about/The\\_Lost\\_City\\_of\\_Dv%C4%81rak%C4%81.html?id=gyFuAAAAAAJ&source=kp\\_book\\_description](https://books.google.com/books/about/The_Lost_City_of_Dv%C4%81rak%C4%81.html?id=gyFuAAAAAAJ&source=kp_book_description)

1255.24 A Bayesian phylogenetic study of the Dravidian language family - <https://royalsocietypublishing.org/doi/10.1098/rsos.171504> - "... Here, we report the results of a Bayesian phylogenetic analysis of cognate-coded lexical data, elicited first hand from native speakers, to investigate the subgrouping of the Dravidian language family, and provide dates for the major points of diversification. Our results indicate that the Dravidian language family is approximately 4500 years old, a finding that corresponds well with earlier linguistic and archaeological studies. ..." - results are arrived at by BEAST 2 Phylogeny modeller - <https://www.beast2.org/> - Cognates are words in different languages of similar meaning.

-----

1256. (THEORY and FEATURE) GIS Urban Sprawl Analytics - Bug resolutions and additional Urban sprawl Facegraph complexity measures for Automatic Urban Delineation - 3 June 2022 - related to 1226 and all sections on GIS Urban Sprawl Analytics, Merit of Large Scale Visuals, Gridded Population Estimators (SEDAC GPW4 and GHSL convex hull estimators), DBSCAN and Neural Network Urban Extent Learners, Computational Geometry, Intrinsic Merit Rankings, R Ricker Population Estimation, Community detection, Social Network Analytics, Space filling by Curves, Unequal Circle and Polynomial packing, Computational Geometry and Polygonal packing by Voronoi Tessellation, Four color theorem, Economic Merit, Computational Economics - GDP estimation from electricity consumption, Jordan Curve Theorem, Weirstrass Theorem, Cellular Automata-SLEUTH-Polya-DynamicFacegraph Urban Growth Models, Preferential attachment,Random Graphs,Dynamic Graphs,NeuronRain CoronaVirus 2019 analyzer (R and Python - GEM,R

Logit,Chaotic ERSIR Cellular Automaton Graph)

-----  
-----  
1256.1 Function urban\_sprawl\_from\_segments() in GISUrbanSprawlAnalytics.py has been updated for changed tuple parameter return values of image\_segmentation() in ImageGraph\_Keras\_Theano.py (indices of segment tuple and maximum\_population\_density have been corrected).

1256.2 Additional Graph complexity measures - HITS Hub-Authorities and Minimum Spanning Forest(Boruvka algorithm) - for Urban sprawl facegraph have been printed in GISUrbanSprawlAnalytics.py. HITS measures are very much necessary for urban sprawls as every major metro area has suburban hubs linked by authority transportation network edges to other suburbs (reduction of internet to transportation network by PageRank and HITS ranking of transportation network vertices). Minimum spanning forest of facegraphs (obtained from Voronoi tessellation-Delaunay triangulation) has been included as implementation of automatic urban delineation algorithm based on Minimum Spanning Tree of Urban sprawl Voronoi Diagrams mentioned in 1226.19.

1256.3 NASA VIIRS imagery of Chennai Metropolitan Area nightlights (17 November 2021) has been re-analyzed and following are logs,contourlabelled images and DOT files for this update:

modified:

testlogs/NASAVIIRSNightLightsChennaiMetropolitanArea\_17November2021-  
contourlabelled.jpg

modified:

testlogs/RemoteSensingGIS/NASAVIIRSNightLightsChennaiMetropolitanArea\_17November  
2021\_ImageNet\_Keras\_Theano\_Segmentation\_FaceGraph.dot  
testlogs/GISUrbanSprawlAnalytics.log.3June2022

-----  
-----  
1257. (THEORY and FEATURE) Medical Imageing and Music Information Retrieval (MIR) - fMRI imagery analysis for music-evoked autobiographical memories - 7 June 2022 - related to 228,385,410,587,588,548,656,868,1218,1223 and all sections on merit of large scale visuals, medical imageing, Evocation WordNet, ThoughtNet and Psychology of Evocation, Music search-Music discovery, Intrinsic Merit of Music, MIR(Music Information Retrieval), Music Similarity and Clustering, AI Music Synthesis, fMRI connectomes - OpenNeuro - Psychology of music, Weighted automata, Chaos, Deep Learning, Dynamic Time Warping-Timeseries analysis, Majority Voting Vs Intrinsic - Condorcet Jury Theorem variants

-----  
-----  
1257.1 Function medical\_imageing() in ImageGraph\_Keras\_Theano.py has been updated to include a clause for fMRI imagery sourced from various experimental study datasets on sensory stimuli affecting human brain, especially how an audio-visual stimulus evokes autobiographical memories of the past. With this support for ECG,MRI and fMRI medical imagery analysis have been added in NeuronRain.

1257.2 Distinguishing human enjoyable music from the rest is the cornerstone of fMRI research having far-reaching implications for music industry, music creativity or music search-music discovery if all 12-note music melody waveforms numbering 68 billion have been already found (from 1223.13). "Is the set of enjoyable music (majority voted, liked by lot) = quality music (naturally meritorious, not voted)" is another open problem in intrinsic merit of music and fits into the realm of Condorcet Jury Theorem variants for bounds on Correctness of Group Decision (Black-Ladha).

1257.3 In this update, an fMRI image for music stimulus (UCDavis dataset imagery - testlogs/medical\_imageing/fMRI\_MusicStimulus\_UCDavis\_janata\_brain\_lg.jpg) on human subjects (music genre of enjoyable-familiar nature evoking memories) has been analyzed by image\_segmentation() and its Chain approximation contours,Voronoi-Delaunay Tessellation-Triangulation,Facegraph,Watershed segments are computed as below:

(Logs)

testlogs/ImageGraph\_Keras\_Theano.MedicalImageing.fMRI\_MusicGenre.7June2022  
(fMRI image from 1257.6)

testlogs/medical\_imageing/fMRI\_MusicStimulus\_UCDavis\_janata\_brain\_lg.jpg  
(facegraph DOT)  
testlogs/medical\_imageing/fMRI\_MusicStimulus\_UCDavis\_janata\_brain\_lg\_ImageNet\_Keras\_Theano\_Segmentation\_FaceGraph.dot  
(Chain approximation contours)  
testlogs/medical\_imageing/fMRI\_MusicStimulus\_UCDavis\_janata\_brain\_lg\_contoursegm  
ented\_7June2022.jpg  
(Voronoi-Delaunay)  
testlogs/medical\_imageing/fMRI\_MusicStimulus\_UCDavis\_janata\_brain\_lg\_medical\_ima  
geing-contourlabelled.jpg  
(Watershed segmented)  
testlogs/medical\_imageing/fMRI\_MusicStimulus\_UCDavis\_janata\_brain\_lg\_segmented.j  
pg

1257.4 Evocation of Memories expressed as texts have been earlier studied and implemented in NeuronRain by various gadgets - ThoughtNet Hypergraph Evocation, Contextual Multi Armed Bandits, Reinforcement Learning and Evocation WordNet - while audio-visual evocation is the best possible formulation of ThoughtNet evocation wherein thoughts are audio-visualized and stored in ThoughtNet Hypergraph hyperedges and hypervertices (Example in Section 385).  
1257.5 If number of all possible music waveform melodies are upperbounded by 68 billion in 12-note scale, number of fMRI visuals of human brain for music sensory stimuli are upperbounded as well at 68 billion thereby narrowing down the size of fMRI dataset.

#### References:

-----  
1257.6 Study Finds Brain Hub That Links Music, Memory and Emotion - "... a golden oldie comes blaring over the radio and suddenly we're transported back - to a memorable high-school dance, or to that perfect afternoon on the beach with friends. But what is it about music that can evoke such vivid memories? ... This fMRI brain scan shows areas that respond to familiar music (green), salient memories (red), and music that is perceived as enjoyable (blue). The yellow area, in the medial prefrontal cortex, is a response both to music familiarity and salient memory. ..." - <https://www.ucdavis.edu/news/study-finds-brain-hub-links-music-memory-and-emotion>  
1257.7 The neural architecture of music-evoked autobiographical memories - [Petr Janata] - <https://pubmed.ncbi.nlm.nih.gov/19240137/>  
1257.8 Forrest Gump Dataset - <https://www.studyforreest.org/> - benchmark neuroscience sensory stimulus fMRI dataset based on movie Forrest Gump which has been set as a standard mix of emotional stimuli simulating reallife  
1257.9 Music Earworm - <https://en.wikipedia.org/wiki/Earworm> - Sticky Music Syndrome  
1257.10 Affect in Music - <https://www.jstor.org/stable/428839> - emotion arising out of music stimulus  
1257.11 Nakai, Koide-Majima, and Nishimoto (2021). Correspondence of categorical and feature-based representations of music in the human brain. Brain and Behavior - <https://pubmed.ncbi.nlm.nih.gov/33164348/> , <https://openneuro.org/datasets/ds003720/versions/1.0.0>

-----  
1258. (THEORY and FEATURE) Intrinsic Merit of Music - Kolmogorov Complexity approximation by Normalized Compression Distance (NCD) - implementation - 8 June 2022 - related to 110,1257 and all sections on Music search-Music discovery, Intrinsic Merit of Music, MIR(Music Information Retrieval), Music Similarity and Clustering, AI Music Synthesis, fMRI connectomes - OpenNeuro - Psychology of music, Weighted automata, Chaos, Deep Learning, Dynamic Time Warping-Timeseries analysis, Majority Voting Vs Intrinsic - Condorcet Jury Theorem variants, Astronomical Datasets, Multiple Sequence Alignment of Strings, Handwriting Recognition  
-----

1258.1 Intrinsic absolute Merit of music (independent of its enjoyability by majority voting) has been defined and implemented earlier by formal language

gadgets - Minimum Description Length (Kraft Inequality) and Weighted Automata learnt from string of music waveform notes based on an axiomatic assumption that quality of music is proportional to fractal nature of notes string formalized by minimum size finite state automata accepting it and Kolmogorov complexity.

1258.2 In this commit, a new approximation of Kolmogorov complexity (or Normalized Information Distance which is Turing undecidable) - Normalized Compression Distance (NCD) - first introduced by [Cilibrasi-Vitanyi] as universal distance measure for datasets in "genomics, virology, languages, literature, music, handwritten digits, astronomy, and combinations of objects from completely different domains, using statistical, dictionary, and block sorting compressors", has been implemented as a function `normalized_compression_distance()` within `MinimumDescLength.py`.

1258.3 `MinimumDescriptionLength.py` and `Entropy.py` have been upgraded to Python 3.7. Usage of `Zlib.compress()` within `MinimumDescLength.py` has been now augmented with a `bytes()` binary cast and encoding to utf-8.

1258.4 Following are excerpts of logs -  
`python-src/music_pattern_mining/testlogs/AudioToBitMatrix.log.KolmogorovComplexityNCD.8June2022` - which compute Minimum Descriptive Lengths (Kraft Inequality) and Normalized Compression Distance for 2 music waveforms of JS Bach:

```

('Merit of Audio - Minimum Descriptive Length and Entropy:',
('725.9117890720116', '1.9348455721183275'))
('Merit of Audio - Minimum Descriptive Length and Entropy:',
('733.1497901326836', '2.49102248187773'))
Normalized Compression Distance (approximation of Kolmogorov Complexity)
between 2 strings: 0.9917355371900827

```

#### References:

1258.5 Clustering by Compression - [Cilibrasi-Vitanyi] - CWI -  
<https://arxiv.org/pdf/cs/0312044.pdf> - Normalized Compression Distance - new Bigdata distance measure - "... A theoretical precursor, the normalized information distance, co-developed by one of the authors, is provably optimal in the sense that it minorizes every computable normalized metric that satisfies a certain density requirement. However, the optimality comes at the price of using the non-computable notion of Kolmogorov complexity. We propose precise notions of similarity metric, normal compressor, and show that the NCD based on a normal compressor is a similarity metric that approximates optimality. ..." - Figure 16 - Clustering of Music Genre (Classic which includes JS Bach, Jazz, Rock and Pop)

1259. (THEORY and FEATURE) Computational Geometric Factorization - 20610 bits huge integer quadcore benchmarks - Spark 3.0.1 + Python 3.7.5 - 10 June 2022 - related to 1254 and all sections on Computational Geometric Factorization, Set Partition to Tile cover reduction by Integer Factorization, Integer Partitions, Histogram Analytics, Neuro fictitious cryptocurrency proof-of-work and Money changing problem

1259.1 Depth of Nick's class `non-uniform circuit (Sequential Iteration)` in `DiscreteHyperbolicFactorizationUpperbound_TileSearch_Optimized.py` has been set to  $O((\log N)^k)$  instead of  $O((\log N)^{2k})$  to remove confusion on depth of the circuit. After this change the pseudocode for polylogarithmic factorization is:  
 Sequentially Iterate for  $O((\log N)^k)$  steps

```

{
 allocate $O(N/(\log N)^k)$ rasterized hyperbolic arc bow segments to each
 parallel processor (theoretically $O(N/(\log N)^k)$ multicores-PRAMS are necessary
 per segment by definition of Nick's class for polysize, logdepth circuit) by
 parallelize() for sequential $O(\log N)$ binary search with in each processor
}

```

which effectively equals  $O(\log N^k) * O(\log N) = O((\log N)^{(k+1)})$  parallel time

(or) logdepth of the non-uniform circuit is  $(k+1)$  for  $O(N/(\log N)^k)$  multicores.  
1259.2 Huge 20610 bits integer has been factorized by  
DiscreteHyperbolicFactorizationUpperbound\_TileSearch\_Optimized.py in quadcore  
after earlier change and some optimizations to Spark config because of following  
exception for large integers which causes Spark crash. Faulthandler python  
package has been imported and enabled:

```
=====
py4j.protocol.Py4JJavaError: An error occurred while calling
z:org.apache.spark.api.python.PythonRDD.collectAndServe.
: org.apache.spark.SparkException: Job aborted due to stage failure: Task 0 in
stage 0.0 failed 1 times, most recent failure: Lost task 0.0 in stage 0.0 (TID
0, ksrinivasan-Acer-One-14-Z422, executor driver): java.net.SocketException:
Connection reset
 at java.net.SocketInputStream.read(SocketInputStream.java:210)
 at java.net.SocketInputStream.read(SocketInputStream.java:141)
 at java.io.BufferedInputStream.fill(BufferedInputStream.java:246)
 at java.io.BufferedInputStream.read(BufferedInputStream.java:265)
 at java.io.DataInputStream.readInt(DataInputStream.java:387)
 at org.apache.spark.api.python.PythonRunner$
$anon$3.read(PythonRunner.scala:628)
 at org.apache.spark.api.python.PythonRunner$
$anon$3.read(PythonRunner.scala:621)
 at
org.apache.spark.api.python.BasePythonRunner$ReaderIterator.hasNext(PythonRunner
.scala:456)
 at
org.apache.spark.InterruptibleIterator.hasNext(InterruptibleIterator.scala:37)
 at scala.collection.Iterator.foreach(Iterator.scala:941)
 at scala.collection.Iterator.foreach$(Iterator.scala:941)
 at
org.apache.spark.InterruptibleIterator.foreach(InterruptibleIterator.scala:28)
 at scala.collection.generic.Growable.$plus$plus$eq(Growable.scala:62)
 at scala.collection.generic.Growable.$plus$pluseq(Growable.scala:53)
 at scala.collection.mutable.ArrayBuffer.
$plus$plus$eq(ArrayBuffer.scala:105)
 at scala.collection.mutable.ArrayBuffer.
$plus$plus$eq(ArrayBuffer.scala:49)
 at scala.collection.TraversableOnce.to(TraversableOnce.scala:315)
 at scala.collection.TraversableOnce.to$(TraversableOnce.scala:313)
 at
org.apache.spark.InterruptibleIterator.to(InterruptibleIterator.scala:28)
 at scala.collection.TraversableOnce.toBuffer(TraversableOnce.scala:307)
 at scala.collection.TraversableOnce.toBuffer$(TraversableOnce.scala:307)
 at
org.apache.spark.InterruptibleIterator.toBuffer(InterruptibleIterator.scala:28)
 at scala.collection.TraversableOnce.toArray(TraversableOnce.scala:294)
 at scala.collection.TraversableOnce.toArray$(TraversableOnce.scala:288)
 at
org.apache.spark.InterruptibleIterator.toArray(InterruptibleIterator.scala:28)
 at org.apache.spark.rdd.RDD.$anonfun$collect$2(RDD.scala:1004)
 at org.apache.spark.SparkContext.
$anonfun$runJob$5(SparkContext.scala:2139)
 at org.apache.spark.scheduler.ResultTask.runTask(ResultTask.scala:90)
 at org.apache.spark.scheduler.Task.run(Task.scala:127)
 at org.apache.spark.executor.Executor$TaskRunner.
$anonfun$run$3(Executor.scala:446)
 at org.apache.spark.util.Utils$.tryWithSafeFinally(Utils.scala:1377)
 at org.apache.spark.executor.Executor$TaskRunner.run(Executor.scala:449)
 at
java.util.concurrent.ThreadPoolExecutor.runWorker(ThreadPoolExecutor.java:1149)
 at
java.util.concurrent.ThreadPoolExecutor$Worker.run(ThreadPoolExecutor.java:624)
 at java.lang.Thread.run(Thread.java:748)
=====
```





[illegible]



$$O(N/(\log N)^{1437}) = 2^{20610}/(\log(20610))^{1437}$$

$$= 2^{20610}$$

----- (for  $\log(20610) = 14.33$ )

$$2^{(1437 \times 14.33)}$$

$$= 2^{(20610 - 20594)}$$

$$= O(2^{(16)}) = 65536 \text{ approximately which is not unusual for cloud computing}$$

mapreduce frameworks (though software version is under the purview of mapreduce class MRC) and supercomputers which are under true Nick's class - Fugaku Supercomputer has 158976 parallel processors

#### References:

-----  
1259.1 Rectification of Hyperbola by two ellipses -

<https://royalsocietypublishing.org/doi/epdf/10.1098/rstl.1811.0007> -

$O(N/(\log N)^k)$  hyperbolic arc tile segments one each per multicore processor in loop earlier are straightline approximations of the hyperbola

1259.2 The hyperbola rectification from Maclaurin to Landen and the Lagrange-Legendre transformation for the elliptic integrals -

<https://arxiv.org/pdf/1209.4909.pdf>

-----  
1260. (THEORY and FEATURE) People Analytics - Unique Identification -

Fingerprint recognition - 17 June 2022 - related to 834,1223,1237 and all

sections on Merit of Large Scale Visuals, Physique Recognition From

Quadrilateral mesh isomorphism, Topological Face and Handwriting recognition,

Product Homotopy, Unique identification, Homeomorphism and Topological

Deformations, Merit of Large Scale Visuals, People Analytics, Computational

Geometry, Graph Edit Distance and Earth mover distance, Graph Isomorphism

(Exact, Approximate and Subgraph), Graph matching, Graph similarity, Image

Search, Quadrilateral Mesh Deformation and Isomorphism, Maximum Common Subgraph

Problem and Approximate Topological Matching, Cybercrime analytics, Forensics-

Predictive Policing, Fraud Analytics, Birthday Paradox, Contextual Name Parsing,

PIPL Name syllable based unique person search, Collision resistant hash

functions, Non Fungible Tokens

-----  
1260.1 Various forms of unique identification namely Face, Physique,

Handwriting, Gender have been either theoretically analyzed or implemented in

NeuronRain through graph theoretic and topological similarity algorithms based

on Product Homotopy, Graph Isomorphism, Dynamic time warping timeseries

similarity (of human physique mobility), Graph Edit Distance, Netrd Graph

distances, TriMesh-QuadMesh and Topological homeomorphic deformations, Voronoi-

Delaunay tessellation-triangulation, Maximum Common Subgraph, Approximate

Topological Matching among others.

1260.2 This update defines a new function fingerprint\_recognition() in

DeepLearning\_ConvolutionNetwork\_BackPropagation.py for matching two images of

fingerprints (fingerprint1.jpeg and fingerprint2.jpeg) based on Kaggle academic

research dataset FVC2000 for fingerprint deeplearning -

[https://www.kaggle.com/datasets/peace1019/fingerprint-dataset-for-fvc2000-db4-b?](https://www.kaggle.com/datasets/peace1019/fingerprint-dataset-for-fvc2000-db4-b?resource=download)

resource=download thereby adding fingerprint dimension to unique identification arsenal.

1260.3 Function fingerprint\_recognition() earlier defined computes contour

segmentation by chain approximation for two fingerprints, finds the Hausdorff

topological distance between two sets of contour polynomials belonging to

either, and clusters the fingerprint contour polynomials of the two images by

KMeans clustering algorithm in ImageGraph\_Keras\_Theano.py

(contours\_kmeans\_clustering())

1260.4 Human fingerprints are topologically significant as every fingerprint

contains clusters of curves or family of polynomials of almost similar

curvature. Contour polynomials-Graph structure from fingerprints could be

extracted by watershed, voronoi-delaunay and chain approximation algorithms in

image\_segmentation() and image\_segmentation\_contours() functions of

ImageGraph\_Keras\_Theano.py

1260.5 DeepLearning\_ConvolutionNetwork\_BackPropagation.py has been refactored as below:

1260.5.1 TopologicalRecognition has been changed from a boolean flag to a string of 3 values - "Fingerprint", "Face" or "Handwriting" which are used within 3 clauses for invocation of face, handwriting or fingerprint recognition routines accordingly

1260.5.2 Graphics for drawing K-Means clustering of contours has been changed from OpenCV drawContours() to Matplotlib plot which differentiates the color coded clusters well.

1260.5.3 Matplotlib show() invocations have been changed to savefig() to write the images for watershed segments, chain approximation contour segments, Voronoi-Delaunay, K-Means clustered contours as JPEG files.

1260.5.4 Directory paths for earlier JPEG images written have been made relative by prefixing ./ and new folder RemoteSensingGIS/ has been created under python-src/testlogs

1260.5.5 Following are the image files and logs for this update:

(logs - clusters and Hausdorff distance between fingerprints)

testlogs/DeepLearning\_ConvolutionNetwork\_BackPropagation.log.17June2022

(k-means clustering) testlogs/fingerprint1-

contourkmeansclustered.jpg

(Voronoi-Delaunay set to False) testlogs/fingerprint1-

contourlabelled.jpg

(Chain approximation contours) testlogs/fingerprint1-

contoursegmented.jpg

(Fingerprint1) testlogs/fingerprint1.jpeg

(k-means clustering) testlogs/fingerprint2-

contourkmeansclustered.jpg

(Voronoi-Delaunay set to True) testlogs/fingerprint2-

contourlabelled.jpg

(Chain approximation contours) testlogs/fingerprint2-

contoursegmented.jpg

(Fingerprint2) testlogs/fingerprint2.jpeg

(DOT)

testlogs/RemoteSensingGIS/fingerprint1\_ImageNet\_Keras\_Theano\_Segmentation\_FaceGraph.apk.dot

(Watershed) testlogs/RemoteSensingGIS/fingerprint1\_segmented.jpg

(DOT)

testlogs/RemoteSensingGIS/fingerprint2\_ImageNet\_Keras\_Theano\_Segmentation\_FaceGraph.apk.dot

(Watershed) testlogs/RemoteSensingGIS/fingerprint2\_segmented.jpg

1260.6 Computational Hardness of unique identification has been studied in theory through collision resistance of hash functions, Minimal Perfect Hash Functions, birthday paradox et al. Designing a dispute-resistant foolproof Unique ID scheme for population and social networks is still a farcry. An example digitally signed unique id string digest for a person: <10-digit fingerprint>:<retinal scan>:<physique or face photo>:<written signature>:<voice>:<ip address or geocoded address>:<timestamp> though theoretically comprehensive, exponentially hard and collision-resistant suffers from lacunae - worn out biometrics-voicemetrics, signature forgery, prosthetics, cosmetic surgically modified eye, face and physiques might mar its efficacy essentially making a compelling case for non-biometric Non Fungible Tokens (unique private event, art and music) as unique id(s).

-----  
1261. (THEORY and FEATURE) Intrinsic merit of Music - Music Information Retrieval - AI Music Synthesis from Weierstrass Fourier Fractal - related to 110,1223,1224,1257,1258 and all sections on Music search-Music discovery, Intrinsic Merit of Music, MIR(Music Information Retrieval), Music Similarity and Clustering, AI Music Synthesis from summation of damped sinusoids, fMRI connectomes - OpenNeuro - Psychology of music, Weighted automata, Chaos, Deep Learning, Dynamic Time Warping-Music Timeseries analysis, Music Evoked Autobiographical Memories, ThoughtNet, Majority Voting (Enjoyable music) Vs Intrinsic (Quality music) - Condorcet Jury Theorem variants - 21 June 2022

-----

1261.1 AudioToBitMatrix.py has been updated to define a new function `weierstrass_fractal_fourier_sinusoids(a,b,n)` which implements celebrated Weierstrass Function, a fractal fourier sinusoidal summation that is continuous everywhere and differentiable nowhere which could be a candidate for AI fractal music synthesis by summation of damped sinusoids. This function computes the summation in a loop subject to the constraint (reference: 1261.4) and returns the fourier series as a huge string length of which is tunable depending on parameters `a` (coefficient), `b` (radian multiple) and `n` (maximum exponent).

1261.2 String for Weierstrass function returned from `weierstrass_fractal_fourier_sinusoids()` is passed on to `notes_to_audio()` as lambda function to evaluate. Weierstrass Function for an example set of parameters is written to `testlogs/AudioToBitMatrix.log.MusicSynthesizer.Weierstrass.log.21June2022` and synthesized music waveform from Weierstrass function for `a=0.5,b=5,n=20` is written to `function_synthesized_music.wav` loadable in Audacity.

1261.3 Music waveforms of arbitrary complexity could be synthesized from Weierstrass function by varying parameters `a,b,n`. Music waveforms are theoretically summation of multiple periodic waveforms - piecewise or continuous - which may be sinusoidal. Synthesizing music from mathematical functions so far is less of AI and more computational - Synthesizing human enjoyable (or discovering melodies from 68 billion 12-note possibilities - 1223.13) music through AI would hypothetically be as follows:

```

for all a,b,n:
{
 1261.3.1 Obtain fMRI imagery for Weierstrass Function synthesized music
 waveform stimulus for a,b,n (or) enumerate all 68 billion 12-note melodies
 1261.3.2 Label the fMRI imagery for "enjoyable" autobiographical memory
 evoking music as "potential candidates" e.g corresponding to "blue" regions of
 cortex in 1257.6
 1261.3.3 Cluster or find similarities in the music waveforms for
 "potential candidates" - patterns found in music waveforms thereof could be
 generating functions for enjoyable music or melodies
}

```

#### References:

-----

1261.4 Weierstrass Function - [https://en.wikipedia.org/wiki/Weierstrass\\_function](https://en.wikipedia.org/wiki/Weierstrass_function)  
 - Continuous everywhere but differentiable nowhere - "...in Weierstrass's original paper, the function was defined as a Fourier series: 
$$f(x) = \sum_{n=0}^{\infty} a^n \cos(b^n \pi x), f(x) = \sum_{n=0}^{\infty} a^n \cos(b^n \pi x),$$
 where 
$$0 < a < 1, \{ \displaystyle b \} b \text{ is a positive odd integer, and } \{ \displaystyle ab > 1 + \frac{3}{2} \pi . \} ab > 1 + \frac{3}{2} \pi .$$
 ...."

1261.5 TensorFlow Magenta - Music and Art by Machine Learning - <https://magenta.tensorflow.org/>

-----

1262. (THEORY and FEATURE) GIS Urban Sprawl Analytics - Moran's I measure of Urban Sprawl Dispersion - 23 June 2022 - related to 1151,1174,1196,1226,1233,1234,1237,1252 and all sections on GIS Urban Sprawl Analytics, Merit of Large Scale Visuals, Gridded Population Estimators (SEDAC GPW4 and GHSL convex hull estimators), DBSCAN and Neural Network Urban Extent Learners, Computational Geometry, Intrinsic Merit Rankings, R Ricker Population Estimation, Community detection, Social Network Analytics, Space filling by Curves, Unequal Circle and Polynomial packing, Computational Geometry and Polygonal packing by Voronoi Tessellation, Four color theorem, Economic Merit, Computational Economics - GDP estimation from electricity consumption, Jordan Curve Theorem, Weierstrass Theorem, Cellular Automata-SLEUTH Urban Growth Models, Automatic Delineation of Urban Growth Boundaries, Preferential attachment, Random Graphs, Dynamic Graphs, Separate Chaining Hash tables, Unmanned Aerial Vehicle Navigation-Autonomous Drone Delivery-Drone EVMs-Passenger Drones, Wiring Problem

-----  
-----  
1262.1 GISUrbanSprawlAnalytics.py has been updated to implement statistical measure of Moran's I in a function urban\_sprawl\_dispersion() called as subroutine from urban\_sprawl\_from\_segments(). Moran's I is proportional to gravity of an urban area and a quantifier of how spatially dispersed an Urban Sprawl GIS (diffusion factor) is in terms of tree canopy(NDVI), building coverage, land usage, transportation network among others.

1262.2 Moran's I ranges from -1 (perfect dispersion) to +1 (lopsided dispersion) with 0 being the inflexion point(random dispersion). Color coded pixels of urban sprawl settlement GIS (SEDAC, HRSL, GHSL) are basically scatterplots of multiple land use segments (29-colored LUIS in 1174.8.5) and Moran's I of those urban sprawl GIS imagery is an analytics measure of equitable distribution of segments in an urban area.

1262.3 Function urban\_sprawl\_dispersion() internally invokes PySAL (Python Spatial Abstraction Library) implementations of Lat2W, Moran's I and Moran's p-norm and a new function image3D\_to\_2D() defined within ImageToBitMatrix.py for flattening 3D OpenCV2 array for an image to 2D array of dimensions height\*width, entries of which are sum of RGB values of the respective pixel ordinates.

1262.4 Urban sprawl diffusion factor (Moran's I dispersion) is computed for (excerpts from testlogs/GISUrbanSprawlAnalytics.log.23June2022.xz):

- 1) GHSL imagery testlogs/GHSL\_GIS\_ChennaiMetropolitanArea.jpg:  
Moran's I of the Urban Sprawl dispersion: 0.8848283189311299  
Moran's p-norm of the Urban Sprawl dispersion: 0.0

- 2) VIIRS imagery

NASAVIIRSNightLightsChennaiMetropolitanArea\_17November2021.jpg

Moran's I of the Urban Sprawl dispersion: 0.99

Moran's p-norm of the Urban Sprawl dispersion: 0.0

1262.5 Invocation of contours\_kmeans\_clustering() has been included in urban\_sprawl\_from\_segments() analytics pipeline and k-means clustering of transit network contours computed from testlogs/GHSL\_GIS\_ChennaiMetropolitanArea.jpg show a distinct 3-cluster layering (big, bigger and biggest) of transportation contours from city centre to suburbs coded in 3 colors automatically delineating urban sprawl boundaries based on transportation contour clusters.

1262.6 Following are logs, DOT and imagery for Watershed segments, Chain approximation contour segments, Voronoi-Delaunay, k-means clustering for this commit:

testlogs/GHSL\_GIS\_ChennaiMetropolitanArea-contourkmeansclustered.jpg

testlogs/GHSL\_GIS\_ChennaiMetropolitanArea-contourlabelled.jpg

testlogs/GHSL\_GIS\_ChennaiMetropolitanArea-contoursegmented.jpg

testlogs/GISUrbanSprawlAnalytics.log.23June2022.xz

testlogs/NASAVIIRSNightLightsChennaiMetropolitanArea\_17November2021-contoursegmented.jpg

testlogs/RemoteSensingGIS/GHSL\_GIS\_ChennaiMetropolitanArea\_ImageNet\_Keras\_Theano\_Segmentation\_FaceGraph.dot

testlogs/RemoteSensingGIS/GHSL\_GIS\_ChennaiMetropolitanArea\_segmented.jpg

References:

-----  
-----  
1262.7 Categorization of 48 Mega-Regions by Spatial Patterns of Population Distribution: The Relationship between Spatial Patterns and Population Change - 48th ISOCARP Congress 2012 - [Yuta Uchiyama, Akiko Okabe] -

[https://www.isocarp.net/Data/case\\_studies/2130.pdf](https://www.isocarp.net/Data/case_studies/2130.pdf) - Clustering of 48 megaregions by Moran's I, M-value and N-value of population density

1262.8 ArcGIS Pro Spatial AutoCorrelation -

<https://pro.arcgis.com/en/pro-app/2.8/tool-reference/spatial-statistics/spatial-autocorrelation.htm>

-----  
-----  
1263. (THEORY and FEATURE) People Analytics - Social Network Analysis (Professional) - Chaotic Hidden Markov Model of Career Transition - JSON

persistence to MongoDB - 24 June 2022 - related to 14,365,711,753,876,1127,1128,1129,1130,1204 and all sections on People Analytics, Intrinsic Merit Versus Fame Equilibrium, BKS Conjecture, Stability and Noise Sensitivity of Interview LTF/PTF, Peres Theorem, Unique Identification, HR Analytics and Automated Recruitment, Question-Answering, Majority Voting, Condorcet Jury Theorem Variants, Margulis-Ruzzo Thresholds, Novelty Detection, Recommender Systems, Urban Sprawl Analytics, AI Question-Answering

-----

1263.1 SocialNetworkAnalysis\_PeopleAnalytics\_ChaoticHMM.py has been changed to read career profile JSONs from MongoDB instead of flatfile. Streaming\_AbstractGenerator.py has been accordingly updated to include a clause for MongoDB-JSON object streaming in addition to existing clause for MongoDB-GIS Visual object streaming - MongoDB client code for database (neuronrainjson) and collections have been made part of the `__init__` and `__iter__` member functions.

1263.2 An example career transition profile JSON of author SocialNetworkAnalysis\_PeopleAnalytics\_ChaoticHMM.json has been populated in a MongoDB database neuronrainjson and collection "bucket2" which is read as an iterable by Streaming\_AbstractGenerator.py

1263.3 Logs for earlier code changes - testlogs/SocialNetworkAnalysis\_PeopleAnalytics\_ChaoticHMM.log.24June2022. Merit of Social or Professional Profiles in candidate recruitment or complexity of Human Interviews/Contests/Question-Answering in its broader theoretical HR analytics context, have been central to the discussions throughout NeuronRain theory drafts supra formalized by a supremacy contrast between Hardness and Goodness of Majority voting and Hardness and Goodness of Intrinsic Merit. Recently there have two significant strides in AI - GPT3 and DALL-E - which are respectively \*) AI text question-answering and \*) text-to-image generation systems (converse of image-to-text ImageNet and could be thought visualizer for ThoughtNet and Autobiographical Memory Evocation) mostly driven by massive datasets and transformer attention sequence pipeline. Computational complexity of Question-Answering (Interview algorithm) has been theoretically analyzed in NeuronRain Design - in [https://github.com/shrinivaasanka/Krishna\\_iResearch\\_DoxygenDocs/blob/master/kuja27\\_website\\_mirrored/site/kuja27/InterviewAlgorithmInPSPACE.pdf](https://github.com/shrinivaasanka/Krishna_iResearch_DoxygenDocs/blob/master/kuja27_website_mirrored/site/kuja27/InterviewAlgorithmInPSPACE.pdf) as Total Quantified Boolean Formulae (TQBF), a PSPACE-complete problem, and as Linear Threshold Functions-Polynomial Threshold Functions.

#### References:

-----

1263.4 GPT3 - OpenAI - <https://arxiv.org/pdf/2005.14165.pdf>, <https://github.com/openai/gpt-3>

1263.5 DALL-E - OpenAI - <https://openai.com/blog/dall-e/>

1263.6 Question answering by humans and machines: A complexity-theoretic view - <https://www.sciencedirect.com/science/article/abs/pii/S0304397518305280> - "... We show that cognitive automata and QA-machines have exactly the same potential in realizing question-answering sessions, provided the resource bounds in one model are sufficient to match the abilities of the other. In particular, polynomially bounded cognitive automata with background intelligence (i.e. human agents) prove to be equivalent to polynomially bounded QA-machines with logarithmic learning space. It generalizes Pippenger's theorem on the computational power of switching circuits (without background intelligence) to a foundational result for question answering in cognitive science. ..."

1263.7 Computational Complexity of GPT3 - <https://lamdalabs.com/blog/demystifying-gpt-3/> - "...the largest language model ever trained. GPT-3 has 175 billion parameters and would require 355 years and \$4,600,000 to train - even with the lowest priced GPU cloud on the market. [1]..."

1263.8 Fault-tolerant circuit-switching networks - [Nick Pippenger, Geng Lin] - <https://dl.acm.org/doi/pdf/10.1145/140901.141867> - Theorem 1 - "if a graph  $G$  has  $k$  failed edges, the probability that the random instance of  $N$  equals  $G$  is  $(2e)^k(1 - 2e)^{(n-k)}$ , where  $n$  is the number of edges in  $N$ ... it is said to be a "rearrangeable  $n$ -network-" if, given any one-to-one correspondence between the

inputs and the outputs, there exists a set of  $n$  vertex-disjoint paths joining each input to its corresponding output; it is said to be an  $n$ -superconcentrator if, for every  $r \leq n$ , every set of  $r$  inputs, and every set of  $r$  outputs, there exists a set of  $r$  vertex-disjoint paths from the given inputs to the given outputs. It is obvious that a non-blocking  $n$ -network is a rearrangeable  $n$ -network and a rearrangeable  $n$ -network is an  $n$ -superconcentrator ... The strategy of the lower bound proof is as follows. We associate with each input a neighborhood containing all vertices within a logarithmic distance of the input. We show that for a large set of inputs, these neighborhoods are disjoint (otherwise two inputs would be shorted by closed failures with high probability). This gives the lower bound for depth ...

**Theorem 1:** Let  $\Phi$  be a  $(1/4, 1/2)$  - $n$ -superconcentrator. For all sufficiently large  $n$ ,  $\Phi$  has size at least  $(1/256)n(\log(n))^2$  and depth at least  $(1/8)\log(n)$ .

" - Circuit-switching circuits are theoretical random graph ancestors of present day Byzantine Fault Tolerant cloud computing (each switch maps to an edge with failure probability) and Cognitive automata Question-Answering machines are fault-tolerant switching circuits augmented with intelligence of the past which is lacking in Switching circuits model. Earlier lowerbound implies depth of Question-Answering circuit is atleast logarithmic and size is atleast polynomial in number ( $n$ ) of vertex disjoint paths which does not rule out the possibility of parallelism in Question-Answering (reallife simulation of parallel Q&A could be non-trivial as interviews are usually sequential one-on-one and not many-on-many).

-----

1264. (THEORY and FEATURE) Space Archaeology - Edge detection for Airborne-Satellite GIS imagery (LIDAR, SAR, LandSat) by Canny Edge Detector - related to 1203, 1232, 1233, 1236, 1237, 1240, 1255 and all sections on Merit of Large Scale Visuals, Physique Recognition From Quadrilateral mesh isomorphism, Topological Face and Handwriting recognition, Archaeology-Topological Script Recognition, Product Homotopy, Homeomorphism and Topological Deformations, People Analytics, Computational Geometry, Graph Edit Distance and Earth mover distance, Graph Isomorphism (Exact, Approximate and Subgraph), Graph matching, Graph similarity, Image Search, Quadrilateral Mesh Deformation and Isomorphism, Maximum Common Subgraph Problem and Approximate Topological Matching, Archaeoastronomical Dating of Scriptures and Mythologies

-----

1264.1 ImageGraph\_Keras\_Theano.py has been updated to implement a new function `image_segmentation_edge_detection()` which internally invokes Canny Edge Detector algorithm of OpenCV2 to detect dominant edges in an image which complements already existing Chain approximation contour segmentation.

1264.2 Canny edge detector applies a Gaussian convolution kernel on an image to magnify prominent pixels along edges of objects in it and thresholds the non-edge pixels which are filtered out leaving only edges in resultant image - following steps summarize Canny Edge Detector:

- 1264.2.1 Noise filtering by Gaussian 5\*5 kernel
- 1264.2.2 Sobel kernel for each pixel to find its first derivative intensity gradient and direction
- 1264.2.3 Non-local maxima pixels based on Gradient are removed.
- 1264.2.4 Hysteresis thresholding to remove edges which are not within minimum and maximum intensity gradient values

1264.3 Space archaeology (Satellite and Airborne) by GIS infrared imagery from Airborne LIDAR-Synthetic Aperture Radar(SAR) and LandSat satellite imagery has met with much success recently in non-invasively penetrating the superficial ground obstacles (Sand dunes, Trees) to map subterranean artefacts (upto few metres depth) which would have otherwise required random digging, thereby furthering Ground Penetrating Radar (GPR) imaging to next level e.g. new structures discovered underground in Mayan sites, Peru, Iram, Egypt. Canny edge detector is useful in archaeology to identify ancient pathways, drains, viaducts (which are edges) constructed by ancient civilizations.

1264.4 An example costly LIDAR 3D imagery of a Mayan pyramid - `testlogs/Mayan_Canaa_Pyramid_Caracol_LIDAR.jpg` - invisible earlier and excavated after LIDAR imaging, has been Canny edge detected by earlier function invoked



as part of image\_segmentation()

1264.5 Following are logs, DOT, image files (Voronoi-Delaunay, Watershed, Chain approximation, Canny Edge Detection) for this update:

testlogs/ImageGraph\_Keras\_Theano.CannyEdgeDetection.log.28June2022  
testlogs/Mayan\_Canaa\_Pyramid\_Caracol\_LIDAR-cannyedgedetection.jpg  
testlogs/Mayan\_Canaa\_Pyramid\_Caracol\_LIDAR-contourlabelled.jpg  
testlogs/Mayan\_Canaa\_Pyramid\_Caracol\_LIDAR-contoursegmented.jpg  
testlogs/Mayan\_Canaa\_Pyramid\_Caracol\_LIDAR.jpg

testlogs/RemoteSensingGIS/Mayan\_Canaa\_Pyramid\_Caracol\_LIDAR\_ImageNet\_Keras\_Theano\_Segmentation\_FaceGraph.dot

testlogs/RemoteSensingGIS/Mayan\_Canaa\_Pyramid\_Caracol\_LIDAR\_segmented.jpg

References:

-----  
1264.6 Space Archaeology - NASA -

<https://earthobservatory.nasa.gov/images/91071/space-archaeology-in-the-realm-of-resolution>

1264.7 Space Archaeology - LIDAR imagery of Canaa Pyramid - Caracol -

<https://earthobservatory.nasa.gov/features/SpaceArchaeology>

1264.8 Egypt: What Lies Beneath - Documentary -

<https://www.discoveryplus.in/videos/egypt-what-lies-beneath/egypts-lost-cities>

1264.9 Satellite Archaeology -

[https://en.wikipedia.org/wiki/Remote\\_sensing\\_\(archaeology\)](https://en.wikipedia.org/wiki/Remote_sensing_(archaeology)) - UAV and Remote sensing imagery aided excavations related to Maya and its Collapse, Peru, Iram, Egypt and Roman

-----  
1265. (THEORY and FEATURE) GIS Urban Sprawl Analytics - Automatic Delineation of Urban Growth Boundaries by KMeans Clustering of Contour Polynomials and Canny Edge Detector - Recomputed - 30 June 2022 - related to

1151, 1174, 1196, 1226, 1233, 1234, 1237, 1252, 1253, 1262 and all sections on GIS Urban Sprawl Analytics, Merit of Large Scale Visuals, Gridded Population Estimators (SEDAC GPW4 and GHSL convex hull estimators), DBSCAN and Neural Network Urban Extent Learners, Computational Geometry, Intrinsic Merit Rankings, R Ricker Population Estimation, Community detection, Social Network Analytics, Space filling by Curves, Unequal Circle and Polynomial packing, Computational Geometry and Polygonal packing by Voronoi Tessellation, Four color theorem, Economic Merit, Computational Economics - GDP estimation from electricity consumption, Jordan Curve Theorem, Weirstrass Theorem, Cellular Automata-SLEUTH Urban Growth Models, Automatic Delineation of Urban Growth Boundaries, Preferential attachment, Random Graphs, Dynamic Graphs, Separate Chaining Hash tables, Unmanned Aerial Vehicle Navigation-Autonomous Drone Delivery-Drone EVMs-Passenger Drones, Wiring Problem

-----  
1265.1 GISUrbanSprawlAnalytics.py has been updated to add 2 new parameters set to 2 by default (which completes faster within an hour, higher number of clusters and iterations are computationally intensive lasting upto few hours) - number of clusters and number of iterations - to function urban\_sprawl\_from\_segments() which are in turn passed onto contours\_kmeans\_clustering() for automatic urban growth boundary delineation by clustering of urban sprawl transportation network contour polynomials.

1265.2 Canny Edge Detector algorithm which is recently introduced in image\_segmentation() could as well be used for detecting transportation network edges (rail, road) from an urban sprawl GIS map apart from Chain approximation contour polynomial segments subject to the constraint that the transportation network edges (roads and rail tracks) must be mostly straightlines.

1265.3 KMeans clustering of contour polynomials and Canny Edge Detection have been computed for Google Maps and GHSL urban transportation GIS images of Chennai urban sprawl - 1)

testlogs/ChennaiMetropolitanAreaTransitNetwork\_GoogleMaps\_20May2022.jpg and 2)  
testlogs/GHSL\_GIS\_ChennaiMetropolitanArea.jpg - by

ImageGraph\_Keras\_Theano.image\_segmentation() and GISUrbanSprawlAnalytics.urban\_sprawl\_from\_segments(). Canny edge detector reasonably approximates curved transportation network edges by piecewise axis-parallel straightlines simulating staircase random walks of multiple 90 degree turns between localities on lattice grid.

1265.4 Deficient color-coding in KMeans contours clustering imagery of testlogs/ChennaiMetropolitanAreaTransitNetwork\_GoogleMaps\_20May2022.jpg has been rectified by earlier recomputation and transportation network contour polynomials have been segregated into 2 clusters (coded by light and dark green color pixels) implicitly delineating a boundary.

1265.5 Following are the imagery and log files affected by this update - Contour Chain Approximation, Canny Edge Detector, KMeans clustering, Voronoi-Delaunay:  
 testlogs/ChennaiMetropolitanAreaTransitNetwork\_GoogleMaps\_20May2022-contourkmeansclustered.jpg  
 testlogs/ChennaiMetropolitanAreaTransitNetwork\_GoogleMaps\_20May2022-contourlabelled.jpg  
 testlogs/ChennaiMetropolitanAreaTransitNetwork\_GoogleMaps\_20May2022-contoursegmented.jpg  
 testlogs/ChennaiMetropolitanAreaTransitNetwork\_GoogleMaps\_20May2022-cannyedgedetection.jpg  
 testlogs/GHSL\_GIS\_ChennaiMetropolitanArea-contourkmeansclustered.jpg  
 testlogs/GHSL\_GIS\_ChennaiMetropolitanArea-cannyedgedetection.jpg  
 testlogs/GISUrbanSprawlAnalytics.log.30June2022.xz

1265.6 Moran's I dispersion and p-norm values for the two images are:  
 testlogs/ChennaiMetropolitanAreaTransitNetwork\_GoogleMaps\_20May2022.jpg - Moran's I of the Urban Sprawl dispersion: 0.6759297613633821  
 testlogs/ChennaiMetropolitanAreaTransitNetwork\_GoogleMaps\_20May2022.jpg - Moran's p-norm of the Urban Sprawl dispersion: 0.0  
 testlogs/GHSL\_GIS\_ChennaiMetropolitanArea.jpg - Moran's I of the Urban Sprawl dispersion: 0.8848283189311299  
 testlogs/GHSL\_GIS\_ChennaiMetropolitanArea.jpg - Moran's p-norm of the Urban Sprawl dispersion: 0.0

#### References:

-----

1265.7 GHSL Atlas of the Human Planet 2016 - [https://ghsl.jrc.ec.europa.eu/documents/Atlas\\_2016.pdf](https://ghsl.jrc.ec.europa.eu/documents/Atlas_2016.pdf) - Section 2.4.3 GHSL Settlement Model: Rural, Urban Cluster, Urban Centre Grids - Section 3.4: City Analysis - Section 3.4.1: 32 Megacities - Canny Edge Detection earlier extracts a lattice grid of transportation network from GIS quite similar to Illustration in Section 2.4.3 of GHSL Atlas

1265.8 Missing millions: undercounting urbanization in India - <https://www.ncbi.nlm.nih.gov/pmc/articles/PMC6934249/> - "... We use a random forest-based model to create a high-resolution (~100 m) population grid from district-level data available from the Indian Census for 2001 and 2011, a novel application of such methods to create temporally consistent population grids. We then apply a community-detection clustering algorithm to construct urban agglomerations for the entire country. Compared with the 2011 official statistics, we estimate 12% more of urban population, but find fewer mid-size cities. We also identify urban agglomerations that span jurisdictional boundaries across large portions of Kerala and the Gangetic Plain...." - parallels could be drawn between Minimum enclosing circles-Voronoi-Delaunay based computational geometric community detection and SEDAC-VIIRS estimates of urban sprawls in 1167,1225 and Random Forest model described in this article.

1265.9 Is cities delineation a pre-requisite for urban modelling? The example of land price determinants in Brussels - Table 1 - Criteria for functional delineations - <https://journals.openedition.org/cybergeogeo/26899> - "... Control variables are the following: Population density, which is the number of inhabitants per square kilometres in each municipality in 2008 (Figure 4), and Income, equal to the median earnings per household in euros for fiscal year 2008, are used as socio-economic indicators. Sources for these data are the DGSIE. The Travel time to the closest main ("IC/IR"2) railway station is used as a local amenities indicator and accounts for the proximity of the municipalities to both the public transport network and to secondary centres with retail

activities. The Forest cover, expressed as the share of the total surface of the municipality covered by forest (CORINE land-cover database, European Environment Agency: <http://www.eea.eu.int>), is used as a green amenities indicator....To compare the different delineations of Brussels, the key variable of the model is the indicator of the accessibility to Brussels, since it will capture the influence of the city on its neighbouring areas. For that purpose, the Travel time to (the CBD of) Brussels, by car, in minutes and congestion included, is used (data from Vandenbulcke et al, 2007). In addition, a gravitational measure of the Accessibility to jobs is also used, and defined as follows: for each municipality *i*, this variable is equal to the log of the Shimmel index (of the travel time by car) between *i* and all other municipalities in Belgium, weighted by the total number of jobs (self-employed excluded) located in these municipalities in 2008..."

-----  
-----  
1266. (THEORY and FEATURE) Astronomical Dataset Analytics - Planetarium Ephemeris Search - SkyField implementation - 7 July 2022 - related to 731,1206,1236,1255 and all sections on Astronomical Dataset Mining, Archaeoastronomical Dating, Sequence Mining, String analytics, Sequence Alignment, Visual Planetarium Search, Archaeology, Reciprocal Recommender Systems based Matrimony analytics in Bipartite Social Networks, Climate and Extreme Weather Event Analytics, Computational Astrophysics, N-Body problem and Gravity Induced Terrestrial Extreme Weather Events, Astronomical Algorithms  
-----  
-----

1266.1 New python 3.7.x script EphemerisSearch.py has been added to NeuronRain AsFer repositories which imports SkyField  
python astronomical algorithms implementation & defines a class EphemerisSearch containing following member functions:  
    `ephem.sky_on_datetime((2022,7,7,1,15,30),"earth","mars")`  
    `ephem.astronomical_event_to_search(planetradeccdict)`  
    `ephem.planetarium_search((2016,6,29,1,15,30),(2022,7,6,1,15,30))`  
1266.2 `__init__()` of EphemerisSearch.py downloads a NASA JPL Ephemeris (DE421 in this example - `de421.bsp`) and loads a timescale based on the ephemeris.  
1266.3 `sky_on_datetime()` accepts a datetime tuple (Year-Month-Day-Hour-Minute-Second shown in earlier example invocation) and converts it to Julian Ephemeris Date (denoted JD or JED) by `utc()`. Two parameters "earth" and "mars" in earlier invocation correspond to planet observed from (Earth) and the planet observed (Mars). Instantaneous Right Ascension and Declination of a planetary body is available by a call of `observe()` on observed from planet to the observed planet at the timepoint argument supplied to `at()`. Function `observe()` returns an astrometric object from which right ascension and declination are obtained by `radec()`.  
1266.4 Function `planetarium_search()` does the main computation by searching the ephemeris for all possible dates with in a range matching the query dictionary of planets-to-radec. This functionality of searching the dates of astronomical events is inherently supported by `find_discrete()` function of SkyField by doing a callback to a boolean function (`radec_match()`) passed on as argument which turns "True" whenever there is a match to ephemeris data on a specific date.  
1266.5 Above facility notwithstanding, use of `find_discrete()` has been made optional by an if-else clause within `planetarium_search()` because of multiple internal exceptions within `find_discrete()` callstack of SkyField and an equivalent native bruteforce search is performed within a datetime range loop and a boolean function `radec_match()` returns True or False depending on ephemeris match for query on that date. Any new algorithm better than bruteforce search of astronomical objects to locate an event could be a breakthrough (Example: Given planetary ephemeris data for an event algorithm has to find the date of the event efficiently without bruteforce search, exploiting Chebyshev polynomial representation of ephemeris : `Chebyshev(date) = Ephemeris` and Inverse of Chebyshev polynomial for ephemeris data could be the `date(s)`).  
1266.6 Ephemeris for datetime "3 July 2016 1 hour 15 minutes 30 seconds" is computed by `sky_on_datetime()` for all solar system planets and made into a query dictionary `planetstoradecdict` by `astronomical_event_to_search()`. Earlier

ephemeris data is searched in two date ranges "29 June 2016 - 6 July 2022" and "29 June 2016BC - 6 July 2022" and match is found in the former as "planetarium\_search(): found matching datetime = 2016-07-03 01:16:38 TT" while the latter throws exception "Exception: ephemeris segment only covers dates 1899-07-28 23:59:18Z through 2053-10-08 23:58:51Z UT" because of DE421 year limitations:

```
ephem.planetarium_search((2016,6,29,1,15,30),(2022,7,6,1,15,30))
ephem.planetarium_search((-2016,6,29,1,15,30),
(2022,7,6,1,15,30),step_days=100)
```

1266.7 Arguments step\_days is similar to find\_discrete() for periodicity filtering of dates to search. In earlier example ephemeris match is computed every 100 days within the range instead of iterating for every day. Full logs of the computation and search are at testlogs/EphemerisSearch.log.7July2022.

1266.8 EphemerisScript.py has multiple uses across NeuronRain - Search of an astronomical event mentioned in an archaeological artifact, N-Body Choreography - Computation of Separation between astronomical bodies (by separation\_from() API), Climate Analytics - analyzing gravitational correlations between periodicities of celestial bodies and terrestrial weather events.

#### References:

-----

1266.9 Astronomical Algorithms -

[https://www.agopax.it/Libri\\_astronomia/pdf/Astronomical%20Algorithms.pdf](https://www.agopax.it/Libri_astronomia/pdf/Astronomical%20Algorithms.pdf) -

Sorting planets by right ascension for example requires quicksort

1266.10 PyEphem - <https://rhodesmill.org/pyephem/>

1266.11 SkyField - <https://rhodesmill.org/skyfield/>

1266.12 AstroPy - <https://docs.astropy.org/en/stable/index.html> - for advanced computational astrophysics models

1266.13 SkyField - Searching for the dates of astronomical events -

<https://rhodesmill.org/skyfield/searches.html>

1266.14 NASA JPL Ephemeris - Chebyshev polynomials -

[https://ssd.jpl.nasa.gov/planets/eph\\_export.html](https://ssd.jpl.nasa.gov/planets/eph_export.html) - DE441 being the latest ranging from year JED -3100015.5, (-13200 AUG 15) to JED 8000016.50, (17191 MAR 15). For wider datetime searches involving archaeoastronomical datings DE441 could be loaded in script earlier.

1266.15 Hurricane Prediction Models - Hurricane Season 2020 Time Lapse -

<https://climate.nasa.gov/news/3184/a-force-of-nature-hurricanes-in-a-changing-climate/> - Thermal Image of Category 5 Hurricane Maria 2017 - Trajectories of Category 4 and Category 5 Atlantic Hurricanes

1266.16 Observed Relationships Between Lunar Tidal Cycles and Formation of Hurricanes and Tropical Storms - NOAA - Gravitational Influence of Sun-Earth-Moon system on Hurricanes least during quadratures (90 degree separation) and highest during syzygies (180 degree separation) -

[https://journals.ametsoc.org/view/journals/mwre/100/6/1520-](https://journals.ametsoc.org/view/journals/mwre/100/6/1520-0493_1972_100_0451_orbltc_2_3_co_2.xml?tab_body=pdf)

0493\_1972\_100\_0451\_orbltc\_2\_3\_co\_2.xml?tab\_body=pdf - "... Visvanathan (1966) showed that de- pressions (winds up to 33 kt) in the Bay of Bengal and Arabian Sea formed more often near first quarter than at other times of the lunar month ..." - Section 7 - Conclusions - "... Hurricane formation has been more frequent near syzygy than at quadrature over a period of 78 yr in the North Atlantic and northwest Pacific Oceans where formation dates are considered to be the best-documented in the world ... Additionally, a correlation coefficient of 0.87 was found between the same dates (after smoothing was performed) and this lunar cycle. This result generally agrees with correlations achieved in other studies of other meteorological phenomena related to lunar tides and indicates that a real relation between the two features may exist. ... Severe tropical storms in the southwest Indian Ocean and Bay of Bengal and Arabian Sea over 75 yr have developed more frequently several days after syzygy and to a lesser extent a few days after quadrature ... we showed that storms developing near quadrature intensified into hurricanes and severe tropical storms less often than those tropical storms that formed during the rest of the synodic month ..."

1266.17 Formation of Depressions in the Indian Seas and Lunar Phase - [T. R. VISVANATHAN] - Nature volume 210, pages 406-407 (1966) - <https://www.nature.com/articles/210406a0>

1266.18 Solar, Lunar and Venus Roles in Some Global Climatic Events - <https://www.scirp.org/journal/paperinformation.aspx?paperid=102705> - Figure 1 - Extraordinary growth of Hurricanes-Typhoons after 1965 - Section 2 - Solar, Lunar and Venus Roles - "... The three underlined with extraordinary values are reduced through dividing by 10. The Sun, Moon and Venus have systematic cyclic direct or indirect link with these hazards which can be seen by their mutual comparison. When compared individually, these hazards mostly show their matching occurrences with the Venus lapses plotted with its y-axis in a respective year domain versus 120 years time span. ... These three celestial bodies have very prominent, direct, short and long cyclic persistent roles on Monsoons, Oceanic tides, Easterlies, Westerly, GAC, IAW formation and propagation, GHT, NAH, Earthquakes, wide spread wildfire, Glaciers and movement of Avalanches, volcanic eruption on the Earth Globe. The common and most important thing in all these is the gravitational pull on the earth and its individual items, particularly loosely tied up with the main earth body like air/atmosphere, water in oceans and ponds, ice glaciers, molten lava, tectonic plates, rocks, mountains ridges, portions of earth plates loosened by earthquakes and volcanic eruptions depending upon their grip of the earth. The activity of this gravity varies much quickly on daily bases with earth rotation about its axes and annually with its rotation around the sun and positional cluster of all these celestial bodies with respect to the earth. ..." - Sequence Mining of HURDAT2 datasets earlier showed a high frequency of Earth-Mercury-Venus laps (inferior conjunction) correlated to occurrence of Hurricanes and Tropical storms.

-----  
-----  
1267. (THEORY and FEATURE) Astronomical Dataset Analytics - Planetarium Ephemeris Search - Longitude-Latitude and AstroPy support - 13 July 2022 - related to 731,1206,1236,1255,1266 and all sections on Astronomical Dataset Mining, Archaeoastronomical Dating, Sequence Mining, String analytics, Sequence Alignment, Visual Planetarium Search, Archaeology, Reciprocal Recommender Systems based Matrimony analytics in Bipartite Social Networks, Climate and Extreme Weather Event Analytics, Computational Astrophysics, N-Body problem, Merit of Large Scale Visuals, Astronomical algorithms

-----  
-----  
1267.1 EphemerisSearch.py has been updated to compute and search for Longitude-Latitude degree position of solar system bodies which is more compatible than Right Ascension-Declination convention. New match function latlon\_match() has been implemented in addition to radec\_match() which invokes SkyField ecliptic\_latlon() for every observed solar system planet to compute their Longitude-Latitude(s).

1267.2 Functions sky\_on\_datetime() and planetarium\_search() take an additional parameter "position" which is valued {"latlon","radec"} to choose between radec\_match() and latlon\_match() within planetarium\_search() and to print radec() or ecliptic\_latlon() within sky\_on\_datetime().

1267.3 latlon\_match() also computes the pairwise degree separation between solar system bodies by SkyField separation\_from() which is crucial for solving an N-Body system particularly for finding correlations between (\*) Sun-Moon-Earth 3-Body syzygies (180 degree separation - reference 1266.16) (\*) Sun-Moon-Earth-Venus Lapses 4-Body System and Tropical storms (reference - 1266.18).

1267.4 The planetary positions from SkyField ephemeris are compared to planetary positions from Maitreya 8t ephemeris and AstroPy ephemeris in planetarium\_search() by subprocess.call() of maitreya8t and astropy\_ephemeris(). AstroPy (for advanced astronomy and cosmology computations) has been integrated and positions of solar system bodies are printed within astropy\_ephemeris().

References:

-----  
1267.5 AstroPy astronomical statistics algorithms - <https://docs.astropy.org/en/stable/stats/index.html>

1267.6 SkyField ICRF separation\_from() - [https://rhodesmill.org/skyfield/api-position.html#skyfield.positionlib.ICRF.separation\\_from](https://rhodesmill.org/skyfield/api-position.html#skyfield.positionlib.ICRF.separation_from)

1267.7 Convert a 3-color image (JPG) to separate FITS images - RGB channel

analysis of Galaxy telescope imagery -  
<https://docs.astropy.org/en/stable/generated/examples/io/split-jpeg-to-fits.html#sphx-glr-generated-examples-io-split-jpeg-to-fits-py> and  
<https://het.as.utexas.edu/HET/Software/Astropy-1.0/io/fits/usage/examples.html>  
1267.8 Hubble Ultra Deep Field - Deepest Image of universe - 13 billion years old - <https://svs.gsfc.nasa.gov/30946> - "... The snapshot includes galaxies of various ages, sizes, shapes, and colors. The smallest, reddest galaxies, about 100, may be among the most distant known, existing when the universe was just 800 million years old. The nearest galaxies - the larger, brighter, well-defined spirals and ellipticals - thrived about 1 billion years ago, when the cosmos was 13 billion years old.....In this image, blue and green correspond to colors that can be seen by the human eye, such as hot, young, blue stars and the glow of Sun-like stars in the disks of galaxies. Red represents near-infrared light, which is invisible to the human eye, such as the red glow of dust-enshrouded galaxies." - RGB analysis of Deep Field images differentiates galaxies by red shift.  
1267.9 AstroPy AstroQuery Hubble Space Telescope Archive - Hubble JPEG Postcards - <https://astroquery.readthedocs.io/en/latest/esa/hubble/hubble.html>  
1267.10 AstroPy Line Search algorithms - Hubble Deep Field North - <https://arxiv.org/pdf/1312.6364.pdf>  
1267.11 All of Hubble in one picture - <https://www.universetoday.com/155549/here-are-all-of-hubbles-observations-in-one-picture/>  
1267.12 AstroPy AstroQuery N-Body Simulation - Solar System with N bodies and Nasa Horizons Data - [https://amor.cms.hu-berlin.de/~rodrigus/Subsites/Jupyter%20Notebooks/Solar\\_System\\_N-Body\\_Simulation.html](https://amor.cms.hu-berlin.de/~rodrigus/Subsites/Jupyter%20Notebooks/Solar_System_N-Body_Simulation.html)

-----  
1268. (THEORY and FEATURE) Astronomy Dataset Analytics - Angular separation of solar system planets during Extreme Weather Events on Earth - an N-Body gravitational pull correlation study - 15 July 2022 - related to 731,1206,1236,1255,1266,1267 and all sections on Astronomical Dataset Mining, Archaeoastronomical Dating, Sequence Mining, String analytics, Sequence Alignment, Visual Planetarium Search, Archaeology, Reciprocal Recommender Systems based Matrimony analytics in Bipartite Social Networks, Climate and Extreme Weather Event Analytics, Computational Astrophysics, N-Body problem, Merit of Large Scale Visuals, Astronomical algorithms  
-----

1268.1 EphemerisSearch.py has been updated to define new function `extreme_weather_events_n_body_analytics()` which iterates through `datetime(s)` of extreme weather events (North Atlantic Hurricanes,Tropical Cyclones,Earthquakes,Typhoons) and computes the angular separation between solar system planets pairwise for each cataclysm.  
1268.2 Patterns in pairwise angular separations between solar system planets are prima facie correlational evidences towards N-Body gravitational influence on terrestrial weather disturbances.  
1268.3 Two sets of occurrences of deadliest natural disasters: (\*) Days of 21st century Tropical storms - sourced from [https://en.wikipedia.org/wiki/List\\_of\\_the\\_deadliest\\_tropical\\_cyclones](https://en.wikipedia.org/wiki/List_of_the_deadliest_tropical_cyclones) and (\*) Days of Top 10 highly studied Earthquakes in seismology literature - sourced from [https://en.wikipedia.org/wiki/Lists\\_of\\_earthquakes](https://en.wikipedia.org/wiki/Lists_of_earthquakes) have been analyzed for syzygies and proximities in angular separations of solar system planets as observed from earth during disasters (references: 1266.16,1266.17,1266.18).  
-----

1268.4 Following are pairwise angular separations for 21st century Tropical storms of Sun-Moon-Venus-Earth 4-body system and Mercury-Venus-Earth 3-body system:  
-----

Angular separations for Sun-Moon : [`<Angle 19deg 07' 47.6">`, `<Angle 155deg 22' 20.7">`, `<Angle 134deg 27' 32.6">`, `<Angle 26deg 59' 51.6">`, `<Angle`

49deg 19' 28.1">, <Angle 12deg 45' 45.4">, <Angle 107deg 32' 09.8">, <Angle 160deg 54' 55.2">, <Angle 151deg 43' 25.6">, <Angle 141deg 05' 03.8">, <Angle 06deg 27' 40.2">, <Angle 19deg 07' 47.6">, <Angle 53deg 28' 49.9">, <Angle 28deg 31' 32.0">]

Angular separations for Sun-Venus : [<Angle 43deg 57' 46.6">, <Angle 29deg 10' 59.9">, <Angle 36deg 59' 32.2">, <Angle 44deg 14' 36.8">, <Angle 07deg 03' 56.2">, <Angle 45deg 56' 16.8">, <Angle 11deg 34' 06.9">, <Angle 02deg 10' 39.4">, <Angle 29deg 51' 11.0">, <Angle 29deg 31' 15.2">, <Angle 47deg 03' 42.9">, <Angle 43deg 57' 46.6">, <Angle 28deg 15' 36.0">, <Angle 40deg 23' 01.5">]

Angular separations for Moon-Venus : [<Angle 25deg 56' 18.5">, <Angle 126deg 18' 14.4">, <Angle 171deg 25' 52.8">, <Angle 71deg 12' 28.8">, <Angle 42deg 17' 33.0">, <Angle 57deg 57' 37.0">, <Angle 95deg 59' 25.6">, <Angle 158deg 54' 48.7">, <Angle 174deg 59' 17.0">, <Angle 169deg 35' 55.4">, <Angle 53deg 28' 04.3">, <Angle 25deg 56' 18.5">, <Angle 25deg 21' 49.9">, <Angle 12deg 06' 55.7">]

Angular separations for Mercury-Venus : [<Angle 26deg 45' 07.7">, <Angle 48deg 40' 16.5">, <Angle 55deg 20' 24.4">, <Angle 34deg 25' 52.6">, <Angle 26deg 55' 31.1">, <Angle 27deg 17' 48.4">, <Angle 23deg 39' 02.2">, <Angle 15deg 51' 03.3">, <Angle 46deg 43' 02.6">, <Angle 14deg 49' 04.4">, <Angle 49deg 46' 07.9">, <Angle 26deg 45' 07.7">, <Angle 11deg 04' 25.7">, <Angle 56deg 38' 59.7">]

-----  
1268.5 Following are pairwise angular separations for Top 10 Earthquakes of Sun-Moon-Earth, Mars-Jupiter-Saturn-Earth systems:  
-----

Angular separations for Sun-Moon : [<Angle 69deg 50' 21.3">, <Angle 91deg 21' 43.4">, <Angle 172deg 17' 32.3">, <Angle 122deg 13' 27.1">, <Angle 64deg 48' 34.3">, <Angle 175deg 09' 29.0">, <Angle 135deg 01' 03.0">, <Angle 159deg 42' 43.8">, <Angle 135deg 18' 23.5">, <Angle 27deg 19' 28.1">]

Angular separations for Jupiter-Saturn : [<Angle 174deg 16' 50.1">, <Angle 140deg 34' 08.6">, <Angle 81deg 18' 02.0">, <Angle 12deg 58' 35.3">, <Angle 106deg 42' 10.3">, <Angle 91deg 42' 19.8">, <Angle 153deg 42' 20.0">, <Angle 156deg 25' 30.7">, <Angle 177deg 42' 21.2">, <Angle 158deg 22' 32.9">]

Angular separations for Mars-Saturn : [<Angle 147deg 08' 00.1">, <Angle 30deg 26' 09.0">, <Angle 124deg 52' 46.6">, <Angle 154deg 45' 04.9">, <Angle 36deg 57' 00.2">, <Angle 171deg 36' 50.7">, <Angle 178deg 35' 59.3">, <Angle 61deg 46' 19.2">, <Angle 79deg 49' 42.8">, <Angle 82deg 21' 37.6">]

Angular separations for Jupiter-Mars : [<Angle 27deg 20' 42.2">, <Angle 170deg 53' 56.1">, <Angle 43deg 35' 24.5">, <Angle 142deg 02' 32.4">, <Angle 69deg 45' 14.5">, <Angle 96deg 19' 42.6">, <Angle 27deg 07' 46.8">, <Angle 141deg 34' 54.5">, <Angle 97deg 52' 51.6">, <Angle 119deg 15' 48.2">]

1268.6 Sun-Moon almost-Syzygies and Mercury-Venus proximities (mostly <30 degrees) are prominent in 1268.4. Jupiter-Saturn, Sun-Moon almost-Syzygies are prominent in 1268.5. More details in testlogs/EphemerisSearch.log.15July2022.

-----  
1269. (THEORY and FEATURE) Majority Voting Versus Query complexity model of Intrinsic Merit of Texts-Audio-Video-People - 18 July 2022 - related to 14,53,318,355,365,420,517,678,682,687,688,1204,1263 and all sections on Intrinsic Merit Rankings of Texts-Publications-Music-Speech-Voice-Images-Videos-People, Intrinsic Merit Versus Fame Equilibrium, BKS Conjecture, Stability and Noise Sensitivity of Interview LTF/PTF, LTF-PTF-TQBF-Switching Circuits models of Question-Answering, Peres Theorem, HR-Talent Analytics and Automated Recruitment, Majority Voting-Boolean composition of Majority+VoterSAT, Condorcet Jury Theorem Variants, Margulis-Ruzzo Thresholds, Novelty Detection, AI Question-Answering, Quantum Computation, Majority+VoterSAT Hardness Amplification Lemma  
-----

-----  
1269.1 Most of the boolean function complexity measures and algorithms (Grover search, Period finding, Element distinctness, Decision Tree, Block

sensitivity, Deterministic and Randomized Certificate complexity, Degree of Polynomial Approximation of Boolean function) have been brought under the purview of what has come to be known as "Query complexity" mostly in quantum computation setting: Compute a function in  $n$  variables  $f(x_1, x_2, x_3, \dots, x_n)$  through set of queries to variables and Query complexity is quantified by number of queries.

1269.2 Every Question-Answering Merit problem which includes Examinations-Contests-Interviews methodologies of judging people merit by asking questions and evaluating answers (in HR-People-Talent Analytics) is theoretically a Query complexity problem which computes a function  $\text{Merit}(x_1, x_2, x_3, \dots, x_n)$  by queries to variables  $x_1, x_2, x_3, \dots, x_n$  where each variable could be a question and value assigned to variable its answer.

1269.3 Query complexity thus generalizes all theoretical models of Question-Answering discussed elsewhere in this design - TQBF, LTF, PTF, Switching Circuits with Background Intelligence. Error in Question-Answering obviously reduces to Error in Query complexity based computation of  $\text{Merit}()$  function (or) Error in Query complexity = Error in computation of  $\text{Merit}()$  function = Error in any Question-Answering system (Examinations-Contests-Interviews)

1269.4 Error in Query complexity model of Intrinsic Merit Question-Answering could be equated to Condorcet Jury Theorem-Margulis-Ruzzo Threshold Majority Voting Group decision error (based on per voter  $p$ -bias) to arrive at a lowerbound (i.e equal error and completeness imply a lowerbound and one side of equality subsumes the other causing a collapse of complexity class) subject to constraints mentioned in tableau of bounded error (BP\*) complexity class scenarios of Majority Voting + VoterSAT composition (Section 517).

#### References:

-----  
1269.5 Understanding Quantum Algorithms via Query Complexity - [Andris Ambainis] - <https://arxiv.org/pdf/1712.06349.pdf> - "... Query complexity is a model of computation in which we have to compute a function  $f(x_1, \dots, x_N)$  of variables  $x_i$  which can be accessed via queries. The complexity of an algorithm is measured by the number of queries that it makes...."

1269.6 Decision Tree model of Query complexity of boolean functions and analogy of computing non-boolean  $\text{Merit}()$  function by adaptive Interview Question-Answering Decision Trees - Examples of Query complexity: Sorting an array, Gradient Descent, Decision tree for maximum element - <http://web.stanford.edu/class/cs354/scribe/lecture01.pdf> - An interview to decide  $\text{Merit}()$  of a candidate could be a decision tree of adaptive Question-Answering in which next question dynamically depends on answers to previous questions and branching to a subtree of the Q&A decision tree depends on threshold scoring of Answer to parent Question node of subtree (or) Set of Q&A are root-to-leaf paths in decision tree. Query complexity of adaptive Q&A is equal to depth of Q&A decision tree.

-----  
1270. (THEORY and FEATURE) Astronomy Dataset Analytics - NASA JPL Horizons Ephemeris Lookup Service support and Hubble Ultra Deep Field imagery RGB analytics - 20 July 2022 - related to 731, 1206, 1236, 1255, 1266, 1267, 1268 and all sections on Astronomical Dataset Mining, Archaeoastronomical Dating, Sequence Mining, String analytics, Sequence Alignment, Visual Planetarium Search, Archaeology, Climate and Extreme Weather Event Analytics, Computational Astrophysics, N-Body problem, Merit of Large Scale Visuals, Astronomical algorithms

-----  
1270.1 EphemerisSearch.py has been updated to define two new functions `jplhorizons_ephemeris()` and `hubble_deep_field_RGB_analytics()` which respectively integrate NASA JPL Horizons Online Ephemeris Lookup API Service and split Hubble Deep Field imagery into RGB Channel for Red-shift distance analysis of Galaxies.  
1270.2 `jplhorizons_ephemeris()` wraps the AstroPy AstroQuery NASA JPL Horizons Ephemeris API lookup service `ephemerides()` for a celestial body id, location (longitude-latitude-elevation) and `epochs(range of dates for ephemeris)`.



1270.3 `jplhorizons_ephemeris()` is invoked within `sky_on_datetime()` if a boolean flag `jplhorizons` is set to True and the arguments are passed on as heterogeneous array `jplhorizonsdata` (`id` is number or name of body, `location` and `epochs` are dictionaries).

1270.4 `hubble_deep_field_RGB_analytics()` function takes an `imagename` which could be either a postcard that can be looked-up by `ESAHubble.get_postcard()` or name of a Hubble Space Telescope Deep Field image already downloaded. Image file is opened in Pillow Image and split into Red-Green-Blue channel ndarrays. Each of RGB channel ndarrays are flattened and histograms are computed per color channel.

1270.5 Percentage of Pixel colors are obtained from RGB histograms which provide a clue to the distribution and distance of the galaxies in Deep Field. Reddest galaxies are farthest away (gravitational red shift) compared to Green and Blue channel galaxies. Each of RGB channel data are written to FITS files analyzable by `fv` tool of NASA GSFC. FITS files created are at present removed because of huge sizes.

1270.6 Sample computations of `hubble_deep_field_RGB_analytics()` for 13 billion light years old Hubble Ultra Deep Field Imagery `HubbleUltraDeepField_heic0611b.jpg` (containing primordial light 800 million years after BigBang and Inflation) from <https://esahubble.org/images/heic0611b/> and `sky_on_datetime()-jplhorizons_ephemeris()` for solar system bodies identified by numeric `id(s)` have been captured (for a date range) at `testlogs/EphemerisSearch.log.20July2022`. Hubble postcard RGB analysis for `J6FL25S4Q` postcard `id` has been commented.

1270.7 Following are the percentage of RGB galaxies by histogram analysis showing slightly higher number of primordial red galaxies than blue and green:

```
('Percentage of Blue Galaxies (Closer) :', 0.0026145)
('Percentage of Green Galaxies (Closer) :', 0.0011199375)
('Percentage of Red Galaxies (Farthest - Red Shift):', 0.0032260625)
```

References:

-----  
1270.8 Deep Field RGB analysis -

<https://docs.astropy.org/en/stable/generated/examples/io/split-jpeg-to-fits.html#sphx-glr-generated-examples-io-split-jpeg-to-fits-py>

1270.9 Deep Field RGB analysis - <https://het.as.utexas.edu/HET/Software/Astropy-1.0/io/fits/usage/examples.html>

1270.10 AstroQuery Hubble -

<https://astroquery.readthedocs.io/en/latest/esa/hubble/hubble.html#module-astroquery.esa.hubble>

1270.11 FV FITS viewer tool -

<https://manpages.ubuntu.com/manpages/focal/man1/fv.1.html>

1270.12 How the Universe Works - Webseries -

<https://www.discoveryplus.in/show/how-the-universe-works>

1270.13 NASA JPL Horizons - <https://ssd.jpl.nasa.gov/horizons/>  
-----

-----  
1271. (THEORY and FEATURE) Astronomy Dataset Analytics - Computation of N-Body Gravitational Acceleration for Solar System bodies on days of Extreme Weather Events (Earthquakes and Hurricanes) - 25 July 2022 - related to 731,1206,1236,1255,1266,1267,1268,1270 and all sections on Astronomical Dataset Mining, Archaeoastronomical Dating, Sequence Mining, String analytics, Sequence Alignment, Visual Planetarium Search, Archaeology, Climate and Extreme Weather Event Analytics, Computational Astrophysics, N-Body problem, Merit of Large Scale Visuals, Astronomical algorithms  
-----

-----  
1271.1 This update implements long pending N-Body Gravitational Acceleration computation for Solar system bodies with respect to observations from Earth for dates of Extreme Weather Events (Earthquakes of high magnitude and Category4-Category5 Hurricanes) thus fulfilling the original goal of NeuronRain which was initially astronomy software.

1271.2 New function `n_body_gravitational_acceleration()` has been implemented to

compute gravitational acceleration of solar system bodies by considering AstroPy JPL Horizons N-Body simulation Jupyter notebook (function `a_t()` for vectorial acceleration) from [https://amor.cms.hu-berlin.de/~rodrigues/Subsites/Jupyter%20Notebooks/Solar\\_System\\_N-Body\\_Simulation.html](https://amor.cms.hu-berlin.de/~rodrigues/Subsites/Jupyter%20Notebooks/Solar_System_N-Body_Simulation.html) as reference.

1271.3 Function `n_body_gravitational_acceleration()` is invoked within `extreme_weather_events_n_body_analytics()` iteratively for Horizons Ephemeris data as Vectors on dates of Extreme Weather Events (JPL Horizons Ephemeris Data Format - `r` is the Vector of 3D location positions of planets, `m` is the Vector of planetary masses and `v` is the Vector of velocities of planets on that day as observed from Earth-Moon barycenter which is center of mass of Earth-Moon situated within Earth and hence seismically sensitive).

=====

1271.4 An example Planetwise gravitational pull (3D components of acceleration) on Earth-Moon Barycenter (Detailed logs:

testlogs/EphemerisSearch.log.25July2022) during Hurricane Katrina (Costliest Cat5 Storm Ever to hit US Eastern Seaboard - 23 August 2005):

`extreme_weather_events_n_body_analytics()`: gravity of Sun at Earth-Moon Barycenter on (2005, 8, 23, 1, 0, 0) : [-4.59023763e-06 -9.57552083e-06 1.33988806e-07]

`extreme_weather_events_n_body_analytics()`: gravity of Moon at Earth-Moon Barycenter on (2005, 8, 23, 1, 0, 0) : [-5.00998359e-03 2.89038032e-03 -1.69038687e-08]

`extreme_weather_events_n_body_analytics()`: gravity of Mars at Earth-Moon Barycenter on (2005, 8, 23, 1, 0, 0) : [-3.06720042e-03 4.51175455e-05 7.63092623e-05]

`extreme_weather_events_n_body_analytics()`: gravity of Mercury at Earth-Moon Barycenter on (2005, 8, 23, 1, 0, 0) : [-0.04877074 -0.0265718 0.00230507]

`extreme_weather_events_n_body_analytics()`: gravity of Jupiter at Earth-Moon Barycenter on (2005, 8, 23, 1, 0, 0) : [ 1.81639208e-04 8.30369383e-05 -4.40933772e-06]

`extreme_weather_events_n_body_analytics()`: gravity of Venus at Earth-Moon Barycenter on (2005, 8, 23, 1, 0, 0) : [ 0.00495958 0.01013055 -0.00014766]

`extreme_weather_events_n_body_analytics()`: gravity of Saturn at Earth-Moon Barycenter on (2005, 8, 23, 1, 0, 0) : [ 3.80719163e-05 -6.09938497e-05 -4.53335739e-07]

`extreme_weather_events_n_body_analytics()`: gravity of Uranus at Earth-Moon Barycenter on (2005, 8, 23, 1, 0, 0) : [-1.37254726e-05 5.37648172e-06 1.97793457e-07]

`extreme_weather_events_n_body_analytics()`: gravity of Neptune at Earth-Moon Barycenter on (2005, 8, 23, 1, 0, 0) : [-4.74401544e-06 4.54907508e-06 1.56547622e-08]

`extreme_weather_events_n_body_analytics()`: gravity of Pluto at Earth-Moon Barycenter on (2005, 8, 23, 1, 0, 0) : [ 6.90750144e-07 6.08469083e-06 -8.50610615e-07]

=====

1271.5 Another example Planetwise gravitational pull on Earth-Moon Barycenter during Sumatra Boxing Day Earthquake (Subduction of India-Burma plates - 9.1-9.3 magnitude - Duration of 8 minutes - 26 December 2004 - Syzygy Day):

`extreme_weather_events_n_body_analytics()`: gravity of Sun at Earth-Moon Barycenter on (2004, 12, 26, 0, 58, 52) : [-8.49202750e-06 -6.83465500e-06 4.02245707e-07]

`extreme_weather_events_n_body_analytics()`: gravity of Moon at Earth-Moon Barycenter on (2004, 12, 26, 0, 58, 52) : [ 4.74835374e-04 -6.08346634e-03 -1.11752400e-06]

`extreme_weather_events_n_body_analytics()`: gravity of Mars at Earth-Moon Barycenter on (2004, 12, 26, 0, 58, 52) : [ 1.84618951e-03 1.52572942e-03 -1.31875566e-05]

`extreme_weather_events_n_body_analytics()`: gravity of Mercury at Earth-Moon Barycenter on (2004, 12, 26, 0, 58, 52) : [ 0.04213648 -0.01067818 -0.00473903]

`extreme_weather_events_n_body_analytics()`: gravity of Jupiter at Earth-Moon Barycenter on (2004, 12, 26, 0, 58, 52) : [ 1.98371660e-04 2.24260649e-05 -4.53163289e-06]

`extreme_weather_events_n_body_analytics()`: gravity of Venus at Earth-Moon Barycenter on (2004, 12, 26, 0, 58, 52) : [ 0.00874993 0.00720906 -0.00040641]

extreme\_weather\_events\_n\_body\_analytics(): gravity of Saturn at Earth-Moon Barycenter on (2004, 12, 26, 0, 58, 52) : [ 2.83958262e-05 -6.65696263e-05 2.86980912e-08]  
 extreme\_weather\_events\_n\_body\_analytics(): gravity of Uranus at Earth-Moon Barycenter on (2004, 12, 26, 0, 58, 52) : [-1.34855345e-05 5.99274945e-06 1.96999535e-07]  
 extreme\_weather\_events\_n\_body\_analytics(): gravity of Neptune at Earth-Moon Barycenter on (2004, 12, 26, 0, 58, 52) : [-4.62705846e-06 4.66464089e-06 1.05755462e-08]  
 extreme\_weather\_events\_n\_body\_analytics(): gravity of Pluto at Earth-Moon Barycenter on (2004, 12, 26, 0, 58, 52) : [ 8.51278012e-07 6.10016758e-06 - 8.98726252e-07]  
 1271.6 Noticeably high values of gravitational force components for Mercury and Venus (sometimes even better than Sun and Moon) in extreme weather events deserves an explanation.

#### References:

-----  
 1271.7 Solar system N-Body simulation in AstroPy-AstroQuery-JPLHorizons - [https://amor.cms.hu-berlin.de/~rodrigus/Subsites/Jupyter%20Notebooks/Solar\\_System\\_N-Body\\_Simulation.html](https://amor.cms.hu-berlin.de/~rodrigus/Subsites/Jupyter%20Notebooks/Solar_System_N-Body_Simulation.html) - N-Body Gravitation Equation - "... For a problem of N bodies indexed by  $i=1, \dots, N$  and known initial positions  $\mathbf{r}_i=(x_i, y_i, z_i)T$ , velocities  $\mathbf{v}_i=(v_x, v_y, v_z)T$ , and masses  $m_i$ , the function giving the gravitational acceleration being exerted by all other  $j$  bodies on a given body  $i$  as per Newton's inverse square law of gravitation is given in vector form by  $\mathbf{a}_i = G \sum_{j=1}^N m_j \frac{\mathbf{r}_j - \mathbf{r}_i}{|\mathbf{r}_j - \mathbf{r}_i|^3} \dots$ "  
 -----

-----  
 1272. (THEORY and FEATURE) Astronomy and Cosmology Datasets Analytics - Hubble eXtreme Deep Field imagery RGB analysis and Distance similarity of N-Body gravitational accelerations - 27 July 2022 - related to 731,1206,1236,1255,1266,1267,1268,1270,1271 and all sections on Astronomical Dataset Mining, Archaeoastronomical Dating, Sequence Mining, String analytics, Sequence Alignment, Visual Planetarium Search, Archaeology, Climate and Extreme Weather Event Analytics, Computational Astrophysics, N-Body problem, Merit of Large Scale Visuals, Astronomical algorithms, Histogram analytics  
 -----

-----  
 1272.1 Pairwise Hausdorff Distance similarity measures of N-Body gravitational accelerations on days of Extreme Weather Events have been computed within extreme\_weather\_events\_n\_body\_analytics() function of EphemerisSearch.py  
 1272.2 Function hubble\_deep\_field\_RGB\_analytics() has been updated to compute RGB channel histograms of Hubble eXtreme Deep Field image (HXDF 2012) from Scikit-Image (skimage) and plot the Histogram and RGB Channel graphics in following files(reference: 1272.5):

testlogs/skimage\_HXDFChannels.jpg  
 testlogs/skimage\_HXDFHistograms.jpg

1272.3 RGB channel histogram analysis of Hubble Ultra Deep Field (HUDF in 1270) has been updated to plot Histogram graphics in file testlogs/HubbleUltraDeepField\_heic0611bHistograms.jpg. Marked deviation in shapes of RGB histogram bins in testlogs/skimage\_HXDFChannels.jpg (HXDF) and testlogs/HubbleUltraDeepField\_heic0611bHistograms.jpg (HUDF) could have contributed to RGB ratio asymmetry in 1270.

1272.4 Following are some excerpts of logs testlogs/EphemerisSearch.log.27July2022 (almost close-enough Pairwise gravity similarities and Mercury-Venus abnormal gravity vectors):

...  
 extreme\_weather\_events\_n\_body\_analytics(): Pairwise Directed hausdorff Distance of Gravitational Acceleration: (0.027206568989690528, 3, 3)  
 extreme\_weather\_events\_n\_body\_analytics(): Pairwise Directed hausdorff Distance of Gravitational Acceleration: (0.02284149980887304, 3, 3)  
 extreme\_weather\_events\_n\_body\_analytics(): Pairwise Directed hausdorff Distance of Gravitational Acceleration: (0.01760670123773365, 3, 3)

```

extreme_weather_events_n_body_analytics(): Pairwise Directed hausdorff Distance
of Gravitational Acceleration: (0.031958191350966725, 3, 3)
extreme_weather_events_n_body_analytics(): Pairwise Directed hausdorff Distance
of Gravitational Acceleration: (0.033769298297935034, 3, 3)
...
Mercury (199) 2455631.5 ... 1.205450513238685 -0.0203938188627328
extreme_weather_events_n_body_analytics(): gravity of Mercury at Earth-Moon
Barycenter on (2011, 3, 11, 5, 46, 23) : [-0.04248091 -0.04133797 0.00052057]
Mercury (199) 2454598.5 ... 0.882339348179382 -0.02192844068446965
extreme_weather_events_n_body_analytics(): gravity of Mercury at Earth-Moon
Barycenter on (2008, 5, 12, 6, 27, 59) : [0.04121007 -0.00578165 -0.004254]
Mercury (199) 2453365.5 ... 0.9338643038989636 0.02207439343425398
extreme_weather_events_n_body_analytics(): gravity of Mercury at Earth-Moon
Barycenter on (2004, 12, 26, 0, 58, 52) : [0.04213787 -0.01067853 -0.00473918]
...
Venus (299) 2455631.5 ... 1.122263766864372 0.006774280431450814
extreme_weather_events_n_body_analytics(): gravity of Venus at Earth-Moon
Barycenter on (2011, 3, 11, 5, 46, 23) : [3.89399938e-03 1.05719009e-02 -
7.99002829e-05]
Venus (299) 2454598.5 ... 1.712807970350092 0.001579916105722341
extreme_weather_events_n_body_analytics(): gravity of Venus at Earth-Moon
Barycenter on (2008, 5, 12, 6, 27, 59) : [-0.00944266 -0.00621917 0.00045984]
Venus (299) 2453365.5 ... 1.518303955991236 0.003995808610124593
extreme_weather_events_n_body_analytics(): gravity of Venus at Earth-Moon
Barycenter on (2004, 12, 26, 0, 58, 52) : [0.00875022 0.0072093 -0.00040642]

```

#### References:

```

1272.5 Hubble eXtreme Deep Field RGB Histogram analytics - https://scientific-
python.readthedocs.io/en/latest/notebooks_rst/5_Image_Processing/02_Examples/
Image_Processing_Tutorial_3.html
1272.6 Hausdorff Distance between 2 sets -
http://cgm.cs.mcgill.ca/~godfried/teaching/cg-projects/98/normand/main.html
1272.7 Hubble Ultra Deep Field Flythrough in 3D - 13 billion light years away -
https://esahubble.org/videos/heic0714g/

```

```

1273. (THEORY and FEATURE) Astronomy and Cosmology Datasets Analytics -
Wilkinson Microwave Anisotropy Probe-Cosmic Microwave Background (WMAP CMB) and
N-Body gravitational accelerations from arbitrary vantage points - 29 July 2022
- related to 148,731,1206,1236,1255,1266,1267,1268,1270,1271,1272 and all
sections on Astronomical Dataset Mining, Archaeoastronomical Dating, Sequence
Mining, String analytics, Sequence Alignment, Visual Planetarium Search,
Archaeology, Climate and Extreme Weather Event Analytics, Computational
Astrophysics, N-Body problem, Merit of Large Scale Visuals, Astronomical
algorithms, Histogram analytics

```

```

1273.1 extreme_weather_events_n_body_analytics() function in EphemerisSearch.py
has been changed to add vantage point of the observation in NASA JPL Horizons
Ephemeris as configurable parameter loc which defaults to "@earth-moon"
barycenter and is invoked for location earth denoted by "@0". By changing loc to
any other solar system body, N-Body gravitational accelerations for other
planets could be found.
1273.2 N-Body gravitational accelerations exerted on Earth during Extreme
Weather Event days have been recomputed for location Earth instead of Earth-Moon
barycenter and the Mercury-Venus high gravity phenomenon remains (Coincidentally
GSP Sequence Mining analysis in Section 148 had found Mercury-Venus pattern in
Seismic events earlier). Periodicities found in Gravitational Acceleration
vectors through Hausdorff Distance earlier (~0.02 or 0.05), if established
beyond doubt, would imply patterns in occurrences of extreme weather events and
their predictability which is impossible at present.
1273.3 New function WMAP_CMB_analytics() has been defined to read Cosmic

```

Microwave Background temperatures data from AstroML WMAP dataset which are footprints of primordial universe before stars-galaxies formation (375000 years after BigBang and Inflation from quantum singularity or 13.77 billion years before present, which stretched the spacetime leaving microwave radiation as traces) and plots the spectrum using HealPy (tool for spherical coordinates) in two images: python-src/testlogs/WMAP\_CMB\_1.jpg and python-src/testlogs/WMAP\_CMB\_2.jpg.

#### References:

-----  
1273.4 WMAP CMB - <https://map.gsfc.nasa.gov/news/index.html>  
1273.5 AstroML - <https://www.astroml.org/index.html> - Machine Learning Algorithms Package for Astronomical Datasets  
1273.6 AstroML Book - <https://press.princeton.edu/books/hardcover/9780691198309/statistics-data-mining-and-machine-learning-in-astronomy>  
1273.7 AstroML WMAP Power Spectrum Analysis - [https://www.astroml.org/examples/datasets/plot\\_wmap\\_power\\_spectra.html](https://www.astroml.org/examples/datasets/plot_wmap_power_spectra.html)  
-----

-----  
1284. (THEORY and FEATURE) NeuronRainApps - Wikipedia Textgraph Question-Answering Bot - 3 August 2022 - related to 1133,1134,1204,1263,1269 and all sections on Intrinsic Merit of Texts, Question-Answering, Embedding in vectorspace, Machine Translation, Transformers Attention Model,Named Entity Recognition and Meaning Representation, Complexity models of Question-Answering (multiple choice,open-ended,adaptive and static) - LTF,PTF,Switching Circuits,TQBF,Markov Chains  
-----

-----  
1284.1 New Question-Answering Bot python implementation QuestionAnswering.py has been added to NeuronRain AstroInfer repositories within NeuronRainApps/QuestionAnswering/ which (\*) takes questions from users as commandline arguments, (\*) parses the question into a question textgraph, (\*) computes dense subgraphs and core numbers of prominent vertices in question textgraph, (\*) searches Wikipedia Corpus through wikipedia python API for top percentile core number vertices in question textgraph to get matching wikipedia pages, (\*) for each matching wikipedia page gets the summary as the text "Answer" to the question, (\*) parses the answer into an answer textgraph and (\*) computes the degree attention of edges of answer textgraph and learns Query-Key-Value weights (by Perceptrons Gradient Descent) through `rlfg_transformers_attention_model()` function in `RecursiveLambdaFunctionGrowth.py`  
1284.2 The `summary()` function of wikipedia python API which wraps MediaWiki PyWikiBot interface of Wikipedia, provides a crisp natural language summary for the question keywords simulating a GPT3-like background intelligence which could be a Turing test.

1284.3 Transformers degree attention learnt for answer textgraph could be helpful in cherrypicking prominent and relevant edges of the textgraph vertices of which are highly interdependent thus aiding a traversal of the answer textgraph to print a natural language answer simulating `summary()` function of MediaWiki API.

1284.4 Following are 5 questions asked through commandline chosen from varied disciplines - Geography,Physics,History,Sports,Archaeology - and the answers from `summary()` and answer textgraph degree attention are printed to logs - Last two questions are sourced from OpenAI GPT3 QA examples - <https://beta.openai.com/examples/default-qa>. Note: Logs correspond to a variant of earlier script which directly searches wikipedia corpus instead of top core number vertices:

```
python3.7 QuestionAnswering.py "which is the largest country in the world"
2>&1 > testlogs/QuestionAnswering.log1.2August2022
python3.7 QuestionAnswering.py "Define Theory of General Relativity" 2>&1
> testlogs/QuestionAnswering.log2.2August2022
python3.7 QuestionAnswering.py "Who is the Father of Indian Freedom Struggle" 2>&1 > testlogs/QuestionAnswering.log3.2August2022
```

GPT3 - python3.7 QuestionAnswering.py "Where were the 1992 Olympics held"  
 2>&1 > testlogs/QuestionAnswering.log4.2August2022  
 GPT3 - python3.7 QuestionAnswering.py "Where is the Valley of Kings?" 2>&1  
 > testlogs/QuestionAnswering.log5.2August2022  
 1284.5 Relevance of answers to questions is along expected lines and multiple answers are allowed per question based on wikipedia matches. For Question 5 earlier following edges have top percentile Query-Key-Value weights laying emphasis on these words in a hypothetical natural language answer (a sentence containing discovery, exploration and land). An example natural language answer could be obtained from edges below by connecting the vertices by a WordNet path between them:

- Query weight for textgraph edge ( discovery , exploration ): 2.0132
- Key weight for textgraph edge ( discovery , exploration ): 5.0504
- Value weight for textgraph edge ( discovery , exploration ): 8.0876
- Query weight for textgraph edge ( discovery , land ): 3.0338
- Key weight for textgraph edge ( discovery , land ): 6.2636
- Value weight for textgraph edge ( discovery , land ): 9.4934

1284.6 Earlier Bot implementation could have sourced answers from Google search but wikipedia corpus has better open API access compared to Google search code for which has since been commented.

-----  
 1285. (THEORY and FEATURE) NeuronRainApps - Wikipedia Textgraph Question-Answering Bot - WordNet Walk on answer textgraph - 4 August 2022 - related to 249,707,829,1133,1134,1204,1263,1269,1284 and all sections on Intrinsic Merit of Texts, Question-Answering, Embedding in vectorspace, Machine Translation, Transformers Attention Model, Named Entity Recognition and Meaning Representation, Complexity models of Question-Answering (multiple choice, open-ended, adaptive and static) - LTF, PTF, Switching Circuits, TQBF, Markov Chains  
 -----

1285.1 In continuation of earlier commit, QuestionAnswering.py has been refactored and enhanced to choose edges of high Query-Key-Values degree attention edges learnt from wikipedia summary answer textgraph and automatically write an answer by concatenating all WordNet walks between vertices of those high degree attention edges.  
 1285.2 AIQuestionAnswering() as a new function within QuestionAnswering.py has been supplied with lot of configurable parameters (questionfraction=5, maxanswers=1, keywordsearch=False, wsheading=False, answerslice d=1, answerfraction=20) to respectively (\*) choose fraction of question textgraph cores (\*) restrict maximum number of answers per question (\*) to choose between dense subgraph core number keyword search of question textgraph and direct question search without question textgraph (\*) to choose between wikipedia summary and page headings for a search() query (\*) choose only a slice of sentences from wikipedia summary() (\*) choose Fraction of sorted Query-Key-Values degree attention for answer WordNet walk.  
 1285.3 rlfg\_transformers\_attention\_model() function of RecursiveLambdaFunctionGrowth.py returns Query-Key-Values and Degree Attention as tuple  
 1285.4 Query-Key-Values attention for answer textgraph are stored in a dictionary of edges-attention, sorted descending and only answerfraction of those edges are chosen to be part of answer generated by concatenating WordNet walks between all pairs of vertices of the chosen edges connected by "is a" relation (WordNetPath.path\_between() is used for WordNet walk between vertices - Section 249).  
 1285.5 Some array overflow errors in Gravit/course\_material/NeuronRain/LinuxKernelAndCloud/code/Transformers\_PerceptronAndGradient.py which is part of Transformers implementation Gravit/course\_material/NeuronRain/LinuxKernelAndCloud/code/Transformers.py have been resolved.  
 1285.6 An excerpt of answer written based on WordNet walk for question "Which is the largest city in the world" (logs have been withheld because of huge sizes (GBs) of Transformer Training iteration logs and only a minimum slice (1

sentence) of wikipedia summary() is used to minimize runtime). Bot generated WordNet walk answer simulates a deep learning human thought process in grasping a question on urban areas, less readability notwithstanding. Though Wikipedia summary() does a reasonably great job of providing very relevant natural language answers to natural language questions, it is not always reliable due to rare exceptions in which case an alternative answer source might have to be resorted to for answer textgraph creation. Question textgraph-Answer textgraph duo is a graph theoretic Meaning Representation, a drastic departure from conventional natural language question-answer pair and is useful in inferring first order logic sentences from lambda functions computed by Recursive Lambda Function Growth algorithm Beta Reduction and multilingual question-answering by mapping textgraph vertices in one language to another (Example: Earlier question is answered in First Order Logic and its equivalent lambda function as "There exist x,y - x and y are cities - For all y, x !=y and x is larger than y")

...

Bot generated answer from textgraph: classified\_ad is a(n)  
 newspaper\_ad.newspaper\_ad is a(n) ad.ad is a(n) promotion.promotion is a(n)  
 message.message is a(n) communication.communication is a(n) act.act is a(n)  
 legal\_document.legal\_document is a(n) document.document is a(n) writing.writing  
 is a(n) written\_communication.written\_communication is a(n) communication.city  
 is a(n) municipality.municipality is a(n)  
 administrative\_district.administrative\_district is a(n) urban\_area.urban\_area is  
 a(n) district.district is a(n) geographical\_area.geographical\_area is a(n)  
 region.region is a(n) location.location is a(n) object.object is a(n)  
 physical\_entity.physical\_entity is a(n) entity.entity is a(n) act.act is a(n)  
 legal\_document.legal\_document is a(n) document.document is a(n) writing.writing  
 is a(n) written\_communication.written\_communication is a(n)  
 communication.communication is a(n) abstraction.abstraction is a(n) entity.state  
 is a(n) political\_unit.political\_unit is a(n) unit.unit is a(n)  
 organization.organization is a(n) social\_group.social\_group is a(n) group.group  
 is a(n) abstraction.abstraction is a(n) act.act is a(n)  
 legal\_document.legal\_document is a(n) document.document is a(n) writing.writing  
 is a(n) written\_communication.written\_communication is a(n)  
 communication.communication is a(n) abstraction.use is a(n) activity.

...

## References:

-----

- 1285.7 Random Walks for Text Semantic Similarity - [Daniel Ramage, Anna N. Rafferty, and Christopher D. Manning] - <https://nlp.stanford.edu/pubs/wordwalk-textgraphs09.pdf>
- 1285.8 Beta Reduction substitutions - <https://www.diderot.one/courses/56/books/275/chapter/3269>
- 1285.9 Tree-Adjoining Grammars - [https://en.wikipedia.org/wiki/Tree-adjoining\\_grammar](https://en.wikipedia.org/wiki/Tree-adjoining_grammar) - Symbols in CFGs are replaced by Tree adjunctions. Earlier question "Which is the largest city in the world" could be parsed by a Tree-Adjoining-Grammar and Lambda Function composition could be learnt from TAG tree by rule: function\_subtreeroot(<leftsubtree>, <rightsubtree>)
- 1285.10 Tree-Adjoining Grammars in Natural Language Processing - <https://www.slideshare.net/jchoi7s/cs571-tree-adjoining-grammar> - TAG tree for example sentence - "John will buy a car". Example TAG Lambda Function composition for "Buy a car": VP(Verb,NP(Disjunction,Noun))
- 1285.11 Tree-Adjoining Grammars - Dissertation - [K Vijayashanker] - <https://repository.upenn.edu/dissertations/AAI8804974/>
- 1285.12 Pumping Lemma for Tree-Adjoining Grammars - [K Vijayashanker] - Dissertation - <https://citeseerx.ist.psu.edu/viewdoc/download?doi=10.1.1.401.1695&rep=rep1&type=pdf> - "... Theorem 4.7 If L is a TAL, then there is a constant n such that if z in L and |z| >= n then z may be written as z=u1v1w1v2u2v3w2v4u3 with v1w1v2v3w2v4 <= n, |v1v2v3v4| >= 1 such that for all i >= 0, z=u1v1^i w1v2^i u2v3^i w2v4^i u3 in L ..." - Pumping Lemma for TALs have far-reaching applications in Natural Language Processing, especially in Sentence summarization and generating natural language answers to queries by Question-Answering bots (two opposing directions) - (\*) A longwinding natural language sentence of the form z=u1v1^i w1v2^i u2v3^i w2v4^i u3 could be summarized by parsing

it into a pumped version of TAG tree and inferring the summary from it as  
 $z = u_1v_1w_1v_2u_2v_3w_2v_4u_3$  (\*) A smaller natural language sentence of the form  
 $z = u_1v_1w_1v_2u_2v_3w_2v_4u_3$  could be pumped and expanded to a long sentence of the form  
 $z = u_1v_1^i w_1v_2^i u_2v_3^i w_2v_4^i u_3$

1285.13 Tree-Adjoining Grammars and Lexicalized Grammars - [Aravind Joshi-Yves Schabes] - <https://core.ac.uk/download/pdf/76362911.pdf> - Figure 3: Derived tree for: "yesterday a man saw Mary" - Tree-Adjoining Grammars are more expressive than CFLs and contained in Context Sensitive Languages - "... CFL  $\subset$  TAL  $\subset$  Indexed Languages  $\subset$  CSL ..."

1285.14 Parikh's Theorem - [https://en.wikipedia.org/wiki/Parikh%27s\\_theorem](https://en.wikipedia.org/wiki/Parikh%27s_theorem) - "... Parikh's theorem in theoretical computer science says that if one looks only at the number of occurrences of each terminal symbol in a context-free language, without regard to their order, then the language is indistinguishable from a regular language.[1] ... Let  $\Sigma = \{a_1, a_2, \dots, a_k\}$  be an alphabet. The Parikh vector of a word is defined as the function  $p: \Sigma^* \rightarrow \mathbb{N}^k$ , given by[1] 
$$p(w) = (|w|_{a_1}, |w|_{a_2}, \dots, |w|_{a_k})$$
 ... " - Parikh Vectors are examples of embedding of CFL words on a vectorspace.

-----  
 1286. (THEORY) Economic Merit and People Analytics - Mechanism Design of Multi-round Majority Voting derived from Simultaneous Ascending Auction - related to 400,790,791 and all sections on Majority Voting, Auction Design, Mechanism Design, Economic Merit, People Analytics, Quantitative Majority Circuit - 8 August 2022  
 -----

1286.1 Traditional mechanism of simultaneous ascending auctions for pricing commodities could be suitably translated to an Election Design Mechanism which allows multiple rounds of voting and flexible values per vote by mapping ascending prices per round (or bidders up the ante every round) to votes by electorate (Price = Vote).

1286.2 Following is a simplified example for Auction Design-to-Election Design translation involving 3 voters, 2 candidates and 3 rounds:

-----  
 Candidate 1:  
 -----

Round1 (all voters vote simultaneously per round by incrementing on previous rounds and votes are ascending monotone):  
 -----

Voter1 - (Round1, 10 votes), (Round2, 20 votes), (Round3, 40 votes)  
 Voter2 - (Round1, 20 votes), (Round2, 30 votes), (Round3, 45 votes)  
 Voter3 - (Round1, 5 votes), (Round2, 15 votes), (Round3, 55 votes - Highest Bidder)

Total votes for Candidate1 at the end of Round3: 140  
 -----

Candidate 2:  
 -----

Round1:  
 -----

Voter1 - (Round1, 5 votes), (Round2, 25 votes), (Round3, 35 votes)  
 Voter2 - (Round1, 15 votes), (Round2, 30 votes), (Round3, 45 votes - Highest Bidder)  
 Voter3 - (Round1, 10 votes), (Round2, 20 votes), (Round3, 30 votes)

Total votes for Candidate2 at the end of Round3: 110

1286.3 Candidate1 wins over Candidate2 (Either by Highest Vote 55 to 45 or Sum of Votes 140 to 110) at the end of Round3. Number of votes per voter per round is arbitrarily non-descending and arbitrary increment-decrement of votes per round per voter is allowed. Multi-round voting relaxes traditional voting by permitting voters to rethink decisions on earlier rounds (if negative votes are allowed, votes can descend in next rounds). Votes for Candidates earlier are stored (as secret ballots) either in a separate chaining hashtable or appended



to a chronological blockchain per voter.

#### References:

-----  
1286.4 Milgrom-Wilson Auction Design with Information Revelation -  
<https://web.stanford.edu/~jdlevin/Econ%20285/SAA%20and%20Spectrum%20Sales.pdf>  
-----

-----  
1287. (THEORY and FEATURE) Merit of Large Scale Visuals - Archaeology - Rebus  
Decipherment of Indus Pashupathi Seal - 9 August 2022 - related to  
1203,1232,1233,1236,1237,1240 and all sections on Merit of Large Scale Visuals,  
Physique Recognition From Quadrilateral mesh isomorphism, Topological Face and  
Handwriting recognition, Archaeology-Topological Script Recognition, Product  
Homotopy, Homeomorphism and Topological Deformations, People Analytics,  
Computational Geometry, Graph Edit Distance and Earth mover distance, Graph  
Isomorphism (Exact, Approximate and Subgraph), Graph matching, Graph  
similarity, Image Search, Quadrilateral Mesh Deformation and Isomorphism, Maximum  
Common Subgraph Problem and Approximate Topological Matching  
-----

-----  
1287.1 ImageGraph\_Keras\_Theano.py has been updated to rebus decipher Indus  
Pashupathi seal or Yogi seal in testlogs/yogic-seal\_0.jpg by ResNet50 and  
ResNet50V2 image object search and predictions (interpreted as Lord Shiva in  
Yogic posture by John Marshall) as below:

```
('Predictions - ', 'ResNet50', ':', [[('n02892201', 'brass', 0.7663543),
('n02910353', 'buckle', 0.09748204), ('n04192698', 'shield', 0.05866886),
('n03903868', 'pedestal', 0.014400147), ('n03929855', 'pickelhaube',
0.010885257)])])
```

```
('Predictions - ', 'ResNet50V2', ':', [[('n02883205', 'bow_tie', 1.0),
('n15075141', 'toilet_tissue', 0.0), ('n02317335', 'starfish', 0.0),
('n02389026', 'sorrel', 0.0), ('n02364673', 'guinea_pig', 0.0)])])
```

1287.2 Following are the sorted PageRanks of the textgraph vertices deep-learned  
from the predictions for Pashupathi seal image through ResNet50:

```
[('brass', 0.2087566573359813), ('pickelhaube', 0.09785508542625027), ('shield',
0.06616892202346995), ('base', 0.05032584032207979), ('buckle',
0.05032584032207979), ('support', 0.026561217769994573), ('foundation',
0.026561217769994573), ('fasten', 0.026561217769994573), ('buckles',
0.026561217769994573), ('structure', 0.023920704153096214), ('covering',
0.023920704153096214), ('protective', 0.023920704153096214), ('helmet',
0.021808293259577533), ('worn', 0.021808293259577533), ('spiked',
0.021808293259577533), ('German', 0.021808293259577533), ('soldiers',
0.021808293259577533), ('usually', 0.01995993372774868), ('means',
0.01995993372774868), ('mouthpiece', 0.01995993372774868), ('blown',
0.01995993372774868), ('cup-shaped', 0.01995993372774868), ('wind',
0.01995993372774868), ('variable', 0.01995993372774868), ('instrument',
0.01995993372774868), ('consists', 0.01995993372774868), ('tube',
0.01995993372774868), ('funnel-shaped', 0.01995993372774868), ('length',
0.01995993372774868)]
```

1287.3 Seat of the posture is identified by

["base","support","structure","pedestal","foundation"]. Posture is identified by  
"buckles" (resembling folded legs of Mulabandhasana). Crescent Moon Crown is  
identified by ["pickelhaube","helmet","worn","spiked"]. Martial nature of the  
seal is deciphered by ["soldiers","shield","protective","instrument","brass"]  
perhaps indicative of a warfare culture.

1287.4 There are some out of place vertices namely "German" originating from  
"pickelhaube" which is German military helmet (Crown in seal is matched to  
German helmet by decode\_predictions()). Apart from earlier figurine motif  
decipherment, ["funnel-shaped","cup-shaped","wind","tube"] seem to indicate  
rebus decipherment of the script on seal - coincidentally funnel-shaped, cup-  
shaped, wind and tube are related to respiratory tract and breathing exercises.  
Possible automated rebus decipherment from earlier predictions is (which is in  
no way a decipherment claim but could assist a manual decipherment): the script  
on seal might be a description on modus operandi of martial (weaponry)

respiratory ritual (which could be yogic posture).  
1287.5 It can be observed from earlier ResNet50 (Version 1 and 2) predictions and the logs testlogs/ImageGraph\_Keras\_Theano.log.PashupathiSeal.9August2022 that ResNet50 produces more meaningful, contextually relevant predictions than ResNet50V2 (except "starfish" for fish shaped script on seal).  
1287.6 Apart from rebus decipherment, Pashupathi seal is image segmented to get Chain approximation contours, Voronoi-Delaunay, Watershed segments, Canny Edge Detection imagery and FaceGraph DOT below:  
testlogs/RemoteSensingGIS/yogic-seal\_0\_ImageNet\_Keras\_Theano\_Segmentation\_FaceGraph.dot  
testlogs/RemoteSensingGIS/yogic-seal\_0\_segmented.jpg  
testlogs/yogic-seal\_0-cannyedgedetection.jpg  
testlogs/yogic-seal\_0-contourlabelled.jpg  
testlogs/yogic-seal\_0-contoursegmented.jpg

#### References:

-----  
1287.7 Statistical analysis (Large Number of Rare Events) of Mahadevan Concordance Table -  
[https://wlv.openrepository.com/bitstream/2436/620846/8/indus\\_new4%20%281%29.pdf](https://wlv.openrepository.com/bitstream/2436/620846/8/indus_new4%20%281%29.pdf)  
-----

-----  
1288. (THEORY and FEATURE) Merit of Large Scale Visuals - Archaeology - Rebus Decipherments of Indus Pashupathi Seals and mining frequent subgraphs from predictions - 10 August 2022 - related to 1203,1232,1233,1236,1237,1240,1287 and all sections on Merit of Large Scale Visuals, Physique Recognition From Quadrilateral mesh isomorphism, Topological Face and Handwriting recognition, Archaeology-Topological Script Recognition, Product Homotopy, Homeomorphism and Topological Deformations, People Analytics, Computational Geometry, Graph Edit Distance and Earth mover distance, Graph Isomorphism (Exact, Approximate and Subgraph), Graph matching, Graph similarity, Image Search, Quadrilateral Mesh Deformation and Isomorphism, Maximum Common Subgraph Problem and Approximate Topological Matching  
-----

-----  
1288.1 In continuation of ResNet50 analysis of Indus-Sarasvati Pashupathi seal in 1287, this update computes the frequent subgraphs in textgraphs of decode\_predictions() for 2 very similar Pashupathi seals (seals 80 and 81 of Plate 4 in Appendix 3 of concordance table)  
python-src/image\_pattern\_mining/ImageNet/testlogs/yogic-seal\_0.jpg and python-src/image\_pattern\_mining/ImageNet/testlogs/yogic-seal\_1.jpg having similar figurines but different script motifs except symbols 59 and 342 of Concordance table which are common to both the seals. By rebus principle, common motifs in two artefacts should result in common predictions corresponding to the common motifs.

1288.2 Following are the frequent subgraphs mined from predictions textgraphs of the two Pashupathi seals which contain prominent vertices for  
brass, buckles, pickelhaube, stupa (a religious structure), shield, helmet etc.,:  
Mined Frequent Subgraph Edges: {('buckles', 'buckle'), ('base', 'support'), ('cup-shaped', 'brass'), ('means', 'brass'), ('spiked', 'pickelhaube'), ('pickelhaube', 'worn'), ('buckle', 'buckle'), ('covering', 'shield'), ('pickelhaube', 'German'), ('Buddhists', 'stupa'), ('shield', 'covering'), ('worn', 'pickelhaube'), ('brass', 'variable'), ('brass', 'means'), ('stupa', 'dome-shaped'), ('support', 'base'), ('stupa', 'shrine'), ('brass', 'instrument'), ('blown', 'brass'), ('stupa', 'erected'), ('pickelhaube', 'soldiers'), ('wind', 'brass'), ('stupa', 'Buddhists'), ('shrine', 'stupa'), ('erected', 'stupa'), ('fasten', 'buckle'), ('soldiers', 'pickelhaube'), ('brass', 'wind'), ('brass', 'usually'), ('brass', 'blown'), ('consists', 'brass'), ('length', 'brass'), ('dome-shaped', 'stupa'), ('mouthpiece', 'brass'), ('instrument', 'brass'), ('brass', 'cup-shaped'), ('foundation', 'base'), ('pickelhaube', 'spiked'), ('brass', 'brass'), ('brass', 'mouthpiece'), ('tube', 'brass'), ('brass', 'funnel-shaped'), ('structure', 'shield'), ('brass', 'length'), ('pickelhaube', 'helmet'), ('buckle', 'fasten'),

('protective', 'shield'), ('shield', 'protective'), ('funnel-shaped', 'brass'), ('variable', 'brass'), ('base', 'foundation'), ('usually', 'brass'), ('shield', 'structure'), ('helmet', 'pickelhaube'), ('buckle', 'buckles'), ('brass', 'tube'), ('brass', 'consists'), ('German', 'pickelhaube')}]  
 1288.3 Insight in earlier common subgraph of the two seals is it has in it buried the meaning of symbols 59 and 342.

#### References:

-----  
 1288.4 The Indus Script:Text,Concordance and Tables - [Iravatham Mahadevan] - TIFR and ASI (1977) -  
<https://ia600906.us.archive.org/34/items/TheIndusScript.TextConcordanceAndTablesIravathanMahadevan/The%20Indus%20Script.%20Text%2C%20Concordance%20and%20Tables%20-Iravathan%20Mahadevan.pdf>  
 1288.5 Deep Learning Indus Script - <https://arxiv.org/pdf/1702.00523.pdf>

-----  
 1289. (THEORY and FEATURE) Astronomy and Cosmology Datasets Analytics - N-Body gravitational accelerations computed for USGS (1900-2012) 8+ magnitude Earthquakes and NOAA HURDAT2 (1851-2012) North Atlantic Hurricanes Datasets - 16 August 2022 - related to  
 17,137,148,445,731,1206,1236,1255,1266,1267,1268,1270,1271,1272,1273 and all sections on Astronomical Dataset Mining, Archaeoastronomical Dating, Sequence Mining, String analytics, Sequence Alignment, Visual Planetarium Search, Archaeology, Climate and Extreme Weather Event Analytics, Computational Astrophysics, N-Body problem, Merit of Large Scale Visuals, Astronomical algorithms, Histogram analytics

-----  
 1289.1 EphemerisSearch.py has been updated to change and add new parameters to function  
 extreme\_weather\_events\_n\_body\_analytics(self,datesofEWEs=None,loc="@earth-moon",angularsep=False,maxiterations=100) for restricting the number of dates of extreme weather events (EWE) iterated, choice of angular separation computation by boolean flag angularsep and 3 types of values for datesofEWEs ("Earthquakes","Hurricanes",User supplied dates of EWEs)  
 1289.2 For datesofEWEs="Earthquakes", datetimes are sourced from USGS 8.0+ earthquakes dataset (1900-2012) which has already been ETled as textfile in python-src/earthquakesFrom1900with8plusmag.pygen.txt. For datesofEWEs="Hurricanes", datetimes are sourced from NOAA Hurricane Dataset HURDAT2 already ETled as textfile in python-src/hurdat2\_1851\_2012-jun2013.pygen.txt. All datetimes are cast to UTC format compatible with JPL Horizons Ephemeris Service. For dateofEWEs supplied by user as array, computations are as usual with no change.  
 1289.3 N-Body Solar system gravitational accelerations are computed at Earth-Moon barycenter for USGS Earthquake datasets and with respect to respective longitude-latitude(s) of formation and zero elevation(sea level) for NOAA HURDAT2 Hurricane datasets (restricted to 100 hurricanes as the dataset is huge containing 50000 hurricanes spanning 161 years). This complements String Encoding and GSP Sequence Mining of USGS and NOAA HURDAT2 datasets in python-src/autogen\_classifier\_dataset/ and documented at asfer-docs/NeuronRain\_Research\_Celestial\_Pattern\_Mining.txt  
 1289.4 Computations of N-Body gravitational accelerations for USGS(Earthquake) and NOAA(Hurricane) datasets have been captured separately in following files:  
     python-src/testlogs/EphemerisSearch.log.Earthquakes.16August2022  
     python-src/testlogs/EphemerisSearch.log.Hurricanes.16August2022  
 1289.5 Following are excerpts of computations respectively for Sendai Earthquake on 11 March 2011 (9.0) and first recorded Hurricane (25 June 1851):

-----  
 -  
 extreme\_weather\_events\_n\_body\_analytics(): gravity of Sun at @earth-moon on (2011, 3, 11, 5, 46, 0) : [-3.60092543e-06 -9.97593306e-06 7.52550118e-08]  
 extreme\_weather\_events\_n\_body\_analytics(): gravity of Moon at @earth-moon on

```
(2011, 3, 11, 5, 46, 0) : [5.93284102e-03 -1.07378201e-03 -6.98565223e-07]
extreme_weather_events_n_body_analytics(): gravity of Mars at @earth-moon on
(2011, 3, 11, 5, 46, 0) : [-2.86408002e-03 1.21006257e-03 9.57056611e-05]
extreme_weather_events_n_body_analytics(): gravity of Mercury at @earth-moon
on (2011, 3, 11, 5, 46, 0) : [-0.04248091 -0.04133797 0.00052057]
extreme_weather_events_n_body_analytics(): gravity of Jupiter at @earth-moon
on (2011, 3, 11, 5, 46, 0) : [-2.35324463e-04 -5.80881981e-05 5.50732456e-06]
extreme_weather_events_n_body_analytics(): gravity of Venus at @earth-moon
on (2011, 3, 11, 5, 46, 0) : [3.89399938e-03 1.05719009e-02 -7.99002829e-05]
extreme_weather_events_n_body_analytics(): gravity of Saturn at @earth-moon
on (2011, 3, 11, 5, 46, 0) : [6.26683011e-05 1.43778659e-05 -2.74496998e-06]
extreme_weather_events_n_body_analytics(): gravity of Uranus at @earth-moon
on (2011, 3, 11, 5, 46, 0) : [-1.47148302e-05 -7.17547152e-08 1.90377268e-07]
extreme_weather_events_n_body_analytics(): gravity of Neptune at @earth-moon
on (2011, 3, 11, 5, 46, 0) : [-5.61349018e-06 3.45933185e-06 5.81269242e-08]
extreme_weather_events_n_body_analytics(): gravity of Pluto at @earth-moon
on (2011, 3, 11, 5, 46, 0) : [-5.46414412e-07 5.75922735e-06 -4.58472382e-07]
```

---

```
extreme_weather_events_n_body_analytics(): gravity of Sun at {'lon': 28.0,
'lat': 94.8, 'elevation': 0.0} on (1851, 6, 25, 0, 0, 0) : [9.38057871e-06
5.60142035e-06 -4.73504468e-07]
extreme_weather_events_n_body_analytics(): gravity of Moon at {'lon': 28.0,
'lat': 94.8, 'elevation': 0.0} on (1851, 6, 25, 0, 0, 0) : [-5.00327362e-04
5.73733377e-03 3.17136748e-06]
extreme_weather_events_n_body_analytics(): gravity of Mars at {'lon': 28.0,
'lat': 94.8, 'elevation': 0.0} on (1851, 6, 25, 0, 0, 0) : [-2.89680838e-03 -
7.70315656e-04 5.57099428e-05]
extreme_weather_events_n_body_analytics(): gravity of Mercury at {'lon':
28.0, 'lat': 94.8, 'elevation': 0.0} on (1851, 6, 25, 0, 0, 0) : [-0.04498039
0.00424941 0.00449187]
extreme_weather_events_n_body_analytics(): gravity of Jupiter at {'lon':
28.0, 'lat': 94.8, 'elevation': 0.0} on (1851, 6, 25, 0, 0, 0) :
[1.79703311e-04 8.78879940e-05 -4.38943473e-06]
extreme_weather_events_n_body_analytics(): gravity of Venus at {'lon': 28.0,
'lat': 94.8, 'elevation': 0.0} on (1851, 6, 25, 0, 0, 0) : [-0.00965776 -
0.0058695 0.0004808]
extreme_weather_events_n_body_analytics(): gravity of Saturn at {'lon': 28.0,
'lat': 94.8, 'elevation': 0.0} on (1851, 6, 25, 0, 0, 0) : [-6.04252762e-05 -
3.29543490e-05 2.97786557e-06]
extreme_weather_events_n_body_analytics(): gravity of Uranus at {'lon': 28.0,
'lat': 94.8, 'elevation': 0.0} on (1851, 6, 25, 0, 0, 0) : [-1.26534427e-05 -
8.24679688e-06 1.33372066e-07]
extreme_weather_events_n_body_analytics(): gravity of Neptune at {'lon':
28.0, 'lat': 94.8, 'elevation': 0.0} on (1851, 6, 25, 0, 0, 0) : [-
6.19751174e-06 2.31563273e-06 9.50902396e-08]
extreme_weather_events_n_body_analytics(): gravity of Pluto at {'lon': 28.0,
'lat': 94.8, 'elevation': 0.0} on (1851, 6, 25, 0, 0, 0) : [-2.02686099e-06 -
1.24640855e-06 7.19837809e-07]
1289.6 It can be observed that the gravitational acceleration vector components
of solar system bodies decrease in value exponentially proportionate to their
distance from earth except Mercury anomaly of which is unusually high.
```

#### References:

```

1289.7 NOAA HURDAT2 - https://www.nhc.noaa.gov/data/
1289.8 USGS Earthquake Hazards Program - https://earthquake.usgs.gov/
1289.9 Tug of sun, moon could be driving plate motions on 'imbalanced' Earth -
Earth-Moon Barycenter wobble - https://source.wustl.edu/2022/01/tug-of-sun-moon-
could-be-driving-plate-motions-on-imbalanced-earth/ and
https://pubs.geoscienceworld.org/books/book/2323/chapter-abstract/131987270/
Links-of-planetary-energetics-to-moon-size-orbit - "... Instead, Earth's plates
might be shifting because the sun exerts such a strong gravitational pull on the
moon that it has caused the moon's orbit around Earth to become elongated. Over
```

time, the position of the barycenter – the center of mass between the orbiting bodies of the Earth and the moon – has moved closer to Earth's surface and now oscillates 600 km per month relative to the geocenter, Hofmeister said. This sets up internal stresses, as the Earth continues to spin...."

-----  
1290. (THEORY and FEATURE) GIS Urban Sprawl Analytics - Facebook (Meta) High Resolution Settlement Layer (HRSL) Population Density Maps - GDAL GeoTIFF to JPEG format Translation - 18 August 2022 - related to 1174,1175,1179,1194,1211 and all sections on GIS Urban Sprawl Analytics, Merit of Large Scale Visuals, Gridded Population Estimators (SEDAC GPW4 and GHSL convex hull estimators), DBSCAN and Neural Network Urban Extent Learners, Computational Geometry, Intrinsic Merit Rankings, R Ricker Population Estimation, Community detection, Social Network Analytics, Space filling by Curves, Unequal Circle and Polynomial packing, Computational Geometry and Polygonal packing by Voronoi Tessellation, Four color theorem, Economic Merit, Computational Economics - GDP estimation from electricity consumption  
-----

-----  
1290.1 GDAL integration which was abandoned due to series of installation issues has been fulfilled after resolving compilation errors based on documentation from <https://mothergeo-py.readthedocs.io/en/latest/development/how-to/gdal-ubuntu-pkg.html> - libgdal-dev has been compiled after setting env:

```
export CPLUS_INCLUDE_PATH=/usr/include/gdal
export C_INCLUDE_PATH=/usr/include/gdal
pip3.7 install GDAL==2.4.2
```

1290.2 GDAL C++-Python bindings are imported from osgeo and new function `translate_geotiff_to_jpeg(geotiff_file, display=True, topx=0, topy=0, bottomx=1000, bottomy=1000)` has been defined which loads a GeoTIFF file by GDAL `Open()` and translates it to jpeg format by GDAL `Translate()`

1290.3 Function earlier optionally displays the GeoTIFF file in a bounding box (`topx, topy, bottomx, bottomy`) and its statistics by Raster X-Y sizes, Bands and `GetStatistics()` if `display=True`.

1290.4 World's most accurate population GIS - Facebook - Data For Good at Meta - HRSL 2021 - "HDX - Pakistan & India: High Resolution Population Density Maps - General" from [https://data.humdata.org/dataset/2c8cfe67-448f-4a27-94b3-aaa944598cba/resource/e3dbe673-4117-4243-93a8-3366c6e6396b/download/population\\_ind\\_pak\\_general.zip](https://data.humdata.org/dataset/2c8cfe67-448f-4a27-94b3-aaa944598cba/resource/e3dbe673-4117-4243-93a8-3366c6e6396b/download/population_ind_pak_general.zip) have been downloaded in GeoTIFF format (523.1 MB) and translated to JPEG format by `translate_geotiff_to_jpeg()`. Display of this high resolution dataset in matplotlib requires 6.92 GB of array memory size per GeoTIFF and might fail in normal desktop configurations and bounding boxes for smaller sizes may not display. This GeoTIFF data set is single band and only grayscale JPEG rendering is possible.

1290.5 Following are the logs and JPG files categorized by grid of longitudes and latitudes translated from HRSL GeoTIFFs:

```
testlogs/GISUrbanSprawlAnalytics.log.18August2022
```

```
testlogs/RemoteSensingGIS/FacebookMetaHRSL_IndiaPak_population_0_lon_70_general-v1.jpg
```

```
testlogs/RemoteSensingGIS/FacebookMetaHRSL_IndiaPak_population_0_lon_80_general-v1.jpg
```

```
testlogs/RemoteSensingGIS/FacebookMetaHRSL_IndiaPak_population_0_lon_90_general-v1.jpg
```

```
testlogs/RemoteSensingGIS/FacebookMetaHRSL_IndiaPak_population_10_lon_70_general-v1.jpg
```

```
testlogs/RemoteSensingGIS/FacebookMetaHRSL_IndiaPak_population_10_lon_80_general-v1.jpg
```

```
testlogs/RemoteSensingGIS/FacebookMetaHRSL_IndiaPak_population_10_lon_90_general
```

-v1.jpg

testlogs/RemoteSensingGIS/FacebookMetaHRSL\_IndiaPak\_population\_20\_lon\_60\_general  
-v1.jpg

testlogs/RemoteSensingGIS/FacebookMetaHRSL\_IndiaPak\_population\_20\_lon\_70\_general  
-v1.jpg

testlogs/RemoteSensingGIS/FacebookMetaHRSL\_IndiaPak\_population\_20\_lon\_80\_general  
-v1.jpg

testlogs/RemoteSensingGIS/FacebookMetaHRSL\_IndiaPak\_population\_20\_lon\_90\_general  
-v1.jpg

testlogs/RemoteSensingGIS/FacebookMetaHRSL\_IndiaPak\_population\_30\_lon\_60\_general  
-v1.jpg

testlogs/RemoteSensingGIS/FacebookMetaHRSL\_IndiaPak\_population\_30\_lon\_70\_general  
-v1.jpg

testlogs/RemoteSensingGIS/FacebookMetaHRSL\_IndiaPak\_population\_30\_lon\_80\_general  
-v1.jpg

#### References:

-----  
1290.6 LandSat 9 imagery - <https://earthexplorer.usgs.gov/>  
1290.7 GDAL python tutorial -  
[https://www.gis.usu.edu/~chrisg/python/2009/lectures/ospy\\_slides4.pdf](https://www.gis.usu.edu/~chrisg/python/2009/lectures/ospy_slides4.pdf)  
1290.8 MotherGeo GDAL installation documentation - <https://mothergeo-py.readthedocs.io/en/latest/development/how-to/gdal-ubuntu-pkg.html>  
1290.9 HDX Facebook - Data for Good at Meta - HRSL - Population Density Maps -  
[https://data.humdata.org/dataset/pakistan-india\\_all-files-high-resolution-population-density-maps](https://data.humdata.org/dataset/pakistan-india_all-files-high-resolution-population-density-maps)  
-----

-----  
1291. (THEORY and FEATURE) GIS Urban Sprawl Analytics - Facebook (Meta) High Resolution Settlement Layer (HRSL) Population Estimation from GDAL-Rasterio Georeferencing - 19 August 2022 - related to 1174,1175,1179,1194,1211,1290 and all sections on GIS Urban Sprawl Analytics, Merit of Large Scale Visuals, Gridded Population Estimators (SEDAC GPW4 and GHSL convex hull estimators), DBSCAN and Neural Network Urban Extent Learners, Computational Geometry, Intrinsic Merit Rankings, R Ricker Population Estimation, Community detection, Social Network Analytics, Space filling by Curves, Unequal Circle and Polynomial packing, Computational Geometry and Polygonal packing by Voronoi Tessellation, Four color theorem, Economic Merit, Computational Economics - GDP estimation from electricity consumption  
-----

-----  
1291.1 New function  
population\_estimate\_from\_raster\_georeferencing(geotiff, longitude=None, latitude=None) has been implemented in GISUrbanSprawlAnalytics.py which imports Rasterio python bindings for GDAL Georeferencing and computes following for a GeoTIFF (invoked for HRSL raster  
testlogs/RemoteSensingGIS/FacebookMetaHRSL\_IndiaPak\_population\_30\_lon\_80\_general-v1.5.tif):

1291.1.1 Coordinate Polygons in the Raster by Rasterio.shapes and Warp() longitude-latitude EPSG:4326 transformations for the polygons which could be the buildings and land usage patterns in zone segment classifications - Residential, Commercial, Industries and Greenery - could be useful for computing land usage percentages.

1291.1.2 Population value for a longitude-latitude from HRSL Raster GeoTIFF Georeferencing (pixels to Coordinate reference frame and viceversa) by index() function which maps to a (row,column) pixel on band 1 of the raster

data.

1291.2 More statistics have been computed within

`translate_geotiff_to_jpeg(geotiff=geotiff, display=True, topx=0, topy=0, bottomx=1000, bottomy=1000)`

1291.3 Smallest size GeoTIFF file has been chosen which contains NaNs as Larger TIFFs are memory intensive and cause segfault. Following are logs, tif and xml files generated:

`testlogs/GISUrbanSprawlAnalytics.log.19August2022`

`testlogs/RemoteSensingGIS/FacebookMetaHRSL_IndiaPak_population_30_lon_80_general-v1.5.tif`

`testlogs/RemoteSensingGIS/FacebookMetaHRSL_IndiaPak_population_30_lon_80_general-v1.5.tif.aux.xml`

`testlogs/RemoteSensingGIS/FacebookMetaHRSL_IndiaPak_population_30_lon_80_general-v1.jpg.aux.xml`

## References:

-----

1291.4 Rasterio Georeferencing 1 -

<https://rasterio.readthedocs.io/en/latest/topics/georeferencing.html> - `index()`

function internally invokes RPC transform while there is an alternative GCP transform

[https://rasterio.readthedocs.io/en/latest/api/rasterio.transform.html#rasterio.transform.from\\_gcps](https://rasterio.readthedocs.io/en/latest/api/rasterio.transform.html#rasterio.transform.from_gcps)

1291.5 Rasterio Georeferencing 2 -

<https://rasterio.readthedocs.io/en/latest/quickstart.html#dataset-georeferencing>

1291.6 Rasterio index -

<https://rasterio.readthedocs.io/en/latest/api/rasterio.io.html#rasterio.io.BufferDatasetWriter.index>

1291.7 Rasterio Transforms -

<https://rasterio.readthedocs.io/en/latest/api/rasterio.enums.html#rasterio.enums.TransformMethod> - options are gcps, affine and rpcs

-----

1292. (THEORY and FEATURE) GIS Urban Sprawl Analytics - Facebook (Meta) High Resolution Settlement Layer (HRSL) and LandSat 9 OLI2-TIRS2 GDAL-Rasterio Georeferencing - Window read - 22 August 2022 - related to

1174, 1175, 1179, 1194, 1211, 1290, 1291 and all sections on GIS Urban Sprawl Analytics, Merit of Large Scale Visuals, Gridded Population Estimators (SEDAC GPW4 and GHSL convex hull estimators), DBSCAN and Neural Network Urban Extent Learners, Computational Geometry, Intrinsic Merit Rankings, R Ricker Population Estimation, Community detection, Social Network Analytics, Space filling by Curves, Unequal Circle and Polynomial packing, Computational Geometry and Polygonal packing by Voronoi Tessellation, Four color theorem, Economic Merit, Computational Economics - GDP estimation from electricity consumption

-----

-----

1292.1 GISUrbanSprawlAnalytics.py has been updated to rename and add parameters to function

`population_estimate_from_raster_georeferencing(geotiff=geotiff, longitude=None, latitude=None)` as generic

`data_from_raster_georeferencing(geotiff=geotiff, shapes=False, longitude=None, latitude=None, bandnum=1, datatype="Population", window_slice=100)` to facilitate window read of huge GeoTIFF raster files which cause `VSIMalloc3()` allocation memory errors within `gdalnodatamaskband.cpp` of GDAL C++ (known issue). Tuning `GDAL_CACHEMAX` does not solve the exception.

1292.2 Boolean flag `shapes` optionally enables or disables masking of the raster to remove unnecessary pixels and computation of polygon shapes from raster.

Parameter `bandnum` determines band number of the raster and `window_slice` configures the number of horizontal and vertical slices to tile huge raster files into smaller rectangular windows. Type of data analyzed is denoted by

"datatype" argument (set to "Population" as default, other value being "Radiance").

1292.3 Rectangular window chunks are read from raster in 2 for loops by raster.read() and longitude-latitude value is searched in each window by index() which throws an exception if search fails. Exception is ignored and exhaustive search resumes(a Duff's device) scanning the whole raster till match is found.

1292.4 Function

```
translate_geotiff_to_jpeg(geotiff,display=True,topx=0,topy=0,bottomx=1000,botomy=1000,bandnum=1) has been updated to replace hardcoded band number. GDAL translate scaleParams are sourced from GetStatistics() as
gdal.Translate("testlogs/RemoteSensingGIS/"+jpegfilename[2] +
".jpg",geotiff,format='JPEG', width=1024, height=0,
scaleParams=[[statistics[0],statistics[1]]], outputType = gdal.GDT_UInt16)
```

1292.5 3 GeoTIFF files (\*) HRSL -  
testlogs/RemoteSensingGIS/FacebookMetaHRSL\_IndiaPak\_population\_10\_lon\_80\_general-v1.5.tif (\*) LandSat 9 OLI2-TIRS2 Chennai Metropolitan Area Downwell Radiance -  
testlogs/RemoteSensingGIS/LC08\_L2SP\_142051\_20220729\_20220806\_02\_T1\_ST\_DRAD.TIF  
(\*) LandSat 9 OLI2-TIRS2 Chennai Metropolitan Area - Band 7 -  
testlogs/RemoteSensingGIS/LC08\_L2SP\_142051\_20220729\_20220806\_02\_T1\_SR\_B7.TIF  
have been translated to JPEG and Georeferenced as below:

```
translate_geotiff_to_jpeg("testlogs/RemoteSensingGIS/FacebookMetaHRSL_IndiaPak_population_10_lon_80_general-v1.5.tif")
```

```
data_from_raster_georeferencing("testlogs/RemoteSensingGIS/FacebookMetaHRSL_IndiaPak_population_10_lon_80_general-v1.5.tif",80.2707,13.0827)
```

```
translate_geotiff_to_jpeg("testlogs/RemoteSensingGIS/LC08_L2SP_142051_20220729_20220806_02_T1_ST_DRAD.TIF")
```

```
data_from_raster_georeferencing("testlogs/RemoteSensingGIS/LC08_L2SP_142051_20220729_20220806_02_T1_ST_DRAD.TIF",bandnum=1,datatype="Radiance")
```

```
translate_geotiff_to_jpeg("testlogs/RemoteSensingGIS/LC08_L2SP_142051_20220729_20220806_02_T1_SR_B7.TIF")
```

```
data_from_raster_georeferencing("testlogs/RemoteSensingGIS/LC08_L2SP_142051_20220729_20220806_02_T1_SR_B7.TIF",bandnum=1,datatype="Radiance")
```

1292.6 LandSat 9 imagery by OLI2-TIRS2 instruments acquired on 29 July 2022 are sourced from USGS EarthExplorer - [https://landsatlook.usgs.gov/gen-browse?size=rrb&type=refl&product\\_id=LC08\\_L1TP\\_142051\\_20220729\\_20220806\\_02\\_T1](https://landsatlook.usgs.gov/gen-browse?size=rrb&type=refl&product_id=LC08_L1TP_142051_20220729_20220806_02_T1)

#### References:

-----

1292.7 LandSat 9 - TIRS-2 and OLI-2 - <https://www.usgs.gov/media/images/landsat-9-oli-2-and-tirs-2-instruments>

1292.8 GDAL2tiles - <https://gdal.org/programs/gdal2tiles.html> - splits TIF file into multiple tiles

-----

1295. (THEORY and FEATURE) GIS Urban Sprawl Analytics - Facebook (Meta) High Resolution Settlement Layer (HRSL) and Global Human Settlement Layer (GHSL) GDAL-Rasterio Georeferencing - Sampling and Mollweide-EPSS transforms reprojections - 25 August 2022 - related to 1174,1175,1179,1194,1211,1290,1291,1292 and all sections on GIS Urban Sprawl Analytics, Merit of Large Scale Visuals, Gridded Population Estimators (SEDAC GPW4 and GHSL convex hull estimators), DBSCAN and Neural Network Urban Extent Learners, Computational Geometry, Intrinsic Merit Rankings, R Ricker Population Estimation, Community detection, Social Network Analytics, Space filling by Curves, Unequal Circle and Polynomial packing, Computational Geometry and Polygonal packing by Voronoi Tessellation, Four color theorem, Economic Merit, Computational Economics - GDP estimation from electricity consumption

-----



```

1295.1 GISUrbanSprawlAnalytics.py now imports fiona transforms and rasterio
sample modules. Function
data_from_raster_georeferencing(geotiff,shapes=False,longitude=None,latitude
=None,bandnum=1,datatype="Population",windowslice=100,sample=False) has been
updated to add sample as a parameter.
1295.2 New if-else clause has been introduced which checks the CRS of the raster
and if crs is (*) EPSG:4326 and if sample is enabled raster is sampled by
sample_gen for data at a longitude-latitude coordinate and if sample is disabled
usual window read scan of whole raster is performed to search for data at
longitude-latitude (*) other than EPSG:4326 which could most likely be
mollweide, EPSG:4326 source longitude-latitude reference system is transformed
to destination mollweide reference system ESRI:54009 by reprojection and data is
sampled by sample_gen at transformed coordinates.
1295.3 data_from_raster_georeferencing() is invoked on two datasets : (*) HRSL
Indian subcontinent population estimate GeoTIFF -
testlogs/RemoteSensingGIS/FacebookMetaHRSL_IndiaPak_population_10_lon_80_general
-v1.5.tif by iterating over a rectangle of longitude-latitude bounding box
ensconcing Chennai Metropolitan Area - bounded by topleft-(80.2,13.0) and
bottomright-(80.3,13.2) to print population data sampled in rectangle -
iteration uses arange() as Python range() is limited to integer values (*) Newly
released GHSL R2022A Built Surface dataset
testlogs/RemoteSensingGIS/GHS_BUILT_S_P2030LIN_GLOBE_R2022A_54009_100_V1_0_R8_C2
6.tif for sampling built surface data at longitude=80.2707,latitude=13.0827 of
Chennai Metropolitan Agglomeration.
1295.4 Following are logs quoted from
testlogs/GISUrbanSprawlAnalytics.log.25August2022 for HRSL and GHSL GeoTIFFs:
...
=====testlogs/RemoteSensingGIS/
FacebookMetaHRSL_IndiaPak_population_10_lon_80_general-
v1.5.tif=====
Raster bounds: BoundingBox(left=79.99819444444445, bottom=12.2554166666660466,
right=86.38041666667178, top=20.006527777777777)
Raster height: 27904
Raster width: 22976
Raster top left - spatial value: (79.99833333333333, 20.00638888888889)
Raster bottom right - spatial value: (86.3805555555556, 12.2552777777771578)
Raster transform: | 0.00, 0.00, 80.00|
| 0.00,-0.00, 20.01|
| 0.00, 0.00, 1.00|
Raster CRS: EPSG:4326
Longitude: 80.290000000000005
Latitude: 13.119999999999997
Population from raster for longitude-latitude: [array([48.887234])]
=====testlogs/RemoteSensingGIS/
GHS_BUILT_S_P2030LIN_GLOBE_R2022A_54009_100_V1_0_R8_C26.tif=====
Raster bounds: BoundingBox(left=7059000.0, bottom=1000000.0, right=7959000.0,
top=2000000.0)
Raster height: 10000
Raster width: 9000
Raster top left - spatial value: (7059050.0, 1999950.0)
Raster bottom right - spatial value: (7959050.0, 999950.0)
Raster transform: | 100.00, 0.00, 7059000.00|
| 0.00,-100.00, 2000000.00|
| 0.00, 0.00, 1.00|
Raster CRS: ESRI:54009
Longitude: 80.2707
Latitude: 13.0827
Source CRS: EPSG:4326
Destination CRS: +proj=moll +lon_0=0 +x_0=0 +y_0=0 +datum=WGS84 +units=m
+no_defs=True
Transformed Coordinates: [[7915402.10721301, 1612214.7819872624]]
BUILT from raster: [array([3699], dtype=uint16)]

```

## References:

-----  
1295.5 GHSL R2022A BUILT-S dataset - [https://jeodpp.jrc.ec.europa.eu/ftp/jrc-opendata/GHSL/GHS\\_BUILT\\_S\\_GLOBE\\_R2022A/GHS\\_BUILT\\_S\\_GLOBE\\_R2022A/GHS\\_BUILT\\_S\\_P2030LIN\\_GLOBE\\_R2022A\\_54009\\_100/V1-0/GHS\\_BUILT\\_S\\_P2030LIN\\_GLOBE\\_R2022A\\_54009\\_100\\_V1\\_0.zip](https://jeodpp.jrc.ec.europa.eu/ftp/jrc-opendata/GHSL/GHS_BUILT_S_GLOBE_R2022A/GHS_BUILT_S_GLOBE_R2022A/GHS_BUILT_S_P2030LIN_GLOBE_R2022A_54009_100/V1-0/GHS_BUILT_S_P2030LIN_GLOBE_R2022A_54009_100_V1_0.zip)  
1295.6 GHSL Data Package 2022 - [https://ghsl.jrc.ec.europa.eu/documents/GHSL\\_Data\\_Package\\_2022.pdf?t=1655995832](https://ghsl.jrc.ec.europa.eu/documents/GHSL_Data_Package_2022.pdf?t=1655995832)  
-----

-----  
1296. (THEORY and FEATURE) GIS Urban Sprawl Analytics - Facebook (Meta) High Resolution Settlement Layer (HRSL) and Global Human Settlement Layer (GHSL) GDAL-Rasterio Georeferencing - Gini Index of Population and Built-Surface - 28 August 2022 - related to 1174,1175,1179,1194,1211,1290,1291,1292,1295 and all sections on GIS Urban Sprawl Analytics, Merit of Large Scale Visuals, Gridded Population Estimators (SEDAC GPW4 and GHSL convex hull estimators), DBSCAN and Neural Network Urban Extent Learners, Computational Geometry, Intrinsic Merit Rankings, R Ricker Population Estimation, Community detection, Social Network Analytics, Space filling by Curves, Unequal Circle and Polynomial packing, Computational Geometry and Polygonal packing by Voronoi Tessellation, Four color theorem, Economic Merit, Computational Economics - GDP estimation from electricity consumption, Poverty alleviation  
-----

-----  
1296.1 GISUrbanSprawlAnalytics.py has been updated to define two new functions (\*) `urbansprawl_gini_coefficient(urbansprawldata)` and (\*) `urban_sprawl_from_raster(longx,latx,longy,laty,raster,dt)` for computing Gini Coefficient measure of inequality in an urban sprawl statistical parameter and to wrap the longitude-latitude urban sprawl bounding box computation of `data_from_raster_georeferencing()` for a raster respectively.

1296.2 `urban_sprawl_from_raster()` is computed on following 2 datasets of GHSL R2022A Built-Surface and Facebook Meta HRSL Indian subcontinent Population for Chennai Metropolitan Area Longitude-Latitude (80.2707,13.0827) Bounding Box - (80.1,13.0) to (80.3,13.2):

`urban_sprawl_from_raster(80.1,13.0,80.3,13.2,"testlogs/RemoteSensingGIS/GHS_BUILT_S_P2030LIN_GLOBE_R2022A_54009_100_V1_0_R8_C26.tif",dt="BUILT-S")`

`urban_sprawl_from_raster(80.1,13.0,80.3,13.2,"testlogs/RemoteSensingGIS/FacebookMetaHRSL_IndiaPak_population_10_lon_80_general-v1.5.tif",dt="Population")`

1296.3 Following excerpts of Gini coefficient computations from `python-src/image_pattern_mining/ImageNet/testlogs/GISUrbanSprawlAnalytics.log.28 August2022` for earlier Built-Surface and Population datasets ignore NaN values by `math.isnan()` filtering. Gini coefficient is defined as ratio of area bounded by hypotenuse and Lorenz curve to total area of right-angle triangle and ranges from 0 (complete equality) to 1 (complete inequality):

Built-Surface - `urbansprawl_gini_coefficient()`: Gini Index of the dataset = 0.48700616284225207 (48.7%)

Population - `urbansprawl_gini_coefficient()`: Gini Index of the dataset = 0.28008540547871624 (28.0%) ignoring NaNs.

1296.4 Disparity of 48.7% and 28% between Built-Surface (less equality) and Population (more equality) implies construction activity is not commensurate and hasn't caught up with burgeoning population.

## References:

-----  
1296.5 Gini coefficient - [https://en.wikipedia.org/wiki/Gini\\_coefficient](https://en.wikipedia.org/wiki/Gini_coefficient)

1296.6 Gini coefficient of income disparity - <https://data.worldbank.org/indicator/SI.POV.GINI>  
-----

-----  
1297. (THEORY and FEATURE) GIS Urban Sprawl Analytics - Facebook (Meta) High Resolution Settlement Layer (HRSL) - Population estimation from GDAL-Rasterio

Georeferencing - 30 August 2022 - related to  
1174,1175,1179,1194,1211,1290,1291,1292,1295,1296 and all sections on GIS Urban  
Sprawl Analytics, Merit of Large Scale Visuals, Gridded Population Estimators  
(SEDAC GPW4 and GHSL convex hull estimators), DBSCAN and Neural Network Urban  
Extent Learners, Computational Geometry, Intrinsic Merit Rankings, R Ricker  
Population Estimation, Community detection, Social Network Analytics, Space  
filling by Curves, Unequal Circle and Polynomial packing, Computational Geometry  
and Polygonal packing by Voronoi Tessellation, Four color theorem, Economic  
Merit, Computational Economics - GDP estimation from Urban sprawl demographics,  
electricity consumption, Poverty alleviation

----- 1297.1

GISUrbanSprawlAnalytics.py has been updated to enhance  
urban\_sprawl\_from\_segments() by adding a clause for looking up population value  
for a pixel in JPEG translation of a GeoTIFF raster by raster.xy() and compute  
population estimation based on it.

1297.2 Within translate\_geotiff\_to\_jpeg(), gdal.Translate() has been changed to  
write JPEG file from GeoTIFF raster after scaling down X and Y sizes by function  
parameter scaledown. Scaling is necessary to reduce JPEG file sizes from actual  
raster dimensions. Scale parameters have been restored to [[0, 255, 0, 65535]]

1297.3 Function

urban\_sprawl\_from\_segments(image,segment,maximum\_population\_density=100000,sqkmt  
ocontourarearatio=0,legend=None,sqkmareatopopulationratio=6.22,voronoi\_delaunay=  
False,number\_of\_clusters=2,maxiterations=2,populationfromraster="None") has been  
updated to include an argument populationfromraster for name of raster TIF file.  
New if clause for reading a raster file has been introduced to find minimum  
enclosing circle of every contour in JPEG translation of TIF file and centroid  
of the enclosing circle. Pixel coordinates of contour centroids are lookedup in  
raster TIF of translated JPEG by xy() to find longitude-latitude after scaling  
up by factor scaleup to restore the coordinates to GeoTIFF dimensions as JPEG  
version is scaled down version of TIFF.

1297.4 Longitude-Latitude earlier is passed on to

data\_from\_raster\_georeferencing() to get population at the centroid coordinates  
within GeoTIFF raster. Scaling up and down earlier might cause some loss in  
pixel coordinate information because of integer division and actual longitude-  
latitude might vary and be inaccurate depending on scaling. Scaling has to be  
resorted to only when size of the raster and translated JPEG are huge and there  
are out of memory errors while loading. Setting scaleup and scaledown to 1  
results in same size of JPEG as raster and doesn't distort the dimensions. Some  
example deviations due to scale up and down which are out 80-87 and 13-20  
longitude-latitude bounding box ambit:

urban\_sprawl\_from\_segments(): raster xy longlat = (87.665000000000613,  
20.006388888888889)

urban\_sprawl\_from\_segments(): raster xy longlat = (87.595555555556163,  
19.950833333333329)

urban\_sprawl\_from\_segments(): raster xy longlat = (87.581666666667273,  
19.923055555555549)

urban\_sprawl\_from\_segments(): raster xy longlat = (87.498333333333933,  
19.992499999999999)

urban\_sprawl\_from\_segments(): raster xy longlat = (87.484444444445043,  
20.006388888888889)

urban\_sprawl\_from\_segments(): raster xy longlat = (87.401111111111703,  
19.992499999999999)

urban\_sprawl\_from\_segments(): raster xy longlat = (87.359444444445033,  
19.950833333333329)

urban\_sprawl\_from\_segments(): raster xy longlat = (87.359444444445033,  
20.006388888888889)

1297.5 Image file tokenization has been changed to remove hardcoded indices and  
replace them by last index of the tokens array in both  
ImageGraph\_Keras\_Theano.py and GISUrbanSprawlAnalytics.py. Array length check in  
contours kmeans clustering has been added.

1297.6 Following are logs, contour-segment-tessellation-edgedetection images and  
some example population estimates computed within  
testlogs/GISUrbanSprawlAnalytics.log.30August2022 for urban sprawl contour

centroid long-lat (83.56,18.20) looking up Meta HRSL EPSG:4326 Raster  
FacebookMetaHRSL\_IndiaPak\_population\_10\_lon\_80\_general-v1.5.tif (not committed)  
bounded by longitudes 80-87 and latitudes 13-20 (unscaled GDAL translated JPEG  
testlogs/RemoteSensingGIS/FacebookMetaHRSL\_IndiaPak\_population\_10\_lon\_80\_general  
-v1.jpg is of size ~25 MB and slow to process which has been scaled to a factor  
of 50):

testlogs/RemoteSensingGIS/FacebookMetaHRSL\_IndiaPak\_population\_10\_lon\_80\_general  
-v1.jpg

testlogs/RemoteSensingGIS/FacebookMetaHRSL\_IndiaPak\_population\_10\_lon\_80\_general  
-v1.jpg.aux.xml

testlogs/FacebookMetaHRSL\_IndiaPak\_population\_10\_lon\_80\_general-v1-  
cannyedgedetection.jpg

testlogs/FacebookMetaHRSL\_IndiaPak\_population\_10\_lon\_80\_general-v1-  
contourkmeansclustered.jpg

testlogs/FacebookMetaHRSL\_IndiaPak\_population\_10\_lon\_80\_general-v1-  
contourlabelled.jpg

testlogs/FacebookMetaHRSL\_IndiaPak\_population\_10\_lon\_80\_general-v1-  
contoursegmented.jpg

testlogs/GISUrbanSprawlAnalytics.log.30August2022

testlogs/RemoteSensingGIS/FacebookMetaHRSL\_IndiaPak\_population\_10\_lon\_80\_general  
-v1\_ImageNet\_Keras\_Theano\_Segmentation\_FaceGraph.dot

testlogs/RemoteSensingGIS/FacebookMetaHRSL\_IndiaPak\_population\_10\_lon\_80\_general  
-v1\_segmented.jpg

=====testlogs/RemoteSensingGIS/  
FacebookMetaHRSL\_IndiaPak\_population\_10\_lon\_80\_general-  
v1.5.tif=====

==  
Raster bounds: BoundingBox(left=79.99819444444445, bottom=12.2554166666660466,  
right=86.380416666667178, top=20.006527777777777)

Raster height: 27904

Raster width: 22976

Raster top left - spatial value: (79.99833333333333, 20.00638888888889)

Raster bottom right - spatial value: (86.38055555555556, 12.2552777777771578)

Raster transform: | 0.00, 0.00, 80.00|

| 0.00, -0.00, 20.01|

| 0.00, 0.00, 1.00|

Raster CRS: EPSG:4326

Longitude: 83.609444444444733

Latitude: 19.77027777777759

Population from raster for longitude-latitude: [array([14.301587])]

urban\_sprawl\_from\_segments(): raster values = [array([14.301587])]

('Convex Hull of Urban Area:', array([[ 19, 259]],

[[ 18, 263]],

[[ 17, 263]],

[[ 17, 259]],

[[ 18, 258]]], dtype=int32))

('Circumference of Urban Area:', 15.899494767189026)

('Approximate circular area of Urban Sprawl:', 12.56)

('Contour Area of Urban Sprawl:', 0.5)

('Ratio of urban sprawl contour area to image area:', 1.952194657233662e-06)

('Square Kilometer Area of Urban Sprawl:', 0.1557377049180328)

('Population of Urban Sprawl (from density):', array([2.22729634]))

('Population of Urban Sprawl (from area):', 0.1508613276001075)

('Centroid of the Urban Sprawl:', (17, 262))

Contour boundary point: [[130 257]]

urban\_sprawl\_from\_segments(): raster xy longlat = (83.56777777778063,

18.200833333333189)

-----  
-----  
1301. (THEORY and FEATURE) GIS Urban Sprawl Analytics - Polya Urn Urban Growth Model - Revised for N color segments - 2 September 2022 - related to 1174,1175,1179,1194,1211,1234,1290,1291,1292,1295,1296,1297 and all sections on GIS Urban Sprawl Analytics, Merit of Large Scale Visuals, Gridded Population Estimators (SEDAC GPW4 and GHSL convex hull estimators), DBSCAN and Neural Network Urban Extent Learners, Computational Geometry, Intrinsic Merit Rankings, R Ricker Population Estimation, Community detection, Social Network Analytics, Space filling by Curves, Unequal Circle and Polynomial packing, Computational Geometry and Polygonal packing by Voronoi Tessellation, Four color theorem, Economic Merit, Computational Economics - GDP estimation from Urban sprawl demographics, electricity consumption, Poverty alleviation  
-----  
-----

1301.1 GISUrbanSprawlAnalytics.py Polya Urn Urban Growth Model function `polya_urn_urban_growth_model(image,ncoloredsegments,segmentedgis,iterations=1000)` has been changed to add image filename parameter and allow arbitrary number of colored contour segments. Contours segmented earlier from a GIS JPEG image are iterated and an n-colored dictionary of colors-to-segments is populated by looking up the color of contour centroid pixel in image ndarray construed as color of the contour segment.

1301.2 Contents of Polya Urn before and after growth (by choosing a random colored segment and replicating it) are printed.

1301.3 GHSL SMOD R2022A Degree of Urbanization JPEG image from [https://ghsl.jrc.ec.europa.eu/ghs\\_smod2022.php](https://ghsl.jrc.ec.europa.eu/ghs_smod2022.php) for Chennai Metro Sprawl `testlogs/RemoteSensingGIS/ChennaiMetropolitanArea_GHSL_R2022A_GHS_SMOD_DegreeOfUrbanisation.jpg` which follows a 3-colored high level zoning (open space-water-vegetation, built space-residential, built space-non-residential) has been segmented for contours,watershed,canny edge detection and grown by Polya Urban Growth Model for 1000 iterations. Non-residential Built space includes both commercial and industrial areas. Following are affected image, DOT and log files:

`testlogs/ChennaiMetropolitanArea_GHSL_R2022A_GHS_SMOD_DegreeOfUrbanisation-cannyedgedetection.jpg`

`testlogs/ChennaiMetropolitanArea_GHSL_R2022A_GHS_SMOD_DegreeOfUrbanisation-contourkmeansclustered.jpg`

`testlogs/ChennaiMetropolitanArea_GHSL_R2022A_GHS_SMOD_DegreeOfUrbanisation-contourlabelled.jpg`

`testlogs/ChennaiMetropolitanArea_GHSL_R2022A_GHS_SMOD_DegreeOfUrbanisation-contoursegmented.jpg`

`testlogs/GISUrbanSprawlAnalytics.log.2September2022`

`testlogs/RemoteSensingGIS/ChennaiMetropolitanArea_GHSL_R2022A_GHS_SMOD_DegreeOfUrbanisation.jpg`

`testlogs/RemoteSensingGIS/ChennaiMetropolitanArea_GHSL_R2022A_GHS_SMOD_DegreeOfUrbanisation_ImageNet_Keras_Theano_Segmentation_FaceGraph.dot`

`testlogs/RemoteSensingGIS/ChennaiMetropolitanArea_GHSL_R2022A_GHS_SMOD_DegreeOfUrbanisation_segmented.jpg`

1301.4 Differentiating Industrial and Commercial segments within Non-residential built space is non-trivial and necessary for 4-colored segmentation. While Polluting Manufacturing industries could be discerned by air quality index (PM2.5,PM10) from a datasource, for example, OpenWeatherMap Longitude-Latitude REST API - <https://openweathermap.org/api/air-pollution>, distinguishing non-polluting Manufacturing-IT-ITES from commercial activity is a problem unless they are of varying building heights or luminosity in NightLights data from



1301.14 LIDAR DEM Flood maps -

<https://www.walshmedicalmedia.com/open-access/lidar-dem-data-for-flood-mapping-and-assessment-opportunities-andchallenges-a-review-2469-4134-1000211.pdf>

1301.15 Triangulated Irregular Network (TIN) based on Constrained Delaunay Triangulation - [https://en.wikipedia.org/wiki/Triangulated\\_irregular\\_network](https://en.wikipedia.org/wiki/Triangulated_irregular_network)

-----  
-----  
1302. (THEORY and FEATURE) NeuronRainApps - Autonomous Driving - Obstacle Lattice from LIDAR Point Cloud Data - 5 September 2022 - related to 1253,1294 and all sections on Async IO, Drone Electronic Voting Machines, GIS and Urban Sprawl Analytics, Merit of Large Scale Visuals, Drone Obstacle Avoidance, Computational Geometry, ADAS-Obstacle avoidance, Autonomous Vehicles, Unmanned Aerial Vehicle Navigation-Autonomous Drone Delivery-Passenger Drones, Wiring Problem

-----  
-----  
1302.1 This commit adds a NeuronRainApps LIDAR usecase for Autonomous Driving - python-src/NeuronRainApps/AutonomousDriving/AutonomousDriving.py - which reads a LIDAR LAS format file, detects Ground and Other Obstacles based on Return Number of LASER pulse and writes a Lattice obstacle matrix which could be read by latticewalks.cpp (NeuronRain Grafit - Section 1294) to compute Obstacle Free optimal lattice walks.

1302.2 Function read\_lidar\_stream() reads a LAS file simple.las (Laspy test dataset - <https://github.com/laspy/laspy/blob/master/tests/data/simple.las>) from LIDAR by laspy utility and finds points within a clearance query range parameter through KDTree representation of LAS point cloud. Rendering of simple.las Point Cloud through <http://lidarview.com/> has been added to repository as PDF file simple.las.pdf showing number of returns and points per return number.

1302.3 It also differentiates points as Ground points and Obstacle points based on return number of the point and total number of returns of a LIDAR pulse reflected from surface. Mostly points of return number equal to number of returns are bottommost and reflected from ground while other points of less return number are obstacles (trees, buildings) which are iterated and populated in a lattice array after scaling (captured in testlogs/AutonomousDriving.log.5September2022). Lattice array requires Terabyte memoryview() allocation and has been commented.

#### References:

-----  
1302.4 Number of Returns and Return number in LIDAR - Graphic illustration - <https://pro.arcgis.com/en/pro-app/latest/help/data/las-dataset/what-is-lidar-.htm> - "... Laser pulses emitted from a lidar system reflect from objects both on and above the ground surface: vegetation, buildings, bridges, and so on. One emitted laser pulse can return to the lidar sensor as one or many returns. Any emitted laser pulse that encounters multiple reflection surfaces as it travels toward the ground is split into as many returns as there are reflective surfaces. The first returned laser pulse is the most significant return and will be associated with the highest feature in the landscape like a treetop or the top of a building. The first return can also represent the ground, in which case only one return will be detected by the lidar system. Multiple returns are capable of detecting the elevations of several objects within the laser footprint of an outgoing laser pulse. The intermediate returns, in general, are used for vegetation structure, and the last return for bare-earth terrain models. ..."

1302.5 Laspy tutorial -

[https://laspy.readthedocs.io/en/latest/complete\\_tutorial.html](https://laspy.readthedocs.io/en/latest/complete_tutorial.html)

1302.6 Memory Requirements of Autonomous Driving -

<https://www.rambus.com/blogs/autonomous-vehicles-memory-requirements-deep-neural-net-limitations/> - DeepTest paper - <https://arxiv.org/pdf/1708.08559.pdf> - Level3 to Level5 full autonomy requires new generations of LPDRAM

1302.7 Memory configuration of Level3-Level5 autonomy -

<https://my.micron.com/insight/on-the-road-to-full-autonomy> - "...The autonomous vehicle is projected to contain more lines of code than any other software





```
13705818346013311833108928252117817790107121301451936108613838402556294473422077
20584667451928017587637898116377574250708847682533578055959395213059298133244667
80566387652974320492163103697723773048880287685485037011832086529810417536909671
26825294474548870111832078730939521984700410407384966407152954148467086458951489
44401910064141750708847004104073849664070891488765593922310340220787309398869849
66413872730969745894667906414074252656324235563264535496622816995877421473488468
46692213040727354833922937707257666024308039229377139824833773683975922781884830
27415325922781830803378846065412516841317362483323621471997952788990785645729289
3475579498302741531914376529541
```

```
xl =
```

```
13705818346013311833108928252117817790107121301451936108613838402556294473422077
20584667451928017587637898116377574250708847682533578055959395213059298133244667
80566387652974320492163103697723773048880287685485037011832086529810417536909671
26825294474548870111832078730939521984700410407384966407152954148467086458951489
44401910064141750708847004104073849664070891488765593922310340220787309398869849
66413872730969745894667906414074252656324235563264535496622816995877421473488468
46692213040727354833922937707257666024308039229377139824833773683975922781884830
27415325922781830803378846065412516841317362483323621471997952788990785645729289
3475579498302741531914376529539
```

```
yl = 67
```

```
Factor point verification: (xl + intervalmidpoint)*yl == number_to_factorize =
True
```

```
Factor point verification: xl*yl == number_to_factorize = False
```

```
('Factors are: (' , 67, ' , ' ,
```

```
13705818346013311833108928252117817790107121301451936108613838402556294473422077
20584667451928017587637898116377574250708847682533578055959395213059298133244667
80566387652974320492163103697723773048880287685485037011832086529810417536909671
26825294474548870111832078730939521984700410407384966407152954148467086458951489
44401910064141750708847004104073849664070891488765593922310340220787309398869849
66413872730969745894667906414074252656324235563264535496622816995877421473488468
46692213040727354833922937707257666024308039229377139824833773683975922781884830
27415325922781830803378846065412516841317362483323621471997952788990785645729289
3475579498302741531914376529541, ') (at ' , 'Wed, 07 Sep 2022 06:54:05 GMT', ')')
nanoseconds elapsed so far in finding all factors: 12204434562 (12.204 seconds)
1303.3 Earlier numbers can be contrasted with FLINT (Fast library for Number
```

```
Theory)-Mathematica-Pari/GP factorization benchmarks quoted from
https://www.flintlib.org/benchmarks.html (which are implementations of some
special case optimized factoring algorithms) from 16 bits to 64 bits on Highend
Octacore-Tencore Intel Xeon E5-2650, 2.00 GHz CPU -
```

```
https://www.intel.in/content/www/in/en/products/sku/64590/intel-xeon-processor-
e52650-20m-cache-2-00-ghz-8-00-gts-intel-qpi/specifications.html - 384 GB RAM
16-Hyperthreaded configuration:
```

n-bits	Mathematica 9.0	Pari/GP 2.5.4	FLINT 2.4 (time in seconds)
16	0.0720	0.0160	0.00476
24	0.108	0.0560	0.0192
32	0.272	0.233	0.0812
40	0.960	0.608	0.199
48	1.87	1.17	0.430
56	2.76	2.28	1.19
64	4.60	4.21	3.86

```

NeuronRain Computational Geometric Factorization (all factors) on Quadcore 2.00
GHZ 4 GB RAM configuration which is trivial compared to Xeon ES-2650 Octacore
(time to first factor):

```

```

67 bits - 4.55 seconds
2232 bits - 12.204 seconds
```

```
References:
```

```

1303.4 CADO-NFS RSA moduli benchmarks - https://cado-nfs.gitlabpages.inria.fr/
1303.5 Integer Factorization Benchmarks -
```

<https://www.mersenneforum.org/showthread.php?t=15109> - performance numbers for CADO-NFS - 110 digit integer (~350 bits integer) requires 27662 seconds to factorize in CADO-NFS (Xeon Haswell CPUs)

-----  
1304. (THEORY and FEATURE) GIS Urban Sprawl Analytics - Polya Urn Urban Growth Model - Weights Learnt - 8 September 2022 - related to 1174,1175,1177,1179,1194,1211,1234,1290,1291,1292,1295,1296,1297,1301 and all sections on GIS Urban Sprawl Analytics, Merit of Large Scale Visuals, Gridded Population Estimators (SEDAC GPW4 and GHSL convex hull estimators), DBSCAN and Neural Network Urban Extent Learners, Computational Geometry, Intrinsic Merit Rankings, R Ricker Population Estimation, Community detection, Social Network Analytics, Space filling by Curves, Unequal Circle and Polynomial packing, Computational Geometry and Polygonal packing by Voronoi Tessellation, Four color theorem, Economic Merit, Computational Economics - GDP estimation from Urban sprawl demographics, electricity consumption, Poverty alleviation, MARA (Multiple Agent Resource Allocation) Facegraph walk coloring DNFSAT algorithm, Preferential Attachment  
-----

-----  
1304.1 GISUrbanSprawlAnalytics.py has been updated to learn replication weights of Polya Urn Urban Growth Model sampling which chooses a random colored segment and replicates it while replacing, through function `learn_polya_urn_growth_weights()`.

1304.2 Function

`learn_polya_urn_growth_weights(ncolorsegments_date1,ncolorsegments_date2)` takes as arguments two n-colored segments of date1(earlier) and date2(later) computed from an urban sprawl segmentation by function `polya_urn_urban_growth_model()` and returns dictionary of replication weights per color as ratio of lengths of corresponding colored bins within Polya Urns of date2 and date1.

1304.3 Function

`polya_urn_urban_growth_model(image,ncoloredsegments,segmentedgis,iterations=1000,replicationweights=None)` additionally takes an optional argument `replicationweights` which is the dictionary of color-to-weights learnt by `learn_polya_urn_growth_weights()`. Polya Urn Growth routine has been rewritten, if learnt replicationweights are supplied, to replicate a randomly sampled contour color segment as many times as the color's weight lookedup within replicationweights which makes the Polya Urn Growth a Randomized Controlled Trial or a predictable randomization learnt from the past - contours of different colors grow at different rates based on past historical growth (typical preferential attachment or Rich-get-richer - a trend which may not be disrupted unless a radical new masterplan is drafted).

1304.4 Percentage Growth of an Urban Sprawl after Polya Urn UGM process is printed as ratio of total number of segments (all colors) before and after Urn growth. Replication weights are learnt from two GHSL GIS Imagery separated by 3 years for Chennai Metropolitan Area Sprawl - `testlogs/GHSL_GIS_ChennaiMetropolitanArea.jpg` (R2019A) and `testlogs/RemoteSensingGIS/ChennaiMetropolitanArea_GHSL_R2022A_GHS_SMOD_DegreeOfUrbanisation.jpg` (R2022A) - and learnt weights are applied to project future growth after 2022 on R2022A

`testlogs/RemoteSensingGIS/ChennaiMetropolitanArea_GHSL_R2022A_GHS_SMOD_DegreeOfUrbanisation.jpg` (Assumption: Same color coding is used across R2019A and R2022A and images approximately have similar scales)

1304.5 Following are 3 trials of Polya Urn Urban Growth Model projections (1000 iterations each) for Chennai Metropolitan Area without and with learnt replication weights quoted from `testlogs/GISUrbanSprawlAnalytics.log.8September2022:`

-----  
Trial 1  
-----

(random - no weights learning) R2019A - Percentage growth of urban sprawl simulated by Polya Urn Urban Growth Model: 24.4270205066345

(random - no weights learning) R2022A - Percentage growth of urban sprawl

simulated by Polya Urn Urban Growth Model: 101.09689213893967  
(predictably random - after weights learning based on 3 years growth)  
R2022A - Percentage growth of urban sprawl simulated by Polya Urn Urban Growth  
Model: 95.7498482088646

-----  
Trial 2  
-----

(random - no weights learning) R2019A - Percentage growth of urban sprawl  
simulated by Polya Urn Urban Growth Model: 25.03015681544029  
(random - no weights learning) R2022A - Percentage growth of urban sprawl  
simulated by Polya Urn Urban Growth Model: 101.64533820840951  
(predictably random - after weights learning based on 3 years growth)  
R2022A - Percentage growth of urban sprawl simulated by Polya Urn Urban Growth  
Model: 76.72727272727273

-----  
Trial 3  
-----

(random - no weights learning) R2019A - Percentage growth of urban sprawl  
simulated by Polya Urn Urban Growth Model: 23.70325693606755  
(random - no weights learning) R2022A - Percentage growth of urban sprawl  
simulated by Polya Urn Urban Growth Model: 103.47349177330896  
(predictably random - after weights learning based on 3 years growth)  
R2022A - Percentage growth of urban sprawl simulated by Polya Urn Urban Growth  
Model: 85.66265060240964  
1304.6 On an average earlier weights-learned Polya Urn Growth predicts 76-95%  
growth of contour segments in Chennai Metropolitan Area based on 3 years growth  
trend (2019-2022) implying proportional future growth of Urban city center and  
Urban metro cluster - From 1174.8.4.3 expanded jurisdiction of Chennai  
Metropolitan Area in 2018 - 8848 sqkm - might witness urban cluster growth of  
76-95% to 17253 sqkms and GHSL (R2019A) city administrative area of Chennai from  
1196.4 and 1253.12 - 940 sqkm - might witness urban center growth of 76-95% to  
1833 sqkms (rough estimate assuming equal area contours).  
1304.7 Allocating new segments projected by weights-learned Polya Urn Model along  
periphery of Facegraph of the Urban sprawl described in 1234.6 adhering to  
DNFSAT Facegraph walk arithmetic progression coloring MARA algorithm in 1177 is  
a sustainable Urban Growth Model assuring equitable growth.

References:

-----  
1304.8 Polya Urn Replacement Matrix -  
[https://warwick.ac.uk/fac/sci/math/people/staff/stefan\\_grosskinsky/rcssm/ws2/cecile.pdf](https://warwick.ac.uk/fac/sci/math/people/staff/stefan_grosskinsky/rcssm/ws2/cecile.pdf) and <https://arxiv.org/pdf/1611.09478.pdf> - For 2 colored Urns, ball  
of color1 is chosen and replaced by a color1 and b color2 balls while ball of  
color2 is chosen and replaced by c color1 and d color2 balls causing a  
replacement matrix  $\begin{bmatrix} a & b \\ c & d \end{bmatrix}$  - such a generic replacement matrix is possible  
in Urban sprawls when segment growths are interdependent e.g if segment of  
color1 grows at rate a, segment of color2 grows at rate b (residential segments  
depend on industrial segments and commercial segments depend on residential  
segments).

-----  
1305. (THEORY and FEATURE) Intrinsic Merit of Music - AI Music Synthesis from  
Sum of Sinusoids - Signal synthesis from librosa tone() - related to  
110,1223,1224,1257,1258,1261 and all sections on Music search-Music discovery,  
Intrinsic Merit of Music, MIR(Music Information Retrieval), Music Similarity and  
Clustering, AI Music Synthesis from summation of damped sinusoids, fMRI  
connectomes - OpenNeuro - Psychology of music, Weighted automata, Chaos, Deep  
Learning, Dynamic Time Warping-Music Timeseries analysis, Music Evoked  
Autobiographical Memories, ThoughtNet, Majority Voting (Enjoyable music) Vs  
Intrinsic (Quality music) - Condorcet Jury Theorem variants - 9 September 2022  
-----

-----  
1305.1 Updated notes\_to\_audio(automaton=False, function=None,

deterministic=True, samplerate=44100, fractal=True, periodicity=100) in AudioToBitMatrix.py to add new parameter periodicity for length of music waveform synthesized and replace existing synthesis code to compute signal waveform from librosa.tone() which produces far superior music rivalling manual composition by keyboard or piano.

1305.2 Lambda function passed on to notes\_to\_audio() is eval()-ed for each point in range determined by periodicity and resultant function values are deemed as frequencies of signal synthesized by librosa.tone() for duration of 0.25 seconds.

1305.3 Signals synthesized for all points of the function in periodicity range are concatenated and written to WAV file.

1305.4 Following are affected logs and function synthesized waveform files for notes\_to\_audio(function='(np.iinfo(np.int16).max\*math.sin(2\*3.1428\*720\*x) + np.iinfo(np.int16).max\*math.sin(2\*3.1428\*1240\*x) + np.iinfo(np.int16).max\*math.sin(2\*3.1428\*2400\*x))', fractal=False, periodicity=35) which is a sum of damped sinusoids of 3 fourier frequencies:  
 function\_synthesized\_music.wav  
 testlogs/AudioToBitMatrix.log.9September2022

1305.5 Synthesized waveform function\_synthesized\_music.wav can be loaded in Audacity for spectral analysis and playing.

1305.6 Human compositions could be simulated in earlier AI function synthesis by learning polynomial interpolations from manually composed music waveforms as training data (e.g SciPy interpolate() - <https://docs.scipy.org/doc/scipy/reference/interpolate.html>) and use a function of learnt interpolation polynomials as baseline for librosa.tone() signal synthesis.

#### References:

-----  
 1305.7 Virtual instruments - Pianoteq Virtual Piano - <https://www.modartt.com/pianoteq>  
 1305.8 Python Music Synthesizer - <https://mdoege.github.io/PySynth/>  
 1305.9 Tensorflow Magenta DDSP-VST Neural Music Synthesizer - <https://magenta.tensorflow.org/ddsp-vst>  
 -----

-----  
 1306. (THEORY and FEATURE) Intrinsic Merit of Music - AI Music Synthesis from Polynomials Learnt from training data - related to 3,110,1223,1224,1257,1258,1261,1305 and all sections on Music search-Music discovery, Intrinsic Merit of Music, MIR(Music Information Retrieval), Music Similarity and Clustering, AI Music Synthesis from summation of damped sinusoids, fMRI connectomes - OpenNeuro - Psychology of music, Weighted automata, Chaos, Deep Learning, Dynamic Time Warping-Music Timeseries analysis, Music Evoked Autobiographical Memories, ThoughtNet, Majority Voting (Enjoyable music) Vs Intrinsic (Quality music) - Condorcet Jury Theorem variants - 12 September 2022  
 -----

-----  
 1306.1 AudioToBitMatrix.py has been updated to implement new function music\_synthesis(training\_music,dur=5,samplerate=44100,polynomial\_interpolation=True) which learns music (based on a boolean flag polynomial\_interpolation) from training music waveforms by (\*) interpolating training music to polynomials by polyfit() and computing a function over interpolated polynomials which is passed on to notes\_to\_audio() for synthesizing new music by tone() (\*) or mapping training music waveforms to array of notes in CDEFGABC notation by hertz-to-notes and synthesizing signal frequencies (by random sampling) from training music notes collated to new music waveform by notes-to-hertz and tone()  
 1306.2 Invocation of SciPy barycentric\_interpolate() which is a recent advance in Lagrange interpolation and could be better than polyfit() has been commented due to slowdown. Function computed over polynomial interpolation of music waveforms is simple summation at present and could be arbitrary. Synthesis by random sampling of notes from training music waveforms is discrete version of continuous polynomial interpolation and randomness could be replaced by a

predictable sampling function. Synthesized music earlier (random notes sampling especially) could be one of the 68 billion 12-note melodies (Section 1223.14). Music synthesis by polynomial interpolation learning as opposed to neural network deep learning (which are threshold circuits) is more algebraic and closer to theoretical gadgets of polynomial threshold functions.

1306.3 Following are logs and synthesized music files from 2 compositions of JS Bach for both the clauses of synthesis - polynomial interpolation and randomly sampled notes:

python-src/music\_pattern\_mining/function\_synthesized\_music.wav

python-src/music\_pattern\_mining/testlogs/AudioToBitMatrix.log.MusicSynthesizer.12September2022

python-src/music\_pattern\_mining/testlogs/AudioToBitMatrix.log2.MusicSynthesizer.12September2022

python-src/music\_pattern\_mining/testlogs/function\_synthesized\_music.interpolation.wav.xz

python-src/music\_pattern\_mining/testlogs/function\_synthesized\_music.random.wav.xz

References:

-----  
1306.4  $O(n)$  complexity Barycentric Interpolation improved over  $O(n^2)$  Lagrange interpolation -

[https://docs.scipy.org/doc/scipy/reference/generated/scipy.interpolate.barycentric\\_interpolate.html#scipy.interpolate.barycentric\\_interpolate](https://docs.scipy.org/doc/scipy/reference/generated/scipy.interpolate.barycentric_interpolate.html#scipy.interpolate.barycentric_interpolate) and

<https://people.maths.ox.ac.uk/trefethen/barycentric.pdf>

1306.5 Polynomial Threshold Functions in terms of Polynomial Interpolations -

Exact and Probabilistic polynomials - idea 1 and idea 2 - All Pairs Hamming Nearest Neighbours - [Ryan Williams (Stanford) Joint with Josh Alman (Stanford) and Timothy M. Chan (Waterloo)] -

<https://simons.berkeley.edu/sites/default/files/docs/6108/simons-threshold-polys-printing.pdf> - Similarity of 2 music waveforms could be an all pairs Hamming nearest neighbours problem where sets A and B are music waveforms.

-----  
1307. (THEORY and FEATURE) Intrinsic Merit of Music - AI Music Synthesis from Polynomials Learnt from training data - PolyFeatures and Carnatic-Hindustani notes support - related to 3,110,1223,1224,1257,1258,1261,1305,1306 and all sections on Music search-Music discovery, Intrinsic Merit of Music, MIR(Music Information Retrieval), Music Similarity and Clustering, AI Music Synthesis from summation of damped sinusoids, fMRI connectomes - OpenNeuro - Psychology of music, Weighted automata, Chaos, Deep Learning, Dynamic Time Warping-Music Timeseries analysis, Music Evoked Autobiographical Memories, Waveshaping, ThoughtNet, Majority Voting (Enjoyable music) Vs Intrinsic (Quality music) - Condorcet Jury Theorem variants - 15 September 2022  
-----

-----  
1307.1 AudioToBitMatrix.py has been updated to import librosa.display and librosa has been upgraded to 0.9.2. Function audio\_to\_notes() has been enhanced to set default duration and print Carnatic and Hindustani notes of a music waveform based on newly added support for Hindustani and Carnatic music in Librosa 0.9.2 through hz\_to\_svara\_c() and hz\_to\_svara\_h() API based on argument "music" set to default "Carnatic" - Index of mela has been hardcoded to 66.

1307.2 Function

music\_synthesis(training\_music,dur=5,samplerate=44100,polynomial\_interpolation=True,polyfeatures=False) has been changed to exploit poly\_features() API of Librosa which fits the spectrogram of a waveform to n-th order polynomial. If boolean flag polyfeatures is set to True, poly\_features() of order-5 is invoked on stft() of the waveform to interpolate the spectrogram to degree-5 polynomial. Spectrogram Interpolation and music waveform are plotted as graphics and order-5

interpolation is chosen by polyfit() of timepoints versus degree-5 interpolation points. Use of polyfeatures refines the structural analysis of music waveform. If polyfeatures is False, behaviour is limited to usual polyfit() earlier. Synthesis by polynomial interpolation is a Waveshaping technique for turning simple sounds to complex sounds.

1307.3 Periodicity has been increased to 100 in notes\_to\_audio(function=synth\_poly\_string[:len(synth\_poly\_string)-1], fractal=False, periodicity=100). Librosa tone() synthesis has been further refined by abs() cast of frequencies.

1307.4 Logs testlogs/AudioToBitMatrix.log.15September2022 capture following invocations:

```
music_synthesis(["testlogs/JSBach_Musicological_Offering.mp4","testlogs/Bach_Flute_Sonata_EFlat.mp4"],dur=10)
audio_to_notes("testlogs/JSBach_Musicological_Offering.mp4", dur=10, music="Carnatic")
```

References:

-----  
1307.5 Chapter 4: The Synthesis of Sound by Computer - Section 4.6 - Waveshaping -

[http://sites.music.columbia.edu/cmc/MusicAndComputers/chapter4/04\\_06.php](http://sites.music.columbia.edu/cmc/MusicAndComputers/chapter4/04_06.php) - Chebyshev polynomial waveshaper - "... Mathematicians like them for lots of different reasons, but computer musicians like them because they can be used to make weird noises, er, we mean music. These Chebyshev polynomials have the property that if you input a sine wave of amplitude 1.0, you get out a sine wave whose frequency is N times the frequency of the input wave. So, they are like frequency multipliers. If the amplitude of the input sine wave is less than 1.0, then you get a complex mix of harmonics. Generally, the lower the amplitude of the input, the lower the harmonic content. This gives musicians a single number, sometimes called the distortion index, that they can tweak to change the harmonic content of a sound..."

1307.6 Chapter 4: The Synthesis of Sound by Computer - Section 4.2 - Additive Synthesis - [http://musicandcomputersbook.com/chapter4/04\\_02.php](http://musicandcomputersbook.com/chapter4/04_02.php)

-----  
1308. (THEORY and FEATURE) Intrinsic Merit of Music - Virtual Piano Implementation and Music Synthesis from 12-notes octave - 16 September 2022 - related to 3,110,1223,1224,1257,1258,1261,1305,1306,1307 and all sections on Music search-Music discovery, Intrinsic Merit of Music, MIR(Music Information Retrieval), Music Similarity and Clustering, AI Music Synthesis from summation of damped sinusoids, Additive Synthesis, fMRI connectomes - OpenNeuro - Psychology of music, Weighted automata, Chaos, Deep Learning, Dynamic Time Warping-Music Timeseries analysis, Music Evoked Autobiographical Memories, Waveshaping, ThoughtNet, Majority Voting (Enjoyable music) Vs Intrinsic (Quality music) - Condorcet Jury Theorem variants  
-----

-----  
1308.1 AudioToBitMatrix.py has been updated to import IPython.display, mir\_eval.sonify and playsound python3.7 packages. Function music\_synthesis(training\_music=None,dur=5,samplerate=44100,polynomial\_interpolation=True,polyfeatures=False,virtual\_piano\_notes=None) has been updated to implement a new clause for Virtual Piano Music Synthesizer implementation based on notes passed on to it through virtual\_piano\_notes. Notes based synthesis is more human than polynomial interpolation and strings of notes alphabets could be programmatically churned out.

1308.2 Notes from virtual\_piano\_notes in usual CDEFGABC 12-note Piano notation [C, C-Sharp (D-Flat), D, D-sharp (E-Flat), E, F, F-Sharp (G-Flat), G, G-Sharp (A-Flat), A, A-Sharp (B-Flat), and B] are converted to frequency domain by note\_to\_hz() and signals are synthesized from them iteratively by librosa.tone(). Synthesized music is written to separate WAV file virtual\_piano\_music.wav and plotted as waveform by waveshow() - commented at present. Invocation of mir\_eval.sonify.pitch\_contour(librosa.times\_like(freq),freq,samplerate,amplitude

s=amps) has also been commented which is a music synthesizer similar to librosa.tone().  
1308.3 New function all\_12notes\_melodies() randomly and iteratively chooses a set of notes from concatenation of 12 notes in C-major,A-minor,... (totalling 60 notes) formats by numpy.random.choice() and music\_synthesis() is invoked on those to synthesize piano music - For Example following set of notes are programmatically created and synthesizer earlier is a DFA state machine over notes alphabet:

```
virtual piano notes: ['F#' 'E' 'F' 'D#' 'F#' 'A#b' 'G' 'C#' 'D' 'F' 'F#'
'A#' 'E' 'G' 'G' 'D'
'G#' 'B' 'B#' 'E#' 'A#' 'G' 'A#' 'D' 'F#' 'D' 'D' 'A' 'F#' 'D' 'A#' 'B'
'F#' 'A#' 'B' 'F#' 'G#' 'C' 'E#' 'B' 'A' 'A#' 'C' 'G#' 'E' 'E#b' 'A#' 'G#'
'A#' 'C' 'D' 'F#' 'E' 'D#' 'D#' 'D#' 'G#' 'D#' 'B' 'A#' 'C#' 'D#' 'A#'
'E' 'E' 'D#' 'A#' 'E#b' 'D' 'F' 'A#' 'C#b' 'B' 'B#b' 'G' 'E#' 'E' 'G' 'C#'
'G#' 'G#' 'G' 'D' 'D#' 'C#' 'A' 'D' 'E' 'D#' 'C#' 'D' 'D' 'G#' 'G#' 'C#'
'F' 'A#' 'A' 'B' 'E']
```

1308.4 Logs testlogs/AudioToBitMatrix.log.16September2022 capture following invocations:

```
all_12notes_melodies(iterations=2,number_of_notes=100)
```

```
music_synthesis(virtual_piano_notes=['A','a','B','B','b','b','C','D','E','B','C',
, 'E','E','e','F','f','C','d','d','d','g','g','g'])
```

1308.5 Function all\_12notes\_melodies() essentially captures the notion of "Music discovery" or "No music is new" enshrined in 68-billion melodies algorithm of 1223.13. For earlier 100 notes (based on 60 repetitive notes) long synthesis possible melodies are  $60^{100}$ .

References:

-----  
1308.6 mir\_eval sonify pitch\_contour() -  
[https://craffel.github.io/mir\\_eval/#module-mir\\_eval.sonify](https://craffel.github.io/mir_eval/#module-mir_eval.sonify)  
1308.7 Piano 101 - <https://www.europeanosnaples.com/piano-keys-101/>  
1308.8 Python Mingus Music Library -  
<http://bspaans.github.io/python-mingus/index.html>  
1308.9 Python Piano - <https://pypi.org/project/py piano/>

-----  
1309. (THEORY and FEATURE) Intrinsic Merit of Music - Virtual Piano Implementation and Music Synthesis from 12-notes octave - Correction to Frequencies - 19 September 2022 - related to 3,110,1223,1224,1257,1258,1261,1305,1306,1307,1308 and all sections on Music search-Music discovery, Intrinsic Merit of Music, MIR(Music Information Retrieval), Music Similarity and Clustering, AI Music Synthesis from summation of damped sinusoids, Additive Synthesis, fMRI connectomes - OpenNeuro - Psychology of music, Weighted automata, Chaos, Deep Learning, Dynamic Time Warping-Music Timeseries analysis, Music Evoked Autobiographical Memories, Waveshaping, ThoughtNet, Majority Voting (Enjoyable music) Vs Intrinsic (Quality music) - Condorcet Jury Theorem variants  
-----

1309.1 New dictionary piano\_notes mapping 12-note octave to frequencies has been introduced to correct the signal synthesis by tone() so that it matches Piano music:

```
piano_notes={'A':440,'B':493.89,'C':261.63,'D':293.67,'E':329.63,'F':349.23,'G':
392,'a':466.17,'c':227.18,'d':311.13,'f':370,'g':415.31}
```

1309.2 Function

```
all_12notes_melodies(iterations=10,number_of_notes=10,keynotes=88,tempo=0.25)
```

has been changed to add clauses and parameters - keynotes and tempo - which respectively define number of keys (88 or 12) to form octave basis and tempo of music synthesized (duration per note).

1309.3 New function get\_piano\_frequencies(virtual\_piano\_notes) returns the array of frequencies for piano notes sequence passed on to it by lookup of piano\_notes dictionary earlier.

#### 1309.4 Function

`music_synthesis(training_music=None, dur=5, samplerate=44100, polynomial_interpolation=True, polyfeatures=False, virtual_piano_notes=None, tempo=1, amplitude=4096)` has been changed to include amplitude as parameter set to 4096 as default, tempo as parameter for `librosa.tone()` and replace `note_to_hz()` by `get_piano_frequencies()` as `note_to_hz()` produces different values simulating a drumbeat.

1309.5 Following notes for "Twinkle Twinkle Little Star" have been synthesized in Virtual Piano and written to `virtual_piano_music.wav` :

```
music_synthesis(virtual_piano_notes=['C', 'C', 'G', 'G', 'A', 'A', 'G', 'F', 'F', 'E', 'E',
, 'D', 'D', 'C', 'G', 'G', 'F', 'F', 'E', 'E', 'D', 'G', 'G', 'F', 'F', 'E', 'E', 'D', 'C', 'C', 'G',
, 'G', 'A', 'A', 'G', 'F', 'F', 'E', 'E', 'D', 'D', 'C', 'C', 'C', 'G', 'G', 'A', 'A', 'G', 'F', 'F',
, 'E', 'E', 'D', 'D', 'C', 'G', 'G', 'F', 'F', 'E', 'E', 'D', 'G', 'G', 'F', 'F', 'E', 'E', 'D', 'C',
, 'C', 'G', 'G', 'A', 'A', 'G', 'F', 'F', 'E', 'E', 'D', 'D', 'C'], tempo=1)
```

#### 1310. (THEORY and FEATURE) Intrinsic Merit of Music - Virtual Piano

Implementation - Carnatic Music Synthesis from 12-notes octave - 20 September 2022 - related to 3,110,1223,1224,1257,1258,1261,1305,1306,1307,1308,1309 and all sections on Music search-Music discovery, Intrinsic Merit of Music, MIR(Music Information Retrieval), Music Similarity and Clustering, AI Music Synthesis from summation of damped sinusoids, Additive Synthesis, fMRI connectomes - OpenNeuro - Psychology of music, Weighted automata, Chaos, Deep Learning, Dynamic Time Warping-Music Timeseries analysis, Music Evoked Autobiographical Memories, Waveshaping, ThoughtNet, Majority Voting (Enjoyable music) Vs Intrinsic (Quality music) - Condorcet Jury Theorem variants

1310.1 Carnatic music svara(s) have been integrated into Piano Notes Frequencies and `piano_notes` is stored in a dictionary of dictionaries of the form genre-note-frequency (including svara subdivisions - frequencies for Gandhara-3, Nishadha-1 and 3, Dhaivadha-3 could be slightly off):

```
piano_notes={"WesternClassical":
{'A':440, 'B':493.89, 'C':261.63, 'D':293.67, 'E':329.63, 'F':349.23, 'G':392, 'a':466.
17, 'c':227.18, 'd':311.13, 'f':370, 'g':415.31}, "Carnatic":{'S':240, 'R1':254.27,
'R2':269.39, 'R3':275, 'G1':285.41, 'G2':302.38, 'G3':311, 'M1':320.36,
'M2':339.41, 'P':359.60, 'D1':380.98, 'D2':403.63, 'D3':415,
'N1':425, 'N2':453.06, 'N3':480}}
```

#### 1310.2 Function

`all_12notes_melodies(iterations=10, number_of_notes=10, keynotes=88, tempo=0.25, musicgenre="WesternClassical")`

has been changed to add music genre as parameter ("WesternClassical" or "Carnatic") and if genre is Carnatic, notes basis is a concatenation of 72 melakarta notes from `librosa.mela_to_svara()` which is randomly sampled to synthesize music. As number of possible melodies in Carnatic are limited to 72000 (Janya or derivatives of 72), synthesis of Carnatic music must be a mathematical function of 72000 derived raaga(s). Existing state-of-the-art in music synthesis is centered around Deep Learning Convolution Neural Networks of huge parameter set and multiple convolution-maxpooling-perceptron layers. An alternative automata theoretic view of music envisages set of notes as language accepted by a finite state automaton. Ramifications of music as automata are enormous - synthesis of new music could be reduced to closure operators of Finite State Machines - Union, Intersection, Difference, Concatenation, Kleene Closure, Reversal, Homomorphism, Inverse Homomorphism - or new music is obtained from operand music FSMs through closures.

#### 1310.3 Function

`get_piano_frequencies(virtual_piano_notes, genre="WesternClassical")` has been changed to add genre of music as parameter.

#### 1310.4 Function

`music_synthesis(training_music=None, dur=5, samplerate=44100, polynomial_interpolation=True, polyfeatures=False, virtual_piano_notes=None, tempo=1, amplitude=4096, musicgenre="WesternClassical")` has been changed to include music genre as parameter



to obtain piano frequencies for Western classical or Carnatic.

1310.5 Function

all\_12notes\_melodies(iterations=5,number\_of\_notes=100,keynotes=12,tempo=0.5, musicgenre="Carnatic") has been invoked for synthesizing randomly sampled music (of 100 notes length) from Carnatic notes for 5 iterations (written to python-src/music\_pattern\_mining/virtual\_piano\_music.wav).

References:

-----  
1310.6 12 notes in Carnatic, Western and Hindustani -

[https://ccrma.stanford.edu/~arvindeh/cmt/the\\_12\\_notes.html](https://ccrma.stanford.edu/~arvindeh/cmt/the_12_notes.html)

1310.7 Closure Properties of Regular Languages -

<http://infolab.stanford.edu/~ullman/ialc/spr10/slides/rs2.pdf>  
-----

-----  
1311. (THEORY and FEATURE) Intrinsic Merit of Music - Deep Learnt Automata and Music Synthesis - a Boolean Composition and Learning Theory perspective - 21 September 2022 - related to

3,110,1223,1224,1257,1258,1261,1305,1306,1307,1308,1309,1310 and all sections on Music search-Music discovery, Intrinsic Merit of Music, MIR(Music Information Retrieval), Music Similarity and Clustering, AI Music Synthesis from summation of damped sinusoids, Additive Synthesis, fMRI connectomes - OpenNeuro - Psychology of music, Weighted automata, Chaos, Deep Learning, Dynamic Time Warping-Music Timeseries analysis, Music Evoked Autobiographical Memories, Waveshaping, ThoughtNet, Majority Voting (Enjoyable music) Vs Intrinsic (Quality music) - Condorcet Jury Theorem variants, Computational Learning Theory, Boolean Function Composition  
-----

-----  
1311.1 Following example is a walkthrough of how a Music Synthesis based on Convolution Neural Network might look like and how formal language models and Boolean function composition might play a key role as Convolution Kernels in Hidden Layer and Maxpooling Layer of CNN, causing a merger of Boolean Function Composition, Computational Learning Theory and Machine Learning.

1311.2 For 7 music waveforms of 7 notes each following is an input 2D matrix of 7\*7=49 notes in CDEFGABC notation:

C-D-E-F-G-A-B

F-D-C-F-D-A-D

C-F-E-G-D-A-B

F-F-E-F-G-A-D

C-C-E-F-G-G-B

F-D-E-F-G-D-B

F-D-E-F-G-D-D

1311.3 For simplistic 1 Convolution Layer Kernel (which is a Majority function returning majority note in receptive field window of 3\*3) of Stride=3 (window jumps 3 elements per entry) and 1 Max Pooling Layer (also a Majority function) - Majority() returns lexicographically maximum note in case of tie:

Convolution Layer for input music earlier - Hidden (Majority function as Convolution Kernel)

C-A-B

F-G-B

F-G-D

Maxpooling Layer (Majority as maximum function)

G

returning G as the most prominent note in 7\*7 input 2D music matrix earlier. For massive input matrices, earlier convolution scales to millions of notes learnt in Maxpooling layer. Choice of Majority function earlier is only an example of how deep structure could be learnt (Usually convolution map kernels are bit matrices and convolution layer is computed by linear algebra of input and convolution kernel) and could be replaced by an arbitrary finite state automata learner per stride which replaces each entry of convolution layer matrix by an automaton learnt from receptive field window alphabets. Maxpooling layer likewise could be any of closure operator on automata (Union, Intersection,

Difference, Concatenation, Kleene Closure, Reversal, Homomorphism, Inverse Homomorphism) in convolution layer.

1311.4 It is obvious that earlier choice of majority function for convolution kernel layer and maxpooling layer indirectly implements a function composition of Majority of Majorities or Depth-2 majority. Replacement of Convolution Kernel and Maxpooling Layer by Automata Learners gives birth to a hybrid Deep Learner of Automata blending the power of Deep Learning, Function composition and Computational Learning Theory in one.

1311.5 Music waveforms could be learnt by simple CNN implementation in NeuronRain - python-src/DeepLearning\_ConvolutionNetwork\_BackPropagation.py by encoding notes to numeric frequencies in input matrix - which implements 1 Convolution Layer of 3 Kernels and 1 Maxpooling layer of 3 Kernels finally flattened and learnt by Perceptron BackPropagation. Massive Music waveform datasets require on-chip implementations of Deep Learning as input could be a million \* million notes matrix.

#### References:

1311.6 Learning and Extracting Finite State Automata with Second-Order Recurrent Neural Networks - <https://clgiles.ist.psu.edu/pubs/NC1992-recurrent-NN.pdf> and <https://direct.mit.edu/neco/article-abstract/4/3/393/5641/Learning-and-Extracting-Finite-State-Automata-with?redirectedFrom=fulltext>

1311.7 Convolution Neural Networks - Graphic Illustrations - <https://towardsdatascience.com/a-comprehensive-guide-to-convolutional-neural-networks-the-eli5-way-3bd2b1164a53>

1312. (THEORY and FEATURE) GIS Urban Sprawl Analytics - Polya Urn Urban Growth Model - Urban sprawl area computation - 22 September 2022 - related to 1174, 1175, 1177, 1179, 1194, 1211, 1234, 1290, 1291, 1292, 1295, 1296, 1297, 1301, 1304 and all sections on GIS Urban Sprawl Analytics, Merit of Large Scale Visuals, Gridded Population Estimators (SEDAC GPW4 and GHSL convex hull estimators), DBSCAN and Neural Network Urban Extent Learners, Computational Geometry, Intrinsic Merit Rankings, R Ricker Population Estimation, Community detection, Social Network Analytics, Space filling by Curves, Unequal Circle and Polynomial packing, Computational Geometry and Polygonal packing by Voronoi Tessellation, Four color theorem, Economic Merit, Computational Economics - GDP estimation from Urban sprawl demographics, electricity consumption, Poverty alleviation, MARA (Multiple Agent Resource Allocation) Facegraph walk coloring DNFSAT algorithm, Preferential Attachment, Fixed Parameter Tractability-Kernelization

1312.1 python-src/image\_pattern\_mining/ImageNet/GISUrbanSprawlAnalytics.py has been updated to compute total area of urban sprawl before and after Polya Urn UGM expansion simulation by sum of contour areas (cv2.contourArea()). Area computation reflects percentage growth of urban sprawl better than number of contour segments.

1312.2 Polya Urn contents are now tuples of the form (<colored\_segment>, <contour\_area>) for facilitating area computation.

1312.3 Function

urban\_sprawl\_from\_raster(79.07, 12.41, 80.3, 13.19, "testlogs/RemoteSensingGIS/GHS\_SMOD\_POP2015\_GLOBE\_R2019A\_54009\_1K\_V2\_0.tif", dt="Degree of Urbanization") has been invoked for computing Degree of Urbanization of Chennai Metropolitan Area for R2019A dataset from R2019A GHS-SMOD DEURBA GeoTIFF raster testlogs/RemoteSensingGIS/GHS\_SMOD\_POP2015\_GLOBE\_R2019A\_54009\_1K\_V2\_0.tif. There is no visual explorer available for R2019A GHS-SMOD as datasets have been replaced by R2022A and Polya Urn UGM has to be populated from settlement classes of the raster pixels instead of contour segments (classes listed in 1312.7). Following are some examples of classes printed from raster for bounding box coordinates:

Degree of Urbanization from raster: [array([30], dtype=int16)]  
Degree of Urbanization from raster: [array([30], dtype=int16)]  
Degree of Urbanization from raster: [array([10], dtype=int16)]

Degree of Urbanization from raster: [array([12], dtype=int16)]  
Degree of Urbanization from raster: [array([12], dtype=int16)]  
Degree of Urbanization from raster: [array([23], dtype=int16)]  
Degree of Urbanization from raster: [array([21], dtype=int16)]  
Degree of Urbanization from raster: [array([21], dtype=int16)]  
Degree of Urbanization from raster: [array([13], dtype=int16)]  
Degree of Urbanization from raster: [array([13], dtype=int16)]  
Degree of Urbanization from raster: [array([12], dtype=int16)]  
Degree of Urbanization from raster: [array([11], dtype=int16)]

1312.4 Dimensions of the longitude-latitude bounding box have been expanded to match R2022A GHS-SMOD Degree of Urbanization imagery.

1312.5 Following are Polya Urn UGM projections for Chennai Metropolitan Area (difference in projections with and without learnt replacement matrix is noticeable):

-----  
---  
R2019A (future projection based on 2019 data - without learnt replacement matrix):  
-----

---  
Percentage growth of urban sprawl simulated by Polya Urn Urban Growth Model (in terms of segments): 24.668275030156817

Percentage growth of urban sprawl simulated by Polya Urn Urban Growth Model (in terms of total area): 4.0728209942696205  
-----

---  
R2022A (future projection based on 2022 data - without learnt replacement matrix):  
-----

---  
Percentage growth of urban sprawl simulated by Polya Urn Urban Growth Model (in terms of segments): 95.9780621572212

Percentage growth of urban sprawl simulated by Polya Urn Urban Growth Model (in terms of total area): 43.19988994359609  
-----

R2022A (future projection based on 2022 data - with learnt Replacement matrix):  
-----

Percentage growth of urban sprawl simulated by Polya Urn Urban Growth Model (in terms of segments): 90.67325509573811

Percentage growth of urban sprawl simulated by Polya Urn Urban Growth Model (in terms of total area): 112.80220836963039 (<- 112% growth projected by learning contour segment replacement - replication weights - from 3 years trend between 2019-2022 as against 43% without learning in previous trial)

#### References and Commentaries:

-----  
1312.6 GHSL R2019A Degree of Urbanization - GHS-SMOD Dataset -

[https://ghsl.jrc.ec.europa.eu/ghs\\_smmod2019.php](https://ghsl.jrc.ec.europa.eu/ghs_smmod2019.php) -

GHS\_SMOD\_POP2015\_GLOBE\_R2019A\_54009\_1K\_V2\_0.tif

1312.7 Legend for GHSL GHS SMOD Degree of Urbanization settlement classes -

Urban centre(city), Urban cluster(metro), Peri-urban, Rural, Water -

[https://ghsl.jrc.ec.europa.eu/documents/GHSL\\_Data\\_Package\\_2019.pdf?t=1637939855](https://ghsl.jrc.ec.europa.eu/documents/GHSL_Data_Package_2019.pdf?t=1637939855)

- "... The settlement grid at level 2 represents these definitions on a single layer grid. Each pixel is classified using the following set of codes (classes) and rules (Table 7):

- Class 30: "Urban Centre grid cell", if the cell belongs to an Urban Centre spatial entity;

- Class 23: "Dense Urban Cluster grid cell", if the cell belongs to a Dense Urban Cluster spatial entity;

- Class 22: "Semi-dense Urban Cluster grid cell", if the cell belongs to a Semi-dense Urban Cluster spatial entity;

- Class 21: "Suburban or per-urban grid cell", if the cell belongs to an Urban Cluster cells at first

hierarchical level but is not part of a Dense or Semi-dense Urban Cluster;  
 - Class 13: "Rural cluster grid cell", if the cell belongs to a Rural Cluster spatial entity;  
 - Class 12: "Low Density Rural grid cell", if the cell is classified as Rural grid cells at first hierarchical level, has more than 50 inhabitant and is not part of a Rural Cluster;  
 - Class 11: "Very low density rural grid cell", if the cell is classified as Rural grid cells at first hierarchical level, has less than 50 inhabitant and is not part of a Rural Cluster;  
 - Class 10: "Water grid cell", if the cell has 0.5 share covered by permanent surface water and is not populated nor built. ..."

1312.8 Table 8 of Logical Formulae for settlement topologies in

[https://ghsl.jrc.ec.europa.eu/documents/GHSL\\_Data\\_Package\\_2019.pdf?t=1637939855](https://ghsl.jrc.ec.europa.eu/documents/GHSL_Data_Package_2019.pdf?t=1637939855)

- could be used directly within DNFSAT MARA for urban sprawl interior (infill) growth - e.g Class 30 is specified by clause  $((P_{dens} \vee B_{dens}) \wedge T_{con}) \wedge P_{min} \vee [iterative\_median\_filter(3-by-3)] \vee [gap\_fill(<15km^2)]$ . It has to be noted that maximizing the number of satisfying Arithmetic Progression n-colored walks on urban sprawl facegraphs specified by DNFSAT MARA in 1177 is a DNFMASAT (conjugate of NP-Hard CNFMASAT) problem shown to be  $W[1]$  Fixed Parameter Tractable - <https://arxiv.org/pdf/1511.05546.pdf> - where  $W[i]$  is the Weft number  $i$  = number of large gates in path from input to output gates of the combinatorial circuit for the algorithm. Simple DNFSAT is trivially in P as it is sufficient to satisfy one clause.

1312.9 Fundamentals of Parameterized Complexity - [Downey-Fellows] -

[https://citeseerx.ist.psu.edu/viewdoc/download?](https://citeseerx.ist.psu.edu/viewdoc/download?doi=10.1.1.456.2729&rep=rep1&type=pdf)

[doi=10.1.1.456.2729&rep=rep1&type=pdf](https://citeseerx.ist.psu.edu/viewdoc/download?doi=10.1.1.456.2729&rep=rep1&type=pdf)

1312.10 ABSDNFSAT and MAXDNFSAT -  $W[1]$  FPT-Hardness -

<https://drops.dagstuhl.de/opus/volltexte/2022/16172/pdf/LIPIcs-SWAT-2022-12.pdf>

-----  
 1313. (THEORY and FEATURE) GIS Urban Sprawl Analytics - Comparison of Raster Data Bounding Boxes between 2 dates - 23 September 2022 - related to 1174,1175,1177,1179,1194,1211,1234,1290,1291,1292,1295,1296,1297,1301,1304,1312 and all sections on GIS Urban Sprawl Analytics, Merit of Large Scale Visuals, Gridded Population Estimators (SEDAC GPW4 and GHSL convex hull estimators), DBSCAN and Neural Network Urban Extent Learners, Computational Geometry, Intrinsic Merit Rankings, R Ricker Population Estimation, Community detection, Social Network Analytics, Space filling by Curves, Unequal Circle and Polynomial packing, Computational Geometry and Polygonal packing by Voronoi Tessellation, Four color theorem, Economic Merit, Computational Economics - GDP estimation from Urban sprawl demographics, electricity consumption, Poverty alleviation, MARA (Multiple Agent Resource Allocation) Facegraph walk coloring DNFSAT algorithm, Preferential Attachment, Fixed Parameter Tractability-Kernelization  
 -----

-----  
 1313.1 New function `compare_raster_data(raster1data,raster2data)` computes dictionary histograms from longitude-latitude rectangle bounding boxes data returned by `urban_sprawl_from_raster()` for 2 GeoTIFF Rasters of 2 time points belonging to same genre. Two Rasters of same datatype (e.g Degree of Urbanization - R2019A and R2022A) are separated by time duration which could be in years. This kind of comparison has no assumption on scale of imagery as same longitude-latitudes are taken into account.

1313.2 Contents of 2 Dictionary histograms are iterated and percentage change of each bin is printed (as  $100 * (earlierdate - laterdate) / earlierdate$ ) - Negative percentages imply expansion and Positive percentages imply contraction. Following 2 rasters from GHSL SMOD R2019A and R2022A are compared for change in urbanization between Chennai Metropolitan Sprawl Bounding Boxes of same dimensions and ordinates separated by 3 years:

```
r1data=urban_sprawl_from_raster(79.07,12.41,80.3,13.19,"testlogs/RemoteSensingGIS/GHS_SMOD_POP2015_GLOBE_R2019A_54009_1K_V2_0.tif",dt="Degree of Urbanization R2019A")
```

```
r2data=urban_sprawl_from_raster(79.07,12.41,80.3,13.19,"testlogs/RemoteSensingGIS/GHS_SMOD_P2030_GLOBE_R2022A_54009_1000_V1_0.tif",dt="Degree of Urbanization R2022A")
```

```
compare_raster_data(r1data,r2data)
```

1313.3 Findings of compare\_raster\_data() from

python-src/image\_pattern\_mining/ImageNet/testlogs/GISUrbanSprawlAnalytics.log.23

September 2022 for R2019A and R2022A earlier in a nutshell (changes of class pixels as per 1312.7 in percentages - negative percentages imply expansion of the class pixels):

```
urbansprawl_gini_coefficient(): Gini Index of the dataset =
```

0.1731406144601959

```
urbansprawl_gini_coefficient(): Gini Index of the dataset =
```

0.1922834751670601

```
compare_raster_data(): raster1hist = defaultdict(<class 'int'>, {13: 1454, 11: 3896, 23: 241, 12: 2353, 30: 1040, 21: 148, 22: 5, 10: 535})
```

```
compare_raster_data(): raster2hist = defaultdict(<class 'int'>, {21: 4047, 11: 1238, 12: 2023, 30: 1504, 23: 260, 10: 573, 13: 14, 22: 13})
```

```
Percentage change in 13 : 99.03713892709766
```

```
Percentage change in 11 : 68.22381930184805
```

```
Percentage change in 23 : -7.883817427385892
```

```
Percentage change in 12 : 14.024649383765405
```

```
Percentage change in 30 : -44.61538461538462
```

```
Percentage change in 21 : -2634.459459459459
```

```
Percentage change in 22 : -160.0
```

```
Percentage change in 10 : -7.102803738317758
```

1313.4 Gini coefficient of inequality has increased from 0.17 to 0.19 in 3 years. Following urban and water classes have undergone expansion between 2019 and 2022 for same Chennai Metropolitan Area bounding box sprawl (by negative percentages earlier coinciding with or even bettering Image Facegraph Polya Urn UGM projections):

- Class 30: "Urban Centre grid cell", if the cell belongs to an Urban Centre spatial entity; (44% expansion in City area)

- Class 23: "Dense Urban Cluster grid cell", if the cell belongs to a Dense Urban Cluster spatial entity; (7% expansion in dense metro area)

- Class 22: "Semi-dense Urban Cluster grid cell", if the cell belongs to a Semi-dense Urban Cluster (160% expansion in semi-dense metro area)

- Class 21: "Suburban or per-urban grid cell", if the cell belongs to an Urban Cluster cells at first (Massive 2634% expansion implying suburban fringe has witnessed an abnormal boom)

- Class 10: "Water grid cell", if the cell has 0.5 share covered by permanent surface water and is not (7% expansion of waterbodies)

1313.5 Following rural classes have contracted between 2019 and 2022 (by positive percentages):

- Class 13: "Rural cluster grid cell", if the cell belongs to a Rural Cluster spatial entity; (99% decrease in rural clusters)

- Class 12: "Low Density Rural grid cell", if the cell is classified as Rural grid cells at first hierarchical level, has more than 50 inhabitant and is not part of a Rural Cluster; (14% decrease in low density rural regions)

- Class 11: "Very low density rural grid cell", if the cell is classified as Rural grid cells at first hierarchical (68% decrease in very low density rural regions)

#### References and Commentaries:

-----

1313.6 GHSL GHS SMOD R2022A Degree of Urbanization Raster dataset -

[https://ghsl.jrc.ec.europa.eu/ghs\\_smod2022.php](https://ghsl.jrc.ec.europa.eu/ghs_smod2022.php)

1313.7 Official Definitions of Cities, Towns and Rural Areas -

<https://blogs.worldbank.org/sustainablecities/how-do-we-define-cities-towns-and-rural-areas>

1313.8 GHSL definitions of urbanization -

<https://ghsl.jrc.ec.europa.eu/degurbaDefinitions.php> - in terms of 4-color theorem segmentation GHSL 3-coloring of (\*) Open spaces-Vegetation-Water (\*)

Built spaces-Residential (\*) Built spaces-Non residential could be widened as  
(\*) Open spaces-Vegetation-Water (\*) Built spaces-Residential (\*) Built spaces-  
Non residential-Commercial Central Business District (\*) Built spaces-Non  
residential-Industrial(Manufacturing and IT-ITES) by splitting Built-Non-  
residential spaces into commercial and industrial as there are Kernel Density  
Estimation algorithms known for identifying city commercial centers.

-----  
1314. (THEORY and FEATURE) Complement Diophantines - Lagrange and Barycentric  
interpolations - 26 September 2022 - related to 323,345,471,735,1160 and all  
sections on Complement Diophantines, Complement Functions, Complementary Sets,  
Quadratic Forms, Riemann Zeta Function, Patterns in Primes, Polynomial  
Reconstruction Problem, Error correcting codes, Computational Learning Theory -  
Multivariate Polynomial Reconstruction over Finite Fields, Lagrange-Taylor-  
Barycentric interpolation, Jones-Sato-Wada-Wiens Theorem, Prime-Composite  
Complementation, Prime Number Theorem, Ulam Spiral, Ramsey 2-coloring of  
integers, Hilbert Tenth Problem, Unique Factorization, Matiyasevich-Robinson-  
Davis-Putnam Theorem, Post's Correspondence Problem, Question-Answering  
-----

1314.1 complement.py has been changed to import barycentric\_interpolate(),  
lagrange() interpolators in SciPy and to plot the complement polynomial in  
matplotlib.

1314.2 Function complement\_diophantine(enumerableset,  
interpol\_algorithm="barycentric") has been changed to add parameter  
"interpolation\_algorithm" and clauses to fit the elements of a complementary set  
to a polynomial by polyfit, barycentric interpolation or Lagrange interpolation  
based on values to interpol\_algorithm={'polyfit','barycentric','lagrange'}.

1314.3 Lagrange interpolated polynomial (Section 3.3.3 - algorithm 1 -  
Decidability of Existence and Construction of a Complement of a given function -  
<https://arxiv.org/abs/1106.4102v1>) interpolated earlier is of arbitrary degree  
and plotted as a graph in matplotlib written as JPEG in testlogs/complement.jpg.

1314.4 There is a Taylor series interpolation variant which approximates a  
function at pre-defined point in terms of existence of derivatives at that  
point. This was mentioned in Google Groups post by author (in ID  
ka\_shrinivaasan@yahoo.com deleted by Yahoo because of cybercrime per author's  
request) in 2003 which mooted the question of Complement of a Function -  
<https://groups.google.com/g/sci.math/c/RqsDNc6SBdk/m/Lgc0wLiFhTMJ> - contents of  
the thread have been saved and committed to  
[python-src/testlogs/ComplementOfAFunction\\_GoogleGroupsThread\\_2003.html](python-src/testlogs/ComplementOfAFunction_GoogleGroupsThread_2003.html)

1314.5 Polynomial interpolations could serve as tools to quantify Question-  
Answering as polynomials where set of ordered pairs

(question(i),score\_for\_answer\_to\_question(i)) are interpolated. Section 864.63  
of NeuronRain Design -

<https://neuronrain-documentation.readthedocs.io/en/latest/> - delves into  
learning theory and complexity lower bounds aspects of Question-Answering in  
multiple choice and boolean setting. Complementation has nice implications for  
Question-Answering in boolean setting E.g. For 10 Questions of Binary Yes-No  
answers, if all 10 questions are answered correctly in the form of a vector  
[1,0,0,1,0,1,1,1,0] and interpolated by a polynomial over GF[2], its complement  
polynomial over GF[2] represents "all wrong answers" defined by complement  
vector [0,1,1,0,1,0,0,0,1].

#### References and Commentaries:

-----  
1314.6 Hardness of Reconstructing Multivariate Polynomials over Finite Fields -  
[Parikshit Gopalan\* Microsoft Research - Silicon Valley. parik@microsoft.com,  
Subhash Khot† New York University and Georgia Tech. khot@cs.nyu.edu, Rishi  
Saket‡ Georgia Tech. saket@cc.gatech.edu] -  
<https://cs.nyu.edu/~khot/papers/polynomial.pdf> - "... We study the polynomial  
reconstruction problem for low-degree multivariate polynomials over finite field  
F[2]. In this problem, we are given a set of points  $x \in \{0, 1\}^n$  and target  
values  $f(x) \in \{0, 1\}$  for each of these points, with the promise that there is a

polynomial over  $F[2]$  of degree at most  $d$  that agrees with  $f$  at  $1 - \epsilon$  fraction of the points. Our goal is to find a degree  $d$  polynomial that has good agreement with  $f$ . We show that it is NP-hard to find a polynomial that agrees with  $f$  on more than  $1 - 2^{-d} + \delta$  fraction of the points for any  $\delta > 0$ ...." - Boolean Question-Answering transcript (Interview of Yes-No answers to questions) could be fit or approximated to a multivariate polynomial over  $GF[2]$ . This result implies even finding an approximation polynomial for Boolean Q&A is NP-Hard. Exact multivariate polynomial interpolation is non-trivial and still an open problem.

1314.7 Taylor series interpolation approximation of a function -

<https://www.uio.no/studier/emner/matnat/math/MAT-INF1100/h10/kompendiet/kap9.pdf>

- Theorem 9.2 - "... The Taylor polynomial of  $f$  of degree  $n$  at  $a$  is unique and can be written as  $T_n(f;a)(x) = f(a) + (x - a)f'(a) + (x - a)^2/2!f''(a) + \dots + (x - a)^n/n!f^{(n)}(a)$ . ..."

1314.8 Complement of a Function - Google Groups Thread - 2003 -

<https://groups.google.com/g/sci.math/c/RqsDNc6SBdk/m/Lgc0wLiFhTMJ>

-----  
1315.(THEORY and FEATURE) Intrinsic Merit of Music - Synthesized Bach from training music waveforms - 27 September 2022 - related to 3,110,134,298,1223,1224,1257,1258,1261,1305,1306,1307,1308,1309,1310,1311 and all sections on Music search-Music discovery, Intrinsic Merit of Music, MIR(Music Information Retrieval), Music Similarity and Clustering, AI Music Synthesis from summation of damped sinusoids, Additive Synthesis, fMRI connectomes - OpenNeuro - Psychology of music, Weighted automata, Chaos, Deep Learning, Dynamic Time Warping-Music Timeseries analysis, Music Evoked Autobiographical Memories, Waveshaping, ThoughtNet, Majority Voting (Enjoyable music) Vs Intrinsic (Quality music) - Condorcet Jury Theorem variants, Computational Learning Theory, Boolean Function Composition, Longest Common Subsequence, Suffix Trees - Longest Repeated Substring  
-----

-----  
1315.1 AudioToBitMatrix.py has been updated to change sharp notes notation in piano\_notes for WesternClassical as:

```
piano_notes={"WesternClassical":
{ 'A':440, 'B':493.89, 'C':261.63, 'D':293.67, 'E':329.63, 'F':349.23, 'G':392, 'A#':466.17, 'C#':227.18, 'D#':311.13, 'F#':370, 'G#':415.31}, "Carnatic":{ 'S':240, 'R1':254.27, 'R2':269.39, 'R3':275, 'G1':285.41, 'G2':302.38, 'G3':311, 'M1':320.36, 'M2':339.41, 'P':359.60, 'D1':380.98, 'D2':403.63, 'D3':415, 'N1':425, 'N2':453.06, 'N3':480}}
```

1315.2 get\_piano\_frequencies() has been changed to tokenize subdivisions of notes which range from 1 to 15 to suit 12-note piano\_notes dictionary lookup earlier - notes of the form <note>-<subdivision\_index> are truncated to <note>.

1315.3 Random sampling synthesis clause within Function music\_synthesis() has been changed to read training music waveforms into synth\_notes\_freq dictionary and iterate through its contents and synthesize new music waveform by chronologically concatenating random time slices from each training waveform. Size of the slice (synthslice) is a function of total duration of clip synthesized.

1315.4 Two music waveforms of JS Bach are passed on as training data to music\_synthesis() and synthesized derivative music waveform in piano is written to virtual\_piano\_music.wav:

```
music_synthesis(["testlogs/JSBach_Musicological_Offering.mp4", "testlogs/Bach_Flute_Sonata_EFlat.mp4"], musicgenre="WesternClassical", dur=60, polynomial_interpolation=False, tempo=0.25)
```

1315.5 Synthesized Bach music in virtual\_piano\_music.wav reasonably simulates a human playing an instrument and derives the patterns in the training Bach music waveforms.

1315.6 NeuronRain has implementations of Longest Common Subsequence (LCS) in C++ (cpp-src/asferlongestcommonsubstring.cpp) and LongestRepeatedSubstring SuffixArray in Python (python-src/StringSearch\_LongestRepeatedSubstring.py) which are other possible algorithms for mining common patterns in notes sequences of music waveforms - Longest Common notes sequence among multiple

training music waveforms and Longest Repeated notes sequence within a music waveform are candidates for synthesized music.

-----  
1316.(THEORY and FEATURE) Astronomy and Cosmology Datasets Analytics - Solar system N-Body Pairwise angular separations computed for NOAA HURDAT2 (1851-2012) North Atlantic Hurricanes Datasets - 28 September 2022 - related to 17,137,148,445,731,1176,1206,1236,1255,1266,1267,1268,1270,1271,1272,1273,1289 and all sections on Astronomical Dataset Mining, Archaeoastronomical Dating, Sequence Mining, String analytics, Sequence Alignment, Visual Planetarium Search, Archaeology, Climate and Extreme Weather Event Analytics, Computational Astrophysics, N-Body problem, Merit of Large Scale Visuals, Astronomical algorithms, Histogram analytics  
-----

-----  
1316.1 python-src/EphemerisSearch.py has been updated to increase maxiterations in extreme\_weather\_events\_n\_body\_analytics(self,datesofEWEs=None,loc="@earth-moon",angularsep=False,maxiterations=200) to 200.

1316.2 Dates of extreme weather events are read in reverse order by readlines() and reverse() (recent dates are analyzed first) as skyfield supports dates between 1899 and 2053 only and extreme weather events have increased in frequency in later half of 20th century and early 21st century.

1316.3 Pairwise angular separations between solar system bodies on extreme weather event dates after 1899 and before 2053 are computed by skyfield.separation\_from() for NOAA North atlantic Hurricanes (HURDAT2) dataset.

ephem.extreme\_weather\_events\_n\_body\_analytics(datesofEWEs="Hurricanes",angularsep=True)

1316.4 Following are Sun-Moon and Mercury-Venus angular separations for some Hurricane formation dates on September-October 2012 showing syzygies and almost-syzygies of Sun-Moon-Earth and ~60 degree separation of Venus-Mercury (from testlogs/EphemerisSearch.log.28September2022) in almost all dates. Gravitational Forces are computed for all solar system bodies including Mercury which mysteriously shows high gravity similar to earlier data:

Angular separations for Sun-Moon : [<Angle 142deg 21' 28.5">, <Angle 139deg 28' 30.8">, <Angle 136deg 34' 47.7">, <Angle 133deg 40' 17.8">, <Angle 130deg 44' 59.4">, <Angle 127deg 48' 50.7">, <Angle 124deg 51' 49.9">, <Angle 121deg 53' 54.9">, <Angle 118deg 55' 03.9">, <Angle 115deg 55' 14.6">, <Angle 112deg 54' 25.1">, <Angle 109deg 52' 33.2">, <Angle 106deg 49' 36.8">, <Angle 103deg 45' 33.9">, <Angle 100deg 40' 22.5">, <Angle 97deg 34' 00.7">, <Angle 94deg 26' 26.8">, <Angle 91deg 17' 39.3">, <Angle 88deg 07' 36.7">, <Angle 84deg 56' 18.1">, <Angle 161deg 45' 59.6">, <Angle 164deg 28' 26.6">, <Angle 167deg 10' 48.0">, <Angle 169deg 52' 47.6">, <Angle 172deg 33' 42.9">, <Angle 175deg 11' 13.6">, <Angle 177deg 32' 40.6">, <Angle 177deg 42' 05.9">, <Angle 178deg 13' 52.5">, <Angle 177deg 59' 38.1">, <Angle 175deg 50' 42.4">, <Angle 173deg 13' 39.3">, <Angle 170deg 30' 54.9">, <Angle 167deg 45' 55.8">, <Angle 164deg 59' 38.6">, <Angle 162deg 12' 24.6">, <Angle 159deg 24' 22.9">, <Angle 156deg 35' 37.6">, <Angle 153deg 46' 10.7">, <Angle 150deg 56' 02.6">, <Angle 148deg 05' 13.4">, <Angle 145deg 13' 42.4">, <Angle 142deg 21' 28.5">, <Angle 139deg 28' 30.8">, <Angle 136deg 34' 47.7">, <Angle 133deg 40' 17.8">, <Angle 130deg 44' 59.4">, <Angle 129deg 17' 01.4">, <Angle 127deg 48' 50.7">, <Angle 127deg 31' 40.4">, <Angle 124deg 51' 49.9">, <Angle 122deg 23' 37.9">, <Angle 121deg 53' 54.9">, <Angle 118deg 55' 03.9">, <Angle 115deg 55' 14.6">, <Angle 112deg 54' 25.1">, <Angle 109deg 52' 33.2">, <Angle 106deg 49' 36.8">, <Angle 103deg 45' 33.9">, <Angle 100deg 40' 22.5">, <Angle 97deg 34' 00.7">, <Angle 94deg 26' 26.8">, <Angle 91deg 17' 39.3">, <Angle 88deg 07' 36.7">, <Angle 84deg 56' 18.1">, <Angle 142deg 21' 28.5">, ...

Angular separations for Mercury-Venus : [<Angle 59deg 59' 56.5">, <Angle 60deg 02' 40.0">, <Angle 60deg 05' 12.9">, <Angle 60deg 07' 35.7">, <Angle 60deg 09' 48.3">, <Angle 60deg 11' 51.3">, <Angle 60deg 13' 44.7">, <Angle 60deg 15' 28.7">, <Angle 60deg 17' 03.7">, <Angle 60deg 18' 29.8">, <Angle 60deg 19' 47.2">, <Angle 60deg 20' 56.1">, <Angle 60deg 21' 56.8">, <Angle 60deg 22' 49.3">, <Angle 60deg 23' 33.9">, <Angle 60deg 24' 10.8">, <Angle 60deg 24'



40.0">, <Angle 60deg 25' 01.9">, <Angle 60deg 25' 16.5">, <Angle 60deg 25' 23.9">, <Angle 58deg 20' 46.9">, <Angle 58deg 28' 08.3">, <Angle 58deg 35' 12.0">, <Angle 58deg 41' 58.7">, <Angle 58deg 48' 28.6">, <Angle 58deg 54' 42.3">, <Angle 59deg 00' 40.2">, <Angle 59deg 01' 09.3">, <Angle 59deg 03' 33.3">, <Angle 59deg 06' 22.6">, <Angle 59deg 11' 49.9">, <Angle 59deg 17' 02.7">, <Angle 59deg 22' 01.1">, <Angle 59deg 26' 45.7">, <Angle 59deg 31' 16.7">, <Angle 59deg 35' 34.5">, <Angle 59deg 39' 39.5">, <Angle 59deg 43' 31.9">, <Angle 59deg 47' 12.0">, <Angle 59deg 50' 40.3">, <Angle 59deg 53' 56.9">, <Angle 59deg 57' 02.2">, <Angle 59deg 59' 56.5">, <Angle 60deg 02' 40.0">, <Angle 60deg 05' 12.9">, <Angle 60deg 07' 35.7">, <Angle 60deg 09' 48.3">, <Angle 60deg 10' 51.0">, <Angle 60deg 11' 51.3">, <Angle 60deg 12' 02.7">, <Angle 60deg 13' 44.7">, <Angle 60deg 15' 12.0">, ...

#### References:

-----  
 1316.5 The Super Cyclone of 1999 and Lunar Alignment Effect - December 2016 - International Journal of Earth Sciences and Engineering 9(6):2338-2347 - Intensified by Full Moon at Perigee in Syzygy - [https://www.researchgate.net/publication/313839574\\_The\\_Super\\_Cyclone\\_of\\_1999\\_and\\_Lunar\\_Alignment\\_Effect](https://www.researchgate.net/publication/313839574_The_Super_Cyclone_of_1999_and_Lunar_Alignment_Effect) - "... The extraordinary intensification of the Super cyclone of 1999 is examined over its entire life period. Luni alignment and particularly full moon at perigee in syzygy stands out as the intensifying cause; ..."  
 1316.6 The Super Cyclone of 1999 - 260-300 kmph - <https://www.hindustantimes.com/india/revisiting-the-super-cyclone-that-hit-odisha-in-1999/story-S0LDY1STwdrVdMravThCZK.html>

-----  
 1317. (THEORY and FEATURE) Computational Geometric Integer Factorization - Multiple Integers - Python 3.10.4 upgrade + Spark 3.0.1 Quadcore Benchmarks - related to 1259,1303 and all sections on Integer Factorization,Computational Geometry,Set Partitions-to-Tile Cover reduction by Lagranges Four Square Theorem and ILP,Primality Testing - 29 September 2022

-----  
 1317.1  
 python-src/DiscreteHyperbolicFactorizationUpperbound\_TileSearch\_Optimized\_MultipleIntegers.py has been upgraded to Python 3.10.4 and 51 consecutive integers from 1000 to 1050, 101 consecutive integers from 10000 to 10100 and 101 integers from 20000 to 20100 have been factorized by Computational Geometric Factorization (253 integers in total).

1317.2 Benchmark runtime numbers for factoring 20000 to 20100 have been plotted as observed curve against a theoretical curve for  $k \cdot \log N \cdot \log N$  for  $k=1$  (testlogs/DiscreteHyperbolicFactorizationUpperbound\_TileSearch\_Optimized\_MultipleIntegers.jpg). Factors are captured in testlogs/DiscreteHyperbolicFactorizationUpperbound\_TileSearch\_Optimized\_MultipleIntegers.log.29September2022 (1000 to 1050), testlogs/DiscreteHyperbolicFactorizationUpperbound\_TileSearch\_Optimized\_MultipleIntegers.log2.29September2022 (10000 to 10100) and testlogs/DiscreteHyperbolicFactorizationUpperbound\_TileSearch\_Optimized\_MultipleIntegers.log3.29September2022 (20000 to 20100). Earlier consecutive integers factorization includes primes.

1317.3 Actual versus theoretical runtime curves of testlogs/DiscreteHyperbolicFactorizationUpperbound\_TileSearch\_Optimized\_MultipleIntegers.jpg are in concurrence and the few spikes could be latencies due to Python Virtual Machine Garbage collection, CPU and Spark scheduling vagaries.

#### References:

-----  
 1317.4 Implementing and Comparing Integer Factorization Algorithms - <https://crypto.stanford.edu/cs359c/17sp/projects/JacquelineSpeiser.pdf>

1317.5 Integer Factoring - [ARJEN K. LENSTRA arjen.lenstra@citicorp.com  
Citibank, N.A.,] -  
[https://www.fdi.ucm.es/profesor/m\\_alonso/Documentos/factorizacion/arjlensfac.pdf](https://www.fdi.ucm.es/profesor/m_alonso/Documentos/factorizacion/arjlensfac.pdf)

-----  
1318. (THEORY and FEATURE) GIS Weather Analytics and Climate Analytics - 3  
October 2022 - related to 148,445,446,463,1165,1171,1176,1266,1289,1316 and all  
sections on Correlation between gravitational effects of Mined Celestial N-Body  
Patterns and terrestrial extreme weather events (or Gravitational effects on  
climate change), Drone natural obstacle avoidance, Drone autonomous online  
shopping delivery, Drone Electronic Voting Machine, Large Scale Visuals  
Recognition, Artificial Intelligence models for Climate Change, Astronomical  
algorithms  
-----

-----  
1318.1 GISWeatherAnalytics.py has been updated to integrate N-Body Gravitational  
Acceleration computation for Solar System bodies implemented in  
EphemerisSearch.py to correlate climate events and gravitational pull of Solar  
system N-Body celestial choreographies on Earth and Ocean surface (especially  
role of Syzygies of solar system bodies). While Sun-Earth-Moon Syzygy has been  
widely studied and found to have high correlation to storm intensification  
(Sections 1266,1289,1316), gravitational influence of rest of Solar system  
planets on Earth has been less studied in literature.

1318.2 Function climate\_analytics(datasource,date="",time="") has been changed  
to include a clause for "n-body-analytics" datasource which accepts an array of  
extreme weather event dates, instantiates Ephemeris object (NASA JPL DE421  
Ephemeris) and invokes extreme\_weather\_events\_n\_body\_analytics() on those dates  
to compute gravitational pull and pairwise angular separation of solar system  
bodies.

1318.3 Function climate\_analytics(datasource="n-body-  
analytics",date=datesofstorms) is invoked for following formation dates of  
storms:

1318.3.1 North Atlantic Hurricanes - Harvey (Category 4 - 17 August 2017),  
Irma (Category 5 - 30 August 2017), Ian (Category 4 - 23 September 2022)

1318.3.2 Bay of Bengal - Very Severe Cyclonic Storms - Amphan (20 May  
2020),Gaja (10 November 2018),Vardah (6 December 2016),Thane (25 December  
2011),Ockhi (29 November 2017)

1318.4 Following are excerpts of angular separations for Sun-Moon and Venus-  
Mercury from testlogs/GISWeatherAnalytics.log.30October2022 for earlier storms:

Angular separations for Venus-Mercury : [<Angle 51deg 49' 11.5">, <Angle  
26deg 43' 05.0">, <Angle 09deg 23' 44.3">, <Angle 04deg 59' 58.7">, <Angle 44deg  
15' 04.4">, <Angle 23deg 56' 21.0">, <Angle 54deg 10' 52.4">, <Angle 31deg 00'  
20.5">]

Angular separations for Sun-Moon : [<Angle 63deg 35' 41.0">, <Angle 97deg  
36' 37.7">, <Angle 33deg 52' 36.9">, <Angle 30deg 22' 33.5">, <Angle 28deg 39'  
00.4">, <Angle 73deg 45' 38.6">, <Angle 04deg 17' 26.3">, <Angle 117deg 39'  
43.0">]

1318.5 Angular separations of Venus-Mercury range from 4 to 54 degrees for all  
storms which could perhaps be anecdotal evidences for 1266.18 indicating a  
synergy of Venus and Mercury and not just Venus. Correlation between lowest  
pressure (millibar) of the storm and angular separations of solar system bodies  
earlier could be of importance.

#### References:

-----  
1318.6 Hurricane Harvey - [https://en.wikipedia.org/wiki/Hurricane\\_Harvey](https://en.wikipedia.org/wiki/Hurricane_Harvey) - 215  
kmph - Lowest pressure - 937 millibar

1318.7 Hurricane Irma - [https://en.wikipedia.org/wiki/Hurricane\\_Irma](https://en.wikipedia.org/wiki/Hurricane_Irma) - 285 kmph  
- Lowest pressure - 914 millibar

1318.8 Hurricane Ian - [https://en.wikipedia.org/wiki/Hurricane\\_Ian](https://en.wikipedia.org/wiki/Hurricane_Ian) - 250 kmph -  
Lowest pressure - 936 millibar

1318.9 Cyclone Thane - [https://en.wikipedia.org/wiki/Cyclone\\_Thane](https://en.wikipedia.org/wiki/Cyclone_Thane) - 165 kmph -  
Lowest pressure - 969 millibar

1318.10 Cyclone Gaja - [https://en.wikipedia.org/wiki/Cyclone\\_Gaja](https://en.wikipedia.org/wiki/Cyclone_Gaja) - 150 kmph - Lowest pressure - 976 millibar  
1318.11 Cyclone Ockhi - [https://en.wikipedia.org/wiki/Cyclone\\_Ockhi](https://en.wikipedia.org/wiki/Cyclone_Ockhi) - 185 kmph - Lowest pressure - 976 millibar  
1318.12 Cyclone Vardah - [https://en.wikipedia.org/wiki/Cyclone\\_Vardah](https://en.wikipedia.org/wiki/Cyclone_Vardah) - 155 kmph - Lowest pressure - 994 millibar  
1318.13 Saffir-Simpson scale of Category 1 to 5 - Lower the pressure, higher is the destructive power - <https://sciencing.com/barometric-pressure-hurricanes-22734.html> - TL;DR - "... The Saffir-Simpson scale ranges from Category 1 hurricanes with a barometric pressure of greater than 980 millibars that cause minimal damage, to Category 5 hurricanes with a central pressure of less than 920 millibars....During their life cycles, each of these storms can expend as much energy as 10,000 nuclear bombs."  
1318.14 Saffir-Simpson scale Hurricane category classification - <https://www.nhc.noaa.gov/aboutsshws.php>  
1318.15 Super Typhoon Haiyan - [https://en.wikipedia.org/wiki/Typhoon\\_Haiyan](https://en.wikipedia.org/wiki/Typhoon_Haiyan) - 315 kmph - Lowest pressure - 895 millibar

-----  
1319. (THEORY and FEATURE) Computational Geometric Integer Factorization - Multiple Integers - Python 3.10.4 upgrade + Spark 3.0.1 Quadcore Benchmarks 2 - Numba JIT optimization - Configurable number of factors - related to 1259,1303,1317 and all sections on Integer Factorization, Computational Geometry, Set Partitions-to-Tile Cover reduction by Lagranges Four Square Theorem and ILP, Primality Testing, RSA Semiprimes - 6 October 2022  
-----

#### 1319.1 Updated

python-src/DiscreteHyperbolicFactorizationUpperbound\_TileSearch\_Optimized.py to import numba JIT (Just In Time)  
python compiler that achieves upto 20X speedup on Numeric Python-Scientific Python and Loops computation.

1319.2 Maximum number of factors found per integer has been made configurable by maxfactors. DiscreteHyperbolicFactorizationUpperbound\_TileSearch\_Optimized.py is a Parallel Planar Point Location Factoring implementation on MapReduce that is inherently capable of finding all factors by parallel invocation of local sequential binary or interpolation search  $((\log N)^k$  sequential binary or interpolation searches of  $\log N$  or  $\log \log N$  time each on  $N/(\log N)^k$  PRAMS-Multicores which is  $NC(k)$  contained in  $DMRC(k-1)$  while traditional factorization is mostly limited to finding one factor alone (all factors of  $N$  can be recursively found by applying same algorithm - whether it is Quadratic Sieve, Dixon, Pollard-Rho or CADO-NFS - on  $N/f(\text{prev})$  where  $f(\text{prev})$  is the last factor found).

1319.3 Restricting the number of factors per integer is necessary for accurate benchmarking as different integers have different number of factors and number of factors has to be same across the board.

1319.4 Function `tilesearch_nonpersistent(y, numfactors=maxfactors)` and `binary_search_interval_nonpersistent(xl, yl, xr, yr, numfactors=3)` have been updated to pass on maxfactors as parameters which is checked by an inequality clause on length of `_value` field of factors Spark accumulator.

1319.5 All functions have been decorated by `@jit(parallel=True)` directive of Numba for enabling parallelism but commented due to compile errors per caveats in Numba documentation -

<https://numba.pydata.org/numba-doc/latest/reference/pysupported.html#pysupported>

1319.6 101 consecutive 22-bits integers from 3203023 have been factorized by restricting the maximum number of factors per integer to 3 and their actual and theoretical  $O(\log N)^2$  for BigO constant 1) runtimes have been plotted in `python-src/testlogs/DiscreteHyperbolicFactorizationUpperbound_TileSearch_Optimized_MultipleIntegers.jpg`:

python3.10

DiscreteHyperbolicFactorizationUpperbound\_TileSearch\_Optimized\_MultipleIntegers.py 3203023 100 2 1 2 >

testlogs/DiscreteHyperbolicFactorizationUpperbound\_TileSearch\_Optimized\_MultipleIntegers.log.60October2022

1319.7 Theoretical and Actual runtime curves in python-src/testlogs/DiscreteHyperbolicFactorizationUpperbound\_TileSearch\_Optimized\_MultipleIntegers.jpg match except spikes caused by Spark Executor while doing a futile search for non-trivial factors in following integers which are primes (independently verified by Google Prime Search e.g <https://www.google.com/search?q=3203117+prime>) - 3203041, 3203047, 3203059, 3203063, 3203071, 3203093, 3203099, 3203107, 3203111, 3203117. It is worth observing to note that spikes for primes in actual runtime curve touch the theoretical curve for upperbound of  $O(\log N * \log N)$ .

#### References:

-----  
1319.7 Numba JIT - <https://numba.readthedocs.io/en/stable/user/jit.html>  
1319.8 Algorithmica - HPC Factorization - <https://en.algorithmica.org/hpc/algorithms/factorization/> - Pollard Rho optimization - "...  $O(\sqrt[4]{n})$ -time Pollard's rho algorithm and optimize it to the point where it can factorize 60-bit semiprimes in 0.3-0.4ms and ~3 times faster than the previous state-of-the-art..."  
1319.9 Efficient Circuit Simulation in MapReduce - [Fabian Frei-Koichi Wada] - <https://arxiv.org/pdf/1907.01624.pdf> - "... We prove that  $NC_{i+1} \subseteq DMRC_i$  for all  $i \in \{0, 1, 2, \dots\}$ , where  $DMRC_i$  is the set of problems solvable by a deterministic MapReduce computation in  $O((\log n)^i)$  rounds ... For every  $i \in \mathbb{N}$ , we have  $NC_i \subseteq EREW_i \subseteq CREW_i \subseteq CRCW_i = AC_i \subseteq NC_{i+1}$ ; ... "  
1319.10 Sorting, Searching, and Simulation in the MapReduce Framework - [Goodrich-Sitchinava-Zhang] - <https://arxiv.org/pdf/1101.1902.pdf> - "... Theorem 3.2: Given an algorithm A in the CRCW PRAM model, with write conflicts resolved according to a commutative semigroup function such that A runs in T steps using P processors and N memory cells, we can simulate A in the I/O-memory-bound MapReduce framework in  $R = O(T \log M P)$  rounds and with  $C = O(T(N + P) \log M(N + P))$  communication complexity ... "  
1319.11 RSA Semiprime Factorization Challenge - [https://en.wikipedia.org/wiki/RSA\\_Factoring\\_Challenge](https://en.wikipedia.org/wiki/RSA_Factoring_Challenge)  
-----

-----  
1320. (THEORY and FEATURE) GIS Urban Sprawl Analytics - R2019A and R2022A - Comparison of Raster Data Bounding Boxes for Chennai Metropolitan Area Sprawl - 7 October 2022 - related to 1174, 1175, 1177, 1179, 1194, 1211, 1234, 1290, 1291, 1292, 1295, 1296, 1297, 1301, 1304, 1312, 1313 and all sections on GIS Urban Sprawl Analytics, Merit of Large Scale Visuals, Gridded Population Estimators (SEDAC GPW4 and GHSL convex hull estimators), DBSCAN and Neural Network Urban Extent Learners, Computational Geometry, Intrinsic Merit Rankings, R Ricker Population Estimation, Community detection, Social Network Analytics, Space filling by Curves, Unequal Circle and Polynomial packing, Computational Geometry and Polygonal packing by Voronoi Tessellation, Four color theorem, Economic Merit, Computational Economics - GDP estimation from Urban sprawl demographics, electricity consumption, Poverty alleviation, MARA (Multiple Agent Resource Allocation) Facegraph walk coloring DNFSAT algorithm, Preferential Attachment, Fixed Parameter Tractability-Kernelization, Automatic Delineation of Urban Sprawls, Cellular Automata-SLEUTH-Polya Urn-Dynamic Facegraph Urban Growth Models  
-----

-----  
1320.1 Exponential 2634% periurbanization-expansion of Chennai Metropolitan Area Sprawl deduced in 1313 from 2019 to 2022 has been re-analyzed by comparing another pair of GHSL SMOD R2019A and R2022A raster datasets.  
1320.2 GISUrbanSprawlAnalytics.py has been updated to compare following pair of rasters from GHSL SMOD Degree of Urbanization - R2019A and R2022A - testlogs/RemoteSensingGIS/GHS\_SMOD\_POP2015\_GLOBE\_R2019A\_54009\_1K\_V2\_0.tif (R2019A) and testlogs/RemoteSensingGIS/GHS\_SMOD\_P2030\_GLOBE\_R2022A\_54009\_1000\_V1\_0\_R8\_C26.tif (Row 8 - Column 26 of R2022A GHSL SMOD dataset obtained from tiled R2022A GUI)



aaaaaaaaaaaaaaaaaaaaaaaaaaaa&pg=V - Earlier expansion numbers compared between R2019A and R2022A are based on 2-dimensional horizontal urbanization. BUILT-V Dataset provides 3-dimensional data of Built-Volume and vertical expansion could be measured by BUILT-V / BUILT-S

-----  
1321. (JIRA,THEORY and FEATURE) Computational Geometric Integer Factorization - Multiple Integers - Python 3.10.4 upgrade + Spark 3.0.1 Quadcore Benchmarks 3 - Numba JIT optimization - Configurable number of factors - Factorization-Primality of Consecutive integers from 999 to 1874 - related to 1259,1303,1319 and all sections on Integer Factorization,Computational Geometry,Set Partitions-to-Tile Cover reduction by Lagranges Four Square Theorem and ILP,Primality Testing,RSA Semiprimes - 7 October 2022  
-----

-----  
1321.1 Logs for factorization of 875 consecutive integers from 999 to 1874 have been committed at  
testlogs/DiscreteHyperbolicFactorizationUpperbound\_TileSearch\_Optimized\_MultipleIntegers.log.7October2022

1321.2 Following example awk script can be used to grep the logs for potential prime integers corresponding to spikes in runtimes (> 100):

grep "in time deltas"

testlogs/DiscreteHyperbolicFactorizationUpperbound\_TileSearch\_Optimized\_MultipleIntegers.log.7October2022 |awk '{if (\$15 > 100) print \$5}'

1193, 1229, 1249, 1277, 1279, 1297, 1301, 1303, 1307, 1319, 1321, 1327, 1361, 1367, 1369, 1373, 1381, 1399, 1409, 1423, 1427, 1429, 1433, 1439, 1447, 1451, 1453, 1459, 1471, 1481, 1483, 1487, 1489, 1493, 1499, 1511, 1523, 1531, 1543, 1549, 1553, 1559, 1567, 1571, 1579, 1583, 1597, 1601, 1607, 1609, 1613, 1619, 1621, 1627, 1637, 1657, 1663, 1667, 1669, 1681, 1693, 1697, 1699, 1709, 1721, 1723, 1733, 1741, 1747, 1753, 1759, 1777, 1783, 1787, 1789, 1801, 1811, 1823, 1831, 1847, 1849, 1861, 1867, 1871, 1873

1321.3 JIRA issue for factorization of squares -

<https://krishnairesearch.atlassian.net/browse/NEUR-1> has been opened for erroneous flagging of squares as primes earlier (1369=37\*37,1681=41\*41)

-----  
1322. (JIRA,THEORY and FEATURE) Computational Geometric Integer Factorization - Multiple Integers - Python 3.10.4 upgrade + Spark 3.0.1 Quadcore Benchmarks 4 - Factorization-SquareRoot-Primality of Consecutive integers from 50000 to 50100 and 9 to 200 - related to 498,601,1226,1259,1303,1319,1321 and all sections on Integer Factorization,Computational Geometry,Set Partitions-to-Tile Cover reduction by Lagranges Four Square Theorem and ILP,Primality Testing,RSA Semiprimes,Almost-Square Bounding Boxes in Large Scale Visual Recognition,Pell's Equation,Brahmagupta's Chakravala,Approximate Factoring by Newton-Raphson Rayshooting queries,Algebraic Geometry of Computational Geometric Factorization - 10 October 2022  
-----

-----  
1322.1 This commit resolves JIRA issue

<https://krishnairesearch.atlassian.net/browse/NEUR-1> concerning problem within python-src/DiscreteHyperbolicFactorizationUpperbound\_TileSearch\_Optimized.py in finding square roots,a very important special case of factorization. It is worth noting that Newton-Raphson square root algorithm is polylogarithmic -

$O((\log N)^k \log \log N)$  - which is used for approximate factor rayshooting queries in algorithm of <https://kuja27.blogspot.com/2018/04/grafit-course-material-newton-raphson.html> - and Computational Geometric Factorization implies general cases of primality testing and factorization are polylogarithmic

$O((\log N)^k \log \log N)$  if interpolation search is employed) as well which includes almost-squares (integer squareroots). Principal Ideal Algebraic Geometry and Differential Calculus involved in computation of arithmetic progression hyperbolic arc rasterization (rectification) are quite similar to Newton-Raphson algorithm:

tile\_segment of length delta (from first derivative - tangent - of hyperbolic arc at x) =  $N/x - N/(x+\text{delta}) = N * [\text{delta}/x(x+\text{delta})]$  or  $N/(x(x+1))$  for delta=1

1322.2 New clause has been added to handle when interval midpoint of binary search is 0 and tile x and y ordinates are equal.

1322.3 Multiple Consecutive integers from 50000 to 50100 have been factorized and following primes have been captured in python-src/testlogs/DiscreteHyperbolicFactorizationUpperbound\_TileSearch\_Optimized\_MultipleIntegers.log.10October2022 (spikes in runtimes):

50021,50023,50033,50047,50051,50053,50069,50077,50087,50093

1322.4 Multiple Consecutive integers from 9 to 200 have been factorized and following square roots have been captured in python-src/testlogs/DiscreteHyperbolicFactorizationUpperbound\_TileSearch\_Optimized\_MultipleIntegers.log2.10October2022 :

('Square root is: ', 3, ' (at ', 'Mon, 10 Oct 2022 09:50:34 GMT', ')')  
('Square root is: ', 4, ' (at ', 'Mon, 10 Oct 2022 09:54:10 GMT', ')')  
('Square root is: ', 5, ' (at ', 'Mon, 10 Oct 2022 09:57:36 GMT', ')')  
('Square root is: ', 6, ' (at ', 'Mon, 10 Oct 2022 10:01:51 GMT', ')')  
('Square root is: ', 7, ' (at ', 'Mon, 10 Oct 2022 10:06:55 GMT', ')')  
('Square root is: ', 8, ' (at ', 'Mon, 10 Oct 2022 10:12:35 GMT', ')')  
('Square root is: ', 9, ' (at ', 'Mon, 10 Oct 2022 10:19:03 GMT', ')')  
('Square root is: ', 10, ' (at ', 'Mon, 10 Oct 2022 10:26:08 GMT', ')')  
('Square root is: ', 11, ' (at ', 'Mon, 10 Oct 2022 10:34:12 GMT', ')')  
('Square root is: ', 12, ' (at ', 'Mon, 10 Oct 2022 10:42:57 GMT', ')')  
('Square root is: ', 13, ' (at ', 'Mon, 10 Oct 2022 10:52:47 GMT', ')')  
('Square root is: ', 14, ' (at ', 'Mon, 10 Oct 2022 11:03:30 GMT', ')')

1322.5 Runtime plot for factoring integers from 9 to 208 has been captured in python-src/testlogs/DiscreteHyperbolicFactorizationUpperbound\_TileSearch\_Optimized\_MultipleIntegers.jpg and spikes correspond to primes - actual runtimes are far upperbounded by theoretical plot for  $O(\log N * \log N)$ .

References:

-----  
1322.6 Complexity of Newton-Raphson Square Root Algorithm -  
[https://courses.csail.mit.edu/6.006/fall11/rec/rec12\\_newton.pdf](https://courses.csail.mit.edu/6.006/fall11/rec/rec12_newton.pdf)

-----  
1323.(THEORY and FEATURE) GIS Urban Sprawl Analytics - R2022A - 3D Urban Sprawl Growth Model from BUILT-V and BUILT-S datasets - Commercial segment (Central Business District) Delineation by average building height - Chennai Metropolitan Area Sprawl Example - 11 October 2022 - related to

1174,1175,1177,1179,1194,1211,1234,1290,1291,1292,1295,1296,1297,1301,1304,1312,1313,1320 and all sections on GIS Urban Sprawl Analytics, Merit of Large Scale Visuals, Gridded Population Estimators (SEDAC GPW4 and GHSL convex hull estimators), DBSCAN and Neural Network Urban Extent Learners, Computational Geometry, Intrinsic Merit Rankings, R Ricker Population Estimation, Community detection, Social Network Analytics, Space filling by Curves, Unequal Circle and Polynomial packing, Computational Geometry and Polygonal packing by Voronoi Tessellation, Four color theorem, Economic Merit, Computational Economics - GDP estimation from Urban sprawl demographics, electricity consumption, Poverty alleviation, MARA (Multiple Agent Resource Allocation) Facegraph walk coloring DNFSAT algorithm, Preferential Attachment, Fixed Parameter Tractability-Kernelization, Automatic Delineation of Urban Sprawls, Cellular Automata-SLEUTH-Polya Urn-Dynamic Facegraph Urban Growth Models

-----  
1323.1 GISUrbanSprawlAnalytics.py has been updated to define new function three\_dimensional\_urban\_growth\_model(rasterdata\_2d,rasterdata\_3d) for computing third dimension (height) from two histograms for 2D raster and 3D raster for any datatype. This function takes as input the data for 2 rasters of 2D (Surface) and 3D (Volume) from urban\_sprawl\_from\_raster(), populates 2 defaultdict() histogram dictionaries from them, sorts the 2 histograms by values of the pixels and computes the third dimension (height) by fraction of maximum elements in the

two histograms (Volume/Surface) which is an estimate of the height. GHSL Data Package 2022 report has more on definitions of ANBHx (Building height), BUVOL (Building volume) and BUSURF (Building surface) in Reference 1323.6.

#### 1323.2 Two rasters

testlogs/RemoteSensingGIS/GHS\_BUILT\_S\_P2030LIN\_GLOBE\_R2022A\_54009\_100\_V1\_0\_R8\_C26.tif (R2022A BUILT-S - 2D surface) and  
testlogs/RemoteSensingGIS/GHS\_BUILT\_V\_P2030LIN\_GLOBE\_R2022A\_54009\_100\_V1\_0\_R8\_C26.tif (R2022A BUILT-V - 3D Volume) are analyzed by  
three\_dimensional\_urban\_growth\_model() to find estimated building height in Chennai Metropolitan Area Sprawl Longitude-Latitude Bounding Box (of size ~130 km \* ~130 km = ~16000 sqkm approximately) delineated by expanse of suburban rail-bus network (Reference 1320.6):

```
r2ddata=urban_sprawl_from_raster(79.271851,12.439259,80.351257,13.568572,"testlogs/RemoteSensingGIS/GHS_BUILT_S_P2030LIN_GLOBE_R2022A_54009_100_V1_0_R8_C26.tif",dt="BUILT_S_R2022A")
```

```
r3ddata=urban_sprawl_from_raster(79.271851,12.439259,80.351257,13.568572,"testlogs/RemoteSensingGIS/GHS_BUILT_V_P2030LIN_GLOBE_R2022A_54009_100_V1_0_R8_C26.tif",dt="BUILT_V_R2022A")
```

```
three_dimensional_urban_growth_model(r2ddata,r3ddata)
```

1323.4 Vertical expansion is defined and analyzed in section 1234 and Reference 1234.8 which delineates based on DBSCAN clustering, has found the ratio of vertical land to surface to be approximately 3.0 as far as European cities (Spain) are concerned. Commercial Central Business District (CBD) of a city typically consists of highrises and CBD could be delineated with in an urban sprawl GIS by aggregating the pixels of high building height values and high NightLights from VIIRS.

1323.5 From testlogs/GISUrbanSprawlAnalytics.log.110ctober2022 and testlogs/GISUrbanSprawlAnalytics.log2.110ctober2022 building height ANBHx has been determined as (in meters):

```
three_dimensional_urban_growth_model(): maximum building height = 18.16121440338903
```

#### References:

-----

1323.6 GHSL GHS BUILT-V(olume) Dataset - R2022A -

[https://ghsl.jrc.ec.europa.eu/documents/GHSL\\_Data\\_Package\\_2022.pdf](https://ghsl.jrc.ec.europa.eu/documents/GHSL_Data_Package_2022.pdf) - Section 2.2.1 Definitions - Section 2.3 - GHS-BUILT-V R2022A - GHS built-up volume grids derived from joint assessment of Sentinel-2, Landsat, and global DEM data, for 1975-2030 (5yrs) interval) - "... The data is made by application of the formula  $BUVOLx = ANBHx * BUSURFx$ , where: the ANBHx is the GHS-BUILT-H R2022A - GHS building height, derived from AW3D30, SRTM30, and Sentinel- 2 composite (2018), the BUSURFx is the GHS-BUILT-S R2022A - GHS built-up surface grid, derived from Sentinel-2 composite and Landsat, multitemporal (1975-2030). ..." - earlier implementation of three\_dimensional\_urban\_growth\_model() computes vertical expansion as  $ANBHx = BUVOLx / BUSURFx$

1323.7 Pesaresi M; Syrris V; Julea A. A New Method for Earth Observation Data Analytics Based on Symbolic Machine Learning. REMOTE SENSING 8 (5); 2016. p. 399. JRC99747 - <https://publications.jrc.ec.europa.eu/repository/handle/JRC99747> and <https://www.mdpi.com/2072-4292/8/5/399/htm> - Machine Learning behind GHSL rasters - Symbolic machine learning is of 2 phases: (1) Sequence Reduction (2) Class Association Rules.

1323.8 Building(s and) cities: Delineating urban areas with a machine learning algorithm - <https://www.sciencedirect.com/science/article/pii/S0094119019300944> - "6 Conclusions ... When comparing our delineated urban areas with other delineations, we find that our urban areas are better measured, being more similar in this regard to commuting-based delineations than to areas delimited by administrative boundaries. ..." - Accuracy of commuting based delineation vindicates suburban transit network bounding box based computation earlier and points to traffic patterns having significant say in delineating urban areas.

1323.9 Microsoft Building Footprints -



<https://github.com/microsoft/USBuildingFootprints>  
1323.10 Meta HRSL - <https://research.fb.com/downloads/high-resolution-settlement-layer-hrsl/>  
1323.11 Multi Resolution Land Characteristics - <https://www.mrlc.gov/data>  
1323.12 Copernicus CLC - <https://land.copernicus.eu/pan-european/corine-land-cover/clc2018>  
1323.13 OpenStreetMap Land Use - <https://osmlanduse.org/#10/80.07793/12.99678/0/>

-----  
-----  
-----  
1324. (JIRA, THEORY and FEATURE) Computational Geometric Integer Factorization - Python 3.10.4, Python 3.7.5, Spark 3.0.1, Spark 3.3.0 Quadcore Benchmarks - Numba JIT enabled for joblib parallelized tiles creation - Semiprimes, Cunningham's Number - related to 498,601,1226,1259,1303,1319,1321,1323 and all sections on Integer Factorization, Computational Geometry, Set Partitions-to-Tile Cover reduction by Lagranges Four Square Theorem and ILP, Primality Testing, RSA Semiprimes, Almost-Square Bounding Boxes in Large Scale Visual Recognition, Pell's Equation, Brahmagupta's Chakravala, Approximate Factoring by Newton-Raphson Rayshooting queries, Algebraic Geometry of Computational Geometric Factorization - 13 October 2022  
-----  
-----  
-----

1324.1

python-src/DiscreteHyperbolicFactorizationUpperbound\_TileSearch\_Optimized.py  
b/python-src/DiscreteHyperbolicFactorizationUpperbound\_TileSearch\_Optimized.py  
has been updated to import joblib Parallel processing framework.

1324.2 Factors accumulator Spark Global variable has been updated within each clause of factor criteria which was printing wrong factors earlier though factors were correctly computed.

1324.3 New function parallel\_tile\_segments() has been defined and Numba JIT decorated for computing tile segments in parallel which is computed sequentially at present.

1324.4 Function SearchTiles\_and\_Factorize(n, k, Parallel\_for="False") has been changed to add a boolean flag Parallel\_for to choose between parallel version and sequential version of for loop. If Parallel\_for is set to False tiles computation for loop is sequential.

1324.5 If Parallel\_for is set to True following commented sequential for-loop code block is replaced by joblib Parallel() processing which parallelly invokes parallel\_tile\_segments() by setting n\_jobs=<number of multicores> followed by Spark parallelize() of the 2D array which is flattened to 1D array by flatMap() and foreach() is invoked in the end - parallel version of a doubly nested for loop. This triply speeds-up the hyperbolic arc bow segmentation by combining Spark Parallelize() + Numba JIT + Joblib Parallel(). Caveat: Following sequential for loop implements  $(\log N)^k$  PRAMS \*  $N/(\log N)^k$  tiles = N which is DMRC simulation of NC necessitated by hardware limitations and not  $N/(\log N)^k$  PRAMS \*  $(\log N)^k$  tiles = N which is true NC though effective work is same. Tile segments computed are stored in a huge 2D array in-memory and number of jobs in joblib have to be set to  $N/(\log N)^k$  equal to number of multicores-PRAMS in NC-DMRC-MapReduce cloud to prevent out of memory errors - requires a Supercomputing or Large cloud infrastructure of massive multicores-PRAMS - for huge integers normal desktop configurations might not work:

#(( $\log N$ )<sup>k</sup> sequential binary or interpolation searches of  $\log N$  or  $\log \log N$  time each on  $N/(\log N)^k$  PRAMS-Multicores

```
#for x in range(int(polylog_n)):
print("tiles_start:", tiles_start)
print("tiles_end:", tiles_end)
tiles = list(range(tiles_start, tiles_end))
print(("len(tiles):", len(tiles)))
spcon.parallelize(tiles).foreach(
tilesearch_nonpersistent)
tiles_start = tiles_end
tiles_end += tiles_per_PRAM
```

```

if len(factors_accum.value) > maxfactors:
break
#Earlier sequential for loop is parallelized by joblib to obtain a
2D array of set of tile segments followed by another nested parallelize() for
each tile segment 1D array
 tile_segments=Parallel(n_jobs=4)(delayed(parallel_tile_segments)
(tiles_per_PRAM,x) for x in range(int(polylog_n)))
 print("tile_segments:",tile_segments)
 spcon.parallelize(tile_segments).flatMap(lambda x:
x).foreach(tilesearch_nonpersistent)
1324.6 Parallel_for is passed on as boolean argument (True or False) from
factorization commandline.
1324.7 Following integers of varied categories have been factorized captured in
respective logs - some of the benchmarks use upgraded Spark 3.3.0:
 1324.7.1
testlogs/DiscreteHyperbolicFactorizationUpperbound_TileSearch_Optimized.log1.120
ctober2022 - Python 3.10.4 + Spark 3.0.1 - Numba JIT Parallel for enabled -
('factors of ', 99999, '(', 16.609626047414267, ' bits integer) =', {1, 3,
33333, 99999})
 1324.7.2
testlogs/DiscreteHyperbolicFactorizationUpperbound_TileSearch_Optimized.log2.120
ctober2022 - Python 3.10.4 + Spark 3.0.1 - Numba JIT Parallel for disabled -
('factors of ', 99999, '(', 16.609626047414267, ' bits integer) =', {1, 3, 813,
271, 369, 33333, 123, 99999})
 1324.7.3
testlogs/DiscreteHyperbolicFactorizationUpperbound_TileSearch_Optimized.log3.120
ctober2022 - Python 3.10.4 + Spark 3.0.1 - Numba JIT Parallel for disabled -
('factors of ', 2137458620009, '(', 40.959033629156515, ' bits integer) =',
{1462001, 2137458620009, 1462009, 1}) - Reference 1324.9
 1324.7.4
testlogs/DiscreteHyperbolicFactorizationUpperbound_TileSearch_Optimized.log4.120
ctober2022 - Python 3.10.4 + Spark 3.0.1 - Numba JIT Parallel for disabled -
random 2070 bits integer - ('factors of ',
99832839829839289382939239728378871872172871827817287187281728718271872817827182
781728718271872871287182718278172179281989819829829829182918938982989289183901809890
89183982939189890839819839891829839182839281398293892839890381908090289891083908
91839028090283098120938183908192839809180923092039029309203920390293203920392093
09230238283818238128983982983982389283982983928839289382983982983982983928398219
839281981208098923819389182390898391831989839898989829839891892893829839289283
98293892898938981983921898391382198391898198319283982382839839130923090302939230
293029039029309203902839289382983828382938982938283982983291909, '(',
2069.5587894854657, ' bits integer) are:') ('Factors are: (' , 7, ', ',
14261834261405612768991319961196981696024695975402469598183104102610267545403883
25453267403883898161245468310311325998545689975689883274134140427041311985972841
55597711848455698691402834270261405597548468771184841834270054558298612841583415
55977004012897585445848311986884691401311560441719861329886274341470457702913156
15604319754831176875569140426283198469140426275548469911854854711997569132628317
11989742588687127483134131177012834169028426284271284261405698841841975691327040
56899127556991283140560271198768885484556885474183426054691405590131870043277032
899004148432758457700405612768997689768991283276897711854755987, ') (at ', 'Wed,
12 Oct 2022 08:27:50 GMT', '))')
 1324.7.5
testlogs/DiscreteHyperbolicFactorizationUpperbound_TileSearch_Optimized.log5.120
ctober2022 - Python 3.7.5 + Spark 3.3.0 - Numba JIT Parallel for disabled -
(12^151 - 1)/11 - 534 bits Cunningham's number -
82219620528659701952660120743076100427390924357073396551677033937335320430502358
02427303275633200540806689460669679221954509396712733084562446289606063026821231
7 - ('Factors are: (' , 3, ', ',
27406540176219900650886706914358700142463641452357798850559011312445106810167452
67475767758544400180268896486889893073984836465570911028187482096535354342273743
9, ') (at ', 'Wed, 12 Oct 2022 10:05:57 GMT', '))') - Reference 1324.11
 1324.7.6
testlogs/DiscreteHyperbolicFactorizationUpperbound_TileSearch_Optimized.log6.120
ctober2022 - Python 3.7.5 + Spark 3.3.0 - Numba JIT Parallel for enabled -

```

Mersenne Semiprime - 8388607 = ( $2^{23} - 1$ ) - ('Factors are: (' , 47, ' ,', 178481, ' ) (at ' , 'Wed, 12 Oct 2022 10:35:48 GMT', ' )') - Reference 1324.8

#### References:

- 1324.8 Mersenne Semiprime -  $2^{23} - 1$  - <https://oeis.org/A244453>  
1324.9 A Fast Factorisation of Semi-Primes Using Sum of Squares - [Anthony Overmars and Sitalakshmi Venkatraman\*] - <https://www.semanticscholar.org/paper/A-Fast-Factorisation-of-Semi-Primes-Using-Sum-of-Overmars-Venkatraman/c1fa2419cd981b3f858bb36fd1c9268dde0067f4> - Example large semiprime in Section 3  
1324.10. New Semi-Prime Factorization and Application in Large RSA Key Attacks - [Anthony Overmars and Sitalakshmi Venkatraman\*] - <https://www.mdpi.com/2624-800X/1/4/33>  
1324.11. <https://krum.rz.uni-mannheim.de/cabench/sieve-record.html> - " ... For  $(12^{151} - 1)/11$ , the researchers chose the polynomials  $12X^5 - 1$  and  $X - 12^{30}$ , with common root  $12^{30}$ . The sieving took eight weeks during April-June, 1993, using 30 SPARC workstations in the OSU Mathematics Department. They gathered 8.98 million relations with large prime bound 100 million. These were used to construct a sparse  $828,077 \times 833,017$  matrix with 26,886,496 nonzero entries. Using a novel Block Lanczos algorithm, the linear algebra took 3.4 hours on one CRAY C90 processor at the Academic Computing Center Amsterdam (SARA). The square root code uses another novel algorithm and took 10.5 hours per dependency, using one processor on an SGI Challenge at CWI. The factors were found on the second dependency. ..."  
1324.12 NeuronRain JIRA issue - <https://krishnairesearch.atlassian.net/browse/NEUR-2>  
-----  
-----  
-----

1325. (JIRA,THEORY and FEATURE) Computational Geometric Integer Factorization - Python 3.10.4 + Spark 3.3.0 Quadcore Benchmarks - Hardware Square root instruction optimization and Semiprime Factorization - related to 498,601,1226,1259,1303,1319,1321,1323,1324 and all sections on Integer Factorization,Computational Geometry,Set Partitions-to-Tile Cover reduction by Lagranges Four Square Theorem and ILP,Primality Testing,RSA Semiprimes,Almost-Square Bounding Boxes in Large Scale Visual Recognition,Pell's Equation,Brahmagupta's Chakravala,Approximate Factoring by Newton-Raphson Rayshooting queries,Algebraic Geometry of Computational Geometric Factorization - 13 October 2022  
-----  
-----  
-----

#### 1325.1

python-src/DiscreteHyperbolicFactorizationUpperbound\_TileSearch\_Optimized.py has been updated to get maximum number of factors from commandline. If argv[5] is set to "all"

factorization is unlimited and all factors (limited by sys.maxsize) are parallel-planar-point-located.

1325.2 tiles\_start is now set to begin from square root of the integer to be factorized instead of 1 earlier (factors are symmetric on either halves of the hyperbolic arc separated by  $(\sqrt{N}, \sqrt{N})$  point) as an optimization because almost all CPUs now support division-square\_root instructions in their instruction sets which are implemented by Digit Recurrence Algorithm of low complexity. GCC square root functions internally invoke square root assembly instructions and it has been assumed that Python math.sqrt() internally is bytecode compiled to CPU sqrt instruction. Being hardware implementation square root might only add a polylogarithmic overhead or even less.

1325.3 Another minor bug has been found and fixed in intervalmidpoint=0 clause which was not printing factors though computed correctly - JIRA issue:

<https://krishnairesearch.atlassian.net/browse/NEUR-3> .

1325.4 Two semiprimes 2505701953 and 2560391 of 32 and 22 bits respectively have been factorized and captured in logs:

#### 1325.4.1

testlogs/DiscreteHyperbolicFactorizationUpperbound\_TileSearch\_Optimized.log.130c  
tober2022 - ('factors of ', 2505701953, '(', 31.222567673873087, ' bits integer)  
are:') - ( ('', 50093, '', 50021, ') (at ', 'Thu, 13 Oct 2022 12:22:32 GMT',  
''))

#### 1325.4.2

testlogs/DiscreteHyperbolicFactorizationUpperbound\_TileSearch\_Optimized.log2.130  
ctoer2022 - ('factors of ', 2560391, '(', 21.287932711849106, ' bits integer)  
are:') - ( ('', 1873, '', 1367, ') (at ', 'Thu, 13 Oct 2022 12:29:13 GMT', ''))

#### References:

-----  
1325.5 Radix-16 Combined Division-Square Root Unit -  
<http://www.imm.dtu.dk/~alna/pubs/ARITH20.pdf>  
1325.6 AN ANALYSIS OF DIVISION ALGORITHMS AND IMPLEMENTATIONS - Stuart F.  
Oberman and Michael J. Flynn -  
<http://i.stanford.edu/pub/cstr/reports/csl/tr/95/675/CSL-TR-95-675.pdf>  
1325.7 Intel Intrinsics Guide - Square Root instruction set -  
[https://www.intel.com/content/www/us/en/docs/intrinsics-guide/index.html#!](https://www.intel.com/content/www/us/en/docs/intrinsics-guide/index.html#!=undefined&text=sqrt&techs=SSE,SSE2&expand=5365,5386,5386&ig_expand=6001,6644,6593,6638)  
=undefined&text=sqrt&techs=SSE,SSE2&expand=5365,5386,5386&ig\_expand=6001,6644,65  
93,6638 - Latency and Throughput data

-----  
1326. (JIRA,THEORY and FEATURE) GIS Urban Sprawl Analytics - R2022A - 3D Urban  
Sprawl Growth Model from BUILT-V and BUILT-S datasets - Mean,Median,Standard  
Deviation of Building Heights - Chennai Metropolitan Area Sprawl Example - 15  
October 2022 - related to  
1174,1175,1177,1179,1194,1211,1234,1290,1291,1292,1295,1296,1297,1301,1304,1312,  
1313,1320,1323 and all sections on GIS Urban Sprawl Analytics, Merit of Large  
Scale Visuals, Gridded Population Estimators (SEDAC GPW4 and GHSL convex hull  
estimators), DBSCAN and Neural Network Urban Extent Learners, Computational  
Geometry, Intrinsic Merit Rankings, R Ricker Population Estimation, Community  
detection, Social Network Analytics, Space filling by Curves, Unequal Circle and  
Polynomial packing, Computational Geometry and Polygonal packing by Voronoi  
Tessellation, Four color theorem, Economic Merit, Computational Economics - GDP  
estimation from Urban sprawl demographics, electricity consumption, Poverty  
alleviation, MARA (Multiple Agent Resource Allocation) Facegraph walk coloring  
DNFSAT algorithm, Preferential Attachment, Fixed Parameter Tractability-  
Kernelization, Automatic Delineation of Urban Sprawls, Cellular Automata-SLEUTH-  
Polya Urn-Dynamic Facegraph Urban Growth Models

#### 1326.1 This commit addresses JIRA issue

<https://krishnairesearch.atlassian.net/browse/NEUR-4> -  
python-src/image\_pattern\_mining/ImageNet/GISUrbanSprawlAnalytics.py has been  
updated to import mean-median-standard deviation functions from statistics.

#### 1326.2 function

three\_dimensional\_urban\_growth\_model(rasterdata\_2d,rasterdata\_3d) has been  
updated to compute heights for each longitude-latitude point in Chennai  
Metropolitan Area bounding box as ratio of following R2022A 3d to 2d rasters -  
BUILT-V and BUILT-S:

```
r2ddata=urban_sprawl_from_raster(79.271851,12.439259,80.351257,13.568572,"testlo
gs/RemoteSensingGIS/
GHS_BUILT_S_P2030LIN_GLOBE_R2022A_54009_100_V1_0_R8_C26.tif",dt="BUILT_S
R2022A")
```

```
r3ddata=urban_sprawl_from_raster(79.271851,12.439259,80.351257,13.568572,"testlo
gs/RemoteSensingGIS/
GHS_BUILT_V_P2030LIN_GLOBE_R2022A_54009_100_V1_0_R8_C26.tif",dt="BUILT_V
R2022A")
```

1326.3 Mean-Median-Standard Deviation of Building Heights are computed through  
statistics module functions. Heights data earlier could be plotted on 3D by

[https://matplotlib.org/2.0.2/mpl\\_toolkits/mplot3d/tutorial.html](https://matplotlib.org/2.0.2/mpl_toolkits/mplot3d/tutorial.html) to obtain a Digital Elevation Model(DEM) graphics for an urban sprawl.  
1326.4 An example delineation algorithm for urban sprawls in 3D DEM Urban Growth Model which complements (\*) Nighttime Lights based delineation (Section 1174) (\*) commuting based delineation guided by suburban transport network (Section 1323.8) and (\*) periurbanization based delineation (Sections 1320.4.1 and 1320.4.2) could be to cluster regions by building heights and include them within an administrative boundary when they reach threshold heights.  
1326.5 Following metrics have been arrived at for BUILT-V and BUILT-S R2022A datasets projected to Chennai Metropolitan Area Sprawl bounding box above (grepped from testlogs/GISUrbanSprawlAnalytics.log.15October2022):

-----  
Gini Index of Inequality  
-----

BUILT-S: `urbansprawl_gini_coefficient()`: Gini Index of the dataset = 0.9031628347857127

BUILT-V: `urbansprawl_gini_coefficient()`: Gini Index of the dataset = 0.9384512498866854  
-----

Mean-Median-Standard Deviation of Heights (BUILT-V/BUILT-S):  
-----

`three_dimensional_urban_growth_model()`: `mean(heights)` = 3.763351991142693  
`three_dimensional_urban_growth_model()`: `median(heights)` = 2.5014084507042256  
`three_dimensional_urban_growth_model()`: `stdev(heights)` = 2.6588372379556384

References:  
-----

1326.6 India Lights API - The Defense Meteorological Satellite Program (DMSP) - <http://api.nightlights.io/>  
1326.7 NASA WorldView Daily NightLights - <https://www.earthdata.nasa.gov/learn/backgrounders/nighttime-lights> and [https://worldview.earthdata.nasa.gov/?v=-218.9957317134641,-81.6598278076184,100.57007868377187,82.92025468333685&l=VIIRS\\_SNPP\\_DayNightBand\\_ENCC,Reference\\_Labels\\_15m\(hidden\),Reference\\_Features\\_15m,Coastlines\\_15m,VIIRS\\_SNPP\\_CorrectedReflectance\\_TrueColor&lg=false&t=2021-05-03-T15%3A25%3A30Z](https://worldview.earthdata.nasa.gov/?v=-218.9957317134641,-81.6598278076184,100.57007868377187,82.92025468333685&l=VIIRS_SNPP_DayNightBand_ENCC,Reference_Labels_15m(hidden),Reference_Features_15m,Coastlines_15m,VIIRS_SNPP_CorrectedReflectance_TrueColor&lg=false&t=2021-05-03-T15%3A25%3A30Z)  
1326.8 Oxfam State of Inequality in India - <https://www.oxfam.org/en/india-extreme-inequality-numbers>  
-----

-----  
1327.(JIRA,THEORY and FEATURE) GIS Weather Analytics and Climate Analytics - 17 October 2022 - Predictions of Extreme Weather Events - related to 148,313,445,446,463,1165,1171,1176,1266,1289,1316,1318 and all sections on Correlation between gravitational effects of Mined Celestial N-Body Patterns and terrestrial extreme weather events (or Gravitational effects on climate change), Drone natural obstacle avoidance, Drone autonomous online shopping delivery, Drone Electronic Voting Machine, Large Scale Visuals Recognition, Artificial Intelligence models for Climate Change, Astronomical algorithms  
-----

-----  
1327.1 This commit resolves two JIRA issues

<https://krishnairesearch.atlassian.net/browse/NEUR-5> and

<https://krishnairesearch.atlassian.net/browse/NEUR-6>

1327.2 `python-src/EphemerisSearch.py` has been updated to import `Angle` and `SkyCoord` from `astropy.coordinates`. New function

`predict_EWE(datefrom,dateto,loc,bodypair,angularsepbounds)` has been implemented to obtain dates range from user for a Longitude-Latitude location, Solar system body pair, range of angular separations between the pair and search the dates range for matching angular separations (`SkyCoord.separation()`) between the pair of celestial bodies by `Angle.is_within_bounds()` which could be potential days of extreme weather events (heavy rain or cyclonic storms in this case).

1327.3 JIRA Bug NEUR-6 raised earlier concerns erroneous overwrite of

datesofEWEs variable and the problem in vectors() invocation on Horizons() object when Longitude-Latitudes are supplied. Problem is due to the lack of support for Longitude-Latitude in vectors\_async() code at [https://astroquery.readthedocs.io/en/latest/\\_modules/astroquery/jplhorizons/core.html](https://astroquery.readthedocs.io/en/latest/_modules/astroquery/jplhorizons/core.html) which raises exception ValueError(('cannot use topographic position in state vectors query')) if location is a dictionary of Longitude-Latitude. As an alternative to dictionary, location could be one of the 2300 pre-defined earth sites in <https://ssd.jpl.nasa.gov/horizons/manual.html#center> which is a numeric id and not in Longitude-Latitude format. But there doesn't seem to be a comprehensive documentation of 2300 earth site codes except 500 which is geocenter.

1327.4 From AstroQuery JPL Horizons documentation

<https://astroquery.readthedocs.io/en/latest/jplhorizons/jplhorizons.html> only following locations are supported by Horizons.vectors() though ephemerides() supports Longitude-Latitude dictionaries for locations but there is no API support to map ephemerides() data to vectors() format:

```

Method location refplane refsistem astropy frame

```

```
.vectors() '@@' 'ecliptic' N/A 'custombarycentricecliptic'
.vectors() '@@' 'earth' N/A 'icrs'
.vectors() '@10' 'ecliptic' N/A 'heliocentriceclipticiau76'
```

1327.5 Because of earlier AstroQuery-AstroPy limitations (or could imply Longitude-Latitude is not necessary for vectors computation) Longitude-Latitude arguments are ignored (ephemerides() invocation has been commented which could be reverted if there is an API support for ephemerides() to vectors() conversion) at present and replaced by hardcoded "@@" as below:

```
obj = Horizons(id=i, location="@@", epochs=Time(str(date[0])
+ "-" + str(date[1]) + "-" + str(date[2])).jd, id_type='id').vectors(refplane="earth")
```

1327.6 predict\_EWE() is invoked to search for matching angular separations between 2 solar system body pairs "Sun-Moon" and "Venus-Mercury" respectively of separation ranges (120-180 degrees) and (0-30 and 0-60 degrees) for dates between 21/10/2022 and 1/12/2022 to match for Sun-Moon-Earth and Venus-Mercury-Earth 3-body syzygies which have been investigated in 1266,1267,1268,1316 and 1318 supra:

```
predict_EWE(datefrom=(2022,10,21,1,00,00), dateto=(2022,12,1,1,00,00), loc='@@', bo
dypair="Sun-Moon", angularsepbounds=('120d', '180d'))
```

```
predict_EWE(datefrom=(2022,10,21,1,00,00), dateto=(2022,12,1,1,00,00), loc='@@', bo
dypair="Venus-Mercury", angularsepbounds=('0d', '30d'))
```

1327.7 Following dates match earlier angular separation bound Syzygy queries which coincide with active North-East Monsoon and Bay of Bengal Cyclone seasons in peninsular India predicting heavy rainfall - this forecast differs from MaitreyaEncHoro\_RuleSearch.py Sequence Mining - Class Association Rule - based forecast of Section 313 and relies only on patterns found from planetarium search of sky for angular separations learnt from HURDAT2 datasets and does not compute N-Body gravitational accelerations for these dates. Of particular significance are the dates 25/10/2022 and 8/11/2022 which are days of Solar and Lunar Eclipse Syzygies :

```
Angular separation of Sun-Moon matches bounds for date: 2022-10-21 00:00:00.000
Angular separation of Sun-Moon matches bounds for date: 2022-10-22 00:00:00.000
Angular separation of Sun-Moon matches bounds for date: 2022-10-23 00:00:00.000
Angular separation of Sun-Moon matches bounds for date: 2022-10-24 00:00:00.000
Angular separation of Sun-Moon matches bounds for date: 2022-10-25 00:00:00.000
Angular separation of Sun-Moon matches bounds for date: 2022-10-26 00:00:00.000
Angular separation of Sun-Moon matches bounds for date: 2022-10-27 00:00:00.000
Angular separation of Sun-Moon matches bounds for date: 2022-10-28 00:00:00.000
Angular separation of Sun-Moon matches bounds for date: 2022-10-29 00:00:00.000
Angular separation of Sun-Moon matches bounds for date: 2022-10-30 00:00:00.000
Angular separation of Sun-Moon matches bounds for date: 2022-10-31 00:00:00.000
Angular separation of Sun-Moon matches bounds for date: 2022-11-01 00:00:00.000
Angular separation of Sun-Moon matches bounds for date: 2022-11-02 00:00:00.000
Angular separation of Sun-Moon matches bounds for date: 2022-11-03 00:00:00.000
```

[illegible]

Angular separation of Venus-Mercury matches bounds for date: 2022-11-21  
00:00:00.000  
Angular separation of Venus-Mercury matches bounds for date: 2022-11-22  
00:00:00.000  
Angular separation of Venus-Mercury matches bounds for date: 2022-11-23  
00:00:00.000  
Angular separation of Venus-Mercury matches bounds for date: 2022-11-24  
00:00:00.000  
Angular separation of Venus-Mercury matches bounds for date: 2022-11-25  
00:00:00.000  
Angular separation of Venus-Mercury matches bounds for date: 2022-11-26  
00:00:00.000  
Angular separation of Venus-Mercury matches bounds for date: 2022-11-27  
00:00:00.000  
Angular separation of Venus-Mercury matches bounds for date: 2022-11-28  
00:00:00.000  
Angular separation of Venus-Mercury matches bounds for date: 2022-11-29  
00:00:00.000  
Angular separation of Venus-Mercury matches bounds for date: 2022-11-30  
00:00:00.000

(  
grepped from :  
python-src/testlogs/EphemerisSearch.log.17October2022 - Python 3.7.5 + AstroPy-  
JPLHorizons - Venus-Mercury 60 degree separation bound search  
python-src/testlogs/EphemerisSearch.log2.17October2022 - Python 3.10.4 +  
AstroPy-JPLHorizons - Venus-Mercury 30 degree separati  
on bound search  
)

#### References:

-----  
1327.8 JAWF Climate Prediction Center - India GFS Precipitation Forecasts - 2  
weeks ensemble -  
[https://www.cpc.ncep.noaa.gov/products/JAWF\\_Monitoring/India/GFS\\_forecasts.shtml](https://www.cpc.ncep.noaa.gov/products/JAWF_Monitoring/India/GFS_forecasts.shtml)  
-----

-----  
1328. (JIRA,THEORY and FEATURE) GIS Urban Sprawl Analytics - R2022A - 3D Urban  
Sprawl Growth Model from BUILT-V and BUILT-S datasets - Digital Elevation Model  
from Matplotlib3D - Chennai Metropolitan Area Sprawl Example - 19 October 2022  
- related to  
1174,1175,1177,1179,1194,1211,1234,1290,1291,1292,1295,1296,1297,1301,1304,1312,  
1313,1320,1323,1326 and all sections on GIS Urban Sprawl Analytics, Merit of  
Large Scale Visuals, Gridded Population Estimators (SEDAC GPW4 and GHSL convex  
hull estimators), DBSCAN and Neural Network Urban Extent Learners, Computational  
Geometry, Intrinsic Merit Rankings, R Ricker Population Estimation, Community  
detection, Social Network Analytics, Space filling by Curves, Unequal Circle and  
Polynomial packing, Computational Geometry and Polygonal packing by Voronoi  
Tessellation, Four color theorem, Economic Merit, Computational Economics - GDP  
estimation from Urban sprawl demographics, electricity consumption, Poverty  
alleviation, MARA (Multiple Agent Resource Allocation) Facegraph walk coloring  
DNFSAT algorithm, Preferential Attachment, Fixed Parameter Tractability-  
Kernelization, Automatic Delineation of Urban Sprawls, Cellular Automata-SLEUTH-  
Polya Urn-Dynamic Facegraph Urban Growth Models  
-----

-----  
1328.1 GISUrbanSprawlAnalytics.py has been changed to plot 3D Digital Elevation  
Model within three\_dimensional\_urban\_growth\_model() by Matplotlib 3D  
plot\_surface() function invoked on (longitudes,latitudes,heights) data from  
ANBHx = BUVOLx / BUSURFx formula for BUILT-H specified by GHSL R2022A datasets  
(BUILT-V & BUILT-S) as (X,Y,Z) points (Section 1323.6).

1328.2 Following matplotlib 3D modules have been imported:  
from mpl\_toolkits.mplot3d import Axes3D  
from matplotlib import cm



from matplotlib.ticker import LinearLocator, FormatStrFormatter  
1328.3 urban\_sprawl\_from\_raster() returns tuple (urbansprawlstatistics,  
(rows,cols)) which includes the shape of bounding box. NaN values for heights  
have been replaced by zeros.  
1328.4 Parameters to  
three\_dimensional\_urban\_growth\_model(rasterdata\_2d,rasterdata\_3d,longx,latx,long  
y,laty) have been expanded to include bounding box long-lat range.  
1328.5 Shape of bounding box and (rows,cols) information are used to create  
meshgrid for X,Y axes and reshape heights Z axis array to 2D plotted by  
ax.plot\_surface(X, Y, heights, cmap=cm.coolwarm, linewidth=0, antialiased=False)  
1328.6 3D Digital Elevation Model (DEM) for Chennai Metropolitan Area Suburban  
Commuting-aligned Bounding Box -  
testlogs/GISUrbanSprawlAnalytics.ChennaiMetropolitanArea\_3D\_DEM.190october2022.jp  
eg - has been plotted from GHSL R2022A BUILT-V and BUILT-S datasets:

```
r2ddata=urban_sprawl_from_raster(79.271851,12.439259,80.351257,13.568572,"testlo
gs/RemoteSensingGIS/
GHS_BUILT_S_P2030LIN_GLOBE_R2022A_54009_100_V1_0_R8_C26.tif",dt="BUILT_S
R2022A")
```

```
r3ddata=urban_sprawl_from_raster(79.271851,12.439259,80.351257,13.568572,"testlo
gs/RemoteSensingGIS/
GHS_BUILT_V_P2030LIN_GLOBE_R2022A_54009_100_V1_0_R8_C26.tif",dt="BUILT_V
R2022A")
```

```


This
work is licensed under a <a rel="license"
href="http://creativecommons.org/licenses/by-nc-nd/4.0/">Creative Commons
Attribution-NonCommercial-NoDerivatives 4.0 International License.
```

```

#####
```

Course Authored By:

```

#####
```

K.Srinivasan

Personal website(research): <https://sites.google.com/site/kuja27/>

NeuronRain Documentation,FAQ,Licensing: [http://neuronrain-  
documentation.readthedocs.io/](http://neuronrain-documentation.readthedocs.io/)

```

#####
```

This is a non-linearly organized, code puzzles oriented, continually updated set  
of course notes on Cloud computing frameworks and BigData analysis.

```


```

7 February 2017

```

```

Apache Spark is a Cloud computing software for processing bigdata. It is based  
on concept of Resilient Distributed Datasets (RDD) which are partitions of a  
dataset executed in parallel. Spark is divided into 2 components: 1) Driver and  
2) Executor. Driver splits the dataset into RDDs and allocates each RDD to an  
executor in parallel. Parallelization can be in two ways: 1) For objects like  
lists,arrays etc., 2) For data in HDFS,cassandra, S3 etc.,

While executing in parallel, there is a necessity to share mutable state across  
executors. This is done in two ways: Broadcast variables and Accumulators (only  
increment is allowed). Spark streaming is a feature that allows realtime  
processing of streaming data by an abstraction of Discretized Streams or  
DStreams. Following code in neuronrain asfer receives generic data from any URL,  
does an ETL on it and stores in RDDs:

<https://github.com/shrinivaasanka/asfer-github-code/blob/master/java-src/>

bigdata\_analytics/spark\_streaming/SparkGenericStreaming.java

There are 2 operations performed on RDDs: 1) Transformations - create a new set or subset of RDDs 2) Actions - do some iteration on transformed RDDs. Spark Streaming allows custom streaming by implementing/overriding receive() method in Receiver interface. Receiver can be started and stopped by onStart() and onStop() methods. Receive method is overridden with customized code to access a remote URL, fetch HTML, parse it and do any ETL operation as deemed fit. From Spark 2.0.0, support for lambda functions (new feature in Java 8) instead of \*.function.\* (Function objects) for RDD transformations has been included. Previous Spark Streaming code demonstrates these features and uses Jsoup GET RESTful API for ETL/scraping of remote URL data.

20 February 2017

-----  
Spark SQL + Hive (Shark) provides synergy of bigdata processing with an SQL storage backend. Hive is implemented on top of Thrift RPC protocol which is modern version of Interface Definition Language based Web Service Architectures like CORBA, Google Protocol buffers, SOAP etc., Streamed data received is an iterable (e.g lines in SparkGenericStreaming.java implementation in [https://github.com/shrinivaasanka/asfer-github-code/blob/master/java-src/bigdata\\_analytics/spark\\_streaming/SparkGenericStreaming.java](https://github.com/shrinivaasanka/asfer-github-code/blob/master/java-src/bigdata_analytics/spark_streaming/SparkGenericStreaming.java)) which is further transformed with map/filter operations quite similar to Java Streams. Java Streams work on similar concept of creating a stream from iterable (arrays, lists etc.,) and applying map/filter transformations. Spark's saveAsTable() saves the streaming data into a hive table in Spark Metastore or Hive metastore (this requires hive-site.xml in Spark conf directory). (MAC currency in AsFer+KingCobra electronic money cloud perfect forwarding move is implemented on Protocol Buffers.)

18 January 2018

-----  
Spark cloud processing framework has support for global variables in two flavours: 1) Accumulators and 2) Broadcast variables. Both of these are mechanisms to reflect global state across Resilient Distributed Data Set nodes in Spark clusters. Accumulators have a single operation add() which incrementally adds a value on a local RDD to the global accumulator variable and is reflected across all nodes in Spark cluster. Both Accumulators and Broadcast variables are instantiated from Spark Context. Broadcast variables are plain read-only global variables which are broadcast as the name suggests to all RDDs in Spark cluster. An example code and logs for how accumulators and broadcast work has been demonstrated in code/Spark\_Broadcast\_Accumulator.py and code/testlogs/Spark\_Broadcast\_Accumulator.log.18January2018. Accumulator constructor can be optionally passed on an object of type AccumulatorParam (or its subclassed types which override add()). Presently accumulators and broadcasts are only way to provide global state across nodes in Spark cluster.

-----  
4 October 2018 - Representational State Transfer - CRUD - RESTful and WebServices in Cloud

-----  
Traditional Client-Server Architecture in Distributed Computing involves client making a socket connection to a listener server, completing a handshake and establishing a two-way message transport. Over the years, with the advent of cloud, every application on web is deemed to be a finite state automaton of 4 states - Create-Read-Update-Delete (CRUD) respective HTTP primitives being PUT, GET, POST, DELETE which create a resource in server, update it, read it and delete. Every resource is identified by a URL or WebService. Though this indirectly wraps the underlying socket communication, benefit is in statelessness of each request - every request is independent of previous request and state is remembered only in client side and server is state oblivious.

Nomenclature RESTful stems from the state getting transferred from client to server for every HTTP request and responded in JSON objects. An example of RESTful API is Facebook Graph API SDK for retrieving user profile information, connections, comments, likes etc., A REST Python Client which GETs/PUTs objects to Facebook wall has been described in code/GRAFIT\_automatic\_wallposter.py. It internally issues HTTP requests to Graph API REST endpoints. Invocation to put\_object() has been commented. This is an updated version of [https://github.com/shrinivaasanka/asfer-github-code/blob/master/python-src/Streaming\\_FacebookData.py](https://github.com/shrinivaasanka/asfer-github-code/blob/master/python-src/Streaming_FacebookData.py) specific to GRAFIT (for Grafit Open Learning facebook profile <https://www.facebook.com/shrinivaasan.ka> which imports @NeuronRain\_Comm - [https://twitter.com/neuronrain\\_comm](https://twitter.com/neuronrain_comm) - automatic commit tweets). RESTful implies every cloud distributed computation is a string from alphabets {GET, POST, PUT, DELETE} amongst the nodes in cloud URL graph.

-----  
5 December 2018 - Apache 2 Web Server, Apache HTTPD modules, Configs and Hooks, Application Servers - example  
-----

-----  
Apache webserver provides facilities to plugin user developed modules. One specific standard example is mod\_ssl which is an SSL plugin module for Apache webserver. An example Apache module implementation and related forum Q&A have been cited in the references. This implementation was a part of Sun Microsystems/Oracle iPlanet Application Server which had a 3-tier J2EE compliant middleware architecture (Clients <-> WebServer <-> ApplicationServer). Application Servers are ancestors of present day cloud implementations which are Service Oriented Architectures. HTTP requests are served by Apache Webserver and responded. Necessity for an Apache module arises when Apache webserver is used as a loadbalancer for a cluster of application servers and requests have to be routed to it. Example module snippet in the reference defines config parameters for Apache webserver - the loadbalancer XML file containing details about cluster of iPlanet Application Servers and Locale. The register\_hooks() function has callback functions for init, name translation (e.g. URL rewriting for session ids and cookies), and handle requests (e.g routing requests to another application server). These config parameters are set by invoking ap\_set\_string\_slot() functions denoted by assignment to take1 structure member (function takes 1 argument)

#### References:

- 1. Apache Modules Mailing list - Apache 1.3.27 and iPlanet Application Server - <https://marc.info/?l=apache-modules&m=105610024116012> (Copyright: Sun Microsystems/Oracle)  
2. Apache Modules Mailing list - Apache 2.0.47 and iPlanet Application Server - <https://marc.info/?l=apache-modules&m=106267009905554> (Copyright: Sun Microsystems/Oracle)  
3. Apache Config Directives - ApacheCon - <http://events17.linuxfoundation.org/sites/events/files/slides/ConfigurationDirectiveAPI.pdf>  
-----

-----  
752. (THEORY and FEATURE) 2 January 2019, 9 January 2019, 8 January 2020, 22 January 2020, 23 January 2020, 29 January 2020, 31 January 2020, 2 February 2020, 4 May 2020, 12 May 2020, 15 May 2020, 2, 3, 4, 7 July 2020, 28 October 2020, 3 November 2020, 2 December 2020, 5 December 2020, 1 January 2021, 29 January 2021, 1 February 2021, 5 March 2021, 1 May 2021, 8 June 2021 - Searching, Indexing, Computational Geometric point location queries, Factorization in Randomized NC - Binary Search Nuances, B-Trees, Sharding - related to 227, 666, 730, 762, 828, 831, 864, 870, 1123 and all sections of People Analytics, Histogram Analytics, Social Network Analysis, Majority Voting, Syllable vectorspace text analytics, Space filling, Cellular automata, Graphical Event Models and Causal Event Models (GEM and CEM) and Computational Geometric Planar

Traditional Binary Search still remains the standard for sifting huge datasets and has undergone significant refinements. Usual Binary Search is centred around midpoint computation and branching:

```
midpoint = (left + right)/2
if query > midpoint:
 search interval [midpoint, right]
else:
 search interval [left, midpoint]
```

Bug in Midpoint computation by previous averaging in some earlier versions of languages like Java caused an overflow error in 32-bit architectures which necessitated replacing it by >>> operator (unsigned right shift):

```
midpoint = (right-left) >>> 1;
```

B-Trees are generalized Binary Search Trees in which each internal and root nodes contain more than one element and every element of a node acts as a separator for values of its subtrees as in example:

```
 2,10
 |
1 ---- 3,9 ---- 11,12
 |
 4,5
```

B+-Trees extend B-Trees by additional linked-list of leaf nodes.

Indexing Bigdata e.g web pages involves storing them as huge set of key-value pairs of the form:

```
word --- (document1, location1), (document2, location2) ...
```

which is termed as posting in inverted indices. Size of an Index in search engine could be unimaginably large requiring partitions into set of rows located across geographically distant servers on cloud. This is horizontal partition based on rows as against vertical partitions of columns in DBMS Normalizations. Each partition is named a Shard.

Fundamental question is: can items in a list be found efficiently by a search graph instead of binary search trees. Lower bound for search is  $\Omega(\log N)$ . Binary Search Trees can be alternatively defined as recursive bipartite graph which is an indefinite recursive fractal bipartition of sets - Example:- Set of integers [2,4,5,1,3,7,9,10,8,6] are represented recursively as bipartite graph by assuming an initial midpoint pivot separator of each subset similar to quicksort which partitions a set into two halves of elements > pivot and elements < pivot in each depth of recursion:

```
pivot 6
[2,3,5,1,4] ----- [7,9,10,8,6]
pivot 3 pivot 8
[[4,5,3]--[2,1]] ---- [[6,8,7]--[10,9]]
pivot 4 pivot 7
[[[4,3]-[5]]--[2,1]] ---- [[[7,8]-[6]]---[[10]-[9]]]
pivot 4 pivot 2 pivot 7
[[[[4]-[3]]-[5]]--[2]-[1]]] ---- [[[[7]-[8]]-[6]]---[[10]-[9]]]
```

Edges are denoted by ----- which connect each parenthesized subset vertex for a subtree obtained by traversing the binary search tree. Last line encodes a recursive bipartite search graph which is the top view of the binary search tree and is a multidimensional tensor - a kind of binary space partition. Searching this tensor locates a point in the nested parentheses by comparing against pivots. Advantage of recursive bipartite graph representation of binary search tree is each subtree can be retrieved by array indexing.

Planar Point Location in Computational Geometry is the most fundamental generalization of conventional one dimensional list search to arbitrary dimensions. Computational Geometric Factorization algorithm implemented in

NeuronRain AstroInfer is a two dimensional parallel geometric search which locates , in polylogarithmic time, factor points with in rectangular faces of planar straight line graph (PSLG) formed by rasterizing (pixel polygon approximation of an algebraic curve on a grid) hyperbolic arc bow on Parallel RAMS - this search involves two phases:

(\*) Locating a rectangle in PSLG polygon subdivision containing factor point in polylogarithmic time by some Parallel RAM Planar Point Location algorithm - PSLG has  $\sim(3N+1)$  vertices and  $\sim 4N$  edges and each polygonal face is a pixel array rectangle of dimensions  $1 * N/[x(x-1)]$

(\*) Binary search the rectangle containing factor point - every rectangle in PSLG of rasterized hyperbolic arc is an arithmetic progression of pixels (ordinate products)

Hardness of Factorization has bearing on susceptibility of cryptographically secure Majority Voting to manipulation and its credibility.

-----  
-  
An example hyperbolic arc rasterization - schematic - pixel array polygonal faces  
(arithmetic progression rectangles marked f denote faces containing factor points):  
-----  
-

```
#####
###f####
#####
#####
#####f###
```

Such a Planar Point Location can be extended to arbitrary dimensions  $> 2$  and any other algebraic curve - E.g. algebraic curve  $uvwxyz=N$  is a 6-dimensional hyperbola and requires rasterization in 6-dimensional hyperplane to locate factor point  $(u,v,w,x,y,z)$ . Multidimensional Point Location factorization is the problem of Factorisatio Numerorum (multiplicative partition).

-----  
-----  
Randomized NC Geometric Search of a 2-dimensional grid and Linear Program Formulation  
-----  
-----

A Grid filling algorithm which maximizes linear program of sum of binary values of ordinate points in Randomized NC has been described in <https://sites.google.com/site/kuja27/Analysis%20of%20a%20Randomized%20Space%20Filling%20Algorithm%20and%20its%20Linear%20Program%20Formulation.pdf> and its Cellular Automaton, Apollonian Gasket-Circle Packing and Factorization-based Set-Partition-to-Lagrangian-Tile-Cover versions have been drafted in NeuronRain AstroInfer Design - <https://github.com/shrinivaasanka/asfer-github-code/blob/master/asfer-docs/AstroInferDesign.txt> . Grid Filling as constraint satisfaction problem which maximizes the number of points hit on a 2-dimensional space is a planar point location geometric search if BigData is visualized as values of ordinates within a 2-dimensional rectangle and a value for a query point has to be found by a parallel pseudorandom generator which simultaneously churns out multiple ordinate points  $(x_i, y_i)$  or circles of small radii centred around random ordinate points within the rectangle (Monte Carlo Simulation). This Randomized NC pseudorandom generator plane sweep covers most of the 2-dimensional rectangle with high probability. Advantage of RNC Grid filling: if query points constitute a meagre percentage of total 2-dimensional rectangular space e.g polynomial curve points, Randomized NC grid filling is able to find query point with high probability in polylogdepth NC without sorting and binary search. It is noteworthy that planar point location for Integer Factorization in exact NC can

also be formulated as less stringent Randomized NC Grid filling which locates a factor on hyperbolic curve with high probability. Chaos theoretic RNC parallel pseudorandom generator defined in <https://sites.google.com/site/kuja27/ChaoticPRG.pdf> could output pseudorandom ordinate bits in parallel.

Probability of hitting a query point within time  $t$  is a Bernoulli trial:  
 Probability of hitting a query point within a rectangle = number of query points or length of query polynomial curve embedded in 2-dimensional plane ( $p$ ) / Area of rectangle of sides  $a$  and  $b$  ( $ab$ ) =  $p/ab$

If in time  $t$  there are  $m$  trials, probability of hitting only query points by pseudorandom sampling =  $(p/ab)^m$ ,  $m$  trials are parallelized by Parallel Chaotic Pseudorandom Bits Generator which generates  $m$  2-dimensional ordinate points simultaneously in Randomized NC.

Previous linear program for maximizing sum of (values are 0 or 1, pseudorandomly flipped)  $q$  ordinates  $x_1 + x_2 + x_3 + \dots + x_q$  is exactly the sum of binary random variables  $X_i$ :  $X_1 + X_2 + \dots + X_q$ . Berry-Esseen Central Limit Theorem - [https://en.wikipedia.org/wiki/Berry-Esseen\\_theorem](https://en.wikipedia.org/wiki/Berry%E2%80%93Esseen_theorem) - implies normalized sum (mean) of random variables tends to a Normal distribution bell curve. Excluding tails of Normal distribution area of bell curve integral( $f(x) \cdot dx$ ) from -left\_tail to +right\_tail is the approximate expected sum of ordinates randomly set to 0 or 1:  $x_1 + x_2 + x_3 + \dots + x_q$

Probability of hitting a query point after  $m$ -th trial (success after  $m-1$  trials):  

$$(1 - [p/ab])^{(m-1)} [p/ab]$$

In the context of factorization, geometric search reduces to finding factor points on a hyperbolic arc bow embedded in 2-dimensional rectangular space. Though less accurate compared to Exact NC-PRAM-BSP computational geometric planar point location, success amplification of RNC pseudorandom factor point location can be achieved by narrowing down the domain of pseudorandom search to a delta-rectangular strip vicinity in lower halfspace created by leading diagonal of the rectangle:

Length of the leading diagonal =  $\sqrt{a^2 + b^2}$

Area of delta-vicinity rectangular strip beneath the leading diagonal which contains the hyperbolic arc =  $\delta \cdot \sqrt{a^2 + b^2}$

Side of the rectangular strip -  $\delta$  - is the distance between tangent of hyperbolic arc at  $(\sqrt{N}, \sqrt{N})$  and line connecting  $(1, N)$  and  $(N, 1)$  which is a very small fraction of area of rectangle  $a \cdot b$ .

Probability of hitting a query point within the rectangular strip = number of query points or length of query polynomial curve embedded in 2-dimensional plane / Area of rectangular strip =  $p / [\delta \cdot \sqrt{a^2 + b^2}] \gg p/[ab]$

Probability of hitting a query point after  $m$ -th trial (success after  $m-1$  trials):  

$$(1 - [p/(\delta \cdot \sqrt{a^2 + b^2})])^{(m-1)} [p/(\delta \cdot \sqrt{a^2 + b^2})]$$
 which amplifies success probability of finding a factor point.

For finding prime factors, number of query points  $p = k \log \log N$  (Hardy-Ramanujan Theorem) and success probability of finding a factor point is substituted for  $p$ :  

$$(1 - [k \log \log N / (\delta \cdot \sqrt{a^2 + b^2})])^{(m-1)} [k \log \log N / (\delta \cdot \sqrt{a^2 + b^2})]$$

For a square embedding of hyperbolic arc  $a=b$  and success probability amplifies to ( $\delta$  is configurable):  

$$(1 - [k \log \log N / (\delta \cdot N \cdot \sqrt{2})])^{(m-1)} [k \log \log N / (\delta \cdot N \cdot \sqrt{2})]$$

Neglecting delta vicinity, obvious randomization is to pseudorandomly choose an x-axis ordinate  $x$  between 1 and  $N$  and compute  $N/x$  which is a random ordered pair  $(x, N/x)$ . For Randomized NC, x-axis is divided to  $N/(\log N)^k$  intervals of width  $(\log N)^k$  each. Each interval is assigned to a PRAM. Thus  $N/(\log N)^k$  pseudorandom ordinate ordered pairs are simultaneously generated by a Chaotic Parallel PRG on  $N/(\log N)^k$  PRAMS which is looped for  $(\log N)^k$  iterations making it an RNC factorization.

NeuronRain AstroInfer implements a sequential Chaotic PRG based on 1-dimensional binary Cellular Automata which grow chaotically by growth rule fraction  $\lambda$ , Undecidable Mandelbrot sets, Logistic and Lehmer-Palmore chaotic PRGs. Spread of memes in Social Networks, pandemics, cybercrimes et al all have common Chaos, Game theory and 2-Dimensional Cellular Automata underpinnings (FTrace analyzer in USBmd is a game theoretic botnet defense model and a design of mechanism to counteract - antigame - as well) - For example Verhulst-Pearl-Reed Logistic Law and its Biological variant ( $\lambda x(1-x)$  and  $N_0 \exp(\lambda(1-Nt))$ ) analysis of CoronaVirus2019 pandemic reveals Bifurcation parameter  $\lambda$  hovering approximately at 4.829487535509905... > 3.57 when chaos sets for a very small initial condition which implies emergence of order in Chaotic spread explained by Period Doubling ratio limit of Bifurcation parameter  $[\lambda(n-1) - \lambda(n-2)] / [\lambda(n) - \lambda(n-1)]$  - Feigenbaum universality constant 1 = 4.669201609... ([https://en.wikipedia.org/wiki/Feigenbaum\\_constants](https://en.wikipedia.org/wiki/Feigenbaum_constants)).

By pandemic cellular automaton model, spread of memes in Social networks can be formulated as RNC space filling problem - social network vertices spreading memes are parallelly chosen random points (people) on a rectangular space effecting a 2-dimensional cellular automaton of 8-neighbours (influenced by meme) per vertex. There are linear stretch PRGs (<https://dl.acm.org/doi/10.1007/s00037-007-0237-6> - [Applebaum-Ishai-Kushilevitz]) subject to assumptions in NC0 from which ordinate points can be computed in NC by splitting bit sequence ( $k \log N$  bit pseudorandom string in NC is split into  $k$   $(x, y)$  ordinates of length  $(\log N/2, \log N/2)$  each). As memes automata evenly cover the surface there is an overlap of neighbours adjoining all or some random points. By increment growth rule, overlapped neighbour vertices are incremented implying a high value vertex (point on grid) has high value neighbours and vice versa simulating any parallel random process (this is in discrete contrast to the continuous plane sweep by circles of small radii mentioned earlier). Thus a cellular automaton leads to a random cellular automaton planar graph (CAGraph):

- (\*) Vertices are randomly chosen and labelled by instantaneous values of points on cellular automaton grid.
- (\*) New edges are created when a point and its neighbours have non-zero value after some generations of increment growth rule
- (\*) Decrement growth rule would conversely obviate edges amongst zero points and neighbours thus simulating Susceptible-Infected-Recovered Erdos-Renyi SIR random graph model.
- (\*) Between every non-zero valued point vertex and its non-zero neighbours (maximum degree = 8) on grid there is an edge
- (\*) Clustering traits of previous CAGraph determine diffusion of a concept in community - strongly connected components of high value vertices are the most influenced giants.

#### References:

- 
- 1. The Art of Computer Programming - Volume 3 - [Donald Knuth] - Sorting and Searching - 6.2.2
- 2. Beautiful Code - Finding Things - [Tim Bray - Sun Microsystems]
- 3. Google AI Blog - [Joshua Bloch] - <https://ai.googleblog.com/2006/06/extra-extra-read-all-about-it-nearly.html>
- 4. Topological Sorting - Fast Parallel Algorithms - [SA Cook] - <https://www.sciencedirect.com/science/article/pii/S0019995885800413> - If set of integers are randomly assigned as labels of a random graph, topological sorting

of vertices by some ordering can be done efficiently in  $NC^2$  and a following binary search can find the element in additional logarithmic time. But the topologically sorted vertex list may not be sorted by total ordering always. Dekel-Nassimi-Sahni algorithm works by Repeated Matrix Multiplication logarithmically many times and sorting by longest paths.

5. Planar Separator Theorem for Graphs - [Richard J. Lipton and Robert Endre Tarjan] - <https://epubs.siam.org/doi/abs/10.1137/0209046> - PSLG from rasterized hyperbolic arc  $xy=N$  can be partitioned to almost equal subgraphs by removing  $O(\sqrt{3N+1})$  vertices - quite useful in parallelizing and fair load balancing the rasterized polygon faces amongst PRAMs for point location queries

-----

1144. (THEORY and FEATURE) Computational Geometric point location queries, Factorization in Randomized NC, SETH, String complexity and distance measures, Causal and Graphical Event Models, Space filling and Cellular automata - related to 752 and all sections of People Analytics, Histogram Analytics, Social Network Analysis, Majority Voting, Syllable vectorspace text analytics, Graphical Event Models and Causal Event Models (GEM and CEM) and Computational Geometric Planar Point Location Factorization in NeuronRain Theory Drafts - 8 June 2021, 21 August 2021

-----

Causal Event Models and Graphical Event Models (CEM and GEM) could be useful for Novel SARS CoronaVirus 2 2019 timeseries analysis. NeuronRain COVID19 analyzer is Python and R based. NeuronRain implements an EventNet GEM based on Recursive Lambda Function Growth Textgraph algorithm. CEM and GEM Integrated Crisis Early Warning System for COVID19 could hypothetically mine news and research articles on COVID19 by Recursive Lambda Function Growth EventNet GEM and grow textgraph from articles which unravels hidden cause-effects of actors and events (on how the keywords in the article are connected) - a random walk on the textgraph implies causality. NeuronRain Cellular Automaton Space Filling ER-SIR graph (CAGraph) has average degree (which depends also on population density) of multiples of 8:

Per day Spread =  $8 * w_1 * I(nfected) - 1 * w_2 * R(ecovered) - 1 * w_3 * S(usceptible) + 1 * w_4 * recovery\_time \dots + constant$

COVID19 ER-SIR graph empirical data show R-number of 406 for 30 days (average degree > 400 - <https://www.hindustantimes.com/india-news/1-covid-patient-can-infect-406-if-physical-distancing-measures-are-not-followed-101619441843605.html>) which makes it a potential expander graph. Random walk on COVID19 CAGraph (ER-SIR random graph) simulates transmission. Infection CAGraph is incidentally a Dynamic Graphical Event Model (GEM) because actors (S, I and R) and causations (infections) are dynamically created and removed - a timeseries of ordered pairs (actor\_infected, time) if viewed as one dimensional stream of data wherein some ordered pair in stream is caused (infected) by some ordered pair in the past. Pandemic SIR ODE model has been invoked to explain diffusion of gossips and memes in social networks. Stanford Prison Experiment (Groups resign to their imposed roles), Stockholm Syndrome (Captive likes captor), Bandwagon effect (Herding - People like an entity because peers like it) and Stanley Milgram Experiment (Power of authority) are oft-cited psychological precedents for explaining how authority, superior or peer opinions can influence decision in social communities (majority voting tends to get correlated swayed by peers) which in a sense is akin to preferential attachment.

Chaotic universality and Ramsey theoretic emergence of monochromatic arithmetic progressions in pseudorandomly colored sequences independently certify "Orderly Disorder" paradox. Recent Chaos Machine PRG by [Maciej A. Czyzewski] has a minimal example implementation of a Push-Hybrid-Pull Chaos Machine PRG computed by non-linear Chaos maps (Butterfly effect, Logistic map, Gingerbreadman map - Chaos Machine source code - <https://eprint.iacr.org/2016/468.pdf>):

Number of prime factors in  $[1, N]$  interval =  $a \log \log N$  for constant  $a$   
 Number of prime factors in unit interval =  $a \log \log N / N$



Number of prime factors in each of  $N/(\log N)^k$  intervals of width  $(\log N)^k = \lceil \log \log N / N \rceil \lceil (\log N)^k \rceil$

Probability of chaotic pseudorandom choice of a prime factor within each  $(\log N)^k$  width interval =  $\lceil \log \log N / N \rceil \lceil (\log N)^k \rceil / (\log N)^k = \log \log N / N =$   
Probability of parallelly locating a prime factor per interval in each Bernoulli trial.

Success amplification - probability of locating a prime factor in each of the  $(\log N)^k$  Bernoulli trial iterations (Randomized NC) in parallel =  $(\log \log N / N)^{\lceil (\log N)^k \rceil}$  which is exponentially small. Suitable choice of constant  $a$  and depth  $k$  of RNC circuit (number of trials) bounds the error and thus in BPNC.

Geometric search can be generic to any dataset beyond numeric including strings and texts. Words in text documents can be embedded in an  $m$ -dimensional vector space  $A^m$  for alphabet  $A$  (or language and script independent syllable space  $A^m$  if texts are syllable hyphenated) and length of longest word  $m$  which is a word embedding kernel for texts. E.g strings "word1" and "word2" in text are embedded as vectors  $[w, o, r, d, 1, \dots]$  and  $[w, o, r, d, 2, \dots]$  of  $m$  dimensions:

Size of the alphabet  $A$  (or syllables) =  $|A|$

Length of the longest word in text (or longest syllable hyphenation) =  $m$

Previous kind of alphabet-syllable word embedding of text in a space of  $A^m$  clusters similar words by usual numeric euclidean distance measures as opposed to levenshtein edit distance. Traditional Latent Semantic Indexing Singular Value Decomposes a term-document matrix and computes low rank approximation for document similarity. Similarly LSI and SVD could be computed for previous word embedding of text which is an  $N \times m$  matrix of word\_id-alphabets for a text of  $N$  words of maximum length  $m$ .

NeuronRain AstroInfer has a polynomial encoding implementation of texts which curve fits a text to a polynomial in  $R^2$  [points on polynomial are ordered pairs (alphabet\_location, alphabet\_unicode)] and PRP error correcting polynomial implementations. Multiple encoded polynomials of texts can be embedded on a 2-D plane and planar point location could be underneath rank() and select() queries on strings. Similarly, People analytics involve intrinsic merit vectors of people e.g [academic credentials, work experience, ...] for people clustering.

Finding closest pair of points in a set of points on a vectorspace has quite a few practical applications in sea and air traffic control and vehicle collision avoidance. Replacing the vehicle points by textual strings on a vectorspace (mentioned earlier) is helpful in finding closest pair of strings within a set of strings. Subquadratic closest pair of points detection is a geometric search problem and distance similarities amongst string datapoints could be ranked (by iteratively removing every closest point to a pivot point and recursively recomputing closest pair algorithm). Subquadratic string distance algorithms are important from complexity theoretic standpoint - Edit distance is a standard measure for string similarity (number of additions and deletions of alphabets necessary to morph one string to another) and subquadratic algorithm for edit distance might nullify SETH. If edit distance is expressible in terms of computational geometric algorithm for closest pair of string points, edit distance could be computed in subquadratic time.

Prerequisite for finding Closest pair of string vehicle datapoints by computational geometric divide and conquer earlier is: Number of strings ( $N$ ) must equal Length of each string( $n$ ) (to attain  $O(n \log n)$  edit distance subquadratic bound).

Example:

-----

string1 - abcde - embedded as point [a,b,c,d,e]

```

string2 - fghij - embedded as point [f,g,h,i,j]
string3 - klmno - embedded as point [k,l,m,n,o]
string4 - pqrst - embedded as point [p,q,r,s,t]
string5 - uvwxy - embedded as point [u,v,w,x,y]

```

Each alphabet is encoded as scalar from 1 to 26 and string vectors are embedded on  $26^n$  vectorspace (similarly for ascii or unicode alphanumeric strings, vectorspace is  $256^n$  or  $512^n$ ):

```

string1 - [a,b,c,d,e] - [1,2,3,4,5]
string2 - [f,g,h,i,j] - [6,7,8,9,10]
string3 - [k,l,m,n,o] - [11,12,13,14,15]

```

Edit distance between string1 and string2 = 5. Euclidean distance between string1 and string2 =  $\sqrt{5^2+5^2+5^2+5^2+5^2} = 5*\sqrt{5}$ . In general,  $\text{euclidean\_distance} \geq \text{function\_of}(\text{edit\_distance})$

Earth mover distance and Word mover distance are current state-of-the-art similarity measures for BigData sets. Recently Earth Mover Distance has been approximated in linear time (Relaxed Word Mover Distance - [Kusner] - <http://proceedings.mlr.press/v37/kusnerb15.pdf>) though exact computation is quadratic or cubic depending on algorithm. If Edit distance is expressible in terms of Earth mover distance, edit distance can be approximated in linear time which is subquadratic (closer to proving SETH is false) and if exact edit distance could be derived from this approximation in subquadratic time SETH is false. Following is an example reduction from Earth mover distance to EDIT distance by tokenizing each string to 1-alphabet arrays or buckets creating a 2D array or histogram per string:

```

abcde - [[a],[b],[c],[d],[e]]
fghijk - [[f],[g],[h],[i],[j],[k]]

```

Earth mover distance or Relaxed Word Mover distance between 2 string histograms earlier is exactly equal to edit distance (work necessary in adding, updating or deleting 1-alphabet buckets for transforming one string to another). NeuronRain AsFer implements Earth Mover Distance similarity measure between two 2D syllabified string tensors.

Edit distance between 2 strings a and b is defined as recurrence solved by dynamic programming in quadratic time by Wagner-Fischer memoization algorithm:  
 $\text{minimum}(d(i-1,j-1), d(i-1,j) + \text{delete}(a_i), d(i,j-1) + \text{insert}(b_j), d(i-1,j-1) + \text{substitute}(a_i, b_j))$

Traditional edit distance dynamic programming recurrence memoization table could be split into quadrants - one of constant size (bottom left) and the other 3 quadrants of variable size. Constant size quadrant of the table could be computed by Earth Mover Distance reduction (LC-RWMD or LC-ACT) in linear time exactly by suitably choosing the number of iterations for 100% accuracy. Rest of the 3 quadrants could be computed by conventional quadratic time edit distance algorithms. Cumulatively total time to compute edit distance is subquadratic (exponent  $k$  in  $O(n^k)$  is  $2-\epsilon < 2$ ) because a constant fraction of tableau is computed in linear time. For example exponent could be 1.9999999.... which adheres to definition of subquadratic though superlinear thus proving SETH is 100% false.

Linear Complexity Approximate Constraints Transfer (LC-ACT) is the generalization of all WMD measures and its accuracy can be controlled by number of iterations( $k$ ). Linear Complexity of LC-ACT is achieved by setting  $k$  to be a constant. LC-ACT has maximum accuracy of 97.83% for 15 iterations for MNIST dataset (<http://yann.lecun.com/exdb/mnist/>). Increasing the constant for number of iterations would asymptotically boost accuracy close to 100%. 99% accuracy of LC-RWMD or LC-ACT for increased iterations implies edit distance is approximable by previous Edit-Distance to EMD reduction in linear time and SETH is false with 99% probability (or) there is an error of +1% or -1%. Deriving exact edit distance from approximate LC-ACT distance in linear time would prove SETH is

100% false. Edit distance from previous dynamic programming recurrence is an integer if weights for delete, insert and substitute primitives are integers. E.g For exact edit distance of 200 between 2 strings, 99% accurate LC-ACT-k computes an approximate distance of 198 or 202 in linear time. Each of the integral values in +1% or -1% error range - 198,199,200,201,202 - have to be sifted for exact edit distance. This requires a verification algorithm in linear time which accepts a numeric argument in the error range and 2 strings and prints if it is exact edit distance between 2 strings. Pseudorandomly choosing one of the integers in error range and repeating the trials might amplify success. Each recursive step in dynamic programming recurrence earlier for edit distance could be computed by LC-ACT-k at 99% accuracy. If definition of subquadratic time allows fractional exponent in runtime  $O(n^k)$  for  $1 \leq k < 2$ , then SETH is still false though ACT is super-linear but still subquadratic and ACT iterations could be increased accordingly for close to 100% accuracy.

Edit distance dynamic programming recurrence could be summarized as:

Edit distance =  $n(s) + n(i) + n(d)$   
 $n(s)$  = number of substitutions  
 $n(i)$  = number of insertions  
 $n(d)$  = number of deletions

Each of the approximate edit distances in LC-ACT error range could be equated to previous summation:

Approximate LC-ACT Edit Distance =  $n(s) + n(i) + n(d)$

For 2 strings of equal lengths  $n(i)$  and  $n(d)$  are zero  $\Rightarrow n(s)$  = approximate edit distance in LC-ACT error range (-1% to +1% error band for 99% accuracy)

Machine Learning solution for deriving exact edit distance from LC-ACT approximate edit distance:

-----  
 Create a training dataset of strings and compute exact edit distances and LC-ACT approximate edit distances for every pair of strings and find the average deviation between exact and approximate edit distances. This learnt deviation could be applied as heuristic correction for exact edit distance to LC-ACT approximate edit distances between 2 arbitrary strings.

References:

- 
1. The Art of Computer Programming - Volume 3 - [Donald Knuth] - Sorting and Searching - 6.2.2
  2. Beautiful Code - Finding Things - [Tim Bray - Sun Microsystems]
  3. Google AI Blog - [Joshua Bloch] - <https://ai.googleblog.com/2006/06/extra-extra-read-all-about-it-nearly.html>
  4. Topological Sorting - Fast Parallel Algorithms - [SA Cook] - <https://www.sciencedirect.com/science/article/pii/S0019995885800413> - If set of integers are randomly assigned as labels of a random graph, topological sorting of vertices by some ordering can be done efficiently in  $NC^2$  and a following binary search can find the element in additional logarithmic time. But the topologically sorted vertex list may not be sorted by total ordering always. Dekel-Nassimi-Sahni algorithm works by Repeated Matrix Multiplication logarithmically many times and sorting by longest paths.
  5. Planar Separator Theorem for Graphs - [Richard J. Lipton and Robert Endre Tarjan] - <https://epubs.siam.org/doi/abs/10.1137/0209046> - PSLG from rasterized hyperbolic arc  $xy=N$  can be partitioned to almost equal subgraphs by removing  $O(\sqrt{3N+1})$  vertices - quite useful in parallelizing and fair load balancing the rasterized polygon faces amongst PRAMs for point location queries
  6. Planar Point Location in sublogarithmic time - [(Late) Mihai Patrascu] and [Timothy Chan] - <https://ieeexplore.ieee.org/document/4031368>
  7. Algorithms - [Cormen-Leiserson-Rivest-Stein] - Page 845 - Number theoretic algorithms - Integer Factorization - 33.9 - Pollard's Rho Heuristic - "...It is infeasible with today's supercomputers and the best algorithms to date to factor

an arbitrary 200-decimal-digit number..."

8. On Implementing an  $O(\log n)$  Planar Point Location Algorithm - [Yifei Zhang, Wei Yu, Decheng Dai] -

<https://dsa.cs.tsinghua.edu.cn/~deng/cg/project/2006f/2006f-b.pdf>

9. Clarkson-Shor Random Sampling, Partitioning Theorem -

<http://courses.cs.tau.ac.il/0368-3249-01/michasodaslid.pdf> - "...Q a set of  $n$

points in the plane  $R$  a random sample of  $r$  points of  $Q$ . Then, with high probability, any triangle that does not contain a point of  $R$  contains at most  $cn/r \cdot \log r$  points of  $Q$  ( $c$  an absolute constant)... For any  $r < n$ ,  $P$  can be partitioned into  $O(r)$  subsets  $P_1, \dots, P_t$ , each of  $\leq n/r$  points, so that any hyperplane  $h$  separates the points of only  $O(r^{1-1/d})$  subsets..." - Query could be a hyperplane or triangle and not necessarily a point. Random sampling is quite necessary in pre-poll and post-poll forecast analytics - if voters are points on a 2-d plane, Clarkson-Shor estimate upperbounds the extent of voters excluded by a random sampling triangle. For plural multipartisan voting, Partitioning theorem has a direct bearing - Set of Voters  $P$  is partitioned to  $r$  subsets of candidates voted for and query hyperplane (forecast sample) separates only a fraction of subsets.

10. SIR ODE model of How Gossips and Rumours spread in Social network -

<https://scholarship.claremont.edu/cgi/viewcontent.cgi?article=1036&context=codee>

11. Random Walks and Diffusion in Networks - Brownian Motion -

<https://www.sciencedirect.com/science/article/pii/S0370157317302946>

12. Finding Closest Pair of Points - Subquadratic  $O(N \log N)$  divide and conquer

algorithm better than naive  $O(N^2)$  brute force for obstacle avoidance - Section

35.4 - Chapter 35: Computational Geometry - Algorithms - [Cormen-Leiserson-Rivest-Stein] - Page 908 - "... System for controlling air or sea traffic might need to know which are the two closest vehicles in order to detect potential collisions ..."

13. Linear Complexity Relaxed Word Mover Distance - LC-RWMD - [Kubilay Atasu-

Thomas Mittelholzer] - IBM Research, Proceedings of the 36th International Conference on Machine Learning, Long Beach, California, PMLR 97, 2019. -

<http://proceedings.mlr.press/v97/atasu19a/atasu19a.pdf> - Figure 2 on computing distance between 2 histograms as transportation cost minimization problem -

Algorithm 3 for ACT - Section 5 - Table 2 - LC-RWMD has average time complexity  $O(vh + nh)$  and average space complexity  $O(nh + vm + vh)$  for  $n$ =Number of database histograms,  $v$ =Size of the vocabulary,  $m$ =Dimensionality of the vectors,  $h$ =Average histogram size - Table 5 on comparison of precisions of various distance measures and maximum precision of approximation is  $> 97\%$  implying EMD-to-EditDistance reduction could be approximated in linear time with  $> 97\%$  accuracy (or SETH is false with  $> 97\%$  probability).

14. Implications of ETH being false -

[https://en.wikipedia.org/wiki/Exponential\\_time\\_hypothesis](https://en.wikipedia.org/wiki/Exponential_time_hypothesis) - "... However, if the exponential time hypothesis fails, it would have no implication for the P versus NP problem. There exist NP-complete problems for which the best known running times have the form  $O(2^{n^c})$  for  $c < 1$ , and if the best possible running time for 3-SAT were of this form, then P would be unequal to NP (because 3-SAT is NP-complete and this time bound is not polynomial) but the exponential time hypothesis would be false...."

15. CGAL 5.2 Planar Point Location Implementation Strategies and Illustrations - C++ - Section 3 and Figure 34.7 -

[https://doc.cgal.org/latest/Arrangement\\_on\\_surface\\_2/index.html](https://doc.cgal.org/latest/Arrangement_on_surface_2/index.html) - CGAL

parallelizes by calls to Intel TBB multicore library - CGAL dependencies -

<https://doc.cgal.org/latest/Manual/thirdparty.html>

16. Minimum Edit Distance Dynamic Programming Table -

<https://web.stanford.edu/class/cs124/lec/med.pdf>

17. Stanford Prison Experiment - [Zimbardo] -

[https://en.wikipedia.org/wiki/Stanford\\_prison\\_experiment](https://en.wikipedia.org/wiki/Stanford_prison_experiment)

-----  
758. (THEORY and FEATURE) 21 January 2019 - FP Growth Algorithm for mining frequent patterns and mining timeout dictionaries example - this section is an extended draft on respective topics in NeuronRain AstroInfer design -

<https://github.com/shrinivaasanka/asfer-github-code/blob/master/asfer-docs/>

AstroInferDesign.txt

Timeout design pattern implemented as a separate chaining/dictionary of timeouts-to-processes has been described in `../AdvancedComputerScienceAndMachineLearning/AdvancedComputerScienceAndMachineLearning.txt`. Discussion there is restricted to a process id present in only one bucket per timeout value. But there are possibilities when same process\_id has to be multilocationed in many timeout buckets e.g multiple threads spawned by a process can have different timer values for varied functionalities and all those threads per process have to be timeouted.

Spark MLlib implements parallel version of FP-Growth algorithm which mines frequent itemsets in multiple baskets with no candidate generation (downward closure) by growing suffix trees. Survival Index Timeout Map is also a set of baskets (buckets) from which frequently occurring process subsets can be mined by Spark FPGrowth. Example Spark code for this has been committed to `code/Spark_FPGrowth_SurvivalIndexTimeout.py` and logs in `code/testlogs/Spark_FPGrowth_SurvivalIndexTimeout.log.21January2019` which demonstrate minimum support for frequent occurrences and minimum confidence for association rules. These frequently occurring process subsets point to some lurking relationship among the colocated processes in some way and thus a measure of system load and behaviour.

Multilocation of process id(s) in multiple time out buckets creates hyperedges amongst the timer bucket vertices and thereby a hypergraph.

References:

1. Spark MLlib Documentation - <https://spark.apache.org/docs/2.3.0/ml-frequent-pattern-mining.html>

19 March 2019 - String Search in Large Files

BigData or Large Text Files on clouds often require a functionality to quickly search for a string of patterns or text. There are standard string matching algorithms like Knuth-Morris-Pratt, Boyer-Moore etc., which are standard algorithms implemented in text editors for "find". For large filesystems, wavelet trees are fast alternatives which support `rank(c,p)` [number of occurrences of character c before position p], `select(c,q)` [q-th occurrence of character c], `access(k)` [access k-th position] operations in  $O(1)$  time for binary vectors. For substring pattern p of size n, repetitive n invocations of `select(p[i],q)` returns all substrings of pattern p in the large text file - Example Pseudocode below for first match:

```
for k in xrange(n):
 pos=wavelettree.select(p[k],1)
 if prevpos + 1 != pos
 return matchfound==false
 prevpos=pos
return matchfound==true
```

26 March 2019 - Example MapReduce in Spark 2.4 Cloud - Bitonic Sequences of Integers

Spark framework parallelizes work by partitioning a bigdata set into Resilient Distributed Datasets which are `map()`-ped to Spark cloud nodes by Spark Executor Driver and local computations in cloud node are unified by `reduce()`. Spark 2.4 + Python Spark

code example in code/Spark\_MapReduce.py defines two functions map() and reduce(). Spark context is instantiated and an array of integers is parallelized to

Spark resilient distributed dataset partitions and map() is invoked per RDD on Map function - Map() which returns a single element array as a tuple. This is followed by reduce() on Reduce function - Reduce() which takes as args two mapped tuples and merges the integer arrays after > or <= checks to create a subarray which is either strictly ascending or descending. Resultant array is checked for sortedness by a function and mapreduces further if not. Logs for this in Spark\_MapReduce.log.26March2019 demonstrate the bitonic sequence n1 + n2 which fluctuate (ascending-descending-ascending):

```
Reduce: (1, [15], 1, [16], 1, [12], 1, [7], 1, [6], 1, [3], 1, [2], 1, [4], 1, [5])
```

```
n1: (1, [15], 1, [16], 1, [12], 1, [7], 1, [6], 1, [3], 1, [2], 1, [4], 1, [5])
```

```
n2: (1, [23], 1, [32])
```

```
Reduce: (1, [15], 1, [16], 1, [12], 1, [7], 1, [6], 1, [3], 1, [2], 1, [4], 1, [5], 1, [23], 1, [32])
```

Bitonic Sequence of Integers:

```
[15, 16, 12, 7, 6, 3, 2, 4, 5, 23, 32]
```

As can be seen, the reduce produces a huge tuple from which an integer array is extracted after typecheck by Python keyword "type".

-----  
757. (THEORY and FEATURE) 16 March 2019 - Set Partitions in SymPy, Survival Index Timeout OS Scheduler

- this section is an extended draft on respective topics in NeuronRain

AstroInfer design -

<https://github.com/shrinivaasanka/asfer-github-code/blob/master/asfer-docs/AstroInferDesign.txt>  
-----

Spark\_FPGrowth\_SurvivalIndexTimeout.py example previously described for FPGrowth mining of dictionaries

has been changed to print all possible partitions of set of processes in OS.

Partition API in SymPy have been invoked for this. OS Scheduler/Timer is in itself a set partition histogram which maps timeout values to subsets of processes. This demonstrates the integer partition and LSH/set partition-separate chaining isomorphism. Logs in

Spark\_FPGrowth\_SurvivalIndexTimeout.log.16April2019 show the all possible permutations of process set partitions. Rank of a partition is printed which is the difference between size of largest part and number of parts (or) equivalently side of largest square in Durfee Diagram.

References:

-----  
1. Durfee Square - [https://en.wikipedia.org/wiki/Durfee\\_square](https://en.wikipedia.org/wiki/Durfee_square)

2. Rank of a partition and Partitions fitting within a rectangle - Gauss Binomial Coefficient - [https://en.wikipedia.org/wiki/Rank\\_of\\_a\\_partition](https://en.wikipedia.org/wiki/Rank_of_a_partition)

3. Ferrers Diagram or Young Tableau of a Partition - [https://en.wikipedia.org/wiki/Partition\\_\(number\\_theory\)#Ferrers\\_diagram](https://en.wikipedia.org/wiki/Partition_(number_theory)#Ferrers_diagram)  
-----

837. (THEORY and FEATURE) People Analytics and Economic merit (Spending Analyzer) - Credit Card Datasets - 9 July 2019 - Fraud Analytics in Spark 2.4.3  
-----

NeuronRain AstroInfer implements a primitive fraud analytics on a credit card transactions dataset -

<https://gitlab.com/shrinivaasanka/asfer-github-code/blob/master/python-src/FraudAnalytics.py> which analyzes <https://www.kaggle.com/mlg-ulb/creditcardfraud> csv dataset. Alternatively Spark provides some basic statistics functions for

analyzing DataFrames of BigData. An example Spark Python code on Spark 2.4.3 at code/Spark\_FraudAnalytics.py does the following :

(\*) Group the transactions by first few columns of cardholder identity and computes average amount withdrawn by aggregating column "Amount"

(\*) Find Frequent Items in the DataFrame

(\*) Describe the columns and compute basic statistics - mean, standard deviation etc.,

```
...
+-----+-----+-----+-----+-----+
+-----+-----+-----+-----+-----+
+-----+-----+-----+-----+-----+
+-----+-----+-----+-----+-----+
|summary| V1| V2| V3|
V4| V5| V6| V7|
V8| V9| Amount|
+-----+-----+-----+-----+-----+
+-----+-----+-----+-----+-----+
+-----+-----+-----+-----+-----+
+-----+-----+-----+-----+-----+
| count| 284807| 284807| 284807|
284807| 284807| 284807| 284807|
284807| 284807| 284807|
| mean|3.742631994571313...|4.949726613980831...|-7.91956258236933...|
2.685625859585728...|-1.52643182031150...|1.813835301123298...|-
1.74517780292937...|-2.00384093565998...|-3.14088095662162...|
88.34961925089794|
| stddev| 1.9586958038574895| 1.6513085794769824| 1.516255005177769|
1.4158685749409246| 1.3802467340314435| 1.3322710897575698|
1.237093598182658| 1.1943529026692032| 1.0986320892243098|250.12010924018742|
| min|-0.00012931370800...|-0.00010296722561...|-0.00010859127517...|-
0.00011921826106...|-0.00010366562678...|-0.00010234903761...|-
0.00010533581684...|-0.00010065655617...|-0.00010181309940...|
0|
| max|7.55406974741191e-05| 9.99769856171626|9.67444968403876e-05|
9.92501936512661|9.99846034625664e-05| 9.91116576052911| 9.97044721041161|
9.90825458583455|9.96754672601408e-05| 999.9|
+-----+-----+-----+-----+-----+
+-----+-----+-----+-----+-----+
+-----+-----+-----+-----+-----+
+-----+-----+-----+-----+-----+
```

756. (THEORY and FEATURE) 21 October 2019 - Advertisement Analytics - Recommender Systems - ALS Collaborative Filtering - this section is an extended draft on respective topics in NeuronRain AstroInfer design - <https://github.com/shrinivaasanka/asfer-github-code/blob/master/asfer-docs/AstroInferDesign.txt>

Collaborative Filtering based Recommender Systems works by plotting a matrix of users versus their item choices and predicting preferences of new users or missing preferences based on inferences from the user-items matrix. Advertisement Analytics by computing PageRank of viewer channel switch graph (converging markov random walk) is explained in [https://github.com/shrinivaasanka/Grafit/blob/master/course\\_material/NeuronRain/AdvancedComputerScienceAndMachineLearning/AdvancedComputerScienceAndMachineLearning.txt](https://github.com/shrinivaasanka/Grafit/blob/master/course_material/NeuronRain/AdvancedComputerScienceAndMachineLearning/AdvancedComputerScienceAndMachineLearning.txt). Spark MLlib predefines a function for alternating least squares (ALS) collaborative filtering on cloud. Code example in SparkRecommenderSystems.py which is a modified version of documentation example in <https://spark.apache.org/docs/latest/ml-collaborative-filtering.html> adapts to channel recommendation systems based on user surveyed matrix of viewer-channel matrix. This is an alternative advertisement analytics. Channel ratings of viewers are read from text file

AdvertisementAnalytics\_RecommenderSystemsCF.txt having fields - viewer, channelid, rating and timestamp.  
 ALS factorizes the user-item matrix into User and Item matrix factors and minimizes a quadratic optimization function:  

$$\text{UserItem} = \text{User} * \text{Item} \text{ (Factorization)}$$

$$(\text{UserItem} - \text{User} * \text{Item})^2 \text{ (Minimization)}$$
 ALS makes either User or Item factor constant alternatingly and converts to a quadratic optimization problem.

-----  
 755. (THEORY and FEATURE) 23 October 2019, 1 November 2019 - Sequence Mining of Astronomical Datasets by Spark PrefixSpan - this section is an extended draft on respective topics in NeuronRain AstroInfer design - <https://github.com/shrinivaasanka/asfer-github-code/blob/master/asfer-docs/AstroInferDesign.txt>  
 -----

NeuronRain Research version of AstroInfer in SourceForge mines astronomical data e.g encoded ephemeris degree locations of celestial bodies, planetary positions on zodiac etc., by native sequential implementation of GSP Sequence Mining algorithm. Spark MLlib provides cloud implementation of an advanced sequence mining algorithm - PrefixSpan which recursively projects a sequence dataset to smaller fine grained datasets and locally mines frequent patterns in smaller databases which are grown (<https://ieeexplore.ieee.org/document/1339268> - Mining sequential patterns by pattern-growth: the PrefixSpan approach - Jian Pei, Sch. of Comput. Sci., Simon Fraser Univ., Burnaby, BC, Canada, Jiawei Han, B. Mortazavi-Asl, Jianyong Wang, H. Pinto, Qiming Chen, U. Dayal, Mei-Chun Hsu). An example code for Spark PrefixSpan pattern mining for encoded astronomical datasets (encoding is numeric 1-to-9 for each of the 9 planets spread across 12 zodiac houses delimited by #) is at code/Spark\_PrefixSpan.py. It prints frequently occurring celestial juxtapositions of planets in the dataset. Large scale mining of celestial data can be used for variety of scientific applications - solving n-body gravitational differential equations, correlating frequent planetary patterns to terrestrial seismic events and weather forecast. Curiously enough, each encoded string of celestial configuration is a set partition and is an instance of balls-bins problem - set of celestial bodies are bucketed by some permutation amongst 12 houses - number of such celestial configurations are governed by Bell and Stirling numbers which is derived as below (background n-body problem choreography analysis is in NeuronRain FAQ - <https://neuronrain-documentation.readthedocs.io/en/latest/>):

Number of ordered partitions of length p of 9 celestial bodies =  $N(p)$   
 $\text{Summation}_{p=1\text{-to-}9(N(p))} = B_9$  - 9th Bell Number (= binomial series summation of Stirling Numbers of second kind) = 7087261  
 Number of all possible choreographic arrangements of 9 celestial bodies amongst 12 zodiac degree divisions =  $\text{Summation}_{p=1\text{-to-}m(12CN(p))}$  which is lowerbounded by  $B_9 \geq 7087261$  = number of celestial patterns to be correlated to terrestrial events. This is a finite number implying repetitive patterns in gravity induced events.

References:

-----  
 1. Sage OrderedSetPartition - [http://doc.sagemath.org/html/en/reference/combinat/sage/combinat/set\\_partition\\_ordered.html](http://doc.sagemath.org/html/en/reference/combinat/sage/combinat/set_partition_ordered.html)  
 -----

754. (THEORY and FEATURE) 18 December 2019, 19 December 2019, 22 July 2020, 23 July 2020 - Intrinsic Performance Ratings and Sports Analytics, Streaming Histogram analytics, Partition distance measures, Random graph streams, Logic and Game theory - this section is an extended draft on respective topics in NeuronRain AstroInfer design - <https://github.com/shrinivaasanka/asfer-github-code/blob/master/asfer-docs/AstroInferDesign.txt>



-----  
-----  
Non-perceptive intrinsic performance rankings (IPR) have been mentioned as one of the multiple classes of measuring intrinsic fitness/merit as part of People Analytics in [https://neuronrain-documentation.readthedocs.io/en/latest/without\\_voting](https://neuronrain-documentation.readthedocs.io/en/latest/without_voting). IPRs are widely used to rank Chess players (e.g Elo ratings). As an alternative bigdata usecase, stream of cricket match statistics is analyzed for intrinsic merit (Example hawkeye statistics - wagon wheel, trajectories, pitch maps - in

<https://www.bcci.tv/events/15305/india-v-west-indies-2019/match/15309/1st-odi?tab=overview#hawkeye>). NeuronRain Set Partition and Histogram analytics implementations elicit patterns from stream of histogram set partitions by multitude of distance measures - earth mover distance, partition rank, correlation among others:

(\*) Batting, Fielding and Bowling figures per match for 11+11=22 players can be plotted as a histogram of player versus runs/wickets.

(\*) Streaming Set partition analytics is a special case of Histogram analytics - stream of histograms can have varied total sum of parts while stream of set partitions have oscillating parts but constant total sum of parts.

(\*) Stream of match statistics histograms (which always have constant 11 parts per team) as time series has the imprint of team performance over the period of time.

(\*) Partition Rank which is defined as maximum part - number of parts is an indicator of skewness in the team performance (maximum runs/wickets scored by a player - 11 per team)

(\*) Durfee square which is the side of largest square inscribed in Ferrer diagram of the match statistics histogram measures if the performance is equitable - larger the square, more players performed nearly equally.

(\*) Time series of Earth mover distance between consecutive match statistics histograms in the stream sheds light on seasonal trend in team performance.

(\*) Patterns in Wagon wheel graphics of shots played per player measures strengths of each player - stream of wagon wheels can be mapped to a histogram of shots and aforementioned metrics apply.

(\*) Clustering of Bowling trajectories/pitch maps extract stereotypes.

Most games have been analyzed for their computational complexity - E.g Go, Chess are either in PSPACE or EXPTIME depending on rules. Cricket on the other hand could be theoretically formulated as two True Quantified Boolean Formulae Satisfiability problems in PSPACE - TQBF1 and TQBF2 - forall and existential quantifiers in each formula symbolize team1 and team2 per innings (adversary-defender game). Batting and Bowling Roles (respectively governed by existential and forall quantifiers) for 22 player statistics variables are interchanged in each innings. Maximum satisfied formula decides the winner and game is undecidable if drawn/tied.

Mining soccer patterns is complex because of random trajectories of the ball which draws a random directed graph on field - trajectory is a brownian motion random walk - whose vertices are 2-colored (bichromatic for vertices belonging to two opponent teams). Consecutive match statistics create a stream of 2-colored random graphs and frequent subgraph patterns in this stream of random trajectory graphs show patterns across matches.

Reference:

- 1.Real Plus Minus of NBA - <http://www.espn.com/nba/statistics/rpm> - Player Efficiency Ratings in Basketball  
2.Go, PSPACE, Combinatorial Game Theory - [https://en.wikipedia.org/wiki/Go\\_and\\_mathematics](https://en.wikipedia.org/wiki/Go_and_mathematics)  
3.Computational Complexity of Games and Puzzles - <https://www.ics.uci.edu/~eppstein/cgt/hard.html>  
4.Why Tennis Is Still Not Ready to Play Moneyball - Sabermetric equivalent of Baseball in Tennis - <https://hdsr.mitpress.mit.edu/pub/uy0zl4i1/release/3>

-----  
-----  
753. (THEORY and FEATURE) Social Network Analytics, People Analytics, Preferential Attachment, Urban Sprawls, Graph Edit Distance and Intrinsic Merit Rankings - 20 February 2020, 26 February 2020, 29 April 2020, 17 May 2020, 18 May 2020, 28 May 2020, 15 August 2020, 24 December 2020 - related to 762, 821, 1128 and all sections on urban planning analytics, GIS analytics among other topics in NeuronRain Theory Drafts  
-----  
-----

NeuronRain AstroInfer codebase has implementations for urban planning analytics including analytics of Remote sensing imagery, GIS 2-D patches extraction, Watershed image segmentation specific to urban sprawls et al. Urban planning analytics could be termed a special category lying in intersection of People analytics and Social Network analytics - difference being people profiles and social profile vertices in world wide web are replaced by real humans and urban clusters. There exists a striking parallel between preferential attachment in social networks and formation and growth of urban agglomerations - Processes underneath why certain social profiles attract more incoming links and why people flock to megapolises (and megalopolises formed by counter magnets) have clustering similarities. Preferential attachment in social networks causes profiles of large followers to be larger or famous become more famous while big cities become megacities. It is self-explanatory that perception underlies preferential attachment (because population is swayed by and gravitates to majority). Average degree of a vertex in Social networks is replaced by population density in Urban sprawls.

On the contrary, rationale for ranking social profiles by their intrinsic least energy merit characterized by inverse lognormal sum of education(E), wealth(W) and valour(V) (energy of social profile vertex is directly proportional to  $1/(\log E + \log W + \log V)$ ) defined and implemented in NeuronRain AstroInfer applies as well to the ability of an urban sprawl to attract population and ranking urban areas absolutely. Some of the following example standard of living factors could be classified into three divisions of lognormal sum (inverse lognormal sum could be broken-up into following finer contributing factors):

- Harbours, Coastal areas (Wealth)
- Infrastructure (Wealth)
- Manufacturing, IT and ITES jobs (Wealth)
- Education and R&D institutions (Education)
- Financial institutions (Wealth)
- Antiquity, Tourism and Culture (Valour)
- Salubrious and Cool climes (less likely)
- ...

Previous division of Social profile vertices into 3 categories may infact be 4 if Wealth category is segregated into Working class and Business profiles:

- (\*) Profiles of Academics and Researchers - Education (E)
- (\*) Profiles of Sports personalities - Valour (V)
- (\*) Profiles of Business - Wealth1 (W1)
- (\*) Profiles of Working class - Wealth2 (W2)

which would consummate to lognormal least energy sum  $\log E + \log V + \log W1 + \log W2$ . On the contrary such a division of social profiles may not be Four color theorem compliant - there is no or least avoidance of colors (categories) of neighbours (though W1 and W2 are repulsive). NeuronRain People Analytics implements Chaotic HMM state machine model for tenure transitions of a profile and an alternative weighted automaton model is put forth (state transitions between organizations are incentivized by weights). Attributing merit to people tenure transitions reduces to rating incentives for choices made e.g:

- (\*) transition from industry to academics is considered nobler than industry-to-industry.
- (\*) transition from academics to industry is majority choice
- (\*) transition from low remuneration to high is a majority choice
- (\*) transition from high remuneration to low is rare
- (\*) transition from employment to entrepreneur is rare and considered less

risk-averse

(\*) transition from low designation to high is majority choice  
Weights of the transitions in Weighted Automata Tenure model are decided by ranking of rarity of choices earlier. Comparing state machines (ChaoticHMM or Weighted Automata) of tenures of two social profiles is the problem of Equivalence of Regular languages (verify if two automata are similar) solved by Table filling algorithm. NeuronRain AstroInfer People Analytics implements career transition analytics based on a weighted automaton derived from graded incentives for previous state transition choices - rare transitions are rewarded. Fluctuating weights between consecutive transitions as points on polynomials could be interpolated to a polynomial career graph and similar profiles could be clustered by distance of those career polynomials e.g Distance between polynomials is defined by inner product spaces - <http://web.mit.edu/18.06/www/Spring17/Orthogonal-Polynomials.pdf>. In the context of "original music score" merit measurement, equivalence of weighted automata of two music compositions is verifiable by Table filling.

GIS imagery of any urban sprawl can be segmented by watershed algorithm or contour detection to following categories (or by approximate color of pixels):

- (\*) Manufacturing, IT and ITES
- (\*) Residential
- (\*) Commercial
- (\*) Agricultural lands, Water bodies (Groundwater and Surfacewater) & Greenery

which correspond to four color cartography of the urban sprawl. By Four color theorem, segments of urban sprawl master plan could be colored by any of the four categories in a way which prevents any neighbor of a segment to be of same category thereby ensuring equitable and sustainable development. Fair Division of resources within an urban sprawl (water, amenities, ...) is a Pareto optimal Multiple Agent Resource Allocation (MARA) problem. An allocation is Pareto optimal if no agent is preferentially treated at the expense of its peers (Envy-free) while a Nash equilibrium occurs when every agent is at its best and can't do better. Four categories or colors of an urban sprawl GIS segmentation earlier correspond to Four agents among whom a resource has to be fairly divided - an analytics alternative to Four color theorem. Segments of an urban sprawl GIS imagery form a Dual graph induced by segment vertices (faces) and their adjacency. Four coloring theorem stems from 4-colorability of unavoidable sets and 1482 reducible configurations. On the lines of TCP congestion control in electronic networks, Bottleneck measures (e.g Expanders, Cheeger constant) of 4-colored FaceGraph of a segmented urban sprawl GIS imagery help in theoretically solving the traffic congestion problem in urban sprawls - Most transport in urban sprawls happens amongst 3 face categories of FaceGraph - Manufacturing-IT-ITES, Residential and Commercial. Four colored Facegraph of segmented urban sprawl GIS imagery has an inherent feature which decongests traffic snarls - every s-t path between vertices of Facegraph is 4-colored (two consecutive vertices in a path avoid same color) implying every route in transport network traverses perfect mix of 4 face categories earlier. Graph Edit Distance between FaceGraphs of 2 urban sprawls is a theoretical measure of similarity which quantifies Urbanization and thus could be used in Ranking Urban agglomerations. FaceGraph as a Flow network (Maxflow-Mincut problem) of face vertices maximizes traffic between source and sink faces through minimum cut edges which if removed would disconnect source from sink. Apart from these population dynamics of urban sprawls are of statistical importance and are necessary for redrawing and expanding urban boundaries. Ricker non-linear logistic  $N(t+1) = N(t)e^{(r(1-N(t)/K))}$  formalizes growth of population from generation t to (t+1) from which future population projections for an urban sprawl could be inferred (implemented as R script in GRAFIT course material). Increasing population implies increasing population density (average degree) for constant sprawl.

Extent of correlation between Rankings of Urban Sprawls by Population (mostly caused by preferential attachment - Urban Area Rankings in Section 675 of <https://github.com/shrinivaasanka/asfer-github-code/blob/master/asfer-docs/AstroInferDesign.txt>) and Intrinsic Lognormal Sum Least Energy Merit is a measure of Fame-Merit coincidence.

## References:

1. Preferential attachment, Bose-Einstein Condensation in Networks, Double Jeopardy in business intelligence (low market share brands have low buyers and low brand loyalty - low market share brand is not necessarily of low merit) - [https://en.wikipedia.org/wiki/Preferential\\_attachment](https://en.wikipedia.org/wiki/Preferential_attachment)
2. Automata - [Hopcroft-Motwani-Ullman] - Page 157 - 4.4.2 - Table Filling algorithm for Equivalence of two automata (NFA and DFA) - If two states are not distinguished by Table filling, they are equivalent
3. NASA SEDAC GIS Population Estimator - <https://sedac.ciesin.columbia.edu/mapping/popest/gpw-v4/> - PDF of 6-colored Terrain Population Density of Settlement Points in Southern India (2015) and Convex Hull Population estimator - Gridded Population of the World (GPW) Version 4 - has been committed to [code/testlogs/NASA\\_SEDAC\\_Population\\_Estimator.6coloredGIS.16August2020.pdf](https://code.testlogs.nasa.gov/testlogs/NASA_SEDAC_Population_Estimator.6coloredGIS.16August2020.pdf)
4. Inner Product Spaces of Polynomials - Examples - <http://www.math.ucdenver.edu/~esulliva/LinearAlgebra/InnerProducts.pdf> - "...  
 $\langle p, q \rangle = p(t_0)q(t_0) + p(t_1)q(t_1) + \dots + p(t_n)q(t_n)$  ..." - For career polynomials of two professional profiles  $p$  and  $q$ ,  $p(t_i)$  and  $q(t_i)$  are the fluctuating weights (value of polynomial) at time  $t_i$  where weight could be any metric including remuneration, designation et al of a profile.

-----  
821. (THEORY and FEATURE) Word Embedding on a Vectorspace - Spark SkipGram Log Likelihood - Text Similarity, Dissimilarity and Merit Measure of Originality - 10 May 2020, 11 May 2020 - related to 762, 815 and all sections on Kernel Lifting, Intrinsic Merit of Academic publications/Large Scale Visuals/Music/People, Psychoanalysis and Shell Turing Machines  
-----

-----  
Word2Vec Embedding in Spark MLLib maps words in a text to vectors in a Vectorspace which facilitates clustering of synonymous words - Words of similar meaning and context are in proximity on the vector space. This kind of kernel lifting from one dimensional text to multidimensional vectorspace of words in Spark MLLib is implemented as a SkipGram. SkipGram maximizes average loglikelihood for a word  $w_t$  and a context training window for  $w_t$  of width  $2k$  -  $w(t-k), \dots, w(t+k)$ :  
$$\frac{1}{T} \sum_{t=1}^T \sum_{j=-k}^k \log p(w(t+j)|w_t)$$
  
Code example Spark\_Word2Vec.py defines a function bibliometrics\_word2vec() which analyzes text file bibliographies from Semantic Scholar (<https://www.semanticscholar.org/author/Ka.-Shrinivaasan/1861803>), DBLP (<https://dblp.dagstuhl.de/pers/hd/s/Shrinivaasan:Ka=>) and Google Scholar (<https://scholar.google.co.in/citations?user=eLZY7CIAAAAJ&hl=en>) profiles of author on quadcore and Python 3.7.5 and tries to find synonyms and clustering similarities (by cosine distance). Sections 762 and 815 propound an alternative merit measure of "Originality" (how dissimilar a work is from other authorships and common theme similarity amongst author's works) which can be best captured by Word2Vec vectorspace embeddings of texts wherein computation of euclidean distance clustering similarity between word vectors is easier. Analyzing academic publications is a field in itself - Bibliometrics and Scientometrics - once touted to be an alternative to peer review. It is worth noting that TextGraph representation of texts offers Graph Isomorphism and Graph Edit Distance as graph theoretic concept similarity alternatives. Originality thus distinguishes seminal papers (differentiated by huge conceptual distance from earlier works), independent of H-index (Fame measure based on voting - citations), which ushered a revolution when they were published. H-index is the Durfee Square of the Integer Partition of Citations amongst papers and approximately equals  $0.54 \cdot \sqrt{N}$  for total citations  $N$ . Concept similarity is defined by archetypes (Thought motif from which copies are made) in Carl Jungian Psychoanalysis (Pattern of Thought in collective unconscious).

## References:

-----  
821.1 H-index - <https://en.wikipedia.org/wiki/H-index>  
821.2 Bibliometrics for Internet Media: Applying H-index to YouTube -  
<https://arxiv.org/abs/1303.0766>  
821.3 Spark MLLib Word2Vec -  
[https://spark.apache.org/docs/latest/api/python/pyspark.ml.html?](https://spark.apache.org/docs/latest/api/python/pyspark.ml.html?highlight=word2vec)  
[highlight=word2vec](https://spark.apache.org/docs/latest/api/python/pyspark.ml.html?highlight=word2vec)  
-----

-----  
822. (FEATURE) Word Embedding of Text on Vectorspace - Merit of Academic Publications - an alternative to H-index - implementation changes - 11 May 2020 - related to 821  
-----

-----  
1. Spark\_Word2Vec.py has been refactored to include separate mapreduce functions for tokenizing the text to words after utf-8 encoding.  
2. To circumvent Spark Java String to Iterable cast error in Word2Vec fit(), list comprehension in mapreduce creates one element arrays per word (instead of array per line earlier).  
3. Parsed data is printed by DataFrame show() and printSchema() - StringType Spark type has been imported.  
4. Google Scholar bibliography has been included.  
5. Spark logs are at testlogs/Spark\_Word2Vec.log.11May2020  
-----

-----  
826. (FEATURE) Spark SkipGram Word2Vec Bibliometrics - increased vocabulary and accuracy - 9,11 June 2020 - related to 821,822  
-----

-----  
1. Spark\_Word2Vec.py has been changed to parse an expanded Bibliography text file (Spark\_Word2Vec\_Bibliography.txt) which is a concatenation of BibTeX from various Bibliography sources (Google Scholar, CiteSeerX, Microsoft Academic, Semantic Scholar, Harvard NASA ADS, DBLP) instead of parsing a single source.  
2. Because of enlarged BibTeX training data, vocabulary of Word2Vec bibliometrics has improved and more meaningful words e.g author, year, Science, merit, title, document have been vectorized  
3. All BibTeX are from author search of self - "Ka Shrinivaasan" - from URLs:  
Google Scholar - [https://scholar.google.co.in/citations?](https://scholar.google.co.in/citations?user=eLZY7CIAAAAJ&hl=en)  
[user=eLZY7CIAAAAJ&hl=en](https://scholar.google.co.in/citations?user=eLZY7CIAAAAJ&hl=en)  
DBLP - <http://dblp.dagstuhl.de/pers/hd/s/Shrinivaasan:Ka=>  
Microsoft Academic - [https://academic.microsoft.com/search?q=ka](https://academic.microsoft.com/search?q=ka%20shrinivaasan&qe=%40%40%40Composite(AA.AuN%3D%3D%27ka%20shrinivaasan%27)&f=&orderBy=4&skip=0&take=10)  
[%20shrinivaasan&qe=%40%40%40Composite\(AA.AuN%3D%3D%27ka%20shrinivaasan%27\)&f=&orderBy=4&skip=0&take=10](https://academic.microsoft.com/search?q=ka%20shrinivaasan&qe=%40%40%40Composite(AA.AuN%3D%3D%27ka%20shrinivaasan%27)&f=&orderBy=4&skip=0&take=10)  
Semantic Scholar - [https://www.semanticscholar.org/author/Ka.-](https://www.semanticscholar.org/author/Ka.-Shrinivaasan/1861803)  
[Shrinivaasan/1861803](https://www.semanticscholar.org/author/Ka.-Shrinivaasan/1861803)  
CiteSeerX - <https://citeseerx.ist.psu.edu/search?q=Ka.+Shrinivaasan>  
NASA/ADS - [https://ui.adsabs.harvard.edu/search/q=author%3A%22Shrinivaasan](https://ui.adsabs.harvard.edu/search/q=author%3A%22Shrinivaasan%2C%20Ka.%22&sort=date%20desc%2C%20bibcode%20desc&p_0)  
[%2C%20Ka.%22&sort=date%20desc%2C%20bibcode%20desc&p\\_0](https://ui.adsabs.harvard.edu/search/q=author%3A%22Shrinivaasan%2C%20Ka.%22&sort=date%20desc%2C%20bibcode%20desc&p_0)  
4. Vector size and Seed size have been set to 5 and 42 respectively  
5. Vocabulary could be further improved by word2vec embedding of entire article instead of BibTeX abstracts which is a concept cloud of vectors.  
-----

-----  
827. (THEORY and FEATURE) Intrinsic Merit of Academic Publications - Bibliometrics - First Order Logic, Monoidal Categories, Girard Geometry of Interactions (GoI), Sequent Calculus, ProofNets - related to 624,821,822,826 - 10,11,13,14,15,16,17 June 2020  
-----

-----

There exists a fine division in quantifying merit of a natural language text and academic publications cutting across disciplines - theoretical and experimental. Natural language texts are measurable by mental representation of meaning and its lambda function approximation (Recursive Lambda Function Growth) whereas every academic publication could be construed as sequence of first order logic formulae connected by logical implications - from conjecture to QED. In Sequent Calculus proof has a tree structure and every line of a proof is a conditional tautology on previous lines. Girard Geometry of Interactions maps every theorem-proof to geometry of logical statements (ProofNets) by defining trip operator (Long Trip Criterion) on proof network. For instance, Coq Theorem Prover has been used to verify proof of Four Color Theorem by [Appel-Haken]. Thus Concept distance for Originality merit measure between any two academic publications could be defined as the distance between their ProofNet GoIs (e.g graph edit distance between ProofNets). On a related note, Distance between two First order logic (FOL) statements is the problem of equivalence of 2 FOL formulae  $F1$  and  $F2$ : If  $F1 == F2$ , distance is 0 else distance is the number of mismatches in truth table - To prove  $F1 == F2$ , both  $F1 \Rightarrow F2$  and  $F2 \Rightarrow F1$  have to be established. There are two other prominent proof calculi - Hilbert and Natural Deduction. Analyzing academic publications and theorem-lemma-proofs therein thus has two facets: 1) Natural Language Processing - Lambda Function approximation, Word2Vec embedding of concepts and their clustering 2) Formal Logic - Proof theory - Sequents, Gentzen Cut-Elimination ( $A \vdash B, C$  and  $D, B \vdash E$  then  $A, D \vdash C, E$ ), ProofNet-GoIs . There is an alternative Category theoretic formalism of Proofs wherein every proof entailment  $A \vdash B$  is a morphism  $A \rightarrow B$  between objects  $A, B$  in a monoidal category  $M$  having a binary operator  $*$  - entailment morphisms thus constitute a ProofNet directed graph (a quiver in Category jargon - <https://ncatlab.org/nlab/show/quiver>). Geometry of Interaction in Linear Logic and Type theory considers  $A \vdash B$  as an endomorphism.

#### References:

- 
- 827.1 Coq Proof Assistant and Four Color Theorem - <https://www.ams.org/notices/200811/tx081101382p.pdf>
  - 827.2 Proof Nets - Sequent Calculus and Girard Geometry of Interactions - [https://en.wikipedia.org/wiki/Proof\\_net](https://en.wikipedia.org/wiki/Proof_net)
  - 827.3 E Theorem prover - <https://www.lehre.dhbw-stuttgart.de/~sschulz/E/E.html>
  - 827.4 Concept Cloud Wordle example for publications - <https://ui.adsabs.harvard.edu/search/q=author%3A%22Shrinivaasan%2C%20Ka.%22&sort=date%20desc%2C%20bibcode%20desc/concept-cloud> - prominent concepts in a set of publications are highlighted
  - 827.5 Equivalence of FOL statements - Biconditional - [http://iiitdm.ac.in/old/Faculty\\_Teaching/Sadagopan/pdf/Discrete/Logic.pdf](http://iiitdm.ac.in/old/Faculty_Teaching/Sadagopan/pdf/Discrete/Logic.pdf) - Indian Institute of Information Technology Design and Manufacturing, Kancheepuram, Chennai 600 127, India
  - 827.6 n-Category Lab - Geometry of Interaction - <https://ncatlab.org/nlab/show/Geometry+of+Interaction>
- 

829. (THEORY and FEATURE) Intrinsic Merit of Academic Publications - Bibliometrics - SkipGram Word2Vec of publication full text - Concept Cloud Wordle - TOP Categories, High Dimensional Inference, Shell Turing Machines and Kernel Lifting, Lambda functions and Beta Reduction, Meaning representation, Graph Edit Distance - related to 827 - 13,14,15,16,17 June 2020, 13 July 2020, 6 December 2020, 25 January 2021, 5 March 2021

-----

- 1.This commit revamps Spark\_Word2Vec.py implementation to parse an entire article text to extract a concept cloud wordle from it by Spark SkipGram Word2Vec. Word2Vec is computationally intensive and corpora-hungry for producing accurate embedding.
- 2.New text file Spark\_Word2Vec\_PublicationFullText.txt is read which contains a

draft publication of author on "Majority Voting" - [https://5d99cf42-a-62cb3a1a-s-sites.googlegroups.com/site/kuja27/IndepthAnalysisOfVariantOfMajorityVotingwithZFAOC\\_2014.pdf](https://5d99cf42-a-62cb3a1a-s-sites.googlegroups.com/site/kuja27/IndepthAnalysisOfVariantOfMajorityVotingwithZFAOC_2014.pdf)

3. Concepts and respective vectors for them are pretty-printed. Concept cloud of full text is quite meaningful and captures the essential words in the text. Clustering of related concepts is implied by Synonyms printed.

4. Recursive Gloss Overlap and Recursive Lambda Function Growth algorithm implementations in NeuronRain could benefit from Word2Vec in filtering less important words while computing textgraphs, euclidean distance among them and their dense subgraph k-cores which serve as unsupervised text classifiers.

5. Extracting a composition of Lambda Functions from Natural Language Text of a Publication and First order logic (FOL) ProofNet representation of Theorems therein are empirically equivalent - former is a Turing machine while the latter is its FOL version. Example Beta Reduction  $((\lambda x. t) s)$  in reference 829.1 translates a natural language sentence to lambda function:

Whiskers disdained catnip  $\Rightarrow$  disdained(Whiskers, catnip)

which could be written as FOL statement:

There exist  $x$  There exist  $y$  ( $x$  disdained  $y$ )

and model {Whiskers, catnip} satisfies it. Recursive Lambda Function Growth algorithm works by Beta Reduction and is motivated by Grounded Cognition in Cognitive Psychology. Thus ProofNet or Category morphisms representation of texts is not just limited to academic publications but pervades any natural language text.

Meanings of Natural Language Texts captured by Recursive Gloss Overlap and Recursive Lambda Function Growth TextGraph representation algorithms could be compared by Graph Edit Distance algorithms which is NP-Hard and APX-Hard (hard to approximate) though there are polynomial approximations for Graph Edit Distance. Graph Edit Distance is the problem of Inexact Graph Matching for dissimilar graphs (while Graph Isomorphism is Exact Graph Matching for similar graphs) solved by computing optimal edit paths through A\*-algorithm. Graph Edit Distance generalizes String edit distance - every string is a connected directed acyclic graph of maximum indegree 1 and outdegree 1.

6. Vectorspace embedding of concepts in an article basically does a kernel lifting of the model to arbitrary dimensional Topological space and from equivalence of Lambda functions-First order logic mentioned earlier, every first order logic statement in the ProofNet is indirectly kernel lifted and implication entailments between them are replaced by monoidal category morphisms between one logical statement embedded in space  $S_1$  to another embedded in  $S_2$  ( $A(S_1) \vdash B(S_2)$  is a morphism  $A(S_1) \rightarrow B(S_2)$  in a theorem monoidal category). Word2Vec typically embeds all concepts in single space and thus  $S_1=S_2$ .

7. Thus every theorem-proof could be stated as TOP category of first order logic objects in some topological space and morphisms amongst them.

8. Spark\_Word2Vec.py has been made Python 3.7 compatible by autopep8 and 2to3.

## References:

- 
- 829.1 Meaning Representation by First order logic and Lambda calculus - <https://www.cs.mcgill.ca/~jcheung/teaching/fall-2015/comp599/lectures/lecture14.pdf>
- 829.2 Logical Representations of Sentence Meaning - Chapter 16 - Speech and Language Processing - [Jurafsky-Martin] - [https://web.stanford.edu/~jurafsky/slp3/edbook\\_oct162019.pdf](https://web.stanford.edu/~jurafsky/slp3/edbook_oct162019.pdf) - Model theory, Curryng and Beta-reduction in Lambda calculus, Tense and Temporal Logics - Modus Ponens on FOL sentences and Lambda function meaning and event representation - Examples: " ... VegetarianRestaurant(AyCaramba)  $\Rightarrow$  Serves(AyCaramba, VegetarianFood) ...  $\exists e$  Eating( $e$ )  $\wedge$  Eater( $e$ , Speaker)  $\wedge$  Eaten( $e$ , TurkeySandwich)  $\wedge$  Meal( $e$ , Lunch)  $\wedge$  Location( $e$ , Desk)..."
- 829.3 Graph Edit Distance - [https://en.wikipedia.org/wiki/Graph\\_edit\\_distance](https://en.wikipedia.org/wiki/Graph_edit_distance)
- 829.4 Graph Edit Distance - Basics and Trends - <https://www.slideshare.net/LucBrun2/graph-edit-distance-basics-trends>
- 829.5 Comparing Stars: On Approximating Graph Edit Distance - Polynomial time approximation of Graph Edit Distance - <https://web.archive.org/web/20170810170852/http://www.vldb.org/pvldb/2/vldb09-568.pdf>

829.6 High Dimensional Inference - Robust Testing of Low Dimensional Functions - k-juntas - <https://eccc.weizmann.ac.il/report/2021/005/> - [Anindya De, Elchanan Mossel, Joe Neeman] - Problem is to distinguish two functions one of which depends on subspace of k dimensions and the other transcends k dimensions - Two functions on different dimensions are two Shell Turing Machines - "...A natural problem in high-dimensional inference is to decide if a classifier  $f: \mathbb{R}^n \rightarrow \{-1, 1\}$  depends on a small number of linear directions of its input data. Call a function  $g: \mathbb{R}^n \rightarrow \{-1, 1\}$  a linear k-junta if it is completely determined by some k-dimensional subspace of the input space. A recent work of the authors showed that linear k-juntas are testable. Thus there exists an algorithm to distinguish between:

1.  $f: \mathbb{R}^n \rightarrow \{-1, 1\}$  which is a linear k-junta with surface area s,
2. f is epsilon-far from any linear k-junta with surface area  $(1+\epsilon)s$ , where the query complexity of the algorithm is independent of the ambient dimension n...."

829.7 Formal Models of Language Learning - [Steven Pinker] - Tree-fitting heuristic - Pages 248-251 -

<https://stevenpinker.com/files/pinker/files/10.1.1.124.5000.pdf> - Has parallels to Recursive Lambda Function Growth Meaning Representation Algorithm

-----  
 836. (THEORY and FEATURE) People Analytics - Theoretical (Drone) Electronic Voting Machines - Population Count - Number of 1s (Decimal parity) in a bitstream - Various algorithms - Parallel computation in Spark - 3 July 2020  
 -----

Finding parity of a boolean string is a major open problem in Computational Complexity which is not known to be in AC0 (constant depth) but in NC1 (log depth parallel computing).

BigData version of parity is the problem of Population Count which pertains to finding number of 1s in a stream of bits. Lot of algorithms for population count have been invented in Hardware and Artificial Intelligence literature - Divide and Conquer, HAKMEM, CSA(Carry Save Adder) etc., . Code example Spark\_PopulationCount.py reads a CSV file containing a huge binary string and computes the number of 1s in it by sequential and parallel mapreduce. String is split into words of length 32 and parallelized to RDDs. Each word is then scanned by a mapbitstream() and population\_count() functions which sequentially compute the function:

$pop(x) = -1 * \text{Summation}(x \ll n)$  for each bit position n.

Bit left shift has been replaced by access to literal in bitstream string. Reduce function reducebitstream() gathers and sums each 32-bit word. Population count gains importance in the context of efficiently counting number of votes in a theoretical Electronic Voting Machine.

References:

- 
- 1.The Quest for an Accelerated Population Count - Beautiful Code - [Oram-Wilson] - Chapter 10 - Population Count by Divide and Conquer, HAKMEM, CSA
  - 2.HAKMEM - [Beeler-Gosper-Schroeppel] - MIT Artificial Intelligence Laboratory AIM 239, February 1972 - <https://w3.pppl.gov/~hammett/work/2009/AIM-239-ocr.pdf>
  - 3.Computer Architecture: A Quantitative approach - [Hennessy - Patterson] - Full Adder of 3 1-bit inputs and 2 1-bit outputs of sum and carry - CSA is sequence of full adders
- 

839. (THEORY and FEATURE) Bibliometrics - Patents as ProofNets and Search - Novelty detection and Originality merit measure, Latent Semantic Analysis, Low Rank Approximation - 6,7,8 July 2020 - related to 829  
 -----

Patents are uniquely granted to individuals and corporations who have invented an original concept which could be underneath any STEM artifact. Patent Search



is a time consuming process and could take years to validate a patent application and involves human effort to find Concept similarity (Novelty detection, Prior art). Novelty detection and Originality are thus synonymous - Latent Semantic Analysis by SVD ( $X = U(\text{Eigen})Z^T$ ) and low rank approximation (choose creamy layer of  $UEZ^T$ ) of term-document matrix of patents mines concept words related to each other. Alternatively, First order logic ProofNet format of patent applications written in natural languages could be an apt model to quantify conceptual distance and patent search. Patent database is a massive open online dataset (MOOD) and Concept similarity search could be automated by a ProofNet distance computations amongst pairs of patent GoIs on a cloud thus replacing humans. This commit computes a Concept Cloud wordle of set of example team software patents author was involved as former staff (Sun Microsystems-Oracle)

#### References:

-----  
839.1 Sun Microsystems-Oracle iPlanet Application Server (iAS) 6.5 patents - <http://patft.uspto.gov/netacgi/nph-Parser?Sect1=PT02&Sect2=HITOFF&p=1&u=%2Fnethtml%2FPT0%2Fsearch-adv.htm&r=0&f=S&l=50&d=PTXT&Query=%22kannan+srinivasan%22+AND+%22sun+microsystems%22>  
839.2 Patent Novelty Detection - <https://www.sciencedirect.com/science/article/abs/pii/S147403461830421X> - Latent Semantic Analysis by Low Rank Approximation of Term-Document matrix  
-----

-----  
840. (THEORY and FEATURE) Fraud Analytics - Cybercrime analyzers - related to 752, 770 (USBWWAN wireless traffic and Ftrace analyzers) - 6,7,8 July 2020  
-----

Cybercrimes are a scourge on society causing immense economic damage. Distinguishing a spoofed email from genuine origin is an artificial intelligence problem and is still less solved. Spam filters and Firewalls in Mail service providers have machine learning algorithm implementations which segregate botnet senders from humans to some extent (Spam folders in mailboxes use Bayesian filters to differentiate frequency of words in human and robot senders). A commonsense workaround to spoofs: As against keyboard typed emails, text could be a handwritten image (scanned or touchscreen stylus written) backed up by a private hardcopy which is digitally watermarked and sent through usual HTTPS/IMAP/POP/SMTP infrastructure. Written emails are less spoof-prone and less forgeable (because of private hardcopy duplication) and introduce an additional layer of reCAPTCHA Turing tests to discern a robot from human. Old school Post office mails are written and stamped hardcopies. Most cybercrimes are difficult to probe not just because of their international impact but as well due to complex traffic routing (e.g Onion routers) which obfuscate IP, munge headers and fudge dates. Parallels between pandemics and cybercrime transmission are fascinating:

(\*) Pandemics are air, vector, contact borne while Cybercrimes are ISP-borne, proliferate by address book lookups (e.g Worm spreads by infecting an id and recursively traversing contacts - contacts per id could be a huge number and thus infection graph could be an expander of high degree)

(\*) Both pandemics and cybercrimes follow Game theoretic (Botnet adversary-defender game), SIR and SIS models of infections

Predominant attacks which render RSA dysfunctional are Radio-Frequency Van Eck Phreaking (capturing RF signals from monitors), Keystroke loggers (Trojan/Malware capturing keystroke signals), SQL and JavaScript XSS Injection attacks which execute malicious code in client side et al. Some example past cybercrime incidents of author's credentials (compromise of linkedin id by password reset, spoofs of yahoo webmail and past institutional affiliation ids) and their traffic pattern (headers) have been committed to [code/testlogs/Cybercrime\\_examples/](#)

Recursive Lambda Function Growth textgraph algorithm implemented in NeuronRain

could be a spam filter - growing a textgraph of an email text and classifying the text by genre of top percentile core number word vertices is a mail segregation mechanism.

#### References:

-----  
840.1 Van Eck Phreaking of Electronic Voting Machines -  
<https://yro.slashdot.org/story/09/11/22/027229/brazilian-breaks-secrecy-of-brazils-e-voting-machines-with-van-eck-phreaking>  
-----

-----  
841. (THEORY and FEATURE) Digital Watermarking of Large Scale Visuals in OpenCV - related to 581,840 and all sections on Large Scale Visual Recognition Analytics, Handwriting Recognition and Fraud analytics - 10,11,12 July 2020  
-----

-----  
This commit implements an OpenCV python function which reads a large scale visual (Video) and a watermark image and writes out a new MP4 video overlaying the watermark image on each frame of the visual. New MP4 video captures the OpenHub, SourceForge, GitHub and GitLab NeuronRain repository profiles of Krishna iResearch Free Open Source Software initiative of the author having both images and text (testlogs/Krishna\_iResearch\_NeuronRain\_Repositories-2020-07-10\_13.17.20.mp4). Function watermark() in DigitalWatermarking.py reads each frame of the video and watermark image in BGRA 4-channel mode (Blue-Green-Red-Alpha). Alpha channel controls the opacity of each pixel. An overlay ndarray is created of the same dimension as each frame of the video. Pixels of overlay array are filled by watermark image. OpenCV addWeighted() function computes a weighted sum of each pixel of watermark and frame images in BGRA 4-color channel - opacity of watermark is controlled by weights. This example watermarks first 2 frames of the video by a Sanskrit name text image (in testlogs/). Alternatively, Image text could be a handwritten signature. Previous watermark is quite primitive and overlay array could be filled by an arbitrary complex pixel cryptographic hash checksum function prior to addWeighted() invocation. Such a steganographic information hiding finds applications in Copyright Protection, Licensing violations, Software Piracy, Currency watermarking, Fraud and Tamper protection, Antitheft Cybercrime software inter alia.

#### References:

-----  
841.1 Digital Watermarking - overview -  
<https://www.sciencedirect.com/topics/computer-science/digital-watermark> - Movie Piracy example - every frame of DVD is copyright watermarked and can be tracked. On the similar lines watermarked open source software repositories should be able to track each fork-off and flag OSS violations if necessary.  
-----

-----  
848. (THEORY and FEATURE) 1 August 2020 - Number crunching - Sublogarithmic Prime power encoding of huge integers by Computational Geometric Factorization and 2060 bits integer factorization quadcore benchmark - related to 2 and all sections on Text Compression and Compressed Sensing, Factorization and its applications, Multiplicative Integer Partitions of NeuronRain Theory Drafts  
-----

-----  
It is often necessary to store numeric bigdata succinctly - Numeric compression vis-a-vis Text Compression. Usual binary storage requires  $\log N$  bits. From Unique Factorization Theorem every integer can be expressed uniquely as product of powers of consecutive primes. Number of prime factors of an integer  $N$  is  $k \log \log N$  by Hardy-Ramanujan theorem. Thus huge integers could be stored as concatenated strings of exponents of consecutive primes (primes are implicit and prior factorization is assumed). Identifying the powers of prime factors is the





\*)  $60466196 = 2^{10} \cdot 3^{10} = 6^{10}$  is 26 bits integer while unique prime factor encoding  $(2,10)(3,10)$  requires only  $2 + 4 + 2 + 4 = 12$  bits (space for ordered pair parenthesization is an additional  $\log \log N$  which has been neglected). If each parenthesis is of 3 bits for "(", ",", and ")" delimiters, total space increases to  $12 + 3 + 3 = 18$  bits in unique factor scheme but still less than 26.

\*) CPU instruction set microcodes might have to compute exponentiation and products of prime exponents which increases per instruction time in spite of compressed space.

-----  
 1129. (THEORY and FEATURE) People Analytics - Feasibility of Automated Talent Recruitment - Fame Versus

Merit - Some Examples - related to 365,420,443,572,613,632,753,1128 and all sections on People Analytics, Fame, Intrinsic Merit, Majority Voting, Sybils, Social Network Analytics, Interview LTF/PTF, BKS Conjecture, Learning LTFs - 28 December 2020  
 -----

From literature cited in the references (1129.1) on Fame versus Merit, there is an empirical and statistical evidence of Fame being exponentially related to Merit:

" ... Fame,  $F$ , grows exponentially with achievement,  $F(A) = \exp(\beta \times A), \dots$ "

and achievement is equivalent to intrinsic merit (e.g academic publications). Fame is modelled as memepool which evolves over time (Diffusion of Opinion in Social Networks) according to differential equation  $d(\text{Fame})/dt = v(\text{Achievement})$ . Resemblance of this DE to Recursive Mistake Correction Tree model of Experiential Learning is uncanny.

Section 1128 defines and implements a weighted state machine model of career transition - every human is non-deterministic indefinite state machine defined by choices made (Legendary "Road not taken"). Following example usecases motivate the necessity for automated objective recruitment of talent vis-a-vis subjective majority voting based choice of candidates in People Analytics (Assumption: Each voter/interviewer uses an Interview LTF which is both subjective and objective multiple choice questionnaire of  $n$  questions denoted by  $q(i)$  and weighted by  $w(i)$  -  $q_1 \cdot w_1 + q_2 \cdot w_2 + \dots + q_n \cdot w_n$ ):

Example 1:

-----  
 If intrinsic merit of a candidate is  $m$  and there are  $k$  voters deciding the candidature (perceived merit or Fame), for each vote being denoted by  $v(i)$ :

$m < v(1) < v(2) < \dots < v(k)$

from assumption - "Intrinsic Merit Lowerbounds Fame in the absence of Sybils" - derived from statistical evidence of exponential separation between the two.  $v(1)$  is the least upperbound Fame for Merit  $m$  implying every voter overrates candidate (Interview LTF succeeds for candidate).

Example 2:

-----  
 If intrinsic merit upperbounds Fame:

$v(1) < v(2) < \dots < v(k) < m$

implying every voter underrates candidate (Interview LTF fails for candidate)

Example 3:

-----  
 If intrinsic merit is an average (weighted mean) of Fame:

$v_1 < v_2 < \dots < v_x < m < v_y < \dots < v_k$

implying some voters underrate while others overrate candidate. This is the most prevalent scenario in real world setting (Interview LTF neither fails nor succeeds for candidate)

Of these, Example usecase1 is supported by statistical evidence. Example1 and Example2 are consensual but yet inaccurate. Previous scenarios demonstrate error probability of real world manual Interview processes which are a mixture of Majority Voting and LTF, thus semi-intrinsic. Replacing manual interviews by objective LTF which is dynamically machine learnt from People profile datasets (e.g Career Transition Automaton, Source Lines of Code for IT domain) minimizes errors and is more absolute. From Computational Learning Theory, LTFs can be learnt in polynomial time in the presence of classification noise.

#### Career Polynomials - Inner Product Spaces - Example 4:

Career Transition of a profile could be plotted as points on polynomials and similarity of two profiles  $p$  and  $q$  could be ascertained by inner product spaces of interpolated career polynomials defined as:

$$\langle p, q \rangle = p(t_0)q(t_0) + p(t_1)q(t_1) + \dots + p(t_n)q(t_n)$$

where  $p(t_i)$  and  $q(t_i)$  are the values (e.g remuneration) of polynomials at time  $t_i$ . Usual algebraic notations of orthonormal basis apply and  $p, q$  are orthogonal if  $\langle p, q \rangle$  is 0 (Gram-Schmidt Orthogonalization). For two profiles making extremely different career choices  $\langle p, q \rangle$  reaches its infimum - Example:

$$p(0) = 0, p(1) = 100000, p(2) = 0, p(3) = 100000$$

$$q(0) = 100000, q(1) = 0, q(2) = 100000, q(3) = 0$$

$\langle p, q \rangle = 0$  (Orthogonal) implying profiles  $p$  and  $q$  made diametrically opposite career choices during similar time points.

#### References:

1129.1 Theory of Aces: Fame by chance or merit? - [Simkin-Roychowdhury] -

<https://arxiv.org/pdf/cond-mat/0310049.pdf> - Equation 2

1129.2 Measuring Celebrity - [Lamport] - Microsoft Research -

<https://lamport.azurewebsites.net/pubs/celebrity.pdf> - "... A preliminary conclusion would be that, in science, fame is based only on publications, but celebrity also depends on TV appearances ..."

1129.3 MEASURING FAME QUANTITATIVELY. V. WHO'S THE MOST FAMOUS OF THEM ALL?

(PART 2) - [Schulman] - dBHa unit of Fame - <https://www.improbable.com/wp-content/uploads/2016/08/MEASURING-FAME-part2-2016-09.pdf>

1129.4 Learning Linear Threshold Functions in the presence of Classification Noise - [Bylander] - <https://citeseerx.ist.psu.edu/viewdoc/download?doi=10.1.1.31.481&rep=rep1&type=pdf>

1129.5 Polynomial time algorithm for learning noisy linear threshold functions - [Blum-Frieze-Kannan-Vempala] - <https://www.math.cmu.edu/~af1p/Texfiles/learn.pdf>

1129.6 Measuring Fame - [Schulman] - <https://www.improbable.com/2009/02/28/measuring-fame-quantitatively-iv-whos-the-most-famous-of-them-all/>

1131.(THEORY and FEATURE) Bibliometrics - Merit of Academic Publications - Transformers Attention Model implementation - related to 702,707

,839 and all sections on Named Entity Recognition, Bibliometrics, Novelty Detection, People Analytics and Embedding in Vector Spaces - 3,4,5,21 January 2021

1.Transformers attention models are recent deep learning advances in NLP replacing Recurrent NNs and LSTMs and are widely used in machine translation and text analytics. BERT and GPT based text writing systems have massive pretrained transformers underneath.

2.Transformers attention model learns Query weights (Q), Key weights (K), Value weights (V) for embedding  $x_i$  for word  $i$  defined by:

$$Q_i = x_i * q_i$$

$$K_i = x_i * k_i$$

$$V_i = x_i * v_i$$

$$\text{Attention}(Q, K, V) = \text{softmax}(Q * K^T / \sqrt{d^k}) * V, d^k = \text{dimension of Keys}$$

vector

$a(i,j)$  = attention of word  $i$  to word  $j = q_i * k_j$

$\text{softmax}(x_i) = e^{x_i} / \text{Sigma}(e^{x_j})$  which normalizes sum to 1

3. Weights are learnt by Gradient Descent Perceptron code for which has been implemented in Transformers\_PerceptronAndGradient.py (invoked by Transformers.py) which is based on PerceptronAndGradient.py in NeuronRain AstroInfer but replicated for Transformer specific enhancements.

4. This commit implements transformer model in Transformers.py and Transformers\_PerceptronAndGradient.py which are invoked from Spark\_Word2vec.py for learning previous attention weights for word2vec embeddings of academic publications. More attention to a word indicates the importance and Novelty associated with it which is particularly necessary in analyzing patent prior art.

5. Transformers object is initialized as:

def

\_\_init\_\_(self, wordembedding, queries, keys, values, expected, dimension)

which are input training gradient descent args for bibliometrics word2vec embedding, prior weights for queries-keys-values, expected attention and dimension of keys vector.

6. Logs testlogs/Spark\_Word2Vec.log.5January2021 for Spark 3.0.1 + Python 3.7.5 execution depict the attention weights learnt by Gradient Descent.

7. Named Entity Recognition PoS Conditional Random Field implementation in NeuronRain has non-statistical alternative which resembles a transformer sequence model pipeline.

References:

-----

1131.1 Transformers -

[https://en.wikipedia.org/wiki/Transformer\\_\(machine\\_learning\\_model\)](https://en.wikipedia.org/wiki/Transformer_(machine_learning_model))

-----  
1140. (THEORY and FEATURE) Teapot Shards and Space filling - related to 135,649,819,752 and all sections on Space filling, Equal and Unequal Circle packing, Grid filling, Integer Linear Programming and Cellular automata, Quantum Versus Classical Computation, Parallel Pseudorandom Generators, Berry-Esseen Central Limit Theorem - 12 May 2021  
-----

-----  
Bocherds Teapot Shards experiment for predicting number of shards teapot would break into has uncanny similarities to Randomized NC Parallel Space Filling of many natural random parallel processes (Rain drops falling at random in parallel, Distribution of randomly strewn sand particles,...). Teapot shards which are randomly created in parallel are of unequal sizes and fill a rectangular space. NeuronRain Randomized NC Cellular automaton parallel PRG space filling algorithm assumes equal sized circles of infinitesimal radii sweeping the 2D plane which is an alternative formulation of Circle Packing Problem. Filling a 2D space at randomly chosen ordinates (which are centroids of circles of small radii) requires classical parallel PRGs (Tygar-Reif, Applebaum Linear stretch PRG in NC). Teapot shards are fragmented at unequal random shapes and predicting number of shards by Quantum computation is equivalent to predicting total number of randomly chosen ordinate points in Classical Parallel PRG Cellular Automaton Grid filling version e.g finding total number of rain drops - rainfall is a massive natural parallel random computation deserving a quantum supremacy analogue and a quantum PRG might be suitable for simulating rain - if randomly chosen ordinate centroids are random variables set to 1 from 0 implying a filling, sampled average of sum of binary random variables converges to expected value (mean) by Central Limit Theorem.

References:

-----

1140.1 Teapot Shards - <https://www.youtube.com/watch?v=sFhhQRxWTIM>

1140.2 Teapot Shards and Quantum supremacy -

<https://www.scottaaronson.com/blog/?p=5460> - "...I do, however, have one

substantive disagreement. At one point, Borchers argues that sampling-based quantum supremacy itself fails his teapot test. For consider the computational problem of predicting how many pieces a teapot will break into if it's dropped on the ground. Clearly, he says, the teapot itself will outperform any simulation running on any existing classical computer at that task, and will therefore achieve "teapot supremacy."...

-----  
1141. (THEORY and FEATURE) Digital Watermarking - refactored - Image and Video functions - related to 841 and all sections on Merit of Large Scale Visuals, Antitamper/Antispoof/Cybercrime analytics, Image Segmentation and Classification, ThoughtNet - 18 May 2021  
-----

DigitalWatermarking.py implementation has been refactored to define 2 separate watermarking functions for Videos and Images which thus far had definition only for Video files (watermark\_video and watermark\_image). Few example group photo image files (Copyright: 95CSE PSG Tech, Coimbatore) of author (.jpg and .png) have been watermarked by Python 3.7.5 + OpenCV2 overlay(). Digital watermarking overlay is a primitive image classifier - overlay of similar segmented images causes high number of superimposed image segments (or) facegraphs of similar segmented images are more isomorphic and high number face vertices of overlaid images get superimposed exactly. Vertices of Facegraphs of the overlaid segmented images are stacked creating a multiplanar graph (in which every vertex is a stack) which is a visual version of ThoughtNet if thoughts are visualized.

-----  
1145. (THEORY and FEATURE) Causal and Graphical Event Models, Collatz Conjecture, Economic Datasets, Complementary Functions and Sequences, Ramsey 2-Coloring, Pseudorandomness, Quantitative Finance, Chaos, Multifractals, Discrete Fourier Transform - related to 1144 and all sections on Economic Merit, Complement functions-sequences, 2-coloring and Event Timeseries analysis - 8 June 2021, 19 June 2021  
-----

Collatz conjecture states:

$x(n+1) = x(n)/2$  if  $x(n)$  is even and  $3x(n) + 1$  if  $x(n)$  is odd and  $\{x(n)\}$  sequence always ends in 1.

Collatz map is a chaotic fractal which exhibits pseudorandomness and generalized Collatz conjecture ( $g(n) = a(i)*n+b(i)$ ,  $n=i \bmod P$  for rational  $a(i)$  and  $b(i)$  and  $g(n)$  is integer) is undecidable. NeuronRain implements a Chaotic PRG based on conventional actuarial and fractal logistic maps (Verhulste-Pearl-Reed and Mandelbrot). Collatz conjecture could be useful for modelling Economic Event Timeseries as Graphical Event Model E.g stock price quote tickers alternately demonstrate ebb and tide which are explained by Chaotic Mandelbrot sets (Multifractals - <https://www.scientificamerican.com/article/multifractals-explain-wall-street/>). Collatz sequence is complementarily 2-colored by odd and even integers determined by rule earlier. Collatz conjecture for economic datasets (quarterly GDP data of Boom-Recession, Demand driven-Supply driven) is a plausible usage for Graphical Event Models by following hypothetical rephrasal:

$x(n+1) = \text{Boom}/2$  (Recession), if  $x(n) = \text{Boom}$  (simulates penalty for supply glut after boom)  
and  
 $3*\text{Recession} + 1$  (Boom) if  $x(n) = \text{Recession}$  (simulates incentive for demand growth after recession)

Stock prices are influenced by global cues and sectorwise stocks fall or rise according to ripple effect of global events making stream of stock quotes an event timeseries for Graphical Event Model. Boom is tentatively defined as  $> 7\%$  GDP growth QoQ while Recession is defined as  $< 2\%$  GDP growth over two



consecutive quarters. Thus GEM and CEM are heavily related to Chaos and Non-linear dynamics. Basic dictum of market event causality cycle goes by: Boom causes supply glut, supply glut causes low demand and recession, and low supply caused by recession spurs demand which is thus a cyclical CEM and GEM.

Multifractal model of stock markets defines stream of multiple local exponents for logistic instead of one exponent. Discrete Fourier Transform of stream of stock quotes could reveal hidden periodicities - For stream  $q_0, q_1, q_2, \dots, q_N$ :

$$X(k) = \text{Sum}_{n=0\_to\_N-1}(x(n) * e^{(2\pi i n k/N)}), \quad k=0,1,2,\dots,N-1$$

$X(k)$  are the Fourier spectrum frequencies.

-----  
1147. (THEORY and FEATURE) ThoughtNet Hypergraph - Difficulty in unique determination of a hyperedge - 24 June 2021 - related to all sections on ThoughtNet Hypergraph Evocation, Evocation WordNet, Contextual Multiarmed Bandit model of ThoughtNet, Reinforcement Learning and Word Sense Disambiguation, Cognitive Psychology  
-----

NeuronRain postulates and implements a Contextual Multiarmed Bandit model of thought evocation named "ThoughtNet" which is a hypergraph of thoughts and every vertex of multiplanar ThoughtNet is a stack. Reinforcement Learning based Contextual Bandit retrieves thought of maximum reward for each evocative. For example, three stack hypervertices  $c_1, c_2, c_3$  of ThoughtNet could be evocatives or modal classes and each hypervertex stack is populated by thoughts  $t_1, t_2, t_3, \dots, t_n$ . Hypergraph nature of ThoughtNet allows a thought hyperedge to connect multiple hypervertices of ThoughtNet. Evocation problem is to uniquely determine a hyperedge on utterances of evocatives  $c_1, c_2$  and  $c_3$ . As opposed to contextual multi armed bandit solution which ranks thoughts evoked by numeric rewards and chooses the maximum, unique thought could be retrieved non-numerically if intersection of sets of hypervertices has size 1. Any intersection of size  $> 1$  would necessitate disambiguation - Example:

$c_1 - \{t_1, t_3, t_7\}$

$c_2 - \{t_1, t_2, t_5, t_6\}$

$c_3 - \{t_1, t_3, t_4, t_5\}$

For previous ThoughtNet hypergraph of three hypervertices  $c_1, c_2, c_3$  and hyperedges  $t_1, t_2, t_3, t_4, t_5, t_6, t_7$ , evocatives  $c_1, c_2, c_3$  uniquely determine  $\{t_1\}$  by intersection while evocatives  $c_1, c_3$  retrieve thoughts  $\{t_1, t_3\}$  which have to be ranked. Datastructure used for intersection (e.g type of hashing) is crucial.

-----  
1151. (THEORY and FEATURE) Graph Theoretic Urban Sprawl Analytics, Konigsberg problem, Edge and Vertex covers, Social Network Analysis, Eulerian circuits, Dense subgraphs and Minimum spanning tree - related to 753 and all sections on Urban Sprawl and GIS analytics, Graph theoretic Merit of Large Scale Visuals, Image segmentation, Drone Navigation, Social Network Analysis - 14,15,16 July 2021  
-----

Graph Theory was born from Euler's analysis of Konigsberg Bridge problem which is an urban transportation feasibility question answered by Eulerian circuits - graphs of even degree vertices and edges belonging to single component - whether people can traverse closed trail of all bridges in city of Konigsberg. Minimum spanning tree (least cost tree of a graph spanning all vertices), Vertex cover (subset of vertices on which atleast one endpoint of every edge is incident), Edge cover (subset of edges on which every vertex is incident) and Eulerian Circuit (graphs of even degree vertices and edges belonging to single component) of Segmented Urban Sprawl GIS Facegraph and Transportation graph are theoretical tools which are useful in planning optimal transportation of an urban sprawl - Every traffic intersection of urban transportation network is a vertex and connecting roads are edges. Vertex cover highlights all important intersections while edge cover is the set of all important roads. Minimum spanning tree is the least cost subset of roads between

any intersection. Dense subgraphs or cores of transportation network are congested clusters of activities. Strongly connected components of transportation network are usually blockade-free. Typically an urban or metropolitan agglomeration is defined as a circle of radius which includes all localities served by suburban public transport (metro, rail or road) connectivity to central business district of the city - by people who commute to work daily. Aforementioned graph theoretic gists of urban transportation graph or facegraph facilitate efficient drone GPS navigation for myriad automatic delivery of services. Urban transportation network is a directed, multiplanar (as intersections might be flyovers or grade separators), multigraph (because of multiple lanes between intersections) or could as well be a hypergraph because carriageways connect multiple vertices (intersections). Air quality index is a pollution measure which is directly proportional to urbanisation and industrialization and optimally spaced-out residential, commercial, manufacturing-IT-ITES and Greenery by Four-color theorem multiple agent resource allocation disperses particulate matter.

#### References:

```

1151.1 Graph Theory - [Douglas B. West]
/*
#####
#####
#
This
work is licensed under a <a rel="license"
href="http://creativecommons.org/licenses/by-nc-nd/4.0/">Creative Commons
Attribution-NonCommercial-NoDerivatives 4.0 International License.
#####
#####
#Course Authored By:
#-----

#K.Srinivasan
#NeuronRain Documentation and Licensing: http://neuronrain-
documentation.readthedocs.io/en/latest/
#Personal website(research): https://sites.google.com/site/kuja27/
#-----

#####
#####
*/
```

This is a non-linearly organized, code puzzles oriented, continually updated set of course notes on C language. Though C is at present rapidly diminishing in usage because of many high level languages and big data tools for cloud processing, a primer in C is essential for grasping nuances of operating system memory management, networking and threading

#### References:

- ```
-----
1. C Puzzle Book - Alan R.Feuer
2. C Programming Language - ANSI C - [Kernighan-Ritchie]
```

2 February 2017

Arithmetic Operators:

```
#include <stdio.h>
```

```
main()
{
```

```

int x;
x = -3 + 4 * 5 - 6; printf("%d\n",x);
x = 3 + 4 % 5 - 6; printf("%d\n",x);
x = -3 * 4 % -6 / 5; printf("%d\n",x);
x = (7 + 6) % 5 / 2; printf("%d\n",x);
}

```

/*

Above prints:

11 (-3 unary operator has precedence over binary, * has precedence over + and -. (-3)+(20) -6 = 11)
 1 (remainder operator (modulus) % has precedence. 3 + (4) - 6 = 1)
 0 ((((-3 * 4) % -6)/5) = (-12 % -6) % (-1) = 0. Operator precedence is same and evaluation is from left to right)
 1 (((13) % 5) / 2 = 3 % 2 = 1)
 */

 10 March 2017

Pointers in C are basic low level primitives of allocating memory and indexing them by contiguous bytes (malloc/free). Most of the vulnerabilities found in software are traced back to memory buffer overruns. Buffer overruns are conditions in which a pointer to a contiguously allocated block of memory goes past the bounds. Two major bugs in modern internet history are OpenSSL's Heartbleed and Cloudflare's Cloudblood both being bugs in array bounds checking crept into software.

1. HeartBleed fix for OpenSSL - <https://git.openssl.org/gitweb/?p=openssl.git;a=commitdiff;h=96db902> - This bug was introduced into OpenSSL in

HeartBeat extensions for SSL connections keep-alive feature. Pointer was getting past without record length checks enforced in the fix commit diffs

2. CloudBleed fix for Cloudflare proxies HTML parsing -

<https://blog.cloudflare.com/incident-report-on-memory-leak-caused-by-cloudflare-parser-bug/>. This is similar to HeartBleed buffer overrun, which happened during equality check for end of buffer pointer (which bypasses an increment check condition within Ragel HTML parser).

 Duff's Device - 7 August 2018

Duff's device is C loop unrolling design pattern which mixes switch and looping for fall throughs. Example code is in code/duffs_device.c which decrements a counter in a loop - switch statement falls through when counter is not divisible by 5 to case statement selected by switch and number for chosen case statement is decremented by fall through to other cases till end. This is an optimized loop unrolling inspired by jmp statements with in loops in assembly language routines. Previous example prints (in "case: counter" format):

```

0: 29
1: 28
2: 27
3: 26
4: 25
0: 24
1: 23
2: 22
3: 21
4: 20
0: 19
1: 18
2: 17
3: 16
4: 15
0: 14
1: 13

```

2: 12
3: 11
4: 10
0: 9
1: 8
2: 7
3: 6
4: 5
0: 4
1: 3
2: 2
3: 1
4: 0

10 February 2020 - C++ Class simulation in C, Function pointers, Private and Public

Example code class_in_c.c simulates object oriented programming of C++ in C. C only has the facility of struct {} declaration which is exploited to declare few private and public variables (variables are structs containing primitive type unions of type "struct variable". A flag to distinguish private variables is part of the struct variable) and member function pointers for class "struct classinc". Member private and public variables are assigned to by set<type>() functions which check private flag of a variable and deny access for private variables. Member function function1() clears the private flag and invokes set<type>() reinstating the private flag after for member variable thus simulating privileged member function access of private. set<type>() functions simulate type overloading. Logs in code/logs/class_in_c.log.10February2020 trace the public and private access by functions pointed to.

7 May 2020 - Simulation of loop by recursion, void typecast, Binary search tree example

Functional programming defines loop imperatives by recursion. Code example recursionasloop.c demonstrates incrementing a counter by recursion without recourse to for loop. Function loop() defines two clauses for simulating increment by recursion and to check if an array representation of a binary tree is indeed a binary search tree by verifying if inorder traversal of the tree is sorted ascending and adheres to subtree comparison ordering. Both int object and int[] array are passed to loop as void* where arg is reinterpret_cast()-ed. Two binary trees one of which is not a BST are tested. Pairwise subtree comparison and loopless increment are printed to logs/recursionasloop.log.7May2020.

6,7,8 June 2020 - Dynamic Nested For Loop (variant of question from UGC NET/SLET/JRF)

Writing hardcoded nested for loops (of constant depth) in C is trivial. But for generalizing loops to arbitrary nested depths is less straightforward because loop body has to be dynamically indented which requires on-the-fly code generation. Code example dynamicnestedloop.c implements a contrived recursive

version of nested looping of arbitrary depth. Function nestedloop() accepts from,to and function pointer to body of the loop. nestedloop() is recursively invoked along with loopbody() till depth is decremented to 0. Subtle difference to usual n depth for loop of range 10 - counter is incremented to $10^n + 10^{(n-1)} + \dots$ instead of 10^n (and thus powerful compared to hardcoded nested for loop) which is filtered by depth==1 check within loopbody(). Removing depth==1 clause increments counter to 1110 and not 1000 (depth 3 nesting). Iterative version of dynamic nesting is again non-trivial.

2,3,4,7 July 2020 - Arrays as Pointers, Recursive exponentiation in binary (variant of questions 22,48 from GATE 2020)

Questions 22 and 48 of GATE 2020 have been merged to code example multidimensionalarrays.c which demonstrate:

- 2-d arrays as objects and their multidimensional pointer dereferencing
- exponentiation function pp(a,b) which raises a to the exponent b after converting b to binary string by modulo 2 division recursively (to-binary function - tob())

pp() function obtains the binary string of b from tob() which is looped through and tot is updated only for bits "1" in binary string of b. Auto variable array arr[] is allocated on stack and dereferenced by tob().

This work is licensed under a Creative Commons Attribution-NonCommercial-NoDerivatives 4.0 International License.

#####

Course Authored By:

K.Srinivasan
Personal website(research): <https://sites.google.com/site/kuja27/>
NeuronRain GitHub and SourceForge Documentation: <http://neuronrain-documentation.readthedocs.io/>

This is a non-linearly organized, continually updated set of course notes on miscellaneous topics in Computer Science (algorithms, datastructures, graph theory etc.,). Puzzles/Problems/Questions are sourced from many text books.

9 February 2017

A graph G with 100 vertices numbered from 1 to 100 has edges between vertices p and q iff $p-q=8$ or $p-q=12$. Number of connected components

of G is:

Number of components of an undirected graph is number of subgraphs with no path between them. Above set of adjacent vertices can be written as merger of 2 arithmetic progressions of common different 8 and 12 as below:

1, 9, 13, 17, 25, 33, 37, 41, 49, ...
2, 10, 14, 18, 26, 34, 38, 42, 50, ...
3, 11, 15, 19, 27, 35, 39, 43, 51, ...
4, 12, 16, 20, 28, 36, 40, 44, 52, ...
5, 13, 17, 21, 29, 37, 41, 45, 53, ...
6, 14, 18, 22, 30, 38, 42, 46, 54, ...
7, 15, 19, 23, 31, 39, 43, 47, 55, ...
8, 16, 20, 24, 32, 40, 44, 48, 56, ...

Further sets are repetitions of the above. Of the previous 8 sets 4 have common elements between them and form a connected component. Thus there are 4 connected components in the graph G. This is equal to GCD of two common differences 4 and 8.

15 February 2017

Linear Programming and Simplex

Linear programming is defined as: Given an objective function to minimize or maximize with set of constraints expressed as inequalities, finding set of solutions which maximize or minimize the objective function. For example following is a linear program:

maximize $x_1 + 6x_2 = P$ (written as $-x_1 - 6x_2 + P = 0$)
subject to constraints:
 $2x_1 + x_2 \leq 10$
 $x_1 + 5x_2 \leq 9$

There are 3 types of solutions possible for a Linear Program:

- *) Basic feasible solution - which is the set of vectors which satisfy the constraints. There are two types of feasible solutions:
 - *) Bounded feasible - the satisfying vectors maximize the objective function to a bounded value
 - *) Unbounded feasible - the satisfying vectors maximize the objective function to an unbounded value
- *) Infeasible - there are no vectors which satisfy the constraints.

Simplex algorithm solves an LP in following tableau steps:

while (there are no negative indicators in ObjF row)

{

- *) Choose least positive pivot row and most negative pivot column as pivots:
 - most negative indicator column is chosen as pivot column
 - divide the last column entries by pivot column entries and choose least positive row as pivot row

| | x1 | x2 | s1 | s2 | P | | |
|----|----|----|----|----|---|----|------------------------------|
| c1 | 2 | 1 | 1 | 0 | 0 | 10 | $10/1 = 10$ |
| c2 | 1 | 5 | 0 | 1 | 0 | 9 | $9/5 = 1.8$ (least positive) |

pivot row - c2)

| ObjF | -1 | -6 | 0 | 0 | 1 | 0 |
|------|----|----|---|---|---|---|
|------|----|----|---|---|---|---|

most negative pivot column (x2)

*) the pivot entry in the intersection of c2 and x2 is 5. Interchanging the row and column variables row2 is x2. Divide by pivot to obtain 1:

| | x1 | c2 | s1 | s2 | P |
|----|----|----|----|----|----|
| c1 | 2 | 1 | 1 | 0 | 10 |

| | | | | | | |
|------|-----|-----|---|-----|---|-----|
| x2 | 1/5 | 5/5 | 0 | 1/5 | 0 | 9/5 |
| ObjF | -1 | -6 | 0 | 0 | 1 | 0 |

and do row operations till all other row entries in pivot column are zero.

*) perform a row mapping operation - $Rc1 = Rc1 - Rx2$:

| | | | | | | |
|------|-----|----|----|------|---|------|
| | x1 | c2 | s1 | s2 | P | |
| c1 | 9/5 | 0 | 1 | -1/5 | 0 | 41/5 |
| x2 | 1/5 | 1 | 0 | 1/5 | 0 | 9/5 |
| ObjF | -1 | -6 | 0 | 0 | 1 | 0 |

*) perform a row mapping operation - $R0bjF = 6Rx2 + R0bjF$:

| | | | | | | |
|------|-----|----|----|------|---|------|
| | x1 | c2 | s1 | s2 | P | |
| c1 | 9/5 | 0 | 1 | -1/5 | 0 | 41/5 |
| x2 | 1/5 | 1 | 0 | 1/5 | 0 | 9/5 |
| ObjF | 1/5 | 0 | 0 | 6/5 | 1 | 54/5 |

(no negative indicators, iteration stops)

}

From previous last iteration feasible solution satisfying the constraints is :
 $x_2=9/5$, $x_1=0$ and maximized objective function value is $54/5$ for $x_1 + 6x_2$
 $= P$

LL,LR and Shift-Reduce Parsers

Parsing with reference to modern programming languages is defined as:
 Given a set of Context Free Grammar Production Rules produce a parse tree in either top-down or bottom-up fashion resulting in a single non-terminal symbol.

LL parsing is Left-Right, Top-Down scanning of the symbols with Leftmost Derivation while LR parsing is Left-Right, Bottom-Up scanning of the symbols with Rightmost Derivation. Shift-reduce parsing which is an LR parsing is implemented with a stack,lookahead symbol(usually 1) and yet to be scanned set of terminals.

Leftmost Derivation applies production rule to leftmost non-terminal in a sentential form(top-down parsing). Rightmost Derivation applies a production rule to rightmost non-terminal in a sentential form(bottom-up parsing)

Example CFG for simple arithmetic operation (+ and *):

$E = E * T$
 $T = E + E$
 $E = id$

Previous CFG is applied to parse a sentence:

$x * x + x$

Leftmost Bottom-Up Derivation Parser:

$x * x + x$
 $E = E * T$
 $E = id * T$ ($E = id$)
 $E = id * E + E$ ($T = E + E$)
 $E = id * id + E$ ($E = id$)
 $E = id * id + id$ ($E = id$)

Rightmost Top-Down Derivation Parser (Complete Reversal of Previous Parsing Steps):

```

E = E * T
E = E * E + E (T = E + E)
E = E * E + id (E = id)
E = E * id + id (E = id)
E = id * id + id (E = id)

```

Bottom-Up Shift-Reduce Parsing with a stack for previous Rightmost Derivation:

| Stack | Lookahead | Yet-to-be-scanned | ProductionRule |
|----------|-----------|-------------------|----------------|
| - | id | * id + id | - |
| (Shift) | | | |
| E | * | * id + id | E = id |
| (Reduce) | | | |
| E | * | id + id | - |
| (Shift) | | | |
| E* | id | + id | E = id |
| (Reduce) | | | |
| E*E | + | id | - |
| (Reduce) | | | |
| E*E | + | id | - |
| (Shift) | | | |
| E*E+ | id | - | E = id |
| (Reduce) | | | |
| E*E+E | - | - | T = E + E |
| (Reduce) | | | |
| E*T | - | - | E = E * T |
| (Reduce) | | | |
| E | - | - | - |

Shift-Reduce parser actions at each step are determined by valid combinations of top of the stack and the lookahead - a pushdown automaton state diagram. Shift step advances to next unscanned symbol and Reduce step applies a production to top of the stack based on lookahead.

 23 February 2017

Evaluate prefix expression:
 *+3+3^3+333

This can be evaluated with two stacks as below by popping topmost and storing it in another stack, evaluating next two operands and operator on first stack and pushing back the result and topmost popped from second stack to first stack:

| | | | | | |
|---|---|-----|-----|-----|--------|
| 3 | 3 | 3 | 3 | 3 | = 2205 |
| 3 | 6 | 729 | 732 | 735 | |
| 3 | 3 | 3 | 3 | * | |
| + | ^ | + | + | | |
| 3 | 3 | 3 | * | | |
| ^ | + | + | | | |
| 3 | 3 | * | | | |
| + | + | | | | |
| 3 | * | | | | |
| + | | | | | |
| * | | | | | |

 An egg dropped from a floor between 1 to 100 breaks if floor value is x or above. With 2 eggs find minimum number of drops required to find the highest floor from which egg does not break.

Binary search on the floors 1 to 100 would require log(100) eggs. With 2 eggs

binary search won't work. For this number 100 is split into intervals of powers of 2 (this is the idea behind logarithmic counters) - 2,4,16,32,64. First egg is dropped sequentially from 2,4,16,32,64th floors. Drop when first egg breaks is denoted as m. Maximum number of drops is 6 for first egg. Then the second egg is sequentially dropped from $2^{(m-1)}$ floor to 2^m floor which is equal to $2^{(m-1)}$. Thus total drops required is $m + 2^{(m-1)}$. For maximum value of $m=6$, this is $6 + 36=42$. Thus with 42 drops, highest floor from where egg does not break can be found. Trivial one level binary search would require 50 ($100/2$) drops for second egg.

28 February 2017

There is a list with integers in range 1..n with length n+1 elements. Find the repeated element (in least space without hash tables)

Brute force requires $O(n)$ space and hash tables require $O(n)$ space too. This list has a pattern that all elements are in range 1..n with one repeat. Sum of this list can be computed in $O(\log N)$ space - single counter incremented - which is $\text{Total} = n(n+1)/2 + \text{repeating_element}$. $\text{Total} - n(n+1)/2$ is the repeating element. Any other value of $|\text{Total} - n(n+1)/2|$ which is not in 1..n indicates more than one repeating element and more than 1 repetition per repeating element. For arbitrary length of list, and multiple repetitive elements, this problem reduces to Element Distinctness Problem which has non-trivial algorithms ($N \log N$ lowerbound with sorting, decision tree model, property testing, quantum etc.,).

6 March 2017

Types of Latches and FlipFlops:

SR latch (Set-Reset):

| S | R | Q |
|---|---|---|
| 1 | 0 | 1 |
| 0 | 1 | 0 |

JK Latch(SR Latch with Toggle Q and !Q states for 00 and 11):

| J | K | Q |
|---|---|---|
| 1 | 0 | 1 |
| 0 | 1 | 0 |

D FlipFlop:

| D | Q |
|---|---|
| 0 | 0 |
| 1 | 1 |

20 September 2017

Bernoulli Trials and Geometric Distribution:

Question: While tossing a coin what is the expected number of coin tosses before Head appears? (i.e expected number of failures before success)

Answer: Probability of head = $\Pr(H) = 1/2$.

Let N be the number of coin tosses before Head appears. N is a Bernoulli trial random variable.

$\Pr(N)$ is the probability of Head appearing after N coin tosses.

$\Pr(N) = (1-\Pr(H))^{(N-1)} \Pr(H)$ (first N-1 tosses is streak of Tails and Nth toss is Head i.e TTTT...TH)

Expected value of N = $E(N) = \sum_{1 \text{ to } \infty} (N * (1-\Pr(H))^{(N-1)} \Pr(H)) = (1/2) + (1/2)^2 + (1/2)^3 + \dots = 1/1-0.5 = 2 = (1-\Pr(H))/\Pr(H)$

Expected value of $N = (1 - \Pr(H)) / \Pr(H) = 0.5 / 0.5 = 1$

This problem has applications in predicting binary streams of 0s and 1s in network traffic. But probability of 1 and 0 need not be a fair coin toss i.e $\Pr(1) \neq \Pr(0)$. If a network packet traffic stream has $\Pr(1) = 0.75$ and $\Pr(0) = 0.25$, Expected number of bits after which bit 1 appears = $(1 - 0.75) / 0.75 = 1/3$ and Expected number of bits before 0 appears = $(1 - 0.25) / 0.25 = 3$

It has to be noted that Expectation of Appearance of Head and Expectation of Failures before Head Appears are two different random variables.

Reference: https://en.wikipedia.org/wiki/Geometric_distribution

13 October 2017

How can all nodes of same level in a binary tree be retrieved (of least time complexity)?

Assuming array representation of a binary tree, each node of the array of size $2^{\lceil \log N \rceil}$ for N tree nodes is filled from the tree top-down and left-right and missing nodes are blank in array. In this array representation, nodes of level l are the consecutive nodes from indices $2^{(l-1)}$ to $(2^l) - 1$ and can be printed by iterating through array.

27 November 2017

847. (THEORY) One way functions - How can a hashmap be inverted i.e keys and values are interchanged? - related to all sections on Hardness Amplification, Locality Sensitive Hashing, Separate Chaining, One-way functions and Parallel algorithms

If the hashmap is perfect hash function, there are programming language supports e.g bidirectional dictionaries - bidict in Python, Ruby Hash#invert - <http://ruby-doc.org/core-1.9.3/Hash.html#method-i-invert>. If the hashmap is not perfect and has collisions each key is mapped to multiple values. Inverting this amounts to unwinding each of the collision buckets as keys and map them to the erstwhile key as value. Brute force algorithm is $O(N)$ time where N is total number of values in the map. An alternative version of this problem is : Given a value v in the map find the key k which maps to v . Theoretically, this problem is parallel to Proving existence of One Way Function which is defined as $\text{Probability}[f(\text{finverse}(y))=y] < \epsilon$ for a function f and its inverse. For a hashmap H , this is equivalently stated as $\text{Probability}[H(H^{-1}(v))=v]$ where H^{-1} is hashmap inverted. Difference is Function has unique range value per domain key while a hashmap has multiple values. Sublinear parallel algorithm to invert a hashmap which is not perfect could be as below:

```
    for each key k in hashmap H1 accessed in parallel
    {
        each element  $v=H1[k]$  in collision bucket is accessed in parallel and
        added as key in a new hashmap H2 as  $H2[v] = k$ 
    }
```

Both keys and buckets are accessed in parallel. Theoretically if hashmap is on a PRAM, previous algorithm is $O(1)$ parallel time and requires $O(N)$ PRAMS.

 2 January 2018 - Find Sum of Bit differences (Distance) between all possible pairs of integers in an array

Example: For array [1,2,3] sum of bit differences for pairs:

distance(1,2) = 01,10 = 2
 distance(1,3) = 01,11 = 1
 distance(2,3) = 10,11 = 1

 4

Trivial bruteforce algorithm has to compute all possible pairs and find the distance of each pair which is $O(NC^2 \log M)$ where N is the size of array and M is the largest integer in array.

Following algorithm finds the bit distance sum in $O(\log M * N)$ time for all pairs of subsets better than above bruteforce:

 (#) Represent the array of size N and largest number M as $N * \log M$ 2-dimensional array.
 (#) For each column ($O(\log M)$):
 {
 Find the number of rows R having same bits - 0 or 1 ($O(N)$).
 /*
 Number of pairs differing in this bit position are :
 Set of all possible pairs - (Set of all possible pairs
 having both 1s + Set of all possible pairs having both 0s)
 This contributes to the sum of distances for all bits
 */
 BitDifferenceSum += $NC^2 - ((N-R)C^2 + RC^2)$
 }

Following example executes above algorithm for array: [5,6,7,8,10] represented as $5 * \text{ceil}(\log_{10})$ 2-dimensional array - there are $5C^2=10$ possible sets of pairs:

0101
 0110
 0111
 1000
 1010

 2+1+3+4+1+3+2+4+3+1=24

There $3C^2+2C^2$ pairs of (1,1) and (0,0) which are subtracted:

$5C^2 - (3C^2+2C^2) + 5C^2 - (3C^2+2C^2) + 5C^2 - (3C^2+2C^2) + 5C^2 - (3C^2+2C^2) = 10-4 + 10-4 + 10-4 + 10-4 = 6+6+6+6 = 24$

An implementation of this algorithm has been included in NeuronRain AsFer Pairwise Encoded String Pattern Mining function in:
<https://github.com/shrinivaasanka/asfer-github-code/blob/master/cpp-src/asferencodestr.cpp>

 9 January 2018 - Find the heavier ball

Question: There are 8 balls of same size. One of them is heavier and all other 7 are of equal lesser weight. Find the heavier ball in just 2 weighings.

Answer: Assuming a balance, split the 8 balls into 2 sets of 4 each placed on

either trays of the balance. One of the trays goes down
 Heavier ball is one of the 4 in going down tray. Split the set having heavier
 element into 2 sets of 2 each placed on either trays. This is
 second weighing. One of the trays goes down. Heavier ball is one of the 2 in
 down tray. Third weighing is not necessary because one ball each
 can be removed from each tray and there are two possibilities: 1) The trays
 level - ball taken from going up tray is heavier, 2) the trays don't level -
 both balls taken are of equal weight and down tray has heavier ball.

Previous problem has deep rooted connection to finding the larger value in a
 balanced search tree. Two trays of the balance are two subtrees of a BST in each
 weighing and query time is $O(\log N)$.

 834. (THEORY and FEATURE) Social Network Analysis - People Analytics - Unique
 Identification - 12 January 2018 - How would you uniquely identify an object
 from a plethora of objects? - Birthday Paradox, Contextual Name Parsing, PIPL
 Name syllable based unique person search - related to all sections of People
 Analytics

 That is, how can a universally unique identifier be created? This is an open-
 ended question. In the context of Public Key Infrastructure,
 creating unique non-repetitive keys has been a challenge - Sections 4.1 and 4.2
 in <https://factorable.net/weakkeys12.conference.pdf> on repetitive and factorable
 keys. Boost C++ has UUID generation algorithm based on
<https://www.itu.int/en/ITU-T/asn1/Pages/UUID/uuids.aspx>. UUID is a misnomer
 because there is a negligible probability of collisions known as birthday
 paradox. Birthday paradox is problem of any two persons in a congregation having
 same birthday. If a unique id is of maximum value N and size of population is M
 ($M < N$):

probability of person2 having different id than person1 = $(N-1)/N$
 probability of person3 having different id than person1 and person2 = $(N-2)/N$
 probability of person4 having different id than person1, person2 and
 person3 = $(N-3)/N$
 ... and so on.

Probability of all persons in population having different UUIDs = $(N-1)(N-2) \dots (N-M) / N * N * N \dots N$
 Probability of some of the population having same UUIDs = $1 - [(N-1)(N-2) \dots (N-M) / N^M]$

This problem has direct bearing on Tabulation Hashing where two objects have
 same hash digest and are hashed to same bucket. Minimizing hash collisions
 therefore requires increase in denominator and lowering numerator i.e $N \gg M$.

This problem is all the more serious in People Analytics where a person has to
 be uniquely identified in ,say, social networks undisputably (e.g there are
 abundant duplicate social profiles of same name, photos etc., and handles are
 sometimes prefixed as "real<name>"). Usually it suffices that N is $\log M$ bit
 integer. Digital Unique IDs stored on cloud often are vulnerable to attacks. An
 example Unique Person Search therefore might involve a decision tree of depth
 $O(\log M)$ and UniqueID is not just an integer but is a concatenation of various
 not-so-forgable human non-digital features (e.g age, voice metric, biometric,
 blood group, height, birthmarks, educational qualifications, work experience,
 circle of human acquaintances, non-invasive unique private event in a person's
 timeline history etc.,)

Name Syllable based Unique Person Search (by scraping PIPL.com data) is
 described and PIPL.com python API search of similar persons is implemented in
 NeuronRain AstroInfer commit <https://gitlab.com/shrinivaasanka/asfer-github-code/commit/d855882c3e8c2f97f6709c6f4a03728f95377ca1> (and in GitHub and

SourceForge AstroInfer repositories). Contextual Name Parsing to parse First and Last Names from Full Name based on ID context has been implemented in NeuronRain AstroInfer commit <https://gitlab.com/shrinivaasanka/asfer-github-code/commit/3ae9054a1311176c87304ed85e3835510657fc8b> (and in GitHub and SourceForge AstroInfer repositories)

835. (THEORY and FEATURE) Unsorted Search - Kernel lifting and Computational Geometric search - 19 January 2018 - How would you find needle in haystack? - related to all sections on Computational Geometric Hyperplanar Point Location, Locality Sensitive Hashing and Shell Turing Machines

Question can be translated to finding a number in a set of unsorted numbers. Trivial brute-force search is of $O(N)$. Can this be improved? There are some ways to go about:

1. Searching set of numbers is one dimensional. If each integer is mapped to a tuple in n -dimensional space, then searching reduces to shooting a ray from origin and doing a sweep line which is computational geometric reduction of search problem. For example, 2387283 is mapped to [2,3,8,7,2,8,3] which is 7 dimensional tuple. Each dimension has maximum of 10 values - 0 to 9. Each number in set is thus a tuple in this space. This has some parallels to kernel trick and Support Vector Machines in Machine Learning which lift data in low dimension to higher dimension (Mercer polynomial Kernels). Previous reduction depends on the radix of the numbers. Representing in hexadecimals, widens the ease of search. This reduction creates a new d -dimensional dataset from one dimensional and distance of any point from origin is the L2 norm upperbounded by $\sqrt{d \cdot 100}$. This shrinks the distance of any point in the haystack from other point from $O(N)$ to $O(\sqrt{d})$.

2. Represent the numbers in dataset as $M \times N$ matrix where N is the size of set and M is the number of digits. Each contiguous subset of columns are transformed into a hashtable of size N corresponding to $O(M^2)$ substrings. Searching the number is then looking up each digit/substring of the query in respective digit's/substring's hashtable. For example, 123,235,534,323,333,343 form the contiguous column subsets:

```
1 2 3 12 23
2 3 5 23 35
5 3 4 53 34
3 2 3 32 23
3 3 3 33 33
3 4 3 34 43
```

Next create 5 hashtables for $3 \times 2 - 1$ digit substrings: [1,2,5,3,3,3], [2,3,3,2,3,4], [3,5,4,3,3,3], [12,23,53,32,33,34], [23,35,34,23,33,43]
Searching 323 then requires 5 lookups for 3,2,3,32,23 in each of previous tables successively.

Searching 545 returns true (false positive) if 4th and 5th contiguous substring columns are not considered which fail the lookup of 54 and 45.
Number of substrings of an integer string of length M is $M + M - 1 + M - 2 + \dots + 1 = M(M - 1)/2$ and each hashtable is for a substring.
Trivial M -length string hashtable is not created (which obviates this algorithm). This is $O(M^2)$ total lookup assuming $O(1)$ per table hash lookup and no sorting is needed. Overhead is the preprocessing step of creating hashtables. If $M \cdot M \ll N$, this $O(M^2)$ lookups is too less than brute force search of $O(N)$.
Number of possible M -digit strings are 10^M which is maximum possible value of N , and $M^2 \ll 10^M$.

Algorithm 1 can search a query point by Algorithm 2.

This algorithm has been implemented in NeuronRain AsFer -
<https://github.com/shrinivaasanka/asfer-github-code/blob/master/python-src/UnsortedSearch.py>

Example unsorted search 1 - <https://github.com/shrinivaasanka/asfer-github-code/blob/master/python-src/testlogs/UnsortedSearch.log.21January2018>

```
.....
...
Is Queried integer 99455 in unsorted array: False
Is Queried integer 43 in unsorted array: True
Is Queried integer 31 in unsorted array: True
Is Queried integer 17 in unsorted array: True
Is Queried integer 3278 in unsorted array: False
Is Queried integer 333 in unsorted array: False
Is Queried integer 29 in unsorted array: True
.....
```

Example unsorted search 2 -
<https://raw.githubusercontent.com/shrinivaasanka/asfer-github-code/1b543857e41824a1ed0e10211ceb1e0906bd670c/python-src/testlogs/UnsortedSearch.log.23March2018>

```
.....
Is Queried integer 99455 in unsorted array: False
Is Queried integer 43 in unsorted array: True
Is Queried integer 31 in unsorted array: True
Is Queried integer 17 in unsorted array: True
Is Queried integer 3278 in unsorted array: False
Is Queried integer 333 in unsorted array: False
Is Queried integer 29 in unsorted array: True
Is Queried integer 327 in unsorted array: False
Is Queried integer 115 in unsorted array: False
.....
```

Previous matrix representation of the unsorted numerical dataset replaces the traditional array storage and requires $O(M^2 \cdot N)$ space. Sequential search time of $O(M^2)$ derived previously can be shrunk to $O(1)$ by searching each substring parallelly in M^2 processors. If number of digits is upperbounded by a constant, storage is $O(N)$ which is of same space complexity as array storage. With respect to overhead of creating hashtables, the benefit of Unsorted Search is the ability to exit the search if prefix or suffix is not found and entire number string need not be matched and is significant optimization for large M . Insertion of an M -digit integer into this Hash storage is $O(M^2)$ for all substrings whereas in traditional lists appending is $O(1)$. But lookup in traditional unsorted list is $O(N)$ and $O(M^2)$ in Unsorted Search of Substring hashtables. Thus the latency of Unsorted Search is only in adding an integer to list and is $O(N \cdot M^2)$ for all integers.

Present implementation in NeuronRain AsFer creates hashtables only for all prefixes and suffixes of strings. Similar to Bloom Filters, Unsorted Search of single digit hashtable lookup can have only False Positives and not False Negatives - if a number does not exist it can be wrongly flagged as match, but if it exists match is always correct. False Positives are removed by matching all prefixes and suffixes. Hashtables for just prefixes and suffixes are sufficient because Set of Unsorted Integers can be stored in a TRIE M -ary Tree datastructure in which numbers in list are marked in internal nodes by a delimiter and all root to nodes paths are the prefixes. Mismatch is flagged by an absence of root-to-node path prefix in TRIE. Maximum size of the TRIE is 10^M .

```
.....
-----
How can a Binary Search Tree be verified? - 12 March 2018
-----
-----
```

An obvious solution is to do an inorder traversal of BST and verify the list of traversed nodes is sorted ascending or descending. This is $O(n)$ for number of

nodes in tree n. Array representation of BST can be directly scanned for sortedness.

850. (THEORY and FEATURE) How would you avert collision of two trains speeding along on same track in opposing directions? - Critical Sections and Synchronization - 3 November 2018, 9 August 2020 - related to all sections on Program Analysis, Software Analytics, Software Transactional Memory, Lockfree datastructures, VIRGO Bakery Algorithm implementation, VIRGO Read-Copy-Update of NeuronRain Theory Drafts

(*) This puzzle is based on P and V Binary Semaphores - Mutexes (Dijkstra):

| | |
|-------------------------|-------------------------|
| Process1(Train1) | Process2(Train2) |
| ----- | |
| P() | P() |
| track(critical_section) | track(critical_section) |
| V() | V() |

(*) P():
while mutex==0
{
 wait()
}

(*) V():
mutex=1

(*) Difference between Binary Semaphores and this puzzle is how to avert collision after both processes have entered critical section by mistake (track) which is more susceptible to happen (e.g signals P and V fail) in real life than operating systems (even in Operating Systems this can occur when atomic instructions for P and V fail theoretically).

(*) In modern architectures, synchronization is supported in hardware by a fine-grained primitive - compare and swap instruction - atomically which has following algorithm:

```
compare_and_swap(p,old,new)
{
    if(p != old)
        return false
    p = new
    return true
}
```

(*) Multiprocessor Hardware support memory fencing instructions, bus locking etc., for serializing instructions issued before fence and to allow maximum of one thread of execution to load and store.

(*) VIRGO32 and VIRGO64 linux kernels of NeuronRain implement various userspace and kernelspace synchronization primitives - Software Transactional Memory Lockfree Userspace C++ usecase, Read-Copy-Update userspace C++ usecase and Bakery algorithm locking synchronization kernel driver which can be module imported (in two variants - 1 or 2 for loops - parametrized)

Some assumptions for solving this puzzle:

(*) Assuming electric traction or maglev, shutting down power supply is an obvious option. But this requires atleast one of the trains to be aware that the other train is on same track or a third party's intervention. Assuming zero-knowledge by everyone (e.g no GPS location info) and both trains are unstoppable, there exists a non-zero probability of collision.

Variant of the previous critical section when two tracks cross

Problem is to cross two tracks by overlap. Railway tracks are undirected cyclic graphs having 2 parallel edges. Overlapping two track edges makes it non-planar and following example gadget schematic creates a planar crossing of two parallel track edges (disconnects the graph at the crossing and adds two point vertices (and)). This is a dimensional critical section which allows a planar intersection (reduces 3D to 2D):



References:

-
- 850.1. Compare and Swap can simulate Lock-free synchronization and mutexes - [Maurice Herlihy] and P and V Semaphores - <https://en.wikipedia.org/wiki/Compare-and-swap> and [https://en.wikipedia.org/wiki/Semaphore_\(programming\)](https://en.wikipedia.org/wiki/Semaphore_(programming))
- 850.2. UNIX Internals: New Frontiers - [Uresh Vahalia - EMC] - Multiprocessor Synchronization Issues - Pages 193,200,201 - Semaphores, Convoys, Necessity of Atomic test_and_set instruction in multiprocessors. Convoys are formed in Semaphores when a queued process in Scheduler waiting on a lock is prevented from being runnable because another process holds the lock.
- 850.3. UNIX - [Maurice J.Bach - AT&T] - Page 396 - Monitors as Synchronization Primitives in Multiprocessor UNIX - Monitors differ from Semaphores by modularizing scope of critical section to subroutine and serializing access by processes.
- 850.4. Operating Systems - [Milan Milenkovic - IBM Corporation] - pages 110-112 - Section 3.4.4 - Compare and Swap instruction in IBM 370 series - Global is copied to Oldreg local registers of interleaving concurrent processes P1,P2,...Pn. Each process computes the local copy of new value of Global in Newreg registers. Condition Oldreg == Global is checked in each process which guarantees Global has not been tampered with by other processes and condition codes are set. Only one process goes beyond this sanity check if condition is satisfied and updates the Global with Newreg local copy. All other processes fail the Global == Oldreg test because Global is updated by only one of the process by its Newreg, and all other local copies of processes are out of sync which branch to loop again to read new value of Global. Similarities to Train collision example earlier have to be noted - Both the trains have to simulate a local copy of the critical section information of the track which, for example, could be Global Positioning System (GPS) location of begin-end of critical section.
- 850.5. Operating Systems - [Silberchatz-Galvin-Gagne] - pages 197-200 - Section 7.3 - TestAndSet and Swap instructions (no comparison) - Synchronization Hardware

1 May 2020 - Insertion in numbered lists

Q: It is trivial to insert an element in unnumbered lists and linked lists. How can an element be inserted in numbered lists without re-ordering - e.g element 6 is inserted in 1,2,3,4,5,6,7,8,9,10 between 6 and 7 making the list 1,2,3,4,5,6,6+1,7+1,8+1,9+1,10+1 (all elements after 6 are re-numbered):

A1: (*) TRIE solution is to append a Dewey decimal suffix to 6 as 6.1 - In previous example 1,2,3,4,5,6,7,8,9,10 becomes 1,2,3,4,5,6,6.1,7,8,9,10 preserving sorted order without renumbering.

A2: (*) List is represented as variable expression array which is lazy evaluated before and after insertion - 1+x,2+x,3+x,4+x,5+x,6+x,7+x,8+x,9+x,10+x for a global shared pointer variable x initialized to 0. All element expressions upto

insertion point are evaluated for $x=0$. After insertion of $6+x$ next to $6+0$, x is incremented by 1 and all element expressions after insertion point are evaluated:

$1+0, 2+0, 3+0, 4+0, 5+0, 6+0, 6+1, 7+1, 8+1, 9+1, 10+1$

This is not a sequential renumbering because global increment of x is reflected at once across all elements of variable array.

849. (THEORY and FEATURE) 29 May 2020 - Probability of Odd number of Heads in Coin Toss - related to all sections on Majority Voting, Efficient Population count, Voting Analytics of NeuronRain Theory Drafts

Q: A coin is tossed n times. What is the chance that the Head will present itself odd number of times (IIT-JEE 1970)

A: Total number of possible toss strings from alphabet $\{H,T\}$ are 2^n . Number of possibilities of odd number of Heads

= number of ways of arranging odd number of Hs in toss string

= number of ways of choosing strings of 1H + number of ways of choosing

strings of 3H + number of ways of choosing strings of 5H + ...

= $(n,1) + (n,3) + (n,5) + \dots = 2^{n-1}$

=> Probability of odd number of heads = $2^{n-1} / 2^n = 0.5$

For binary strings H and T are replaced by 1 and 0 and previous probability corresponds to a randomly chosen binary string to be of odd parity. Bipartisan (2-colored) voting patterns are random binary strings.

846. (THEORY) 2,3,4 June 2020 - Union of Probabilities, Bayes Rule, Venn Diagrams, Pairwise and Mutual independence - related to all sections on Majority Voting and Correlated Majority, Statistical dependence of voters

Q: Three outcomes of an experiment are w_1, w_2 and w_3 such that w_1 is twice as likely as w_2 which is twice likely as w_3 . What are the probabilities of w_1, w_2 and w_3 (UPSC Civil Services - IAS(Main) - 2003)

A: $P(w_1) = 2P(w_2), P(w_2) = 2P(w_3)$

Straightforward solution neglecting dependence of outcomes:

$4P(w_3) + 2P(w_3) + P(w_3) = 1$

$P(w_3) = 1/7, P(w_2) = 2/7$ and $P(w_1) = 4/7$

Dependent events (if "as likely as" implies dependence):

=> By union bound for dependent events w_1, w_2 and w_3 , $P(w_1 \cup w_2 \cup w_3) = P(w_1) + P(w_2) + P(w_3) - P(w_1 \cap w_2 \cap w_3) = 1$

$7P(w_3) - P(w_1 \cap w_2 \cap w_3) = 1$

By Bayes Rule for Total Probability if W is the total outcome event space, probability of total outcome:

$P(W) = \sum(P(W/W_i) * P(W_i))$

from which per event conditional probability is derived as:

$P(W_i/W) = P(W \cap W_i) / P(W)$

By General Multiplication Chain Rule for dependent events:

$$P(w_1 \wedge w_2 \wedge w_3) = P(w_1 / (w_2 \wedge w_3)) * P(w_2 / w_3) * P(w_3)$$

=> $7P(w_3) - P(w_1 / (w_2 \wedge w_3)) * P(w_2 / w_3) * P(w_3) = 1$ solving which requires knowledge of conditional probabilities

$P(w_1 \wedge w_2 \wedge w_3)$ is the intersection of three circles for $P(w_1)$, $P(w_2)$ and $P(w_3)$ in Venn Diagram - overlap of circles is the dependence of events.

Independent events - Pairwise and Mutual:

if the outcomes of experiment are mutually independent, $P(w_1 \wedge w_2 \wedge w_3) = P(w_1)P(w_2)P(w_3) = 8P(w_3) = 8/7 > 1$ for $P(w_3) = 1/7$ implying outcomes are not mutually independent (which is stricter than pairwise independence for w_1 - w_2 , w_2 - w_3 and w_1 - w_3)

References:

846.1. Probability and Statistics with Reliability, Queueing and Computer Science Applications - [Kishor Shridharbhai Trivedi] - Chapter 1 - Page 33 - Problem 4 - General Multiplication Rule (GMR)

846.2. Correlated Majority Voting - https://en.wikipedia.org/wiki/Condorcet_jury_theorem#Correlated_votes - "...Condorcet's theorem assumes that the votes are statistically independent. But real votes are not independent: voters are often influenced by other voters, causing a peer pressure effect... In a jury comprising an odd number of jurors $\{n\}$, let p be the probability of a juror voting for the correct alternative and c be the (second-order) correlation coefficient between any two correct votes. If all higher-order correlation coefficients in the Bahadur representation[6] of the joint probability distribution of votes equal to zero, and $(p, c) \in \mathcal{B}_n$ is an admissible pair, then: The probability of the jury collectively reaching the correct decision (Condorcet probability) under simple majority is given by: $P(n, p, c) = I_p\left(\frac{n+1}{2}, \frac{n+1}{2}\right) + 0.5c(n-1)(0.5-p)\frac{\partial I_p\left(\frac{n+1}{2}, \frac{n+1}{2}\right)}{\partial p}$, where I_p is the regularized incomplete beta function...."

830. (THEORY and FEATURE) Set Partition Analytics, Voting Analytics, Ramsey 2-coloring - m men and n women are to be seated in a row so that no two women sit together. If $m > n$, show that the number of ways in which they can be seated is $m! (m+1)! / (m-n+1)!$ - (Question from IIT-JEE 1983) - related to all sections of NeuronRain Theory Drafts on Set Partitions, Theoretical Electronic Voting Machines, Ramsey coloring of sequences, Complementary Sets, Avoidance Patterns in Primes - 18 June 2020, 19 June 2020

A1) m men can be seated in $m!$ ways and for each such permutation, n women can be seated in $(m+1)P_n = (m+1)! / (m+1-n)!$ ways. Multiplying, total number of such arrangements are $m! * (m+1)! / (m-n+1)!$

A2) But previous answer assumes set of m men is partitioned into m parts of size 1 each. Generalizing it to a set partition of m males of arbitrary sized parts (unrestricted set partition) no two women might still sit together - a woman sandwiched between any 2 male parts - if number of male parts exceed number of women:
- m men could be partitioned in $B(m)$ ways where $B(m)$ is the Bell number =

number of partitions of a set of size m = Sum of Stirling numbers of second kind

- Number of ways m men could be partitioned into k parts = Stirling number of second kind $\{m, k\} = \frac{1}{k!} \sum_{i=0}^k (-1)^i \binom{k}{i} (k-i)^m$
- n women could be seated in each of the k vacancies for all $k > n$ and each of k vacancies (parts) are created in $\{m, k\}$ ways
- Total arrangements possible = $\sum_k \{m, k\} k^n$ for all $k > n$

A3) Problem is symmetric:

- instead of partitioning m males first, n females could be partitioned in $\{n, 1\}$ ways where $\{n, 1\}$ is the Stirling number of second kind for number of partitions of size 1 parts (or $n!$).
- m males could be partitioned into k parts in $\{m, k\}$ ways (from A2)
- k parts of set of males could be seated in $(n+1)$ vacancies between each female - including extra seat beyond end of row - in $\sum_k (n+1)^k$ ways for all $k = n, n+1$ and each of the k parts could be found in $\{m, k\}$ ways
- k should not be less than n because it might juxtapose two women
- Total arrangements possible = $\{n, 1\} \sum_k \{m, k\} (n+1)^k$ for all $k = n, n+1$

A2 and A3 are equivalent:

$\sum_k \{m, k\} k^n$ for all $k > n = \{n, 1\} \sum_k \{m, k\} (n+1)^k$ for all $k = n, n+1$

Computer Science Theory Applications of such an avoidance are numerous - biased binary strings, patterns in primes, 2-colored sequences, bipartisan voting patterns are some of them (by replacing men-women by 0-1 or Red-Blue colors).

845. (THEORY) Finding average number of comparisons per element in a Binary Search Tree - based on question 2 of ETS GRE Major Field Test model - Computer Science Subject GRE - https://www.ets.org/Media/Tests/MFT/pdf/mft_samp_questions_compsci.pdf - DFS traversal of a Binary Search Tree - 21,22 July 2020 - related to 751,768

Following is an example of a complete binary search tree which stores a sorted array of integers in adjacency list:

```

      8 - 4,12
     /  \
    4 - 2,6
   /  \
  12 - 10,14
 /  \
2 - 1,3
6 - 5,7
10 - 9,11
14 - 13,15

```

Inorder traversal of the BST produces the sorted list 1,2,3,4,5,6,7,8,9,10,11,12,13,14,15. Problem is to find the average number of comparisons required to find an element. Generic expression for average number of comparisons could be derived as:

Number of comparisons per root-to-leaf traversal * Number of root-to-leaf traversals

Total number of elements in Binary search tree

Average root-to-leaf depth of the search tree = d

Number of comparisons per root-to-leaf traversal = $1 + 2 + 3 + \dots + d = \frac{d(d+1)}{2}$ by Gauss Formula

Number of root-to-leaf traversals = $2^{(d-1)}$

Total number of elements in Binary search tree = $2^d - 1$

=> Average number of comparisons per element of the Binary Search Tree = $\frac{d(d+1)}{2}$

* $2^{(d-1)} / [2 * (2^d - 1)]$

For previous example $d=4$ (including root) \Rightarrow Average comparisons = $4 * 5 * 8 / [2 * 15] = 80/15 = 5.33$ while Worst case number of comparisons is $O(\log N) \sim 4k$ which is counterintuitive because worst case complexity is exceeded by average case complexity (unless $k > 1$).

Previous is an approximate estimate which does not subtract overlapping traversals - Every root-to-leaf DFS traversal left-to-right marks the nodes "visited" for which comparisons have been already computed. Comparisons for visited nodes must be excluded from total comparisons. In previous example following is the DFS traversal which marks the visited nodes and number of comparisons per root-to-leaf traversal in parentheses:

8-4-2-1 (1+2+3+4=10) - 4 nodes
8-4-2 (visited), 3 (4) - 1 node
8-4 (visited), 6-5 (3+4=7) - 2 nodes
8-4-6 (visited), 7 (4) - 1 node
8 (visited), 12-10-9 (2+3+4=9) - 3 nodes
8-12-10 (visited), 11 (4) - 1 node
8-12 (visited), 14-13 (3+4=7) - 2 nodes
8-12-14 (visited), 15 (4) - 1 node

Thus there are 49 total unique comparisons for 15 nodes ignoring the visited nodes and thus average comparisons = $49/15 \sim 3.2666...$

\Rightarrow worst case complexity $4k$ is more than average case complexity $3.2666...$ for $k \geq 1$.

(PUZZLE) Elementary Number Theoretic Zero Knowledge Proofs - 16 June 2022 - Predict the integer

Q: $(BE)^2 = MPB$ for different integers B,E,M,P. Which is the correct value of M amongst 4,1,3,6?? (UPSC Civil Services - Mental ability)

A: All 4 possibilities can be tried and proved by contradiction:

1) $M=4$:

BEBE = MPB

BEE = MP

BEE = 4P

$\Rightarrow E=2$ and $B=P$ (or) $B=4$ and $M=4$ (contradiction, $B=M$ or $B=P$, no two integers can be equal)

2) $M=1$:

BEE = $1 * P$

$\Rightarrow BEBE = M(BEE)B$ (no contradiction, B,E,P can be different)

3) $M=3$:

BEE = $3P$

$\Rightarrow EE$ cannot equal 3

$\Rightarrow EE = P$ and $B = 3$ (contradiction, $B=M$, no two integers can be equal)

4) $M=6$:

BEE = $6P$

$\Rightarrow BEE = 2 * 3 * P$

$\Rightarrow P$ has to be either 2 or 3

$\Rightarrow BEE = 2 * 3 * 3$ or $BEE = 2 * 3 * 2$

$\Rightarrow B=2$ and $E=3$ and $P=3$ (or) $B=3$ and $E=2$ and $P=2$ (contradiction, $E=P$, no two integers can be equal)

All choices except $M=1$ are contradictory forcing $M=1$.

```

/*
#####
#####
#<a rel="license" href="http://creativecommons.org/licenses/by-nc-nd/4.0/"></a><br />This
work is licensed under a <a rel="license"
href="http://creativecommons.org/licenses/by-nc-nd/4.0/">Creative Commons
Attribution-NonCommercial-NoDerivatives 4.0 International License</a>.
#####
#####
#Course Authored By:
#-----
#-----
#K.Srinivasan
#NeuronRain Documentation and Licensing: http://neuronrain-
documentation.readthedocs.io/en/latest/
#Personal website(research): https://sites.google.com/site/kuja27/
#-----
#-----
#####
#####
*/

```

This is a non-linearly organized, code puzzles oriented, continually updated set of course notes on C++ language. This complements NeuronRain course materials on Linux Kernel, Cloud, BigData Analytics and Machine Learning and covers fundamentals of C++.

22 February 2017

An example on C++ templates and Runtime type identification:

Example code snippet in code/templates.cpp implements a simple templated book class with book type string as template parameter. Template book is instantiated with template and typename keywords and type T can be any subject type passed in as template parameter. Template class EBook derives from base class Book<T>. A subtlety in this example is absence of default constructor for Book<T> causes following compiler error:

```

g++ -g -o templates -I/usr/local/include -L/usr/local/lib -std=c++14 *.cpp
templates.cpp: In instantiation of 'EBook<T>::EBook(T) [with T =
std::__cxx11::basic_string<char>]':
templates.cpp:47:28:   required from here
templates.cpp:36:2: error: no matching function for call to
'Book<std::__cxx11::basic_string<char> >::Book()'
    {
    ^
templates.cpp:18:2: note: candidate: Book<T>::Book(T) [with T =
std::__cxx11::basic_string<char>]
    Book(T type)
    ^
templates.cpp:18:2: note:   candidate expects 1 argument, 0 provided
templates.cpp:8:7: note: candidate: Book<std::__cxx11::basic_string<char>
>::Book(const Book<std::__cxx11::basic_string<char> >&)
    class Book
    ^
templates.cpp:8:7: note:   candidate expects 1 argument, 0 provided
templates.cpp:8:7: note: candidate: Book<std::__cxx11::basic_string<char>
>::Book(Book<std::__cxx11::basic_string<char> >&&)

```

templates.cpp:8:7: note: candidate expects 1 argument, 0 provided

Adding default constructor:

```
    Book()
    {
    }
```

removes compilation error and following is printed:

Instantiating Book of type Maths
template type:NSt7__cxx1112basic_stringIcSt11char_traitsIcESaIcEEE
Instantiating Book of type ComputerScience
template type:NSt7__cxx1112basic_stringIcSt11char_traitsIcESaIcEEE
Instantiating Book of type Physics
template type:NSt7__cxx1112basic_stringIcSt11char_traitsIcESaIcEEE
Instantiating Book of type History
template type:NSt7__cxx1112basic_stringIcSt11char_traitsIcESaIcEEE
Instantiating EBook of type English
Read book
Read book
Read book
Read book
Read book

In above example, read_book() is a virtual function in superclass Book which can be overridden in derived classes. Previous output indicates how dynamic polymorphism works and read_book() of Book<T> is invoked from derived class EBook<T>. Type information is printed by typeid keyword of C++. This example is built using G++ with C++14 standard compiler option.

858. (THEORY and FEATURE) 17 July 2017, 9 August 2020 - Self-Aware Software, Quines - related to all sections on Formal Languages, Program Analysis, Software Analytics

Question: How can a program print its source itself as output ? [Quine - self-aware code]

Answer: Theoretically, there exists a lambda function with a fixed point i.e $f(x)=x$. Unix/Linux binaries are stored in ELF format which have debugging information embedded in DWARF entries (as set of DIES - Debugging Information Entries). There are utilities like objdump and dwarfdump which display the DIES. For example, following is the DWARF dump of asfer executable pointing to the compilation source directory in DW_AT_comp_dir:

```
root@Inspiron-1545:/media/shrinivaasanka/6944b01d-ff0d-43eb-8699-cca469511742/home/shrinivaasanka/Krishna_iResearch_OpenSource/GitHub/asfer-github-code/cpp-src# objdump --dwarf=info asfer |more
```

```
asfer:      file format elf32-i386
```

Contents of the .debug_info section:

```
Compilation Unit @ offset 0x0:
  Length:      0x16f7e (32-bit)
  Version:      4
  Abbrev Offset: 0x0
  Pointer Size: 4
<0><b>: Abbrev Number: 1 (DW_TAG_compile_unit)
  <c>   DW_AT_producer      : (indirect string, offset: 0x35560): GNU C++14
5.2.1 20151010 -mtune=generic -march=i686 -g -std=c++14 -fstack-pro
tector-strong
  <10>  DW_AT_language      : 4      (C++)
```



```
str:9abcddefgjks
str:9abcddefgjks
str:9abcddefgjks
str:9abcddefgjks
str:9abcddefgjks
str:9abcddefgjks
str:9abcddefgjks
str:9abcddefgjks
```


2 October 2017 - Placement New and Operator Overloading

C++ provides mechanisms to override default storage allocation by overloading operator new. There are two types of operator new(): Plain overload and Placement Overload. Placement new supplies storage as argument to operator new. Code example in code/placement_new.cpp illustrates this as below (this has been compiled to C++2017 standard). Older ways of overriding pointer this have been described in comments. Recent compilers do not allow direct *this overrides and prefer operator new. Operator new facility is useful for writing new storage allocators and memory debuggers which can instrument and bypass default memory allocation for profiling. This example also explains the rvalue reference operator && for *this. Rvalue references alias the right side of an assignment while Lvalue references(&) alias the left side of assignment.

```
=====
auto allocation
=====
this...0xffa08a90
overwriting this...
rvaluethis :0xffa08a90
=====
operator new:
=====
operator new overloaded and this is from a heap allocator
this...0x96a3e18
overwriting this...
rvaluethis :0x96a3e18
operator delete overloaded and this is freed to a heap allocator
=====
placement operator new:
=====
this...0xffa08aa8
overwriting this...
rvaluethis :0xffa08aa8
```


21 December 2017 - Rvalue References in C++ and Move semantics

Rvalue references were introduced in C++11 standard specification. Cloud move implementation of NeuronRain Neuro Currency applies the move semantics and rvalue references (client, server and header in https://github.com/shrinivaasanka/asfer-github-code/blob/master/cpp-src/cloud_move/). Traditionally lvalue refers to LHS of an assignment operator and rvalue to RHS of it. For example:

```
int x=5
assigns rvalue 5 to lvalue x. Lvalue references are declared by alias operator &
as:
int& y=x
and Rvalue references are declared by && operator:
int&& y=10
```


Move semantics in C++ specify moving an object by move constructor (std::move() and operator= overload) vis-a-vis copying an object by copy constructor. Move constructor is defined in Neuro currency as:

```
T& operator=(cloudmove<T>&& rvalue) {  
    ...  
}
```

and this move constructor is invoked by:

```
cloudmove<currency::Currency> currency_src(&c1,"localhost");  
cloudmove<currency::Currency> currency_dest(&c2,"localhost");  
...  
currency_dest = std::move(currency_src);
```

Move differs from Copy by returning rvalue of the argument to std::move() and renders the operand currency_src nullified by moving the resources to lvalue currency_dest.

7 August 2018 - Substring/Regular Expression Matcher

Matching a substring within a larger string is regular expression matching problem of writing a DFA. Deterministic Finite State Automaton are usually state transition tables on a graph. String is looped through and state transition table is looked up for next state till accept is reached. Designing this as a recursion saves lot of lines of code. An example recursive regexp substring matcher is in code/regexp.cpp which prints all matching positions of a substring as below:

```
:regexp matchks does not match at 0  
:regexp matchks does not match at 1  
:regexp matchks does not match at 2  
:regexp matchks does not match at 3  
:regexp matchks does not match at 4  
:regexp matchks does not match at 5  
:regexp matchks does not match at 6  
:regexp matchks does not match at 7  
:regexp matchks does not match at 8  
:regexp matchks does not match at 9  
:regexp matchks does not match at 10  
:regexp matchks matches at 11  
:regexp atchks matches at 12  
:regexp tchks matches at 13  
:regexp chks matches at 14  
:regexp hks does not match at 15  
:regexp matchks does not match at 16  
:regexp matchks does not match at 17  
:regexp matchks does not match at 18  
:regexp matchks does not match at 19  
:regexp matchks does not match at 20  
:regexp matchks matches at 21  
:regexp atchks matches at 22  
:regexp tchks matches at 23  
:regexp chks matches at 24  
:regexp hks matches at 25  
:regexp ks matches at 26  
:regexp s matches at 27
```


7 September 2018 - Unordered Map, Hash table buckets and Auto Iterator

C++ supports hashtables via unordered_map which is initialized either by emplace() or by {{...}} notation.

C++ from 2011 has new kind of iterators similar to Java 8 which automatically identify the type by auto keyword:

```
auto& it: <container>
```

Bucket containing an entry in the map is accessed by bucket() member function. An example code which populates

an unordered_map by process-clocks ticks pairs, auto iterates them and prints the buckets is committed in:

code/unordered_map_auto_iter.cpp and logs are committed to

code/logs/unordered_map_auto_iter.log. 7 September 2018.

10 September 2018 - Unordered Map and for_each()

Previous example for auto iterator has been changed to iterate the unordered map by for_each() primitive

from <algorithm>. This is C++ equivalent of map() in python which invokes a function on each element of the container. Unordered map has std::pair<> elements accessed by .first and .second members.

855. (THEORY and FEATURE) 24 September 2018, 9 August 2020 - Fowler-Noll-Vo Hashing, Custom Hash Functions in unordered_map, Nested Template Classes - related to all sections on Locality Sensitive Hashing, Separate Chaining Bucketization

FNV or Fowler-Noll-Vo Hashing is a non-cryptographic hash algorithm which has high dispersion and minimizes collisions in same bucket. It iterates through literals in text and multiplies their unicode values by a prime and XORs with an offset. This has avalanche effect - hash is very sensitive to small change in input. An example FNV implementation based on Boost C++ example has been added to course material at code/fnv.cpp. This defines a namespace class and nested fnv templated struct through which prime number and offsets can be passed as arguments. FNV hashing is widely used in search engines, text processing, MS Visual Studio, memcache etc.,

References:

855.1. Boost FNV example -

https://www.boost.org/doc/libs/1_68_0/libs/unordered/examples/fnv1.hpp

855.2. Fowler-Noll-Vo - FNV - Hashing: <http://www.isthe.com/chongo/tech/comp/fnv/>

855.3. Go Lang FNV package - <https://golang.org/pkg/hash/fnv/>

5 October 2018 - C++ Move-Assign Threads, Unordered Map Rehash and Concurrent Access

In C++ threads can be created in C++ specific move-assign paradigm which moves RHS thread object to LHS and destroys LHS. Move-assign is done by std::thread() operator= overloaded function which takes thread function

and arguments to it as parameters. An example C++ source file threads.cpp has been committed in code/ which

creates 50 thread objects, move-assigns thread objects to them by invoking a function to populate an unordered

map. populate_hashmap() waits for few nanoseconds, makes a key-value pair and places them in unordered map.

Load factor (number of items/number of buckets ratio) is recomputed to by

invoking `max_load_factor()` and `rehash()` functions alternately for odd and even values. This is a contrived example to demonstrate concurrent accesses to a container in C++. Logs for this example are in `code/logs/threads.log`. 50 October 2018.

854. (THEORY and FEATURE) 28 October 2018, 9 August 2020 - Three Distances Theorem and Fibonacci Hashing - related to all sections on Locality Sensitive Hashing, Separate Chaining Bucketization

Three Distances Theorem - Proof of Steinhaus Conjecture:

If $\Phi = (\sqrt{5}-1)/2$, and sequences of points $\{\Phi\}$, $\{2\Phi\}$, $\{3\Phi\}$, ... are plotted in $[0...1]$ y-interval, and successive line segments are inserted in $[0...1]$ y-interval from $(k, \{k\Phi\})$ to $(n, \{k\Phi\})$ the line segments are of sets of 3 lengths. $\{k\Phi\}$ is the fraction obtained subtracting the integer $\text{floor}(k\Phi)$ from $k\Phi$

An example C++ code which implements this as a hash function to an `unordered_map` has been described in `code/threedistances.cpp`.

Following are the size of each line segment sets grepped from log:

`grep "big " logs/threedistances.log.28October2018 |wc -l`
68
`grep "bigger " logs/threedistances.log.28October2018 |wc -l`
66
`grep "biggest " logs/threedistances.log.28October2018 |wc -l`
66

References:

854.1. The Art of Computer Programming - Volume 3 - Sorting and Searching - Page 518 - [Don Knuth] - Proof of Steinhaus Conjecture - Theorem S - [Vera Turan Sos]

1 November 2018, 2 November 2018, 3 November 2018 - Polymorphism, RTTI, Pure Virtual Functions, Friend classes, Scope Resolution operator, protected and private members, Initializers in Constructors, const correctness

C++ specifies polymorphic classes by deriving a base super class by syntax:

`class <derived> : <qualifier> <super>`

code example in `code/polymorphism.cpp` defines a base class `Animal` and 2 derived classes: `Tiger` and `Lion`.

Keyword `protected` in derived classes imply the derived class access to base class's protected members. Base

class `Animal` has a private member which is accessible by the derived classes through friend class declarations

in base class. There are two virtual functions in base class one of which is declared pure and makes `Animal`

an Abstract Data Type. Derived classes `Tiger` and `Lion` implement the pure virtual function in abstract base

class and override the other virtual function. Runtime Type Identification

(RTTI) is from `typeid` infrastructure provided by C++ standard for inferring the type of the object at runtime - `typeid()` keyword prints the `typename`

of the object. Constructor Initializers are mentioned by a list of variables

suffixed by `()` operators and values assigned to private member variables. `Const` qualifier informs the compiler that the function should not alter

the variables (immutables).

Scope resolution operator `::` resolves the private (by friendship) and protected members of the super class (by protected derivative classing). Header `cxxabi.h` has been included for C++ ABI name demangling of RTTI typenames. const disambiguation has been demonstrated by two functions `legs()` with `const` and without `const` qualifier. Both `legs()` are invoked by base class pointer `Animal* (->legs())` and as member invocation `(.legs())` and difference in behaviour is obvious from logs/polymorphism.log.3November2018.

References:

-
- 1. The C++ Programming Language - [Bjarne Stroustrup]
- 2. Essential C++ - C++ in depth series : Bjarne Stroustrup - [Stanley Lippman, Dreamworks] - const example - Section 5.9 - Page 161 - Previous example differs because of g++-6 idiosyncrasy: `const Animal*` is required to invoke `legs()` having `const` qualifier.

29 November 2018 - Pointers and References (Lvalue and Rvalue)

An example C++ code for miscellaneous permutations of pointers and aliases usage has been committed at `code/pointerstew.cpp`. C++ pointers which are supersets of C pointers have additional facilities for aliasing to an object location in the form of right value references (&& operator) and left value references (& operator). References or aliases do not consume extra memory storage as opposed to pointers which are object memory locations themselves. Points-to and Reference-to graph of the variables declared in `pointerstew.cpp` is below (legend: pointer #####>, rvaluereferences: =====>, lvaluereferences: ----->):

```
psptr #####> ps <===== psrvalueref
pint1 #####> ps.rvalueref1 =====> ps.x
pint2 #####> ps.lvalueref2 -----> ps.x
func1() parameter y =====> forwarded rvalue of arg to func1()
```

Assigning an lvalue to rvalue of same datatype throws following GCC error:
`pointerstew.cpp: In function 'int main()':`
`pointerstew.cpp:33:28: error: cannot bind 'pointerstew' lvalue to 'pointerstew&&'`
`pointerstew&& psrvalueref=ps;`

Logs for this example code have some surprising values for rvalue references. Assigning values directly to rvalue references corrupts the rvalue in GCC (shown in logs):

```
int&& rvalueref1=1;
whereas std::forward<int>(1) is required to forward the rvalue to lvalue for any
assignment and across function invocations as parameters:
int&& rvalueref1=std::forward<int>(x);
```

`func1()` has been overloaded with parameters and without them. Difference between effect of post-increment of rvalue (`ps.rvalueref1++;`) with and without `std::forward()` (previous two ways of initializing `rvalueref1` within `pointerstew` object) is evident. One time `std::move` of rvalue and `std::forward()` of rvalue is demonstrated by static value of `xx` across multiple invocations in `std::move()` while rvalues always reflect `x` dynamically.

References:

-
- 1. C++ Programming Language - [Bjarne Stroustrup]
- 2. C Puzzles - Pointer Stew - [Alan Feuer]

856. (THEORY and FEATURE) 26 December 2018 - Bridge and Iterator Design Patterns
- related to all sections on Software Analytics, Program Analysis, Survival
Index Timeout and Scheduler of NeuronRain Theory Drafts

Bridge is a design pattern mentioned in Gang-of-Four catalog of C++ Design
Patterns. Bridge separates implementations and the interfaces by defining
implementation itself as an abstract data type. Iterators are the patterns to
enumerate iterable containers - arrays, hashmaps, linkedlists etc., C++ code
example bridgeiteratordesignpatterns.cpp which demonstrates how timeout pattern
described in
https://github.com/shrinivaasanka/Grafit/blob/master/course_material/NeuronRain/AdvancedComputerScienceAndMachineLearning/AdvancedComputerScienceAndMachineLearning.txt fits as an amalgamation of Bridge
and Iterator Design Patterns, has been committed in C++/code. Timeout is a
dictionary of timeout values to lists of objects to timeout. Timeout as a
pattern has universal occurrence across whole gamut of software engineering.
Code example defines following classes - Timeout and TCPTimeout are interfaces
and TimeoutImp and TCPTimeoutImp are implementations which are bridged by a
pointer reference Timeout holds to TimeoutImp. This Decoupling is by passing any
derivative TimeoutImp object in TCPTimeout constructor which in turns assigns to
timeoutimp reference in Timeout. timeout() overridden virtual member function in
TCPTimeout invokes imptimeout() unaware of implementation TimeoutImp :

Timeout ----- implemented-by ----- TimeoutImp
(derived by TCPTimeoutImp)
(derived by TCPTimeout)

References:

856.1.Design Patterns - Elements of Reusable Object Oriented Software - [1995] -
[Erich Gamma - Richard Helm - Ralph Johnson - John Vlissides] - Bridge and
Iterator Patterns - Page 160 - Shared Strings Class - [Coplén] and [Stroustrup]

851. (THEORY and FEATURE) 12 February 2019, 9 August 2020 - Software
Transactional Memory - related to Program Analysis, Software Analytics, Software
Transactional Memory, Lockfree datastructures, Bakery Algorithm, Read-copy-
update sections of NeuronRain Theory Drafts

Software Transactional Memory is supported by C++ by synchronized blocks of
compound statements and transaction_safe directive in function declaration.
Software Transaction Memory is the intrinsic facility for transactional rollback
or commit of set of statements similar to RDBMS - either all are executed or
none. An example transactional memory code has been committed to
code/softwaretransactionalmemory.cpp. It declares two functions - function1()
executing a synchronized block and function2() declared transaction_safe which
is a tighter restriction preventing unsafe code. Compiler error flagged for
unsafe function calls have been added in code comments. Curious statement in the
code is:

```
t=std::thread([]{for(int n=0; n < 10;n++) function1(n);});
```

which is a lambda expression doing null capture by [] operator and just invoking
the function function1() within lambda expression loop block. Auto iterator
variable t is assigned to the thread object. Logs in
logs/softwaretransactionalmemory.log.12February2019 show serialized execution of
10 threads instantiated. VIRGO32 and VIRGO64 kernels implement a Bakery
algorithm locking primitive as kernel driver while in userspace VIRGO system
calls could be wrapped by C++ transaction memory primitives.

References:

851.1.C++ Lambda Expressions - <https://en.cppreference.com/w/cpp/language/lambda>
851.2.C++ Software Transactional Memory -
https://en.cppreference.com/w/cpp/language/transactional_memory

15 February 2019 - Lambda Functions and Capture, Functional Programming -
std::function

C++ supports lambda functional programming constructs similar to other languages like Python and Java.

An example C++ code which dynamically creates lambda functions and returns them is shown in code/lambdafunctions.cpp. It defines a struct and member function dynamicfunctions() which populates an unordered_map of string-to-int by parameters defined by () operator. It also captures this object from its present scope by [] operator which is internally accessed by on-the-fly lambda function block for the hashmap member. Capturing is intended for data communication between lambda function block and external scope. Member function dynamicfunctions() is returned as std::function object function1 returning int and taking (string,int) as arguments. Returned dynamic function object function1 is invoked like any other function by passing (string,int) arguments twice. Resultant hashmap is printed by auto iterator. Logs for this are committed to logs/lambdafunctions.log.15February2019.

852. (THEORY and FEATURE) 23 February 2019,9 August 2020 - Concurrency, Promise and Future Asynchronous I/O - related to Program Analysis, Software Analytics, Software Transactional Memory, Lockfree datastructures, Bakery Algorithm, Read-copy-update, Drone Autonomous Delivery sections of NeuronRain Theory Drafts

C++ facilitates asynchronous communication between concurrent threads by Promise and Future. Promise is instantiated by std::promise template and passed on as arguments to threads similar to shared_ptr which are shared mutables within thread functions. Future associated to Promise is acquired at a later time point asynchronously and value set by threads is readable. Code example at code/promisefuture.cpp describes two fictitious train threads having access to Promise and sets the nanoseconds time duration between present and an epoch as its value. std::chrono high resolution clock is invoked for time duration in nanoseconds. Future value for this Promise is later read by get() on Future object. Logs are shown in logs/promisefuture.log.23February2019. C++ SDK asynchronous I/O code for Drone telemetry could be augmented by Promise and Future code blocks.

853. (THEORY and FEATURE) 6 February 2020, 9 August 2020 - Read-Copy-Update mentioned in VIRGO Design Document of NeuronRain Theory Drafts has been implemented in userspace - related to Program Analysis, Software Analytics, Software Transactional Memory, Lockfree datastructures, Bakery Algorithm, Read-copy-update sections of NeuronRain Theory Drafts

Read-Copy-Update (RCU) has been mentioned as a feature in VIRGO32 and VIRGO64 design documents. Read-Copy-Update which is an efficient synchronization primitive implemented in most OS kernels works quite similar to local CPU caches of global RAM memory:

- (*) READ - Read the variable
- (*) COPY - Copy it to a temporary variable
- (*) UPDATE - Update the temporary variable
- (*) WRITEBACK - Write back temporary variable to the actual source

Advantage of Read-Copy-Update is the lack of necessity of mutexes:

(*) multiple concurrent readers have access to an older version of variable while a writer updates the copy of it

(*) older version of the variable is updated by new after all existing reads of older versions are done and no new read is allowed.

(*) older version is updated by the new version of the writer's working copy.

All the previous steps require no synchronization though it has to be ensured no new reads are performed while older version is updated. This kind of lockfree synchronization is quite useful for multiple readers of a linked list while some writer removes an element of the linked list. [Example of such a necessity is the WCET EDF Survival Index Scheduler design in GRAFIT course material - https://github.com/shrinivaasanka/Grafit/blob/master/course_material/NeuronRain/AdvancedComputerScienceAndMachineLearning/AdvancedComputerScienceAndMachineLearning.txt - which is a set partition of linked list of process id(s) where frequently process id(s) are read by almost every component of OS kernel and deleted by scheduler]. Writer marks the node to delete and updates the links bypassing the deleted node. Thus both node pointed to by new link and deletion-marked node of the linked list are available to existing readers. After all existing queued reads are over, node marked for deletion is really deleted. Efficiency stems from the fact that no locks are necessary for concurrent RCU.

Code example in code/readupdatecopy.cpp implements a C++ class and wraps the RCU assign functionality as its operator= overloaded member function. As evident from example synchronized blocks for software transactional memory and mutexes have been commented. It can be compiled by commandline - g++ -g readcopyupdate.cpp -fgnu-tm -lpthread -o readcopyupdate. Three kinds of copy have been shown - invoking operator=, copy assign of RCU object and copy assign of members. Third clause for copy assign of member has the following schematic:

```
        valuecopy=value; //READ and COPY
        cout<<"COPY: valuecopy="<<valuecopy<<endl;
        valuecopy=rvalue.value; //UPDATE
        cout<<"UPDATE: lvaluecopy
updated="<<valuecopy<<endl;
        value=valuecopy; //WRITEBACK

=====

value
| (READ)
V
(COPY) valuecopy <- rvalue.value (UPDATE)
|
V
value (WRITEBACK)
```

Logs in code/logs/readcopyupdate.log.6February2020 demonstrate a concurrent read-write by RCU of 200 threads. This code example is in effect a userspace implementation of RCU in VIRGO linux kernel (and is a spillover code of VIRGO repositories in GRAFIT) because reads and writes in thread functions can be replaced by syscall invocations of virgo_get() and virgo_set() preceded and succeeded by a global virgo_malloc() and virgo_free() respectively and no kernel codechange is necessary.

References:

853.1.Read-Copy-Update - <https://en.wikipedia.org/wiki/Read-copy-update>

857. (THEORY and FEATURE) 28 April 2020 - Name filter - C++ STL containers and algorithms - copy, copy_if, shared_ptr, tokenizer - related to all sections on People Analytics, Named Entity Recognition, Name filters (learning proper nouns in a text)

C++ Standard Templates Library implements algorithms for manipulating containers - for copying, filtering and erasure. A contrived example C++ name filter class has been defined in namefilter.cpp which accepts a textfile and parses it to filter the words having a substring name pattern. An example list of names from linkedin profile of author is namefiltered for a certain prefix. Lines are tokenized by stringstream iterator and copied to a vector by copy(). Name filter is done twice - for non-zero length of strings in lambda function capture of copy_if() and in auto iterator loop by find() of the pattern. Shared pointers are C++ STL facility for refcounted pointers. Wordcount of the strings containing pattern is incremented via a shared_ptr. Arbitrary filtering implementation can be plugged-in to lambda function capture block of copy_if() - Most names are of persons, organizations, locations and namefiltering or proper noun extraction has multiple solutions:

(*) NER PoS tagging by Conditional Random Fields(Supervised-costly- requires culture neutral training corpora e.g
<https://www.aclweb.org/anthology/P95-1032.pdf>)

(*) Natural Language Dictionary or Ontology lookup(Unsupervised-preferred- no training data-if word is not in dictionary or semantic network - WordNet, ConceptNet, NameNet -
<https://pdfs.semanticscholar.org/56f9/cf53333a46c9ea355578f6b7b9424a4737e2.pdf> - it is most likely a proper noun) are some of them. NeuronRain AstroInfer People Analytics implements dictionary filter.

1 November 2020, 2 November 2020 - Mediator-Colleague Design Pattern - C++ example

Mediator Design Pattern encapsulates the set of colleague objects and a director object which mediates the interactions between colleague objects. Colleagues do not interact among themselves directly but are moderated by the mediator object. C++ code example mediatordesignpattern.cpp implements two classes for director-mediator and colleagues - colleague objects invoke the singleton mediator for interaction amongst them and do not communicate with each other. Such a pattern is necessary in GUI event oriented programming - set of widgets which do not know each other notify a mediator about an event and mediator acts accordingly issuing further directives.

References:

1..Design Patterns - Elements of Reusable Object Oriented Software - [1995] - [Erich Gamma - Richard Helm - Ralph Johnson - John Vlissides] - Mediator Behavioural Pattern - Page 273

25 November 2020 - Reference wrappers, Arrays of references, Array move, C++ Array Objects, Reference to C++ Array object, Array Rotation

Code example arraymove.cpp demonstrates the following on C++ bounded array objects:

- (*) Define a primitive integer array
- (*) Perform memmove() on elements of integer array
- (*) Instantiate a vector from integer array (copies array to a vector)

- (*) Rotate the vector data and print them (would not affect source array)
- (*) Define & alias operator to std::string type as
reference_wrapper<string> object - from <functional> library
- (*) Define array object of reference_wrapper<string> objects
- (*) Invoke a function and pass bounded array object of
reference_wrapper<string> objects by reference to function - (&array)[length]
- (*) Perform memmove() on elements of array object of
reference_wrapper<string> objects
- (*) auto iterate the memmove()-ed integer array object and
reference_wrapper<string> array objects

References:

- 1.Clockwise-Spiral rule for C type inference -
<http://c-faq.com/decl/spiral.anderson.html>
- 2.C++ Reference wrapper -
https://en.cppreference.com/w/cpp/utility/functional/reference_wrapper
- 3.C++ Rotate - <https://en.cppreference.com/w/cpp/algorithm/rotate>

1222. (THEORY and FEATURE) 22 December 2020 - Russian Peasant Multiplication in Linear Time by BitShift operator - related to
1221 and all sections on Integer Factorization, Succinct Datastructures, Numeric Compression, Arithmetic Circuits

Code example russianpeasant.cpp implements the Russian Peasant Multiplication Algorithm for 2 integers which is in Linear time ($\Theta(n)$). It takes two integers as commandline arguments and casts them to type "unsigned long long" by strtoull(). Linear complexity product is obtained by Carry-Save adder, Parity and Majority Functions. Russian Peasant Algorithm works by:

- (*) Bit shifting right operand a and Bit shifting left operand b by 1 till one of the operands reaches single bit
- (*) Add all rows for Left shifted values of b for which corresponding right shifted rows of a are odd to get the product $a*b$.

Logs logs/russianpeasant.log.22December2020 show few example products by Russian Peasant algorithm.

Conventional multiplication is quadratic time - $O(n^2)$. Russian Peasant Algorithm dating back to 1800 BC used in Egypt and other Fast linear time multiplication circuits invert efficient circuits for factorization (non-uniform NC-PRAM-BSP Computational Geometric algorithm implemented in NeuronRain) and viceversa. Reverse engineering the steps of Russian Peasants algorithm bottom-up could be another direction of research for efficient factorization but non-trivial - for example:

- (*) Double the column left and Halve the column right from bottom to top
- (*) and guess the least significant bits for odd left column rows

References:

1. Algorithms - [Cormen-Leiserson-Rivest-Stein] - Chapter 29 - Arithmetic Circuits - Section 29.4.2 - Clocked Circuits - Faster Russian Peasant Multiplication Circuit in Linear Time -
<http://staff.ustc.edu.cn/~csli/graduate/algorithms/book6/chap29.htm>

1293. (THEORY and FEATURE) NeuronRainApps - Obstacle Free Lattice Walks -
Usecase implementation of Autonomous Driving ADAS algorithm in

Section 864 - item 59 - related to 1253 and all sections on Async IO, Drone Electronic Voting Machines, GIS and Urban Sprawl Analytics, Merit of Large Scale Visuals, Drone Obstacle Avoidance, Computational Geometry, ADAS-Obstacle avoidance, Autonomous Vehicles, Unmanned Aerial Vehicle Navigation-Autonomous Drone Delivery-Passenger Drones, Wiring Problem

1293.1 A primitive C++ template class usecase implementation latticewalks.cpp has been added to repository which computes all possible walks within a grid lattice or grid graph from bottom row to top row allowing obstacles - supplements ADAS Lattice walks algorithm in Section 864 - item 59 of NeuronRain conceptual graph - <https://neuronrain-documentation.readthedocs.io/en/latest/>.
1293.2 Lattice walks are computed by two functions findlatticewalks() and findlatticewalks2() which respectively consider lattice walks as Vector of Vectors and Vector of Point<int> template class. Lattice is binary Vector of Vectors wherein obstacles are marked as 1.

References:

1293.3 Efficient all path score computations on grid graphs (Lattices) - "...given a grid graph, to compute the maximum weights of paths between every pair of a vertex on the first row of the graph and a vertex on the last row of the graph. ..." - <https://www.sciencedirect.com/science/article/pii/S0304397513005215>

1294. (THEORY and FEATURE) NeuronRainApps - Obstacle Free Lattice Walks - Usecase implementation of Autonomous Driving ADAS algorithm in Section 864 - item 59 - All Pairs Paths in Grid Lattice - related to 1253 and all sections on Async IO, Drone Electronic Voting Machines, GIS and Urban Sprawl Analytics, Merit of Large Scale Visuals, Drone Obstacle Avoidance, Computational Geometry, ADAS-Obstacle avoidance, Autonomous Vehicles, Unmanned Aerial Vehicle Navigation-Autonomous Drone Delivery-Passenger Drones, Wiring Problem

1294.1 latticewalks.cpp has been changed to print paths between all pairs of vertices by iterating through walk counts computed in 1293 (logs/latticewalks.log.24August2022).
1294.2 findlatticewalks2() has been updated to iteratively decrement walks datastructure, extract (x,y) coordinate from walks and populate all pairs paths (set of all multiple 90 degree turn walks between any pair of vertices in grid graph).
1294.3 Outermost while loop in findlatticewalks2() stops when walks matrix contains only -1 or 0 entries.
1294.4 Most autonomous driving solutions employ deep learning and neural networks while finding Obstacle Free Lattice Walks in ADAS is pure theory. Earlier usecase implementation of 2D Lattice Grid with obstacles could be suitably changed to a 3D LiDAR Point Cloud Data (a 3D Lattice Grid) after a preprocessing to identify obstacle points on 3D Lattice.

References:

1294.5 Autonomous Driving by LiDAR Perception Point Cloud Library - <https://towardsdatascience.com/an-algorithmic-implementation-of-an-autonomous-driving-lidar-perception-stack-with-pcl-4d5928bcebc7> - Latency concerns - "... The scan rate may vary from 10 to 25 scans per second in real-life cases which leads to the maximal latency of any processing stage ranging from 100 ms to 40 ms. If for any possible incoming point cloud any of the stages, for example, clusterization, lags over 100 ms (for 10 scans per second rate), either a frame drop will happen, or the total latency of the pipeline will start to grow arbitrarily ..."
1294.6 Efficient LiDAR sensing - <https://www.csail.mit.edu/news/more-efficient-lidar-sensing-self-driving-cars> - "... A typical 64-channel sensor, for example,

produces more than 2 million points per second. Due to the additional spatial dimension, the state-of-the-art 3D models require 14x more computation at inference time compared to its 2D image counterpart. This means that, in order to navigate effectively, engineers first typically have to collapse the data into 2D - the side effect of this is that it introduces significant information loss. But a team from MIT has been working on a self-driving system that uses machine learning so that custom hand-tuning isn't needed. Their new end-to-end framework can navigate autonomously using only raw 3D point cloud data and low-resolution GPS maps, ..."

#####

This work is licensed under a Creative Commons Attribution-NonCommercial-NoDerivatives 4.0 International License.

#####

Course Authored By:

Srinivasan Kannan
(also known as: Shrinivaasan Kannan, Shrinivas Kannan)
Ph: 9791499106, 9003082186
Krishna iResearch Open Source Products Profiles:
http://sourceforge.net/users/ka_shrinivaasan,
<https://github.com/shrinivaasanka>,
https://www.openhub.net/accounts/ka_shrinivaasan
Personal website(research): <https://sites.google.com/site/kuja27/>
emails: ka.shrinivaasan@gmail.com, shrinivas.kannan@gmail.com,
kashrinivaasan@live.com

#####

This is a non-linearly organized, code puzzles oriented, continually updated set of course notes on Java language. This complements NeuronRain course materials on Linux Kernel, Cloud, BigData Analytics and Machine Learning and covers fundamentals of Java.

7 February 2017

Generics in Java are equivalents of Standard Templates Library/Boost in C++ with facility to parametrize Classes and Function signatures. Java Generics define a variable, class, interface and function with syntax:

```
variablename<T1,T2,...> v;  
classname<T1,T2,...> { };  
interfacename<T1,T2,...> { };  
T1 functionname(T2 t2,...);
```

Spark Streaming code in

https://github.com/shrinivaasanka/asfer-github-code/blob/master/java-src/bigdata_analytics/spark_streaming/SparkGenericStreaming.java uses Generic JavaDStream with type parameter <String> and JavaPairDStream with parameter <String, Integer>. Diamond notation ignores typenames and runtime inference is done for following declaration:

```
T1<T2,T3> t1 = new T1<>();
```

which automatically infers type as T1<T2,T3>.

21 May 2019

Lambda functions in Java are illustrated by LambdaExpressions.java which implements a functional interface and a lambda expression to print N consecutive numbers without looping. Function recursion() implements the recursive part while lambda expression just consists of printing an integer which is captured from argument to lambda function. Logs for this code example are in testlogs/LambdaExpressions.log.21May2019.

NEURONRAIN KingCobra - Module for Kernelspace Messaging and Computational Economics

This program is free software: you can redistribute it and/or modify it under the terms of the GNU General Public License as published by the Free Software Foundation, either version 3 of the License, or (at your option) any later version.

This program is distributed in the hope that it will be useful, but WITHOUT ANY WARRANTY; without even the implied warranty of MERCHANTABILITY or FITNESS FOR A PARTICULAR PURPOSE. See the GNU General Public License for more details.

You should have received a copy of the GNU General Public License along with this program. If not, see <<http://www.gnu.org/licenses/>>.

#-----

#K.Srinivasan
#NeuronRain Documentation and Licensing: <http://neuronrain-documentation.readthedocs.io/en/latest/>
#Personal website(research): <https://acadpdrafts.readthedocs.io/en/latest/>
#-----

*****/

Theoretical Interludes, Design Notes and ToDo (long term with no deadline)

[This is a major research oriented subsystem of NeuronRain and inspired by COBRA project (done by the author in his BE (1995-1999) along with few other esteemed classmates.

http://sourceforge.net/projects/acadpdrafts/files/Excerpts_Of_PSG_BE_FinalProject_COBRA_done_in_1999.pdf/download.)]

[KingCobra though a misnomer is expanded as Cloud With ARBiters MimicKING containing the anagram]

1072. (THEORY) There is a cloud of nodes which execute a set of services from randomly created clients.

1073. (THEORY) This cloud could be on NeuronRain (AsFer+USBmd+VIRGO+KingCobra) platform or any other opensource cloud platforms like Hadoop Cluster.

1074. (THEORY) The Clients are publishers of Service requests which are of many types - miscellaneous types of Service that could be dynamically added through other kernel modules and invoked through a switch-case or embedded in function itself. Identified by unique id(s) for different types of services (for example Problem reports, Suggestions etc.,)

1075. (THEORY) The Services on the Cloud are Subscribers to these requests of specific type. Thus this is the conventional publisher-subscriber model.

1076. (THEORY) The requests flow through cloud using a workqueue (which could be a lowlevel Linux workqueue or VIRGO queue or some other queuing middleware software like ActiveMQ). The publishers enqueue and Subscribers dequeue the requests.

1077. (THEORY) The difference is that the Cloud has nodes that "deceive" or "corrupt".

1078. (THEORY) Service requests - are published by the clients in the need of a service which could be defined by markup file. These requests are scheduled and routed by the middleware to competent authority which services it (with or without timeframe) and replies to the client.

1079. (THEORY) Problem reports - are published by clients which are "dissatisfied" by the quality of service by the cloud. These are analyzed by "arbiters" in the cloud which find the faulting node(s) and take action. This allows manual intervention but minimizes it.

1080. (THEORY) Suggestions - are enhancement requests sent by clients and require manual intervention.

1081. (THEORY) Cloud nodes have a Quality of Service metric calculated by a model.

1082. (THEORY) The cloud has a reporting structure of nodes - either as a graph or tree. The graph is dynamically reorganized by weighting the Quality of Service of each node.

1083. (THEORY) The difficult part of the above is using Arbiters to find "faulty" nodes based on problem reports from clients.

1084. (THEORY) Brewer's CAP conjecture proved by [GilbertLynch] as a theorem (still debated) states that only 2 of the 3 (Consistency of data, Availability of data and Partition tolerance when some nodes or messages are lost) can be guaranteed and not all 3 are simultaneously achievable.

1085. (THEORY) CAP theorem does not seem to apply to the above faulty scenario with corrupt nodes under Consistency or Availability or Partition Tolerance. This is because a corrupt node can have any 2 of the 3 - it can give consistent data, is available with success response or can make the cloud work with missing data in partition tolerance but yet can "corrupt" the cloud. Probably this needs to be defined as a new attribute called Integrity.

1086. (THEORY) As "corruption" is more conspicuous with monetary element, if above services are "charged" with a logical currency (e.g. bitcoin), then corruption in cloud is defineable approximately as (but not limited to)- "Undue favour or harm meted out to a client not commensurate with the charge for the service (or) unreasonable extra logical currency demanded to execute the service of same quality (or) deliberate obstruction of justice to a client with malevolent and unholy collusion with other cloud nodes with feigned CAP".

1087. (THEORY) Identifying criminal nodes as in (15) above seems to be beyond the ambit of CAP. Thus CAP with Integrity further places a theoretical limit on "pure" cloud. If Integrity is viewed as a Byzantine problem with faulty or corrupt processes in a distributed system, and if resilience factor is r_f (expected number of faulty nodes), then most algorithms can ensure a "working" cloud only if resilience is $\sim 30\%$ or less ($3 \cdot r_f + 1$) of the total number of cloud nodes. Probably this could apply to Integrity also that places a limit of 30% on "corrupt nodes" for the Cloud to work with sanity. Translating this to a Governance problem, a corruption-free administration is achievable with a maximum limit of 30% "corrupt" elements.

1088. (THEORY and FEATURE) Analytics on the Problem reports sent to the cloud queue give a pattern of corrupt nodes. Intrinsic Merit ranking with Citation

graph maxflow considering cloud as a flow network where a node positively or negatively cites or "opines" about a node, as mentioned in <http://arxiv.org/abs/1006.4458> (author's Master's thesis) and http://www.nist.gov/tac/publications/2010/participant.papers/CMI_IIT.proceedings.pdf (published by the author during PhD) give a p2p ranking of cloud nodes that can be used for analysis though may not be reliable fully. AsFer has bigdata analytics functionality that fits well to this point to analyse the problem reports with machine learning algorithms and set the key-value pairs that are read by VIRGO kernel_analytics module and exported kernelwide. The persisted REQUEST_REPLY.queue with the logged request-reply IPs and timestamps can be mined with AsFer bigdata capability (e.g. Spark)

1089. (THEORY) Policing the cloud nodes with arbiters - This seems to be limited by CAP theorem and Integrity as above. Also this is reducible to perfect inference problem in <http://sourceforge.net/p/asfer/code/HEAD/tree/AstroInferDesign.txt> and drafts in <https://sites.google.com/site/kuja27/>

1090. (THEORY) Brooks-Iyengar algorithm for sensors in all cloud nodes is an improved Byzantine Fault Tolerant algorithm.

1091. (THEORY) BitCoin is a Byzantine Fault Tolerant protocol.

1092. (THEORY) Byzantine Fault Tolerance in Clouds is described in <http://www.computer.org/csdl/proceedings/cloud/2011/4460/00/4460a444-abs.html>, <http://www.eurecom.fr/~vukolic/ByzantineEmpire.pdf> which is more on Cloud of Clouds - Intercloud with cloud nodes that have malicious or corrupt software. Most of the key-value(get/set) implementations do not have byzantine nodes (for example CAP without Byzantine nodes in Amazon Dynamo: <http://www.eurecom.fr/~michiard/teaching/slides/clouds/cap-dynamo.pdf>)

1093. (THEORY) Related to point 18 - The problem of fact finding or fault finding using a cloud police has the same limitation as the "perfect inference" described in <http://sourceforge.net/p/asfer/code/HEAD/tree/AstroInferDesign.txt>. "Money trail" involving the suspect node in point 28 is important to conclude something about the corruption. In real world tracking money trail is a daunting task. In cloud that abides by CAP, missing messages on trail can prevent reaching a conclusion thereby creating benefit-of-doubt. Also fixing exact value for a transaction that involves MAC currency message is undecidable - a normative economics problem can never be solved by exact theoretical computer science.

1094. (THEORY) Reference article on cloud BFT for Byzantine, Corrupt brokers - Byzantine Fault-Tolerant Publish/Subscribe: A Cloud Computing Infrastructure (www.ux.uis.no/~meling/papers/2012-bftps-srds.pdf)

1095. KingCobra messaging request-response design - options

1095a. Implementing a message subscription model in kernelspace where clients publish the message that is queued-in to subscribers' queue (Topic like implementation - use of ActiveMQ C implementation if available).

1095b. (DONE-minimal implementation) At present a minimum kernelspace messaging system that queues remote request and handles through workqueue handler is in place. This responds to the client once the Kingcobra servicerequest function finishes processing the request(reply_to_publisher() in KingCobra driver). Unlike the usual messaging server, in which client publishes messages of a particular type that are listened to by interested clients, one option is to continue the status-quo of KingCobra as a peer-to-peer messaging system. Thus every VIRGO node is both a kernelspace messaging client and server that can both publish and listen. Every message in the cloud can have a universally unique id

assigned by a timestamp server - <https://tools.ietf.org/html/rfc4122> (similar to bitcoin protocol) so that each message floating in the cloud is unique across the cloud (or) no two messages on the VIRGO cloud are same. The recipient node executing `kingcobra_servicerequest_kernelspace()` parses the unique-id (example naive unique-id is `<ip-address:port>#localtimestampofmachine` which is a simplified version of RFC4122) from the incoming remote request and responds to the remote client through kernel socket connection that gets queued-in the remote client and handled similar to incoming remote request. To differentiate request and response-for-request response messages are padded with a string "REPLY:<unique-id-of-message>" and requests are padded with "REQUEST:<unique-id-of-message>". This is more or less similar to TCP flow-control with SEQ numbers but state-less like UDP. Simple analogy is post-office protocol with reference numbers for each mail and its reply. Thus there are chronologically two queues: (1) queue at the remote VIRGO cloud service node for request (2) queue at the remote client for response to the request sent in (1). Thus any cloudnode can have two types of messages - REQUEST and REPLY. Following schematic diagram has been implemented so far.

 1300a.(DONE) KingCobra - VIRGO queue - VIRGO cpupooling , mempooling and queue service drivers interaction schematic diagram:


```

KingCobraClient =====><REQUEST:id>===== VIRGO
cpupooling service =====> VIRGO Queue =====> KingCobraService
      ||
      ||
      ||
      ||
      <===== VIRGO Queue <===== VIRGO cpupooling service
=====<REPLY:id>===== V

```

```

KingCobraClient =====><REQUEST:id>===== VIRGO
mempooling service =====> VIRGO Queue =====> KingCobraService
      ||
      ||
      ||
      ||
      <===== VIRGO Queue <===== VIRGO mempooling service
=====<REPLY:id>===== V

```

```

KingCobraClient =====><REQUEST:id>===== VIRGO Queue
service =====> KingCobraService
      ||
      ||
      ||
      ||
      <===== VIRGO Queue service
=====<REPLY:id>===== V

```

1300b. (ONGOING) `kingcobra_servicerequest_kernelspace()` distinguishes the "REQUEST" and "REPLY" and optionally persists them to corresponding on-disk filesystem. Thus a disk persistence for the queued messages can either be implemented in 1) VIRGO queue driver 2) `workqueue.c` (kernel itself needs a rewrite (or) 3) KingCobra driver. Option (2) is difficult in the sense that it could impact the kernel as-a-whole whereas 1) and 3) are modularized. At present Option 3 persistence within KingCobra driver has been implemented.

1300c. Above option 1095b implements a simple p2p queue messaging in kernel. To get a Topic-like behaviour in VIRGO queue might be difficult as `queue_work()`

kernel function has to be repeatedly invoked for the same work_struct on multiple queues which are subscribers of that message in AMQ protocol. Moreover creating a queue at runtime on need basis looks difficult in kernel which is usually done through some CLI or GUI interface in ActiveMQ and other messaging servers.

1096. (ONGOING) For the timestamp service, EventNet described in <http://sourceforge.net/p/asfer/code/HEAD/tree/AstroInferDesign.txt> is a likely implementation choice. AsFer already has a primitive text files based EventNet graph implementation in place. Periodic topological sort (quite expensive) of EventNet gives logical ordering and thus a logical timestamp of the cloud events.

784. (THEORY - Neuro Cryptocurrency Implemented in AstroInfer - this section is an extended draft on respective topics in NeuronRain AstroInfer Design - <https://github.com/shrinivaasanka/asfer-github-code/blob/master/asfer-docs/AstroInferDesign.txt>) MESSAGE-AS-CURRENCY PROTOCOL: If each message payload is also construed as a currency carrier, each message id can be mapped to a unique currency or a coin with fixed denomination. This is similar to each currency note having a serial number as unique id. Uniqueness is guaranteed since there can be only one message (or coin) with that id on the cloud. This simulates a scenario - "Sender of the message pays the Receiver with a coin having the unique id and Receiver acknowledges receipt". This is an alternative to BitCoin protocol. Double spending is also prohibited since at any point in time the message or "coin" with unique id can be sent by only one node in the cloud. Unique Cloudwide Timestamp server mimicks the functionality of "Mint". There is a difference here between conventional send-receive of messages - Once a message is sent to remote cloud node, no copy of it should exist anywhere in the cloud. That is, every MAC currency message is a cloudwide singleton. In pseudocode this is expressible as:

```
m1=MAC_alloc(denomination)
m2=m1 (---- this is disallowed)
```

Linux kernel allocation functions - kmalloc() - have a krefs functionality for reference counting within kernel. Refcount for MAC message can never exceed 1 across cloud for above singleton functionality - this has to be a clause everywhere for any unique MAC id. This requires a cloudwide krefs rather. Buyer decrements cloudwide kref and Seller increments it. In C++ this is done by std::move() and often required in "Perfect Forwarding" - http://thbecker.net/articles/rvalue_references/section_07.html - within single addressspace. By overloading operator=() with Type&& rvalue reference, the necessary networking code can be invoked that does the move which might include serialization. But unfortunately C++ and Linux kernel are not compatible. The Currency object has to be language neutral and thus Google Protocol Buffers which have C,C++,Java, Python .proto files compilers support might be useful but yet the move semantics in Kernel/C is non-trivial that requires cloudwide transactional kernel memory as mentioned in (31) below. A C++ standalone userspace client-server cloud object move implementation based on std::move() over network of Protocol Buffer Currency Objects has been added to AsFer repository at - http://sourceforge.net/p/asfer/code/HEAD/tree/cpp-src/cloud_move which can optionally be upcall-ed to userspace from VIRGO and KingCobra drivers. This C++ implementation is invoked in userspace with call_usermodehelper() from VIRGO Queue Messaging via the kernel workqueue handler.

784.1 Schematic Diagram for Cloud Perfect Forwarding with AsFer+VIRGOQueue+KingCobraUserspace:

Telnet or other client =====> VIRGO Queue Service Listener =====>
VIRGO Workqueue Handler

|
| [KernelSpace]
V

AsFer Cloud Perfect Forwarding Client <===== KingCobra Userspace shell


```

script(call_usermodehelper)
      |
Virtual Currency      |
      V               |
      AsFer Cloud Perfect Forwarding Server
<=====

```

References:

784.2 An example distributed transactional memory implementation in cloud - <http://infinispan.org/tutorials/simple/tx/> and <http://www.cloudtm.eu/> - these are in userspace cloud (C++ and Java) and may not have cloud move functionality - move has to be simulated in a transaction: replicate data, delete in one endpoint and create in other endpoint

1097. (THEORY) SIMULATING A VIRTUAL ECONOMY with above MAC protocol (Message-as-currency): If each message sent is considered as "money" element and cloud nodes and clients are the consumers and producers of "electronic money", the timestamp "Mint" becomes a virtual Federal Reserve or Central Bank that controls the "electronic money" circulation in the cloud. Infact any REPLY messages could be mapped to a Service a client derives by s(p)ending the REQUEST "money message". Thus value(REQUEST) should equal value(REPLY) where value() is a function that measures the value of a money denomination and the value of goods and/or services for that money. For example Rs.10000 or \$10000 has no meaning if it doesn't translate into a value (analogy: erstwhile Gold Standard).When the value() function gets skewed phenomena like Inflation arise. Thus above model could also have a notion of value() and "electronic money inflation". Thus any "message money" with a unique id assigned by the cloud unique id(or logical timestamp) server can exist at most in only one node in the cloud. Money trail can be implemented by prefixing a header to the incoming message money in each cloud node that receives the money which traces the "path" taken. Cloud has to implement some Byzantine Fault Tolerant protocol. The value() function to some extent can measure the "deceit" as above. When a Buyer and Seller's value() functions are at loggerheads then that is starting point of "cloud corruption" at either side and might be an undecidable problem.

785. (THEORY - this section is an extended draft on respective topics in NeuronRain AstroInfer Design - <https://github.com/shrinivaasanka/asfer-github-code/blob/master/asfer-docs/AstroInferDesign.txt>) TRADING WITH ABOVE KINGCOBRA MAC protocol - somewhat oversimplified:

```

-----
Unique MAC id MINT
      ||
----money trail-----
|
V
....
Buyer ===== sends MAC message (REQUEST id) =====> Seller (stores the
MAC in local cash reserve and prepends money trail)
||                                     ||
<===== sends the goods and services (REPLY id) ==

```

In the above schematic, money with unique id in cloud reaches a buyer after many buyer-seller transitions called "money trail". The MAC currency is prefixed by each node to create a chain. Buyer then sends a request to the seller through MAC virtual currency and seller replies with goods and services. Seller prepends the money trail chain. When a transaction occurs the whole cloud need not be notified about it except only buyer and seller. MAC Mint could create a bulk of money denominations and circulate them in cloud economy.

References:

785.1 Price fixing for items in Buyer-Seller-Trader networks - Trading Networks - Market Equilibrium and Walrasian Model of Price fixing - <http://www.cs.cornell.edu/~eva/traders.pdf>
785.2 Algorithmic Game Theory - Market Equilibrium for Price - Equilibrium is a strategic standoff - both players can't better their own present by changing strategies e.g Buyer-Sellers are market players and equilibrium price is the one where both buyer and seller can't gain by varying it - <http://www.cis.upenn.edu/~mkearns/nips02tutorial/nips.pdf>. Buyer-Seller payoff matrix pictures the bargaining problem.
785.3 Price-setting in Trading networks - Chapter 11 - <https://www.cs.cornell.edu/home/kleinber/networks-book/networks-book.pdf>

1098. (THEORY) VALUE FOR ELECTRONIC MONEY: How is above MAC money earned - This again requires linking value to money (as money is not a value by itself and only a pointer to valuable item or resource). Thus any buyer can "earn" MAC money by something similar to a barter.

786. (THEORY and IMPLEMENTATION - this section is an extended draft on respective topics in NeuronRain AstroInfer Design - <https://github.com/shrinivaasanka/asfer-github-code/blob/master/asfer-docs/AstroInferDesign.txt>) FIXING VALUE FOR MAC MONEY: To delineate corruption as discussed in 27 above with value() disparity between MAC money and REPLY goods and services, an arbiter node in cloud has to "judge" the value of MAC sent by buyer and goods and services from seller and proclaim if corruption exists. Thus value() function itself has to be some kind of machine learning algorithm. This is related to or same as points 12 to 23 above. For example, while buying an item for few million bucks, value() has to take as input the description of the item and calculate the value "ideally" which is difficult. Because there are no perfect references to evaluate and only a weighted average of available market price range has to be taken as a reference which is error-prone. value() function can be recursively defined as ("Reductionism" and a variant of Ricardo Labor theory of value - value of a commodity is proportional to cost of labor required to make it - e.g Software is approximately valued by lines of code, concept patent innovations and manhours):

|value(i) = summation(value(ingredients of i)) + cost(integrating the ingredients to create item i) |

Obviously the above recursion combinatorially explodes into exponential number of nodes in the recursion tree. Ideally recursion has to go deep upto quarks and leptons that makeup the standard model. If for practical purposes, recursion depth is restricted to t then size of value() tree is $O(m^t)$ where m is average number of ingredients per component. Hence any algorithm computing the value() recursion has to be exponential in time. Computation of value() in the leaf nodes of the recursion is most crucial as they percolate bottom-up. If leaf nodes of all possible items are same (like quarks and leptons making up universe) then such atomic ingredient has to have "same" value for all items. Only the integration cost varies in the levels of the tree. For infinite case, value() function is conjectured to be undecidable - probably invoking some halting problem reduction. But above value() function could be Fixed Parameter Tractable in parameter recursion depth - t but yet could only be an approximation. A Turing machine computing value() function exactly might loop forever and thus Recursively Enumerable and not Recursive. A CVXPY implementation for Pricing Market Equilibrium has been implemented in KingCobra.

787. (THEORY - this section is an extended draft on respective topics in NeuronRain AstroInfer Design - <https://github.com/shrinivaasanka/asfer-github-code/blob/master/asfer-docs/AstroInferDesign.txt>) Buyer-Seller and MAC electronic money transaction schematic:

```

-----
      Buyer      A-----<id><refcnt:0>-----> Seller
<id><refcnt:1> (increments refcnt)
  (<id><refcnt:1> |
   <id><refcnt:0> |
   after decrement |
   refcnt          |
  )----->

```

Above has to be transactional (i.e atomic across cloud nodes)

1099. (THEORY) MAC protocol reaper

Reaper thread in each cloud node harvests the zero refcounted allocations and invokes destructors on them. Same MAC id cannot have kref count of 1 or above in more than one cloud node due to the transaction mentioned previously.

1100. (THEORY) Cloud Policing With Arbiters - Revisited:

When a suspect node is analyzed when a complaint problem is filed on it, (1) it is of foremost importance on how flawless is the arbiter who investigates on that and is there a perfect way to choose a perfect arbiter. In the absence of the previous credibility of entire cloud judiciary is blown to smithereens and falls apart. (2) Assuming a perfect arbiter which is questionable, next thing is to analyze the credibility of the node who sulked. This is nothing but the Citation problem in <http://arxiv.org/abs/1106.4102> and http://www.nist.gov/tac/publications/2010/participant.papers/CMI_IIT.proceedings.pdf where a node can positively or negatively cite another node a "Societal Norm" which can be faulted and citations/opinions could be concocted with malafide intent(perjury). This is rather a generalization of PageRank algorithm with negative citations. Thus Perfect Cloud Arbitration could be an unsolvable problem. (3) Even if both arbiter and complainant are perfect which is again questionable, there are still loopholes - lack of evidences or implicated witnesses might portray a negative impression of a positive node. Thus there are 3 tiers of weakenings in cloud arbitration and there could be more. P(Good) series in <https://sites.google.com/site/kuja27/> precisely addresses this problem.

788. (THEORY) MAC Money Flow as MaxFlow problem - this section is an extended draft on respective topics in NeuronRain AstroInfer Design - <https://github.com/shrinivaasanka/asfer-github-code/blob/master/asfer-docs/AstroInferDesign.txt>

Transactions happening in a cloud are edges between the nodes involved (buyer and seller). Thus it creates a huge directed graph. Flow of money in this graph can be modelled as Flow network. Minimum Cut of this graph shows crucial nodes in the graph which play vital role in cloud economy removal of which paralyzes the cloud (could be Central bank and other financial institutions). This graph has bidirectional edges where one direction is for money and the opposite direction is for Goods and Services. In the Flow network sum of flows is zero. But in the Money Flow Network each node is having a cash reserve ratio (CRR) due to commercial transactions which is confidential and privy to that node only and thus sum of flows can not be zero. Hub nodes in the Money Flow graph which can be obtained by getting k-core or D-core of the graph by some graph peeling algorithms are crucial nodes to the economy that contribute to Money circulation.

1101. (THEORY) Cycles and components in above MAC Money Flow Graph:

Above graph of money transactions could be cyclic which implies a supply chain. Strongly connected components of this graph are most related nodes that are in

same industry.

1102. (THEORY) STOCK TRADING:

One of the component in above MAC Money Flow Graph of cloud could be a virtual Stock Exchange. Based on the financial and securities transactions of constituent organizations in the graph, index of the exchange varies.

789. (THEORY) Analysis of Poverty and Alleviation through above money flow graph - this section is an extended draft on respective topics in NeuronRain AstroInfer Design - <https://github.com/shrinivaasanka/asfer-github-code/blob/master/asfer-docs/AstroInferDesign.txt>

Weights of the edges of money flow graph are the denominations of the transaction. Thus high value edges and low value edges divide the Graph logically into Rich and Poor strata (Bourgeoisie and Proletariat subgraphs). Equitable graph is the one which does not have too much of value difference between Rich and Poor sets of edges - a utopian to achieve. Mathematically, it is an optimization LP problem that seeks to minimize $\text{sum}(\text{RichEdges}) - \text{sum}(\text{PoorEdges})$ or $\text{Sum}(\text{RichVertices}) - \text{sum}(\text{PoorVertices})$ - without harming either - to be precise. This requires money flow to be programmed to find a feasible solution to this LP subject to constraints like work-pay parity etc., (there could be more variables and constraints to this LP). Due to CRR above Vertices also can be Rich and Poor in addition to Rich Edges and Poor Edges.

Previous Linear Program could be weighted to : $\text{Sum}(w(i) * \text{RichEdges}) - \text{Sum}(w(k) * \text{PoorEdges})$. Money Flow Graph (or Money Trail as it is commonly termed) is a potential expander of high regularity. Some constraints could be imposed on this Poverty Alleviation Linear Program e.g Number of Rich edges (x) must be atleast a non-negligible fraction of Number of poor edges (y) which guarantees equitable money trail:

$R(i) = \text{Rich Edges}$

$P(i) = \text{Poor Edges}$

minimize:

$\text{Poverty} = \text{Sum}_{1_to_x}(w(i) * R(i)) - \text{Sum}_{1_to_y}(w(k) * P(i))$

subject to constraint:

$x \geq \text{epsilon} * y, 0 < \text{epsilon} < 1$

References:

789.1 J-PAL case study of social programs fund flow reforms - <https://www.povertyactionlab.org/case-study/fund-flow-reforms-improved-social-program-delivery-india>

790. (THEORY) Demand and Supply and Value() function - Quantitative Majority Circuit - this section is an extended draft on respective topics in NeuronRain AstroInfer Design - <https://github.com/shrinivaasanka/asfer-github-code/blob/master/asfer-docs/AstroInferDesign.txt>

Alternative to the recursive definition of value() function above can be done through Demand and Supply - more the demand and less the supply, price increases and vice-versa. This is quite subjective compared to absolute recursive definition above. To simulate demand and supply, the weights of the money edges (-> direction) in the bidirectional graph change and fluctuate dynamically over time for unchanging weights of the Goods and Services edges (<- direction) between any pair of Buyer-Seller vertices. This makes Money and G&S Flow graph a

Dynamic Graph with edge weight update primitive. Parallels can be drawn between majority voting and Demand-Supply pricing - Candidates are replaced by commodities and Votes for candidates are replaced by Consumers demanding a product - but difference being the dynamism and inverse proportionality of demand-supply - Number of demanding consumers (voter leaves of majority circuit) increase with dwindling availability of commodity (Candidate voted for) which is a special variation of voting. Every commodity vertex and its buyer neighborhood in Money Trail graph could be translated to a majority voting circuit. In essence, leaves of majority circuit for demand-supply dynamically bloat or shrink depending on quantity of commodity which is a quantitative weighted version of majority circuit vis-a-vis conventional qualitative boolean and non-boolean (set partition/LSH) majority neglecting volume of a candidate. This quantitative dynamic majority circuit gadget can formalize any economic process which has fluctuating demand-supply underneath. In the context of social networks, demand-supply inverse relationship defines a least energy Intrinsic Fitness constraint - Vertex or commodity in a Market Bipartite Graph (edges between two sets - buyers and commodities) of least availability attracts most buyers and thus has most merit. Szemerédi's Regularity Lemma implies any graph can be approximately partitioned as union of bipartite graphs by which Money Trail graph can be decomposed as union of Bipartite graphs of random edge densities (buyers and sellers). Quantum of a commodity vertex in Buy-Sell Market Bipartite Graph could be represented by gradation of its color (darkest-most available to lightest-least available) which is dynamically recomputed. Section 727 of NeuronRain Unified Theory Drafts delves into Fame-Merit counterpart of this problem - Bipartite decomposition of WWW. BWBP model of majority has an advantage of constant width 5 of variable length = 4^{depth} - Length of Quantitative majority BWBP varies depending on demand-supply.

References:

 790.1 Barrington Theorem - Majority can be computed by Bounded Width Branching Program (BWBP) of width 5 and length 4^d -
<http://www.ccs.neu.edu/home/viola/classes/gems-08/lectures/le11.pdf>
 790.2 Szemerédi Regularity Lemma - Section 1.3 -
<http://www.math.ucsd.edu/~fan/teach/262/read/reg.pdf> - "...the Regularity Lemma provides us with an approximation of an arbitrary dense graph with the union of a constant number of random-looking bipartite graphs..."

 791.(THEORY) Hidden or Colored Money - this section is an extended draft on respective topics in NeuronRain AstroInfer Design -
<https://github.com/shrinivaasanka/asfer-github-code/blob/master/asfer-docs/AstroInferDesign.txt>

 In an ideal Cloud with only MAC currencies, colored money can co-exist if (not limited to) some money trails are missing, due to "cloud corruption", systemic failure, hardware and network issues etc.,. Probably this is the direct consequence of CAP theorem and can be conjectured to be undecidable. Hidden money is to some extent dependent on quantity of net flow (if non-zero) and how much of this net flow is contributed by Rich vertices and Edges. Money Circulation with Colored money can be formulated as Network Flow Problem with Time horizon and storage at nodes. Time horizon implies a certain flow has to happen before a stop time. Flow conservation is affected by this Dynamic Flow because of storage at nodes and money entering a node need not be equal to money leaving. Thus not all Hidden/Colored money is illegal in theoretical terms. As mentioned in 39.1, storage is simulated with a closed loop at nodes so that flow conservation is not seemingly violated. Profiteering is achieved by money flows over time in financial markets by assigning a multiplicative factor at each edge which accrues through a cycle and comes back to start node in cycle with a magnification in value. Blockchain techniques maintain ledgers which record all transactions globally thus decimating hidden unaccounted wealth if any. KingCobra experimental MAC currency relies on unique global identifier and

global refcounts with atomic cloud transactions in linux kernel. Money Flow Graph mentioned in 34-39 has striking resemblance to Money Flow Markets already studied in Algorithmic Game Theory (AGT). 39.3 primarily devotes to Pricing and Equilibrium of Edges in Money Flow Graphs and not much on Colored Money Flow. An algorithm to find colored money flow could be a major advance in AGT. Prima facie there exists no zero-knowledge blackbox proof algorithm to find colored money because all storage data is a prerequisite which is impossible to know. Money trail for MAC currency described in 22,27,28 requires tracking of currencies. There are recent dollar and euro bills issued with Radio Frequency ID tags (RFID).

Total storage of money in Flow Market Graph = | Incoming money flow at Source - Incoming money flow at Sink | i.e Flow conservation is no longer obeyed.

There is a special vertex in Money Flow Market designated as Direct Taxation Hub which has incoming direct tax money flow edges from all other vertices in Flow market. Colored money is then approximately the taxed storage money estimated above minus the net flow of money received at Taxation Hub.

Colored Money = | Total storage money * Direct Taxation rate - Incoming Flow at Direct Taxation Hub Node |

Colored Money = | Incoming money flow at Source * Direct Taxation rate - Incoming money flow at Sink * Direct Taxation rate - Incoming Flow at Direct Taxation Hub Node |

Previous is an approximate naive zero-knowledge estimation of Colored money in Money Flow Market. This assumes that there is always a sink in Money Flow Market which is not necessarily valid unless notes are returned to mint. Satellite RFID Tracking technologies though invasive and intrusive like previous can present a rough figure of total money circulation in Source and Sink.

Above estimate is for direct taxation and resultant evasion. For indirect taxes (on Goods and Services etc.), there is no direct impact on the money component and only G&S are affected. Combining Goods, Services and Income into one (direct+indirect) taxation could have a negative effect on Colored money because incentive to hide money no longer exists. For example, if only Goods and Services consumed by high-income brackets are preferentially taxed at high percentage replacing tax on income, income is also indirectly taxed in addition to G&S. Thus there is no necessity to tax income and any advantage of such direct taxation is indirectly usurped by preferential G&S taxation. Previous zero-knowledge estimate then becomes:

Colored Money = | Total Goods and Services * Taxation rate - Incoming Flow at Indirect Taxation Hub Node |

Colored Money = | GDP² * Tax-to-GDP ratio - Incoming Flow at Indirect Taxation Hub Node | where GDP is assumed to be equal to Total Goods and Services.

References:

-
- 791.1 Network Flows over time over Storage Area Networks (SAN) - <https://hal.inria.fr/inria-00071643/document>
 - 791.2 Network Flow - [GoldbergTardosTarjan] - <http://www.cs.cornell.edu/~eva/network.flow.algorithms.pdf>
 - 791.3 Algorithmic Game Theory - Flow Markets - [TimRoughGarden] - <http://theory.stanford.edu/~tim/books.html>
 - 791.4 RFID tagged currencies - \$100 bill - <http://www.businessinsider.in/New-Smart-Paper-Could-Put-An-End-To-Dark-Money/articleshow/21134569.cms>
 - 791.5 Cons of RFID currencies - <http://www.prisonplanet.com/022904rfidtagsexplode.html>
 - 791.6 Mechanism Design and Machine Learning - <https://www.cs.cmu.edu/~mblum/search/AGTML35.pdf> - Design of algorithms for maximizing gain in auctions involving sellers and buyers
 - 791.7 Financial and Economic Networks -

<https://supernet.isenberg.umass.edu/bookser/innov-ch1.pdf>

1103. Commits as on 1 March 2014

Example java Publisher and Listeners that use ActiveMQ as the messaging middleware have been committed to repository for an ActiveMQ queue instance created for KingCobra. For multiple clients this might have to be a Topic rather than Queue instance. Request types above and a workflow framework can be added on this. This will be a JMS compliant implementation which might slow down compared to a linux workqueue or queue implementation being done in VIRGO.

1104. Commits as on 17 March 2014

KingCobra userspace library and kernelspace driver module have been implemented that are invoked 1) either in usermode by call_usermodehelper()
2) or through intermodule invocation through exported symbols in KingCobra kernel module, by the workqueue handler in VIRGO workqueue implementation.

1105. Commits as on 22 March 2014

Minimalistic Kernelspace messaging server framework with kernel workqueue, handler and remote cloud client has been completed - For this VIRGO clone cpupooling driver has been added a clause based on a boolean flag, to direct incoming request from remote client to VIRGO linux workqueue which is popped by workqueue handler that invokes a servicerequest function on the KingCobra kernel module. (Build notes: To remove any build or symbol errors, Module.symvers from VIRGO queue has to be copied to VIRGO clouddex and built to get a unified VIRGO clouddex Module.symvers that has exported symbol definitions for push_request()). End-to-end test with telnet path client sending a request to VIRGO clouddex service, that gets queued in kernel workqueue, handled by workqueue handler that finally invokes KingCobra service request function has been done and the kern.log has been added to repository at drivers/virgo/queuing/test_logs/

1106. Commits as on 29 March 2014

Initial commits for KingCobra Request Response done by adding 2 new functions parse_ip_address() and reply_to_publisher() in kingcobra_servicerequest_kernelspace()

1107. Commits as on 30 March 2014

Both VIRGO cpupooling and mempooling drivers have been modified with use_as_kingcobra_service boolean flag for sending incoming remote cloud node requests to VIRGO queue which is serviced by workqueue handler and KingCobra service as per the above schematic diagram and replied to.

1108. Commits as on 6 April 2014

Fixes for REQUEST and REPLY headers for KingCobra has been made in virgo_clouddex_mempool recvfrom() if clause and in request parser in KingCobra with strsep(). This has been implemented only in VIRGO mempool codepath and not in VIRGO clone.

1109. Commits as on 7 April 2014

New function parse_timestamp() has been added to retrieve the timestamp set by the VIRGO mempool driver before pushing the request to VIRGO queue driver

1110. Commits as on 29 April 2014

Initial commits for disk persistence of KingCobra request-reply queue messages have been done with addition of new boolean flag `kingcobra_disk_persistence`. VFS calls are used to open and write to the queue.

1111. Commits as on 26 August 2014

KingCobra driver has been ported to 3.15.5 kernel and bugs related to a `kernel_recvmsg()` crash, timestamp parsing etc., have been fixed. The random crashes were most likely due to incorrect parameters to `filp_open()` of disk persistence file and filesystem being mounted as read-only.

Version 14.9.9 release tagged on 9 September 2014

Version 15.1.8 release tagged on 8 January 2015

1112. Commits as on 17 August 2015

KingCobra + VIRGO Queuing port of Linux Kernel 4.1.5 :

- changed the `REQUEST_REPLY.queue` disk persisted queue path to `/var/log/kingcobra/REQUEST_REPLY.queue`
- kernel built sources, object files
- `kern.log` with logs for telnet request sent to VIRGO queue driver, queued in kernel work queue and handler invocation for the KingCobra service request kernel function for the popped request; disk persisted `/var/log/kingcobra/REQUEST_REPLY.queue`

1113. Commits as on 14 October 2015

AsFer Cloud Perfect Forwarding binaries are invoked through `call_usermodehelper()` in VIRGO queue. KingCobra commands has been updated with a clause for cloud perfect forwarding.

1114. Commits as on 15 October 2015

- Updated KingCobra module binaries and build generated sources
- `kingcobra_usermode_log.txt` with "not found" error from output redirection (`kingcobra_commands.c`). This error is due to need for absolute path. But there are "alloc_fd: slot 1 not NULL!" after `fd_install()` is uncommented in `virgo_queue.h` `call_usermodehelper()` code. The `kern.log` with these errors has been added to testlogs
- `kingcobra_commands.c` has been changed to invoke absolute path executable. With uncommenting of `fd_install` and `set_ds` code in `virgo_queue` the return code of `call_usermodehelper()` is 0 indicating successful invocation

1115. Commits as on 10 January 2016

NeuronRain KingCobra research version 2016.1.10 released.

1116. NEURONRAIN VIRGO Commits for `virgo_clone()/telnet -> VIRGO cpupooling -> VIRGO Queue -> KingCobra`

- as on 12 February 2016

VIRGO commit:

<https://github.com/shrinivaasanka/virgo-linux-github-code/commit/72d9cfc90855719542cdb62ce40b798cc7431b3d>

Commit comments:

Commits for Telnet/System Call Interface to VIRGO CPUPooling -> VIRGO Queue -> KingCobra

*) This was commented earlier for the past few years due to a serious kernel panic in previous kernel versions - <= 3.15.5
*) In 4.1.5 a deadlock between VIRGO CPUPooling and VIRGO queue driver init was causing following error in "use_as_kingcobra_service" clause :
- "gave up waiting for virgo_queue init, unknown symbol push_request()"
*) To address this a new boolean flag to selectively enable and disable VIRGO Queue kernel service mode "virgo_queue_reactor_service_mode" has been added.
*) With this flag VIRGO Queue is both a kernel service driver and a standalone exporter of function symbols - push_request/pop_request
*) Incoming request data from telnet/virgo_clone() system call into cpupooling kernel service reactor pattern (virgo cpupooling listener loop) is treated as generic string and handed over to VIRGO queue and KingCobra which publishes it.
*) This resolves a long standing deadlock above between VIRGO cpupooling "use_as_kingcobra_service" clause and VIRGO queue init.
*) This makes virgo_clone() syscall/telnet both synchronous and asynchronous - requests from telnet client/virgo_clone() system call can be either synchronous RPC functions executed on a remote cloud node in kernelspace (or) an asynchronous invocation through "use_as_kingcobra_service" clause path to VIRGO Queue driver which enqueues the data in kernel workqueue and subsequently popped by KingCobra.
*) Above saves an additional code implementation for virgo_queue syscall paths - virgo_clone() handles, based on config selected, incoming data passed to it either as a remote procedure call or as a data that is pushed to VIRGO Queue/KingCobra pub-sub kernelspace
*) Kernel Logs and REQUEST_REPLY.queue for above commits have been added to kingcobra c-src/testlogs/

1117. Commits - KingCobra 64 bit and VIRGO Queue + KingCobra telnet requests - 17 April 2017

*) Rebuilt KingCobra 64bit kernel module
*) telnet requests to VIRGO64 Queueing module listener driver are serviced by KingCobra servicerequest
*) Request_Reply queue persisted for this VIRGO Queue + KingCobra routing has been committed to c-src/testlogs.
*) kern.log for this routing has been committed in VIRGO64 queueing directory
) Similar to other drivers struct socket reinterpret cast to int has been removed and has been made const in queuesvc kernel thread

779. (FEATURE-DONE) Commits - CVXPY implementation for Eisenberg-Gale Convex Program - 18 August 2017 - - this section is an extended draft on respective topics in NeuronRain AstroInfer Design -
<https://github.com/shrinivaasanka/asfer-github-code/blob/master/asfer-docs/AstroInferDesign.txt>

- (*) First commits for Convex Optimized Market Equilibrium Prices
- (*) Imports CVXPY Convex Program solver
- (*) Objective function is a logistic variant of Eisenberg-Gale Convex Program i.e uses $\text{money} * \log(1+e^{\text{utility}})$ instead of $\text{money} * \log(\text{utility})$ because of curvature error (log is error flagged as concave and logistic is convex per:
<http://www.cvxpy.org/en/latest/tutorial/functions/index.html#vector-matrix-functions>)
- (*) Formulates constraints and objective functions based on <http://www.cs.cmu.edu/~sandholm/cs15-892F13/algorithmic-game-theory.pdf> - Page 106 and Equation 5.1
- (*) But, For all installed solvers ECOS, ECOS_BB, SCS, LS solved convex program prints value as None despite all constraints and objective functions being convex. Also `is_dcp()` prints "not a disciplined convex program". Logs in testlogs/.
- (*) Obviously it should have worked. Therefore this is only a partial implementation commit.
- (*) This implementation uses numpy randomly initialized arrays for Money each buyer has and per-good utility(happiness) each buyer has.
- (*) Replacing money with perceived merit values translates this Market Equilibrium - Intrinsic Value versus Market Price - to Merit Equilibrium - Intrinsic Merit versus Perceived Merit. This has been already described in NeuronRain AsFer Design Documents:

-
<http://sourceforge.net/p/asfer/code/HEAD/tree/asfer-docs/AstroInferDesign.txt>
 and
 - <https://github.com/shrinivaasanka/asfer-github-code/blob/master/asfer-docs/AstroInferDesign.txt>

780. (FEATURE-DONE - this section is an extended draft on respective topics in NeuronRain AstroInfer Design - <https://github.com/shrinivaasanka/asfer-github-code/blob/master/asfer-docs/AstroInferDesign.txt>) Commits - Convex Optimization - DCCP - 21 August 2017

- (*) `import dccp` has been added
- (*) DCCP is the recent advancement and generalization of DCP for convex-concave programs
- (*) `method='dccp'` has been added as parameter to `solve()`
- (*) Objective function has been changed to `log()` from `logistic()` - curvature is concave which is in conflict with definition of Eisenberg-Gale convex program in textbooks. Reason for this contradiction is unknown.
- (*) But DCCP overcomes the DCP limitation and `solve()` prints converged solutions for objective functions
- (*) logs have been committed to testlogs/
- (*) CVXOPT solver has been installed but it does not solve the Eisenberg-Gale objective function. Only SCS solver works - by default applies KKT conditions indirectly.

1118. (FEATURE-DONE) Commits - Convex Optimization - DCCP - 22 August 2017

- (*) Verbose set to True for printing Splitting Conic Solver progress information
- (*) logs committed to testlogs/

1119. (FEATURE-DONE) Commits - Convex Optimization update - 29 August 2017

(*) Removed hardcoded variable values in objective and constraints
(*) In the context of pricing, ECOS Error Metrics print the matrices of market clearing prices for goods
(Reference - pages 3072 and 3073 of
https://web.stanford.edu/~boyd/papers/pdf/ecos_ecc.pdf - KKT conditions in ECOS solver)

778. (FEATURE-DONE) Convex Optimization - Pricing Computation - 30 August 2017 - this section is an extended draft on respective topics in NeuronRain AstroInfer Design - <https://github.com/shrinivaasanka/asfer-github-code/blob/master/asfer-docs/AstroInferDesign.txt>

(*) Prices of Goods/Services have been computed explicitly from Karush-Kuhn-Tucker Conditions (1,2,3 and especially 4)
(*) References:
- Pages 106-108 of
<http://www.cs.cmu.edu/~sandholm/cs15-892F13/algorithmic-game-theory.pdf>)
- KKT conditions and Conic Optimization-
<https://arxiv.org/pdf/1312.3039.pdf>
(*) logs committed to testlogs/

1120. (FEATURE-DONE) KingCobra Kernelspace Messaging Driver for 4.13.3 64-bit kernel - 24 September 2017

(*) KingCobra driver in GitHub and SourceForge at present are 32-bit based on mainline 4.1.5 kernel
(*) Both USB-md and KingCobra kernel modules are subsidiaries of VIRGO kernel
(*) There is a necessity for 64-bit version of KingCobra for interoperability to VIRGO64 64-bit kernel on mainline version 4.13.3
(*) This requires separate repository for KingCobra because of significant kernel function changes between 4.1.5 and 4.13.3 and idiosyncrasies of 64-bit
(*) KingCobra driver has been rebuilt on 4.13.3 64-bit kernel after some changes to function prototypes and new kingcobra64 repository is initialized with these commits
(*) KingCobra kernel sockets have been TLS-ed by kernel_setsockopt(TX_TLS) newly introduced in 4.13 kernel.
(*) After this complete request-reply traffic from VIRGO64 system calls to VIRGO64 queueing and KingCobra is encrypted.

1121. (FEATURE-DONE) Commits - telnet - VIRGO64Queue - KingCobra64 - 25 September 2017

(*) Disk persisted KingCobra64 REQUEST-REPLY Queue written by VIRGO64 Queue to KingCobra64 telnet invocation after 4.13.3 64-bit KTLS upgrade has been committed

1122. (FEATURE-DONE) VIRGO64 Queueing Kernel Module Listener - KingCobra64 - 4.13.3 - 6 October 2017

(*) telnet client connection to VIRGO64 Queue and a subsequent workqueue routing (pub/sub) to KingCobra64 has been tested on 4.13.3
(*) TX_TLS socket option has not been disabled and is a no-op because it has no effect on the socket.
(*) REQUEST_REPLY.queue for this routing from VIRGO64 queue and persisted by KingCobra64 has been committed to KingCobra64 repositories in GitHub and SourceForge

777. (FEATURE-DONE) KingCobra64 Neuro Electronic Currency transactional cloud move - Perfect Forward - 17 January 2018 - this section is an extended draft on respective topics in NeuronRain AstroInfer Design - <https://github.com/shrinivaasanka/asfer-github-code/blob/master/asfer-docs/AstroInferDesign.txt>

(#) Neuro Currency cloud perfect forward has been made transactional by wrapping it by Python Transaction Manager (widely used in Zope Python Application Server)
(#) imports transaction python package and invokes begin() and commit() on subprocess call to neuro cloud move client and server

776. (FEATURE) Concurrent Managed Workqueue(CMWQ), VIRGO64 Queueing and KingCobra64 messaging - 12 June 2019 - this section is an extended draft on respective IoT messaging and kernel analytics topics in NeuronRain AstroInfer Design - <https://github.com/shrinivaasanka/asfer-github-code/blob/master/asfer-docs/AstroInferDesign.txt>

1. Existing workqueue underneath VIRGO64 queueing and requests routed by it to KingCobra64 messaging are old legacy workqueues which have been revamped to Concurrent Managed Workqueue which supports concurrent messaging and lot of other options in queue creation.
2. create_workqueue() in VIRGO64 Queueing has been changed to alloc_workqueue() of Concurrent Managed Workqueue.
3. VIRGO64 Queueing request routing to KingCobra64 messaging has been tested with CMWQ and queueing log and kingcobra64 Request-Reply Queue have been committed to respective testlogs of the drivers
4. reading from stream has been disabled in virgo_kernel_analytics.h
5. Reference - CMWQ documentation - <https://www.kernel.org/doc/html/v4.11/core-api/workqueue.html>
6. Byzantine Fault Tolerance in KingCobra64 persisted queue can be made available by performant CMWQ and routing to the Replicas of REQUEST_REPLY.queue by any of the practical BFT protocols available.
7. Most important application of CMWQ based VIRGO64-KingCobra64 is in the context of kernelspace hardware messaging in IoT,Drones and other analytics driven embedded systems.
8. An example usecase which is a mix of sync and async I/O in kernelspace:
 - (*) Analytics Variables computed by userspace machine learning are read over socket stream by kernel_analytics driver and exported kernelwide
 - (*) Some interested Drone driver in kernel (example PXRC) reads the analytics variables synchronously and sends reply messages asynchronously to VIRGO64 Queueing driver over kernel sockets.
 - (*) VIRGO Queueing routes the queued messages to KingCobra64 driver

1216. (THEORY and FEATURE) Algorithmic Trading in Fictitious Neuro Cryptocurrency - EventNet Graphical Event Model (GEM) HyperLedger implementation - 14 February 2022 - related to 690,789,790,791,1213,1214,1215 and all sections

on Computational Economics - Theory of Value (economic merit), Algorithmic trading, Quantitative Majority Circuit simulation of Demand-Supply, Bounded Width Branching Programs, Algorithmic Game Theory and Mechanism Design, Money Trail, Poverty Alleviation, Graphical Event Models and Causal Event Models, Timeseries analysis, Integer Factorization and Money Changing Program ILP Proof of Work for Neuro Cryptocurrency, Byzantine Fault Tolerance

1216.1 This commit implements a new Python 3.8 source file Neuro_EventNetGEM_HyperLedger.py defining a class for Neuro Cryptocurrency transactional hyperledger. Class member function algorithmic_trading(self,commodity, quantity, neuro_currency, buyer, seller, type) simulates an algorithmic trading activity of buy and sell for a commodity of specified quantity and updates EventNet GEM HyperLedger.

1216.2 Buy-Sell transactions are uniquely identified by the Boost UUID of Neuro Cryptocurrency paid,commodity name and type of transaction. Commodity could include Stock quotes analyzed earlier by Timeseries (ARMA and ARIMA) in NeuronRain AstroInfer where high frequency algorithmic trading aided by machine learning is used widely in practice.

1216.3 Following EventNet GEM convention two text files Neuro_HyperLedger_EventNetGEMEdges.txt and Neuro_HyperLedger_EventNetGEMVertices.txt are updated for each transaction and the actors concerned (buyer-seller). Direction of edge in money trail graph is determined by parenthesized ordered pair of actors.

1216.4 4 sample Neuro transactions (of few trillion Neuros) have been written to Neuro_HyperLedger_EventNetGEMVertices.txt and Neuro_HyperLedger_EventNetGEMEdges.txt respectively below:

```
commodity1:buy:#ff1f984d-ab18-4e69-9a3b-85ddd3c2cce7:10000000000000 -
buyer1,seller1 - (buyer1,seller1)#
commodity2:buy:#ff1f984d-ab18-4e79-1a3b-85ddd3c6cde7:20000000000000 -
buyer2,seller2 - (buyer2,seller2)#
commodity3:sell:#ff2f984d-ab18-5e79-1a3b-85ddd4c1cde7:30000000000000 -
buyer3,seller3 - (buyer3,seller3)#
commodity4:sell:#ff2f994d-ab18-5e79-5a3b-85ddd4c3cde7:90000000000000 -
buyer4,seller4 - (buyer4,seller4)#
---
```

(buyer1,seller1)
(buyer2,seller2)
(buyer3,seller3)
(buyer4,seller4)

1216.5 EventNet GEM for Neuro Cryptocurrency transactions plays the role of blocks added to blockchain for each unique transaction and explicitly stores the causality information for every transaction event. EventNet storage for Neuro HyperLedger could be a NoSQL cloud backend of low latency which makes it truly distributed.

1216.6 Neuro cryptocurrency Boost UUIDs for some denomination minted by Pseudorandom Choice, Integer Factorization and Money Changing Problem Integer Linear Program Proof of Work of varied complexity classes ranging from Bounded Probabilistic Polynomial, Nick's class to NP-Complete have to be digitally signed, a pre-requisite assumed herein.

References:

1216.7 Bitcoin Blockchain Hyperledgering - https://en.wikipedia.org/wiki/Blockchain#/media/File:Bitcoin_Block_Data.svg - Byzantine Fault Tolerant - Does not encode causality explicitly as Graphical model though transaction merkle tree has details of the participants.

#####

#####

This work is licensed under a Creative Commons

Attribution-NonCommercial-NoDerivatives 4.0 International License.

#####

Course Authored By:

Srinivasan Kannan

(also known as: Shrinivaasan Kannan, Shrinivas Kannan)

Ph: 9791499106, 9003082186

Krishna iResearch Open Source Products Profiles:

http://sourceforge.net/users/ka_shrinivaasan,

<https://github.com/shrinivaasanka>,

https://www.openhub.net/accounts/ka_shrinivaasan

Personal website(research): <https://sites.google.com/site/kuja27/>

emails: ka.shrinivaasan@gmail.com, shrinivas.kannan@gmail.com,

kashrinivaasan@live.com

#####

This is a non-linearly organized, continually updated set of course notes on
Linux Kernel and Cloud

and supplements NeuronRain USBmd, VIRGO Linux and KingCobra Design Notes in:

NeuronRain Enterprise Version Design Documents:

USBmd USB and WiFi network analytics - https://github.com/shrinivaasanka/usb-md-github-code/blob/master/USBmd_notes.txt

VIRGO Linux -

<https://github.com/shrinivaasanka/virgo-linux-github-code/blob/master/virgo-docs/VirgoDesign.txt>

KingCobra KernelSpace Messaging - <https://github.com/shrinivaasanka/kingcobra-github-code/blob/master/KingCobraDesignNotes.txt>

NeuronRain Research Version Design Documents:

USBmd USB and WiFi network analytics -
https://sourceforge.net/p/usb-md/code-0/HEAD/tree/USBmd_notes.txt

VIRGO Linux -

<https://sourceforge.net/p/virgo-linux/code-0/HEAD/tree/trunk/virgo-docs/VirgoDesign.txt>

KingCobra KernelSpace Messaging -

<https://sourceforge.net/p/kcobra/code-svn/HEAD/tree/KingCobraDesignNotes.txt>

17 March 2017

VIRGO Linux Kernel Build Steps

VIRGO Linux kernel is an overlay of VIRGO codebase on kernel mainline (presently 4.1.5) source tree. Building a custom kernel for VIRGO

is required for building new system calls and kernel modules in it. Shell script for building kernel mainline is in:

https://github.com/shrinivaasanka/virgo-linux-github-code/blob/master/buildscript_4.1.5.sh

https://sourceforge.net/p/virgo-linux/code-0/HEAD/tree/trunk/buildscript_4.1.5.sh
h

VIRGO Linux kernel has following new system calls:

Cloud RPC system call:

virgo_clone()

Cloud Kernel Memory Cache (kernelspace equivalent of memcache):

virgo_malloc()

virgo_get()

virgo_set()

virgo_free()

Cloud File System:

virgo_open()

virgo_close()

virgo_read()

virgo_write()

VIRGO Linux kernel has following new kernel modules (kernelsocket listeners) corresponding to previous system call clients:

-
1. cpupooling virtualization - VIRGO_clone() system call and VIRGO cpupooling driver by which a remote procedure can be invoked in kernelspace.(port: 10000)
 2. memorypooling virtualization - VIRGO_malloc(), VIRGO_get(), VIRGO_set(), VIRGO_free() system calls and VIRGO memorypooling driver by which kernel memory can be allocated in remote node, written to, read and freed - A kernelspace memcache-ing.(port: 30000)
 3. filesystem virtualization - VIRGO_open(), VIRGO_read(), VIRGO_write(), VIRGO_close() system calls and VIRGO cloud filesystem driver by which file IO in remote node can be done in kernelspace.(port: 50000)
 4. config - VIRGO config driver for configuration symbols export.
 5. queueing - VIRGO Queuing driver kernel service for queuing incoming requests, handle them with workqueue and invoke KingCobra service routines in kernelspace.(port: 60000)
 6. cloudsync - kernel module for synchronization primitives (Bakery algorithm etc.,) with exported symbols that can be used in other VIRGO cloud modules for critical section lock() and unlock()
 7. utils - utility driver that exports miscellaneous kernel functions that can be used across VIRGO Linux kernel
 8. EventNet - eventnet kernel driver to vfs_read()/vfs_write() text files for EventNet vertex and edge messages (port: 20000)
 9. Kernel_Analytics - kernel module that reads machine-learnt config key-value pairs set in /etc/virgo_kernel_analytics.conf. Any machine learning software can be used to get the key-value pairs for the config. This merges three facets - Machine Learning, Cloud Modules in VIRGO Linux-KingCobra-USBmd , Mainline Linux Kernel
 10. SATURN program analysis wrapper driver.
- and userspace test cases for the above.

Prerequisites for building VIRGO Linux kernel are similar to mainline kernel:
apt install libncurses5-dev gcc make git exuberant-ctags bc libssl-dev

Presently VIRGO kernel is 32-bit. Building 64 bit linux kernel requires long mode CPU flag (lm) in /proc/cpuinfo. Also booting a 64 bit kernel built on 32 bit kernel could cause init to fail as "init not found". This is because init is a symbolic link to systemd binary when kernel boots up which is 32-bit and not 64-bit. For this menuconfig in Kbuild provides IA32 Emulation config parameter.

Bootting a custom kernel could also cause partition issues while grub is updated sometimes with error "no such partition" and could drop to grub rescue> prompt. This can be remedied by:

1. grub rescue> ls

which lists the partitions in format (hd0, msdos<#number>)

2. grub rescue> set root=(hd0, msdos<#number>) {for each such partition}

3. grub rescue> set prefix=(hd0, msdos<#number>)/boot/grub

```
4. grub rescue> insmod normal
5. grub rescue> normal
which boots grub normally. This has to be persisted with:
6. update-grub2
7. grub-install /dev/sda
on reboot
```

Some grub errors can be debugged by adding kernel boot parameters in /boot/grub/grub.cfg or at boot time edit of the entry with "... \$vt_handoff". Appending options "debug init=<path-to-systemd>" to this line might help.

Sometimes repetitive builds and grub updates also cause a rare file system corruption as below which causes root shell drop:

```
ALERT! <diskid> does not exist
Boot args (cat /proc/cmdline)
- Check rootdelay
- Check root
Missing modules (cat /proc/modules, ls /dev)
Dropping to root shell
(initramfs)
This is remedied by:
(initramfs) modprobe dm-mod
(initramfs) lvm
lvm> vgchange -ay
lvm> exit
(initramfs) exit
```

followed by:
mount -o remount,rw /dev/sda<number> <mount_point_directory>

Complete documentation of VIRGO Linux with Design Documents is in:
<https://github.com/shrinivaasanka/virgo-linux-github-code/tree/master/virgo-docs/>
<https://sourceforge.net/p/virgo-linux/code-0/HEAD/tree/trunk/virgo-docs/>

20 March 2017

VIRGO Linux 64 bit build - continued:

*) After configuring IA32 simulation and a successful build, there could still be initramfs errors because of i915 drivers mismatch as below:

"Possible missing firmware ----- for i915"

*) Previous error requires installation of latest linux i915 graphics drivers (though there may not be a matching hardware for it) listed in <https://01.org/linuxgraphics/downloads/firmware>: for Kabylake, Skylake, Broxton graphics processors

*) update-initramfs has to be done again for correct /boot initrd image to be created for 4.10.3 after updating i915 drivers previously listed

*) In some cases image may be hidden in grub boot menu. For this an already available boot-repair tool scans the /boot images and reinstalls grub menu.

*) On successful 64 bit build, uname -a should have x86_64 as below:

```
Linux kashrinivaasan-Inspiron-1545 4.10.3 #1 SMP Fri Mar 17 18:30:40 IST 2017
x86_64 x86_64 x86_64 GNU/Linux
```


24 September 2017

NeuronRain VIRGO64 presently has been ported to 4.13.3 Linux Kernel. Also the accompanying USBmd and KingCobra kernel modules have been

split into 32-bit and 64-bit versions and separate repositories have been created for them in SourceForge and GitHub. 4.13.3 kernel has transport layer security enshrined in kernel which is essential for securing kernelspace cloud traffic. A detailed FAQ on technical aspects of VIRGO 64-bit version and KTLS is in <http://neuronrain-documentation.readthedocs.io/en/latest/> .

Logging Servers and Clients - Some Implementation Examples - 28 September 2018

In large cloud installations, there often arises a need to log frequently occurring network event traces to log files realtime minimizing network latency. Example 1 in references is the Trace utility implemented in an application server (Java) for logging Global and Local JTS Transaction (XA) events with facility for Trace Levels. Example 2 describes sequential and parallel implementations of a logging server in a network and logging clients connecting to this server. Reactor pattern is a Listener on pending socket descriptors (select/poll) and events to be serviced. Example 3 in the references: NeuronRain VIRGO32 and VIRGO64 Linux Kernels implement a kernel service module and logging client utility kernel function for writing EventNet log messages to EventNet Edges and Vertices files sent from remote cloud nodes by `eventnet_log()` - implements Acceptor-Worker Kernel Threads (Router-Dealer) pattern. Example 4 is the ZeroMQ Publish-Subscribe protocol for designing a log collector subscriber and log client publishers.

References:

- 1.Oracle Glassfish Java EE - (Earlier Sun Microsystems iPlanet Application Server - IAS) - JTS XA Transaction Logging - <https://github.com/javaee/glassfish/blob/master/appserver/transaction/jts/src/main/java/com/sun/jts/trace> and <https://github.com/javaee/glassfish/tree/master/appserver/transaction/jts/src/main/java/com/sun/jts/utils> - IAS_JTS_TRACE - authors: "mailto:k.venugopal@sun.comi,kannan.srinivasan@sun.com" - "...public static void setTraceWriter(PrintWriter traceWriter) { m_traceWriter = traceWriter; }..." - Wrapper Facade pattern - wraps a writer object
- 2.Beautiful Code - Chapter 26 - Labor-Saving Architecture - An Object Oriented Framework for Networked Architecture - Concurrent Logging Servers in C++ - Reactor Pattern for Logging Concurrent Events
- 3.EventNet Kernel Service Module and EventNet Logging Client function in NeuronRain VIRGO Linux Kernel - <https://gitlab.com/shrinivaasanka/virgo64-linux-github-code/tree/master/linux-kernel-extensions/drivers/virgo/eventnet> and https://gitlab.com/shrinivaasanka/virgo64-linux-github-code/blob/master/linux-kernel-extensions/drivers/virgo/utils/virgo_generic_kernelsock_client.c - `eventnet_log()`
- 4.ZeroMQ Pub-Sub for distributed logging - <http://zguide.zeromq.org/php:chapter8#toc31>

Linux Kernel Development (System calls and Drivers) - some low level architecture specific issues - 14 May 2019

Following are few architecture specific idiosyncracies and heisen bugs that could cause harrowing experience while writing new kernel system calls and drivers (32 bit versus 64 bit, dual core versus quad core versus octa core):

- 1.strcpy() buffer overflow (kernel has its own implementation of glibc string library in include/linux) - there is a documented intel x86_64 buffer overrun error in some chips
- 2.char * to const char* cast requirement

3. (u8*) cast for sin_addr in kernel sockets
4. memcpy() versus copy_to_user() or copy_from_user() - in some architectures memcpy() works while in others copy_xxx() pairs work without crashes
5. Requirement for __user qualifier macro for some system call parameters passed to copy_from_user() and copy_to_user()
6. Correct location of kernel glibc string library headers in Makefile paths
7. strcpy() instead of strncpy() - works some times
8. Usage of BUF_SIZE (buffer size as macro) instead of strlen()
9. kstrdup() might crash sometimes in strlen() which can be replaced by strncpy() and strcat()
10. User memory access warning/error in KASAN because of copy_from_user() and copy_to_user() (access_ok() assertions crash)
11. memcpy() is less secure than copy_xxx() pairs
12. __put_user() and strncpy_from_user() might sometimes circumvent crashes
13. Setting the segment correctly - get_fs()/set_ds(KERNEL_DS) must correctly encapsulate kernel data access.
14. copy_user_generic() avoids crashes in some cases if previous do not work
15. cast char to unsigned long long which bypasses lot of buffer issues and __put_user() supports only unsigned long long
16. unsigned long long has the advantage of abstracting any datatype.
17. Being compatible for both 32 and 64 bits simultaneously could be a problem - u8 and const char* cast
18. memcpy() could fail in certain multicores
19. strncpy_from_user() in place of copy_from_user() creates stabler kernel syscalls and driver builds
20. __put_user() in place of copy_to_user() is stabler in some multicores
21. unsigned long long is sometimes stabler than char __user*
22. sizeof() might have to be replaced by BUF_SIZE macro for all copy functions
23. in4_pton() might fail in some cases while in_aton() might work

 Linux Kernel Development (System calls and Drivers) - some low level
 architecture specific issues 2 - 10 June 2019

Following are some architecture specific problems while invoking kernel sockets (e.g simulating a telnet client and server within kernel):

1. System calls (especially written new) often involve userspace strings passed on to kernel (and sometimes transported to a remote kernel by kernel sockets) which are mandated to be marked as "const __user char**"
2. __user pointer marked as previous informs the kernel that a userspace data has to be handled by kernel by copying it to kernelspace
3. Accessing __user pointers directly within system calls and kernel modules (e.g in printk) creates a fault because a userspace pointer is accessed in kernel space illegitimately.
4. Special functions like copy_from_user()/strncpy_from_user() are meant for copying userspace __user pointed data to kernelspace pointers.
5. This userspace to kernelspace copy requires setting kernel data segments appropriately by set_ds(KERNEL_DS) followed by the invocation and resetting the datasegment to status quo ante.
6. Buffers used within the kernel modules and system calls for copying user buffers must have sufficient size and strlen() may not work for strings which are not null terminated causing overflow.
7. copy_to_user() causes weird faults and there is no equivalent strncpy_to_user() for out parameters in system calls which might necessitate __put_user() to a generic data type e.g unsigned long long and reinterpret-cast to a char literal. Sequential invocation of these creates an array of chars or strings.
8. -32, -107, -101 errors are often witnessed in kernel_connect() which is probably caused by in4_pton()

05/03/2020
(6) LinkedIn
6
Search
Try Premium Free
for 1 Month
Manage synced and imported contacts
370 Connections
Sort by: First name
Your contact import is ready
Search by name
Search with filters
Connect with your contacts and never lose touch
Continue
Aarthi Prashanth
Senior Manager-TA
Abdullah Abdul Khadir
Software Engineer
Abha Walvekar
HR and Operations Executive at EAI Systems
Abhishek Porwal
Talent Acquisition Manager at Sumo Logic
Message
Message
Message
Message
About
Addhyan Pandey
Director Data Science at Cars.com
More options
Help Center
Advertising
Message
Privacy & Terms
Business Services
Get the LinkedIn app
More
LinkedIn Corporation © 2020
Addlin Sofia
HR Systems Professional
Adhavan Veeraiyan
Senior Developer
Message
Message
Messaging
<https://www.linkedin.com/mynetwork/invite-connect/connections/>
1/38
05/03/2020
(6) LinkedIn
Aditi Singh
Search
Director at OSTtalent
Aditya Sen
LYNKERSOFT
Message
6
Try Premium Free
for 1 Month
Manage synced and imported contacts
Message
Your contact import is ready
Connect with your contacts and never lose touch
Adlin Asha
Talent Acquisition

Adwait Gaikwad
Student at Chennai Mathematical Institute
Ajay Kumar
Technology & Product Hiring @ Licious - Born to Meat
Ajay V
Technology Hiring | TiVo
Ajmal Khan
Managing Director and Co-founder at ChennaiSoft Consultancy Services
Message
Continue
More options
Message
Message
Message
Message
About
Help Center
Advertising
Privacy & Terms
Business Services
Get the LinkedIn app
Alagappan (Alan) Ramu
Lead Software Engineer at Applied Data Finance
Alex Rose, PHR
Expert Resume Writer & Experienced Recruiter
Alik Saring
Principal Software Engineer at EMC Corporation
<https://www.linkedin.com/mynetwork/invite-connect/connections/>
Message
More
LinkedIn Corporation © 2020
Message
Message
Messaging
2/38
05/03/2020
(6) LinkedIn
6
Search
Amaresan Balakrishnan
Software Engineering Sr Mgr at Juniper Networks
Message
Manage synced and imported contacts
Anamika Krishnamoorthy
Human Resources Manager at HELYXON HEALTHCARE SOLUTIONS PRIVATE LIMITE
D
Your contact import is ready
Message
Connect with your contacts and never lose touch
Continue
Anand Vaidhyanathan
Principal Consultant - NFV, 5G Orchestration & OSS at Hewlett Packard Enterprise
Try Premium Free
for 1 Month
More options
Message
Anand - Freelancer Online Trainer - Hourly Project Support
Provides Online Training, Freelancers, resources for short & long-term projects,
hou
rly/per-project work. +91-9500192218
Anbu Ganesh
Founder & CEO - CanGo Networks - OptiGo
Aneek Maiti
Mathematics research scholar

Message
Message
Message
About
Angelin N
Human Resources at Workfreaks.in
Message
Help Center
Advertising
Privacy & Terms
Business Services
Get the LinkedIn app
More
LinkedIn Corporation © 2020
Angeline T.
Head of Integrated Resourcing - Singapore, Philippines & Thailand at Shell
Anshul Khandelwal
Products, ML, AI, Software Architecture and Engineering
Message
Message
Messaging
<https://www.linkedin.com/mynetwork/invite-connect/connections/3/38>
05/03/2020
(6) LinkedIn
Senior Associate TAG
Search
Archana Mishra
Technical Recruiter at Akidev Corporation
Message
Message
6
Try Premium Free
for 1 Month
Manage synced and imported contacts
Your contact import is ready
Arihide Fukuda
Vymo Solution Director
Arpith Siromoney
Software Engineer at Stripe
Arulraj V
Technical Lead at The Fabric
Arun Kumar Sudhakar
Senior Business Specialist at A.P. Moller - Maersk
Asha TB
Technical Recruiter at BMC(I)Pvt Ltd
Connect with your contacts and never lose touch
Message
Continue
Message
Message
Message
Message
About
Help Center
Advertising
Ashish Gupta
Deputy Director at BT
Ashutosh Kinikar
Senior Recruiter
Ashwini Kumar
Assistant Product Manager at Qwiksilver Souldtions
<https://www.linkedin.com/mynetwork/invite-connect/connections/>
More options

Privacy & Terms
Business Services
Get the LinkedIn app
More
Message
LinkedIn Corporation © 2020
Message
Message
Messaging
4/38
05/03/2020
(6) LinkedIn
Search
Aysha David
Underwriting Associate at Accenture
6
Try Premium Free
for 1 Month
Message
Manage synced and imported contacts
Baba Weedy
Independent Recruiter
Message
Your contact import is ready
Connect with your contacts and never lose touch
Babu Jayaraj
Principal Architect at Jio
Bala. Dutt
Principal Engineer at Intuit
balaji narayana
Team lead Talent Acquisition at Altimetrik
Balaji R
Engineering Leader | Scrum Master | Agile Coach | Fintech
Balasubbhramaniyam Ayyaswaami
Head of Online Business at Pepipost
Continue
Message
More options
Message
Message
Message
About
Message
Help Center
Advertising
Privacy & Terms
Business Services
Get the LinkedIn app
Bavani T
HR I Recruiter I Headhunter I Employer Branding
Benjamin Booth
Product Management & Software Engineering
LinkedIn Corporation © 2020
Message
Message
Messaging
Berlin Fernandez
<https://www.linkedin.com/mynetwork/invite-connect/connections/>
More
M
5/38
05/03/2020
(6) LinkedIn
Senior Executive Human Resources at Encore Software Services, Inc.

Search
Bhavya Shriyan
In search of Right Talent!!!
Bhuvaneshwari V
HR Recruiter & Web researcher
Message
6
Message Manage synced and imported contacts
Message Connect with your contacts and never lose touch
Your contact import is ready
Continue
Bhuvaneshwari Selvaraj
Software Development Manager at Amazon
Bound Tech Solutions
CEO Bound Tech Solutions
Try Premium Free
for 1 Month
More options
Message
Message
Brahmaiah M
SAP HCM & Success Factors Certified Consultant. at itelligence India Software
Solutions Pvt Ltd
Brahmaiah Thumbeti
Founder and CEO at Jiosmart Private Limited
Message
Message
About
Help Center
Advertising
Brinda Murali
Manager - Leadership hiring
Message
Privacy & Terms
Business Services
Get the LinkedIn app
More
LinkedIn Corporation © 2020
C MANI
system administrator at Sanpra Infotech Pvt. Ltd.
Cheris Mehta
Founder & Designated Partner at TalentHome Solutions LLP
Message
Message
Messaging
<https://www.linkedin.com/mynetwork/invite-connect/connections/6/38>
05/03/2020
(6) LinkedIn
Chester Cuaresma
Search
Lead Software Engineer at Software AG (formerly webMethods)
Try Premium Free
for 1 Month
Manage synced and imported contacts
Chitra Sudalaikannan
CEO of my life| I Love myself | Simple | Elegant| Dreamer| Achiever| UI UX
Designer|
Front End Developer| E'neur| Dancer
6
Message
Message
Your contact import is ready

Connect with your contacts and never lose touch

Deepak Nair

HR Business Partner at CanGo Networks

Deepu Ponnappan (MBA. CCNP. JNCIA. ITIL. CEH, Prince2)

Global Technical Specialist at AT&T

Devika Kakkar

HR Consultant at Consultant

Dhritiparna Dhar

Head of Talent Acquisition - Zendrive

Dineshkumar Baktavachalam

Looking for new opportunities

Continue

Message

More options

Message

Message

Message

Message

About

Help Center

Advertising

Privacy & Terms

Business Services

Get the LinkedIn app

Diptaishik Choudhury

Student at Chennai Mathematical Institute

Divya S

Hiring for React JS and Fullstack developer position - Singapore location

Dr Sridevi Srivatsa

Research

<https://www.linkedin.com/mynetwork/invite-connect/connections/>

Message

More

LinkedIn Corporation © 2020

Message

Message

Messaging

7/38

05/03/2020

(6) LinkedIn

6

Search

Try Premium Free

for 1 Month

Dr. Amita Navnish

Strategic Human Resources (HR) Professional having an International experience and passion to drive results for children at #UNICEF. #Hope & #Happiness #ForEv...

Dr. Harichandra Reddy

CEO & Founder of INTENT InfoTech

Message

Message

Manage synced and imported contacts

Your contact import is ready

Connect with your contacts and never lose touch

Continue

Dr. Pedro Dujon Malode

IJIRUSA JOURNALS, Content Editors, Writers, Research, Thesis Guidance

Elena DSouza

🔗 HR Recruiter 🔗 Mays Consultants 🔗 ▶ LinkedIn Hiring Specialist ◀

Firnaz M

Product Innovation & Business Strategy at Adzis, Inc.

G R Karpagam Rangaraju

Professor at PSG College of Technology

Message
Message
Message
Message
About
G.Deepthi Rani
Sr Associate at Honeywell Tech. Solution Lab, Bangalore
More options
Help Center
Advertising
Message
Privacy & Terms
Business Services
Get the LinkedIn app
More
LinkedIn Corporation © 2020
Ganesan Gurumurthy
Principal Architect
Gaurav Bansal
Senior Engineer at DNV GL
Message
Message
Messaging
<https://www.linkedin.com/mynetwork/invite-connect/connections/8/38>
05/03/2020
(6) LinkedIn
Gayatri Patil
Connecting talent with top product companies like Google, Amazon, PhonePe
Search
Message
Gayatri Verma Thirty thousands Plus Followers
International Recruitment- IT,Oil & Gas,Healthcare,Legal, Banking- India KSA UAE
K
uwait UK Ireland Germany Canada
6
Try Premium Free
for 1 Month
Manage synced and imported contacts
Message
Your contact import is ready
Connect with your contacts and never lose touch
Girish B V
General Manager at Aarvi Encon Limited
Gopa Kumar GopalaKrishnan
Talent Acquisition Lead at Sandhata Technologies
Gopalan Priyaranjan
Software Lead/Head at AgShift
Gopalan Raman GPLN
Senior Director, Human Resources
Goutham- Looking for MAC OS Architect Düsseldorf/Essen German...
Delivery Lead at Avance Consulting
Message
Continue
More options
Message
Message
Message
Message
About
Help Center
Advertising
Privacy & Terms
Business Services

Get the LinkedIn app
Govind Bhone
Software Engineer at Trading Technologies
Gulen Chongtham
IT Consultant at Tata Consultancy Services Ltd
Harini Vijay
Senior Manager - Recruitment at Han Digital Solution (p) Ltd
<https://www.linkedin.com/mynetwork/invite-connect/connections/>
Message
More
LinkedIn Corporation © 2020
Message
Message
Messaging
9/38
05/03/2020
(6) LinkedIn
6
Search
Harsha Aswath
Senior Software Engineer at Netflix
Try Premium Free
for 1 Month
Message
Manage synced and imported contacts
Harun Prasad Paramasivam
Chief Development Officer at tappit
Message
Your contact import is ready
Connect with your contacts and never lose touch
Continue
Hema M
Relationship Executive at New Era India
IndosHRservices Consultants
IndosHRservices
Jagadish G (SSM)
Sr IT Recuriter at PTC
Jagan D
Senior Talent Acquisition Manager at Cienra
Message
Message
Message
Message
About
Jaganathan Jagan
retired from Food Corporation Of India at Food Corporation of India
More options
Message
Help Center
Advertising
Privacy & Terms
Business Services
Get the LinkedIn app
More
LinkedIn Corporation © 2020
James Clarke
injury data specialist
James Schaum
IT Consultant - Looking for IT Infrastructure opportunity (LION 29K+)
Message
Message
Messaging
<https://www.linkedin.com/mynetwork/invite-connect/connections/>
10/38

05/03/2020
(6) LinkedIn
Europe/Americas at ZBX
Search
Janani Jayaram
HR Consultant
Message
Message
6
Try Premium Free
for 1 Month
Manage synced and imported contacts
Your contact import is ready
Janeesh A
Odoo Consultant at Steigend IT Solutions | Odoo Developer
Jayadev Mahalingam
The Entrepreneur
Jayanthi P
Currently Hiring Technical Writer (6 Months - 1 years) at Hyderabad
John P Thomas
Executive Recruiting | Searchologist | TA Brand Ambassador
Jose Mathew
Engineering Manager, AI/ML applications at Adobe
Message
Connect with your contacts and never lose touch
Continue
Message
Message
Message
Message
About
Help Center
Advertising
JOSHUA IMMANUAL
Senior Executive HR@ EASi
K Venu Gopal
Director Of Engineering at Rakuten
Kala Krishnaswamy
Correspondent & Principal at Sriniketan's Matriculation School "JINGLE BELLS"
<https://www.linkedin.com/mynetwork/invite-connect/connections/>
More options
Message
Privacy & Terms
Business Services
Get the LinkedIn app
More
LinkedIn Corporation © 2020
Message
Message
Messaging
11/38
05/03/2020
(6) LinkedIn
Kalpana Karunamurthi
Search
Senior Director of Engineering at SAP
6
Try Premium Free
for 1 Month
Message
Manage synced and imported contacts
Kalyan Hadoop
Apache Hive Contributor at The Apache Software Foundation
Message

Your contact import is ready
Connect with your contacts and never lose touch
Kamal Kaanth Chettiaar
Founder and CEO at WeRecruit Talent Pvt. Ltd.
Kannan Rajagopalan
Independent Management Consulting Professional
Karthick Chandran
Manager Recruitment at Amazon.com
Karthik Chandrasekhar
Doctor of Philosophy in Mathematics, Assistant Professor at PES University
Karthik Muralitharan
Deputy Manager - IMS - CoE/Practice Hiring Specialist at Hexaware Technologies
Continue
Message
More options
Message
Message
Message
Message
About
Help Center
Advertising
Privacy & Terms
Business Services
Get the LinkedIn app
Kavita S. Sunil
Word weaver. Storyteller. Lifelong learner
Kiran Balivada
LEARN > RECRUIT > REPEAT *Nothing will work unless you do.*
Message
LinkedIn Corporation © 2020
Message
Messaging
Kiran T
<https://www.linkedin.com/mynetwork/invite-connect/connections/>
More
Message
12/38
05/03/2020
(6) LinkedIn
Founder & CEO at Stealth Mode Startup
Search
Krishna Gopinathan
CEO at Applied Data Finance
Message
6
Message Manage synced and imported contacts
Message Connect with your contacts and never lose touch
Your contact import is ready
Krishnakumar Narayanan
Co-Founder, COO @ CoreStack. We Deliver Continuous Compliance Assurance & Operations Automation for Your Cloud.
Kruthi Patwari
Head - HR & Finance at Yantriks
Kumar Mangesh
Sales Consultant || Travel & Expense Management || Enterprise Selling
Kunal Singh
Sr. Consultant in US IT Staffing
Laxman M D
Head Talent Acquisition - Angulus IT Services (P) Ltd
Continue
Message
Message
Message

Area Office at LIC HFL

Help Center

Advertising

Laxmi CTC

LIC HFL Rajaji Nagar

More options

Message

About

Hiring Sr. Technical Consultant-Adobe Campaign for Noida & Bangalore. Email at hr

@careertrackers.in

Try Premium Free

for 1 Month

Message

Privacy & Terms

Business Services

Get the LinkedIn app

More

LinkedIn Corporation © 2020

Message

Lucky K

Urgent Requirement!! Android Developer positions with BOSE...Share profiles to lu

cky@infyshine.com

Message

Messaging

<https://www.linkedin.com/mynetwork/invite-connect/connections/>

13/38

05/03/2020

(6) LinkedIn

Madhan P

Search

Sr Product Manager at MicroFocus / Novell

6

Message

Try Premium Free

for 1 Month

Manage synced and imported contacts

Madhavi Kamatagi

HR at PharmEasy

Message

Your contact import is ready

Connect with your contacts and never lose touch

MALATHI RANGANATHAN

Independent Facilities Services Professional

Continue

Message

More options

Malcolm Dsouza

Senior Digital Marketing Executive | Digital Marketing Consultant | Digital Strategis

t

Malvika Gaharwar

Recruiter at OpenSea Software Technologies Pvt. Ltd.

Manas Jalahalli Umapathy

Talent Acquisition Business Partner at Grab

Message

Message

Message

Manasi Karri

Connecting talent with right jobs | Message me if you are exploring new opportuni

ties

Message

About
Help Center
Advertising
Privacy & Terms
Business Services
Get the LinkedIn app
Manish Patnaik
Team Lead (India Operations) at eTeki Inc
Manisha Dhawan
Manager- (Recruitment) - IT Hiring expert
Manjula Dilip
Business Account Manager
<https://www.linkedin.com/mynetwork/invite-connect/connections/>
Message
More
LinkedIn Corporation © 2020
Message
Message
Messaging
14/38
05/03/2020
(6) LinkedIn
6
Search
Manjunath Velusamy
District Youth Wing Secretary & Spokesperson-Trichy Zone at Aiadm
Mary Shamini
Senior Consultant at Strivex Consulting P Ltd
Message
Manage synced and imported contacts
Message
Your contact import is ready
Connect with your contacts and never lose touch
Continue
Meenu Singh
Recruitment Evangelist - Top Product Companies!
Megavarnan Govindaswamy
Author, Founder & CEO at EONE Technologies
Megh Makwana
Hiring: Angular / Reactjs / BD / BA / Flutter-Android / Laravel -Yii
Mohamed Althaf
Senior Executive - HR at HCL Technologies
Sr HR Recruiter at High Noon Corporation
More options
Message
Message
Message
Message
About
Mohammed (👉👈)
Try Premium Free
for 1 Month
Message
Help Center
Advertising
Privacy & Terms
Business Services
Get the LinkedIn app
More
LinkedIn Corporation © 2020
Mohan Akula Chandrasekar
Recruitment Consultant at Capgemini Technology India Pvt Ltd
Monica Weslie
Director at Talent Hire Consulting

Message
Message
Messaging
<https://www.linkedin.com/mynetwork/invite-connect/connections/15/38>
05/03/2020
(6) LinkedIn
Mukesh Garg
Staff Software Engineer at Intuit
Search
Muktha Shivakumar
Recruitment Lead - Leadership Hiring at Gallagher
Message
Message
6
Try Premium Free
for 1 Month
Manage synced and imported contacts
Your contact import is ready
Connect with your contacts and never lose touch
Murali Krishna
Freelance Recruiter Hiring for various Product, Tech start-ups and companies across India
Message
Continue
More options
Murali Krishnan
Technical Manager - Identity & Access Management at Standard Chartered Global Business Services
Murali Naru
IT Analyst(Hadoop Developer) at Tata Consultancy Services
Muthu Kumar
Talent Acquisition (We are Hiring)
Muthu Kumar Raju
ITIL/Business Process Consultant
Message
Message
Message
Message
About
Help Center
Advertising
Muzaffar Maqbool
Director at IndosHRservices
Nagendra HK
Senior Principal Engineer at Dell EMC
Nagendra Kumar
Senior Consultant at Arcadis
<https://www.linkedin.com/mynetwork/invite-connect/connections/>
Privacy & Terms
Business Services
Get the LinkedIn app
Message
More
LinkedIn Corporation © 2020
Message
Message
Messaging
16/38
05/03/2020
(6) LinkedIn
6
Search

Nanda gopal
Plant Head at Sheet Metal
Try Premium Free
for 1 Month
Message
Manage synced and imported contacts
Narasimha Reddy Dwarsala
Quality Manager at Oracle India Pvt. Ltd
Narayan Bethmangalkar
Senior Director of Engineering at Software AG
Narayanan Govindarajan
Technical Leader in Big Data and Search
Narendra K Jha
Software Engineer 2 at Zynga Games
Naureen Sheikh
Managing Partner at Dreams Placement
Naveen Damaraju
Senior Delivery Manager at Kaarya Consulting Services Pvt. Ltd.
Naveen Paulkandasamy
Director of Platform Engineering at Unravel Data
Navoneel Raichaudhuri
Quantitative Analyst (AVP) - Equity Algo Trading at Citi
Neeraj Malik
<https://www.linkedin.com/mynetwork/invite-connect/connections/>
Message
Your contact import is ready
Connect with your contacts and never lose touch
Continue
More options
Message
Message
Message
Message
About
Message
Help Center
Advertising
Privacy & Terms
Business Services
Get the LinkedIn app
More
LinkedIn Corporation © 2020
Message
Message
Messaging
17/38
05/03/2020
(6) LinkedIn
Director at Reis Staffing & HR Services Pvt. Ltd
Search
Neethu Shibu
Human Resources at Mastech InfoTrellis, Inc.
Message
Message
Neha Kukerja
HR Consultant at Self
Neha Modi
Freelance Recruiter
Neha Sharma _ We are hiring..
Talent Acquisition Specialist _Volantis Technologies
Neha Garg
Senior IT Recruiter at Confidential
Manage synced and imported contacts
Message

Connect with your contacts and never lose touch

Continue

Founder, Big Recruit Consulting

Nibedita Roy Choudhury

Actively looking for a analyst role in financial sector

Nibha Singh

Talent Acquisition Lead

More options

Message

Message

Message

Message

About

Help Center

Advertising

Nevenka Dhadwal

Try Premium Free

for 1 Month

Your contact import is ready

Neha Gupta

Recruitment @ Paytm | Hiring Java Leads/Architects/Principal Engineers/Engineeri
ng Managers

6

Message

Privacy & Terms

Business Services

Get the LinkedIn app

More

LinkedIn Corporation © 2020

Message

Message

Messaging

[https://www.linkedin.com/mynetwork/invite-connect/connections/
18/38](https://www.linkedin.com/mynetwork/invite-connect/connections/18/38)

05/03/2020

(6) LinkedIn

Nidisha Sree M

Search

Career Coach | Conscious Careers| L& D Person| For a happy
growth programs in IoT | Data Science |AI

Now focus- custom

Nikhil Jadhav

Talent Acquisition Consultant at Tata Communications

6

Message

Try Premium Free

for 1 Month

Manage synced and imported contacts

Message

Your contact import is ready

Connect with your contacts and never lose touch

Nirosha Nisha Yadav

Working In Aisan Auto Parts

Continue

Message

More options

Nisha .

Hiring for PHP Developers, .Net Developers and Business Development Executive-
Ahmedabad

Message

Nishant Bhardwaj

Talent Acquisition| Employer Branding | Social Media Hiring | Leadership Hiring
| Ca

mpus Recruitment
Nishant Singh
SAP S4 Fashion PTP Consultant at Deloitte Consulting
Nithya Ramakrishnan
Talent Acquisition
Message
Message
Message
About
Help Center
Advertising
Privacy & Terms
Business Services
Get the LinkedIn app
Padma Reddy
COO Global R&D; Head, Software AG India
Parthan S Ramanujam
Lead Ruby Developer at iPRO Group Pty Ltd
Parthasarathy Mani
<https://www.linkedin.com/mynetwork/invite-connect/connections/>
Message
More
LinkedIn Corporation © 2020
Message
Message
Messaging
19/38
05/03/2020
(6) LinkedIn
Founder at Vingsfire HRIM Pvt Ltd
Search
Pavithra N J Achar
Recruitment Specialist (Malaysia)
Pavithra Rajappa
Data Analyst
6
Message
Manage synced and imported contacts
Your contact import is ready
Message
Connect with your contacts and never lose touch
Continue
Pawan Verma
Talent Acquisition Manager at Vegazva Group
Piyush Jain
Team Lead at Software AG
Poornima KS
Talent Search Manager @ Kalpavrksha Associates
Prabhakar Ramadass
Product Management at Amazon
Search Executive at Executive Search
More options
Message
Message
Message
Message
About
Prabhu K
Try Premium Free
for 1 Month
Help Center
Advertising
Message
Privacy & Terms

Business Services
Get the LinkedIn app
More
LinkedIn Corporation © 2020
Prakash Kewalramani
Career Strategist, Career Shaper & Motivator since 25 years
Prakash Khemani
Data and Distributed Systems
Message
Message
Messaging
<https://www.linkedin.com/mynetwork/invite-connect/connections/20/38>
05/03/2020
(6) LinkedIn
Pranita Shukla
Search
Deputy Brand Manager at LODHA Group
Message
Try Premium Free
for 1 Month
Manage synced and imported contacts
Prashant K Lal
IoT, RPA, NFV, Digitisation, Physical Web, Web Scaled Hyper Converged Architecture, PWA, c-RIM, OpenSource, R&D, Cloud Comp...
6
Message
Your contact import is ready
Connect with your contacts and never lose touch
Prasid Mitra
Software Engineer at Galileo
Pratapan J Karoor
Freelance IT Consultant
Prathima V
Actively Looking For Recruiter Roles!!
Pratish Gandhi
CEO, Co-Founder, Credy | Y Combinator alum | ex Goldman Sachs
Praveen Jain
Self Employed
Message
Continue
More options
Message
Message
Message
Message
About
Help Center
Advertising
Privacy & Terms
Business Services
Get the LinkedIn app
Praveen Jesudhas
Manager, Data Science at Tiger Analytics
Praveen Sam Sambath
DevOps Specialist at plusautomate
Preethi C
Hr Executive at Digit88 Technologies(Looking for change)
<https://www.linkedin.com/mynetwork/invite-connect/connections/>
Message
More
LinkedIn Corporation © 2020
Message
Message

Messaging
21/38
05/03/2020
(6) LinkedIn
6
Search
Prem Kumar
Team Manager at ManpowerGroup
Message
Manage synced and imported contacts
Prem Kumar U
"Time spent on hiring, is time well spent."
Message
Your contact import is ready
Connect with your contacts and never lose touch
Continue
Premkumar Raja - CSPO @
Technical Project Manager
Prince .
IT Recruiter
PRIYA KOTTE
IT Recruiter at US Tech Solutions
Priya Singh
Executive Search - Specialist
Ex Talent Acquisition Manager at Medlife.com
More options
Message
Message
Message
Message
About
Priyanka .K.G
Try Premium Free
for 1 Month
Message
Help Center
Advertising
Privacy & Terms
Business Services
Get the LinkedIn app
More
LinkedIn Corporation © 2020
Priyanka K
Asst. Manager - Recruitment & Client Relations at Attune Consulting
Message
PRIYANKA KURUP
30k connections. Hiring for RPA AutomationAnywhere Technical Architect. Send resumes to priyanka.k@careator.com
Message
Messaging
<https://www.linkedin.com/mynetwork/invite-connect/connections/>
22/38
05/03/2020
(6) LinkedIn
P i
Lookingk S D th
for new opportunities in HR (Generalist)
Search
Message
Professor K M Mehata
Senior Professor ,School of Computing Sciences,Hindustan University,Padur,Chennai-603103
Message
6

Try Premium Free
for 1 Month
Manage synced and imported contacts
Your contact import is ready
Raajsupramanian Muralidharan
Application Architect at Inland Revenue Authority of Singapore (IRAS)
RADHA G
Senior HR Partner at CONTUS
Radhakrishnan RK
OpenstackCloud Engineer at Cloudenablers
Radhakrishnan RK
OpenstackEngineer
Ragavendran J
HCL Tech
Connect with your contacts and never lose touch
Message
Continue
Message
Message
Message
Message
About
Help Center
Advertising
Raghuraman Rajagopalan
Co-Founder at Sporfy I Tech Play
Ragukumar G
Assistant professor at Kamaraj college,Tuticorin
Rahul Kumar (Jha)
IAAS Officer Trainee at Government of India
<https://www.linkedin.com/mynetwork/invite-connect/connections/>
More options
Privacy & Terms
Business Services
Get the LinkedIn app
Message
More
LinkedIn Corporation © 2020
Message
Message
Messaging
23/38
05/03/2020
(6) LinkedIn
Rahul Rathore
Search
Certified Microsoft Professional- Data Science ; Python, R, Machine Learning,
Deep
Learning, IoT, Cloud (Azure, AWS)
Raja Nagendra Kumar
Is #BadCode endangering rapid product evolution!!
6
Try Premium Free
for 1 Month
Message
Manage synced and imported contacts
Message
Your contact import is ready
Connect with your contacts and never lose touch
Rajagopalareddy Kommareddy
Assistant Manager at IDC Technologies, Inc.
Continue
More options
Message

rajeev kumar
Founder of TheCyberAll Social Entrepreneur Looking for LIKE MINDED PEOPLE. M
essage me OR WhatsApp me @ +91-9980105333
Rajesh s
Sr.Executive-HR
Rajesh Vaidyanathan
Delivery Manager at Career Soft Solutions
Rajesh Kumar Sahoo
Automation Lead in AI & Embedded Systems at Harman
Message
Message
Message
About
Message
Help Center
Advertising
Privacy & Terms
Business Services
Get the LinkedIn app
Rajyalaxmi Kuchalakanti
Technical Recruiter at ZEN3
More
LinkedIn Corporation © 2020
Message
Rama Chandra Prasath S
Understand the devilish details, deliver the angelic promise. Nurture a culture
of c
ommitment.
Message
Messaging
Raman Soraiyur V
<https://www.linkedin.com/mynetwork/invite-connect/connections/>
M
24/38
05/03/2020
(6) LinkedIn
Principal Consultant, Sai Veera & Associates
Search
Message
6
Try Premium Free
for 1 Month
Rameshwar Pratap, Ph.D.
Assistant Professor at School of Computing and Electrical Engineering (SCEE),
IIT
Mandi
Message
Manage synced and imported contacts
Your contact import is ready
Ravikant Dubey
Tech IT Recruiter at Interec IT Global Executive Search
Ravishankara Shastry
Independent Researcher at An AI company
Rebecca B
SDE Hiring at Amazon - Virginia, Boston, Seattle, Sunnyvale, Toronto, Vancouver!
Reena Rayen J
Director - Compliance at Global Analytics India Private Limited
Remi Guha
IT Recruiter at Arminus
Message
Connect with your contacts and never lose touch
Continue
Message
Message

Message
Message
About
Help Center
Advertising
Revathy Shanmugam
Connecting Job Seeker with opportunity
More options
Message
Privacy & Terms
Business Services
Get the LinkedIn app
More
LinkedIn Corporation © 2020
Rinku Bhadra
HR and Admin Specialist at Self-Employed
Rinku Chauhan
Lets Grow Together!
Message
Message
Messaging
<https://www.linkedin.com/mynetwork/invite-connect/connections/25/38>
05/03/2020
(6) LinkedIn
Rohan Sinha
Search
Assistant Manager at State Bank of India
Try Premium Free
for 1 Month
Manage synced and imported contacts
Rohit Swami
SWE Intern at InterviewBit • Data Scientist Nanodegree Graduate • Machine Learning • Deep Learning
6
Message
Message
Your contact import is ready
Connect with your contacts and never lose touch
Rupa Bang
Director, Recruitment - Pramati Technologies
Rupali Patkar
Talent Acquisition Partner (Technology & Sales hiring)
Continue
Message
More options
Message
Sabapathy Arumugam
Co-Founder and CTO at CoreStack, We Deliver Continuous Compliance Assurance & Operations Automation for Your Cloud
Sai Sree Jn
HR Recruiter at Top Mentor
Sakthi Chokkalingam
Director of IT
Message
Message
Message
About
Help Center
Advertising
Privacy & Terms
Business Services
Get the LinkedIn app
Saldin Samuel

Creator at apiplatform.io, YCombinator SUS 2019, Accel Rebound 2019

Sam Charles Daniel

Music Teacher at Cluny Convent

Message

<https://www.linkedin.com/mynetwork/invite-connect/connections/>

LinkedIn Corporation © 2020

Message

Samaksh Gupta

30K Connects- Lead- Talent Acquisition- APAC (Analytics- Lateral + Campus Hiring)

More

Message

Messaging

26/38

05/03/2020

(6) LinkedIn

at EXL

Search

Sameeullah Rashid

Looking for an Opportunity

Sandeep Kumar

Taking a break

6

Message

Manage synced and imported contacts

Your contact import is ready

Message

Connect with your contacts and never lose touch

Continue

Sandeep Kumar

Engineering Manager at Software AG

Sandeep Kumar

Headhunter

Sandhya Edupuganti

Software Development Manager, Amazon Mexico and Amazon Canada

Sandipan Bhattacharyya

Director - Research Scientist | AmEX | INSEAD | Chennai Mathematical Institute

More options

Message

Message

Message

Message

About

Sandish Kumar H N

Senior Software Engineer (Distributed Systems) at Aruba, a Hewlett Packard Enterprise company

Try Premium Free

for 1 Month

Help Center

Advertising

Message

Privacy & Terms

Business Services

Get the LinkedIn app

More

LinkedIn Corporation © 2020

Saranya Anandh

Managing Director - Gladwin Analytics® | Hiring Big Data and Analytics leaders for leading MNCs & Successful Startups.

saranya meena

HR Recruiter

Message

Message

Messaging
<https://www.linkedin.com/mynetwork/invite-connect/connections/27/38>
05/03/2020
(6) LinkedIn
Saraswathy Sudhakar
Search
saraswathy@ampvl.com
Saravana Kesavan Gurunathan
BI Developer at Visual BI Solutions
Message
6
Try Premium Free
for 1 Month
Manage synced and imported contacts
Message
Your contact import is ready
Connect with your contacts and never lose touch
Saravana Kumar Mvk
AVP - Enterprise Practice at GFI Informatique India Pvt Ltd.
Message
Continue
More options
Saravanan Govardhanan
Associate Quality Lead at CNSI
Saravanan K
Looking out for a job change - available immediately
Sathya Seelan
Sr. Software Engineer at KGISL
Satya Sai
Senior IT Recruiter at ENRATEC CONSULTANCY SERVICES PRIVATE LIMITED
Message
Message
Message
Message
About
Help Center
Advertising
Seema Alevoor
Developer at Oracle
Selva Velu
Business Partner at Quotient Technology Inc.
<https://www.linkedin.com/mynetwork/invite-connect/connections/>
Business Services
Get the LinkedIn app
Satyabrat Chowdhury
VP Engineering @ CoreStack. We Deliver Continuous Compliance Assurance & Operations Automation for Your Cloud.
Privacy & Terms
Message
More
LinkedIn Corporation © 2020
Message
Message
Messaging
28/38
05/03/2020
(6) LinkedIn
6
Search
Selvakumar Rathinam
Microsoft Certified Solution Expert (Cloud Platform) TOGAF 9.2 Certified .NET Azure Solution Architect

shaheen banu
Recruitments-HR at Zarlina Systems
Message
Manage synced and imported contacts
Your contact import is ready
Message
Connect with your contacts and never lose touch
Continue
Shahzad Ali
Talent Acquisition Lead at Lecan Solutions Private Limited
Shakila Savithri Rengan
Python Development Lead at Turing Eye
Shaline Udmale
Principal - Digital, Technology and Analytics
Shalini Srivastava
Senior Consultant (Recruitments) at Amazon Web Services
Account Manager
More options
Message
Message
Message
Message
About
Shankar Darna
Try Premium Free
for 1 Month
Message
Help Center
Advertising
Privacy & Terms
Business Services
Get the LinkedIn app
More
LinkedIn Corporation © 2020
Shanker Perumal
Director of Engineering at Visa
Sharda Bareja
Account Manager -Technology Hiring at Randstad India
Message
Message
Messaging
<https://www.linkedin.com/mynetwork/invite-connect/connections/29/38>
05/03/2020
(6) LinkedIn
Postdoctoral Research Fellow at University of Michigan
Search
Shashi Dagar
Leadership Hiring !!
Message
Message
6
Try Premium Free
for 1 Month
Manage synced and imported contacts
Your contact import is ready
Sheetal (khushi) Raheja
Associated with Zen3 Infosolutions as Head Client Relations & Delivery, & a membe
r of "GGA-Global Goodwill ambassador"
Shiva Paramasivam
Staff Software Engineer
Shiva Rajendran
Manager | Engineering | GainCredit

Shiva Reddy PV
Chief Talent Advisor at The Finder India
Shivashankar Subramanian
Research Intern at IBM
Connect with your contacts and never lose touch
Message
Continue
Message
Message
Message
Message
About
Help Center
Advertising
Shobhit Tulsyan
Senior Software Engineer at Akamai Technologies
Shonam Godara
Placament Database IT at HR Advisors
Simontini Das
Lead Recruitment at PureSoftware Ltd
<https://www.linkedin.com/mynetwork/invite-connect/connections/>
More options
Privacy & Terms
Business Services
Get the LinkedIn app
More
Message
LinkedIn Corporation © 2020
Message
Message
Messaging
30/38
05/03/2020
(6) LinkedIn
Search
Sivakumar Malli
Entrepreneur
6
Try Premium Free
for 1 Month
Message
Manage synced and imported contacts
Smita Acharya
HR Recruiter at Consultancy
Message
Your contact import is ready
Connect with your contacts and never lose touch
Snehan Snehan
Hiring Civil3D, Rail Strs, Revit,Arch, BIM, RCC,GIS, SewerCAD, StormCAD, MX
Road,
AECosim,Landscape, AutoCAD, IT Skills
Som - Looking for Analyst
Consultant at Osttalent.com
Sonal Kumar
Founding Partner
Soosai Agnel Jude
Senior Leadership, Diversity & Strategic Talent Hunter
Sreekanth Nair Sreekanth.pa@gmail.com
Looking out for Executive Secretary to the CEO Mumbai:- a Top Financial firm
Continue
More options
Message
Message
Message

Message
About
Message
Help Center
Advertising
Privacy & Terms
Business Services
Get the LinkedIn app
Sreelekha Unnikrishnan
Sr Recruitment Specialist at Confidential
Sreeram Chandrasekar
Product Engineering at Cadence Design Systems
LinkedIn Corporation © 2020
Message
Message
Messaging
Sri Vaishnavi
<https://www.linkedin.com/mynetwork/invite-connect/connections/>
More
M
31/38
05/03/2020
(6) LinkedIn
Talent Acquisition Specialist at Vivriti Capital
Search
Sridhar Satuloori
Software Development Professional
Message
6
Try Premium Free
for 1 Month
Message Manage synced and imported contacts
Message Connect with your contacts and never lose touch
Your contact import is ready
Sridharan Natarajan
Staff Engineer at Samsung India Software Operations
Continue
Srinivas Ramprasad M
Founder Director Persept Solar Pvt. Ltd.
Sripriya Sampath
Sr. Recruiter, AWS, Annapurna Labs
Sriram Seshadri
Senior Product Manager at OYE Fintech Pvt. Ltd
Srividhya Pazhaniraja
Lead Talent Acquisition Expert/ Lead Recruiter at Infosys Ltd
Message
Message
Message
Message
About
Help Center
Advertising
Srujana Odnala
Senior Talent Acquisition Specialist at Optum
More options
Message
Privacy & Terms
Business Services
Get the LinkedIn app
More
LinkedIn Corporation © 2020
Steve Dashiell
Founder at Dash Innovations, LLC
Subhaga, looking for Data Science experts

Consultant at osttalent

Message

Message

Messaging

<https://www.linkedin.com/mynetwork/invite-connect/connections/32/38>

05/03/2020

(6) LinkedIn

Subramanian Kannappan

Search

Program Manager

6

Message

Try Premium Free

for 1 Month

Manage synced and imported contacts

Sudalai Rajkumar

Data Scientist | Kaggle Grandmaster

Message

Your contact import is ready

Connect with your contacts and never lose touch

Sudeshna Kolay

Attended Institute of Mathematical Sciences

Sudhakaran Packianathan

Head IT at Atech Network Systems Pvt. Ltd.

Sundar M

.

Sunil Mohanty

Distributed Systems | Cloud | File Systems | Data Protection | Machine Learning

Sunita M R

Counselor at MiDNA Global

Continue

Message

More options

Message

Message

Message

Message

About

Help Center

Advertising

Privacy & Terms

Business Services

Get the LinkedIn app

Surabhi Aswal

Talent Lead at Climate Corporation

Surabhi N

Strategic Recruiter at eCommerce

Suresh BV

Managing Consultant at AHC Consulting

<https://www.linkedin.com/mynetwork/invite-connect/connections/>

Message

More

LinkedIn Corporation © 2020

Message

Message

Messaging

33/38

05/03/2020

(6) LinkedIn

6

Search

Suresh Kumar M

Director at JLL India

Suresh Mali
Looking for interns (BE any dicipline) starting immidiate, if interested
contact me
Message
Message
Manage synced and imported contacts
Your contact import is ready
Connect with your contacts and never lose touch
Continue
Suresh Mynampati
Hiring Global Leaders!
Suresh Rukmangathan
Software Architect at Hewlett Packard Enterprise
Suresh Somanathan
Director - Sales at Career Soft Solutions Pvt. Ltd.
Susmitha Srinath
Building a team of passionate and talented people @Windcave Limited!!
CSR Project Implementation
More options
Message
Message
Message
Message
About
SWARNALI Dhar
Try Premium Free
for 1 Month
Help Center
Advertising
Message
Privacy & Terms
Business Services
Get the LinkedIn app
More
LinkedIn Corporation © 2020
Swathi Balaji
HR Strategist - Business Partner with a growing Startup in Chennai
Swati Agrawal
Key Account Manager l Training Coordination l Sourcing l 11000+ Connection
Message
Message
Messaging
<https://www.linkedin.com/mynetwork/invite-connect/connections/34/38>
05/03/2020
(6) LinkedIn
Founder at HireXL (A Hiring and Assessment platform) Recruitment consultant for Search
Fast Growing Startups
Message
Tahir Majeed (LION) - Hiring is ON
Hiring Experts in ERP / CRM / DWH / BI / Bigdata / Data Scientist / Data Analyst / AI
/ Machine Learning /
Taranga Phukan
Employed at HCL Technologies
Tarun K D
Hiring for Enterprise Sales-APAC & Enterprise Account Executive-US south
Try Premium Free
for 1 Month
Manage synced and imported contacts
Message
Your contact import is ready
Connect with your contacts and never lose touch

Tanushree D
Talent Acquisition Lead with a Global market leader product development company.

6

Message

Continue

More options

Message

Message

Thamba Meshach W

Associate Professor @ PEC & Research Scholar at Anna University, Chennai in Computer Science & Engineering

Thiruvalluvar NB

Founder & Managing Director at CoreStack

Message

Message

About

Help Center

Advertising

Privacy & Terms

Business Services

Get the LinkedIn app

Timothy Ruff

Co-founder, Evernym. Co-inventor, Sovrin.

Message

More

LinkedIn Corporation © 2020

Trisha Anand

Hiring Super Senior Tech Leads (Backend/Devops & Frontend) for Mumbai/Delhi/Bangalore

Vaidehi Patel

Sales and Marketing Executive at Brij & Co.

<https://www.linkedin.com/mynetwork/invite-connect/connections/>

Message

Message

Messaging

35/38

05/03/2020

(6) LinkedIn

6

Search

Varsha Menon

Co-Founder at Jumpfrog

Try Premium Free

for 1 Month

Message

Manage synced and imported contacts

Varun Kumar

Senior Software Engineer at Crayon Data

Your contact import is ready

Message

Connect with your contacts and never lose touch

Continue

Veena Ramakrishna

Director Niche Hiring

Velmurugan Sundararajan

Sr Principal Engineer at VVDN Technologies

Vengatagiri Venkatesan

Head of Integration & Ecosystem Growth at numberz

Venkataramanan R

Part of a growing start-up at Pipesort Technologies

Message

Message

Message

Message
About
Venkatesh Raman
Professor at IMSc, Chennai
More options
Message
Help Center
Advertising
Privacy & Terms
Business Services
Get the LinkedIn app
More
LinkedIn Corporation © 2020
Vidya Ravi
Senior Manager, Talent Acquisition at Philips Innovation Campus, Bangalore
Vignesh Gopalakrishnan
Lead Developer at Visual BI Solutions
Message
Message
Messaging
<https://www.linkedin.com/mynetwork/invite-connect/connections/36/38>
05/03/2020
(6) LinkedIn
Courier Boy to CEO | Tech Startup | 30K Connections
Search
Vijaya Kiran
Spearheading HR and Recruitment @ OKCredit
Message
Message
6
Try Premium Free
for 1 Month
Manage synced and imported contacts
Your contact import is ready
Vijaya Kumari
Human Resources Executive at Altimetrik India Pvt Ltd
Vinay Kapoor
Rekindling my passions Self, Silence & Peace
Vinaya Mekala
Certified Internet Recruiter
VinayKumar S
Assistant Manager - Talent Aquisition at Techwave
Message
Connect with your contacts and never lose touch
Continue
More options
Message
Message
Message
Vinod Joshi
Consulting COO for a Staffing Company, Consulting VP -Sales for a Software Consulting and Product Engineering Companies
Message
About
Help Center
Advertising
Vinod Kumar Devi
Lead Architect at Cura Technologies Inc.
Vinod kumar Pandurangan
Director of Engineering, Product Development at Oracle
Vinoth kumar
Manager-Sales - Solar Division at Elma International, Bangalore.
<https://www.linkedin.com/mynetwork/invite-connect/connections/>

Privacy & Terms
Business Services
Get the LinkedIn app
More
Message
LinkedIn Corporation © 2020
Message
Message
Messaging
37/38
05/03/2020
(6) LinkedIn
Search
Vinoth Raj SR
TAG Business Partner - Enterprise Application Services (IPM) at Cognizant
6
Try Premium Free
for 1 Month
Message
Manage synced and imported contacts
Vishal Byakod
Head of India Development Centre, Cleo
Message
Your contact import is ready
Connect with your contacts and never lose touch
Vivek Nayak
Senior Finance Director at Software AG
Vivekananda Venkateswaran
Staff Engineer at VMware
Continue
Message
More options
Message
Yogita Malviya
Recruitment Specialist || InterviewBit and Scaler Academy || Startup Enthusiast
{Hiring Now!}
Gopireddy N
Sr. IT Recruitment Specialist at GlobalHunt
Message
Message

About
Help Center
Advertising
Privacy & Terms
Business Services
Get the LinkedIn app
More
LinkedIn Corporation © 2020
Messaging
<https://www.linkedin.com/mynetwork/invite-connect/connections/>
38/38

This work is licensed under a Creative Commons Attribution-NonCommercial-NoDerivatives 4.0 International License.
#####

#####

Course Authored By:

#####

#####

K.Srinivasan

NeuronRain Documentation and Licensing: <http://neuronrain-documentation.readthedocs.io/en/latest/>

Personal website(research): <https://sites.google.com/site/kuja27/>

This is a non-linearly organized, code puzzles oriented, continually updated set of course notes on Python language. This complements NeuronRain course materials on Linux Kernel, Cloud, BigData Analytics and Machine Learning and covers fundamentals of Python.

6 February 2017

Code Reference:

<https://github.com/shrinivaasanka/asfer-github-code/blob/master/python-src/CNFSATSolver.py>

Python's object oriented paradigm is quite similar to most of the languages like Java and C++ but the difference in number of lines code for same algorithm between Python and C++/Java is what makes it favourable for Natural Language Processing and writing microservices (services with small functionality which are interconnected). Python is more Haskell or LISP functional language-like and achieves both worlds of functional programming and imperative procedural programming by Lambda on-the-fly functions. Previous code demonstrates some of the minimum basic features of Python:

- Python Classes
- Tuples
- Lists
- List Slicing
- Set operations on python objects
- Control structures (for, if)
- Python object member functions and self keyword

Python classes are defined with class <class>(<baseclass>) and member functions are defined with def <function>(). Base class by default is object unless explicitly stated. Tuples are ordered pairs of arbitrary dimensions equivalent to vectorspaces in mathematics defined with (). Lists are equivalent to arrays in C defined with [] subscripts. Accessing an element in both tuples and lists are by [] subscript. Concepts of slicing is central to list comprehension in Python. Slicing can return a contiguous subset of a list by [<start>:<end>] notation. When either start or end is ignored implicit list start and end are assumed. For loops in python can iterate over any "iterable" object. Iterables include lists, dictionaries and user defined containers. if..else..elif is the python equivalent of conditional clauses with truth values being boolean keywords "True" or "False" which are builtins. Python classes denote self keyword to be the present object instantiated (equivalent to "this" in C++)

27 February 2017 - Python Generators and Yield

Python has a notion of iterables where any sequential data structure can be made to return an element and resume from where it left to return the next element in the sequence. This is quite useful for problems which need to remember the last element accessed and resume from next element (can be contrasted with static keyword in C/C++ which live across function invocations with global scope) - typical streaming scenario.

Streaming Abstract Generator implemented in :
https://github.com/shrinivaasanka/asfer-github-code/blob/master/python-src/Streaming_AbstractGenerator.py
 is based on this idiom. It basically is facade frontend abstraction for multiple backend streaming datasources. It overrides the `__iter__()` method to access an element and yield it instead of returning it. User of this class, instantiates with desired data storage constructor arguments and iterates through it without any knowledge of how the data is accessed. In python terms, data is "generated" and "yielded" iteratively in a loop accessing consecutive elements. No storage is allocated by generator explicitly and backend client objects for HBase/Cassandra/Spark/Hive/File datasources handle them internally.

This is a typical example of Iterator/Facade design pattern listed in Gof4.

 844. (THEORY and FEATURE) 6 January 2018, 18 July 2020 - Currying and Partial Function Application in Python - related to all sections on Recursive Lambda Function Growth algorithm implementation for learning lambda functions from Natural Language Texts and Text analytics

Python has functional programming (Haskell) equivalents of Currying and Partial Application support. Currying converts a function of n parameters to n functions of one parameter each invoked in nesting, and returns a function in each function. Partial Application Function is similar to currying but takes 2 arguments instead of 1 in currying, and returns a function. Code examples for these are below - committed to code/Currying.py and code/PartialFunctionApplication.py

 Currying.py:

```
1
2
3
4
5
6
=====
Curried :
=====
6 5 4 3 2 1
```

 PartialFunctionApplication.py:

=====

```
Equivalent Partially applied functions
=====
1 2 3 4 5 6
1 2 3 4 5 6
1 2 3 4 5 6
1 2 3 4 5 6
1 2 3 4 5 6
1 2 3 4 5 6
```

Currying by Partial Functions (as Beta reduction) are used in Recursive Lambda Function Growth - Graph Tensor Neuron Network algorithm implementation of NeuronRain which converts a natural language text to tree composition of functions of 2 arguments (a function operator acting on two operands) by traversing a random walk or cycle of the textgraph. Example:
 maximum_per_random_walk_graph_tensor_neuron_network_intrinsic_merit=

```
('one((integer(digit,(definite_quantity(abstraction,(measure(number,
(command(act,(speech_act(psychological_feature,(order(abstraction,(event(order,
(speech_act(event,(act(abstraction,(digit(three,(psychological_feature(number,
(abstraction(measure,
(definite_quantity(integer,command))))))))))))))))))))))',
10.804699467199468)
```


 7 August 2018 - Python Dictionaries

Python dictionaries are the hashtable implementations using linear probing(open addressing) to find next available slot (preferred to Chaining/Buckets). Open addressing in python applies the following function recurrently to find next available slot:

```
x = 5*x + perturb + 1
perturb >> PERTURB_SHIFT (some constant)
```

This function has been found to be optimal in python benchmarks. Simulating buckets/chaining in builtin dictionaries is therefore done by an alternative dictionary implementation defaultdict() which initializes the dictionary to a default key whose type is defined by argument to constructor. An example, chaining/buckets has been described in code/Dictionaries.py which prints :

```
['__class__', '__cmp__', '__contains__', '__delattr__', '__delitem__',
'__doc__', '__eq__', '__format__', '__ge__', '__getattr__', '__getitem__',
'__gt__', '__hash__', '__init__', '__iter__', '__le__', '__len__', '__lt__',
'__ne__', '__new__', '__reduce__', '__reduce_ex__', '__repr__', '__setattr__',
'__setitem__', '__sizeof__', '__str__', '__subclasshook__', 'clear', 'copy',
'fromkeys', 'get', 'has_key', 'items', 'iteritems', 'iterkeys', 'itervalues',
'keys', 'pop', 'popitem', 'setdefault', 'update', 'values', 'viewitems',
'viewkeys', 'viewvalues']
{0: 0, 1: 1, 2: 4, 3: 9, 4: 16, 5: 25, 6: 36, 7: 49, 8: 64, 9: 81}
defaultdict(<type 'list'>, {0: [0], 1: [1, 81], 4: [4, 64], 5: [25], 6: [16,
36], 9: [9, 49]})
```

References:

- -----
 1. CPython PyDictObject source - code comments -
<https://github.com/python/cpython/blob/master/Objects/dictobject.c>
 2. Beautiful Code - [Greg wilson]

 7 October 2018 - Python Reflection, Derived Classes and Class Methods

Python has support for reflection in the form of function and code objects. Python function objects are accessed by __func__ member of any function considered as an object. Python classmethods are decorators declared before defining a function by @classmethod annotation and defined as class method and defined by def <func>(cls, ...) declarative containing cls keyword. Class methods are useful for defining a classwide method common to all instances . This is different from static keyword in other languages and there is a @staticmethod decorator in python, the static equivalent. Class methods called on derived class take derived class objects for cls. An example for reflection and class methods is in code/Reflection.py and logs in code/logs/Reflection.log.7October2018

13 March 2019 - Async/Await - Asynchronous IO in Python 3.7

Python 3.7 supports asynchronous invocations of coroutines by `async` and `await` pairs of keywords similar to promise-future in C++. An example Chatbot Client and Server in `AsyncIO_Client.py` and `AsyncIO_Server.py` define two classes for Chat Server and Client which implement `connection_made()` and `data_received()` interface functions. Notable feature in 3.7 is the "`async def`" for function declarations in lieu of `@asyncio` coroutine decorators in previous versions of Python 3. Both client and server instantiate a loop object and invoke `create_connection()` and `create_server()` respectively for client and server by `await` semantics. Notion is to make client-server transport completely event driven by `await` and non-blocking by `async`. This example applies as a pattern to any algorithm doing `asyncio`. Logs in `logs/AsyncIO_ClientServer.log.13March2019` show a sample chat.

References:

1. Python 3.7 documentation - Async/Await -
<https://docs.python.org/3/library/asyncio-protocol.html>

14 November 2019, 23 April 2020 - Multidimensional Array Slicing - List comprehension, `slice()` function and NumPy - and StringIO

Python has in-built `slice()` function which is an iterator for array indices to `slice`. Numeric Python
NumPy has library support for multidimensional array slicing by subscripts. Code example `code/Slicing.py` demonstrates 5 variants of slicing of a 2 dimensional ndarray parsed from a string text. Text of multiple lines separated by newline "`\n`" is read by `StringIO` object by `genfromtxt()` and parsed to a multidimensional array by delimiter `,`. Five different slicings in the example are:

1. `slicedarray1` - equal slices for 2 dimensions by `slice()`
2. `slicedarray2` - unequal slices for 2 dimensions by `slice()` - only larger slice is effected
3. `slicedarray3` - `slice()` for one dimension and tuple of indices for the other - only indices from tuple are effected
4. `slicedarray4` - equal slices of 2 dimensions with an added step parameter - only one dimension is sliced
5. tuple of indices for both the dimensions raises Python error:
Traceback (most recent call last):
File "`Slicing.py`", line 23, in `<module>`
 `slicedarray3=parsedarray[(0,3),(0,3)]`
IndexError: index 3 is out of bounds for axis 0 with size 2

Code example chooses either `Slicing` or `List comprehension` to extract a slice by a flag - `List comprehension` being the most fundamental Python primitive is the obvious choice for slicing. Following list comprehension:

```
slicedarray5=[row[2:5] for row in parsedarray]
extracts a rectangular slice:
[['1', '2', '3', '4', '5', '6', '7', '8'], ['9', '10', '11', '12', '13',
'14', '15', '16']]
slicedarray5 - list comprehension:
[['3', '4', '5'], ['11', '12', '13']]
```

14 December 2019 - Rounding off, Floating point division, Python 2.7 and Python 3.7.5, PDB

Following code snippet defined within a class of code/RoundOff.py demonstrates difference in division behaviour between Python 2.7 and Python 3.7.5 by disassembly of Python bytecode in PDB debugger:

```
    x1 = (1-2)/2
    x2 = (2-1)/2
```

=====
Python 2.7
=====

=====
python RoundOff.py
('x1:', -1)
('x2:', 0)
=====

=====
Python 3.7.5
=====

=====
python3.7m RoundOff.py
x1: -0.5
x2: 0.5

Python 3.7.5 does auto type promotion to float while Python 2.7 rounds off to floor. PDB is imported by -m pdb in commandline and disassembler is imported as dis in pdb. Roundoff class is loaded in PDB. PDB Python VM bytecode disassembly shows absence of binary divide opcode in Python 3.7.5

26 June 2020 - Object Marshalling and Unmarshalling - Python Serialization and Persistence

Python has variety of infrastructure to support serialization and deserialization of objects - some of them being Pickle, Marshal, DBM and Shelve modules. While pickling is widely used, marshal, dbm and shelve are lowlevel alternatives - marshal is most widely used for persisting compiled binaries (.pyc) and restricted to python types while shelve and DBM depend on file and linux database backends and can persist arbitrary user defined types as persistence dictionaries of name-values. Thus lookup is easier making them powerful than pickle and marshal. Code example Marshal.py demonstrates the serialization and deserialization of an example Python 3.7 class and primitive list datatypes. Class Marshal defines __init__(), marshal(), unmarshal() and sync() functions which respectively wrap following shelve innards:

- init - opening a file persistence by shelve.open() in writeback=True mode and retrieve serializer dict
- marshal - populating serializer dict by object name ("array1" and "exampleobject1") and object.
- unmarshal - retrieval of a persisted object by object name from serializer dict
- sync - which synchronizes the persistence if writeback=True

Marshal databases and logs are in:
code/MarshalDB.bak
code/MarshalDB.dat
code/MarshalDB.dir
code/logs/Marshal.log.26June2020

Fields of deserialized Example() object and array are printed by print():

```
Marshalling object: array1
Shelve serializer: [('array1', [1, 2, 3]), ('exampleobject1', <__main__.Example
object at 0xb7396aec>)]
Unmarshalling object: array1
Shelve serializer: [('array1', [1, 2, 3]), ('exampleobject1', <__main__.Example
object at 0xb7396aec>)]
[1, 2, 3]
Marshalling object: exampleobject1
Shelve serializer: [('array1', [1, 2, 3]), ('exampleobject1', <__main__.Example
object at 0xb7396aec>)]
Unmarshalling object: exampleobject1
Shelve serializer: [('array1', [1, 2, 3]), ('exampleobject1', <__main__.Example
object at 0xb746188c>)]
field1: field1
field2: [1, 2, 3, 4, 5, 6, 7, 8, 9, 10]
```

30 July 2020 - Pointers, C-types, Copy-On-Write, Mutables, Immutables in Python 3.7.5

Python compiles to bytecodes which are executed on Python Virtual Machine. Basic datatype objects are immutable while iterables are mutable in python. Code example Pointers.py defines a function to simulate pointers on Python by importing ctypes C wrapper library and instantiating pointers to some string and integer objects by c_wchar_p() and c_void_p(). Illegal access Exception while assigning to immutable string literal is handled and pointer to string is created by writing a copy (Copy-On-Write) of original string which is different from C pointers. Similarly pointer copy to an integer data is assigned to while leaving the original unchanged. An alternative to C-type string creation by create_string_buffer() is demonstrated.

```
Logs from code/logs/Pointers.log.30July2020 :
Immutable - sentence1: This is a sentence
Exception: 'str' object does not support item assignment
Pointer to sentence1 string: c_wchar_p(3075052112)
Changed pointer copy of sentence1: This is different sentence
sentence2 - RAM contents after create_string_buffer(): b'\x00\x00\x00\x00\x00\x00\x00\x00\x00\x00\x00\x00'
Pointer to integer1: c_void_p(200)
immutable - integer1: 100
Changed pointer copy of integer1: 200
```

References:

1. Python 3.8.5 documentation - <https://docs.python.org/3/library/ctypes.html>

862. (THEORY and FEATURE) NeuronRainApps - NeuronRain Usecases - MAVSDK Python Async I/O Drone Simulator - related to 637,713,722 and all sections on Drone Autonomous Delivery, Drone Electronic Voting Machines, Large Scale Visuals/Urban Sprawl/GIS Analytics, VIRGO PXRC Flight Controller Kernel Driver - 18 August 2020

1. This commit implements Drone_MAVSDK_Client.py and Drone_MAVSDK_Server.py asynchronous Drone I/O by importing MAVSDK (Micro Air Vehicle SDK) Python library which contains an interface for drone telemetry - mavsdk_server. Earlier NeuronRainApps usecase implementations for Autonomous Online Shopping Delivery (and Conceptual Set Partition Drone Electronic Voting Machines) depend on

Dronecode Python SDK which might alternatively import MAVSDK.

2. Asynchronous I/O Chatbot Python class example has been augmented to import mavsdk and defines a new asynchronous function drone_async_io() which takes a Drone System object, Drone port, Drone action as arguments and accordingly async-invokes (await) MAVSDK internal functions for those actions.

3. Because of absence of a licensed Drone, this is a conceptual-only usecase implementation of a Drone simulator and "No System" exceptions are thrown which are handled and printed. Standalone product-specific Simulators (e.g jMAVSIM, Gazebo and AirSim for PX4 -

<https://dev.px4.io/v1.9.0/en/simulation/jmavsim.html>, ROS-Simulator -

https://dev.px4.io/v1.9.0/en/simulation/ros_interface.html) could be used for development testing.

4. Drone action clauses for "info", "takeoff", "arm", "camera", "goto_location" have been implemented in drone_async_io() which respectively print flight information, control takeoff, arm the AV, control camera video streaming, and pass on Longitude-Latitude-Altitude-Yaw GPS destination data for autopilot of the AV.

5. drone_async_io() is an async member of DroneMAVSDKClient class. Drone object is instantiated by System() and drone_async_io() initializes connect() to mavsdk_server Drone server port.

863. (THEORY and FEATURE) MAVSDK Python jMAVSIM Drone flight simulator - Proof-of-Concept implementation related to 862 and all sections on Drone Autonomous Delivery, Drone EVMs, Large Scale Visuals/Urban Sprawl/GIS Analytics, VIRGO PXRC Flight controller kernel driver - 26 August 2020

1. This commit revamps Drone_MAVSDK_Client.py earlier to define a new command "all" in drone_async_io() which connects to a drone, prints its flight information, arms, takes-off, navigates, streams visuals to ground station and lands a drone - everything in a simulator (jMAVSIM)

2. Before arming the drone its connection state, UUID and GPS health checks are preferable code for which has been introduced in 2 async iterators. "If" clause for Command "all" is a ubiquitous pattern which might be frequently necessary in Drone Autonomous Delivery and Drone electronic voting machines.

3. Drone_MAVSDK_Client.py connects to a PX4 jMAVSIM flight simulator which can be installed by instructions in

https://dev.px4.io/v1.9.0/en/setup/dev_env_linux.html (Section on JMAVSIM and Gazebo simulation) and <https://dev.px4.io/v1.9.0/en/simulation/jmavsim.html>. PX4 Firmware, ROS and ECL dependencies are installed by sourcing shell script

https://raw.githubusercontent.com/PX4/Devguide/v1.9.0/build_scripts/ubuntu_sim.sh which clones PX4 dependencies and creates build scripts. PX4 jMAVSIM SITL (Software in the loop) is built by target "make --debug px4_sitl jmavsim" in PX4/Firmware source which starts the Simulator GUI and SITL CLI pxh> prompt.

4. Drone_MAVSDK_Client.py is either executed from apython (asynchronous python CLI installed by aioconsole) or usual python commandline interface which connects to jMAVSIM GUI server.

5. jMAVSIM flight simulation logs for a multirotor aerial vehicle is at code/logs/PX4_Drone_JMAVSIM_Flight_Simulation.log.26August2020 which shows the jMAVSIM server side logs for GPS, arm, vertical takeoff, navigation and vertical landing. Camera streaming is failed with Error "DENIED".

6. drone_async_io() might be significantly augmented and imported across every Drone dependent analytics code in NeuronRain which can be developed and tested on a 3D Virtual Reality simulation without a real drone.

7. Efficient Drone Autonomous Delivery is an NP-complete Travelling Salesman-Hamiltonian Cycle problem which traverses lowest cost circuit connecting set of delivery points on a transportation network graph.

8. Drone FOSS Code Repositories and References:

8.1 MAVSDK Python - <https://github.com/mavlink/MAVSDK-Python>

8.2 PX4 Drone Autopilot Firmware - <https://github.com/PX4/Firmware>

8.3 PX4 Estimation and Control - <https://github.com/PX4/ec1>
8.4 PX4 JMAVSIM - <https://github.com/PX4/jMAVSim>
8.5 Auterion MAVSDK Java - Android Client - QGroundControl - <https://auterion.com/getting-started-with-mavsdk-java/>
8.6 PX4-ROS-Gazebo simulator - Graphic Illustration - MAVROS - https://dev.px4.io/v1.9.0/en/simulation/ros_interface.html
8.7 PX4: A node-based multithreaded open source robotics framework for deeply embedded platforms
- "...Our system architecture is centered around a publish-subscribe object request broker on top of a POSIX application programming interface. This allows to reuse common Unix knowledge and experience, including a bash-like shell. We demonstrate with a vertical takeoff and landing (VTOL) use case that the system modularity is well suited for novel and experimental vehicle platforms. We also show how the system architecture allows a direct interface to ROS and ..." - <https://ieeexplore.ieee.org/document/7140074>
9. jMAVSIM replay logs have been committed to code/logs/jMAVSIM_replay_logs/

5 September 2020, 7 September 2020 - Python Decorators, Static Type Checking, Type Hints, Mypy and IDE typecheckers, Final constant type hint, final decorator in Python 3.8

Python traditionally implements Duck typing or Dynamic typing and types of objects could be checked at runtime by `type()` and `isinstance()`. Decorators in Python are features which could be used to instrument another function and return a wrapped new function having additional code. Lack of support for static type checking and constant definitions in Python have been answered in Python 3.8 which implements series of PEPs for final decorator for final methods which cannot be overridden in derived classes and Final type hint which aids Typecheckers (mypy, PyCharm IDE) to statically analyze code and flag type errors.
Code example Decorators.py defines two classes - Base and Derived - which import various typecheck artefacts from typing module. Class BaseDecorated defines a constant `var1` by type hint Final and a method `cannotoverride()` by @final decorator which can be type-enforced by linters in mypy (<http://mypy-lang.org/>) and PyCharm. Both base and derived classes define member functions to which argument type hints and return type hints are annotated by ":" and "->" operators. Most importantly member function `funcdecorator()` defines an inner function `wrapper()` which takes a function argument and instruments additional code around it and returns a new decorated function by `typing.cast()` typecasting. Declaration of T defines a Callable type variable (TypeVar) of arbitrary number of arguments specified by Any. Logs code/logs/Decorators.log.5September2020 capture the decorator callstack.

866. (THEORY and FEATURE) A* (A-Star) Best First Search Algorithm Implementation - Python 3.8.5 - 8 September 2020, 27 October 2020 - related to all sections on Drone Autonomous Delivery Navigation, Drone Obstacle Avoidance, Drone Electronic Voting Machines and Graph Analytics

1.This commit implements the standard A-Star Path Finding algorithm widely used in Robotics as a general purpose graph search implementation which could be invoked by multitude of NeuronRain code dependent on Graph Analytics as well as a routine prerequisite for motion planning in NeuronRain Drone Navigation.
2.A-Star algorithm of [Hart-Nilsson-Raphael] described in https://en.wikipedia.org/wiki/A*_search_algorithm is the reference for this implementation in Python 3.8.5.

3.This implementation uses a plain list in place of a Priority Queue for Open set (Discovered nodes)

4.A-Star algorithm improves upon Dijkstra's Shortest Path by finding the path which minimizes the cost function with the help of a heuristic:
 $\text{argmin}(f(n) = g(n) + \text{heuristic}(n))$
 where $f(n)$ is the fscore map, $g(n)$ is the cost of traversing to node n (gscore map) from start and $\text{heuristic}(n)$ is the estimated cost of traversing to end vertex from n .

5.Logs in code/logs/AStar_BestFirstSearch.log.8September2020 compute the Best First Search Path [3,6,7] from node 3 to node 7 in an 8 vertex graph denoted by adjacency matrix which marks lack of edges by -1.

6.Navigation in Drone Autonomous Delivery and EVMs is a TSP-Hamiltonian Cycle NP-complete problem wherein Drone has to efficiently visit set of all delivery points-voter residences once while A-Star motion planning is necessary for finding the least cost trajectory between longitude-latitude-altitude of any two delivery points or voter residences (by looking up the addresses in a map service e.g Google Maps).

References:

 866.1 Finding Closest Pair of Points - $O(N \log N)$ divide and conquer algorithm better than naive $O(N^2)$ brute force for obstacle avoidance - Section 35.4 - Chapter 35: Computational Geometry - Algorithms - [Cormen-Leiserson-Rivest-Stein] - Page 908 - "... System for controlling air or sea traffic might need to know which are the two closest vehicles in order to detect potential collisions ..." - quite relevant for Drone swarms

 871. (THEORY and FEATURE) Generating all possible permuted strings of an alphabet - related to 843 and all sections on Social networks, Bipartite and General Graph Maximum Matching, Symmetric Group, Permanent, Boolean majority, Ramsey coloring - Number of Perfect (Mis)Matchings - 28 October 2020

 1.Related to a question in IIT-JEE: Find sum of integers > 10000 having only 0,2,4,6,8 as digits without repetition (implies < 99999 because more digits would repeat).
 2.This commit implements Permutations.py utility which generates all possible permutations of a list of integers and creates permuted integers from them. Generating permutations is required in section 843 for perfect (mis)matches.
 3.In the function genpermutations() random permutation is obtained from `numpy.random.permutation()` and its numeric equivalent is hashed to a dictionary iteratively till all permutations are generated (which is $N!$).
 4.Finding sum of the permuted integers is tricky and makes use of the fact that every digit in the list of permutation is independently and identically distributed - For example, there are 120 ($5!$) integer permutations of 0,2,4,6,8 and each of [0,2,4,6,8] occurs $120/5 = 24$ times per digit in the permutations.
 5.Thus per digit sum is $24*8 + 24*6 + 24*4 + 24*2 + 24*0 = 480$ and following schematic depicts carry forward:

```

53+ 53+ 52+ 48+
|  |  |  |  |
....(480 for each digit)
|  |  |  |  |
-----
533 3  2  8  0

```

and sum of the permuted integers is 5333280.

6.Permutations.py demonstrates this fact and prints:

```

('summation:', 5333280)
('permutations:', defaultdict(<type 'int'>, {46082: 56, 24068: 97, 20486: 24,
86024: 36, 82604: 75, 60428: 15, 62480: 52, 4628: 81, 24086: 70, 86042: 65,
64028: 40, 24608: 85, 80426: 43, 8246: 107, 26804: 95, 84026: 35, 60482: 55,
8264: 41, 4682: 78, 80462: 28, 64082: 80, 42068: 9, 24860: 91, 2648: 110, 84062:
39, 62048: 99, 42086: 21, 24680: 100, 68204: 77, 42608: 71, 6248: 116, 84602:

```

```

86, 2684: 108, 82046: 82, 46208: 51, 48260: 44, 84620: 7, 68240: 57, 20648: 79,
82460: 58, 4268: 61, 40628: 8, 42680: 2, 6842: 62, 86204: 83, 4286: 68, 46280:
109, 20684: 102, 82640: 30, 46802: 69, 26840: 113, 4826: 120, 86240: 6, 64208:
31, 46820: 76, 24806: 14, 8426: 63, 84206: 13, 80624: 3, 28406: 18, 4862: 98,
80642: 72, 8462: 96, 64280: 32, 62084: 48, 6428: 49, 2846: 89, 64802: 92, 84260:
27, 26408: 22, 28460: 26, 2864: 12, 68402: 104, 64820: 114, 42806: 17, 68420:
54, 6284: 90, 40268: 53, 6482: 34, 62804: 115, 60248: 105, 40286: 84, 82064: 93,
42860: 64, 20846: 106, 26480: 4, 80246: 10, 62840: 47, 40826: 29, 60284: 20,
40682: 118, 20864: 67, 86402: 37, 80264: 60, 28046: 88, 86420: 101, 60824: 119,
48026: 94, 40862: 112, 28064: 74, 2468: 42, 60842: 19, 8624: 45, 2486: 103,
68024: 5, 28604: 66, 48062: 33, 26048: 25, 8642: 23, 62408: 59, 68042: 11,
46028: 16, 48206: 117, 48602: 50, 28640: 46, 26084: 38, 82406: 1, 48620: 87,
6824: 73, 20468: 111}))
('numbers:', 120)

```

1149. (THEORY and FEATURE) ThoughtNet Evocation of Thought Hyperedges by Set Intersection of Hypervertices - related to 620,1147 and all sections of ThoughtNet Hypergraph Evocation, Contextual Multiarmed Bandits, Reinforcement Learning, Word Sense Disambiguation, Balls-Bins Problem - 28 June 2021, 29 June 2021, 30 June 2021, 1 July 2021

1.This commit implements HypergraphIntersections.py which computes the ThoughtNet hyperedge thought evocations from evocative modal classes of hypervertices within the function hypervertices_intersections(). This code is a non-machine learning alternative to ThoughtNet Hypergraph Contextual Multiarmed Bandit Reinforcement Learning implementation in NeuronRain AstroInfer and demonstrates unique intersection example mentioned in 1147.

2.Function hypervertices_intersections() could be imported in NeuronRain AsFer ThoughtNet as graph theoretic evocation alternative to Contextual Multiarmed bandits.

3.hypervertices_intersections() takes the hypergraph encoded as dictionary and the evocative modal classes (which could be learnt from some machine learning classifier including unsupervised dense subgraph core number classifier implemented in NeuronRain) as arguments.

4.For example, some fictitious news headlines have been populated as thought hyperedges which connect some or all of hypervertices 'water','air' and 'agriculture' assigned by a classifier:

```

'water':['flood caused by storms wrought havoc','water scarcity hits
crops','cost effective sea water desalination would benefit agriculture'],
'air':['flood caused by storms wrought havoc','air traffic flourished in last
financial year','air pollution hits new high'],
'agriculture':['water scarcity hits crops','cost effective sea water
desalination would benefit agriculture']

```

5.Thoughts evoked for some set of modal classes are:

```

hypervertices intersection of ['water', 'air'] : {'flood caused by storms
wrought havoc'}

```

```

hypervertices intersection of ['water', 'agriculture'] : {'water scarcity hits
crops', 'cost effective sea water desalination would benefit agriculture'}

```

```

hypervertices intersection of ['water', 'air', 'agriculture'] : set()

```

6.One of the evocations is not unique and multiple thoughts are evoked which might be difficult to assign numeric weights (as implemented in the Contextual Multiarmed Bandit Reinforcement Learning version) and thoughts could be a partial ordering instead of total ordering (all thoughts evoked might be equally important). Complexity of unique evocation increases proportional to number of hyperedges incident per hypervertex (or average degree of ThoughtNet hypergraph)

7.ThoughtNet Hypergraph is a variant of Balls-Bins (Coupon Collector) problem in which each bin is a hypervertex and balls connected by a hyperedge (each

hyperedge connecting similarly labelled balls across hypervertices is uniquely colored) are thoughts pigeonholed to modal class bins.

References:

1149.1 Modality Effect in Psychology -

https://en.wikipedia.org/wiki/Modality_effect - "...Modality can refer to a number of characteristics of the presented study material. However, this term is usually used to describe the improved recall of the final items of a list when that list is presented verbally in comparison with a visual representation. The effect is seen in free recall (recall of list items in any given order), serial recall (recall of list items in the order of study), short-term sentence recall (recall specific words from sentences with similar meanings) and paired associate recall (recall of a pair from presentation of one of its members)...."
- ThoughtNet evocation by multiarmed bandit could be likened to a serial recall while evocation by intersection could be a free recall.

1153. (THEORY and FEATURE) ThoughtNet Evocation of Thought Hyperedges by Set Intersection of Hypervertices - related to 620,1147,1149 and all sections of ThoughtNet Hypergraph Evocation, Contextual Multiarmed Bandits, Reinforcement Learning, Word Sense Disambiguation, Balls-Bins
Problem - NeuronRain implementation of set intersection by hashing - 26 July 2021

1153.1 HypergraphIntersections.py has been refactored to define a native implementation of set intersection by Python 3.8 collections defaultdict() in function neuronrain_setintersection()

1153.2 Elements of set1 are populated in an instance of defaultdict() and elements of set2 are lookedup in defaultdict of set1 and returned as intersection of set1 and set2 if present in defaultdict of set1.

1153.3 Boolean flag for choice between python intersection implementation and NeuronRain intersection implementation has been introduced.

1163. (THEORY and FEATURE) Drone Electronic Voting Machine - Set Partition Analytics electronic_voting_machine() invocation - PX4 SITL JMAVSIM simulation - Geocoding integration for address to longitude-latitude translation - related to all sections on Majority Voting, Drone Electronic Voting Machines, Set Partition Analytics - 8 September 2021

1163.1 Drone_MAVSDK_Client.py has been updated to import electronic_voting_machine() set partition EVM implementation from Streaming_SetPartitionAnalytics.py and geopy Geocoding service for address to longitude-latitude lookup - geopy Geocoding service looksup the Nominatim Geocoding from OpenStreetMap

1163.2 drone_async_io() has been changed to accept additional arguments for address of the voter, id proof context and list of candidates as array.

1163.3 New command "drone_EVM" has been introduced which geocodes the voter address and navigates to voter longitude and latitude by goto_location() followed by invocation of electronic_voting_machine() which takes voter id proof context and candidates list as arguments and simulates a random vote for some candidate at the voter address.

1163.4 PX4 JMAVSIM drone simulation (VTOL and navigation) has been captured as video logs/DroneEVM_PX4_JMAVSIM_Flight_Simulation_8September2021.mp4 (uploaded at <https://kuja27.blogspot.com/2021/09/drone-electronic-voting-machine-px4.html>)

1163.5 PX4 SITL JMAVSIM, MAVSDK Client and Server simulation logs are at:

logs/DroneEVM_PX4_JMAVSIM_Flight_Simulation.log.8September2021

logs/Drone_MAVSDK_Client.log.8September2021

logs/Drone_MAVSDK_Server.log.8September2021

logs/jMAVSIM_replay_logs/2021-09-07/
1163.6 Command "goto_location" has been updated similarly for address to longitude-latitude translation. Simulation earlier is limited in scope because realworld franchise exercise would have two unpredictable asynchronous halves: (*) landing at voter address (*) taking off after voting. Presently electronic_voting_machine() has been invoked synchronously without async def and await event driven program pairing which would necessitate a rewrite or asynchronous counterpart of Streaming_SetPartitionAnalytics subclassing asyncio.Protocol (or Python events Model-View-Controller GUI pattern).

1164. (THEORY and FEATURE) Drone Electronic Voting Machine - Set Partition Analytics electronic_voting_machine_asynchronous() wrapper definition and invocation - PX4 SITL JMAVSIM simulation - Fictitious address - related to all sections on Majority Voting, Async IO, Drone Electronic Voting Machines, Set Partition Analytics - 29 September 2021

1164.1 Drone_MAVSDK_Client.py has been updated to navigate to a fictitious address by introducing an imaginary address "fictitious" for PX4 simulation because of rate limiting errors in REST calls to OpenStreetMap Nominatim Geocoding address-to-longlat lookup.

1164.2 New asynchronous function electronic_voting_machine_asynchronous() has been async def-ed which is the async wrapper over electronic_voting_machine() synchronous function in Streaming_SetPartitionAnalytics.py

1164.3 This new asynchronous Drone EVM function wrapper electronic_voting_machine_asynchronous() is await-ed within "drone_EVM" command of drone_async_io()

1164.4 Drone_MAVSDK_Client.py has been PEP8 formatted by autopep8.

1164.5 PX4 jMAVSIM simulation console SITL, drone Client and Server logs for this commit are at:

code/logs/DroneEVM_PX4_JMAVSIM_Flight_Simulation.log.29September2021

code/logs/Drone_MAVSDK_Client.log.29September2021

code/logs/Drone_MAVSDK_Server.log.29September2021

1164.6 MP4 video for jMAVSIM PX4 drone VTOL and navigation is similar to earlier simulations and has not been committed.

(CODE PUZZLE) Mixed Python Arrays - Remove and Simulated Remove - 25 May 2022

Mixed datatypes within python lists are problematic while performing index() or remove() primitives which throw exception:

The truth value of an array with more than one element is ambiguous. Use a.any() or a.all()

This fact has been demonstrated in code/MixedPythonArrays.py (Python 3.8) by 2 types of removes on a heterogeneous array of a defaultdict(list) containing python list objects and Numeric Python NDArray objects - (*) by direct remove() which fails with earlier ambiguity exception and (*) simulated remove which iterates through array elements, does equality test for truth value of matching element to remove and excludes the element while copying to a temporary array. Temporary array (having excluded an element) replaces earlier array. Simulated remove earlier (commented) can be condensed to one line list comprehension. Previous simulated remove has been implemented in NeuronRain AstroInfer image analytics code -

asfer-github-code/python-src/image_pattern_mining/ImageNet/ImageGraph_Keras_Theano.py - def

contours_kmeans_clustering(imagefile, segment, number_of_clusters=3, maxiterations=3) - while handling remove of an element from mixed Python arrays containing contour ndarray int32 datatypes and python list objects. Two removes are shown in code/logs/MixedPythonArrays.log.25May2022 for a mixed array element of a defaultdict - initial element of the list is a normal python list while rest are

```

ndarrays and exception is encountered while removing array([[[ 1, 2]], [[11,
12]]], dtype=int32):
    defaultdict(<class 'list'>, {0: [[100, 200], array([[[ 1, 2]], [[11,
12]]], dtype=int32), array([[[4, 5]]], dtype=int32), array([[[7, 8]]],
dtype=int32), array([[[10, 11]]], dtype=int32), array([[[13, 14]]],
dtype=int32)])})

```

Python 3.10.x - Memory View and Buffer for different datatypes - 6 September 2022

Code snippet Python/MemoryView.py demonstrates the memoryview() built-in function of Python 3.10.x and how it wraps the C memory view of Python objects through bytearray() buffer protocol. It also explains the usages of string binary encode(), bit_length(), to_bytes() and Big Endian-Little Endian storages.

References:

1. Python memoryview() documentation -
<https://docs.python.org/3/library/stdtypes.html#memoryview>

```

/*
#####
#####
#<a rel="license" href="http://creativecommons.org/licenses/by-nc-nd/4.0/"></a><br />This
work is licensed under a <a rel="license"
href="http://creativecommons.org/licenses/by-nc-nd/4.0/">Creative Commons
Attribution-NonCommercial-NoDerivatives 4.0 International License</a>.
#####
#####
#Course Authored By:
#-----
#K.Srinivasan
#NeuronRain Documentation and Licensing: http://neuronrain-
documentation.readthedocs.io/en/latest/
#Personal website(research): https://sites.google.com/site/kuja27/
#-----
#####
#####
*/

```

823. (THEORY and FEATURE) People Analytics - Social Network and Urban Sprawl Analytics - Ricker - Population Dynamics - Functions, Loops, Variables, Timeseries and Plots in R - 22,23,24,25,26 May 2020, 2,3,4 June 2020 - related to 487,572,770

R along with SAS is a standard BigData analytics programming language having MATLAB capabilities. Code example Ricker.R in code/ defines a function ricker() which computes the Ricker Chaotic Biological logistic function for population dynamics ($N_t * \exp(r(1 - N_t/K))$) a variant of [Robert May] logistic for pandemic non-linear dynamics modelling (Initial condition is per generation and $K=1$). The code example demonstrates assignment of variables by "<->" operator, for loop block, list initialization by ":", initialization of timeseries by ts and plotting graphics by plot(). Function block by "<- function()" has been

commented which can be run as main. R scripts could be executed either by RStudio or Rscript CLI. R Graphics plot from RStudio and logs from Rscript have been committed.

References:

- 1.R for Beginners - [Emmanuel Paradis] -
https://cran.r-project.org/doc/contrib/Paradis-rdebuts_en.pdf
- 2.Biological Logistic - [Robert May] -
http://abel.harvard.edu/archive/118r_spring_05/docs/may.pdf - equation 4
-

824. (FEATURE) People Analytics - Social Network Analysis - CoronaVirus2019 analyzer - Statistics in R - Data Frames, Factors, Histograms, Fitting a Probability Distribution - 27 May 2020, 2,3,4 June 2020 - related to 487,572,770

R is the prominent choice for data science because of immense builtins for statistical analysis. Contrived Code example FileIOVectStats.R demonstrates analysis of CoronaVirus2019 dataset from <https://www.worldometers.info/coronavirus/> by computing following metrics from it:

- Histogram
- ECDF - Cumulative Density Function
- Stem
- Rug
- Find the correlation to Bell curve - Shapiro-Wilk test
- Find the correlation to Bell curve - Kolmogorov-Smirnov (KS) test
- T-two sample test
- Mean, Median, Quantiles summary

COVID2019 data requires preprocessing of the text data and R script executes the following:

- attaching a dataframe by attach()
- instantiate Data Frame after reading the data file by read.table()
- summary() from dataframe
- accessing each field of read.table() dataframe by [[]] operator
- converting string fields to numeric by as.numeric()
- splitting sample into two for T-test
- instantiate a factor object (which categorizes the data)

Statistical tests - Shapiro, KS, T-test - try to find the proximity of the dataset to normal distribution.

Histogram bucketization of COVID2019 shows an initial huge bucket followed by almost equal sized buckets.

825. (THEORY and FEATURE) People Analytics - Social Network Analysis - CoronaVirus2019 analyzer - Correlation coefficients in R - Concatenation of Vectors, c() function, Vector arithmetic, Correlation of two datasets - related to 487,572,770 - 2,3,4 June 2020

R provides various facilities for creating sequences - seq(), array(), c(), data.frame(), vector(). Code example VerhulstPearlReed.R analyzes the correlation between a Chaotic sequence from Verhulst-Pearl-Reed logistic law (and biological logistic) and CoronaVirus2019 dataset, both of same length. Spread of memes, fads, epidemics and diffusion of concepts in community is a Chaotic process which can be modelled by Erdos-Renyi random graphs and Cellular automata. Though Chaotic fractal datasets (Mandelbrot) are undecidable, from social network analysis literature it is evident that emergence of giant components in scalefree (Pareto 80-20 rule - number of vertices of degree r is proportional to $1/r^k$ - high degree vertices are least and low degree vertices are numerous) random graphs are inevitable. Approximate correlation to onset of

Chaos could be deciphered by varying initial condition and bifurcation parameter(λ) of logistic and finding maximum correlation to CoronaVirus2019 dataset. COVID2019 dataset is scaled to decimals in interval $[0,1]$ by vector division feature of R which applies division by maximum element to each element of sequence. Vector division could also be performed on dataframe objects (commented). Scale-normalized dataset is then correlated to Chaotic sequence by Kendall, Spearman, Pearson coefficients (~45% maximum). Concatenation is done by `c()` function within for loop which reassigns the vector after concatenating next element. Double precision arithmetic has been coerced. Factor objects of both logistics are printed which show the levels of data. Graphics are plotted by `timeseries plot()` function (most recent to the left) - Chaotic sequence oscillates heavily by period doubling. Low p-value implies null hypothesis (no correlation) can be rejected with high confidence. Maximum correlation occurs at $\lambda=4.0$ and initial condition= 0.000000000000001 and for increasing λ both logistics coincide (resemble a heaviside step function). Return value is a concatenated vector by `c()`.

References:

825.1 R and S documentation -
<https://www.rdocumentation.org/packages/base/versions/3.6.2/topics/c>

828. (THEORY and FEATURE) People Analytics - Social Network Analysis - CoronaVirus2019 analyzer - Linear Models - 11,12 June 2020, 26 July 2021 - related to 487,572,752,770,823,824,825

R has variety of builtins for Linear Regression and Logistic Regression - Linear Models - `lm()` and `glm()` functions. Code example LinearModels.R computes linear model `lm()` and generalized linear model `glm()` for CoronaVirus2019 dataset which correlate per-day and total fields by various family of fit measures - gaussian, gamma, poisson, binomial and link functions - logit, identity, log, inverse, $1/\mu^2$. It also demonstrates matrix creation by `cbind()` which combines vectors and `$` notation for dataframe fields. Summary including linear.predictor for each model is printed to testlogs/LinearModels.log.11June2020. Pandemics as Social network fad diffusion are traditionally fit to Chaos, Cellular automata, ERSIR random graph model, SIS random graph model, exponential or poisson distributions. An example Theoretical regression model which explains the spread based on population density (average degree in urban sprawl social networks) could be:

Per day Spread = $\text{weight1} * \text{total_infected} - \text{weight2} * \text{total_recovered} - \text{weight3} * \text{deaths} + \text{weight4} * \text{recovery_time} \dots + \text{constant}$
for variables `total_infected`, `deaths`, `recovery time` and `total_recovered` and weights `weights3=1`, `weight4`, `weight1=average_degree` and `weight2=1` (spread is en masse and depends on degree of network and recovery time but recovery benefits only individual). By CAGraph social network concept diffusion model, `weight1=average_degree=8` for 2 dimensional cellular automaton increment growth rule. Linear model is dependent mostly on recovery time which then becomes:
Per day Spread = $8 * \text{total_infected} - 1 * \text{total_recovered} - 1 * \text{deaths} + \text{weight4} * \text{recovery_time} \dots + \text{constant}$

References:

828.1 Scaling and Fame - Large Numbers -
<https://rjlipton.wpcomstaging.com/2021/06/29/scaling-and-fame/> - Tao and Strogatz - Small world networks and Pandemic - Strength of weak ties - "...The sum over pairs $\{(X,Y)\}$ of the number of pairs $\{(A,B)\}$ between them who would be affected equals the sum over edges $\{(A,B)\}$ of the number of pairs $\{(X,Y)\}$ they can be struck by: both are equal to the number of paths of length $\{3\}$ in the graph...."

831. (THEORY and FEATURE) People Analytics - Social Network Analysis -
CoronaVirus2019 analyzer - Cellular Automaton Graph (CAGraph) - Regression
Models of Diffusion - Iteratively Re-Weighted Least Squares (IWLS) - 22,23,24,25
June 2020 - related to 678,740,762,828,830 and all sections on Business
Intelligence, Voting Analytics, Urban Sprawl Analytics, Random Walks on
Expanders of NeuronRain Theory Drafts

1. In continuation of R CoronaVirus2019 models earlier, Cellular Automaton Graph
diffusion logit in 828 has been implemented by glm() and lm() utilities of R
library.

2. Two R functions in CAGraphLogit.R - cagraphlogit() and cagraphprojections() -
respectively learn a regression model from COVID19 data and project it to a
later datapoint to obtain per day global spread.

3. glm() and lm() functions learn the model:

Perdiem ~ Infected + Deaths + Recovered + RecoveryTime

based on Susceptible-Infected-Recovered (SIR) data gathered from few giant
geographic clusters.

4. Logs of code/testlogs/CAGraphLogit.log.24June2020 detail the predictors,
coefficients and fitted model.

5. Regression model coefficients are learnt by Iteratively Re-Weighted Least
Squares implementations of glm() and lm(). CoronaVirus2019 dataset has been
chosen as a representational dataset because of its unprecedented global scale
and randomness which could simulate any other random process involving people
including business, economy and majority voting (Preferential attachment of high
market share brands versus Double Jeopardy of low market share brands - new
products gain market share by word of mouth and promos, spread of opinions as
opposed to pandemics decide elections than individual rational decision making -
correlated majority or statistical dependence of voters - CJT for Correlated
Majority -

<https://www.sciencedirect.com/science/article/abs/pii/S016726819400068P> ,
Markets' spikes and corrections are explained by Bounded rationality and
Irrational exuberance).

6. All learnt weights have been multiplied by 400 except total_infected which is
multiplied by $8 \times 400 = 3200$ as 2-dimensional Cellular Automaton Graph heuristics
for High degree Expander graphs (from Section 740, degree 400 graphs are
Expanders which facilitate huge spread subject to $|eigenvalue(k)|/d$ -regularity
 $\leq 1/10$) - Rationale being Spread in an Urban Sprawl social network is a Random
walk on Expander Cellular Automaton Graph. Function cagraphprojections()
computes the following global spread per day from the learnt model applying
signs (and multiplications by 8 and 400) for each dependent variable of recent
COVID19 SIR data (by abs() of weights to ignore signs and without abs()). Model
could be refined by incorporating additional dependent variables:

[1] "Per day spread(abs):"

[1] 121087.5

[1] "Per day spread:"

[1] 149975.7

7. Section 830 has a derivation for number of possible arrangements or 2-
colorings of people subject to avoidance criteria. Number of possible
arrangements of people (uniquely identified by integers) bijectively equal
number of possible complementary equations or complement diophantines defined on
the integer sequences (Complementary Equations, Functional equations, Beatty
sequences, Taichi - partition of Integer sequences -
<https://cs.uwaterloo.ca/journals/JIS/VOL10/Kimberling/kimberling26.pdf>). In the
context of diffusion in social network, 2-coloring reduces to Infected-
Uninfected. An example combinatorial avoidance: Infected and Uninfected couldn't
be juxtaposed.

8. Section 762 defines least square model for variables in business and
econometric datasets - By replacing the variables of COVID19 analyzer, similar
models could be learnt for those datasets as well.

870. (THEORY and FEATURE) People Analytics - Social Network Analysis -
CoronaVirus2019 Analyzer - Exponential Fit in R - related to 744,831
and all sections on Chaos, Cybercrime analyzers, Game theoretic Cybersecurity,
Pseudorandomness, Random walks on Cellular Automata and Expander Graphs - 11
October 2020, 12 October 2020

1. CoronaVirus2019 dataset has been thus far fit to non-exponential probability
distributions and Chaotic non-linear models.
2. Chaotic models suffer from theoretical limitations of computational
undecidability thereby prohibiting accurately learnt models.
3. This commit implements exponential fit of CoronaVirus2019 dataset till 11
October 2020, by `lm()` applying logarithmic version of:
$$\text{Fatalities} = A \cdot \exp(B \cdot \text{days})$$

which is $\log_2(\text{Fatalities}) = \log A + B \cdot \text{days}$ (R linear model is used for learning
non-linear exponential model)
4. Logs code/testlogs/Exponential.log.12October2020 print the exponential fit
model.
5. Previous exponential model is the solution for differential equation
 $d(\text{Fatalities})/\text{Fatalities} = B \cdot d(\text{days})$ which is similar to DEs in
Erdos-Renyi Susceptible-Infected-Recovered random graph epidemic model.
6. Differential equation in (5) implies rate of change of fatalities depends on
instantaneous fatalities (Geometric progression or evolving m-ary tree).
7. From coefficients in logs, COVID19 dataset is fit to $A=11.27683950$ and
 $B=0.04250611$

1231. (THEORY and FEATURE) People Analytics - Social Network Analysis -
CoronaVirus2019 analyzer - Recomputed Spearman, Kendall Tau, Pearson Correlation
coefficients of COVID19 dataset and Verhulste-Pearl-Reed Logistic in R - related
to 487,572,770 and all sections on People Analytics, Urban Sprawl Analytics,
Social Network Analysis, ERSIR-SIS model of pandemic/cybercrimes/opinions,
Cellular Automaton Graph model of Social Networks - 30 March 2022

1231.1 COVID19 dataset has been updated to latest daily death toll data from
<https://www.worldometers.info/coronavirus/coronavirus-death-toll/> and Lambda of
theoretical chaotic dataset in VerhulstePearlReedLogistic.R has been revised to
1.079487535509905.

1231.2 Spearman, Kendall and Pearson correlation coefficients between updated
COVID19 dataset (daily data for the past 2.25 years) and chaotic dataset (of
lambda 1.079487535509905) have been recomputed.

1231.3 Following are the summary of tau, rho and product-moment correlation
coefficients for Kendall, Spearman and Pearson between Chaotic data and actual
COVID19 pandemic data (full logs at
code/testlogs/VerhulstPearlReedLogistic.log.30March2022):

Kendall's rank correlation tau

```
data: coronavirus2019scaled and rev(vprlogistic)
z = 42.254, p-value < 2.2e-16
alternative hypothesis: true tau is greater than 0
sample estimates:
tau
1
```

Spearman's rank correlation rho

```
data: coronavirus2019scaled and rev(vprlogistic)
S = 0, p-value < 2.2e-16
alternative hypothesis: true rho is greater than 0
sample estimates:
```

$$\rho_1$$

Pearson's product-moment correlation

```
data: coronavirus2019scaled and rev(vprlogistic)
t = 65.863, df = 795, p-value < 2.2e-16
alternative hypothesis: true correlation is greater than 0
95 percent confidence interval:
 0.9097611 1.0000000
sample estimates:
      cor
0.9193034
```

1231.4 Earlier correlations shed some light on trend of the pandemic and how it has evolved over 2+ years - First and foremost, lamda of Verhulste-Pearl-Reed Logistic has come down from 4.829487535509905 2 years ago, to 1.079487535509905 and 2 of 3 correlation coefficients are 100% (and the third correlation coefficient is 92%) for lowest p-value at 10^{-16} which is a drastic drop of 3.75, implying the pandemic has reversed from being chaotic to predictable (after almost 5 peak waves). Few other values of lambda (plus and minus) were tried and highest correlation (for atleast 2 of 3 coefficients) of 100% happens at 1.079487535509905.

1231.5 R plots for VPR logistic, May logistic have been redrawn -
code/VerhulstPearlReedLogistic_Rplots.pdf.

1235. (THEORY and FEATURE) People Analytics - Social Network Analysis - CoronaVirus2019 analyzer - Recomputed Spearman, Kendall Tau, Pearson Correlation coefficients for revised COVID19 dataset (Lancet,WHO estimates) and corrections to Verhulste-Pearl-Reed and May Logistic code in R - related to 487,572,770,1231 and all sections on People Analytics, Urban Sprawl Analytics, Social Network Analysis, ERSIR-SIS model of pandemic/cybercrimes/opinions, Cellular Automaton Graph model of Social Networks - 18 April 2022

1235.1 course_material/Programming/R/code/VerhulstPearlReedLogistic.R has been updated to add a scaling multiplicand to daily COVID19 death toll vector data which is multiplied by Verhulste-Pearl-Reed and May Logistics R implementations as an adjustment for revised excess daily mortalities.

1235.2 Scaling multiplicand has been hardcoded to 3.0 to account for the huge gap estimated between official (6.2 million) and actual COVID19 global death tolls (till March 2022) by Lancet and WHO COVID19 analyzer models (Lancet - 18 million, WHO - 15 million) implying a triplication of death figures.

1235.3 Some bugs in R plot of May logistic and computation May Logistic have been resolved. Function `verhulstpearlreedlaw()` has been changed to pass on two bifurcation parameters each for Verhulste-Pearl-Reed (quadratic chaos) and May Logistic (exponential chaos). Revised COVID19 daily death toll multiplied by 3 has been fit to VPR and May logistics for bifurcation parameters of 0.34 and 0.26 respectively where maximum correlations occur (2 of 3 correlation coefficients except Pearson attain 100% each in VPR model) - detailed logs at `code/testlogs/VerhulstPearlReedLogistic.log`. 18 April 2022. Lambda value of 4.82 has dropped to 0.34 in 2 years which is a reversal of chaotic bifurcation by ~4.5 (or) reproduction number of COVID19 has tapered:

```
corcoeff <-  
verhulstpearlreedlaw("./VerhulstPearlReedLogistic.dat",0.34,0.26,0.000000000000000  
1)
```

References:

1235.4 Lancet COVID19 estimates - paper -
[https://www.thelancet.com/journals/lancet/article/PIIS0140-6736\(21\)02796-3/](https://www.thelancet.com/journals/lancet/article/PIIS0140-6736(21)02796-3/)

fulltext - Bayesian spline ensemble expected deathtoll model implemented in Python 3.7.7, Stata and R
1235.5 Lancet COVID19 estimates - PDF - Figure 1 on excess and official deathtolls, Table of countrywise actual and official deathtolls - <https://www.thelancet.com/action/showPdf?pii=S0140-6736%2821%2902796-3>
1235.6 WHO COVID19 excess mortality model - <https://www.nytimes.com/2022/04/16/health/global-covid-deaths-who-india.html>, <https://www.who.int/news-room/questions-and-answers/item/global-excess-deaths-associated-with-the-COVID-19-pandemic>

1241. (THEORY and FEATURE) People Analytics - Social Network Analysis - CoronaVirus2019 analyzer - Excess Mortality Model implementation - related to 487,572,770,831,1150,1231,1235 and all sections on People Analytics, Urban Sprawl Analytics, Social Network Analysis, ERSIR-SIS model of pandemic/cybercrimes/opinions, Cellular Automaton Graph model of Social Networks - 18 May 2022

1241.1 CAGraphLogit.R has been updated to define two new R functions `cagraphexcessmortalityratemodel()` and `cagraphemrprojections()` to implement excess COVID19 mortality estimation for Cellular Automaton Grid S-I-R model described in 1150.

1241.2 Following two regressions have been computed in Poisson distribution family and later used to extrapolate excess COVID19 mortalities:

```
if(emrmodel==1)
{
  coronavirus2019emr <- glm(deaths ~ seropositivity * mortalityrate *
totalpopulation - mortalityrate * recovered, family = poisson())
}
else
{
  coronavirus2019emr <- glm(deaths ~ totalpopulation * unvaccinated *
seropositivity * mortalityrate, family = poisson())
}
```

1241.3 CAGraphLogit.dat has been extended for additional fields - TotalPopulation, SeroPositivity, Unvaccinated, MortalityRate (populated approximately due to lack of data for intermediary dates) and earlier 2 models are learnt by `glm()` fit.

1241.4 Following are excess deathtoll estimates predicted from 2 models for India data available from Worldometer (till 31 March 2022):

MODEL 1:

```
[1] "Excess Mortalities:"
(Intercept)
10573454
```

MODEL 2:

```
[1] "Excess Mortalities:"
[1] 6912560
```

1241.5 Earlier two models are two different interpretations of projected deathtolls. MODEL 2 has been already explained in 1150 while the MODEL 1 is based on following reasoning. MODEL 2 is more in line with other excess death estimator models and straightforward to compute (Terminology for Susceptible is different from usual SIR convention - "Susceptible" has been used to connote "possible mortality"):

```
Pr(Uninfected) + Pr(Infected) = 1
Pr(Infected) = Pr(Susceptible) + Pr(Recovered)
=> Pr(Uninfected) + Pr(Susceptible) + Pr(Recovered) = 1
Seropositivity = Pr(Infected)
Pr(Uninfected) = 1 - Pr(Infected)
Pr(Uninfected) = 1 - Seropositivity
```

```

Pr(Susceptible) = 1 - Pr(Uninfected) - Pr(Recovered)
=> Pr(Susceptible) = Seropositivity - Pr(Recovered)
=> Pr(Deaths) = Pr(Susceptible) * MortalityRate ('Deaths' are certain
'Susceptibilities')
=> Pr(Deaths) = Seropositivity * MortalityRate - Pr(Recovered) *
MortalityRate
    After multiplying probabilities by Total population:
=> Estimated Deaths = Totalpopulation * Seropositivity * MortalityRate -
Recovered * MortalityRate
@article{k2010few,
  title={Few Algorithms for ascertaining merit of a document and their
applications},
  author={K Shrinivaasan, Balaraman Ravindran, Madhavan Mukund},
  journal={arXiv preprint arXiv:1006.4458},
  year={2010}
}

```

```

@article{shrinivaasan2011decidability,
  title={Decidability of Existence and Construction of a Complement of a given
Function},
  author={Shrinivaasan, K},
  journal={arXiv preprint arXiv:1106.4102},
  year={2011},
  publisher={acknowledgement: advised by Meena Mahajan, Institute of
Mathematical~...}
}

```

```

@inproceedings{k2010update,
  title={Update summarization with Interview Algorithm -
http://www.nist.gov/tac/publications/2010/participant.papers/CMI\
_IIT.proceedings.pdf},
  author={K Shrinivaasan, Balaraman Ravindran, Madhavan Mukund},
  booktitle={NIST TAC 2010},
  year={2010},
  organization={NIST}
}

```

```

@article{shrinivaasan2013indepth,
  title={Indepth analysis of a variant of Majority Voting and relation to
Zermelo-Fraenkel Set Theory With Axiom of Choice (ZFC)},
  author={Shrinivaasan, Ka},
  year={2013}
}

```

Decidability of Existence and Construction of a Complement of a given Function
Ka. Shrinivaasan
Mathematics, Computer Science
ArXiv
2011
This article de nes a complement of a function and conditions for existence of
such a complement function and presents few algorithms to construct a
complement.

Cite

Save

Feed

TAC 2010 Summarization Track - Update Summarization with Interview Algorithm
Ka. Shrinivaasan
Computer Science
TAC
2010

Existing models for ranking documents(mostly in world wide web) are prestige
based. In this article, alternative graph-theoretic schemes to objectively judge

the merit of a document independent of... Continue Reading
View PDF

Cite

Save

Feed

Few Algorithms for ascertaining merit of a document and their applications

Ka. Shrinivaasan

Computer Science

ArXiv

2010 (First Publication: 23 June 2010)

Existing models for ranking documents(mostly in world wide web) are prestige based. In this article, three algorithms to objectively judge the merit of a document are proposed-1) Citation graph... Continue Reading

```
@article{DBLP:journals/corr/abs-1106-4102,  
  author    = {Ka. Shrinivaasan},  
  title     = {Decidability of Existence and Construction of a Complement of a  
given  
              Function},  
  journal   = {CoRR},  
  volume    = {abs/1106.4102},  
  year      = {2011},  
  url       = {http://arxiv.org/abs/1106.4102},  
  archivePrefix = {arXiv},  
  eprint    = {1106.4102},  
  timestamp = {Mon, 13 Aug 2018 01:00:00 +0200},  
  biburl    = {https://dblp.org/rec/journals/corr/abs-1106-4102.bib},  
  bibsource = {dblp computer science bibliography, https://dblp.org}  
}
```

```
@inproceedings{DBLP:conf/tac/Shrinivaasan10,  
  author    = {Ka. Shrinivaasan},  
  title     = {{TAC} 2010 Summarization Track - Update Summarization with  
Interview  
              Algorithm},  
  booktitle = {Proceedings of the Third Text Analysis Conference, {TAC} 2010,  
Gaithersburg,  
              Maryland, USA, November 15-16, 2010},  
  year      = {2010},  
  crossref  = {DBLP:conf/tac/2010},  
  url       = {https://tac.nist.gov/publications/2010/participant.papers/CMI\  
_IIT.proceedings.pdf},  
  timestamp = {Tue, 20 Aug 2019 13:25:20 +0200},  
  biburl    = {https://dblp.org/rec/conf/tac/Shrinivaasan10.bib},  
  bibsource = {dblp computer science bibliography, https://dblp.org}  
}
```

```
@article{DBLP:journals/corr/abs-1006-4458,  
  author    = {Ka. Shrinivaasan},  
  title     = {Few Algorithms for ascertaining merit of a document and their  
applications},  
  journal   = {CoRR},  
  volume    = {abs/1006.4458},  
  year      = {2010},  
  url       = {http://arxiv.org/abs/1006.4458},  
  archivePrefix = {arXiv},  
  eprint    = {1006.4458},  
  timestamp = {Mon, 13 Aug 2018 01:00:00 +0200},  
  biburl    = {https://dblp.org/rec/journals/corr/abs-1006-4458.bib},  
  bibsource = {dblp computer science bibliography, https://dblp.org}  
}
```

```
@proceedings{DBLP:conf/tac/2010,  
  title      = {Proceedings of the Third Text Analysis Conference, {TAC} 2010,  
Gaithersburg,  
    Maryland, USA, November 15-16, 2010},  
  publisher  = {{NIST}},  
  year       = {2010},  
  url        = {https://tac.nist.gov/publications/2010/papers.html},  
  timestamp  = {Tue, 20 Aug 2019 13:25:20 +0200},  
  biburl     = {https://dblp.org/rec/conf/tac/2010.bib},  
  bibsource  = {dblp computer science bibliography, https://dblp.org}  
}
```

6/9/2020

ka shrinivaasan - Search Results | Microsoft Academic

Microsoft
Academic

▣

ka shrinivaasan

▣ ▣ Sign up /
Sign in

CLEAR ALL

FILTER BY: ▣

▣ Time

▣

▣ Top Topics

▣

▣ Publication Types

▣

⌵ Top Authors

▣

} Top Journals

▣

⌵ Ka. Shrinivaasan
PUBLICATIONS (2)

▣

CITATIONS* (0)

Authors with similar name

⌵ Ka. Shrinivaasan
PUBLICATIONS (1)

▣

CITATIONS* (0)

Showing 13* of 3 (2.102 seconds)

VIEW □ □ □

SORT BY

SALIENCY □

□ Decidability of Existence and Construction of a
Complement of a given Function

0 citations*

2011

Ka. Shrinivaasan

□ Mathematics

□ Discrete mathematics

□ Decidability

□

□

Feedback

□

[https://academic.microsoft.com/search?q=ka%20shrinivaasan&qe=%40%40%40Composite\(AA.AuN%3D%3D%27ka%20shrinivaasa...](https://academic.microsoft.com/search?q=ka%20shrinivaasan&qe=%40%40%40Composite(AA.AuN%3D%3D%27ka%20shrinivaasa...)

1/2

6/9/2020

ka shrinivaasan - Search Results | Microsoft Academic

▫ TAC 2010 Summarization Track Update
Summarization with Interview Algorithm.

0 citations*

2010 THEORY AND APPLICATIONS OF
CATEGORIES

Ka. Shrinivaasan

▫ Information retrieval

▫ Data mining

▫ Computer science

View More (1+) ▫

▫

▫

▫ Few Algorithms for ascertaining merit of a
document and their applications

▫

▫

0 citations*

2010

Ka. Shrinivaasan

▫ World Wide Web

▫ Information retrieval

▫ Computer science

▫

▫

▫

▫

FAQ

Contact Us

Privacy and Cookies

Terms of Use

Trademarks

Specific Terms

* Estimated Count

© 2020 Microsoft

[https://academic.microsoft.com/search?q=ka%20shrinivaasan&qe=%40%40%40Composite\(AA.AuN%3D%3D%27ka%20shrinivaasa...](https://academic.microsoft.com/search?q=ka%20shrinivaasan&qe=%40%40%40Composite(AA.AuN%3D%3D%27ka%20shrinivaasa...)

2/2

```
@ARTICLE{2011arXiv1106.4102S,
  author = {{Shrinivaasan}, Ka.},
  title = "{Decidability of Existence and Construction of a Complement of
a given Function}",
  journal = {arXiv e-prints},
  keywords = {Computer Science - Logic in Computer Science},
  year = 2011,
  month = jun,
  eid = {arXiv:1106.4102},
  pages = {arXiv:1106.4102},
archivePrefix = {arXiv},
  eprint = {1106.4102},
  primaryClass = {cs.LO},
  adsurl = {https://ui.adsabs.harvard.edu/abs/2011arXiv1106.4102S},
  adsnote = {Provided by the SAO/NASA Astrophysics Data System}
}
```

```
@ARTICLE{2010arXiv1006.4458S,
  author = {{Shrinivaasan}, Ka.},
  title = "{Few Algorithms for ascertaining merit of a document and their
applications}",
  journal = {arXiv e-prints},
  keywords = {Computer Science - Information Retrieval},
  year = 2010,
  month = jun,
  eid = {arXiv:1006.4458},
  pages = {arXiv:1006.4458},
archivePrefix = {arXiv},
  eprint = {1006.4458},
  primaryClass = {cs.IR},
  adsurl = {https://ui.adsabs.harvard.edu/abs/2010arXiv1006.4458S},
  adsnote = {Provided by the SAO/NASA Astrophysics Data System}
}
```

6/9/2020
Documents

CiteSeerX – Search Results – Ka. Shrinivaasan
Authors

Tables

Donate

DMCA

MetaCart

Results 1 2 of 2

Sign up

Log in

Tools

Ka.Shrinivaasan

Sorted by:
Relevance

by Dr. Madhavan Mukund Cmi , 2010

"... algorithms for ascertaining merit of documents and their applications ..."
Abstract Add to MetaCart

Try your query at:

TAC 2010 Summarization Track Update Summarization with Interview Algorithm
by unknown authors

"... Existing models for ranking documents(mostly in world wide web) are prestige based. In this article, alternative graphtheoretic schemes to objectively judge the merit of a document independent of any external factors (like link graph) and without probabilistic inference are proposed and application ..."
Abstract Add to MetaCart

Results 1 2 of 2

Powered by:
About CiteSeerX

[Submit and Index Documents](#)

[Privacy Policy](#)

[Help](#)

[Data](#)

[Source](#)

[Contact Us](#)

Developed at and hosted by The College of Information Sciences and Technology
© 20072019 The Pennsylvania State University

<https://citeseerx.ist.psu.edu/search?q=Ka.+Shrinivaasan>

1/1

6/9/2020
Documents

CiteSeerX – Search Results – Ka. Shrinivaasan
Authors

Tables

Donate

DMCA

MetaCart

Results 1 2 of 2

Sign up

Log in

Tools

Ka.Shrinivaasan

Sorted by:
Relevance

by Dr. Madhavan Mukund Cmi , 2010
"... algorithms for ascertaining merit of documents and their applications ..."
Abstract Add to MetaCart

Try your query at:

TAC 2010 Summarization Track Update Summarization with Interview Algorithm
by unknown authors
"... Existing models for ranking documents(mostly in world wide web) are prestig
e based. In this article, alternative graphtheoretic
schemes to objectively judge the merit of a document independent of any external
factors (like link graph) and without probabilistic
inference are proposed and application ..."
Abstract Add to MetaCart

Results 1 2 of 2

Powered by:
About CiteSeerX

Submit and Index Documents

Privacy Policy

Help

Data

Source

Contact Us

Developed at and hosted by The College of Information Sciences and Technology
© 20072019 The Pennsylvania State University

<https://citeseerx.ist.psu.edu/search?q=Ka.+Shrinivaasan>

1/1

```
@article{DBLP:journals/corr/abs-1106-4102,
  author   = {Ka. Shrinivaasan},
  title    = {Decidability of Existence and Construction of a Complement of a
given
              Function},
  journal  = {CoRR},
  volume   = {abs/1106.4102},
  year     = {2011},
  url      = {http://arxiv.org/abs/1106.4102},
  archivePrefix = {arXiv},
  eprint   = {1106.4102},
  timestamp = {Mon, 13 Aug 2018 01:00:00 +0200},
  biburl   = {https://dblp.org/rec/journals/corr/abs-1106-4102.bib},
  bibsource = {dblp computer science bibliography, https://dblp.org}
}
```

```
@inproceedings{DBLP:conf/tac/Shrinivaasan10,
  author   = {Ka. Shrinivaasan},
  title    = {{TAC} 2010 Summarization Track - Update Summarization with
Interview
              Algorithm},
  booktitle = {Proceedings of the Third Text Analysis Conference, {TAC} 2010,
Gaithersburg,
              Maryland, USA, November 15-16, 2010},
  year     = {2010},
  crossref = {DBLP:conf/tac/2010},
  url      = {https://tac.nist.gov/publications/2010/participant.papers/CMI\
_IIT.proceedings.pdf},
  timestamp = {Tue, 20 Aug 2019 13:25:20 +0200},
  biburl   = {https://dblp.org/rec/conf/tac/Shrinivaasan10.bib},
  bibsource = {dblp computer science bibliography, https://dblp.org}
}
```

```
@article{DBLP:journals/corr/abs-1006-4458,
  author   = {Ka. Shrinivaasan},
  title    = {Few Algorithms for ascertaining merit of a document and their
applications},
  journal  = {CoRR},
  volume   = {abs/1006.4458},
  year     = {2010},
  url      = {http://arxiv.org/abs/1006.4458},
  archivePrefix = {arXiv},
  eprint   = {1006.4458},
  timestamp = {Mon, 13 Aug 2018 01:00:00 +0200},
  biburl   = {https://dblp.org/rec/journals/corr/abs-1006-4458.bib},
  bibsource = {dblp computer science bibliography, https://dblp.org}
}
```

```
@proceedings{DBLP:conf/tac/2010,
  title    = {Proceedings of the Third Text Analysis Conference, {TAC} 2010,
Gaithersburg,
              Maryland, USA, November 15-16, 2010},
  publisher = {{NIST}},
  year     = {2010},
  url      = {https://tac.nist.gov/publications/2010/papers.html},
  timestamp = {Tue, 20 Aug 2019 13:25:20 +0200},
  biburl   = {https://dblp.org/rec/conf/tac/2010.bib},
  bibsource = {dblp computer science bibliography, https://dblp.org}
}
```

```
@article{k2010few,
  title={Few Algorithms for ascertaining merit of a document and their
applications},
  author={K Shrinivaasan, Balaraman Ravindran, Madhavan Mukund},
```

```
journal={arXiv preprint arXiv:1006.4458},
year={2010}
}
```

```
@article{shrinivaasan2011decidability,
  title={Decidability of Existence and Construction of a Complement of a given
Function},
  author={Shrinivaasan, K},
  journal={arXiv preprint arXiv:1106.4102},
  year={2011},
  publisher={acknowledgement: advised by Meena Mahajan, Institute of
Mathematical~...}
}
```

```
@inproceedings{k2010update,
  title={Update summarization with Interview Algorithm -
http://www.nist.gov/tac/publications/2010/participant.papers/CMI\
_IIT.proceedings.pdf},
  author={K Shrinivaasan, Balaraman Ravindran, Madhavan Mukund},
  booktitle={NIST TAC 2010},
  year={2010},
  organization={NIST}
}
```

```
@article{shrinivaasan2013indepth,
  title={Indepth analysis of a variant of Majority Voting and relation to
Zermelo-Fraenkel Set Theory With Axiom of Choice (ZFC)},
  author={Shrinivaasan, Ka},
  year={2013}
}
6/9/2020
```

ka shrinivaasan - Search Results | Microsoft Academic

Microsoft
Academic

□

ka shrinivaasan

□ □ Sign up /
Sign in

CLEAR ALL

FILTER BY: □

□ Time

□

□ Top Topics

□

□ Publication Types

□

∞ Top Authors

□

} Top Journals

□

⌘ Ka. Shrinivaasan
PUBLICATIONS (2)

□

CITATIONS* (0)

Authors with similar name
⌘ Ka. Shrinivaasan
PUBLICATIONS (1)

□

CITATIONS* (0)

Showing 13* of 3 (2.102 seconds)

VIEW □ □ □

SORT BY

SALIENCY □

□ Decidability of Existence and Construction of a
Complement of a given Function

0 citations*

2011

Ka. Shrinivaasan

□ Mathematics

□ Discrete mathematics

□ Decidability

□

□

Feedback

□

[https://academic.microsoft.com/search?q=ka%20shrinivaasan&qe=%40%40%40Composite\(AA.AuN%3D%3D%27ka%20shrinivaasa...](https://academic.microsoft.com/search?q=ka%20shrinivaasan&qe=%40%40%40Composite(AA.AuN%3D%3D%27ka%20shrinivaasa...)

1/2

6/9/2020

ka shrinivaasan - Search Results | Microsoft Academic

▫ TAC 2010 Summarization Track Update
Summarization with Interview Algorithm.

0 citations*

2010 THEORY AND APPLICATIONS OF
CATEGORIES

Ka. Shrinivaasan

▫ Information retrieval

▫ Data mining

▫ Computer science

View More (1+) ▫

▫

▫

▫ Few Algorithms for ascertaining merit of a
document and their applications

▫

▫

0 citations*

2010

Ka. Shrinivaasan

▫ World Wide Web

▫ Information retrieval

▫ Computer science

▫

▫

▫

▫

FAQ

Contact Us

Privacy and Cookies

Terms of Use

Trademarks

Specific Terms

* Estimated Count

© 2020 Microsoft

[https://academic.microsoft.com/search?q=ka%20shrinivaasan&qe=%40%40%40Composite\(AA.AuN%3D%3D%27ka%20shrinivaasa...](https://academic.microsoft.com/search?q=ka%20shrinivaasan&qe=%40%40%40Composite(AA.AuN%3D%3D%27ka%20shrinivaasa...)

```
@ARTICLE{2011arXiv1106.4102S,
  author = {{Shrinivaasan}, Ka.},
  title = "{Decidability of Existence and Construction of a Complement of
a given Function}",
  journal = {arXiv e-prints},
  keywords = {Computer Science - Logic in Computer Science},
  year = 2011,
  month = jun,
  eid = {arXiv:1106.4102},
  pages = {arXiv:1106.4102},
archivePrefix = {arXiv},
  eprint = {1106.4102},
  primaryClass = {cs.LO},
  adsurl = {https://ui.adsabs.harvard.edu/abs/2011arXiv1106.4102S},
  adsnote = {Provided by the SAO/NASA Astrophysics Data System}
}
```

```
@ARTICLE{2010arXiv1006.4458S,
  author = {{Shrinivaasan}, Ka.},
  title = "{Few Algorithms for ascertaining merit of a document and their
applications}",
  journal = {arXiv e-prints},
  keywords = {Computer Science - Information Retrieval},
  year = 2010,
  month = jun,
  eid = {arXiv:1006.4458},
  pages = {arXiv:1006.4458},
archivePrefix = {arXiv},
  eprint = {1006.4458},
  primaryClass = {cs.IR},
  adsurl = {https://ui.adsabs.harvard.edu/abs/2010arXiv1006.4458S},
  adsnote = {Provided by the SAO/NASA Astrophysics Data System}
}
```

7/8/2020

Patent Database Search Results: "kannan srinivasan" AND "sun microsystems" in US Patent Collection

Searching US Patent Collection...
Results of Search in US Patent Collection db for:
("kannan srinivasan" AND "sun microsystems"): 9 patents.
Hits 1 through 9 out of 9
Jump To

Refine Search

PAT.

NO.

1 8,521,875

2 8,145,759

3 7,743,083

4 7,739,252

5 7,640,545

6 7,610,305

7 7,165,061

8 7,134,008

9 7,082,432

"kannan srinivasan" AND "sun microsystems"

Title

Identity for data sources
Dynamically configurable resource pool
Common transaction manager interface for local and global transactions
Read/write lock transaction manager freezing
Transaction manager freezing
Simultaneous global transaction and local transaction management in an application server
Transaction optimization of readonly data sources
Utility for configuring and verifying data sources
Specifying transaction manager type at various application levels

<http://patft.uspto.gov/netacgi/nph-Parser?Sect1=PT02&Sect2=HITOFF&p=1&u=%2Fnetacgi%2FPT02%2Fsearch-adv.htm&r=0&f=...>
1/1

7/8/2020
United States Patent: 8521875

(1 of 9)
United States Patent
Dutt , et al.
8,521,875
August 27, 2013
Identity for data sources
Abstract
Various embodiments of a networked computer system in which an application server associates an identity with each data source included in the system are disclosed. The networked computer system may include several backend systems, each including one or more data resources, and the identity of a data source may be unique to a data resource. When an application requests a connection to a data resource, the application server may ascertain the identity of the associated data source and compare this identity to identities of data sources with existing connections. If a match is found, the application server may provide an existing connection to the application, whereas if no match is found the application server may provide a new connection. The identity of a data source may include one or more data source configuration properties. In some embodiments, the identity may include database name, URL, and user name.
Inventors: Dutt; Bala (Bangalore, IN), Kumar; Ajay (Bangalore, IN), K; Venugopal Rao (Karnataka, IN), Bhogi; Sankara R. (Bangalore, IN), Kannan; Srinivasan (Bangalore, IN)
Applicant:
Name
City

State Country Type

Dutt; Bala

Bangalore

Kumar; Ajay

Bangalore

K; Venugopal Rao Karnataka

Bhogi; Sankara R. Bangalore

Kannan; Srinivasan Bangalore

Assignee:

Family ID:

Appl. No.:

Filed:

N/A

N/A

N/A

N/A

N/A

IN

IN

IN

IN

IN

Oracle America, Inc. (Redwood City, CA)

34226108

10/655,346

September 4, 2003

Prior Publication Data

<http://patft.uspto.gov/netacgi/nph-Parser?Sect1=PT02&Sect2=HITOFF&p=1&u=%2Fmetahtml%2FPT0%2Fsearch-adv.htm&r=1&f...>

1/17

7/8/2020

United States Patent: 8521875

Document Identifier

US 20050055325 A1

Current U.S. Class:

Current CPC Class:

Current International Class:

Field of Search:

Publication Date

Mar 10, 2005

709/225; 707/609; 709/203; 707/607; 709/223

G06F 16/25 (20190101)

G06F 15/173 (20060101); G06F 15/16 (20060101); G06F

7/00 (20060101)

;709/225,223,203 ;707/607,609

References Cited [Referenced By]

U.S. Patent Documents

4502116

5335343

5504899

5504900

5586312

5630081

5701480

6011791

6038587

6041354

6105067

6154787

6157927

6233587

6243737

6272675

6317773

6338112
6374243
6411956
6421661
6421688
6442618
6496828
6519679
6687729
6687831
6704737
6728958
February 1985
August 1994
April 1996
April 1996
December 1996
May 1997
December 1997
January 2000
March 2000
March 2000
August 2000
November 2000
December 2000
May 2001
June 2001
August 2001
November 2001
January 2002
April 2002
June 2002
July 2002
July 2002
August 2002
December 2002
February 2003
February 2004
February 2004
March 2004
April 2004
Fowler et al.
Lampson et al.
Raz
Raz
Johnson et al.
Rybicki et al.
Raz
Okada et al.
Phillips et al.
Biliris et al.
Batra
Urevig et al.
Schaefer et al.
Tandon
Flanagan et al.
Schrab et al.
Cobb et al.
Wipfel et al.
Kobayashi et al.
Ng
Doan et al.
Song
Phillips et al.

Cochrane et al.
Devireddy et al.
Sievert et al.
Albaugh et al.
Nixon et al.
Klein et al.
<http://patft.uspto.gov/netacgi/nph-Parser?Sect1=PT02&Sect2=HITOFF&p=1&u=%2Fmetahtml%2FPT0%2Fsearch-adv.htm&r=1&f...>
2/17
7/8/2020
6832238
6854646
6862573
6873995
6950848
6981221
7065563
7080119
7082432
7089566
7134008
7165061
2002/0124083
2003/0033398
2003/0036919
2003/0046342
2003/0055968
2004/0030739
2004/0088413
2004/0153349
2004/0153383
2004/0153450
2004/0172385
2004/0215473
2004/0215894
2004/0216109
2005/0015353
2005/0015425
2005/0055324
2005/0066155
United States Patent: 8521875
December 2004
February 2005
March 2005
March 2005
September 2005
December 2005
June 2006
July 2006
July 2006
August 2006
November 2006
January 2007
September 2002
February 2003
February 2003
March 2003
March 2003
February 2004
May 2004
August 2004
August 2004
August 2004
September 2004

October 2004
 October 2004
 October 2004
 January 2005
 January 2005
 March 2005
 March 2005
 Sharma et al.
 Ieshima et al.
 Kendall et al.
 Benson et al.
 Yousefi'zadeh
 Neudeck et al.
 Islam et al.
 Felt et al.
 Bhogi et al.
 Johnson
 Dutt et al.
 K et al.
 Jeyaraman et al.
 Carlson et al.
 Felt et al.
 Felt et al.
 Hochmuth et al.
 Yousefi'zadeh
 Bhogi et al.
 K. et al.
 K. et al.
 K. et al.
 Dayal
 Bhogi et al.
 Bhogi et al.
 Bhogi et al.
 Kumar et al.
 Kumar et al.
 Godeby et al.
 Dutt et al.
 Other References
 Manolis Marazakis, "Distributed Systems", University of Crepe; Sep. 2002, pp. 1-31. cited by applicant .
 Oracle9i JDBC Developer's Guide and Reference (Mar. 2002, retrieved from <http://www.stanford.edu/dept/itss/docs/oracle/9i/java.920/a96654/toc.htm> on Sep. 6, 2005). cited by applicant .
 Kannegaard (J2EE BluePrints, Mar. 20, 2000 retrieved from <http://java.sun.com/blueprints/guidelines/designing.sub.enterprise.sub.applications/apmTOC.html> on Sep. 6, 2005). cited by applicant .
 BEA WebLogic Enterprise 5.1, BEA Systems, Inc., 2000, (13 Pages). cited by applicant .
 "Simplified Guide to the Java TM 2 Platform Enterprise Edition," Sun Microsystems, Inc., <http://patft.uspto.gov/netacgi/nph-Parser?Sect1=PT02&Sect2=HITOFF&p=1&u=%2Fnethtml%2FPT0%2Fsearch-adv.htm&r=1&f...>
 3/17
 7/8/2020
 United States Patent: 8521875
 1999, (13 Pages). cited by applicant .
 Dogac et al., "METU Interoperable Database System," Demo Description, In Proc. of ACM
 Sigmod Intl. Conf. on Management of Data, Jun. 1996, (6 Pages). cited by applicant .
 "Interface DataSource," DataSource (Java 2 Platform, SE v1.4.1), 2002, (1 Page). cited by

applicant .
 "Initial Context," JNDI 1.2.1 Specification: Class Initial Context,
<http://java.sun.com/products/jndi/1.2/javadoc/javax/naming/InitialContext.html>,
 Jul. 14,
 1999, (1 Page). cited by applicant .
 JNDIJava.TM. Naming & Directory Interface.TM., Sun Microsystems, Inc.,
<http://java.sun.com/jndi>, May 15, 2003, (2 Pages). cited by applicant .
 "iPlanet Application Server 6.0 Administration Guide: Chapter 9 Administering
 Transactions," <http://docs.sun.com/source/816578410/adtrans.htm>, Sep. 5, 2000,
 (11 Pages).
 cited by applicant .
 Breitbart et al., "Replication and Consistency Being Lazy Helps Sometimes," PODS
 '97, Jun.
 1997, (pp. 173184). cited by applicant .
 Patricia SerranoAlvarado et al. "Mobile Transaction Supports for DBMS". In
 17iemes
 Journees Bases de Donnees Avancees, Agadir, Maroc, Oct. 2001, (19 Pages). cited
 by
 applicant .
 Liu et al., "Designing a Test Suite for Empiricallybased Middleware Performance
 Prediction," Australian Computer Society, Inc., (2002), (8 Pages). cited by
 applicant .
 "Java .TM. 2SDK, Enterprise Edition 1.3.1 Configuration Guide,"
<http://java.sun.com/j2ee/sdk.sub.1.3/techdocs/release/ConfigGuide.html>, Jan. 3,
 2002, (16
 Pages). cited by applicant .
 Ellis et al., :JDBC .TM. 3.0 SpecificationFinal Release, Sun Microsystems, Inc.,
 Oct. 2001,
 (190 pages). cited by applicant .
 "iPlanet Application Server 6.0 Administration Guide: Chapter 4 Logging Server
 Messages,"
<http://docs.sun.com/source/816572010/adlog.htm>, Sep. 5, 2000, (21 Pages). cited
 by
 applicant .
 "JDBC .TM. Data Access APIThe JDBC API Universal Data Access for the Enterprise,"
java.sun.com, Aug. 10, 2003, (5 Pages). cited by applicant .
 "Connection Pooling," Advanced Programming for the Java 2 Platform, Aug. 16,
 2002, (4
 Pages). cited by applicant .
 Siva Visveswaram, "Manage Access to Shared, ServerSide Resources for High
 Performance
 Dive Into Connection Pooling with J2EE," JavaWorld, Oct. 2000, (8 Pages). cited
 by
 applicant.
 Primary Examiner: Tiv; Backhean
 Assistant Examiner: Chou; Alan S
 Attorney, Agent or Firm: Kowert; Robert C. Meyertons, Hood, Kivlin, Kowert &
 Goetzel, P.C.
 Claims
 What is claimed is:
 1. A system, comprising: an application server; and one or more of backend
 systems coupled to the
 application server; wherein the one or more backend systems comprises a
 plurality of distinct data
 resources; wherein the application server comprises: an application configured
 to initiate requests for
 connections with the plurality of distinct data resources; a plurality of data
 sources configured to provide
[http://patft.uspto.gov/netacgi/nph-Parser?Sect1=PT02&Sect2=HITOFF&p=1&u=](http://patft.uspto.gov/netacgi/nph-Parser?Sect1=PT02&Sect2=HITOFF&p=1&u=%2Fnetacgi%2FPT02%2Fsearch-adv.htm&r=1&f...)
[%2Fnetacgi%2FPT02%2Fsearch-adv.htm&r=1&f...](http://patft.uspto.gov/netacgi/nph-Parser?Sect1=PT02&Sect2=HITOFF&p=1&u=%2Fnetacgi%2FPT02%2Fsearch-adv.htm&r=1&f...)
 4/17
 7/8/2020
 United States Patent: 8521875
 connections with the plurality of distinct data resources; and wherein the

application server is configured to associate an identity with each of the plurality of data sources and to use the identity to determine whether one of the plurality of data sources provides connections to the same data resource as another of the plurality of data sources, wherein each identity is unique to one of the plurality of distinct data resources, and wherein multiple ones of the data sources have the same identity.

2. The system as recited in claim 1, wherein in response to the application requesting a connection from one of the plurality of data sources, a data source ID manager is configured to ascertain the identity of the data source from which the connection was requested and determine whether the identity matches the identity of any other of the plurality of data sources.

3. The system as recited in claim 2, wherein the data source ID manager is further configured to determine whether any of the data sources with matching identities previously supplied a connection to the application and, if a connection was previously supplied, to return the previously supplied connection to the application.

4. The system as recited in claim 3, wherein if no connection from a data source with a matching identity exists, the data source is configured to forward the request to a corresponding data source to obtain a new connection.

5. The system as recited in claim 4, wherein the connection is a local connection.

6. The system as recited in claim 1, wherein the identity comprises values for one or more data source properties.

7. The system as recited in claim 6, wherein the identity comprises database name, URL, and user name.

8. The system as recited in claim 1, wherein one or more of the plurality of data sources is a data source proxy, wherein the application server is configured to instantiate the data source proxy for an abstract name of a data resource used by an application; ascertain an identity for a true data source; and use the identity to link the proxy to the true data source.

9. The system as recited in claim 8, wherein multiple data source proxies correspond to the same data source identity, wherein in response to the application requesting connections with a same data resource from multiple data source proxies, the data source proxies from which the connections were requested are configured to forward the connection requests to the data source whose identity corresponds to said proxies.

10. The system as recited in claim 1, wherein in response to a request to instantiate a data source corresponding to an abstract name, the application server is configured to determine an identity for the proposed data source, determine whether any existing data source has a matching identity, instantiate the proposed data source only if no existing data source with matching identity is found.

11. The system as recited in claim 1, wherein the application server further comprises a transaction manager; wherein in response to a request to commit a transaction the transaction manager is configured to identify a number of data resources participating in the transaction according to connections supplied

for unique data source identities; wherein if the number of data resources participating in the transaction is two or more the transaction manager is configured to commit the transaction utilizing a twophase commit protocol; and wherein if only one data resource participating in the transaction the transaction manager is configured to commit the transaction utilizing a onephase commit optimization.

<http://patft.uspto.gov/netacgi/nph-Parser?Sect1=PT02&Sect2=HITOFF&p=1&u=%2Fmetahtml%2FPT0%2Fsearch-adv.htm&r=1&f...>

5/17

7/8/2020

United States Patent: 8521875

12. A method, comprising: receiving notification of a request for a connection; ascertaining an identity of a data source associated with the request, wherein the data source is configured to provide the connection to one of a plurality of distinct data resources, and wherein said identity is unique to said one of said plurality of distinct data resources; comparing said identity with respective identities of multiple data sources with existing connections, wherein the identity of each of the multiple data sources is unique to a specific one of said plurality of distinct data resources; providing an existing connection if an identity match is found with one of the data sources with existing connections; and providing a new connection if no identity match is found.

13. The method as recited in claim 12, wherein the identity comprises values for one or more data source property.

14. The method as recited in claim 13, wherein the identity comprises database name, URL, and user name.

15. The method of claim 12, further comprising: creating one or more data source proxies, wherein multiple data source proxies correspond to the same data source identity; each data source proxy associated with the same data source identity forwarding connection requests to the same data source whose identity corresponds to said proxies.

16. The method of claim 12, further comprising: in response to a request to commit a transaction, identifying the number of data resources participating in the transaction according to the number of unique data source identities used to establish data resource connections; and if the number of data resources participating in the transaction is two or more, committing the transaction utilizing a twophase commit protocol, and if only one data resource is participating in the transaction, committing the transaction utilizing a onephase commit optimization.

17. A method, comprising: receiving a request for a connection with a participant in a transaction; ascertaining an identity of a local data source associated with the request; attempting to identify a data source that is already participating in the transaction whose identity matches the identity of the data source associated with the request, wherein said attempting comprises comparing the ascertained identity to identities for a plurality of data sources, wherein each of the plurality of data sources is configured to provide a connection with one of a plurality of distinct data resources, and wherein each identity is

unique to one of the plurality of distinct data resources; sharing an existing connection associated with the identity if a data source with a matching identity is found; and providing a new connection if no data source with a matching identity is found.

18. A nontransitory computer accessible medium comprising program instructions, wherein the program instructions are computerexecutable to: receive notification of a request for a connection; ascertain an identity of a data source associated with the request; determine whether the identity of a data source from among a plurality of local and global data sources each having an existing connection matches the identity of a data source associated with the request, wherein each of the plurality of local and global data sources is configured to provide a connection with one of a plurality of distinct data resources, and wherein each of the plurality of local and global data sources has an identity unique to one of the plurality of distinct data resources; provide the existing connection if an identity match is found; and provide a new connection if no identity match is found.

19. The nontransitory computer accessible medium as recited in claim 18, wherein the identity comprises values for one or more data source properties.

<http://patft.uspto.gov/netacgi/nph-Parser?Sect1=PT02&Sect2=HITOFF&p=1&u=%2Fnethtml%2FPT0%2Fsearch-adv.htm&r=1&f...>

6/17

7/8/2020

United States Patent: 8521875

20. The nontransitory computer accessible medium as recited in claim 19, wherein the identity comprises database name, URL, and user name.

21. The nontransitory computer accessible medium as recited in claim 18, wherein the program

instructions are further computerexecutable to: create one or more data source proxies, wherein multiple data source proxies correspond to the same data source identity; wherein each data source proxy associated with the same data source identity forwards connection requests to the same data source whose identity corresponds to said proxies.

22. The nontransitory computer accessible medium as recited in claim 18, wherein the program

instructions are further computerexecutable to: in response to a request to commit a transaction, identify the number of data resources participating in the transaction according to the number of unique data source identities used to establish data resource connections; and if the number of data resources participating in the transaction is two or more, commit the transaction utilizing a twophase commit protocol, and if only one data resource is participating in the transaction, commit the transaction utilizing a onephase commit optimization.

23. A nontransitory computer accessible medium comprising program instructions, wherein the program

instructions are computerexecutable to: receive a request for a connection with a participant in a transaction; ascertain an identity of a local data source associated with the request; attempt to identify a data source that is already participating in the transaction whose identity matches the identity of the data source associated with the request, wherein to attempt to identify comprises

comparing the ascertained identity to identities for a plurality of data sources, wherein each of the plurality of data sources is configured to provide a connection with one of a plurality of distinct data resources, and wherein each identity is unique to one of the plurality of distinct data resources; share an existing connection associated with the identity if a data source with matching identity is found; and provide a new connection if no data source with matching identity is found.

Description

BACKGROUND OF THE INVENTION

1. Field of the Invention

The invention relates to computer systems and computer software, and more particularly to identifying data sources in computer systems.

2. Description of the Related Art

Large business systems may include application servers that run multiple applications and/or multiple copies of the same application concurrently. Some or all of these applications may be transaction oriented and may be capable of conducting many transactions simultaneously. Each transaction may require at least one connection for each data resource to be accessed and each connection requires a certain amount of system resources. Given the potentially large number of data resources and applications involved in transactions, the amount of system resources devoted to connections required to support the transactions could be substantial.

http://patft.uspto.gov/netacgi/nph-Parser?Sect1=PT02&Sect2=HIT0FF&p=1&u=%2Fnethtml%2FPT02%2Fsearch-adv.htm&r=1&f...

7/17

7/8/2020

United States Patent: 8521875

Data sources in Java Database Connectivity (JDBC) are the connection factories through which connections to different databases may be obtained. The function of these data source objects is to hide backend database configuration specific details from the application and offer a uniform interface for obtaining connections, as defined in the JDBC specifications. For example, when it is determined that an application needs to communicate with a specific database resident on a backend system, the application server may typically instantiate a data source object corresponding to the database. The data source object may be associated with a connection pool including one or more connections to the database. In order to minimize the amount of database configuration specific information required by an application in order to obtain a connection, both the data source object and the application may use an abstract name to refer to the database. In this way, a developer writing application code may only need to know the abstract name for a database in order to obtain a connection to it. Typically to obtain a connection to a database where `my_database` is an abstract name referring to a specific database on a backend system, application code would create a `datasource` object with `my_database` and call `get_connection` on the object. The data source object associated with the abstract name, `my_database`, will supply a connection to the desired database corresponding to the abstract name.

A Java code example is as follows: `DataSource ds=new DataSource(abstract_name); ds.getConnection();`

Some applications may be large and complex and may be implemented by more than one developer. As a developer implements communications in a particular portion of an application, he may use abstract names to refer to the data sources that are to be accessed. These abstract names often aid the developer in recalling some characteristic of the data to be accessed. Developers implementing different portions of an application may use different abstract names for the same data resource. In a typical application server, a separate data source object is instantiated for each abstract name of a data resource to be accessed by an application. For example, a company may have a database for storing human resources (HR) information resident on a backend system. A large application for manipulating the HR information may be written by several developers. One section of the application written by a first developer may require access to employee name information from the HR database and may use the abstract name "employee_names" to obtain a connection to the HR database. Another section of the application written by a second developer may require access to employee serial number information from the HR database and may use the abstract name "empnumber" to obtain a connection. Yet another section of the application written by a third developer may require access to employee salary information from the HR database and may use the abstract name "salary" to obtain a connection. When the application is executed, the three sections obtain three different connections from data source objects associated with the three different abstract names corresponding to the singular HR database. This situation results in an inefficient use of system communication resources due to the lack of a standard method for discovering whether multiple data source entities refer to the same backend data resource. For a transactional application this connection redundancy can result in the use of a more burdensome twophase commit protocol, when if it were known that all connections were with the same data resource, a lesscostly singlephase commit protocol could be used.

SUMMARY

Various embodiments of a networked computer system in which an application server associates an identity with each data source included in the system are disclosed. The networked computer system may include several backend systems, each including one or more data resources, and the identity of a data

<http://patft.uspto.gov/netacgi/nph-Parser?Sect1=PT02&Sect2=HITOFF&p=1&u=%2Fnethtml%2FPT0%2Fsearch-adv.htm&r=1&f...>

8/17

7/8/2020

United States Patent: 8521875

source may be unique to a data resource. When an application requests a connection to a data resource, the application server may ascertain the identity of the associated data source and compare this identity to identities of data sources with existing connections. If a match is found, the application server may provide an existing connection to the application, whereas if no match is found

the application server may provide a new connection. The identity of a data source may include one or more data source configuration parameters. In some embodiments, the identity may include database name, uniform resource locator (URL), and user name. In one embodiment, the data sources may be Java Data Base Connectivity (JDBC) DataSources and may be connection factories through which connection to different data resources (e.g. data bases) can be retrieved. These DataSource objects may hide data base specific configuration and offer a uniform interface for getting new connections as defined in JDBC. A global data source may be an XADataSource similar to a DataSource except that it is used to retrieve XAConnections. As described below, a unique identity may be established across DataSource and XADataSource objects and may be used to determine if two data source entities refer to the same backend data resource in order to facilitate connection sharing. By determining data source identities, a connection once retrieved from a data source may be shared across multiple uses in an application or transaction. The identity of both local and global data sources may be defined by a subset of properties used to configure the data source. For example, when a driver for a data base is specified, a subset of properties may be linked as that data source's identity. In one embodiment, the subset of properties may be data base name, URL and user name. For data sources participating in a transaction, the identity of each requested data source may be compared to the identities of any data sources already participating in the transaction. If a match is found, the existing data source connection is used by the application. This may allow some transaction to be treated as local transactions (and thus use a more efficient commit protocol) that otherwise would have been treated as global transactions.

BRIEF DESCRIPTION OF THE DRAWINGS

A better understanding of the present invention can be obtained when the following detailed description is considered in conjunction with the following drawings, in which:

FIG. 1 illustrates components of an application server, according to one embodiment.

FIG. 2 illustrates components of an application server, according to another embodiment.

FIG. 3 is a flowchart of one embodiment of a method of operating a data source ID manager.

FIG. 4 illustrates a logical representation of data source configuration data, according to one embodiment.

FIG. 5 is a flow chart of a method of configuring an application server, according to one embodiment.

FIG. 6 illustrates components of a networked, transactional computer system, according to one embodiment.

FIG. 7 is a flow chart of a method for operating a transaction manager, according to one embodiment.

<http://patft.uspto.gov/netacgi/nph-Parser?Sect1=PT02&Sect2=HITOFF&p=1&u=%2Fnethtml%2FPT0%2Fsearch-adv.htm&r=1&f...>

9/17

7/8/2020

United States Patent: 8521875

FIG. 8 illustrates an exemplary computer system, according to one embodiment. While the invention is susceptible to various modifications and alternative forms, specific embodiments thereof are shown by way of example in the drawings and will herein be described in detail. It should be understood, however, that the drawings and detailed description thereto are not intended to limit the invention to the particular form disclosed, but on the contrary, the intention is to cover all modifications, equivalents, and alternatives falling within the spirit and scope of the present invention as defined by the appended claims. Note, the headings are for organizational purposes only and are not meant to be used to limit or interpret the description or claims. Furthermore, note that the word "may" is used throughout this application in a permissive sense (i.e., having the potential to, being able to), not a mandatory sense (i.e., must). The term "include" and derivations thereof mean "including, but not limited to." The term "connected" means "directly or indirectly connected," and the term "coupled" means "directly or indirectly coupled."

DETAILED DESCRIPTION OF EMBODIMENTS

FIG. 1 is a block diagram illustrating components of application server 140, according to one embodiment. Application server 140 may include application program(s) 100, data source ID manager 130, data source objects 150, 152, and 154, and data source properties 160, among other components. Typically, an application server 140 may include a data source for each abstract name for a data resource with which application programs 100 requires communication. Some data sources may provide only local connections. Such data sources may be referred to as local data sources. A local connection, for example may be used in transactions involving only one data resource. For example, data source 150 may provide local connections to database 180 resident on backend system 170. Other data sources may provide global connections, or both global and local connections. Such data sources may be referred to as global data sources. Global connections may be used, for example, in transactions involving multiple distinct data resources. Data source 152 may be an XA data source supporting distributed transactions and providing global XA connections, which are also associated with database 180 resident on backend system 170.

In one embodiment, the data sources may be Java Data Base Connectivity (JDBC) DataSources and may be connection factories through which connection to different data resources (e.g. data bases) can be retrieved. These DataSource objects may hide data base specific configuration and offer a uniform interface for getting new connections as defined in JDBC. A global data source may be an XADataSource similar to a DataSource except that it is used to retrieve XAConnections. As described below, a unique identity may be established across DataSource and XADataSource objects and may be used to determine if two data source entities refer to the same backend data resource in order to facilitate connection sharing. By determining data source identities, a connection once retrieved from a data source

may be shared across multiple uses in an application or transaction. The identity of both local and global data sources may be defined by a subset of properties used to configure the data source. For example, when a driver for a data base is specified, a subset of properties may be linked as that data source's identity.

For data sources participating in a transaction, the identity of each requested data source may be compared to the identities of any data sources already participating in the transaction. If a match is found, the existing data source connection is used by the application. This may allow some transaction to be treated as local transactions (and thus use a more efficient commit protocol) that otherwise would have been treated as global transactions.

<http://patft.uspto.gov/netacgi/nph-Parser?Sect1=PT02&Sect2=HITOFF&p=1&u=%2Fnethtml%2FPT0%2Fsearch-adv.htm&r=1&...>

10/17

7/8/2020

United States Patent: 8521875

In some embodiments, a data source ID manager 130 may be included to determine data source

identities. For example, an application 100 may request a connection with a data resource 180 according

to an abstract name associated with the data resource. The application may specify a data source to

provide the connection. Data source ID manager 130 may receive or intercept the application request and

determine a unique data source ID for the specified data source. In one embodiment, data source ID

manager 130 may determine the data source ID from a set of data source properties for the specified data

source. In one embodiment, a configuration utility may have been used to configure the data sources and

to indicate which data source properties 160 should be used to uniquely identify each data source. Data

source ID manager 130 may determine which data sources have the same data source identity. For

example, data sources 150 and 152 may both have data source identity 190 and therefore, may both be

capable of supplying connections to the same data resource.

Data source ID manager 130 may determine whether any data source having a matching data source ID

has previously supplied a connection of the requested type that is still available to the application, and if

so, return or cause to be returned the previously supplied connection to the application. For example, for

a request to access database 180, if a connection has previously been supplied from either data source

150 or 152, the data source ID manager may return this connection to the application. If no connection

exists, data source ID manager 130 may cause the appropriate data source to obtain a new connection.

In other embodiments, as depicted in FIG. 2 the data source ID manager may intercept connection

requests from data sources to a connection repository of the application server, e.g. connection pool 235.

If an application 200 requests a connection with a data resource 280 according an abstract name

associated with the data resource from data source 250, data source 250 may return a connection to the

application in response to the request. To return the connection, data source 250 may request a

connection to data resource 280 from connection pool 235. Data source ID manager

230 may receive or intercept the request and determine a unique ID for the data source. In one embodiment, data source ID manager 230 may use a particular set of data source properties to determine a data source identity 290 associated with the request and determine which other data sources have the same data source identity 290. For example, data source 252 may also have data source identity 290 and therefore, may be capable of supplying connections of the requested type. Data source ID manager 230 may determine whether a data source with a matching ID, e.g. data source 252, has previously supplied a connection that is still active of the requested type to the application. If a connection has previously been supplied from data source 252, the data source ID manager may return or cause to be returned this connection to data source 250 to be sent to the application. If no connection has been supplied previously, data source ID manager 230 may forward the connection request to connection pool 235 for a new connection. By sharing previously supplied connections, across data sources with matching data source identities, the data source ID manager 130 may eliminate redundant connections. In still other embodiments, upon receiving a request for a connection, data source ID manager may determine a unique data source identity associated with the request (e.g. from a predetermined set of properties for that data source), as described above. The data source ID manager may compare the data source identity associated with the request with the identities of available data sources to determine whether a data source exists that is capable of supplying connections of the requested type. If no such data source exists, the data source ID manager may instantiate a data source associated with the abstract name to supply the necessary connection. If a data source with a matching data source ID already exists, the data source ID manager may forward the request to that data source. In another embodiment, the data source ID manager may create data source proxies for each different data source specified by an application (e.g. according to each different abstract name for data resources used in the application. For each data source referenced by the application having matching data source IDs, the data source ID

<http://patft.uspto.gov/netacgi/nph-Parser?Sect1=PT02&Sect2=HITOFF&p=1&u=%2Fmetahtml%2FPT0%2Fsearch-adv.htm&r=1&...>

11/17
7/8/2020

United States Patent: 8521875

manager may configure the data source proxies as proxies to the same true data source. In this way, redundant connections may be eliminated through eliminating redundant data sources.

FIG. 3 is a flowchart of a method using data source IDs in an application server to improve efficiency of operation, according to one embodiment. At 300, an application may issue a request for a connection to a data resource. As depicted in block 310, a unique data source identity corresponding to the request may be ascertained. For example, data source property information may be retrieved from a data source properties object. The data source ID may be based on the information or values

for a predetermined set of the data source properties for the requested data source. In decision block 320, the ascertained data source ID may be compared to data source IDs for other data sources in the application server. If a data source has already been established with a matching ID, a connection from the data source with a matching ID may be returned to the application, as shown in block 330. For example, the data source having a matching ID might have multiple connections pooled and the application server might choose any one of them to be returned. If no identity match is found at 320, a new connection may be obtained and returned to the application, as depicted at 340.

FIG. 4 illustrates a logical representation of data source configuration properties 200, according to one embodiment. In any given implementation, data source configuration information 200 may not necessarily be stored in the format illustrated. An application running on an application server may require communications with various data resources such as databases. Some of these data resources may reside on backend systems networked to the application server. The application server may include configuration information to establish successful communications with each of the data resources with which the application interacts. Data source configuration information 200 may include a plurality of data source entries 220. A data source entry may include the information needed to connect an application to a database that is managed by a database driver. Data source objects may work with a naming directory interface service in such a way that a connection may be instantiated and managed independently of the applications that use it. In this manner, connection information, such as path and port number, may be quickly changed in the properties of the data source object, without requiring code changes in the applications that use the data resource.

In some embodiments, data source configuration information 200 may be included in an object. This object may include one or more methods that receive requests for information included in data source entries 220. For example, an application or a component of an application server may need to retrieve data from a database residing on a backend system remote from the application server on which the application is running. The application server may be coupled to the backend system by a network. In order to access the required data, the application may need to establish a network connection with the database. In some cases, the application may only include an abstract designation or name for the desired database. The application may generate a request for information necessary to connect to the database. A function included in the object may use the abstract designation supplied by the application to identify and return property information from a corresponding data source entry 220. Data source entry 220A may include a number of properties used to configure a data source, such as DB Name field 221A. DB Name field 221A may store a name for the database as provided by a naming directory interface service. URL field 223A may include the URL of the database.

A URL is the address of a resource available on the Internet. The URL includes the protocol of the resource (e.g. http:// or ftp://), along with the domain name (IP address) and the hierarchical name for the resource. User Name field 225A may include a name that the database recognizes as being authorized to access and or modify

http://patft.uspto.gov/netacgi/nph-Parser?Sect1=PT02&Sect2=HITOFF&p=1&u=%2Fmetahtml%2FPT0%2Fsearch-adv.htm&r=1&...

12/17

7/8/2020

United States Patent: 8521875

data. Class Name field 227A may include specific information about the database driver associated with the database. Password field 229A may include information that the database may use to authenticate the user specified by User Name field 225A. Abstract Name field 239A may include a string of character data that serves as an alias for the database. The abstract name may allow an application programmer to easily associate the type of data stored in the database but may contain little or no information needed to instantiate a network connection with the database. Many other types and/or combinations of types of properties and/or information may be included in a data source entry 210.

Identity 210 may include a subset of the information fields of data source entry 210. Typically, data

source configuration information 200 may include multiple data source entries 210 corresponding to a

particular data resource. For example, different components of an application may access a data resource

for different reasons and may refer to that data resource by different abstract designations 239. Data

source configuration information 200 may include a data source entry 220 corresponding to each abstract

designation included in an application. A data source ID manager may be configured to identify a subset

of the information included in a data source entry 220 as the data source identity 220 for that data source

entry. In some embodiments, a configuration utility may be provided by the application server to

configure the data source properties. The configuration utility may also be used to specify the particular

set of properties that should be used to identify a particular data source.

Different sets of properties may

be specified for different types of data source, e.g. from different vendors or for different types of

backend data resource.

The data source entries 220 corresponding to a particular data resource may all include the same identity

210. In the illustrated embodiment, identity 210 may include the DB Name field 221, the URL field 223,

and the User Name field 225. In other embodiments, the identity may include a greater or lesser number

of information fields and/or other combinations of information fields included in the data source entry.

The identity may incorporate less than all of the information included in an information field of the data

source entry. The data source manager may combine and/or reorder entire information fields or portions

of information fields included in the data source entry, in order to produce the data source identity 220.

Regardless of format, the information included in the identity is sufficient to identify all data sources for

a single data resource uniquely with respect to data sources for other data resources in a networked computer system.

An application server may use proxies in conjunction with data source identities in order to eliminate the instantiation of redundant data sources. When the application server is prepared to instantiate a data

source associated with an abstract name, the data source ID manager may determine the identity of the

data source. The data source ID manager may compare the identity of the data source to be instantiated

with the identities of existing data sources. If no existing data source has a matching identity, the

application server may proceed with the instantiation of the new data source.

However, if a data source

with a matching identity does exist, the application server may instantiate a proxy for the new data source

in the naming directory space instead. The proxy for the new data source may receive connection

requests intended for the new data source and route them to the existing data source with the matching

identity. In this way the allocation of system resources to a redundant data source may be avoided.

FIG. 5 is a flow chart of a method of configuring an application server, according to one embodiment. At

500, a data source proxy may be instantiated corresponding to each data resource reference (e.g. abstract

name) used in an application. Data source identities may be determined for each abstract data source

reference in the application, as shown in block 510.

Each data source proxy may be linked to a data source with a matching identity, as illustrated at 520. For

example, multiple abstract names for data resources included in an application may refer to the same data

<http://patft.uspto.gov/netacgi/nph-Parser?Sect1=PT02&Sect2=HITOFF&p=1&u=%2Fmetahtml%2FPT0%2Fsearch-adv.htm&r=1&...>

13/17

7/8/2020

United States Patent: 8521875

resource e.g. a particular database on a backend system. A single data source may be included in the

application server to provide connections to that database. All data source proxies whose associated

abstract names correspond to the identity of the data source may be linked to that data source. The

application may then obtain a connection to the data resource using any abstract name linked to the data

source, as illustrated at block 530.

In addition to conserving resources in the application server by eliminating redundant data sources, the

association of identities with data sources may also improve the efficiency of transactions in multitier

applications, as described below.

Some application programs, particularly business applications, may require that the results of sets of data

modifying operations must be committed to permanent storage atomically, that is either together or not at

all, in order for the data to remain consistent and to maintain data integrity.

Such a set of operations may

be referred to as a transaction. An application may designate operations to be included in a transaction by

including a statement to initiate a transaction, designating an identity for the transaction, and concluding

the operations included in the transactions with a command to commit the

database operations to permanent storage.

An example of an application in which a transaction may be beneficial is a banking application in which funds are transferred from one account to another. The application may accomplish the transfer by performing a withdrawal from one account and a deposit to another account. If the withdrawal operation completes but the deposit operation does not, the first account may reflect an improper balance. Conversely, if the deposit operation completes, but the withdrawal fails, the second account may show an improper balance. In the case of such a set of interdependent operations, neither the withdrawal nor the deposit should complete unless both can complete. By including both the withdrawal and deposit operations in a transaction, the application may designate that the operations are required to complete atomically.

In some cases, a transaction may be limited in scope to operations, which modify data in only one database on a single backend system. Such operations may be referred to as local transactions and the database or backend resource manager may itself, manage such transactions using a singlephase commit protocol. In other instances, a transaction may span multiple databases, backend systems, and/or resource managers. These transactions may be referred to as distributed or global transactions. Global transactions may require transaction coordination by a transaction manager external to the backend systems involved in the transaction. The transaction manager may coordinate a global transaction using a twophase commit protocol.

FIG. 6 illustrates a networked computer system, according to one embodiment. The networked computer system may support the execution of threetier applications. A threetier application is an application that may be organized into three major parts, each of which may be distributed within a networked computer system. The three parts (tiers) may include: one or more clients 760, one or more servers 740, and one or more backend systems 770 (e.g. databases) along with their management functions 785. In the first tier, a client may be a program running on a user's computer that includes a graphical user interface, applicationspecific entry forms, and/or interactive windows for interacting with an application. An exemplary client may be a web browser that allows a user to access the Internet. In the second tier, a server may be a program such as an application server that contains the business logic for an application such as banking transactions or purchasing merchandise for the user of a client. The server may be running on one or more computers.

A plurality of client systems may connect to one or more servers as components of a network 750. An

<http://patft.uspto.gov/netacgi/nph-Parser?Sect1=PT02&Sect2=HITOFF&p=1&u=%2Fmetahtml%2FPT0%2Fsearch-adv.htm&r=1&...>

14/17

7/8/2020

United States Patent: 8521875

exemplary network of this type is the Internet. Clients may submit requests to servers. In some instances

a server 740 may be able to fulfill a request using only resources available within the server itself. In other cases, the server may need to access resources in other networked computer systems in order to fulfill the client's request. For example, server 740 may request data on the behalf of client 760 from a database 780 residing on a backend system 770. This request may require the establishment of a connection between the server 740 and a backend system 770. A connection is a set of computer system resources and parameters, which allows communications between two or more entities within the system. The third tier of a threetier application may include one or more backend systems 770. A backend system 770 may include one or more databases 780 and programs that facilitate access to the data they contain, designated resource managers 785. Databases on backend systems may be referred to as data sources. In order to perform a particular function, an application 720 may need to retrieve and/or alter data in multiple databases resident on multiple backend systems. A set of two or more related operations that must be coordinated together atomically may be referred to as a transaction. A transaction involving more than one data source may be referred to as a distributed or global transaction.

FIG. 7 is a flow chart illustrating a method for transaction management, according to one embodiment. As illustrated by block 800, after a transaction has been initiated, the data source ID manager may determine identities of data sources supplying connections to transaction participants to ensure that redundant connections are avoided for communicating with any data resource participating in the transaction. At some point, the application may request that the transaction manager commit the state of the transaction, as indicated at block 810. As shown by decision block 820, the transaction manager may determine whether more than one unique data resource is participating in the transaction by checking the number of unique connections being used. If multiple unique data resources have been enlisted, the transaction manager may use a twophase commit protocol to coordinate the transaction as indicated in block 830, whereas a onephase commit optimization may be used for a transaction communicating with a single data resource, as shown at 840. For example, in the case where an application communicates with a single data resource using a plurality of abstract names, the data source ID manager may ensure that only a single connection is enlisted in the transaction. Thus, the transaction manager may coordinate the transaction as a local transaction rather than a global transaction. This may reduce the amount of resources and time needed to execute the transaction.

FIG. 8 illustrates one embodiment of a computer system 1000 that may include an application server 1005 utilizing data source identities as described herein. Computer system 1000 may include many different components such as memory 1010, a central processing unit (CPU) or processor 1020, and an input/output (I/O) interface 1025. Interconnect 1015 is relied upon to communicate data from one component to another. For example, interconnect 1015 may be a pointtopoint

interconnect, a shared bus, a combination of point-to-point interconnects and one or more buses, and/or a bus hierarchy including a system bus, CPU bus, memory bus and I/O buses such as a peripheral component interconnect (PCI) bus.

The computer system 1000 preferably includes a memory medium on which computer programs according to various embodiments may be stored. The term "memory medium" may include an installation medium, e.g., a CDROM, or floppy disk; a computer system memory such as DRAM, SRAM, EDO DRAM, SDRAM, DDR SDRAM, Rambus RAM, etc., or a nonvolatile memory such as a magnetic media, e.g., a hard drive 1030, or optical storage. The memory medium may include other types of memory as well, or combinations thereof. In addition, the memory medium may be located in a first computer in which the programs are executed, or may be located in a second different computer, which connects to the first computer over a network. In the latter instance, the second computer provides the program instructions to the first computer for execution.

<http://patft.uspto.gov/netacgi/nph-Parser?Sect1=PT02&Sect2=HITOFF&p=1&u=%2Fnethtml%2FPT0%2Fsearch-adv.htm&r=1&...>

15/17

7/8/2020

United States Patent: 8521875

Also, the computer system 1000 may take various forms, including a personal computer system, mainframe computer system, workstation, network appliance, Internet appliance, personal digital assistant (PDA), television system or other device. In general, the term "computer system" can be broadly defined to encompass any device having a processor, which executes instructions from a memory medium. The memory medium preferably stores a software program or programs for event-triggered transaction processing as described herein. The software program(s) may be implemented in any of various ways, including procedure-based techniques, component-based techniques, and/or object-oriented techniques, among others. For example, the software program may be implemented using ActiveX controls, C++ objects, JavaBeans, Microsoft Foundation Classes (MFC), or other technologies or methodologies, as desired.

Memory 1010 may store program instructions accessed by the CPU 1020. For example, instructions and data implementing an application server 1005 may be stored in memory 1010.

Application server 1005

may include one or more applications, data sources, data source proxies, transaction managers, and/or a data source ID manager.

Computer system 1000 may further include other software and hardware components, such as an input/output (I/O) interface 1025, that may be coupled to various other components and memory 1010.

The CPU 1020 may acquire instructions and/or data through the I/O interface 1025. Through the I/O

interface 1025, the CPU 1020 may also be coupled to one or more I/O components.

As illustrated, I/O

components may include a hard disk drive 1030, a network adapter 1035, a display adapter 1040 and/or a

removable storage adapter 1045. Some components 1030 to 1045 may be coupled to the I/O interface 1025. In addition, the computer system 1000 may include one or more of a particular type of component. The computer system 1000 may include one or more components coupled to the system through a component other than the I/O interface 1025. Some computer systems may include additional and/or other components such as application software (e.g., stored in memory 1010), other CPUs, video monitors or other displays, track balls, mice, keyboards, printers, plotters, scanners, or other types of I/O devices for use with computer system 1000. Various embodiments may further include receiving, sending or storing instructions and/or data implemented in accordance with the foregoing description upon a carrier medium. Generally speaking, a carrier medium may include storage media or memory media such as magnetic or optical media, e.g., disk or CDROM, volatile or nonvolatile media such as RAM (e.g. SDRAM, DDR SDRAM, RDRAM, SRAM, etc.), ROM, etc. as well as transmission media or signals such as electrical, electromagnetic, or digital signals, conveyed via a communication medium such as network and/or a wireless link. The various methods as illustrated in the figures and described herein represent exemplary embodiments of methods. The methods may be implemented in software, hardware, or a combination thereof. The order of method may be changed, and various elements may be added, reordered, combined, omitted, modified, etc. Various modifications and changes may be made as would be obvious to a person skilled in the art having the benefit of this disclosure. It is intended that the invention embrace all such modifications and changes and, accordingly, the above description to be regarded in an illustrative rather than a restrictive sense.

* * * * *

<http://patft.uspto.gov/netacgi/nph-Parser?Sect1=PT02&Sect2=HITOFF&p=1&u=%2Fnethtml%2FPT0%2Fsearch-adv.htm&r=1&...>

16/17

7/8/2020

United States Patent: 8521875

<http://patft.uspto.gov/netacgi/nph-Parser?Sect1=PT02&Sect2=HITOFF&p=1&u=%2Fnethtml%2FPT0%2Fsearch-adv.htm&r=1&...>

17/17

Indepth analysis of a variant of Majority Voting and relation to Zermelo-Fraenkel Set Thoery With Axiom of Choice (ZFC) - Updated Draft

SrinivasanKannan(alias)Ka.Shrinivaasan(alias)Shrinivaskannan

IndependentOpenSourceDeveloper, ResearcherandConsultant

P h : 9789346927, 9003082186, 9791165980

KrishnaiResearchOpenSourceP roducts : [http : //sourceforge.net/users/ka_shrinivaasan](http://sourceforge.net/users/ka_shrinivaasan),

[https : //www.ohloh.net/accounts/ka_shrinivaasan](https://www.ohloh.net/accounts/ka_shrinivaasan)

ResearchW ebsite : <https://sites.google.com/site/kuja27/>
(ka.shrinivaasan@gmail.com, shrinivas.kannan@gmail.com, kashrinivaasan@live.com)
February 8, 2014

Abstract

As a generalization on Majority voting and pseudorandom choice, a BPNC majority voting circuit with oracle access to a choice function is presented and the choice function (which in the infinite case would be a choice function for ZFC) is defined in this article.

1

Majority voting circuit and pseudorandom choice are in BPNC

It is a known result that $BPNC_k$ is contained in BPP. Earlier a majority voting circuit with BPP

voter oracle circuit lying in $N C_1 BP P$ was explained. It was also mentioned that instead of an oracle

voter, the majority voting circuit can be formulated alternatively as a non-uniform BPNC circuit.

But pseudorandom choice was shown to be in BPP using Nisan's Pseudo random generator. Since

BPNC is contained in BPP, this probably gives a counterintuitive result that majority voting is

more efficient compared to a pseudorandom choice but both have a same bounded error derived

using $P(\text{Good})$ expression. But recently there are pseudorandom generators constructed in NC_0

with linear stretch. Thus there is a symmetry for the LHS and RHS of the $P(\text{good})$ equation with

both Pseudorandom choice with bounded error and Majority voting with bounded error lying in

BPNC class. But the caveat is that the majority voting is non-uniform. This is an improved bound

as against $N C_1 BP P$ oracle circuit for majority voting and BPP machine for pseudorandom choice.

2

Majority and Parity

By the result of Furst, Saxe and Sipser Parity is not in AC_0 . It is also proved by Hastad's switching

lemma implying Parity cannot be computed by constant depth circuits of polynomial size and

unbounded fanin. There is a simple reduction from parity to majority function where sum of bits

are computed by a 3-to-2 way addition of 3 numbers and parity (XOR) is used in the computation.

Thus parity function forms the building block of entire majority voting circuit. Since parity is not

computable in AC_0 , the majority circuit with bounded error cannot be computed in constant depth

and this justifies the BPNC bound obtained above.

13

Zermelo-Fraenkel-Axiom-of-Choice (ZFC) and its relevance to majority voting

Axiom of choice in set theory postulates that given a set X (possibly infinite) of non-empty sets, there

always exists a choice function that chooses one element from each element-set in X . Though existence of choice function for infinite case is controversial, AOC has been pushed

into Zermelo-Fraenkel

Set theory to make it ZFC set theory (ZF with AOC). Now let us consider a majority voting scenario

where the voting population is partitioned into subsets called constituencies and there exists

a choice function that chooses one representative element from each constituency. Thus set of representatives

from each constituency chosen by choice function form an electoral

collegium denoted

as EC. This EC can be modelled as a majority voting circuit with each chosen representative of EC

as an input to the majority circuit. Thus we have a voting system with two levels.

4

Definition of a choice function and circuits for choice function computation

Let m be the size of voting citizens in a constituency and

$q \ll m$ be the number of candidates.

Each of the q candidates get votes $v(i)$ for $i=1,2,3,\dots,q$.

Thus $v(1) + v(2) + v(3) + \dots + v(q) = m$

Above is a partition of voting population. The choice function C is defined as follows:

$C(m,q) = \text{index } \max I$ of the biggest valued part in the integer partition of m as defined above, where $1 < \max I < q$

By Axiom of Choice, there exists a choice function for choosing a representative from each

constituency in infinite case. But it needs to be well-defined that the above choice function always

returns a unique index of biggest part in the partition. Unfortunately partition of votes as defined

by the choice function can have multiple similar valued biggest parts (which requires a tie- breaker

criterion) and might return a set in the absence of a tiebreaker. Thus any voting system similar to

above choice function allowing a tie has an inherent limitation. A turing machine computing the

choice function for a constituency takes as input the voting population and candidates, initiates

a voting on candidates, computes a partition of the voting population into votes for individual

candidates, sorts the parts in the partition and outputs the index of the candidate with largest

vote (assuming a tiebreaker). Aggregating votes for candidates involves addition NC1 circuits for

each of the candidates where voters cast their vote by giving inputs into the NC1 circuit of the

corresponding candidate. Outputs of each of the addition circuits form a partition of the voting

population. These outputs are parts in the partition which can be sorted using a sorting network to

get the largest indexed candidate part. For voting with bounded error these addition NC1 circuits

are BPNC circuits with error and feed to a sorting network of polynomial size and logdepth (AKS

sorting circuits). Thus the choice function oracle circuit is in BPNC of polylog depth and polynomial

size.5

Circuit for majority voting with constituencies as described above

The non-uniform NC1 majority voting circuit can be modified to query a choice function oracle

described above and get the inputs(representatives) for majority gate collegium. Using BPNC

choice function described above as oracle for electoral collegium, we obtain a BP N C BP N C circuit.

It is not known if BPNC is low for itself like BPP. Thus a BPNC circuit with oracle access to a

BPNC choice function has been arrived at for the special case of majority voting with constituencies

and electoral collegium.

6

Future directions

Handwritten notes on perfect voter decidability and relation to Arrow's

Impossibility Theorem, NP-

Completeness of Democracy, Relation between hash functions and integer partitions by the author in

references below might further strengthen the above result. For instance, for above Choice function,

a hash function that unequally distributes is needed (no two keys have equally long buckets of

values hashed into them). Thus number of such hash functions indirectly give all possible voting

patterns with unique elected choice. If coalitions are also mathematically defined, more fine-grained

complexity model for practical multiparty majority voting can be obtained.

7

Acknowledgements

I dedicate this article to God.

8

Bibliography

References

[1] On Type-2 Probabilistic Quantifiers, Automata, Languages and Programming: 23rd interna-

tional colloquium, ICALP

[2] Pseudorandom generators with linear stretch in NC₀, Benny Applebaum, Yuval Ishai, Eyal

Kushilevitz, Computer science department, Technion, Israel.

[3] Various resources on Choice functions and Zermelo-Fraenkel-Axiom-of-Choice set theory

[4] TAC 2010 – Update summarization through interview algorithm - [http://www.nist.gov/tac/publications/2010/participant.papers/CM I I](http://www.nist.gov/tac/publications/2010/participant.papers/CM%20I%20IT.proceedings.pdf)

IT.proceedings.pdf

:

[5] Few Algorithms for ascertaining merit of a document and their applications - [http :](http://arxiv.org/abs/1006.4458)

[//arxiv.org/abs/1006.4458](http://arxiv.org/abs/1006.4458)

[6] Various resources on Integer Partitioning

[7] Parity not in AC₀ - Furst, Saxe and Sipser

[8] Hastad's Switching Lemma, John Hastad's PhD thesis, MIT

[9] Majority is in non-uniform NC₁, Mix Barrington

[10] Sorting networks of Ajtai-Komlos-Szemerédi [11] Integer Partitions and Hash Functions - [https : //sites.google.com/site/kuja27/IntegerP artitionAndHashF u](https://sites.google.com/site/kuja27/IntegerPartitionAndHashFunction)

0

[12] Informal notes - 3 :
on Minimum Convex Hulls of Implication Ran-
dom

Growth

Networks

and

Perfect

Voter

Decidability

-

[https](https://sites.google.com/site/kuja27/ImplicationRandomGraphConvexHullsAndPerfectVoterProblem2014-01-11.pdf?attredirects=0)

:

[//sites.google.com/site/kuja27/ImplicationRandomGraphConvexHullsAndP erf ectV](https://sites.google.com/site/kuja27/ImplicationRandomGraphConvexHullsAndPerfectVoterProblem2014-01-11.pdf?attredirects=0)

oterP roblem 2 014-

01 - 11.pdf ?attredirects = 0

[13] Informal notes - 2 :

on Minimum Convex Hulls of Implication Graphs and

Hidden Markov Model on class nodes of Concept Hypergraph - [https](https://sites.google.com/site/kuja27/NotesOnConceptHypergraphHMMAandImplicationRandomGraphConvexHulls2012-30.pdf?attredirects=0)

:

[//sites.google.com/site/kuja27/N otesOnConceptHypergraphHM M a nd I](https://sites.google.com/site/kuja27/NotesOnConceptHypergraphHMMAandImplicationRandomGraphConvexHulls2012-30.pdf?attredirects=0)

mplicationGraphConvexHulls 2 01

12 - 30.pdf ?attredirects = 0

[14] Informal

notes

-
1
:
on
Implication
Graphs,
Error
proba-
bility
of
Majority
Voting
and
P
Versus
NP
Question
http
:
//sourceforge.net/projects/acadpdr/fts/files/ImplicationGraphsP
GoodEquationAndPNotEqualTONPQ
[15] Lower Bounds for Majority Voting and Pseudorandom Choice - https
:
//sites.google.com/site/kuja27/LowerBoundsForMajorityVotingP
seudorandomChoice.pdf?attredirects
0
[16] Circuit For Computing Error Probability of Majority Voting and Pseudorandom
Choice - https :
//sites.google.com/site/kuja27/CircuitForComputingErrorProbabilityOfM
ajorityVoting.pdf?attredirect
0
[17] Interview Algorithm is in $IP=PSPACE$ - https :
//sites.google.com/site/kuja27/InterviewAlgorithmInPSPACE
0
Decidability of Existence and Construction of a Complement of a given Function
Ka. Shrinivaasan
Mathematics, Computer Science
ArXiv
2011
This article defines a complement of a function and conditions for existence of
such a complement function and presents few algorithms to construct a
complement.

Cite

Save

Feed

TAC 2010 Summarization Track - Update Summarization with Interview Algorithm

Ka. Shrinivaasan

Computer Science

TAC

2010

Existing models for ranking documents (mostly in world wide web) are prestige
based. In this article, alternative graph-theoretic schemes to objectively judge
the merit of a document independent of... Continue Reading

View PDF

Cite

Save

Feed

Few Algorithms for ascertaining merit of a document and their applications

Ka. Shrinivaasan
Computer Science
ArXiv

2010 (First Publication: 23 June 2010)

Existing models for ranking documents(mostly in world wide web) are prestige based. In this article, three algorithms to objectively judge the merit of a document are proposed-1) Citation graph... Continue Reading

#!/

##* NEURONRAIN USB-md - Wireless Network and USB Stream Data Analytics
##* This program is free software: you can redistribute it and/or modify
##* it under the terms of the GNU General Public License as published by
##* the Free Software Foundation, either version 3 of the License, or
##* (at your option) any later version.

##*

##* This program is distributed in the hope that it will be useful,
##* but WITHOUT ANY WARRANTY; without even the implied warranty of
##* MERCHANTABILITY or FITNESS FOR A PARTICULAR PURPOSE. See the
##* GNU General Public License for more details.

##*

##* You should have received a copy of the GNU General Public License
##* along with this program. If not, see <<http://www.gnu.org/licenses/>>.

##*

##-----

K.Srinivasan

#NeuronRain Documentation and Licensing: <http://neuronrain-documentation.readthedocs.io/en/latest/>

#Personal website(research): <https://sites.google.com/site/kuja27/>

##-----

##*****
*****/

1298. (THEORY and FEATURE) Program Analysis and Software analytics - USBmd
driver - motivations, network traffic analytics,
cybercrime analytics

USBmd driver is an experimental modified version of already existing USB driver
in linux.

Purpose of this modified version is for doing more sophisticated debugging of
USB endpoints and devices and as
USB packet sniffer. Technical Necessity for this was created due to prolonged
data theft, id spoofing and cybercrime that has been happening
in author's personal electronic devices for years that resulted in a Cybercrime
Police Complaint also few years ago.

There were also such incidents while developing open source code (some code
commits have description of these mysterious occurrences). There is no
comprehensive USB debugger available on linux to sift bad traffic though there
are strong evidences of such cybercrime and datatheft through other sources.
Author is inclined to believe that such recurring events of datatheft that
defies all logic can have no other intent but to cause malafide theft or loss of
private data and an act of defamation among other things.

This is also done as a technical learning exercise to analyze USB Hosts, packets
and USB's interaction,if any, with wireless devices including
mobiles, wireless LANs(radiotap) etc.,

The pattern mining of numeric dataset designed for AstroInfer can apply here also since USB bitstream can be analyzed using algorithms for numerical dataset mining. Also Discrete Fourier Transform used for analyzing data for frequencies (periodicities if any) can be used for USB data , for example USB wireless traffic.

```
new UMB driver bind - 27 Feb 2014 (for Bus id 7)
```

Following example commandlines install umb.ko module, unbind the existing option driver from bus-device id and bind the umb.ko to that bus id:

1055. Commits as on 29 July 2014

Driver has been ported and built on 3.15.5 kernel. Also a driver build script has been committed.

USBmd version 14.9.9 has been release tagged on 9 September 2014

USBmd Version 15.1.8 has been release tagged on 8 January 2015

<http://sourceforge.net/p/usb-md/code-0/HEAD/tree/Adding%20new%20vendor%20and%20product%20IDs%20to%20an%20existing%20USB%20driver%20on%20Linux.html> has steps to add new vendor-id.

1056. USB debug messages from "cat /sys/kernel/debug/usb/devices" for UMB bound
above:

```
E: Ad=06(0) Atr=02(Bulk) MxPS= 64 IvL=0ms
I:* If#= 3 Alt= 0 #EPs= 2 Cls=08(stor.) Sub=06 Prot=50 Driver=usb-storage
E: Ad=87(I) Atr=02(Bulk) MxPS= 64 IvL=0ms
E: Ad=08(0) Atr=02(Bulk) MxPS= 64 IvL=0ms
```

1057. usbmon, libpcap tcpdump and wireshark (or vusb-analyzer) debugging

```
*mount -t debugfs none_debugs /sys/kernel/debug
*modprobe usbmon
*ls /sys/kernel/debug/usb/usbmon/
```

```
0s  0u      1s  1t      1u  2s      2t  2u      3s  3t      3u  4s      4t  4u
      5s  5t      5u  6s      6t  6u      7s  7t      7u  8s      8t  8u
```

```
*cat /sys/kernel/debug/usb/usbmon/8t > usbmon.mon (any of the above usbmon debug logs)
```

```
*vusb-analyzer usbmon.mon
```

```
ef728540 3811287714 S Ci:001:00 s a3 00 0000 0001 0004 4 <
ef728540 3811287743 C Ci:001:00 0 4 = 00010000
ef728540 3811287752 S Ci:001:00 s a3 00 0000 0002 0004 4 <
ef728540 3811287763 C Ci:001:00 0 4 = 00010000
f50f6540 3811287770 S Ii:001:01 -115 2 <
f50f6540 3811287853 C Ii:001:01 -2 0
f5390540 3814543695 S Ci:001:00 s a3 00 0000 0001 0004 4 <
f5390540 3814543715 C Ci:001:00 0 4 = 00010000
f5390540 3814543756 S Ci:001:00 s a3 00 0000 0002 0004 4 <
f5390540 3814543767 C Ci:001:00 0 4 = 00010000
f50f6540 3814543805 S Ii:001:01 -115 2 <
```

```
*modprobe usbmon
*ls /dev/usbmon[1-8]
*tcpdump -i usbmon1 -w usbmon.pcap
tcpdump: listening on usbmon1, link-type USB_LINUX_MMAPPED (USB with padded Linux header), capture size 65535 bytes
^C86 packets captured
86 packets received by filter
```

```
*wireshark usbmon.pcap (loads on wireshark)
```

1058. Dynamic Debug - dev_dbg() and dev_vdbg()

USB Debugging References:

- Texas Instruments -
http://elinux.org/images/1/17/USB_Debugging_and_Profiling_Techniques.pdf

NeuronRain version 15.6.15 release tagged

1059. Commits as on 11 July 2015

```
usbmd kernel module has been ported to Linux Kernel 4.0.5
```

1060. Commits as on 26 November 2015

```
- Updated USB-md driver with a lookup of VIRGO kernel_analytics config variable exported by kernel_analytics module in umb_read() as default.
```

- New header file umb.h has been added that externs the VIRGO kernel_analytics config array variables
- Module.symvers has been imported from VIRGO kernel_analytics and clean target has been commented in build script after initial build as make clean removes Module.symvers.
- kern.log with umb_read() and umb_write() have been added with following commandlines:
 - cat /dev/umb0 - invokes umb_read() but there are kernel panics sometimes
 - cat <file> > /dev/umb0 - invokes umb_write()
 where umb0 is usb-md device name registered with /sys/bus/usb as below:
 - insmod umb.ko
 - echo -n "7-1:1.0" > /sys/bus/usb/drivers/option/unbind
 - echo -n "7-1:1.0" > /sys/bus/usb/drivers/umb/bind
- Updated build generated sources and object files have been added

 1061. Commits as on 27 November 2015

New folder usb_wwan_modified has been added that contains the USB serial, option and wireless USB modem WWAN drivers from kernel mainline instrumented with lot of printk()s so that log messages are written to kern.log. Though dev_dbg dynamic debugging can be used by writing to /sys/kernel/debug/<...>/dynamic_debug printk()s are sufficient for now. This traces through the USB connect and data transfer code:

- probe
- buffer is copied from userspace to kernelspace
- URB is allocated in kernel
- buffer is memcopied to URB
- usb send/receive bulk pipe calls
- usb_fill_bulk_urb

Almost all buffers like in and out buffers in URBs, portdata, interfacedata, serial_data, serial_port_data are printed to kern.log. This log is analyzable by AsFer machine learning code for USB debugging similar to usbmon logs.

These are initial commits only and usb-serial.c, usb_wwan.c, option.c and serial.h might be significantly altered going forward.

 1062. Commits as on 30 November 2015

Added usb.h from kernel mainline, instrumented with printk() to print transfer_buffer in usb_fill_[control/bulk/interrupt]_urb() functions. kern.log for this has been added in usb_wwan_modified/testlogs.

 1063. Commits as on 1 December 2015

- new kernel function print_buffer() has been added in usb.h that prints contents of char buffer in hex
- Above print_buffer() is invoked to print transfer_buffer in usb_wwan.c, usb-serial.c, option.c
- kern.log with print_buffer() output has been added - This dumps similar to wireshark, usbmon and other usb analyzers.

 1064. Commits as on 2 December 2015

- changed print_buffer() printk() to print a delimiter in each byte for AsFer Machine Learning code processing
- add a parser script for kern.log to print print_buffer() lines
- parsed kern.log with print_buffer() lines has been added
- Added an Apache Spark MapReduce python script to compute byte frequency in

parsed print_buffer() kern.log

879. (FEATURE) NeuronRain USBmd Debug and Malafide Traffic Analytics

As mentioned in commit notes above, USB incoming and outgoing data transfer_buffer are dumped byte-by-byte. Given this data various analytics can be performed most of which are already implemented in AsFer codebase:

- frequency of bytes
 - most frequent sequence of bytes
 - bayesian and decision tree inference
 - deep learning
 - perceptrons
 - streaming algorithms for USB data stream
- and so on.

1065. Commits as on 3 December 2015

- Apache Spark script for analyzing the USBWWAN byte stream logs has been updated with byte counts map-reduce functions from print_buffer() logs and temp DataFrame Table creation with SparkSQL.
- logs for the script have been added in usb_wwan_modified/python-src/testlogs/Spark_USBWWANLogMapReduceParser.out.3December2015
- kern.log parser shellscript has been updated

1066. AsFer commits for USBmd as on 4 December 2015

All the Streaming_<>.py Streaming Algorithm implementations in AsFer/python-src/ have been updated with:

- hashlib ripemd160 hash MD algorithm for hash functions and return hexdigest()
- USBWWAN byte stream data from USBmd print_buffer() logs in usb-md/usb_wwan_modified/testlogs/ has been added as a Data Storage and Data Source
- logs for the above have been added to asfer/python-src/testlogs/
- Streaming Abstract Generator has been updated with USB stream data iterable and parametrized for data source and storage
- Some corrections to the asfer/python-src/Streaming_<> scripts

1067. Commits as on 7 December 2015

- added Spark Mapreduce and DataFrame log for USBWWAN byte stream
 - added a parsed kern.log with only bytes from USBWWAN stream
 - Added dict() and sort() for query results and printed cardinality of the stream data set which is the size of the dict.
- An example log has been added which prints the cardinality as ~250. In contrast, LogLog and HyperLogLog counter estimations approximate the cardinality to 140 and 110 respectively

880. (FEATURE) AsFer commits for USBmd as on 11 December 2015 - USBWWAN stream data backend in MongoDB

Dependency Injection code commits for MongoDB backend - With this MongoDB is also a storage backend for AsFer algorithms similar to MySQL:

- Abstract_DBBBackend.py has been updated for both MySQL and MongoDB injections
- MongoDB configuration and backend connect/query code has been added. Backend is either populated by Robomongo or pymongo reading from the

Streaming Abstract Generator iterable framework.

- With this AsFer supports both SQL(MySQL) and NoSQL(file,hive,hbase,cassandra backends in Streaming Abstract Generator).
- log with a simple NoSQL table with StreamingData.txt and USBWWAN data has been added to testlogs/.
- MongoDB configuration has a database(asfer-database) and a collection(asfer-collection).
- MongoDB_DBBBackend @provides pymongo.collection.Collection which is @inject-ed to Abstract_DBBBackend

1068. Commits as on 10 January 2016

NeuronRain USBmd enterprise version 2016.1.10 released.

1069. Commits - 4 August 2016

- 1.New build script for drivers/usb top level folder has been added.
- 2.Copyleft notices updated
- 3.print_buffer() in usb.h has been #ifdef-ed based on a build time flag to suppress the buffer bytes dump preferentially so that kern.log is not flooded.
- 4.Flag PRINT_BUFFER has to be defined with #define somewhere within KBuild makefiles or externally.
- 5..ko files rebuilt
6. Miscellaneous code changes to suppress kbuild warnings - cast etc.,
7. PRINT_BUFFER block changed to print the bytes in single line for each buffer

1070. Commits - 13 July 2017 - usb-storage driver last sector access slab out of bounds error in 64-bit - committed for analysis
- this error was frequently witnessed in VIRGO 32-bit stability issues and panics - ISRA looks like a GCC optimization of a function invocation (Interprocedural Scalar Replacement of Aggregates)

Jul 13 15:03:36 localhost kernel: [9837.497280]
=====

Jul 13 15:03:36 localhost kernel: [9837.499787]
=====

Jul 13 15:03:36 localhost kernel: [9837.499822] BUG: KASAN: slab-out-of-bounds in last_sector_hacks.isra.1.part.2+0xc9/0x1d0 [usb_storage] at addr ffff88007cdaa758

Jul 13 15:03:36 localhost kernel: [9837.499831] Read of size 8 by task usb-storage/6243

Jul 13 15:03:36 localhost kernel: [9837.499844] CPU: 0 PID: 6243 Comm: usb-storage Tainted: G B 4.10.3 #18

Jul 13 15:03:36 localhost kernel: [9837.499849] Hardware name: Dell Inc. Inspiron 1545 /0J037P, BIOS A14 12/07/2009

Jul 13 15:03:36 localhost kernel: [9837.499851] Call Trace:

Jul 13 15:03:36 localhost kernel: [9837.499863] dump_stack+0x63/0x8b

Jul 13 15:03:36 localhost kernel: [9837.499870] kasan_object_err+0x21/0x70

Jul 13 15:03:36 localhost kernel: [9837.499877]

kasan_report.part.1+0x219/0x4f0

Jul 13 15:03:36 localhost kernel: [9837.499893] ?

last_sector_hacks.isra.1.part.2+0xc9/0x1d0 [usb_storage]

Jul 13 15:03:36 localhost kernel: [9837.499899] kasan_report+0x25/0x30

```

Jul 13 15:03:36 localhost kernel: [ 9837.499906] __asan_load8+0x5e/0x70
Jul 13 15:03:36 localhost kernel: [ 9837.499922]
last_sector_hacks.isra.1.part.2+0xc9/0x1d0 [usb_storage]
Jul 13 15:03:36 localhost kernel: [ 9837.499938]
usb_stor_invoke_transport+0x1a1/0x960 [usb_storage]
Jul 13 15:03:36 localhost kernel: [ 9837.499946] ?
migrate_swap_stop+0x2e0/0x2e0
Jul 13 15:03:36 localhost kernel: [ 9837.499963] ?
usb_stor_port_reset+0xb0/0xb0 [usb_storage]
Jul 13 15:03:36 localhost kernel: [ 9837.499973] ?
wait_for_completion_interruptible+0x1a7/0x260
Jul 13 15:03:36 localhost kernel: [ 9837.499981] ?
wait_for_completion_killable+0x2a0/0x2a0
Jul 13 15:03:36 localhost kernel: [ 9837.499989] ?
raise_softirq_irqoff+0xba/0xd0
Jul 13 15:03:36 localhost kernel: [ 9837.499995] ? wake_up_q+0x80/0x80
Jul 13 15:03:36 localhost kernel: [ 9837.500011]
usb_stor_transparent_scsi_command+0xe/0x10 [usb_storage]
Jul 13 15:03:36 localhost kernel: [ 9837.500017]
usb_stor_control_thread+0x344/0x510 [usb_storage]
Jul 13 15:03:36 localhost kernel: [ 9837.500017] ?
usb_stor_disconnect+0x120/0x120 [usb_storage]
Jul 13 15:03:36 localhost kernel: [ 9837.500017] ?
default_wake_function+0x2f/0x40
Jul 13 15:03:36 localhost kernel: [ 9837.500017] ? __wake_up_common+0x78/0xc0
Jul 13 15:03:36 localhost kernel: [ 9837.500017] kthread+0x178/0x1d0
Jul 13 15:03:36 localhost kernel: [ 9837.500017] ?
usb_stor_disconnect+0x120/0x120 [usb_storage]
Jul 13 15:03:36 localhost kernel: [ 9837.500017] ?
kthread_create_on_node+0xd0/0xd0
Jul 13 15:03:36 localhost kernel: [ 9837.500017] ret_from_fork+0x2c/0x40
Jul 13 15:03:36 localhost kernel: [ 9837.500017] Object at ffff88007cdaa668, in
cache kmalloc-192 size: 192
Jul 13 15:03:36 localhost kernel: [ 9837.500017] Allocated:
Jul 13 15:03:36 localhost kernel: [ 9837.500017] PID = 6277
Jul 13 15:03:36 localhost kernel: [ 9837.500017] save_stack_trace+0x1b/0x20
Jul 13 15:03:36 localhost kernel: [ 9837.500017] save_stack+0x46/0xd0
Jul 13 15:03:36 localhost kernel: [ 9837.500017] kasan_kmalloc+0xad/0xe0
Jul 13 15:03:36 localhost kernel: [ 9837.500017]
kmem_cache_alloc_trace+0xef/0x210
Jul 13 15:03:36 localhost kernel: [ 9837.500017] kernfs_fop_open+0x14b/0x540
Jul 13 15:03:36 localhost kernel: [ 9837.500017] do_dentry_open+0x39a/0x560
Jul 13 15:03:36 localhost kernel: [ 9837.500017] vfs_open+0x84/0xd0
Jul 13 15:03:36 localhost kernel: [ 9837.500017] path_openat+0x4ab/0x1e10
Jul 13 15:03:36 localhost kernel: [ 9837.500017] do_filp_open+0x122/0x1c0
Jul 13 15:03:36 localhost kernel: [ 9837.500017] do_sys_open+0x17c/0x2c0
Jul 13 15:03:36 localhost kernel: [ 9837.500017] compat_Sys_open+0x1b/0x20
Jul 13 15:03:36 localhost kernel: [ 9837.500017] do_fast_syscall_32+0x188/0x300
Jul 13 15:03:36 localhost kernel: [ 9837.500017]
entry_SYSENTER_compat+0x4c/0x5b
Jul 13 15:03:36 localhost kernel: [ 9837.500017] Freed:
Jul 13 15:03:36 localhost kernel: [ 9837.500017] PID = 6277
Jul 13 15:03:36 localhost kernel: [ 9837.500017] save_stack_trace+0x1b/0x20
Jul 13 15:03:36 localhost kernel: [ 9837.500017] save_stack+0x46/0xd0
Jul 13 15:03:36 localhost kernel: [ 9837.500017] kasan_slab_free+0x71/0xb0
Jul 13 15:03:36 localhost kernel: [ 9837.500017] kfree+0x9e/0x1e0
Jul 13 15:03:36 localhost kernel: [ 9837.500017] kernfs_fop_release+0x87/0xa0
Jul 13 15:03:36 localhost kernel: [ 9837.500017] __fput+0x177/0x350
Jul 13 15:03:36 localhost kernel: [ 9837.500017] __fput+0xe/0x10
Jul 13 15:03:36 localhost kernel: [ 9837.500017] task_work_run+0xa0/0xc0
Jul 13 15:03:36 localhost kernel: [ 9837.500017]
exit_to_usermode_loop+0xc5/0xd0
Jul 13 15:03:36 localhost kernel: [ 9837.500017] do_fast_syscall_32+0x2ef/0x300
Jul 13 15:03:36 localhost kernel: [ 9837.500017]

```

```

entry_SYSENTER_compat+0x4c/0x5b
Jul 13 15:03:36 localhost kernel: [ 9837.500017] Memory state around the buggy
address:
Jul 13 15:03:36 localhost kernel: [ 9837.500017] ffff88007cdaa600: fc fc fc fc
fc fc fc fc fc fc fc fc fb fb fb
Jul 13 15:03:36 localhost kernel: [ 9837.500017] ffff88007cdaa680: fb fb fb fb
fb fb fb fb fb fb fb fb fb fb fb
Jul 13 15:03:36 localhost kernel: [ 9837.500017] >ffff88007cdaa700: fb fb fb fb
fb fc fc fc fc fc fc fc fc fc fc
Jul 13 15:03:36 localhost kernel: [ 9837.500017]
^
Jul 13 15:03:36 localhost kernel: [ 9837.500017] ffff88007cdaa780: fc fc fc fc
fc fc fc fc fc fc fc fc fc fc fc
Jul 13 15:03:36 localhost kernel: [ 9837.500017] ffff88007cdaa800: fc fc fc fc
fc fc fc fc fc fc fc fc fc fc fc
Jul 13 15:03:36 localhost kernel: [ 9837.500017]
=====
Jul 13 15:03:37 localhost kernel: [ 9837.668157]
=====
Jul 13 15:03:37 localhost kernel: [ 9837.668191] BUG: KASAN: slab-out-of-bounds
in last_sector_hacks.isra.1.part.2+0xc9/0x1d0 [usb_storage] at addr
ffff88007cdaa758
Jul 13 15:03:37 localhost kernel: [ 9837.668200] Read of size 8 by task usb-
storage/6243
Jul 13 15:03:37 localhost kernel: [ 9837.668213] CPU: 1 PID: 6243 Comm: usb-
storage Tainted: G B 4.10.3 #18
Jul 13 15:03:37 localhost kernel: [ 9837.668218] Hardware name: Dell Inc.
Inspiron 1545 /0J037P, BIOS A14 12/07/2009
Jul 13 15:03:37 localhost kernel: [ 9837.668220] Call Trace:
Jul 13 15:03:37 localhost kernel: [ 9837.668233] dump_stack+0x63/0x8b
Jul 13 15:03:37 localhost kernel: [ 9837.668240] kasan_object_err+0x21/0x70
Jul 13 15:03:37 localhost kernel: [ 9837.668247]
kasan_report.part.1+0x219/0x4f0
Jul 13 15:03:37 localhost kernel: [ 9837.668263] ?
last_sector_hacks.isra.1.part.2+0xc9/0x1d0 [usb_storage]
Jul 13 15:03:37 localhost kernel: [ 9837.668269] kasan_report+0x25/0x30
Jul 13 15:03:37 localhost kernel: [ 9837.668277] __asan_load8+0x5e/0x70
Jul 13 15:03:37 localhost kernel: [ 9837.668292]
last_sector_hacks.isra.1.part.2+0xc9/0x1d0 [usb_storage]
Jul 13 15:03:37 localhost kernel: [ 9837.668308]
usb_stor_invoke_transport+0x1a1/0x960 [usb_storage]
Jul 13 15:03:37 localhost kernel: [ 9837.668316] ?
migrate_swap_stop+0x2e0/0x2e0
Jul 13 15:03:37 localhost kernel: [ 9837.668332] ?
usb_stor_port_reset+0xb0/0xb0 [usb_storage]
Jul 13 15:03:37 localhost kernel: [ 9837.668343] ?
wait_for_completion_interruptible+0x1a7/0x260
Jul 13 15:03:37 localhost kernel: [ 9837.668351] ?
wait_for_completion_killable+0x2a0/0x2a0
Jul 13 15:03:37 localhost kernel: [ 9837.668360] ?
raise_softirq_irqoff+0xba/0xd0
Jul 13 15:03:37 localhost kernel: [ 9837.668366] ? wake_up_q+0x80/0x80
Jul 13 15:03:37 localhost kernel: [ 9837.668382]
usb_stor_transparent_scsi_command+0xe/0x10 [usb_storage]
Jul 13 15:03:37 localhost kernel: [ 9837.668398]
usb_stor_control_thread+0x344/0x510 [usb_storage]
Jul 13 15:03:37 localhost kernel: [ 9837.668415] ?
usb_stor_disconnect+0x120/0x120 [usb_storage]
Jul 13 15:03:37 localhost kernel: [ 9837.668422] ?
default_wake_function+0x2f/0x40
Jul 13 15:03:37 localhost kernel: [ 9837.668430] ? __wake_up_common+0x78/0xc0
Jul 13 15:03:37 localhost kernel: [ 9837.668436] kthread+0x178/0x1d0
Jul 13 15:03:37 localhost kernel: [ 9837.668454] ?
usb_stor_disconnect+0x120/0x120 [usb_storage]

```

```

Jul 13 15:03:37 localhost kernel: [ 9837.668460] ?
kthread_create_on_node+0xd0/0xd0
Jul 13 15:03:37 localhost kernel: [ 9837.668466] ret_from_fork+0x2c/0x40
Jul 13 15:03:37 localhost kernel: [ 9837.668472] Object at ffff88007cdaa668, in
cache kmalloc-192 size: 192
Jul 13 15:03:37 localhost kernel: [ 9837.668478] Allocated:
Jul 13 15:03:37 localhost kernel: [ 9837.668483] PID = 6277
Jul 13 15:03:37 localhost kernel: [ 9837.668494] save_stack_trace+0x1b/0x20
Jul 13 15:03:37 localhost kernel: [ 9837.668500] save_stack+0x46/0xd0
Jul 13 15:03:37 localhost kernel: [ 9837.668506] kasan_kmalloc+0xad/0xe0
Jul 13 15:03:37 localhost kernel: [ 9837.668513]
kmem_cache_alloc_trace+0xef/0x210
Jul 13 15:03:37 localhost kernel: [ 9837.668520] kernfs_fop_open+0x14b/0x540
Jul 13 15:03:37 localhost kernel: [ 9837.668527] do_dentry_open+0x39a/0x560
Jul 13 15:03:37 localhost kernel: [ 9837.668532] vfs_open+0x84/0xd0
Jul 13 15:03:37 localhost kernel: [ 9837.668538] path_openat+0x4ab/0x1e10
Jul 13 15:03:37 localhost kernel: [ 9837.668544] do_filp_open+0x122/0x1c0
Jul 13 15:03:37 localhost kernel: [ 9837.668549] do_sys_open+0x17c/0x2c0
Jul 13 15:03:37 localhost kernel: [ 9837.668554] compat_Sys_open+0x1b/0x20
Jul 13 15:03:37 localhost kernel: [ 9837.668561] do_fast_syscall_32+0x188/0x300
Jul 13 15:03:37 localhost kernel: [ 9837.668568]
entry_SYSENTER_compat+0x4c/0x5b
Jul 13 15:03:37 localhost kernel: [ 9837.668570] Freed:
Jul 13 15:03:37 localhost kernel: [ 9837.668575] PID = 6277
Jul 13 15:03:37 localhost kernel: [ 9837.668583] save_stack_trace+0x1b/0x20
Jul 13 15:03:37 localhost kernel: [ 9837.668589] save_stack+0x46/0xd0
Jul 13 15:03:37 localhost kernel: [ 9837.668594] kasan_slab_free+0x71/0xb0
Jul 13 15:03:37 localhost kernel: [ 9837.668599] kfree+0x9e/0x1e0
Jul 13 15:03:37 localhost kernel: [ 9837.668605] kernfs_fop_release+0x87/0xa0
Jul 13 15:03:37 localhost kernel: [ 9837.668611] __fput+0x177/0x350
Jul 13 15:03:37 localhost kernel: [ 9837.668616] ____fput+0xe/0x10
Jul 13 15:03:37 localhost kernel: [ 9837.668623] task_work_run+0xa0/0xc0
Jul 13 15:03:37 localhost kernel: [ 9837.668629]
exit_to_usermode_loop+0xc5/0xd0
Jul 13 15:03:37 localhost kernel: [ 9837.668635] do_fast_syscall_32+0x2ef/0x300
Jul 13 15:03:37 localhost kernel: [ 9837.668642]
entry_SYSENTER_compat+0x4c/0x5b
Jul 13 15:03:37 localhost kernel: [ 9837.668644] Memory state around the buggy
address:
Jul 13 15:03:37 localhost kernel: [ 9837.668655] ffff88007cdaa600: fc fc fc fc
fc fc fc fc fc fc fc fc fb fb fb
Jul 13 15:03:37 localhost kernel: [ 9837.668664] ffff88007cdaa680: fb fb fb fb
fb fb fb fb fb fb fb fb fb fb fb
Jul 13 15:03:37 localhost kernel: [ 9837.668674] >ffff88007cdaa700: fb fb fb fb
fb fc fc fc fc fc fc fc fc fc fc
Jul 13 15:03:37 localhost kernel: [ 9837.668680]
^
Jul 13 15:03:37 localhost kernel: [ 9837.668689] ffff88007cdaa780: fc fc fc fc
fc fc fc fc fc fc fc fc fc fc fc
Jul 13 15:03:37 localhost kernel: [ 9837.668698] ffff88007cdaa800: fc fc fc fc
fc fc fc fc fc fc fc fc fc fc fc
Jul 13 15:03:37 localhost kernel: [ 9837.668704]
=====
Jul 13 15:03:37 localhost NetworkManager[745]: <info> [1499938417.1889]
address 192.168.1.100

```

```

-----
1071. Commits - 13 August 2017 - Suspicious use-after-free error flagged by
Kernel Address Sanitizer - committed for analysis
This error precedes last_sector_hacks ISRA error above in USB storage driver.
-----

```

```

Aug 13 14:53:17 localhost kernel: [ 47.797146] BUG: KASAN: use-after-free in

```

```

sr_probe+0x7e0/0xb20 at addr ffff88000009637e
Aug 13 14:53:17 localhost kernel: [ 47.797146] Read of size 1 by task
kworker/u4:1/37
Aug 13 14:53:17 localhost kernel: [ 47.797146] page:ffffea0000002580 count:0
mapcount:0 mapping: (null) index:0x0
Aug 13 14:53:17 localhost kernel: [ 47.797146] flags: 0x0()
Aug 13 14:53:17 localhost kernel: [ 47.797146] raw: 0000000000000000
0000000000000000 0000000000000000 00000000ffffffff
Aug 13 14:53:17 localhost kernel: [ 47.797146] raw: ffffefa00000025a0
ffffefa00000025a0 0000000000000000 0000000000000000
Aug 13 14:53:17 localhost kernel: [ 47.797146] page dumped because: kasan: bad
access detected
Aug 13 14:53:17 localhost kernel: [ 47.797146] CPU: 1 PID: 37 Comm:
kworker/u4:1 Tainted: G B 4.10.3 #18
Aug 13 14:53:17 localhost kernel: [ 47.797146] Hardware name: Dell Inc.
Inspiron 1545 /0J037P, BIOS A14 12/07/2009
Aug 13 14:53:17 localhost kernel: [ 47.797146] Workqueue: events_unbound
async_run_entry_fn
Aug 13 14:53:17 localhost kernel: [ 47.797146] Call Trace:
Aug 13 14:53:17 localhost kernel: [ 47.797146] dump_stack+0x63/0x8b
Aug 13 14:53:17 localhost kernel: [ 47.797146]
kasan_report.part.1+0x4bc/0x4f0
Aug 13 14:53:17 localhost kernel: [ 47.797146] ? sr_probe+0x7e0/0xb20
Aug 13 14:53:17 localhost kernel: [ 47.797146] ? scsi_mode_select+0x370/0x370
Aug 13 14:53:17 localhost kernel: [ 47.797146] kasan_report+0x25/0x30
Aug 13 14:53:17 localhost kernel: [ 47.797146] __asan_load1+0x47/0x50
Aug 13 14:53:17 localhost kernel: [ 47.797146] sr_probe+0x7e0/0xb20
Aug 13 14:53:17 localhost kernel: [ 47.797146] ?
kernfs_next_descendant_post+0x93/0xf0
Aug 13 14:53:17 localhost kernel: [ 47.797146] ? sr_block_ioctl+0xe0/0xe0
Aug 13 14:53:17 localhost kernel: [ 47.797146] ?
sysfs_do_create_link_sd.isra.2+0x7c/0xc0
Aug 13 14:53:17 localhost kernel: [ 47.797146]
driver_probe_device+0x40b/0x670
Aug 13 14:53:17 localhost kernel: [ 47.797146]
__device_attach_driver+0xd9/0x160
Aug 13 14:53:17 localhost kernel: [ 47.797146] ? __driver_attach+0x120/0x120
Aug 13 14:53:17 localhost kernel: [ 47.797146] bus_for_each_drv+0x107/0x180
Aug 13 14:53:17 localhost kernel: [ 47.797146] ? bus_rescan_devices+0x20/0x20
Aug 13 14:53:17 localhost kernel: [ 47.797146] __device_attach+0x17e/0x200
Aug 13 14:53:17 localhost kernel: [ 47.797146] ? device_bind_driver+0x80/0x80
Aug 13 14:53:17 localhost kernel: [ 47.797146] ?
kobject_uevent_env+0x1ec/0x7f0
Aug 13 14:53:17 localhost kernel: [ 47.797146] device_initial_probe+0x13/0x20
Aug 13 14:53:17 localhost kernel: [ 47.797146] bus_probe_device+0xfe/0x120
Aug 13 14:53:17 localhost kernel: [ 47.797146] device_add+0x5f1/0x9f0
Aug 13 14:53:17 localhost kernel: [ 47.797146] ?
device_private_init+0xc0/0xc0
Aug 13 14:53:17 localhost kernel: [ 47.797146] ?
scsi_dh_add_device+0xd4/0x130
Aug 13 14:53:17 localhost kernel: [ 47.797146] scsi_sysfs_add_sdev+0xd1/0x350
Aug 13 14:53:17 localhost kernel: [ 47.797146] do_scan_async+0xfd/0x230
Aug 13 14:53:17 localhost kernel: [ 47.797146] ? scsi_scan_host+0x250/0x250
Aug 13 14:53:17 localhost kernel: [ 47.797146] async_run_entry_fn+0x84/0x270
Aug 13 14:53:17 localhost kernel: [ 47.797146] ?
pwq_dec_nr_in_flight+0x8c/0x110
Aug 13 14:53:17 localhost kernel: [ 47.797146] process_one_work+0x2c6/0x7d0
Aug 13 14:53:17 localhost kernel: [ 47.797146] worker_thread+0x90/0x850
Aug 13 14:53:17 localhost kernel: [ 47.797146] kthread+0x178/0x1d0

```

- Commits 1

(*) Upgraded Spark version to 2.1.0 on Hadoop 2.7
(*) Changed to SparkContext text file instead of reading the input kernel log in python I/O
(*) Added flatMap to front of MapReduce chain of transformations for tokenizer
(*) Changed the input kernel log to 64bit 4.10.3 Kernel Address Sanitizer enabled kern.log which prints lot of debugging information on memory accesses especially for USBWWAN and USB Storage drivers.
(*) This is an alternative to traditional promiscuous USB Analyzers like WireShark to get kernel stack traces for USB and WLAN operations.
(*) Particularly useful in malware related untoward memory access and traffic analysis
(*) Unifies Kernel Address Sanitizer, USB storage/WLAN driver and Spark Cloud for analytics
(*) Logs for this have been committed to testlogs/ and python-src/testlogs

882. (FEATURE-DONE) Spark Cloud Analytics for Linux Kernel 4.10.3 64 bit with Kernel Address Sanitizer debug logging enabled - 15 August 2017

- Commits 2

(*) Added a substring match filter to RDD map/reduce transformations chain
(*) Presently hardcoded as "+0x" which extracts all kernel functions invoked from Kernel Address Sanitizer kern.log and their frequencies

Previous profiling prints following top kernel function invocations:

(u'last_sector_hacks.isra.1.part.2+0xc9/0x1d0', 159),
(u'usb_stor_disconnect+0x120/0x120', 106),
(u'save_stack+0x46/0xd0', 106),
(u'save_stack_trace+0x1b/0x20', 106),
(u'entry_SYSENTER_compat+0x4c/0x5b', 85),
(u'kthread+0x178/0x1d0', 74),

implying heavy dependence on last_sector_hacks.isra gcc optimization. Discussion on <https://groups.google.com/forum/#!topic/linux.kernel/IYBXrW7K2Vc> shows it to be an old kernel bug.

883. (FEATURE-DONE) Commits - 24 September 2017 - USB-md driver for USB and Wireless LAN analytics for 4.13.3 64-bit kernel

(*) USB-md driver in GitHub and SourceForge at present are 32-bit based on mainline 4.1.5 kernel
(*) Both USB-md and KingCobra kernel modules are subsidiaries of VIRGO kernel
(*) There is a necessity for 64-bit version of USB-md for interoperability to VIRGO64 64-bit kernel on mainline version 4.13.3
(*) This requires separate repository for USB-md because of significant kernel function changes between 4.1.5 and 4.13.3 and idiosyncrasies of 64-bit
(*) USB-md driver has been rebuilt on 4.13.3 64-bit kernel after some changes to function prototypes and new usb-md64 repository is initialized with these commits

884. USBWWAN Kernel Log Spark Analyzer Update - Refactoring to a new python function - 18 June 2018

1. Spark Log Analyzer Spark_USBWWANLogMapReduceParser.py has been changed to modularize the pattern extraction by defining a new function accepting kern.log file, pattern and filter and also creates Spark DataFrame SQL table and queries it.
2. This is similar to NeuronRain AsFer log_mapreducer()

769. (FEATURE) USBWWAN analytics - USBmon and FTrace logs analysis - 15 November 2018 - this section is an extended draft on respective topics in NeuronRain AstroInfer design -
<https://github.com/shrinivaasanka/asfer-github-code/blob/master/asfer-docs/AstroInferDesign.txt>

1. Logs Analysis for 2 standard kernel tracing facilities have been included - USBmon and FTrace. USBmon is the kernel debugfs tracing facility and FTrace is the Kernel functions tracing utility accessible from user space. (Kernel Address Sanitizer - KASAN - is only enabled in kernelspace via KBuild config and kernel build transparent to userspace)

2. USBmon traces are enabled by debugfs in /sys/kernel/debug/usb/usbmon and can be loaded in Wireshark in libpcap format or usbmon pseudodevices can be viewed in tcpdump:

```
467 ls /sys/kernel/debug/  
468 modprobe usbmon  
472 dumpcap -D  
474 ls /dev/usbmon0  
475 ls -l /dev/usbmon*  
487 tcpdump -i usbmon1  
488 tcpdump -i usbmon2  
489 tcpdump -i usbmon0  
490 tcpdump -i usbmon3  
491 tcpdump -i usbmon4
```

```
520 cat /sys/kernel/debug/usb/usbmon/1t 2>&1 > usbmon.mon
```

3. FTrace for function graph analysis are enabled by (Kernel.org FTrace Documentation: <https://www.kernel.org/doc/Documentation/trace/ftrace.txt>):

```
536 ls /sys/kernel/debug/tracing/current_tracer  
537 echo nop > /sys/kernel/debug/tracing/current_tracer  
538 echo 0 > /sys/kernel/debug/tracing/tracing_on  
539 echo $$ > /sys/kernel/debug/tracing/set_ftrace_pid  
541 echo function > /sys/kernel/debug/tracing/current_tracer  
545 echo 1 > /sys/kernel/debug/tracing/tracing_on  
557 ls -l /sys/kernel/debug/tracing/trace  
561 cat /sys/kernel/debug/tracing/set_graph_function  
562 cat /sys/kernel/debug/tracing/trace_options  
563 echo funcgraph-duration > /sys/kernel/debug/tracing/trace_options  
566 cat /sys/kernel/debug/tracing/set_graph_function  
567 cat /sys/kernel/debug/tracing/trace_options  
568 cat /sys/kernel/debug/tracing/trace_options  
569 echo funcgraph-cpu 2>&1 > /sys/kernel/debug/tracing/trace_options  
620 cat /sys/kernel/debug/tracing/set_ftrace_pid  
624 echo 7379 > /sys/kernel/debug/tracing/set_ftrace_pid  
625 cat /sys/kernel/debug/tracing/trace 2>&1 > ftrace.log.15November2018  
639 export JAVA_HOME=/media/Ubuntu2/jdk1.8.0_171/  
640 export PATH=/usr/bin:$PATH
```

```
671 /media/Ubuntu2/spark-2.3.1-bin-hadoop2.7/bin/spark-submit
```

```
Spark_USBWWANLogMapReduceParser.py 2>&1 >
```

```
testlogs/Spark_USBWWANLogMapReduceParser.FTraceAndUSBMon.log.15November2018
```

4. FTrace traces for specific userspace threads/processes are enabled by previous example commandlines and available through /sys/kernel/debug/tracing/trace (circular buffer). Function graph traces show kernel function invocations as call graph edges (denoted by fn2 <- fn1)

5. Spark_USBWWANLogMapReduceParser.py has been changed to invoke log analyzer for USBmon and FTrace logs for patterns Bi(BULK IN) and usb from USBmon and FTrace logs respectively:
- usbmon.15November2018.mon
- ftrace.ping.log.15November2018 (ftraces for ping of an IP address)
6. Logs for Spark Analyzer have been committed to Spark_USBWWANLogMapReduceParser.FTraceAndUSBMon.log.15November2018 which analyze the USBmon logs and WLAN traffic for IP address ping.

770. (THEORY and FEATURE) Program Analysis and Software Analytics - USBmd FTrace Kernel Function CallGraph Generation for Analysis - 22 November 2018 - this section is an extended draft on respective topics in NeuronRain AstroInfer design - <https://github.com/shrinivaasanka/asfer-github-code/blob/master/asfer-docs/AstroInferDesign.txt>

1. New bash shell script usb_md_ftrace.sh has been committed to repository which writes out an ftrace.log file containing kernel function call graph sequences for an executable code. It is invoked as:

\$usb_md_ftrace.sh <executable-to-trace>

usb_md_ftrace.sh summarizes previously mentioned ftrace options enabling commands into single file with an option for commandline argument of an executable to trace.

2. usb_wwan_modified/python-src/Spark_USBWWANLogMapReduceParser.py has been changed to include a new function ftrace_callgraph_dot() which parses an ftrace log generated by usb_md_ftrace.sh for command:

\$usb_md_ftrace.sh traceroute <ip-address>

3. ftrace_callgraph_dot() parses each line of ftrace.log and adds them as edges in a NetworkX Directed Graph. DOT file for this call graph is written to

Spark_USBWWANLogMapReduceParser.ftrace_callgraph.dot

4. As a novelty, PageRank and Degree Centrality measures of the call graph NetworkX DiGraph are printed which show the prominently active regions of the kernel for traceroute. PageRank/Degree Centrality of kernel function callgraph is quite useful by treating every function caller as a voter to function callee. Theoretically, this centrality in kernel throws light on suspicious, malevolent invocations particularly involving memory and locking. In this traceroute ftrace example, lock and kmalloc functions have high centrality, and USB URB related functions are way down the ranking. More the ranking, deeper the function is in callstack trace in kernel.

5. Lot of functions have ISRA optimization of GCC. ISRA is known to cause signed int bugs (0 was erroneously promoted to 1 in loops) and ISRA has been disabled in ARM kernel: <https://patchwork.kernel.org/patch/7113091/> by -fno-ipa-sra GCC flag. This kind of instability could be the reason for 32-bit VIRGO heisenbugs in string functions in older kernels.

6. Previous FTrace kernel call graph analysis is not only limited to USBmd WLAN analytics but can be applied to any executable requiring kernel profiling. Usual profilers measure time spent in the function whereas this graph theoretic analysis is superior and finds kernel bottlenecks and malicious patterns by analyzing call graphs within kernel.

7. Malicious code (e.g virus, worms, root-kits, bots, keystroke loggers) are usually associated with high cpu and memory footprint causing abnormal traffic. Analyzing infected kernel callgraph patterns might help in identifying the root cause.

8. FTrace kernel function call graph complements already implemented Program Analyzers: SATURN CFG driver in VIRGO kernels (accessible only in kernelspace) and Valgrind/KCachegrind/Callgrind userspace call graph analyzer in AsFer. By this kernel activity is partially visible and can be analyzed graph theoretically from userspace.

9. Outbreak of epidemics have been analyzed as Game Theoretic problem

(<https://blogs.cornell.edu/info2040/2016/09/16/game-theory-in-the-context-of-epidemics/>) - on how people behave in epidemics and their conclusion - "faster information limits disease spread". Cybercrimes are epidemics counterpart in cloud of computers only difference being damage inflicted on intellectual property than humans and adversaries are hackers/malicious code in place of viri. This makes Cybercrimes a multi-player adversarial game involving Hackers/Malicious code Versus Aggrieved. Translating the previous conclusion to cybercrimes: Faster information about malicious code limits the damage.

```
/
*****
*****
#-----
-----
#NEURONRAIN VIRGO - Cloud, Machine Learning and Queue augmented Linux Kernel
Fork-off
#This program is free software: you can redistribute it and/or modify
#it under the terms of the GNU General Public License as published by
#the Free Software Foundation, either version 3 of the License, or
#(at your option) any later version.
#This program is distributed in the hope that it will be useful,
#but WITHOUT ANY WARRANTY; without even the implied warranty of
#MERCHANTABILITY or FITNESS FOR A PARTICULAR PURPOSE. See the
#GNU General Public License for more details.
#You should have received a copy of the GNU General Public License
#along with this program. If not, see <http://www.gnu.org/licenses/>.
#-----
-----
#K.Srinivasan
#NeuronRain Documentation and Licensing: http://neuronrain-
documentation.readthedocs.io/en/latest/
#Personal website(research): https://sites.google.com/site/kuja27/
#-----
-----
*****
*****/
```

885. VIRGO is an operating system kernel forked off from Linux kernel mainline to add cloud functionalities (system calls, modules etc.,) within kernel itself with machine learning, analytics, debugging, queueing support in the deepest layer of OSI stack i.e AsFer, USBmd, KingCobra together with VIRGO constitute the previous functionalities. Presently there seems to be no cloud implementation with fine-grained cloud primitives (system calls, modules etc.,) included in kernel itself though there are coarse grained clustering and SunRPC implementations available. VIRGO complements other Clustering and application layer cloud Oses like cloudstack, openstack etc., in these aspects - CloudStack and OpenStack can be deployed on a VIRGO Linux Kernel Cloud - OpenStack nova compute, neutron network, cinder/swift storage subsystems can be augmented to have additional drivers that invoke lowlevel VIRGO syscall and kernel module primitives (assuming there are no coincidental replications of functionalities) thereby acting as a foundation to application layer cloud.

886. Remote Device Invocation , which is an old terminology for Internet-Of-Things has already been experimented in SunRPC and KOrbit CORBA-in-linux-kernel kernel modules in old linux kernels (<http://www.csn.ul.ie/~mark/fyp/fypfinal.html> - with Solaris MC and example Remote Device Client-Server Module implementation). VIRGO Linux with the larger encompassing NeuronRain suite is an effort to provide a unified end-to-end application-to-kernel machine-learning propelled cloud and internet-of-things framework.

887. Memory pooling:

Memory pooling is proposed to be implemented by a new `virgo_malloc()` system call that transparently allocates a block of virtual memory from memory pooled from virtual memory scattered across individual machines part of the cloud.

888. CPU pooling or cloud ability in a system call:

`Clone()` system call is linux specific and internally it invokes `sys_clone()`. All `fork()`, `vfork()` and `clone()` system calls internally invoke `do_fork()`. A new system call `virgo_clone()` is proposed to create a thread transparently on any of the available machines on the cloud. This creates a thread on a free or least-loaded machine on the cloud and returns the results.

`virgo_clone()` is a wrapper over `clone()` that looks up a map of machines-to-loadfactor and get the host with least load and invokes `clone()` on a function on that gets executed on the host. Usual cloud implementations provide userspace API that have something similar to this - `call(function, host)`. Loadfactor can be calculated through any of the prominent loadbalancing algorithm. Any example userspace code that uses `clone()` can be replaced with `virgo_clone()` and all such threads will be running in a cloud transparently. Presently Native POSIX threads library (NPTL) and older LinuxThreads thread libraries internally use `clone()`.

Kernel has support for kernel space sockets with `kernel_accept()`, `kernel_bind()`, `kernel_connect()`, `kernel_sendmsg()` and `kernel_recvmsg()` that can be used inside a kernel module. Virgo driver implements `virgo_clone()` system call that does a `kernel_connect()` to a remote kernel socket already `__sock_create()`-d, `kernel_bind()`-ed and `kernel_accept()`-ed and does `kernel_sendmsg()` of the function details and `kernel_recvmsg()` after function has been executed by `clone()` in remote machine. After `kernel_accept()` receives a connection it reads the function and parameter details. Using these `kthread_create()` is executed in the remote machine and results are written back to the originating machine. This is somewhat similar to SunRPC but adapted and made lightweight to suit `virgo_clone()` implementation without any external data representation.

Experimental Prototype

`virgo_clone()` system call and a kernel module `virgocloudexec` which implements Sun RPC interface have been implemented.

VIRGO - loadbalancer to get the host:ip of the least loaded node

889. Loadbalancer option 1 - Centralized loadbalancer registry that tracks load:

`Virgo_clone()` system call needs to lookup a registry or map of host-to-load and get the least loaded host:ip from it. This requires a load monitoring code to run periodically and update the map. If this registry is located on a single machine then simultaneous `virgo_clone()` calls from many machines on the cloud could choke the registry. Due to this, loadbalancer registry needs to run on a high-end machine. Alternatively, each machine can have its own view of the load and multiple copies of load-to-host registries can be stored in individual machines. Synchronization of the copies becomes a separate task in itself (Cache coherency). Either way gives a tradeoff between accuracy, latency and efficiency.

Many application level userspace load monitoring tools are available but as `virgo_clone()` is in kernel space, it needs to be investigated if kernel-to-kernel loadmonitoring can be done without userspace data transport. Most Cloud API explicitly invoke a function on a host. If this functionality is needed, `virgo_clone()` needs to take host:ip address as extra argument, but it reduces transparent execution.

(Design notes for LB option 1 handwritten by myself are at
: <http://sourceforge.net/p/virgo-linux/code-0/HEAD/tree/trunk/virgo-docs/MiscellaneousOpenSourceDesignAndAcademicResearchNotes.pdf>)

890. Loadbalancer option 2 - Linux Psuedorandom number generator based load balancer(experimental) instead of centralized registry that tracks load:

Each virgo_clone() client has a PRG which is queried (/dev/random or /dev/urandom) to get the id of the host to send the next virgo_clone() function to be executed

Expected number of requests per node is derived as:

expected number of requests per node =
summation(each_value_for_the_random_variable_for_number_of_requests *
probability_for_each_value) where random variable ranges from 1 to k where N is
number of processors and k is the number of requests to be distributed on N
nodes

=expected number of requests per node = $(\text{math.pow}(N, k+2) - k * \text{math.pow}(N, 2) + k * \text{math.pow}(N, 1) - 1) / (\text{math.pow}(N, k+3) - 2 * \text{math.pow}(N, k+2) + \text{math.pow}(N, k+1))$

This loadbalancer is dependent on efficacy of the PRG and since each request is uniformly, identically, independently distributed use of PRG would distribute requests evenly. This obviates the need for loadtracking and coherency of the load-to-host table.

(Design notes for LB option 2 handwritten by myself at
:http://sourceforge.net/p/virgo-linux/code-0/HEAD/tree/trunk/virgo-docs/
MiscellaneousOpenSourceDesignAndAcademicResearchNotes.pdf)

(python script in virgo-python-src/)

891. Implemented VIRGO Linux components (as on 7 March 2016)

1. cpupooling virtualization - VIRGO_clone() system call and VIRGO cpupooling driver by which a remote procedure can be invoked in kernelspace.(port: 10000)
2. memorypooling virtualization - VIRGO_malloc(), VIRGO_get(), VIRGO_set(), VIRGO_free() system calls and VIRGO memorypooling driver by which kernel memory can be allocated in remote node, written to, read and freed - A kernelspace memcache-ing.(port: 30000)
3. filesystem virtualization - VIRGO_open(), VIRGO_read(), VIRGO_write(), VIRGO_close() system calls and VIRGO cloud filesystem driver by which file IO in remote node can be done in kernelspace.(port: 50000)
4. config - VIRGO config driver for configuration symbols export.
5. queueing - VIRGO Queuing driver kernel service for queuing incoming requests, handle them with workqueue and invoke KingCobra service routines in kernelspace.(port: 60000)
6. cloudsync - kernel module for synchronization primitives (Bakery algorithm etc.,) with exported symbols that can be used in other VIRGO cloud modules for critical section lock() and unlock()
7. utils - utility driver that exports miscellaneous kernel functions that can be used across VIRGO Linux kernel
8. EventNet - eventnet kernel driver to vfs_read()/vfs_write() text files for EventNet vertex and edge messages (port: 20000)
9. Kernel_Analytics - kernel module that reads machine-learnt config key-value pairs set in /etc/virgo_kernel_analytics.conf. Any machine learning software can be used to get the key-value pairs for the config. This merges three facets - Machine Learning, Cloud Modules in VIRGO Linux-KingCobra-USBmd , Mainline Linux Kernel
10. Testcases and kern.log testlogs for the above
11. SATURN program analysis wrapper driver.

Thus VIRGO Linux at present implements a minimum cloud OS (with cloud-wide cpu, memory and file system management) over Linux and potentially fills in a gap to integrate both software and hardware into cloud with machine learning and analytics abilities that is absent in application layer cloud implementations. Thus VIRGO cloud is an IoT operating system kernel too that enables any hardware to be remote controlled. Data analytics using AsFer can be done by just invoking requisite code from a kernelspace driver above and creating an updated driver binary (or) by kernel_analytics module which reads the userland machine-learned config.

VIRGO Features (list is quite dynamic and might be rewritten depending on feasibility - longterm with no deadline)

892. (FEATURE - DONE-minimum separate config file support in client and kernel service)1. More Sophisticated VIRGO config file and read_virgo_config() has to be invoked on syscall clients virgo_clone and virgo_malloc also. Earlier config was being read by kernel module only which would work only on a single machine. A separate config module kernel service has been added for future use while exporting kernel-wide configuration related symbols. VIRGO config files have been split into /etc/virgo_client.conf and /etc/virgo_cloud.conf to delink the cloud client and kernel service config parameters reading and to do away with oft occurring symbol lookup errors and multiple definition errors for num_cloud_nodes and node_ip_addrs_in_cloud - these errors are frequent in 3.15.5 kernel than 3.7.8 kernel. Each VIRGO module and system call now reads the config file independent of others - there is a read_virgo_config<module>_<client_or_service>() function variant for each driver and system call. Though at present smacks of a replicated code, in future the config reads for each component (system call or module) might vary significantly depending on necessities. New kernel module config has been added in drivers/virgo. This is for future prospective use as a config export driver that can be looked up by any other VIRGO module for config parameters. include/linux/virgo_config.h has the declarations for all the config variables declared within each of the VIRGO kernel modules. Config variables in each driver and system call have been named with prefix and suffix to differentiate the module and/or system call it serves. In geographically distributed cloud virgo_client.conf has to be in client nodes and virgo_cloud.conf has to be in cloud nodes. For VIRGO Queue - KingCobra REQUEST-REPLY peer-to-peer messaging system same node can have virgo_client.conf and virgo_cloud.conf. Above segregation largely simplifies the build process as each module and system call is independently built without need for a symbol to be exported from other module by pre-loading it.(- from commit comments done few months ago)

893. (FEATURE - Special case implementation DONE) 2. Object Marshalling and Unmarshalling (Serialization) Features - Feature 4 is a marshalling feature too as Python world PyObjects are serialized into VIRGO linux kernel and unmarshalled back bottom-up with CPython and Boost::Python C++ invocations - CPython and Boost internally take care of serialization.

894. (FEATURE - DONE) Virgo_malloc(), virgo_set(), virgo_get() and virgo_free() syscalls that virtualize the physical memory across all cloud nodes into a single logical memory behemoth (NUMA visavis UMA). (There are random crashes in copy_to_user and copy_from_user in syscall path for VIRGO memory pooling commands that were investigated but turned out to be mystery). These crashes have either been resolved or occur less in 3.15.5 and 4.1.5 kernels.

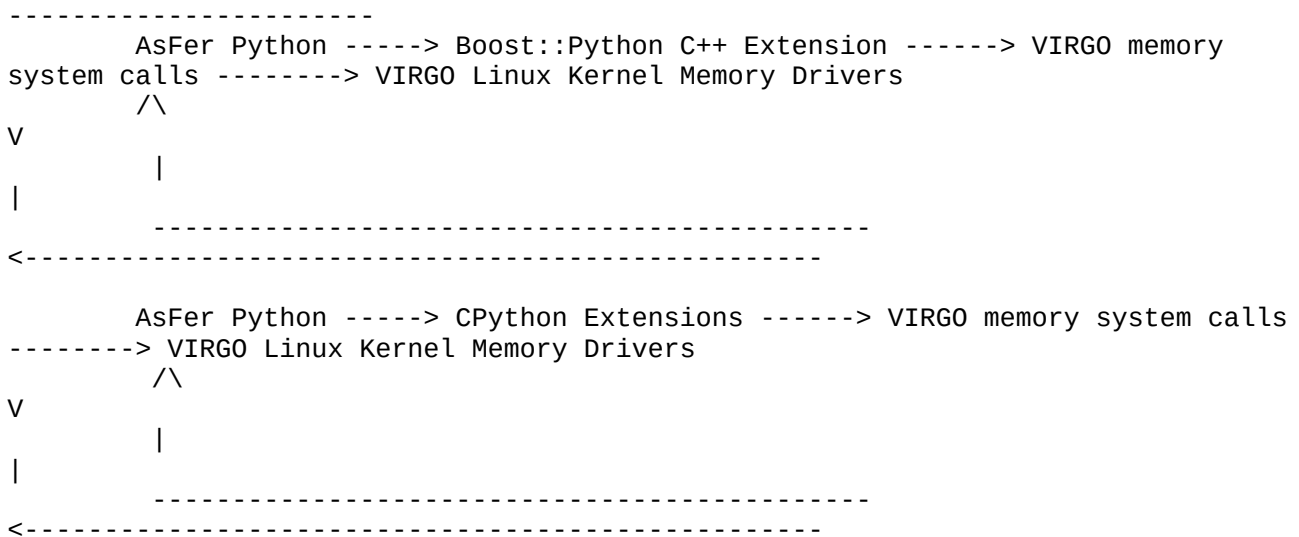
Initial Design Handwritten notes committed at: <http://sourceforge.net/p/virgo-linux/code-0/210/tree/trunk/virgo-docs/>

VIRGO_Memory_Pooling_virgomalloc_initial_design_notes.pdf

895. (FEATURE - DONE) Integrated testing of AsFer-VIRGO Linux Kernel request

roundtrip - invocation of VIRGO linux kernel system calls from AsFer Python via C++ or C extensions - Commits for this have been done on 29 January 2016. This unifies userlevel applications and kernelspace modules so that AsFer Python makes VIRGO linux kernel an extension. Following is schematic diagram and More details in commit notes below.

895.1 Schematic Diagram:



896. (FEATURE - DONE) Multithreading of VIRGO clouDEXEC kernel module (if not already done by kernel module subsystem internally)

897. (FEATURE - DONE) Sophisticated queuing and persistence of CPU and Memory pooling requests in Kernel Side (by possibly improving already existing kernel workqueues). Either open source implementations like ZeroMQ/ActiveMQ can be used or Queuing implementation has to be written from scratch or both. ActiveMQ supports REST APIs and is JMS implementation. This feature has been marked completed because recently NeuronRain AsFer backend has been updated to support KingCobra REQUEST_REPLY.queue as a datasource for Streaming Abstract Generator. By enabling use_as_kingcobra_service=1 in cpupooling and memorypooling VIRGO drivers, any incoming CPU and Memory related request can be routed to KingCobra by linux workqueue in VIRGO queue and disk persisted (/var/log/REQUEST_REPLY.queue) by KingCobra servicerequest recipient. Also Kafka Publisher/Subscriber have been implemented in NeuronRain AsFer which invoke Streaming Abstract Generator with KingCobra REQUEST_REPLY.queue as datasource to publish persisted already received CPU and Memory requests to Kafka Message Queue. Thus queuing and persistence for VIRGO CPU and Memory is in place. ZeroMQ does not have persistence and is used for NeuronRain client side Router-Dealer concurrent request servicing pattern.

898. (FEATURE - DONE-Minimum Functionality - this section is an extended draft on respective topics in NeuronRain AstroInfer design - <https://github.com/shrinivaasanka/asfer-github-code/blob/master/asfer-docs/AstroInferDesign.txt>) Integration of Asfer(AstroInfer) algorithm codes into VIRGO which would add machine learning capabilities into VIRGO - That is, VIRGO cloud subsystem which is part of a linux kernel installation "learns" and "adapts" to the processes that are executed on VIRGO. This catapults the power of the Kernel and Operating System into an artificially (rather approximately naturally) intelligent computing platform (a software "brain"). For example VIRGO can "learn" about "execution times" of processes and suitably act for future processes. PAC Learning of functions could be theoretical basis for this. Initial commits for Kernel Analytics Module which reads the /etc/virgo_kernel_analytics.conf config have been done. This config file virgo_kernel_analytics.conf having csv(s) of key-value pairs of analytics variables is set by AsFer or any other Machine Learning code. With this VIRGO Linux Kernel is endowed with abilities to dynamically evolve than being just a platform for user code. Implications are huge - for example, a config variable

"MaxNetworkBandwidth=255" set by the ML miner in userspace based on a Perceptron or Logistic Regression executed on network logs can be read by a kernel module that limits the network traffic to 255Mbps. Thus kernel is no longer a static predictable blob behemoth. With this, VIRGO is an Internet-of-Things kernel that does analytics and based on analytics variable values integrated hardware can be controlled across the cloud through remote kernel module function invocation. This facility has been made dynamic with Boost::Python C++ and CPython extensions that permit flow of objects from machine learnt AsFer kernel analytics variables to VIRGO Linux Kernel memory drivers via VIRGO system calls directly and back - Commits on 29 January 2016 - this should obviate re-reading /etc/virgo_kernel_analytics.conf and is an exemplary implementation which unifies C++/Python into C/Kernel.

Example scenario 898.1 without implementation:

- Philips Hue IoT mobile app controlled bulb - <http://www2.meethue.com/en-xx/>
- kernel_analytics module learns key-value pairs from the AsFer code and exports it VIRGO kernel wide
- A driver function with in bulb embedded device driver can be invoked through VIRGO cpupooling (invoked from remote virgo_clone() system_call) based on if-else clause of the kernel_analytics variable i.e remote_client invokes virgo_clone() with function argument "lights on" which is routed to another cloud node. The recipient cloud node "learns" from AsFer kernel_analytics that Voltage is low or Battery is low from logs and decides to switch in high beam or low beam.

Example scenario 898.2 without implementation:

- A swivel security camera driver is remotely invoked via virgo_clone() in the VIRGO cloud.
- The camera driver uses a machine learnt variable exported by kernel_analytics-and-AsFer to pan the camera by how much degrees.

Example scenario 898.3 without implementation - probably one of the best applications of NeuronRain IoT OS:

- Autonomous Driverless Automobiles - a VIRGO driver for a vehicle which learns kernel analytics variables (driving directions) set by kernel_analytics driver and AsFer Machine Learning. A naive algorithm for Driverless Car (with some added modifications over A-Star and Motion planning algorithms):
 - AsFer analytics receives obstacle distance data 360+360 degrees (vertical and horizontal) around the vehicle (e.g ultrasound sensors) which is updated in a Spark DataFrame table with high frequency (100 times per second).
 - VIRGO Linux kernel on vehicle has two special drivers for Gear-Clutch-Break-Accelerator-Fuel(GCBAF) and Steering listening on some ports.
 - AsFer analytics with high frequency computes threshold variables for applying break, clutch, gear, velocity, direction, fuel changes which are written to kernel_analytics.conf realtime based on distance data from Spark table.
 - These analytics variables are continuously read by GCBAF and Steering drivers which autopilot the vehicle.
 - Above applies to Fly-by-wire aeronautics too with appropriate changes in analytics variables computed.
 - The crucial parameter is the response time in variable computation and table updates which requires a huge computing power unless the vehicle is hooked onto a Spark cloud in motion by wireless which process the table and compute analytic variables.

E.g. Autopilot in Tesla Cars processes Petabytes of information (Smooth-as-Silk algorithm) from sensors which are fed to neural networks computed on a cloud - <https://www.teslarati.com/tesla-firmware-v8-1-17-22-26-autopilot-2-0-smooth->

`silk-update-video/`.

References for Machine Learning + Linux Kernel

898.4 KernTune -

[http://repository.uwc.ac.za/xmlui/bitstream/handle/10566/53/Yi_KernTune\(2007\).pdf?sequence=3](http://repository.uwc.ac.za/xmlui/bitstream/handle/10566/53/Yi_KernTune(2007).pdf?sequence=3)

898.5 Self-learning, Predictive Systems -

<https://icri-ci.technion.ac.il/projects/past-projects/machine-learning-for-architecture-self-learning-predictive-computer-systems/>

898.6 Linux Process Scheduling and Machine Learning -

<http://www.cs.ucr.edu/~kishore/papers/tencon.pdf>

898.7 Network Latency and Machine Learning -

https://users.soe.ucsc.edu/~slukin/rtt_paper.pdf

898.8 Machine Learning based Meta-Scheduler for Multicore processors -

[https://books.google.co.in/books?id=1GWcHmCrl0QC&pg=PA528&lpg=PA528&dq=linux+kernel+machine+learning&source=bl&ots=zfJsq_uu5q&sig=mMIUZ-](https://books.google.co.in/books?id=1GWcHmCrl0QC&pg=PA528&lpg=PA528&dq=linux+kernel+machine+learning&source=bl&ots=zfJsq_uu5q&sig=mMIUZ-oyJIwZXtYj4HntrQE8NSk&hl=en&sa=X&ved=0CCAQ6AEwATgKahUKewjs9sqF9vPIAhVBFZQKHbNtA6A)

[oyJIwZXtYj4HntrQE8NSk&hl=en&sa=X&ved=0CCAQ6AEwATgKahUKewjs9sqF9vPIAhVBFZQKHbNtA6A](https://books.google.co.in/books?id=1GWcHmCrl0QC&pg=PA528&lpg=PA528&dq=linux+kernel+machine+learning&source=bl&ots=zfJsq_uu5q&sig=mMIUZ-oyJIwZXtYj4HntrQE8NSk&hl=en&sa=X&ved=0CCAQ6AEwATgKahUKewjs9sqF9vPIAhVBFZQKHbNtA6A)

899. A Symmetric Multi Processing subsystem Scheduler that virtualizes all nodes in cloud (probably this would involve improving the loadbalancer into a scheduler with priority queues)

900. (FEATURE - ONGOING) Virgo is an effort to virtualize the cloud as a single machine - Here cloud is not limited to servers and desktops but also mobile devices that run linux variants like Android, and other Mobile OSes. In the longterm, Virgo may have to be ported or optimized for handheld devices.

Boost::Python AsFer-VIRGO system call invocations implemented in NeuronRain is framework for implementing python applications interfacing with kernel. If deployed on Mobile processors (e.g by overlaying Android Kernel with VIRGO layer) there are IDEs like QPython to develop python apps for Android.

901. (FEATURE - DONE) Memory Pooling Subsystem Driver - `Virgo_malloc()`, `Virgo_set()`, `Virgo_get()` and `Virgo_free()` system calls and their Kernel Module Implementations. In addition to syscall path, telnet or userspace socket client interface is also provided for both VIRGO CPU pooling(`virgo_clone()`) and VIRGO Memory Pooling Drivers.

902. (FEATURE - DONE) Virgo Cloud File System with `virgo_cloud_open()`, `virgo_cloud_read()` , `virgo_cloud_write()` and `virgo_cloud_close()` commands invoked through telnet path has been implemented that transcends disk storage in all nodes in the cloud. It is also fanciful feature addition that would make VIRGO a complete all-pervading cloud platform. The remote telnet clients send the file path and the buf to be read or data to be written. The Virgo File System kernel driver service creates a unique Virgo File Descriptor for each struct file* opened by `filp_open()` and is returned to client. Earlier design option to use a hashmap (`linux/hashmap.h`) looked less attractive as file descriptor is an obvious unique description for open file and also map becomes unscalable. The kernel upcall path has been implemented (`paramIsExecutable=0`) and may not be necessary in most cases and all above cloudfs commands work in kernelspace using VFS calls.

903. (FEATURE - DONE) VIRGO Cloud File System commands through syscall paths - `virgo_open()`, `virgo_close()`, `virgo_read()` and `virgo_write()`. All the syscalls have been implemented with testcases and more bugs fixed. After fullbuild and testing, `virgo_open()` and `virgo_read()` work and `copy_to_user()` is working.

904. (FEATURE - DONE) VIRGO memory pooling feature is also a distributed key-value store similar to other prominent key-store software like BigTable implementations, Dynamo, memory caching tools etc., but with a difference that VIRGO mempool is implemented as part of Linux Kernel itself thus circumventing

userspace latencies. Due to Kernel space VIRGO mempool has an added power to store and retrieve key-value pair in hardware devices directly which otherwise is difficult in userspace implementations.

905. VIRGO memory pooling can be improved with disk persistence for in-memory key-value store using `virgo_malloc()`, `virgo_set()`, `virgo_get()` and `virgo_free()` calls. Probably this might be just a set of invocations of read and write ops in disk driver or using `sysfs`. Probably this could be redundant as the VIRGO filesystem primitives have been implemented that write to a remote host's filesystem in kernelspace.

906. (FEATURE-DONE) Socket Debugging, Program Analysis and Verification features for user code that can find bugs statically. Socket `skbuff` debug utility and SATURN Program Analysis Software has been integrated into NEURONRAIN VIRGO Linux Kernel.

907. (FEATURE - DONE-Minimum Functionality) Operating System Logfile analysis using Machine Learning code in AstroInfer for finding patterns of processes execution and learn rules from the log. Kernel_Analytics VIRGO module reads `/etc/virgo_kernel_analytics.conf` config key-value pairs which are set by AsFer or other Machine Learning Software. At present an Apache Spark usecase that mines Uncomplicated Fire Wall logs in `kern.log` for most prominent source IP has been implemented in AsFer codebase :
<http://sourceforge.net/p/asfer/code/704/tree/python-src/SparkKernelLogMapReduceParser.py> . This is set as a key-value config in `/etc/virgo_kernel_analytics.conf` read and exported by `kernel_analytics` module.

908. (USERSPACE C++ usecase implemented in GRAFIT course material - <https://gitlab.com/shrinivaasanka/Grafit>) Implementations of prototypical Software Transactional Memory and LockFree Datastructures for VIRGO memory pooling.

909. Scalability features for Multicore machines - references:
(<http://halobates.de/lk09-scalability.pdf>,
<http://pdos.csail.mit.edu/papers/linux:osdi10.pdf>)

910. (USERSPACE C++ usecase implemented in GRAFIT course material - <https://gitlab.com/shrinivaasanka/Grafit>) Read-Copy-Update algorithm implementation for VIRGO memory pooling that supports multiple simultaneous versions of memory for readers - widely used in redesigned Linux Kernel.

911. (FEATURE - SATURN integration - minimum functionality DONE) Program Comprehension features as an add-on described in :
<https://sites.google.com/site/kuja27/PhDThesisProposal.pdf?attredirects=0>.
SATURN program analysis has been integrated into VIRGO linux with a stub driver.

912. (FEATURE - DONE) Bakery Algorithm implementation - `cloudsync` kernel module

913. (FEATURE - minimal EventNet Logical Clock primitive implemented in AstroInfer and this section is an extended draft on respective topics in NeuronRain AstroInfer design - <https://github.com/shrinivaasanka/asfer-github-code/blob/master/asfer-docs/AstroInferDesign.txt>) Implementation of Distributed Systems primitives for VIRGO cloud viz., Logical Clocks, Termination Detection, Snapshots, Cache Coherency subsystem etc., (as part of `cloudsync` driver module). Already a simple timestamp generation feature has been implemented for KingCobra requests with `<ipaddress>:<localmachinetimestamp>` format

914. (FEATURE - minimum functionality DONE - this section is an extended draft on respective packing/filling/tiling topics in NeuronRain AstroInfer design specific to kernel SLAB allocator - <https://github.com/shrinivaasanka/asfer-github-code/blob/master/asfer-docs/AstroInferDesign.txt>) Enhancements to `kmem` if it makes sense, because it is better to rely on `virgo_malloc()` for per machine memory management and wrap it around with a cloudwide VIRGO Unique ID based address lookup implementation of which is already in place.

Kernel Malloc syscall `kmalloc()` internally works as follows:

- `kmem_cache_t` object has pointers to 3 lists
- These 3 lists are full objects SLAB list, partial objects SLAB list and free objects SLAB list - all are lists of objects of same size and `cache_cache` is the global list of all caches created thus far.
- Any `kmalloc()` allocation searches partial objects SLAB list and allocates a memory block with `kmem_cache_alloc()` from the first SLAB available - returned to caller.
- Any `kfree()` returns an object to a free SLAB list
- Full SLABs are removed from partial SLAB list and appended to full SLAB list
- SLABs are virtual memory pages created with `kmem_cache_create`
- Each SLAB in SLABs list has blocks of similar sized objects (e.g. multiples of two). Closest matching block is returned and fragmentation is minimized (incidentally this is the knapsack and packing optimization LP problem and thus NP-complete).

KERNELSPACE:

VIRGO address translation table already implements a tree registry of vtables each of capacity 3000 that keep track of `kmalloc()` allocations across all cloud nodes. Implementation of SLAB allocator for `kmalloc()` creates a `kmem_cache(s)` of similar sized objects and `kmem_cache_alloc()` allocates from these caches. `kmalloc()` already does lot of per-machine optimizations. VIRGO vtable registry tree maintained in VIRGO memory syscall end combined with per-machine `kmalloc()` `cache_cache` already look sufficient. Instrumenting `kmem_cache_create()` with `#ifdef SLAB_CLOUD_MALLOC` flags to do RPC looks superfluous. Hence marking this action item as done. Any further optimization can be done on top of existing VIRGO address translation table struct - e.g bookkeeping flags, function pointers etc.,.

USERSPACE: `sbrk()` and `brk()` are no longer used internally in `malloc()` library routines. Instead `mmap()` has replaced it

(<http://web.eecs.utk.edu/courses/spring2012/cs360/360/notes/Malloc1/lecture.html>,

<http://web.eecs.utk.edu/courses/spring2012/cs360/360/notes/Malloc1/diff.html>).

915. (FEATURE - ONGOING) Cleanup the code and remove unnecessary comments.

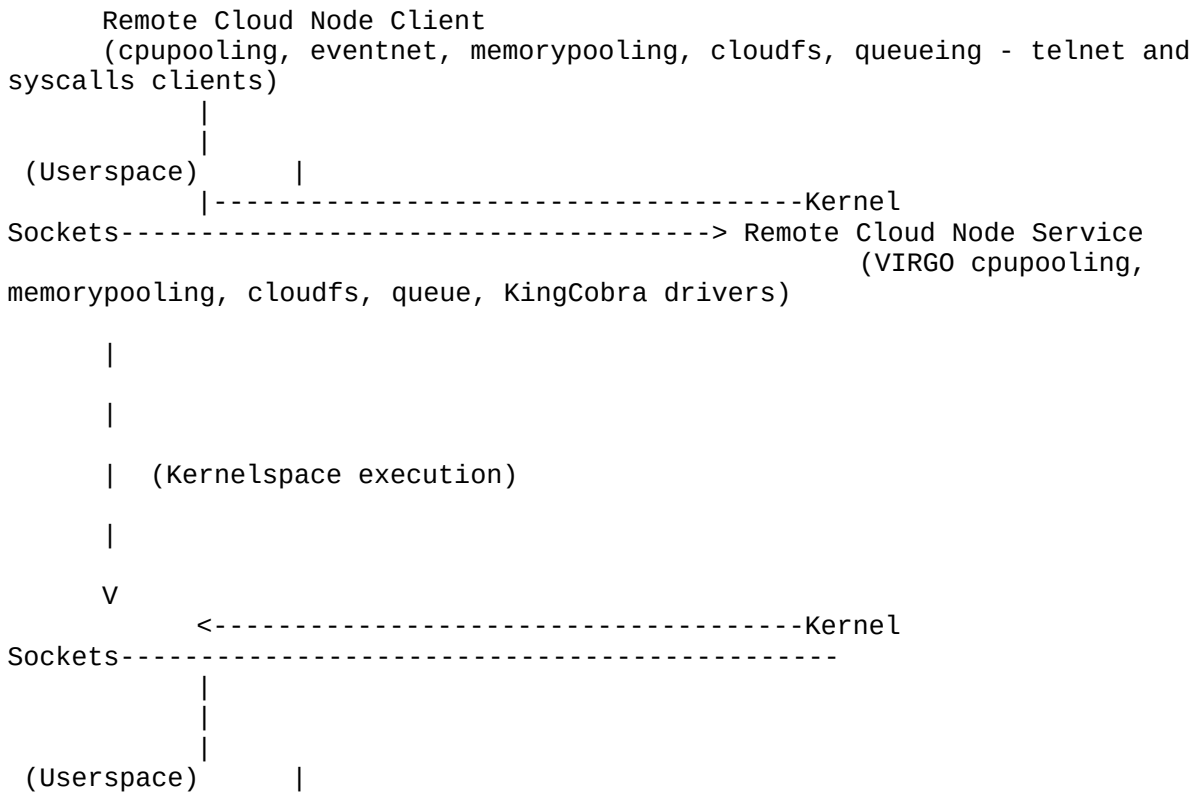
916. (FEATURE - DONE) Documentation - This design document is also a documentation for commit notes and other build and debugging technical details. Doxygen html cross-reference documentation for AsFer, USBmd, VIRGO, KingCobra and Acadpdrfts has been created along with summed-up design document and committed to GitHub Repository at https://github.com/shrinivaasanka/Krishna_iResearch_DoxygenDocs

917. (FEATURE - DONE) Telnet path to `virgo_cloud_malloc`, `virgo_cloud_set` and `virgo_cloud_get` has been tested and working. This is similar to `memcached` but stores key-value in kernelspace (and hence has the ability to write to and retrieve from any device driver memory viz., cards, handheld devices). An optional todo is to write a script or userspace socket client that connects to VIRGO mempool driver for these commands.

918. Augment the Linux kernel workqueue implementation (<http://lxr.free-electrons.com/source/kernel/workqueue.c>) with disk persistence if feasible and doesn't break other subsystems - this might require additional persistence flags in `work_struct` and additional `#ifdefs` in most of the queue functions that write and read from the disk. Related to item 6 above.

919. (FEATURE - DONE) VIRGO queue driver with native userspace queue and kernel workqueue-handler framework that is optionally used for KingCobra and is invoked through VIRGO cpupooling and memorypooling drivers. (Schematic in <http://sourceforge.net/p/kcobra/code-svn/HEAD/tree/KingCobraDesignNotes.txt> and http://sourceforge.net/p/acadpdrfts/code/ci/master/tree/Krishna_iResearch_opensourceproducts_archdiagram.pdf)

920. (FEATURE - DONE) KERNELSPACE EXECUTION ACROSS CLOUD NODES which geographically distribute userspace and kernelspace execution creating a logical abstraction for a cloudwide virtualized kernel:



921. (FEATURE - DONE) VIRGO platform as on 5 May 2014 implements a minimum set of features and kernelsocket commands required for a cloud OS kernel: CPU virtualization(virgo_clone), Memory virtualization(virgo_malloc,virgo_get,virgo_set,virgo_free) and a distributed cloud file system(virgo_open,virgo_close,virgo_read,virgo_write) on the cloud nodes and thus gives a logical view of one unified, distributed linux kernel across all cloud nodes that splits userspace and kernelspace execution across cloud as above.

922. (FEATURE - DONE) VIRGO Queue standalone kernel service has been implemented in addition to paths in schematics above. VIRGO Queue listens on hardcoded port 60000 and enqueues the incoming requests to VIRGO queue which is serviced by KingCobra:

VIRGO Queue client(e.g telnet) -----> VIRGO Queue kernel service ---> Linux Workqueue handler -----> KingCobra

923. (FEATURE - DONE) EventNet kernel module service:
VIRGO eventnet client (telnet) -----> VIRGO EventNet kernel service -----> EventNet graph text files

924. (FEATURE - DONE) Related to point 22 - Reuse EventNet cloudwide logical time infinite graph in AsFer in place of Logical clocks. At present the eventnet driver listens on port 20000 and writes the edges and vertices files in kernel using vfs_read()/vfs_write(). These text files can then be read by the AsFer code to generate DOT files and visualize the graph with graphviz.

925. (FEATURE - OPTIONAL) The kernel modules services listening on ports could return a JSON response when connected instead of plaintext, conforming to REST protocol. Additional options for protocol buffers which are becoming a standard data interchange format.

926. (FEATURE-Minimum Functionality DONE) Pointer Swizzling and Unswizzling of VIRGO addressspace pointers to/from VIRGO Unique ID (VUID). Presently VIRGO memory system calls implement a basic minimal pointer address translation to unique kmem location identifier.

CODE COMMIT RELATED NOTES

927. VIRGO code commits as on 16/05/2013

1. VIRGO clouddex driver with a listener kernel thread service has been implemented and it listens on port 10000 on system startup through /etc/modules load-on-bootup facility

2. VIRGO clouddex virgo_clone() system call has been implemented that would kernel_connect() to the VIRGO clouddex service listening at port 10000

3. VIRGO clouddex driver has been split into virgo.h (VIRGO typedefs), virgoclouddexsvc.h(VIRGO clouddex service that is invoked by module_init() of VIRGO clouddex driver) and virgo_clouddex.c (with module ops definitions)

4. VIRGO does not implement SUN RPC interface anymore and now has its own virgo ops.

5. Lot of Kbuild related commits with commented lines for future use have been done viz., to integrate VIRGO to Kbuild, KBUILD_EXTRA_SYMBOLS for cross-module symbol reference.

928. VIRGO code commits as on 20/05/2013

1. test_virgo_clone.c testcase for sys_virgo_clone() system call works and connections are established to VIRGO clouddex kernel module.

2. Makefile for test_virgo_clone.c and updated buildscript.sh for headers_install for custom-built linux.

929. VIRGO code commits as on 6/6/2013

1. Message header related bug fixes

930. VIRGO code commits as on 25/6/2013

1.telnet to kernel service was tested and found working

2.GFP_KERNEL changed to GFP_ATOMIC in VIRGO clouddex kernel service

931. VIRGO code commits as on 1/7/2013

1. Instead of printing iovec, printing buffer correctly prints the messages

2. wake_up_process() added and function received from virgo_clone() syscall is executed with kernel_thread and results returned to virgo_clone() syscall client.

932. commit as on 03/07/2013

PRG loadbalancer preliminary code implemented. More work to be done

933. commit as on 10/07/2013

Tested PRG loadbalancer read config code through telnet and virgo_clone. VFS code to read from virgo_cloud.conf commented for testing

934. commits as on 12/07/2013

PRG loadbalancer prototype has been completed and tested with test_virgo_clone and telnet and symbol export errors and PRG errors have been fixed

935. commits as on 16/07/2013

read_virgo_config() and read_virgo_clone_config()(replica of read_virgo_config()) have been implemented and tested to read the virgo_cloud.conf config parameters(at present the virgo_cloud.conf has comma separated list of ip addresses. Port is hardcoded to 10000 for uniformity across all nodes). Thus minimal cloud functionality with config file support is in place. Todo things include function pointer lookup in kernel service, more parameters to cloud config file if needed, individual configs for virgo_clone() and virgo kernel service, kernel-to-userspace upcall and execution instead of kernel space, performance tuning etc.,

936. commits as on 17/07/2013

moved read_virgo_config() to VIRGOcloudexec's module_init so that config is read at boot time and exported symbols are set beforehand.
Also commented read_virgo_clone_config() as it is redundant

937. commits as on 23/07/2013

Lack of reflection kind of facilities requires map of function_names to pointers_to_functions to be executed on cloud has to be lookedup in the map to get pointer to function. This map is not scalable if number of functions are in millions and size of the map increases linearly. Also having it in memory is both CPU and memory intensive. Moreover this map has to be synchronized in all nodes for coherency and consistency which is another intensive task. Thus name to pointer function table is at present not implemented. Suitable way to call a function by name of the function is yet to be found out and references in this topic are scarce.

If parameterIsExecutable is set to 1 the data received from virgo_clone() is not a function but name of executable
This executable is then run on usermode using call_usermodehelper() which internally takes care of queueing the workstruct and executes the binary as child of keventd and reaps silently. Thus workqueue component of kernel is indirectly made use of.
This is sometimes more flexible alternative that executes a binary itself on cloud and is preferable to clone()ing a function on cloud. Virgo_clone() syscall client or telnet needs to send the message with name of binary.

If parameterIsExecutable is set to 0 then data received from virgo_clone() is name of a function and is executed in else clause using dlsym() lookup and pthread_create() in user space. This unifies both call_usermodehelper() and creating a userspace thread with a fixed binary which is same for any function. The dlsym lookup requires mangled function names which need to be sent by virgo_clone or telnet. This is far more efficient than a function pointer table.

call_usermodehelper() Kernel upcall to usermode to exec a fixed binary that would inturn execute the cloneFunction in userspace by spawning a pthread. cloneFunction is name of the function and not binary.

This clone function will be `dlsym()`ed and a pthread will be created by the fixed binary. Name of the fixed binary is hardcoded herein as "virgo_kernelupcall_plugin". This fixed binary takes clone function as argument. For testing libvirgo.so has been created from `virgo_cloud_test.c` and separate build script to build the cloud function binaries has been added.

- Ka.Shrinivaasan (alias) Shrinivas Kannan (alias) Srinivasan Kannan (<https://sites.google.com/site/kuja27>)

938. commits as on 24/07/2013

test_virgo_clone unit test case updated with mangled function name to be sent to remote cloud node. Tested with test_virgo_clone end-to-end and all features are working. But sometimes kernel_connect hangs randomly (this was observed only today and looks similar to blocking vs non-blocking problem. Origin unknown).

- Ka.Shrinivaasan (alias) Shrinivas Kannan (alias) Srinivasan Kannan (<https://sites.google.com/site/kuja27>)

939. commits as on 29/07/2013

Added kernel mode execution in the clone_func and created a sample kernel_thread for a cloud function. Some File IO logging added to upcall binaries and parameterIsExecutable has been moved to virgo.h

940. commits as on 30/07/2013

New usecase virgo_cloud_test_kernelspace.ko kernel module has been added. This exports a function virgo_cloud_test_kernelspace() and is accessed by virgo_cloudeexec kernel service to spawn a kernel thread that is executed in kernel addressspace. This Kernel mode execution on cloud adds a unique ability to VIRGO cloud platform to seamlessly integrate hardware devices on to cloud and transparently send commands to them from a remote cloud node through virgo_clone().

Thus above feature adds power to VIRGO cloud to make it act as a single "logical device driver" though devices are in geographically in a remote server.

941. commits as on 01/08/2013 and 02/08/2013

Added Bash shell commandline with -c option for call_usermodehelper upcall clauses to pass in remote virgo_clone command message as arguments to it. Also tried output redirection but it works some times that too with a fatal kernel panic.

Ideal solutions are :

1. either to do a copy_from_user() for message buffer from user address space (or)
2. somehow rebuild the kernel with fd_install() pointing stdout to a VFS file* struct. In older kernels like 2.6.x, there is an fd_install code with in kmod.c (___call_usermodehelper()) which has been redesigned in kernel 3.x versions and fd_install has been removed in kmod.c .
3. Create a Netlink socket listener in userspace and send message up from kernel Netlink socket.

All the above are quite intensive and time consuming to implement. Moreover doing FileIO in usermode helper is strongly discouraged in kernel docs

Since Objective of VIRGO is to virtualize the cloud as single execution

"machine", doing an upcall (which would run with root abilities) is redundant often and kernel mode execution is sufficient. Kernel mode execution with intermodule function invocation can literally take over the entire board in remote machine (since it can access PCI bus, RAM and all other device cards)

As a longterm design goal, VIRGO can be implemented as a separate protocol itself and sk_buff packet payload from remote machine can be parsed by kernel service and kernel_thread can be created for the message.

942. commits as on 05/08/2013:

Major commits done for kernel upcall usermode output logging with fd_install redirection to a VFS file. With this it has become easy for user space to communicate runtime data to Kernel space. Also a new strip_control_M() function has been added to strip \r\n or " ".

943. 11 August 2013:

Open Source Design and Academic Research Notes uploaded to http://sourceforge.net/projects/acadp drafts/files/MiscellaneousOpenSourceDesignAndAcademicResearchNotes_2013-08-11.pdf/download

944. commits as on 23 August 2013

New Multithreading Feature added for VIRGO Kernel Service - action item 5 in ToDo list above (virgo_clouddriver module). All dependent headers changed for kernel threadlocalizing global data.

945. commits as on 1 September 2013

GNU Copyright license and Product Owner Profile (for identity of license issuer) have been committed. Also Virgo Memory Pooling - virgo_malloc() related initial design notes (handwritten scanned) have been committed(http://sourceforge.net/p/virgo-linux/code-0/HEAD/tree/trunk/virgo-docs/VIRGO_Memory_Pooling_virgomalloc_initial_design_notes.pdf)

946. commits as on 14 September 2013

Updated virgo malloc design handwritten notes on kmalloc() and malloc() usage in kernelspace and userspace execution mode of virgo_clouddriver service (http://sourceforge.net/p/virgo-linux/code-0/HEAD/tree/trunk/virgo-docs/VIRGO_Memory_Pooling_virgomalloc_design_notes_2_14September2013.pdf). As described in handwritten notes, virgo_malloc() and related system calls might be needed when a large scale allocation of kernel memory is needed when in kernel space execution mode and large scale userspace memory when in user modes (function and executable modes). Thus a cloud memory pool both in user and kernel space is possible.

947. VIRGO virtual addressing

VIRGO virtual address is defined with the following datatype:

```
struct virgo_address
{
    int node_id;
    void* addr;
};
```

VIRGO address translation table is defined with following datatype:

```

struct virgo_addr_transtable
{
    int node_id;
    void* addr;
};

```

----- 948. VIRGO memory pooling prototypical implementation -----

VIRGO memory pooling implementation as per the design notes committed as above is to be implemented as a prototype under separate directory under drivers/virgo/memorypooling and \$LINUX_SRC_ROOT/virgo_malloc. But the underlying code is more or less similar to drivers/virgo/cpupooling and \$LINUX_SRC_ROOT/virgo_clone.

virgo_malloc() and related syscalls and virgo mempool driver connect to and listen on port different from cpupooling driver. Though all these code can be within cpupooling itself, mempooling is implemented as separate driver and co-exists with cpupooling on bootup (/etc/modules). This enables clear demarcation of functionalities for CPU and Memory virtualization.

949. Commits as on 17 September 2013 -----

Initial untested prototype code - virgo_malloc and virgo mempool driver - for VIRGO Memory Pooling has been committed - copied and modified from virgo_clone client and kernel driver service.

950. Commits as on 19 September 2013 -----

3.7.8 Kernel full build done and compilation errors in VIRGO malloc and mempool driver code and more functions code added

951. Commits as on 23 September 2013 -----

Updated virgo_malloc.c with two functions, int_to_str() and addr_to_str(), using kmalloc() with full kernel re-build.
(Rather a re-re-build because some source file updates in previous build got deleted somehow mysteriously. This could be related to Cybercrime issues mentioned in https://sourceforge.net/p/usb-md/code-0/HEAD/tree/USBmd_notes.txt)

952. Commits as on 24 September 2013 -----

Updated syscall*.tbl files, staging.sh, Makefiles for virgo_malloc(), virgo_set(), virgo_get() and virgo_free() memory pooling syscalls. New testcase test_virgo_malloc for virgo_malloc(), virgo_set(), virgo_get(), virgo_free() has been added to repository. This testcase might have to be updated if return type and args to virgo_malloc+ syscalls are to be changed.

953. Commits as on 25 September 2013 -----

All build related errors fixed after kernel rebuild some changes made to function names to reflect their names specific to memory pooling. Updated /etc/modules also has been committed to repository.

954. Commits as on 26 September 2013 -----

Circular dependency error in standalone build of cpu pooling and memory pooling drivers fixed and datatypes and declarations for CPU pooling and Memory Pooling drivers have been segregated into respective header files (virgo.h and virgo_mempool.h with corresponding service header files) to avoid any dependency error.

955. Commits as on 27 September 2013

Major commits for Memory Pooling Driver listen port change and parsing VIRGO memory pooling commands have been done.

956. Commits as on 30 September 2013

New parser functions added for parameter parsing and initial testing on virgo_malloc() works with telnet client with logs in test_logs/

957. Commits as on 1 October 2013

Removed strcpy in virgo_malloc as ongoing bugfix for buffer truncation in syscall path.

958. Commits as on 7 October 2013

Fixed the buffer truncation error from virgo_malloc syscall to mempool driver service which was caused by sizeof() for a char*. BUF_SIZE is now used for size in both syscall client and mempool kernel service.

959. Commits as on 9 October 2013 and 10 October 2013

Mempool driver kernelspace virgo mempool ops have been rewritten due to lack of facilities to return a value from kernel thread function. Since mempool service already spawns a kthread, this seems to be sufficient. Also the iov.iov_len in virgo_malloc has been changed from BUF_SIZE to strlen(buf) since BUF_SIZE causes the kernel socket to block as it waits for more data to be sent.

960. Commits as on 11 October 2013

sscanf format error for virgo_cloud_malloc() return pointer address and sock_release() null pointer exception has been rectified. Added str_to_addr() utility function.

961. Commits as on 14 October 2013 and 15 October 2013

Updated todo list.

Rewritten virgo_cloud_malloc() syscall with:

- mutexed virgo_cloud_malloc() loop
- redefined virgo address translation table in virgo_mempool.h
- str_to_addr(): removed (void**) cast due to null sscanf though it should have worked

962. Commits as on 18 October 2013

Continued debugging of null sscanf - added str_to_addr2() which uses simple_strtoll() kernel function for scanning pointer as long long from string and casting it to void*. Also more %p qualifiers where added in str_to_addr() for debugging.

Based on latest test_virgo_malloc run, simple_strtoll() correctly parses the address string into a long long base 16 and then is reinterpret_cast to void*. Logs in test/

963. Commits as on 21 October 2013

Kern.log for testing after vtranstable addr fix with simple_strtoll() added to repository and still the other %p qualifiers do not work and only simple_strtoll() parses the address correctly.

964. Commits as on 24 October 2013

Lot of bugfixes made to virgo_malloc.c for scanning address into VIRGO transtable and size computation. Testcase test_virgo_malloc.c has also been modified to do reinterpret cast of long long into (struct virgo_address*) and corresponding test logs have been added to repository under virgo_malloc/test.

Though the above sys_virgo_malloc() works, the return value is a kernel pointer if the virgo_malloc executes in the Kernel mode which is more likely than User mode (call_usermodehelper which is circuitous). Moreover copy_from_user() or copy_to_user() may not be directly useful here as this is an address allocation routine. The long long reinterpret cast obfuscates the virgo_address(User or Kernel) as a large integer which is a unique id for the allocated memory on cloud. Initial testing of sys_virgo_set() causes a Kernel Panic as usual probably due to direct access of struct virgo_address*. Alternatives are to use only long long for allocation unique-id everywhere or do copy_to_user() or copy_from_user() of the address on a user supplied buffer. Also vtranstable can be made into a bucketed hash table that maps each alloc_id to a chained virgo malloc chunks than the present sequential addressing which is more similar to open addressing.

965. Commits as on 25 October 2013

virgo_malloc.c has been rewritten by adding a userspace __user pointer to virgo_get() and virgo_set() syscalls which are internally copied with copy_from_user() and copy_to_user() kernel function to get and set userspace from kernelspace. Header file syscalls.h has been updated with changed syscalls prototypes. Two functions have been added to map a VIRGO address to a unique virgo identifier and viceversa for abstracting hardware addresses from userspace as mentioned in previous commit notes. VIRGO cloud mempool kernelspace driver has been updated to use virgo_mempool_args* instead of void* and VIRGO clouddex mempool driver has been updated accordingly during intermodule invocation. The virgo_malloc syscall client has been updated to modified signatures and return types for all mempool alloc, get, set, free syscalls.

966. Commits as on 29 October 2013

Miscellaneous ongoing bugfixes for virgo_set() syscall error in copy_from_user().

967. Commits as on 2 November 2013

Due to an issue which corrupts the kernel memory, presently telnet path to VIRGO mempool driver has been tested after commits on 31 October 2013 and 1 November 2013 and is working but again there is an issue in kstrtoul() that returns the wrong address in virgo_cloud_mempool_kernelspace.ko that gives the address for data to set.

968. Commits as on 6 November 2013

New parser function virgo_parse_integer() has been added to virgo_cloud_mempool_kernelspace driver module which is carried over from lib/kstrtoux.c and modified locally to add an if clause to discard quotes and unquotes. With this the telnet path commands for virgo_malloc() and virgo_set() are working. Today's kern.log has been added to repository in test_logs/.

969. Commits as on 7 November 2013

In addition to virgo_malloc and virgo_set, virgo_get is also working through telnet path after today's commit for "virgodata:" prefix in virgo_cloud_mempool_kernelspace.ko. This prefix is needed to differentiate data

and address so that toAddressString() can be invoked to sprintf() the address in virgo_clouddexec_mempool.ko. Also mempool command parser has been updated to strcmp() virgo_cloud_get command also.

970. Commits as on 11 November 2013

More testing done on telnet path for virgo_malloc, virgo_set and virgo_get commands which work correctly. But there seem to be unrelated kmem_cache_trace_alloc panics that follow each successful virgo command execution. kern.log for this has been added to repository.

971. Commits as on 22 November 2013

More testing done on telnet path for virgo_malloc, virgo_set and virgo_set after commenting kernel socket shutdown code in the VIRGO clouddexec mempool sendto code. Kernel panics do not occur after commenting kernel socket shutdown.

972. Commits as on 2 December 2013

Lots of testing were done on telnet path and syscall path connection to VIRGO mempool driver and screenshots for working telnet path (virgo_malloc, virgo_set and virgo_get) have been committed to repository. Intriguingly, the syscall path is suddenly witnessing series of broken pipe errors, blocking errors etc., which are mostly Heisenbugs.

973. Commits as on 5 December 2013

More testing on system call path done for virgo_malloc(), virgo_set() and virgo_get() system calls with test_virgo_malloc.c. All three syscalls work in syscall path after lot of bugfixes. Kern.log that has logs for allocating memory in remote cloud node with virgo_malloc, sets data "test_virgo_malloc_data" with virgo_set and retrieves data with virgo_get.

VIRGO version 12.0 tagged.

974. Commits as on 12 March 2014

Initial VIRGO queueing driver implemented that flips between two internal queues: 1) a native queue implemented locally and 2) wrapper around linux kernel's workqueue facility 3) push_request() modified to pass on the request data to the workqueue handler using container_of on a wrapper structure virgo_workqueue_request.

975. Commits as on 20 March 2014

- VIRGO queue with additional boolean flags for its use as KingCobra queue
- KingCobra kernel space driver that is invoked by the VIRGO workqueue handler

976. Commits as on 30 March 2014

- VIRGO mempool driver has been augmented with use_as_kingcobra_service flags in CPU pooling and Memory pooling drivers

977. Commits as on 6 April 2014

- VIRGO mempool driver recvfrom() function's if clause for KingCobra has been updated for REQUEST header formatting mentioned in KingCobra design notes

978. Commits as on 7 April 2014

- generate_logical_timestamp() function has been implemented in VIRGO mempool driver that generates timestamps based on 3 boolean flags. At present

machine_timestamp is generated and prepended to the request to be pushed to VIRGO queue driver and then serviced by KingCobra.

979. Commits as on 25 April 2014

- client ip address in VIRGO mempool recvfrom KingCobra if clause is converted to host byte order from network byte order with ntohs()

980. Commits as on 5 May 2014

- Telnet path commands for VIRGO cloud file system - virgo_cloud_open(), virgo_cloud_read(), virgo_cloud_write(), virgo_cloud_close() has been implemented and test logs have been added to repository (drivers/virgo/cloudfs/ and cloudfs/testlogs) and kernel upcall path for paramIsExecutable=0

981. Commits as on 7 May 2014

- Bugfixes to tokenization in kernel upcall plugin with strsep() for args passed on to the userspace

982. Commits as on 8 May 2014

- Bugfixes to virgo_cloud_fs.c for kernel upcall (parameterIsExecutable=0) and with these the kernel to userspace upcall and writing to a file in userspace (virgofstest.txt) works. Logs and screenshots for this are added to repository in test_logs/

983. Commits as on 6 June 2014

- VIRGO File System Calls Path implementation has been committed. Lots of Linux Full Build compilation errors fixed and new integer parsing functionality added (similar to driver modules). For the timebeing all syscalls invoke loadbalancer. This may be further optimized with a sticky flag to remember the first invocation which might be usually virgo_open syscall to get the VFS descriptor that is used in subsequent syscalls.

984. Commits as on 3 July 2014

- More testing and bugfixes for VIRGO File System syscalls have been done. virgo_write() causes kernel panic.

985. 7 July 2014 - virgo_write() kernel panic notes:

warning within <http://lxr.free-electrons.com/source/arch/x86/kernel/smp.c#L121>:

```
static void native_smp_send_reschedule(int cpu)
{
    if (unlikely(cpu_is_offline(cpu))) {
        WARN_ON(1);
        return;
    }
    apic->send_IPI_mask(cpumask_of(cpu), RESCHEDULE_VECTOR);
}
```

This is probably a fixed kernel bug in <3.7.8 but recurring in 3.7.8:

- <http://lkml.iu.edu/hypermail/linux/kernel/1205.3/00653.html>
- http://www.kernelhub.org/?p=3&msg=74473&body_id=72338
- <http://lists.openwall.net/linux-kernel/2012/09/07/22>
- https://bugzilla.kernel.org/show_bug.cgi?id=54331
- <https://bbs.archlinux.org/viewtopic.php?id=156276>

986. Commits as on 29 July 2014

All VIRGO drivers(cloudfs, queuing, cpupooling and memorypooling) have been built on 3.15.5 kernel with some Makefile changes for ccflags and paths

Commits as on 17 August 2014

987. (FEATURE - DONE) VIRGO Kernel Modules and System Calls major rewrite for 3.15.5 kernel - 17 August 2014

1. VIRGO config files have been split into /etc/virgo_client.conf and /etc/virgo_cloud.conf to delink the cloud client and kernel service config parameters reading and to do away with oft occurring symbol lookup errors and multiple definition errors for num_cloud_nodes and node_ip_addrs_in_cloud - these errors are frequent in 3.15.5 kernel than 3.7.8 kernel.

2. Each VIRGO module and system call now reads the config file independent of others - there is a read_virgo_config_<module>_<client_or_service>() function variant for each driver and system call. Though at present smacks of a replicated code, in future the config reads for each component (system call or module) might vary significantly depending on necessities.

3. New kernel module config has been added in drivers/virgo. This is for future prospective use as a config export driver that can be looked up by any other VIRGO module for config parameters.

4. include/linux/virgo_config.h has the declarations for all the config variables declared within each of the VIRGO kernel modules.

5. Config variables in each driver and system call have been named with prefix and suffix to differentiate the module and/or system call it serves.

6. In geographically distributed cloud virgo_client.conf has to be in client nodes and virgo_cloud.conf has to be in cloud nodes. For VIRGO Queue - KingCobra REQUEST-REPLY peer-to-peer messaging system same node can have virgo_client.conf and virgo_cloud.conf.

7. Above segregation largely simplifies the build process as each module and system call is independently built without need for a symbol to be exported from other module by pre-loading it.

8. VIRGO File system driver and system calls have been tested with above changes and the virgo_open(),virgo_read() and virgo_write() calls work with much less crashes and freeze problems compared to 3.7.8 (some crashes in VIRGO FS syscalls in 3.7.8 where already reported kernel bugs which seem to have been fixed in 3.15.5). Today's kern.log test logs have been committed to repository.

988. Committed as on 23 August 2014

Commenting use_as_kingcobra_service if clauses temporarily as disabling also doesnot work and only commenting the block works for VIRGO syscall path. Quite weird as to how this relates to the problem. As this is a heisenbug further testing is difficult and sufficient testing has been done with logs committed to repository. Probably a runtime symbol lookup for kingcobra causes the freeze.

For forwarding messages to KingCobra and VIRGO queues, cpupooling driver is sufficient which also has the use_as_kingcobra_service clause.

989. Committed as on 23 August 2014 and 24 August 2014

As cpupooling driver has the same crash problem with kernel_accept() when KingCobra has been enabled, KingCobra clauses have been commented in both cpupooling and mempooling drivers. Instead queueing driver has been updated with a kernel service infrastructure to accept connections at port 60000. With this following paths are available for KingCobra requests:

VIRGO cpupooling or mempooling =====> VIRGO Queue =====> KingCobra
(or)
VIRGO Queue kernel service =====> KingCobra

990. Committed as on 26 August 2014

- - all kmallocs have been made into GFP_ATOMIC instead of GFP_KERNEL
- moved some kingcobra related header code before kernel_recvmsg()
- some header file changes for set_fs()

This code has been tested with modified code for KingCobra and the standalone kernel service that accepts requests from telnet directly at port 60000, pushes to virgo_queue and is handled to invoke KingCobra servicerequest kernelspace function, works (the kernel_recvmsg() crash was most probably due to Read-Only filesystem -errno printed is -30)

VIRGO version 14.9.9 has been release tagged on 9 September 2014

991. Committed as on 26 November 2014

New kernel module cloudsync has been added to repository under drivers/virgo that can be used for synchronization(lock() and unlock()) necessities in VIRGO cloud. Presently Bakery Algorithm has been implemented.

992. Committed as on 27 November 2014

virgo_bakery.h bakery_lock() has been modified to take 2 parameters - thread_id and number of for loops (1 or 2)

993. Committed as on 2 December 2014

VIRGO bakery algorithm implementation has been rewritten with some bugfixes. Sometimes there are soft lockup errors due to looping in kernel time durations for which are kernel build configurable.

994. Committed as on 17 December 2014

Initial code commits for VIRGO EventNet kernel module service:

1.EventNet Kernel Service listens on port 20000

2.It receives eventnet log messages from VIRGO cloud nodes and writes the log messages after parsing into two text files /var/log/eventnet/EventNetEdges.txt and /var/log/eventnet/EventNetVertices.txt by VFS calls

3.These text files can then be processed by the EventNet implementations in

AsFer (python pygraph and
C++ boost::graph based)

4.Two new directories virgo/utils and virgo/eventnet have been added.

5.virgo/eventnet has the new VIRGO EventNet kernel module service implementation that listens on port 20000.

6.virgo/utils is the new generic utilities driver that has a virgo_eventnet_log() exported function which connects to EventNet kernel service and sends the vertex and edge eventnet log messages which are parsed by kernel service and written to the two text files above.

7.EventNet log messages have two formats:

- Edge message - "eventnet_edgmsg#<id>#<from_event>#<to_event>"
- Vertex message - "eventnet_vertextmsg#<id>-<partakers csv>-<partaker conversations csv>"

8.The utilities driver Module.symvers have to be copied to any driver which are then merged with the symbol files of the corresponding driver. Target clean has to be commented while building the unified Module.symvers because it erases symvers carried over earlier.

9.virgo/utils driver can be populated with all necessary utility exported functions that might be needed in other VIRGO drivers.

10.Calls to virgo_eventnet_log() have to be #ifdef guarded as this is quite network intensive.

995. Commits as on 18 December 2014

Miscellaneous bugfixes, logs and screenshot

- virgo_clouddexec_eventnet.c - eventnet messages parser errors and eventnet_func bugs fixed
- virgo_cloud_eventnet_kernelspace.c - filp_open() args updated due to vfs_write() kernel panics. The vertexmessage vfs_write is done after looping through the vertice textfile and appending the conversation to the existing vertex.Some more code has to be added.
- VIRGO EventNet build script updated for copying Module.symvers from utils driver for merging with eventnet Module.symvers during Kbuild
- Other build generated sources and kernel objects
- new testlogs directory with screenshot for edgmsg sent to EventNet kernel service and kern.log with previous history for vfs_write() panics due to permissions and the logs for working filp_open() fixed version
- vertex message update

996. Commits as on 2,3,4 January 2015

- fixes for virgo eventnet vertex and edge message text file vfs_write() errors
- kern.logs and screenshots

VIRGO version 15.1.8 release tagged on 8 January 2015

772. (FEATURE) Commits as on 3 March 2015 - Initial commits for Kernel Analytics Module which reads the /etc/virgo_kernel_analytics.conf config (and) VIRGO memorypooling Key-Value Store Architecture Diagram - - this section is an extended draft on respective topics in NeuronRain AstroInfer design - <https://github.com/shrinivaasanka/asfer-github-code/blob/master/asfer-docs/AstroInferDesign.txt>

- Architecture of Key-Value Store in memorypooling (virgo_malloc,virgo_get,virgo_set,virgo_free) has been uploaded as a diagram at

http://sourceforge.net/p/virgo-linux/code-0/HEAD/tree/trunk/virgo-docs/VIRGOlinuxKernel_KeyValueStore_and_Modules_Interaction.jpg

- new kernel_analytics driver for AsFer <=> VIRGO+USBmd+KingCobra interface has been added.

- virgo_kernel_analytics.conf having csv(s) of key-value pairs of analytics variables is set by AsFer or any other Machine Learning code. With this VIRGO Linux Kernel is endowed with abilities to dynamically evolve than being just a platform for user code. Implications are huge - for example, a config variable "MaxNetworkBandwidth=255" set by the ML miner in userspace based on a Perceptron or Logistic Regression executed on network logs can be read by a kernel module that limits the network traffic to 255Mbps. Thus kernel dynamically changes behaviour.

- kernel_analytics Driver build script has been added

997. Commits as on 6 March 2015

- code has been added in VIRGO config module to import EXPORTed kernel_analytics config key-pair array set by Apache Spark (mined from Uncomplicated Fire Wall logs) and manually and write to kern.log.

NeuronRain version 15.6.15 release tagged

998. Portability to linux kernel 4.0.5

The VIRGO kernel module drivers are based on kernel 3.15.5. With kernel 4.0.5 kernel which is the latest following

compilation and LD errors occur - this is on cloudfs VIRGO File System driver :
- msghdr has to be user_msghdr for iov and iov_len as there is a segregation of msghdr

- modules_install throws an error in scripts/Makefile.modinst while overwriting already installed module

999. Commits as on 9 July 2015

VIRGO cpupooling driver has been ported to linux kernel 4.0.5 with msghdr changes as mentioned previously

with kern.log for VIRGO cpupooling driver invoked in parameterIsExecutable=2 (kernel module invocation) added in testlogs

1000. Commits as on 10,11 July 2015

VIRGO Kernel Modules:

- memorypooling

- cloudfs
- utils
- config
- kernel_analytics
- cloudsync
- eventnet
- queuing

along with cpupooling have been ported to Linux Kernel 4.0.5 - Makefile and header files have been updated wherever required.

1001. Commits as on 20,21,22 July 2015

Due to SourceForge Storage Disaster(<http://sourceforge.net/blog/sourceforge-infrastructure-and-service-restoration/>), the github replica of VIRGO is urgently updated with some important changes for msg_iter, iovec etc., in 4.0.5 kernel port specifically for KingCobra and VIRGO Queueing. These have to be committed to SourceForge Krishna_iResearch repository at http://sourceforge.net/users/ka_shrinivaasan once SourceForge repos are restored.

Time to move on to the manufacturing hub? GitHub ;-)

1002. VIRGO Queueing Kernel Module Linux Kernel 4.0.5 port:

- msg_iter is used instead of user_msghdr
- kvec changed to iovec
- Miscellaneous BUF_SIZE related changes
- kern.logs for these have been added to testlogs
- Module.symvers has been recreated with KingCobra Module.symvers from 4.0.5 KingCobra build
- clean target commented in build script as it wipes out Module.symvers
- updated .ko and .mod.c

1003. KingCobra Module Linux Kernel 4.0.5 port

- vfs_write() has a problem in 4.0.5
- the filp_open() args and flags which were working in 3.15.5 cause a kernel panic implicitly and nothing was written to logs
- It took a very long time to figure out the reason to be vfs_write and filp_open
- O_CREAT, O_RDWR and O_LARGEFILE cause the panic and only O_APPEND is working, but does not do vfs_write(). All other VIRGO Queue + KingCobra functionalities work viz., enqueueing, workqueue handler invocation, dequeueing, invoking kingcobra kernelspace service request function from VIRGO queue handler, timestamp, timestamp and IP parser, reply_to_publisher etc.,
- As mentioned in Greg Kroah Hartman's "Driving me nuts", persistence in Kernel space is a bad idea but still seems to be a necessary stuff - yet only vfs calls are used which have to be safe
- Thus KingCobra has to be in-memory only in 4.0.5 if vfs_write() doesn't work
- Intriguingly cloudfs filesystems primitives - virgo_cloud_open, virgo_cloud_read, virgo_cloud_write etc., work perfectly and append to a file.
- kern.logs for these have been added to testlogs
- Module.symvers has been recreated for 4.0.5
- updated .ko and .mod.c

Due to SourceForge outage and for a future code diversification

NeuronRain codebases (AsFer, USBmd, VIRGO, KingCobra)
in <http://sourceforge.net/u/userid-769929/profile/> have been
replicated in GitHub also - <https://github.com/shrinivaasanka>
excluding some huge logs due to Large File Errors in GitHub.

1004. Commits as on 30 July 2015

VIRGO system calls have been ported to Linux Kernel 4.0.5 with commented gcc
option -Wimplicit-function-declaration,
msghdr and iovec changes similar to drivers mentioned in previous commit notes
above. But Kernel 4.1.3 has some Makefile and build issues.
The NeuronRain codebases in SourceForge and GitHub would henceforth be mostly
and always out-of-sync and not guaranteed to be replicas - might get diversified
into different research and development directions (e.g one codebase might be
more focussed on IoT while the other towards enterprise bigdata analytics
integration with kernel and training which is yet to be designed- depend on lot
of constraints)

1005. Commits as on 2,3 August 2015

- new .config file added which is created from menuconfig
- drivers/Kconfig has been updated with 4.0.5 drivers/Kconfig for trace event
linker errors

Linux Kernel 4.0.5 - KConfig is drivers/ has been updated to resolve RAS driver
trace event linker error. RAS was not included in KConfig earlier.

- link-vmlinux.sh has been replaced with 4.0.5 kernel version

1006. Commits as on 12 August 2015

VIRGO Linux Kernel 4.1.5 port - related code changes - some important notes:

- Linux Kernel 4.0.5 build suddenly had a serious root shell drop error in
initramfs which was not resolved by:
 - adding rootdelay in grub
 - disabling uuid for block devices in grub config
 - mounting in read/write mode in recovery mode
 - no /dev/mapper related errors
 - repeated exits in root shell
- delay before mount of root device in initrd scripts
- mysteriously there were some firmware microcode bundle executions in
ieucodetool
- Above showed a serious grub corruption or /boot MBR bug or 4.0.5 VIRGO kernel
build problem
- Linux 4.0.x kernels are EOL-ed
- Hence VIRGO is ported to 4.1.5 kernel released few days ago
- Only minimum files have been changed as in commit log for Makefiles and
syscall table and headers and a build script has been added
for 4.1.5:

Changed paths:

- A buildscript_4.1.5.sh
- M linux-kernel-extensions/Makefile
- M linux-kernel-extensions/arch/x86/syscalls/Makefile
- M linux-kernel-extensions/arch/x86/syscalls/syscall_32.tbl
- M linux-kernel-extensions/drivers/Makefile
- M linux-kernel-extensions/include/linux/syscalls.h

- Above minimum changes were enough to build an overlay-ed Linux Kernel with
VIRGO codebase

1007. Commits as on 14,15,16 August 2015

Executed the minimum end-end telnet path primitives in Linux kernel 4.1.5 VIRGO code:

- cpu virtualization
 - memory virtualization
 - filesystem virtualization (updated filp_open flags)
- and committed logs and screenshots for the above.

1008. Commits as on 17 August 2015

VIRGO queue driver:

- Rebuilt Module.symvers
- kern.log for telnet request to VIRGO Queue + KingCobra queueing system in kernelspace

1009. Commits as on 25,26 September 2015

VIRGO Linux Kernel 4.1.5 - memory system calls:

- updated testcases and added logs for syscalls invoked separately(malloc,set,get,free)
- The often observed unpredictable heisen kernel panics occur with 4.1.5 kernel too. The logs are 2.3G and only grepped output is committed to repository.
- virgo_malloc.c has been updated with kstrdup() to copy the buf to iov.iov_base which was earlier crashing in copy_from_iter() within tcp code. This problem did not happen in 3.15.5 kernel.
- But virgo_clone syscall code works without any changes to iov_base as above which does a strcpy() which is an internal memcpy() though. So what causes this crash in memory system calls alone is a mystery.
- new insmod script has been added to load the VIRGO memory modules as necessary instead of at boot time.
- test_virgo_malloc.c and its Makefile has been updated.

VIRGO Linux Kernel 4.1.5 - filesystem calls- testcases and logs:

-
- added insmod script for VIRGO filesystem drivers
 - test_virgo_filesystem.c has been updated for syscall numbers in 4.1.5 VIRGO kernel
 - virgo_fs.c syscalls code has been updated for iov.iov_base kstrdup() - without this there are kernel panics in copy_from_iter(). kern.log testlogs have been added, but there are heisen kernel panics. The virgo syscalls are executed but not written to kern.log due to these crashes. Thus execution logs are missing for VIRGO filesystem syscalls.

1010. Commits as on 28,29 September 2015

VIRGO Linux Kernel 4.1.5 filesystem syscalls:

- Rewrote iov_base code with a separate iovbuf set to iov_base and strcpy()-ing the syscall command to iov_base similar to VIRGO memory syscalls
- Pleasantly the same iovbuf code that crashes in memory syscalls works for VIRGO FS without crash. Thus both virgo_clone and virgo_filesystem syscalls work without issues in 4.1.5 and virgo_malloc() works erratically in 4.1.5 which remains as issue.

- kern.log for VIRGO FS syscalls and virgofstest text file written by virgo_write() have been added to repository

VIRGO Linux 4.1.5 kernel memory syscalls:

- rewrote the iov_base buffer code for all VIRGO memory syscalls by allocating separate iovbuf and copying the message to it - this just replicates the virgo_clone syscall behaviour which works without any crashes mysteriously.
- did extensive repetitive tests that were frequented by numerous kernel panics and crashes
- The stability of syscalls code with 3.15.5 kernel appears to be completely absent in 4.1.5
- The telnet path works relatively better though
- Difference between virgo_clone and virgo_malloc syscalls despite having same kernel sockets code looks like a non-trivial bug and a kernel stability issue.
- kernel OOPS traces are quite erratic.
- Makefile path in testcase has been updated

1011. Commits as on 4 October 2015

VIRGO Linux Kernel 4.1.5 - Memory System Calls:

- replaced copy_to_user() with a memcpy()
- updated the testcase with an example VUID hardcoded.
- str_to_addr2() is done on iov_base instead of buf which was causing NULL parsing
- kern.log with above resolutions and multiple VIRGO memory syscalls tests - malloc, get, set
- With above VIRGO malloc and set syscalls work relatively causing less number of random kernel panics
- return values of memory calls set to 0
- in virgo_get() syscall, memcpy() of iov_base is done to data_out userspace pointer
- kern.log with working logs for syscalls - virgo_malloc(), virgo_set(), virgo_get() but still there are random kernel panics
- Abridged kern.log for VIRGO Memory System Calls with 4.1.5 Kernel - shows example logs for virgo_malloc(), virgo_set() and virgo_get()

1012. Commits as on 14 October 2015

VIRGO Queue Workqueue handler usermode clause has been updated with 4.1.5 kernel paths and kingcobra in user mode is enabled for invoking KingCobra Cloud Perfect Forwarding.

1013. Commits as on 15 October 2015

- Updated VIRGO Queue kernel binaries and build generated sources
- virgo_queue.h has been modified for call_usermodehelper() - set_ds() and fd_install() have been uncommented for output redirection. Output redirection works but there are "alloc_fd: slot 1 not NULL!" errors at random (kern.log in kingcobra testlogs) which seems to be a new feature in 4.1.5 kernel. This did not happen in 3.7.8-3.15.5 kernels

1014. Commits as on 3 November 2015

- kern.log for VIRGO kernel_analytics+config drivers which export the analytics variables from /etc/virgo_kernel_analytics.conf kernel-wide and print them in config driver has been added to config/testlogs

1015. Commits as on 10 January 2016

NeuronRain VIRGO enterprise version 2016.1.10 released.

NeuronRain - AsFer commits for VIRGO - C++ and C Python extensions
- Commits as on 29 January 2016

1016. (FEATURE - DONE) Python-C++-VIRGOKernel and Python-C-VIRGOKernel
boost::python and cpython implementations:

- It is a known idiom that Linux Kernel and C++ are not compatible.
- In this commit an important feature to invoke VIRGO Linux Kernel from
userspace python libraries via two alternatives have been added.
- In one alternative, C++ boost::python extensions have been added to
encapsulate access to VIRGO memory system calls - virgo_malloc(), virgo_set(),
virgo_get(), virgo_free(). Initial testing reveals that C++ and Kernel are not
too incompatible and all the VIRGO memory system calls work well though
initially there were some errors because of config issues.
- In the other alternative, C Python extensions have been added that replicate
boost::python extensions above in C - C Python with Linux kernel
works exceedingly well compared to boost::python.
- This functionality is required when there is a need to set kernel analytics
configuration variables learnt by AsFer Machine Learning Code
dynamically without re-reading /etc/virgo_kernel_analytics.conf.
- This completes a major integration step of NeuronRain suite - request travel
roundtrip to-and-fro top level machine-learning C++/python
code and rock-bottom C linux kernel - bull tamed ;-).
- This kind of python access to device drivers is available for Graphics Drivers
already on linux (GPIO - for accessing device states)
- logs for both C++ and C paths have been added in cpp_boost_python_extensions/
and cpython_extensions.
- top level python scripts to access VIRGO kernel system calls have been added
in both directories:
 CPython - python cpython_extensions/asferpythonextensions.py
 C++ Boost::Python - python
cpp_boost_python_extensions/asferpythonextensions.py
- .so, .o files with build commandlines(asferpythonextensions.build.out) for
"python setup.py build" have been added
in build lib and temp directories.
- main implementations for C++ and C are in
cpp_boost_python_extensions/asferpythonextensions.cpp and
cpython_extensions/asferpythonextensions.c

Commits as on 12 February 2016

1017. Commits for Telnet/System Call Interface to VIRGO CPUPooling -> VIRGO
Queue -> KingCobra

*) This was commented earlier for the past few years due to a serious kernel
panic in previous kernel versions - <= 3.15.5
*) In 4.1.5 a deadlock between VIRGO CPUPooling and VIRGO queue driver init was
causing following error in "use_as_kingcobra_service" clause :
 - "gave up waiting for virgo_queue init, unknown symbol push_request()"

*) To address this a new boolean flag to selectively enable and disable VIRGO Queue kernel service mode "virgo_queue_reactor_service_mode" has been added.

*) With this flag VIRGO Queue is both a kernel service driver and a standalone exporter of function symbols - push_request/pop_request

*) Incoming request data from telnet/virgo_clone() system call into cpupooling kernel service reactor pattern (virgo cpupooling listener loop) is treated as generic string and handed over to VIRGO queue and KingCobra which publishes it.

*) This resolves a long standing deadlock above between VIRGO cpupooling "use_as_kingcobra_service" clause and VIRGO queue init.

*) This makes virgo_clone() syscall/telnet both synchronous and asynchronous - requests from telnet client/virgo_clone() system call can be either synchronous RPC functions executed on a remote cloud node in kernelspace (or) an asynchronous invocation through "use_as_kingcobra_service" clause path to VIRGO Queue driver which enqueues the data in kernel workqueue and subsequently popped by KingCobra.

*) Above saves an additional code implementation for virgo_queue syscall paths - virgo_clone() handles, based on config selected, incoming data passed to it either as a remote procedure call or as a data that is pushed to VIRGO Queue/KingCobra pub-sub kernelspace.

Prerequisites:

- insmod kingcobra_main_kernelspace.ko
- insmod virgo_queue.ko compiled with flag virgo_queue_reactor_service_mode=1 (when virgo_queue_reactor_service_mode=0, listens on port 60000 for direct telnet requests)
- insmod virgo_cloud_test_kernelspace.ko
- insmod virgo_clouddexec.ko (listens on port 10000)

Schematic Diagram

VIRGO clone system call/telnet client ---> VIRGO cpupooling(compiled with use_as_kingcobra_service=1) -----> VIRGO Queue kernel service (compiled with virgo_queue_reactor_service_mode=1) ---> Linux Workqueue handler -----> KingCobra

1018. Commits as on 15 February 2016 - Kernel Analytics - VIRGO Linux Kernelwide imports

- Imported Kernel Analytics variables into CloudFS kernel module - printed in driver init()
- Module.symvers from kernel_analytics has been merged with CloudFS Module.symvers
- Logs for above has been added in cloudfs/test_logs/
- Makefile updated with correct fs path
- Copyleft notices updated

1019. Commits as on 15 February 2016 - Kernel Analytics - VIRGO Linux Kernelwide imports

- Kernel Analytics driver exported variables have been imported in CPU virtualization driver
- Module.symvers from kernel_analytics has been merged with Module.symvers in cpupooling

- kern.log for this import added to cpupooling/virgocloudexec/test_logs/

1020. Commits as on 15 February 2016 - Kernel Analytics - VIRGO Linux Kernelwide imports

- Imported kernel analytics variables into memory virtualization driver init() , exported from kernel_analytics driver
- build shell script updated
- logs added to test_logs/
- Module.symvers from kernel_analytics has been merged with memory driver Module.symvers
- Makefile updated

1021. Commits as on 15 February 2016 - Kernel Analytics - VIRGO Linux Kernelwide imports

- Imported kernel analytics variables into VIRGO Queueing Driver
- logs for this added in test_logs/
- Makefile updated
- Module.symvers from kernel_analytics has been merged with Queueing driver's Module.symvers
- .ko, .o and build generated sources

Commits as on 16,17 February 2016

1022. (FEATURE-DONE) Socket Buffer Debug Utility Function - uses linux skbuff facility

- In this commit a multipurpose socket buffer debug utility function has been added in utils driver and exported kernelwide.
- It takes a socket as function argument does the following:
 - dereference the socket buffer head of skbuff per-socket transmit data queue
 - allocate skbuff with alloc_skb()
 - reserve head room with skb_reserve()
 - get a pointer to data payload with skb_put()
 - memcpy() an example const char* to skbuff data
 - Iterate through the linked list of skbuff queue in socket and print headroom and data pointers
 - This can be used as a packet sniffer anywhere within VIRGO linux network stack
- Any skb_*() functions can be plugged-in here as deemed necessary.
- kern.log(s) which print the socket internal skbuff data have been added to a new testlogs/ directory
- .cmd files generated by kbuild

1023. (FEATURE-DONE) Commits as on 24 February 2016

skbuff debug function in utils/ driver:
(*) Added an if clause to check NULLity of skbuff headroom before doing skb_alloc()
(*) kern.log for this commit has been added testlogs/
(*) Rebuilt kernel objects and sources

Commits as on 29 February 2016

771. (FEATURE-DONE) Software Analytics - SATURN Program Analysis added to VIRGO Linux kernel drivers - this section is an extended draft on respective topics in NeuronRain AstroInfer design - <https://github.com/shrinivaasanka/asfer-github-code/blob/master/asfer-docs/AstroInferDesign.txt>

- SATURN (saturn.stanford.edu) Program Analysis and Verification software has been integrated into VIRGO Kernel as a Verification+SoftwareAnalytics subsystem
- A sample driver that can invoke an exported function has been added in drivers
- saturn_program_analysis
- Detailed document for an example null pointer analysis usecase has been created in virgo-docs/VIRGO_SATURN_Program_Analysis_Integration.txt
-
linux-kernel-extensions/drivers/virgo/saturn_program_analysis/saturn_program_analysis_trees/error.txt is the error report from SATURN
- SATURN generated preproc and trees are in
linux-kernel-extensions/drivers/virgo/saturn_program_analysis/preproc and
linux-kernel-extensions/drivers/virgo/saturn_program_analysis/
saturn_program_analysis_trees/

1024. Commits as on 10 March 2016

- SATURN analysis databases (.db) for locking, memory and CFG analysis.
- DOT and PNG files for locking, memory and CFG analysis.
- new folder saturn_calypso_files/ has been added in saturn_program_analysis/
with new .clp files virgosaturncfg.clp and virgosaturnmemory.clp
- SATURN alias analysis .db files

1025.(FEATURE-DONE) NEURONRAIN - ASFER Commits for VIRGO - CloudFS systems calls integrated into Boost::Python C++ and Python CAPI invocations

AsFer Commits as on 30 May 2016

VIRGO CloudFS system calls have been added (invoked by unique number from syscall_32.tbl) for C++ Boost::Python interface to VIRGO Linux System Calls. Switch clause with a boolean flag has been introduced to select either VIRGO memory or filesystem calls.
kern.log and CloudFS textfile Logs for VIRGO memory and filesystem invocations from AsFer python have been committed to testlogs/

1026. AsFer Commits as on 31 May 2016

Python CAPI interface to NEURONRAIN VIRGO Linux System Calls has been updated to include File System open, read, write primitives also.
Rebuilt extension binaries, kern.logs and example appended text file have been committed to testlogs/. This is exactly similar to
commits done for Boost::Python C++ interface. Switch clause has been added to select memory or filesystem VIRGO syscalls.

(BUG - STABILITY ISSUES) Commits - 25 July 2016 - Static Analysis of VIRGO Linux kernel for investigating heisencrashes

Initial Documentation for Smatch and Coccinelle kernel static analyzers executed on VIRGO Linux kernel - to be updated periodically with further analysis.

(BUG - STABILITY ISSUES) Commits - 1 August 2016 - VIRGO Linux Stability Issues - Ongoing Random oops and panics investigation

-
1. GFP_KERNEL has been replaced with GFP_ATOMIC flags in kmem allocations.
 2. NULL checks have been introduced in lot of places involving strcpy, strcat, strcmp etc., to circumvent buffer overflows.
 3. Though this has stabilized the driver to some extent, still there are OOPS in unrelated places deep with in kernel where paging datastructures are accessed - kmalloc somehow corrupts paging
 4. OOPS are debugged via gdb as:
 - 4.1 gdb ./vmlinux /proc/kcore
 - or
 - 4.2 gdb <loadable_kernel_module>.ofollowed by
 - 4.3 l *(address+offset in OOPS dump)
 5. kern.log(s) for the above have been committed in tar.gz format and have numerous OOPS occurred during repetitive telnet and syscall invocation(boost::python C++) invocations of virgo memory system calls.
 6. Paging related OOPS look like an offshoot of set_fs() encompassing the filp_open VFS calls.
-

(BUG-STABILITY ISSUES) Commits - 26 September 2016 - Ongoing Random Panic investigation

Further analysis on direct VIRGO memory cache primitives telnet invocation - problems are similar to Boost::Python AsFer VIRGO system calls invocations.

(BUG-STABILITY ISSUES) Commits - 27 September 2016 - Ongoing Random Panic investigation

Analysis of VIRGO memory cache primitives reveal more inconsistencies in cacheline flushes between CPU and GPU.

1027. Commits - 20 March 2017 and 21 March 2017 - VIRGO Linux 64-bit build based on 4.10.3 kernel

-
- *) moved virgoeventnetclient_driver_build.sh to virgoutils_driver_build.sh in utils/ driver
 - *) Updated VIRGO Linux Build Steps for 4.10.3
 - *) New repository has been created for 64-bit VIRGO Linux kernel based on 4.10.3

mainline kernel in GitHub and imported in SourceForge:

<https://github.com/shrinivaasanka/virgo64-linux-github-code>

<https://sourceforge.net/p/virgo64-linux/>

*) Though it could have been branched off from existing VIRGO repository (32-bit) which is based on 4.1.5 mainline kernel, creating a separate repository for 64-bit 4.10.3 VIRGO kernel code was simpler because:

- there have been directory path changes for syscall entries in 4.10.3 and some other KBuild entities

- Some script changes done for 4.1.5 in modpost and vmlinux phases are not required

- having two VIRGO branches one with 4.1.5 code and 32-bit driver .ko binaries and other with 4.10.3 code and 64-bit driver .ko

binaries could be unmanageable and commits could go into wrong branch

- 4.10.3 64-bit VIRGO kernel build is still in experimental phase and it is not known if 64-bit 4.10.3 build solves earlier panic problems in 4.1.5

- If necessary one of these two repositories could be made branch of the other later

1028. Commits - 27 March 2017 Ongoing analysis of VIRGO 64 bit linux kernel based on 4.10.3 kernel mainline

*) Prima facie, 64 bit kernel is quite finicky and importunate compared to 32 bit and 64 bit specific idiosyncrasies are to the fore.

*) During the past 1 week, quite a few variants of kernel and drivers builds were tried with KASAN enabled and without KASAN (Google Kernel Address Sanitizer)

*) KASAN shows quite huge number of user memory accesses which later translate to panics.

*) Most nagging of these was kernel_recvmsg() panic.

*) Added and updated skbuff socket debug utility driver with a new debug function and to print more fields of skbuff

*) KASAN was complaining about _asan_load8 (loading 8 userspace bytes)

*) All erroneous return data types in VIRGO mempool ops structure have been corrected in VIRGO headers

*) all type casts have been sanitized

*) Changed all kernel stack allocations to kernel heap kzallocs

*) This later caused a crash in inet_sendmsg in kernel_sendmsg()

*) gdb64 disassemble showed a trapping instruction:

testb \$0x6,0x91(%14) with corresponding source line:

sg = !!((sk->sk_route_caps & NETIF_F_SG)

in tcp_sendmsg() (net/ipv4/tcp.c)

*) changed kernel_sendmsg() to sock->ops->sendmsg()

*) These commits are still ongoing analysis only.

*) Screenshots for these have been added to debug-info/

1029. Continued analysis of VIRGO 64-bit linux kernel built on 4.10.3 mainline - Commits - 30 March 2017

*) Previous commit was crashing inside tcp_sendmsg()

*) GDB64 disassembly shows NULL values for register R12 which is added with an offset 91 and is an operand in testb

*) Protected all kernel_sendmsg() and kernel_recvmsg() in both system calls side and drivers side with

oldfs=get_fs(), set_ds(KERNEL_DS) and set_fs(oldfs)

blocks without which there are random kernel_sendmsg and kernel_recvmsg hangs

*) Removed init_net and sock_create_kern usage everywhere and replaced them with sock_create calls

- *) Tried MSG_FASTOPEN flags but it does not help much in resolving tcp_sendmsg() NULL pointer dereference issue. MSG_FASTOPEN just speeds up the message delivery by piggybacking the message payload before complete handshake is established (SYN, SYN-ACK, SYN-ACK-ACK) in SYN-ACK itself. But eventually it has to be enabled as fast open is becoming a standard.
- *) Kasan reports have been enabled.
- *) Added more debug code in skbuff debug utility functions in utils driver to check if sk->prot is a problem.
- *) Replaced kernel_sendmsg with a sock->ops->sendmsg() in mempool sendto function which otherwise crashes in tcp_sendmsg().
- *) With sock->ops->sendmsg() systemcalls <----> drivers two-way request-reply works but still there are random -32 (broken pipe) and -104 (Connection Reset by Peer) errors
- *) Logs for working sys_virgo_malloc() call with correctly returned VIRGO Unique ID for memory allocated has been committed to test_logs in virgocloudexecmempool
- *) sock->ops->sendmsg() in mempool driver sendto function requires a MSG_NOSIGNAL flag which prevents SIGPIPE signal though not fully
- *) Reason for random broken pipe and connection reset by peer errors in mempool sendto is unknown. Both sides have connections open and there is no noticeable traffic.
- *) While socket communications in 32 bit VIRGO kernel syscalls and drivers work with no issues, why 64-bit has so many hurdles is puzzling. Reasons could be 64 bit address alignment issues, 64 bit specific #ifdefs in kernel code flow, major changes from 4.1.5 to 4.10.3 kernels etc.,
- *) NULL values for register R12 indicate already freed skbuff data which are accessed/double-freed. Kernel TCP engine has a circular linked list of skbuff write queue which is iterated in skbuff utils driver debug functions.
- *) TCP engine clones the head data of skbuff queue, transmits it and waits for an ACK or timeout. Data is freed only if ACK or timeout occurs. And head of the queue is advanced to next element in write queue and this continues till write queue is empty waiting for more messages.
- *) If ACK is not received, head data is cloned again and retransmitted by sequence number flow control.

 1030. Continued Analysis of VIRGO 64 bit based on 4.10.3 linux kernel - Commits
 - 1 April 2017, 3 April 2017

- *) kernel_sendmsg() has been replaced with sock->ops->sendmsg() because kernel_sendmsg() is quite erratic in 4.10.3 64 bit
- *) There were connection reset errors in system calls side for virgo_malloc/. This was probably because sock->ops->sendmsg() requires MSG_DONTWAIT and MSG_NOSIGNAL flags and sendmsg does not block.
- *) sock release happens and virgo_malloc syscalls receives -104 error
- *) Temporarily sock_release has been commented. Rather socket timeout should be relied upon which should do automatic release of socket resources
- *) Similar flags have been applied in virgo_malloc syscalls too.
- *) Logs with above changes do not have reset errors as earlier.
- *) virgo set/get still crashes because 64 bit id is truncated which would require data type changes for 64 bit
- *) test_virgo_malloc test case has been rebuilt with -m64 flag for invocation of 64 bit syscalls by numeric ids

 1031. Continued Analysis of VIRGO 64 bit 4.10.3 kernel - commits - 10 April 2017

```

-----
*) There is something seriously wrong with 4.10.3 kernel sockets in 64 bit build
VIRGO send/recv messages and even accept/listen too.
*) All kernel socket functionalities which work well in 4.1.5 32 bit VIRGO ,
have random hangs, panics in 4.10.3 VIRGO64 build mostly
in inet_recvmmsg/sendmsg code path
*) KASAN shows attempts to access user address which occurs despite
set_fs(KERNEL_DS)
*) Crash stack is similar to previous crashes in tcp_sendmsg()
*) Tried different address and protocol families for kernel socket accept
(TCP,UDP,RAW sockets)
*) With Datagram sockets, kernel_listen() mysteriously fails with -95 error in
kernel_bind(operation not supported)
*) With RAW sockets, kernel_listen() fails with -93 error for AF_PACKET
(protocol not supported)
*) tcpdump pcap sniffer doesn't show anything unruly.
*) This could either be a problem with kernel build (unlikely), Kbuild .config
or could have extraneous reasons. But .config for
4.1.5 and 4.10.3 are similar.
*) Only major difference between 4.10.3 and 4.1.5 is init_net added in
sock_create_kern() internally
*) datatype of VIRGO Unique ID has been changed to unsigned long long (_u64)
*) tried with INADDR_LOOPBACK in place of INADDR_ANY
*) also tried with disabled multi(homing) in /etc/hosts.conf
*) Above random kernel socket hangs occur across all VIRGO system calls and
drivers transport.
*) Utils kernel socket client to EventNet kernel service also has similar
inet_recvmmsg/inet_sendmsg panic problems.
-----

```

```

-----
1032. Commits - 11 April 2017 - EventNet and Utils Drivers 64bit
-----

```

```

*) EventNet driver works in 64 bit VIRGO Linux
*) An example eventnet logging with utils virgo_eventnet_log() works now without
tcp_sendmsg() related stalls in previous builds
*) Return Datatypes for all EventNet operations have been sanitized (struct
socket* was returned as int in 32 build and reinterpret-cast to
struct socket*. This reinterpret cast does not work in 64 bit) in eventnet
header.
*) utils eventnet log in init() has been updated with a meaningful edge update
message
*) kern.log for this has been added to eventnet/testlogs
-----

```

```

-----
1033. Commits - 17 April 2017 - VIRGO64 Memory, CPU, FileSystem, EventNet kernel
module drivers
-----

```

```

*) telnet requests to VIRGO memory(kernelmemcache), cpu and filesystem modules
work after resolving issues with return value types
*) commented le32_to_cpu() and print_buffer() which was suppressing lot of log
messages.
*) VIRGO <driver> ops structures have been updated with correct datatypes.
*) reinterpret cast of struct socket* to int has been completely done away with
which could have caused 64bit specific panics
*) lot of kern.log(s) and screen captures have been added for telnet requests in
testlogs/ of respective <driver> directory
*) Prima facie 64bit telnet requests to VIRGO module listeners are relatively
stabler than 32bit
*) Previous code changes should be relevant to 32 bit VIRGO kernel too.

```

*) tcp_sendmsg()/tcp_recvmsg() related hangs could be mostly related to corrupted skbuff queue within each socket.
*) This is because replacing kernel_<send/recv>msg() with sock_<send/recv>msg() causes return value to be 0 while socket release crashes within skbuff related kernel functions.
*) To make socket state immutable, in VIRGO memory driver header files, client socket has been declared as const type.

1034. Commits - KingCobra 64 bit and VIRGO Queue + KingCobra telnet requests - 17 April 2017

*) Rebuilt KingCobra 64bit kernel module
*) telnet requests to VIRGO64 Queueing module listener driver are serviced by KingCobra servicerequest
*) Request_Reply queue persisted for this VIRGO Queue + KingCobra routing has been committed to c-src/testlogs.
*) kern.log for this routing has been committed in VIRGO64 queueing directory
) Similar to other drivers struct socket reinterpret cast to int has been removed and has been made const in queuesvc kernel thread

1035. Commits - VIRGO64 system calls - kernel module listeners - testcases and system calls updates - 18 April 2017

*) All testcases have been rebuilt
*) VIRGO kernel memcache,cpu and filesystem system calls have been updated with set_fs()/get_fs() blocks for kernel_sendmsg() and kernel_recvmsg()
*) Of these virgo_clone() system call testcase (test_virgo_clone) works flawlessly and there are no tcp_sendmsg()/tcp_recvmsg() related kernel panics.
*) VIRGO memcache and filesystem system call testcases have usual tcp_sendmsg()/tcp_recvmsg() despite the kernel socket code being similar to VIRGO clone system call
*) Logs for VIRGO clone system call to CPU kernel driver module have been committed to virgo_clone/test/testlogs

1036. Commits - VIRGO64 Kernel MemCache and FileSystem system calls to VIRGO Memory and FileSystem Drivers - 19 April 2017

*) Changed iovec in virgo_clone.c to kvec
*) test_virgo_filesystem.c and test_virgo_malloc.c VIRGO system calls testcases have been changed with some additional printf(s) in userspace
*) virgo_malloc.c has been updated with BUF_SIZE in iov_len and memset to zero initialize the buffer. tcp_sendmsg()/tcp_recvmsg() pair were getting stuck in copy_from_iter_full() memcpy with a NULL Dereference. memcpy() was reading past the buffer bound causing an overrun. strlen() didnt work for iov_len.
*) virgo_fs.c virgo_write() memcpy has been changed back to copy_from_user() thereby restoring status quo ante (commented more than 3 years ago because of a kernel panic in older versions of 32 bit VIRGO kernel)
*) Logs for VIRGO kmemcache and filesystem system calls have been committed to respective system call directories.
*) With this all VIRGO64 functionalities work in both telnet and system calls requests routes end-to-end from clients to kernel modules with kernel sockets issues resolved fully.

*) Major findings are:

- VIRGO 4.10.3 64 bit kernel is very much stable compared to 32 bit 4.1.5 kernel
- there are no i915 related errors which happened in VIRGO 32 bit 4.1.5 kernel
- Repetitive telnet and system calls requests to VIRGO modules are stable and there are no kernel panics like 4.1.5 32 bit kernel.
- Google Kernel Address Sanitizer is quite helpful in finding stack overruns, null derefs, user memory accesses etc.,
- 64 bit kernel is visibly faster than 32 bit.
- Virgo Unique ID is now extended to 2^64 with unsigned long long.

1037. Commits - VIRGO64 memory and filesystem calls to memory and filesystem drivers requests routing - 20 April 2017

*) Changed return value of virgo_cloud_free_kernelspace() to a string literal "kernel memory freed"

*) Logs for VIRGO64 memory and filesystem calls to memory and filesystem drivers requests routing have been committed in test_logs of both driver directories

1038. Commits - 27 April 2017

Residual logs for VIRGO 64 bit 4.10.3 kernel committed.

1039. Commits - 25 May 2017

*) Changed LOOPBACK to INADDR_ANY for VIRGO64 kernel memcache listen port

*) All VIRGO64 RPC, kernel memcache, cloud filesystem primitives have been retested

*) VIRGO64 mempool binaries have been rebuilt

1040. Commits - 31 August 2017 - NeuronRain ReadTheDocs Documentation - VIRGO64 System calls and Drivers
(<http://neuronrain-documentation.readthedocs.io/en/latest/>)

(*) New directory systemcalls_drivers/ has been added to virgo-docs/ and representative VIRGO64

system calls and drivers functionality logs have been committed for demonstration purpose.

(*) VIRGO64 cloudfs driver has been rebuilt after changing virgofstest.txt file creation filp_open() call

(*) Screenshots and logs for VIRGO64 Clone, Kernel MemCache and Cloud FS SystemCalls-Drivers interaction, socket transport debug messages and Kernel Address Sanitizer have been committed in virgo-docs/systemcalls_drivers

1041. Commits - 23 September 2017 - Major VIRGO mainline kernel version Upgrade for Kernel Transport Layer Security - 4.10.3 to 4.13.3

(*) Recently released mainline kernel version 4.13 integrates SSL/TLS into kernelspace- KTLS - for the first time.

(*) KTLS is a standalone kernel module af_ktls (<https://github.com/ktls>) implemented by RedHat and Facebook for optimizing SSL handshake within kernelspace itself and reduce userspace-kernelspace switches.

(*) sendfile() system call in linux which is used for file transmission (combining read+write) from one fd to another uses this KTLS optimization in kernelspace in af_ktls codebase (af_ktls tool)

(*) VIRGO Linux kernel fork-off requires this kernelspace TLS functionality to fully secure traffic from system call client to remote cloud node's kernel module listeners

(*) Hence VIRGO64 linux kernel mainline base is urgently upgraded from 4.10.3 to 4.13.3

(*) All system calls and kernel module code in VIRGO64 now have #include(s) for tls.h and invoke kernel_setsockopt() on the client-server kernelspace sockets for SOL_TLS and TLS_TX options and have been rebuilt.

(*) VIRGO64 RPC clone/kmemcache/cloudfs system calls to kernel module listeners have been tested with this new KTLS socket option, on rebuilt VIRGO64 kernel overlay-ed on 4.13.3 64-bit linux kernel

(*) 4.13 mainline kernel also has SMB CIFS bug fixes for recent malware attacks (WannaCry etc.,) which further ensures security of VIRGO64 linux fork-off kernelspace traffic.

(*) New buildscript for 4.13.3 linux kernel has been committed

(*) testlogs for VIRGO64 system calls and driver listeners KTLS transport have been committed in virgo-docs/systemcalls_drivers/kern.log.VIRGO64_SystemCalls_Drivers.4.13.3_KTLS_kernelsockets.22September2017

(*) After this upgrade, complete system calls to driver listener traffic is SSL enabled implicitly.

(*) Updated kernel object files for 4.13.3 build are part of this commit.

 1042. Commits - Remnant commits for 4.13.3 upgrade - 24 September 2017

 Updated init.h and syscalls.h headers for virgo system calls

 1043. Commits - VIRGO64 4.13.3 KTLS Upgrade - System Calls-Driver Listeners End-to-End encrypted traffic testing - 25 September 2017

 (*) VIRGO64 CPU/KMemCache/CloudFS system calls have been invoked by userspace testcases and all primitives work after 4.13.3 KTLS upgrade

(*) Some small modifications to system calls code have been made and rebuilt to remove redundant iovbuf variables in printk(s)

(*) test_virgo_filesystem.c testcase has been updated and rebuilt

(*) kern.log(s) for CPU/KMemCache/CloudFS systemcalls to driver listeners invocations have been committed to respective system call directories

(*) virgofstest.txt written to by virgo_write() has also been committed. But a weird behaviour is still observed similar to previous linux kernel versions (4.1.5 and 4.10.3): Repetitive invocations are required to flush the filesystem buffer to force write the file.

(*) No DRM GEM i915 panics are observed and stability of VIRGO64 + 4.13.3 linux kernel is more or equal to VIRGO64 + 4.10.3 linux kernel

 1044. Commits - VIRGO64 VIRGO_KTLS branch creation and rebase of master to previous commit - 30 September 2017

 (*) New branch VIRGO_KTLS has been created after previous commit on 25 September

2017 and all 5 commits after 25 September 2017 till 28 September 2017 have been branched to VIRGO_KTLS (which has the #ifdef for crypto_info, reads from /etc/virgo_ktls.conf and a new ktls driver module)

(*) Following are the commit hashes and commandlines in GitHub and SourceForge:

```
git branch -b VIRGO_KTLS
git branch master
git rebase -i <SHA1_on_25September2017>
git rebase --continue
git commit --amend
git push --force
```

```
-----
1958 git checkout -b
1959 git checkout -b VIRGO_KTLS
1960 ls
1961 git checkout VIRGO_KTLS
1962 git push origin VIRGO_KTLS
1963 git status
1964 git checkout
1965 git checkout -b
1966 git branch
1967 git branch master
1968 git branch -h
1969 git branch
1970 git checkout master
1975 git checkout -b
1976 git checkout -b VIRGO_KTLS
1979 git push origin VIRGO_KTLS
1990 git rebase -i bb661e908cba2a5357414e89166f29086a28bdf0
1991 git status
1992 git rebase -i bb661e908cba2a5357414e89166f29086a28bdf0
1996 git rebase --continue
1997 git commit --amend
2019 git rebase -i bb661e908cba2a5357414e89166f29086a28bdf0
2029 git rebase --continue
2037 git push --force
2091 git rebase -i bb661e908cba2a5357414e89166f29086a28bdf0
2092 git rebase --continue
2093 git commit --amend
2094 git push --force
2110 git branch
2111 git branch master
2112 git checkout master
2113 git branch
2114 git rebase -i e76b4089633223f610fddc0e0eaff8c2cef8b9f1
2115 git commit --amend
2116 git rebase --continue
2117 git push --force
-----
```

KTLS in 4.13.3 has support for only private symmetric encryption. It does not support Public Key Encryption yet. Since this might take a while mainstream VIRGO64 code might change a lot for other features. Therefore, VIRGO_KTLS specific crypto_info code has been branched off and would parallelly evolve if PKI features are available on KTLS in next versions of Linux kernel.

1045. Commits - 1 October 2017

kern.log(s) for VIRGO64 systemcalls-driver 4.13.3 64-bit upgrade tests on master branch after reversal and rebase of master HEAD yesterday for

branching to VIRGO_KTLS. There is a weird General Protection Fault in intel atomic commit work not seen thus far. Also -32 and -107 socket errors are frequent after reversal though code remains same. But all virgo clone/kmemcache/fs systemcalls functionalities work in invocations after GPF.

1046. Commits - VIRGO64 Utils and EventNet Drivers Update for tcp_sendmsg()
stack out-of-bounds error - 3 October 2017

(*) Utils Generic Socket Client function virgo_eventnet_log() for EventNet kernel module listener was repeatedly failing in kernel_connect() emitting -32 and -107 errors.
(*) kernel_connect() was guarded by set_fs() and get_fs() memory segment routines to prevent any memory corruption. After this stack out-of-bounds error was reported by kernel address sanitizer in tcp_sendmsg() and copy_from_iter_full() implying the message buffer was not properly read within kernel.
(*) After replacing strlen(buf) by BUF_SIZE in msg flags before kernel_connect() stack out-of-bounds error has been remedied and Utils to EventNet virgo_eventnet_log() doesn't crash in tcp_sendmsg()
(*) kern.log for this has been committed in drivers/virgo/utils/testlogs/
(*) Both eventnet and utils drivers have been rebuilt

1047. VIRGO64 system calls-drivers on linux kernel 4.13.3 - miscellaneous bugfixes - 5 October 2017

(*) kernel_setsockopt() for KTLS has been commented in all system calls and drivers because KTLS functionality has been branched to VIRGO_KTLS
(*) In virgo_clone.c, iov.iov_len has been set to BUF_SIZE
(*) kernel_connect() has been guarded by set_fs()/get_ds() in VIRGO64 system call clients
(*) test_virgo_malloc.c testcase has been updated
(*) There was a weird problem in in4_pton(): sin_addr.saddr was not set correctly from string IP address and this was randomly occurring only in virgo_set()
(*) in4_pton() is implemented in net/core/utils.c and reads the string IP address digits and sums up the ASCII values to hex representation of the address. Bitwise operations within this functions were failing randomly.
(*) Repeated builds were done trying different possible fixes but didn't work e.g casting saddr to (u8*)
(*) There is an alternative in_aton() function which takes only String IP address and returns address as __be32
(*) After in_aton() in virgo_set() random faulty address conversion does not occur - in_aton() is differently implemented compared to in4_pton()
(*) msg_hdr has been initialized to NULL in virgo_set()
(*) Lot of debug printk()s have been added
(*) kern.log (.tar.gz) for RPC clone/KMemCache/Filesystem systemcalls-driver has been committed to virgo-docs/systemcalls_drivers
(*) VIRGO Linux build steps have been updated for example commandlines to overlay mainline kernel tree by VIRGO64 source

commit 4e6681ade4ddbf1bed17f7c115b59a5ebf884256
Author: K.Srinivasan <ka.shrinivaasan@gmail.com>
Date: Fri Oct 6 11:36:15 2017 +0530

1048. VIRGO64 Queueing Kernel Module Listener - KingCobra64 - 4.13.3 - 6 October

2017

(*) telnet client connection to VIRGO64 Queue and a subsequent workqueue routing (pub/sub) to KingCobra64 has been tested on 4.13.3
(*) TX_TLS socket option has not been disabled and is a no-op because it has no effect on the socket.
(*) REQUEST_REPLY.queue for this routing from VIRGO64 queue and persisted by KingCobra64 has been committed to KingCobra64 repositories in GitHub and SourceForge

commit d4e95b58474838d65da9c69944c6287acbdfe72c
Author: K.Srinivasan <ka.shrinivaasan@gmail.com>
Date: Fri Oct 6 11:05:21 2017 +0530

1049. VIRGO64 System Calls to Drivers and Telnet Client to Drivers on 4.13.3 linux kernel - master branch (after KTLS has been reverted and branched to VIRGO_KTLS) - test case logs - 6 October 2017

(*) VIRGO64 System calls - Clone, KMemCache and Filesystem system call primitives to Driver listeners invocations have been tested by respective test_<syscall> unit testcases
(*) VIRGO64 Telnet Clients to Driver listeners invocations have been tested by telnet connections
(*) Master branches in SourceForge and GitHub VIRGO64 do not have KTLS provisions. Only VIRGO_KTLS branch has crypto_info and setsockopt() for TX_TLS for kernel sockets.
(*) It has been already mentioned in NeuronRain Documentation in <https://neuronrain-documentation.readthedocs.io/en/latest/> on securing VIRGO cloud nodes in the absence of KTLS - most obvious solution is to install VPN client-servers in all nodes which create Virtual IPs on a secure tunnel (e.g OpenVPN).
(*) VIRGO64 system call clients and driver listeners should read these Virtual IPs from /etc/virgo_client.conf and /etc/virgo_cloud.conf and cloud traffic is confined to the VPN tunnel.

1050. VIRGO64 SystemCalls-Drivers endtoend invocations unit case tests - on 4.13.3 - VIRGO64 main branch - 11 October 2017

(*) VIRGO64 systemcalls have been invoked from unit test cases (test_<system_call>) in a loop of few hundred iterations
(*) No DRM GEM i915 panics or random crashes are observed and stability is good
(*) This is probably the first loop iterative testing of VIRGO system calls and drivers.
(*) Kernel logs for this have been committed to virgo-docs/systemcalls_drivers directory.
(*) Note on concurrency: Presently mutexing within system calls have been commented because in past linux versions mutexing within kernel was causing strange panic issues. As a design choice and feature-stability tradeoff (stability is more important than introducing additional code) mutexing has been lifted up to userspace. It is upto the user applications invoking the system calls to synchronize multiple user threads invoking VIRGO64 system calls i.e VIRGO64 system calls are not re-entrant. This would allow just one kernel thread (mapped 1:1 to a user thread) to execute in kernel space. Mostly this is relevant only to kmemcache system calls which have global in-kernel-memory address translation tables and next_id variable. VIRGO clone/filesystem calls do not have global in-kernel-memory datastructures.

1051. VIRG064 SystemCalls-Drivers concurrent invocations - 2 processes having shared mutex - 14 October 2017

(*) VIRG064 systemcalls are invoked in a function which is called from 2 processes concurrently
(*) Mutexes between the processes are PTHREAD_PROCESS_SHARED attribute set.
(*) test_virgo_malloc.c unit testcase has been enhanced to fork() a process and invoke systemcalls in a function for 100 iterations each
(*) Logs for the Virgo Unique IDs malloc/set/get/free in the systemcalls side and kern.logs for the drivers have been committed to test/testlogs/
(*) No DRM GEM i915 crashes were observed
(*) test_virgo_malloc.c testcase demonstrates the coarse grained critical section lock/unlock for kmemcache systemcalls and is a template that should be followed for any userspace application.

775. (FEATURE) VIRG064 Kernel Analytics - Streaming Implementation - 13 December 2017 - this section is an extended draft on respective topics in NeuronRain AstroInfer design -
<https://github.com/shrinivaasanka/asfer-github-code/blob/master/asfer-docs/AstroInferDesign.txt>

(#) Presently kernel analytics config have to be read from a file storage. This is a huge performance bottleneck when frequency of analytics variables written to is realtime. For example autonomous vehicles/drones write gigabytes of navigation data in few minutes.
(#) Because of this /etc/virgo_kernel_analytics.conf grows tremendously. File I/O in linux kernel module is also fragile and not recommended.
(#) Previous latency limitations necessitate an alternative high performance analytics config variable read algorithm
(#) This commit introduces new streaming kernel analytics config reading function - It connects to a kernel analytics streaming IP address on hardcoded port 64000 and reads analytics key-value pairs in an infinite loop.
(#) These read key-value pairs are stored in a kernel global ring buffer exported symbol (by modulus operator). Because of circular buffer, older kernel analytics variables are overwritten repetitively.
(#) kernel socket message flags are set to MSG_MORE | MSG_FASTOPEN | MSG_NOSIGNAL for high response time. MSG_FASTOPEN works with no panic in 4.13.3 64-bit which was a problem in previous kernel versions.
(#) kern.log for this has been committed to kernel_analytics/testlogs/
(#) include/linux/virgo_kernel_analytics.h header file has been updated for declarations related to streaming analytics.
(#) Webserver used for this is netcat started on port 64000 as:
 nc -l 64000
 >k1=v1
 >k2=v2
 ...

1052. VIRG064 Kernel Analytics - Reading Stream of Analytic Variables made a kernel thread - 13 December 2017

(#) This is sequel to previous commit for Stream reading Kernel Analytics variables over a network socket
(#) read_streaming_virgo_kernel_analytics_conf() function is invoked in a separate kernel thread because module init is blocked

(#) VIRGO64 config module was loaded and exported kernel analytics variables read over socket by previous spin-off kernel thread are imported in VIRGO64 config init.
(#) kern.log for this has been committed to testlogs/
(#) Pre-requisite: Webservice serving kernel_analytics variables must be started before kernel_analytics module is loaded in kernel.
(#) By this a minimum facility for live reading analytics anywhere on cloud (it can be userspace or kernelspace) and exporting them to modules on a local cloud node kernel has been achieved - ideal for cloud-analytics-driven IoT

1053. VIRGO64 System Calls - Drivers - Kernel Analytics Streaming - on 4.13.3 kernel - 15 December 2017

(#) VIRGO64 System Calls to Drivers invocations on 4.13.3 kernel have been executed after enabling streaming kernel analytics
(#) VIRGO64 RPC/KMemCache/CloudFS Drivers import, streamed variable-value pairs exported from kernel_analytics read from netcat webservice
(#) VIRGO64 KMemCache testcase has 2 concurrent processes invoking kememcache systemcalls in a loop.
(#) kern.log for this has been committed to virgo-docs/systemcalls_drivers
(#) virgofstest.txt written by CloudFS systemcalls-drivers invocation is also committed to virgo-docs/systemcalls_drivers

1054. VIRGO64 system calls and drivers - Quadcore 64bit - Known Issues - documentation only - 26 May 2019

1. VIRGO64 system calls to drivers interactions so far have been tested only on dual core 64 bit architecture.
2. In quad core 64 bit there have been random -32, -107, -101 errors in kernel_connect() from system call clients to driver services in almost all three types of VIRGO64 system calls - clone/kmemcache/filesystem - to respective drivers
3. These errors do not occur if following in4_pton() invocation is changed to in_aton() before kernel_connect() in system call clients and kernel is rebuilt with following change before kernel_connect():

```
/*in4_pton(vaddr->hstprt->hostip, strlen(vaddr->hstprt->hostip),  
(u8*)&sin.sin_addr.s_addr, '\0', NULL);*/  
sin.sin_addr.s_addr=in_aton(vaddr->hstprt->hostip);
```

4. Since this problem occurs erratically and only on quadcore 64-bit and reasons for these random -32, -101, -107 errors are still unknown, no commit for this code change has been made and this issue is left as documented known issue.
5. Most likely the u8* cast causes client socket address corruption.
6. Because of random -32, -101, -107 errors, in quadcore, system calls sometimes do not transmit client side commandline primitive strings to driver services.

773. (FEATURE) Linux Kernel 5.1.4, PXRC Drone/UAV/Flight Controller, UVC Video WebCam driver, Kernel Analytics, NeuronRain Usecases - 28 May 2019 - this section is an extended draft on respective topics in NeuronRain AstroInfer design - <https://github.com/shrinivaasanka/asfer-github-code/blob/master/asfer-docs/AstroInferDesign.txt>

1. Two analytics usecases mentioned in NeuronRainUsecases.txt in NeuronRain

AsFer asfer-docs/ have been illustrated in this commit by
 2 example drivers for PXRC Drone controller Driver and UVC Video WebCam Driver.
 2. PXRC Phoenix RC flight controller is part of linux kernel from 4.17 and kernel major version has been bumped to 5.x.x recently.
 3. Linux kernel 5.1.4 has been built by a new build script - buildscript_5.1.4.sh.
 4. Linux kernel 5.1.4 has recent versions of PXRC drone controller driver and a UVC video webcam driver (<http://www.ideasonboard.org/uvc/faq/>)
 5. New directory linux-kernel-5.1.4-extensions/ has been created for VIRGO64 code built on kernel mainline version 5.1.4. No branch is created for version 5.1.4 because pxrc driver is part of kernel only from 4.17 while code in linux-kernel-extensions/ is based on kernel 4.13.3 for dual core 64-bit architecture.
 6. New VIRGO64 build on 5.1.4 kernel is necessary only for PXRC, UVC and kernel_analytics drivers while other VIRGO64 drivers have not been ported to 5.1.4 and are still on 4.13.3 kernel.
 7. Two drivers for PXRC and UVC Webcam in 5.1.4 have been committed under linux-kernel-5.1.4-extensions/drivers/media/usb/uvc and linux-kernel-5.1.4-extensions/drivers/input/joystick
 8. VIRGO64 kernel_analytics driver for 5.1.4 has been committed under linux-kernel-5.1.4-extensions/drivers/virgo/kernel_analytics.
 9. Porting VIRGO64 kernel_analytics driver from 4.13.3 to 5.1.4 required changing vfs_read() of /etc/virgo_kernel_analytics.conf to kernel_read() in config file read.
 10. Drivers code for PXRC is in drivers/input/joystick/pxrc.c has been instrumented with few printk() statements that print the virgo_kernel_analytics_conf array variable-value pairs exported by VIRGO64 kernel_analytics driver. Kernel analytics variables are imported by #include of virgo_config.h
 11. Drivers code for UVC Video WebCam is in drivers/media/usb/uvc. File drivers/media/usb/uvc/uvc_video.c has been instrumented with lot of uvc_trace() statements which print kernel_analytics driver exported analytics variable "match" and its boolean value. Kernel analytics variables are imported by #include of virgo_config.h. Variable "match" has been set to "True" assuming a face recognition or retinal scan match by userspace analytics and /etc/virgo_kernel_analytics.conf has been written to.
 12. UVC Video WebCam traces are enabled by:
 echo 0xffff > /sys/module/uvcvideo/parameters/trace
 13. Example kern.log(s) for PXRC and UVC drivers are committed under drivers/input/joystick/testlogs/kern.log.pxrc.28May2019 and drivers/media/usb/uvc/kern.log.uvcvideo.28May2019 which show UVC traces printing the imported kernel analytics variable "match=True" and PXRC driver registration. No other PXRC traces are printed because of lack of drones and drone licensing dependency
 14. Both UVC and PXRC drivers, VIRGO64 kernel_analytics driver and linux kernel 5.1.4 have been built on quadcore 64-bit architecture.
 15. This example import of VIRGO64 kernel analytics variables into PXRC drone and UVC webcam drivers demonstrate passing of userspace analytics information to kernel for suitable action.
 16. Driver build shell scripts have been committed to UVC and PXRC driver directories.

 774. (FEATURE) Concurrent Managed Workqueue(CMWQ), VIRGO64 Queueing and KingCobra64 messaging - 12 June 2019 - this section is an extended draft on respective topics in NeuronRain AstroInfer design and KingCobra design - <https://github.com/shrinivaasanka/asfer-github-code/blob/master/asfer-docs/AstroInferDesign.txt>, <https://github.com/shrinivaasanka/kingcobra64-github-code/blob/master/KingCobraDesignNotes.txt>

1. Existing workqueue underneath VIRGO64 queueing and requests routed by it to

KingCobra64 messaging are old legacy workqueues which have been revamped to Concurrent Managed Workqueue which supports concurrent messaging and lot of other options in queue creation.

2. `create_workqueue()` in VIRGO64 Queueing has been changed to `alloc_workqueue()` of Concurrent Managed Workqueue.
3. VIRGO64 Queueing request routing to KingCobra64 messaging has been tested with CMWQ and queueing log and kingcobra64 Request-Reply Queue have been committed to respective testlogs of the drivers
4. reading from stream has been disabled in `virgo_kernel_analytics.h`
5. Reference - CMWQ documentation - <https://www.kernel.org/doc/html/v4.11/core-api/workqueue.html>
6. Byzantine Fault Tolerance in KingCobra64 persisted queue can be made available by performant CMWQ and routing to the Replicas of `REQUEST_REPLY.queue` by any of the practical BFT protocols available.
7. Most important application of CMWQ based VIRGO64-KingCobra64 is in the context of kernelspace hardware messaging in IoT, Drones and other analytics driven embedded systems.
8. An example usecase which is a mix of sync and async I/O in kernelspace:
 - (*) Analytics Variables computed by userspace machine learning are read over socket stream by `kernel_analytics` driver and exported kernelwide
 - (*) Some interested Drone driver in kernel (example PXRC) reads the analytics variables synchronously and sends reply messages asynchronously to VIRGO64 Queueing driver over kernel sockets.
 - (*) VIRGO Queueing routes the queued messages to KingCobra64 driver

Srinivasan Kannan (alias) Ka.Shrinivaasan (alias) Shrinivas Kannan
<http://sites.google.com/site/kuja27>

1242. Coding Conventions and Best Practices followed in NeuronRain Architecture and Development

There are no strict standard conventions or practices followed in NeuronRain commits but following are some guiding principles:

1. NeuronRain repositories are spread across SourceForge(<https://sourceforge.net/u/userid-769929/>), GitHub(<https://github.com/shrinivaasanka/>) and GitLab(<https://gitlab.com/shrinivaasanka/>) - though they do not differ much at present, NeuronRain SourceForge focuses on Astronomical Datasets, NeuronRain GitHub is for Generic Datasets and Clouds and NeuronRain GitLab is intended for Drone Development. Every source file has copyleft header and attributions.
2. Presently there are no Continuous Integration/Unit testing framework. But every code change is tested manually and logs are captured suffixing timestamps in separate testlogs/ folder within C/C++/Java/Python source directories.
3. Development model followed is somewhat similar to Agile (but only a Single person team - K.Srinivasan - <https://sites.google.com/site/kuja27/> - Deleted and Mirrored at https://github.com/shrinivaasanka/Krishna_iResearch_DoxygenDocs/tree/master/kuja27_website_mirrored) and small incremental changes are frequent compared to rare big feature additions/changes especially in Python/MachineLearning code.
4. Code documentation - comments are profusely littered wherever necessary. NeuronRain FAQ simulates an enduser and asks questions on h(is/er) behalf and answers them.
5. Architectural choices are more important than implementation - no complicated overengineering - Occam's Razor.
6. VIRGO32 and VIRGO64 linux kernel base mainline PPA versions are not frequently

updated having reached minimum stability.

7. Benchmarks on Single/Multicore/Clusters are committed for salient Cloud implemented features (Factorization, Intrinsic Merit/Fitness, VIRGO system calls-drivers etc.,)

8. Code Reviews are Self-Reviews (GitHub and GitLab review tool comments by Author) only based on QE/QA logs. Entire NeuronRain repositories are architected and developed by 1 person team (K.Srinivasan - <https://acadpdrafts.readthedocs.io/en/latest/>) without any peer review. NeuronRain development is free, open and transparent not-for-profit charity effort. Comprehensive logs are committed along with almost every code change in NeuronRain repositories in Sourceforge, GitHub and GitLab available for public review.

9. To err is human - erroneous commits are corrected as and when found. Bug Tracking is minimal and there are no strict timelines for resolution. Following are bug tracking pages for all Krishna iResearch - NeuronRain repositories:

SourceForge - NeuronRain Research -

https://sourceforge.net/u/ka_shrinivaasan/tickets/

GitHub - NeuronRain Green -

https://github.com/shrinivaasanka/Krishna_iResearch_DoxygenDocs/issues

GitLab - NeuronRain Antariksh -

https://gitlab.com/shrinivaasanka/Krishna_iResearch_DoxygenDocs/-/issues

(Deprecated) AsFer GitHub issues page -

<https://github.com/shrinivaasanka/asfer-github-code/issues?q=is%3Aissue+is%3Aclosed>).

JIRA Bug Tracking - <https://krishnairesearch.atlassian.net/>

10. NeuronRain architecture and development has two worlds - userspace(AsFer)

cloud/machine learning and kernelspace(VIRGO/KingCobra/USBmd)

cloud/Embedded/IoT/Drones/Robotics - connected by kernel_analytics.conf and live reading of remote sockets for analytics variables from kernel_analytics module.

AsFer has more activity compared to others.

11. No strict deadlines/releases but repositories are source-released periodically.

12. Bug Reports/Pull Requests are encouraged at Issues tracking pages (item 9) but resolution depends on feasibility and time availability.

13. Each NeuronRain repository has a design document updated periodically for commits and related technical notes. Though "git log" is sufficient, design document delves into theoretical aspects of the implementation which are related to publications and draft publications of the author. Commits for multiple dates are sometimes batched and dates of commits might be out of sync with dates of code commentaries in design documents. NeuronRain design documents have unified numbering for theory content because of strongly connected conceptual graph aligned to the 32-bit and 64-bit codebases - AstroInfer(Machine Learning), USBmd(Software Analytics and Program Analyzer), VIRGO(IoT, Scheduler/Kernel Analytics and Program Analyzer), KingCobra(Kernelspace messaging and Algorithmic economics), GRAFIT(course materials overlap theory of NeuronRain), Krishna_iResearch_DoxygenDocs(NeuronRain FAQ), Acadpdrafts(publications and drafts for implementations in NeuronRain).

14. In essence any good software relies on the basic thumbrule: concept feature --- design/algorithm for feature --- choice of software for implementation of the algorithm --- how much value this new feature adds to existing implementation .

15. Any software is the result of immense human effort. NeuronRain is an academic FOSS research and development product which includes implementations and later non-peer reviewed expansions of author's publications and contributed as charity - https://arxiv.org/user/698017/pwc_link,

https://arxiv.org/user/626007/pwc_link,

https://tac.nist.gov/publications/2010/participant.papers/CMI_IIT.proceedings.pdf

(<https://cs.paperswithcode.com/paper/decidability-of-existence-and-construction-of>, <https://paperswithcode.com/paper/few-algorithms-for-ascertaining-merit-of-a>) - an alpha or beta version in state of flux - and

integration of nightly build setup, QA/QE test suites and formal installation packages for OS platforms are pending. There is no mobile app for NeuronRain though it can be installed on Android which is a linux-forkoff just like any other OS. NeuronRain has not been tested on Production-grade

Datasets/Cloud/Drones and largescale institutional-commercial-corporate deployments if any are cautioned against per FAQ,Licensing and Documentation URLs in 17 and 18 - especially VIRGO linux kernel system calls and drivers (kernel space cloud RPC) are sensitive to hardware-architectural idiosyncracies and mainline linux kernel versions. Drone code has been tested only on JMAVSIM flight simulator. Algorithmic fairness of ML datasets is not vouchsafed. Neuro Cryptocurrency Rig has been implemented only for academic use. Dependency OSS licenses are strictly respected and periodically updated in Requirements.txt. More details at Disclaimer in NeuronRain Documentation and Licensing - <https://neuronrain-documentation.readthedocs.io/en/latest/>
16.Copyrights for Images, Audios, Videos, Manual or Spider Crawled Websites, News articles and Social Network Profiles for testing purposes have been attributed to the respective source - Most of them are related to the author excluding oriental and western classical music clips.
17.NeuronRain Documentation - <https://neuronrain-documentation.readthedocs.io/en/latest/>
18.NeuronRain Documentation Repositories (updated more frequently):
18.1 GitHub - https://github.com/shrinivaasanka/Krishna_iResearch_DoxygenDocs
18.2 GitLab - https://gitlab.com/shrinivaasanka/Krishna_iResearch_DoxygenDocs
18.3 SourceForge - https://sourceforge.net/u/userid-769929/Krishna_iResearch_DoxygenDocs/ci/master/tree/
19.OpenHub Source Code Analyzer Profile - https://www.openhub.net/accounts/ka_shrinivaasan,
https://www.openhub.net/accounts/ka_shrinivaasan/positions
20.NeuronRain commits twitter handle - https://twitter.com/neuronrain_comm
21.Author's website - <https://acadpdrfts.readthedocs.io/en/latest/> - Mirror of deleted <https://sites.google.com/site/kuja27/> portal is at https://github.com/shrinivaasanka/Krishna_iResearch_DoxygenDocs/tree/master/kuja27_website_mirrored

#-----

#NEURONRAIN ASFER - Software for Mining Large Datasets
#This program is free software: you can redistribute it and/or modify
#it under the terms of the GNU General Public License as published by
#the Free Software Foundation, either version 3 of the License, or
#(at your option) any later version.
#This program is distributed in the hope that it will be useful,
#but WITHOUT ANY WARRANTY; without even the implied warranty of
#MERCHANTABILITY or FITNESS FOR A PARTICULAR PURPOSE. See the
#GNU General Public License for more details.
#You should have received a copy of the GNU General Public License
#along with this program. If not, see <<http://www.gnu.org/licenses/>>.
#-----

#Copyleft (Copyright+):
#Srinivasan Kannan
#(also known as: Shrinivaasan Kannan, Shrinivas Kannan)
#Ph: 9791499106, 9003082186
#Krishna iResearch Open Source Products Profiles:
#http://sourceforge.net/users/ka_shrinivaasan,
#<https://github.com/shrinivaasanka>,
#https://www.openhub.net/accounts/ka_shrinivaasan
#Personal website(research): <https://sites.google.com/site/kuja27/>
#emails: ka.shrinivaasan@gmail.com, shrinivas.kannan@gmail.com,
#kashrinivaasan@live.com
#-----

(*) ./asfer - C++ binary and doClustering=true in asfer.conf - clusters the string encoded celestial configurations by KMeans and kNN clustering algorithms

(*) python AsferClassifierPreproc.py - #autogenerated words.txt and words-frequency.txt needed for NaiveBayesClassifier

(*) geonames.py - #Geolocation Service JSON Request and Response for timezone Offset #Copyright - <https://gist.github.com/pamelafox/2288222/download#>
#Simplified and modified for AstroInfer

(*) python asfer_dataset_seggregator.py - #Partitions the parsed datasets which contain date-time-long-lat data based on classifier output grepped #by the invoker shell script - asfer_dataset_seggregator.sh - and writes the names of parsed dataset files into
#text files with names of regular expression "EventClassDataSet_<class>.txt"

(*) python MaitreyaToEnchoroClassified.py - #Reads the segregated parsed dataset files generated by asfer_dataset_aggregator.sh and invokes maitreya_textclient #for all date-time-long-lat data within all parsed datasets for a particular event class - "EventClassDataSet_<class>.txt"
#and also creates autogenerated asfer.enchoros.<class>.zodiacal and asfer.enchoros.<class>.asrelative encoded files

(*) python SequenceMining.py - #This class Implements Sequence Mining for encoded strings - at present Apriori GSP algorithm has been #implemented - uses Downward Closure - superset is frequent only if subset is frequent #SourceForge version is specialized for Mining Astronomical Datasets - read from files with .enchoros suffix. #It predicts pattern in swiss ephemeris encoded astronomical datasets corresponding to weather phenomena. #GitHub version is generic to all string patterns.

Prerequisites - Dataset Classification and Preprocessing

- create/add articles on earthquakes and hurricanes as training dataset for NaiveBayesian Classifier

- tuples in

python-src/autogen_classifier_dataset/AsferClassifierPreproc.py has to be updated to include new articles for creating updated NaiveBayesian training data

- training data for NaiveBayesian classifier - words.txt, word-frequency.txt, training-set.txt, topics.txt, test-set.txt - have to be re-created by executing python-src/autogen_classifier_dataset/AsferClassifierPreproc.py

- execute python asfer_dataset_seggregator.sh - invokes NaiveBayesian classifier to classify datasets into files of names EventClassDataSet_<class>.txt

- execute python MaitreyaToEnchoroClassified.py - creates asfer.enchoros.<class>.zodiacal and asfer.enchoros.<class>.asrelative encoded files read from "EventClassDataSet_<class>.txt"

- rename asfer.enchoros.<class>.zodiacal and asfer.enchoros.<class>.asrelative to asfer.enchoros.* input file read by respective implementations

String encoded celestial datasets can be analyzed in multiple ways as below:

(*) Clustering - kMeans and kNN - Unsupervised

- by enabling clustering in asfer.conf config file and executing ./asfer

C++ binary having suitable asfer.anchors input files (input files have to be rewritten by respective string encoded outputs from ephemeris script mentioned above in autogen_classifier_dataset/ directory)

(*) NaiveBayesian and DecisionTree Classifiers - Supervised

- execute python AsferClassifierPreproc.py to create training data for weather/celestial events
- execute ./asfer C++ binary.
- This classifies the datasets in multiple categories

(*) BioPython and ClustalOmega sequence alignment mining - uses Third Party opensource packages to extract common subsequences in celestial string encoded data - corresponds to astronomical conjunctions.

(*) Needleman-Wunsch multiple sequence alignment mining - aligns the celestial data strings and extracts common subsequences which correspond to astronomical conjunctions in sky.

(*) Sequence Mining - Apriori GSP

- execute python SequenceMining.py - mines common subsequences in celestial string encoded data - correspond to astronomical conjunctions in sky

(*) Spark PrefixSpan Sequence Mining

- Spark Cloud implementation - PrefixSpan mining of encoded Astronomical datasets -

https://github.com/shrinivaasanka/Grafit/blob/master/course_material/NeuronRain/LinuxKernelAndCloud/code/Spark_PrefixSpan.py (in SourceForge, GitLab Grafit repositories as well)

#-----

#NEURONRAIN ASFER - Software for Mining Large Datasets

#This program is free software: you can redistribute it and/or modify
#it under the terms of the GNU General Public License as published by
#the Free Software Foundation, either version 3 of the License, or
#(at your option) any later version.

#This program is distributed in the hope that it will be useful,
#but WITHOUT ANY WARRANTY; without even the implied warranty of
#MERCHANTABILITY or FITNESS FOR A PARTICULAR PURPOSE. See the
#GNU General Public License for more details.

#You should have received a copy of the GNU General Public License
#along with this program. If not, see <<http://www.gnu.org/licenses/>>.

#-----

#K.Srinivasan

#NeuronRain Documentation and Licensing: <http://neuronrain-documentation.readthedocs.io/en/latest/>

#Personal website(research): <https://sites.google.com/site/kuja27/>

#-----

1244. Following are NeuronRain Usecases (some of which have been implemented in NeuronRain while others have dependencies):

1. Software Analytics - Scheduler Analytics - Psutil Deep Learning of Scheduler Classes and writing to /etc/kernel_analytics.conf or /etc/sysctl.conf (kernel.sched.*)

2. Software Analytics - Software Analytics - Psutil Deep Learning of Systemwide Memory/IO/CPU load.

3. Software Analytics - Userspace and Kernel space Program Analyzers
4. Software Analytics - Kernel Analytics - Analysis of kernel logs
5. Software Analytics - Wireless Network Traffic Analytics
6. Drones/Unmanned Aerial Vehicles - Deep Learning of GIS imagery by Video ImageNet-EventNet Tensor Products Algorithm for prominent features (convex hulls, bounding boxes etc.,) in terrestrial images and navigation accordingly - Drone Online Shopping Delivery example
7. Drones/Unmanned Aerial Vehicles - Kernel Analytics for Drone and Robotic OSes (<https://github.com/Dronecode>, <https://github.com/Dronecode/DronecodeSDK>, <https://github.com/Dronecode/DronecodeSDK-Python>) - Drone Online Shopping Delivery example
8. Streaming Analytics - Streams from various datasources
9. Advertisement Analytics - by Spark Structured Streaming, PageRank
10. Merit ranking and Analytics of Text, Audio/Music, Video, People
11. Histogram-Set Partition Analytics - Streams of business intelligence histograms, voting histograms, hashtable or dictionaries
12. Medical Imaging Analytics - find patterns in ECG, MRI, Scan medical images for diagnosis
13. Image Analytics - Webcam or retinal scan driver captures face or retinal scan image, compares them for match (face or retinal scan as password) in userspace deep learning analytics, exports match = True or False as kernel analytics variables which are read and exported by kernel_analytics VIRGO32 and VIRGO64 drivers and read by some other authentication driver in kernel and message is logged in /var/log/kern.log
14. Drones/Flights/UAVs - Change pxrc flight controller driver for reading analytics variables exported by kernel_analytics VIRGO32 and VIRGO64 drivers
15. Astronomy analytics - Sequence Mining and N-Body equation solver for gravitational acceleration-extreme weather events correlation, Space imagery analysis

NeuronRain Licensing is explained in FAQ: <http://neuronrain-documentation.readthedocs.io/en/latest/>

1245. NeuronRain Depends on Following Opensource C, Python, Java and C++ packages - Copyright/Copyleft licenses apply per respective codebases below:

1. Boost C++ and Python libraries (1.64.0)
2. g++
3. Python NLTK
4. NetworkX 2.5
5. Matplotlib
6. Scrapy
7. R-Python (rpy2)
8. Maitreya's Dreams 8 (for ephemeris and text client)
9. Hadoop
10. Spark 2.4.3, Spark 3.0.1 and pyspark client
11. Hive and Hive Client (thrift or pyhs2)
12. Cassandra and Cassandra Cluster client
13. HBase and HBase client (happybase)
14. Python-LinkedIn
15. Python Twitter
16. Biopython
17. ClustalOmega
18. BeautifulSoup
19. Google Protocol Buffer libraries 3.5 / libprotobuf15
20. Pig
21. SVMLight (there is also a NeuronRain AsFer Support Vector Machines implementation alternative)
22. MySQLdb
23. Python Injector
24. R
25. Python Tornado
26. Linux Kernel Mainline 32 bit (4.1.5) - for VIRGO

27. MongoDB and pymongo
28. Cython
29. SATURN Program Analyzer
30. MemCached, pymemcache (Python 3.x) and Python-memcache (Python 2.x - <https://github.com/linsomniac/python-memcached/>)
31. Bidict
32. Java 1.8
33. Python Jellyfish
34. Python Enchant
35. Python ystockquote
36. Python geonames (Maitreya's Dreams - location-to-timezone lookup)
37. Python zlib
38. Neo4j Graph Database
39. py2neo python client for Neo4j
40. Python OAuth2
41. Redis and Python Redis
42. Passlib SHA256 encryption library
43. ZeroMQ
44. Kafka and Confluent Kafka Python client
45. Spark 2.3.0 + Hadoop 2.7 for Java Spark Streaming
46. Jsoup Java HTML parser
47. PILlow Python Imaging Library
48. ConceptNet 5.7
49. NumPy
50. SciPy 1.1.0
51. Linux Kernel Mainline 64 bit (4.13.3) - for VIRG064
52. CvxPy
53. SymPy
54. Python transaction 2.1.2
55. OpenSSL development libraries for C++
56. DictDiffer - <https://github.com/inveniosoftware/dictdiffer>
57. Python 2.7.x, 3.4, 3.6, 3.7.5, 3.8.5, 3.9.0
58. Facebook SDK for Python 3.4
59. Empath (<https://arxiv.org/pdf/1602.06979.pdf>)
60. Scikit-Learn
61. Pandas
62. librosa - Python Audio Library - 0.9.2
63. Psutils - Python process utility
64. FlameGraph - <https://github.com/brendangregg/FlameGraph>
65. Valgrind/Callgrind/KCachegrind
66. GraphFrames/GraphX Spark Package - <https://graphframes.github.io/>
67. Theano
68. Keras (Theano and TensorFlow backends)
69. OpenCV 3.4.3 - opencv-python - cv2
70. PyPDF2
71. FTrace (for kernel functions call graphs)
72. PyDictionary
73. Optional - Not tested - DronecodesDK (Python - only for usecases in NeuronRainApps/Drones and Autonomous Drone Electronic Voting Machines)
74. Optional - Not tested - Helicamera Drones (Hardware e.g PX4 MAVLink Hexacopters - only for usecases in NeuronRainApps/Drones and Autonomous Drone Electronic Voting Machines)
75. AudioRead
76. Scikit-SPLearn - <http://dev.pages.lis-lab.fr/scikit-splearn/index.html>
77. Python SpeechRecognition
78. Python PocketSphinx
79. Swig
80. ALSA development library
81. PulseAudio development library
82. Kaggle Datasets - CreditCard Transactions and LinkedIn Profiles
83. googletrans
84. Goslate
85. PIPL.com Python API (requires API key)
86. Python Human Name Parser

87. PyHyphen - for syllables in strings
88. TensorLy - for Video EventNet Tensor Decomposition to Rank-x tensors
89. autopep8 - for PEP8 python coding convention -
<https://pypi.org/project/autopep8/>
90. 2to3 - for upgrading python 2.x to 3.x -
<https://docs.python.org/2/library/2to3.html>
91. CVXOPT - Convex Program for Market Equilibrium - KingCobra-AstroInfer Neuro
cryptocurrency and transactional cloud move
92. Linux Kernel Mainline 64 bit (5.1.4) - for VIRGO64 PXRC Drone Telemetry
93. PX4 Firmware and ECL - installed by ubuntu_sim.sh - Drone Simulator
94. PX4 SITL - JMAVSIM - Drone Simulator
95. MAVSDK-Python
96. TensorFlow for Python
97. TensorFlow I/O for Python
98. CVXOPT GLPK for Integer Linear Programming
99. Python geopy (OpenStreetMap Nominatim Geocoding - for Drone address-to-
longitude-latitude lookup)
100. Optional - QGroundControl - <http://qgroundcontrol.com/> - QGC - for Drone
code (MAVSDK-PX4-SITL-JMAVSIM simulation)
101. Robomongo3T and Studio3T - for MongoDB GIS imagery bulk upload to GridFS
102. Python OpenWeatherMap - PyOWM - Weather Forecast
103. CliMetLab - ECMWF Climate Dataset Library
104. Optional - MetView 5.0 - ECMWF datasets
105. Optional - MetView Python - ECMWF datasets - MARS Retrieve
106. Shapely - Computational Geometry python library
107. Dlib - Face landmark detection
108. Netrd - Graph Similarity
109. PyVis - Graph Visualization
110. GMSH - FEM - Trimesh and Quadmesh
111. PySAL - Python Spatial Abstraction Library
112. SkyField - Python Astronomy Library
113. PyEphem - Python Astronomy Library - NASA JPL ephemeris (Optional)
114. AstroPy - Python Astronomy and Cosmology Library
115. jplephem - NASA JPL ephemeris - dependency for AstroPy
116. Scikit-Image - Hubble eXtreme Deep Field
117. Numba and Numba CUDA - Python and NumPy JIT optimizing fast bytecode
compiler for CPUs and GPUs (optional)
118. AstroPy-AstroQuery - <https://astroquery.readthedocs.io/en/latest/> - NASA
JPL Horizons Online Ephemeris REST API Service
119. AstroML - AstroPy + AstroQuery + Machine Learning
120. HealPy - for AstroML
121. Wikipedia Python API - PyWikiBot wrapper
122. GDAL C++ - <https://gdal.org/> - Installation of GDAL is complex and there
are lot of dependencies - <https://trac.osgeo.org/gdal/wiki/BuildingOnUnix>
123. GDAL Python bindings to GDAL C++ - Installation instructions at
[https://motheregeo-py.readthedocs.io/en/latest/development/how-to/gdal-ubuntu-
pkg.html](https://motheregeo-py.readthedocs.io/en/latest/development/how-to/gdal-ubuntu-pkg.html)
124. Rasterio - Has dependency on GDAL C -
<https://rasterio.readthedocs.io/en/latest/>
125. Fiona - GeoTIFF transforms - <https://fiona.readthedocs.io/en/latest/>
126. Laspy - LIDAR utility - <https://laspy.readthedocs.io/en/latest/>
127. IPython notebook (optional)
128. Jupyter notebook (optional)
129. Python mir_eval - https://craffel.github.io/mir_eval/
130. Python Playsound
131. Joblib - <https://joblib.readthedocs.io/en/latest/>

=====

=====
Coccinelle Static Analysis of NEURONRAIN VIRGO Linux Kernel

=====

=====
Analyzed on 25 July 2016:

1. Coccinelle static analyzer is an ubuntu package installable from APT.

2. Report for Static Analysis of virgo_malloc and virgo_filesystem syscalls are generated by following commandlines:

```
-----  
-----  
root@shrinivaasanka-Inspiron-1545:/media/shrinivaasanka/0fc4d8a2-1c74-42b8-8099-9ef78d8c8ea2/home/kashrinivaasan/linux-4.1.5# make coccicheck MODE=report  
M=virgo_filesystem/virgo_fs.c
```

Please check for false positives in the output before submitting a patch.
When using "patch" mode, carefully review the patch before submitting it.

```
virgo_filesystem/virgo_fs.c:470:12-16: WARNING: casting value returned by memory  
allocation function to (char *) is useless.  
virgo_filesystem/virgo_fs.c:479:12-16: WARNING: casting value returned by memory  
allocation function to (char *) is useless.  
root@shrinivaasanka-Inspiron-1545:/media/shrinivaasanka/0fc4d8a2-1c74-42b8-8099-9ef78d8c8ea2/home/kashrinivaasan/linux-4.1.5# make coccicheck MODE=report  
M=virgo_malloc/virgo_malloc.c
```

Please check for false positives in the output before submitting a patch.
When using "patch" mode, carefully review the patch before submitting it.

```
virgo_malloc/virgo_malloc.c:563:12-16: WARNING: casting value returned by memory  
allocation function to (char *) is useless.  
virgo_malloc/virgo_malloc.c:554:12-16: WARNING: casting value returned by memory  
allocation function to (char *) is useless.  
-----  
-----
```

```
kashrinivaasan@kashrinivaasan-Inspiron-1545:~/linux-3.7.8$ ls  
arch      crypto      firmware    ipc          lib           modules.builtin  
net        scripts     sound       virt  
block     Documentation  fs          Kbuild      MAINTAINERS  modules.order  
README     security     System.map  vmlinux  
COPYING    drivers      include     Kconfig     Makefile     Module.symvers  
REPORTING-BUGS signing_key.priv tools        vmlinux.o  
CREDITS    extra_certificates init         kernel      mm           Module.symvers.orig  
samples    signing_key.x509 usr          x509.genkey  
kashrinivaasan@kashrinivaasan-Inspiron-1545:~/linux-3.7.8$ make  
make[1]: Nothing to be done for `all'.  
make[1]: Nothing to be done for `relocs'.  
CHK      include/generated/uapi/linux/version.h  
CHK      include/generated/utsrelease.h  
CALL     scripts/checksyscalls.sh  
CHK      include/generated/compile.h  
PASYSMS  arch/x86/realmode/rm/pasyms.h  
LDS      arch/x86/realmode/rm/realmode.lds  
LD       arch/x86/realmode/rm/realmode.elf  
RELOCS   arch/x86/realmode/rm/realmode.relocs  
OBJCOPY  arch/x86/realmode/rm/realmode.bin  
AS       arch/x86/realmode/rmpiggy.o  
LD       arch/x86/realmode/built-in.o  
VDSOSYM  arch/x86/vdso/vdso32-int80-syms.lds  
VDSOSYM  arch/x86/vdso/vdso32-sysenter-syms.lds  
VDSOSYM  arch/x86/vdso/vdso32-syms.lds  
LD       arch/x86/vdso/built-in.o  
LD       arch/x86/built-in.o  
LINK     vmlinux  
LD       vmlinux.o  
MODPOST  vmlinux.o  
WARNING: modpost: Found 2 section mismatch(es).  
To see full details build your kernel with:  
'make CONFIG_DEBUG_SECTION_MISMATCH=y'  
GEN      .version
```

```

CHK      include/generated/compile.h
UPD      include/generated/compile.h
CC       init/version.o
LD       init/built-in.o
KSYM     .tmp_kallsyms1.o
KSYM     .tmp_kallsyms2.o
LD       vmlinux
SORTEX   vmlinux
sort done marker at 9333c4
SYSMAP   System.map
VOFFSET  arch/x86/boot/voffset.h
OBJCOPY  arch/x86/boot/compressed/vmlinux.bin
RELOCS   arch/x86/boot/compressed/vmlinux.relocs
GZIP     arch/x86/boot/compressed/vmlinux.bin.gz
MKPIGGY  arch/x86/boot/compressed/piggy.S
AS       arch/x86/boot/compressed/piggy.o
CC       arch/x86/boot/compressed/eboot.o
AS       arch/x86/boot/compressed/efi_stub_32.o
LD       arch/x86/boot/compressed/vmlinux
ZOFFSET  arch/x86/boot/zoffset.h
AS       arch/x86/boot/header.o
CC       arch/x86/boot/version.o
LD       arch/x86/boot/setup.elf
OBJCOPY  arch/x86/boot/setup.bin
OBJCOPY  arch/x86/boot/vmlinux.bin
BUILD    arch/x86/boot/bzImage
Setup is 16844 bytes (padded to 16896 bytes).
System is 5147 kB
CRC 51a4c3e5
Kernel: arch/x86/boot/bzImage is ready (#2)
  Building modules, stage 2.
  MODPOST 3834 modules
WARNING: modpost: Found 13 section mismatch(es).
To see full details build your kernel with:
'make CONFIG_DEBUG_SECTION_MISMATCH=y'
kashrinivaasan@kashrinivaasan-Inspiron-1545:~/linux-3.7.8$

```

```

kashrinivaasan@kashrinivaasan-Inspiron-1545:~/linux-3.7.8/drivers/usb/usb-md$
sudo make -C /lib/modules/`uname -r`/build/ M=`pwd`
[sudo] password for kashrinivaasan:
kashrinivaasan@kashrinivaasan-Inspiron-1545:~/linux-3.7.8/drivers/usb/usb-md$
sudo make -C /lib/modules/`uname -r`/build/ M=`pwd`
[sudo] password for kashrinivaasan:
make: Entering directory `/usr/src/linux-headers-3.7.8-030708-generic'
CC [M] /home/kashrinivaasan/linux-3.7.8/drivers/usb/usb-md/umb.o
/home/kashrinivaasan/linux-3.7.8/drivers/usb/usb-md/umb.c:78: warning:
initialization from incompatible pointer type
/home/kashrinivaasan/linux-3.7.8/drivers/usb/usb-md/umb.c: In function
'umb_write_bulk_callback':
/home/kashrinivaasan/linux-3.7.8/drivers/usb/usb-md/umb.c:139: warning: format
'%s' expects type 'char *', but argument 2 has type 'int'
/home/kashrinivaasan/linux-3.7.8/drivers/usb/usb-md/umb.c:139: warning: too few
arguments for format
/home/kashrinivaasan/linux-3.7.8/drivers/usb/usb-md/umb.c: In function
'umb_write':
/home/kashrinivaasan/linux-3.7.8/drivers/usb/usb-md/umb.c:162: warning: passing
argument 6 of 'usb_fill_bulk_urb' from incompatible pointer type
include/linux/usb.h:1442: note: expected 'usb_complete_t' but argument is of
type 'void (*)(struct urb *, struct pt_regs *)'
/home/kashrinivaasan/linux-3.7.8/drivers/usb/usb-md/umb.c: In function
'umb_exit':
/home/kashrinivaasan/linux-3.7.8/drivers/usb/usb-md/umb.c:186: warning: 'return'
with a value, in function returning void
/home/kashrinivaasan/linux-3.7.8/drivers/usb/usb-md/umb.c: In function

```

```

'umb_probe':
/home/kashrinivaasan/linux-3.7.8/drivers/usb/usb-md/umb.c:230: warning: 'return'
with a value, in function returning void
/home/kashrinivaasan/linux-3.7.8/drivers/usb/usb-md/umb.c:196: warning: unused
variable 'retval'
/home/kashrinivaasan/linux-3.7.8/drivers/usb/usb-md/umb.c: In function
'umb_disconnect':
/home/kashrinivaasan/linux-3.7.8/drivers/usb/usb-md/umb.c:236: warning: unused
variable 'minor'
/home/kashrinivaasan/linux-3.7.8/drivers/usb/usb-md/umb.c: In function
'umb_release':
/home/kashrinivaasan/linux-3.7.8/drivers/usb/usb-md/umb.c:271: warning: no
return statement in function returning non-void
Building modules, stage 2.
MODPOST 1 modules
LD [M] /home/kashrinivaasan/linux-3.7.8/drivers/usb/usb-md/umb.ko
make: Leaving directory `/usr/src/linux-headers-3.7.8-030708-generic'
kashrinivaasan@kashrinivaasan-Inspiron-1545:~/linux-3.7.8/drivers/usb/usb-md$
sudo make -C /lib/modules/`uname -r`/build/ M=`pwd` clean
make: Entering directory `/usr/src/linux-headers-3.7.8-030708-generic'
CLEAN /home/kashrinivaasan/linux-3.7.8/drivers/usb/usb-md/.tmp_versions
CLEAN /home/kashrinivaasan/linux-3.7.8/drivers/usb/usb-md/Module.symvers
make: Leaving directory `/usr/src/linux-headers-3.7.8-030708-generic'
kashrinivaasan@kashrinivaasan-Inspiron-1545:~/linux-3.7.8/drivers/usb/usb-md$
sudo make -C /lib/modules/`uname -r`/build/ M=`pwd`
make: Entering directory `/usr/src/linux-headers-3.7.8-030708-generic'
LD /home/kashrinivaasan/linux-3.7.8/drivers/usb/usb-md/built-in.o
CC [M] /home/kashrinivaasan/linux-3.7.8/drivers/usb/usb-md/umb.o
/home/kashrinivaasan/linux-3.7.8/drivers/usb/usb-md/umb.c:78: warning:
initialization from incompatible pointer type
/home/kashrinivaasan/linux-3.7.8/drivers/usb/usb-md/umb.c: In function
'umb_write_bulk_callback':
/home/kashrinivaasan/linux-3.7.8/drivers/usb/usb-md/umb.c:139: warning: format
'%s' expects type 'char *', but argument 2 has type 'int'
/home/kashrinivaasan/linux-3.7.8/drivers/usb/usb-md/umb.c:139: warning: too few
arguments for format
/home/kashrinivaasan/linux-3.7.8/drivers/usb/usb-md/umb.c: In function
'umb_write':
/home/kashrinivaasan/linux-3.7.8/drivers/usb/usb-md/umb.c:162: warning: passing
argument 6 of 'usb_fill_bulk_urb' from incompatible pointer type
include/linux/usb.h:1442: note: expected 'usb_complete_t' but argument is of
type 'void (*)(struct urb *, struct pt_regs *)'
/home/kashrinivaasan/linux-3.7.8/drivers/usb/usb-md/umb.c: In function
'umb_exit':
/home/kashrinivaasan/linux-3.7.8/drivers/usb/usb-md/umb.c:186: warning: 'return'
with a value, in function returning void
/home/kashrinivaasan/linux-3.7.8/drivers/usb/usb-md/umb.c: In function
'umb_probe':
/home/kashrinivaasan/linux-3.7.8/drivers/usb/usb-md/umb.c:230: warning: 'return'
with a value, in function returning void
/home/kashrinivaasan/linux-3.7.8/drivers/usb/usb-md/umb.c:196: warning: unused
variable 'retval'
/home/kashrinivaasan/linux-3.7.8/drivers/usb/usb-md/umb.c: In function
'umb_disconnect':
/home/kashrinivaasan/linux-3.7.8/drivers/usb/usb-md/umb.c:236: warning: unused
variable 'minor'
/home/kashrinivaasan/linux-3.7.8/drivers/usb/usb-md/umb.c: In function
'umb_release':
/home/kashrinivaasan/linux-3.7.8/drivers/usb/usb-md/umb.c:271: warning: no
return statement in function returning non-void
Building modules, stage 2.
MODPOST 1 modules
CC /home/kashrinivaasan/linux-3.7.8/drivers/usb/usb-md/umb.mod.o
LD [M] /home/kashrinivaasan/linux-3.7.8/drivers/usb/usb-md/umb.ko

```



```

make: Leaving directory `/usr/src/linux-headers-3.7.8-030708-generic'
kashrinivaasan@kashrinivaasan-Inspiron-1545:~/linux-3.7.8/drivers/usb/usb-md$ ls
-lrt
total 132
-rwxr-xr-x 1 kashrinivaasan kashrinivaasan 117 Feb 17 18:24 Makefile
-rwxr-xr-x 1 kashrinivaasan kashrinivaasan 5763 Feb 17 18:24 Kconfig
-rw-rw-r-- 1 kashrinivaasan kashrinivaasan 7606 Feb 17 18:29 umb.c
-rw-r--r-- 1 root          root          5512 Apr  5 11:06 umb.o
-rw-r--r-- 1 root          root           66 Apr  5 11:06 modules.order
-rw-r--r-- 1 root          root            8 Apr  5 11:06 built-in.o
-rw-r--r-- 1 root          root        3368 Apr  5 11:06 umb.mod.o
-rw-r--r-- 1 root          root        1552 Apr  5 11:06 umb.mod.c
-rw-r--r-- 1 root          root       7472 Apr  5 11:06 umb.ko
-rw-r--r-- 1 root          root            0 Apr  5 11:06 Module.symvers
kashrinivaasan@kashrinivaasan-Inspiron-1545:~/linux-3.7.8/drivers/usb/usb-md$

```

```

437  ls
438  cd usb
439  ls
440  cd core
441  ls
442  sudo make -C /lib/modules/`uname -r`/build/ M=`pwd` modules
443  ls
444  strip --strip-debug usbcore.ko
445  cd /lib
446  ls
447  find . -exec grep usbcore.ko
448  find . -exec grep usbcore.ko /dev/null {} \;
449  cd modules/3.2.0-29-generic-pae/modules.builtin:kernel/drivers/usb/core
450  ls
451  cd modules/3.2.0-29-generic-pae/kernel/drivers/
452  ls
453  cd usb
454  ls
455  cd wusbcore/
456  ls
457  pwd
458  cd
459  ls
460  pwd
461  cd /usr/src
462  ls
463  cd linux-source-3.2.0/
464  ls
465  cd linux-source-3.2.0/
466  ls
467  pwd
468  cd drivers
469  ls
470  cd usb
471  ls
472  cd core
473  ls
474  cd
475  sudo apt-get install build-essential bin86 kernel-package libqt3-headers
libqt3-mt-dev wget libncurses5 libncurses5-dev
476  pwd
477  cd /usr/src
478  ls
479  cd linux-source-3.2.0/
480  ls
481  cd linux-source-3.2.0/
482  ls
483  cd drivers/

```

```
484 ls
485 cd usb
486 ls
487 cd core
488 ls
489 pwd
490 sudo make -C /lib/modules/`uname -r`/build/ M=`pwd` modules
491 cd /usr/src/linux-headers-3.2.0-32-generic-pae
492 ls
493 cd drivers
494 ls
495 cdusb
496 cd usb
497 ls
498 cd core
499 ls
500 make
501 pwd
502 cd ..
503 ls
504 cd ..
505 ls
506 pwd
507 cd ..
508 ls
509 sudo make -C /lib/modules/`uname -r`/build/ M=`pwd` modules
510 [wd
511 ;s
512 la
513 ls
514 cd drivers
515 s
516 ls
517 cd usb
518 ls
519 cd core
520 sudo make -v -C /lib/modules/`uname -r`/build/ M=`pwd` modules
521 sudo make -C /lib/modules/`uname -r`/build/ M=`pwd` modules
522 cd /lib
523 ls
524 cd modules/
525 ls
526 cd 3.2.0-32-generic-pae/
527 ls
528 cd build
529 ls
530 cd drivers
531 ls
532 cd usb/
533 ls
534 cd core/
535 ls
536 pwd
537 cd ../../../../
538 ls
539 cd kernel/
540 ls
541 cd drivers/
542 ls
543 cd usb/
544 ls
545 pwd
546 cd ../../..
547 ls
```

```
548 cd build
549 ls
550 ls lib
551 ls
552 cd drivers
553 s
554 ls
555 cd usb
556 ls
557 cd core/
558 ls
559 cd ../../..
560 ls
561 cd sound
562 cd ..
563 ls
564 strip --strip-debug usbcore.ko
565 ls
566 make
567 cd
568 tcpdump
569 tcpdump -h
570 ifconfig
571 sudo wireshark
572 pwd
573 ls
574 cd /usr
575 ls
576 cd src
577 ls
578 cd modules/
579 ls
580 cd ..
581 ls
582 cd linux-
583 cd
584 locate bluez
585 cd /usr/share/doc
586 ls
587 cd bluez
588 ls
589 cd examples/
590 ls
591 ./monitor-bluetooth
592 cd
593 ls
594 cd /usr/src
595 ls
596 cd linux-source-3.2.0/
597 ls
598 cd linux-source-3.2.0/
599 ls
600 cd drivers
601 ls
602 cd usb
603 ls
604 cd core
605 ls
606 sudo perl -pi.bak -e 's/16384/131072/' devio.c
607 make -C /lib/modules/`uname -r`/build/ M=`pwd` modules
608 sudo make -C /lib/modules/`uname -r`/build/ M=`pwd` modules
609 cd /usr/src
610 ls
611 cd linux-source-3.2.0/
```

```

612 ls
613 cd linux-source-3.2.0/
614 ls
615 mv * ..
616 sudo mv * ..
617 ls
618 pwd
619 cd ..
620 ls
621 ls linux-source-3.2.0
622 rm -rf linux-source-3.2.0
623 sudo rm -rf linux-source-3.2.0
624 ls
625 cd drivers
626 ls
627 cd usb
628 ls
629 cd core
630 ls
631 sudo perl -pi.bak -e 's/16384/131072/' devio.c
632 sudo make -C /lib/modules/`uname -r`/build/ M=`pwd` modules
633 ls
634 pwd
635 ls ../..
636 ls
637 ls /lib/modules
638 sudo make -C /lib/modules/`uname -r`/build/ M=`pwd` modules
639 uname -r
640 sudo make -C /lib/modules/linux-source-3.2.0/build/ M=`pwd` modules
641 hostname:~/lkmpg-examples/02-HelloWorld# make
642 make -C /lib/modules/2.6.11/build M=/root/lkmpg-examples/02-HelloWorld
modules
643 make[1]: Entering directory `/usr/src/linux-2.6.11'
644   CC [M] /root/lkmpg-examples/02-HelloWorld/hello-1.o
645   Building modules, stage 2.
646   MODPOST
647   CC      /root/lkmpg-examples/02-HelloWorld/hello-1.mod.o
648   LD [M] /root/lkmpg-examples/02-HelloWorld/hello-1.ko
649 make[1]: Leaving directory `/usr/src/linux-2.6.11'
650 hostname:~/lkmpg-examples/02-HelloWorld#
651
652 sudo apt-get build-dep linux-source-3.2.0-generic-pae
653 sudo apt-get build-dep linux-source-3.2.0-32-generic-pae
654 ls
655* sudo make -C /lib/modules/`uname -r`/build/ M=`pwd` modules
656 pwd
657 sudo apt-get build-dep linux-source-3.2.0-32
658 sudo apt-get build-dep linux-source-3.2.0
659 cd
660 ls
661 cd italc-2.0.0/
662 ls
663 sudo aptitude install libitalc italc-client italc-master
664 sudo apt-get install libitalc italc-client italc-master
665 italc
666 git
667 sudo apt-get install git
668 uname -r
669 ls
670 pwd
671 cd /usr/src
672 ls
673 cd linux-source-3.2.0/
674 ls

```

```

675 pwd
676 cd ..
677 ls
678 mkdir modifiedUSBdriver
679 sudo mkdir modifiedUSBdriver
680 ls
681 pwd
682 cd modifiedUSBdriver/
683 ls
684 cp /boot/config-`uname -r` .config
685 sudo cp /boot/config-`uname -r` .config
686 sudo cp /boot/config-`uname -r` .config
687 ls
688 ls -al
689 ls -al
690 pwd
691 uname -r
692 cp /usr/src/linux-headers-3.2.0-32-generic-pae/Module.symvers .
693 sudo cp /usr/src/linux-headers-3.2.0-32-generic-pae/Module.symvers .
694 ls
695 cd ..
696 ls
697 cd linux-source-3.2.0/
698 ls
699 pwd
700 sudo make EXTRAVERSION=-32-generic 0=/usr/src/modifiedUSBdriver oldconfig
701 sudo make EXTRAVERSION=-32-generic 0=/usr/src/modifiedUSBdriver
oldconfigls
702 pwd
703 uname -r
704 sudo make EXTRAVERSION=-32-generic-pae 0=/usr/src/modifiedUSBdriver
oldconfig
705 sudo apt-get build-dep --no-install-recommends linux-image-$(uname -r)
706 sudo apt-get build-dep --no-install-recommends linux-image-$(uname -r)
707 apt-get source linux-image-$(uname -r)
708 sudo apt-get source linux-image-$(uname -r)
709 ls
710 pwd
711 ls
712 cd /usr/src
713 ls
714 cd modifiedUSBdriver/
715 ls
716 uname -r
717 cp /usr/src/linux-headers-3.2.0-32-generic-pae/Module.symvers .
718 sudo cp /usr/src/linux-headers-3.2.0-32-generic-pae/Module.symvers .
719 cp /boot/config-`uname -r` .config
720 sudo cp /boot/config-`uname -r` .config
721 pwd
722 ls
723 cd ..
724 ls
725 ls -lrt
726 cd linux-source-3.2.0/
727 ls
728 ls -lrt
729 make EXTRAVERSION=-32-generic-pae 0=/usr/src/modifiedUSBdriver oldconfig
730 ls
731 pwd
732 cd
733 ls
734 cd modifiedUSBdriver/
735 ls
736 ls -l

```

```
737 pwd
738 rm -rf *
739 sudo rm -rf *
740 ls
741 pwd
742 sudo cp /usr/src/linux-headers-3.2.0-32-generic-pae/Module.symvers .
743 sudo cp /boot/config-`uname -r` .config
744 ls-l
745 ls -l
746 vi Module.symvers
747 ls
748 vi .config
749 ls
750 cd
751 ls
752 cd linux-3.2.0/
753 ls
754 make mrproper
755 sudo make mrproper
756 ls
757 ls -a
758 zcat /proc/config.gz > .config
759 sudo zcat /proc/config.gz > .config
760 ls
761 ls -al
762 ls
763 pwd
764 lsmod
765 ls
766 cd ..
767 ls
768 mv modifiedUSBdriver/ ~
769 sudo mv modifiedUSBdriver/ ~
770 cd
771 ls
772 cd modifiedUSBdriver/
773 ls
774 cd ..
775 ls
776 rm -rf modifiedUSBdriver/
777 cd /usr/src
778 ls
779 sudo mv modifiedUSBdriver/ ~
780 cd ~/linux-3.2.0/
781 ls
782 sudo make EXTRAVERSION=-32-generic-pae
0=/home/kashrinivaasan/modifiedUSBdriver oldconfig
783 gcc
784 gcc -v
785 apt-get install gcc
786 sudo apt-get install gcc
787 sudo apt-get upgrade gcc
788 sudo make EXTRAVERSION=-32-generic-pae
0=/home/kashrinivaasan/modifiedUSBdriver oldconfig
789 sudo make EXTRAVERSION=-32-generic-pae
0=/home/kashrinivaasan/modifiedUSBdriver oldconfig|more
790 locate config.gz
791 pwd
792 ls
793 cd /usr/src
794 ls
795 ls -lrt
796 cd
797 ls
```

```

798 ls -lrt
799 cd linux-3.2.0/
800 ls
801 pwd
802 make O=/home/kashrinivaasan/modifiedUSBdriver menuconfig
803 sudo make O=/home/kashrinivaasan/modifiedUSBdriver menuconfig
804 pwd
805 cd
806 cd /usr/src
807 ls
808 cd linux-source-3.2.0/
809 ls
810 ls -lrt
811 sudo make O=/home/kashrinivaasan/modifiedUSBdriver menuconfig
812 ls
813 pwd
814 cd
815 ls
816 cd linux-3.2.0/
817 ls
818 sudo make O=/home/kashrinivaasan/modifiedUSBdriver menuconfig
819 make mrproper
820 ls
821 sudo make mrproper
822 ls
823 sudo make O=/home/kashrinivaasan/modifiedUSBdriver menuconfig
824 sudo make O=/home/kashrinivaasan/modifiedUSBdriver menuconfig 2>&1 >
brokenbuild.txt
825 sudo make O=/home/kashrinivaasan/modifiedUSBdriver menuconfig 2>&1 >
~/brokenbuild.txt
826 ls
827 cd
828 ls
829 vi brokenbuild.txt
830 cd linux-3.2.0/
831 sudo make O=/home/kashrinivaasan/modifiedUSBdriver menuconfig 2>
~/brokenbuild.txt
832 cd ..
833 vi brokenbuild.txt
834 locate sys
835 locate types.h
836 ls
837 cd /usr/include/
838 ls
839 cd
840 ls
841 cd linux-3.2.0/
842 ls
843 cd include/
844 ls
845 pwd
846 cd ..
847 ls
848 find . -name types.h
849 ls
850 pwd
851 apt-get install libc6-dev
852 sudo apt-get install libc6-dev
853 dpkg -L libc6-dev
854 dpkg -L libc6-dev|grep tpes.h
855 dpkg -L libc6-dev|grep types.h
856 dpkg -L libc6-dev|grep mman.h
857 dpkg -L libc6-dev|grep stat.h
858 cd

```

```

859 ls
860 cd modifiedUSBdriver/
861 ls
862 cd scripts/
863 ls
864 cd basic/
865 ls
866 ls -al
867 pwd
868 cd ../../
869 ls
870 vi .config
871 ls
872 pwd
873 cd
874 ls
875 pwd
876 cd linux-3.2.0/
877 ls
878 cd include/
879 ls
880 cd
881 ls
882 pwd
883 sudo apt-get build-dep --no-install-recommends linux-image-$(uname -r)
884 apt-get source linux-image-$(uname -r)
885 ls
886 ls -lrt
887 ls
888 mv modifiedUSBdriver/ linuxbuild
889 ls
890 cd linux
891 cd linuxbuild/
892 ls
893 sudo cp /usr/src/linux-headers-3.2.0-32-generic-pae/Module.symvers .
894 sudo cp /boot/config-`uname -r` .config
895 pwd
896 ls
897 cd ~/linux-3.2.0/
898 ls
899 sudo make EXTRAVERSION=-32-generic-pae O=/home/kashrinivaasan/linuxbuild
oldconfig
900 pwd
901 ls
902 locate i386
903 locate i386|grep sys
904 ls
905 pwd
906 make menuconfig
907 ls
908 pwd
909 ls
910 cd
911 ls
912 vi brokenbuild.txt
913 cd linux-3.2.0/
914 ls
915 make O=/home/kashrinivaasan/linuxbuild menuconfig
916 sudo make O=/home/kashrinivaasan/linuxbuild menuconfig
917 sudo make -v O=/home/kashrinivaasan/linuxbuild menuconfig
918 sudo make -verbose O=/home/kashrinivaasan/linuxbuild menuconfig
919 sudo make -g O=/home/kashrinivaasan/linuxbuild menuconfig
920 sudo make -d O=/home/kashrinivaasan/linuxbuild menuconfig
921 sudo make -d O=/home/kashrinivaasan/linuxbuild menuconfig 2>

```



```
~/brokenbuild.txt
922 ls
923 pwd
924 cd
925 ls
926 vi brokenbuild.txt
927 pwd
928 ls
929 cd linuxbuild/
930 ls
931 cd ..
932 ls
933 pwd
934 cd linux-3.2.0/
935 ls
936 sudo make -d O=/home/kashrinivaasan/linuxbuild menuconfig
937 sudo make O=/home/kashrinivaasan/linuxbuild menuconfig
938 pwd
939 cd
940 cd linuxbuild/
941 ls
942 cp /usr/src/linux-headers-3.2.0-35-generic-pae/Module.symvers .
943 sudo cp /usr/src/linux-headers-3.2.0-35-generic-pae/Module.symvers .
944 sudo cp /boot/config-`uname -r` .config
945 pwd
946 cd ~/linux-3.2.0/
947 ls
948 make EXTRAVERSION=-35-generic O=~/linuxbuild oldconfig
949 sudo make EXTRAVERSION=-35-generic O=~/linuxbuild oldconfig
950 cd
951 ls
952 vi brokenbuild.txt
953 pwd
954 cd /usr/include/
955 ls
956 cd i386-linux-gnu/
957 ls
958 ls -lrt
959 pwd
960 cd
961 ls
962 cd linuxbuild/
963 ls
964 vi Module.symvers
965 ls
966 vi .config
967 ls
968 pwd
969 cd
970 ls
971 cd /usr/include
972 ls
973 pwd
974 ln -s sys i386-linux-gnu/sys
975 sudo ln -s sys i386-linux-gnu/sys
976 ls
977 sudo ln -s asm i386-linux-gnu/asm
978 ls
979 ls -lrt
980 ls -lrt
981 cd sys
982 ls
983 cd i386-linux-gnu/
984 ls
```

```
985 cd sys
986 pwd
987 cd ../../
988 ls
989 ln
990 ln -h
991 ln --help
992 man ln
993 ls
994 ln -s i386-linux-gnu/asm asm
995 sudo ln -s i386-linux-gnu/asm asm
996 ls asm
997 sudo ln -s i386-linux-gnu/sys sys
998 ls sys
999 pwd
1000 ls -al
1001 ls -lrt
1002 ls i386-linux-gnu/
1003 sudo ln -s i386-linux-gnu/bits bits
1004 sudo ln -s i386-linux-gnu/gnu gnu
1005 ls
1006 pwd
1007 ls -lrt
1008 ls
1009 pwd
1010 cd
1011 ls
1012 cd linux-3.2.0/
1013 ls
1014 sudo make O=/home/kashrinivaasan/linuxbuild menuconfig
1015 sudo make clean
1016 sudo make O=/home/kashrinivaasan/linuxbuild menuconfig
1017 pwd
1018 cd -
1019 cd /usr/include/
1020 ls
1021 ls -lrt
1022 ls i386-linux-gnu/
1023 sudo ln -s i386-linux-gnu/fpu_control.h fpu_control.h
1024 ls -lrt
1025 pwd
1026 ls
1027 ls -lrt
1028 cd
1029 ls
1030 cd linux
1031 cd linux-3.2.0/
1032 ls
1033 sudo make O=/home/kashrinivaasan/linuxbuild menuconfig
1034 locate crt1.o
1035 export LD_LIBRARY_PATH=/usr/lib/i386-linux-gnu/:$LD_LIBRARY_PATH
1036 sudo make O=/home/kashrinivaasan/linuxbuild menuconfig
1037 sudo make -d O=/home/kashrinivaasan/linuxbuild menuconfig
1038 pwd
1039 cd
1040 locate crt1.o
1041 sudo ln -s /usr/lib/i386-linux-gnu/crt1.o /usr/lib/crt1.o
1042 ls -lrt /usr/lib
1043 pwd
1044 ls
1045 cd linux-3.2.0/
1046 ls
1047 sudo make -d O=/home/kashrinivaasan/linuxbuild menuconfig
1048 sudo make O=/home/kashrinivaasan/linuxbuild menuconfig
```

```

1049 export LD_LIBRARY_PATH=/usr/lib:/usr/lib/i386-linux-gnu/:$LD_LIBRARY_PATH
1050 sudo make O=/home/kashrinivaasan/linuxbuild menuconfig
1051 locate crt1.o
1052 ls -lrt /usr/lib
1053 ls -lrt /usr/lib/i386-linux-gnu/
1054 ls -lrt /usr/lib/i386-linux-gnu/*crt*
1055 sudo ln -s /usr/lib/i386-linux-gnu/crt1.o /usr/lib/crt1.o
1056 sudo ln -s /usr/lib/i386-linux-gnu/crtn.o /usr/lib/crtn.o
1057 sudo ln -s /usr/lib/i386-linux-gnu/gcrt1.o /usr/lib/gcrt1.o
1058 sudo ln -s /usr/lib/i386-linux-gnu/Mcrt1.o /usr/lib/Mcrt1.o
1059 sudo ln -s /usr/lib/i386-linux-gnu/Scrt1.o /usr/lib/Scrt1.o
1060 ls -lrt /usr/lib
1061 sudo make O=/home/kashrinivaasan/linuxbuild menuconfig
1062 apt-get install ncurses
1063 sudo apt-get install ncurses
1064 sudo apt-get install ncurses-devel
1065 sudo apt-get install libncurses5-dev
1066 sudo make O=/home/kashrinivaasan/linuxbuild menuconfig
1067 make EXTRAVERSION=-35-generic O=~/.linuxbuild oldconfig
1068 sudo make EXTRAVERSION=-35-generic O=~/.linuxbuild oldconfig
1069 sudo make EXTRAVERSION=-35-generic O=~/.linuxbuild prepare
1070 sudo make EXTRAVERSION=-35-generic O=~/.linuxbuild outputmakefile
1071 sudo make EXTRAVERSION=-35-generic O=~/.linuxbuild archprepare
1072 sudo make EXTRAVERSION=-35-generic O=~/.linuxbuild modules SUBDIRS=scripts
1073 pwd
1074 ls
1075 sudo make EXTRAVERSION=-35-generic O=~/.linuxbuild modules
SUBDIRS=drivers/usb/
1076 ls
1077 pwd
1078 cd ls
1079 ls
1080 cd drivers
1081 ls
1082 cd usb/core
1083 ls
1084 cd
1085 cd linuxbuild/
1086 ls
1087 cd drivers/
1088 ls
1089 cd usb
1090 ls
1091 cd core
1092 ls
1093 cd ..
1094 ls
1095 cd wusbcore/
1096 ls
1097 pwd
1098 cd ..
1099 ls
1100 cd core
1101 ls
1102 cd ..
1103 ls
1104 pwd
1105 cd
1106 ls
1107 cd linux-3.2.0/
1108 sudo make EXTRAVERSION=-35-generic O=~/.linuxbuild
1109 ls
1110 sudo make EXTRAVERSION=-35-generic O=~/.linuxbuild
SUBDIRS=drivers/usb/core

```

```
1111 vi drivers/usb/core/usb.c
1112 ls
1113 sudo make EXTRAVERSION=-35-generic O=~/.linuxbuild
SUBDIRS=drivers/usb/core
1114 sudo make EXTRAVERSION=-35-generic O=~/.linuxbuild SUBDIRS=drivers/usb/
1115 pwd
1116 ls
1117 pwd
1118 cd /media/OS_
1119 ls
1120 find . -name *.jhd
1121 pwd
1122 ls
1123 cd linux-3.2.0/
1124 ls
1125 sudo make EXTRAVERSION=-35-generic O=~/.linuxbuild SUBDIRS=drivers/usb/
1126 sudo make EXTRAVERSION=-35-generic O=~/.linuxbuild
SUBDIRS=drivers/usb/core
1127 sudo make -d EXTRAVERSION=-35-generic O=~/.linuxbuild
SUBDIRS=drivers/usb/core
1128 pwd
1129 chmod -R 755 *
1130 sudo chmod -R 755 *
1131 sudo make -d EXTRAVERSION=-35-generic O=~/.linuxbuild modules
SUBDIRS=drivers/usb/core
1132 sudo make EXTRAVERSION=-35-generic O=~/.linuxbuild modules
SUBDIRS=drivers/usb/core
1133 vi drivers/usb/core/usb.c
1134 ls -lrt
1135 pwd
1136 cd drivers/usb/core
1137 ls
1138 vi usb.c
1139 ls
1140 pwd
1141 ls -lrt
1142 id
1143 sudo vi usb.c
1144 pwd
1145 cd ../../
1146 ls
1147 pwd
1148 cd ..
1149 ls
1150 sudo make EXTRAVERSION=-35-generic O=~/.linuxbuild modules
SUBDIRS=drivers/usb/core
1151 sudo make EXTRAVERSION=-35-generic O=~/.linuxbuild modules
SUBDIRS=drivers/usb/wusb
1152 sudo make EXTRAVERSION=-35-generic O=~/.linuxbuild modules
SUBDIRS=drivers/usb/wusbcore
1153 sudo make EXTRAVERSION=-35-generic O=~/.linuxbuild modules
SUBDIRS=drivers/usb/core
1154 ls
1155 pwd
1156 cd drivers
1157 ls
1158 cd usb
1159 ls
1160 cd core
1161 ls
1162 pwd
1163 sudo chmod -R 755 *
1164 pwd
1165 cd
```

```
1166 cd linuxbuild/
1167 ls
1168 cd drivers/
1169 ls
1170 cd usb
1171 ls
1172 cd core
1173 ls
1174 sudo vi modules.order
1175 sudo vi modules.builtin
1176 sudo vi modules.order
1177 ls
1178 pwd
1179 cd ../..
1180 ls
1181 pwd
1182 cd ..
1183 ls
1184 pwd
1185 sudo make EXTRAVERSION=-35-generic O=~/.linuxbuild modules
SUBDIRS=drivers/usb/core
1186 vi drivers/usb/core/
1187 vi drivers/usb/core/modules.order
1188 pwd
1189 chmod -R 755 drivers/usb/core/*
1190 sudo chmod -R 755 drivers/usb/core/*
1191 vi drivers/usb/core/modules.order
1192 cd drivers/usb/core
1193 lks
1194 ls
1195 ls -lrt
1196 vi modules.builtin
1197 vi modules.order
1198 ls
1199 sudo vi modules.order
1200 cd ../../..
1201 ls
1202 sudo make EXTRAVERSION=-35-generic O=~/.linuxbuild modules
SUBDIRS=drivers/usb/core
1203 vi modules.order
1204 vi modules.builtin
1205 cd drivers/usb
1206 ls
1207 cd core
1208 ls
1209 ls -lrt
1210 cd ..
1211 ls
1212 vi modules.order
1213 ls
1214 pwd
1215 ls -lrt
1216 pwd
1217 cd ..
1218 ls
1219 vi modules.order
1220 ls
1221 cd ..
1222 ks
1223 ls
1224 vi modules.order
1225 grep modules.order *
1226 pwd
1227 vi Makefile
```

```
1228 ls
1229 ls /lib/modules/
1230 ls /lib/modules/3.2.0-35-generic-pae/
1231 ls /lib/modules/3.2.0-35-generic-pae/build
1232 ls /lib/modules/3.2.0-35-generic-pae/build/drivers
1233 ls /lib/modules/3.2.0-35-generic-pae/build/drivers/usb/core/
1234 ls /lib/modules/3.2.0-35-generic-pae/build/drivers/usb/wusbcore/
1235 ls
1236 vi Makefile
1237 ls
1238 pwd
1239 cd
1240 cd linux-3.2.0/
1241 ls
1242 cd drivers/
1243 ls
1244 cd usb/core/
1245 ls
1246 vi driver.c
1247 ls
1248 pwd
1249 vi Makefile
1250 ls
1251 pwd
1252 vi Kconfig
1253 pwd
1254 cd ../wusbcore/
1255 ls
1256 vi reservation.c
1257 ls
1258 vi Makefile
1259 pwd
1260 grep wusbcore.ko
1261 grep wusbcore.ko *
1262 pwd
1263 cd ..
1264 ls
1265 cd core
1266 ls
1267 grep usbcore.ko *
1268 vi devio.c
1269 ls
1270 vi quirks.c
1271 ls
1272 vi driver.c
1273 ls
1274 grep pr_info *
1275 vi usb.c
1276 ls
1277 vi hub.c
1278 pwd
1279 cd ..
1280 ls
1281 cd wusbcore/
1282 ls
1283 vi wa-xfer.c
1284 vi mmc.c
1285 ls
1286 vi wusbhc.c
1287 vi wa-nep.c
1288 pwd
1289 vi pal.c
1290 pwd
1291 cd ..
```

```
1292 ls
1293 vi README
1294 cd core
1295 ls
1296 cd ..
1297 ls
1298 cd ..
1299 ls
1300 cd ..
1301 ls
1302 cd Documentation/
1303 ls
1304 vi BUG-HUNTING
1305 vi parport-lowlevel.txt
1306 cd ..
1307 ls
1308 pwd
1309 cd usb
1310 ls
1311 cd Documentation/usb
1312 ls
1313 vi WUSB-Design-overview.txt
1314 ls
1315 pwd
1316 vi usb-help.txt
1317 vi usb-serial.txt
1318 ls
1319 vi ./drivers/usb/wusbcore/.wusbcore.ko.cmd
1320 cd drivers
1321 ls
1322 cd usb
1323 ls
1324 cd core
1325 ls
1326 sudo make EXTRAVERSION=-35-generic O=~/.linuxbuild modules
1327 sudo make EXTRAVERSION=-35-generic O=~/.linuxbuild
1328 cd
1329 cd drivers/usb/core
1330 cd linux-3.2.0/usb/core
1331 ls
1332 cd linux-3.2.0/drivers/usb/core
1333 ls
1334 sudo make EXTRAVERSION=-35-generic O=~/.linuxbuild
1335 sudo make EXTRAVERSION=-35-generic O=~/.linuxbuild modules
1336 cd ../wusbcore/
1337 ls
1338 sudo make EXTRAVERSION=-35-generic O=~/.linuxbuild modules
1339 sudo make EXTRAVERSION=-35-generic O=~/.linuxbuild
1340 sudo make EXTRAVERSION=-35-generic O=~/.linuxbuild M=`pwd`
1341 cd ../../..
1342 sudo make EXTRAVERSION=-35-generic O=~/.linuxbuild modules
SUBDIRS=drivers/usb/core
1343 sudo make -d EXTRAVERSION=-35-generic O=~/.linuxbuild modules
SUBDIRS=drivers/usb/core
1344 sudo make -d EXTRAVERSION=-35-generic O=~/.linuxbuild modules
SUBDIRS=drivers/usb/wusbcore
1345 sudo make -d EXTRAVERSION=-35-generic O=~/.linuxbuild modules
1346 sudo make -d EXTRAVERSION=-35-generic O=~/.linuxbuild modules
SUBDIRS=drivers/usb/core
1347 sudo make -d EXTRAVERSION=-35-generic O=~/.linuxbuild modules
SUBDIRS=drivers/usb/wusbcore
1348 sudo make -d EXTRAVERSION=-35-generic O=~/.linuxbuild modules
SUBDIRS=drivers/usb/wusbcore 2> wusbcorebuild.txt
1349 ls -lrt
```

```
1350 sudo vi wusbcorebuild.txt
1351 sudo make -d EXTRAVERSION=-35-generic O=~/.linuxbuild modules
SUBDIRS=drivers/usb/wusbcore 2> wusbcorebuild.txt
1352 ls -l
1353 sudo chmod -R 755 wusbcorebuild.txt
1354 sudo make -d EXTRAVERSION=-35-generic O=~/.linuxbuild modules
SUBDIRS=drivers/usb/wusbcore 2> wusbcorebuild.txt
1355 ls -l
1356 sudo make -d EXTRAVERSION=-35-generic O=~/.linuxbuild modules
SUBDIRS=drivers/usb/wusbcore | more
1357 ls
1358 sudo make EXTRAVERSION=-35-generic O=~/.linuxbuild modules
SUBDIRS=drivers/usb/wusbcore | more
1359 sudo make EXTRAVERSION=-35-generic O=~/.linuxbuild modules
SUBDIRS=drivers/usb/wusbcore
1360 pwd
1361 vi Makefile
1362 cd /
1363 cd media/OS
1364 cd media/OS_
1365 ls
1366 find . -name Root
1367 cat /proc/bus/usb/devices
1368 lsmod
1369 lsmod|grep usb
1370 lsmod | grep usb
1371 dmesg
1372 dmesg|grep usbcore
1373 dmesg|grep wusbcore
1374 dmesg|grep usbcore
1375 cd linux-3.2.0/
1376 ls
1377 cd drivers/
1378 ls
1379 cd usb/core
1380 ls
1381 fc -l
1382 history
1383 history
1384 history 2>&1 ~/.linuxbuildcommandlines.txt
1385 history 2>&1 > ~/.linuxbuildcommandlines.txt
1386 cd
1387 ls
1388 vi linuxbuildcommandlines.txt
1389 ls
1390 pwd
1391 cd linuxbuild/
1392 cd
1393 cd linux-3.2.0/
1394 ls
1395 cd drivers/
1396 ls
1397 cd usb
1398 ls
1399 pwd
1400 ls
1401 cd core
1402 ls
1403 fc -l
1404 man fc
1405 fc -h
1406 fc -lnr
1407 ls
1408 vi Makefile
```



```

1409 sudo vi usb.c
1410 sudo vi hub.c
1411 grep printk *
1412 vi hub.c
1413 ls
1414 grep ratelimit *.c
1415 sudo wireshark &
1416 grep init *.c
1417 ls
1418 grep main *.c
1419 grep __init *.c
1420 vi usb.c
1421 ls
1422 vi hub.c
1423 ls
1424 pwd
1425 cd ../../..
1426 sudo make EXTRAVERSION=-35-generic O=~/.linuxbuild modules
SUBDIRS=drivers/usb/wusbcore clean
1427 cd -
1428 ls
1429 sudo make -C /lib/modules/`uname -r`/build/ M=`pwd` modules clean
1430 sudo make -C /lib/modules/`uname -r`/build/ M=`pwd` clean
1431 ls
1432 sudo make -C /lib/modules/`uname -r`/build/ M=`pwd`
1433 ls
1434 fc -l
1435 history
1436 history 2>&1 > ~/.linuxbuildcommandlines.txt

```

```
VIRGO cpupooling driver ----- 10000
```

```
VIRGO EventNet driver ----- 20000
```

```
VIRGO memorypooling driver ----- 30000
```

```
VIRGO filesystems driver ----- 50000
```

```
VIRGO queueing driver ----- 60000
```

```

    and KingCobra
kernel_analytics
config
utils
virgo_queueing
kingcobra
cpupooling
memorypooling
cloudfs
eventnet

```

In pre-4.x.x Linux kernels these modules are boot time loaded from /etc/modules
 In post-4.x.x Linux kernels due to systemd, the modules are boot time loaded
 from /lib/modules-load.d/virgo_modules.conf

```
=====
```

Smatch Static Analysis of NEURONRAIN VIRGO Linux Source Tree

```
=====
```

Analyzed on 25 July 2016:

```
-----
```

1. Smatch (<http://smatch.sourceforge.net/>) finds bugs in linux kernel code statically.

2. Article by Dan Carpenter on Smatch -

https://blogs.oracle.com/linuxkernel/entry/smatch_static_analysis_tool_overview

3. Smatch kchecker was run as an example on virgo_malloc system call with

following logs (commandline: `$/root/smatch/smatch/smatch_scripts/kchecker - spammy virgo_malloc/virgo_malloc.c`)

```
-----
CHK      include/config/kernel.release
CHK      include/generated/uapi/linux/version.h
CHK      include/generated/utsrelease.h
CHK      include/generated/bounds.h
CHK      include/generated/asm-offsets.h
CALL     scripts/checksyscalls.sh
CHECK    scripts/mod/empty.c
CHECK    virgo_malloc/virgo_malloc.c
include/linux/virgo_mempool.h:36:9: warning: preprocessor token
LINUX_KERNEL_4_x_x redefined
n:1:9: this was the original definition
virgo_malloc/virgo_malloc.c:72:9: warning: preprocessor token BUF_SIZE redefined
include/linux/virgo_mempool.h:97:9: this was the original definition
virgo_malloc/virgo_malloc.c:83:63: warning: non-ANSI function declaration of
function 'get_least_loaded_hostport_from_cloud_mempool'
virgo_malloc/virgo_malloc.c:115:45: warning: non-ANSI function declaration of
function 'get_host_from_cloud_Loadtrack_mempool'
virgo_malloc/virgo_malloc.c:124:39: warning: non-ANSI function declaration of
function 'get_host_from_cloud_PRG_mempool'
virgo_malloc/virgo_malloc.c:164:9: warning: mixing declarations and code
virgo_malloc/virgo_malloc.c:168:9: warning: mixing declarations and code
virgo_malloc/virgo_malloc.c:175:9: warning: mixing declarations and code
virgo_malloc/virgo_malloc.c:242:9: warning: mixing declarations and code
virgo_malloc/virgo_malloc.c:244:9: warning: mixing declarations and code
virgo_malloc/virgo_malloc.c:258:9: warning: mixing declarations and code
virgo_malloc/virgo_malloc.c:264:9: warning: mixing declarations and code
virgo_malloc/virgo_malloc.c:390:25: warning: mixing declarations and code
virgo_malloc/virgo_malloc.c:476:9: warning: mixing declarations and code
virgo_malloc/virgo_malloc.c:503:9: warning: mixing declarations and code
virgo_malloc/virgo_malloc.c:509:9: warning: mixing declarations and code
virgo_malloc/virgo_malloc.c:659:50: warning: non-ANSI function declaration of
function 'virgomemorypooling_read_virgo_config_client'
virgo_malloc/virgo_malloc.c:683:9: warning: mixing declarations and code
virgo_malloc/virgo_malloc.c:686:9: warning: mixing declarations and code
virgo_malloc/virgo_malloc.c:709:9: warning: mixing declarations and code
virgo_malloc/virgo_malloc.c:96 get_least_loaded_hostport_from_cloud_mempool()
error: potential null dereference 'hopo'. (kmalloc returns null)
virgo_malloc/virgo_malloc.c:189 sys_virgo_get() warn: inconsistent indenting
virgo_malloc/virgo_malloc.c:289 sys_virgo_set() warn: inconsistent indenting
virgo_malloc/virgo_malloc.c:522 sys_virgo_free() warn: inconsistent indenting
CC       virgo_malloc/virgo_malloc.o
-----
```

VIRGO Linux Build Steps

1. Download and build 4.1.5 kernel from www.kernel.org mainline (build commandlines as in `buildscript.sh`)
2. Overlay the virgo-linux source tree (from `linux-kernel-extensions` subtree) on linux kernel src root.
3. Invoke the driver build scripts in each driver folder to build with path updates.
4. For USBmd and KingCobra drivers also above steps are sufficient.
5. Test cases in `virgo_clone`, `virgo_malloc` and `virgo_filesystem` can be invoked for syscall paths and for telnet path the ports listed in `ModuleListenPorts.txt` can be used.

-
6. Changes required for building overlayed 4.1.5 linux kernel - documented in github commit diffs of 12 August 2015 :

<https://github.com/shrinivaasanka/virgo-linux-github-code/commit/6916585c04e4df5>

1ca75384aacee18fa9c13de10

<https://github.com/shrinivaasanka/virgo-linux-github-code/commit/6916585c04e4df51ca75384aacee18fa9c13de10>

- *) buildscript_4.1.5.sh (build script for 4.1.5)
- *) linux-kernel-extensions/Makefile
- *) linux-kernel-extensions/arch/x86/syscalls/Makefile
- *) linux-kernel-extensions/arch/x86/syscalls/syscall_32.tbl
- *) linux-kernel-extensions/drivers/Makefile
- *) linux-kernel-extensions/include/linux/syscalls.h

Above minimum changes were enough to build an overlay-ed Linux Kernel with VIRGO codebase

7. Changes required for building overlayed 4.10.3 VIRGO 64-bit linux kernel:

- copy linux-kernel-extensions/virgo_<syscalls> to linux-4.10.3
- copy linux-kernel-extensions/drivers/virgo to linux-4.10.3/drivers
- copy linux-kernel-extensions/drivers/kingcobra to linux-4.10.3/drivers
- Build each driver in linux-4.10.3/drivers/virgo/<driver> with <drivername>_driver_build.sh

- Some drivers require Module.symvers to be copied from other exporting drivers e.g kingcobra, virgo/kernel_analytics

- Copy Module.symvers from exporting driver to importing driver
- Comment clean make target and compile with driver build script.
- This appends symbols to Module.symvers
- sock_create_kern() compilation errors have been fixed by additional &init_net parameter to it (mainline added it in 2015)
- changes in linux-4.10.3/Makefile:

- core-y := usr/ virgo_clone/ virgo_malloc/ virgo_filesystem/

- changes in linux-4.10.3/arch/x86/entry/syscalls/syscall_64.tbl:

#VIRGO system calls

| | | | |
|-----|----|--------------|------------------|
| 548 | 64 | virgo_clone | sys_virgo_clone |
| 549 | 64 | virgo_malloc | sys_virgo_malloc |
| 550 | 64 | virgo_set | sys_virgo_set |
| 551 | 64 | virgo_get | sys_virgo_get |
| 552 | 64 | virgo_free | sys_virgo_free |
| 553 | 64 | virgo_open | sys_virgo_open |
| 554 | 64 | virgo_close | sys_virgo_close |
| 555 | 64 | virgo_read | sys_virgo_read |
| 556 | 64 | virgo_write | sys_virgo_write |

- changes in linux-4.10.3/include/linux/syscalls.h:
asmlinkage long sys_virgo_clone(char* func, void *child_stack, int flags, void *arg);
asmlinkage long sys_virgo_malloc(int size,unsigned long __user *vuid);
asmlinkage long sys_virgo_set(unsigned long vuid, const char __user *data_in);
asmlinkage long sys_virgo_get(unsigned long vuid, char __user *data_out);
asmlinkage long sys_virgo_free(unsigned long vuid);
asmlinkage long sys_virgo_open(char* filepath);
asmlinkage long sys_virgo_read(long vfsdesc, char __user *data_out, int size, int pos);
asmlinkage long sys_virgo_write(long vfsdesc, const char __user *data_in, int size, int pos);
asmlinkage long sys_virgo_close(long vfsdesc);

8. Additional information on linux build and grub issues have been updated in GRAFIT Open Learning Course Notes at:

https://github.com/shrinivaasanka/Grafit/blob/master/course_material/

NeuronRain/LinuxKernelAndCloud/LinuxKernelAndCloud.txt

9. Presently VIRGO Linux Kernel is based on mainline 4.1.5 kernel (32-bit) and 4.10.3 kernel (64-bit). As newer kernel versions are released, there are changes in kernel functions and data structures. This could cause a working VIRGO linux build in version v to break in version v+delta (For example sock_create_kern() changes from 4.1.5 to 4.10.3). Certifying and Porting VIRGO linux code base on each and every kernel version is beyond the scope of NeuronRain design goals - it is left to the end-user of NeuronRain. There is a possibility that VIRGO kernel completely becomes a self-sufficient kernel with no need for overlay build on linux mainline. Crucial reason for 64-bit of VIRGO on 4.10.3 is the randomly witnessed i915 related panics in 4.1.5 virgo system calls and drivers. Mainline 4.10.3 kernel has major updates to i915 intel graphics drivers. It is still to be verified if upgrade to 4.10.3 and 64-bit addressing in any way resolves these random virgo_<syscall> panics.

```
/
*****
*****
#-----
-----
#NEURONRAIN VIRGO - Cloud, Machine Learning and Queue augmented Linux Kernel
Fork-off
#This program is free software: you can redistribute it and/or modify
#it under the terms of the GNU General Public License as published by
#the Free Software Foundation, either version 3 of the License, or
#(at your option) any later version.
#This program is distributed in the hope that it will be useful,
#but WITHOUT ANY WARRANTY; without even the implied warranty of
#MERCHANTABILITY or FITNESS FOR A PARTICULAR PURPOSE. See the
#GNU General Public License for more details.
#You should have received a copy of the GNU General Public License
#along with this program. If not, see <http://www.gnu.org/licenses/>.
#-----
-----
#Copyleft (Copyright+):
#Srinivasan Kannan (alias) Ka.Shrinivaasan (alias) Shrinivas Kannan
#Ph: 9791499106, 9003082186
#Krishna iResearch Open Source Products Profiles:
#http://sourceforge.net/users/ka_shrinivaasan,
#https://github.com/shrinivaasanka,
#https://www.openhub.net/accounts/ka_shrinivaasan
#Personal website(research): https://sites.google.com/site/kuja27/
#emails: ka.shrinivaasan@gmail.com, shrinivas.kannan@gmail.com,
#kashrinivaasan@live.com
#-----
-----
*****
*****/
```

1. SATURN (<http://saturn.stanford.edu/>) is a Program Analysis Software for Verification of Large Scale Linux Software.

2. There are quite a few other softwares already available :

2.1 SLAM (Windows) and Yogi - Sriram Rajamani, Microsoft Research -
<http://research.microsoft.com/en-us/projects/slam/>

2.2 BLAST - <http://forge.ispras.ru/projects/blast/> which is part of Linux Driver Verification Project
(<http://forge.ispras.ru/projects/ldv>)

3. SATURN has been integrated into VIRGO Linux Kernel drivers/ pursuant to the author's old PhD thesis proposal in 2011
(<https://sites.google.com/site/kuja27/PhDThesisProposal.pdf>) which was later

dropped because of penchant for Complexity+MachineLearning and lack of feasibility. But now It finds relevance as a fundamental ingredient in Software Analytics subsystem of NeuronRain AsFer and VIRGO. SATURN error reports leveraged with AsFer Machine Learning makes a hitherto unusual combination - Formal Logic Verification + Data Analytics.

4. saturn_program_analysis has been added as a new VIRGO kernel module in drivers/ with an example driver implementation adapted from kernel_analytics. It can be overwritten with inline code or an exported function invocation from external driver and thus can do analysis of any arbitrary C subroutine.

5. SATURN installed from above url requires OCAML, libstr etc., for build to succeed with NATIVECAML unset in \$CLPA_HOME/clpa/cil/Makefile.

6. Following changes are required in \$CLPA_HOME/clpa/build-intercept/ - New file interceptor.config with following lines added for source files:
intercept_home=/media/shrinivaasanka/0fc4d8a2-1c74-42b8-8099-9ef78d8c8ea2/home/kashrinivaasan/linux-4.1.5/drivers/virgo/saturn_program_analysis
intercept_scripts=/home/shrinivaasanka/clpa/build-intercept/
intercept_library=/home/shrinivaasanka/clpa/build-intercept/libintercept.so

----- 7. Program Analysis with SATURN - steps -----

SATURN intercepts the linux kernel driver build and creates analysis tree directory (saturn_program_analysis_trees). Intercepted build creates .db files in trees which are extracted with clpa-extract to generate a report (errors.txt). It can then be analyzed for algorithms like null pointer detection, aliases etc., from calypso (.clp) files in analysis/. Following does null pointer analysis.

```
$/home/shrinivaasanka/clpa/bin/clpa-intercept make -C /lib/modules/`uname -r`/build/ M=`pwd` clean
$/home/shrinivaasanka/clpa/bin/clpa-intercept make -C /lib/modules/`uname -r`/build/ M=`pwd`
$/home/shrinivaasanka/clpa/bin/clpa-intercept make -C /lib/modules/`uname -r`/build/ M=`pwd` modules_install
$/home/shrinivaasanka/clpa/bin/clpa-extract ../saturn_program_analysis_trees/virgo_saturn_program_analysis.ko
$/home/shrinivaasanka/clpa/bin/clpa --no-fixpoint --timeout 60
/home/shrinivaasanka/clpa/analysis/null/null.clp
```

Following commandlines do memory, locking analysis and create Graphviz renderable DOT files:

```
/home/shrinivaasanka/clpa/bin/clpa --no-fixpoint --timeout 60
/home/shrinivaasanka/clpa/analysis/memory/base01/run.clp
/home/shrinivaasanka/clpa/bin/clpa --stats memory_deltas --timeout 60
/home/shrinivaasanka/clpa/analysis/memory/base02/run.clp
/home/shrinivaasanka/clpa/bin/clpa --list-stats
/home/shrinivaasanka/clpa/bin/clpa --stats memory_deltas --stats sat_counts --timeout 60 /home/shrinivaasanka/clpa/analysis/memory/base02/run.clp
/home/shrinivaasanka/clpa/bin/clpa --list-debug
/home/shrinivaasanka/clpa/bin/clpa --stats memory_deltas --stats sat_counts --timeout 60 /home/shrinivaasanka/clpa/analysis/memory/ptdot.clp
/home/shrinivaasanka/clpa/bin/clpa --stats memory_deltas --stats sat_counts --timeout 60 /home/shrinivaasanka/clpa/analysis/smemory/memory.clp
/home/shrinivaasanka/clpa/bin/clpa --stats memory_deltas --stats sat_counts --timeout 60 /home/shrinivaasanka/clpa/analysis/smemory/paths.clp
/home/shrinivaasanka/clpa/bin/clpa --stats memory_deltas --stats sat_counts --timeout 60 /home/shrinivaasanka/clpa/analysis/locking/locking.clp
```

Following does CFG and memory analysis and plots a DOT graph for dataflow:

```
/home/shrinivaasanka/clpa/bin/clpa
/home/shrinivaasanka/clpa/analysis/virgosaturnmemory.clp
```

```
/home/shrinivaasanka/clpa/bin/clpa
/home/shrinivaasanka/clpa/analysis/virgosaturncfg.clp
```

```
-----
8. NULL pointer Error report from SATURN - from
$VIRGO_LINUX_ROOT/linux-kernel-extensions/drivers/virgo/
saturn_program_analysis/saturn_program_analysis_trees/error.txt
-----
```

blue

```
925 blue __arg0 of function /media/shrinivaasanka/0fc4d8a2-1c74-42b8-8099-
9ef78d8c8ea2/home/kashrinivaasan/linux-4.1.5/include/linux/
mmzone.h:__section_mem_map_addr can evaluate to NULL
/media/shrinivaasanka/0fc4d8a2-1c74-42b8-8099-9ef78d8c8ea2/home/kashrinivaasan/
linux-4.1.5/include/linux/mmzone.h:__section_mem_map_addr
(925:/media/shrinivaasanka/0fc4d8a2-1c74-42b8-8099-9ef78d8c8ea2/home/
kashrinivaasan/linux-4.1.5/include/linux/mm.h), final site of dereference is:
(1151:/media/shrinivaasanka/0fc4d8a2-1c74-42b8-8099-9ef78d8c8ea2/home/
kashrinivaasan/linux-4.1.5/include/linux/mmzone.h)
/media/shrinivaasanka/0fc4d8a2-1c74-42b8-8099-9ef78d8c8ea2/home/kashrinivaasan/
linux-4.1.5/include/linux/mm.h
Null pointer is passed to a function which dereferences it.
None
```

blue

```
205 blue __arg0 of function /media/shrinivaasanka/0fc4d8a2-1c74-42b8-8099-
9ef78d8c8ea2/home/kashrinivaasan/linux-4.1.5/include/linux/
mmzone.h:__section_mem_map_addr can evaluate to NULL
/media/shrinivaasanka/0fc4d8a2-1c74-42b8-8099-9ef78d8c8ea2/home/kashrinivaasan/
linux-4.1.5/include/linux/mmzone.h:__section_mem_map_addr
(205:/media/shrinivaasanka/0fc4d8a2-1c74-42b8-8099-9ef78d8c8ea2/home/
kashrinivaasan/linux-4.1.5/include/linux/scatterlist.h), final site of
dereference is: (1151:/media/shrinivaasanka/0fc4d8a2-1c74-42b8-8099-
9ef78d8c8ea2/home/kashrinivaasan/linux-4.1.5/include/linux/mmzone.h)
/media/shrinivaasanka/0fc4d8a2-1c74-42b8-8099-9ef78d8c8ea2/home/kashrinivaasan/
linux-4.1.5/include/linux/scatterlist.h
Null pointer is passed to a function which dereferences it.
None
```

orange

```
382 orange (INCONSISTENT USE) Possible null dereference of variable dst. This
variable is checked for Null at lines: 386
/media/shrinivaasanka/0fc4d8a2-1c74-42b8-8099-9ef78d8c8ea2/home/kashrinivaasan/
linux-4.1.5/include/net/dst.h
Inconsistency error
None
```

blue

```
1471 blue __arg0 of function /media/shrinivaasanka/0fc4d8a2-1c74-42b8-8099-
9ef78d8c8ea2/home/kashrinivaasan/linux-4.1.5/include/linux/
mmzone.h:__section_mem_map_addr can evaluate to NULL
/media/shrinivaasanka/0fc4d8a2-1c74-42b8-8099-9ef78d8c8ea2/home/kashrinivaasan/
linux-4.1.5/include/linux/mmzone.h:__section_mem_map_addr
(1471:/media/shrinivaasanka/0fc4d8a2-1c74-42b8-8099-9ef78d8c8ea2/home/
kashrinivaasan/linux-4.1.5/include/linux/mm.h), final site of dereference is:
(1151:/media/shrinivaasanka/0fc4d8a2-1c74-42b8-8099-9ef78d8c8ea2/home/
kashrinivaasan/linux-4.1.5/include/linux/mmzone.h)
/media/shrinivaasanka/0fc4d8a2-1c74-42b8-8099-9ef78d8c8ea2/home/kashrinivaasan/
linux-4.1.5/include/linux/mm.h
Null pointer is passed to a function which dereferences it.
None
```

```

#/  

*****  

*****  

#* UMB - Universal Modified Bus Driver - simple USB driver for debugging  

#* This program is free software: you can redistribute it and/or modify  

#* it under the terms of the GNU General Public License as published by  

#* the Free Software Foundation, either version 3 of the License, or  

#* (at your option) any later version.  

#*  

#* This program is distributed in the hope that it will be useful,  

#* but WITHOUT ANY WARRANTY; without even the implied warranty of  

#* MERCHANTABILITY or FITNESS FOR A PARTICULAR PURPOSE. See the  

#* GNU General Public License for more details.  

#*  

#* You should have received a copy of the GNU General Public License  

#* along with this program. If not, see <http://www.gnu.org/licenses/>.  

#*  

#-----  

-----  

#Copyleft (Copyright+):  

#Srinivasan Kannan (alias) Ka.Shrinivaasan (alias) Shrinivas Kannan  

#Ph: 9791499106, 9003082186  

#Krishna iResearch Open Source Products Profiles:  

#http://sourceforge.net/users/ka\_shrinivaasan,  

#https://github.com/shrinivaasanka,  

#https://www.openhub.net/accounts/ka\_shrinivaasan  

#Personal website(research): https://sites.google.com/site/kuja27/  

#emails: ka.shrinivaasan@gmail.com, shrinivas.kannan@gmail.com,  

#kashrinivaasan@live.com  

#-----  

-----  

#*****  

*****/

```

USBmd driver is an experimental modified version of already existing USB driver in linux.

Purpose of this modified version is for doing more sophisticated debugging of USB endpoints and devices and as USB packet sniffer. Technical Necessity for this was created due to prolonged data theft, id spoofing and cybercrime that has been happening in author's personal electronic devices for years that resulted in a Cybercrime Police Complaint also few years ago.

There were also such incidents while developing open source code (some code commits have description of these mysterious occurrences). There is no comprehensive USB debugger available on linux to sift bad traffic though there are strong evidences of such cybercrime and datatheft through other sources. Author is inclined to believe that such recurring events of datatheft that defies all logic can have no other intent but to cause malafide theft or loss of private data and an act of defamation among other things.

This is also done as a technical learning exercise to analyze USB Hosts, packets and USB's interaction,if any, with wireless devices including mobiles, wireless LANs(radiotap) etc.,

In the longterm USBmd might have to be integrated into VIRGO. As VIRGO would have the synergy of AstroInfer machine learning codebase for "learning" from datasets, this USBmd driver can have the added ability of analyzing large USB traffic (as a dataset) using some decision making algorithms and evolve as an anti-cybercrime, anti-plagiarism and anti-theft tool to single out "malevolent" traffic that would save individuals and organisations from the

The pattern mining of numeric dataset designed for AstroInfer can apply here also since USB bitstream can be analyzed using algorithms for numerical dataset mining. Also Discrete Fourier Transform used for analyzing data for frequencies (periodicities if any) can be used for USB data, for example USB wireless traffic.

Following example commandlines install umb.ko module, unbind the existing option driver from bus-device id and bind the umb.ko to that bus id:

```
=====
Commits as on 29 July 2014
```

USBmd version 14.9.9 has been release tagged on 9 September 2014

USBmd version 15.1.8 has been release tagged on 8 January 2015

USB debug messages from "cat /sys/kernel/debug/usb/devices" for UMB bound above:

usbmon, libpcap tcpdump and wireshark (or vusb-analyzer) debugging

```
*mount -t debugfs none debugs /sys/kernel/debug
```



```
*modprobe usbmon
*ls /sys/kernel/debug/usb/usbmon/
```

```
0s 0u      1s 1t      1u 2s      2t 2u      3s 3t      3u 4s      4t 4u
      5s 5t      5u 6s      6t 6u      7s 7t      7u 8s      8t 8u
```

```
*cat /sys/kernel/debug/usb/usbmon/8t > usbmon.mon (any of the above usbmon debug logs)
```

```
*vusb-analyzer usbmon.mon
```

```
ef728540 3811287714 S Ci:001:00 s a3 00 0000 0001 0004 4 <
ef728540 3811287743 C Ci:001:00 0 4 = 00010000
ef728540 3811287752 S Ci:001:00 s a3 00 0000 0002 0004 4 <
ef728540 3811287763 C Ci:001:00 0 4 = 00010000
f50f6540 3811287770 S Ii:001:01 -115 2 <
f50f6540 3811287853 C Ii:001:01 -2 0
f5390540 3814543695 S Ci:001:00 s a3 00 0000 0001 0004 4 <
f5390540 3814543715 C Ci:001:00 0 4 = 00010000
f5390540 3814543756 S Ci:001:00 s a3 00 0000 0002 0004 4 <
f5390540 3814543767 C Ci:001:00 0 4 = 00010000
f50f6540 3814543805 S Ii:001:01 -115 2 <
```

```
*modprobe usbmon
```

```
*ls /dev/usbmon[1-8]
```

```
*tcpdump -i usbmon1 -w usbmon.pcap
```

```
tcpdump: listening on usbmon1, link-type USB_LINUX_MMAPPED (USB with padded Linux header), capture size 65535 bytes
```

```
^C86 packets captured
```

```
86 packets received by filter
```

```
*wireshark usbmon.pcap (loads on wireshark)
```

```
-----
Dynamic Debug - dev_dbg() and dev_vdbg()
-----
```

```
USB Debugging References:
```

```
-----
- Texas Instruments -
```

```
http://elinux.org/images/1/17/USB\_Debugging\_and\_Profiling\_Techniques.pdf
```

```
-----
NeuronRain version 15.6.15 release tagged
-----
```

```
-----
Commits as on 11 July 2015
-----
```

```
usbmd kernel module has been ported to Linux Kernel 4.0.5
```

```
-----
Commits as on 26 November 2015
-----
```

```
- Updated USB-md driver with a lookup of VIRGO kernel_analytics config variable exported by kernel_analytics module in umb_read() as default.
```

```
- New header file umb.h has been added that externs the VIRGO kernel_analytics config array variables
```

```
- Module.symvers has been imported from VIRGO kernel_analytics and clean target has been commented in build script after initial build as make clean removes Module.symvers.
```

```
- kern.log with umb_read() and umb_write() have been added with following commandlines:
```

- cat /dev/umb0 - invokes umb_read() but there are kernel panics sometimes
- cat <file> > /dev/umb0 - invokes umb_write()

where umb0 is usb-md device name registered with /sys/bus/usb as below:

- insmod umb.ko
- echo -n "7-1:1.0" > /sys/bus/usb/drivers/option/unbind
- echo -n "7-1:1.0" > /sys/bus/usb/drivers/umb/bind
- Updated build generated sources and object files have been added

Commits as on 27 November 2015

New folder usb_wwan_modified has been added that contains the USB serial, option and wireless USB modem WWAN drivers from kernel mainline instrumented with lot of printk()s so that log messages are written to kern.log. Though dev_dbg dynamic debugging can be used by writing to /sys/kernel/debug/<...>/dynamic_debug printk()s are sufficient for now. This traces through the USB connect and data transfer code:

- probe
- buffer is copied from userspace to kernelspace
- URB is allocated in kernel
- buffer is memcopied to URB
- usb send/receive bulk pipe calls
- usb_fill_bulk_urb

Almost all buffers like in and out buffers in URBs, portdata, interfacedata, serial_data, serial_port_data are printed to kern.log. This log is analyzable by AsFer machine learning code for USB debugging similar to usbmon logs.

These are initial commits only and usb-serial.c, usb_wwan.c, option.c and serial.h might be significantly altered going forward.

Commits as on 30 November 2015

Added usb.h from kernel mainline, instrumented with printk() to print transfer_buffer in usb_fill_[control/bulk/interrupt]_urb() functions. kern.log for this has been added in usb_wwan_modified/testlogs.

Commits as on 1 December 2015

- new kernel function print_buffer() has been added in usb.h that prints contents of char buffer in hex
- Above print_buffer() is invoked to print transfer_buffer in usb_wwan.c, usb-serial.c, option.c
- kern.log with print_buffer() output has been added - This dumps similar to wireshark, usbmon and other usb analyzers.

Commits as on 2 December 2015

- changed print_buffer() printk() to print a delimiter in each byte for AsFer Machine Learning code processing
- add a parser script for kern.log to print print_buffer() lines
- parsed kern.log with print_buffer() lines has been added
- Added an Apache Spark MapReduce python script to compute byte frequency in parsed print_buffer() kern.log

(ONGOING) NeuronRain USBmd Debug and Malafide Traffic Analytics

As mentioned in commit notes above, USB incoming and outgoing data transfer_buffer are dumped byte-by-byte. Given this data various analytics can be performed most of which are already implemented in AsFer codebase:

- frequency of bytes
 - most frequent sequence of bytes
 - bayesian and decision tree inference
 - deep learning
 - perceptrons
 - streaming algorithms for USB data stream
- and so on.

Commits as on 3 December 2015

- Apache Spark script for analyzing the USBWWAN byte stream logs has been updated with byte counts map-reduce functions from print_buffer() logs and temp DataFrame Table creation with SparkSQL.
- logs for the script have been added in usb_wwan_modified/python-src/testlogs/Spark_USBWWANLogMapReduceParser.out.3December2015
- kern.log parser shellscript has been updated

AsFer commits for USBmd as on 4 December 2015

All the Streaming_<>.py Streaming Algorithm implementations in AsFer/python-src/ have been updated with:

- hashlib ripemd160 hash MD algorithm for hash functions and return hexdigest()
- USBWWAN byte stream data from USBmd print_buffer() logs in usb-md/usb_wwan_modified/testlogs/ has been added as a Data Storage and Data Source
- logs for the above have been added to asfer/python-src/testlogs/
- Streaming Abstract Generator has been updated with USB stream data iterable and parametrized for data source and storage
- Some corrections to the asfer/python-src/Streaming_<> scripts

Commits as on 7 December 2015

- added Spark Mapreduce and DataFrame log for USBWWAN byte stream
 - added a parsed kern.log with only bytes from USBWWAN stream
 - Added dict() and sort() for query results and printed cardinality of the stream data set which is the size of the dict.
- An example log has been added which prints the cardinality as ~250. In contrast, LogLog and HyperLogLog counter estimations approximate the cardinality to 140 and 110 respectively

AsFer commits for USBmd as on 11 December 2015 - USBWWAN stream data backend in MongoDB

Dependency Injection code commits for MongoDB backend - With this MongoDB is also a storage backend for AsFer algorithms similar to MySQL:

- Abstract_DBBBackend.py has been updated for both MySQL and MongoDB injections
- MongoDB configuration and backend connect/query code has been added. Backend is either populated by Robomongo or pymongo reading from the Streaming Abstract Generator iterable framework.
- With this AsFer supports both SQL(MySQL) and NoSQL(file,hive,hbase,cassandra backends in Streaming Abstract Generator).
- log with a simple NoSQL table with StreamingData.txt and USBWWAN data has been added to testlogs/.
- MongoDB configuration has a database(asfer-database) and a collection(asfer-collection).
- MongoDB_DBBBackend @provides pymongo.collection.Collection which is @inject-ed to Abstract_DBBBackend

Commits as on 10 January 2016

NeuronRain USBmd enterprise version 2016.1.10 released.

Commits - 4 August 2016

- 1.New build script for drivers/usb top level folder has been added.
 - 2.Copyleft notices updated
 - 3.print_buffer() in usb.h has been #ifdef-ed based on a build time flag to suppress the buffer bytes dump preferentially so that kern.log is not flooded.
 - 4.Flag PRINT_BUFFER has to be defined with #define somewhere within KBuild makefiles or externally.
 - 5..ko files rebuilt
 6. Miscellaneous code changes to suppress kbuild warnings - cast etc.,
 7. PRINT_BUFFER block changed to print the bytes in single line for each buffer
-

Commits - 13 July 2017 - usb-storage driver last sector access slab out of bounds error in 64-bit - committed for analysis
- this error was frequently witnessed in VIRGO 32-bit stability issues and panics - ISRA looks like a GCC optimization of a function invocation (Interprocedural Scalar Replacement of Aggregates)

Jul 13 15:03:36 localhost kernel: [9837.497280]
=====

Jul 13 15:03:36 localhost kernel: [9837.499787]
=====

Jul 13 15:03:36 localhost kernel: [9837.499822] BUG: KASAN: slab-out-of-bounds in last_sector_hacks.isra.1.part.2+0xc9/0x1d0 [usb_storage] at addr ffff88007cdaa758

Jul 13 15:03:36 localhost kernel: [9837.499831] Read of size 8 by task usb-storage/6243

Jul 13 15:03:36 localhost kernel: [9837.499844] CPU: 0 PID: 6243 Comm: usb-storage Tainted: G B 4.10.3 #18

Jul 13 15:03:36 localhost kernel: [9837.499849] Hardware name: Dell Inc. Inspiron 1545 /0J037P, BIOS A14 12/07/2009

Jul 13 15:03:36 localhost kernel: [9837.499851] Call Trace:

Jul 13 15:03:36 localhost kernel: [9837.499863] dump_stack+0x63/0x8b

Jul 13 15:03:36 localhost kernel: [9837.499870] kasan_object_err+0x21/0x70

Jul 13 15:03:36 localhost kernel: [9837.499877]

kasan_report.part.1+0x219/0x4f0

Jul 13 15:03:36 localhost kernel: [9837.499893] ?

last_sector_hacks.isra.1.part.2+0xc9/0x1d0 [usb_storage]

Jul 13 15:03:36 localhost kernel: [9837.499899] kasan_report+0x25/0x30

Jul 13 15:03:36 localhost kernel: [9837.499906] __asan_load8+0x5e/0x70

Jul 13 15:03:36 localhost kernel: [9837.499922]

last_sector_hacks.isra.1.part.2+0xc9/0x1d0 [usb_storage]

Jul 13 15:03:36 localhost kernel: [9837.499938]

usb_stor_invoke_transport+0x1a1/0x960 [usb_storage]

Jul 13 15:03:36 localhost kernel: [9837.499946] ?

migrate_swap_stop+0x2e0/0x2e0

Jul 13 15:03:36 localhost kernel: [9837.499963] ?

usb_stor_port_reset+0xb0/0xb0 [usb_storage]

```

Jul 13 15:03:36 localhost kernel: [ 9837.499973] ?
wait_for_completion_interruptible+0x1a7/0x260
Jul 13 15:03:36 localhost kernel: [ 9837.499981] ?
wait_for_completion_killable+0x2a0/0x2a0
Jul 13 15:03:36 localhost kernel: [ 9837.499989] ?
raise_softirq_irqoff+0xba/0xd0
Jul 13 15:03:36 localhost kernel: [ 9837.499995] ? wake_up_q+0x80/0x80
Jul 13 15:03:36 localhost kernel: [ 9837.500011]
usb_stor_transparent_scsi_command+0xe/0x10 [usb_storage]
Jul 13 15:03:36 localhost kernel: [ 9837.500017]
usb_stor_control_thread+0x344/0x510 [usb_storage]
Jul 13 15:03:36 localhost kernel: [ 9837.500017] ?
usb_stor_disconnect+0x120/0x120 [usb_storage]
Jul 13 15:03:36 localhost kernel: [ 9837.500017] ?
default_wake_function+0x2f/0x40
Jul 13 15:03:36 localhost kernel: [ 9837.500017] ? __wake_up_common+0x78/0xc0
Jul 13 15:03:36 localhost kernel: [ 9837.500017] kthread+0x178/0x1d0
Jul 13 15:03:36 localhost kernel: [ 9837.500017] ?
usb_stor_disconnect+0x120/0x120 [usb_storage]
Jul 13 15:03:36 localhost kernel: [ 9837.500017] ?
kthread_create_on_node+0xd0/0xd0
Jul 13 15:03:36 localhost kernel: [ 9837.500017] ret_from_fork+0x2c/0x40
Jul 13 15:03:36 localhost kernel: [ 9837.500017] Object at ffff88007cdaa668, in
cache kmalloc-192 size: 192
Jul 13 15:03:36 localhost kernel: [ 9837.500017] Allocated:
Jul 13 15:03:36 localhost kernel: [ 9837.500017] PID= 6277
Jul 13 15:03:36 localhost kernel: [ 9837.500017] save_stack_trace+0x1b/0x20
Jul 13 15:03:36 localhost kernel: [ 9837.500017] save_stack+0x46/0xd0
Jul 13 15:03:36 localhost kernel: [ 9837.500017] kasan_kmalloc+0xad/0xe0
Jul 13 15:03:36 localhost kernel: [ 9837.500017]
kmem_cache_alloc_trace+0xef/0x210
Jul 13 15:03:36 localhost kernel: [ 9837.500017] kernfs_fop_open+0x14b/0x540
Jul 13 15:03:36 localhost kernel: [ 9837.500017] do_dentry_open+0x39a/0x560
Jul 13 15:03:36 localhost kernel: [ 9837.500017] vfs_open+0x84/0xd0
Jul 13 15:03:36 localhost kernel: [ 9837.500017] path_openat+0x4ab/0x1e10
Jul 13 15:03:36 localhost kernel: [ 9837.500017] do_filp_open+0x122/0x1c0
Jul 13 15:03:36 localhost kernel: [ 9837.500017] do_sys_open+0x17c/0x2c0
Jul 13 15:03:36 localhost kernel: [ 9837.500017] compat_Sys_open+0x1b/0x20
Jul 13 15:03:36 localhost kernel: [ 9837.500017] do_fast_syscall_32+0x188/0x300
Jul 13 15:03:36 localhost kernel: [ 9837.500017]
entry_SYSENTER_compat+0x4c/0x5b
Jul 13 15:03:36 localhost kernel: [ 9837.500017] Freed:
Jul 13 15:03:36 localhost kernel: [ 9837.500017] PID = 6277
Jul 13 15:03:36 localhost kernel: [ 9837.500017] save_stack_trace+0x1b/0x20
Jul 13 15:03:36 localhost kernel: [ 9837.500017] save_stack+0x46/0xd0
Jul 13 15:03:36 localhost kernel: [ 9837.500017] kasan_slab_free+0x71/0xb0
Jul 13 15:03:36 localhost kernel: [ 9837.500017] kfree+0x9e/0x1e0
Jul 13 15:03:36 localhost kernel: [ 9837.500017] kernfs_fop_release+0x87/0xa0
Jul 13 15:03:36 localhost kernel: [ 9837.500017] __fput+0x177/0x350
Jul 13 15:03:36 localhost kernel: [ 9837.500017] ____fput+0xe/0x10
Jul 13 15:03:36 localhost kernel: [ 9837.500017] task_work_run+0xa0/0xc0
Jul 13 15:03:36 localhost kernel: [ 9837.500017]
exit_to_usermode_loop+0xc5/0xd0
Jul 13 15:03:36 localhost kernel: [ 9837.500017] do_fast_syscall_32+0x2ef/0x300
Jul 13 15:03:36 localhost kernel: [ 9837.500017]
entry_SYSENTER_compat+0x4c/0x5b
Jul 13 15:03:36 localhost kernel: [ 9837.500017] Memory state around the buggy
address:
Jul 13 15:03:36 localhost kernel: [ 9837.500017] ffff88007cdaa600: fc fc fc fc
fc fc fc fc fc fc fc fc fb fb fb
Jul 13 15:03:36 localhost kernel: [ 9837.500017] ffff88007cdaa680: fb fb fb fb
fb fb fb fb fb fb fb fb fb fb fb
Jul 13 15:03:36 localhost kernel: [ 9837.500017] >ffff88007cdaa700: fb fb fb fb
fb fc fc fc fc fc fc fc fc fc fc

```

```

Jul 13 15:03:36 localhost kernel: [ 9837.500017]
^
Jul 13 15:03:36 localhost kernel: [ 9837.500017] ffff88007cdaa780: fc fc fc fc
fc fc fc fc fc fc fc fc fc fc fc fc
Jul 13 15:03:36 localhost kernel: [ 9837.500017] ffff88007cdaa800: fc fc fc fc
fc fc fc fc fc fc fc fc fc fc fc fc
Jul 13 15:03:36 localhost kernel: [ 9837.500017]
=====
Jul 13 15:03:37 localhost kernel: [ 9837.668157]
=====
Jul 13 15:03:37 localhost kernel: [ 9837.668191] BUG: KASAN: slab-out-of-bounds
in last_sector_hacks.isra.1.part.2+0xc9/0x1d0 [usb_storage] at addr
ffff88007cdaa758
Jul 13 15:03:37 localhost kernel: [ 9837.668200] Read of size 8 by task usb-
storage/6243
Jul 13 15:03:37 localhost kernel: [ 9837.668213] CPU: 1 PID: 6243 Comm: usb-
storage Tainted: G      B          4.10.3 #18
Jul 13 15:03:37 localhost kernel: [ 9837.668218] Hardware name: Dell Inc.
Inspiron 1545                /0J037P, BIOS A14 12/07/2009
Jul 13 15:03:37 localhost kernel: [ 9837.668220] Call Trace:
Jul 13 15:03:37 localhost kernel: [ 9837.668233] dump_stack+0x63/0x8b
Jul 13 15:03:37 localhost kernel: [ 9837.668240] kasan_object_err+0x21/0x70
Jul 13 15:03:37 localhost kernel: [ 9837.668247]
kasan_report.part.1+0x219/0x4f0
Jul 13 15:03:37 localhost kernel: [ 9837.668263] ?
last_sector_hacks.isra.1.part.2+0xc9/0x1d0 [usb_storage]
Jul 13 15:03:37 localhost kernel: [ 9837.668269] kasan_report+0x25/0x30
Jul 13 15:03:37 localhost kernel: [ 9837.668277] __asan_load8+0x5e/0x70
Jul 13 15:03:37 localhost kernel: [ 9837.668292]
last_sector_hacks.isra.1.part.2+0xc9/0x1d0 [usb_storage]
Jul 13 15:03:37 localhost kernel: [ 9837.668308]
usb_stor_invoke_transport+0x1a1/0x960 [usb_storage]
Jul 13 15:03:37 localhost kernel: [ 9837.668316] ?
migrate_swap_stop+0x2e0/0x2e0
Jul 13 15:03:37 localhost kernel: [ 9837.668332] ?
usb_stor_port_reset+0xb0/0xb0 [usb_storage]
Jul 13 15:03:37 localhost kernel: [ 9837.668343] ?
wait_for_completion_interruptible+0x1a7/0x260
Jul 13 15:03:37 localhost kernel: [ 9837.668351] ?
wait_for_completion_killable+0x2a0/0x2a0
Jul 13 15:03:37 localhost kernel: [ 9837.668360] ?
raise_softirq_irqoff+0xba/0xd0
Jul 13 15:03:37 localhost kernel: [ 9837.668366] ? wake_up_q+0x80/0x80
Jul 13 15:03:37 localhost kernel: [ 9837.668382]
usb_stor_transparent_scsi_command+0xe/0x10 [usb_storage]
Jul 13 15:03:37 localhost kernel: [ 9837.668398]
usb_stor_control_thread+0x344/0x510 [usb_storage]
Jul 13 15:03:37 localhost kernel: [ 9837.668415] ?
usb_stor_disconnect+0x120/0x120 [usb_storage]
Jul 13 15:03:37 localhost kernel: [ 9837.668422] ?
default_wake_function+0x2f/0x40
Jul 13 15:03:37 localhost kernel: [ 9837.668430] ? __wake_up_common+0x78/0xc0
Jul 13 15:03:37 localhost kernel: [ 9837.668436] kthread+0x178/0x1d0
Jul 13 15:03:37 localhost kernel: [ 9837.668454] ?
usb_stor_disconnect+0x120/0x120 [usb_storage]
Jul 13 15:03:37 localhost kernel: [ 9837.668460] ?
kthread_create_on_node+0xd0/0xd0
Jul 13 15:03:37 localhost kernel: [ 9837.668466] ret_from_fork+0x2c/0x40
Jul 13 15:03:37 localhost kernel: [ 9837.668472] Object at ffff88007cdaa668, in
cache kmalloc-192 size: 192
Jul 13 15:03:37 localhost kernel: [ 9837.668478] Allocated:
Jul 13 15:03:37 localhost kernel: [ 9837.668483] PID = 6277
Jul 13 15:03:37 localhost kernel: [ 9837.668494] save_stack_trace+0x1b/0x20
Jul 13 15:03:37 localhost kernel: [ 9837.668500] save_stack+0x46/0xd0

```

```

Jul 13 15:03:37 localhost kernel: [ 9837.668506] kasan_kmalloc+0xad/0xe0
Jul 13 15:03:37 localhost kernel: [ 9837.668513]
kmem_cache_alloc_trace+0xef/0x210
Jul 13 15:03:37 localhost kernel: [ 9837.668520] kernfs_fop_open+0x14b/0x540
Jul 13 15:03:37 localhost kernel: [ 9837.668527] do_dentry_open+0x39a/0x560
Jul 13 15:03:37 localhost kernel: [ 9837.668532] vfs_open+0x84/0xd0
Jul 13 15:03:37 localhost kernel: [ 9837.668538] path_openat+0x4ab/0x1e10
Jul 13 15:03:37 localhost kernel: [ 9837.668544] do_filp_open+0x122/0x1c0
Jul 13 15:03:37 localhost kernel: [ 9837.668549] do_sys_open+0x17c/0x2c0
Jul 13 15:03:37 localhost kernel: [ 9837.668554] compat_Sys_open+0x1b/0x20
Jul 13 15:03:37 localhost kernel: [ 9837.668561] do_fast_syscall_32+0x188/0x300
Jul 13 15:03:37 localhost kernel: [ 9837.668568]
entry_SYSENTER_compat+0x4c/0x5b
Jul 13 15:03:37 localhost kernel: [ 9837.668570] Freed:
Jul 13 15:03:37 localhost kernel: [ 9837.668575] PID = 6277
Jul 13 15:03:37 localhost kernel: [ 9837.668583] save_stack_trace+0x1b/0x20
Jul 13 15:03:37 localhost kernel: [ 9837.668589] save_stack+0x46/0xd0
Jul 13 15:03:37 localhost kernel: [ 9837.668594] kasan_slab_free+0x71/0xb0
Jul 13 15:03:37 localhost kernel: [ 9837.668599] kfree+0x9e/0x1e0
Jul 13 15:03:37 localhost kernel: [ 9837.668605] kernfs_fop_release+0x87/0xa0
Jul 13 15:03:37 localhost kernel: [ 9837.668611] __fput+0x177/0x350
Jul 13 15:03:37 localhost kernel: [ 9837.668616] ____fput+0xe/0x10
Jul 13 15:03:37 localhost kernel: [ 9837.668623] task_work_run+0xa0/0xc0
Jul 13 15:03:37 localhost kernel: [ 9837.668629]
exit_to_usermode_loop+0xc5/0xd0
Jul 13 15:03:37 localhost kernel: [ 9837.668635] do_fast_syscall_32+0x2ef/0x300
Jul 13 15:03:37 localhost kernel: [ 9837.668642]
entry_SYSENTER_compat+0x4c/0x5b
Jul 13 15:03:37 localhost kernel: [ 9837.668644] Memory state around the buggy
address:
Jul 13 15:03:37 localhost kernel: [ 9837.668655] ffff88007cdaa600: fc fc fc fc
fc fc fc fc fc fc fc fc fb fb fb
Jul 13 15:03:37 localhost kernel: [ 9837.668664] ffff88007cdaa680: fb fb fb fb
fb fb fb fb fb fb fb fb fb fb fb
Jul 13 15:03:37 localhost kernel: [ 9837.668674] >ffff88007cdaa700: fb fb fb fb
fb fc fc fc fc fc fc fc fc fc fc
Jul 13 15:03:37 localhost kernel: [ 9837.668680]
^
Jul 13 15:03:37 localhost kernel: [ 9837.668689] ffff88007cdaa780: fc fc fc fc
fc fc fc fc fc fc fc fc fc fc fc
Jul 13 15:03:37 localhost kernel: [ 9837.668698] ffff88007cdaa800: fc fc fc fc
fc fc fc fc fc fc fc fc fc fc fc
Jul 13 15:03:37 localhost kernel: [ 9837.668704]
=====
Jul 13 15:03:37 localhost NetworkManager[745]: <info> [1499938417.1889]
address 192.168.1.100

```

```

-----
Commits - 13 August 2017 - Suspicious use-after-free error flagged by Kernel
Address Sanitizer - committed for analysis
This error precedes last_sector_hacks ISRA error above in USB storage driver.
-----

```

```

Aug 13 14:53:17 localhost kernel: [ 47.797146] BUG: KASAN: use-after-free in
sr_probe+0x7e0/0xb20 at addr ffff88000009637e
Aug 13 14:53:17 localhost kernel: [ 47.797146] Read of size 1 by task
kworker/u4:1/37
Aug 13 14:53:17 localhost kernel: [ 47.797146] page:ffffea0000002580 count:0
mapcount:0 mapping: (null) index:0x0
Aug 13 14:53:17 localhost kernel: [ 47.797146] flags: 0x0()
Aug 13 14:53:17 localhost kernel: [ 47.797146] raw: 0000000000000000
0000000000000000 0000000000000000 00000000ffffff
Aug 13 14:53:17 localhost kernel: [ 47.797146] raw: fffffea00000025a0

```

```

ffffea000000025a0 0000000000000000 0000000000000000
Aug 13 14:53:17 localhost kernel: [ 47.797146] page dumped because: kasan: bad
access detected
Aug 13 14:53:17 localhost kernel: [ 47.797146] CPU: 1 PID: 37 Comm:
kworker/u4:1 Tainted: G B 4.10.3 #18
Aug 13 14:53:17 localhost kernel: [ 47.797146] Hardware name: Dell Inc.
Inspiron 1545 /0J037P, BIOS A14 12/07/2009
Aug 13 14:53:17 localhost kernel: [ 47.797146] Workqueue: events_unbound
async_run_entry_fn
Aug 13 14:53:17 localhost kernel: [ 47.797146] Call Trace:
Aug 13 14:53:17 localhost kernel: [ 47.797146] dump_stack+0x63/0x8b
Aug 13 14:53:17 localhost kernel: [ 47.797146]
kasan_report.part.1+0x4bc/0x4f0
Aug 13 14:53:17 localhost kernel: [ 47.797146] ? sr_probe+0x7e0/0xb20
Aug 13 14:53:17 localhost kernel: [ 47.797146] ? scsi_mode_select+0x370/0x370
Aug 13 14:53:17 localhost kernel: [ 47.797146] kasan_report+0x25/0x30
Aug 13 14:53:17 localhost kernel: [ 47.797146] __asan_load1+0x47/0x50
Aug 13 14:53:17 localhost kernel: [ 47.797146] sr_probe+0x7e0/0xb20
Aug 13 14:53:17 localhost kernel: [ 47.797146] ?
kernfs_next_descendant_post+0x93/0xf0
Aug 13 14:53:17 localhost kernel: [ 47.797146] ? sr_block_ioctl+0xe0/0xe0
Aug 13 14:53:17 localhost kernel: [ 47.797146] ?
sysfs_do_create_link_sd.isra.2+0x7c/0xc0
Aug 13 14:53:17 localhost kernel: [ 47.797146]
driver_probe_device+0x40b/0x670
Aug 13 14:53:17 localhost kernel: [ 47.797146]
__device_attach_driver+0xd9/0x160
Aug 13 14:53:17 localhost kernel: [ 47.797146] ? __driver_attach+0x120/0x120
Aug 13 14:53:17 localhost kernel: [ 47.797146] bus_for_each_drv+0x107/0x180
Aug 13 14:53:17 localhost kernel: [ 47.797146] ? bus_rescan_devices+0x20/0x20
Aug 13 14:53:17 localhost kernel: [ 47.797146] __device_attach+0x17e/0x200
Aug 13 14:53:17 localhost kernel: [ 47.797146] ? device_bind_driver+0x80/0x80
Aug 13 14:53:17 localhost kernel: [ 47.797146] ?
kobject_uevent_env+0x1ec/0x7f0
Aug 13 14:53:17 localhost kernel: [ 47.797146] device_initial_probe+0x13/0x20
Aug 13 14:53:17 localhost kernel: [ 47.797146] bus_probe_device+0xfe/0x120
Aug 13 14:53:17 localhost kernel: [ 47.797146] device_add+0x5f1/0x9f0
Aug 13 14:53:17 localhost kernel: [ 47.797146] ?
device_private_init+0xc0/0xc0
Aug 13 14:53:17 localhost kernel: [ 47.797146] ?
scsi_dh_add_device+0xd4/0x130
Aug 13 14:53:17 localhost kernel: [ 47.797146] scsi_sysfs_add_sdev+0xd1/0x350
Aug 13 14:53:17 localhost kernel: [ 47.797146] do_scan_async+0xfd/0x230
Aug 13 14:53:17 localhost kernel: [ 47.797146] ? scsi_scan_host+0x250/0x250
Aug 13 14:53:17 localhost kernel: [ 47.797146] async_run_entry_fn+0x84/0x270
Aug 13 14:53:17 localhost kernel: [ 47.797146] ?
pwq_dec_nr_in_flight+0x8c/0x110
Aug 13 14:53:17 localhost kernel: [ 47.797146] process_one_work+0x2c6/0x7d0
Aug 13 14:53:17 localhost kernel: [ 47.797146] worker_thread+0x90/0x850
Aug 13 14:53:17 localhost kernel: [ 47.797146] kthread+0x178/0x1d0

```

```

-----
(FEATURE-DONE) Spark Cloud Analytics for Linux Kernel 4.10.3 64 bit with Kernel
Address Sanitizer debug logging enabled - 15 August 2017
- Commits 1
-----

```

```

-----
(*) Upgraded Spark version to 2.1.0 on Hadoop 2.7
(*) Changed to SparkContext text file instead of reading the input kernel log in
python I/O
(*) Added flatMap to front of MapReduce chain of transformations for tokenizer
(*) Changed the input kernel log to 64bit 4.10.3 Kernel Address Sanitizer
enabled kern.log which prints lot of debugging information on

```


memory accesses especially for USBWWAN and USB Storage drivers.
(*) This is an alternative to traditional promiscuous USB Analyzers like WireShark to get kernel stack traces for USB and WLAN operations.
(*) Particularly useful in malware related untoward memory access and traffic analysis
(*) Unifies Kernel Address Sanitizer, USB storage/WLAN driver and Spark Cloud for analytics
(*) Logs for this have been committed to testlogs/ and python-src/testlogs

(FEATURE-DONE) Spark Cloud Analytics for Linux Kernel 4.10.3 64 bit with Kernel Address Sanitizer debug logging enabled - 15 August 2017
- Commits 2

(*) Added a substring match filter to RDD map/reduce transformations chain
(*) Presently hardcoded as "+0x" which extracts all kernel functions invoked from Kernel Address Sanitizer kern.log and their frequencies

Previous profiling prints following top kernel function invocations:

```
(u'last_sector_hacks.isra.1.part.2+0xc9/0x1d0', 159),  
(u'usb_stor_disconnect+0x120/0x120', 106),  
(u'save_stack+0x46/0xd0', 106),  
(u'save_stack_trace+0x1b/0x20', 106),  
(u'entry_SYSENTER_compat+0x4c/0x5b', 85),  
(u'kthread+0x178/0x1d0', 74),
```

implying heavy dependence on last_sector_hacks.isra gcc optimization. Discussion on <https://groups.google.com/forum/#!topic/linux.kernel/IYBXrW7K2Vc> shows it to be an old kernel bug.

USBWWAN Kernel Log Spark Analyzer Update - Refactoring to a new python function - 18 June 2018

1. Spark Log Analyzer Spark_USBWWANLogMapReduceParser.py has been changed to modularize the pattern extraction by defining a new function accepting kern.log file, pattern and filter and also creates Spark DataFrame SQL table and queries it.
2. This is similar to NeuronRain AsFer log_mapreducer()

(FEATURE) USBWWAN analytics - USBmon and FTrace logs analysis - 15 November 2018

1. Logs Analysis for 2 standard kernel tracing facilities have been included - USBmon and FTrace. USBmon is the kernel debugfs tracing facility and FTrace is the Kernel functions tracing utility accessible from user space. (Kernel Address Sanitizer - KASAN - is only enabled in kernelspace via KBuild config and kernel build transparent to userspace)
2. USBmon traces are enabled by debugfs in /sys/kernel/debug/usb/usbmon and can be loaded in wireshark in libpcap format or usbmon pseudodevices can be viewed in tcpdump:

```
467 ls /sys/kernel/debug/  
468 modprobe usbmon  
472 dumpcap -D  
474 ls /dev/usbmon0  
475 ls -lrt /dev/usbmon*  
487 tcpdump -i usbmon1
```

```

488 tcpdump -i usbmon2
489 tcpdump -i usbmon0
490 tcpdump -i usbmon3
491 tcpdump -i usbmon4
520 cat /sys/kernel/debug/usb/usbmon/1t 2>&1 > usbmon.mon
3. FTrace for function graph analysis are enabled by (Kernel.org FTrace
Documentation: https://www.kernel.org/doc/Documentation/trace/ftrace.txt):
536 ls /sys/kernel/debug/tracing/current_tracer
537 echo nop > /sys/kernel/debug/tracing/current_tracer
538 echo 0 > /sys/kernel/debug/tracing/tracing_on
539 echo $$ > /sys/kernel/debug/tracing/set_ftrace_pid
541 echo function > /sys/kernel/debug/tracing/current_tracer
545 echo 1 > /sys/kernel/debug/tracing/tracing_on
557 ls -lrt /sys/kernel/debug/tracing/trace
561 cat /sys/kernel/debug/tracing/set_graph_function
562 cat /sys/kernel/debug/tracing/trace_options
563 echo funcgraph-duration > /sys/kernel/debug/tracing/trace_options
566 cat /sys/kernel/debug/tracing/set_graph_function
567 cat /sys/kernel/debug/tracing/trace_options
568 cat /sys/kernel/debug/tracing/trace_options
569 echo funcgraph-cpu 2>&1 > /sys/kernel/debug/tracing/trace_options
620 cat /sys/kernel/debug/tracing/set_ftrace_pid
624 echo 7379 > /sys/kernel/debug/tracing/set_ftrace_pid
625 cat /sys/kernel/debug/tracing/trace 2>&1 > ftrace.log.15November2018
639 export JAVA_HOME=/media/Ubuntu2/jdk1.8.0_171/
640 export PATH=/usr/bin:$PATH
671 /media/Ubuntu2/spark-2.3.1-bin-hadoop2.7/bin/spark-submit

```

Spark_USBWWANLogMapReduceParser.py 2>&1 >

testlogs/Spark_USBWWANLogMapReduceParser.FTraceAndUSBMon.log.15November2018

4. FTrace traces for specific userspace threads/processes are enabled by previous example commandlines and available through /sys/kernel/debug/tracing/trace (circular buffer). Function graph traces show kernel function invocations as call graph edges (denoted by fn2 <- fn1)

5. Spark_USBWWANLogMapReduceParser.py has been changed to invoke log analyzer for USBmon and FTrace logs for patterns Bi(BULK IN) and usb from USBmon and FTrace logs respectively:

- usbmon.15November2018.mon
- ftrace.ping.log.15November2018 (ftraces for ping of an IP address)

6. Logs for Spark Analyzer have been committed to Spark_USBWWANLogMapReduceParser.FTraceAndUSBMon.log.15November2018 which analyze the USBmon logs and WLAN traffic for IP address ping.

7. include/linux/serial.h has been committed (similar to other versions of USBmd - 32 and 64 bits - in SourceForge, GitHub and GitLab)

(FEATURE) USBmd FTrace Kernel Function CallGraph Generation for Analysis - 22 November 2018

1. New bash shell script usb_md_ftrace.sh has been committed to repository which writes out an ftrace.log file containing kernel function call graph sequences for an executable code. It is invoked as:

```
$usb_md_ftrace.sh <executable-to-trace>
```

usb_md_ftrace.sh summarizes previously mentioned ftrace options enabling commands into single file with an option for commandline argument of an executable to trace.

2. usb_wwan_modified/python-src/Spark_USBWWANLogMapReduceParser.py has been changed to include a new function ftrace_callgraph_dot() which parses an ftrace log generated by usb_md_ftrace.sh for command:

```
$usb_md_ftrace.sh traceroute <ip-address>
```

3. ftrace_callgraph_dot() parses each line of ftrace.log and adds them as edges

in a NetworkX Directed Graph. DOT file for this call graph is written to Spark_USBWWANLogMapReduceParser.ftrace_callgraph.dot

4. As a novelty, PageRank and Degree Centrality measures of the call graph NetworkX DiGraph are printed which show the prominently active regions of the kernel for traceroute . PageRank/Degree Centrality of kernel function callgraph is quite useful by treating every function caller as a voter to function callee. Theoretically, this centrality in kernel throws light on suspicious, malevolent invocations particularly involving memory and locking. In this traceroute ftrace example, lock and kmalloc functions have high centrality, and USB URB related functions are way down the ranking. More the ranking, deeper the function is in callstack trace in kernel.

5. Lot of functions have ISRA optimization of GCC. ISRA is known to cause signed int bugs (0 was erroneously promoted to 1 in loops) and ISRA has been disabled in ARM kernel: <https://patchwork.kernel.org/patch/7113091/> by -fno-ipa-sra GCC flag. This kind of instability could be the reason for 32-bit VIRGO heisenbugs in string functions in older kernels.

6. Previous FTrace kernel call graph analysis is not only limited to USBmd WLAN analytics but can be applied to any executable requiring kernel profiling. Usual profilers measure time spent in the function whereas this graph theoretic analysis is superior and finds kernel bottlenecks and malicious patterns by analyzing call graphs within kernel.

7. Malicious code (e.g virus, worms, root-kits, bots, keystroke loggers) are usually associated with high cpu and memory footprint causing abnormal traffic. Analyzing infected kernel callgraph patterns might help in identifying the root cause.

8. FTrace kernel function call graph complements already implemented Program Analyzers: SATURN CFG driver in VIRGO kernels (accessible only in kernelspace) and Valgrind/KCachegrind/Callgrind userspace call graph analyzer in AsFer. By this kernel activity is partially visible and can be analyzed graph theoretically from userspace.

9. Outbreak of epidemics have been analyzed as Game Theoretic problem (<https://blogs.cornell.edu/info2040/2016/09/16/game-theory-in-the-context-of-epidemics/>) - on how people behave in epidemics and their conclusion - "faster information limits disease spread". Cybercrimes are epidemics counterpart in cloud of computers only difference being damage inflicted on intellectual property than humans and adversaries are hackers/malicious code in place of viri. This makes Cybercrimes a multi-player adversarial game involving Hackers/Malicious code Versus Aggrieved. Translating the previous conclusion to cybercrimes: Faster information about malicious code limits the damage.

/

#-----

#NEURONRAIN VIRGO - Cloud, Machine Learning and Queue augmented Linux Kernel Fork-off

#This program is free software: you can redistribute it and/or modify

#it under the terms of the GNU General Public License as published by

#the Free Software Foundation, either version 3 of the License, or

##(at your option) any later version.

#This program is distributed in the hope that it will be useful,

#but WITHOUT ANY WARRANTY; without even the implied warranty of

#MERCHANTABILITY or FITNESS FOR A PARTICULAR PURPOSE. See the

#GNU General Public License for more details.

#You should have received a copy of the GNU General Public License

#along with this program. If not, see <<http://www.gnu.org/licenses/>>.

#-----

#Copyleft (Copyright+):

#Srinivasan Kannan (alias) Ka.Shrinivaasan (alias) Shrinivas Kannan

#Ph: 9791499106, 9003082186

#Krishna iResearch Open Source Products Profiles:

#http://sourceforge.net/users/ka_shrinivaasan,

```
#https://github.com/shrinivaasanka,
#https://www.openhub.net/accounts/ka_shrinivaasan
#Personal website(research): https://sites.google.com/site/kuja27/
#emails: ka.shrinivaasan@gmail.com, shrinivas.kannan@gmail.com,
#kashrinivaasan@live.com
#-----
-----
*****
*****/
```

VIRGO is an operating system kernel forked off from Linux kernel mainline to add cloud functionalities (system calls, modules etc.,) within kernel itself with machine learning, analytics, debugging, queueing support in the deepest layer of OSI stack i.e AsFer, USBmd, KingCobra together with VIRGO constitute the previous functionalities. Presently there seems to be no cloud implementation with fine-grained cloud primitives (system calls, modules etc.,) included in kernel itself though there are coarse grained clustering and SunRPC implementations available. VIRGO complements other Clustering and application layer cloud OSes like cloudstack, openstack etc., in these aspects - CloudStack and OpenStack can be deployed on a VIRGO Linux Kernel Cloud - OpenStack nova compute, neutron network, cinder/swift storage subsystems can be augmented to have additional drivers that invoke lowlevel VIRGO syscall and kernel module primitives (assuming there are no coincidental replications of functionalities) thereby acting as a foundation to application layer cloud.

Remote Device Invocation , which is an old terminology for Internet-Of-Things has already been experimented in SunRPC and KORbit CORBA-in-linux-kernel kernel modules in old linux kernels (<http://www.csn.ul.ie/~mark/fyp/fypfinal.html> - with Solaris MC and example Remote Device Client-Server Module implementation). VIRGO Linux with the larger encompassing NeuronRain suite is an effort to provide a unified end-to-end application-to-kernel machine-learning propelled cloud and internet-of-things framework.

Memory pooling:

Memory pooling is proposed to be implemented by a new virgo_malloc() system call that transparently allocates a block of virtual memory from memory pooled from virtual memory scattered across individual machines part of the cloud.

CPU pooling or cloud ability in a system call:

Clone() system call is linux specific and internally it invokes sys_clone(). All fork(),vfork() and clone() system calls internally invoke do_fork(). A new system call virgo_clone() is proposed to create a thread transparently on any of the available machines on the cloud.This creates a thread on a free or least-loaded machine on the cloud and returns the results.

virgo_clone() is a wrapper over clone() that looks up a map of machines-to-loadfactor and get the host with least load and invokes clone() on a function on that gets executed on the host. Usual cloud implementations provide userspace API that have something similar to this - call(function,host). Loadfactor can be calculated through any of the prominent loadbalancing algorithm. Any example userspace code that uses clone() can be replaced with virgo_clone() and all such threads will be running in a cloud transparently.Presently Native POSIX threads library(NPTL) and older LinuxThreads thread libraries internally use clone().

Kernel has support for kernel space sockets with kernel_accept(), kernel_bind(), kernel_connect(), kernel_sendmsg() and kernel_recvmsg() that can be used inside a kernel module. Virgo driver implements virgo_clone() system call that does a kernel_connect() to a remote kernel socket already __sock_create()-d, kernel_bind()-ed and kernel_accept()-ed and does kernel_sendmsg() of the function details and kernel_recvmsg() after function has been executed by clone() in remote machine. After kernel_accept() receives a connection it reads

the function and parameter details. Using these `kthread_create()` is executed in the remote machine and results are written back to the originating machine. This is somewhat similar to SunRPC but adapted and made lightweight to suit `virgo_clone()` implementation without any external data representation.

Experimental Prototype

`virgo_clone()` system call and a kernel module `virgocloudexec` which implements Sun RPC interface have been implemented.

VIRGO - loadbalancer to get the host:ip of the least loaded node

Loadbalancer option 1 - Centralized loadbalancer registry that tracks load:

`Virgo_clone()` system call needs to lookup a registry or map of host-to-load and get the least loaded host:ip from it. This requires a load monitoring code to run periodically and update the map. If this registry is located on a single machine then simultaneous `virgo_clone()` calls from many machines on the cloud could choke the registry. Due to this, loadbalancer registry needs to run on a high-end machine. Alternatively, each machine can have its own view of the load and multiple copies of load-to-host registries can be stored in individual machines. Synchronization of the copies becomes a separate task in itself (Cache coherency). Either way gives a tradeoff between accuracy, latency and efficiency.

Many application level userspace load monitoring tools are available but as `virgo_clone()` is in kernel space, it needs to be investigated if kernel-to-kernel loadmonitoring can be done without userspace data transport. Most Cloud API explicitly invoke a function on a host. If this functionality is needed, `virgo_clone()` needs to take host:ip address as extra argument, but it reduces transparent execution.

(Design notes for LB option 1 handwritten by myself are at
: <http://sourceforge.net/p/virgo-linux/code-0/HEAD/tree/trunk/virgo-docs/MiscellaneousOpenSourceDesignAndAcademicResearchNotes.pdf>)

Loadbalancer option 2 - Linux Psuedorandom number generator based load balancer(experimental) instead of centralized registry that tracks load:

Each `virgo_clone()` client has a PRG which is queried (`/dev/random` or `/dev/urandom`) to get the id of the host to send the next `virgo_clone()` function to be executed

Expected number of requests per node is derived as:

expected number of requests per node =
summation(each_value_for_the_random_variable_for_number_of_requests *
probability_for_each_value) where random variable ranges from 1 to k where N is
number of processors and k is the number of requests to be distributed on N
nodes

=expected number of requests per node = $(\text{math.pow}(N, k+2) - k * \text{math.pow}(N, 2) + k * \text{math.pow}(N, 1) - 1) / (\text{math.pow}(N, k+3) - 2 * \text{math.pow}(N, k+2) + \text{math.pow}(N, k+1))$

This loadbalancer is dependent on efficacy of the PRG and since each request is uniformly, identically, independently distributed use of PRG would distribute requests evenly. This obviates the need for loadtracking and coherency of the load-to-host table.

(Design notes for LB option 2 handwritten by myself at
: <http://sourceforge.net/p/virgo-linux/code-0/HEAD/tree/trunk/virgo-docs/MiscellaneousOpenSourceDesignAndAcademicResearchNotes.pdf>)

(python script in virgo-python-src/)

```
*****
*****
Implemented VIRGO Linux components (as on 7 March 2016)
*****
*****
1. cpupooling virtualization - VIRGO_clone() system call and VIRGO cpupooling
driver by which a remote procedure can be invoked in kernelspace.(port: 10000)
2. memorypooling virtualization - VIRGO_malloc(), VIRGO_get(), VIRGO_set(),
VIRGO_free() system calls and VIRGO memorypooling driver by which kernel memory
can be allocated in remote node, written to, read and freed - A kernelspace
memcache-ing.(port: 30000)
3. filesystem virtualization - VIRGO_open(), VIRGO_read(), VIRGO_write(),
VIRGO_close() system calls and VIRGO cloud filesystem driver by which file IO in
remote node can be done in kernelspace.(port: 50000)
4. config - VIRGO config driver for configuration symbols export.
5. queueing - VIRGO Queueing driver kernel service for queuing incoming requests,
handle them with workqueue and invoke KingCobra service routines in kernelspace.
(port: 60000)
6. cloudsync - kernel module for synchronization primitives (Bakery algorithm
etc.,) with exported symbols that can be used in other VIRGO cloud modules for
critical section lock() and unlock()
7. utils - utility driver that exports miscellaneous kernel functions that can
be used across VIRGO Linux kernel
8. EventNet - eventnet kernel driver to vfs_read()/vfs_write() text files for
EventNet vertex and edge messages (port: 20000)
9. Kernel_Analytics - kernel module that reads machine-learnt config key-value
pairs set in /etc/virgo_kernel_analytics.conf. Any machine learning software can
be used to get the key-value pairs for the config. This merges three facets -
Machine Learning, Cloud Modules in VIRGO Linux-KingCobra-USBmd , Mainline Linux
Kernel
10. Testcases and kern.log testlogs for the above
11. SATURN program analysis wrapper driver.
```

Thus VIRGO Linux at present implements a minimum cloud OS (with cloud-wide cpu, memory and file system management) over Linux and potentially fills in a gap to integrate both software and hardware into cloud with machine learning and analytics abilities that is absent in application layer cloud implementations. Thus VIRGO cloud is an IoT operating system kernel too that enables any hardware to be remote controlled. Data analytics using AsFer can be done by just invoking requisite code from a kernelspace driver above and creating an updated driver binary (or) by kernel_analytics module which reads the userland machine-learnt config.

```
*****
*****
VIRGO ToDo and NiceToHave Features (list is quite dynamic and might be rewritten
depending on feasibility - longterm with no deadline)
*****
*****
```

(FEATURE - DONE-minimum separate config file support in client and kernel service)1. More Sophisticated VIRGO config file and read_virgo_config() has to be invoked on syscall clients virgo_clone and virgo_malloc also. Earlier config was being read by kernel module only which would work only on a single machine. A separate config module kernel service has been added for future use while exporting kernel-wide configuration related symbols. VIRGO config files have been split into /etc/virgo_client.conf and /etc/virgo_cloud.conf to delink the cloud client and kernel service config parameters reading and to do away with oft occurring symbol lookup errors and multiple definition errors for num_cloud_nodes and node_ip_addrs_in_cloud - these errors are frequent in 3.15.5 kernel than 3.7.8 kernel. Each VIRGO module and system call now reads the config

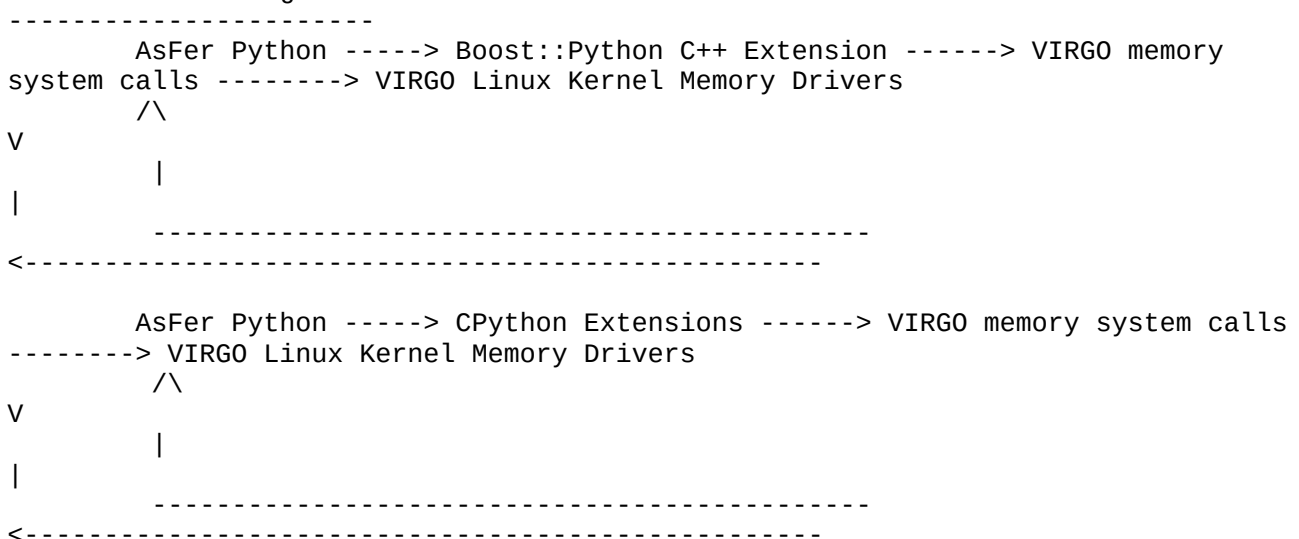
file independent of others - there is a `read_virgo_config<module>_<client_or_service>()` function variant for each driver and system call. Though at present smacks of a replicated code, in future the config reads for each component (system call or module) might vary significantly depending on necessities. New kernel module config has been added in `drivers/virgo`. This is for future prospective use as a config export driver that can be looked up by any other VIRGO module for config parameters. `include/linux/virgo_config.h` has the declarations for all the config variables declared within each of the VIRGO kernel modules. Config variables in each driver and system call have been named with prefix and suffix to differentiate the module and/or system call it serves. In geographically distributed cloud `virgo_client.conf` has to be in client nodes and `virgo_cloud.conf` has to be in cloud nodes. For VIRGO Queue - KingCobra REQUEST-REPLY peer-to-peer messaging system same node can have `virgo_client.conf` and `virgo_cloud.conf`. Above segregation largely simplifies the build process as each module and system call is independently built without need for a symbol to be exported from other module by pre-loading it. (- from commit comments done few months ago)

(FEATURE - Special case implementation DONE) 2. Object Marshalling and Unmarshalling (Serialization) Features - Feature 4 is a marshalling feature too as Python world PyObjects are serialized into VIRGO linux kernel and unmarshalled back bottom-up with CPython and Boost::Python C++ invocations - CPython and Boost internally take care of serialization.

(FEATURE - DONE) 3. `virgo_malloc()`, `virgo_set()`, `virgo_get()` and `virgo_free()` syscalls that virtualize the physical memory across all cloud nodes into a single logical memory behemoth (NUMA visavis UMA). (There are random crashes in `copy_to_user` and `copy_from_user` in syscall path for VIRGO memory pooling commands that were investigated but turned out to be mystery). These crashes have either been resolved or occur less in 3.15.5 and 4.1.5 kernels. Initial Design Handwritten notes committed at: http://sourceforge.net/p/virgo-linux/code-0/210/tree/trunk/virgo-docs/VIRGO_Memory_Pooling_virgomalloc_initial_design_notes.pdf

(FEATURE - DONE) 4. Integrated testing of AsFer-VIRGO Linux Kernel request roundtrip - invocation of VIRGO linux kernel system calls from AsFer Python via C++ or C extensions - Commits for this have been done on 29 January 2016. This unifies userlevel applications and kernelspace modules so that AsFer Python makes VIRGO linux kernel an extension. Following is schematic diagram and More details in commit notes below.

4.1 Schematic Diagram:



(FEATURE - DONE) 5. Multithreading of VIRGO cloudexec kernel module (if not already done by kernel module subsystem internally)

(FEATURE - DONE) 6. Sophisticated queuing and persistence of CPU and Memory pooling requests in Kernel Side (by possibly improving already existing kernel workqueues). Either open source implementations like ZeroMQ/ActiveMQ can be used or Queuing implementation has to be written from scratch or both. ActiveMQ supports REST APIs and is JMS implementation. This feature has been marked completed because recently NeuronRain AsFer backend has been updated to support KingCobra REQUEST_REPLY.queue as a datasource for Streaming Abstract Generator. By enabling use_as_kingcobra_service=1 in cpupooling and memorypooling VIRGO drivers, any incoming CPU and Memory related request can be routed to KingCobra by linux workqueue in VIRGO queue and disk persisted (/var/log/REQUEST_REPLY.queue) by KingCobra servicerequest recipient. Also Kafka Publisher/Subscriber have been implemented in NeuronRain AsFer which invoke Streaming Abstract Generator with KingCobra REQUEST_REPLY.queue as datasource to publish persisted already received CPU and Memory requests to Kafka Message Queue. Thus queuing and persistence for VIRGO CPU and Memory is in place. ZeroMQ does not have persistence and is used for NeuronRain client side Router-Dealer concurrent request servicing pattern.

(FEATURE - DONE-Minimum Functionality) 7. Integration of Asfer(AstroInfer) algorithm codes into VIRGO which would add machine learning capabilities into VIRGO - That is, VIRGO cloud subsystem which is part of a linux kernel installation "learns" and "adapts" to the processes that are executed on VIRGO. This catapults the power of the Kernel and Operating System into an artificially (rather approximately naturally) intelligent computing platform (a software "brain"). For example VIRGO can "learn" about "execution times" of processes and suitably act for future processes. PAC Learning of functions could be theoretical basis for this. Initial commits for Kernel Analytics Module which reads the /etc/virgo_kernel_analytics.conf config have been done. This config file virgo_kernel_analytics.conf having csv(s) of key-value pairs of analytics variables is set by AsFer or any other Machine Learning code. With this VIRGO Linux Kernel is endowed with abilities to dynamically evolve than being just a platform for user code. Implications are huge - for example, a config variable "MaxNetworkBandwidth=255" set by the ML miner in userspace based on a Perceptron or Logistic Regression executed on network logs can be read by a kernel module that limits the network traffic to 255Mbps. Thus kernel is no longer a static predictable blob behemoth. With this, VIRGO is an Internet-of-Things kernel that does analytics and based on analytics variable values integrated hardware can be controlled across the cloud through remote kernel module function invocation. This facility has been made dynamic with Boost::Python C++ and CPython extensions that permit flow of objects from machine learnt AsFer kernel analytics variables to VIRGO Linux Kernel memory drivers via VIRGO system calls directly and back - Commits on 29 January 2016 - this should obviate re-reading /etc/virgo_kernel_analytics.conf and is an exemplary implementation which unifies C++/Python into C/Kernel.

Example scenario 1 without implementation:

- Philips Hue IoT mobile app controlled bulb - <http://www2.meethue.com/en-xx/>
- kernel_analytics module learns key-value pairs from the AsFer code and exports it VIRGO kernel wide
- A driver function with in bulb embedded device driver can be invoked through VIRGO cpupooling (invoked from remote virgo_clone() system_call) based on if-else clause of the kernel_analytics variable i.e remote_client invokes virgo_clone() with function argument "lights on" which is routed to another cloud node. The recipient cloud node "learns" from AsFer kernel_analytics that Voltage is low or Battery is low from logs and decides to switch in high beam or low beam.

Example scenario 2 without implementation:

- A swivel security camera driver is remotely invoked via virgo_clone() in the VIRGO cloud.

- The camera driver uses a machine learnt variable exported by kernel_analytics-and-AsFer to pan the camera by how much degrees.

Example scenario 3 without implementation - probably one of the best applications of NeuronRain IoT OS:

- Automatic Driverless Automobiles - a VIRGO driver for a vehicle which learns kernel analytics variables (driving directions) set by kernel_analytics driver and AsFer Machine Learning. A naive algorithm for Driverless Car (with some added modifications over A-Star and Motion planning algorithms):

- AsFer analytics receives obstacle distance data 360+360 degrees (vertical and horizontal) around the vehicle (e.g ultrasound sensors) which is updated in a Spark DataFrame table with high frequency (100 times per second).

- VIRGO Linux kernel on vehicle has two special drivers for Gear-Clutch-Break-Accelerator-Fuel(GCBAF) and Steering listening on some ports.

- AsFer analytics with high frequency computes threshold variables for applying break, clutch, gear, velocity, direction, fuel changes which are written to kernel_analytics.conf realtime based on distance data from Spark table.

- These analytics variables are continuously read by GCBAF and Steering drivers which autopilot the vehicle.

- Above applies to Fly-by-wire aeronautics too with appropriate changes in analytics variables computed.

- The crucial parameter is the response time in variable computation and table updates which requires a huge computing power unless the vehicle is hooked onto a Spark cloud in motion by wireless which process the table and compute analytic variables.

References for Machine Learning + Linux Kernel

7.1 KernTune -

[http://repository.uwc.ac.za/xmlui/bitstream/handle/10566/53/Yi_KernTune\(2007\).pdf?sequence=3](http://repository.uwc.ac.za/xmlui/bitstream/handle/10566/53/Yi_KernTune(2007).pdf?sequence=3)

7.2 Self-learning, Predictive Systems -

<https://icri-ci.technion.ac.il/projects/past-projects/machine-learning-for-architecture-self-learning-predictive-computer-systems/>

7.3 Linux Process Scheduling and Machine Learning -

<http://www.cs.ucr.edu/~kishore/papers/tencon.pdf>

7.4 Network Latency and Machine Learning -

https://users.soe.ucsc.edu/~slukin/rtt_paper.pdf

7.5 Machine Learning based Meta-Scheduler for Multicore processors -

<https://books.google.co.in/books?>

[id=1GwCmCr10QC&pg=PA528&lpg=PA528&dq=linux+kernel+machine+learning&source=bl&ots=zfJsqu5q&sig=mMIUZ-oyJIwZXtYj4HntrQE8NSk&hl=en&sa=X&ved=0CCAQ6AEwATgKahUKEwjs9sqF9vPIAhVBFZQKHbNtA6A](https://books.google.co.in/books?id=1GwCmCr10QC&pg=PA528&lpg=PA528&dq=linux+kernel+machine+learning&source=bl&ots=zfJsqu5q&sig=mMIUZ-oyJIwZXtYj4HntrQE8NSk&hl=en&sa=X&ved=0CCAQ6AEwATgKahUKEwjs9sqF9vPIAhVBFZQKHbNtA6A)

8. A Symmetric Multi Processing subsystem Scheduler that virtualizes all nodes in cloud (probably this would involve improving the loadbalancer into a scheduler with priority queues)

(FEATURE - ONGOING) 9. Virgo is an effort to virtualize the cloud as a single machine - Here cloud is not limited to servers and desktops but also mobile devices that run linux variants like Android, and other Mobile OSes. In the longterm, Virgo may have to be ported or optimized for handheld devices.

Boost::Python AsFer-VIRGO system call invocations implemented in NeuronRain is framework for implementing python applications interfacing with kernel. If deployed on Mobile processors (e.g by overlaying Android Kernel with VIRGO layer) there are IDEs like QPython to develop python apps for Android.

(FEATURE - DONE) 10. Memory Pooling Subsystem Driver - Virgo_malloc(),

Virgo_set(), Virgo_get() and Virgo_free() system calls and their Kernel Module Implementations. In addition to syscall path, telnet or userspace socket client interface is also provided for both VIRGO CPU pooling(virgo_clone()) and VIRGO Memory Pooling Drivers.

(FEATURE - DONE) 11. Virgo Cloud File System with virgo_cloud_open(), virgo_cloud_read() , virgo_cloud_write() and virgo_cloud_close() commands invoked through telnet path has been implemented that transcends disk storage in all nodes in the cloud. It is also fanciful feature addition that would make VIRGO a complete all-pervading cloud platform. The remote telnet clients send the file path and the buf to be read or data to be written. The Virgo File System kernel driver service creates a unique Virgo File Descriptor for each struct file* opened by filp_open() and is returned to client. Earlier design option to use a hashmap (linux/hashmap.h) looked less attractive as file descriptor is an obvious unique description for open file and also map becomes unscalable. The kernel upcall path has been implemented (paramIsExecutable=0) and may not be necessary in most cases and all above cloudfs commands work in kernelspace using VFS calls.

(FEATURE - DONE) 12. VIRGO Cloud File System commands through syscall paths - virgo_open(),virgo_close(),virgo_read() and virgo_write(). All the syscalls have been implemented with testcases and more bugs fixed. After fullbuild and testing, virgo_open() and virgo_read() work and copy_to_user() is working.

(FEATURE - DONE) 13. VIRGO memory pooling feature is also a distributed key-value store similar to other prominent key-store software like BigTable implementations, Dynamo, memory caching tools etc., but with a difference that VIRGO mempool is implemented as part of Linux Kernel itself thus circumventing userspace latencies. Due to Kernel space VIRGO mempool has an added power to store and retrieve key-value pair in hardware devices directly which otherwise is difficult in userspace implementations.

14. VIRGO memory pooling can be improved with disk persistence for in-memory key-value store using virgo_malloc(),virgo_set(),virgo_get() and virgo_free() calls. Probably this might be just a set of invocations of read and write ops in disk driver or using sysfs. Probably this could be redundant as the VIRGO filesystem primitives have been implemented that write to a remote host's filesystem in kernelspace.

15. (FEATURE-DONE) Socket Debugging, Program Analysis and Verification features for user code that can find bugs statically. Socket skbuff debug utility and SATURN Program Analysis Software has been integrated into NEURONRAIN VIRGO Linux Kernel.

16(FEATURE - DONE-Minimum Functionality). Operating System Logfile analysis using Machine Learning code in AstroInfer for finding patterns of processes execution and learn rules from the log. Kernel_Analytics VIRGO module reads /etc/virgo_kernel_analytics.conf config key-value pairs which are set by AsFer or other Machine Learning Software. At present an Apache Spark usecase that mines Uncomplicated Fire Wall logs in kern.log for most prominent source IP has been implemented in AsFer codebase : <http://sourceforge.net/p/asfer/code/704/tree/python-src/SparkKernelLogMapReduceParser.py> . This is set as a key-value config in /etc/virgo_kernel_analytics.conf read and exported by kernel_analytics module.

17. Implementations of prototypical Software Transactional Memory and LockFree Datastructures for VIRGO memory pooling.

18. Scalability features for Multicore machines - references:
(<http://halobates.de/lk09-scalability.pdf>,
<http://pdos.csail.mit.edu/papers/linux:osdi10.pdf>)

19. Read-Copy-Update algorithm implementation for VIRGO memory pooling that supports multiple simultaneous versions of memory for readers - widely used in

redesigned Linux Kernel.

20. (FEATURE - SATURN integration - minimum functionality DONE) Program Comprehension features as an add-on described in :
<https://sites.google.com/site/kuja27/PhDThesisProposal.pdf?attredirects=0>.
SATURN program analysis has been integrated into VIRGO linux with a stub driver.

21. (FEATURE - DONE) Bakery Algorithm implementation - cloudsync kernel module

22. (FEATURE - ONGOING) Implementation of Distributed Systems primitives for VIRGO cloud viz., Logical Clocks, Termination Detection, Snapshots, Cache Coherency subsystem etc., (as part of cloudsync driver module). Already a simple timestamp generation feature has been implemented for KingCobra requests with <ipaddress>:<localmachinetimestamp> format

23. (FEATURE - minimum functionality DONE) Enhancements to kmem if it makes sense, because it is better to rely on virgo_malloc() for per machine memory management and wrap it around with a cloudwide VIRGO Unique ID based address lookup implementation of which is already in place.

Kernel Malloc syscall kmalloc() internally works as follows:

- kmem_cache_t object has pointers to 3 lists
- These 3 lists are full objects SLAB list, partial objects SLAB list and free objects SLAB list - all are lists of objects of same size and cache_cache is the global list of all caches created thus far.
- Any kmalloc() allocation searches partial objects SLAB list and allocates a memory block with kmem_cache_alloc() from the first SLAB available - returned to caller.
- Any kfree() returns an object to a free SLAB list
- Full SLABs are removed from partial SLAB list and appended to full SLAB list
- SLABs are virtual memory pages created with kmem_cache_create
- Each SLAB in SLABs list has blocks of similar sized objects (e.g. multiples of two). Closest matching block is returned and fragmentation is minimized (incidentally this is the knapsack and packing optimization LP problem and thus NP-complete).

KERNELSPACE:

VIRGO address translation table already implements a tree registry of vtables each of capacity 3000 that keep track of kmalloc() allocations across all cloud nodes. Implementation of SLAB allocator for kmalloc() creates a kmem_cache(s) of similar sized objects and kmem_cache_alloc() allocates from these caches. kmalloc() already does lot of per-machine optimizations. VIRGO vtable registry tree maintained in VIRGO memory syscall end combined with per-machine kmalloc() cache_cache already look sufficient. Instrumenting kmem_cache_create() with #ifdef SLAB_CLOUD_MALLOC flags to do RPC looks superfluous. Hence marking this action item as done. Any further optimization can be done on top of existing VIRGO address translation table struct - e.g bookkeeping flags, function pointers etc.,.

USERSPACE: sbrk() and brk() are no longer used internally in malloc() library routines. Instead mmap() has replaced it

(<http://web.eecs.utk.edu/courses/spring2012/cs360/360/notes/Malloc1/lecture.html>,

<http://web.eecs.utk.edu/courses/spring2012/cs360/360/notes/Malloc1/diff.html>).

24.(FEATURE - ONGOING) Cleanup the code and remove unnecessary comments.

25.(FEATURE - DONE) Documentation - This design document is also a documentation for commit notes and other build and debugging technical details. Doxygen html cross-reference documentation for AsFer, USBmd, VIRGO, KingCobra and Acadpdrfts has been created along with summed-up design document and committed to GitHub Repository at https://github.com/shrinivaasanka/Krishna_iResearch_DoxygenDocs

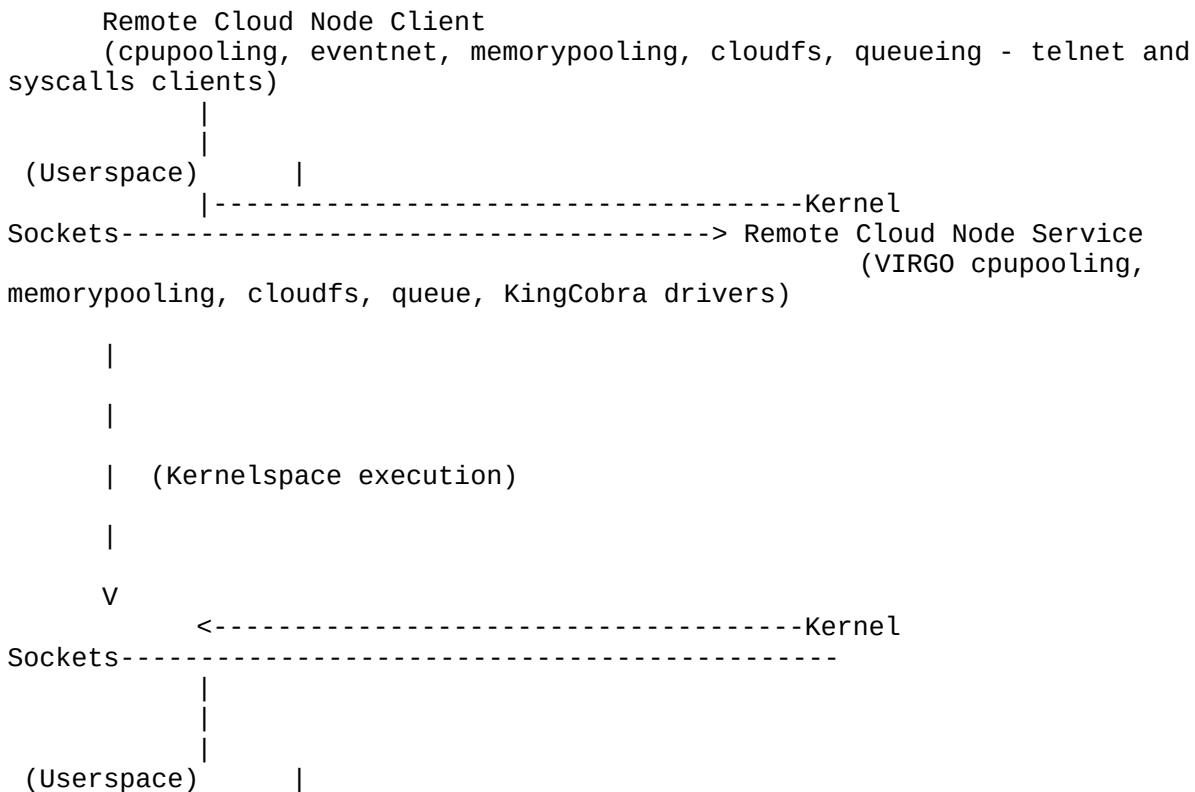
26. (FEATURE - DONE) Telnet path to virgo_cloud_malloc, virgo_cloud_set and virgo_cloud_get has been tested and working. This is similar to memcached but

stores key-value in kernelspace (and hence has the ability to write to and retrieve from any device driver memory viz., cards, handheld devices). An optional todo is to write a script or userspace socket client that connects to VIRGO mempool driver for these commands.

27. Augment the Linux kernel workqueue implementation (<http://lxr.free-electrons.com/source/kernel/workqueue.c>) with disk persistence if feasible and doesn't break other subsystems - this might require additional persistence flags in work_struct and additional #ifdefs in most of the queue functions that write and read from the disk. Related to item 6 above.

28.(FEATURE - DONE) VIRGO queue driver with native userspace queue and kernel workqueue-handler framework that is optionally used for KingCobra and is invoked through VIRGO cpupooling and memorypooling drivers. (Schematic in <http://sourceforge.net/p/kcobra/code-svn/HEAD/tree/KingCobraDesignNotes.txt> and http://sourceforge.net/p/acadpdrafts/code/ci/master/tree/Krishna_iResearch_opensourceproducts_archdiagram.pdf)

29.(FEATURE - DONE) KERNELSPACE EXECUTION ACROSS CLOUD NODES which geographically distribute userspace and kernelspace execution creating a logical abstraction for a cloudwide virtualized kernel:



30. (FEATURE - DONE) VIRGO platform as on 5 May 2014 implements a minimum set of features and kernelsocket commands required for a cloud OS kernel: CPU virtualization(virgo_clone), Memory virtualization(virgo_malloc,virgo_get,virgo_set,virgo_free) and a distributed cloud file system(virgo_open,virgo_close,virgo_read,virgo_write) on the cloud nodes and thus gives a logical view of one unified, distributed linux kernel across all cloud nodes that splits userspace and kernelspace execution across cloud as above.

31. (FEATURE - DONE) VIRGO Queue standalone kernel service has been implemented in addition to paths in schematics above. VIRGO Queue listens on hardcoded port 60000 and enqueues the incoming requests to VIRGO queue which is serviced by KingCobra:

VIRGO Queue client(e.g telnet) -----> VIRGO Queue kernel service ---> Linux
Workqueue handler -----> KingCobra

32. (FEATURE - DONE) EventNet kernel module service:

VIRGO eventnet client (telnet) -----> VIRGO EventNet kernel service ----->
EventNet graph text files

33. (FEATURE - DONE) Related to point 22 - Reuse EventNet cloudwide logical time infinite graph in AsFer in place of Logical clocks. At present the eventnet driver listens on port 20000 and writes the edges and vertices files in kernel using vfs_read()/vfs_write(). These text files can then be read by the AsFer code to generate DOT files and visualize the graph with graphviz.

34. (FEATURE - OPTIONAL) The kernel modules services listening on ports could return a JSON response when connected instead of plaintext, conforming to REST protocol. Additional options for protocol buffers which are becoming a standard data interchange format.

35. (FEATURE-Minimum Functionality DONE) Pointer Swizzling and Unswizzling of VIRGO addressspace pointers to/from VIRGO Unique ID (VUID). Presently VIRGO memory system calls implement a basic minimal pointer address translation to unique kmem location identifier.

CODE COMMIT RELATED NOTES

VIRGO code commits as on 16/05/2013

1. VIRGO clouddriver with a listener kernel thread service has been implemented and it listens on port 10000 on system startup through /etc/modules load-on-bootup facility

2. VIRGO clouddriver virgo_clone() system call has been implemented that would kernel_connect() to the VIRGO clouddriver service listening at port 10000

3. VIRGO clouddriver has been split into virgo.h (VIRGO typedefs), virgoclouddriverv.h(VIRGO clouddriver service that is invoked by module_init() of VIRGO clouddriver driver) and virgo_clouddriver.c (with module ops definitions)

4. VIRGO does not implement SUN RPC interface anymore and now has its own virgo ops.

5. Lot of Kbuild related commits with commented lines for future use have been done viz., to integrate VIRGO to Kbuild, KBUILD_EXTRA_SYMBOLS for cross-module symbol reference.

VIRGO code commits as on 20/05/2013

1. test_virgo_clone.c testcase for sys_virgo_clone() system call works and connections are established to VIRGO clouddriver kernel module.

2. Makefile for test_virgo_clone.c and updated buildscript.sh for headers_install for custom-built linux.

VIRGO code commits as on 6/6/2013

1. Message header related bug fixes

VIRGO code commits as on 25/6/2013

1. telnet to kernel service was tested and found working
2. GFP_KERNEL changed to GFP_ATOMIC in VIRGO clouDEXEC kernel service

VIRGO code commits as on 1/7/2013

1. Instead of printing iovector, printing buffer correctly prints the messages
2. wake_up_process() added and function received from virgo_clone() syscall is executed with kernel_thread and results returned to virgo_clone() syscall client.

commit as on 03/07/2013

PRG loadbalancer preliminary code implemented. More work to be done

commit as on 10/07/2013

Tested PRG loadbalancer read config code through telnet and virgo_clone. VFS code to read from virgo_cloud.conf commented for testing

commits as on 12/07/2013

PRG loadbalancer prototype has been completed and tested with test_virgo_clone and telnet and symbol export errors and PRG errors have been fixed

commits as on 16/07/2013

read_virgo_config() and read_virgo_clone_config()(replica of read_virgo_config()) have been implemented and tested to read the virgo_cloud.conf config parameters(at present the virgo_cloud.conf has comma separated list of ip addresses. Port is hardcoded to 10000 for uniformity across all nodes). Thus minimal cloud functionality with config file support is in place. Todo things include function pointer lookup in kernel service, more parameters to cloud config file if needed, individual configs for virgo_clone() and virgo kernel service, kernel-to-userspace upcall and execution instead of kernel space, performance tuning etc.,

commits as on 17/07/2013

moved read_virgo_config() to VIRGOclouDEXEC's module_init so that config is read at boot time and exported symbols are set beforehand.
Also commented read_virgo_clone_config() as it is redundant

commits as on 23/07/2013

Lack of reflection kind of facilities requires map of function_names to pointers_to_functions to be executed on cloud has to be lookedup in the map to get pointer to function. This map is not scalable if number of functions are in millions and size of the map increases linearly. Also having it in memory is both CPU and memory intensive. Moreover this map has to be synchronized in all nodes for coherency and consistency which is another intensive task. Thus name to pointer function table is at present not implemented. Suitable way to call a function by name of the function is yet to be found out and references in this topic are scarce.

If parameterIsExecutable is set to 1 the data received from virgo_clone() is not a function but name of executable
This executable is then run on usermode using call_usermodehelper() which internally takes care of queueing the workstruct

and executes the binary as child of keventd and reaps silently. Thus workqueue component of kernel is indirectly made use of. This is sometimes more flexible alternative that executes a binary itself on cloud and is preferable to clone()ing a function on cloud. Virgo_clone() syscall client or telnet needs to send the message with name of binary.

If parameterIsExecutable is set to 0 then data received from virgo_clone() is name of a function and is executed in else clause using dlsym() lookup and pthread_create() in user space. This unifies both call_usermodehelper() and creating a userspace thread with a fixed binary which is same for any function. The dlsym lookup requires mangled function names which need to be sent by virgo_clone or telnet. This is far more efficient than a function pointer table.

call_usermodehelper() Kernel upcall to usermode to exec a fixed binary that would inturn execute the cloneFunction in userspace by spawning a pthread. cloneFunction is name of the function and not binary. This clone function will be dlsym()ed and a pthread will be created by the fixed binary. Name of the fixed binary is hardcoded herein as "virgo_kernelupcall_plugin". This fixed binary takes clone function as argument. For testing libvirgo.so has been created from virgo_cloud_test.c and separate build script to build the cloud function binaries has been added.

- Ka.Shrinivaasan (alias) Shrinivas Kannan (alias) Srinivasan Kannan
(<https://sites.google.com/site/kuja27>)

commits as on 24/07/2013

test_virgo_clone unit test case updated with mangled function name to be sent to remote cloud node. Tested with test_virgo_clone end-to-end and all features are working. But sometimes kernel_connect hangs randomly (this was observed only today and looks similar to blocking vs non-blocking problem. Origin unknown).

- Ka.Shrinivaasan (alias) Shrinivas Kannan (alias) Srinivasan Kannan
(<https://sites.google.com/site/kuja27>)

commits as on 29/07/2013

Added kernel mode execution in the clone_func and created a sample kernel_thread for a cloud function. Some File IO logging added to upcall binaries and parameterIsExecutable has been moved to virgo.h

commits as on 30/07/2013

New usecase virgo_cloud_test_kernelspace.ko kernel module has been added. This exports a function virgo_cloud_test_kernelspace() and is accessed by virgo_cloudexec kernel service to spawn a kernel thread that is executed in kernel addressspace. This Kernel mode execution on cloud adds a unique ability to VIRGO cloud platform to seamlessly integrate hardware devices on to cloud and transparently send commands to them from a remote cloud node through virgo_clone().

Thus above feature adds power to VIRGO cloud to make it act as a single "logical device driver" though devices are in geographically in a remote server.

commits as on 01/08/2013 and 02/08/2013

Added Bash shell commandline with -c option for call_usermodehelper upcall

clauses to pass in remote virgo_clone command message as arguments to it. Also tried output redirection but it works some times that too with a fatal kernel panic.

Ideal solutions are :

1. either to do a copy_from_user() for message buffer from user address space (or)
2. somehow rebuild the kernel with fd_install() pointing stdout to a VFS file* struct. In older kernels like 2.6.x, there is an fd_install code with in kmod.c (___call_usermodehelper()) which has been redesigned in kernel 3.x versions and fd_install has been removed in kmod.c .
3. Create a Netlink socket listener in userspace and send message up from kernel Netlink socket.

All the above are quite intensive and time consuming to implement. Moreover doing FileIO in usermode helper is strongly discouraged in kernel docs

Since Objective of VIRGO is to virtualize the cloud as single execution "machine", doing an upcall (which would run with root abilities) is redundant often and kernel mode execution is sufficient. Kernel mode execution with intermodule function invocation can literally take over the entire board in remote machine (since it can access PCI bus, RAM and all other device cards)

As a longterm design goal, VIRGO can be implemented as a separate protocol itself and sk_buff packet payload from remote machine can be parsed by kernel service and kernel_thread can be created for the message.

commits as on 05/08/2013:

Major commits done for kernel upcall usermode output logging with fd_install redirection to a VFS file. With this it has become easy for user space to communicate runtime data to Kernel space. Also a new strip_control_M() function has been added to strip \r\n or " ".

11 August 2013:

Open Source Design and Academic Research Notes uploaded to http://sourceforge.net/projects/acadpdrafts/files/MiscellaneousOpenSourceDesignAndAcademicResearchNotes_2013-08-11.pdf/download

commits as on 23 August 2013

New Multithreading Feature added for VIRGO Kernel Service - action item 5 in ToDo list above (virgo_cloudeexec driver module). All dependent headers changed for kernel threadlocalizing global data.

commits as on 1 September 2013

GNU Copyright license and Product Owner Profile (for identity of license issuer) have been committed. Also Virgo Memory Pooling - virgo_malloc() related initial design notes (handwritten scanned) have been committed(http://sourceforge.net/p/virgo-linux/code-0/HEAD/tree/trunk/virgo-docs/VIRGO_Memory_Pooling_virgomalloc_initial_design_notes.pdf)

commits as on 14 September 2013

Updated virgo malloc design handwritten nodes on kmalloc() and malloc() usage in kernelspace and userspace execution mode of virgo_cloudeexec service (http://sourceforge.net/p/virgo-linux/code-0/HEAD/tree/trunk/virgo-docs/VIRGO_Memory_Pooling_virgomalloc_design_notes_2_14September2013.pdf). As described in handwritten notes, virgo_malloc() and related system calls might be

needed when a large scale allocation of kernel memory is needed when in kernel space execution mode and large scale userspace memory when in user modes (function and executable modes). Thus a cloud memory pool both in user and kernel space is possible.

VIRGO virtual addressing

VIRGO virtual address is defined with the following datatype:

```
struct virgo_address
{
    int node_id;
    void* addr;
};
```

VIRGO address translation table is defined with following datatype:

```
struct virgo_addr_transtable
{
    int node_id;
    void* addr;
};
```

VIRGO memory pooling prototypical implementation

VIRGO memory pooling implementation as per the design notes committed as above is to be implemented as a prototype under separate directory under drivers/virgo/memorypooling and \$LINUX_SRC_ROOT/virgo_malloc. But the underlying code is more or less similar to drivers/virgo/cpupooling and \$LINUX_SRC_ROOT/virgo_clone.

virgo_malloc() and related syscalls and virgo mempool driver connect to and listen on port different from cpupooling driver. Though all these code can be within cpupooling itself, mempooling is implemented as separate driver and co-exists with cpupooling on bootup (/etc/modules). This enables clear demarcation of functionalities for CPU and Memory virtualization.

Commits as on 17 September 2013

Initial untested prototype code - virgo_malloc and virgo mempool driver - for VIRGO Memory Pooling has been committed - copied and modified from virgo_clone client and kernel driver service.

Commits as on 19 September 2013

3.7.8 Kernel full build done and compilation errors in VIRGO malloc and mempool driver code and more functions code added

Commits as on 23 September 2013

Updated virgo_malloc.c with two functions, int_to_str() and addr_to_str(), using kmalloc() with full kernel re-build.
(Rather a re-re-build because some source file updates in previous build got deleted somehow mysteriously. This could be related to Cybercrime issues mentioned in https://sourceforge.net/p/usb-md/code-0/HEAD/tree/USBmd_notes.txt)

Commits as on 24 September 2013

Updated syscall*.tbl files, staging.sh, Makefiles for virgo_malloc(), virgo_set(), virgo_get() and virgo_free() memory pooling syscalls. New testcase test_virgo_malloc for virgo_malloc(), virgo_set(), virgo_get(), virgo_free() has been added to repository. This testcase might have to be

updated if return type and args to virgo_malloc+ syscalls are to be changed.

Commits as on 25 September 2013

All build related errors fixed after kernel rebuild some changes made to function names to reflect their names specific to memory pooling. Updated /etc/modules also has been committed to repository.

Commits as on 26 September 2013

Circular dependency error in standalone build of cpu pooling and memory pooling drivers fixed and datatypes and declarations for CPU pooling and Memory Pooling drivers have been segregated into respective header files (virgo.h and virgo_mempool.h with corresponding service header files) to avoid any dependency error.

Commits as on 27 September 2013

Major commits for Memory Pooling Driver listen port change and parsing VIRGO memory pooling commands have been done.

Commits as on 30 September 2013

New parser functions added for parameter parsing and initial testing on virgo_malloc() works with telnet client with logs in test_logs/

Commits as on 1 October 2013

Removed strcpy in virgo_malloc as ongoing bugfix for buffer truncation in syscall path.

Commits as on 7 October 2013

Fixed the buffer truncation error from virgo_malloc syscall to mempool driver service which was caused by sizeof() for a char*. BUF_SIZE is now used for size in both syscall client and mempool kernel service.

Commits as on 9 October 2013 and 10 October 2013

Mempool driver kernelspace virgo mempool ops have been rewritten due to lack of facilities to return a value from kernel thread function. Since mempool service already spawns a kthread, this seems to be sufficient. Also the iov.iov_len in virgo_malloc has been changed from BUF_SIZE to strlen(buf) since BUF_SIZE causes the kernel socket to block as it waits for more data to be sent.

Commits as on 11 October 2013

sscanf format error for virgo_cloud_malloc() return pointer address and sock_release() null pointer exception has been rectified. Added str_to_addr() utility function.

Commits as on 14 October 2013 and 15 October 2013

Updated todo list.

Rewritten virgo_cloud_malloc() syscall with:

- mutexed virgo_cloud_malloc() loop
- redefined virgo address translation table in virgo_mempool.h
- str_to_addr(): removed (void**) cast due to null sscanf though it should have worked

Commits as on 18 October 2013

Continued debugging of null sscanf - added str_to_addr2() which uses simple_strtoll() kernel function for scanning pointer as long long from string and casting it to void*. Also more %p qualifiers where added in str_to_addr() for debugging.

Based on latest test_virgo_malloc run, simple_strtoll() correctly parses the address string into a long long base 16 and then is reinterpret_cast to void*. Logs in test/

Commits as on 21 October 2013

Kern.log for testing after vtranstable addr fix with simple_strtoll() added to repository and still the other %p qualifiers do not work and only simple_strtoll() parses the address correctly.

Commits as on 24 October 2013

Lot of bugfixes made to virgo_malloc.c for scanning address into VIRGO transtable and size computation. Testcase test_virgo_malloc.c has also been modified to do reinterpret cast of long long into (struct virgo_address*) and corresponding test logs have been added to repository under virgo_malloc/test.

Though the above sys_virgo_malloc() works, the return value is a kernel pointer if the virgo_malloc executes in the Kernel mode which is more likely than User mode (call_usermodehelper which is circuitous). Moreover copy_from_user() or copy_to_user() may not be directly useful here as this is an address allocation routine. The long long reinterpret cast obfuscates the virgo_address(User or Kernel) as a large integer which is a unique id for the allocated memory on cloud. Initial testing of sys_virgo_set() causes a Kernel Panic as usual probably due to direct access of struct virgo_address*. Alternatives are to use only long long for allocation unique-id everywhere or do copy_to_user() or copy_from_user() of the address on a user supplied buffer. Also vtranstable can be made into a bucketed hash table that maps each alloc_id to a chained virgo malloc chunks than the present sequential addressing which is more similar to open addressing.

Commits as on 25 October 2013

virgo_malloc.c has been rewritten by adding a userspace __user pointer to virgo_get() and virgo_set() syscalls which are internally copied with copy_from_user() and copy_to_user() kernel function to get and set userspace from kernelspace. Header file syscalls.h has been updated with changed syscalls prototypes. Two functions have been added to map a VIRGO address to a unique virgo identifier and viceversa for abstracting hardware addresses from userspace as mentioned in previous commit notes. VIRGO cloud mempool kernelspace driver has been updated to use virgo_mempool_args* instead of void* and VIRGO clouddex mempool driver has been updated accordingly during intermodule invocation. The virgo_malloc syscall client has been updated to modified signatures and return types for all mempool alloc, get, set, free syscalls.

Commits as on 29 October 2013

Miscellaneous ongoing bugfixes for virgo_set() syscall error in copy_from_user().

Commits as on 2 November 2013

Due to an issue which corrupts the kernel memory, presently telnet path to VIRGO mempool driver has been tested after commits on 31 October 2013 and 1 November 2013 and is working but

again there is an issue in kstrtoul() that returns the wrong address in virgo_cloud_mempool_kernelspace.ko that gives the address for data to set.

Commits as on 6 November 2013

New parser function virgo_parse_integer() has been added to virgo_cloud_mempool_kernelspace driver module which is carried over from lib/kstrtoux.c and modified locally to add an if clause to discard quotes and unquotes. With this the telnet path commands for virgo_malloc() and virgo_set() are working. Today's kern.log has been added to repository in test_logs/.

Commits as on 7 November 2013

In addition to virgo_malloc and virgo_set, virgo_get is also working through telnet path after today's commit for "virgodata:" prefix in virgo_cloud_mempool_kernelspace.ko. This prefix is needed to differentiate data and address so that toAddressString() can be invoked to sprintf() the address in virgo_cloudexec_mempool.ko. Also mempool command parser has been updated to strcmp() virgo_cloud_get command also.

Commits as on 11 November 2013

More testing done on telnet path for virgo_malloc, virgo_set and virgo_get commands which work correctly. But there seem to be unrelated kmem_cache_trace_alloc panics that follow each successful virgo command execution. kern.log for this has been added to repository.

Commits as on 22 November 2013

More testing done on telnet path for virgo_malloc, virgo_set and virgo_get after commenting kernel socket shutdown code in the VIRGO cloudexec mempool sendto code. Kernel panics do not occur after commenting kernel socket shutdown.

Commits as on 2 December 2013

Lots of testing were done on telnet path and syscall path connection to VIRGO mempool driver and screenshots for working telnet path (virgo_malloc, virgo_set and virgo_get) have been committed to repository. Intriguingly, the syscall path is suddenly witnessing series of broken pipe errors, blocking errors etc., which are mostly Heisenbugs.

Commits as on 5 December 2013

More testing on system call path done for virgo_malloc(), virgo_set() and virgo_get() system calls with test_virgo_malloc.c. All three syscalls work in syscall path after lot of bugfixes. Kern.log that has logs for allocating memory in remote cloud node with virgo_malloc, sets data "test_virgo_malloc_data" with virgo_set and retrieves data with virgo_get.

VIRGO version 12.0 tagged.

Commits as on 12 March 2014

Initial VIRGO queueing driver implemented that flips between two internal queues: 1) a native queue implemented locally and 2) wrapper around linux kernel's workqueue facility 3) push_request() modified to pass on the request data to the workqueue handler using container_of on a wrapper structure virgo_workqueue_request.

Commits as on 20 March 2014

-
- VIRGO queue with additional boolean flags for its use as KingCobra queue
 - KingCobra kernel space driver that is invoked by the VIRGO workqueue handler

Commits as on 30 March 2014

-
- VIRGO mempool driver has been augmented with use_as_kingcobra_service flags in CPU pooling and Memory pooling drivers

Commits as on 6 April 2014

-
- VIRGO mempool driver recvfrom() function's if clause for KingCobra has been updated for REQUEST header formatting mentioned in KingCobra design notes

Commits as on 7 April 2014

-
- generate_logical_timestamp() function has been implemented in VIRGO mempool driver that generates timestamps based on 3 boolean flags. At present machine_timestamp is generated and prepended to the request to be pushed to VIRGO queue driver and then serviced by KingCobra.

Commits as on 25 April 2014

-
- client ip address in VIRGO mempool recvfrom KingCobra if clause is converted to host byte order from network byte order with ntohs()

Commits as on 5 May 2014

-
- Telnet path commands for VIRGO cloud file system - virgo_cloud_open(), virgo_cloud_read(), virgo_cloud_write(), virgo_cloud_close() has been implemented and test logs have been added to repository (drivers/virgo/cloudfs/ and cloudfs/testlogs) and kernel upcall path for paramIsExecutable=0

Commits as on 7 May 2014

-
- Bugfixes to tokenization in kernel upcall plugin with strsep() for args passed on to the userspace

Commits as on 8 May 2014

-
- Bugfixes to virgo_cloud_fs.c for kernel upcall (parameterIsExecutable=0) and with these the kernel to userspace upcall and writing to a file in userspace (virgofstest.txt) works. Logs and screenshots for this are added to repository in test_logs/

Commits as on 6 June 2014

-
- VIRGO File System Calls Path implementation has been committed. Lots of Linux Full Build compilation errors fixed and new integer parsing functionality added (similar to driver modules). For the timebeing all syscalls invoke loadbalancer. This may be further optimized with a sticky flag to remember the first invocation which might be usually virgo_open syscall to get the VFS descriptor that is used in subsequent syscalls.

Commits as on 3 July 2014

-
- More testing and bugfixes for VIRGO File System syscalls have been done. virgo_write() causes kernel panic.

7 July 2014 - virgo_write() kernel panic notes:

warning within <http://lxr.free-electrons.com/source/arch/x86/kernel/smp.c#L121>:

static void native_smp_send_reschedule(int cpu)

```

{
    if (unlikely(cpu_is_offline(cpu))) {
        WARN_ON(1);
        return;
    }
    apic->send_IPI_mask(cpumask_of(cpu), RESCHEDULE_VECTOR);
}

```

This is probably a fixed kernel bug in <3.7.8 but recurring in 3.7.8:

- <http://lkml.iu.edu/hypermail/linux/kernel/1205.3/00653.html>
- http://www.kernelhub.org/?p=3&msg=74473&body_id=72338
- <http://lists.openwall.net/linux-kernel/2012/09/07/22>
- https://bugzilla.kernel.org/show_bug.cgi?id=54331
- <https://bbs.archlinux.org/viewtopic.php?id=156276>

Commits as on 29 July 2014

All VIRGO drivers(cloudfs, queuing, cpupooling and memorypooling) have been built on 3.15.5 kernel with some Makefile changes for ccflags and paths

Commits as on 17 August 2014

(FEATURE - DONE) VIRGO Kernel Modules and System Calls major rewrite for 3.15.5 kernel - 17 August 2014

-
1. VIRGO config files have been split into /etc/virgo_client.conf and /etc/virgo_cloud.conf to delink the cloud client and kernel service config parameters reading and to do away with oft occurring symbol lookup errors and multiple definition errors for num_cloud_nodes and node_ip_addrs_in_cloud - these errors are frequent in 3.15.5 kernel than 3.7.8 kernel.
 2. Each VIRGO module and system call now reads the config file independent of others - there is a read_virgo_config_<module>_<client_or_service>() function variant for each driver and system call. Though at present smacks of a replicated code, in future the config reads for each component (system call or module) might vary significantly depending on necessities.
 3. New kernel module config has been added in drivers/virgo. This is for future prospective use as a config export driver that can be looked up by any other VIRGO module for config parameters.
 4. include/linux/virgo_config.h has the declarations for all the config variables declared within each of the VIRGO kernel modules.
 5. Config variables in each driver and system call have been named with prefix and suffix to differentiate the module and/or system call it serves.
 6. In geographically distributed cloud virgo_client.conf has to be in client nodes and virgo_cloud.conf has to be in cloud nodes. For VIRGO Queue - KingCobra REQUEST-REPLY peer-to-peer messaging system same node can have virgo_client.conf and virgo_cloud.conf.
 7. Above segregation largely simplifies the build process as each module and system call is independently built without need for a symbol to be exported from other module by pre-loading it.
 8. VIRGO File system driver and system calls have been tested with above changes and the virgo_open(), virgo_read() and virgo_write() calls work with much less

crashes and freeze problems compared to 3.7.8 (some crashes in VIRGO FS syscalls in 3.7.8 where already reported kernel bugs which seem to have been fixed in 3.15.5). Today's kern.log test logs have been committed to repository.

Committed as on 23 August 2014

Commenting use_as_kingcobra_service if clauses temporarily as disabling also doesnot work and only commenting the block works for VIRGO syscall path. Quite weird as to how this relates to the problem. As this is a heisenbug further testing is difficult and sufficient testing has been done with logs committed to repository. Probably a runtime symbol lookup for kingcobra causes the freeze. For forwarding messages to KingCobra and VIRGO queues, cpupooling driver is sufficient which also has the use_as_kingcobra_service clause.

Committed as on 23 August 2014 and 24 August 2014

As cpupooling driver has the same crash problem with kernel_accept() when KingCobra has benn enabled, KingCobra clauses have been commented in both cpupooling and mempooling drivers. Instead queueing driver has been updated with a kernel service infrastructure to accept connections at port 60000. With this following paths are available for KingCobra requests:

```
VIRGO cpupooling or mempooling =====> VIRGO Queue =====> KingCobra
                                   (or)
VIRGO Queue kernel service =====> KingCobra
```

Committed as on 26 August 2014

- all kmallocs have been made into GFP_ATOMIC instead of GFP_KERNEL
- moved some kingcobra related header code before kernel_recvmg()
- some header file changes for set_fs()

This code has been tested with modified code for KingCobra and the standalone kernel service that accepts requests from telnet directly at port 60000, pushes to virgo_queue and is handled to invoke KingCobra servicerequest kernelspace function, works (the kernel_recvmg() crash was most probably due to Read-Only filesystem -errno printed is -30)

VIRGO version 14.9.9 has been release tagged on 9 September 2014

Committed as on 26 November 2014

New kernel module cloudsnc has been added to repository under drivers/virgo that can be used for synchronization(lock() and unlock()) necessities in VIRGO cloud. Presently Bakery Algorithm has been implemented.

Committed as on 27 November 2014

virgo_bakery.h bakery_lock() has been modified to take 2 parameters - thread_id and number of for loops (1 or 2)

Committed as on 2 December 2014

VIRGO bakery algorithm implementation has been rewritten with some bugfixes.
Sometimes there are soft lockup errors due to looping in kernel time durations
for which are kernel build configurable.

Committed as on 17 December 2014

Initial code commits for VIRGO EventNet kernel module service:

- 1.EventNet Kernel Service listens on port 20000
- 2.It receives eventnet log messages from VIRGO cloud nodes and writes the log messages
after parsing into two text files /var/log/eventnet/EventNetEdges.txt and
/var/log/eventnet/EventNetVertices.txt by VFS calls
- 3.These text files can then be processed by the EventNet implementations in
AsFer (python pygraph and
C++ boost::graph based)
- 4.Two new directories virgo/utils and virgo/eventnet have been added.
- 5.virgo/eventnet has the new VIRGO EventNet kernel module service implementation
that listens on
port 20000.
- 6.virgo/utils is the new generic utilities driver that has a
virgo_eventnet_log()
exported function which connects to EventNet kernel service and sends the vertex
and edge eventnet
log messages which are parsed by kernel service and written to the two text
files above.
- 7.EventNet log messages have two formats:
 - Edge message - "eventnet_edgmsg#<id>#<from_event>#<to_event>"
 - Vertex message - "eventnet_vertxmsg#<id>-<partakers csv>-<partaker
conversations csv>"
- 8.The utilities driver Module.symvers have to be copied to any driver which are
then merged with the symbol files of the corresponding driver. Target clean has
to be commented while
building the unified Module.symvers because it erases symvers carried over
earlier.
- 9.virgo/utils driver can be populated with all necessary utility exported
functions that might be needed
in other VIRGO drivers.
- 10.Calls to virgo_eventnet_log() have to be #ifdef guarded as this is quite
network intensive.

Commits as on 18 December 2014

Miscellaneous bugfixes, logs and screenshot

- virgo_clouddexec_eventnet.c - eventnet messages parser errors and eventnet_func
bugs fixed
- virgo_cloud_eventnet_kernelspace.c - filp_open() args updated due to
vfs_write() kernel panics. The vertexmessage vfs_write is done after looping
through the vertice textfile and appending the conversation to the existing
vertex.Some more code has to be added.
- VIRGO EventNet build script updated for copying Module.symvers from utils

driver for merging with eventnet Module.symvers during Kbuild

- Other build generated sources and kernel objects
- new testlogs directory with screenshot for edgemsg sent to EventNet kernel service and kern.log with previous history for vfs_write() panics due to permissions and the logs for working filp_open() fixed version
- vertex message update

Commits as on 2,3,4 January 2015

- fixes for virgo eventnet vertex and edge message text file vfs_write() errors
- kern.logs and screenshots

VIRGO version 15.1.8 release tagged on 8 January 2015

Commits as on 3 March 2015 - Initial commits for Kernel Analytics Module which reads the /etc/virgo_kernel_analytics.conf config (and) VIRGO memorypooling Key-Value Store Architecture Diagram

- Architecture of Key-Value Store in memorypooling (virgo_malloc, virgo_get, virgo_set, virgo_free) has been uploaded as a diagram at http://sourceforge.net/p/virgo-linux/code-0/HEAD/tree/trunk/virgo-docs/VIRGOlinuxKernel_KeyValueStore_and_Modules_Interaction.jpg
- new kernel_analytics driver for AsFer <=> VIRGO+USBmd+KingCobra interface has been added.
- virgo_kernel_analytics.conf having csv(s) of key-value pairs of analytics variables is set by AsFer or any other Machine Learning code. With this VIRGO Linux Kernel is endowed with abilities to dynamically evolve than being just a platform for user code. Implications are huge - for example, a config variable "MaxNetworkBandwidth=255" set by the ML miner in userspace based on a Perceptron or Logistic Regression executed on network logs can be read by a kernel module that limits the network traffic to 255Mbps. Thus kernel dynamically changes behaviour.
- kernel_analytics Driver build script has been added

Commits as on 6 March 2015

- code has been added in VIRGO config module to import EXPORTed kernel_analytics config key-pair array set by Apache Spark (mined from Uncomplicated Fire Wall logs) and manually and write to kern.log.

NeuronRain version 15.6.15 release tagged

Portability to linux kernel 4.0.5

The VIRGO kernel module drivers are based on kernel 3.15.5. With kernel 4.0.5 kernel which is the latest following compilation and LD errors occur - this is on cloudfs VIRGO File System driver :

- msghdr has to be user_msghdr for iov and iov_len as there is a segregation of msghdr
- modules_install throws an error in scripts/Makefile.modinst while overwriting already installed module

Commits as on 9 July 2015

VIRGO cpupooling driver has been ported to linux kernel 4.0.5 with msghdr changes as mentioned previously
with kern.log for VIRGO cpupooling driver invoked in parameterIsExecutable=2 (kernel module invocation)
added in testlogs

Commits as on 10,11 July 2015

VIRGO Kernel Modules:

- memorypooling
- cloudfs
- utils
- config
- kernel_analytics
- cloudsync
- eventnet
- queuing

along with cpupooling have been ported to Linux Kernel 4.0.5 - Makefile and header files have been updated wherever required.

Commits as on 20,21,22 July 2015

Due to SourceForge Storage Disaster(<http://sourceforge.net/blog/sourceforge-infrastructure-and-service-restoration/>), the github replica of VIRGO is urgently updated with some important changes for msg_iter, iovec etc., in 4.0.5 kernel port specifically for KingCobra and VIRGO Queueing. These have to be committed to SourceForge Krishna_iResearch repository at http://sourceforge.net/users/ka_shrinivaasan once SourceForge repos are restored.
Time to move on to the manufacturing hub? GitHub ;-)

VIRGO Queueing Kernel Module Linux Kernel 4.0.5 port:

- msg_iter is used instead of user_msghdr
- kvec changed to iovec
- Miscellaneous BUF_SIZE related changes
- kern.logs for these have been added to testlogs
- Module.symvers has been recreated with KingCobra Module.symvers from 4.0.5 KingCobra build
- clean target commented in build script as it wipes out Module.symvers
- updated .ko and .mod.c

KingCobra Module Linux Kernel 4.0.5 port

- vfs_write() has a problem in 4.0.5
- the filp_open() args and flags which were working in 3.15.5 cause a kernel panic implicitly and nothing was written to logs
- It took a very long time to figure out the reason to be vfs_write and filp_open
- O_CREAT, O_RDWR and O_LARGEFILE cause the panic and only O_APPEND is working, but does not do vfs_write(). All other VIRGO Queue + KingCobra functionalities work viz., enqueueing, workqueue handler invocation, dequeueing, invoking kingcobra kernelspace service request function from VIRGO queue handler, timestamp, timestamp and IP parser,

reply_to_publisher etc.,
- As mentioned in Greg Kroah Hartman's "Driving me nuts", persistence in Kernel space is a bad idea but still seems to be a necessary stuff - yet only vfs calls are used which have to be safe
- Thus KingCobra has to be in-memory only in 4.0.5 if vfs_write() doesn't work
- Intriguingly cloudfs filesystems primitives - virgo_cloud_open, virgo_cloud_read, virgo_cloud_write etc., work perfectly and append to a file.
- kern.logs for these have been added to testlogs
- Module.symvers has been recreated for 4.0.5
- updated .ko and .mod.c

Due to SourceForge outage and for a future code diversification NeuronRain codebases (AsFer, USBmd, VIRGO, KingCobra) in <http://sourceforge.net/u/userid-769929/profile/> have been replicated in GitHub also - <https://github.com/shrinivaasanka> excluding some huge logs due to Large File Errors in GitHub.

Commits as on 30 July 2015

VIRGO system calls have been ported to Linux Kernel 4.0.5 with commented gcc option -Wimplicit-function-declaration, msghdr and iovec changes similar to drivers mentioned in previous commit notes above. But Kernel 4.1.3 has some Makefile and build issues.
The NeuronRain codebases in SourceForge and GitHub would henceforth be mostly and always out-of-sync and not guaranteed to be replicas - might get diversified into different research and development directions (e.g one codebase might be more focussed on IoT while the other towards enterprise bigdata analytics integration with kernel and training which is yet to be designed- depend on lot of constraints)

Commits as on 2,3 August 2015

- new .config file added which is created from menuconfig
- drivers/Kconfig has been updated with 4.0.5 drivers/Kconfig for trace event linker errors
Linux Kernel 4.0.5 - KConfig is drivers/ has been updated to resolve RAS driver trace event linker error. RAS was not included in KConfig earlier.
- link-vmlinux.sh has been replaced with 4.0.5 kernel version

Commits as on 12 August 2015

VIRGO Linux Kernel 4.1.5 port - related code changes - some important notes:

- Linux Kernel 4.0.5 build suddenly had a serious root shell drop error in initramfs which was not resolved by:
 - adding rootdelay in grub
 - disabling uuid for block devices in grub config
 - mounting in read/write mode in recovery mode
 - no /dev/mapper related errors
 - repeated exits in root shell
 - delay before mount of root device in initrd scripts
- mysteriously there were some firmware microcode bundle executions in ieucodetool
- Above showed a serious grub corruption or /boot MBR bug or 4.0.5 VIRGO kernel build problem
- Linux 4.0.x kernels are EOL-ed
- Hence VIRGO is ported to 4.1.5 kernel released few days ago

- Only minimum files have been changed as in commit log for Makefiles and syscall table and headers and a build script has been added

for 4.1.5:

Changed paths:

A buildscript_4.1.5.sh

M linux-kernel-extensions/Makefile

M linux-kernel-extensions/arch/x86/syscalls/Makefile

M linux-kernel-extensions/arch/x86/syscalls/syscall_32.tbl

M linux-kernel-extensions/drivers/Makefile

M linux-kernel-extensions/include/linux/syscalls.h

- Above minimum changes were enough to build an overlay-ed Linux Kernel with VIRGO codebase

Commits as on 14,15,16 August 2015

Executed the minimum end-end telnet path primitives in Linux kernel 4.1.5 VIRGO code:

- cpu virtualization
 - memory virtualization
 - filesystem virtualization (updated filp_open flags)
- and committed logs and screenshots for the above.

Commits as on 17 August 2015

VIRGO queue driver:

- Rebuilt Module.symvers
- kern.log for telnet request to VIRGO Queue + KingCobra queueing system in kernelspace

Commits as on 25,26 September 2015

VIRGO Linux Kernel 4.1.5 - memory system calls:

- updated testcases and added logs for syscalls invoked separately(malloc,set,get,free)
- The often observed unpredictable heisen kernel panics occur with 4.1.5 kernel too. The logs are 2.3G and only grepped output is committed to repository.
- virgo_malloc.c has been updated with kstrdup() to copy the buf to iov.iov_base which was earlier crashing in copy_from_iter() within tcp code. This problem did not happen in 3.15.5 kernel.
- But virgo_clone syscall code works without any changes to iov_base as above which does a strcpy() which is an internal memcpy() though. So what causes this crash in memory system calls alone is a mystery.
- new insmod script has been added to load the VIRGO memory modules as necessary instead of at boot time.
- test_virgo_malloc.c and its Makefile has been updated.

VIRGO Linux Kernel 4.1.5 - filesystem calls- testcases and logs:

- added insmod script for VIRGO filesystem drivers
- test_virgo_filesystem.c has been updated for syscall numbers in 4.1.5 VIRGO kernel
- virgo_fs.c syscalls code has been updated for iov.iov_base kstrdup() - without this there are kernel panics in copy_from_iter(). kern.log testlogs have been added, but there are heisen kernel panics. The virgo syscalls are executed but not written to kern.log due to these crashes.

Thus execution logs are missing for VIRGO filesystem syscalls.

Commits as on 28,29 September 2015

VIRGO Linux Kernel 4.1.5 filesystem syscalls:

-
- Rewrote iov_base code with a separate iovbuf set to iov_base and strcpy()-ing the syscall command to iov_base similar to VIRGO memory syscalls
 - Pleasantly the same iovbuf code that crashes in memory syscalls works for VIRGO FS without crash. Thus both virgo_clone and virgo_filesystem syscalls work without issues in 4.1.5 and virgo_malloc() works erratically in 4.1.5 which remains as issue.
 - kern.log for VIRGO FS syscalls and virgofstest text file written by virgo_write() have been added to repository

VIRGO Linux 4.1.5 kernel memory syscalls:

-
- rewrote the iov_base buffer code for all VIRGO memory syscalls by allocating separate iovbuf and copying the message to it - this just replicates the virgo_clone syscall behaviour which works without any crashes mysteriously.
 - did extensive repetitive tests that were frequented by numerous kernel panics and crashes
 - The stability of syscalls code with 3.15.5 kernel appears to be completely absent in 4.1.5
 - The telnet path works relatively better though
 - Difference between virgo_clone and virgo_malloc syscalls despite having same kernel sockets code looks like a non-trivial bug and a kernel stability issue.
 - kernel OOPS traces are quite erratic.
 - Makefile path in testcase has been updated

Commits as on 4 October 2015

VIRGO Linux Kernel 4.1.5 - Memory System Calls:

-
- replaced copy_to_user() with a memcpy()
 - updated the testcase with an example VUID hardcoded.
 - str_to_addr2() is done on iov_base instead of buf which was causing NULL parsing
 - kern.log with above resolutions and multiple VIRGO memory syscalls tests - malloc, get, set
 - With above VIRGO malloc and set syscalls work relatively causing less number of random kernel panics
 - return values of memory calls set to 0
 - in virgo_get() syscall, memcpy() of iov_base is done to data_out userspace pointer
 - kern.log with working logs for syscalls - virgo_malloc(), virgo_set(), virgo_get() but still there are random kernel panics
 - Abridged kern.log for VIRGO Memory System Calls with 4.1.5 Kernel - shows example logs for virgo_malloc(), virgo_set() and virgo_get()

Commits as on 14 October 2015

VIRGO Queue Workqueue handler usermode clause has been updated with 4.1.5 kernel paths and kingcobra in user mode is enabled for invoking KingCobra Cloud Perfect Forwarding.

Commits as on 15 October 2015

- Updated VIRGO Queue kernel binaries and build generated sources
- virgo_queue.h has been modified for call_usermodehelper() - set_ds() and fd_install() have been uncommented for output redirection. Output redirection works but there are "alloc_fd: slot 1 not NULL!" errors at random (kern.log in kingcobra testlogs) which seems to be a new feature in 4.1.5 kernel. This did not happen in 3.7.8-3.15.5 kernels

Commits as on 3 November 2015

- kern.log for VIRGO kernel_analytics+config drivers which export the analytics variables from /etc/virgo_kernel_analytics.conf kernel-wide and print them in config driver has been added to config/testlogs

Commits as on 10 January 2016

NeuronRain VIRGO enterprise version 2016.1.10 released.

NeuronRain - AsFer commits for VIRGO - C++ and C Python extensions
- Commits as on 29 January 2016

(FEATURE - DONE) Python-C++-VIRGOKernel and Python-C-VIRGOKernel boost::python and cpython implementations:

- It is a known idiom that Linux Kernel and C++ are not compatible.
- In this commit an important feature to invoke VIRGO Linux Kernel from userspace python libraries via two alternatives have been added.
- In one alternative, C++ boost::python extensions have been added to encapsulate access to VIRGO memory system calls - virgo_malloc(), virgo_set(), virgo_get(), virgo_free(). Initial testing reveals that C++ and Kernel are not too incompatible and all the VIRGO memory system calls work well though initially there were some errors because of config issues.
- In the other alternative, C Python extensions have been added that replicate boost::python extensions above in C - C Python with Linux kernel works exceedingly well compared to boost::python.
- This functionality is required when there is a need to set kernel analytics configuration variables learnt by AsFer Machine Learning Code dynamically without re-reading /etc/virgo_kernel_analytics.conf.
- This completes a major integration step of NeuronRain suite - request travel roundtrip to-and-fro top level machine-learning C++/python code and rock-bottom C linux kernel - bull tamed ;-).
- This kind of python access to device drivers is available for Graphics Drivers already on linux (GPIO - for accessing device states)
- logs for both C++ and C paths have been added in cpp_boost_python_extensions/ and cpython_extensions.
- top level python scripts to access VIRGO kernel system calls have been added in both directories:
 CPython - python cpython_extensions/asferpythonextensions.py
 C++ Boost::Python - python
cpp_boost_python_extensions/asferpythonextensions.py
- .so, .o files with build commandlines(asferpythonextensions.build.out) for "python setup.py build" have been added in build lib and temp directories.
- main implementations for C++ and C are in
cpp_boost_python_extensions/asferpythonextensions.cpp and
cpython_extensions/asferpythonextensions.c

Commits as on 12 February 2016

Commits for Telnet/System Call Interface to VIRGO CPUPooling -> VIRGO Queue -> KingCobra

*) This was commented earlier for the past few years due to a serious kernel panic in previous kernel versions - <= 3.15.5
*) In 4.1.5 a deadlock between VIRGO CPUPooling and VIRGO queue driver init was causing following error in "use_as_kingcobra_service" clause :
- "gave up waiting for virgo_queue init, unknown symbol push_request()"
*) To address this a new boolean flag to selectively enable and disable VIRGO Queue kernel service mode "virgo_queue_reactor_service_mode" has been added.
*) With this flag VIRGO Queue is both a kernel service driver and a standalone exporter of function symbols - push_request/pop_request
*) Incoming request data from telnet/virgo_clone() system call into cpupooling kernel service reactor pattern (virgo cpupooling listener loop) is treated as generic string and handed over to VIRGO queue and KingCobra which publishes it.
*) This resolves a long standing deadlock above between VIRGO cpupooling "use_as_kingcobra_service" clause and VIRGO queue init.
*) This makes virgo_clone() syscall/telnet both synchronous and asynchronous - requests from telnet client/virgo_clone() system call can be either synchronous RPC functions executed on a remote cloud node in kernelspace (or) an asynchronous invocation through "use_as_kingcobra_service" clause path to VIRGO Queue driver which enqueues the data in kernel workqueue and subsequently popped by KingCobra.
*) Above saves an additional code implementation for virgo_queue syscall paths - virgo_clone() handles, based on config selected, incoming data passed to it either as a remote procedure call or as a data that is pushed to VIRGO Queue/KingCobra pub-sub kernelspace.

Prerequisites:

- insmod kingcobra_main_kernelspace.ko
- insmod virgo_queue.ko compiled with flag virgo_queue_reactor_service_mode=1 (when virgo_queue_reactor_service_mode=0, listens on port 60000 for direct telnet requests)
- insmod virgo_cloud_test_kernelspace.ko
- insmod virgo_cloudexec.ko (listens on port 10000)

Schematic Diagram

VIRGO clone system call/telnet client ---> VIRGO cpupooling(compiled with use_as_kingcobra_service=1) -----> VIRGO Queue kernel service (compiled with virgo_queue_reactor_service_mode=1) ---> Linux Workqueue handler -----> KingCobra

Commits as on 15 February 2016 - Kernel Analytics - VIRGO Linux Kernelwide imports

- Imported Kernel Analytics variables into CloudFS kernel module - printed in driver init()
- Module.symvers from kernel_analytics has been merged with CloudFS

Module.symvers

- Logs for above has been added in cloudfs/test_logs/
- Makefile updated with correct fs path
- Copyleft notices updated

Commits as on 15 February 2016 - Kernel Analytics - VIRGO Linux Kernelwide imports

-
- Kernel Analytics driver exported variables have been imported in CPU virtualization driver
 - Module.symvers from kernel_analytics has been merged with Module.symvers in cpupooling
 - kern.log for this import added to cpupooling/virgocloudexec/test_logs/

Commits as on 15 February 2016 - Kernel Analytics - VIRGO Linux Kernelwide imports

-
- Imported kernel analytics variables into memory virtualization driver init() , exported from kernel_analytics driver
 - build shell script updated
 - logs added to test_logs/
 - Module.symvers from kernel_analytics has been merged with memory driver
- Module.symvers
- Makefile updated

Commits as on 15 February 2016 - Kernel Analytics - VIRGO Linux Kernelwide imports

-
- Imported kernel analytics variables into VIRGO Queueing Driver
 - logs for this added in test_logs/
 - Makefile updated
 - Module.symvers from kernel_analytics has been merged with Queueing driver's
- Module.symvers
- .ko, .o and build generated sources

Commits as on 16,17 February 2016

(FEATURE-DONE) Socket Buffer Debug Utility Function - uses linux skbuff facility

- In this commit a multipurpose socket buffer debug utility function has been added in utils driver and exported kernelwide.
- It takes a socket as function argument does the following:
 - dereference the socket buffer head of skbuff per-socket transmit data queue
 - allocate skbuff with alloc_skb()
 - reserve head room with skb_reserve()
 - get a pointer to data payload with skb_put()
 - memcpy() an example const char* to skbuff data
 - Iterate through the linked list of skbuff queue in socket and print headroom and data pointers
 - This can be used as a packet sniffer anywhere within VIRGO linux network stack
- Any skb_*() functions can be plugged-in here as deemed necessary.
- kern.log(s) which print the socket internal skbuff data have been added to a

new testlogs/ directory
- .cmd files generated by kbuild

(FEATURE-DONE) Commits as on 24 February 2016

skbuff debug function in utils/ driver:
(*) Added an if clause to check NULLity of skbuff headroom before doing
skb_alloc()
(*) kern.log for this commit has been added testlogs/
(*) Rebuilt kernel objects and sources

Commits as on 29 February 2016

(FEATURE-DONE) Software Analytics - SATURN Program Analysis added to VIRGO Linux
kernel drivers

- SATURN (saturn.stanford.edu) Program Analysis and Verification software has
been
integrated into VIRGO Kernel as a Verification+SoftwareAnalytics subsystem
- A sample driver that can invoke an exported function has been added in drivers
- saturn_program_analysis
- Detailed document for an example null pointer analysis usecase has been
created in virgo-docs/VIRGO_SATURN_Program_Analysis_Integration.txt
-
linux-kernel-extensions/drivers/virgo/saturn_program_analysis/saturn_program_ana
lysis_trees/error.txt is the error report from SATURN
- SATURN generated preproc and trees are in
linux-kernel-extensions/drivers/virgo/saturn_program_analysis/preproc and
linux-kernel-extensions/drivers/virgo/saturn_program_analysis/
saturn_program_analysis_trees/

Commits as on 10 March 2016

- SATURN analysis databases (.db) for locking, memory and CFG analysis.
- DOT and PNG files for locking, memory and CFG analysis.
- new folder saturn_calypso_files/ has been added in saturn_program_analysis/
with new .clp files virgosaturncfg.clp and virgosaturnmemory.clp
- SATURN alias analysis .db files

(FEATURE-DONE) NEURONRAIN - ASFER Commits for VIRGO - CloudFS systems calls
integrated into Boost::Python C++ and Python CAPI invocations

AsFer Commits as on 30 May 2016

VIRGO CloudFS system calls have been added (invoked by unique number from
syscall_32.tbl) for C++ Boost::Python interface to
VIRGO Linux System Calls. Switch clause with a boolean flag has been introduced
to select either VIRGO memory or filesystem calls.
kern.log and CloudFS textfile Logs for VIRGO memory and filesystem invocations
from AsFer python have been committed to testlogs/

AsFer Commits as on 31 May 2016

Python CAPI interface to NEURONRAIN VIRGO Linux System Calls has been updated to include File System open, read, write primitives also.
Rebuilt extension binaries, kern.logs and example appended text file have been committed to testlogs/. This is exactly similar to commits done for Boost::Python C++ interface. Switch clause has been added to select memory or filesystem VIRGO syscalls.

(BUG - STABILITY ISSUES) Commits - 25 July 2016 - Static Analysis of VIRGO Linux kernel for investigating heisencrashes

Initial Documentation for Smatch and Coccinelle kernel static analyzers executed on VIRGO Linux kernel - to be updated periodically with further analysis.

(BUG - STABILITY ISSUES) Commits - 1 August 2016 - VIRGO Linux Stability Issues - Ongoing Random oops and panics investigation

1. GFP_KERNEL has been replaced with GFP_ATOMIC flags in kmem allocations.
2. NULL checks have been introduced in lot of places involving strcpy, strcat, strcmp etc., to circumvent buffer overflows.
3. Though this has stabilized the driver to some extent, still there are OOPS in unrelated places deep with in kernel where paging datastructures are accessed - kmalloc somehow corrupts paging
4. OOPS are debugged via gdb as:
 4.1 gdb ./vmlinux /proc/kcore
 or
 4.2 gdb <loadable_kernel_module>.o
 followed by
 4.3 l *(address+offset in OOPS dump)
5. kern.log(s) for the above have been committed in tar.gz format and have numerous OOPS occurred during repetitive telnet and syscall invocation(boost::python C++) invocations of virgo memory system calls.
6. Paging related OOPS look like an offshoot of set_fs() encompassing the filp_open VFS calls.

(BUG-STABILITY ISSUES) Commits - 26 September 2016 - Ongoing Random Panic investigation

Further analysis on direct VIRGO memory cache primitives telnet invocation - problems are similar to Boost::Python AsFer VIRGO system calls invocations.

(BUG-STABILITY ISSUES) Commits - 27 September 2016 - Ongoing Random Panic investigation

Analysis of VIRGO memory cache primitives reveal more inconsistencies in

cacheline flushes between CPU and GPU.

Srinivasan Kannan (alias) Ka.Shrinivaasan (alias) Shrinivas Kannan
<http://sites.google.com/site/kuja27>

KingCobra - A Research Software for Distributed Request Service on Cloud with Arbiters

This program is free software: you can redistribute it and/or modify it under the terms of the GNU General Public License as published by the Free Software Foundation, either version 3 of the License, or (at your option) any later version.

This program is distributed in the hope that it will be useful, but WITHOUT ANY WARRANTY; without even the implied warranty of MERCHANTABILITY or FITNESS FOR A PARTICULAR PURPOSE. See the GNU General Public License for more details.

You should have received a copy of the GNU General Public License along with this program. If not, see <<http://www.gnu.org/licenses/>>.

#-----
#-----
#Copyleft (Copyright+):
#Srinivasan Kannan
#(also known as: Ka.Shrinivaasan, Shrinivas Kannan)
#Ph: 9791499106, 9003082186
#Krishna iResearch Open Source Products Profiles:
#http://sourceforge.net/users/ka_shrinivaasan,
#<https://github.com/shrinivaasanka>,
#https://www.openhub.net/accounts/ka_shrinivaasan
#Personal website(research): <https://sites.google.com/site/kuja27/>
#emails: ka.shrinivaasan@gmail.com, shrinivas.kannan@gmail.com,
#kashrinivaasan@live.com
#-----
#-----

*****/

Theoretical Interludes, Design Notes and ToDo (long term with no deadline)

[This is a major research oriented subsystem of NeuronRain and inspired by COBRA project (done by the author in his BE (1995-1999) along with few other esteemed classmates.

http://sourceforge.net/projects/acadpdrafts/files/Excerpts_Of_PSG_BE_FinalProject_COBRA_done_in_1999.pdf/download.)]

[KingCobra though a misnomer is expanded as Cloud With ARBiters MimicKING containing the anagram]

1. (THEORY) There is a cloud of nodes which execute a set of services from randomly created clients.
2. (THEORY) This cloud could be on iCloud (AsFer+USBmd+VIRGO) platform or any other opensource cloud platforms like Hadoop Cluster.
3. (THEORY) The Clients are publishers of Service requests which are of many

types - miscellaneous types of Service that could be dynamically added through other kernel modules and invoked through a switch-case or embedded in function itself. Identified by unique id(s) for different types of services (for example Problem reports, Suggestions etc.,)

4. (THEORY) The Services on the Cloud are Subscribers to these requests of specific type. Thus this is the conventional publisher-subscriber model.

5. (THEORY) The requests flow through cloud using a workqueue (which could be a lowlevel Linux workqueue or VIRGO queue or some other queuing middleware software like ActiveMQ). The publishers enqueue and Subscribers dequeue the requests.

6. (THEORY) The difference is that the Cloud has nodes that "deceive" or "corrupt".

7. (THEORY) Service requests - are published by the clients in the need of a service which could be defined by markup file. These requests are scheduled and routed by the middleware to competent authority which services it (with or without timeframe) and replies to the client.

8. (THEORY) Problem reports - are published by clients which are "dissatisfied" by the quality of service by the cloud. These are analyzed by "arbiters" in the cloud which find the faulting node(s) and take action. This allows manual intervention but minimizes it.

9. (THEORY) Suggestions - are enhancement requests sent by clients and require manual intervention.

10. (THEORY) Cloud nodes have a Quality of Service metric calculated by a model.

11. (THEORY) The cloud has a reporting structure of nodes - either as a graph or tree. The graph is dynamically reorganized by weighting the Quality of Service of each node.

12. (THEORY) The difficult part of the above is using Arbiters to find "faulty" nodes based on problem reports from clients.

13. (THEORY) Brewer's CAP conjecture proved by [GilbertLynch] as a theorem (still debated) states that only 2 of the 3 (Consistency of data, Availability of data and Partition tolerance when some nodes or messages are lost) can be guaranteed and not all 3 are simultaneously achievable.

14. (THEORY) CAP theorem does not seem to apply to the above faulty scenario with corrupt nodes under Consistency or Availability or Partition Tolerance. This is because a corrupt node can have any 2 of the 3 - it can give consistent data, is available with success response or can make the cloud work with missing data in partition tolerance but yet can "corrupt" the cloud. Probably this needs to be defined as a new attribute called Integrity.

15. (THEORY) As "corruption" is more conspicuous with monetary element, if above services are "charged" with a logical currency (e.g. bitcoin), then corruption in cloud is defineable approximately as (but not limited to)- "Undue favour or harm meted out to a client not commensurate with the charge for the service (or) unreasonable extra logical currency demanded to execute the service of same quality (or) deliberate obstruction of justice to a client with malevolent and unholy collusion with other cloud nodes with feigned CAP".

16. (THEORY) Identifying criminal nodes as in (15) above seems to be beyond the ambit of CAP. Thus CAP with Integrity further places a theoretical limit on "pure" cloud. If Integrity is viewed as a Byzantine problem with faulty or corrupt processes in a distributed system, and if resilience factor is r_f (expected number of faulty nodes), then most algorithms can ensure a "working" cloud only if resilience is $\sim 30\%$ or less ($3 \cdot r_f + 1$) of the total number of cloud

nodes. Probably this could apply to Integrity also that places a limit of 30% on "corrupt nodes" for the Cloud to work with sanity. Translating this to a Governance problem, a corruption-free administration is achievable with a maximum limit of 30% "corrupt" elements.

17. (THEORY-ONGOING) Analytics on the Problem reports sent to the cloud queue give a pattern of corrupt nodes. Intrinsic Merit ranking with Citation graph maxflow considering cloud as a flow network where a node positively or negatively cites or "opines" about a node, as mentioned in <http://arxiv.org/abs/1006.4458> (author's Master's thesis) and http://www.nist.gov/tac/publications/2010/participant.papers/CMI_IIT.proceedings.pdf (published by the author during PhD) give a p2p ranking of cloud nodes that can be used for analysis though may not be reliable fully. AsFer has bigdata analytics functionality that fits well to this point to analyse the problem reports with machine learning algorithms and set the key-value pairs that are read by VIRGO kernel_analytics module and exported kernelwide. The persisted REQUEST_REPLY.queue with the logged request-reply IPs and timestamps can be mined with AsFer bigdata capability (e.g. Spark)

18. (THEORY) Policing the cloud nodes with arbiters - This seems to be limited by CAP theorem and Integrity as above. Also this is reducible to perfect inference problem in <http://sourceforge.net/p/asfer/code/HEAD/tree/AstroInferDesign.txt> and drafts in <https://sites.google.com/site/kuja27/>

19. (THEORY) Brooks-Iyengar algorithm for sensors in all cloud nodes is an improved Byzantine Fault Tolerant algorithm.

20. (THEORY) BitCoin is a Byzantine Fault Tolerant protocol.

21. (THEORY) Byzantine Fault Tolerance in Clouds is described in <http://www.computer.org/csdl/proceedings/cloud/2011/4460/00/4460a444-abs.html>, <http://www.eurecom.fr/~vukolic/ByzantineEmpire.pdf> which is more on Cloud of Clouds - Intercloud with cloud nodes that have malicious or corrupt software. Most of the key-value(get/set) implementations do not have byzantine nodes (for example CAP without Byzantine nodes in Amazon Dynamo: <http://www.eurecom.fr/~michiard/teaching/slides/clouds/cap-dynamo.pdf>)

22. (THEORY) Related to point 18 - The problem of fact finding or fault finding using a cloud police has the same limitation as the "perfect inference" described in <http://sourceforge.net/p/asfer/code/HEAD/tree/AstroInferDesign.txt>. "Money trail" involving the suspect node in point 28 is important to conclude something about the corruption. In real world tracking money trail is a daunting task. In cloud that abides by CAP, missing messages on trail can prevent reaching a conclusion thereby creating benefit-of-doubt. Also fixing exact value for a transaction that involves MAC currency message is undecidable - a normative economics problem can never be solved by exact theoretical computer science.

23. (THEORY) Reference article on cloud BFT for Byzantine, Corrupt brokers - Byzantine Fault-Tolerant Publish/Subscribe: A Cloud Computing Infrastructure (www.ux.uis.no/~meling/papers/2012-bftps-srdsw.pdf)

24. KingCobra messaging request-response design - options

24a. Implementing a message subscription model in kernelspace where clients publish the message that is queued-in to subscribers' queue (Topic like implementation - use of ActiveMQ C implementation if available).

24b. (DONE-minimal implementation) At present a minimum kernelspace messaging system that queues remote request and handles through workqueue handler is in

place. This responds to the client once the Kingcobra servicerequest function finishes processing the request(reply_to_publisher() in KingCobra driver). Unlike the usual messaging server, in which client publishes messages of a particular type that are listened to by interested clients, one option is to continue the status-quo of KingCobra as a peer-to-peer messaging system. Thus every VIRGO node is both a kernelspace messaging client and server that can both publish and listen. Every message in the cloud can have a universally unique id assigned by a timestamp server - <https://tools.ietf.org/html/rfc4122> (similar to bitcoin protocol) so that each message floating in the cloud is unique across the cloud (or) no two messages on the VIRGO cloud are same. The recipient node executing kingcobra_servicerequest_kernelspace() parses the unique-id (example naive unique-id is <ip-address:port>#localtimestampofmachine which is a simplified version of RFC4122) from the incoming remote request and responds to the remote client through kernel socket connection that gets queued-in the remote client and handled similar to incoming remote request. To differentiate request and response-for-request response messages are padded with a string "REPLY:<unique-id-of-message>" and requests are padded with "REQUEST:<unique-id-of-message>". This is more or less similar to TCP flow-control with SEQ numbers but state-less like UDP. Simple analogy is post-office protocol with reference numbers for each mail and its reply. Thus there are chronologically two queues: (1) queue at the remote VIRGO cloud service node for request (2) queue at the remote client for response to the request sent in (1). Thus any cloudnode can have two types of messages - REQUEST and REPLY. Following schematic diagram has been implemented so far.

 24c.(DONE) KingCobra - VIRGO queue - VIRGO cpupooling , mempooling and queue service drivers interaction schematic diagram:


```

KingCobraClient =====><REQUEST:id>===== VIRGO
cpupooling service =====> VIRGO Queue =====> KingCobraService
    ||
    ||
    ||
    ||
    <===== VIRGO Queue <===== VIRGO cpupooling service
====<REPLY:id>===== V

```

```

KingCobraClient =====><REQUEST:id>===== VIRGO
mempooling service =====> VIRGO Queue =====> KingCobraService
    ||
    ||
    ||
    ||
    <===== VIRGO Queue <===== VIRGO mempooling service
====<REPLY:id>===== V

```

```

KingCobraClient =====><REQUEST:id>===== VIRGO Queue
service =====> KingCobraService
    ||
    ||
    ||
    ||
    <===== VIRGO Queue service
=====<REPLY:id>===== V

```

24d. (ONGOING) kingcobra_servicerequest_kernelspace() distinguishes the "REQUEST" and "REPLY" and optionally persists them to corresponding on-disk filesystem. Thus a disk persistence for the queued messages can either be

implemented in 1) VIRGO queue driver 2) workqueue.c (kernel itself needs a rewrite (or) 3) KingCobra driver. Option (2) is difficult in the sense that it could impact the kernel as-a-whole whereas 1) and 3) are modularized. At present Option 3 persistence within KingCobra driver has been implemented.

24e. Above option 24b implements a simple p2p queue messaging in kernel. To get a Topic-like behaviour in VIRGO queue might be difficult as queue_work() kernel function has to be repeatedly invoked for the same work_struct on multiple queues which are subscribers of that message in AMQ protocol. Moreover creating a queue at runtime on need basis looks difficult in kernel which is usually done through some CLI or GUI interface in ActiveMQ and other messaging servers.

25. (ONGOING) For the timestamp service, EventNet described in <http://sourceforge.net/p/asfer/code/HEAD/tree/AstroInferDesign.txt> is a likely implementation choice. AsFer already has a primitive text files based EventNet graph implementation in place. Periodic topological sort (quite expensive) of EventNet gives logical ordering and thus a logical timestamp of the cloud events.

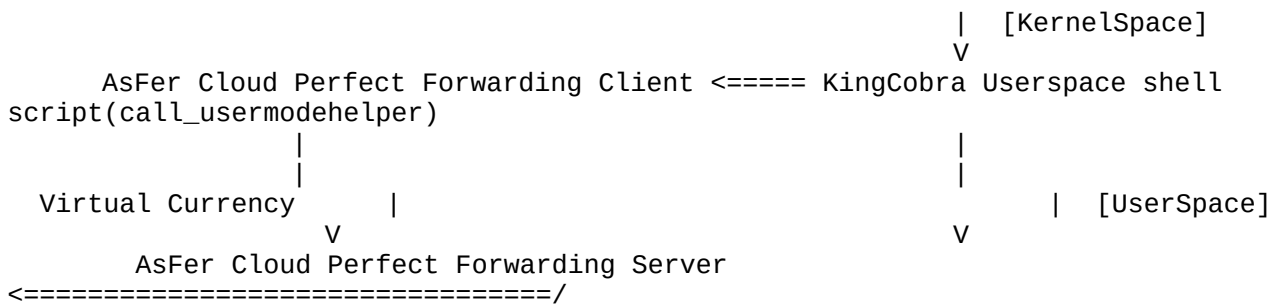
26. (THEORY - ONGOING Implementation) MESSAGE-AS-CURRENCY PROTOCOL: If each message payload is also construed as a currency carrier, each message id can be mapped to a unique currency or a coin with fixed denomination. This is similar to each currency note having a serial number as unique id. Uniqueness is guaranteed since there can be only one message (or coin) with that id on the cloud. This simulates a scenario - "Sender of the message pays the Receiver with a coin having the unique id and Receiver acknowledges receipt". This is an alternative to BitCoin protocol. Double spending is also prohibited since at any point in time the message or "coin" with unique id can be sent by only one node in the cloud. Unique Cloudwide Timestamp server mimicks the functionality of "Mint". There is a difference here between conventional send-receive of messages - Once a message is sent to remote cloud node, no copy of it should exist anywhere in the cloud. That is, every MAC currency message is a cloudwide singleton. In pseudocode this is expressible as:

```
m1=MAC_alloc(denomination)
m2=m1 (---- this is disallowed)
```

Linux kernel allocation functions - kmalloc() - have a krefs functionality for reference counting within kernel. Refcount for MAC message can never exceed 1 across cloud for above singleton functionality - this has to be a clause everywhere for any unique MAC id. This requires a cloudwide krefs rather. Buyer decrements cloudwide kref and Seller increments it. In C++ this is done by std::move() and often required in "Perfect Forwarding" - http://thbecker.net/articles/rvalue_references/section_07.html - within single addressspace. By overloading operator=() with Type&& rvalue reference, the necessary networking code can be invoked that does the move which might include serialization. But unfortunately C++ and Linux kernel are not compatible. The Currency object has to be language neutral and thus Google Protocol Buffers which have C, C++, Java, Python .proto files compilers support might be useful but yet the move semantics in Kernel/C is non-trivial that requires cloudwide transactional kernel memory as mentioned in (31) below. A C++ standalone userspace client-server cloud object move implementation based on std::move() over network of Protocol Buffer Currency Objects has been added to AsFer repository at - http://sourceforge.net/p/asfer/code/HEAD/tree/cpp-src/cloud_move which can optionally be upcall-ed to userspace from VIRGO and KingCobra drivers. This C++ implementation is invoked in userspace with call_usermodehelper() from VIRGO Queue Messaging via the kernel workqueue handler.

26.1 Schematic Diagram for Cloud Perfect Forwarding with AsFer+VIRGOQueue+KingCobraUserspace:

```
-----
Telnet or other client =====> VIRGO Queue Service Listener =====>
VIRGO Workqueue Handler
```

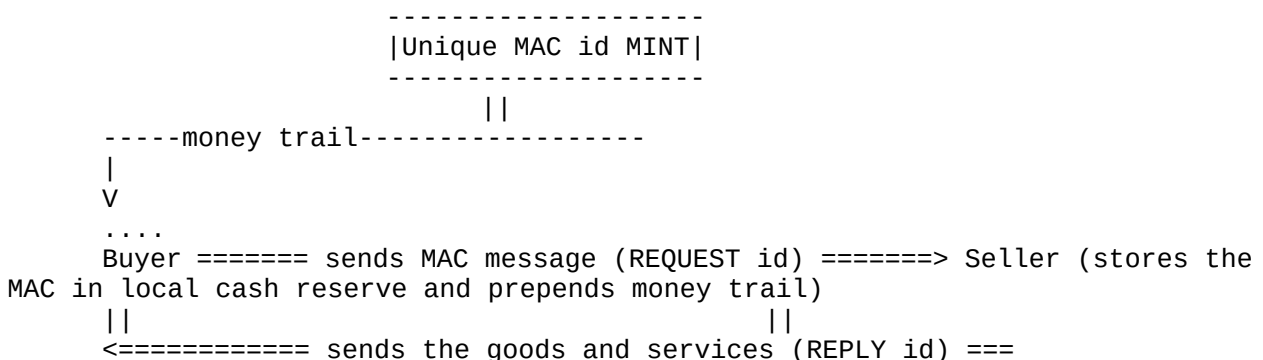


References:

 26.2 An example distributed transactional memory implementation in cloud - <http://infinispan.org/tutorials/simple/tx/> and <http://www.cloudtm.eu/> - these are in userspace cloud (C++ and Java) and may not have cloud move functionality - move has to be simulated in a transaction: replicate data, delete in one endpoint and create in other endpoint

27. (THEORY) SIMULATING A VIRTUAL ECONOMY with above MAC protocol (Message-as-currency): If each message sent is considered as "money" element and cloud nodes and clients are the consumers and producers of "electronic money", the timestamp "Mint" becomes a virtual Federal Reserve or Central Bank that controls the "electronic money" circulation in the cloud. Infact any REPLY messages could be mapped to a Service a client derives by s(p)ending the REQUEST "money message". Thus value(REQUEST) should equal value(REPLY) where value() is a function that measures the value of a money denomination and the value of goods and/or services for that money. For example Rs.10000 or \$10000 has no meaning if it doesn't translate into a value (analogy: erstwhile Gold Standard).When the value() function gets skewed phenomena like Inflation arise. Thus above model could also have a notion of value() and "electronic money inflation". Thus any "message money" with a unique id assigned by the cloud unique id(or logical timestamp) server can exist at most in only one node in the cloud. Money trail can be implemented by prefixing a header to the incoming message money in each cloud node that receives the money which traces the "path" taken. Cloud has to implement some Byzantine Fault Tolerant protocol. The value() function to some extent can measure the "deceit" as above. When a Buyer and Seller's value() functions are at loggerheads then that is starting point of "cloud corruption" at either side and might be an undecidable problem.

28. (THEORY) TRADING WITH ABOVE KINGCOBRA MAC protocol - somewhat oversimplified:



In the above schematic, money with unique id in cloud reaches a buyer after many buyer-seller transitions called "money trail". The MAC currency is prefixed by each node to create a chain. Buyer then sends a request to the seller through MAC virtual currency and seller replies with goods and services. Seller prepends the money trail chain. When a transaction occurs the whole cloud need not be notified about it except only buyer and seller. MAC Mint could create a bulk of money denominations and circulate them in cloud economy.

References:

28.1 Price fixing for items in Buyer-Seller-Trader networks - Trading Networks - Market Equilibrium and Walrasian Model of Price fixing - <http://www.cs.cornell.edu/~eva/traders.pdf>
28.2 Algorithmic Game Theory - Market Equilibrium for Price - Equilibrium is a strategic standoff - both players can't better their own present by changing strategies e.g Buyer-Sellers are market players and equilibrium price is the one where both buyer and seller can't gain by varying it - <http://www.cis.upenn.edu/~mkearns/nips02tutorial/nips.pdf>. Buyer-Seller payoff matrix picturises the bargaining problem.
28.3 Price-setting in Trading networks - Chapter 11 - <https://www.cs.cornell.edu/home/kleinber/networks-book/networks-book.pdf>

29. (THEORY) VALUE FOR ELECTRONIC MONEY: How is above MAC money earned - This again requires linking value to money (as money is not a value by itself and only a pointer to valuable item or resource). Thus any buyer can "earn" MAC money by something similar to a barter.

30. (THEORY and IMPLEMENTATION) FIXING VALUE FOR MAC MONEY: To delineate corruption as discussed in 27 above with value() disparity between MAC money and REPLY goods and services, an arbiter node in cloud has to "judge" the value of MAC sent by buyer and goods and services from seller and proclaim if corruption exists. Thus value() function itself has to be some kind of machine learning algorithm. This is related to or same as points 12 to 23 above. For example, while buying an item for few million bucks, value() has to take as input the description of the item and calculate the value "ideally" which is difficult. Because there are no perfect references to evaluate and only a weighted average of available market price range has to be taken as a reference which is error-prone. value() function can be recursively defined as("Reductionism"):

|value(i) = summation(value(ingredients of i)) + cost(integrating the ingredients to create item i) |

Obviously the above recursion combinatorially explodes into exponential number of nodes in the recursion tree. Ideally recursion has to go deep upto quarks and leptons that makeup the standard model. If for practical purposes, recursion depth is restricted to t then size of value() tree is $O(m^t)$ where m is average number of ingredients per component. Hence any algorithm computing the value() recursion has to be exponential in time. Computation of value() in the leaf nodes of the recursion is most crucial as they percolate bottom-up. If leaf nodes of all possible items are same (like quarks and leptons making up universe) then such atomic ingredient has to have "same" value for all items. Only the integration cost varies in the levels of the tree. For infinite case, value() function is conjectured to be undecidable - probably invoking some halting problem reduction. But above value() function could be Fixed Parameter Tractable in parameter recursion depth - t but yet could only be an approximation. A Turing machine computing value() function exactly might loop forever and thus Recursively Enumerable and not Recursive. A CVXPY implementation for Pricing Market Equilibrium has been implemented in KingCobra.

31. (THEORY) Buyer-Seller and MAC electronic money transaction schematic:

Buyer A-----<id><refcnt:0>-----> Seller
<id><refcnt:1> (increments refcnt)
 (<id><refcnt:1> |
 <id><refcnt:0> |
 after decrement |
 refcnt |
)----->

Above has to be transactional (i.e atomic across cloud nodes)

32. (THEORY) MAC protocol reaper

Reaper thread in each cloud node harvests the zero refcounted allocations and invokes destructors on them. Same MAC id cannot have kref count of 1 or above in more than one cloud node due to the transaction mentioned previously.

33. (THEORY) Cloud Policing With Arbiters - Revisited:

When a suspect node is analyzed when a complaint problem is filed on it, (1) it is of foremost importance on how flawless is the arbiter who investigates on that and is there a perfect way to choose a perfect arbiter. In the absence of the previous credibility of entire cloud judiciary is blown to smithereens and falls apart. (2) Assuming a perfect arbiter which is questionable, next thing is to analyze the credibility of the node who sulked. This is nothing but the Citation problem in <http://arxiv.org/abs/1106.4102> and http://www.nist.gov/tac/publications/2010/participant.papers/CMI_IIT.proceedings.pdf where a node can positively or negatively cite another node a "Societal Norm" which can be faulted and citations/opinions could be concocted with malafide intent(perjury). This is rather a generalization of PageRank algorithm with negative citations. Thus Perfect Cloud Arbitration could be an unsolvable problem. (3) Even if both arbiter and complainant are perfect which is again questionable, there are still loopholes - lack of evidences or implicated witnesses might portray a negative impression of a positive node. Thus there are 3 tiers of weakenings in cloud arbitration and there could be more. P(Good) series in <https://sites.google.com/site/kuja27/> precisely addresses this problem.

34. (THEORY) MAC Money Flow as MaxFlow problem:

Transactions happening in a cloud are edges between the nodes involved (buyer and seller). Thus it creates a huge directed graph. Flow of money in this graph can be modelled as Flow network. Minimum Cut of this graph shows crucial nodes in the graph which play vital role in cloud economy removal of which paralyzes the cloud (could be Central bank and other financial institutions). This graph has bidirectional edges where one direction is for money and the opposite direction is for Goods and Services. In the Flow network sum of flows is zero. But in the Money Flow Network each node is having a cash reserve ratio (CRR) due to commercial transactions which is confidential and privy to that node only and thus sum of flows can not be zero. Hub nodes in the Money Flow graph which can be obtained by getting k-core or D-core of the graph by some graph peeling algorithms are crucial nodes to the economy that contribute to Money circulation.

35. (THEORY) Cycles and components in above MAC Money Flow Graph:

Above graph of money transactions could be cyclic which implies a supply chain. Strongly connected components of this graph are most related nodes that are in same industry.

36. (THEORY) STOCK TRADING:

One of the component in above MAC Money Flow Graph of cloud could be a virtual Stock Exchange. Based on the financial and securities transactions of constituent organizations in the graph, index of the exchange varies.

37. (THEORY) Analysis of Poverty and Alleviation through above money flow graph:

Weights of the edges of money flow graph are the denominations of the transaction. Thus high value edges and low value edges divide the Graph logically into Rich and Poor strata(Bourgeoisie and Proletariat subgraphs). Equitable graph is the one which does not have too much of value difference between Rich and Poor sets of edges - a utopian to achieve. Mathematically, it

is an optimization LP problem that seeks to minimize $\text{sum}(\text{RichEdges}) - \text{sum}(\text{PoorEdges})$ or $\text{Sum}(\text{RichVertices}) - \text{sum}(\text{PoorVertices})$ - without harming either - to be precise. This requires money flow to be programmed to find a feasible solution to this LP subject to constraints like work-pay parity etc., (there could be more variables and constraints to this LP) . Due to CRR above Vertices also can be Rich and Poor in addition to Rich Edges and Poor Edges.

38.(THEORY) Demand and Supply and Value() function:

Alternative to the recursive definition of value() function above can be done through Demand and Supply - more the demand and less the supply, price increases and vice-versa. This is quite subjective compared to absolute recursive definition above. To simulate demand and supply, the weights of the money edges (-> direction) in the bidirectional graph change and fluctuate dynamically over time for unchanging weights of the Goods and Services edges (<- direction) between any pair of Buyer-Seller vertices. This makes Money and G&S Flow graph a Dynamic Graph with edge weight update primitive.

39.(THEORY) Hidden or Colored Money:

In an ideal Cloud with only MAC currencies, colored money can co-exist if (not limited to) some money trails are missing, due to "cloud corruption", systemic failure, hardware and network issues etc.,. Probably this is the direct consequence of CAP theorem and can be conjectured to be undecidable. Hidden money is to some extent dependent on quantity of net flow (if non-zero) and how much of this net flow is contributed by Rich vertices and Edges. Money Circulation with Colored money can be formulated as Network Flow Problem with Time horizon and storage at nodes. Time horizon implies a certain flow has to happen before a stop time. Flow conservation is affected by this Dynamic Flow because of storage at nodes and money entering a node need not be equal to money leaving. Thus not all Hidden/Colored money is illegal in theoretical terms. As mentioned in 39.1, storage is simulated with a closed loop at nodes so that flow conservation is not seemingly violated. Profiteering is achieved by money flows over time in financial markets by assigning a multiplicative factor at each edge which accrues through a cycle and comes back to start node in cycle with a magnification in value. Blockchain techniques maintain ledgers which record all transactions globally thus decimating hidden unaccounted wealth if any. KingCobra experimental MAC currency relies on unique global identifier and global refcounts with atomic cloud transactions in linux kernel. Money Flow Graph mentioned in 34-39 has striking resemblance to Money Flow Markets already studied in Algorithmic Game Theory(AGT). 39.3 primarily devotes to Pricing and Equilibrium of Edges in Money Flow Graphs and not much on Colored Money Flow. An algorithm to find colored money flow could be a major advance in AGT. Prima facie there exists no zero-knowledge blackbox proof algorithm to find colored money because all storage data is a prerequisite which is impossible to know. Money trail for MAC currency described in 22,27,28 requires tracking of currencies. There are recent dollar and euro bills issued with Radio Frequency ID tags (RFID).

Total storage of money in Flow Market Graph = | Incoming money flow at Source - Incoming money flow at Sink | i.e Flow conservation is no longer obeyed.

There is a special vertex in Money Flow Market designated as Direct Taxation Hub which has incoming direct tax money flow edges from all other vertices in Flow market. Colored money is then approximately the taxed storage money estimated above minus the net flow of money received at Taxation Hub.

Colored Money = | Total storage money * Direct Taxation rate - Incoming Flow at Direct Taxation Hub Node|

Colored Money = | Incoming money flow at Source * Direct Taxation rate - Incoming money flow at Sink * Direct Taxation rate - Incoming Flow at Direct Taxation Hub Node |

Previous is an approximate naive zero-knowledge estimation of Colored money in

Money Flow Market. This assumes that there is always a sink in Money Flow Market which is not necessarily valid unless notes are returned to mint. Satellite RFID Tracking technologies though invasive and intrusive like previous can present a rough figure of total money circulation in Source and Sink.

Above estimate is for direct taxation and resultant evasion. For indirect taxes (on Goods and Services etc.), there is no direct impact on the money component and only G&S are affected. Combining Goods, Services and Income into one (direct+indirect) taxation could have a negative effect on Colored money because incentive to hide money no longer exists. For example, if only Goods and Services consumed by high-income brackets are preferentially taxed at high percentage replacing tax on income, income is also indirectly taxed in addition to G&S. Thus there is no necessity to tax income and any advantage of such direct taxation is indirectly usurped by preferential G&S taxation. Previous zero-knowledge estimate then becomes:

Colored Money = | Total Goods and Services * Taxation rate - Incoming Flow at Indirect Taxation Hub Node|

Colored Money = | GDP^2 * Tax-to-GDP ratio - Incoming Flow at Indirect Taxation Hub Node| where GDP is assumed to be equal to Total Goods and Services.

References:

-
- 39.1 Network Flows over time over Storage Area Networks (SAN) - <https://hal.inria.fr/inria-00071643/document>
- 39.2 Network Flow - [GoldbergTardosTarjan] - <http://www.cs.cornell.edu/~eva/network.flow.algorithms.pdf>
- 39.3 Algorithmic Game Theory - Flow Markets - [TimRoughGarden] - <http://theory.stanford.edu/~tim/books.html>
- 39.4 RFID tagged currencies - \$100 bill - <http://www.businessinsider.in/New-Smart-Paper-Could-Put-An-End-To-Dark-Money/articleshow/21134569.cms>
- 39.5 Cons of RFID currencies - <http://www.prisonplanet.com/022904rfidtagsexplode.html>
- 39.6 Mechanism Design and Machine Learning - <https://www.cs.cmu.edu/~mblum/search/AGTML35.pdf> - Design of algorithms for maximizing gain in auctions involving sellers and buyers
- 39.7 Financial and Economic Networks - <https://supernet.isenberg.umass.edu/bookser/innov-ch1.pdf>

Commits as on 1 March 2014

Example java Publisher and Listeners that use ActiveMQ as the messaging middleware have been committed to repository for an ActiveMQ queue instance created for KingCobra. For multiple clients this might have to be a Topic rather than Queue instance. Request types above and a workflow framework can be added on this. This will be a JMS compliant implementation which might slow down compared to a linux workqueue or queue implementation being done in VIRGO.

Commits as on 17 March 2014

KingCobra userspace library and kernelspace driver module have been implemented that are invoked 1) either in usermode by call_usermodehelper() 2) or through intermodule invocation through exported symbols in KingCobra kernel module, by the workqueue handler in VIRGO workqueue implementation.

Commits as on 22 March 2014

Minimalistic Kernelspace messaging server framework with kernel workqueue, handler and remote cloud client has been completed - For this VIRGO clone cpupooling driver has been added a clause based on a boolean flag, to direct incoming request from remote client to VIRGO linux workqueue which is

popped by workqueue handler that invokes a servicerequest function on the KingCobra kernel module. (Build notes: To remove any build or symbol errors, Module.symvers from VIRGO queue has to be copied to VIRGO clouddex and built to get a unified VIRGO clouddex Module.symvers that has exported symbol definitions for push_request()). End-to-end test with telnet path client sending a request to VIRGO clouddex service, that gets queued in kernel workqueue, handled by workqueue handler that finally invokes KingCobra service request function has been done and the kern.log has been added to repository at drivers/virgo/queuing/test_logs/

Commits as on 29 March 2014

Initial commits for KingCobra Request Response done by adding 2 new functions parse_ip_address() and reply_to_publisher() in kingcobra_servicerequest_kernelspace()

Commits as on 30 March 2014

Both VIRGO cpupooling and mempooling drivers have been modified with use_as_kingcobra_service boolean flag for sending incoming remote cloud node requests to VIRGO queue which is serviced by workqueue handler and KingCobra service as per the above schematic diagram and replied to.

Commits as on 6 April 2014

Fixes for REQUEST and REPLY headers for KingCobra has been made in virgo_clouddex_mempool recvfrom() if clause and in request parser in KingCobra with strsep(). This has been implemented only in VIRGO mempool codepath and not in VIRGO clone.

Commits as on 7 April 2014

New function parse_timestamp() has been added to retrieve the timestamp set by the VIRGO mempool driver before pushing the request to VIRGO queue driver

Commits as on 29 April 2014

Initial commits for disk persistence of KingCobra request-reply queue messages have been done with addition of new boolean flag kingcobra_disk_persistence. VFS calls are used to open and write to the queue.

Commits as on 26 August 2014

KingCobra driver has been ported to 3.15.5 kernel and bugs related to a kernel_recvmmsg() crash, timestamp parsing etc., have been fixed. The random crashes were most likely due to incorrect parameters to filp_open() of disk persistence file and filesystem being mounted as read-only.

Version 14.9.9 release tagged on 9 September 2014

Version 15.1.8 release tagged on 8 January 2015

Commits as on 17 August 2015

KingCobra + VIRGO Queuing port of Linux Kernel 4.1.5 :

- changed the REQUEST_REPLY.queue disk persisted queue path to /var/log/kingcobra/REQUEST_REPLY.queue
- kernel built sources, object files
- kern.log with logs for telnet request sent to VIRGO queue driver, queued in kernel work queue and handler invocation for the KingCobra service request kernel function for the popped request; disk persisted /var/log/kingcobra/REQUEST_REPLY.queue

Commits as on 14 October 2015

AsFer Cloud Perfect Forwarding binaries are invoked through call_usermodehelper() in VIRGO queue. KingCobra commands has been updated with a clause for cloud perfect forwarding.

Commits as on 15 October 2015

- Updated KingCobra module binaries and build generated sources
- kingcobra_usermode_log.txt with "not found" error from output redirection (kingcobra_commands.c). This error is due to need for absolute path. But there are "alloc_fd: slot 1 not NULL!" after fd_install() is uncommented in virgo_queue.h call_usermodehelper() code. The kern.log with these errors has been added to testlogs
- kingcobra_commands.c has been changed to invoke absolute path executable. With uncommenting of fd_install and set_ds code in virgo_queue the return code of call_usermodehelper() is 0 indicating successful invocation

Commits as on 10 January 2016

NeuronRain KingCobra enterprise version 2016.1.10 released.

NEURONRAIN VIRGO Commits for virgo_clone()/telnet -> VIRGO cpupooling -> VIRGO Queue -> KingCobra
- as on 12 February 2016

VIRGO commit:
<https://github.com/shrinivaasanka/virgo-linux-github-code/commit/72d9cfc90855719542cdb62ce40b798cc7431b3d>

Commit comments:

Commits for Telnet/System Call Interface to VIRGO CPUPooling -> VIRGO Queue -> KingCobra

- *) This was commented earlier for the past few years due to a serious kernel panic in previous kernel versions - <= 3.15.5
- *) In 4.1.5 a deadlock between VIRGO CPUPooling and VIRGO queue driver init was causing following error in "use_as_kingcobra_service" clause :
 - "gave up waiting for virgo_queue init, unknown symbol push_request()"
- *) To address this a new boolean flag to selectively enable and disable VIRGO Queue kernel service mode "virgo_queue_reactor_service_mode" has been added.
- *) With this flag VIRGO Queue is both a kernel service driver and a standalone exporter of function symbols - push_request/pop_request
- *) Incoming request data from telnet/virgo_clone() system call into cpupooling kernel service reactor pattern (virgo cpupooling listener loop) is treated as generic string and handed over to VIRGO queue and KingCobra which publishes it.

- *) This resolves a long standing deadlock above between VIRGO cpupooling "use_as_kingcobra_service" clause and VIRGO queue init.
- *) This makes virgo_clone() syscall/telnet both synchronous and asynchronous - requests from telnet client/virgo_clone() system call can be either synchronous RPC functions executed on a remote cloud node in kernelspace (or) an asynchronous invocation through "use_as_kingcobra_service" clause path to VIRGO Queue driver which enqueues the data in kernel workqueue and subsequently popped by KingCobra.
- *) Above saves an additional code implementation for virgo_queue syscall paths - virgo_clone() handles, based on config selected, incoming data passed to it either as a remote procedure call or as a data that is pushed to VIRGO Queue/KingCobra pub-sub kernelspace
- *) Kernel Logs and REQUEST_REPLY.queue for above commits have been added to kingcobra c-src/testlogs/

 Commits - KingCobra 64 bit and VIRGO Queue + KingCobra telnet requests - 17 April 2017

- *) Rebuilt KingCobra 64bit kernel module
- *) telnet requests to VIRGO64 Queueing module listener driver are serviced by KingCobra servicerequest
- *) Request_Reply queue persisted for this VIRGO Queue + KingCobra routing has been committed to c-src/testlogs.
- *) kern.log for this routing has been committed in VIRGO64 queueing directory
- *) Similar to other drivers struct socket* reinterpret cast to int has been removed and has been made const in queuesvc kernel thread

 (FEATURE-DONE) Commits - CVXPY implementation for Eisenberg-Gale Convex Program - 18 August 2017

- (*) First commits for Convex Optimized Market Equilibrium Prices
- (*) Imports CVXPY Convex Program solver
- (*) Objective function is a logistic variant of Eisenberg-Gale Convex Program i.e uses money * log(1+e^utility) instead of money * log(utility) because of curvature error (log is error flagged as concave and logistic is convex per:
<http://www.cvxpy.org/en/latest/tutorial/functions/index.html#vector-matrix-functions>)
- (*) Formulates constraints and objective functions based on
<http://www.cs.cmu.edu/~sandholm/cs15-892F13/algorithmic-game-theory.pdf> - Page 106 and Equation 5.1
- (*) But, For all installed solvers ECOS, ECOS_BB, SCS, LS solved convex program prints value as None despite all constraints and objective functions being convex. Also is_dcp() prints "not a disciplined convex program". Logs in testlogs/.
- (*) Obviously it should have worked. Therefore this is only a partial implementation commit.
- (*) This implementation uses numpy randomly initialized arrays for Money each buyer has and per-good utility(happiness) each buyer has.
- (*) Replacing money with perceived merit values translates this Market Equilibrium - Intrinsic Value versus Market Price - to Merit Equilibrium - Intrinsic Merit versus Perceived Merit. This has been already described in NeuronRain AsFer Design Documents:

-
<http://sourceforge.net/p/asfer/code/HEAD/tree/asfer-docs/AstroInferDesign.txt>
 and
 - <https://github.com/shrinivaasanka/asfer-github-code/blob/master/asfer-docs/AstroInferDesign.txt>

(FEATURE-DONE) Commits - Convex Optimization - DCCP - 21 August 2017

(*) import dccp has been added
(*) DCCP is the recent advancement and generalization of DCP for convex-concave programs
(*) method='dccp' has been added as parameter to solve()
(*) Objective function has been changed to log() from logistic() - curvature is concave which is in conflict with definition of eisenberg-gale convex program in textbooks. Reason for this contradiction is unknown.
(*) But DCCP overcomes the DCP limitation and solve() prints converged solutions for objective functions
(*) logs have been committed to testlogs/
(*) CVXOPT solver has been installed but it does not solve the Eisenberg-Gale objective function. Only SCS solver works - by default applies KKT conditions indirectly.

(FEATURE-DONE) Commits - Convex Optimization - DCCP - 22 August 2017

(*) Verbose set to True for printing Splitting Conic Solver progress information
(*) logs committed to testlogs/

(FEATURE-DONE) Commits - Convex Optimization update - 29 August 2017

(*) Removed hardcoded variable values in objective and constraints
(*) In the context of pricing, ECOS Error Metrics print the matrices of market clearing prices for goods
(Reference - pages 3072 and 3073 of https://web.stanford.edu/~boyd/papers/pdf/ecos_ecc.pdf - KKT conditions in ECOS solver)

(FEATURE-DONE) Convex Optimization - Pricing Computation - 30 August 2017

(*) Prices of Goods/Services have been computed explicitly from Karush-Kuhn-Tucker Conditions (1,2,3 and especially 4)
(*) References:
- Pages 106-108 of <http://www.cs.cmu.edu/~sandholm/cs15-892F13/algorithmic-game-theory.pdf>
- KKT conditions and Conic Optimization-
<https://arxiv.org/pdf/1312.3039.pdf>
(*) logs committed to testlogs/

NEURONRAIN

நியூரான் ரெயின்

.. image:: Krishna_iResearch-logos.jpeg

NeuronRain is a new linux kernel fork-off from mainline kernel (presently overlayed on kernel 4.1.5 32 bit and kernel 4.13.3 64 bit) augmented with

Machine Learning, Analytics, New system call primitives and Kernel Modules for cloud RPC, Memory and Filesystem. It differs from usual CloudOSes like OpenStack, VMs and containers in following ways:

- (*) Mostly available CloudOSes are application layer deployment/provisioning (YAML etc.,) focussed while NeuronRain is not about deploying applications but to bring the cloud functionality into Linux kernel itself.

- (*) There are application layer memcache softwares available for bigdata processing.

- (*) There have been some opensource projects for linux kernel on GitHub to provide memcache functionality for kernelspace memory.

- (*) NeuronRain VIRGO32 and VIRGO64 kernels have new system calls and kernel drivers for remote cloning a process, memcache kernel memory and remote file I/O with added advantage of reading analytics variables in kernel.

- (*) Cloud RPCs, Cloud Kernel Memcache and Filesystems are implemented in Linux kernel with kernelspace sockets

- (*) Linux kernel has access to Machine Learnt Analytics(in AsFer) with VIRGO linux kernel_analytics driver

- (*) Assumes already encrypted data for traffic between kernels on different machines.

- (*) Advantages of kernelspace Cloud implementation are: Remote Device Invocation (recently known as Internet of Things), Mobile device clouds, High performance etc.,.

- (*) NeuronRain is not about VM/Containerization but VMs, CloudOSes and Containers can be optionally rewritten by invoking NeuronRain VIRGO systemcalls and drivers - thus NeuronRain Linux kernel is the bottommost layer beneath VMs, Containers, CloudOSes.

- (*) Partially inspired by old Linux Kernel components - Remote Device Invocation and SunRPC

- (*) VIRGO64 kernel based on 4.13.3 mainline kernel, which is 64 bit version of VIRGO32, has lot of stability/panic issues resolved which were random and frequent in VIRGO32 and has Kernel Transport Layer Security (KTLS) integrated into kernel tree.

NeuronRain - Repositories:

NeuronRain repositories are in:

- (*) NeuronRain Research - http://sourceforge.net/users/ka_shrinivaasan - astronomy datasets

- (*) NeuronRain Green - <https://github.com/shrinivaasanka> - generic datasets

- (*) NeuronRain Antariksh - <https://gitlab.com/shrinivaasanka> - Drone development

NeuronRain Documentation Repositories:

- (*) https://github.com/shrinivaasanka/Krishna_iResearch_DoxygenDocs

- (*) https://gitlab.com/shrinivaasanka/Krishna_iResearch_DoxygenDocs

- (*)

https://sourceforge.net/u/userid-769929/Krishna_iResearch_DoxygenDocs/ci/master/tree/

NeuronRain Version:

Previously, each NeuronRain repository source in SourceForge, GitHub and GitLab was snapshotted periodically by a version number convention

<year>.<month>.<day>. Because total number of repositories in NeuronRain spread across SourceForge, GitHub and GitLab is huge, release tagging each repository is arduous and therefore individual repository source tagging is hereinafter discontinued. Every NeuronRain source code release for SourceForge, GitHub and

GitLab repositories henceforth would be notified in this documentation page and latest commit on the date of release (inferred from <year>#<month>#<day>) has to be construed as the latest source release. Latest NeuronRain Research, Green and Antariksh version is 2022#10#01.

NeuronRain - Features:

****VIRGO system calls from include/linux/syscalls.h****

```
asmlinkage long sys_virgo_clone(char* func, void *child_stack, int flags, void *arg);
```

```
asmlinkage long sys_virgo_malloc(int size,unsigned long long __user *vuid);
```

```
asmlinkage long sys_virgo_set(unsigned long long vuid, const char __user *data_in);
```

```
asmlinkage long sys_virgo_get(unsigned long long vuid, char __user *data_out);
```

```
asmlinkage long sys_virgo_free(unsigned long long vuid);
```

```
asmlinkage long sys_virgo_open(char* filepath);
```

```
asmlinkage long sys_virgo_read(long vfsdesc, char __user *data_out, int size, int pos);
```

```
asmlinkage long sys_virgo_write(long vfsdesc, const char __user *data_in, int size, int pos);
```

```
asmlinkage long sys_virgo_close(long vfsdesc);
```

****VIRGO Kernel Modules in drivers/virgo****

1. cpupooling virtualization - VIRGO_clone() system call and VIRGO cpupooling driver by which a remote procedure can be invoked in kernelspace.(port: 10000)

2. memorypooling virtualization - VIRGO_malloc(), VIRGO_get(), VIRGO_set(), VIRGO_free() system calls and VIRGO memorypooling driver by which kernel memory can be allocated in remote node, written to, read and freed - A kernelspace memcache-ing.(port: 30000)

3. filesystem virtualization - VIRGO_open(), VIRGO_read(), VIRGO_write(), VIRGO_close() system calls and VIRGO cloud filesystem driver by which file IO in remote node can be done in kernelspace.(port: 50000)

4. config - VIRGO config driver for configuration symbols export.

5. queueing - VIRGO Queuing driver kernel service for queuing incoming requests, handle them with workqueue and invoke KingCobra service routines in kernelspace. (port: 60000)

6. cloudsync - kernel module for synchronization primitives (Bakery algorithm etc.,) with exported symbols that can be used in other VIRGO cloud modules for critical section lock() and unlock()

7. utils - utility driver that exports miscellaneous kernel functions that can be used across VIRGO Linux kernel

8. EventNet - eventnet kernel driver to vfs_read()/vfs_write() text files for EventNet vertex and edge messages (port: 20000)

9. Kernel_Analytics - kernel module that reads machine-learnt config key-value pairs set in /etc/virgo_kernel_analytics.conf (and from a remote cloud as stream

of key-value pairs in VIRGO64). Any machine learning software can be used to get the key-value pairs for the config. This merges three facets - Machine Learning, Cloud Modules in VIRGO Linux-KingCobra-USBmd , Mainline Linux Kernel

10. SATURN program analysis wrapper driver.

11. KTLS config driver - for Kernel Transport Layer Security - only in VIRGO_KTLS branch of VIRGO64 repositories

Apart from aforementioned drivers, PXRC flight controller and UVC video drivers from kernel 5.1.4 have been changed to import kernel_analytics exported analytics variables and committed to VIRGO64.

Complete list of Features of NeuronRain (Research and Enterprise) are detailed in:

<https://sites.google.com/site/kuja27/>

CV_of_SrinivasanKannan_alias_KaShrinivaasan_alias_ShrinivasKannan.pdf (Deleted and Mirrored at

https://github.com/shrinivaasanka/Krishna_iResearch_DoxygenDocs/blob/master/kuja27_website_mirrored/site/kuja27/

CV_of_SrinivasanKannan_alias_KaShrinivaasan_alias_ShrinivasKannan.pdf)

Previous system calls and drivers do not have internal mutexes and synchronization is left to the userspace. Quoting Commit Notes from hash <https://github.com/shrinivaasanka/virgo64-linux-github-code/commit/ad59cbb0bec23ced72109f8c5a63338d1fd84beb> :

"... Note on concurrency: Presently mutexing within system calls have been commented because in past linux versions mutexing within kernel was causing strange panic issues. As a design choice and feature-stability tradeoff (stability is more important than introducing additional code) mutexing has been lifted up to userspace. It is upto the user applications invoking the system calls to synchronize multiple user threads invoking VIRGO64 system calls i.e VIRGO64 system calls are not re-entrant. This would allow just one kernel thread (mapped 1:1 to a user thread) to execute in kernel space. Mostly this is relevant only to kmemcache system calls which have global in-kernel-memory address translation tables and next_id variable. VIRGO clone/filesystem calls do not have global in-kernel-memory datastructures. ...". An example pthread mutex code doing VIRGO64 system calls invocation in 2 parallel concurrent processes within a critical section lock/unlock is at https://github.com/shrinivaasanka/virgo64-linux-github-code/blob/master/linux-kernel-extensions/virgo_malloc/test/test_virgo_malloc.c. Synchronization in userspace for system calls-drivers RPC is easier to analyze and modify user application code if there are concurrency issues than locking within kernelspace in system calls and drivers. This would also remove redundant double locking in userspace and kernelspace. Another advantage of doing synchronization in userspace is the flexibility in granularity of the critical section - User can decide when to lock and unlock access to a resource e.g permutations of malloc/set/get/free kmemcache primitive sequences can be synchronized as desired by an application.

NeuronRain - Architecture Diagrams:

.. image:: NeuronRainVIRGOArchitecture.jpg

https://github.com/shrinivaasanka/Krishna_iResearch_DoxygenDocs/blob/master/Krishna_iResearch_opensourceproducts_archdiagram.pdf

https://github.com/shrinivaasanka/Krishna_iResearch_DoxygenDocs/blob/master/NeuronRain_Architecture_Diagrams_29September2016.pdf

Products in NeuronRain Suite (Research,Green,Antariksh):

AsFer - AstroInfer was initially intended, as the name suggests, for pattern mining of Astronomical Datasets to predict natural weather disasters. It is focussed on mining patterns in texts and strings. It also has implementations of algorithms for analyzing merit of text, PAC learning, Polynomial reconstruction,

List decoding, Factorization etc., which are later expansions of publications by the author (K.Srinivasan - <http://dblp.dagstuhl.de/pers/hd/s/Shrinivaasan:Ka=>) after 2012. Presently AsFer in SourceForge, GitHub and GitLab has implementations for prominently used machine learning algorithms.

USBmd - Wireless data traffic and USB analytics - analyzes internet traffic and USB URB data packets for patterns by AsFer machine learning (e.g FTrace, USBmon, Wireshark/Tcpdump PCAP, USBWWAN and kern.log Spark MapReduce) implementations and Graph theoretic algorithms on kernel function call graphs. It is also a module in VIRGO linux kernel.

VIRGO Linux Kernel - Linux kernel fork-off based on 4.1.5 (32 bit) and 4.13.3 (64 bit) has new system calls and drivers which abstract cloud RPC, kernel memcache and Filesystem. These system calls are kernelspace socket clients to kernelspace listeners modules for RPC, Kernelspace Memory Cacheing and Cloud Filesystems. These new system calls can be invoked by user applications written in languages other than C and C++ also (e.g. Python). Simply put VIRGO is a kernelspace cloud while present cloud OSes concentrate on userspace applications. Applications on VIRGO kernel are transparent to how cloud RPC works in kernel. This pushes down the application layer socket transport to the kernelspace and applications need not invoke any userspace cloud libraries e.g make REST http GET/POST requests by explicitly specifying hosts in URL. Most of the cloud webservice applications use REST for invoking a remote service and response is returned as JSON. This is no longer required in VIRGO linux kernel. Application code is just needed to invoke VIRGO system calls, and kernel internally loadbalances the requests to cloud nodes based on config files. VIRGO system call clients and driver listeners converse in TCP kernelspace sockets. Responses from remote nodes are presently plain texts and can be made as JSON responses optionally. Secure kernel socket families like AF_KTLS are available as separate linux forks. If AF_KTLS is in mainline, all socket families used in VIRGO kernel code can be changed to AF_KTLS from AF_INET and thus security is implicit. VIRGO cloud is defined by config files (virgo_client.conf and virgo_cloud.conf) containing comma separated list of IP addresses in constituent machines of the cloud abstracted from userspace. It also has a kernel_analytics module that reads periodically computed key-value pairs from AsFer and publishes as global symbols within kernel. Any kernel driver including network, I/O, display, paging, scheduler etc., can read these analytics variables and dynamically change kernel behaviour. Good example of userspace cloud library and RPC is gRPC - <https://developers.googleblog.com/2015/02/introducing-grpc-new-open-source-http2.html> which is a recent cloud RPC standard from Google. There have been debates on RPC versus REST in cloud community. REST is stateless protocol and on a request the server copies its "state" to the remote client. RPC is a remote procedure invocation protocol relying on serialization of objects. Both REST and RPC are implemented on HTTP by industry standard products with some variations in syntaxes of the resource URL endpoints. VIRGO linux kernel does not care about how requests are done i.e REST or RPC but where the requests are done i.e in userspace or kernelspace and prefers kernelspace TCP request-response transport. In this context it differs from traditional REST and RPC based cloud - REST or RPC are userspace wrappers and both internally have to go through TCP, and VIRGO kernel optimizes this TCP bottleneck. Pushing down cloud transport primitives to kernel away from userspace should theoretically be faster because

- (*) cloud transport is initiated lazy deep into kernel and not in userspace which saves serialization slowdown

- (*) lot of wrapper application layer overheads like HTTP, HTTPS SSL handshakes are replaced by TCP transport layer security (assuming AF_KTLS sockets)

- (*) disk I/O in VIRGO file system system-calls and driver is done in kernelspace closer to disk than userspace - userspace clouds often require file persistence

- (*) repetitive system call invocations in userspace cloud libraries which cause frequent userspace-kernelspace switches are removed.

- (*) best suited for interacting with remote devices than remote servers because direct kernelspace-kernelspace remote device communication is possible

with no interleaved switches to userspace. This makes it ideal for IoT.

(*) VIRGO kernel memcache system-calls and driver facilitate abstraction of kernelspaces of all cloud nodes into single VIRGO kernel addressspace.

(*) VIRGO clone system-call and driver enable execution of a remote binary or a function in kernelspace i.e kernelspace RPC

An up-to-date description of how RPC ruled the roost, fell out of favour and reincarnated in latest cloud standards like Finagle/Thrift/gRPC is in <http://dist-prog-book.com/chapter/1/rpc.html> - RPC is Not Dead: Rise, Fall and the Rise of Remote Procedure Calls. All these recent RPC advances are in userspace while VIRGO linux kernel abstracts RPC and loadbalancing within system calls itself requiring no user intervention (it is more than mere Remote Procedure Call - a lightweight Remote Resource System Call - a new paradigm in itself).

KingCobra - This is a VIRGO module and implements message queueing and pub-sub model in kernelspace. This also has a userspace facet for computational economics (Pricing, Electronic money protocol buffer implementation etc.,)

Following are frequently updated design documents and theoretical commentaries for NeuronRain code commits which have been organized into numbered non-linear section vertices and edges amongst them are mentioned by "related to <section>" phrase. NeuronRain Design is a unification of following repository specific documents (sections are numbered uniquely and spread out in multiple repository specific documents):

NeuronRain Green - GitHub - Repositories and Design Documents which include course material (repositories suffixed 64 are for 64-bit and others are 32-bit on different linux versions)

AsFer - <https://github.com/shrinivaasanka/asfer-github-code/blob/master/asfer-docs/AstroInferDesign.txt>

USBmd - https://github.com/shrinivaasanka/usb-md-github-code/blob/master/USBmd_notes.txt

USBmd64 - https://github.com/shrinivaasanka/usb-md64-github-code/blob/master/USBmd_notes.txt

VIRGO Linux - <https://github.com/shrinivaasanka/virgo-linux-github-code/blob/master/virgo-docs/VirgoDesign.txt>

VIRGO64 Linux - <https://github.com/shrinivaasanka/virgo64-linux-github-code/blob/master/virgo-docs/VirgoDesign.txt>

KingCobra - <https://github.com/shrinivaasanka/kingcobra-github-code/blob/master/KingCobraDesignNotes.txt>

KingCobra64 - <https://github.com/shrinivaasanka/kingcobra64-github-code/blob/master/KingCobraDesignNotes.txt>

GRAFIT - <https://github.com/shrinivaasanka/Grafit/blob/master/README.md>

Acadpdrafts - <https://github.com/shrinivaasanka/acadpdrafts-github-code/blob/master/index.rst>

Krishna_iResearch_DoxygenDocs - https://github.com/shrinivaasanka/Krishna_iResearch_DoxygenDocs/blob/master/index.rst

NeuronRain Antariksh - GitLab - Repositories and Design Documents which include course material (repositories suffixed 64 are for 64-bit and others are 32-bit on different linux versions)

AsFer - <https://gitlab.com/shrinivaasanka/asfer-github-code/blob/master/asfer-docs/AstroInferDesign.txt>

USBmd -
https://gitlab.com/shrinivaasanka/usb-md-github-code/blob/master/USBmd_notes.txt

USBmd64 - https://gitlab.com/shrinivaasanka/usb-md64-github-code/blob/master/USBmd_notes.txt

VIRGO Linux -
<https://gitlab.com/shrinivaasanka/virgo-linux-github-code/blob/master/virgo-docs/VirgoDesign.txt>

VIRGO64 Linux -
<https://gitlab.com/shrinivaasanka/virgo64-linux-github-code/blob/master/virgo-docs/VirgoDesign.txt>

KingCobra -
<https://gitlab.com/shrinivaasanka/kingcobra-github-code/blob/master/KingCobraDesignNotes.txt>

KingCobra64 -
<https://gitlab.com/shrinivaasanka/kingcobra64-github-code/blob/master/KingCobraDesignNotes.txt>

GRAFIT - <https://gitlab.com/shrinivaasanka/Grafit/-/blob/master/README.md>

Acadpdrafts - <https://gitlab.com/shrinivaasanka/acadpdrafts-github-code>

Krishna_iResearch_DoxygenDocs -
https://gitlab.com/shrinivaasanka/Krishna_iResearch_DoxygenDocs/-/blob/master/index.rst

NeuronRain Research - Repositories and Design Documents which include course material (repositories suffixed 64 are for 64-bit and others are 32-bit on different linux versions)

AsFer -
<https://sourceforge.net/p/asfer/code/HEAD/tree/asfer-docs/AstroInferDesign.txt>

USBmd - https://sourceforge.net/p/usb-md/code-0/HEAD/tree/USBmd_notes.txt

USBmd64 - https://sourceforge.net/p/usb-md64/code/ci/master/tree/USBmd_notes.txt

VIRGO Linux -
<https://sourceforge.net/p/virgo-linux/code-0/HEAD/tree/trunk/virgo-docs/VirgoDesign.txt>

VIRGO64 Linux -
<https://sourceforge.net/p/virgo64-linux/code/ci/master/tree/virgo-docs/VirgoDesign.txt>

KingCobra -

<https://sourceforge.net/p/kcobra/code-svn/HEAD/tree/KingCobraDesignNotes.txt>

KingCobra64 -

<https://sourceforge.net/p/kcobra64/code/ci/master/tree/KingCobraDesignNotes.txt>

GRAFIT -

https://sourceforge.net/u/ka_shrinivaasan/Grafit/ci/master/tree/README.md

Acadpdrafts - <https://sourceforge.net/projects/acadpdrafts/>

Krishna_iResearch_DoxygenDocs -

https://sourceforge.net/u/ka_shrinivaasan/Krishna_iResearch_DoxygenDocs/ci/master/tree/index.rst

NeuronRain Acadpdrafts - Drafts and Publications:

Academic Publications, Preprints and Draft publications of the Author are at portal <https://acadpdrafts.readthedocs.io> (which replaces erstwhile

<https://sites.google.com/site/kuja27>) unifying :

(*) publications in [https://scholar.google.co.in/citations?](https://scholar.google.co.in/citations?hl=en&user=eLZY7CIAAAAJ)

[hl=en&user=eLZY7CIAAAAJ](https://scholar.google.co.in/citations?hl=en&user=eLZY7CIAAAAJ)

(*) publication drafts in <https://sites.google.com/site/kuja27/> (Deleted and Mirrored at

https://github.com/shrinivaasanka/Krishna_iResearch_DoxygenDocs/blob/master/kuja27_website_mirrored/site/kuja27/) and

(*) publication drafts in

<https://sourceforge.net/projects/acadpdrafts/files/>

(*) Research Profiles - <https://sites.google.com/site/kuja27/CV.pdf>

(Deleted and Mirrored at

https://github.com/shrinivaasanka/Krishna_iResearch_DoxygenDocs/blob/master/kuja27_website_mirrored/site/kuja27/CV.pdf)

Some Implementations in AsFer in GitLab, GitHub and Sourceforge are related to aforementioned publications and drafts

Free GRAFIT (portmanteau of Graph-Merit) course material:

Online free course material in:

(*) GitHub - <https://github.com/shrinivaasanka/Grafit>

(*) Sourceforge -

<https://sourceforge.net/u/userid-769929/Grafit/ci/master/tree/>

(*) GitLab - <https://gitlab.com/shrinivaasanka/Grafit>

also refer to implementations in previous NeuronRain GitHub, GitLab and Sourceforge repositories and implement some additional example analytics - Advertisement Analytics by PageRank and Collaborative Filtering, PrefixSpan Astronomical Analytics of Celestial bodies, FPGrowth frequent itemset analytics, Set Partition Rank etc.,. Some of NeuronRain Sourceforge, GitHub and GitLab code commits and course material link to <https://kuja27.blogspot.in> which is meant for additional NeuronRain theory, expository graphics and large MP4 audio-visuals related to NeuronRain code commits in GitHub-GitLab-SourceForge repositories.

(*) GitHub Virtual Classroom for GRAFIT -

<https://classroom.github.com/classrooms/8086998-https-github-com-shrinivaasanka-grafit>

(*) GRAFIT course material in Moodle -

<https://moodle.org/pluginfile.php/4765687/user/private/Grafit-master.zip?forcedownload=1>

BRIHASPETHI - Private Virtual Classrooms and JAIMINI Closed Source Private Repositories:

GitHub - Private repositories of virtual classrooms for various commercial online courses (BigData, Machine Learning, Topics in Mathematics and Computer Science,...) and JAIMINI Closed Source Derivative of NeuronRain - <https://github.com/Brihaspathi> - requires GitHub student logins

SourceForge - <https://sourceforge.net/projects/jaimini/>

GitLab - <https://gitlab.com/shrinivaasanka/jaimini>

Atlassian BitBucket - https://bitbucket.org/ka_shrinivaasan/ (NeuronRain repositories imported as course material supplement to BRIHASPATHI - <https://github.com/Brihaspathi> - Virtual classrooms)

Bug tracking pages for NeuronRain repositories:

SourceForge - NeuronRain Research - https://sourceforge.net/u/ka_shrinivaasan/tickets/

GitHub - NeuronRain Green - https://github.com/shrinivaasanka/Krishna_iResearch_DoxygenDocs/issues

GitLab - NeuronRain Antariksh - https://gitlab.com/shrinivaasanka/Krishna_iResearch_DoxygenDocs/-/issues

(Deprecated) AsFer GitHub issues page - <https://github.com/shrinivaasanka/asfer-github-code/issues?q=is%3Aissue+is%3Aclosed>).

JIRA Bug Tracking - <https://krishnairesearch.atlassian.net/>

FAQ

****What is the meaning of name "NeuronRain"?****

Earlier the repositories in GitHub and SourceForge were named "iCloud" but it was in conflict with an already existing mobile cloud platform. Hence different name had to be chosen. All these codebases are targeted at a machine learning powered cloud. AsFer implements almost all prominent machine learning and deep learning neural network algorithms among others. It was intended to be named "NeuronCloud" but because of astronomical weather forecasting origins (both have clouds - weather and linux), and rain realises cloud, it has been named "NeuronRain".

****How does machine learning help in predicting weather vagaries? How does NeuronRain research version approach this?****

794. Computational Astrophysics - Astronomical Datasets Analytics - this section is an extended unifying draft of theory and feature in AstroInfer, USBmd, VIRGO, KingCobra, GRAFIT, Acadpdrafts, Krishna_iResearch_DoxygenDocs

It is an unusual application of machine learning to predict weather from astronomical data. Disclaimer here is this is not astrology but astronomy. It is long known that earth is influenced by gravitational forces of nearby ethereal bodies (e.g high tides associated with lunar activity, ElNino-La Nina pairs correlated to Sun spot cycles and Solar maxima etc.,). NeuronRain research version in SourceForge uses Swiss Ephemeris (based on NASA JPL Ephemeris - <http://ssd.jpl.nasa.gov/horizons.cgi>) implementation in a third-party opensource code (Maitreya's Dreams) to compute celestial degree locations of planets in Solar system. It mines historic data of weather disasters (Typhoons, Hurricanes, Earthquakes) for patterns in astronomical positions of celestial bodies and their connections to heightened weather disturbances on earth. Prominent

algorithm used is sequence mining which finds common patterns in string encoded celestial information. This sequence mining along with other bioinformatics tools extracts class association rules for weather patterns. Preliminary analysis shows this kind of pattern mining of astronomical data coincides reasonably with actual observations. There is a python script in asfer codebase which iterates through sequence mined rules and searches a celestial configuration matching it. Most weather models are fluid dynamics based while this is a non-conventional astronomy based analysis. Most accurate Medium Range Numeric Weather Prediction model in use at present is ECMWF - OpenIFS - <https://confluence.ecmwf.int/display/OIFS/OpenIFS+Home> . High correlation between low sunspot activity and high number of hurricanes has been studied - Sunspot-hurricane link - <https://www.nature.com/articles/news.2008.1136> . Gravitational influences amongst celestial bodies and their resultant orbital vicissitudes are formulated by set of differential equations and solutions to them known as N-Body Problem (http://en.wikipedia.org/wiki/N-body_problem - 2-body problem and restricted 3-body problems have already been solved by Sundman, Poincare, Kepler - $n \geq 4$ is chaotic). Hierarchical N-Body Symplectic Integration Package - HNBody - <https://janus.astro.umd.edu/HNBody/> - is an approximate N-Body differential equations solver and a sample orbital integration computation of few solar system planets for 50000 years is in <https://janus.astro.umd.edu/HNBody/examples/index.html>. N-Body solver benchmarks for various programming languages and multicores are at <https://benchmarksgame-team.pages.debian.net/benchmarksgame/description/nbody.html#nbody>. Solar system is a set of celestial bodies with mutual gravitational influences. Sequence mining of string encoded celestial configurations, mines patterns in planetary conjunctions ([http://en.wikipedia.org/wiki/Conjunction_\(astronomy\)](http://en.wikipedia.org/wiki/Conjunction_(astronomy))) vis-a-vis weather/geological vagaries on earth. Each such pattern is an instance of N-Body problem and its solutions pertain to gravitational influences for such a celestial configuration. Solving N-Body problem for $N > 3$ is non-trivial and no easy solutions are known. Solar system in this respect is 9-Body problem of 9 known planets and their mutual gravitational influences affecting Earth, ignoring asteroids/comets/KuiperBeltObjects. N-body problem has set of special solutions which are equally spaced-out configurations of celestial bodies on single orbit which need not be ellipsoid, known as n-body choreography e.g planets on vertices of equilateral triangles (https://en.wikipedia.org/wiki/N-body_choreography). Finding such periodic celestial arrangement of planets aligned on an orbit is a pattern mining problem. Celestial arrangement is also a set partition (string encoded) problem - house divisions are bins/buckets and 9 planets are partitioned into some of the 12 houses. Number of possible celestial ordered partitions are lowerbounded by 9-th ordered Bell number (7087261) which is a binomial series summation of Stirling numbers of second kind - it is a lowerbound because set of all possible ordered partitions of 9 planets have to be permuted amongst 12 houses. Thus machine learning helps in solving N-Body problem indirectly by mining 9-body choreography patterns in planetary positions and how they correlate to gravity induced events on Earth obviating N-Body differential equations. Disclaimer is this kind of forecast drastically differs from conventions and it does not prove but only correlates astronomical gravity influences and events on Earth. Proof requires solving the differential equations for N-Body and match them with mined celestial patterns which is daunting. As mentioned earlier, preliminary mined correlation analysis shows emergence of similar celestial conjunction patterns for similar genre of terrestrial events. Meaning of celestial bodies named Rahu and Ketu is the imaginary Lunar nodes (http://en.wikipedia.org/wiki/Lunar_node) which are points on zodiac where Ecliptic of the Sun (path of Sun observed from earth) crosses the Path of Moon which happens approximately $2 \times (12 \text{ or } 13)$ times per year. Chandler Wobble (<https://image.gsfc.nasa.gov/poetry/ask/a11435.html>) which is periodic movement of earth's pole by 0.7 arcseconds every 14 months influenced by Sun, Moon tidal forces causing earth crust rearrangements and seismic events. Phases of Moon affect rainfall patterns on earth (New York Times Archive 1962 - <https://www.nytimes.com/1962/09/07/archives/moon-phases-found-to-affect-rainfall.html>). More details on correlations between celestial n-body configurations and terrestrial weather vagaries can be found in Chapters 9 and 10 of "Planetary Influences on Human Affairs" by B.V.Raman (Chandler Wobble, Sun spots and Solar maxima, Orbit of moon in relation to earthquake epicentres, Uranus

causing earthquakes - [Tomaschek] - <https://www.nature.com/articles/184177a0> , MIT study of rainfall correlated to lunar phases among other factors). Stresses induced on earth by an extraterrestrial mass are proportional to Gravitational Field Gradient $-2GMm/r^3$ - USGS - https://www.usgs.gov/faqs/can-position-moon-or-planets-affect-seismicity-are-there-more-earthquakes-morning-in-evening-at-a-qt-news_science_products=0#qt-news_science_products .

****Is it possible to do accurate long term weather forecasting? Are there theoretical limitations? How does NeuronRain weather forecast overcome it?****

795. Computational Astrophysics - Astronomical Datasets Analytics - (this section is an extended unifying draft of theory and feature in AstroInfer, USBmd, VIRGO, KingCobra, GRAFIT, Acadp drafts, Krishna_iResearch_DoxygenDocs)

No and Yes. Both N-Body problem of solar system and failure of long term weather forecast have their basis in Chaos theory e.g Poincare Maps for 3-body problems define chaos in the orbits in system of 3 bodies while Lorenz attractors depict sensitive dependence on initial conditions specifically in weather forecast (Butterfly effect). This presents a natural limitation. All existing weather models suffer due to Chaos. But NeuronRain does not have any Chaos theoretic limitation. It just mines patterns in sky and tries to correlate them with weather events on earth accuracy of which depends on how the pattern-event correlations match solutions to N-Body problem. N-Body problem rests on Newton's Law of Gravitation. It is not just gravity but electromagnetic fields of other celestial objects also influence earth. So it is not exact astrophysics but computational learning model for astrophysics with failure probability.

****Can you cite an example machine learnt celestial pattern correlated to a terrestrial event?****

796. Computational Astrophysics - Astronomical Datasets Analytics - Correlation of Celestial N-body choreographies and Extreme Weather Events on Earth (this section is an extended unifying draft of theory and feature in AstroInfer, USBmd, VIRGO, KingCobra, GRAFIT, Acadp drafts, Krishna_iResearch_DoxygenDocs)

Sequence Mined Class Association Rules in <http://sourceforge.net/p/asfer/code/HEAD/tree/python-src/MinedClassAssociationRules.txt> and <http://github.com/shrinivaasanka/asfer-github-code/blob/master/python-src/MinedClassAssociationRules.txt> created by SequenceMining of string encoded celestial configuration show prominent celestial conjunctions when large magnitude Earthquakes or Hurricanes occur. One of the mined rule is Sun + Moon also known as New Moon. High probability of earthquakes due to Moon's gravitational effects during New Moon days (especially eclipses when Earth-Sun-Moon are aligned in line) is known (<http://www.scientificamerican.com/article/moon-s-gravity-linked-to-big-earthquakes/>). Other prominent mined rule is juxtaposition of Mercury-Sun-Venus (intercuspal and intracuspal) which highly correlates to heightened hurricane-typhoon-tropical cyclone events. Sun-Moon factor influencing ocean currents and causing earthquakes is plausible and known but Mercury-Venus, which are distant celestial systems having negligible gravitational effects, affecting tropical monsoons is an intriguing coincidental pattern. Likely explanation is: Mercury-Sun-Venus-Earth is a 4 body system. Mercury is always +/-15 degrees approximately from Sun and Venus is always +/- 60 degrees approximately from Sun on the zodiac. This 4 body system which is close to earth is quite periodic

almost annually exerting gravitational influence. Astrological explanation for effects of planetary conjunctions on earth is debunked excluding hightides - <https://image.gsfc.nasa.gov/poetry/venus/q189.html> - nevertheless miniscule influence on tides might snowball to chaos by sensitive dependence on initial conditions which doomed long term weather forecasts e.g storm surge or tidal surge associated with low pressure areas. Meteorological variables have a similar recurrence format of Aforecast = Ainitial + F(A)Δt which resembles Chaotic Verhulste logistic $X(n+1) = \text{Lambda} * Xn * (1 - Xn)$. References: (*) Numeric Weather Prediction - <https://rams.atmos.colostate.edu/at540/fall03/fall03Pt7.pdf> (*) Equation 1 and Section 3.1 on exceptional ocean waves - "Fluid mechanics and thermodynamics of tropical cyclones" - https://www.math.nyu.edu/chaos_teaching/hurricanes/LighthillFMTc98.pdf. Similar explanation holds for Mars-Earth et al system too. There is an empirical evidence of Jupiter-Venus 2-body system affecting climate on Earth in a cycle of 405000 years - Empirical evidence for stability of the 405-kiloyear Jupiter-Venus eccentricity cycle over hundreds of millions of years - <https://www.pnas.org/content/pnas/115/24/6153.full.pdf>.

****What is the historic timeline evolution of NeuronRain repositories?****

Initial design of a cognitive inference model (uncommitted) was during 2003 though original conceptualization occurred during 1998-99 to design a distributed linux. Coincidentally, an engineering team project done by the author was aligned in this direction - a distributed cloud-like execution system - though based on application layer CORBA (https://sourceforge.net/projects/acadp drafts/files/Excerpts_Of_PSG_BE_FinalProject_COBRA_done_in_1999.pdf/download). Since 1999, author has worked in various IT companies (<https://sourceforge.net/projects/acadp drafts/files/AllRelievingLetters.pdf/download>) and studied further (MSc and an incomplete PhD at CMI/IMSc/IIT, Chennai, India - 2008-2011). It was a later thought to merge machine learning analytics and a distributed linux kernel into a new linux fork-off driven by BigData analytics. Commits into Sourceforge and GitHub repositories are chequered with fulltime work and Study tenures. Thus it is pretty much parallel charity effort from 2003 alongside mainstream official work. Presently author does not work for any and works fulltime on NeuronRain code commits and related independent academic research only with no monetary benefit accrued. Significant commits have been done from 2013 onwards and include implementations for author's publications done till 2011 and significant expansion of them done after 2012 till present. Initially AstroInfer was intended for pattern mining Astronomical Datasets for weather prediction. In 2015, NeuronRain was replicated in SourceForge and GitHub after a SourceForge outage and since then SourceForge NeuronRain repos have been made specialized for academic research and astronomy while GitHub NeuronRain repos are for production cloud deployments.

****Why is NeuronRain code separated into multiple repositories?****

Reason is NeuronRain integrates multiple worlds into one and it was difficult to manage them in single repository - AsFer implements only userspace machine learning, USBmd is only for USB and WLAN debugging, VIRGO kernel is specially for new systemcalls and drivers, KingCobra is for kernelspace messaging/pubsub. Intent was to enable end-user to use any of the repositories independent of the other. But the boundaries among them have vanished as below:

- (*) AsFer invokes VIRGO systemcalls
- (*) AsFer implements publications and drafts in acadp drafts
- (*) USBmd invokes AsFer machine learning
- (*) VIRGO Queueing forwards to KingCobra
- (*) VIRGO is dependent on AsFer for kernel analytics
- (*) KingCobra is dependent on AsFer Neuro MAC Protocol Buffer currency implementation

(*) Graft course materials refer to all these repositories and all NeuronRain repositories are strongly interdependent now. Each repository of NeuronRain can be deployed independent of the other - for example, VIRGO linux kernel and kernel_analytics module in it can learn analytic variables from

any other third-party Machine Learning framework not necessarily from AstroInfer - TensorFlow, Weka, RapidMiner etc., Only prerequisite is /etc/kernel_analytics.conf should be periodically updated by set of key-value pairs of machine-learned analytic variables written to it. But flipside of using third-party machine-learning software in lieu of AsFer is lack of implementations specialized and optimized for NeuronRain. NeuronRain Research repos in SourceForge is astronomy specific while NeuronRain Green repos in GitHub and GitLab are for generic datasets (GitHub and GitLab repos of NeuronRain might diversify and be specialized for cloud and drones/IoTs)

****NeuronRain repositories have implementations for your publications and drafts. Are they reviewed? Could you explain about them?****

Only arXiv articles and TAC 2010 publications below are reviewed and guided by faculty - Profs. Balaraman Ravindran(IIT, Chennai), Madhavan Mukund(CMI) and Meena Mahajan (IMSc) [Co-Authors in <https://scholar.google.co.in/citations?hl=en&user=eLZY7CIAAAAJ>] while the author was doing PhD till 2011 in CMI/IMSc/IIT, Chennai:

- 2011 - Decidability of Complementarity - <http://arxiv.org/abs/1106.4102>
- 2010 - Algorithms for Intrinsic Merit - <http://arxiv.org/abs/1006.4458>
- 2010 - NIST TAC 2010 version of Algorithms for Intrinsic Merit - http://www.nist.gov/tac/publications/2010/participant.papers/CMI_IIT.proceedings.pdf

Important Cautionary Legal Disclaimer: All other theory drafts (excluding earlier publications) in NeuronRain design documents and <http://sites.google.com/site/kuja27> (Deleted and Mirrored at https://github.com/shrinivaasanka/Krishna_iResearch_DoxygenDocs/blob/master/kuja27_website_mirrored/site/kuja27/ - Linked by new expanded portal <https://acadp drafts.readthedocs.io>) including theorem-proofs thereof are non-peer-reviewed, private, unvetted and unaffiliated research of the author (K. Srinivasan - <https://sites.google.com/site/kuja27/> - Deleted and Mirrored at https://github.com/shrinivaasanka/Krishna_iResearch_DoxygenDocs/blob/master/kuja27_website_mirrored/site/kuja27/ - Linked by new expanded portal <https://acadp drafts.readthedocs.io>) aligned to features of NeuronRain codebases and as well significant expansions of previous publications (Refer to "NeuronRain Licensing" section of FAQ). Author is an independent professional and because of certain speculations and confusions about its monetization-commercialization by an anonymous entity and conflicts-violations brought to notice, it is hereby clarified that NeuronRain codebases, architecture and development are private, independent, non-commercial, academic research and charity initiatives of author subject to NeuronRain licensing terms (GPL 3.0 and CC 4.0) and have nothing to do with any of the organizations and academic institutions (government or private) author may or may not have worked/affiliated with in the past including but not limited to any commercial derived clones of NeuronRain that might be in circulation by aforementioned entity with which author has no relationship (business and otherwise) - author contributes to NeuronRain codebases as a noble charity gesture motivated towards academic enlightenment without monetary or royalty benefit from any external funding source. Cloning NeuronRain for production-commercial deployments is cautioned against because of certain known technical issues (mostly with respect to fragile low level linux kernelspace RPC - Refer BestPractices.txt in NeuronRain AstroInfer source code - VIRG032 and VIRG064 linux kernel system calls and drivers are sensitive to hardware-architectural idiosyncracies and mainline linux kernel versions - what works in previous mainline kernel version may not work in next because of subtle system call interface changes in kernelspace sockets causing regressions (example of an issue found in 4.1.5 and fixed in 4.10.3 i915 GEM drivers - DMA panics - <https://github.com/shrinivaasanka/asfer-github-code/issues/1>). Another issue is the non-reentrant nature of VIRGO system calls - Mutexing within VIRGO system calls have been disabled per commit hash comments <https://github.com/shrinivaasanka/virgo64-linux-github-code/commit/ad59cbb0bec23ced72109f8c5a63338d1fd84beb> . Because of earlier technicality, mainline version of VIRG032 and VIRG064 hasn't been QAed and updated since

4.13.3 (for system calls and drivers excluding PXRC) and 5.1.4 (for PXRC) and mainline kernel upgrade underneath and build is left to enduser) though academic usage is encouraged. Author has no involvement in any alleged commercialization of NeuronRain fork-off by aforementioned anonymous entity and bears no responsibility for misgivings caused - NeuronRain is not for sale and would remain as academic charity forever, safeguarding sanctity and spirit of FOSS though design and code of NeuronRain is being derived, cloned or extended by author within BRIHASPATI organization (JAIMINI closedsource repositories in GitHub, GitLab and SourceForge) and used as textbook reference for BRIHASPATI commercial online classrooms and repositories (reference: BRIHASPATI print media advertisements - THE HINDU - 20 March 2022 and 26 June 2022 - https://github.com/shrinivaasanka/Krishna_iResearch_DoxygenDocs/blob/master/TheHinduAdvt_TrichyEdition_2022-03-20.jpg , https://github.com/shrinivaasanka/Krishna_iResearch_DoxygenDocs/blob/master/TheHinduAdvt_AllIndiaEdition_2022-06-26.jpg). Bugs-Issues for all NeuronRain repositories can be filed in NeuronRain JIRA - <https://krishnairesearch.atlassian.net/jira/software/projects/NEUR/boards/1> . Neuro Protocol Buffer Perfect Forward (Cloud Object Move) Cryptocurrency implemented in NeuronRain is only an academic research effort for modelling money changing problem and optimal denomination, economic networks, transaction hyperledgering and money trail. Neuro is a fictitious cryptocurrency and not a legal tender and cannot be used as a commercial denomination. Academic use of Neuro is subject to government regulations and statute.

****Is there a central theme connecting the publications, drafts and their implementations mentioned previously?****

 781. (THEORY and FEATURE) Social Choice, Complexity and Learning theoretic motivations for Intrinsic Merit - this section is an extended unifying draft of theory and feature in AstroInfer, USBmd, VIRGO, KingCobra, GRAFIT, Acadp drafts, Krishna_iResearch_DoxygenDocs

 Yes. All these drafts revolve around the fundamental philosophical/mathematical question - Which choice is better? Group Social Choice by Majority or Any Choice function other than Majority? Is it possible to determine merit intrinsically unpolluted by mass opinions? This problem has been studied for centuries e.g Condorcet Jury Theorem. Drafts and publications above are efforts in this direction translating this question to problems requiring measurement of merit and ranking of text etc., in World Wide Web and Human Social Networks. These drafts bridge the usual chasm between Theoretical Computer Science and Engineering side of it like Machine Learning by concepts drawn from Boolean social choice, Pseudorandomness, Boolean Satisfiability, Learning theory etc.,. Notion of Complementing a Function has origins in computability theory (Hilbert's tenth problem, Solutions to Diophantine Equations, MRDP theorem etc.,) and closely relates to Ramsey Theory of Coloring sequences of real/integer lines. Complementing a function is also another facet of social choice e.g Complement of a social choice function - "Who voted in favour" is a complement of a social choice function - "Who did not vote in favour". In complexity parlance, complementation is reminiscent of the definition of C and Co-C complexity classes for some class C. Integer partition and Locality Sensitive Hashing are theoretical gadgets for a multipartisan voting - votes are partitioned among candidates and each candidate has similar voters chained in an LSH bucket together. LSH Hash function of 2 buckets is nothing but the boolean majority function in tabulation and each bucket has a generating function which are mutually complement functions. Complement Functions are special subsets of Diophantine Equations in which two complementary sets (or sets in an exact cover) are defined by Diophantine Equations. Integer Factorization is also a diophantine problem e.g. Brahmagupta's Chakravala and Solutions to Pell Equation etc., Integer Factorization is a peripheral requirement for integer partitioning

- each number can be partitioned in as many ways as sum of products of frequencies of partition and size of partition - defined by coefficients in partition generating function. Space filling/Circle filling algorithms are packing constraint satisfaction problems which can be social choice functions too (each packing problem is an objective function of a voter maximized by a candidate). Complement Functions can be generalized to Diophantine Equations for sets in exact cover and are thus special subproblems of Space filling/Packing/Tiling problems (e.g Pentominoes tiling exact cover of plane). These drafts describe a parallel PRG cellular automaton algorithm for space filling. Last but not the least, Complement Function generalizes the well-known patterns in primes problem (which is related to real part of non-trivial zeros of Riemann Zeta Function) - a function complementing integer factorization implies pattern in primes. Prime-Composite complementation is also related to Jones-Sato-Wada-Wiens Theorem - <http://www.math.ualberta.ca/~wiens/home%20page/pubs/diophantine.pdf> - set of primes is exactly the set of values of a polynomial in 25 degree - 26 variables - because primes are recursively enumerable Diophantine set. Pattern in primes is also a problem related to energy levels of Erbium nuclei - Freeman Dyson and Montgomery statistics - http://seedmagazine.com/content/article/prime_numbers_get_hitched/ . Intrinsic merit versus perceived merit dichotomy has immense complexity theoretic ramifications which are analyzed in the drafts which have to be read with the caveat: equating majority and non-majority social choices subsume all classes of complexity zoo under equal goodness (in the context of Condorcet Jury Theorem Group Decision vis-a-vis a non-conventional social choice) and completeness assumptions. Intrinsic merit is about objectively determining value of an entity (text, academic papers, audio-visuals and humans too) whereas Condorcet Jury Theorem and its later enhancements are about correctness of subjective Majority Voting Decision. Notion of Intrinsic Merit already has been widely studied in the name of Intrinsic Fitness of a vertex in Social Networks (ability to attract links) - e.g Bianconi-Barabasi Network Bose-Einstein Fitness and its later derivative papers. Previous publications till 2010 devote only to intrinsic merit of text documents and later draft expansions after 2011 generalize it to merit of any(text, audio, visuals, people). Most of the literature assumes a probability distribution of fitness/merit and not finding it. These drafts are efforts in this direction to pinpoint how to quantize intrinsic fitness/merit. Obviously defining intrinsic merit is a difficult problem, but there are precedents to solving it e.g individual social merit is measured by examinations/question-answering/contests etc., not much by voting. Both these problems reduce to satisfying a boolean formula (e.g 3SAT) of arbitrary complexity class because "judging" implies extent of constraints satisfied e.g Voters have varied 3CNFs to rank a candidate making it subjective while Intrinsic merit requires an absolute 3CNF. Finding an absolute CNF is the leitmotif of all Intrinsic Merit algorithms implemented in NeuronRain - this is computational learning theory problem viz., PAC Learning, MB Learning etc., All Deep Learning algorithms including BackPropagation, Convolution, Recurrent Neural Networks etc., learn from errors and iteratively minimize. Neural networks are theoretically equivalent to threshold AC=NC=TC circuits. Learning theory goes beyond just constructing formulas and places limits on what is efficiently learnable. Merit computed by these can be translated to variables in a CNF. NeuronRain implements a Least Square Approximate MaxSAT solver to rank the targets by the percentage of clauses satisfied.

 864. (THEORY and FEATURE) Conceptual Graph of Theory aligned to Features of NeuronRain

1. Intrinsic Merit is a Non-majority Social Choice Function and quantifies merit of text, audio/music, visuals, people and economies. Intrinsic merit is omnipresent - wherever rankings are required intrinsic merit finds place vis-a-vis perceptive/fame rankings. Intrinsic merit is defined as any good, incorruptible, error-resilient mathematical function for quantifying merit of an

entity which does not depend on popular perception and majority voting where goodness has wider interpretations - sensitivity, block sensitivity, noise sensitivity/stability, randomized decision tree evaluation being one of them but not limited to in boolean setting and BKS conjecture implies there is a stabler function than majority (example: examinations, interviews and contests are objective threshold functions for evaluating people which do not involve subjective voting; counterexample: stock market indices though mathematically derived are not intrinsic since they are computed from perceptive human valuations of market, but high frequency algorithmic trading platforms and quantitative finance algorithms might find equilibrium pricing solutions between perception and absolute). An alternative measure of merit is "Originality" of an entity which distinguishes from rest. Following classes of merit have been defined in the drafts and most of them are implemented(excluding dependencies):

1.1 Alphanumeric Text(WordNet, ConceptNet, compressed sensing and vowelless string complexity, text restoration, Numeric compression by unique integer factorization, syllabification and TeX hyphenation, language independent phonetic syllable vector embedding of strings - String tensors, recursive gloss overlap, recursive lambda function growth, Question-Answering[Interview algorithm, LTFs, PTFs, Cognitive automata-Switching circuits with background intelligence], Reduction between Question-Answering and Boolean and Non-Boolean Query complexity measures (certificate complexity, decision trees, polynomial degree, block sensitivity - classical and quantum), Coh-Metrix, Berlekamp-Welch error correction, Polynomial text encoding, Named Entity Recognition, Sentiment Analysis, Graph Mining, Graph Edit Distance between Text graphs, Locality Sensitive Hashing, Unsorted search, Set Partition Analytics, FP Growth frequent itemset mining, Machine translation, Originality by Word2Vec embedding, Bibliometrics-merit of academic publications by Meaning Representation in first order logic and Beta reduction of Lambda calculus, Novelty detection and Patent search, Multilingual strings-code switching),

1.2 Alphanumeric Text(String Analytics - Longest Repeated Substring-SuffixArray-LongestCommonPrefix, BioPython/ClustalOmega Multiple Sequence Alignment, Sequence Mining, Minimum Description Length, Entropy, Support Vector Machines, Knuth-Morris-Pratt string match, Needleman-Wunsch alignment, Longest common substring, KNN clustering, KMeans clustering, Decision Tree, Bayes, Edit Distance, Earth Mover Distance, Linear Complexity Relaxed Word Mover Distance, PrefixSpan - astronomical, binary, numeric and generic encoded string datasets - astronomical datasets and algorithmic usecases include (*) USGS Earthquakes and NOAA HURDAT2 datasets (*) Cosmology - Deep Field Space Telescope Visuals - Hubble and WMAP imagery - AstroPy-AstroQuery interface of JPL Horizon Ephemeris service and AstroML astronomical machine learning algorithms integration (*) SkyField-AstroPy JPL Ephemeris queries for positions of celestial bodies (*) Maitreya 8t - encoded strings of celestial bodies obtained from ephemeris corresponding to various extreme weather events (*) Ephemeris Search for astronomical events in SkyField-AstroPy (*) correlation of terrestrial climate events and gravitational influence of solar system N-body orbit choreographies-Syzygies, Conjunctions, Quadratures - implementation of N-Body equation solver to gauge gravitational accelerations of solar system bodies on Earth-Moon barycenter on days of extreme weather events (*) correlation of extreme weather events and celestial bodies by Sequence mining of astronomical datasets to get Class Association Rules,

1.3 Audio-speech(Speech-to-Text and recursive lambda function growth, Graph Edit Distance),

1.4 Audio-music(Music Information Retrieval-MIR, mel frequency cepstral coefficients, Learning weighted automata from music notes waveform, Graph Edit Distance between weighted automata, Equivalence of Weighted automata by Table filling, Kullback-Leibler and Jensen-Shannon divergence, Novelty detection and Originality of a score by waveform distance, AI music synthesis by functions-automata-fractals and polynomial interpolations of training music waveforms, AI music synthesis by Virtual Piano from random 12-notes string, Deep Learnt Automata, Dynamic Time Warping distance similarity between music timeseries, Music synthesis from sum of damped sinusoids, Weierstrass Function - Fractal Fourier summation, Music evoked autobiographical memories, Normalized Compression Distance-Kolmogorov Complexity, Contours of Functional MRI medical imaging for music stimuli -

<https://openneuro.org/datasets/ds000171/versions/00001>) - AI Music Synthesizer from mathematical functions is the converse of Learning weighted automata from music notes wherein innate fractal self-similar structure of music is exploited by machine learning to churn out music - JS Bach + Fractals = New Music - <https://www.nytimes.com/1991/04/16/science/j-s-bach-fractals-new-music.html>, https://link.springer.com/chapter/10.1007/978-3-642-78097-4_3. Learning a polynomial from music waveform as against weighted automaton learning (graph structure of music) could extract algebraic structure of music - NeuronRain implements a Degree 5 (Quintic) polynomial learner for music waveforms - Unsolvability of Quintic polynomial (Degree ≥ 5) by Abel-Ruffini Theorem intuitively means roots of polynomial learnt from music waveform could not be expressed as formulae on radicals - tough nut to crack and could be irreducible. Earth Mover Distance Triple Sequence from moves of Towers of Hanoi Single Bin Sorted LIFO histogram exhibits a Collatz-like Chaotic structure suitable for Music and Financial Timeseries modelling ending always in (0,0,0) for 3 buckets.

1.5 Visuals-images(Compressed Sensing,ImageNet ImageGraph algorithm, Graph Edit Distance between FaceGraphs of segmented images, GIS Remote Sensing Analytics, Weather analytics, Climate analytics, Clustering Analytics of celestial bodies in sky imagery from planetarium software and their correlation to extreme weather events - visual analogue of textual astronomical datasets, Modularity-Community Detection, Urban planning analytics (3D UGM - Digital Elevation Models - Mapping and 3D modelling using quadrotor drone and GIS software - <https://journalofbigdata.springeropen.com/articles/10.1186/s40537-021-00436-8>, 2D UGM - Dynamic Facegraph, Cellular Automata and Polya Urn Urban Growth [by Learnt Replacement matrix] Models), Automatic Delineation of Urban Growth Boundaries, Gini Coefficient of Inequality, Moran's I measure of Urban Sprawl Dispersion-Diffusion Factor, Canny Edge Detection-Transportation Network Lattice Grid, Ocean Floor Bathymetry GIS, Machine Learning models of Urban Extent-NASA SEDAC GPW,Facebook HRSL,European Union GHSL R2019A-R2022A and NASA VIIRS NightLights, USGS LandSat9 TIRS-2/OLI-2 imagery, Voronoi Tessellation, Delaunay Triangulation, GMSH Trimesh-Quadmesh, Preferential attachment, Face and Handwriting Recognition, Neural network clustering, DBSCAN Clustering, DICOM-Medical imageing-ECG-MRI-fMRI-EEG-CTSCAN-PET-Doppler-XRay, Convex Hull, Patches Extraction-RGB and 2-D, Segmentation, Random forests, Autonomous Driving-LIDAR point cloud data, Flood vulnerability detection from GIS and LiDAR DEM, Drone Aerial Imagery Analytics, Astronomy-Cosmology Datasets-Deep Field Visuals from Space Telescopes) - GHSL rasters are mosaics created from Symbolic Machine Learning which is quite akin to Multiple Sequence Alignment and Class Association Rules based learning implemented for Astronomical Pattern Mining in NeuronRain. GDP and other socioeconomic indicators can be estimated from GIS Imagery analytics,

1.6 Visuals-videos(ImageNet VideoGraph EventNet Tensor products algorithm for measuring Tensor Rank connectivity merits of movies,youtube videos and Large Scale Visuals, Graph Edit Distance between Video EventNet, Sentiment analysis of predictions textgraphs for youtube and movie videos by Empath-MarkovRandomFields Recursive Gloss Overlap Belief Propagation-SentiWordNet, Topological Sort for video summary, Digital watermarking, Drone Aerial Video Streaming Analytics, GIS Imagery Contour graphs for A-Star motion planning and Road Geometry Airspace Drone obstacle avoidance),

1.7 People(Social and Professional Networks) - experiential and intrinsic(recursive mistake correction tree, Question-Answering in Interviews/Examinations/Contests),

1.8 People(Social and Professional Networks) - lognormal least energy(inverse lognormal sum of education-wealth-valour,Sports Analytics-Intrinsic Performance Ratings-IPR e.g Elo ratings,Real Plus Minus, Non-perceptive Rankings in Sports, Wealth, Research and Academics),

1.9 People(Professional Networks)-analytics(attritions, tenure histogram set partitions - correlations, set partition analytics, analytics driven automatic recruitment of talent - an alternative to manual Interviews, Career transition score, Career Polynomials and Inner Product Spaces, Chaotic Hidden Markov Model and Weighted automata model of Tenures, Originality of a profile measured by tenure choices-equivalence of state transition automata, Novelty detection-Innovation-Patents, Fibonaccian Search of sorted unique id(s)),

1.10 People-election analytics(Boyer-Moore Streaming majority, set partition EVMS, drone electronic voting machine by autonomous delivery, voting analytics, efficient population count, pre-poll and post-poll forecast analytics, Bertrand ballot theorem, Arrow and Gibbard-Satterthwaite No-Go Theorems on Impossibility of Fair Voting satisfying criteria for 3 or more candidates),

1.11 People(Social and Professional Networks)-unique person search (similar name clustering by phonetic syllable vectorspace embedding of names - String Tensors, People profiles as Tensors, Graph Edit Distance, contextual name parsing, unique person identification from multiple datasources viz., LinkedIn, Twitter, Facebook, PIPL.com, Emails)

1.12 People(Social and Professional Networks, Archaeology-Civilizations)-face and handwriting recognition (textual, topological and graph theoretic handwriting and face recognition-physique recognition by dynamic time warping on physical mobility timeseries-gender recognition, fingerprint recognition for unique identification, Feasibility of Non Fungible Tokens as non-biometric unique id alternatives e.g Neuro fictitious Cryptocurrency Boost UUIDs, Decipherment of ancient scripts by Rebus principle topological script recognition - Chain Approximation Contour polynomials clustering/Homeomorphism/Product Homotopy/Pasting Lemma/Graph Edit Distance and Earth mover distance/Gromov-Hausdorff distance/Multiple Netrd Graph distances/Graph matching/Exact-Approximate Graph and Subgraph Isomorphisms/Trimesh-Quadmesh/Bezier-animated Mesh Deformations/Dynamic Time Warping/Common Subgraph Problem/Approximate Topological Matching between Dlib face landmark detected and segmented Image Voronoi tessellation FaceGraphs, Delaunay Triangulation graphs and Quadrilateral Mesh Graphs/Euler Characteristic of 2D and 3D Voronoi tessellations), Sentiment Analysis based Reciprocal Recommender Systems for Bipartite Social Network Graphs - Matrimonial and other Match making Services, Gale-Shapley Stable Marriage Problem, Hall's Marriage Theorem, Physique recognition by Dynamic Time Warping Timeseries similarity of trimesh-quadmesh sequences of full body video footages - claimed to be more accurate than face recognition. Decipherment of ancient writing systems is a harder problem of handwriting recognition where no prior training data are available for an AI model to decipher an unknown inscription on potsherds-painted_gray_ware into natural language and Rebus principle is often resorted to e.g Asko Parpola's Rebus decipherment of Indus script - four conditions for Rebus principle - <https://www.harappa.com/content/indus-script-6> - [Iravatham Mahadevan] - The Indus Script: Texts, Concordance and Tables - <https://www.harappa.com/content/indus-script-texts-concordance-and-tables>. Rebus principle topological script recognition from textgraph of ImageNet predictions of inscription imagery could extract deeplearnt meanings of individual script pictograms graph theoretically and serve as a validation of a decipherment - For example following fictitious undeciphered inscriptions:

Inscription1 - ABCD - ImageNet prediction Textgraph1

Inscription2 - BFGH - ImageNet prediction Textgraph2

Inscription3 - KBPQ - ImageNet prediction Textgraph3

isolate the meanings of common pictogram B in three ways by 1) Set intersection between Textgraph1-Textgraph2 (extracts textgraphX for B) 2) Set intersection between Textgraph2-Textgraph3 (extracts textgraphY for B) or 3) Frequent subgraphs mined (GSpan) in Textgraph1, Textgraph2 and Textgraph3 - For a valid Rebus decipherment textgraphX and textgraphY for pictogram B must concur or be highly isomorphic and a non-trivial Frequent subgraph is found by GSpan between 3 Textgraphs (based on natural language assumption that any word, syllable or letter is used recurrently with almost same meaning throughout - for instance, multiple occurrences of word "Elephant" in an English text have same meaning) - any high deviation could be a false decipherment in natural language logossyllabic terms.

1.13 Economic merit(Financial Fraud Analytics, Quantitative Finance, Stock Market Tickers ARMA-ARIMA timeseries analysis, Economic Networks, Dynamic Time Warping similarity of financial timeseries - similarity of timeseries implies an indirect causality, Graph Edit Distance between economic networks, Poverty alleviation Linear Program, Neuro Cryptocurrency Proof-of-Work Hardness, Colored Money as Flow Conservation Problem, Production Networks-Supply Chain, Human Development Index, Gross Domestic Product, Purchasing Manager Index,

Social Progress Index, Intrinsic Pricing Vs Demand-Supply Market Equilibrium, Quantitative Majority circuit, Bargaining problem, Product Recommendations-Collaborative Filtering-ALS, Brand loyalty switch graph, media analytics, Granger causality, Graphical Event Models-Graphical Causal Models - advertisement analytics, business analytics, logistic regression and Gravity model in economic networks for predicting trade between nations based on GDP as fitness measure, Software Valuations) - Demand-Supply pricing and Auction Design for commodity are majority driven while Theory of Value (Labor Theory of Value by Adam Smith and Ricardo and Scarcity Theory of Value - https://www.researchgate.net/publication/302454600_Samuelson_and_the_93_Scarcity_Theory_of_Value/link/5cbb1e2c92851c8d22f822d2/download) is an example of intrinsic economic merit. Spectrum Auction widely used for pricing wireless spectrum allocations to highest bidder is a multi-round voting mechanism (vote for a commodity is proportional to its bidding price per round - Section 790 of NeuronRain Design formalizes this notion by Quantitative Majority Circuit gadget in which number of leaves of majority circuit changes simulating increase or dearth in demand depending on supply of commodity) on band of frequencies - <https://www.cramton.umd.edu/papers2005-2009/cramton-spectrum-auction-design.pdf> - two types of spectrum auctions are followed by governments: 1) traditional - Simultaneous ascending auction 2) recent - Combinatorial clock auctions. Cryptocurrency mining rigs award currencies by Proof of Work proportional to hardness (which could be a function of labour necessary to produce a commodity from scratch) of computation performed and hence reinstate the glory of Labour Theory of Value in new avatar. An example derivation of intrinsic pricing for two factors labour and land from Samuelson-Stolper theorem - https://en.wikipedia.org/wiki/Stolper%E2%80%93Samuelson_theorem - Price of Cloth and Wheat in two-good economy. GDP can be estimated by linear or logistic regression on various independent variables sourced from GIS imagery analytics (e.g Electricity consumption from NASA VIIRS NightLights)

1.14 Streaming Analytics for different types of streaming datasources - Spark streaming, many NoSQL DBs and other backends - text, audio, video, people, numeric, frequent subgraphs, A-star graph best first search for Drone motion planning, histograms for music spectrograms-set partitions-business intelligence, OS scheduler runqueue etc., - by standard streaming algorithms (LogLog counter, HyperLogLog counter, Bloom Filter, CountMinSketch, Boyer-Moore majority, CountMeanMinSketch, Approximate counting, Distinct Elements)

1.15 Deep Learning Analytics for different types of datasources - text, PSUtils OS Scheduler analytics - ThoughtNet Reinforcement Learning, Recommender Systems, LSTM/GRU Recurrent Neural Networks, Convolution Networks, BackPropagation

1.16 Computational Learning Theory Analytics - Complement Diophantine Learning, PAC Learning from numeric and binary encoded datasets

1.17 Time Series Analysis for different types of datasources - Leaky Bucket, ARMA and ARIMA, miscellaneous statistics functions based on R and PythonR (Economic merit - Poverty alleviation example by timeseries correlation of poverty and financial deepening - https://www.researchgate.net/publication/287580802_Financial_development_and_poverty_alleviation_Time_series_evidence_from_Pakistan, Granger causality)

1.18 Fame-Merit Equilibrium (any Semantic Network) - applies to all previous merit measures and how they relate to perceptions. In the absence of 100% good intrinsic merit function, it is often infeasible to ascertain merit exactly. But Market Equilibrium Pricing in algorithmic economics solves this problem approximately by finding an equilibrium point between intrinsic and perceived price of a commodity. Similar Intrinsic (Merit) Versus Perceived (Fame) equilibria can be defined for every class of merit above and solution is only approximate. [Conjecture: Fame-Merit equilibrium and Converging Markov Random Walk (PageRank) rankings should coincide - Both are two facets of mistake-minimizing Nash equilibrium per Condorcet Jury Theorem for infinite jury though algorithmically different - former is a convex program and latter is a Markov chain. Convex Optimization has been shown to be solved by Random Walks - <https://www.mit.edu/~dbertsim/papers/Optimization/Solving%20Convex%20Programs%20by%20Random%20Walks.pdf>]

2. Complement Functions are subset of Diophantine Equations (e.g Beatty functions). Polynomial Reconstruction Problem/List decoding/Interpolation which

retrieve a polynomial (exact or approximate) for set of message points is indeed a Diophantine Representation/Diophantine Approximation problem for the complementary sets (e.g. approximating Real Pi by Rational Continued Fractions). Undecidability of Complement Diophantine Representation follows from MRDP theorem and Post's Correspondence Problem. Prime-Composite complementation is a special diophantine problem of finding patterns in primes which relies on non-trivial zeroes of Riemann Zeta Function (Riemann Hypothesis). ABC Conjecture can be rephrased as a complementation problem. Riemann Hypothesis has Diophantine representation by Davis-Matiyasevich-Robinson Theorem.

3. Factorization has a Diophantine Representation (Brahmagupta's Chakravala and Pell Equation: $x^2 - y^2 = N = (x+y)(x-y)$). Four major problems are solved by NeuronRain MapReduce-NC-PRAM-BSP-Multicore Computational Geometric Factorization: (*) Factorization of composites for which no polynomial time algorithms known (*) Primality Testing which is known to be $O((\log N)^6)$ by an improved version of AKS primality test - [Pomerance-Lenstra] - <https://math.dartmouth.edu/~carlp/aks041411.pdf> (*) Finding Square Roots - known to be $O((\log N)^k \log \log N)$ by Newton-Raphson algorithm (*) Pell's equation (which so far has only a quantum polynomial time algorithm known - <https://arxiv.org/abs/quant-ph/0302134>)

4. Tiling/Filling/Packing is a generalization of Complement Functions (Exact Cover).

5. Majority Function has a Tabulation Hashing definition (e.g Electronic Voting Machines) i.e Hash table of candidates as keys and votes per candidate as chained buckets

6. Integer Partitions and Tabulation Hashing are isomorphic e.g partition of an integer 21 as 5+2+3+4+5+2 and Hash table of 21 values partitioned by keys on bucket chains of sizes 5,2,3,4,5,2 are bijective. Both Set Partitons and Hash tables are exact covers quantified by Bell Numbers/Stirling Numbers. Partitions/Hashing is a special case of Multiple Agent Resource Allocation problem. Thus hash tables and partitions create complementary sets defined by Diophantine equations. Pareto Efficient resource allocation by Multi Agent Graph Coloring - coloring partition of vertices of a graph - finds importance in GIS and Urban Sprawl analytics, Resource Scheduling in Operating Systems (allocating processors to processes), Resource allocation in People Analytics (allocating scarce resources - jobs, education - to people) by a Social welfare function e.g Envy-Free, Pareto efficient Multi Agent Graph Fair Coloring of Social Networks to identify communities, allocate resources to communities of social networks in proportion to size of each community.

7. Ramsey Coloring and Complementation are equivalent. Ramsey coloring and Complement Diophantines can quantify intrinsic merit of texts.

8. Graph representation of Texts and Lambda Function Composition are Formal Language and Algorithmic Graph Theory Models e.g parenthesization of a sentence creates a Lambda Function Composition Tree of Part-of-Speech.

9. Majority Function - Voter SAT is a Boolean Function Composition Problem and is related to an open problem - KRW conjecture - and hardness of this composition is related to another open problem - P Vs NP and Knot Theory. Theoretical Electronic Voting Machine (which is a LSH/set partition for multipartisan election) for two candidates is the familiar Boolean Majority Circuit whose leaves are the binary voters (and their VoterSATs in Majority+VoterSAT circuit composition). Pseudorandom shuffle of leaves of Boolean majority circuit simulates paper ballot which elides chronology. Pseudorandomly shuffled Electorate Leaves of the Boolean Majority Circuit are thus Ramsey 2-colored (e.g Red-Candidate0, Blue-Candidate1) by the candidate indices voted for. Pseudorandom shuffle and Ramsey coloring are at loggerheads - arithmetic progression order arises in pseudorandomly shuffled bichromatic electorate disorder and voters of same candidate are equally spaced out which facilitates approximate inference of voting pattern. Hardness of inversion in the context of boolean majority is tantamount to difficulty in unravelling the voters who voted in favour of a candidate - $\text{voters_for(candidate)}$ - pseudorandom shuffle of leaves of boolean majority circuit must minimize arithmetic progressions emergence which amplifies hardness of the function $\text{voters_for(candidate)}$.

10. Majority Versus Non-Majority Social Choice comparison arises from Condorcet Jury Theorem (recent proof of Condorcet Jury Theorem in the context of

Strength of Weak Learnability - Majority Voting in Learning theory - AdaBoost Ensemble Classifier - <https://arxiv.org/pdf/2002.03153.pdf>) and Margulis-Russo Threshold phenomenon in Boolean Social Choice i.e how individual decision correctness affects group decision correctness. Equating the two social choices has enormous implications for Complexity theory because all complexity classes are subsumed by Majority-VoterSAT boolean function composition. Depth-2 majority (Majority+Majority composition) social choice function - boolean and non-boolean - is an instance of Axiom of Choice (AOC) stated as "for any collection of nonempty sets X , there exists a function f such that $f(A)$ is in A , for all A in X ". Depth-2 majority (both boolean and non-boolean voters set-partition induced by candidate voted for), which is the conventional democracy, chooses one element per constituency electorate set A of set of constituencies X in the leaves, at Depth-1.

11. Intrinsic Merit Ranking can be defined as a MAXSAT problem. Random matrix based LSMR/LSQR SAT solver approximately solves MAXSAT in polynomial time on an average. Ranking of texts based on distance similarity is also a problem solved by collision-supportive Locality Sensitive Hashing - similar texts are clustered in a bucket chain.

12. Question-Answering/Interview Intrinsic Merit is a QBFSAT problem. Question-Answering is also a Linear or Polynomial Threshold Function in Learning theory perspective

13. Pseudorandom Choice is a Non-Majority Social Choice Function

14. Voter SAT can be of any complexity class - 3SAT, QBFSAT etc.,

15. Space Filling by circles is a vast area of research - Circle Packing. Parallel Circle Packing unifies three fields - Parallel Pseudorandom Generators (classical or quantum PRGs - ordinates on 2-D plane are generated in parallel and at random which is underneath most natural processes - including but not limited to Rain, Teapot Shards, Agriculture), 0-1 Integer Linear Programming and Circle Packing. Efficient parallel circle packing has computational geometric importance - geometric search where each circle is a query which might contain expected point - planar point location. Random Close Packing and Circle Packing are Constraint Satisfaction/SAT Problems. Polynomial packing which generalizes circle packing to arbitrary closed curves sparsely or closely packed on a surface finds applications in GIS analytics of Urban sprawl contour polynomials embedded on a space forming a finite multiply connected region - <https://www.sciencedirect.com/topics/engineering/simply-connected-region>. Closely packed Urban sprawl contour polynomials can be approximated by Voronoi diagram tessellation polygons (follows from Jordan curve theorem and Weierstrass theorem for approximation of a function by polynomials)

16. Intrinsic Merit is the equivalent of Intrinsic Fitness in Social Networks and Experiential learning is defined in terms of intrinsic merit and mistake bound learning. Recursive Lambda Function Growth Algorithm for creating lambda function composition trees from random walks of Definition Graphs of Text simulates Human Brain Connectomes. High Expander Definition Graphs are intrinsically better connected and meritorious because average links incident per vertex or sets of vertices is high from definition of Expander Graphs. This parallels Bose-Einstein Condensation in Networks in which least energy nodes attract most links. An algorithm for EventNet and ImageNet Graph based Intrinsic Merit for Large Scale Visuals and Audio has been described in AstroInfer Design Documents (EventNet Tensor Products Algorithm) and has been implemented in AstroInfer for the hardest Video Merit - Large Scale Visual Recognition Challenge (LSVR). Images can be ranked by Exact-Approximate Graph-Subgraph isomorphism percentage of their Voronoi facegraphs thus implementing an intrinsic merit image search engine.

17. Intrinsic Merit versus Perceived Merit and Non-Majority Versus Majority Social Choice are equivalent - Absolute Versus Subjective - and can be defined in terms of Mechanism Design/Flow Market Equilibrium in Algorithmic Economics. In Social Networks this is well-studied Fame Versus Merit Problem. Intrinsic Merit in the context of economies pertains to affixing value to commodities - the old school of labour theory of value (LTV) does not depend on perception in deciding value but only on labour involved in making a commodity while Demand-Supply pricing is a perception on the contrary: Demand or Fame for a commodity in effect is the result of perceived majority desire for a commodity - a majority voting for it. Market Equilibria (Eisenberg-Gale, Fisher et al)

which are the basis for Fame-Merit equilibrium assume equal demand and supply. Condorcet Jury Theorem which bounds correctness of majority decision and its later variants thus find importance in economics because CJT implies Nash equilibrium - or in other words labour theory of value might coincide with demand-supply curve as jurors (consumers constituting demand) minimize their mistakes and market corrections happen.

18. Money Changing Problem/Coin Problem/Combinatorial Schur Theorem for Partitions and Tabulation Hashing are equivalent i.e expressing an integer as a linear combination of products, which defines distribution of buckets in a hash table.

19. ThoughtNet/EventNet are theoretical reinforcement learning simulations of Cognitive Evocation, Cause-Effect ordering and events involving actors in Clouds. ThoughtNet is a (contextual multiarmed bandit and hypervertex intersection) Hypergraph which evokes thought/knowledge of maximum potential. Potential of thoughts/knowledge in Hypergraph is proportional to their intrinsic merit. Name ThoughtNet is a misnomer because it focuses only on evocation and doesn't exactly reflect human thought in its fullest power which is a far more complicated, less-understood open problem. Name ThoughtNet was chosen to differentiate between another evocation framework - Evocation WordNet (<https://wordnet.princeton.edu/sites/wordnet/files/jbj-jeju-fellbaum.pdf> - "...assigned a value of "evocation" representing how much the first concept brings to mind the second..."). Music Evoked Autobiographical Memories (MEAM) have been studied in the context of fMRI imagery of human brain and how areas of brain respond to music stimuli of varied genre. Music Evoked Autobiographical Memories can be explained by ThoughtNet model of thought evocation which is at present restricted to textual encoding of thoughts and storing them in ThoughtNet Hypergraph. Evocation WordNet already formalizes text evoked autobiographical memories. Along the lines of Text and Audio (Speech-Voice-Music) Evocation, following autobiographical memories could be postulated based on ThoughtNet:

19.1 Visual (Image or Video) evoked autobiographical memories of the past - Visuals thoughts are stored in ThoughtNet Hypergraph and evoked when a similar visual is seen by subject

19.2 People evoked autobiographical memories of the past - Memories of People are stored in ThoughtNet Hypergraph and evoked when similar events involving people are interacted.

20. Neuro Electronic Currency is an experimental, minimal, academic, fictitious cryptocurrency for modelling Intrinsic Merit and Optimal denomination in economic networks (AstroInfer and KingCobra repositories - Intrinsic and Market Equilibrium Pricing, Perfect Forward-Zero Copy Move e.g C++ move constructor https://en.cppreference.com/w/cpp/language/move_constructor, Google Cloud Object Move API - <https://cloud.google.com/storage/docs/renaming-copying-moving-objects#move>). EventNet is an economic network for Money Flow Markets/Trade. Intrinsic merit in economic network is the economic influence of each vertex in trade. Optimal Denomination Problem/Money Changing Problem/Knapsack Problem is an open research area in economics and theoretical computer science ([Kozen] - <https://www.cs.cornell.edu/~kozen/Papers/change.pdf>, <https://www.jstor.org/stable/2673933?seq=1>). Monetary transactions are events leaving a trail of causality footprints and could be formulated as Graphical Event Models and Causal Event Models including NeuronRain-native GEM implementation - EventNet. A minimal Global EventNet Graphical Event Model HyperLedger has been implemented for high frequency algorithmic trading of commodities in NeuronRain KingCobra as blockchain equivalent which include stocks and put-call derivatives forward tradings betting on a futuristic price of a commodity. High Frequency Trading platforms are prone to Order Flow Toxicity (insider information possessed by one party causing disadvantage to counter party) leading to a crash - Academic Research on Flash Crash of 2010 - https://en.wikipedia.org/wiki/2010_flash_crash#Academic_research. Neuro Cryptocurrency mining rig implements following Proof of Work algorithms of varying complexity classes:

20.1 BPP - Pseudorandom choice of Boost UUID Hashes of leading "ff" hexadecimal digits

20.1 BPP + P + MRC-NC + NP-Hard - Pseudorandom integer partition of an integer equalling the value of Neuro cryptocurrency is reduced to a Square

tile cover of a rectangle of area equal to value of Neuro cryptocurrency by Lagrange Sum of Four Squares Theorem reduction, Factor sides of the rectangle are found by Computational Geometric Factorization and factor sides of the rectangle are equated to 2 Money Changing Problem Frobenius Coin Diophantines solved as 2 Integer Linear Programs. Integer Partition to Rectangular Square Tile Cover reduction is a kernel lifting from 1 dimensional vector of partitions to 2 dimensional area.

21. Text sentences are Ramsey colored by Part-of-Speech tags and alphabet positions. Similarly graph representation of texts are Ramsey edge-colored by relations (e.g WordNet, ConceptNet relations). Text-graph complement to convert cliques to independent sets and vice-versa is a special application of Complement Functions. Coloring texts by vowel-consonant and alphabets creates 2-coloring and 255 coloring respectively and imply existence of monochromatic APs in texts. Vowel-consonant 2-coloring and vowelless string complexity are equivalent to Compressed Sensing sketches i.e extracted APs are sketches compressing text.

22. Shell Turing Machines are experimental novelty in definition of Turing computability which introduce dimension of truth as an additional parameter in addition to tapes, alphabets, head of tape etc., to simulate hierarchy of truths across dimensions E.g 2-D Turing Machine has no knowledge about concept of Volume which is defined only in a 3-D Turing Machine. This has similarities to Tarski Truth Undefinability - Object language versus Meta Language and parallels Goedel Incompleteness. Shell Turing machines have applications in intrinsic merit definitions in the context of word2vec embeddings of words in vector spaces. NeuronRain implements a word2vec embedding of academic publication bibliographies (bibliometrics) for originality merit measure. Colloquial example: Two Turing machines computing name of "Tallest building" on two vector spaces (or universe of discourses in First Order Logic) of different dimensions - "Country" and "World" - Country is a subspace of World - might return two different results though question is same. Formally, Shell Turing Machines have parallels to Turing Degrees which are measures of unsolvability of a set. Turing Degree is an equivalence class and two Turing machines X and Y have degrees defined by partial order $d(X) > d(Y)$ meaning X solves a more difficult set than Y. Essentially, Shell Turing machines defined over two vector spaces of two dimensions $d_1 > d_2$ can be construed as two machines of varying Turing degrees. Reduction from Turing degrees to Dimensions of Shell Turing Machines: Shell Turing machines defined on vector space of dimension $d+x$ have oracle access to a shell Turing machine on vector space of dimension d creating a Turing jump. Hilbert Machines defined on Hilbert Spaces, Eilenberg Linear Machines defined on vector spaces are examples of Shell Turing Machines - <http://citeseerx.ist.psu.edu/viewdoc/download?doi=10.1.1.36.73&rep=rep1&type=pdf> - "... The notion of a linear machine goes back at least 25 years to Eilenberg [14]. The basic idea is to base a machine (or automata) not just on a non-interpretable set of symbols but instead use a linear structure. That means, that the data this type of machines operates on are vectors in some vector space ..." , <https://www.nap.edu/read/10169/chapter/9#107> - "...One of my fonder memories comes from sitting next to Sammy in the early 1960s when Frank Adarns gave one of his first lectures on how every functor on finite-dimensional vector spaces gives rise to a natural transformation on the K-functor...". Shell Turing Machines go farther than mere embedding of Turing machines in a vectorspace - they delve into feasibility of exporting truth values of logical statements embedded in space S_1 to another space S_2 by linear transformations. There is a close resemblance between Shell Turing Machines and Category of Topological Spaces (Top) - https://en.wikipedia.org/wiki/Category_of_topological_spaces - Top is a category of topological spaces as its objects and morphisms are continuous functions (e.g computable by a Turing machine) amongst the topological space objects - Top formalizes a multiverse/universe in computational physics: Multiverse is a Top category of universes each of which is an object in Top category and linear transformations are morphisms amongst the universes - each morphism can be imagined as conduit Turing Machine exporting truth of logical statements between two universe topological space objects. TOP category abstraction of Shell Turing Machines has weird implication: For n-level nested kernel lifting by Conduit Turing Machines, truth values could be exported only upto (n-1) levels. There is no outward kernel

lifting from outermost TOP category space - Proof is by contradiction: If there is a lifting from biggest space to bigger-than-the-biggest space, bigger-than-the-biggest space dons the mantle of biggest TOP space (in other words, there is no exit possible from the biggest outermost shell - leaving it would imply entering a bigger shell, an anomaly).

23. Pseudorandomness and Random Close Packing are equivalent - a random close packing is generated by a pseudorandom generator e.g shaking a container of balls shuffles the centroids of balls at random. Cellular Automaton algorithm uses Parallel PRGs to simulate Filling of Space by random strewing of solids/liquids. Computational Chaos is a randomness source - <https://sites.google.com/site/kuja27/ChaoticPRG.pdf> (Deleted and Mirrored at https://github.com/shrinivaasanka/Krishna_iResearch_DoxygenDocs/blob/master/kuja27_website_mirrored/site/kuja27/ChaoticPRG.pdf) defines an RNC pseudorandom generator based on [Palmore-Herring] Chaotic PRG - <https://dl.acm.org/citation.cfm?id=71608>. Chaos Machines are randomness extractors for pseudorandom oracles -

https://en.wikipedia.org/wiki/Chaos_machine, Czyzewski Chaos Machine [2016] - <https://eprint.iacr.org/2016/468>, Merkle-Damgard construction - https://en.wikipedia.org/wiki/Merkle%E2%80%93Damgard%3A5rd_construction.

Conventional Buy-Sell monetary transactions create Money Trail EventNet Graphs whose edges are labelled by currency unique id(s)/commodities and vertices are any economic entity - people, financial instruments, institutions. Because of its sheer magnitude and unpredictability, Money Trail graph is a potential expander graph having least Cheeger constant (low eigenvalues, high regularity and less bottleneck) and thus a candidate for Expander Graph Random Walk Pseudorandom Generators e.g Blockchain Distributed Ledger (Bitcoin - [Satoshi Nakamoto]) is a consensus replicated money trail graph -

<http://documents.worldbank.org/curated/en/177911513714062215/pdf/122140-WP-PUBLIC-Distributed-Ledger-Technology-and-Blockchain-Fintech-Notes.pdf>

24. A random integer partition can be generated by a Pseudorandom generator. This extends the Partition-HashTable isomorphism to PRG-Partition-Hashtable transitive equivalence: PRG produces random partitions of integer, random partitions map to random buckets in tabulation hashing.

25. Computational Geometric Parallel RAM Factorization applies datastructures (e.g Parallel construction of segment trees/wavelet trees/interval trees/k-d trees) and algorithms (Planar Point Location, ray shooting queries) from Computational Geometry and Number Theory. Factorization in number theory is a multiplicative partition problem - Factorisatio Numerorum - as opposed to additive partitions. Quantum Computational version of Computational Geometric factorization has also been described in the context of quantum to classical decoherence. Computational Geometric Parallel RAM Factorization allocates $O((\log N)^k)$ arithmetic progression line segments (or a PSLG formed by a pixel array polygon) of a rasterized hyperbolic arc, to $O(N/(\log N)^k)$ PRAM-multicore processors which could be binary or interpolation searched in $O((\log N)^{(k+1)})$ or $O((\log N)^k \log \log N)$ parallel RAM time. Parallel Rasterization of hyperbolic curve which creates line segments of pixels from hyperbola in parallel could be performed by advanced GPU architectures - e.g NVIDIA CUDA - illustrations - https://research.nvidia.com/sites/default/files/pubs/2011-08_High-Performance-Software-Rasterization/laine2011hpg_paper.pdf.

26. Program Analysis is a converse of complement diophantine problem and is an approximation of Rice Theorem which ordains any non-trivial property of recursively enumerable sets is Undecidable

27. Software Analytics based on static and dynamic analyses (SATURN CFG/Valgrind CallGraphs/FlameGraphs/Points-to Graphs/FTrace) and applying Centrality/Graph Mining/Latent Semantic Indexing/Graph Edit Distance/Graph Isomorphism on them is a Program Analysis problem. Various Program Analyzers in userspace and kernelspace have been implemented in AstroInfer, USBmd and VIRGO linux kernel repositories which use Degree centrality, PageRank, Cyclomatic Complexity measures, Graph Isomorphism, Degree Sequence EMD Similarity among others. Some userspace usecases for Read-Copy-Update, Software Transactional Memory - Lockfree - synchronization have also been implemented for wrapping VIRGO32 and VIRGO64 kernelspace RPC cloud system calls. VIRGO32 and VIRGO64 linux kernels feature a kernelspace Bakery algorithm kernel driver

implementation for Cloud synchronization. GRAFIT course materials have some spillover analytics implementations and catechisms for classroom pedagogy - notable of them being Earliest Deadline First Worst Case Execution Time (EDF WCET Survival Index Timeout) OS Scheduler which depends on static code analyzers - IPET, CFG, SyntaxTree, LongestPath - or Master Theorem for WCET approximation.

28. Automated Debugging (e.g delta debugging, streaming common program state subgraphs) and Debug Analytics (finding minimum size program state automaton for isolating and resolving buggy code changes - finding and resolving bugs are two different problems because resolution of bug might necessitate major refactoring and rewrites) is a Software Analytics problem. Epidemics are modelled by Chaotic Strange attractors and Game theory (adversarial game between pestilence and infected) and Cybercrimes are epidemics infecting electronics. Software Analytics for Cybercrime forensics therefore have game theoretic reasoning (adversarial game between criminals and affected)

29. Set Partitions (Complementary Sets, LSH Partitions, Separate Chaining Hash tables, Histograms, Electronic Voting Machines etc.,) have a reduction to Space Filling/Packing by Exact Square Tile Cover of Rectangle from a fundamental result in number theory - Lagrange Four Square Theorem. This kind of square tile cover of a rectangle can be written as a non-linear quadratic programming optimization which solves integer factorization indirectly. Lagrangian Square Tiles are arranged in rectangle found by computational geometric factorization which is also an instance of NP-Hard exact Coin Problem/Money Changing Problem/Integer Linear Programming and polynomial time approximation problem by least squares (e.g LSMR). NeuronRain implements both Exact (CVXOPT GLPK Integer Linear Programming) and Approximate (LSMR least squares) reductions from set partitions to square tile cover by computational geometric factorization.

30. Computational Geometric Factorization by Parallel Planar Point Location rectifies a hyperbolic continuous curve to set of straightline segments as part of factorization which are searched. Each rectified segment is an arithmetic progression definable by an arithmetic progression diophantine or generating functions and set of these diophantines represent the exact cover (set of subsets) of points on rectified hyperbolic curve. Arithmetic progressions arise in Ramsey theory while arbitrarily coloring integer sequences. This rectification of a hyperbola by axis-parallel line segments is a union of arithmetic progressions.

31. Question-Answering Interview Intrinsic Merit as a threshold function (linear or polynomial) is related to an open problem in boolean functions - BKS conjecture. BKS conjecture predicts existence of a function which is more resilient or stabler than majority function. Stability is a measure of incorruptibility of a function. Question-Answering can also be formulated by a TQBF (Totally Quantified Boolean Formula) Satisfiability problem.

32. Category Theory is the most fundamental abstraction of mathematics. Morphisms and Functors of Categories on algebraic topological spaces can be formulated as Shell Turing Machines on some topological space defined on objects embedded in topological space.

33. EventNet Logical Clock which has been applied for EventNet Tensor Products merit of Large Scale Visuals can be formalised by Category Theory - as Event Categories and Morphisms amongst Actors with in an Event and Causation Functors across Events. EventNet causality has an unusual connection to one-way functions, Quantum computation and Bell non-locality of hidden variables (QM predicts Future influences Past - <https://www.sciencealert.com/quantum-physics-theory-predicts-future-might-influence-the-past-retrocausality>), Pseudorandom generators, Hardness amplification, $P \neq NP$ and Retrocausality/time reversal - EventNet causality DAG can be partitioned to past, present and future components by 2 cuts/vertex separators and if Retrocausality is false there exist atleast two one way future functions defined on the partition ($f_1(\text{past})=\text{present}$, $f_2(\text{present})=\text{future}$) which are hard to invert ruling out bidirectional time. Partitioning EventNet DAG into more than 2 disjoint components gives birth to multiple one way functions (not just 2) - for every vertex separated component triple (px, py, pz) of EventNet DAG partition two one-way future functions $f_1(px) = py$ and $f_2(py) = pz$ which are hard to invert could be defined - Falsification of Retrocausality and bidirectional arrow of time implies Hardness amplification. Tensor Decomposition of EventNet implies time has component basis similar to any vectorspace.

34. Shell Turing Machines have connections to Diophantine Equations - set of languages of all Shell Turing Machines cover the set of Recursively Enumerable languages and MRDP theorem equates Diophantine Equations and Recursively Enumerable sets. Relation between dimension of topological space of a Shell Turing Machine and (degree, number of unknowns) of its Diophantine representation is an open problem. Set Partitions to Lagrangian Four Square Theorem Tile Cover Reduction for Rectangle Square tile filling by Computational Geometric Factorization is a Shell Turing Machine Kernel Lifting from one dimensional partition space to 2 dimensional square tile cover space. Shell Turing Machines are universal category of topological spaces (TOP) abstractions for any computation in STEM(Science-Technology-Engineering-Mathematics) e.g. Support Vector Machine Kernels, Reproducing Kernel Hilbert Space (functions embedded in Hilbert space), Hilbert Quantum Machines, Linear Machines, Word Embeddings for BigData sets, NP-Hard Set partitions to Lagrange's Sum of Four Square Theorem Square tile cover Integer Linear Program 1 dimension to 2 dimension kernel lifting implemented in NeuronRain as Neuro cryptocurrency proof-of-work(POW).

35. ThoughtNet Modal Hypergraph Evocation Model and Randomized versions of Electronic Voting Machines/Integer Partitions/Set Partitions/Locality Sensitive Hashing/Linear Programs are instances of Coupon Collector Balls-Bins problem.

36. Conventional Search Engine Rankings are scalar total orderings while in reality two URLs may not be totally comparable which makes search results per query to be partial ordered sets - each URL is assigned a merit vector of features and one URL might be better in some feature dimensions and other URL in rest. Galois connections can be defined between partial ordered search results of two different queries. An exception to this is Zorn's Lemma which is equivalent to Axiom of Choice (AOC) stated as - "a partial ordered set containing upperbounds for every totally ordered subset of it (chain) has atleast one maximal element". Implications of Zorn's lemma and AOC for search engine results poset are immediate - maximal ranked element of the search query results exists if every totally ordered chain of the results poset have an upperbound which implies unique oneupmanship might arise. Search Engine Intrinsic Merit Rankings are as well instances of Envy-Free Multiple Agent Resource Allocation (MARA) or Fair Division problem - every URL is fairly rated.

37. Shell Turing Machines Kernel Lifting and their Category of Topological Spaces version are in a sense space filling gadgets e.g Each Shell Turing Machine is embedded in an n-sphere topological space bubble and Environment(Truth values) Kernel Lifting Export Morphisms are defined between them - visually a "Graph of Nested Pearls" or an n-dimensional nested Apollonian Gasket - Shell Topological space bubbles can be nested creating a tree of spaces.

38. Linear Programming formulation of Pseudorandom RNC Space filling is an algorithmic version of Berry-Esseen Central Limit Theorem - Sum (and Average) of random variables tend to Normal distribution.

39. Multiple variants of Computational Geometric Space filling algorithms mentioned in NeuronRain theory drafts are:

39.1 Pseudorandom space filling linear programming algorithm in RNC of a rectangle by ordinate points generated by parallel PRG or circles of small radii around them which simulates natural processes by Berry-Esseen Central Limit Theorem

39.2 Cellular Automaton space filling algorithm in NC which simulates natural processes. An one dimensional Chaotic Cellular Automata PRG has been implemented in NeuronRain

39.3 Random Closed Packing of balls in a container which is a Structural Topology problem

39.4 Constraint Satisfaction, Linear Programming, Circle Packing and Apollonian Gasket, Circle Packing Theorem for Graph Planarity, Thue's theorem, Kepler's theorem, Apollonian Networks - planar dual graphs of finite Apollonian Gasket (which has chromatic number ≤ 4 by Four Color Theorem)

39.5 Shell Turing Machines Category of Topological Spaces (TOP) which are non-nested and nested n-sphere shell spaces filling n-dimensional space having export Conduit Turing Machine morphisms amongst them, define hierarchy of environment of truths and linear transformation lifting between

spaces - Section 1228 of NeuronRain Design describes a Kernel lift random walk in tree of TOP Category Shell Turing Machines by UNIX Shell Tree Game Example.

39.6 Set partitions to Lagrangian Four Square Theorem square tile cover of rectangle sides of which are found by factorization

39.7 Set partitions to n-dimensional space cover by Chinese Remainder Theorem

39.8 Apart from monochromatic fillings above, Planar Multichromatic Filling (Coloring) of a Contiguous Disjoint Space Partition Cover is the most obvious byproduct of Four Color Theorem e.g Watershed algorithm for image segmentation which partitions an image into irregular multicolored segments. For every segmented image, there is a Voronoi tessellation available considering the centroids of the segments as points on a planar subdivision. Every Voronoi diagram of segmented image is a facegraph - facets of tessellation are faces of the graph containing segment centroids. Pareto efficient Multi Agent coloring of a Voronoi diagram facegraph has far reaching applications in Urban sprawl analytics, fair division, computational economics and multiple agent resource allocation(MARA). NeuronRain theory states (without implementation) a 4-color theorem based MARA for Urban sprawl analytics by analyzing facegraphs of segmented Urban sprawl GIS as 4-colored Residential, Commercial, Manufacturing-IT-ITES, Greenery faces. Naive areawise MARA for 4-colored segmented urban sprawls could be 25% each though standards mandate 33% area for greenery. Urban land use 4-coloring MARA has been formulated as MAXDNFSAT for maximizing number of arithmetic progression 4-colored facegraph walks encoded as DNF clauses, a problem known to be Fixed Parameter Tractable (FPT) - W[1]-Hard.

40. Algorithms for Problems of - *) Planar Point Location Computational Geometric Factorization in NC, Quantum NC and Randomized NC *) Hyperplanar point location for algebraic curves on arbitrary dimensional space *) Pseudorandom linear program space filling (e.g monte carlo sampling, cellular automaton, circle packing, random closed packing, set partition to lagrangian tile cover of rectangle by factorization and arbitrary n-dimensional space by Chinese remainder theorem) in Randomized NC which simulates many natural processes by Berry-Esseen Central Limit Theorem *) Vector space embedding and kernel lifting of intrinsic merit feature vectors in text, audio, video, people, econometric analytics *) Chaotic non-linear pseudorandom generators in Randomized NC *) Kernel lifting by Shell Turing Machine Category of Topological spaces and environment Export Morphisms amongst shell spaces - unify fields of Computational Geometry, Sorting, Geometric Search, Pseudorandomness, Chaos, Category Theory, Algebra, Set Partitions, Topology, Quantum Computation, Probabilistic Methods, Turing Degrees, Linear Programs, Formal languages, Software analytics, Kernels and Linear Transformations between vector spaces, Fame-Merit Rankings, Operating Systems theory, Parallel computing and theory of Nick's class.

41. Bibliometrics is the problem of intrinsic merit of academic publications - a machine learning alternative to peer-review and a subclass of broader textual merit. NeuronRain defines and implements SkipGram word2vec embedding of academic publications (BibTex). Every academic article proving a result could also be viewed as a set of first order logic statements as opposed to natural language text which abide by various Proof calculi - Sequent, ProofNets (Geometry of Interactions-GoI) - and conceptual distance between 2 publications could be derived from graph edit-distance between their ProofNet-GoIs. Proof entailments could also be represented as TOP Category of first order logic statements and morphisms among them (Quiver) which applies to any natural language text. Word2Vec embedding prepares the groundwork by embedding concepts - model for the FOL statements - in a topological space. Meaning representation (MR) could be done by translating a natural language text to Lambda Functions and First order logic statements. Recursive Lambda Function Growth algorithm in NeuronRain learns a lambda function composition via beta reduction from natural language texts.

42. Cellular Automaton Space filling algorithm which has Parallel PRG plane sweep and Increment Growth rule underneath it, has widespread applications in Chaotic modelling of natural processes, diffusion of memes, fads, pandemics, concepts and cybercrimes in a community. NeuronRain envisages a new random graph model based on 2-dimensional Cellular Automaton - CAGraph - which could be another social network model similar to Erdos-Renyi

Susceptible-Infected-Recovered, Susceptible-Infected-Susceptible random graph models. Logistic/Linear Regression models for diffusion could be inferred from CAGraph.

43. Universally Unique Identifier Generation is a challenge in Cloud Computing (Algorithms for UUID creation - RFC 4122 - <https://tools.ietf.org/html/rfc4122#section-4.3>). There are known vulnerabilities in RSA cryptosystem which could churn similar repetitive semiprime moduli for digital certificates of different users (<https://blog.keyfactor.com/the-irony-and-dangers-of-predictable-randomness>) and efficient integer factorization for RSA grade huge PKI semiprimes weakens ecommerce. Unique ID creation for NeuronRain VIRGO cloud system calls, Unique Identification in NeuronRain People Analytics and Boost UUID for NeuronRain KingCobra Neuro protocol buffer cryptocurrency depend on cloudwise unique ID creation.

44. In Social Networks and State issued Unique ID databases, Searching sorted unique id(s) is a daunting task and advanced search techniques - Fibonacci search, Interpolation search - are better suited to architectures having costly numeric division instruction sets. Fibonacci search and Interpolation search could also be used in place of binary search in Computational Geometric Factorization. Interpolation search assumes the range of the elements are predetermined and in Computational Geometric Planar Point Location Factorization, range of each tile segment/pixel polygon array/interval can be computed by elementary calculus thus enabling interpolation search which is $O(\log \log N)$. This implies local tile search optimization in factorization - which assigns $O((\log N)^k)$ segments to $O(N/(\log N)^k)$ PRAMs and each PRAM sequentially binary searches $O((\log N)^k)$ implicitly sorted tile arithmetic progressions - could be $O((\log N)^k \log \log N)$ an improvement from $O((\log N)^{(k+1)})$.

45. Finding Closest Pair of Points in a set of points is a Computational Geometric Problem and finds use in Air and Sea Vehicle Collision Avoidance. Theoretically if strings are embedded in a vectorspace of alphabets finding closest pair of string points is an edit distance alternative. Finding closest pair of points is a perfect fit for People Analytics if People profiles are points on a vectorspace - particularly for measuring extent of how much crowd flocks to a social profile vertex, distances of neighbours and its resultant impact on spread of memes, gossips and even cybercrimes/pandemics.

46. Almost every BigData set is multidimensional and could be formalized by Tensors - EventNet Logical Clock for Causality in Cloud, Video EventNet Tensor Products for Merit of Large Scale Visuals having EventNet Logical Clock underneath, Alphabet-Syllable Vectorspace Embedding of Textual strings, People Profiles for Social Network, Human Resource and Talent Analytics are implemented as Tensors in NeuronRain.

47. Finding distance between two tensors of unequal dimensions is a non-trivial problem e.g. Computation of distance between two String Syllable Hyphenated 2D Tensors of unequal rows and columns - $[[\text{"ten"}], [\text{"sion"}]]$ and $[[\text{"at"}], [\text{"ten"}], [\text{"tion"}]]$ - requires histogram distance measures (Earth Mover Distance, Word Mover Distance, ...) because each syllable hyphenated string is a histogram set-partition of the string and each syllable is a bucket. Conventional Edit Distance measure for two strings is 1-dimensional and does not give weightage to acoustics while Earth Mover Distance between two Syllable hyphenated strings is 2-dimensional and more phonetic. In complexity theoretic terms, bound for edit distance is quadratic while Earth mover distance is cubic though there are recent linear complexity EMD and WMD approximation measures - LC-RWMD - Linear Complexity Relaxed Word Mover Distance - <https://www.ibm.com/blogs/research/2019/07/earth-movers-distance/>, <https://www.ibm.com/blogs/research/2018/11/word-movers-embedding/>. Subquadratic string distance measures if reduced to edit distance imply SETH is false. Closest Pair of N Points algorithm in Computational Geometry is subquadratic $O(N \log N)$ which could be applied to syllable hyphenated String tensor point sets. Towers of Hanoi Problem concerns hardness of moving a single bucket histogram of disks (Animation: <http://towersofhanoi.info/Animate.aspx>) sorted by descending radii bottom-top to itself preserving sorted order always (Fixed point computation) and only exponential time ($2^N - 1$ for N disks) algorithms are known for it. Weird counterintuitive fact about Towers of Hanoi: Earth mover distance upon completion of aforementioned exponential number of fixed point

moves is 0 - Histogram remains identical after complete move though partial intermediate moves (require minimum 3 single bucket histograms of sorted order) could have Earth mover distance > 0 - or Sequence of EMDs between 3 histograms sinusoidally fluctuates over time for $2^N - 1$ moves before eventually reaching 0 (3 histograms unite to 1), a feature strikingly reminiscent of Collatz conjecture. Towers of Hanoi is NP-Hard (Every problem in NP is polytime many-one reducible to Towers of Hanoi) but not known to be in NP (no NP algorithm has been found). Technically, NP-Hard class is unaffected irrespective of $P \neq NP$ or $P = NP$ - https://en.wikipedia.org/wiki/NP-hardness#/media/File:P_np_np-complete_np-hard.svg. Previous reduction from Towers of Hanoi histograms to EMD sequence is a #P-Complete parsimonious reduction bijection preserving number of solutions -

https://en.wikipedia.org/wiki/Parsimonious_reduction#Examples_of_parsimonious_reduction_in_proving_#P-completeness. Towers of Hanoi and other problems in NP-Hard class and #P-Complete problems are thus obvious choice for cryptocurrency proof-of-work (POW) as the hardness (or labour value) of cryptocurrency is insulated from and independent of $P \neq NP$ or $P = NP$. NeuronRain implements Towers of Hanoi (Single Bin Sorted LIFO Histogram) NP-Hard problem as Neuro Cryptocurrency Proof-Of-Work, a harder alternative to NP-Complete ILP Proof-Of-Work.

48. Graph Edit Distance (GED) is the most fundamental clustering similarity measure which pervades Text-Audio-Visual-People Graph Analytics and Program Analyzers in NeuronRain. Graph Edit Distance generalizes String Edit Distance - every String (and thus Text) is a connected, directed acyclic graph of maximum degree 1 and alphabets are its vertices. Graph Edit Distance between EventNet of a Video and ImageNet ImageGraphs of Images quantifies visual similarity. Graph Edit Distance between weighted automata of two music clips differentiates music (In theory, automata can be checked for equivalence by Table filling algorithm) while GED between Speech-to-Text textgraphs measures audio similarity. Graph Edit Distance between Social Community Graphs, Connections Graph and proper noun filtered (e.g dictionary filter) Textgraphs of People Profiles measures People similarity. Graph Edit Distance between Control Flow Graphs from SATURN, Program Slice Dependency Graphs, FTrace Kernel callgraphs, Valgrind/KCacheGrind/Callgrind userspace callgraphs identify similar codeflow and malwares. While Graph Isomorphism finds similar graphs by vertex relabelling (Exact Graph Matching), Graph Edit Distance generalizes to dissimilar graphs (Inexact Graph Matching).

49. Transformers are recent advances in Text analytics - NeuronRain Textgraph implementations for Recursive Lambda Function Growth and Named Entity Recognition extend transformers to textgraph vertices degree attention for inferring importance of word vertices of textgraphs. A Question-Answering Bot has been implemented in NeuronRain which takes natural language questions from users and queries wikipedia corpus for answer summary to create a rephrased deep-learned natural language answer by WordNet walk on edges chosen based on top percentile Transformers Degree attention Query-Key-Values from wikipedia summary textgraph.

50. Graphical Event Models (OGEM, PGEM) decipher graph dependency amongst timeseries of real life events (politics, economic and other bigdata streams). EventNet theory and implementation in NeuronRain is a Graphical Event Model for interevent and intraevent actor-model causality. EventNet Tensor Product algorithm for Videos is a Graphical Event Model based on ImageNet for extracting dependencies between frames (Video is a timeseries stream of frames). EventNet Graphical Event Model (GEM) is a 2-dimensional Tensor of interevent and intraevent causalities. Probabilistic EventNet GEM can be learnt from timeseries of events (news articles on socioeconomics and politics) - Learning Bayesian model GEM on example timeseries datasets is described in <http://www.contrib.andrew.cmu.edu/org/cfe/simplicity-workshop-2014/workshop%20talks/Meek2014.pdf>. Tensor Decomposition of EventNet GEM (decomposition of a Tensor into sum of rank-one product tensors - <https://www.kolda.net/publication/TensorReview.pdf>) has enormous implications for timeseries causality - real life event causalities in Tensor notation could be classified into linearly independent low rank tensor components.

51. Digital Watermarking overlay of segmented large scale visuals is in a sense a primitive image classifier - vertices of facegraphs of similar segmented images when overlayed on one another are highly superimposed and isomorphic (and

thus a measure of similarity) creating a multiplanar graph in which each vertex is a stack - a visual version of ThoughtNet.

52. Integer Partitions and String complexity measures are related - Every string is encoded in some alphabet (ASCII or Unicode) having a numeric value and thus every string is a histogram set partition whose bins have sizes equal to ASCII or Unicode values of alphabets which partition the sum of ASCII or Unicode values of constituent alphabets of a string. This enables partition distance (a kind of earth mover distance - e.g. Optimal transport and integer partitions - <https://arxiv.org/pdf/1704.01666.pdf>) between string histograms as a distance measure between strings apart from usual edit distance measures.

53. Byzantine Fault Tolerance (BFT) has theoretical implications for mitigating faults including cybercrimes in electronic networks and containment of pandemics in social networks modelled by Cellular automaton graphs.

54. Economic Merit - fluctuations in economy and stock markets are modelled by Chaotic multifractals wherein single exponent is not sufficient and behaviour around any point is defined by a local exponent. NeuronRain envisages Collatz conjecture model of market vagaries which is a 2-colored pseudorandom sequence of odd and even integers always ending in 1.

55. Graph theory originated from an urban sprawl analytics problem - Euler circuit and Closed trail of Seven bridges of Königsberg. Variety of Urban sprawl metrics could be derived from FaceGraph of segmented GIS imagery - Built-up area (impervious surface (IS) land cover derived from satellite imagery), Urbanized area (built-up area + urbanized open space (OS)), Urbanized OS (non-IS pixels in which more than 50% of the neighborhood is built-up), Buildable (does not contain water or excessive slope), Urban footprint (built-up area + urbanized open space + peripheral open space), Peripheral OS (non-IS pixels that are within 100 meters of the built-up area), Open space (OS - the sum of the urbanized and peripheral OS) (from URBAN SPRAWL METRICS: AN ANALYSIS OF GLOBAL URBAN EXPANSION USING GIS - [by Shlomo Angel , Jason Parent , Daniel Civco] - Table 3 of metrics for measuring urban extent - <https://citeseerx.ist.psu.edu/viewdoc/summary?doi=10.1.1.586.5052>). Polya Urn Urban Growth Model (which simulates the growth of new segments along periphery of urban sprawl facegraph by Rich-get-richer preferential attachment) and DNFSAT MARA arithmetic progression n-segment coloring of all-pair walks in facegraph (which is a Constraint Satisfaction Problem for interior of urban sprawl facegraph) together stipulate a stringent condition for exterior and interior of urban area (and often less satisfiable theoretical fancy because DNFSAT MARA mandates that the segments of same color are equally spaced-out by arithmetic progression hops as interior segments change and new segments along urban sprawl periphery are attached by Polya Urn process dynamically) for equitable and sustainable urban growth - for instance arithmetic progression 4-coloring of facegraph all-pair walks is disturbed when interior segments develop and new segment faces from Polya Urn growth are added to periphery (Example: openness, urbanness, infill, extension, leapfrog, reflectance, urban fringe, ribbon development, scatter development segmentation of Bangkok metro area - https://proceedings.esri.com/library/userconf/proc08/papers/papers/pap_1692.pdf) of urban sprawl facegraph and 4-coloring has to be recomputed causing re-classification of few segments. Earlier instance of DNFSAT MARA by arithmetic progression coloring of facegraph walks is just one example of how MARA could be implemented in urban sprawls and DNFSAT could be derived from any other arbitrary constraints on graph complexity measures that are satisfiable in practice. Real-life problems of urban areas are solvable by vertex cover, edge cover, maxflow-mincut, leaky bucket model of traffic, strongly connected components, dense subgraphs of transportation network graphs aiding efficient drone navigation. NeuronRain implements ranking of Urban Sprawls from segmented Contour polynomial areas bounding urban sprawls based on NASA VIIRS NightLights imagery which is a polynomial variant of Space filling problem usually limited to Packing by Circles and Chaotic Mandelbrot set curves. Delaunay triangulation graph of SEDAC and VIIRS Urban sprawl contours approximates transportation graph and could be an estimator of Euler Circuit and Hamiltonian for efficient drone navigation. Design of Urban transportation networks could be formulated by a reduction from Global wiring and Detailed wiring 0-1 Integer Linear Programming NP-Hard problems mostly used to solve layouts in logic gate arrays in chip design - [Randomized Algorithms - Rajeev Motwani and Prabhakar Raghavan -

Section 4.3 - Pages 79-81 - simplified for nets containing at most one 90 degree turn and each net is an optimal path-to-be-found connecting two logic gates]: Edges of urban transportation networks are carriageways (wires) connecting two urban centres or two suburbs within an urban centre (logic gate vertices) and number of turns in each carriageway and their angles are indefinite. Finding optimal layout of transportation network carriageways for unrestricted turns is harder than one 90 degree turn version, in which case multi-turn carriageway could be approximated by multiple one 90 degree turn segments and encoded as 0-1 linear program variables - monotonic walks on lattice grids (random walk from bottom-left to top-right on $m \times n$ grid) are of multiple 90 degree turns which could approximate unrestricted-angle-and-multiple-turn carriageways connecting 2 urban centres. Optimal alignment of a carriageway could be its monotonic random walk (multiple 90 degree turn) approximation of least root mean square error between turn points on lattice walk and straightline connecting 2 urban centres (Illustration:

<https://www.statisticshowto.com/probability-and-statistics/regression-analysis/rmse-root-mean-square-error/>). Public transit data (daily transport patterns) are available through OpenStreetMap PTNA - <https://ptna.openstreetmap.de/>. On the other hand, pedestrian networks are as important as transportation networks. There have been some recent Pedestrian network construction algorithms based on inputs from GPS Traces feature of OpenStreetMap (<https://www.openstreetmap.org/traces>) for inferring pedestrian geometric patterns -

<https://www.sciencedirect.com/science/article/abs/pii/S0968090X12001179>

56. Quantum Circuits in Deutsch Model could be translated to classical Parallel RAMs by Memory Peripheral Model which maps quantum circuits to PRAM instruction set -

https://uwspace.uwaterloo.ca/bitstream/handle/10012/16060/Schanck_John.pdf. This bridges a missing link between Quantum and Classical computations which might resolve lot of conflicts involving derandomization of Shor BQP Factorization to P and NC, Classical PRAM-NC-BSP and Quantum NC Computational Geometric factorizations described and implemented in NeuronRain.

57. In NeuronRain complement implementation, Complement Diophantines are learnt by Least Squares and Lagrangian interpolations which are total functions while Lagrange Four Square Theorem complement map is a partial surjective function (not all domain tuples are mapped to a point in complementary set)

58. MapReduce cloud parallel computing framework (on which Hadoop, Spark are based) has separate complexity class MRC (MapReduce Class) defined for itself:

58.1 [Karloff-Suri-Vassilvitskii] -

<http://theory.stanford.edu/~sergei/papers/soda10-mrc.pdf> - Section 4.1, Theorem 4.1 and Theorem 7.1. DMRC is a generic version MRC which allows deterministic randomization (Las Vegas algorithms which always return correct answers). Most problems in NC are in DMRC but converse is not true unless $NC=P$. CREW PRAM algorithms can be simulated by MapReduce class (MRC). Thus NeuronRain MapReduce implementations including Spark Computational Geometric Factorization and Recursive Gloss Overlap Interview Algorithm for intrinsic merit are in MRC though the computational geometric factorization algorithm is in NC-PRAM-BSP which is a limitation of Cloud computing and MapReduce software though Supercomputers running proprietary software might be in exact NC e.g Fugaku Supercomputer - <https://www.bnl.gov/modsim2019/files/talks/SatoshiMatsuoka.pdf> - ARM - Exascale - Petaflop. It is known that $SAC=NC=AC=TC$ or Nick's Class-Bounded Fanin, Semi-unbounded Fanin, Unbounded Fanin and Threshold Circuits (made of Majority gates - theoretical formalism of Neural networks) are equivalent - http://users.uoa.gr/~glentaris/papers/MPLA_thesis_lentaris.pdf - and thereby Neural Networks can compute Integer Factorization in parallel, an unusual connection between Number Theory and Machine Learning (or Factorization is computationally learnable from training data).

58.2 [Fish-Kun-Lelkes-Reysin] - class of regular languages (and all of sublogarithmic space) is in constant round MRC - https://www.researchgate.net/publication/266376763_On_the_Computational_Complexity_of_MapReduce/link/56cc71e908aee3cee54375d6/download.

58.3 Simulating BSP+PRAM in MapReduce -

<https://www.cs.utah.edu/~jeffp/teaching/cs7960/L18-MR-simulate.pdf>

58.4 Complexity Measures for Map-Reduce and Comparison to Parallel Computing - <https://users.cs.duke.edu/~kamesh/mapreduce.pdf>

58.5 Efficient Circuit Simulation in MapReduce - [Fabian Frei-Koichi Wada] - <https://arxiv.org/pdf/1907.01624.pdf> - "... Relying on the standard MapReduce model introduced by Karloff et al. a decade ago, we develop an intricate simulation technique to show that any problem in NC (i.e., a problem solved by a logspace-uniform family of Boolean circuits of polynomial size and a depth polylogarithmic in the input size) can be solved by a MapReduce computation in $O(T(n)/\log n)$ rounds, where n is the input size and $T(n)$ is the depth of the witnessing circuit family. Thus, we are able to closely relate the standard, uniform NC hierarchy modeling parallel computations to the deterministic MapReduce hierarchy DMRC by proving that $NC_{i+1} \subseteq DMRC_i$ for all $i \in \mathbb{N}$..." - NC circuit of depth $O((\log N)^{i+1})$ is in $DMRC_i$ which is an improvement over 58.1. Computational Geometric Factorization Spark MapReduce implementation in NeuronRain is of polylogdepth or runtime $O((\log N)^{k+1})$ and thus in $NC^2=DMRC_1$ for $k=1$. Due to this result, underlying parallel hardware model (Multicore-PRAM-BSP-logP) is abstracted and MapReduce frameworks are sufficient to implement NC.

58.6 Sorting, Searching, and Simulation in the MapReduce Framework - [Goodrich-Sitchinava-Zhang] - <https://arxiv.org/pdf/1101.1902.pdf> - "... Lemma 4.3: Given a set X of N indexed comparable items, we can sort them in $O(\log M(N))$ rounds and $O(N^2 \log M(N))$ communication complexity in the MapReduce model. ..." - Computational Geometric Factorization implemented in NeuronRain is a Parallel Planar Point Location Binary Search algorithm which does not require sorting as every rectified hyperbolic arc segment is locally binary (or interpolation) searched. Even if sorting is necessary, by this result, factors could be found in $O(\log M(N) + \log N)$ time having an additional sequential binary search overhead after sorting.

59. Almost all Autonomous Drone Delivery Problems including Drone Electronic Voting Machines, Online Shopping Delivery, Autonomous Combat Drone Swarms are NP-Complete which have to navigate along Hamiltonians optimally on surface and aerial transportation graphs. NeuronRain theory describes a Graph Masking Drone Obstacle Avoidance algorithm by dynamically overlaying segmented (convexhull) weather GIS imagery on terrestrial transportation graph for weather obstacles which is crucial for faultless delivery of payload carried by drones. Graph Masking which is a computational geometric planar intersection problem of graph and convex hull polygons, removes (or masks) subgraphs below aerial weather obstacles (e.g cloud) from transportation graph thereby creating a stripped-down topologically punctured transportation graph which bypasses weather obstacles. Optimal best route in this masked transportation graph could be found by A* Best First Search Robotic Motion Planning algorithm. Segmenting wind speed and temperature obstacle convex hulls from Weather GIS imagery is non-trivial because of high fluidity of atmosphere. Obstacles for UAVs are two fold - Natural (Inclement weather, Mountains) and Artificial (Man-made structures). Artificial obstacles can be avoided by choosing airstrip directly above surface transportation graph edges (Road network) as airspace above roads is usually free of obstacles and structures except interchanges which could be bypassed by raising drone altitude to atleast the maximum height of the structures. Natural obstacles (Rains, Wind, Heat) are not so obvious to tackle - Though cloud formations in Weather GIS are somewhat static and can be bounded by convex hull polygon boxes, segmenting wind and heat obstacle convex hulls requires sensors transmitting wind speed and temperature either from Satellite GIS or from points on Road network. Gathering wind and heat data along the points on transportation graph minimizes number of sensors. Onboard sensors in Drones for wind and heat may not be sufficient because drone has to learn obstacle data which are located at some distance ahead from drones so as to backtrack and realign the mission trajectory. Obstacle Avoidance Algorithms in Drone Navigation apply as well with some modifications to Advanced Driver Assistance Systems (ADAS) for self-driving surface transport automobiles (e.g lane detection, collision detection). An example primitive self-driving collision detection algorithm for LIDAR sensor and GPS based ADAS (requires a realtime OS kernel for low response time - a primitive C++ and Python usecase for LIDAR PCD generated obstacle-free lattice walks has been implemented in NeuronRain AstroInfer-Grafit repositories - Sections 1294 and 1302 - obstacles

in lattice have been marked based on LiDAR data):

while destination not reached:

{

(*) Find obstacles and their distances within a 3D spherical volume (3D grid) of constant clearance radius (e.g of few meters) centered around the vehicle from LIDAR sensor inputs (This spherical 3D volume dynamically moves as vehicle at its center is driven)

(*) Transportation network carriageways are instances of wiring problem and can be approximated by multiple 90 degree turn lattice walks on 2D grid extensible to 3D lattice grid. An optimal lattice walk minimizes root mean square error between GPS map route connecting source and destination and the actual multi-turn lattice walk trajectory of the vehicle.

(*) Compute the most optimal multiple-90-degree-turn lattice walk fragment within the clearance 3D grid volume which does not intersect with obstacles sensed by LIDAR. Vehicle is driven along this obstacle-free lattice walk fragment. If there is an intersection vehicle stops or waits till such an obstacle-free lattice walk fragment is found.

(*) Recompute 3D clearance volume for new location of the vehicle - Frequency or duration between successive computations of 3D spherical lattice walk grid must be less than (radius of the 3D spherical grid / maximum vehicular velocity) e.g for maximum velocity of 100 km/h and 10 metre radius 3D grid, frequency = $20/100000 \times 3600 = 0.72$ seconds (for 20 metre diameter).

}

60. Two Set Partitions are classified as Complementary Partitions or Connected Partitions if their least upperbound is the unpartitioned set - <https://royalsocietypublishing.org/doi/pdf/10.1098/rspa.1988.0018> . There is another definition of Category Theoretic Complementary Set Partitions which finds use in Deep Learning Recommender Systems and Computational advertising - <https://arxiv.org/pdf/1909.02107.pdf> - each pair of elements of partitioned set S are distinguished (present in different equivalence classes of partition sets) by atleast one partition. Conjugate Partitions are kind of complementary set partitions whose Ferrer Diagrams are inverted along diagonal (rows and columns of Ferrer Diagram are interchanged) - [https://en.wikipedia.org/wiki/Partition_\(number_theory\)#Conjugate_and_self-conjugate_partitions](https://en.wikipedia.org/wiki/Partition_(number_theory)#Conjugate_and_self-conjugate_partitions). NeuronRain definition of complementary set partition differs - Set Partition S is complementary to Set Partition S' if there exists an equidepth (all buckets have equal size) set partition E and $E / S = S'$. E, S and S' have same number of buckets and buckets of S' fill the buckets of S to make rectangular equidepth E. Complement of Set Partition version of boolean majority function (2 buckets for votes to 0 and 1) is another boolean majority set partition function inverting the output. In other words, complementary set partitions S, S' split an equidepth partition E into two and each of the complementary set partitions S and S' could be written as equidepth partitions by rearranging items in buckets. Example of NeuronRain definition of Complementary set partitions:

| | | |
|----|---|----------------|
| | | 1 2 3 |
| S | = | 6 7 8 9 |
| | | 11 12 |
| | | 4 5 |
| S' | = | 10 |
| | | 13 14 15 |
| E | = | 1 2 3 4 5 |
| | | 6 7 8 9 10 |
| | | 11 12 13 14 15 |

size(E) = $3 \times 5 = 15 = \text{size}(S) + \text{size}(S') = 9 + 6$

size(S) = 9 which can be rearranged to an equidepth partition as 3×3

size(S') = 6 which can be rearranged to an equidepth partition as 2×3

For 20 voters indexed by integers 1 to 20:

| | |
|--------|-------------------------------|
| E = 0: | 1 2 3 4 5 6 7 8 9 10 |
| 1: | 11 12 13 14 15 16 17 18 19 20 |

Set Partition version of Boolean Majority (0 wins):

S = 0: 1 2 3 4 5 6

1: 11 12

Set Partition Version of Complementary Boolean Majority (1 wins):

S' = 0: 7 8 9 10

1: 13 14 15 16 17 18 19 20

61. NeuronRain theorizes and implements multiple Logical clocks for (unidirectional and bidirectional) Timeout and Graphic Event Models-Causal Event Models:

61.1 EventNet GEM Tensor - a Graphical Event Model of events and actors per event for capturing Causality relationship between events on Cloud (e.g Money Trail - Monetary Transactions, Causality between frames of video in Large Scale Visuals). EventNet logical clocks do not rule out cycles and retrocausality and can be decomposed as linear function of Tensor component basis implying time could be multidimensional similar to any topological space.

61.2 Survival Index Based Timeout for OS Schedulers - Unidirectional (Downward clockticks) Dynamic Hashing based Process Timeout mechanism for OS Scheduler - derived from an earlier proprietary Survival Index Transaction Timeout Manager (Sun Microsystems-Oracle: patent pending) implemented in iPlanet Application Server (iAS) now opensourced as Eclipse GlassFish and Oracle GlassFish - <https://projects.eclipse.org/proposals/eclipse-glassfish>, <https://www.oracle.com/middleware/technologies/glassfish-server.html>

61.3 Expirable C++ Objects - Reference Counting of objects (mostly images and Neuro currencies) which is a bidirectional logical clock of increment and decrement (Upward and Downward clockticks) - Object is reaped by Garbage collector when refcount reaches 0. Collatz conjecture defined as: $\{x(n+1) = x(n)/2 \text{ if } x(n) \text{ is even and } 3x(n) + 1 \text{ if } x(n) \text{ is odd and } \{x(n)\} \text{ sequence always ends in 1}\}$ is a bidirectional clock and might be useful to simulate lifetime reference count (trajectory of ups and downs) of an object. EMD sequence for Towers of Hanoi intermediate computations mentioned earlier (47) is a Collatz-like sequence of exponential number of elements terminating always in 0 and could be another instance of bidirectional refcount clock.

61.4 KingCobra Atomic Transactional Refcounting within linux kernel for cloud RPC - reference count of an object is globally persisted within move semantics - For an object move over VIRGO64 cloud kernelspace RPC, sender decrements global refcount of object and receiver increments its global refcount within an atomic transactional block - requires XA transactional Linux kernel supporting 2-phase commit. An example Userspace Distributed Reference Counting framework - Ray Actor Model - <https://docs.ray.io/en/master/ray-core/memory-management.html> - maintains a global ledger of objects, ip-addresses and processes holding references to those objects.

62. Factorization and Multiplication (Mutual Nick's Class reducibility of Division, Multiplication and Iterated integer addition - [Beame-Cook-Hoover] Theorem - Wallace Tree Circuits and FFTs - <https://courses.cs.washington.edu/courses/cse532/08sp/lect08.pdf>) are mutual inverses - Efficient circuits for linear complexity integer multiplications have been devised making room for the possibility of efficient factorization e.g Russian Peasant or Egyptian multiplication example multiplication of $101 * 115 = 11615$ is a tableau of 2 columns that could be written as product of factor and sum of exponents of 2 (Right columns in Rows of odd Left columns are added) - Tableau is of size $O(\log(\text{factor}))$:

| | |
|-----|--------|
| 101 | 115 + |
| 50 | 230 |
| 25 | 460 + |
| 12 | 920 |
| 6 | 1840 |
| 3 | 3680 + |
| 1 | 7360 + |

Last row of the tableau always ends in 1 and right column is of the form $115 * (1 + 2^2 + 2^5 + 2^6)$ [a decimal factor multiplied by another binary factor written as exponential sum - 110011 is the binary for 101]. Hardness of inverting the tableau bottom-up (to get the factors) involves a non-trivial efficient guessing (from number theory estimates - quite similar to number theoretic ray shooting query optimization in NC-PRAM-BSP-Multicore NeuronRain

Computational Geometric Factorization) of bottom row-right column(7360 above) and reversing the computation from bottom to top - Irreversibility of the tableau might imply an One-Way function and Hardness amplification.

63. Reduction could be arrived at between Question-Answering algorithms to compute Merit() function in non-boolean setting and Query complexity in classical and quantum boolean setting by defining Question-Answering as a Query complexity problem of computing function Merit($q_1, q_2, q_3, \dots, q_n$) of an entity (People-Audio-Visuals-Texts) by series of queries - set of ordered pairs $\{(q_i, a_i)\}$ of Question variables $q_1, q_2, q_3, \dots, q_n$ and respective answer values $a_1, a_2, a_3, \dots, a_n$. Query complexity model unifies all theoretical models of Question-Answering earlier by LTF, PTF, TQBF and Switching circuits. Adaptive Question-Answering which dynamically changes future questions depending on answers to past questions is Discrete Time Markov Chain wherein Question(n) depends on (Question($n-1$), Answer($n-1$)) and every adaptive Interview is a traversal from root-to-leaf of a decision tree whose vertices are questions and branching to a subtree of a question(n) is chosen depending on answer(n) to question(n). Generalized $N \times N$ version of Chess is PSPACE-complete though limited 50-move version of Chess is not - Alternating Questions and Answers simulate role of alternating moves by two players in Chess - interrogator and respondent. Decision tree or Game Tree (https://en.wikipedia.org/wiki/Game_tree) in 50-move Chess is of depth 50 and for maximum of m possible configurations per move (known as branching factor), size of Game tree is $(m^{50}-1)/(m-1)$. AI Chess Engines solve Game tree by a minimax algorithm which predicts or looks-ahead certain number of moves (also known as "plies" - Deep Blue look ahead was 12) and alpha-beta pruning to maximize gain. Most games including Chess, Go, Hex, Generalized Geography among others have been shown to be PSPACE-complete in $N \times N$ versions by reduction from TQBF where formula could be an AND-of-OR - <https://people.csail.mit.edu/rrw/6.045-2020/lec21-color.pdf>. Of these Generalized Geography (which is about player2 trying to name geographic location which starts from last letter of previous name uttered by player1) fits well into adaptive Question-Answering as present geographic location (or a question(n) from player2) name depends on previous name (or answer($n-1$) from player1) effectively reducing Question-Answering to an adversarial game alternated between two players. Multiple choice Question-Answering are easier to formulate as TQBF than open-ended Question-Answering - Threshold Circuits, LTFs and PTFs are theoretical models of Two Choice (Boolean Yes-No) Question-Answering. TQBF Chess reduction earlier is an OR of limited multiple choices a player could make per move (Questions are move choices made by player1 and Answers are countermove choices made by player2 in response to player1 at round N), ANDed for all moves. Primitive automated Question-Answering could be devised by Recursive Lambda Function Growth and Recursive Gloss Overlap Meaning Representation Algorithms which extract a TextGraph from natural language texts - Dense subgraphs and high degree vertices of textgraphs for a "Question" (which are the crux of the question) obtained from these algorithms could be searched in a background intelligence database (search engine) and the text results could be unified into an "Answer" textgraph by Recursive Lambda Function Growth and Recursive Gloss Overlap algorithms. Multiple Choice Question-Answering could be simulated by Two-Choice Boolean Question-Answering gadgets - LTFs, PTFs and TQBFs - by allocating one LTF, PTF or TQBF per binary digit of the decimal answer choice. For example, usual Four-Choice Question-Answering convention followed by Admission Tests to educational institutions could be simulated by 2 LTFs, PTFs or TQBFs encoding 4 answer choices - 0(00), 1(01), 2(10), 3(11) - LTF1 example: $a_{11}x_{11} + a_{12}x_{12} + \dots + a_{1n}x_{1n}$, LTF2 example: $a_{21}x_{21} + a_{22}x_{22} + \dots + a_{2n}x_{2n}$. For answer choice 4 for question 1, x_{11} and x_{21} are set to 1 to get binary string 11 corresponding to decimal 4. Such Admission Tests, which are non-STEM (e.g Medicine, Language), could be solved by a Question-Answering Bot which searches a corpus and matches the open-ended answer with one of the choices (similar to one implemented in NeuronRain for open-ended natural language answers). STEM Admission Tests require solving a given mathematical problem for which querying a corpus may not be sufficient. There are sensitivity upperbounds available for Polynomial Threshold Functions (PTFs) which are defined as $f(x_1, x_2, \dots, x_n) = \text{sign}(\text{Degree } d \text{ polynomial on } x_1, x_2, \dots, x_n)$ thanks to result by [Harsha-Klivans-Mekha] - Bounding the Sensitivity of Polynomial Threshold Functions -

<http://theoryofcomputing.org/articles/v010a001/v010a001.pdf>,
https://booleanzoo.weizmann.ac.il/index.php/Polynomial_threshold#:~:text=4%20References-,Definition,is%20the%20linear%20threshold%20function - "... • The average sensitivity of f is at most $O(n^{1-1/(4d+6)})$. (We also give a combinatorial proof of the bound $O(n^{1-1/2^d})$. • The noise sensitivity of f with noise rate δ is at most $O(\delta^{1/(4d+6)})$..." PTFs being polynomials of degree d over reals in n variables are best suited models of examinations/contests/interviews which map non-boolean Question-Answer transcript of length n to a boolean sign of the PTF. Upperbound of two sensitivity measures for PTFs earlier defined as "... the average sensitivity of a Boolean function f measures the expected number of bit positions that change the sign of f for a randomly chosen input, and the noise sensitivity of f measures the probability over a randomly chosen input x that f changes sign if each bit of x is flipped independently with probability δ ..." indirectly also bound the failure probabilities of realworld examinations/contests/interviews which could be written as polynomials over reals and are vulnerable to corruption of answer values input to question variables. Possible ways of sabotaging a realworld examinations/contests/interviews include: (*) corrupted question (*) wrong question (*) corrupted answer (*) wrong answer which are bound to change the expected outcome of an admission test. Decision lists, Decision trees and DNFs can be computed by a PTF formed from Chebyshev polynomials which are valued between $[-1,1]$ for interval $[-1,1]$ and exponential outside $[-1,1]$ - <https://www.cs.utexas.edu/~klivans/f07lec5.pdf> - Theorem 1: "If all $c \in C$ have PTF degree d then C is learnable in the Mistake Bound model in time and mistake bound $n^{O(d)}$ " implies admission tests as Question-Answering PTFs are Mistake Bound learnable in time degree-exponential in number of questions (or reallife human formulation of framing Questions for corresponding Answers is exponentially hard). Average sensitivity bound in [Harsha-Klivans-Mekha] is directly proportional to degree of the PTF. If a non-STEM Multiple-Choice Question-Answering transcript is expressible as CNF (AND of OR constant depth) PTF degree of such a CNF is lowerbounded in <https://www.cs.cmu.edu/~odonnell/papers/ptf-degree.pdf> - [O'Donnell-Servedio] - improving [Minsky-Papert] Perceptron (<https://direct.mit.edu/books/book/3132/PerceptronsAn-Introduction-to-Computational-Perceptrons>: An Introduction to Computational Geometry (1969) - "... Section 3.2 One-in-a-box theorem - Theorem 3.2: Let A, A^r , be disjoint subsets of \mathbb{R}^n and define the predicate $\phi = \bigwedge_{i=1}^n x_i \in A_i$, for every A_i , $1 \leq i \leq n$, that is, there is at least one point of X in each A_i . If for all i , $|A_i| \geq 4m^2$ then the order of ϕ is $> m$. *This theorem is used to prove the theorem in §5.1. Because §5.7 gives an independent proof (using Theorem 3.1.1), this section can be skipped on first reading. [60] 3.2 Algebraic Theory of Linear Parallel Predicates: Corollary: If $\phi = \bigwedge_{i=1}^n \bigvee_{j=1}^m x_j \in A_{ij}$ the order of ϕ is at least $1/4|R|^{1/3}$..." result:"... More recently, Klivans and Servedio [17] showed that any polynomial-size DNF formula (equivalently, CNF formula) has a polynomial threshold function of degree $O(n^{1/3} \log n)$... We prove an "XOR lemma" for polynomial threshold function degree and use this lemma to obtain an $\Omega(n^{1/3} \log n^{2d/3})$ lower bound on the degree of an explicit Boolean circuit of polynomial size and depth $d + 2$. This is the first improvement on Minsky and Papert's $\Omega(n^{1/3})$ lower bound for any constant-depth circuit. ...". Example: For following 2 questions and 4 answer choices CNF is formulated as:
 Question1: Which is the largest city by area?
 Options: a1) Chongqing b1) Tokyo c1) Sao Paulo d1) New York (Answer: a1)
 Question2: Which is the largest country by area?
 Options: a2) Brazil b2) Russia c2) USA d2) China (Answer: b2)
 CNF for 2 QAs earlier: $(a1 \vee !b1 \vee !c1 \vee !d1) \wedge (!a2 \vee b2 \vee !c2 \vee !d2)$
 Computing Merit Score for earlier CNF formulation of Multiple-Choice question-answering is a MAXSAT problem (finding maximum number of satisfiable clauses or correctly answered questions) which is NP-Hard. An open-ended Question-Answering could be reduced to earlier 4-choice CNF MAXSAT format by grading the answers in 4 ranges of satisfaction percentages: 0-25%, 25-50%, 50-75%, 75-100% (Grading in academics fit into this multiple choice CNF of grade variables - A+, A, B+, B, C, D, E, F, ...). STEM multiple choice Question-Answering admission tests on the other hand would not depend on corpus queries but instead on theorem provers and equation solvers and are non-trivial AI problems. Combining upper

and lower bounds from [Harsha-Klivans-Mekha] and [O'Donnell-Servedio] average sensitivity of CNF Question-Answering is lowerbounded by $\Omega(n^{1-1/(4(n^{1/3}\log n^{2d/3})+6)})$. Degree of a monomial in PTF roughly corresponds to difficulty of a question for that monomial. CNF format of Multiple-Choice question-answering could be learnt in Mistake-Bound Learning model in $\Omega(n^{1/3}\log n^{2d/3})$ and $O(n^{1/3}\log n)$ combining earlier results on PTF degree of CNF which is phenomenally hard perhaps hinting at hardness of framing questions for answer samplespace (or answer-questioning) in real life examinations and fall in the category of $O(n^n)$ or $O(n!)$ complexity problems (e.g Travelling Salesman Problem is $O(n!)$). It is worth contrasting techniques of Polynomial Interpolations over Reals and Learning a Concept class in Boolean setting which is an interpolation of a Polynomial Threshold Function or Linear Threshold Function over $GF(2)$: Barycentric Interpolation of learning a polynomial over reals (<https://people.maths.ox.ac.uk/trefethen/barycentric.pdf>) is of linear time complexity and Question-Answering could be even represented as set of ordered pairs of (question(i),score_for_answer_to_question(i)) over reals and learnt by a polynomial interpolation algorithm. Statistical Query Dimension is defined (due to [Blum]) as minimum number of statistical queries required to learn a Boolean concept class. Halfspace intersections which are intersections of halfspaces over arbitrary dimensions are known to formalize any convex set (<https://www.cs.umd.edu/class/spring2020/cmsc754/Lects/lect06-duality.pdf>) and Question-Answering could be written in terms of halfspace intersections by reduction: exact answer(i) to question(i) is a line separating a plane and any deviating answer(i) to question(i) is either in upper halfplane or lower halfplane and intersection of halfplanes for all questions and answers represents a transcript - in other words sign of polynomial is ternary: + and - correspond to wrong answer halfplanes while 0 is exact answer line. By a result due to [Klivans-Sherstov] - Unconditional Lower Bounds for Learning Intersections of Halfspaces - <https://www.cs.utexas.edu/~klivans/mlj07-sq.pdf> - any statistical-query algorithm for learning the intersection of \sqrt{n} halfspaces in n dimensions must make $2^{\Omega(\sqrt{n})}$ queries implying exponential lowerbound of Question-Answering in Boolean setting. The exponential separation between polynomial interpolation over Reals (R) and $GF(2)$ or Z_2 is counterintuitive while conventional wisdom would suggest the contrary. Another contradiction between polynomial interpolation in 1 variable over reals and Boolean concept class mistake bound learning arises from Theorem 1: "If all $c \in C$ have PTF degree d then C is learnable in the Mistake Bound model in time and mistake bound $n^{O(d)}$ " of <https://www.cs.utexas.edu/~klivans/f07lec5.pdf> - again real univariate polynomial interpolation is exponentially faster than boolean degree- d PTF learning. Contradiction could be perhaps reconciled by the fact that univariate real polynomials correspond to univariate boolean functions and multivariate boolean PTFs and LTFs must be matched with multivariate polynomial interpolations. More generic Polynomial interpolation over several variables is a difficult problem involving Haar spaces - Definition 1.1 - <http://pcmap.unizar.es/~gasca/investig/GSSurvey.pdf>. In the context of admission tests, Polynomial interpolation over reals of Question-Answering transcript (set of ordered pairs of the form [question(i),score_for_answer_to_question(i)]) creates a family of polynomials for set of candidates ranked and ranking could be by any distance measure between polynomials including total score - it is obvious to note that integral of the polynomial (area under polynomial) per candidate is the total score per candidate. In NeuronRain, Complexity upper and lower bounds of Interviews-Contests-Examinations (Problem of People intrinsic merit or Talent analytics) have been investigated through earlier multiple theoretical models of Question-Answering: 1) QBFSAT 2) Linear Threshold Function 3) Polynomial Threshold Function 4) CNFSAT 5) Polynomial Interpolation over Reals 6) Halfspace intersections. Answers to Multiple Choice Questions which are words or phrases in most cases, could be embedded on a vectorspace (e.g Word2Vec) and Halfspace intersections could be defined over those word embeddings by unique straightlines passing through correct answer choice word vector to each question which intersect to form a convex polytope separating interior and exterior vector halfspaces of wrong answer choices.

64. Mining patterns in Astronomy Datasets has been less studied in BigData - NeuronRain (originally intended to be an astronomy software) brings astronomy and cosmology datasets (Ephemeris data of celestial bodies, Gravitational pull

and Correlation of Celestial N-Body choreographies to terrestrial extreme weather events, Climate analytics, Satellite weather GIS imagery, Space Telescope Deep Field Imagery of Cosmos) into machine learning and artificial intelligence mainstream. For example, Red-Green-Blue channel histogram analysis of Hubble Ultra Deep Field in NeuronRain seems to show an anomaly in percentage of Red (Farthest-Redshift), Green(Farther), Blue(Far) galaxies - ratio of Red:Green:Blue galaxies are 3:1:2 while intuition would suggest the contrary 1:2:3 (Deep Field is a light cone search and Red-Blue-Green channels of Deep Field are circular intersections of the light cone at different time points of past. As galaxies would appear more spread out proportionate to distance in expanding spacetime, Red-Green-Blue circular disks should theoretically contain increasing number of galaxies in order $\text{Red} < \text{Green} < \text{Blue}$). Possibly this contradiction could be explained by Einstein Field Equations - https://en.wikipedia.org/wiki/Einstein_field_equations - accounting for per body spacetime curvature and light cone of deep field is warped. Example Python RGB Analysis and Histogram plots of Hubble eXtreme Deep Field (2012) imagery is documented in https://scientific-python.readthedocs.io/en/latest/notebooks_rst/5_Image_Processing/02_Examples/Image_Processing_Tutorial_3.html

****What are some unusual applications of Factorization implemented in NeuronRain?

861. Computational Geometric Factorization - Applications to Numeric Compression and Space filling

by Tile cover - related to 814 and all sections on Factorization, Compressed Sensing, Integer Partitions and Space Filling, Goldbach Conjecture, Primality Testing, Fermat's Sum of Two Squares Theorem

Integer Factorization and Discrete logarithm problem traditionally have been a mere theoretical fancy. But following are some unusual connections of an efficient factorization of huge integers to other seemingly unrelated silos:
(*) Partitions of an integer N which are one dimensional could be lifted to a 2-dimensional square tile cover of a rectangle by Lagranges Four Square Theorem whose sides are the factors of N .

(*) Sublogarithmic Numeric compression of huge integers by Unique Integer Factorization has benefits for memory intensive ecommerce websites which transact millions of PKI Diffie-Hellman exchanges per day - mostly 2048 bits semiprimes

(*) Sublogarithmic Numeric compression by Unique factorization is helpful in designing better CPU instruction sets - registers can have lesser number of bits

(*) Even Goldbach Conjecture (every even integer > 2 is sum of 2 odd primes) and Odd Goldbach Conjecture (every odd integer > 5 is sum of three odd primes - which has been proved for odd integers > 7 because 7 can be partitioned only as $3+2+2$) are the greatest unsolved problems of Number theory. Even Integers upto $4 \cdot 10^{18}$ and Odd Integers upto $8.37 \cdot 10^{26}$ have been computationally verified for truth of 2 Goldbach conjectures by many variants of Segmented Sieve of Eratosthenes which is $O(N \log \log N)$ sequential time - Algorithm 1.1 to generate all primes in interval (A, B) -

<https://www.ams.org/journals/mcom/2014-83-288/S0025-5718-2013-02787-1/S0025-5718-2013-02787-1.pdf> - Prerequisite for this algorithm is a list of prime integers $< \sqrt{B}$ and first prime $> \sqrt{B}$. Factorization in NC-PRAM-BSP implies Primality testing is in NC which is already proved to be in larger class P by AKS primality test. This list of primes for segmented Eratosthenes sieve can be efficiently found in $O(\sqrt{B} \cdot (\log B)^k)$ parallel RAM time by Computational Geometric Factorization Primality test.

(*) Even Goldbach conjecture could be written as a reduction of integer partition to square tile cover of a rectangle:

(*) Even Goldbach Conjecture: $N = 2n = P + Q$ for all positive integers n and odd primes P and Q .

(*) Computational Geometric Factorization by parallel RAM planar factor point location on hyperbola $N = xy$ (factors x and y) could be equated to some random integer partition of $N = p_1 + p_2 + p_3 + \dots + p_k$

(*) Previous partition $N = p_1 + p_2 + p_3 + \dots + p_k$ is expanded by Lagrange Four Square Theorem as Sum of Squares (SOS) i.e. $N = 2n = P + Q = xy = p_1 + p_2 + p_3 + \dots + p_k = p_1a^2 + p_1b^2 + p_1c^2 + p_1d^2 + \dots + p_kd^2$ in which each part p_i is written as sum of 4 squares $p_ia^2 + p_ib^2 + p_ic^2 + p_id^2 = p_i$.

(*) If Even Goldbach conjecture is True, Primes P and Q can be written as two sum of squares one per prime: $N = 2n = P + Q = xy = p_1 + p_2 + p_3 + \dots + p_k = p_1a^2 + p_1b^2 + p_1c^2 + p_1d^2 + \dots + p_kd^2 = \text{SOS}(P) + \text{SOS}(Q)$.

(*) If Even Goldbach conjecture is True, earlier sum of $\text{SOS}(P)$ and $\text{SOS}(Q)$ of length $4k$ could be written as twice of another $\text{SOS}(R)$ of length m :

$N = 2n = P + Q = xy = (\text{length-}k \text{ random partition of } N) p_1 + p_2 + p_3 + \dots + p_k = (\text{Sum of 4 Squares of each } p_i \text{ of length } 4k) p_1a^2 + p_1b^2 + p_1c^2 + p_1d^2 + \dots + p_kd^2 = (\text{length } 4k-l) \text{SOS}(P) + (\text{length } l) \text{SOS}(Q) = 2*(r_1^2 + r_2^2 + r_3^2 + \dots + r_m^2) = (\text{length } m) 2*\text{SOS}(R)$.

(*) Geometric intuition for SOS formulation of Goldbach conjecture earlier which is a Universal Quadratic Form

(https://en.wikipedia.org/wiki/Quadratic_form): Necessary condition for Goldbach conjecture to be true is "4k squares must be coalesceable to 8 squares segregated into 2 equal-area rectangles composed of 4 squares each".

(*) Universal Quadratic Form version of Goldbach conjecture earlier leads to 15 and 290 theorems by [Conway-Schneeberger] and [Manjul Bhargava]-
https://en.wikipedia.org/wiki/15_and_290_theorems - which stipulate conditions for integer matrix representation of the quadratic form (if an integer matrix of quadratic form represents upto 15 or 290, then it represents all integers) perhaps implying limited number of solutions that could be verified for earlier Quadratic Form algorithmically sufficient to prove Goldbach Conjecture.

(*) Bhargava's prime-universality criterion theorem asserts that an integer-matrix quadratic form represents all prime numbers if and only if it represents all numbers in this sequence - <https://oeis.org/A154363>. If there exists such an integer-matrix quadratic form (PrimeUniversalQF) representing all prime numbers, Even Goldbach conjecture [$N = 2n = P + Q$] Quadratic Form earlier could be simplified (which may not be a universal quadratic form) without random partition as $N = 2n = \text{PrimeUniversalQF}(P) + \text{PrimeUniversalQF}(Q)$. Random partitions have the advantage of choosing arbitrary size squares. Algorithmic verification of Even Goldbach conjecture through factorization consists of solving 2 Integer Linear Programs equated to factors 2 and n for sides of the rectangle covered by set-partition-to-lagrange-four-square-theorem square tiles quite similar to CVXOPT ILP implementation
https://github.com/shrinivaasanka/asfer-github-code/blob/master/python-src/Streaming_SetPartitionAnalytics.py.

(*) Every variable bin depth histogram defined on a square integer grid is a geometric representation of a quadratic form having integer matrix. E.g. Following 6-bin histogram is represented by quadratic form $2x_1^2 + 4x_2^2 + 2x_3^2 + 3x_4^2 + x_5^2 + x_6^2 = 16$ (each # is a square cell on grid of dimensions $1*1$ and @ is of dimensions 2) for bin depth variable values $x_1=x_2=x_3=x_4=x_5=1$ and $x_6=2$:

```
x1 ##-----
x2 #####-----
x3 ##-----
x4 ###-----
x5 #-----
x6 @@-----
```

(*) Usual distance measures between histograms (Earth Mover Distance et al) apply as well to Quadratic forms represented by histograms similar to the one depicted earlier (or integer partitions) a sequitur from IntegerPartitions-Histogram-QuadraticForm bijection.

(*) Chen's theorem - https://en.wikipedia.org/wiki/Chen's_theorem - states that every sufficiently large even number is either *) a sum of two primes or *) a sum of prime and semiprime - closer to proving Goldbach conjecture. Consequence of Chen's theorem which has implications for keypair creation and semiprime factorization: semiprime

factorization could be written as difference of an even number and a prime.

(*) In Additive Number Theory, Fermat's Sum of Two Squares Theorem - https://en.wikipedia.org/wiki/Fermat%27s_theorem_on_sums_of_two_squares - states that Every odd prime p can be written as sum of two squares x^2 and y^2 if $p \equiv 1 \pmod{4}$. Such primes are termed Pythagorean Primes. Previous Sum of Squares expansion is a generic case of Fermat's Theorem on Sum of Two Squares.

(*) By Fermat's Sum of Two Squares Theorem, Previous partition to Sum of Squares reduction solves a special case of Even Goldbach Conjecture if $P \equiv 1 \pmod{4}$, $Q \equiv 1 \pmod{4}$ and thus $SOS(P) = a_1^2 + b_1^2$ and $SOS(Q) = a_2^2 + b_2^2 \Rightarrow N = 2n = xy = P + Q = SOS(P) + SOS(Q) = a_1^2 + b_1^2 + a_2^2 + b_2^2$ which is Lagrange Sum of 4 squares.

(*) Finding factor pair p and q of integer $N=pq$ such that ratio p/q is closest to 1 is non-trivial problem of almost-square factorization of N (factor sides of rectangle of area N are almost equal - an integer equivalent of real square root algorithm). Such an almost-square is best suited for solutions to two ILPs (equated to factors) of square tile packing of rectangle of area N .

****Why is Intrinsic Merit necessary? Are there counterexamples to perceptive voting based ranking? Why is voting based merit judgement anachronistic?***

797. Intrinsic Merit versus Majority Voting - Fame-Merit usecases - (this section is an extended unifying draft of theory and feature in AstroInfer, USBmd, VIRGO, KingCobra, GRAFIT, Acadpdrfts, Krishna_iResearch_DoxygenDocs)

Following counterexamples on merit-fame

```
(prestige)
```

 anachronism and Q&A already mentioned in AstroInfer Design Document are quoted herewith as they are pertinent to this question:

*) Performance of an academic personality is measured first by accolades, awards, grades etc., which form the societal opinion - prestige (citations). That is prestige is created from intrinsic merit. But measuring merit from prestige is anachronistic because merit precedes prestige. Ideally prestige and intrinsic merit should coincide when the algorithms are equally error-free. In case of error, prestige and merit are two intersecting worlds where documents without merit might have prestige and vice-versa. Size of the set-difference is measure of error. *) Soccer player, Cricket player or a Tennis player is measured intrinsically by number of goals scored, number of runs/wickets or number of grandslams won respectively and not subjectively by extent of votes or fan following to them (incoming edges). Here reality and perception coincide often and an intrinsically best player by records is also most revered. Any deviation is because of human prejudice. Here intrinsic merit precedes social prestige. *) Merits of students are judged by examinations (question-answering) and not by majority voting by faculty. Thus question-answering or interview is an algorithm to measure intrinsic merit objectively. Here again best student in terms of marks or grades is also the most favoured. Any deviation is human prejudice. Interview of a document is how relevant it is to a query measured by graph edit distance between recursive gloss overlap graphs of query and text. Here also intrinsic merit precedes social prestige. Caveat is these examples do not prove voting is redundant but only exemplify that Voting succeeds only when all voters decide merit with high degree of accuracy (Condorcet Jury Theorem). *) Legal System rests on this absoluteness - People frame law, reach consensus on its clauses and Everyone agrees and accepts Law as a standard. *) Most obvious counterexample to perceptive ranking is the pricing in money flow markets. Same Good and Service is differentially priced by different Sellers. Widely studied question in algorithmic economics is how to fix an absolute price for commodity. There are only equilibrium convex program solutions available (Nash, Fisher, Eisenberg-Gale) where buyer-seller may reach an agreement point which is not necessarily intrinsic. This problem is parallel to existence of Intrinsic Merit/Fitness in world wide web and social networks. *) Stock buy-sell decisions are often influenced by Credit Rating agencies which is also an intrinsic merit assessment in financial markets. *) Darwin's Theory of

Natural Selection and Survival of the Fittest is one of the oldest scientific example for Intrinsic merit or fitness in anthropology - Nature makes beings to compete with each other for survival, less fit become extinct and the fittest of them emerge victorious and evolve. *) Economic Networks for Shock Propagation(<https://economics.mit.edu/files/9790>) - Gravity Model of Economic Networks and GDP as intrinsic fitness measure in World Trade Web - <https://www.nature.com/articles/srep15758> and <https://arxiv.org/pdf/1409.6649.pdf> (A GDP-driven model for the binary and weighted structure of the International Trade Network) *) Human Development Index Rankings of Countries which is a geometric mean of Life Expectancy Index, Education Index and Income Index - http://hdr.undp.org/sites/default/files/hdr_2013_en_technotes.pdf - is an intrinsic macroeconomics merit measure. *) Software Cost Estimation models - COCOMO (Constructive Cost Model), Function Point Analysis and SLOC are intrinsic merit measures for software effort valuations though disputed - e.g OpenHub Open Source Analyzer estimated cost of GitHub NeuronRain AsFer repository - https://www.openhub.net/p/asfer-github-code/estimated_cost - by COCOMO formula per <https://en.wikipedia.org/wiki/COCOMO> - "... $E = a_i(KLoC)^{b_i}(EAF)$ where E is the effort applied in person-months, KLoC is the estimated number of thousands of delivered lines of code for the project, and EAF is the factor calculated above..."

****Why should intrinsic merit be judged only by mapping a text to a graph?****

 798. Cognition and Neuro-Psycho-Linguistic motivations for Intrinsic Merit - (this section is an extended unifying draft of theory and feature in AstroInfer, USBmd, VIRGO, KingCobra, GRAFIT, Acadpdrafts, Krishna_iResearch_DoxygenDocs)

 This is not the only possible objective intrinsic merit judgement. There could be other ways too. Disclaimer is intrinsic merit assumes cerebral representation of sensory reception (words, texts, visuals, voices etc.,) and its complexity to be the closest to ideal judgement. Simulating cerebral representation of meaning by a neural network therefore approximates intrinsic merit well (BRAIN initiative - circuit diagram of neurons - <http://www.braininitiative.org/achievements/making-the-connection/> - neurons for similar tasks are closely connected). Usually cognition of text or audio-visuals, can be approximated by bottom-up recursive lambda function composition tree evaluation on each random walk of the Definition Graph. Graph representation of a text can be easily made into a Graph Neural Network, a recent advance in Deep Learning, and thus closely resembles internal neural synaptic activation in brain on reading a text. AstroInfer implements this as Graph Neuron Tensor Network (GNTN) on lambda composition tree of random walks on definition graph which is a merger of Graph Neural Networks(GNN) and Neural Tensor Network(NTN). Neural Tensor Networks formalize similarity of two vertices connected by a relation as a Tensor Neuron and are ideally suitable for ontologies like WordNet. Intrinsic Merit can also have errors similar to Perceptive Majority Vote Ranking. But Intrinsic Merit has an inherent cost advantage compared to aggregating votes.

Intrinsic Merit in the context of psychology has its origins in various types of cognition - Grounded Cognition, Embodied Cognition etc., - Embodied Cognition puts forth revolutionary concept of "body influencing mind and cognition is not limited to cerebral cortices" while Grounded cognition defines how language is understood. Following excerpts from psychology literature illustrate cognition:

*) Barsalou's Grounded Cognition - <https://www.slideshare.net/jeannan/on-barsalou's-grounded-cognition>

*) Grounded Cognition - <http://matt.colorado.edu/teaching/highcog/readings/b8.pdf> - 1) "...Phrasal structures embed recursively.(e.g The dog the cat chased howled). Propositions extracted from linguistic utterances represent meaning beyond surface

structure.e.g extracting chase(cat,dog) from either "The cat chased the dog" or "The dog was chased by the cat"... 2) "...as an experience occurs (e.g easing into a chair) brain captures states across modalities and integrates them with a multimodal representation stored in memory (e.g how a chair looks and feels,the action of sitting,introspections of comfort and relaxations). Later on when knowledge is needed to represent a category (e.g chair) multimodal representations captured during experiences are reactivated to simulate how brain represented perception, action and introspection associated with it ...". Recursive phrasal structure in Grounded cognition and Currying/Beta reduction in Lambda calculus have uncanny similarities.

*) Embodied Cognition - <https://blogs.scientificamerican.com/guest-blog/a-brief-guide-to-embodied-cognition-why-you-are-not-your-brain/>

ThoughtNet and Recursive Lambda Function Growth algorithms in NeuronRain exactly implement previous grounded cognition theory - Language sentences are parsed into a recursive tree of lambda function compositions and each lambda function subtree composition can be simulated by composing images from a semantic network e.g ImageNet for approximate movie representation of meaning. ThoughtNet Hypergraph vertices are categories (modalities or classes) and each thought/sentence/experience is pigeonholed to classes (or modalities by a classifier). Previous example experience "easing into a chair" can be a hyperedge sprawling the modal classes "comfort","chair","sitting" which are ThoughtNet hypervertices for modals. Any future experience of chair or sitting might evoke this experience based on its merit potential by Contextual Multi Armed Bandit.

References:

798.1 Compilers - [Ravi Sethi-Aho-Ullman] - Page 387 - Type inferences, Currying and applying function predicates to arguments

Wouldn't cerebral representation vary from person to person and thus be subjective?

799. Cognition and Neuro-Psycho-Linguistic motivations for Intrinsic Merit - (this section is an extended unifying draft of theory and feature in AstroInfer,USBmd,VIRGO,KingCobra,GRAFIT,Acadpdrafts,Krishna_iResearch_DoxygenDocs)

There are standardized event related potential (ERP) datasets (N400,LAN,P600 etc., - <https://www.ncbi.nlm.nih.gov/pmc/articles/PMC3822000/>) and Event Related Functional MRI datasets gathered from multiple neuroscience experiments on human subjects. Such ERP data are similar for most brains. Variation in potential occurs because cerebral cortex and its sulci&gyri vary from person to person. It has been found that cortex and complexity of gray matter determine intelligence and grasping ability. Intrinsic merit should therefore be based on best brain potential data. ERP is non invasive compared to fMRI. An example of how ERP related to "meaningfulness"/"semantic correctness" of two texts - meaningful and meaningless - is plotted in <https://brainlang.georgetown.edu/research/erplab>.

Isn't perception based ranking enough? Why is such an intrusive objective merit required?

800. Social network centrality motivations for Intrinsic Merit - (this section is an extended unifying draft of theory and feature in AstroInfer,USBmd,VIRGO,KingCobra,GRAFIT,Acadpdrafts,Krishna_iResearch_DoxygenDocs)

Perception majority voting based ranking is accurate only if all voters have decision correctness probability > 0.5 from Condorcet Jury Theorem. PageRank works well in most cases because incoming edges vote mostly with $>50\%$ correctness. This correctness is accumulated by a Markov Chain Random Walk recursively - vote from a good vertex to another vertex implies voted vertex is good (Bonacich Power Centrality) and so on. Initial goodness is based on weight of an edge. Markov iteration stabilizes the goodness. Probability that goodness of stationary Markov distribution < 0.5 can be obtained by a tail bound and should be exponentially meagre.

****Can Intrinsic Merit for a human social network vertex, a text document or any other entity be precisely defined as opposed to a probability distribution for Intrinsic Fitness defined for Social network vertices?****

801. Social networks, Bipartite and General Graph Maximum Matching, Permanent, Boolean majority, LTF, PTF, Votes aggregation, KRW Conjecture and Majority-VoterSAT Boolean Composition, Communication Complexity, BKS Conjecture, Condorcet Jury Theorem, Sharp Thresholds, Preferential attachment versus Fit-get-richer, Correlated Majority, Boolean Sensitivity measures, Majority Hardness Amplification Lemma - motivations for Intrinsic Merit - (related to Sections 14, 555, 678, 682 and an extended unifying draft of theory and feature in AstroInfer, USBmd, VIRGO, KingCobra, GRAFIT, Acadp drafts, Krishna_iResearch_DoxygenDocs)

Boolean Composition of Majority Voting and VoterSATs and its Goodness in the context of Karchmer-Raz-Wigderson [1995] conjecture and various versions of Condorcet Jury Theorem have been researched extensively in NeuronRain Theory Drafts. In section 682, Depth of the Majority and VoterSAT composition is lower bounded by $(= \text{CommunicationComplexity}(\text{Majority}+\text{Voter})) \geq 5.3 \cdot \log m + n - 2 \cdot \log m - 10$ for m voters having SATs of n variables each which is logdepth in number of voters if number of VoterSAT variables is constant. Recent result extends the range of inner functions handled by KRW conjecture e.g VoterSATs composed to Majority - <https://eccc.weizmann.ac.il/report/2020/099/>. If equal Goodness of *) Majority+SAT composition social choice by CJT variants and *) a non-majority social choice e.g LTFs and PTFs, implies lowerbound (this assumption pervades throughout the NeuronRain theory drafts because Goodness plays the role of error probability which is crucial if both LHS or RHS are not complete problems for some probabilistic complexity class - if LHS or RHS is a complete problem in any deterministic class lowerbound is obvious because Goodness is 100% either side) and if LHS non-majority social choice is a P-complete problem (every problem in P is reduced to it), every problem in P is in BPNC which is larger class than NC1. But KRW conjecture implies P is not in NC1. Combining the two previous logdepth lowerbound for Majority+VoterSAT composition implies: P is not in NC1 but could be in BPNC (P is known to be in BPP). Many realworld elections are both sequential and parallel comprising numerous sequential queueues of voters which vote in parallel. Social Networks could be viewed as Correlated Majority Voting gadgets - Herding phenomenon - decision of a voter vertex is influenced by its neighbours which could be likened to Block sensitivity. Majority Hardness Amplification Lemma in 678 upperbounds the amplified hardness of Majority+VoterSAT composition by $\leq 2 \cdot \text{sensitivity}$ and by proof of Sensitivity conjecture, Block sensitivity $\leq \text{poly}(\text{sensitivity})$. Complete social network graph is solved for maximum matching such that no two edges in matching have common vertices and two voter vertices of opposing allegiance are pitted against for every edge in matching. Matching in Bipartite graphs is solvable by permanent while for General graphs maximum matching is equal to size of minimum odd vertex cover (Theorem 7.2 - <https://www.cs.tau.ac.il/~zwick/grad-algo-0910/match.pdf>). Literature on Social network intrinsic fitness does not define but only relates why preferential attachment happens in networks i.e Why certain social people profiles are highly regarded and attract audience. Earlier Scale-Free networks defined degree of vertex exponentially (Power Law) which is Rich-Get-Richer in random graphs

(Erdos-Renyi model) i.e if a vertex has huge degree already it would have greater ability to attract future links. Recent advances place more importance on Fit-Get-Richer idiom and express fitness as a function of degree (a posteriori estimation). Defining Exact Fitness is a void in literature still and Intrinsic merit algorithms for texts fit in right there. These algorithms are not probabilistic. For humans, defining merit independent of perception has a long drawn tradition - talk to h(im/er) directly and judge and don't rely on popular opinions. This requires a consensus on who judges merit and how. Previous counterexamples assume that such an Intrinsic, Absolute standard exists e.g Examination/Interviews/Contests/Law are accepted standards to assess human merit - All students are asked same questions, All candidates are asked same questions, All contestants have equal levelled opportunities, All plaintiffs have equal freedom to defend - Thus proving/disproving existence of absolute consensus standard is tantamount to proving/disproving human intrinsic merit. Following statements of First order logic give an inkling of philosophical challenge in defining intrinsic merit:

If 99% voters agree to a fact it is imperfect - Falsehood
(Majority) e.g Social choice

If 100% voters agree to a fact it is perfect - Truth (Consensus)
e.g speed of Electromagnetic waves from Maxwell equations

Ultimately, intrinsic merit existence reduces to consensus problem to measure merit - when everyone agrees on how to decide merit, perception gives way to intrinsic: Assuming a scored question-answering by threshold functions (PTF or LTF) which is intrinsic way of judging merit of a candidate and multiple evaluators arriving at multiple scores for the same candidate, conclusion is called into question and a consensus is needed as opposed to majority evaluated score - Condorcet Jury Theorem implies if each LTF or PTF of an evaluator is > 50% good, final group evaluation tends to 100% or consensus. Goodness of majority voting is then reduced to Goodness of Individual Threshold functions. Finding a 100% good threshold function (which is stable and resilient to correlation) is the holy grail of Intrinsic merit - BKS "majority is least stable" conjecture implies such a function stabler than majority exists for all correlation probabilities. If BKS conjecture is disproved, it amounts to saying voting is better than intrinsic evaluation debunking any socially accepted standards of merit e.g examinations, contests, interviews which are threshold functions. Similar reasoning applies to Buy-Sell Market Equilibrium and determining intrinsic price of a commodity - Following references expound theory of Threshold phenomenon in majority voting and economics:

(*) Wisdom of Crowds - Vote Aggregation and averages -
https://aidanlyon.com/epac_woc.pdf - "... There are now many well-documented and contemporary examples of the so-called Wisdom of Crowds : Amazon's product recommendations. • Wikipedia and Intellipedia. • Netflix's movie recommendation algorithm. • Prediction markets. • Online citizen science. • Google's PageRank algorithm ..." and "...A famous theorem, known as the Condorcet 1785 jury theorem (rediscovered by Black (1963)), shows that as you add more and more people to the crowd and aggregate their judgements using the majority rule, then if each person has a greater than 50% chance of being right, and if they make their judgements independently of one another, then the probability that the collective judgement is correct will approach certainty. ..."

(*) Threshold Phenomena and Influences - [Gil Kalai-Safra] -
<http://www.cs.tau.ac.il/~safra/PapersAndTalks/muligil.old.pdf> - "...The reason usually given for the interest of CJT to economics and political science is that it can be interpreted as saying that even if agents receive very poor (yet independent) signals, indicating which of two choices is correct, majority voting nevertheless results in the correct decision being taken with high probability, as long as there are enough agents, and the agents vote according to their signal. This is referred to in economics "asymptotically complete aggregation of information" ..." and "...In particular, if there is a sharp threshold then there always is a Nash-equilibrium point for which the probability of mistakes tends to zero as the number of jurors grows..." - CJT implying Nash equilibrium is crucial economically because jurors (buyers) minimize their mistakes in evaluating price of a commodity intrinsically.

(*) Boolean composition of leaves of Boolean majority circuit and individual VoterSATs has a curious implication when all voters are quantum voters (all VoterSATs are in BQP): By Condorcet Jury Theorem and its later versions by [Black] and [Ladha] and Margulis-Russo sharp threshold at $p\text{-bias} > 0.5$, infinite majority + BQP VoterSAT boolean composition tends to goodness 1 or quantum world derandomizes to P (by phenomena of Decoherence, Wavefunction collapse) implying one of the superimposed quantum states of some amplitude (defined in Hilbert space) is chosen for certainty by nature. Majority is in non-uniform NC1 and thus in P which in turn is in BPP and the larger class BQP which implies boolean majority is in BQP. If boolean composition of BQP majority function and BQP voter SATs are relativizable (conjectural assumption: boolean composition is equivalent to oracle access Turing machines) as BQP^{BQP} (BQP majority function having oracle access to BQP voter SATs) and since BQP is low for itself, $BQP^{BQP} = BQP$. By CJT-Black-Ladha-Margulis-Russo threshold theorems for infinite majority quantum boolean composition tends to 100% goodness or in other words BQP asymptotically dissipates quantum error and derandomizes to P.

**Aren't there counterexamples to Intrinsic Merit examples mentioned previously? For example, aren't there brilliant scientists faring poorly in examinations? Aren't there bright candidates rejected by Interviews? And vice-versa? How do you explain it?*

 802. Question-Answering, Deficiencies in Sampling and Approximating Intrinsic Merit - why examinations fail, People Analytics, Partial Ordered Rankings - (this section is an extended unifying draft of theory and feature in AstroInfer, USBmd, VIRGO, KingCobra, GRAFIT, Acadpdrafts, Krishna_iResearch_DoxygenDocs)

 Probably this is the best question of this FAQ. These counterexamples imply the examination/interview system is flawed and violates consensus. Accuracy of Question-Answer based merit judgement depends on how efficiently the system samples merit from past history of the subject. This can be equivalently stated as Merit Summarization Problem (similar to text summarization). If merit features are represented on a metric vector space, sampling should construct an efficient summary subspace of merit metric space. Clustering/Partitioning this space by a computational geometric algorithm e.g Voronoi tessellation, Delaunay triangulation etc., or a Clustering algorithm yields strong regions of merit. Question-Answering should therefore concentrate on these merit clusters - examples: 1) each candidate is presented with questions based on past strengths (2) academic examinations source questions from set of historically high scoring subjects of a student. If points in this merit space are connected as a dependency graph, strongly connected components of the graph are closely related regions of merit and a component graph is the merit summary in which each vertex is a strongly connected component. Theoretically, question answering reduces to a polynomial round QBFSAT and is a PSPACE problem (unbounded QBFSAT is EXP-complete). Traditional question-answering is time-bounded and intrinsic merit need not depend on time restrictions - answering a question depends on how much instantaneous insight or epiphany a person has within limited time in responding. This insight depends on both natural merit and past learning. It is against definition of merit itself because merit is absolute and independent of time while only experiential learning grows over time. Problem therefore is how efficient and time-independent the QBF is and this error in QBF is the failure probability of Intrinsic Merit. Probably above counterexamples could have succeeded in unbounded, better-formed QBF. A nice academic example of unboundedness: Graduate/Doctoral studies give more importance to assignments, quizzes, take-home exams in deciding course credit and merit which are less time-bounded compared to conventional 3 hour tests. Someone failing in a 3 hour test might succeed in (3+x)th hour and time limit shouldn't constrain someone from proving their innate ability. But traditionally intelligence is measured by how fast a person solves a problem e.g puzzles and this is based on assumption that all contestants have similar cerebral activity simultaneously in the

duration of contest. This assumption is questionable - if problem solving faculty (periods of peak creativity or insight) of brain is plotted as a curve against time for each individual, it is not necessary that curves of any two individuals should coincide. One person might have peak cerebral activity/insight at time t (during the contest) and another might have peak activity/insight at $t+dt$ (outside the duration of contest) and thus the intelligence quotient test fails to capture the merit of the latter. Most standard examinations follow objective multiple choice question-answering convention and thus are intrinsic and absolute. Some variants of examinations are personalized and adaptive - questions dynamically change based on answers to past questions - from complexity theoretic standpoint LTF, PTF or TQBF are not static but dynamic - values (answers) for future variables (questions) in threshold function or TQBF change depending on values (answers) assigned to past variables (questions). Complexity ramifications of dynamic LTF, PTF and TQBF are less known. But the question of if past merit history can be efficiently constructed and sampled is itself non-trivial. Because this implies personalization in deciding merit. For instance, academic and work credentials in a curriculum vitae/resume has to be mapped to a graph or merit vector. Even if merit clusters are conceivable, aforementioned limitation because of peak cerebral activity has to be accounted for accurate definition of intrinsic merit. Mind Mapping and Concept Mapping Software create wordled semantic graphs of concept vertices from a knowledgebase which is an example of Merit cluster (https://en.wikipedia.org/wiki/Mind_map). NeuronRain AstroInfer Design mentions a Banach Fixed Point Theorem Contraction Map procedure to sample knowledge which is applicable to Talent analytics, Human Resource Analytics and People Analytics. Apart from these, NeuronRain People Analytics suggests and implements Domain Specific Talent Analytics for automatic machine learnt talent recruitment minimizing manual errors E.g. Number of Source Lines of Code written by a Software Professional is an intrinsic merit measure which reflects the overall technical knowhow of a candidate garnered over a long period of time thus capturing merit better than manual interviews of short durations. Career transition of a profile is modelled as Weighted automaton and interpolated as Polynomial. Similarity of 2 people profiles is determined by Inner Product Spaces of the career polynomials. Partial Ordered Intrinsic Merit Rankings of search engine query results and Galois Connection between posets mooted in NeuronRain AstroInfer Design best suits People analytics where merit vectors of two individuals may not be a linear ordering but a partial one - both could be outstanding in their own right. As an aside some of the established university rankings (QS ranking, NIRF-India) are mixtures of intrinsic merit and perception and depend on a formula which gives percentage weightages to reputation-perception, academic citations, research, faculty and students and thus are mostly majority voted and not purely intrinsic. Rankings of academic institutions, which are academic People Talent analytics measures, have been contentious and marred by lack of absolute merit metrics to quantify quality of people than infrastructure (e.g Rapport of Faculty-Students, Clarity of students, Quality of teaching) and dependence on Fame (popular perception). Statistically, Rank Correlation coefficients (e.g Spearman - https://statweb.stanford.edu/~cgates/PERSI/papers/77_04_spearmans.pdf) of the following pairs of rankings would dispel myths of Fame and Merit (it has been conjectured earlier that Fame-Merit Equilibrium Convex Program and PageRank Fame Markov Random Walk should coincide):

(*) Rank Correlation coefficient between Hardness rankings of admission tests to institutions Versus Overall Rankings of institutions - high correlation implies high quality students are admitted to the institution by tough admission tests who automatically catapult the quality of institution - quality of institution is decided by quality of students and admission criteria than teaching (e.g Institutes ranked high by NIRF 2021 have the toughest admission procedures choosing the best students)

(*) Rank Correlation coefficient between Qualification rankings of faculty (research profile, number of papers and citations) Versus Overall Ranking of institutions - high correlation implies quality of institution is decided by quality of faculty than difficulty of admission tests

And the latter correlation is preferable for People Talent-Merit analytics as

measure of value added by institution. In complexity theoretic terms, ranking of academic admission tests by difficulty reduces to ranking of complexity class hardness measures (different from Stability, Sensitivity measures which bound incorruptibility of a function) of question-answering by LTFs, PTFs and TQBFs e.g PSPACE-complete for TQBF SAT, NP-complete when value (answer) of each boolean variable (question) in threshold function is decided by some 3SAT formula. Satisfiability algorithms for threshold circuits (equivalent to threshold functions) have been analyzed in <https://arxiv.org/abs/1806.06290> and <https://drops.dagstuhl.de/opus/volltexte/2018/9450/>

****How measurable are Intrinsic merit and Creativity? Is there any perfect metric to quantify these?****

803. Question-Answering, Approximating Natural Language by Tree of Lambda Functions (Turing Machine), fMRI and Connectomes, Church-Turing Thesis, Sanskrit grammar example - (this section is an extended unifying draft of theory and feature in AstroInfer, USBmd, VIRGO, KingCobra, GRAFIT, Acadpdrafts, Krishna_iResearch_DoxygenDocs)

There are metrics but not necessarily perfect. This requires a detailed anecdotal clarification. Consider for example two sentences: "You saved the nation" and "You shaved the nation". Both are grammatically correct but latter is semantically discordant. First sentence is obviously more meaningful because WordNet distance between "save" and "nation" is less than "shave" and "nation". Representing these sentences as a lambda function yields 2 functions: save(nation) and shave(nation) i.e verb acts as a function on the object. Best natural language closer to realising lambda function composition without significant loss of information is Sanskrit which has peculiar grammatical structure and brevity. Panini's sanskrit grammar notation has similarities to Backus-Naur Form of Context Free Grammars. An example sanskrit sentence below can be arbitrarily shuffled without loss of meaning (Reference: Conversational Sanskrit - Cycle 35 - by N.D.Krishnamurthy, U.P.Upadhyaya, Jayanthi Manohar, N.Shailaja):

api asmin maargae vaahanam na sthaapayitavyam ? - Are vehicular parkings prohibited in this road?
is equivalent to:

asmin maargae na sthaapayitavyam vaahanam api ?

Lambda composition tree of this sentence might look like:

api(asmin(maargae(na(sthaapayitavyam(vaahanam)))))?

where each parenthesis is a lambda function on an object argument and evaluated right-to-left. Previous example of currying grows a tree of 1 parameter lambda functions. Recursive Lambda Function Growth algorithm is therefore a natural language counterpart of compilers for Context Free Grammars - Recursive Lambda Function Growth compiles a natural language to a tree of lambda functions while Programming Language Compilers translate a context free language (high level code) to machine language (assembly instructions). This lambda tree and wordnet relevance distance combine approximates quantitative complexity of cerebral meaning representation well. Creativity or Genius has contextual interpretations in academics/art/music/linguistics : Creativity in academics is measured by how influential a research paper is on future articles and how it is confirmed by experimental science. For example, Einstein's papers on Special and General relativity grew in influence over the past 100 years because of its experimental validity (Eddington Eclipse Experiment, Gravitational Lensing, Discovery of Black Holes, Precession of Equinox in Mercury's Orbit, Gravitational Waves found by CERN-LIGO etc.,) and citations were the result of these experimental proofs. Thus incoming hyperlinks or Fame is a result of Proved Intrinsic Merit (or) merit in science is defined as experimental establishment of a theory and citations automatically ensue. Creativity/Originality/Merit in art and music is far more complex to define e.g What made Mozart or Van Gogh famous? It is not known if there is an experimental proof for merit of music and art. But art and

music are known to stimulate neural activity in humans and cure illness. Only an fMRI or an ERP dataset on these stimuli could quantify merit. Functional MRI datasets for audio and music stimuli of different genres of music collected from human subjects are available in public domain at OpenfMRI - <https://openfmri.org/dataset/ds000113b/>, <https://www.openfmri.org/dataset/ds000171/>. These also contain respiratory and heartbeat information on hearing music stimuli. There have been recent fMRI datasets like Human Connectome Project - <https://www.humanconnectome.org/> - studying brain connectivity and its relevance to Intelligence Quotient.

References:

-
- 803.1 Panini-Backus Form suggested - Ashtadhyayi - [Ingerman] - <https://dl.acm.org/doi/10.1145/363162.363165>
- 803.2 Compilers - [Ravi Sethi-Aho-Ullman] - Page 82
- 803.3 Structured compilers due to [Ammann U.], The development of a compiler Proc. Int. Symposium on Computing - North-Holland-1973 - Algol - BNF of the If-Else Clause and its type inference - <http://citeseerx.ist.psu.edu/viewdoc/download?doi=10.1.1.34.9856&rep=rep1&type=pdf>
- 803.4 Panini-Backus Form - [Don Knuth] - Ashtadhyayi written in Grantha Tamil script - <https://blogs.scientificamerican.com/roots-of-unity/a-feat-of-mathematical-eponymy/>
- 803.5 Backus-Naur Form Context Free Grammar Parse Tree for Natural Language Poetry - Tamil - <https://wiki2.org/en/Venpa>

****NeuronRain design documents and drafts refer to something called EventNet and ThoughtNet. What are they?***

804. EventNet, Actor Pattern, ThoughtNet, Contextual Multi Armed Bandits, Reinforcement Learning, Evocation, Neurolinguistics - (this section is an extended unifying draft of theory and feature in AstroInfer, USBmd, VIRGO, KingCobra, GRAFIT, Acadpdrafts, Krishna_iResearch_DoxygenDocs)

EventNet is a new protocol envisaged to picturise cause-effect relations in cloud. It is a directed graph of event nodes each of which is an occurrence involving set of actors. This can be contrasted against actors pattern in Akka(<http://doc.akka.io/docs/akka/current/scala/guide/actors-intro.html>) which has interacting actor objects. EventNet is graph of not just actors but events involving actors. ThoughtNet is another equivalent formalism to connect related concepts than events. This is a theoretically strengthened version of cognitive inference model mentioned as uncommitted earlier in 2003. Basically ThoughtNet is a non-planar Hypergraph of concepts. Each vertex in ThoughtNet is essentially a stack because multiple hyperedges go through a vertex and these edges can be imagined as stacked upon one another. Rough analogy is a source versioning system which maintains versions of code at multiple time points. This model closely matches human evocative cognitive inference because upon sensory perception of a stimulus, brain's associative evocation finds all possible matching thoughts and disambiguates them. Each set of evocations correspond to hyperedges transiting a stack vertex in ThoughtNet. ThoughtNet inherently has a temporal fingerprint because top most hyperedges of all stack vertices are the newest and deeper down the stack thoughts get older. Each hyperedge has a related potential and disambiguation depends on it. In machine learning jargon, ThoughtNet is a Contextual Multi-Armed Bandit Reinforcement Learning Data Structure - an agent interacts with environment and its actions have rewards - each stack vertex is a multi-armed bandit environment and each element of the stack is an arm. Evocation scans the stack vertex to choose an arm followed by an action and most potent evocative thought fetches highest reward. Choice of a highest rewarding arm is the disambiguation and depends on rewards for past evocation choices. Thus multi-armed bandit iteratively learns from past

disambiguation to make future choices(a generalization of hidden markov model where present state depends on previous state). This is a computational psychoanalytic framework and has some similarities to Turing machines/Pushdown automata with stack and tapes - but alphabet and languages are thoughts not just symbols. ThoughtNet can be simulated by a Turing Machine of hypergraph storage and computation state transition defined by evocative actions. Each actor in EventNet has a ThoughtNet. Thus EventNet and ThoughtNet together formalise causation, human evocation and action. New memories in human brain are acquired by Hippocampus and removal of Hippocampus causes difficulty in acquiring new memory though old memories remain (Reference: Limbic System and Hippocampus - Phantoms in Human Brain: Probing the mysteries of human mind - V.S.Ramachandran and Sandra Blakeslee). Broca's Area in brain processes Lexical-Grammatical aspects of sensory reception and forwards to Limbic System for emotional reaction - <https://www.ncbi.nlm.nih.gov/pubmed/19833971> by [Sahin NT1, Pinker S, Cash SS, Schomer D, Halgren E.] lists fMRI Local Field Potentials experimental observations for lexical-grammatical-phonological regular and irregular verb inflections (200-320-450ms). ThoughtNet theoretically simulates Broca's Area, Hippocampus and Limbic system and accumulates memories on hypergraph. Word inflections are sourced and normalized from WordNet Synsets. Sensory Stimulus for example is a Galvanic Skin Response. Evocative action based on stimulus by Limbic system is simulated by retrieval of the most potent thought hyperedge bandit arm and respectively defined action for the arm. NeuronRain grows ThoughtNet by creating vertex for each class of a thought hyperedge found by a classifier and storing the hyperedge across these class vertices. Example: Sentences "There is heavy flooding", "Typhoon wrought havoc","Weather is abnormal" are classified into 3 classes "Disaster","Water","Flooding" found by a classifier. An example stimulus "Flooding" evokes all these sentences. Following diagrams explain it:

.. image:: NeuronRain_ThoughtNet.jpg

.. image:: NeuronRain_EventNet.jpg

****Why is a new Linux kernel required for cloud? There are Cloud operating systems already.****

 1198. (THEORY and FEATURE) Machine Learning enabled VIRGO32 and VIRGO64 Linux Kernels - Userspace interface to Kernelspace Cloud System calls and Drivers - related to all sections of Drone Autonomous Delivery, IoT and Kernel Analytics, Program Analysis, Software Analytics

Because, most commercial cloud operating systems are deployment oriented and cloud functionality is in application layer outside kernel. User has to write the boilerplate application layer RPC code. NeuronRain VIRGO provides system calls and kernel modules which obfuscate and encapsulate the RPC code and inherent analytics ability within linux kernel itself. For example, virgo_clone() , virgo_malloc(), virgo_open() system calls transparently converse with remote cloud nodes with no user knowledge, configured in virgo conf files - this feature is unique in NeuronRain. Application developer (Python/C/C++) has to just invoke the system call from userspace to embark on cloud. This is not possible in present linux distros. Linux and unix system calls do not mostly use kernel sockets in system call kernelspace code and do not have kernel level support for cloud and analytics a void not compensated by even Cloud operating systems like openstack.

****Fedora and Ubuntu Linux distros have optimized Linux Kernels for Cloud e.g linux-aws for AWS. Is VIRGO Linux kernel similar to them?****

 1199. (THEORY and FEATURE) Machine Learning enabled VIRGO32 and VIRGO64 Linux

Kernels - Performance Optimizations - Kernelspace Cloud System calls and Drivers
- related to all sections of Drone Autonomous Delivery, IoT and Kernel
Analytics, Program Analysis, Software Analytics

No. Amazon Machine Image (AMI) for virtual machine hypervisors have optimized linux kernel packages available for Fedora and Ubuntu. AWS has a network throughput enhancement named ENA (Elastic Network Adapter) which are device drivers (<https://github.com/amzn/amzn-drivers>) written to take advantage of Linux kernel Gigabit ethernet drivers. ENA has features for hardware checksums of TCP packets, Multiple packet message queues, Packet Steering to a specific port etc.,. VIRGO Linux kernel does not presently do any ethernet optimization. But message flags for kernel sockets send and receive between system call clients (virgo_xxxxxx() system calls in RPC/KMemCache/FileSystem) and Kernel Module Listeners can be optimized by having MSG_FASTOPEN to piggyback payload on SYN packets in SYN-ACK-SYNACK 3-way handshake. MSG_FASTOPEN was experimented but it had to be reverted because of some random kernel panics in kernel versions before 4.13.3. Presently MSG_FASTOPEN flag has been found to be working in kernel_analytics VIRGO64 module on 4.13.3 64-bit kernel for streaming analytics variables realtime from a remote webservice. Fedora and Ubuntu AMIs leverage ENA for better response time. Ubuntu press release at <https://insights.ubuntu.com/2017/04/05/ubuntu-on-aws-gets-serious-performance-boost-with-aws-tuned-kernel/> details the enhancements. Notable among them is the CONFIG_NO_HZ_FULL Kconfig parameter which reduces scheduler clockticks. Clocksource is also a performance parameter - Changing to TSC clocksource improves CPU performance (Netflix EC2 performance tuning for linux kernel - <http://www.brendangregg.com/blog/2015-03-03/performance-tuning-linux-instances-on-ec2.html>). These are already available mainline configurables and VIRGO kernel does not have anything new on that front. VIRGO kernel's main goal is to introduce new system calls and drivers for accessing resources/devices on remote cloud nodes and all traffic happens only among kernelspaces of cloud nodes underneath userspace applications - there are no userspace sockets.

****What languages, libraries and third-party packages are used in NeuronRain?****

AsFer machine learning implementations are written in C++/Python/Java(Spark-streaming). USBmd VIRGO kernel module is written in C and Python(Spark). VIRGO linux kernel is forked off from mainline <http://www.kernel.org> PPA and new systemcalls and drivers are written in C/Python(Some utility scripts, Userspace boost::python invocation of systemcalls). KingCobra VIRGO kernel module is written in C/Java/Python(Pricing)/C++(protocol buffers for Neuro MAC electronic currency).

Requirements.txt in:

<https://sourceforge.net/p/asfer/code/HEAD/tree/asfer-docs/Requirements.txt>
<https://github.com/shrinivaasanka/asfer-github-code/blob/master/asfer-docs/Requirements.txt>

has continuously updated list of opensource packages/libraries dependencies - this file implicitly attributes copyright/copyleft to respective original contributors.

****How do VIRGO system calls and driver listeners differ from SunRPC?****

1200. (THEORY and FEATURE) Machine Learning enabled VIRGO32 and VIRGO64 Linux Kernels - SunRPC,ORB in Kernel,Kernelspace Cloud System calls and Drivers - related to all sections of Drone Autonomous Delivery, IoT and Kernel Analytics, Program Analysis, Software Analytics

SunRPC is one of the oldest ingredient of linux kernel making kernelspace TCP transport. SunRPC is used by lot of distributed protocols e.g NFS. SunRPC kernel

sockets code in

<http://elixir.free-electrons.com/linux/latest/source/net/sunrpc/svcsock.c> is an example of how kernelspace request-response happens. SunRPC is like a traditional ORB, requiring compilation of stubs and implementations done in server side. Services register to portmap to get a random port to run. Client discover the services via portmap and invoke remote functions. XML-RPC is a later advancement which uses XML encoded transport between client and server. XML-RPC is the ancestor of SOAP and present industry standard JSON-REST.

Comparison of SunRPC and XML-RPC in http://people.redhat.com/rjones/secure_rpc/ shows how performant SunRPC is. SunRPC uses XDR for data representation. VIRGO presently does not have service registry, discovery, stub generation like SunRPC because it delegates all those complexities to kernel and user does not need to do any registration, service discovery or stub implementation. User just needs to know the unique name of the executable or function (and arguments) in the remote cloud node. All cloud nodes must have replicated binaries which is the simplest registration. Ports are hardcoded and hence no discovery is required. Only linux 32-bit (4.1.5) and 64-bit (4.13.3) datatypes are supported. In this respect, VIRGO differs from any traditional RPC protocols.

Marshalling/Unmarshalling have been ignored because, goal of VIRGO is not just RPC, but a logically unified kernel address-space and filesystems of all cloud nodes - kernel address spaces of all cloud nodes are stored in a VIRGO address translation table by VIRGO system calls. VIRGO system calls at present have a plain round-robin and a random-number based loadbalancing schemes. Research paper on userspace versus kernelspace remote procedure calls in [http://citeseerx.ist.psu.edu/viewdoc/download?](http://citeseerx.ist.psu.edu/viewdoc/download?doi=10.1.1.32.4304&rep=rep1&type=pdf)

[doi=10.1.1.32.4304&rep=rep1&type=pdf](http://citeseerx.ist.psu.edu/viewdoc/download?doi=10.1.1.32.4304&rep=rep1&type=pdf) has experimental results proving kernelspace RPC has a non-trivial speedup compared to userspace RPC in Amoeba OS. Most prominent cloud implementations (JSON-RPC or JSON-REST) do userspace RPCs presently and rarely use SunRPC-NFS style of kernelspace RPCs. Article in <http://www.csn.ul.ie/~mark/fyp/fypfinal.html> - CORBA in the kernel? - compares two mechanisms for kernelspace RPC - CORBA-kORBit and SunRPC. Quoting from it: "... One application of this idea is that the user should be able to use a physical device attached to any of the nodes in the cluster as if it were physically attached to the node the user was operating from. ...". VIRGO linux kernel systemcalls/drivers try to achieve exactly this where "physical device" is CPU, Kernel Memory and Filesystem in a remote cloud node. This is a typical feature required for a cloud of embedded systems. In this respect, VIRGO is a hybrid of cloud and cluster for parallelism. VIRGO does not invoke SunRPC code at present and just derives the concept, though original intention was to wrap the system calls and drivers on SunRPC. Reason is the considerable code changes required in existing SunRPC socket code in kernel - thus VIRGO systemcalls and drivers were written from scratch.

****Doesn't VIRGO expose the kernel address space directly to application user e.g Kernel Memcache system calls?****

860. (THEORY and FEATURE) VIRGO32 and VIRGO64 Kernelspace RPC Memory Allocation System Calls - Memory

Allocator and Defragmentation Bounds - related to all sections of Drone

Autonomous Delivery, IoT and

Kernel Analytics, Program Analysis, Software Analytics, VIRGO memory allocator of NeuronRain Theory Drafts

VIRGO system calls, especially kmemcache

virgo_malloc()/virgo_get()/virgo_set()/virgo_free() system calls, allocate a contiguous kernel memory in a remote cloud node's kernel address space but refer to the memory locations only by VIRGO Unique ID which abstracts the user from kernel internals. Similarly, VIRGO cloudfs systemcalls virgo_open(), virgo_read(), virgo_write(), virgo_close() read/write to a file in remote cloud node by VFS kernelspace functions. VIRGO Unique ID for a memory location is translated by the system call to actual kernel address in remote node which is

not exposed to the user. VIRGO system calls wrap kernel space RPC calls to remote OS kernel memory allocators by an internal memory map datastructure - vtranstable - VIRGO Address Translation Table. Most of the available memory allocators in kernel are SLAB, SLOB and SLUB. Computational complexity bounds of Dynamic storage allocators place limitation on implementing any memory allocator:

(*) Robson bounds - Memory allocation and Defragmentation guarantees - SQLite - <https://www.sqlite.org/malloc.html#nofrag> - $N = M * (1 + (\log_2 n) / 2) - n + 1$ (N - number of memory pools in allocator, M - Maximum memory requirement, n - ratio of largest to smallest memory allocation)

(*) Memory Defragmentation is NP-Hard - Theorem 3.2 - Heap defragmentation in bounded time - <https://pdfs.semanticscholar.org/0b76/95751ec6ed1029bc15ba389798aa8897dc85.pdf> [J. M. Robson. "Bounds for Some Functions Concerning Dynamic Storage Allocation". Journal of the Association for Computing Machinery, Volume 21, Number 8, July 1974, pages 491-499.]

As mentioned in earlier question of this FAQ on similarities to SunRPC/NFS/kORBit and elsewhere, VIRGO system calls try to unify kernel address spaces of all constituent nodes in the cluster/cloud mainly targeting IoT and embedded hardware. This requires mutual trust amongst the nodes of the cloud - e.g. KTLS, OpenVPN Virtual IPs, Access Controlled Lists - which is presently a prerequisite and KTLS is still in flux. Assuming availability of a secure trusted cloud, for example an office intranet having IoT devices in Servers, UPS, Lighting, Security CCTV cameras etc., which have their device memory addresses mmap()-ed to kernel address space, VIRGO kmemcache and cloudfs system calls can directly access kernel space address or storage of these devices which is permissible in trusted cloud. Presently this kind of IoT is done in userspace protocols like MQTT/MAVlink. Most apt application of VIRGO system calls is the wireless cloud of drones/autonomous vehicles/fly-by-wire which require low latency - VIRGO system calls writing to kernel space of remote vehicles in cloud for navigation/flight should theoretically be faster than userspace protocols (some research examples on AmoebaOS cited previously) because direct access to kernel space bypasses lot of roundtrip of the packets from userspace to kernel space and viceversa. Motivation for KTLS was precisely to cut this overhead (<https://netdevconf.org/1.2/papers/ktls.pdf> - Figure 1 and 2 - send file implementation in kernel space by Facebook bypassing userspace). There have been some efforts to port memcached (<http://memcached.org/>) cacheing server to linux kernel - kmemcached in-kernel server - <https://github.com/achivetta/kmemcached> - which has similar motivation.

****Linux side of NeuronRain does everything in kernel space transparent to userspace. Wouldn't this prohibit userspace cloud because end consumers are applications in userspace? Why should transport be abstracted and submerged within kernel and re-emerge to userspace? Doesn't it affect response time?***

1197. (THEORY and FEATURE) Machine Learning enabled VIRGO32 and VIRGO64 Linux Kernels - SunRPC and Kernel space Cloud System calls and Drivers - related to all sections of Drone Autonomous Delivery, IoT and Kernel Analytics, Program Analysis, Software Analytics

SunRPC is one of the oldest ingredient of linux kernel making kernel space TCP transport. SunRPC is used by lot of distributed protocols e.g. NFS. SunRPC kernel sockets code in <http://elixir.free-electrons.com/linux/latest/source/net/sunrpc/svcsock.c> is an example of how kernel space request-response happens. SunRPC is like a traditional ORB, requiring compilation of stubs and implementations done in server side. Services register to portmap to get a random port to run. Client discover the services via portmap and invoke remote functions. XML-RPC is a later advancement which uses XML encoded transport between client and server. XML-RPC is the ancestor of SOAP and present industry standard JSON-REST.

Comparison of SunRPC and XML-RPC in http://people.redhat.com/rjones/secure_rpc/ shows how performant SunRPC is. SunRPC uses XDR for data representation. VIRGO presently does not have service registry, discovery, stub generation like SunRPC because it delegates all those complexities to kernel and user does not need to do any registration, service discovery or stub implementation. User just needs to know the unique name of the executable or function (and arguments) in the remote cloud node. All cloud nodes must have replicated binaries which is the simplest registration. Ports are hardcoded and hence no discovery is required. Only linux 32-bit (4.1.5) and 64-bit (4.13.3) datatypes are supported. In this respect, VIRGO differs from any traditional RPC protocols.

Marshalling/Unmarshalling have been ignored because, goal of VIRGO is not just RPC, but a logically unified kernel address-space and filesystems of all cloud nodes - kernel address spaces of all cloud nodes are stored in a VIRGO address translation table by VIRGO system calls. VIRGO system calls at present have a plain round-robin and a random-number based loadbalancing schemes. Research paper on userspace versus kernelspace remote procedure calls in <http://citeseerx.ist.psu.edu/viewdoc/download?doi=10.1.1.32.4304&rep=rep1&type=pdf> has experimental results proving kernelspace RPC has a non-trivial speedup compared to userspace RPC in Amoeba OS. Most prominent cloud implementations (JSON-RPC or JSON-REST) do userspace RPCs presently and rarely use SunRPC-NFS style of kernelspace RPCs. Article in <http://www.csn.ul.ie/~mark/fyp/fypfinal.html> - CORBA in the kernel? - compares two mechanisms for kernelspace RPC - CORBA-kORBit and SunRPC. Quoting from it: "... One application of this is idea is that the user should be able to use a physical device attached to any of the nodes in the cluster as if it were physically attached to the node the user was operating from. ...". VIRGO linux kernel systemcalls/drivers try to achieve exactly this where "physical device" is CPU, Kernel Memory and Filesystem in a remote cloud node. This is a typical feature required for a cloud of embedded systems. In this respect, VIRGO is a hybrid of cloud and cluster for parallelism. VIRGO does not invoke SunRPC code at present and just derives the concept, though original intention was to wrap the system calls and drivers on SunRPC. Reason is the considerable code changes required in existing SunRPC socket code in kernel - thus VIRGO systemcalls and drivers were written from scratch.

End consumers are not necessarily only userspace applications. NeuronRain VIRGO systemcalls/driver listeners communicate in kernelspace which is prime necessity for embedded systems cloud e.g cloud of devices like IoT. That's why it has been reiterated NeuronRain is mainly for kernelspace clouds and not for userspace which already has many frameworks. For example, KingCobra pub-sub depends on linux work-queue for enqueueing a message and servicing it. This kind of kernel space messaging is a requirement for device clouds which receive and queue event interrupts. Another example is the kmemcache system calls/drivers functionality which allocates/sets/gets/frees kernel memory in a remote cloud node. This is most sought after feature in device clouds than application layer clouds.

Userspace clouds cannot control remote devices unless some kind of REST/RPC message is sent/received. By implementing RPCs within system calls, every cloud node has direct access to remote cloud's kernel memory. It has to be noted this does not compromise security despite AF_KTLS sockets being still experimental. Because all system calls have processor support for privileged mode execution. Access to remote kernel memory can happen only by invoking system calls because the memory locations are translated to a unique id in a table privy to system calls and stored in kernelspace. Vulnerability of this communication between kernelspaces is as bad as traditional transport and there is no additional performance overhead. Even if AF_KTLS is not available in near future (which is OpenSSL integrated into kernel), messages can be encrypted by userspace and sent and decrypted in the other end though limited in scope relative to Diffie-Hellman SSL handshake. Presently AF_KTLS is available as separate kernel module (<https://netdevconf.org/1.2/papers/ktls.pdf>, https://github.com/ktls/af_ktls) which exports AF_KTLS socket family symbol kernel-wide. Regarding when transport abstraction to kernel and re-emergence to userspace is required, please refer to GlusterFS architecture documentation and diagrams at: <http://docs.gluster.org/en/latest/Quick-Start-Guide/Architecture/>. Diagram for simple file listing ls command is pertinent to this question - ls command originates in userspace dives into kernel VFS, is intercepted by FUSE kernel

module and is redirected by upcall to userspace. All VIRGO linux kernel driver listeners support upcalls to userspace which have downcall-upcall request flow similar to GlusterFS (NeuronRain RPC is shown in draw.io JGraph architecture diagram: https://github.com/shrinivaasanka/Krishna_iResearch_DoxygenDocs/blob/master/NeuronRainVIRGOArchitecture.jpg). GlusterFS is userspace filesystem meant for cloud storage. It implements FileSystem in Userspace (FUSE) paradigm. Userspace filesystem performs better than kernelspace per GlusterFS documentation. VIRGO kernel_analytics module does in reverse what FUSE kernel module does in GlusterFS, but for analytics - VIRGO kernel_analytics reads in realtime, a periodically updated userspace analytics config file and exports into kernel. [EDIT - 21 September 2017, 23 September 2017]: In a Recent Development, KTLS has been integrated into linux kernel version 4.13 mainline - <https://github.com/torvalds/linux/blob/master/Documentation/networking/tls.txt> , <https://opensourceforu.com/2017/09/linux-4-13-enhanced-security/>). Because of this important feature required for VIRGO cloud security, all system calls and kernel module listeners of VIRGO64 have been forward ported to 4.13.3 (in separate branch - VIRGO_KTLS - https://github.com/shrinivaasanka/virgo64-linux-github-code/tree/VIRGO_KTLS and https://sourceforge.net/p/virgo64-linux/code/ci/VIRGO_KTLS/tree/) including KTLS setsockopt() related client-server kernel socket code changes in a compile time VIRGO_KTLS #ifdef option. This finally makes all VIRGO64 kernelspace systemcalls-drivers network traffic encrypted. KTLS enabled VIRGO64 is built by including -DVIRGO_KTLS in system calls and driver Makefiles. Cryptographic handshake information is created by Userspace libraries like GNUTLS and written in /etc/virgo_ktls.conf key-value pairs (For GNUTLSget_record state the tuples are IV,SequenceNumber,Cipher,Salt). Wrapper KTLS module driver/virgo/ktls and system calls read /etc/virgo_ktls.conf and set crypto_info for all kernel sockets by kernel_setsockopt(). By default, VIRGO_KTLS option in Makefiles are commented. Every userspace handshake has to overwrite /etc/virgo_ktls.conf. Presently, GNUTLS is not tested in kernelspace and only example ktls config crypto_info variables have been exported to kernelspace. Master branches of VIRGO64 in both SourceForge and GitHub do not have KTLS because KTLS is a nascent functionality forcing changes to existing non-TLS kernel sockets code flow and does not have public key encryption yet. An alternative to KTLS is to have fully-secure Virtual Private Network Tunnel clients and servers (e.g OpenVPN) across all VIRGO64 cloud nodes. This secures L2 and L3 TCP/IP by assigning Virtual IP addresses to the nodes and all systemcalls-drivers traffic happens across these Virtual IPs within a secure Tunnel without KTLS. SunRPC is one of the oldest ingredient of linux kernel making kernelspace TCP transport. SunRPC is used by lot of distributed protocols e.g NFS. SunRPC kernel sockets code in <http://elixir.free-electrons.com/linux/latest/source/net/sunrpc/svcsock.c> is an example of how kernelspace request-response happens. SunRPC is like a traditional ORB, requiring compilation of stubs and implementations done in server side. Services register to portmap to get a random port to run. Client discover the services via portmap and invoke remote functions. XML-RPC is a later advancement which uses XML encoded transport between client and server. XML-RPC is the ancestor of SOAP and present industry standard JSON-REST. Comparison of SunRPC and XML-RPC in http://people.redhat.com/rjones/secure_rpc/ shows how performant SunRPC is. SunRPC uses XDR for data representation. VIRGO presently does not have service registry, discovery, stub generation like SunRPC because it delegates all those complexities to kernel and user does not need to do any registration, service discovery or stub implementation. User just needs to know the unique name of the executable or function (and arguments) in the remote cloud node. All cloud nodes must have replicated binaries which is the simplest registration. Ports are hardcoded and hence no discovery is required. Only linux 32-bit (4.1.5) and 64-bit (4.13.3) datatypes are supported. In this respect, VIRGO differs from any traditional RPC protocols. Marshalling/Unmarshalling have been ignored because, goal of VIRGO is not just RPC, but a logically unified kernel address-space and filesystems of all cloud nodes - kernel address spaces of all cloud nodes are stored in a VIRGO address translation table by VIRGO system calls. VIRGO system calls at present have a plain round-robin and a random-number based loadbalancing schemes. Research paper on userspace versus kernelspace remote procedure calls in

<http://citeseerx.ist.psu.edu/viewdoc/download?doi=10.1.1.32.4304&rep=rep1&type=pdf> has experimental results proving kernelspace RPC has a non-trivial speedup compared to userspace RPC in Amoeba OS. Most prominent cloud implementations (JSON-RPC or JSON-REST) do userspace RPCs presently and rarely use SunRPC-NFS style of kernelspace RPCs. Article in <http://www.csn.ul.ie/~mark/fyp/fypfinal.html> - CORBA in the kernel? - compares two mechanisms for kernelspace RPC - CORBA-kORBit and SunRPC. Quoting from it: "... One application of this idea is that the user should be able to use a physical device attached to any of the nodes in the cluster as if it were physically attached to the node the user was operating from. ...". VIRGO linux kernel systemcalls/drivers try to achieve exactly this where "physical device" is CPU, Kernel Memory and Filesystem in a remote cloud node. This is a typical feature required for a cloud of embedded systems. In this respect, VIRGO is a hybrid of cloud and cluster for parallelism. VIRGO does not invoke SunRPC code at present and just derives the concept, though original intention was to wrap the system calls and drivers on SunRPC. Reason is the considerable code changes required in existing SunRPC socket code in kernel - thus VIRGO systemcalls and drivers were written from scratch.

****How does machine learning and analytics help in kernel?****

A lot. NeuronRain analytics can learn key-value pairs which can be read by kernel_analytics kernel module dynamically. Kernel thus is receptive to application layer a feature hitherto unavailable. Earlier OS drove applications - this is reversed by making applications drive kernel behaviour.

****Are there existing examples of machine learning being used in Linux kernel?****

805. Program Analysis, Software Analytics, OS Kernel and Scheduler Analytics, Online Streaming Classifiers, Self-Healing - (this section is an extended unifying draft of theory and feature in AstroInfer, USBmd, VIRGO, KingCobra, GRAFIT, Acadp drafts, Krishna_iResearch_DoxygenDocs)

Yes. There have been some academic research efforts, though not commercial, to write a machine learning scheduler for linux kernel. Linux kernel presently has Completely Fair Scheduler (CFS) which is based on Red-Black Tree insertion and deletion indexed by execution time. It is "fair" in the sense it treats running and sleeping processes equally. If incoming processes are treated as a streaming dataset, a hypothetical machine learning enabled scheduler could ideally be a "Multilabel Streaming Dataset Classifier" partitioning the incoming processes in the scheduler queue into "Highest, Higher, High, Normal, Low, Lower, Lowest" priority labels assigning time slices dynamically according to priority classifier. It is unknown if there is a classifier algorithm for streaming datasets (though there are streaming majority, frequency estimator, distinct elements streaming algorithms). In supervised classification, such algorithm might require some information in the headers of the executables and past history as training data, neural nets for example. Unsupervised classifier for scheduling (i.e scheduler has zero knowledge about the process) requires definition of a distance function between processes - similar processes are clustered around a centroid in Voronoi cells. An example distance function between two processes is defined by representing processes on a feature vector space:
process1 = <pid1, executabletype1, executablename1, size1, cpu_usage1, memory_usage1, disk_usage1>
process2 = <pid2, executabletype2, executablename2, size2, cpu_usage2, memory_usage2, disk_usage2>
distance(process1, process2) = euclidean_distance(process1, process2)
Psutils Dictionary Encoding of a process and Diff edit distance between two processes has been implemented in <https://github.com/shrinivaasanka/asfer->

github-code/blob/master/python-src/software_analytics/DeepLearning_SchedulerAnalytics.py. Socket Streaming Analytics Server of Process Statistics has been implemented in https://github.com/shrinivaasanka/asfer-github-code/blob/master/python-src/software_analytics/ which analyzes stream of process JSON dictionary data and can write out analytics variables read/exported by VIRGO Linux kernel_analytics driver which in turn are readable by OS Scheduler (requires Scheduler rewrite). This is an ideal solution for self-healing OS kernels which learn from process performance in userspace and change scheduler behaviour dynamically. Analytics variables can be directly written to /etc/sysctl.conf or by sysctl if alternative to /etc/kernel_analytics.conf is preferred. Sysctl has config variables for VM Paging, Scheduler, Networking among others which are read by kernel live (kernel.sched.*)- if kernel provides comprehensive sysctl variables for Scheduler policy, it removes necessity for Scheduler rewrite. Presently sysctl apparently exports Round Robin timeslicing only. Similarly, USBmd 32 and 64 bit drivers for Wireless LAN traffic analytics can directly write learnt analytic variables to /etc/sysctl.conf (<https://www.kernel.org/doc/Documentation/networking/ip-sysctl.txt> lists various TCP tuning configs - net.* - e.g Corking consecutive frequent read/writes into one read/write, SYNACK retries, fastopen, receive buffer size). GRAFIT Course Material in https://github.com/shrinivaasanka/Grafit/blob/c8290348b916e5b35044c3834f56a825b4db23e4/course_material/NeuronRain/AdvancedComputerScienceAndMachineLearning/AdvancedComputerScienceAndMachineLearning.txt describe an example performance analytics of OS Scheduler (clockticks-to-processes) hypothetically implemented as LSH. Simulating this in a linux kernel may not be straightforward. But there are performance tools like perf (<http://www.brendangregg.com/perf.html#SchedulerAnalysis>) and SAR which can create a streaming text dataset of kernel scheduler runqueue after some script processing and write kernel.sched.* variables based on analytics. NeuronRain Theory Drafts include a Worst Case Execution Time scheduler which depends on apriori knowledge of maximum execution times of process executables - Linux kernel 4.x implements an Earlier Deadline First scheduler for realtime executables (SCHED_DEADLINE - sched/deadline.c) based on Constant Bandwidth Server (CBS) and Greedy Reclamation of Unused Bandwidth (CBS and GRUB) algorithms which "reserve" resources for processes and "reclaim" if not used.

****Who can deploy NeuronRain?****

 832. NeuronRain Usecases - Drones - UAV Autonomous Delivery and GPS Navigation, Kernel Analytics - (this section is an extended unifying draft of theory and feature in AstroInfer, USBmd, VIRGO, KingCobra, GRAFIT, Acadpdrafts, Krishna_iResearch_DoxygenDocs)

 Anyone interested in dynamic analytics driven kernel. For example, realtime IoT kernels operating on smart devices, autonomous driverless vehicles, robots, drones, embedded systems etc.,. There are already linux distros for drones and unmanned aerial vehicles (<https://www.dronecode.org/>) and automobiles (Automotive Grade Linux - <https://www.automotivelinux.org/>). For example autonomous vehicles and drones have linux kernel drivers for LIDAR sensors for navigation which can be analytics driven. Linux kernel tree has support for LIDAR sensors and GARMIN GPS USB drivers (pulsedlight LIDAR driver - <https://github.com/torvalds/linux/commits/master/drivers/iio/proximity/pulsedlight-lidar-lite-v2.c>, GARMIN GPS USB drivers - http://elixir.free-electrons.com/linux/latest/source/drivers/usb/serial/garmin_gps.c). LIDAR sensor and GPS drivers can import kernel_analytics exported variables - from UAV autopilot, drone navigation for example. Present implementation of kernel_analytics driver in VIRGO32 and VIRGO64 reads /etc/kernel_analytics.conf by VFS kernel functions. In autonomous driving this file has to be overwritten in high frequency by machine learning userspace code. Intense File I/O in kernel

modules is strongly advised against. Some realtime alternatives to this have been minimally implemented e.g perpetual reading of analytics variables from a streaming socket in a local or remote cloud node in kernelspace - something similar to Spark Streaming in Kernelspace. This would remove disk latency and necessity for storage of analytics variables - kernel_analytics driver reads the variables from socket and exports them kernelwide in an infinite loop. VIRGO64 kernel_analytics module has an optional function implemented to read stream of config variable-value pairs connecting to an analytics server and stored in a circular buffer exported kernelwide. For realtime low latency requirements viz., autonomous vehicles, patching linux kernel with realtime PREEMPT_RT (<https://git.kernel.org/pub/scm/linux/kernel/git/rt/linux-rt-devel.git/tree/>) is suggested (though this has not been tested). NeuronRain is a generic machine learning, kernelspace cloud system calls and drivers for analytics powered linux fork-off which integrates cloud and machine learning features into kernel itself more than being IoT specific e.g ARM has a linux fork-off - <https://github.com/ARM-software/linux> and Machine Learning Library based on GoogLeNet Deep Learning - <https://github.com/ARM-software/ComputeLibrary>. Zephyr RTOS Linux supports most of the IoT boards - <https://github.com/zephyrproject-rtos/zephyr> - overlaying NeuronRain system calls and drivers source tree on Zephyr is probably the best usecase for kernel analytics driven IoT.

****How does NeuronRain compare against other Cloud IoT platforms?****

833. NeuronRain Usecases - IoT and Kernel Analytics - (this section is an extended unifying draft of theory and feature in AstroInfer, USBmd, VIRGO, KingCobra, GRAFIT, Acadpdrafts, Krishna_iResearch_DoxygenDocs)

Prominent cloud platforms for IoT include Google Cloud IoT (<https://cloud.google.com/iot-core/>), AWS IoT (<https://aws.amazon.com/iot-platform/>), Microsoft Azure(<https://azure.microsoft.com/en-in/suites/iot-suite/>) among others. Almost all of these implement an RPC standard named MQTT (over TCP/IP stack) a pub-sub message broker protocol for device-device communications e.g for processing data from sensors connected to cloud. Data from sensors is ingested in broker and processed by machine learning analytics. There are Eclipse IoT projects (<https://iot.eclipse.org/>) implementing MQTT protocol for embedded device clouds e.g Mosquitto (<https://mosquitto.org/>). MQTT pub-sub is in userspace. NeuronRain does not have MQTT and implements a system call-to-kernel module kernelspace socket RPC in VIRGO linux, machine learning analytics in AsFer and USBmd kernel module and device pub-sub in KingCobra kernel module. On the other hand IoT combined with machine learning is a modern version of SCADA which acquires data from devices and graphically presents them - For example https://sourceforge.net/projects/acadpdrafts/files/BEInternship1998SAIL_PSGTechPresentation.pdf/download is a SCADA code written in DEC VAX VMS Fortran Graphics (SAIL - 1998) for sourcing realtime data from steel furnaces and smelters connected by optic fibres (SAILNET) which are equipped with Programmable Logic Controller sensors. While SCADA is a supervised, controlled data acquisition, IoT + Machine Learning is an unsupervised data acquisition (ETL) and learning methodology.

References:

833.1 ActiveWorks-webMethods-SoftwareAG Broker Server - Oldest Publish-Subscribe Model MQ and XML implementation - 1995 - <https://www.pcmag.com/encyclopedia/term/activeworks>
833.2 ActiveWorks-webMethods-SoftwareAG Broker Server - Message Queue Broker - Forums - <https://tech.forums.softwareag.com/tag/managing-webmethods-broker>

****How does Neuro MAC electronic money in KingCobra differ from other**

cryptocurrencies?**

806. EventNet HyperLedger, Neuro Cryptocurrency, Money Trails, Money Changing Problem - Optimal Denomination, Market dynamics - (this section is an extended unifying draft of theory and feature in AstroInfer, USBmd, VIRGO, KingCobra, GRAFIT, Acadp drafts, Krishna_iResearch_DoxygenDocs)

Disclaimer: MAC protocol buffer implementation of a fictitious electronic currency - Neuro - in AsFer/KingCobra is an off-shoot of Equilibrium Pricing implementation in KingCobra and is still evolving (e.g a minimal proof of work, boost UUID globally unique hashes per protocol buffer currency object have been implemented). Intent of this fictitious currency is to create a virtual economic network e.g Stock Market, Money Market Flow Dynamics, Money Trail EventNet Graph, Buy-Sell Equilibrium for pricing etc., and draw analytics inferences from them (e.g Graph Mining). It tries to simulate realworld currency transactions in software by C++ idiom of zero-copy Perfect Forwarding - only one instance of an object exists globally at any instant - notion of singleton added to unique timestamp. This is how currency having unique id flows across an economic network in realworld - two copies of a bill create counterfeit - and ideal for obliterating double-spending. Traditional cryptocurrencies like bitcoin use blockchain technology - a chronologically increasing linked list of transaction blocks - to maintain a global ledger of bitcoin transactions which can be lookedup publicly. Mint/Fed in Bitcoin proliferates by process of mining SHA hashes having some specific qualities - certain leading digits must be 0 and a non-trivial computation has to be performed to attain this least probable hashcash - known as Proof-of-Work computation. Bitcoins are awarded based on complexity of proof-of-work. Bitcoin network hashcash proof-of-work is power intensive requiring hundreds of megawatts of electricity (Bitcoin GPU mining rigs worldwide consume 126.09 terawatts of power annually - <https://www.cnet.com/personal-finance/crypto/heres-how-much-electricity-it-takes-to-mine-bitcoin-and-why-people-are-worried/>). KingCobra Neuro MAC currency does not envisage a global transaction ledger. It only relies on singleton-ness of a currency protobuf object. Optimal denominations which minimize the number of currency notes-coins - usually decimal multiples of 1,2,5 - could be simulated by Neuro protobuf currency objects. Most cloud object move protocols mimic move by copy-delete and do not implement equivalent of C++ std::move(). Every Neuro MAC transaction is a Client-Server Network Perfect Forwarding which "moves" (and not copies) a fictional currency protocol buffer object over network from sender to receiver (code for this is in cpp-src/cloud_move/ directory of AsFer and invoked in a shell script and python transaction code in KingCobra. Compile time option -DOPENSSL enables SSL client-server socket transport). This global object uniqueness is sufficient for unique spending. Ledgering can be optionally implemented by tracking the trail of transactions as a linked list in Currency Protocol Buffer. EventNet described in this documentation and implemented in AsFer fits in as global Neuro MAC transaction hyperledger graph where each vertex in EventNet has actors (Buyers and Sellers) in transaction and direction of edge indicates flow of Neuro MAC. Minimal EventNet HyperLedger has been implemented in NeuronRain which encodes causality of every buy-sell transaction. Platform neutrality of Protocol Buffer was the reason for its choice as Currency format. Neuro Cryptocurrency minted by Proof of Work algorithms have been assigned a Visual representation for network transmission secured by Digital Watermarking signatures. Expirable C++ objects implementation in NeuronRain which is meant for restricting number of views of a visual sent over network driven by privacy concerns, could be a wrapper for Neuro Visual Currency to upperbound the number of transactions a currency UUID (generated by Boost UUID or SHA256) is part of - a timeout feature, resulting in truncation of money trail after some hops - UUID has to be regenerated after timelapse.

Is NeuronRain production deployment ready? Is it scalable?

807. NeuronRain - Scalability Benchmarks and Caution - (this section is an extended unifying draft of theory and feature in AstroInfer, USBmd, VIRGO, KingCobra, GRAFIT, Acadpdrfts, Krishna_iResearch_DoxygenDocs)

Presently complete GitHub, GitLab and SourceForge repositories for NeuronRain are contributed (committed, designed and quality assured) by a single person without any funding (K.Srinivasan - <http://sites.google.com/site/kuja27> - Deleted and Mirrored at https://github.com/shrinivaasanka/Krishna_iResearch_DoxygenDocs/blob/master/kuja27_website_mirrored/site/kuja27/) with no team or commercial entity involved in it. This requires considerable time and effort to write a bug-free code. Though functionalities are tested sufficiently there could be untested code paths. Automated unit testing framework has not been integrated yet. Note of caution: though significant code has gone in GitHub, GitLab and Sourceforge repositories there is still a lot to be done in terms of cleaning, documentation, standards, QA etc., So it is upto the end-user to decide. There are no scalability benchmarks as of now though some AsFer Spark Cloud implementations - Recursive Gloss Overlap Intrinsic Merit, Computational Geometric Factorization, Video EventNet Tensor Products-Tensor Rank Decomposition and Approximate Least Squares SAT Solver have been benchmarked on Python 2.7.x and Python 3.x - quadcore and single node cluster. All Python 2.7 source files of NeuronRain can be upgraded to Python 3.x by autopep8 PEP8 compliance and 2to3-2.7 upgrade utilities. Python 3.x is faster and preferable to Python 2.x for computationally intensive code. VIRGO system calls-kernel modules transport has been tested on a 2 node cluster. Presently, NeuronRain is almost like a beta version. Deployments on large clouds for academic research are encouraged (e.g VIRGO system calls/drivers and kernel analytics for IoT and Drones, Spark Recursive Gloss Overlap Interview Intrinsic Merit, Graph Tensor Neuron Network Recursive Lambda Function Growth Intrinsic Merit, Video EventNet Tensor Products, Spark Computational Geometric Factorization on large clusters- specifically Bitonic Sort and Local Segment Binary Search, Approximate least squares CNF SAT solver for millions of variables and clauses). Production/Commercial deployments are subject to caveats and licensing terms mentioned in this FAQ and BestPractices.txt in NeuronRain AstroInfer SourceForge, GitHub and GitLab repositories (e.g Drones require aviation license compliance in respective countries) and utmost caution is advised.

****Are there any demonstrative tutorial usecases/examples on how NeuronRain VIRGO system calls and drivers work?****

Some reference screen and kernel logs have been committed to:

-
https://github.com/shrinivaasanka/virgo64-linux-github-code/tree/master/virgo-docs/systemcalls_drivers
- https://sourceforge.net/p/virgo64-linux/code/ci/master/tree/virgo-docs/systemcalls_drivers/

which demonstrate the system call testcases for VIRGO clone, kmemcache and filesystem listener drivers.
virgo-docs/ in URLs above have detailed description of System Calls and Drivers in commit notes. VIRGO64 is the 64-bit version of VIRGO repositories but overlay-ed on top of 4.13.3 mainline kernel. 64-bit VIRGO kernel has lot of bug fixes and is stabler than 32-bit VIRGO kernel. This anomaly between 32 bit 4.1.5 and 64 bit 4.13.3 linux kernels was a frustrating, deplorable issue to debug. Mainly, 32 bit kernels were frequently crashing in DRM GEM i915 intel graphics drivers. Quite a few i915 bug fixes went in 4.9 and 4.10 kernels which could have been the reason for stabler 64-bit VIRGO kernel. Apart from these testlogs/ or test_logs/ folders in all NeuronRain repositories contain manually captured testcase logs appended with historic date/time stamp suffix. Course material in

https://github.com/shrinivaasanka/Grafit/tree/master/course_material/NeuronRain
have complementary information on NeuronRain meant for academic classroom teaching.

****How applicable is NeuronRain for Drones/Robots?****

808. (THEORY and FEATURE) Machine Learning Enabled VIRGO32 and VIRGO64 linux kernels - Drone Telemetry in Linux kernel - NeuronRain Usecases - NeuronRainApps - Autonomous Delivery, Drone Electronic Voting Machines, Kernel Analytics and Dynamic Mission Plans, GIS Urban Sprawl Analytics, Road geometry and Homotopy, Cellular automaton graph, Social network analysis, Space filling, Circle Packing, Pandemic/Memes/Fads/Opinions/Cybercrime analytics, 8 Queens Problem, Graph Hamiltonians - related to 713 - this section is an extended unifying draft of theory and feature in NeuronRain repositories - AstroInfer, USBmd, VIRGO, KingCobra, GRAFIT, Acadp drafts, Krishna_iResearch_DoxygenDocs

Drones have distinct software and hardware for mission plan (route map), flight and ground control often different from mainstream linux kernel. Mission plans are uploaded to drone by special protocols like MAVlink and userspace SDKs are available for it. Drone control userspace C++ code example in https://github.com/Dronecode/DronecodeSDK/blob/develop/example/fly_qgc_mission/fly_qgc_mission.cpp uses DronecodeSDK in userspace and there is no necessity for kernel_analytics kernel module to read analytics variables into kernelspace from userspace Machine Learning code. Application code can directly instantiate /etc/kernel_analytics.conf File locally/Socket Streaming Iterable in https://gitlab.com/shrinivaasanka/asfer-github-code/blob/master/python-src/Streaming_AbstractGenerator.py on a remote host and at port 64001 (in Python) and read analytics variables for drone navigation augmenting flight plan - Quite useful when static mission plans require dynamic changes (obstacle avoidance for instance) after upload to drone e.g Military Reconnaissance, Autonomous Combat (https://auterion.com/wp-content/uploads/2020/05/PR-Auterion-awarded-contract-by-DIU-to-strengthen-PX4-ecosystem-4_29_19.pdf), Autonomous Online Shopping Delivery, Autonomous Drone Electronic Voting Machines, Autonomous Search and Rescue Drones. For robots, there are already linux add-on operating systems in development e.g ROS - <http://www.ros.org/> which could benefit by kernel_analytics and VIRGO32/VIRGO64 system calls and drivers. Recent linux kernel versions from 4.17.x onwards support PhoenixRC flight controller (<https://github.com/torvalds/linux/blob/master/drivers/input/joystick/pxrc.c>) and thus drone telemetry is part of linux kernel. Kernel Analytics navigation variables exported by VIRGO32 and VIRGO64 kernel_analytics drivers can be imported in pxrc drone driver and input_set_abs_params() is invoked for appropriate setting of ordinates, rudder, throttle values. NeuronRain AstroInfer has a partial untested drone implementation (DroneSDK Python code and PXRC linux kernel driver code have not been executed on a Drone and Flight controller because of lack of licensed unmanned aerial vehicle) and usecases description for Autonomous Online Shopping Delivery, Drone Electronic Voting Machines which assumes a GPS-ROS-Google Maps navigation algorithm (e.g <https://journalofbigdata.springeropen.com/articles/10.1186/s40537-019-0214-3>, Google geocoding - Address to Longitude-Latitude and viceversa- <https://developers.google.com/maps/documentation/geocoding/overview> - Highrise addresses might require altitude for 3D navigation) etc. DroneSDKs for Python rely on asynchronous I/O for drone communication. NeuronRain GRAFIT repositories have an example Asynchronous I/O implementation of a Python 3.x ChatBot Client-Server which can be adapted to invoke MAVSDK Drone Telemetry API and make decisions by performing NeuronRain machine learning analytics (by replacing the await call to wait for drone.connect() - https://github.com/shrinivaasanka/Grafit/blob/master/course_material/Programming/Python/code/AsyncIO_Client.py and AsyncIO_Server.py). Example Drone code in <https://github.com/mavlink/MAVSDK-Python/> import mavsdk and connect to drone via await drone.connect(system_address="udp://:14540"). MAVSDK protocol

[illegible]

- 02: open spaces, medium vegetation surfaces $0.3 < \text{NDVI} \leq 0.5$
- 03: open spaces, high vegetation surfaces $\text{NDVI} > 0.5$
- 04: open spaces, water surfaces $\text{LAND} < 0.5$
- 05: open spaces, road surfaces
- 11: built spaces, residential, building height $\leq 3\text{m}$
- 12: built spaces, residential, $3\text{m} < \text{building height} \leq 6\text{m}$
- 13: built spaces, residential, $6\text{m} < \text{building height} \leq 15\text{m}$
- 14: built spaces, residential, $15\text{m} < \text{building height} \leq 30\text{m}$
- 15: built spaces, residential, building height $> 30\text{m}$
- 21: built spaces, non-residential, building height $\leq 3\text{m}$
- 22: built spaces, non-residential, $3\text{m} < \text{building height} \leq 6\text{m}$
- 23: built spaces, non-residential, $6\text{m} < \text{building height} \leq 15\text{m}$
- 24: built spaces, non-residential, $15\text{m} < \text{building height} \leq 30\text{m}$
- 25: built spaces, non-residential, building height $> 30\text{m}$.

Segregating Non-residential as Commercial or Central Business District (CBD) and Industrial (Manufacturing-IT-ITES) splits earlier 3-color classification into desired 4-coloring and there are kernel density based clustering solutions suggested for identifying CBD : 1) Building an Urban Spatial Structure from Urban Land Use Data: An Example Using Automated Recognition of the City Centre - <https://www.mdpi.com/2220-9964/6/4/122/htm> 2) Delimitating Urban Commercial Central Districts by Combining Kernel Density Estimation and Road Intersections: A Case Study in Nanjing City, China - <https://www.mdpi.com/2220-9964/8/2/93/htm> . Moran's I and Gini Index are measures of dispersion and unequal lopsided distribution of growth within an urban sprawl. Graph connecting nightlights circular vertices by edges, could be an aerial transportation graph for autonomous delivery Drones between cities. Electricity Consumption and NightLights are mostly limited to Residential, Commercial and Manufacturing-IT-ITES regions of an urban sprawl and Agricultural land-Greenery-Waterbodies are excluded because of almost nil night lighting. Thus only 3 of the 4 colors of an Urban sprawl FaceGraph are covered by NightLights urban sprawl estimation excluding Farm lands which could be an error-free guideline for Urban planning and Expansion. There is an unusual theoretical aspect to NASA VIIRS NightLights urban area circles - Circular Urban areas of varied radii are packed (close or loose) on 2 dimensional space of a nation which makes it a variant of Space filling or Unequal Circle packing problem. Some bustling urban areas in VIIRS imagery of India 2017 are not heavily lit which could be inferred as "NightLights imply urbanization while converse may not be true (or) NightLights sprawl lowerbounds an Urban sprawl". NeuronRain implements ranking of urban sprawls based on areas of segmented Contour polynomials. Circles or contour polynomials bounding urban areas unequally fill the 2D space and ratio of sum of urban contour areas to area of the country is the urbanization percentage metric. Set of Urban area contours could be grouped by unsupervised clustering algorithms (e.g Neural Networks, DBSCAN, Voronoi Tessellation) using euclidean distances amongst their centroids from which juxtaposed urban area contour polynomials that might coalesce to form megalopolises with high probability could be found. Distance similarity between (difference in number and area of urban sprawl contour polynomials) VIIRS imagery of 2012 and 2016 is a measure of urban expansion, creation of new urban sprawls and merger of adjoining urban areas and suburbs which should be commensurate with rate of growth of GDP between 2012 and 2016. As a space filling problem, this is equivalent to finding distance between 2 temporally separate unequal polynomial (or circle) packings of a 2D surface. As opposed to 4-colored segmented facegraphs of Urban sprawl GIS imagery (Residential, Commercial, Manufacturing-IT-ITES, Greenery) for resource allocation, transportation network graph (e.g retrieved from Google Roads API) could be basis for urban sprawl analytics based on which drones could navigate. Transportation network graph of urban sprawls is topologically and geometrically different from theoretical graphs - edges (rail, roads) between intersections or localities are not necessarily straight lines but are curves of arbitrary shapes, though drone and UAV navigation is mostly along straightlines except obstacle avoidance. In other words, edges (roads) are embedded on a 2D plane (with the exception of multiplanar intersections) which is a product homotopy in topological terms (Analogy: In NeuronRain handwriting recognition by Product Homotopy, Pasting lemma merges paths defined by all possible curve fragments of

written alphabets between points x_0 - x_1 and x_1 - x_2). 8 Queens Problem in algorithmic theory which is about dynamic programming based optimal placement of 8 queens on a 64 square chequered chessboard so that none of the paths of queens collide, could be adapted to obstacle avoidance in drone navigation and autonomous vehicles. Queen moves on 8 directions on chessboard cellular automaton grid separated by 45 degrees quite similar to cellular automaton graph model of how pandemics/memes/fads/opinions/cybercrimes spread in social and electronic networks - in order to avoid infection in ER-SIR model, human vertices in a social-urban-sprawl network (which is a floating population) might choose routes found by N-Queen problem (N =average population density, significantly intractable compared to 8 queens). On the contrary, problem of autonomous combat between 2 sets of adversarial drone swarms (https://en.wikipedia.org/wiki/Unmanned_combat_aerial_vehicle) could be theoretically shown to be a PSPACE-complete problem, by an oversimplified reduction from $N*N$ Chess (On the complexity of Chess - $N*N$ Chess is proved to be PSPACE-complete -

<https://www.sciencedirect.com/science/article/pii/S0022000083900302>) in which each set (Black and White) has 1 King, at least 1 Queen (q) and N^h pawns ($h > 0$) - 2 sets of Adversarial Drone swarms each of size ($N^h + q + 1$) navigate along $N*N$ 2-dimensional Cellular Automaton Chess Grid. Earlier PSPACE-complete reduction from Chess is too simplistic because actual drone combat is chaotic and drone navigations are along 26 directions at least on 3-dimensional cellular automaton grid (8 directions on 2D plane + 9-up + 9-down). Almost all Drone Delivery problems are NP-Complete Hamiltonian problems which involve optimal tour mission plans along edges and vertices of an aerial or surface transportation graph. NASA Mars Rover Collaborative Information Portal is an example of hugely successful Robotic Drone Rover which has a scalable streamer service (Service Oriented Architecture) for Mission data transport between Mars Rover File Servers and multiple clients on Earth (Reference: Beautiful Code - Chapter 20 - Highly Reliable Enterprise System for NASA's Mars Rover Mission). UAVs for Drone EVMs, Autonomous Delivery et al., might similarly have to service multithreaded, parallel terrestrial MAVSDK clients which issue imaging commands e.g TAKE_PHOTO. Mars Rover which has been designed for unpredictable terrains and weather could be suitable as platform for online shopping delivery. Online shopping delivery which is still in conceptual stages of R&D has to focus on UAV transport of FMCG, Home appliances and Groceries in the range of 1 kg to 100 kg which are mostly sensitive to handle. Manned drones on the other hand are the holy grail of drone human transport (References on manned drones, flight time (20 minutes) and payload (220 kg): https://en.wikipedia.org/wiki/Passenger_drone, <https://lucidcam.com/how-much-weight-can-a-drone-carry/>, <http://www.onemandrone.com/about>, <https://www.droneblog.com/how-long-does-a-drone-battery-last-what-you-need-to-know/>). NeuronRain theoretical VREPAT (Voter Received Encrypted Paper Audit Trail) voting machine for Drone EVMs envisages an One Time Password facility (preferably non-digital: Currency OTP) and Voter Receipt of an Encrypted Audit Trail for ensuring free, fair and unique Vote.

****Can NeuronRain be deployed on Mobile processors?****

Presently mobile OSes are not supported. But that should not be difficult. Similar to Android which is a linux variant, NeuronRain can be cross-compiled for a mobile architecture.

****Are there any realworld usecases for applicability of machine learning in linux kernel?****

809. NeuronRain Usecases - Program Analysis, Kernel Analytics, Software Analytics, Fraud Analytics, Network Traffic and Cybercrimes/Malware/Worms/Bots/Virus Analyzers, Faraday Cageing - (this section is an extended unifying draft of theory and feature in AstroInfer, USBmd, VIRGO, KingCobra, GRAFIT, Acadpdrfts, Krishna_iResearch_DoxygenDocs) - related to all sections on Cybercrime analytics

Yes. Some usecases are described in https://github.com/shrinivaasanka/Grafit/blob/master/EnterpriseAnalytics_with_NeuronRain.pdf. Apart from these, Pagefault data and on-demand paging reference pattern for each application can be analyzed for unusual behaviour and malware infection. Malware have abnormal address reference patterns than usual applications. Antivirus example: Malicious code attacks could be isolated by comparison of Valgrind/Callgrind/FTrace callgraphs (and their centrality measures) of infected and clean kernels for some commandlines - Graph similarity measures include isomorphism, edit distance, GSpan-frequent subgraphs among others. Cybercrimes mostly are categorized to: viri, worms, spoofs, identity thefts, phishing attacks by injecting script malware in HTML/DOM, Keystroke loggers capturing RF from keyboards, DDOS attacks bringing down a network, Van Eck phreaking by RF (radio frequency) emissions from monitors of electronic devices (example: RF emissions in GHz range from certain classes of Li-ion batteries, LED bulbs and other electronic instruments interfere with mobile broadband spectrum and cause RF resonance boom. LED lights simulate natural white light by mixing Red-Blue-Green LED lights on Phosphor alloy ballast and are known to cause Blue light hazards which are spikes in blue light high frequency emission - 440 nanometers or 681346.49545 GHz - colliding with mobile spectrum in GHz band - https://www.archlighting.com/technology/blue-light-hazard-and-leds-fact-or-fiction_o). RF Resonance boom hazards by mobile spectrum-LED-battery-electromagnetic devices RF transmission collision could be mitigated by replacing LEDs by plasma and filament lighting (tubelights and tungsten) and Faraday Cageing - insulators like wood, plastic, paper prohibit radio frequencies and concrete walls curtail less - though less feasible in practice because of their abundance and indispensability. Most datacentres storing unique IDs of users on cloud have many feet thick concrete walls. Cybercrime and Fraud Analytics in NeuronRain focuses mostly on: USBWWAN and Kernel Ftrace callgraph traffic analysis, Digital watermarking of visuals, Spending analysis and outlier detection for credit card and financial datasets, Susceptible-Infected-Recovered Cellular Automaton Random Graph model of Cybercrimes (which is presently based on CoronaVirus 2019 pandemic dataset and could be replaced by Cybercrime or any other bigdata) - spread of XSS worms by recursive address book lookups in social networks/mail services and less immune ISP infrastructure is exactly similar to SIR random graphs of pandemics.

1146. (THEORY and FEATURE) Parallels between Biological Pandemics and Electronic Cybercrimes, Cellular Automaton Graph, Period Three Theorem, Social Network Analysis, Byzantine Fault Tolerance, Antivirus software versus vaccination, Consensus - related to all sections on Cybercrime analytics, Chaos, Cellular Automaton Graph Space filling model of Cybercrimes and Pandemics in Electronic and Social networks - 10,12,16,17 June 2021

Spread of Pandemics in social networks and Cybercrimes in IT systems have similarities - NeuronRain envisages Cellular Automaton Graph chaotic spacefilling for modelling transmission of pandemics and cybercrimes. By Period three theorem in non-linear dynamics any sequence having periodicity 3 could have indefinite number of larger periodicities. COVID19 cellular automaton infection graph if viewed as sequence of SIR data already has exhibited 2 peaks and a third peak would theoretically imply indefinite number of further waves. Cellular automaton graph model of pandemics and cybercrimes connects points on grid through which disease or cybercrime is transmitted - Increment and Decrement growth rules increase and decrease point values depending on whether neighbour nodes are Susceptible (Increment and Decrement), Infected (Increment) or Recovered (Decrement). CAGraph is dynamic graph and edges are removed if values reach zero and created if values are non-zero. Byzantine Fault Tolerance (BFT) in distributed systems formalize the resilience and tolerance of a cloud of IT systems in the event of faulty nodes (e.g affected by cybercrimes). BFT solution by [Lamport-Shostak-Pease -

<https://web.archive.org/web/20170205142845/http://lampport.azurewebsites.net/pubs/byz.pdf>] for 2 Generals, 1 Traitor problem guarantees fault-tolerant cloud (i.e nodes of the cloud reach consensus on the message) if $t < n/3$ for a distributed system of n nodes and t faulty nodes. Each node broadcasts a message to peer nodes which could be corrupted by cybercrimes. Proof of $t < n/3$ bound is by following reasoning:

(*) For 3 groups of nodes P,Q and R - P is Faulty (33%) and Q and R are Honest (67%). P sends corrupted messages to Q and R. Q cannot discern if the corruption happened at P or R while R cannot distinguish if corrupt message was originated from P or Q.

Byzantine Fault Tolerance for previous cybercrime example could be reduced to Pandemic Cellular Automaton ER-SIR CAGraph social network by following:

(*) Pandemic is vector borne (Air, Water, Faeces[Potential intestinal infection and faecal-oral transmission of SARS-CoV-2-<https://www.nature.com/articles/s41575-021-00416-6>], Saliva, Phlegm, Animals) and 3 social groups of nodes in ER-SIR CAGraph could be P(Infected), Q(Uninfected), R(Uninfected) and role of corrupted message in BFT solution is accomplished by disease bearing vectors. P infects (virus is the message) Q and R. Q cannot discern if infection originated from P or R while R cannot distinguish if infection originated from P or Q.

From previous BFT reduction, it could be sufficient if 67% neighbours of a node in CAGraph are protected (by vaccination in social network or by securing nodes in electronic network) so as to contain cybercrimes or pandemics - BFT reduction is obvious if CAGraph has lot of triangles - vertices of each triangle enact 2 generals,1 traitor BFT solution. Each vertex of CAGraph has 8 neighbours and 67% of its (5.28) uninfected neighbours are sufficient for fault tolerance in social network and electronic network. Most IT systems are connected by grids and CAGraph formalism readily applies (There are some non-BFT solutions to resolve fault - e.g failed ATM transactions could be reconciled if network of ATMs keep track of serial numbers of currency dispensed and thereby maintaining money trail audit). COVID19 has fatality rate of 1% implying 99% population is protected statistically despite infection while vaccine efficacy has a maximum of 95% which is a paradox. While social distancing might contain spread in human social networks, proximity is irrelevant for IT systems.

1148. (THEORY and FEATURE) Decidability of Intrinsic Merit in general case - related to 801 and all sections on Merit versus Fame, LTFs and PTFs, BKS Conjecture, Consensus versus Intrinsic merit, Byzantine Fault Tolerance, Condorcet Jury Theorem and its variants, Complexity theoretic aspects of merit, Quantum Computation - 24 June 2021

By BKS conjecture, there exists an LTF or PTF which is stabler than boolean majority and thus resilient to voting errors. Defining merit has been a subject of debate and following are two accepted ways of it:

(1148.1) By consensus - everyone agrees on merit of an entity judged (or) everyone votes "yes"

(1148.2) No voting - there is an absolute 100% perfect universal LTF or PTF which everyone uses as a standard to measure merit (quest for such an LTF or PTF is elusive and hinges on BKS Conjecture) - realworld examples of LTFs/PTFs are contests,interviews,examinations which are far from being errorfree.

In Byzantine Fault Tolerance which tolerates faults by consensus,all nodes in a cloud agree on value of a message despite corruption - in other words:

(*) Consensus does not imply intrinsic merit - universal agreement on some value does not imply merit

(*) But converse is true - Intrinsic merit implies Consensus - everyone must agree

Hypothetically assume a majority voting on merit of an entity by infinite number of voters - Each voter votes on merit of an entity as "Good" or "Bad". By CJT-

Black-Ladha-Margulis-Russo theorems on sharp thresholds if each voter decides correctly on merit by $> 50\%$ probability, group decision tends to 100% and everyone agrees on merit in the infinity. This is counterintuitive because if infinite majority is a recursively enumerable problem (RE - Turing machine computing infinite majority might loop forever), merit has a definitive outcome (if p -bias is 0 for all voters) and 100% consensus on merit is attained by 1148.1. By a recent result $RE=MIP^*$ and eventually recursively enumerable infinite majority problem is solvable by quantum computers.

1152. (THEORY and FEATURE) Integer Factorization, Boolean Majority-VoterSAT composition, KRW Conjecture, CJT-Black-Ladha-Margulis-Russo sharp thresholds for majority, BQP as VoterSAT, Derandomization, Quantum decoherence - a hypothetical scenario - related to 801 and all sections on Factorization, KRW communication complexity and Majority Voting - 19 July 2021, 20 July 2021, 21 July 2021, 5 September 2021

1152.1 Quoting 801:

"...Boolean composition of leaves of Boolean majority circuit and individual VoterSATs has a curious implication when all voters are quantum voters (all VoterSATs are in BQP): By Condorcet Jury Theorem and its later versions by [Black] and [Ladha] and Margulis-Russo sharp threshold at p -bias > 0.5 , infinite majority + BQP VoterSAT boolean composition tends to goodness 1 or quantum world derandomizes to P (by phenomena of Decoherence, Wavefunction collapse) implying one of the superimposed quantum states of some amplitude (defined in Hilbert space) is chosen for certainty by nature. Majority is in non-uniform NC1 and thus in P which in turn is in BPP and the larger class BQP which implies boolean majority is in BQP. If boolean composition of BQP majority function and BQP voter SATs are relativizable (conjectural assumption: boolean composition is equivalent to oracle access Turing machines) as BQP^{BQP} (BQP majority function having oracle access to BQP voter SATs) and since BQP is low for itself, $BQP^{BQP} = BQP$. By CJT-Black-Ladha-Margulis-Russo threshold theorems for infinite majority quantum boolean composition tends to 100% goodness or in other words BQP asymptotically dissipates quantum error and derandomizes to P...."

1152.2 Conjecture: Boolean composition of BQP majority and BQP voter SATs is relativizable - Draft Proof outline: Compute boolean majority function on a BQP Turing machine whose leaves have oracle access to infinite number of BQP VoterSAT Turing machines. This oracle machine simulates boolean composition as BQP^{BQP} relativization.

1152.3 Some peculiar conclusion is arrived at if all VoterSATs depend on Shor's BQP factorization: Every voter factorizes same integer N by Shor's BQP factorization and votes 1 if factors are correct and 0 if factors are wrong. By definition of BQP more than $2/3$ of infinite voters factorize N correctly (67%).

1152.4 But CJT and its variants for infinite majority imply 100% correct factorization because each VoterSAT has p -bias error $\leq 1/3$ and group decision correctness (whether factors of N are right or not) tends to 100% probability implying Shor's BQP factorization derandomizes to P (or) success of BQP factorization is amplified to exact and CJT implies quantum decoherence.

1152.5 Factorization is known to be in complexity class ZPP^{BQNC} (<https://arxiv.org/abs/quant-ph/0006004>, ZPP = intersection of one-sided error classes RP and coRP). Thus factorization has been already shown to have semiclassical algorithm querying quantum oracle. If VoterSATs for every voter are in ZPP^{BQNC} , depth-2 infinite majority voting earlier is in nonuniform $NC^{ZPP^{BQNC}}$. By definition of ZPP and $BQNC$, each voter finds factors correctly in at least 67% of the trials (ZPP returns 100% correct answer but with polynomial overhead while $BQNC$ is $> 67\%$ correct) and therefore by Condorcet Jury Theorem and Margulis-Russo thresholds, infinite majority asymptotically decides factors 100% correctly, potentially derandomizing semiclassical ZPP^{BQNC} to classical P or NC.

1152.6 Previous derandomization algorithm is relevant to any bounded error VoterSAT and not just limited to BQP factorization.

NeuronRain Licensing:

How is NeuronRain code licensed? Can it be used commercially? Is technical support available?

(*) NeuronRain repositories are spread across following SourceForge, GitHub and GitLab URLs:

(*) NeuronRain Research -
http://sourceforge.net/users/ka_shrinivaasan

(*) NeuronRain Green - <https://github.com/shrinivaasanka>

(*) NeuronRain Green (replicated) -
<https://gitlab.com/shrinivaasanka>

(*) All repositories of NeuronRain (in Sourceforge, GitLab and GitHub) excluding Grafit course materials, Krishna_iResearch_DoxygenDocs NeuronRain PDF/HTML documentation and NeuronRain Design Documents are GPLv3 copyleft licensed.

(*) Grafit course materials (includes NeuronRain Design Documents) and Krishna_iResearch_DoxygenDocs PDF/HTML documentation (in SourceForge, GitLab and GitHub) are Creative Commons 4.0 NCND licensed.

(*) As per license terms, NeuronRain code has no warranty. Any commercial derivative is subject to clauses of GPLv3 copyleft licensing. Please refer to <https://www.gnu.org/licenses/gpl-faq.html#GPLCommercially> for licensing terms for commercial derivatives ("Free means freedom, not price"). GPLv3 copyleft license mandates any derived source code to be open sourced (Sections on Conveying Verbatim Copies, Conveying Modified Source and Non-Source versions - <https://www.gnu.org/licenses/gpl-3.0.en.html>). Present model followed is as below:

(*) NeuronRain repositories also have implementations of author's publications and drafts - respective GPLv3 and Creative Commons 4.0 NCND clauses apply

(*) Premium Technical support for NeuronRain codebases is provided only on direct request based on feasibility and time constraints.

(*) GPLv3 license terms do not prohibit pricing.

(*) Commercial derivatives (for individuals or organizations who clone NeuronRain repositories and make modifications for commercial use) if any have to be GPLv3 copyleft and Creative Commons 4.0 NCND compliant.

(*) Drone code (Autonomous Delivery, EVM) in NeuronRain is a conceptual implementation only (Python DroneSDK and Linux Kernel PXRC Flight Controller driver code have not been tested on a licensed drone but only on JMAVSIM simulator)

What is dual licensing?

Closedsource, proprietary, premium version derived and completely different from NeuronRain Open Source codebases is in research, architecture and development - JAIMINI. Some features of JAIMINI have been Opensourced and made part of NeuronRain. Only opensource codebases of NeuronRain in SourceForge, GitHub and GitLab are copyleft licensed under GPL v3 and Creative Commons 4.0 NCND. Dual licensing implies dichotomous licensing - NeuronRain is free (open) and free (without price) while Closedsource is at premium.

Who owns NeuronRain repositories?

NeuronRain GitHub, GitLab and SourceForge repositories licenses for Krishna iResearch Open Source Products repositories at:

http://sourceforge.net/users/ka_shrinivaasan,

<https://github.com/shrinivaasanka>,

<https://gitlab.com/shrinivaasanka>,

https://www.openhub.net/accounts/ka_shrinivaasan

Krishna iResearch GitHub Organization: <https://github.com/Krishna-iResearch>

Personal website(research): <https://sites.google.com/site/kuja27/> (Deleted because of Google Classic Sites Discontinuation and Mirrored at

https://github.com/shrinivaasanka/Krishna_iResearch_DoxygenDocs/blob/master/

kuja27_website_mirrored/site/kuja27/ and similar relative paths in GitLab and SourceForge)

****are owned by:****

P.R.S.Kannan and Alamelu Kannan (alias Rukmini Kannan)

[Dedicated to memory of late P.R.S.Kannan -

https://twitter.com/ka_shrinivaasan/status/1504761670794883073]

Emails: preskannan@gmail.com, alamelukannan1941@gmail.com

Licensing 1 - Creative Commons 4.0 No Derivatives Non Commercial for NeuronRain Krishna_iResearch_DoxygenDocs SourceForge, GitHub and GitLab HTML/PDF documentations and Grafit Open Learning Course Notes (GRAFIT open learning course material includes all NeuronRain Design Documents which are frequently updated commentaries on NeuronRain code commits and related theory) : https://github.com/shrinivaasanka/Krishna_iResearch_DoxygenDocs/blob/master/Creative%20Commons%20%E2%80%94%20Attribution-NonCommercial-NoDerivatives%204.0%20International%20%E2%80%94%20CC%20BY-NC-ND%204.0.html (replicated in SourceForge and GitLab)

Licensing 2 - GPL v3.0 for other NeuronRain GitLab, GitHub and SourceForge repositories (excluding GRAFIT open learning repositories, NeuronRain Design Documents and Krishna_iResearch_DoxygenDocs HTML/PDF documentation which are Creative Commons 4.0 NCND licensed): [https://github.com/shrinivaasanka/Krishna_iResearch_DoxygenDocs/blob/master/The%20GNU%20General%20Public%20License%20v3.0%20-%20GNU%20Project%20-%20Free%20Software%20Foundation%20\(FSF\).html](https://github.com/shrinivaasanka/Krishna_iResearch_DoxygenDocs/blob/master/The%20GNU%20General%20Public%20License%20v3.0%20-%20GNU%20Project%20-%20Free%20Software%20Foundation%20(FSF).html) (replicated in SourceForge and GitLab)

Previous license ownership attribution supersedes all other copyleft notice headers within NeuronRain GitLab, GitHub and SourceForge source code files and design documents.

****and contributed by:****

Author:

K.Srinivasan

Emails: ka.shrinivaasan@gmail.com, shrinivas.kannan@gmail.com, kashrinivaasan@live.com

NeuronRain mailing lists: <https://sourceforge.net/p/virgo-linux/mailman/virgo-linux-mailing-list/> (not recently updated),

<https://in.groups.yahoo.com/neo/groups/grafitopenlearning/info> (archived because of Verizon-Oath-Yahoo-Apollo groups shutdown)

Contributor has no government, industry and academic affiliations (as JRF) and does not accrue any monetary benefit for Opensource research and development effort (contribution is a charity). Name "Krishna iResearch" is non-funded, not a commercially registered entity but only a profile name registered in SourceForge and later in GitHub and GitLab. Because of certain cybercrimes, mistaken identity and copyleft violation problems in the past (and possibility of a signature forgery too which is neither confirmed nor denied), sumptuous id proofs of the author have been uploaded to <https://sourceforge.net/projects/acadpdrafts/files/> and https://sites.google.com/site/kuja27/CV_of_SrinivasanKannan_alias_KaShrinivaasan_alias_ShrinivasKannan.pdf (Deleted and Mirrored at https://github.com/shrinivaasanka/Krishna_iResearch_DoxygenDocs/blob/master/kuja27_website_mirrored/site/kuja27/CV_of_SrinivasanKannan_alias_KaShrinivaasan_alias_ShrinivasKannan.pdf)